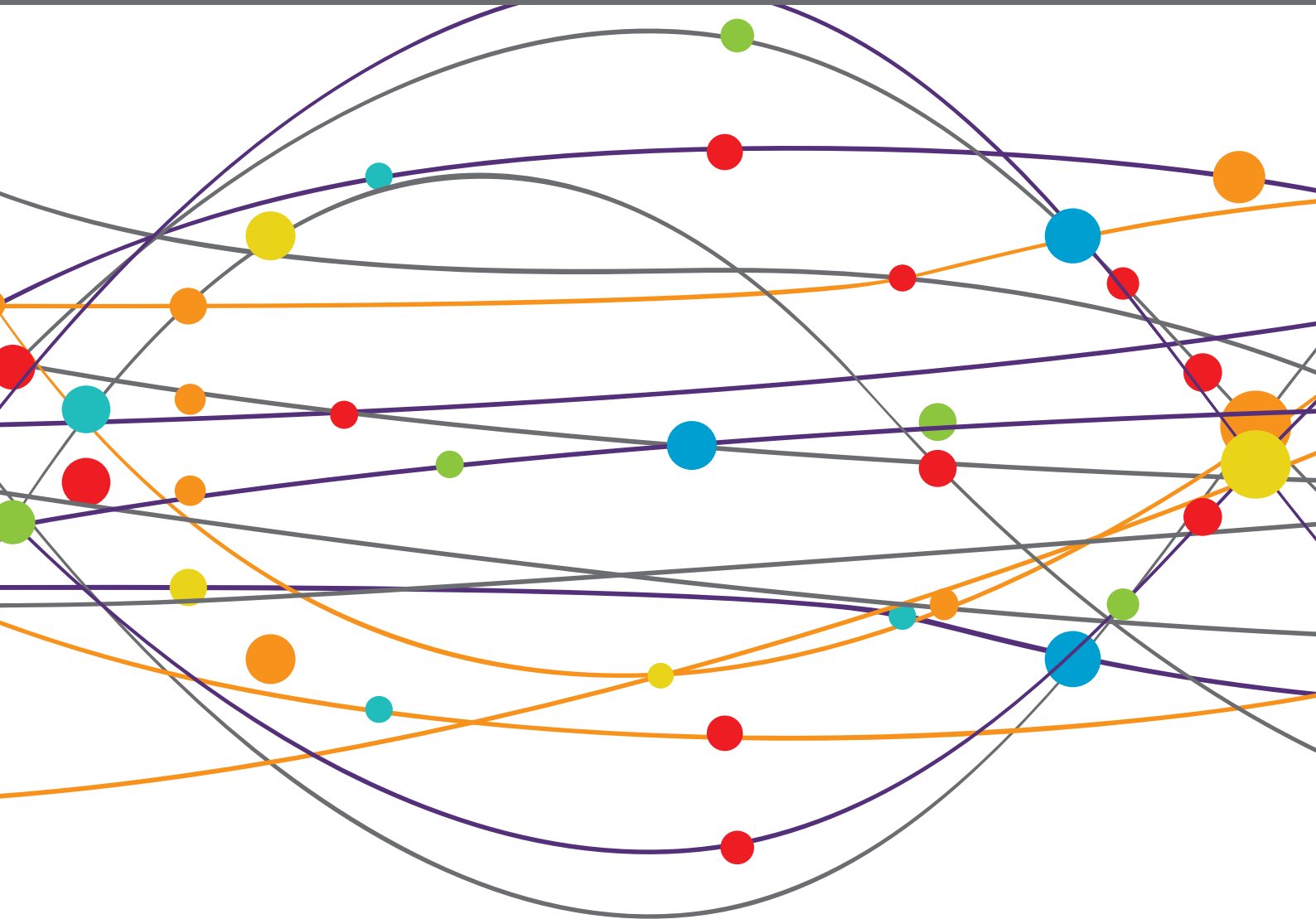


OROFACIAL FUNCTIONS: FROM NEURAL MECHANISMS TO REHABILITATION

EDITED BY: Teresa Lever, Limor Avivi-Arber and Kazutaka Takahashi
PUBLISHED IN: Frontiers in Neurology, Frontiers in Neuroscience,
Frontiers in Physiology, Frontiers in Cellular Neuroscience,
Frontiers in Human Neuroscience,
Frontiers in Aging Neuroscience and
Frontiers in Integrative Neuroscience





frontiers

Frontiers eBook Copyright Statement

The copyright in the text of individual articles in this eBook is the property of their respective authors or their respective institutions or funders. The copyright in graphics and images within each article may be subject to copyright of other parties. In both cases this is subject to a license granted to Frontiers.

The compilation of articles constituting this eBook is the property of Frontiers.

Each article within this eBook, and the eBook itself, are published under the most recent version of the Creative Commons CC-BY licence.

The version current at the date of publication of this eBook is CC-BY 4.0. If the CC-BY licence is updated, the licence granted by Frontiers is automatically updated to the new version.

When exercising any right under the CC-BY licence, Frontiers must be attributed as the original publisher of the article or eBook, as applicable.

Authors have the responsibility of ensuring that any graphics or other materials which are the property of others may be included in the CC-BY licence, but this should be checked before relying on the CC-BY licence to reproduce those materials. Any copyright notices relating to those materials must be complied with.

Copyright and source acknowledgement notices may not be removed and must be displayed in any copy, derivative work or partial copy which includes the elements in question.

All copyright, and all rights therein, are protected by national and international copyright laws. The above represents a summary only. For further information please read Frontiers' Conditions for Website Use and Copyright Statement, and the applicable CC-BY licence.

ISSN 1664-8714

ISBN 978-2-83250-043-9

DOI 10.3389/978-2-83250-043-9

About Frontiers

Frontiers is more than just an open-access publisher of scholarly articles: it is a pioneering approach to the world of academia, radically improving the way scholarly research is managed. The grand vision of Frontiers is a world where all people have an equal opportunity to seek, share and generate knowledge. Frontiers provides immediate and permanent online open access to all its publications, but this alone is not enough to realize our grand goals.

Frontiers Journal Series

The Frontiers Journal Series is a multi-tier and interdisciplinary set of open-access, online journals, promising a paradigm shift from the current review, selection and dissemination processes in academic publishing. All Frontiers journals are driven by researchers for researchers; therefore, they constitute a service to the scholarly community. At the same time, the Frontiers Journal Series operates on a revolutionary invention, the tiered publishing system, initially addressing specific communities of scholars, and gradually climbing up to broader public understanding, thus serving the interests of the lay society, too.

Dedication to Quality

Each Frontiers article is a landmark of the highest quality, thanks to genuinely collaborative interactions between authors and review editors, who include some of the world's best academicians. Research must be certified by peers before entering a stream of knowledge that may eventually reach the public - and shape society; therefore, Frontiers only applies the most rigorous and unbiased reviews.

Frontiers revolutionizes research publishing by freely delivering the most outstanding research, evaluated with no bias from both the academic and social point of view. By applying the most advanced information technologies, Frontiers is catapulting scholarly publishing into a new generation.

What are Frontiers Research Topics?

Frontiers Research Topics are very popular trademarks of the Frontiers Journals Series: they are collections of at least ten articles, all centered on a particular subject. With their unique mix of varied contributions from Original Research to Review Articles, Frontiers Research Topics unify the most influential researchers, the latest key findings and historical advances in a hot research area! Find out more on how to host your own Frontiers Research Topic or contribute to one as an author by contacting the Frontiers Editorial Office: frontiersin.org/about/contact

OROFACIAL FUNCTIONS: FROM NEURAL MECHANISMS TO REHABILITATION

Topic Editors:

Teresa Lever, University of Missouri, United States

Limor Avivi-Arber, Faculty of Dentistry, University of Toronto, Canada

Kazutaka Takahashi, The University of Chicago, United States

Citation: Lever, T., Avivi-Arber, L., Takahashi, K., eds. (2022). Orofacial Functions: From Neural Mechanisms to Rehabilitation. Lausanne: Frontiers Media SA. doi: 10.3389/978-2-83250-043-9

Table of Contents

- 08** *Mandibular Vertical Growth Deficiency After Botulinum-Induced Hypotrophy of Masticatory Closing Muscles in Juvenile Nonhuman Primates*
Hak-Jin Kim, Hye-Jin Tak, Joo-Won Moon, Sang-Hoon Kang, Seong Taek Kim, Jinquan He, Zhenguo Piao and Sang-Hwy Lee
- 21** *The Adult Ts65Dn Mouse Model of Down Syndrome Shows Altered Swallow Function*
Tiffany J. Glass, Luke Carmichael V. Valmadrid and Nadine P. Connor
- 32** *A Dynamic Jaw Model With a Finite-Element Temporomandibular Joint*
Benedikt Sagl, Martina Schmid-Schwap, Eva Piehslinger, Michael Kundi and Ian Stavness
- 44** *TRPV1 and TRPV1-Expressing Nociceptors Mediate Orofacial Pain Behaviors in a Mouse Model of Orthodontic Tooth Movement*
Sheng Wang, Martin Kim, Zayd Ali, Katherine Ong, Eung-Kwon Pae and Man-Kyo Chung
- 55** *Corrigendum: TRPV1 and TRPV1-Expressing Nociceptors Mediate Orofacial Pain Behaviors in a Mouse Model of Orthodontic Tooth Movement*
Sheng Wang, Martin Kim, Zayd Ali, Katherine Ong, Eung-Kwon Pae and Man-Kyo Chung
- 57** *Multimodal Sensory Stimulation of the Masseter Muscle Reduced Precision but Not Accuracy of Jaw-Opening Movements*
Birgitta Wiesinger, Birgitta Häggman-Henrikson, Anton Eklund, Anders Wänman and Fredrik Hellström
- 66** *Effects of Chronic and Experimental Acute Masseter Pain on Precision Biting Behavior in Humans*
Samaa Al Sayegh, Annie Borgwardt, Krister G. Svensson, Abhishek Kumar, Anastasios Grigoriadis and Nikolaos Christidis
- 76** *Preceding Administration of Minocycline Suppresses Plastic Changes in Cortical Excitatory Propagation in the Model Rat With Partial Infraorbital Nerve Ligation*
Manabu Zama, Satoshi Fujita, Yuka Nakaya, Morio Tonogi and Masayuki Kobayashi
- 85** *Peripheral and Central Mechanisms of Persistent Orofacial Pain*
Masamichi Shinoda, Asako Kubo, Yoshinori Hayashi and Koichi Iwata
- 95** *The Better to Eat You With: Bite Force in the Naked Mole-Rat (Heterocephalus glaber) Is Stronger Than Predicted Based on Body Size*
Natalee J. Hite, Cody Germain, Blake W. Cain, Mason Sheldon, Sai Saketh Nandan Perala and Diana K. Sarko
- 109** *Effect of Sudden Deprivation of Sensory Inputs From Periodontium on Mastication*
Anastasios Grigoriadis, Abhishek Kumar, Magnus K. Åberg and Mats Trulsson

- 118 ***Specific Vagus Nerve Lesion Have Distinctive Physiologic Mechanisms of Dysphagia***
François D. H. Gould, Andrew R. Lammers, Christopher J. Mayerl and Rebecca Z. German
- 126 ***Genetic Taster Status as a Mediator of Neural Activity and Swallowing Mechanics in Healthy Adults***
Angela M. Dietsch, Ross M. Westemeyer, William G. Pearson Jr. and Douglas H. Schultz
- 137 ***Tongue Force Training Induces Plasticity of the Lingual Motor Cortex in Young Adult and Aged Rats***
Miranda J. Cullins, Julie M. Wenninger, Jared S. Cullen, John A. Russell, Jeffrey A. Kleim and Nadine P. Connor
- 145 ***Functional Adaptation of Oromotor Functions and Aging: A Focused Review of the Evidence From Brain Neuroimaging Research***
Chia-Shu Lin
- 161 ***Subcortical Brain Abnormalities and Clinical Relevance in Patients With Hemifacial Spasm***
Hui Xu, Chenguang Guo, Feifei Luo, Romina Sotoodeh, Ming Zhang and Yuan Wang
- 169 ***Functional Analysis of Rhythmic Jaw Movements Evoked by Electrical Stimulation of the Cortical Masticatory Area During Low Occlusal Loading in Growing Rats***
Phyo Thura Aung, Chiho Kato, Yasunori Abe, Takuya Ogawa, Hideyuki Ishidori, Akiyo Fujita, Hidemasa Okihara, Satoshi Kokai and Takashi Ono
- 185 ***Persistent Feeding and Swallowing Deficits in a Mouse Model of 22q11.2 Deletion Syndrome***
Lauren Welby, Hailey Caudill, Gelila Yitsege, Ali Hamad, Filiz Bunyak, Irene E. Zohn, Thomas Maynard, Anthony-Samuel LaMantia, David Mendelowitz and Teresa E. Lever
- 202 ***Prefrontal Consolidation and Compensation as a Function of Wearing Denture in Partially Edentulous Elderly Patients***
Noriyuki Narita, Tomohiro Ishii, Sunao Iwaki, Kazunobu Kamiya, Masakazu Okubo, Takeshi Uchida, Ikuo Kantake and Koh Shibutani
- 217 ***Functional Connectivity Evoked by Orofacial Tactile Perception of Velocity***
Yingying Wang, Fatima Sibaii, Rebecca Custead, Hyuntaek Oh and Steven M. Barlow
- 230 ***An fMRI Study of the Brain Network Involved in Teeth Tapping in Elderly Adults***
T. Kobayashi, H. Fukami, E. Ishikawa, K. Shibata, M. Kubota, H. Kondo and Y. Sahara
- 247 ***Model-Based and Model-Free Analyses of the Neural Correlates of Tongue Movements***
Peter Sörös, Sarah Schäfer and Karsten Witt
- 262 ***A Systematic Review of Physical Rehabilitation of Facial Palsy***
Annabelle Vaughan, Danielle Gardner, Anna Miles, Anna Copley, Rachel Wenke and Susan Coulson

- 275 Masticatory Adaptation to Occlusal Changes**
Pierre Bourdiol, Martine Hennequin, Marie-Agnes Peyron and Alain Woda
- 292 The Effect of Granisetron on Sensory Detection and Pain Thresholds in Facial Skin of Healthy Young Males**
Malin Ernberg, Anna Wieslander Fältmars, Milad Hajizadeh Kopayeh, Sofia Arzt Wallén, Therese Cankalp and Nikolaos Christidis
- 302 Swallow Motor Pattern Is Modulated by Fixed or Stochastic Alterations in Afferent Feedback**
Suzanne N. King, Tabitha Y. Shen, M. Nicholas Musselwhite, Alyssa Huff, Mitchell D. Reed, Ivan Poliacek, Dena R. Howland, Warren Dixon, Kendall F. Morris, Donald C. Bolser, Kimberly E. Iceman and Teresa Pitts
- 313 Characterizing Motor Control of Mastication With Soft Actor-Critic**
Amir H. Abdi, Benedikt Sagl, Venkata P. Srungarapu, Ian Stavness, Eitan Prisman, Purang Abolmaesumi and Sidney Fels
- 330 A Case of Recurrent Painful Ophthalmoplegic Neuropathy**
Yaping Yan, Bo Zhang, Zhuocong Lou, Kaiming Liu, Ming Lou, Meiping Ding and Yongfeng Xu
- 335 Different Therapeutic Effects of CO₂ and Diode Laser Irradiation on Tooth Movement-Related Pain**
Takako Tsuchiya, Naoya Hasegawa, Misato Yugawa, Au Sasaki, Naoto Suda and Kazunori Adachi
- 350 Differentiation of Feeding Behaviors Based on Masseter and Supra-Hyoid Muscle Activity**
Fumiko Uehara, Kazuhiro Hori, Kazuhiro Murakami, Jumpei Okawa and Takahiro Ono
- 358 Toll-Like Receptor 4 in the Rat Caudal Medulla Mediates Tooth Pulp Inflammatory Pain**
Helena F. Filippini, Graziella R. Molska, Maryam Zanjir, Yamini Arudchelvan, Siew-Ging Gong, Maria M. Campos, Limor Avivi-Arber and Barry J. Sessle
- 369 Functional Connectivity Between the Trigeminal Main Sensory Nucleus and the Trigeminal Motor Nucleus**
Mohammed Slaoui Hasnaoui, Isabel Arsenault, Dorly Verdier, Sami Obeid and Arlette Kolta
- 391 Brain Cortex Activity in Children With Anterior Open Bite: A Pilot Study**
Claudia Restrepo, Paola Botero, David Valderrama, Kelly Jimenez and Rubén Manrique
- 399 Effect of Deep Brain Stimulation on Swallowing Function: A Systematic Review**
Huiyan Yu, Kazutaka Takahashi, Lisa Bloom, Samuel D. Quaynor and Tao Xie
- 412 Modulation of Intermuscular Beta Coherence in Different Rhythmic Mandibular Behaviors**
Evan R. Usler, Xiaomei Wei, Meg Simione, Brian Richburg, Kaila L. Stipancic and Jordan R. Green
- 422 Chewing Efficiency, Global Cognitive Functioning, and Dentition: A Cross-sectional Observational Study in Older People With Mild Cognitive Impairment or Mild to Moderate Dementia**
Suzanne Delwel, Andrea B. Maier, Donya Parvaneh, Jesse Meijers, Erik J. A. Scherder and Frank Lobbezoo

- 432 *Small Posterior Cranial Fossa and Cerebellopontine Cistern Volumes Are Associated With Bilateral Trigeminal Neuralgia***
Jiayu Liu, Ruen Liu, Bo Liu, Jingru Zhou, Cungang Fan, Feng Jiao, Dongliang Wang, Fang Li and Bo Hei
- 439 *Hyperalgesia and Central Sensitization in Subjects With Chronic Orofacial Pain: Analysis of Pain Thresholds and EEG Biomarkers***
Andrea Baroni, Giacomo Severini, Sofia Straudi, Sergio Buja, Silvia Borsato and Nino Basaglia
- 450 *The Pain-to-Well-Being Relationship in Patients Experiencing Chronic Orofacial Pain***
Kanokporn Bhalang, Beat Steiger, Nenad Lukic, Aleksandra Zumbrunn Wojczyńska, Ray S. Hovijitra and Dominik A. Ettlin
- 463 *Adaptive Stress Coping in Awake Bruxism***
Xabier Ander Soto-Goñi, Francisco Alen, Leticia Buiza-González, Danielle Marcolino-Cruz, Teresa Sánchez-Sánchez, Ignacio Ardizzone-García, Fernando Aneiros-López and Laura Jiménez-Ortega
- 472 *Neuromotor Speech Recovery Across Different Behavioral Speech Modifications in Individuals Following Facial Transplantation***
Marziye Eshghi, Bridget J. Perry, Brian Richburg, Hayden M. Ventresca, Bohdan Pomahac and Jordan R. Green
- 484 *Electromyographic Patterns and the Identification of Subtypes of Awake Bruxism***
Ubirakitan Maciel Monteiro, Vinicius Belém Rodrigues Barros Soares, Caio Belém Rodrigues Barros Soares, Tiago Coimbra Costa Pinto, Rosana Christine Cavalcanti Ximenes and Marcelo Araújo Cairrão Rodrigues
- 492 *Functional Magnetic Resonance Connectivity in Patients With Temporomandibular Joint Disorders***
Felice Festa, Chiara Rotelli, Antonio Scarano, Riccardo Navarra, Massimo Caulo and Monica Macri
- 502 *Risk Score for Predicting Dysphagia in Patients After Neurosurgery: A Prospective Observational Trial***
Li Zeng, Yu Song, Yan Dong, Qian Wu, Lu Zhang, Lei Yu, Liang Gao and Yan Shi
- 511 *The Role of White Matter in the Neural Control of Swallowing: A Systematic Review***
Ann Alvar, Rachel Hahn Arkenberg, Bethany McGowan, Hu Cheng and Georgia A. Malandraki
- 539 *Coordination of Respiration, Swallowing, and Chewing in Healthy Young Adults***
Naohito Hao, Anna Sasa, Sirima Kulvanich, Yuta Nakajima, Kouta Nagoya, Jin Magara, Takanori Tsujimura and Makoto Inoue
- 554 *Event-Related Desynchronization and Corticomuscular Coherence Observed During Volitional Swallow by Electroencephalography Recordings in Humans***
Satoko Koganemaru, Fumiya Mizuno, Toshimitsu Takahashi, Yuu Takemura, Hiroshi Irisawa, Masao Matsushashi, Tatsuya Mima, Takashi Mizushima and Kenji Kansaku

563 Effectiveness of Standard Oral Care Plan During Hospital Stay in Individuals With Brain Injury

Simple F. Kothari, Gustavo G. Nascimento, Mille B. Jakobsen, Jørgen F. Nielsen and Mohit Kothari

572 Functional Role of Suprahyoid Muscles in Bolus Formation During Mastication

Anna Sasa, Sirima Kulvanich, Naohito Hao, Reiko Ita, Masahiro Watanabe, Taku Suzuki, Jin Magara, Takanori Tsujimura and Makoto Inoue

586 A Strength Endurance Exercise Paradigm Mitigates Deficits in Hypoglossal-Tongue Axis Function, Strength, and Structure in a Rodent Model of Hypoglossal Motor Neuron Degeneration

Erika R. Murphy, Rebecca Thompson, Kate L. Osman, Chandler Haxton, Margaret Brothers, Li Lee, Kristen Warncke, Catherine L. Smith, Amy N. Keilholz, Ali Hamad, Mojgan Golzy, Filiz Bunyak, Lixin Ma, Nicole L. Nichols and Teresa E. Lever



Mandibular Vertical Growth Deficiency After Botulinum-Induced Hypotrophy of Masticatory Closing Muscles in Juvenile Nonhuman Primates

Hak-Jin Kim¹, Hye-Jin Tak², Joo-Won Moon², Sang-Hoon Kang³, Seong Taek Kim⁴, Jinquan He⁵, Zhenguo Piao⁵ and Sang-Hwy Lee^{6*}

¹ Department of Oral and Maxillofacial Surgery, College of Dentistry, Yonsei University, Seoul, South Korea, ² Oral Science Research Center, College of Dentistry, Yonsei University, Seoul, South Korea, ³ Department of Oral and Maxillofacial Surgery, National Health Insurance Service, Ilsan Hospital, Goyang, South Korea, ⁴ Department of Oral Medicine, College of Dentistry, Yonsei University, Seoul, South Korea, ⁵ Department of Oral and Maxillofacial Surgery, Stomatology Hospital of Guangzhou Medical University, Guangzhou, China, ⁶ Department of Oral and Maxillofacial Surgery, Oral Science Research Center, College of Dentistry, Yonsei University, Seoul, South Korea

OPEN ACCESS

Edited by:

Limor Avivi-Arber,
University of Toronto, Canada

Reviewed by:

Susan W. Herring,
University of Washington,
United States
Masayoshi Kawakami,
Nara Medical University, Japan

*Correspondence:

Sang-Hwy Lee
sanghwy@yuhs.ac

Specialty section:

This article was submitted to
Craniofacial Biology and Dental
Research,
a section of the journal
Frontiers in Physiology

Received: 08 January 2019

Accepted: 08 April 2019

Published: 26 April 2019

Citation:

Kim H-J, Tak H-J, Moon J-W,
Kang S-H, Kim ST, He J, Piao Z and
Lee S-H (2019) Mandibular Vertical
Growth Deficiency After
Botulinum-Induced Hypotrophy
of Masticatory Closing Muscles
in Juvenile Nonhuman Primates.
Front. Physiol. 10:496.
doi: 10.3389/fphys.2019.00496

The purpose of this study was to investigate the relationship between masticatory muscular hypotrophy and mandibular growth in juvenile nonhuman primates (cynomolgus monkeys, *Macaca fascicularis*). We hypothesized that botulinum toxin (BTX)-induced neuro-muscular junctional block and its resultant hypotrophy of masticatory muscles would produce mandibular growth disturbances in size and shape. Ten male cynomolgus monkeys were divided into three groups: group I (control; $n = 3$), group II (unilateral BTX; $n = 4$), and group III (bilateral BTX; $n = 3$). The unilateral or bilateral muscular hypotrophy of major masticatory closing muscles was induced by synchronous BTX application to masseter, medial pterygoid, and temporal muscle. Mandibular growth was tracked by linear, angular, area and volume measurements using three-dimensional (3D) computed tomography imaging before BTX treatment and after 3 and 6 months. After unilateral hypotrophy of masticatory muscles in group II, vertical growth deficiency was prominent on the BTX side, with compensatory overgrowth on the control side. The bilateral muscular hypotrophy in group III also showed smaller ramal height and width than that of control (group I) and control side (group II). Moreover, ramal sagittal angles (posterior tilt) increased on the BTX side of both groups II and III, but coronal angles (lateral tilt) did so on the BTX side of group II, resulting in asymmetry. The results confirmed our hypothesis that functional activity of masticatory closing muscles is closely related to mandibular growth in size and shape of juvenile nonhuman primates. In addition, the focused growth disturbances on the ramal height and posterior-lateral tilt suggested the possible role of masticatory closing muscles for ramal vertical and angular growth vector of the mandible.

Keywords: masticatory muscles, craniofacial, growth, botulinum toxin, computed tomography, mandible, monkey

INTRODUCTION

The bone-muscle relationship may be viewed in terms of structure and function (Cianferotti and Brandi, 2014). Some studies have reported aberrant craniofacial structure after experimental muscular function changes (Boyd et al., 1967; Navarro et al., 1995). However, these growths were also influenced by the secondary effects of scar tissues and their subsequent contractures. This issue can be avoided by the introduction of botulinum toxin (BTX), which blocks the nerve endings of the muscles without scarring (Babuccu et al., 2009) and is now regarded as an effective experimental tool for the control of muscle activity similar to that in a clinical environment.

The masticatory muscles power the orofacial system, their structures being closely related to the growth and functions of the teeth, jaw, and joints (Dixon et al., 1997). Although the inhibition of mandibular growth following treatment of BTX to the masticatory muscles has already been addressed (Sakurai et al., 2007; Tsai et al., 2009; Kun-Darbois et al., 2015), the results of these studies may not be comprehensive in that their muscular environments were unnatural, with singular muscular paralysis and two-dimensional analyses. The unilateral singular paralysis of the masticatory muscle may be causing minor structural changes in the mandible and zygoma (Matic et al., 2007) and provoke compensatory work by the medial pterygoid or other muscle (Rafferty et al., 2012). We thus need to consider the simultaneous inhibition of the major masticatory closing muscles, including the masseter, temporal, and medial pterygoid muscles, in order to observe the genuine effect of masticatory muscular inactivity on mandibular growth.

We also paid attention to the possible compensatory reaction of the biological system in terms of bilaterality; the mandibular structure consists of right and left hemi-mandible with articulating joints which are essentially reciprocal, one side of the hemi-mandible influencing and being influenced by the other side (Rafferty et al., 2012). The unilateral masticatory hypofunction may therefore not necessarily produce the same phenotype as that of the bilateral hypofunctional model. In addition, the growth of the nonBTX side in unilateral hypotrophy may not match that of the normal control without any masticatory hypofunction.

Finally, we considered a primate model system to mirror the association between growth and function in human. To infer how human mandibular growth would be impacted by masticatory muscle hypotrophy, we looked for an animal model with craniofacial growth pattern similar to that of human. Investigations to date have documented such similarity in nonhuman hominoids, whose mastication, nasal breathing and orthostatic position affect the mechanical properties of the skeletal system and the mode of facial bone growth (Moss, 1968; Losken et al., 1994). However, they are difficult to work with, which inevitably led us to utilize a primate model system, specifically the cynomolgus monkey, to evaluate masticatory muscle-related growth and function in humans.

The purpose of this study was to investigate the relationship between masticatory muscular function and mandibular skeletal

growth. We hypothesized that the mandible would undergo differential growth disturbances in size and shape due to BTX-induced unilateral or bilateral hypotrophy of masticatory muscles. We also introduced synchronous BTX treatments to unilateral or bilateral major masticatory closing muscles to prevent compensatory masticatory muscle function. Three-dimensional (3D) changes in the size and shape of the mandible were obtained by measuring and comparing serial computed tomographic (CT) images.

MATERIALS AND METHODS

Animals and Animal Care

This study was approved by the Animal Experimental Ethics Committee of Southern Medical University, Guangzhou, China (2014-024). All experiments were performed under protocols to meet the requirements of the Association for Assessment and Accreditation of Laboratory Animal Care International and the Experimental Animal Center of Southern Medical University. Male cynomolgus monkeys (*Macaca fascicularis*) were used, preliminary power analysis being performed to get the proper sample size for three groups (G*Power 3.1, Heinrich-Heine-Universität Düsseldorf, Germany; $\alpha = 0.05$, power = 0.95; total $N = 20$ hemi-mandibles). They had complete deciduous dentitions and first permanent molars in occlusion, indicating their juvenile period (McNamara and Graber, 1975).

The animal care was performed by full-time attending veterinarians under the Guide for the Care and Use of Laboratory Animals of the National Institutes of Health. The animals were housed individually in stainless steel cages (85 cm × 92 cm × 100 cm) under a 12 h light-dark cycle at 25–27°C. They were provided with a diet of vitamin enriched biscuits, fruits, and water until they were satisfied. They were also provided with social interactions with neighboring animals and attending veterinarians and given toys and trees for play stimulation. During all experimental periods, they were closely monitored on a regular basis throughout the day by the attending veterinarians as well as the experimental operators to ensure their health and welfare.

For the experimental BTX treatments, the animals were sedated by intramuscular (IM) injection with ketamine HCl (Ketamine, 5–10 mg/Kg, IM) and rompun (Xylazine, 1–2 mg/Kg, IM), with glycopyrrolate (Robinul, 0.004 mg/Kg, IM). Tramadol (50 mg) was given intramuscularly after intervention to alleviate suffering. After 24 weeks of experiments, the animals were sacrificed by a method consistent with the American Veterinary Medical Association Guidelines for the Euthanasia of Animals (IV administration of pentobarbital overdose, >100 mg/Kg) to collect the samples necessary for the histological examination.

Experimental Design and BTX

The predictor variables were the elapsed time and side of BTX injection; the outcome variables were mandibular structure-related dimensional parameters. Ten monkeys aged 18–24 months (mean age, 22 months), weighing between 2.0 and 3.1 Kg (average 2.44 Kg), were divided into three groups based on the

side of BTX injection: group I (control; $n = 3$; mean age 21.0 months), group II (unilateral BTX; $n = 4$; mean age 21.8 months), and group III (bilateral BTX; $n = 3$; mean age 26.7 months) (**Supplementary Table S4**). The age differences between the groups were not significantly correlated with outcome variables (by Pearson's product-moment correlation coefficients; details not shown), and the mandibular growth curve by Schneiderman (Schneiderman, 1992) showed a marked decrease in skeletal growth after 4 years old, excluding the possible influence of group age differences.

The masseter, temporal, and medial pterygoid muscles were selected for simultaneous injections of BTX. A total of 20 units/Kg of BTX A (Botulax®, Hugel Inc., Chuncheon, Korea, 50 U/ml) was injected into the targeted masticatory muscles. The ratio of the BTX dose to masseter, temporalis, and medial pterygoid muscle was 5:4:3, based on the size and function of the muscle and the therapeutic dose (Bhidayasiri et al., 2006). The muscles on the right (BTX) side were injected for group II (unilateral), and on both sides for group III (bilateral). The masseter and temporalis muscle had two points of injection, while the medial pterygoid had one point. The same amount of normal saline was injected into both sides for group I (control) or into the control side for group II (unilateral). Later, the mandible of group I (control), BTX side of group II (unilateral), control side of group II (unilateral), and group III (bilateral) were independently evaluated for comparison of morphological changes.

Eleven titanium mini-screws (1.2×3 mm self-drilling screws; Gssem Co., Korea) were placed at the mandible, maxilla, and cranium as reference markers for 3D superimposition (Bjork, 1955; McNamara and Graber, 1975).

3D Morphometric Analysis

3D Imaging

CTs were taken (Aquilion, Toshiba, Japan) at T0 (initial time point just before BTX injection), T1 (3 months after BTX injection), and T2 (6 months after BTX) under sedation. The working condition for CT scan was set to 120 kVp, 150 mA, 0.3 mm of pixel size, and less than 0.5 mm of slice thickness. To maintain the maximum occlusion, the subjects were placed in prone position with the mandible set into a head stabilizer designed for the purpose. CT data were stored in DICOM file format and 3D reconstruction of the mandible and skull and their analyses were performed using software (Mimics and 3-matic, Materialize Co., Leuven, Belgium; Simplant, Materialize Dental Co., Leuven, Belgium).

Morphometric Reference Points

Our reference points were selected based on reviews of the morphometric reference points reported so far (Moss and Simon, 1968; Park et al., 2010; Markic et al., 2015), mainly with the aim of facilitating 3D measurements (**Supplementary Figures S1A,B**). These included the condyle, gonion, and other points for anatomical description as well as nasion, porion, and others for the construction of reference planes. These are detailed in **Supplementary Table S1**.

Reference Planes

The reference planes were defined for linear, angular, area and volume measurements as follows (**Supplementary Figures S1C–E** and **Supplementary Table S2**): Frankfort horizontal plane (as the horizontal reference plane), the midsagittal plane (MSP; as the sagittal reference plane), and the coronal plane. The mandibular occlusal plane was set as passing through the mandibular first molars and central incisors (**Supplementary Figure S1D**), while the mandibular inferior border plane (IBP) was set as passing through the menton-gonion line and running perpendicular to the ramal plane (**Supplementary Figure S1E**). The mandibular ramal plane runs parallel to the mandibular ramus and passes through the ramus posterior point, sigmoid notch, and ramus anterior point (**Supplementary Figure S1E**), while the ramus anterior plane is perpendicular to mandibular occlusal plane (**Supplementary Figure S1H**). Details are described in **Supplementary Table S2**.

3D Measurements

The dimensional changes of the mandible were evaluated in terms of relative growth increments as well as absolute value changes in lengths, angles, areas and volumes (**Supplementary Tables S5–S10**). Relative growth rates were calculated by the ratio of measurements at each time period to the size at T0, and then compared with the interval changes from T0 to T1 and T2 (**Figures 3–5**). We confirmed the possible association between the right and left side of hemi-mandible in group I (control) and group III (bilateral) by paired *t*-test, showing that their differences were not statistically significant ($p > 0.05$; details not shown). We therefore used the hemi-mandibles of groups I and III as independent variables, the average values of right and left side thus being used for statistical analysis.

Mandibular unit size

The mandible was divided into five units in accordance with the concept of mandibular units or module (**Figure 1A**; Moss and Young, 1960; Moss, 1968). Each unit was designed to represent developmental characteristics and measured in-line by connecting reference points, as shown in **Figure 1A**. 3D mandibular unit analysis was performed based on previous reports (Moore, 1973; Delaire, 1990; Park et al., 2010). Lengths were measured for body unit [between the inferior alveolar foramen (IAF) and mental foramen (MF)], condylar unit (condyle point (Con)-IAF), coronoid unit (coronoid point (Cor)-IAF), and others.

Mandibular size

The mandible height was measured in terms of distance to each reference point from IBP (**Figure 1B**). Anterior-posterior (AP) dimension was evaluated as the distance from infradentale (Id) to the reference points (**Figure 1B**). The mandibular width was measured between the bilateral reference points to obtain condylar width (Con-Con), coronoid width (Cor-Cor) or mandibular first molar width (Mn6-Mn6) (**Figure 1C**).

Mandibular angles

The angles of the mandibular structure were also measured between the reference plane and the ramal axis (Con-Go),

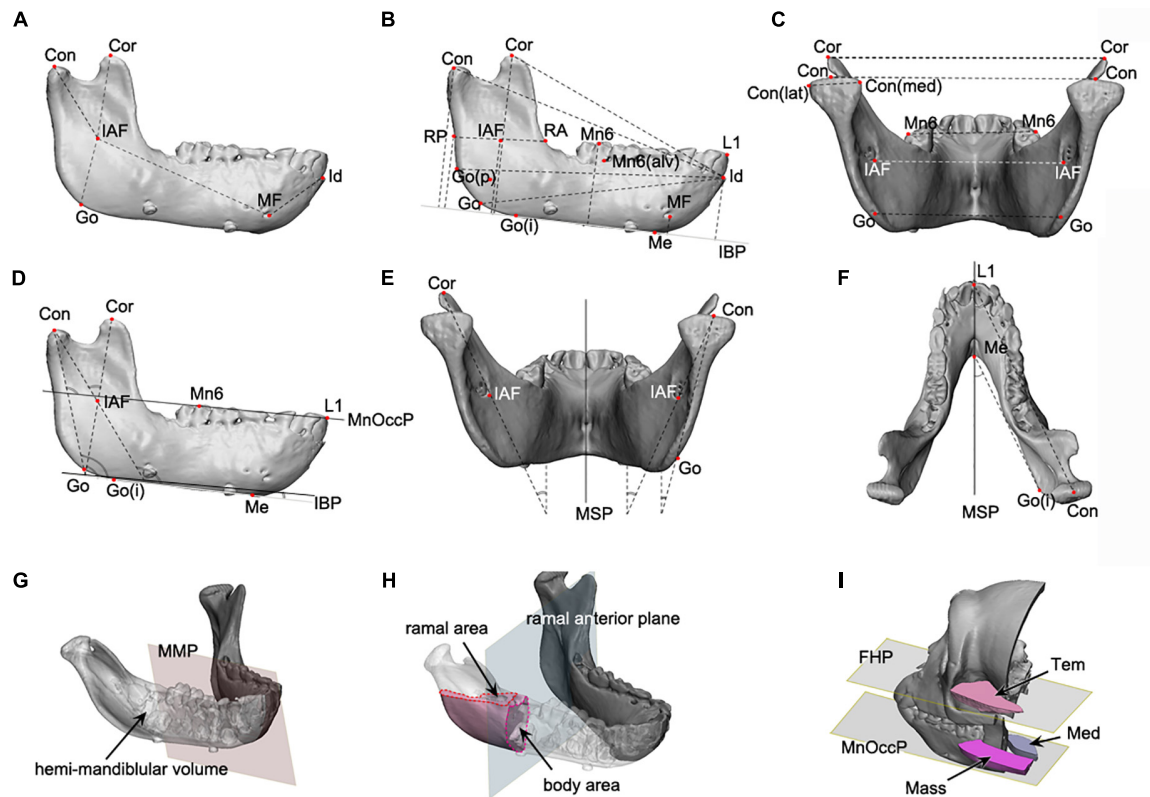


FIGURE 1 | The mandibular linear, angular, area, and volume measurements applied to this study. **(A–C)** The linear measurements; **(D–F)**, the angular measurements; **(G,H)**, the volume and area measurement; **(A)** the mandibular unit measurements, including the condylar and body unit; **(B)** the mandibular length and height measurements; **(C)** the transverse length measurements; **(D)** the angular measurements on the sagittal plane; **(E)** the angular measurements on the coronal plane; **(F)** the angular measurements on the Frankfort horizontal plane; **(G)** the volume measurement of hemi-mandible, produced by the division of mandibular model by mandibular median plane; **(H)** the measurement of cross-sectional area for ramus and body, at the level of mandibular occlusal plane for ramus and ramal anterior plane for body; **(I)** the measurement of cross-sectional area of temporal, medial pterygoid, and masseter muscle, at the mandibular occlusal plane and FHP. Abbreviations are defined in **Supplementary Tables S1–S3**. Abbreviations for reference points) IAF, inferior alveolar foramen; Con, condyle; Cor, coronoid; Go, gonion; MF, mental foramen; Id, infradentale; Mn6, lower 1st molar; Id, infradentale; Go(p), gonion posterior point; Go(i), gonion inferior point; RA, ramus anterior point; RP, ramus posterior point; Me, menton; Con(med), condylar medial point; Con(lat), condylar lateral point; MF, mental foramen; Li, lower incisor point. Abbreviations for planes: MSP, midsagittal plane; MnOccP, mandibular occlusal plane; IBP, mandibular inferior border plane; FHP, Frankfort horizontal plane; CP, coronal plane; MMP, mandibular median plane; MRP, mandibular ramal plane; RAP, ramus anterior plane. Abbreviations for measurements: IAF-Con, condylar unit; IAF-Cor, coronoid unit; IAF-Go, angular unit; IAF-MF, body unit; Id-MF, symphyseal unit; IBP-Con, condylar height; IBP-Cor, coronoid height; IBP-Go, angular height; IBP-IAF, mandibular foramen height; IBP-Mn6, mandibular molar height; Id-Con, condylar length; Id-Cor, coronoid length; IAF-Go(p), angular length; RA-RP, ramal breadth; Con(med)-Con(lat), condylar head size; Con-Con, condylar width; Cor-Con, coronoid width; Go-Go, angular width; MF-MF, mental width; Mn6-Mn6, molar width.

mandibular unit (Con-IAF and Cor-IAF), or mandibular border lines (gonion inferior point – Me) (**Figures 1D–F**).

Mandibular volumes and areas

The hemi-mandibular volumes and cross-sectional areas of the ramus (at the level of mandibular occlusal plane) and the body (on the ramus anterior plane) were measured on the constructed 3D models (**Figures 1G,H**).

Masticatory muscular areas

The cross-sectional areas of masseter, medial pterygoid, and temporalis on the reference planes (including mandibular occlusal plane for masseter and medial pterygoid and FHP for temporalis) were measured on the 3D model constructed from CT images using the soft tissue setting (**Figure 1I**).

Assessment of Interval Growth

3D-reconstructed mandibular models for three subsequent time periods were superimposed to verify the chronologic changes using the best-fit algorithm of the software. Three superimposition methods using different registration points were tried to achieve the most accurate picture of dimensional changes (**Supplementary Figure S2**): the mandibular reference screws, mandibular foramen-mental foramen (IAF-MF), and cranial reference screws. The inter-surface distance between the models was also calculated and color-coded for comparison, based on the superimposition using mandibular reference screws (**Figure 6**).

Histological Analysis

Following CT evaluation and euthanasia, the head parts of subjects were fixed at room temperature in 10% formalin solution

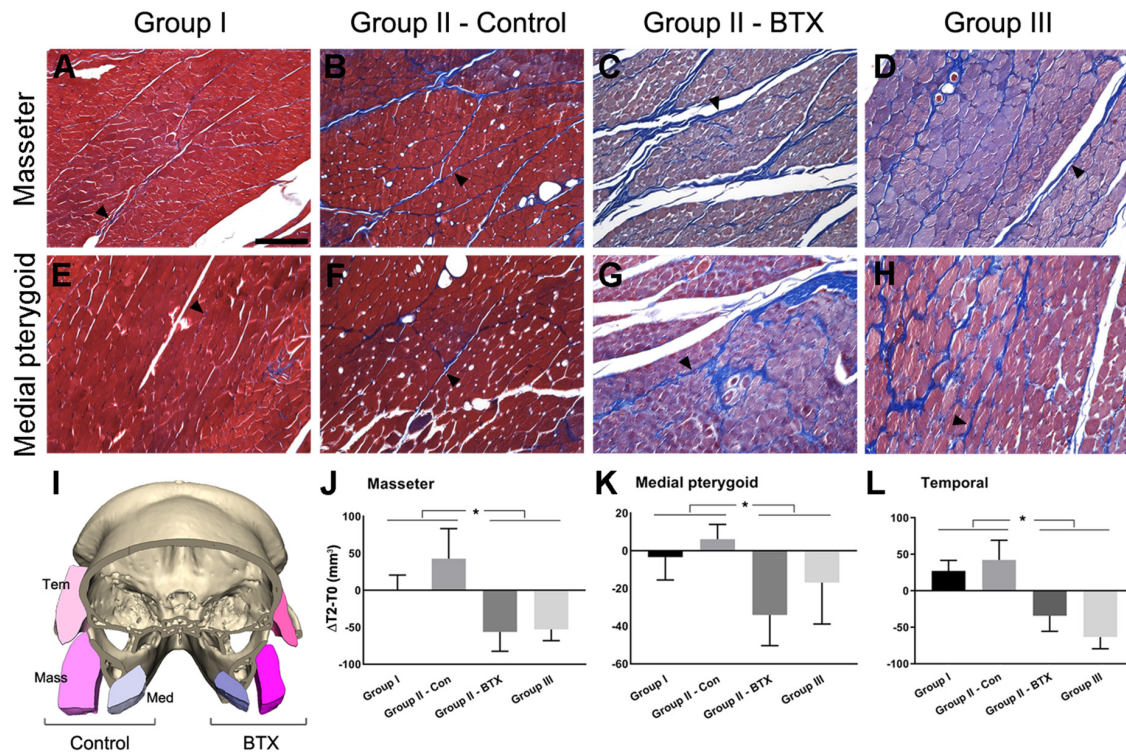


FIGURE 2 | Histological and measurement analysis of masticatory muscles. (A–H) Masson's trichrome staining of masseter (A–D) and medial pterygoid muscle (E–H) after 6 months of BTX treatments; (I), the comparison of cross-sectional area of muscles in control and the BTX side of group II (unilateral); (J–L), the area measurement of cross-sectional area of muscles and their comparison; (A,E) the masseter and medial pterygoid muscles in group I (control), showing reddish myofibers in compact alignment, being encapsulated by thin blue perimysium (arrowhead for perimysium); (B,F) the muscles from the control side of group II, showing the similar arrangements of myofibers with more perimysia and dilated vessels; (C,D,G,H) masseter and medial pterygoid muscle in group III (bilateral) and on the BTX side of group II (unilateral), which shows the hypotrophic changes with decreased myofiber size and increased perimysia; (I) the muscles in the BTX-treated side of group II (unilateral) showed a marked decrease in size as compared with those on the saline-injected control side; (J–L) masseter, medial pterygoid, and temporalis muscles of group I and control side of group II (unilateral) showed statistically significant greater increments between T0 and T2 than those of group III (bilateral) and the BTX side of group II (unilateral). *Significant when $p < 0.05$. Scale bar = 50 μm (A).

and decalcified in 0.5 M ethylenediaminetetraacetic acid solution at pH 7.4 for 1 year at 4°C. After decalcification, axial sections of masseter and medial pterygoid muscle around the middle point region between ramus anterior and posterior point were obtained. Masson's trichrome staining (Histoperfect™, Masson's Trichrome Staining Kit, BBC Biochemical, Stanwood, WA, United States) were used to examine the histological condition of masticatory muscles (Figures 2A–H).

Statistical Analysis and Methods Error

Statistical analyses were performed to compare the measurements between the groups. Linear mixed model analysis was used to compare the results in terms of groups, BTX treatments, and time period for bilaterality of mandible. The two-way analysis of variance (ANOVA) test was applied for comparison of measurements between the bilateral structures and verified by *post hoc* analysis with the Bonferroni correction procedure, using Statistical Package for the Social Sciences (SPSS, Version 24, IBM Co.) and Prism (Version 8, Graphpad Co.).

The possible error associated with the methods when assigning reference points on 3D CT was also calculated in each dimension of X, Y, and Z according to Dahlberg's formula

(Dahlberg, 1949). One author (H-JK) digitized each of 5 reference points on 3D CT images 20 times. To evaluate intra-observer variability, a reliability analysis with the determination of the intraclass correlation coefficient (ICC) was calculated with 95% confidence intervals.

RESULTS

Body Weight

The mean body weight for all three groups increased from 2.44 Kg (T0) to 2.67 Kg (T2). Specifically, group I (control) gained 0.31 Kg of body weight over 6 months (T2–T0), while weight gain in group II (unilateral) was 0.24 Kg and 0.15 Kg in group III (bilateral). There was no increase in body weight in group III (bilateral) during the first 3 months (T1–T0). While group II (unilateral) and group III (bilateral) gained 0.24 and 0.15 Kg, respectively, Pearson's correlation analysis revealed no statistically significant difference between body weight and dimensional measurements ($p > 0.05$; details not shown). Subjects in group I (control) had no difficulties feeding, those from group II (unilateral) mainly chewed on the control side,

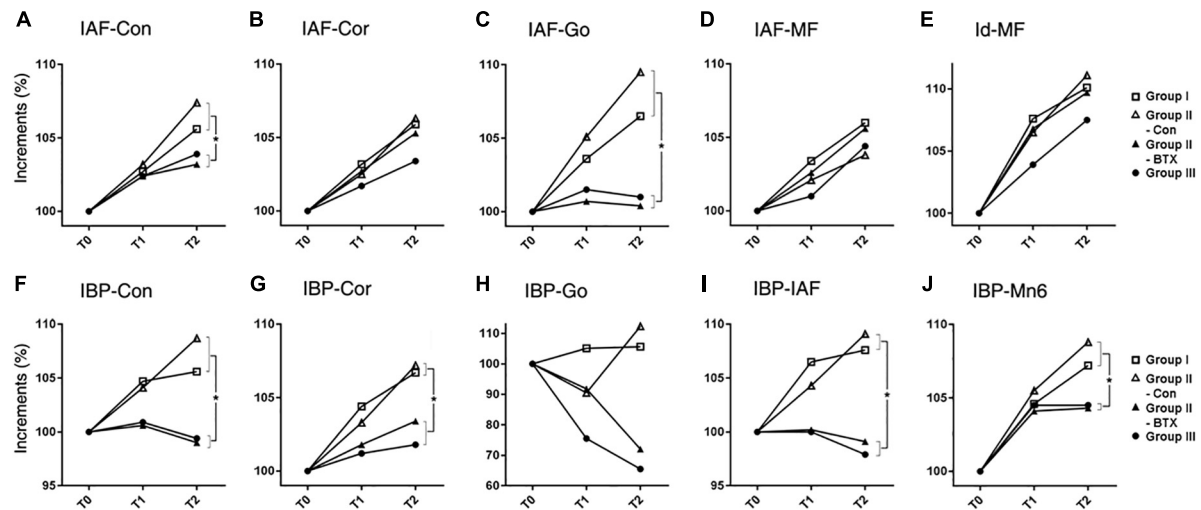


FIGURE 3 | Time-dependent incremental changes in mandibular measurements (A–E) mandibular unit size, (F–J) mandibular height. Abbreviations: IAF, inferior alveolar foramen; Con, condyle; Cor, coronoid; Go, gonion; MF, mental foramen; Id, infradentale; IBP, mandibular inferior border plane; Mn6, lower 1st molar. Abbreviations: IAF-Con, condylar unit; IAF-Cor, coronoid unit; IAF-Go, angular unit; IAF-MF, body unit; Id-MF, symphyseal unit; IBP-Con, condylar height; IBP-Cor, coronoid height; IBP-Go, angular height; IBP-IAF, mandibular foramen height; IBP-Mn6, mandibular molar height. □ for group I (control), Δ for control side of group II (unilateral), ▲ for BTX side of group II (unilateral), ● for group III (bilateral). *Significant when $p < 0.05$, to compare saline- and BTX-treatment by linear mixed model analysis; units in incremental percent (T2–T0/T0).

and those from group III (bilateral) temporarily could not eat properly. Group III was thus fed with a full liquid diet through the nasogastric tube for about 2 weeks, followed by normal feeding.

Histological Analysis

The histological evaluation by Masson's trichrome staining showed that the masseter and medial pterygoid muscles in group I (control) had red plump myofibers encapsulated by thin or indistinct perimysium (Figures 2A,E; arrowhead for perimysium). The same muscles on BTX side revealed a degenerative hypotrophic change of myofibrils with a decrease in the myofibrillar diameters as well as an increase in the collagen fibers forming perimysium around the myofibers (Figures 2C,D,G,H; arrowheads for perimysium).

3D Measurements and Analysis

The mandibular structures were measured and their periodic increments (T2–T0) as well as percentage change with respect to initial values (T2–T0/T0) were calculated to compare time-dependent changes.

Mandibular Unit Size

The increased length at T0–T2 was greatest at the body unit (IAF-MF; 2.0 mm) and least at the angular unit (IAF-Go; 0.8 mm) for group I (control) (Figure 3 and Supplementary Table S5). The relative increase in mandibular unit length for group I (control) was greater than that of other groups, except for the four units on the control side of group II (unilateral). The condylar (IAF-Con) and angular unit (IAF-Go) on the group I (control) and control side of group II (unilateral) showed significantly greater growth increments than on the BTX side of group II (unilateral) and group III (bilateral) ($p = 0.01$ for condylar unit

and $p = 0.04$ for angular unit). In contrast, the body (IAF-MF) and coronoid unit (IAF-Cor) showed no significant changes for all groups.

Mandibular Size

The periodic increment from T0 to T2 was greatest at the condylar height (IBP-Con) and coronoid height (IBP-Cor) (2.4 mm each) on the control side of group II (unilateral), and least at the angular height (IBP-Go; -0.8 mm) in group III (bilateral) (Supplementary Table S6). The relative growth rate for the coronoid height (IBP-Cor), IAF height (IBP-IAF), and molar height (IBP-Mn6) in group I (control) and the control side of group II (unilateral) was significantly greater than those in group III (bilateral) ($p < 0.05$ for condylar and alveolar height; $p < 0.01$ for coronoid and molar height) (Figure 3).

AP length increments in condylar (Id-Con) and coronoid length (Id-Cor) were not significantly different for all groups, while those of ramal breadth (RA-RP) for group I (control) and control side of group II (unilateral) were significantly greater than those on the group III (bilateral) and BTX side of group II (unilateral) ($p = 0.01$) (Figure 4 and Supplementary Table S7). In addition, the coronoid length (Id-Cor) and condylar head size [Con(med)-Con(lat)] in T2 were significantly greater than that of T0 ($p < 0.05$).

The transverse length at the condylar width (Con-Con) of group I (control) or control side of group II (unilateral) was significantly greater than that of group III (bilateral) and BTX side of group II (unilateral) ($p < 0.0001$ for condylar width and 0.016 for body width) (Figure 4 and Supplementary Table S8). The ramus width (RA-RA) and molar width (Mn6-Mn6) from T0 to T2 were significantly different for all groups.

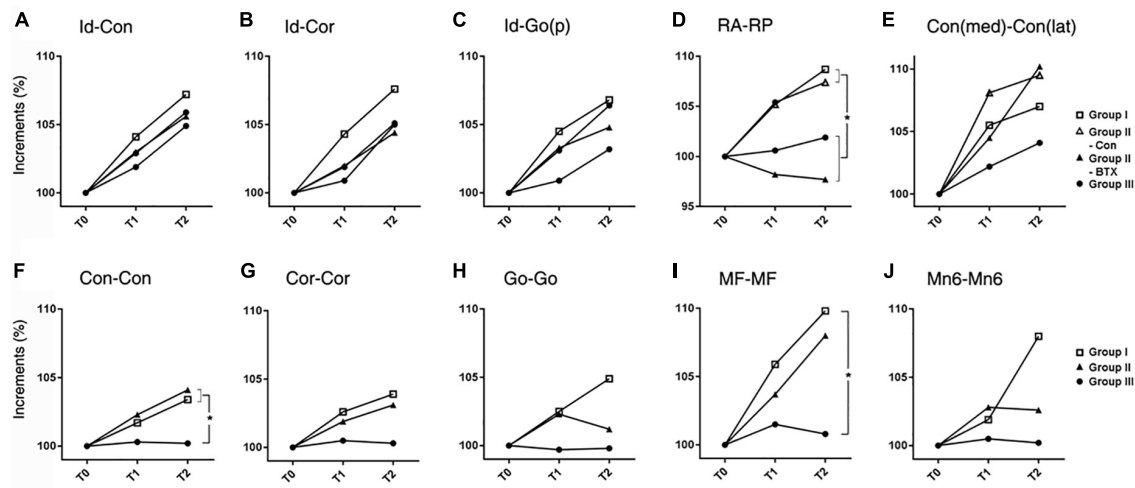


FIGURE 4 | Time-dependent differential changes in mandibular size (A–E) mandibular AP length, (F–J) mandibular transverse length. Abbreviations: Id, infradentale; Con, condyle; Cor, coronoid; Go(p), gonion posterior point; RA, ramus anterior point; RP, ramus posterior point; Con (med), condylar medial point; Con (lat), condylar lateral point; MF, mental foramen; Mn6, lower 1st molar. Abbreviations: Id-Con, condylar length; Id-Cor, coronoid length; IAF-Go(p), angular length; RA-RP, ramal breadth; Con(med)-Con(lat), condylar head size; Con-Con, condylar width; Cor-Cor, coronoid width; Go-Go, angular width; MF-MF, mental width; Mn6-Mn6, molar width. □ for group I (control), Δ for control side of group II (unilateral), ▲ for BTX side of group II (unilateral), ● for group III (bilateral). *Significant when $p < 0.05$, to compare saline- and BTX-treatment by linear mixed model analysis; units in incremental percent (T2-T0/T0).

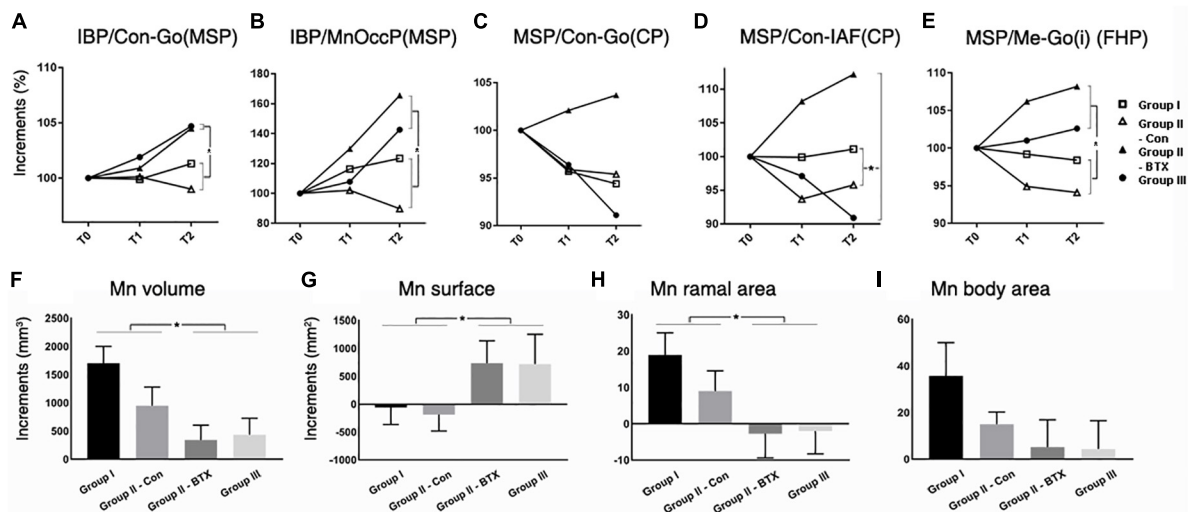


FIGURE 5 | Time-dependent differential changes in mandibular angle and volume measurements for four groups. Abbreviations: IBP, mandibular inferior border plane; Con, condyle; Go, gonion; MSP, midsagittal plane; CP, coronal plane; IAF, inferior alveolar foramen; MnOccP, mandibular occlusal plane; Me, menton; Go(i), gonion inferior point; FHP, Frankfort horizontal plane. Abbreviations: Con-Go, ramal axis; Con-IAF, condylar unit; Me-Go(i), mandibular inferior border line. □ for group I (control), Δ for control side of group II (unilateral), ▲ for BTX side of group II (unilateral), ● for group III (bilateral). *Significant when $p < 0.05$, to compare saline- and BTX-treatment by linear mixed model analysis; units in incremental percent (T2-T0/T0) for (A–E), and units in mm³ of increments from T0 to T2 (T2-T0) for (F–I).

Mandibular Angles

The angle between the ramal axis (Con-Go) and the IBP on MSP for group III (bilateral) and BTX side of group II (unilateral) was significantly greater than that for group I (control) and control side of group II (unilateral) ($p = 0.001$) (Figure 5 and Supplementary Table S9). The angle between the condylar axis (Con-IAF) and MSP on the coronal plane on the group III (bilateral) and BTX side of group II (unilateral)

increased significantly by time periods, more so than that for group I (control) and control side of group II (unilateral) ($p = 0.004$ for condylar axis). In addition, the angle between MSP and the mandibular inferior border (Me-gonion inferior) on FHP for group III (bilateral) and BTX side of group II (unilateral) was greater than that of group I (control) and control side of group II (unilateral) ($p < 0.0001$) (Figures 1F, 5E and Supplementary Table S9).

Mandibular Volumes and Areas

The periodic increment of hemi-mandibular volumes from T0 to T2 was the greatest in group I (1702 mm³) and the least on BTX side of group II (949 mm³) (Figure 5F and Supplementary Table S10). In addition, the volume increments of BTX treatments in group III (bilateral) and BTX side of group II (unilateral) were significantly smaller than those of saline treatments in group I (control) and control side of group II (unilateral). The difference between the BTX and

control sides was also statistically significant for ramal cross-sectional area (Figure 5H and Supplementary Table S10), but insignificant for body cross-sectional area (Figure 5I and Supplementary Table S10).

Masticatory Muscular Areas

The cross-sectional areas between T0 and T2 on masseter, medial pterygoid, and temporalis in group I and control side of group II (unilateral) mostly increased, more so on the control side of

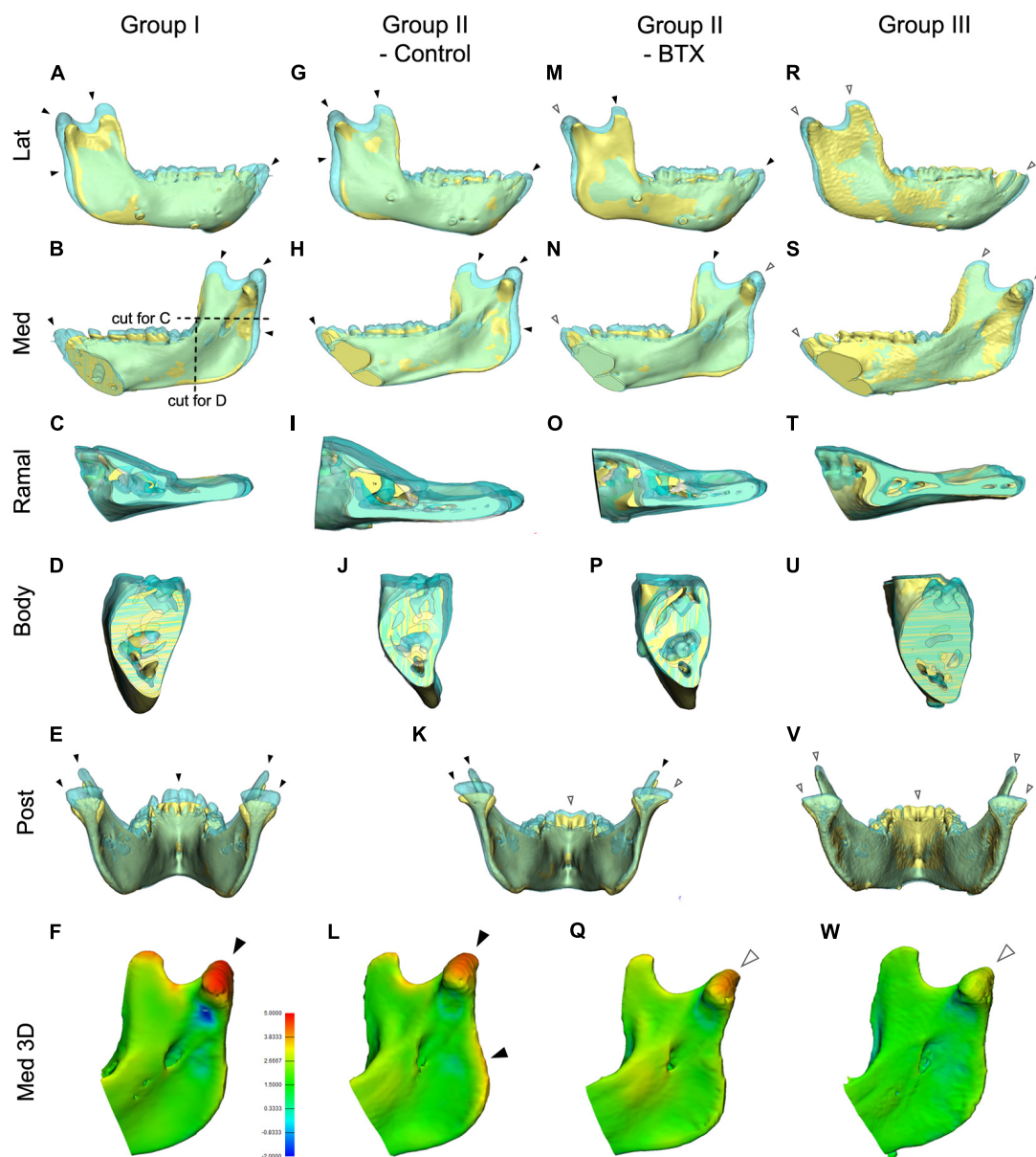


FIGURE 6 | Comparison of mandibular growth of the four groups between stages T0 and T2 based on superimposition at the mandibular screws.

(A–E,G–K,M–P,R–V) The lateral, medial, cross-sectional ramus and body, and posterior sides of the superimposition or section were visualized to compare states T0 and T2. The blue model represents stage T2 mandible, the yellow stage T0. (F,L,Q,W) 3D comparison with color-coding to visualize growth-related changes inserted color diagram for figure (L) shows the inter-surface distance of the two models. Red indicates bony apposition; blue shows resorption. Arrowheads in (A–W); black for marked growth between T0 and T2; white for less evident changes. Color coding for (F,L,Q,W); in orange and red color for 3.8–5.0 mm; in light and dark blue for –0.9 to –2.0 mm.

group II (**Figures 2I–L** and **Supplementary Table S10**). However, those from group III (bilateral) and the BTX side of group II (unilateral) all decreased and were significantly different from saline-treated both sides of group I and the control side of group II (**Figures 2J–L** and **Supplementary Table S10**).

Assessment of Interval Growth

Three methods of superimposition in group I (control) yielded different growth measurements (marked with arrowheads; **Figure 6**). Cranial superimposition by craniomaxillary reference screws (red circles; **Supplementary Figure S2**) revealed relatively static condylar and posterior ramal regions, with the main direction of growth being at the symphysis and the inferior border (**Supplementary Figure S2B**). The superimposition at the mandibular foramen and mental foramen showed growth mainly in the condyle, coronoid, posterior ramus, and symphyseal regions, coming midway between the other two methods and matching well with the previously mentioned measurement results (**Supplementary Figure S2C**). On the other hand, the registration at the mandibular reference screws (marked with red circles) indicated the static inferior border region and the main direction of growth were in the condylar and coronoid regions (**Supplementary Figure S2A**). We finally chose the fixed screw-based superimposition method to evaluate growth changes.

Figure 6 shows the superimposed mandibular models of stages T0 and T2 based on screw superimposition for comparison of dimensional changes among the four groups. The lateral and medial views for group I (control) and the control side of group II (unilateral) showed greater dimensions at T2 for the condylar, coronoid, posterior ramus, and symphyseal regions (shown in blue and indicated by black arrowheads), showing marked growth in the superior, posterior, and anterior growth directions (**Figures 6A–L**). They also showed less evident changes in the inferior border, dentoalveolus, and lateral ramus regions, indicating less growth in the inferior, lateral, and dental areas (shown in blue and indicated by white arrowheads). In addition, the control side of group II (unilateral) had more growth in the posterior ramus and angular regions than did group I (control) (**Figures 6A–E, G–K**). The same views of the BTX side of group II (unilateral) and group III (bilateral) presented a minimal inter-surface distance in all corresponding regions, including the inferior border, compared to that in group I (control) (**Figures 6K, M–Q** for group II (BTX); **Figures 6R–W** for group III (bilateral)). In addition, group III (bilateral) had the least eruption at the anterior teeth without accompanying open bite. These changes were also confirmed by color-coded distance measurements as seen in **Figures 6F, LQ, W**.

The posterior and cross-sectional views in group I (control) showed greater increments and lateral-posterior direction of growth in the condylar, coronoid, and posterior ramus and maintaining angular interrelationships and sectional area of body being insignificant changes (**Figures 6B–E**). This condylar lateral expansive growth with increased width was not found in group II (unilateral) or group III (bilateral) (**Figures 6I–K, O, P**). Moreover, the BTX side of group II (unilateral) showed a lateral tilt of condyle and posterior ramus with a lateral elongated condylar head (**Figure 6K**).

Methods Error

The methods error when assigning reference points was 0.05 mm on average, the ICC being 0.972 (by Cronbach's alpha).

DISCUSSION

This study aimed to evaluate the association between masticatory muscle function and mandibular growth in juvenile primates. The function of major masticatory closing muscles was simultaneously interrupted by BTX treatment in the unilateral or bilateral muscles of growing cynomolgus monkeys. Mandibular growth evaluated with 3D CT data at three time points over 6 months showed dimensional and angular changes in skeletal structural growth, mainly in the ramal area in the vertical dimension.

The mandibular and craniofacial growths of nonhuman primates, especially genus *Macaca*, have been studied in depth (Siegel et al., 1985). The juvenile monkey at age 18–24 months has a deciduous dentition with the first permanent molars in full occlusion (McNamara and Graber, 1975). The growth velocity of the *Macaca* mandible peaks at 3 years of age on average, and drops after 4 years old (McNamara and Graber, 1975). The ages of our models ranged 21–27 months and the experiments continued for 6 months, covering a period of rapid juvenile growth without significant differences in growth speed among groups.

The mandible is a U-shaped structure mainly consisting of the ramal and body parts. The ramal structure, particularly in mammals, consists of one angular region and two processes, forming a Y-shape. The plump masticatory muscles, i.e., masseter, temporal and medial pterygoid muscles, envelop the ramus and provide stability and mobility as well as the main blood supply to the ramus (Cohen, 1960; Saka et al., 2002).

The normal growth and maintenance of the mandibular skeletal structure is influenced by various genetic as well as epigenetic factors such as masticatory muscular force and function, bite force, chewing pattern, and diet (Dechow and Carlson, 1990). The decreased loading with soft diet influences the internal structure, bone mass, cortical thickness, and morphology of mandible (Kiliaridis, 1995). It also results in a posteriorly rotated mandible, reduced ramal size, more posteriorly directed growth of the condyle, and a shorter vertically angular process (Bouvier and Hylander, 1984; Kiliaridis et al., 1985; Yamada and Kimmel, 1991), or limited vertical displacement (Kono et al., 2017), similar to the results of BTX treatments in our group III (bilateral).

BTX paralyzes muscles by blocking acetylcholine release at the neuro-muscular junction, their recovery being accomplished by motor axon sprouts (Angaut-Petit et al., 1990). The time elapsed for the recovery varies by animal (Pickett, 2012), but the partial or complete recovery of masticatory function comes around 3 months in human, mouse, and rabbit (Poliachik et al., 2010; Park et al., 2013). However, some studies report a delay in muscular and skeletal recovery of 3 or 6 months after BTX to monkey masseter (Capra et al., 1991), mouse limb muscle (Grimston et al., 2007) and human calf muscles (Polak et al., 2002). In addition, our evaluations of muscles morphologically,

histologically, radiographically, and functionally at the end of experiment clearly indicated incomplete recovery of masticatory muscles after 6 months. Furthermore, incremental changes in body weight and the major measurement variables showed no clear evidence suggesting prominent muscular recovery after 3 months of BTX treatment.

The most common physiological test to determine jaw muscle activity is electromyography, but muscle measurement (length, thickness, cross-sectional area, and volume) constitutes an alternative method using ultrasonography, computed tomography, or magnetic resonance imaging. The cross-sectional area of jaw muscle and bite force magnitude are closely related (van Spronsen et al., 1989). In order to determine the state of the tested masticatory muscles, we measured the cross-sectional area of three masticatory muscles at the level of the mandibular occlusal plane and FHP on CT images of T0 and T2. The masticatory muscles all decreased in cross-sectional area with statistical significance by BTX treatment, augmenting the histological evaluation of muscle hypotrophy.

The functional relationship between muscle and bone can be observed throughout mandibular growth, development, and aging (Hamrick, 2010). It has long been advocated that function and form are closely related (Sugiyama et al., 2002), and that functional stress patterns bone morphology (Wolff, 1892). Moss described the skeletal unit as being biomechanically supported and/or protected by its related functional matrix (Moss, 1968), and Frost suggested that bone strength and mass are controlled by mechanically-loaded strain (Frost, 1998). A significant association was proved between mandibular shape and muscle cross-sectional areas, such as the association between the larger muscular cross-sectional area and more trapezoidal ramus and rectangular body with more massive coronoid (Sella-Tunis et al., 2018). Our results showing reduced muscular and mandibular skeletal cross-sectional areas in BTX treatment groups also support this functional relationship between muscle and bone.

Our measurement results showed that the ramus, especially in the vertical dimension, was the main region for structural changes following BTX treatment, with remarkable structural differences between the BTX- and saline-applied angular, condylar, coronoid, and posterior ramus regions after 6 months. This was first evidenced by measurements of the angular region, including the angular unit (IAF-Go) and mandibular foramen height (IBP-IAF). For example, the mandibular angular unit lengths (IAF-Go) of group III (bilateral) and the BTX side of group II (unilateral) showed stagnant growth (0.1 mm, 0.8% each), while the lengths of group I (control) and the control side of group II (unilateral) increased (0.8 mm, 6.5%; 1.2 mm, 9.5%) (**Supplementary Table S5**). These regional changes were, similarly, observed in the superimpositions and color-coded measurements of 3D models for group II (unilateral) and group III (bilateral) (**Figure 6**). This result was consistent with reports of other studies that the ramus height decreased after BTX injection into the masticatory muscles of rats and rabbits (Kwon et al., 2007; Tsai et al., 2009).

The mandibular angle is the region of masseter and medial pterygoid muscle attachment. It is known as a secondary and mechanically obligatory region that can respond to the functional demands of these muscles (Moss and Simon, 1968). Normal remodeling in the angular region in primates has already been reported (McNamara and Graber, 1975), despite a gradual decrease with age (Bravo et al., 1989). We assumed that BTX decreased muscle function, thereby inhibiting growth in the mandibular angle area, while the compensatory action of the control side of group II (unilateral) accelerated growth in the angular region.

The most prominent incremental change in normal growth as well as in BTX-induced hypoplastic growth was in the condylar and coronoid regions, and it was again in the vertical dimension. This was evidenced in the results for the condylar unit (IAF-Con), condylar height (IBP-Con), and coronoid height (IBP-Cor). For instance, the condylar height (IBP-Con) of group III (bilateral) and the BTX side of group II (unilateral) showed stagnation or slight decrease (-0.2 mm, -0.7%; -0.3 mm, -1.1%, respectively), while group I (control) and the control side of group II (unilateral) showed a distinct increase (1.6 mm, 5.6%; 2.4 mm, 8.6%) (**Supplementary Table S6**). The condylar head had more distinct BTX-related inhibitory undergrowth (as shown in yellow-orange color of **Figures 6Q,W**) and compensatory overgrowth (shown in red, **Figure 6L**) than did the coronoid or other regions. This suggests a stronger association between masticatory function and growth of the condyle than of the coronoid or other regions, though the coronoid has the major masticatory muscle attachment. This may be related to reports that the chondrogenic growth potential of the condylar head, especially the articular portion, under indirect loading is greater than that of the coronoid region (Miyazaki et al., 2016).

One more interesting result was the remarkable growth on the control side of group II (unilateral), possibly induced by compensatory unilateral mastication on the contralateral side. Many previous studies applied BTX unilaterally, using the other side as the control (Kwon et al., 2007; Tsai et al., 2009). However, our results clearly showed the presence of compensatory function and point out the need to differentiate the effects of muscular hypotrophy and compensatory outcomes. In addition, unbalanced growth on the nonBTX side may accentuate asymmetrical growth in that it accompanies decreased growth on the BTX side. A possible etiopathogenic association with human asymmetric growth needs further clarification.

The BTX-induced vertical dimensional changes in the anterior part of the mandible were less evident than those in the ramal part. The indices for anterior vertical dimension, such as the mental foramen height (IBP-MF), incisor height (IBP-Id) and molar height (IBP-Mn6), demonstrated similar small increases within the range of 0.2–1.2 mm (4.3–15.3%) in group III (bilateral) and the BTX side of group II (unilateral), as compared with a range of 0.2–1.6 mm (5.4–8.5%) in group I (control) and the control side of group II (unilateral). The cross-sectional areas of the body region were not significantly different for all groups, as compared with ramus region results. These indifferent growth increments in the anterior mandibular part might indicate less involvement of masticatory muscles in this region than in the

ramus region. It is not clear whether they are related to the limited contribution of masticatory muscle or functional matrix that mainly envelop the ramal region (Hohl, 1983).

The normal growth ranges in the AP dimension were relatively greater than those in the vertical dimension. While the condylar height (IBP-Con) and the coronoid height (IBP-Cor) in group I (control) showed a 1.6 and 1.3 mm increase over 6 months, the condylar AP length (Id-Con) and angular AP length [Id-Go (p)] in group I increased by 4.5 and 4.4 mm. Our AP growth increments were similar to those of a previous study (Schneiderman, 1992), which reported 3.77 mm at the same point per 6 months between 1.5 and 3.5 years of age. However, the AP dimension growth changes in the BTX-treatment groups were not so different from those in the control group. The lengths of the condylar AP (Id-Con), angular AP (Id-gonion posterior point), coronoid AP (Id-Cor) and the symphyseal unit (Id-MF) on the BTX-treated side showed growth increments similar to those of the control side. These results indicate a smaller contribution of masticatory muscle to AP growth (Kiliaridis, 1995).

One more notable finding regarding AP length again concerns the ramus. The ramal breadths (RA-RP) of group I (control) and the control side of group II (unilateral) increased (1.6 mm, 8.6%; 1.2 mm, 7.4%), but decreased 0.4 mm (2.3%) on the BTX side of group II (unilateral) and increased only 0.4 mm (1.8%) for group III (bilateral) (**Supplementary Table S7**). These changes are also evident in the superimposed 3D models and their cross-sectional views, which show a lack of apposition on the posterior border of ramus on the BTX side of group II (unilateral) and group III (bilateral). Bone resorption, which has been well documented on the anterior border of ramus and apposition on the posterior border, is related to the progressive process of mandibular relocation and tooth eruption (Krarup et al., 2005). These changes suggest the contribution of masticatory muscle to the control of ramal breadth either directly or indirectly.

The angulations of the ramus [IBP/Con-Go (MSP)] and occlusal plane [IBP/MnOccP (MSP)] on the sagittal plane for group I (control) and control side of group II (unilateral) were markedly constant during the whole experimental period (**Figures 5, 6** and **Supplementary Table S9**), the condyle showing limited changes within the ranges of 0.8 and 1.9 degrees. However, angulations on the BTX side of group II (unilateral) and group III (bilateral) were significantly different in that they increased 3.1–5.2 degrees over the same period. They indicate that hypotrophy of the masticatory muscles induced a more posterior tilt of the ramus/condyle and a greater clockwise rotation of the occlusal plane. They also suggest the effect of masticatory muscle loading on the sagittal relationship between the ramus and body, as well as between the body and dentoalveolus. Although underlying pathogeneses remain unclear, muscular function may be involved; further evaluation is planned in this regard.

Angular measurements on the coronal plane were similar to those on the sagittal plane in that the angulation of group I subjects were relatively unchanged over the experiment period (**Figure 6** and **Supplementary Table S9**). This meant a constant lateral and superior axis of growth along the condylar and ramal

axes on the coronal plane. The condylar growth direction is well known to be V-shaped (Enlow and Harris, 1964). The condyle of group I subjects grew in the posterior-superior direction with an almost 1:1 ratio of horizontal and vertical displacement, as previously reported (McNamara and Graber, 1975; Nanda et al., 1987).

However, the altered masticatory muscle function also accompanied angular changes of the mandible on the coronal plane, as seen in the condylar unit angle (MSP/Con-IAF (CP)); these increased on the BTX side of group II (unilateral) and group III with statistical significance. These results suggest the coincidental development of mandibular asymmetry and lateral tilting due to unilateral muscular function. The phenotype of human asymmetry closely matches that of group II (unilateral) in presenting a ramus canted toward the short ramal side. Greater lateral angulation on the BTX side may be amplified by the lateral path of closure due to BTX-induced unilateral mastication (Lepley et al., 2010).

CONCLUSION

The impact of masticatory muscle function on mandibular growth was investigated. Following BTX-induced synchronous hypotrophy of the masticatory muscles of juvenile nonhuman primates, the ramus growth decreased mainly in the vertical dimension with compensatory growth on the control side of unilateral treatment. The BTX side of unilateral treatment showed increased posterior tilt (increased sagittal angles) and lateral tilt (increased coronal angles) of the ramus. However, AP growth following unilateral or bilateral BTX-treatment was similar to that of group I (control), except at the ramal breadth.

In conclusion, BTX-induced masticatory muscle hypotrophy resulted in a decrease in the size of the mandible and also a change in its form, particularly in the vertical dimension and in the posterior-lateral angulation of the ramus. It also accompanied compensatory growth of the nonBTX side ramus that might accentuate asymmetrical growth of the hypofunctional mandible.

ETHICS STATEMENT

This study was approved by the Animal Experimental Ethics Committee of Southern Medical University, Guangzhou, China (2014-024). All experiments were performed under protocols to meet the requirements of the Association for Assessment and Accreditation of Laboratory Animal Care International and the Experimental Animal Center of Southern Medical University.

AUTHOR CONTRIBUTIONS

H-JK, ZP, and S-HL designed the study. H-JK, J-WM, H-JT, JH, and ZP did the experiments and data acquisition. J-WM, H-JT, S-HK, STK, H-JK, and S-HL performed analysis and interpretation of data. H-JK and S-HL wrote the draft of the manuscript. S-HK and STK contributed to revise and all authors

approve the manuscript to be published and agreed on all aspects of the work.

FUNDING

This work was supported by the National Research Foundation of Korea (NRF) grant funded by the Korean Government (NRF-2017R1A2B4005319).

SUPPLEMENTARY MATERIAL

The Supplementary Material for this article can be found online at: <https://www.frontiersin.org/articles/10.3389/fphys.2019.00496/full#supplementary-material>

FIGURE S1 | The reference points and planes for the measurements. **(A,B)** the mandibular landmark points designed for measurements, revealed on the lateral **(A)** and posterior **(B)** views; **(C–E)** the cranial and mandibular reference planes used in this study. Abbreviations are defined in **Supplementary Tables S1, S2**. Abbreviations: IAF, inferior alveolar foramen; Con, condyle; Cor, coronoid; Go, gonion; MF, mental foramen; Id, infradentale; Mn6, lower 1st molar; Id, infradentale; Go(p), gonion posterior point; Go(i), gonion inferior point; RA, ramus anterior point; RP, ramus posterior point; Me, menton; Con(med), condylar medial point; Con(lat), condylar lateral point; MF, mental foramen; Li, lower incisor point.

REFERENCES

- Angaut-Petit, D., Molgo, J., Comella, J. X., Faille, L., and Tabti, N. (1990). Terminal sprouting in mouse neuromuscular junctions poisoned with botulinum type A toxin: morphological and electrophysiological features. *Neuroscience* 37, 799–808. doi: 10.1016/0306-4522(90)90109-h
- Babuccu, B., Babuccu, O., Yurdakan, G., and Ankarali, H. (2009). The effect of the Botulinum toxin-A on craniofacial development: an experimental study. *Ann. Plast. Surg.* 63, 449–456. doi: 10.1097/SAP.0b013e31818d4559
- Bhidayasiri, R., Cardoso, F., and Truong, D. D. (2006). Botulinum toxin in blepharospasm and oromandibular dystonia: comparing different botulinum toxin preparations. *Eur. J. Neurol.* 13(Suppl. 1), 21–29. doi: 10.1111/j.1468-1331.2006.01441.x
- Bjork, A. (1955). Facial growth in man, studied with the aid of metallic implants. *Acta Odontol. Scand.* 13, 9–34. doi: 10.3109/00016355509028170
- Bouvier, M., and Hylander, W. L. (1984). The effect of dietary consistency on gross and histologic morphology in the craniofacial region of young rats. *Am. J. Anat.* 170, 117–126. doi: 10.1002/aja.1001700109
- Boyd, T. G., Castelli, W. A., and Huelke, D. F. (1967). Removal of the temporalis muscle from its origin: effects on the size and shape of the coronoid process. *J. Dent. Res.* 46, 997–1001. doi: 10.1177/00220345670460056401
- Bravo, L. A., Nielsen, I. L., and Miller, A. J. (1989). Changes in facial morphology in *Macaca mulatta*: a cephalometric study from 1.5 to 5 years of age. *Am. J. Orthod. Dentofacial. Orthop.* 96, 26–35. doi: 10.1016/0889-5406(89)90225-4
- Capra, N. F., Bernanke, J. M., and Porter, J. D. (1991). Ultrastructural changes in the masseter muscle of *Macaca fascicularis* resulting from intramuscular injections of botulinum toxin type A. *Arch. Oral Biol.* 36, 827–836. doi: 10.1016/0003-9969(91)90032-p
- Cianferotti, L., and Brandi, M. L. (2014). Muscle-bone interactions: basic and clinical aspects. *Endocrine* 45, 165–177. doi: 10.1007/s12020-013-0026-8
- Cohen, L. (1960). Further studies into the vascular architecture of the mandible. *J. Dent. Res.* 39, 936–946. doi: 10.1177/00220345600390052801
- Dahlberg, G. (1949). Standard error and medicine. *Acta Genet. Stat. Med.* 1, 313–321. doi: 10.1159/000150653
- Dechow, P. C., and Carlson, D. S. (1990). Occlusal force and craniofacial biomechanics during growth in rhesus monkeys. *Am. J. Phys. Anthropol.* 83, 219–237. doi: 10.1002/ajpa.1330830211

Abbreviations: MSP, midsagittal plane; MnOccP, mandibular occlusal plane; IBP, mandibular inferior border plane; FHP, Frankfort horizontal plane; CP, coronal plane; MMP, mandibular median plane; MRP, mandibular ramal plane.

FIGURE S2 | Comparison of three superimposition methods showing different growth patterns for group I (control) model. **(A)** the mandibular registration at the screws on the inferior border showing the superior growth direction in the condylar and coronoid regions; **(B)** the cranial screw-based cranial superimposition showing the main growth direction at the symphysis and on the inferior border; **(C)** superimposition at the mandibular and mental foramen showing growth in the condyle, coronoid, posterior ramus, and symphyseal regions. Red circles indicate the position of reference screws and points of superimpositions.

TABLE S1 | The landmark points and their descriptions used in this study.

TABLE S2 | The reference planes and their descriptions used in this study.

TABLE S3 | Mandibular measurements for height, length, width, angles, areas, and volume.

TABLE S4 | Age and change of body weight by group.

TABLE S5 | The measurements of mandibular unit.

TABLE S6 | Mandibular height measurements.

TABLE S7 | Mandibular length measurements.

TABLE S8 | Mandibular width measurements.

TABLE S9 | Mandibular angular measurements.

TABLE S10 | Mandibular volume and area measurements.

- Delaire, J. (1990). The role of the condyle in the growth of the mandible and in facial balance. *Rev. Stomatol. Chir. Maxillofac.* 91, 179–192.
- Dixon, A. D., Hoyte, D. A. N., and Ronning, O. (1997). *Fundamentals of Craniofacial Growth*. Boca Raton, FL: CRC Press LLC.
- Enlow, D. H., and Harris, D. B. (1964). A study of the postnatal growth of the human mandible. *Am. J. Orthod.* 50, 25–50. doi: 10.1016/s0002-9416(64)80016-6
- Frost, H. M. (1998). From Wolff's law to the mechanostat: a new "face" of physiology. *J. Orthop. Sci.* 3, 282–286. doi: 10.1007/s007760050054
- Grimston, S. K., Silva, M. J., and Civitelli, R. (2007). Bone loss after temporarily induced muscle paralysis by Botox is not fully recovered after 12 weeks. *Ann. N. Y. Acad. Sci.* 1116, 444–460. doi: 10.1196/annals.1402.009
- Hamrick, M. (2010). JMNI special issue: basic science and mechanisms of muscle-bone interactions. *J. Musculoskelet. Neuronal Interact.* 10, 1–2.
- Hohl, T. H. (1983). Masticatory muscle transposition in primates: effects on craniofacial growth. *J. Maxillofac. Surg.* 11, 149–156. doi: 10.1016/s0301-0503(83)80038-1
- Kiliaridis, S. (1995). Masticatory muscle influence on craniofacial growth. *Acta Odontol. Scand.* 53, 196–202. doi: 10.3109/00016359509005972
- Kiliaridis, S., Engström, C., and Thilander, B. (1985). The relationship between masticatory function and craniofacial morphology: I. A cephalometric longitudinal analysis in the growing rat fed a soft diet. *Eur. J. Orthod.* 7, 273–283. doi: 10.1093/ejo/7.4.273
- Kono, K., Tanikawa, C., Yanagita, T., Kamioka, H., and Yamashiro, T. (2017). A Novel Method to Detect 3D Mandibular Changes Related to Soft-Diet Feeding. *Front. Physiol.* 8:567. doi: 10.3389/fphys.2017.00567
- Krupar, S., Darvann, T. A., Larsen, P., Marsh, J. L., and Kreiborg, S. (2005). Three-dimensional analysis of mandibular growth and tooth eruption. *J. Anat.* 207, 669–682. doi: 10.1111/j.1469-7580.2005.00479.x
- Kun-Darbois, J. D., Libouban, H., and Chappard, D. (2015). Botulinum toxin in masticatory muscles of the adult rat induces bone loss at the condyle and alveolar regions of the mandible associated with a bone proliferation at a muscle enthesis. *Bone* 77, 75–82. doi: 10.1016/j.bone.2015.03.023
- Kwon, T. G., Park, H. S., Lee, S. H., Park, I. S., and An, C. H. (2007). Influence of unilateral masseter muscle atrophy on craniofacial morphology in growing rabbits. *J. Oral Maxillofac. Surg.* 65, 1530–1537. doi: 10.1016/j.joms.2006.10.059

- Lepley, C., Throckmorton, G., Parker, S., and Buschang, P. H. (2010). Masticatory performance and chewing cycle kinematics—are they related? *Angle Orthod.* 80, 295–301. doi: 10.2319/061109-333.1
- Losken, A., Mooney, M. P., and Siegel, M. I. (1994). Comparative cephalometric study of nasal cavity growth patterns in seven animal models. *Cleft Palate Craniofac. J.* 31, 17–23. doi: 10.1597/1545-1569(1994)031<0017:ccsonc>2.3.co;2
- Markic, G., Muller, L., Patcas, R., Roos, M., Lochbuehler, N., Peltomaki, T., et al. (2015). Assessing the length of the mandibular ramus and the condylar process: a comparison of OPG, CBCT, CT, MRI, and lateral cephalometric measurements. *Eur. J. Orthod.* 37, 13–21. doi: 10.1093/ejo/cjv008
- Matic, D. B., Yazdani, A., Wells, R. G., Lee, T. Y., and Gan, B. S. (2007). The effects of masseter muscle paralysis on facial bone growth. *J. Surg. Res.* 139, 243–252. doi: 10.1016/j.jss.2006.09.003
- McNamara, J. A. Jr., and Graber, L. W. (1975). Mandibular growth in the rhesus monkey (*Macaca mulatta*). *Am. J. Phys. Anthropol.* 42, 15–24.
- Miyazaki, M., Yonemitsu, I., Takei, M., Kure-Hattori, I., and Ono, T. (2016). The imbalance of masticatory muscle activity affects the asymmetric growth of condylar cartilage and subchondral bone in rats. *Arch. Oral Biol.* 63, 22–31. doi: 10.1016/j.archoralbio.2015.11.020
- Moore, W. J. (1973). An experimental study of the functional components of growth in the rat mandible. *Acta Anat.* 85, 378–385. doi: 10.1159/000144005
- Moss, M. L. (1968). Functional cranial analysis of mammalian mandibular ramal morphology. *Acta Anat.* 71, 423–447. doi: 10.1159/000143198
- Moss, M. L., and Simon, M. R. (1968). Growth of the human mandibular angular process: a functional cranial analysis. *Am. J. Phys. Anthropol.* 28, 127–138. doi: 10.1002/ajpa.1330280211
- Moss, M. L., and Young, R. W. (1960). A functional approach to craniology. *Am. J. Phys. Anthropol.* 18, 281–292. doi: 10.1002/ajpa.1330180406
- Nanda, R., Baume, R. M., Tanne, K., and Sugawara, J. (1987). Longitudinal study of craniofacial growth in *Macaca fascicularis*. *Am. J. Phys. Anthropol.* 73, 215–225. doi: 10.1002/ajpa.1330730208
- Navarro, M., Delgado, E., and Monje, F. (1995). Changes in mandibular rotation after muscular resection. Experimental study in rats. *Am. J. Orthod. Dentofacial Orthop.* 108, 367–379. doi: 10.1016/s0889-5406(95)70034-x
- Park, H. U., Kim, B. I., Kang, S. M., Kim, S. T., Choi, J. H., and Ahn, H. J. (2013). Changes in masticatory function after injection of botulinum toxin type A to masticatory muscles. *J. Oral Rehabil.* 40, 916–922. doi: 10.1111/joor.12111
- Park, W., Kim, B. C., Yu, H. S., Yi, C. K., and Lee, S. H. (2010). Architectural characteristics of the normal and deformity mandible revealed by three-dimensional functional unit analysis. *Clin. Oral Investig.* 14, 691–698. doi: 10.1007/s00784-009-0349-2
- Pickett, A. (2012). Animal studies with botulinum toxins may produce misleading results. *Anesth. Analg.* 115:736; author reply 736–737.
- Polak, F., Morton, R., Ward, C., Wallace, W. A., Doderlein, L., and Siebel, A. (2002). Double-blind comparison study of two doses of botulinum toxin A injected into calf muscles in children with hemiplegic cerebral palsy. *Dev. Med. Child Neurol.* 44, 551–555. doi: 10.1111/j.1469-8749.2002.tb00328.x
- Poliachik, S. L., Bain, S. D., Threet, D., Huber, P., and Gross, T. S. (2010). Transient muscle paralysis disrupts bone homeostasis by rapid degradation of bone morphology. *Bone* 46, 18–23. doi: 10.1016/j.bone.2009.10.025
- Rafferty, K. L., Liu, Z. J., Ye, W., Navarrete, A. L., Nguyen, T. T., Salamati, A., et al. (2012). Botulinum toxin in masticatory muscles: short- and long-term effects on muscle, bone, and craniofacial function in adult rabbits. *Bone* 50, 651–662. doi: 10.1016/j.bone.2011.11.015
- Saka, B., Wree, A., Henkel, K. O., Anders, L., and Gundlach, K. K. (2002). Blood supply of the mandibular cortex: an experimental study in Gottingen minipigs with special reference to the condyle. *J. Craniomaxillofac. Surg.* 30, 41–45. doi: 10.1054/jcms.2001.0257
- Sakurai, M., Yonemitsu, I., Muramoto, T., and Soma, K. (2007). Effects of masticatory muscle force on temporomandibular joint disc growth in rats. *Arch. Oral Biol.* 52, 1186–1193. doi: 10.1016/j.archoralbio.2007.07.003
- Schneiderman, E. D. (1992). *Facial Growth in the Rhesus Monkey: A Longitudinal Cephalometric Study*. Princeton, NJ: Princeton University Press.
- Sella-Tunis, T., Pokhraj, A., Sarig, R., O'higgins, P., and May, H. (2018). Human mandibular shape is associated with masticatory muscle force. *Sci. Rep.* 8:6042. doi: 10.1038/s41598-018-24293-3
- Siegel, M. I., Doyle, W. J., Gest, T. R., and Ingraham, A. S. (1985). A comparison of craniofacial growth in normal and cleft palate rhesus monkeys. *Cleft Palate J.* 22, 192–196.
- Sugiyama, T., Yamaguchi, A., and Kawai, S. (2002). Effects of skeletal loading on bone mass and compensation mechanism in bone: a new insight into the “mechanostat” theory. *J. Bone Miner Metab.* 20, 196–200. doi: 10.1007/s007740200028
- Tsai, C. Y., Chiu, W. C., Liao, Y. H., and Tsai, C. M. (2009). Effects on craniofacial growth and development of unilateral botulinum neurotoxin injection into the masseter muscle. *Am. J. Orthod. Dentofacial Orthop.* 135, 142.e1–142.e6. doi: 10.1016/j.ajodo.2008.06.020
- van Spronsen, P. H., Weijs, W. A., Valk, J., Prahl-Andersen, B., and Van Ginkel, F. C. (1989). Comparison of jaw-muscle bite-force cross-sections obtained by means of magnetic resonance imaging and high-resolution CT scanning. *J. Dent. Res.* 68, 1765–1770. doi: 10.1177/00220345890680120901
- Wolff, J. (1892). *Das Gesetz der Transformation der Knochen*. Berlin: A Hirschwald.
- Yamada, K., and Kimmel, D. B. (1991). The effect of dietary consistency on bone mass and turnover in the growing rat mandible. *Arch. Oral Biol.* 36, 129–138. doi: 10.1016/0003-9969(91)90075-6

Conflict of Interest Statement: The authors declare that the research was conducted in the absence of any commercial or financial relationships that could be construed as a potential conflict of interest.

Copyright © 2019 Kim, Tak, Moon, Kang, Kim, He, Piao and Lee. This is an open-access article distributed under the terms of the Creative Commons Attribution License (CC BY). The use, distribution or reproduction in other forums is permitted, provided the original author(s) and the copyright owner(s) are credited and that the original publication in this journal is cited, in accordance with accepted academic practice. No use, distribution or reproduction is permitted which does not comply with these terms.



The Adult Ts65Dn Mouse Model of Down Syndrome Shows Altered Swallow Function

Tiffany J. Glass^{1*}, Luke Carmichael V. Valmadrid¹ and Nadine P. Connor^{1,2}

¹ Department of Surgery, University of Wisconsin–Madison, Madison, WI, United States, ² Department of Communication Sciences and Disorders, University of Wisconsin–Madison, Madison, WI, United States

OPEN ACCESS

Edited by:

Teresa Lever,
University of Missouri, United States

Reviewed by:

Elisa L. Hill-Yardin,
RMIT University, Australia
Makoto Inoue,
Niigata University, Japan
Gaya Balasuriya,
RMIT University, Australia, contributed
to the review of EH-Y

*Correspondence:

Tiffany J. Glass
glass@surgery.wisc.edu

Specialty section:

This article was submitted to
Neurodegeneration,
a section of the journal
Frontiers in Neuroscience

Received: 09 May 2019

Accepted: 13 August 2019

Published: 29 August 2019

Citation:

Glass TJ, Valmadrid LCV and
Connor NP (2019) The Adult Ts65Dn
Mouse Model of Down Syndrome
Shows Altered Swallow Function.
Front. Neurosci. 13:906.
doi: 10.3389/fnins.2019.00906

There are increased risks for deglutition disorders in people with Down syndrome (DS). Although mouse models have been used to study the biological underpinnings of DS in other areas, relatively little is known about swallowing phenotypes in these models. We hypothesized that swallowing performance would be affected in adult mouse models of DS, relative to typical control mice. Videofluoroscopic swallow studies (VFSS) were conducted on adults of two mouse models of DS: Ts65Dn and Dp(16)1Yey, and evaluated in comparison with age-matched controls. Relative to other groups, adult Ts65Dn showed significantly slower swallow rates, longer inter-swallow intervals (ISI), and greater numbers of jaw excursion cycles preceding each swallow. In contrast, adult Dp(16)1Yey mice showed swallowing performance similar to control mice. Exploratory quantitative analyses of the intrinsic tongue (transverse muscle), and extrinsic tongue muscles [genioglossus (GG), styloglossus (SG), and hyoglossus (HG)] showed no significant differences between genotype groups in myosin heavy chain isoform profiles. Collectively, these findings suggest that while swallowing is typical in adult Dp(16)1Yey, swallowing in adult Ts65Dn is atypical due to unknown causes. The finding that adult Ts65Dn may have utility as a model of dysphagia provides new opportunities to elucidate biological underpinnings of dysphagia associated with DS.

Keywords: deglutition, deglutition disorders, swallow, Down syndrome, mouse, VFSS, Ts65Dn, Dp(16)1Yey

INTRODUCTION

Down syndrome (DS), typically caused by a trisomy of the 21st chromosome, is associated with increased risks for feeding challenges and deglutition disorders across the lifespan (Lazenby, 2008). These can coincide with medical comorbidities (Dinan and Golden, 1990; Zárate et al., 2001; Prasher et al., 2004; Abanto et al., 2011), craniofacial differences (Hashimoto et al., 2014), sensory differences (Frazier and Friedman, 1996), and behavioral differences (Homer and Carbajal, 2015). In patients with DS in which impairment of deglutition is suspected, videofluoroscopic swallow studies (VFSS) may detect swallowing impairments (O'Neill and Richter, 2013; Jackson et al., 2016). While clinical studies have reported both oral motor dysfunction and pharyngeal phase dysphagia in children with DS (Jackson et al., 2016), it is also known that adults with DS are likely to experience several additional risk factors for swallowing disorders (Lazenby, 2008).

Dysphagia associated with DS in later life stages can coincide with multiple challenges including an increased prevalence of age-related comorbidities (Yang et al., 2002; Cipriani et al., 2018), unique health care and support needs (Carling-Jenkins et al., 2012; Capone et al., 2018), and communication impairments associated with the syndrome that may obstruct self-reporting of symptoms (Lazenby, 2008; Capone et al., 2018). One avenue for addressing this research challenge may be the use of animal models, which offer opportunities to explore aspects of pathophysiology of feeding and swallowing that cannot be studied in patient populations (German et al., 2017).

Recent work has refined the application of experimental VFSS for the quantitative study of swallowing performance in animal models of swallowing disorders. For example, VFSS has been used to detect and characterize swallowing differences in rat models of aging and Parkinson disease (Russell et al., 2013; Cullen et al., 2018), mouse models of presbyphagia (Lever et al., 2015b), and ALS (Lever et al., 2010). This validated experimental paradigm offers new opportunities for similar evaluation of swallowing differences in mouse models of DS. The Ts65Dn and Dp(16)1Yey mouse models of DS are both used for translational research (Liu et al., 2011). While Ts65Dn models DS through a partial trisomy comprised of a distal portion of mouse chromosome 16 and a centromeric portion of mouse chromosome 17 (Davisson et al., 1993; Duchon et al., 2011), Dp(16)1Yey features a typical karyotype with a duplication of the entire mouse chromosome 16 region that is syntenic to the human 21st chromosome (Li et al., 2007). While these models are generally regarded as having utility for the study of biological differences associated with DS, relatively little is known about their feeding and swallowing phenotypes.

Our prior work suggested normal swallowing performance in juvenile (5–6-week-old) Ts65Dn mice, as assessed by swallow rates (Glass and Connor, 2016). However, because impairments associated with DS are known to change with age (Bayen et al., 2018), we hypothesized that swallowing performance would be affected in adult mouse models of DS. We report the outcomes of VFSS and initial tongue muscle characterization of two adult mouse models of DS: Ts65Dn and Dp(16)1Yey.

METHODS

Mice

All husbandry and experimental procedures involving live mice were carried out with approval from the University of Wisconsin School of Medicine and Public Health Animal Care and Use Committee (IACUC) and were conducted in accordance with the Guide for the Care and Use of Laboratory Animals (8th ed.) (The National Academies Press, 2011). Mice were weaned at 3 weeks of age and raised on a hard pellet diet. Ts65Dn were maintained from The Jackson Laboratory mouse stock number 005252, by pairing Ts65Dn females with B6EiC3Sn.BLiAF1/J males (stock number 003647). Dp(16)1Yey mice were assessed in the same genetic background, as achieved through multiple backcrosses to B6EiC3Dn.BLiAF1. Dp(16)1Yey used in the present study were generated by mating Dp(16)1Yey females

to B6EiC3Sn.BLiAF1/J males. Genotypes were determined by separated PCR or by Transnetyx as previously reported (Glass and Connor, 2016).

Mice were analyzed in videofluoroscopic swallowing assays in comparison to age-matched euploid sibling controls (Ts65Dn) and WT sibling controls [Dp(16)] at 5 months (19–22 weeks) of age (9–13 mice per group). This is an age immediately preceding the onset of age-related neurodegeneration and associated cognitive decline reported to occur in Ts65Dn at 6 months of age (Holtzman et al., 1996; Hunter et al., 2003). These groups subsisted on Harlan Teklad diet 7913, which is a hard food pellet. Separately, male and female Ts65Dn mice were evaluated in videofluoroscopic swallowing assays in comparison to euploid controls, in groups comprised of mice spanning an adult age range (9–36 weeks of age, 7 mice per group). This age range encompasses early adulthood through late maturity, and was anticipated to provide a preliminary indication of whether swallowing phenotypes differed with sex and age. Video-recording assays of mastication of hard food pellets were also performed on male mice across an adult age range (8–44 weeks of age, 13–14 mice per group). All age range groups subsisted on Harlan Teklad diet 8604, which is a hard food pellet. Following behavioral experiments, mice were weighed, euthanized with CO₂, and muscles were isolated and stored at –80°C for subsequent analysis.

Videofluoroscopic Swallow Studies

Videofluoroscopic swallow studies assays were performed as previously described (Glass and Connor, 2016). Mice were identified by alphanumeric codes to mask genotype identities to workers during VFSS assays. The food used for imaging was a 2:1 mixture of Fritos Mild Cheddar CheeseTM dip and 40% weight/volume barium suspension. Mice were acclimated to cheese mixtures daily for a few days immediately prior to VFSS, and all food was withheld overnight prior to the VFSS study. On the day of data acquisition, each mouse was placed alone in a cage and was imaged during continuous volitional eating at 30 fps with an Artis Zee system (Siemens Healthcare, Forchheim, Germany). The duration of VFSS acquisition for each mouse was limited to the amount of time required to record several visible swallows, typically at least 10 s. For all experiments, each mouse generated VFSS data for only one time point. Following VFSS, mice were weighed.

Videofluoroscopic Analysis

Videofluoroscopic swallow studies footage was manually analyzed in ImageJ using measures as previously described, to quantify measures of oral and pharyngeal function (Lever et al., 2015a,b). These measures included swallow rate (the number of swallows per 2 s of eating), inter-swallow interval (ISI, the number of seconds elapsed between two successive swallows), jaw excursion rate (JER, the number of cycles of jaw opening and closing per second), and jaw cycle:swallow ratio (JSR, the number of jaw excursion cycles per ISI). In these studies of a puree consistency, the JSR measure is analogous to the lick-swallow ratio (LSR) previously described in analysis of drinking (Lever et al., 2015a,b), however, in the present study the

JSR acronym was used to accommodate the possibility that with a puree consistency jaw cycles may indicate other oral processing movements and/or licking. These measures were obtained using a minimum of three and a maximum of five separate measurements for each mouse, which were then averaged to generate each final data point. Intrarater and interrater reliability for this study were evaluated through interclass correlation coefficients (ICC). Values of 0.90 or greater were obtained for all measures, which indicated robust agreement for evaluation of VFSS (Nordin et al., 2017).

Mastication Rate Analysis

To supplement VFSS analysis which evaluated swallowing performance during consumption of puree, high-speed videorecording was used in separate sessions to evaluate mastication of a hard food pellet. Food was removed from the cage the evening prior to the assay and restored the following morning at the start of the assay. Mice were videorecorded at 60 fps in lateral profile while eating. Video footage was manually analyzed in Adobe Photoshop CC to quantify mastication rate as previously described (Lever et al., 2009). The analysis began on a frame with the jaw maximally closed, and the rater counted the number of subsequent mastication cycles (jaw fully open and then closed) that occurred during the next 59 consecutive frames. This provided the number of chewing cycles per second. The mastication rate for each mouse was determined from the average of four to five different 1-second periods of continuous chewing.

Immunofluorescence and Microscopy of Intrinsic Tongue Muscles

Intrinsic tongues were examined through tissue sections due to the unique anatomical specialization and complex interdigitation of these muscles (Cullins and Connor, 2017). Tongues of adult mice were embedded in OCT (Optimum Cutting Temperature) in plastic cassettes, and frozen through immersion in isopentane cooled in liquid nitrogen. Tissue was sectioned at 10 μ m onto slides and unfixed tissue sections were incubated overnight at 4°C with primary antibodies mouse IgG1 SC-71 (applied at 1:1), mouse IgM BF-F3 (applied at 1:1; Developmental Studies Hybridoma Bank), or rabbit anti-Laminin (applied at 1:200; Sigma, L9393), to detect myosin heavy chain isoform (MyHC) 2a, MyHC 2b, and myofiber borders, respectively. In each technical staining iteration, mouse soleus and extensor digitorum longus (EDL) muscle sections were processed concurrently as biological positive and negative controls for MyHC isoform staining. After PBS washes, slides were incubated for 1 h at room temperature with fluorescent secondary antibodies from Thermo Fisher Scientific (goat anti-mouse IgM AF350, A31552 (1:50), donkey anti-rabbit IgG AF488 A21206 (1:1000), goat anti-mouse IgG1 AF568, A21124, 1:300), rinsed, mounted, and imaged. Imaging was performed on an epifluorescence Olympus Bx53 microscope with a motorized stage and CellSens software. Optimal image exposure settings for all isoforms were experimentally determined for each image acquisition session through evaluation of biological positive control staining for

MyHC 2b (EDL muscle), biological positive control staining for MyHC 2a (soleus muscle), biological negative control staining for MyHC 2b (soleus muscle), and technical negative control slides with all primary antibodies omitted to control for autofluorescence. Tissue sections were imaged through semi-automated acquisition to generate composites of multiple fields of view acquired with a 20 \times objective. One large composite image was obtained from one section from each intrinsic tongue.

Quantitative Image Analysis

Quantitative analyses of myofibers of the transverse intrinsic tongue muscle were performed on images cropped to isolate one large region of interest within the blade of the tongue. Analyzed regions were located within an area bordered anteriorly by the tongue tip, posteriorly by the frenulum (posterior limit of ventral tongue mucosa), superiorly by the superior longitudinal (SL) muscle, and inferiorly by the inferior longitudinal (IL) muscle (Figure 3A). Regions of interest were analyzed through the MATLAB Application SMASH as previously described (Smith and Barton, 2014). Laminin staining was used for the semi-automated detection of myofibers, allowing myofiber size to be quantified. MyHC signal was used to calculate the percentage of fibers positive for each isoform. At least several hundred myofibers located in the blade of the tongue were analyzed to produce one average data point for each mouse.

MyHC Protein Analysis of Extrinsic Tongue Muscles

Total protein was isolated from homogenized extrinsic tongue muscles of adult mice using methods previously described (Adreani et al., 2006). Following sample protein quantification through a Bradford protein concentration assay (Thermo Fisher Scientific), MyHC profiles of extrinsic tongue muscles were analyzed through separation by sodium dodecyl sulfate polyacrylamide gel electrophoresis (SDS-PAGE) (Adreani et al., 2006), and silver staining to visualize protein isoform bands. Stained gels were digitally scanned using a flatbed scanner and band signal intensity was quantified using UN-SCAN-IT gel analysis software (Silk Scientific). Each mouse muscle sample was analyzed in duplicate.

Statistics

GraphPad Prism 7.04 was used to perform one- or two-way ANOVAs as applicable, with Tukey's *post hoc* tests. One-way analysis of variance was used to evaluate the impact of genotype (euploid, Ts65Dn, WT, and Dp(16)1Yey) on swallowing measures for male 5-month-old mice, and two-way analysis of variance was used to evaluate the impact of genotype (euploid, Ts65Dn) and sex (male, female) on swallowing measures for groups comprised of Ts65Dn mice and controls spanning the adult age range. An unpaired *t*-test was used to evaluate mastication rates in male Ts65Dn and male euploid controls. IBM SPSS Statistics software was used to calculate ICC values to evaluate VFSS interrater and intrarater reliability. An α -level of 0.05 defined statistical significance.

RESULTS

VFSS

5-Month-Old Ts65Dn and Dp(16)1Yey

Analysis of total body weight revealed statistically significant differences in weight between genotype groups [$F(3,54) = 13.76$, $p < 0.0001$]. *Post hoc* tests confirmed that the Ts65Dn group weighed significantly less than both euploid control ($p < 0.0001$) and Dp(16)1Yey ($p = 0.0006$) groups (Figure 1A). There was a significant main effect of genotype on swallow rate [$F(3,39) = 8.07$, $p = 0.0003$], and *post hoc* testing indicated that the Ts65Dn group showed significantly lower swallow rates than the Dp(16)1Yey group ($p \leq 0.05$). Inter-swallow intervals (ISI) are closely related to swallow rate, and provide a supplementary, independent measure for comparison of swallow speed differences between groups. There were corresponding significant differences between genotype groups for ISI [$F(3,44) = 9.31$, $p < 0.0001$]. *Post hoc* testing revealed that the Ts65Dn group showed significantly longer ISIs than both euploid ($p \leq 0.001$) and Dp(16)1Yey groups ($p \geq 0.01$). In analysis of the JSR, there were significant differences between genotypes for the number of jaw cycles per swallow [$F(3,41) = 5.45$, $p = 0.003$]. *Post hoc* testing indicated that the Ts65Dn group completed significantly more jaw cycles per swallow than both euploid ($p \leq 0.01$) and Dp(16)1Yey groups ($p \geq 0.05$). However, there were no significant differences between genotype groups for jaw excursion rates, [$F(3,43) = 0.79$, $p = 0.50$] (Figures 1C–F). Collectively, these analyses indicate normal jaw cycle speeds in the Ts65Dn group, but a greater number of jaw cycles preceding each swallow (JSR), associated with increases in the amount of time elapsed between swallows (ISI). That results in overall reductions in swallow rates.

Male and Female Ts65Dn Across an Adult Age Range

In a separate analysis of swallow rates and ISIs across an adult age range in male and female Ts65Dn, two-way ANOVAs revealed significant main effects for genotype, but not for sex, in the absence of significant interactions between genotype and sex. Ts65Dn across an adult age range showed slower swallow rates than euploid controls [$F(1,23) = 4.61$, $p = 0.04$]. Similarly, ISIs were of significantly longer duration in the adult Ts65Dn than in the adult euploid [$F(1,26) = 5.14$, $p = 0.03$] (Figures 2A,B). Finally, video analysis of male mice eating standard hard chow pellets revealed no significant differences between Ts65Dn and euploid controls in mastication rates [$t(25) = 0.36$, $p = 0.72$] (Figure 2C).

Tongue Muscle Analysis

Intrinsic Tongue Muscles in Ts65Dn and Dp(16)1Yey

Following VFSS, mice were euthanized and intrinsic tongue muscles of Ts65Dn and Dp(16)1Yey were evaluated by immunofluorescence staining and microscopy. While the majority of intrinsic tongue myofibers were positive for MyHC 2b, anterior-to-posterior anatomical distributions of MyHC isoforms were qualitatively observed in the mouse intrinsic

tongue, with the greatest preponderance of MyHC 2b in the anterior tongue, and an increasing prevalence of MyHC 2a in the posterior regions of the tongue (Figure 3A). Exploratory analysis of myofiber cross-sectional area (CSA) of the transverse muscle (Figures 3B,C) revealed no significant differences between genotype groups for either CSA of MyHC 2a positive fibers [$F(3,18) = 1.73$, $p = 0.20$], nor prevalence of MyHC 2a positive fibers [$F(3,18) = 1.44$, $p = 0.27$].

Extrinsic Tongue MyHC Isoform Profiles Across the Adult Age Range

The genioglossus (GG) is an extrinsic tongue muscle involved in tongue protrusion, and the styloglossus (SG) and hyoglossus (HG) are involved in tongue retrusion. The GG, SG, and HG were assessed in male Ts65Dn and euploid control mice across the adult age range to assess the likelihood that genotype-specific MyHC isoform differences were present in these muscles in adult mice. No significant differences in proportion of MyHC isoforms were found between the Ts65Dn genotype and euploid controls for extrinsic tongue muscles [$F(1,37) = 0.004$, $p = 0.95$]. However, significant differences were found between extrinsic tongue muscles [$F(2,37) = 10.35$, $p = 0.0003$]. Specifically, the HG muscle had greater levels of MyHC 2b than the SG and GG muscles, across both genotypes (Figure 4).

DISCUSSION

A variety of feeding and swallowing challenges can occur at relatively high frequency in individuals with DS. These include reduced mastication rates (Smith et al., 2013), inefficient oral processing (Hennequin et al., 2015), and silent aspiration (aspiration of food or liquid into the trachea or lungs, in the absence of a protective cough reflex) (Jackson et al., 2016). In mice, eating involves cycles of oral processing to collect a consolidated food bolus at the region of the epiglottic vallecula, or the base of the tongue. Through food procurement and oral processing, the size of the consolidated bolus gradually increases and ultimately triggers a swallow in which the entire bolus is released from the vallecular region and proceeds through the esophagus (Figure 1B). The present study tested the hypothesis that adult mouse models of DS demonstrate abnormal feeding and swallowing performance. It was found that adult Ts65Dn swallow more slowly than Dp(16)1Yey and control mice, with longer inter-swallow interval times. Ts65Dn also showed significant increases in the JSR, which is the number of jaw cycles preceding each swallow. However, jaw excursion rates and mastication rates (measures of jaw cycle speed) were both unaffected in adult Ts65Dn. In this study, jaw excursion rates were measured by VFSS during consumption of puree, whereas mastication rates were measured by analysis of videorecordings during consumption of a hard food pellet. Therefore these were two methodologically independent measures of jaw cycle speed. The presence of typical jaw cycle speeds in Ts65Dn suggests that reduced swallow rates do not occur in the context of slower rhythmic jaw movement, but rather involve a greater number of oral movements prior to

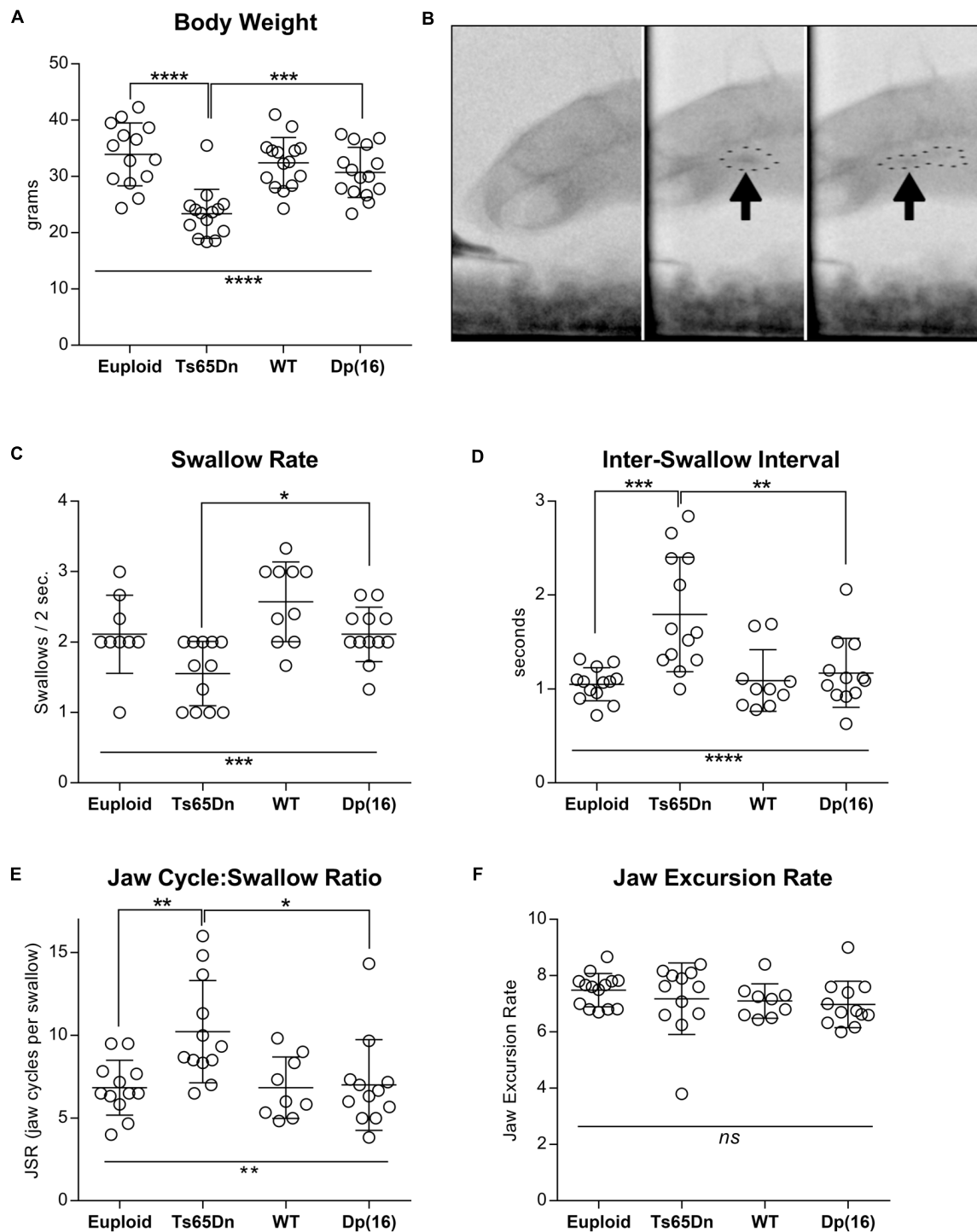


FIGURE 1 | Videofluoroscopic swallow studies analysis in 5-month-old male Ts65Dn and Dp(16) mice. **(A)** Total body weight of mice analyzed through VFSS. **(B)** Stills from VFSS footage of adult mice. Arrows and dotted outlines show a food bolus immediately prior to initiation of a swallow (left), and immediately after initiation of a swallow (right). **(C)** VFSS Swallow rate, **(D)** VFSS Inter-swallow Interval, **(E)** VFSS Jaw Cycle:Swallow Ratio, **(F)** Jaw Excursion Rate. Each symbol indicates the average of 3–5 separate iterations for a single mouse. Mean and SD are shown. * $p \leq 0.05$, ** $p \leq 0.01$, *** $p \leq 0.001$, and **** $p \leq 0.0001$.

each swallow. Collectively, these differences indicate increased oral processing times prior to each swallow, and/or delayed initiation of the swallow.

The presence of increased oral processing times prior to each swallow is compatible with the possibility of inefficient oral processing, or differences in the oral movements responsible for

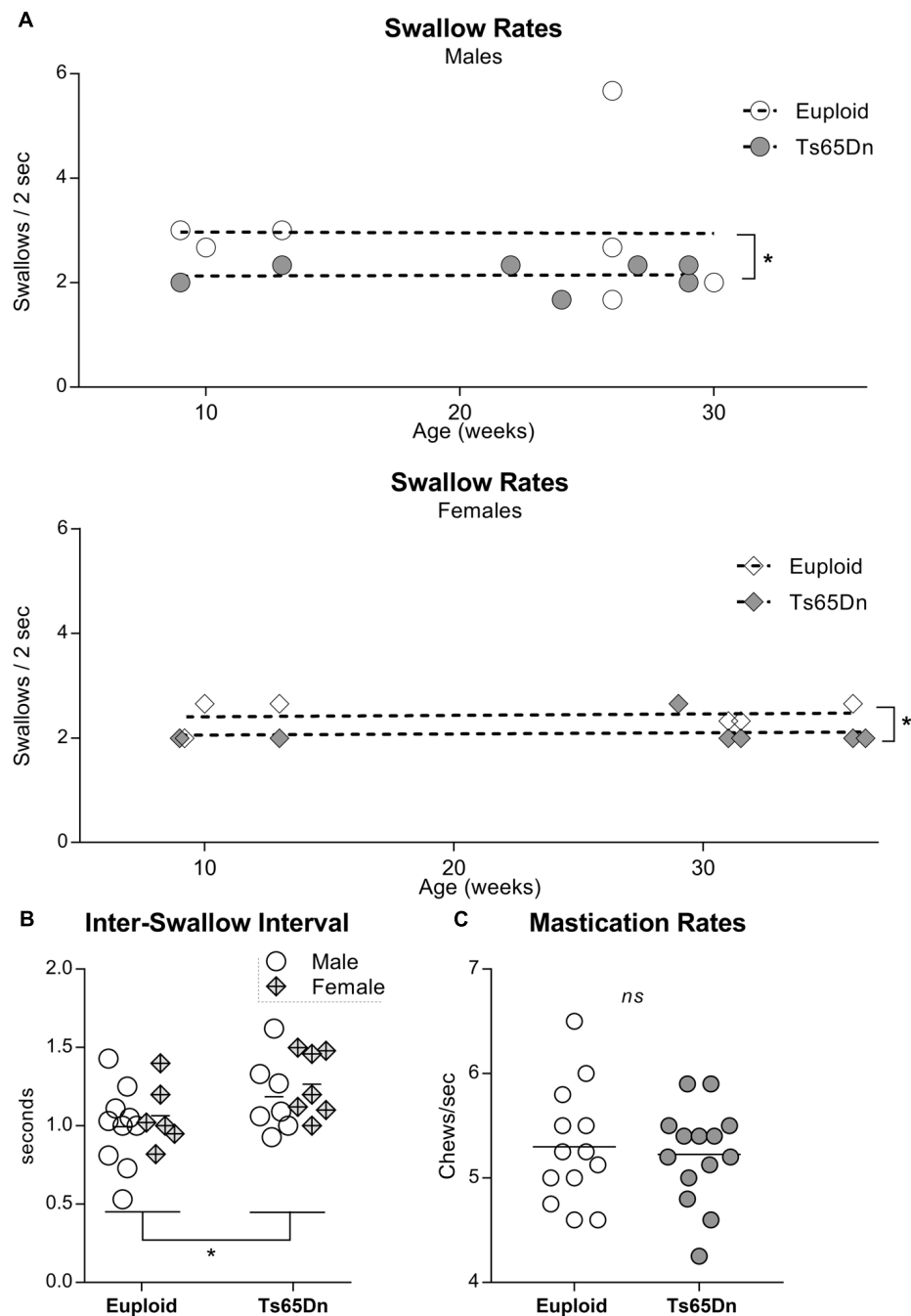
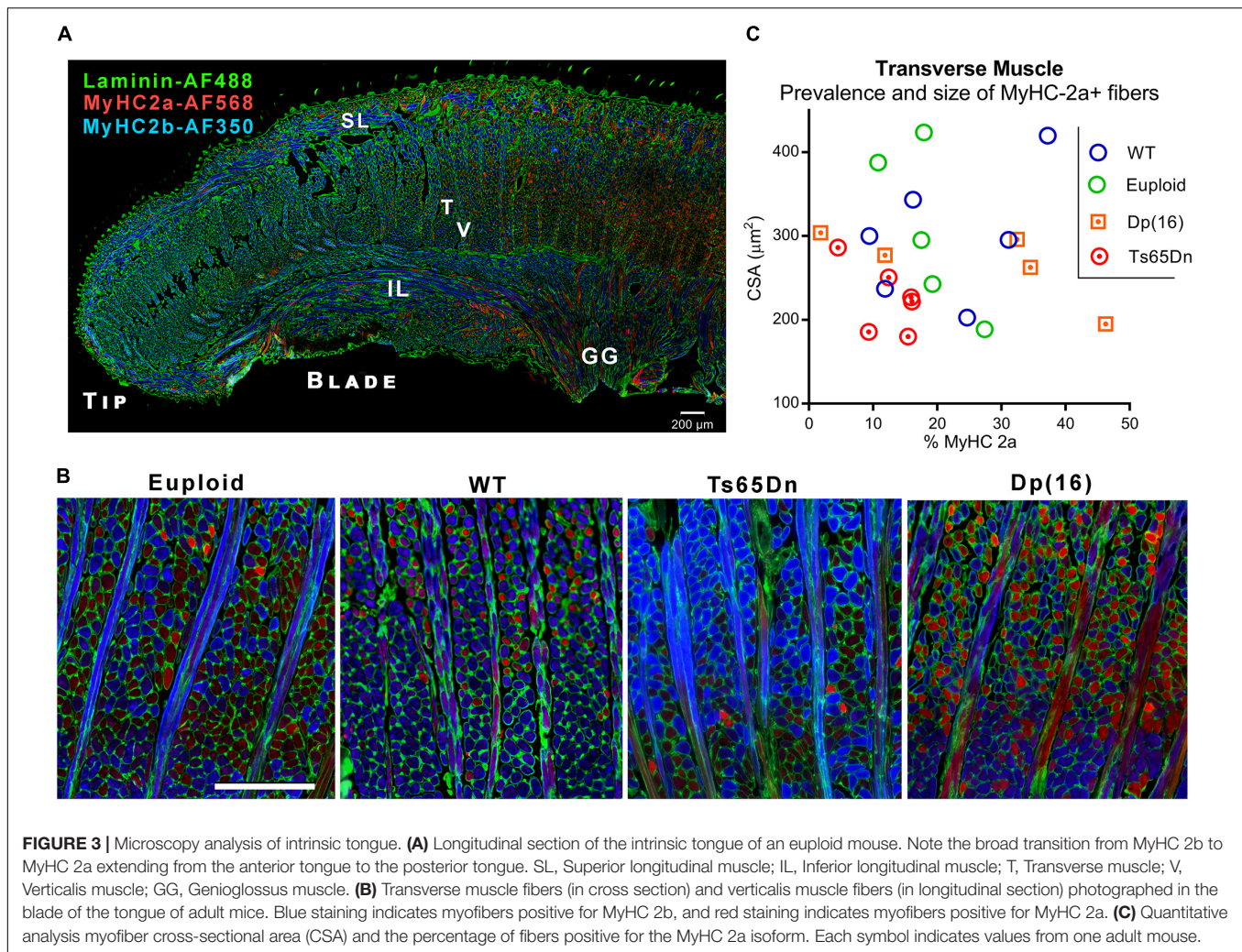


FIGURE 2 | Videofluoroscopic swallow studies analysis of male and female Ts65Dn mice across an adult age range. Each symbol indicates the average of 3–5 separate iterations of the measure for a single mouse. **(A)** Swallow rates for each sex, distributed across an adult age range. **(B)** ISI measurements from mice in panel **(A)**. **(C)** Mastication rates assessed from analysis of high-speed video footage of adult male mice eating hard food pellets. * $p \leq 0.05$.

procuring the food, forming the bolus, and conveying it to the oropharynx. If elicitation of the swallow requires a minimum bolus size and Ts65Dn mice require a greater number of oral movement cycles to achieve the requisite bolus size, delayed initiation of the swallow could result. Alternatively, a second potential cause of the difference in swallowing outcomes between

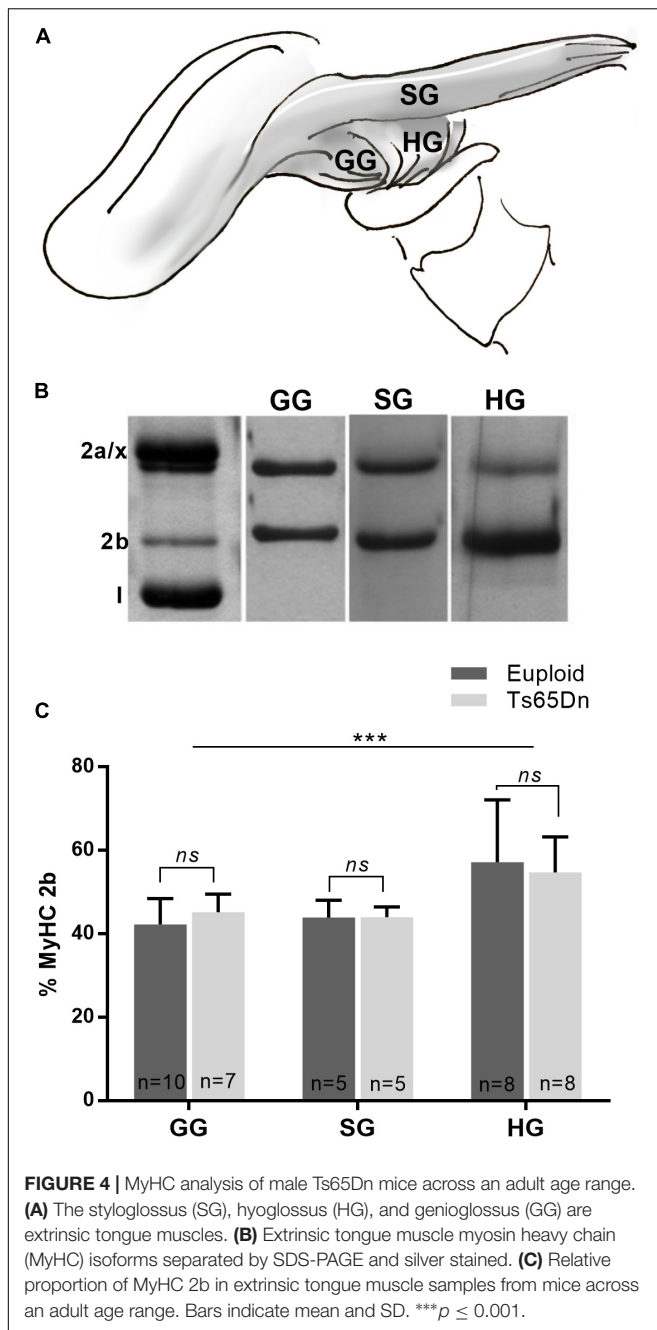
genotypes could involve reduced sensitivity to the characteristics of the bolus that trigger the swallow, or increases in the threshold volume of the bolus required to trigger the swallow, as has been previously reported to occur in aging humans (Shaker et al., 1994; Miller, 2002). However, the image resolution in this VFSS study was not conducive to direct quantification of



either bolus size or tongue movement. There are opportunities for future work to overcome these types of limitations through the use of VFSS systems with improved imaging capabilities, higher imaging speeds, and through supplemental experimental strategies for quantification of swallowing measures (Lever et al., 2015a; German et al., 2017).

Differences of masticatory function, and/or lingual function may influence oral processing. Prior work has identified MyHC profile differences of the digastric muscle (a muscle involved in jaw movement and chewing), in both juvenile and adult Ts65Dn (Glass and Connor, 2016). However, that work also found that juvenile Ts65Dn with atypical digastric muscle MyHC nevertheless had typical swallowing speeds as evaluated by VFSS (Glass and Connor, 2016). It is therefore possible that atypical MyHC profiles of digastric muscles in adult Ts65Dn are unlikely to be the primary cause of the significant differences in swallow rates seen in adult mice. This suggests a possibility that differences in lingual function, rather than differences in masticatory function, may be of interest as a possible factor in reduced swallowing speeds in adult Ts65Dn. Significant differences in swallow rates without the means

to conclusively rule out lingual processing deficits through VFSS analysis parameters alone prompted interest in examining supplemental indicators of tongue muscle function. The extrinsic tongue muscles are responsible for tongue protrusion and retraction. Alterations in the movements of these extrinsic tongue muscles are sometimes accompanied by alterations of MyHC isoform profiles. We evaluated the MyHC isoform profiles of these muscles to determine whether the adult Ts65Dn exhibit biochemical signatures of altered extrinsic tongue muscle function. We found that adult Ts65Dn showed no differences in MyHC isoform profiles of these muscles as compared to euploid controls. This result was similar to prior analyses of MyHC profiles of extrinsic tongue muscles in younger Ts65Dn and euploid controls at 5–6 weeks of age, which also showed no significant differences between genotypes in analysis of GG and SG MyHC (Glass and Connor, 2016). It has been previously suggested that in murine VFSS assays of drinking, jaw cycle rates are directly representative of lick rates (Lever et al., 2015b), which are accomplished through cycles of tongue protrusion (GG), and retraction (SG and HG). Therefore, normal jaw cycle rates in Ts65Dn seen in this study, in conjunction with normal



extrinsic tongue muscle MyHC profiles, provide complementary support for the conclusion that extrinsic tongue muscle function in Ts65Dn was not detectably impaired during these VFSS assays.

The intrinsic tongue muscles (SL, IL, transverse, and verticalis) may act synergistically with the extrinsic muscles to achieve protrusion and retrusion (McClung and Goldberg, 2000), and additionally alter intrinsic tongue shape which helps to form the bolus and propel it posteriorly along the length of the tongue (Hiimae and Palmer, 2003). However, the muscular organization of the mammalian intrinsic tongue is complex. In addition to regional MyHC profile gradients, prior studies

have proposed the existence of multiple functionally distinct neuromuscular compartments spanning the length of the tongue (Mu and Sanders, 1999; Hiimae and Palmer, 2003). While our exploratory inquiry examined the transverse muscle of the intrinsic tongue, several questions remain for future work. First, it remains to be determined whether each intrinsic tongue muscle is developmentally and anatomically typical in Ts65Dn. Secondly, incidental observation indicated a prevalence of MyHC 2b in the anterior tongue, and increasing numbers of MyHC 2a-positive myofibers in the posterior tongue (Figure 2A). To our knowledge this phenomenon has not been reported previously in mice, however, it has been reported previously in rats (Cullins and Connor, 2017). Because MyHC 2b is associated with faster contraction velocity and lower fatigue resistance as compared to MyHC 2a, (Talmadge et al., 1993; Rivero et al., 1999) it may be speculated that an anterior-to-posterior MyHC shift could have implications for tongue function. Prior studies of the intrinsic tongue in rats have found alterations in spatial gradients of MyHC profiles at older ages associated with reduced bolus speeds and reduced bolus size as determined through VFSS (Russell et al., 2013; Cullins and Connor, 2017). Because the spatial distribution of MyHC profiles in the intrinsic tongue is anticipated to be of functional significance (Stål et al., 2003), has been shown to change with aging (Cullins and Connor, 2017), and DS is associated with hallmarks of age-related functional decline (Wisniewski et al., 1978), future studies evaluating the spatiotemporal distribution of myofiber types in the intrinsic tongue in mouse models of DS may support improved understanding of functional changes in tongue movement across the lifespan in DS.

Delayed swallows in Ts65Dn are also compatible with the possibility is that Ts65Dn may experience reduced oropharyngeal sensation, which prior studies have suggested may occur in DS as evidenced by high rates of silent aspiration (Jackson et al., 2016). Impaired oropharyngeal sensation, if present, could be expected to delay swallow initiation in mice due to, among other things, reduced sensitivity to bolus size. Prior studies in mouse models of DS have reported significant reductions in innervation density of many structures (Patel et al., 2015); however, relatively little is currently known about the innervation densities of the tongue, larynx, and pharynx of Ts65Dn and Dp(16)1Yey. Studies of the peripheral innervation densities of structures involved in swallowing would conceivably be of value for efforts to identify biological mechanisms of impairment contributing to silent aspiration in DS. Similarly, it may be of interest to consider the potential role of central nervous system differences in swallowing phenotypes of Ts65Dn. For example, Ts65Dn shows a variety of GABAergic phenotypes (Deidda et al., 2015; Contestabile et al., 2017), while a recent study in typical rats has shown that GABA receptor ligands can modify murine swallowing function (Tsujimura et al., 2017). However, measures of central nervous system function were not evaluated in the present study and it is currently not known whether differences of the central nervous system impact swallowing in Ts65Dn.

While considering swallowing performance, it may be worth noting that both Ts65Dn and Dp(16)1Yey have been previously suggested to have potential utility as models of

gastrointestinal abnormalities associated with DS. Ts65Dn has been suggested to have functional differences of the jejunum (Cefalu et al., 1998), and prior work in the Dp(16)1Yey model identified annular pancreas or malrotation of the intestines to be present at or below an incidence of 26% of E18.5 embryos (Li et al., 2007). It is possible, however, that pups with significant gastrointestinal abnormalities have relatively greater likelihood of perinatal or juvenile mortality. Therefore, mice with significant gastrointestinal phenotypes may or may not have been represented among the adults evaluated in the present study.

Ts65Dn and Dp(16)1Yey may in some ways offer complementary strengths and weaknesses as models of DS, however, neither model is an ideal genetic recapitulation of DS. Three different mouse chromosomes (Mmu) collectively provide regions that are syntenic to the human chromosome 21. Neither Ts65Dn nor Dp(16)1Yey comprehensively model DS through contributions from all three of these mouse chromosomes (Herault et al., 2012). Historically, Ts65Dn has been the most extensively studied mouse model of DS, and features an extra chromosome composed of a distal portion of Mmu 16, and a small centromeric portion of Mmu 17 that is not related to DS. Thus, not only does Ts65Dn incompletely model effects arising from all of the genes on Mmu 16 that are homologous to those on human chr 21, but due to contributions from unrelated genes on Mmu 17 there is an additional risk that it also may conceivably show phenotypes that are etiologically irrelevant to phenotypes of DS in humans (Gupta et al., 2016). By comparison, the Dp(16)1Yey model features a large genetic duplication that includes the full range of genes on Mmu 16 that are homologous to genes on human chr 21, thus may offer comparatively superior fidelity in modeling the gene-dosage effects in DS. However, unlike Ts65Dn, Dp(16)1Yey does not involve an extra chromosome. This bears mentioning as it has been speculated that some phenotypes of DS may be influenced by disruptions intrinsic to the presence of an additional chromosome, rather than through gene-dosage effects alone (Shapiro, 1983; Herault et al., 2012). Since Ts65Dn and Dp(16)1Yey were analyzed concurrently on the same genetic background in the present study, differences in their respective swallowing phenotypes may be attributable to functional differences in Ts65Dn caused by the contributions from Mmu 17 which are arguably not translationally relevant to DS, or may be caused by the additional partial chromosome itself in Ts65Dn, which could be of potential translational relevance to DS. Regardless, identification of swallowing phenotypes in mouse models of DS may expand opportunities for the study of dysphagia in DS to follow murine-based approaches to basic and translational research, as have been commonly used for investigations of intellectual disability in this syndrome.

Finally, it has been previously proposed that licking motor patterns in adult mice may bear some resemblance to feeding patterns in human infants (Lever et al., 2015a), in which rhythmic sucks precede each swallow (suck/swallow cycles) (Gewolb et al., 2001; Lau, 2015). The age of Ts65Dn predominately studied here (5 months) also approaches the age at which biological indicators of adult-onset neurodegeneration and age-related memory and learning impairments appear in this model (Holtzman et al.,

1996; Hyde and Crnic, 2001; Hunter et al., 2003). Intriguingly, increased swallow durations characterized by increased oral processing times and delays in swallow initiation have been reported to occur in dysphagia associated with Alzheimer's disease in the general population (Lazenby, 2008). The fact that juvenile Ts65Dn have shown normal swallow rates (Glass and Connor, 2016), while adult Ts65Dn show significantly slower swallow rates than euploid controls, suggests an age-related or maturational component to the etiology of this swallowing phenotype. Therefore, the study of feeding and swallowing in adult Ts65Dn may be anticipated to have relevance to a broad range of chronological, developmental, and biological research questions involved in feeding challenges associated with DS.

DATA AVAILABILITY

The raw data supporting the conclusion of this manuscript will be made available by the authors, without undue reservation, to any qualified researcher.

ETHICS STATEMENT

All husbandry and experimental procedures involving live mice were carried out with approval from the University of Wisconsin School of Medicine and Public Health Animal Care and Use Committee (IACUC) and were conducted in accordance with the Guide for the Care and Use of Laboratory Animals (8th ed.).

AUTHOR CONTRIBUTIONS

TG and NC conceived and designed the study, and contributed reagents, materials, and analysis tools. TG and LV performed the experiments and analyzed the data. TG performed the statistical analysis. All authors wrote and edited the manuscript.

FUNDING

This work was supported by the National Institute on Deafness and Other Communication Disorders (NIDCD) F32 DC014885, R01 DC008149, R01 DC014358, and Jerome Lejeune Foundation, Agreement #1326 (URL: <https://lejeunefoundation.org/>).

ACKNOWLEDGMENTS

The authors gratefully acknowledge the assistance of Dr. Alberto C. Costa and Melissa Stasko, Case Western Reserve University, who supplied initial breeding pairs of Dp(16)1Yey mice in the mixed background used to generate mice used in this research. The SC-71 and BF-F3 antibodies developed by S. Schiaffino were obtained from the Developmental Studies Hybridoma Bank, created by the NICHD of the NIH and maintained at Department of Biology, The University of Iowa, Iowa City, IA, United States.

REFERENCES

- Abanto, J., Ciamponi, A. L., Franciscini, E., Murakami, C., de Rezende, N. P., and Gallotini, M. (2011). Medical problems and oral care of patients with Down syndrome: a literature review. *Spec. Care Dentist.* 31, 197–203. doi: 10.1111/j.1754-4505.2011.00211.x
- Adreani, C. M., Li, Z. B., Lehar, M., Southwood, L. L., Habecker, P. L., Flint, P. W., et al. (2006). Myosin heavy chain composition in normal and atrophic equine laryngeal muscle. *Vet. Pathol.* 43, 881–889.
- Bayen, E., Possin, K. L., Chen, Y., Cleret de Langavant, L., and Yaffe, K. (2018). Prevalence of aging, dementia, and multimorbidity in older adults with Down syndrome. *JAMA Neuro.* 75, 1399–1406. doi: 10.1001/jamaneurol.2018.2210
- Capone, G. T., Chicoine, B., Bulova, P., Stephens, M., Hart, S., Crissman, B., et al. (2018). Co-occurring medical conditions in adults with Down syndrome: a systematic review toward the development of health care guidelines. *Am. J. Med. Genet. A* 176, 116–133. doi: 10.1002/ajmg.a.38512
- Carling-Jenkins, R., Torr, J., Iacono, T., and Bigby, C. (2012). Experiences of supporting people with Down syndrome and Alzheimer's disease in aged care and family environments. *J. Intellect. Dev. Disabil.* 37, 54–60. doi: 10.3109/13668250.2011.645473
- Cefalu, J. A., Croom, W. J., Eisen, E. J., Jones, E. E., Daniel, L. R., and Taylor, I. L. (1998). Jejunal function and plasma amino acid concentrations in the segmental trisomic Ts65Dn mouse. *Growth Dev. Aging* 62, 47–59.
- Cipriani, G., Danti, S., Carlesi, C., and Di Fiorino, M. (2018). Aging with Down syndrome: the dual diagnosis: Alzheimer's disease and Down syndrome. *Am. J. Alzheimers Dis. Other Dement.* 33, 253–262. doi: 10.1177/1533317518761093
- Contestabile, A., Magara, S., and Cancedda, L. (2017). The GABAergic hypothesis for cognitive disabilities in Down syndrome. *Front. Cell Neurosci.* 11:54. doi: 10.3389/fncel.2017.00054
- Cullen, K. P., Grant, L. M., Kelm-Nelson, C. A., Brauer, A. F. L., Bickelhaupt, L. B., Russell, J. A., et al. (2018). Pink1 $-/-$ rats show early-onset swallowing deficits and correlative brainstem pathology. *Dysphagia* 33, 749–758.
- Cullins, M. J., and Connor, N. P. (2017). Alterations of intrinsic tongue muscle properties with aging. *Muscle Nerve* doi: 10.1002/mus.25605 [Epub ahead of print].
- Davison, M. T., Schmidt, C., Reeves, R. H., Irving, N. G., Akeson, E. C., Harris, B. S., et al. (1993). Segmental trisomy as a mouse model for Down syndrome. *Prog. Clin. Biol. Res.* 384, 117–133.
- Deidda, G., Parrini, M., Naskar, S., Bozarth, I. F., Contestabile, A., and Cancedda, L. (2015). Reversing excitatory GABAAR signaling restores synaptic plasticity and memory in a mouse model of Down syndrome. *Nat. Med.* 21, 318–326. doi: 10.1038/nm.3827
- Dinan, T. G., and Golden, T. (1990). Orofacial dyskinesia in Down's syndrome. *Br. J. Psychiatry* 157, 131–132.
- Duchon, A., Raveau, M., Chevalier, C., Nalesso, V., Sharp, A. J., and Herault, Y. (2011). Identification of the translocation breakpoints in the Ts65Dn and Ts1Cje mouse lines: relevance for modeling Down syndrome. *Mamm. Genome* 22, 674–684. doi: 10.1007/s00335-011-9356-0
- Frazier, J. B., and Friedman, B. (1996). Swallow function in children with Down syndrome: a retrospective study. *Dev. Med. Child Neurol.* 38, 695–703.
- German, R. Z., Crompton, A. W., Gould, F. D., and Thexton, A. J. (2017). Animal models for dysphagia studies: what have we learnt so far. *Dysphagia* 32, 73–77. doi: 10.1007/s00455-016-9778-7
- Gewolb, I. H., Vice, F. L., Schwietzer-Kenney, E. L., Taciak, V. L., and Bosma, J. F. (2001). Developmental patterns of rhythmic suck and swallow in preterm infants. *Dev. Med. Child Neurol.* 43, 22–27.
- Glass, T. J., and Connor, N. P. (2016). Digastric muscle phenotypes of the Ts65Dn mouse model of Down syndrome. *PLoS One* 11:e0158008. doi: 10.1371/journal.pone.0158008
- Gupta, M., Dhanasekaran, A. R., and Gardiner, K. J. (2016). Mouse models of Down syndrome: gene content and consequences. *Mamm. Genome* 27, 538–555.
- Hashimoto, M., Igari, K., Hanawa, S., Ito, A., Takahashi, A., Ishida, N., et al. (2014). Tongue Pressure during swallowing in adults with Down syndrome and its relationship with palatal morphology. *Dysphagia* 29, 509–518. doi: 10.1007/s00455-014-9538-5
- Hennequin, M., Mazille, M. N., Cousson, P. Y., and Nicolas, E. (2015). Increasing the number of inter-arch contacts improves mastication in adults with Down syndrome: a prospective controlled trial. *Physiol. Behav.* 145, 14–21. doi: 10.1016/j.physbeh.2015.03.034
- Herault, Y., Duchon, A., Velot, E., Maréchal, D., and Brault, V. (2012). The in vivo Down syndrome genomic library in mouse. *Prog. Brain Res.* 197, 169–197. doi: 10.1016/B978-0-444-54299-1.00009-1
- Hiimae, K. M., and Palmer, J. B. (2003). Tongue movements in feeding and speech. *Crit. Rev. Oral Biol. Med.* 14, 413–429.
- Holtzman, D. M., Santucci, D., Kilbridge, J., Chua-Couzens, J., Fontana, D. J., Daniels, S. E., et al. (1996). Developmental abnormalities and age-related neurodegeneration in a mouse model of Down syndrome. *Proc. Natl. Acad. Sci. U.S.A.* 93, 13333–13338.
- Homer, E., and Carbajal, P. (2015). Swallowing and feeding services in the schools: from therapy to the dinner table. *Perspect. Swallow. Swallow. Disord.* 24, 151–161.
- Hunter, C. L., Bimonte, H. A., and Granholm, A. C. (2003). Behavioral comparison of 4 and 6 month-old Ts65Dn mice: age-related impairments in working and reference memory. *Behav. Brain Res.* 138, 121–131.
- Hyde, L. A., and Crnic, L. S. (2001). Age-related deficits in context discrimination learning in Ts65Dn mice that model Down syndrome and Alzheimer's disease. *Behav. Neurosci.* 115, 1239–1246.
- Jackson, A., Maybee, J., Moran, M. K., Wolter-Warmerdam, K., and Hickey, F. (2016). Clinical characteristics of dysphagia in children with Down Syndrome. *Dysphagia* 31, 663–671. doi: 10.1007/s00455-016-9725-7
- Lau, C. (2015). Development of suck and swallow mechanisms in infants. *Ann. Nutr. Metab.* 66(Suppl. 5), 7–14. doi: 10.1159/000381361
- Lazenby, T. (2008). The impact of aging on eating, drinking, and swallowing function in people with Down's syndrome. *Dysphagia* 23, 88–97.
- Lever, T. E., Braun, S. M., Brooks, R. T., Harris, R. A., Littrell, L. L., Neff, R. M., et al. (2015a). Adapting human videofluoroscopic swallow study methods to detect and characterize dysphagia in murine disease models. *J. Vis. Exp.* 97:52319. doi: 10.3791/52319
- Lever, T. E., Brooks, R. T., Thombs, L. A., Littrell, L. L., Harris, R. A., Allen, M. J., et al. (2015b). Videofluoroscopic validation of a translational murine model of presbyphagia. *Dysphagia* 30, 328–342. doi: 10.1007/s00455-015-9604-7
- Lever, T. E., Gorsek, A., Cox, K. T., O'Brien, K. F., Capra, N. F., Hough, M. S., et al. (2009). An animal model of oral dysphagia in amyotrophic lateral sclerosis. *Dysphagia* 24, 180–195. doi: 10.1007/s00455-008-9190-z
- Lever, T. E., Simon, E., Cox, K. T., Capra, N. F., O'Brien, K. F., Hough, M. S., et al. (2010). A mouse model of pharyngeal dysphagia in amyotrophic lateral sclerosis. *Dysphagia* 25, 112–126. doi: 10.1007/s00455-009-9232-1
- Li, Z., Yu, T., Morishima, M., Pao, A., LaDuca, J., Conroy, J., et al. (2007). Duplication of the entire 22.9 Mb human chromosome 21 syntenic region on mouse chromosome 16 causes cardiovascular and gastrointestinal abnormalities. *Hum. Mol. Genet.* 16, 1359–1366.
- Liu, C., Belichenko, P. V., Zhang, L., Fu, D., Kleschevnikov, A. M., Baldini, A., et al. (2011). Mouse models for Down syndrome-associated developmental cognitive disabilities. *Dev. Neurosci.* 33, 404–413. doi: 10.1159/000329422
- McClung, J. R., and Goldberg, S. J. (2000). Functional anatomy of the hypoglossal innervated muscles of the rat tongue: a model for elongation and protrusion of the mammalian tongue. *Anat. Rec.* 260, 378–386.
- Miller, A. J. (2002). Oral and pharyngeal reflexes in the mammalian nervous system: their diverse range in complexity and the pivotal role of the tongue. *Crit. Rev. Oral Biol. Med.* 13, 409–425.
- Mu, L., and Sanders, I. (1999). Neuromuscular organization of the canine tongue. *Anat. Rec.* 256, 412–424.
- Nordin, N. A., Miles, A., and Allen, J. (2017). Measuring competency development in objective evaluation of videofluoroscopic swallowing studies. *Dysphagia* 32, 427–436. doi: 10.1007/s00455-016-9776-9
- O'Neill, A. C., and Richter, G. T. (2013). Pharyngeal dysphagia in children with Down syndrome. *Otolaryngol. Head Neck Surg.* 149, 146–150. doi: 10.1177/0194599813483445
- Patel, A., Yamashita, N., Ascaño, M., Bodmer, D., Boehm, E., Bodkin-Clarke, C., et al. (2015). RCAN1 links impaired neurotrophin trafficking to aberrant development of the sympathetic nervous system in Down syndrome. *Nat. Commun.* 6:10119. doi: 10.1038/ncomms10119
- Prasher, V. P., Metsegharun, T., and Haque, S. (2004). Weight loss in adults with Down syndrome and with dementia in Alzheimer's disease. *Res. Dev. Disabil.* 25, 1–7.

- Rivero, J. L., Talmadge, R. J., and Edgerton, V. R. (1999). Interrelationships of myofibrillar ATPase activity and metabolic properties of myosin heavy chain-based fibre types in rat skeletal muscle. *Histochem. Cell Biol.* 111, 277–287.
- Russell, J. A., Ciucci, M. R., Hammer, M. J., and Connor, N. P. (2013). Videofluorographic assessment of deglutitive behaviors in a rat model of aging and Parkinson disease. *Dysphagia* 28, 95–104. doi: 10.1007/s00455-012-9417-x
- Shaker, R., Ren, J., Zamir, Z., Sarna, A., Liu, J., and Sui, Z. (1994). Effect of aging, position, and temperature on the threshold volume triggering pharyngeal swallows. *Gastroenterology* 107, 396–402.
- Shapiro, B. L. (1983). Down syndrome—a disruption of homeostasis. *Am. J. Med. Genet.* 14, 241–269.
- Smith, C. H., Teo, Y., and Simpson, S. (2013). An observational study of adults with Down syndrome eating independently. *Dysphagia* 29, 52–60. doi: 10.1007/s00455-013-9479-4
- Smith, L. R., and Barton, E. R. (2014). SMASH - semi-automatic muscle analysis using segmentation of histology: a MATLAB application. *Skelet Muscle* 4:21. doi: 10.1186/2044-5040-4-21
- Stål, P., Marklund, S., Thornell, L. E., De Paul, R., and Eriksson, P. O. (2003). Fibre composition of human intrinsic tongue muscles. *Cells Tissues Organs* 173, 147–161.
- Talmadge, R. J., Roy, R. R., and Edgerton, V. R. (1993). Muscle fiber types and function. *Curr. Opin. Rheumatol.* 5, 695–705.
- The National Academies Press. (2011). *Guide for the Care and use of Laboratory Animals*. Washington, D.C: The National Academies Press.
- Tsujimura, T., Sakai, S., Suzuki, T., Ujihara, I., Tsuji, K., Magara, J., et al. (2017). Central inhibition of initiation of swallowing by systemic administration of diazepam and baclofen in anaesthetized rats. *Am. J. Physiol. Gastrointest. Liver Physiol.* 312, G498–G507. doi: 10.1152/ajpgi.00299.2016
- Wisniewski, K., Howe, J., Williams, D. G., and Wisniewski, H. M. (1978). Precocious aging and dementia in patients with Down's syndrome. *Biol. Psychiatry* 13, 619–627.
- Yang, Q., Rasmussen, S. A., and Friedman, J. M. (2002). Mortality associated with Down's syndrome in the USA from 1983 to 1997: a population-based study. *Lancet* 359, 1019–1025.
- Zárate, N., Mearin, F., Hidalgo, A., and Malagelada, J. R. (2001). Prospective evaluation of esophageal motor dysfunction in Down's syndrome. *Am. J. Gastroenterol.* 96, 1718–1724.

Conflict of Interest Statement: The authors declare that the research was conducted in the absence of any commercial or financial relationships that could be construed as a potential conflict of interest.

Copyright © 2019 Glass, Valmadrid and Connor. This is an open-access article distributed under the terms of the Creative Commons Attribution License (CC BY). The use, distribution or reproduction in other forums is permitted, provided the original author(s) and the copyright owner(s) are credited and that the original publication in this journal is cited, in accordance with accepted academic practice. No use, distribution or reproduction is permitted which does not comply with these terms.



A Dynamic Jaw Model With a Finite-Element Temporomandibular Joint

Benedikt Sagl^{1*}, Martina Schmid-Schwap¹, Eva Piehlslinger¹, Michael Kundi² and Ian Stavness³

¹ Department of Prosthodontics, University Clinic of Dentistry, Medical University of Vienna, Vienna, Austria, ² Institute of Environmental Health, Medical University of Vienna, Vienna, Austria, ³ Department of Computer Science, University of Saskatchewan, Saskatoon, SK, Canada

OPEN ACCESS

Edited by:

Kazutaka Takahashi,
University of Chicago, United States

Reviewed by:

Yukihiro Michiwaki,
Musashino Red Cross Hospital,
Japan
Alexandros Efthimis Tsouknidas,
University of Western Macedonia,
Greece

*Correspondence:

Benedikt Sagl
benedikt.sagl@meduniwien.ac.at

Specialty section:

This article was submitted to
Craniofacial Biology and Dental
Research,
a section of the journal
Frontiers in Physiology

Received: 23 May 2019

Accepted: 28 August 2019

Published: 13 September 2019

Citation:

Sagl B, Schmid-Schwap M,
Piehlslinger E, Kundi M and Stavness I
(2019) A Dynamic Jaw Model With
a Finite-Element Temporomandibular
Joint. *Front. Physiol.* 10:1156.
doi: 10.3389/fphys.2019.01156

The masticatory region is an important human motion system that is essential for basic human tasks like mastication, speech or swallowing. An association between temporomandibular disorders (TMDs) and high temporomandibular joint (TMJ) stress has been suggested, but *in vivo* joint force measurements are not feasible to directly test this assumption. Consequently, biomechanical computer simulation remains as one of a few means to investigate this complex system. To thoroughly examine orofacial biomechanics, we developed a novel, dynamic computer model of the masticatory system. The model combines a muscle driven rigid body model of the jaw region with a detailed finite element model (FEM) disk and elastic foundation (EF) articular cartilage. The model is validated using high-resolution MRI data for protrusion and opening that were collected from the same volunteer. Joint stresses for a clenching task as well as protrusive and opening movements are computed. Simulations resulted in mandibular positions as well as disk positions and shapes that agree well with the MRI data. The model computes reasonable disk stress patterns for dynamic tasks. Moreover, to the best of our knowledge this model presents the first ever contact model using a combination of EF layers and a FEM body, which results in a clear decrease in computation time. In conclusion, the presented model is a valuable tool for the investigation of the human TMJ and can potentially help in the future to increase the understanding of the masticatory system and the relationship between TMD and joint stress and to highlight potential therapeutic approaches for the restoration of orofacial function.

Keywords: jaw modeling, temporomandibular joint, finite-element modeling, musculoskeletal modeling, computational biomechanics

INTRODUCTION

The masticatory system is an incredibly complex musculoskeletal system, comprised of two bony structures, the mandible and the skull, which are connected by two temporomandibular joints (TMJs). The masticatory system is frequently used in everyday tasks like speaking and chewing, but a variety of complications can lead to dysfunction of the TMJs. Disorders of the TMJ are grouped as temporomandibular disorders (TMDs) (Schiffman et al., 2014) and are prevalent in roughly 20%

of the population (Solberg et al., 1979). Problems range from reduced quality of live up to severe impairment of the above-mentioned essential functions.

One unique feature of the masticatory system is that it encompasses two separate joints that articulate the mandible and hence allow a multitude of different movement patterns with six degrees of freedom including rotation as well as translation (Drake et al., 2014). Moreover, a dynamic, cartilaginous disk is located between the mandibular condyle and the articular fossa. This TMJ disk plays a crucial role in force absorption and lubrication of the joint (Koolstra et al., 2007; Tanaka and Koolstra, 2008; Koolstra and Tanaka, 2009; Nickel et al., 2009; Stankovic et al., 2013) and additionally increases the complexity of mandibular dynamics. Previous literature suggests that many cases of TMD are associated with increased load on the TMJ (Detamore and Athanasiou, 2003; Ingawale and Goswami, 2009), which highlights the importance of the detailed investigation of TMJ loads using realistic, dynamic loading scenarios. Additionally, the small size and complex organization of the TMJ make *in vivo* investigations of joint forces impossible due to patient safety restrictions. This leaves computational biomechanics as one of the few possibilities to gain knowledge on the internal workings of the TMJ.

Historically speaking, computational models of the masticatory region can be separated into two categories. On the one hand, there are rigid body models which have been extensively used for most of the history of masticatory computational modeling (Throckmorton and Throckmorton, 1985; Koolstra and van Eijden, 1995; Trainor et al., 1995; Peck et al., 2000). These dynamic models are a valuable tool for the investigation of complex movements or muscle activation patterns. Rigid body models have been used previously to investigate a variety of tasks, including open-close movements (Tuijt et al., 2010) and mastication (Hannam et al., 2008). Moreover, they have been used to investigate changes of function due to surgery (de Zee et al., 2009; Stavness et al., 2010) or the effect of morphological changes on the involved structures (Marková and Gallo, 2016). Their main drawback is that they use quite simple representations of the TMJ itself, consisting of a combination of planes or spline functions and completely lacking a TMJ disk (Curtis, 2011; Hannam, 2011). Hence, these models cannot appropriately capture the forces applied to the different joint structures.

The second category of jaw simulations are finite element (FE) models. FE models of the masticatory region generally are comprised of detailed meshes of the structures of the TMJ and enable the use of sophisticated material models (Lamela et al., 2011; Commisso et al., 2016). While this set up allows researchers to compute more realistic force patterns of the joint, simulations often solely focus on the TMJ itself; neglecting or drastically simplifying the dentition as well as muscle force calculations. Additionally, due to the high computational cost of these models, typically static- or quasi-static simulations are performed (Mori et al., 2010; Commisso et al., 2014; Hattori-Hara et al., 2014). However, tasks that are most likely to create high forces in the joint, like mastication or tooth grinding, have important dynamic characteristics and hence cannot be

appropriately modeled using a static or quasi-static set-up. This problem becomes more apparent when investigating the wide range of functional and parafunctional movements, which are performed many times during the course of a single day and involve large translations and rotations.

Overall, the above-mentioned facts highlight the need for representations of dynamic jaw movement and muscle forces, while also having a detailed representation of TMJ and disk mechanics. Such a model enables the dynamic investigation of functional or non-functional movements; giving detailed joint stress or strain predictions that are transferable to the *in vivo* situation. To the best of our knowledge only two models exist that fit this description. The model proposed by Koolstra and van Eijden is the only previous attempt of a dynamic musculoskeletal model of the full masticatory system with a FE model of the TMJ (Koolstra and van Eijden, 2005). Nonetheless, the model includes a quite coarse joint representation, most likely due to the computational limitations at the time of publication. Moreover, the model was created for the right side of the TMJ and mirrored. This neglects the effect of facial asymmetries, which are very common in humans. The second model developed by Martinez Choy et al. (2017) proposes a full FEM modeling approach, containing meshes of all involved structures as well as Hill-type muscles. The model was built using data from various literature sources and the anatomy was based on the (Koolstra and van Eijden, 2005) model, using a mirrored jaw setup. The model was used for the investigation of a chewing cycle. A similar modeling approach has been previously used for the evaluation of mastication in mice (Tsouknidas et al., 2017). Due to the full FEM approach a long simulation time on even the most powerful PCs is to be expected, even though no simulation time was reported. These long simulation times limit the applicability of the model in a clinical setting.

The aim of this project was to create a comprehensive rigid body model, derived from medical imaging data, encompassing the whole masticatory region combined with a detailed representation of the TMJ, while keeping simulation times reasonably short. To validate the model, we computed opening and protrusion movements and compared mandibular end position as well as disk position and deformation to high-resolution MRI data from the same volunteer. Moreover, we report clenching stresses to more thoroughly investigate the behavior of the model. Simulation times are also reported and compared to previous models. Overall, this project presents a unique tool for the investigation of the workings of the jaw region that is well-suited for future analysis of the effect of various masticatory functions, parafunctions and dysfunctions and consequently could give valuable input for the development of novel treatment strategies of orofacial sensorimotor impairments.

Related Work

Rigid Body Modeling of the TMJ

Early computational investigations of the masticatory region were mostly performed using two-dimensional rigid body models. These investigations focused on static investigations

of joint reaction forces utilizing muscle force estimations derived from maximum bite force estimations (Greaves, 1978; Throckmorton and Throckmorton, 1985). While these investigations are a valuable tool for the examination of bite performance and the mechanical efficiency of masticatory muscles, they cannot be used for dynamic investigations and are an oversimplification of the three-dimensional masticatory system. An early example of a three-dimensional dynamic model was published by Koolstra and van Eijden (1997). The TMJ was modeled as purely elastic, frictionless contact between a sphere (simplified condyle) and a spline surface representing the articular fossa. Their model used contact points on the lower teeth and a flat surface mimicking the occlusal surface of the upper dentition. Moreover, the presented model includes a muscle model that connects muscle force to muscle activation, muscle length and a force-velocity curve. Tooth contact was modeled as contact between points representing the tip of the lower teeth and a plane that represented the occlusal plane. In a more recent iteration of the model (Tuijt et al., 2010) the TMJ surfaces were modeled as 3D shell type meshes. An ellipsoid was used for the condyle and the fossa was modeled using a third-degree polynomial in the sagittal plane, combined with a second-degree polynomial for the mediolateral curve. In this model a tangent plane approximation of the fossa mesh around a contact point was used. Penetrating vertices were defined, and point-to-plane distance was calculated to derive the joint reaction force for each penetrating vertex. The upper teeth were modeled as single bite plane and the lower dentition was modeled using points for an incisor and the two second molars.

Peck et al. (2000) also used an ellipsoidal shape to approximate the condyle and a combination of multiple linear plates to model the condylar path along the fossa. Again, contact was monitored by interpenetration of the two geometrical shapes. In the case of constant contact an instantaneous constraint was added to simulate sliding along the surfaces. Dentition was simulated as a flat occlusal plane and muscles were modeled as Hill-type actuators (Hill, 1953). The Stavness et al. (2006) model can be seen as most recent version of this “model family.” The model uses a bilateral or unilateral point constraint, sitting in the anatomical center of the condyle and a combination of three rigid, frictionless surfaces. These surfaces define the movement of the mandible in the anterior-posterior and medial-lateral directions. de Zee et al. (2007) used a comparable approach modeling the TMJ by using a single unilateral, planar constraint that was angled downwards and canted medially. In a more recent version, the group used an elastic contact foundation model to solve contact between the condyle and the fossa articularis using a Force Dependent Kinematics approach to track movement data and compute muscle, ligament and contact forces (Andersen et al., 2017).

Finite Element Modeling of the TMJ

Nagahara et al. (1999) investigated the stress distribution and displacement during static clenching. This early investigation used a CT scan of a cadaver for bony structures and the TMJ disk was digitized after extraction. Muscle forces were modeled using external forces in the direction of the main closing muscles. Perez

del Palomar and Doblaré created FEM simulations of mouth opening as well as lateral movements (Pérez del Palomar and Doblaré, 2006a,b). The models were built from medical scans of a patient and used a porohyperelastic material model for the TMJ disk. No muscle representations were included, and the movements were simulated by prescribed translation of the mandible. While the model used for opening simulations only contains one half of the masticatory system, the model for lateral movements contains both joints. Mori et al. (2010) built a model from 1.5T MRI images of a volunteer. The cartilaginous and ligamentous structures were modeled using a Kelvin material model and retrodiscal tissue and the TMJ capsule were included. Moreover, the articular cartilage was included as uniform layer. Mandible movement was constrained to only allow movement in the sagittal plane and clenching was simulated using an external load. Hattori-Hara et al. (2014) created a model of the TMJ from a CT scan and a 1.5T MRI of a patient for the investigation of unilateral disk displacement during static clenching. The model includes the bony structures and TMJ disk. Articular cartilage and capsule were modeled as uniform layers. Muscle forces were modeled as external forces and distributed over the insertion of the muscles. Commisso et al. (2014) created a model of the mandible and TMJ from a human cadaver. The model includes cube like teeth that are connected to the mandible with a layer of elements mimicking the periodontal ligament. A quasi-linear viscoelastic material was used for the TMJ disk. Forces were applied as external load at the insertion area of each respective muscle. They used the model to simulate sustained clenching as well as rhythmic masticatory muscle activity. In a more recent study they used the same model to investigate the lateral pterygoid muscle during a unilateral mastication cycle (Commisso et al., 2015). For this purpose, they used a two-step setup. They estimated muscle forces using a Hill-type muscle model, while neglecting force-length as well as force-velocity dependencies. These calculated muscle forces were applied to the muscle insertion areas as external forces. Martinez Choy et al. (2017) proposed a full FEM modeling approach, containing detailed meshes of all involved structures as well as Hill-type muscles. The model was built using data from various literature sources and used for the investigation of a chewing cycle.

Recently, co-simulation techniques have been proposed to use musculoskeletal models to define boundary conditions for static FEM simulations. Examples of modeled joint systems include tibial loading while load carrying (Xu et al., 2019) or patellofemoral cartilage stresses during a stair climb task (Pal et al., 2019). Currently, no such approach has been reported for jaw models, even though the recent, more sophisticated rigid body models are theoretically capable of driving such a modeling strategy (Andersen et al., 2017). Nevertheless, this approach does not fully solve the presented problems. While using such a technique potentially decreases the simulation time needed, the use of two different modeling toolkits increases the complexity of model setup and therefore decreases the likelihood of clinical use. Moreover, the use of forces computed with a simple joint set-up might not necessarily compute the correct motion and reaction forces when applied to a more complex FEM joint. To the best of our knowledge the only previous dynamic rigid body

model that incorporated a FEM TMJ was published by Koolstra and van Eijden (2005). The mandible was modeled as dynamic rigid body with 12 Hill-type actuators attached and the TMJ disks were included as FE models with tetrahedral elements and an edge length of approximately 0.5 mm. The articular cartilage was represented as a uniform layer using a FE approach. The model was built from cadaver data of the right TMJ and mirrored for the left side. A maximum jaw opening of 3 cm was achieved. **Table 1** presents an overview of the literature review.

MATERIALS AND METHODS

Data were acquired from one symptom-free volunteer. Ethics approval was obtained from the institutional review board of the Medical University of Vienna and written informed consent was obtained. The detailed data acquisition and processing workflow has been extensively explained in a previous publication (Sagl et al., 2019b). In brief, we collected a single full skull CT scan for bony structures as well as a full skull MRI scan for the definition of muscle paths. Additionally, high resolution TMJ MRI volumes were created to enable accurate representations of the TMJ disks. MRI scans were acquired using a TSE-T1 sequence on a Siemens Magnetom 3T machine and a 64-channel head coil, achieving a resolution of 0.17 mm and a slice thickness of 1 mm. High-resolution scans were collected in different static positions, using silicone bite blocks for defined jaw postures verified with the help of a jaw tracking system. These scans were used for model validation as described below. Bony structures were segmented from the CT scan, while the TMJ disk was manually segmented from the MRI scans by an expert specialized in TMD and TMJ-MRI for all positions. To enable realistic maximum opening behavior with a static hyoid, the respective mesh was moved 7 mm posteriorly and 7 mm downwards, which lies in the range of previously reported literature values (Muto and Kanazawa, 1994).

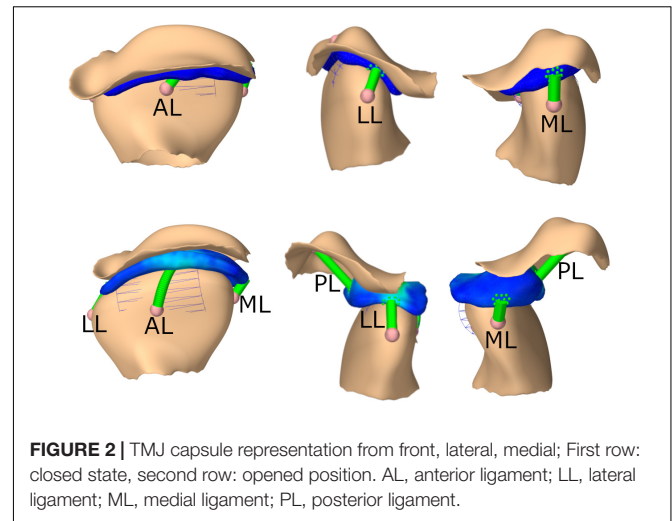
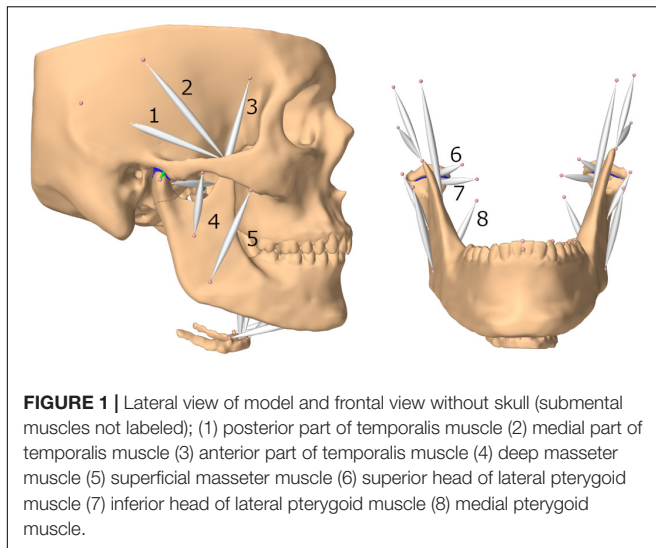
The model was developed using the opensource ArtiSynth Modeling Toolkit¹ (Lloyd et al., 2012). Boney structures were modeled as rigid bodies. Inertial properties of the mandible were estimated from mesh geometry with an assumed mandibular mass of 200 g (Langenbach and Hannam, 1999). The hyoid and skull were kept static for all presented simulations and therefore no inertia properties had to be defined.

Muscles were represented as Hill-type point-to-point muscles (Hill, 1953; Peck et al., 2000; Hannam et al., 2008). Since these muscle models apply forces in the one-dimensional direction of the force vectors defined by an origin and insertion point, larger muscles were split up into multiple models to more accurately mimic activation of muscle compartments. The included muscles are: posterior, medial and anterior parts of the temporal muscle, superior and inferior head of the lateral pterygoid muscle, superficial and deep masseter muscles, medial pterygoid muscle, anterior digastric muscle, geniohyoid muscle, anterior and posterior mylohyoid muscle (**Figure 1**). Cross-sectional areas, velocity-force and length-force behavior were defined with the

¹ www.artisynth.org

TABLE 1 | Overview of features of computer models of the jaw region.

| | Point Constraint | Geometric Contact | FEM Disc | Deformable Articular Cartilage | FEM Capsule/Ligaments | Teeth can be in and leave contact | Dynamic | Muscle driven | Individually Modeled Joints | Reported Simulation Time |
|--------------------------------------|------------------|-------------------|----------|--------------------------------|-----------------------|-----------------------------------|---------|---------------|-----------------------------|--------------------------|
| Koolstra and van Eijden, 1997 | × | ✓ | × | × | × | ✓ | ✓ | ✓ | × | × |
| Tuijt et al., 2010 | × | ✓ | × | × | × | ✓ | ✓ | ✓ | × | × |
| Peck et al., 2000 | × | ✓ | × | × | × | ✓ | ✓ | ✓ | × | × |
| Hannam et al., 2008 | ✓ | × | × | × | × | ✓ | ✓ | ✓ | × | × |
| de Zee et al., 2007 | ✓ | × | × | × | × | ✓ | ✓ | ✓ | ✓ | × |
| Andersen et al., 2017 | × | ✓ | × | × | × | ✓ | ✓ | ✓ | ✓ | × |
| Nagahara et al., 1999 | × | × | ✓ | × | × | × | × | × | × | × |
| Pérez del Palomar and Doblaré, 2006a | × | × | ✓ | × | ✓ | × | × | × | ✓ | × |
| Pérez del Palomar and Doblaré, 2006b | × | × | ✓ | × | ✓ | × | × | × | ✓ | × |
| Mori et al., 2010 | × | × | ✓ | ✓ | ✓ | × | × | × | ✓ | × |
| Hattori-Hara et al., 2014 | × | × | ✓ | ✓ | ✓ | ✓ | × | × | ✓ | × |
| Commisso et al., 2014 + 15) | × | × | ✓ | × | ✓ | ✓ | × | × | ✓ | × |
| Martinez Choy et al., 2017 | × | × | ✓ | ✓ | ✓ | ✓ | ✓ | ✓ | × | × |
| Koolstra and van Eijden, 2005 | × | × | ✓ | ✓ | × | ✓ | ✓ | ✓ | × | × |
| Our model | × | × | ✓ | ✓ | × | ✓ | ✓ | ✓ | ✓ | ✓ |



help of previous literature (Langenbach and Hannam, 1999; Peck et al., 2000; Hannam et al., 2008).

The TMJ disks were modeled as FEM with roughly 6000 first-order tetrahedral elements for the right and 8000 for the left disk and an estimated weight of 0.006 kg. The volumetric meshes were created using the tetgen library and the previously segmented and processed disk surface meshes (Si, 2015). A hyperelastic Mooney–Rivlin material with material constants taken from literature (Beek et al., 2001; Koolstra and van Eijden, 2005) ($C_1 = 9 \cdot 10^5 Pa$ and $C_2 = 9 \cdot 10^2 Pa$), was used. The strain energy function for this material is:

$$W(I_1, I_2) = C_1(I_1 - 3) + C_2(I_2 - 3), \quad (1)$$

where C_1 and C_2 are material constants and I_1 and I_2 are the first and the second invariant of the left Cauchy–Green deformation tensor B . Simulations were computed using a first-order Backward Euler implicit integrator.

Additionally, four axial springs mimic the biomechanics of the TMJ capsule. One connects the disk and the condyle anteriorly, one medially, one laterally and one connects the skull and disk posteriorly. The ligaments were modeled as inextensive cables, using an elongation stiffness of 250 MPa once the tendon slack length was exceeded. For the posterior ligaments the slack length was 7.5 mm longer than the initial length of the ligament, for the anterior ligaments the slack length was 4 mm longer and for the medial the slack length was 1.9 mm and for the lateral ligament 2.5 mm longer than the initial length. These slack lengths were determined to ensure best simulation results for various movements. A wrapping cylinder was added on both sides to make the anterior ligament wrap around the mandibular condyle. Since attaching the axial springs to a single node of the FEM would lead to unstable and incorrect simulation results, we used a distributed FEM attachment, spreading out the applied force over approximately 20 nodes per ligament; an approach similar to previous literature (Fernandez et al., 2014). An overview of the joint set-up can be found in **Figure 2**.

To speed up simulations, articular cartilage was modeled as an elastic foundation (EF) contact model (Blankevoort et al., 1991; Bei and Fregly, 2004), as opposed to full FEM for the contact surfaces. EF contact can be seen as an elastic layer bonded to a rigid substrate. This is achieved by distributing springs over the surface of the rigid body, modeling the elastic layer with a predefined thickness. EF contact approaches speed up contact calculation by neglecting the effect of contact forces applied at one location at all other locations. This simplification speeds up simulations substantially and has proven to be a valuable tool for elastic layers that are connected to a rigid body (Bei and Fregly, 2004). The EF layers had a thickness of 0.4 mm (Hansson et al., 1977) and contact pressure between the surface mesh of the temporomandibular disk (TD) and the articular cartilage mesh (AC) was computed using:

$$p(d) = K \ln \left(1 - \frac{d}{h} \right), K \equiv \frac{-(1-\nu)E}{(1+\nu)(1-2\nu)} \quad (2)$$

where E is the elastic modulus, ν is the Poisson's ratio of the contact, d represents the depth of penetration and h is the cartilage thickness. Contact pressure is non-linear with respect to d and linear with respect to E . We based our elastic modulus on previous literature values for an articular cartilage Mooney–Rivlin material (Koolstra and van Eijden, 2005) and estimated E using $6 \cdot C_1$ (Nazari et al., 2011). For our simulations, we used an elastic modulus of 2.7 MPa and a Poisson's ratio of 0.49. Contact between the TD and the AC is computed by finding the FEM nodes of the TD that penetrate the AC mesh. For each penetrating node a contact, with a penetration depth d and normal direction n , is defined. Equation (2) is then used to determine the appropriate nodal response force f , according to

$$f = p(d)An$$

Here A denotes the surface area associated with the contact (estimated by splitting the total mesh penetration area over all penetrating vertices).

Since usually contact forces are stiff, very small timesteps or the use of an implicit integrator are required to keep simulations stable using an EF approach. To additionally increase stability, our implementation uses a constraint regularization scheme that does not use penalty forces to simulate contact, but rather uses point constraints, based on the contact normal directions. A “contact force behavior,” which implements the EF approach, is then used to regularize, or “soften” the contact. Full details are given in Servin et al. (2006).

To validate the model, we performed multiple forward-dynamics simulation tasks. First, we computed a postural rest position. Additionally, an active maximum opening movement was performed (bilateral maximal activation of lateral pterygoid, anterior digastric, geniohyoid, and mylohyoid muscles) as well as an incisal edge-to-edge protrusion movement (bilateral maximal activation of lateral pterygoid muscles, with lower activation of jaw closing and opening muscles for stabilization). Maximal activation of the jaw closing muscles was used to simulate a clenching behavior. Simulated end positions of the mandible and TMJ disks for active opening and protrusion were compared to the respective meshes segmented from the high-resolution MRI images of the same volunteer. Additionally, differences in deformation of the TMJ disks were visualized using these MRI data. Moreover, to check the mesh quality, we computed the mean values for the ratio of the radius of the circumscribed sphere to the shortest edge length as well as for the maximal dihedral angle for both disks to measure quality of the created first-order tetrahedral elements.

As an additional verification of the mesh used in the model, the opening task was simulated with different numbers of mesh elements. For this purpose, the surface meshes of both disks were remeshed, using Meshmixer (Autodesk, Inc.), to have an edge length of 0.5/0.45/0.4/0.35/0.3 mm respectively. This led to disk models with numbers of elements varying from approximately 7500 to 20000 elements for the left disk. The overall trend in stress maps for the left disk was compared between the simulations to check for consistency. Furthermore, we performed a trend validation, describing TMJ disk stress and qualitatively comparing it to previous work.

To investigate the effect of the chosen material constants for the FEM disks, a sensitivity analysis consisting of 15 simulations was performed, including changes of both material constants over a range of one negative and positive order of magnitude for C1 and two negative and positive orders of magnitude for C2.

RESULTS

A postural rest position simulation, with a steady-state activity of 0.08% for the closer muscles (masseter, temporalis, and medial pterygoid muscles) (Langenbach and Hannam, 1999), produced a mouth with an inter-incisal separation of 5 mm. For maximum opening an inter-incisal gap of 30 mm was achieved.

To more thoroughly validate the workings of our model the mandibular positions of the opening and protrusion simulation tasks were compared to high resolution meshes gathered from medical imaging data of the same volunteer. Data were

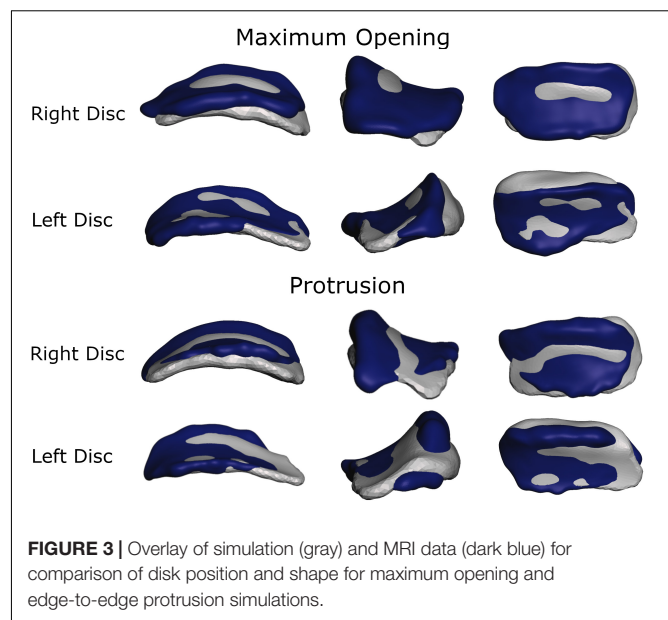


FIGURE 3 | Overlay of simulation (gray) and MRI data (dark blue) for comparison of disk position and shape for maximum opening and edge-to-edge protrusion simulations.

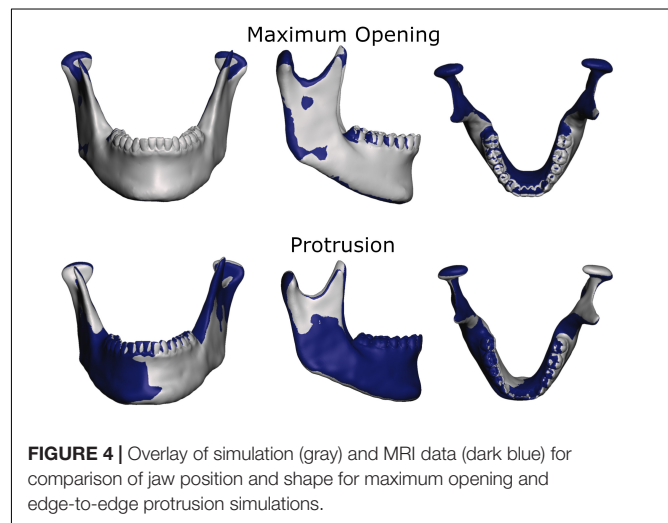


FIGURE 4 | Overlay of simulation (gray) and MRI data (dark blue) for comparison of jaw position and shape for maximum opening and edge-to-edge protrusion simulations.

TABLE 2 | Hausdorff distances for opening simulation.

| | Mandible | Discus right | Discus left |
|-----------------------|--------------------|----------------------|----------------------|
| Minimum distance [mm] | 6×10^{-7} | 7.7×10^{-5} | 1.2×10^{-5} |
| Maximum distance [mm] | 1.57 | 3.43 | 2.9 |
| Mean distance [mm] | 0.42 | 0.84 | 0.61 |
| RMS [mm] | 0.53 | 1.1 | 0.88 |

collected for maximum mouth opening and a protrusive position. **Figures 3, 4** show that mandible as well as disk positions for both simulation tasks fit the recorded data very well. For the disks only minor differences in shape can be observed. A detailed Hausdorff distance analysis is presented in **Tables 2, 3** for opening and protrusion, respectively.

Von Mises and maximum principal stresses on the disk and contact pressures on the articular cartilage are plotted

TABLE 3 | Hausdorff distances for protrusion simulation.

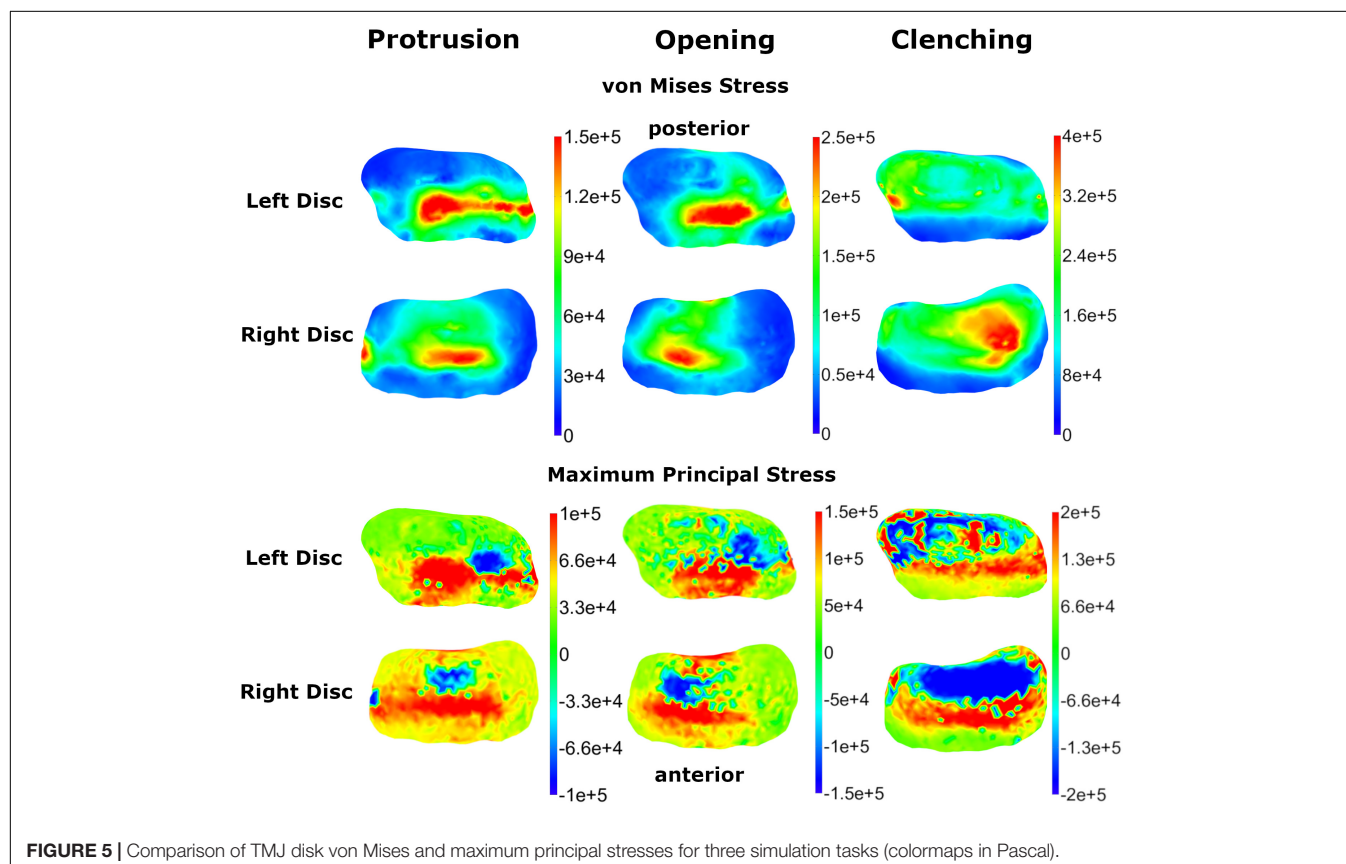
| | Mandible | Discus right | Discus left |
|-----------------------|----------------------|--------------------|--------------------|
| Minimum distance [mm] | 1.1×10^{-6} | 4×10^{-5} | 1×10^{-6} |
| Maximum distance [mm] | 1.1 | 3.1 | 2.12 |
| Mean distance [mm] | 0.35 | 0.79 | 0.41 |
| RMS [mm] | 0.42 | 1.03 | 0.56 |

in **Figures 5, 6** for opening, protrusion and clenching tasks. The results show that the maximum disk stresses during opening occur in the central joint area, with a computed maximum von Mises value of around 250 kPa and a maximum principal stress of 150 kPa. For protrusion, some stress can be seen on the lateral side of the disk, additional to the central area, with maximal von Mises stresses of 150 kPa and maximum principal stresses of 100 kPa. A maximum von Mises stress of 500 kPa and a maximum principal stress of 250 kPa was observed for the clenching simulation, with highest stresses over the area of the disk that is in direct contact with the articular fossa. Overall, the maximum principal stress maps show more noise than the von Mises stress maps, which is consistent with previous literature (Koolstra and van Eijden, 2005). Maximum principal stresses generally show tensile stresses in the intermediate area of the disk, which has the highest von Mises stresses. Comparing our results, we can see that contact pressures are roughly one order of magnitude higher

than the maximum principal stresses in the disk. This difference of one order of magnitude has been previously reported for maximum principal stresses of FEM disk and FEM articular cartilage (Koolstra and van Eijden, 2005). The computed quality measures resulted in a mean ratio for the radius of the circumscribed sphere to the shortest edge length of 2.25 for the left disk and 1.85 for the right disk. The mean maximal dihedral angle was 113° for the left disk and 110.9° for the right disk, respectively.

The sensitivity analysis of material properties showed that the values of the FEM parameters do not have a major influence on the mandibular end position during an opening movement (**Figure 7**). Only a slight shift of the mid-incisal point with a maximum of 0.24 mm laterally, 0.25 mm anterior-posteriorly and a maximum variation of 1.45 mm in z-direction was observed. A sensitivity analysis for mesh size was also conducted. **Figure 8** shows the stress maps of the left disk for the end position of an opening movement using different amounts of mesh elements. The mean difference for meshes finer than 8000 elements (as used in our model) was 2.7% and the stress distributions were consistent between all mesh configurations (**Figure 8**).

The average execution time of a 1 s forward simulation, encompassing 1000 timesteps, was 441.03 s with a standard deviation of 1.75 s over 400 repeated simulations. Simulations were performed on a workstation PC with an Intel Xeon E5-2660 processor and 96 Gb RAM.



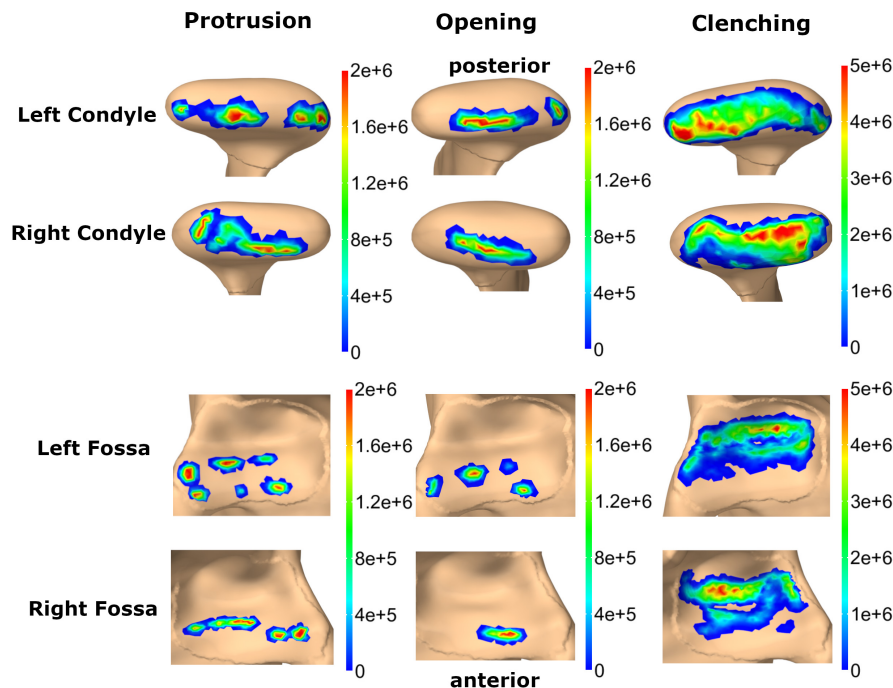


FIGURE 6 | Comparison of contact pressure maps for fossa articularis and mandibular condyle for three simulation tasks (colormaps in Pascal).

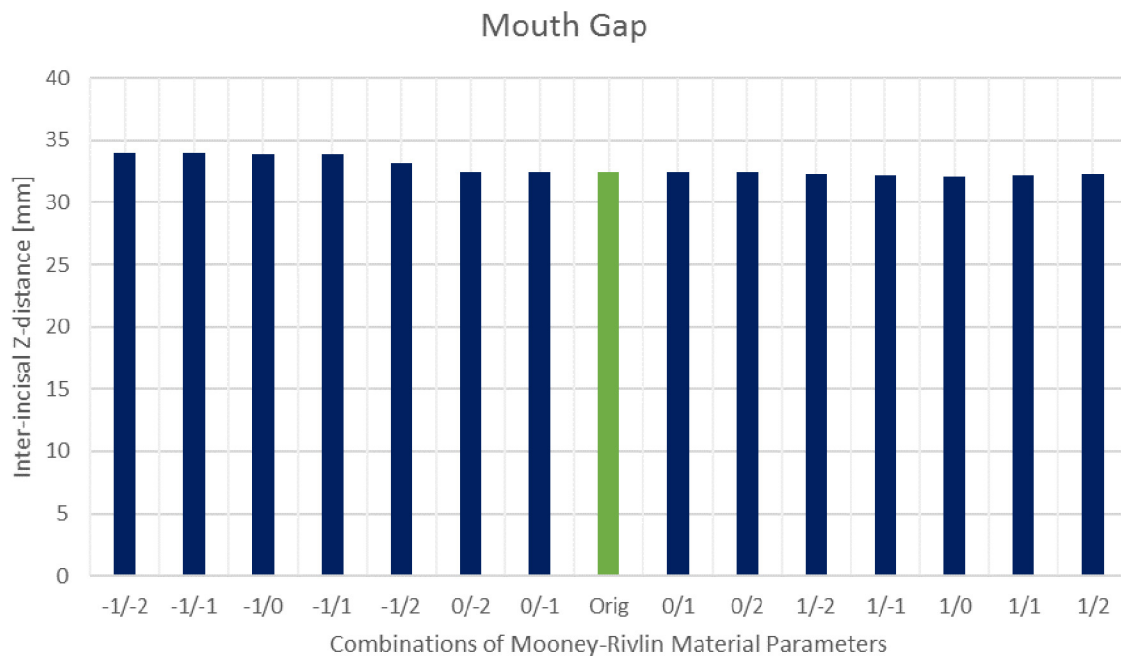
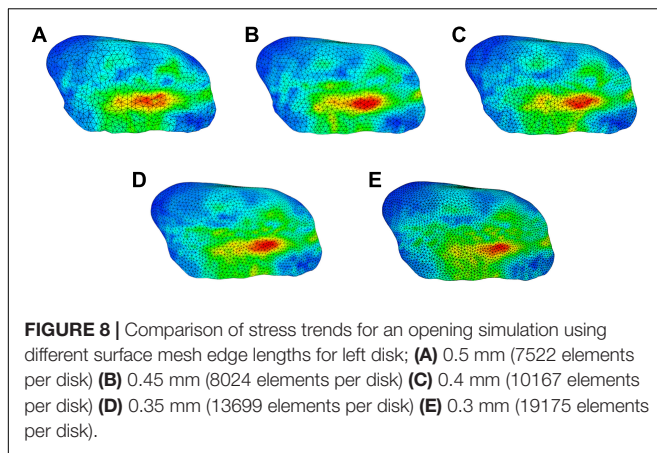


FIGURE 7 | Inter-incisal distance in Z-direction for different Mooney-Rivlin material parameter combinations.

DISCUSSION

This paper presents a novel rigid body model of the complete masticatory region in combination with a detailed FEM TMJ disk and an EF representation of articular cartilage. This

combination presents a novel contact formulation that has not been presented previously. The model allows for the simulation of complex movement tasks as well as high force tasks, like clenching and grinding, while achieving reasonable simulation times. This combination of complexity and computational



performance helps to bring biomechanical simulations closer to clinical relevancy and enables the use of large-scale sensitivity analysis for the investigation of uncertainty in predictions of modeling parameters.

To validate our model, we compared the results of basic simulation tasks to literature values as well as high-resolution image data. The recorded inter-incisal separation for passive opening was 5 mm, which is consistent with literature values of 3 ± 2 (Langenbach and Hannam, 1999; Stavness et al., 2006). Moreover, the Hausdorff distance between the simulated mandible maximum opening position and the recorded position from MRI was extremely close, with a mean Hausdorff distance of 0.42 mm. Similar accuracy can be seen for TMJ disk positions. For maximum opening, we used a forward simulation that fully activated opening muscles and held the maximal position for 0.25 s to let the disk deform, since the position was also held for some time during MRI acquisition. For protrusion, the MRI data does not represent a maximum protrusion posture, because this position caused discomfort for the volunteer. Instead a protrusive movement until the upper and lower incisors were edge-to-edge was performed. Activation of the lateral pterygoid muscles alone was not able to protrude the mandible and hold it in this submaximal position, hence we added low level activation of the jaw closing and opening muscles to stabilize the mandible. The muscle activation levels were found by using a forward-dynamics tracking simulation that moved and held the mandible at the desired protrusive position. The resulting simulations show that our model performs well and that the computed positions for both disks and the mandible are close to the actual data for the opening and protrusion tasks.

While the computed maximum inter-incisal gap of 30 mm agrees with previous simulation studies (Peck et al., 2000; Koolstra and van Eijden, 2005; Stavness et al., 2006), it is not in the range reported for *in vivo* studies. Wide mouth opening *in vivo* is facilitated by a translation of the hyoid together with backwards rotation of the head (Muto and Kanazawa, 1994). By translating the hyoid bone in our model caudally and posteriorly we achieve a mouth opening that fits very well with the maximum opening of the volunteer recorded in the MRI in a lying position without head rotation. Hence, it is

a reasonable assumption that the computed maximum mouth opening is correct and for a larger mouth gap a head rotation would have to be added.

Two major challenges of biomechanical computer investigations are the limited amount of information on properties of human tissues and the large amount of required computational power. In our opinion, one way of tackling these goals is by using appropriately complex representations for the level of information on various anatomical structures. In the case of the presented model we use a full FEM approach for the TMJ disk, which is a well-studied tissue with many investigations on its structure, composition and mechanical properties (Detamore and Athanasiou, 2003; Tanaka et al., 2008; Stankovic et al., 2013). On the other hand, TMJ articular cartilage is not as well-defined and hence we decided to speed up simulation by using a simplified elastic contact foundation approach, which has proven to be a valuable tool for modeling of cartilage layer attached to a bone (Blankevoort et al., 1991; Bei and Fregly, 2004). By using this combination of FEM and EF contact, an approach that to the best of our knowledge has not been presented previously, we can compute realistic deformation patterns for the disk and cartilage layers, while achieving simulation times much shorter than a full FEM simulation. Of course, if future research will more clearly define mechanical properties of other involved structures and a specific research question requires this step, our model and software toolkit are capable of using a full FEM approach for all parts of the model, albeit at a higher computational cost.

One limitation of the current iteration of the model is the use of a Mooney–Rivlin material for the TMJ disk. Previous investigations have shown that the disk demonstrates hyperelastic as well as viscoelastic properties and a variety of material models of different complexity have been suggested (Koolstra et al., 2007; Commisso et al., 2015, 2016). The Mooney–Rivlin material was used in the previous combined rigid body – FEM jaw model (Koolstra and van Eijden, 2005) and hence we used it for model testing. The sensitivity analysis of the material parameters also showed that the model computes quite similar mouth openings for a large range of material properties, which suggests that the dynamic behavior of the mandible is not extremely sensitive to the material properties of the TMJ disk. Moreover, the sensitivity analysis showed that larger changes of the C1 material constant of the Mooney–Rivlin material have a bigger influence on the stability of the simulations. Extremely stiff C1 (two orders of magnitudes higher) and extremely soft C1 (two orders of magnitudes lower) tend to create unstable simulations, while changes of two orders of magnitude for C2 still lead to stable simulations with only small differences in mandible position. To further improve the investigation of joint loads and disk deformation we nevertheless plan on implementing a more complex, poroelastic material model in the future.

To further verify our simulation results we performed a mesh independent grid test. The use of a complex contact model in combination with rigid body– FEM attachments makes a traditional mesh convergence study difficult to perform. For example, the number and location of attachment vertices changes

for different mesh set-ups (and consequently different node locations), which inherently leads to differences in attachment between the meshes. Also, the contact force is distributed over all interpenetrating vertices, which again changes between meshes. The complexity of this problem is supported by the fact that previous models of the human masticatory system did not include a mesh independent grid analysis (Koolstra and van Eijden, 2005; Mori et al., 2010; Comisso et al., 2014, 2015; Hattori-Hara et al., 2014; Martinez Choy et al., 2017). Additionally, the purpose of the presented model and the large amount of uncertainty in measured parameters of the jaw region will permit a larger amount of error. For example, material properties of the components are largely based off of animal studies (Tanaka et al., 2002; Koolstra et al., 2007; Singh and Detamore, 2008) and the use of patient specific geometry infers a non-negligible amount of variation as well. For these reasons, the stress values computed by the model should only be used for comparative investigations (Tsouknidas et al., 2013).

In this study, we report von Mises and maximum principal stresses for three simulations tasks. In agreement with the point made in the previous paragraph, clenching stress values in literature change in the order of 1–2 magnitudes for different material models and simulation set-ups, which makes a direct comparison of results difficult. Generally, our computed trends agree with previous studies, as described in Section “Results”. As expected, clenching created high von Mises stresses over the whole disk surface which is in contact with the articular surfaces. The highest stresses were located around the latero-posterior region, consistent with the overall muscle force direction of the closing muscles. For opening and protrusion the presented von Mises stress patterns are reasonable in the context of the disk movements, which were validated using MRI data of the volunteer. Conceptually, von Mises stresses are strongly related to tissue strain and are hardly comparable to contact pressures. Articular cartilage contact pressures in our simulation are computed as pressure in the normal direction of the surface and are hence closer related to principal stresses of the disk.

The presented dynamic model highlights some unique possibilities for future investigations. For example, detailed investigations of joint loads for muscle driven mastication cycles are possible, as well as studies on the effect of TMDs, like disk dislocation, on tasks like chewing or speaking. Another problem of interest is the investigation of tooth grinding and its possible connection to increased TMJ loads. We previously presented an optimization approach that enables the use of movement as well as constraint reaction forces for forward-dynamics tracking simulations (Sagl et al., 2019a). The combination of this optimization approach with the presented model allows for a detailed investigation of muscle activation patterns and the joint loads during dynamic tooth grinding tasks. Additionally, computational modeling of the masticatory system has proven to be a useful instrument for many orofacial applications outside of the more traditional fields of dentistry. Possibilities include the use for the investigation novel TMJ total joint replacement devices (Detamore et al., 2007; Ackland et al., 2015, 2018; Omid

et al., 2018) as well as areas of orofacial function like speech (Anderson et al., 2015; Harandi et al., 2017) and swallowing (Mayer et al., 2016; Wang et al., 2018).

CONCLUSION

This paper presents a novel computer model of the masticatory region that combines rigid body bones and Hill-type muscles with a detailed representation of the TMJ. The model allows for the investigation of dynamic tasks of the jaw apparatus, while enabling detailed investigation of stresses on the cartilage layers of the joint. The unique combination of a FEM disk and two EF articular cartilage layers allows us to keep simulation times reasonable, which is of utmost importance for the translation of computational biomechanics to the clinical practice. This will potentially lead to the development of therapeutic interventions for the restoration of orofacial functions and an increase in quality of life for TMD patients.

DATA AVAILABILITY

The datasets generated for this study are available on request to the corresponding author.

ETHICS STATEMENT

The studies involving human participants were reviewed and approved by the Institutional Review Board of the Medical University of Vienna. The patients/participants provided their written informed consent to participate in this study.

AUTHOR CONTRIBUTIONS

BS, MS-S, EP, MK, and IS conceived and designed the study, and analyzed and interpreted the data. BS and IS developed the computer model. BS drafted the manuscript. All authors edited the manuscript.

FUNDING

This research has been funded by the Medical Scientific Fund of the Mayor of the City of Vienna (PN 17109) and the Vienna School of Interdisciplinary Dentistry (PN SA670KV001).

ACKNOWLEDGMENTS

This research was undertaken thanks in part to input from John Lloyd and the ArtiSynth team. The authors also want to thank Prof. Rudolf Slavicek for his feedback during the project.

REFERENCES

- Ackland, D., Robinson, D., Lee, P. V. S., and Dimitroulis, G. (2018). Design and clinical outcome of a novel 3D-printed prosthetic joint replacement for the human temporomandibular joint. *Clin. Biomech.* 56, 52–60. doi: 10.1016/j.clinbiomech.2018.05.006
- Ackland, D. C., Moskaljuk, A., Hart, C., Vee Sin Lee, P., and Dimitroulis, G. (2015). Prosthesis loading after temporomandibular joint replacement surgery: a musculoskeletal modeling study. *J. Biomech. Eng.* 137:041001. doi: 10.1115/1.4029503
- Andersen, M. S., de Zee, M., Damsgaard, M., Nolte, D., and Rasmussen, J. (2017). Introduction to force-dependent kinematics: theory and application to mandible modeling. *J. Biomech. Eng.* 139:091001. doi: 10.1115/1.4037100
- Anderson, P., Harandi, N. M., Moisis, S., Stavness, I., and Fels, S. (2015). “A comprehensive 3D biomechanically-driven vocal tract model including inverse dynamics for speech research,” in *Proceedings of the Annual Conference of the International Speech Communication Association, INTERSPEECH*, Dresden, 2395–2399.
- Beek, M., Aarnts, M. P., Koolstra, J. H., Feilzer, A. J., and Van Eijden, T. M. G. J. (2001). Dynamic properties of the human temporomandibular joint disc. *J. Dent. Res.* 80, 876–880. doi: 10.1177/00220345010800030601
- Bei, Y., and Fregly, B. J. (2004). Multibody dynamics simulation of knee contact mechanics. *Med. Eng. Phys.* 26, 777–789. doi: 10.1038/nature13314.A
- Blankevoort, L., Kuiper, J. H., Huijskes, R., and Grootenboer, H. J. (1991). Articular contact in a three-dimensional model of the knee. *J. Biomech.* 24, 1019–1031. doi: 10.1016/0021-9290(91)90019-J
- Commisso, M. S., Calvo-Gallego, J. L., Mayo, J., Tanaka, E., and Martínez-Reina, J. (2016). Quasi-Linear viscoelastic model of the articular disc of the temporomandibular joint. *Exp. Mech.* 56, 1169–1177. doi: 10.1007/s11340-016-0161-2
- Commisso, M. S., Martínez-Reina, J., and Mayo, J. (2014). A study of the temporomandibular joint during bruxism. *Int. J. Oral Sci.* 6, 116–123. doi: 10.1038/ijos.2014.4
- Commisso, M. S., Martínez-Reina, J., Ojeda, J., and Mayo, J. (2015). Finite element analysis of the human mastication cycle. *J. Mech. Behav. Biomed. Mater.* 41, 23–35. doi: 10.1016/j.jmbbm.2014.09.022
- Curtis, N. (2011). Craniofacial biomechanics: an overview of recent multibody modelling studies. *J. Anat.* 218, 16–25. doi: 10.1111/j.1469-7580.2010.01317.x
- de Zee, M., Cattaneo, P. M., Svensson, P., Pedersen, T. K., Melsen, B., Rasmussen, J., et al. (2009). Prediction of the articular eminence shape in a patient with unilateral hypoplasia of the right mandibular ramus before and after distraction osteogenesis-A simulation study. *J. Biomech.* 42, 1049–1053. doi: 10.1016/j.jbiomech.2009.02.027
- de Zee, M., Dalstra, M., Cattaneo, P. M., Rasmussen, J., Svensson, P., and Melsen, B. (2007). Validation of a musculo-skeletal model of the mandible and its application to mandibular distraction osteogenesis. *J. Biomech.* 40, 1192–1201. doi: 10.1016/j.jbiomech.2006.06.024
- Detamore, M. S., and Athanasiou, K. A. (2003). Structure and function of the temporomandibular joint disc: implications for tissue engineering. *J. Oral Maxillofac. Surg.* 61, 494–506. doi: 10.1053/joms.2003.50096
- Detamore, M. S., Athanasiou, K. A., and Mao, J. (2007). A call to action for bioengineers and dental professionals: directives for the future of TMJ bioengineering. *Ann. Biomed. Eng.* 35, 1301–1311. doi: 10.1007/s10439-007-9298-6
- Drake, R., Vogl, W., and Mitchell, A. (2014). *Gray's Anatomy for Students*, 3rd Edn. London: Churchill Livingstone.
- Fernandez, J., Sartori, M., Lloyd, D., Munro, J., and Shim, V. (2014). Bone remodelling in the natural acetabulum is influenced by muscle force-induced bone stress. *Int. J. Numer. Method Biomed. Eng.* 30, 28–41. doi: 10.1002/cnm.2586
- Greaves, W. S. (1978). The jaw lever system in ungulates: a new model. *J. Zool.* 184, 271–285. doi: 10.1111/j.1469-7998.1978.tb03282.x
- Hannam, A. G. (2011). Current computational modelling trends in craniomandibular biomechanics and their clinical implications. *J. Oral Rehabil.* 38, 217–234. doi: 10.1111/j.1365-2842.2010.02149.x
- Hannam, A. G., Stavness, I., Lloyd, J. E., and Fels, S. (2008). A dynamic model of jaw and hyoid biomechanics during chewing. *J. Biomech.* 41, 1069–1076. doi: 10.1016/j.jbiomech.2007.12.001
- Hansson, T., Öberg, T., Carlsson, G. E., and Kopp, S. (1977). Thickness of the soft tissue layers and the articular disk in the temporomandibular joint. *Acta Odontol. Scand.* 35, 77–83. doi: 10.3109/00016357709055993
- Hattori-Hara, E., Mitsui, S. N., Mori, H., Arafurue, K., Kawaoka, T., Ueda, K., et al. (2014). The influence of unilateral disc displacement on stress in the contralateral joint with a normally positioned disc in a human temporomandibular joint: an analytic approach using the finite element method. *J. Cranio Maxillof. Surg.* 42, 2018–2024. doi: 10.1016/j.jcms.2014.09.008
- Hill, A. V. (1953). The mechanics of active muscle. *Proc. R. Soc. Lond. B Biol. Sci.* 141, 104–117. doi: 10.1098/rspb.1953.0027
- Ingawale, S., and Goswami, T. (2009). Temporomandibular joint: disorders, treatments, and biomechanics. *Ann. Biomed. Eng.* 37, 976–996. doi: 10.1007/s10439-009-9659-4
- Koolstra, J. H., and Tanaka, E. (2009). Tensile stress patterns predicted in the articular disc of the human temporomandibular joint. *J. Anat.* 215, 411–416. doi: 10.1111/j.1469-7580.2009.01127.x
- Koolstra, J. H., Tanaka, E., and Van Eijden, T. M. (2007). Viscoelastic material model for the temporomandibular joint disc derived from dynamic shear tests or strain-relaxation tests. *J. Biomech.* 40, 2330–2334. doi: 10.1016/j.jbiomech.2006.10.019
- Koolstra, J. H., and van Eijden, T. M. (2005). Combined finite-element and rigid-body analysis of human jaw joint dynamics. *J. Biomech.* 38, 2431–2439. doi: 10.1016/j.jbiomech.2004.10.014
- Koolstra, J. H., and van Eijden, T. M. G. J. (1995). Biomechanical analysis of jaw-closing movements. *J. Dent. Res.* 74, 1564–1570. doi: 10.1177/00220345950740091001
- Koolstra, J. H., and van Eijden, T. M. G. J. (1997). The jaw open-close movements predicted by biomechanical modelling. *J. Biomech.* 30, 943–950. doi: 10.1016/S0021-9290(97)00058-4
- Lamela, M. J., Prado, Y., Fernández, P., Fernández-Canteli, A., and Tanaka, E. (2011). Non-linear viscoelastic model for behaviour characterization of the temporomandibular joint discs. *Exp. Mech.* 51, 1435–1440. doi: 10.1007/s11340-011-9465-4
- Langenbach, G. E. J., and Hannam, A. G. (1999). The role of passive muscle tensions in a three-dimensional dynamic model of the human jaw. *Arch. Oral Biol.* 44, 557–573. doi: 10.1016/S0003-9969(99)00034-5
- Lloyd, J. E., Stavness, I., and Fels, S. (2012). “ArtiSynth: a fast interactive biomechanical modeling toolkit combining multibody and finite element simulation,” in *Soft Tissue Biomechanical Modeling for Computer Assisted Surgery*, ed. Y. Payan, (Heidelberg: Springer), 355–394. doi: 10.1007/8415_2012_126
- Harandi, N. M., Woo, J., Stone, M., Abugharbieh, R., and Fels, S. (2017). Variability in muscle activation of simple speech motions: a biomechanical modeling approach. *J. Acoust. Soc. Am.* 141, 2579–2590. doi: 10.1121/1.4978420
- Marková, M., and Gallo, L. M. (2016). The influence of the human TMJ eminence inclination on predicted masticatory muscle forces. *Hum. Mov. Sci.* 49, 132–140. doi: 10.1016/j.humov.2016.06.012
- Martinez Choy, S. E., Lenz, J., Schweizerhof, K., Schmitter, M., and Schindler, H. J. (2017). Realistic kinetic loading of the jaw system during single chewing cycles: a finite element study. *J. Oral Rehabil.* 44, 375–384. doi: 10.1111/joor.12501
- Mayer, C., Roewer-Despres, F., Stavness, I., and Gick, B. (2016). Does swallowing bootstrap speech learning? *Can. Acoust. Acoust. Can.* 44, 194–195.
- Mori, H., Horiuchi, S., Nishimura, S., Nikawa, H., Murayama, T., Ueda, K., et al. (2010). Three-dimensional finite element analysis of cartilaginous tissues in human temporomandibular joint during prolonged clenching. *Arch. Oral Biol.* 55, 879–886. doi: 10.1016/j.archoralbio.2010.07.011
- Muto, T., and Kanazawa, M. (1994). Positional change of the hyoid bone at maximal mouth opening. *Oral Surgery Oral Med. Oral Pathol.* 77, 451–455. doi: 10.1016/0030-4220(94)90222-4
- Nagahara, K., Murata, S., Nakamura, S., and Tsuchiya, T. (1999). Displacement and stress distribution in the temporomandibular joint during clenching. *Angle Orthod.* 69, 372–379. doi: 10.1043/0003-32191999069<0372:DASDIT>2.3.CO;2
- Nazari, M. A., Perrier, P., Chabanas, M., Payan, Y., and Yohan, P. (2011). *Shaping by Stiffening: a Modeling Study for Lips*. Available at: <https://hal.archives-ouvertes.fr/hal-00565466> (accessed May 15, 2019).

- Nickel, J., Spilker, R., Iwasaki, L., Gonzalez, Y., McCall, W., Ohrbach, R., et al. (2009). Static and dynamic mechanics of the temporomandibular joint: plowing forces, joint load and tissue stress. *Orthod. Craniofac. Res.* 12, 159–167. doi: 10.1111/j.1601-6343.2009.01449.x
- Omidi, A., Ali Nazari, M., and Jeannine, C. (2018). “A 3D Finite Element Model of Mastication Muscles to Study the Jaw Movement for TMJ Prosthesis Performance Evaluation,” in *Proceedings of the 2017 24th National and 2nd International Iranian Conference on Biomedical Engineering (ICBME)*, Tehran, doi: 10.1109/ICBME.2017.8430268
- Pal, S., Besier, T. F., Gold, G. E., Fredericson, M., Delp, S. L., and Beaupre, G. S. (2019). Patellofemoral cartilage stresses are most sensitive to variations in vastus medialis muscle forces. *Comput. Methods Biomech. Biomed. Eng.* 22, 206–216. doi: 10.1080/10255842.2018.1544629
- Peck, C. C., Langenbach, G. E. J., and Hannam, A. G. (2000). Dynamic simulation of muscle and articular properties during human wide jaw opening. *Arch. Oral Biol.* 45, 963–982. doi: 10.1016/S0003-9969(00)00071-76
- Pérez del Palomar, A., and Doblaré, M. (2006a). 3D Finite element simulation of the opening movement of the mandible in healthy and pathologic situations. *J. Biomech. Eng.* 128:242. doi: 10.1115/1.2165697
- Pérez del Palomar, A., and Doblaré, M. (2006b). Finite element analysis of the temporomandibular joint during lateral excursions of the mandible. *J. Biomech.* 39, 2153–2163. doi: 10.1016/j.jbiomech.2005.06.020
- Sagl, B., Dickerson, C. R., and Stavness, I. (2019a). Fast forward-dynamics tracking simulation: application to upper limb and shoulder modeling. *IEEE Trans. Biomed. Eng.* 66, 335–342. doi: 10.1109/TBME.2018.2838020
- Sagl, B., Schmid-Schwap, M., Piehlsinger, E., Kronnerwetter, C., Kundi, M., Trattinig, S., et al. (2019b). In vivo prediction of temporomandibular joint disc thickness and position changes for different jaw positions. *J. Anat.* 234, 718–727. doi: 10.1111/joa.12951
- Schiffman, E., Ohrbach, R., Truelove, E., Look, J., Anderson, G., Goulet, J.-P., et al. (2014). Diagnostic criteria for temporomandibular disorders (DC/TMD) for clinical and research applications: recommendations of the international RDC/TMD Consortium Network* and Orofacial Pain Special Interest Group†. *J. Oral Facial Pain Headache* 28, 6–27. doi: 10.11607/jop.1151
- Servin, M., Lacoursière, C., and Melin, N. (2006). “Interactive Simulation of Elastic Deformable Materials,” in *Proceedings of SIGRAD Conference*, Skövde.
- Si, H. (2015). TetGen, a delaunay-based quality tetrahedral mesh generator. *ACM Trans. Math. Softw.* 41, 1–36. doi: 10.1145/2629697
- Singh, M., and Detamore, M. S. (2008). Tensile properties of the mandibular condylar cartilage. *J. Biomech. Eng.* 130:011009. doi: 10.1115/1.2838062
- Solberg, W. K., Woo, M. W., and Houston, J. B. (1979). Prevalence of mandibular dysfunction in young adults. *J. Am. Dent. Assoc.* 98, 25–34. doi: 10.14219/jada.archive.1979.0008
- Stankovic, S., Vlajkovic, S., Boskovic, M., Radenkovic, G., Antic, V., and Jevremovic, D. (2013). Morphological and biomechanical features of the temporomandibular joint disc: an overview of recent findings. *Arch. Oral Biol.* 58, 1475–1482. doi: 10.1016/j.archoralbio.2013.06.014
- Stavness, I., Hannam, A. G., Lloyd, J. E., and Fels, S. (2006). “An integrated dynamic jaw and laryngeal model constructed from CT data,” in *Lecture Notes in Computer*, eds M. Harders, and G. Székely, (Berlin: Springer), 169–177. doi: 10.1007/11790273_19
- Stavness, I., Hannam, A. G., Lloyd, J. E., and Fels, S. (2010). Predicting muscle patterns for hemimandibulectomy models. *Comput. Methods Biomech. Biomed. Eng.* 13, 483–491. doi: 10.1080/10255841003762034
- Tanaka, E., del Pozo, R., Sugiyama, M., and Tanne, K. (2002). Biomechanical response of retrodiscal tissue in the temporomandibular joint under compression. *J. Oral Maxillofac. Surg.* 60, 546–551. doi: 10.1053/joms.2002.31853
- Tanaka, E., Detamore, M. S., Tanimoto, K., and Kawai, N. (2008). Lubrication of the temporomandibular joint. *Ann. Biomed. Eng.* 36, 14–29. doi: 10.1007/s10439-007-9401-z
- Tanaka, E., and Koolstra, J. H. (2008). Biomechanics of the temporomandibular joint. *J. Dent. Res.* 87, 989–991. doi: 10.1177/154405910808701101
- Throckmorton, G. S., and Throckmorton, L. S. (1985). Quantitative calculations of temporomandibular joint reaction forces-I. The importance of the magnitude of the jaw muscle forces. *J. Biomech.* 18, 445–452. doi: 10.1016/0021-9290(85)90279-9
- Trainor, P. G. S., McLachlan, K. R., and McCall, W. D. (1995). Modelling of forces in the human masticatory system with optimization of the angulations of the joint loads. *J. Biomech.* 28, 829–843. doi: 10.1016/0021-9290(94)00128-Q
- Tsouknidas, A., Jimenez-Rojo, L., Karatsis, E., Michailidis, N., and Mitsiadis, T. A. (2017). A Bio-Realistic finite element model to evaluate the effect of masticatory loadings on mouse mandible-related tissues. *Front. Physiol.* 8:273. doi: 10.3389/fphys.2017.00273
- Tsouknidas, A., Savvakis, S., Asaniotis, Y., Anagnostidis, K., Lontos, A., and Michailidis, N. (2013). The effect of kyphoplasty parameters on the dynamic load transfer within the lumbar spine considering the response of a bio-realistic spine segment. *Clin. Biomech.* 28, 949–955. doi: 10.1016/j.CLINBIOMECH.2013.09.013
- Tuijt, M., Koolstra, J. H., Lobbezoo, F., and Naeije, M. (2010). Differences in loading of the temporomandibular joint during opening and closing of the jaw. *J. Biomech.* 43, 1048–1054. doi: 10.1016/j.jbiomech.2009.12.013
- Wang, J., Ho, A. K., Papadopoulos-Nydam, G., Rieger, J., Inamoto, Y., Fels, S., et al. (2018). Simulated volume loss in the base of tongue in a virtual swallowing model. *Comput. Methods Biomech. Biomed. Eng. Imaging Vis.* 7, 389–395. doi: 10.1080/21681163.2017.1382392
- Xu, C., Reifman, J., Baggaley, M., Edwards, W. B., and Unnikrishnan, G. (2019). Individual differences in women during walking affect tibial response to load carriage: the importance of individualized musculoskeletal finite-element models. *IEEE Trans. Biomed. Eng.* doi: 10.1109/tbme.2019.2917415 [Epub ahead of print].

Conflict of Interest Statement: The authors declare that the research was conducted in the absence of any commercial or financial relationships that could be construed as a potential conflict of interest.

Copyright © 2019 Sagl, Schmid-Schwap, Piehlsinger, Kundi and Stavness. This is an open-access article distributed under the terms of the Creative Commons Attribution License (CC BY). The use, distribution or reproduction in other forums is permitted, provided the original author(s) and the copyright owner(s) are credited and that the original publication in this journal is cited, in accordance with accepted academic practice. No use, distribution or reproduction is permitted which does not comply with these terms.



TRPV1 and TRPV1-Expressing Nociceptors Mediate Orofacial Pain Behaviors in a Mouse Model of Orthodontic Tooth Movement

Sheng Wang¹, Martin Kim¹, Zayd Ali¹, Katherine Ong¹, Eung-Kwon Pae² and Man-Kyo Chung^{1*}

¹Program in Neuroscience, Center to Advance Chronic Pain Research, Department of Neural and Pain Sciences, School of Dentistry, University of Maryland, Baltimore, MD, United States, ²Department of Orthodontic and Pediatric Dentistry, School of Dentistry, University of Maryland, Baltimore, MD, United States

OPEN ACCESS

Edited by:

Limor Avivi-Arber,
University of Toronto, Canada

Reviewed by:

Koichi Iwata,
Nihon University, Japan
Kaj Fried,
Karolinska Institute (KI), Sweden

*Correspondence:

Man-Kyo Chung
mchung@umaryland.edu

Specialty section:

This article was submitted to
Craniofacial Biology and Dental
Research,
a section of the journal
Frontiers in Physiology

Received: 21 May 2019

Accepted: 04 September 2019

Published: 20 September 2019

Citation:

Wang S, Kim M, Ali Z, Ong K, Pae E-K
and Chung M-K (2019) TRPV1 and
TRPV1-Expressing Nociceptors
Mediate Orofacial Pain Behaviors
in a Mouse Model of Orthodontic
Tooth Movement.
Front. Physiol. 10:1207.
doi: 10.3389/fphys.2019.01207

Orthodontic force produces mechanical irritation and inflammation in the periodontium, which is inevitably accompanied by pain. Despite its prevalence, treatment of orthodontic pain is ineffective. Elucidating underlying neural mechanisms is critical to improving the management of orthodontic pain. We have assessed the contribution of transient receptor potential vanilloid subtype 1 (TRPV1) and the TRPV1-expressing subset of nociceptive afferents to pain behaviors induced by orthodontic force in mice. Microfocus X-ray computed tomography analysis showed that application of an orthodontic force of 10 g to the maxillary first molar produced reliable tooth movement in mice. Mouse grimace scale (MGS) was evaluated as an indication of non-evoked spontaneous pain and bite force (BF) was measured for assessing bite-evoked nocifensive behaviors. Orthodontic force increased MGS and decreased BF, both of which were interpreted as increased levels of pain. These behaviors peaked at 1d and returned near to the sham level at 7d. Retrograde labeling and immunohistochemical assays showed TRPV1-expressing peptidergic afferents are abundantly projected to the periodontium. Direct injection of resiniferatoxin into trigeminal ganglia (TG) decreased TRPV1-expressing afferents by half in the targeted region of TG. The chemical ablation of TRPV1-expressing afferents significantly attenuated orthodontic pain behaviors assessed by MGS and BF. Consistently, the knockout of TRPV1 also attenuated orthodontic force-induced changes in MGS and BF. These results suggest that TRPV1 and TRPV1-expressing trigeminal nociceptors constitute a primary pathway mediating orthodontic pain behaviors in mice. This model will be useful for mechanistic studies on orthodontic pain aimed at developing novel approaches for painless orthodontics.

Keywords: orthodontic tooth movement, trigeminal ganglia, TRPV1, peptidergic nociceptors, periodontium, behavioral assays

INTRODUCTION

Pain and discomfort are the major side effects of orthodontic treatment. Fixed orthodontic appliances produce pain in 94% of patients (Scheurer et al., 1996). Pain and soreness induced by orthodontic adjustment peaks after 24 h, and gradually declines, and resolution occurs within a week (Ngan et al., 1989; Scheurer et al., 1996). Pain during biting and chewing also peaks after 24 h, creating a major functional discomfort in daily life (Scheurer et al., 1996). Pain management during orthodontic treatment is often not effective, significantly affecting the patient's compliance to treatment (Sergl et al., 1998). Peripheral and central mechanisms of orthodontic pain are under active investigation (Long et al., 2016) and better understanding of neurobiological mechanisms should help to better manage orthodontic pain.

Orthodontic force induces a variety of morphological and neurochemical responses of the peripheral and central nervous system (Long et al., 2016; Kobayashi and Horinuki, 2017). For mechanistic determination of orthodontic pain, it is critical to elucidate causal contributions of neural components in animal models involving pain behaviors. In rats, placement of a coil spring between the maxillary first molar and incisors produces changes in grimace scale and facial grooming (Yang et al., 2009; Liao et al., 2014). These behaviors are inhibited by morphine (Liao et al., 2014; Gao et al., 2016), indicating that these behaviors are relevant to nociception. A recent study also suggested that measuring changes in biting force in rats provides a functional surrogate outcome for biting-induced pain by orthodontic force (Long et al., 2019). However, similar models for assessing orthodontic pain behaviors have not been well established in mice, precluding the use of various genetic tools available in mice for mechanistic study of orthodontic pain.

The peripheral and central ascending pain pathways and neuronal circuitry that mediate orthodontic pain are not well defined. Orthodontic force should lead to the activation of periodontal nociceptors. However, the identity of the nociceptor subpopulation responsible for orthodontic pain is not well known. Periodontal ligament (PDL) contains A δ and C nociceptive terminals (Byers, 1985). One of the well-defined populations of nociceptors is a peptidergic nociceptor containing the neuropeptides such as calcitonin gene-related peptide (CGRP). Peptidergic nociceptors project into the PDL in mice (Sarram et al., 1997). However, the role of periodontal peptidergic afferents in spontaneous pain or function-related pain evoked by orthodontic force is unknown.

Peptidergic afferents are enriched with transient receptor potential vanilloid subtype 1 (TRPV1), a receptor for capsaicin and noxious heat (Caterina et al., 2000; Cavanaugh et al., 2011). Although TRPV1 contributes to thermal hyperalgesia in skin (Caterina et al., 2000), TRPV1 mediates spontaneous pain and mechanical hyperalgesia during orofacial muscle inflammation (Chung et al., 2016; Wang et al., 2017a). The role of TRPV1 in non-evoked pain upon the application of orthodontic force was also suggested. Pharmacological inhibition or knockdown of TRPV1 attenuates facial grooming or grimace scale induced by orthodontic force in rats (Gao et al., 2016; Guo et al., 2019a).

However, it is not known if TRPV1 contributes to other modalities of orthodontic pain, such as bite-evoked pain. Given the differential contribution of TRPV1 to spontaneous pain and bite-evoked pain under muscle inflammation (Wang et al., 2017a), it is important to determine the role of TRPV1 in bite-evoked nocifensive behaviors during orthodontic tooth movement.

In this study, we have determined the contribution of TRPV1 and TRPV1-expressing afferents to orthodontic pain behaviors in a mouse model of orthodontic tooth movement. We have assessed a mouse model of orthodontic pain using two different behavioral measurements. In combination with targeted chemical ablation of specific neuronal subtypes and genetic inhibition, we tested the hypothesis that TRPV1 and TRPV1-expressing trigeminal nociceptors constitute a major pathway for transduction of orthodontic pain.

MATERIALS AND METHODS

Experimental Animals

C57BL/6 mice (The Jackson Laboratory, Bar Harbor, Maine), TRPV1 KO mice (Caterina et al., 2000), TRPV1-Cre mice (Jax #017769) (Cavanaugh et al., 2011), and Rosa26-mT/mG (Jax #007576) (Muzumdar et al., 2007; Wang et al., 2017b) were used. In experiments involving behavioral assays, 12-week-old mice were used for stable measurement of bite force (BF) behaviors (Wang et al., 2017a). Orthodontic pain shows limited or no clear sex difference (Jones, 1984; Ngan et al., 1989; Scheurer et al., 1996), whereas mouse behavioral assays, especially BF measurement, are influenced by sex; when both male and female mice are included in pain assays, variation of the data increases (Guo et al., 2019b). To facilitate establishing a model of orthodontic pain in mice, we have focused on male mice without attempting to determine sex differences at this time. All animal procedures were consistent with the NIH Guide for the Care and Use of Laboratory Animals (Publication 85-23, Revised 1996), and were performed according to a University of Maryland-approved Institutional Animal Care and Use Committee protocol.

Experimental Orthodontic Tooth Movement

To produce orthodontic forces in mice, a coil spring was placed between maxillary first molar and maxillary incisors (Figure 1A). The animals were anesthetized with ketamine (100–150 mg/kg) and xylazine (10–16 mg/kg). A 0.010-in stainless steel ligature wire was looped around the first molar, and a second ligature wire was looped around maxillary incisors. We used two nickel-titanium orthodontic coil springs (Xu Jia Chuang Spring; Guangdong, China) exerting different forces: a 2 g spring (wire diameter: 0.1 mm; outer diameter: 1.6 mm; length: 1.8 mm) exerts 2 ± 0.2 g force, whereas a 10 g spring (wire diameter: 0.15 mm; outer diameter: 1.8 mm; length: 2.2 mm) exerts 10 ± 1 g force upon activation of 1 mm. In the group with orthodontic force (OF), the coil spring was extended mesially and ligated to the incisors. In the sham group, the orthodontic spring was irreversibly deformed by extension beyond elastic limit and ligated so

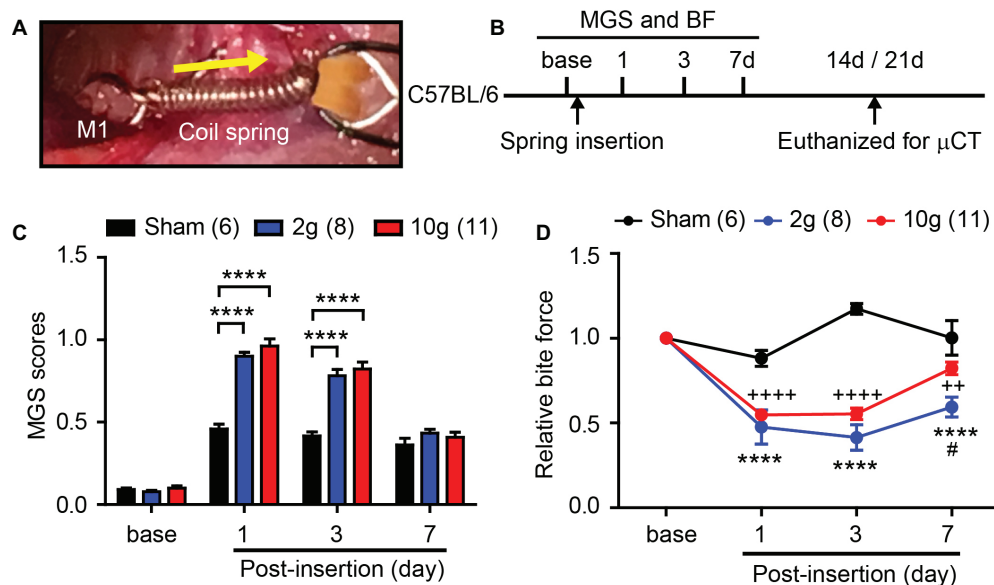


FIGURE 1 | Orthodontic force induces spontaneous and bite-evoked pain behaviors in mice. **(A)** Ni-Ti closed coil spring was placed between the left maxillary first molar (M1) and incisors (INC). The spring was activated to exert 2 or 10 g force in the orthodontic force group. In the sham group, the spring did not produce active force. Arrow, direction of orthodontic force. **(B)** Timeline of experiment. In adult C57BL/6 mice, behavioral assays were performed before and after the placement of an orthodontic spring. BF assay was performed immediately after video recording for facial grimace assay on each day. The mice were euthanized for μ CT at 14d, with the exception that five mice in the 2 g group and all mice in the sham group were euthanized at 21d. BF, bite force assay; MGS, mouse grimace scale; μ CT, micro-CT. **(C)** Comparison of MGS scores at different time points. Numbers within parentheses represent number of animals. **** $p < 0.0001$ in two-way repeated-measure (RM) ANOVA followed by Bonferroni *post hoc* test. **(D)** Comparison of relative BF at different time points. **** $p < 0.0001$ (2 g vs. sham), ** $p < 0.01$, **** $p < 0.001$ (10 g vs. sham), * $p < 0.05$ (2 g vs. 10 g) in Bonferroni *post hoc* test following two-way RM ANOVA.

that the spring delivered no force. To secure the ligature wires, self-etching primer and light-cured adhesive resin cement (Transbond; 3 M Unitek, Monrovia, California) were applied to the palatal surfaces of the maxillary incisors and first molars. After spring insertion, the animals were supplied with soft diet (Dietgel recovery; ClearH2O; Portland, ME). The appliances were inspected daily, and additional bonding material was applied as necessary.

Microfocus Computed Tomography

The animals were anesthetized by ketamine/xylazine, and euthanized by transcardial perfusion using 3.7% paraformaldehyde. Maxillae were hemisected, and microfocus computed tomography (μ CT) images were obtained using a Siemens Inveon Micro-PET/SPECT/CT (Siemens, Ann Arbor, MI) with 9 μ m spatial resolution. Siemens Inveon Research Workplace 4.2 software was used for image acquisition and processing, 2-D and 3-D image viewing, and quantitative analysis. The intermolar distance was measured as the distance between the most distal point of the maxillary first molar crown and the most mesial point of the maxillary second molar crown. The measurements were performed in the sagittal plane because this plane showed the most root structure, permitting estimation of angulation of the long axis of the tooth. The two-dimensional images were magnified 10 times for more precise line drawings at the closest proximity of the two convex molar crown surfaces. Bone volume fraction in the furcation region of the maxillary first molar was assessed as a quantitative analysis of alveolar bone changes.

The region of interest for the total interradicular alveolar bone space [tissue volume (TV)] in the furcation region was defined as previously described (Yadav et al., 2015). Within the region of interest, total amount of actual interradicular alveolar bone volume (BV) was calculated, which was divided by TV to calculate bone volume fraction.

Microinjection Into Trigeminal Ganglia

To selectively ablate TRPV1-expressing trigeminal nociceptors, resiniferatoxin (RTX) was directly injected into trigeminal ganglia (TG). RTX is a highly efficacious agonist of TRPV1, and the activation of TRPV1 by RTX leads to ablation of nociceptor terminals or soma upon localized injection (Karai et al., 2004; Chung and Campbell, 2016). The animals were anesthetized using ketamine/xylazine and placed in a Kopf stereotaxic apparatus. A midline incision of 3–5 mm and an opening to the skull were made. A 0.5- μ l Hamilton micro-syringe was used for microinjection. The micro-syringe needle was placed in the left TG regions according to the stereotaxic coordinates of the mouse brain (0.2 mm posterior to bregma, 1.3 mm lateral to the midline, and 6.5 mm deep) for targeting ophthalmic/maxillary (V1/V2) region. RTX (50 ng/0.5 μ l; Sigma-Aldrich) was dissolved in phosphate buffered saline (PBS) containing 1% dimethyl sulfoxide and 10% Tween-80. Mice injected with vehicle (0.5 μ l) served as a control group. Injection was performed at a rate of 0.5 μ l/min and the injection needle was held in the tissue for 2 min to allow diffusion before removal.

Measurement of Mouse Grimace Scale and Bite Force Measurement

Mouse grimace scale (MGS) and BF were performed as previously described (Wang et al., 2017a, 2018; Guo et al., 2019b). All behavioral assays and video analysis were performed in a blinded manner. For MGS assay, the mice were videotaped for 30 min in each experimental time point and 10 images per 30 min session were manually captured. The scores of the five action units in each photograph were averaged, and a mean MGS score was obtained from the 10 images, which was presumed to reflect the level of spontaneous pain. For BF assay, mice were placed in a modified 60-ml plastic syringe with a wide opening at one end to accommodate the head of the mouse. To minimize stress, the mouse was released immediately from the syringe if it vigorously moved or tried to hide inside the syringe. The syringe containing the mouse was held manually and moved slowly at 0.5–1 cm/s toward bite plates so that the mouse could bite the plates. Spike 2 software was used to measure the voltage changes from transducer displacement. SigmaPlot 8.0 was used to convert the voltage change into force based on calibration using standard weights. Bite force was recorded for 120 s per session and the top five force measurements were averaged.

Measurement of Eye-Wiping Behavior

To functionally verify the effective ablation of TRPV1-expressing afferents by intra-TG injection of RTX, we performed an eye-wiping test using capsaicin. The animals were placed in a plastic container (9 cm × 9 cm × 13 cm) with two-mirrored back walls to allow the video camera to record a four-sided view. Two drops (20 µl) of 0.03% capsaicin solution were placed onto the left conjunctiva of the eye. The number of eye wipes with the ipsilateral forepaw in a 5-min window was counted.

Retrograde Labeling of Periodontal Afferents

In C57BL/6 mice anesthetized by Ketamine/Xylazine, fluorogold (FG; Fluorochrome) was injected into gingiva around maxillary first molar to retrogradely label periodontal afferents in TG. FG was dissolved in 0.9% saline at a concentration of 4%. A 50-µl Hamilton syringe was used to slowly inject 5 µl of tracer into five sites (1 µl per site) at gingiva around disto-buccal groove, buccal groove, mesial groove, palatal groove, and disto-palatal groove of the maxillary first molar. The mice were euthanized 7 days following the injection by transcardial perfusion for further histological study. Four ganglia were analyzed for quantification.

Immunohistochemistry of Trigeminal Ganglia and Maxillae

Immunohistochemical assays of TG and maxillae were performed as previously described (Chung et al., 2011, 2012; Wang et al., 2017a). Maxillae were decalcified in 10% EDTA (pH 7.4) for 7 days at 4°C. Tissues were cryoprotected and cryosectioned at 12 µm for TG and 30 µm for decalcified maxillae. Conventional immunohistochemical procedures were performed with rabbit anti-TRPV1 (1:1,000; a generous gift from Dr. Michael Caterina at Johns Hopkins University), guinea pig anti-CGRP (1:1,000;

Penninsula Labs), or rabbit green fluorescent protein (GFP; 1:1,000, Invitrogen). We verified the specificity of the primary antibodies by using genetically engineered mice lacking the expression of the target gene or by omitting the primary antibody (Chung et al., 2012). The sections were further incubated with appropriate secondary antibodies (Invitrogen). Tooth sections were stained with 4',6-diamidino-2-phenylindole (DAPI) to visualize the cellular nuclei. For classification of neuronal size in TG sections, we measured the cross-sectional area of the neurons in ImageJ and followed the criteria described elsewhere (small, < 300 µm²; medium, 300–600 µm²; large, > 600 µm²) (Ichikawa et al., 2006). For counting TG neurons, Nissl staining was performed using NeuroTrace 500/525 green fluorescent Nissl Stain (Invitrogen). Four to five images from V1/V2 regions and three to four images from mandibular (V3) regions were taken from each TG.

Statistical Analysis

Data are presented as mean ± standard error of the mean. Statistical comparisons were performed using Student's *t*-test or analysis of variance (ANOVA) followed by Bonferroni *post hoc* test as indicated in figure legends. The criterion for statistical significance was $p < 0.05$. All statistical analyses were performed using Prism (GraphPad Software, La Jolla, CA).

RESULTS

A 10 g Orthodontic Force Reliably Produces Pain and Tooth Movement in Mice

In mice, the range of orthodontic force used for producing tooth movement is between 3 and 50 g (Yan et al., 2015; Rangiani et al., 2016; Yadav et al., 2016; Liu et al., 2017; Odagaki et al., 2018). Using two coil springs exerting either 2 or 10 g (Figure 1A), we performed an experiment (Figure 1B) to determine the amount of orthodontic force required to effectively produce pain and tooth movement. Mouse grimace scale (MGS) scores among three groups (sham, 2 g, and 10 g) showed significant difference over 7 days following procedure (Figure 1C; interaction of time and group effect, $F_{6,66} = 14.61$, $p < 0.0001$). At baseline, there were no differences in MGS scores between groups (Figure 1C). At 1d and 3d after spring insertion, MGS scores of 2 and 10 g groups were similar and significantly higher than those of the sham group. At 7d, there were no differences in MGS scores among the three groups. Changes in bite force (BF) were also analyzed (Figure 1D) and three groups showed significant difference over 7 days following procedure (Figure 1D; interaction of time and group effect, $F_{6,60} = 15.67$, $p < 0.0001$). At 1d and 3d, BF of 2 and 10 g groups was significantly reduced compared to the sham group. At 7d, BF had partially recovered toward the baseline in both 2 and 10 g groups, but remained significantly lower than that of the sham group. Interestingly, the recovery in the 2 g group was slower than in the 10 g group, such that at 7d, BF was significantly lower in the 2 g group than in the 10 g group.

All mice in the 10 g group and five mice in 2 g group were euthanized 14d after spring insertion. All mice in the

sham group and five mice in the 2 g group were euthanized 21d after spring insertion. Micro-CT analysis was performed to evaluate the extent of tooth movement (**Figure 2**). The sham group did not produce tooth movement during the 3 weeks (**Figures 2A,D**). The 2 g spring produced $25.1 \pm 8.4 \mu\text{m}$ ($n = 5$) of mesial movement of the first molar during 2 weeks, which was not significantly different from the amount during 3 weeks ($30.4 \pm 13.6 \mu\text{m}$; $n = 5$; $p > 0.7$; Student's *t*-test). When, the 2 g data from the two time points were pooled, the three groups (sham, 2 g, and 10 g) showed significant difference in tooth movement ($F_{2,27} = 10.6$, $p = 0.0004$). Intermolar distances in 2 g group were not significantly different from sham ($p = 0.076$; **Figure 2D**). Among 10 samples in the 2 g group, three showed no tooth movement. Although 3 g force produces tooth movement well in juvenile 5-week-old mice (Rangiani et al., 2016), 2 g force was not as effective in our 12-week-old mice. In contrast, the 10 g spring produced $59 \mu\text{m}$ of tooth movement after 2 weeks, which was significantly different from sham or 2 g groups (**Figures 2C,D**; $p = 0.0013$ vs. sham; $p = 0.037$ vs. 2 g). In comparison of bone volume fraction, the three groups showed significant difference (**Figure 2E**; $F_{2,25} = 8.78$, $p = 0.0013$). Both 2 and 10 g springs produced significantly reduced bone volume fraction (BV/TV) compared to sham, which indicates active bone remodeling has occurred in both groups. However, there was no difference between 2 and 10 g groups. Based on these results, we regarded 10 g as the force of choice to reliably produce tooth movement during a 2-week period, and 10 g was used in the remainder of studies.

Periodontium Is Innervated by TRPV1-Expressing Peptidergic Afferents

To determine the major primary afferents subpopulation transducing orthodontic pain, we determined neurochemical properties of primary afferents projected to periodontium (**Figure 3**). We injected the retrograde labeling tracer fluorogold (FG) into

gingiva around the maxillary first molars in mice. FG-labeled TG neurons showed various sizes and neurochemical properties (**Figure 3A**). Among 313 FG-labeled neurons, small-, medium-, and large-sized afferents compose 44, 44, and 12%, respectively ($372 \pm 11 \mu\text{m}^2$; **Figure 3B**). When these data were compared with published data from FG-labeled pulpal afferents (Chung et al., 2011), the size of periodontal afferents was significantly smaller than pulpal afferents ($586 \pm 33 \mu\text{m}^2$; $n = 99$; $p < 0.0001$; **Figure 3B**, red dotted line). When the extent of co-localization of FG, CGRP, and TRPV1 was determined (**Figure 3C**), 23% of the periodontal afferents expressed CGRP and 28% of periodontal afferents expressed TRPV1. Eighty-one percent of CGRP-expressing periodontal afferents were co-expressed with TRPV1.

We further determined the neurochemical properties of nerve terminals within PDL by immunohistochemical labeling of afferent terminals in decalcified periodontal tissues (**Figure 4**). CGRP-expressing terminals were densely projected into the PDL (**Figure 4A**), which is consistent with previous reports (Sarram et al., 1997). We also attempted immunohistochemical labeling of TRPV1-expressing nerve terminals in decalcified periodontium. However, we were not able to observe convincing TRPV1 labeling of nerve terminals within PDL. As an indirect approach, we took advantage of TRPV1-Cre mice for GFP labeling of TRPV1-lineage neurons (Cavanaugh et al., 2011). In this mouse line, approximately half of GFP-expressing neurons express TRPV1 in ganglia (Cavanaugh et al., 2011). TRPV1-Cre line was crossed with R26-mT/mG line to express membrane-bound GFP from TRPV1-lineage afferents. To maximize labeling of nerve terminals, we performed immunohistochemical labeling of GFP using a specific antibody. In this line, tdTomato is also expressed from all neuronal and non-neuronal cells other than TRPV1-lineage afferents. Under this condition, GFP-expressing nerve terminals were clearly visible in the PDL (**Figure 4B**). GFP-expressing terminals were often observed in close proximity with blood vessels within the PDL (Arrows in **Figure 4C**). The thickness

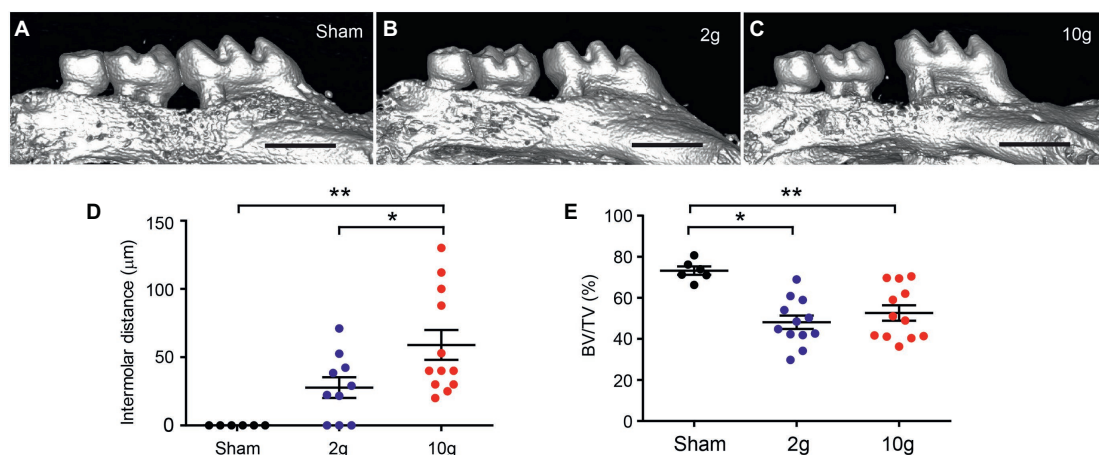


FIGURE 2 | Orthodontic force of 10 g produces reliable tooth movement in mice. (**A–C**) Examples of 3D constructed μCT images of sham (**A**), 2 g (**B**), and 10 g (**C**) force groups. Intermolar distance was measured as 49 and 86 μm in (**B** and **C**), respectively. Scale bar, 1 mm. * $p < 0.05$; ** $p < 0.005$ in Holm-Sidak's multiple comparison post-test following one-way ANOVA. (**D,E**) Comparison of intermolar distances (**D**) and bone volume fraction (**E**). BV/TV, bone volume/tissue volume; * $p < 0.05$, ** $p < 0.005$ in Holm-Sidak's multiple comparison post-test following one-way ANOVA.

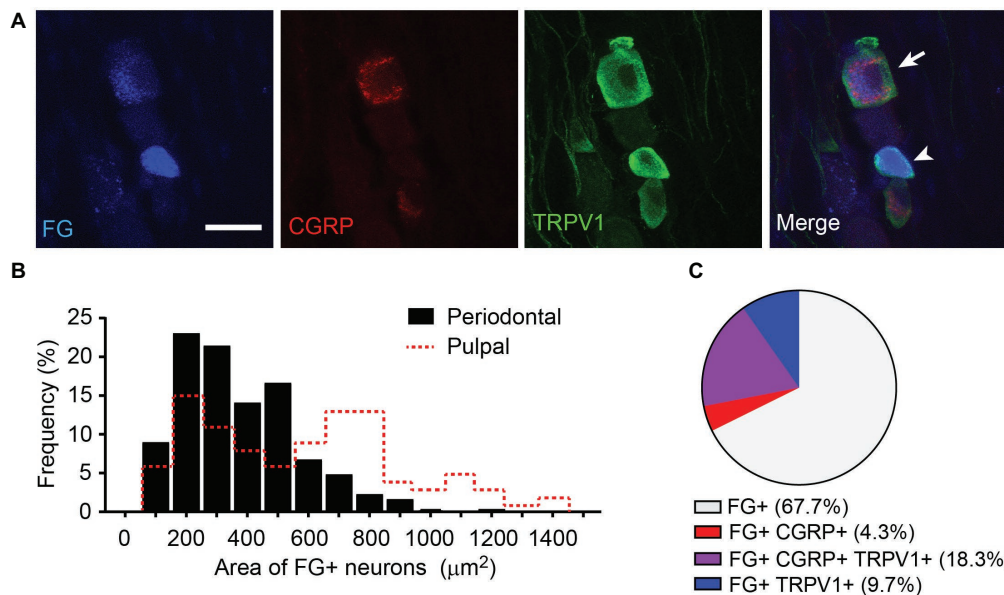


FIGURE 3 | Neurochemical properties of retrogradely labeled periodontal afferents in mice. **(A)** Representative images of periodontal afferents retrogradely labeled using fluorogold (FG) co-labeled with TRPV1 and CGRP. Arrowhead, FG+ TRPV1+ neuron; arrow, FG+ TRPV1+ CGRP+ neuron; scale bar, 30 μm. **(B)** Distribution of cross-sectional area of FG-labeled periodontal afferents ($n = 313$). Size distribution of FG+ pulpal afferents in mice (red dotted line) was derived from published data (Chung et al., 2011) for comparison. **(C)** Proportion of TRPV1+ and CGRP+ afferents among FG-labeled periodontal afferents. A total of 313 FG+ neurons were analyzed.

of the GFP-expressing axonal terminals was various and there was a subpopulation of fine terminals (arrowheads in **Figures 4B,C**) that are presumably unmyelinated C fibers. These results suggest that TRPV1-expressing peptidergic afferents constitute a major subset of afferents in the periodontium including PDL and likely mediate orthodontic pain.

Ablation of TRPV1-Expressing Nociceptors Attenuates Orthodontic Pain Behaviors

For selective ablation of TRPV1-expressing nociceptors, we injected RTX to one side of TG (**Figure 5A**). After a week, behavioral assays were performed before and after insertion of the spring. MGS scores among groups showed significant difference over 7 days following procedure (**Figure 5B**; interaction of time and group effect, $F_{9,69} = 16.1$, $p < 0.0001$). There were no differences in MGS scores between groups at baseline (**Figure 5B**). At 1d, the group receiving vehicle and subjected to 10 g OF (Veh/OF) had significantly higher MGS scores than mice receiving vehicle and sham treatment (Veh/Sham). RTX-treated mice receiving OF (RTX/OF) also had increased MGS compared to sham (RTX/Sham). RTX/OF mice exhibited significantly lower MGS scores than Veh/OF mice. At 3d, the trend was similar to the 1d result. At 7d, the Veh/OF group but not the RTX/OF group showed significant differences in MGS compared to sham controls.

In the BF assay (**Figure 5C**), changes in bite force showed significant difference over 7 days following procedure (interaction of time and group effect, $F_{9,72} = 7.814$, $p < 0.0001$). The Veh/OF group showed a significant reduction in BF compared to

the Veh/Sham group at 1d. In contrast, RTX-treated groups showed no significant differences in BF between OF and sham groups. BF reduction was significantly less in the RTX/OF group compared to the Veh/OF group at both 1d and 3d. At 3d, the Veh/sham group showed a recovery in BF to levels similar to RTX-treated groups, while Veh/OF group continued to exhibit a significant reduction in BF compared to the RTX/OF group. At 7d, there were no significant differences between BF among experimental groups.

After pain measurements were completed, the mice underwent the capsaicin eye-wiping test. Following application of capsaicin to the ipsilateral eye, RTX-treated mice exhibited significantly fewer eye wipes than controls (**Figure 5D**; $t(11) = 10.08$, $p < 0.0001$). In the post-mortem immunohistochemical staining, substantial reduction in TRPV1 expression was observed in RTX mice compared to controls (**Figure 5E**). These results validate ablation of trigeminal TRPV1-expressing afferents.

To estimate the efficacy of ablating TRPV1-expressing afferents by intra-TG injection of RTX, we injected RTX into V1/V2 area of left side TG of four C57BL/6 mice (**Figure 6**). After a week, the mice were euthanized, and we compared the proportion of TRPV1-expressing afferents between RTX-injected TG and the uninjected contralateral TG (**Figure 6A**). To label all neurons, including ones not expressing TRPV1, Nissl staining was performed. As an internal control, we also compared TRPV1-expressing afferents in V3 region. Uninjected contralateral TG showed that TRPV1-expressing neurons account for 24% of all the Nissl-positive neurons in V1/V2 region and 22% in V3 region (**Figures 6A,B**). In contrast, the proportion of TRPV1-expressing neurons

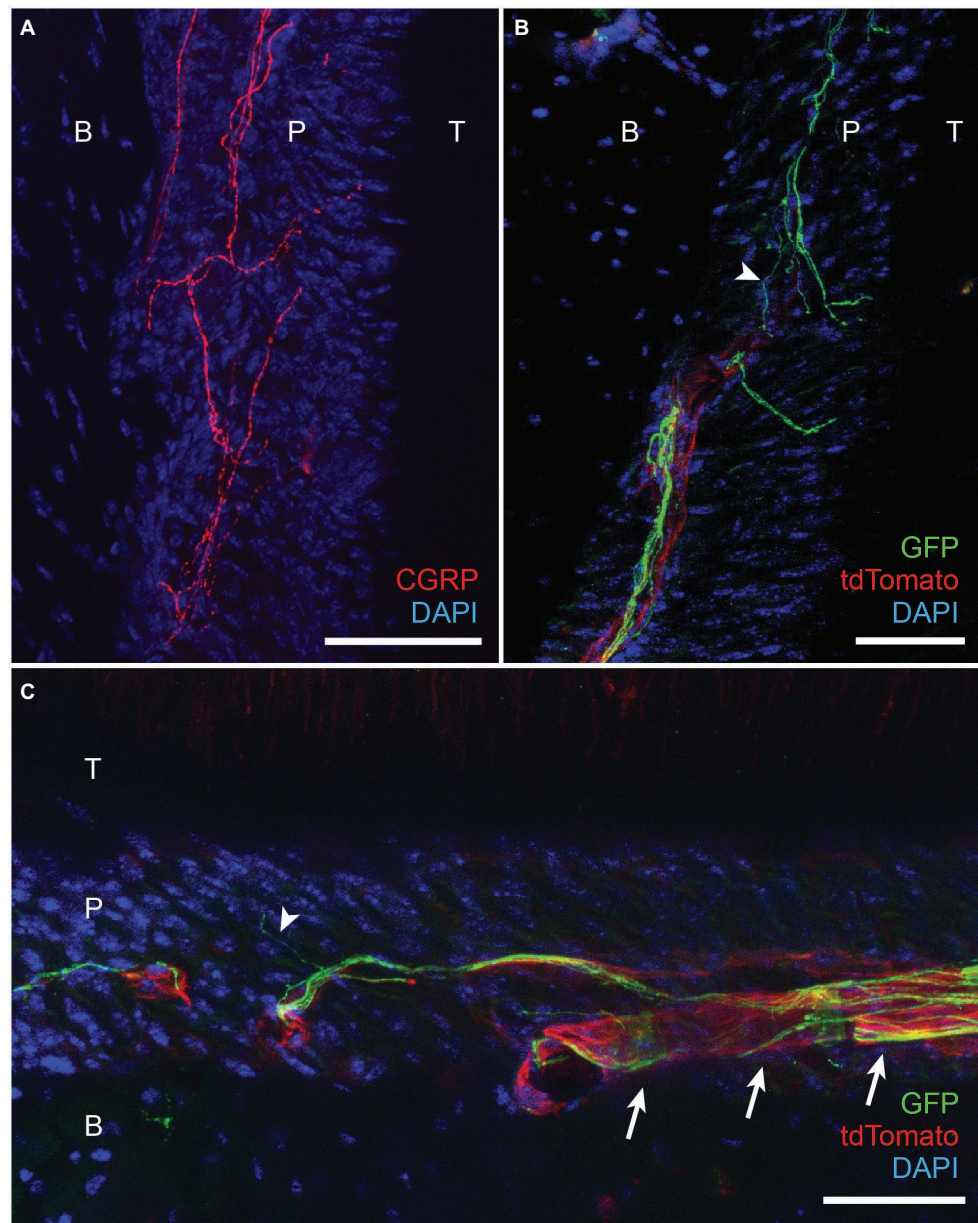


FIGURE 4 | Projection of CGRP-expressing and TRPV1-lineage afferents to periodontal ligaments in mice. **(A)** Immunohistochemical labeling of CGRP in periodontium from C57BL/6 mice. T, tooth; P, periodontal ligament; B, alveolar bone; scale bar, 30 μ m. **(B)** Immunohistochemical labeling of GFP in TRPV1-GFP mice (TRPV1-Cre X Rosa26-mT/mG) labeling TRPV1-lineage neurons. B, bone; P, PDL; T, tooth; scale bar, 50 μ m. In this mouse line, tdTomato labels all neuronal and non-neuronal cells except TRPV1-lineage afferents. Arrowhead, an example of fine GFP-expressing terminal. **(C)** Immunohistochemical labeling of GFP in TRPV1-GFP mice labeling TRPV1-lineage neurons. Scale bar, 50 μ m; arrowhead, an example of fine GFP-expressing terminal; arrows, examples of GFP-expressing nerve terminals associated with blood vessel.

was reduced to approximately half (12%) in V1/V2 region of RTX-injected mice, which was significantly different from contralateral TG (**Figure 6B**; $t(6) = 12$, $p < 0.0001$). The proportion of TRPV1-expressing neurons in the untargeted V3 region of RTX-injected mice was 22%, which was not significantly different from V3 region of contralateral TG ($p > 0.96$). These results suggest that intra-TG injection of RTX produces ablation of approximately half of TRPV1-expressing neurons in V1/V2 region of TG.

Genetic Inhibition of TRPV1 Attenuates Orthodontic Pain Behaviors

To determine the roles of TRPV1 in orthodontic pain, we evaluated MGS and BF in TRPV1 KO or WT littermates subjected to 10 g OF or sham (**Figure 7A**). MGS scores among groups showed significant difference over 7 days following procedure (**Figure 7B**; interaction of time and group effect, $F_{9,54} = 15.38$, $p < 0.0001$). There were no differences in MGS scores between groups at baseline. At 1d, WT mice subjected

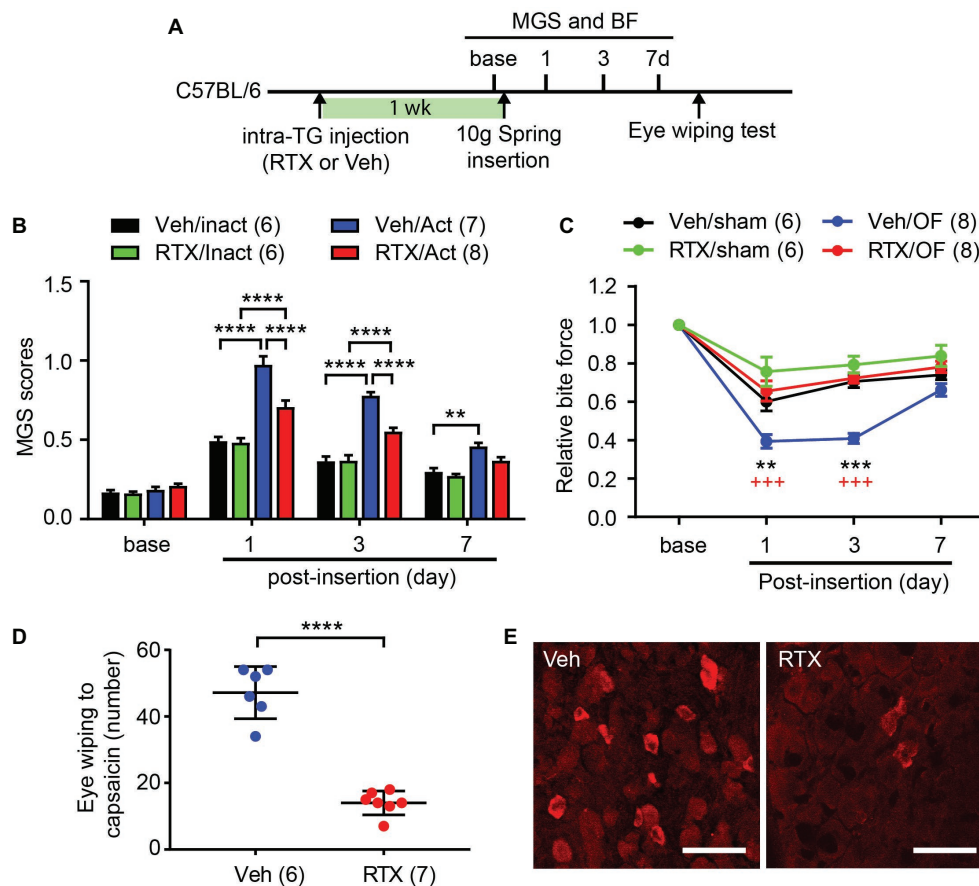


FIGURE 5 | Chemical ablation of TRPV1-expressing trigeminal afferents attenuates orthodontic pain behaviors. **(A)** Timeline of experiment. Resiniferatoxin (RTX, 50 ng in 0.5 μ l PBS) or vehicle (Veh) was stereotactically injected into left trigeminal ganglia (TG) in adult C57BL/6 mice 1 week before the placement of the 10 g spring. **(B)** Comparison of MGS scores at different time points. Numbers within parentheses represent number of animals. ** $p < 0.01$, **** $p < 0.0001$ in Bonferroni *post hoc* test following two-way RM ANOVA. OF, 10 g orthodontic force; RTX, resiniferatoxin; Veh, vehicle. **(C)** Comparison of relative BF at different time points. ** $p < 0.01$, *** $p < 0.0001$ (vs. Veh/sham), *** $p < 0.001$ (vs. RTX/OF) in Bonferroni *post hoc* test following two-way RM ANOVA. **(D)** Number of eye-wiping motions measured over 5 min following the application of capsaicin (0.03% in 20 μ l) to the ipsilateral eye in mice with intra-TG injection of vehicle or RTX. **** $p < 0.0001$, Student's *t*-test. **(E)** Immunohistochemical labeling of TRPV1 in TG from mice injected with Veh or RTX into TG. Scale bar, 50 μ m.

to 10 g OF (WT/OF) showed significantly higher MGS scores than WT mice receiving sham treatment (WT/Sham). In contrast, changes in MGS in TRPV1 KO mice receiving OF (KO/OF) did not show significant difference compared to sham (KO/Sham). Consequently, KO/OF mice exhibited significantly lower MGS scores than WT/OF mice. At 3d, the trend was similar to the 1d result. At 7d, the WT/OF group and the KO/OF group did not show significant differences in MGS compared to sham controls.

In the BF assay (Figure 7C), changes in bite force showed significant difference over 7 days following procedure (interaction of time and group effect, $F_{9,54} = 9.882$, $p < 0.0001$). The WT/OF group showed a significant reduction in BF compared to the WT/Sham group at 1d. KO/OF group also showed significantly reduced BF compared to KO/sham group. BF reduction in the KO/OF group was significantly less than reduction in the WT/OF group at both 1d and 3d. At 7d, BF of WT/OF and KO/OF had further recovered toward levels in sham groups. However, the BF of WT/OF and KO/OF were significantly lower than that of WT/sham and KO/sham groups, respectively.

There were no significant differences between BF in WT/OF and KO/OF groups.

DISCUSSION

We have established a mouse model of orthodontic pain, and have tested two orthodontic force levels, 2 and 10 g. The 2 g force was great enough to produce comparable levels of pain as the 10 g force, but was not sufficient to produce consistent tooth movement. Therefore, we regarded 10 g as a minimum orthodontic force producing reliable tooth movement with maximal levels of pain in the mouse model. In clinic, orthodontic force induces spontaneous pain and chewing-evoked pain, which is resolved in approximately 1 week (Scheurer et al., 1996). Our mouse model reflects similar clinical characteristics: MGS and BF may reflect spontaneous pain and chewing-evoked pain, respectively, and orthodontic force-induced changes in MGS and BF lasted approximately a week. Thus, our mouse model mimics clinically relevant pain evoked by a reasonable force that produces orthodontic tooth movement.

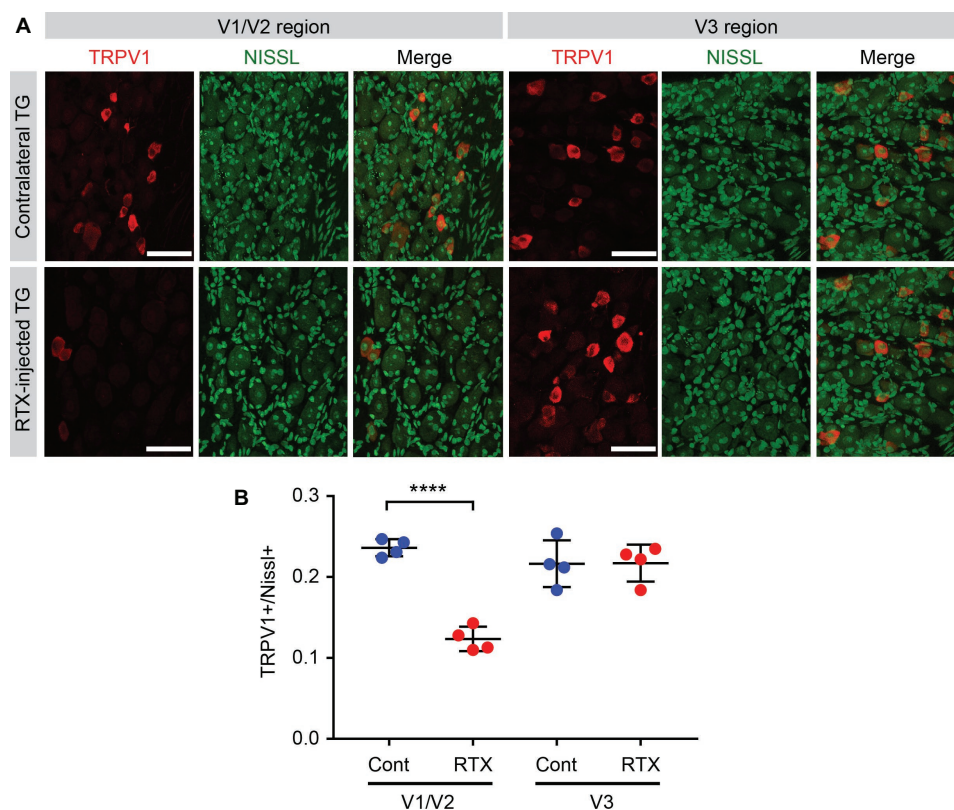


FIGURE 6 | Efficacy of ablation of TRPV1-expressing nociceptors by intra-TG injection of RTX. **(A)** Immunohistochemical labeling of TRPV1 (red), Nissl staining (green), and merged images in ophthalmic/maxillary (V1/V2) area or mandibular (V3) area of TG from RTX-injected or uninjected contralateral side. **(B)** Proportion of TRPV1-expressing neurons among Nissl+ neurons. **** $p < 0.0001$ in Student's t -test. $N = 4$ ganglia in each group.

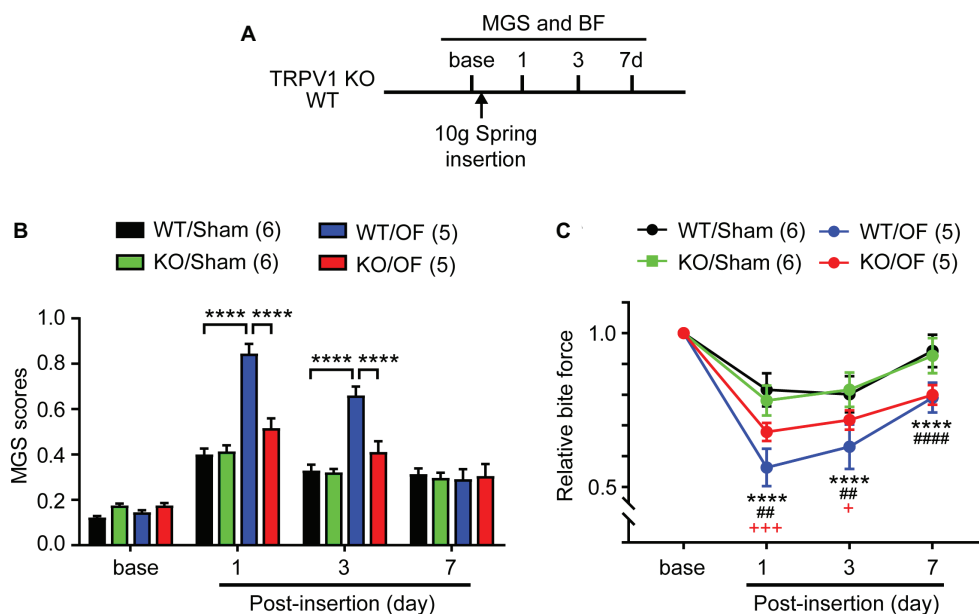


FIGURE 7 | TRPV1 KO attenuates orthodontic pain behaviors. **(A)** Timeline of experiment. The 10 g spring was placed in TRPV1 KO and sham. **(B)** MGS before and 1, 3, and 7d after the application of 10 g orthodontic force (OF) or sham. **** $p < 0.0001$ in Bonferroni *post hoc* test following two-way RM ANOVA. **(C)** Relative BF from the same mice used for measuring MGS in A. **** $p < 0.0001$ (WT/sham vs. WT/OF); ** $p < 0.01$, **** $p < 0.0001$ (KO/Sham vs. KO/OF); * $p < 0.05$, *** $p < 0.001$ (WT/OF vs. KO/OF) in Bonferroni *post hoc* test following two-way RM ANOVA.

We determined the neurochemical properties of afferents retrogradely labeled from periodontium including gingiva, alveolar bone, and periodontal ligament. The size distribution showed that majority of periodontal afferents are small to medium diameter. The size of periodontal afferents is apparently larger than facial skin afferents, similar to dural afferents but smaller than pulpal afferents (Chung et al., 2011; Huang et al., 2012). We found that 28% of TG afferents retrogradely labeled from mouse periodontium contained TRPV1 and 23% of periodontal afferents contained CGRP. The proportion of TRPV1-expressing periodontal afferents in mice is comparable to the proportion of TRPV1-expressing periodontal ligament afferents in rats (~25%) (Gibbs et al., 2011) and higher than in pulpal afferents in mice (~10%) (Chung et al., 2011). The proportion of CGRP-expressing afferents in mouse periodontal afferents is similar to the proportion in pulpal afferents (28%), lower than in mouse facial skin afferents (~30%) but higher than in dural afferents (~15%) (Chung et al., 2012; Huang et al., 2012). Importantly, the peptidergic periodontal afferents were highly colocalized with TRPV1. Therefore, chemical ablation of TRPV1-expressing afferents should affect a majority of peptidergic afferents that project to periodontium.

Using targeted chemical ablation, we found that TRPV1-expressing trigeminal nociceptors are major contributors to pain behaviors evoked by orthodontic force in mice. TRPV1-expressing afferents are responsible for thermal, but not mechanical, sensitivity in skin (Cavanaugh et al., 2009). In deep tissues, such as masseter muscle, however, TRPV1-expressing afferents mediate spontaneous pain as well as bite-evoked pain under inflammation (Wang et al., 2017a). Since orthodontic force induces inflammation in periodontium to produce inflammatory mediators and cytokines (Long et al., 2016; Kobayashi and Horinuki, 2017), it is likely that changes in MGS and BF involve peripheral sensitization of periodontal afferent terminals. Indeed, non-steroidal anti-inflammatory drugs (NSAIDs) reduce orthodontic pain in patients and rodents (Bartzela et al., 2009; Shibasaki et al., 2009). Pharmacological inhibition or knockdown of TRPV1 attenuates spontaneous pain behaviors, such as grimace scale or face grooming, induced by orthodontic forces in rats (Gao et al., 2016; Guo et al., 2019a). Our experiments using genetic knockout of TRPV1 further support the contribution of TRPV1 to spontaneous pain behaviors evoked by orthodontic force. We also showed that knockout of TRPV1 attenuated BF reduction evoked by orthodontic force. This is in contrast to the results from inflamed masseter muscle, in which TRPV1 substantially contributes to MGS whereas it only marginally affects BF (Wang et al., 2017a). These results suggest that inhibiting TRPV1 can affect different modalities of orthodontic pain and that the contribution of TRPV1 to bite-evoked pain is context-dependent. The source of such different contribution of TRPV1 to bite-evoked nocifensive behaviors following masseter inflammation versus orthodontic tooth movement is not clear. It is possible that the extent of injury produced by masseter inflammation is more extensive than orthodontic tooth movement and, therefore, involves greater peripheral and central components that are independent of TRPV1.

Despite the clear role of TRPV1 and TRPV1-expressing afferents in orthodontic pain behaviors, we do not exclude possible contributions of other molecules and neurochemically distinct subtypes of nociceptors. Partial attenuation of MGS and BF by the ablation of TRPV1-expressing afferents or knockout of TRPV1 supports this notion. It is highly likely that other TRP channels enriched in peptidergic afferents, for example TRPA1, play additional or overlapping roles in orthodontic pain behaviors as in the case of masseter hyperalgesia (Wang et al., 2018). These possibilities need to be determined in the future.

Determining the mechanisms of orthodontic pain addresses a critical clinical problem in orthodontics. A major concern in the field is that conventional analgesics such as NSAIDs adversely affect orthodontic tooth movement (Bartzela et al., 2009). Therefore, understanding mechanisms of orthodontic pain should help in the development of new approaches for attenuating pain without deleteriously affecting orthodontic tooth movement.

In conclusion, our data support the hypothesis that TRPV1 and TRPV1-expressing trigeminal nociceptors constitute a major pathway for transduction of orthodontic pain. This study established a new mouse model of orthodontic pain, well suited to mechanistic studies aimed at developing novel approaches for painless orthodontics.

DATA AVAILABILITY STATEMENT

All datasets generated for this study are included in the manuscript/supplementary files.

ETHICS STATEMENT

The animal study was reviewed and approved by All animal procedures were consistent with the NIH Guide for the Care and Use of Laboratory Animals (Publication 85-23, Revised 1996), and were performed according to a University of Maryland-approved Institutional Animal Care and Use Committee protocol.

AUTHOR CONTRIBUTIONS

SW, E-KP, and M-KC designed the experiments. SW, MK, ZA, and KO performed the experiments and analyzed the data. SW, E-KP, and M-KC wrote the manuscript. All authors edited the manuscript and approved the final version.

FUNDING

This study was supported in part by National Institute of Dental and Craniofacial Research R01 DE023846 and R01 DE027731 to M-KC.

ACKNOWLEDGMENTS

The authors thank Dr. Abrar Bakhsh for assisting in data analysis and John Joseph for critical reading of the manuscript.

REFERENCES

- Bartzela, T., Turp, J. C., Motschall, E., and Maltha, J. C. (2009). Medication effects on the rate of orthodontic tooth movement: a systematic literature review. *Am. J. Orthod. Dentofac. Orthop.* 135, 16–26. doi: 10.1016/j.ajodo.2008.08.016
- Byers, M. R. (1985). Sensory innervation of periodontal ligament of rat molars consists of unencapsulated Ruffini-like mechanoreceptors and free nerve endings. *J. Comp. Neurol.* 231, 500–518.
- Caterina, M. J., Leffler, A., Malmberg, A. B., Martin, W. J., Trafton, J., Petersen-Zeitz, K. R., et al. (2000). Impaired nociception and pain sensation in mice lacking the capsaicin receptor. *Science* 288, 306–313. doi: 10.1126/science.288.5464.306
- Cavanaugh, D. J., Chesler, A. T., Braz, J. M., Shah, N. M., Julius, D., and Basbaum, A. I. (2011). Restriction of transient receptor potential vanilloid-1 to the peptidergic subset of primary afferent neurons follows its developmental downregulation in nonpeptidergic neurons. *J. Neurosci.* 31, 10119–10127. doi: 10.1523/JNEUROSCI.1299-11.2011
- Cavanaugh, D. J., Lee, H., Lo, L., Shields, S. D., Zylka, M. J., Basbaum, A. I., et al. (2009). Distinct subsets of unmyelinated primary sensory fibers mediate behavioral responses to noxious thermal and mechanical stimuli. *Proc. Natl. Acad. Sci. USA* 106, 9075–9080. doi: 10.1073/pnas.0901507106
- Chung, M. K., Asgar, J., Jennifer, P., and Ro, J. Y. (2016). Transcriptome analysis of trigeminal ganglia following masseter muscle inflammation in rats. *Mol. Pain* 12, 1–11. doi: 10.1177/1744806916668526
- Chung, M. K., and Campbell, J. N. (2016). Use of capsaicin to treat pain: mechanistic and therapeutic considerations. *Pharmaceuticals* 9:E66. doi: 10.3390/ph9040066
- Chung, M. K., Jue, S. S., and Dong, X. (2012). Projection of non-peptidergic afferents to mouse tooth pulp. *J. Dent. Res.* 91, 777–782. doi: 10.1177/0022034512450298
- Chung, M. K., Lee, J., Duraes, G., and Ro, J. Y. (2011). Lipopolysaccharide-induced pulpitis up-regulates TRPV1 in trigeminal ganglia. *J. Dent. Res.* 90, 1103–1107. doi: 10.1177/0022034511413284
- Gao, Y., Liu, Y., Zhu, K., Zhang, Z., Qiao, H., Lu, Z., et al. (2016). Blocking of TRPV-1 in the parodontium relieves orthodontic pain by inhibiting the expression of TRPV-1 in the trigeminal ganglion during experimental tooth movement in rats. *Neurosci. Lett.* 628, 67–72. doi: 10.1016/j.neulet.2016.06.007
- Gibbs, J. L., Melnyk, J. L., and Basbaum, A. I. (2011). Differential TRPV1 and TRPV2 channel expression in dental pulp. *J. Dent. Res.* 90, 765–770. doi: 10.1177/0022034511402206
- Guo, R., Zhou, Y., Long, H., Shan, D., Wen, J., Hu, H., et al. (2019a). Transient receptor potential Vanilloid 1-based gene therapy alleviates orthodontic pain in rats. *Int. J. Oral Sci.* 11:11. doi: 10.1038/s41368-019-0044-3
- Guo, W., Zou, S., Mohammad, Z., Wang, S., Yang, J., Li, H., et al. (2019b). Voluntary biting behavior as a functional measure of orofacial pain in mice. *Physiol. Behav.* 204, 129–139. doi: 10.1016/j.physbeh.2019.02.024
- Huang, D., Li, S., Dhaka, A., Story, G. M., and Cao, Y. Q. (2012). Expression of the transient receptor potential channels TRPV1, TRPA1 and TRPM8 in mouse trigeminal primary afferent neurons innervating the dura. *Mol. Pain* 8:66. doi: 10.1186/1744-8069-8-66
- Ichikawa, H., Matsuo, S., Terayama, R., Yamaai, T., and Sugimoto, T. (2006). Aspartate-immunoreactive primary sensory neurons in the mouse trigeminal ganglion. *Brain Res.* 1082, 67–72. doi: 10.1016/j.brainres.2006.01.092
- Jones, M. L. (1984). An investigation into the initial discomfort caused by placement of an archwire. *Eur. J. Orthod.* 6, 48–54. doi: 10.1093/ejo/6.1.48
- Karai, L., Brown, D. C., Mannes, A. J., Connelly, S. T., Brown, J., Gandal, M., et al. (2004). Deletion of vanilloid receptor 1-expressing primary afferent neurons for pain control. *J. Clin. Invest.* 113, 1344–1352. doi: 10.1172/JCI20449
- Kobayashi, M., and Horinuki, E. (2017). Neural mechanisms of nociception during orthodontic treatment. *J. Oral Sci.* 59, 167–171. doi: 10.2334/josnusd.16-0847
- Liao, L., Long, H., Zhang, L., Chen, H., Zhou, Y., Ye, N., et al. (2014). Evaluation of pain in rats through facial expression following experimental tooth movement. *Eur. J. Oral Sci.* 122, 121–124. doi: 10.1111/eos.12110
- Liu, Y., Zhang, T., Zhang, C., Jin, S. S., Yang, R. L., Wang, X. D., et al. (2017). Aspirin blocks orthodontic relapse via inhibition of CD4(+) T lymphocytes. *J. Dent. Res.* 96, 586–594. doi: 10.1177/0022034516685527
- Long, H., Shan, D., Huang, R., Liu, H., Zhou, Y., Gao, M., et al. (2019). Bite force measurements for objective evaluations of orthodontic tooth movement-induced pain in rats. *Arch. Oral Biol.* 101, 1–7. doi: 10.1016/j.archoralbio.2019.02.002
- Long, H., Wang, Y., Jian, F., Liao, L. N., Yang, X., and Lai, W. L. (2016). Current advances in orthodontic pain. *Int. J. Oral Sci.* 8, 67–75. doi: 10.1038/ijos.2016.24
- Muzumdar, M. D., Tasic, B., Miyamichi, K., Li, L., and Luo, L. (2007). A global double-fluorescent Cre reporter mouse. *Genesis* 45, 593–605. doi: 10.1002/dvg.20335
- Ngan, P., Kess, B., and Wilson, S. (1989). Perception of discomfort by patients undergoing orthodontic treatment. *Am. J. Orthod. Dentofac. Orthop.* 96, 47–53. doi: 10.1016/0889-5406(89)90228-X
- Odagaki, N., Ishihara, Y., Wang, Z., Ei Hsu Hlaing, E., Nakamura, M., Hoshijima, M., et al. (2018). Role of osteocyte-PDL crosstalk in tooth movement via SOST/Sclerostin. *J. Dent. Res.* 97, 1374–1382. doi: 10.1177/0022034518771331
- Rangiani, A., Jing, Y., Ren, Y., Yadav, S., Taylor, R., and Feng, J. Q. (2016). Critical roles of periostin in the process of orthodontic tooth movement. *Eur. J. Orthod.* 38, 373–378. doi: 10.1093/ejo/cjv071
- Sarram, S., Lee, K. F., and Byers, M. R. (1997). Dental innervation and CGRP in adult p75-deficient mice. *J. Comp. Neurol.* 385, 297–308. doi: 10.1002/(SICI)1096-9861(19970825)385:2<297::AID-CNE8>3.0.CO;2-X
- Scheurer, P. A., Firestone, A. R., and Burgin, W. B. (1996). Perception of pain as a result of orthodontic treatment with fixed appliances. *Eur. J. Orthod.* 18, 349–357. doi: 10.1093/ejo/18.1.349
- Sergl, H. G., Klages, U., and Zentner, A. (1998). Pain and discomfort during orthodontic treatment: causative factors and effects on compliance. *Am. J. Orthod. Dentofac. Orthop.* 114, 684–691. doi: 10.1016/S0889-5406(98)70201-X
- Shibazaki, T., Yozgatian, J. H., Zeredo, J. L., Gonzales, C., Hotokezaka, H., Koga, Y., et al. (2009). Effect of celecoxib on emotional stress and pain-related behaviors evoked by experimental tooth movement in the rat. *Angle Orthod.* 79, 1169–1174. doi: 10.1023/121108-629R.1
- Wang, S., Brigoli, B., Lim, J., Karley, A., and Chung, M. K. (2018). Roles of TRPV1 and TRPA1 in spontaneous pain from inflamed masseter muscle. *Neuroscience* 384, 290–299. doi: 10.1016/j.neuroscience.2018.05.048
- Wang, S., Lim, J., Joseph, J., Wei, F., Ro, J. Y., and Chung, M. K. (2017a). Spontaneous and bite-evoked muscle pain are mediated by a common nociceptive pathway with differential contribution by TRPV1. *J. Pain* 18, 1333–1345. doi: 10.1016/j.jpain.2017.06.005
- Wang, S., Wang, S., Asgar, J., Joseph, J., Ro, J. Y., Wei, F., et al. (2017b). Ca(2+) and calpain mediate capsaicin-induced ablation of axonal terminals expressing transient receptor potential vanilloid 1. *J. Biol. Chem.* 292, 8291–8303. doi: 10.1074/jbc.M117.778290
- Yadav, S., Dobie, T., Assefnia, A., Gupta, H., Kalajzic, Z., and Nanda, R. (2015). Effect of low-frequency mechanical vibration on orthodontic tooth movement. *Am. J. Orthod. Dentofac. Orthop.* 148, 440–449. doi: 10.1016/j.ajodo.2015.03.031
- Yadav, S., Dobie, T., Assefnia, A., Kalajzic, Z., and Nanda, R. (2016). The effect of mechanical vibration on orthodontically induced root resorption. *Angle Orthod.* 86, 740–745. doi: 10.2319/090615-599.1
- Yan, Y., Liu, F., Kou, X., Liu, D., Yang, R., Wang, X., et al. (2015). T cells are required for orthodontic tooth movement. *J. Dent. Res.* 94, 1463–1470. doi: 10.1177/0022034515595003
- Yang, Z., Luo, W., Hou, J., Zhao, Z., Jian, F., Wamalwa, P., et al. (2009). Development of a behavior model of pain induced by experimental tooth movement in rats. *Eur. J. Oral Sci.* 117, 380–384. doi: 10.1111/j.1600-0722.2009.00639.x

Conflict of Interest: The authors declare that the research was conducted in the absence of any commercial or financial relationships that could be construed as a potential conflict of interest.

Copyright © 2019 Wang, Kim, Ali, Ong, Pae and Chung. This is an open-access article distributed under the terms of the Creative Commons Attribution License (CC BY). The use, distribution or reproduction in other forums is permitted, provided the original author(s) and the copyright owner(s) are credited and that the original publication in this journal is cited, in accordance with accepted academic practice. No use, distribution or reproduction is permitted which does not comply with these terms.



Corrigendum: TRPV1 and TRPV1-Expressing Nociceptors Mediate Orofacial Pain Behaviors in a Mouse Model of Orthodontic Tooth Movement

OPEN ACCESS

Approved by:
Frontiers Editorial Office,
Frontiers Media SA, Switzerland

***Correspondence:**
Man-Kyo Chung
mchung@umaryland.edu

Specialty section:
This article was submitted to
Craniofacial Biology and Dental
Research,
a section of the journal
Frontiers in Physiology

Received: 10 October 2019

Accepted: 11 October 2019

Published: 22 October 2019

Citation:
Wang S, Kim M, Ali Z, Ong K, Pae E-K
and Chung M-K (2019) Corrigendum:
TRPV1 and TRPV1-Expressing
Nociceptors Mediate Orofacial Pain
Behaviors in a Mouse Model of
Orthodontic Tooth Movement.
Front. Physiol. 10:1353.
doi: 10.3389/fphys.2019.01353

Sheng Wang¹, Martin Kim¹, Zayd Ali¹, Katherine Ong¹, Eung-Kwon Pae² and Man-Kyo Chung^{1*}

¹ Program in Neuroscience, Center to Advance Chronic Pain Research, Department of Neural and Pain Sciences, School of Dentistry, University of Maryland, Baltimore, MD, United States, ² Department of Orthodontic and Pediatric Dentistry, School of Dentistry, University of Maryland, Baltimore, MD, United States

Keywords: orthodontic tooth movement, trigeminal ganglia, TRPV1, peptidergic nociceptors, periodontium, behavioral assays

A Corrigendum on

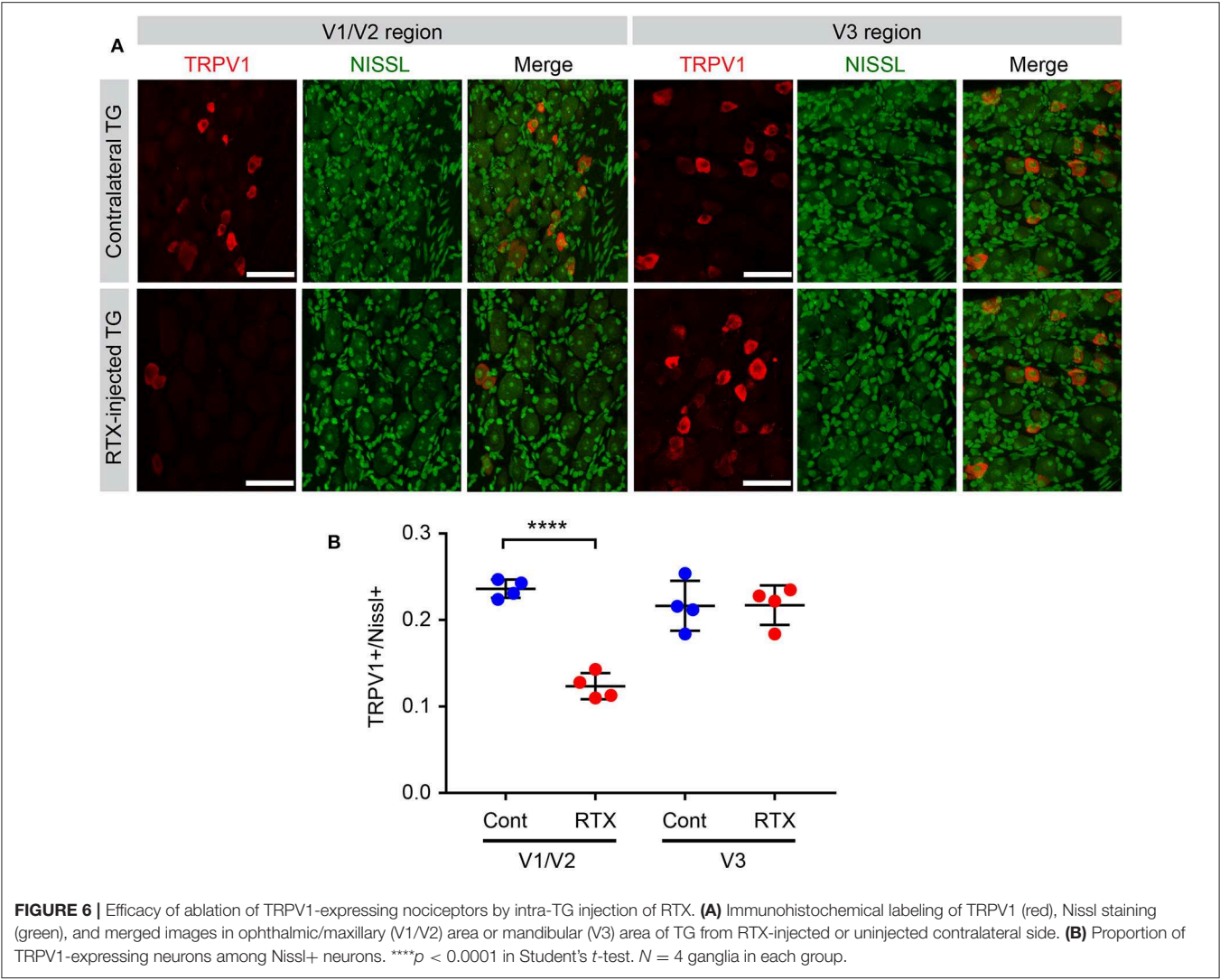
TRPV1 and TRPV1-Expressing Nociceptors Mediate Orofacial Pain Behaviors in a Mouse Model of Orthodontic Tooth Movement

by Wang, S., Kim, M., Ali, Z., Ong, K., Pae, E.-K., and Chung, M.-K. (2019). *Front. Physiol.* 10:1207. doi: 10.3389/fphys.2019.01207

In the original article, there was a mistake in **Figure 6** as published. The X-axis of panel B was labeled incorrectly. The corrected **Figure 6** appears below.

The authors apologize for this error and state that this does not change the scientific conclusions of the article in any way. The original article has been updated.

Copyright © 2019 Wang, Kim, Ali, Ong, Pae and Chung. This is an open-access article distributed under the terms of the Creative Commons Attribution License (CC BY). The use, distribution or reproduction in other forums is permitted, provided the original author(s) and the copyright owner(s) are credited and that the original publication in this journal is cited, in accordance with accepted academic practice. No use, distribution or reproduction is permitted which does not comply with these terms.





Multimodal Sensory Stimulation of the Masseter Muscle Reduced Precision but Not Accuracy of Jaw-Opening Movements

Birgitta Wiesinger^{1,2*}, Birgitta Häggman-Henrikson^{1,3}, Anton Eklund¹, Anders Wänman¹ and Fredrik Hellström⁴

¹ Department of Odontology, Clinical Oral Physiology, Umeå University, Umeå, Sweden, ² Department of Research and Development, Västernorrland County Council, Umeå University, Sundsvall, Sweden, ³ Department of Orofacial Pain and Jaw Function, Malmö University, Malmö, Sweden, ⁴ Centre for Musculoskeletal Research, Gävle University College, Umeå, Sweden

OPEN ACCESS

Edited by:

Kazutaka Takahashi,
The University of Chicago,
United States

Reviewed by:

Greg Murray,
The University of Sydney, Australia
Yoshihide Satoh,
The Nippon Dental University, Japan
Kensuke Yamamura,
Niigata University, Japan

*Correspondence:

Birgitta Wiesinger
birgitta.h@wiesinger.se;
birgitta.wiesinger@umu.se

Specialty section:

This article was submitted to
Perception Science,
a section of the journal
Frontiers in Neuroscience

Received: 14 August 2019

Accepted: 25 September 2019

Published: 10 October 2019

Citation:

Wiesinger B,
Häggman-Henrikson B, Eklund A,
Wänman A and Hellström F (2019)
Multimodal Sensory Stimulation of the
Masseter Muscle Reduced Precision
but Not Accuracy of Jaw-Opening
Movements.
Front. Neurosci. 13:1083.
doi: 10.3389/fnins.2019.01083

A functional integration between the trigeminal and craniocervical sensorimotor systems has been demonstrated, with simultaneous jaw and head-neck movements during jaw opening-closing. We previously showed that pain induction in the masseter muscle increased the relative contribution of the neck component of integrated jaw-neck movements. Induced pain or manipulation of proprioception by vibration did not affect accuracy during a jaw-opening task in men. It is not known how multimodal sensory stimulation, with a combination of pain induction and vibration, affects jaw-opening accuracy and precision. The aim was to investigate how jaw-neck movements, and specifically accuracy and precision of jaw-opening, are affected during concomitant nociceptive and proprioceptive stimulation of the masseter muscle. Twenty-one healthy men performed jaw-opening to a target position, defined as 75% of individual maximum jaw opening, during control (Ctr), vibration of masseter muscles (Vib), pain induction in the masseter (Pain), and concomitant vibration and pain induction in the masseter muscle (VibPain). Simultaneous jaw and head movements were recorded with an optoelectronic system and amplitudes calculated for each jaw opening-closing cycle. Accuracy of jaw movements was defined as the achievement of the target position. Precision of jaw movements was defined as the cycle-to-cycle variability from the mean of cycles 2–10 (coefficient of variation, CV). Differences between the trials were analyzed with Friedman's test, Dunn's test, and Benjamini-Hochberg correction. There were no significant differences between the trials for jaw movement amplitudes. For head movements, amplitudes for cycles 2–10 were larger during Pain compared to Ctr and Vib (both $p = 0.034$), and larger during VibPain compared to Ctr ($p = 0.034$) and Vib ($p = 0.035$). There were no differences in accuracy of jaw movements between the trials. For precision of jaw movements, the cycle-to-cycle variability was larger during VibPain compared to Ctr ($p = 0.027$) and Vib ($p = 0.018$). For integrated jaw-neck motor

strategy, there was a difference between pain and non-pain trials, but no differences between unimodal and multimodal stimulation trials. For achievement of jaw-opening to a target position, the results show no effect on accuracy, but a reduced precision of jaw movements during combined proprioceptive and nociceptive multimodal stimulation.

Keywords: sensorimotor control, multimodal sensory stimulation, accuracy, precision, jaw movements, head-neck movements, pain, vibration

INTRODUCTION

Jaw function, including jaw opening, biting, and chewing, incorporates functional integration between the jaw and neck sensorimotor system. Thus, in healthy humans, head and jaw movements are coordinated during jaw-opening tasks in both single and rhythmical movements (Eriksson et al., 2000; Zafar et al., 2000). The coordination of movements is characterized by head extension during jaw-opening and head flexion during jaw-closing (Eriksson et al., 1998). These integrated jaw and head movements involve jaw and neck muscles, among others, the masseter, temporal, sternocleidomastoid, and trapezius muscles (Häggman-Henrikson et al., 2013). The simultaneous jaw and head-neck movements during jaw opening-closing tasks (Eriksson et al., 2000; Kohno et al., 2001) have been suggested to be based in a functional relationship between the trigeminal and craniocervical sensorimotor systems (Eriksson et al., 2000), also seen during jaw clenching (Clark et al., 1993), and in the trigeminocervical reflex (Sartucci et al., 1986). It has been proposed that this functional integration between the trigeminal and cervical regions can optimize performance during jaw function, such as jaw opening (Häggman-Henrikson et al., 2006).

We previously demonstrated that experimental pain in healthy individuals can alter jaw-neck motor behavior, underlining the sensorimotor relationship between the jaw and neck regions (Wiesinger et al., 2013). The relationship between trigeminal and craniocervical sensorimotor systems has a neuroanatomical basis, as the subnucleus caudalis in the trigeminal brainstem nuclear complex receives converging sensory inputs from deep and superficial trigeminal, facial, and upper cervical nerves. The subnucleus caudalis is also anatomically overlapping with the upper cervical dorsal horn, since it extends caudally to the upper spinal cord (Sessle et al., 1986). Sensory information from masseter muscle spindles is processed by neurons in the trigeminal mesencephalic nucleus (MesV). These neurons project through synaptic pathways to the trigeminal motor nucleus (Shigenaga et al., 1988), affecting multiple motor neurons including both jaw-opening and jaw-closing muscles (Zhang et al., 2012), as well as the motor nucleus in the cervical spine (Dessem and Luo, 1999). This convergence of various afferent inputs in the subnucleus caudalis may contribute to the regulation of trigeminal motor function (Romaniello et al., 2000).

The study of sensorimotor interactions and coordination has often been conducted by external manipulation of different sensory signals (modalities) and observation of changes in motor control. Common manipulations are experimentally induced

pain by injection of hypertonic saline (HS) (Graven-Nielsen et al., 2000), glutamate, or capsaicin (Wang et al., 2010) in humans, or activation of nociceptors by bradykinin (Hellström et al., 2000) or HS (Capra and Ro, 2000) in animals. To manipulate another modality, Loucks and De Nil (2006, 2012) and Wiesinger et al. (2014) used vibration stimulation of proprioceptors, mainly muscle spindles within the masseter muscle. Research with concomitant stimulation of different sensory modalities related to nociception and proprioception in the trigeminal system, using motor control as an outcome, is limited. However, there are studies evaluating motor control outcomes such as balance, postural control, and speed of gait in combination with vibration of neck muscles in patients with neck pain (Beinert et al., 2015; Wannaprom et al., 2018). Vibration affects motor performance (evaluated by balance and speed of gait) differently depending on presence of pain, with decreased motor performance during vibration in healthy individuals and increased performance in patients with neck pain (Wannaprom et al., 2018). Similar results were previously shown for cervical joint position sense, and dynamic and static postural stability in patients with neck pain (Beinert et al., 2015). In the case of integrated jaw and head movements, no studies have investigated the effect of vibration on motor control output in patients with jaw or neck pain or during experimentally induced pain in healthy participants. In our previous study (Wiesinger et al., 2013), where experimental pain was induced by HS injection in the masseter muscle in men, the results showed that the relative contribution of the neck component of the movements increased during pain, indicating an altered strategy for jaw-neck motor control, which is in line with the notion that pain leads to adaptations in motor control with a wide spectrum of adaptation mechanisms, including redistribution of activity within and between muscles, as well as changes at different levels of the motor system (review by Hodges, 2011).

When performing a motor task to a specific target position, the outcome of the task can be assessed by both the accuracy, that is, achievement of the target position, and precision, that is, reproducibility of the performance of the task. In our previous study, nociceptive stimulation by pain induction in the masseter muscle affected the jaw-neck motor strategy, but did not affect the accuracy during a jaw-opening task to a predefined target amplitude (Wiesinger et al., 2013). Also, when manipulating a different sensory modality, proprioception, by vibration of the masseter muscles, neither the accuracy, nor the precision during the jaw-opening task was affected (Wiesinger et al., 2014).

Thus, previous studies suggest a high stability in the jaw-neck motor system during a jaw-opening task when manipulating

separate sensory modalities in the masseter muscle in men. It is not known how concomitant multimodal sensory stimulation affects jaw-opening accuracy and precision.

The aim of the present study was to investigate how jaw-neck movements, and specifically accuracy and precision of jaw opening, are affected by concomitant nociceptive and proprioceptive stimulation of the masseter muscle in men.

MATERIALS AND METHODS

Participants

Healthy men were invited to participate in the study. Originally, data for 21 men were collected; out of these, a total of seven were excluded: three due to a necessary change in study design, three due to incorrect application of the vibrator, and one due to a time delay in the start of the movement recording during the pain trial. To retain the statistical power, eight more participants were therefore recruited for a second data collection. Of these, one participant was excluded due to inability to follow given instructions. Thus, the final analysis is based on 21 healthy men aged 20–34 years ($SD = 3.9$).

A screening questionnaire and a clinical examination of the jaw function were used to determine eligibility for the study. Exclusion criteria were both self-reported – symptoms in the jaw (joint sounds during jaw opening-closing/chewing; pain/tiredness; difficult opening wide; jaw locking); pain in the head, neck, shoulder, or back; ear disease; hearing loss; neurological disorders; impaired balance; diabetes; muscle and joint disease; tumor; body mass index ≥ 30 ; elite athletes or persons with very low level of physical activity – as well as established by clinical examination – signs and symptoms of temporomandibular disorder (TMD) according to Research Diagnostic Criteria Axis I (Dworkin and LeResche, 1992). The participants had to abstain from alcohol and analgesics 24 h prior to the experiment. They were informed about the test procedures and that the injection was expected to cause pain of a short duration, but not about the specific aims of the investigation. All participants provided written, informed consent. The study was conducted according to the Declaration of Helsinki. The Regional Ethical Review Board in Umeå approved the investigation.

Experimental Procedure and Set-Up

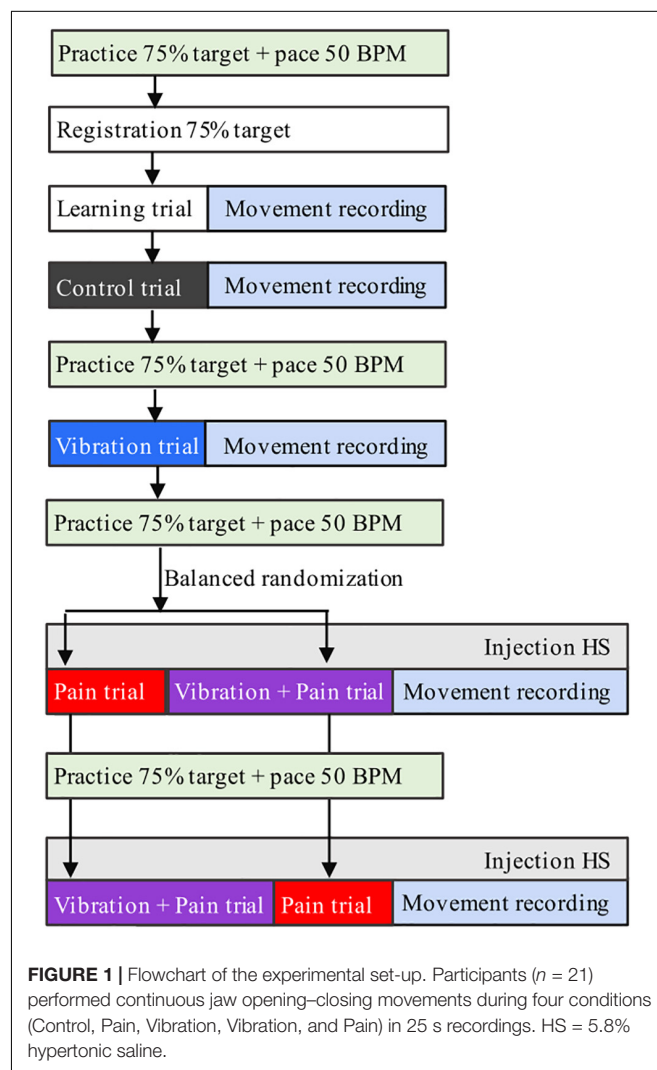
The participants performed continuous jaw opening-closing movements from light tooth contact, in the intercuspal position, to a predefined, individual target position, with eyes closed. The target jaw opening position was defined as 75% of the individual maximum jaw opening, as measured with a ruler.

The motor task was performed under four conditions: (1) control (Ctr), (2) vibration of the masseter muscle (Vib), (3) pain induction in the masseter muscle (Pain), and (4) concomitant vibration and pain induction in the masseter muscle (VibPain). The order of Pain and VibPain was randomized in a balanced design, and there was 30 min resting time between the pain injections. The subjects performed one learning trial before the Ctr trial; this was not used in the analysis. The recording

time for each trial was 25 s. The four trials were performed in one experimental session. The motor task was performed three times during each trial, only the first recording was used in the analysis.

Participants practiced the individual jaw-opening target before each trial, using a cellular plastic block cut to the individual 75% target position. The target position was registered twice with the optoelectronic recording system (MacReflex®, Qualisys), while the subjects held the plastic block between their front teeth. The jaw opening-closing pace was also practiced before each trial, with a metronome set at 50 beats/min. The subjects were instructed to try to maintain a similar speed during the trials, while their main task was to achieve the 75% target position in each jaw opening-closing cycle.

The participants were seated in an upright position in a chair with back support but without headrest, to allow for free head-neck movements. Before and throughout the experiments, they were given standardized information about the procedure. A flowchart of the experimental set-up is shown in **Figure 1**.



Vibration

Bilateral vibration of the masseter muscles was performed with a custom-made device, which has previously been described in detail (Wiesinger et al., 2014). The device was fitted at the start of the session and remained in place until the end. Two plexiglass tubes, attached with an adjustable headband, contained electrical motors and mounted weights, causing vibrations of the tubes. Rubber feet positioned on the bellies of the masseter transmitted the vibrations to the masseter muscles. The application pressure was 2 N on each side, and the vibration frequency was 80 Hz. The vibrators were activated 2 s after the start of movement recording, and the subjects were verbally instructed to start the motor task 1 s after the start of the vibrators.

Experimental Pain

Pain was induced with unilateral injections of HS (0.2 ml, 5.8%) with a 27G \times 3/4" needle into the mid-portion of the masseter muscle over 15 s. The first injection was given on the right side and the second injection, 30 min later, on the left side, regardless of whether the trial included vibration or not (VibPain or Pain). The movement recording started 60 s after the injection of HS, and the subjects started the task 2 s after the start of movement recording.

Participants rated their pain intensity on a 100 mm visual analog scale (VAS), ranging from 0 (no pain) to 100 (worst pain imaginable) 15 and 30 s after the injection, 5 s after the movement recording, and then repeatedly every 15 s up to 4 min 45 s after the injection. Pain rating was not performed during movement recording.

Concomitant Vibration and Pain Induction

The movement recording started 60 s after injection of HS, the vibrators were activated 2 s after the start of movement recording, and the subjects started the task 1 s after activation of the vibrators.

Movement Recording

Movements of the jaw and the head were simultaneously recorded in three dimensions with a wireless optoelectronic system (MacReflex®, Qualisys) at a sampling rate of 50 Hz. A tripod of retro-reflective markers was attached to the bridge of the nose, and a single marker at the tip of the chin. Two cameras acted as illuminators and detectors of the reflective markers. The set-up enabled movements to be recorded with a spatial resolution of 0.02 mm, within a working volume of 45 cm \times 55 cm \times 50 cm. Details of the set-up have been described previously (Eriksson et al., 2000; Wiesinger et al., 2013).

Jaw and Head Movements

To enable mathematical compensation of the jaw movements for the associated head–neck movements, reference markers were positioned on the head during the recordings. This marker arrangement allowed us to perform a calculation of the jaw movements in relation to the head, thereby compensating for simultaneously occurring head–neck movements. Definitions of

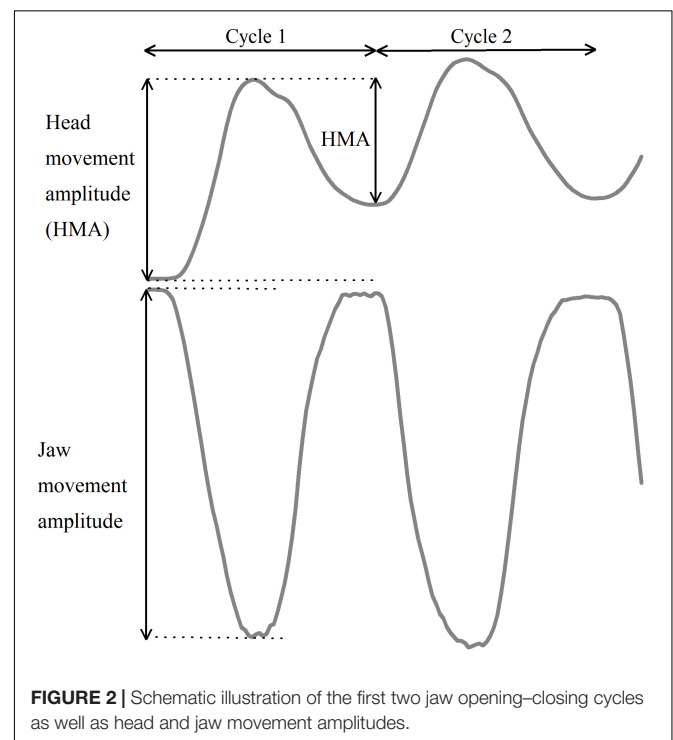
head and jaw movement amplitudes and Cycle 1 are defined in Figure 2.

The movement amplitudes for the jaw and head were calculated for each jaw opening–closing cycle. Since the first head movement cycle did not follow the same pattern as the following cycles, the movement amplitude for the first movement cycle was analyzed separately for both jaw and head amplitudes for each individual. The average amplitudes of the jaw and head movements for cycles 2–10 were calculated for each participant in each trial.

The starting point for the jaw movement cycle was defined as the time point at which the mandible began the downward jaw-opening movement. For each movement cycle, the jaw movement amplitude was defined as the distance from the starting position to the most inferior position of the jaw (i.e., at the shift from the jaw-opening phase to the jaw closing phase). For each corresponding movement cycle, the head movement amplitude was defined as the distance between the starting position and the most superior position of the head. The accuracy of the jaw movements was defined as the achievement of the individual 75% target position, and expressed as percentage of target amplitude. The precision of the jaw movements was defined as the intra-individual cycle-to-cycle variability from the mean of Cycles 2–10 of each trial, that is, the coefficient of variation (CV).

Analysis

Rated pain intensities at specific time points in Pain and VibPain were compared with Wilcoxon matched pairs test. Accuracy of jaw movement amplitudes at different trials was calculated as the percentage of the individual 75% target position. The CV for



Cycles 2–10 was calculated for each trial. The overall differences between the trials (Control, Vib, Pain, and VibPain) in Cycle 1 and Cycles 2–10, respectively, were analyzed with Friedman's test for movement amplitudes, accuracy, and precision. In case of a significant Friedman's test, *post hoc* comparisons were performed with Dunn's test. Benjamini–Hochberg correction (Benjamini and Hochberg, 1995) was used to correct the *p*-values for multiple comparisons. Interquartile range was calculated for all variables. The significance level was set at 0.05.

RESULTS

Pain Intensity

The HS injections initiated local pain in all participants. The pattern for the rated pain intensity was similar for the Pain and VibPain trials with no differences between the trials for specific time points (Figure 3).

Movement Amplitudes

There were no significant differences between the different trials for jaw movement amplitudes for Cycle 1 ($p = 0.074$) or Cycles 2–10 ($p = 0.164$) (Figure 4 and Table 1). For head movement amplitudes, there was no overall significant difference between the trials for Cycle 1 ($p = 0.074$), but an overall statistically significant difference for Cycles 2–10 ($p = 0.009$). After corrected Dunn's tests the head movement amplitudes for Cycles 2–10 were significantly larger during Pain compared to Control and to Vib (both $p = 0.034$), and significantly larger during VibPain

compared to Control ($p = 0.034$) and to Vib ($p = 0.035$). There was no difference between Pain and VibPain trials (Figure 5 and Table 1).

Jaw Opening Accuracy and Precision

For accuracy of jaw movements there were no overall differences between the trials for Cycle 1 ($p = 0.102$) or Cycles 2–10 ($p = 0.164$). For precision of jaw movements there was an overall significant difference between the trials ($p = 0.014$). After corrected Dunn's test the CV was significantly larger during VibPain compared to both Ctr ($p = 0.027$) and to Vib ($p = 0.018$). Table 2 shows the accuracy and precision of jaw movements during the different trials.

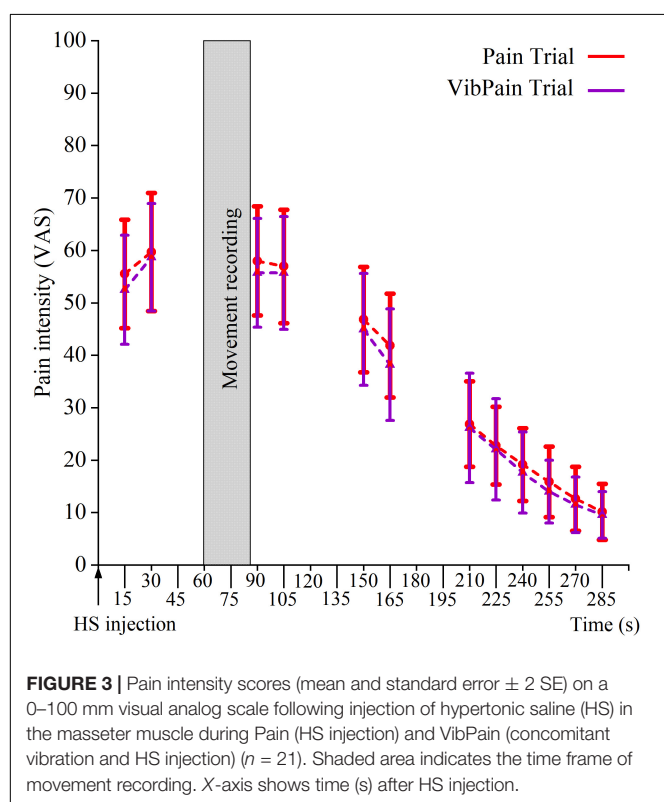
DISCUSSION

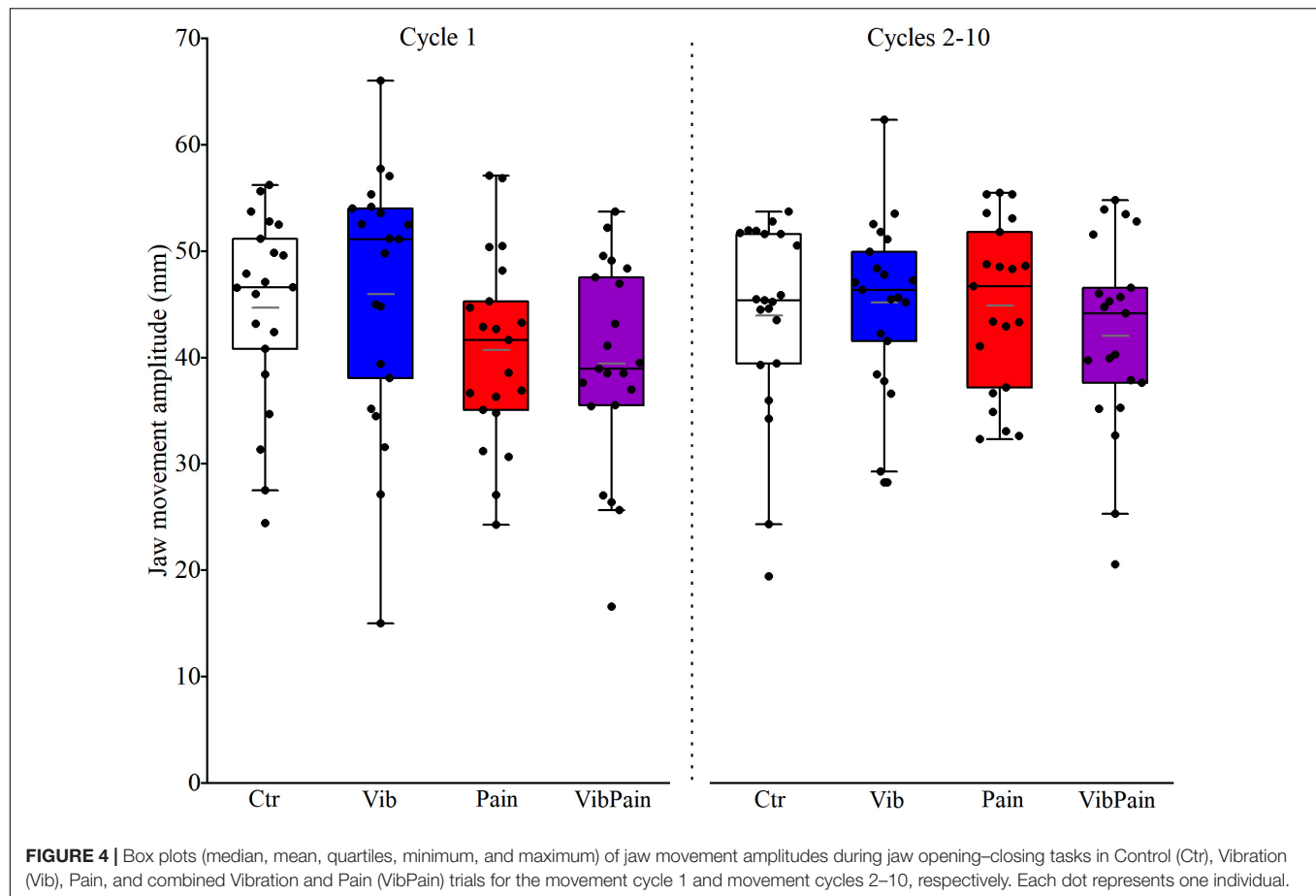
Main Findings

In this study, integrated jaw and head movements during a jaw-opening task were evaluated during concomitant manipulations of two sensory modalities, proprioception by vibration of the masseter muscle and nociception by HS injections in the masseter muscle. For the integrated jaw–neck motor strategy, there was an overall difference between pain and non-pain trials, but no additional difference between unimodal and multimodal stimulation trials. For the achievement of the jaw opening task to a target position, the results show no overall difference between trials for jaw movement accuracy, but an overall reduced jaw movement precision during multimodal stimulation with vibration and pain induction combined, compared to unimodal stimulation.

Jaw and Neck Motor Strategy

We have previously shown that experimental pain in healthy individuals altered jaw–neck motor strategy during a jaw-opening task to a target position. The pain-induced change in motor strategy was expressed as an increase of the relative component of the head movements compared to the jaw movements, which remained unchanged (Wiesinger et al., 2013) in both men and women (Wiesinger et al., 2016). This finding, that jaw movement amplitudes remained unchanged during pain induction, despite other reports of reduced jaw amplitudes during experimental pain, was interpreted as an example of task-dependent effects of pain on motor behavior (Sae-Lee et al., 2008). In another study (Wiesinger et al., 2014), we reported that jaw and head movement amplitudes were not affected by vibration of the masseter muscle, indicating a high stability of the jaw–neck motor system. For the combined multimodal stimulation with pain and vibration in the present study, the overall findings were similar to the pain trials, with no change in jaw movement amplitudes, but larger head movement amplitudes compared to the control and vibration trials. This lack of difference in jaw and neck motor strategy, between unimodal and multimodal stimulation trials indicate a general stability of the jaw–neck system. The increase in the relative neck component in pain trials compared to non-pain trials, combined with the stability of jaw movement amplitudes and maintained





task achievement, points to goal-oriented performance by the multi joint jaw–neck motor system to ensure the execution of functional jaw tasks.

Accuracy

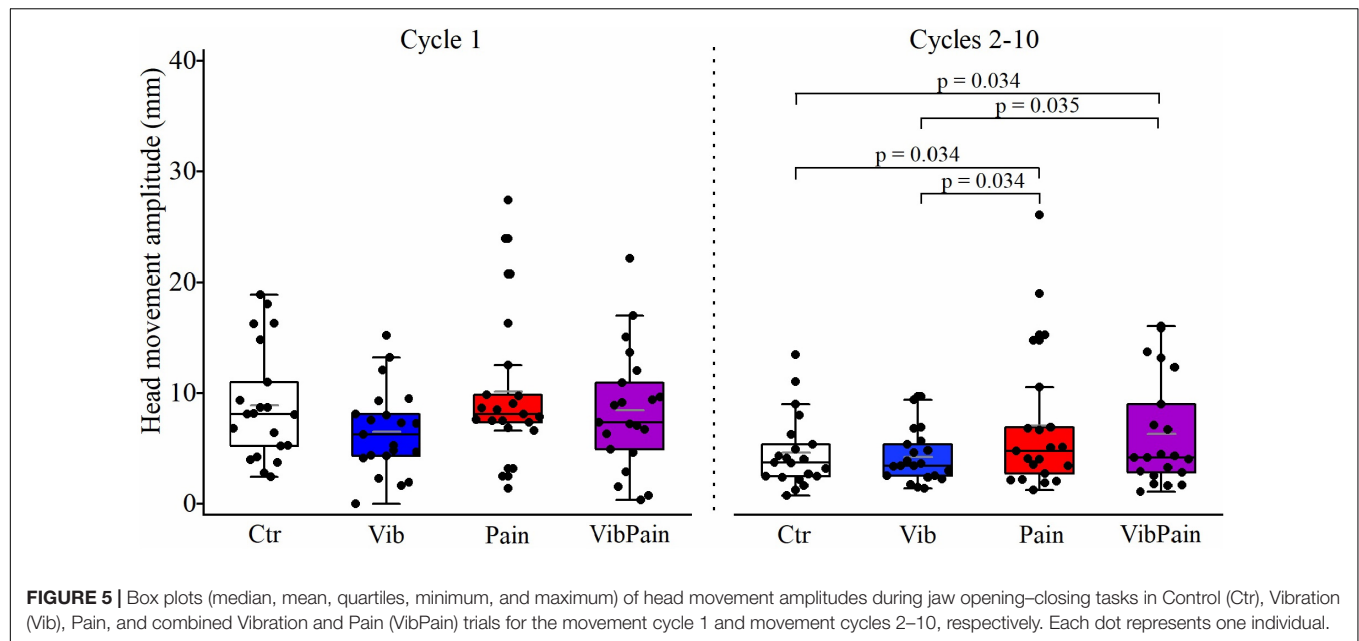
In our previous studies of jaw opening to a target position, where, as described above, experimental pain in healthy men altered jaw–neck motor strategy, the accuracy of achieving

the jaw-opening target position was not affected (Wiesinger et al., 2013). Neither was the accuracy of jaw opening affected by vibration (Wiesinger et al., 2014). Vibration can affect muscle spindles, sensory organs that convey information on muscle length related to body and limb movement and position movements, as well as other rapidly adapting afferents (Goodwin et al., 1972; Roll et al., 1989). A human study concluded that vibrations with frequencies of 80–100 Hz activated the largest number of muscle spindle endings (Roll et al., 1989). It has previously been reported that vibration can decrease the accuracy of target movements in both extra-trigeminal (Inglis and Frank, 1990) and trigeminal areas (Loucks and De Nil, 2006, 2012), presumably by increased firing of muscle spindles causing an illusion of larger muscle extension than actually performed. In terms of achievement of the target position in our previous study, an undershoot was seen in the control trial, but only for women in the pain trial, and with large individual variations (Wiesinger et al., 2016). Our finding in the present study that vibration did not affect the undershoot meant that we could therefore not confirm previous reports of increased undershoot when vibrating executing muscles. The experimental set-up and the vibration device used in our experiments have also been utilized in another study, where an effect on fine motor control was demonstrated during a bite–hold task (Kumar et al., 2019), indicating that our experimental set-up

TABLE 1 | Jaw and head movement amplitudes (mm) with interquartile range (IQR) for the different trials.

| | Trial | Cycle 1 | Cycles 2–10 |
|-------------|---------|--------------|--------------|
| | | Median (IQR) | Median (IQR) |
| Jaw | Ctr | 46.6 (12.2) | 45.4 (12.3) |
| | Vib | 51.1 (17.4) | 46.4 (10.6) |
| | Pain | 41.7 (11.8) | 46.7 (15.5) |
| | VibPain | 39.0 (12.5) | 44.2 (12.6) |
| Head | Ctr | 8.1 (8.2) | 3.7 (3.4) |
| | Vib | 6.2 (4.5) | 3.4 (3.1) |
| | Pain | 8.1 (4.1) | 4.8 (6.3)* |
| | VibPain | 7.4 (6.7) | 4.2 (8.0)* |

IQR = interquartile range. *Significant difference from Ctr and Vib after corrected Dunn's test.



does affect the proprioception. Taken together, the results from the above studies indicate that for vibration, as for experimental pain (Sae-Lee et al., 2008), the effects, or lack thereof, on jaw motor behavior may be task dependent. Furthermore, the results indicate an overriding stability of the jaw system when performing a goal-orientated task, jaw-opening to a target position, during unimodal stimulation with experimental pain and vibration, as well as multimodal stimulation with both pain and vibration.

Precision

The precision of jaw opening, as evaluated by the cycle-to-cycle variability, was reduced in the multimodal trial with concomitant pain induction and vibration, compared to the control and unimodal vibration trials. Our finding of a reduced precision, in combination with no change in accuracy, is in line with a study by Kumar et al. (2017) where a dissociation between accuracy and precision was found during a biting task,

although they reported dynamic changes for both accuracy and precision. Furthermore, the authors reported differences between trigeminal and non-trigeminal systems, where the lack of visual feedback was discussed as a possible contributing factor.

Multimodal Stimulation With Pain and Vibration

In the present study, a difference in jaw and neck motor strategy between pain and non-pain trials was found, but no additional difference between uni- and multi-modal stimulations. Also, there was no difference in perceived pain intensity between uni- and multi-modal stimulations. This is in contrast to findings in other body regions, where activation of large myelinated fiber by vibration generally produced an analgesic effect (Lundeberg et al., 1988; Kakigi and Shibasaki, 1992; Ward et al., 1996; Weerakkody et al., 2003; Gay et al., 2015).

The analgesic effect produced by activation of large myelinated fibers during vibration is mediated by receptors located in the skin responding to different vibration frequencies. In the present study the vibration frequency was 80 Hz. It has been suggested that the Pacinian channels should be responsible for the analgesic effect in stimulation ranges from 60 to 400 Hz (Pertovaara, 1979). This could explain the lack of analgesic effect seen in this study, since the skin in the orofacial area lacks functional Pacinian channels (Barlow, 1987; Hollins et al., 1991) or demonstrated afferents from Pacinian corpuscles (Johansson et al., 1988). However, spontaneous TMD pain is shown to be reduced by 100 Hz vibration applied in the orofacial area; thus, the Pacinian corpuscles cannot be essential for the analgesic effect, and other receptors could be involved, for instance, the Meissner's corpuscles (Roy et al., 2003). The Meissner's corpuscles are mainly activated by frequencies of 20–50 Hz (Gilman, 2002), which is lower than the 80 Hz used in the present study. In the present study, acute pain stimulation by injection of HS in

TABLE 2 | Percentage achievement of the individual target position (accuracy) for Cycle 1 and Cycles 2–10, as well as cycle-to-cycle variability (precision) for Cycles 2–10, during the different trials.

| Trial | Accuracy | | Precision |
|---------|---------------------------|-------------------------------|----------------------------------|
| | Cycle 1 % Median (IQR) | Cycles 2–10 % Median (IQR) | Cycles 2–10 % Median CV (IQR) |
| Ctr | 95.8 (26.9) | 92.9 (21.6) | 5.5 (6.0) |
| Vib | 102.5 (21.1) | 97.6 (16.7) | 5.9 (4.1) |
| Pain | 84.1 (27.9) | 97.0 (27.4) | 6.4 (3.3) |
| VibPain | 82.8 (32.8) | 91.9 (20.4) | 7.4 (5.9)* |

CV = coefficient of variation, IQR = interquartile range. *Significant difference from Ctr and Vib after corrected Dunn's test.

the masseter muscle was used in healthy individuals, as opposed to the study of Roy et al. (2003), where individuals with chronic TMD were used. It cannot be ruled out that the barrage of tactile afferent information evoked by the vibration may have had effects on the central processing of nociceptive information. Chronic TMD is suggested to include alternations in processing of nociceptive information (review by Chichorro et al., 2017); thus, it is not clear if responses to vibration during acute and chronic pain in the orofacial area would be the same.

CONCLUSION

For the integrated jaw and neck motor strategy, there was a difference between pain and non-pain trials, but no additional differences between unimodal and multimodal stimulation trials. For the achievement of jaw opening to a target position, the results show no effect on accuracy, but a reduced precision of jaw movements during multimodal stimulation with combined proprioceptive and nociceptive stimulation.

DATA AVAILABILITY STATEMENT

The datasets generated for this study are available on request to the corresponding author.

REFERENCES

- Barlow, S. M. (1987). Mechanical frequency detection thresholds in the human face. *Exp. Neurol.* 96, 253–261. doi: 10.1016/0014-4886(87)90044-6
- Beinert, K., Preiss, S., Huber, M., and Taube, W. (2015). Cervical joint position sense in neck pain. Immediate effects of muscle vibration versus mental training interventions: a RCT. *Eur. J. Phys. Rehabil. Med.* 51, 825–832.
- Benjamini, Y., and Hochberg, Y. (1995). Controlling the false discovery rate: a practical and powerful approach to multiple testing. *J. R. Stat. Soc. Ser. B* 57, 289–300. doi: 10.1111/j.2517-6161.1995.tb02031.x
- Capra, N. F., and Ro, J. Y. (2000). Experimental muscle pain produces central modulation of proprioceptive signals arising from jaw muscle spindles. *Pain* 86, 151–162. doi: 10.1016/s0304-3959(00)00231-1
- Chichorro, J. G., Porreca, F., and Sessle, B. (2017). Mechanisms of craniofacial pain. *Cephalalgia* 37, 613–626. doi: 10.1177/0333102417704187
- Clark, G. T., Browne, P. A., Nakano, M., and Yang, Q. (1993). Co-activation of sternocleidomastoid muscles during maximum clenching. *J. Dent. Res.* 72, 1499–1502. doi: 10.1177/00220345930720110701
- Dessem, D., and Luo, P. (1999). Jaw-muscle spindle afferent feedback to the cervical spinal cord in the rat. *Exp. Brain Res.* 128, 451–459. doi: 10.1007/s002210050868
- Dworkin, S. F., and LeResche, L. (1992). Research diagnostic criteria for temporomandibular disorders: review, criteria, examinations and specifications, critique. *J. Craniomandib. Disord.* 6, 301–355.
- Eriksson, P. O., Häggman-Henrikson, B., Nordh, E., and Zafar, H. (2000). Co-ordinated mandibular and head-neck movements during rhythmic jaw activities in man. *J. Dent. Res.* 79, 1378–1384. doi: 10.1177/00220345000790060501
- Eriksson, P. O., Zafar, H., and Nordh, E. (1998). Concomitant mandibular and head-neck movements during jaw opening-closing in man. *J. Oral Rehabil.* 25, 859–870. doi: 10.1046/j.1365-2842.1998.00333.x
- Gay, A., Aimonetti, J. M., Roll, J. P., and Ribot-Ciscar, E. (2015). Kinesthetic illusions attenuate experimental muscle pain, as do muscle and cutaneous stimulation. *Brain Res.* 1615, 148–156. doi: 10.1016/j.brainres.2015.04.041

ETHICS STATEMENT

This study involving human participants was reviewed and approved by the Regional Ethical Review Board in Umeå. The participants provided their written informed consent to participate in this study.

AUTHOR CONTRIBUTIONS

BW, BH-H, AW, and FH contributed to the conception and design of the study. BW, BH-H, and AE conducted the experiments. BW performed the statistical analysis. BW and FH wrote the first draft of the manuscript. All authors contributed to the manuscript revision, read, and approved the submitted version.

FUNDING

This study was supported by grants from Region Västernorrland, Research and Development.

ACKNOWLEDGMENTS

The authors thank Erling Englund for statistical advice.

- Gilman, S. (2002). Joint position sense and vibration sense: anatomical organisation and assessment. *J. Neurol. Neurosurg. Psychiatry* 73, 473–477. doi: 10.1136/jnnp.73.5.473
- Goodwin, G. M., McCloskey, D. I., and Matthews, P. B. (1972). Proprioceptive illusions induced by muscle vibration: contribution by muscle spindles to perception? *Science* 175, 1382–1384. doi: 10.1126/science.175.4028.1382
- Graven-Nielsen, T., Svensson, P., and Arendt-Nielsen, L. (2000). Effect of muscle pain on motor control: a human experimental approach. *Adv. Physiother.* 2, 26–38. doi: 10.1080/140381900443418
- Häggman-Henrikson, B., Nordh, E., and Eriksson, P. O. (2013). Increased sternocleidomastoid, but not trapezius, muscle activity in response to increased chewing load. *Eur. J. Oral Sci.* 121, 443–449. doi: 10.1111/eos.12066
- Häggman-Henrikson, B., Nordh, E., Zafar, H., and Eriksson, P. O. (2006). Head immobilization can impair jaw function. *J. Dent. Res.* 85, 1001–1005. doi: 10.1177/154405910608501105
- Hellström, F., Thunberg, J., Bergenheim, M., Sjölander, P., Pedersen, J., and Johansson, H. (2000). Elevated intramuscular concentration of bradykinin in jaw muscle increases the fusimotor drive to neck muscles in the cat. *J. Dent. Res.* 79, 1815–1822. doi: 10.1177/00220345000790101401
- Hodges, P. W. (2011). Pain and motor control: from the laboratory to rehabilitation. *J. Electromyogr. Kinesiol.* 21, 220–228. doi: 10.1016/j.jelekin.2011.01.002
- Hollins, M., Delemos, K. A., and Goble, A. K. (1991). Vibrotactile adaptation on the face. *Percept. Psychophys.* 49, 21–30. doi: 10.3758/bf03211612
- Inglis, J. T., and Frank, J. S. (1990). The effect of agonist/antagonist muscle vibration on human position sense. *Exp. Brain Res.* 81, 573–580. doi: 10.1007/bf02423506
- Johansson, R. S., Trulsson, M., Olsson, K. A., and Westberg, K. G. (1988). Mechanoreceptor activity from the human face and oral mucosa. *Exp. Brain Res.* 72, 204–208. doi: 10.1007/bf00248518
- Kakigi, R., and Shibasaki, H. (1992). Mechanisms of pain relief by vibration and movement. *J. Neurol. Neurosurg. Psychiatry* 55, 282–286. doi: 10.1136/jnnp.55.4.282

- Kohno, S., Matsuyama, T., Medina, R. U., and Arai, Y. (2001). Functional-rhythmical coupling of head and mandibular movements. *J. Oral Rehabil.* 28, 161–167. doi: 10.1046/j.1365-2842.2001.00636.x
- Kumar, A., Tanaka, Y., Grigoriadis, A., Grigoriadis, J., Trulsson, M., and Svensson, P. (2017). Training-induced dynamics of accuracy and precision in human motor control. *Sci. Rep.* 7:6784. doi: 10.1038/s41598-017-07078-y
- Kumar, A., Tanaka, Y., Takahashi, K., Grigoriadis, A., Wiesinger, B., Svensson, P., et al. (2019). Vibratory stimulus to the masseter muscle impairs the oral fine motor control during biting tasks. *J. Prosthodont. Res.* 63, 354–360. doi: 10.1016/j.jpor.2018.10.011
- Loucks, T. M., and De Nil, L. F. (2006). Anomalous sensorimotor integration in adults who stutter: a tendon vibration study. *Neurosci. Lett.* 402, 195–200. doi: 10.1016/j.neulet.2006.04.002
- Loucks, T. M., and De Nil, L. F. (2012). Oral sensorimotor integration in adults who stutter. *Folia Phoniatrica et Logopedica.* 64, 116–121. doi: 10.1159/000338248
- Lundeberg, T., Abrahamsson, P., Bondesson, L., and Haker, E. (1988). Effect of vibratory stimulation on experimental and clinical pain. *Scand. J. Rehabil. Med.* 20, 149–159.
- Pertovaara, A. (1979). Modification of human pain threshold by specific tactile receptors. *Acta Physiol. Scand.* 107, 339–341. doi: 10.1111/j.1748-1716.1979.tb06485.x
- Roll, J. P., Vedel, J. P., and Ribot, E. (1989). Alteration of proprioceptive messages induced by tendon vibration in man: a microneurographic study. *Exp. Brain Res.* 76, 213–222.
- Romaniello, A., Svensson, P., Cruccu, G., and Arendt-Nielsen, L. (2000). Modulation of exteroceptive suppression periods in human jaw-closing muscles induced by summation of nociceptive and non-nociceptive inputs. *Exp. Brain Res.* 132, 306–313. doi: 10.1007/s002210000353
- Roy, E. A., Hollins, M., and Maixner, W. (2003). Reduction of TMD pain by high-frequency vibration: a spatial and temporal analysis. *Pain* 101, 267–274. doi: 10.1016/s0304-3959(02)00332-9
- Sae-Lee, D., Whittle, T., Peck, C. C., Forte, A. R., Klineberg, I. J., and Murray, G. M. (2008). Experimental jaw-muscle pain has a differential effect on different jaw movement tasks. *J. Orofac. Pain* 22, 15–29.
- Sartucci, F., Rossi, A., and Rossi, B. (1986). Trigemino cervical reflex in man. *Electromyogr. Clin. Neurophysiol.* 26, 123–129.
- Sessle, B. J., Hu, J. W., Amano, N., and Zhong, G. (1986). Convergence of cutaneous, tooth pulp, visceral, neck and muscle afferents onto nociceptive and non-nociceptive neurones in trigeminal subnucleus caudalis (medullary dorsal horn) and its implications for referred pain. *Pain* 27, 219–235. doi: 10.1016/0304-3959(86)90213-7
- Shigenaga, Y., Sera, M., Nishimori, T., Suemune, S., Nishimura, M., Yoshida, A., et al. (1988). The central projection of masticatory afferent fibers to the trigeminal sensory nuclear complex and upper cervical spinal cord. *J. Comp. Neurol.* 268, 489–507. doi: 10.1002/cne.902680403
- Wang, K., Svensson, P., Sessle, B. J., Cairns, B. E., and Arendt-Nielsen, L. (2010). Interactions of glutamate and capsaicin-evoked muscle pain on jaw motor functions of men. *Clin. Neurophysiol.* 121, 950–956. doi: 10.1016/j.clinph.2010.01.015
- Wannaprom, N., Treleaven, J., Jull, G., and Uthakhip, S. (2018). Neck muscle vibration produces diverse responses in balance and gait speed between individuals with and without neck pain. *Musculoskelet Sci. Pract.* 35, 25–29. doi: 10.1016/j.msksp.2018.02.001
- Ward, L., Wright, E., and McMahon, S. B. (1996). A comparison of the effects of noxious and innocuous counterstimuli on experimentally induced itch and pain. *Pain* 64, 129–138. doi: 10.1016/0304-3959(95)00080-1
- Weerakkody, N. S., Percival, P., Hickey, M. W., Morgan, D. L., Gregory, J. E., Canny, B. J., et al. (2003). Effects of local pressure and vibration on muscle pain from eccentric exercise and hypertonic saline. *Pain* 105, 425–435. doi: 10.1016/s0304-3959(03)00257-4
- Wiesinger, B., Haggman-Henrikson, B., Hellstrom, F., Englund, E., and Wanman, A. (2016). Does induced masseter muscle pain affect integrated jaw-neck movements similarly in men and women? *Eur. J. Oral Sci.* 124, 546–553. doi: 10.1111/eos.12315
- Wiesinger, B., Haggman-Henrikson, B., Hellstrom, F., and Wanman, A. (2013). Experimental masseter muscle pain alters jaw-neck motor strategy. *Eur. J. Pain* 17, 995–1004. doi: 10.1002/j.1532-2149.2012.00263.x
- Wiesinger, B., Haggman-Henrikson, B., Wanman, A., Lindkvist, M., and Hellstrom, F. (2014). Jaw-opening accuracy is not affected by masseter muscle vibration in healthy men. *Exp. Brain Res.* 232, 3501–3508. doi: 10.1007/s00221-014-4037-4033
- Zafar, H., Nordh, E., and Eriksson, P. O. (2000). Temporal coordination between mandibular and head-neck movements during jaw opening-closing tasks in man. *Arch. Oral Biol.* 45, 675–682. doi: 10.1016/s0003-9969(00)00032-7
- Zhang, J., Luo, P., Ro, J. Y., and Xiong, H. (2012). Jaw muscle spindle afferents coordinate multiple orofacial motoneurons via common premotor neurons in rats: an electrophysiological and anatomical study. *Brain Res.* 1489, 37–47. doi: 10.1016/j.brainres.2012.10.021

Conflict of Interest: The authors declare that the research was conducted in the absence of any commercial or financial relationships that could be construed as a potential conflict of interest.

Copyright © 2019 Wiesinger, Haggman-Henrikson, Eklund, Wänman and Hellström. This is an open-access article distributed under the terms of the Creative Commons Attribution License (CC BY). The use, distribution or reproduction in other forums is permitted, provided the original author(s) and the copyright owner(s) are credited and that the original publication in this journal is cited, in accordance with accepted academic practice. No use, distribution or reproduction is permitted which does not comply with these terms.



Effects of Chronic and Experimental Acute Masseter Pain on Precision Biting Behavior in Humans

Samaa Al Sayegh^{1,2*}, Annie Borgwardt¹, Krister G. Svensson³, Abhishek Kumar^{1,2}, Anastasios Grigoriadis^{1,2} and Nikolaos Christidis^{1,2}

¹ Division of Oral Diagnostics and Rehabilitation, Department of Dental Medicine, Karolinska Institutet, Huddinge, Sweden,

² Scandinavian Center for Orofacial Neurosciences, Huddinge, Sweden, ³ Swedish Armed Forces Headquarters, Medical Service, Stockholm, Sweden

OPEN ACCESS

Edited by:

Limor Avivi-Arber,
University of Toronto, Canada

Reviewed by:

Greg Murray,
The University of Sydney, Australia
Diana K. Sarko,
Southern Illinois University
Carbondale, United States

*Correspondence:

Samaa Al Sayegh
samaa.al.sayegh@ki.se

Specialty section:

This article was submitted to
Craniofacial Biology and Dental
Research,
a section of the journal
Frontiers in Physiology

Received: 09 July 2019

Accepted: 15 October 2019

Published: 29 October 2019

Citation:

Al Sayegh S, Borgwardt A, Svensson KG, Kumar A, Grigoriadis A and Christidis N (2019) Effects of Chronic and Experimental Acute Masseter Pain on Precision Biting Behavior in Humans. *Front. Physiol.* 10:1369. doi: 10.3389/fphys.2019.01369

Chronic pain in the orofacial region is common worldwide. Pain seems to affect the jaw motor control. Hence, temporomandibular disorders (TMD) are often accompanied by pain upon chewing, restricted mouth opening and impaired maximal bite forces. However, little is known on the effects of pain, in particular the effects of chronic jaw muscle pain on precision biting. The aim of the study was to investigate the effect of chronic and acute jaw muscle pain on oral motor control during precision biting in humans. Eighteen patients with chronic masseter muscle pain and 18 healthy participants completed the experiment. All participants were examined according to the Diagnostic Criteria for TMD. Experimental acute pain was induced by bilateral, simultaneous sterile hypertonic saline infusions into the healthy masseter muscles. A standardized hold and split biting task was used to assess the precision biting. The data was analyzed with non-parametric statistical tests. The results showed no significant differences in the hold forces, split forces, durations of split or peak split rates within or between the pain and pain-free conditions. The mean split rate increased significantly compared to baseline values both in the chronic patients and the pain-free condition. However, this increase was not evident in the experimental acute pain condition. Further, there were no significant differences in the mean split rates between the conditions. The data suggest that jaw muscle pain does not seem to alter precision biting in humans, however, the possibility that a nociceptive modulation of spindle afferent activity might have occurred but compensated for cannot be ruled out.

Keywords: jaw motor control, chronic pain, myalgia, experimental pain, hypertonic saline

Abbreviations: ANOVA, analysis of variance; au, arbitrary units; cm, centimeter; CNS, central nervous system; CPG, central pattern generator; DC-TMD, diagnostic criteria for temporomandibular disorders; EMG, electromyographic muscle activity; G, gram; GAD-7, generalized anxiety disorder scale-7; GCP-7, graded chronic pain scale-7; Hz, hertz; IQR, interquartile range; mg, milligram; min, minute; ml, milliliter; mm, millimeter; N, Newton; NRS, numeric rating scale; PHQ-15, the patient health questionnaire for physical symptoms-15; PHQ-9, the patient health questionnaire for depression-9; PMR, periodontal mechanoreceptor; PSS-10, perceived stress scale-10; s, second; SCON, Scandinavian Center for Orofacial Neurosciences; SD, standard deviation; TMD, temporomandibular disorders; TMJ, temporomandibular joint; US, United States; USD, United States dollar; μ l, microliter.

INTRODUCTION

Chronic pain is a large and worldwide health problem with approximately 20% of the population reporting chronic pain of moderate to severe intensity (Breivik et al., 2006). The orofacial region is one of the most frequent locations for chronic pains, with a prevalence of 5–33% worldwide (Macfarlane et al., 2001, 2002, 2004; Isong et al., 2008; Schiffman et al., 2014). The most common diagnosis of the temporomandibular disorders (TMD) is masticatory muscle pain, i.e., myalgia (LeResche, 1997). Previous studies have shown that pain affects jaw motor control (Lund et al., 1991; Svensson and Graven-Nielsen, 2001; Murray and Peck, 2007) hence TMD is often accompanied by pain upon chewing, restricted mouth opening and impaired maximal (premolar/molar) bite force (Felićio et al., 2002; Goiato et al., 2017; Xu et al., 2017). In the past, different theories have attempted to explain how pain and jaw function interrelate (Parker, 1990; Lund et al., 1991; Stohler, 1999; Svensson and Graven-Nielsen, 2001; Lobbezoo et al., 2006; Murray and Peck, 2007; Svensson and Kumar, 2016). However, several studies have either failed to or have presented contrary data to the fundamentals of these theories (Stohler et al., 1988; Lund et al., 1991; Svensson et al., 1997, 1998; Svensson and Graven-Nielsen, 2001; Sae-Lee et al., 2008a,b). This contrasting evidence in the association between pain-related TMD and masticatory muscle function led to the integrated pain adaptation model which was presented in 2007 (Murray and Peck, 2007). Accordingly, pain is biopsychosocial and the relationship between pain and function may be more complex than proposed by the previous theories (Ohrbach et al., 2011, 2013; Bair et al., 2013). The theory proposes that just as an individual's experience of pain varies, so will also an individual's motor response.

Most evidence for how pain and jaw function interact comes from studies where pain was induced by injecting chemical substances in healthy subjects (Svensson and Graven-Nielsen, 2001; Graven-Nielsen, 2006; Kumar et al., 2015a,b). The use of pain models to mimic clinical pain is essential in research because the cause of pain is known and the effect can be controlled in such models. However, even if these pain models resemble clinical TMD-pain it is not certain that the induced pain can be exactly compared with the real, chronic TMD-condition. During a chronic pain condition changes in the nervous system occur causing central sensitization, which in turn may affect the motor function (Woolf and Walters, 1991; Woolf and Salter, 2000; Latremoliere and Woolf, 2009). Therefore, there is a greater need for studies that aim to investigate the mechanisms behind chronic musculoskeletal pain as well as further investigations of the contrasting evidence for the association between pain-related TMD and masticatory muscle function.

Human biting and chewing behaviors are controlled by a complex sensory-motor regulation involving the face primary motor cortex, the cortical masticatory area, and the central pattern generator (CPG) and coordinated by the sensory information from the periodontal mechanoreceptors (PMRs), jaw muscle spindles, articular temporomandibular joint (TMJ) receptors, and pulpal mechanoreceptors as well as other orofacial features (Dellow and Lund, 1971; Nozaki et al., 1986; Lund, 1991;

Trulsson and Johansson, 1996a, 2002; Türker, 2002; Lund and Kolta, 2006; Trulsson, 2006; van der Bilt et al., 2006; Grigoriadis et al., 2014; Kumar et al., 2014). Further, orofacial pain may be a potential modifier of mastication and jaw motor control (Clark et al., 1984) and therefore it is of great importance to investigate how pain affects human jaw function. Therefore, the aim of the study was to investigate the effect of chronic pain on oral motor force control during precision biting and compare it with experimentally induced acute pain in healthy controls. Our hypothesis was that chronic jaw muscle pain would affect the precise biting behavior and this would be reflected in the higher holding forces during the biting task (Capra et al., 2007), similar to the higher forces caused by alterations of the PMRs (Svensson and Trulsson, 2011). Furthermore, we also hypothesized that the duration of the split phase should increase in chronic pain patients due to the fear of pain increase (Nicholas, 2007). On the other hand, the experimental acute pain model was not hypothesized to alter the fine motor control and would not affect the hold force and split duration in healthy participants similarly to other previously used models (Kumar et al., 2015a).

MATERIALS AND METHODS

This controlled, experimental, clinical study was conducted at the Department of Dental Medicine, Karolinska Institutet, Huddinge, Sweden. The study was performed in accordance with the declaration of Helsinki and approved by the Regional Ethical Review Board in Stockholm (DNR: 2014/1394-3). The chronic TMD-pain patients were recruited at the Specialist Clinic at the University Dental Clinic, Karolinska Institutet, Huddinge, Sweden and Eastmaninstitutet Folkandvården Stockholms län AB, Stockholm, Sweden. The healthy participants were recruited at the Department of Dental Medicine or the University Dental Clinic, Karolinska Institutet, Huddinge, Sweden. Before inclusion, all participants were given both verbal as well as written information about this study and an informed written consent was obtained.

Participants

A sample size calculation revealed that 17 participants in each group was required to show a mean (SD) difference of 30% between the groups, with a power of 80% and a significance level of 0.05 (Svensson and Trulsson, 2011). Hence, 22 patients (mean age \pm SD = 34 \pm 12 years) with chronic myalgia including myofascial pain with referred pain in the masseter muscles with/without temporal myalgia were recruited in the study. Additionally, 22 pain-free, sex- and age-matched healthy volunteers (mean age \pm SD = 33 \pm 11 years), were also included in the study as controls. Therefore, the patient group comprised of 16 women (mean age \pm SD = 35 \pm 13 years) and six men (mean age \pm SD = 30 \pm 7 years), the control group also comprised of 16 women (mean age \pm SD = 34 \pm 13 years) and six men (mean age \pm SD = 30 \pm 6 years). The healthy controls also acted as the experimental acute pain group.

Further, out of the 22 included participants in each group 18 participants (14 women and 4 men) from the chronic patient

group and 18 participants (12 women and 6 men) from the control group provided complete data for the analysis. The four remaining participants in each group had either incomplete data or were identified as outliers. This data was handled as missing data in the statistical analyses (identification of outliers is described further below).

The inclusion criteria for participation in the study were: (a) age over 18 years; (b) intact natural central incisors with normal relation to antagonistic teeth; (c) individuals capable to protrude the lower jaw in order to be able to perform the hold and split task. Exclusion criteria were: (1) a diagnosis of arthralgia, degenerative joint disease painful jaw clicking or locking according to (DC/TMD) (Schiffman et al., 2014); (2) clinically visible dental pathology or mobility, toothache, severe malocclusions, tooth wear grade 3 = exposure of pulp or secondary dentine according to the simplified scoring criteria for tooth wear index I (López-Frías et al., 2012), (3) earlier trauma to the anterior teeth; (4) root-canal treatments in the anterior teeth, orthodontic retainer, fixed prosthodontics (implants, bridges, crowns) in the anterior teeth, dentures; (5) systemic inflammatory diseases (i.e., rheumatoid arthritis, fibromyalgia, etc.), neuropathic pain or neurological disease; (6) whiplash associated disorder; (7) use of any medication that might influence the response of pain i.e., analgesics during 24 h preceding the experiment, use of cannabinoids, or any medication that might influence the neurological function; (8) allergy to any of the substances or food used in the experiment; (9) pregnancy or lactation; and (10) cognitive or physical disability that prevent participation.

Additional inclusion criteria for patient group were: (d) a diagnosis of local myalgia or myofascial pain or myofascial pain with referred pain in the masseter muscle according to the diagnostic criteria for temporomandibular disorders (DC/TMD); (e) a pain duration of at least 3 months; (f) current pain with a minimum score of 3 according to numeric rating scale (NRS 0–10).

For the healthy individuals the additional inclusion criteria were: (d) good general health. Additional exclusion criteria were: (11) a diagnosis of myalgia or myofascial pain according to the DC/TMD; (12) additional palpatory tenderness of the masseter, temporalis muscles or over the TMJ.

Experimental Protocol

Participants answered questionnaires regarding anxiety (generalized anxiety disorder scale-7; GAD-7) (Löwe et al., 2008), depression (the patient health questionnaire for depression-9; PHQ-9) (Kroenke et al., 2001), physical symptoms (PHQ-15, the patient health questionnaire for physical symptoms-15) (Kroenke et al., 2002), and stress (PSS-10, perceived stress scale-10) (Nordin and Nordin, 2013). Patients with myalgia answered questionnaires regarding chronic pain (graded chronic pain scale-7; G-7) (Von Korff et al., 1992). Prior to the inclusion, all participants were clinically examined according to DC/TMD. The experimental protocol and time points of assessments are illustrated in **Figure 1A** for the chronic pain and **1B** for the pain-free and experimental acute pain. During the single experimental session of about 1 h, the chronic pain patients as well as the

pain-free healthy controls were asked to perform ten trials of a standardized hold and split biting task (Trulsson and Johansson, 1996b) after performing five training trials. In order to simulate the experimental acute pain condition, simultaneous bilateral infusions of 0.4 ml of sterile hypertonic saline (58.5 mg/ml) into both masseter muscles were performed in the healthy controls during 20 s. The infusions were performed by an infusion pump (infusion rate 1200 μ l/min; Harvard Infusion Pump 22, Harvard Apparatus, Great Britain) (Christidis et al., 2008), as shown in **Figure 1C**. The healthy controls were asked to perform ten trials while in pain. For all participants in all condition-groups, pain intensity was recorded before the task (for the experimental acute pain condition immediately after injection), at peak pain and at the end of the task. The experimental acute pain participants were also instructed to inform when the pain intensity was below the level of three on the 11-graded NRS-scale (0–10). While the chronic pain patients were asked to comment if their pain increased, decreased or remained unchanged after performing the hold and split task. After the task, all participants were asked to mark the maximum pain spread on a pain drawing. In the digital analysis, the scanned pain areas (i.e., the marks on the pain drawings) were analyzed in arbitrary units (au). Pain drawings provided visual illustration and quantitatively described the pattern and location of pain as well as referred pain (Wright, 2000). Three examiners (SA, AB, and KS) led the trials and were trained together in giving the instructions in the same manner according to a standardized protocol.

Hold and Split Task

The hold and split task simulated the natural behavior of positioning/holding and contracting the jaw muscles to apply the optimum force needed for splitting food. The task was firstly described by Trulsson and Johansson in 1996 (Trulsson and Johansson, 1996b) using peanuts as test food. Many studies embraced the same methodology later on using a custom-built apparatus (Umeå University, Physiology Section, IMB, Umeå, Sweden) of the same design (Johnsen et al., 2007; Svensson and Trulsson, 2009, 2011; Kumar et al., 2014, 2015a, 2017, 2019). The apparatus consisted of 11 cm-long plastic-covered metal handle with a diameter of 7 mm connected to two duralumin blocks that terminate in two parallel rectangular plates. The total weight of the plates was 48 g and the stiffness between the plates was 50 N/mm while the total length of the apparatus was 17 cm. The upper duralumin block contained strain gauge force transducers for assessment of the forces applied to the plate (DC 200 Hz). The apparatus was designed to insure that the force assessment is independent of where the force was applied to the plate (Svensson and Trulsson, 2009). A half of a roasted and salted peanut (Estrella salta jordnötter; Estrella AB, Angered, Sweden) was placed on the free-end of the plate. A less than 0.1 mm thin piece of plastic-coated fabric tape on the top of the upper plate prevents the peanut from slipping while the apparatus was being positioned. The lower plate, which was placed with 8 mm distance between surfaces from the upper plate, was equipped with a piece of plexiglass designed to function as an anterior stop while positioning of the lower incisors. Participants used their preferred hand to place the apparatus between the upper

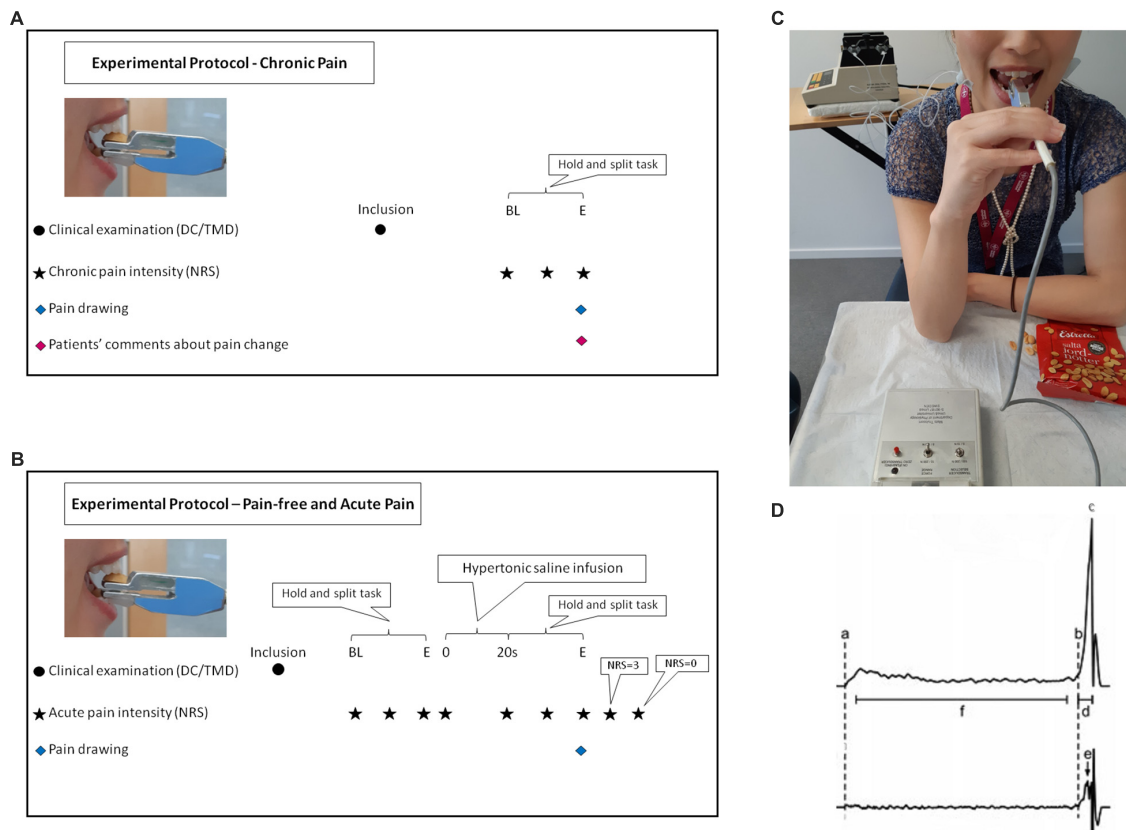


FIGURE 1 | Flow-chart illustrates the experimental protocol for chronic pain (A). BL, baseline before the task; BL, start of the task; E, end of the task. Flow-chart illustrates the experimental protocol for pain-free and experimental acute pain (B). BL, baseline before the task; s, second; E, end of the task. DC/TMD, Diagnostic criteria for temporomandibular disorders; NRS, numeric rating scale. Participant performing the hold and split task and the equipment used during the experiment (C). Estrella half peanut was placed on force transducer during acute induced pain in the masseter muscles bilaterally by infusion of hypertonic saline with Harvard infusion pump. A written informed consent was obtained from the participant in the figure for the publication of the image. A representative schematic force profile (upper trace) and force rate profile (lower trace) of one hold and split trial as shown in the WinZoom program (D). (a) Initial contact with the food, (b) Initiation of splitting, (c) the split force and end of the split phase, (d) duration of the split phase, (e) peak rate of split force, and (f) hold phase, interval beginning 0.2 s after initial contact with the food and ending 0.2 s prior to the onset of the split phase.

and lower right or left central incisors in order to hold the apparatus in a horizontal position. The participants placed the lower plate on the lower incisor and slid the apparatus until the anterior stop was reached and the edge of the upper antagonist central incisor was positioned near the middle of the peanut, as shown in **Figure 1C**. The participants were instructed to hold the peanut between their incisors and not to use more force than necessary to control the peanut (Trulsson and Gunne, 1998). After approximately 3–5 s, the participants were asked to split the peanut. The forces applied by the incisors were continuously monitored during the task. If the peanut was dropped before the holding phase, a new trial with a new peanut was recorded. On the other hand, if the peanut was dropped before splitting, the trial was observed as a failure.

Data Analyses

The force data were collected and analyzed using a customized software (WinSC/WinZoom v1.52.0.1; Umeå University, Umeå, Sweden) with 12-bit resolution at 800 Hz. Force rates were obtained by symmetrical numerical time differentiation ± 5

points from/to the force signal. The initial contact (a) and the onset of the split phase (b) were both reliably identified from the force-rate signal. The beginning of the split phase was detected at the point at which the force rate exceeded 5 N/s, the minimum rate of force increase that could be reliably detected in a single trial. The hold force was measured as the mean value of the force during the interval (f) – beginning 0.2 s after initial contact with the food (a) and ending 0.2 s before the onset (b) of the split phase. The split phase was characterized by a distinct rapid increase in force (b to c), which eventually split the food morsel. The split force/the end of the split phase (c) was defined as the peak force prior to the moment the morsel split, indicated by a rapid decrease in the force. The duration of the split phase (d) was defined as the time from the onset of the split phase (b) to the end of the split phase (c). The mean split force rate was defined as the force increase from the onset (b) to the end (c) of the split phase, divided by the duration of the split phase (d). The peak split force rate (e) defined as the max split force rate (steepest slope in the split phase profile) was identified by the

WinZoom program. This is schematically shown in **Figure 1D** (Svensson and Trulsson, 2009).

Incomplete force trials as well as trials that were observed as failures due to dropping the peanut before splitting were handled as missing data. The peanut slippage was observed five times in the chronic condition (two patients), while this occurred once in the pain-free condition and once during acute pain condition (the same participant). Since the participants were not allowed to train more than five times before performing the hold and split task all trials' profiles were manually checked and outliers were detected by using Adjusted Boxplot Method for skewed distributions (Brys et al., 2004, 2005; Hubert and Vandervieren, 2008). Outliers were handled as missing data. In all the three conditions (chronic pain, pain-free and experimental acute pain) only the first five "inlying" trials were included in the analyses (as for the pain conditions only trials during pain intensity of $\text{NRS} \geq 3$). One participant from the healthy group did not answer the questionnaires hence; psychosocial data for that particular participant was handled as missing data.

The normality of the entire data was evaluated by using the Adjusted Boxplot Method and the Shapiro-Wilk test. The data showed a non-normal distribution with majority of the variables skewed to the right. Therefore, non-parametric tests were used to analyze the data. For each participant, data from all five included trials provided a participant median for each measurement and all data are further presented as group median (IQR, interquartile range). The data were analyzed with the SigmaStat software (version14.0; Systat Software Inc., San Jose, CA, United States) and for all tests, the level of significance was set at $P < 0.05$. Comparisons of psychosocial variables were done with Mann-Whitney Rank Sum test. For within condition's comparisons, the non-parametric Friedman's analysis of variance (ANOVA) for repeated measures and Tukey *post hoc* test for the associated multiple comparisons were used to test changes in all variables versus the baseline value of each variable (the first trial for each participant and condition was considered as baseline). For between conditions' comparisons, Wilcoxon Signed Rank test and Mann-Whitney Rank Sum test were used. The variables included in the analyses were therefore conditions (chronic, pain-free, acute) and trials (Macfarlane et al., 2001, 2002; Breivik et al., 2006; Isong et al., 2008; Schiffman et al., 2014). For descriptive purposes, sex (men, women) was an additional variable included in the analyses. Spearman correlation test was applied to detect any correlation between force and pain variables.

RESULTS

Psychosocial Characteristics

There were no significant differences between the chronic pain patients and the healthy participants regarding any of the psychosocial symptoms (Mann-Whitney Rank Sum test; $P > 0.05$) (**Table 1**).

Pain Characteristics

Majority of the chronic pain patients (61%) were diagnosed with local myalgia in the masseter muscles (with/without temporal

myalgia) and 39% were diagnosed with myofascial pain with referred pain in the masseter muscles (with/without temporal myalgia) according to DC/TMD. 61% of the chronic patients had low pain intensity and low grade of disability (GCPS-7), 33% had high pain intensity and low grade of disability, about 6% had moderately limiting high disability and none of them had severely limiting high disability. The pain intensity, pain area and pain duration in the chronic patients are presented in **Table 1**.

The induced experimental acute pain intensity, pain area, and pain duration in the healthy participants are presented in **Table 1**.

Force Characteristics

Healthy participants, both during pain-free and experimental acute pain condition, as well as chronic pain patients applied low forces during the hold phase followed by a rapid-ramp increase in force until the peanut split. There were no significant differences in the hold forces (pain-free: 0.99 N, acute pain: 1.46 N, chronic pain: 1.00 N) and the split forces (pain-free: 28.95 N, acute pain: 27.35 N, chronic pain: 30.79 N) within (Friedman/Tukey; $P > 0.05$) (**Table 2**) or between the conditions (Wilcoxon Signed Rank and Mann-Whitney Rank Sum; $P > 0.05$) (**Table 3**). Further, there were also no significant differences in the durations of split (pain-free: 0.26 s, acute pain: 0.30 s, chronic pain: 0.30 s) and the peak split force rates (pain-free: 307.38 N/s, acute pain: 285.28 N/s, chronic pain: 278.34 N/s) both within (Friedman/Tukey; $P > 0.05$) (**Table 2**) and between the conditions (Wilcoxon Signed Rank and Mann-Whitney Rank Sum; $P > 0.05$) (**Table 3**). The mean split force rate increased significantly compared to baseline values both in the chronic condition and the pain-free condition (Friedman/Tukey; $P = 0.04$ and 0.01 , respectively) (**Table 2**). This increase in rate was not evident in the experimental acute pain condition (Friedman; $P = 0.11$) (**Table 2**). Observations of the mean split rates revealed no significant differences (pain-free: 99.76 N/s, acute pain: 82.07 N/s, chronic pain: 83.62 N/s) between the conditions (Wilcoxon Signed Rank and Mann-Whitney Rank Sum; $P > 0.05$) (**Table 3**).

Pain Intensity in Relation to Force Variables

The worst reported pain intensity during trial ($\text{NRS} = 4.25$) in the chronic condition correlated negatively with the hold force (1.00 N) (Spearman correlation; $P = 0.04$). The pain intensity 20s after infusion ($\text{NRS} = 7.00$), and the worst reported pain intensity during trial ($\text{NRS} = 7.00$) showed a negative correlation with the duration of the split phase in the experimental acute pain condition (0.30 s) (Spearman correlation; $P < 0.05$).

DISCUSSION

The findings of the present study showed that neither experimental acute pain nor chronic muscular pain affects the human jaw motor control during a standardized precision biting task involving "holding" and "splitting" of peanuts with anterior teeth. The findings seem to indicate that jaw muscle

TABLE 1 | Pain and psychosocial data.

| | All | Women | Men |
|--|-----------------|------------------|-------------------|
| Chronic pain patients | | | |
| Pain intensity (NRS) | 3.50 (1.50) | 3.50 (1.00) | 3.50 (1.75) |
| Peak pain intensity (NRS) | 4.25 (3.50) | 4.25 (3.50) | 4.50 (3.50) |
| Pain area (au) | 584.84 (745.53) | 537.89 (639.169) | 851.90 (1354.763) |
| Pain duration (months) | 72.00 (85.50) | 90.00 (78) | 39.00 (25.50) |
| Experimental acute pain in healthy participants | | | |
| Pain intensity after 20 s infusion (NRS) | 7.00 (2.25) | 6.50 (1.75) | 7.50 (1.38) |
| Peak pain intensity (NRS) | 7.00 (1.625) | 7.00 (2.625) | 7.00 (1.625) |
| Pain area (au) | 195.99 (278.50) | 185.75 (277.50) | 323.73 (168.79) |
| Pain duration to NRS = 3 s | 216 (184.50) | 244.00 (184.50) | 202.00 (97.25) |

| | All patients | All healthy participants | P-value | Female patients | Healthy women | P-value | Male patients | Healthy men | P-value |
|---------------------|---------------|--------------------------|---------|-----------------|---------------|---------|---------------|--------------|---------|
| GAD-7 ¹ | 22.22 (55.56) | 16.67 (66.67) | 1.00 | 16.67 (38.89) | 11.11 (38.89) | 0.70 | 5.56 (16.67) | 5.56 (16.67) | 1.00 |
| PHQ-9 ² | 19.44 (30.56) | 8.33 (68.06) | 0.34 | 16.67 (27.78) | 5.56 (33.33) | 0.49 | 5.56 (8.33) | 2.78 (18.06) | 0.89 |
| PHQ-15 ³ | 27.78 (19.44) | 16.67 (43.06) | 0.69 | 22.22 (16.67) | 13.89 (25) | 0.89 | 5.56 (8.33) | 2.78 (18.06) | 0.89 |
| PSS-10 ⁴ | 38.89 (16.67) | 27.78 (22.22) | 1.00 | 27.78 (16.67) | 22.22 (22.22) | 0.70 | 5.56 (5.56) | 11.11 (5.56) | 0.70 |

Data are expressed as median (IQR, interquartile range). The forces were assessed in Newton (N), the duration in Seconds (s), and the rates in Newton per Seconds (N/s). P-values refer to the comparisons between trials by Friedman's ANOVA and Tukey post hoc test. ¹GAD-7: Generalized Anxiety Disorder (7 Questions). ²PHQ-9: The Patient Health Questionnaire for Depression (9 Questions). ³PHQ-15: The Patient Health Questionnaire for Physical Symptoms (15 Questions). ⁴PSS-10: Perceived Stress Scale Scoring (10 Questions).

TABLE 2 | Changes compared to baseline values in force, duration and rate variables in the three conditions.

| Variable | Chronic | | | Pain-free | | | Experimental acute | | |
|--------------------------|-----------------|-----------------|---------|-----------------|-----------------|---------|--------------------|-----------------|---------|
| | Trial 1 | Trial 5 | P-value | Trial 1 | Trial 5 | P-value | Trial 1 | Trial 5 | P-value |
| Hold force (N) | 0.84 (1.13) | 1.09 (1.02) | 0.85 | 0.99 (1.47) | 1.14 (1.08) | 0.43 | 1.29 (1.28) | 1.76 (1.56) | 0.12 |
| Split force (N) | 30.05 (14.09) | 29.42 (7.71) | 0.66 | 30.78 (14.94) | 28.83 (7.72) | 0.91 | 27.19 (14.49) | 27.46 (14.78) | 0.67 |
| Duration of Split (s) | 0.47 (0.56) | 0.28 (0.38) | 0.07 | 0.32 (0.34) | 0.27 (0.28) | 0.08 | 0.41 (0.53) | 0.24 (0.20) | 0.054 |
| Split force increase (N) | 24.69 (19.40) | 27.00 (15.83) | 0.92 | 29.50 (7.91) | 26.12 (6.89) | 0.46 | 24.40 (13.36) | 22.89 (11.01) | 0.51 |
| Mean split rate (N/s) | 63.62 (60.08) | 69.59 (102.83) | 0.04* | 85.23 (45.68) | 128.83 (119.56) | 0.01* | 59.56 (66.23) | 85.99 (79.06) | 0.11 |
| Peak split rate (N/s) | 226.89 (285.29) | 370.36 (290.28) | 0.15 | 226.89 (145.03) | 396.22 (254.0) | 0.06 | 266.93 (285.29) | 238.36 (215.21) | 0.37 |

Data are expressed as median (IQR, interquartile range). The forces were assessed in Newton (N), the duration in Seconds (s), and the rates in Newton per Seconds (N/s). P-values refer to the comparisons between trials by Friedman's ANOVA and Tukey post hoc test. *Significant difference $P < 0.05$.

TABLE 3 | Comparisons between the three conditions regarding force, duration, and rate variables.

| Variable | Chronic | Pain-free | P-value | Experimental acute | Pain-free | P-value | Chronic | Experimental acute | P-value |
|--------------------------|-----------------|-----------------|---------|--------------------|-----------------|---------|-----------------|--------------------|---------|
| Hold force (N) | 1.00 (1.30) | 0.99 (1.13) | 0.99 | 1.46 (0.94) | 0.99 (1.13) | 0.06 | 1.00 (1.30) | 1.46 (0.94) | 0.28 |
| Split force (N) | 30.79 (5.28) | 28.95 (5.62) | 0.19 | 27.35 (7.50) | 28.95 (5.62) | 0.55 | 30.79 (5.28) | 27.35 (7.50) | 0.07 |
| Duration of split (s) | 0.30 (0.22) | 0.26 (0.21) | 0.32 | 0.30 (0.20) | 0.26 (0.21) | 0.33 | 0.30 (0.22) | 0.30 (0.20) | 0.99 |
| Split force increase (N) | 27.70 (11.01) | 28.09 (5.09) | 0.83 | 23.43 (7.32) | 28.09 (5.09) | 0.01* | 27.70 (11.01) | 23.43 (7.32) | 0.12 |
| Mean split rate (N/s) | 83.62 (80.63) | 99.76 (57.61) | 0.28 | 82.07 (55.51) | 99.76 (57.61) | 0.12 | 83.62 (80.63) | 82.07 (55.51) | 0.84 |
| Peak split rate (N/s) | 278.34 (240.24) | 307.38 (228.56) | 0.40 | 285.28 (142.84) | 307.38 (228.56) | 0.10 | 278.34 (240.24) | 285.28 (142.84) | 0.94 |

Data are expressed as median (IQR, interquartile range). The forces were assessed in Newton (N), the duration in Seconds (s), and the rates in Newton per Seconds (N/s). P-values refer to the comparisons between conditions by Wilcoxon Signed Rank and Mann-Whitney Rank Sum tests. *Significant difference $P < 0.05$.

pain does not alter the sensorimotor regulation and precision control of the jaws.

The PMRs are innervated by fibers terminating in subnucleus interpolaris. The signaling in these fibers is faster and probably not affected by noxious stimuli from trigeminal facial areas that terminate more caudally in subnucleus caudalis. The rostral projections are larger in diameter and thereby faster than the more caudally located ones (Capra and Dessem, 1992). Further, the muscle spindles are innervated by efferent nerve fibers, motoneurons, which receive information from the central nervous system (CNS). The motoneurons convey nervous impulses to produce muscular effect, causing muscle fibers to shorten and contract. To enhance contraction either the firing frequency of each neuron increases or more motor units are activated/recruited (McComas, 1998; Loeb and Ghez, 2000; Miles, 2004). The fine-tuning of this activity is achieved by sensory information from orofacial receptors including the PMRs and muscle spindles to the CNS. The results seem to indicate that the presence of healthy PMRs and pulpal receptors provide the CNS with accurate sensory information despite the muscular pain. There is a possibility that a nociceptive modulation of spindle afferent activity might have occurred (Capra et al., 2007) but compensated for, hence resulting in undetectable effect on the force parameters in the present study. Activity along slower conducting nociceptive afferents could still modify the activity of faster afferents via intra-nuclear connections within the trigeminal brainstem sensory nuclear complex. Some masseter nociceptive afferents might provide axon collaterals to the rostral trigeminal subnuclei (Capra and Dessem, 1992). Nevertheless, this study did not assess nociceptive afferent activity. Furthermore, a potential effect of the experimentally induced pain (Nash et al., 2010; Minami et al., 2013) might have been compensated by other unaffected muscle parts/muscles. This assumption could be applicable on the chronic pain condition as well. The chronic pain patients may over time have developed compensating motor and behavioral strategies (Mohn et al., 2011; Fillingim et al., 2018).

Hold Phase

The fact that all the conditions showed no significant differences in the hold forces compared to the baseline trials indicated no trial order effect within the conditions. This is in line with results from previous studies where the hold and split task was used (Kumar et al., 2014; Zhang et al., 2016). The hold force in the pain-free condition was found to be 0.99 N in this study and in line with the previously mentioned study (Kumar et al., 2014) as well as earlier reports where the hold force for peanuts in healthy participants with natural dentition during normal conditions varied between 0.59 and 0.79 N (Trulsson and Johansson, 1996b; Trulsson and Gunne, 1998; Johnsen et al., 2007; Svensson and Trulsson, 2009, 2011).

The chronic pain patients applied similar hold force as the pain-free participants. During the holding phase in pain-free healthy individuals, it has been hypothesized that the PMRs besides the afferent nerve fibers in muscle spindles play a role in signaling the early contact-state information about the peanut in a predictive feed-forward manner in order to activate the

motor commands that are needed for initiating the split phase (Svensson and Trulsson, 2009, 2011). The jaw muscle activity increases in response to an increased food hardness. It was shown that the destruction of either periodontal or muscle afferents in animals, reduced such increase in jaw muscle activity (Lavigne et al., 1987; Morimoto et al., 1989; Hidaka et al., 1997). However, chronic muscle pain did not seem to have any effect on the forces during the holding phase in this study. One probable explanation could be that the presence of healthy PMRs are of greater importance in oral fine motor control than the muscle spindles (Kumar et al., 2019).

Split Phase

The split phase was characterized by a sudden rapid ramp increase in the bite force. When the peanut was split, the force dropped down and an unloading of the teeth occurred (Svensson and Trulsson, 2009, 2011). The unloading contributes to a reflex response in the masseter muscle activity that results in stopping the jaw closing movement (Turker and Jenkins, 2000). All conditions showed no differences in the split force and duration of split phase compared to baseline values. This finding is in line with previous studies where experimental acute pain did not show any robust effects on the split forces (Kumar et al., 2014, 2015a). It was previously suggested that split forces and duration of split are mainly dependent on the mechanical properties of the food and the bevel of the incisal edges during biting with anterior teeth (Johnsen et al., 2007; Svensson and Trulsson, 2009, 2011; Kumar et al., 2014, 2015c, 2017). In healthy individuals in previous studies, the split forces varied between 17.6 and 35.9 N and the duration of the split phase varied between 0.22 and 0.34 s (Trulsson and Johansson, 1996b; Svensson and Trulsson, 2009, 2011). In our study the split force was 28.95 N and the duration of the split phase was 0.26 s in healthy pain-free participants. Our findings were within the range of the previous results.

The significant increase in the mean split force rate in the pain-free individuals and chronic pain patients indicates that reaching to the split of the peanut from the initiation of the split phase was faster compared to baseline. On the other hand, no statistically significant difference in the mean split force rate in the acute condition compared to baseline may indicate that the high intensity of the induced pain and the protective effect of the acute pain affected the rate. However, the differences were only found within the conditions (not between them) and there were no differences in the duration of the split (one of the two variables that the mean split force rate depends on) in all the three conditions. Further statistical analyses showed that there was a significant difference in the split force increase (the other variable that the mean split force rate depends on) between the acute and the pain-free conditions where the acute condition showed a smaller increase (**Table 3**). This significant difference could not be found between the chronic and the pain-free conditions or between the chronic and acute conditions. Moreover, no significant differences could be found within the three groups in the split force increase (**Table 2**). Therefore, this finding should be considered with caution and further investigations would be needed in order to make a more conclusive interpretation. It was suggested that the individual's reaction to pain might depend on

the specifics of the performed task (Sae-Lee et al., 2008a,b). An individual's confidence that they can manage pain (self-efficacy beliefs) predicts avoidance behavior (Nicholas, 2007) and the ability to persist with a task (Turner et al., 2005). The smaller split force increase in the acute condition could be an indication that the participants could predict the split force needed easier than the two other condition groups. The acute condition group did not need to increase the mean split force rate as much as the other two condition groups since the split force onset was already high and more approximate to the split force needed. That is in line with the significant increase in the mean split force rate in the pain-free and chronic conditions. A possible explanation could be a training effect since the participants in the acute condition were the same persons as in the pain-free condition. However, the previously cited studies (Kumar et al., 2014, 2015a; Zhang et al., 2016) did not report any findings about rate variables. There were no significant differences in the mean and peak split force rates between the three conditions indicating that the pain did not impair the neural control needed for achieving the necessary force magnitude needed for splitting the peanut.

For the acute jaw muscle pain, the results confirms our hypothesis and are in line with previous studies using other experimental jaw muscle pain models and in other populations which had shown that experimental acute pain had no detectable or robust effect on the hold and split forces and on the variability of the forces, duration of the split phase, electromyographic muscle activity (EMG) or jaw movement amplitude in comparison with healthy controls during biting and mastication (Svensson et al., 1997; Kumar et al., 2015a,b) indicating the absence of motor impairment even in subjects who reported moderate to intense levels of pain. Interestingly, the results showed that this was the case even for the chronic jaw muscle pain which was contradictory to our hypothesis. On the other hand, this is in line with results from a previous study (Goiato et al., 2017) showing that maximal bite forces in the incisor region was similar prior to and after jaw muscle pain relief, suggesting that the presence of pain did not affect the maximal forces in this region.

Study Limitations and Strengths

The baseline pain intensity in chronic pain patients was rather low, none of them had a severely limiting high disability according to GCPS-7 and pain catastrophizing according to pain catastrophizing scale-13 (PCS-13) (Boonstra et al., 2016) was not assessed in this study which could be considered as a limitation. The fact that there were no significant differences between chronic patients and healthy participants regarding the psychosocial characteristics minimized the possible confounding effect, and therefore could be considered a strength of the current study.

Incisors were used in this study in order to minimize confounding factors as it had earlier been reported that participants felt it was easier to master the task when anterior teeth were used compared to posterior teeth (Johnsen et al., 2007). It had been also shown that the masseter muscle was significantly more active (higher EMG) than the temporal muscle during tasks involving incisal biting and jaw protrusion (Farella et al., 2008)

and that biting in a protrusive position was accompanied by the highest activation of the masseter muscle (Lu et al., 2013). One can assume that there would be a practicing bias in the experimental acute pain condition since the same individuals performed the task twice, pain-free and while in experimental acute pain. However, the circumstances differed and a previous study showed that there was no apparent or optimization of jaw motor control when this specific task was repeated up to sixty times, in participants with healthy periodontium (Kumar et al., 2014).

Conclusion

The current study shows that jaw muscle pain does not seem to alter precision biting in humans. Specifically, chronic myalgia in the jaw muscles as well as experimentally induced acute pain did not show any effects on the hold or split forces when compared to healthy pain-free individuals. However, a possibility that a nociceptive modulation of spindle afferent activity might have occurred but compensated for cannot completely be ruled out.

DATA AVAILABILITY STATEMENT

The datasets for this study will be made available by the authors, without undue reservations, to any qualified researcher.

ETHICS STATEMENT

The studies involving human participants were reviewed and approved by the Regional Ethical Review Board in Stockholm (DNR: 2014/1394-3). The patients/participants provided their written informed consent to participate in this study.

AUTHOR CONTRIBUTIONS

SA wrote the manuscript, performed the research, analyzed the data, and made the tables and figures. AB performed the research and participated in manuscript editing. KS participated in the design of the project, performed the research, and participated in manuscript editing. AK participated in data analyses and manuscript editing. AG designed the project and participated in manuscript editing. NC designed the project, and participated in data analyses, making the figures, and manuscript editing.

FUNDING

The study was funded from the Stockholm County Council and the Karolinska Institutet (SOF; Styrgruppen för Odontologisk Forskning).

ACKNOWLEDGMENTS

We are grateful to Reika Makita for the contribution as a model in **Figure 1**.

REFERENCES

- Bair, E., Ohrbach, R., Fillingim, R. B., Greenspan, J. D., Dubner, R., Diatchenko, L., et al. (2013). Multivariable modeling of phenotypic risk factors for first-onset TMD: the OPFERA prospective cohort study. *J. Pain* 14(12 Suppl.), T102–T115. doi: 10.1016/j.jpain.2013.09.003
- Boonstra, A. M., Stewart, R. E., Kōke, A. J., Oosterwijk, R. F., Swaan, J. L., Schreurs, K. M., et al. (2016). Cut-Off points for mild, moderate, and severe pain on the numeric rating scale for pain in patients with chronic musculoskeletal pain: variability and influence of sex and catastrophizing. *Front. Psychol.* 7:1466. doi: 10.3389/fpsyg.2016.01466
- Breivik, H., Collett, B., Ventafridda, V., Cohen, R., and Gallacher, D. (2006). Survey of chronic pain in Europe: prevalence, impact on daily life, and treatment. *Eur. J. Pain* 10, 287–333.
- Brys, G., Hubert, M., and Rousseeuw, P. J. (2005). A robustification of independent component analysis. *J. Chemom.* 19, 364–375. doi: 10.1002/cem.940
- Brys, G., Hubert, M., and Struyf, A. (2004). A robust measure of skewness. *J. Comput. Graph. Stat.* 13, 996–1017. doi: 10.1198/106186004x12632
- Capra, N. F., and Dessem, D. (1992). Central connections of trigeminal primary afferent neurons: topographical and functional considerations. *Crit. Rev. Oral Biol. Med.* 4, 1–52. doi: 10.1177/10454411920040010101
- Capra, N. F., Hisley, C. K., and Masri, R. M. (2007). The influence of pain on masseter spindle afferent discharge. *Arch. Oral Biol.* 52, 387–390. doi: 10.1016/j.archoralbio.2006.10.011
- Christidis, N., Ioannidou, K., Milosevic, M., Segerdahl, M., and Ernberg, M. (2008). Changes of hypertonic saline-induced masseter muscle pain characteristics, by an infusion of the serotonin receptor type 3 antagonist granisetron. *J. Pain* 9, 892–901. doi: 10.1016/j.jpain.2008.05.002
- Clark, G. T., Jacobson, R., and Beemsterboer, P. L. (1984). Interdental thickness discrimination in myofascial pain dysfunction subjects. *J. Oral Rehabil.* 11, 381–386. doi: 10.1111/j.1365-2842.1984.tb00589.x
- Dellow, P. G., and Lund, J. P. (1971). Evidence for central timing of rhythmic mastication. *J. Physiol.* 215, 1–13. doi: 10.1113/jphysiol.1971.sp009454
- Farella, M., Palla, S., Erni, S., Michelotti, A., and Gallo, L. M. (2008). Masticatory muscle activity during deliberately performed oral tasks. *Physiol. Meas.* 29, 1397–1410. doi: 10.1088/0967-3334/29/12/004
- Felício, C. M., Mazzetto, M. O., and Perri Angote Dos Santos, C. (2002). Masticatory behavior in individuals with temporomandibular disorders. *Minerva Stomatol.* 51, 111–120.
- Fillingim, R. B., Slade, G. D., Greenspan, J. D., Dubner, R., Maixner, W., Bair, E., et al. (2018). Long-term changes in biopsychosocial characteristics related to temporomandibular disorder: findings from the OPFERA study. *Pain* 159, 2403–2413. doi: 10.1097/j.pain.0000000000001348
- Goiato, M. C., Zuim, P. R. J., Moreno, A., Dos Santos, D. M., da Silva, E. V. F., de Caxias, F. P., et al. (2017). Does pain in the masseter and anterior temporal muscles influence maximal bite force? *Arch. Oral Biol.* 83, 1–6. doi: 10.1016/j.archoralbio.2017.06.029
- Graven-Nielsen, T. (2006). Fundamentals of muscle pain, referred pain, and deep tissue hyperalgesia. *Scand. J. Rheumatol. Suppl.* 122, 1–43. doi: 10.1080/03009740600865980
- Grigoriadis, A., Johansson, R. S., and Trulsson, M. (2014). Temporal profile and amplitude of human masseter muscle activity is adapted to food properties during individual chewing cycles. *J. Oral Rehabil.* 41, 367–373. doi: 10.1111/joor.12155
- Hidaka, O., Morimoto, T., Masuda, Y., Kato, T., Matsuo, R., Inoue, T., et al. (1997). Regulation of masticatory force during cortically induced rhythmic jaw movements in the anesthetized rabbit. *J. Neurophysiol.* 77, 3168–3179. doi: 10.1152/jn.1997.77.6.3168
- Hubert, M., and Vandervieren, E. (2008). An adjusted boxplot for skewed distributions. *Comput. Stat. Data Anal.* 52, 5186–5201. doi: 10.1016/j.csda.2007.11.008
- Isong, U., Gansky, S. A., and Plesh, O. (2008). Temporomandibular joint and muscle disorder-type pain in U.S. adults: the national health interview survey. *J. Orofac. Pain* 22, 317–322.
- Johnsen, S. E., Svensson, K. G., and Trulsson, M. (2007). Forces applied by anterior and posterior teeth and roles of periodontal afferents during hold-and-split tasks in human subjects. *Exp. Brain Res.* 178, 126–134. doi: 10.1007/s00221-006-0719-9
- Kroenke, K., Spitzer, R. L., and Williams, J. B. (2001). The PHQ-9: validity of a brief depression severity measure. *J. Gen. Intern. Med.* 16, 606–613. doi: 10.1046/j.1525-1497.2001.016009606.x
- Kroenke, K., Spitzer, R. L., and Williams, J. B. (2002). The PHQ-15: validity of a new measure for evaluating the severity of somatic symptoms. *Psychosom. Med.* 64, 258–266. doi: 10.1097/00006842-200203000-00008
- Kumar, A., Castrillon, E., Svensson, K. G., Baad-Hansen, L., Trulsson, M., and Svensson, P. (2015a). Effects of experimental craniofacial pain on fine jaw motor control: a placebo-controlled double-blinded study. *Exp. Brain Res.* 233, 1745–1759. doi: 10.1007/s00221-015-4245-5
- Kumar, A., Castrillon, E., and Svensson, P. (2015b). Can experimentally evoked pain in the jaw muscles or temporomandibular joint affect anterior bite force in humans? *J. Oral Facial Pain Headache* 29, 31–40. doi: 10.11607/ofph.1268
- Kumar, A., Grigoriadis, J., Trulsson, M., Svensson, P., and Svensson, K. G. (2015c). Effects of short-term training on behavioral learning and skill acquisition during intraoral fine motor task. *Neuroscience* 306, 10–17. doi: 10.1016/j.neuroscience.2015.06.065
- Kumar, A., Castrillon, E., Trulsson, M., Svensson, K. G., and Svensson, P. (2017). Fine motor control of the jaw following alteration of orofacial afferent inputs. *Clin. Oral Investig.* 21, 613–626. doi: 10.1007/s00784-016-1939-4
- Kumar, A., Svensson, K. G., Baad-Hansen, L., Trulsson, M., Isidor, F., and Svensson, P. (2014). Optimization of jaw muscle activity and fine motor control during repeated biting tasks. *Arch. Oral Biol.* 59, 1342–1351. doi: 10.1016/j.archoralbio.2014.08.009
- Kumar, A., Tanaka, Y., Takahashi, K., Grigoriadis, A., Wiesinger, B., Svensson, P., et al. (2019). Vibratory stimulus to the masseter muscle impairs the oral fine motor control during biting tasks. *J. Prosthodont. Res.* 63, 354–360. doi: 10.1016/j.jpor.2018.10.011
- Latremoliere, A., and Woolf, C. J. (2009). Central sensitization: a generator of pain hypersensitivity by central neural plasticity. *J. Pain* 10, 895–926. doi: 10.1016/j.jpain.2009.06.012
- Lavigne, G., Kim, J. S., Valiquette, C., and Lund, J. P. (1987). Evidence that periodontal pressoreceptors provide positive feedback to jaw closing muscles during mastication. *J. Neurophysiol.* 58, 342–358. doi: 10.1152/jn.1987.58.2.342
- LeResche, L. (1997). Epidemiology of temporomandibular disorders: implications for the investigation of etiologic factors. *Crit. Rev. Oral Biol. Med.* 8, 291–305. doi: 10.1177/10454411970080030401
- Lobbezoo, F., van Selms, M. K., and Naeije, M. (2006). Masticatory muscle pain and disordered jaw motor behaviour: literature review over the past decade. *Arch. Oral Biol.* 51, 713–720. doi: 10.1016/j.archoralbio.2006.03.012
- Loeb, G. E., and Ghez, C. (2000). “The motor unit and Muscle action,” in *Principles of Neural Science*, eds E. R. Kandel, J. Schwartz, and T. M. Jessell, (New York, NY: McGraw-Hill Companies Inc.).
- López-Frías, F. J., Castellanos-Cosano, L., Martín-González, J., Llamas-Carreras, J. M., and Segura-Egea, J. J. (2012). Clinical measurement of tooth wear: tooth wear indices. *J. Clin. Exp. Dent.* 4, e48–e53. doi: 10.4317/jced.50592
- Löwe, B., Decker, O., Müller, S., Brähler, E., Schellberg, D., Herzog, W., et al. (2008). Validation and standardization of the generalized anxiety disorder screener (GAD-7) in the general population. *Med. Care* 46, 266–274. doi: 10.1097/MLR.0b013e31816d0d93
- Lu, S., Baad-Hansen, L., Zhang, Z., and Svensson, P. (2013). One hour jaw muscle training does not evoke plasticity in the corticomotor control of the masseter muscle. *Arch. Oral Biol.* 58, 1483–1490. doi: 10.1016/j.archoralbio.2013.06.012
- Lund, J. P. (1991). Mastication and its control by the brain stem. *Crit. Rev. Oral Biol. Med.* 2, 33–64. doi: 10.1177/10454411910020010401
- Lund, J. P., Donga, R., Widmer, C. G., and Stohler, C. S. (1991). The pain-adaptation model: a discussion of the relationship between chronic musculoskeletal pain and motor activity. *Can. J. Physiol. Pharmacol.* 69, 683–694. doi: 10.1139/y91-102
- Lund, J. P., and Kolta, A. (2006). Generation of the central masticatory pattern and its modification by sensory feedback. *Dysphagia* 21, 167–174. doi: 10.1007/s00455-006-9027-6
- Macfarlane, T. V., Blinkhorn, A. S., Davies, R. M., Kincey, J., and Worthington, H. V. (2004). Predictors of outcome for orofacial pain in the general population: a four-year follow-up study. *J. Dent. Res.* 83, 712–717. doi: 10.1177/154405910408300911
- Macfarlane, T. V., Blinkhorn, A. S., Davies, R. M., Ryan, P., Worthington, H. V., and Macfarlane, G. J. (2002). Orofacial pain: just another chronic pain?

- Results from a population-based survey. *Pain* 99, 453–458. doi: 10.1016/s0304-3959(02)00181-1
- Macfarlane, T. V., Glenny, A. M., and Worthington, H. V. (2001). Systematic review of population-based epidemiological studies of oro-facial pain. *J. Dent.* 29, 451–467. doi: 10.1016/s0300-5712(01)00041-0
- McComas, A. J. (1998). Oro-facial muscles: internal structure, function and ageing. *Gerodontology* 15, 3–14. doi: 10.1111/j.1741-2358.1998.00003.x
- Miles, T. S. (2004). "Mastication," in *Clinical Oral Physiology*, eds T. S. Miles, N. Birgitte, and P. Svensson, (Copenhagen: Quintessence Publishing Company Ltd.).
- Minami, I., Akhter, R., Albersen, I., Burger, C., Whittle, T., Lobbezoo, F., et al. (2013). Masseter motor unit recruitment is altered in experimental jaw muscle pain. *J. Dent. Res.* 92, 143–148. doi: 10.1177/0022034512470832
- Mohn, C., Vassend, O., and Knardahl, S. (2011). Psychophysiological responses to pain stimulation and cognitive tasks in female temporomandibular disorder patients. *Scand. J. Pain* 2, 72–82. doi: 10.1016/j.sjpain.2010.12.001
- Morimoto, T., Inoue, T., Masuda, Y., and Nagashima, T. (1989). Sensory components facilitating jaw-closing muscle activities in the rabbit. *Exp. Brain Res.* 76, 424–440.
- Murray, G. M., and Peck, C. C. (2007). Orofacial pain and jaw muscle activity: a new model. *J. Orofac. Pain* 21, 263–278.
- Nash, P. G., Macefield, V. G., Klineberg, I. J., Gustin, S. M., Murray, G. M., and Henderson, L. A. (2010). Changes in human primary motor cortex activity during acute cutaneous and muscle orofacial pain. *J. Orofac. Pain* 24, 379–390.
- Nicholas, M. K. (2007). The pain self-efficacy questionnaire: taking pain into account. *Eur. J. Pain* 11, 153–163. doi: 10.1016/j.ejpain.2005.12.008
- Nordin, M., and Nordin, S. (2013). Psychometric evaluation and normative data of the Swedish version of the 10-item perceived stress scale. *Scand. J. Psychol.* 54, 502–507. doi: 10.1111/sjop.12071
- Nozaki, S., Iriki, A., and Nakamura, Y. (1986). Localization of central rhythm generator involved in cortically induced rhythmical masticatory jaw-opening movement in the guinea pig. *J. Neurophysiol.* 55, 806–825. doi: 10.1152/jn.1986.55.4.806
- Ohrbach, R., Bair, E., Fillingim, R. B., Gonzalez, Y., Gordon, S. M., Lim, P. F., et al. (2013). Clinical orofacial characteristics associated with risk of first-onset TMD: the OPERA prospective cohort study. *J. Pain* 14(12 Suppl.), T33–T50. doi: 10.1016/j.jpain.2013.07.018
- Ohrbach, R., Fillingim, R. B., Mulkey, F., Gonzalez, Y., Gordon, S., Gremillion, H., et al. (2011). Clinical findings and pain symptoms as potential risk factors for chronic TMD: descriptive data and empirically identified domains from the OPERA case-control study. *J. Pain* 12(11 Suppl.), T27–T45. doi: 10.1016/j.jpain.2011.09.001
- Parker, M. W. (1990). A dynamic model of etiology in temporomandibular disorders. *J. Am. Dent. Assoc.* 120, 283–290. doi: 10.14219/jada.archive.1990.0045
- Sae-Lee, D., Whittle, T., Forte, A. R., Peck, C. C., Byth, K., Sessle, B. J., et al. (2008a). Effects of experimental pain on jaw muscle activity during goal-directed jaw movements in humans. *Exp. Brain Res.* 189, 451–462. doi: 10.1007/s00221-008-1439-0
- Sae-Lee, D., Whittle, T., Peck, C. C., Forte, A. R., Klineberg, I. J., and Murray, G. M. (2008b). Experimental jaw-muscle pain has a differential effect on different jaw movement tasks. *J. Orofac. Pain* 22, 15–29.
- Schiffman, E., Ohrbach, R., Truelove, E., Look, J., Anderson, G., Goulet, J. P., et al. (2014). Diagnostic criteria for temporomandibular disorders (DC/TMD) for clinical and research applications: recommendations of the international RDC/TMD consortium network* and orofacial pain special interest group†. *J. Oral Facial Pain Headache* 28, 6–27. doi: 10.11607/jop.1151
- Stohler, C. S. (1999). Craniofacial pain and motor function: pathogenesis, clinical correlates, and implications. *Crit. Rev. Oral Biol. Med.* 10, 504–518. doi: 10.1177/10454411990100040601
- Stohler, C. S., Ashton-Miller, J. A., and Carlson, D. S. (1988). The effects of pain from the mandibular joint and muscles on masticatory motor behaviour in man. *Arch. Oral Biol.* 33, 175–182. doi: 10.1016/0003-9969(88)90042-8
- Svensson, K. G., and Trulsson, M. (2009). Regulation of bite force increase during splitting of food. *Eur. J. Oral Sci.* 117, 704–710. doi: 10.1111/j.1600-0722.2009.00691.x
- Svensson, K. G., and Trulsson, M. (2011). Impaired force control during food holding and biting in subjects with tooth- or implant-supported fixed prostheses. *J. Clin. Periodontol.* 38, 1137–1146. doi: 10.1111/j.1600-051X.2011.01781.x
- Svensson, P., and Graven-Nielsen, T. (2001). Craniofacial muscle pain: review of mechanisms and clinical manifestations. *J. Orofac. Pain* 15, 117–145.
- Svensson, P., Graven-Nielsen, T., Matre, D., and Arendt-Nielsen, L. (1998). Experimental muscle pain does not cause long-lasting increases in resting electromyographic activity. *Muscle Nerve* 21, 1382–1389. doi: 10.1002/(sici)1097-4598(199811)21:11<1382::aid-mus4>3.0.co;2-5
- Svensson, P., Houe, L., and Arendt-Nielsen, L. (1997). Bilateral experimental muscle pain changes electromyographic activity of human jaw-closing muscles during mastication. *Exp. Brain Res.* 116, 182–185. doi: 10.1007/pl00005738
- Svensson, P., and Kumar, A. (2016). Assessment of risk factors for oro-facial pain and recent developments in classification: implications for management. *J. Oral Rehabil.* 43, 977–989. doi: 10.1111/joor.12447
- Trulsson, M. (2006). Sensory-motor function of human periodontal mechanoreceptors. *J. Oral Rehabil.* 33, 262–273. doi: 10.1111/j.1365-2842.2006.01629.x
- Trulsson, M., and Gunne, H. S. (1998). Food-holding and -biting behavior in human subjects lacking periodontal receptors. *J. Dent. Res.* 77, 574–582. doi: 10.1177/00220345980770041001
- Trulsson, M., and Johansson, R. S. (1996a). Encoding of tooth loads by human periodontal afferents and their role in jaw motor control. *Prog. Neurobiol.* 49, 267–284. doi: 10.1016/s0301-0082(96)00016-0
- Trulsson, M., and Johansson, R. S. (1996b). Forces applied by the incisors and roles of periodontal afferents during food-holding and -biting tasks. *Exp. Brain Res.* 107, 486–496.
- Trulsson, M., and Johansson, R. S. (2002). Orofacial mechanoreceptors in humans: encoding characteristics and responses during natural orofacial behaviors. *Behav. Brain Res.* 135, 27–33. doi: 10.1016/s0166-4328(02)00151-1
- Türker, K. S. (2002). Reflex control of human jaw muscles. *Crit. Rev. Oral Biol. Med.* 13, 85–104. doi: 10.1177/154411130201300109
- Turker, K. S., and Jenkins, M. (2000). Reflex responses induced by tooth unloading. *J. Neurophysiol.* 84, 1088–1092. doi: 10.1152/jn.2000.84.2.1088
- Turner, J. A., Ersek, M., and Kemp, C. (2005). Self-efficacy for managing pain is associated with disability, depression, and pain coping among retirement community residents with chronic pain. *J. Pain* 6, 471–479. doi: 10.1016/j.jpain.2005.02.011
- van der Bilt, A., Engelen, L., Pereira, L. J., van der Glas, H. W., and Abbink, J. H. (2006). Oral physiology and mastication. *Physiol. Behav.* 89, 22–27.
- Von Korff, M., Ormel, J., Keefe, F. J., and Dworkin, S. F. (1992). Grading the severity of chronic pain. *Pain* 50, 133–149. doi: 10.1016/0304-3959(92)90154-4
- Woolf, C. J., and Salter, M. W. (2000). Neuronal plasticity: increasing the gain in pain. *Science* 288, 1765–1769.
- Woolf, C. J., and Walters, E. T. (1991). Common patterns of plasticity contributing to nociceptive sensitization in mammals and Aplysia. *Trends Neurosci.* 14, 74–78. doi: 10.1016/0166-2236(91)90024-o
- Wright, E. F. (2000). Referred craniofacial pain patterns in patients with temporomandibular disorder. *J. Am. Dent. Assoc.* 131, 1307–1315. doi: 10.14219/jada.archive.2000.0384
- Xu, L., Fan, S., Cai, B., Fang, Z., and Jiang, X. (2017). Influence of sustained submaximal clenching fatigue test on electromyographic activity and maximum voluntary bite forces in healthy subjects and patients with temporomandibular disorders. *J. Oral Rehabil.* 44, 340–346. doi: 10.1111/joor.12497
- Zhang, H., Kumar, A., Kothari, M., Luo, X., Trulsson, M., Svensson, K. G., et al. (2016). Can short-term oral fine motor training affect precision of task performance and induce cortical plasticity of the jaw muscles? *Exp. Brain Res.* 234, 1935–1943. doi: 10.1007/s00221-016-4598-4

Conflict of Interest: The authors declare that the research was conducted in the absence of any commercial or financial relationships that could be construed as a potential conflict of interest.

Copyright © 2019 Al Sayegh, Borgwardt, Svensson, Kumar, Grigoriadis and Christidis. This is an open-access article distributed under the terms of the Creative Commons Attribution License (CC BY). The use, distribution or reproduction in other forums is permitted, provided the original author(s) and the copyright owner(s) are credited and that the original publication in this journal is cited, in accordance with accepted academic practice. No use, distribution or reproduction is permitted which does not comply with these terms.



Preceding Administration of Minocycline Suppresses Plastic Changes in Cortical Excitatory Propagation in the Model Rat With Partial Infraorbital Nerve Ligation

Manabu Zama^{1,2}, Satoshi Fujita^{1,3}, Yuka Nakaya^{1,3}, Morio Tonogi^{2,3} and Masayuki Kobayashi^{1,3,4*}

¹ Department of Pharmacology, Nihon University School of Dentistry, Tokyo, Japan, ² Department of Oral and Maxillofacial Surgery, Nihon University School of Dentistry, Tokyo, Japan, ³ Division of Oral and Craniomaxillofacial Research, Dental Research Center, Nihon University School of Dentistry, Tokyo, Japan, ⁴ Molecular Dynamics Imaging Unit, RIKEN Center for Life Science Technologies, Kobe, Japan

OPEN ACCESS

Edited by:

Kazutaka Takahashi,
University of Chicago, United States

Reviewed by:

Angel Nunez,
Autonomous University of
Madrid, Spain
Myeounghoon Cha,
Yonsei University, South Korea
Sascha R. Alles,
University of New Mexico,
United States

*Correspondence:

Masayuki Kobayashi
kobayashi.masayuki@nihon-u.ac.jp

Specialty section:

This article was submitted to
Headache Medicine and Facial Pain,
a section of the journal
Frontiers in Neurology

Received: 21 August 2019

Accepted: 14 October 2019

Published: 05 November 2019

Citation:

Zama M, Fujita S, Nakaya Y, Tonogi M
and Kobayashi M (2019) Preceding
Administration of Minocycline
Suppresses Plastic Changes in
Cortical Excitatory Propagation in the
Model Rat With Partial Infraorbital
Nerve Ligation.
Front. Neurol. 10:1150.
doi: 10.3389/fneur.2019.01150

Neuropathic pain is known to be attributable to the injured nerve, a postoperative problem induced by surgery. The infraorbital nerve (ION), a branch of the trigeminal nerve, innervates to the facial and oral regions and conveys somatosensory information to the central nervous system. The partial ligation of ION (pl-ION) is a method to mimic chronic trigeminal neuropathic pain and behavioral abnormality. To counteract induction of such abnormal pain, the effective pharmacological treatment is desired. Although recent studies have revealed the molecular mechanisms regarding chronic pain, estimation of the effectiveness of the pharmacological treatment has not been well-provided especially in the central nervous system so far. Here we examined whether pl-ION induces plastic changes in the cerebral cortex and investigated effects of minocycline on the cortical plastic changes. We performed the pl-ION to Wistar male rats (4–5 weeks old), and confirmed a mechanical nocifensive behavior in response to the mechanical stimulation with von-Frey filaments. The withdrawal threshold to mechanical stimuli of the whisker pad was decreased 1 day (1 d) after pl-ION, which continued up to 14 d after pl-ION, suggesting that pl-ION model rats presented allodynia and enhanced the response sustained at least for 14 d after pl-ION. Next, cerebrocortical activities were evaluated 3 d after pl-ION (3d-pl-ION) by the optical imaging with a voltages-sensitive dye, RH1691, to quantify the response to electrical stimulation of the whisker pad skin, mandibular molar dental pulp, and mentum skin. Electrical stimulation to the whisker pad skin induced smaller excitation in the primary sensory cortex (S1) of 3d-pl-ION in comparison to that in the sham. In contrast, cerebral cortical responses to the mandibular molar dental pulp and mentum skin stimuli increased both in S1, and the secondary somatosensory and insular oral region (S2/IO) after pl-ION. Administration of minocycline (30 mg/kg/d) from 1 d before to 2 d after pl-ION partially recovered the pl-ION-induced changes in cortical excitation in S1 and S2/IO in 3d-pl-ION. These results suggest that somatosensory and insular cortical excitation is changed by pl-ION, and the preceding injection of minocycline counteracts the plastic changes in the cortical activities.

Keywords: insular cortex, somatosensory cortex, orofacial pain, referred pain, microglia

INTRODUCTION

The trigeminal nerve has three major branches, the ophthalmic, maxillary, and mandibular nerves. The infraorbital nerve (ION) is a branch of the maxillary nerve, which innervates to the middle part of the maxillofacial region including the whisker pad. Partial ligation of ION (pl-ION) induces changes in spontaneous behaviors and responses to mechanical stimulation (1, 2). The animal with pl-ION shows lower threshold for a brisk withdrawal of the head responding to mechanical stimulation of the ipsilateral whisker pad, and allodynia starts from 1 day (1 d) after pl-ION and sustains more than 3 weeks (2). Interestingly, allodynia also occurs in the surrounding region of the pl-ION and in the contralateral whisker pad (2), indicating that ectopic pain occurs in the pl-ION model.

The dorsal part of the insular cortex (IC) around the middle cerebral artery (MCA) and the adjacent secondary somatosensory cortex (S2) receive sensory information from the oral structures including the dental pulp (3, 4) and the periodontal ligament (5, 6). The S2 and IC related to the sensation in the oral structure (S2/IO) project to the limbic structures such as amygdala (7, 8) and lateral hypothalamic area (7). In addition, the recent anatomical studies have demonstrated the descending projections to the trigeminal caudal subnucleus (medullary dorsal horn; Vc), which receives nociceptive inputs from the orofacial structures (9) and transmits these information to the higher brain regions including the parabrachial nucleus and thalamus (10). Therefore, S2/IO is considered to play a key role in nociceptive information processing of the oral structures (11).

Recent studies have demonstrated that disturbance of nociceptive inputs induces plastic changes not only in the peripheral but also in the central nervous system including the cerebral cortex, and such plastic changes in the cortex may be a part of mechanisms underlying the refractory pain (12). Indeed, trigeminal nerve injury causes plastic changes in neural responses of S2/IO. We have demonstrated that 1–2 weeks after transection of the inferior alveolar nerve, a branch of the mandibular nerve, S2/IO shows hyperexcitability responding to electrical stimulation of the upper molar pulp, which is innervated by the maxillary nerve (13). A part of the mechanisms for this plastic change occur in the local circuits of S2/IO. This finding suggests a possibility that hyperexcitability of S2/IO may trigger chronic pain even after recovery of the peripheral nervous system that is directly damaged.

Not a few studies in terms of the injury models of the trigeminal nerve have reported the substances that suppress pain-related behaviors. Activation of microglial cells is considered to be a key process that induces neuropathic pain. A variety of cytokines and neurotrophic factors have been reported to induce neuroplastic changes and central sensitization noted above (14, 15). However, little information is available how these drugs affect on neural activities in the cerebral cortex. Taking that the cortical responses reflect integrated information from the peripheral nerve to the cerebral cortex, clarification of drug effects on cortical responses provides critical information of the mechanisms for suppression of nociception.

Minocycline is one of the microglial inhibitors, and the present study aimed to elucidate the effect of minocycline application to the pl-ION model on hyperexcited cortical activities in S1/2 and IC. We performed an *in vivo* optical imaging with RH1691, a voltage-sensitive dye, under urethane anesthesia. The amplitude of optical signals mediated by the voltage-sensitive dye correlates to the membrane potential and reflects excitatory and inhibitory postsynaptic potentials in real time (16), and thus, we can quantify the spatiotemporal patterns of neural excitation with a high resolution. The findings obtained from this study shed light on a new approach to prevent chronic pain induced by peripheral nerve injury.

MATERIALS AND METHODS

The Animal Experimentation Committee of Nihon University approved the present experiments, which were performed according to the institutional guidelines for the care and use of experimental animals described in the National Institute of Health *Guide for the Care and Use of Laboratory Animals*. All efforts were made to minimize animal suffering and to reduce the number of animals used.

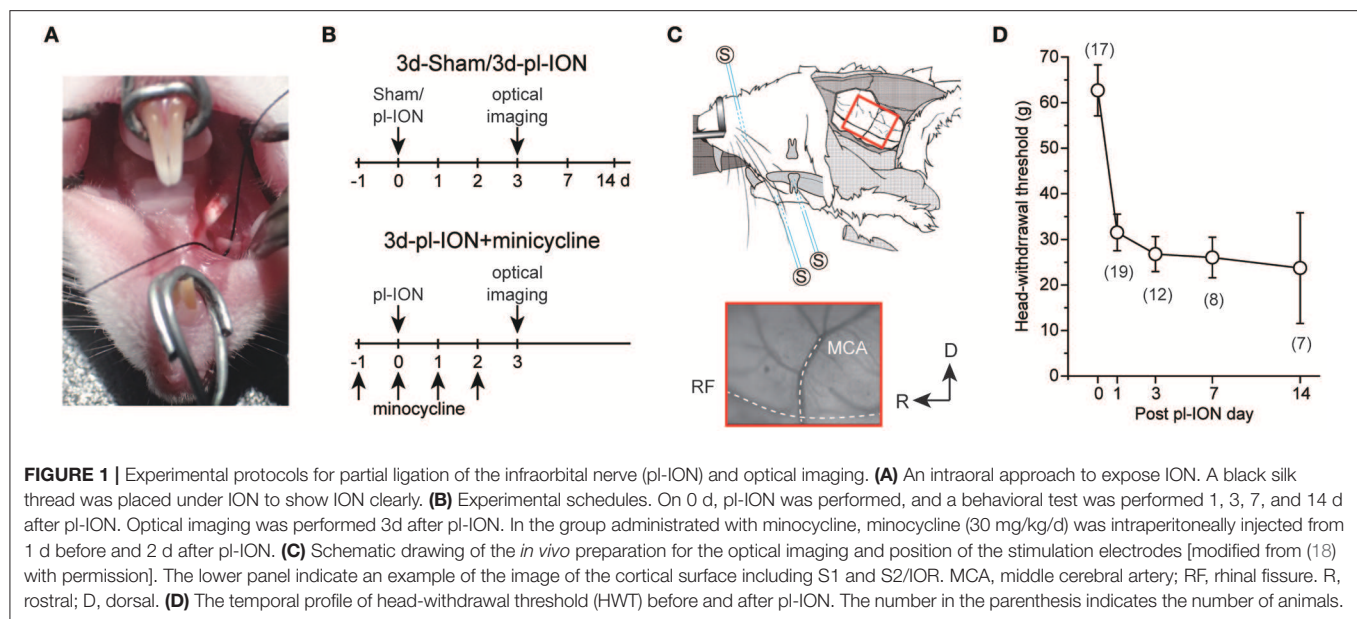
Animals

Four to 5-week-old male Wistar rats (Sankyo Labo, Tokyo, Japan) were anesthetized with intraperitoneal (i.p.) administration of butorphanol (2.5 mg/kg, Meiji Seika Pharma, Tokyo, Japan), medetomidine (0.375 mg/kg, Zenozak, Fukushima, Japan), and midazolam (2.0 mg/kg, Sandoz, Tokyo, Japan) dissolved in saline. A pl-ION was performed via the oral cavity (17). Briefly, gingivobuccal fold was incised to expose the ION (**Figure 1A**). An one-half to one-third thickness of the ION was trapped and ligated tightly by 5–0 silk. The incision was sutured with 5–0 silk. The sham operation was identical except for nerve ligation.

In the model of minocycline treatment, minocycline hydrochloride (30 mg/kg/d, i.p.; Sigma-Aldrich, St Louis, USA) was daily administered from 1 d before pl-ION to 2 d after pl-ION. The 3d-pl-ION received saline injection instead of minocycline.

Behavioral Test

The head-withdrawal threshold (HWT) to mechanical stimulation of the ipsilateral whisker pad skin was measured using von Frey filaments (4, 8, 15, 26, 30, 40, 50, 60, and 100 g of force; North Coast Medical, Morgan Hill, USA) before and 1, 3, 7, and 14 d after pl-ION (**Figure 1B**). The animals were restrained around the trunk with a cloth to calm them and were treated gently during the experiments. Training sessions were performed for at least 7 consecutive days. Each stimulus was applied five times in each series of trials. HWT for mechanical stimulation was determined as the minimum pressure intensity that evoked head-withdrawal behavior in response to more than 3 of 5 stimuli. All behavioral tests were performed under blinded conditions.



In vivo Cerebrocortical Imaging

Optical imaging was performed as previously described (3–6, 13, 19–21). Briefly the sham and pl-ION model rats were anesthetized with urethane (1.5 g/kg, i.p.), and then, atropine methyl bromide was administered (0.5 mg/kg, i.p.). The toe pinch reflex was monitored to check the depth of anesthesia, and additional urethane was administered as needed. Body temperature was kept at 37°C using a rectal probe and heating pad (BWT-100, Bio Research Center, Osaka, Japan). The local anesthetic, lidocaine (2% gel, AstraZeneca, Tokyo, Japan), was administered to the incised skin. The anesthetized rats were fixed to a custom-made stereotaxic snout frame (Narishige, Tokyo, Japan), which was tilted 60° laterally, and a craniotomy was performed (Figure 1C).

RH1691 (1 mg/ml; Optical Imaging, New York) in saline was applied to the cortical surface for 1 h. This application method of RH1691 stains cells between the cortical surface and the deeper layer III. Thus, the optical signals reflect changes in the membrane potential of neurons in layers I–III (3). Changes in RH1691 fluorescence were measured using the CCD camera (MiCAM02, Brainvision, Tokyo, Japan), which was mounted on a stereomicroscope (Leica Microsystems, Wetzlar, Germany). The cortical surface was illuminated through a 632-nm excitation filter and a dichroic mirror using a tungsten-halogen lamp (CLS150XD, Leica Microsystems). The fluorescent emission was captured through an absorption filter ($\lambda > 650$ -nm longpass, Andover, Salem, MA). The size and resolution of the image captured with the CCD camera was $6.4 \times 4.8 \text{ mm}^2$ and 184×124 pixels, respectively.

To remove signals due to acute bleaching of the dye, values without stimuli were subtracted from each recording with stimulation. The sampling interval was 4 ms (250 Hz), and the acquisition time was 500 ms, which was mostly longer than 90–10% decay time of optical signals responding to the stimulation.

Forty consecutive images were averaged to improve signal to noise ratio.

Stimulation of the Skin and Dental Pulp

To quantify the cortical excitation responding to electrical stimulation of the regions innervated by the maxillary and mandibular nerves, we inserted bipolar electrodes, which were made from enamel-coated copper wire (diameter = 80 μm), into the whisker pad skin, mandibular first molar pulp (Figure 1C), and mentum skin (3). Five rectangular voltage pulses (5 V, 100- μs duration, 20 ms interstimulus interval) were applied by a stimulator (STG2008, Multi-Channel Systems, Reutlingen, Germany) at 0.05 Hz to obtain stable cortical responses.

Data Analysis

The optical imaging data were processed and analyzed using Brain Vision Analyzer software (Brainvision, Tokyo, Japan). Changes in the intensity of fluorescence (ΔF) of each pixel relative to the initial intensity of fluorescence (F) were calculated ($\Delta F/F$), and the ratio was processed with a spatial filter (9×9 pixels). A significant response was defined as a signal exceeding seven times the SD of the baseline noise, as previously described (3). Images were aligned across multiple rats using the rhinal fissure and MCA as landmarks. In a part of animals, the rhinal fissure and the MCA could not be aligned with the other animals due to angioplasty; therefore, we excluded the results obtained from these animals. We estimated the spatial profiles of excitation using the initial and maximum responses. The initial response was obtained by outlining the excitation evoked in the first frame that exhibited a significant increase in the optical signal. The maximum response was defined as the outline of the excitatory response in the frame with the maximum amplitude of the optical signal in the center of the initial response. We defined the peak amplitude at the maximum amplitude of an optical response at the point of the initial response.

Statistics

The data are expressed as the mean \pm SEM. Student's *t*-test was used in the analyses. In multiple comparisons, we applied the Bonferroni correction with a Bonferroni-corrected probability value of $P < 0.016$ considered statistically significant.

RESULTS

Temporal Changes in HWT of pl-ION Models

Head-withdrawal reflex elicited by mechanical stimulation using von Frey filaments was examined to evaluate nociceptive threshold in pl-ION models. HWT of nociceptive responses to the application of von Frey filaments showed a significant decrease 1–14 d after pl-ION in comparison to that before pl-ION, indicating the development of mechanical hyperalgesia (Figure 1D). Clinically, it is considered that treatments of neuropathic pain are more effective in the earlier period, and thus, we focused on the profile 3 d after pl-ION in the following analyses.

Cortical Responses to Electrical Stimulation of the Whisker Pad Skin

ION innervates to the whisker pad skin, and pl-ION injured a part of ION. To examine the effect of pl-ION on the cortical activities, we first stimulated the whisker pad skin using a bipolar electrode.

The responses were consistently observed in the barrel field that involves both S1 and S2 responding to electrical stimuli at 5 V (Figures 2A,B) as previously reported (3, 22). The excitation in S1 and S2 frequently expanded beyond the field of view, and thus we quantified only the amplitude of excitation in the initially evoked response region. Because of the difficulty in identifying the border between S1 and S2, we quantified the amplitude in the initial region of excitation as the representative amplitude in S1/S2. For the comparison to the excited regions responding to whisker pad skin stimulation, we first imaged IC around MCA, which corresponds to IOR, and then moved the field of view dorsally to image the barrel cortex.

The peak amplitudes of cortical excitation in S1/S2 of 3d-Sham were $0.89 \pm 0.08\%$ ($N = 18$). Cortical excitation 3 d after pl-ION was significantly reduced to $0.60 \pm 0.07\%$ ($N = 13$; $P < 0.016$, Student's *t*-test with Bonferroni correction; Figure 2C). There was little difference in the evoked S1/S2 regions between 3d-Sham and 3d-pl-ION as shown in Figure 2D. These results suggest that pl-ION decreases somatosensory sensation 3d after the treatment.

Cortical Responses to Electrical Stimulation of the Mandibular Molar Pulp

The mandibular first molar pulp is innervated by the inferior alveolar nerve, a branch of the mandibular nerve, which is adjacent to the maxillary nerve but is not injured in the present experimental condition. To test whether pl-ION induces ectopic pain as previously reported in similar nerve injury models

(13, 23), we examined the profiles of cortical responses to the mandibular molar pulp stimulation.

The initial responses to electrical stimulation of the mandibular molar pulp were detected in two cortical regions: the rostroventral part of S1 and dorsocaudal part in reference to the cross point of the rhinal fissure and MCA (Figures 3A,B). The latter corresponds to S2/IOF as previously we reported (3, 4). Excitation spread to the surrounding cortical regions in a concentric manner. Similar to the case of the whisker pad skin stimulation, we stimulated the molar pulps at 5 V because the responses in S1 and S2/IOF was consistently observed at 5 V (3).

In 3d-Sham, the peak amplitudes of cortical excitation in S1 and S2/IOF were $0.27 \pm 0.05\%$ ($N = 13$) and $0.21 \pm 0.04\%$ ($N = 13$), respectively. Cortical excitation 3 d after pl-ION was facilitated in both S1 and S2/IOF (Figure 3E). In 3d-pl-ION, the peak amplitude of cortical excitation in S1 was significantly larger than that in 3d-Sham ($0.54 \pm 0.08\%$, $N = 13$; $P < 0.016$, Student's *t*-test with Bonferroni correction). Similarly, S2/IOF showed larger cortical excitation in 3d-pl-ION than that of the Sham ($0.55 \pm 0.06\%$, $N = 13$; $P < 0.001$, Student's *t*-test with Bonferroni correction). These results suggest that ectopic pain occurs in 3d-pl-ION.

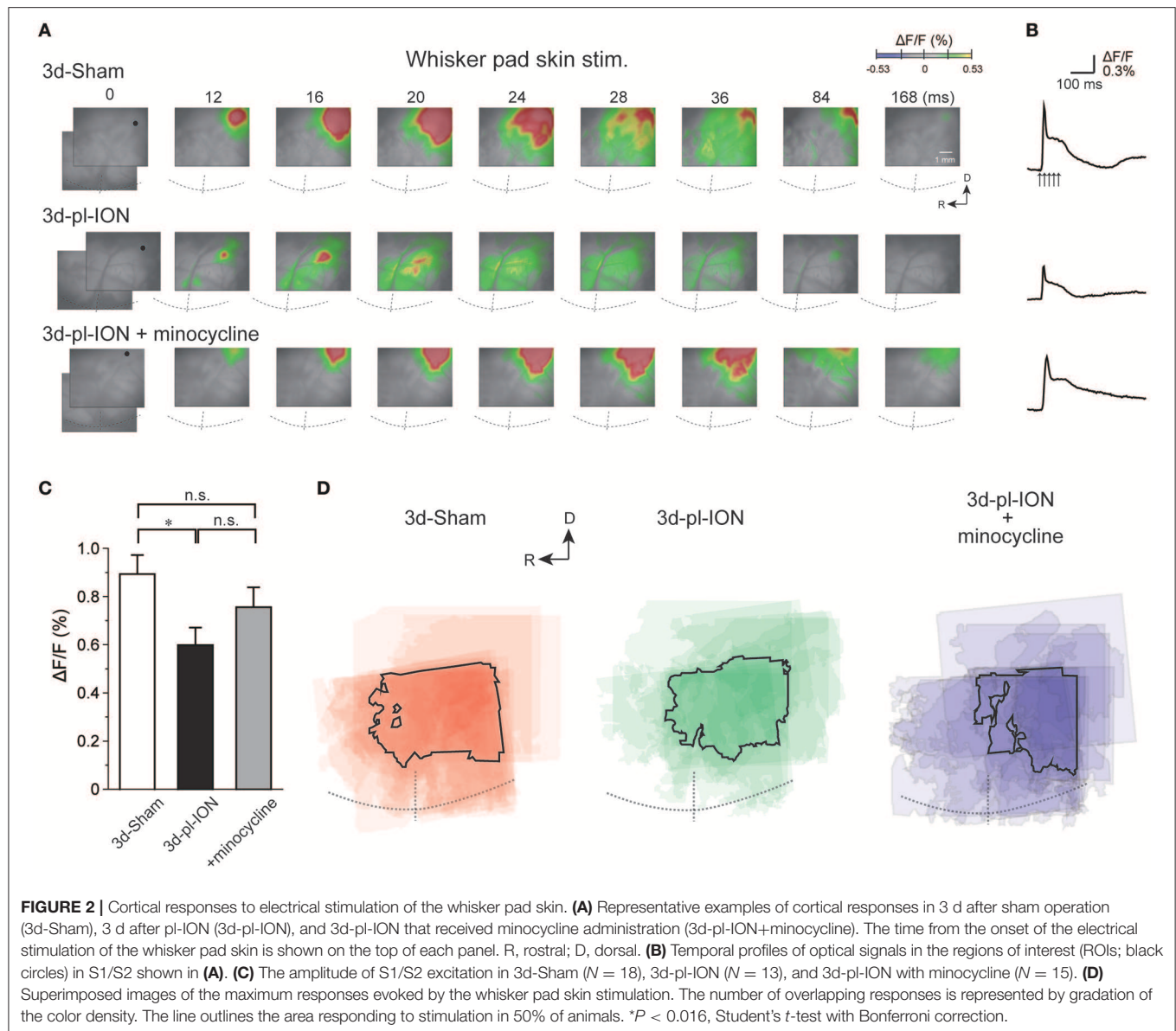
Cortical Responses to Electrical Stimulation of the Mentum Skin

The skin is consistently stimulated, whereas the dental pulps are protected from mechanical stimulation by the dentin and enamel. These differences might cause a distinct effect of pl-ION on evoked cortical responses between the skin and dental pulps, although stimulation of the dental pulps by the bipolar electrodes has an advantage to restrict the stimulated region. We, therefore, examined the cortical responses to stimulating the mentum skin, which is innervated by the mental nerve, a branch of the mandibular nerve.

In 3d-Sham, the peak amplitudes of cortical excitation in S1 and S2/IOF were $0.36 \pm 0.05\%$ ($N = 7$) and $0.17 \pm 0.07\%$ ($N = 7$), respectively. Cortical excitation 3 d after pl-ION was facilitated in both S1 and S2/IOF (Figures 3C,D,F). In 3d-pl-ION, the peak amplitude of cortical excitation in S1 was significantly larger than that in 3d-Sham ($0.59 \pm 0.04\%$, $N = 15$; $P < 0.016$, Student's *t*-test with Bonferroni correction). Similarly, S2/IOF in 3d-pl-ION showed larger cortical responses to the mentum skin stimulation than that in 3d-Sham ($0.46 \pm 0.05\%$, $N = 15$; $P < 0.001$, Student's *t*-test with Bonferroni correction). These results suggest ectopic pain occurs 3d-pl-ION that not only in the dental pulp but also in the skin.

Minocycline Partially Recovers Abnormal Cortical Responses to Electrical Stimulation of the Orofacial Regions

In the experiment of whisker pad stimulation, administration of minocycline (30 mg/kg; i.p.) once a day from a day before and 0, 1, and 2 d after pl-ION (Figure 1B) tended to recover pl-ION-induced change in the amplitude of the cortical excitation in S1/S2 to 3d-Sham though the difference was not significant ($0.76 \pm 0.08\%$, $N = 15$; $P = 0.17$, Student's *t*-test



with Bonferroni correction; **Figure 2**). Indeed, no significant difference was detected in the comparison to 3d-Sham and to 3d-pl-ION with minocycline ($P = 0.24$, Student's t -test with Bonferroni correction).

On the other hand, minocycline decreased pl-ION-induced hyperexcitation of cortical responses to mandibular molar pulp and mentum skin stimulation (**Figure 3**). In minocycline-administered animals, mandibular molar pulp stimulation induced comparable cortical excitation in S1 compared to that of 3d-Sham ($0.38 \pm 0.05\%$, $N = 14$; $P = 0.15$, Student's t -test with Bonferroni correction), though this amplitude was not different from that in 3d-pl-ION ($P = 0.09$, Student's t -test with Bonferroni correction). In S2/IOR, the group of 3d-pl-ION with minocycline showed a tendency of slightly higher amplitude of cortical excitation ($0.36 \pm 0.05\%$, $N = 14$) to that in 3d-Sham

($P = 0.03$, Student's t -test with Bonferroni correction), and this amplitude was significantly smaller than that in 3d-pl-ION ($P < 0.016$, Student's t -test with Bonferroni correction).

In terms of mentum skin stimulation, minocycline suppressed the pl-ION-induced increase of cortical responses in S1 ($0.44 \pm 0.04\%$, $N = 15$; $P < 0.016$; Student's t -test with Bonferroni correction). In addition, there was no significant difference in the amplitude between 3d-Sham and 3d-pl-ION + minocycline ($P = 0.18$, Student's t -test with Bonferroni correction). On the other hand, in the group of 3d-pl-ION with minocycline, excitation in S2/IOR ($0.32 \pm 0.03\%$, $N = 15$) had a tendency of smaller amplitude of cortical excitation to that in 3d-pl-ION ($P = 0.05$, Student's t -test with Bonferroni correction), though this amplitude was significantly larger than that in 3d-Sham ($P < 0.016$, Student's t -test with Bonferroni correction).

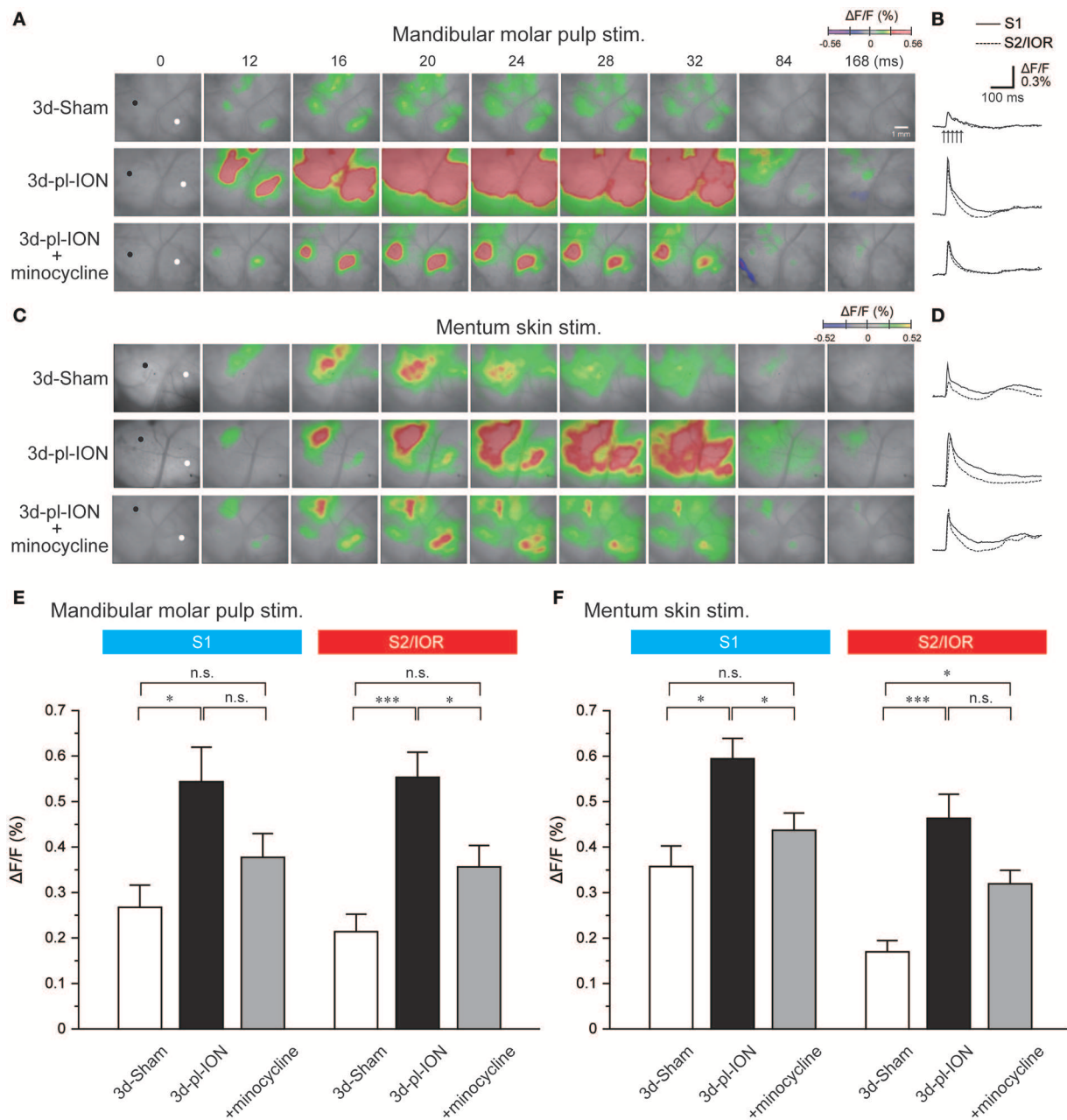
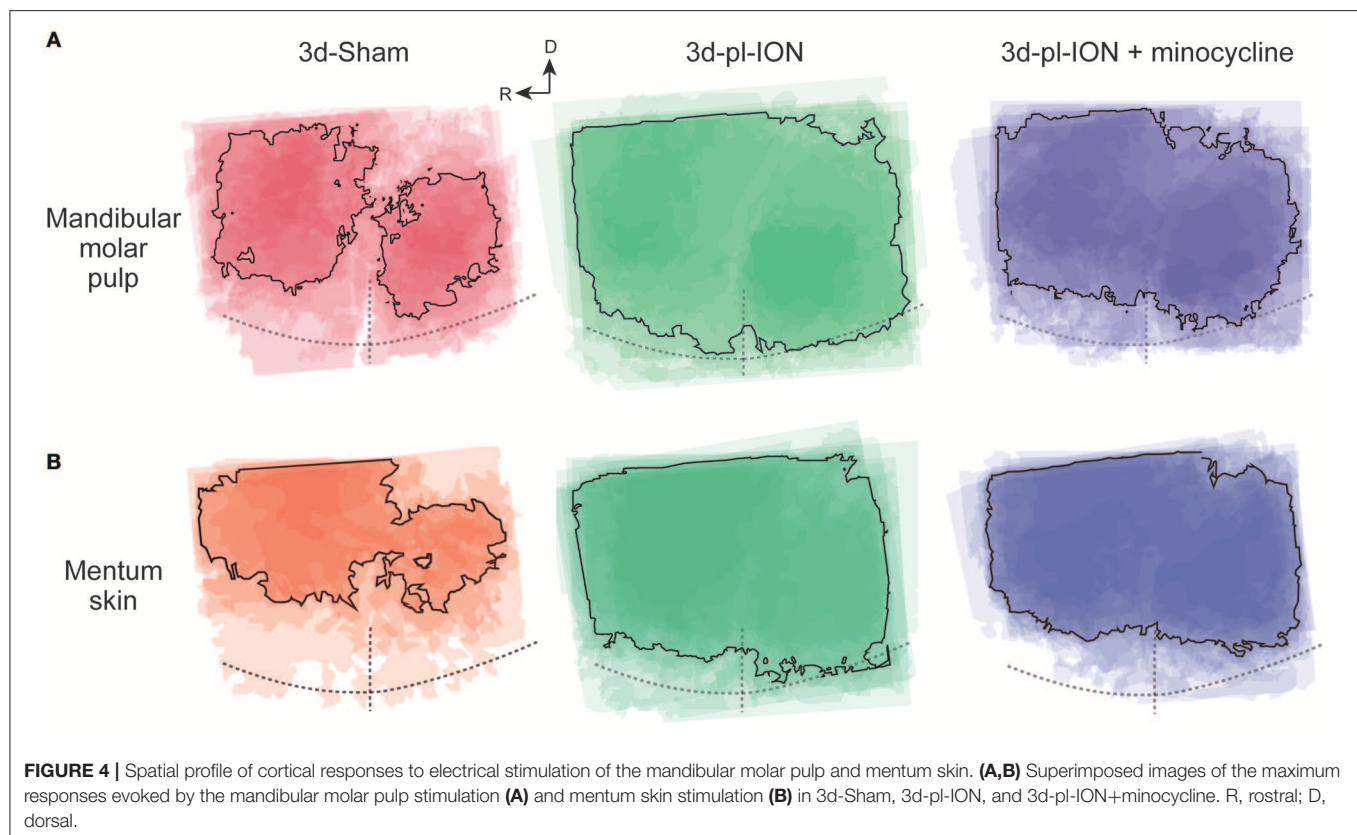


FIGURE 3 | Cortical responses to electrical stimulation of the mandibular molar pulp and mentum skin. **(A)** Representative examples of cortical responses in 3d-Sham, 3d-pl-ION, and 3d-pl-ION+minocycline to mandibular molar pulp stimulation. The time from the onset of the electrical stimulation of the whisker pad skin is shown on the top of each panel. **(B)** Temporal profiles of optical signals in the ROIs: black circles in S1 (thick lines) and white circles in S2/IOR (dotted lines) shown in **(A)**. **(C)** Representative examples of cortical responses in 3d-Sham, 3d-pl-ION, and 3d-pl-ION+minocycline to mentum skin stimulation. **(D)** Temporal profiles of optical signals in the ROIs: black circles in S1 (thick lines) and white circles in S2/IOR (dotted lines) shown in **(C)**. **(E)** The amplitude of S1 (blue) and S2/IOR (red) excitation in 3d-Sham ($N = 13$), 3d-pl-ION ($N = 13$), and 3d-pl-ION with minocycline ($N = 14$) in response to stimulation of the mandibular molar pulp. **(F)** The amplitude of S1 (blue) and S2/IOR (red) excitation in 3d-Sham ($N = 7$), 3d-pl-ION ($N = 15$), and 3d-pl-ION with minocycline ($N = 15$) in response to stimulation of the mentum skin. * $P < 0.016$, *** $P < 0.001$, n.s., not significant (Student's t -test with Bonferroni correction).

These results suggest that minocycline suppresses pl-ION-induced facilitative neural activities, which may be a part of mechanism for inducing ectopic pain.

Effects of pl-ION and Minocycline on the Area of Cortical Excitation

Accompanied with the analysis of the amplitude of cortical excitation responding to orofacial stimulation, the area of



excitation was analyzed in the Sham, pl-ION model, and minocycline-administered model. Although the excited area should be quantified by measuring the pixels whose signals exceeded the threshold, the cortical excitation frequently propagated to the dorsal S1 and S2 especially in 3d-pl-ION (Figure 4). Therefore, the accurate quantification of the excited area could not be done in the present study. Alternatively, the areas of excitation were merged at the timing when the excitation amplitude reached the peak, and we specified the outline of the excited areas overlapped in $\geq 50\%$ animals.

In term of the stimulation of uninjured branches of mandibular nerves, the area analysis showed the similar tendency, i.e., a facilitative effect of pl-ION and a suppressive effect of minocycline in consistent with the analysis of the amplitude (Figure 4). In 3d-pl-ION, the excited area responding to electrical stimulation of the mandibular molar pulp and mentum skin expanded especially toward the dorsal region, which corresponds to S1 and S2. On the other hand, minocycline administration reduced the facilitative expansion of excitatory area by pl-ION (Figure 4), which corresponded to the analysis of the amplitude of the cortical excitation.

DISCUSSION

The present study demonstrated the plastic changes in the spatiotemporal excitation patterns in S1/2 and IC of the model with pl-ION. The response to the whisker pad skin stimulation, which activates regions innervated by injured

ION, was suppressed, whereas S1/2 and IC responses were facilitated to the stimulation of the mandibular molar pulp and mentum skin, which are innervated by adjacent branches of the maxillary nerve including ION. These changes are considered to underlie the ectopic pain induced by pl-ION. Administration of minocycline partially inhibited these cortical changes, suggesting that suppression of microglial activation may be effective to suppress ectopic pain induction.

Hypoexcitation in S1/S2 Responding to Whisker Pad Skin Stimulation

According to our previous study, electrical stimulation of the whisker pad skin in control rats induced excitation rather in the dorsal region compared to the cortical responses to the mandibular molar pulp and mentum skin (3) (Figures 2–4). This area corresponds to the barrel cortex, which is clearly presented by flat mount sections (3). It is known that whisker sensation is processed in both S1 and S2 with the barrel structure in layer IV (24), and the somatotopic map showed these fields symmetrically organized. Therefore, it is difficult to discriminate whether the excited region is located in S1 or S2 by the view of the cortical surface, and we did not discriminate between S1 and S2 excited regions in the experiment of stimulating the whisker pad stimulation. While several recordings showed a clear excitation in S2/ION responding to whisker pad skin stimulation, most cases showed a faint activation in S2/ION, and thus, we did not analyzed the excitation kinetics in S2/ION.

The treatment of pl-ION injures a part of nerve fibers of ION, and therefore, it is reasonable that 3d-pl-ION showed lower excitation in S1/S2 responding to whisker pad stimulation. However, behavioral studies including the present study have demonstrated the hyperexcitability of neural activities in the primary and secondary neurons (25, 26). This seems to contradict to the result of suppressive cortical excitation in 3d-pl-ION. A possible explanation for the discrepancy is that pl-ION increases spontaneous neural activities of the secondary neurons in Vc (27), and these activities may induce continuous excitation of the cortical neurons. Indeed, Latremoliere et al. (14) reported an increase in spontaneous behaviors correlating to pain: an increment of face-grooming activity. If this is the case, the present optical imaging technique cannot estimate the increase in the baseline activities, because we quantified the differences between evoked and baseline signals as mentioned in the Materials and Methods. This discrepancy should be further explored by another method such as *in vivo* Ca^{2+} imaging.

Hyperexcitation in S1 and S2/IOR Responding to Mandibular Dental Pulp and Mentum Skin Stimulation

In contrast to the responses to the whisker pad skin stimulation, mandibular molar pulp stimulation and mentum skin stimulation in pl-ION models induced larger excitatory responses in S1 and S2/IOR than those in controls. Because S1 exhibits a clear somatotopy, the expanded excitatory propagation in S1 is a possible underlying mechanism for the enlargement of the receptive field in the orofacial area and lower capacity to detect the stimulated region. In addition, larger response in S1 may contribute to hypersensitivity responding to mechanical sensation.

On the other hand, S2/IOR is likely to detect nociception rather than touch (11). For example, electrical and mechanical stimuli of the periodontal ligaments induce excitation principally in S2/IOR and S1, respectively (5, 19). According to this idea, larger excitation in S2/IOR may reflect higher sensitivity to nociceptive inputs, which would cause hyperalgesia and allodynia. These results are consistent with behavioral findings of the decrease in HWT reported in this and previous studies (17, 28).

The mechanisms for abnormal pain induced by pl-ION have been explored. Shinoda et al. (17) demonstrated an involvement of P2X_3 receptors expressed in the trigeminal ganglion neurons. Several neurochemical marker expressions including calcitonin gene-related peptide and substance P, and NK1 receptors are also changed in Vc, where the secondary neurons exist (2). In contrast, little information has been obtained with respect to the contribution of higher brain regions to abnormal pain induced by pl-ION. We consider that not only the primary and secondary neurons but also the cerebrocortical neurons and their local circuits may be changed by pl-ION, because the transection model of the inferior alveolar nerve shows hyperexcitation, which accompanies plastic changes in excitatory and inhibitory synaptic transmission in the cortical circuits (13).

Minocycline Relieves Trigeminal Neuropathic Pain

Minocycline is a popular tetracycline, which inhibits protein synthesis of bacteria by a blockade of tRNA binding to ribosomal subunit (30S). In the nervous system, minocycline is known to inhibit activation of microglia, and cytokines and other bioactive substances have been reported to be involved in modulation of microglial activities: interleukin (IL)-1, IL-1 β , IL-6, nitric oxide, prostaglandin, and so on (14, 29, 30).

It has been explored whether minocycline administration relieves neuropathic pain that occurs in the orofacial regions innervated by the trigeminal nerve (14, 23, 31). The inferior alveolar nerve and mental nerve transection model that shows hypersensitivity estimated by mechanical stimulation of the whisker pad show minocycline-dependent suppression of hypersensitivity possibly by inhibiting p38 mitogen-activated protein kinase in microglia of Vc (31). Shibuta et al. (23) demonstrated that minocycline suppresses activation of microglia in parallel to the attenuation of Vc neuronal activities in the pl-ION model showing mechanical allodynia. The present results that minocycline partially recovers cortical activity changes induced by pl-ION corroborate these previous reports.

We consider that inhibition of microglial activation before pl-ION is critical in minocycline-induced recovery of cortical response changes by pl-ION. Our pilot study suggests that the effect of minocycline application started just after ION and sequential application once a day (1 mg/kg) had little effect on cortical responses. This issue should be further examined in the future.

DATA AVAILABILITY STATEMENT

All datasets generated for this study are included in the article.

ETHICS STATEMENT

The animal study was reviewed and approved by The Animal Experimentation Committee of Nihon University.

AUTHOR CONTRIBUTIONS

MK designed the research. MZ performed the research. SF and MZ analyzed the data. MZ, YN, MT, and MK wrote the paper.

FUNDING

This work was supported by the Japan Society for the Promotion of Science KAKENHI (25293379 and 19H03821 to MK, 19K10064 to SF); AMED to MK; and the Sato Fund and Dental Research Center at Nihon University School of Dentistry.

ACKNOWLEDGMENTS

We thank Prof. Noriaki Koshikawa for helpful discussion.

REFERENCES

- Vos BP, Strassman AM, Maciewicz RJ. Behavioral evidence of trigeminal neuropathic pain following chronic constriction injury to the rat's infraorbital nerve. *J Neurosci.* (1994) 14:2708–23. doi: 10.1523/JNEUROSCI.14-05-02708.1994
- Xu M, Aita M, Chavkin C. Partial infraorbital nerve ligation as a model of trigeminal nerve injury in the mouse: behavioral, neural, and glial reactions. *J Pain.* (2008) 9:1036–48. doi: 10.1016/j.jpain.2008.06.006
- Nakamura H, Kato R, Shirakawa T, Koshikawa N, Kobayashi M. Spatiotemporal profiles of dental pulp nociception in rat cerebral cortex: an optical imaging study. *J Comp Neurol.* (2015) 523:1162–74. doi: 10.1002/cne.23692
- Nakamura H, Shirakawa T, Koshikawa N, Kobayashi M. Distinct excitation to pulpal stimuli between somatosensory and insular cortices. *J Dent Res.* (2016) 95:180–7. doi: 10.1177/0022034515611047
- Horinuki E, Shinoda M, Shimizu N, Koshikawa N, Kobayashi M. Orthodontic force facilitates cortical responses to periodontal stimulation. *J Dent Res.* (2015) 94:1158–66. doi: 10.1177/0022034515586543
- Horinuki E, Yamamoto K, Shimizu N, Koshikawa N, Kobayashi M. Sequential changes in cortical excitation during orthodontic treatment. *J Dent Res.* (2016) 95:897905. doi: 10.1177/0022034516641276
- Allen GV, Saper CB, Hurley KM, Cechetto DF. Organization of visceral and limbic connections in the insular cortex of the rat. *J Comp Neurol.* (1991) 311:1–16. doi: 10.1002/cne.903110102
- Shi CJ, Cassell MD. Cascade projections from somatosensory cortex to the rat basolateral amygdala via the parietal insular cortex. *J Comp Neurol.* (1998) 399:469–1. doi: 10.1002/(SICI)1096-9861(19981005)399:4<469::AID-CNE3>3.0.CO;2-#
- Takemura M, Sugiyo S, Moritani M, Kobayashi M, Yonehara N. Mechanisms of orofacial pain control in the central nervous system. *Arch Histol Cytol.* (2006) 69:79–100. doi: 10.1679/aohc.69.79
- Mitchell JL, Silverman MB, Aicher SA. Rat trigeminal lamina I neurons that project to thalamic or parabrachial nuclei contain the mu-opioid receptor. *Neuroscience.* (2004) 128:571–82. doi: 10.1016/j.neuroscience.2004.07.026
- Kobayashi M, Horinuki E. Neural mechanisms of nociception during orthodontic treatment. *J Oral Sci.* (2017) 59:167–71. doi: 10.2334/josnusd.16-0847
- Qiu S, Chen T, Koga K, Guo YY, Xu H, Song Q, et al. An increase in synaptic NMDA receptors in the insular cortex contributes to neuropathic pain. *Sci Signal.* (2013) 6:ra34. doi: 10.1126/scisignal.2003778
- Fujita S, Yamamoto K, Kobayashi M. Trigeminal nerve transection-induced neuroplastic changes in the somatosensory and insular cortices in a rat ectopic pain model. *eNeuro.* (2019) 6:ENEURO.0462-18.2019. doi: 10.1523/ENEURO.0462-18.2019
- Latremoliere A, Mauborgne A, Masson J, Bourgoin S, Kayser V, Hamon M, et al. Differential implication of proinflammatory cytokine interleukin-6 in the development of cephalic versus extracephalic neuropathic pain in rats. *J Neurosci.* (2008) 28:8489–501. doi: 10.1523/JNEUROSCI.2552-08.2008
- Taylor AM, Ribeiro-Da-Silva A. GDNF levels in the lower lip skin in a rat model of trigeminal neuropathic pain: implications for nonpeptidergic fiber reinnervation and parasympathetic sprouting. *Pain.* (2011) 152:1502–10. doi: 10.1016/j.pain.2011.02.035
- Berger T, Borgdorff A, Crochet S, Neubauer FB, Lefort S, Fauvet B, et al. Combined voltage and calcium epifluorescence imaging *in vitro* and *in vivo* reveals subthreshold and suprathreshold dynamics of mouse barrel cortex. *J Neurophysiol.* (2007) 97:3751–62. doi: 10.1152/jn.01178.2006
- Shinoda M, Kawashima K, Ozaki N, Asai H, Nagamine K, Sugiura Y. P2X3 receptor mediates heat hyperalgesia in a rat model of trigeminal neuropathic pain. *J Pain.* (2007) 8:588–97. doi: 10.1016/j.jpain.2007.03.001
- Fujita S, Adachi K, Koshikawa N, Kobayashi M. Spatiotemporal dynamics of excitation in rat insular cortex: intrinsic corticocortical circuit regulates caudal-rostral excitatory propagation from the insular to frontal cortex. *Neuroscience.* (2010) 165:278–92. doi: 10.1016/j.neuroscience.2009.09.073
- Kaneko M, Horinuki E, Shimizu N, Kobayashi M. Physiological profiles of cortical responses to mechanical stimulation of the tooth in the rat: an optical imaging study. *Neuroscience.* (2017) 358:170–80. doi: 10.1016/j.neuroscience.2017.06.042
- Kaneko M, Fujita S, Shimizu N, Motoyoshi M, Kobayashi M. Experimental tooth movement temporally changes neural excitation and topographical map in rat somatosensory cortex. *Brain Res.* (2018) 1698:62–9. doi: 10.1016/j.brainres.2018.06.022
- Zama M, Hara Y, Fujita S, Kaneko T, Kobayashi M. Somatotopic organization and temporal characteristics of cerebrocortical excitation in response to nasal mucosa stimulation with and without an odor in the rat: an optical imaging study. *Neuroscience.* (2018) 377:77–86. doi: 10.1016/j.neuroscience.2018.02.042
- Remple MS, Henry EC, Catania KC. Organization of somatosensory cortex in the laboratory rat (*Rattus norvegicus*): evidence for two lateral areas joined at the representation of the teeth. *J Comp Neurol.* (2003) 467:105–18. doi: 10.1002/cne.10909
- Shibuta K, Suzuki I, Shinoda M, Tsuboi Y, Honda K, Shimizu N, et al. Organization of hyperactive microglial cells in trigeminal spinal subnucleus caudalis and upper cervical spinal cord associated with orofacial neuropathic pain. *Brain Res.* (2012) 1451:74–86. doi: 10.1016/j.brainres.2012.02.023
- Woolsey TA, Van Der Loos H. The structural organization of layer IV in the somatosensory region (SI) of mouse cerebral cortex. The description of a cortical field composed of discrete cytoarchitectonic units. *Brain Res.* (1970) 17:205–42. doi: 10.1016/0006-8993(70)90079-X
- Toyama M, Kudo C, Mukai C, Inoue M, Oyamaguchi A, Hanamoto H, et al. Trigeminal nervous system sensitization by infraorbital nerve injury enhances responses in a migraine model. *Cephalalgia.* (2017) 37:1317–28. doi: 10.1177/0333102416678387
- Zhang Q, Zhu MD, Cao DL, Bai XQ, Gao YJ, Wu XB. Chemokine CXCL13 activates p38 MAPK in the trigeminal ganglion after infraorbital nerve injury. *Inflammation.* (2017) 40:762–9. doi: 10.1007/s10753-017-0520-x
- Martin YB, Malmierca E, Avendano C, Nunez A. Neuronal disinhibition in the trigeminal nucleus caudalis in a model of chronic neuropathic pain. *Eur J Neurosci.* (2010) 32:399–408. doi: 10.1111/j.1460-9568.2010.07302.x
- Kubo A, Shinoda M, Katagiri A, Takeda M, Suzuki T, Asaka J, et al. Oxytocin alleviates orofacial mechanical hypersensitivity associated with infraorbital nerve injury through vasopressin-1A receptors of the rat trigeminal ganglia. *Pain.* (2017) 158:649–59. doi: 10.1097/j.pain.0000000000000808
- Yrjanheikki J, Tikka T, Keinanen R, Goldsteins G, Chan PH, Koistinaho J. A tetracycline derivative, minocycline, reduces inflammation and protects against focal cerebral ischemia with a wide therapeutic window. *Proc Natl Acad Sci USA.* (1999) 96:13496–500. doi: 10.1073/pnas.96.23.13496
- Stirling DP, Koochesfahani KM, Steeves JD, Tetzlaff W. Minocycline as a neuroprotective agent. *Neuroscientist.* (2005) 11:308–22. doi: 10.1177/1073858405275175
- Piao ZG, Cho IH, Park CK, Hong JP, Choi SY, Lee SJ, et al. Activation of glia and microglial p38 MAPK in medullary dorsal horn contributes to tactile hypersensitivity following trigeminal sensory nerve injury. *Pain.* (2006) 121:219–31. doi: 10.1016/j.pain.2005.12.023

Conflict of Interest: The authors declare that the research was conducted in the absence of any commercial or financial relationships that could be construed as a potential conflict of interest.

Copyright © 2019 Zama, Fujita, Nakaya, Tonogi and Kobayashi. This is an open-access article distributed under the terms of the Creative Commons Attribution License (CC BY). The use, distribution or reproduction in other forums is permitted, provided the original author(s) and the copyright owner(s) are credited and that the original publication in this journal is cited, in accordance with accepted academic practice. No use, distribution or reproduction is permitted which does not comply with these terms.



Peripheral and Central Mechanisms of Persistent Orofacial Pain

Masamichi Shinoda[†], Asako Kubo[†], Yoshinori Hayashi and Koichi Iwata*

Department of Physiology, Nihon University School of Dentistry, Tokyo, Japan

OPEN ACCESS

Edited by:

Kazutaka Takahashi,
The University of Chicago,
United States

Reviewed by:

Paul Durham,
Missouri State University,
United States
Jianguo Gu,
The University of Alabama
at Birmingham, United States

Phillip R. Kramer,
Texas A&M University, United States

*Correspondence:

Koichi Iwata
iwata.kouichi@nihon-u.ac.jp

[†] These authors have contributed
equally to this work

Specialty section:

This article was submitted to
Perception Science,
a section of the journal
Frontiers in Neuroscience

Received: 16 August 2019

Accepted: 30 October 2019

Published: 13 November 2019

Citation:

Shinoda M, Kubo A, Hayashi Y
and Iwata K (2019) Peripheral
and Central Mechanisms of Persistent
Oral Pain.
Front. Neurosci. 13:1227.
doi: 10.3389/fnins.2019.01227

Neuroplastic changes in the neuronal networks involving the trigeminal ganglion (TG), trigeminal spinal subnucleus caudalis (Vc), and upper cervical spinal cord (C1/C2) are considered the mechanisms underlying the ectopic orofacial hypersensitivity associated with trigeminal nerve injury or orofacial inflammation. It has been reported that peripheral nerve injury causes injury discharges in the TG neurons, and a barrage of action potentials is generated in TG neurons and conveyed to the Vc and C1/C2 after trigeminal nerve injury. Long after trigeminal nerve injury, various molecules are produced in the TG neurons, and these molecules are released from the soma of TG neurons and are transported to the central and peripheral terminals of TG neurons. These changes within the TG cause neuroplastic changes in TG neurons and they become sensitized. The neuronal activity of TG neurons is further accelerated, and Vc and C1/C2 neurons are also sensitized. In addition to this cascade, non-neuronal glial cells are also involved in the enhancement of the neuronal activity of TG, Vc, and C1/C2 neurons. Satellite glial cells and macrophages are activated in the TG after trigeminal nerve injury and orofacial inflammation. Microglial cells and astrocytes are also activated in the Vc and C1/C2 regions. It is considered that functional interaction between non-neuronal cells and neurons in the TG, Vc, and C1/C2 regions is a key mechanism involved in the enhancement of neuronal excitability after nerve injury or inflammation. In this article, the detailed mechanisms underlying ectopic orofacial hyperalgesia associated with trigeminal nerve injury and orofacial inflammation are addressed.

Keywords: orofacial ectopic pain, trigeminal ganglion, trigeminal spinal subnucleus caudalis and upper cervical spinal cord, satellite cell, macrophage, microglia, astrocyte

INTRODUCTION

Trigeminal nerve injury and orofacial inflammation are known to frequently cause persistent pain that can spread to adjacent orofacial regions innervated by the uninjured trigeminal nerve branches. Peripheral and central mechanisms are considered to be involved in the persistent ectopic orofacial pain associated with trigeminal nerve injury or orofacial inflammation (Imbe et al., 2001).

Abbreviations: ATP, adenosine triphosphate; BDNF, brain-derived neurotrophic factor; CCL2, chemokine C-C motif ligand 2; CGRP, calcitonin gene-related peptide; DRG, dorsal root ganglion; ERK, extracellular signal-regulated kinase; FKN, fractalkine; GFAP, glial fibrillary acidic protein; iNOS, inducible nitric oxide synthase; LIF, leukemia inhibitory factor; MAPK, mitogen-activated protein kinase; Nav, voltage-gated sodium channel; NGF, nerve growth factor; nNOS, neuronal nitric oxide synthase; NOS, nitric oxide synthase; RVM, rostro-ventral medulla; SGC, satellite glial cell; SP, substance P; TG, trigeminal ganglion; TNF, tumor necrosis factor; TNFR, TNF receptor; Vc, trigeminal spinal subnucleus caudalis; Vi, trigeminal subnucleus interpolaris.

Orofacial ectopic pain is defined as pain spreading from injured branch regions to uninjured branch areas following trigeminal nerve injury or orofacial inflammation. Orofacial ectopic persistent pain is sometimes difficult to diagnose and treat. After tooth extraction or tooth-pulp inflammation, ectopic persistent pain occurs in the uninjured and non-inflamed areas of the orofacial regions (Chiang et al., 2011).

Following trigeminal nerve injury, primary afferent neurons are significantly activated, and a barrage of action potentials is generated in TG neurons and conveyed to the central nervous system. Background activity is also augmented in TG neurons, resulting in the increment of baseline activity in the primary afferent neurons. nNOS expression in the sensitized primary afferent neurons accelerates NO synthesis, and NO is released from the sensitized primary afferent neurons. Neuronal excitability in the uninjured trigeminal nerve branches is altered by NO signaling, the injured neurons and increased excitability of uninjured neurons together contribute to persistent pain (Sugiyama et al., 2013). The soma of a primary afferent neuron is known to be tightly surrounded by SGCs in the TG. Connexins are the primary components of gap junctions organized into two hemichannels called connexons and contribute to binding SGCs. Connexin 43 (Cx43), which is the primary gap junction protein, is known to modulate transportation of small molecules between SGCs. Following trigeminal nerve injury, SGC activation via gap junctions composed of Cx43 propagates throughout the TG, resulting in the sensitization of uninjured TG neurons responsible for ectopic orofacial pain (Kaji et al., 2016). The gap between the soma of primary afferent neurons and the SGCs is only 20 nm, and these cells communicate with each other by releasing chemical messengers. Various molecules are released from TG neurons and cause activation of SGCs, and activated SGCs also generate many molecules that are released from SGCs in the TG, leading to acceleration of TG neuronal activity (Chiang et al., 2011).

Non-neuronal cells such as macrophages are accumulated in the TG after trigeminal nerve injury and orofacial inflammation. Two types of macrophages, M1 and M2, are activated and infiltrate in the injured and inflamed sites and the TG. Macrophages release various cytokines and chemokines, and these molecules are involved in the modulation of TG neuronal activity. M1 and M2 are known to be differentially involved in the modulation of inflammation and to have pro- and anti-inflammatory actions, respectively. Therefore, SGCs, macrophages, and TG neurons functionally communicate with each other, resulting in the enhancement of the TG neuronal excitability responsible for ectopic orofacial pain. Long after the acceleration of primary afferent activity, TG neurons are sensitized, and TG neuronal activity is further enhanced. These peripheral mechanisms are considered to be involved in the ectopic orofacial pain associated with trigeminal nerve injury and orofacial inflammation (Ji et al., 2016; Batbold et al., 2017; Iwata et al., 2017).

Orofacial noxious information is sent to the Vi and Vc transition zone (Vi/Vc), Vc, and upper cervical spinal cord (C1/C2) via trigeminal nerve fibers (Okamoto et al., 2009; Chiang et al., 2011; Ren and Dubner, 2011). These nuclei

have different functions in the processing of orofacial noxious information. Neurotransmitters and neuropeptides are released from the central terminals of the primary afferent neurons and affect the excitability of Vi/Vc, Vc, and C1/C2 nociceptive neurons. After trigeminal nerve injury, the Vi/Vc, Vc, and C1/C2 nociceptive neuronal activities are strongly enhanced, and microglial cells are also activated. Microglial cell activation is reportedly caused by ATP binding to P2X₄ receptors in microglial cells (Inoue and Tsuda, 2018). Activated microglial cells release BDNF, which binds to the TrkB receptor expressed in second-order neurons in the spinal dorsal horn, resulting in the neuronal hyperexcitability responsible for ectopic orofacial pain (Chiang et al., 2011). Macrophages are also activated and infiltrate in the Vi/Vc, Vc, and C1/C2 regions following trapezius muscle inflammation. The cleavage of FKN from the central terminals of primary afferents innervating the trapezius muscle was enhanced following trapezius muscle inflammation, and microglia in the Vc and C1/C2 were activated via FKN signaling (Kiyomoto et al., 2013). Furthermore, interleukin-1 beta (IL-1 β) release was accelerated through p38 phosphorylation followed by microglial activation, and the excitability of the Vc and C1/C2 neurons was enhanced via IL-1 β signaling. Trapezius muscle inflammation has been shown to contribute to the hyperexcitability of Vc and C1/C2 neurons receiving inputs from the uninjured orofacial region (Chiang et al., 2011; Kiyomoto et al., 2013; Iwata et al., 2017).

Astrocytes, which are non-neuronal glial cells, are also known to be activated by glutamate uptake with late-onset compared to microglial cells in the Vc. In the central nervous system, these cells also communicate with each other and functionally affect the excitability of Vi/Vc, Vc, and C1/C2 neurons, resulting in the enhancement of the neuronal activity responsible for ectopic orofacial pain (Okada-Ogawa et al., 2009).

It is highly likely that the functional interaction among neurons, immune cells, and glial cells is involved in the enhancement of neuronal excitability in the peripheral and central nervous systems, resulting in the ectopic orofacial pain associated with trigeminal nerve injury and orofacial inflammation. These findings raise the possibility that molecules causing functional changes in neuron–glial interaction following trigeminal nerve injury and orofacial inflammation may be a promising therapeutic target for the treatment of ectopic orofacial pain. In this article, the involvement of functional interaction among TG neurons, immune cells, and glial cells in orofacial pathological pain is reviewed and discussed based on the results of recent animal studies.

PERIPHERAL SENSITIZATION

Satellite Glia–Neuron Communication

Satellite glial cells, which surround the soma of TG neurons, are essential components evoking orofacial pain following nerve injury or inflammation (Hanani et al., 2002; Hanani, 2005; Dublin and Hanani, 2007). Activation of SGCs is characterized by an increase in the expression level of GFAP in SGCs under pathological conditions, whereas this is not observed under

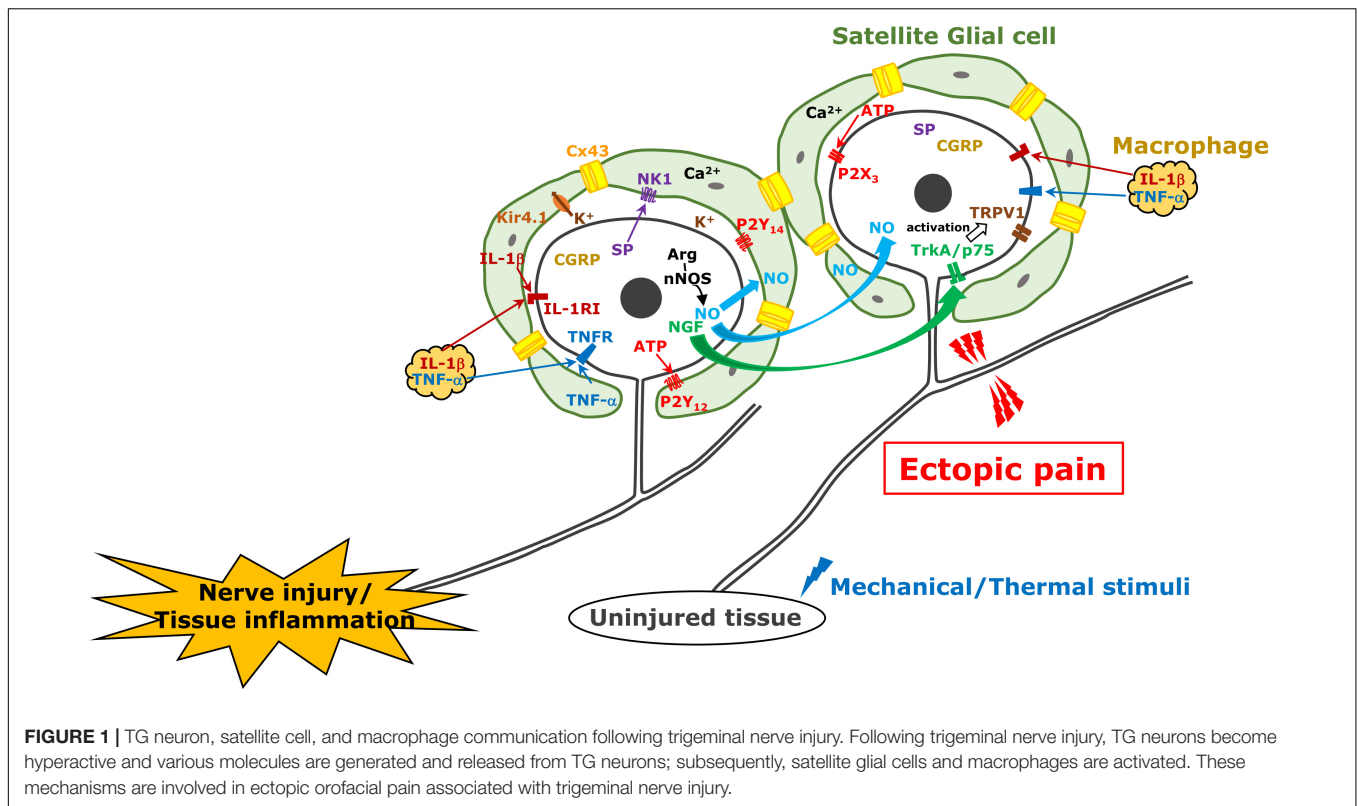
non-pathological conditions. GFAP upregulation is observed in the injured trigeminal nerve branch associated with the development of hyperalgesia (Vit et al., 2006; Katagiri et al., 2012). It is believed that neuropeptide such as SP or CGRP is synthesized in TG neurons by various noxious stimuli and is released from neuronal soma as well as peripheral and central terminals, bind their receptors expressed on SGCs, and GFAP expression in SGCs is upregulated after nerve injury or inflammation (Takeda et al., 2005; Vause et al., 2007; Mikuzuki et al., 2017; Zhang et al., 2019). Activated SGCs could release cytokines such as IL-1 β in the gap between SGCs and the neuronal soma (Takeda et al., 2007; Lin et al., 2019), that cause acceleration of neuronal excitation. In *in vitro* experiment, SP or CGRP application to the cultured trigeminal SGCs provoke to release some cytokines including IL-1 β , TNF α , or IL-6 (Ceruti et al., 2011; Afroz et al., 2019; Zhang et al., 2019). The expression increase of IL-1 β in SGCs upregulates voltage-gated Nav1.7 expression in the TG neurons via the cyclooxygenase-2/prostaglandin E2/E prostanoic acid 2 receptor pathway following temporomandibular joint inflammation (Zhang et al., 2018). It has also been reported in the *in vitro* study that multiple cytokines are released from SGCs by the stimulatory effect of CGRP (Vause and Durham, 2010). Purinergic receptors are also involved in SGCs activation. Increase of P2Y₁₂ receptor expression in SGC upregulates GFAP expression in SGCs and enhances TG neuronal excitability following trigeminal nerve injury (Katagiri et al., 2012). Recent findings from a report show activation of P2Y₁₄ receptor expressing in trigeminal SGCs upregulates GFAP, IL-1 β , and chemokine CCL2 in SGCs via ERK and p38 MAPK activation *in vitro* (Lin et al., 2019), that could cause neuronal excitation (Figure 1).

In TG unlike DRG, neuronal cell bodies are known to be localized in each innervating region (i.e., V1–V3) (Thalakoti et al., 2007). Activation of SGCs surrounding neuronal soma of injured nerve branch spreads into the TG region where the soma of uninjured nerve branches localizes in, that resulting in ectopic orofacial hyperalgesia. The first report was demonstrated in 2007 about neuronal–glial communication through gap junction in the development of sensitization within the TG (Thalakoti et al., 2007). The gap junctions provide direct links and exchange of small molecules and ions between cells under numerous physiological processes. It is believed that this propagation mechanism of activated SGCs is based on gap junctional communication between SGCs. Poulsen et al. (2015) and Feldman-Goriachnik and Hanani (2017) reported that 19–50% of SGCs showed coupling among SGCs around different TG neurons isolated from uninjured mice by dye injection. The former also shows that the dye coupling among SGCs is increased to 44% in neuropathic pain induced by oxaliplatin treatment and the coupling is reversed by gap junction blocker application (Poulsen et al., 2015). Cx43 belongs to the connexin family of proteins in mammals and is not expressed in neurons but in SGCs in the TG (Ohara et al., 2008). The number of Cx43-immunopositive neurons increases in the TG following trigeminal nerve injury in rats, and they are involved in ectopic mechanical allodynia (Kaji et al., 2016). After 3rd branch nerve injury, mechanical hypersensitivity was shown

in the upper eyelid skin and whisker pad skin innervated by an uninjured 1st and 2nd branches, respectively, and this sensitization was sustained for at least 2 weeks associated with increase of Cx43 and GFAP protein expression in SGCs surrounding TG neurons innervating uninjured region. The intra-TG injection of the connexin-mimetic peptide attenuates the ectopic hyperalgesia and expressions of both GFAP and Cx43. The detailed relationship between SGCs coupling with the intercellular passage of neuromediators such as Ca²⁺, inositol triphosphate and ATP, and glial activation remains unclear (Chen et al., 2008), although Ca²⁺ quickly passes through gap junctions between glial cells and provokes intercellular calcium waves, which induce increase of glutamate release, reduction of inwardly rectifying potassium channel 4.1 expression, and activation of small-conductance calcium-activated potassium channel 3, increasing neuronal excitability (Vit et al., 2006, 2008; Giugliano, 2009). Cx43 and SGC activation also contributes to ectopic tooth hypersensitivity following inflammation (Komiya et al., 2018). Increase of Cx43 expression and SGC activation are observed under tooth-pulp inflammation. Increased sensitivity to capsaicin in the adjacent tooth pulp to the inflamed one is associated with upregulation of Cx43 and GFAP expression in the SGCs surrounding the soma of TG innervating these teeth via the IL-1 β mechanism (Figure 1).

Connexin 43 is believed to play a pivotal role in the propagation of SGC activation mentioned above, which is the basis of ectopic pain. However, increase of gap junction between SGCs in primary cultures of mice TG by the chemotherapeutic agent oxaliplatin (third generation platinum analog) treatment is reported to be independent of Cx43 (Poulsen et al., 2015). More recently, it was reported that there were possible couplings between SGCs, neuron–neuron, and neuron–SGC in TG (Spray et al., 2019). They indicate other connexin types besides Cx43 may be candidates for these couplings.

Nitric oxide is a free radical endogenous gas produced by NOS from L-arginine (Snyder, 1992). There are three types of NOS as follows: nNOS in neurons, iNOS in immunological cells, and endothelial NOS in vascular endothelial cells. NO plays a pivotal role as an endothelial-derived relaxing factor. A unique feature of NO is that it spreads quickly through the cell membrane and its *in vivo* half-life is very short (approximately 1 s) because it is rapidly converted to oxidized nitrogen dioxide. Some evidences have also shown that NO acts as a neuromodulator in the nervous system (Fan et al., 2012). NO activates soluble guanylate cyclase to increase intracellular cGMP concentration. cGMP activates cGMP-dependent protein kinase G, which activates and modulates numerous types of target molecules by phosphorylation (Fan et al., 2012). Freeman et al. (2008) demonstrated NO-proton injection into temporomandibular joint elicit increase of phosphorylated ERK and MAPK in neurons and SGCs located in not only V3 but also V1/V2 regions of the ganglion. Upregulation of nNOS is accompanied by abnormal pain following peripheral nerve injury (Sugiyama et al., 2013). Under the 3rd branch of the trigeminal nerve transection, the mechanical hyperalgesia of the whisker pad skin innervated by the 2nd branch of trigeminal nerve was observed over 6 weeks (Iwata et al., 2001). The expression of nNOS was



upregulated in TG neurons innervating the mandibular region, while that in the TG neurons innervating the whisker pad skin did not change even in the presence of mechanical hyperalgesia. The inhibition of nNOS attenuates the mechanical hyperalgesia of the whisker pad skin (Sugiyama et al., 2013) and intra-TG administration of L-arginine causes mechanical hyperalgesia within 2 h after its injection. These results suggest that nNOS expression increases in the neuronal soma of the injured nerve branch; it accelerates NO production and is rapidly diffused into the entire TG, affecting the excitability of uninjured TG neurons. It has also been reported in the *in vitro* study that CGRP in TG neurons is involved in iNOS synthesis in SGCs via MAP kinase signaling (Li et al., 2008; Vause and Durham, 2009). Although it is currently unclear whether NO directly activates TG neurons or indirectly activates via activation of SGCs or macrophages, neuronal NO-protein kinase G signaling can be involved in ectopic orofacial mechanical allodynia (Fan et al., 2012; **Figure 1**).

Macrophage–Neuron Communication

At the site of inflammation, nerve injury, or trauma, many types of immune cells including granulocytes, monocytes, lymphocytes, and macrophages are accumulated and activated to initiate tissue repair. Among them, macrophages are richly populated at the site of a lesion and release mediators such as cytokines, chemokines, and neuropeptides (Lee and Zhang, 2012). Nociceptive neuronal hyperexcitation, which leads to intractable pain hypersensitivity, is induced by various cellular and molecular processes related to peripheral

inflammation, nerve injury, or trauma. Several mediators released from macrophages bind to their receptors on nociceptive primary afferent neurons, which cause nociceptive neuronal hyperexcitation, which leads to intractable inflammatory and neuropathic pain (Ji et al., 2016). For instance, local-infiltrated macrophages release inflammatory mediators such as TNF α , NGF, LIF, IL-1 β , and IL-6 in the inflammatory locus (Zelenka et al., 2005). Moreover, macrophages are also activated by TNF α , which is further conducive to the secretion of inflammatory mediators including IL-1 β and TNF α under inflammatory conditions (Mika et al., 2013). TNFR-1 and TNFR-2 are expressed in small DRG neurons, which are considered to be nociceptive primary afferents, TNF α signaling via TNFR-1 and TNFR-2 induces the sensitization of Nav1.8 through protein kinase C activation followed by the promotion of action potential generation and pain hypersensitivity (Guillouet et al., 2011; Leo et al., 2015). The p75 neurotrophin and TrkA receptors act as NGF receptors in nociceptive primary neurons (Meakin and Shooter, 1992). It has been reported that NGF signaling in nociceptive primary afferent neurons enhances the magnitude of the tetrodotoxin-resistant sodium current, decreases in voltage threshold for Nav1.8 activation, and delayed rectifier potassium currents, which accounts for mechanical hypersensitivity in inflamed tissue (Gold et al., 1996; Zhang et al., 2002; Belkouch et al., 2014). Furthermore, the NGF/TrkA complex is internalized in inflamed tissue and transported to the soma, resulting in upregulated expression of Nav1.8 and transient receptor potential vanilloid 1, which plays a crucial role in heat hypersensitivity (Xue et al., 2007; Shinoda et al., 2011).

IL-6 signaling also activates the Janus kinase/phosphoinositide 3-kinase signaling pathway in DRG neurons, which results in functional upregulation of transient receptor potential vanilloid 1, followed by cancerous pain hypersensitivity (Fang et al., 2015). Prolonged IL-1 β exposure increases DRG neuronal excitability, resulting in pain hypersensitivity by attenuation of the potassium current depending on potassium channel functional alternation *in vitro* (Stemkowski et al., 2015). Small DRG neurons reportedly express the LIF receptor, and pain behaviors are induced by the plantar administration of LIF, while it has been reported that local injection of LIF suppresses inflammatory pain hypersensitivity and IL-1 β (Banner et al., 1998; Spofford et al., 2011; **Figure 1**).

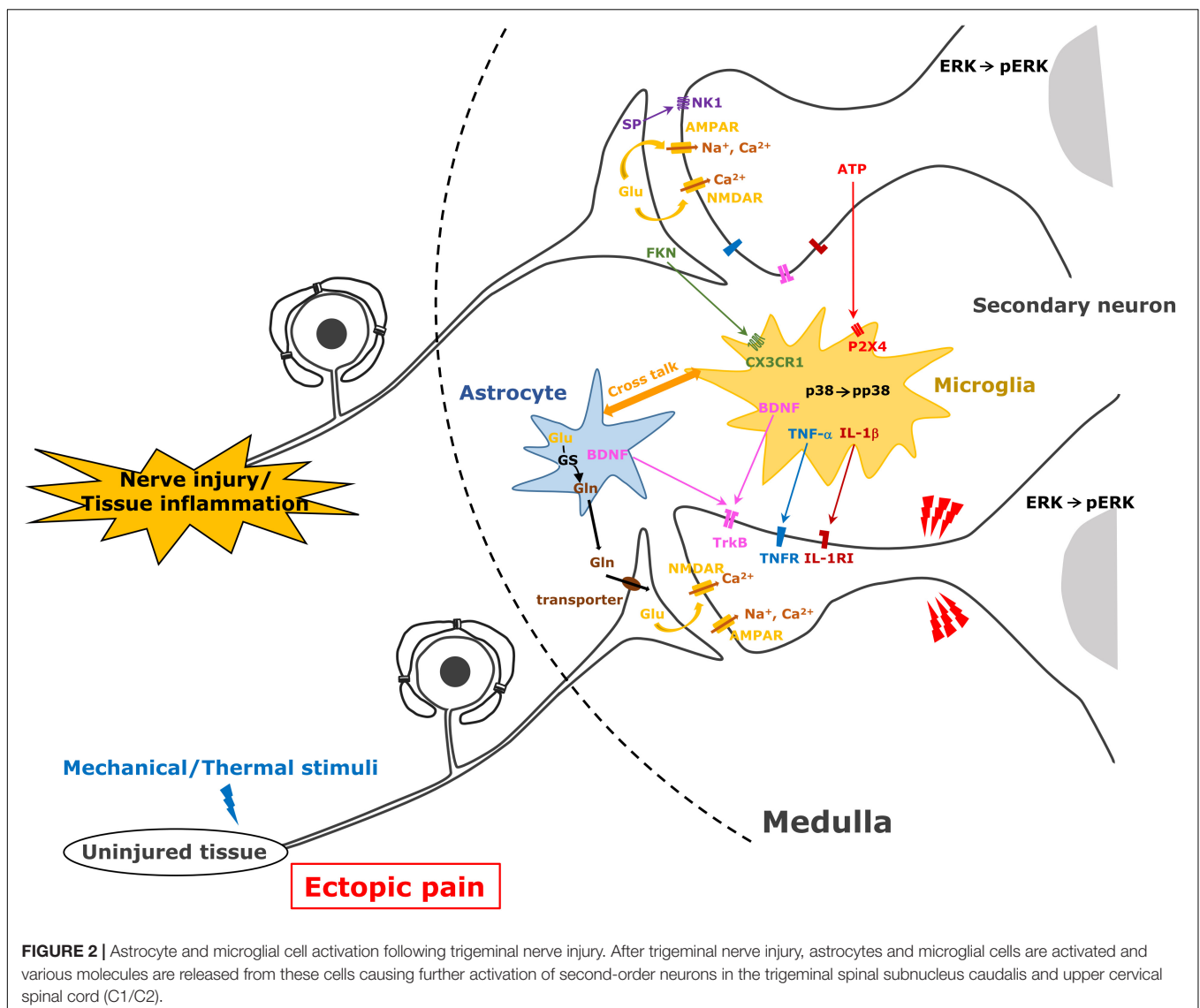
Additionally, activated macrophages do not only infiltrate at the site of inflammation, nerve injury, or trauma but also in the DRG (Ji et al., 2016). Aside from the DRG, the infiltration of non-neuronal immune cells, such as macrophages into the TG, and their activation in the TG are upregulated following orofacial pathogenesis including peripheral trigeminal nerve trauma and orofacial inflammation (Iwata and Shinoda, 2019). Incidentally, most of the macrophages serving as mononuclear phagocytes are supplied from the bone marrow, released from the blood vessels, and migrate into various tissues (Doulatov et al., 2010). Previous studies have indicated that peripheral nerve injury induces increase and activation of resident and proliferated macrophages in the DRG (Lu and Richardson, 1993; Komori et al., 2011; Donegan et al., 2013). The infiltrated and activated macrophages exhibit characteristic morphological structures involving a larger soma and thicker ramifications, which encourages changes in the microenvironment (Harvey et al., 2015). Morphological structural changes indicate their activation (Harvey et al., 2015). Moreover, the migrated macrophages mainly differentiate into two populations that have discrete morphological and functional profiles corresponding to the microenvironment of the migrating sites (Sprangers et al., 2016). Classically activated phenotype called M1 macrophages possess the capacity to secrete numerous pro-inflammatory cytokines and chemokines that participate in the local inflammatory reaction at the early stage. M1 macrophages are activated by interferon- γ , TNF α , or lipopolysaccharides (Laskin et al., 2011; Brown et al., 2012). In contrast, M2 macrophages possess opposite attributes pertaining to the anti-inflammatory response and the advancement of tissue repair and they are activated by IL-4 and IL-13 (Laskin et al., 2011; Franco and Fernandez-Suarez, 2015). IL-4 and IL-13 signaling in M2 macrophages induces the phosphorylation of signal transducer and activator of transcription 6, and the facilitation of signal transducer and activator of transcription 6-mediated gene transcription is involved in the polarization of macrophages (Waqas et al., 2019). M1 and M2 macrophages are activated at and infiltrate the sites of peripheral nerve trauma and inflammation and also at the sensory ganglion (Komori et al., 2011). The infiltrated and activated macrophages that are known to be differentially involved in the modulation of inflammation release numerous chemical mediators such as cytokines and chemokines. Furthermore, functional cell-to-cell communication between macrophages and TG neurons through some chemical

mediators allows for the augmentation of the sensory neuronal excitability in the TG (Iwata et al., 2017). Extended periods of enhancement of sensory neuronal excitability amplify functional cell-to-cell communication leading to neuronal hyperexcitability, resulting in the hyperexcitability of nociceptive neurons in the central nervous system. These plastic changes in cell-to-cell communication in the TG are implicated as a cause of orofacial intractable pain hypersensitivity following orofacial pathogenesis such as trigeminal nerve trauma or inflammation (Chiang et al., 2011). Following peripheral nerve injury, the signaling of CCL2, which is released from the soma of injured neurons via the C-C chemokine receptor type 2 in macrophages, results in macrophage proliferation and its activation in the DRG (Abbadie et al., 2003; Kwon et al., 2015; Liu et al., 2016). Moreover, the increment of CCL2 expression in the soma of TG neurons and the infiltration of macrophages in the TG by peripheral nerve injury never occur under conditions of toll-like receptor 2 deficit, suggesting that the signaling of CCL2 released from injured neurons via toll-like receptor 2 potentiates the abundance of activated macrophage infiltration in the TG after trigeminal nerve trauma (Kim et al., 2011). TNF α in the DRG is considered to derive from macrophages, and the release of TNF α is regulated by intracellular signaling cascades such as ERK and p38 MAPK cascades (Wagner and Myers, 1996; Raghavendra et al., 2003; Wang et al., 2012). Moreover, it has long been known that peripheral nerve injury amplifies SP synthesis in DRG neurons, and synthesized SP was released throughout the DRG (Fu et al., 2013). Some reports have suggested that SP is released into the TG by exocytosis and that it binds the neurokinin 1 receptor expressed in macrophages, which also facilitates TNF α exocytosis from the infiltrated and activated macrophages in the TG through the ERK 1/2 and p38 MAPK signaling pathway (Bardelli et al., 2005; Sun et al., 2008; Matsumoto et al., 2013). Together with these reports, TNF α or SP released by exocytosis from proliferated and activated macrophages following trigeminal nerve injury and enhanced TNF α or SP signaling in the TG lead to TG neuronal hyperexcitability, resulting in orofacial pain hypersensitivity (Batbold et al., 2017; **Figure 1**).

CENTRAL SENSITIZATION OF CENTRAL NERVOUS SYSTEM NEURONS

Orofacial noxious information is sent to the Vc and C1/C2 with the somatotopic organization via primary afferent TG neurons (Noma et al., 2008). The first branch of the trigeminal nerve projects to the ventral portion of the Vc and C1/C2, the third projects to their dorsal part, while the second branch projects to their middle part. Orofacial noxious stimuli cause activation of nociceptive neurons in these areas according to the regions innervated by each branch of the trigeminal nerve (Iwata et al., 1998; Noma et al., 2008). However, the receptive fields of each nociceptive neuron change their innervation areas, expanding the receptive fields beyond the other branch regions after trigeminal nerve injury or orofacial inflammation (Iwata et al., 1999, 2001). Nociceptive neurons in the Vc and

It has also been reported that Vi and Vc transition zone (Vi/Vc) has a unique function for orofacial nociception. Many of nociceptive neurons in this area responded to noxious stimulation of the TMJ (Chichorro et al., 2017). Based on c-Fos studies, the number of c-Fos positive neurons did not increase in this area, whereas that was increased in C1/C2 area following noxious stimulation of the TMJ (Bereiter and Okamoto, 2011). Further, noxious responses of TMJ neurons in Vi/Vc altered according to the gender differences, suggesting that TMJ neurons in this area are involved in gender-related TMJ pain. Furthermore, many Vc/C1 neurons respond to dural stimulation, and some of them also respond to bright light stimulation to the eye (Okamoto et al., 2010; Hitomi et al., 2017a).



Some bright light-responsive neurons in this area increased in their response magnitude following noxious dural stimulation (Hitomi et al., 2017b). It is also known that many neurons responding to corneal stimulation could be found in this area (Kumar et al., 2018). It is highly likely that nociceptive neurons in this area are involved in multiple sensory functions related to dural pain and corneal pain as well orofacial pain.

After trigeminal nerve injury or orofacial inflammation, various molecules are released from the primary afferent terminals, and these molecules contribute to the activation of microglial cells and astrocytes (Okada-Ogawa et al., 2009; Shibuta et al., 2012). ATP and glutamate are essential molecules for the activation of microglial cells and astrocytes, respectively. P2X₄ receptor expression is known to be significantly enhanced in microglial cells in the spinal dorsal horn after sciatic nerve injury (Inoue and Tsuda, 2018). After peripheral nerve injury, the accumulation of ATP released from primary afferent terminals or blood vessels is strongly accelerated in the spinal dorsal horn, and ATP binds to the P2X₄ receptor expressed in the microglial cells (Inoue and Tsuda, 2018). As P2X₄ is a cation permeable purinergic receptor, ATP binding to the P2X₄ receptor causes activation of the intracellular signal cascade (Inoue and Tsuda, 2018). Ca²⁺ influx causes p38 phosphorylation and various proteins are produced. Cleaved FKN from the primary afferent terminals is also known to be involved in the activation of microglial cells after peripheral nerve injury or inflammation. FKN binds to the FKN receptor expressed in the microglial cells involved in microglial cell activation (Kiyomoto et al., 2013). FKN binding to its receptor also causes p38 phosphorylation in microglial cells, resulting in the production of various cytokines (Kiyomoto et al., 2013).

Activated microglial cells produce various pro-inflammatory cytokines (IL-1 β , TNF α , and IL-6), BDNF, and ATP and activated astrocytes produce CCL2, glutamine, and NF- κ B and release these molecules under the trigeminal neuropathic state (Iwata et al., 2011, 2017; Goto et al., 2016). Conversely, after orofacial inflammation, activated microglial cells produce various cytokines and BDNF, and activated astrocytes produce BDNF and glutamine (Chiang et al., 2011). These molecules are considered to be involved in modulation of Vc and C1/C2 nociceptive neuronal activity (Figure 2).

Astrocytes are also activated following trigeminal nerve injury or orofacial inflammation in the Vc and C1/C2 (Okada-Ogawa et al., 2009; Tsuboi et al., 2011). Glutamine-glutamate shuttle in the activated astrocytes is considered a key mechanism involving modulation of neuronal activity in the Vc and C1/C2. After the activation of astrocytes, glutamine is produced by the action of glutamine synthetase in astroglial cells and released from these cells (Chiang et al., 2011; Figure 2). Glutamine is transferred from the primary afferent terminals of the trigeminal nerve via the glutamine transporter, and then glutamate release is accelerated, resulting in the hyperactivation of Vc and C1/C2 neurons. Activated astrocytes also release CCL2 and NF- κ B, and these molecules are also known to be involved in the modulation

of the excitability of Vc and C1/C2 nociceptive neurons (Iwata et al., 2017).

There is a large number of interneurons in the Vc and C1/C2 and many of them are classified as GABAergic or glycinergic interneurons involved in excitability decrease in the vicinity of GABAergic neurons (Okada-Ogawa et al., 2015). After trigeminal nerve injury, the number of inhibitory interneurons in the Vc and C1/C2 regions is reduced, resulting in enhanced excitability of nociceptive neurons (Okada-Ogawa et al., 2015). Furthermore, KCC2 downregulation occurs in Vc and C1/C2 neurons, and the chloride ion is accumulated in nociceptive neurons, resulting in the enhancement of nociceptive neuronal activity by inhibitory interneurons acting as excitatory.

INVOLVEMENT OF DESCENDING MODULATION

Severe inflammation in the orofacial region causes strong activation of the descending pathways as well as ascending noxious pathways (Gu et al., 2011; Okubo et al., 2013). The RVM in the reticular formation is a critical area involved in the descending modulatory system (Lau and Vaughan, 2014; Martins and Tavares, 2017). Three types of neurons, ON cells, OFF cells, and neutral cells, are differentially involved in the modulation of nociceptive neurons in the Vc and C1/C2 (Hitomi et al., 2017a). Many serotonergic neurons that exist in the RVM are involved in the modulation of Vc and C1/C2 nociceptive transmission. The descending system appropriately alters the excitability of nociceptive neurons in the Vc and C1/C2 under normal conditions, contributing to the sensory-discriminative aspect of orofacial pain. After orofacial deep tissue inflammation, microglial cells are activated in the RVM, and the excitability of ON cells further accelerating, and Vc and medullary neuronal activities becoming strongly enhanced, resulting in orofacial hyperalgesia (Wei et al., 2008). These findings suggest that the glial cell activation in RVM is also involved in the modulation of descending inhibitory and excitatory systems associated with orofacial inflammation.

AUTHOR CONTRIBUTIONS

MS, AK, YH, and KI wrote the manuscript. All authors have read and approved the final manuscript.

FUNDING

This study was supported in part by research grants from the Sato and Uemura Funds from the Nihon University School of Dentistry, the Dental Research Center at Nihon University School of Dentistry, and the KAKENHI (Grant-in-Aid for Scientific Research [C] 25462968, 19K10049, 18K09541, and 16K11566).

REFERENCES

- Abbadie, C., Lindia, J. A., Cumiskey, A. M., Peterson, L. B., Mudgett, J. S., Bayne, E. K., et al. (2003). Impaired neuropathic pain responses in mice lacking the chemokine receptor CCR2. *Proc. Natl. Acad. Sci. U.S.A.* 100, 7947–7952. doi: 10.1073/pnas.1331358100
- Afroz, S., Arakaki, R., Iwasa, T., Oshima, M., Hosoki, M., Inoue, M., et al. (2019). CGRP induces differential regulation of cytokines from satellite glial cells in trigeminal ganglia and orofacial nociception. *Int. J. Mol. Sci.* 20:26. doi: 10.3390/ijms20030711
- Banner, L. R., Patterson, P. H., Allchorne, A., Poole, S., and Woolf, C. J. (1998). Leukemia inhibitory factor is an anti-inflammatory and analgesic cytokine. *J. Neurosci.* 18, 5456–5462. doi: 10.1523/jneurosci.18-14-05456.1998
- Bardelli, C., Gunella, G., Varsaldi, F., Balbo, P., Del Boca, E., Bernardone, I. S., et al. (2005). Expression of functional NK1 receptors in human alveolar macrophages: superoxide anion production, cytokine release and involvement of NF-kappaB pathway. *Br. J. Pharmacol.* 145, 385–396. doi: 10.1038/sj.bjp.0706198
- Batbold, D., Shinoda, M., Honda, K., Furukawa, A., Koizumi, M., Akasaka, R., et al. (2017). Macrophages in trigeminal ganglion contribute to ectopic mechanical hypersensitivity following inferior alveolar nerve injury in rats. *J. Neuroinflammation* 14:249. doi: 10.1186/s12974-017-1022-3
- Belkouch, M., Dansereau, M. A., Tetreault, P., Biet, M., Beaudet, N., Dumaine, R., et al. (2014). Functional up-regulation of Nav1.8 sodium channel in Abeta afferent fibers subjected to chronic peripheral inflammation. *J. Neuroinflammation* 11:45. doi: 10.1186/1742-2094-11-45
- Bereiter, D. A., and Okamoto, K. (2011). Neurobiology of estrogen status in deep craniofacial pain. *Int. Rev. Neurobiol.* 97, 251–284. doi: 10.1016/B978-0-12-385198-7.00010-2
- Brown, B. N., Ratner, B. D., Goodman, S. B., Amar, S., and Badylak, S. F. (2012). Macrophage polarization: an opportunity for improved outcomes in biomaterials and regenerative medicine. *Biomaterials* 33, 3792–3802. doi: 10.1016/j.biomaterials.2012.02.034
- Ceruti, S., Villa, G., Fumagalli, M., Colombo, L., Magni, G., Zanardelli, M., et al. (2011). Calcitonin gene-related peptide-mediated enhancement of purinergic neuron/glia communication by the algogenic factor bradykinin in mouse trigeminal ganglia from wild-type and R192Q Cav2.1 Knock-in mice: implications for basic mechanisms of migraine pain. *J. Neurosci.* 31, 3638–3649. doi: 10.1523/JNEUROSCI.6440-10.2011
- Chen, Y., Zhang, X., Wang, C., Li, G., Gu, Y., and Huang, L. Y. (2008). Activation of P2X7 receptors in glial satellite cells reduces pain through downregulation of P2X3 receptors in nociceptive neurons. *Proc. Natl. Acad. Sci. U.S.A.* 105, 16773–16778. doi: 10.1073/pnas.0801793105
- Chiang, C. Y., Dostrovsky, J. O., Iwata, K., and Sessle, B. J. (2011). Role of glia in orofacial pain. *Neuroscientist* 17, 303–320. doi: 10.1177/1073858410386801
- Chichorro, J. G., Porreca, F., and Sessle, B. (2017). Mechanisms of craniofacial pain. *Cephalalgia* 37, 613–626. doi: 10.1177/0333102417704187
- Donegan, M., Kernisant, M., Cua, C., Jasmin, L., and Ohara, P. T. (2013). Satellite glial cell proliferation in the trigeminal ganglia after chronic constriction injury of the infraorbital nerve. *Glia* 61, 2000–2008. doi: 10.1002/glia.22571
- Doulavov, S., Notta, F., Eppert, K., Nguyen, L. T., Ohashi, P. S., and Dick, J. E. (2010). Revised map of the human progenitor hierarchy shows the origin of macrophages and dendritic cells in early lymphoid development. *Nat. Immunol.* 11, 585–593. doi: 10.1038/ni.1889
- Dublin, P., and Hanani, M. (2007). Satellite glial cells in sensory ganglia: their possible contribution to inflammatory pain. *Brain Behav. Immun.* 21, 592–598. doi: 10.1016/j.bbi.2006.11.011
- Fan, W., Huang, F., Wu, Z., Zhu, X., Li, D., and He, H. (2012). The role of nitric oxide in orofacial pain. *Nitric Oxide* 26, 32–37. doi: 10.1016/j.niox.2011.11.003
- Fang, D., Kong, L. Y., Cai, J., Li, S., Liu, X. D., Han, J. S., et al. (2015). Interleukin-6-mediated functional upregulation of TRPV1 receptors in dorsal root ganglion neurons through the activation of JAK/PI3K signaling pathway: roles in the development of bone cancer pain in a rat model. *Pain* 156, 1124–1144. doi: 10.1097/j.pain.0000000000000158
- Feldman-Goriachnik, R., and Hanani, M. (2017). The effects of endothelin-1 on satellite glial cells in peripheral ganglia. *Neuropeptides* 63, 37–42. doi: 10.1016/j.npep.2017.03.002
- Franco, R., and Fernandez-Suarez, D. (2015). Alternatively activated microglia and macrophages in the central nervous system. *Prog. Neurobiol.* 131, 65–86. doi: 10.1016/j.pneurobio.2015.05.003
- Freeman, S. E., Patil, V. V., and Durham, P. L. (2008). Nitric oxide-proton stimulation of trigeminal ganglion neurons increases mitogen-activated protein kinase and phosphatase expression in neurons and satellite glial cells. *Neuroscience* 157, 542–555. doi: 10.1016/j.neuroscience.2008.09.035
- Fu, C., Yin, Z., Yu, D., and Yang, Z. (2013). Substance P and calcitonin gene-related peptide expression in dorsal root ganglia in sciatic nerve injury rats. *Neural Regen. Res.* 8, 3124–3130. doi: 10.3969/j.issn.1673-5374.2013.33.006
- Giugliano, M. (2009). Calcium waves in astrocyte networks: theory and experiments. *Front. Neurosci.* 3:160–161. doi: 10.3389/fneuro.01.019.2009
- Gold, M. S., Reichling, D. B., Shuster, M. J., and Levine, J. D. (1996). Hyperalgesic agents increase a tetrodotoxin-resistant Na⁺ current in nociceptors. *Proc. Natl. Acad. Sci. U.S.A.* 93, 1108–1112. doi: 10.1073/pnas.93.3.1108
- Goto, T., Oh, S. B., Takeda, M., Shinoda, M., Sato, T., Gunjikake, K. K., et al. (2016). Recent advances in basic research on the trigeminal ganglion. *J. Physiol. Sci.* 66, 381–386. doi: 10.1007/s12576-016-0448-1
- Gu, M., Miyoshi, K., Dubner, R., Guo, W., Zou, S., Ren, K., et al. (2011). Spinal 5-HT(3) receptor activation induces behavioral hypersensitivity via a neuronal-glial-neuronal signaling cascade. *J. Neurosci.* 31, 12823–12836. doi: 10.1523/JNEUROSCI.1564-11.2011
- Guillouet, M., Gueret, G., Rannou, F., Giroux-Metges, M. A., Gioux, M., Arvieux, C. C., et al. (2011). Tumor necrosis factor-alpha downregulates sodium current in skeletal muscle by protein kinase C activation: involvement in critical illness polyneuropathy. *Am. J. Physiol. Cell Physiol.* 301, C1057–C1063. doi: 10.1152/ajpcell.00097.2011
- Hanani, M. (2005). Satellite glial cells in sensory ganglia: from form to function. *Brain Res. Brain Res. Rev.* 48, 457–476. doi: 10.1016/j.brainresrev.2004.09.001
- Hanani, M., Huang, T. Y., Cherkas, P. S., Ledda, M., and Pannese, E. (2002). Glial cell plasticity in sensory ganglia induced by nerve damage. *Neuroscience* 114, 279–283. doi: 10.1016/s0306-4522(02)00279-8
- Harvey, L. D., Yin, Y., Attarwala, I. Y., Begum, G., Deng, J., Yan, H. Q., et al. (2015). Administration of DHA reduces endoplasmic reticulum stress-associated inflammation and alters microglial or macrophage activation in traumatic brain injury. *ASN Neuro* 7:1759091415618969.
- Hitomi, S., Kross, K., Kurose, M., Porreca, F., and Meng, I. D. (2017a). Activation of dura-sensitive trigeminal neurons and increased c-Fos protein induced by morphine withdrawal in the rostral ventromedial medulla. *Cephalalgia* 37, 407–417. doi: 10.1177/0333102416648655
- Hitomi, S., Okada-Ogawa, A., Sato, Y., Shibuta-Suzuki, I., Shinoda, M., Imamura, Y., et al. (2017b). Enhancement of ERK phosphorylation and photic responses in Vc/C1 neurons of a migraine model. *Neurosci. Lett.* 647, 14–19. doi: 10.1016/j.neulet.2017.03.023
- Imbe, H., Iwata, K., Zhou, Q. Q., Zou, S., Dubner, R., and Ren, K. (2001). Orofacial deep and cutaneous tissue inflammation and trigeminal neuronal activation. Implications for persistent temporomandibular pain. *Cells Tissues Organs* 169, 238–247. doi: 10.1159/000047887
- Inoue, K., and Tsuda, M. (2018). Microglia in neuropathic pain: cellular and molecular mechanisms and therapeutic potential. *Nat. Rev. Neurosci.* 19, 138–152. doi: 10.1038/nrn.2018.2
- Iwata, K., Imai, T., Tsuboi, Y., Tashiro, A., Ogawa, A., Morimoto, T., et al. (2001). Alteration of medullary dorsal horn neuronal activity following inferior alveolar nerve transection in rats. *J. Neurophysiol.* 86, 2868–2877. doi: 10.1152/jn.2001.86.6.2868
- Iwata, K., Imamura, Y., Honda, K., and Shinoda, M. (2011). Physiological mechanisms of neuropathic pain: the orofacial region. *Int. Rev. Neurobiol.* 97, 227–250. doi: 10.1016/B978-0-12-385198-7.00009-6
- Iwata, K., Katagiri, A., and Shinoda, M. (2017). Neuron-glia interaction is a key mechanism underlying persistent orofacial pain. *J. Oral. Sci.* 59, 173–175. doi: 10.2334/josn.16-0858
- Iwata, K., and Shinoda, M. (2019). Role of neuron and non-neuronal cell communication in persistent orofacial pain. *J. Dent. Anesth. Pain Med.* 19, 77–82. doi: 10.17245/jdpm.2019.19.2.77
- Iwata, K., Takahashi, O., Tsuboi, Y., Ochiai, H., Hibiya, J., Sakaki, T., et al. (1998). Fos protein induction in the medullary dorsal horn and first segment of the spinal cord by tooth-pulp stimulation in cats. *Pain* 75, 27–36. doi: 10.1016/s0304-3959(97)00201-7

- Iwata, K., Tashiro, A., Tsuboi, Y., Imai, T., Sumino, R., Morimoto, T., et al. (1999). Medullary dorsal horn neuronal activity in rats with persistent temporomandibular joint and perioral inflammation. *J. Neurophysiol.* 82, 1244–1253. doi: 10.1152/jn.1999.82.3.1244
- Ji, R. R., Chamesian, A., and Zhang, Y. Q. (2016). Pain regulation by non-neuronal cells and inflammation. *Science* 354, 572–577. doi: 10.1126/science.aaf8924
- Kaji, K., Shinoda, M., Honda, K., Unno, S., Shimizu, N., and Iwata, K. (2016). Connexin 43 contributes to ectopic orofacial pain following inferior alveolar nerve injury. *Mol. Pain* 12:1744806916633704. doi: 10.1177/1744806916633704
- Katagiri, A., Shinoda, M., Honda, K., Toyofuku, A., Sessle, B. J., and Iwata, K. (2012). Satellite glial cell P2Y12 receptor in the trigeminal ganglion is involved in lingual neuropathic pain mechanisms in rats. *Mol. Pain* 8:23. doi: 10.1186/1744-8069-8-23
- Kim, D., You, B., Lim, H., and Lee, S. J. (2011). Toll-like receptor 2 contributes to chemokine gene expression and macrophage infiltration in the dorsal root ganglia after peripheral nerve injury. *Mol. Pain* 7:74. doi: 10.1186/1744-8069-7-74
- Kiyomoto, M., Shinoda, M., Okada-Ogawa, A., Noma, N., Shibuta, K., Tsuboi, Y., et al. (2013). Fractalkine signaling in microglia contributes to ectopic orofacial pain following trapezius muscle inflammation. *J. Neurosci.* 33, 7667–7680. doi: 10.1523/JNEUROSCI.4968-12.2013
- Komiyama, H., Shimizu, K., Noma, N., Tsuboi, Y., Honda, K., Kanno, K., et al. (2018). Role of neuron-glial interaction mediated by IL-1 β in ectopic tooth pain. *J. Dent. Res.* 97, 467–475. doi: 10.1177/0022034517741253
- Komori, T., Morikawa, Y., Inada, T., Hisaoka, T., and Senba, E. (2011). Site-specific subtypes of macrophages recruited after peripheral nerve injury. *Neuroreport* 22, 911–917. doi: 10.1097/WNR.0b013e32834cd76a
- Kumar, V., Sur, V. P., Guha, R., Konar, A., and Hazra, S. (2018). Estrogen modulates corneal nociception and maintains corneal homeostasis in rat eye. *Cornea* 37, 508–514. doi: 10.1097/ICO.0000000000001437
- Kwon, M. J., Shin, H. Y., Cui, Y., Kim, H., Thi, A. H., Choi, J. Y., et al. (2015). CCL2 Mediates Neuron-Macrophage Interactions to Drive Proregenerative Macrophage Activation Following Preconditioning Injury. *J. Neurosci.* 35, 15934–15947. doi: 10.1523/JNEUROSCI.1924-15.2015
- Laskin, D. L., Sunil, V. R., Gardner, C. R., and Laskin, J. D. (2011). Macrophages and tissue injury: agents of defense or destruction? *Annu. Rev. Pharmacol. Toxicol.* 51, 267–288. doi: 10.1146/annurev.pharmtox.010909.105812
- Lau, B. K., and Vaughan, C. W. (2014). Descending modulation of pain: the GABA disinhibition hypothesis of analgesia. *Curr. Opin. Neurobiol.* 29, 159–164. doi: 10.1016/j.conb.2014.07.010
- Lee, S., and Zhang, J. (2012). Heterogeneity of macrophages in injured trigeminal nerves: cytokine/chemokine expressing vs. phagocytic macrophages. *Brain Behav. Immun.* 26, 891–903. doi: 10.1016/j.bbi.2012.03.004
- Leo, M., Argalski, S., Schafers, M., and Hagenacker, T. (2015). Modulation of voltage-gated sodium channels by activation of tumor necrosis factor receptor-1 and receptor-2 in small DRG neurons of rats. *Mediators Inflamm.* 2015:124942. doi: 10.1155/2015/124942
- Li, J., Vause, C. V., and Durham, P. L. (2008). Calcitonin gene-related peptide stimulation of nitric oxide synthesis and release from trigeminal ganglion glial cells. *Brain Res.* 1196, 22–32. doi: 10.1016/j.brainres.2007.12.028
- Lin, J., Liu, F., Zhang, Y. Y., Song, N., Liu, M. K., Fang, X. Y., et al. (2019). P2Y14 receptor is functionally expressed in satellite glial cells and mediates interleukin-1 β and chemokine CCL2 secretion. *J. Cell Physiol.* 234, 21199–21210. doi: 10.1002/jcp.28726
- Liu, X. J., Liu, T., Chen, G., Wang, B., Yu, X. L., Yin, C., et al. (2016). TLR signaling adaptor protein MyD88 in primary sensory neurons contributes to persistent inflammatory and neuropathic pain and neuroinflammation. *Sci. Rep.* 6:28188. doi: 10.1038/srep28188
- Lu, X., and Richardson, P. M. (1993). Responses of macrophages in rat dorsal root ganglia following peripheral nerve injury. *J. Neurocytol.* 22, 334–341. doi: 10.1007/bf01195557
- Martins, I., and Tavares, I. (2017). Reticular formation and pain: the past and the future. *Front. Neuroanat.* 11:51. doi: 10.3389/fnana.2017.00051
- Matsumoto, K., Nakajima, T., Sakai, H., Kato, S., Sagara, A., Arakawa, K., et al. (2013). Increased expression of 5-HT $_3$ and NK 1 receptors in 5-fluorouracil-induced mucositis in mouse jejunum. *Dig. Dis. Sci.* 58, 3440–3451. doi: 10.1007/s10620-013-2709-7
- Meakin, S. O., and Shooter, E. M. (1992). The nerve growth factor family of receptors. *Trends Neurosci.* 15, 323–331. doi: 10.1016/0166-2236(92)90047-c
- Mika, J., Zychowska, M., Popielek-Barczyk, K., Rojewska, E., and Przewlocka, B. (2013). Importance of glial activation in neuropathic pain. *Eur. J. Pharmacol.* 716, 106–119. doi: 10.1016/j.ejphar.2013.01.072
- Mikuzuki, L., Saito, H., Katagiri, A., Okada, S., Sugawara, S., Kubo, A., et al. (2017). Phenotypic change in trigeminal ganglion neurons associated with satellite cell activation via extracellular signal-regulated kinase phosphorylation is involved in lingual neuropathic pain. *Eur. J. Neurosci.* 46, 2190–2202. doi: 10.1111/ejn.13667
- Noma, N., Tsuboi, Y., Kondo, M., Matsumoto, M., Sessle, B. J., Kitagawa, J., et al. (2008). Organization of pERK-immunoreactive cells in trigeminal spinal nucleus caudalis and upper cervical cord following capsaicin injection into oral and craniofacial regions in rats. *J. Comp. Neurol.* 507, 1428–1440. doi: 10.1002/cne.21620
- Ohara, K., Shimizu, K., Matsuura, S., Ogiso, B., Omagari, D., Asano, M., et al. (2013). Toll-like receptor 4 signaling in trigeminal ganglion neurons contributes tongue-referred pain associated with tooth pulp inflammation. *J. Neuroinflammation* 10:139. doi: 10.1186/1742-2094-10-139
- Ohara, P. T., Vit, J. P., Bhargava, A., and Jasmin, L. (2008). Evidence for a role of connexin 43 in trigeminal pain using RNA interference in vivo. *J. Neurophysiol.* 100, 3064–3073. doi: 10.1152/jn.90722.2008
- Okada-Ogawa, A., Nakaya, Y., Imamura, Y., Kobayashi, M., Shinoda, M., Kita, K., et al. (2015). Involvement of medullary GABAergic system in extraterritorial neuropathic pain mechanisms associated with inferior alveolar nerve transection. *Exp. Neurol.* 267, 42–52. doi: 10.1016/j.expneurol.2015.02.030
- Okada-Ogawa, A., Suzuki, I., Sessle, B. J., Chiang, C. Y., Salter, M. W., Dostrovsky, J. O., et al. (2009). Astroglia in medullary dorsal horn (trigeminal spinal subnucleus caudalis) are involved in trigeminal neuropathic pain mechanisms. *J. Neurosci.* 29, 11161–11171. doi: 10.1523/JNEUROSCI.3365-09.2009
- Okamoto, K., Bereiter, D. F., Tashiro, A., and Bereiter, D. A. (2009). Ocular surface-evoked Fos-like immunoreactivity is enhanced in trigeminal subnucleus caudalis by prior exposure to endotoxin. *Neuroscience* 159, 787–794. doi: 10.1016/j.neuroscience.2008.12.015
- Okamoto, K., Tashiro, A., Chang, Z., and Bereiter, D. A. (2010). Bright light activates a trigeminal nociceptive pathway. *Pain* 149, 235–242. doi: 10.1016/j.pain.2010.02.004
- Okubo, M., Castro, A., Guo, W., Zou, S., Ren, K., Wei, F., et al. (2013). Transition to persistent orofacial pain after nerve injury involves supraspinal serotonin mechanisms. *J. Neurosci.* 33, 5152–5161. doi: 10.1523/JNEUROSCI.3390-12.2013
- Poulsen, J. N., Warwick, R., Duroux, M., Hanani, M., and Gazerani, P. (2015). Oxaliplatin enhances gap junction-mediated coupling in cell cultures of mouse trigeminal ganglia. *Exp. Cell Res.* 336, 94–99. doi: 10.1016/j.yexcr.2015.05.009
- Raghavendra, V., Tanga, F., Rutkowski, M. D., and Deleo, J. A. (2003). Anti-hyperalgesic and morphine-sparing actions of propentofylline following peripheral nerve injury in rats: mechanistic implications of spinal glia and proinflammatory cytokines. *Pain* 104, 655–664. doi: 10.1016/s0304-3959(03)00138-6
- Ren, K., and Dubner, R. (2008). Neuron-glia crosstalk gets serious: role in pain hypersensitivity. *Curr. Opin. Anaesthesiol.* 21, 570–579. doi: 10.1097/ACO.0b013e32830eddbf
- Ren, K., and Dubner, R. (2011). The role of trigeminal interpolaris-caudalis transition zone in persistent orofacial pain. *Int. Rev. Neurobiol.* 97, 207–225. doi: 10.1016/B978-0-12-385198-7.00008-4
- Shibuta, K., Suzuki, I., Shinoda, M., Tsuboi, Y., Honda, K., Shimizu, N., et al. (2012). Organization of hyperactive microglial cells in trigeminal spinal subnucleus caudalis and upper cervical spinal cord associated with orofacial neuropathic pain. *Brain Res.* 1451, 74–86. doi: 10.1016/j.brainres.2012.02.023
- Shinoda, M., Asano, M., Omagari, D., Honda, K., Hitomi, S., Katagiri, A., et al. (2011). Nerve growth factor contribution via transient receptor potential vanilloid 1 to ectopic orofacial pain. *J. Neurosci.* 31, 7145–7155. doi: 10.1523/JNEUROSCI.0481-11.2011
- Snyder, S. H. (1992). Nitric oxide: first in a new class of neurotransmitters. *Science* 257, 494–496. doi: 10.1126/science.1353273

- Spofford, C. M., Mohan, S., Kang, S., Jang, J. H., and Brennan, T. J. (2011). Evaluation of leukemia inhibitory factor (LIF) in a rat model of postoperative pain. *J. Pain* 12, 819–832. doi: 10.1016/j.jpain.2011.02.351
- Sprangers, S., De Vries, T. J., and Everts, V. (2016). Monocyte Heterogeneity: Consequences for Monocyte-Derived Immune Cells. *J. Immunol. Res.* 2016:1475435. doi: 10.1155/2016/1475435
- Spray, D. C., Iglesias, R., Shraer, N., Suadicani, S. O., Belzer, V., Hanstein, R., et al. (2019). Gap junction mediated signaling between satellite glia and neurons in trigeminal ganglia. *Glia* 67, 791–801. doi: 10.1002/glia.23554
- Stemkowski, P. L., Noh, M. C., Chen, Y., and Smith, P. A. (2015). Increased excitability of medium-sized dorsal root ganglion neurons by prolonged interleukin-1beta exposure is K(+) channel dependent and reversible. *J. Physiol.* 593, 3739–3755. doi: 10.1113/jp270905
- Sugiyama, T., Shinoda, M., Watase, T., Honda, K., Ito, R., Kaji, K., et al. (2013). Nitric oxide signaling contributes to ectopic orofacial neuropathic pain. *J. Dent. Res.* 92, 1113–1117. doi: 10.1177/0022034513509280
- Sun, J., Ramnath, R. D., Zhi, L., Tamizhselvi, R., and Bhatia, M. (2008). Substance P enhances NF-kappaB transactivation and chemokine response in murine macrophages via ERK1/2 and p38 MAPK signaling pathways. *Am. J. Physiol. Cell Physiol.* 294, C1586–C1596. doi: 10.1152/ajpcell.00129.2008
- Takeda, M., Tanimoto, T., Kadoi, J., Nasu, M., Takahashi, M., Kitagawa, J., et al. (2007). Enhanced excitability of nociceptive trigeminal ganglion neurons by satellite glial cytokine following peripheral inflammation. *Pain* 129, 155–166. doi: 10.1016/j.pain.2006.10.007
- Takeda, M., Tanimoto, T., Nasu, M., Ikeda, M., Kadoi, J., and Matsumoto, S. (2005). Activation of NK1 receptor of trigeminal root ganglion via substance P paracrine mechanism contributes to the mechanical allodynia in the temporomandibular joint inflammation in rats. *Pain* 116, 375–385. doi: 10.1016/j.pain.2005.05.007
- Thalakoti, S., Patil, V. V., Damodaram, S., Vause, C. V., Langford, L. E., Freeman, S. E., et al. (2007). Neuron-glia signaling in trigeminal ganglion: implications for migraine pathology. *Headache* 47, 1008–1023. doi: 10.1111/j.1526-4610.2007.00854.x
- Tsuboi, Y., Iwata, K., Dostrovsky, J. O., Chiang, C. Y., Sessle, B. J., and Hu, J. W. (2011). Modulation of astroglial glutamine synthetase activity affects nociceptive behaviour and central sensitization of medullary dorsal horn nociceptive neurons in a rat model of chronic pulpitis. *Eur. J. Neurosci.* 34, 292–302. doi: 10.1111/j.1460-9568.2011.07747.x
- Vause, C., Bowen, E., Spierings, E., and Durham, P. (2007). Effect of carbon dioxide on calcitonin gene-related peptide secretion from trigeminal neurons. *Headache* 47, 1385–1397.
- Vause, C. V., and Durham, P. L. (2009). CGRP stimulation of iNOS and NO release from trigeminal ganglion glial cells involves mitogen-activated protein kinase pathways. *J. Neurochem.* 110, 811–821. doi: 10.1111/j.1471-4159.2009.06154.x
- Vause, C. V., and Durham, P. L. (2010). Calcitonin gene-related peptide differentially regulates gene and protein expression in trigeminal glia cells: findings from array analysis. *Neurosci. Lett.* 473, 163–167. doi: 10.1016/j.neulet.2010.01.074
- Vit, J. P., Jasmin, L., Bhargava, A., and Ohara, P. T. (2006). Satellite glial cells in the trigeminal ganglion as a determinant of orofacial neuropathic pain. *Neuron Glia Biol.* 2, 247–257. doi: 10.1017/s1740925x07000427
- Vit, J. P., Ohara, P. T., Bhargava, A., Kelley, K., and Jasmin, L. (2008). Silencing the Kir4.1 potassium channel subunit in satellite glial cells of the rat trigeminal ganglion results in pain-like behavior in the absence of nerve injury. *J. Neurosci.* 28, 4161–4171. doi: 10.1523/JNEUROSCI.5053-07.2008
- Wagner, R., and Myers, R. R. (1996). Endoneurial injection of TNF-alpha produces neuropathic pain behaviors. *Neuroreport* 7, 2897–2901.
- Wang, C. L., Lu, C. Y., Pi, C. C., Zhuang, Y. J., Chu, C. L., Liu, W. H., et al. (2012). Extracellular polysaccharides produced by *Ganoderma formosanum* stimulate macrophage activation via multiple pattern-recognition receptors. *BMC Complement Altern Med.* 12:119. doi: 10.1186/1472-6882-12-119
- Waqas, S. F. H., Ampem, G., and Roszer, T. (2019). Analysis of IL-4/STAT6 signaling in macrophages. *Methods Mol. Biol.* 1966, 211–224. doi: 10.1007/978-1-4939-9195-2_17
- Wei, F., Guo, W., Zou, S., Ren, K., and Dubner, R. (2008). Supraspinal glial-neuronal interactions contribute to descending pain facilitation. *J. Neurosci.* 28, 10482–10495. doi: 10.1523/JNEUROSCI.3593-08.2008
- Xue, Q., Jong, B., Chen, T., and Schumacher, M. A. (2007). Transcription of rat TRPV1 utilizes a dual promoter system that is positively regulated by nerve growth factor. *J. Neurochem.* 101, 212–222. doi: 10.1111/j.1471-4159.2006.04363.x
- Zelenka, M., Schafers, M., and Sommer, C. (2005). Intraneural injection of interleukin-1beta and tumor necrosis factor-alpha into rat sciatic nerve at physiological doses induces signs of neuropathic pain. *Pain* 116, 257–263. doi: 10.1016/j.pain.2005.04.018
- Zhang, P., Bi, R. Y., and Gan, Y. H. (2018). Glial interleukin-1beta upregulates neuronal sodium channel 1.7 in trigeminal ganglion contributing to temporomandibular joint inflammatory hypernociception in rats. *J. Neuroinflammation* 15:117. doi: 10.1186/s12974-018-1154-0
- Zhang, Y., Song, N., Liu, F., Lin, J., Liu, M., Huang, C., et al. (2019). Activation of mitogen-activated protein kinases in satellite glial cells of the trigeminal ganglion contributes to substance P-mediated inflammatory pain. *Int. J. Oral Sci.* 11:24. doi: 10.1038/s41368-019-0055-0
- Zhang, Y. H., Vasko, M. R., and Nicol, G. D. (2002). Ceramide, a putative second messenger for nerve growth factor, modulates the TTX-resistant Na(+) current and delayed rectifier K(+) current in rat sensory neurons. *J. Physiol.* 544, 385–402. doi: 10.1111/j.2002.00385.x

Conflict of Interest: The authors declare that the research was conducted in the absence of any commercial or financial relationships that could be construed as a potential conflict of interest.

Copyright © 2019 Shinoda, Kubo, Hayashi and Iwata. This is an open-access article distributed under the terms of the Creative Commons Attribution License (CC BY). The use, distribution or reproduction in other forums is permitted, provided the original author(s) and the copyright owner(s) are credited and that the original publication in this journal is cited, in accordance with accepted academic practice. No use, distribution or reproduction is permitted which does not comply with these terms.



The Better to Eat You With: Bite Force in the Naked Mole-Rat (*Heterocephalus glaber*) Is Stronger Than Predicted Based on Body Size

Natalee J. Hite¹, Cody Germain², Blake W. Cain³, Mason Sheldon², Sai Saketh Nandan Perala⁴ and Diana K. Sarko^{5*}

¹ Department of Physiology, School of Medicine, Southern Illinois University, Carbondale, IL, United States, ² Southern Illinois University, Carbondale, IL, United States, ³ School of Medicine, Southern Illinois University, Carbondale, IL, United States,

⁴ Department of Electrical and Computer Engineering, Southern Illinois University, Carbondale, IL, United States,

⁵ Department of Anatomy, School of Medicine, Southern Illinois University, Carbondale, IL, United States

OPEN ACCESS

Edited by:

Limor Avivi-Arber,
University of Toronto, Canada

Reviewed by:

Phillip Cox,
University of York, United Kingdom
Elias Manjarrez,
Meritorious Autonomous University
of Puebla, Mexico

*Correspondence:

Diana K. Sarko
dsarko38@siu.edu

Received: 26 September 2019

Accepted: 19 November 2019

Published: 04 December 2019

Citation:

Hite NJ, Germain C, Cain BW, Sheldon M, Perala SSN and Sarko DK (2019) The Better to Eat You With: Bite Force in the Naked Mole-Rat (*Heterocephalus glaber*) Is Stronger Than Predicted Based on Body Size. *Front. Integr. Neurosci.* 13:70. doi: 10.3389/fnint.2019.00070

Naked mole-rats (*Heterocephalus glaber*) are subterranean rodents that utilize their incisors for feeding, chisel-tooth digging of complex tunnel systems, social interactions, and defense in their eusocial colony structure. Previous studies have shown that naked mole-rats have morphological and anatomical adaptations that predict strong bite forces, namely, skulls that are relatively tall and wide, in addition to impressive masticatory musculature. However, no studies to date have directly measured bite force in this species or analyzed the relationship between bite force and social caste. In the current study, we assessed adult naked mole-rat maximum bite force in relation to body mass, in addition to considering each animal's position within the eusocial hierarchy (i.e., dominant versus subordinate). Each animal was permitted to freely interact with a piezo-resistive bite force sensor. Our results showed that bite force was correlated with body mass in subordinate but not in dominant naked mole-rats, and that subordinate animals exhibited a shorter latency in producing their first bite. Maximum bite force was significantly influenced by caste. In comparing bite force with available data from previous studies across 82 additional mammalian species, subordinate naked mole-rats exhibited a bite force that was 65% higher than predicted for their body size, comparable to Tasmanian devils and exceeding bite force values for all of the carnivorans included for comparison. These results supported the hypothesis that the naked mole-rat's bite force would exceed predictions based on body size due to the behavioral importance and specialization of the naked mole-rat incisors. This study provides insight into the differences in bite force across species, and the significant role that social and ecological factors might play in the evolutionary relationship between bite force performance and underlying anatomical structures.

Keywords: naked mole-rat, incisor, bite force, bite force quotient, bite frequency, bite latency, piezo-resistive sensor, eusocial

INTRODUCTION

The maximum bite force across different taxa varies according to a wide range of factors including ecological niche, diet, and behavioral use of dentition. Anatomical characteristics such as body mass have proven to be significant predictors of bite force (Wroe et al., 2005; Anderson et al., 2008; Freeman and Lemen, 2008a; Marshall et al., 2012). In addition, the size of masticatory muscles for a particular species and related behavioral demands—e.g., attack and acquisition of prey, excavating tubers, digging underground tunnel systems—influence and co-vary with the strength of biting capabilities (Wroe et al., 2005; Christiansen and Wroe, 2007; Freeman and Lemen, 2008b; Becerra et al., 2014). Feeding habits in particular show a strong relationship with bite force capabilities (Wroe et al., 2005; Christiansen and Wroe, 2007; Maestri et al., 2016). Strong bite force estimates based on cranial morphology have been shown for predators that rely on the ability to effectively incapacitate and dismember prey (Christiansen and Wroe, 2007). In contrast, low bite force estimates were found for insectivores relying on a diet composed of prey that are less difficult to overpower and to consume (Aguirre et al., 2002, 2003; Wroe et al., 2005). Relatively high bite force quotients (BFQs) (comparisons to predicted bite forces across a range of taxa with different body masses based on linear regression analyses) have also been attributed to osteophages, tasked with breaking down bone material, as well as to herbivores that predominantly ingest geophytes and other hard vegetables (Herrel et al., 2002; Erickson et al., 2003; Herrel and O'Reilly, 2005; Wroe et al., 2005; Lappin et al., 2017).

Naked mole-rats (*Heterocephalus glaber*) are a subterranean species that uses their continuously erupting incisors to dig tunnels, defend their colony, show dominance among conspecifics, and consume foods ranging from vegetables to geophytes and the bones of ungulates found near and within their tunnels (Brett, 1991). Naked mole-rats exhibit skull morphological characteristics associated with strong bite forces (Figure 1A), including large head height and cranial width (McIntosh and Cox, 2016). Previous studies have shown that naked mole-rats also have large musculature of the head and neck that facilitates feeding, digging, and social behaviors that rely on use of the incisors (Cox and Faulkes, 2014; McIntosh and Cox, 2016; Cain et al., 2019). The musculature of the jaw is responsible for approximately 25% of their total body mass (Sherman et al., 1992). The size of the muscles of mastication, in particular the masseter and temporalis muscles as seen in Figure 1B, are large compared to other species such as mice (Figure 1C). The enlarged temporalis muscles of naked mole-rats extend far medially compared to other species, meeting at the midline (Figures 1B,C). Digital dissection using microCT techniques demonstrated that the total mass of masticatory muscles in naked mole-rats was 75% of what is seen in rats, despite rats having approximately five times the body mass (Cox and Jeffery, 2011; Cox and Faulkes, 2014). Although skull measures and large muscles of mastication predict a strong bite force for naked mole-rats, and studies of other African mole-rat species have

demonstrated strong bite forces (Fukomys; Van Daele et al., 2008), bite force has not been directly measured in naked mole-rats to date.

Beyond any direct bite force assessment in naked mole-rats, the influence of hierarchical social status on bite force has not been explored. As a eusocial species, naked mole-rats assume various roles within a colony. These roles range from dominant (e.g., queen, breeder) to subordinate (e.g., forager, defender, caretaker) (Sherman et al., 1992; Faulkes and Bennett, 2001). Hierarchical status is related to differences in body mass (Sherman et al., 1992) and might also be associated with differing reliance on masticatory strength used to accomplish the tasks demanded by each role such as colony defense or caring for pups (Sherman et al., 1991; Anderson et al., 2008). In the current study, we utilized piezo-resistive force sensors paired with a Raspberry Pi system and customized software to directly measure bite force from the incisors in freely behaving naked mole-rats. We then analyzed maximum bite force, bite frequency, and bite latency in relation to body mass, sex, and caste, and compared naked mole-rat maximum bite force with that of other mammalian taxa.

MATERIALS AND METHODS

Animals

Nineteen adult (≥ 1 year old) naked mole-rats [*H. glaber* (Rüppell, 1842), RRID: NCBITaxon 10181], including 10 subordinate animals (five males and five females) and nine dominant animals (five males and four females), were used in this study (Table 1). The nine dominant animals consisted of all colony founders. Founders were the naked mole-rats used to initially establish our two separate laboratory colonies, and subsequently populate each respective colony; therefore, these were also the oldest colony members. The subordinate naked mole-rats were offspring of the founding group members. Body masses for the naked mole-rats included in the present study ranged from 32.4 to 94.1 g (Table 1; Braintree Scientific compact portable scale model CB 1001 with 0.1 g precision). Naked mole-rats were maintained in two separate laboratory breeding colonies, each with one queen. They were housed at ambient temperatures of approximately 27.8–30°C and at least 40% relative humidity, with free access to food. For complete housing details, see Artwohl et al. (2002). All aspects of this research complied with our protocol approved by the Institutional Animal Care and Use Committee at Southern Illinois University, Carbondale, IL, United States, and were in accordance with the National Institutes of Health Guide for the Care and Use of Laboratory Animals (NIH Publication Nos. 8023 and 1978).

Force Sensor Preparation and Calibration

We utilized FlexiForce type A201 force sensors (111N sensors; Tekscan; Boston, MA, United States) to assess naked mole-rat bite force. Per the manufacturer, each sensor has the following typical performance: linearity (error) of $<\pm 3\%$ of full scale, repeatability of $<\pm 2.5\%$, hysteresis of $<4.5\%$ of full scale, drift of $<5\%$ /logarithmic time, response time $<5\mu\text{sec}$, and an operating

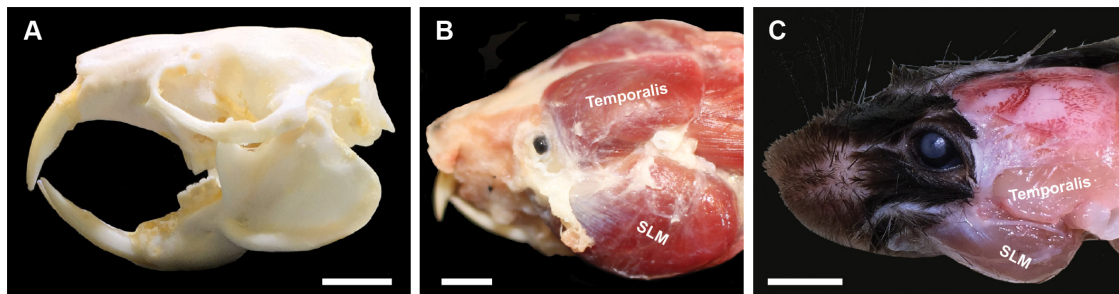


FIGURE 1 | Naked mole-rat skull (A) and masticatory musculature (B) compared to that of a mouse (C). (A) The naked mole-rat skull is characterized by large cranial width and head height, factors predictive of stronger bite forces (McIntosh and Cox, 2016). (B) Naked mole-rats also have large temporalis and masseter muscles, associated with strong jaw closure (biting), with the dorsal attachment site of the temporalis muscle extending toward the midline. (C) By comparison, the mouse has much smaller masticatory muscles, with the dorsal attachment of the temporalis muscle limited to a far lateral extent of the skull. Masseter nomenclature follows Becerra et al. (2014) for the *m. masseter lateralis, pars superficial* (superficial lateral masseter). SLM = superficial lateral masseter. Scale bar = 5 mm.

temperature range of -0 to 60°C . A protective coating of Plasti-Dip (Plasti-Dip International; Blaine, MN, United States) was added to prolong the life of the sensor and to maintain its responsiveness for multiple bite interactions. Plasti-Dip was applied in two coats to the distal 50 mm length of the force sensor. Each coat was given 48 h to completely cure before the coated force sensor was calibrated and utilized in experimental sessions. Each Plasti-Dipped bite force sensor was approximately 1.5 mm thick, 15 mm long, and 15 mm wide (see the inset in **Supplementary Figure S1C**).

In order to create calibration force curves, force sensors were conditioned following the manufacturer's recommended parameters. Conditioning consisted of applying 110% of maximum load to the sensor until voltage response stabilized (approximately 3 s), repeated five times. A universal testing machine (UTM), specifically the Material Testing Systems (MTS) Insight 30SL Model Number 820.030-SL (MTS Systems Corporation, Eden Prairie, MN, United States), was used to calibrate our sensors. To maintain consistent force application and to achieve precise alignment, custom aluminum fixtures matching the average footprint of naked mole-rat upper and lower incisors were fabricated by the machine shop at Southern Illinois University. Setup of the UTM followed the manufacturer's guidelines, and the force sensor was placed between the fabricated fixture interfaces. After sensor conditioning, known forces were applied to the sensor via the UTM, and the force sensor responses were recorded. A voltage per newton (V/N) curve was then directly created from the response data (**Supplementary Figure S1A**). The V/N ratio changes in a manner that is dependent on the input voltage resistance of the force sensor. Once the V/N ratio was calculated, bite forces measured by the probe was then converted from voltage to newton. Calibrated force sensors were paired with a Raspberry Pi Model B (Adafruit; New York City, NY, United States) using customized Python (version 3.0) software for bite force data acquisition (see **Supplementary Figure S1C** for detailed circuit connections).

Bite Force Data Collection and Analysis

Each animal was placed in a chamber similar to its permanent housing chambers and was allowed to acclimate

TABLE 1 | Descriptive statistics (values shown are mean \pm SEM) and range for body mass, maximum bite force, bite frequency (inclusive and stringent analyses), and bite latency in naked mole-rats separated by caste.

| | Subordinate | Dominant |
|-------------------------------------|------------------------|-------------------------------------|
| Animals | $n = 10$ | $n = 9$ |
| | Five male, five female | Five male, four female (two queens) |
| Age (yrs) | 1.68 ± 0.38 | 3.74 ± 0.21 |
| Body mass (g) | 56.05 ± 12.84 | 74.26 ± 10.68 |
| Range | 32.4–76.6 | 54–94.1 |
| Maximum bite force (N) | 21.07 ± 8.89 | 19.82 ± 4.68 |
| Range | 7.74–35.95 | 13.88–28.25 |
| Bite frequency (# bites/min) | | |
| Inclusive criteria | 4.29 ± 1.70 | 3.39 ± 0.92 |
| Range | 2.05–7.75 | 2.07–5.15 |
| Stringent criteria | 1.37 ± 0.54 | 0.97 ± 0.31 |
| Range | 0.51–2.39 | 0.51–1.54 |
| Bite latency (min) | 1.44 ± 1.12 | 2.48 ± 1.66 |
| Range | 0.40–3.58 | 0.81–6.41 |

g = grams, *min* = minutes, *N* = newton, and *yrs* = years.

for several minutes. Next, the force sensor was inserted through a small opening at the blocked terminal end of a PVC tunnel tube to allow the animal to interact freely with the force sensor. Slightly agitating the force sensor to attract the animal's attention generally proved effective at eliciting biting behaviors, and naked mole-rats were motivated to bite when the opening of a tunnel was blocked. Bite force measurements were then recorded for approximately 20 min after which the animal was returned to its permanent housing chamber. Five trials of approximately 20 min each were run for each animal.

The force sensor raw voltage data were sampled at 128 Hz (**Supplementary Figure S1B**). Data for each force sensor probe was adjusted by first subtracting the baseline "noise" voltage readings from the force sensor output, which were then converted from raw voltage output to newton values using the conversion factor for the specific probe utilized

TABLE 2 | Descriptive statistics (maximum bite force, body mass, residuals, and bite force quotients) across mammalian species, including data from the present study for naked mole-rats.

| Species | BF (N) | BM (g) | MV or C | Tooth | Residuals ¹ : Rodentia | Residuals ² : Rodentia | Residuals ¹ : Mammalia | Residuals ² : Mammalia | BFQ ₁ | BFQ ₂ |
|---|--------------------|--------------------|---------|-------|-----------------------------------|-----------------------------------|-----------------------------------|-----------------------------------|------------------|------------------|
| Rodentia | | | | | | | | | | |
| <i>Heterocephalus glaber</i> (naked mole-rat) castes combined | 20.48 ^a | 64.67 ^a | MV | I | | 0.0930 | | 0.1814 | | 152 |
| <i>Heterocephalus glaber</i> (naked mole-rat) dominant only | 19.82 ^a | 74.26 ^a | MV | I | 0.0273 | | 0.1133 | | 130 | |
| <i>Heterocephalus glaber</i> (naked mole-rat) subordinate only | 21.07 ^a | 56.05 ^a | MV | I | 0.1266 | | 0.2169 | | 165 | |
| <i>Chinchilla laniger</i> (long-tailed chinchilla) | 23.5 ^f | 639 ^f | MV | I | −0.3943 | −0.3923 | −0.3385 | −0.3367 | 46 | 46 |
| <i>Ctenomys australis</i> (sand dune tucú-tucú) | 68.7 ^f | 315 ^f | MV | I | 0.2368 | 0.2391 | 0.3026 | 0.3046 | 201 | 202 |
| <i>Dipodomys ordii</i> (Ord's kangaroo rat) | 13.98 ^d | 63 ^d | MV | I | −0.0789 | −0.0758 | 0.0097 | 0.0124 | 102 | 103 |
| <i>Fukomys micklemi</i> (African mole-rat) | 41 ^c | 89 ^c | MV | I | 0.3077 | 0.3107 | 0.3914 | 0.3940 | 246 | 248 |
| <i>Fukomys whytei</i> (African mole-rat) | 31 ^c | 78 ^c | MV | I | 0.2171 | 0.2201 | 0.3027 | 0.3053 | 201 | 202 |
| <i>Geomys bursarius</i> (plains pocket gopher) | 50.61 ^d | 153 ^d | MV | I | 0.2726 | 0.2753 | 0.3487 | 0.3510 | 223 | 224 |
| <i>Microtus ochrogaster</i> (prairie vole) | 12.88 ^d | 34 ^d | MV | I | 0.0295 | 0.0330 | 0.1269 | 0.1298 | 134 | 135 |
| <i>Mus musculus</i> (Gough Island mouse) | 5.36 ^b | 28.60 ^b | MV | I | −0.3109 | −0.3073 | −0.2110 | −0.2080 | 62 | 62 |
| <i>Mus musculus</i> (strain: Watkins Star Line B) | 3.92 ^b | 19.06 ^b | MV | I | −0.3520 | −0.3482 | −0.2464 | −0.2432 | 57 | 57 |
| <i>Neotoma floridana</i> (eastern woodrat) | 30.26 ^d | 321 ^d | MV | I | −0.1237 | −0.1214 | −0.0582 | −0.0561 | 87 | 88 |
| <i>Octodon degus</i> (common degus) | 21.9 ^f | 206 ^f | MV | I | −0.1606 | −0.1581 | −0.0888 | −0.0865 | 82 | 82 |
| <i>Onychomys leucogaster</i> (grasshopper mouse) | 24.7 ^e | 50 ^e | MV | I | 0.2222 | 0.2255 | 0.3142 | 0.3169 | 206 | 207 |
| <i>Perognathus flavescens</i> (plains pocket mouse) | 4.64 ^d | 6.5 ^d | MV | I | −0.0276 | −0.0233 | 0.0933 | 0.0969 | 124 | 125 |
| <i>Peromyscus leucopus</i> (white-footed mouse) | 10 ^d | 23 ^d | MV | I | 0.0108 | 0.0145 | 0.1138 | 0.1169 | 130 | 131 |
| <i>Peromyscus maniculatus</i> (deer mouse) | 12.9 ^e | 21 ^e | MV | I | 0.1427 | 0.1464 | 0.2469 | 0.2500 | 177 | 178 |
| <i>Rattus norvegicus</i> (Norway/common rat) | 47 ^g | 555 ^g | MV | I | −0.0603 | −0.0583 | −0.0026 | −0.0007 | 99 | 100 |
| <i>Reithrodontomys megalotis</i> (western harvest mouse) | 7.67 ^d | 12 ^d | MV | I | 0.0575 | 0.0615 | 0.1703 | 0.1736 | 148 | 149 |
| <i>Sciurus niger</i> (fox squirrel) | 72.95 ^d | 588 ^d | MV | I | 0.1171 | 0.1191 | 0.1740 | 0.1759 | 149 | 150 |
| <i>Sigmodon hispidus</i> (hispid cotton rat) | 19.87 ^d | 105 ^d | MV | I | −0.0455 | −0.0426 | 0.0359 | 0.0384 | 109 | 109 |
| <i>Spermophilus tridecemlineatus</i> (13-lined ground squirrel) | 21.05 ^d | 144 ^d | MV | I | −0.0942 | −0.0915 | −0.0173 | −0.0149 | 96 | 97 |
| <i>Zapus hudsonius</i> (meadow jumping mouse) | 7.63 ^d | 24.5 ^d | MV | I | −0.1214 | −0.1178 | −0.0193 | −0.0163 | 96 | 96 |
| Didelphimorphia | | | | | | | | | | |
| <i>Didelphis virginiana</i> (opossum) | 442 ^h | 5000 ^h | MV | M | | | 0.42629968 | 0.4273 | 267 | 267 |
| <i>Monodelphis domestica</i> (gray short-tailed opossum) | 21 ^h | 90 ^h | MV | M | | | 0.09811479 | 0.1007 | 125 | 126 |
| Carnivora | | | | | | | | | | |
| <i>Acinonyx jubatus</i> (Felidae) cheetah | 472 ⁱ | 29500 ⁱ | C | Ca | | | 0.0152025 | 0.0155 | 104 | 104 |
| <i>Alopex lagopus</i> (Canidae) Arctic fox | 178 ^j | 8200 ^j | C | Ca | | | −0.091228 | −0.0905 | 81 | 81 |
| <i>Canis alpinus</i> (Canidae) Dhole, wild dog | 314 ⁱ | 16500 ⁱ | C | Ca | | | −0.0179014 | −0.0174 | 96 | 96 |
| <i>Canis aureus</i> (Canidae) golden jackal | 165 ^j | 7700 ^j | C | Ca | | | −0.1085817 | −0.1078 | 78 | 78 |
| <i>Canis domesticus</i> (Labrador retriever) | 732 ^j | 2864 ^j | MV | Ca | | | 0.20160883 | 0.2019 | 159 | 159 |
| <i>Canis latrans</i> (Canidae) coyote | 275 ^j | 19800 ^j | C | Ca | | | −0.1206555 | −0.1202 | 76 | 76 |
| <i>Canis lupus dingo</i> (Canidae) dingo | 313 ^j | 17500 ^j | C | Ca | | | −0.0338603 | −0.0334 | 92 | 93 |
| <i>Canis lupus hallstromi</i> (Canidae) New Guinea singing dog | 235 ^j | 12300 ^j | C | Ca | | | −0.071005 | −0.0704 | 85 | 85 |

(Continued)

TABLE 2 | Continued

| Species | BF (N) | BM (g) | MV or C | Tooth | Residuals ¹ : Rodentia | Residuals ² : Rodentia | Residuals ¹ : Mammalia | Residuals ² : Mammalia | BFQ ₁ | BFQ ₂ |
|---|-------------------|---------------------|------------|-------|--------------------------------------|--------------------------------------|--------------------------------------|--------------------------------------|------------------|------------------|
| <i>Canis lupus lupus</i> (Canidae) common wolf | 593 ⁱ | 34700 ⁱ | C | Ca | | | 0.07410479 | 0.0743 | 119 | 119 |
| <i>Crocuta crocuta</i> (Hyaenidae) spotted hyena | 1569 ⁱ | 69100 ⁱ | C | Ca | | | 0.01862516 | 0.0186 | 104 | 104 |
| <i>Dasyurus maculatus</i> (Dasyuridae) spotted-tail quoll | 153 ⁱ | 3000 ⁱ | C | Ca | | | 0.09208918 | 0.0933 | 124 | 124 |
| <i>Dasyurus viverrinus</i> (Dasyuridae) eastern quoll | 65 ⁱ | 870 ⁱ | C | Ca | | | 0.02690553 | 0.0286 | 106 | 107 |
| <i>Felis concolor</i> (Felidae) cougar | 472 ⁱ | 34500 ⁱ | C | Ca | | | −0.0235762 | −0.0234 | 95 | 95 |
| <i>Felis sylvestris</i> (Felidae) wildcat | 56 ⁱ | 2800 ⁱ | C | Ca | | | −0.3273262 | −0.3261 | 47 | 47 |
| <i>Felis yagouaroundi</i> (Felidae) jaguarundi/eyra | 127 ⁱ | 7100 ⁱ | C | Ca | | | −0.2021689 | −0.2013 | 63 | 63 |
| <i>Genetta tigrina</i> (Viverridae) Cape genet | 73 ⁱ | 6200 ⁱ | C | Ca | | | −0.4090781 | −0.4082 | 39 | 39 |
| <i>Hyaena hyaena</i> (Hyaenidae) striped hyena | 545 ⁱ | 40800 ⁱ | C | Ca | | | −0.002663 | −0.0025 | 99 | 99 |
| <i>Lycaon pictus</i> (Canidae) African hunting/painted dog | 428 ⁱ | 18900 ⁱ | C | Ca | | | 0.0829776 | 0.0834 | 121 | 121 |
| <i>Lynx rufus</i> (Felidae) bobcat | 98 ⁱ | 2900 ⁱ | C | Ca | | | −0.0929795 | −0.0918 | 81 | 81 |
| <i>Meles meles</i> (Mustelidae) badger | 244 ⁱ | 11400 ⁱ | C | Ca | | | −0.035863 | −0.0352 | 92 | 92 |
| <i>Neofelis nebulosa</i> (Felidae) clouded leopard | 595 ⁱ | 34400 ⁱ | C | Ca | | | 0.07771769 | 0.0779 | 120 | 120 |
| <i>Panthera leo</i> (Felidae) lion | 1768 ⁱ | 294600 ⁱ | C | Ca | | | 0.01877883 | 0.0182 | 104 | 104 |
| <i>Panthera onca</i> (Felidae) jaguar | 1014 ⁱ | 83200 ⁱ | C | Ca | | | 0.09049162 | 0.0904 | 123 | 123 |
| <i>Panthera pardus</i> (Felidae) leopard | 467 ⁱ | 43100 ⁱ | C | Ca | | | −0.0833255 | −0.0832 | 83 | 83 |
| <i>Panthera tigris</i> (Felidae) tiger | 1525 ⁱ | 186900 ⁱ | C | Ca | | | 0.06727106 | 0.0668 | 117 | 117 |
| <i>Proteles cristatus</i> (Hyaenidae) aardwolf | 151 ⁱ | 9300 ⁱ | C | Ca | | | −0.1938489 | −0.1931 | 64 | 64 |
| <i>Sarcophilus harrisii</i> (Dasyuridae) Tasmanian devil | 418 ⁱ | 12000 ⁱ | C | Ca | | | 0.18521922 | 0.1858 | 153 | 153 |
| <i>Urocyon cinereoargenteus</i> (Canidae) gray fox | 114 ⁱ | 5300 ⁱ | C | Ca | | | −0.1766497 | −0.1757 | 67 | 67 |
| <i>Ursus americanus</i> (Ursidae) American black bear | 541 ⁱ | 105200 ⁱ | C | Ca | | | −0.2404583 | −0.2407 | 57 | 57 |
| <i>Ursus arctos</i> (Ursidae) brown bear | 751 ⁱ | 128800 ⁱ | C | Ca | | | −0.1481451 | −0.1484 | 71 | 71 |
| <i>Ursus thibetanus</i> (Ursidae) Asian black bear | 312 ⁱ | 77200 ⁱ | C | Ca | | | −0.4028536 | −0.4030 | 40 | 40 |
| <i>Vulpes vulpes</i> (Canidae) red fox | 164 ⁱ | 8100 ⁱ | C | Ca | | | −0.1237652 | −0.1230 | 75 | 75 |
| Chiroptera | | | | | | | | | | |
| <i>Cynopterus brachyotis</i> (lesser short-nosed fruit bat) | 12 ^k | 44 ^k | MV | Ca | | | 0.03232018 | 0.0351 | 108 | 108 |
| <i>Eidolon helvum</i> (straw-colored fruit bat) | 92 ^k | 272 ^k | MV | M | | | 0.39405996 | 0.3962 | 248 | 249 |
| <i>Pteropus poliocephalus</i> (gray-headed flying fox) | 117 ^k | 820 ^k | MV | M | | | 0.02799251 | 0.0297 | 107 | 107 |
| <i>Pteropus vampyrus</i> (large/greater flying fox) | 163 ^k | 1166 ^k | MV | M | | | 0.07088074 | 0.0724 | 118 | 118 |
| <i>Rousettus egyptiacus</i> (Egyptian fruit bat) | 32 ^k | 179 ^k | MV | M | | | −0.1156485 | −0.1134 | 77 | 77 |
| <i>Artibeus jamaicensis</i> (Jamaican fruit bat) | 19 ^k | 45 ^k | MV | Ca | | | 0.2263265 | 0.2291 | 168 | 169 |
| <i>Carollia perspicillata</i> (Seba's short-tailed bat) | 4 ^k | 18 ^k | MV | Ca | | | −0.2234219 | −0.2203 | 60 | 60 |
| <i>Desmodus rotundus</i> (common vampire bat) | 9 ^l | 41 ^l | MV | Ca | | | −0.0751281 | −0.0723 | 84 | 85 |
| <i>Eptesicus furinalis</i> (Argentine brown bat) | 7 ^l | 9 ^l | MV | Ca | | | 0.19129354 | 0.1947 | 155 | 157 |
| <i>Erophylla sezekorni</i> (buffy flower bat, in the leaf-nosed bat family) | 3 ^k | 17 ^k | MV | Ca | | | −0.3342038 | −0.3310 | 46 | 47 |

(Continued)

TABLE 2 | Continued

| Species | BF (N) | BM (g) | MV or C | Tooth | Residuals ¹ : Rodentia | Residuals ² : Rodentia | Residuals ¹ : Mammalia | Residuals ² : Mammalia | BFQ ₁ | BFQ ₂ |
|---|-------------------|-------------------|---------|-------|-----------------------------------|-----------------------------------|-----------------------------------|-----------------------------------|------------------|------------------|
| <i>Glossophaga soricina</i> (Pallas's long-tongued bat) | 1 ^l | 11 ^k | MV | Ca | | | −0.7035062 | −0.7001 | 20 | 20 |
| <i>Micronycteris minuta</i> (white-bellied big-eared bat) | 2 ^l | 8 ^l | MV | Ca | | | −0.3236022 | −0.3201 | 47 | 48 |
| <i>Mimon crenulatum</i> (striped hairy-nosed bat) | 7 ^l | 16 ^l | MV | Ca | | | 0.04878841 | 0.0520 | 112 | 113 |
| <i>Molossus rufus</i> (black mastiff bat) | 8 ^l | 29 ^l | MV | Ca | | | −0.0405156 | −0.0375 | 91 | 92 |
| <i>Monophyllus redmani</i> (Leach's single leaf bat/greater Antillean long-tongued bat) | 1 ^k | 13 ^k | MV | Ca | | | −0.7448819 | −0.7416 | 18 | 18 |
| <i>Myotis albescens</i> (silver-tipped myotis) | 2 ^l | 5 ^l | MV | Ca | | | −0.2071926 | −0.2035 | 62 | 63 |
| <i>Myotis nigricans</i> (black myotis) | 1 ^l | 4 ^l | MV | Ca | | | −0.4529548 | −0.4492 | 35 | 36 |
| <i>Myotis simus</i> (velvety myotis) | 3 ^l | 8 ^l | MV | Ca | | | −0.147511 | −0.1440 | 71 | 72 |
| <i>Noctilio leporinus</i> (greater bulldog/fisherman bat) | 20 ^l | 63 ^l | MV | Ca | | | 0.16526608 | 0.1679 | 146 | 147 |
| <i>Noctilio albiventris</i> (lesser bulldog bat) | 12 ^l | 34 ^l | MV | Ca | | | 0.09617882 | 0.0991 | 125 | 126 |
| <i>Phyllostomus elongatus</i> (lesser spear-nosed bat) | 15 ^l | 35 ^l | MV | Ca | | | 0.18590925 | 0.1888 | 153 | 154 |
| <i>Phyllostomus discolor</i> (pale spear-nosed bat) | 22 ^l | 37 ^l | MV | Ca | | | 0.33847724 | 0.3414 | 218 | 219 |
| <i>Sturnira lilium</i> (little yellow-shouldered bat) | 8 ^l | 20 ^l | MV | Ca | | | 0.05151258 | 0.0546 | 113 | 113 |
| <i>Tonatia silvicola</i> (white-throated round-eared bat) | 22 ^l | 27 ^l | MV | Ca | | | 0.41651593 | 0.4195 | 261 | 263 |
| <i>Uroderma bilobatum</i> (tent-making bat) | 10 ^l | 23 ^l | MV | Ca | | | 0.11380662 | 0.1169 | 130 | 131 |
| Primate | | | | | | | | | | |
| <i>Homo sapiens</i> (humans) | 749 ^o | 2874 ^p | MV | I | | | 0.04659657 | 0.0466 | 111 | 111 |
| <i>Pongo pygmaeus</i> (orangutan) | 1712 ^m | 3233 ⁿ | C | M | | | 0.41337255 | 0.4134 | 259 | 259 |

¹Naked mole-rat castes separated (subordinate, dominant); ²Naked mole-rat castes combined (subordinate + dominant). ^aHite et al., 2019; ^bParmenter et al., 2019; ^cVan Daele et al., 2008; ^dFreeman and Lemen, 2008a; ^eWilliams et al., 2009; ^fBecerra et al., 2014; ^gRobins, 1977; ^hThomason et al., 1990; ⁱWroe et al., 2005; ^jEllis et al., 2008; ^kDumont and Herrel, 2003; ^lAguirre et al., 2002; ^mLucas et al., 1994; ⁿSilva and Downing, 1995; ^oVan Eijden, 1991; ^pRuff, 1994. Bite force data cited from previous studies were either directly measured values from behavioral studies or calculated values based on skull morphology parameters or other factors (categorical nomenclature follows Van Daele et al., 2008). BF = bite force, BM = body mass, BFQ = bite force quotient, C = calculated value, Ca = canine, g = grams, I = incisor, M = molar, MV = measured value, and N = newton.

during behavioral testing based on the calibration curve for that probe, as described above regarding the V/N ration. The maximum bite force was extracted from each experimental session (trial) for five total trials per animal. The largest bite force across all five trials per animal was used for analysis of maximum bite force (Table 1). For comparisons with other rodent species and across mammalian orders, data were log transformed to normalize the distribution of the sample values (Table 2).

All statistical analyses were performed using IBM SPSS Statistics version 26. In order to further facilitate cross-species comparisons for taxa spanning a wide range of body masses, we also calculated BFQs by applying our linear regression analyses for Mammalia (Table 2) following similar BFQ analyses from previous studies (Wroe et al., 2005; Christiansen and Wroe, 2007). To calculate BFQ, the following equation was used for separated naked mole-rat castes (dominant and subordinate; Table 2):

$$BFQ_1 = 100 \left(\frac{BF}{10^{0.5703(\log_{10} BM) + 0.1096}} \right)$$

where BF is bite force and BM is body mass. For combined naked mole-rat castes (Table 2), the following equation was used:

$$BFQ_2 = 100 \left(\frac{BF}{10^{0.5712(\log_{10} BM) + 0.1053}} \right)$$

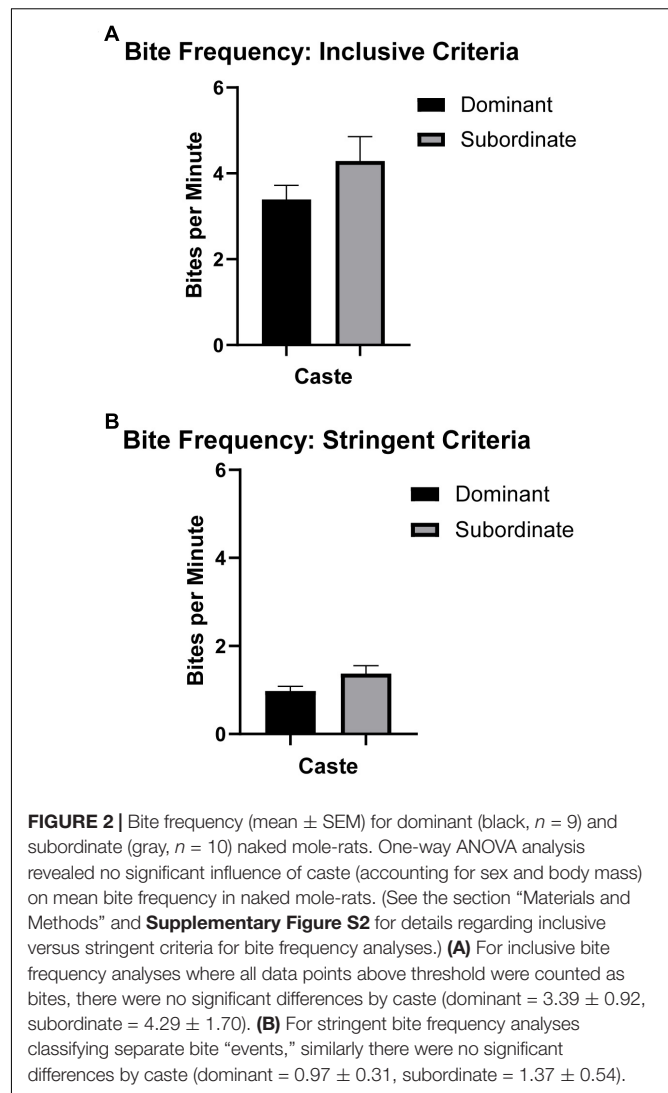
For bite latency and bite frequency analyses, comparisons were made using the mean values across the five trials per animal (Table 1). We used Matlab to locate the first data point that passed the force threshold (at least two standard deviations above the mean of all recorded force sensor data for that session from the start time of each trial) to qualify as a bite and to assess latency. In addition, two separate bite frequency analyses were performed using Matlab to quantify the number of individual bites that occurred per experimental session above the force threshold. The first was an inclusive bite frequency analysis in which all points above threshold were counted (Supplementary Figure S2A). The second applied more stringent criteria and required a minimum distance of 50 acquired data points between any point surpassing the threshold in order to assess separate bite

events (**Supplementary Figure S2B**). The values acquired in Matlab for bite latency, inclusive bite frequency, and stringent bite frequency were imported into SPSS Statistics version 26 for further statistical analyses. Separate ANOVA analyses used either bite frequency, bite latency, or bite force as the dependent variable; sex and caste as fixed factors; and body mass as a covariate in testing for the main effect of caste on each dependent variable. Age was not included in analyses due to its significant correlation with body mass (Spearman correlation coefficient of 0.570, $p = 0.011$).

RESULTS

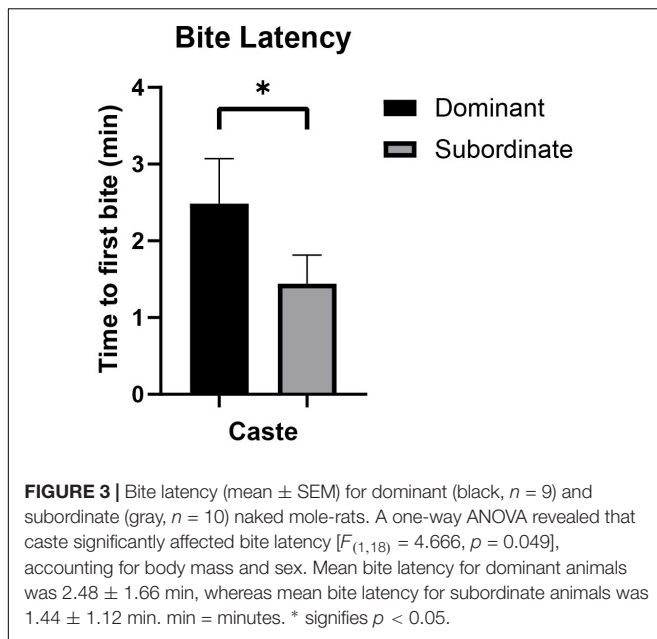
Qualitative Assessment of Biting Behaviors in Naked Mole-Rats

Overarching trends observed during bite force assessments characterized naked mole-rat biting behaviors as defensive, exploratory, digging, or chewing. One such behavior was a tendency to bite the edge of the probe and to exhibit what appeared to be defensive biting behavior. Upon grasping the probe's edge between its upper and lower incisors, the naked mole-rat would simultaneously run backward and twist its head as if attempting to tear away part of the probe (similar to the manner in which a person might twist their head while biting to tear off a piece of tough food matter such as beef jerky). A second noteworthy behavior in naked mole-rats was a tendency to gnaw on the probe in what appeared to be exploratory biting rather than defensive behavior. During exploratory biting, rather than retreating backward through its tunnel system and twisting its head, the animal kept the probe between its upper and lower incisors while continuously applying pressure to the probe and pulling on it, paired with bracing and pressing of the forelimbs and occasionally even lifting the hindlimbs off the ground. As each experimental session progressed, animals more frequently exhibited a forelimb digging motion targeting the site where the probe emerged through a slot at the tunnel's terminal. If the probe was temporarily removed, animals would occasionally place their upper incisors within the slot of the tunnel terminal and would gnaw at the edges, keeping the upper incisors in place while scraping the lower incisors along the tunnel's edge in a chisel-tooth digging fashion (Olivares et al., 2004; Samuels and Van Valkenburgh, 2009; McIntosh and Cox, 2016). If food was offered in place of the probe at the tunnel's terminal, the naked mole-rat would tear off parts of the food (e.g., sweet potato) with its incisors and retreat backward through the tunnel to the larger housing chamber where it grasped the food between its forepaws to steady it during consumption. The upper incisors were used to hold the food item in place while the lower incisors were moved in such a way so as to dislodge and scoop smaller pieces of the food that could be consumed with multiple smaller bites using the molars. Naked mole-rats likely modulate bite force across these different categories of biting behaviors in order to optimize outcomes, with defensive behaviors associated with the strongest bite forces in order to effectively protect the colony.



Naked Mole-Rat Bite Frequency and Bite Latency With Respect to Caste

Bite frequency and bite latency (**Table 1**) were analyzed to assess differences between castes that might indicate differences in motivation to bite (e.g., high bite frequency or short bite latency potentially indicating increased motivation and/or decreased inhibition to bite). Bite frequency ANOVA analyses found no significant differences in bite frequency between dominant versus subordinate animals whether the analysis was based on more inclusive criteria [$F_{(1,18)} = 1.431$, $p = 0.251$; **Figure 2A**] or more stringent criteria [$F_{(1,18)} = 2.765$, $p = 0.119$; **Figure 2B**], adjusting for body mass and sex. (Also see **Supplementary Figure S2** for an illustration of each bite frequency criterion applied to representative data.) Thus, these values can be combined across castes to yield an average bite frequency of 3.895 bites/min using inclusive criteria and 1.185 bites/min using stringent criteria. In contrast, quantification of latency to first bite showed significant effects of caste when body mass and sex were accounted for [$F_{(1,18)} = 4.666$, $p = 0.049$; **Figure 3**]. Dominant naked mole-rats



took nearly twice as long to produce their first bite compared to subordinate animals (2.48 ± 1.66 s versus 1.44 ± 1.12 s, respectively; **Table 1**).

Naked Mole-Rat Maximum Bite Force With Respect to Caste

For the naked mole-rats included in this study, body mass—shown by previous studies in other species to be a key predictor of maximum bite force—was distributed across a relatively wide range of 32.4–94.1 g (**Table 1**). The maximum bite forces produced also varied across a wide range of 7.74–35.95 N, with an average maximum bite force of 19.82 ± 4.68 N in dominant naked mole-rats and 21.07 ± 8.89 N in subordinate naked mole-rats (**Table 1**). When naked mole-rats were separated by caste, distinct differences in maximum bite force were observed with respect to body mass. Initial correlation assessments of each group showed that maximum bite force was significantly and positively correlated with body mass in subordinate animals (Spearman correlation coefficient of 0.7212, $p = 0.019$; **Figure 4A**), as predicted based on other species. However, in dominant animals, maximum bite force was not correlated with body mass (Spearman correlation coefficient of 0.1833, $p = 0.637$; **Figure 4B**). Thus, whereas bite force increased with body mass in subordinate animals, it remained similar irrespective of body mass in dominant animals. ANOVA analysis further confirmed that maximum bite force showed a significant main effect of caste [$F_{(1,18)} = 6.212$, $p = 0.026$], adjusting for body mass and sex, indicating that a naked mole-rat's role within the eusocial hierarchy was significantly interrelated with maximum bite force when the comparison between castes was conducted on a body mass-corrected bite force measure. There was also a significant main effect of body mass on bite force [$F_{(1,18)} = 10.800$, $p = 0.005$]. Sex approached but did not reach a significant effect on bite force [$F_{(1,18)} = 4.298$, $p = 0.057$], and there was

no significant interaction between caste and sex on bite force measures [$F_{(1,18)} = 0.209$, $p = 0.654$].

Maximum Bite Force in Naked Mole-Rats Compared to Other Mammalian Species

There was a significant, positive allometric relationship between maximum bite force and body mass analyzed across naked mole-rats and 21 additional species of Rodentia whether naked mole-rat castes were separated ($y = 0.5376x + 0.2571$, $R^2 = 0.7061$, $p < 0.001$; **Figure 5A** and **Table 2**) or combined ($y = 0.5388x + 0.2518$, $R^2 = 0.7090$, $p < 0.001$; **Figure 5B** and **Table 2**). Compared to other rodents, when naked mole-rats were separated by caste (**Figure 5A**), subordinate naked mole-rats exhibited bite forces that exceeded predicted values (residual of 0.1266) whereas dominant naked mole-rats exhibited bite forces that more closely approximated predicted values (residual of 0.0273; **Table 2**). This equated to a predicted bite force of 15.74 N for subordinate animals compared to our directly measured average value of 21.07 N, which was 34% greater than the predicted subordinate bite force. Dominant animals were predicted to have a bite force of 18.61 N, compared to our directly measured average value of 19.82 N, which was only 6.5% greater than predicted and more closely matched the predicted dominant bite force. Combining subordinate and dominant castes to be grouped together (**Figure 5B**) brought the naked mole-rat residual to 0.0930 (**Table 2**) with a predicted bite force of 16.53 N, compared to our directly measured average value of 20.48 N for the combined castes, which was 24% greater than the predicted bite force. Thus, naked mole-rats exhibited a bite force that was stronger than predicted for their body mass compared to other rodent species, and this was primarily driven by the performance of subordinate naked mole-rats.

The significant, positive relationship between bite force and body mass was also found when the Rodentia comparison was broadened to encompass additional mammalian orders for a total of 83 mammalian species, including naked mole-rats separated by caste ($y = 0.5703x + 0.1096$, $R^2 = 0.9244$, $p < 0.001$; **Figure 6** and **Table 2**). Within this scope, naked mole-rat bite force exceeded predicted values for each caste when separated (residual of 0.2169 for subordinate naked mole-rats, residual of 0.1133 for dominant naked mole-rats). The cross-order mammalian comparison generated a predicted bite force of 12.79 N for subordinate naked mole-rats (compared to our directly measured average value of 21.07 N, which was 65% greater than the predicted subordinate bite force) and 15.27 N for dominant naked mole-rats (compared to our directly measured average value of 19.82 N, which was 30% greater than the predicted dominant bite force). Combining subordinate and dominant castes ($y = 0.5712x + 0.1053$, $R^2 = 0.9252$, $p < 0.001$) generated a residual of 0.1814 and a predicted bite force of 13.49 N for naked mole-rats (compared to our directly measured average value of 20.48 N for the combined castes, which was 52% greater than the predicted bite force). Overall, in comparison to a wide range of mammalian species spanning multiple orders, naked mole-rat bite force remained much stronger than predicted based on body size, particularly for subordinate animals.

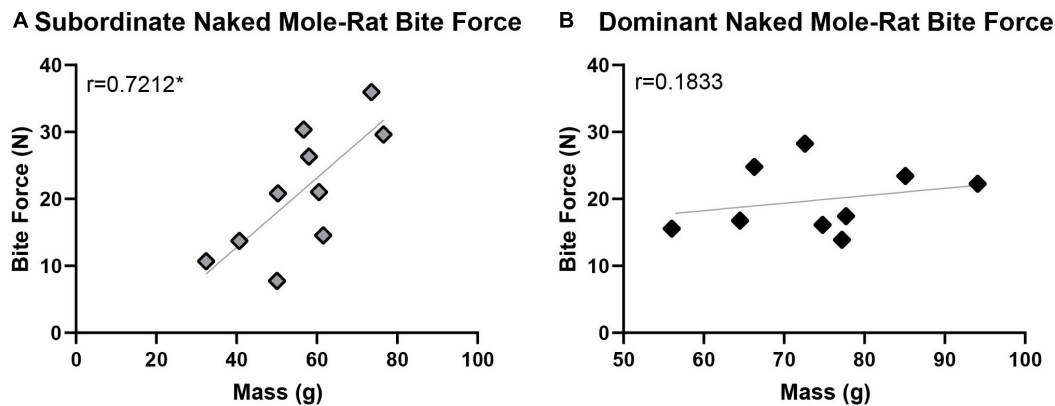


FIGURE 4 | Maximum bite force was significantly correlated with body mass in subordinate naked mole-rats (**A**; $n = 10$; $r = 0.7212$, $p = 0.019$) but not in dominant naked mole-rats (**B**; $n = 9$; $r = 0.1833$, $p = 0.637$). ANOVA analysis further confirmed that maximum bite force was significantly influenced by caste, adjusting for body mass and sex [$F_{(1,18)} = 6.212$, $p = 0.026$]. Black represents dominant naked mole-rats and gray represents subordinate naked mole-rats. * signifies $p < 0.05$.

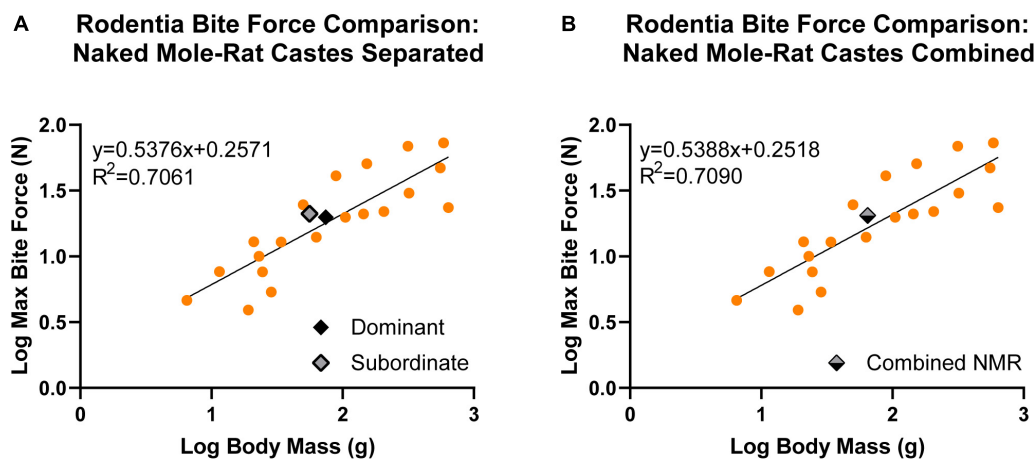


FIGURE 5 | Linear regression analyses comparing maximum bite force to body mass in naked mole-rats together with 21 additional rodent species (data from other rodent species obtained from previous studies; see **Table 2** for associated references). Data were log transformed to normalize the distribution of the sample values. There was a significant, positive allometric relationship between bite force and body mass across Rodentia. (**A**) When naked mole-rats were separated by caste ($y = 0.5376x + 0.2571$), subordinate animals (gray, $n = 10$) were above the regression line (residual = 0.1266) whereas dominant animals (black, $n = 9$) fell closer to the regression line (residual = 0.0273). (**B**) When dominant and subordinate castes were combined (gray/black; $y = 0.5388x + 0.2518$), naked mole-rats exhibited bite forces above the regression line (residual = 0.0930). g = grams, N = newton, and NMR = naked mole-rat.

Although BFQ results were similar for other mammalian species whether they were based on linear regression analyses that included naked mole-rat castes as separated (BFQ₁, **Table 2**) or combined (BFQ₂, **Table 2**), we included both sets of values for completeness and to enable either set of values to be applied to and compared with future studies. Species with BFQs of approximately 100 have bite forces equal to those predicted by the cross-species comparison for their body size (Wroe et al., 2005; Christiansen and Wroe, 2007). Subordinate and dominant naked mole-rats exhibited BFQs that exceeded predicted values (164.78 and 129.79, respectively) whereas grouping castes together produced a naked mole-rat BFQ of 151.74, altogether indicating that naked mole-rat bite force was much greater than predicted based on body mass in comparison to other mammals spanning a wide range of body masses and bite forces (**Table 2**).

DISCUSSION

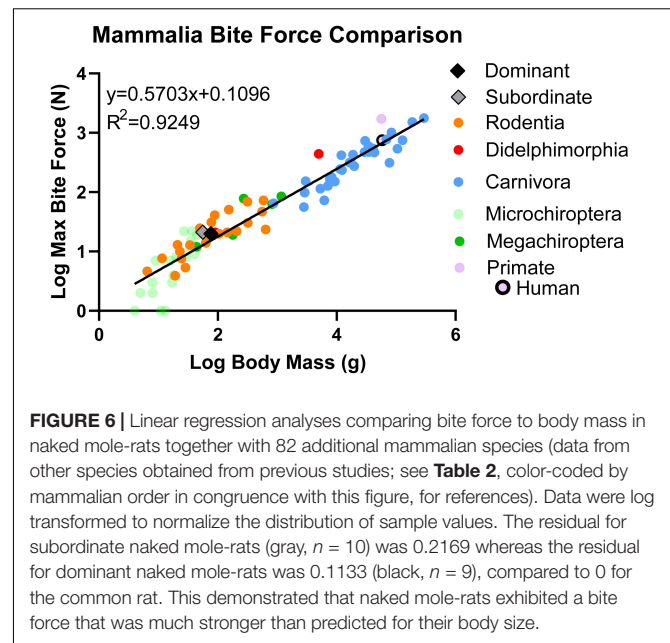
Naked mole-rats were assessed across multiple variables including bite frequency, bite latency, and maximum bite force in order to characterize their biting behaviors in relation to body mass and caste. Other studies that have assessed mammalian bite frequency have focused on chewing behaviors rather than the defensive or exploratory bites that predominantly characterized naked mole-rat biting behaviors in our study. Chewing frequency has been shown to negatively correlate with body mass in mammals, with a ceiling effect imposed by masticatory muscle capabilities (Druzinsky, 1993; Virot et al., 2017). Mammalian species studied for chewing frequency included lions (1.43 ± 0.41 Hz), orangutans (1.21 ± 0.24 Hz), humans (1.71 ± 0.42 Hz), and a

chinchilla (4.24 ± 0.59 Hz) (Virot et al., 2017). Bite frequency, as measured in the current study, does not directly compare to chewing frequency, with naked mole-rats averaging a bite frequency of approximately 1 bite/min using stringent analysis criteria (Table 1, Supplementary Figure S2B, and Figure 2B). Bite frequency was not associated with caste. In contrast to bite frequency in naked mole-rats, bite latency was significantly associated with caste. Dominant animals took nearly twice as long to initially bite the force sensor compared to subordinate animals (Table 1 and Figure 3). Very few studies have characterized mammalian bite frequency and bite latency, particularly with respect to the relationship of each of these variables with body mass or social hierarchical status. Social behaviors attributable to lower-ranking versus high-ranking animals may in part drive the influence of caste on bite latency. Subordinate animals may have a higher motivation and/or less inhibition to initiate biting behaviors, whereas dominant animals with a more established position in the colony hierarchy may exhibit less motivation and/or greater inhibition to initiate biting behaviors. Bite latency has been examined in rodents using behavioral tests of aggression which showed that shorter bite latencies were associated with increased aggression (Koolhaas et al., 2013). Latency to bite has not been previously analyzed with respect to body mass and caste, rendering it difficult to compare the relationships between these variables in naked mole-rats to those observed in other species.

The average bite force was 21.07 ± 8.89 N in subordinate naked mole-rats and 19.82 ± 4.68 N in dominant naked mole-rats (Table 1). Bite force was positively and significantly correlated with body mass in subordinate but not in dominant naked mole-rats (Figure 4). When assessed with 21 additional species of Rodentia (Figure 5 and Table 2) or expanded to 82 additional species of Mammalia (Figure 6 and Table 2), naked mole-rat bite force exceeded the values predicted based on body size, particularly for subordinate animals.

Naked Mole-Rat Bite Force Compared to Other Mammalian Species

The maximum bite force of naked mole-rats was greater than expected based on predicted values, whether these comparisons were limited to other rodents (Figure 5) or expanded across mammalian orders (Figure 6). Subordinate and dominant naked mole-rats exhibited BFQ values of 165 and 130, respectively (Table 2), whereas a measured bite force that matched predictions based on body size would have produced BFQ values of 100 (Wroe et al., 2005; Christiansen and Wroe, 2007). For their body size, subordinate naked mole-rats outperformed all of the carnivorans included for comparison, such as American black bears (BFQ of 57), lions (BFQ of 104), and wolves (BFQ of 119), all of which require strong bite forces in order to shear the muscle and crack the bones of their prey (Table 2). Subordinate naked mole-rat bite force was comparable to the value calculated for Tasmanian devils (BFQ of 153; Table 2). Like some of the carnivorans in the Mammalia comparisons, naked mole-rats occasionally consume bone, a feat associated with large bite forces (Wroe et al., 2005; Christiansen and Wroe, 2007). Often,



species with higher than predicted bite forces are also animals that hunt prey larger than themselves (Christiansen and Wroe, 2007). Naked mole-rats share some similarities with these species in that they require stronger bite forces for adversaries such as snakes that far exceed their own average body size (Sherman et al., 1991). In addition, reliance on different biting strategies also affects maximum bite force. Wroe et al. (2005) categorized distinct biting strategies for mammals, distinguishing between those that used static versus kinetic bites, the latter of which requires more force. The kinetic bites consisted of stabbing bites targeted at the neck and ones that sheared with their canines.

Naked mole-rats outperformed humans as well, with a human BFQ of 111 that closely approximated the value predicted for their body size (Table 2). If the bite force exhibited by subordinate naked mole-rats were extrapolated to the body mass of humans (2874 g; Table 2; Van Eijden, 1991), a human-sized naked mole rat would exhibit a bite force of 1110 N—48% greater than the measured human bite force. By comparison, an American black bear-sized naked mole-rat would produce a bite force of 1553 N, or 187% greater than the calculated black bear bite force; a lion-sized naked mole rat would yield a bite force of 2794 N, or 58% stronger than the lion's calculated bite force; and a wolf-sized naked mole-rat would produce a bite force of 825 N, or 39% stronger than the wolf's calculated bite force (Table 2; Wroe et al., 2005).

Although naked mole-rats exhibited higher BFQs than the majority of other mammalian species included for comparison in the present study, they were out-performed by certain species including orangutans (Lucas et al., 1994), several bat species (Aguirre et al., 2002; Dumont and Herrel, 2003), and opossums (Thomason et al., 1990), in addition to several rodent species (Table 2). These rodent species included other species of subterranean mole-rats, the African mole-rats (*Fukomys micklemi* and *Fukomys whytei*, Van Daele et al., 2008), as well

as the plains pocket gopher (Freeman and Lemen, 2008a), the grasshopper mouse (Williams et al., 2009), and the sand dune tuco-tuco (*Ctenomys australis*, Becerra et al., 2014). *C. australis* is a subterranean species that relies on both chisel- and scratch-tooth digging (Becerra et al., 2013). Socially, *C. australis* is highly aggressive, territorial, and solitary (Becerra et al., 2013)—traits shared with the ground-dwelling, carnivorous grasshopper mouse (Satoh and Iwaku, 2006; Williams et al., 2009) as well as with the fossorial pocket gopher (Freeman and Lemen, 2008a). Naked mole-rats, by comparison, are subterranean chisel-tooth diggers that are eusocial and can be aggressive as needed for colony defense or intraspecific competition. Chisel-tooth diggers are characterized by well-developed head and neck musculature utilized in biting, as well as adaptations in skull morphology such as large zygomatic arches and temporal fosse that facilitate usage of the incisors as chisel-like tools (Samuels and Van Valkenburgh, 2009). McIntosh and Cox (2016) classified chisel-tooth diggers as more capable of producing stronger bites than their scratch-digging counterparts based on dental and skull morphology related to increased behavioral reliance on and utilization of masticatory musculature.

Bite force can also be influenced by masticatory muscle variations, such as the microstructural composition and relative size of the temporalis and masseter muscles (Olivares et al., 2004), as well as differences in craniofacial morphology and gape (McIntosh and Cox, 2016). Such variations, together with divergent evolutionary pressures, likely contribute to the discrepancies in predicted versus actual bite force, and differing BFQ values (Table 2). Maximum gape is dictated by skull and muscular parameters in that gape increases with increased resting and stretch length of masticatory muscles, increased size of the temporalis muscles, increased jaw length, increased condyle length, and decreased condyle height (Satoh and Iwaku, 2006; Cox and Faulkes, 2014). Variations in gape, in turn, strongly influence bite force such that bite force negatively scales with gape angle (Dumont and Herrel, 2003; Santana, 2016). Bite force also varies according to the tooth being assessed, with higher bite forces associated with molars compared to incisors (Dumont and Herrel, 2003). Due to these factors, differences observed in our cross-mammalian comparison were likely affected by, and must be considered within the context of, the tooth being assessed for bite force (canine, molar, or incisor) and associated gape differences (Table 2).

Naked Mole-Rat Bite Force and Body Mass: Relationship to Behavioral Roles Within the Eusocial Colony Structure

Maximum bite force was correlated with body mass for subordinate naked mole-rats (Figure 4A), as predicted based on the relationship between body mass and bite force demonstrated in a wide range of other taxa (Thomason et al., 1990; Lucas et al., 1994; Aguirre et al., 2002; Dumont and Herrel, 2003; Thompson et al., 2003; Wroe et al., 2005; Freeman and Lemen, 2008a; Ellis et al., 2009; Williams et al., 2009; Becerra et al., 2014). However, in dominant naked mole-rats, bite force remained fairly constant and was not correlated with body mass (Figure 4B). Further

analysis confirmed that bite force was significantly influenced by caste. However, it should be noted that the dominant naked mole-rats in our sample are also inherently larger and older animals, and it may be the case that the correlation with bite force weakens at higher body masses rather than differences between dominant and subordinate naked mole-rats being due exclusively to caste-specific influences. When dominant and subordinate groups were combined, naked mole-rats exhibited a maximum bite force that exceeded the predicted value based on their body mass. Separating these groups by caste demonstrated that this difference was primarily driven by subordinate naked mole-rats, such that these animals exhibited bite forces well beyond those predicted for their body mass whereas dominant naked mole-rats more closely adhered to predicted values.

The eusocial colony structure of naked mole-rats is related to behavioral and body size differences between castes, as well as differing role requirements for animals within each caste. Within the present study, the dominant group was composed solely of founding members of each naked mole-rat colony. Previous studies have shown significant differences in body mass between larger naked mole-rats that established a colony (i.e., founders) versus smaller animals that were subsequently birthed into the colony, in addition to body mass fluctuations in response to changes in or disruption of the eusocial hierarchy (O’Riain and Jarvis, 1998). The first litter of a nascent colony responded most strongly to social structure changes within the colony, such as death of a male breeder, with distinct increases in body mass. O’Riain and Jarvis (1998) were also able to show that the subsequent litters (referred to in the current study as subordinates) maintained smaller body sizes unless particular animals diverged to defensive or breeding roles within the colony, at which point these animals greatly increased in body mass as a direct result of assuming a new role in the social hierarchy. When naked mole-rats were classified as breeders (more dominant) and non-breeders (more subordinate), behaviors involving utilization of the incisors such as nest building, digging, transporting food, and defense were associated with differences in body mass (Sherman et al., 1991).

As opposed to dominant naked mole-rats, subordinate animals exhibited a significant correlation between body mass and bite force. This may be related to the broad spectrum of behavioral roles and associated differences in body mass observed in subordinate naked mole-rats. Larger non-breeding subordinate animals engage in chisel-tooth digging required for excavating new tunnels. The largest of the subordinate naked mole-rats have been observed to be “volcanoers,” animals that hold positions at the openings of underground tunnels to the surface in order to kick out dirt (which takes on the outward appearance of sandy volcanoes). This is by necessity a defensive behavioral role due to the proximity to the surface rendering these animals vulnerable to predators. The large body size of these animals may also be related to the strong musculature needed to move large volumes of dirt, as is required for tunnel “volcanoing” (Hamilton, 1928). The larger subordinate animals perform tasks that require more forceful utilization of masticatory musculature than their smaller counterparts that tend to focus on nesting behaviors, thereby aligning with the

positive significant correlation of body mass with bite force. As described above, differences in gape between smaller versus larger animals may also have contributed to the bite force differences observed. However, our bite force sensors were small (1.5 mm thick) relative to the head size of naked mole-rats (see the inset in **Supplementary Figure S1C**) and should have produced minimal differences in gape across the naked mole-rats examined. Nonetheless, the influence of gape angle on bite force would be more pronounced in subordinate naked mole-rats, with the same bite force sensor requiring a proportionately larger gape in these smaller animals and potentially reducing bite force performance compared to the larger, dominant naked mole-rats.

Caveats of the Present Study

In vivo measurements from freely behaving animals, as used in the current study, can elicit highly variable responses depending on the motivation level of the animals and how successful the experimental conditions are at eliciting a true maximum bite force. As such, in spite of care being taken to elicit a true maximum bite force, any sub-optimal experimental conditions may underestimate an animal's actual capabilities. A number of factors can impact biting behaviors. One such variable is ambient temperature, which has been shown to alter biting behaviors in reptiles due to their inability to thermoregulate (Anderson et al., 2008), a quality also characterizing naked mole-rats (Johansen et al., 1976). In addition, *in vivo* bite forces are often elicited as defensive behavioral responses, thus making the effectiveness of experimental conditions in eliciting defensive behaviors a factor in accurately capturing true maximum bite force. Under our experimental conditions, the force sensor probe was combined with a blocked tunnel exit. This was perceived as an agitation and possibly also as a threat, given that our observations indicate that naked mole-rats become aggressive when a tunnel exit is blocked. One role of subordinate animals is that of defenders of the colony, making defensive biting behaviors more likely to be elicited from subordinate animals. Conversely, the dominant naked mole-rats may have been less motivated to bite under such conditions due to their minimal role in defense-related behaviors associated with their higher status in the eusocial hierarchy of the colony (Sherman et al., 1991). Previous studies have shown a positive correlation between defensive biting frequency and body mass, particularly for non-breeding subordinate males that participate in aggressive behaviors such as incisor fencing, biting, shoving, tugging, and open-mouth gaping (Sherman et al., 1991). The lack of an animate threat beyond a blocked tunnel exit could potentially have resulted in diminished defensive biting behaviors elicited in the present study compared to studies in which predators (e.g., snakes) and conspecifics were presented (Sherman et al., 1991). Finally, our comparisons to other mammalian species were weighted toward larger carnivorans for which there are disproportionately more existing data in the literature than for non-predatory species such as ungulates. This over-representation of carnivorans, in addition to differences in the teeth being assessed for bite force calculations (canines, molars, or incisors) and associated gape angle differences as described above, may have skewed our regression analyses (**Table 2** and **Figure 6**). However, naked

mole-rats out-performed all carnivorans included in the present analyses, and the addition of ungulates would very likely serve to increase rather than diminish our reported BFQ values for naked mole-rats.

Bite Force Methodological Differences and Future Directions

Previous studies assessing bite force have relied on a range of different methodologies. These have included: bite force directly measured from freely behaving animals; bite force directly measured in anesthetized animals, elicited via electrical stimulation of masticatory muscles; and bite force values that are predicted based on extrapolations from skull morphology parameters. Variations in BFQs among species may be attributed in part to the methodologies of the studies performed. Across studies, there are differences in how a bite was either directly measured or calculated (annotated as MV for directly measured values or C for calculated values in **Table 2** for cross-species comparisons included in the present study). The specific teeth assessed for bite force can also differ (i.e., molars, incisors, or canines), in addition to the environmental conditions and the animal's motivation to perform, as described above (Thomason et al., 1990; Van Eijden, 1991; Aguirre et al., 2002; Dumont and Herrel, 2003; Thompson et al., 2003; Van Daele et al., 2008; Ellis et al., 2009; Williams et al., 2009). Some bite force studies focused on wild animals that were momentarily restrained within their natural habitat and were (relatively) freely behaving, whereas others assessed wild or laboratory animals in a laboratory setting. In calculated bite force measurements, variations in the specific skull morphology parameters may have resulted in differences in extrapolated bite force predictions (Lucas et al., 1994; Wroe et al., 2005). In the present study, we feel that accurately representative naked mole-rat bite force values were obtained given that the relatively long experimental trials offered ample opportunity for the animals to produce a maximum bite force (five trials of approximately 20 min each, compared to other studies in which five total bites were recorded and the maximum was analyzed, e.g., Van Daele et al., 2008). In addition, our results are consistent with other studies predicting high bite force values for *H. glaber* based on skull morphology and cranial musculature (Cox and Faulkes, 2014; McIntosh and Cox, 2016). Future studies involving electrical stimulation of masticatory muscles, individually and in combination, would be useful in elucidating the extent to which each muscle contributes to overall bite force in naked mole-rats. In addition, intracortical microstimulation (ICMS) electrophysiological experiments targeting primary motor cortex could delineate mototopy and characterize evoked jaw movements that subserve bite force capabilities. Finally, further behavioral studies would be needed to link bite force differences to distinct hierarchical roles (e.g., defender or caretaker) in the naked mole-rat colony. This would be of particular interest in relation to: (1) longitudinal studies focused on specific animals with naturally changing social roles over time, particularly if a subordinate animal transitioned to dominant status, or (2) experimental interventions (e.g., removal of a queen, or removing animals from an established colony to start a new

colony) causing shifts in social status that could then be directly related to bite force changes.

CONCLUSION

Previous studies have shown that naked mole-rats possess qualities (biting style, skull shape, and masticatory muscle size) indicative of the potential to produce powerful bite forces. This study supported these hypotheses by demonstrating that naked-mole rats produce maximum bite forces that greatly surpass the bite force predicted for their body mass. Subordinate naked mole-rats in particular drive this increase in measured bite force compared to predicted values with their significant, positive allometric relationship of bite force to body mass, biting with forces 65% stronger than the capacity indicated by their body mass based on mammalian cross-species comparisons. This places naked mole-rat bite force performance well above most mammalian species studied to date, surpassing even carnivores such as lions, wolves, and bears that traditionally epitomize bite strength.

DATA AVAILABILITY STATEMENT

The datasets generated for this study are available on request to the corresponding author.

ETHICS STATEMENT

All experiments were performed under a protocol approved by the Southern Illinois University Institutional Animal Care and Use Committee and in accordance with the National Institutes of Health Guide for the Care and Use of Laboratory Animals (NIH Publication Nos. 8023 and 1978).

AUTHOR CONTRIBUTIONS

DS, BC, and SP contributed to experimental design. NH, CG, and MS collected data for the study. NH, DS, CG, and MS analyzed the data. NH and DS interpreted the data and

prepared the manuscript figures. NH and DS drafted and revised the manuscript.

ACKNOWLEDGMENTS

The authors would like to thank David Kukla for assistance with preliminary data, Jayasimha Sai Koduri for assistance with early stages of customized Python programming for bite force data acquisition, and Rebecca Embalabala for helpful edits in drafting the manuscript.

SUPPLEMENTARY MATERIAL

The Supplementary Material for this article can be found online at: <https://www.frontiersin.org/articles/10.3389/fnint.2019.00070/full#supplementary-material>

FIGURE S1 | Bite force sensor calibration with representative data collection from one experimental trial session and data collection system schematic. **(A)** A calibration curve was generated prior to using each force sensor for data collection, and shows the standardized force (N) applied to a piezo-resistive force sensor (Tekscan; Boston, MA, United States), as well as the resulting force sensor digital input. The representative sensor responded well within the manufacturer's $\pm 3\%$ linearity specifications ($R^2 = 0.9918$). **(B)** Data acquired from a representative bite force experimental session (one trial) is shown for one dominant adult naked mole-rat (female, 1RW, 74 g). Data were sampled at 128 Hz. **(C)** Top left inset of a naked mole-rat biting a force sensor that has been coated in protective Plasti-Dip, along with a schematic of the bite force measurement data collection system. A = 201 Flexiforce sensor (Tekscan; Boston, MA, United States), B = Tekscan Flexiforce Quickstart Board (Tekscan; Boston, MA, United States), C = Adafruit Powerboost 1000C (Adafruit; New York City, NY, United States), D = Adafruit 16bit I2C ADC + PGA ADS1115 (Adafruit; New York City, NY, United States), and E = Raspberry Pi Model B v1.2 (Adafruit; New York City, NY, United States). GND = ground, SCL = serial clock, SDA = serial data, and V = voltage.

FIGURE S2 | Illustration of two separate criteria applied in determining bite force frequency. Representative bite force data are shown from a single trial for a dominant adult female naked mole-rat (1RW). **(A)** Inclusive bite frequency criteria: illustration of data points included in the number of bites used to determine bite frequency (gray circles). All points above threshold (at least two standard deviations above the mean) were included to generate the number of bites per trial. This bite frequency was then averaged for each animal across five trials. **(B)** Stringent bite frequency criteria: illustration of data points included in analyses. Red circles represent points above threshold with a minimum of 50 acquired data points between each designated bite event.

REFERENCES

- Aguirre, L. F., Herrel, A., Van Damme, R., and Matthysen, E. (2002). Ecomorphological analysis of trophic niche partitioning in a tropical savannah bat community. *Proc. R. Soc. Lond. Ser. B Biol. Sci.* 269, 1271–1278. doi: 10.1098/rspb.2002.2011
- Aguirre, L. F., Herrel, A., Van Damme, R., and Matthysen, E. (2003). The implications of food hardness for diet in bats. *Funct. Ecol.* 17, 201–212. doi: 10.1002/jmor.20424
- Anderson, R. A., McBrayer, L. D., and Herrel, A. (2008). Bite force in vertebrates: opportunities and caveats for use of a nonpareil whole-animal performance measure. *Biol. J. Linn. Soc.* 93, 709–720. doi: 10.1111/j.1095-8312.2007.00905.x
- Artwohl, J., Hill, T., Comer, C., and Park, T. (2002). Naked mole-rats: unique opportunities and husbandry challenges. *Lab Anim.* 31, 32–36.
- Becerra, F., Casinos, A., and Vassallo, A. I. (2013). Biting performance and skull biomechanics of a chisel tooth digging rodent (*Ctenomys tuconax*; *Caviomorpha*; *Octodontoidea*). *J. Exp. Zool. Part A Ecol. Genet. Physiol.* 319, 74–85. doi: 10.1002/jez.1770
- Becerra, F., Echeverría, A. I., Casinos, A., and Vassallo, A. I. (2014). Another one bites the dust: bite force and ecology in three caviomorph rodents (*Rodentia*, *Hystricognathi*). *J. Exp. Zool. Part A Ecol. Genet. Physiol.* 321, 220–232. doi: 10.1002/jez.1853
- Brett, R. A. (1991). "The ecology of naked mole-rat colonies: burrowing, food and limiting factors," in *The Biology of the Naked Mole-Rat*, eds P. W. Sherman, J. U. M. Jarvis, and R. D. Alexander, (New Jersey, NJ: Princeton University Press), 137–184.
- Cain, B. W., Reynolds, T., and Sarko, D. K. (2019). Superficial, suprahyoid, and infrahyoid neck musculature in naked mole-rats (*Heterocephalus glaber*):

- relative size and potential contributions to independent movement of the lower incisors. *J. Morphol.* 280, 1185–1196. doi: 10.1002/jmor.21022
- Christiansen, P., and Wroe, S. (2007). Bite forces and evolutionary adaptations to feeding ecology in carnivores. *Ecology* 88, 347–358.
- Cox, P. G., and Faulkes, C. G. (2014). Digital dissection of the masticatory muscles of the naked mole-rat, *Heterocephalus glaber* (Mammalia, Rodentia). *PeerJ* 2:e448. doi: 10.7717/peerj.448
- Cox, P. G., and Jeffery, N. (2011). Reviewing the morphology of the jaw-closing musculature in squirrels, rats, and guinea pigs with contrast-enhanced microCT. *Anat. Rec. Adv. Integr. Anat. Evol. Biol.* 294, 915–928. doi: 10.1002/ar.21381
- Druzinsky, R. E. (1993). The time allometry of mammalian chewing movements: chewing frequency scales with body mass in mammals. *J. Theor. Biol.* 160, 427–440.
- Dumont, E. R., and Herrel, A. (2003). The effects of gape angle and bite point on bite force in bats. *J. Exp. Biol.* 206, 2117–2123. doi: 10.1242/jeb.00375
- Ellis, J. L., Thomason, J. J., Kebreab, E., and France, J. (2008). Calibration of estimated biting forces in domestic canids: comparison of post-mortem and *in vivo* measurements. *J. Anat.* 212, 769–780. doi: 10.1111/j.1469-7580.2008.00911.x
- Ellis, J. L., Thomason, J., Kebreab, E., Zubair, K., and France, J. (2009). Cranial dimensions and forces of biting in the domestic dog. *J. Anat.* 214, 362–373. doi: 10.1111/j.1469-7580.2008.01042.x
- Erickson, G. M., Lappin, A. K., and Vliet, K. A. (2003). The ontogeny of bite-force performance in American alligator (*Alligator mississippiensis*). *J. Zool.* 260, 317–327. doi: 10.1017/S0952836903003819
- Faulkes, C. G., and Bennett, N. C. (2001). Family values: group dynamics and social control of reproduction in African mole-rats. *Trends Ecol. Evol.* 16, 184–190. doi: 10.1016/S0169-5347(01)02116-2
- Freeman, P. W., and Lemen, C. A. (2008a). A simple morphological predictor of bite force in rodents. *J. Zool.* 275, 418–422. doi: 10.1111/j.1469-7998.2008.00459.x
- Freeman, P. W., and Lemen, C. A. (2008b). Measuring bite force in small mammals with a piezo-resistive sensor. *J. Mammal.* 89, 513–517. doi: 10.1644/07-mamm-a-101r.1
- Hamilton, W. J. (1928). *Heterocephalus: the Remarkable African Burrowing Rodent*. New York, NY: Macmillan.
- Herrel, A., and O'Reilly, J. C. (2005). Ontogenetic scaling of bite force in lizards and turtles. *Physiol. Biochem. Zool.* 79, 31–42. doi: 10.1086/498193
- Herrel, A., O'Reilly, J. C., and Richmond, A. M. (2002). Evolution of bite performance in turtles. *J. Evol. Biol.* 15, 1083–1094. doi: 10.1046/j.1420-9101.2002.00459.x
- Hite, N. J., Germain, C., Cain, B. W., Sheldon, M., Perala, S. S. N., and Sarko, D. K. (2019). The better to eat you with: bite force in the naked mole-rat (*Heterocephalus glaber*) is stronger than predicted based on body size. *Front. Integr. Neurosci.* 13:70. doi: 10.3389/fnint.2019.00070
- Johansen, K., Lykkeboe, G., Weber, R. E., and Maloiy, G. M. O. (1976). Blood respiratory properties in the naked mole rat *Heterocephalus glaber*, a mammal of low body temperature. *Respir. Physiol.* 28, 303–314. doi: 10.1016/0034-5687(76)90025-9
- Koolhaas, J. M., Coppens, C. M., de Boer, S. F., Buwalda, B., Meerlo, P., and Timmermans, P. J. A. (2013). The resident-intruder paradigm: a standardized test for aggression, violence and social stress. *J. Vis. Exp.* 4:e4367. doi: 10.3791/4367
- Lappin, A. K., Wilcox, S. C., Moriarty, D. J., Stoeppler, S. A. R., Evans, S. E., and Jones, M. E. H. (2017). Bite force in the horned frog (*Ceratophrys cranwelli*) with implications for extinct giant frogs. *Sci. Rep.* 7:11963. doi: 10.1038/s41598-017-11968-1
- Lucas, P. W., Peters, C. R., and Arrandale, S. R. (1994). Seed-breaking forces exerted by orangutans with their teeth in captivity and a new technique for estimating forces produced in the wild. *Am. J. Phys. Anthropol.* 94, 365–378. doi: 10.1002/ajpa.1330940306
- Maestri, R., Patterson, B. D., Fornel, R., Monteiro, L. R., and de Freitas, T. R. O. (2016). Diet, bite force and skull morphology in the generalist rodent morphotype. *J. Evol. Biol.* 29, 2191–2204. doi: 10.1111/jeb.12937
- Marshall, C. D., Guzman, A., Narazaki, T., Sato, K., Kane, E. A., and Sterba-Boatwright, B. D. (2012). The ontogenetic scaling of bite force and head size in loggerhead sea turtles (*Caretta caretta*): implications for durophagy in neritic, benthic habitats. *J. Exp. Biol.* 215, 4166–4174. doi: 10.1242/jeb.074385
- McIntosh, A. F., and Cox, P. G. (2016). Functional implications of craniomandibular morphology in African mole-rats (*Rodentia: Bathyergidae*). *Biol. J. Linn. Soc.* 117, 447–462. doi: 10.1111/bij.12691
- Olivares, A. I., Verzi, D. H., and Vassallo, A. I. (2004). Masticatory morphological diversity and chewing modes in South American caviomorph rodents (family Octodontidae). *J. Zool.* 263, 167–177. doi: 10.1017/S095283690400500X
- O'Riain, M. J., and Jarvis, J. U. M. (1998). The dynamics of growth in naked mole-rats: the effects of litter order and changes in social structure. *J. Zool.* 246, 49–60. doi: 10.1017/S0952836998009066
- Parmenter, M. D., Nelson, J. P., Weigel, S. E., Gray, M. M., Payseur, B. A., and Vinyard, C. J. (2019). Masticatory apparatus performance and functional morphology in the extremely large mice from gough island. *Anat. Rec.* 1–13. doi: 10.1002/ar.24053 [Epub ahead of print]
- Robins, M. W. (1977). Biting loads generated by the laboratory rat. *Arch. Oral Biol.* 22, 43–47.
- Ruff, C. B. (1994). Morphological adaptation to climate in modern and fossil hominids. *Am. J. Phys. Anthropol.* 37, 65–107.
- Rüppell, E. (1842). Säugethiere aus der Ordnung der Nager, beobachtet im nordöstlichen Africa. *Mus. Senck.* 3, 99–101.
- Samuels, J. X., and Van Valkenburgh, B. (2009). Craniodental adaptations for digging in extinct burrowing beavers. *J. Vertebr. Paleontol.* 29, 254–268. doi: 10.1080/02724634.2009.10010376
- Santana, S. E. (2016). Quantifying the effect of gape and morphology on bite force: biomechanical modelling and *in vivo* measurements in bats. *Funct. Ecol.* 30, 557–565. doi: 10.1111/1365-2435.12522
- Satoh, K., and Iwaku, F. (2006). Jaw muscle functional anatomy in northern grasshopper mouse, *Onychomys leucogaster*, a carnivorous murid. *J. Morphol.* 267, 987–999. doi: 10.1002/jmor
- Sherman, P. W., Jarvis, J. U. M., and Alexander, R. D. (1991). *The Biology of the Naked Mole-Rat*. Princeton, NJ: Princeton University Press.
- Sherman, W., Jarvis, J. U. M., and Braude, S. H. (1992). *Naked Mole Rats*. Available at: https://www.researchgate.net/profile/Stan_Braude/publication/260566942_Naked_Mole_Rats/links/5716678308aefeb022c36cc/Naked-Mole-Rats.pdf (accessed June 14, 2019).
- Silva, M., and Downing, J. A. (1995). *CRC Handbook of Mammalian Body Masses*. Boca Raton, FL: CRC Press.
- Thomason, J., Russell, A. P., and Morgeli, M. (1990). Forces of biting, body size, and masticatory muscle tension in the opossum *Didelphis virginiana*. *Can. J. Zool.* 68, 318–324.
- Thompson, E. N., Biknevicius, A. R., and German, R. Z. (2003). Ontogeny of feeding function in the gray short-tailed opossum *Monodelphis domestica*: empirical support for the constrained model of jaw biomechanics. *J. Exp. Biol.* 206, 923–932. doi: 10.1242/jeb.00181
- Van Daele, P. A., Herrel, A., and Adriaens, D. (2008). Biting performance in teeth-digging African mole-rats (Fukomys, Bathyergidae, Rodentia). *Physiol. Biochem. Zool.* 82, 40–50. doi: 10.1086/594379
- Van Eijden, T. M. (1991). Three-dimensional analyses of human bite-force magnitude and moment. *Arch. Oral Biol.* 36, 535–539.
- Virost, E., Ma, G., Clanet, C., and Jung, S. (2017). Physics of chewing in terrestrial mammals. *Sci. Rep.* 7, 6–11. doi: 10.1038/srep43967
- Williams, S. H., Peiffer, E., and Ford, S. (2009). Gape and bite force in the rodents *Onychomys leucogaster* and *Peromyscus maniculatus*: does jaw-muscle anatomy predict performance? *J. Morphol.* 270, 1338–1347. doi: 10.1002/jmor.10761
- Wroe, S., McHenry, C., and Thomason, J. (2005). Bite club: comparative bite force in big biting mammals and the prediction of predatory behaviour in fossil taxa. *Proc. R. Soc. B Biol. Sci.* 272, 619–625. doi: 10.1098/rspb.2004.2986

Conflict of Interest: The authors declare that the research was conducted in the absence of any commercial or financial relationships that could be construed as a potential conflict of interest.

Copyright © 2019 Hite, Germain, Cain, Sheldon, Perala and Sarko. This is an open-access article distributed under the terms of the Creative Commons Attribution License (CC BY). The use, distribution or reproduction in other forums is permitted, provided the original author(s) and the copyright owner(s) are credited and that the original publication in this journal is cited, in accordance with accepted academic practice. No use, distribution or reproduction is permitted which does not comply with these terms.



Effect of Sudden Deprivation of Sensory Inputs From Periodontium on Mastication

Anastasios Grigoriadis^{1,2*}, Abhishek Kumar^{1,2}, Magnus K. Åberg³ and Mats Trulsson^{1,2}

¹ Section of Oral Rehabilitation, Division of Oral Diagnostics and Rehabilitation, Department of Dental Medicine, Karolinska Institutet, Huddinge, Sweden, ² Scandinavian Center for Orofacial Neurosciences, Huddinge, Sweden, ³ Department of Environmental Science and Analytical Chemistry, Stockholm University, Stockholm, Sweden

Objective: To investigate the effect of sudden deprivation of sensory inputs from the periodontium on jaw kinematics and time-varying activation profile of the masseter muscle.

Methods: Fourteen (age range: 22–26 years; four men) healthy and natural dentate volunteers participated in a single experimental session. During the experiment, the participants were asked to eat six hard visco-elastic test food models, three each before and after an anesthetic intervention. The movements of the jaw in three dimensions and electromyographic (EMG) activity of the masseter muscle on the chewing side were recorded.

Results: The results of the study showed no significant differences in the number of chewing cycles ($P = 0.233$) and the duration of chewing sequence ($P = 0.198$) due to sudden deprivation of sensory inputs from the periodontium. However, there was a significant increase in the jaw opening velocity ($P = 0.030$) and a significant increase in the duration of occlusal phase ($P = 0.004$) during the anesthetized condition. The EMG activity of the jaw closing phase was significantly higher during the control condition [116.5 arbitrary units (AU)] than anesthetized condition (93.9 AU). The temporal profile of the masseter muscle showed a biphasic increase in the excitatory muscle drive in the control condition but this increase was virtually absent during the anesthetized condition.

Conclusion: Sudden deprivation of sensory inputs from the periodontium affects the jaw kinematics and jaw muscle activity, with a clear difference in the time-varying activation profile of the masseter muscle. The activation profile of the masseter muscle shows that periodontal mechanoreceptors contribute to approximately 20% of the EMG activity during the jaw closing phase.

Keywords: temporal profile, jaw muscle activity, periodontal mechanoreceptors, viscoelastic hard food, muscle activation, jaw kinematics

INTRODUCTION

The rhythmic masticatory movements of the jaws help in the physical breakdown of food morsels into smaller particles and form a soft bolus suitable for swallowing. The central pattern generators located in the brain stem are responsible for generating the basic rhythmic jaw movements (Dellow and Lund, 1971; Lund, 1991; Lund et al., 1998). The afferent sensory information from

OPEN ACCESS

Edited by:

Limor Avivi-Arber,
University of Toronto, Canada

Reviewed by:

Makoto Inoue,
Niigata University, Japan
Greg Murray,
The University of Sydney, Australia

*Correspondence:

Anastasios Grigoriadis
Anastasios.Grigoriadis@ki.se

Specialty section:

This article was submitted to
Systems Biology,
a section of the journal
Frontiers in Neuroscience

Received: 14 June 2019

Accepted: 25 November 2019

Published: 10 December 2019

Citation:

Grigoriadis A, Kumar A, Åberg MK
and Trulsson M (2019) Effect
of Sudden Deprivation of Sensory
Inputs From Periodontium on
Mastication.
Front. Neurosci. 13:1316.
doi: 10.3389/fnins.2019.01316

in and around the oral cavity modify and fine-tune the jaw movements. One important class of somatosensory receptors is located in the collagen fibers within the periodontal ligament space of the tooth root. These primary afferent receptors are called periodontal mechanoreceptors (PMRs). The PMRs are efficient in encoding specific information for modulating the jaw motor neuron activity responsible for regulation of forces and jaw movements during chewing (Lund, 1991; Trulsson, 2006). Specifically, it is suggested that the sensory information from the PMRs are used by the central nervous system to optimize food positioning between the teeth and regulate the force levels and force vectors involved in biting. Further, the forces required in regulating the masticatory movements can also be influenced by the motor cortex (Sessle, 2006; Sessle et al., 2007, 2013; Avivi-Arber et al., 2011). Thus, mastication is a semiautomatic, subconscious activity that can be brought to conscious control according to the specifics of task demand (Westberg and Kolta, 2011).

The jaw muscle activity adapts to the changing properties/hardness of the food during the masticatory sequence. The jaw muscle activity is generally higher while chewing harder food than chewing softer food (Peyron et al., 2002; Grigoriadis et al., 2011, 2014; Iguchi et al., 2015; Grigoriadis and Trulsson, 2018). However, people lacking PMRs as in case of patients with implant supported bridges show an impaired adaptation to food hardness (Grigoriadis et al., 2011). While both “implant patient” and the “naturally dentate” groups show similar behavior in chewing soft food morsels, the implant patient group particularly demonstrate signs of impairment while chewing harder food (Grigoriadis et al., 2011). It has been previously shown that the adaptation to the physical characteristics of the food (including its rheological properties) is caused by changes in the muscle commands that alter jaw kinematics and chewing forces (Ottenhoff et al., 1992, 1993; Grigoriadis et al., 2011). These studies have shown that a major fraction of the observed jaw muscle activity also referred to as the “additional muscle activity” is used to overcome the resistance offered by the food hardness during the act of chewing (Ottenhoff et al., 1992, 1993). While a smaller fraction of this muscle activity is also utilized to move the jaw. However, the muscle build up for the jaw movements can partially also occur in anticipation to the tooth food contact (Westberg and Kolta, 2011).

Studies on anesthetized rabbits indicate that the component of “additional muscle activity” that precedes the early tooth–food contact during chewing is unaffected by blocking the PMRs. Likewise, other animal studies suggest that signals from muscle spindles are most important during the early phases of force generation, whereas inputs from both muscle spindles and PMRs are important during the later phases (Lavigne et al., 1987; Morimoto et al., 1989). Previously, we have shown impaired force control and impaired spatial regulation in healthy young adults after anesthesia of the teeth during biting tasks (Trulsson and Johansson, 1996; Grigoriadis et al., 2017; Kumar et al., 2017). We have previously also described the chewing sequence, chewing cycle, and time-varying activation profile of the masseter muscle and how food hardness affects the profile during natural chewing in healthy participants (Grigoriadis et al., 2014). Subsequently,

it was shown that unlike natural dentate participants who demonstrate increased ability to adapt jaw muscle activity according to the food hardness, the implant prosthesis patients fail to adapt/increase the jaw muscle activity (Grigoriadis et al., 2011). However, the degree of contribution of the PMRs in the regulation of jaw muscle activity during chewing has not been studied. Therefore, in the current study we investigated the effect of sudden deprivation of sensory inputs from the periodontium on jaw kinematics and time-varying activation profile of the masseter muscle. We hypothesized that sudden deprivation of sensory inputs would alter the jaw movement kinetics and jaw muscle activity along with changes in the time-varying activation profile of the masseter muscles similar to the findings from implant patients in the previous studies (Grigoriadis et al., 2011; Grigoriadis and Trulsson, 2018).

MATERIALS AND METHODS

Study Participants

The study included 14 (age range: 22–26 years; four men) healthy and natural dentate participants with at least 28 permanent teeth. At the time of the experiment none of the participants reported, nor indicated, any problems or dysfunctions related to biting or chewing behavior. The Regional Ethical Review Board, Stockholm, Sweden, approved the study and all participants gave written informed consent in accordance with the Declaration of Helsinki II, prior to the start of the experiment.

Experimental Protocol

The participants voluntarily participated in a single experimental session. During the experiment the participants were asked to chew and swallow a hard visco-elastic test food models three times each (total six trials) before and after an anesthetic intervention. The participants were also asked about their preferred chewing side and were instructed to chew only on the preferred chewing side throughout the experiment. The recipe for the preparation of the visco-elastic model foods has been previously described in detail, see Grigoriadis et al. (2011) for more information. The test food model was cylindrical (20 mm × 10 mm) in shape with a hardness of about 129 ± 21 kPa. Before the start of each trial, the experimenter placed the test food morsel on the extended tongue of the participant. The participants were asked to hold the test food between the tongue and the palate with the mouth closed and their teeth in maximum intercuspation for about 2–4 s. Further, the experimenter signaled the participants to start chewing and place the teeth back again in intercuspation once the morsel was swallowed. Between trials, the participants were free to drink, rest, speak, and rinse the mouth if they desired to. The participants were not given any specific information regarding the objective of the study prior to the start of the experiment.

Anesthetic Intervention

A computer-assisted system for local anesthesia (The Wand®, Milestone Scientific, Livingston, NJ, United States) was used to anesthetize the teeth on the preferred chewing side of both

the jaws. Anesthesia was achieved by local infiltration and periodontal injections of approximately 6×1.8 ml anesthetic solution (Citanest®, Dentsply Sirona, Sweden). The participants were asked to confirm the subjective symptoms associated with local anesthesia and these symptoms were objectively evaluated by lack of response to light touch and pressure to the anesthetized teeth.

Recording Jaw Movements and Muscle Activity

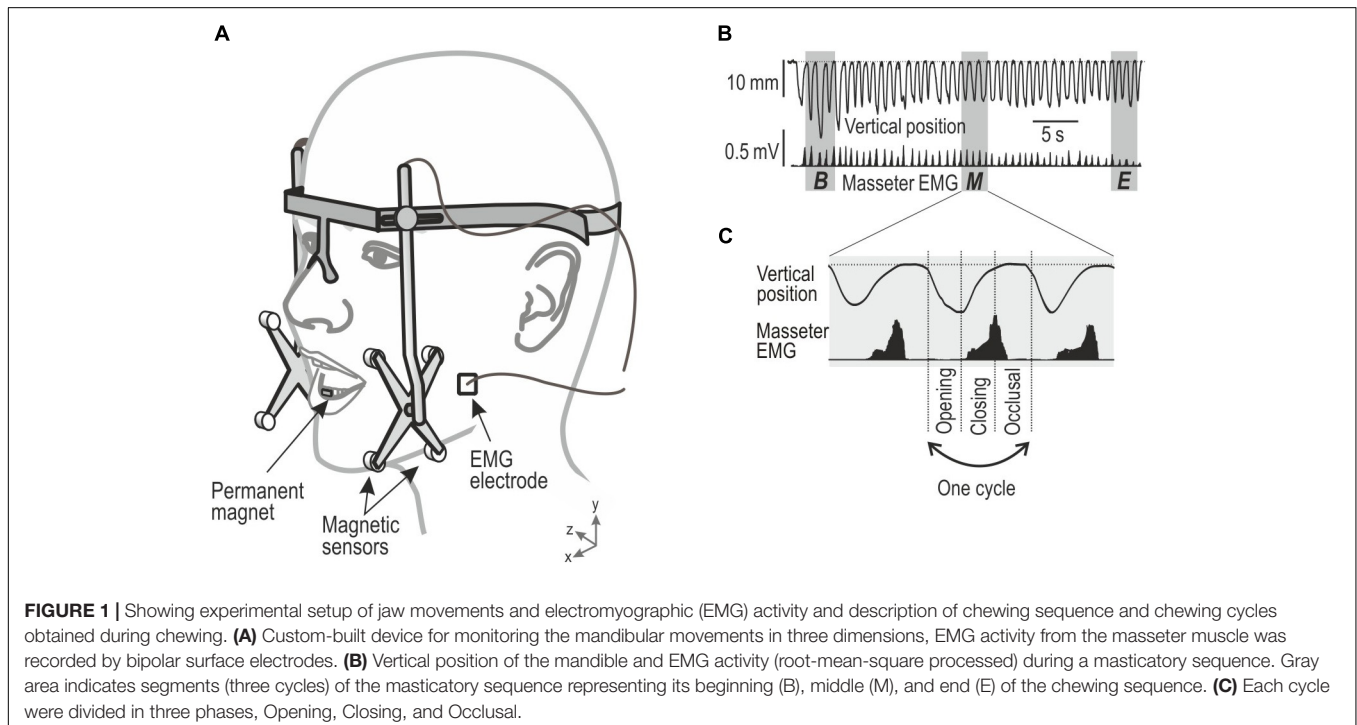
The apparatus and the general description of the armamentariums used in the current experiment have been described in detail in our earlier publications; see Grigoriadis et al. (2011, 2014), Svensson et al. (2013), Kumar A. et al. (2015), and Grigoriadis and Trulsson (2018). Briefly, movements of the lower jaw in reference to the upper jaw were measured using a custom built three dimensional, jaw movement tracking equipment (Department of Integrative Medical Biology, Umeå University, Umeå, Sweden). The labial surface of mandibular central incisors was etched and a small magnet ($10 \times 5 \times 5$ mm) was attached with dental composites. A lightweight frame equipped with eight magnetic sensors (four on each side) that tracked the position of the magnet in all three dimensions (accuracy: 0.1 mm; bandwidth: 0–100 Hz) was attached to the head of the participant in a spectacle-like frame (**Figure 1A**). The frame was further secured with adjustable straps. The electromyographic (EMG) activity of the masseter muscle was recorded with customized, bipolar, surface electrodes (Department of Integrative Medical Biology, Umeå University, Umeå, Sweden). The skin over the masseter muscle was cleansed thoroughly with alcohol and electrodes (2 mm in diameter

and 12 mm apart) were carefully placed on the muscle after palpation. The data acquired was stored using the SC/ZOOM microcomputer-based data acquisition and analyzed with customized software (SC/ZOOM, v. 3.1.02, Physiology Section, IMB, Umeå University, Umeå, Sweden). Further, the data acquired was transferred to Matlab (Version R2010b, The MathWorks, Inc.) for analysis.

Data Analysis

The outcome variables and the areas of interest were similar to our previous studies (Grigoriadis et al., 2014; Grigoriadis and Trulsson, 2018). The jaw movement kinematics were established to study the number of chewing cycles and the duration of the chewing sequence during each trial. The vertical and lateral amplitude of the jaw movements during a single chewing cycle along with the peak velocity of the jaw during jaw opening and jaw closing were also measured in the vertical and lateral dimension. The analysis was focused on three segments that represented the beginning, middle, and end of each chewing sequence (**Figure 1B**). Each segment was represented by the mean of three consecutive cycles in the beginning, middle, and the end of the chewing sequence. The first and the last cycle of the sequence were excluded due to great intra-individual variability across trials. Thus, the first and the last segment represented about second to fourth cycles during the onset and offset of the chewing sequence, respectively. The segment representing the middle of the sequence included the three cycles located in its center.

Each chewing cycle consisted of a jaw-opening phase, followed by a jaw closing phase and an occlusal phase (**Figure 1C**). The start of the jaw-opening phase was characterized by the



opening of the jaw from the occlusal state by 1 mm. The occlusal state was characterized for each participant as the minimum jaw opening recorded during each trial, including the periods when the participants' teeth were in maximum intercuspation. The jaw opening phase ended at peak jaw opening and was followed by the jaw closing phase which subsequently ended when the jaw reached the same vertical jaw position as when the jaw opening phase begun (Grigoriadis et al., 2014). Finally, the occlusal phase, started at the end of the closing phase, and ended at the beginning of the jaw-opening phase of the subsequent chewing cycle (Grigoriadis et al., 2014).

The EMG signals were sampled at 3.2 kHz and thereafter the root mean square (RMS) of the EMG signals was processed over a moving time window corresponding to 100 samples (31 ms). The RMS-processed signals were integrated during each phase of each chewing cycle giving each phase a measure corresponding to the area under the RMS-processed EMG signal. The total EMG activity for each chewing cycle was also computed as the sum of the integrated electromyograms for each of the three phases (Grigoriadis et al., 2011). The EMG data obtained from the mean EMG activity averaged across all chewing cycles were normalized to facilitate cross comparison of the EMG activity across participants. Specifically, the time-varying RMS processed EMG signals from each participant and each muscle was divided by the mean value of the EMG activity recorded from the muscle during all chewing cycles performed by the participant. This normalization allowed evaluation of relative effects of segment of the masticatory sequence on the time-varying activity in each of the four muscles recorded. To preserve phase information while combining data from different chewing cycles, the time base was normalized by scaling each phase of each cycle to the mean duration of that phase (Grigoriadis et al., 2011).

Statistical Analysis

The data were checked for the assumptions of normal distribution with Shapiro–Wilk test and histogram plots. The data pertaining to the number of chewing cycles, duration of chewing cycle, jaw opening velocity, occlusal, and jaw-opening and jaw-closing duration did not appear to be normally distributed hence, non-parametric Wilcoxon sign-ranked tests were applied to test the differences between the conditions. All normally distributed data, i.e., frequency/rhythm of chewing, vertical and lateral jaw movements, and jaw closing velocity were analyzed with Student's *t*-tests. The normally distributed data for the EMG activity of the masseter muscle were analyzed with two-way analysis of variance model (ANOVA) with repeated measures. The factors in ANOVA were conditions (two levels; control and anesthetized) and segments (three levels; beginning, middle, and end). *Post hoc* comparisons were done with Tukey's HSD test. A *P*-value of <0.05 was decided to be significant. The percent changes in EMG activation between the control and anesthetized conditions during the jaw closing phase were calculated as (EMG activity during the jaw closing phase in the control condition – EMG activity during the jaw closing phase in the anesthetized condition)/EMG activity during the jaw closing phase in the control condition × 100.

RESULTS

The participants were able to perform the chewing task in a reliable manner under both the conditions, as instructed. All the participants confirmed the subjective symptoms related to local anesthesia after the anesthetic intervention. We have previously reported the quantitative parameters of jaw-movements, integrated EMG activity during the chewing cycles, and the adaptation of jaw muscle activity to food hardness in these healthy adults (Grigoriadis et al., 2014). In the current study, we will focus on the effect of anesthetic intervention on these parameters and compare them with control condition from the previous study (Grigoriadis et al., 2014). **Table 1** presents the mean and standard deviations of all the outcome variables related to chewing sequence and jaw kinematics during both conditions.

Chewing Sequence

There were no significant differences in the number of chewing cycles ($P = 0.233$), the duration of chewing sequence ($P = 0.198$), and the subsequent frequency/rhythm of chewing ($P = 0.424$) between the anesthesia and control conditions.

Jaw Kinematics

There were no significant differences in the vertical and lateral jaw amplitudes between the anesthesia and control conditions at the beginning ($P = 0.196$ and $P = 0.053$, respectively), middle ($P = 0.352$, and $P = 0.379$, respectively), and end ($P = 0.486$, and $P = 0.379$) of the chewing sequence. However, there was a significant increase in the jaw opening velocity at the middle ($P = 0.030$) of the chewing sequence during the anesthetized condition, and a significant increase in the duration of occlusal phase ($P = 0.004$) but a significant decrease in the jaw opening phase ($P = 0.009$) during the anesthetized condition than the control condition, at the beginning of the chewing sequence.

EMG Activity

The EMG activity of the masseter muscle on the chewing side during the control and anesthetized conditions was evaluated. The results showed an overall significant effect of condition with EMG activity lower in the anesthetized condition than the control condition (main effect; $F = 5.39$, $P = 0.037$). Further, there was a significant decrease in the EMG activity in the middle and end in comparison to the beginning of the chewing sequence (main effect; $F = 33.82$, $P < 0.001$). However, there was no significant interaction between the conditions and the segments ($F = 0.83$, $P = 0.447$).

Temporal Profile of the EMG Activity

The time dependent changes in the EMG activation are captured in the temporal profile of the EMG activity (**Figures 2A–C**). The temporal profile in the beginning of the chewing sequence during both the conditions showed a similar “bell-shaped” curve. The temporal profile at the beginning of the chewing sequence was characterized by an initial slow and later steep increase in the EMG activity during the jaw-closing phase and a clear peak followed by a declining EMG activity during the occlusal

TABLE 1 | Showing mean and standard deviations of all the outcome variables related to chewing sequence and jaw kinematics.

| | | Control | | | Anesthesia | | |
|------------------|--------------------------------|-------------|-------------|-------------|-------------|-------------|-------------|
| Chewing sequence | 1. Number of cycles | 26.9 ± 13.8 | | | 27.7 ± 15.2 | | |
| | 2. Duration of sequence (s) | 20.1 ± 10.4 | | | 21.0 ± 10.9 | | |
| | 3. Rhythm (Hz) | 1.4 ± 0.3 | | | 1.4 ± 0.3 | | |
| | | Beginning | Middle | End | Beginning | Middle | End |
| Jaw kinematics | 4. Vertical amplitude (mm) | 17.6 ± 2.9 | 14.4 ± 2.3 | 13.0 ± 2.1 | 16.9 ± 2.6 | 14.8 ± 2.0 | 13.3 ± 2.2 |
| | 5. Lateral amplitude (mm) | 8.2 ± 1.4 | 6.7 ± 1.2 | 6.3 ± 1.5 | 7.4 ± 1.3 | 7.0 ± 1.2 | 6.2 ± 1.3 |
| | 6. Jaw opening velocity (mm/s) | 86.1 ± 28.2 | 78.8 ± 22.4 | 72.7 ± 18.7 | 93.4 ± 31.2 | 87.9 ± 23.7 | 76.0 ± 20.5 |
| | 7. Jaw closing velocity (mm/s) | 97.3 ± 29.1 | 84.6 ± 21.6 | 73.0 ± 14.0 | 88.9 ± 22.2 | 87.4 ± 21.7 | 73.4 ± 17.3 |
| | 8. Occlusal duration (s) | 0.3 ± 0.1 | 0.3 ± 0.1 | 0.3 ± 0.1 | 0.4 ± 0.1 | 0.3 ± 0.1 | 0.4 ± 0.1 |
| | 9. Opening duration (s) | 0.3 ± 0.1 | 0.2 ± 0.1 | 0.2 ± 0.1 | 0.2 ± 0.1 | 0.2 ± 0.1 | 0.2 ± 0.1 |
| | 10. Closing duration (s) | 0.3 ± 0.1 | 0.2 ± 0.03 | 0.2 ± 0.03 | 0.3 ± 0.1 | 0.2 ± 0.04 | 0.2 ± 0.04 |

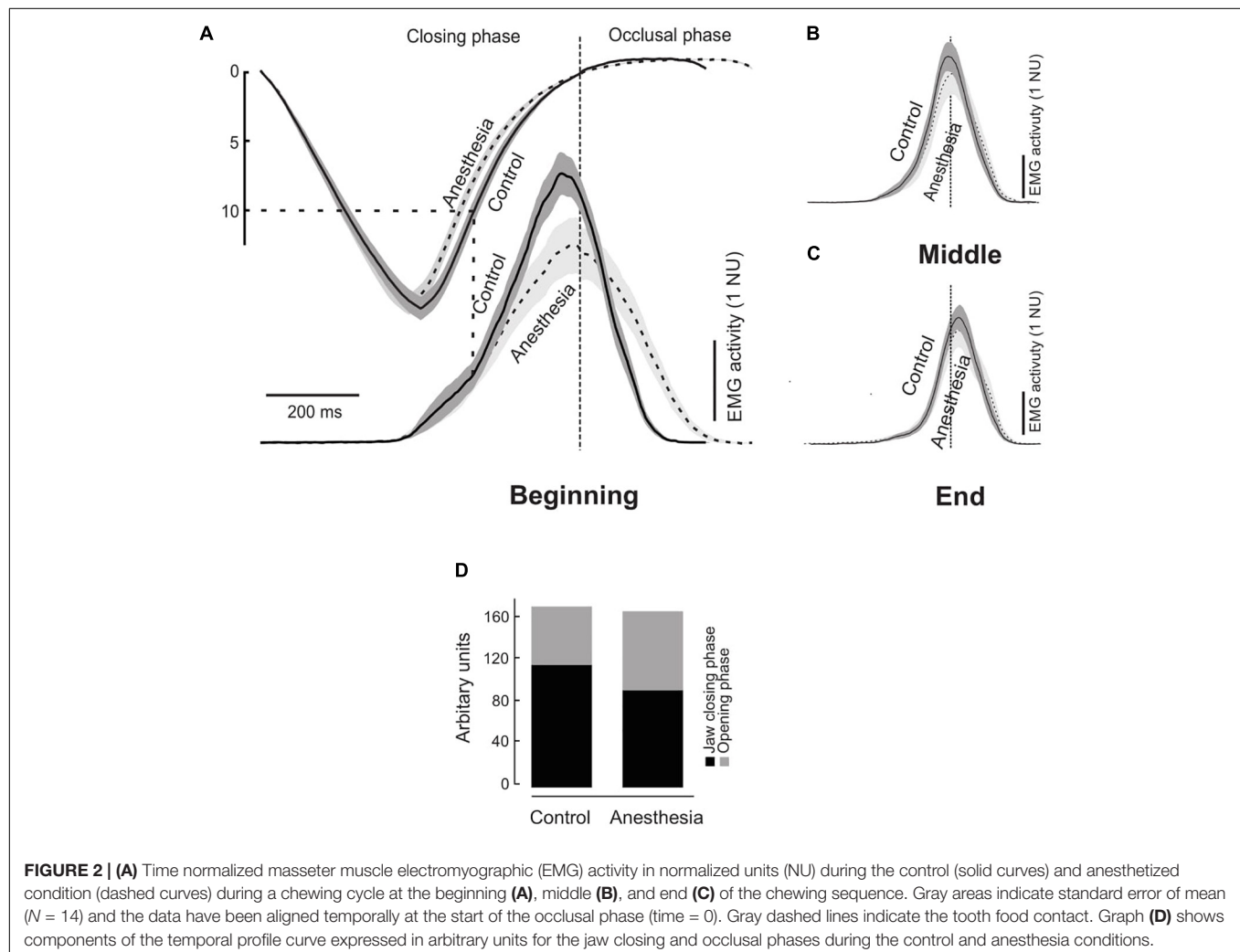


FIGURE 2 | (A) Time normalized masseter muscle electromyographic (EMG) activity in normalized units (NU) during the control (solid curves) and anesthetized condition (dashed curves) during a chewing cycle at the beginning **(A)**, middle **(B)**, and end **(C)** of the chewing sequence. Gray areas indicate standard error of mean ($N = 14$) and the data have been aligned temporally at the start of the occlusal phase (time = 0). Gray dashed lines indicate the tooth food contact. Graph **(D)** shows components of the temporal profile curve expressed in arbitrary units for the jaw closing and occlusal phases during the control and anesthesia conditions.

phase (**Figure 2A**). Both the curves appeared to be similar yet there were some noteworthy and distinct differences, which are discussed below.

A detailed analysis of the components of the temporal profile showed significantly lower peak of the EMG activity

(highest point on the temporal profile of the EMG activity) expressed in arbitrary units (AU) during the anesthetized condition than the control condition ($P = 0.003$) (**Figure 2A**). Further, in the control condition the EMG activity during the jaw-closing phase (116.5 AU) was significantly higher than the

occlusal phase (55.9 AU) ($P < 0.001$) (**Figure 2D**). However, there was no such difference in the anesthetized condition during jaw closing and occlusal phase (93.9 and 76.0 AU, respectively) ($P = 0.198$) (**Figure 2D**). The percent changes in EMG activation during the jaw closing phase were assessed by calculating the relative differences in the EMG activation between both the conditions. It was incidental that the EMG activity of the jaw-closing phase was approximately 20% lower during the anesthetized condition than the control ($P = 0.009$) but there was no such difference during the occlusal phase ($P = 0.056$).

The temporal profile activation of the masseter muscle on the chewing side during the beginning, middle, and end of the chewing sequence has been illustrated in **Figures 2A–C**, respectively. As reported earlier (Grigoriadis et al., 2014), the temporal profile on visual inspection showed a biphasic excitatory drive during the jaw closing phase in the control condition during the beginning of the chewing sequence. This biphasic excitatory drive clearly demonstrated an “early” and a “late” component during a single chewing cycle. The point of transition between the early and late component of the excitatory muscle drive occurred after the maximum jaw opening roughly corresponding to the size of the food morsel (~11 mm). This transition is an indication of the time during the initial tooth food contact. However, the biphasic muscle drive was virtually absent during the anesthetized condition in the beginning of the masticatory sequence. Note that the cue to visually identify the biphasic phase is the exact time point when the tooth comes in contact with the food. During the initial stages of the chewing cycle the food dimensions are intact and food size is known (10 mm approximately in current experiment). However, since the food is cut and divided into several smaller pieces it is difficult to estimate the size of the food morsel and subsequently identify the occurrence of biphasic phases later in the chewing sequence. Hence, in the current study we have described the temporal profile of the jaw muscle activation only during the beginning of the chewing sequence.

DISCUSSION

We have previously shown altered motor function between naturally dentate controls and dental prosthesis patients during various biting (Trulsson and Gunne, 1998; Svensson et al., 2013) and chewing tasks (Grigoriadis et al., 2011, 2015). It has been suggested that the impaired masticatory performance in prosthodontic patients is primarily due to the lack of sensory information from the PMRs and neuromuscular coordination (Kapur et al., 1990; Grigoriadis et al., 2011, 2016). The results of the present study showed no significant effects of anesthesia on the number of chewing cycles and the duration of chewing sequence in young adults chewing elastic model food. However, sudden deprivation of sensory inputs from PMRs resulted in a significant increase in the jaw opening velocity, and duration of occlusal phase with a significant decrease in the duration of jaw-opening phases. Although deprivation of sensory inputs also resulted in an overall decrease in the EMG activity this decrease was not evident at the beginning of the masticatory

sequence. On comparing the time-varying activation profile during the jaw closing phase the participants demonstrated a clear biphasic excitatory muscle drive in the control condition. However, this biphasic muscle drive was diminished and virtually absent in the anesthetized condition. Further, the difference in time-varying activation profile showed that PMRs contribute to approximately 20% of the EMG activity during the jaw closing phase. A previous study suggested that muscle spindle from the jaws is responsible for the facilitatory responses during the jaw closing phase in animals (Komuro et al., 2001). Another animal study suggested that periodontal afferents are responsible for the quick buildup of masticatory forces, but other afferents (e.g., muscle spindles) contribute to the hardness-dependent change of masticatory forces, especially during cortically induced rhythmic jaw movements (Hidaka et al., 1997). It is further suggested that low-threshold somatosensory receptors in skin, mucosa, periodontium, temporomandibular joint, etc. and their afferent inputs to the central nervous system are also suggested to contribute to the jaw muscle activity and jaw movement (Trulsson, 2006). However, our results indicate that a fraction (i.e., 20%) of the EMG activity during the jaw closing phase is also contributed by the PMRs.

Chewing Sequence

Studies have suggested that face motor cortex plays a strategic role in most aspects of chewing and swallowing. Further, the face somatosensory cortex appears to guide these behaviors, but has a more limited role in chewing and swallowing (Sessle, 2006; Avivi-Arber et al., 2011). Dellow and Lund (1971) have demonstrated that the basic pattern/rhythm of mastication can be generated even in decelerate paralyzed animals. Under normal conditions, the sensory inputs to generate the basic rhythm of jaw opening and jaw closing are not conditionally required. However, sensory inputs are essential to adapt or to fine-tune the masticatory movements and forces according to the properties of the masticated food, or to compensate for the sudden perturbations (Lund, 1991). Animals deprived of afferent inputs can still chew, but their chewing movements appear clumsy (Morimoto et al., 1989). In agreement with these findings, our results showed that there were no significant effects of anesthesia on the number of chewing cycles and duration of the chewing sequence and the rhythm of masticatory movements. While, on the one hand, studies in humans have shown uncompromised chewing rhythm due to food hardness or with advancements in age (Horio and Kawamura, 1989; Bishop et al., 1990; Peyron et al., 2002). On the other hand, studies have also shown a decrease in chewing rhythm with an increase in tooth loss (Slagter et al., 1993) or altered masticatory pattern. However, in the current study we observed that chewing can occur without optimum sensory input and the rhythm of the chewing sequence is not compromised by a sudden deprivation of sensory inputs due to local anesthesia. These results are similar to the findings of the previous studies where there was no significant difference in the number of chewing cycles and the duration of the chewing sequence between natural dentate and people with bimaxillary implant prosthesis (Grigoriadis et al., 2011).

Jaw Kinematics

In the current study, sudden deprivation of sensory inputs did not alter the vertical and lateral jaw movement amplitudes but caused an increase in jaw opening velocity, duration of occlusal phase with a significant decrease in duration of jaw-opening phase. These findings are contrary to the observations in patients with implant-supported prosthesis who demonstrate smaller lateral displacement of the mandible during the first chewing cycle (Grigoriadis et al., 2015). It was suggested that the “chopping-like” movement of the mandible observed in patients with implant or tooth supported prosthesis are to facilitate proper positioning of the food on the dental arch. In the process, the prosthesis patients tend to have a narrower, shortened dental arch in comparison to the natural dentate (Grigoriadis et al., 2015). However, there was no change in the amplitude of the lateral jaw movement after sudden deprivation of sensory information in the current study. This result could imply that narrower jaw movement is perhaps a learnt/adjusted behavior and a compensatory mechanism in dental prosthesis users. It is suggested that this behavior is exhibited to counter/minimize food escape from between the teeth, during chewing, compared to the momentaneous loss of sensory inputs in the current study. Previously, it has been shown that more number of food morsels escaped from between the teeth in dental prosthesis users than natural dentate controls (Grigoriadis et al., 2016). The somatosensory awareness due to the somatic sensations arising from the oral cavity provides information about the state and structure of the oral cavity along with the objects in the oral cavity (Haggard and de Boer, 2014). Lack of such information leads to decrease in somatosensory awareness and hence increase in the food escape. Further, it is also suggested that the slower jaw opening and longer duration of the occlusal phase in the current study could be due to the lack of appropriate sensory information from the PMRs during the tooth–food contact.

Jaw Muscle Activity

Electromyographic recordings from the jaw muscles are good indicators for studying masticatory sequence patterns and movement strategies used to chew different food (Veyrune et al., 2007). The adaptation of the jaw movements to the properties of the food requires that the central nervous system have sufficient information related to forces acting on the teeth, the position and movements of the jaws, and the current state of the jaw muscles. Although several different types of mechanoreceptors in the orofacial tissues may contribute to this information (Trulsson and Johansson, 2002), the muscle spindles in the jaw closing muscles and the PMRs are considered as prime contributors (Trulsson, 2006; Turker et al., 2006; Kumar et al., 2017). Strong pressures generated during the jaw-closing phase of mastication cause the jaw closing motor neurons to fire at a higher frequency leading to accentuated jaw muscle activity. However, animal studies have shown that reduced sensory inputs from either PMRs or muscle afferents result in decrease in the accentuated jaw muscle activity required in response to increased food hardness (Lavigne et al., 1987; Morimoto et al., 1989). It was suggested that PMRs may be responsible for the sensory

inputs regarding the initial tooth food contact especially at the beginning of the chewing sequence (Grigoriadis et al., 2011, 2014; Grigoriadis and Trulsson, 2018).

A strong relationship between food hardness and jaw muscle activity has been observed in humans chewing on elastic model food with controlled hardness (Peyron et al., 2002; Veyrune et al., 2007; Grigoriadis et al., 2014). The jaw muscle activity and the jaw movements adapt to the changing properties of the food during the masticatory sequence. Progression of a chewing sequence is typically characterized by an initial overall increase with a gradual decrease in the jaw muscle activity, as the chewing sequence progresses. Similarly, in the current study, we observed a higher EMG activity during the beginning of the chewing sequence and a significant decrease in the EMG activity as the food was crushed. This gradual decrease in EMG activity was evident in both the anesthetized and control conditions. Previous studies have shown that PMRs provide vital information to the jaw closing motoneurons during the beginning of the chewing sequence (Grigoriadis et al., 2011; Grigoriadis and Trulsson, 2018). However, the current study results show no significant interactions in the EMG activity between the condition and segments. This result implies that sudden deprivation of sensory inputs does not affect the EMG activity especially at the beginning of the chewing sequence.

Temporal Profile of the Jaw Muscle Activation

It was suggested that recruitment patterns of different motor units and activation dynamics greatly influence the temporal profile and magnitude of muscle force development in a muscle (Lee et al., 2011). As mentioned above (see the section “Results”) the temporal profile showed greater EMG activity during the jaw-closing phase than the occlusal phase in the control condition. However, this difference in EMG activity between the phases was absent during anesthesia due to the sudden deprivation of sensory inputs from the PMRs. This finding suggests that a major fraction of the EMG activity in the control condition is used to overcome the resistance and crush food during the jaw-closing phase. While in the absence of sensory inputs from the PMRs the ability to increase the jaw muscle activity during the jaw closing phase is compromised. As a result, the participants were also no longer able to produce the characteristic biphasic increase in the excitatory masseter muscle drive during the anesthetized condition. In other words, they failed to generate a distinct augmentation of the jaw muscle drive during the tooth food contact at the beginning of the masticatory sequence. The lack of excitatory muscle drive in the anesthetized condition suggests that the inputs from the PMRs are critical in overcoming the resistance provided by the food during the initial tooth food contact. In the current study, the PMRs contributed to approximately 20% of the EMG activity during the jaw closing phase which was evident in the relative changes of the EMG activation between both the conditions. Therefore, lack of sensory information during the jaw closing phase compromises the regulation of masticatory forces responsible for boosting the power to overcome the resistance of the food during chewing

in accordance with the animal studies (Lavigne et al., 1987; Inoue et al., 1989). These findings are similar to the observations in dental implant-supported prosthesis users where the distinct biphasic muscle drive was clearly absent in the beginning of the masticatory sequence (Grigoriadis and Trulsson, 2018). Further, previous studies have also suggested that the participants with reduced/alterd sensory inputs fail to regulate the bite forces according to the specifics of the task (Kumar et al., 2017). Therefore, it is hypothesized that people with dental implants to a large degree behave like people with natural teeth with anesthesia in accordance with the previous findings (Trulsson and Johansson, 1996).

Methodological limitations are quite apparent in human experimental and clinical studies. One such limitations in the current study was the absence of an “actual” control group where normal saline would have been injected instead of the local anesthetic solution thus mimicking the exact mechanical stimulation of the needle and the pressure of flow of the fluid in the interstitial tissue during the control condition. Further, the unequal distribution of men and women among the study participants and relatively small sample size may also be a methodological concerns in these studies. Future studies should be directed at including an actual control group with equal number of men and women participants and with a relatively larger sample size in a randomized controlled study design. However, paired design where each participants was his/her own control and the normalization of EMG parameters in order to allow for cross comparison between the conditions would be positive attributes of the current study.

CONCLUSION

In conclusion, sudden deprivation of sensory inputs from the PMRs affects the jaw kinematics but causes no changes in the number of chewing cycles or duration of chewing sequence. Despite the absence of changes in the EMG activity of the masseter muscle, time-varying activation profile showed absence of biphasic excitatory muscle drive in the anesthetized condition. Further, the time-varying activation profile of the masseter muscle showed that PMRs contribute to approximately 20% of the EMG activity during the jaw closing phase. Hence, sensory

inputs from PMRs are responsible for the discrepancy in the activation profile of the masseter muscles during the beginning of the chewing sequence.

DATA AVAILABILITY STATEMENT

The datasets generated for this study are available on request to the corresponding author.

ETHICS STATEMENT

The studies involving human participants were reviewed and approved by the Regional Ethical Review Board in Stockholm. The patients/participants provided their written informed consent to participate in this study.

AUTHOR CONTRIBUTIONS

AG performed the experiments, analyzed the data, made the figures, and prepared the first draft of the manuscript. AK analyzed the data, made the table, and drafted and edited the manuscript. MÅ analyzed the data and edited the final draft. MT conceived and designed the study, helped in data analysis, and edited several versions of the manuscript. All authors have substantially contributed and approved the final version of the manuscript.

FUNDING

This work was funded by the Strategic Research Program in Neuroscience at the Karolinska Institutet and received grant from the Stockholm County Council and Karolinska Institutet (SOF: Styrgruppen för Odontologisk Forskning).

ACKNOWLEDGMENTS

The authors are thankful to G. Westling and A. Bäckström for their technical support.

REFERENCES

- Avivi-Arber, L., Martin, R., Lee, J. C., and Sessle, B. J. (2011). Face sensorimotor cortex and its neuroplasticity related to orofacial sensorimotor functions. *Arch. Oral. Biol.* 56, 1440–1465. doi: 10.1016/j.archoralbio.2011.04.005
- Bishop, B., Plesh, O., and McCall, W. D. (1990). Effects of chewing frequency and bolus hardness on human incisor trajectory and masseter muscle activity. *Arch. Oral Biol.* 35, 311–318. doi: 10.1016/0003-9969(90)90048-f
- Dellow, P. G., and Lund, J. P. (1971). Evidence for central timing of rhythmical mastication. *J. Physiol.* 215, 1–13. doi: 10.1113/jphysiol.1971.sp009454
- Grigoriadis, A., Johansson, R. S., and Trulsson, M. (2011). Adaptability of mastication in people with implant-supported bridges. *J. Clin. Periodontol.* 38, 395–404. doi: 10.1111/j.1600-051X.2010.01697.x
- Grigoriadis, A., Johansson, R. S., and Trulsson, M. (2014). Temporal profile and amplitude of human masseter muscle activity is adapted to food properties during individual chewing cycles. *J. Oral Rehabil.* 41, 367–373. doi: 10.1111/joor.12155
- Grigoriadis, A., and Trulsson, M. (2018). Excitatory drive of masseter muscle during mastication with dental implants. *Sci. Rep.* 8:8597. doi: 10.1038/s41598-018-26926-z
- Grigoriadis, J., Kumar, A., Svensson, P., Svensson, K. G., and Trulsson, M. (2017). Perturbed oral motor control due to anesthesia during intraoral manipulation of food. *Sci. Rep.* 7:46691. doi: 10.1038/srep46691
- Grigoriadis, J., Trulsson, M., and Svensson, K. G. (2015). Motor behavior during the first chewing cycle in subjects with fixed tooth- or implant-supported prostheses. *Clin. Oral Implants Res.* 27, 473–480. doi: 10.1111/clr.12559
- Grigoriadis, J., Trulsson, M., and Svensson, K. G. (2016). Motor behavior during the first chewing cycle in subjects with fixed tooth- or implant-supported prostheses. *Clin. Oral Implants Res.* 27, 473–480. doi: 10.1111/clr.12559

- Haggard, P., and de Boer, L. (2014). Oral somatosensory awareness. *Neurosci. Biobehav. Rev.* 47, 469–484. doi: 10.1016/j.neubiorev.2014.09.015
- Hidaka, O., Morimoto, T., Masuda, Y., Kato, T., Matsuo, R., Inoue, T., et al. (1997). Regulation of masticatory force during cortically induced rhythmic jaw movements in the anesthetized rabbit. *J. Neurophysiol.* 77, 3168–3179. doi: 10.1152/jn.1997.77.6.3168
- Horio, T., and Kawamura, Y. (1989). Effects of texture of food on chewing patterns in the human subject. *J. Oral Rehabil.* 16, 177–183. doi: 10.1111/j.1365-2842.1989.tb01331.x
- Iguchi, H., Magara, J., Nakamura, Y., Tsujimura, T., Ito, K., and Inoue, M. (2015). Changes in jaw muscle activity and the physical properties of foods with different textures during chewing behaviors. *Physiol. Behav.* 152, 217–224. doi: 10.1016/j.physbeh.2015.10.004
- Inoue, T., Kato, T., Masuda, Y., Nakamura, T., Kawamura, Y., and Morimoto, T. (1989). Modifications of masticatory behavior after trigeminal deafferentation in the rabbit. *Exp. Brain Res.* 74, 579–591.
- Kapur, K. K., Garrett, N. R., and Fischer, E. (1990). Effects of anaesthesia of human oral structures on masticatory performance and food particle size distribution. *Arch. Oral Biol.* 35, 397–403. doi: 10.1016/0003-9969(90)90187-f
- Komuro, A., Morimoto, T., Iwata, K., Inoue, T., Masuda, Y., and Kato, T. (2001). Putative feed-forward control of jaw-closing muscle activity during rhythmic jaw movements in the anesthetized rabbit. *J. Neurophysiol.* 86, 2834–2844. doi: 10.1152/jn.2001.86.6.2834
- Kumar, A., Castrillon, E., Trulsson, M., Svensson, K. G., and Svensson, P. (2017). Fine motor control of the jaw following alteration of orofacial afferent inputs. *Clin. Oral Investig.* 21, 613–626. doi: 10.1007/s00784-016-1939-4
- Kumar, A., Grigoriadis, J., Trulsson, M., Svensson, P., and Svensson, K. G. (2015). Effects of short-term training on behavioral learning and skill acquisition during intraoral fine motor task. *Neuroscience* 306, 10–17. doi: 10.1016/j.neuroscience.2015.06.065
- Lavigne, G., Kim, J. S., Valiquette, C., and Lund, J. P. (1987). Evidence that periodontal pressoreceptors provide positive feedback to jaw closing muscles during mastication. *J. Neurophysiol.* 58, 342–358. doi: 10.1152/jn.1987.58.2.342
- Lee, S. S. M., Miara, B. M. D., Arnold, A. S., Biewener, A. A., and Wakeling, J. M. (2011). EMG analysis tuned for determining the timing and level of activation in different motor units. *J. Electromyogr. Kinesiol.* 21, 557–565. doi: 10.1016/j.jelekin.2011.04.003
- Lund, J. P. (1991). Mastication and its control by the brain stem. *Crit. Rev. Oral Biol. Med.* 2, 33–64. doi: 10.1177/10454411910020010401
- Lund, J. P., Kolta, A., Westberg, K. G., and Scott, G. (1998). Brainstem mechanisms underlying feeding behaviors. *Curr. Opin. Neurobiol.* 8, 718–724. doi: 10.1016/s0959-4388(98)80113-x
- Morimoto, T., Inoue, T., Masuda, Y., and Nagashima, T. (1989). Sensory components facilitating jaw-closing muscle activities in the rabbit. *Exp. Brain Res.* 76, 424–440.
- Ottenhoff, F. A., van der Bilt, A., van der Glas, H. W., and Bosman, F. (1992). Control of elevator muscle activity during simulated chewing with varying food resistance in humans. *J. Neurophysiol.* 68, 933–944. doi: 10.1152/jn.1992.68.3.933
- Ottenhoff, F. A., van der Bilt, A., van der Glas, H. W., and Bosman, F. (1993). Control of human jaw elevator muscle activity during simulated chewing with varying bolus size. *Exp. Brain Res.* 96, 501–512. doi: 10.1007/bf00234118
- Peyron, M. A., Lassauzay, C., and Woda, A. (2002). Effects of increased hardness on jaw movement and muscle activity during chewing of visco-elastic model foods. *Exp. Brain Res.* 142, 41–51. doi: 10.1007/s00221-001-0916-5
- Sessle, B., Avivi-Arber, L., and Murray, G. (2013). “Motor Control of Masticatory Muscles,” in *Craniofacial Muscles*, eds L. K. McLoon, and F. Andrade, (New York, NY: Springer New York), 111–130. doi: 10.1007/978-1-4614-4466-4_7
- Sessle, B. J. (2006). Mechanisms of oral somatosensory and motor functions and their clinical correlates. *J. Oral Rehabil.* 33, 243–261. doi: 10.1111/j.1365-2842.2006.01623.x
- Sessle, B. J., Adachi, K., Avivi-Arber, L., Lee, J., Nishiura, H., Yao, D., et al. (2007). Neuroplasticity of face primary motor cortex control of orofacial movements. *Arch. Oral Biol.* 52, 334–337. doi: 10.1016/j.archoralbio.2006.11.002
- Slagter, A. P., Bosman, F., van der Glas, H. W., and van der Bilt, A. (1993). Human jaw-elevator muscle activity and food comminution in the dentate and edentulous state. *Arch. Oral Biol.* 38, 195–205. doi: 10.1016/0003-9969(93)90028-k
- Svensson, K. G., Grigoriadis, J., and Trulsson, M. (2013). Alterations in intraoral manipulation and splitting of food by subjects with tooth- or implant-supported fixed prostheses. *Clin. Oral Implants Res.* 24, 549–555. doi: 10.1111/j.1600-0501.2011.02418.x
- Trulsson, M. (2006). Sensory-motor function of human periodontal mechanoreceptors. *J. Oral Rehabil.* 33, 262–273. doi: 10.1111/j.1365-2842.2006.01629.x
- Trulsson, M., and Gunne, H. S. (1998). Food-holding and -biting behavior in human subjects lacking periodontal receptors. *J. Dent. Res.* 77, 574–582. doi: 10.1177/00220345980770041001
- Trulsson, M., and Johansson, R. S. (1996). Forces applied by the incisors and roles of periodontal afferents during food-holding and -biting tasks. *Exp. Brain Res.* 107, 486–496.
- Trulsson, M., and Johansson, R. S. (2002). Orofacial mechanoreceptors in humans: encoding characteristics and responses during natural orofacial behaviors. *Behav. Brain Res.* 135, 27–33. doi: 10.1016/s0166-4328(02)00151-1
- Turker, K. S., Johnsen, S. E., Sowman, P. F., and Trulsson, M. (2006). A study on synaptic coupling between single orofacial mechanoreceptors and human masseter muscle. *Exp. Brain Res.* 170, 488–500. doi: 10.1007/s00221-005-0231-7
- Veyrune, J. L., Lassauzay, C., Nicolas, E., Peyron, M. A., and Woda, A. (2007). Mastication of model products in complete denture wearers. *Arch. Oral Biol.* 52, 1180–1185. doi: 10.1016/j.archoralbio.2007.04.016
- Westberg, K. G., and Kolta, A. (2011). The trigeminal circuits responsible for chewing. *Int. Rev. Neurobiol.* 97, 77–98. doi: 10.1016/B978-0-12-385198-7.00004-7

Conflict of Interest: The authors declare that the research was conducted in the absence of any commercial or financial relationships that could be construed as a potential conflict of interest.

Copyright © 2019 Grigoriadis, Kumar, Åberg and Trulsson. This is an open-access article distributed under the terms of the Creative Commons Attribution License (CC BY). The use, distribution or reproduction in other forums is permitted, provided the original author(s) and the copyright owner(s) are credited and that the original publication in this journal is cited, in accordance with accepted academic practice. No use, distribution or reproduction is permitted which does not comply with these terms.



Specific Vagus Nerve Lesion Have Distinctive Physiologic Mechanisms of Dysphagia

François D. H. Gould^{1*†}, Andrew R. Lammers^{2†}, Christopher J. Mayerl³ and Rebecca Z. German³

¹ Department of Cell Biology and Neuroscience, Rowan University School of Osteopathic Medicine, Stratford, NJ, United States, ² School of Health Sciences, Cleveland State University, Cleveland, OH, United States, ³ Department of Anatomy and Neurobiology, NEOMED, Rootstown, OH, United States

OPEN ACCESS

Edited by:

Teresa Lever,
University of Missouri, United States

Reviewed by:

Makoto Inoue,
Niigata University, Japan
Takanori Tsujimura,
Niigata University Graduate School of
Medical and Dental Sciences, Japan

*Correspondence:

François D. H. Gould
gouldf@rowan.edu

[†]These authors share first authorship

Specialty section:

This article was submitted to
Neurorehabilitation,
a section of the journal
Frontiers in Neurology

Received: 19 August 2019

Accepted: 26 November 2019

Published: 12 December 2019

Citation:

Gould FDH, Lammers AR, Mayerl CJ
and German RZ (2019) Specific Vagus
Nerve Lesion Have Distinctive
Physiologic Mechanisms of
Dysphagia. *Front. Neurol.* 10:1301.
doi: 10.3389/fneur.2019.01301

Swallowing is complex at anatomical, functional, and neurological levels. The connections among these levels are poorly understood, yet they underpin mechanisms of swallowing pathology. The complexity of swallowing physiology means that multiple failure points may exist that lead to the same clinical diagnosis (e.g., aspiration). The superior laryngeal nerve (SLN) and the recurrent laryngeal nerve (RLN) are branches of the vagus that innervate different structures involved in swallowing. Although they have distinct sensory fields, lesion of either nerve is associated clinically with increased aspiration. We tested the hypothesis that despite increased aspiration in both case, oropharyngeal kinematic changes and their relationship to aspiration would be different in RLN and SLN lesioned infant pigs. We compared movements of the tongue and epiglottis in swallows before and after either RLN or SLN lesion. We rated swallows for airway protection. Posterior tongue ratio of safe swallows changed in RLN ($p = 0.01$) but not SLN lesioned animals. Unsafe swallows post lesion had different posterior tongue ratios in RLN and SLN lesioned animals. Duration of epiglottal inversion shortened after lesion in SLN animals ($p = 0.02$) but remained unchanged in RLN animals. Thus, although SLN and RLN lesion lead to the same clinical outcome (increased aspiration), the mechanisms of failure of airway protection are different, which suggests that effective therapies may be different with each injury. Understanding the specific pathophysiology of swallowing associated with specific neural insults will help develop targeted, disease appropriate treatments.

Keywords: dysphagia, superior laryngeal nerve, recurrent laryngeal nerve, kinematics, animal model

INTRODUCTION

Many different types of neurological damage lead to similar outcomes of dysphagia or deglutitive disorders, such as failure to propel the bolus, aspiration, or pharyngeal residue. For example, dysphagia is often associated with cortical injuries or conditions, such as stroke, amyotrophic lateral sclerosis, and cerebral palsy, and with midbrain conditions, such as Parkinson's disease (1). Dysphagia may also result from disorders that affect the myoneural junctions, such as myasthenia gravis. Similarly, injury to branches of the vagus nerve, whose axons synapse within the medulla and pons of the brainstem, also frequently result in dysphagia (2–4). Swallowing is a complex, coordinated process involving 25 paired muscles, and five cranial nerves (sensory

and motor) all coordinated by multiple brainstem and cortical loci (5). The temporal sequence of events is critical for the efficient passing of a bolus from the oral cavity into the esophagus, while simultaneously avoiding the airway (6, 7). It is this complex and integrated process that presents many different failure points leading to the same outcome. Yet understanding *where* and *how* that process is interrupted and compromised is necessary to design interventions to correct the outcome. Furthermore, the *where* and *how* is likely to be specific to the type of neurological insult, even if the outcome is not.

The laryngeal branches of the vagus nerve, which arise from or send fibers to several nuclei within the medulla of the brainstem, have different roles in swallowing. The superior laryngeal nerve's (SLN) sensory branch innervates the valleculae and structures superior to the vocal folds. The sensory signals from the SLN are carried in the vagus nerve to the nodose ganglion, and then synapse in the nucleus of the solitary tract. Clinical and experimental data demonstrate that stimulation of the SLN can initiate the swallow (5, 8–11). The recurrent laryngeal nerve (RLN) innervates the muscles of the vocal folds and laryngeal mucosa below the vocal folds. Motor neurons innervating the laryngeal muscles are located in the nucleus ambiguus. Sensory signals from the lower laryngeal mucosa travel to the nucleus of the solitary tract in the brainstem. The sensory portion of the RLN is known to be important in eliciting the cough reflex (12). Both clinically and experimentally, lesion of either the RLN or the SLN leads to increased aspiration (13–15).

Although insult to either SLN or RLN results in increased aspiration (16, 17), these two lesions impact the size and shape of the bolus in infant animal models differently (13, 18, 19). After surgical transection of the right SLN, the volume of the bolus was greater (13), although bolus size was not associated with increased aspiration. When the right RLN was cut, however, the bolus area was *smaller* post lesion, with evidence suggestive of an airway protection effect. Before RLN lesion, bolus size, and the success or failure of airway protection were unrelated. After lesion, however, smaller bolus size was associated with safer swallows (19).

Bolus size prior to a swallow is a result of oropharyngeal kinematics, and how the tongue processes food to form that bolus. Thus, the movements of the tongue are also part of the biomechanics that drive the swallow. How such kinematics differ between these two lesions is not clear, and how those kinematics produce the performance failure that is dysphagia is also unknown. The movements of the tongue are intricately tied to the kinematics of the hyoid bone and jaw during swallowing (20), as well as bolus volume (21). In this chapter, we present unpublished data comparing swallow duration and tongue movement during the swallow before and after transection of the SLN or RLN in infant pigs. Because bolus size prior to a swallow is a result of oropharyngeal kinematics, we hypothesize that tongue movement and swallow duration will also differ between SLN and RLN lesions.

METHODS

The data used for this paper were collected in two locations over 5 years, with resulting slight differences in protocols, which

are described below where relevant. We will indicate where this impacts on our conclusions.

Animals

Data on SLN lesions were collected at Johns Hopkins University School of Medicine on five infant pigs (Tom Morris farms, Reisterstown, MD) in 2010 and 2011. Pigs were delivered to the vivarium at 2–3 weeks of age and weighed 4–5 kg at the start of experiments. Pigs were trained to drink a pig milk replacement solution (Land O' Lakes Solustart, St. Paul, MN) five times a day via a bottle fitted with a modified nipple. All procedures were approved by the Johns Hopkins University IACUC (protocol SW10M212). Some raw data from these pigs were generated for previous publications (13, 22), but a fifth pig that had not hitherto been digitized was added for this paper.

Data on the RLN lesions was collected at Northeast Ohio Medical University (NEOMED) in 2014 on six infant pigs (Michael Fanning Farm, Howe, IN) aged 5–14 days on arrival. Pigs were trained to feed on the same milk replacer and bottle as the pigs used for superior laryngeal nerve studies. All procedures were approved by the NEOMED IACUC committee (protocol 13–011). Data presented in this paper were originally generated for a previous publication (23).

Procedures and Surgeries

Pigs in both groups underwent similar procedures as the studies were designed to mirror each other. Under isoflurane anesthesia (2–5%), radiopaque markers were implanted intraorally into the tongue, soft palate, and the gingiva under the hard palate. A radiopaque hemoclip (Weck Ligation Solutions, NC) was attached to the tip of the epiglottis. Subsequently, pigs underwent surgery under full aseptic conditions to implant EMG electrodes and identify the relevant nerve on the right side (RLN or SLN). Pigs were intubated and maintained in a stable plane of anesthesia throughout (0.5–3% isoflurane). During the surgery, radiopaque markers were sutured to the hyoid bone and thyroid cartilage. Prior to implantation of electrodes, the appropriate nerve was located and marked with loosely tied suture. For the SLN lesion, the nerve was identified on the right side originating from the vagus nerve in the carotid sheath and followed caudally on the surface of the thyrohyoid membrane. Two pieces of loose suture were tied close to where the SLN emerged from the carotid sheath in the carotid triangle (13, 22). For the RLN, the recurrent portion nerve was identified on the right side coursing lateral and dorsal to the trachea, deep to the infrahyoid muscles. The nerve was traced until it was seen entering the larynx by passing deep and dorsal to the cricothyroid muscle under the thyroid shield. In its long section close to the trachea, the nerve was loosely tied with suture for future identification. After nerve identification, marking of the hyoid and thyroid and EMG electrode implantation, the incision was closed with suture. One to four hours after surgical recovery, animals were taken to the fluoroscopy suite for recording as detailed below. As these recordings were pre-lesion, they constituted control recordings for each animal.

Thirty-six to seventy-two hours after the initial surgery, animals underwent a second surgery. A second incision was made on the right side lateral to the initial incision above the area

TABLE 1 | Summary of the IMPAS scale.

| Score | What happens |
|-------|---|
| 1 | Normal swallow |
| 2 | Some penetration that is cleared during the swallow |
| 3 | Some penetration that is not cleared during the swallow |
| 4 | A lot of penetration that is not cleared during the swallow |
| 5 | Aspiration with a successful attempt to clear |
| 6 | Aspiration with an unsuccessful attempt to clear |
| 7 | Aspiration with no attempt to clear |

where the nerve had been located. Using the suture placed around the nerve, the target nerve in each case (SLN, including both internal and external branches, or RLN) was located, then ligated in two places and fully transected with scissors, and the ends displaced to prevent regrowth. Data collected after this surgery were postlesion data. Animals received analgesics and antibiotics from before the first surgery and continuously throughout the experiments as needed.

Videofluoroscopy

Pigs were recorded in lateral view feeding unrestrained in a plexiglass box. The SLN pre- and post-lesion pigs were filmed at either 60 frames per second (Allura FD20, Philips Healthcare, Best, The Netherlands) or 30 frames per second (Infinix-I, Toshiba Corporation, Tokyo, Japan). The RLN pre- and post-lesion pigs were filmed on a modified C-arm (GE9400 C-Arm) connected to a high speed (100 frames per second) digital video camera (XC 1M digital video camera, Xcitex, Cambridge, MA). Pigs were filmed drinking milk mixed with barium to visualize swallows. Videos were saved as AVI files for subsequent analysis.

Scoring of Swallows for Airway Protection

Control and lesion swallows for both groups of pigs were assessed for effectiveness of airway protection using the Infant Mammalian Penetration Aspiration Scale (IMPAS) (24). This validated, ordinal ranking scale scores infant liquid swallows for penetration and aspiration from 1 (no milk enters the airway at any point) to 7 (silent aspiration: milk passes below the vocal folds and no attempt is made to clear the milk) (Table 1). Swallows were scored by individuals trained together in using the IMPAS scale at NEOMED. Training followed the protocol described in Holman et al. (24) to ensure agreement between raters.

Digitizing of Markers

One hundred and seventy-seven control and lesion swallows were identified from the SLN lesion pigs, and 113 control and lesion swallows for the RLN pigs. X and Y coordinates of the tongue, epiglottis, hard and soft palate, hyoid, and thyroid cartilage markers were digitized using either manual or automated marker tracking in specialized software (ProAnalyst, Xcitex, MA) for all frames of each swallow. Marker coordinates were then translated, rotated, and scaled to the two markers in the hard palate so that the hard palate became the horizontal axis with the anterior hard palate marker as the origin of the reference system. This transformation ensures that movements of the other

markers are now described relative to a fixed hard palate, which removes the effect of full head motions during feeding (23, 25).

After rotation, two swallow-specific kinematic metrics were calculated from the digitized X/Y coordinates. *Duration of epiglottal flip* was calculated as the time between when the epiglottis begins its caudal movement to when it returns to its resting position, which is considered to be equivalent to the duration of the pharyngeal swallow (22). *Posterior tongue ratio* was calculated as the ratio of the distance traveled by the posterior tongue marker from the beginning of epiglottal movement to the time when the epiglottis reaches its most caudal point to the total distance traveled by the posterior tongue marker throughout the duration of epiglottal flip (23).

Analysis

Because of the low number of aspiration events seen in the SLN sample, we combined IMPAS scores of 3, 4, and 7 into a single category for subsequent analysis. No scores of 5 or 6 were observed. Furthermore, because of the low number of more serious penetration and aspiration levels in control animals (scores 3–7), we subdivided our test of the effect of lesion on kinematics into two subtests, following Gould et al. (23). First, we tested the hypothesis that the impact of RLN and SLN lesion on posterior tongue ratio in safe (IMPAS 1 and 2) swallows would differ, using a mixed model with nerve (SLN or RLN), condition (control or lesion), and airway protection outcome (1 and 2) as fixed factors and individual as a random factor. Secondly, we tested the hypothesis that the relationship between swallow safety and posterior tongue ratio in post lesion swallows only would be different for RLN and SLN groups. Once again we used a mixed model, with airway protection outcome (safe swallows with IMPAS scores of 1 or 2 vs. unsafe swallows with IMPAS scores of 3–7) and nerve group (SLN and RLN) as fixed factors and individual as a random factor. Because of the differences in the treatment of the SLN and RLN groups of pigs, we nested condition and airway protection within nerve group in all analyses. Where significant main effects were observed, we used *post hoc* pairwise Tukey tests on the least squares means to determine what the significant differences were. We carried out an identical set of analyses on swallow duration (i.e., duration of epiglottal flip).

To test our hypothesis that epiglottal flip duration would differ between RLN and SLN lesion, we used a mixed model with condition (control or lesion) nested within nerve (SLN or RLN), and individual as a random factor. All analyses were done in R (26), using the packages lme4, lmerTest, and emmeans. We reported the variance of the random factor as an absolute and a percentage of total variation in the model for each test.

RESULTS

The Effect of Nerve Lesion on Posterior Tongue Ratio for Safe Swallows Is Different for RLN and SLN Lesions

There is a significant main effect of nerve group (SLN vs. RLN) and the nerve group-condition interaction (pre- vs. post-lesion for each nerve group) on posterior tongue ratio in safe swallows

TABLE 2 | Results of mixed model analysis of the effects of RLN vs. SLN lesion on posterior tongue ratio in safe swallows (IMPAS 1 or 2).

| Factor | F (numerator df, denominator df) | P-value |
|-------------------------------|----------------------------------|--------------|
| Nerve group | 7.85 (1, 10.17) | 0.018 |
| Nerve group: condition | 5.16 (2, 137.2) | 0.007 |
| Nerve group:IMPAS | 0.02 (2, 139.79) | 0.985 |
| Nerve group:condition:IMPAS | 0.67 (2, 136.64) | 0.513 |

Bold indicates statistically significant effects.

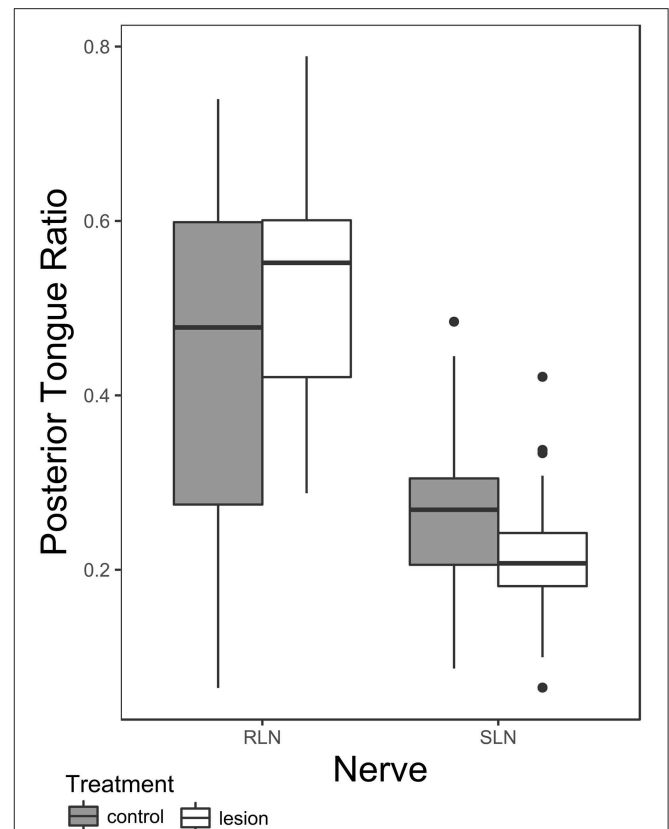
(Table 2). *Post hoc* pairwise tests on the least squares means of treatment within nerve group reveal a significant effect of RLN lesion on posterior tongue ratio [t ratio (138.53) = -2.577 , $p = 0.01$], but no effect of SLN lesion [t ratio (135.88) = 1.897 , $p = 0.06$]. Furthermore, the polarity of change between the pre and post lesion means is different between the two groups: posterior tongue ratio tends to increase in RLN lesion (pre lesion mean 0.43 ± 0.037 standard error (SE); post lesion mean 0.51 ± 0.039 SE), and tends to decrease in SLN lesion (pre lesion mean 0.27 ± 0.05 SE; post lesion mean 0.21 ± 0.05 SE) (Figure 1). The controls for the two treatments are different, reflecting the significant nerve group factor. The variance of the individual factor was 0.006, representing 9.31% of total variation in the model.

Post Lesion, the Difference in Posterior Tongue Ratio in Safe and Unsafe Swallows Is Not the Same in SLN vs. RLN Lesioned Animals

Posterior tongue ratio differed significantly between SLN and RLN lesions. After the lesion surgery, the posterior tongue ratio was higher in the RLN lesion group compared with the SLN lesion group. Furthermore, nerve group—airway protection interaction on posterior tongue ratio in lesioned animals was also significant (Table 3 and Figure 2). *Post hoc* pairwise tests within nerve group indicate a significant difference between swallows with an IMPAS score 1 (mean 0.51 ± 0.051 SE) and swallows with IMPAS score of 3 to 7 (mean 0.38 ± 0.042 SE) in RLN lesioned animals [t ratio (109.63) = 2.657 , $p = 0.044$] but in SLN lesioned animals there is no significant difference in posterior tongue ratio between swallows with different airway protection outcomes. The variance of the individual random factor was 0.006, representing 20% of the variation in the total model.

Epiglottal Flip Duration Shortens in SLN Lesioned Swallows, Not RLN Lesioned Swallows

There is a significant effect of nerve group-condition interaction on epiglottal flip duration (Table 4 and Figure 3). *Post hoc* tests within nerve group reveal a significant shortening of epiglottal flip duration in SLN lesioned animals [t -ratio (277.08) = 2.343 , $p = 0.02$, pre lesion mean 0.24 ± 0.022 SE, post lesion mean 0.23 ± 0.022 SE], but no significant effect in RLN lesioned animals. The variance of the individual random factor was 0.003, representing 56.52% of the variation in the sample.

**FIGURE 1 |** Box plot comparing posterior tongue ratio pre- and post lesion in SLN or RLN lesioned animals. Note that the data presented here includes only safe swallows (i.e., IMPAS 1 and 2). The box represents 50% of the data, with the line near the middle representing the median. Whiskers extend to 1.5 times the interquartile range from the median. Dots are outliers.**TABLE 3 |** Results of mixed model analysis of the effect of RLN and SLN lesion on posterior tongue ratio and airway protection in lesion swallows only.

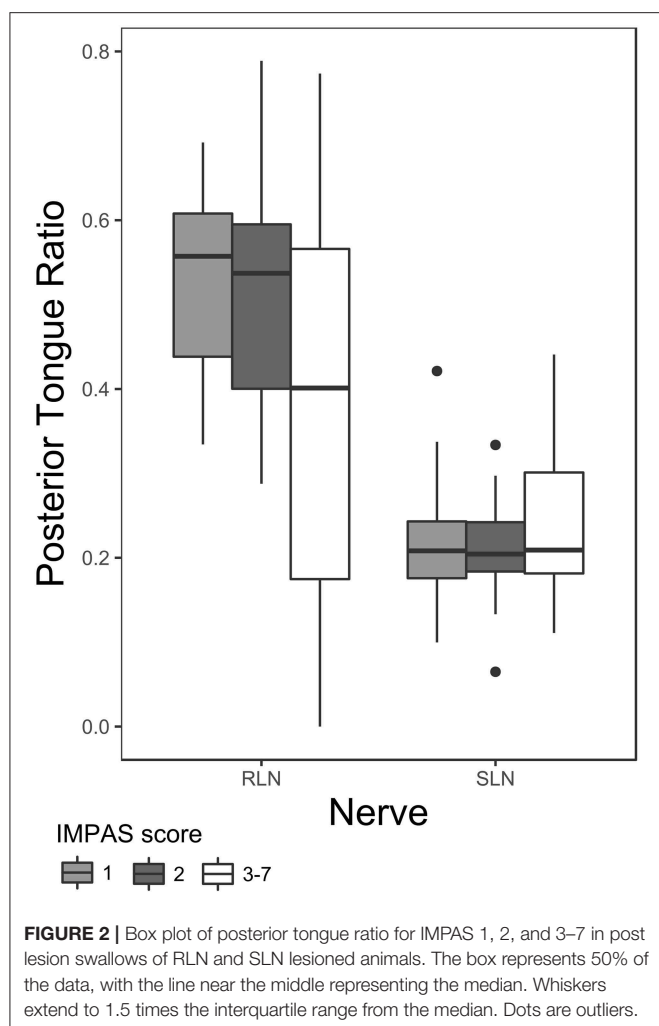
| Factor | F (numerator df, denominator df) | P-value |
|---------------------------|----------------------------------|--------------|
| Nerve group | 13.57 (1, 16.37) | 0.002 |
| Nerve group: IMPAS | 2.52 (4, 115.2) | 0.045 |

Bold indicates statistically significant effects.

DISCUSSION

Despite Both Resulting in Increased Aspiration, RLN and SLN Lesions Have Different Effects on Swallowing Physiology

The results of this study show that similar patterns to what is found with bolus size also apply to swallowing mechanics and kinematics, namely movement of the posterior tongue and duration of epiglottal inversion. Our results agree with previous studies that documented that RLN and SLN lesion affected bolus size differently (13, 19). Furthermore, how all these swallow parameters relate to airway protection deficits after lesion of



either nerve also differs, indicating the specific mechanism of aspiration in SLN and RLN lesion is different.

Based on the results of this study, and the work by Ding et al. (13) and Gould et al. (19), we can propose hypotheses associated with the specific neurological functions of the SLN and RLN that could explain these differences. The increase in bolus size following SLN lesion matches the SLN's role as a swallow trigger (5, 9–11). Unilateral SLN lesion will therefore result in decreased sensitivity to the swallow stimulus by reducing the pool of available sensory receptors, thus requiring a bigger bolus to trigger the swallow. Large boluses are generally associated with longer swallow transit times (27); while our data indicated that swallow duration after SLN lesion was *shorter*, the study by Ding et al. (22) found *longer* swallow durations after transecting the SLN. Our own contradictory result around swallow duration likely resulted from using some different individuals in the analysis. Such variation was consistently found in all of the RLN lesion studies (14, 19, 23) as well as other studies of sensory disruption (25). Thus, in these animals, variation in response to insult seems to characterize dysphagia.

However, although the SLN is important in triggering the swallow response, its sensitivity is highly modulated by oral

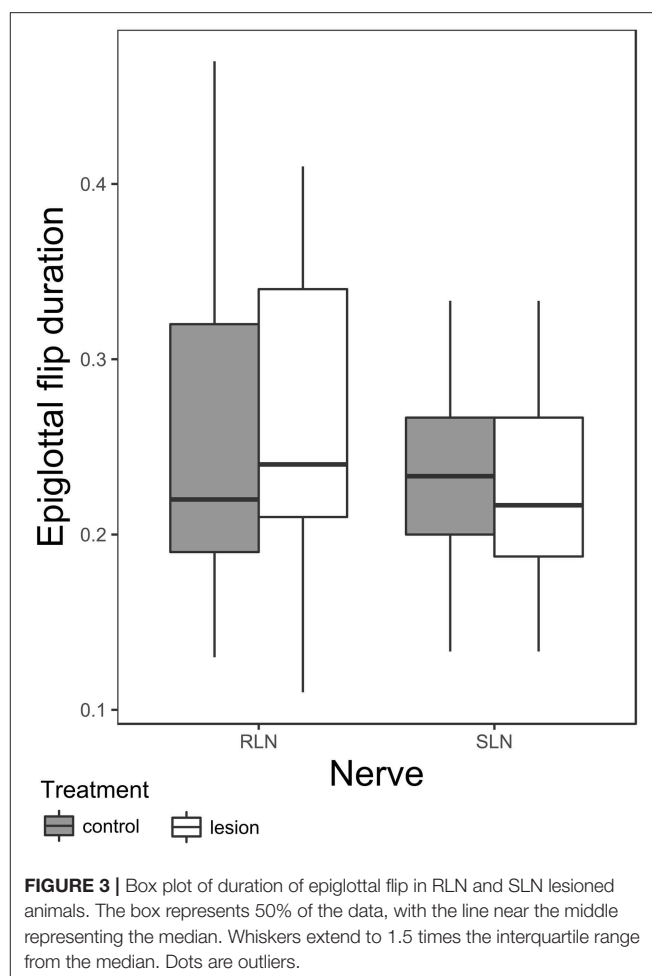


TABLE 4 | Results of mixed model analysis of the effect of RLN and SLN lesion on duration of epiglottal flip.

| Factor | F (numerator df, denominator df) | P-value |
|-------------------------------|----------------------------------|--------------|
| Nerve group | 0.016 (1, 11.03) | 0.9 |
| Nerve group: condition | 3.32 (2, 277.15) | 0.037 |

Bold indicates statistically significant effects.

sensation arising from the trigeminal and glossopharyngeal nerves. For example, palatal anesthesia modifies both swallowing kinematics and airway protection (24), and oral stimulation through rhythmic delivery affects bolus volume that trigger swallowing (28). Thus, the impact of unilateral SLN lesion on swallowing function, bolus volume, and airway protection in otherwise neurologically intact animals will be modified by other oral sensory pathways. Further studies looking at the impact of different oral sensory stimuli on animals with SLN lesion will be necessary to clarify these relationships.

High levels of inter-individual variability itself has implications for neural control (29). Posterior tongue ratio does not seem to change pre- to post-lesion in the SLN lesioned animals, nor to differ between safe and unsafe swallows. This suggests that the relative timing of the movements of different

structures during the early stages of the pharyngeal swallow is not affected by SLN lesion. Indeed, none of the parameters examined in this study are strongly associated with airway protection, suggesting that the mechanism of aspiration after SLN lesion is related to physiological parameters not captured in this study, and are more likely linked to increased bolus sizes (13). These results suggest that the larger bolus, coupled with the sensory deficit resulting from unilateral SLN transection, is simply more difficult to control. This hypothesis requires further testing.

In contrast, the pattern for the RLN suggests a more subtle, but more widespread disruption of swallowing coordination (6). Bolus volume is on average smaller post lesion, and here larger boluses are associated with failure of airway protection after RLN lesion (19). Furthermore, there is a change in the relative timing of tongue movement post lesion, which is also associated with airway protection, particularly to achieve safe swallows. Thus, in the RLN lesioned animals, we see changes in efficiency (as safe swallows require smaller boluses) tied to changes in the relative timing of movements in the early part of the pharyngeal swallow. Because these changes are related to airway protection outcomes, it seems more likely that the mechanism of aspiration is related to kinematics and bolus formation early in the swallow. Indeed, work on the effects of RLN lesion on patterns of muscle activation, both duration and timing, in swallowing has shown changes in the timing of muscle contraction for muscles located in the floor of the mouth, and which are active early in the swallow sequence before bolus formation (30). However, a complete comparison requires similar data for the SLN lesion animals.

Further supporting the idea that the mechanism of aspiration in RLN and SLN lesion animals are different, the time of aspiration in each case differs. In SLN lesioned animals, aspiration tends to occur *during* the swallow (22). However, in RLN lesioned animals aspiration can occur either during or *after* the swallow (14). Here again, differences in the details of the timing of events suggest differences in underlying mechanism of airway protection failure.

These hypotheses for the neural origin of kinematic differences between RLN and SLN lesioned pigs also suggest that different interventions may be effective to modify swallowing in each case. If the reduced sensitivity hypothesis is correct for explaining the patterns we see in the SLN lesioned animals, then either controlling bolus volume directly through regulated feeding, or increasing sensitivity of the valleculae by using other stimuli in conjunction with volume [i.e., capsaicin (31, 32)] are likely to be most effective for restoring normal swallow function. In the case of RLN lesion, however, restoring something like normal function is likely to involve interventions that harness sensory motor mechanisms that establish coordination between tongue and pharyngeal components of swallowing, such as entrained milk delivery (28) or motor learning (33–35).

Limitations of This Study and Unknowns

The way in which the data presented in this study were collected means that some caution must be taken in interpreting these results. The two groups of pigs are different in their control kinematics. As these groups of animals were collected several

years apart in two different locations, a number of factors may account for this. The SLN lesioned pigs were older by several days than the RLN lesioned pigs. Pigs reach weaning age in about 25 days, and show maturation of certain feeding behaviors in that time (36, 37). In particular, the (younger) RLN pigs were considerably variable in all studies (14, 19, 23). Thus, the younger age of the RLN pigs may account for the greater variation in control kinematics seen in this study. The specific statistical model used here, which controls for individual variation and, by using nesting, does not pool the RLN and SLN control data, goes some way to mitigating this variation. As a proportion of total variance in the model, the importance of individual variation varies depending on what aspect of oropharyngeal function is being measured (tongue vs. epiglottal flip) and whether post-lesion only animals are being examined.

Technical differences, most notable the different maximum frame rate available for the SLN vs. the RLN pigs, also are a limitation. In particular this means that meaningful differences in kinematics between SLN and RLN pigs can only be measured to the precision of the slower frame rate (30–60 fps). Finally, airway protection, a major variable in our data set, is not experimenter controlled, but occurs *ad hoc* among animals. Rates of aspiration after RLN lesion are quite irregular among individuals (14). This variability limits our ability to look at fine grain differences between penetration and aspiration in this study, as the SLN lesioned pigs available for this work, while showing penetration, showed limited aspiration.

A Better Etiology of Dysphagia Is Needed, One That Is Based on Functional Damage Effects Instead of Gross Outcomes

When discussing dysphagia in the context of neurological disorders, a significant list of conditions where dysphagia occurs is often presented (as indeed at the beginning of this paper). Knowing the prevalence and occurrence of dysphagia across different patient populations is important for epidemiology and public health. Yet, as this study shows, a diagnosis of dysphagia is insufficient for understanding the specific pathophysiology behind dysphagia in a given condition. Furthermore, the diagnostic endpoint (e.g., aspiration or residue), may result from very different processes going wrong within the swallow. On the other hand, when pathophysiology is identified and studied, for example tongue weakness in Parkinson's disease (38–40), its relationship to the diagnostic symptoms, again aspiration or residue, is often unclear. What is missing is a classification of dysphagia that accounts for the steps between neurological insult, pathophysiology, and diagnostic criterion, so that therapies can be developed that specifically target the disordered physiology.

Clinically, our work suggests that knowing how specific nerve lesions affect swallowing function in the context of aspiration could help inform treatment selection. As an example, the difference in bolus size between SLN and RLN lesioned suggests that bolus size restriction might be more useful in one type of lesion than another to prevent aspiration. Thus, when evaluating treatments, studies need to account as best as possible for the etiology of the dysphagia, as different etiologies may respond

better or worse to different treatments. Further, the category “dysphagia,” or even “deglutitive disorders,” is very broad. Sorting out the specific, and possibly different, functional deficits in conditions that appear superficially similar is a critical first step in determining differences in the mechanisms that generate the pathophysiology. Understanding the mechanism, in turn, is critical for the design of effective interventions.

Our work on SLN and RLN lesions shows how a strictly experimental, systematic, basic science approach can provide the framework for beginning to understand these issues (6, 13, 14, 19, 22, 23). Animal model work is particularly well-suited to the hierarchical study of insult, pathophysiology, and disease (41). Indeed, the literature on animal models of neurological disorders increasingly combines attempts to model the complete disorder with targeted approaches seeking to reproduce a particular part of the neurological disorder to test hypotheses about pathophysiology (42). In our own work, we are currently working on steps to test interventions in infant pigs based on what we have learnt through the systematic analysis of the relationship between specific nerve lesions, pathophysiology, and dysphagic outcomes (43, 44). In order to build this systematic understanding of the relationship between specific neural insults, pathophysiology, and dysphagia in a context that will ultimately improve human health, collaborations between clinical researchers, human physiologists, and animal model workers are essential.

REFERENCES

- Logemann JA. *Evaluation and Treatment of Swallowing Disorders*. Austin, TX: PRO-ED (1998). p. 432. doi: 10.1097/00020840-199812000-00008
- Jabbour J, Martin T, Beste D, Robey T. Pediatric vocal fold immobility: natural history and the need for long-term follow-up. *JAMA Otolaryngol Neck Surg.* (2014) 140:428–33. doi: 10.1001/jamaoto.2014.81
- Jafari S, Prince RA, Kim DY, Paydarfar D. Sensory regulation of swallowing and airway protection: a role for the internal superior laryngeal nerve in humans. *J Physiol.* (2003) 550:287–304. doi: 10.1113/jphysiol.2003.039966
- Setlur J, Hartnick CJ. Management of unilateral true vocal cord paralysis in children. *Curr Opin Otolaryngol Head Neck Surg.* (2012) 20:497–501. doi: 10.1097/MOO.0b013e3283590b56
- Jean A. Brain stem control of swallowing: neuronal network and cellular mechanisms. *Physiol Rev.* (2001) 81:929–69. doi: 10.1152/physrev.2001.81.2.929
- Gross A, Ohlemacher J, German R, Gould FDH. LVC timing in infant pig swallowing and the effect of safe swallowing. *Dysphagia.* (2018) 33:51–62. doi: 10.1007/s00455-017-9832-0
- Young JL, Macrae P, Anderson C, Taylor-Kamara I, Humbert IA. The sequence of swallowing events during the chin-down posture. *Am J Speech Lang Pathol.* (2015) 24:659–70. doi: 10.1044/2015_AJSLP-15-0004
- Lang IM, Medda BK, Babaei A, Shaker R. Role of peripheral reflexes in the initiation of the esophageal phase of swallowing. *AJP Gastrointest Liver Physiol.* (2014) 306:G728–37. doi: 10.1007/978-94-017-8771-0
- Sasaki CT, Hundal JS, Kim Y-H. Protective glottic closure: biomechanical effects of selective laryngeal denervation. *Ann Otol Rhinol Laryngol.* (2005) 114:271–5. doi: 10.1177/000348940511400404
- Suzuki T, Yoshihara M, Sakai S, Tsuji K, Nagoya K, Magara J, et al. Effect of peripherally and cortically evoked swallows on jaw reflex responses in anesthetized rabbits. *Brain Res.* (2018) 1694:19–28. doi: 10.1016/j.brainres.2018.05.002

DATA AVAILABILITY STATEMENT

The datasets generated for this study are available on request to the corresponding author.

ETHICS STATEMENT

The animal study was reviewed and approved by NEOMED IACUC.

AUTHOR CONTRIBUTIONS

FG, AL, and RG designed the study and performed experiments. FG and AL collected data and analyzed data. FG, AL, CM, and RG wrote and edited manuscript.

FUNDING

This work was funded by NIH grant R01 DC009980 to RG.

ACKNOWLEDGMENTS

We acknowledge the work of Peng Ding on collecting data used in this paper, as well as students and staff at both Johns Hopkins and NEOMED who assisted with animal care, surgical procedures, and data collection.

- Takahashi K, Shingai T, Saito I, Yamamura K, Yamada Y, Kitagawa J. Facilitation of the swallowing reflex with bilateral afferent input from the superior laryngeal nerve. *Neurosci Lett.* (2014) 562:50–3. doi: 10.1016/j.neulet.2014.01.017
- Canning BJ. Anatomy and neurophysiology of the cough reflex: ACCP evidence-based clinical practice guidelines. *Chest.* (2006) 129:33S–47. doi: 10.1378/chest.129.1_suppl.33S
- Ding P, Campbell-Malone R, Holman SD, Lukasik SL, Thexton AJ, German RZ. The effect of unilateral superior laryngeal nerve lesion on swallowing threshold volume. *Laryngoscope.* (2013) 123:1942–7. doi: 10.1002/lary.24051
- Gould FDH, Lammers AR, Ohlemacher J, Ballester A, Fraley L, Gross A, et al. The physiologic impact of unilateral Recurrent Laryngeal Nerve (RLN) lesion on infant oropharyngeal and esophageal performance. *Dysphagia.* (2015) 30:714–22. doi: 10.1007/s00455-015-9648-8
- Varaldo E, Ansaldo GL, Mascherini M, Cafiero F, Minuto MN. Neurological complications in thyroid surgery: a surgical point of view on laryngeal nerves. *Front Endocrinol.* (2014) 5:108. doi: 10.3389/fendo.2014.00108
- Liu J, Hai Y, Kang N, Chen X, Zhang Y. Risk factors and preventative measures of early and persistent dysphagia after anterior cervical spine surgery: a systematic review. *Eur Spine J.* (2018) 27:1209–18. doi: 10.1007/s00586-017-5311-4
- Tsujimura T, Suzuki T, Yoshihara M, Sakai S, Koshi N, Ashiga H, et al. Involvement of hypoglossal and recurrent laryngeal nerves on swallowing pressure. *J Appl Physiol.* (1985) 124:1148–54. doi: 10.1152/japplphysiol.00944.2017
- Ding P, Fung GS-K, Lin M, Holman SD, German RZ. The effect of bilateral superior laryngeal nerve lesion on swallowing: a novel method to quantitate aspirated volume and pharyngeal threshold in videofluoroscopy. *Dysphagia.* (2014) 30:47–56. doi: 10.1007/s00455-014-9572-3
- Gould FDH, Yglesias B, Ohlemacher J, German RZ. Pre-pharyngeal swallow effects of recurrent laryngeal nerve lesion on bolus shape and airway protection in an infant pig model. *Dysphagia.* (2017) 32:362–73. doi: 10.1007/s00455-016-9762-2

20. Matsuo K, Palmer JB. Kinematic linkage of the tongue, jaw, and hyoid during eating and speech. *Arch Oral Biol.* (2010) 55:325–31. doi: 10.1016/j.archoralbio.2010.02.008
21. Tasko SM, Kent RD, Westbury JR. Variability in tongue movement kinematics during normal liquid swallowing. *Dysphagia.* (2002) 17:126–38. doi: 10.1007/s00455-001-0112-6
22. Ding P, Campbell-Malone R, Holman SD, Lukasik SL, Fukuhara T, Gierbolini-Norat EM, et al. Unilateral superior laryngeal nerve lesion in an animal model of *Dysphagia* and its effect on sucking and swallowing. *Dysphagia.* (2013) 28:404–12. doi: 10.1007/s00455-013-9448-y
23. Gould FDH, Ohlemacher J, Lammers AR, Gross A, Ballester A, Fraley L, et al. Central nervous system integration of sensorimotor signals in oral and pharyngeal structures: oropharyngeal kinematics response to recurrent laryngeal nerve lesion. *J Appl Physiol.* (2016) 120:495–502. doi: 10.1152/jappphysiol.00946.2015
24. Holman SD, Campbell-Malone R, Ding P, Gierbolini-Norat EM, Griffioen AM, Inokuchi H, et al. Development, reliability, and validation of an infant mammalian penetration–aspiration scale. *Dysphagia.* (2013) 28:178–87. doi: 10.1007/s00455-012-9427-8
25. Holman SD, Campbell-Malone R, Ding P, Gierbolini-Norat EM, Lukasik SL, Waranch DR, et al. Swallowing kinematics and airway protection after palatal local anesthesia in infant pigs: swallowing after palatal anesthesia. *Laryngoscope.* (2014) 124:436–45. doi: 10.1002/lary.24204
26. R Core Team. *R: A Language and Environment for Statistical Computing.* Vienna: R Foundation for Statistical Computing (2015). Available online at: <http://www.R-project.org/> (accessed November 10, 2019).
27. Shibata S, Inamoto Y, Saitoh E, Kagaya H, Aoyagi Y, Ota K, et al. The effect of bolus volume on laryngeal closure and UES opening in swallowing: kinematic analysis using 320-row area detector CT study. *J Oral Rehabil.* (2017) 44:974–81. doi: 10.1111/joor.12573
28. German RZ, Crompton AW, Owerkowicz T, Thexton AJ. Volume and rate of milk delivery as determinants of swallowing in an infant model animal (*Sus scrofa*). *Dysphagia.* (2004) 19:147–54. doi: 10.1007/s00455-004-0001-x
29. Frigon A. Chapter 7—interindividual variability and its implications for locomotor adaptation following peripheral nerve and/or spinal cord injury. *Prog Brain Res.* (2011) 188:101–18. doi: 10.1016/B978-0-444-53825-3.00012-7
30. DeLozier KR, Gould FDH, Ohlemacher J, Thexton AJ, German RZ. Impact of recurrent laryngeal nerve lesion on oropharyngeal muscle activity and sensorimotor integration in an infant pig model. *J Appl Physiol.* (2018) 125:159–66. doi: 10.1152/jappphysiol.00963.2017
31. Kondo E, Jinnouchi O, Nakano S, Ohnishi H, Kawata I, Okamoto H, et al. Aural stimulation with capsaicin ointment improved swallowing function in elderly patients with dysphagia: a randomized, placebo-controlled, double-blind, comparative study. *Clin Interv Aging.* (2017) 12:1921–8. doi: 10.2147/CIA.S138357
32. Shin S, Shutoh N, Tonai M, Ogata N. The effect of capsaicin-containing food on the swallowing response. *Dysphagia.* (2016) 31:146–53. doi: 10.1007/s00455-015-9668-4
33. Humbert IA, Christopherson H, Lokhande A, German R, Gonzalez-Fernandez M, Celnik P. Human hyolaryngeal movements show adaptive motor learning during swallowing. *Dysphagia.* (2013) 28:139–45. doi: 10.1007/s00455-012-9422-0
34. Humbert IA, German RZ. New directions for understanding neural control in swallowing: the potential and promise of motor learning. *Dysphagia.* (2013) 28:1–10. doi: 10.1007/s00455-012-9432-y
35. Park SH, Casamento-Moran A, Singer ML, Ernster AE, Yacoubi B, Humbert IA, et al. Integration of visual feedback and motor learning: corticospinal vs. corticobulbar pathway. *Hum Mov Sci.* (2018) 58:88–96. doi: 10.1016/j.humov.2018.01.002
36. Ballester A, Gould FDH, Bond L, Stricklen B, Ohlemacher J, Gross A, et al. Maturation of the coordination between respiration and deglutition with and without recurrent laryngeal nerve lesion in an animal model. *Dysphagia.* (2018) 33:627–35. doi: 10.1007/s00455-018-9881-z
37. Crompton AW, German RZ, Thexton AJ. Development of the movement of the epiglottis in infant and juvenile pigs. *Zoology.* (2008) 111:339–49. doi: 10.1016/j.zool.2007.10.002
38. Ciucci MR, Russell JA, Schaser AJ, Doll EJ, Vinney LM, Connor NP. Tongue force and timing deficits in a rat model of Parkinson disease. *Behav Brain Res.* (2011) 222:315–20. doi: 10.1016/j.bbr.2011.03.057
39. De Letter M, Santens P, Van Borsel J. The effects of levodopa on tongue strength and endurance in patients with Parkinson's disease. *Acta Neurol Belg.* (2003) 103:35–8.
40. Umamoto G, Tsuboi Y, Kitashima A, Furuya H, Kikuta T. Impaired food transportation in Parkinson's disease related to lingual bradykinesia. *Dysphagia.* (2011) 26:250–5. doi: 10.1007/s00455-010-9296-y
41. German RZ, Crompton AW, Gould FDH, Thexton AJ. Animal models for *Dysphagia* studies: what have we learnt so far. *Dysphagia.* (2017) 32:73–7. doi: 10.1007/s00455-016-9778-7
42. Lind LA, Murphy ER, Lever TE, Nichols NL. Hypoglossal motor neuron death via Intralingual CTB-saporin (CTB-SAP) injections mimic aspects of Amyotrophic Lateral Sclerosis (ALS) related to dysphagia. *Neuroscience.* (2018) 390:303–16. doi: 10.1016/j.neuroscience.2018.08.026
43. Gould FDH, Gross A, German RZ, Richardson JR. Evidence of oropharyngeal dysfunction in feeding in the rat rotenone model of Parkinson's Disease. *Parkinson's Dis.* (2018) 2018:6537072. doi: 10.1155/2018/6537072
44. Mayerl CJ, Gould FDH, Bond LE, Stricklen BM, Buddington RK, German RZ. Preterm birth disrupts the development of feeding and breathing coordination. *J Appl Physiol.* (2019) 126:1681–6. doi: 10.1152/jappphysiol.00101.2019

Conflict of Interest: The authors declare that the research was conducted in the absence of any commercial or financial relationships that could be construed as a potential conflict of interest.

Copyright © 2019 Gould, Lammers, Mayerl and German. This is an open-access article distributed under the terms of the Creative Commons Attribution License (CC BY). The use, distribution or reproduction in other forums is permitted, provided the original author(s) and the copyright owner(s) are credited and that the original publication in this journal is cited, in accordance with accepted academic practice. No use, distribution or reproduction is permitted which does not comply with these terms.



Genetic Taster Status as a Mediator of Neural Activity and Swallowing Mechanics in Healthy Adults

Angela M. Dietsch^{1,2*}, Ross M. Westemeyer¹, William G. Pearson Jr.³ and Douglas H. Schultz²

¹ Department of Special Education and Communication Disorders, University of Nebraska–Lincoln, Lincoln, NE, United States, ² Center for Brain, Biology and Behavior, University of Nebraska–Lincoln, Lincoln, NE, United States,

³ Department of Cellular Biology & Anatomy, Medical College of Georgia, Augusta University, Augusta, GA, United States

OPEN ACCESS

Edited by:

Teresa Lever,
University of Missouri, United States

Reviewed by:

Julie M. Barkmeier-Kraemer,
The University of Utah, United States
Erin Kamarunas,
James Madison University,
United States

*Correspondence:

Angela M. Dietsch
angela.dietsch@unl.edu

Specialty section:

This article was submitted to
Systems Biology,
a section of the journal
Frontiers in Neuroscience

Received: 31 July 2019

Accepted: 26 November 2019

Published: 17 December 2019

Citation:

Dietsch AM, Westemeyer RM,
Pearson WG Jr and Schultz DH
(2019) Genetic Taster Status as
a Mediator of Neural Activity
and Swallowing Mechanics in Healthy
Adults. *Front. Neurosci.* 13:1328.
doi: 10.3389/fnins.2019.01328

As part of a larger study examining relationships between taste properties and swallowing, we assessed the influence of genetic taster status (GTS) on measures of brain activity and swallowing physiology during taste stimulation in healthy men and women. Twenty-one participants underwent videofluoroscopic swallowing study (VFSS) and functional magnetic resonance imaging (fMRI) during trials of high-intensity taste stimuli. The precisely formulated mixtures included sour, sweet-sour, lemon, and orange taste profiles and unflavored controls. Swallowing physiology was characterized via computational analysis of swallowing mechanics plus other kinematic and temporal measures, all extracted from VFSS recordings. Whole-brain analysis of fMRI data assessed blood oxygen responses to neural activity associated with taste stimulation. Swallowing morphometry, kinematics, temporal measures, and neuroimaging analysis revealed differential responses by GTS. Supertasters exhibited increased amplitude of most pharyngeal movements, and decreased activity in the primary somatosensory cortex compared to nontasters and midtasters. These preliminary findings suggest baseline differences in swallowing physiology and the associated neural underpinnings associated with GTS. Given the potential implications for dysphagia risk and recovery patterns, GTS should be included as a relevant variable in future research regarding swallowing function and dysfunction.

Keywords: swallowing, sensorimotor integration, taste, sensory perception, physiology, morphometry, genetic taster status, functional MRI

INTRODUCTION

Within the swallowing literature, the influence of taste stimulation on swallowing biomechanics has been an area of interest in healthy populations (Ding et al., 2003; Palmer et al., 2005; Pelletier and Dhanaraj, 2006; Leow et al., 2007; Wahab et al., 2011; Nagy et al., 2014b) and persons with swallowing impairments, or dysphagia (Pelletier and Lawless, 2003; Lee et al., 2012; Pauloski et al., 2012; Dietsch et al., 2019). Taste is particularly salient to swallowing, as gustation is important in eating and drinking behaviors and is mediated by multiple cranial nerves and neural structures that are integral in the swallowing response (Simon et al., 2006; Steele and Miller, 2010). Gustatory sensation is hypothesized to have a feed-forward effect on swallowing movement (Ding et al., 2003),

as enhanced sensory stimulation may elicit faster and/or stronger swallowing responses. This theory is strengthened by studies reporting taste-related increases in neural activation in the cortical swallowing network (Babaei et al., 2010; Humbert and Joel, 2012); however, the evidence lacks consensus regarding taste's effects on swallowing physiology and underlying neural activation.

Beneficial effects on the biomechanics of swallowing from a variety of taste stimuli in healthy people and persons with dysphagia include faster temporal parameters (Ding et al., 2003; Leow et al., 2007; Cola et al., 2010; Lee et al., 2012; Pauloski et al., 2012; Steele et al., 2012; Gatto et al., 2013) and more efficient/greater magnitudes of swallowing movements (Pelletier and Lawless, 2003; Palmer et al., 2005; Pelletier and Dhanaraj, 2006; Leow et al., 2007; Miura et al., 2009; Plonk et al., 2011; Wahab et al., 2011; Lee et al., 2012; Todd et al., 2012a,b; Nagy et al., 2014a,b; Pelletier and Steele, 2014; Dietsch et al., 2019). Although taste has shown positive effects on swallowing performance, these effects are not always statistically significant, may be conditional on certain taste stimuli, and/or may only be present at high concentrations of taste or with an interaction of multiple sensory inputs. Several studies report taste having negative or no effect on swallowing physiology in healthy adults (Butler et al., 2004; Hiss et al., 2004; Chee et al., 2005; Miyaoka et al., 2005, 2006) and persons with dysphagia (Hamdy et al., 2003) suggesting that positive results of taste on swallowing may be inconsistent for reasons that have not yet been elucidated.

Interpretation of the current literature is challenging for a multitude of reasons, which involve differences in (a) taste stimuli used, (b) measurement in swallowing outcomes, and (c) participant demographics. A paucity of evidence in the structural and functional neural representation of taste and swallowing also adds to the challenge in elucidating the relationship between these sensory inputs and motor outcomes. In addition to these issues, factors such as age, sex, and genetic predisposition create potentially significant sources of variability in modulating taste's influence on brain activity and swallowing physiology (Bartoshuk et al., 1986, 1994; Bartoshuk, 2000; Kim et al., 2003).

Genetic taster status (GTS) is an inherited relative sensitivity to taste stimulation. It is assessed via chromosomal expression of the *TAS2R38* gene (Reed et al., 1999; Bartoshuk, 2000; Kim et al., 2003), density of the fungiform papillae on the tongue (Bartoshuk, 1993; Bartoshuk et al., 1994; Essick et al., 2003), and/or perceptual sensitivity to the bitter compound 6-n-Propylthiouracil (PROP; Bartoshuk, 1991; Smutzer et al., 2013). There are three broad classifications of GTS: nontasters, midtasters, and supertasters (Bartoshuk, 1991). Roughly half of the population are midtasters, one in four persons are supertasters, and women are more likely than men to be supertasters (Bartoshuk et al., 1994). GTS also influences perception of taste intensities, as supertasters report more intense reactions to taste stimuli in comparison to the other taster groups (Ko et al., 2000; Dietsch et al., 2014; Nagy et al., 2014a,b; Pelletier and Steele, 2014). This difference in oral perception could be a result of PROP tasters having higher amounts of gustatory papillae and taste pores (Bartoshuk et al., 1994; Bartoshuk, 2000; Essick et al., 2003) and thus experiencing increased sensory

stimulation, and possibly a different combination of gustatory, chemosensory, and somatosensory input from oral stimuli, compared to nontasters (Karrer et al., 1992). These genetic, anatomical, and perceptual differences among GTS groups may manifest in different abilities and responses to taste stimuli in terms of both neural activation and swallowing movements.

A few studies have investigated GTS effects on neural activity using a range of neuroimaging designs and taste stimuli. Using magnetic resonance imaging (MRI), Bembich et al. (2010) reported significantly greater hemodynamic responses in areas of the prefrontal cortex (PFC) within supertasters after administration of PROP strips compared to nontasters, indicating the PFC's active role in conscious processing of intense bitter tastes. Eldeghaidy et al. (2011) further investigated other brain regions that may be differentially activated based on GTS, and reported significant positive correlations between blood oxygen level-dependent (BOLD) responses and GTS in primary and secondary somatosensory cortices (SI, SII) the anterior cingulate cortex, and the anterior-, mid-, and posterior-insula after varied concentrations of isoviscous and isosweet fat emulsions. A functional near infrared spectroscopy (fNIRS) study by Mulheren et al. (2016) found no significant differences in hemodynamic activity among GTS groups in the sensorimotor cortices using sweet and sour stimuli. Similar to the neuroimaging literature, the evidence of an effect of GTS on swallowing biomechanics is also mixed. Supertasters have demonstrated stronger submental muscle activation (Pelletier and Steele, 2014), higher anterior lingual pressure generation (Nagy et al., 2014b; Pelletier and Steele, 2014), and longer swallow apnea durations (Plonk et al., 2011) in a variety of taste-intense stimuli compared with nontasters; however, other studies have reported GTS having no effects on these parameters (Todd et al., 2012a; Nagy et al., 2014a).

As part of a larger study, GTS was considered as a relevant factor in discerning the effects of taste stimulation on brain activity and swallowing physiology, as clarifying these relationships has important potential implications for dysphagia management. Specifically, the current study examines whether and how GTS influences neural hemodynamic responses and swallowing biomechanics within the same participants using standardized taste stimuli. It was hypothesized that general labeled magnitude scale (gLMS) scores, as an indicator of GTS, would be (H_1) positively correlated to the magnitude of component swallowing movements and (H_2) associated with differences in BOLD activity in taste- and swallowing-related neural areas.

MATERIALS AND METHODS

Participants

This study included healthy adult volunteers recruited from the community via posters in local businesses and places of worship as well as in public buildings on the university campus. Volunteers were excluded from study participation if they had a history of neurological, taste, or swallowing disorders; injuries or surgeries to the orofacial region (aside from

TABLE 1 | Participant demographics.

| Group | Women | Men | Total N |
|-------------|-------|-----|---------|
| Nontaster | 2 | 7* | 9 |
| Midtaster | 4* | 2 | 6 |
| Supertaster | 5 | 1** | 6 |
| Total N | 11 | 10 | 21 |

Twenty-one adult volunteers ranging 19–49 years of age (mean = 27.66) were distributed across sex and genetic taster status. *One participant from this group excluded from MRI analysis due to technical issues. **Excluded from CASM analysis as an extreme statistical outlier.

routine wisdom tooth extraction), or could not safely undergo MRI due to embedded metal or claustrophobia. The study protocol was approved by the primary investigator's Institutional Review Board (#16762) and all participants provided written informed consent.

Twenty-one healthy adults (11 women, 10 men; mean age 27.66 years, range 19–49 years) participated in both data collection sessions. Distribution across sex and GTS is shown in **Table 1** and is consistent with overall population distribution in that proportionately more women than men are supertasters, and more men than women are nontasters (Bartoshuk et al., 1994).

Stimuli

Five custom-mixed stimuli were prepared in distilled water for the functional magnetic resonance imaging (fMRI) trials and in a 40% weight/volume barium sulfate in distilled water mixture for the videofluoroscopic swallowing study (VFSS) trials. These included (1) intense sour, (2) sweet-sour, (3) lemon, (4) orange, and (5) unflavored (McBride and Johnson, 1987; Pelletier et al., 2004; Dietsch et al., 2019). All of the stimuli fell within the viscosity range for thin liquids according to the flow test methods and criteria recommended by the International Dysphagia Diet Standardization Initiative (Hanson et al., 2019). **Table 2** delineates the composition of each tastant type.

Procedures

Participants underwent one session of data collection for VFSS, and another for MRI. These sessions were completed

as proximately as scheduling allowed (mean 4.2 days, range 0–9 days). The MRI session was completed first for 16 participants and after the VFSS session for five participants.

Neuroimaging data were collected on a research-dedicated Siemens 3T MAGNETOM Skyra with 32-channel head coil. After positioning a participant in the scanner bed, investigators used medical tape to secure a short length of tubing (Skarda 1/8" OD clear food-grade urethane) to the participant's lower face with the tip of the tube in the anterior portion of the participant's oral cavity. This tubing was the endpoint for a custom-made stimulus dispensing system comprised of a series of modular pumps (Harvard Apparatus, Holliston, MA, United States) controlled by a PowerLab 16/35 (AD Instruments, Colorado Springs, CO, United States) and LabChart software (V. 8.1.13, AD Instruments, Colorado Springs, CO, United States). During functional image acquisition, TR pulses from the Siemens scanner were recorded within the LabChart software to enable precise registration of each volume to stimulus dispensation during analysis. Taste stimuli were administered in four counterbalanced blocks per functional run. Within each block, a single tastant was presented four times (3 ml per trial dispensed over 5 s with 15–30 s between onset of trials, see **Figure 1**), followed by two presentations of distilled water to rinse the oral cavity before starting the next tastant block. Four functional runs (430 volumes per run, gradient-echo T2*-weighted imaging pulse sequence with GeneRalized Autocalibrating Partial Parallel Acquisition [GRAPPA] multi-band acceleration factor = 3, voxel size 2.5 mm³, field of view = 210 mm², TR = 1 s, TE = 29.8 ms, flip angle = 60°, bandwidth = 2052 Hz/Px, echo spacing = 0.59 ms, interleaved) plus an anatomical T1 sequence (voxel size = 1 mm³, field of view = 256 mm², phase encoding = anterior-posterior, TR = 2.20 s, TE = 3.37 ms, TI = 0.91 s, flip angle = 7°, bandwidth = 200 Hz/Px, echo spacing = 7.9 ms) were collected per participant as part of the larger study protocol.

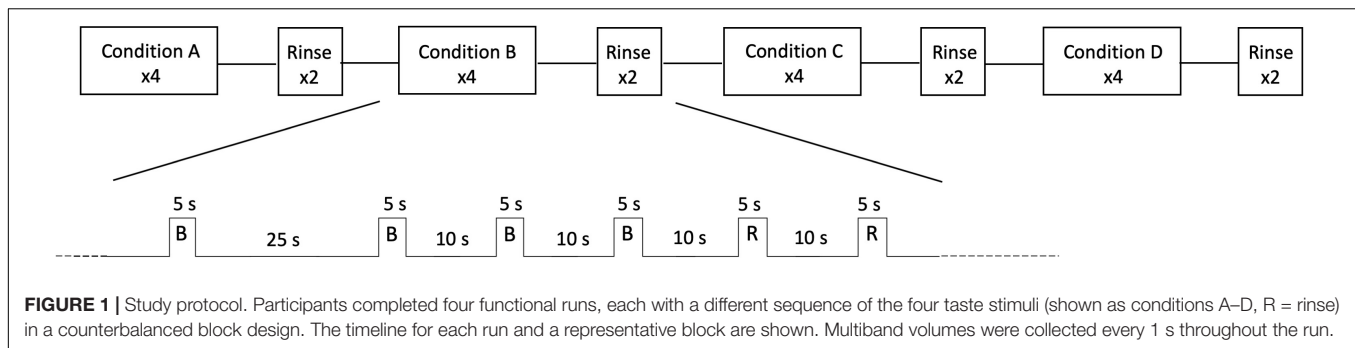
Videofluoroscopic data were acquired at a local hospital by research personnel and cooperating radiology staff. Participants were seated with a lateral view that captured all relevant anatomical landmarks. Two trials of each stimulus were administered in a counterbalanced order via syringe at 45–55°F, for a total of ten 5-ml trials per participant. Immediately prior to each trial, the participant rinsed the oral cavity with tap water until no taste was discernable. Then, the syringe tip for the next trial was placed between the participant's lips, emptied, and immediately withdrawn. Participants were prompted to swallow normally as soon as the syringe was removed from the oral cavity. Fluoroscopic swallowing images were captured at 30 pulses/s, and digitally recorded at 30 frames/s for further analysis.

In order to determine GTS, testing using a film impregnated with PROP (Sigma-Aldrich) was completed at the conclusion of their first data collection session. The researcher provided a simple explanation that taste perception is genetically influenced, and that the individual's perception of the film could help us determine their genetic taste status. Then participants dissolved the PROP-impregnated strip on their tongue and then indicated the intensity of any associated taste on a gLMS (Smutzer et al., 2013). The intensity ratings were used by researchers to classify

TABLE 2 | Taste stimuli.

| Tastant | Citric acid | Sucrose | Lemon extract | Orange extract |
|------------|--------------------------------------|--------------------------------------|------------------------------------|-------------------------------------|
| Sour | 2.7% wt/vol | N/A | N/A | N/A |
| Sweet-Sour | 1.11% wt/vol | 8% wt/vol | N/A | N/A |
| Lemon | 1.11% wt/vol | 8% wt/vol | 1% vol/vol | N/A |
| Orange | 1.11% wt/vol | 8% wt/vol | N/A | 1% vol/vol |
| Source | Fisher Scientific Citric Acid USP | C&H Granulated Pure Cane Sugar | McCormick Pure Lemon Extract | McCormick Pure Orange Extract |

All taste stimuli were precisely mixed using food- or pharmaceutical-grade materials. Distilled water served as the solvent for the neuroimaging trial stimuli. So the contrast would be visible on x-ray, a 40% weight/volume (wt/vol) barium sulfate (Fisher Scientific) suspension prepared in the lab served as the solvent for the videofluoroscopic swallowing trial stimuli.



participants' GTS during data analysis according to the criteria validated by Smutzer et al. (2013). Participants were not provided with information about the different GTS groups, how those groups typically perceive PROP, or their own GTS at any point during data collection.

Analysis

VFSS Analysis

Each taste trial was clipped from the VFSS recording and coded such that researchers were blinded to stimulus type and GTS during data extraction. Oropharyngeal swallowing physiology of taste trials was assessed using a method called computational analysis of swallowing mechanics (CASM; May et al., 2017). CASM is the morphometric analysis of coordinate data mapping frame-by-frame displacement of anatomical landmarks. First, researchers who had achieved post-training interrater reliability of $r \geq 0.95$ used a MATLAB-based semi-automated software tool to track twelve key anatomical landmarks frame by frame (Natarajan et al., 2015). Four of these anatomical landmarks (genial tubercle of mandible; posterior margin of hard palate; anterior tubercle of atlas; and the anterior inferior margin of C2) represent three relatively fixed levers within the skeletal structure surrounding the oropharyngeal swallow. They provide a reference framework for alignment of landmarks during the Procrustean fit portion of the analysis. Along with the anterior inferior margin of C4, they also are used to assess the relative posture of the cervical vertebrae during swallows. The remaining eight landmarks (anterior inferior margin of the hyoid; superior border of the upper esophageal sphincter (UES); anterior and posterior margins of the vocal folds; pit of the vallecula; and attachment of the superior and middle pharyngeal constrictors) represent the attachment points and foci of movement trajectory for muscle groups underlying pharyngeal swallowing mechanics (Hosseini et al., 2019). Considered together, these landmarks create a constellation representing overall pharyngeal shape changes during swallowing. The analysis process reveals whether the shape changes are associated with assigned grouping variables (such as GTS) as well as the magnitude and direction of coordinate shifts that contribute to the shape change. Ten percent of the study data were re-extracted to check for reliability; intra- and interrater correlation coefficients for CASM coordinate data were 0.933 and 0.975, respectively. Next, coordinates were compiled and imported into MorphoJ (Klingenberg, 2011). A Procrustes fit was performed to control for camera

and subject position. An evaluation of the 3,607 sets of 12 coordinates representing pharyngeal stage swallowing against a multivariate distribution curve indicated that three sets of coordinates were found to be statistical outliers and excluded from analysis. A morphometric principal component analysis was performed to visually inspect the distribution of the sample. All data points from one subject, a male supertaster, lay outside of a 0.95 confidence interval of all other subjects and was therefore excluded from the analysis. To determine whether GTS impacted swallowing mechanics, a morphometric canonical variate analysis of coordinate data representing pharyngeal swallowing mechanics by GTS categories was performed in MorphoJ (Klingenberg, 2011). Ratings from PROP testing were used to stratify participants: nontasters = $gLMS \leq 20$, midtasters = $gLMS 21-40$, supertasters = $gLMS \geq 41$ (Smutzer et al., 2013). *Post hoc* discriminant function analysis yielded eigenvectors representing pairwise differences in pharyngeal phase mechanics by tastant. Eigenvector results were scaled using Mahalanobis distance in MorphoJ. A matrix transformation using MATLAB was performed on an exported eigenvector file (scaled vector graph) that aligns C1 and C4 vertebrae coordinates in order to visualize functional anatomical differences in swallow mechanics by tastant.

A second set of analyses of the VFSS images used more traditional kinematic and timing measures to further explore the effects of GTS on swallowing physiology. Pharyngeal constriction ratio (PCR; Leonard et al., 2006) was used to assess the magnitude of pharyngeal constriction by comparing pharyngeal volume at rest and at peak constriction. The pharyngeal phase duration was measured from the first frame of upward/forward movement of the hyoid to the frame in which the UES closes behind the bolus tail (Leonard et al., 2000). The UES distension was defined as the distance between the inferior and posterior opening of the UES when a majority of the bolus was passing through it. The parameters for each of these three measures were extracted from VFSS images and evaluated via a series of analyses of variance (ANOVA); significant alpha levels were set at 0.05 for the ANOVAs and Bonferroni adjusted to 0.0167 for *post hoc* testing.

MRI Preprocessing

Functional imaging reconstruction, processing, and analysis was conducted using Analysis of Functional Neuroimages (AFNI; Cox, 1996). Anatomical images were reconstructed and segmented using the standard FreeSurfer processing pipeline

(Fischl et al., 2004; Desikan et al., 2006). Anatomical images were then non-linearly warped to MNI152_2009 template space using the AFNI program 3dQwarp, and the skull was removed. Echo-planar images for each run were despiked (spikes in each voxel's time series are truncated), slice time corrected, aligned to the anatomical images and transformed to MNI space. Each volume was then registered to the volume with the minimum outlier fraction. Functional images were spatially smoothed using a 4 mm full-width at half maximum Gaussian filter, and skull stripped. The time course of each voxel was scaled to a mean of 100. We then ran a general linear model using the six motion estimates from volume registration as regressors of no interest. Additionally, we used up to third-order polynomials to model baseline and drift. Pairs of volumes where the Euclidean norm of the motion derivatives exceeded 0.4 were "scrubbed" and eliminated from further analysis. Finally, we modeled hemodynamic response functions using the "BLOCK" basis function at the onset time for each tastant as well as the rinse. The duration of the function was 6 s. Data from two participants (a female midtaster and a male nontaster) were excluded from further analysis due to technical issues with matching timelines of stimuli dispensation to image acquisition.

MRI Analysis

Beta values for rinse trials were subtracted from the beta value for each tastant. An ANOVA was conducted in AFNI using the 3dMVM program (Chen et al., 2014) with tastant as a within-subject factor, and GTS treated as a continuous between-subjects factor. A cluster-based approach was used to correct for multiple comparisons (Forman et al., 1995). We estimated the spatial smoothness of the residuals for each participant using a Gaussian plus mono-exponential function implemented with 3dFWHMx. The spatial autocorrelation function values were determined for each participant using the "-acf" option, and the mean values across participants (0.761, 2.956, 11.06) were calculated (Cox et al., 2017). Ten thousand random maps with these smoothness parameters were generated and thresholded at a voxel-wise $p < 0.001$. The largest surviving cluster from each of these simulations was recorded, and this distribution was used to estimate the probability of a false positive. Based on these estimations, we applied a cluster threshold to our data at a voxel-wise p -value of 0.001 and a minimum cluster size of ten contiguous voxels which resulted in a corrected two-tailed alpha of $p < 0.05$.

RESULTS

Swallowing Physiology Outcomes

Multivariate morphometric canonical variate analysis of the VFSS recordings by GTS showed statistically significant differences ($P < 0.0001$) in swallow mechanics across all comparisons (Figure 2) with Mahalanobis distances as follows: nontaster vs. midtaster ($D = 2.40$), midtaster vs. supertaster ($D = 2.90$), nontaster vs. supertaster ($D = 3.44$).

In the subsequent discriminant function analysis, eigenvectors illustrate the differences in supertaster pharyngeal swallowing

mechanics compared to those of nontasters (Figure 3, left panel) and midtasters (Figure 3, right panel). As depicted by the length and direction of the eigenvectors, supertasters demonstrated greater pharyngeal constriction and increased head and neck flexion than either of the other groups. Additionally, the CASM results indicated increased laryngeal elevation, anterior hyoid excursion, and pharyngeal shortening in supertasters as compared to nontasters.

The three kinematic and timing variables analyzed via one-way ANOVAs further characterized the impact of taster status group on swallowing physiology (Table 3). Consistent with the results from the CASM, supertasters had significantly smaller PCR values than midtasters and nontasters, indicating they had the largest average magnitude of pharyngeal constriction across taster groups. Additionally, supertasters had the shortest pharyngeal phase duration of swallowing; it was significantly shorter than for midtasters but not nontasters. Although there were no significant mean differences of GTS and UES distension, supertasters had the largest value of UES distension ($M = 23.208$, $SD = 8.126$) with midtasters ($M = 20.389$, $SD = 4.684$) and nontasters ($M = 21.285$, $SD = 5.507$) having similar UES distension values.

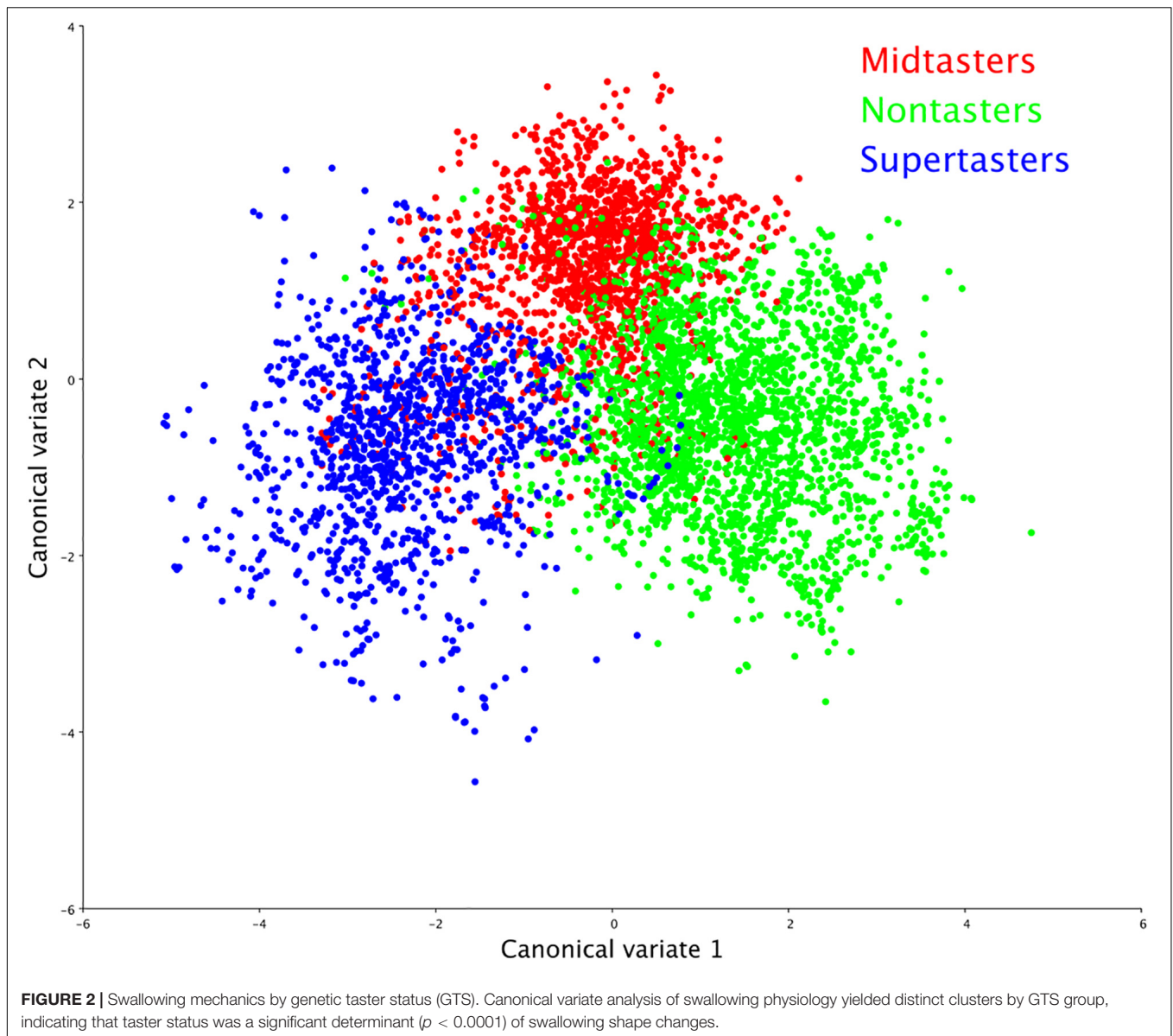
MR Outcomes

The whole-brain neuroimaging analysis identified regions where BOLD activity varied as a function of GTS as measured by gLMS intensity ratings for the PROP strip. The analysis revealed two clusters of BOLD signal associated with main effects of GTS. Their coordinates, cluster size, and effect descriptions are summarized in Table 4. The smaller cluster was located in the superior temporal gyrus (STG), a region implicated in a broad range of functions including swallowing (Martin et al., 2004; Shibamoto et al., 2007; Peck et al., 2010). The larger cluster was located in the left post-central gyrus, specifically in a portion of S1 associated with orofacial sensation (Haggard and de Boer, 2014). Within this area of S1, participants' gLMS intensity rating for the PROP strip testing (a reflection of GTS) accounted for 53% of the variance in hemodynamic response in this key region ($F[1,17] = 19.17$, $p < 0.0001$). As depicted in Figure 4 (right panel), higher PROP gLMS ratings, reflecting greater sensitivity to taste, were associated with lower BOLD activation during trials that involved tastant presentations as compared to during the control condition.

DISCUSSION

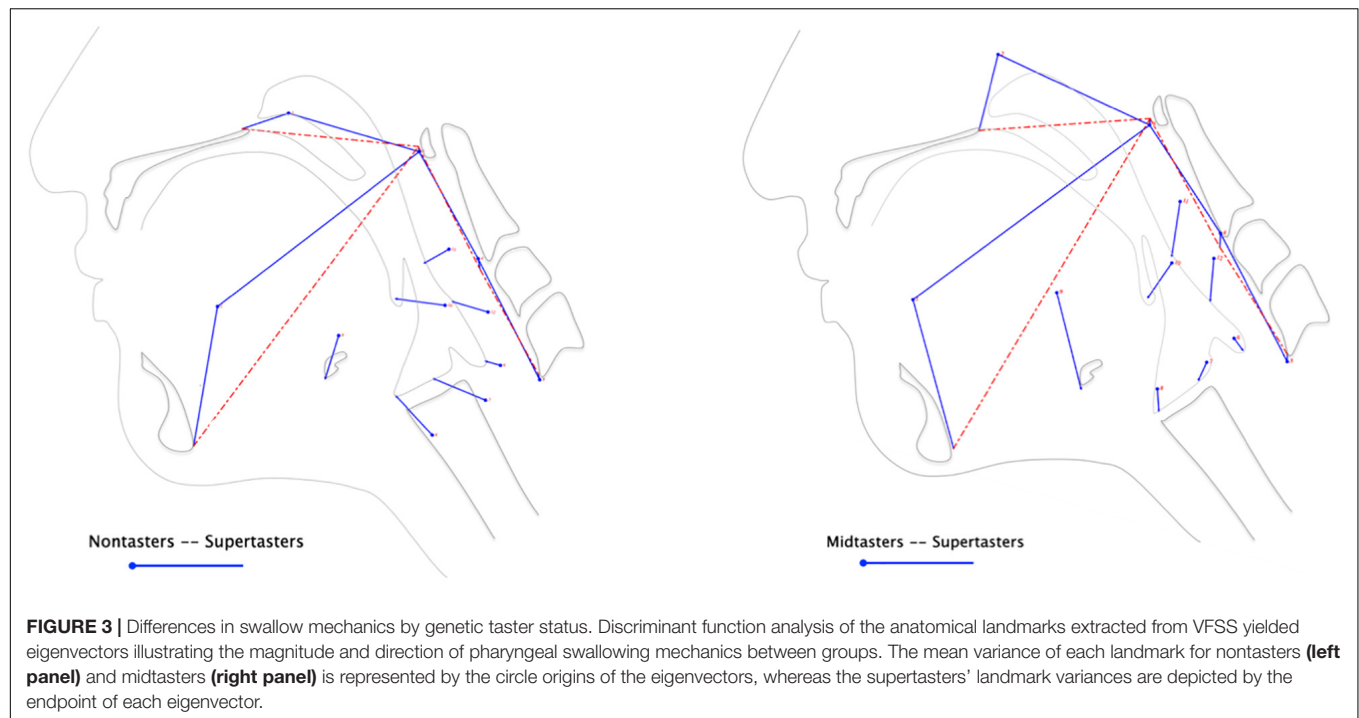
The present analysis assessed the relationships between GTS, swallowing physiology, and neural activity in healthy adults in response to precisely mixed taste stimuli. The results supported our hypotheses, with supertasters exhibiting greater amplitudes of critical swallowing movements (H_1) and a different pattern of neural activation (H_2) compared to mid- and nontasters.

Analysis of swallowing physiology via CASM and other kinematic/timing variables confirmed previous reports of GTS-dependent differences in swallowing movements. Overall, supertaster status was associated with greater magnitude of



swallowing movements compared to mid- and nontasters, as evidenced by CASM's discriminant function analysis eigenvectors and the kinematic pharyngeal constriction findings. In addition to the movement parameters, supertasters had the shortest pharyngeal swallow phase duration (the time required to move the bolus through the pharynx), suggesting more efficient swallowing physiology than both mid- and nontasters. This may seem counterintuitive initially, and some studies have reported increased pharyngeal constriction to be associated with longer contraction of the relevant musculature (Inamoto et al., 2018; Molfenter et al., 2018). However, these findings involved within-subject comparisons of swallowing dynamics across varying conditions or cues that yielded different levels of effort in the swallows, i.e., the same basic motor plan executed to varying endpoints. In contrast, Steele et al. (2019) reported that whereas pharyngeal constriction ratios were

significantly different during normal-effort swallows of varying bolus consistencies, healthy swallowers exhibited less than 20% variability in the timing parameters of those swallows. In the present study, we report across-subject comparisons, which may have introduced variability in the speed and acceleration of component movements from one person's motor plan to another's. This would confound the stability of the larger amplitude/longer duration relationship. Additionally, our measure of duration was not based on timing of component movements or muscle contractions, but on how fast the bolus completed the pharyngeal phase (spanning from the first frame of hyolaryngeal excursion to when the UES closes behind the bolus tail; Leonard et al., 2000). So even though the duration of pharyngeal movements/contractions may be longer for those exhibiting greater magnitudes of constriction (supertasters), that is not directly tied to the speed with which they moved the bolus.



Although we did not measure speed or acceleration of component movements, perhaps the baseline swallowing mechanics of the supertasters included greater speed and magnitude of pharyngeal constriction, leading to faster propulsion of the bolus through the pharynx and into the UES.

Neuroimaging also delineated GTS-linked differences, though the reduced activation in S1 and STG for supertasters as compared to mid- and nontasters may seem counterintuitive; one might expect the increased sensory input inherent to supertasters to be associated with increased S1 and STG activation. Broader consideration of the extant literature in the fields of cognitive psychology, sensory processing, and neuroscience, however, offers several possible explanations for these findings.

Researchers in cognitive psychology, for example, note that more intelligent individuals exhibit smaller activation amplitude

while performing cognitive tasks than lower intelligence individuals (Haier et al., 1992; Neubauer and Fink, 2009). This finding has been referred to as the Neural Efficiency Hypothesis. Further evidence of this hypothesis has suggested that it is sensitive to other variables such as task demands (Dunst et al., 2014), and gender (Lipp et al., 2012). In addition to more efficient brain activation patterns, other studies have suggested that this efficiency effect may also be apparent in updates to brain network communication (Schultz and Cole, 2016; Zuo et al., 2018). If applied to taste stimulation, this neural efficiency phenomenon could suggest that by virtue of their higher density of taste receptors, supertasters are relatively more adept at processing taste-related sensation and thus need to devote fewer neural resources than mid- and nontasters, or that their neural patterns for processing the gustatory, chemosensory, and somatosensory inputs associated with taste are simply different than their counterparts. Prior studies have identified increased activity in the STG during swallows at higher effort levels (Peck et al., 2010) and of more complex boluses (Shibamoto et al., 2007). The lower STG activations in supertasters, combined with their generation of greater movement magnitudes more quickly than their mid- and nontaster counterparts in this study, suggest that perhaps supertasters are more efficient at motor aspects of swallowing as well.

The sensory processing literature offers other possible explanations for the lower S1 and STG activations in supertasters. Abundant evidence supports that S1 has a critical role in pain perception (Bushnell et al., 1999), and undergoes neuroplastic changes in response to pain (see Kim et al., 2017 scoping review). For example, persons with acute low back pain exhibited

TABLE 3 | Analyses of variance for kinematic and timing variables across genetic taster groups.

| Variable | df | F | p | Effect description |
|-------------------------------------|--------|-------|--------|---|
| Pharyngeal constriction ratio (PCR) | 2, 182 | 5.191 | 0.006 | *Supertasters < Midtasters *Supertasters < Nontasters Midtasters = Nontasters |
| Pharyngeal phase duration (PPD) | 2, 180 | 9.305 | <0.001 | *Supertasters < Midtasters Supertasters = Nontasters Midtasters > Nontasters |
| UES distension | 2, 190 | 2.991 | 0.053 | N/A |

*Post hoc pairwise comparisons for significant main effects revealed that supertasters exhibited more efficient swallows (lower PCR and PPD) than mid- and nontasters. *Denotes a statistically significant relationship at Bonferroni-adjusted alpha levels of 0.0167.*

TABLE 4 | Main effects of genetic taster status.

| Cluster | Coordinates (MNI152-2009) | | | Volume (mm ³) | F(1,17) | R ² | Effect description |
|-------------------------|---------------------------|-----|-----|---------------------------|---------|----------------|---|
| | RL | AP | IS | | | | |
| Post-central gyrus | −50 | −32 | 51 | 203 | 19.17 | 0.530 | Higher gLMS → more negative beta weight |
| Superior temporal gyrus | 26 | 5 | −32 | 156 | 21.57 | 0.560 | Higher gLMS → more negative beta weight |

Two clusters survived whole brain analysis and cluster-based correction for multiple comparisons. Higher scores on the general labeled magnitude scale (gLMS) during 6-n-Propylthiouracil testing were associated with supertaster status. RL = right/left, AP = anterior/posterior, IS = inferior/superior.

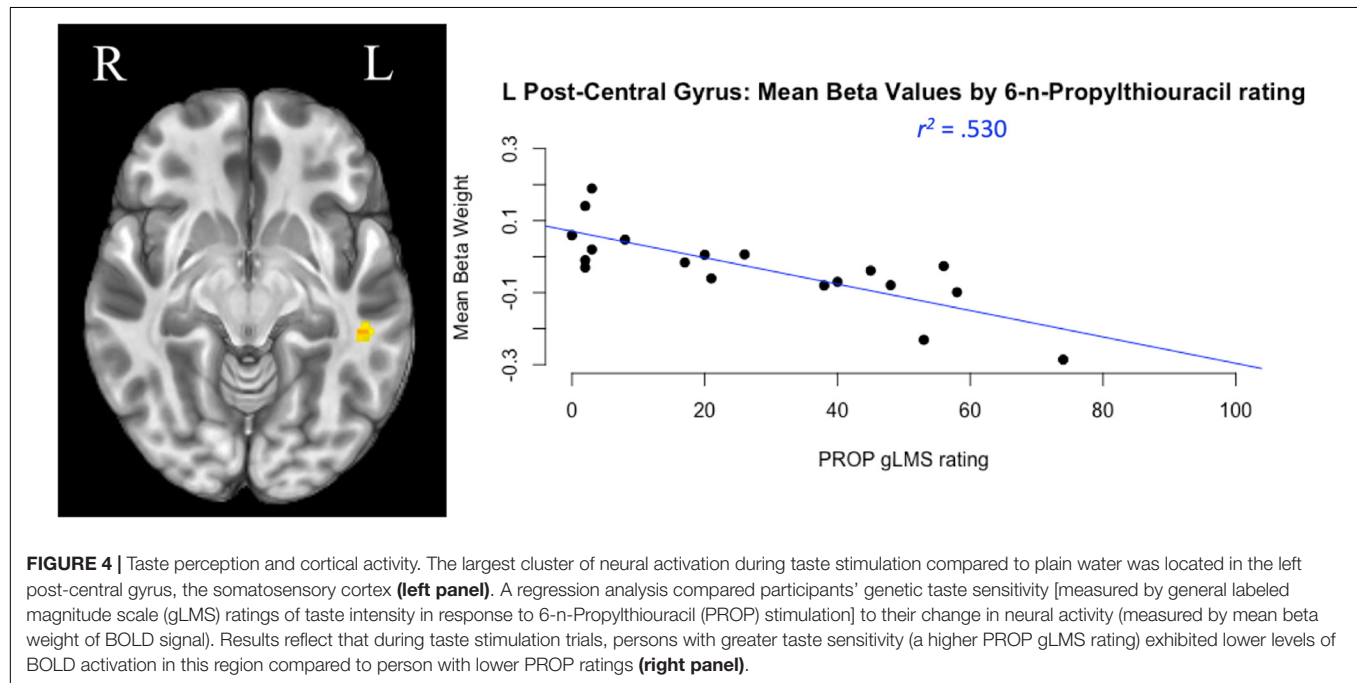


FIGURE 4 | Taste perception and cortical activity. The largest cluster of neural activation during taste stimulation compared to plain water was located in the left post-central gyrus, the somatosensory cortex (**left panel**). A regression analysis compared participants' genetic taste sensitivity [measured by general labeled magnitude scale (gLMS) ratings of taste intensity in response to 6-n-Propylthiouracil (PROP) stimulation] to their change in neural activity (measured by mean beta weight of BOLD signal). Results reflect that during taste stimulation trials, persons with greater taste sensitivity (a higher PROP gLMS rating) exhibited lower levels of BOLD activation in this region compared to person with lower PROP ratings (**right panel**).

smaller activations in the sensorimotor cortex than pain-free peers in response to non-noxious afferent inputs (Chang et al., 2019), suggesting that decreased S1 activations may be a rapidly developing compensatory response to discomfort. Similarly, individuals with chronic pain disorders exhibited reduced resting state activity in STG (Zhao et al., 2017). Perhaps supertasters' neural systems perceive intense taste-related stimulation, which may include somatosensory and chemesthetic (and possibly nociceptive for certain stimuli such as capsaicin or intense sour) components, as uncomfortable or noxious. To compensate, supertasters' neural networks might downregulate S1 and STG activity in response to taste stimulation in the same way that persons with pain downregulate other tactile stimuli. Additionally, it is well-established that pain perception and S1 activation are also modulated by attentional factors (Zeidan et al., 2011) and enhancement of other sensory modalities (Sharma et al., 2016). Under this principle, supertasters' inherent sensitivity to taste stimuli could yield a neural network that de-prioritizes somatosensory/chemesthetic information in favor of gustatory inputs, resulting in comparatively less S1 activity than mid- and nontasters.

A third consideration involves the extant neuroscience literature regarding taste-related sensation, or rather the gaps that

exist in our current understanding of the complex underlying networks. Investigators using various stimuli and neuroimaging technologies have identified a range of brain regions and timing patterns that appear to be involved in the processing of taste stimuli generally (Babaei et al., 2010; Humbert and Joel, 2012), and specifically with regard to GTS (Bembich et al., 2010; Eldeghaidy et al., 2011; Mulheren et al., 2016). While all of these contributions are valuable, a clear picture of the neural pathways for processing of the multimodal inputs associated with taste stimulation, much less one that accounts specifically for GTS, has yet to emerge. Another study reporting GTS-related differences in S1 activation showed opposite effects to ours, with greater activation in S1 for supertasters (Eldeghaidy et al., 2011). However, the trials of fat emulsions used in that work have different mouth-coating and dispersive qualities than our taste stimuli (Drewnowski, 1992). In addition to contrasting taste stimuli, different prioritization of gustatory, chemosensory, and somatosensory inputs by supertasters could contribute to differing somatosensory-specific S1 activation patterns.

The baseline differences in swallowing physiology and neural activation in healthy persons demonstrated by these results may help explain the disparate results in previous studies of swallowing function. If people have genetic differences in

their baseline swallowing movements and responses to oral sensation, GTS could be a confounding variable in capturing outcomes of enhanced sensory stimulation on swallowing, or in responding to particular sensorimotor intervention strategies. Additionally, symptoms of dysphagia could manifest differently even in persons with similar neurological or structural insults due to variations in baseline swallowing movements and neural networks associated with their GTS. If so, GTS could influence the severity and prognosis of dysphagia, and therefore may be an important variable to consider in dysphagia assessment and management. Further investigation is necessary to determine whether the incidence of dysphagia is different across GTS groups, and whether there are fundamental differences in the functional and anatomical neural connections that could influence one's susceptibility to taste- and swallowing-related impairments and responsiveness to specific interventions.

The present results support that supertasters require less S1 activation and similar M1 activation in order to achieve greater amplitude and efficiency of swallowing movements. In other words, supertasters may be neurologically predisposed to produce more optimized swallows at baseline compared to non- and midtasters. While this raises intriguing questions about the role of GTS in the risk of developing dysphagia as well as the potential to recover from it, additional work is necessary to address limitations of the current work and further examine the underlying mechanisms. For example, CASM comparisons would benefit from an increased sample size that would enable stratification by sex to account for morphological differences that may affect functional anatomy as represented by the eigenvectors. This may improve the precision of vectors indicating how the multiple elements of pharyngeal swallowing mechanics are impacted by GTS. Larger sample size could also increase the statistical power to detect additional shifts and/or clusters of BOLD signal change in other brain regions. Also, the incorporation of genetic testing in future work will allow for more precise assessment of taster status haplotype than is possible with the PROP testing utilized here. Additionally, the tastants used here were developed to mirror those that elicited the most efficacious swallowing mechanics in previous studies, but it is possible that other tastant types may have similar or even better effects. Although other studies reported no differences in measures of taste perception and swallowing physiology for the barium and non-barium versions of sweet, sour, and unflavored taste stimuli similar to the formulas used here (Dietsch et al., 2014; Nagy et al., 2014a), the stimuli in the fMRI and VFSS are not identical because of their barium status, which may have impacted the respective results in unappreciated ways. Likewise, the fact that some participants underwent VFSS first whereas others completed the MRI first could have confounded results. Finally, the current work focuses on swallowing mechanics and neural activity in healthy persons, so further work is necessary to assess whether these relationships hold in persons with dysphagia. Nonetheless, these findings raise questions about whether supertasters may also require less neural recruitment to adapt the swallowing motor plan based on the intraoral stimulus being swallowed, which may have significant implications for treatment selection for individuals with dysphagia.

In summary, the current study offers a unique contribution to the extant literature by using GTS as a covariate in both neuroimaging and swallowing physiology data from the same participants using standardized taste stimuli. Comparison of swallowing mechanics revealed increased amplitude and efficiency of swallowing physiology in supertasters compared to mid- and nontasters. Further, S1 activation inversely correlated to PROP rating, such that supertasters appear to devote fewer neural resources to somatosensory aspects of oral stimulation than mid/nontasters. The influence of GTS on swallowing biomechanics and neural substrates is a compelling new finding, and these preliminary results suggest that GTS may be a relevant consideration in future swallowing-related research.

DATA AVAILABILITY STATEMENT

The raw data supporting the conclusions of this article will be made available by the authors, without undue reservation, to any qualified researcher who makes reasonable and scientifically feasible requests. Data sharing will occur after appropriate institutional data use agreements have been completed.

ETHICS STATEMENT

This study was conducted under the guidance and approval of the Institutional Review Board of the University of Nebraska–Lincoln, with written informed consent from all participants in accordance with the Declaration of Helsinki.

AUTHOR CONTRIBUTIONS

AD conceptualized the study, obtained funding, designed the study, constructed the requisite equipment, recruited the participants, collected the data, oversaw all the analyses, and wrote the manuscript. RW helped to recruit participants, collect data, and analyze data, and wrote portions of the manuscript. WP designed and conducted the morphometric analysis. DS designed and conducted the neuroimaging analysis, and wrote portions of the manuscript. All authors contributed to the manuscript editing, revision, read, and approved the submitted version.

FUNDING

This research was funded by the internal funding including a Layman Award (WBS# 26-1710-0159-001) from the University of Nebraska–Lincoln (PI: Dietsch).

ACKNOWLEDGMENTS

The authors thank Megan Asselin, Rachel Feuker, Jake Greenwood, Makenzie Logan, Megan Rovang, and Kaytlin Tippin for their contributions to the equipment development, stimulus preparation, and protocol testing.

REFERENCES

- Babaei, A., Kern, M., Antonik, S., Mepani, R., Ward, B. D., Li, S., et al. (2010). Enhancing effects of flavored nutritive stimuli on cortical swallowing network activity. *Am. J. Physiol. Gastrointest. Liver Physiol.* 299, G422–G429. doi: 10.1152/ajpgi.00161.2010
- Bartoshuk, L. (1991). Sweetness: history, preference, and genetic variability. *Food Technol.* 45, 108–113.
- Bartoshuk, L. (1993). The biological basis of food perception and acceptance. *Food Qual Prefer.* 4, 21–32. doi: 10.1016/0950-3293(93)90310-3
- Bartoshuk, L. M. (2000). Comparing sensory experiences across individuals: recent psychophysical advances illuminate genetic variation in taste perception. *Chem. Sens.* 25, 447–460. doi: 10.1093/chemse/25.4.447
- Bartoshuk, L. M., Duffy, V. B., and Miller, I. J. (1994). PTC/PROP tasting: anatomy, psychophysics, and sex effects. *Physiol. Behav.* 56, 1165–1171. doi: 10.1016/0031-9384(94)90361-1
- Bartoshuk, L. M., Rifkin, B., Marks, L. E., and Bars, P. (1986). Taste and aging. *J. Gerontol.* 41, 51–57.
- Bembich, S., Lanzara, C., Clarici, A., Demarini, S., Tepper, B. J., Gasparini, P., et al. (2010). Individual differences in prefrontal cortex activity during perception of bitter taste using fNIRS methodology. *Chem. Sens.* 35, 801–812. doi: 10.1093/chemse/bjq080
- Bushnell, M. C., Duncan, G. H., Hofbauer, R. K., Ha, B., Chen, J.-I., and Carrier, B. (1999). Pain perception: is there a role for primary somatosensory cortex? *Proc Natl Acad Sci U.S.A.* 96, 7705–7709. doi: 10.1073/pnas.96.14.7705
- Butler, S. G., Postima, G. N., and Fischer, E. (2004). Effects of viscosity, taste, and bolus volume on swallowing apnea duration of normal adults. *Otolaryngol. Head Neck Surg.* 131, 860–863. doi: 10.1016/j.otohns.2004.06.706
- Chang, W. J., Buscemi, V., Liston, M. B., McAuley, J. H., Hodges, P. W., and Schabrun, S. M. (2019). Sensorimotor cortical activity in acute low back pain: a cross-sectional study. *J. Pain* 20, 819–829. doi: 10.1016/j.jpain.2019.01.006
- Chee, C., Arshad, S., Singh, S., Mistry, S., and Hamdy, S. (2005). The influence of chemical gustatory stimuli and oral anaesthesia on healthy human pharyngeal swallowing. *Chem. Sens.* 30, 393–400. doi: 10.1093/chemse/bji034
- Chen, G., Adelman, N. E., Saad, Z. S., Leibenluft, E., and Cox, R. W. (2014). Applications of multivariate modeling to neuroimaging group analysis: a comprehensive alternative to univariate general linear model. *Neuroimage* 99, 571–588. doi: 10.1016/j.neuroimage.2014.06.027
- Cola, P. C., Gatto, A. R., Silva, R. G., Spadotto, A. A., Schelp, A. O., and Henry, M. A. C. (2010). The influence of sour taste and cold temperature in pharyngeal transit duration in patients with stroke. *Arq. Gastroenterol.* 47, 18–21. doi: 10.1590/S0004-28032010000100004
- Cox, R. W. (1996). AFNI: software for analysis and visualization of functional magnetic resonance neuroimages. *Comput. Biomed. Res.* 29, 162–173. doi: 10.1006/cbmr.1996.0014
- Cox, R. W., Chen, G., Glen, D. R., Reynolds, R. C., and Taylor, P. A. (2017). FMRI clustering in AFNI: false-positive rates redux. *Brain Connect.* 7, 152–171. doi: 10.1089/brain.2016.0475
- Desikan, R. S., Ségonne, F., Fischl, B., Quinn, B. T., Dickerson, B. C., Blacker, D., et al. (2006). An automated labeling system for subdividing the human cerebral cortex on MRI scans into gyral based regions of interest. *Neuroimage* 31, 968–980. doi: 10.1016/j.neuroimage.2006.01.021
- Dietsch, A. M., Dorris, H. D., Pearson, W. G., Dietrich-Burns, K. E., and Solomon, N. P. (2019). Taste manipulation and swallowing mechanics in trauma-related sensory-based dysphagia. *J. Speech Lang. Hear. Res.* 62, 2703–2712. doi: 10.1044/2019_JSLHR-S-18-0381
- Dietsch, A. M., Solomon, N. P., Steele, C. M., and Pelletier, C. A. (2014). The effect of barium on perceptions of taste intensity and palatability. *Dysphagia* 29, 96–108. doi: 10.1007/s00455-013-9487-4
- Ding, R., Logemann, J. A., Larson, C. R., and Rademaker, A. W. (2003). The effects of taste and consistency on swallow physiology in younger and older healthy individuals: a surface electromyographic study. *J. Speech Lang. Hear. Res.* 46, 977–989. doi: 10.1044/1092-4388(2003)076
- Drewnowski, A. (1992). Sensory properties of fats and fat replacements. *Nutr. Rev.* 50, 17–20. doi: 10.1111/j.1753-4887.1992.tb01285.x
- Dunst, B., Benedek, M., Jauk, E., Bergner, S., Koschutnig, K., Sommer, M., et al. (2014). Neural efficiency as a function of task demands. *Intelligence* 42, 22–30. doi: 10.1016/j.intell.2013.09.005
- Eldegaidy, S., Marciani, L., McGlone, F., Hollowood, T., Hort, J., Head, K., et al. (2011). The cortical response to the oral perception of fat emulsions and the effect of taster status. *J. Neurophysiol.* 105, 2572–2581. doi: 10.1152/jn.00927.2010
- Essick, G. K., Chopra, A., Guest, S., and McGlone, F. (2003). Lingual tactile acuity, taste perception, and the density and diameter of fungiform papillae in female subjects. *Physiol. Behav.* 80, 289–302. doi: 10.1016/j.physbeh.2003.08.007
- Fischl, B., Salat, D. H., van der Kouwe, A. J. W., Makris, N., Ségonne, F., Quinn, B. T., et al. (2004). Sequence-independent segmentation of magnetic resonance images. *Neuroimage* 23, S69–S84. doi: 10.1016/j.neuroimage.2004.07.016
- Forman, S. D., Cohen, J. D., Fitzgerald, M., Eddy, W. F., Mintun, M. A., and Noll, D. C. (1995). Improved assessment of significant activation in functional magnetic resonance imaging (fMRI): use of a cluster-size threshold. *Magn. Reson. Med.* 33, 636–647. doi: 10.1002/mrm.1910330508
- Gatto, A. R., Cola, P. C., da Silva, R. G., Spadotto, A. A., Ribeiro, P. W., Schelp, A. O., et al. (2013). Sour taste and cold temperature in the oral phase of swallowing in patients after stroke. *Codas* 25, 163–167. doi: 10.1590/S2317-17822013000200012
- Haggard, P., and de Boer, L. (2014). Oral somatosensory awareness. *Neurosci. Biobehav. Rev.* 47, 469–448. doi: 10.1016/j.neubiorev.2014.09.015
- Haier, R. J., Siegel, B., Tang, C., Abel, L., and Buchsbaum, M. S. (1992). Intelligence and changes in regional cerebral glucose metabolic rate following learning. *Intelligence* 16, 415–426. doi: 10.1016/0160-2896(92)90018-m
- Hamdy, S., Jilani, S., Price, V., Parker, C., Hall, N., and Power, M. (2003). Modulation of human swallowing behaviour by thermal and chemical stimulation in health and after brain injury. *Neurogastroenterol. Motil.* 15, 69–77. doi: 10.1046/j.1365-2982.2003.00390.x
- Hanson, B., Steele, C. M., Lam, P., and Cichero, J. A. Y. (2019). Fluid testing methods recommended by IDDSI. *Dysphagia* 34, 716–717. doi: 10.1007/s00455-018-9957-9
- Hiss, S. G., Strauss, M., Treole, K., and Stuart, A. (2004). Effects of age, gender, bolus volume, bolus viscosity, and gustation on swallowing apnea onset relative to lingual propulsion onset in normal adults. *J. Speech Lang. Hear. Res.* 47, 572–583. doi: 10.1044/1092-4388(2004)044
- Hosseini, P., Tadavarthi, Y., Martin-Harris, B., and Pearson, W. G. (2019). Functional modules of pharyngeal swallowing mechanics. *Laryngoscope Invest. Otolaryngol.* 4, 341–346. doi: 10.1002/lio2.273
- Humbert, I. A., and Joel, S. (2012). Tactile, gustatory, and visual biofeedback stimuli moderate neural substrates of deglutition. *Neuroimage* 59, 1485–1490. doi: 10.1016/j.neuroimage.2011.08.022
- Inamoto, Y., Saitoh, E., Ito, Y., Kagaya, H., Aoyagi, Y., Shibata, S., et al. (2018). The Mendelsohn maneuver and its effects on swallowing: kinematic analysis in three dimensions using dynamic area detector CT. *Dysphagia* 33, 419–430. doi: 10.1007/s00455-017-9870-7
- Karrer, T., Bartoshuk, L. M., Conner, E., Fehrenbaker, S., Grubin, D., and Snow, D. (1992). PROP status and its relationship to the perceived burn intensity of capsaicin at different tongue loci. *Chem. Sens.* 17:649. doi: 10.1093/chemse/17.5.589
- Kim, U. K., Jorgenson, E., Coon, H., Leppert, M., Risch, N., and Drayna, D. (2003). Positional cloning of the human quantitative trait locus underlying taste sensitivity to phenylthiocarbamide. *Science* 299, 1221–1225. doi: 10.1126/science.1080190
- Kim, W., Kim, S. K., and Nabekkura, J. (2017). Functional and structural plasticity in the primary somatosensory cortex associated with chronic pain. *J. Neurochem.* 141, 499–506. doi: 10.1111/jnc.14012
- Klingenberg, C. P. (2011). MorphoJ: an integrated software package for geometric morphometrics. *Mol. Ecol. Resour.* 11, 353–357. doi: 10.1111/j.1755-0998.2010.02924.x
- Ko, C. W., Hoffman, H. J., Lucchina, L. A., Snyder, D. J., Weiffenbach, J. M., and Bartoshuk, L. M. (2000). Differential perceptions of intensity for the four basic taste qualities in PROP supertasters versus nontasters. *Chem. Sens.* 25, 639–640. doi: 10.1093/chemse/25.5.639
- Lee, K. L., Kim, D. Y., Kim, W. H., Kim, E. J., Lee, W. K., Hahn, S. J., et al. (2012). The influence of sour taste on dysphagia in brain injury: blind study. *Ann. Rehabil. Med.* 36, 365–370. doi: 10.5535/arm.2012.36.3.365
- Leonard, R., Belafsky, P. C., and Rees, C. J. (2006). Relationship between fluoroscopic and manometric measures of pharyngeal constriction: the pharyngeal constriction ratio. *Ann. Otol. Rhinol. Laryngol.* 115, 897–901. doi: 10.1177/000348940611501207

- Leonard, R. J., Kendall, K. A., McKenzie, S., Goncalves, M. I., and Walker, A. (2000). Structural displacements in normal swallowing: a videofluoroscopic study. *Dysphagia* 15, 146–152. doi: 10.1007/s004550010017
- Leow, L. P., Huckabee, M.-L., Sharma, S., and Tooley, T. P. (2007). The influence of taste on swallowing apnea, oral preparation time, and duration and amplitude of submental muscle contraction. *Chem. Sens.* 32, 119–128. doi: 10.1093/chemse/bjl037
- Lipp, I., Benedek, M., Fink, A., Koschutnig, K., Reishofer, G., Bergner, S., et al. (2012). Investigating neural efficiency in the visuo-spatial domain: an fmri study. *PLoS One* 7:e51316. doi: 10.1371/journal.pone.0051316
- Martin, R. E., MacIntosh, B. J., Smith, R. C., Barr, A. M., Stevens, T. K., Gati, J. S., et al. (2004). Cerebral areas processing swallowing and tongue movement are overlapping but distinct: a functional magnetic resonance imaging study. *J. Neurophysiol.* 92, 2428–2443. doi: 10.1152/jn.01144.2003
- May, N. H., Pisegna, J. M., Marchina, S., Langmore, S. E., Kumar, S., Pearson, W. G. Jr. (2017). Pharyngeal swallowing mechanics secondary to hemispheric stroke. *J. Stroke Cerebrovasc. Dis.* 26, 952–961. doi: 10.1016/j.jstrokecerebrovasdis.2016.11.001
- McBride, R. L., and Johnson, R. L. (1987). Perception of sugar-acid mixtures in lemon juice drink. *Food Sci Technol Int.* 22, 399–408. doi: 10.1111/j.1365-2621.1987.tb00503.x
- Miura, Y., Morita, Y., Koizumi, H., and Shingai, T. (2009). Effects of taste solutions, carbonation, and cold stimulus on the power frequency content of swallowing submental surface electromyography. *Chem. Sens.* 34, 325–331. doi: 10.1093/chemse/bjp005
- Miyaoka, Y., Ashida, I., Inagaki, D., and Kawakami, S. (2005). Differentiation of activity patterns in the suprahyoid muscles during swallowing of foods with five taste qualities. *J. Sens. Stud.* 20, 473–483. doi: 10.1111/j.1745-459x.2005.00041.x
- Miyaoka, Y., Haishima, K., Takagi, M., Haishima, H., Asari, J., and Yamada, Y. (2006). Influences of thermal and gustatory characteristics on sensory and motor aspects of swallowing. *Dysphagia* 21, 38–48. doi: 10.1007/s00455-005-9003-6
- Molfenter, S. M., Hsu, C.-Y., Lu, Y., and Lazarus, C. L. (2018). Alterations to swallowing physiology as the result of effortful swallowing in healthy seniors. *Dysphagia* 33, 3800–3388. doi: 10.1007/s00455-017-9863-6
- Mulheren, R. W., Kamarunas, E., and Ludlow, C. L. (2016). Sour taste increases swallowing and prolongs hemodynamic responses in the cortical swallowing network. *J. Neurophys.* 116, 2033–2042. doi: 10.1152/jn.00130.2016
- Nagy, A., Steele, C. M., and Pelletier, C. A. (2014b). Differences in swallowing between high and low concentration taste stimuli. *Biomed. Res. Int.* 2014:813084. doi: 10.1155/2014/813084
- Nagy, A., Steele, C. M., and Pelletier, C. A. (2014a). Barium versus nonbarium stimuli: differences in taste intensity, chemesthesis, and swallowing behavior in healthy adult women. *J. Speech Lang. Hear. Res.* 57, 758–767. doi: 10.1044/2013_JSLHR-S-13-0136
- Natarajan, R., Stavness, I., and Pearson, W. (2015). Semi-automatic tracking of hyolaryngeal coordinates in videofluoroscopic swallowing studies. *Comput. Methods Biomech. Biomed. Eng.* 5, 379–389. doi: 10.1080/21681163.2015.1046190
- Neubauer, A. C., and Fink, A. (2009). Intelligence and neural efficiency. *Neurosci. Biobehav. Rev.* 33, 1004–1023. doi: 10.1016/j.neubiorev.2009.04.001
- Palmer, P. M., McCulloch, T. M., Jaffe, D., and Neel, A. T. (2005). Effects of a sour bolus on the intramuscular electromyographic (EMG) activity of muscles in the submental region. *Dysphagia* 20, 210–217. doi: 10.1007/s00455-005-0017-x
- Pauloski, B. R., Logemann, J. A., Rademaker, A. W., Lundy, D., Sullivan, P. A., Newman, L. A., et al. (2012). Effects of enhanced bolus flavors on oropharyngeal swallow in patients treated for head and neck cancer. *Head Neck.* 35, 1124–1131. doi: 10.1002/hed.23086
- Peck, K. K., Branski, R. C., Lazarus, C., Cody, V., Kraus, D., Haupage, S., et al. (2010). Cortical activation during swallowing rehabilitation maneuvers: a unctinal MRI study of healthy controls. *Laryngoscope* 120, 2153–2159. doi: 10.1002/lary.21125
- Pelletier, C. A., and Dhanaraj, G. E. (2006). The effect of taste and palatability on lingual swallowing pressure. *Dysphagia* 21, 121–128. doi: 10.1007/s00455-006-9020-0
- Pelletier, C. A., and Lawless, H. T. (2003). Effect of citric acid and citric acid-sucrose mixtures on swallowing in neurogenic oropharyngeal dysphagia. *Dysphagia* 18, 231–241. doi: 10.1007/s00455-003-0013-y
- Pelletier, C. A., Lawless, H. T., and Horne, J. (2004). Sweet-sour mixture suppression in older and young adults. *Food Qual. Prefer.* 15, 105–116. doi: 10.1016/S0950-3293(03)00037-5
- Pelletier, C. A., and Steele, C. M. (2014). Influence of the perceived taste intensity of chemesthetic stimuli on swallowing parameters given age and genetic taste differences in healthy adult women. *J. Speech Lang. Hear. Res.* 57, 46–56. doi: 10.1044/1092-4388(2013/13-0005)
- Plonk, D. P., Butler, S. G., Grace-Martin, K., and Pelletier, C. A. (2011). Effects of chemesthetic stimuli, age, and genetic taste groups on swallowing apnea duration. *Otolaryngol. Head Neck Surg.* 145, 618–622. doi: 10.1177/0194599811407280
- Reed, D. R., Nanthakumar, E., North, M., Bell, C., Bartoshuk, L. M., and Price, R. A. (1999). Localization of a gene for bitter-taste perception to human chromosome 5p15. *Am. J. Hum. Genet.* 64, 1478–1480. doi: 10.1086/302367
- Schultz, D. H., and Cole, M. W. (2016). Higher intelligence is associated with less task-related brain network reconfiguration. *J. Neurosci.* 36, 8551–8561. doi: 10.1523/JNEUROSCI.0358-16.2016
- Sharma, A., Glick, H., Campbell, J., Torres, J., Dorman, M., and Zeitler, D. M. (2016). Cortical plasticity and reorganization in pediatric single-sided deafness pre- and postcochlear implantation: a case study. *Otol. Neurotol.* 37, e26–e34. doi: 10.1097/MAO.0000000000000904
- Shibamoto, I., Tanaka, T., Fujishima, I., Katagiri, N., and Uematsu, H. (2007). Cortical activation during solid bolus swallowing. *J. Med. Dent. Sci.* 54, 25–30. doi: 10.11480/jmds.540104
- Simon, S. A., de Araujo, I. E., Gutierrez, R., and Nicolelis, M. A. L. (2006). The neural mechanisms of gustation: a distributed processing code. *Nat. Rev. Neurosci.* 7, 890–901. doi: 10.1038/nm2006
- Smutzer, G., Desai, H., Coldwell, S. E., and Griffith, J. W. (2013). Validation of edible taste strips for assessing PROP taste perception. *Chem. Sens.* 38, 529–530. doi: 10.1093/chemse/bjt023
- Steele, C. M., and Miller, A. J. (2010). Sensory input pathways and mechanisms in swallowing: a review. *Dysphagia* 25, 323–333. doi: 10.1007/s00455-010-9301-5
- Steele, C. M., Peladeau-Pigeon, M., Barbon, C. A. E., Guida, B. T., Namasivayam-MacDonald, A. M., Nascimento, W. V., et al. (2019). Reference values for healthy swallowing across the range from thin to extremely thick liquids. *J. Speech Lang. Hear. Res.* 62, 1338–1363. doi: 10.1044/2019_JSLHR-S-18-0448
- Steele, C. M., van Lieshout, P. H. H., and Pelletier, C. A. (2012). The influence of stimulus taste and chemesthesis on tongue movement timing in swallowing. *J. Speech Lang. Hear. Res.* 55, 262–275. doi: 10.1044/1092-4388(2011/11-0012)
- Todd, J. T., Butler, S. G., Plonk, D. P., Grace-Martin, K., and Pelletier, C. A. (2012a). Effects of chemesthetic stimuli mixtures with barium on swallowing apnea duration. *Laryngoscope* 122, 2248–2251. doi: 10.1002/lary.23511
- Todd, J. T., Butler, S. G., Plonk, D. P., Grace-Martin, K., and Pelletier, C. A. (2012b). Main taste effects on swallowing apnea duration in healthy adults. *Otolaryngol. Head Neck Surg.* 147, 678–683. doi: 10.1177/0194599812450839
- Wahab, N. A., Jones, R. D., and Huckabee, M.-L. (2011). Effects of olfactory and gustatory stimuli on the biomechanics of swallowing. *Physiol. Behav.* 102, 485–490. doi: 10.1016/j.phybeh.2010.11.030
- Zeidan, F., Martucci, K. T., Kraft, R. A., Gordon, N. S., McHaffie, J. G., and Coghill, R. C. (2011). Brain mechanisms supporting the modulation of pain by mindfulness meditation. *J. Neurosci.* 31, 5540–5548. doi: 10.1523/jneurosci.5791-10.2011
- Zhao, Z., Huang, T., Tang, C., Ni, K., Pan, X., Yan, C., et al. (2017). Altered resting-state intra- and inter- network functional connectivity in patients with persistent somatoform pain disorder. *PLoS One* 12:e0176494. doi: 10.1371/journal.pone.0176494
- Zuo, N., Yang, Z., Liu, Y., Li, J., and Jiang, T. (2018). Core networks and their reconfiguration patterns across cognitive loads. *Hum. Brain Mapp.* 39, 3546–3557. doi: 10.1002/hbm.24193

Conflict of Interest: The authors declare that the research was conducted in the absence of any commercial or financial relationships that could be construed as a potential conflict of interest.

Copyright © 2019 Dietsch, Westemeyer, Pearson and Schultz. This is an open-access article distributed under the terms of the Creative Commons Attribution License (CC BY). The use, distribution or reproduction in other forums is permitted, provided the original author(s) and the copyright owner(s) are credited and that the original publication in this journal is cited, in accordance with accepted academic practice. No use, distribution or reproduction is permitted which does not comply with these terms.



Tongue Force Training Induces Plasticity of the Lingual Motor Cortex in Young Adult and Aged Rats

Miranda J. Cullins^{1*}, Julie M. Wenninger¹, Jared S. Cullen¹, John A. Russell¹, Jeffrey A. Kleim² and Nadine P. Connor¹

¹ Department of Surgery, University of Wisconsin-Madison, Madison, WI, United States, ² School of Biological and Health Systems Engineering, Arizona State University, Tempe, AZ, United States

OPEN ACCESS

Edited by:

Limor Avivi-Arber,
University of Toronto, Canada

Reviewed by:

Bryan Kolb,
University of Lethbridge, Canada
Kazunori Adachi,
Meikai University, Japan

*Correspondence:

Miranda J. Cullins
mcullins@wisc.edu

Specialty section:

This article was submitted to
Neurodegeneration,
a section of the journal
Frontiers in Neuroscience

Received: 26 July 2019

Accepted: 02 December 2019

Published: 19 December 2019

Citation:

Cullins MJ, Wenninger JM, Cullen JS, Russell JA, Kleim JA and Connor NP (2019) Tongue Force Training Induces Plasticity of the Lingual Motor Cortex in Young Adult and Aged Rats. *Front. Neurosci.* 13:1355. doi: 10.3389/fnins.2019.01355

Tongue exercise programs are used clinically for dysphagia in aged individuals and have been shown to improve lingual strength. However, the neural mechanisms of age-related decline in swallowing function and its association with lingual strength are not well understood. Using an established rat model of aging and tongue exercise, we hypothesized that the motor cortex of aged rats would have a smaller lingual motor map area than young adult rats and would increase in size as a function of tongue exercise. Over 8 weeks, rats either underwent a progressive resistance tongue exercise program (TE), learned the task but did not exercise (trained controls, TC), or were naïve untrained controls (UC). Cortical motor map areas for tongue and jaw were determined using intracortical microstimulation (ICMS). Rats in the TE and TC groups had a significantly larger motor cortex region for the tongue than the UC group. Lingual cortical motor area was not correlated with protrusive tongue force gains and did not differ significantly with age. These results suggest that learning a novel tongue force skill was sufficient to induce plasticity of the lingual motor cortex yet increasing tongue strength with progressive resistance exercise did not significantly expand the lingual motor area beyond the gains that occurred through the skilled learning component.

Keywords: tongue, exercise, plasticity, motor cortex, age

INTRODUCTION

Dysphagia is a common condition among aged individuals and is associated with serious health problems, reduced quality of life, and high healthcare costs (Sura et al., 2012; Westmark et al., 2018). Age related changes in swallowing function (presbyphagia), including lingual weakness (Robbins et al., 1995; Hara et al., 2018) and increased swallow durations (Shaw et al., 1995; Nicosia et al., 2000; Namasivayam-MacDonald et al., 2018), may predispose aged individuals to developing dysphagia (Humbert and Robbins, 2008). The mechanisms of age-related decline in swallowing function and its association with lingual strength are not well understood. Determining the underlying causes of declines in oral-motor function with age may lead to more targeted approaches to treat or prevent dysphagia in aged individuals.

An overwhelming body of evidence suggests that CNS changes contribute substantially to sarcopenia, the age-related loss of skeletal muscle mass, strength, and function (Clark and Manini, 2008; Kwan, 2013; Tieland et al., 2018). Age-related reductions in muscle strength and motor

control have been associated with motor cortex atrophy and reduced excitability (Clark and Taylor, 2011), but whether such motor cortex changes contribute to declines in lingual motor function are not known. Our previous studies in rats have found age-related changes in neuromuscular junctions in tongue muscles (Hodges et al., 2004; Johnson and Connor, 2011), hypoglossal motor neurons (Schwarz et al., 2009; Behan et al., 2012; Schaser et al., 2012), and the lingual muscles themselves (Ota et al., 2005; Connor et al., 2008; Nagai et al., 2008; Schaser et al., 2011; Cullins and Connor, 2017). In this study we sought to determine whether age is associated with changes in the motor cortex representation of the tongue and jaw. The topographical organization and excitability of the motor cortex can be assessed by using intracortical microstimulation (ICMS) to map cortically driven muscle activation.

Motor cortex plasticity may also be induced by rehabilitative exercises for dysphagia such as tongue exercise. Skilled motor learning has been shown to induce plasticity in the motor cortex, with functional improvements corresponding to increased cortical motor map representation and reduced stimulation thresholds of the involved muscles (Nudo et al., 1996; Kleim et al., 1998; Tennant et al., 2012). Tongue training programs are used clinically for dysphagia in aged individuals and have been shown to improve lingual strength (Robbins et al., 2005; Yeates et al., 2008; Park and Kim, 2016; Rogus-Pulia et al., 2016). There is evidence in young-adult humans and monkeys that tongue-task training induces cortical plasticity (Svensson et al., 2003, 2006; Baad-Hansen et al., 2009; Komoda et al., 2015). However, cortical plasticity may be reduced with age (Seidler et al., 2010; Tennant et al., 2012), and the impact of age on the relationship between tongue training and motor cortex plasticity is not known.

We hypothesized that, compared to young adult rats, the motor cortex of aged rats would have a smaller lingual motor map area and increased lingual motor threshold, assessed by ICMS. We further hypothesized that the cortical movement representation of the tongue would be expanded and movement thresholds reduced as a function of tongue exercise training in young adult and aged rats.

MATERIALS AND METHODS

Animals

This study was performed in compliance with the Guide for Care and Use of Laboratory Animals (8th edition, 2011, National Academies Press) and approved by the Animal Care and Use Committee of the University of Wisconsin School of Medicine and Public Health. Male Fischer 344/Brown Norway rats were obtained from the National Institute on Aging colony (Harlan Laboratories, Indianapolis, IN, United States). Young adult (9 months old at study completion) and old (32 months at study completion) rats were randomly assigned to one of three groups: (1) untrained controls (UC; $n = 7$ young adult, $n = 8$ old) naïve to the tongue force task; (2) trained controls (TC) that learned the tongue force task and performed maximum force testing ($n = 9$ young adult, 9 old), or (3) trained exercise (TE) that underwent the 8-week tongue exercise paradigm described below

($n = 9$ young adult, 9 old). Each group consisted of 10 rats, but final numbers reflect losses due to surgical complications or age-related health concerns. The rats were housed in pairs in standard polycarbonate cages on a 12:12-h light-dark reversed light cycle.

Tongue Exercise

The clinically based progressive rat tongue exercise training methods have been detailed previously (Connor et al., 2009) and have been shown to increase voluntary tongue force in young and aged rats in a number of studies (Connor et al., 2009; Schaser et al., 2012; Kletzien et al., 2013; Krekeler and Connor, 2017; Cullins et al., 2018). This well-established training paradigm was originally developed based on several studies that used operant conditions in rats to assess licking function (Fowler and Mortell, 1992; Moss et al., 2001; Stanford et al., 2003; Smittkamp et al., 2008). TC and TE rats were water restricted to 3 h/day then trained to press their tongue against an instrumented disk to receive a water reward. Maximum voluntary tongue force was determined at baseline, 4-, and 8-weeks by incrementally increasing the reward force thresholds by 0.002 N after each successful press. This process was repeated over the course of 3 days, and the average of the 10 highest forces was used to determine an individual rat's maximum voluntary tongue force. The TE group underwent a progressive resistance training program, performed 5 days/week for a total of 8 weeks. Rats exercised at water reward thresholds of 50% max (weeks 1–2), 60% max (weeks 3–4), 70% max (weeks 5–6), and 80% max (weeks 7–8). Force thresholds for weeks 1–4 were calculated from baseline maximums; maximum force testing was repeated in week 4 and the new individual maximums were used to calculate thresholds for weeks 5–8. Each exercise session lasted 10 min. The TC group learned the tongue pressing task and underwent maximum tongue force testing but did not perform progressive tongue exercise. They were placed in the operandum 5 days/week and were allowed to briefly lick water from the disk before they were removed. Body weights were recorded daily to monitor the effects of the water restriction and training paradigms.

Intracortical Microstimulation (ICMS)

Intracortical Microstimulation was adapted from previously published techniques (Kleim et al., 1998) which have been used to map the orolingual motor area in a rat model of Parkinson disease (Plowman and Kleim, 2011; Plowman et al., 2014). Rats were anesthetized by intraperitoneal (IP) injection (70 mg/kg ketamine and 9 mg/kg xylazine). The plane of anesthesia was monitored for presence of moderate toe-pinch response and maintained either by supplemental IP doses of ketamine (0.1cc as needed) or a femoral i.v. catheter infusion of ketamine (40 mg/kg/hr, adjusted as needed). Anesthesia by infusion was found to be easier to maintain. Anesthesia type (IP or IV) was included as a covariate in the statistical analysis. However, anesthesia type was not found to have any significant influence on map size ($p = 0.554$; combined jaw and tongue area \pm SD: IP = $1.91 \pm 1.04 \text{ mm}^2$, $N = 26$; IV = $2.18 \pm 0.83 \text{ mm}^2$, $N = 25$). Animals were placed in a stereotaxic apparatus and the skull and dura were removed from 5 to 6 mm rostral and 2–3 mm caudal to Bregma, over the left motor cortex; up to 5 mm lateral. A small

puncture was made in the cisterna magna prior to removing the skull and dura to prevent edema. Warm silicone oil was placed on the cortical surface. A digital image of the cortical surface was taken and a 250 μm grid was superimposed onto the image and used as a guide to select and track stimulation sites. A glass microelectrode filled with 3.5 M saline solution and a platinum wire (600–800 k Ω) controlled by a hydraulic microdrive was used to make systematic penetrations across the cortex using the cortical surface image and grid as a guide. At each penetration site, the electrode was lowered to approximately 1550 μm from the surface to correspond with cortical layer V. Stimulation consisted of thirteen 200 μs cathodal pulses delivered at 350 Hz from an electrically isolated stimulation circuit. Rats were maintained in a prone position with the forelimb consistently supported. At each site the stimulating current was gradually increased until a movement was detected, up to 60 μA . Once movement was detected, the stimulating current was gradually lowered until the movement disappeared then increased again to establish the movement threshold at which a motor response occurred 6 of 10 stimulations. If more than one muscle group was activated at the threshold current, that site was considered positive for both and included in the map size calculation for each (ex: jaw + tongue or jaw + neck). If no movement could be detected at 60 μA , the site was determined to be non-responsive. The initial penetration site was randomly selected. Once movement of any sort (including elbow or neck) was established at the initial penetration, sites likely to border tongue or jaw motor areas were targeted. The jaw and tongue map areas are typically bordered rostrally and laterally by non-responsive sites, and caudally and medially by sites activating the vibrissae, neck, and forelimb (Neafsey et al., 1986). The next penetration site, regardless of response, was selected at least 2 grid lengths from the previous activation site whenever possible to avoid temporary threshold changes due to recent adjacent stimulation. Movements of the tongue and jaw were differentiated visually and confirmed as needed by accelerometers attached to the tongue and jaw.

The procedure was continued until the entire jaw and tongue representations were mapped, as both the tongue and jaw muscles contribute to swallowing and may be activated by the tongue force task. Representation area was calculated by multiplying the number of stimulation sites by 0.0625 mm².

Statistical Analysis

Motor cortical representations of the tongue and jaw were assessed by MANCOVA. Independent variables were age and treatment (UC, TC, TE), and dependent variables were tongue and jaw area. Anesthesia type (IP or IV) and weight were included as covariates. Rats grow throughout their lifespan, so old rats typically weigh more than young rats (Turturro et al., 1999). Weight was included as a covariate based on previous studies that found body weight and brain volume to be correlated in the rat (Bailey et al., 2004; Oguz et al., 2013; Welniak-Kaminska et al., 2019). Over the course of the 8-week training paradigm old rats lost on average 7% of their body weight and young rats gained 12%. Mapping occurred at the end of the study and weight at the time of mapping was used. Estimated marginal

means and standard errors are reported with the covariate body weight at 575 g. Movement thresholds of the tongue and jaw were also assessed by MANCOVA. Independent variables were age and treatment (UC, TC, TE), dependent variables were mean tongue and jaw thresholds (μA), and anesthesia type (IP or IV) was included as a covariate. The Pillai's trace test statistics are reported. MANCOVA was followed by individual univariate ANCOVAs.

A 2-way and repeated measures ANOVA were used to assess change in maximum tongue force from baseline to 8 weeks by age and treatment group with weight included as a covariate. A Pearson correlation was used to assess the relationship between tongue motor representation area and change in maximum tongue force.

RESULTS

Tongue Cortical Area

Examples of tongue and jaw representations in the motor cortex determined by ICMS are shown in **Figure 1**. MANCOVA results indicated a significant main effect of treatment group (UC, TC, TE) across the dependent variables of Tongue and Jaw motor cortical area [Pillai's Trace = 0.473, $F(4,86) = 6.668$, $p < 0.001$, $\eta_p^2 = 0.237$]. There was not a significant main effect for age [Pillai's Trace = 0.104, $F(2,42) = 2.43$, $p = 0.101$], or an age-treatment interaction [Pillai's Trace = 0.065, $F(4,86) = 0.725$, $p = 0.577$].

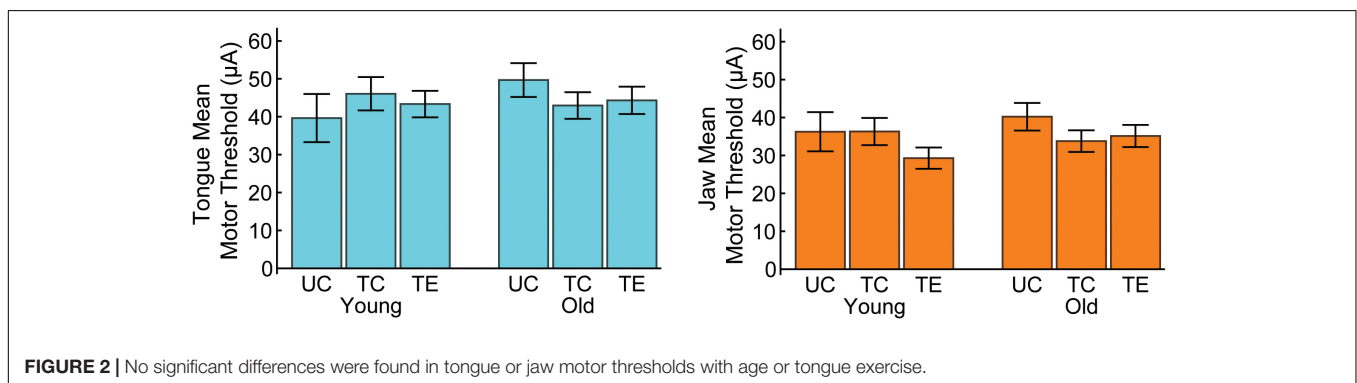
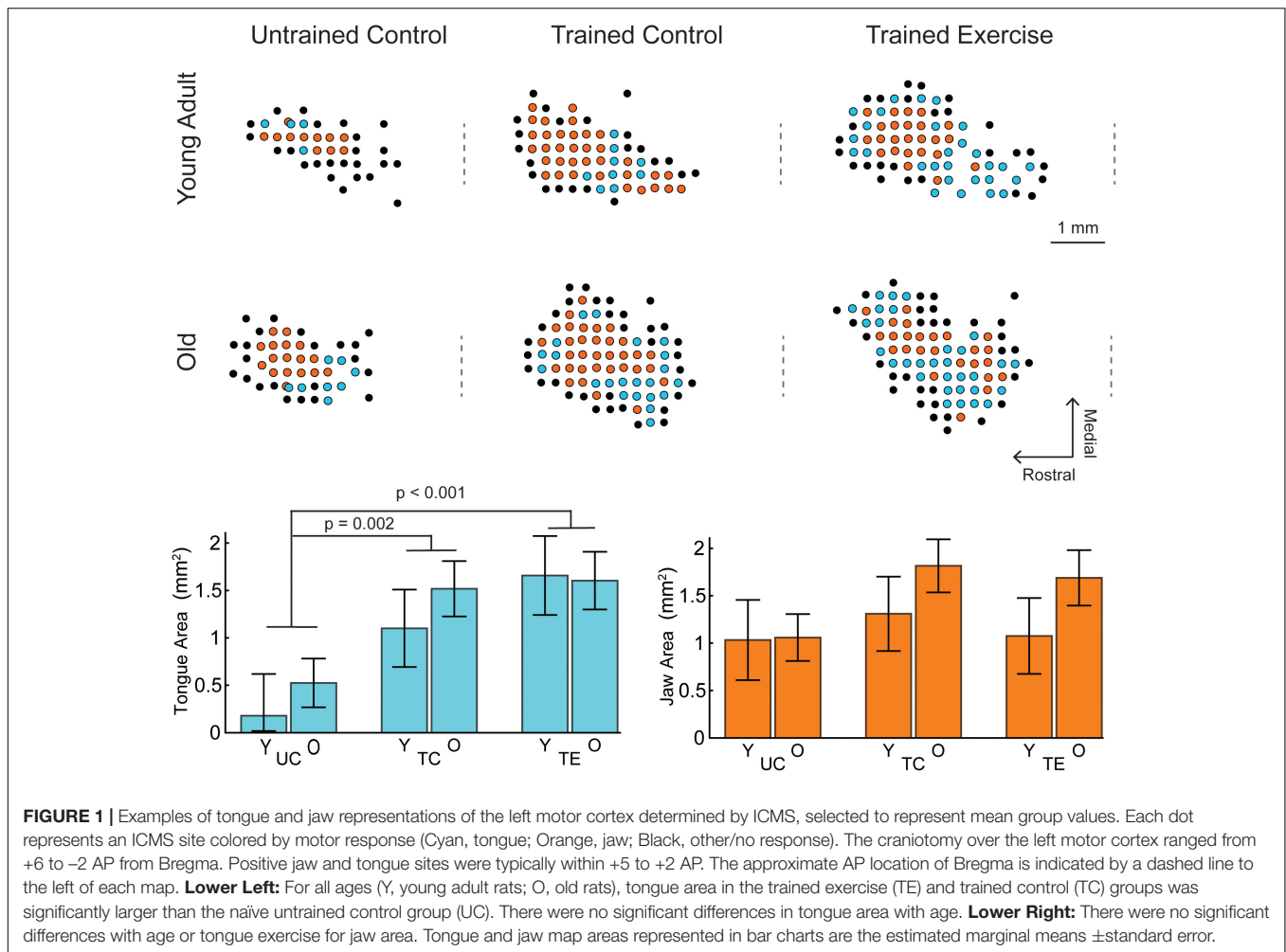
The MANCOVA treatment results were followed up with univariate ANCOVA tests which indicated a significant treatment effect for tongue area [$F(2,43) = 9.537$, $p < 0.001$, $\eta_p^2 = 0.307$] but not jaw area [$F(2,43) = 1.680$, $p = 0.198$, $\eta_p^2 = 0.072$]. Pairwise comparisons indicated that the area of tongue motor cortical representation was significantly larger in each of the trained groups (TC = 1.31 mm² \pm 0.31 SE, TE = 1.63 mm² \pm 0.32 SE) compared to the untrained control group (0.352 mm² \pm 0.27 SE; $p = 0.002$ and $p < 0.001$ respectively; estimated marginal means reported at weight = 575 g). The mean tongue area of the exercise group was not significantly larger than the trained control group ($p = 0.143$).

Movement Thresholds

The effects of age and treatment on movement thresholds, the mean minimum stimulation current that elicited jaw or tongue movement, was evaluated in a separate MANCOVA with anesthesia (IP or IV) as a covariate. No significant age [Pillai's Trace = 0.027, $F(2,35) = 0.475$, $p < 0.63$, $\eta_p^2 = 0.026$], treatment [Pillai's Trace = 0.068, $F(4,72) = 0.64$, $p = 0.64$, $\eta_p^2 = 0.034$], or interaction effects [Pillai's Trace = 0.10, $F(4,72) = 0.95$, $p = 0.44$, $\eta_p^2 = 0.05$] were found for tongue and jaw motor thresholds (**Figure 2**).

Tongue Force

A 2-way ANOVA was used to determine the effects of age and exercise (TE, TC) on the change in maximum tongue force (8 weeks – baseline). The main effect of exercise was significant $F(1,31) = 72.76$, $p < 0.001$, $\eta_p^2 = 0.701$; the change in maximum

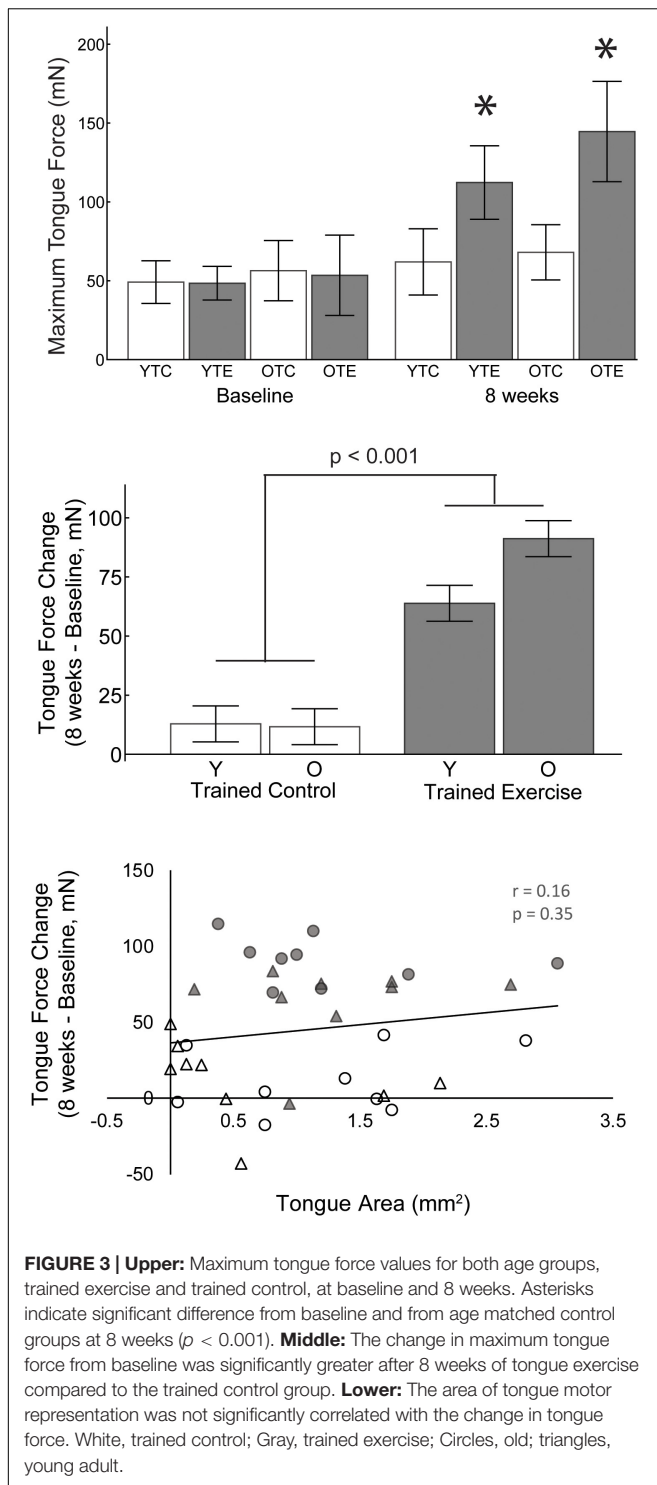


tongue force was significantly greater after 8 weeks of tongue exercise (TE group) compared to the trained control (TC) group ($77.66 \text{ mN} \pm 5.43 \text{ SE}$, $12.11 \text{ mN} \pm 5.43 \text{ SE}$). Age and age-treatment interaction effects were not significant [$F(1,31) = 0.889$, $p = 0.353$, $\eta_p^2 = 0.028$, $F(1,31) = 3.54$, $p = 0.069$, $\eta_p^2 = 0.102$].

Tongue force was not significantly correlated with tongue motor area (Figure 3; $r = 0.16$, $p = 0.35$) and variance in the cortical map size accounted for very little variance ($<3\%$, $r^2 = 0.026$) in increased tongue force.

DISCUSSION

This study found that rats that performed protrusive tongue force training and testing, with or without progressive resistance exercise, had a significantly larger motor cortex region representing the tongue than the untrained control group. No significant differences with age or changes in motor threshold were found. A previous study that assessed total cortical orolingual movement area (jaw, tongue, and lips combined) in



the rat after shorter tongue force training protocol (4–6 day), in contrast to our results, found a decreased motor threshold, but no change in motor area (Guggenmos et al., 2009). Motor area expansions can occur at the expense of the area of adjacent muscle groups (Kleim et al., 1998), thus motor area changes due to tongue training may not be detected when measuring

the total oral-lingual motor area. We found that tongue training specifically increased tongue representation, though we did not find a significant reduction in jaw area (Figure 1). Additional contributing factors may include differences in the training paradigms and timing of motor cortex assessment.

Skilled Motor Learning vs. Strength

Studies of skilled, unskilled, and strength-based forearm reaching tasks in rats have found that only skilled motor learning induces plasticity of the motor cortex, in which case increased area is associated with motor gains (Kleim et al., 1998; Remple et al., 2001). Our study is in agreement with these results in that both groups that learned the tongue force task (trained control and trained exercise) had an increased area of tongue representation in the motor cortex, but the exercise group did not have a significantly larger tongue area than the trained control group (Figure 1). It is worth noting that the trained control group, which learned the task and underwent maximum force testing, experienced a small yet significant increase in maximum tongue force from baseline (Figure 3). Furthermore, tongue area was not predictive of maximum tongue force (Figure 3). Plasticity contributing to lingual force gains may be encoded outside of the motor cortex; some studies have suggested that plasticity relevant to limb strength training occurs in the spinal cord (Sale et al., 1983; Griffin and Cafarelli, 2005). Similarly, a previous study from our lab found that the tongue training paradigm increased neuroplasticity associated neurotrophins in the tongue motor nuclei of the brainstem (Schaser et al., 2012, 2016).

Movement Thresholds

We hypothesized the aged group would have increased movement thresholds because age has been associated with reduced excitability of the motor cortex (Bhandari et al., 2016). However, we did not find any significant differences in the average threshold (minimum stimulation current) that induced tongue or jaw movement (Figure 2). We also did not find a significant change in threshold with tongue training. Reports on motor training threshold changes with ICMS have been mixed (Remple et al., 2001; Guggenmos et al., 2009) and it has been suggested that motor threshold decreases occur after the map area has returned to baseline (Tennant et al., 2012). This may explain why we did not find a change in threshold with training, as the tongue motor map area was still significantly expanded at the end of the study.

Motor Plasticity With Age

We hypothesized that plasticity of the motor cortex would be reduced with age, but our results did not support this hypothesis. A previous study using ICMS and skilled reaching reported that aged animals can learn new motor tasks, but do so without motor map expansions (Tennant et al., 2012). In our study the difference in tongue motor area between the trained exercise and untrained groups appears smaller in the aged vs. young rats (Figure 1), but these differences were not significant. Neuroplasticity in aged individuals has also been described as a critical mechanism of preserving motor function, including mastication, by recruiting additional brain regions beyond the

sensorimotor areas to compensate for declining peripheral and CNS tissues (Clark and Taylor, 2011; Avivi-Arber and Sessle, 2018). Future studies could determine whether tongue exercise training also induces plasticity in the functional connectivity of brain regions activated during swallowing.

Timing

Previous studies on skilled reaching have suggested that reorganization of cortical motor maps may be transient, and return to baseline after the initial learning period, despite maintaining the skill (Molina-Luna et al., 2008; Tennant et al., 2012). Our results appear to differ as we found significantly increased map size after 8 weeks of training. This difference may be due to the tongue training task being progressive over the course of training. In the previous studies of skilled reaching, the majority of performance gains occurred the first week of training. In the current study, the tongue exercise reward threshold was increased every other week and terminated with 3 days of peak voluntary force testing in both training groups. Thus, our results suggest that if the motor task continues to be challenging and produce performance gains, the motor map expansion may continue over a longer time frame. Additionally, the current study investigates the corticobulbar rather than corticospinal system, and the pattern of experience dependent plasticity may differ between these two systems.

Limitations

This study established that a clinically based lingual exercise program is sufficient to induce plasticity of the motor cortex, but no assessments of swallowing function were included. Thus, we cannot address whether the lingual motor cortex plasticity induced by tongue training transfers any benefits to swallowing function. This will be an important topic to address in future studies as clinical tongue strengthening trials have shown improvements in swallowing related outcomes (Rogus-Pulia et al., 2016), but the efficacy of tongue exercise as a treatment for dysphagia is not well established (Langmore and Pisegna, 2015). Dysphagia etiology may also be a key factor in establishing the biological mechanisms by which tongue exercise may improve swallowing function. Therefore, it may be advisable to address these questions of plasticity specificity and transference in specific disease models with established swallowing deficits such as Parkinson's (Russell et al., 2013) and stroke (Cullins and Connor, 2019).

We did not find any significant differences in jaw and tongue motor area with age, but this comparison may have been limited by two different factors. First, we assessed cortical area by stimulating at a constant superficial cortical depth within layer V of the M1 motor region. However, other studies have reported

ICMS can evoke tongue and jaw movements from multiple depths within layers 5 and 6 of M1, the adjacent S1 region, and the gustatory insular cortex (Neafsey et al., 1986; Adachi et al., 2007; Avivi-Arber et al., 2010a,b, 2015). Additionally, cortical thinning may occur with age (Salat et al., 2004). Thus, more accurate orolingual motor maps and aging comparisons may require measuring the total 3D cortical volume that can elicit movements of tongue and jaw. In addition to mapping deeper sites, lingual EMG recordings may be used to improve detection of sites that evoke more subtle twitches of the tongue (Adachi et al., 2007; Avivi-Arber et al., 2010a,b). An additional limitation in our age group comparison was that rats continue to grow with age thus the aged group weighed more than the young adult group. Weight was included as a covariate because brain volume may increase with body weight, but this may still be a confounding factor for age group comparisons.

Conclusion

We found that tongue training induced plasticity of the motor cortex in both young and aged rats, but further studies are needed to establish the relevance of lingual motor plasticity for dysphagia rehabilitation.

DATA AVAILABILITY STATEMENT

The datasets generated for this study are available on request to the corresponding author.

ETHICS STATEMENT

The animal study was reviewed and approved by the Animal Care and Use Committee of the University of Wisconsin, School of Medicine and Public Health.

AUTHOR CONTRIBUTIONS

NC and JK designed and supervised the study. JW, JR, JC, and MC collected, analyzed, and interpreted the data. MC wrote the manuscript with input from all authors. All authors approved the manuscript.

FUNDING

This study was funded by the following NIH grants: R01DC008149, R01DC014358, R37CA225608, T32DC009401, F32HD094527, and K99HD098300.

REFERENCES

- Adachi, K., Lee, J.-C., Hu, J. W., Yao, D., and Sessle, B. J. (2007). Motor cortex neuroplasticity associated with lingual nerve injury in rats. *Somatosens. Mot. Res.* 24, 97–109. doi: 10.1080/08990220701470451
- Avivi-Arber, L., Lee, J.-C., and Sessle, B. J. (2010a). Cortical orofacial motor representation: effect of diet consistency. *J. Dent. Res.* 89, 1142–1147. doi: 10.1177/0022034510373767
- Avivi-Arber, L., Lee, J.-C., and Sessle, B. J. (2010b). Effects of incisor extraction on jaw and tongue motor representations within face sensorimotor cortex of adult rats. *J. Comp. Neurol.* 518, 1030–1045. doi: 10.1002/cne.22261

- Avivi-Arber, L., Lee, J.-C., and Sessle, B. J. (2015). Dental occlusal changes induce motor cortex neuroplasticity. *J. Dent. Res.* 94, 1757–1764. doi: 10.1177/0022034515602478
- Avivi-Arber, L., and Sessle, B. J. (2018). Jaw sensorimotor control in healthy adults and effects of ageing. *J. Oral Rehabil.* 45, 50–80. doi: 10.1111/joor.12554
- Baad-Hansen, L., Blicher, J. U., Lapitskaya, N., Nielsen, J. F., and Svensson, P. (2009). Intra-cortical excitability in healthy human subjects after tongue training. *J. Oral Rehabil.* 36, 427–434. doi: 10.1111/j.1365-2842.2009.01955.x
- Bailey, S. A., Zidell, R. H., and Perry, R. W. (2004). Relationships between organ weight and body/brain weight in the rat: what is the best analytical endpoint? *Toxicol. Pathol.* 32, 448–466. doi: 10.1080/01926230490465874
- Behan, M., Moeser, A. E., Thomas, C. F., Russell, J. A., Wang, H., Levenson, G. E., et al. (2012). The effect of tongue exercise on serotonergic input to the hypoglossal nucleus in young and old rats. *J. Speech Lang. Hear. Res.* 55, 919–929. doi: 10.1044/1092-4388(2011/11-0091)
- Bhandari, A., Radhu, N., Farzan, F., Mulsant, B. H., Rajji, T. K., Daskalakis, Z. J., et al. (2016). A meta-analysis of the effects of aging on motor cortex neurophysiology assessed by transcranial magnetic stimulation. *Clin. Neurophysiol.* 127, 2834–2845. doi: 10.1016/j.clinph.2016.05.363
- Clark, B. C., and Manini, T. M. (2008). Sarcopenia \neq dynapenia. *J. Gerontol. A Biol. Sci. Med. Sci.* 63, 829–834. doi: 10.1093/gerona/63.8.829
- Clark, B. C., and Taylor, J. L. (2011). Age-related changes in motor cortical properties and voluntary activation of skeletal muscle. *Curr. Aging Sci.* 4, 192–199. doi: 10.2174/1874609811104030192
- Connor, N. P., Ota, F., Nagai, H., Russell, J. A., and Levenson, G. (2008). Differences in age-related alterations in muscle contraction properties in rat tongue and hindlimb. *J. Speech Lang. Hear. Res.* 51, 818–827. doi: 10.1044/1092-4388(2008/059)
- Connor, N. P., Russell, J. A., Wang, H., Jackson, M. A., Mann, L., and Kluender, K. (2009). Effect of tongue exercise on protrusive force and muscle fiber area in aging rats. *J. Speech Lang. Hear. Res.* 52, 732–744. doi: 10.1044/1092-4388(2008/08-0105)
- Cullins, M. J., and Connor, N. P. (2017). Alterations of intrinsic tongue muscle properties with aging: aging intrinsic tongue muscles. *Muscle Nerve* 56, E119–E125. doi: 10.1002/mus.25605
- Cullins, M. J., and Connor, N. P. (2019). Reduced tongue force and functional swallowing changes in a rat model of post stroke dysphagia. *Brain Res.* 1717, 160–166. doi: 10.1016/j.brainres.2019.04.023
- Cullins, M. J., Krekeler, B. N., and Connor, N. P. (2018). Differential impact of tongue exercise on intrinsic lingual muscles. *Laryngoscope* 128, 2245–2251. doi: 10.1002/lary.27044
- Fowler, S. C., and Mortell, C. (1992). Low doses of haloperidol interfere with rat tongue extensions during licking: a quantitative analysis. *Behav. Neurosci.* 106, 386–395. doi: 10.1037//0735-7044.106.2.386
- Griffin, L., and Cafarelli, E. (2005). Resistance training: cortical, spinal, and motor unit adaptations. *Can. J. Appl. Physiol.* 30, 328–340. doi: 10.1139/h05-125
- Guggenmos, D. J., Barbay, S., Bethel-Brown, C., Nudo, R. J., and Stanford, J. A. (2009). Effects of tongue force training on orolingual motor cortical representation. *Behav. Brain Res.* 201, 229–232. doi: 10.1016/j.bbr.2009.02.020
- Hara, K., Tohara, H., Kobayashi, K., Yamaguchi, K., Yoshimi, K., Nakane, A., et al. (2018). Age-related declines in the swallowing muscle strength of men and women aged 20–89 years: a cross-sectional study on tongue pressure and jaw-opening force in 980 subjects. *Arch. Gerontol. Geriatr.* 78, 64–70. doi: 10.1016/j.archger.2018.05.015
- Hodges, S. H., Anderson, A. L., and Connor, N. P. (2004). Remodeling of neuromuscular junctions in aged rat genioglossus muscle. *Ann. Otol. Rhinol. Laryngol.* 113, 175–179. doi: 10.1177/000348940411300301
- Humbert, I. A., and Robbins, J. (2008). Dysphagia in the elderly. *Phys. Med. Rehabil. Clin. N. Am.* 19, 853–866. doi: 10.1016/j.pmr.2008.06.002
- Johnson, A. M., and Connor, N. P. (2011). Effects of electrical stimulation on neuromuscular junction morphology in the aging rat tongue. *Muscle Nerve* 43, 203–211. doi: 10.1002/mus.21819
- Kleim, J. A., Barbay, S., and Nudo, R. J. (1998). Functional reorganization of the rat motor cortex following motor skill learning. *J. Neurophysiol.* 80, 3321–3325. doi: 10.1152/jn.1998.80.6.3321
- Kletzien, H., Russell, J. A., Levenson, G. E., and Connor, N. P. (2013). Differential effects of targeted tongue exercise and treadmill running on aging tongue muscle structure and contractile properties. *J. Appl. Physiol.* 114, 472–481. doi: 10.1152/japplphysiol.01370.2012
- Komoda, Y., Iida, T., Kothari, M., Komiyama, O., Baad-Hansen, L., Kawara, M., et al. (2015). Repeated tongue lift movement induces neuroplasticity in corticomotor control of tongue and jaw muscles in humans. *Brain Res.* 1627, 70–79. doi: 10.1016/j.brainres.2015.09.016
- Krekeler, B. N., and Connor, N. P. (2017). Age-related changes in mastication are not improved by tongue exercise in a rat model: age-related changes in mastication. *Laryngoscope* 127, E29–E34. doi: 10.1002/lary.26045
- Kwan, P. (2013). Sarcopenia, a neurogenic syndrome? *J. Aging Res.* 2013:791679. doi: 10.1155/2013/791679
- Langmore, S. E., and Pisegna, J. M. (2015). Efficacy of exercises to rehabilitate dysphagia: a critique of the literature. *Int. J. Speech Lang. Pathol.* 17, 222–229. doi: 10.3109/17549507.2015.1024171
- Molina-Luna, K., Hertler, B., Buitrago, M. M., and Luft, A. R. (2008). Motor learning transiently changes cortical somatotopy. *Neuroimage* 40, 1748–1754. doi: 10.1016/j.neuroimage.2007.11.018
- Moss, S. J., Wang, G., Chen, R., Pal, R., and Fowler, S. C. (2001). 3-acetylpyridine reduces tongue protrusion force but does not abolish lick rhythm in the rat. *Brain Res.* 920, 1–9. doi: 10.1016/s0006-8993(01)02790-1
- Nagai, H., Russell, J. A., Jackson, M. A., and Connor, N. P. (2008). Effect of aging on tongue protrusion forces in rats. *Dysphagia* 23, 116–121. doi: 10.1007/s00455-007-9103-6
- Namasivayam-MacDonald, A. M., Barbon, C. E. A., and Steele, C. M. (2018). A review of swallow timing in the elderly. *Physiol. Behav.* 184, 12–26. doi: 10.1016/j.physbeh.2017.10.023
- Neafsey, E. J., Bold, E. L., Haas, G., Hurley-Gius, K. M., Quirk, G., Sievert, C. F., et al. (1986). The organization of the rat motor cortex: a microstimulation mapping study. *Brain Res. Rev.* 11, 77–96. doi: 10.1016/0165-0173(86)90011-1
- Nicosia, M. A., Hind, J. A., Roecker, E. B., Carnes, M., Doyle, J., Dengel, G. A., et al. (2000). Age effects on the temporal evolution of isometric and swallowing pressure. *J. Gerontol. A Biol. Sci. Med. Sci.* 55, M634–M640.
- Nudo, R. J., Milliken, G. W., Jenkins, W. M., and Merzenich, M. M. (1996). Use-dependent alterations of movement representations in primary motor cortex of adult squirrel monkeys. *J. Neurosci.* 16, 785–807. doi: 10.1523/jneurosci.16-02-00785.1996
- Oguz, I., Yaxley, R., Budin, F., Hoogstoel, M., Lee, J., Maltbie, E., et al. (2013). Comparison of magnetic resonance imaging in live vs. post mortem rat brains. *PLoS One* 8:e71027. doi: 10.1371/journal.pone.0071027
- Ota, F., Connor, N. P., and Konopacki, R. (2005). Alterations in contractile properties of tongue muscles in old rats. *Ann. Otol. Rhinol. Laryngol.* 114, 799–803. doi: 10.1177/000348940511401010
- Park, T., and Kim, Y. (2016). Effects of tongue pressing effortful swallow in older healthy individuals. *Arch. Gerontol. Geriatr.* 66, 127–133. doi: 10.1016/j.archger.2016.05.009
- Plowman, E. K., and Kleim, J. A. (2011). Behavioral and neurophysiological correlates of striatal dopamine depletion: a rodent model of Parkinson's disease. *J. Commun. Disord.* 44, 549–556. doi: 10.1016/j.jcomdis.2011.04.008
- Plowman, E. K., Maling, N., Thomas, N. J., Fowler, S. C., and Kleim, J. A. (2014). Targeted motor rehabilitation dissociates corticobulbar versus corticospinal dysfunction in an animal model of Parkinson's disease. *Neurorehabil. Neural Repair* 28, 85–95. doi: 10.1177/1545968313498648
- Remple, M. S., Bruneau, R. M., VandenBerg, P. M., Goertzen, C., and Kleim, J. A. (2001). Sensitivity of cortical movement representations to motor experience: evidence that skill learning but not strength training induces cortical reorganization. *Behav. Brain Res.* 123, 133–141. doi: 10.1016/s0166-4328(01)00199-1
- Robbins, J., Gangnon, R. E., Theis, S. M., Kays, S. A., Hewitt, A. L., and Hind, J. A. (2005). The effects of lingual exercise on swallowing in older adults. *J. Am. Geriatr. Soc.* 53, 1483–1489. doi: 10.1111/j.1532-5415.2005.53467.x
- Robbins, J., Levine, R., Wood, J., Roecker, E. B., and Luschei, E. (1995). Age effects on lingual pressure generation as a risk factor for dysphagia. *J. Gerontol. A Biol. Sci. Med. Sci.* 50, M257–M262.
- Rogus-Pulia, N., Rusche, N., Hind, J. A., Zielinski, J., Gangnon, R., Safdar, N., et al. (2016). Effects of device-facilitated isometric progressive resistance oropharyngeal therapy on swallowing and health-related outcomes in older adults with dysphagia. *J. Am. Geriatr. Soc.* 64, 417–424. doi: 10.1111/jgs.13933

- Russell, J. A., Ciucci, M. R., Hammer, M. J., and Connor, N. P. (2013). Videofluorographic assessment of deglutitive behaviors in a rat model of aging and Parkinson disease. *Dysphagia* 28, 95–104. doi: 10.1007/s00455-012-9417-x
- Salat, D. H., Buckner, R. L., Snyder, A. Z., Greve, D. N., Desikan, R. S. R., Busa, E., et al. (2004). Thinning of the cerebral cortex in aging. *Cereb. Cortex* 14, 721–730. doi: 10.1093/cercor/bbh032
- Sale, D. G., MacDougall, J. D., Upton, A. R., and McComas, A. J. (1983). Effect of strength training upon motoneuron excitability in man. *Med. Sci. Sports Exerc.* 15, 57–62.
- Schaser, A. J., Ciucci, M. R., and Connor, N. P. (2016). Cross-activation and detraining effects of tongue exercise in aged rats. *Behav. Brain Res.* 297, 285–296. doi: 10.1016/j.bbr.2015.10.030
- Schaser, A. J., Stang, K., Connor, N. P., and Behan, M. (2012). The effect of age and tongue exercise on BDNF and TrkB in the hypoglossal nucleus of rats. *Behav. Brain Res.* 226, 235–241. doi: 10.1016/j.bbr.2011.09.027
- Schaser, A. J., Wang, H., Volz, L. M., and Connor, N. P. (2011). Biochemistry of the anterior, medial, and posterior genioglossus in the aged rat. *Dysphagia* 26, 256–263. doi: 10.1007/s00455-010-9297-x
- Schwarz, E. C., Thompson, J. M., Connor, N. P., and Behan, M. (2009). The effects of aging on hypoglossal motoneurons in rats. *Dysphagia* 24, 40–48. doi: 10.1007/s00455-008-9169-9
- Seidler, R. D., Bernard, J. A., Burutolu, T. B., Fling, B. W., Gordon, M. T., Gwin, J. T., et al. (2010). Motor control and aging: links to age-related brain structural, functional, and biochemical effects. *Neurosci. Biobehav. Rev.* 34, 721–733. doi: 10.1016/j.neubiorev.2009.10.005
- Shaw, D. W., Cook, I. J., Gabb, M., Holloway, R. H., Simula, M. E., Panagopoulos, V., et al. (1995). Influence of normal aging on oral-pharyngeal and upper esophageal sphincter function during swallowing. *Am. J. Physiol.* 268, G389–G396.
- Smittkamp, S. E., Brown, J. W., and Stanford, J. A. (2008). Time-course and characterization of orolingual motor deficits in B6SJL-Tg(SOD1-G93A)1Gur/J mice. *Neuroscience* 151, 613–621. doi: 10.1016/j.neuroscience.2007.10.017
- Stanford, J. A., Vorontsova, E., Surgener, S. P., Gerhardt, G. A., and Fowler, S. C. (2003). Aged Fischer 344 rats exhibit altered orolingual motor function: relationships with nigrostriatal neurochemical measures. *Neurobiol. Aging* 24, 259–266. doi: 10.1016/s0197-4580(02)00083-0
- Sura, L., Madhavan, A., Carnaby, G., and Crary, M. A. (2012). Dysphagia in the elderly: management and nutritional considerations. *Clin. Interv. Aging* 7, 287–298. doi: 10.2147/CIA.S23404
- Svensson, P., Romaniello, A., Arendt-Nielsen, L., and Sessle, B. J. (2003). Plasticity in corticomotor control of the human tongue musculature induced by tongue-task training. *Exp. Brain Res.* 152, 42–51. doi: 10.1007/s00221-003-1517-2
- Svensson, P., Romaniello, A., Wang, K., Arendt-Nielsen, L., and Sessle, B. J. (2006). One hour of tongue-task training is associated with plasticity in corticomotor control of the human tongue musculature. *Exp. Brain Res.* 173, 165–173. doi: 10.1007/s00221-006-0380-3
- Tennant, K. A., Adkins, D. L., Scalco, M. D., Donlan, N. A., Asay, A. L., Thomas, N., et al. (2012). Skill learning induced plasticity of motor cortical representations is time and age-dependent. *Neurobiol. Learn. Mem.* 98, 291–302. doi: 10.1016/j.nlm.2012.09.004
- Tieland, M., Trouwborst, I., and Clark, B. C. (2018). Skeletal muscle performance and ageing. *J. Cachexia Sarcopenia Muscle* 9, 3–19. doi: 10.1002/jcsm.12238
- Turturro, A., Witt, W. W., Lewis, S., Hass, B. S., Lipman, R. D., and Hart, R. W. (1999). Growth curves and survival characteristics of the animals used in the biomarkers of aging program. *J. Gerontol. A Biol. Sci. Med. Sci.* 54, B492–B501.
- Welniak-Kaminska, M., Fiedorowicz, M., Orzel, J., Bogorodzki, P., Modlinska, K., Stryjek, R., et al. (2019). Volumes of brain structures in captive wild-type and laboratory rats: 7T magnetic resonance in vivo automatic atlas-based study. *PLoS One* 14:e0215348. doi: 10.1371/journal.pone.0215348
- Westmark, S., Melgaard, D., Rethmeier, L. O., and Ehlers, L. H. (2018). The cost of dysphagia in geriatric patients. *Clinicoecon. Outcomes Res.* 10, 321–326. doi: 10.2147/CEOR.S165713
- Yeates, E. M., Molfenter, S. M., and Steele, C. M. (2008). Improvements in tongue strength and pressure-generation precision following a tongue-pressure training protocol in older individuals with dysphagia: three case reports. *Clin. Interv. Aging* 3, 735–747. doi: 10.2147/cia.s3825

Conflict of Interest: The authors declare that the research was conducted in the absence of any commercial or financial relationships that could be construed as a potential conflict of interest.

Copyright © 2019 Cullins, Wenninger, Cullen, Russell, Kleim and Connor. This is an open-access article distributed under the terms of the Creative Commons Attribution License (CC BY). The use, distribution or reproduction in other forums is permitted, provided the original author(s) and the copyright owner(s) are credited and that the original publication in this journal is cited, in accordance with accepted academic practice. No use, distribution or reproduction is permitted which does not comply with these terms.



Functional Adaptation of Oromotor Functions and Aging: A Focused Review of the Evidence From Brain Neuroimaging Research

Chia-Shu Lin^{1,2,3*}

¹ Department of Dentistry, School of Dentistry, National Yang-Ming University, Taipei, Taiwan, ² Institute of Brain Science, School of Medicine, National Yang-Ming University, Taipei, Taiwan, ³ Brain Research Center, National Yang-Ming University, Taipei, Taiwan

OPEN ACCESS

Edited by:

Limor Avivi-Arber,
University of Toronto, Canada

Reviewed by:

Steven M. Barlow,
University of Nebraska–Lincoln,
United States
Inga Teismann,
Clemens Hospital, Germany

*Correspondence:

Chia-Shu Lin
winzlin@ym.edu.tw

Received: 12 August 2019

Accepted: 05 December 2019

Published: 09 January 2020

Citation:

Lin C-S (2020) Functional Adaptation of Oromotor Functions and Aging: A Focused Review of the Evidence From Brain Neuroimaging Research.
Front. Aging Neurosci. 11:354.
doi: 10.3389/fnagi.2019.00354

“Practice makes perfect” is a principle widely applied when one is acquiring a new sensorimotor skill to cope with challenges from a new environment. In terms of oral healthcare, the traditional view holds that restoring decayed structures is one of the primary aims of treatment. This assumes that the patient’s oromotor functions would be recovered back to normal levels after the restoration. However, in older patients, such a structural–functional coupling after dental treatment shows a great degree of individual variations. For example, after prosthodontic treatment, some patients would adapt themselves quickly to the new dentures, while others would not. In this Focused Review, I argue that the functional aspects of adaptation—which would be predominantly associated with the brain mechanisms of cognitive processing and motor learning—play a critical role in the individual differences in the adaptive behaviors of oromotor functions. This thesis is critical to geriatric oral healthcare since the variation in the capacity of cognitive processing and motor learning is critically associated with aging. In this review, (a) the association between aging and the brain-stomatognathic axis will be introduced; (b) the brain mechanisms underlying the association between aging, compensatory behavior, and motor learning will be briefly summarized; (c) the neuroimaging evidence that suggests the role of cognitive processing and motor learning in oromotor functions will be summarized, and critically, the brain mechanisms underlying mastication and swallowing in older people will be discussed; and (d) based on the current knowledge, an experimental framework for investigating the association between aging and the functional adaptation of oromotor functions will be proposed. Finally, I will comment on the practical implications of this framework and postulate questions open for future research.

Keywords: aging, mastication, swallowing, adaptation, brain plasticity, motor learning

INTRODUCTION

Pierre Fauchard, known as the father of modern dentistry, wrote in his classic textbook *The Surgeon Dentist, a Treatise on Teeth* that teeth are the primary object of dental therapy (Fauchard, 1946). At that time, dental treatment would follow a relatively simple logic: because most of the oral diseases related the teeth and oral cavity, as Fauchard’s textbook has focused (Lynch et al., 2006),

the primary aim of dental treatment is to manage the patients' teeth. However, in the modern days, the stomatognathic system is considered as an assembly composed of 'the mouth, teeth, jaws, pharynx, and related structures as they relate to mastication, deglutition, and speech' (PubMed¹). The modern view holds that not only the individual anatomical components (e.g., the teeth or the tongue) but also the interaction between these components would play a key role in oral functions.

From the view of functional physiology, one may place a greater emphasis on the functions of the stomatognathic system, i.e., focusing on how the individuals improve their functional performance when facing environmental stress (Frisancho, 1993). Based on this view, a critical challenge of managing sensorimotor disorders is whether the patients adapt themselves to a new oral condition. In dental practice, for example, installing a new denture may not necessarily improve the patients' satisfaction of oromotor functions (Carlsson and Omar, 2010) or significantly improve their nutritional status (Toniazzo et al., 2018). It should be noted that restoring the anatomical deficits would still be the primary aim of dental treatment. However, the notion that oral sensorimotor functions would be fully regained, as long as anatomical deficits are well-restored, may be oversimplified. In terms of oral functions, what is ignored here is the role of functional adaptation, which generally refers to 'the process whereby the organism has attained a beneficial adjustment to the environment' (Frisancho, 1993). As the saying goes, 'practice makes perfect': the issues about how individuals acquire new oral sensorimotor skills, and the mechanisms underlying the individual difference of adaptation, require further investigation.

In this review, I will focus on individual differences in oral sensorimotor functions. I argue that functional adaptation is associated with the brain mechanisms of cognitive processing and motor learning and that these variations in brain signatures of cognitive processing and motor learning may underlie the individual differences in oral sensorimotor adaptation. The brain-stomatognathic mechanisms underlying sensorimotor adaptation may provide important insight into the age-related changes in oral functions and contribute to the clinical management of geriatric patients. The article will be organized into four sections:

- (1) The age-related changes in the stomatognathic system will be recapitulated, and the concept of the 'brain-stomatognathic axis' (BSA) will be defined. The association between aging and the individual differences in the BSA will be highlighted.
- (2) The general framework concerning the association between aging, adaptation, and compensation will be reviewed. I will focus on the concept of 'motor learning' and explain why it plays a key role in sensorimotor adaptation in older people. The brain mechanisms of motor learning from recent neuroimaging evidence will be discussed.
- (3) Recent neuroimaging findings [primarily based on magnetic resonance imaging (MRI)] regarding aging and

the brain mechanism of mastication and swallowing will be systematically discussed. Specifically, the role of functional adaptation and the individual differences in the oromotor functions will be highlighted.

- (4) Finally, a research model for oral sensorimotor adaptation will be proposed. I will focus on using neuroimaging methods to quantify the individual differences in compensatory mechanisms in older people. Further investigation may provide important insight into the age-related changes in oral functions and contribute to the clinical management of geriatric patients.

AGING AND THE BRAIN-STOMATOGNATHIC AXIS

Aging and the Coupling Between Brain Structure and Functions

Broadly defined as 'the gradual irreversible changes in structure and function of an organism that occur as a result of the passage of time' (PubMed¹), the effect of aging is associated with both structural and functional changes. However, it does not necessarily mean that aging has the same effect on all the structural and functional aspects. In terms of the cognitive abilities of elderly people, the decline of perceptual speed is a life-long change, gradually decreasing by year; in contrast, the decline of verbal memory is a late-life change, i.e., occurring in the later periods of life (Hedden and Gabrieli, 2004). In terms of the variations in brain morphology, as age increases, the brain does not change in size homogeneously. For example, the prefrontal cortex and the medial temporal lobe (where the hippocampus resides) show a more pronounced decrease in size (Curiati et al., 2009; Lemaitre et al., 2012), but the primary sensory cortices (e.g., the visual cortex and the somatosensory cortex) are less sensitive to the aging effect (Lemaitre et al., 2012). Notably, there is a critical coupling between functional and structural variations. The size of the prefrontal cortex and perceptual speed, which is associated with prefrontal functions (Muller-Oehring et al., 2013), showed a similar age-related trend. The size of the hippocampus and verbal memory, which is associated with hippocampal functions, also showed a similar age-related trend (Hackert et al., 2002). The structural-functional coupling suggests that in elderly people, variations in brain signatures are critically related to individual differences in mental functions.

Age-Related Changes in the Stomatognathic System: A View From the Brain-Stomatognathic Axis

As age increased, the individuals showed significant changes in several biomechanical features of the stomatognathic system (for a detailed review, please see Avivi-Arber and Sessle, 2018). In general, these changes included a decrease in the maximal bite force (Ikebe et al., 2005), the maximum tongue pressure (Utanohara et al., 2008), and the rate of oral diadochokinesis (Ben-David and Icht, 2018). Similar to the age-related changes in the brain, the changes in oral functions are also coupled

¹ Medical Subject Headings (Online). Available at: <https://www.ncbi.nlm.nih.gov/mesh/68000375> (accessed August 12, 2019).

with structural alterations. For example, the age-related reduction in tongue pressure may be associated with the decreased fiber size of the intrinsic tongue muscle (Cullins and Connor, 2017). An age-related increase in sensory threshold was also identified, including an increased threshold in thermal pain, touch, and two-point discrimination in the orofacial regions (Heft and Robinson, 2010). An age-related decrease in the intrafusal fibers of muscle spindles, a critical proprioceptor for sensory feedback from the jaw-closing muscles, may account for the decreased masticatory functions (Winarakwong et al., 2004). In general, these age-related changes in structure and biomechanical features contributed to worse masticatory performance (Morita et al., 2018).

It should be noted that while the biomechanical features showed an overall age-related reduction, these changes did not fully account for the individual variations in the oral sensorimotor performance of the older people. The results collected from a local community in Taipei, Taiwan revealed a heterogeneous effect of aging: while some parameters showed a significant age-related decline (e.g., oral mixing ability, the efficiency of saliva swallowing) (Lin et al., 2017a, 2019), others did not (e.g., number of masticatory cycles, unstimulated salivary flow rate, and masseter muscle volume) (Lin et al., 2017a, 2019). Notably, the stomatognathic parameters *per se* may not fully explain the individual differences in a certain function. For example, more saliva does not necessarily reflect a higher swallowing frequency (Persson et al., 2018; Lin et al., 2019), and the number of chewing strokes before swallowing was not significantly associated with masticatory performance (Fontijn-Tekamp et al., 2004). Therefore, regarding the individual differences in oral sensorimotor functions, one may consider the contribution from features other than the stomatognathic system. Since aging has a profound effect on the brain (Curiati et al., 2009; Lemaitre et al., 2012), variations in brain signatures, including brain morphology and intrinsic connectivity, should be considered when one interprets the individual differences in oral sensorimotor functions.

The Brain-Stomatognathic Axis Focuses on Individual Differences in Age-Related Changes

The concept of the BSA has been proposed to emphasize that when explaining the individual differences in oral sensorimotor functions, one needs to consider the brain and the stomatognathic system as a closely coupled assembly. Moreover, the BSA should be considered a complex adaptive system so that feeding behaviors can dynamically respond to environmental changes (Holland, 1982). At the conceptual level, research on the BSA is different from research on the brain mechanisms underlying oral sensorimotor functions, which have been gradually unraveled at the cause-effect level, thanks to the systematic investigation of animal research (Sessle, 2006; Avivi-Arber and Sessle, 2018). The BSA is rooted in the background of the neuroanatomical infrastructure of the stomatognathic system, but it focuses on how the brain and the stomatognathic system, as a whole, respond to challenges in feeding behaviors.

Moreover, the BSA highlights the individual differences in such a behavioral adaptation.

There are several practical reasons why the issues of the BSA need to be highlighted. First, many geriatric disorders have posed great challenges in dental practice, including dysphagia (Rommel and Hamdy, 2016), stroke (Schimmel et al., 2017) and dementia (Daly et al., 2018), and most of these disorders are associated with the disruption in the brain functions. Second, since the BSA focused on unraveling the individual differences in oral sensorimotor functions, the framework would be particularly suitable in diagnosis and outcome evaluation of oral sensorimotor functions, which has posed a great challenge in clinical practice, e.g., assessing patients with dementia for pain (Delwel et al., 2019) and masticatory ability (Weijenberg et al., 2019). Third, from the experimental perspective, the advent of neuroimaging techniques has made it feasible to quantify individual brain signatures based on a large sample size (Dubois and Adolphs, 2016). Neuroimaging research has proven useful in unraveling the brain mechanisms underlying the individual variations of sensorimotor functions, which I will elaborate in the following section. In general, the focus on the BSA will meet the increasing demand for dental researchers to translate research findings to clinical practice, especially for managing geriatric and special needs patients.

AGING AND ADAPTATIONS IN MOTOR ACTION

The Theoretical Framework of Adaptation, Reserve, and Compensation

In terms of geriatric medicine, a discrepancy may exist between one's anatomical condition (structure) and the actual performance (function). For example, in patients with Alzheimer's disease, why do some people behave better than others? A critical underlying factor is the individual differences in 'reserve'—the variation in brain signatures and cognitive experience—which would underlie the "differential susceptibility to functional impairment" in the presence of a disorder (Barulli and Stern, 2013). For example, an increased brain size and a rich life experience of cognitive ability are associated with a lesser chance for elderly patients to develop severe disabilities (for detailed reviews, see Barulli and Stern, 2013 and Cabeza et al., 2018). Critically, these brain and cognitive reserves are associated with individual differences in compensation, a notion that interprets how functional status is maintained under an (anatomically) aging status (Cabeza et al., 2018). The compensatory mechanisms are crucial in explaining how people adapt to the environment. Through compensation, individuals can functionally adapt to a changing environment by recruiting neural resources (Cabeza et al., 2018), rather than drastically modifying the anatomical apparatus. Such an adaptive coupling between the brain and behavior, primarily based on brain plasticity (Pascual-Leone et al., 2005), is the key to the BSA being regarded as a complex adaptive system (Holland, 1982).

Adaptation of the Stomatognathic Structure

In order to cope with the environmental stress, the adaptation from the functional aspects (i.e., the brain functions) and from the structural aspects (i.e., the alterations in the peripheral anatomical device) would play a key role. The age-related changes in the masseter, the primary jaw-closing muscle in the stomatognathic system, would demonstrate the adaptation of the stomatognathic structure. Evidence from clinical research revealed that the increased age was associated with the delayed latency in muscle reflex (Peddireddy et al., 2006) and lower maximal isometric voluntary contraction in elderly women (Gaszynska et al., 2017). The structural and functional features of the masseter also related to systemic factors. For example, masseter thickness was positively correlated with grip force (Yamaguchi et al., 2018). Notably, these general decreases in biomechanical features occurred in the individual with normal aging. However, not all the structural and functional features showed the consistent age-related 'degradation' or 'degeneration.' For example, the age-related change in the size of the masseter and its muscle fibers was not pronounced, evidenced by both human and animal research (Norton et al., 2001; Lin et al., 2017a; Daboul et al., 2018). Evidence from animal research revealed that the older subjects showed more nerve terminal branches at the neuromuscular junction of the masseter, compared to the younger subjects (Elkerdany and Fahim, 1993). As the age increased, the masseter may show the plasticity or remodeling at the neuromuscular junction (Elkerdany and Fahim, 1993). In terms of oral rehabilitation, the adaptive process can also be examined by assessing masticatory performance and muscle work, which showed an initial decrease after denture installation, and then a full recovery back to the original status (Eberhard et al., 2018). The human masseter may be less vulnerable to the age-related degeneration, due to its major role in feeding behavior (Avivi-Arber and Sessle, 2018).

Motor Control, Motor Learning, and 'Relearning'

The control of an action, which is predominantly mandated by the primary motor cortex, is associated with complicated cognitive processing, such as memory and choice-making (Ebbesen and Brecht, 2017). Motor control is generally defined as 'the process of transforming sensory inputs into consequent motor outputs' (Wolpert et al., 2001) and motor learning is about the process of refining this association, in order to adapt sensorimotor transformations for environmental challenges (Wolpert et al., 2001). Behind these 'transformations' is the complicated mechanism of building a predictive model that can bidirectionally match a motor command and the corresponding sensory outcomes. Under such a computational framework, motor learning can be regarded as a process of acquiring such a forward/inverse model (Wolpert et al., 1998, 2001). Critically, the model can be reshaped to respond to environmental changes so that the performance can be dynamically improved (Wolpert et al., 2001). This association between learning and oromotor functions is manifested in patients who wear a new set of

dentures. While the stomatognathic structure is restored (e.g., by replacing the missing teeth with prosthesis), patients need to learn how to chew with the new dentures. From the computational view of brain functions, the individuals need to relearn this chewing action, i.e., building a new model of sensorimotor transformation, in contrast to the old one (i.e., their experience of chewing without dentures).

What are the brain correlates associated with motor learning? When people learn a new motor skill, the prefrontal cortex, the secondary motor area, and the cerebellum show distinct activation (Lage et al., 2015). The prefrontal cortex is critical to cognitive processing, such as attending to a movement, switching from one movement to another, and monitoring of the progression of a movement (for a detailed review on the prefrontal functions, see Ridderinkhof et al., 2004). The secondary motor area consists of the supplementary motor area and the premotor cortex (Marvel et al., 2019). While the activation of the primary motor cortex is associated with the execution of movement, the activation of the secondary motor area is associated with planning or preparation of movement (Marvel et al., 2019), which can be guided by external cues or by memory (Heuninckx et al., 2010). As shown in the following section, cumulating evidence has consistently revealed that older people engage an extended brain region when learning a new motor skill, including the prefrontal area, the supplementary area, and the premotor cortex. The pattern of brain activation may be associated with an increased cognitive effort, e.g., a greater demand for multisensory integration and attentional control during movement (Ward, 2006; Seidler et al., 2010). The cerebellum is a critical component in forming the predictive model of motor learning (Wolpert et al., 1998). It receives the error between the actual and the anticipated action and gives a new motor command that is corrected for the error message (Wolpert et al., 1998). The cerebellum integrates and fine-tunes sensory and motor information for refining the models so that movement can be automatically performed (Ramnani, 2014; Schmähmann, 2019). Compared to the basal ganglia, the cerebellum plays a dominant role in sensorimotor adaptation, i.e., modulating motor commands on the basis of sensory feedback, via error-based learning (Bostan and Strick, 2018). Furthermore, the cerebellum has an extensive connection with the prefrontal and the parietal lobes as well as the motor areas (Stoodley, 2012). The age-related changes in cerebellar morphology may be associated with both motor and cognitive declines in older people (Bernard and Seidler, 2014; Schmähmann, 2019).

Age-Related Changes in the Brain Signatures of Motor Learning

Evidence from neuroimaging research has revealed that older people, compared to younger people, showed greater activation of the primary and secondary motor areas, the cerebellum, and the prefrontal cortex when they are acquiring a new motor skill (Mattay et al., 2002; Heuninckx et al., 2005; Wu and Hallett, 2005; Rowe et al., 2006). This age-related activation is associated with increased task complexity (Heuninckx et al., 2005) and reduced response time of a motor task (Mattay et al., 2002). The findings

suggest that when coping with a more challenging environment (i.e., a difficult motor task), older people would compensate for their performance by recruiting more extended brain regions beyond the primary motor cortex (Ward, 2006). This difference in brain mechanisms may reflect a decreased automaticity in older people, i.e., performing one motor task without being interfered with by another task (Ward, 2006). Comparing brain activation before and after motor learning, younger, but not older, people showed reduced activation of the cerebellum, a region critically related to automaticity of movement (Wu and Hallett, 2005). During the retention of a learned skill, older subjects showed a smaller deactivation of the frontal lobe (Berghuis et al., 2019). The extended engagement with the prefrontal areas implied that the older subjects demanded more cognitive efforts in learning a skill.

Importantly, the age-related changes in the brain mechanisms of motor learning were manifested not only in regional activation but also in the interregional connections. Aging is related to increased local effective connectivity within the motor network, centered at the premotor cortex (Rowe et al., 2006). In the older subjects, better motor performance was associated with an increased resting-state functional connectivity between the cerebellum and the primary and secondary motor areas (Seidler et al., 2015). Similarly, an increased connectivity between the primary motor cortex and the premotor/prefrontal cortex was associated with a faster psychomotor speed (Michely et al., 2018). The local connectivity efficiency of the primary somatosensory and motor cortices was correlated with gait stability in older, but not younger, subjects (Di Scala et al., 2019). The findings suggest that the increased performance in older people is associated with a greater role of premotor and prefrontal areas. Moreover, at the scale of the whole-brain connectome, older people showed a stronger, not weaker, connection between the prefrontal cortex and the sensorimotor module of the orofacial part (Chan et al., 2014). Decreased segregation in brain networks plays a key role in age-related declines in motor performance (King et al., 2018). The findings suggest that the age-related difference in the architecture of the functional connectivity of the brain may be associated with individual differences in motor performance.

MOTOR LEARNING AND AGING: RESEARCH EVIDENCE FROM MASTICATION AND SWALLOWING

Brain Mechanisms of Mastication

For decades, the brain mechanisms of mastication have been systematically investigated, primarily via animal research (for detailed reviews, see Sessle, 2006; Avivi-Arber and Sessle, 2018). The following sections will focus on recent findings based on neuroimaging methods, primarily based on the MRI. As a non-invasive brain imaging method, functional MRI has identified several brain regions associated with mastication that have been consistently reported by animal research (Lin, 2018). Moreover, neuroimaging findings have revealed

more complicated mechanisms underlying the adaptation of oromotor functions.

Recent functional MRI findings of mastication in older people are summarized in **Table 1**. One of the earliest neuroimaging studies on human mastication was performed by Onozuka and colleagues, who asked subjects to chew gum during the MRI scan (Onozuka et al., 2002). The study consistently identified an increased activation of the primary somatosensory and motor cortices, which plays a key role in motor control and has also been found in animal research (Avivi-Arber and Sessle, 2018). The activation at the somatosensory region, which was also found during the adaptation of facial tactile stimuli (Custead et al., 2017) and stimulation of periodontal ligament (Trulsson et al., 2010), especially highlighted the role of sensory feedback in mastication. Interestingly, pronounced activation was also found in the supplementary motor area and the cerebellum (Onozuka et al., 2002), and an increased functional connectivity between the motor areas and the cerebellum was found during chewing (Quintero et al., 2013b). Moreover, the prefrontal activation was found only during jaw movement, but not during hand movement, in the older subjects (Fang et al., 2005). Further studies revealed that the primary motor cortex was dominantly engaged when a chewing block was initiated or terminated (Quintero et al., 2013a). While activation of the primary motor cortex was identified in both the younger and the older subjects, activation of the prefrontal cortex was more pronounced in the older than the younger subjects (Onozuka et al., 2003). The increased functional connectivity between the motor areas and the prefrontal cortex was also reported (Quintero et al., 2013b). Consistently, imaging meta-analysis also revealed a common coactivation of the primary somatosensory/motor cortex, the secondary motor area, the prefrontal cortex, and the cerebellum (Lin, 2018). The findings revealed that beyond the primary somatosensory and motor cortices, an extended network of cognitive processing and motor learning is critical to chewing.

Notably, activation of the prefrontal cortex was frequently associated with activation of the secondary motor area, including the supplementary motor area and the premotor cortex. The supplementary motor area plays a pivotal role in preparation and planning of voluntary movements (Thickbroom et al., 2000) and the premotor cortex, together with the parietal lobe and the somatosensory area, is critical to the integration of polymodal motion processing with movement (Bremner et al., 2001). The connectivity between the prefrontal cortex, the supplementary motor cortex, and the premotor cortex, is critical to attention to action (Rowe et al., 2002). The coactivation of these cognitive regions (i.e., the prefrontal cortex, the premotor cortex, and the supplementary motor area) has been identified not only on healthy subjects (Onozuka et al., 2002, 2003) but also on the patients receiving a denture, which may suggest an adaptive experience of using a denture (Yan et al., 2008; Kimoto et al., 2011; Shoi et al., 2014).

These functional MRI studies revealed the brain activation associated with the processing of mastication. Recent neuroimaging findings have revealed that individual differences in masticatory performance were associated with intrinsic brain signatures, such as gray matter volume and resting-state

TABLE 1 | Results of literature search of the recent neuroimaging findings (from 2000 January 1 to present) of aging and oromotor functions.

| ID | Source | Subjects (disease/treatment) | Age (year) (mean or range) | Imaging methods | Major findings |
|---|-----------------------|---------------------------------|-------------------------------|--|--|
| (A) Summary of recent neuroimaging findings of aging and masticatory functions¹ | | | | | |
| 1 | Lin et al., 2015 | Healthy, OA | 64.2 | sMRI, rs-fMRI | '... in the premotor cortex, a reduction of GMV and rsFC would reflect declined masticatory performance. The positive correlation between DLPFC connectivity and masticatory performance implies that masticatory ability is associated with cognitive function in the elderly' (Lin et al., 2015). |
| 2 | Lin et al., 2017b | Healthy, OA vs. YA | 64.4 | rs-fMRI | '... in OA, higher masticatory performance is associated with a widespread pattern of mastication-related hubs. Such a widespread engagement of multiple brain regions associated with the MPI may reflect an increased demand in sensorimotor integration, attentional control and monitoring for OA to maintain good mastication' (Lin et al., 2017b). |
| 3 | Fang et al., 2005 | Healthy, OA vs. YA | 60–70 | fMRI | 'For movements of the face (chewing, opening and closing of mouth), the prefrontal cortex was activated in the old age group but finger and hand movements never activated the prefrontal cortex in any age' (Fang et al., 2005). |
| 4 | Onozuka et al., 2003 | Healthy, OA vs. YA | 65–73 | fMRI | 'In all subjects, chewing resulted in a bilateral increase in the BOLD signals in the sensorimotor cortex, cerebellum, thalamus, supplementary motor area, and insula, and a unilateral increase in the right prefrontal area. In the first three regions, the signal increases were attenuated in an age-dependent manner, whereas, in the right prefrontal area, the converse was seen. The remaining two regions showed no significant differences with ages. These results indicate that chewing causes regional increases in neuronal activity in the brain, some of which are age-dependent' (Onozuka et al., 2003). |
| 5 | Shoi et al., 2014 | Prosthesis | 66.1 | fMRI | 'Brain activation during gum chewing with the full dental arch occurred in the middle frontal gyrus, primary sensorimotor cortex extending to the pre-central gyrus, supplementary motor area, putamen, insula, and cerebellum. However, middle frontal gyrus activation was not observed during gum chewing with the shortened dental arch. These results suggest that shortened dental arch affects human brain activity in the middle frontal gyrus during gum chewing, and the decreased middle frontal gyrus activation may be associated with decreased masticatory function' (Shoi et al., 2014). |
| 6 | Luraschi et al., 2013 | Prosthesis | 70.3 | fMRI | 'The right and the left precentral gyrus (PRCG) and post-central gyrus (POCG) were identified with significant activation across all three functional tasks. A statistically significant increase in the level of activity between T0 and T2 (POCG: $P = 0.022$; PRCG: $P = 0.017$) was found during jaw clenching tasks' (Luraschi et al., 2013). |
| 7 | Kimoto et al., 2011 | Prosthesis | 64–79 | fMRI | '... the gum-chewing task in elderly edentulous patients resulted in differential neural activity in the frontal pole within the prefrontal cortex between the 2 prosthodontic therapies-mandibular CD and IOD' (Kimoto et al., 2011). |
| 8 | Yan et al., 2008 | Prosthesis | 48–72 | fMRI | 'Increased blood oxygen level dependent signals in the primary sensorimotor cortex were found in patients with implant-supported fixed dentures. Other activated areas included prefrontal cortex, Broca's area, premotor cortex, supplementary motor area, superior temporal gyrus, insular, basal ganglion, and hippocampus... Activation of the primary sensorimotor cortex in patients with implant-supported dentures might explain the improved tactile, stereognostic ability, and mastication functions, which are more similar to the natural dentition' (Yan et al., 2008). |
| 9 | Miyamoto et al., 2005 | Prosthesis | 56.9 | Near-infrared optical topography | 'Results revealed a significantly ($P < 0.001$; paired t -test) increased cerebral regional blood volume during maximum voluntary clenching task by implant-retained prosthesis. There were no statistically significant differences between patients with and without prosthesis in the latency to the maximum regional blood volume after the task. Conclusively, clenching can be effective for increasing cerebral blood volume; accordingly maintenance of normal chewing might prevent the brain from degenerating' (Miyamoto et al., 2005). |

(Continued)

TABLE 1 | Continued

| ID | Source | Subjects (disease/treatment) | Age (year) (mean or range) | Imaging methods | Major findings |
|--|------------------------------|---------------------------------|-------------------------------|--------------------|---|
| (B) Summary of recent neuroimaging findings of aging and swallowing functions² | | | | | |
| 10 | Humbert et al., 2011 | Alzheimer's disease | 74.3 | fMRI | 'Disease-related differences were evident where the AD group had significantly greater BOLD response in the insula/operculum than the old. These findings have significant clinical implications for control of swallowing across the age span and in neurodegenerative disease. Greater activation in the insula/operculum for the AD group supports previous studies where this region is associated with initiating swallowing. The AD group may have required more effort to "turn off" swallowing centers to reach the intentional swallowing off-state' (Humbert et al., 2011). |
| 11 | Humbert et al., 2010 | Alzheimer's disease | 74.3 | fMRI | '... the AD group had significantly lower Blood-Oxygen-Level-Dependent (BOLD) response in many cortical areas that are traditionally involved in normal swallowing (i.e., pre and post-central gyri, Rolandic and frontal opercula). There were no regions where the AD group showed more brain activity than the healthy controls during swallowing, and only 13% of all active voxels were unique to the AD group, even at this early stage. This suggests that the AD group is not recruiting new regions, nor are they compensating within regions that are active during swallowing' (Humbert et al., 2010). |
| 12 | Lin et al., 2019 | Healthy, OA | 69.1 | sMRI | 'In healthy older adults, swallowing efficiency was positively correlated with cerebellar GMV. The findings suggested that in older people, structural variations of the brain may play a key role in individual differences in swallowing performance' (Lin et al., 2019). |
| 13 | Lowell et al., 2012 | Healthy | 52 | fMRI | 'The greater connectivity from the left hemisphere insula to brain regions within and across hemispheres suggests that the insula is a primary integrative region for volitional swallowing in humans' (Lowell et al., 2012). |
| 14 | Martin et al., 2007 | Healthy | 74.2 | fMRI | 'Activation of the post-central gyrus was lateralized to the left hemisphere for saliva and water swallowing, consistent with our findings in young female subjects. Comparison of saliva and water swallowing revealed a fourfold increase in the brain volume activated by the water swallow compared to the saliva swallow, particularly within the right premotor and prefrontal cortex. This task-specific activation pattern may represent a compensatory response to the demands of the water swallow in the face of age-related diminution of oral sensorimotor function' (Martin et al., 2007). |
| 15 | Windel et al., 2015 | Healthy, OA vs. YA | 64 | fMRI | 'The results indicate that the highly automated swallowing network retains its functionality with age. However, seniors with higher SCR during swallowing appear to also engage areas involved in attention control and emotional regulation, possibly suggesting increased attention and emotional demands during task performance' (Windel et al., 2015). |
| 16 | Malandraki et al., 2011 | Healthy, OA vs. YA | 70.2 | fMRI | 'Both groups showed activations in the major motor areas involved in the initiation and execution of movement; however, areas involved in sensory processing, sensorimotor integration and/or motor coordination and control, showed reduced or limited activity in the elderly' (Malandraki et al., 2011). |
| 17 | Teismann et al., 2010 | Healthy, OA vs. YA | 71.6 | MEG | 'The main finding of this study was an increase of somatosensory cortical activation during swallowing execution in elderly subjects compared to the young control group. This effect was present in both hemispheres. These results point to adaptive cerebral changes in response to aging effects on the complex process of swallowing. Our finding underlines the relevance of age matched control groups in neuroimaging studies related to deglutition or other complex sensorimotor processes' (Teismann et al., 2010). |
| 18 | Humbert et al., 2009 | Healthy, OA vs. YA | 72.3 | fMRI | 'The group of older adults recruited more cortical regions than young adults, including the pericentral gyri and inferior frontal gyrus pars opercularis and pars triangularis (primarily right-sided). Saliva swallows elicited significantly higher BOLD responses in regions important for swallowing compared to water and barium... These findings suggest that older adults without neurological insult elicit more cortical involvement to complete the same swallowing tasks as younger adults' (Humbert et al., 2009). |
| 19 | Suntrup-Krueger et al., 2017 | Stroke | 73.7 | CT/MRI | 'This study gives new insights on the cortical representation of single components of swallowing and airway protection behaviors. The lesion model may help to risk-stratify patients for dysphagia and pneumonia based on their brain scan' (Suntrup-Krueger et al., 2017). |

(Continued)

TABLE 1 | Continued

| ID | Source | Subjects (disease/treatment) | Age (year) (mean or range) | Imaging methods | Major findings |
|----|-----------------------|---------------------------------|-------------------------------|--------------------|--|
| 20 | Galovic et al., 2017 | Stroke | 75.6 | dMRI | '... early swallowing recovery is influenced by white matter lesions disrupting thalamic and corticobulbar projection fibers. Late recovery is determined by specific cortical lesions affecting association fibers. This knowledge may help clinicians to identify patients at risk of prolonged swallowing problems that would benefit from enteral tube feeding' (Galovic et al., 2017). |
| 21 | Mihai et al., 2016 | Stroke | 56.6 | fMRI/dMRI | 'Overall, patients showed decreased fMRI-activation in the entire swallowing network apart from an increase of activation in the contralesional primary somatosensory cortex (S1). Moreover, fMRI activation in contralesional S1 correlated with initial dysphagia score. Finally, when lesions of the pyramidal tract were more severe, recovered swallowing appeared to be associated with asymmetric activation of the ipsilesional anterior cerebellum. Taken together, our data support a role for increased contralesional somatosensory resources and ipsilesional anterior cerebellum feed forward loops for recovered swallowing after dysphagia following stroke' (Mihai et al., 2016). |
| 22 | Galovic et al., 2016 | Stroke | 71,76 | MRI | 'Mild impairment of oral intake correlates with damage to a widespread operculo-insular swallowing network. However, specific lesions of the anterior insula lead to severe impairment and tube dependency and clinicians might consider early enteral tube feeding in these patients' (Galovic et al., 2016). |
| 23 | Suntrup et al., 2015 | Stroke | 73.7 | CT/MRI | 'In particular, right hemispheric lesions of the pre- and post-central gyri, opercular region, supramarginal gyrus and respective subcortical white matter tracts were related to dysphagia, with post-central lesions being especially associated with severe swallowing impairment. ... Distinct brain lesion locations are related to the incidence, severity and pattern of swallowing dysfunction' (Suntrup et al., 2015). |
| 24 | Li et al., 2014 | Stroke | 65.2 | rs-fMRI, dMRI | Stroke patients with dysphagia exhibited dysfunctional connectivity mainly in the sensorimotor-insula-putamen circuits based on seed-based analysis of the left and right M1 and SMA and decreased connectivity in the bilateral swallowing-related ROIs functional connectivity network. Additionally, white matter tract connectivity analysis revealed that the mean fractional anisotropy of the white matter tract was significantly reduced, especially in the left-to-right SMA and in the corticospinal tract' (Li et al., 2014). |
| 25 | Momosaki et al., 2012 | Stroke | 66.1 | SPECT | 'The rCBF in Brodmann areas 4 and 24 was significantly lower in the dysphagia group. The highest area under the curve was found in Brodmann area 4. In this area, 80% sensitivity and 60% specificity for discriminating dysphagia were achieved with an optimal cutoff value. When analyzed with novel methods, SPECT imaging can be useful for predicting the risk of dysphagia and subsequent aspiration in post-stroke patients' (Momosaki et al., 2012). |
| 26 | Teismann et al., 2011 | Stroke | 63.5 | MEG | 'Our results demonstrate strong bilateral reduction of cortical swallowing activation in dysphagic patients with hemispheric stroke. In hemispheric stroke without dysphagia, bilateral activation was found. In the small group of patients with brainstem stroke we observed a reduction of cortical activation and a right hemispheric lateralization' (Teismann et al., 2011). |
| 27 | Li et al., 2009 | Stroke | 70.9 | fMRI | 'Cerebral activation during swallowing tasks was localized to the precentral, post-central and anterior cingulate gyri, insula and thalamus in all groups. Activation of volitional swallowing in dysphagic unilateral hemispheric stroke patients might require reorganization of the dominant hemispheric motor cortex, or a compensatory shift in activation to unaffected areas of the hemisphere' (Li et al., 2009). |

¹According to a PubMed-based search with the following combination of keywords: (aging OR age-related OR older OR elderly) AND (chew* OR masticat*) AND (neuroimaging OR "brain imaging" OR MRI) AND brain, with the publication date from 2000/01/01. ²According to a PubMed-based search with the following combination of keywords: (aging OR age-related OR older OR elderly) AND (swallow* OR deglut*) AND (neuroimaging OR "brain imaging" OR MRI) AND brain, with the publication date from 2000/01/01. CT, computed tomography; dMRI, diffusion magnetic resonance imaging; fMRI, functional magnetic resonance imaging; MEG, magnetoencephalography; OAs, older adults; sMRI, structural magnetic resonance imaging; SPECT, single photon emission computed tomography; rCBF, regional cerebral blood flow; rs, resting-state, structural magnetic resonance imaging; YA, younger adults.

functional connectivity. In older subjects, the masticatory performance was positively correlated with gray matter volume of the premotor cortex and the lateral prefrontal cortex (Lin et al., 2015) and an increased connectivity between these motor areas and the cerebellum (Lin et al., 2015). Moreover, when investigating the association between functional connectivity and masticatory performance, one could identify a qualitatively different pattern: in the older subjects, those who had a higher chewing performance showed a stronger connectivity between the core sensorimotor regions and the non-primary areas (e.g., the prefrontal and the parietal areas and the insula) (Lin et al., 2017b). It is noteworthy that the prefrontal cortex is one of the brain regions that showed the greatest degree of age-related volumetric decline (Curiati et al., 2009; Lemaitre et al., 2012). Therefore, the findings suggest that in older people, in addition to the age-related decline in structure or biomechanical features (e.g., tooth loss or the decreased biting force), the individual variation in masticatory performance may be associated with brain functions of cognitive processing and learning.

Brain Mechanisms of Swallowing

Much neuroimaging evidence regarding swallowing has been reported over the past decades. A synthesis from imaging meta-analysis revealed that water swallowing and saliva swallowing are associated with different patterns of brain activation (Soros et al., 2009). Water swallowing requires a higher degree of sensory-motor integration, which shows a higher activation at the parietal lobe. In contrast, saliva swallowing is more associated with the premotor areas, which are crucial for the initiation and control of movements (Soros et al., 2009). Notably, this pattern of brain activation revealed an age-related difference. The primary somatosensory cortex showed a lower activation in the older subjects, compared to the younger subjects (Malandraki et al., 2011). In the older subjects, water swallowing was engaged with stronger activation of the right premotor and prefrontal cortices compared to saliva swallowing (Martin et al., 2007). To complete the same swallowing tasks, the older subjects showed more cortical involvement as the younger subjects (Humbert et al., 2009). Another critical finding revealed that older subjects showed longer reaction times and higher skin conductance responses (SCRs) during swallowing (Windel et al., 2015). Importantly, a stronger SCR was associated with greater brain activation in areas related to sensorimotor and emotional processing, suggesting increased cognitive-affective regulation during task performance (Windel et al., 2015). In stroke patients with dysphagia, there was a distinct activation and lesion locations of the primary somatosensory and motor cortices (Li et al., 2009; Suntrup et al., 2015) and the insula (Galovic et al., 2016) and changes in the connection of these regions (Li et al., 2014). Furthermore, the pattern of brain activation differed substantially between healthy controls and the patients with cognitive impairment. During swallowing, the patients with Alzheimer's disease showed a lower activation of the primary somatosensory and motor cortices and no recruitment of new brain regions, suggesting insufficient compensation (Humbert et al., 2010). In contrast, they showed a higher activation of the insula, when intentionally inhibit swallowing

(Humbert et al., 2011). These findings from both healthy and disease groups revealed that in older people, swallowing is associated with the brain regions of cognitive processing and motor learning.

Notably, these neuroimaging findings were largely based on functional MRI, which investigated the swallowing-related brain signals by contrasting different task conditions (e.g., saliva swallows vs. resting). The relatively lower temporal resolution (by seconds) poses a limitation on experimental design and data interpretation of fMRI research. In contrast, the magnetoencephalography (MEG) study is superior in recording the brain signals at a higher temporal resolution (by milliseconds). It can be synchronized with other assessments, such as electromyography, for recording the brain signals associated at different stages of swallowing. In one study, the whole-brain MEG scan was associated with electromyography and revealed a bilateral increased somatosensory activation in the elderly subjects, compared to the younger controls (Teismann et al., 2010). Moreover, the same method revealed that during swallowing execution, the cortical activation was lower in the stroke patients with dysphagia vs. without dysphagia (Teismann et al., 2011). The findings extended the previous results from fMRI research, demonstrating the changes in brain activity synchronized with swallowing movement.

Recent neuroimaging evidence has also revealed that the gray matter volume of the posterior cerebellum was associated with an increased swallowing performance (Lin et al., 2019). Notably, part of the identified posterior cerebellum (the cerebellar crus and lobule VII) did not directly connect with the primary sensorimotor area but with the prefrontal cortex and the posterior parietal lobe (Schmahmann, 2019). Therefore, the findings suggest that swallowing performance may partly reflect individual variations in the cognitive control of swallowing. Notably, in the study, swallowing performance was quantified by the repetitive saliva swallowing task (RSST), a simple and safe test that represents the number of voluntary swallow in 30 s (Oguchi et al., 2000a,b). Recent findings from Sweden and Taiwan revealed that RSST scores were not significantly associated with the degree of saliva secretion (Persson et al., 2018; Lin et al., 2019). These findings together suggest that in older people, individual differences in swallowing performance may be attributed to variations in brain signatures, rather than the peripheral conditions (e.g., saliva secretion) *per se*.

FUNCTIONAL ADAPTATION OF OROMOTOR SKILLS – AN HYPOTHETICAL EXPERIMENTAL FRAMEWORK

Functional Adaptation of Oromotor Skills: Why Do We Need More Evidence?

While the current neuroimaging evidence has provided a general picture of the brain signatures associated with the individual differences in the BSA, it is difficult to directly translate these research findings to clinical applications. From the perspective

of clinical practice, a crucial question is to quantify the degree of individual differences and to provide a better prediction of the outcome of adaptation on an individual basis. The critical issues are to clarify (a) what functional performance is regained, (b) what structural impairment is compensated for, and (c) what brain regions (or networks) are associated with the individual differences in the adaptation. These goals can be achieved only with a valid experimental design. In the following section, I will propose three conditions of experimental design that may facilitate the design of a neuroimaging study about the functional adaptation of oromotor functions.

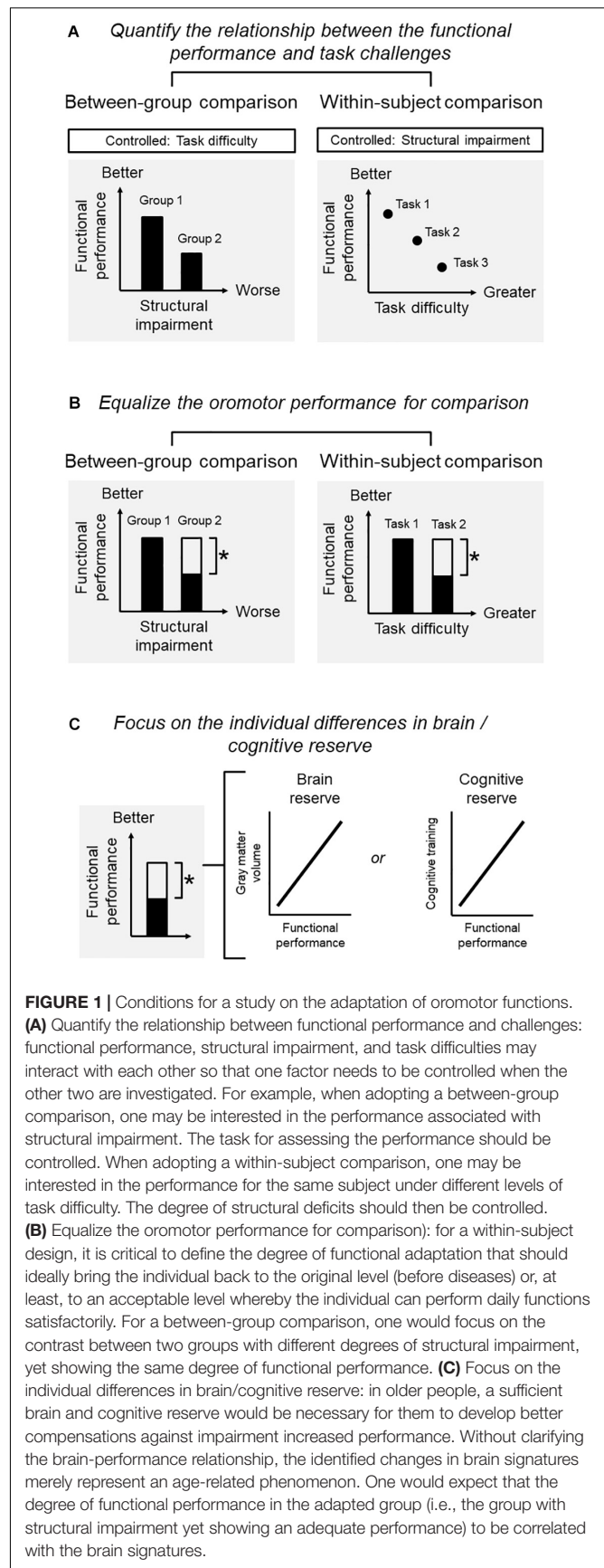
Proposed Conditions for a Study on the Adaptation of Oromotor Functions

Quantify the Relationship Between Functional Performance and Challenges (Figure 1A)

A primary condition is to quantify the relationship between functional performance, structural impairment, and task difficulties, depending on the purpose of the research. Notably, these factors may interact with each other so that one should control one of the factors when examining the association between the other two factors. For example, when adopting a between-group comparison, one may be interested in the masticatory performance associated with structural impairment. Here, the task difficulty for assessing masticatory performance should be controlled. When adopting a within-subject comparison, one may be interested in the performance for the same subject under different levels of task difficulty. The degree of structural impairment should then be controlled (Figure 1A).

Equalize the Oromotor Performance for Comparison (Figure 1B)

In older people, the ‘overactivation’ of some brain regions (e.g., the prefrontal recruitment during chewing) would indicate a compensatory process or ‘working harder’ than their younger counterparts (Reuter-Lorenz and Cappell, 2008). However, such an ‘overactivation’ may represent maladaptive neuroplasticity of sensorimotor functions, rather than an underlying compensation (Sessle, 2019). Therefore, the use of the term ‘compensation’ should be confined to situations where a substantial degree of functional performance was regained against the observed structural impairment. For a within-subject design, it is critical to define the degree of functional adaptation that should ideally bring the individual back to the original level (before diseases) or, at least, to an acceptable level whereby the individual can perform daily functions satisfactorily. The same principle applies to between-group comparisons (e.g., younger vs. older subjects). For example, a neuroimaging study reported that younger and older subjects showed different degrees of brain activation when consolidating acquired motor skills into memory. The specific changes in the older group could be interpreted as a compensatory mechanism for adapting their functions only when the two groups showed a similar degree of motor learning (e.g., the same learning rate) (Berghuis et al., 2019). Therefore, the between-group comparison would focus



on the contrast between two groups with different degrees of structural impairment, yet showing the same degree of functional performance (Figure 1B).

Focus on the Individual Differences in Brain/Cognitive Reserve (Figure 1C)

As shown previously, in older people, a sufficient brain and cognitive reserve would be necessary for them to develop better compensations against impairment (Cabeza et al., 2018). Theoretically, to claim that the changes in brain signatures are associated with the compensation on a certain performance, one needs to identify the association between the changes of the brain and the increased performance. Without clarifying the brain-performance relationship, the identified changes in brain signatures merely represent an age-related phenomenon (Cabeza et al., 2018). Clinically, it would be more important to differentiate those who are capable of compensation from those who cannot, via an assessment of their brain/cognitive profiles. Since the individual capacity of compensation is associated with brain and cognitive reserve, one would expect that the degree of functional performance in the adapted group (i.e., the group with structural impairment yet showing an adequate performance) to be correlated with the brain signatures, e.g., gray matter volume or intrinsic connectivity. Notably, such a correlation holds only in the adapted group but not in the non-adapted group (i.e., the group with structural impairment and showing insufficient performance).

Brain Mechanisms of Functional Adaptation of Mastication: An Example of Neuroimaging Research

To illustrate how the three proposed conditions are applied to clinical research, I will propose an example study about mastication. The aim of this research is to understand (a) the potential mechanisms that could explain why some individuals can maintain their masticatory performance, even if they have a poorer status of teeth contact, and (b) whether the identified brain signatures can predict individual differences in functional adaptation.

Quantify the Relationship Between Functional Performance and Challenges

We first clarify the association between functional performance and challenges. In our case, we adopted a between-group design, and the sample was subgrouped by the degree of structural impairment based on the Eichner Index, which reflects the degree of posterior contact, and the masticatory performance (Figure 2A). The subgroup with fewer teeth contact would have a lower masticatory performance, based on the previous findings (Ikebe et al., 2012). The task of assessing functional performance (gum-chewing) was standardized for both groups.

Equalize the Oromotor Performance for Comparison

Our next step is to equalize the functional performance between the subgroups. Because we aimed to understand how masticatory function is maintained in the condition of structural impairment, each group was further subgrouped by masticatory performance

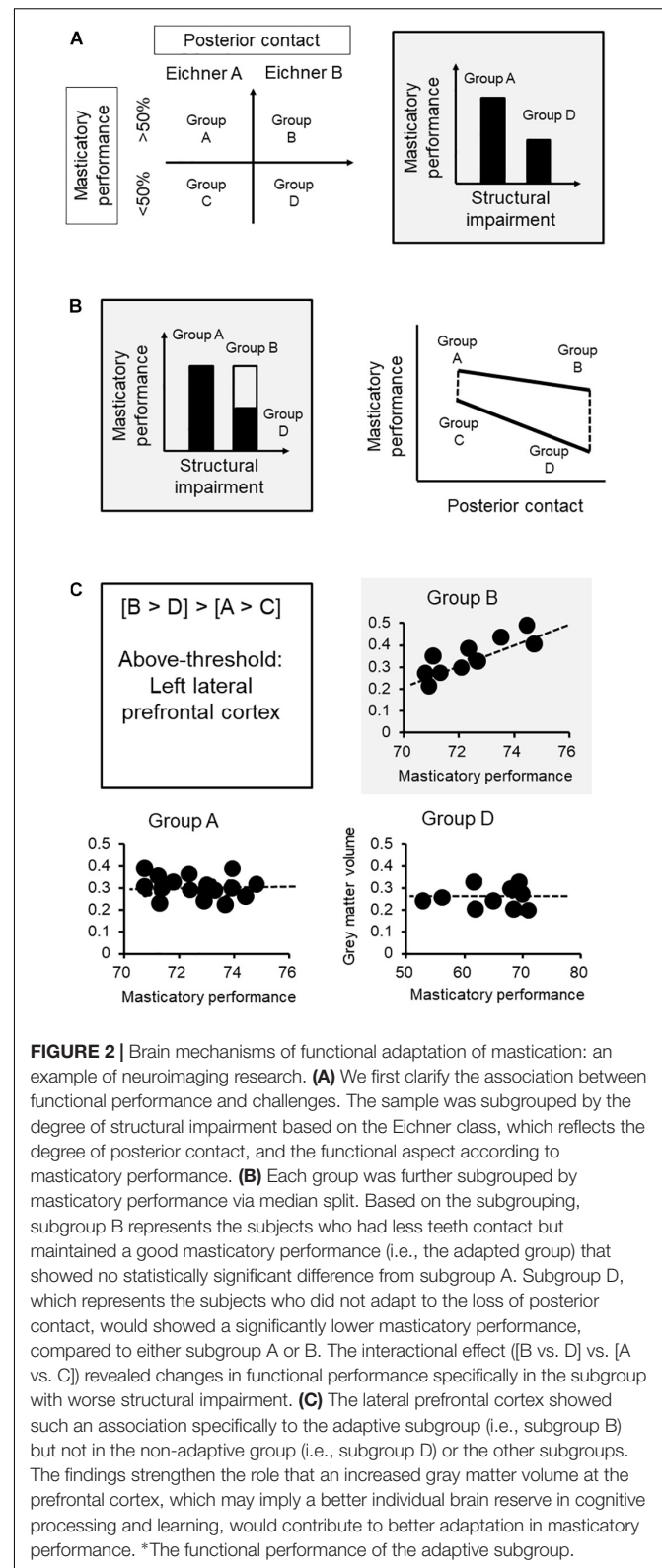


FIGURE 2 | Brain mechanisms of functional adaptation of mastication: an example of neuroimaging research. **(A)** We first clarify the association between functional performance and challenges. The sample was subgrouped by the degree of structural impairment based on the Eichner class, which reflects the degree of posterior contact, and the functional aspect according to masticatory performance. **(B)** Each group was further subgrouped by masticatory performance via median split. Based on the subgrouping, subgroup B represents the subjects who had less teeth contact but maintained a good masticatory performance (i.e., the adapted group) that showed no statistically significant difference from subgroup A. Subgroup D, which represents the subjects who did not adapt to the loss of posterior contact, would show a significantly lower masticatory performance, compared to either subgroup A or B. The interactional effect ([B vs. D] vs. [A vs. C]) revealed changes in functional performance specifically in the subgroup with worse structural impairment. **(C)** The lateral prefrontal cortex showed such an association specifically to the adaptive subgroup (i.e., subgroup B) but not in the non-adaptive group (i.e., subgroup D) or the other subgroups. The findings strengthen the role that an increased gray matter volume at the prefrontal cortex, which may imply a better individual brain reserve in cognitive processing and learning, would contribute to better adaptation in masticatory performance. *The functional performance of the adaptive subgroup.

via median split (Figure 2A). Based on the subgrouping, subgroup B represents the subjects who had fewer teeth contact but maintained a good masticatory performance (i.e., the adapted

group) that showed no statistically significant difference from subgroup A (**Figure 2B**). Subgroup D, which represents the subjects who did not adapt to the loss of posterior contact, would show a significantly lower masticatory performance, compared to either subgroup A or B. Notably, what we are interested in is the brain signature that will reflect the interaction between the structural and functional factors. The contrast between subgroups A and B or between subgroups C and D only revealed the changes explained by structural impairment. In contrast, the interactional effect ([B vs. D] vs. [A vs. C]) revealed changes in functional performance specifically in the subgroup with worse structural impairment (**Figure 2B**). For example, in the current case, the gray matter volume at the lateral prefrontal cortex reflected the interactional effect of functional adaptation (**Figure 2B**).

Focus on the Individual Differences in Brain/Cognitive Reserve

If the brain signature is associated with functional adaptation, we may expect that variations in this signature would explain individual variations in functional adaptation. Critically, since the brain signature specifically reflects individual differences in performance, a significant correlation would be identified only in the subgroup showing adaptation (i.e., subgroup B) but not in the other subgroups (**Figure 2C**). In this case, the lateral prefrontal cortex showed such an association specifically to the adaptive subgroup (i.e., subgroup B) but not in the non-adaptive group (i.e., subgroup D) or the other subgroups. The findings strengthen the role that an increased gray matter volume at the prefrontal cortex, which may imply a better individual brain reserve in cognitive processing and learning, would contribute to better adaptation in masticatory performance.

Statistical Considerations

The hypothetical experimental framework should be investigated with careful considerations from research design and statistical analysis. First of all, the example that was proposed previously is a cross-sectional observational research. It may help to identify the brain region associated with the individual variations in adaptation. However, it does not disclose the dynamic process of functional adaptation, which should be identified through a longitudinal observation. Secondly, either for a cross-sectional or a longitudinal design, the independent and dependent variables and potentially confounding factors need to be clarified. For example, when it comes to *what functional performance is regained*, one should clarify how masticatory performance is assessed: a self-report of chewing experience or the results from objective assessment (e.g., oral mixing tests or cutting/crunching tests). Third, all the observed variables may covariate with some confounding factors. For example, an increased degree of structural impairment, such as tooth loss, may be associated with orofacial pain. And some general factors, such as general physical ability (e.g., grip force) and the use of medication may be associated with oral functions (Morita et al., 2018; Yamaguchi et al., 2018). These factors should be carefully considered in the statistical model. Finally, it should be noted that either the within-subject or between-group

comparison should be interpreted on the basis of an adequate statistical power and a proper estimation of effect size. The under-powered results suffer from an increased risk of type II error. The lack of adequate statistical power may be associated with a small sample size, which is not uncommon in neuroimaging research (Button et al., 2013). The estimation of the training-related effect size is particularly critical from the clinical perspective. A task that leads to a small effect size – even being statistically significant – would still be clinically insignificant.

PRACTICAL IMPLICATIONS AND FURTHER CONSIDERATIONS

Implications for Geriatric Patients With Neurological Disorders

There is an urgent demand for dentists to focus on geriatric patients with neurological disorders, including dementia and stroke. These disorders have posed a great challenge to clinical management because they may interfere with regular dental assessments or therapies, which successfully work in healthy older patients. For example, dysphagia remains a huge challenge in patients with dementia (Boccardi et al., 2016). Notably, patients with dementia have a problem with the cognitive aspects of swallowing. For example, they may require a cue from the other person to initiate eating (Priefer and Robbins, 1997). The score from the Mini-Mental State Examination was inversely associated with the suspected rate of aspiration (Rosler et al., 2015). Even when they receive training in swallowing, they may be less able to follow these instructions and keep doing them regularly (Wirth et al., 2016). The recent findings regarding cognitive processing and motor learning of oromotor functions can provide a better evaluation of the oral sensorimotor functions, which could be pivotal to formulate evidence-based clinical management of geriatric and special needs patients.

Implications for the Neuroplasticity of Oral Rehabilitation

Evidence from animal research has revealed that the sensorimotor cortices show a plastic effect that responds to changes in oral functions (Avivi-Arber et al., 2011; Avivi-Arber and Sessle, 2018). In mice, a widespread change in the volumes of multiple cortical brain regions, including the areas associated with sensorimotor, cognitive and emotional functions, were identified, following the extraction of molar teeth (Avivi-Arber et al., 2017). Brain plasticity can also be identified in human subjects with oromotor training or prosthetic treatment (Kumar et al., 2018). It should be noted that this effect implies a cause-effect relationship, i.e., the changes in brain capacity respond to experienced demands (Lindenberger et al., 2017). However, most of the cross-sectional neuroimaging studies primarily revealed correlational but not causal results (Poldrack and Farah, 2015). Nevertheless, these cross-sectional findings from human subjects would be valuable for further animal and neuroimaging research based on intervention. When a sensorimotor intervention is

adopted to elucidate the cause-effect relationship of learning and brain plasticity, the protocol of the intervention should be clearly defined. For example, the intervention can be a tactile stimulus (e.g., repetitive sensory stimulation), which improved tactile performance and revealed a corresponding plastic effect on brain structure and intrinsic functional network (Heba et al., 2017; Schmidt-Wilcke et al., 2018). In terms of orofacial research, the intervention can be a standardized training protocol, e.g., the food biting task (Kumar et al., 2019), or a pre- vs. post-treatment comparison of denture installation (Luraschi et al., 2013). Notably, either repetitive stimulation or the use of denture has revealed brain plasticity at the somatosensory region (Luraschi et al., 2013; Heba et al., 2017; Schmidt-Wilcke et al., 2018). Such a convergent finding would strengthen the role of sensory feedback in adaptation in sensorimotor functions, helping to clarify the cause-effect relationship between learning and plasticity.

Implications for Geriatric Patients With Normal Aging

It is noteworthy that functional adaptation would be a general issue for all geriatric dental patients, not just for those with severe physical/cognitive impairment. Indeed, most elderly patients were satisfied with their dentures (Carlsson and Omar, 2010), and through the advent of implant dentistry, masticatory functions can be substantially improved (for a detailed review, see Trulsson et al., 2012). However, there are still pronounced individual differences in their experience of improvement. For example, a randomized controlled trial revealed that an implant-supported overdenture, compared to the denture with conventional relines, improved one's maximum bite force. However, the scores of masticatory performance and the nutritional scale did not show a significant difference between the

two therapies (Muller et al., 2013). In elderly people of Eichner Index C (i.e., without occlusal contact), a great variation in masticatory performance was shown (Ikebe et al., 2012). The clinical findings imply that even under the same condition of structural impairment (e.g., being edentulous), older people may adapt to this challenge to different degrees.

CONCLUSION

This Focused Review highlighted that the functional aspects of adaptation—which would be predominantly associated with the brain mechanisms of cognitive processing and motor learning—play a critical role in the individual differences in the adaptive behaviors of oromotor functions. Issues about how individuals acquire new oral sensorimotor skills and the mechanisms underlying the individual differences in adaptation require further investigation. Understanding the brain-stomatognathic mechanisms underlying sensorimotor adaptation may provide important insight into the age-related changes in oral functions and contribute to the clinical management of dental patients.

AUTHOR CONTRIBUTIONS

C-SL conceived and wrote the review.

FUNDING

C-SL was funded by the Ministry of Science and Technology of Taiwan (MOST 105-2628-B-010-008-MY4 and MOST 107-2314-B-010-030-MY2).

REFERENCES

- Avivi-Arber, L., Martin, R., Lee, J. C., and Sessle, B. J. (2011). Face sensorimotor cortex and its neuroplasticity related to orofacial sensorimotor functions. *Arch. Oral Biol.* 56, 1440–1465. doi: 10.1016/j.archoralbio.2011.04.005
- Avivi-Arber, L., Seltzer, Z., Friedel, M., Lerch, J. P., Moayed, M., Davis, K. D., et al. (2017). Widespread volumetric brain changes following tooth loss in female mice. *Front. Neuroanat.* 10:121. doi: 10.3389/fnana.2016.00121
- Avivi-Arber, L., and Sessle, B. J. (2018). Jaw sensorimotor control in healthy adults and effects of ageing. *J. Oral Rehabil.* 45, 50–80. doi: 10.1111/joor.12554
- Barulli, D., and Stern, Y. (2013). Efficiency, capacity, compensation, maintenance, plasticity: emerging concepts in cognitive reserve. *Trends Cogn. Sci.* 17, 502–509. doi: 10.1016/j.tics.2013.08.012
- Ben-David, B. M., and Icht, M. (2018). The effect of practice and visual feedback on oral-diadochokinetic rates for younger and older adults. *Lang. Speech* 61, 113–134. doi: 10.1177/0023830917708808
- Berghuis, K. M. M., Fagioli, S., Maurits, N. M., Zijdwind, I., Marsman, J. B. C., Hortobagyi, T., et al. (2019). Age-related changes in brain deactivation but not in activation after motor learning. *Neuroimage* 186, 358–368. doi: 10.1016/j.neuroimage.2018.11.010
- Bernard, J. A., and Seidler, R. D. (2014). Moving forward: age effects on the cerebellum underlie cognitive and motor declines. *Neurosci. Biobehav. Rev.* 42, 193–207. doi: 10.1016/j.neubiorev.2014.02.011
- Boccardi, V., Ruggiero, C., Patrini, A., and Marano, L. (2016). Diagnostic assessment and management of dysphagia in patients with Alzheimer's disease. *J. Alzheimers Dis.* 50, 947–955. doi: 10.3233/JAD-150931
- Bostan, A. C., and Strick, P. L. (2018). The basal ganglia and the cerebellum: nodes in an integrated network. *Nat. Rev. Neurosci.* 19, 338–350. doi: 10.1038/s41583-018-0002-7
- Bremmer, F., Schlack, A., Shah, N. J., Zafiris, O., Kubischik, M., Hoffmann, K., et al. (2001). Polymodal motion processing in posterior parietal and premotor cortex: a human fMRI study strongly implies equivalencies between humans and monkeys. *Neuron* 29, 287–296. doi: 10.1016/s0896-6273(01)00198-2
- Button, K. S., Ioannidis, J. P., Mokrysz, C., Nosek, B. A., Flint, J., Robinson, E. S., et al. (2013). Power failure: why small sample size undermines the reliability of neuroscience. *Nat. Rev. Neurosci.* 14, 365–376. doi: 10.1038/nrn3475
- Cabeza, R., Albert, M., Belleville, S., Craik, F. I. M., Duarte, A., Grady, C. L., et al. (2018). Maintenance, reserve and compensation: the cognitive neuroscience of healthy ageing. *Nat. Rev. Neurosci.* 19, 701–710. doi: 10.1038/s41583-018-0068-2
- Carlsson, G. E., and Omar, R. (2010). The future of complete dentures in oral rehabilitation. A critical review. *J. Oral Rehabil.* 37, 143–156. doi: 10.1111/j.1365-2842.2009.02039.x
- Chan, M. Y., Park, D. C., Savalia, N. K., Petersen, S. E., and Wig, G. S. (2014). Decreased segregation of brain systems across the healthy adult lifespan. *Proc. Natl. Acad. Sci. U.S.A.* 111, E4997–E5006. doi: 10.1073/pnas.1415122111
- Cullins, M. J., and Connor, N. P. (2017). Alterations of intrinsic tongue muscle properties with aging. *Muscle Nerve* 56, E119–E125. doi: 10.1002/mus.25605
- Curiati, P. K., Tamashiro, J. H., Squarzon, P., Duran, F. L., Santos, L. C., Wajngarten, M., et al. (2009). Brain structural variability due to aging and gender in cognitively healthy elders: results from the Sao Paulo ageing and health study. *AJNR Am. J. Neuroradiol.* 30, 1850–1856. doi: 10.3174/ajnr.A1727

- Custead, R., Oh, H., Wang, Y., and Barlow, S. (2017). Brain encoding of saltatory velocity through a pulsed pneumotactile array in the lower face. *Brain Res.* 1677, 58–73. doi: 10.1016/j.brainres.2017.09.025
- Daboul, A., Schwahn, C., Bulow, R., Kiliaridis, S., Kocher, T., Klinke, T., et al. (2018). Influence of age and tooth loss on masticatory muscles characteristics: a population based MR imaging study. *J. Nutr. Health Aging* 22, 829–836. doi: 10.1007/s12603-018-1029-1
- Daly, B., Thompsell, A., Sharpling, J., Rooney, Y. M., Hillman, L., Wanyonyi, K. L., et al. (2018). Evidence summary: the relationship between oral health and dementia. *Br. Dent. J.* 223, 846–853. doi: 10.1038/sj.bdj.2017.992
- Delwel, S., Scherder, E. J. A., De Baat, C., Binnekade, T. T., Van Der Wouden, J. C., Hertogh, C., et al. (2019). Orofacial pain and its potential oral causes in older people with mild cognitive impairment or dementia. *J. Oral Rehabil.* 46, 23–32. doi: 10.1111/joor.12724
- Di Scala, G., Dupuy, M., Guillaud, E., Doat, E., Barse, E., Dillhareguy, B., et al. (2019). Efficiency of sensorimotor networks: posture and gait in young and older adults. *Exp. Aging Res.* 45, 41–56. doi: 10.1080/0361073X.2018.1560108
- Dubois, J., and Adolphs, R. (2016). Building a science of individual differences from fMRI. *Trends Cogn. Sci.* 20, 425–443. doi: 10.1016/j.tics.2016.03.014
- Ebbesen, C. L., and Brecht, M. (2017). Motor cortex - to act or not to act? *Nat. Rev. Neurosci.* 18, 694–705. doi: 10.1038/nrn.2017.119
- Eberhard, L., Oh, K., Eiffler, C., Rammelsberg, P., Kappel, S., Schindler, H. J., et al. (2018). Adaptation to neuromuscular complete dentures-is the nas system outcome-oriented or effort-oriented? *Clin. Oral Investig.* 22, 2309–2317. doi: 10.1007/s00784-017-2331-8
- Elkerdany, M. K., and Fahim, M. A. (1993). Age changes in neuromuscular junctions of masseter muscle. *Anat. Rec.* 237, 291–295. doi: 10.1002/ar.1092370215
- Fang, M., Li, J., Lu, G., Gong, X., and Yew, D. T. (2005). A fMRI study of age-related differential cortical patterns during cued motor movement. *Brain Topogr.* 17, 127–137. doi: 10.1007/s10548-005-4446-5
- Fauchard, P. (1946). *The Surgeon Dentist, Treatise on the Teeth*. Oxford: Butterworth & Company.
- Fontijn-Tekamp, F. A., Van Der Bilt, A., Abbink, J. H., and Bosman, F. (2004). Swallowing threshold and masticatory performance in dentate adults. *Physiol. Behav.* 83, 431–436. doi: 10.1016/j.physbeh.2004.08.026
- Frisancho, A. R. (1993). *Human Adaptation and Accommodation*. Ann Arbor, MI: The University of Michigan Press.
- Galovic, M., Leisi, N., Muller, M., Weber, J., Tettenborn, B., Brugger, F., et al. (2016). Neuroanatomical correlates of tube dependency and impaired oral intake after hemispheric stroke. *Eur. J. Neurol.* 23, 926–934. doi: 10.1111/ene.12964
- Galovic, M., Leisi, N., Pastore-Wapp, M., Zbinden, M., Vos, S. B., Mueller, M., et al. (2017). Diverging lesion and connectivity patterns influence early and late swallowing recovery after hemispheric stroke. *Hum. Brain Mapp.* 38, 2165–2176. doi: 10.1002/hbm.23511
- Gaszynska, E., Kopacz, K., Fronczek-Wojciechowska, M., Padula, G., and Szatko, F. (2017). Electromyographic analysis of masticatory muscles in elderly women - a pilot study. *Clin. Interv. Aging* 12, 111–116. doi: 10.2147/CIA.S118338
- Hackert, V. H., Den Heijer, T., Oudkerk, M., Koudstaal, P. J., Hofman, A., and Breteler, M. M. (2002). Hippocampal head size associated with verbal memory performance in nondemented elderly. *Neuroimage* 17, 1365–1372. doi: 10.1006/nimg.2002.1248
- Heba, S., Lenz, M., Kalisch, T., Hoffken, O., Schweizer, L. M., Glaubitz, B., et al. (2017). Regionally specific regulation of sensorimotor network connectivity following tactile improvement. *Neural Plast.* 2017:5270532. doi: 10.1155/2017/5270532
- Hedden, T., and Gabrieli, J. D. (2004). Insights into the ageing mind: a view from cognitive neuroscience. *Nat. Rev. Neurosci.* 5, 87–96. doi: 10.1038/nrn1323
- Heft, M. W., and Robinson, M. E. (2010). Age differences in orofacial sensory thresholds. *J. Dent. Res.* 89, 1102–1105. doi: 10.1177/0022034510375287
- Heuninckx, S., Wenderoth, N., Debaere, F., Peeters, R., and Swinnen, S. P. (2005). Neural basis of aging: the penetration of cognition into action control. *J. Neurosci.* 25, 6787–6796. doi: 10.1523/jneurosci.1263-05.2005
- Heuninckx, S., Wenderoth, N., and Swinnen, S. P. (2010). Age-related reduction in the differential pathways involved in internal and external movement generation. *Neurobiol. Aging* 31, 301–314. doi: 10.1016/j.neurobiolaging.2008.03.021
- Holland, J. H. (1982). *Adaptation in Natural and Artificial Systems: an Introductory Analysis With Applications to Biology, Control, and Artificial Intelligence*. Cambridge, MA: MIT Press.
- Humbert, I. A., Fitzgerald, M. E., McLaren, D. G., Johnson, S., Porcaro, E., Kosmatka, K., et al. (2009). Neurophysiology of swallowing: effects of age and bolus type. *Neuroimage* 44, 982–991. doi: 10.1016/j.neuroimage.2008.10.012
- Humbert, I. A., McLaren, D. G., Kosmatka, K., Fitzgerald, M., Johnson, S., Porcaro, E., et al. (2010). Early deficits in cortical control of swallowing in Alzheimer's disease. *J. Alzheimers Dis.* 19, 1185–1197. doi: 10.3233/JAD-2010-1316
- Humbert, I. A., McLaren, D. G., Malandraki, G., Johnson, S. C., and Robbins, J. (2011). Swallowing intentional off-state in aging and Alzheimer's disease: preliminary study. *J. Alzheimers Dis.* 26, 347–354. doi: 10.3233/JAD-2011-110380
- Ikebe, K., Matsuda, K., Kagawa, R., Enoki, K., Okada, T., Yoshida, M., et al. (2012). Masticatory performance in older subjects with varying degrees of tooth loss. *J. Dent.* 40, 71–76. doi: 10.1016/j.jdent.2011.10.007
- Ikebe, K., Nokubi, T., Morii, K., Kashiwagi, J., and Furuya, M. (2005). Association of bite force with ageing and occlusal support in older adults. *J. Dent.* 33, 131–137. doi: 10.1016/j.jdent.2004.09.002
- Kimoto, K., Ono, Y., Tachibana, A., Hirano, Y., Otsuka, T., Ohno, A., et al. (2011). Chewing-induced regional brain activity in edentulous patients who received mandibular implant-supported overdentures: a preliminary report. *J. Prosthodont. Res.* 55, 89–97. doi: 10.1016/j.jpor.2010.09.006
- King, B. R., Van Ruitenbeek, P., Leunissen, I., Cuyper, K., Heise, K. F., Santos Monteiro, T., et al. (2018). Age-related declines in motor performance are associated with decreased segregation of large-scale resting state brain networks. *Cereb. Cortex* 28, 4390–4402. doi: 10.1093/cercor/bhx297
- Kumar, A., Kothari, M., Grigoriadis, A., Trulsson, M., and Svensson, P. (2018). Bite or brain: implication of sensorimotor regulation and neuroplasticity in oral rehabilitation procedures. *J. Oral Rehabil.* 45, 323–333. doi: 10.1111/joor.12603
- Kumar, A., Koullia, N., Jongenburger, M., Koutris, M., Lobbezoo, F., Trulsson, M., et al. (2019). Behavioral learning and skill acquisition during a natural yet novel biting task. *Physiol. Behav.* 211:112667. doi: 10.1016/j.physbeh.2019.112667
- Lage, G. M., Ugrinowitsch, H., Apolinario-Souza, T., Vieira, M. M., Albuquerque, M. R., and Benda, R. N. (2015). Repetition and variation in motor practice: a review of neural correlates. *Neurosci. Biobehav. Rev.* 57, 132–141. doi: 10.1016/j.neubiorev.2015.08.012
- Lemaitre, H., Goldman, A. L., Sambataro, F., Verchinski, B. A., Meyer-Lindenberg, A., Weinberger, D. R., et al. (2012). Normal age-related brain morphometric changes: nonuniformity across cortical thickness, surface area and gray matter volume? *Neurobiol. Aging* 33, 617.e1–617.e9. doi: 10.1016/j.neurobiolaging.2010.07.013
- Li, S., Luo, C., Yu, B., Yan, B., Gong, Q., He, C., et al. (2009). Functional magnetic resonance imaging study on dysphagia after unilateral hemispheric stroke: a preliminary study. *J. Neurol. Neurosurg. Psychiatry* 80, 1320–1329. doi: 10.1136/jnnp.2009.176214
- Li, S., Ma, Z., Tu, S., Zhou, M., Chen, S., Guo, Z., et al. (2014). Altered resting-state functional and white matter tract connectivity in stroke patients with dysphagia. *Neurorehabil. Neural Repair* 28, 260–272. doi: 10.1177/1545968313508227
- Lin, C. S. (2018). Meta-analysis of brain mechanisms of chewing and clenching movements. *J. Oral Rehabil.* 45, 627–639. doi: 10.1111/joor.12657
- Lin, C. S., Wu, C. Y., Wang, D. H., Lin, H. H., Lo, K. C., Lo, W. L., et al. (2019). Brain signatures associated with swallowing efficiency in older people. *Exp. Gerontol.* 115, 1–8. doi: 10.1016/j.exger.2018.11.007
- Lin, C. S., Wu, C. Y., Wu, S. Y., Chuang, K. H., Lin, H. H., Cheng, D. H., et al. (2017a). Age- and sex-related differences in masseter size and its role in oral functions. *J. Am. Dent. Assoc.* 148, 644–653. doi: 10.1016/j.adaj.2017.03.001
- Lin, C. S., Wu, C. Y., Wu, S. Y., Lin, H. H., Cheng, D. H., and Lo, W. L. (2017b). Age-related difference in functional brain connectivity of mastication. *Front. Aging Neurosci.* 9:82. doi: 10.3389/fnagi.2017.00082
- Lin, C. S., Wu, S. Y., Wu, C. Y., and Ko, H. W. (2015). Gray matter volume and resting-state functional connectivity of the motor cortex-cerebellum network reflect the individual variation in masticatory performance in healthy elderly people. *Front. Aging Neurosci.* 7:247. doi: 10.3389/fnagi.2015.00247
- Lindenberger, U., Wenger, E., and Lovden, M. (2017). Towards a stronger science of human plasticity. *Nat. Rev. Neurosci.* 18, 261–262. doi: 10.1038/nrn.2017.44
- Lowell, S. Y., Reynolds, R. C., Chen, G., Horwitz, B., and Ludlow, C. L. (2012). Functional connectivity and laterality of the motor and sensory components

- in the volitional swallowing network. *Exp. Brain Res.* 219, 85–96. doi: 10.1007/s00221-012-3069-9
- Luraschi, J., Korgaonkar, M. S., Whittle, T., Schimmel, M., Muller, F., and Klineberg, I. (2013). Neuroplasticity in the adaptation to prosthodontic treatment. *J. Orofac. Pain* 27, 206–216. doi: 10.11607/jop.1097
- Lynch, C. D., O'sullivan, V. R., and McGillicuddy, C. T. (2006). Pierre Fauchard: the 'father of modern dentistry'. *Br. Dent. J.* 201, 779–781.
- Malandraki, G. A., Perlman, A. L., Karampinos, D. C., and Sutton, B. P. (2011). Reduced somatosensory activations in swallowing with age. *Hum. Brain Mapp.* 32, 730–743. doi: 10.1002/hbm.21062
- Martin, R., Barr, A., Macintosh, B., Smith, R., Stevens, T., Taves, D., et al. (2007). Cerebral cortical processing of swallowing in older adults. *Exp. Brain Res.* 176, 12–22. doi: 10.1007/s00221-006-0592-6
- Marvel, C. L., Morgan, O. P., and Kronemer, S. I. (2019). How the motor system integrates with working memory. *Neurosci. Biobehav. Rev.* 102, 184–194. doi: 10.1016/j.neubiorev.2019.04.017
- Mattay, V. S., Fera, F., Tessitore, A., Hariri, A. R., Das, S., Callicott, J. H., et al. (2002). Neurophysiological correlates of age-related changes in human motor function. *Neurology* 58, 630–635. doi: 10.1212/wnl.58.4.630
- Michely, J., Volz, L. J., Hoffstaedter, F., Tittgemeyer, M., Eickhoff, S. B., Fink, G. R., et al. (2018). Network connectivity of motor control in the ageing brain. *Neuroimage Clin.* 18, 443–455. doi: 10.1016/j.nicl.2018.02.001
- Mihai, P. G., Otto, M., Domin, M., Platz, T., Hamdy, S., and Lotze, M. (2016). Brain imaging correlates of recovered swallowing after dysphagic stroke: a fMRI and DWI study. *Neuroimage Clin.* 12, 1013–1021. doi: 10.1016/j.nicl.2016.05.006
- Miyamoto, I., Yoshida, K., Tsuboi, Y., and Iizuka, T. (2005). Rehabilitation with dental prosthesis can increase cerebral regional blood volume. *Clin. Oral Implants Res.* 16, 723–727. doi: 10.1111/j.1600-0501.2005.01171.x
- Momosaki, R., Abo, M., Kakuda, W., and Uruma, G. (2012). Which cortical area is related to the development of dysphagia after stroke? A single photon emission computed tomography study using novel analytic methods. *Eur. Neurol.* 67, 74–80. doi: 10.1159/000333778
- Morita, K., Tsuka, H., Kato, K., Mori, T., Nishimura, R., Yoshida, M., et al. (2018). Factors related to masticatory performance in healthy elderly individuals. *J. Prosthodont. Res.* 62, 432–435. doi: 10.1016/j.jpor.2018.03.007
- Muller, F., Duvernoy, E., Loup, A., Vazquez, L., Herrmann, F. R., and Schimmel, M. (2013). Implant-supported mandibular overdentures in very old adults: a randomized controlled trial. *J. Dent. Res.* 92, 154S–160S. doi: 10.1177/0022034513509630
- Muller-Oehring, E. M., Schulte, T., Rohlfing, T., Pfefferbaum, A., and Sullivan, E. V. (2013). Visual search and the aging brain: discerning the effects of age-related brain volume shrinkage on alertness, feature binding, and attentional control. *Neuropsychology* 27, 48–59. doi: 10.1037/a0030921
- Norton, M., Versteegden, A., Maxwell, L. C., and McCarter, R. M. (2001). Constancy of masseter muscle structure and function with age in F344 rats. *Arch. Oral Biol.* 46, 139–146. doi: 10.1016/s0003-9969(00)00107-2
- Oguchi, K., Saitoh, E., Baba, M., Kusodo, S., Tanaka, T., and Onogi, K. (2000a). The repetitive saliva swallowing test (RSST) as a screening test of functional dysphagia (2) validity of RSST. *Jpn. J. Rehabil. Med.* 37, 383–388. doi: 10.2490/jjrm1963.37.383
- Oguchi, K., Saitoh, E., Mizuno, M., Baba, M., Okui, M., and Suzuki, M. (2000b). The repetitive saliva swallowing test (RSST) as a screening test of functional dysphagia (1) normal values of RSST. *Jpn. J. Rehab. Med.* 37, 375–382. doi: 10.2490/jjrm1963.37.375
- Onozuka, M., Fujita, M., Watanabe, K., Hirano, Y., Niwa, M., Nishiyama, K., et al. (2002). Mapping brain region activity during chewing: a functional magnetic resonance imaging study. *J. Dent. Res.* 81, 743–746. doi: 10.1177/0810743
- Onozuka, M., Fujita, M., Watanabe, K., Hirano, Y., Niwa, M., Nishiyama, K., et al. (2003). Age-related changes in brain regional activity during chewing: a functional magnetic resonance imaging study. *J. Dent. Res.* 82, 657–660. doi: 10.1177/154405910308200817
- Pascual-Leone, A., Amedi, A., Fregni, F., and Merabet, L. B. (2005). The plastic human brain cortex. *Annu. Rev. Neurosci.* 28, 377–401.
- Peddireddy, A., Wang, K., Svensson, P., and Arendt-Nielsen, L. (2006). Influence of age and gender on the jaw-stretch and blink reflexes. *Exp. Brain Res.* 171, 530–540. doi: 10.1007/s00221-005-0300-y
- Persson, E., Wardh, I., and Ostberg, P. (2018). Repetitive saliva swallowing test: norms, clinical relevance and the impact of saliva secretion. *Dysphagia* 34, 271–278. doi: 10.1007/s00455-018-9937-0
- Poldrack, R. A., and Farah, M. J. (2015). Progress and challenges in probing the human brain. *Nature* 526, 371–379. doi: 10.1038/nature15692
- Priefer, B. A., and Robbins, J. (1997). Eating changes in mild-stage Alzheimer's disease: a pilot study. *Dysphagia* 12, 212–221. doi: 10.1007/pl00009539
- Quintero, A., Ichescio, E., Myers, C., Schutt, R., and Gerstner, G. E. (2013a). Brain activity and human unilateral chewing: an fMRI study. *J. Dent. Res.* 92, 136–142. doi: 10.1177/0022034512466265
- Quintero, A., Ichescio, E., Schutt, R., Myers, C., Peltier, S., and Gerstner, G. E. (2013b). Functional connectivity of human chewing: an fMRI study. *J. Dent. Res.* 92, 272–278. doi: 10.1177/0022034512472681
- Ramrani, N. (2014). Automatic and controlled processing in the corticocerebellar system. *Prog. Brain Res.* 210, 255–285. doi: 10.1016/B978-0-444-63356-9.00010-8
- Reuter-Lorenz, P. A., and Cappel, K. A. (2008). Neurocognitive aging and the compensation hypothesis. *Curr. Direct. Psychol. Sci.* 17, 177–182. doi: 10.1111/j.1467-8721.2008.00570.x
- Ridderinkhof, K. R., Van Den Wildenberg, W. P., Segalowitz, S. J., and Carter, C. S. (2004). Neurocognitive mechanisms of cognitive control: the role of prefrontal cortex in action selection, response inhibition, performance monitoring, and reward-based learning. *Brain Cogn.* 56, 129–140. doi: 10.1016/j.bandc.2004.09.016
- Rommel, N., and Hamdy, S. (2016). Oropharyngeal dysphagia: manifestations and diagnosis. *Nat. Rev. Gastroenterol. Hepatol.* 13, 49–59. doi: 10.1038/nrgastro.2015.199
- Rosler, A., Pfeil, S., Lessmann, H., Hoder, J., Befahr, A., and Von Renteln-Kruse, W. (2015). Dysphagia in dementia: influence of dementia severity and food texture on the prevalence of aspiration and latency to swallow in hospitalized geriatric patients. *J. Am. Med. Dir. Assoc.* 16, 697–701. doi: 10.1016/j.jamda.2015.03.020
- Rowe, J., Stephan, K. E., Friston, K., Frackowiak, R., Lees, A., and Passingham, R. (2002). Attention to action in Parkinson's disease: impaired effective connectivity among frontal cortical regions. *Brain* 125, 276–289.
- Rowe, J. B., Siebner, H., Filipovic, S. R., Cordivari, C., Gerschlag, W., Rothwell, J., et al. (2006). Aging is associated with contrasting changes in local and distant cortical connectivity in the human motor system. *Neuroimage* 32, 747–760. doi: 10.1016/j.neuroimage.2006.03.061
- Schimmel, M., Ono, T., Lam, O. L., and Muller, F. (2017). Oro-facial impairment in stroke patients. *J. Oral Rehabil.* 44, 313–326. doi: 10.1111/joor.12486
- Schmahmann, J. D. (2019). The cerebellum and cognition. *Neurosci. Lett.* 688, 62–75. doi: 10.1016/j.neulet.2018.07.005
- Schmidt-Wilcke, T., Wulms, N., Heba, S., Pleger, B., Puts, N. A., Glaubit, B., et al. (2018). Structural changes in brain morphology induced by brief periods of repetitive sensory stimulation. *Neuroimage* 165, 148–157. doi: 10.1016/j.neuroimage.2017.10.016
- Seidler, R., Erdeniz, B., Koppelmans, V., Hirsiger, S., Merillat, S., and Jancke, L. (2015). Associations between age, motor function, and resting state sensorimotor network connectivity in healthy older adults. *Neuroimage* 108, 47–59. doi: 10.1016/j.neuroimage.2014.12.023
- Seidler, R. D., Bernard, J. A., Burutolu, T. B., Fling, B. W., Gordon, M. T., Gwin, J. T., et al. (2010). Motor control and aging: links to age-related brain structural, functional, and biochemical effects. *Neurosci. Biobehav. Rev.* 34, 721–733. doi: 10.1016/j.neubiorev.2009.10.005
- Sessle, B. J. (2006). Mechanisms of oral somatosensory and motor functions and their clinical correlates. *J. Oral Rehabil.* 33, 243–261. doi: 10.1111/j.1365-2842.2006.01623.x
- Sessle, B. J. (2019). Can you be too old for oral implants? An update on ageing and plasticity in the oro-facial sensorimotor system. *J. Oral Rehabil.* 46, 936–951. doi: 10.1111/joor.12830
- Shoi, K., Fueki, K., Usui, N., Taira, M., and Wakabayashi, N. (2014). Influence of posterior dental arch length on brain activity during chewing in patients with mandibular distal extension removable partial dentures. *J. Oral Rehabil.* 41, 486–495. doi: 10.1111/joor.12169
- Soros, P., Inamoto, Y., and Martin, R. E. (2009). Functional brain imaging of swallowing: an activation likelihood estimation meta-analysis. *Hum. Brain Mapp.* 30, 2426–2439. doi: 10.1002/hbm.20680

Stoodley, C. J. (2012). The cerebellum and cognition: evidence from functional imaging studies. *Cerebellum* 11, 352–365. doi: 10.1007/s12311-011-0260-7

Suntrup, S., Kemmling, A., Warnecke, T., Hamacher, C., Oelenberg, S., Niederstadt, T., et al. (2015). The impact of lesion location on dysphagia incidence, pattern and complications in acute stroke. Part 1: dysphagia incidence, severity and aspiration. *Eur. J. Neurol.* 22, 832–838. doi: 10.1111/ene.12670

Suntrup-Krueger, S., Kemmling, A., Warnecke, T., Hamacher, C., Oelenberg, S., Niederstadt, T., et al. (2017). The impact of lesion location on dysphagia incidence, pattern and complications in acute stroke. Part 2: Oropharyngeal residue, swallow and cough response, and pneumonia. *Eur. J. Neurol.* 24, 867–874. doi: 10.1111/ene.13307

Teismann, I. K., Steinstraeter, O., Schwindt, W., Ringelstein, E. B., Pantev, C., and Dziewas, R. (2010). Age-related changes in cortical swallowing processing. *Neurobiol. Aging* 31, 1044–1050. doi: 10.1016/j.neurobiolaging.2008.07.001

Teismann, I. K., Suntrup, S., Warnecke, T., Steinstrater, O., Fischer, M., Floel, A., et al. (2011). Cortical swallowing processing in early subacute stroke. *BMC Neurol.* 11:34. doi: 10.1186/1471-2377-11-34

Thickbroom, G. W., Byrnes, M. L., Sacco, P., Ghosh, S., Morris, I. T., and Mastaglia, F. L. (2000). The role of the supplementary motor area in externally timed movement: the influence of predictability of movement timing. *Brain Res.* 874, 233–241. doi: 10.1016/s0006-8993(00)02588-9

Toniazzo, M. P., Amorim, P. S., Muniz, F., and Weidlich, P. (2018). Relationship of nutritional status and oral health in elderly: systematic review with meta-analysis. *Clin. Nutr.* 37, 824–830. doi: 10.1016/j.clnu.2017.03.014

Trulsson, M., Francis, S. T., Bowtell, R., and Mcglone, F. (2010). Brain activations in response to vibrotactile tooth stimulation: a psychophysical and fMRI study. *J. Neurophysiol.* 104, 2257–2265. doi: 10.1152/jn.00565.2010

Trulsson, M., Van Der Bilt, A., Carlsson, G. E., Gotfredsen, K., Larsson, P., Muller, F., et al. (2012). From brain to bridge: masticatory function and dental implants. *J. Oral Rehabil.* 39, 858–877. doi: 10.1111/j.1365-2842.2012.02340.x

Utanohara, Y., Hayashi, R., Yoshikawa, M., Yoshida, M., Tsuga, K., and Akagawa, Y. (2008). Standard values of maximum tongue pressure taken using newly developed disposable tongue pressure measurement device. *Dysphagia* 23, 286–290. doi: 10.1007/s00455-007-9142-z

Ward, N. S. (2006). Compensatory mechanisms in the aging motor system. *Ageing Res. Rev.* 5, 239–254. doi: 10.1016/j.arr.2006.04.003

Weijenbergh, R. A. F., Delwel, S., Ho, B. V., Van Der Maarel-Wierink, C. D., and Lobbezoo, F. (2019). Mind your teeth-the relationship between mastication and cognition. *Gerodontology* 36, 2–7. doi: 10.1111/ger.12380

Winarakwong, L., Muramoto, T., Soma, K., and Takano, Y. (2004). Age-related changes and the possible adaptability of rat jaw muscle spindles: immunohistochemical and fine structural studies. *Arch. Histol. Cytol.* 67, 227–240. doi: 10.1679/aohc.67.227

Windel, A. S., Mihai, P. G., and Lotze, M. (2015). Neural representation of swallowing is retained with age. A functional neuroimaging study validated by classical and Bayesian inference. *Behav. Brain Res.* 286, 308–317. doi: 10.1016/j.bbr.2015.03.009

Wirth, R., Dziewas, R., Beck, A. M., Clave, P., Hamdy, S., Heppner, H. J., et al. (2016). Oropharyngeal dysphagia in older persons - from pathophysiology to adequate intervention: a review and summary of an international expert meeting. *Clin. Interv. Aging* 11, 189–208. doi: 10.2147/CIA.S97481

Wolpert, D. M., Ghahramani, Z., and Flanagan, J. R. (2001). Perspectives and problems in motor learning. *Trends Cogn. Sci.* 5, 487–494. doi: 10.1016/s1364-6613(00)01773-3

Wolpert, D. M., Miall, R. C., and Kawato, M. (1998). Internal models in the cerebellum. *Trends Cogn. Sci.* 2, 338–347. doi: 10.1016/s1364-6613(98)01221-2

Wu, T., and Hallett, M. (2005). The influence of normal human ageing on automatic movements. *J. Physiol.* 562, 605–615. doi: 10.1113/jphysiol.2004.076042

Yamaguchi, K., Tohara, H., Hara, K., Nakane, A., Kajisa, E., Yoshimi, K., et al. (2018). Relationship of aging, skeletal muscle mass, and tooth loss with masseter muscle thickness. *BMC Geriatr.* 18:67. doi: 10.1186/s12877-018-0753-z

Yan, C., Ye, L., Zhen, J., Ke, L., and Gang, L. (2008). Neuroplasticity of edentulous patients with implant-supported full dentures. *Eur. J. Oral Sci.* 116, 387–393. doi: 10.1111/j.1600-0722.2008.00557.x

Conflict of Interest: The author declares that the research was conducted in the absence of any commercial or financial relationships that could be construed as a potential conflict of interest.

Copyright © 2020 Lin. This is an open-access article distributed under the terms of the Creative Commons Attribution License (CC BY). The use, distribution or reproduction in other forums is permitted, provided the original author(s) and the copyright owner(s) are credited and that the original publication in this journal is cited, in accordance with accepted academic practice. No use, distribution or reproduction is permitted which does not comply with these terms.



Subcortical Brain Abnormalities and Clinical Relevance in Patients With Hemifacial Spasm

Hui Xu^{1,2}, Chenguang Guo¹, Feifei Luo^{1,2}, Romina Sotoodeh³, Ming Zhang^{1*} and Yuan Wang^{1*}

¹ Department of Medical Imaging, The First Affiliated Hospital of Xi'an Jiaotong University, Xi'an, China, ² Key Laboratory of Biomedical Information Engineering of Education Ministry, Institute of Biomedical Engineering, Xi'an Jiaotong University, Xi'an, China, ³ Faculty of Dentistry, McGill University, Montreal, QC, Canada

OPEN ACCESS

Edited by:

Teresa Lever,
University of Missouri, United States

Reviewed by:

Matteo Bologna,
Sapienza University of Rome, Italy
Hao Song,
University of Freiburg, Germany
Guang Hui Bai,
Second Affiliated Hospital and Yuying
Children's Hospital of Wenzhou
Medical University, China

*Correspondence:

Ming Zhang
zhangming01@mail.xjtu.edu.cn
Yuan Wang
wangyuan8003@126.com

Specialty section:

This article was submitted to
Movement Disorders,
a section of the journal
Frontiers in Neurology

Received: 21 June 2019

Accepted: 16 December 2019

Published: 15 January 2020

Citation:

Xu H, Guo C, Luo F, Sotoodeh R,
Zhang M and Wang Y (2020)
Subcortical Brain Abnormalities and
Clinical Relevance in Patients With
Hemifacial Spasm.
Front. Neurol. 10:1383.
doi: 10.3389/fneur.2019.01383

Purpose: Hemifacial spasm (HFS), a rare neuromuscular movement disorder, is characterized by unilateral, irregular, and paroxysmal facial muscle contractions. To explore the central neural mechanisms of HFS, we conducted vertex-wise shape analyses to investigate volume and shape alterations of subcortical structures, which could help to better understand the abnormality in distinct subcortical regions and determine alternative biomarkers of HFS.

Methods: Thirty patients with HFS and 30 age- and sex-matched healthy controls provided written informed consent. T1-weighted structural magnetic resonance imaging (MRI) data were collected from all participants. Vertex-wise shape analyses were performed to assess the volume and shape alterations of subcortical structures following HFS. *Post hoc* correlations with spasm severity and measures of mood dysfunction were applied to characterize subcortical brain alterations.

Results: Compared with healthy controls, patients with HFS showed increased volume in the right caudate specifically. Furthermore, patients exhibited significant shape atrophy in the anterior medial aspect of left pallidum, together with shape expansion in the anterior ventrolateral aspect of right caudate head. In addition, shape alteration in right caudate was positively correlated with both anxiety and depression severity in patients with HFS.

Conclusions: This is the first study to employ vertex-wise shape analysis to investigate subcortical brain abnormalities in patients with HFS. Our findings provide compelling evidence for subcortical brain alterations specific to HFS, and further may shed light on the pathophysiology of HFS and apply to the translational medicine.

Keywords: hemifacial spasm, orofacial muscle contractions, subcortical brain abnormalities, affective symptoms, translational medicine

INTRODUCTION

Hemifacial spasm (HFS), a rare neuromuscular movement disorder, is characterized by unilateral, irregular, and paroxysmal facial muscle contractions (1, 2). Its spasms usually start in the orbicularis oculi muscle of the eyelid (3). As this disorder progresses, spasms spread to the orbicularis oris around lips and buccinator muscles at the cheekbone (4). HFS is not a life threatening condition with low incidence in the general population (5), but it is more prevalent among older adults and

inevitably causes social embarrassment and mental distress, which can affect patients' functioning and quality of life (6). Notably, patients with HFS demonstrate negative emotional symptoms, which have been reported to be related to brain structural alterations (7).

Subcortical structures including the basal ganglia and parts of the limbic system (8) have vital roles in learning, attention, memory, motor control, as well as emotion (9). Furthermore, they are integrally involved in cognitive executive functions through their structural and functional connectivity with high-order cortical areas (10). Prior studies have revealed alterations of subcortical regions in various psychiatric disorders including autism spectrum disorders (11), depression (12), and schizophrenia (13). However, little is known about the contribution of subcortical abnormalities to the progress of HFS, and it is not clear whether those alterations cause or result from HFS symptoms. To date, only one study has observed subcortical alterations in HFS, which demonstrated reduced gray matter volume in the thalamus, putamen, pallidum, and amygdala in patients with HFS compared to healthy volunteers (7). The data were processed by voxel-based morphometry (VBM) and traditional volumetric (i.e., total volume) approach with inherent limitations. Furthermore, the findings reflect a mix of variations in shape, volume, and position of subcortical structures, and depend on smoothing extents and accurate classification of tissue type.

Vertex-wise shape analysis has been applied in studies of subcortical morphology in various disorders (14–16), and has been approved to overcome the limitations from the VBM and traditional volumetric approach. This method uses a joint shape and appearance model to robustly determine the subcortical boundary. It then provides a local and direct measure of geometric change that does not depend on the tissue-type classification or arbitrary smoothing extent (17). To date, vertex-wise shape analysis has not been performed to characterize subcortical brain abnormalities in HFS condition.

Hence, in current study, we conducted vertex-wise shape analyses to investigate volume and shape alterations of subcortical structures in patients with HFS compared with matched healthy controls. The objectives of this study are to: (1) identify subcortical volume alterations in patients with HFS, (2) identify subcortical shape abnormalities in patients with HFS. Finally, we will test whether these subcortical abnormalities are associated with clinical data.

MATERIALS AND METHODS

Participants

Thirty patients with HFS (18 females, mean age 48.80 ± 11.73 years) were recruited from neurological clinics. The diagnosis of HFS was assessed by two experienced neurologists according to the following criteria as typical hemifacial muscle spasms with involuntary and intermittent onset and no neurological deficit or sensory loss. Exclusion criteria were: secondary HFS caused by tumors and cysts, significant premorbid psychiatric or neurological history, alcohol or substance misuse, and MRI contra-indicators (e.g., metal implants, claustrophobia). Thirty

age- and sex-matched healthy controls were recruited (18 females, mean age 49.77 ± 11.61 years). Participants had no history of psychiatric or neurological illness, alcohol or substance misuse. This study was conducted in accordance with the Declaration of Helsinki and had full ethical approval from the ethics committee of the first affiliated hospital of Xi'an Jiaotong University. Each participant gave written informed consent.

Neuropsychological Assessment

All subjects underwent a structured clinical interview and completed a brief psychological assessment. The Hamilton Anxiety Rating Scale (HAM-A) was used to evaluate anxiety symptoms (18, 19), and the Hamilton Depression Rating Scale (HAM-D) measured feelings of depression (20). The obtained data were reviewed by a psychiatrist who was blinded to the experimental groups. In addition, patients with HFS were also assessed by Cohen evaluation scale (21) to quantify severity of facial muscle contraction [0–4 scale: 0 = none; 1 = increased blinking caused by external stimuli; 2 = mild, noticeable fluttering, not incapacitating; 3 = moderate, very noticeable spasm, mildly incapacitating; 4 = severely incapacitating (unable to drive, read, etc.)].

MRI Data Acquisition

Neuroimaging data from patients with HFS and healthy controls were acquired on a 3.0-T scanner (Signa HDxt; GE Medical Systems, Waukesha, WI, USA) with an 8-channel phased-array head coil. For each subject, a T1-weighted high-resolution structural image was acquired using axial fast spoiled gradient recalled sequence with the following parameters: field of view (FOV) = $256 \text{ mm} \times 256 \text{ mm}$, matrix size = 256×256 , time of repetition (TR) = 10.7 ms, time of echo (TE) = 4.9 ms, flip angle (FA) = 15° , voxel size = $1.00 \times 1.00 \times 1.0 \text{ mm}^3$, and scan duration = 4 min and 51 s. Next, a resting-state functional magnetic resonance image scan and a diffusion tensor image scan were carried out immediately after the survey, but they were not discussed in this study.

Statistical Analysis of Demographical and Clinical Variables

Demographical and clinical characteristics of all subjects were analyzed using SPSS 25.0 software (Statistical Package for Social Sciences, Release 25.0, IBM, Chicago, IL), and parametric and non-parametric statistics were used as appropriate. Group differences in age, HAM-A score, HAM-D score were evaluated using independent samples *t*-tests; chi-square test was used to estimate sex difference between groups.

Vertex-Wise Shape Analyses

MRI data analysis was processed using FSL tools (FMRIB Software Library v6.0, <https://fsl.fmrib.ox.ac.uk/fsl/>) (22). First, brain tissue volume, normalized for participant head size, was estimated with SIENAX (Structural Image Evaluation, using Normalization, of Atrophy) (23), part of FSL. By using SINEAX, the volumes of neocortical gray matter (GM), total GM, white matter (WM), cerebral spinal fluid (CSF), total intracranial volume (TIV), and a volumetric scaling factor were acquired.

Second, FSL-integrated registration and segmentation toolbox (FIRST, part of FSL, <https://fsl.fmrib.ox.ac.uk/fsl/fslwiki/FIRST>) (17), a model based automated registration and segmentation tool, was used to specifically investigate neuroanatomical alterations of subcortical structures in shape. Briefly, all subcortical structures were segmented, from high-resolution structural images, based on shape and appearance models using Gaussian assumptions combined with a Bayesian probabilistic approach (17). Then, the volumetric labels in terms of meshes were automatically parameterized using deformable surfaces of each subcortical structure. And the normalized intensities along the surface of meshes were sampled and modeled. Finally, a shape appearance model was performed based on multivariate Gaussian assumptions. The shape was expressed as a mean with modes of variation. Quality of segmentation and registration of all subcortical structures were manually checked and confirmed for each subject.

For the normalized volume of brain tissue (GM, total GM, WM, CSF, and TIV) from SIENAX, we conducted a univariate mixed ANOVA with normalized volume as a dependent variable, group (patients with HFS and healthy controls) as a between-subjects factor and brain tissue as a within-subjects factor. SPSS 25.0 software was used for this statistical analysis.

Vertex-wise shape analyses of subcortical structures were performed using a general linear model (GLM) with permutation-based non-parametric testing (5,000 times permutation using randomize) to examine group differences. Maps showing significant group differences between patients with HFS and healthy controls were generated by thresholding the images of *t* statistics with cluster-based family-wise error (FWE) correction of $P < 0.05$.

Quality Control of Structural MRI

For anatomical data, we checked the image quality to ensure that there was no apparent motion artifact in each subject. All scans were field inhomogeneity corrected. During the structural MRI analysis, we inspected any artifact that could affect the processing, including segmentation, normalization, etc. All structural MR images from each participant were good for further analysis, so we included all participants (30 patients with HFS and 30 healthy controls, details seen in Table 1) in this study.

Volumetric Analyses

The absolute volumes of subcortical structures were calculated from FIRST using *fslstats* command (<https://fsl.fmrib.ox.ac.uk/fsl/fslwiki/Fslutils>). Then, normalized volumes of subcortical structures were obtained by multiplying those absolute volumes by a volumetric scaling factor of each subject from SIENAX.

To investigate volumetric alterations of subcortical structures in HFS, three-way mixed ANOVA with a between-subjects factor “group” (patients with HFS and healthy controls) and two within-subjects factors “hemispheres” (left and right) and “subcortical structures” (accumbens, amygdala, caudate, hippocampus, pallidum, putamen, and thalamus) was performed on normalized volumes. *Post hoc* analysis of simple-simple effect was carried out with Bonferroni corrections using SPSS

TABLE 1 | Demographics and clinical variables of patients with HFS and healthy controls.

| | Patients with HFS (SD) | Healthy controls (SD) | Significance, <i>P</i> -value |
|-----------------------------|------------------------|-----------------------|-------------------------------|
| Age (years) | 48.80 (11.73) | 49.77 (11.61) | $t_{58} = 0.32, P = 0.75$ |
| Sex (female/male) | 18/12 | 18/12 | $\chi^2 < 0.01, P > 0.99$ |
| Duration of disease (years) | 3.38 (3.53) | NA | NA |
| Scores of Cohen | 2.93 (0.74) | NA | NA |
| Scores of HAM-A | 5.23 (2.66) | 0.23 (0.57) | $t_{58} = 10.06, P < 0.01^*$ |
| Scores of HAM-D | 4.97 (2.77) | 0.23 (0.77) | $t_{58} = 9.01, P < 0.01^*$ |

HFS, hemifacial spasm; SD, Standard Deviation; Scores of Cohen, spasm severity rating via the Cohen evaluation scale; HAM-A, Hamilton Anxiety Rating Scale; HAM-D, Hamilton Depression Rating Scale; NA, not applicable. *Significant difference between patient and control groups.

25.0 software, and a threshold of $P < 0.05$ was considered statistically significant.

Correlation Analyses

To examine whether subcortical structures alterations would be associated with clinical parameters, non-parametric Spearman correlation analyses were performed between volume index or vertex index and clinical parameters in patients with HFS. The significance threshold was Bonferroni corrected for multiple comparisons. Therefore, findings were considered significant if the *P* value was < 0.0042 based on a *P* value $< 0.05/(3 \text{ subcortical abnormality indexes} \times 4 \text{ clinical variables per subcortical abnormality index})$.

RESULTS

Demographics and Neuropsychological Assessment

Patients with HFS and healthy controls were matched well for age (48.80 ± 11.73 years old for patients and 49.77 ± 11.61 years old for controls, $t_{58} = 0.32, P = 0.75$) and sex (60% female patients vs. 60% female controls, $\chi^2_1 < 0.01, P > 0.99$). In addition, patients with HFS reported significant levels of anxiety ($t_{58} = 10.06, P < 0.01$) and felt more depressed ($t_{58} = 9.01, P < 0.01$) than healthy controls, which were measured by HAM-A and HAM-D, respectively. Patients with HFS had moderate spasm severity (2.93 ± 0.74) with a mean disease duration of 3.38 years. Demographic and clinical data were all presented in Table 1.

Measures of Brain Tissue Volume

A 2×5 (Groups \times Brain Tissue) mixed measures ANOVA was performed to examine group differences according to brain tissue volume. Notably, there was no significant Group-by-Brain Tissue interaction [$F_{(4, 9)} = 1.218, P = 0.303$], reflecting the fact that there were no significant group differences in brain tissue (GM, total GM, WM, CSF, and TIV) volume.

Volume Alteration in Right Caudate

The $2 \times 2 \times 7$ (Groups \times Hemispheres \times Subcortical Structures) mixed measures ANOVA of subcortical volumes

revealed a significant Groups-by-Hemispheres-by-Subcortical Structures interaction effect [$F_{(6, 812)} = 9.13, P < 0.001$, **Table 2**]. A *post hoc* analysis was then performed on the interaction effect with Bonferroni adjustment and confirmed a significant difference in right caudate with greater volume in patients with HFS compared with healthy controls [$F_{(1, 825)} = 4.09, P = 0.043$, **Figure 1**]. Other subcortical structures did not show any volume alterations in HFS patients.

Shape Abnormalities in Left Pallidum and Right Caudate

Vertex-wise shape analyses revealed areas of significant shape atrophy in the anterior medial aspect of left pallidum in patients with HFS compared to healthy controls ($P < 0.05$, FWE

corrected; **Figure 2** and **Table 3**). Besides, patients with HFS exhibited significant shape expansion in the anterior ventrolateral aspect of right caudate head in contrast to healthy controls ($P < 0.05$, FWE corrected; **Figure 3** and **Table 3**). There were no significant alterations in other subcortical structures in patients compared to controls.

Subcortical Abnormalities Correlation With Clinical Parameters

Shape alterations in right caudate was positively correlated with both anxiety ($\rho = 0.861, P < 0.001$, Bonferroni corrected, **Figure 4**) and depression scale ($\rho = 0.723, P < 0.001$, Bonferroni corrected, **Figure 4**) in patients with HFS. No other significant correlations were observed in patients with HFS between other clinical parameters (disease duration, spasm severity) and subcortical structural alterations (all $P > 0.05$).

DISCUSSION

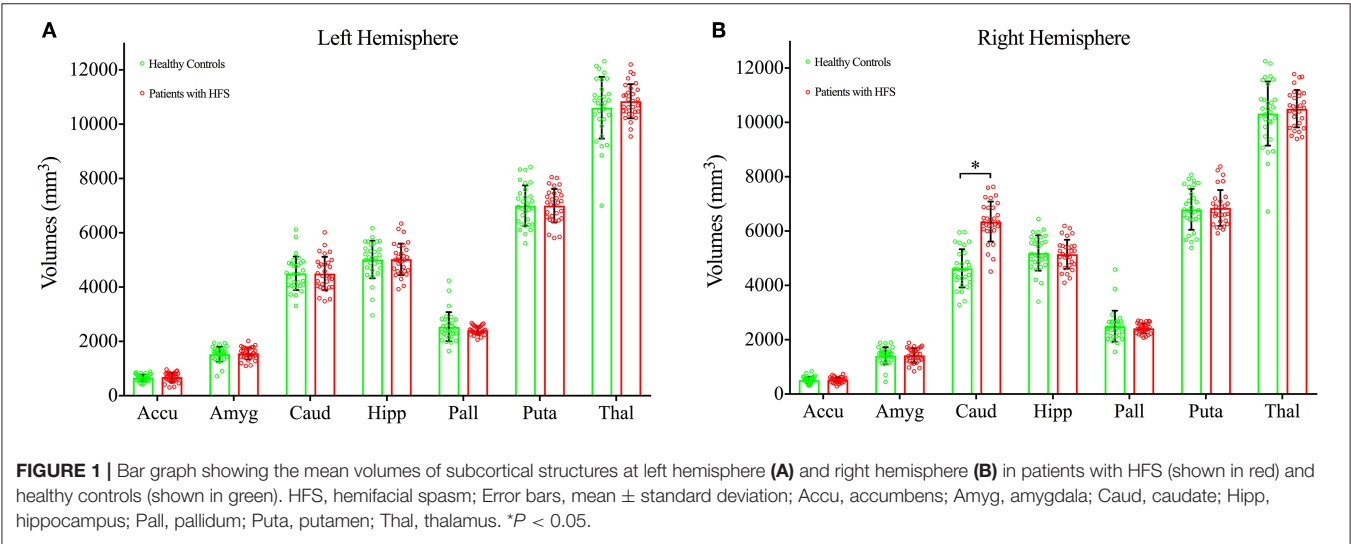
To our knowledge, this is the first study to employ vertex-wise shape analysis to investigate subcortical morphologic abnormalities in patients with HFS. The goal of this study was to examine subcortical aberrations in distinct subcortical regions and determine informative biomarkers of HFS. Among subcortical structures, we found increased volume specifically in the right caudate in patients with HFS compared with healthy controls. Moreover, patients with HFS exhibited significant shape atrophy in the anterior medial aspect of left pallidum, along with shape expansion in the anterior ventrolateral aspect of right caudate head when compared to healthy controls. In addition, more severe affective symptoms were associated with increased shape expansion in the anterior ventrolateral aspect of right caudate head in patients with HFS, providing support for the evidence that subcortical brain abnormalities reflect emotional disorders in patients with HFS (7).

Specifically, we observed that patients with HFS showed shape atrophy in anterior medial aspect of the left pallidum, which is known to link to motor abilities (24, 25). The

TABLE 2 | Normalized volumes (mm³) of subcortical structures in patients with HFS and healthy controls.

| Hemisphere | Subcortical structures | Patients with HFS (SD) | Healthy controls (SD) |
|------------|------------------------|------------------------|-----------------------|
| Left | Accumbens | 683.47 (172.25) | 660.86 (125.34) |
| | Amygdala | 1561.99 (225.25) | 1537.49 (274.04) |
| | Caudate | 4505.34 (614.87) | 4509.03 (618.91) |
| | Hippocampus | 5027.18 (583.45) | 5020.36 (690.21) |
| | Pallidum | 2411.15 (156.19) | 2545.55 (538.50) |
| | Putamen | 7002.80 (614.24) | 7002.59 (748.26) |
| | Thalamus | 10848.63 (630.63) | 10607.66 (1136.85) |
| Right | Accumbens | 522.71 (103.95) | 519.07 (127.30) |
| | Amygdala | 1422.99 (272.76) | 1413.56 (317.02) |
| | Caudate | 6350.62 (738.88) | 4632.59 (703.44) |
| | Hippocampus | 5151.10 (535.87) | 5193.64 (652.86) |
| | Pallidum | 2418.75 (186.37) | 2498.08 (568.78) |
| | Putamen | 6854.08 (659.67) | 6802.52 (752.00) |
| | Thalamus | 10507.01 (688.90) | 10332.04 (1180.14) |

HFS, hemifacial spasm; SD, Standard Deviation.



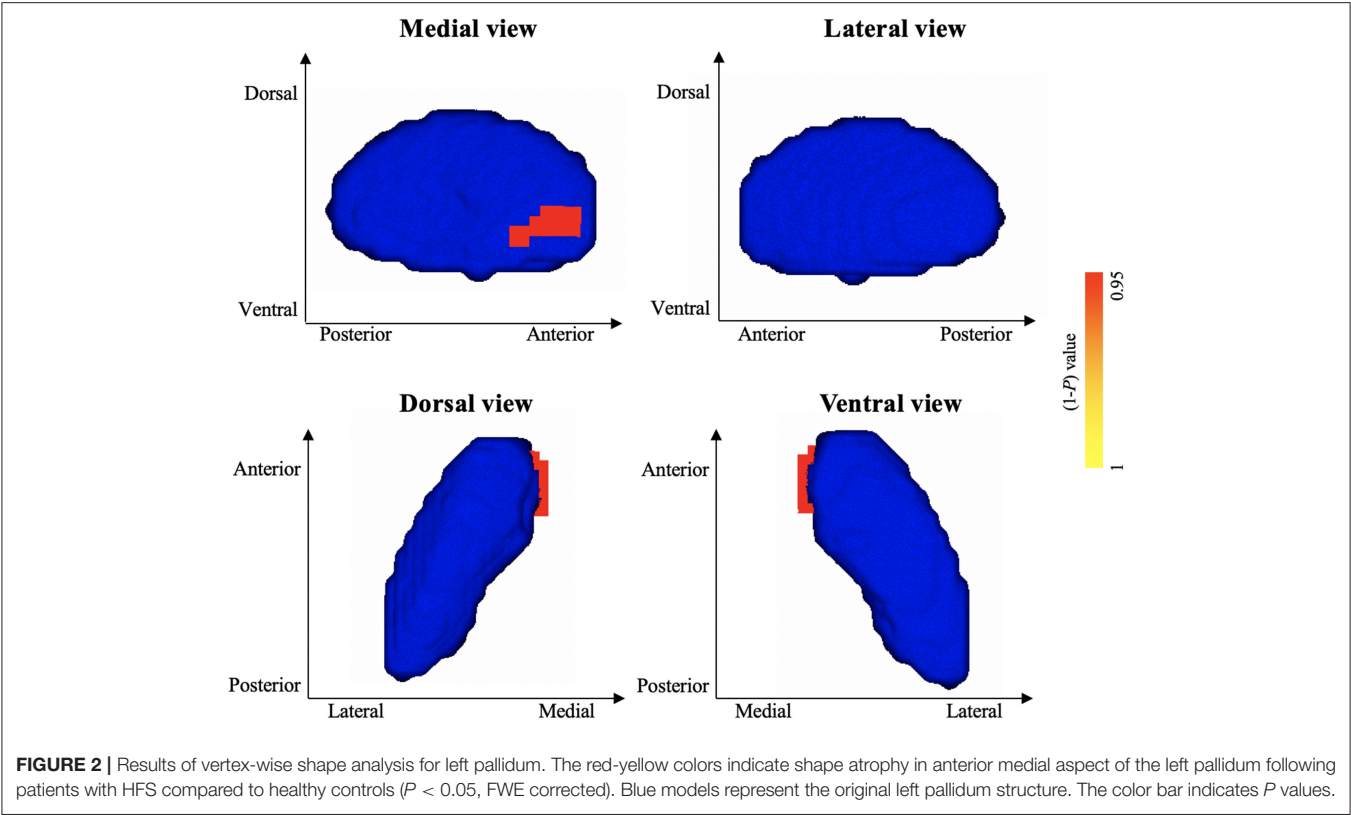


TABLE 3 | Shape abnormalities in left pallidum and right caudate following patients with HFS compared to healthy controls.

| Subcortical structure | Side | Vertices | Peak MNI coordinates | | | t | p^a |
|-------------------------------|------|----------|----------------------|----|----|-------|-------|
| | | | x | y | z | | |
| SHAPE ATROPHY IN HFS | | | | | | | |
| Pallidum | L | 23 | −11 | 5 | −3 | 3.841 | 0.027 |
| SHAPE EXPANSION IN HFS | | | | | | | |
| Caudate | R | 57 | 20 | 22 | −1 | 3.076 | 0.047 |

MNI, Montreal Neurological Institute; HFS, hemifacial spasm; L, left; R, right. ^a $P < 0.05$, family-wise error corrected.

pallidum is a hub inside the basal ganglia with widespread projections to all the other subcortical structures of the motor circuit (26) and receives highly convergent and topographically organized projections from the dorsal striatum (26). Pallidum alterations have been previously reported in other movement-related disorders (27, 28). To date, only one study that used VBM method reported volume alterations in the pallidum in patients with HFS (7). Possible explanations for this discrepancy may be the presence of focal disease related morphological changes within subcortical structures which does not affect the global brain volume significantly. Moreover, vertex-wise shape analyses permitted detection of shape deformations in localized areas among subcortical structures (17, 29). Shape atrophy of the left pallidum was found in HFS group, although no significant relationship was discovered between shape alteration of left pallidum and spasm severity. As the disorder progresses, spasms

inevitably cause severe dysfunction of facial muscles (4). Further research is needed to determine whether pallidum abnormality is associated with other movement functions in HFS.

Furthermore, we detected increased right caudate volume following HFS. Previous studies have observed caudate volume reduction in various disorders and its associations with mood symptoms (30, 31). However, our finding of the larger-than-normal volume of caudate was inconsistent with these previous findings. This discrepancy might be owing to social phobia and depression accompanied by HFS, which may, in turn, have a cumulative effect on the caudate morphology. Moreover, patients with HFS also exhibited shape expansion in the anterior ventrolateral aspect of right caudate head. It should be noted that the ventral caudate is well-known as a vital component of the ventral striatum, and its related-neural circuits are involved in emotional processing (32, 33). Hence, shape expansion of ventral caudate in HFS may be due to the mood dysfunctions suffered by patients inducing ventral caudate alterations as this disorder progresses.

In addition, shape alteration in the right caudate was positively correlated with both anxiety and depression scale in patients with HFS, supporting an interaction that links mood dysfunctions to subcortical morphologic abnormalities in HFS. Previous studies have proved that caudate abnormality was significantly associated with depression severity in late-life depressive disorder (30) and anxiety levels in generalized anxiety disorder (34). The right caudate volume and shape abnormalities suggest that the caudate plays a critical role in mood characteristic of HFS, even though the temporal or pathophysiologic nature of caudate alterations

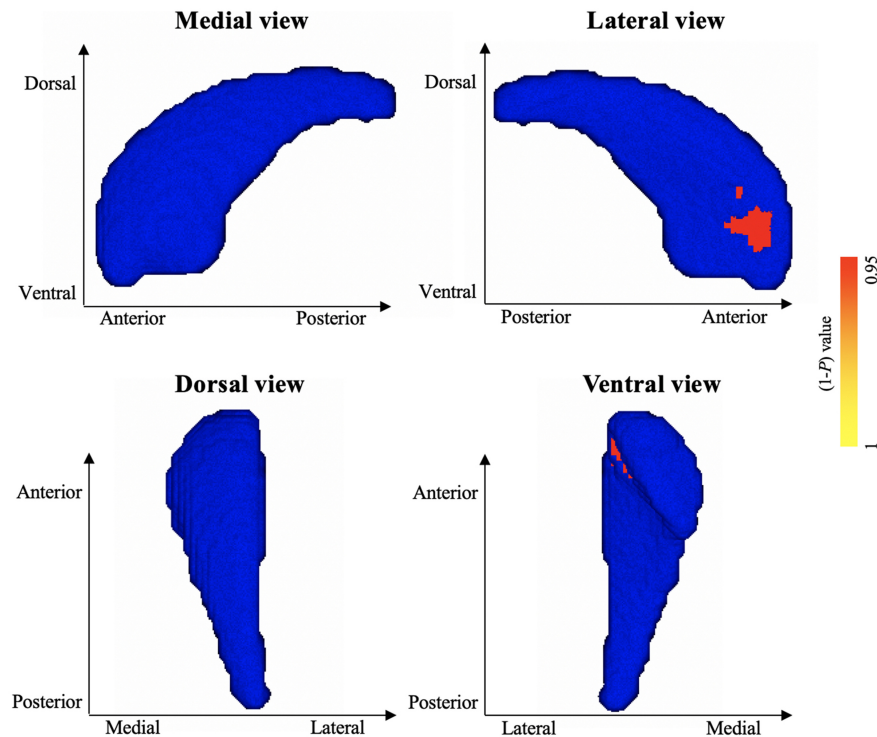


FIGURE 3 | Results of vertex-wise shape analysis for right caudate. The red-yellow colors indicate shape expansion in anterior ventrolateral aspect of the right caudate head in patients with HFS compared with healthy controls ($P < 0.05$, FWE corrected). Blue models represent the original right caudate structure. The color bar indicates P values.

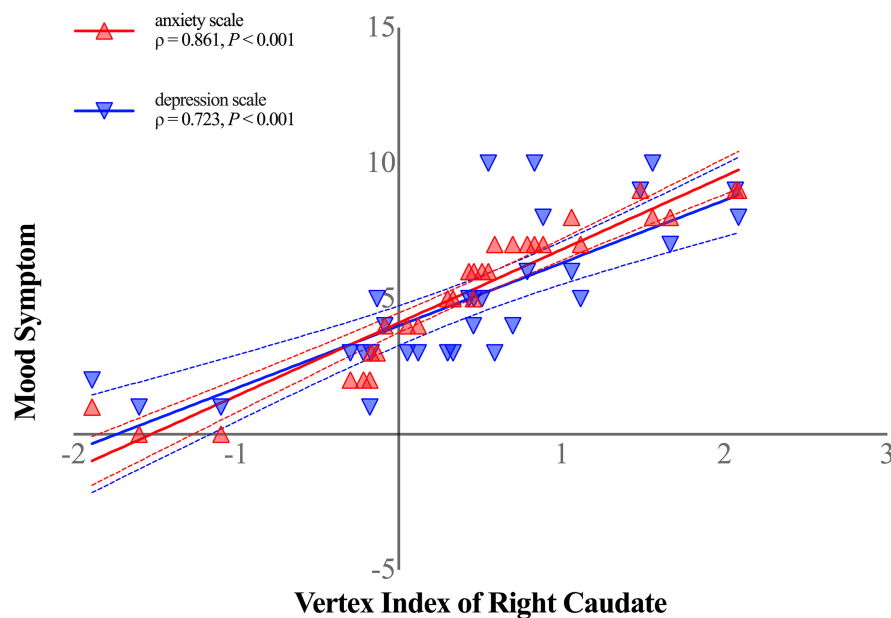


FIGURE 4 | Shape alterations in right caudate was positively correlated with anxiety symptom (shown in red-filled triangle; $\rho = 0.861, P < 0.001$, Bonferroni corrected) and depression symptom (shown in blue-filled upside-down triangle; $\rho = 0.723, P < 0.001$, Bonferroni corrected) in patients with HFS. Curved dashed lines indicate 95% confidence intervals. The vertex index of anterior ventrolateral aspect of the right caudate head represented shape alterations in patients with HFS. The anxiety symptom was measured by Hamilton Anxiety Scale, and Hamilton Depression Scale was performed to assess patients' depression symptom.

in HFS have not been previously reported. It is unknown whether mood dysfunction leads to cellular alteration or vice versa in caudate as HFS progresses. However, because these relationships were identified in HFS, our findings suggest that caudate abnormalities could be important for further study of trans-diagnostic brain-behavior relations in HFS.

Several limitations of this study bear acknowledgment here. First, the sample size of both groups is small. Future work with larger samples is needed to confirm these findings and improve the reliability of the results. Furthermore, the affected side of HFS need to be considered with a large sample size of patients in future work. Second, we could not examine whether subcortical abnormalities observed herein precede HFS symptoms, precipitating their development, or instead represent sequelae of mood dysfunctions in our cross-sectional design. Prospective longitudinal studies are needed to delineate causes from consequences in the underlying mechanism of subcortical brain alterations in HFS.

In summary, this is the first study to employ vertex-wise shape analysis in HFS, which can reveal precisely subtle and localized alterations among subcortical structures. Compared with healthy controls, patients with HFS showed increased volume specifically in the right caudate. In addition, patients with HFS exhibited significant shape atrophy in the anterior medial aspect of left pallidum together with shape expansion in the anterior ventrolateral aspect of right caudate head. Moreover, shape alterations in right caudate were positively correlated with both anxiety and depression scale in patients with HFS. Taken together, our findings provide compelling evidence for subcortical brain abnormalities specific to HFS, and further may shed light on the pathophysiology of HFS and apply to the translational medicine.

REFERENCES

- Jannetta PJ. Typical or atypical hemifacial spasm. *J Neurosurg.* (1998) 89:346–7. doi: 10.3171/jns.1998.89.2.0346
- Colosimo C, Bologna M, Lamberti S, Avanzino L, Marinelli L, Fabbrini G, et al. A comparative study of primary and secondary hemifacial spasm. *Arch Neurol Chicago.* (2006) 63:441–4. doi: 10.1001/archneur.63.3.441
- Pleger B. The structure of facial spasms. *Clin Neurophysiol.* (2016) 127:1003–4. doi: 10.1016/j.clinph.2015.08.003
- Au WL, Tan LC, Tan AK. Hemifacial spasm in Singapore: clinical characteristics and patients' perceptions. *Ann Acad Med Singapore.* (2004) 33:324–8.
- Barker FG II, Jannetta PJ, Bissonette DJ, Shields PT, Larkins MV, Jho HD. Microvascular decompression for hemifacial spasm. *J Neurosurg.* (1995) 82:201–10. doi: 10.3171/jns.1995.82.2.0201
- Xu H, Guo C, Li H, Gao L, Zhang M, Wang Y. Structural and functional amygdala abnormalities in hemifacial spasm. *Front Neurol.* (2019) 10:393. doi: 10.3389/fneur.2019.00393
- Bao F, Wang Y, Liu J, Mao C, Ma S, Guo C, et al. Structural changes in the CNS of patients with hemifacial spasm. *Neuroscience.* (2015) 289:56–62. doi: 10.1016/j.neuroscience.2014.12.070
- Johnson MH. Subcortical face processing. *Nat Rev Neurosci.* (2005) 6:766–74. doi: 10.1038/nrn1766
- van Schouwenburg MR, den Ouden HE, Cools R. The human basal ganglia modulate frontal-posterior connectivity during attention shifting. *J Neurosci.* (2010) 30:9910–8. doi: 10.1523/JNEUROSCI.1111-10.2010
- Fischi-Gomez E, Vasung L, Meskaldji DE, Lazeyras F, Borradori-Tolsa C, Hagmann P, et al. Structural brain connectivity in school-age preterm infants provides evidence for impaired networks relevant for higher order cognitive skills and social cognition. *Cereb Cortex.* (2015) 25:2793–805. doi: 10.1093/cercor/bhu073
- Hoogman M, Buitelaar JK, Faraone SV, Shaw P, Franke B, ENIGMA-ADHD working group. Subcortical brain volume differences in participants with attention deficit hyperactivity disorder in children and adults - Authors' reply. *Lancet Psychiatry.* (2017) 4:440–1. doi: 10.1016/S2215-0366(17)30200-6
- Schmaal L, Veltman DJ, van Erp TG, Samann PG, Frodl T, Jahanshad N, et al. Subcortical brain alterations in major depressive disorder: findings from the ENIGMA Major Depressive Disorder working group. *Mol Psychiatry.* (2016) 21:806–12. doi: 10.1038/mp.2015.69
- Rimol LM, Hartberg CB, Nesvag R, Fennema-Notestine C, Hagler DJ Jr, Pung CJ, et al. Cortical thickness and subcortical volumes in schizophrenia and bipolar disorder. *Biol Psychiatry.* (2010) 68:41–50. doi: 10.1016/j.biopsych.2010.03.036
- Opel N, Redlich R, Zwanzger P, Grotegerd D, Arolt V, Heindel W, et al. Hippocampal atrophy in major depression: a function of childhood maltreatment rather than diagnosis? *Neuropsychopharmacology.* (2014) 39:2723–31. doi: 10.1038/npp.2014.145
- Mao CP, Yang HJ. Smaller amygdala volumes in patients with chronic low back pain compared with healthy control individuals. *J Pain.* (2015) 16:1366–76. doi: 10.1016/j.jpain.2015.08.012

DATA AVAILABILITY STATEMENT

The datasets generated for this study are available on request to the corresponding author.

ETHICS STATEMENT

Written informed consent was obtained from all subjects prior to participation in accordance with the Declaration of Helsinki. This study was approved by the Ethical Committee of the first affiliated hospital of Xi'an Jiaotong University.

AUTHOR CONTRIBUTIONS

YW, MZ, and HX contributed to study concept/design, analysis and interpretation of data, statistical analysis, and drafting manuscript. CG and FL contributed to data acquisition, interpretation, and manuscript revision. HX and RS contributed to statistical analysis and language help.

FUNDING

This study was funded by the Natural Science Foundation of Shaanxi Province (No. 2018JM7026), Xi'an Science and Technology Project [No. 201805102YX10SF36(3)], and Fundamental Research Funds for the Central Universities in Xi'an Jiaotong University (No. xjj2018272).

ACKNOWLEDGMENTS

We thank Dr. Faxiu Bao for her assistance with recruiting HFS patients.

16. Husoy AK, Pintzka C, Eikenes L, Haberg AK, Hagen K, Linde M, et al. Volume and shape of subcortical grey matter structures related to headache: a cross-sectional population-based imaging study in the Nord-Trøndelag Health Study. *Cephalalgia*. (2019) 39:173–84. doi: 10.1177/0333102418780632
17. Patenaude B, Smith SM, Kennedy DN, Jenkinson M. A Bayesian model of shape and appearance for subcortical brain segmentation. *Neuroimage*. (2011) 56:907–22. doi: 10.1016/j.neuroimage.2011.02.046
18. Maier W, Buller R, Philipp M, Heuser I. The Hamilton Anxiety Scale: reliability, validity and sensitivity to change in anxiety and depressive disorders. *J Affect Disord*. (1988) 14:61–8. doi: 10.1016/0165-0327(88)90072-9
19. Wang Y, Cao D-y, Remeniuk B, Krimmel S, Seminowicz DA, Zhang M. Altered brain structure and function associated with sensory and affective components of classic trigeminal neuralgia. *Pain*. (2017) 158:1561–70. doi: 10.1097/j.pain.0000000000000951
20. Hamilton M. A rating scale for depression. *J Neurol Neurosurg Psychiatry*. (1960) 23:56–62. doi: 10.1136/jnnp.23.1.56
21. Cohen DA, Savino PJ, Stern MB, Hurtig HI. Botulinum injection therapy for blepharospasm: a review and report of 75 patients. *Clin Neuropharmacol*. (1986) 9:415–29. doi: 10.1097/00002826-198610000-00002
22. Jenkinson M, Beckmann CF, Behrens TE, Woolrich MW, Smith SM. Fsl. *Neuroimage*. (2012) 62:782–90. doi: 10.1016/j.neuroimage.2011.09.015
23. Smith SM, Zhang Y, Jenkinson M, Chen J, Matthews PM, Federico A, et al. Accurate, robust, and automated longitudinal and cross-sectional brain change analysis. *Neuroimage*. (2002) 17:479–89. doi: 10.1006/nimg.2002.1040
24. DeVito JL, Anderson ME. An autoradiographic study of efferent connections of the globus pallidus in *Macaca mulatta*. *Exp Brain Res*. (1982) 46:107–17. doi: 10.1007/BF00238104
25. Hardman CD, Halliday GM. The external globus pallidus in patients with Parkinson's disease and progressive supranuclear palsy. *Mov Disord*. (1999) 14:626–33. doi: 10.1002/1531-8257(199907)14:4<626::AID-MDS1012>3.0.CO;2-U
26. Schwab BC, van Wezel RJA, van Gils SA. Sparse pallidal connections shape synchrony in a network model of the basal ganglia. *Eur J Neurosci*. (2017) 45:1000–12. doi: 10.1111/ejn.13324
27. Saini J, Bagepally BS, Sandhya M, Pasha SA, Yadav R, Thennarasu K, et al. Subcortical structures in progressive supranuclear palsy: vertex-based analysis. *Eur J Neurol*. (2013) 20:493–501. doi: 10.1111/j.1468-1331.2012.03884.x
28. Rahayel S, Postuma RB, Montplaisir J, Bedetti C, Brambati S, Carrier J, et al. Abnormal gray matter shape, thickness, and volume in the motor cortico-subcortical loop in idiopathic rapid eye movement sleep behavior disorder: association with clinical and motor features. *Cereb Cortex*. (2018) 28:658–71. doi: 10.1093/cercor/bhx137
29. Smith Y, Kiehl JZ. Anatomy of the dopamine system in the basal ganglia. *Trends Neurosci*. (2000) 23 (10 Suppl.):S28–33. doi: 10.1016/S1471-1931(00)00023-9
30. Butters MA, Aizenstein HJ, Hayashi KM, Meltzer CC, Seaman J, Reynolds CF III, et al. Three-dimensional surface mapping of the caudate nucleus in late-life depression. *Am J Geriatr Psychiatry*. (2009) 17:4–12. doi: 10.1097/JGP.0b013e31816ff72b
31. Koo M-S, Levitt JJ, McCarley RW, Seidman LJ, Dickey CC, Niznikiewicz MA, et al. Reduction of caudate nucleus volumes in neuroleptic-naïve female subjects with schizotypal personality disorder. *Biol Psychiatry*. (2006) 60:40–8. doi: 10.1016/j.biopsych.2005.09.028
32. Postuma RB, Dagher A. Basal ganglia functional connectivity based on a meta-analysis of 126 positron emission tomography and functional magnetic resonance imaging publications. *Cereb Cortex*. (2006) 16:1508–21. doi: 10.1093/cercor/bhj088
33. Xu H, Zhao T, Luo F, Zheng Y. Dissociative changes in gray matter volume following electroconvulsive therapy in major depressive disorder: a longitudinal structural magnetic resonance imaging study. *Neuroradiology*. (2019) 61:1297–308. doi: 10.1007/s00234-019-02276-z
34. Hilbert K, Pine DS, Muehlhan M, Lueken U, Steudte-Schmiedgen S, Beesdo-Baum K. Gray and white matter volume abnormalities in generalized anxiety disorder by categorical and dimensional characterization. *Psychiatry Res*. (2015) 234:314–20. doi: 10.1016/j.psychres.2015.10.009

Conflict of Interest: The authors declare that the research was conducted in the absence of any commercial or financial relationships that could be construed as a potential conflict of interest.

Copyright © 2020 Xu, Guo, Luo, Sotoodeh, Zhang and Wang. This is an open-access article distributed under the terms of the Creative Commons Attribution License (CC BY). The use, distribution or reproduction in other forums is permitted, provided the original author(s) and the copyright owner(s) are credited and that the original publication in this journal is cited, in accordance with accepted academic practice. No use, distribution or reproduction is permitted which does not comply with these terms.



Functional Analysis of Rhythmic Jaw Movements Evoked by Electrical Stimulation of the Cortical Masticatory Area During Low Occlusal Loading in Growing Rats

Phyo Thura Aung, Chiho Kato*, Yasunori Abe, Takuya Ogawa, Hideyuki Ishidori, Akiyo Fujita, Hidemasa Okihara, Satoshi Kokai and Takashi Ono

Department of Orthodontic Science, Graduate School of Medical and Dental Sciences, Tokyo Medical and Dental University, Tokyo, Japan

OPEN ACCESS

Edited by:

Limor Avivi-Arber,
University of Toronto, Canada

Reviewed by:

Arlotte Kolta,
Université de Montréal, Canada
Alexandros E. Tsouknidas,
University of Western Macedonia,
Greece

*Correspondence:

Chiho Kato
katorts@tmd.ac.jp

Specialty section:

This article was submitted to
Craniofacial Biology and Dental
Research,
a section of the journal
Frontiers in Physiology

Received: 30 August 2019

Accepted: 16 January 2020

Published: 31 January 2020

Citation:

Aung PT, Kato C, Abe Y, Ogawa T, Ishidori H, Fujita A, Okihara H, Kokai S and Ono T (2020) Functional Analysis of Rhythmic Jaw Movements Evoked by Electrical Stimulation of the Cortical Masticatory Area During Low Occlusal Loading in Growing Rats. *Front. Physiol.* 11:34. doi: 10.3389/fphys.2020.00034

The maturation of rhythmic jaw movements (RJMs) and related neuromuscular control has rarely been studied in animals, though this process is essential for regulating the development of stomatognathic functions. Previous studies have shown that occlusal hypofunction during growth alters masticatory performance. However, little is known about patterns of cortically-induced RJMs under conditions of soft-diet feeding during development. The aim of this study is to clarify the effect of low occlusal loading on the pattern of cortically induced RJMs and related neuromuscular responses in growing rats. Sixty-four 2-week-old male albino Wistar rats were randomly divided into two groups and fed on either a normal diet (control) or soft diet (experimental) soon after weaning. At 5, 7, 9, and 11 weeks of age, electromyographic (EMG) activity was recorded from the right masseter and anterior digastric muscles along with corresponding kinematic images in RJMs during repetitive intracortical microstimulation of the left cortical masticatory area (CMA). Rats in both groups showed an increase in gape size and lateral excursion until 9 weeks of age. The vertical jaw movement speed in both groups showed no significant difference between 5 and 7 weeks of age but increased with age from 9 to 11 weeks. Compared to the control group, the average gape size and vertical speed were significantly lower in the experimental group, and the pattern and rhythm of the jaw movement cycle were similar between both groups at each recording age. EMG recordings showed no age-related significant differences in onset latency, duration, and peak-to-peak amplitude. Moreover, we found significantly longer onset latency, smaller peak-to-peak amplitude, and greater drop-off mean and median frequencies in the experimental group than in the control group, while there was no significant difference in the duration between groups. These findings indicate that a lack of enough occlusal function in infancy impedes the development of patterns of RJMs and delays the neuromuscular response from specific stimulation of the CMA.

Keywords: rhythmic jaw movements, cortical masticatory area, intracortical microstimulation, electromyography, soft diet, rat

INTRODUCTION

Mastication involves complex neuromuscular interactions between central and peripheral control mechanisms. The masticatory process is assisted by the coordinated movement of the tongue, jaw, and masticatory muscles, followed by the appropriate positioning of the jaw during opening and closing (Nakamura and Katakura, 1995). With growth-related changes, modifications of masticatory functions occur in response to varying functional demands. The critical step for the development of mastication appears to begin around the weaning period because the main feeding process changes from sucking to chewing. Subsequently, many morphological changes occur, including tooth eruption, an increase in muscle mass and jaw growth, and maturation of the nervous system (Herring, 1985).

Masticatory movements are generated by neural mechanisms originating in the brain. Research into typical rhythmic jaw movements (RJMs) is essential for understanding the development of masticatory functions in mammals. RJMs are generated by interconnected neural systems termed the masticatory central pattern generator (CPG), which is located in the brainstem (Lund, 1991). In order to produce the complex and variable patterns of mastication-like behavior, the CPG can be modulated by inputs from peripheral afferents as well as higher centers such as the cortical masticatory area (CMA) (Lund et al., 1981; Lund, 1991; Nakamura and Katakura, 1995). RJMs can be generated at the cortical level through repetitive intracortical microstimulation of the CMA (Avivi-Arber et al., 2011; Avivi-Arber and Sessle, 2018). In addition, intracortical microstimulation of the CMA can evoke orofacial movements and electromyographic (EMG) activity within the orofacial muscles (Neafsey et al., 1986). The CMA is composed of areas encompassing the sensorimotor cortex, which also evokes RJMs when it is stimulated with repetitive electrical stimulation. Several studies have reported that different areas of the CMA evoke different RJM patterns and jaw muscle EMG activity in rats (Sasamoto et al., 1990; Satoh et al., 2007; Maeda et al., 2014), guinea pigs (Isogai et al., 2012), rabbits (Lund et al., 1984), and monkeys (Huang et al., 1989). Moreover, stimulation of the postero-lateral region of the CMA induces grinding movements that resemble natural chewing patterns in rats (Sasamoto et al., 1990).

Daily masticatory muscle activity is associated with the development of the masticatory system. Currently, modern dietary forms tend to be soft and easily digested, which dramatically influences the growth of a normal stomatognathic system (Proffit et al., 1998). Prolonged changes in masticatory function could lead to altered craniofacial morphology (Hichijo et al., 2014; Kufley et al., 2017), development of muscle fibers of masticatory muscles (Grunheid et al., 2009; Kawai et al., 2010), and neuronal connections in the hippocampus (Okihara et al., 2014; Aneagawa et al., 2015). Recent studies have suggested that changes in masticatory function have an influence in motor representations within the sensorimotor cortex (Avivi-Arber et al., 2010a,b, 2015). With regards to masticatory functions, previous studies have shown that changes in loading force produce alterations in masticatory patterns and rhythm when

chewing normal or soft food (Yamada et al., 2006; Fujishita et al., 2015). However, the development of RJMs in association with the CMA have been rarely described to date, in relation to changing occlusal function during maturation.

Our aim was to evaluate the developmental course of specific RJMs that are evoked by stimulation of the CMA, and to examine the effect of changing occlusal loading on cortically-induced RJMs and associated neuromuscular responses during development. Jaw movement regulation is of key importance for masticatory performance during early chewing. Thus, we hypothesized that the effect of decreased occlusal loading through feeding with a soft diet might negatively affect the regulation of RJMs evoked by the CMA during development. We examined both jaw movement trajectories and EMG activities of the jaw muscles of rats fed on a soft diet. These findings were compared with a control group fed a normal diet and across age groups to examine whether low occlusal loading impeded the maturation of jaw movements during the period when the development of a mechanism of mastication is activated.

MATERIALS AND METHODS

Animal Model and Surgical Preparation

This study was performed according to the recommendations of the guide for the Institutional Animal Care and Use Committee (A2017-135A and A2018-028A) in compliance with the Animal Care Standards of Tokyo Medical and Dental University.

Sixty-four albino Wistar rats were used in this study (male, 2-weeks-old). All young cubs were examined and confirmed to be weaning to prevent any experience of chewing a solid diet from being included in the experimental group. Immediately after weaning, infants were divided into two equally-sized groups receiving: normal diet (control), fed with ordinary chow pellet (CE-2, CLEA, Inc., Tokyo, Japan) ($n = 32$); and soft diet (experimental), fed with powder pellet (<0.02 mm diameter) ($n = 32$) until 11 weeks of age. Both groups were weighed weekly throughout the entire experimental period.

All rats underwent the experimental procedure at 5, 7, 9, or 11 weeks of age ($n = 8$ per group per time point). Ketamine-HCl [100 mg/kg, intraperitoneal (IP)] injection was administered initially for the craniotomy and EMG electrode insertion. Supplementary doses were injected whenever necessary to maintain a constant level of anesthesia according to checks of vibrissa movements, pinch-withdrawal, and corneal reflexes throughout the experiments. The local anesthetic lidocaine hydrochloride (2%) was injected into the subcutaneous space below the planned surgical areas. Body temperature was maintained at 37–38°C using a thermo-regulated heating pad.

To record EMG activity from the jaw muscles, a midline incision was made along the neck from the mandible on the ventral surface to the rostral portion to expose the right side of masseter (jaw-closer) and anterior digastric (jaw-opener) muscles. Bipolar EMG electrodes (40 gauge, single-stranded, Teflon insulated stainless-steel wires, 2 mm inter-electrode distance) were then inserted into the muscles to record EMG activity.

To stimulate the cerebral cortex, part of the left frontal and parietal bones were drilled using a dental bar to expose the outer surface of the masticatory cortex, and the dura mater was covered with paraffin liquid oil (37°C). The lower incisors were ground to approximately 1 mm to minimize interference of jaw and tongue movements, especially at 9 and 11 weeks of age. The rat was then secured in a stereotaxic apparatus (models SN-2 and Sm-15M; Narishige Scientific Instruments, Tokyo, Japan). A fine glass-insulated tungsten microelectrode (shaft diameter 100 μ m, impedance 1–3 M Ω at 1 kHz; Unique Medical, Tokyo, Japan) was inserted vertically into the masticatory area of the cerebral cortex. Electrical stimulation (0.5 ms duration, 20 Hz, 180 μ A, 7 s) was applied to the left CMA (0–2 mm rostral, 4–5.5 mm lateral to Bregma, 4–5 mm ventral). A reference electrode was attached to the exposed neck muscle. RJMs were determined by the mandibular movements and rhythmic bursts of the anterior digastric and masseter EMG activities. Three trials of stimulation were performed at each stimulation site.

Recording of Jaw Movements and EMG Activity

For recording sessions, a wire (0.7 mm thick) attached to a marker was placed between the lower incisors attached with dental resin. A digital high-speed HAS-U1M camera (DITECT, Corp., Tokyo, Japan) was set directly in front of the marker to detect jaw movements. During stimulation, a videotape of the jaw movements was recorded, and 2D motion analysis system software (Dipp-motion V, DITECT, Corp., Tokyo, Japan) was used to refine the marker position of the jaw movements.

Signals of EMG activity were filtered and amplified using a multichannel amplifier (MEG-6108; Nihon Kohden, Tokyo, Japan; 1000x gain, bandpass 0.3–3 kHz), and all EMG waveforms were rectified and averaged. Data were analyzed offline using the CED 1401 interface and Spike2 software for Windows, version 5.21 (Cambridge Electronic Design, Cambridge, United Kingdom). EMG responses of each muscle were analyzed in a fast sweep. To analyze the specific characteristics of the EMG, the sonogram was calculated based on the peak root-mean-square EMG activity, and the power spectrum was displayed using fast Fourier transform.

The RJMs and EMG activities were stored on a computer disk. Jaw movement patterns during stimulation were observed from the frontal plane. The jaw movement parameters measured were: (1) gape size (vertical excursion between maximum opening and maximum closing), (2) lateral excursion (horizontal distance between minimum jaw-opening position and the most lateral jaw position), (3) speed of vertical jaw movements (rate of jaw movement distance per s), (4) changes in the vertical jaw movement pattern (the 13 points traced with an interval of 10 ms along the path of one cycle of jaw movement), (5) jaw-opening duration (time between maximum closing and subsequent maximum opening), (6) jaw-closing duration (time between maximum opening and subsequent maximum closing), (7) total cycle duration (duration between two consecutive

maximum openings), (8) rhythm of jaw movements during stimulation (total cycle duration of the jaw movement during stimulation at each time point per s), (9) changes in amplitude of vertical jaw movements (gape size) in relation to the time in the sequence (total duration of stimulation divided into three equal periods: early, middle, and late, corresponding to the first, second, and third, for 2 s respectively). Jaw muscle activity was analyzed in terms of (1) onset latency (interval between the onset of the stimulus and the onset of the first response), (2) duration (interval between the onset and offset of the first response), (3) peak-to-peak amplitude (amplitude from baseline to the positive peak of the first response), (4) median frequency from the power spectrum (the EMG power spectrum divided into two halves with equal amplitude) and (5) mean frequency of the power spectrum (average frequency which is calculated as the sum of product of the EMG power spectrum and the frequency divided by the total sum of the power spectrum) (Phinyomark et al., 2012). The mean values of data for each parameter were measured from 10 chewing cycles. The EMG bursts were identified when the rectified EMG exceeded the mean by 2SD. All values are expressed as mean \pm standard deviation.

Statistical Analysis

Significant differences between control and experimental groups were determined by using an unpaired *t*-test, and repeated measures multivariate analysis for intergroup and intragroup comparisons of jaw movement trajectories and EMG activities. Simple *post hoc* tests using the Sidak adjustment were performed for multiple comparisons. Statistical analysis was performed with SPSS for Windows, version 23 (SPSS, Inc., Chicago, IL, United States), and *p*-values less than 0.05 or 0.01 were considered to be statistically significant.

Histological Identification of Electrode Position

After the experiment had been completed and rats remained on the stereotaxic apparatus, they were anesthetized with Ketamine-HCl (20 mg/kg, IP) and the electrode was reinserted into some of the cortical areas at which RJMs had been induced and electrical lesions were created by passing currents (30 μ A for 20 s) through the stimulating electrode. The rats were then deeply anesthetized and perfused with 100 ml of phosphate-buffered saline (PBS; pH 7.4) through the left cardiac ventricle followed by 300 ml of fixative solution of 4% paraformaldehyde. Serial coronal sections of the brain (50 μ m thick) were cut and counterstained with hematoxylin-eosin stain. The locations of the electrode tips were confirmed under a light microscope and verified using the reference (Paxinos and Watson, 2007) (Figure 1).

RESULTS

Body Weight

Body weights of the rats in both groups increased gradually throughout the experimental period, and there were no

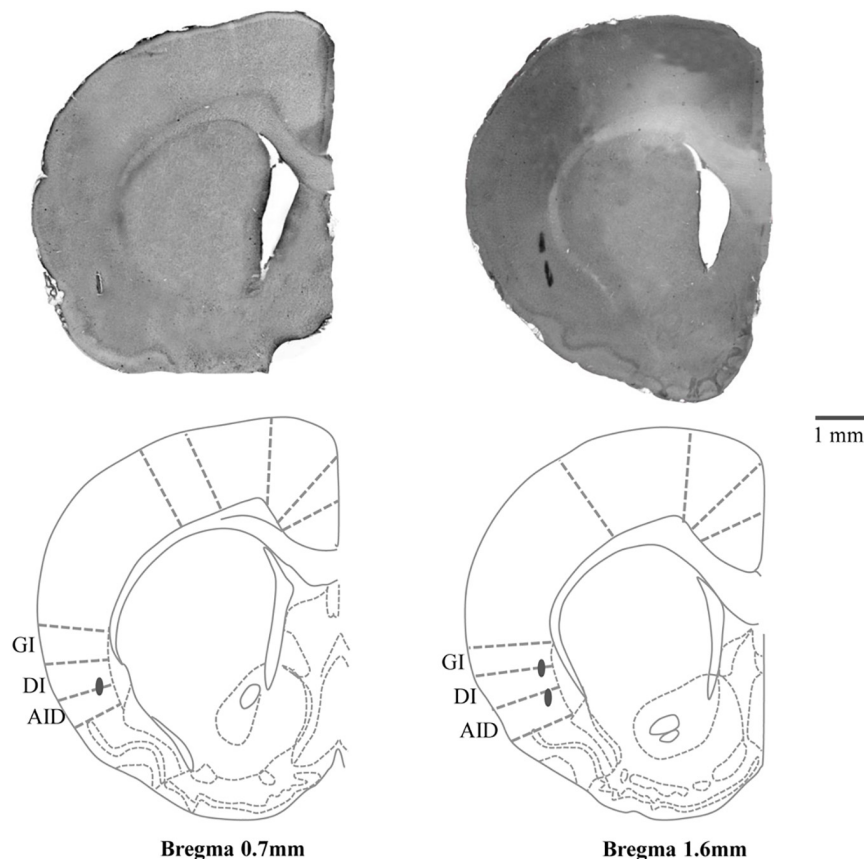


FIGURE 1 | Hematoxylin-eosin stained coronal section (50 μ m) with schematic drawing of the stimulation sites in the posterolateral part of left cortical masticatory area (CMA). Gray circles indicate the electrolytic lesions of the stimulation sites. Relative distances from Bregma in the rostral (0.7 and 1.6 mm anterior to the Bregma) direction are depicted. Template from the brain atlas (Paxinos and Watson, 2007), illustrating the left insular cortices (posterolateral part of CMA) showing the location of stimulation sites. Gl, granular insular cortex; DI, dysgranular insular cortex; AID, dorsal part of the agranular insular cortex.

significant differences in mean body weight between groups at any time point (**Figure 2**).

Jaw Movement Trajectories During Stimulation

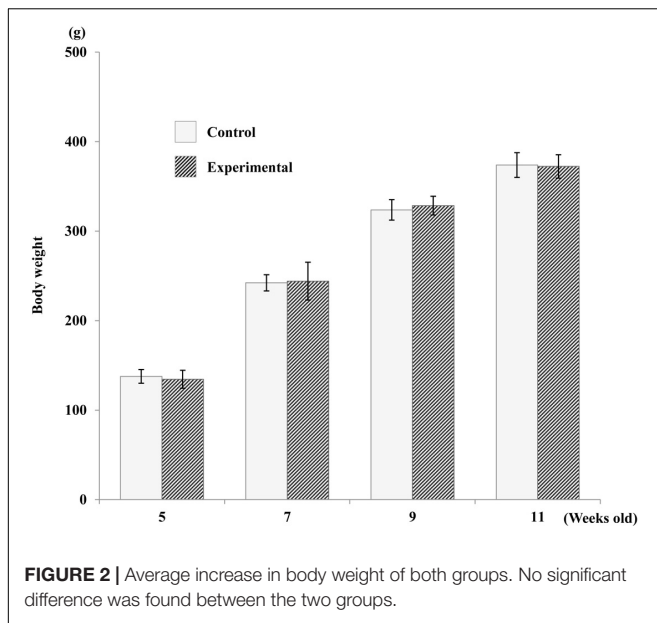
Typical EMG activity with the inset enlargement of raw data for both groups during stimulation are shown in **Figure 3**, and the representative recordings of RJM trajectories of both groups are shown in **Figure 4**. The jaw position was stable at rest and the distance between the upper and lower incisors was approximately 2–2.5 mm before stimulation.

During the repetitive electrical stimulation, the characteristics of the jaw movement patterns and the EMG were similar to those reported in previous studies (Sasamoto et al., 1990; Satoh et al., 2007). The gape size of jaw movements in the control group was significantly larger than those in the experimental group at each recording age (**Figure 5A**). Relative to the control group, the gape size at weeks 7, 9, and 11 was significantly larger ($p < 0.01$) than at week 5; at week 11, it was significantly larger ($p = 0.034$) than at week 7, but there were no significant differences of gape size between weeks 7 and 9, and weeks 9 and 11. Similarly, in the

experimental group, the gape size of the jaw movement at weeks 7, 9, and 11 was significantly larger ($p < 0.05$) than at week 5, and significantly larger ($p < 0.05$) at weeks 9 and 11 than at week 7, but there was no significant difference between weeks 9 and 11.

With regards to the lateral movement, the excursion in the control group was significantly larger ($p < 0.01$) than in the experimental group at weeks 9 and 11, while there was no significant difference between groups at weeks 5 and 7 (**Figure 5B**). Intragroup comparison of the control group showed that the lateral excursion at weeks 9 and 11 was significantly larger ($p < 0.05$) than at weeks 5 and 7, while there were no differences between weeks 5 and 7, or weeks 9 and 11. Intragroup comparison of the experimental group showed that the lateral excursion at weeks 9 and 11 was significantly larger ($p < 0.05$) than at week 5, and that of week 11 was significantly larger ($p < 0.05$) than week 7. There were no significant differences between weeks 5 and 7, or weeks 9 and 11.

The overall development of vertical mandibular speed showed an increase with age in both groups (**Figure 5C**). Compared to the control group, the vertical mandibular speed was significantly smaller ($p < 0.01$) in the experimental group at each recording age. Intragroup comparison within the control group showed that



the speed at week 9 was significantly larger ($p < 0.05$) than at week 5, and that of week 11 was significantly larger ($p < 0.05$) than weeks 5, 7, and 9. There were no significant differences between weeks 5 and 7, or weeks 7 and 9. Similarly intragroup comparison within the experimental group showed that the speed at week 9 was significantly larger ($p < 0.05$) than at week 5, and that of week 11 was significantly larger ($p < 0.05$) than at week 5, 7, and 9. There was no significant difference between weeks 5 and 7, or weeks 7 and 9.

Regarding the pattern of vertical jaw movement, the jaw movement paths were similar between both groups at all ages. A majority of traces overlapped along the path at week 5, except the traces at the maximum jaw-opening position, referred to as gape size, which were significantly different ($p < 0.05$) between both groups. The jaw movement paths at weeks 7, 9, and 11 were significantly increased ($p < 0.01$) in terms of gape size in the control group compared to the experimental group (Figure 6). Comparison of the jaw movement duration showed that there were no significant differences between the control and experimental groups in the jaw-opening, jaw-closing, and total cycle durations (Figure 7). Intragroup comparison revealed no significant effects of age on these parameters in either the control or the experimental group at any recording age. There were no significant differences in the rhythm of movement between the both groups at all ages (Figure 8).

In terms of time-dependent changes in the jaw movement sequences, we measured and compared vertical jaw movement between the early, middle, and late periods for each age in both groups. As described above, the amplitude of vertical jaw movement, as well as the gape size, was significantly smaller in the experimental group at all ages. Comparison of vertical movements among the early, middle, and late periods at 5 weeks of age showed that there were no significant differences in either group (Figure 9A). At 7 weeks of age, there were no significant differences among the early, middle, and late periods

in the control group; however, in the experimental group, the jaw movement during the late period of the sequence was significantly smaller ($p < 0.05$) than that during the early and middle periods (Figure 9B). At 9 weeks of age, the jaw movement during the middle and late period was significantly larger ($p < 0.05$) than during the early period in the control group. Conversely, the late period of the sequence in the experimental group was significantly smaller ($p < 0.05$) than the early and middle periods (Figure 9C). At 11 weeks of age, the early period of the sequence in the control group was significantly smaller ($p < 0.05$) than the middle; however, there were no significant differences between both the early and late, as well as the middle and late periods. In contrast, the late period in the experimental group was significantly smaller ($p < 0.05$) than the middle period; however, there were no significant differences between both the early and late, as well as the early and middle periods (Figure 9D).

Electromyographic Activities During Stimulation

During the sustained stimulation, the EMG activities in the anterior digastric muscle were recorded, however, no activities were seen in the masseter muscle at any age. The EMG onset latency, duration, and peak-to-peak amplitude of the anterior digastric muscles are shown in Figure 10. Compared to the control group, the onset latency was significantly longer, and the peak-to-peak amplitude was significantly smaller in the experimental group at each recording age, but there were no significant differences in intragroup comparisons at weeks 5, 7, 9, and 11 in either the control or the experimental group. In terms of duration no significant differences in EMG were observed between the two groups, or for the intragroup comparisons at any recording age.

A visual comparison of the EMG spectrum showed that a higher median frequency was observed during the early period of contraction in both groups, which shifted toward lower frequencies during the late period of contraction. The median frequency generated in the experimental group was significantly reduced compared to that of the control group at all ages (Figure 11). Similarly, the mean frequencies generated in the control group were significantly higher than those in the experimental groups during the stimulation period at all ages (Figure 12).

DISCUSSION

In the current study, we investigated the developmental course of cortically-evoked RJMs, comparing normal conditions to altered occlusal loading forces provided by a soft diet and assessing the neuromuscular responses of jaw-opening and jaw-closing muscles during maturation. The stimulus intensity required for CMA stimulation to elicit RJMs in rats has been shown to vary between 50 and 300 μA , and the threshold for RJMs evoked from the posterior part of the CMA is higher during repetitive stimulation (Sasamoto et al., 1990; Satoh et al., 2006b, 2007; Maeda et al., 2014; Tsujimura et al., 2016). Furthermore, it has been noted that a stimulus intensity of up to 300 μA used to

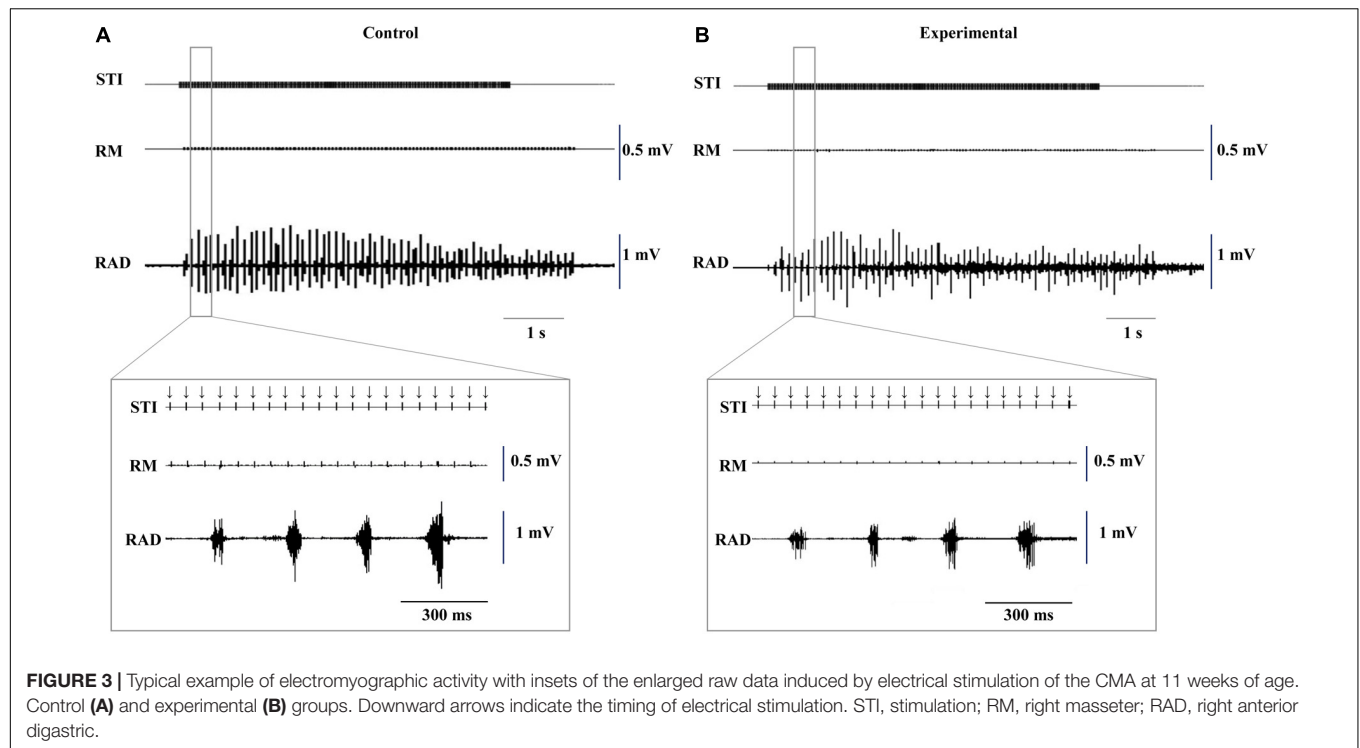


FIGURE 3 | Typical example of electromyographic activity with insets of the enlarged raw data induced by electrical stimulation of the CMA at 11 weeks of age. Control (A) and experimental (B) groups. Downward arrows indicate the timing of electrical stimulation. STI, stimulation; RM, right masseter; RAD, right anterior digastric.

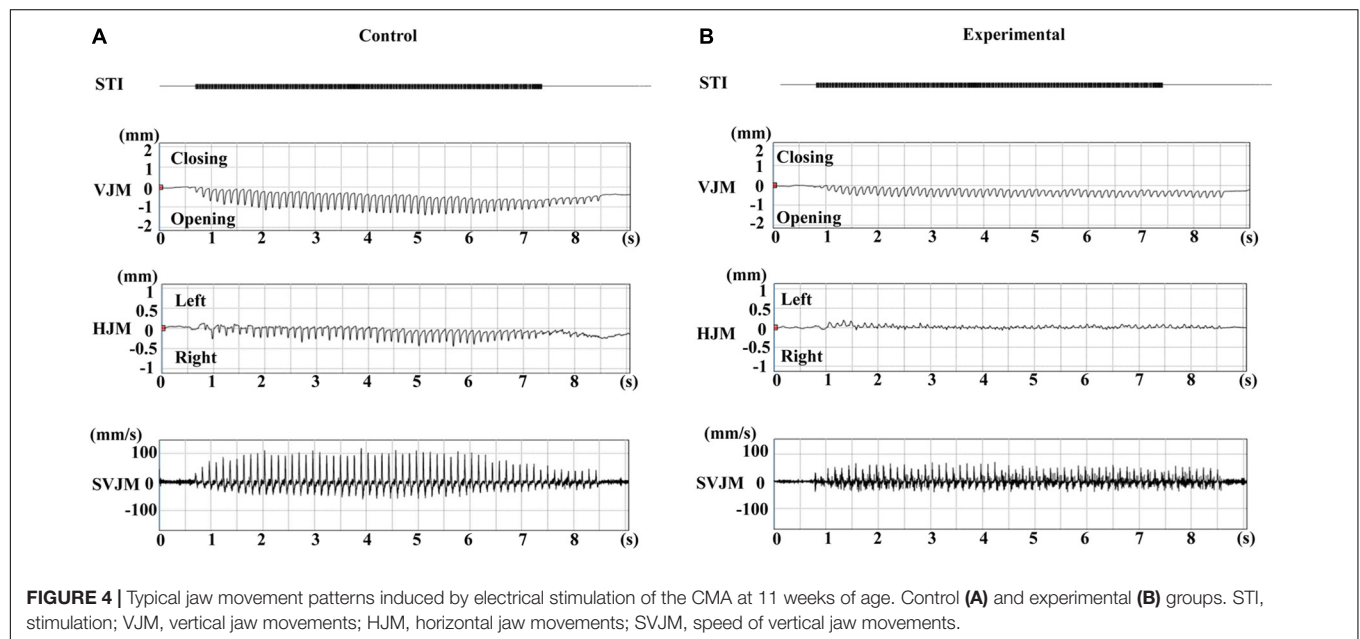


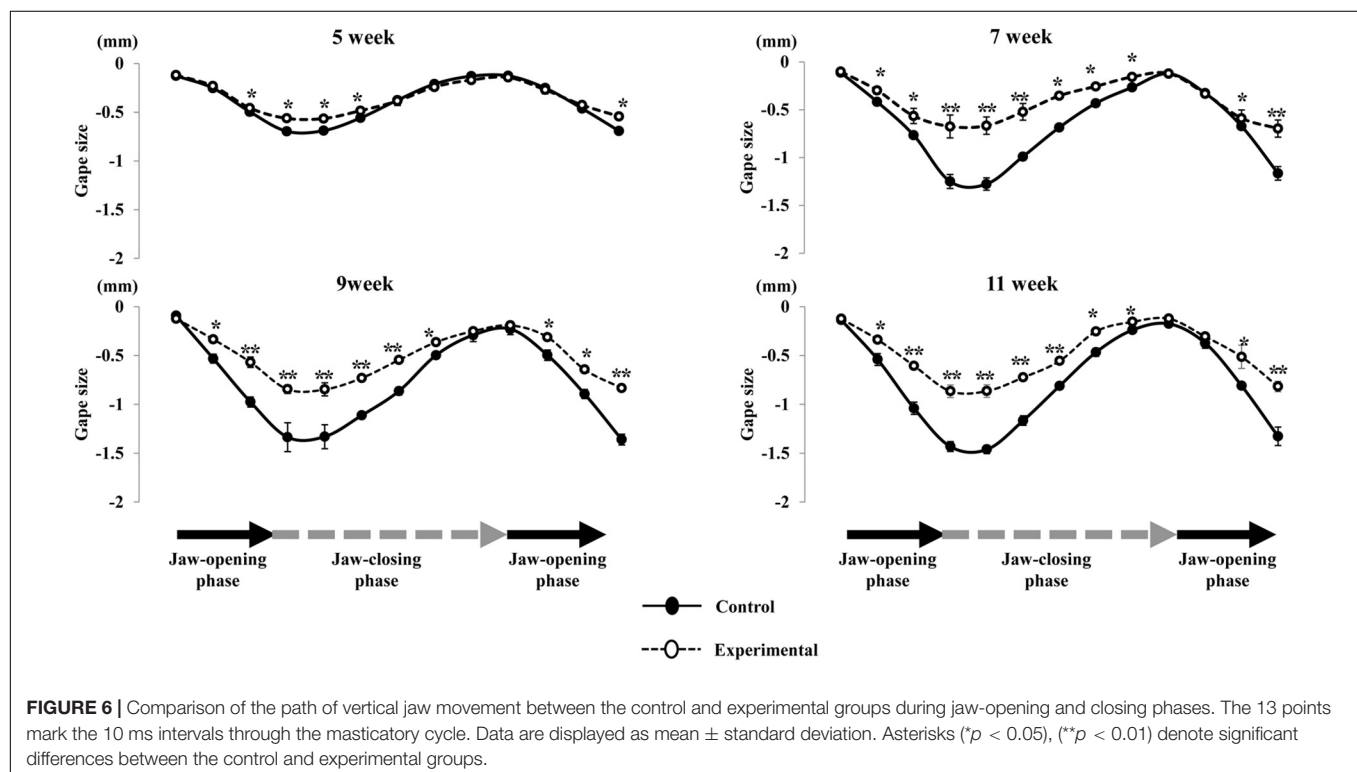
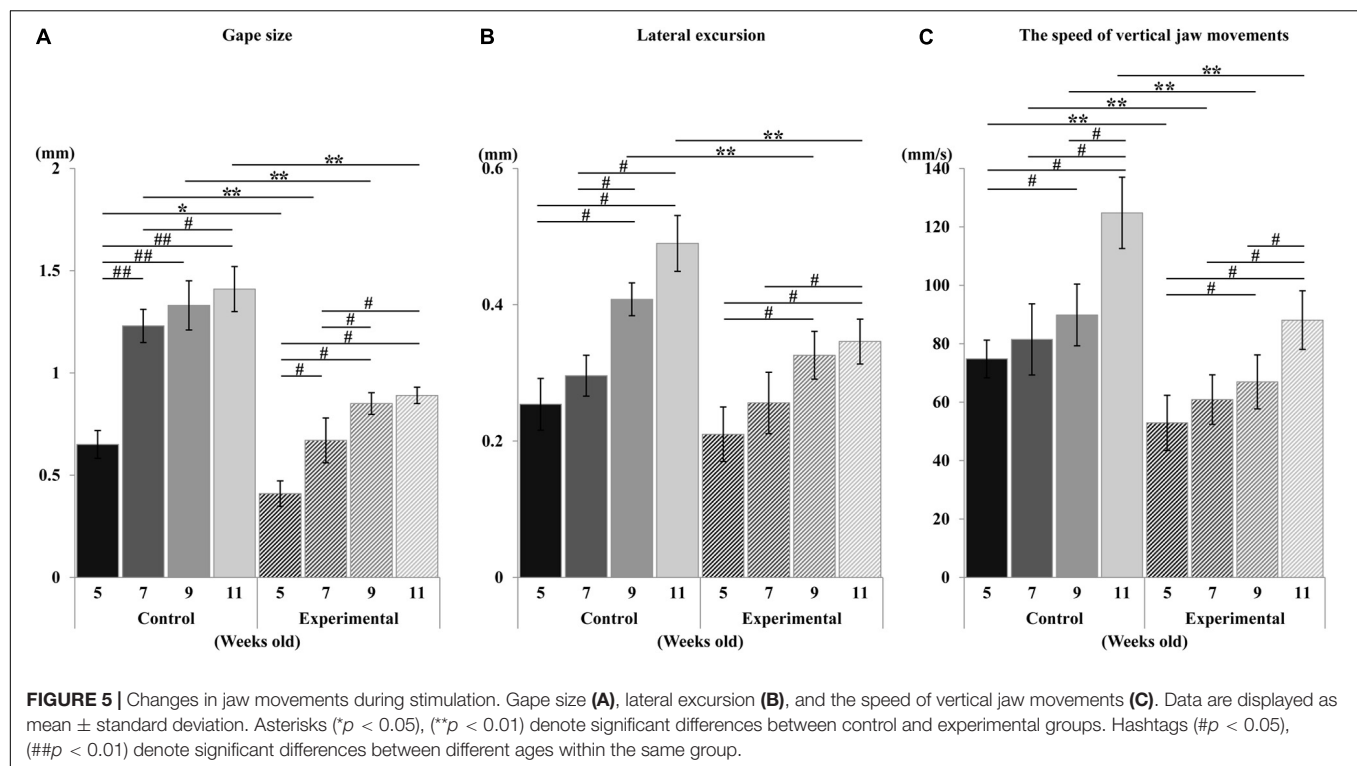
FIGURE 4 | Typical jaw movement patterns induced by electrical stimulation of the CMA at 11 weeks of age. Control (A) and experimental (B) groups. STI, stimulation; VJM, vertical jaw movements; HJM, horizontal jaw movements; SVJM, speed of vertical jaw movements.

evoke RJMs in rats does not appear to have any noxious effects during repetitive stimulation (Satoh et al., 2006a,b, 2007). In our study, the CMA was stimulated and RJMs subsequently identified through mandibular movements and rhythmic bursts of EMG activity. The current stimulus intensity used in our experiment was designated as the threshold required to elicit RJMs. We used a constant current strength (180 μ A) to compare the cortically evoked RJMs and found that long-term alteration of the masticatory load at an early age affected the developmental

course of jaw movements and the neuromuscular response of the masticatory muscle.

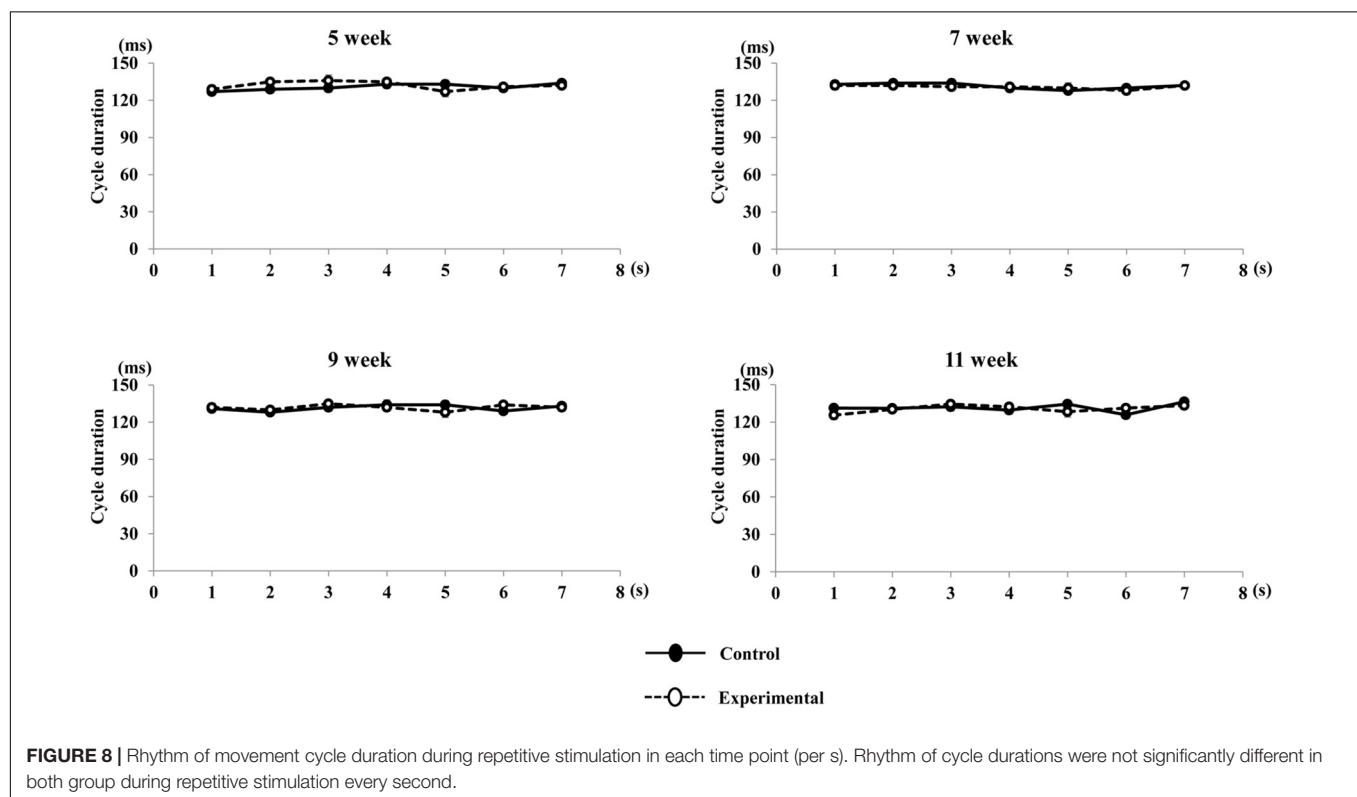
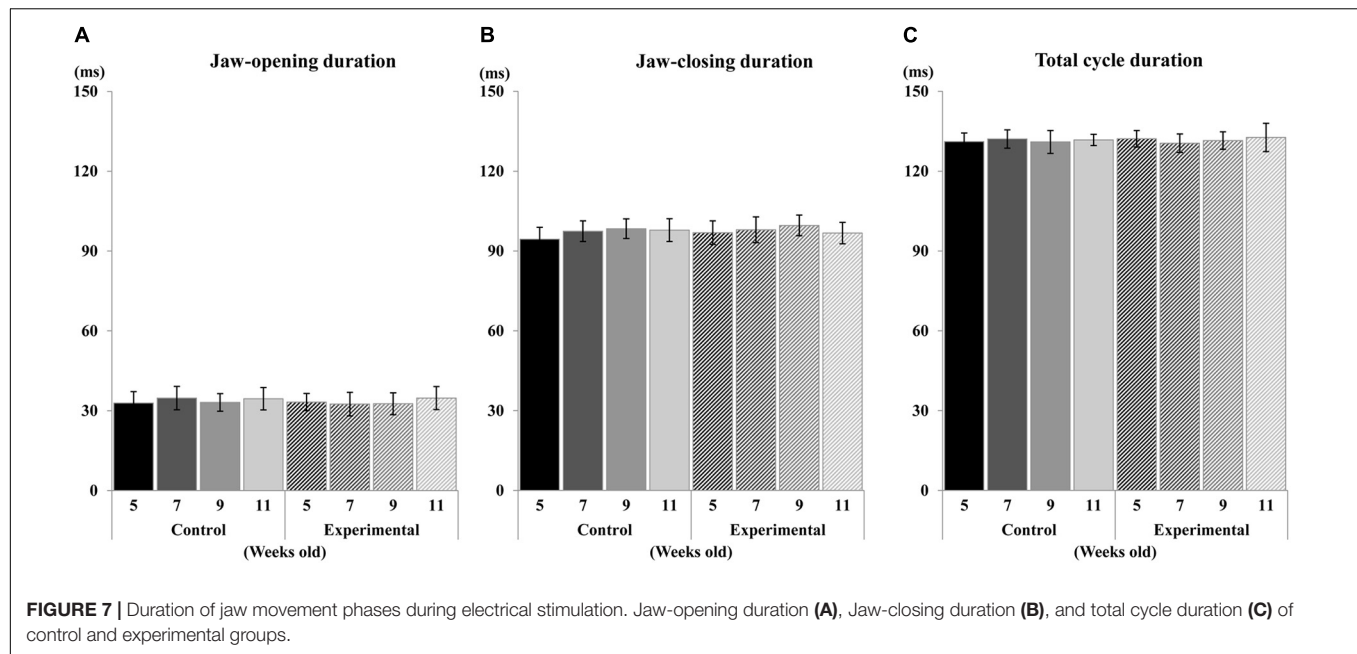
Growth-Related Changes in Cortically-Induced Jaw Movements

In our study, low-frequency long-train stimulation of the posterolateral part of the CMA evoked simple vertical RJMs in both groups. The gape size of jaw movement was smallest in



each group at week 5, and it increased until 9 weeks of age in both the control and the experimental groups, while there was no significant difference between weeks 9 and 11. Previous study have reported that the masticatory movements in rats appeared

at approximately 3 weeks of age (Westneat and Hall, 1992). Since all repetitive neuronal bursts for rhythmical mastication were detected at approximately 13–17 days in rats (Brocard et al., 2006), the initial masticatory patterns developed at approximately



12 days, and the adult masticatory movements were established between 18 and 21 days (Westneat and Hall, 1992). However, facial morphological development continued after 3 weeks of age in rats. The variations in mandibular and condylar growth positively correlated with the maximum jaw movement capacity (Fukui et al., 2002). A recent three-dimensional study has reported that the natural growth rate of the mandible was greatest

between 4 and 8 weeks of age, and reached a plateau after 9 weeks of age in rats (Kim et al., 2018). A report on the development of jaw movements in children and adolescents showed that the maximum jaw-opening movement was less stable during an early age, and increased until the age of 17 years (Hirsch et al., 2006). Thus, we considered that orofacial morphological development could affect the pattern of RJMs during maturation.

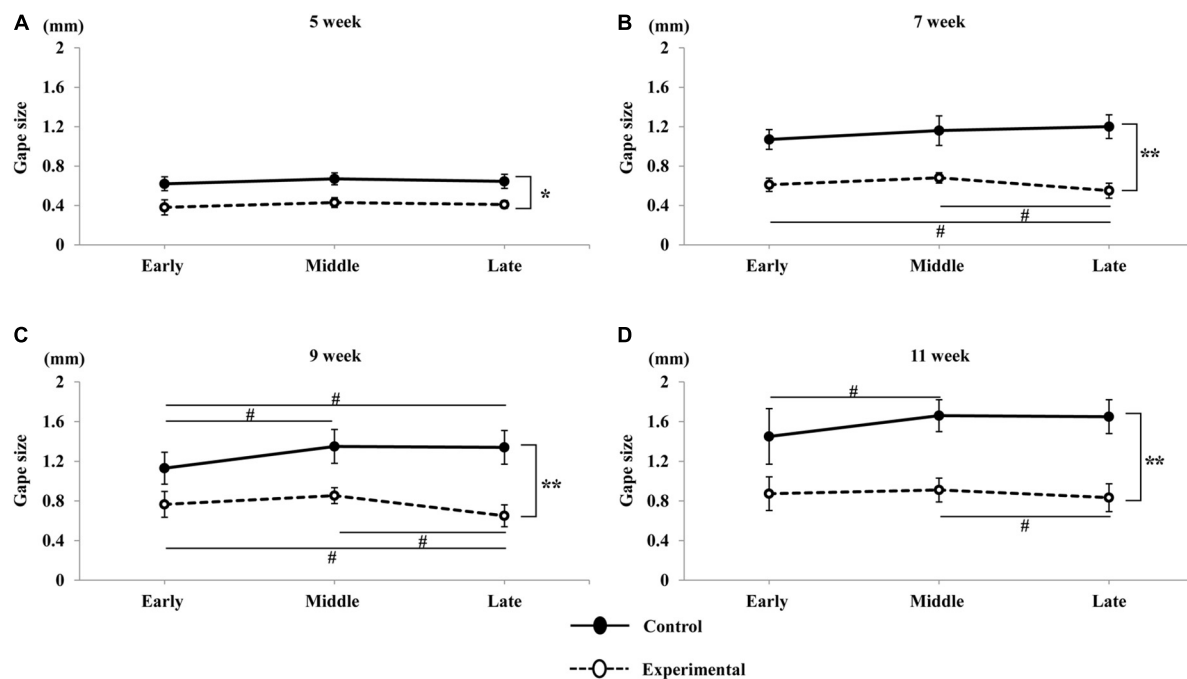


FIGURE 9 | Variations in gape size of jaw movements with time in the sequence. Total duration of the stimulation sequence was divided into three equal periods: early, middle, and late, corresponding to the first, second, and third for 2 s respectively. Jaw movements at 5 weeks of age (A), 7 weeks of age (B), 9 weeks of age (C), and 11 weeks of age (D) in the control and experimental groups. Data are displayed as mean \pm standard deviation. Asterisks (* $p < 0.05$), (** $p < 0.01$) denote significant differences between the control and experimental groups. Hashtags (# $p < 0.05$) denote significant differences between the sequences at each age.

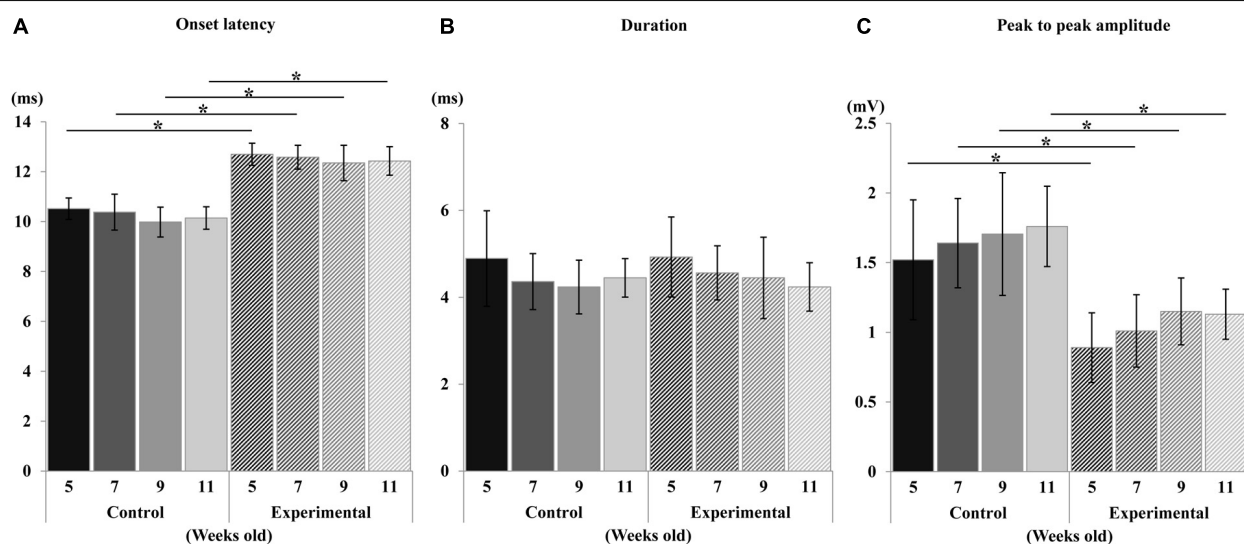


FIGURE 10 | Changes in electromyographic activity. Onset latency (A), duration (B), and peak-to-peak amplitude (C) of control and experimental groups. Data are displayed as mean \pm standard deviation. Asterisks (* $p < 0.05$) denote significant differences between the control and experimental groups.

Lateral excursion movements were small at weeks 5 and 7 in the control group. During stimulation, the jaw movement deviated slightly toward the right side (i.e., the side contralateral to the stimulation) followed by grinding movements during the jaw-closing phase, but this type of movement was small at 5 and 7 weeks of age. A previous

study reported that the size of the mandibular condyle and fossa did not increase between weeks 4 and 8, although body weight of the rats increased (Kato et al., 2015). Thus, the decreased lateral movements may be related to the shape of the temporomandibular joint that would restrict lateral movements at this age.

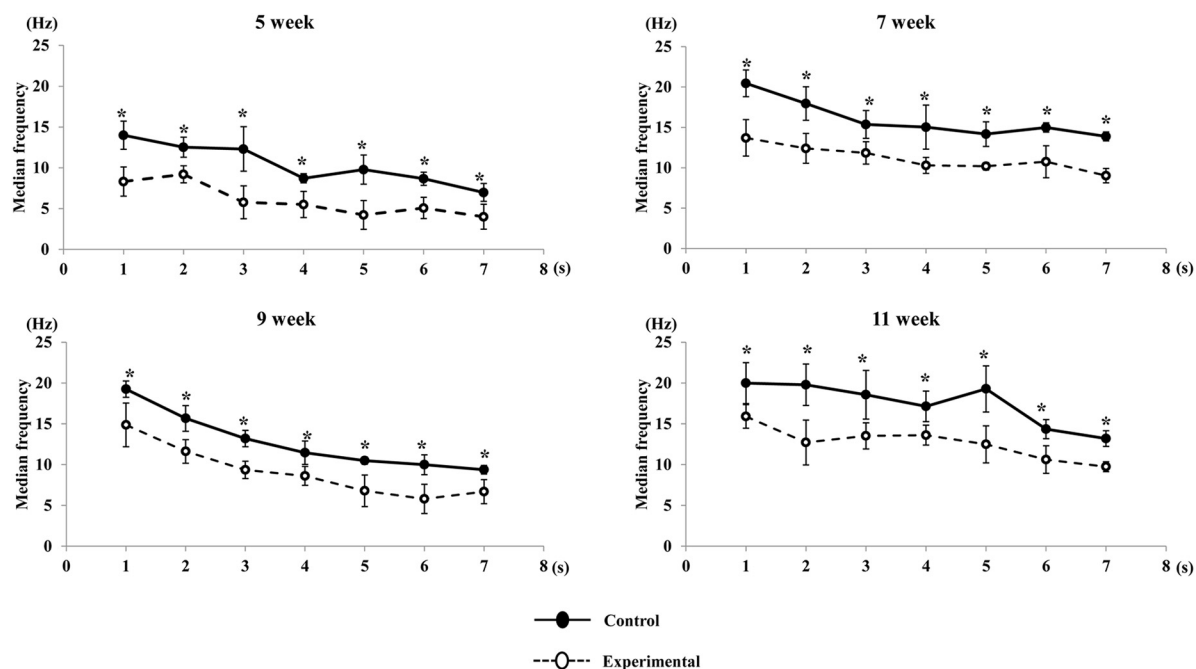


FIGURE 11 | Changes in median frequency of the anterior digastric muscle during stimulation in each time point (per s) at each age. Data are displayed as mean \pm standard deviation. Asterisks ($*p < 0.05$) denote significant differences between the control and experimental groups.

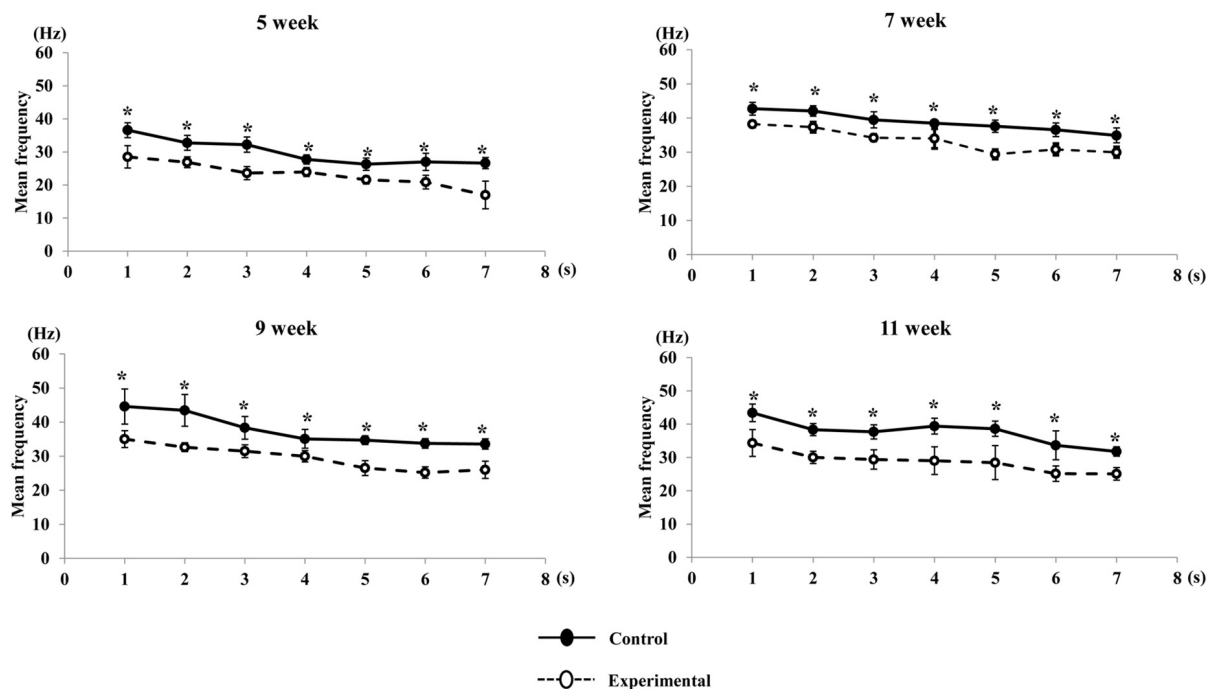


FIGURE 12 | Changes in mean frequency of the anterior digastric muscle during stimulation in each time point (per s) at each age. Data are displayed as mean \pm standard deviation. Asterisks ($*p < 0.05$) denote significant differences between the control and experimental groups.

During constant stimulation, we noticed that the speed of vertical movements is augmented with age. In our study, the speed of vertical jaw movements increased until 9 weeks, then

peaked at 11 weeks of age in both the control and experimental groups. A previous study suggested that the speed of the jaw movements is reflected in the amount of muscle force produced

during mastication (Watanabe and Watanabe, 2001; Anderson et al., 2002). Moreover, the force and power output of a muscle mainly depends on the muscle fiber size and length. The skeletal muscle fibers of rat undergo intense growth from 3 to 10 weeks of age, with an increase in the number and size of myofibers, and attain stable growth after 10 weeks (Tamaki and Uchiyama, 1995). This suggests that changes in morphology of muscles may also affect the speed of jaw movements.

The patterns of the vertical movement were similar in both the control and experimental groups, with the exception of the gape size of jaw movements, which differed significantly with age. Many previous electrophysiological studies have reported that different sites in the CMA evoke different patterns of jaw movement (Sasamoto et al., 1990; Gerstner and Goldberg, 1991; Isogai et al., 2012; Uchino et al., 2015). Vertical RJMs have been shown to be induced by stimulating the ventrolateral area of the CMA (i.e., the agranular cortex) (Enomoto et al., 1995; Masuda et al., 2002; Isogai et al., 2012). It is likely that that stimulating the same effective site of the CMA may evoke these patterns of jaw movement.

The duration of parameters of RJMs including jaw-opening and jaw-closing showed no significant differences between ages in both the control and experimental groups. Moreover, the total cycle duration was also consistent depending on the stimulus interval during stimulation. The timing and sequence of contractions of the jaw-opening and jaw-closing muscles are associated with the development of the masticatory CPG, which generates the RJMs (Lund and Kolta, 2006; Morquette et al., 2012). It has been shown that in rats, repetitive bursting neurons are detected postnatal days 9 to 12, and rapidly increase in activity up until postnatal day 14, after which it remains constant (Brocard et al., 2006; Morquette et al., 2012). This result may suggest that the masticatory CPG maintains the cycle duration that resembles the set duration of the stimulus interval to the CMA until it reaches the mature level.

Effects of Low Occlusal Loading on Cortically-Induced Jaw Movements

During electrical stimulation of the CMA, the gape size was significantly smaller in the experimental group than in the control group at each recording age. The difference between the gape size at week 5 in both groups had a lower level of significance than at weeks 7, 9, and 11. It has been reported that being raised with a soft diet during the optimum learning period prevents masticatory function from reaching a normal level (Fujishita et al., 2015). Our findings were consistent with this previous report, as the maximum gape size during opening did not reach a normal level in rats fed a soft diet. Moreover, the opening capacity of the jaw is associated with the coactivation of the jaw muscles and the neuromuscular response from the brain. A previous study has reported that changes in occlusal loading are responsible for the variation in the maturation of sensory afferents such as the muscle spindles and periodontal mechanoreceptors, thereby affecting the capacity for modulatory sensory feedback from the masticatory CPG (Lund and Kolta, 2006). Altered sensory inputs of the oral

receptors and muscle spindles have been shown to result in decreased synaptic density in the cerebral cortex, which impairs the strengthening of synapses and causes sensory deprivation of the cerebral cortex (Yamamoto and Hirayama, 2001; Bhatt, 2010). Morphological studies have also reported that the number of cross-sectional muscle fibers and mitochondria per unit in muscles was significantly reduced in growing rats fed on a soft diet (Sato and Konishi, 2004; Kawai et al., 2010). In addition, decreases in the proportion of cross-sectional areas of both type 1 and 2 fibers in jaw-closing muscles, and type 2 fibers only in jaw-opening muscles, were found in animals during training with low occlusal force (Langenbach et al., 2003; Kitagawa et al., 2004). Changes in the oxidative capacity of muscle fibers, due to lower muscle usage after 2 weeks feeding on a soft diet, have been shown to significantly reduce the motor properties of jaw muscles in rats (Liu et al., 1998). In addition, varying masticatory loading directly affects the mandibular remodeling process, which causes changes in the morphology of the mandible (Renaud et al., 2010; Tsouknidas et al., 2017). Hence, the decreased vertical jaw movement observed in our study might be influenced by morphological changes and diminished activities of mechanoreceptors from the oro-facial regions.

The lateral excursion at 9 and 11 weeks of age was more significantly reduced in the experimental group than in the control group. Rats exhibit a smaller mandibular condyle and thinner cartilage when fed a soft diet during growth (Kato et al., 2015). Previous studies have reported that there was a regressive change in the trabecular structure when being fed a soft diet, which can reduce the resistance of the mandibular condyle to mechanical loading, and increase the occurrence temporomandibular deformation (Ogawa et al., 2016; Kono et al., 2017). In addition, alterations in occlusal stimuli followed by consumption of a soft diet may result in a decrease in the response of the mechanoreceptors of the temporomandibular joint (Ishida et al., 2009). Therefore, these findings demonstrated that the low occlusal loading during growth has a significant influence on the shape of the temporomandibular joint and its mechanoreceptors, resulting in the observed reduction in the lateral excursion.

The speed of vertical jaw movements was lower in the experimental group than in the control, at each recording age. The contraction velocity of jaw muscles is known to depend on the amount of force that is generated during muscle contraction. It has been reported that changing the consistency of food to a softer form may reduce the masticatory muscle load, and thus decrease tetanic isometric tension force during muscle contraction (Kiliaridis and Shyu, 1988). Moreover, rats raised on a soft diet show a decrease in muscle fiber conduction velocity, which delays muscle contraction time, affecting the speed of movement (Murakami et al., 2014). Human studies have also suggested that the velocity of muscle contractions during jaw-opening and jaw-closing was significantly decreased when consuming food of a softer consistency (Watanabe and Watanabe, 2001; van der Bilt and Abbink, 2017). It is possible that changing the occlusal loading with a softer diet may result in lesser masticatory force, which causes the slower speed of jaw movements observed in our study.

With regards to the similar masticatory pattern observed in our study, a human study has suggested that the path of the masticatory pattern is affected by muscle, TMJ form, and the inclination of the occlusal plane (Tomonari et al., 2017). However, rats raised on a soft diet have been shown to have a similar pattern of masticatory movement regardless of food consistency (Fujishita et al., 2015). This may be due to the different characteristics of the masticatory system between humans and rodents, since rats have limited lateral movement and diverge widely in the sagittal plane (Utsumi et al., 2010). In our study, a similar pattern of jaw movement was observed, with the exception of the gape size, which was small in rats fed a soft diet. At week 5, a majority of traces overlapped along the path between the both groups, and the low significant difference observed at the maximum gape size showed that the effect of low occlusal loading appeared 2 weeks after being fed a soft diet. The maximum gape size of jaw movement at weeks 7, 9, and 11 were more significantly reduced in rats fed a soft diet, suggesting that changes in food consistency have a larger effect on masticatory function and sensory feedback during the developmental period, resulting in a decreased gape size. However, this did not show any influence on the masticatory pattern during the electrophysiological study.

Phases of jaw movements including jaw-opening, jaw-closing, and total cycle duration were not statistically different between the experimental and the control groups. Also, no significant difference was observed in the rhythm of jaw cycle duration between both groups. When repetitive electrical stimulation is delivered to the corticobulbar tract, duration is mainly controlled by the activation of jaw-opening and jaw-closing motoneurons, which are part of the circuitry of the masticatory CPG (Morquette et al., 2012). One diet-related study reported that changing to a soft diet alters the motor unit activity of muscles due to impairment of morphological and metabolic properties of muscle, but found no changes in soma diameter and enzymatic activity of motoneurons (Miyata et al., 1993). Therefore, it appears unlikely that low occlusal loading could affect the response properties of jaw motoneurons in the masticatory CPG. Rather, stimulus of the CMA could directly activate the masticatory CPG through the corticobulbar tracts, resulting in the stable duration of jaw movements observed across both groups during stimulation in the present study.

In the present study, we divided the total duration of vertical jaw movements into 3 periods of equal duration to evaluate changes in jaw movements during constant stimulation. The amplitude of jaw movements was less stable in the experimental group during stimulation. In the late period, jaw movements during stimulation were not as marked as in the early and middle periods at 7, 9, and 11 weeks of age, which is reflected by the reduced EMG activity of the anterior digastric muscle. It has been reported that the jaw movement rhythm is mainly controlled by the activity of the jaw-opening muscles (Lund, 1991). More than 90% of fibers in the jaw-opening muscles are composed of fast-contracting or type 2 fibers (Cobos et al., 2001). In addition, a lesser proportion of type 1 and type 2B fibers, and a greater proportion of type 2A fibers have been found in developing rats

fed on a soft diet (Kitagawa et al., 2004; Kawai et al., 2010). This may be due to the diminished activity of masticatory muscles resulting in a shift of fiber-type that caused conversion to type 2A fibers. Generally, type 1 fibers are optimally suited for sustained contraction force and type 2B fibers are suited for sudden and powerful contraction of large force (Grunheid et al., 2009). It is likely that the incremental shift in fiber-type may also be reflected in the stable jaw movements during stimulation, particularly in the late period.

Growth-Related Changes and Effects of Low Occlusal Loading on Muscular Work

In our study, only activity of the anterior digastric muscle, and not the masseter muscle, was observed. Further, the anterior digastric activity during stimulation comprised of clusters that were time-locked to each stimulus pulse. Previous studies have reported that the posterior part of the CMA might correspond to the unilateral RJMs with time-locked activity of the anterior digastric muscle in guinea pigs (Gerstner and Goldberg, 1991; Enomoto et al., 1995), and that stimulation of the rostral part of the somatosensory cortex can evoke sustained jaw-opening with elevated anterior digastric activity in rats (Uchino et al., 2015). However, low-frequency long-train stimulation of the deep part of the CMA evokes RJMs with alternating activities of the anterior digastric and masseter muscles (Isogai et al., 2012). This may be associated with site dependent differences in the cytoarchitecture of the cortical areas, and the connection patterns between the granular and agranular cortex and the thalamic nuclei (Haque et al., 2010; Isogai et al., 2012); RJMs with alternating activity of the masseter and anterior digastric muscles were induced from the rostral part of granular cortex, and vertical RJMs with only the anterior digastric activity were induced from the agranular cortex (Isogai et al., 2012). It is likely that the stimulation in our study mostly induced the agranular region of the cortex, which elicited activity in anterior digastric muscle, but not the masseter muscle.

The EMG activity showed that the onset latency of the anterior digastric muscle in the experimental group was significantly delayed than in the control group, but there was no significant difference among ages in either the control or the experimental group. Measuring the onset latency is the best way to assess the muscle fiber conduction velocity during stimulation (Beck, 2006). In stimulated muscle contractions in rats, the latency was delayed at 3 weeks of age, however, the delay in latency disappeared from 5 weeks of age onwards (Seki et al., 2002; Changsiripun et al., 2012). In addition, alterations of peripheral sensory regulation due to occlusal hypofunction affect the conduction velocity of muscle fibers (Seki et al., 2002; Changsiripun et al., 2009). Therefore, we may assume that low occlusal loading caused by consumption of a soft diet may reduce the conduction velocity of the muscle resulting in delayed maturation of muscle responses, but this is not a consequence of the experimental period.

The duration of the contractions of the anterior digastric muscle did not differ between groups. During stimulated muscle contractions, the duration of jaw muscle contraction is controlled by the masticatory CPG in response to repetitive

electrical stimulation of CMA (Lund, 1991; Lund and Kolta, 2006; Morquette et al., 2012). Moreover, it has been reported that altering the masticatory load does not affect the duration of muscle contraction in studies of the rat (Changsiripun et al., 2009) and humans (Anderson et al., 2002). Stimulation of the CMA induces the excitatory activation of jaw muscles through corticobulbar projections to the masticatory CPG, suggesting that the masticatory CPG maintains muscle contraction duration resulting in a stable cycle of jaw movements with differing occlusal force.

The peak-to-peak amplitude was significantly larger in the control group than the experimental group at all ages. Greater muscle force produces greater excursion of the mandible throughout the jaw movement cycle (Anderson et al., 2002). Measuring the peak-to-peak amplitude is a way to assess voluntary contraction force determined by the number of muscle fibers and the proportional number of motor units activated by electrical stimulation (Keenan et al., 2005; Kamen and Gabriel, 2010). A corresponding reduction in motor unit activity had been found with occlusal hypofunction (Miyata et al., 1993). In addition, input-output properties of the motor unit can be altered by the alteration in the functional sensitivity of oral mechanoreceptors when the masticatory conditions change (Shi et al., 2006; Ishida et al., 2009). Oral receptors, including periodontal afferents and muscle fibers, are major input sources for the CPG, exciting neurons throughout the lateral brainstem during mastication. It has been suggested that their output can be influenced by hardness-related feedback. Most of the neurons that activate during jaw-opening are excited by periodontal feedback, and the neurons that activate during jaw-closing are excited by spindle afferents (Lund and Kolta, 2006). The periodontal receptors are sensitive to changing forces, and specific changes in the distribution and shape of nerve terminals were found in periodontal afferents after changes in occlusal force (Piancino et al., 2017). A previous study has suggested that abolishing the signal information from periodontal receptors and muscle spindle receptors can completely diminish the activity of muscles and reduce the build-up speed of the masticatory force during mastication (Trulsson, 2006). In our study, the peak to peak amplitude from the anterior digastric muscle was significantly decreased in rats fed a soft diet at all ages, although we could not obtain measurements from the masseter muscle. It is believed that long-term low occlusal loading may have differential effects on burst generating neurons, resulting in decreased EMG activity during stimulation of the CMA.

In this study, we also performed a power spectral analysis with a visual representation of the power spectrum in the EMG signal. A frequency analysis of how the EMG signal varies with the time has been used to monitor muscle fatigue during muscle contraction (Cifrek et al., 2009). In this analysis, the mean and median frequencies are generally measured as a gold standard for the assessment of muscle fatigue (Phinyomark et al., 2012). The mean frequency is used to determine changes in muscle fatigue over time, whereas the median frequency measures two equal halves of the spectrum during muscle contraction (Cifrek et al., 2009). The contribution of muscle fibers to the varying size of the EMG power spectrum is associated with variations

in the proportion of muscle fiber diameter. In addition, the distribution of muscle fibers during activation also affects the EMG power spectrum (Gerdle et al., 2000). It is likely that the larger the muscle fibers with fast conduction velocities, the higher the frequency in the EMG spectrogram (Seven et al., 2013). In the anterior digastric muscle of the rat, a significant proportion of type 2B, fast contracting, fibers are found in peripheral regions, and a lower proportion of type 1, slow contracting, fibers are found in the central regions (Cobos et al., 2001). The transition from type 1 to type 2 fibers may occur during reduced masticatory loading, followed by a reduction in muscle fiber size (Tsai et al., 2012). In the present study, the higher mean/median EMG burst frequencies observed during early contraction reflect the activation of larger type 2B fast contraction fibers. The shift to lower frequencies in the late contraction period suggests that a larger muscle force was generated in the early contraction period during stimulation, and the muscle force tended to reduce in the late contraction period. On the other hand, the low occlusal loading by feeding a soft diet resulted in decreased force generation during contraction, due to altered muscle fiber size and conduction velocity, which causes muscle fatigue during dynamic muscle contraction.

In summary, the findings of our study provided further evidence that decreasing occlusal loading through consumption of a soft diet induces smaller patterns of cortically-evoked jaw movements. Changes in occlusal functions are associated with neuroplasticity in the jaw and tongue motor representations within the somatosensory cortex (Avivi-Arber et al., 2010b, 2015). Neural signals from the CMA induce projections to the brainstem reticular formation and trigeminal motor nuclei, which induces various trigeminal actions to orofacial regions (Morquette et al., 2012). Cortical inputs to motoneuron pools provide a direct pathway for voluntary control of jaw muscles and fine control of voluntary bite force (Nordstrom, 2007). The masticatory CPG mainly regulates the rhythmic trigeminal activity of masticatory movements, and peripheral sensory information may modulate the central motor command (Nakamura and Katakura, 1995). Our results suggest that consuming a soft diet during early development inhibits the motor performance of higher brain centers, and masticatory functions never reach the normal levels during the experimental period. In our study, we only investigated the RJM trajectories and EMG activities from 5 to 11 weeks of age in rats. The functional properties of oral mechanoreceptors (i.e., periodontal and temporomandibular joint mechanoreceptors) and trigeminal neurons in the brainstem are mature by an age of 5 weeks in rats (Nasution et al., 2002; Ishida et al., 2009; Hiranuma et al., 2013). In addition, the craniofacial growth maturation of the rats reaches a plateau in approximately 79 days (Abed et al., 2007). Thus, we believe that it is important to learn the masticatory function and associated neuromuscular control from the brain, particularly from the CMA, around these time periods. However, it remains controversial whether the low occlusal function actually affects the functional activity of the masticatory CPG since we found no significant changes in the duration and rhythm of jaw movements between the groups in our study. Therefore, further studies are needed to explore the effects of alterations in oral functions on

the functional configuration of the masticatory CPG in rats fed with foods of different consistencies.

CONCLUSION

The present study shows that (1) the pattern of cortically-induced RJMs become stable after 9 weeks of age in rats; (2) changing the loading force alters the maturation and pattern of cortically induced RJMs during growth; (3) with decreased occlusal function, the masticatory CPG maintains the duration of jaw movement sequences during growth, in accordance with the stimulus interval that is applied to CMA; and (4) long-term low occlusal loading generates downward shifts in frequency with localized muscle fatigue. Collectively, the present findings suggest that alteration of occlusal loading force during the several weeks after weaning significantly modulates the regulation of cortically-induced RJMs and the neuromuscular response of jaw muscles during development. Therefore, an appropriate ingestion behavior during the growing period should be essential for the normal growth and development of the craniofacial complex, as well as for the maturation of masticatory functions.

DATA AVAILABILITY STATEMENT

The raw data supporting the conclusions of this article will be made available by the authors, without undue reservation, to any qualified researcher.

REFERENCES

- Abed, G. S., Buschang, P. H., Taylor, R., and Hinton, R. J. (2007). Maturation and functional related differences in rat craniofacial growth. *Arch. Oral Biol.* 52, 1018–1025. doi: 10.1016/j.archoralbio.2007.05.008
- Anderson, K., Throckmorton, G. S., Buschang, P. H., and Hayasaki, H. (2002). The effects of bolus hardness on masticatory kinematics. *J. Oral Rehabil.* 29, 689–696. doi: 10.1046/j.1365-2842.2002.00862.x
- Anegawa, E., Kotorii, N., Ishimaru, Y., Okuro, M., Sakai, N., and Nishino, S. (2015). Chronic powder diet after weaning induces sleep, behavioral, neuroanatomical, and neurophysiological changes in mice. *PLoS One* 10:e0143909. doi: 10.1371/journal.pone.0143909
- Avivi-Arber, L., Lee, J. C., and Sessle, B. J. (2010a). Cortical orofacial motor representation: effect of diet consistency. *J. Dent. Res.* 89, 1142–1147. doi: 10.1177/0022034510373767
- Avivi-Arber, L., Lee, J. C., and Sessle, B. J. (2010b). Effects of incisor extraction on jaw and tongue motor representations within face sensorimotor cortex of adult rats. *J. Comp. Neurol.* 518, 1030–1045. doi: 10.1002/cne.22261
- Avivi-Arber, L., Lee, J. C., Sood, M., Lakschevitz, F., Fung, M., Barashi-Goza, M., et al. (2015). Long-term neuroplasticity of the face primary motor cortex and adjacent somatosensory cortex induced by tooth loss can be reversed following dental implant replacement in rats. *J. Comp. Neurol.* 523, 2372–2389. doi: 10.1002/cne.23793
- Avivi-Arber, L., Martin, R., Lee, J. C., and Sessle, B. J. (2011). Face sensorimotor cortex and its neuroplasticity related to orofacial sensorimotor functions. *Arch. Oral Biol.* 56, 1440–1465. doi: 10.1016/j.archoralbio.2011.04.005
- Avivi-Arber, L., and Sessle, B. J. (2018). Jaw sensorimotor control in healthy adults and effects of ageing. *J. Oral Rehabil.* 45, 50–80. doi: 10.1111/joor.12554

ETHICS STATEMENT

The animal study was reviewed and approved by the Institutional Animal Care and Use Committee (A2017-135A and A2018-028A) in compliance with the Animal Care Standards of Tokyo Medical and Dental University.

AUTHOR CONTRIBUTIONS

All authors conceived and designed the experiments, interpreted results of experiments, approved the final version of the manuscript. PA, CK, and YA performed the experiments. PA, CK, and TOn analyzed the data. PA and CK prepared the figures and drafted the manuscript. PA, CK, SK, and TOn edited and revised the manuscript.

FUNDING

This study was financially funded in part by Grant-in-Aid for Scientific Research 15K11338 and 15K20581 from the Japanese Ministry of Education, Culture, Sports, Science, and Technology.

ACKNOWLEDGMENTS

We express our gratitude to Dr. Akira Nishiyama and Dr. Narumi Katsuyama for their valuable comments in this study. We are also thankful to Project Assistant Professor Masako Akiyama for her statistical expertise.

- Beck, R. (2006). “Muscle fiber conduction velocity,” in *Wiley Encyclopedia of Biomedical Engineering*, ed. M. Akay, (Hoboken, NJ: John Wiley & Sons, Inc). doi: 10.1002/9780471740360.ebs0306
- Bhatt, S. (2010). The neurobiology of orthodontics: treatment of malocclusion through neuroplasticity. *Br. Dent. J.* 208, 433–433. doi: 10.1038/sj.bdj.2010.427
- Brocard, F., Verdier, D., Arsenault, I., Lund, J. P., and Kolta, A. (2006). Emergence of intrinsic bursting in trigeminal sensory neurons parallels the acquisition of mastication in weanling rats. *J. Neurophysiol.* 96, 2410–2424. doi: 10.1152/jn.00352.2006
- Changsiripun, C., Yabushita, T., and Soma, K. (2009). Masticatory function and maturation of the jaw-opening reflex. *Angle Orthod.* 79, 299–305. doi: 10.2319/021408-91.1
- Changsiripun, C., Yabushita, T., and Soma, K. (2012). Differences in maturation of the jaw-opening reflex between rats that received early- and late-masticatory stimulation. *J. Oral Rehabil.* 39, 879–887. doi: 10.1111/joor.12000
- Cifrek, M., Medved, V., Tonkovic, S., and Ostojic, S. (2009). Surface EMG based muscle fatigue evaluation in biomechanics. *Clin. Biomech.* 24, 327–340. doi: 10.1016/j.clinbiomech.2009.01.010
- Cobos, A. R., Segade, L. A., and Fuentes, I. (2001). Muscle fibre types in the suprahyoid muscles of the rat. *J. Anat.* 198(Pt 3), 283–294. doi: 10.1046/j.1469-7580.2001.19830283.x
- Enomoto, S., Kohase, H., and Nakamura, Y. (1995). Dual brain stem projection from the cortical masticatory area in guinea-pig. *Neuroreport* 6, 1573–1577. doi: 10.1097/00001756-199507310-00027
- Fujishita, A., Koga, Y., Utsumi, D., Nakamura, A., Yoshimi, T., and Yoshida, N. (2015). Effects of feeding a soft diet and subsequent rehabilitation on the development of the masticatory function. *J. Oral Rehabil.* 42, 266–274. doi: 10.1111/joor.12248

- Fukui, T., Tsuruta, M., Murata, K., Wakimoto, Y., Tokiwa, H., and Kuwahara, Y. (2002). Correlation between facial morphology, mouth opening ability, and condylar movement during opening-closing jaw movements in female adults with normal occlusion. *Eur. J. Orthod.* 24, 327–336. doi: 10.1093/Ejo/24.4.327
- Gerdle, B., Karlsson, S., Crenshaw, A. G., Elert, J., and Friden, J. (2000). The influences of muscle fibre proportions and areas upon EMG during maximal dynamic knee extensions. *Eur. J. Appl. Physiol. Occup. Physiol.* 81, 2–10. doi: 10.1007/Pl00013792
- Gerstner, G. E., and Goldberg, L. J. (1991). Genioglossus EMG activity during rhythmic jaw movements in the anesthetized guinea pig. *Brain Res.* 562, 79–84. doi: 10.1016/0006-8993(91)91189-8
- Grunheid, T., Langenbach, G. E., Korfage, J. A., Zentner, A., and van Eijden, T. M. (2009). The adaptive response of jaw muscles to varying functional demands. *Eur. J. Orthod.* 31, 596–612. doi: 10.1093/ejo/cjp093
- Haque, T., Yamamoto, S., Masuda, Y., Kato, T., Sato, F., Uchino, K., et al. (2010). Thalamic afferent and efferent connectivity to cerebral cortical areas with direct projections to identified subgroups of trigeminal premotoneurons in the rat. *Brain Res.* 1346, 69–82. doi: 10.1016/j.brainres.2010.05.034
- Herring, S. W. (1985). The ontogeny of mammalian mastication. *Am. Zool.* 25, 339–349. doi: 10.1093/icb/25.2.339
- Hichijo, N., Kawai, N., Mori, H., Sano, R., Ohnuki, Y., Okumura, S., et al. (2014). Effects of the masticatory demand on the rat mandibular development. *J. Oral Rehabil.* 41, 581–587. doi: 10.1111/joor.12171
- Hiranuma, M., Kokai, S., Fujita, K., Ishida, T., Shibata, M., Naito, S., et al. (2013). Effects of a liquid diet on the response properties of temporomandibular joint nociceptive neurons in the trigeminal subnucleus caudalis of growing rats. *Orthod. Craniofac. Res.* 16, 214–222. doi: 10.1111/ocr.12023
- Hirsch, C., John, M. T., Lautenschlager, C., and List, T. (2006). Mandibular jaw movement capacity in 10–17-yr-old children and adolescents: normative values and the influence of gender, age, and temporomandibular disorders. *Eur. J. Oral Sci.* 114, 465–470. doi: 10.1111/j.1600-0722.2006.00402.x
- Huang, C. S., Hiraba, H., and Sessle, B. J. (1989). Input-output relationships of the primary face motor cortex in the monkey (*Macaca fascicularis*). *J. Neurophysiol.* 61, 350–362. doi: 10.1152/jn.1989.61.2.350
- Ishida, T., Yabushita, T., and Soma, K. (2009). Effects of a liquid diet on temporomandibular joint mechano-receptors. *J. Dent. Res.* 88, 187–191. doi: 10.1177/0022034508328626
- Isogai, F., Kato, T., Fujimoto, M., Toi, S., Oka, A., Adachi, T., et al. (2012). Cortical area inducing chewing-like rhythmical jaw movements and its connections with thalamic nuclei in guinea pigs. *Neurosci. Res.* 74, 239–247. doi: 10.1016/j.neures.2012.10.009
- Kamen, G., and Gabriel, D. (2010). *Essentials of Electromyography*. Champaign, IL: Human Kinetics.
- Kato, T., Takahashi, S., and Domon, T. (2015). Effects of a liquid diet on the temporomandibular joint of growing rats. *Med. Princ. Pract.* 24, 257–262. doi: 10.1159/000370072
- Kawai, N., Sano, R., Korfage, J. A., Nakamura, S., Kinouchi, N., Kawakami, E., et al. (2010). Adaptation of rat jaw muscle fibers in postnatal development with a different food consistency: an immunohistochemical and electromyographic study. *J. Anat.* 216, 717–723. doi: 10.1111/j.1469-7580.2010.01235.x
- Keenan, K. G., Farina, D., Maluf, K. S., Merletti, R., and Enoka, R. M. (2005). Influence of amplitude cancellation on the simulated surface electromyogram. *J. Appl. Physiol.* 98, 120–131. doi: 10.1152/jappphysiol.00894.2004
- Kiliaridis, S., and Shyu, B. C. (1988). Isometric muscle tension generated by masseter stimulation after prolonged alteration of the consistency of the diet fed to growing rats. *Arch. Oral Biol.* 33, 467–472. doi: 10.1016/0003-9969(88)90026-X
- Kim, H. J., Park, K. M., Tak, H. J., Choi, J. W., Kang, S. H., Park, W., et al. (2018). Three-dimensional growth pattern of the rat mandible revealed by periodic live micro-computed tomography. *Arch. Oral Biol.* 87, 94–101. doi: 10.1016/j.archoralbio.2017.12.012
- Kitagawa, Y., Mitera, K., Ogasawara, T., Nojyo, Y., Miyauchi, K., and Sano, K. (2004). Alterations in enzyme histochemical characteristics of the masseter muscle caused by long-term soft diet in growing rabbits. *Oral Dis.* 10, 271–276. doi: 10.1111/j.1601-0825.2004.01020.x
- Kono, K., Tanikawa, C., Yanagita, T., Kamioka, H., and Yamashiro, T. (2017). A novel method to detect 3D mandibular changes related to soft-diet feeding. *Front. Physiol.* 8:567. doi: 10.3389/fphys.2017.00567
- Kufley, S., Scott, J. E., and Ramirez-Yanez, G. (2017). The effect of the physical consistency of the diet on the bone quality of the mandibular condyle in rats. *Arch. Oral Biol.* 77, 23–26. doi: 10.1016/j.archoralbio.2017.01.015
- Langenbach, G., van de Pavert, S., Savalle, W., Korfage, H., and van Eijden, T. (2003). Influence of food consistency on the rabbit masseter muscle fibres. *Eur. J. Oral Sci.* 111, 81–84. doi: 10.1034/j.1600-0722.2003.00008.x
- Liu, Z. J., Ikeda, K., Harada, S., Kasahara, Y., and Ito, G. (1998). Functional properties of jaw and tongue muscles in rats fed a liquid diet after being weaned. *J. Dent. Res.* 77, 366–376. doi: 10.1177/00220345980770020501
- Lund, J. P. (1991). Mastication and its control by the brain stem. *Crit. Rev. Oral Biol. Med.* 2, 33–64. doi: 10.1177/10454411910020010401
- Lund, J. P., and Kolta, A. (2006). Generation of the central masticatory pattern and its modification by sensory feedback. *Dysphagia* 21, 167–174. doi: 10.1007/s00455-006-9027-6
- Lund, J. P., Rossignol, S., and Murakami, T. (1981). Interactions between the jaw-opening reflex and mastication. *Can. J. Physiol. Pharmacol.* 59, 683–690. doi: 10.1139/y81-104
- Lund, J. P., Sasamoto, K., Murakami, T., and Olsson, K. A. (1984). Analysis of rhythmical jaw movements produced by electrical stimulation of motor-sensory cortex of rabbits. *J. Neurophysiol.* 52, 1014–1029. doi: 10.1152/jn.1984.52.6.1014
- Maeda, N., Kobashi, M., Mitoh, Y., Fujita, M., Minagi, S., and Matsuo, R. (2014). Differential involvement of two cortical masticatory areas in submandibular salivary secretion in rats. *Brain Res.* 1543, 200–208. doi: 10.1016/j.brainres.2013.11.024
- Masuda, Y., Tachibana, Y., Inoue, T., Iwata, K., and Morimoto, T. (2002). Influence of oro-facial sensory input on the output of the cortical masticatory area in the anesthetized rabbit. *Exp. Brain Res.* 146, 501–510. doi: 10.1007/s00221-002-1221-7
- Miyata, H., Sugiura, T., Kawai, Y., and Shigenaga, Y. (1993). Effect of soft diet and aging on rat masseter muscle and its motoneuron. *Anat. Rec.* 237, 415–420. doi: 10.1002/ar.1092370315
- Morquette, P., Lavoie, R., Fhima, M. D., Lamoureux, X., Verdier, D., and Kolta, A. (2012). Generation of the masticatory central pattern and its modulation by sensory feedback. *Prog. Neurobiol.* 96, 340–355. doi: 10.1016/j.pneurobio.2012.01.011
- Murakami, K., Fujisawa, H., Onobe, J., and Sato, Y. (2014). Relationship between muscle fiber conduction velocity and the force-time curve during muscle twitches. *J. Phys. Ther. Sci.* 26, 621–624. doi: 10.1589/jpts.26.621
- Nakamura, Y., and Katakura, N. (1995). Generation of masticatory rhythm in the brainstem. *Neurosci. Res.* 23, 1–19. doi: 10.1016/0168-0102(95)90003-9
- Nasution, F. H., Toda, K., and Soma, K. (2002). Functional maturation of periodontal mechanoreceptors during development in rats. *Brain Res. Dev. Brain Res.* 139, 307–312. doi: 10.1016/s0165-3806(02)00543-6
- Neafsey, E. J., Bold, E. L., Haas, G., Hurley-Gius, K. M., Quirk, G. F., Sievert, C. F., et al. (1986). The organization of the rat motor cortex: a microstimulation mapping study. *Brain Res.* 396, 77–96. doi: 10.1016/s0006-8993(86)80191-3
- Nordstrom, M. A. (2007). Insights into the bilateral cortical control of human masticatory muscles revealed by transcranial magnetic stimulation. *Arch. Oral Biol.* 52, 338–342. doi: 10.1016/j.archoralbio.2006.09.013
- Ogawa, K., Kiguchi, Y., Yamamoto-Nemoto, S., Hirai, N., Sawamoto, K., and Shimizu, T. (2016). Loss of masticatory function affects growth and development of the mandibular condyle in rats. *Open J. Stomatol.* 6, 261–273. doi: 10.4236/ojst.2016.612032
- Okihara, H., Ito, J., Kokai, S., Ishida, T., Hiranuma, M., Kato, C., et al. (2014). Liquid diet induces memory impairment accompanied by a decreased number of hippocampal neurons in mice. *J. Neurosci. Res.* 92, 1010–1017. doi: 10.1002/jnr.23383
- Paxinos, G., and Watson, C. (2007). *The Rat Brain in Stereotaxic Coordinates*, 6th Edn. Cambridge, MA: Academic Press.
- Phinyomark, A., Thongpanja, S., Hu, H., Phukpattaranont, P., and Limsakul, C. (2012). *The Usefulness of Mean and Median Frequencies in Electromyography Analysis*. London: InTech, 195–220. doi: 10.5772/50639
- Piancino, M. G., Isola, G., Cannavale, R., Cutroneo, G., Vermiglio, G., Bracco, P., et al. (2017). From periodontal mechanoreceptors to chewing motor control: a systematic review. *Arch. Oral Biol.* 78, 109–121. doi: 10.1016/j.archoralbio.2017.02.010

- Proffit, W. R., Fields, H. W. Jr., and Moray, L. J. (1998). Prevalence of malocclusion and orthodontic treatment need in the United States: estimates from the NHANES III survey. *Int. J. Adult Orthodon. Orthognath. Surg.* 13, 97–106.
- Renaud, S., Auffray, J. C., and de la Porte, S. (2010). Epigenetic effects on the mouse mandible: common features and discrepancies in remodeling due to muscular dystrophy and response to food consistency. *BMC Evol. Biol.* 10:28. doi: 10.1186/1471-2148-10-28
- Sasamoto, K., Zhang, G., and Iwasaki, M. (1990). Two types of rhythmical jaw movements evoked by stimulation of the rat cortex. *Jpn. J. Physiol.* 32, 57–68. doi: 10.2330/joralbiosci1965.32.57
- Sato, I., and Konishi, K. (2004). Effects of soft diet on rat masseter muscle mitochondrial development. *Okajimas Folia Anat. Jpn.* 81, 67–74. doi: 10.2535/ofaj.81.67
- Satoh, Y., Ishizuka, K., and Murakami, T. (2006a). Effect of orofacial motor cortex stimulation on neuronal activity in the red nucleus. *Brain Res.* 1123, 119–124. doi: 10.1016/j.brainres.2006.09.032
- Satoh, Y., Ishizuka, K., and Murakami, T. (2006b). Modulation of cortically induced rhythmical jaw movements by stimulation of the red nucleus in the rat. *Brain Res.* 1087, 114–122. doi: 10.1016/j.brainres.2006.03.001
- Satoh, Y., Ishizuka, K., and Murakami, T. (2007). Changes in cortically induced rhythmic jaw movements after lesioning of the red nucleus in rats. *Brain Res.* 1165, 60–70. doi: 10.1016/j.brainres.2007.06.008
- Seki, Y., Ishii, N., Toda, K., and Soma, K. (2002). Influence of occlusal hypofunction induced by opposed tooth loss on periodontal mechanoreceptors in rat molars. *Jpn. J. Biol.* 44, 66–74. doi: 10.2330/joralbiosci1965.44.66
- Seven, Y. B., Mantilla, C. B., Zhan, W. Z., and Sieck, G. C. (2013). Non-stationarity and power spectral shifts in EMG activity reflect motor unit recruitment in rat diaphragm muscle. *Respir. Physiol. Neurobiol.* 185, 400–409. doi: 10.1016/j.resp.2012.08.020
- Shi, L., Atsumi, Y., Kodama, Y., Honma, S., and Wakisaka, S. (2006). Requirement of proper occlusal force for morphological maturation of neural components of periodontal Ruffini endings of the rat incisor. *Arch. Oral Biol.* 51, 681–688. doi: 10.1016/j.archoralbio.2006.02.006
- Tamaki, T., and Uchiyama, S. (1995). Absolute and relative growth of rat skeletal muscle. *Physiol. Behav.* 57, 913–919. doi: 10.1016/0031-9384(94)00359-D
- Tomonari, H., Kwon, S., Kuninori, T., and Miyawaki, S. (2017). Differences between the chewing and non-chewing sides of the mandibular first molars and condyles in the closing phase during chewing in normal subjects. *Arch. Oral Biol.* 81, 198–205. doi: 10.1016/j.archoralbio.2017.05.006
- Trulsson, M. (2006). Sensory-motor function of human periodontal mechanoreceptors. *J. Oral Rehabil.* 33, 262–273. doi: 10.1111/j.1365-2842.2006.01629.x
- Tsai, C. Y., Lin, Y. C., Su, B., Yang, L. Y., and Chiu, W. C. (2012). Masseter muscle fibre changes following reduction of masticatory function. *Int. J. Oral Maxillofac. Surg.* 41, 394–399. doi: 10.1016/j.ijom.2011.10.016
- Tsouknidas, A., Jimenez-Rojo, L., Karatsis, E., Michailidis, N., and Mitsiadis, T. A. (2017). A bio-realistic finite element model to evaluate the effect of masticatory loadings on mouse mandible-related tissues. *Front. Physiol.* 8:273. doi: 10.3389/fphys.2017.00273
- Tsujimura, T., Tsuji, K., Magara, J., Sakai, S., Suzuki, T., Nakamura, Y., et al. (2016). Differential response properties of peripherally and cortically evoked swallows by electrical stimulation in anesthetized rats. *Brain Res. Bull.* 122, 12–18. doi: 10.1016/j.brainresbull.2016.02.015
- Uchino, K., Higashiyama, K., Kato, T., Haque, T., Sato, F., Tomita, A., et al. (2015). Jaw movement-related primary somatosensory cortical area in the rat. *Neuroscience* 284, 55–64. doi: 10.1016/j.neuroscience.2014.09.072
- Utsumi, D., Nakamura, A., Matsuo, K., Zeredo, J. L., Koga, Y., and Yoshida, A. (2010). Motor coordination of masseter and temporalis muscle during mastication in mice. *J. Stomat. Occlusion Med.* 3, 187–194. doi: 10.1007/s12548-011-0068-6
- van der Bilt, A., and Abbink, J. H. (2017). The influence of food consistency on chewing rate and muscular work. *Arch. Oral Biol.* 83, 105–110. doi: 10.1016/j.archoralbio.2017.07.011
- Watanabe, K., and Watanabe, M. (2001). Activity of jaw-opening and jaw-closing muscles and their influence on dentofacial morphological features in normal adults. *J. Oral Rehabil.* 28, 873–879. doi: 10.1111/j.1365-2842.2001.00738.x
- Westneat, M. W., and Hall, W. G. (1992). Ontogeny of feeding motor patterns in infant rats: an electromyographic analysis of suckling and chewing. *Behav. Neurosci.* 106, 539–554. doi: 10.1037//0735-7044.106.3.539
- Yamada, M., Koga, Y., Okayasu, I., Sanefuji, K., Yamada, Y., Oi, K., et al. (2006). Influence of soft diet feeding on development of masticatory function. *J. Jpn. Soc. Stomatognath. Funct.* 12, 118–125. doi: 10.7144/sgf.12.118
- Yamamoto, T., and Hirayama, A. (2001). Effects of soft-diet feeding on synaptic density in the hippocampus and parietal cortex of senescence-accelerated mice. *Brain Res.* 902, 255–263. doi: 10.1016/S0006-8993(01)02410-6

Conflict of Interest: The authors declare that the research was conducted in the absence of any commercial or financial relationships that could be construed as a potential conflict of interest.

Copyright © 2020 Aung, Kato, Abe, Ogawa, Ishidori, Fujita, Okihara, Kokai and Ono. This is an open-access article distributed under the terms of the Creative Commons Attribution License (CC BY). The use, distribution or reproduction in other forums is permitted, provided the original author(s) and the copyright owner(s) are credited and that the original publication in this journal is cited, in accordance with accepted academic practice. No use, distribution or reproduction is permitted which does not comply with these terms.



Persistent Feeding and Swallowing Deficits in a Mouse Model of 22q11.2 Deletion Syndrome

Lauren Welby^{1†}, Hailey Caudill^{2†}, Gelila Yitsege^{3,4}, Ali Hamad⁵, Filiz Bunyak⁵, Irene E. Zohn^{2,3,4,6}, Thomas Maynard⁷, Anthony-Samuel LaMantia^{7,8}, David Mendelowitz² and Teresa E. Lever^{1*}

¹ Department of Otolaryngology Head and Neck Surgery, School of Medicine, University of Missouri, Columbia, MO, United States, ² Department of Pharmacology and Physiology, School of Medicine and Health Sciences, The George Washington University, Washington, DC, United States, ³ Center for Genetic Medicine and the Center for Neuroscience Research, Children's National Medical Center, Children's National Health Systems, Washington, DC, United States, ⁴ School of Medicine and Health Sciences, Institute for Neuroscience, The George Washington University, Washington, DC, United States, ⁵ Department of Electrical Engineering and Computer Science, University of Missouri, Columbia, MO, United States, ⁶ Departments of Pediatrics, School of Medicine and Health Sciences, The George Washington University, Washington, DC, United States, ⁷ Laboratory of Developmental Disorders and Genetics, Virginia Tech-Carilion School of Medicine, The Fralin Biomedical Research Institute, Roanoke, VA, United States, ⁸ Department of Biology, Virginia Tech, Blacksburg, VA, United States

OPEN ACCESS

Edited by:

Emilia Michou,
University of Manchester,
United Kingdom

Reviewed by:

Tiffany J. Glass,
University of Wisconsin, United States
Toshi Tomoda,
Centre for Addiction and Mental
Health (CAMH), Canada

*Correspondence:

Teresa E. Lever
LeverTE@health.missouri.edu

[†]These authors have contributed
equally to this work

Specialty section:

This article was submitted to
Neurorehabilitation,
a section of the journal
Frontiers in Neurology

Received: 24 October 2019

Accepted: 06 January 2020

Published: 31 January 2020

Citation:

Welby L, Caudill H, Yitsege G,
Hamad A, Bunyak F, Zohn IE,
Maynard T, LaMantia A-S,
Mendelowitz D and Lever TE (2020)
Persistent Feeding and Swallowing
Deficits in a Mouse Model of 22q11.2
Deletion Syndrome.
Front. Neurol. 11:4.
doi: 10.3389/fneur.2020.00004

Disrupted development of oropharyngeal structures as well as cranial nerve and brainstem circuits may lead to feeding and swallowing difficulties in children with 22q11.2 deletion syndrome (22q11DS). We previously demonstrated aspiration-based dysphagia during early postnatal life in the *LgDel* mouse model of 22q11DS along with disrupted oropharyngeal morphogenesis and divergent differentiation and function of cranial motor and sensory nerves. We now ask whether feeding and swallowing deficits persist in adult *LgDel* mice using methods analogous to those used in human patients to evaluate feeding and swallowing dysfunction. Compared to wild-type mice, videofluoroscopic swallow study revealed that *LgDel* mice have altered feeding and swallowing behaviors, including slower lick rates, longer inter-lick intervals, and longer pharyngeal transit times with liquid consistency. Transoral endoscopic assessment identified minor structural anomalies of the palate and larynx in one-third of the *LgDel* mice examined. Video surveillance of feeding-related behaviors showed that *LgDel* mice eat and drink more frequently. Furthermore, *LgDel* animals engage in another oromotor behavior, grooming, more frequently, implying that divergent craniofacial and cranial nerve structure and function result in altered oromotor coordination. Finally, *LgDel* mice have significantly increased lung inflammation, a potential sign of aspiration-based dysphagia, consistent with results from our previous studies of early postnatal animals showing aspiration-related lung inflammation. Thus, oromotor dysfunction, feeding, and swallowing difficulties and their consequences persist in the *LgDel* 22q11DS mouse model. Apparently, postnatal growth and/or neural plasticity does not fully resolve deficits due to anomalous hindbrain, craniofacial, and cranial nerve development that prefigure

perinatal dysphagia in 22q11DS. This new recognition of persistent challenges with feeding and swallowing may provide opportunities for improved therapeutic intervention for adolescents and adults with 22q11DS, as well as others with a history of perinatal feeding and swallowing disorders.

Keywords: 22q11 deletion syndrome, DiGeorge syndrome, pediatric dysphagia, dysphagia, deglutition, feeding, mouse model

INTRODUCTION

Almost all infants with 22q11.2 Deletion Syndrome (22q11DS) have pediatric dysphagia—perinatal difficulties with suckling, feeding, and swallowing (1). As a consequence, many children with 22q11DS have recurrent naso-sinus and respiratory infections, impaired speech development, and failure to thrive (2, 3). Clinically significant dysphagia continues in approximately one-third of individuals with 22q11DS as they mature, and approximately half will require enteral feeding interventions (1). Our previous work demonstrates that newborn *LgDel* mice—a genomically accurate 22q11DS model that carries a heterozygous deletion of 28 contiguous genes on mouse chromosome 16, orthologous to the minimal 1.5 MB critical region on human chromosome 22 deleted in 22q11DS (4, 5)—exhibit multiple signs of pediatric dysphagia (6, 7). It is not clear, however, whether maturation or compensatory changes including neural circuit plasticity correct or at least diminish presumed developmental pathology. Thus, we asked whether dysphagic symptoms continue into maturity in adult *LgDel* mice using high resolution video and fluorographic analysis of oromotor function and feeding-related behaviors.

Several clinically significant 22q11DS phenotypes, including pediatric dysphagia, emerge during infancy and early life (2, 8–10). Many of these phenotypes reflect disruptions of the developmental program for embryonic pharyngeal morphogenesis (11). Nevertheless, feeding difficulties in 22q11DS are apparently independent of palatal and/or cardiac disruption and instead reflect poor coordination of the suck/swallow/breathing pattern (1), implicating altered neural circuit differentiation in this 22q11DS clinical complication. Disrupted patterning of the embryonic hindbrain, as well as divergent development of cranial nerves (CNs) V, IX, and X precede these anomalies (7). Despite these developmentally established differences, it remains unclear whether apparently related perinatal feeding and swallowing difficulties are mostly resolved subsequently, or whether they persist, introducing ongoing challenges for essential oromotor behaviors throughout life.

Accordingly, we characterized feeding and swallowing related behaviors as well as oropharyngeal and craniofacial morphology in adult *LgDel* mice and wild type (WT) controls and assessed additional signs of aspiration-related swallowing difficulties. We assessed functional phenotypes related to dysphagia using fluoroscopic and endoscopic approaches as well as automated video-based monitoring and computational analysis of baseline feeding behaviors. We found that *LgDel* adult mice have persistent oromotor control difficulties, disrupted feeding, and aspiration-related lung inflammation. These studies establish

methods for continued analysis of the consequences of underlying developmental origins of dysphagia and a preclinical model so that rational strategies of treatment and prevention can be devised.

METHODS

Animals

All mice in this study were offspring from a Del(16Dgcr2-Hira)1Rak (*LgDel*) colony maintained at The George Washington University. Wild-type (WT) and *LgDel* littermates were obtained by crossbreeding heterozygous C57BL/6N *LgDel* males with adult C57BL/6N WT females. Following genotyping by PCR (12) at weaning, 32 colony offspring were allocated to this study: 16 *LgDel* (11 males and five females) and 16 WT (10 males and six females). Mice were subsequently ear punched for identification and group housed (based on sex and litter) without experimental testing until approximately 3 months of age. At that time, 22 mice (11 *LgDel*: six males and five females; 11 WT: five males and six females) were shipped to the University of Missouri and following a 2-week quarantine period, were processed for fluoroscopic (13–15) and endoscopic (16–19) assessments of deglutition-related structure and function. The remaining 10 mice (5 *LgDel* and 5 WT, all males) were retained at The George Washington University for video surveillance of feeding and grooming activity using automated behavioral analysis (HomeCageScan 3.0; CleverSys Inc., Reston, VA) and Capture Star software (Version 1; CleverSys Inc.). Mice were housed in accordance with NIH and Institutional Animal Care and Use Committee guidelines, under standard local light/dark cycle conditions at The George Washington University (14/10 h) and the University of Missouri (12/12 h).

Experimental Procedures

Mice underwent experimental procedures described below between 3 and 4 months of age, followed by euthanasia for post-mortem assessment of lung tissue and cranial bones. The genotypes of all mice were blinded until all data collection was completed; *unblinding occurred* following data entry for statistical analysis.

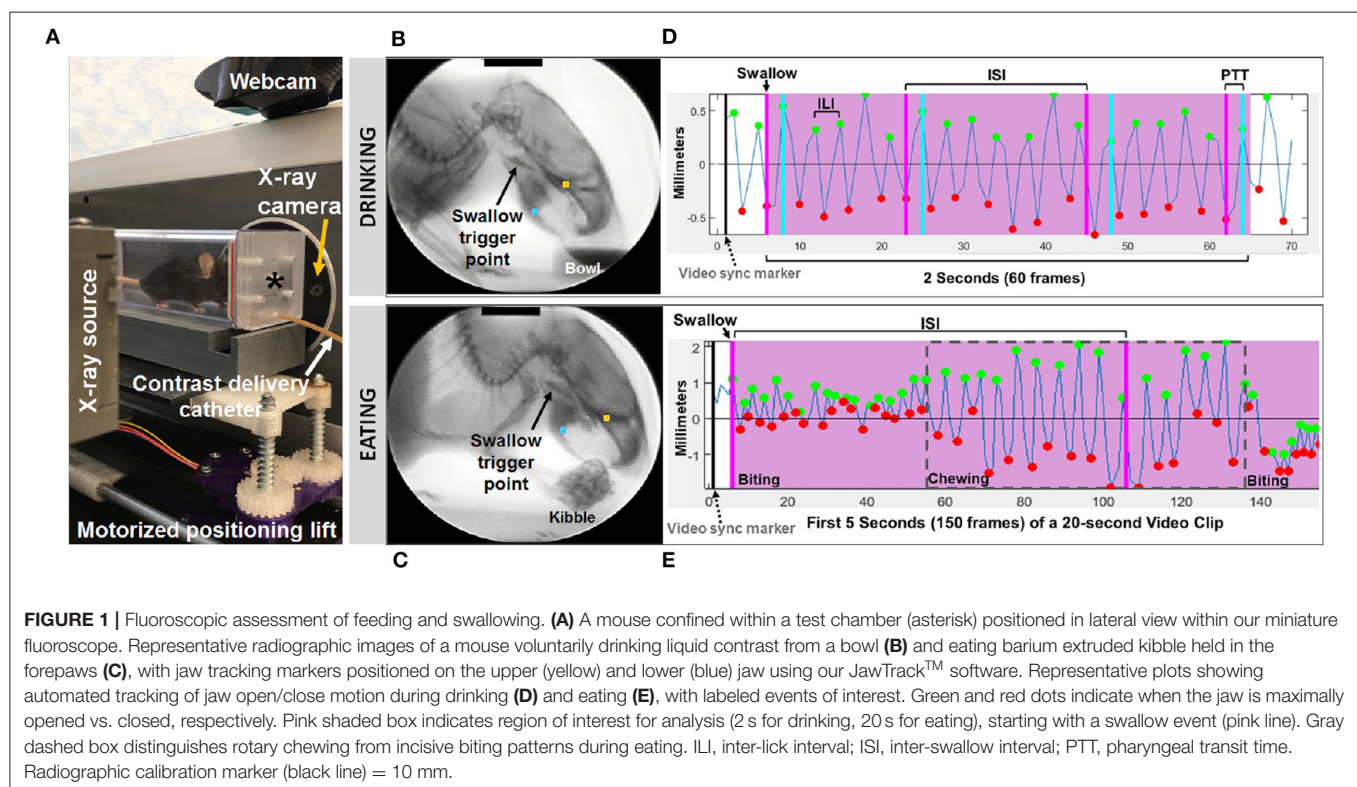
Fluoroscopic Assessment of Feeding and Swallowing

Mice ($n = 11$ WT, 11 *LgDel*, mixed sexes, 3–4 months of age) underwent videofluoroscopic swallow study testing (VFSS) at the University of Missouri using custom equipment and an established protocol (13–15). Following 2-week behavioral conditioning to optimize performance, VFSS testing was

performed separately for drinking vs. eating, spaced 1 week apart. For each test (drinking vs. eating), mice were individually subjected to ~2 min of low dose radiation (~30 kV and ~0.2 mA) using our miniaturized fluoroscope (The LabScope, Glenbrook Technologies, Randolph, NJ). The night prior to testing, mice were weighed (grams) and then underwent either a water restriction (12 h) to motivate voluntary drinking or a food restriction (4–6 h) to motivate voluntary eating, both in the home cage. A VFSS test chamber with one endcap removed was placed in the home cage overnight for mice to voluntarily explore; this same test chamber was used during VFSS testing the following morning. During testing, mice were enclosed within the test chamber and positioned within the lateral plane of the fluoroscope (**Figure 1**). For drinking, our established thin liquid oral contrast agent (Omnipaque, GE Healthcare, 350 mg iodine/mL; diluted to a 25% solution with deionized water and 3% chocolate flavoring) was administered via a custom syringe delivery device into a custom bowl, secured to the test chamber end-cap closest to the radiation source. For eating, peanut butter flavored kibble (circular shape, ~10 mm diameter × 5 mm thick) extruded with barium (40% weight/volume, manufactured in collaboration with AFB International, St. Charles, MO), which retains a dry, crunchy consistency, was used for fluoroscopic assessment of mastication-related behaviors. For each mouse, a half piece of kibble (~10 × 5 × 5 mm) was placed in the chamber bowl. Throughout testing, the fluoroscope was activated via foot pedal only when the mouse was actively drinking or eating, visualized in real-time using a webcam (Logitech, HD Pro C920) positioned above the test chamber. A custom, remote-controlled

platform was used to maintain the mouse's head and neck in the fluoroscopy field of view while drinking and eating.

Approximately 30 s to 1 min of video was captured separately for drinking and eating episodes, digitally recorded at 30 frames per second (fps) and saved as AVI files. From these videos, five 2 s episodes of uninterrupted drinking and one 20 s episode of uninterrupted eating were identified; the start frame coincided with a swallow event, identified as abrupt movement of the bolus from the vallecular space (i.e., the stereotypical swallow trigger point in mice) to the esophagus. These “episodes” were spliced from the raw video using Pinnacle Studio (version 14; Pinnacle Systems, Inc., Mountain View, CA), with five frames added to each end to provide contextual information as needed during subsequent frame-by-frame analysis using our custom VFSS analysis software, JawTrack™. This software (© Copyright 2019 by The Curators of the University of Missouri) provides an interactive interface that permits automated tracking of jaw motion during drinking and eating in rodents based on the location of manually placed markers on the upper and lower jaw in the first frame of each video clip. The distance (in pixels) between the two markers is automatically converted into mm for each video frame, based on manual tracing of the 10 mm calibration marker at the top of the first video frame image displayed in the interface. Following jaw tracking, the interface displays a graph of cyclic jaw opening and closing motion (distance over time), synchronized with the video. Jaw tracking events (i.e., maximally opened or closed jaw) are manually reviewed and easily edited within the interface. Further, bolus flow events of interest (e.g., swallowing) can be manually added



via makers within the jaw tracking graph. Once all events are edited/added, a set of VFSS metrics (**Table 1**) is automatically calculated and displayed in the interface as well as automatically exported into an Excel spreadsheet for subsequent use in statistical analysis. The only exception is mastication rate, which required manual identification of rotary chewing behaviors in the graphic display. Also of note, pharyngeal transit time was not included during eating, as bolus flow through the distal pharynx and proximal esophagus was typically obscured by the shoulders and arms while mice ate kibble from the forepaws.

Endoscopic Assessment of Upper Airway Structure and Function

Within 1 week after completing VFSS testing, the same 22 mice underwent transoral endoscopy for gross assessment of craniofacial structure and function using our established protocol and custom equipment (16–19). The night prior to endoscopy, mice were food restricted for 4–6 h to prevent post-prandial retention of food in the pharynx that may interfere with testing. Mice were anesthetized with ketamine-xylazine (90 mg/kg ketamine, 11.25 mg/kg xylazine, subcutaneous injection) followed by a single dose of ketamine (1/2 the original dose) to maintain light sedation (i.e., only local limb movement in response to toe pinch) while secured in ear bars in dorsal recumbency within our custom murine endoscopy suite. Core body temperature was maintained at $37 \pm 0.2^\circ\text{C}$ using a rectal thermocouple (DC Temperature Control System; FHC, Bowdoin, ME). Mice spontaneously breathed room air during the entire procedure, which lasted ~30 min.

Endoscopy was performed using a miniature endoscope (sialendoscope; R11573A; Karl Storz). A custom laryngoscope was used to secure the endoscope to a custom micromanipulator, which permitted precise manual control. The tongue was gently

retracted as the endoscope was guided via micromanipulator into the oral cavity, then slowly advanced to visualize the pharynx and larynx. The larynx was maintained in the endoscope field of view for approximately 10 s to visualize spontaneous abduction and adduction motion during each inspiratory and expiratory phase of the respiratory cycle, respectively. Using our previously published methods (19), we then assessed the laryngeal adductor reflex (LAR) by delivering up to five air puffs per mouse, targeting the arytenoid mucosa near the dorsal commissure. Air pulses (4 mm Hg, 250 ms duration) were delivered via the sialendoscope working channel using our custom air pulse generating device, with stimuli spaced at least 10 s apart. Responses were scored as present or absent. A present response was identified by abrupt, brief glottic closure (i.e., bilateral arytenoid medialization) immediately following air pulse delivery. The entire endoscopic procedure was video recorded at 30 fps and saved as MPEG files.

At a later time, the videos were viewed via Pinnacle Studio (version 14; Pinnacle Systems) to identify gross structural and functional anomalies. LAR events were analyzed frame-by-frame to identify the start and end frame, which was used to calculate LAR duration (ms). From each video, a 10 s episode of uninterrupted vocal fold motion during spontaneous breathing was spliced from the raw video for objective analysis using our custom laryngeal motion analysis software, VFtrackTM. This software (© Copyright 2017 by The Curators of the University of Missouri) provides an interactive interface that permits automated tracking of laryngeal motion during breathing, based on manually placed markers on the left and right glottal edge (near the vocal process) and dorsal commissure (midline between the arytenoids) in the first frame of each video clip. Using these three points, two separate lines are automatically drawn along the left and right glottal edge. The location of the left and right points is automatically adjusted to be equidistant from

TABLE 1 | VFSS metrics and operational definitions.

| | VFSS metrics | Operational definitions | Units |
|----------|-------------------------|---|-------|
| Drinking | Lick rate | Number of jaw open/close cycles per second, calculated separately for each second of a 2 s video clip, then averaged. | #/s |
| | Inter-lick interval | Time between successive lick cycles throughout a 2 s video clip. | ms |
| | Swallow rate | Number of swallows in each second of a 2 s video clip, converted to a rate (swallows/second), then averaged. | #/s |
| | Inter-swallow interval | Time between successive swallow pairs throughout a 2 s video clip, then averaged. | ms |
| | Lick-swallow ratio | Number of jaw open/close cycles between each successive swallow pair throughout a 2 s video clip, then averaged. | n/a |
| | Pharyngeal transit time | Bolus flow time through the pharynx for each successive swallow, then averaged. The start frame is the “rest frame” that immediately precedes visible transfer of the bolus from the vallecula (swallow trigger point). The end frame is when the tail of the bolus enters the esophagus. | ms |
| | Jaw closing velocity | Speed at which the jaw closes during each jaw cycle throughout a 2 s video clip, then averaged. | mm/s |
| Eating | Jaw opening velocity | Speed at which the jaw opens during each jaw cycle throughout a 2 s video clip, then averaged. | mm/s |
| | Mastication rate | Number of jaw open/close cycles per second during three separate 1 s episodes of rotary mastication, then averaged. | #/s |
| | Swallow rate | Number of swallows in each second of a 20 s video clip, converted to a rate (swallows/second), then averaged. | #/s |
| | Inter-swallow interval | Time between successive swallow pairs throughout a 20 s video clip, then averaged. | s |

All video clips depict uninterrupted drinking or eating behaviors, beginning with a swallow event (i.e., rest frame immediately preceding bolus flow from the vallecula). For each mouse, five 2 s episodes of drinking and one 20 s episode of eating were analyzed via JawTrackTM.

the dorsal commissure point, using the furthest left/right point as the reference. The adjusted points are then automatically tracked in all subsequent video frames and graphically displayed in the interface as a cyclic waveform representing the oscillatory motion of the larynx during breathing. Using the interface, glottal tracking events can be manually reviewed in synchrony with the video and edited as needed. Following manual review and editing, a set of laryngeal motion metrics (**Table 2**) is automatically calculated and displayed in the interface, as well as automatically exported into an Excel spreadsheet for subsequent use in statistical analysis. A summary of the entire endoscopic test and analysis process is shown in **Figure 2**.

Craniofacial Imaging

While still anesthetized from endoscopy, photographic (Apple iPhone 6 Plus) and radiographic (LabScope) images were obtained for gross assessment of craniofacial structures and features. Mice were photographed from the front, left lateral, and right lateral positions, followed by fluoroscopic imaging in the lateral and axial planes. Images of *LgDel* mice were compared side-by-side with WT mice to identify visibly obvious abnormalities in craniofacial structure and symmetry.

Post-mortem Assessment of Lung Tissue and Cranial Bones

Following imaging and while still anesthetized, mice were euthanized by pentobarbital overdose (390 mg/ml + sodium phenytoin 50 mg/ml, intraperitoneal injection), followed by cardiac perfusion with saline and then 4% paraformaldehyde (PFA). The lungs (with trachea attached) and skulls were collected and shipped to The George Washington University on dry ice for processing. Lungs were washed in phosphate-buffered saline, equilibrated in 30% sucrose, and then embedded in optimal cutting temperature (OCT) compound. Frozen lung tissue was sectioned at 20 microns via cryostat (Leica CM1950) and stained with Hematoxylin and Eosin (H&E). Images were acquired using an Olympus BX63 Upright Microscope equipped with a DP80 digital camera and cellSens imaging software using the 10X and 20X objectives. Hemorrhages were digitally quantified in Adobe Photoshop (20). Five images were taken

for each sample, each adjusted in Adobe Photoshop using the following methods: (1) the Magic Wand tool was used to select and remove the background from the image; (2) under the Hue/Saturation tool, the red channel was selected and increased to +100; (3) the blue channel was selected and maximally decreased, and the lightness was increased to +100; and (4) the brightness and contrast were changed to 150 and 100, respectively. These color adjustments isolated the darker red/purple hues of blood vessels and clumps of neutrophils. The threshold was then set to 130 to completely isolate the inflamed pixels. An inflammation ratio for each image was calculated by comparing the number of pixels within the threshold and the total number of pixels before editing. The five inflammation ratios per sample were averaged together to obtain a representative inflammation ratio for each mouse.

For bone analysis, fixed cranial bones were isolated by multiple digestions (3–4 days each, until tissue was removed, over a period of ~3 weeks) with proteinase K (200 µg/ml) at 60°C in buffer (20 mM Tris, 10 mM CaCl₂, 400 mM NaCl, 1% Sodium dodecyl sulfate, pH 8.0). Bones were imaged on a Leica M420 microscope with a 5MP digital camera. Mandibles were imaged laterally, and pixel measurements between cardinal points were made in Adobe Photoshop and converted to millimeter measurements by scaling to a micrometer imaged in the same imaging session.

Video Surveillance of Feeding and Grooming Activity

A separate cohort consisting of 10 male mice (5 WT, 5 *LgDel*, 3–4 months of age) collected from multiple litters, was assessed using an automated behavioral analysis system (HomeCageScan 3.0; CleverSys Inc., Reston, VA) and Capture Star software (Version 1; CleverSys Inc.) that permits real-time detection and analysis of a variety of unconstrained rodent behaviors (21). For this study, we focused on detection and analysis of drinking, eating, and grooming behaviors for comparison with non-oromotor-based behaviors (**Figure 3**). Testing entailed placing individual mice into a clean shoebox-style acrylic cage with a filter top. Within each cage, a wire top feeder provided free access to

TABLE 2 | Laryngeal motion metrics and operational definitions.

| Laryngeal motion metrics | Operational definitions | Units |
|--|--|---------|
| Mean motion range ratio (MMRR) | Ratio of the right and left VF motion range (i.e., amplitude) during each respiratory cycle throughout a 10 s video clip, then averaged. | n/a |
| Open close cycle ratio (OCCR) | Ratio of the number of right and left VF motion cycles (i.e., frequency) throughout a 10 s video clip, then averaged. | n/a |
| Motion correlation coefficient (Mcorr) | Comparison of left and right VF motion direction (i.e., motion correlation coefficient) in each video frame throughout a 10 s clip, then averaged. Values range from –1 to 1, where values close to –1 represent a negative correlation (i.e., VF motion in opposite directions; normal function), values close to 1 represent a positive correlation (i.e., VF motion in the same direction; paradoxical motion), and values close to 0 represent minimal correlation (i.e., little to no VF motion). | n/a |
| VF angle | Measurement of VF maximum and minimum angle for each respiratory cycle throughout a 10 s video clip, then averaged. | degrees |
| Respiratory rate | Number of VF motion cycles per minute throughout a 10 s video clip, then averaged. VF abduction = inspiration; VF adduction = expiration. | #/min |

For each mouse, one 10 s video clip of spontaneous breathing under anesthesia was analyzed via VFTrack™.

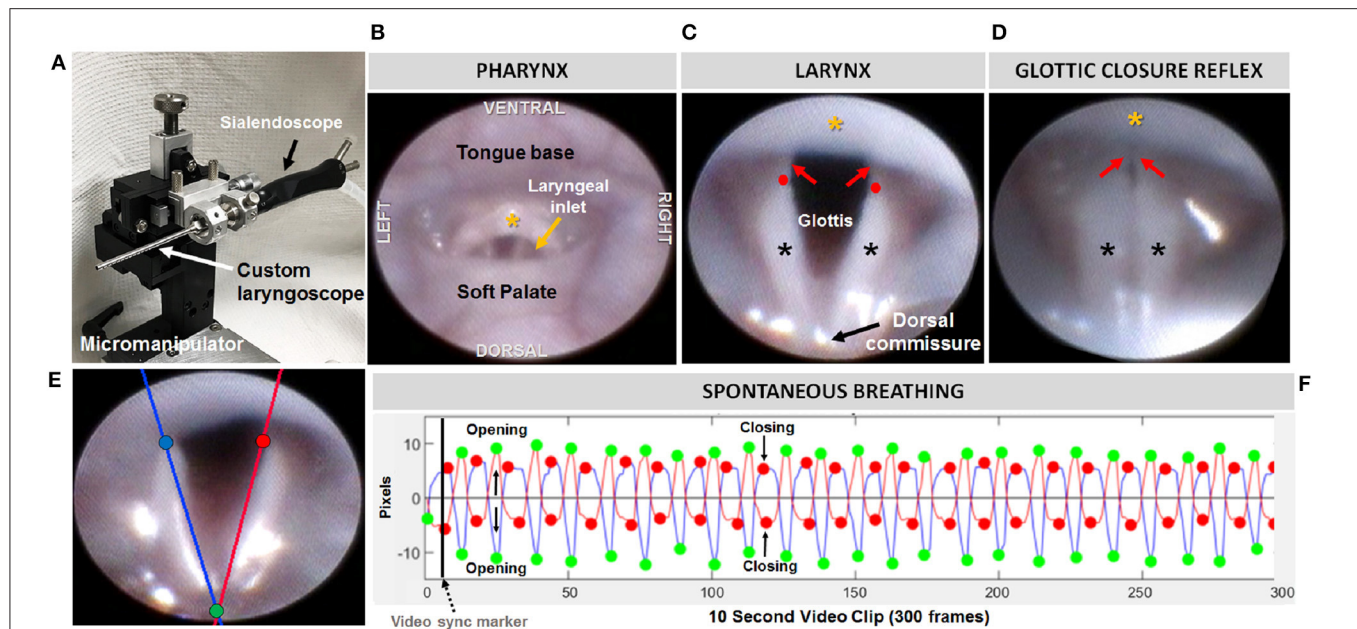


FIGURE 2 | Endoscopic assessment of upper airway structure and function. **(A)** Modified sialendoscope with micromanipulator control for precise transoral insertion. Representative endoscopic images of a mouse pharynx **(B)** and larynx **(C)** with labeled structures. In mice, the glottal edge is formed predominantly by the arytenoids (black asterisks); the proportionately smaller vocal folds (red arrows) are nearly obscured by the epiglottis (yellow asterisk); red dots indicate the location of the arytenoid vocal process. **(D)** Air pulse stimulation of the arytenoid mucosa near the dorsal commissure evokes the glottic closure reflex (i.e., laryngeal adductor reflex, LAR), identified by brief, bilateral medialization of the arytenoids and vocal folds. **(E)** Tracking lines positioned along the left (blue) and right (red) glottal edge using our VFTrack™ software, based on the location of three manually placed markers within the software interface: blue (left arytenoid vocal process), red (right arytenoid vocal process), and green (dorsal commissure). **(F)** Representative plot showing automated tracking of glottal edge open/close motion during spontaneous breathing under light sedation. Green and red dots indicate when the glottis is maximally opened during inspiration vs. maximally closed during expiration, respectively.

standard rodent pellets in a U-shaped hopper and water from a standard spout bottle. Each cage was placed into one of the four chambers (stacked 2 X 2) within the monitoring system, each equipped with one infrared camera positioned exterior to the right or left side of the cage, depending upon chamber assignment, for side-view recording. The position of all four cameras was adjusted within each chamber to maintain a consistent field of view within and between cages. To maximize visibility within the cage, enrichment material was limited to a thin layer of cobb bedding on the cage floor and half of a nestlet (i.e., nesting material). Mice were acclimated to the cage for 24 h, followed by 72 consecutive hours of video recording (30 fps, MPG file format) and real-time detection and analysis of drinking, eating, and grooming activity (frequency and duration; **Table 3**). Prior to recording, the following parameters were manually defined within the software: location of the food hopper and waterspout, and interior cage perimeter (i.e., free-space accessible to the mouse). It should be noted that all mice appeared healthy prior to and following the recording, with no evidence of barbering, hair loss, or skin lesions due to chewing. Additionally, eating and drinking occurred while the mice were rearing on hind legs due to the location of the food hopper and waterspout, as shown in **Figure 3**, which allowed the software to readily detect these behaviors for analysis. For each mouse, the automatically detected and analyzed drinking, eating, and grooming data (frequency and duration) from the 72 h of video recording were exported to Excel as three 24 h periods (bins), each including chronological event classification

(drinking, eating, or grooming), along with the corresponding timestamp, frequency, and duration of each event. At a later time, the data were “spot checked” for accuracy at ~6 h intervals by manually comparing the automated event classification with the corresponding timestamp in the video recording. Data from the three 24 h bins were averaged for each mouse for statistical analysis.

Statistical Analysis

After verifying a normal data distribution for each variable, independent samples *t*-tests were used to explore differences between the two genotypes (WT and *LgDel*), using averaged data when applicable. Outliers were identified but not removed from the dataset. Statistical analyses were performed using IBM SPSS Statistics 24. Variability within genotype was reported as the mean \pm standard error of mean (SEM) for each variable, and two-sided *p* values of 0.05 or less were considered statistically significant. Mandibular measurements were assessed by 2-way ANOVA (genotype x side, GraphPad PRISM) to account for measurements of both left and right bones.

RESULTS

Fluoroscopic Assessment of Feeding and Swallowing

We first asked whether the oral or pharyngeal phases of feeding and swallowing in *LgDel* mice differed from their WT counterparts. All 22 mice subjected to VFSS testing voluntarily

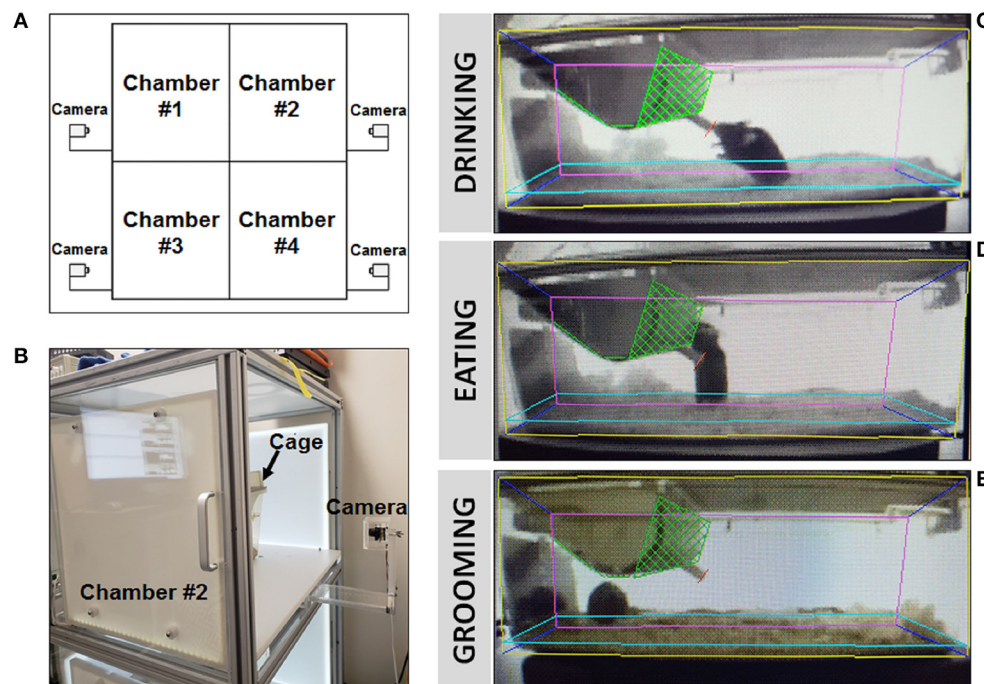


FIGURE 3 | Behavioral video surveillance of murine activity via HomeCageScan. **(A)** Schematic of CleverSys Inc. HomeCageScan chamber and camera set-up made up of four separate chambers, each with its own camera for behavioral recording. One mouse/cage was placed into each chamber, up to 4 animals at a time to be analyzed. **(B)** Enlarged image for detail of the cameras used to record all behaviors attached to each chamber. **(C–E)** Specific parameters for each standard size cage were manually defined prior to recording in order to ensure accurate analysis: yellow—area of the proximal lateral cage wall, pink—area of the distal lateral cage wall, dark blue—area of the front and back cage walls, light blue—area and height of the bedding, green—food container, red—drinking spout. All three images were taken from the same animal. **(C)** Still image of “drinking” behavior recorded and analyzed by the software. **(D)** Still image of “eating” behavior recorded and analyzed by the software. **(E)** Still image of “grooming” behavior recorded and analyzed by the software.

participated, resulting in 110 drinking-based video clips (2 s each) and 22 eating-based video clips (20 s each) for frame-by-frame analysis of VFSS metrics (**Table 1**) using JawTrackTM. Body weight prior to VFSS testing was not significantly different between groups ($p = 0.373$; WT: 22.39 ± 0.55 ; *LgDel*: 21.83 ± 0.26). We analyzed both male and female mice; however, we have not separated the samples by sex for this study. Some behavioral sex differences have been described in individuals with 22q11DS: males tend to be more withdrawn, have more somatic complaints, and are more likely to have anxiety and depression than females (22). Nevertheless, the incidence of dysphagia and other airway abnormalities in 22q11DS does not differ between males and females (1, 10, 23–26). In addition, our previous research with adult C57BL/6J mice revealed no significant differences in swallowing function between sexes (13). Compared to WT mice, *LgDel* mice had altered swallowing behaviors during drinking (**Table 4**; **Figure 4**). Specifically, *LgDel* mice had significantly slower lick rates ($p = 0.035$; WT: 8.71 ± 0.18 ; *LgDel*: 8.07 ± 0.22 ; **Figure 4A**), longer inter-lick intervals ($p = 0.046$; WT: 114.43 ± 2.30 ; *LgDel*: 121.91 ± 2.65 ; **Figure 4B**), and longer pharyngeal transit times ($p = 0.013$; WT: 85.82 ± 1.91 ; *LgDel*: 94.36 ± 2.50 ; **Figure 4C**). All other drinking- and eating-based VFSS metrics were not statistically different between genotypes ($p > 0.05$; **Table 4**). Thus, there are significant differences in distinct, measurable aspects of the

oral and pharyngeal phases of feeding and swallowing in adult *LgDel* mice.

Transoral Endoscopy

We next asked whether oropharyngeal dysmorphology accompanies these functional differences in *LgDel* adult feeding and swallowing. Minor structural anomalies of the palate and larynx were identified in four of the 11 *LgDel* mice (36%) that underwent transoral endoscopic assessment. All of the WT mice appeared structurally normal. Specifically, one *LgDel* mouse had an asymmetric soft palate, two had extraneous laryngeal mucosa along the medial edge of the glottis, and another had a narrowed larynx without any visible aryepiglottic folds (**Figure 5**). Laryngeal adductor reflex (LAR) testing was successful in only eight mice (4 WT and 4 *LgDel*), mainly attributed to the laryngoscope diameter (2.0 mm outer diameter) being slightly too large to pass through the laryngeal inlet for targeted air pulse delivery to the dorsal commissure of the larynx. The LAR was evoked in all 4 WT mice but only three of the four *LgDel* mice. For the seven mice with LAR responses, no difference in LAR duration was identified between WT and *LgDel* mice ($p = 0.197$). VFtrackTM analysis of the 10 s endoscopic video clips revealed that laryngeal motion metrics were not significantly different between WT and *LgDel* mice ($p > 0.05$), as summarized in **Table 5**. In other words, laryngeal motion

TABLE 3 | HomeCageScan metrics and operational definitions.

| HomeCageScan metrics | | | Operational definitions | Units |
|----------------------|-------------------|-----------|---|-------------|
| Oromotor | Drinking | Frequency | Number of times that the animal's snout is in close proximity to the defined water spout in the act of drinking. | events/bin |
| | | Duration | The length of time the animal spends drinking as analyzed by the animal's snout being within close proximity to the defined water spout starting from a non-drinking position, to active drinking, until finished. | seconds/bin |
| | Eating | Frequency | Number of times that the animal's snout is at/near the defined food hopper in the act of eating. | events/bin |
| | | Duration | The length of time the animal spends eating as analyzed by the animal's snout being at/near the defined food hopper from a non-eating position, to active eating, until finished. | seconds/bin |
| | Grooming | Frequency | The number of times the animal's snout is in close proximity to its body and the body deforms into a grooming position while making specific grooming movements with its head, paws, and body. | events/bin |
| | | Duration | The length of time an animal spends in a grooming position, with the animal's snout in close proximity to its body and making specific grooming movements with its head, paws, and body. | seconds/bin |
| Non-Oromotor | Walking Slowly | Frequency | The number of times that the animal makes any sideways movement that does not have a definite directional component. | events/bin |
| | Come Down | Duration | The length of time an animal spends moving from a fully reared up position to a low position. | seconds/bin |
| | Hang vertically | Duration | The length of time and animal spends moving from a hang cuddled position to a hang vertical position (note: the hang cuddled position involves the animal having all four limbs at the top of the cage in a horizontal position). | seconds/bin |
| | from hang cuddled | | | |

Each "bin" represents a 24 h period of data collection.

TABLE 4 | VFSS summary statistics.

| VFSS metrics | | p-value | Mean (\pm SEM) | |
|--------------|------------------------------|--------------|-------------------|----------------|
| | | | WT | LgDel |
| Drinking | Lick rate (#/s) | 0.035 | 8.71 (0.18) | 8.07 (0.22) |
| | Inter-lick interval (ms) | 0.046 | 114.43 (2.30) | 121.91 (2.65) |
| | Swallow rate (#/s) | 0.508 | 1.68 (0.11) | 1.77 (0.08) |
| | Inter-swallow interval (ms) | 0.356 | 752.91 (56.22) | 690.18 (35.35) |
| | Lick-swallow ratio | 0.228 | 4.47 (0.36) | 3.85 (0.34) |
| | Pharyngeal transit time (ms) | 0.013 | 85.82 (1.91) | 94.36 (2.50) |
| | Jaw closing velocity (mm/s) | 0.255 | 14.39 (0.77) | 13.19 (0.67) |
| | Jaw opening velocity (mm/s) | 0.883 | 13.71 (0.71) | 13.55 (0.79) |
| Eating | Mastication rate (#/s) | 0.852 | 8.26 (0.31) | 8.167 (0.42) |
| | Swallow rate (#/s) | 0.228 | 0.31 (0.08) | 0.27 (0.02) |
| | Inter-swallow interval (s) | 0.840 | 4.01 (0.60) | 4.17 (0.43) |

Bold p-values denote statistical significance (<0.05); SEM, standard error of the mean; VFSS, videofluoroscopic swallow study; WT, wild-type.

in *LgDel* mice was bilaterally symmetric during spontaneous breathing under light anesthesia, without detectable aberrations in motion range or frequency. Thus, structural anomalies of the palate, glottis and larynx, at moderate penetrance, accompany functional disruption feeding and swallowing in *LgDel* mice. Nevertheless, the consequences of these anomalies for baseline laryngeal reflexes and function during breathing are uncertain; few differences were detected between *LgDel* and WT for these measures.

Craniofacial Imaging

It seemed possible that partially penetrant, but significant, oropharyngeal functional and structural anomalies in *LgDel*

adult mice might occur in concert with extrinsic craniofacial anomalies. Facial photography and skull radiographs revealed structural anomalies of the eyes, premaxilla, nasal spine, incisors, and/or snout in two of the 11 *LgDel* mice (18%; **Table 6; Figure 6**). One of these mice was previously identified via endoscopy as having soft palate asymmetry. This brings the final count to five of the 11 *LgDel* mice (45%) identified with anomalies based upon assessment of craniofacial structure and function. To confirm these *in vivo* assessments we isolated the mandible, nasal, frontal and zygomatic bones of the dorsal skull of one of these mice, and saw significant bone dysmorphology that parallels the live craniofacial malformations (**Figure 6**). Thus, in agreement with initial measures of quantitative changes in the size and structure of the mandible in juvenile *LgDel* mice (7), there is evidence of variable extrinsic craniofacial dysmorphology in *LgDel* adults.

To assess whether the mandibles of the *LgDel* animals we analyzed were morphologically distinct from our WT sample for this study, we performed a multi-point morphometric assay, measuring the distance between cardinal points (7). The results of these measures that assess dorsal-ventral and anterior-posterior lengths in this relatively small sample of adult male mice of both genotypes were significantly more variable than in the much larger cohort of younger mice we analyzed previously (7), and did not reach statistical significance. On further inspection, there was one morphological distinction between *LgDel* and WT mandibles: the shape and size of the mandibular notch (i.e., the curved depression between the coronoid process and the head of the mandible) appeared altered. An additional measurement of the distance between the tip of the coronoid and the mandibular head confirmed this difference ($p < 0.005$ by two-way ANOVA; **Figure 6**).

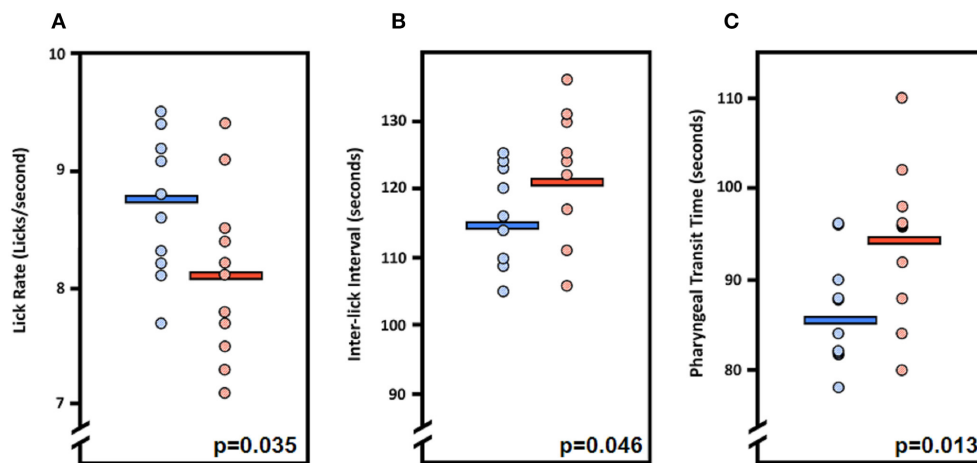


FIGURE 4 | Fluoroscopic evidence of feeding and swallowing deficits in *LgDel* mice. Analysis of fluoroscopic videos using our JawTrack™ software revealed that three of the eight VFSS metrics investigated were statistically significant between *LgDel* mice (red) and WT controls (blue). Specifically, *LgDel* mice had (A) slower lick rates, (B) longer inter-lick intervals, and (C) longer pharyngeal transit times when voluntarily drinking thin liquid contrast.

Video Surveillance of Feeding and Grooming Activity

The evidence for selective disruption of feeding and swallowing mechanics, and related anatomical anomalies, suggested that ongoing feeding or other orofacial behaviors observed in mice housed in standard conditions without any manipulations or special modes of measurement might differ in *LgDel* vs. WT mice. We used an automated video recording and coding system (HomeCageScan; see Methods) to observe and quantify natural feeding-related behaviors with no additional intervention. We recorded several spontaneous behaviors in the home cage over a period of 72 h. Review of the quantitative data and corresponding video recording at ~6 h intervals for each mouse revealed that automated detection/classification of drinking, eating, and grooming behaviors via HomeCageScan was accurate. All three classes of behaviors were altered in *LgDel* compared to WT mice, based upon the reported mean and SEM values and corresponding statistical analysis (Table 7; Figure 7). The drinking frequency (events/bin) was 1.2 times higher for *LgDel* animals compared to WT mice ($p = 0.0006$; WT: 82.32 ± 4.8 ; *LgDel*: 102.72 ± 3.36 ; Figure 7A), with an associated 2-fold increase in drinking duration (seconds/24 h; $p < 0.0001$; WT: 107.40 ± 6.00 ; *LgDel*: 223.2 ± 4.80 ; Figure 7B). Similarly, the eating frequency was 2.3 times higher for *LgDel* animals compared to WT mice ($p < 0.0001$; WT: 456.00 ± 19.20 ; *LgDel*: $1,070.88 \pm 30.72$; Figure 7C), with an associated 2.8-fold increase in eating duration ($p < 0.0001$; WT: 442.20 ± 18.60 ; *LgDel*: $1,257.60 \pm 30.60$; Figure 7D). Disparities in grooming habits were also observed between the two groups of mice. While the grooming frequency was 1.2 times higher for *LgDel* animals compared to WT mice ($p < 0.0001$; WT: 386.64 ± 15.36 ; *LgDel*: 484.56 ± 5.52 ; Figure 7E), the grooming duration was not found to be significantly different between the two groups of animals ($p = 0.6297$; WT: $12,168.60 \pm 427.80$; *LgDel*: $11,948.40 \pm 103.80$; Figure 7F). We also evaluated non-romotor behaviors

including walking slowly, come down duration, and duration of hanging vertically from a cuddled position, which did not differ in the *LgDel* animals vs. WT mice (Figures 7G–I). It is apparent that the *LgDel* mice have ongoing challenges in drinking, eating, and grooming, all of which require oromotor coordination, in their standard environment.

Post-mortem Assessment of Lung Tissue and Cranial Bones

Our previous studies established increased inflammation and the presence of milk proteins in the lungs as a signal of aspiration-based dysphagia in neonatal *LgDel* mice (6, 7). In H&E stained sections, lung inflammation appears as increased blood vessel dilation with pooling of blood in the tissue (27). To evaluate inflammation in the lungs of mice previously evaluated by fluoroscopic assessment of feeding and swallowing, dissected lungs were assessed for histological evidence of inflammation (Figure 8). *LgDel* lungs showed significantly greater evidence of inflammation, including dilated blood vessels and cellular accumulations of eosin stained proteins and erythrocytes. We found a >4-fold increased lung inflammation in *LgDel* compared to control mice ($p = 0.0016$; WT: $0.78 \pm 0.13\%$; *LgDel*: $3.93 \pm 0.85\%$; Figure 8). There was no correlation between lick rate and lung inflammation as determined by plotting lick rate vs. lung inflammation, followed by linear regression. For example, the most affected *LgDel* mutant for lick rate was the most normal of the mutants in terms of inflammation but the second highest *LgDel* mouse for lick rate. The *LgDel* mouse with the most apparent craniofacial abnormalities had a lick rate of 7.2 Hz and was near the mean in terms of inflammation (3.34%).

To assess the mandibles, we performed a multi-point morphometric assay to measure the distance between cardinal points, as performed previously (7), using the male cohort of tested mice. The results of these measures—designed to assess dorsal-ventral and rostral-caudal lengths—were significantly

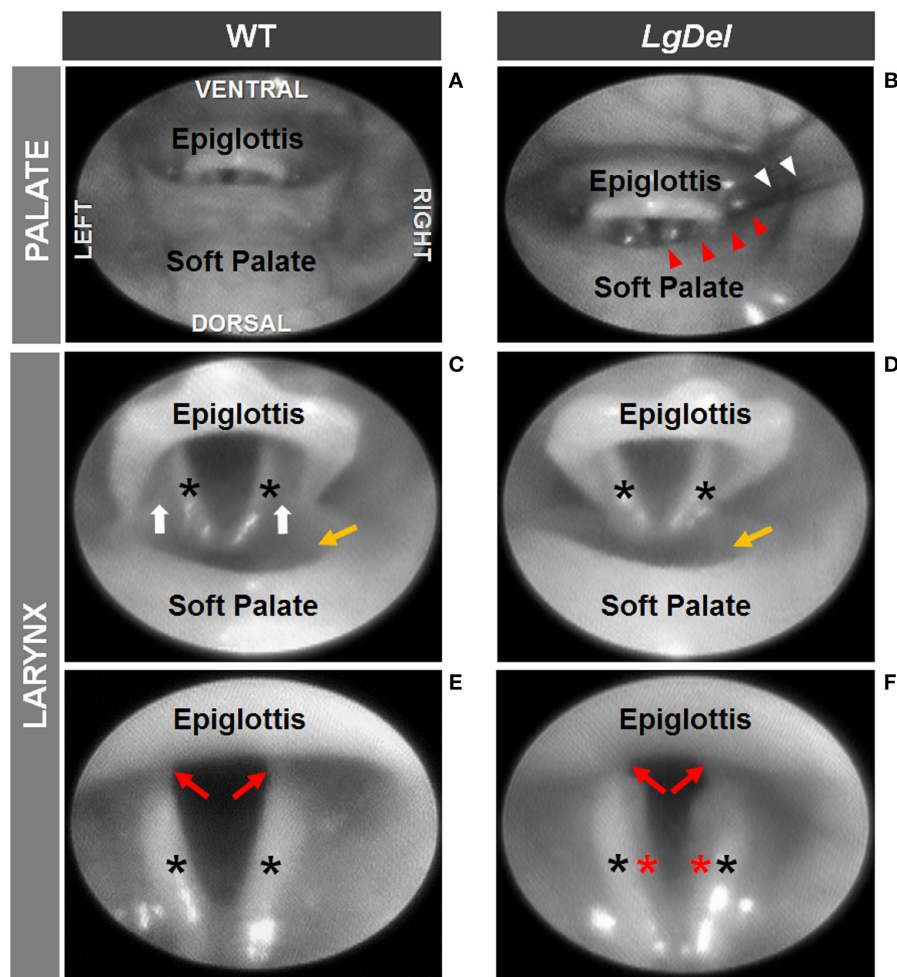


FIGURE 5 | Endoscopic evidence of palatal and laryngeal anomalies in *LgDel* mice. Representative images showing advancement of the endoscope into the pharynx (A,B) and laryngeal inlet (C,D) to visualize the glottis (E,F). Compared to WT mice (A,C,E), *LgDel* mice displayed several minor structural anomalies, including soft palate asymmetry (red arrowheads), and in this mouse, strands of fur (white arrowheads) were found lodged within the laryngeal inlet (B); narrowed epiglottis with visibly absent aryepiglottic folds (D); and extraneous mucosa (red asterisk) along the medial edge of the arytenoids (F). Black asterisks, arytenoid mucosa; white arrows, aryepiglottic folds; red arrows, vocal folds; yellow arrow, laryngeal pouch. Images were adjusted for color, brightness, and contrast to enhance visualization of key features.

more variable than a previously tested younger cohort and did not reach statistical significance. On further inspection, it appeared that there was a morphological distinction between *LgDel* and WT mandibles, particularly in the shape of the sigmoid (i.e., mandibular) notch. An additional measurement of the distance between the tip of the coronoid process and the condyle revealed a significant difference between groups ($p < 0.005$). Images from isolated skull bones are included in **Figure 6**, which illustrate dysmorphology similar to our findings via facial photographs and skull radiographs.

DISCUSSION

We characterized functional, structural, and baseline behavioral correlates of feeding and swallowing in adult *LgDel* mice to determine if dysphagia recognized perinatally in *LgDel* pups is

TABLE 5 | Laryngeal motion summary statistics.

| Laryngeal motion metrics | p-value | Mean (±SEM) | |
|--|---------|---------------|----------------|
| | | WT | <i>LgDel</i> |
| Mean motion range ratio (MMRR) | 0.194 | 0.90 (0.06) | 0.77 (0.07) |
| Open close cycle ratio (OCCR) | 0.236 | 0.94 (0.05) | 1.01 (0.02) |
| Motion correlation coefficient (Mcorr) | 0.952 | −0.86 (0.23) | −0.85 (0.04) |
| Average VF angle (degrees) | 0.253 | 33.57 (1.40) | 30.60 (2.10) |
| Respiratory rate (#/min) | 0.092 | 165.26 (6.48) | 143.61 (10.40) |

Bold p-values denote statistical significance (<0.05). WT, wild-type.

followed by sustained difficulties in feeding and swallowing in maturity. We found that lick rate is slower and the inter-lick interval is longer in *LgDel* adult mice, both of which are correlates

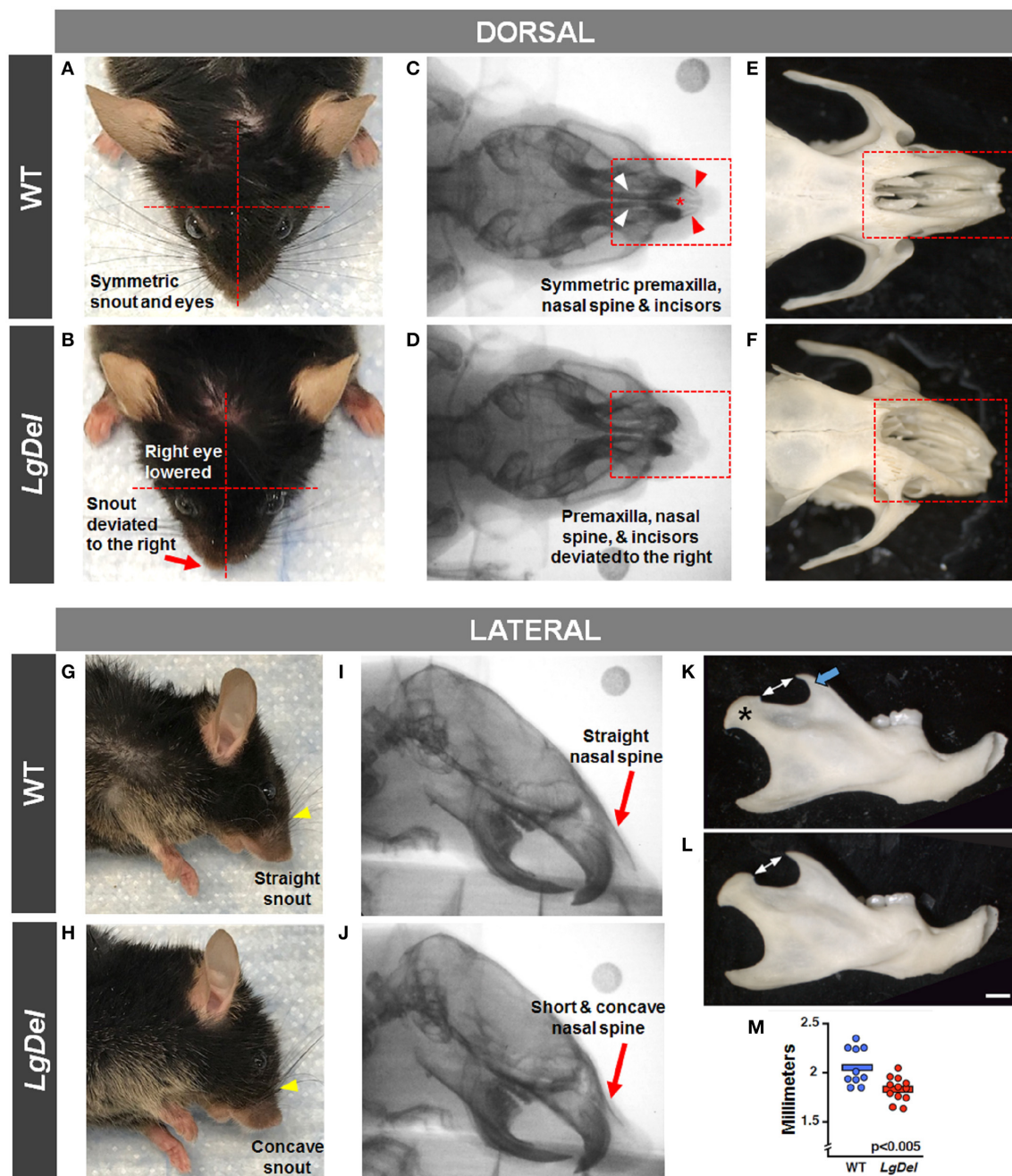


FIGURE 6 | Craniofacial anomalies in *LgDel* mice identified via facial photographs, skull radiographs, and bone morphology. Representative images of a WT mouse in dorsal and lateral view (**A,G**) and skull bones (**C,E,I**) showing symmetric facial features. Some *LgDel* mice had facial asymmetry involving the eyes and snout (**B,H**), and skull abnormalities involving the nasal spine, premaxilla, and incisors (**D,F,J**). The mouse depicted here displayed all of these abnormalities; however, this phenotype had low penetrance. Representative examples of right mandible from WT (**K**) and *LgDel* (**L**) mice showing difference in morphology of the coronoid process (blue arrow) and condyle (asterisk). (**M**) Quantification shows *LgDel* mice have a significantly shorter distance between the coronoid process and the head of the mandible than their WT counterparts ($p < 0.005$). Scale bar = 1 mm.

of impaired feeding and oral stage dysphagia. The increase in pharyngeal transit time is an indicator of motility issues during the pharyngeal stage of swallowing. These functional changes are accompanied by variably penetrant oropharyngeal

dysmorphology and extrinsic craniofacial anomalies in adult *LgDel* mice. These specific disruptions in feeding, swallowing, and related oropharyngeal and craniofacial structures were paralleled by altered homeostatic drinking, eating, and grooming,

TABLE 6 | Individual *LgDel* mice with craniofacial structural and functional anomalies.

| Mouse | Palate | Larynx | Face | LAR |
|-------|-----------------------|--|---|--------|
| 1 | — | Extraneous laryngeal mucosa along the medial edge of the glottis | — | — |
| 2 | — | Extraneous laryngeal mucosa along the medial edge of the glottis | — | Absent |
| 3 | Soft palate asymmetry | — | Snout asymmetry | NT |
| 4 | — | — | Asymmetry of the eyes, premaxilla, nasal spine, incisors, and snout | NT |
| 5 | — | Narrowed larynx, aryepiglottic folds not visible | — | NT |

LAR, laryngeal adductor reflex (i.e., glottic closure reflex); NT, not tested.

TABLE 7 | Feeding and grooming activity summary statistics.

| VFSS metrics | | p-value | Mean (\pm SEM) | |
|--------------|-------------------------|-------------------|-------------------|---------------|
| | | | WT | <i>LgDel</i> |
| Drinking | Frequency (events/hour) | 0.001 | 3.43 (0.20) | 4.28 (0.14) |
| | Duration (minutes/24 h) | <0.0001 | 1.79 (0.10) | 3.72 (0.08) |
| Eating | Frequency (events/hour) | <0.0001 | 19.00 (0.80) | 44.63 (1.28) |
| | Duration (minutes/24 h) | <0.0001 | 7.37 (0.31) | 20.96 (0.51) |
| Grooming | Frequency (events/hour) | <0.0001 | 16.11 (0.64) | 20.19 (0.23) |
| | Duration (minutes/24 h) | 0.630 | 202.81 (7.13) | 199.14 (1.73) |

Bold p-values denote statistical significance (<0.05); SEM, standard error of the mean; WT, wild-type.

all of which require oromotor coordination. Finally, *LgDel* mice had far more frequent signs of lung inflammation consistent with food and/or liquid aspiration than WT counterparts. Together, these anomalies demonstrate that the developmental disruptions associated with perinatal feeding and swallowing difficulties in *LgDel* mouse pups are maintained, resulting in a high frequency of feeding and swallowing difficulties in adulthood.

Persistent Feeding Difficulties and Oropharyngeal Dysphagia

Deficits in lick rate, rhythm (inter-lick interval), and pharyngeal transit time in *LgDel* mice are indicative of tongue dysfunction, which corresponds with our previous finding of altered CN XII neurodevelopment in this model (28). Aside from the tongue, numerous pharyngeal muscles contribute to the pharyngeal stage of swallowing, with motor innervation supplied by CN IX and X, both of which have been shown to have divergent development from normal in *LgDel* mice (7). Prolonged pharyngeal transit times correspond to impaired pharyngeal constriction (i.e., pharyngeal squeeze) by the tongue and pharyngeal muscles during swallowing, which is associated with increased laryngeal penetration of liquids and aspiration pneumonia risk in dysphagic patients (29–31). Importantly, CN IX and X also

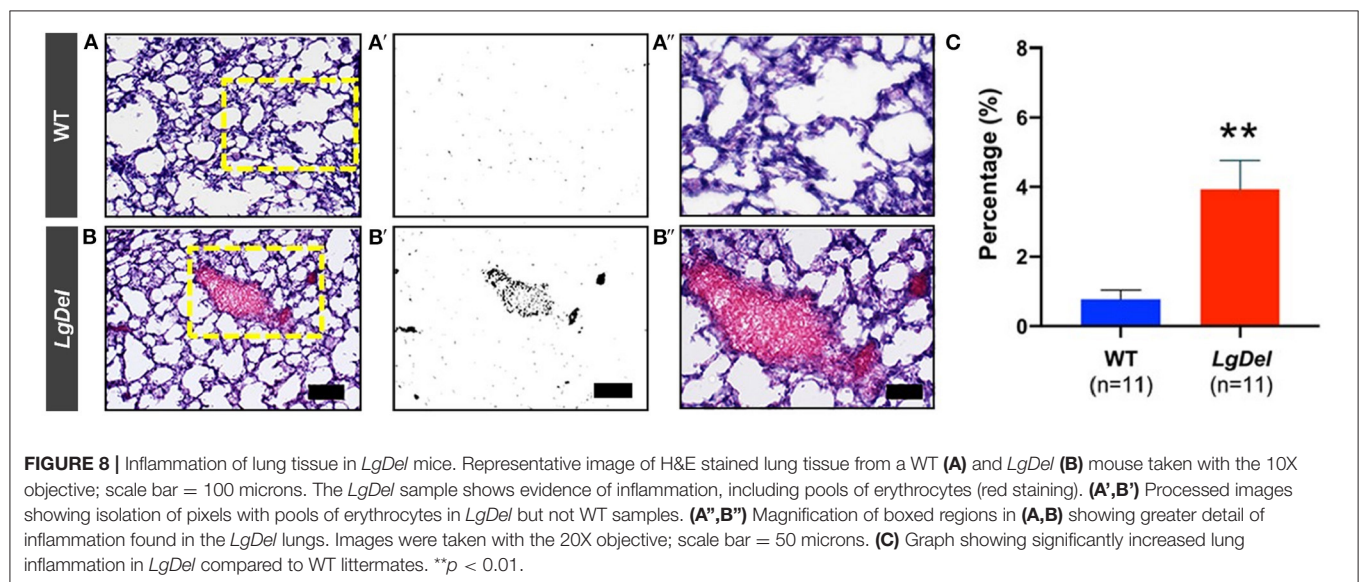
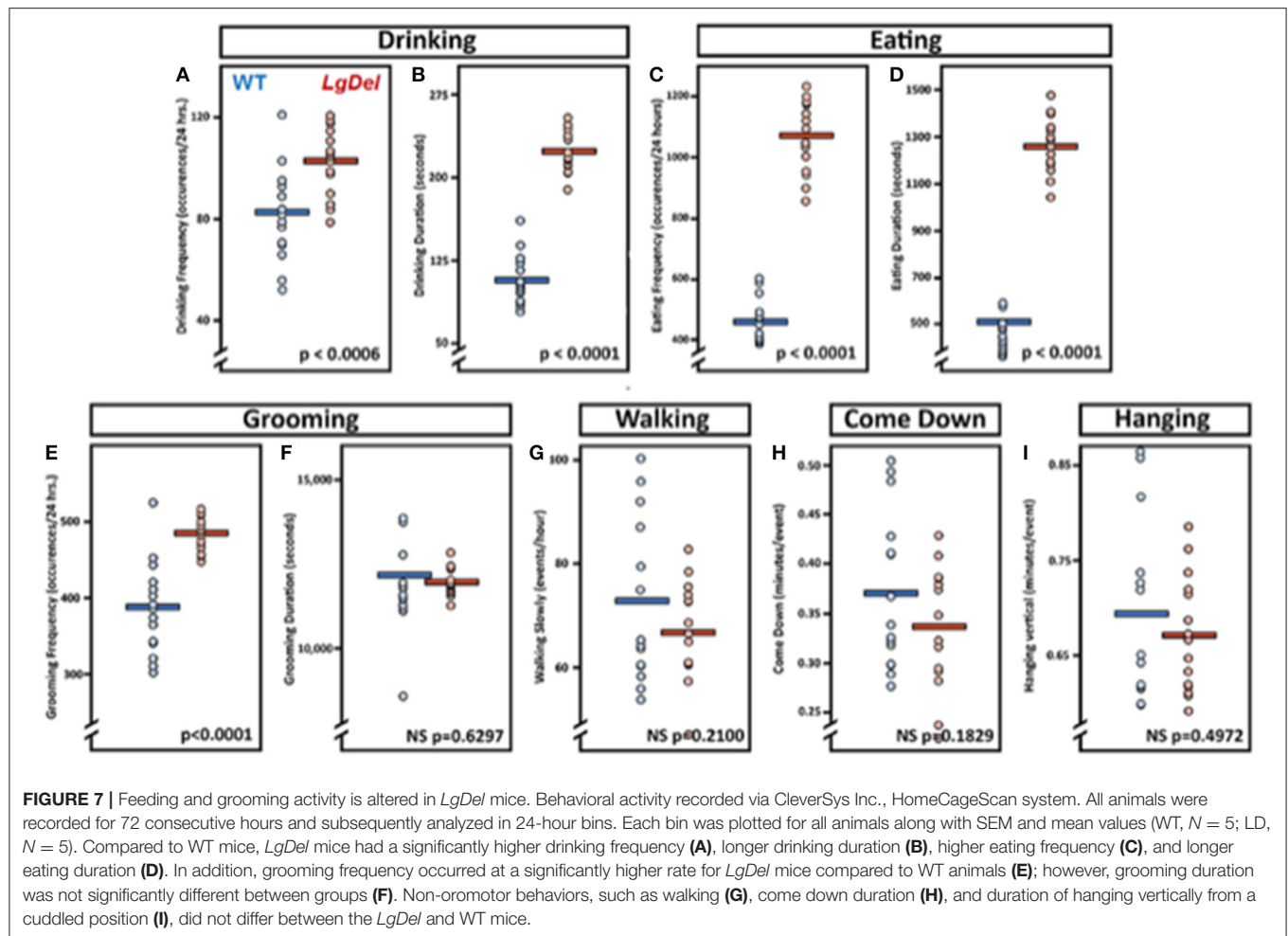
provide sensory innervation to pharynx and larynx. Clinical evaluation of laryngeal sensory function entails delivering puffs of air to the laryngeal mucosa to evoke the laryngeal adductor reflex (LAR or glottic closure reflex). A normal response is abrupt, brief (<1 s) adduction of the vocal folds to protect the airway (19, 32). Our finding of an absent LAR in one *LgDel* mouse suggests that laryngeal sensory impairment may exist in some cases; however, testing with a larger sample size is needed to rule out effects from anesthesia, which is essential for performing LAR testing in mice. Importantly, none of the mice in this study demonstrated laryngeal penetration or aspiration while voluntarily drinking and eating during videofluoroscopic testing. This finding was not unexpected, as the larynx in mice resides in the nasopharynx (similar to human infants), which inherently protects the larynx from the path of the bolus (13–15). Regardless, *LgDel* mice display other deficits in feeding and swallowing that can serve as robust outcome measures in future preclinical therapeutic studies with this model.

In addition to CN IX, X, and XII deficits, CN V develops anomalously in *LgDel* mice (7). CN V provides motor innervation to the muscles involved in opening and closing of the jaw during drinking (licking) and eating (mastication). Although lick rate and rhythm were impaired in *LgDel* mice, the velocity of jaw open/close motion during drinking was indistinguishable from controls. Further, the mastication rate of *LgDel* mice during rotary chewing was no different from controls. However, alterations in jaw opening/closing velocity during chewing cannot be ruled out at this time, as this measure was not quantifiable using our JawTrack™ software. To answer this question, machine learning approaches are currently being incorporated into our software to permit automated detection and quantification of various masticatory patterns (e.g., biting, rotary chewing) in future work with this mouse model.

People with 22q11DS commonly have hypocalcemia due to parathyroid hypoplasia, and as a result, may experience paresthesias, tetany, muscle weakness, dysphagia, and fatigue (33). Therefore, it is important to note that while parathyroid hypoplasia has been established in the *LgDel* mice (34), calcium homeostasis has not been fully evaluated in this model. Although past studies and this study clearly demonstrate craniofacial and neurological origins of dysphagia, hypocalcemia could exacerbate the dysphagic deficits seen in the *LgDel* mice and therefore warrants further investigation.

Variability in Oropharyngeal Anomalies in *LgDel* Mice Parallels That in 22q11DS

We found substantial, but in some cases variably, penetrant disruptions of several functional and anatomical measures of feeding and swallowing in adult *LgDel* mice. This variability accords with the variable penetrance of most 22q11 clinical phenotypes across individuals with 22q11DS, including variable penetrance and expressivity of features that may impact feeding and swallowing such as craniofacial abnormalities, congenital heart defects, and anomalies of the gastrointestinal tract (35). One limitation in the evaluation of craniofacial abnormalities associated with 22q11DS is the lack of established criteria



for what is considered “normal” vs. “abnormal.” This is not helped by the fact that the identification of such anomalies

is extremely subjective and limited by the quality of the photographs, radiographs, and recorded videos. Additional

imaging and analytic approaches like those developed to assess cranial dysmorphology in mice with Down syndrome and other developmental disorders (36, 37) may be necessary to resolve this issue with appropriate quantitative and statistical precision. Though some progress has been made on digital diagnosis of 22q11DS (38).

Incomplete Compensation for Developmental Disruptions Due to 22q11 Deletion

Both the frequency and the duration of eating and drinking were increased in adult *LgDel* mice, suggesting that these mice require more time and effort to ingest an equal amount of sustenance compared to WT littermates. Similarly, the *LgDel* mice groomed more frequently, but for the same cumulative duration as WT mice. This may signify that in order for the *LgDel* animals to achieve the same amount of grooming, they have to groom more frequently for shorter periods of time throughout the day, possibly due to fatigue and dysregulated tongue movement. These outcomes are supported by the decrease in lick rate observed in *LgDel* mice during VFSS with liquid consistency. Thus, with a diminished lick rate, the *LgDel* mice spend more time eating and/or drinking in order to achieve sufficient nourishment throughout the day and to maintain body weight. Although the oromotor deficits detected via HomeCageScan testing of only male mice appear to be more pronounced compared to the VFSS data obtained from male and female mice, we expect this “discrepancy” may be explained by differences in the types of behaviors assessed by each test rather than sex differences. HomeCageScan assessed the presence/absence of spontaneous oromotor behaviors over time whereas VFSS assessed characteristics of specific oromotor behaviors, specifically drinking and eating. However, we intend to investigate this hypothesis using a larger sample size of males and females in our future investigations with this model.

Additionally, other examined parameters unrelated to feeding and swallowing showed insignificant differences between the *LgDel* and WT mice as determined via HomeCageScan analysis, including walking slowly, coming down, and hanging vertically from a hang cuddled position (see **Table 3** for definitions). Significant defects in the behaviors involving oromotor coordination, such as drinking, eating, and grooming coincide with the observed structural and functional issues within the *LgDel* mice. At the same time, the lack of significant differentiation in unrelated oromotor behaviors (walk slowly, come down, hang vertical from hang cuddled) indicate specificity of dysfunction in drinking and eating, as those actions that were not different in *LgDel* and WT mice do not involve known impairments associated with dysphagia and/or 22q11DS.

LgDel mice eat and drink more frequently and for longer durations. They may do so because of an underlying disruption of neural circuitry to execute the behavior or as a compensatory mechanism to minimize discomfort. Lack of coordination, slower execution (i.e., diminished lick rate) and fatigue would support the former possibility, particularly if cranial motor neurons are compromised or circuit integrity is altered (28).

Moreover, altered nociceptive or mechanoreceptive innervation may also contribute to discomfort, thus supporting the latter mechanism. Finally, it is not unimaginable that slower nutrient intake over a longer duration may help the animals ingest food with fewer issues. This work suggests that feeding and swallowing difficulties observed in pediatric dysphagia are likely not fully resolved as the child develops further, leading to possible weight loss, food avoidance, aspiration, as well as frequent or chronic lung, naso-sinus or middle ear infections. Many of the oropharyngeal structural and cranial sensory-motor issues associated with dysphagia are due to underlying neurodevelopmental abnormalities; however, some of these difficulties may be ameliorated with slower nutrient intake. Similarly, fatigue involving suboptimal oropharyngeal structures or motor innervation for feeding and swallowing may be addressed by eating or drinking smaller amounts more frequently throughout the day. It would be an advantage in future work to use the same cohort of mice for VFSS, endoscopy, and behavioral assessments in order to investigate relationships between variables within the same mice.

It should be noted that mice are social animals by nature; therefore, it is possible that isolating mice from one another for 4 days during HomeCageScan testing may cause anxiety-related behaviors such as pacing or increased movement (39). However, such behaviors did not greatly vary between bins for individual animals, suggesting that anxiety level was not a confounding variable in this study. In addition, mice were rearing while eating and drinking during HomeCageScan testing, which was a necessary condition for automated detection of these behaviors; drinking and eating near the cage floor is too non-distinctive from other behaviors (e.g., grooming) for accurate quantitative video analysis. This rearing posture likely results in a more complicated task involving both oromotor and gross axial coordination and balance. This may be a confounding factor, given that children with 22q11DS are known to have marked neuromotor deficits affecting static and dynamic balance (40, 41) associated with diminished cerebellar volume (42). However, upon careful review of the HomeCageScan videos, there was no obvious evidence of balance or coordination deficits in either group of mice. It may be of interest in future work to investigate potential coordination and balance deficits and associated etiologies in this mouse model.

Persistent Lung Inflammation in *LgDel* Mice

As pups, the *LgDel* mice showed evidence of aspiration and inflammation based on the presence of murine milk proteins, neutrophils, macrophages, and the accumulation of red blood cells within the lung tissue (7). The *LgDel* mice in this study also showed substantial lung inflammation, but it is not clear whether this was acute, chronic, or both. Thus, it is uncertain if the same degree of dysphagia seen in the *LgDel* pups, which appears to be acute during early life (6, 7), persists into adulthood or if the characteristics of feeding and swallowing difficulties change with growth, maturation, and behavioral compensation. People with 22q11DS can be immunocompromised, which may chronically

impair their ability to clear aspiration-based infections (43). *LgDel* mice have not been evaluated immunologically, and they may also be immunocompromised to some degree, preventing them from adequately clearing aspirated milk and accompanying bacteria as pups. Like many other features of 22q11DS, the severity of immunological dysfunction is highly variable. Our finding that none of the mice in this study aspirated during videofluoroscopic testing may suggest that lung inflammation may be maintained from infancy rather than caused by ongoing aspiration during eating and drinking. In adults, however, aspiration may be more sporadic, thus not easily detected with a single episode of videofluorography. Thus, the lung inflammation may reflect a somewhat chronic state due to occasional aspiration events. In addition, videofluoroscopy lacks the visual resolution to permit detection of micro-aspiration associated with gastric reflux, which is the major pathogenetic mechanism of aspiration pneumonia (44). Typically developing mice cannot vomit or spontaneously reflux gastric contents, and therefore micro-aspiration is unlikely (45). Although unknown, it is possible that the major neurodevelopmental anomalies in *LgDel* mice may alter esophageal and gastric function, thus making gastric reflux and micro-aspiration possible. To address this knowledge gap, future studies should include histological assays of the lungs to detect the presence of proteins that are found in the adult mouse diet.

Anomalous Feeding and Swallowing Throughout Life

The retention of feeding and swallowing deficits beyond the perinatal period in individuals with syndromic or non-syndromic neurodevelopmental disorders has not been considered thoroughly. We suggest that these sometimes subtle, but nevertheless significant difficulties in managing food intake and deglutition may establish subclinical challenges or clinical signs of diminished nutrition and weight regulation and increased ongoing aspiration-related naso-sinus or respiratory infections throughout the lifespan. Further, individuals with 22q11DS may be more vulnerable to age-related feeding difficulties or in extreme cases, oropharyngeal dysphagia due to early onset Parkinson's disease for which 22q11DS is a genetic risk factor (46, 47). Finally, additional neurological complications like traumatic brain injury or stroke—causes for acute dysphagia after a lifetime of optimal feeding in non-syndromic individuals—may occur with similar, or even enhanced frequency in individuals with 22q11DS vs. typical adults, and exacerbate chronic, sub-clinical feeding and swallowing difficulties.

The relationship between perinatal dysphagia due to 22q11 deletion and continued oropharyngeal dysfunction and feeding and swallowing difficulties may extend to other syndromic and non-syndromic neurodevelopmental disorders. Indeed, later arising issues with food avoidance, food preferences, and diminished or disordered food intake in clinically diagnosed disorders like autistic spectrum disorder or attention deficit-hyperactivity disorder may reflect undiagnosed perinatal feeding difficulties that are never fully corrected, due either to lack of intervention during a critical period

or the degree of developmental disruption that established anomalies in oropharyngeal and craniofacial structures as well as neural circuits critical for feeding and swallowing. Thus, additional attention to issues of oropharyngeal competence and related behaviors should be considered more carefully in the management of a broad range of neurodevelopmental disorders throughout the lifespan.

Our results allow us to begin to understand how the severity of this neurodevelopmental disease may change with compensation in maturity, both behaviorally and biologically. Our findings in mice suggest there may be slight improvements observed over time in individuals with 22q11DS. Nevertheless, it appears that the majority of the deficits that occur during development are either stable or not fully corrected. Significant oropharyngeal motor disruptions and continued evidence of partially penetrant craniofacial anomalies most likely are due to early hindbrain and craniofacial patterning disruption, which cannot be effectively or fully corrected by developmental or post-natal compensatory mechanisms. Lung inflammation, which may be persistent, or acute and recurring due to occasional aspiration, is a less definitive, although suggestive, observation. Abnormalities in lick rate/rhythm and pharyngeal transit time suggest that the consequences of pathological cranial nerve or brainstem development remain unresolved as the animals mature. Further, the increased frequency and duration at which the *LgDel* animals spent eating and drinking corroborates this supposition. This work has therefore provided a deeper understanding of developmental to behavioral dimensions of dysphagia associated with 22q11DS, and provides a foundation for future work to identify effective therapeutic interventions.

DATA AVAILABILITY STATEMENT

The datasets generated for this study are available on request to the corresponding author.

ETHICS STATEMENT

This animal study was reviewed and approved by the Institutional Animal Care and Use Committee (IACUC) at the University of Missouri – Columbia and The George Washington University.

AUTHOR CONTRIBUTIONS

LW and TL performed and analyzed fluoroscopic and endoscopic assessments, facial photographs, and skull radiographs, and performed post-mortem tissue collection. TL performed statistical analysis of the fluoroscopic and endoscopic data. HC conducted and analyzed all HomeCageScan behavioral data and performed the statistical analysis. GY imaged and analyzed the lung samples for evidence of inflammation. AH, FB, and TL developed and applied the JawTrack™ and VFtrack™ software to the fluoroscopic and endoscopic videos collected during this study. IZ contributed to the conception and design of the study. DM contributed to the conception and design of the behavioral aspects of this study. LW, HC, IZ, A-SL, and TL drafted the

initial manuscript, figures, and legends. All authors contributed to manuscript revision and approved the submitted version.

FUNDING

The behavioral and craniofacial analysis for this work were supported by the Eunice Kennedy Shriver National Institute of Child Health & Human Development of the National Institutes of Health (5P01HD083157). The microscopic analysis for this study was conducted at the CRI Light Microscopy and Image Analysis Core, supported by the Intellectual and Developmental

Disabilities Research Center Award (U54HD090257) through the Eunice Kennedy Shriver National Institute of Child Health and Human Development of the National Institutes of Health.

ACKNOWLEDGMENTS

We graciously thank Kate Osman (Lever Lab) for assistance with behavioral conditioning and post-mortem collection of tissue samples, Maggie Brothers (Lever Lab) for assisting with analysis of VFSS videos, and Megan Maynard (LaMantia/Maynard Lab) for assisting with measurements of cranial bones.

REFERENCES

- Eicher PS, McDonald-McGinn DM, Fox CA, Driscoll DA, Emanuel BS, Zackai EH. Dysphagia in children with a 22q11.2 deletion: unusual pattern found on modified barium swallow. *J Pediatr.* (2000) 137:158–64. doi: 10.1067/mpd.2000.105356
- Vantrappen G, Devriendt K, Swillen A, Rommel N, Vogels A, Eyskens B, et al. Presenting symptoms and clinical features in 130 patients with the velocardio-facial syndrome. The Leuven experience. *Genet Couns.* (1999) 10:3–9.
- Ryan AK, Goodship JA, Wilson DI, Philip N, Levy A, Seidel H, et al. Spectrum of clinical features associated with interstitial chromosome 22q11 deletions: a European collaborative study. *J Med Genet.* (1997) 34:798–804. doi: 10.1136/jmg.34.10.798
- Meechan DW, Rutz HL, Fralish MS, Maynard TM, Rothblat LA, LaMantia AS. Cognitive ability is associated with altered medial frontal cortical circuits in the LgDel mouse model of 22q11.2DS. *Cereb Cortex.* (2015) 25:1143–51. doi: 10.1093/cercor/bht308
- Maynard TM, Gopalakrishna D, Meechan DW, Paronett EM, Newbern JM, LaMantia AS. 22q11 Gene dosage establishes an adaptive range for sonic hedgehog and retinoic acid signaling during early development. *Hum Mol Genet.* (2013) 22:300–12. doi: 10.1093/hmg/ddt429
- LaMantia AS, Moody SA, Maynard TM, Karpinski BA, Zohn IE, Mendelowitz D, et al. Hard to swallow: developmental biological insights into pediatric dysphagia. *Dev Biol.* (2016) 409:329–42. doi: 10.1016/j.ydbio.2015.09.024
- Karpinski BA, Maynard TM, Fralish MS, Nuwayhid S, Zohn IE, Moody SA, et al. Dysphagia and disrupted cranial nerve development in a mouse model of DiGeorge (22q11) deletion syndrome. *Dis Model Mech.* (2014) 7:245–57. doi: 10.1242/dmm.012484
- McDonald-McGinn DM, Kirschner R, Goldmuntz E, Sullivan K, Eicher P, Gerdes M, et al. The Philadelphia story: the 22q11.2 deletion: report on 250 patients. *Genet Couns.* (1999) 10:11–24.
- Motzkun B, Marion R, Goldberg R, Shprintzen R, Saenger P. Variable phenotypes in velocardiofacial syndrome with chromosomal deletion. *J Pediatr.* (1993) 123:406–10. doi: 10.1016/S0022-3476(05)81740-8
- McDonald-McGinn DM, Sullivan KE, Marino B, Philip N, Swillen A, Vorstman JA, et al. 22q11.2 deletion syndrome. *Nat Rev Dis Primers.* (2015) 1:15071. doi: 10.1038/nrdp.2015.71
- Saitta SC, Harris SE, Gaeth AP, Driscoll DA, McDonald-McGinn DM, Maisenbacher MK, et al. Aberrant interchromosomal exchanges are the predominant cause of the 22q11.2 deletion. *Hum Mol Genet.* (2004) 13:417–28. doi: 10.1093/hmg/ddh041
- Meechan DW, Tucker ES, Maynard TM, LaMantia AS. Diminished dosage of 22q11 genes disrupts neurogenesis and cortical development in a mouse model of 22q11 deletion/DiGeorge syndrome. *Proc Natl Acad Sci USA.* (2009) 106:16434–45. doi: 10.1073/pnas.0905696106
- Lever TE, Braun SM, Brooks RT, Harris RA, Littrell LL, Neff RM, et al. Adapting human videofluoroscopic swallow study methods to detect and characterize dysphagia in murine disease models. *J Vis Exp.* (2015) 97:e52319. doi: 10.3791/52319
- Lever T, Brooks R, Thombs L, Littrell L, Harris R, Allen M, et al. Videofluoroscopic validation of a translational murine model of presbyphagia. *Dysphagia.* (2015) 30:328–42. doi: 10.1007/s00455-015-9604-7
- Osman KL, Kohlberg S, Mok A, Brooks R, Lind LA, McCormack K, et al. Optimizing the translational value of mouse models of ALS for Dysphagia Therapeutic Discovery. *Dysphagia.* (2019). doi: 10.1007/s00455-019-10034-9. [Epub ahead of print].
- Haney MM, Hamad A, Leary E, Bunyak F, Lever TE. Automated quantification of vocal fold motion in a recurrent laryngeal nerve injury mouse model. *Laryngoscope.* (2019) 129:E247–54. doi: 10.1002/lary.27609
- Haney MM, Hamad A, Woldu HG, Ciucci M, Nichols N, Bunyak F, et al. Recurrent laryngeal nerve transection in mice results in translational upper airway dysfunction. *J Comp Neurol.* (2019) 528:574–96. doi: 10.1002/cne.24774
- Mok A, Allen J, Haney MM, Deninger I, Ballenger B, Caywood V, et al. A surgical mouse model for advancing laryngeal nerve regeneration strategies. *Dysphagia.* (2019). doi: 10.1007/s00455-019-10045-6. [Epub ahead of print].
- Shock LA, Gallemore BC, Hinkel CJ, Szwedczyk MM, Hopewell BL, Allen MJ, et al. Improving the utility of laryngeal adductor reflex testing: a translational tale of mice and men. *Otolaryngol Head Neck Surg.* (2015) 153:94–101. doi: 10.1177/0194599815578103
- Tang XN, Berman AE, Swanson RA, Yenari MA. Digitally quantifying cerebral hemorrhage using Photoshop and Image J. *J Neurosci Methods.* (2010) 190:240–3. doi: 10.1016/j.jneumeth.2010.05.004
- Adamah-Biassi EB, Stepien I, Hudson RL, Dubocovich ML. Automated video analysis system reveals distinct diurnal behaviors in C57BL/6 and C3H/HeN mice. *Behav Brain Res.* (2013) 243:306–12. doi: 10.1016/j.bbr.2013.01.003
- Sobin C, Kiley-Brabeck K, Monk SH, Khuri J, Karayiorgou M. Sex differences in the behavior of children with the 22q11 deletion syndrome. *Psychiatry Res.* (2009) 166:24–34. doi: 10.1016/j.psychres.2008.03.023
- Dyce O, McDonald-McGinn D, Kirschner RE, Zackai E, Young K, Jacobs IN. Otolaryngologic manifestations of the 22q11.2 deletion syndrome. *Arch Otolaryngol Head Neck Surg.* (2002) 128:1408–12. doi: 10.1001/archotol.128.12.1408
- Grasso F, Cirillo E, Quaremba G, Graziano V, Gallo V, Cruoglio L, et al. Otolaryngological features in a cohort of patients affected with 22q11.2 deletion syndrome: a monocentric survey. *Am J Med Genet A.* (2018) 176:2128–34. doi: 10.1002/ajmg.a.40518
- Jones JW, Tracy M, Perryman M, Arganbright JM. Airway anomalies in patients with 22q11.2 deletion syndrome: a 5-year review. *Ann Otol Rhinol Laryngol.* (2018) 127:384–9. doi: 10.1177/0003489418771711
- Wong NS, Feng Z, Rappazzo C, Turk C, Randall C, Ongkasuwan J. Patterns of dysphagia and airway protection in infants with 22q11.2-deletion syndrome. *Laryngoscope.* (2019) doi: 10.1002/lary.28317. [Epub ahead of print].
- Pober JS, Sessa WC. Inflammation and the blood microvascular system. *Cold Spring Harb Perspect Biol.* (2014) 7:a016345. doi: 10.1101/cshperspect.a016345
- Wang X, Bryan C, LaMantia AS, Mendelowitz D. Altered neurobiological function of brainstem hypoglossal neurons in DiGeorge/22q11.2 deletion syndrome. *Neuroscience.* (2017) 359:1–7. doi: 10.1016/j.neuroscience.2017.06.057
- Aviv JE, Spitzer J, Cohen M, Ma G, Belafsky P, Close LG. Laryngeal adductor reflex and pharyngeal squeeze as predictors of laryngeal penetration and aspiration. *Laryngoscope.* (2002) 112:338–41. doi: 10.1097/00005537-200202000-00025

30. Kaneoka A, Pisegna JM, Inokuchi H, Ueha R, Goto T, Nito T, et al. Relationship between laryngeal sensory deficits, aspiration, and pneumonia in patients with dysphagia. *Dysphagia*. (2018) 33:192–9. doi: 10.1007/s00455-017-9845-8
31. Onofri SM, Cola PC, Berti LC, da Silva RG, Dantas RO. Correlation between laryngeal sensitivity and penetration/aspiration after stroke. *Dysphagia*. (2014) 29:256–61. doi: 10.1007/s00455-013-9504-7
32. Aviv JE, Kim T, Sacco RL, Kaplan S, Goodhart K, Diamond B, et al. FEESST: a new bedside endoscopic test of the motor and sensory components of swallowing. *Ann Otol Rhinol Laryngol*. (1998) 107:378–87. doi: 10.1177/000348949810700503
33. Schafer AL, Shoback D. Hypocalcemia: definition, etiology, pathogenesis, diagnosis and management. In: Rose CJ, editor. *Primer on the Metabolic Bone Diseases and Disorders of Mineral Metabolism*. Ames, IA: John Wiley & Sons (2013). p. 572–8.
34. Merscher S, Funke B, Epstein JA, Heyer J, Puech A, Lu MM, et al. TBX1 is responsible for cardiovascular defects in velo-cardio-facial/DiGeorge syndrome. *Cell*. (2001) 104:619–29. doi: 10.1016/S0092-8674(01)00247-1
35. Morrow BE, McDonald-McGinn DM, Emanuel BS, Vermeesch JR, Scambler PJ. Molecular genetics of 22q11.2 deletion syndrome. *Am J Med Genet A*. (2018) 176:2070–81. doi: 10.1002/ajmg.a.40504
36. Singh N, Dutka T, Reeves RH, Richtsmeier JT. Chronic up-regulation of sonic hedgehog has little effect on postnatal craniofacial morphology of euploid and trisomic mice. *Dev Dyn*. (2016) 245:114–22. doi: 10.1002/dvdy.24361
37. Motch Perrine SM, Stecko T, Neuberger T, Jabs EW, Ryan TM, Richtsmeier JT. Integration of brain and skull in prenatal mouse models of apert and crouzon syndromes. *Front Hum Neurosci*. (2017) 11:369. doi: 10.3389/fnhum.2017.00369
38. Kruszka P, Addissie YA, McGinn DE, Porras AR, Biggs E, Share M, et al. 22q11.2 deletion syndrome in diverse populations. *Am J Med Genet A*. (2017) 173:879–88. doi: 10.1002/ajmg.a.38199
39. Kappel S, Hawkins P, Mendl MT. To group or not to group? Good practice for housing male laboratory mice. *Animals*. (2017) 7:E88. doi: 10.3390/ani7120088
40. Sobin C, Monk SH, Kiley-Brabeck K, Khuri J, Karayiorgou M. Neuromotor deficits in children with the 22q11 deletion syndrome. *Mov Disord*. (2006) 21:2082–9. doi: 10.1002/mds.21103
41. Oskarsdottir S, Belfrage M, Sandstedt E, Viggedal G, Uvebrant P. Disabilities and cognition in children and adolescents with 22q11 deletion syndrome. *Dev Med Child Neurol*. (2005) 47:177–84. doi: 10.1017/S0012162205000320
42. Haenssler AE, Baylis A, Perry JL, Kollara L, Fang X, Kirschner R. Impact of cranial base abnormalities on cerebellar volume and the velopharynx in 22q11.2 deletion syndrome. *Cleft Palate Craniofac J*. (2019) 1055665619874175. doi: 10.1177/1055665619874175. [Epub ahead of print].
43. McDonald-McGinn DM, Sullivan KE. Chromosome 22q11.2 deletion syndrome (DiGeorge syndrome/velocardiofacial syndrome). *Medicine*. (2011) 90:1–18. doi: 10.1097/MD.0b013e3182060469
44. Mandell LA, Niederman MS. Aspiration Pneumonia. *N Engl J Med*. (2019) 380:651–63. doi: 10.1056/NEJMra1714562
45. He J, Fang Y, Chen X. Surgical models of gastroesophageal reflux with mice. *J Vis Exp*. (2015) 102:e53012. doi: 10.3791/53012
46. Butcher NJ, Marras C, Pondal M, Rusjan P, Boot E, Christopher L, et al. Neuroimaging and clinical features in adults with a 22q11.2 deletion at risk of Parkinson's disease. *Brain*. (2017) 140:1371–83. doi: 10.1093/brain/awx053
47. Dufournet B, Nguyen K, Charles P, Grabli D, Jacquette A, Borg M, et al. Parkinson's disease associated with 22q11.2 deletion: Clinical characteristics and response to treatment. *Rev Neurol*. (2017) 173:406–10. doi: 10.1016/j.neurol.2017.03.021

Conflict of Interest: The authors declare that the research was conducted in the absence of any commercial or financial relationships that could be construed as a potential conflict of interest.

Copyright © 2020 Welby, Caudill, Yitsege, Hamad, Bunyak, Zohn, Maynard, LaMantia, Mendelowitz and Lever. This is an open-access article distributed under the terms of the Creative Commons Attribution License (CC BY). The use, distribution or reproduction in other forums is permitted, provided the original author(s) and the copyright owner(s) are credited and that the original publication in this journal is cited, in accordance with accepted academic practice. No use, distribution or reproduction is permitted which does not comply with these terms.



Prefrontal Consolidation and Compensation as a Function of Wearing Denture in Partially Edentulous Elderly Patients

Noriyuki Narita^{1*}, Tomohiro Ishii², Sunao Iwaki³, Kazunobu Kamiya², Masakazu Okubo², Takeshi Uchida⁴, Ikuo Kantake^{4,5} and Koh Shibutani⁵

¹ Research Institute of Oral Science, Nihon University School of Dentistry at Matsudo, Matsudo, Japan, ² Department of Removable Prosthodontics, Nihon University School of Dentistry at Matsudo, Matsudo, Japan, ³ Automotive Human Factors Research Center, National Institute of Advanced Industrial Science and Technology, Tsukuba, Japan, ⁴ Dental Support Co. Ltd., Chiba, Japan, ⁵ Department of Anesthesiology, Nihon University School of Dentistry at Matsudo, Matsudo, Japan

OPEN ACCESS

Edited by:

Kazutaka Takahashi,
The University of Chicago,
United States

Reviewed by:

Yuji Masuda,
Matsumoto Dental University, Japan
Gianluca Tartaglia,
University of Milan, Italy
Shunsuke Minakuchi,
Tokyo Medical and Dental University,
Japan

*Correspondence:

Noriyuki Narita
narita.noriyuki@nihon-u.ac.jp

Received: 27 September 2019

Accepted: 23 December 2019

Published: 31 January 2020

Citation:

Narita N, Ishii T, Iwaki S,
Kamiya K, Okubo M, Uchida T,
Kantake I and Shibutani K (2020)
Prefrontal Consolidation
and Compensation as a Function
of Wearing Denture in Partially
Edentulous Elderly Patients.
Front. Aging Neurosci. 11:375.
doi: 10.3389/fnagi.2019.00375

Background: The cognitive effects of wearing a denture are not well understood. This study was conducted to clarify the effects of denture use on prefrontal and chewing muscle activities, occlusal state, and subjective chewing ability in partially edentulous elderly individuals.

Methods: A total of 16 partially edentulous patients were enrolled. Chewing-related prefrontal cortex and jaw muscle activities were simultaneously examined using a functional near-infrared spectroscopy (fNIRS) device and electromyography, under the conditions of unwearing, and wearing a denture. Occlusal state and masticatory score were also determined under both conditions. Using multiple linear regression analysis, associations between prefrontal and chewing activities with wearing were examined using change rates.

Results: Chewing rhythmicity was maintained under both conditions. As compared with unwearing, the wearing condition was associated with improved prefrontal cortex and chewing muscle activities, occlusal state in regard to force and area, and masticatory score. Also, prefrontal activities were positively associated with burst duration and peak amplitude in masseter (Mm) and temporal muscle activities, as well as masticatory scores. In contrast, prefrontal activities were negatively associated with occlusal force.

Conclusion: Wearing a denture induced a positive association between burst duration and peak amplitude in Mm and temporal muscle activities and prefrontal activity, which may indicate a parallel consolidation of prefrontal cortex and rhythmical chewing activities, as well as masticatory scores. On the other hand, denture use induced a negative association of occlusal force with prefrontal activities, which might suggest that prefrontal compensative associations for the physiocognitive acquisition depended on biomechanical efficacy gained by wearing a denture.

Keywords: prefrontal cortex, consolidation, compensation, chewing activity, denture wearing, elderly

INTRODUCTION

Epidemiologic studies have suggested associations between cognitive ability and oral conditions, such as number of teeth (Luo et al., 2015; Li et al., 2017; Oh et al., 2018) and dental occlusion (Ono et al., 2010; Franco et al., 2012; Takeuchi et al., 2015). Furthermore, occlusal force (Takeshita et al., 2016; Ikebe et al., 2018) and chewing ability have been shown to have effects on cognitive ability (Chen et al., 2015; Natalie et al., 2015; Seraj et al., 2017). Oral reconstruction by means of wearing a denture may induce cortical activation in prefrontal, sensorimotor, and sensory association cortices during chewing performance (Kimoto et al., 2011; Kamiya et al., 2016) and might also contribute to antiaging cognitive activation in the prefrontal cortex of elderly edentulous patients (Banu et al., 2016).

Denture use is considered to have effects on not only physical activity but also cognitive demands in aged individuals (Cerutti-Kopplin et al., 2015; Shin et al., 2019). Thus, a well-fitting denture may help to maintain cognitive ability and prevent its decline otherwise caused by tooth loss in elderly edentulous patients. On the other hand, in individuals with tooth loss who do not wear a denture, cognitive decline might be accelerated with age.

The association of a higher cognitive node with biomechanical state caused by wearing a denture remains unknown, though a functional association of prefrontal activity with chewing ability in elderly patients has been proposed (Lin et al., 2016). The present study was conducted to clarify the biomechanical efficacy of wearing a denture based on the associations of prefrontal cortex activities with physical chewing activities in partially edentulous elderly patients.

In addition to investigations of chewing-related prefrontal participation under wearing a denture and tooth loss conditions, studies that used a cognitive task demanding consolidation or compensation by prefrontal cortex activities during physical task performances have been presented (Bhambhani et al., 2006; Tsujii et al., 2013; Moriya et al., 2016; Mirelman et al., 2017; Hawkins et al., 2018). Thus, the elucidation of the relationships between consolidated or compensated prefrontal activities and physical chewing activities in partially edentulous elderly patients would help with evaluation of the efficacy and quality of wearing a denture in the process of oral neurorehabilitation. The present is the first known study to explore the possibility of neurorehabilitation by use of a denture in partially edentulous elderly subjects.

Functional near-infrared spectroscopy has been used to reveal the hemodynamic response to stimulus-induced cortical activation in order to evaluate the neurobiology in exercise and cognition (Bhambhani et al., 2006; Tsujii et al., 2013; Moriya et al., 2016), and chewing cognition was also examined by fNIRS in both young and aged subjects (Hasegawa et al., 2013; Kamiya et al., 2016; Yokoyama et al., 2017) as well as psychiatric patients with persistent occlusal dysesthesia (Narita et al., 2019). fNIRS

was used in the present investigation, as it is considered suitable for examinations of prefrontal and chewing activities with and without wearing a denture in clinical situations.

MATERIALS AND METHODS

Participants

A total of 16 partially edentulous patients {nine males and seven females; mean age 64.0 ± 6.2 years [mean \pm standard deviation (SD)]} undergoing treatments at the Prosthodontics Department of Nihon University School of Dentistry at Matsudo Hospital were enrolled in this study. The G*Power 3 software package (non-commercial program downloaded from the University of Dusseldorf, Germany) (Faul et al., 2007) was used to determine the sample size, which established parameters with a significance level of 0.05, statistical power of 0.8, and effect size of 0.25 (medium effect). From those findings, the number of subjects needed to detect significant differences in this study was concluded to be 16. Statistical results were obtained with the power of the performed test at $\alpha = 0.050$. The mean (\pm SD) numbers of the remaining, lost, and prosthetic teeth in the present patients were 17.9 ± 3.2 , 10.2 ± 3.2 , and 9.8 ± 3.4 , respectively (Figure 1). Based on Eichner's intermaxillary tooth contact classification (Eichner, 1955), we divided the subjects into three groups (B2, $n = 8$; B3, $n = 4$; and B4, $n = 4$), with B2 indicating two supporting zones, B3 indicating one supporting zone, and B4 indicating no supporting zones (Figure 1). None of the patients noted prosthesis conditions, such as discomfort or pain, or had difficulties with chewing performance and symptoms of temporomandibular joint or masticatory muscle dysfunction such as jaw pain or jaw movement difficulties. Individual patterns of tooth loss in each patient, as well as details of their tooth defects and partial denture-wearing condition, are presented in Figure 1. This study was conducted in accordance with the Declaration of Helsinki and approved by the Ethics Committee of Nihon University School of Dentistry at Matsudo (EC 14-13-010-1). Prior to beginning the examinations, all patients provided written informed consent for participation.

Experimental Procedures

Each patient received sufficient prosthodontic treatment in the form of conventional removable partial denture prostheses during the 3 months prior to beginning the study. Masticatory score, occlusal state, and jaw muscle and prefrontal activities during chewing were determined to elucidate changes in chewing ability, occlusal force or occlusal area, jaw muscle activity, and prefrontal activity during chewing caused by wearing a denture. Measurements were conducted under the conditions of rest (Rest), without use of a denture (Unwearing), and while wearing a denture (Wearing). With the patient comfortably seated in a quiet room, masticatory muscle and prefrontal activities were recorded during gum chewing simultaneously using fNIRS and EMG devices under the Unwearing and Wearing conditions, while those were also recorded at Rest without gum chewing. Chewing ability and occlusal force and area were evaluated using the food intake questionnaire and the pressure-sensitive sheets under the

Abbreviations: AD, anterior digastric; BA, pars triangularis Broca's area; DLPFC, dorsolateral prefrontal cortex; EMG, electromyography; FPA, frontopolar area; fMRI, functional magnetic resonance imaging; fNIRS, functional near-infrared spectroscopy; IPG, inferior prefrontal gyrus; Mm, masseter; OFC, orbitofrontal cortex; Ta, anterior temporal.

| Subject (age, sex) | Eichner's index | Remaining teeth/ lost teeth/ prosthetic teeth | Subject (age, sex) | Eichner's index | Remaining teeth/ lost teeth/ prosthetic teeth |
|-----------------------|--------------------|--|-----------------------|--------------------|--|
| A (52, f) | B2 | 654321 1234567 7654321 1234567 22 6 5 | I (60, f) | B3 | 7654321 1234567 654321 1234567 20 8 7 |
| B (57, f) | B2 | 7654321 1234567 7654321 1234567 17 11 11 | J (65, f) | B3 | 7654321 1234567 654321 23456 18 10 7 |
| C (62, f) | B2 | 7654321 1234567 7654321 1234567 18 10 10 | K (67, m) | B3 | 7654321 123456 7654321 1234567 18 10 9 |
| D (60, m) | B2 | 7654321 1234567 7654321 1234567 13 15 15 | L (72, m) | B3 | 7654321 1234567 7654321 1234567 21 7 7 |
| E (67, m) | B2 | 7654321 1234567 7654321 1234567 11 17 17 | M (60, f) | B4 | 7654321 1234567 4321 123456 17 11 7 |
| F (69, m) | B2 | 7654321 1234567 7654321 1234567 18 10 10 | N (63, f) | B4 | 7654321 1234567 7654321 1234567 14 14 14 |
| G (74, m) | B2 | 7654321 1234567 7654321 1234567 22 6 6 | O (60, m) | B4 | 7654321 1234567 7654321 1234567 18 10 10 |
| H (74, m) | B2 | 7654321 1234567 7654321 1234567 22 6 6 | P (62, m) | B4 | 7654321 1234567 7654321 1234567 17 11 11 |

FIGURE 1 | Age, gender, and dental state in partially edentulous patients. Age, gender, and dental state for each of the 16 partially edentulous patients (A–P) are shown. Subjects A–H, I–L, and M–P were classified as B2, B3, and B4, respectively, according to Eichner's intermaxillary tooth contact classification. The remaining teeth are indicated in black and prosthetic teeth in red.

Unwearing and Wearing conditions, respectively (Hirai et al., 1994; Miura et al., 1998).

Chewing Task

Chewing sessions consisted of four different chewing performances, as follows: (1) chewing on the left side under Unwearing, (2) chewing on the left side under Wearing, (3) chewing on the right side under Unwearing, and (4) chewing on the right side under Wearing. The four chewing sessions were performed randomly to avoid the influence of task sequence on the results. Each session included five chewing trials, with the trial conducted for 10 s with gum chewing and separated from the succeeding chewing trial by a 40-s rest phase. One piece of chewing gum (Freezone, Lotte Corporation, Japan) was used for the chewing task under both the Unwearing and Wearing conditions. The patients were instructed to be quiet until given a verbal cue (pre-task period), and then a verbal cue was given to start gum chewing for 10 s (task period) until a verbal cue to stop chewing was given, after which they were instructed to remain quiet for 20 s (post-task period). In addition, the patients performed a Rest session without a chewing task and were asked to remain quiet during that time.

Masticatory Score

Masticatory score, determined based on results of self-assessed chewing ability under the Unwearing and Wearing conditions, was used to evaluate subjective chewing ability (Hirai et al., 1994;

Miura et al., 1998). Each patient rated their ability to chew 35 different food items according to the following scale: 2, can be eaten easily; 1, can be eaten with difficulty; 0, cannot be eaten (Hirai et al., 1994; Miura et al., 1998).

Occlusal State

In order to evaluate occlusal state, bilateral maximal occlusal force, occlusal area, average pressure, and maximum pressure were examined under the Unwearing and Wearing conditions using 97- μ m-thick pressure-sensitive sheets (Dental Prescale 50H R-type, Fuji Film Co., Tokyo, Japan), with the patients asked to perform maximal clenching in an intercuspal position after placement of the sheet. Values for those parameters were obtained by use of analytic equipment (Occluzer FPD703, Fuji Film Co., Tokyo, Japan).

Masticatory Muscle EMG Activity

Masticatory muscle EMG activities from the left and right masseter (Mm, jaw closing), anterior temporal (Ta, jaw closing), and anterior digastric (AD, jaw opening) muscles were recorded using a multichannel EMG device (Polygraph Bioelectric Amplifier 1253A, San-ei MED, Tokyo, Japan) during chewing under the Unwearing and Wearing conditions. Electrodes were positioned bilaterally on the center of the muscle parallel with the direction of the muscle fibers and an interelectrode distance of 20 mm, with a ground electrode attached to the left earlobe. Amplified EMG signals were digitized with 16-bit resolution

using an A/D converter [APA16-32/2(OB) F, CONTEC, Tokyo, Japan] and then downloaded to a personal computer at a sampling rate of 1 kHz.

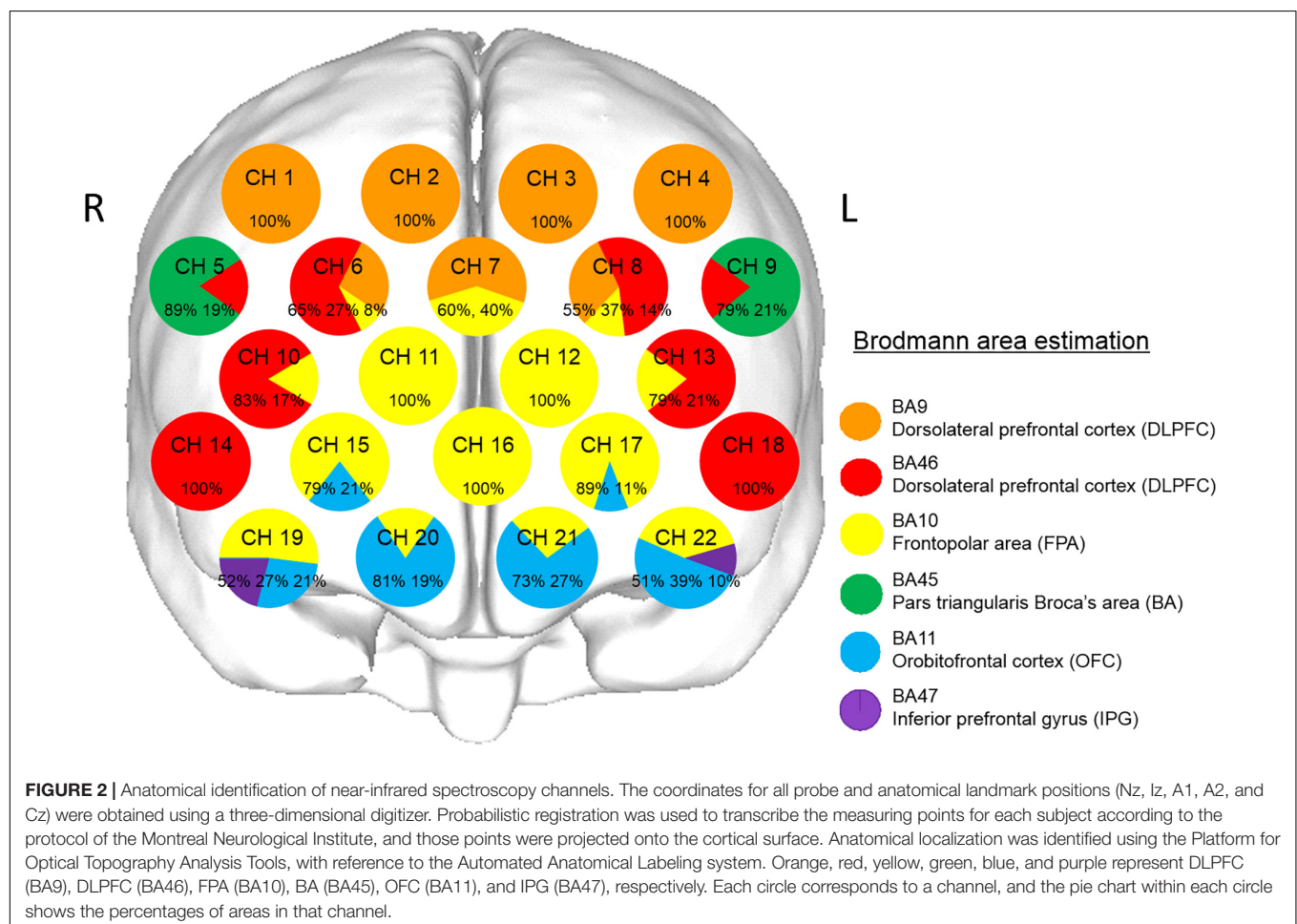
Prefrontal fNIRS During Chewing Performance

A 22-channel fNIRS device (ETG-100, Hitachi Medical Co., Chiba, Japan), which utilizes near-infrared light at wavelengths of 780 and 830 nm (Strangman et al., 2002), was used to assess the activity of the prefrontal cortex during chewing performance. Each fNIRS probe was fitted with a 3×5 thermoplastic shell and placed in the prefrontal region, with the bottom lines of the probes set according to Fp1 and Fp2, with referral to the international 10–20 system (Klem et al., 1999). Change in oxygenated hemoglobin concentration [(oxy-Hb)] was used as an indicator of change of brain activity, as previously validated (Hoshi et al., 2001). Change in [oxy-Hb] has been shown to have a strong correlation with blood-oxygenation-level-dependent signals measured by fMRI (Toronov et al., 2001). The sampling interval was 0.1 s. During the measurements, the patients were instructed to open their eyes and gaze at a point in front of them. Each trial was repeated five times, and [oxy-Hb] was measured during chewing performance on the left and right sides under

the Unwearing and Wearing conditions, as well as during Rest. The obtained [oxy-Hb] values were averaged using the “integral mode” of the ETG-100 software. Measurement baselines were corrected using linear fitting (Sawa et al., 2012), which was performed by connecting the pre-task baseline (mean of final 20 s of the pre-task period) with the post-task baseline (mean of final 20 s of the post-task period).

Anatomic Localization of fNIRS Channels

The coordinates for all probe and anatomical landmark (Nz, Iz, A1, A2, and Cz) positions were obtained using a three-dimensional digitizer (3SPACE ISOTRAK2, Polhemus, United States) and then transcribed into Montreal Neurological Institute standard brain space (Collins et al., 1994; Brett et al., 2002) using probabilistic registration (Okamoto and Dan, 2005; Singh et al., 2005). The probe positions were projected onto the cortical surface, with Platform for Optical Topography Analysis Tools (POTATo, Hitachi, Japan) used to identify the anatomic localization corresponding to each probe coordinate, with reference to the Brodmann area (Tzourio-Mazoyer et al., 2002; Okamoto and Dan, 2005; Singh et al., 2005; **Figure 2**). Representative anatomical identification of the fNIRS channels is shown in **Figure 2**. Those channels were localized in



the dorsolateral prefrontal cortex (DLPFC, BA9 and BA46), frontopolar area (FPA, BA10), pars triangularis Broca's area (BA, BA45), orbitofrontal cortex (OFC, BA11), and inferior prefrontal gyrus (IPG, BA47).

Data and Statistical Analyses

Averaging of Masticatory Muscle and Prefrontal Cortex Activities During Chewing Performance

Masticatory muscle activities, such as number of chewing strokes, cycle duration, burst duration, inter-burst duration, area, mean amplitude, and peak amplitude, were averaged using data obtained for right- and left-side chewing. Those results showed no significant differences in regard to the number of remaining teeth, chewing muscle activities, or prefrontal [oxy-Hb] values between right- and left-side chewing under the Unwearing and Wearing conditions (**Supplementary Material**).

Comparing Masticatory Score, Masticatory Muscle Activities, Occlusal Force, Occlusal Area, Average Pressure, and Max Pressure Between Unwearing and Wearing Conditions

A paired *t*-test or Wilcoxon's signed rank test was used for comparing masticatory score, masticatory muscle activities, occlusal force, occlusal area, average pressure, and max pressure between Unwearing and Wearing conditions, depending on normality test results.

Comparing Prefrontal [oxy-Hb] Values Between the Rest, Unwearing, and Wearing Conditions

Furthermore, averaged data for prefrontal [oxy-Hb] were accumulated during chewing periods (10 s) from all 22 channels under [oxy-Hb] values. One-way repeated-measures ANOVA and Tukey's test or Friedman's repeated-measures ANOVA on ranks and Dunn's test were applied for analyzing prefrontal [oxy-Hb] values obtained during chewing periods in order to compare between the Rest, Unwearing, and Wearing conditions, depending on normality test results.

Multiple Linear Regression Analysis Dependent Variable (Prefrontal Activities) and Independent Variables (Occlusal States and Chewing Activities)

Change rate (difference between Wearing and Unwearing values, divided by the Unwearing value) was used to standardize the prefrontal [oxy-Hb] values as dependent variables and to standardize values for masticatory score, burst duration, peak amplitude, and occlusal force as independent variables.

Multiple linear regression was performed using a model corresponding to each variable, with the following equation:

$$Y = a_1x_1 + a_2x_2 + a_3x_3 + a_4x_4 + c$$

where *Y* is the dependent variable; *x*₁, *x*₂, *x*₃, and *x*₄ are independent variables; *a*₁, *a*₂, *a*₃, and *a*₄ are regression coefficients; and *c* is the error term with an *N*(0, σ^2) distribution.

When performing multiple regression analysis, an important assumption is that the independent variables are truly independent of each other; i.e., there is no relationship among

any of the independent variables used to estimate ordinary least squares. However, in some applications of regression, independent variables are in fact related to each other, which is termed a multicollinearity problem (Chatterjee and Hadi, 2006). For the present study, correlation analysis by Pearson's correlation coefficient was used to check for a multicollinearity problem among the independent variables. Variables with a correlation coefficient (*r*) of ≥ 0.5 were considered to be strongly correlated with each other. To avoid multicollinearity, separate models were built using variables with lower levels of correlation with each other (*r* < 0.5). Evaluations of the multivariate models were conducted using coefficients of determination (*r*). Any intercorrelation between the four independent variables, change rates in the masticatory score, occlusal force, burst duration, and peak amplitude of Mm or Ta between the Unwearing and Wearing conditions, was subjected to bivariate correlation coefficient evaluation. In the present study, a correlation was found between the muscle activities of Mm or Ta; thus, they were considered separately in the model.

The statistical software package SigmaPlot 12.5 (Systat Software Inc., CA, United States) was used for all analyses, and *p* values less than 0.05 were considered to be statistically significant. Results are expressed as the Mean \pm SD, *p* value, or power of the performed test.

RESULTS

Effects of Wearing a Denture on Masticatory Score, Occlusal State, and Masticatory Muscle EMG Activities

Masticatory Score

Masticatory score under the Wearing condition were significantly (*p* < 0.001, paired *t*-test, power of performed two-tailed test with

TABLE 1 | Masticatory scores under Unwearing and Wearing conditions.

| | Unwearing | | Wearing | | <i>P</i> value |
|-------------------|-----------|------|---------|-----|----------------|
| | Mean | SD | Mean | SD | |
| Masticatory score | 48.0 | 23.1 | 81.3 | 9.5 | <0.001*** |

***Significant difference between Unwearing and Wearing conditions (paired *t*-test, *p* < 0.001).

TABLE 2 | Occlusal states under the Unwearing and Wearing conditions.

| Occlusal states | Unwearing | | Wearing | | <i>p</i> value |
|--|-----------|-------|---------|-------|----------------|
| | Mean | SD | Mean | SD | |
| Occlusal force (N) | 289.3 | 105.9 | 620.0 | 132.5 | <0.001*** |
| Occlusal contact area (mm ²) | 6.6 | 2.6 | 14.2 | 3.7 | <0.001*** |
| Average pressure (MPa) | 43.3 | 5.7 | 42.9 | 5.5 | 0.89 |
| Maximum pressure (MPa) | 100.6 | 14.3 | 104.6 | 12.3 | 0.130 |

***Significant difference between the Unwearing and Wearing conditions (paired *t*-test, *p* < 0.001). Paired *t*-test is indicated in normal font, and Wilcoxon's signed rank test is indicated in bold font.

$\alpha = 0.050$: 1.000) increased as compared with those under the Unwearing condition (Table 1).

Occlusal State

Occlusal force under the Wearing condition was significantly ($p < 0.001$, paired t -test, power of performed two-tailed test with $\alpha = 0.050$: 1.000) increased as compared with that under the Unwearing condition (Table 2). Additionally, the occlusal contact area under the Wearing condition was significantly ($p < 0.001$, paired t -test, power of performed two-tailed test with $\alpha = 0.050$: 1.000) increased as compared with that under the Unwearing condition (Table 2). Average and max pressure were not significantly (paired t -test and Wilcoxon's signed rank test, respectively) different between these conditions (Table 2).

Masticatory Muscle EMG Activities During Chewing Performance

The number of chewing strokes for Mm under the Wearing condition was not significantly (paired t -test) different as compared to that under the Unwearing condition, and cycle duration for AD EMG activity was also not significantly (paired t -test) different between the conditions (Table 3). Burst duration for Mm EMG activity under the Wearing was significantly ($p = 0.010$, paired t -test, power of performed two-tailed test with $\alpha = 0.050$: 0.615) elongated as compared with that under the Unwearing condition. Under the Wearing condition, burst duration for Ta EMG activity was not significantly (paired t -test) different with that under Unwearing condition, and the inter-burst duration for Mm and Ta EMG activities was also not significantly (paired t -test) different between these conditions (Table 3). In contrast, the areas for Mm and Ta under the Wearing condition were significantly ($p \leq 0.001$, Wilcoxon's signed rank test) increased, and the mean amplitude for Mm EMG activity under the Wearing condition was also significantly ($p = 0.001$, Wilcoxon's signed rank test) increased as compared with that under the Unwearing condition (Table 3). Also, the mean amplitude for Ta EMG activity under the Wearing

condition was significantly ($p = 0.044$, paired t -test, power of performed two-tailed test with $\alpha = 0.050$: 0.539) increased as compared with that under the Unwearing condition, while the peak amplitude for Mm EMG activity was not significantly (paired t -test) different between these conditions (Table 3). Finally, peak amplitude for Ta EMG activity under the Wearing condition was significantly ($p = 0.012$, paired t -test, power of performed two-tailed test with $\alpha = 0.050$: 0.759) increased as compared with that under the Unwearing condition (Table 3).

Grand Average Waveforms for Changes in Prefrontal [oxy-Hb]

The grand averaged waveforms for changes in prefrontal [oxy-Hb] and prefrontal deoxygenated hemoglobin concentration [(deoxy-Hb)] under the Rest, Unwearing, and Wearing conditions are shown in Figures 3A–C, respectively. Unwearing resulted in slight changes in prefrontal [oxy-Hb] during the chewing period as compared with Rest (Figures 3A,B). In contrast, under the Wearing condition, marked and broad increases in prefrontal [oxy-Hb] were found during the task period, as compared to Rest and Unwearing conditions (Figures 3A–C).

Topographical Changes in Prefrontal [oxy-Hb] During 10-s Task Periods Under Rest, Unwearing, and Wearing Conditions

Topographical maps for changes in prefrontal [oxy-Hb] in the pre-task, task, and post-task periods under the Rest, Unwearing, and Wearing conditions are shown in Figures 3A–C, respectively. An equivocal change in prefrontal [oxy-Hb] throughout the Rest condition was noted (Figure 3A), while slight changes in prefrontal [oxy-Hb] presented during chewing under the Unwearing condition in the pre-task, task, and post-task periods, as compared with the Rest condition

TABLE 3 | Masticatory muscle EMG activities under the Unwearing and Wearing conditions.

| Masticatory muscle EMG activities | | Unwearing | | Wearing | | p value |
|-----------------------------------|----|-----------|--------|---------|--------|-----------|
| | | Mean | SD | Mean | SD | |
| Number of chewing strokes | Mm | 63.28 | 13.44 | 65.16 | 13.34 | 0.55 |
| Cycle duration (ms) | AD | 837.28 | 123.56 | 838.71 | 173.34 | 0.55 |
| Burst duration (ms) | Mm | 306.54 | 87.03 | 344.67 | 72.93 | 0.03* |
| | Ta | 282.19 | 67.71 | 297.80 | 59.95 | 0.49 |
| Inter-burst duration (ms) | Mm | 535.75 | 102.93 | 503.19 | 121.81 | 0.96 |
| | Ta | 561.60 | 100.59 | 545.19 | 132.23 | 0.26 |
| Area (mV·s) | Mm | 0.01 | 0.01 | 0.02 | 0.01 | <0.001+++ |
| | Ta | 0.01 | 0.00 | 0.02 | 0.01 | <0.001+++ |
| Mean amplitude (mV) | Mm | 0.04 | 0.03 | 0.06 | 0.04 | 0.001+++ |
| | Ta | 0.04 | 0.02 | 0.05 | 0.03 | 0.04* |
| Peak amplitude (mV) | Mm | 0.10 | 0.07 | 0.13 | 0.08 | 0.34 |
| | Ta | 0.07 | 0.04 | 0.09 | 0.05 | 0.01* |

*Significant difference between the Unwearing and Wearing conditions (paired t -test, $p < 0.05$). +++Significant difference between the Unwearing and Wearing conditions (Wilcoxon's signed rank test, $p < 0.001$).

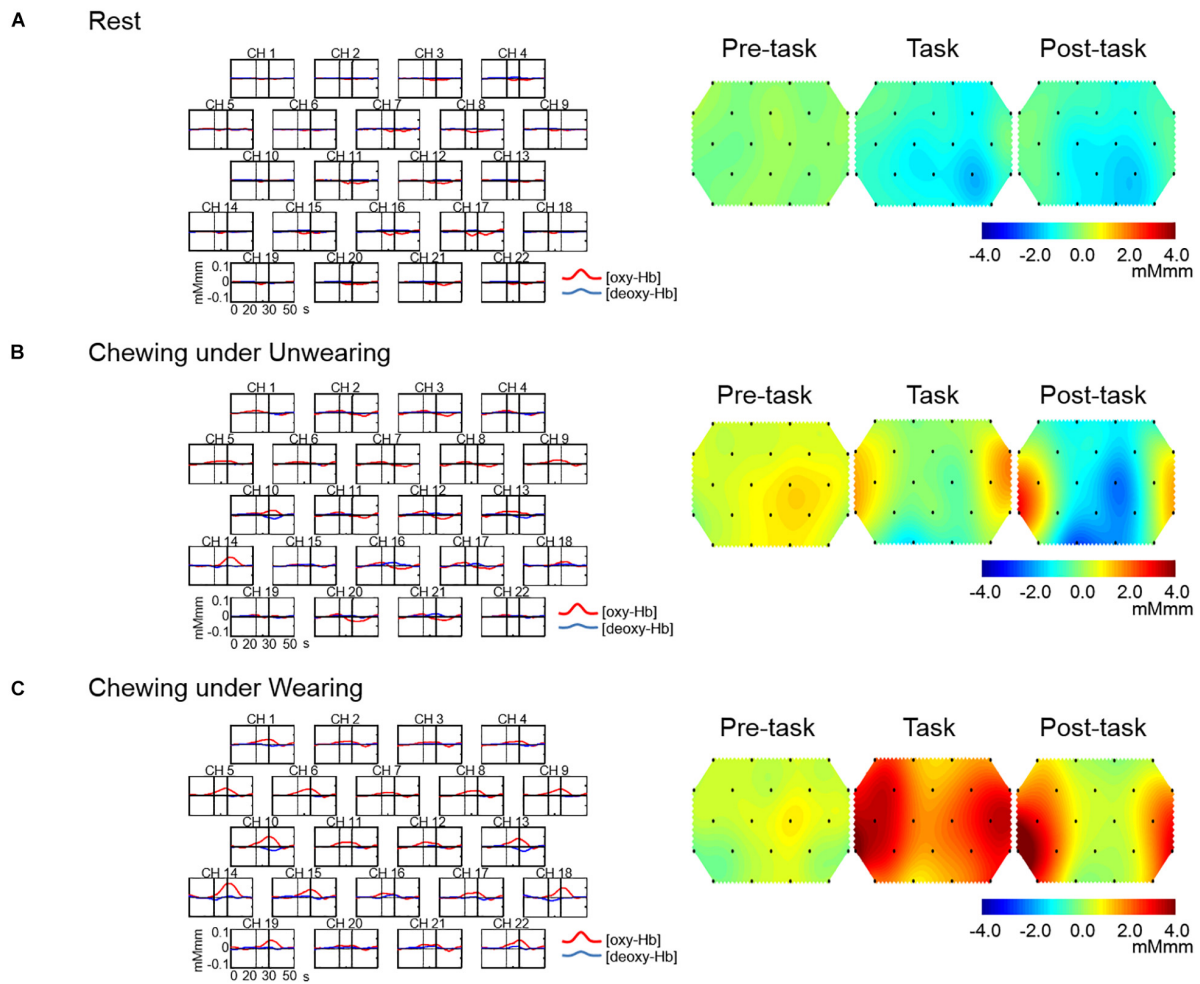


FIGURE 3 | Grand average waveforms for oxygenated hemoglobin concentration ([oxy-Hb]) and deoxygenated hemoglobin concentration ([deoxy-Hb]) and topographical maps showing changes in [oxy-Hb] during Rest and chewing under Unwearing and Wearing conditions. On the left are grand average changes in [oxy-Hb] (red line) and [deoxy-Hb] (blue line) for each of the 22 measurement channels during the Rest condition (A), chewing under the Unwearing (B), and Wearing (C) conditions. The x-axis indicates time (s) and the y-axis hemodynamic change (mMmm). Vertical lines at 20 and 30 s indicate the start and end of the 10-s chewing period. On the right are 10-s topographical maps showing changes in [oxy-Hb] preceding (pre-task), during (task), and following (post-task) rest (A), chewing under the Unwearing (B), and Wearing (C) conditions. There was little change in [oxy-Hb] throughout the Rest session (A), while there was a slight increase during the chewing period under the Unwearing (B) condition and marked increases during chewing and post-chewing under the Wearing (C) condition.

(Figures 3A,B). In contrast, a marked increase in prefrontal [oxy-Hb] during the chewing session under the Wearing condition in the task and post-task periods as compared to the Rest and Unwearing conditions was noted (Figures 3A–C).

Accumulated Prefrontal [oxy-Hb] During the Task Period

Prefrontal [oxy-Hb] in the task periods under the Rest, Unwearing, and Wearing conditions was analyzed using one-way repeated-measures ANOVA and Friedman's repeated-measures ANOVA on ranks in R-DLPFC (CH 1, power of performed test with $\alpha = 0.050$: 0.963), R-DLPFC (CH 2), L-DLPFC (CH 3 and CH 4), R-BA/DLPFC (CH 5, power of performed test with $\alpha = 0.050$: 1.000), R-DLPFC/FPA (CH 6), RL-DLPFC/FPA (CH 7, power of performed test with $\alpha = 0.050$: 0.760),

L-DLPFC/FPA (CH 8, power of performed test with $\alpha = 0.050$: 0.981), L-BA/DLPFC (CH 9, power of performed test with $\alpha = 0.050$: 0.943), R-DLPFC/FPA (CH 10), R-FPA (CH 11), L-FPA (CH 12), L-DLPFC/FPA (CH 13, power of performed test with $\alpha = 0.050$: 0.972), R-DLPFC (CH 14, power of performed test with $\alpha = 0.050$: 0.893), R-FPA/OFC (CH 15), RL-FPA (CH 16), L-FPA/OFC (CH 17), L-DLPFC (CH 18), R-FPA/OFC/IPG (CH 19), R-OFC/FPA (CH 20), L-OFC/FPA (CH 21), and L-OFC/FPA/IPG (CH 22, power of performed test with $\alpha = 0.050$: 0.717).

Unwearing as Compared With Rest

During the chewing session under the Unwearing condition, a significant ($p < 0.01$, one-way repeated-measures ANOVA and Tukey's test, Friedman's repeated-measures ANOVA on

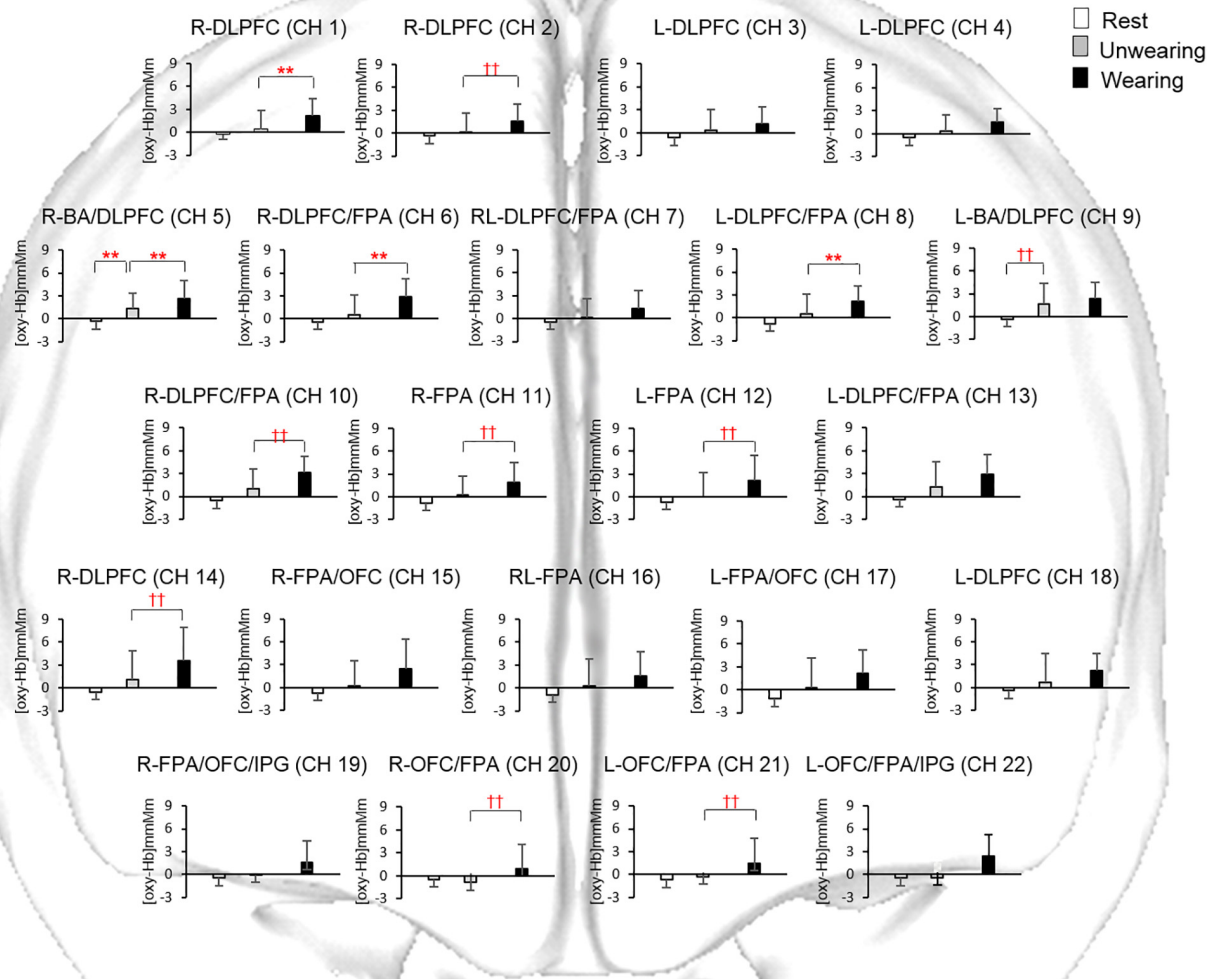


FIGURE 4 | Accumulated oxygenated hemoglobin concentration [oxy-Hb] under the Rest condition and during chewing under the Unwearing and Wearing conditions. Statistical analyses were performed using one-way repeated measures ANOVA and pairwise multiple comparison procedures of Tukey's test, as well as Dunn's test. **Significant difference between Rest and Unwearing, and between Unwearing and Wearing conditions (one-way repeated-measures ANOVA and Tukey's test, $p < 0.01$). ††Significant difference between Rest and Unwearing, and between Unwearing and Wearing conditions (Friedman's repeated-measures ANOVA on ranks and Dunn's test, $p < 0.01$). Accumulated [oxy-Hb] under Unwearing significantly increased for BA/DLPFC (CH 5, 9) as compared to Rest condition. Accumulated [oxy-Hb] under Wearing also significantly increased for DLPFC (CH 1, 2, 14), BA/DLPFC (CH 5), DLPFC/FPA (CH 6, 8, 10), FPA (CH 11, 12), and FPA/OFC (CH 20, 21) as compared to Unwearing condition.

ranks, and Dunn's test) increase in accumulated prefrontal [oxy-Hb] in RL-DLPFC/BA (CH 5, 9) was noted during the task period as compared with that under the Rest condition (Figure 4).

Wearing as Compared With Rest

During the chewing session under the Wearing condition, significant ($p < 0.05$, one-way repeated-measures ANOVA and Tukey's test and Dunn's test) increases in accumulated prefrontal [oxy-Hb] in R-DLPFC (CH 1, 2, 14), L-DLPFC (CH 3, 4, 18), R-DLPFC/FPA (CH 6, 10), RL-DLPFC/FPA (CH 7), L-DLPFC/FPA (CH 8), L-DLPFC/FPA (CH 13), R-DLPFC/BA (CH 5), L-DLPFC/BA (CH 9), R-FPA (CH 11), L-FPA (CH 12), RL-FPA (CH 16), R-FPA/OFC (CH 15),

L-FPA/OFC (CH 17), R-OFC/FPA (CH 20), R-OFC/FPA (CH 21), R-FPA/OFC/IPG (CH 19), and L-FPA/OFC/IPG (CH 22) were seen, as compared with that under the Rest condition (Figure 4).

Wearing as Compared With Unwearing

During the chewing session under the Wearing condition, significant ($p < 0.01$, one-way repeated-measures ANOVA and Tukey's test and Dunn's test) increases in accumulated prefrontal [oxy-Hb] in R-DLPFC (CH 1, 2), R-DLPFC/BA (CH 5), R-DLPFC/FPA (CH 6, 10), L-DLPFC/FPA (CH 8), R-FPA (CH 11), L-FPA (CH 12), R-OFC/FPA (CH 20), and L-OFC/FPA (CH 21) were seen, as compared with that under the Unwearing condition (Figure 4).

Inter-Correlations Among the Four Independent Variables Related to Increases in Masticatory Score, Burst Duration, and Peak Amplitude for Mm or Ta Between Wearing and Unwearing

Intercorrelations among the four independent variables related to change rates in masticatory score, burst duration, and peak amplitude for Mm or Ta in the Wearing condition, as well as occlusal force, were examined using a bivariate correlation coefficient between the independent variables, with no significant intercorrelations found between them (Tables 4, 5). After the desired variables were entered into the regression model, significant relationships were assessed between dependent variables related to change rates in prefrontal [oxy-Hb] and independent variables related to change rates in masticatory score, burst duration, and ratio of peak amplitudes for Mm or Ta in the Wearing condition, as well as increases in occlusal force.

Multiple Linear Regression Analysis of Independent Variables Related to Masticatory Score, Burst Duration, and Peak Amplitude in Mm, as Well as Occlusal Force, and Dependent Variables Related to Prefrontal [oxy-Hb]

The change rate in burst duration in the Wearing condition was significantly and positively associated with a change rate in prefrontal [oxy-Hb] during the chewing task in R-FPA (CH 11) ($p = 0.014$, power of performed test with $\alpha = 0.050$: 0.999), L-FPA (CH 12) ($p = 0.002$, power of performed test with $\alpha = 0.050$: 0.983), and L-FPA/OFC (CH 17) ($p = 0.005$, power of performed test with $\alpha = 0.050$: 0.967) (Table 6 and Figure 5A).

The change rate in peak amplitude in the Wearing condition was significantly and positively associated with the change rate in prefrontal [oxy-Hb] during the chewing task in R-FPA (CH 11) ($p = 0.003$, power of performed test with $\alpha = 0.050$: 0.999) (Table 6 and Figure 5B).

The change rate in masticatory score in the Wearing condition was significantly and positively associated with the change rate in prefrontal [oxy-Hb] during the chewing task in R-FPA (CH 11) ($p = 0.001$, power of performed test with $\alpha = 0.050$: 0.999) (Table 6 and Figure 5C).

Multiple Linear Regression Analysis of Independent Variables Related to Burst Duration and Peak Amplitude in Ta, Occlusal Force, and Masticatory Score and Dependent Variables of Prefrontal [oxy-Hb]

The change rates in burst duration in the Wearing condition were significantly and positively associated with the change rates in prefrontal [oxy-Hb] during the chewing task in L-FPA (CH 12) ($p = 0.003$, power of performed test with $\alpha = 0.050$: 0.985) (Table 7 and Figure 6A).

TABLE 4 | Bivariate Pearson's correlation coefficients between independent variables of masticatory score, burst duration [masseter (Mm)], peak amplitude (Mm), and occlusal force in the regression analyses.

| Independent variables | Masticatory score | Burst duration (Mm) | Peak amplitude (Mm) | Occlusal force |
|-----------------------|-------------------|---------------------|---------------------|----------------|
| Masticatory score | | −0.070 | −0.098 | −0.349 |
| Burst duration (Mm) | | | 0.222 | −0.246 |
| Peak amplitude (Mm) | | | | −0.127 |

TABLE 5 | Bivariate Pearson's correlation coefficients between independent variables of masticatory score, burst duration [anterior temporal (Ta)], peak amplitude (Ta), and occlusal force in the regression analyses.

| Independent variables | Masticatory score | Burst duration (Ta) | Peak amplitude (Ta) | Occlusal force |
|-----------------------|-------------------|---------------------|---------------------|----------------|
| Masticatory score | | 0.127 | −0.209 | −0.349 |
| Burst duration (Ta) | | | −0.467 | −0.149 |
| Peak amplitude (Ta) | | | | 0.365 |

The change rates in peak amplitude in the Wearing condition were significantly and positively associated with the change rate in prefrontal [oxy-Hb] during the chewing task in L-FPA (CH 12) ($p = 0.004$, power of performed test with $\alpha = 0.050$: 0.985) (Table 7 and Figure 6B).

The change rate in occlusal force in the Wearing condition was significantly negatively associated with the change rate in prefrontal [oxy-Hb] during the chewing task in L-FPA (CH 12) ($p = 0.034$, power of performed test with $\alpha = 0.050$: 0.985) (Table 7 and Figure 6C).

DISCUSSION

This study primarily defined the consistent chewing rhythm formation under Unwearing and Wearing conditions. As compared to the Unwearing condition in our subjects, the Wearing condition resulted in improved masticatory score, occlusal state in regard to force and area, jaw muscle activities in regard to burst duration, area, mean amplitude, and prefrontal activities in DLPFC/FPA/OFC during chewing. In addition, a positive association of the burst duration and peak amplitude of Mm and temporal muscle activities with the prefrontal activities in the Wearing condition was noted as well as masticatory score, while a negative association of occlusal force with prefrontal activities was also noted in the Wearing condition.

Furthermore, the patients investigated in this study presented a masticatory score greater than 80 in subjective evaluations of chewing ability, as well as sufficient occlusal force and masticatory muscle activities under the Wearing condition (Tallgren and Tryde, 1991; Hirai et al., 1994; Miura et al., 1998; Aras et al., 2009). It is therefore conceivable that these positive and negative associations can be considered to reflect the physiological stomatognathic functioning in partially edentulous elderly patients.

TABLE 6 | Multiple linear regression for association of prefrontal oxygenated hemoglobin concentration [(oxy-Hb)] with masticatory score, burst duration [masseter (Mm)], and peak amplitude (Mm).

| Independent variables | Channel (Brodmann area) | Coefficients | Std. error | Standardized coefficients | p value |
|-----------------------|-------------------------|--------------|------------|---------------------------|---------|
| Burst duration (Mm) | CH 11 (R-FPA) | 2.550 | 0.876 | 0.427 | 0.014* |
| | CH 12 (L-FPA) | 8.231 | 2.031 | 0.758 | 0.002** |
| | CH 17 (L-FPA/OFC) | 9.261 | 2.654 | 0.697 | 0.005** |
| Peak amplitude (Mm) | CH 11 (R-FPA) | 0.417 | 0.111 | 0.534 | 0.003** |
| Masticatory score | CH 11 (R-FPA) | 0.164 | 0.039 | 0.631 | 0.001** |

*Significant association of prefrontal [oxy-Hb] (multiple linear regression analysis, $p < 0.05$). **Significant association of prefrontal [oxy-Hb] (multiple linear regression analysis, $p < 0.01$).

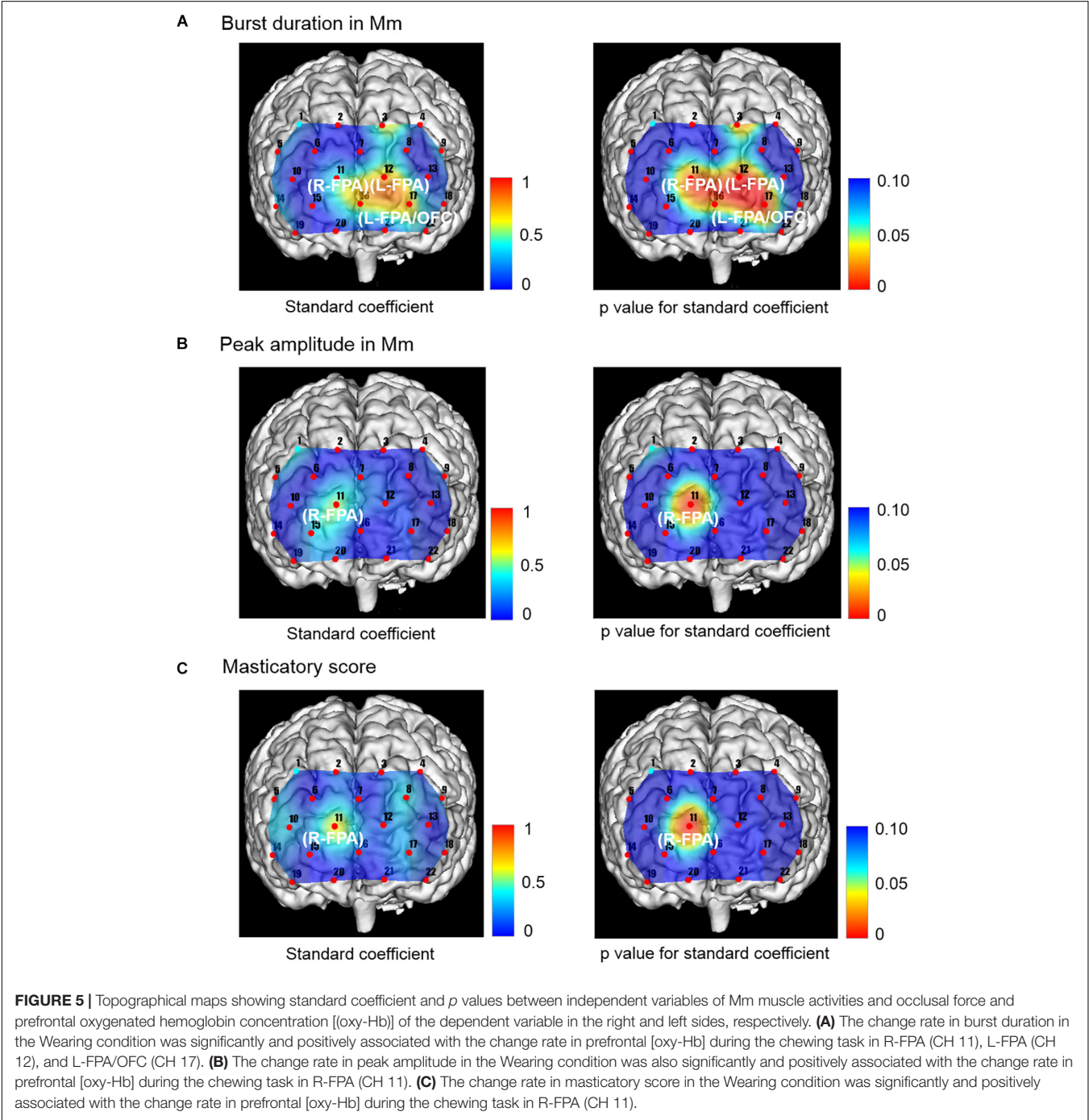


TABLE 7 | Multiple linear regression for association of prefrontal oxygenated hemoglobin concentration [(oxy-Hb)] with burst duration [anterior temporal (Ta)], peak amplitude (Ta), and occlusal force.

| Independent variables | Channel (Brodmann area) | Coefficients | Std. error | Standardized coefficients | p value |
|-----------------------|-------------------------|--------------|------------|---------------------------|---------|
| Burst duration (Ta) | CH 12 (L-FPA) | 6.223 | 1.654 | 0.743 | 0.003** |
| Peak amplitude (Ta) | CH 12 (L-FPA) | 2.896 | 0.811 | 0.749 | 0.004** |
| Occlusal force | CH 12 (L-FPA) | -1.239 | 0.513 | -0.475 | 0.034* |

*Significant association of prefrontal [oxy-Hb] (multiple linear regression analysis, $p < 0.05$). **Significant association of prefrontal [oxy-Hb] (multiple linear regression analysis, $p < 0.01$).

Positive Associations Between Chewing and Prefrontal Activities by Wearing a Denture

The present study found that wearing a denture induces a positive association of burst duration and peak amplitude of jaw muscle activities and masticatory score with prefrontal activities in FPA/OFC. Considering the consistent chewing rhythmicity by the Wearing and Unwearing conditions, the elongated burst duration and increased peak amplitude seen with consistent rhythmic chewing may suggest the enhanced chewing automaticity based on central rhythm and pattern generation in partially edentulous elderly patients (Lund, 1991; Nakamura and Katakura, 1995; Clark, 2015) and associated sensory facilitation by wearing a denture (Morimoto et al., 1989; Hidaka et al., 1999; Grigoriadis and Trulsson, 2018). Furthermore, the prefrontal cortex associated with basal ganglia and sensorimotor cortices may be involved in automatic and habitual control (Takakusaki et al., 2004; Hikosaka and Isoda, 2010; Redgrave et al., 2010) in parallel with the top-down controlling in movement execution (Narayanan and Laubach, 2006; Kamigaki, 2019), sensory percepts (Gilbert and Sigman, 2007; Okamoto et al., 2011; Raos and Savaki, 2017), reward (Horst and Laubach, 2013), and attention (Small et al., 2003).

The prefrontal acceleration caused by wearing a denture may be also supported by the research results showing a positive correlation between chewing ability and jaw closing muscle activities in partially edentulous elderly patients in regard to increased burst duration and peak amplitude, when wearing a denture (Fueki et al., 2008; Kamiya et al., 2016), as well as the finding of chewing-related prefrontal activities (Kamiya et al., 2016; Lin et al., 2016).

Moreover, it has been reported that physical exercise promotes prefrontal physiological and cognitive activities in aged individuals (Bhambhani et al., 2006; Tsujii et al., 2013; Moriya et al., 2016). Such prefrontal positive activation may also be effective to retrieve cognitive activity in aged edentulous individuals by the consolidation of interplay between the hippocampus and prefrontal activities induced by wearing a denture (Preston and Eichenbaum, 2013; Chen et al., 2015; Weilbacher and Gluth, 2016).

Taken together, the finding of elongated burst duration and increased peak amplitude of Mm and temporal muscle activities with consistent chewing rhythmicity by wearing a denture, as well as masticatory score, may be associated with the cognitive prefrontal consolidation in partially edentulous elderly patients, which might occur under usage of good-fitting denture that does

not cause unnecessary distraction (Schneider and Shiffrin, 1977; Shiffrin and Schneider, 1977).

Negative Association of Chewing With Prefrontal Activities Under the Wearing Condition

Our results in this study suggested that wearing a denture induced negative associations of the biomechanical factors in occlusal force with prefrontal activities in FPA.

Findings obtained in previous studies indicate that acceleration of prefrontal cortex activities during usual gait may be induced in older healthy individuals with poor gait speed and/or stride length, as compared with healthy young adults (Mirelman et al., 2017; Hawkins et al., 2018). It is therefore assumed that older adults with poor gait may rely on prefrontal cognition even when moving under a usual gait. Considering this compensative prefrontal participation in old adults, the poor acquisition of biomechanical structure in occlusal force by wearing a denture may be also interpreted as the association of compensative prefrontal recruitments involved in top-down generation of appropriate chewing force in partially edentulous elderly patients.

Standardization of Jaw Muscle Activities

Standardization of jaw muscle activities during chewing is essential for the critical evaluation of the effects of denture wearing. In the present study, change rates were applied for standardization of chewing-related jaw muscle activities between the Wearing and Unwearing conditions. In addition, in order to define the multiple prefrontal associations with chewing activities, comprehensive standardization was conducted using change rates for prefrontal fNIRS, occlusal force, and mastication score as subjective chewing ability, as well as burst duration and peak amplitude of jaw muscle activities. The results revealed specific prefrontal activation induced by wearing a denture in partially edentulous elderly patients associated with chewing activities.

Ferrario et al. (2004) reported a method for standardization of chewing muscle activities, referred to as jaw muscle EMG activity, under maximum voluntary teeth clenching and used that to compare the effects of two types of denture prostheses. There is no best way to normalize muscle activities, though Halaki and Ginn (2012) suggested obtaining reference values for normalization of EMG activities using the following: (1) maximum activation level during maximum contractions, (2) peak or mean activation level obtained during the task under investigation, (3) activation level during submaximal isometric

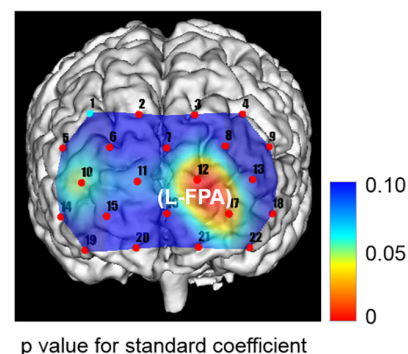
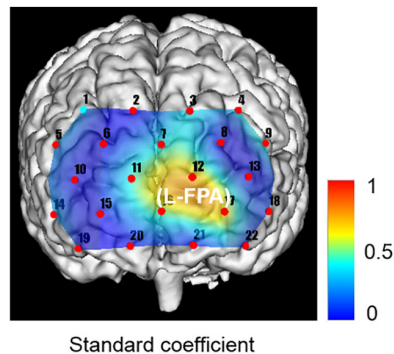
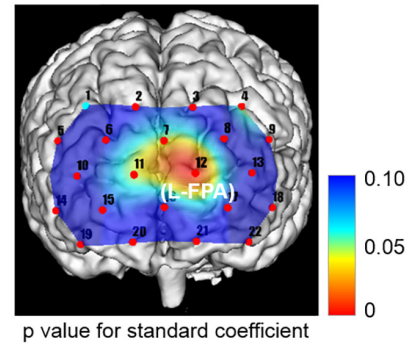
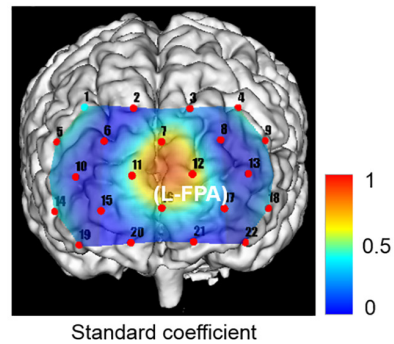
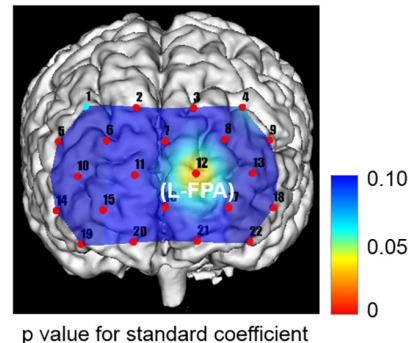
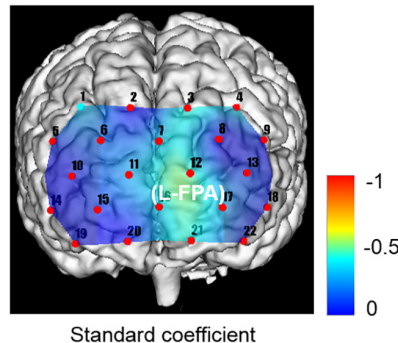
A Burst duration in Ta**B Peak amplitude in Ta****C Occlusal force**

FIGURE 6 | Topographical maps showing standard coefficient and p values between independent variables of Ta muscle activities and occlusal force and prefrontal oxygenation hemoglobin concentration [(oxy-Hb)] of the dependent variable in right and left sides, respectively. **(A)** The change rates in burst duration in the Wearing condition were significantly and positively associated with the change rates in prefrontal [oxy-Hb] in L-FPA (CH 12). **(B)** The change rates in peak amplitude in the Wearing condition were significantly and positively associated with the change rate in prefrontal [oxy-Hb] during the chewing task in L-FPA (CH 12). **(C)** The change rate in occlusal force in the Wearing condition was significantly negatively associated with change rate in prefrontal [oxy-Hb] during the chewing task in L-FPA (CH 12).

contractions, and (4) peak-to-peak amplitude of maximum muscle activation. An additional examination may be needed with another method for standardization of jaw muscle activities during chewing performance.

Measuring fNIRS for Prefrontal Cortex Activities During Chewing Performance

Artifacts in fNIRS can be caused by contractions of temporal muscle blood flow during chewing performance

(Schecklmann et al., 2017); thus, scrupulous attention is required to protect the interfusion of muscle artifacts during fNIRS measurements. In this regard, we consider it necessary to comment regarding possible artifact interfusion in the present fNIRS examinations. A previous report presented averaged recording data for masticatory muscle activities and fNIRS obtained during both right- and left-side chewing in order to exclude functional laterality (Kamiya et al., 2016), and the present study also averaged the bilateral fNIRS data. Recently, the dissociated prefrontal cortex activities were presented

during chewing performance in patients complaining of oral dysesthesia as compared with healthy controls, even though jaw muscle activities were not different between those two groups (Narita et al., 2019).

In the present study, significant associations of prefrontal fNIRS with jaw muscle activities and occlusal force and masticatory score were noted. Specifically, prefrontal fNIRS was positively associated with burst duration and peak amplitude of the Mm and temporal muscles as well as masticatory score, whereas prefrontal fNIRS was negatively associated with occlusal force (Figures 5, 6). Notably, prefrontal fNIRS was positively associated with burst duration and peak amplitude of temporal muscle activity (Figures 6A,B) and negatively with occlusal force in the same prefrontal localization (Figure 6C). When prefrontal fNIRS data become contaminated by jaw muscle blood flow during chewing performance, these conflicting positive and negative associations cannot simultaneously occur in the same region of the prefrontal cortex and also may not be associated with the bilaterally averaged chewing activities examined in the present study.

The present results also demonstrated separable functional localizations in regard to the associations of prefrontal activities with the peak amplitude of Mm and temporal muscle activities. A prefrontal association of peak amplitude in the Mm muscle was presented in the right FPA, whereas that in temporal muscle was presented in the left FPA (Figures 5B, 6B). In consideration of possible involvement of multiple brain areas in rhythmical chewing, including prefrontal higher cognition, sensorimotor cortices, and subcortical areas (Quintero et al., 2013; Lin et al., 2016, 2017), an additional study that utilizes whole-brain network analysis may be necessary to more appropriately interpret functional laterality in regard to the association of the prefrontal cortex with chewing activities in partially edentulous elderly patients when wearing a denture.

CONCLUSION

This study was conducted to clarify the efficacy of wearing a denture in partially edentulous elderly patients from the viewpoint of associations between prefrontal and chewing activities in regard to chewing ability, occlusal force, and chewing muscle activities. Our results show that wearing a denture improves prefrontal activity, occlusal state, chewing muscle activities, and masticatory score, as compared with not wearing one. Additionally, the prefrontal activities were positively associated with burst duration and peak amplitude of Mm and temporal muscle activities and masticatory score by wearing a denture. In contrast, the prefrontal activities were negatively associated with occlusal force by wearing a denture.

In consideration of prefrontal cognitive activation caused by physical exercise (Bhambhani et al., 2006; Tsujii et al., 2013; Moriya et al., 2016), the positive relationships between the temporal burst duration and peak amplitude in Mm and temporal muscle activities, as well as masticatory score, and the associated

prefrontal activation induced by wearing a denture may be considered as the prefrontal consolidation under the condition of the enhanced chewing automaticity in partially edentulous elderly patients. On the other hand, the negative relationships between the occlusal force and the prefrontal activations shown by wearing a denture could be interpreted as the prefrontal compensative participation in order to precisely generate the biomechanical occlusal force during chewing performance in partially edentulous elderly patients (Spraker et al., 2009; Derosière et al., 2014).

Findings obtained in this study warrant further investigations for the better understanding of oral neurorehabilitation based on Eichner's intermaxillary tooth contact classification in the individual elderly patient.

DATA AVAILABILITY STATEMENT

The datasets generated for this study are available on request to the corresponding author.

ETHICS STATEMENT

The present study protocol was approved by the Ethics Committee of Nihon University School of Dentistry at Matsudo (EC 14-13-010-1), and all patients provided written informed consent prior to participation.

AUTHOR CONTRIBUTIONS

NN designed the study and wrote the manuscript. KK collected the data. TI and KK analyzed the obtained data. SI, MO, TU, IK, and KS contributed to the data interpretation.

FUNDING

This work was supported by the Dental Support Co. Ltd. and the JSPS KAKENHI (Grant No. 21592473).

ACKNOWLEDGMENTS

We would like to thank Shingo Kawasaki for the excellent technical assistance.

SUPPLEMENTARY MATERIAL

The Supplementary Material for this article can be found online at: <https://www.frontiersin.org/articles/10.3389/fnagi.2019.00375/full#supplementary-material>

REFERENCES

- Aras, K., Hasanreisioğlu, U., and Shinogaya, T. (2009). Masticatory performance, maximum occlusal force, and occlusal contact area in patients with bilaterally missing molars and distal extension removable partial dentures. *Int. J. Prosthodont.* 22, 204–209.
- Banu, R. F., Veeravalli, P. T., and Kumar, V. A. (2016). Comparative evaluation of changes in brain activity and cognitive function of edentulous patients, with dentures and two-implant supported mandibular overdenture-pilot study. *Clin. Implant Dent. Relat. Res.* 18, 580–587. doi: 10.1111/cid.12336
- Bhambhani, Y., Maikala, R., Farag, M., and Rowland, G. (2006). Reliability of near-infrared spectroscopy measures of cerebral oxygenation and blood volume during handgrip exercise in nondisabled and traumatic brain-injured subjects. *J. Rehabil. Res. Dev.* 43, 845–856.
- Brett, M., Johnsrude, I. S., and Owen, A. M. (2002). The problem of functional localization in the human brain. *Nat. Rev. Neurosci.* 3, 243–249. doi: 10.1038/nrn756
- Cerutti-Kopplin, D., Emami, E., Hilgert, J. B., Hugo, F. N., and Padilha, D. M. P. (2015). Cognitive status of edentate elders wearing complete denture: does quality of denture matter? *J. Dent.* 43, 1071–1075. doi: 10.1016/j.jdent.2015.07.008
- Chatterjee, S., and Hadi, A. S. (2006). *Regression Analysis by Example*, 4th Edn. New York, NY: John Wiley & Sons.
- Chen, H., Iinuma, M., Onozuka, M., and Kubo, K. (2015). Chewing maintains hippocampus-dependent cognitive function. *Int. J. Med. Sci.* 12, 502–509. doi: 10.7150/ijms.11911
- Clark, D. J. (2015). Automaticity of walking: functional significance, mechanisms, measurement and rehabilitation strategies. *Front. Hum. Neurosci.* 9:246. doi: 10.3389/fnhum.2015.00246
- Collins, D. L., Neelin, P., Peters, T. M., and Evans, A. C. (1994). Automatic 3D intersubject registration of MR volumetric data in standardized Talairach space. *J. Comput. Assist. Tomogr.* 18, 192–205. doi: 10.1097/00004728-199403000-00005
- Derosière, G., Alexandre, F., Bourdillon, N., Mandrick, K., Ward, T. E., and Perrey, S. (2014). Similar scaling of contralateral and ipsilateral cortical responses during graded unimanual force generation. *Neuroimage* 85(Pt 1), 471–477. doi: 10.1016/j.neuroimage.2013.02.006
- Eichner, K. (1955). Über eine gruppeneinteilung der lückengebisse für die prothetik. *Dtsch. Zahnärztl. Z.* 10, 1831–1834.
- Faul, F., Erdfelder, E., Lang, A. G., and Buchner, A. G. (2007). Power 3: a flexible statistical power analysis program for the social, behavioral, and biomedical sciences. *Behav. Res. Methods* 39, 175–191. doi: 10.3758/bf03193146
- Ferrario, V. F., Tartaglia, G. M., Maglione, M., Simion, M., and Sforza, C. (2004). Neuromuscular coordination of masticatory muscles in subjects with two types of implant-supported prostheses. *Clin. Oral Implants Res.* 15, 219–225. doi: 10.1111/j.1600-0501.2004.00974.x
- Franco, A. L., de Andrade, M. F., Segalla, J. C., Gonçalves, D. A., and Camparis, C. M. (2012). New approaches to dental occlusion: a literature update. *Cranio* 30, 136–143. doi: 10.1179/crn.2012.020
- Fueki, K., Sugiura, T., Yoshida, E., and Igarashi, Y. (2008). Association between food mixing ability and electromyographic activity of jaw-closing muscles during chewing of a wax cube. *J. Oral Rehabil.* 35, 345–352. doi: 10.1111/j.1365-2842.2008.01849.x
- Gilbert, C. D., and Sigman, M. (2007). Brain states: top-down influences in sensory processing. *Neuron* 54, 677–696. doi: 10.1016/i.neuron.2007.05.019
- Grigoriadis, A., and Trulsson, M. (2018). Excitatory drive of masseter muscle during mastication with dental implants. *Sci. Rep.* 8:8597. doi: 10.1038/s41598-018-26926-z
- Halaki, M., and Ginn, K. (2012). “Normalization of EMG signals: to normalize or not to normalize and what to normalize to?” in *Computational Intelligence in Electromyography Analysis—A Perspective on Current Applications and Future Challenges*, ed. G. R. Naik, (London: InTech), 175–194.
- Hasegawa, Y., Tachibana, Y., Sakagami, J., Zhang, M., Urade, M., and Ono, T. (2013). Flavor-enhanced modulation of cerebral blood flow during gum chewing. *PLoS One* 8:e66313. doi: 10.1371/journal.pone.0066313
- Hawkins, K. A., Fox, E. J., Daly, J. J., Rose, D. K., Christou, E. A., McGuirk, T. E., et al. (2018). Prefrontal over-activation during walking in people with mobility deficits: interpretation and functional implications. *Hum. Mov. Sci.* 59, 46–55. doi: 10.1016/j.humov.2018.03.010
- Hidaka, O., Morimoto, T., Kato, T., Masuda, Y., Inoue, T., and Takada, K. (1999). Behavior of jaw muscle spindle afferents during cortically induced rhythmic jaw movements in the anesthetized rabbit. *J. Neurophysiol.* 82, 2633–2640. doi: 10.1152/jn.1999.82.5.2633
- Hikosaka, O., and Isoda, M. (2010). Switching from automatic to controlled behavior: cortico-basal ganglia mechanisms. *Trends Cogn. Sci.* 14, 154–161. doi: 10.1016/j.tics.2010.01.006
- Hirai, T., Ishijima, T., Koshino, H., and Anzai, T. (1994). Age-related change of masticatory function in complete denture wearers: evaluation by a sieving method with peanuts and a food intake questionnaire method. *Int. J. Prosthodont.* 7, 454–460.
- Horst, N. K., and Laubach, M. (2013). Reward-related activity in the medial prefrontal cortex is driven by consumption. *Front. Neurosci.* 7:56. doi: 10.3389/fnins.2013.00056
- Hoshi, Y., Kobayashi, N., and Tamura, M. (2001). Interpretation of near-infrared spectroscopy signals: a study with a newly developed perfused rat brain model. *J. Appl. Physiol.* 90, 1657–1662. doi: 10.1152/jappl.2001.90.5.1657
- Ikebe, K., Gondo, Y., Kamide, K., Masui, Y., Ishizaki, T., Arai, Y., et al. (2018). Occlusal force is correlated with cognitive function directly as well as indirectly via food intake in community-dwelling older Japanese: from the SONIC study. *PLoS One* 13:e0190741. doi: 10.1371/journal.pone.0190741
- Kamigaki, T. (2019). Prefrontal circuit organization for executive control. *Neurosci. Res.* 140, 23–36. doi: 10.1016/j.neures.2018.08.017
- Kamiya, K., Narita, N., and Iwaki, S. (2016). Improved prefrontal activity and chewing performance as function of wearing denture in partially edentulous elderly individuals: functional near-infrared spectroscopy study. *PLoS One* 11:e0158070. doi: 10.1371/journal.pone.0158070
- Kimoto, K., Ono, Y., Tachibana, A., Hirano, Y., Otsuka, T., Ohno, A., et al. (2011). Chewing-induced regional brain activity in edentulous patients who received mandibular implant-supported overdentures: a preliminary report. *J. Prosthodont. Res.* 55, 89–97. doi: 10.1016/j.jpor.2010.09.006
- Klem, G. H., Lüders, H. O., Jasper, H. H., and Elger, C. (1999). The ten-twenty electrode system of the International Federation. The International Federation of Clinical Neurophysiology. *Electroencephalogr. Clin. Neurophysiol. Suppl.* 52, 3–6.
- Li, J., Xu, H., Pan, W., and Wu, B. (2017). Association between tooth loss and cognitive decline: a 13-year longitudinal study of Chinese older adults. *PLoS One* 12:e0171404. doi: 10.1371/journal.pone.0171404
- Lin, C. S., Wu, C. Y., Wu, S. Y., Lin, H. H., Cheng, D. H., and Lo, W. L. (2017). Age-related difference in functional brain connectivity of mastication. *Front. Aging Neurosci.* 9:82. doi: 10.3389/fnagi.2017.00082
- Lin, C. S., Wu, S. Y., Wu, C. Y., and Ko, H. W. (2016). Gray matter volume and resting-state functional connectivity of the motor cortex-cerebellum network reflect the individual variation in masticatory performance in healthy elderly people. *Front. Aging Neurosci.* 7:247. doi: 10.3389/fnagi.2015.00247
- Lund, J. P. (1991). Mastication and its control by the brain stem. *Crit. Rev. Oral Biol. Med.* 2, 33–64. doi: 10.1177/10454411910020010401
- Luo, J., Wu, B., Zhao, Q., Guo, Q., Meng, H., Yu, L., et al. (2015). Association between tooth loss and cognitive function among 3063 Chinese older adults: a community-based study. *PLoS One* 10:e0120986. doi: 10.1371/journal.pone.0120986
- Mirelman, A., Maidan, I., Bernad-Elazari, H., Shustack, S., Giladi, N., and Hausdorff, J. M. (2017). Effects of aging on prefrontal brain activation during challenging walking conditions. *Brain Cogn.* 115, 41–46. doi: 10.1016/j.bandc.2017.04.002
- Miura, H., Araki, Y., Hirai, T., Isogai, E., Hirose, K., and Umenain, T. (1998). Evaluation of chewing activity in the elderly person. *J. Oral Rehabil.* 25, 190–193. doi: 10.1046/j.1365-2842.1998.00237.x
- Morimoto, T., Inoue, T., Masuda, Y., and Nagashima, T. (1989). Sensory components facilitating jaw-closing muscle activities in the rabbit. *Exp. Brain Res.* 76, 424–440. doi: 10.1007/bf00247900
- Moriya, M., Aoki, C., and Sakatani, K. (2016). Effects of physical exercise on working memory and prefrontal cortex function in post-stroke patients. *Adv. Exp. Med. Biol.* 923, 203–208. doi: 10.1007/978-3-319-38810-6_27
- Nakamura, Y., and Katakura, N. (1995). Generation of masticatory rhythm in the brainstem. *Neurosci. Res.* 23, 1–19. doi: 10.1016/0168-0102(95)90003-9

- Narayanan, N. S., and Laubach, M. (2006). Top-down control of motor cortex ensembles by dorsomedial prefrontal cortex. *Neuron* 52, 921–931. doi: 10.1016/j.neuron.2006.10.021
- Narita, N., Kamiya, K., Makiyama, Y., Iwaki, S., Komiyama, O., Ishii, T., et al. (2019). Prefrontal modulation during chewing performance in oroclusal dysesthesia patients: a functional near-infrared spectroscopy study. *Clin. Oral Investig.* 23, 1181–1196. doi: 10.1007/s00784-018-2534-7
- Natalie, S., Sophie, M. K., and Sandrine, T. (2015). The impact of mastication on cognition: evidence for intervention and the role of adult hippocampal neurogenesis. *Nutr. Aging* 3, 115–123. doi: 10.3233/NUA-150054
- Oh, B., Han, D. H., Han, K. T., Liu, X., Ukken, J., Chang, C., et al. (2018). Association between residual teeth number in later life and incidence of dementia: a systematic review and meta-analysis. *BMC Geriatr.* 18:48. doi: 10.1186/s12877-018-0729-z
- Okamoto, M., and Dan, I. (2005). Automated cortical projection of head-surface locations for transcranial functional brain mapping. *Neuroimage* 26, 18–28. doi: 10.1016/j.neuroimage.2005.01.018
- Okamoto, M., Wada, Y., Yamaguchi, Y., Kyutoku, Y., Clowney, L., Singh, A. K., et al. (2011). Process-specific prefrontal contributions to episodic encoding and retrieval of tastes: a functional NIRS study. *Neuroimage* 54, 1578–1588. doi: 10.1016/j.neuroimage.2010.08.016
- Ono, Y., Yamamoto, T., Kubo, K. Y., and Onozuka, M. (2010). Occlusion and brain function: mastication as a prevention of cognitive dysfunction. *J. Oral Rehabil.* 37, 624–640. doi: 10.1111/j.1365-2842.2010.02079.x
- Preston, A. R., and Eichenbaum, H. (2013). Interplay of hippocampus and prefrontal cortex in memory. *Curr. Biol.* 23, R764–R773. doi: 10.1016/j.cub.2013.05.041
- Quintero, A., Ichesco, E., Schutt, R., Myers, C., Peltier, S., and Gerstner, G. E. (2013). Functional connectivity of human chewing: an fMRI study. *J. Dent. Res.* 92, 272–278. doi: 10.1177/0022034512472681
- Raos, V., and Savaki, H. E. (2017). The Role of the prefrontal cortex in action perception. *Cereb. Cortex* 27, 4677–4690. doi: 10.1093/cercor/bhw261
- Redgrave, P., Rodriguez, M., Smith, Y., Rodriguez-Oroz, M. C., Lehericy, S., Bergman, H., et al. (2010). Goal-directed and habitual control in the basal ganglia: implications for Parkinson's disease. *Nat. Rev. Neurosci.* 11, 760–772. doi: 10.1038/nrn2915
- Sawa, M., Yamashita, H., Fujimaki, K., Okada, G., Takahashi, T., and Yamawaki, S. (2012). Depressive symptoms and apathy are associated with psychomotor slowness and frontal activation. *Eur. Arch. Psychiatry Clin. Neurosci.* 262, 493–499. doi: 10.1007/s00406-012-0296-9
- Schecklmann, M., Mann, A., Langguth, B., Ehli, A. C., Fallgatter, A. J., and Haeussinger, F. B. (2017). The temporal muscle of the head can cause artifacts in optical imaging studies with functional near-infrared spectroscopy. *Front. Hum. Neurosci.* 11:456. doi: 10.3389/fnhum.2017.00456
- Schneider, W., and Shiffrin, R. M. (1977). Controlled and automatic human information processing: I. Detection, search and attention. *Psychol. Rev.* 84, 1–66. doi: 10.1037//0033-295x.84.1.1
- Seraj, Z., Al-Najjar, D., Akl, M., Aladle, N., Altijani, Y., Zaki, A., et al. (2017). The effect of number of teeth and chewing ability on cognitive function of elderly in UAE: a pilot study. *Int. J. Dent.* 2017:5732748. doi: 10.1155/2017/5732748
- Shiffrin, R. M., and Schneider, W. (1977). Controlled and automatic human information processing: II. Perceptual learning, automatic attending and a general theory. *Psychol. Rev.* 84, 127–190. doi: 10.1037//0033-295x.84.2.127
- Shin, M. S., Shin, Y. J., Karna, S., and Kim, H. D. (2019). Rehabilitation of lost teeth related to maintenance of cognitive function. *Oral Dis.* 25, 290–299. doi: 10.1111/odi.12960
- Singh, A. K., Okamoto, M., Dan, H., Jurcak, V., and Dan, I. (2005). Spatial registration of multichannel multi-subject fNIRS data to MNI space without MRI. *Neuroimage* 27, 842–851. doi: 10.1016/j.neuroimage.2005.05.019
- Small, D. M., Gitelman, D. R., Gregory, M. D., Nobre, A. C., Parrish, T. B., and Mesulam, M. M. (2003). The posterior cingulate and medial prefrontal cortex mediate the anticipatory allocation of spatial attention. *Neuroimage* 18, 633–641. doi: 10.1016/s1053-8119(02)00012-5
- Spraker, M. B., Corcos, D. M., and Vaillancourt, D. E. (2009). Cortical and subcortical mechanisms for precisely controlled force generation and force relaxation. *Cereb. Cortex* 19, 2640–2650. doi: 10.1093/cercor/bhp015
- Strangman, G., Culver, J. P., Thompson, J. H., and Boas, D. A. (2002). A quantitative comparison of simultaneous BOLD fMRI and NIRS recordings during functional brain activation. *Neuroimage* 17, 719–731. doi: 10.1006/nimg.2002.1227
- Takakusaki, K., Saitoh, K., Harada, H., and Kashiwayanagi, M. (2004). Role of basal ganglia-brainstem pathways in the control of motor behaviors. *Neurosci. Res.* 50, 137–151. doi: 10.1016/j.neures.2004.06.015
- Takeshita, H., Ikebe, K., Gondo, Y., Inagaki, H., Masui, Y., Inomata, C., et al. (2016). Association of occlusal force with cognition in independent older Japanese people. *JDR Clin. Trans. Res.* 1, 69–76. doi: 10.1177/2380084416636604
- Takeuchi, K., Izumi, M., Furuta, M., Takeshita, T., Shibata, Y., Kageyama, S., et al. (2015). Posterior teeth occlusion associated with cognitive function in nursing home older residents: a cross-sectional observational study. *PLoS One* 10:e0141737. doi: 10.1371/journal.pone.0141737
- Tallgren, A., and Tryde, G. (1991). Chewing and swallowing activity of masticatory muscles in patients with a complete upper and a partial lower denture. *J. Oral Rehabil.* 18, 285–299. doi: 10.1111/j.1365-2842.1991.tb00060.x
- Toronov, V., Webb, A., Choi, J. H., Wolf, M., Michalos, A., Gratton, E., et al. (2001). Investigation of human brain hemodynamics by simultaneous near-infrared spectroscopy and functional magnetic resonance imaging. *Med. Phys.* 28, 521–527. doi: 10.1118/1.1354627
- Tsuji, T., Komatsu, K., and Sakatani, K. (2013). Acute effects of physical exercise on prefrontal cortex activity in older adults: a functional near-infrared spectroscopy study. *Adv. Exp. Med. Biol.* 765, 293–298. doi: 10.1007/978-1-4614-4989-8_41
- Tzourio-Mazoyer, N., Landeau, B., Papathanassiou, D., Crivello, F., Etard, O., Delcroix, N., et al. (2002). Automated anatomical labeling of activations in SPM using a macroscopic anatomical parcellation of the MNI MRI single-subject brain. *Neuroimage* 15, 273–289. doi: 10.1006/nimg.2001.0978
- Weißbacher, R. A., and Gluth, S. (2016). The interplay of hippocampus and ventromedial prefrontal cortex in memory-based decision making. *Brain Sci.* 7:4. doi: 10.3390/brainsci7010004
- Yokoyama, T., Sato, M., Natsui, S., Kuboyama, N., Suzuki, K., Inaba, H., et al. (2017). Effect of gum chewing frequency on oxygenation of the prefrontal cortex. *Percept. Mot. Skills* 124, 58–71. doi: 10.1177/003151251668307

Conflict of Interest: TU and IK were employed by company Dental Support Co. Ltd. and have no potential conflicts of interest with respect to the research, authorship, and/or publication of this article.

The remaining authors declare that the research was conducted in the absence of any commercial or financial relationships that could be construed as a potential conflict of interest.

Copyright © 2020 Narita, Ishii, Iwaki, Kamiya, Okubo, Uchida, Kantake and Shibutani. This is an open-access article distributed under the terms of the Creative Commons Attribution License (CC BY). The use, distribution or reproduction in other forums is permitted, provided the original author(s) and the copyright owner(s) are credited and that the original publication in this journal is cited, in accordance with accepted academic practice. No use, distribution or reproduction is permitted which does not comply with these terms.



Functional Connectivity Evoked by Orofacial Tactile Perception of Velocity

Yingying Wang^{1,2,3,4*}, Fatima Sibaii^{1,4}, Rebecca Custead⁵, Hyuntaek Oh^{4,5} and Steven M. Barlow^{2,4,5}

¹ Neuroimaging for Language, Literacy and Learning Laboratory, Department of Special Education and Communication Disorders, University of Nebraska-Lincoln, Lincoln, NE, United States, ² Center for Brain, Biology and Behavior, University of Nebraska-Lincoln, Lincoln, NE, United States, ³ Nebraska Center for Research on Children, Youth, Families and Schools, University of Nebraska-Lincoln, Lincoln, NE, United States, ⁴ Biomedical Engineering, University of Nebraska-Lincoln, Lincoln, NE, United States, ⁵ Communication Neuroscience Laboratory, Department of Special Education and Communication Disorders, University of Nebraska-Lincoln, Lincoln, NE, United States

OPEN ACCESS

Edited by:

Kazutaka Takahashi,
University of Chicago, United States

Reviewed by:

Christian Wallraven,
Korea University, South Korea
Yusuke Takatsuru,
Gunma University, Japan
Sanne Kikkert,
ETH Zürich, Switzerland

*Correspondence:

Yingying Wang
yingying.wang@unl.edu

Specialty section:

This article was submitted to
Perception Science,
a section of the journal
Frontiers in Neuroscience

Received: 07 October 2019

Accepted: 19 February 2020

Published: 06 March 2020

Citation:

Wang Y, Sibaii F, Custead R, Oh H
and Barlow SM (2020) Functional
Connectivity Evoked by Orofacial
Tactile Perception of Velocity.
Front. Neurosci. 14:182.
doi: 10.3389/fnins.2020.00182

The cortical representations of orofacial pneumotactile stimulation involve complex neuronal networks, which are still unknown. This study aims to identify the characteristics of functional connectivity (FC) evoked by three different saltatory velocities over the perioral and buccal surface of the lower face using functional magnetic resonance imaging in twenty neurotypical adults. Our results showed a velocity of 25 cm/s evoked stronger connection strength between the right dorsolateral prefrontal cortex and the right thalamus than a velocity of 5 cm/s. The decreased FC between the right secondary somatosensory cortex and right posterior parietal cortex for 5-cm/s velocity versus all three velocities delivered simultaneously (“All ON”) and the increased FC between the right thalamus and bilateral secondary somatosensory cortex for 65 cm/s vs “All ON” indicated that the right secondary somatosensory cortex might play a role in the orofacial tactile perception of velocity. Our results have also shown different patterns of FC for each seed (bilateral primary and secondary somatosensory cortex) at various velocity contrasts (5 vs 25 cm/s, 5 vs 65 cm/s, and 25 vs 65 cm/s). The similarities and differences of FC among three velocities shed light on the neuronal networks encoding the orofacial tactile perception of velocity.

Keywords: functional connectivity, orofacial, pneumotactile stimulation, fMRI, saltatory velocity, cortical representation

INTRODUCTION

The human somatosensory system decodes tactile stimuli from peripheral sensory receptors through a complex process involving interactions between bottom-up thalamocortical and top-down corticocortical/cortico-thalamo-cortical pathways (Avivi-Arber et al., 2011; Lundblad et al., 2011; Zembrzycki et al., 2013; Hwang et al., 2017). Studies of cortical representations of tactile stimulation of different body parts have identified the primary (SI) and secondary (SII) somatosensory cortices, as well as the supplementary motor area responsible for sensory processing (Ibáñez et al., 1995; Backes et al., 2000; Grodd et al., 2001; Backlund et al., 2003; Paus et al., 2006; Backlund Wasling et al., 2008; Bjørnsdotter et al., 2009; Ackerley et al., 2012; Zembrzycki et al., 2013; Akselrod et al., 2017; Custead et al., 2017; Oh et al., 2017; Yeon et al., 2017). SI, which is

located in the postcentral gyrus, processes complex information about the location, velocity, and other characteristics of tactile stimulation from the thalamus through the thalamocortical axons. Damage to the SI (e.g., by stroke, traumatic brain injury, etc.) could result in orofacial sensory and motor deficits; the recovery of such damage to the sensorimotor system requires characterizing the neuronal connections (both structural and functional connectivity) (Nudo, 2013). Therefore, the neuronal connections among cortical regions are critical for understanding the cortical plasticity after injuries to the somatosensory system.

Tactile sensation is detected by cutaneous mechanoreceptors in the skin and is then projected to afferent neurons or sensory nerves, via the spinal cord, toward the central nervous system (Jenkins and Lumpkin, 2017). Pacinian corpuscles, a type of cutaneous mechanoreceptors that usually detect rapid vibrations (about 200–300 Hz) in both glabrous and hairy skin (e.g., palm and arm, respectively), were considered to be virtually absent from the facial skin based on psychophysical methods (Barlow, 1987), and the cutaneous mechanoreceptors in the facial skin have high densities and are slow adapting, with small receptive fields (Johansson and Olsson, 1976; Johansson et al., 1988).

Vibrotactile adaption has been observed in both the hands and face (Hollins et al., 1991). Individual mechanoreceptors in the facial skin responded differently to brush stimuli moving at different velocities (Edin et al., 1995). Nevertheless, it has been argued that the central nervous system might not be able to decode velocity of movement across the skin in humans (Edin et al., 1995). However, animal studies have suggested that rat SI neurons could process complex tactile stimuli such as direction and velocity of motion (Moore et al., 1999; Krupa et al., 2001; Ferezou et al., 2007; Tomita et al., 2012; Zembrzycki et al., 2013). Furthermore, neuroimaging studies also indicated that there are different cortical representations for different tactile stimuli in humans (e.g., location, type of motion, direction, velocity, etc.) (Reed et al., 2004; Miyamoto et al., 2006; Backlund Wasling et al., 2008; Eickhoff et al., 2008; Bjornsdotter et al., 2009; Moulton et al., 2009; Avivi-Arber et al., 2011; Grabski et al., 2012; Huang et al., 2012; Khoshnejad et al., 2014; Yang et al., 2014; Custead et al., 2015, 2017; Hwang et al., 2017; Oh et al., 2017; Yeon et al., 2017).

The cross-modality plasticity theory suggested that somatosensory stimuli could evoke neural responses to promote learning of new motor skills (Sanes and Donoghue, 2000; Nasir et al., 2013; Ladda et al., 2014) and performing motor tasks more accurately (Pearson, 2000). The integration of the orofacial sensory and motor system has been suggested to be critical for motor learning and motor control for sucking, swallowing, and producing speech sounds (Barlow and Bradford, 1996; Barlow, 1998; Sessle et al., 2005, 2007; Barlow and Estep, 2006; Barlow and Stumm, 2010; Smith, 2016). If passive pneumotactile stimulation could effectively evoke changes in the neuronal connections and positively impact motor learning, there may be a paradigm shift in early neurorehabilitation protocols to improve functional recovery after brain injury (e.g., due to stroke, traumatic brain injury, etc.).

The cortical representations of moving tactile stimulation have mostly been investigated on the hand. Brushing over the right

thumb once every one and a half second and using electric stimuli to the median nerve in seven healthy participants, Lin et al. identified the different shapes of waveforms of somatosensory evoked fields in SI using magnetoencephalography (MEG) (Lin and Kajola, 2003). A functional magnetic resonance imaging (fMRI) study compared active touch, self-touch, and passive touch of both the glabrous palm and hairy arm, using a stroking velocity between 6 and 8 cm/s and demonstrated specialization of cortical regions for processing of somatosensory information (Ackerley et al., 2012). They found that moving tactile stimulation of the glabrous palm activated more extensive cortical areas of the right SI (subarea Brodmann area BA 3, contralateral) than that of the hairy arm. Moreover, active stroking evoked positive blood-oxygenation level dependent (BOLD) signals in the left SI (ipsilateral), whereas passive stroking evoked negative BOLD signals. More recently, a fMRI study identified the left SI, left superior temporal gyrus (STG), and the left precentral gyrus (preG) as being involved in encoding saltatory pneumotactile velocity stimulation of the glabrous hand, using stimuli at 5, 25, and 65 cm/s (Oh et al., 2017). The velocity of 25 cm/s evoked the most extensive BOLD signal among all velocity settings.

However, for the face, the cortical representations of moving tactile stimulation have not been well studied. Not knowing the neural substrates of perceiving moving stimulation on the face has limited our understanding of velocity and directional encoding in the sensory domain. In our previous fMRI study, we identified a putative neural somatosensory velocity network with bilateral SI, bilateral cerebellum, bilateral middle occipital gyrus, left MI, right SII, right STG, and right SMG, right inferior frontal gyrus (IFG), which had not been reported previously (Custead et al., 2017). Custead et al. used a univariate generalized linear model (GLM) to determine brain regions with specific responses to the pneumotactile stimulation at each voxel. The univariate GLM approach assumes that each voxel in the brain is functionally specialized rather than functionally integrated (Stephan et al., 2006). However, this perspective limits our understanding of how different brain regions communicate with each other, which is essential for understanding complex neuronal networks (Tononi et al., 1998). Task-based functional connectivity (FC) measured by evaluating the correlation between time series of BOLD signals among brain regions does not measure structural connections (e.g., axonal projections), but represents the functional coupling between two or more spatially or anatomically distinct areas of the brain (Stevens, 2009; Hermundstad et al., 2013). To date, little is known about the functional connectivity (FC) evoked by the orofacial tactile perception of velocity.

The present study therefore aimed to identify the characteristics of FC evoked by pneumotactile stimuli, at three saltatory velocities (5, 25, and 65 cm/s), on the non-glabrous lower face, as an extension to our previous work, in order to enhance our understanding of the neural networks responsible for encoding the velocity of tactile stimulation (Custead et al., 2017). We hypothesized that there would be different patterns of FC corresponding to the three velocities.

The pneumotactile stimulator used in this study (GalileoTM) overcomes the technical challenges of automatically applying

tactile stimulation to the face without eliciting pain sensation during fMRI (Custead et al., 2017). A single chambered tactile cell (TAC-Cell) or multiple TAC-Cells of the Galileo system can be placed on both glabrous and hairy skin through adhesive tape collars, and are compatible with many neuroimaging techniques, such as MRI, functional near-infrared spectroscopy (fNIRS), MEG, and electroencephalography (EEG). The in-house computer software allows the Galileo system to deliver saltatory tactile stimuli at a variety of settings (amplitude, velocity, etc.). Unlike other pneumotactile stimulators (Dresel et al., 2008; Huang et al., 2012), the Galileo with TAC-Cells is easy to set up and program for various applications. This pneumotactile stimulator has been used to examine the neural substrates of the human somatosensory system and has effectively activated SI, SII, and the PPC (Popescu et al., 2013; Custead et al., 2017; Oh et al., 2017).

Based on our previous work and other studies in the literature (Blatow et al., 2007; Huang et al., 2012; Custead et al., 2017), we here chose 10 regions-of-interest (ROIs), including the bilateral SI, SII, PPC, dorsolateral prefrontal cortex, and thalamus for hypothesis-driven ROI-to-ROI FC analysis, to examine whether the FC of our hypothesized networks differ across the three stimulation velocities. Then, four ROIs, including the bilateral SI and SII, were chosen for data-driven Seed-to-Voxel FC analysis to examine which cortical areas are functionally connected to either SI or SII, and whether this differ across the three stimulation velocities.

MATERIALS AND METHODS

Participants

Twenty healthy, right-handed, native English-speaking adults (15 females), 18–30 years of age (mean \pm SD: 22.3 ± 1.7), agreed to participate in the study after providing written informed consent. All participants reported the right hand as the preferred hand and had no history of neurological or psychiatric disorders, or any chronic illness or scheduled medications. The study was approved by the Institutional Review Board at the University of Nebraska-Lincoln.

Stimulus Device

Pneumotactile stimuli were delivered to the facial skin by a multichannel pneumatic amplifier and tactile array known as the Galileo SomatosensoryTM system (Epic Medical Concepts & Innovations, Inc., Mission, Kansas, KS, United States). The Galileo system utilizes TAC-Cells made from acetyl thermoplastic homopolymer, which uses tiny volumes of compressed air to deform the surface of the skin rapidly. The TAC-Cells are MRI-safe and incorporate a small capsule with a sealing flange. In **Figure 1**, the placement of seven TAC-Cells on a representative participant was shown from the upper and lower lips to the right lateral cheek of the face. Before using double-adhesive tape collars to secure each TAC-Cell, ten percent concentration of tincture of Benzoin was applied to the skin for improvement of adhesion. For each participant, the distances between each TAC-Cell were

measured and taken into consideration for designing the velocity trains traversing in a repeating medial-to-lateral direction on the face. For all conditions, the Galileo system was programmed to generate biphasic pulses with a duration of 60 ms, frequency of 1 Hz, 10 ms rise/fall, amplitude from -5 to 28 kPa (Custead et al., 2017; Oh et al., 2017). Our in-house software program generated air pressure pulses to five channels sequentially for 5, 25, 65 cm/s conditions and simultaneously for “All ON” condition. The Galileo system was located outside the MRI suite and delivered pneumotactile stimuli through polyurethane tubing into the MRI suite. Participants described the sensory experience as a moving sequence of discrete ‘taps’ or ‘raindrops’ on their lower face without any discomfort (Custead et al., 2017).

Paradigms

We used a block design, and each twenty-second task block was followed by a twenty-second resting block (Custead et al., 2017; Oh et al., 2017) (see **Figure 2**). The twenty-second block of either 5 cm/s, or 25 cm/s, or 65 cm/s, or “All ON”, or “All OFF” was randomized. The different velocities represented the different speeds of the air pressure pulses traveling (saltation) through channels (see **Figure 1**). For instance, the 5 cm/s represented that the air pressure pulses went through all channels sequentially within approximately 5 s in total (starting at channel 1, about 1 s at channel 2, 2 s at channel 3, 3 s at channel 4, and about 5 s at channel 5). The 25 cm/s meant that the pressure pulses went through all channels sequentially within approximately 2 s in total. The 65 cm/s represented that the air pressure pulses went through all channels sequentially within about 1.5 s in total. The “All ON” indicated that the air pressure pulses went through all channels simultaneously. The “All OFF” meant that no air pressure pulse went through all channels, which is equivalent to the resting period. During the fMRI scan, visual countdown task was used to maintain the participants’ vigilance using E-Prime 2.0 software (Psychology Software Tools, Pittsburgh, PA, United States). The participants were directed to pay attention to the number shown on the screen for only 0.5 s to minimize brain activation in the primary visual cortex. A declining countdown from 20 to 1 represented the remaining time in seconds for the tactile stimulation.

Data Acquisition

All images were acquired on a 3.0 T Siemens Skyra whole-body MRI system (Siemens Medical Solutions, Erlangen, Germany) with a 32-channel head coil. A high-resolution T1-weighted three-dimensional anatomical scan was acquired using magnetization-prepared rapid gradient-echo sequences (MPRAGE) with the following parameters: TR/TE/TA = 2.4 s/3.37 ms/5:35 min, flip angle = 7° , field of view = 256×256 mm, spatial resolution = $1 \times 1 \times 1$ mm³, number of slices = 192. Following the MPRAGE anatomical scan, three sessions of functional MRI (fMRI) scans were recorded using a T2*-weighted echo planar imaging (EPI) sequence with the following parameters: TR/TE/TA = 2.5 s/30 ms/800 s, voxel size = $2.5 \times 2.5 \times 2.5$ mm³, flip angle = 83° , number of slices = 41, number of volumes = 320.

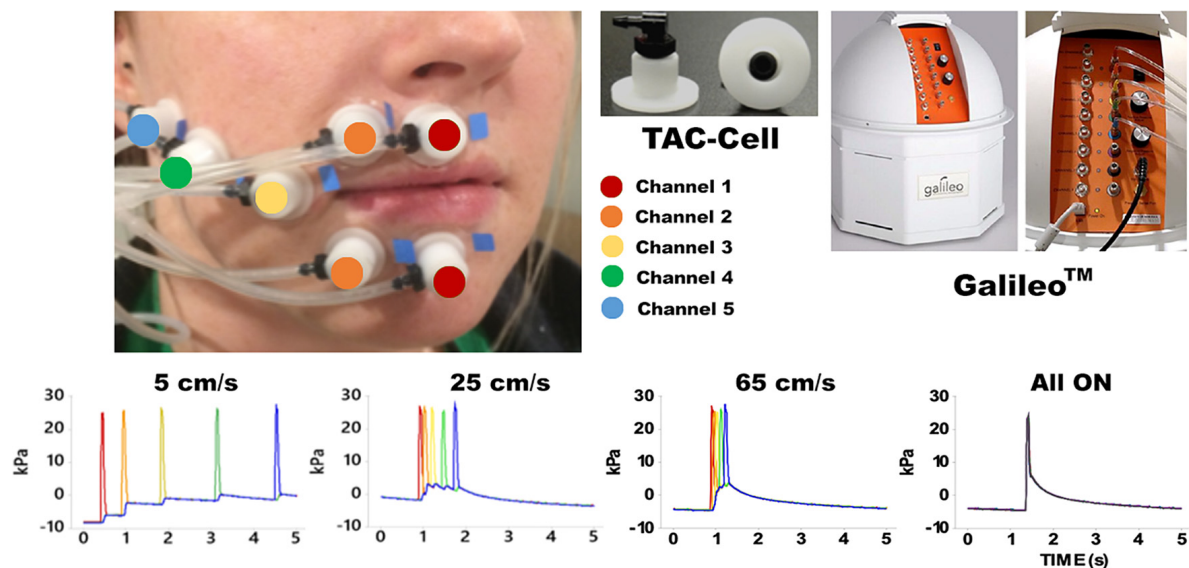


FIGURE 1 | Shows the experimental configuration for the Galileo somatosensory stimulator with pneumatic velocity arrays aligned on the participant from the right philtral column to the right buccal face. White flanged surface of the TAC-Cell was adhered to skin surface with double adhesive colars and 7 TAC-Cells form 5 channels in five colors (red: channel 1 placed two TAC-Cells on the median upper and lower lips; orange: channel 2 placed two TAC-Cells next to the TAC-Cells of channel 1; yellow: channel 3 placed a TAC-Cells next to the channel 2; green: channel 4 placed a TAC-Cell next to channel 3; blue: channel 5 placed a TAC-Cell next to channel 4). The bottom four graphs show the time courses for each velocity and All ON.

Each Run consists of twenty 40-s block (4 blocks for each condition).

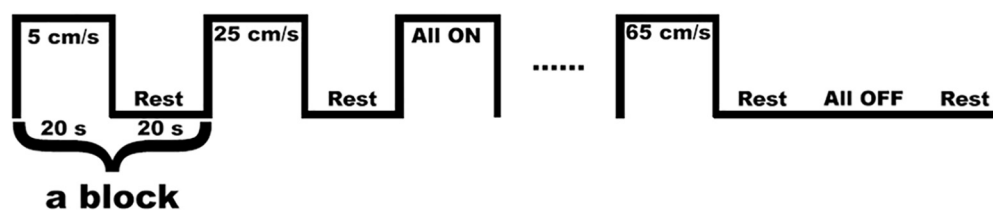


FIGURE 2 | One run of the fMRI in-scan paradigm indicates a series of pneumotactile saltatory stimuli traversed the skin in a repeating medial-to-lateral direction. There are twenty 40 s long blocks in one run. Each block consisted of one 20 s block of task stimuli presentation and 20 s block of rest. There are five possible task blocks (5, 25, 65 cm/s, All ON, All OFF) randomly presented.

The first TR pulse from the MRI scanner during fMRI data acquisition went through a Berkeley Nucleonics pulse generator (Model 645), which was in charge of sending triggers to the Galileo system to produce a velocity sequence every 40 s. The Galileo system generated a velocity condition for 20 s, then wait for 20 s to initiate the next velocity sequence. To reduce the effect of fatigue, we did three runs separately and gave optional breaks between runs. Each run consisted of 20 blocks, and 20 blocks consisted of four sets of randomly presented five conditions (5, 25, 65 cm/s, “All ON”, “All OFF”) (see **Figure 2**). Each run includes four blocks of 5 cm/s (80 s and 52 TR), four blocks of 25 cm/s (80 s and 52 TR), four blocks of 65 cm/s (80 s and 52 TR), four blocks of “All ON” (80 s and 52 TR), four blocks of “All OFF” (80 s and 52 TR). In total, each condition block lasted 960 s with 480 s condition segment and 480 s rest segment. Nineteen participants completed all three runs, while one participant only completed two runs.

Data Analysis

The CONN toolbox (Whitfield-Gabrieli and Nieto-Castanon, 2012)¹ was used for pre-processing all images and compute brain connectivity using both seed-based and region-of-interests (ROIs)-based approaches. The CONN toolbox used Statistical Parametric Mapping (SPM12)² toolbox to pre-process all image volumes, including functional realignment, structural segmentation and normalization, ART-based scrubbing, and smoothing. First, the functional data were realigned to the first scan and to correct for interscan head movement. The functional realignment process in the CONN toolbox automatically generated the first-level covariate with six rigid-body parameters that quantified the estimated motion for each participant and each run. The functional realignment covariate

¹<http://www.nitrc.org/projects/conn>

²<https://www.fil.ion.ucl.ac.uk/spm/software/spm12/>

can be used in the GLM to regress out the residual movement-related effects from the time series. Second, the structural image was segmented into gray matter (GM), white matter (WM), and cerebrospinal fluid (CSF) in the individual participant's space, and normalized to the Montreal Neurological Institute (MNI) space. The transformation matrix between the segmented MRI to MNI space was saved and used to coregister functional images to the normalized structural MRI. The Artifact Rejection Toolbox (ART³)-based scrubbing built-in CONN toolbox was applied to outlier detection and scrubbing to compute confound regressors using default parameters (global threshold: 9 stand-deviations above or below the mean, motion threshold: 2 mm translation and 2° rotation in any direction). The ART-based scrubbing technique detected an outlier if the largest voxel movement between volumes exceeded the thresholds. Only three outliers were identified and treated as nuisance regressors in the first-level GLM analysis. Finally, all coregistered fMRI data were smoothed with an isotropic Gaussian kernel of 8 mm full-width-at-half-maximum (FWHM).

The task-related functional connectivity was computed in the CONN toolbox. For each participant, CONN implemented CompCor to identify the top five principal components associated with segmented WM and CSF (Behzadi et al., 2007). These components were entered as confounds along with realignment parameters and nuisance regressors from ART-based scrubbing in the first-level GLM analysis. The residual time courses were linearly detrended (no despiking) and temporally filtered using a band-pass filter (0.008–0.09 Hz) during the denoising process in the CONN toolbox.

For the ROI-to-ROI analyses, we studied FC between ROIs for different velocities (5, 25, 65 cm/s, “All ON”). We computed the strength and significance of bivariate Pearson correlation among pairs of ten ROIs for each participant. Five bilateral ROIs (see **Table 1**) were created using MNI coordinates in the CONN toolbox and the MNI coordinates were based on our previous work (Custead et al., 2017; Oh et al., 2017). The ROI-to-ROI correlation coefficients were obtained by calculating all possible correlation coefficients between the time series of each pair of ROIs. For ROI-to-ROI connectivity, significant connections were identified by calculating the False Discovery Rate (FDR)-corrected two-sided *p*-value (*q*) at *q* < 0.05 thresholds for seed-level correction. The FDR seed-level correction applied FDR separately for each ROI and corrected across the multiple comparisons from having multiple target ROIs.

For seed-based FC analyses, a whole-brain approach was used to identify cortical areas that were differentially connected with bilateral SI and SII among four conditions (5, 25, 65 cm/s, and “All ON”). The four seeds (see **Table 1**) were chosen based on the literature (Lin and Kajola, 2003; Pastor et al., 2004; Reed et al., 2004; Dresel et al., 2008; Ackerley et al., 2012; Popescu et al., 2013; Custead et al., 2017; Oh et al., 2017; Yeon et al., 2017) because bilateral SI and SII were most consistently identified across imaging studies with different parameters. We chose to compute all possible cross-correlation coefficients between the time series of the seeds and all residual voxels in the brain, and

TABLE 1 | Regions Of Interest.

| Name | Description | Coordinates in MNI space | | |
|------------------|-------------|--------------------------|--------|--------|
| | | X (mm) | Y (mm) | Z (mm) |
| Left hemisphere | | | | |
| Left SI | ROI & Seed | −55 | −19 | 24 |
| Left SII | ROI & Seed | −48 | −24 | 16 |
| Left PPC | ROI | −56 | −31 | 32 |
| Left DLPFC | ROI | −27 | 32 | 36 |
| Left Thalamus | ROI | −9 | −17 | 6 |
| Right hemisphere | | | | |
| Right SI | ROI & Seed | 56 | −13 | 29 |
| Right SII | ROI & Seed | 48 | −24 | 16 |
| Right PPC | ROI | 56 | −31 | 32 |
| Right DLPFC | ROI | 30 | 35 | 34 |
| Right Thalamus | ROI | 10 | −19 | 6 |

MNI, Montreal Neurological Institute; ROI, region of interest; SI, primary somatosensory cortex; SII, supplementary somatosensory cortex; PPC, Posterior Parietal Cortex; DLPFC, dorsolateral Prefrontal Cortex.

then convert them to Z-scores. At the second-level analysis in the CONN toolbox, we compared FC patterns among different tactile stimuli. To control for multiple comparison, the CONN toolbox implemented the Cluster Size Statistic (CSS) (Ing and Schwarzbauer, 2014). FC maps between all voxel pairs for all participants under all conditions were generated, and then *T*-statistics were calculated between connectivity values taken under different velocity conditions. A cluster-forming threshold was set at voxel-level *p* < 0.001 and CSS only counted those with cluster-level FDR-corrected *p* < 0.05 as significant, which is a multiple-comparison correction at the whole-brain level to control the false discoveries among significant clusters below 5% rate (Friston et al., 1994).

RESULTS

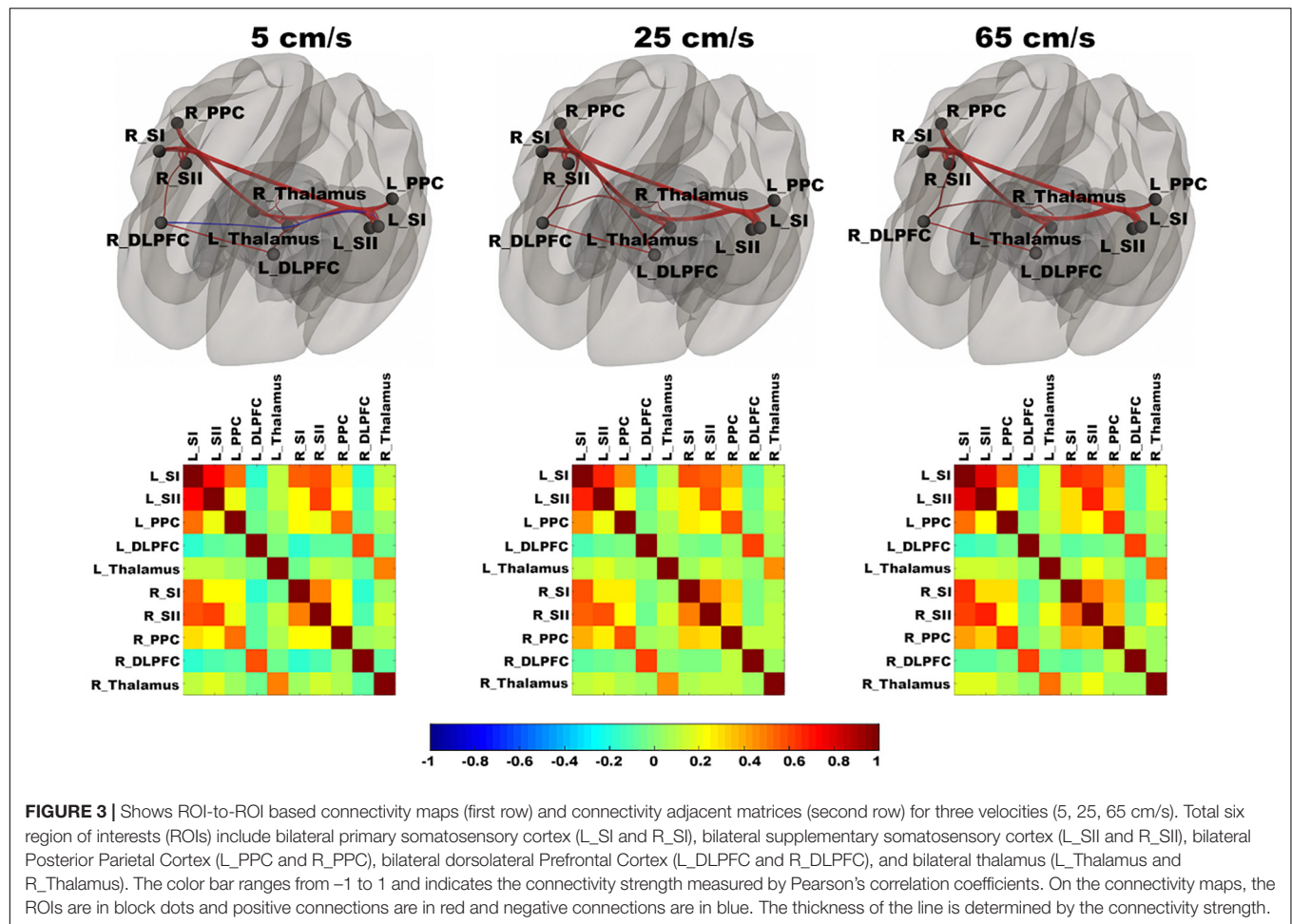
ROI-Based FC

In **Figure 3**, functional networks for each velocity (5, 25, and 65 cm/s) were overlaid onto three-dimensional rendered brain on the first row and task-related FC matrices for each velocity were plotted on the second row. Comparing 5 and 25 cm/s task conditions, increased FC was identified between the right DLPFC and the right thalamus (see **Figure 4**). There is no significant difference of FC between 5 and 65 cm/s and between 25 and 65 cm/s for all ROI-to-ROI pairs. The contrast of 5 cm/s vs “All ON” task condition showed significant decreased FC between the right SII and the right PPC and the contrast 65 cm/s vs “All ON” task condition revealed increased FC between the right thalamus and the left SII and between the right thalamus and the right SII (see **Figure 5**).

Seed-Based FC

The seed-to-voxel analyses assessed FCs between four seed regions covering bilateral SI and SII and all other voxels in the brain (cluster size > 35, cluster size FDR-corrected). In **Table 2**

³http://www.nitrc.org/projects/artifact_detect/

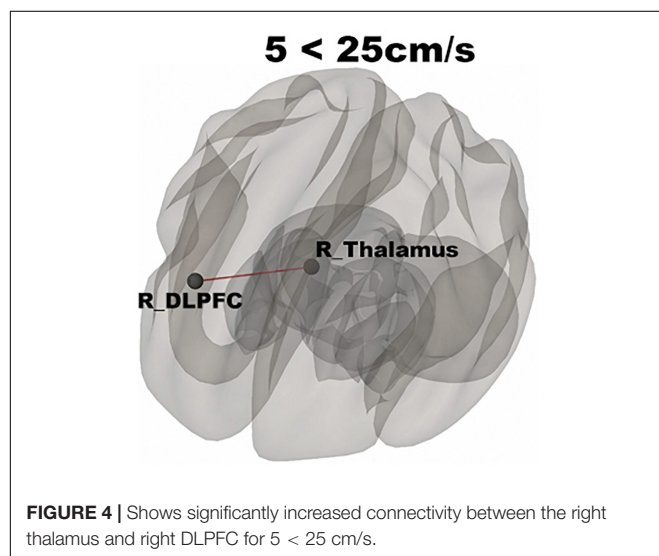


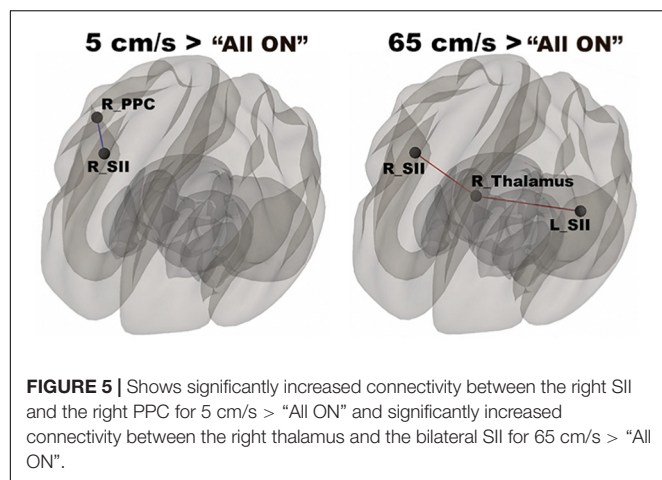
and **Figure 6**, for the left SI seed, results revealed increased FC in the left PostCG and left SMG for 5 > 25 cm/s, in the right pMTG, right cerebellum 6, and right AG for 5 > 65 cm/s, in the bilateral

iLOC, right sLOC, right FG, right Cerebellum 6 for 25 > 65 cm/s. For the left SII seed, increased FCs were only in the left SPL and right sLOC for 25 > 65 cm/s. In **Table 2** and **Figure 7**, for the right SI seed, increased FCs were shown in the left iLOC and right pMTG along with decreased FCs in the right IC for 5 > 65 cm/s, and increased FCs were also observed in the bilateral iLOC along with decreased FC in the left cerebellum crus II for 25 > 65 cm/s. For the right SII seed, decreased FC was present in the right SFG for both 5 > 65 cm/s and 25 > 65 cm/s. Additionally, increased FCs were shown in the left SPL and sLOC for 25 > 65 cm/s.

DISCUSSION

The present study examined FC evoked by the orofacial tactile perception of velocity using fMRI in 20 neurotypical adults. This study attempted to identify FC evoked by novel saltatory pneumotactile stimuli using TAC-Cells with the Galileo system, which has not been reported previously. Our findings suggested that there were more similarities in ROI-to-ROI neuronal networks in the contralateral cortical areas (on the opposite side to the stimuli) and more differences in FC patterns in the ipsilateral cortical areas (on the same side as the stimuli). The 5 cm/s velocity evoked weaker FC between the right thalamus





and the right DLPFC than did the 25 cm/s velocity, indicating that a velocity of 25 cm/s evoked stronger FC in the ipsilateral cortical regions. During the “All ON” condition, all TAC-Cells were stimulated simultaneously at 1 Hz, without varying velocity. The decreased FC between the right SII and right PPC for contrasting 5 cm/s with the “All ON” condition, and the increased FC between the right thalamus and bilateral SII for contrasting 65 cm/s with the “All ON” condition, demonstrated the FC pattern evoked by orofacial tactile perception of velocity. Our Seed-to-Voxel approach identified different cortical network patterns for each seed at various velocity contrasts (5 vs 25 cm/s, 5 vs 65 cm/s, and 25 vs 65 cm/s), suggesting that specialized FC patterns are responsible for discriminating different velocities of orofacial tactile stimuli.

Effects of Velocity

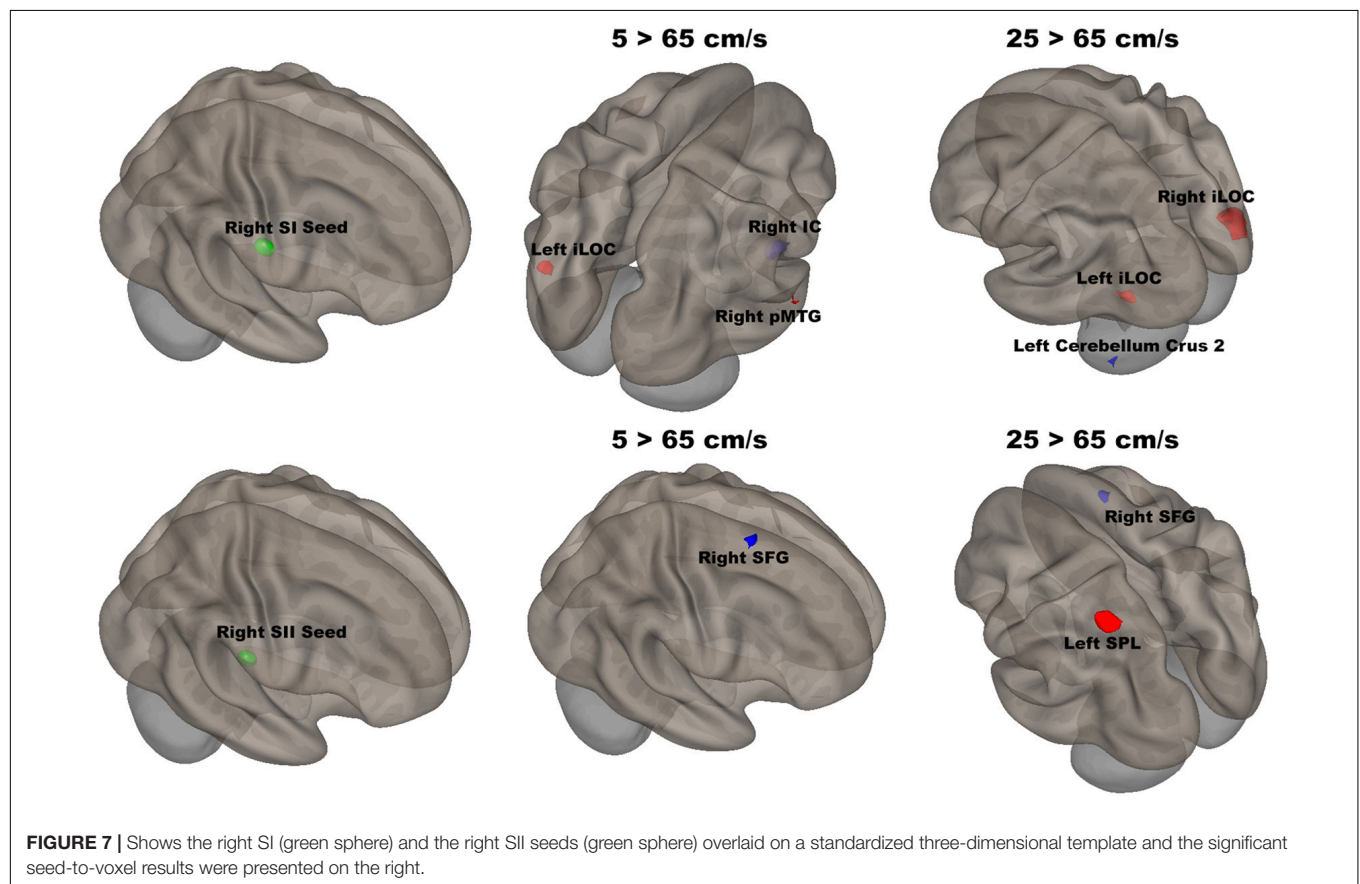
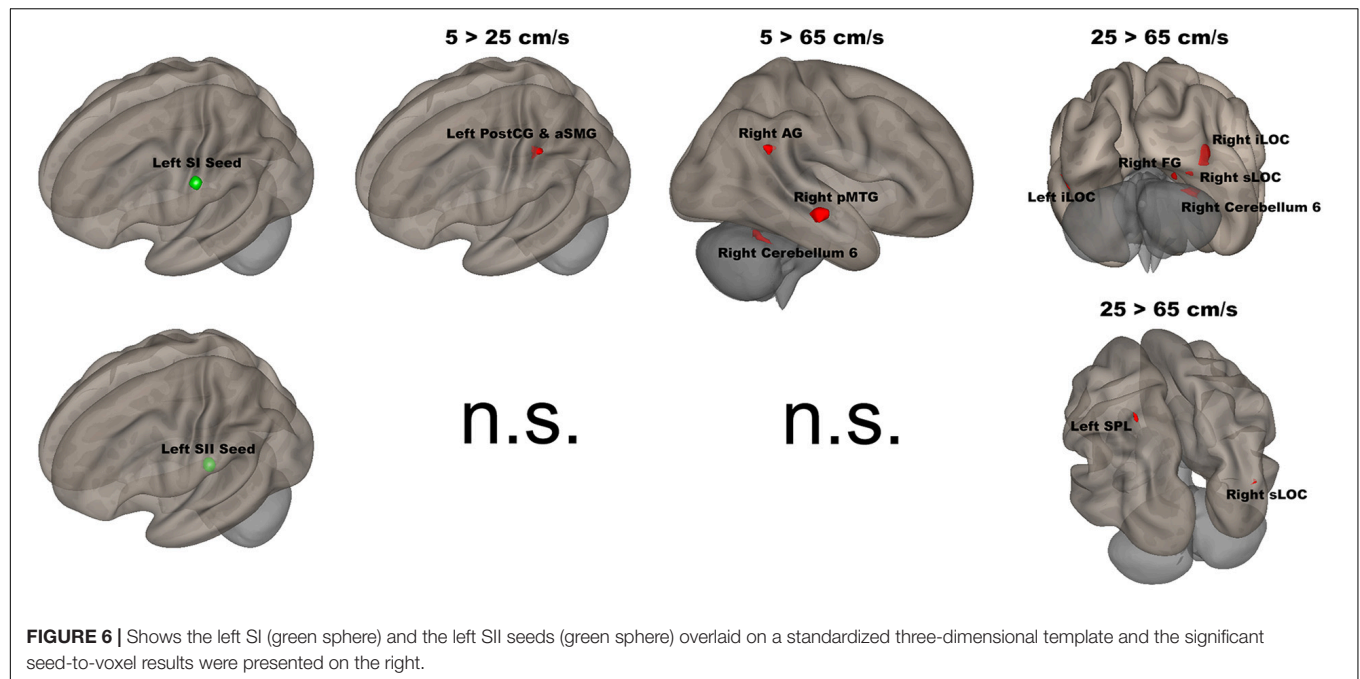
In this study, the right side of the lower face was passively stimulated with air pulses from a spatial array of TAC-Cells, which produced a 2–3 mm deflection of the skin surface. Unlike the glabrous hand, the facial skin is non-glabrous and lacks Pacinian afferents (Barlow, 1987). Hairly skin also lacks Meissner afferents and contains both slowly conducting unmyelinated C-tactile afferents and fast-conducting myelinated A β fibers (Nordin, 1990; Ackerley et al., 2014). The Merkel afferents, a population of slow-adapting type 1 (SA1) afferents, were stimulated in the right lower face, and then their first-order afferents produced action potentials, which were carried by the first-order A β axons into the ipsilateral main sensory trigeminal nucleus to release neurotransmitters to the second-order afferents. The second-order afferents generated action potentials that were conducted by their axons into the contralateral pons, to the ventral trigeminal lemniscus. The action potentials arrived at the contralateral thalamus and released neurotransmitters to the third-degree afferents in the core of the ventral posteromedial nucleus (VPM) of the thalamus. Finally, the third-degree VPM afferents released neurotransmitters to the cortical neurons in the SI and initiated the higher-order processing of the spatiotemporal information about the tactile stimuli delivered to the face (Norrssell and Olausson, 1994; Lundblad et al., 2011).

TABLE 2 | Seed-to-voxel results of changes in functional connectivity related to each velocity.

| Region | Coordinates in MNI space | | | Voxels |
|--|--------------------------|--------|--------|--------|
| | X (mm) | Y (mm) | Z (mm) | |
| 1. Left SI seed | | | | |
| Contrast: 5 > 25 cm/s | | | | |
| Left PostCG (35), aSMG (22) | −38 | −36 | 42 | 57 |
| Contrast: 5 > 65 cm/s | | | | |
| Right pMTG | 70 | −22 | −12 | 155 |
| Right Cerebellum 6 | 34 | −54 | −24 | 73 |
| Right AG | 60 | −52 | 26 | 64 |
| Contrast: 25 > 65 cm/s | | | | |
| Left iLOC (140) | −36 | −78 | 2 | 140 |
| Right iLOC (490), sLOC (138), FG (64) | 40 | −82 | −6 | 692 |
| Right FG (53), Right Cerebellum 6 (46) | 34 | −60 | −22 | 99 |
| 2. Left SII seed | | | | |
| Contrast: 25 > 65 cm/s | | | | |
| Left SPL | −32 | −52 | 68 | 42 |
| Right sLOC | 36 | −84 | 18 | 42 |
| 3. Right SI seed | | | | |
| Contrast: 5 > 65 cm/s | | | | |
| Left iLOC | −42 | −72 | 2 | 78 |
| Right pMTG | 64 | −24 | −4 | 40 |
| Contrast: 5 < 65 cm/s | | | | |
| Right IC | 40 | −4 | −6 | 109 |
| Contrast: 25 > 65 cm/s | | | | |
| Left iLOC | −38 | −78 | 0 | 96 |
| Right iLOC | 46 | −82 | −4 | 298 |
| Contrast: 25 < 65 cm/s | | | | |
| Left Cerebellum Crus II | −38 | −66 | −54 | 34 |
| 4. Right SII seed | | | | |
| Contrast: 5 < 65 cm/s | | | | |
| Right SFG | 18 | 8 | 66 | 76 |
| Contrast: 25 > 65 cm/s | | | | |
| Left SPL | −30 | −58 | 62 | 147 |
| Contrast: 25 < 65 cm/s | | | | |
| Right SFG | 18 | 12 | 48 | 50 |

PostCG, Postcentral Gyrus; aSMG, anterior Supramarginal Gyrus; pMTG, posterior Middle Temporal Gyrus; AG, Angular Gyrus; iLOC, inferior Lateral Occipital Cortex; sLOC, superior Lateral Occipital Cortex; FG, Fusiform Gyrus; SPL, Superior Parietal Lobule; IC, Insular Cortex; SFG, Superior Frontal Gyrus.

Our ROI-to-ROI results presented greater similarity of FC across the three velocities in the contralateral hemisphere. The only difference in connection strength was between the right DLPFC, and the right thalamus, and the 5 cm/s velocity evoked weaker FC than did the 25 cm/s. The right DLPFC has been associated with many high-level functions, such as alerting, cognitive control, emotional regulation, and working memory (Critchley et al., 2001; Mannarelli et al., 2015; Schaal et al., 2017; Wang et al., 2018; Yang et al., 2018). A case report has shown that a patient with a thalamic lesion in the region of the right intralaminar nuclei was conspicuously slow, inflexible, and lacked concentration, suggesting that the right thalamus is critical for healthy cognitive functions (Van Der Werf et al., 1999). Our



paradigm used a fixed block length. Thus, there were more air pulses delivered for the 25 cm/s blocks than for the 5 cm/s blocks. The 5 cm/s velocity, which had the lowest temporal density

of tactile stimulation, required little attention during the task, leading to weaker FC between the attention region (right DLPFC) and important hub region (right thalamus). Interestingly, there

were no differences in the FC connection strength between the right DLPFC and the right thalamus for contrasts of 5 vs 65 cm/s, or 25 vs 65 cm/s. This result indicated that a 65 cm/s velocity, the highest velocity used in this study, exceeded the optimal range of velocity. The optimal velocity range for moving tactile stimuli was 3–30 cm/s for the hand and 3–25 cm/s for the face (Langford et al., 1973; Whitsel et al., 1978, 1986; Dreyer et al., 1979; Essick et al., 1987, 1988; Edin et al., 1995). Additionally, the results of our previous study indicated that a velocity of 5 cm/s evoked the most extensive brain activation (Custead et al., 2017), indicating that there were sufficient data from three runs for the lowest temporal density of pneumotactile stimulation (5 cm/s) to evoke cortical activation. For 25- and 65-cm/s velocities, the higher temporal density of air-pulse stimulation did not elicit more BOLD responses in the brain, suggesting that adaptation or repetition-suppressing processes may play a role (Hollins et al., 1991; Popescu et al., 2013; Yang et al., 2014; Custead et al., 2017). Additionally, the 65-cm/s velocity exceeded the optimal range of velocity for the face and was processed differently in higher-order cortical levels of cortex in an animal study (Darian-Smith et al., 1984). High velocities have high temporal density, but have low perception accuracy (Lamb, 1983; Custead et al., 2017), whereas the 5-cm/s velocity might be processed as discrete stimuli to the facial skin, rather than as a constant motion across the skin (Wacker et al., 2011; Depeault et al., 2013). A recent study evaluated tactile pleasantness by stroking a soft brush over the skin and concluded that middle velocities, from 1 to 10 cm/s, were the preferred velocities, based on the pleasantness ratings (Ackerley et al., 2014). No participant in this study reported discomfort or pain sensation. Thus, pain-related neuronal networks did not influence our results.

In the “All ON” condition, the multichannel TAC-Cells were stimulated simultaneously. The contrasts of each velocity with the “All ON” condition revealed differences in FC strengths caused by the effects of the velocities of the tactile stimuli. For 5 cm/s vs “All ON” conditions, there was reduced FC between the right SII and the right PPC. Our previous results showed bilateral activation patterns when comparing 5 cm/s vs “All ON” (Custead et al., 2017). Our previous GLM results were limited to the strength of BOLD signals and could not determine the FC between a pair of cortical areas, while the present FC analysis allowed us to understand FC by calculation of Pearson’s correlation coefficients using time courses from pairs of cortical areas. A previous fMRI study has reported the representations of six body parts (face, fingers, legs, shoulders, lips, and toes) in the superior PPC (Huang et al., 2012). The right SII is connected reciprocally with the right (ipsilateral) SI (Karhu and Tesche, 1999). The “All ON” condition contains the highest temporal density of pneumotactile stimuli, and the fast A β fibers were used to carry the sensory information. The 5-cm/s velocity contained the lowest temporal density, and the slow C-tactile fibers were probably used to pass the sensory information. Therefore, the faster conduction from the peripheral nervous system (PNS) for the “All ON” condition allowed faster information flow between the right PPC and the right SII and led to stronger FC than the 5-cm/s velocity. For the 65 cm/s vs “All ON” conditions, there was increased

FC between the right thalamus and bilateral SII. The 65-cm/s velocity is not optimal for evoking functional networks in brain supporting velocity encoding, but the 65-cm/s velocity elicited increased FC in the right thalamus. Our results support the role of the thalamus as an integrative hub for functional brain networks (Hwang et al., 2017). An early animal study found that SII receives substantial inputs from topographically appropriate regions within the ipsilateral ventrobasal nucleus and from the ipsilateral posterior group (Carvell and Simons, 1987), which indicated that SII in mice may complement the function of SI by helping to define the overall sensory context in which detailed tactile discriminations are made. Our findings suggested that the right SII was involved in both low and high velocities and might play an important role in discriminating the velocity of orofacial tactile stimuli (Carvell and Simons, 1987; Tommerdahl et al., 2005a). Moreover, there was no statistically significant difference in connection strength for the 25 cm/s vs “All ON” conditions. This unexpected finding indicated that the three velocities were processed differently at the CNS-level, and that different processes at the PNS level might be the driving force. Determining how the three velocities were processed in the PNS was beyond the scope of the present study.

Our Seed-to-Voxel analyses were limited to four seeds only, since the bilateral SI and SII were most commonly activated during tactile stimulation (Karhu and Tesche, 1999; Simoes and Hari, 1999; Backes et al., 2000; Lin and Kajola, 2003; Simoes et al., 2003; Inui et al., 2004; Blatow et al., 2007; Dresel et al., 2008; Eickhoff et al., 2008; Garraghty et al., 2009; Tommerdahl et al., 2010; Hu et al., 2012; Popescu et al., 2013; Vahdat et al., 2014; Venkatesan et al., 2014; Avanzini et al., 2016). Although more seeds could be added, the power of this study would have been affected due to the relatively small number of participants. The changes in FC patterns for different velocities and four seeds (bilateral SI and SII) suggested that each velocity is unique, and might be used based on the sensitivity and spatial specificity needed for the specific neurotherapeutic applications.

The left (contralateral) SI seed had stronger FC with the left PostCG/aSMG in the comparison of 5 vs 25 cm/s. The left PostCG/aSMG were reported to demonstrate significant increases in BOLD signals for 5 cm/s vs “All OFF” condition in our previous fMRI study (Custead et al., 2017). More specifically, the low velocity (5 cm/s) evoked both stronger FC and BOLD signals in the left PostCG/aSMG than did the mid-range velocity (25 cm/s). Lamb et al. reported that increases in stimulus velocity could lead to sufficient loss of spatiotemporal information to decrease discrimination accuracy (Lamb, 1983). FC was increased between the left SI seed and the right AG, right pMTG, and right cerebellum 6 for 5-cm/s velocity vs 65-cm/s velocity. The right AG has been related to numerical representation (Gobel et al., 2001). Our visual paradigm was a visual number countdown task. During the 5 cm/s blocks, the number countdown task-evoked time courses in the right AG that correlated with the time courses of BOLD signals in the left SI. The stronger FC between the left SI and the right FG for 5-cm/s velocity vs 65-cm/s velocity indicated that temporal accuracy was higher for the slowest velocity. The right pMTG has been shown to be involved in the frontoparietal network, which positively modulated cognitive

tasks (Jolles et al., 2013). The low velocity evoked the largest spatial extent of activation in the comparison of 5 cm/s with the “All OFF” condition (Custead et al., 2017), which corresponded with the stronger FC between the left SI and right pMTG for 5-cm/s velocity vs 65-cm/s velocity. FC was increased between the left SI seed with the right FG, right sLOC, bilateral iLOC, and right cerebellum 6 for 25-cm/s velocity as compared to 65-cm/s velocity. The right FG, right sLOC, and bilateral iLOC cover the spatial extent of the occipital lobe, suggesting more involvement of visual attention for 25-cm/s velocity than for 65-cm/s velocity. The right cerebellum 6 was activated for both 5 vs 65 cm/s and 25 vs 65 cm/s. The right cerebellum 6 region is located at the right lobule VI of the cerebellum and is involved in the sensorimotor network (Bellebaum and Daum, 2007; Habas et al., 2009; Stoodley et al., 2012; Picerni et al., 2013; Guo et al., 2015), in line with our findings.

The left SII showed significantly increased FC only between the left SPL and right sLOC for 25 cm/s as compared to 65 cm/s. There were clear differences in FC patterns between the left SI and SII, in agreement with other studies (Backes et al., 2000). There were more similarities in FC patterns between 5 and 25 cm/s conditions in the left SII than for the left SI. Both velocities were within the optimal velocity range. The differences in FC between 25 and 65 cm/s conditions is likely to be driven by the 25-cm/s velocity, since there was no difference in FC for 5 vs 65 cm/s or 5 vs 25 cm/s. The left SII has been suggested to participate in the high-order processing of somatosensory stimuli (Backes et al., 2000), which was supported by our results.

There was significantly increased FC between the right SI seed and the left iLOC and right pMTG, as well as decreased FC between the right SI seed and right IC for 5 cm/s as compared to 65 cm/s. The right IC has been shown to be involved in inhibiting sensorimotor responses as part of the attention network (Corbetta and Shulman, 2002; Custead et al., 2017). The fastest velocity with the highest temporal density led to more repetition and required more control over response suppression. FC between the right SI seed and the bilateral iLOC was significantly increased, and FC between the right SI and the left cerebellum crus II was significantly decreased, for 25 cm/s as compared to 65 cm/s. The cerebellar involvement is consistent with the putative role of the cerebellum in feedforward control of sensory-guided movements at 5 cm/s (Custead et al., 2017).

The right SII showed significantly weaker FC with the right SFG for both 5 vs 65 cm/s and 25 vs 65 cm/s, but there was no difference for 5 vs 25 cm/s conditions. Thus, the noted FC difference was driven by the highest velocity. The right SFG plays a role in executive function, supporting bottom-up attention (Jolles et al., 2013). The increases in velocity required more bottom-up attention or alertness. Moreover, the right SII showed significantly stronger FC with the left SPL and weaker FC with the right SFG for 25 cm/s as compared to 65 cm/s. Somatosensory stimuli are processed in the left SPL, which is also involved in sensorimotor integration (Ruben et al., 2001). Weaker FC with the left SPL for 25 than for 65 cm/s might be due to the higher temporal density of the highest velocity stimulation. In other words, there are more somatosensory stimuli delivered in 20 s for the 65 cm/s than for either 5 or 25 cm/s stimuli.

Laterality

Both contralateral and ipsilateral FC of both SI and SII during unilateral or bilateral activation have been reported in animal (Tommerdahl et al., 2005a,b) and human studies (Tommerdahl et al., 2006; Akselrod et al., 2017). Neurons in SII most often have bilateral receptive fields, unlike neurons in SI (Whitsel et al., 1969). Our ROI-to-ROI results showed stronger FC between the right thalamus and bilateral SII for 65 cm/s as compared to the “All ON” condition, supporting the view of the involvement of bilateral SII in unilateral stimulation. The present study demonstrated that FC was reduced between the right PPC and the right SII for 5 cm/s as compared to the “All ON” condition, suggesting that right SII activity evoked by the slow velocity is critical for neuronal encoding of orofacial tactile perception of velocity. We also observed changes in FC in both hemispheres, in alignment with our previous report on bilateral cortical responses (Custead et al., 2017). The different velocities evoked different brain connectivity patterns that were mostly noted in the right (contralateral) hemisphere, supporting the involvement of interhemispheric connections for complex pneumotactile stimulation.

Limitations

This study had several limitations. First, a major limitation was that the imaging modality measured relatively slow hemodynamic responses, in the order of seconds. fMRI data can provide some indirect measures to decode how the sensory system perceives stimuli with different velocities. However, humans can make sensory decisions in less than 200 ms, which relies primarily on rapid synaptic neurotransmission on a time scale of milliseconds (Kohn et al., 2002). Thus, electrophysiology-based imaging approaches (i.e., MEG, EEG) are more suitable for studying the dynamic information of this rapidly changing system (Puts et al., 2019). Second, the relatively small sample size and wider age range of our participants could have limited the power of this study. Third, the FC analyses in the present study could not allow conclusions about the causal relationships between cortical regions and about whether the cortical network supporting higher-order processing of the facial tactile stimuli involved serial or parallel processing. Lastly, no behavioral measures were collected to assess individual differences in perception ability.

CONCLUSION AND FUTURE DIRECTIONS

In this study, cortical connectivity patterns associated with various tactile stimulation velocities were studied using fMRI, which has not been reported previously. Our results demonstrated both similarities and differences in the neuronal networks across the three velocities. Animal and human studies have shown that passively evoked sensory stimulation can enhance neuronal activity after stroke (Whitaker et al., 2007). Therefore, the present study has implications for applying passive pneumotactile stimuli, with various velocities, to bolster functional recovery during sensorimotor rehabilitation.

For instance, if this is combined with physical therapy for stroke patients or brain-injury survivors, it might induce more brain plasticity during sensorimotor rehabilitation (Small et al., 2002; Luft et al., 2005; da Guarda and Conforto, 2014). In future, a large cohort study should investigate age- and sex-effects on the perception of velocity (Venkatesan et al., 2015). Moreover, the effect of placement of TAC-Cells (right side vs left side, etc.) on the face should be investigated. Finally, stroke survivors could be included as a comparison group in future studies. Rehabilitation protocols for stroke survivors can be designed using the Galileo system, and the efficacy thereof could be assessed using fMRI, or MEG, or both.

DATA AVAILABILITY STATEMENT

The raw data supporting the conclusions of this article will be made available by the authors, without undue reservation, to any qualified researcher.

ETHICS STATEMENT

The study was reviewed and approved by the Institutional Review Board at University of Nebraska-Lincoln. Written informed consent was obtained from each participant in accordance with the Declaration of Helsinki.

REFERENCES

- Ackerley, R., Carlsson, I., Wester, H., Olausson, H., and Backlund Wasling, H. (2014). Touch perceptions across skin sites: differences between sensitivity, direction discrimination and pleasantness. *Front. Behav. Neurosci.* 8:54. doi: 10.3389/fnbeh.2014.00054
- Ackerley, R., Hassan, E., Curran, A., Wessberg, J., Olausson, H., and Mcglone, F. (2012). An fMRI study on cortical responses during active self-touch and passive touch from others. *Front. Behav. Neurosci.* 6:51. doi: 10.3389/fnbeh.2012.00051
- Akselrod, M., Martuzzi, R., Serino, A., Van Der Zwaag, W., Gassert, R., and Blanke, O. (2017). Anatomical and functional properties of the foot and leg representation in areas 3b, 1 and 2 of primary somatosensory cortex in humans: a 7T fMRI study. *Neuroimage* 159, 473–487.
- Avanzini, P., Abdollahi, R. O., Sartori, I., Caruana, F., Pelliccia, V., Casaceli, G., et al. (2016). Four-dimensional maps of the human somatosensory system. *Proc. Natl. Acad. Sci. U.S.A.* 113, E1936–E1943.
- Avivi-Arber, L., Martin, R., Lee, J. C., and Sessle, B. J. (2011). Face sensorimotor cortex and its neuroplasticity related to orofacial sensorimotor functions. *Arch. Oral Biol.* 56, 1440–1465.
- Backes, W., Mess, W., Van Kranen-Mastenbroek, V., and Reulen, J. (2000). Somatosensory cortex responses to median nerve stimulation: fMRI effects of current amplitude and selective attention. *Clin. Neurophysiol.* 111, 1738–1744.
- Backlund, H., Wiklund Fernström, K., Starck, G., Ekholm, S., and Olausson, H. (2003). “Directional sensibility of the human hairy skin: an fMRI study,” in *Proceedings of the Abstract for the 33rd Annual Meeting of the Society for Neuroscience*, New Orleans, LA.
- Backlund Wasling, H., Lundblad, L., Loken, L., Wessberg, J., Wiklund, K., Norrsell, U., et al. (2008). Cortical processing of lateral skin stretch stimulation in humans. *Exp. Brain Res.* 190, 117–124.
- Barlow, S. M. (1987). Mechanical frequency detection thresholds in the human face. *J. Exp. Neurol.* 96, 253–261.
- Barlow, S. M. (1998). Real time modulation of speech-orofacial motor performance by means of motion sense. *J. Commun. Disord.* 31, 511–534.

AUTHOR CONTRIBUTIONS

YW proposed and performed connectivity analysis, and drafted the manuscript. SB contributed to the conception, design, and data collection of the study, and revising the manuscript critically for important intellectual content. RC and HO carried out the experiment and data collection. FS organized and pre-processed the data. All authors read and approved the submitted version and agree to be accountable for all aspects of the work.

FUNDING

This work was supported by funds from the Barkley Trust (SB and YW), Nebraska Tobacco Settlement Biomedical Research Development, College of Education and Human Sciences, and the Office of Research and Economic Development.

ACKNOWLEDGMENTS

We thank the families for their participation. We also thank the supports for undergraduate research assistants from the UNL UCARE program funded in part by gifts from the Pepsi Quasi Endowment and Union Bank & Trust. We also thank Editage (www.editage.com) for English language editing.

- Barlow, S. M., and Bradford, P. T. (1996). Comparison of perioral reflex modulation in the upper and lower lip. *J. Speech Lang. Hear. Res.* 39, 55–75.
- Barlow, S. M., and Estep, M. (2006). Central pattern generation and the motor infrastructure for suck, respiration, and speech. *J. Commun. Disord.* 39, 366–380.
- Barlow, S. M., and Stumm, S. (2010). “Speech production: adult,” in *Encyclopedia of Neuroscience*, ed. L. R. Squire (Amsterdam: Elsevier Ltd), 247–254.
- Behzadi, Y., Restom, K., Liau, J., and Liu, T. T. (2007). A component based noise correction method (CompCor) for BOLD and perfusion based fMRI. *Neuroimage* 37, 90–101.
- Bellebaum, C., and Daum, I. (2007). Cerebellar involvement in executive control. *Cerebellum* 6, 184–192.
- Bjornsdotter, M., Loken, L., Olausson, H., Vallbo, A., and Wessberg, J. (2009). Somatotopic organization of gentle touch processing in the posterior insular cortex. *J. Neurosci.* 29, 9314–9320.
- Blatow, M., Nennig, E., Durst, A., Sartor, K., and Stippich, C. (2007). fMRI reflects functional connectivity of human somatosensory cortex. *Neuroimage* 37, 927–936.
- Carvell, G. E., and Simons, D. J. (1987). Thalamic and corticocortical connections of the second somatic sensory area of the mouse. *J. Compar. Neurol.* 265, 409–427.
- Corbetta, M., and Shulman, G. L. (2002). Control of goal-directed and stimulus-driven attention in the brain. *Nat. Rev. Neurosci.* 3, 201–215.
- Critchley, H. D., Mathias, C. J., and Dolan, R. J. (2001). Neural activity in the human brain relating to uncertainty and arousal during anticipation. *Neuron* 29, 537–545.
- Custead, R., Oh, H., Rosner, A. O., and Barlow, S. M. (2015). Adaptation of the cortical somatosensory evoked potential following pulsed pneumatic stimulation of the lower face in adults. *Brain Res.* 1622, 81–90.
- Custead, R., Oh, H., Wang, Y., and Barlow, S. (2017). Brain encoding of saltatory velocity through a pulsed pneumotactile array in the lower face. *Brain Res.* 1677, 58–73.
- da Guarda, S. N. F., and Conforto, A. B. (2014). Effects of somatosensory stimulation on corticomotor excitability in patients with unilateral cerebellar infarcts and healthy subjects—preliminary results. *Cereb. Ataxias* 1:16.

- Darian-Smith, I., Goodwin, A., Sugitani, M., and Heywood, J. (1984). "The tangible features of textured surfaces: their representation in the monkey's somatosensory cortex," in *Dynamic Aspects of Neocortical Function*, eds G. M. Edelman, W. E. Gall, and W. M. Cowan (New York, NY: Wiley), 475–500.
- Depeault, A., Meftah, E. M., and Chapman, C. E. (2013). Neuronal correlates of tactile speed in primary somatosensory cortex. *J. Neurophysiol.* 110, 1554–1566.
- Dresel, C., Parzinger, A., Rimpau, C., Zimmer, C., Ceballos-Baumann, A. O., and Haslinger, B. (2008). A new device for tactile stimulation during fMRI. *Neuroimage* 39, 1094–1103.
- Dreyer, D. A., Duncan, G. H., Wong, C. L., and Whitsel, B. L. (1979). Factors influencing capacity to judge direction of tactile stimulus movement on the face. *J. Dent. Res.* 58, 2052–2057.
- Edin, B. B., Essick, G. K., Trulsson, M., and Olsson, K. A. (1995). Receptor encoding of moving tactile stimuli in humans. I. Temporal pattern of discharge of individual low-threshold mechanoreceptors. *J. Neurosci.* 15, 830–847.
- Eickhoff, S. B., Grefkes, C., Fink, G. R., and Zilles, K. (2008). Functional lateralization of face, hand, and trunk representation in anatomically defined human somatosensory areas. *Cereb. Cortex* 18, 2820–2830.
- Essick, G., Franzen, O., and Whitsel, B. (1988). Discrimination and scaling of velocity of stimulus motion across the skin. *Somatos. Motor Res.* 6, 21–40.
- Essick, G., Starr, G., Dolan, P., and Afferica, T. (1987). Evaluation of directional sensitivity within the mental nerve distribution. *J. Dental Res.* 93, 157–157.
- Ferezou, I., Haiss, F., Gentet, L. J., Aronoff, R., Weber, B., and Petersen, C. C. (2007). Spatiotemporal dynamics of cortical sensorimotor integration in behaving mice. *Neuron* 56, 907–923.
- Friston, K. J., Worsley, K. J., Frackowiak, R. S., Mazziotta, J. C., and Evans, A. C. (1994). Assessing the significance of focal activations using their spatial extent. *Hum. Brain Mapp.* 1, 210–220.
- Garraghty, P. E., Pons, T. P., and Kaas, J. H. (2009). Ablations of areas 3b (SI Proper) and 3a of somatosensory cortex in marmosets deactivate the second and parietal ventral somatosensory areas. *Somatos. Motor Res.* 7, 125–135.
- Gobel, S., Walsh, V., and Rushworth, M. F. (2001). The mental number line and the human angular gyrus. *Neuroimage* 14, 1278–1289.
- Grabski, K., Lamalle, L., Vilain, C., Schwartz, J. L., Vallee, N., Tropres, I., et al. (2012). Functional MRI assessment of orofacial articulators: neural correlates of lip, jaw, larynx, and tongue movements. *Hum. Brain Mapp.* 33, 2306–2321.
- Grodd, W., Hulsmann, E., Lotze, M., Wildgruber, D., and Erb, M. (2001). Sensorimotor mapping of the human cerebellum: fMRI evidence of somatotopic organization. *Hum. Brain Mapp.* 13, 55–73.
- Guo, W., Liu, F., Chen, J., Wu, R., Zhang, Z., Yu, M., et al. (2015). Resting-state cerebellar-cerebral networks are differently affected in first-episode, drug-naïve schizophrenia patients and unaffected siblings. *Sci. Rep.* 5:17275.
- Habas, C., Kamdar, N., Nguyen, D., Prater, K., Beckmann, C. F., Menon, V., et al. (2009). Distinct cerebellar contributions to intrinsic connectivity networks. *J. Neurosci.* 29, 8586–8594.
- Hermundstad, A. M., Bassett, D. S., Brown, K. S., Aminoff, E. M., Clewett, D., Freeman, S., et al. (2013). Structural foundations of resting-state and task-based functional connectivity in the human brain. *Proc. Natl. Acad. Sci. U.S.A.* 110, 6169–6174.
- Hollins, M., Delemos, K. A., and Goble, A. K. (1991). Vibrotactile adaptation on the face. *Percept. Psychophys.* 49, 21–30.
- Hu, L., Zhang, Z. G., and Hu, Y. (2012). A time-varying source connectivity approach to reveal human somatosensory information processing. *Neuroimage* 62, 217–228.
- Huang, R. S., Chen, C. F., Tran, A. T., Holstein, K. L., and Sereno, M. I. (2012). Mapping multisensory parietal face and body areas in humans. *Proc. Natl. Acad. Sci. U.S.A.* 109, 18114–18119.
- Hwang, K., Bertolero, M. A., Liu, W. B., and D'Esposito, M. (2017). The human thalamus is an integrative hub for functional brain networks. *J. Neurosci.* 37, 5594–5607.
- Ibáñez, V., Deiber, M.-P., Sadato, N., Toro, C., Grissom, J., Woods, R. P., et al. (1995). Effects of stimulus rate on regional cerebral blood flow after median nerve stimulation. *Brain* 118, 1339–1351.
- Ing, A., and Schwarzbauer, C. (2014). Cluster size statistic and cluster mass statistic: two novel methods for identifying changes in functional connectivity between groups or conditions. *PLoS ONE* 9:e98697. doi: 10.1371/journal.pone.0098697
- Inui, K., Wang, X., Tamura, Y., Kaneoke, Y., and Kakigi, R. (2004). Serial processing in the human somatosensory system. *Cereb. Cortex* 14, 851–857.
- Jenkins, B. A., and Lumpkin, E. A. (2017). Developing a sense of touch. *Development* 144, 4078–4090.
- Johansson, R. S., and Olsson, K. A. (1976). Microelectrode recordings from human oral mechanoreceptors. *Brain Res.* 118, 307–311.
- Johansson, R. S., Trulsson, M., Olsson, K., and Westberg, K.-G. (1988). Mechanoreceptor activity from the human face and oral mucosa. *Exp. Brain Res.* 72, 204–208.
- Jolles, D. D., Van Buchem, M. A., Crone, E. A., and Rombouts, S. A. (2013). Functional brain connectivity at rest changes after working memory training. *Hum. Brain Mapp.* 34, 396–406.
- Karhu, J., and Tesche, C. (1999). Simultaneous early processing of sensory input in human primary (SI) and secondary (SII) somatosensory cortices. *J. Neurophysiol.* 81, 2017–2025.
- Khoshnejad, M., Piche, M., Saleh, S., Duncan, G., and Rainville, P. (2014). Serial processing in primary and secondary somatosensory cortex: a DCM analysis of human fMRI data in response to innocuous and noxious electrical stimulation. *Neurosci. Lett.* 577, 83–88.
- Kohn, A., Metz, C., Tommerdahl, M. A., and Whitsel, B. L. (2002). Stimulus-evoked modulation of sensorimotor pyramidal neuron EPSPs. *J. Neurophysiol.* 88, 3331–3347.
- Krupa, D. J., Matell, M. S., Brisben, A. J., Oliveira, L. M., and Nicolelis, M. A. (2001). Behavioral properties of the trigeminal somatosensory system in rats performing whisker-dependent tactile discriminations. *J. Neurosci.* 21, 5752–5763.
- Ladda, A. M., Pfannmoeller, J. P., Kalisch, T., Roschka, S., Platz, T., Dinse, H. R., et al. (2014). Effects of combining 2 weeks of passive sensory stimulation with active hand motor training in healthy adults. *PLoS ONE* 9:e84402. doi: 10.1371/journal.pone.0084402
- Lamb, G. D. (1983). Tactile discrimination of textured surfaces: psychophysical performance measurements in humans. *J. Physiol.* 338, 551–565.
- Langford, N., Hall, R. J., and Monty, R. A. (1973). Cutaneous perception of a track produced by a moving point across the skin. *J. Exp. Psychol.* 97, 59–63.
- Lin, Y. Y., and Kajola, M. (2003). Neuromagnetic somatosensory responses to natural moving tactile stimulation. *Can. J. Neurol. Sci.* 30, 31–35.
- Luft, A. R., Manto, M.-U., and Taib, N. O. B. (2005). Modulation of motor cortex excitability by sustained peripheral stimulation: the interaction between the motor cortex and the cerebellum. *Cerebellum* 4:90.
- Lundblad, L. C., Olausson, H. W., Hermansson, A. K., and Wasling, H. B. (2011). Cortical processing of tactile direction discrimination based on spatiotemporal cues in man. *Neurosci. Lett.* 501, 45–49.
- Mannarelli, D., Pauletti, C., Grippo, A., Amantini, A., Augugliaro, V., Curra, A., et al. (2015). The role of the right dorsolateral prefrontal cortex in phasic alertness: evidence from a contingent negative variation and repetitive transcranial magnetic stimulation study. *Neural Plast.* 2015:410785.
- Miyamoto, J. J., Honda, M., Saito, D. N., Okada, T., Ono, T., Ohyama, K., et al. (2006). The representation of the human oral area in the somatosensory cortex: a functional MRI study. *Cereb. Cortex* 16, 669–675.
- Moore, C. I., Nelson, S. B., and Sur, M. (1999). Dynamics of neuronal processing in rat somatosensory cortex. *Trends Neurosci.* 22, 513–520.
- Moulton, E. A., Pendse, G., Morris, S., Aiello-Lammens, M., Becerra, L., and Borsook, D. (2009). Segmentally arranged somatotopy within the face representation of human primary somatosensory cortex. *Hum. Brain Mapp.* 30, 757–765.
- Nasir, S. M., Darainy, M., and Ostry, D. J. (2013). Sensorimotor adaptation changes the neural coding of somatosensory stimuli. *J. Neurophysiol.* 109, 2077–2085.
- Nordin, M. (1990). Low-threshold mechanoreceptive and nociceptive units with unmyelinated (C) fibres in the human supraorbital nerve. *J. Physiol.* 426, 229–240.
- Norrsell, U., and Olausson, H. (1994). Spatial cues serving the tactile directional sensibility of the human forearm. *J. Physiol.* 478(Pt 3), 533–540.
- Nudo, R. J. (2013). Recovery after brain injury: mechanisms and principles. *Front. Hum. Neurosci.* 7:887. doi: 10.3389/fnhum.2013.00887
- Oh, H., Custead, R., Wang, Y., and Barlow, S. (2017). Neural encoding of saltatory pneumotactile velocity in human glabrous hand. *PLoS ONE* 12:e0183532. doi: 10.1371/journal.pone.0183532
- Pastor, M. A., Day, B. L., Macaluso, E., Friston, K. J., and Frackowiak, R. S. (2004). The functional neuroanatomy of temporal discrimination. *J. Neurosci.* 24, 2585–2591.

- Paus, R., Schmelz, M., Biro, T., and Steinhoff, M. (2006). Frontiers in pruritus research: scratching the brain for more effective itch therapy. *J. Clin. Invest.* 116, 1174–1186.
- Pearson, K. (2000). Motor systems. *Curr. Opin. Neurobiol.* 10, 649–654.
- Picerni, E., Petrosini, L., Piras, F., Laricchiuta, D., Cutuli, D., Chiapponi, C., et al. (2013). New evidence for the cerebellar involvement in personality traits. *Front. Behav. Neurosci.* 7:133. doi: 10.3389/fnbeh.2013.00133
- Popescu, E. A., Barlow, S. M., Venkatesan, L., Wang, J., and Popescu, M. (2013). Adaptive changes in the neuromagnetic response of the primary and association somatosensory areas following repetitive tactile hand stimulation in humans. *Hum. Brain Mapp.* 34, 1415–1426.
- Puts, N. A. J., Edden, R. A. E., Muthukumaraswamy, S., Singh, K. D., and McGonigle, D. J. (2019). Induced and evoked properties of vibrotactile adaptation in the primary somatosensory cortex. *Neural Plast.* 2019:5464096.
- Reed, C. L., Shoham, S., and Halgren, E. (2004). Neural substrates of tactile object recognition: an fMRI study. *Hum. Brain Mapp.* 21, 236–246.
- Ruben, J., Schwiemann, J., Deuchert, M., Meyer, R., Krause, T., Curio, G., et al. (2001). Somatotopic organization of human secondary somatosensory cortex. *Cereb. Cortex* 11, 463–473.
- Sanes, J. N., and Donoghue, J. P. (2000). Plasticity and primary motor cortex. *Annu. Rev. Neurosci.* 23, 393–415.
- Schaal, N. K., Kretschmer, M., Keitel, A., Krause, V., Pfeifer, J., and Pollok, B. (2017). The significance of the right dorsolateral prefrontal cortex for pitch memory in non-musicians depends on baseline pitch memory abilities. *Front. Neurosci.* 11:677. doi: 10.3389/fnins.2017.00677
- Sessle, B., Adachi, K., Avivi-Arber, L., Lee, J., Nishiura, H., Yao, D., et al. (2007). Neuroplasticity of face primary motor cortex control of orofacial movements. *Arch. Oral Biol.* 52, 334–337.
- Sessle, B. J., Yao, D., Nishiura, H., Yoshino, K., Lee, J. C., Martin, R. E., et al. (2005). Properties and plasticity of the primate somatosensory and motor cortex related to orofacial sensorimotor function. *Clin. Exp. Pharmacol. Physiol.* 32, 109–114.
- Simoës, C., and Hari, R. (1999). Relationship between responses to contra- and ipsilateral stimuli in the human second somatosensory cortex SII. *Neuroimage* 10, 408–416.
- Simoës, C., Jensen, O., Parkkonen, L., and Hari, R. (2003). Phase locking between human primary and secondary somatosensory cortices. *Proc. Natl. Acad. Sci. U.S.A.* 100, 2691–2694.
- Small, S., Hlustik, P., Noll, D., Genovese, C., and Solodkin, A. (2002). Cerebellar hemispheric activation ipsilateral to the paretic hand correlates with functional recovery after stroke. *Brain* 125, 1544–1557.
- Smith, A. (2016). The control of orofacial movements in speech. *Crit. Rev. Oral Biol. Med.* 3, 233–267.
- Stephan, K. E., Mattout, J., David, O., and Friston, K. J. (2006). Models of functional neuroimaging data. *Curr. Med. Imaging Rev.* 2, 15–34.
- Stevens, M. C. (2009). The developmental cognitive neuroscience of functional connectivity. *Brain Cognit.* 70, 1–12.
- Stoodley, C. J., Valera, E. M., and Schmahmann, J. D. (2012). Functional topography of the cerebellum for motor and cognitive tasks: an fMRI study. *Neuroimage* 59, 1560–1570.
- Tomita, A., Kato, T., Sato, F., Haque, T., Oka, A., Yamamoto, M., et al. (2012). Somatotopic direct projections from orofacial areas of primary somatosensory cortex to pons and medulla, especially to trigeminal sensory nuclear complex, in rats. *Neuroscience* 200, 166–185.
- Tommerdahl, M., Favorov, O. V., and Whitsel, B. L. (2010). Dynamic representations of the somatosensory cortex. *Neurosci. Biobehav. Rev.* 34, 160–170.
- Tommerdahl, M., Simons, S. B., Chiu, J. S., Favorov, O., and Whitsel, B. (2005a). Response of SI cortex to ipsilateral, contralateral and bilateral flutter stimulation in the cat. *BMC Neurosci.* 6:29. doi: 10.1186/1471-2202-6-29
- Tommerdahl, M., Simons, S. B., Chiu, J. S., Tannan, V., Favorov, O., and Whitsel, B. (2005b). Response of SII cortex to ipsilateral, contralateral and bilateral flutter stimulation in the cat. *BMC Neurosci.* 6:11. doi: 10.1186/1471-2202-6-11
- Tommerdahl, M., Simons, S. B., Chiu, J. S., Favorov, O., and Whitsel, B. L. (2006). Ipsilateral input modifies the primary somatosensory cortex response to contralateral skin flutter. *J. Neurosci.* 26, 5970–5977.
- Tononi, G., Edelman, G. M., and Sporns, O. (1998). Complexity and coherency: integrating information in the brain. *Trends Cognit. Sci.* 2, 474–484.
- Vahdat, S., Darainy, M., and Ostry, D. J. (2014). Structure of plasticity in human sensory and motor networks due to perceptual learning. *J. Neurosci.* 34, 2451–2463.
- Van Der Werf, Y. D., Weerts, J. G., Jolles, J., Witter, M. P., Lindeboom, J., and Scheltens, P. (1999). Neuropsychological correlates of a right unilateral lacunar thalamic infarction. *J. Neurol. Neurosurg. Psychiatry* 66, 36–42.
- Venkatesan, L., Barlow, S. M., and Kieweg, D. (2015). Age- and sex-related changes in vibrotactile sensitivity of hand and face in neurotypical adults. *Somatos. Motor Res.* 32, 44–50.
- Venkatesan, L., Barlow, S. M., Popescu, M., and Popescu, A. (2014). Integrated approach for studying adaptation mechanisms in the human somatosensory cortical network. *Exp. Brain Res.* 232, 3545–3554.
- Wacker, E., Spitzer, B., Lutzkendorf, R., Bernarding, J., and Blankenburg, F. (2011). Tactile motion and pattern processing assessed with high-field fMRI. *PLoS ONE* 6:e24860. doi: 10.1371/journal.pone.0024860
- Wang, J., Tian, J., Hao, R., Tian, L., and Liu, Q. (2018). Transcranial direct current stimulation over the right DLPFC selectively modulates subprocesses in working memory. *PeerJ* 6:e4906.
- Whitaker, V. R., Cui, L., Miller, S., Yu, S. P., and Wei, L. (2007). Whisker stimulation enhances angiogenesis in the barrel cortex following focal ischemia in mice. *J. Cereb. Blood Flow Metab.* 27, 57–68.
- Whitfield-Gabrieli, S., and Nieto-Castanon, A. (2012). Conn: a functional connectivity toolbox for correlated and anticorrelated brain networks. *Brain Connect.* 2, 125–141.
- Whitsel, B., Dreyer, D., and Hollins, M. (1978). Representation of moving stimuli by somatosensory neurons. *Fed. Proc.* 37, 2223–2227.
- Whitsel, B. L., Franzen, O., Dreyer, D. A., Hollins, M., Young, M., Essick, G. K., et al. (1986). Dependence of subjective traverse length on velocity of moving tactile stimuli. *Somatosens. Res.* 3, 185–196.
- Whitsel, B. L., Petrucelli, L. M., and Werner, G. (1969). Symmetry and connectivity in the map of the body surface in somatosensory area II of primates. *J. Neurophysiol.* 32, 170–183.
- Yang, J., Yu, Y., Kunita, A., Huang, Q., Wu, J., Sawamoto, N., et al. (2014). Tactile priming modulates the activation of the fronto-parietal circuit during tactile angle match and non-match processing: an fMRI study. *Front. Hum. Neurosci.* 8:926. doi: 10.3389/fnhum.2014.00926
- Yang, L.-C., Ren, P., and Ma, Y.-Y. (2018). Anodal transcranial direct-current stimulation over the right dorsolateral prefrontal cortex influences emotional face perception. *Neurosci. Bull.* 34, 842–848.
- Yeon, J., Kim, J., Ryu, J., Park, J. Y., Chung, S. C., and Kim, S. P. (2017). Human brain activity related to the tactile perception of stickiness. *Front. Hum. Neurosci.* 11:8. doi: 10.3389/fnhum.2017.00008
- Zembrzycki, A., Chou, S. J., Ashery-Padan, R., Stoykova, A., and O'leary, D. D. (2013). Sensory cortex limits cortical maps and drives top-down plasticity in thalamocortical circuits. *Nat. Neurosci.* 16, 1060–1067.

Conflict of Interest: The authors declare that the research was conducted in the absence of any commercial or financial relationships that could be construed as a potential conflict of interest.

Copyright © 2020 Wang, Sibaii, Custead, Oh and Barlow. This is an open-access article distributed under the terms of the Creative Commons Attribution License (CC BY). The use, distribution or reproduction in other forums is permitted, provided the original author(s) and the copyright owner(s) are credited and that the original publication in this journal is cited, in accordance with accepted academic practice. No use, distribution or reproduction is permitted which does not comply with these terms.



An fMRI Study of the Brain Network Involved in Teeth Tapping in Elderly Adults

T. Kobayashi^{1†}, H. Fukami^{2,3†}, E. Ishikawa², K. Shibata², M. Kubota¹, H. Kondo¹ and Y. Sahara^{2*}

¹ Department of Prosthodontics and Oral Implantology, School of Dentistry, Iwate Medical University, Morioka, Japan,

² Department of Physiology, School of Dentistry, Iwate Medical University, Shiwa-gun, Japan, ³ Department of Oral Health Sciences, Faculty of Nursing and Health Care, Baika Women's University, Osaka, Japan

OPEN ACCESS

Edited by:

Kazutaka Takahashi,
The University of Chicago,
United States

Reviewed by:

Angela M. Dietsch,
University of Nebraska-Lincoln,
United States
Geoffrey Gerstner,
University of Michigan, United States
Corinne A. Jones,
The University of Texas at Austin,
United States

*Correspondence:

Y. Sahara
ysahara@iwate-med.ac.jp

[†]These authors have contributed
equally to this work

Received: 19 August 2019

Accepted: 03 February 2020

Published: 17 March 2020

Citation:

Kobayashi T, Fukami H, Ishikawa E, Shibata K, Kubota M, Kondo H and Sahara Y (2020) An fMRI Study of the Brain Network Involved in Teeth Tapping in Elderly Adults. *Front. Aging Neurosci.* 12:32. doi: 10.3389/fnagi.2020.00032

Cortical activity during jaw movement has been analyzed using various non-invasive brain imaging methods, but the contribution of orofacial sensory input to voluntary jaw movements remains unclear. In this study, we used functional magnetic resonance imaging (fMRI) to observe brain activities during a simple teeth tapping task in adult dentulous (AD), older dentulous (OD), and older edentulous subjects who wore dentures (OEd) or did not wear dentures (OE) to analyze their functional network connections. (1) To assess the effect of age on natural activation patterns during teeth tapping, a comparison of groups with natural dentition—AD and OD—was undertaken. A general linear model analysis indicated that the major activated site in the AD group was the primary sensory cortex (SI) and motor cortex (MI) ($p < 0.05$, family wise error corrected). In the OD group, teeth tapping induced brain activity at various foci ($p < 0.05$, family wise error corrected), including the SI, MI, insula cortex, supplementary motor cortex (SMC)/premotor cortex (PMA), cerebellum, thalamus, and basal ganglia in each group. (2) Group comparisons between the OD and OEd subjects showed decreased activity in the SI, MI, Brodmann's area 6 (BA6), thalamus (ventral posteromedial nucleus, VPM), basal ganglia, and insular cortex ($p < 0.005$, uncorrected). This suggested that the decreased S1/M1 activity in the OEd group was related to missing teeth, which led to reduced periodontal afferents. (3) A conjunction analysis in the OD and OEd/OE groups revealed that commonly activated areas were the MI, SI, cerebellum, BA6, thalamus (VPM), and basal ganglia (putamen; $p < 0.05$, FWE corrected). These areas have been associated with voluntary movements. (4) Psychophysiological interaction analysis (OEd vs OE) showed that subcortical and cortical structures, such as the MI, SI, DLPFC, SMC/PMA, insula cortex, basal ganglia, and cerebellum, likely function as hubs and form an integrated network that participates in the control of teeth tapping. These results suggest that oral sensory inputs are involved in the control of teeth tapping through feedforward control of intended movements, as well as feedback control of ongoing movements.

Keywords: fMRI, teeth tapping, denture, sensory input, voluntary movement

INTRODUCTION

Orofacial muscles are involved in several behaviors, including elemental (e.g., tongue protrusion and jaw opening) and semiautomatic (e.g., mastication and swallowing) movements. Many tasks demand complex refined control of the musculature. Animal studies have indicated that chewing involves interactions between sensory feedback and an intrinsic rhythmical neural pattern. Signals from cortical masticatory areas trigger the central pattern generator and execute a coordinated rhythmical jaw movements (for reviews, see Dubner et al., 1978; Lund and Kolta, 2006; Avivi-Arber et al., 2011; Morquette et al., 2012; Avivi-Arber and Sessle, 2018). Although subcortical and cortical motor regions play central roles in orofacial movements, the underlying brain circuitry that initiates and brings about jaw movements remains poorly understood.

Direct investigation of the human cerebral cortical areas involved in jaw movements is possible due to the advent of non-invasive visualizing techniques such as fMRI, PET, and MEG. Initial PET-based exploration of the cortical areas related to mastication showed that the sensorimotor areas of the cortex were strongly activated and this was followed by activation of the supplementary motor areas, insulae, striatum, and Cb (Momose et al., 1997). Using fMRI, patterns of brain activation associated with mandibular movements (Ishikawa, 2002) during teeth clenching (Tamura et al., 2002; Byrd et al., 2009; Iida et al., 2010) and chewing (Onozuka et al., 2002; Tamura et al., 2003) have been identified, and there is agreement that an experimental task evoked concurrent activity in multiple brain regions. Studies that relate a behavior to activity in a single area or to a specific connection have been faced with difficulties. Neither the interconnections of a network have been identified, nor is it known whether these areas comprise a cohesive functional network.

In elderly adults, reduced masticatory performance is thought to be associated with changes in brain structures and/or functions. The MRI methods have been providing important evidences on how the brain changes with age at various gross anatomical and functional levels (Grady, 2012): (1) Healthy aging is known to be associated with GMV reductions and functional alterations in several regions that are crucial for higher cognitive function, i.e., the prefrontal, medial temporal, and parietal cortices. (2) Diffusion MRI methods have shown age-related changes in white matter connectivity between prefrontal and posterior cortical regions and within posterior sensory cortices. Therefore, reduced activity in elderly adults can be assumed to reflect a reduced level of functioning (Grady, 2012). On the other

hand, functional MRI studies have also shown that there are additional cortical activations (for reviews, see D'Esposito et al., 2003; Humbert et al., 2009; Grady, 2012). Because synchronized and coherent fluctuations of BOLD signals have been shown to be important for studying underlying neuronal networks of the human brain (Fox and Raichle, 2007), some recent investigations have begun to assess the brain networks and identify connections between these areas (Quintero et al., 2013; Lin et al., 2017; Michely et al., 2018).

The aim of this study was to understand the neural control mechanism of a complex behavior such as orofacial movement. While older human subjects performed a simple dental tapping task in an MRI environment, we examined how subcortical and cortical areas are activated and how they function together to produce behavior. In this study, we applied the PPI analysis for assessing the functional relevance of tapping task-activated areas. We predicted that the effect of denture wearing (peripheral sensory inputs) influences voluntary motor responses in the cortex during the teeth tapping task. fMRI allowed confirmation of the basic findings that have been characterized in non-human animal studies, and these findings have been extended to behaviors observed in humans.

MATERIALS AND METHODS

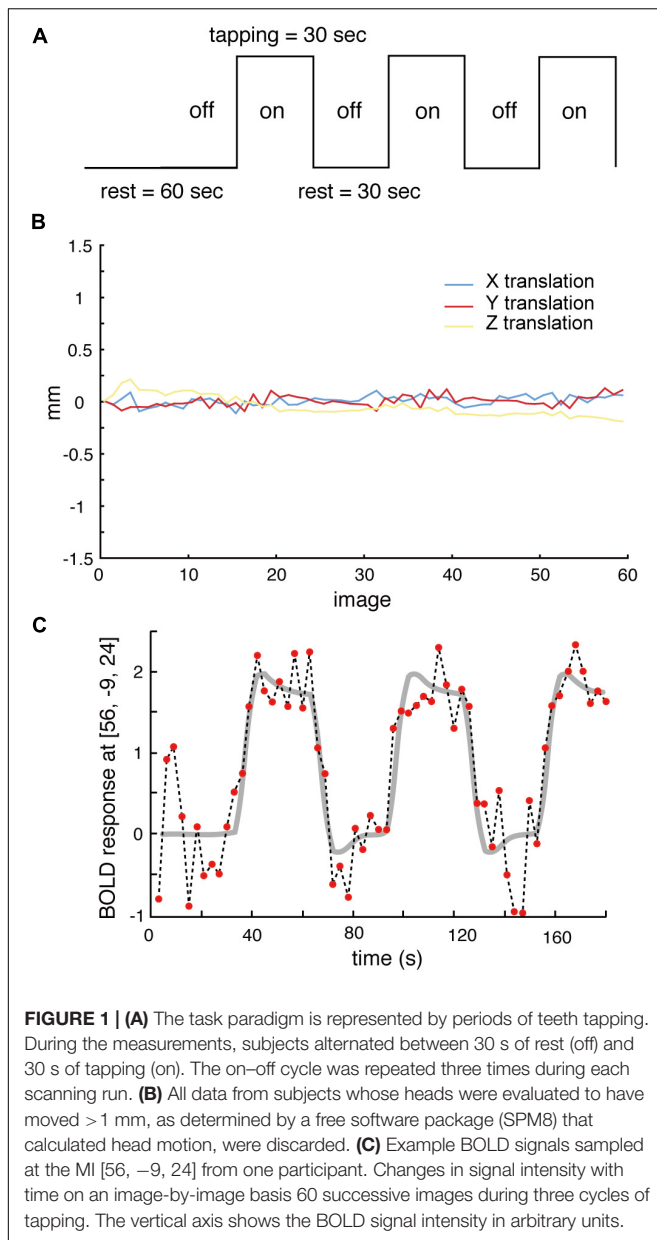
Subjects

Three groups of healthy subjects were included in this study: (1) an AD group (5 males and 4 females, mean age = 30.7 years, range: 26–40 years); (2) an OD group (6 males and 7 females, mean age = 81.8 years, range: 80–83 years); and (3) an OED group (7 males and 8 females, mean age = 79.1, range: 71–88 years). To reduce unidentified variance between the subject groups, careful characterization and selection of the subjects was undertaken. All subjects (1) were right-handed; (2) cleared the International Classification of Impairments, Disabilities, and Handicaps test and the Active-Daily Living Score (ADI Score) test; (3) had no history of neurologic or psychiatric disease; and (4) had no history of oral surgery, dental implants, head and neck cancer, and temporomandibular joint disorders. The dental states of the subjects in the OD group were Eichner A-1 type. The subjects' dentures were fabricated using traditional techniques, and all patients were satisfied with their daily denture use at the point of examinations (~3 months). After a full de-briefing, written informed consent was obtained from each subject. The experimental protocol for the use of human subjects was approved by the Medical Ethics Committee of Iwate Medical University (approval # 01071 and 01254).

Task Paradigm

During scanning, participants lay on their backs in the scanner. They were instructed (1) to keep the lower jaw in a rest position during the rest stage and (2) to perform a teeth tapping task, i.e., light tapping of the upper and lower teeth together with self-paced timing (~1 Hz). We employed a block design in this experiment (Figure 1A). The task comprised 30 s in a resting position (off) followed by 30 s of teeth tapping (on), i.e.,

Abbreviations: AD, adult dentulous; BA6, Brodmann area 6; Bg, basal ganglia; BOLD, blood-oxygen-level dependent; Cb, cerebellum; DLPFC, dorso-lateral prefrontal cortex; EPI, echo-planar imaging; FA, flip angle; fMRI, functional magnetic resonance imaging; FOV, field of view; FWE, family wise error; GLM, general linear model; GMV, gray matter volume; MEG, magnetoencephalography; MI, primary motor cortex; MNI, Montreal Neurological Institute; NIRS, near-infrared spectroscopy; OD, older dentulous; OE, older edentulous; OED, OE/denture wear; PET, positron emission tomography; PMA, premotor area; PPI, psychophysiological interaction; SI, primary somatosensory cortex; SMC, supplementary motor cortex; TE, echo time; Th, thalamus; TR, time interval; VL, ventrolateral nucleus; VPM, ventroposteromedial nucleus.



continuous tapping throughout the entire 30 s block. This task was repeated three times in a run. Therefore, a total duration of each scan was 210 s (dummy 30 s + task 180 s). A single fMRI trial included two runs for the AD and OD groups. The OE group performed the task with and without dentures. Within these trials, the order was randomized yet equal for both conditions to counter ordering effects and to maintain comparability. During the tapping task without dentures (sham teeth tapping), the subjects were instructed to mimic the teeth tapping movements, but were told not to bring the gums into contact. For data analysis, the first 10 volumes were discarded because of unstable magnetization. To minimize motions during the measurements, the head of the examinee was fixed in a supine position. All data from subjects whose head moved > 1 mm, which was determined

by a motion correction procedure in SPM8 (**Figure 1B**), were rejected. Imaging data of four elderly subjects (two males and two females of OE/OEd group) were excluded from all analyses.

Image Acquisition

Adults and two groups of elderly adult subjects (aged > 80 years); i.e., people with >20 teeth remaining (OD group) and the OE/OEd group, underwent fMRI during the teeth tapping task using EPI with a 3T MRI scanner. For each subject, functional images were acquired with a 3.0-T Signa HDxt system (GE Medical Systems, Milwaukee, WI, United States). The fMRI data were acquired using the gradient-EPI sequence (Bandettini et al., 1992) with the following BOLD imaging parameters: each volume comprised 24 oblique slices (in the axial orientation), each slice was 5 mm thick, and there was no gap. The TR was 3000 ms with a FA of 60° and 30 ms of TE. The FOV was 240 mm and the in-plane matrix size was 64 × 64 pixels (i.e., resolution 3.75 × 3.75 × 5 mm). T1-weighted images for anatomical details were obtained with the 3D-SPGR pulse sequence: TR 7.584 ms; TE 1.56 ms; FOV 240 mm; matrix 128 × 128; and 148 slices. The resolution of T1-weighted images was 1.875 × 1.875 × 1.4 mm.

Data Analysis

The MRI data were converted to an ANALYZE format and examined using MATLAB (R2007b, Mathworks, Natick, MA, United States) and SPM8 (Wellcome Department of Cognitive Neurology, London, United Kingdom, <http://www.fil.ion.ucl.ac.uk/spm/>).

First, 60 images from each trial were automatically realigned to the first image to correct for movements (Friston et al., 1994, 1995, 1998). Then, the images from two runs were co-registered with the T1-weighted anatomical image and normalized into a standard stereotaxic space that corresponded to the MNI template (provided by the MNI; Evans et al., 1994). To increase the signal-to-noise ratio, all functional images were smoothed with an 8-mm full-width at half-maximum isotropic Gaussian kernel filter.

General Linear Model

Statistical analyses were based on the GLM (Friston et al., 1995). Data were analyzed for each subject individually in the first level of analysis and individual contrast images were used for a random-effects analysis that assessed group effects. The statistical threshold for comparisons of the main effect of each condition was set ($p < 0.05$) using the FWE correction provided by SPM8. The cluster level was set at 10.

The resulting areas of activation were characterized regarding peak height and spatial extent (>10 voxels). Functional images were generated based on a two-tailed t -test that compared the resting and active conditions on a pixel-by-pixel basis. The results were considered significant at $p < 0.05$. The FWE rate corrected for the whole brain volume. Significant voxels were expressed with their coordinates in Talairach's space transformed from MNI coordinates (Talairach Daemon client software version 1.1; Research Imaging Center, University of Texas Health Science Center). Anatomical maps were created using the Anatomy Toolbox to identify the location, intensity,

and activated voxels in the anatomical regions. Images were first evaluated at the single-subject level and then group statistics were computed. The activation regions of the three groups were determined and compared using a one-way ANOVA. Conjunction analysis was performed to analyze the brain regions activated in all three groups.

PPI Analysis

To test the increase in sensory input induced by denture wearing on functional connectivity, PPI analyses were performed. PPI analysis provides a way to determine how neural activity from a seed region interacts with a psychological state to stimulate different levels of neural activity in other parts of the brain (Friston et al., 1997; Bingel et al., 2007; Kim and Horwitz, 2008). Subject-specific seed regions were determined by analyzing each OE individual subject's contrasts for tapping with dentures (OEd) and no dentures (OE, sham tapping) displayed at $p < 0.05$ referring for a value of conjunction analysis. Seed regions were defined as 10-mm spheres around the peak voxel rate of the activated cluster. The psychological variable was defined as the contrast of denture wearing vs no-denture wearing. In the first-level analysis, the PPI regressor was extracted from each subject. The PPI regressor consisted of the convolution of two functions, i.e., hemodynamic function convolved task regressor (denture wearing vs no-denture wearing) and the BOLD time course extracted from the seed ROI. This regressor was used to identify the individual effect of sensory modulation on connectivity. The second-level analysis was a group-level analysis. PPI results are reported at a statistical threshold of $p < 0.005$ (uncorrected) with a cluster size threshold of five voxels.

RESULTS

Comparison of Teeth Tapping in Young and Elderly Adults

We compared the two groups with natural dentition—AD and OD—to assess the effect of age on natural activation patterns during teeth tapping. As shown in **Figure 2A** (upper), the major activated site in the AD group was the primary sensory cortex and motor cortex. Small sites of activation were found in the association cortex. In the OD group, additional areas were activated and then compared with the AD group [**Figure 2A** (lower)]. The activated areas that were found bilaterally were the motor/somatosensory cortices, temporal association cortex, and parietal association cortex.

As shown in the **Figure 2B**, activated regions from uncorrected results provided some additional cortical activations to FWE-corrected results, as has been seen in other fMRI studies (Onozuka et al., 2003; Fang et al., 2005). Since fMRI studies rely on the detection of a weak signal in the presence of substantial noise, many statistical tests may lead to false-positive results regardless of the analytical approach. However, it has also been pointed out that standard corrections, such as Bonferroni's methods, are too strict and may eliminate true activation.

MRI Results During a Teeth Tapping Task in the OD and OE Groups

Statistical maps of brain regions with significant increases in BOLD contrast during a teeth tapping task in the OD and OE groups are shown in **Figures 3, 4**, respectively. Teeth tapping tasks in elderly adults recruited various subcortical and cortical foci, and the locations of the most significant foci of activation are summarized in **Table 1**, in which MNI coordinates of anatomical regions with maximum t -values are shown. Activated areas of the OD group were found bilaterally in the SI, MI, prefrontal cortex, temporal association area, and SMC. Activation foci were also revealed in cortical areas such as the insula (INS) and cingulate gyrus. Significant subcortical activation was present in the putamen and substantia nigra of the Bg, ventral posteromedial nucleus (VPM), and ventral lateral (VL) nucleus of the Th, amygdala, and cerebellar cortex. However, tapping tasks in the OE group recruited relatively smaller areas in the MI, SI, BA6, and prefrontal cortex than the OD group. The dorso-lateral area of the prefrontal cortex (DLPFC) was activated in the OD and OEd groups, but not in the OE groups.

Differences in Teeth Tapping in the OD and OEd Groups

We compared the brain activation patterns in the OEd to OD groups while they were performing the teeth tapping tasks. Group comparison analysis (OD > OEd) showed that activated areas were different in the SI, MI, SMC, Th (VPM), Bg (putamen and substantia nigra), and insula (**Figures 5A,B**; for coordinates and t -values, see **Table 2**).

The initial representation of oral somatosensory input is strictly somatotopically organized with the orofacial region (face SI) represented most laterally (Haggard and de Boer, 2014). In accord with the functional representation in the precentral gyrus, where the superior-inferior gradient was established by the sensory homunculus with the lips located dorsally to the teeth and the teeth dorsally to the tongue, the areas representing maximum tapping without dentures tended to be observed inferio-anterior to those while tapping with dentures. In addition, the mean percent signal changes also demonstrated significant between-group differences in the SI regions (**Figure 5C**). Thus, the reduction in brain map size and reduced response strength are best explained as that caused by reduced sensory inputs (Godde et al., 2002) and could be related to missing teeth, which leads to reduced periodontal afferents.

Identification of Common Activated Areas in the OD and OEd/OE Groups

To identify the brain regions that were activated during tapping tasks in the OD and OEd/OE groups, a conjunction analysis (Friston et al., 1999) was conducted. A conjunction analysis revealed that teeth tapping induced activation in the MI, SI, SMC/PMA, VPM in the Th, Cb, and putamen in the Bg ($p < 0.05$, FWE corrected), as shown in **Figure 6** and **Table 3** (for coordinates and t -values). These areas have

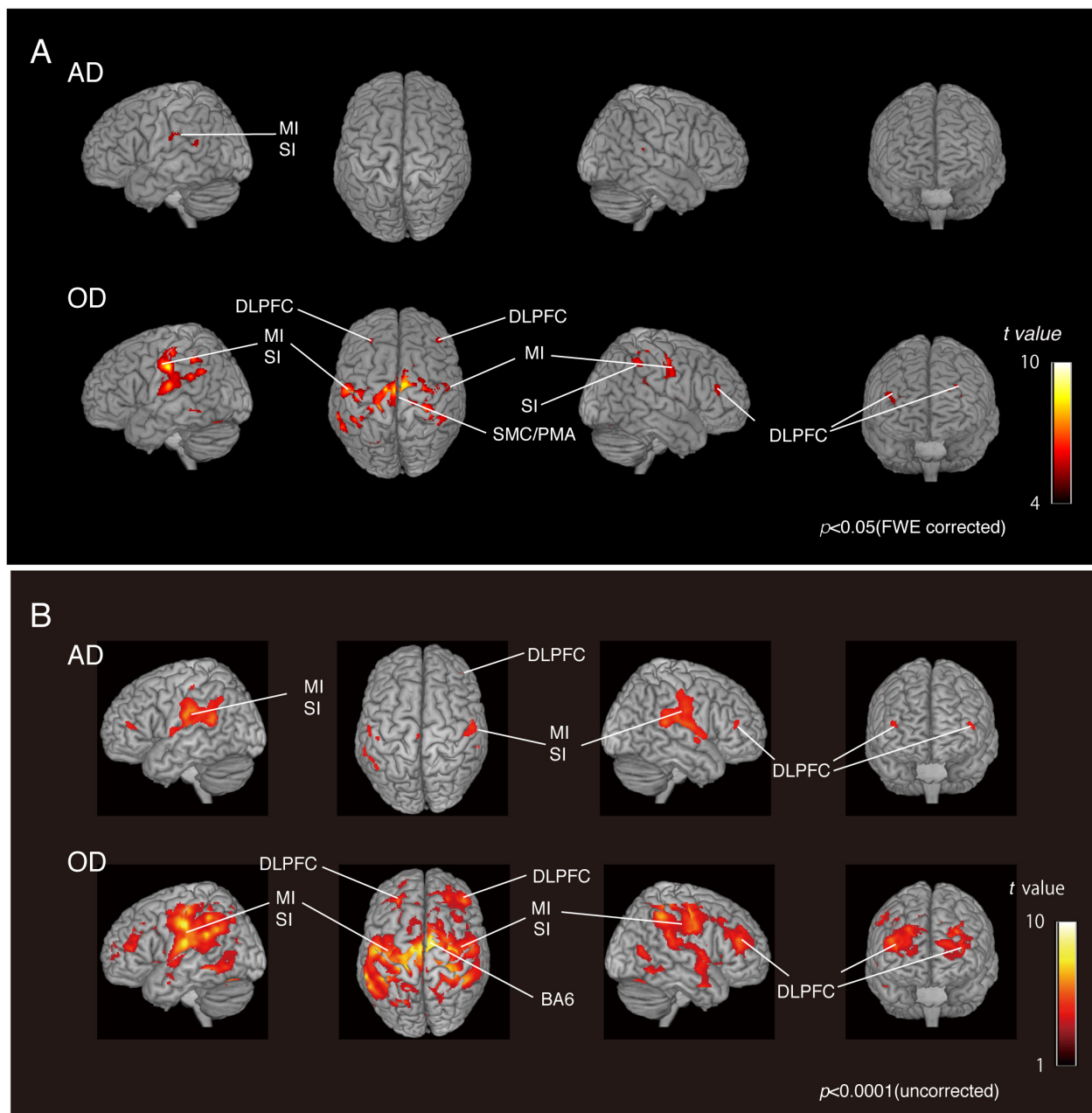


FIGURE 2 | BOLD activation pattern. **(A)** Surface projection of statistical parametric maps superimposed onto a standard MNI template brain ($p < 0.05$, FWE corrected). Significant increases in signals associated with tapping in the AD group (**upper section**) and OD group (**lower section**). The color bar shows the *t*-values. **(B)** Surface projection of statistical parametric maps superimposed onto a standard MNI template brain ($p < 0.0001$, uncorrected). Significant increases in signals associated with tapping in the AD group (**upper section**) and OD group (**lower section**). The color bar shows the *t*-values. Activated regions from uncorrected results provide some additional cortical activations to FWE corrected results (**A**), suggesting that the vast number of statistical tests may lead to false positive results regardless of the analysis approach used.

been shown to be regions that are involved in voluntary movements of primates. MI and PMA/SMC have been suggested to be involved in motor planning and initiation (for reviews, see Hoshi and Tanji, 2007; Nachev et al., 2008), and the Bg and Cb are well-known subcortical centers that provide a loop that is essential to the smooth execution

of skilled movements (Caligiore et al., 2017; Bostan and Strick, 2018). Furthermore, preparatory activity has been identified in the MI, premotor and supplemental motor cortex, parietal cortex, frontal eye field, striatum, motor-related Th, superior colliculus, and Cb in non-human primates (Svoboda and Li, 2018).

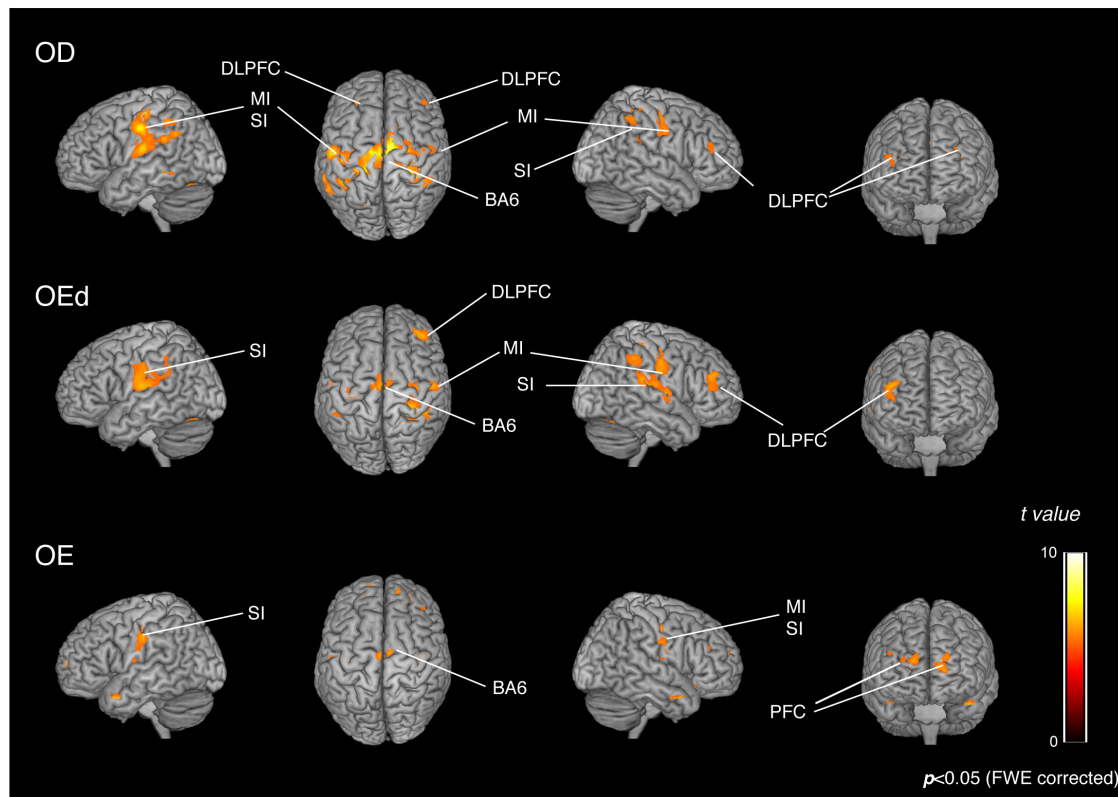


FIGURE 3 | Teeth tapping induced activated regions on the cortex in the OD (**top**), OEd (**middle**), and OE (**bottom**) groups. Surface projection of statistical parametric maps (GLM analysis) superimposed onto a standard MNI template brain ($p < 0.05$, FWE corrected). The color bar shows the t -values. Teeth tapping activated various foci, including the sensorimotor cortex, BA6, and prefrontal cortex.

Functional Connectivity Analysis During the Dental Tapping Task

To determine the functional relevance of tapping task-activated areas, we performed a PPI analysis. The effect of denture wearing on connectivity modulations was assessed; i.e., our prediction was that peripheral sensory inputs influence voluntary motor responses in the cortex during tapping tasks. Subject-specific seed regions were identified by searching for tapping contrasts for each OE individual subject with dentures in (OEd) and dentures out (OE, sham tapping), evaluated at $p < 0.05$ referring for a value of conjunction analysis. Seed regions included the MI, SI, PMA/SMC, putamen in the Bg, and cerebellar cortex (Figures 7, 8 and Table 4).

First, we seeded the SI region for PPI analysis. The responses of the Th (VPM), Bg (putamen), and PMA/SMC showed a stronger connectivity with the SI under OE conditions versus OEd conditions. As shown in Figure 7, tapping with dentures enhanced the connectivity to the VPM nuclei in the Th, putamen in the Bg, SMC, Cb, and the DLPFC ($p < 0.05$). The correlation coefficient between the activity in a seed (SI) and targets was shown under OE (red dots) conditions versus OEd (black dots) conditions.

By seeding the VPM nucleus of the Th for PPI analysis, we confirmed that tapping while wearing dentures enhanced the

connectivity to the S1 ($p < 0.05$, Table 4), which tells us that somatosensory afferent pathways that contribute to perception (i.e., trigeminal sensory nuclear complex–posteromedial ventral nucleus of the Th–SI pathway).

The increased functional connections from the SI were also detected in the Bg, Cb, PMA/SMC, and DLPFC, which are thought to be primarily involved in voluntary movements. Indeed, tapping with dentures enhanced connectivity from the putamen to the M1/S1, PMA/SMC, and the cingulate cortex, but it decreased connectivity to the VL nucleus in the Th ($p < 0.05$, Figure 8 and Table 4). The brain's circuits for voluntary action are known to consist of loops rather than linear chains; thus, this may correspond to the cerebral cortex–Bg–cerebral cortex loop (Alexander et al., 1986; Middleton and Strick, 2002).

When we defined a seed on the cerebellar cortex, functional connections were observed in the VL nucleus in the Th, M1, S1, PMA/SMC, cingulate cortex, and DLPFC ($p < 0.05$, Figure 8 and Table 4). The major influence of the Cb on movement is known through its connections in the VL nuclei of the Th, which connects directly to the motor and premotor cortex (i.e., cerebellar loop).

When defining a seed on the MI, no effective connectivity sites were detected ($p < 0.05$ uncorrected). However, when

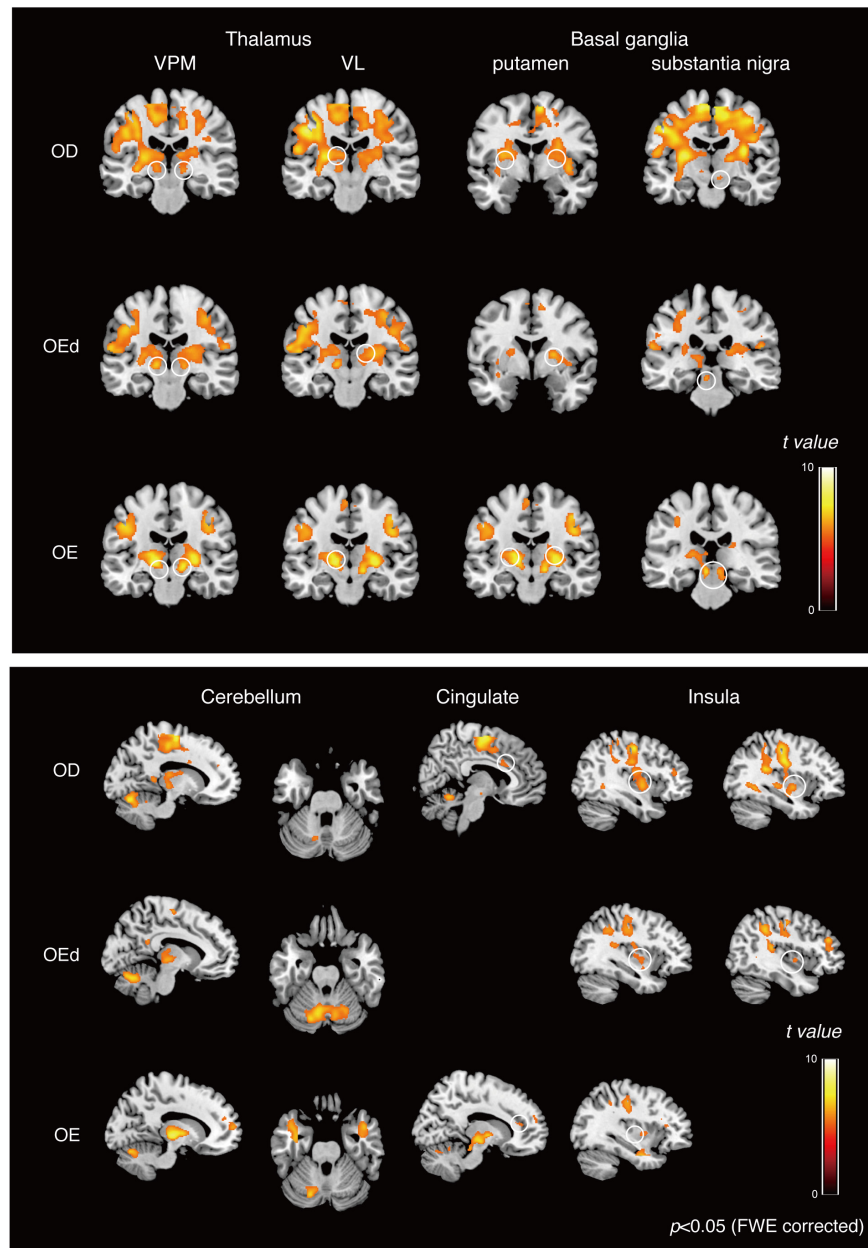


FIGURE 4 | Teeth tapping activated foci in the cortical and subcortical areas in the OD (top), OEd (middle), and OE (bottom) groups. Results from GLM analysis were superimposed onto a standard MNI template brain ($p < 0.05$, FWE corrected). The color bar shows the t -values. Activated regions, the thalamus (VPM and VL), basal ganglia (putamen and substantia nigra, shown on the coronal planes), cerebellum (shown on the sagittal and coronal planes), cingulate, and insula (shown on the sagittal planes). The color bar shows the t -values.

defining a seed on the PMA/SMC (i.e., BA6), there was effective connectivity with BA5, the DLPFC, and Cb ($p < 0.05$ uncorrected, Table 4). This suggests that the MI receives, as in non-human primates, two broad classes of inputs: the Bg-pre-SMA pathway-MI pathway and the parietal-premotor-MI pathway (Picard and Strick, 1996).

Results of the functional connection analyses are summarized in Figure 9, which demonstrate that subcortical and cortical structures, such as the MI, SI, SMC/PMA, DLPFC, Bg, Cb,

and insula cortex, probably function as hubs that form an integrated network and participate in generating and/or controlling teeth tapping.

DISCUSSION

Although teeth tapping appears to be a simple mechanical action, the neural machinery underlying it is surprisingly complex.

TABLE 1 | Significantly activated regions during tapping in the AD, OD, OE, and OEd groups.

| | Activated area | Brodmann's area | MNI coordinates | | | t-value |
|-----|-----------------------------|-----------------|-----------------|-----|-----|---------|
| | | | x | y | z | |
| AD | Primary motor cortex (M1) | 4 | -51 | -19 | 24 | 4.77 |
| | | | 47 | -12 | 25 | 4.69 |
| | Primary sensory cortex (S1) | 1, 2, 3 | -47 | -45 | 16 | 5.62 |
| | | | -45 | -25 | 30 | 6.51 |
| OD | Primary motor cortex (M1) | 4 | -47 | -16 | 37 | 6.76 |
| | | | 32 | -36 | 54 | 7.3 |
| | Primary sensory cortex (S1) | 1, 2, 3 | -39 | -16 | 52 | 7.07 |
| | | | 33 | -39 | 54 | 7.34 |
| | Supplementary/premotor area | 6 | -11 | -12 | 61 | 6.71 |
| | | | 8 | -7 | 61 | 6.48 |
| | Thalamus | | | | | |
| | VPM | | -14 | -22 | -2 | 6.03 |
| | | | 15 | -23 | -3 | 5.66 |
| | VL | | -14 | -19 | 9 | 5.41 |
| | Basal ganglia | | | | | |
| | Putamen | | -29 | -2 | 9 | 5.97 |
| | | | 21 | -2 | 12 | 5.73 |
| | Substantia nigra | | 8 | -13 | -11 | 4.87 |
| | DLPFC | 9 | -27 | 29 | 30 | 4.99 |
| | Cerebellum | | -14 | -65 | -28 | 5.73 |
| | Cingulate cortex | 24 | 6 | 16 | 27 | 5.59 |
| | Insula | | 38 | -3 | 0 | 6.48 |
| | | | -36 | -5 | -4 | 6.15 |
| OE | Primary motor cortex (M1) | 4 | -47 | -16 | 37 | 5.78 |
| | | | 45 | -10 | 28 | 5.76 |
| | Primary sensory cortex (S1) | 1, 2, 3 | 28 | -21 | 42 | 5.26 |
| | | | 39 | -18 | 42 | 6.43 |
| | Supplementary/premotor area | 6 | -5 | -10 | 60 | 5.19 |
| | | | 8 | -7 | 63 | 5.25 |
| | Thalamus | | | | | |
| | VPM | | -15 | -16 | 0 | 6.49 |
| | | | 15 | -18 | -3 | 6.00 |
| | VL | | -15 | -14 | 2 | 8.23 |
| | Basal ganglia | | | | | |
| | Putamen | | 26 | -15 | 1 | 6.18 |
| | | | -6 | -25 | -9 | 7.10 |
| | Substantia nigra | | -14 | -65 | -26 | |
| | Cerebellum | | -14 | -65 | -26 | |
| | Cingulate cortex | 24 | 12 | 37 | 15 | 5.44 |
| | Insula | | -35 | 0 | 1 | 5.61 |
| OEd | Primary motor cortex (M1) | 4 | -51 | -12 | 24 | 6.96 |
| | | | 53 | -12 | 39 | 6.70 |
| | Primary sensory cortex (S1) | 1, 2, 3 | -45 | -18 | 36 | 7.02 |
| | | | 32 | -36 | 52 | 6.72 |
| | Supplementary/premotor area | 6 | 45 | -12 | 30 | 7.07 |
| | | | -3 | -10 | -61 | 6.56 |
| | Thalamus | | | | | |
| | VPM | | -13 | -19 | 1 | 6.57 |
| | | | 15 | -21 | -1 | 6.39 |

(Continued)

TABLE 1 | Continued

| Activated area | Brodmann's area | MNI coordinates | | | t-value |
|------------------|-----------------|-----------------|-----|-----|---------|
| | | x | y | z | |
| VL | | 15 | -17 | 10 | 5.47 |
| Basal ganglia | | | | | |
| Putamen | | 22 | 0 | 7 | 6.31 |
| | | -22 | 3 | 7 | 5.22 |
| Substantia nigra | | -4 | -27 | -15 | 6.17 |
| DLPFC | 9 | 41 | 41 | 24 | 6.70 |
| Cerebellum | | -10 | -63 | -24 | 7.13 |
| Insula | | 40 | -3 | -2 | 5.57 |
| | | -36 | -3 | -2 | 5.53 |

$p < 0.05$ FWE corrected.

Using fMRI methods, we demonstrated how elderly adults recruit various cortical and subcortical foci, including the MI, SI, prefrontal cortex, temporal association area, PFC/SMC, INS, the putamen and substantia nigra of the Bg, VPM and VL nucleus of the Th, cerebellar cortex, and amygdala, to produce tapping. When combining functional connection analyses to assess how representative foci of the cerebral cortex that are involved in the tapping task act together to execute tapping, we showed that subcortical and cortical structures, such as the MI, SI, SMC/PMA, DLPFC, Bg, Cb, and insula cortex, probably function as hubs that form an integrated network and participate in generating and/or controlling teeth tapping. All of

these results support the idea that peripheral orofacial sensory inputs can notify the motor system about the current state of the body, such as its position, and movement of the teeth and jaw, and that they can allow the control of teeth tapping, for example, feedforward control of intended movements and feedback control of ongoing movements via the cerebello-cerebral loop, which can be used to correct errors that occur during movement, and feedback via the Bg-pre-SMA-MI circuit (the Bg loop), which can be used to promote smooth execution of tapping movements. This knowledge may help in explaining the increased recruitment of brain regions in the elderly compared with the young.

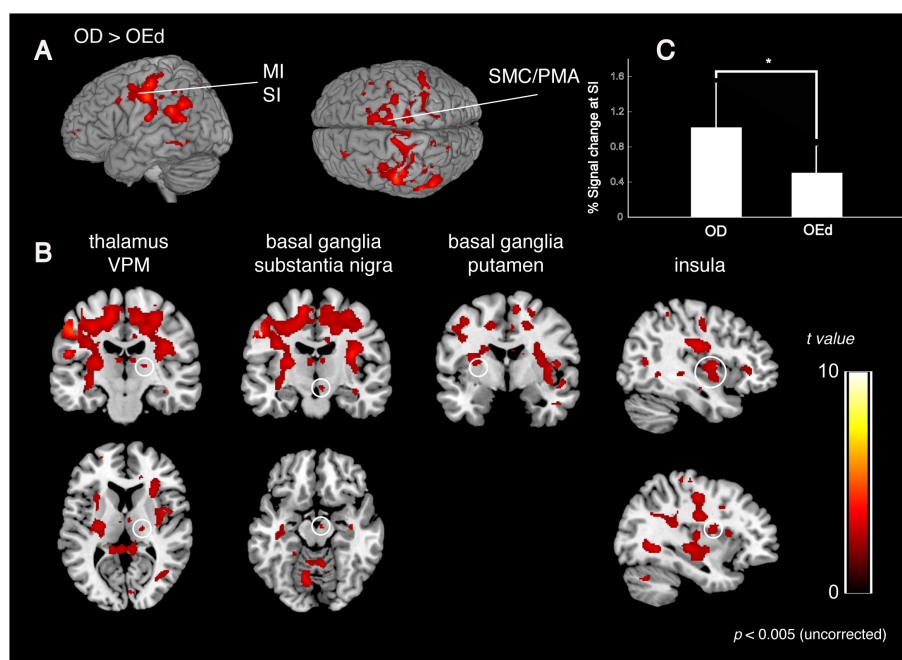


FIGURE 5 | Comparison between OD and OEd groups. **(A,B)** Results from group comparisons between OD and OEd ($OD > OEd$) are shown. Activated areas were decreased in the MI, SI, thalamus (VPM), basal ganglia, and insula cortex ($p < 0.005$, uncorrected). The color bar shows the t -values. **(C)** The reduction of BOLD response strengths in the SI ($*p < 0.05$). The reduction of representation areas and BOLD response strengths can be related to missing teeth, which leads to reduced periodontal afferents.

TABLE 2 | Significantly activated regions during tapping (OD > OEd).

| | Activated area | Brodmann's area | MNI coordinates | | | t-value |
|----------|-----------------------------|-----------------|-----------------|-----|-----|---------|
| | | | x | y | z | |
| OD - OEd | Primary motor cortex (MI) | 4 | -51 | -15 | 41 | 4.98 |
| | Primary sensory cortex (SI) | 1, 2, 3 | -45 | -16 | 51 | 4.42 |
| | Supplementary/premotor area | 6 | 12 | -14 | 62 | 2.96 |
| | Thalamus | | | | | |
| | VPM | | -18 | -17 | 8 | 2.36 |
| | Basal ganglia | | | | | |
| | Putamen | | -29 | -2 | 9 | 2.24 |
| | Substantia nigra | | 5 | -12 | -14 | 2.56 |
| | Insula | | 39 | -2 | 6 | 3.12 |
| | | | -35 | 0 | 15 | 2.67 |

$p < 0.005$ uncorrected.

How the Brain Transforms Sensory Input Into Motor Output Through a Cascade of Sensorimotor Transformations

How Does the Cerebral Cortex Use Sensory Information From the External World to Organize Teeth Tapping Movements?

Neural processes by which the brain controls goal-oriented behaviors, such as tasks involving arm movements and eye movements in non-human primates (for reviews, see Schwartz, 2016; Gallivan et al., 2018), have been studied well and have been reported that (1) perceptual mechanisms generate a unified sensory representation of the external world and the individual within it; (2) cognitive processes use this internal replica of the world to decide on a course of action; and (3) the selected

motor plan is relayed to action systems for implementation. Teeth tapping movements may share some of the motor-visual task pathways. However, there are crucial differences between the mouth and other body parts regarding neural machinery, in terms of repetitive movements, the target, the types of sensory information being processed, and the types of joints and muscle units involved (Iida et al., 2010).

How Does the Brain Construct an Internal Representation of External Physical Events During Teeth Tapping?

Here, we showed changes in the activation of specific regions in the brain in the “OD vs OEd” condition, as well as in the “denture in vs out” condition. Taking into account the topographic arrangements of the body, these areas correspond to the most lateral aspect of orofacial regions (face SI). *What specific sensorimotor changes might create the brain regional activation?* “OD vs OEd” condition provides changes in periodontal afferents. Iida et al. (2012) reported similar cortical activation patterns during teeth tapping tasks in young adults, but they did not detect any difference in “sham teeth tapping vs teeth tapping task.” Therefore, the relationship between periodontal sensation and the resulting changes in tapping under experimentally anesthetized conditions remains to be examined. “Denture in (OEd) vs out (OE)” condition provides the following: (1) a hard vertical stop during tooth tapping, (2) changes in afferent inputs from the joints and muscles, (3) cover/mask mechanoreceptor input from periodontal ligaments and/or the alveolar ridge, and (4) changes in mechanoreceptor input from the tongue, lips, and cheeks due to material bulk. In fact, some oral sensory inputs are generated by the active movement of oral tissues, such as the contact between different surfaces in the mouth, e.g., the palate and tongue or upper and lower teeth, is rich and constant. The somatosensory experience of the mouth itself comes from the perceived object sensed by the oral tissues (for a review, see Haggard and de Boer, 2014), even though the underlying processing mechanisms of the oral sensory information remain unclear.

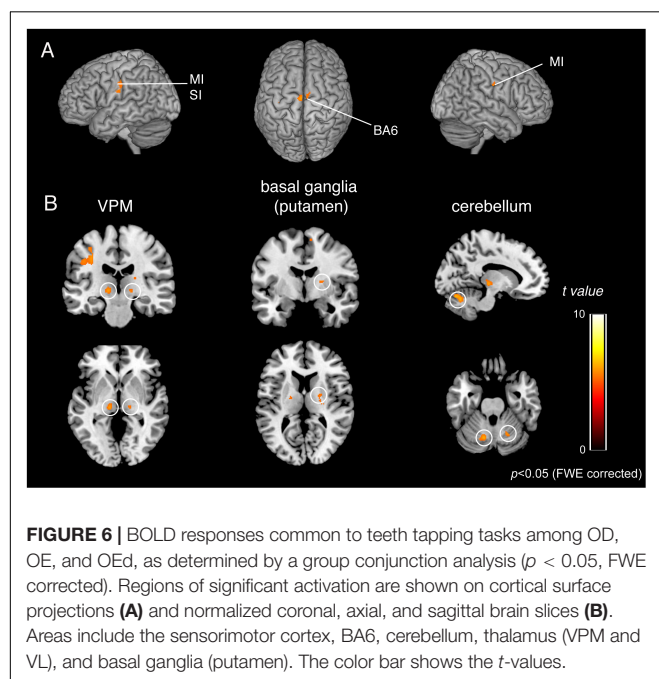


TABLE 3 | Significantly activated regions during tapping (conjunction analysis).

| | Activated area | Brodmann's area | MNI coordinates | | | t-value |
|-------------|-----------------------------|-----------------|-----------------|-----|-----|---------|
| | | | x | y | z | |
| Conjunction | Primary motor cortex (Ml) | 4 | -51 | -10 | 23 | 6.26 |
| | | | 45 | -12 | 30 | 6.18 |
| | Primary sensory cortex (Sl) | 1, 2, 3 | -51 | -15 | 24 | 6.26 |
| | Supplementary/premotor area | 6 | 9 | -5 | 63 | 5.77 |
| | Thalamus | | -14 | -21 | -2 | 6.1 |
| | | | 15 | -8 | -2 | 5.63 |
| | Basal ganglia | | | | | |
| | Putamen | | -20 | -5 | 11 | 5.39 |
| | | | 20 | -5 | -26 | 5.61 |
| | Cerebellum | | -14 | -66 | -27 | 6.44 |

p < 0.05 FWE corrected.

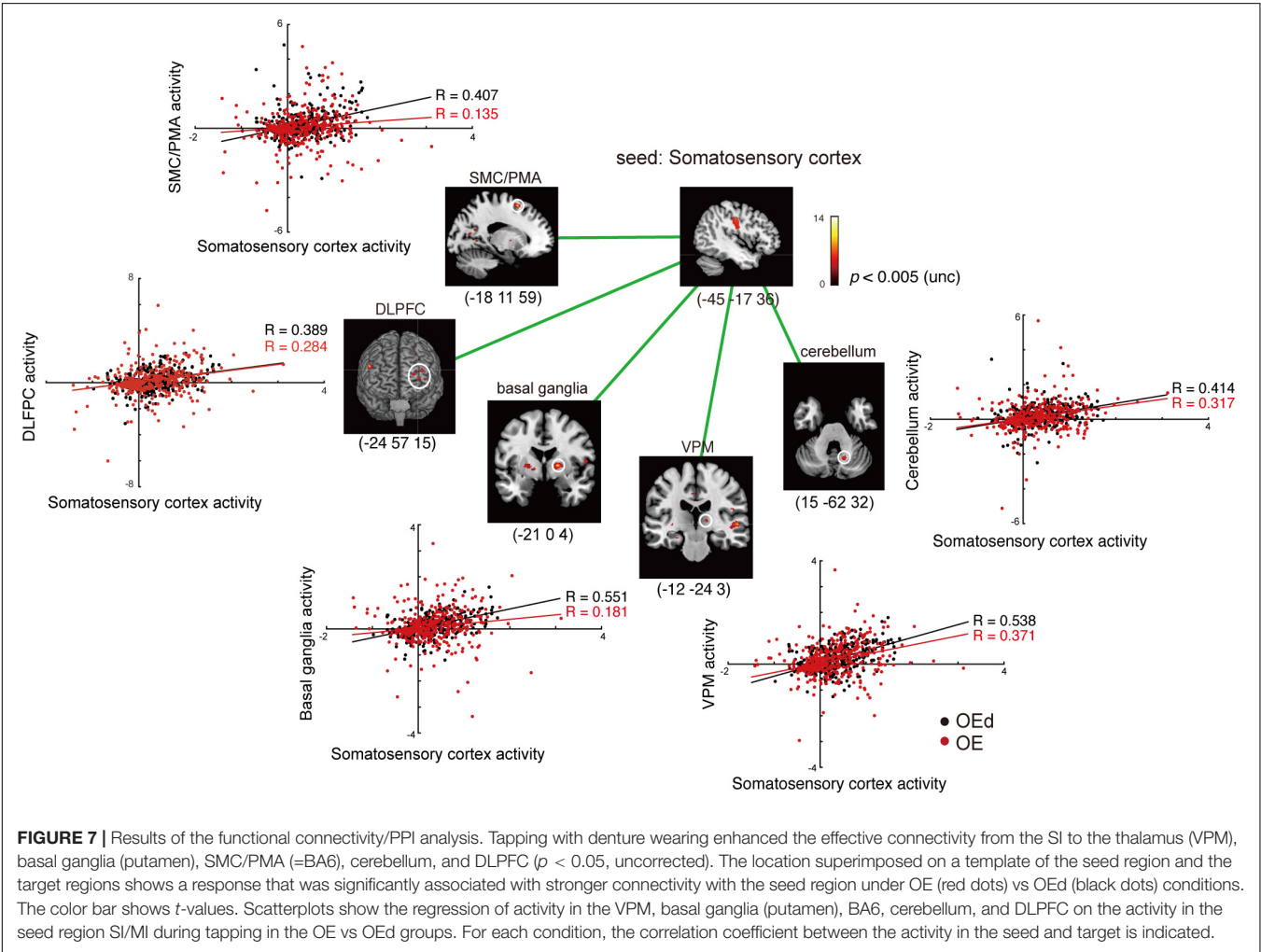


TABLE 4 | Anatomical location and MNI coordinates of PPI analysis (OEd vs OE; $p < 0.005$ uncorrected on the cluster level).

| | | MNI coordinates | | | t-value |
|---------------------------------|-----------------------------------|-----------------|-----|-----|---------|
| | Activated area | x | y | z | |
| PPI seed: left SI | Supplementary/premotor area (BA6) | -18 | 11 | 59 | 10.05 |
| | Thalamus | | | | |
| | VPM | -12 | -24 | 3 | 5.05 |
| | | 14 | -23 | 6 | 4.02 |
| | Basal ganglia | | | | |
| | Putamen | 18 | -2 | 5 | 12.55 |
| | | -21 | 0 | 4 | 4.22 |
| | Cerebellum | 15 | -62 | 32 | 6.25 |
| PPI seed: right BG | DLPFC | -24 | 57 | 15 | 5.67 |
| | Supplementary/premotor area (BA6) | 12 | -21 | 66 | 4.63 |
| | Thalamus | | | | |
| | VL | 14 | -6 | -9 | 4.4 |
| | MI | 38 | -30 | 59 | 4.18 |
| | SI | 48 | -21 | 52 | 4.25 |
| | Cingulate cortex | -6 | 32 | 37 | 3.77 |
| | | 51 | -18 | 22 | 5.77 |
| PPI seed: left cerebellum | Supplementary/premotor area (BA6) | 32 | -15 | 60 | 8.12 |
| | Thalamus | | | | |
| | VL | 14 | -15 | 9 | 3.58 |
| | MI | -3 | -19 | 67 | 3.58 |
| | SI | -15 | -39 | 70 | 3.58 |
| | Cingulate cortex | 6 | -15 | 43 | 3.88 |
| | DLPFC | 41 | 11 | 33 | 4.25 |
| | | -20 | 42 | 37 | 4.42 |
| PPI seed: right BA6 | Cerebellum | -11 | -75 | -17 | 3.78 |
| | VPM | 15 | -24 | 2 | 3.55 |
| PPI seed: left VPM | SI | 47 | -25 | 56 | 3.45 |
| | Supplementary/premotor area (BA6) | 8 | -20 | 63 | 5.34 |
| PPI seed: left insula | Supplementary/premotor area (BA6) | -36 | 8 | 54 | 4.84 |
| | SI | -41 | -25 | 51 | 4.58 |
| | Cingulate cortex | -2 | -1 | 36 | 4 |
| | PFC | -42 | 41 | 16 | 3.66 |

 $p < 0.005$ uncorrected

From studies in unanesthetized monkeys, short-train intracortical microstimulation (ICMS) was shown to evoke elemental movements, such as jaw opening and tongue protrusion, when applied to the face MI or face SI (Huang et al., 1989). It suggests that the face SI has a role in sensorimotor integration as well as the generation and control of orofacial movements.

How Can Sensory Feedback Be Used During Teeth Tapping Movements?

To decide on a course of action, the motor system requires information about the target object as well as the current status of the body, including its motion, posture, and location relative to

the target. During hand movements, vision and proprioception provide the most prominent sources of feedback, yet they have inherent temporal delays that limit their use during very rapid corrections. Prediction can compensate for such delays and thus increase the accuracy of sensory feedback with hand movements; i.e., motor commands are copied and conveyed internally to the Cb where they are used to generate rapid predictions of the sensory consequences of motor actions (forward models; for reviews, see Scott, 2004; Scott et al., 2015). Therefore, information about the environment encoded in the sensory cortices is sent to motor systems in a feedforward fashion (for reviews, see Azim and Alstermark, 2015; Schwartz, 2016; Gallivan et al., 2018), and these sensorimotor transformations are strongly shaped by

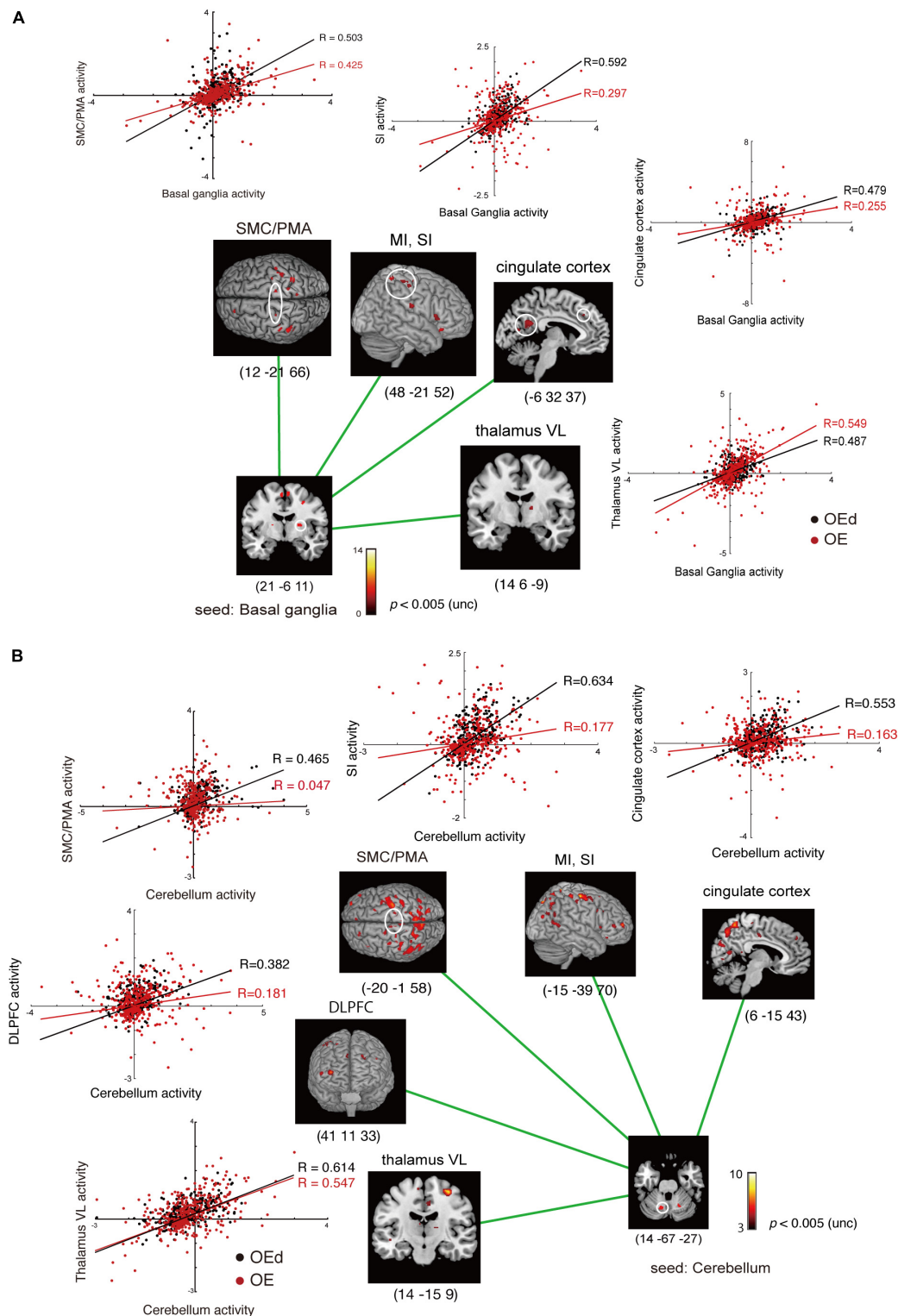


FIGURE 8 | Results of the functional connectivity/PPI analysis. The location superimposed on a template of the seed regions [basal ganglia **(A)** and cerebellum **(B)**] and the target regions shows neural responses that were significantly associated with stronger connectivity with the seed region under OE vs OEd conditions. For each condition, the correlation coefficient between the activity in the seed and targets is indicated. The color bar shows t -values. Co-activation plot in panel **(A)** shows the changes in coupling between dentures in vs dentures out; activity in the SI/MI, SMC/PMA, thalamus (VL), and cingulate cortex becomes more sensitive to inputs from the basal ganglia (putamen) with dentures. Co-activation plot in panel **(B)** shows that the activity in the cerebellum positively predicted activity in the VL, DLPFC, SMC/PMA (=BA6), SI/MI, and cingulate cortex with dentures.

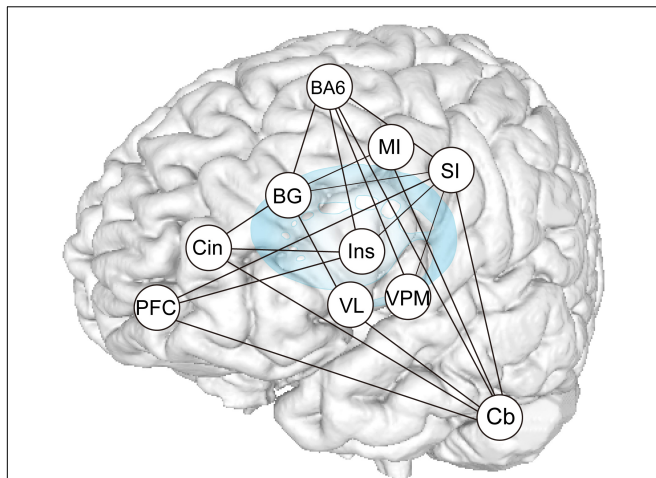


FIGURE 9 | Summary of PPI analysis. Increases or decreases in functional connectivity for dentures in vs dentures out between seed regions within the distributed teeth tapping networks of the brains of elderly adult and areas related to representation, as indicated in the conjunction analysis. The sensory information used to control voluntary actions is processed in pathways that are distinct from the afferent pathways (that contribute to perception). Much oral sensory information may serve to allow for the planning and/or execution of motor acts (teeth tapping). Feedback via the cerebellar loop can be used to correct errors that arise during movement (i.e., essential smooth execution of tapping movements) and feedback via the basal ganglia loop can be used to promote sequential and rhythmical tapping.

feedback from the prefrontal and association cortices to early sensory cortices. Our results support the idea that feedforward signals and sensory feedback via the cerebellar loop can be used to correct errors that arise during movement (Dean et al., 2010; Caligiore et al., 2017; Sokolov et al., 2017) and that the Cb can influence movements not only at the level of MI but also through interactions with premotor cortical areas and sensorimotor regions of the Bg (Bostan and Strick, 2018). It is important to note that the spatial location of a target can often be provided by visual input rather than somatosensation with hand movements, but within the mouth, somatosensation is the most important and vision plays a minimal role. Some oral sensory inputs are often generated by the contact between different surfaces in the mouth, such as the palate and tongue or upper and lower teeth. The somatosensory experience of the mouth itself comes from the perceived object sensed by the oral tissues (for a review, see Haggard and de Boer, 2014). Considering that the planning and execution of voluntary movements rely on sensorimotor transformations, the nervous system may have several different modes of control that use prediction and sensory feedback to different extents.

How Can Voluntary Action Be Executed?

A key feature of voluntary motor behaviors is that voluntary action depends on sequencing elementary movements to form a purposeful action, and the sequence of elementary movements is thought to involve parallel computations in multiple cortical areas and subcortical nuclei. To produce movements, signals from the cortex must reach motor neurons in the limbs and

trunk. In humans, 30–40% of the corticospinal tract axons originate from neurons in the MI, whereas the rest of the axons have origins mainly in the SMA and PMC and in the parietal areas lying posterior to the precentral sulcus (Chouinard and Paus, 2006; Verstynen et al., 2011). Based on the finding that patients with damage to the MI are unable to independently move their fingers and can only grasp a cup clumsily, the corticospinal system is considered to not only control all aspects of body and limb movement but also have a special role in the fractionated movements necessary for skilled motor acts (for a review, see Ebbesen and Brecht, 2017). The activity of the majority of pyramidal tract neurons in the motor cortex correlates positively with movement and force (Evarts, 1968; Georgopoulos et al., 1982), suggesting a role for the motor cortex in movement initiation (Georgopoulos et al., 1982). On the other hand, damage to certain premotor cortical areas results in neurological syndromes. Both non-human primate studies and observations in humans imply a major role of the SMA in movement inhibition, and lesions to this area evoke involuntary and strange movements (for a review, see Ebbesen and Brecht, 2017). In primates and rodents, most corticobulbar and corticospinal neurons have inhibitory connections with motor neurons (Bradbury and McMahon, 2006; Isa et al., 2013).

Interestingly, long-train ICMS from the face MI and the face SI of sub-primates and non-human primates can evoke semiautomatic movements such as mastication, swallowing, and facial whisking, whereas a single transcranial magnetic stimulation of the face MI can activate one or more orofacial muscles (for a review, see Avivi-Arber and Sessle, 2018). It is considered that these semiautomatic movements are mediated by a subcortical central pattern generator (Gao et al., 2001). Animal studies have shown an intrinsic rhythmical neural pattern such that signals from cortical masticatory areas trigger the central pattern generator and execute a coordinated rhythmical pattern of jaw movements (Masuda et al., 2002; Lund and Kolta, 2006; Morquette et al., 2012). During active behavior, it is possible that the motor cortex may initiate or suppress motor programs that were initiated reflexively from subcortical circuits, such as the Bg and brainstem (Ebbesen and Brecht, 2017).

Neural Plasticity in Oral Function

Reduced activity in elderly adults can reasonably be assumed to reflect a reduced level of functioning (Grady, 2012); however, fMRI studies have provided ample evidence for additional cortical activations in some brain areas of elderly adults (D'Esposito et al., 2003; Heuninckx et al., 2008; Grady, 2012; Samanez-Larkin and Knutson, 2015; Michely et al., 2018). During teeth tapping movements, we found an increased recruitment of brain regions in the elderly compared with young participants. An increased activity in elderly adults led to the suggestion that additional frontal activity can compensate for reduced activity elsewhere in the brain, which is beneficial to cognitive performance (for a review, see Cabeza et al., 2018). *Can age-related increases in brain activity during tapping movements be interpreted as compensation for declines in oral sensory inputs to the brain?* Alterations in oral structure and/or function (e.g., chewing and swallowing) have been shown to reshape the

brain regions related to oral sensorimotor functions through a process known as neuroplasticity (Sessle et al., 2007; Avivi-Arber et al., 2011; Lin et al., 2016, 2017; Avivi-Arber and Sessle, 2018). Anatomically, connections from early sensory cortices were shown to be relayed to intermediate-level representations in the parietal lobe and then to the lateral part of the premotor cortex, which in turn projects to the MI (Rizzolatti et al., 1998). Functionally, the parietal lobe was shown to extract sensory information about the external sensory body, which is useful for the planning and guidance of movements (for reviews, see Romo et al., 2012; Azim and Alstermark, 2015; Svoboda and Li, 2018). Thus, the parietal-premotor circuit may guide teeth tapping using current oral sensory inputs.

Other interpretations of over-recruited activity in elderly adults are also possible. For example, a lack of efficiency in the use of neural resources or reduction in the selectivity of responses (which is known as dedifferentiation) can sometimes be observed with poorer performance (over-recruitment; for reviews, see Grady, 2012; Cabeza et al., 2018). Interestingly, studies employing animal models have revealed that the motor effects of motor cortical lesions greatly change over time; the acute effects of motor cortex lesions in primates and human patients are muscle weakness and slow or reduced movement. In contrast, the chronic effects are spastic hypertonia and clonus (Ebbesen and Brecht, 2017). These deficits are due to a lack of controlled movements and compromised inhibition of movement and are not due to the inability to generate movement. Indeed, numerous animal studies and classic neuropsychological studies have pointed to a major role for the frontal and prefrontal cortex in the inhibitory control of movement (for a review, see Ebbesen and Brecht, 2017). Detecting individual variations in masticatory function and/or long-term experience of mastication in the brain signatures may have a clue to understand neural mechanisms of age-related recruitment of brain regions in the elderly.

Limitation

Although the present network analysis shows strong task-based connections between many brain regions, including MI, SI, Cb, Bg, VPM, SMC/PMA, and DLPPFC, one may point out the absence of a model. In a sense, our analysis is descriptive in nature, which is similar to the functional connectivity analysis. PPI looks very similar to comparing correlations with a seed region; however, the crucial difference is that the summary statistic reports effective connectivity, but not functional connectivity (Stephan et al., 2007; Friston, 2011). Functional connectivity analyses, e.g., principal or independent component analysis (ICA), usually entail finding the predominant pattern of correlations, or establishing that a particular correlation between two areas is significant. In contrast, effective connectivity corresponds to the intuitive notion of coupling or directed causal influence. Thus, the results of PPI may be treated in a way to identify regions whose effective connectivity with the reference region differs significantly. One can then interpret the areas that are activated by a certain task component as the element of a distributed system, though one does not still characterize how the local computations are bound together by context-dependent interactions among these areas. Another

effective connectivity analysis, direct causal model (DCM), could help model comparison or optimization, although the fluctuations in the fMRI measure are typically very slow (< 1 Hz), and connectivity does not necessarily reflect monosynaptic connections (Stephan et al., 2007; Michely et al., 2018).

Contemporary theories have emphasized on how interactions among distributed neuronal populations and brain areas enable flexible cognitive operations and complex behaviors (Sporns and Betzel, 2016). Thus, analytic advancements in network science and statistics can be beneficent to quantify and represent the structural and functional connectivity of the brain and to make a feasible model for deducing its organizational properties (Bullmore and Sporns, 2009; Bassett and Sporns, 2015; Petersen and Sporns, 2015; Avena-Koenigsberger et al., 2018; see also Arce-McShane et al., 2016), even though the underlying brain circuitry that initiates and executes jaw movements remains uncertain.

DATA AVAILABILITY STATEMENT

Because of the large size of the dataset, the raw data will be made available by the authors to any researcher who makes scientifically feasible requests. The sharing of the data will occur after appropriate institutional data use agreements have been completed.

ETHICS STATEMENT

The studies involving human participants were reviewed and approved by Medical Ethics Committee of Iwate Medical University. The patients/participants provided their written informed consent to participate in this study.

AUTHOR CONTRIBUTIONS

TK, HF, HK, and YS conceived and designed the study. TK and MK performed the fMRI recordings. HF, EI, KS, and YS analyzed the data. TK, HF, EI, KS, and YS generated the figure. TK, HF, and YS contributed to draft writing of the manuscript. All authors approved the manuscript for publication and agreed on all aspects of the work.

FUNDING

This work was supported by a Grant-in-Aid for Scientific Research (Nos. 50382635, 15K11172 to TK and 18K09706 to YS) from the Japan Society for the Promotion of Science; a Grant-in-Aid for Strategic Medical Science Research (S1491001, 2014–2018) from the Ministry of Education, Culture, Sports, Science and Technology of Japan (to TK and YS); a grant from the Keiryokai Research Foundation (Nos. 107 to TK and 122 to HF); and a grant from the Food Science Institute Foundation (to YS).

ACKNOWLEDGMENTS

We would like to thank Mrs. Y. Matsumura and T. Metoki, as well as Dr. S. Higuchi, for technical assistance; Drs. H. Toya, T.

Suzuki, A. Sakuraba, and M. Kimura (Iwate Medical University School of Dentistry) for analyzing the data; Drs. M. Sasaki, K. Tohyama, and K. Nakajima for reading the manuscript; and Enago (www.enago.jp) for the English language review.

REFERENCES

- Alexander, G. E., DeLong, M. R., and Strick, P. L. (1986). Parallel organization of functionally segregated circuits linking basal ganglia and cortex. *Ann. Rev. Neurosci.* 9, 357–381. doi: 10.1146/annurev.ne.09.030186.002041
- Arce-McShane, F. I., Ross, C. F., Takahashi, K., Sessle, B. J., and Hatsopoulos, N. G. (2016). Primary motor and sensory cortical areas communicate via spatiotemporally coordinated networks at multiple frequencies. *Proc. Natl. Acad. Sci. U.S.A.* 113, 5083–5088. doi: 10.1073/pnas.1600788113
- Avena-Koenigsberger, A., Misisic, B., and Sporns, O. (2018). Communication dynamics in complex brain networks. *Nat. Rev. Neurosci.* 19, 17–33.
- Avivi-Arber, L., Martin, R., Lee, J.-C., and Sessle, B. J. (2011). Facesensorimotor cortex and its neuroplasticity related to orofacial sensorimotor functions. *Arch. Oral Biol.* 56, 1440–1465. doi: 10.1016/j.archoralbio.2011.04.005
- Avivi-Arber, L., and Sessle, B. J. (2018). Jaw sensorimotor control in healthy adults and effects of ageing. *J. Oral Rehabil.* 45, 50–80. doi: 10.1111/joor.12554
- Azim, E., and Alstermark, B. (2015). Skilled forelimb movements and internal copy motor circuits. *Curr. Opin. Neurobiol.* 33, 16–24. doi: 10.1016/j.conb.2014.12.009
- Bandettini, P. A., Wong, E. C., Hinks, R. S., Tikofsky, R. S., and Hyde, J. S. (1992). Time course EPI of human brain function during task activation. *Magn. Reson. Med.* 25, 390–397. doi: 10.1002/mrm.1910250220
- Bassett, D. S., and Sporns, O. (2015). Network neuroscience. *Nat. Neurosci.* 18, 353–364.
- Bingel, U., Rose, M., Gläscher, J., and Büchel, C. (2007). fMRI reveals how pain modulates visual objects processing in the ventral visual stream. *Neuron* 55, 157–167. doi: 10.1016/j.neuron.2007.05.032
- Bostan, A. C., and Strick, P. L. (2018). The basal ganglia and the cerebellum: nodes in an integrated network. *Nat. Rev. Neurosci.* 19, 338–350. doi: 10.1038/s41583-018-0002-7
- Bradbury, E., and McMahon, S. B. (2006). Spinal cord repair strategies: why do they work? *Nat. Rev. Neurosci.* 7, 644–653. doi: 10.1038/nrn1964
- Bullmore, E., and Sporns, O. (2009). Complex brain networks: graph theoretical analysis of structure and functional systems. *Nat. Rev. Neurosci.* 10, 186–198. doi: 10.1038/nrn2575
- Byrd, K. E., Romito, L. M., Dziedzic, M., Wong, D., and Talavage, T. M. (2009). fMRI study of brain activity elicited by oral parafunctional movements. *J. Oral Rehabil.* 36, 346–361. doi: 10.1111/j.1365-2842.2009.01947.x
- Cabeza, R., Albert, M., Belleville, S., Craik, F. I. M., Duarte, A., Grady, C. L., et al. (2018). Maintenance, reserve and compensation: the cognitive neuroscience of healthy ageing. *Nat. Rev. Neurosci.* 19, 701–710. doi: 10.1038/s41583-018-0068-2
- Caligiore, D., Pezzullo, G., Baldassarre, G., Bostan, A. C., Strick, P. L., Doya, K., et al. (2017). Consensus paper: toward a system-level view of cerebellar function: the interplay between cerebellum, basal ganglia, and cortex. *Cerebellum* 16, 203–229. doi: 10.1007/s12311-016-0763-3
- Chouinard, P. A., and Paus, T. (2006). The primary motor and premotor areas of the human cerebral cortex. *Neuroscientist* 12, 143–152. doi: 10.1177/1073858405284255
- Dean, P., Porrill, J., Ekerot, C.-F., and Jörntell, H. (2010). The cerebellar microcircuit as an adaptive filter: experimental and computational evidence. *Nat. Rev. Neurosci.* 11, 30–43. doi: 10.1038/nrn2756
- D'Esposito, M., Deouell, L. Y., and Gazzaley, A. (2003). Alterations in the BOLD fMRI signal with aging and diseases: a challenge for neuroimaging. *Nat. Rev. Neurosci.* 4, 863–872. doi: 10.1038/nrn1246
- Dubner, R., Sessle, B. J., and Storey, A. T. (1978). *The Neural Basis of Oral and Facial Function*. New York, NY: Plenum Press.
- Ebbesen, C. L., and Brecht, M. (2017). Motor cortex – to act or not to act? *Nat. Rev. Neurosci.* 18, 694–705. doi: 10.1038/nrn.2017.119
- Evans, A. C., Kamber, M., Collins, D. L., and MacDonald, D. (1994). *An MRI-Based Probabilistic Atlas of Neuroanatomy*. New York, NY: Plenum Press, 263–274.
- Evarts, E. V. (1968). Relation of pyramidal tract activity to force exerted during voluntary movement. *J. Neuro Physiol.* 31, 14–27. doi: 10.1152/jn.1968.31.1.14
- Fang, M., Li, J., Lu, G., Gong, X., and Yew, D. T. (2005). A fMRI study of age-related differential cortical patterns during cued motor movement. *Brain Topogr.* 17, 127–137. doi: 10.1007/s10548-005-4446-5
- Fox, M. D., and Raichle, M. E. (2007). Spontaneous fluctuations in brain activity observed with functional magnetic resonance imaging. *Nat. Rev. Neurosci.* 8, 700–711. doi: 10.1038/nrn2201
- Friston, K. J. (2011). Functional and effective connectivity: a review. *Brain Connect.* 1, 13–36. doi: 10.1089/brain.2011.0008
- Friston, K. J., Ashburner, J., Frith, C. D., Poline, J.-B., Heather, J. D., and Frackowiak, R. S. J. (1995). Spatial registration and normalization of images. *Hum. Brain Mapp.* 3, 165–189. doi: 10.1002/hbm.460030303
- Friston, K. J., Büchel, C., Morris, J., Rolls, E., and Dolan, R. J. (1997). Psychophysiological and modulatory interactions in neuroimaging. *Neuroimage* 6, 218–219.
- Friston, K. J., Fletcher, P., Josephs, O., Holmes, A., Rugg, M. D., and Turner, R. (1998). Event-related fMRI: characterizing differential responses. *Neuroimage* 7, 30–40. doi: 10.1006/nimg.1997.0306
- Friston, K. J., Holmes, A. P., Price, C. J., Büchel, C., and Worsley, K. J. (1999). Multisubject fMRI studies and conjunction analyses. *Neuroimage* 10, 385–386.
- Friston, K. J., Holmes, A. P., Worsley, K. J., Poline, J.-P., Frith, C. D., and Frackowiak, R. S. J. (1994). Statistical parametric maps in functional imaging: a general linear approach. *Hum. Brain Mapp.* 2, 189–210. doi: 10.1002/hbm.460020402
- Gallivan, J. P., Chapman, C. S., Wolpert, D. M., and Flanagan, J. R. (2018). Decision-making in sensorimotor control. *Nat. Rev. Neurosci.* 19, 519–534. doi: 10.1038/s41583-018-0045-9
- Gao, P., Bermejo, R., and Zeigler, H. P. (2001). Whisker deafferentation and whisker patterns: behavioral evidence for a central pattern generator. *J. Neurosci.* 21, 5374–5380. doi: 10.1523/jneurosci.21-14-05374.2001
- Georgopoulos, A. P., Kalaska, J. F., Caminiti, R., and Massey, J. T. (1982). On the relations between the direction of two-dimensional arm movements and cell discharge in primate motor cortex. *J. Neurosci.* 2, 1527–1537. doi: 10.1523/jneurosci.02-11-01527.1982
- Godde, B., Berkefeld, T., David-Jurgens, M., and Dinse, H. R. (2002). Age-related changes in primary somatosensory cortex of rats: evidence for parallel degenerative and plastic-adaptive processes. *Neurosci. Biobehav. Rev.* 26, 743–752. doi: 10.1016/s0149-7634(02)00061-1
- Grady, C. (2012). The cognitive neuroscience of aging. *Nat. Rev. Neurosci.* 13, 491–505.
- Haggard, P., and de Boer, L. (2014). Oral somatosensory awareness. *Neurosci. Biobehav. Rev.* 47, 469–484. doi: 10.1016/j.neubiorev.2014.09.015
- Heuninckx, S., Wenderoth, N., and Swinnen, S. P. (2008). Systems neuroplasticity in the aging brain: recruiting additional neural responses for successful motor performance in elderly persons. *J. Neurosci.* 28, 91–99. doi: 10.1523/jneurosci.3300-07.2008
- Hoshi, E., and Tanji, J. (2007). Distinctions between dorsal and ventral premotor areas: anatomical connectivity and functional properties. *Curr. Opin. Neurobiol.* 17, 234–242. doi: 10.1016/j.conb.2007.02.003
- Huang, C. S., Hiraba, H., Murray, G. M., and Sessle, B. J. (1989). Topographical distribution and functional properties of cortically induced rhythmic jaw movements in the monkey (*Macaca fascicularis*). *J. Neurophysiol.* 61, 635–650. doi: 10.1152/jn.1989.61.3.635
- Humbert, I. A., Fitzgerald, M. E., McLaren, D. G., Johnson, S., Porcaro, E., Kosmatka, K., et al. (2009). Neurophysiology of swallowing: effects of age and bolus type. *Neuroimage* 44, 982–991. doi: 10.1016/j.neuroimage.2008.10.012
- Iida, T., Kato, M., Komiyama, O., Suzuki, H., Asano, T., Kuroki, T., et al. (2010). Comparison of cerebral activity during teeth clenching and first clenching: a

- functional magnetic resonance imaging study. *Eur. J. Oral Sci.* 118, 635–641. doi: 10.1111/j.1600-0722.2010.00784.x
- Iida, T., Sakayanagi, M., Svensson, P., Komiya, O., Hirayama, T., Kaneda, T., et al. (2012). Influence of periodontal afferent inputs for human cerebral blood oxygenation during jaw movements. *Exp. Brain Res.* 216, 375–384. doi: 10.1007/s00221-011-2941-3
- Isa, T., Kinoshita, M., and Nishimura, Y. (2013). Role of direct vs indirect pathways from the motor cortex to spinal motoneurons in the control of hand dexterity. *Front. Neurol.* 4:191. doi: 10.3389/fneur.2013.00191
- Ishikawa, T. (2002). Brain regions activated during the mandibular movement tasks in functional magnetic resonance imaging. *Kokubyo Gakkai Zasshi* 69, 39–48. doi: 10.5357/koubyou.69.39
- Kim, J., and Horwitz, B. (2008). Investigating the neural basis for fMRI-based functional connectivity in a block design: application to interregional correlations and psycho-physiological interactions. *Magn. Reson. Image* 26, 583–593. doi: 10.1016/j.mri.2007.10.011
- Lin, C.-S., Wu, C.-Y., Wu, S.-Y., Lin, H.-H., Cheng, D.-H., and Lo, W.-L. (2017). Age-related difference in functional brain connectivity of mastication. *Front. Aging Neurosci.* 9:82. doi: 10.3389/fnagi.2017.00082
- Lin, C.-S., Wu, S.-Y., Wu, C.-Y., and Ko, H.-W. (2016). Gray Matter volume and resting-state functional connectivity of the motor cortex-cerebellum network reflect the Individual variation in masticatory performance in healthy elderly people. *Front. Aging Neurosci.* 7:247. doi: 10.3389/fnagi.2015.00247
- Lund, J. P., and Kolta, A. (2006). Generation of the central masticatory pattern and its modification by sensory feedback. *Dysphagia* 21, 167–174. doi: 10.1007/s00455-006-9027-6
- Masuda, Y., Tachibana, Y., Inoue, T., Iwata, K., and Morimoto, T. (2002). Influence of oro-facial sensory input on the output of the cortical masticatory area in the anesthetized rabbit. *Exp. Brain Res.* 146, 501–510. doi: 10.1007/s00221-002-1221-7
- Michely, J., Volz, L. J., Hoffstaedter, F., Tittgemeyer, M., Eickhoff, S. B., Fink, G. R., et al. (2018). Network connectivity of motor control in the ageing brain. *Neuroimage Clin.* 18, 443–455. doi: 10.1016/j.nicl.2018.02.001
- Middleton, F. A., and Strick, P. L. (2002). Basal-ganglia ‘projections’ to the prefrontal cortex of the primate. *Cereb. Cortex* 12, 1047–1211.
- Momose, T., Nishikawa, J., Watanabe, T., Sasaki, Y., Senda, M., Kubota, K., et al. (1997). Effect of mastication on regional cerebral blood flow in humans examined by positron-emission tomography with 15O-labelled water and magnetic resonance imaging. *Arch. Oral Biol.* 42, 57–61. doi: 10.1016/s0003-9969(96)00081-7
- Morquette, P., Lavoie, R., Fhima, M.-D., Lamoureux, X., Verdier, D., and Kolta, A. (2012). Generation of the masticatory central pattern and its modulation by sensory feedback. *Progr. Neurobiol.* 96, 340–355. doi: 10.1016/j.pneurobio.2012.01.011
- Nachev, P., Kennard, C., and Husain, M. (2008). Functional role of the supplementary and pre-supplementary motor areas. *Nat. Rev. Neurosci.* 9, 856–869. doi: 10.1038/nrn2478
- Onozuka, M., Fujita, M., Watanabe, K., Hirano, Y., Niwa, M., Nishiyama, K., et al. (2002). Mapping brain region activity during chewing: a functional magnetic resonance imaging study. *J. Dent Res.* 81, 743–746. doi: 10.1177/154405910208101104
- Onozuka, M., Fujita, M., Watanabe, K., Hirano, Y., Niwa, M., Nishiyama, K., et al. (2003). Age-related changes in brain regional activity during chewing: a functional magnetic resonance imaging studies. *J. Dent Res.* 82, 657–660. doi: 10.1177/154405910308200817
- Petersen, S. E., and Sporns, O. (2015). Brain networks and cognitive architectures. *Neuron* 88, 207–218.
- Picard, N., and Strick, P. L. (1996). Motor areas of the medial wall: a review of their location and functional activation. *Cereb. Cortex* 6, 342–353. doi: 10.1093/cercor/6.3.342
- Quintero, A., Ichescio, E., Schutt, R., Myers, C., Peltier, S., and Gerstner, G. E. (2013). Functional connectivity of human chewing: an fMRI study. *J. Dent Res.* 92, 272–278. doi: 10.1177/0022034512472681
- Rizzolatti, G., Luppino, G., and Matelli, M. (1998). The organization of the cortical motor system: new concepts. *Electroencephalogr. Clin. Neurophysiol.* 106, 283–296. doi: 10.1016/s0013-4694(98)00022-4
- Romo, R., Lemus, L., and de Lafuente, V. (2012). Sense, memory, and decision-making in the somatosensory cortical network. *Curr. Opin. Neurobiol.* 22, 914–919. doi: 10.1016/j.conb.2012.08.002
- Samanez-Larkin, G. R., and Knutson, B. (2015). Decision making in the ageing brain: changes in affective and motivational circuits. *Nat. Rev. Neurosci.* 16, 278–289. doi: 10.1038/nrn3917
- Schwartz, A. B. (2016). Movement: how the brain communicates with the world. *Cell* 164, 1122–1136.
- Scott, S. H. (2004). Optimal feedback control and the neural basis of volitional motor control. *Nat. Rev. Neurosci.* 5, 534–546.
- Scott, S. H., Cluff, T., Lowrey, C. R., and Takei, T. (2015). Feedback control during voluntary motor actions. *Curr. Opin. Neurobiol.* 33, 85–94. doi: 10.1016/j.conb.2015.03.006
- Sessle, B. J., Adachi, K., Avivi-Arber, L., Lee, J., Nishiura, H., Yao, D., et al. (2007). Neuroplasticity of face primary motor cortex control of orofacial movements. *Arch. Oral Biol.* 52, 334–337. doi: 10.1016/j.archoralbio.2006.11.002
- Sokolov, A., Miall, R. C., and Ivry, R. B. (2017). The cerebellum: adaptive prediction for movement and cognition. *Trends Cognit. Sci.* 21, 313–332. doi: 10.1016/j.tics.2017.02.005
- Sporns, O., and Betzel, R. F. (2016). Modular brain networks. *Ann. Rev. Psychol.* 67, 613–640. doi: 10.1146/annurev-psych-122414-033634
- Stephan, K. E., Harrison, L. M., Kiebel, S. J., David, O., Penny, W. D., and Friston, K. J. (2007). Dynamic causal models of neural system dynamics: current state and future extensions. *J. Biosci.* 32, 129–144. doi: 10.1007/s12038-007-0012-5
- Svoboda, K., and Li, N. (2018). Neural mechanisms of movement planning: motor cortex and beyond. *Curr. Opin. Neurobiol.* 49, 33–41. doi: 10.1016/j.conb.2017.10.023
- Tamura, T., Kanayama, T., Yoshida, S., and Kawasaki, T. (2002). Analysis of brain activity during clenching by fMRI. *J. Oral Rehabil.* 30, 614–622.
- Tamura, T., Kanayama, T., Yoshida, S., and Kawasaki, T. (2003). Functional magnetic resonance imaging of human jaw movements. *J. Oral Rehabil.* 30, 614–622. doi: 10.1046/j.1365-2842.2003.01054.x
- Verstynen, T., Jarco, K., Pathak, S., and Schneider, W. (2011). In vivo mapping of microstructural somatotopies in the human corticospinal pathways. *J. Neurophysiol.* 105, 336–346. doi: 10.1152/jn.00698.2010

Conflict of Interest: The authors declare that the research was conducted in the absence of any commercial or financial relationships that could be construed as a potential conflict of interest.

Copyright © 2020 Kobayashi, Fukami, Ishikawa, Shibata, Kubota, Kondo and Sahara. This is an open-access article distributed under the terms of the Creative Commons Attribution License (CC BY). The use, distribution or reproduction in other forums is permitted, provided the original author(s) and the copyright owner(s) are credited and that the original publication in this journal is cited, in accordance with accepted academic practice. No use, distribution or reproduction is permitted which does not comply with these terms.



Model-Based and Model-Free Analyses of the Neural Correlates of Tongue Movements

Peter Sörös^{1,2*}, Sarah Schäfer¹ and Karsten Witt^{1,2}

¹ Neurology, School of Medicine and Health Sciences, University of Oldenburg, Oldenburg, Germany, ² Research Center Neurosensory Science, University of Oldenburg, Oldenburg, Germany

OPEN ACCESS

Edited by:

Kazutaka Takahashi,
University of Chicago, United States

Reviewed by:

Georgia Malandraki,
Purdue University, United States
Chia-shu Lin,
National Yang-Ming University, Taiwan
Yingying Wang,
University of Nebraska-Lincoln,
United States

*Correspondence:

Peter Sörös
peter.soros@gmail.com

Specialty section:

This article was submitted to
Brain Imaging Methods,
a section of the journal
Frontiers in Neuroscience

Received: 20 October 2019

Accepted: 02 March 2020

Published: 24 March 2020

Citation:

Sörös P, Schäfer S and Witt K (2020)
Model-Based and Model-Free
Analyses of the Neural Correlates of
Tongue Movements.
Front. Neurosci. 14:226.
doi: 10.3389/fnins.2020.00226

The tongue performs movements in all directions to subserve its diverse functions in chewing, swallowing, and speech production. Using task-based functional MRI in a group of 17 healthy young participants, we studied (1) potential differences in the cerebral control of frontal (protrusion), horizontal (side to side), and vertical (elevation) tongue movements and (2) inter-individual differences in tongue motor control. To investigate differences between different tongue movements, we performed voxel-wise multiple linear regressions. To investigate inter-individual differences, we applied a novel approach, spatio-temporal filtering of independent components. For this approach, individual functional data were decomposed into spatially independent components and corresponding time courses using independent component analysis. A temporal filter (correlation with the expected brain response) was used to identify independent components time-locked to the tongue motor tasks. A spatial filter (cross-correlation with established neurofunctional systems) was used to identify brain activity not time-locked to the tasks. Our results confirm the importance of an extended bilateral cortical and subcortical network for the control of tongue movements. Frontal (protrusion) tongue movements, highly overlearned movements related to speech production, showed less activity in the frontal and parietal lobes compared to horizontal (side to side) and vertical (elevation) movements and greater activity in the left frontal and temporal lobes compared to vertical movements (cluster-forming threshold of $Z > 3.1$, cluster significance threshold of $p < 0.01$, corrected for multiple comparisons). The investigation of inter-individual differences revealed a component representing the tongue primary sensorimotor cortex time-locked to the task in all participants. Using the spatial filter, we found the default mode network in 16 of 17 participants, the left fronto-parietal network in 16, the right fronto-parietal network in 8, and the executive control network in four participants (Pearson's $r > 0.4$ between neurofunctional systems and individual components). These results demonstrate that spatio-temporal filtering of independent components allows to identify individual brain activity related to a specific task and also structured spatiotemporal processes representing known neurofunctional systems on an individual basis. This novel approach may be useful for the assessment of individual patients and results may be related to individual clinical, behavioral, and genetic information.

Keywords: tongue, motor control, cortex, cerebellum, speech production, swallowing, functional magnetic resonance imaging, independent component analysis

INTRODUCTION

The human tongue is a unique muscular and sensory organ with critical roles in several motor tasks, such as chewing, swallowing, respiration, and speech (Sawczuk and Mosier, 2001; Hiimeae and Palmer, 2003), in addition to its somatosensory (Pardo et al., 1997; Sakamoto et al., 2010) and gustatory functions (Kobayakawa et al., 2005; Hummel et al., 2010).

To subserve its distinct motor tasks, the tongue contains intrinsic and extrinsic muscle fibers (Schumacher, 1927; Abd-El-Malek, 1939), which are extensively interwoven (Gaige et al., 2007). Intrinsic fibers originate and insert within the tongue itself, while extrinsic fibers are attached to bony structures, such as the mandible, hyoid bone, or styloid process (Sanders and Mu, 2013). This complex biomechanical architecture is the basis for the tongue's ability to move and alter its shape in all three dimensions (Kier and Smith, 1985). Moreover, adult human tongues, compared to the tongues of other mammals, are characterized by a higher proportion of slow-twitch (type I) muscle fibers, which are associated with fine motor control (Sanders et al., 2013). Intrinsic and extrinsic tongue muscles are innervated by the lateral and medial divisions of the hypoglossal nerve (cranial nerve XII), with different components of the musculature being supplied by different hypoglossal branches (Mu and Sanders, 2010) and controlled by distinct hypoglossal subnuclei (McClung and Goldberg, 2002).

The cortical and subcortical control of tongue movements has been studied thoroughly in animals and humans using various invasive and non-invasive techniques. These electrophysiologic, neuroimaging, and lesion studies suggest that voluntary (e.g., speech-related) and semi-automatic (e.g., swallowing-related) tongue movements (Martin et al., 1997) are controlled by the lateral primary sensorimotor cortex (Takai et al., 2010), supplementary motor area, basal ganglia, and cerebellum (Corfield et al., 1999; Shinagawa et al., 2003; Martin et al., 2004; Watanabe et al., 2004).

Using functional magnetic resonance imaging (fMRI), researchers investigated (1) isolated voluntary tongue movements, such as frontal (protrusion) (Arima et al., 2011), horizontal (side to side) (Riecker et al., 2000), and vertical (elevation) tongue movements (Martin et al., 2004) and (2) tongue movements as part of speaking (Riecker et al., 2005; Sörös et al., 2006), singing (Ozdemir et al., 2006; Jungblut et al., 2012), and swallowing (Sörös et al., 2009; Lowell et al., 2012). A detailed comparison of the neural correlates of different tongue movements in all three directions has not been performed yet [but see the study by Watanabe et al. (2004), comparing tongue protrusions in different directions with tongue retraction]. Moreover, almost all fMRI studies on tongue movements present only group analyses [one notable exception is the study by Martin et al. (2004), Table 5, presenting individual brain activation in all studied participants]. Finally, almost all fMRI studies on tongue motor control have been performed on older scanner hardware and with relatively small sample sizes. Our literature review was based on a systematic search

of the PubMed¹ and Google Scholar² databases with the search terms “tongue fMRI” or “tongue functional magnetic resonance imaging.” The detailed presentation of this systematic review is beyond the scope of the present study.

The first aim of the present study was to identify and compare brain activity associated with different tongue movements. Following previous research, we simplified the wide range of different tongue movements and shapes and only studied movements along the three main axes of the body: frontal (protrusion) tongue movements, horizontal (side to side) tongue movements, and vertical (elevation) tongue movements. These tongue movements are used in different tongue motor tasks, primarily during chewing, swallowing, and speaking (Sawczuk and Mosier, 2001; Hiimeae and Palmer, 2003; Ferrand, 2018). Frontal (protrusion) tongue movements are almost exclusively used in speech production and singing, e.g., during the production of dental consonants (Ladefoged and Maddieson, 1996). Horizontal (side to side) tongue movements are used during chewing to position the food in the oral cavity and to form the bolus in preparation for swallowing (Hiimeae and Palmer, 2003). Vertical (elevation) tongue movements, finally, are used in both speech production [e.g., during the production of high vowels (Ladefoged and Maddieson, 1996)] and the oral phase of swallowing (Hiimeae and Palmer, 2003).

The second aim of this study was to investigate inter-individual similarities and differences in tongue movement-related brain activity. The number of swallows (Rudney et al., 1995) and of words produced per day (Mehl et al., 2007) varies considerably between individuals. Moreover, the biomechanics of articulation (Weirich et al., 2013) and of swallowing (Kennedy et al., 2010) is characterized by substantial inter-individual variability. To investigate individual brain activity, we performed an independent component analysis (ICA) of individual task-based fMRI data sets. ICA decomposes four-dimensional data into spatial maps and associated time courses (Beckmann et al., 2006). Compared to a model-based analysis, an advantage of ICA is the ability to detect unknown, not necessarily time-locked brain activity in fMRI data. This is of particular importance for experimental designs, in which the exact timing of events cannot be recorded (McKeown et al., 1998a; Calhoun et al., 2002). Moreover, ICA is able to separate brain activity from noise, such as artifacts induced by head motion or physiological processes (McKeown et al., 1998b). With a novel approach, spatio-temporal filtering of independent components, we identified individual components whose time courses were highly correlated with the expected brain response and whose spatial patterns were highly correlated with one of the established neurofunctional networks described by Smith et al. (2009).

Investigating differences in tongue motor control between different movements and across individuals is expected to deepen our knowledge not only of physiological but also of pathological tongue movements. The ultimate goal of this line of research is to understand the disruption of the supranuclear control of speech-

¹www.ncbi.nlm.nih.gov/pubmed

²scholar.google.com

and swallowing-related tongue movements in diseases, such as amyotrophic lateral sclerosis (ALS, Kollewé et al., 2011; Shellikeri et al., 2016) and Parkinson's disease (Van Lieshout et al., 2011) on an individual, personalized basis.

METHODS

Participants

Twenty young healthy individuals have been investigated for the present study. Three participants were excluded from the data analysis (two because of excessive head motion, one because of widespread, most likely artifactual signal increase in the first-level analysis of the horizontal tongue movement condition). For the final data analysis, the MRI data of 17 participants (nine women, eight men) have been investigated. Mean age \pm standard deviation (SD) of included participants was 25.9 ± 3.3 years (minimum: 20, maximum: 34 years). All participants met the following criteria: (1) no history of neurological disorders (such as dementia, movement disorder, stroke, epilepsy, multiple sclerosis, traumatic brain injury, migraine), psychiatric disorders (such as schizophrenia or major depression), or cancer, (2) no impaired kidney or liver function, (3) no use of psychotropic medication (in particular, antidepressants, antipsychotics, benzodiazepines, and opioids), (4) no substance abuse, (5) no excessive head motion (<1 mm relative mean displacement and <3 mm absolute mean displacement) during fMRI. Handedness was determined with the Edinburgh Handedness Inventory–Short Form (Veale, 2014). Right handedness was present in 13 individuals (handedness scores: 62.5–100), mixed handedness was found in four individuals (handedness scores: 33.3–50). Seven participants have had an MRI scan before for diagnostic or research purposes, 10 participants have never been within an MRI scanner. All data sets presented here have been acquired for this study and have not been analyzed or published previously. All participants were students of the University of Oldenburg and were recruited through an advertisement on the University's student portal or word-of-mouth communication, thus representing a convenience sample. All participants gave written informed consent for participation in the study. A compensation of 10 € per hour was provided. The study was approved by the Medical Research Ethics Board, University of Oldenburg, Germany (2017-072).

Experimental Paradigm and Tongue Movements

The data for the present study were collected as part of a larger project on oral and speech-language functions. **Table 1** summarizes the order in which the four different tasks were performed. The total MRI measurement time was ~ 45 min.

For the investigation of the neural correlates of tongue movements, participants were visually cued to perform one of three different repetitive tongue movements (**Figure 1**): (1) frontal (protrusion) tongue movements; participants were instructed to push the tip of the tongue against the surface of the maxillary incisors and then retract the tongue to the rest position, similar to the English /th/ sound, (2) horizontal (side

TABLE 1 | Structural and functional sequences used for the entire project (scan 4: tongue movements).

| No. | Sequence | Time of acquisition |
|-----|------------------------------------|---------------------|
| 1 | T1-weighted MPRAGE | 6:16 min |
| 2 | T2*-weighted (syllable production) | 9:16 min |
| 3 | T2*-weighted (tongue twister) | 8:31 min |
| 4 | T2*-weighted (tongue movements) | 9:21 min |
| 5 | T2*-weighted (sentence production) | 9:14 min |

to side) tongue movements; participants were instructed to move the tongue against the right and left mandibular pre-molars, and (3) vertical (elevation) tongue movements; participants were instructed to elevate the tongue and to press it against the hard palate (the roof of the mouth), similar to the beginning of the oral phase of swallowing (Dodds, 1989).

Before the fMRI measurement, all participants underwent a short training outside the scanner to familiarize themselves with the different tongue movements and the visual cues. During the training, the participants were first shown a sheet of paper with the three visual cues (**Figure 1**) and were instructed how to perform the respective movement. The experimenter then demonstrated the required movements herself with open mouth and asked the participants to perform all movements with closed mouth, without performing head or jaw movements. The experimenter watched all participants closely and made sure that no visible head or jaw movements were produced. For all conditions, participants performed rhythmic and self-paced movements. Participants were asked to choose a relaxed and pleasant movement frequency. Our aim was to keep the movement effort comparable across participants. Finally, a short version of the fMRI paradigm (two blocks of 15 s duration for each tongue movement in pseudorandomized order) was presented on the screen of a PC to give the participants further opportunity to train the required tongue movements.

Visual cues were presented by the MATLAB toolbox Cogent Graphics (developed by John Romaya, Laboratory of Neurobiology, Wellcome Department of Imaging Neuroscience, London, UK)³ on a PC and projected through an LCD projector onto a screen mounted within the scanner bore behind the head coil. Participants were able to see the cues via a mirror attached to the head coil. Visual cues were shown in blocks of 15 s duration with a 15 s rest condition (during which a fixation cross was presented) after every third tongue movement block. The remaining tongue movement blocks were separated by a shorter rest condition of 3 s. **Figure 2** visualizes the experimental paradigm. Behavioral performance during fMRI was not recorded.

MRI Data Acquisition

MR images of the entire brain were acquired at 3 Tesla on a Siemens MAGNETOM Prisma whole-body scanner (Siemens, Erlangen, Germany) with the XR gradient system (gradient

³www.vislab.ucl.ac.uk/cogent_graphics.php

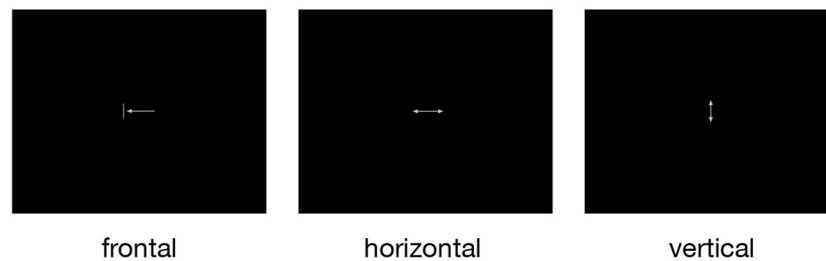


FIGURE 1 | The three pictograms used to cue frontal (protrusion), horizontal (side to side), and vertical (elevation) tongue movements. All symbols were simple and small to minimize eye movements and visual processing. During rest periods, a small fixation cross was shown.

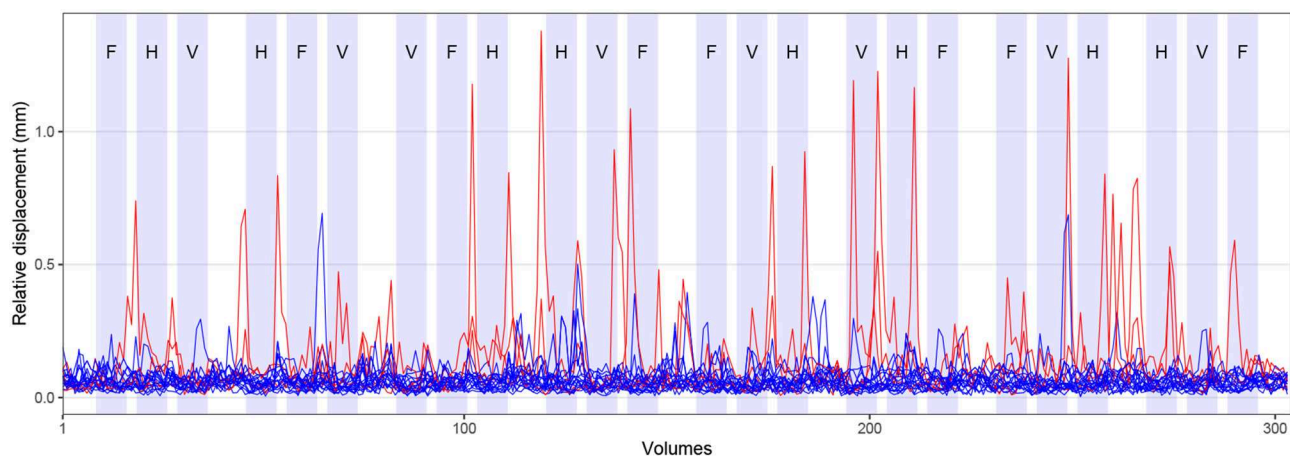


FIGURE 2 | Experimental paradigm and head motion. Blocks of tongue movement are shown in light blue; F: frontal (protrusion), H: horizontal (side to side), and V: vertical (elevation) movements; duration 15 s each. Mean relative displacement, the distance between one volume and the following volume, during all fMRI measurements is displayed with blue (17 included participants) and red lines (three excluded participants). Data from individual participants are superimposed.

strength: 80 mT/m, gradient rise time: 200 T/m/s on all three gradient axes simultaneously) and a 64-channel head/neck receive-array coil. This coil enhances the signal-to-noise ratio of the peripheral image, primarily corresponding to the cortex of the human brain. The scanner is located at the Neuroimaging Unit, School of Medicine and Health Sciences, University of Oldenburg, Germany⁴.

For structural brain imaging, Siemens' 3-dimensional T1-weighted magnetization prepared rapid gradient echo (MPRAGE) sequence (Brant-Zawadzki et al., 1992) was used (TR: 2,000 ms, TE: 2.07 ms, flip angle 9°, isotropic voxel size: $0.75 \times 0.75 \times 0.75 \text{ mm}^3$, 224 axial slices, time of acquisition: 6:16 min). For functional imaging, Siemens' ep2d_bold T2*-weighted gradient-echo echo-planar sequence was used (TR: 1,800 ms, TE: 30 ms, flip angle 75°, isotropic voxel size: $3 \times 3 \times 3 \text{ mm}^3$, 33 slices, time of acquisition: 9:21 min). Structural and functional measurements used in-plane acceleration (generalized autocalibrating partial parallel acquisition, GRAPPA) with an acceleration factor of 2 (Griswold et al., 2002). Before every functional sequence, extended 3-dimensional B0 shimming

and true-form B1 shimming was applied. Siemens' pre-scan normalization filter was deactivated during functional sequences.

MRI Data Analysis

Pre-processing of Structural Images

Pre-processing of T1-weighted images was done with the *antsBrainExtraction.sh* script, part of Advanced Normalization Tools (ANTs, version 2.1)⁵ (Tustison et al., 2014). This script performs (1) bias field correction to minimize the effects of magnetic field inhomogeneity using the N4 algorithm (Tustison et al., 2010) and (2) brain extraction using a hybrid segmentation/template-based strategy (Tustison et al., 2014). The script was used together with brain templates derived from the OASIS-1 study⁶. For quality control, all brain extracted structural MR images were visually inspected after using ANTs.

Pre-processing of Functional Images

Pre-processing of fMRI data was carried out using FEAT (version 6.00), part of FMRIB's Software Library (FSL)⁷ (Smith

⁴uol.de/en/medicine/biomedicum/neuroimaging-unit

⁵stnava.github.io/ANTs/

⁶www.oasis-brains.org

⁷fsl.fmrib.ox.ac.uk/fsl/fslwiki/

et al., 2004; Woolrich et al., 2009; Jenkinson et al., 2012). Pre-processing included removal of the first four recorded volumes to allow for signal equilibration in addition to the two dummy volumes measured, but not recorded, as part of the *ep2d_bold* sequence (304 volumes were retained). Standard head motion correction was performed by volume-realignment to the middle volume using MCFLIRT (Jenkinson et al., 2002). Mean relative displacement (the distance between one volume and the following volume) of all participants is shown in **Figure 2**. Brain extraction of functional images was done with FSL's brain extraction tool, BET (Smith, 2002). Spatial smoothing with a Gaussian kernel of 5 mm full width at half maximum (FWHM) and grand-mean intensity normalization of the entire data set by a single multiplicative factor were also performed. Slice time correction was not conducted (as e.g., in Beckmann et al., 2006).

After completion of standard data pre-processing, but without temporal filtering, ICA-based automatic removal of motion artifacts (FSL's ICA-AROMA version 0.3 beta)⁸ was used to identify and remove motion-related ICA components from FMRI data (Pruim et al., 2015). Here, the non-aggressive option was used, performing a partial component regression. First, ICA-AROMA carries out probabilistic ICA of individual subjects' MRI data using FSL's MELODIC (Beckmann and Smith, 2004). Second, ICA-AROMA employs four theoretically motivated temporal and spatial criteria to select motion-related components from MELODIC's output. These criteria include (1) high-frequency content of the time courses of independent components, (2) correlation between the time courses of independent components and motion correction parameters, (3) representation of independent components at the edge of the brain, and (4) representation of independent components within cerebrospinal fluid (for a detailed description, see Pruim et al., 2015). Finally, ICA-AROMA removes these components from the initial data set through an ordinary least squares regression using FSL's *fsl_regfilt* command (Pruim et al., 2015). Decomposition of individual data sets created between 47 and 68 independent components (mean: 60 components). To determine the optimal number of components for every data set, MELODIC uses Bayesian principal component analysis (Beckmann and Smith, 2004). Of these components, between 18 and 39 (mean: 30) components were identified as noise and regressed out applying the aforementioned four temporal and spatial features. ICA-AROMA has been validated for resting state and task-based FMRI data, demonstrating that this approach effectively removes motion artifacts, while increasing sensitivity to the signal of interest (Pruim et al., 2015).

Following ICA-AROMA, data were high-pass filtered (Gaussian-weighted least-squares straight-line fitting, $\sigma = 45$ s). Registration of functional to high-resolution structural images was carried out using FLIRT (Jenkinson et al., 2002). Registration from high-resolution structural to Montreal Neurological Institute (MNI152) standard space was further refined using 12-parameter affine transformation and non-linear registration with a warp resolution of 10 mm in FNIRT⁹.

Model-Based Individual and Group FMRI Analysis

For first-level model-based analysis, functional data sets were analyzed with a general linear model-based time-series analysis using voxel-wise multiple linear regressions (Friston et al., 1995; Monti, 2011) as implemented in FEAT. The time courses of the three movement conditions were convolved with a gamma hemodynamic response function (using the standard settings: phase: 0 s, standard deviation: 3 s, mean lag: 6 s) and served as regressors of interest. The temporal derivative of each primary regressor was included as a regressor of no interest to improve the model fit when the timing was not exactly correct (e.g., if tongue movements were started or stopped with a slight delay). Regressors of interest (experimental conditions) and regressors of no interest (temporal derivatives) formed the design matrix used for voxel-wise multiple linear regressions. Motion parameters derived from initial head motion correction via volume-realignment were not included in the design matrix because ICA-AROMA was used for additional head motion correction.

To remove temporal autocorrelations, time-series pre-whitening was used (Woolrich et al., 2001). After generating parameter estimates (PEs) for every primary regressor and every participant, the following contrasts of parameter estimates (COPEs) were calculated: (1) frontal > rest, (2) horizontal > rest, (3) vertical > rest, (4) horizontal > frontal, (5) vertical > frontal, (6) frontal > vertical, (7) horizontal > vertical, (8) frontal > horizontal, and (9) vertical > horizontal.

For higher-level analysis, mixed-effects group analysis maps were generated by FLAME (stages 1 and 2) for all contrasts. FLAME uses a fully Bayesian inference technique in a two-stage process: a fast approach using maximum *a posteriori* estimates and a slower, more accurate approach using Markov Chain Monte Carlo methods (Woolrich et al., 2004). *Z* statistic images were thresholded non-parametrically using a cluster-forming threshold of $Z > 3.1$ and a (corrected) cluster significance threshold of $p < 0.01$ assuming a Gaussian random field for the *Z*-statistics. No additional correction for multiple contrasts was performed. Local maxima (peaks of brain activation) were identified within the *Z* statistic images using FSL's *cluster* command (maximum number of local maxima: 100, minimum distance between local maxima: 20 mm). The anatomical location of each local maximum was determined with FSL's *atlasquery* command and the following probabilistic atlases:¹⁰ (1) Harvard-Oxford cortical structural atlas (48 cortical areas), (2) Harvard-Oxford subcortical structural atlas (21 subcortical areas), and (3) Probabilistic cerebellar atlas (28 regions) (Diedrichsen et al., 2009). Because we report local maxima of brain activation, the extent of activation cannot be determined.

Model-Free Individual FMRI Analysis

A single-session probabilistic ICA was conducted to decompose every pre-processed individual FMRI data set into 20 independent spatial components and corresponding time courses using MELODIC (version 3.14). The data sets fed

⁸github.com/maartenmennes/ICA-AROMA

⁹fsl.fmrib.ox.ac.uk/fsl/fslwiki/FNIRT

¹⁰fsl.fmrib.ox.ac.uk/fsl/fslwiki/Atlases

into ICA were the pre-processed data sets used for first-level model-based analysis (i.e., after denoising with ICA-AROMA). Of note, these data sets contained brain activity associated with all three tongue movements. A low-dimensional decomposition into 20 components was chosen for later comparison with a well-established set of published networks. MELODIC performs linear decomposition (Comon, 1994) of the original fMRI signal using the FastICA technique (Hyvärinen, 1999) and variance-normalization of the associated timecourses. Spatial maps were thresholded using a Gaussian mixture model approach at a posterior probability level of $p < 0.5$ (Beckmann and Smith, 2004).

Spatio-Temporal Filtering of Independent Components

To identify spatial components whose activity was time-locked to tongue movements, FSL's GLM Setup program was used to convolve the time course of all three movement conditions with a gamma hemodynamic response function (as for model-based analysis). The resulting time course, representing the expected brain activity, was correlated with all ICA time courses of all participants. Similarly, Kokkonen et al. (2009) analyzed task-based fMRI activity associated with left and right finger tapping with ICA and correlated ICA time courses with motor task timing. In our study, a significant ($p < 0.05$) Pearson's correlation coefficient of $r > 0.4$ or $r < -0.4$ between time courses indicated temporal significance.

To identify relevant spatial components not time-locked to the tongue motor tasks, the spatial maps obtained for every participant were cross-correlated with ten established neural networks¹¹ (Smith et al., 2009). These ten networks have been derived from resting state fMRI data of healthy adults after performing a low-dimensional decomposition with 20 components (ten components were identified as brain activity, ten components as potentially artifactual). Importantly, Smith et al. (2009) also analyzed the results of 1687 task-based fMRI studies available through the BrainMap database¹². Both analyses resulted in a similar set of major brain networks, demonstrating a close correspondence between resting and task-based brain activation. A significant Pearson's correlation coefficient of $r > 0.4$ between components indicated spatial significance. The cross-correlation of study-specific spatial components with established networks (e.g., developed by Smith et al., 2009 or Yeo et al., 2011) has been performed previously for the analysis of resting-state fMRI data (e.g., by Reineberg et al., 2015 and Sörös et al., 2019).

RESULTS

Head Motion

Across all included participants, the average mean absolute displacement of the head (relative to the middle volume) was 0.7 mm (SD: 0.4 mm, min: 0.2 mm, max: 1.9 mm). The average mean relative displacement (compared to the following volume) was 0.3 mm (SD: 0.2 mm, min: 0.1 mm, max: 0.7 mm). The

time course of the mean relative displacement of all participants is shown in **Figure 2** (17 included participants in blue, three excluded participants in red). Comparing the time course of head displacement with the experimental paradigm, we did not find evidence for task-related head motion.

Model-Based Group fMRI Analysis

Compared to rest, the three tongue movements were associated with similar bilateral brain activity (**Figure 3A**). Major regions of cortical activation were the lateral pre- and post-central gyrus, supplementary motor cortex, anterior cingulate gyrus, and the frontal cortex of both hemispheres. Activation was also found in the bilateral insulae, basal ganglia, thalamus, amygdala, and cerebellum. For visualization of subcortical brain activity, **Figure 4** shows axial slices for frontal (protrusion) tongue movements > rest. **Table 2** lists the coordinates in MNI space and the corresponding Z value of significant local maxima of brain activation for the contrast frontal > rest.

Contrasts between different tongue movements resulted in significant activation in several cortical areas (**Figure 3B**, **Table 3**). Horizontal tongue movements were associated with greater activation in the bilateral superior parietal lobule (vs. frontal movements) and in the bilateral pre- and post-central gyri as well as in the left inferior frontal gyrus (vs. vertical movements). The contrast vertical > frontal movements demonstrated greater activation in the bilateral precentral and the right post-central gyri, as well as the left supramarginal gyrus and the left superior parietal lobule. The reverse contrast, frontal > vertical movements, showed greater activation in the left frontal and temporal lobes. The contrasts frontal > horizontal and vertical > horizontal did not result in significant activation.

Model-Free Individual fMRI Analysis

The individual brain activity of all 17 participants is presented in **Figure 5**. Temporally filtered (time-locked) independent components are shown on the left (**Figure 5A**), spatially filtered components on the right (**Figure 5B**). In all participants, the fMRI data set contained one bilateral sensorimotor component (**Figure 5A**, first column) positively correlated with the expected brain activity (graph in the first row), representing the tongue primary sensorimotor cortex. In four participants, another frontal or parietal component (**Figure 5A**, second column) was positively correlated with the expected brain activity. In seven participants, a bilateral occipital component (**Figure 5A**, third column) was negatively correlated with the expected brain activity.

Spatial filtering of independent components revealed inter-individually variable patterns of brain activity during tongue movements. Spatial cross-correlations with established neural networks (shown in the first row of **Figure 5B**) (Smith et al., 2009) identified between one and three visual networks in all participants (except P2, who showed a visual component after temporal filtering). In addition, the default mode network and the left fronto-parietal network were active in all but one participant. Of note, the default mode network was not negatively correlated with the expected brain activity associated with tongue movements. The right fronto-parietal network was

¹¹www.fmrib.ox.ac.uk/datasets/brainmap+rsns/

¹²www.brainmap.org

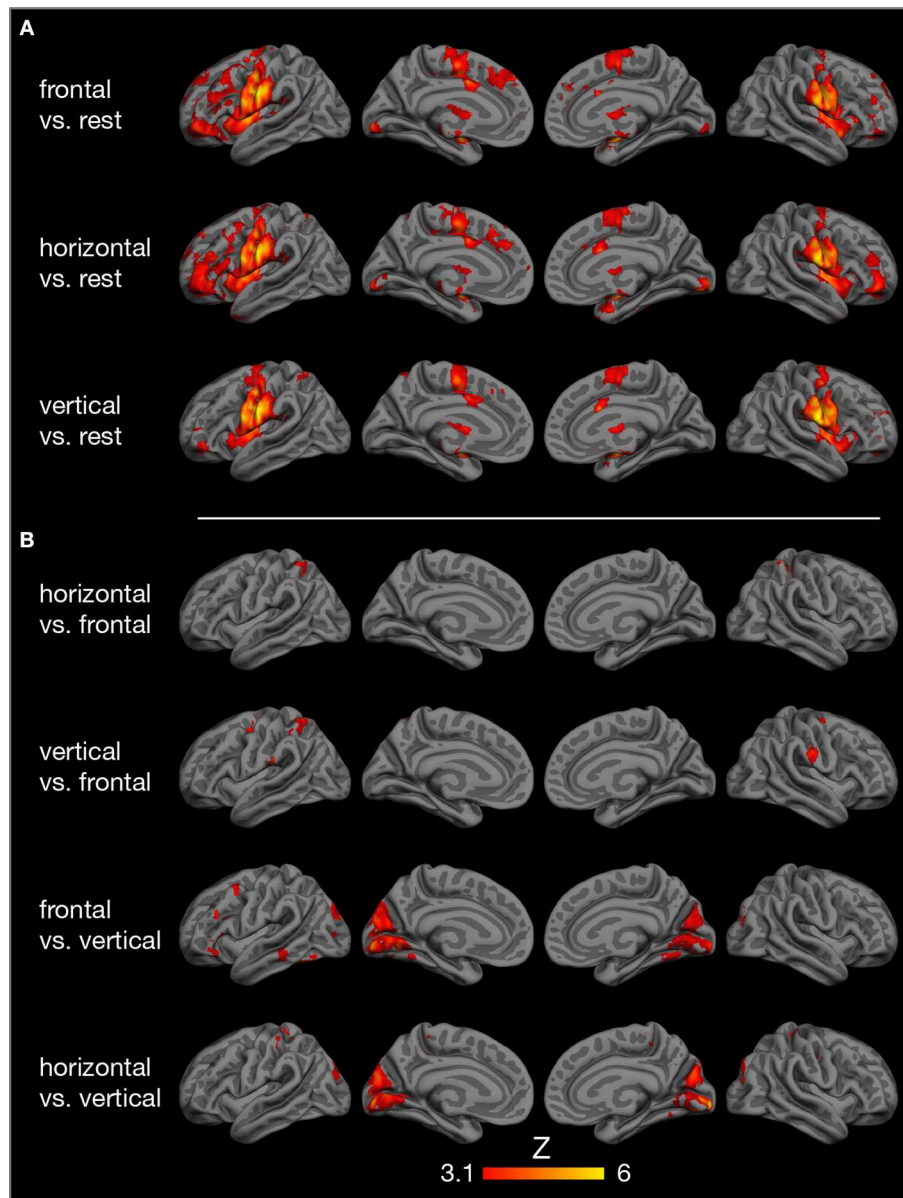


FIGURE 3 | Results of model-based group analysis. Brain activity associated with tongue movements averaged across 17 participants after cluster-based thresholding and correction for multiple comparisons ($Z > 3.1$, $p < 0.01$) is shown in red-yellow. Activated areas were projected onto the semi-inflated pial surface of the *fsaverage* brain, reconstructed by FreeSurfer (Fischl, 2012). **(A)** Tongue movements > rest, **(B)** contrasts between tongue movements.

active in eight participants and the executive control network in four participants. In four participants, a superior sensorimotor network, comprising the hand sensorimotor cortex and the supplementary motor area, was found.

DISCUSSION

Main results of the present task-based fMRI study on the neural correlates of tongue movements were: (1) All three tongue movements under investigation were controlled by the same neurofunctional system, consisting of the bilateral

tongue primary sensorimotor cortex, supplementary motor cortex, anterior cingulate gyrus, basal ganglia, thalamus, and cerebellum. (2) Distinct tongue movements also involved more specialized regions, such as the prefrontal, posterior parietal, and temporal cortices. (3) Using a novel approach to characterize inter-individual differences in task-based fMRI data, spatio-temporal filtering of independent components, we found consistent activation of the tongue primary sensorimotor cortex in all participants, but also remarkable variability, e.g., in fronto-parietal and executive control networks.

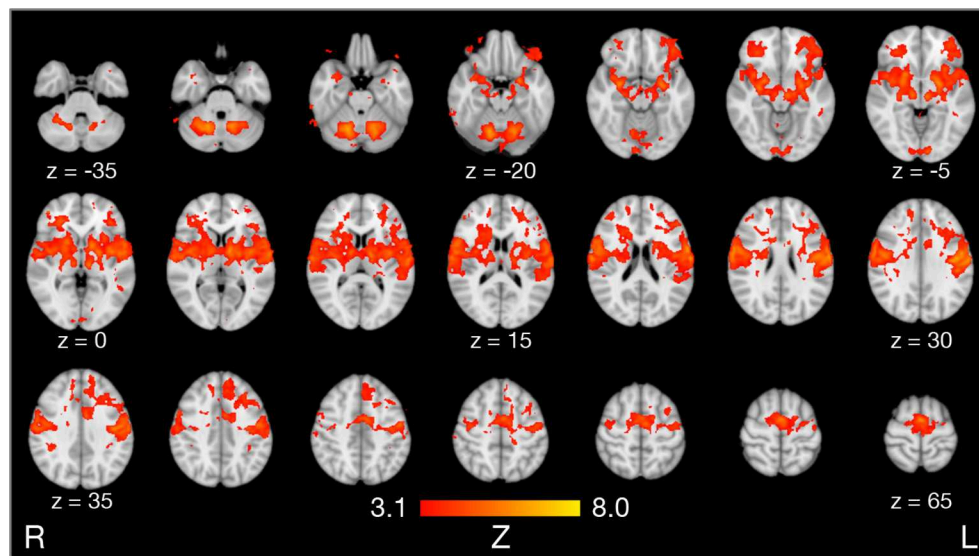


FIGURE 4 | Results of model-based group analysis. Brain activity associated with frontal tongue movements vs. rest averaged across 17 participants after cluster-based thresholding and correction for multiple comparisons ($Z > 3.1$, $p < 0.01$) is shown in red-yellow. Brain activity is projected onto axial slices of the MNI152 standard space template in radiological convention (the left hemisphere is seen on the right).

Model-Based Group FMRI Analysis

The present study demonstrates the core cortical [lateral primary motor cortex (Fesl et al., 2003), supplementary motor area, cingulate motor area] and subcortical regions (basal ganglia, thalamus, cerebellum) of the tongue motor system, corroborating several previous FMRI studies (Corfield et al., 1999; Shinagawa et al., 2003; Martin et al., 2004; Watanabe et al., 2004; Brown et al., 2008; Malandraki et al., 2009). The tongue motor system was very similar for all three tongue movements under investigation (Figure 3). The local maxima of precentral activation (Table 2) correspond well to activation maxima reported in the literature, e.g., by Arima et al. (2011) for tongue protrusion and by Fesl et al. (2003) for horizontal tongue movements, supporting our interpretation that the precentral brain activation seen here represents the primary tongue motor cortex. Our results also demonstrate the involvement of the lateral primary somatosensory cortex, reflecting the extensive mechanosensory (Kaas et al., 2006) and proprioceptive innervation of the tongue (Adatia and Gehring, 1971).

Moreover, the bilateral insular cortex was active during all three tongue movements. The insulae are not regarded as motor areas *per se*, but as areas of polymodal sensory, motor, cognitive, and affective integration. The insular cortex is involved in processing somatosensory (Sörös et al., 2008; Pugnaghi et al., 2011), gustatory (Small, 2010), and nociceptive stimuli (Xu et al., 2019). In addition, insular activity is associated with voluntary and semi-voluntary oro-facial movements, such as jaw opening and closing (Wong et al., 2011), speech production (Simonyan and Fuertringer, 2015; Tourville et al., 2019), and swallowing (Sörös et al., 2009; Leopold and Daniels, 2010; Malandraki et al., 2011). Importantly, insular activity is not specific for oro-facial

movements, but has been found in simple finger movements as well (Turesky et al., 2016).

Tongue motor control was also associated with activity in prefrontal areas, critical for motor planning (Svoboda and Li, 2018), and in posterior parietal areas, involved in processing and perception of action-related information (Culham and Valyear, 2006). Parietal activity has also been found in previous FMRI studies during frontal tongue movements (tapping of the tip of the tongue against the alveolar ridge) (Malandraki et al., 2009) and a series of spatially complex tongue movements (pressing the inside of a left or right, upper or lower incisor, canine, or molar tooth with the tip of the tongue) (Watanabe et al., 2004).

Comparing brain activity between different tongue movements resulted in complex patterns of activation differences (Table 3). Speech-related frontal (protrusion) tongue movements were associated with less activation in parts of the bilateral superior parietal lobule (vs. horizontal, side to side movements) and in parts of the bilateral precentral gyrus, right post-central gyrus, and the left posterior parietal cortex (vs. vertical, elevation movements). We may speculate that, in most humans, speech-related tongue movements are probably some of the most overlearned movements (Ziegler, 2003) and therefore are performed with less neural resources than less extensively trained tongue movements. Similarly, complex and relatively unfamiliar sequential finger movements are associated with increased FMRI activity compared with repetitive movements of the same fingers (Wexler et al., 1997). Remarkably, frontal (protrusion) tongue movements were associated with increased activity in parts of the left frontal and temporal lobes compared with vertical (elevation) movements. Again, we may speculate that frontal (protrusion) tongue movements, usually performed in the context of overt speech production, activate areas critical

TABLE 2 | Local maxima in brain activation: stereotaxic coordinates in MNI space, Z values, and corresponding brain regions for the contrast frontal tongue movement > rest.

| Region | Side | x (mm) | y (mm) | z (mm) | Z value |
|--------------------------------------|------|--------|--------|--------|---------|
| Precentral gyrus | L | -60 | 2 | 20 | 6.24 |
| | R | 58 | 8 | 8 | 5.00 |
| | R | 42 | -10 | 52 | 4.56 |
| Supplementary motor cortex | | 0 | -4 | 64 | 6.22 |
| Superior frontal gyrus | | 0 | 32 | 46 | 6.00 |
| Middle frontal gyrus | L | -12 | 16 | 56 | 5.03 |
| | L | -50 | 16 | 38 | 4.36 |
| Inferior frontal gyrus, pars triang. | L | -26 | 20 | 38 | 5.31 |
| | L | -48 | 28 | 16 | 5.14 |
| Frontal operculum | R | 34 | 16 | 10 | 4.65 |
| Frontal orbital cortex | L | -34 | 18 | -12 | 5.02 |
| Frontal pole | R | 36 | 42 | 20 | 4.51 |
| Post-central gyrus | L | -42 | -16 | 32 | 6.56 |
| | R | 62 | -6 | 28 | 6.17 |
| Supramarginal gyrus, post. div. | L | -38 | -50 | 42 | 4.49 |
| | R | 34 | -38 | 36 | 5.44 |
| Central opercular cortex | L | -60 | -20 | 12 | 5.78 |
| Middle temporal gyrus | L | -54 | -54 | 0 | 3.97 |
| Lingual gyrus | L | -14 | -78 | -2 | 3.94 |
| | R | 6 | -92 | -16 | 6.76 |
| Cingulate gyrus, ant. div. | L | -8 | 1 | 37 | 4.65 |
| | R | 6 | 0 | 36 | 3.53 |
| Insular cortex | L | -40 | -4 | 2 | 5.81 |
| | R | 42 | -4 | 4 | 5.21 |
| Putamen | R | 22 | 8 | -2 | 5.51 |
| Pallidum | L | -13 | 4 | 0 | 5.63 |
| | L | -10 | -2 | 4 | 5.93 |
| Thalamus | R | 14 | -4 | 8 | 5.45 |
| | L | -26 | -4 | -16 | 5.77 |
| Amygdala | R | 28 | -2 | -16 | 5.65 |
| | L | -16 | -64 | -22 | 6.08 |
| Cerebellum lobule VI | L | -16 | -64 | -22 | 6.08 |
| | R | 16 | -66 | -22 | 6.60 |

to speech-language production, such as the left inferior frontal gyrus (Flinker et al., 2015), even when performed in isolation.

Unexpectedly, we found increased brain activity in the occipital lobe in the contrasts frontal vs. vertical and horizontal vs. vertical movements (**Figure 3, Table 3**). Because previous fMRI studies do not report occipital activity, we are reluctant to attribute this activity to tongue movement. Still, it may be possible that frontal and horizontal tongue movements, exploring the oral cavity with the densely innervated tip of the tongue, contribute to the development of oral awareness (Haggard and de Boer, 2014) and activate not only somatosensory but also visual cortices. An alternative explanation would be that the different visual stimuli used to cue the three tongue movements (**Figure 1**) may have induced different activation patterns in visual areas.

Overall, the differences of brain activity during the three different tongue movement conditions need to be interpreted

TABLE 3 | Local maxima in brain activation: stereotaxic coordinates in MNI space, Z values, and corresponding brain regions for the contrasts horizontal > frontal, vertical > frontal, frontal > vertical, and horizontal > vertical tongue movements.

| Region | Side | x (mm) | y (mm) | z (mm) | Z value |
|--------------------------------------|------|--------|--------|--------|---------|
| Horizontal > frontal | | | | | |
| Superior parietal lobule | L | -32 | -50 | 58 | 4.75 |
| | R | 26 | -48 | 66 | 4.98 |
| Vertical > frontal | | | | | |
| Precentral gyrus | L | -26 | -12 | 62 | 5.29 |
| | R | 32 | -6 | 66 | 4.59 |
| Post-central gyrus | R | 52 | -20 | 34 | 6.70 |
| | R | 32 | -34 | 36 | 4.67 |
| Central opercular cortex | L | -60 | -20 | 16 | 4.72 |
| Supramarginal gyrus, ant. div. | L | -44 | -34 | 38 | 5.03 |
| Superior parietal lobule | L | -34 | -48 | 52 | 4.69 |
| Frontal > vertical | | | | | |
| Middle frontal gyrus | L | -46 | 10 | 46 | 4.56 |
| Inferior frontal gyrus, pars triang. | L | -46 | 24 | 12 | 4.95 |
| Frontal orbital cortex | L | -42 | 30 | -16 | 4.29 |
| Middle temporal gyrus, post. div. | L | -60 | -36 | -10 | 4.33 |
| Inferior temporal gyrus, temp-occ. | L | -42 | -50 | -16 | 4.47 |
| Cuneal cortex | R | 2 | -78 | 22 | 5.56 |
| Lateral occipital cortex | L | -20 | -86 | 20 | 4.79 |
| | R | 28 | -82 | 12 | 4.85 |
| Intracalcarine cortex | R | 8 | -64 | 8 | 4.45 |
| Lingual gyrus | L | -10 | -78 | 0 | 5.35 |
| Occipital pole | | 0 | -96 | -4 | 6.33 |
| | R | 24 | -96 | -8 | 3.87 |
| Occipital fusiform gyrus | L | -32 | -72 | -12 | 4.29 |
| | R | 26 | -66 | -6 | 4.97 |
| Horizontal > vertical | | | | | |
| Precentral gyrus | L | -22 | -26 | 58 | 4.74 |
| | L | -40 | -16 | 46 | 4.60 |
| | R | 22 | -28 | 68 | 4.97 |
| Inferior frontal gyrus, pars triang. | L | -54 | 28 | -10 | 4.53 |
| | L | -2 | -38 | 58 | 4.83 |
| Post-central gyrus | R | 38 | -26 | 50 | 4.67 |
| | L | -2 | -20 | 44 | 4.23 |
| Cingulate gyrus, post. div. | L | -2 | -20 | 44 | 4.23 |
| | L | -6 | -88 | 22 | 5.05 |
| Cuneal cortex | R | 10 | -70 | 20 | 5.17 |
| | L | -10 | -90 | -2 | 5.65 |
| Occipital pole | R | 16 | -98 | -6 | 8.61 |
| | R | 26 | -60 | -16 | 5.16 |

with caution. As we do not have EMG recordings of tongue activity during fMRI, we cannot be sure that tongue movements were produced with the same velocity and pressure. Differences in motion parameters could well explain the subtle differences of brain activity seen here (Wexler et al., 1997).

Model-Free Individual fMRI Analysis

Almost all task-based and resting-state fMRI studies only present group analyses of brain activity. Recently, individual differences

in brain structure and function have attracted growing attention (Kanai and Rees, 2011; Finn et al., 2015; Dubois and Adolphs, 2016). The study of individual differences of the neural control of tongue movements is expected to improve our understanding of tongue motor impairment, e.g., in amyotrophic lateral sclerosis (Kollewe et al., 2011) or Parkinson's disease (Van Lieshout et al., 2011), and help in the assessment of the efficacy of treatment options, such as tongue motor training (Arima et al., 2011; Komoda et al., 2015).

To investigate inter-individual differences in tongue movement-related brain activity, we used a novel approach, spatio-temporal filtering of independent components. First, ICA

was employed to perform a low-dimensional decomposition of every single fMRI data set of 9:21 min duration. ICA carried out a model-independent separation of the original data into components that are related to brain activity, physiological extra-cerebral processes (such as respiration or blood pulsation), and imaging artifacts (such as head motion or susceptibility artifacts). The primary advantage of a model-free ICA was the detection of previously unexpected patterns of brain activity (McKeown et al., 1998b). In the traditional general linear model-based analysis of fMRI time series, these patterns of activity would be considered as noise and discarded (Monti, 2011).

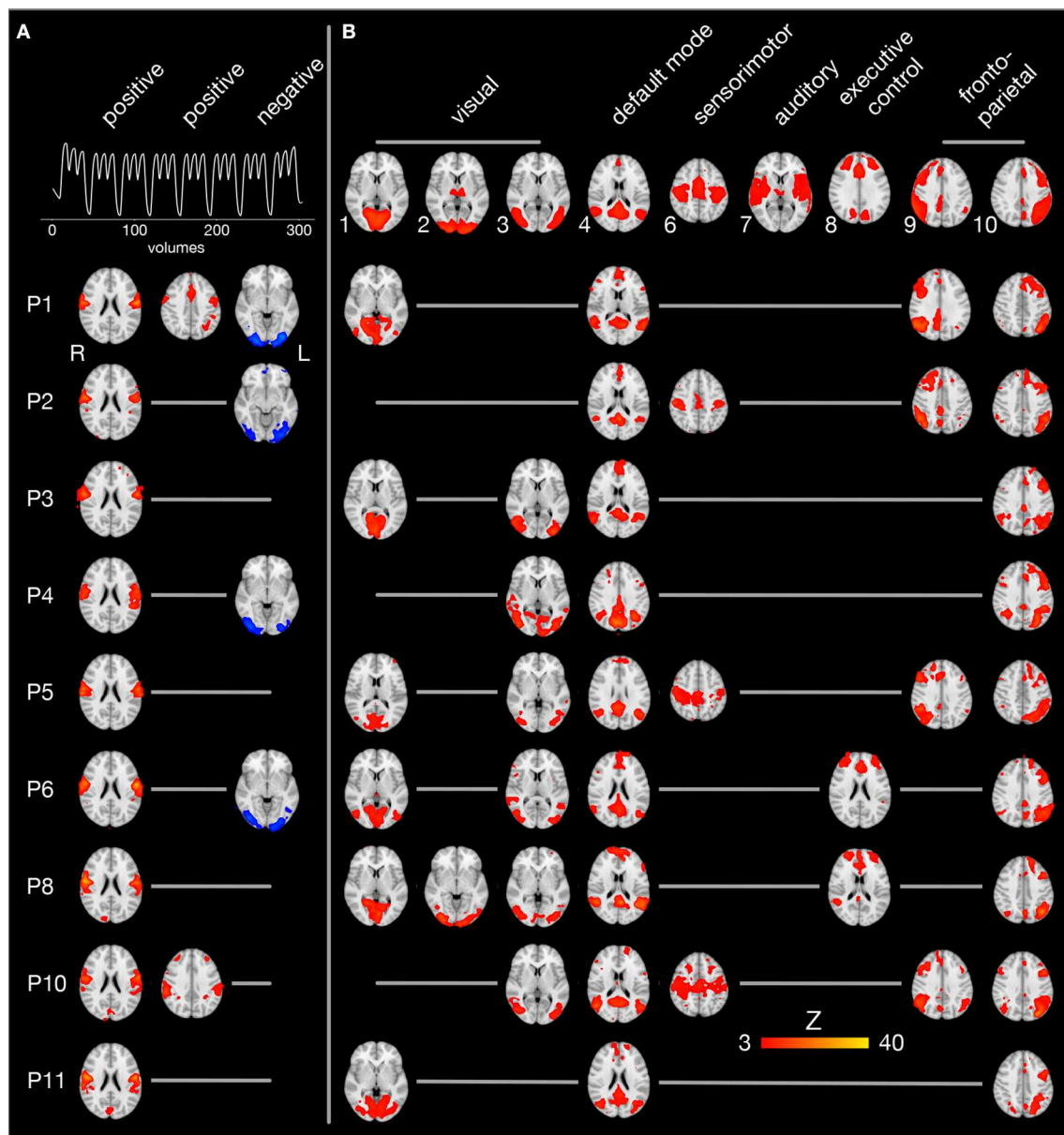


FIGURE 5 | Continued

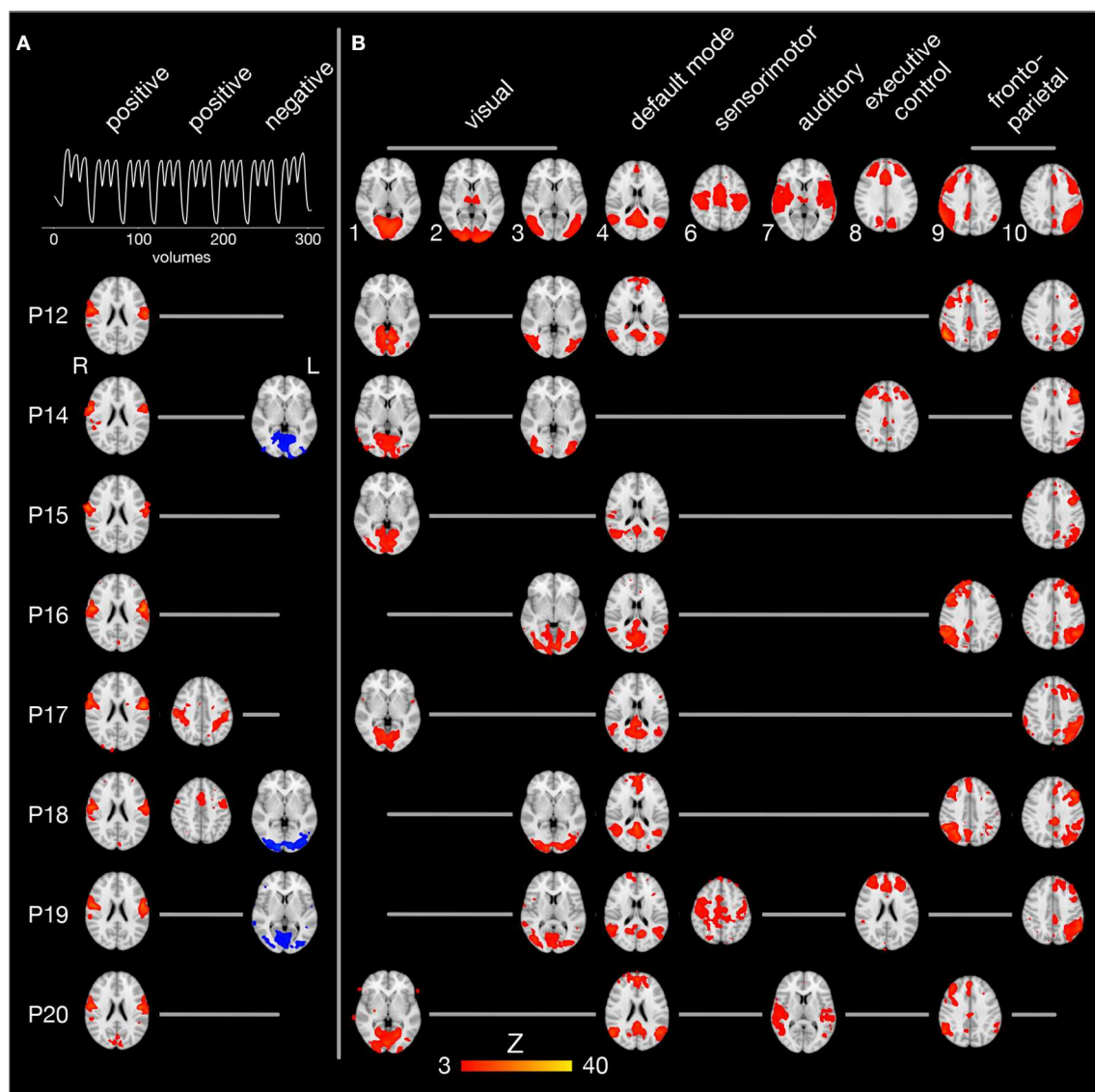


FIGURE 5 | Spatio-temporal filtering of individual ICA components. The results of the single-session independent component analyses of all 17 participants (one participant per row) are summarized. Brain images are shown in radiological convention (the left hemisphere is seen on the right) after registration to the MNI152 standard space template. **(A)** The three columns on the left display components whose time course is significantly correlated with the expected brain activity (first row). The first and second column show positively correlated ($r > 0.4, p < 0.05$), the third column negatively correlated components (blue, $r < -0.4, p < 0.05$). **(B)** The upper row illustrates 9 of 10 established brain networks identified in resting state FMRI data (Smith et al., 2009). For every single participant, independent components are displayed that are spatially correlated with one of the established networks. Network 5 from the study by Smith et al. (2009) (consisting of large parts of the cerebellum) is not shown because it was not significantly correlated with cerebellar activity in one of the present FMRI data sets.

Second, we used a temporal filter to identify independent components whose time course was correlated with the expected brain response (for the use of correlation as a filter technique, see Mwangi et al., 2014). This approach demonstrated that the activation of the lateral primary sensorimotor cortex was found in all 17 participants. Tongue movement is, similar to e.g., finger tapping (Engström et al., 2004), a very robust sensorimotor paradigm.

Third, we applied a spatial filter, i.e., we cross-correlated the independent components obtained for our participants with a set

of ten established components (interpreted as neural networks). These canonical networks were derived from resting state FMRI data (Smith et al., 2009). Of importance, an analysis of task-based brain activation performed for the same study identified similar networks, demonstrating a close correspondence between resting and task-based brain activation (Smith et al., 2009). A study by Calhoun et al. (2008) investigated neural networks in rest and during an auditory oddball task, finding the same 11 networks in both conditions with one additional network (anterior cingulate) only present during rest.

Nine of 10 canonical networks (Smith et al., 2009) were also found in our task-based data sets of tongue movement. In 16 participants, the default mode network was active, a large-scale neural network, including the posterior cingulate cortex, precuneus, medial prefrontal gyrus, and inferior parietal cortex (Greicius et al., 2003). In 16 participants, the left fronto-parietal network and in eight participants, the right fronto-parietal network was active. Fronto-parietal networks have been shown to subserve attentional mechanisms (Markett et al., 2014) and are probably involved in a wide variety of other tasks.

Results from spatio-temporal filtering of independent components suggest that large-scale neural networks are active during simple tongue movements. Activation of these networks is not time-locked to tongue movement and thus is not detectable in model-based fMRI analysis. Of major importance, not all established networks appear to be active in all individuals. At present, it is unclear if the pattern of neural networks seen here is specific for tongue movement or, more likely, reflecting motor control in general. Moreover, it is undetermined which factors contribute to the physiological activation or deactivation of specific networks in different individuals during tongue motor control. In addition, we do not know if the pattern of neural networks found in a single individual is stable over time or may change depending on internal states or external stimulation. Results from resting state fMRI suggest that at least the major heteromodal association networks, such as the default mode network and the fronto-parietal networks, are stable over time (Zuo and Xing, 2014).

Knowledge of the neural basis of pathological tongue movements is very limited (Mohammadi et al., 2009; Kollwe et al., 2011; Shen et al., 2015). We assume that spatio-temporal filtering of independent components may be able to determine individual patterns of brain activity related to functional impairment. Of importance, this approach may differentiate between impaired activation of the primary tongue motor cortex and disorders of large-scale association networks. For clinical use, this approach may assist in detecting disordered tongue motor control in an early stage of neurodegenerative disease and may help monitoring efficacy of pharmacological treatment, non-invasive brain stimulation, or training. Recently, resting state and task-based fMRI were used to predict a cognitive trait (fluid intelligence, reading comprehension) (Greene et al., 2018; Jiang et al., 2020). Both studies found that functional connectivity based on task-based fMRI has higher prediction performance than the results of resting state fMRI. Similarly, the results of spatio-temporal filtering of independent components may be used to predict clinical parameters and may be correlated with individual behavioral, clinical, and genetic information.

Limitations and Directions for Future Research

Our study has limitations that need to be addressed. The sample size of our study (17 participants included in final data analysis) is relatively small, at least compared to the recommendation of $n = 30$ for a typical task-based fMRI study (Turner et al., 2018). However, our literature search identified only one fMRI study of tongue motor control with a larger sample size ($n = 24$, Watanabe

et al., 2004). Nevertheless, a larger sample size would have been helpful for the robust identification of differences between tongue movements in the model-based analysis and of inter-individual differences in the model-free analysis.

We did not record tongue motion during fMRI. Using surface EMG, it is possible to record electric activity of the suprahyoid muscles and then identify different tongue movements with high accuracy using a support vector machine algorithm for pattern recognition (Sasaki et al., 2016). To ensure that the behavioral performance was as similar as possible across participants, we gave detailed instructions and performed a training session before fMRI scanning. Of note, recording EMG activity would have been helpful to refine the time course of expected brain responses for model-based analysis on an individual basis. By contrast, EMG recordings would have not been used for model-free ICA (Calhoun and de Lacy, 2017). Moreover, we did not record potential jaw movements that may have been occurred during tongue movements. Recording the opening and closing of the jaw is possible with e.g., a fiber-optic sensor attached to the chin (Sörös et al., 2010).

Our experimental paradigm included regular rest periods of 15 s duration after every third tongue movement block (Figure 2). During this rest period, the hemodynamic response curve is supposed to reach the pre-movement baseline. To keep the entire duration of the tongue movement experiment shorter than 10 min (we also acquired data for three separate speech production experiments), while still recording eight blocks of 15 s length per movement condition, we chose shorter rest periods of 3 s each between the remaining tongue movement blocks. During this shorter rest period, the hemodynamic response curve has not reached the baseline. Thus, we cannot rule out the possibility that BOLD activity from one tongue block was carried over to the next block. This may have impaired our ability to detect differences between tongue movements in model-based analysis. Of note, model-free ICA does not require specific rest periods and ICA results should not be affected by shorter rest periods.

For future research on tongue motor control, we recommend to (1) replicate our investigation of different tongue movements with a larger sample size to increase statistical power and reproducibility, (2) use different stimuli (e.g., auditory instructions) to cue tongue movements in order to determine whether certain tongue movements are associated with activity in the visual cortex, (3) record surface EMG from the suprahyoid muscles during the pre-scan training session and during fMRI, (4) study tongue motor control in younger and older individuals because disorders of tongue movement are often related to diseases prevalent in the elderly and differences in brain activation between younger and older individuals have been shown for speech motor tasks (Sörös et al., 2011; Tremblay et al., 2017), (5) correlate inter-individual differences in brain activity determined with spatio-temporal filtering of independent components with age, sex, and behavioral parameters of tongue movement in a larger sample of healthy younger and older individuals, and (6) investigate the neural correlates of tongue movements in patients with neurogenic dysarthria and dysphagia on an individual basis and correlate fMRI results with etiology, disease severity, and behavioral performance.

DATA AVAILABILITY STATEMENT

The datasets generated for this study are available on request to the corresponding author.

ETHICS STATEMENT

The studies involving human participants were reviewed and approved by Medical Research Ethics Board, University of Oldenburg, Germany. The participants provided their written informed consent to participate in this study.

AUTHOR CONTRIBUTIONS

PS and SS designed the study, acquired the MRI data, and performed the data analysis. SS recruited the participants. PS prepared the figures and wrote the manuscript. SS and KW revised the manuscript and participated in the interpretations

of the findings. PS conceived the spatio-temporal filtering of independent components approach.

FUNDING

This work was supported by the Neuroimaging Unit, University of Oldenburg, funded by grants from the German Research Foundation (DFG, 3T MRI INST 184/152-1 FUGG and MEG INST 184/148-1 FUGG).

ACKNOWLEDGMENTS

The authors wish to thank Katharina Grote and Gülsen Yanc for assisting with MRI data acquisition. The authors also appreciate the work of Sarah Schumacher, Miriam Treutler, and Zoe Tromberend, who performed the speech production experiments for this project.

REFERENCES

- Abd-El-Malek, S. (1939). Observations on the morphology of the human tongue. *J. Anat.* 73, 201–210.
- Adatia, A., and Gehring, E. (1971). Proprioceptive innervation of the tongue. *J. Anat.* 110, 215–220.
- Arima, T., Yanagi, Y., Niddam, D., Ohata, N., Arendt-Nielsen, L., Minagi, S., et al. (2011). Corticomotor plasticity induced by tongue-task training in humans: a longitudinal fMRI study. *Exp. Brain Res.* 212, 199–212. doi: 10.1007/s00221-011-2719-7
- Beckmann, C., Jenkinson, M., Woolrich, M., Behrens, T., Flitney, D., Devlin, J., et al. (2006). Applying FSL to the FIAC data: model-based and model-free analysis of voice and sentence repetition priming. *Hum. Brain Mapp.* 27, 380–391. doi: 10.1002/hbm.20246
- Beckmann, C., and Smith, S. (2004). Probabilistic independent component analysis for functional magnetic resonance imaging. *IEEE Trans. Med. Imaging* 23, 137–152. doi: 10.1109/TMI.2003.822821
- Brant-Zawadzki, M., Gillan, G., and Nitz, W. (1992). MP RAGE: a three-dimensional, T1-weighted, gradient-echo sequence—initial experience in the brain. *Radiology* 182, 769–775. doi: 10.1148/radiology.182.3.1535892
- Brown, S., Ngan, E., and Liotti, M. (2008). A larynx area in the human motor cortex. *Cereb. Cortex* 18, 837–845. doi: 10.1093/cercor/bhm131
- Calhoun, V., and de Lacy, N. (2017). Ten key observations on the analysis of resting-state functional MR imaging data using independent component analysis. *Neuroimaging Clin. N. Am.* 27, 561–579. doi: 10.1016/j.nic.2017.06.012
- Calhoun, V., Kiehl, K., and Pearson, G. (2008). Modulation of temporally coherent brain networks estimated using ICA at rest and during cognitive tasks. *Hum. Brain Mapp.* 29, 828–838. doi: 10.1002/hbm.20581
- Calhoun, V., Pekar, J., McGinty, V., Adali, T., Watson, T., and Pearson, G. (2002). Different activation dynamics in multiple neural systems during simulated driving. *Hum. Brain Mapp.* 16, 158–167. doi: 10.1002/hbm.10032
- Comon, P. (1994). Independent component analysis, a new concept. *Signal Process.* 36, 287–314. doi: 10.1016/0165-1684(94)90029-9
- Corfield, D., Murphy, K., Josephs, O., Fink, G., Frackowiak, R., Guz, A., et al. (1999). Cortical and subcortical control of tongue movement in humans: a functional neuroimaging study using fMRI. *J. Appl. Physiol.* 86, 1468–1477. doi: 10.1152/jappl.1999.86.5.1468
- Culham, J., and Valyear, K. (2006). Human parietal cortex in action. *Curr. Opin. Neurobiol.* 16, 205–212. doi: 10.1016/j.conb.2006.03.005
- Diedrichsen, J., Balsters, J., Flavell, J., Cussans, E., and Ramnani, N. (2009). A probabilistic MR atlas of the human cerebellum. *Neuroimage* 46, 39–46. doi: 10.1016/j.neuroimage.2009.01.045
- Dodds, W. (1989). Physiology of swallowing. *Dysphagia* 3, 171–178. doi: 10.1007/BF02407219
- Dubois, J., and Adolphs, R. (2016). Building a science of individual differences from fMRI. *Trends Cogn. Sci.* 20, 425–443. doi: 10.1016/j.tics.2016.03.014
- Engström, M., Ragnehed, M., Lundberg, P., and Söderfeldt, B. (2004). Paradigm design of sensory-motor and language tests in clinical fMRI. *Neurophysiol. Clin.* 34, 267–277. doi: 10.1016/j.neucli.2004.09.006
- Ferrand, C. (2018). *Speech Science. An Integrated Approach to Theory and Clinical Practice*. Boston, MA: Pearson Education.
- Fesl, G., Moriggl, B., Schmid, U., Naidich, T., Herholz, K., and Yousry, T. (2003). Inferior central sulcus: variations of anatomy and function on the example of the motor tongue area. *Neuroimage* 20, 601–610. doi: 10.1016/S1053-8119(03)00299-4
- Finn, E., Shen, X., Scheinost, D., Rosenberg, M., Huang, J., Chun, M., et al. (2015). Functional connectome fingerprinting: identifying individuals using patterns of brain connectivity. *Nat. Neurosci.* 18, 1664–1671. doi: 10.1038/nn.4135
- Fischl, B. (2012). Freesurfer. *Neuroimage* 62, 774–781. doi: 10.1016/j.neuroimage.2012.01.021
- Flinker, A., Korzeniewska, A., Shestyuk, A., Franaszczuk, P., Dronkers, N., Knight, R., et al. (2015). Redefining the role of Broca's area in speech. *Proc. Natl. Acad. Sci. U.S.A.* 112, 2871–2875. doi: 10.1073/pnas.1414491112
- Friston, K. J., Holmes, A. P., Worsley, K. J., Poline, J.-P., Frith, C. D., and Frackowiak, R. S. (1995). Statistical parametric maps in functional imaging: a general linear approach. *Hum. Brain Mapp.* 2, 189–210. doi: 10.1002/hbm.460020402
- Gaige, T., Benner, T., Wang, R., Wedeen, V., and Gilbert, R. (2007). Three dimensional myoarchitecture of the human tongue determined *in vivo* by diffusion tensor imaging with tractography. *J. Magn. Reson. Imaging* 26, 654–661. doi: 10.1002/jmri.21022
- Greene, A., Gao, S., Scheinost, D., and Constable, R. (2018). Task-induced brain state manipulation improves prediction of individual traits. *Nat. Commun.* 9:2807. doi: 10.1038/s41467-018-04920-3
- Greicius, M., Krasnow, B., Reiss, A., and Menon, V. (2003). Functional connectivity in the resting brain: a network analysis of the default mode hypothesis. *Proc. Natl. Acad. Sci. U.S.A.* 100, 253–258. doi: 10.1073/pnas.0135058100
- Griswold, M., Jakob, P., Heidemann, R., Nittka, M., Jellus, V., Wang, J., et al. (2002). Generalized autocalibrating partially parallel acquisitions (GRAPPA). *Magn. Reson. Med.* 47, 1202–1210. doi: 10.1002/mrm.10171
- Haggard, P., and de Boer, L. (2014). Oral somatosensory awareness. *Neurosci. Biobehav. Rev.* 47, 469–484. doi: 10.1016/j.neubiorev.2014.09.015
- Hiimeae, K., and Palmer, J. (2003). Tongue movements in feeding and speech. *Crit. Rev. Oral Biol. Med.* 14, 413–429. doi: 10.1177/154411130301400604

- Hummel, T., Genow, A., and Landis, B. (2010). Clinical assessment of human gustatory function using event related potentials. *J. Neurol. Neurosurg. Psychiatry* 81, 459–464. doi: 10.1136/jnnp.2009.183699
- Hyvärinen, A. (1999). Fast and robust fixed-point algorithms for independent component analysis. *IEEE Trans. Neural Netw.* 10, 626–634. doi: 10.1109/72.761722
- Jenkinson, M., Bannister, P., Brady, M., and Smith, S. (2002). Improved optimization for the robust and accurate linear registration and motion correction of brain images. *Neuroimage* 17, 825–841. doi: 10.1006/nimg.2002.1132
- Jenkinson, M., Beckmann, C., Behrens, T., Woolrich, M., and Smith, S. (2012). FSL. *Neuroimage* 62, 782–790. doi: 10.1016/j.neuroimage.2011.09.015
- Jiang, R., Zuo, N., Ford, J., Qi, S., Zhi, D., Zhuo, C., et al. (2020). Task-induced brain connectivity promotes the detection of individual differences in brain-behavior relationships. *Neuroimage* 207:116370. doi: 10.1016/j.neuroimage.2019.116370
- Jungblut, M., Huber, W., Pustelniak, M., and Schnitker, R. (2012). The impact of rhythm complexity on brain activation during simple singing: an event-related fMRI study. *Restor. Neurol. Neurosci.* 30, 39–53. doi: 10.3233/RNN-2011-0619
- Kaas, J., Qi, H., and Iyengar, S. (2006). Cortical network for representing the teeth and tongue in primates. *Anat. Rec. A Discov. Mol. Cell. Evol. Biol.* 288, 182–190. doi: 10.1002/ar.a.20267
- Kanai, R., and Rees, G. (2011). The structural basis of inter-individual differences in human behaviour and cognition. *Nat. Rev. Neurosci.* 12, 231–242. doi: 10.1038/nrn3000
- Kennedy, D., Kieser, J., Bolter, C., Swain, M., Singh, B., and Waddell, J. (2010). Tongue pressure patterns during water swallowing. *Dysphagia* 25, 11–19. doi: 10.1007/s00455-009-9223-2
- Kier, W., and Smith, K. (1985). Tongues, tentacles and trunks: the biomechanics of movement in muscular-hydrostats. *Zool. J. Linn. Soc.* 83, 307–324. doi: 10.1111/j.1096-3642.1985.tb01178.x
- Kobayakawa, T., Wakita, M., Saito, S., Gotow, N., Sakai, N., and Ogawa, H. (2005). Location of the primary gustatory area in humans and its properties, studied by magnetoencephalography. *Chem. Senses* 30, i226–i227. doi: 10.1093/chemse/bjh196
- Kokkonen, S., Nikkinen, J., Remes, J., Kantola, J., Starck, T., Haapea, M., et al. (2009). Preoperative localization of the sensorimotor area using independent component analysis of resting-state fMRI. *Magn. Reson. Imaging* 27, 733–740. doi: 10.1016/j.mri.2008.11.002
- Kollewe, K., Münte, T., Samii, A., Dengler, R., Petri, S., and Mohammadi, B. (2011). Patterns of cortical activity differ in ALS patients with limb and/or bulbar involvement depending on motor tasks. *J. Neurol.* 258, 804–810. doi: 10.1007/s00415-010-5842-7
- Komoda, Y., Iida, T., Kothari, M., Komiyama, O., Baad-Hansen, L., Kawara, M., et al. (2015). Repeated tongue lift movement induces neuroplasticity in corticomotor control of tongue and jaw muscles in humans. *Brain Res.* 1627, 70–79. doi: 10.1016/j.brainres.2015.09.016
- Ladefoged, P., and Maddieson, I. (1996). *The Sounds of the World's Languages*. Oxford: Blackwell.
- Leopold, N., and Daniels, S. (2010). Supranuclear control of swallowing. *Dysphagia* 25, 250–257. doi: 10.1007/s00455-009-9249-5
- Lowell, S., Reynolds, R., Chen, G., Horwitz, B., and Ludlow, C. (2012). Functional connectivity and laterality of the motor and sensory components in the volitional swallowing network. *Exp. Brain Res.* 219, 85–96. doi: 10.1007/s00221-012-3069-9
- Malandraki, G., Johnson, S., and Robbins, J. (2011). Functional MRI of swallowing: from neurophysiology to neuroplasticity. *Head Neck* 33, S14–20. doi: 10.1002/hed.21903
- Malandraki, G., Sutton, B., Perlman, A., Karampinos, D., and Conway, C. (2009). Neural activation of swallowing and swallowing-related tasks in healthy young adults: an attempt to separate the components of deglutition. *Hum. Brain Mapp.* 30, 3209–3226. doi: 10.1002/hbm.20743
- Markett, S., Reuter, M., Montag, C., Voigt, G., Lachmann, B., Rudorf, S., et al. (2014). Assessing the function of the fronto-parietal attention network: insights from resting-state fMRI and the attentional network test. *Hum. Brain Mapp.* 35, 1700–1709. doi: 10.1002/hbm.22285
- Martin, R., MacIntosh, B., Smith, R., Barr, A., Stevens, T., Gati, J., et al. (2004). Cerebral areas processing swallowing and tongue movement are overlapping but distinct: a functional magnetic resonance imaging study. *J. Neurophysiol.* 92, 2428–2443. doi: 10.1152/jn.01144.2003
- Martin, R., Murray, G., Kemppainen, P., Masuda, Y., and Sessle, B. (1997). Functional properties of neurons in the primate tongue primary motor cortex during swallowing. *J. Neurophysiol.* 78, 1516–1530. doi: 10.1152/jn.1997.78.3.1516
- McClung, J., and Goldberg, S. (2002). Organization of the hypoglossal motoneurons that innervate the horizontal and oblique components of the genioglossus muscle in the rat. *Brain Res.* 950, 321–324. doi: 10.1016/S0006-8993(02)03240-7
- McKeown, M., Jung, T., Makeig, S., Brown, G., Kindermann, S., Lee, T., et al. (1998a). Spatially independent activity patterns in functional MRI data during the stroop color-naming task. *Proc. Natl. Acad. Sci. U.S.A.* 95, 803–810. doi: 10.1073/pnas.95.3.803
- McKeown, M., Makeig, S., Brown, G., Jung, T., Kindermann, S., Bell, A., et al. (1998b). Analysis of fMRI data by blind separation into independent spatial components. *Hum. Brain Mapp.* 6, 160–188. doi: 10.1002/(SICI)1097-0193(1998)6:3<160::AID-HBM5>3.0.CO;2-1
- Mehl, M., Vazire, S., Ramírez-Esparza, N., Slatcher, R., and Pennebaker, J. (2007). Are women really more talkative than men? *Science* 317:82. doi: 10.1126/science.1139940
- Mohammadi, B., Kollewe, K., Samii, A., Krampfl, K., Dengler, R., and Münte, T. (2009). Decreased brain activation to tongue movements in amyotrophic lateral sclerosis with bulbar involvement but not Kennedy syndrome. *J. Neurol.* 256, 1263–1269. doi: 10.1007/s00415-009-5112-8
- Monti, M. (2011). Statistical analysis of fMRI time-series: a critical review of the GLM approach. *Front. Hum. Neurosci.* 5:28. doi: 10.3389/fnhum.2011.00028
- Mu, L., and Sanders, I. (2010). Human tongue neuroanatomy: nerve supply and motor endplates. *Clin. Anat.* 23, 777–791. doi: 10.1002/ca.21011
- Mwangi, B., Tian, T., and Soares, J. (2014). A review of feature reduction techniques in neuroimaging. *Neuroinformatics* 12, 229–244. doi: 10.1007/s12021-013-9204-3
- Ozdemir, E., Norton, A., and Schlaug, G. (2006). Shared and distinct neural correlates of singing and speaking. *Neuroimage* 33, 628–635. doi: 10.1016/j.neuroimage.2006.07.013
- Pardo, J., Wood, T., Costello, P., Pardo, P., and Lee, J. (1997). PET study of the localization and laterality of lingual somatosensory processing in humans. *Neurosci. Lett.* 234, 23–26. doi: 10.1016/S0304-3940(97)00650-2
- Pruim, R., Mennes, M., van Rooij, D., Llera, A., Buitelaar, J., and Beckmann, C. (2015). ICA-AROMA: a robust ICA-based strategy for removing motion artifacts from fMRI data. *Neuroimage* 112, 267–277. doi: 10.1016/j.neuroimage.2015.02.064
- Pugnaghi, M., Meletti, S., Castana, L., Francione, S., Nobili, L., Mai, R., et al. (2011). Features of somatosensory manifestations induced by intracranial electrical stimulations of the human insula. *Clin. Neurophysiol.* 122, 2049–2058. doi: 10.1016/j.clinph.2011.03.013
- Reineberg, A., Andrews-Hanna, J., Depue, B., Friedman, N., and Banich, M. (2015). Resting-state networks predict individual differences in common and specific aspects of executive function. *Neuroimage* 104, 69–78. doi: 10.1016/j.neuroimage.2014.09.045
- Riecker, A., Ackermann, H., Wildgruber, D., Meyer, J., Dogil, G., Haider, H., et al. (2000). Articulatory/phonetic sequencing at the level of the anterior perisylvian cortex: a functional magnetic resonance imaging (fMRI) study. *Brain Lang.* 75, 259–276. doi: 10.1006/brln.2000.2356
- Riecker, A., Mathiak, K., Wildgruber, D., Erb, M., Hertrich, I., Grodd, W., et al. (2005). fMRI reveals two distinct cerebral networks subserving speech motor control. *Neurology* 64, 700–706. doi: 10.1212/01.WNL.0000152156.90779.89
- Rudney, J., Ji, Z., and Larson, C. (1995). The prediction of saliva swallowing frequency in humans from estimates of salivary flow rate and the volume of saliva swallowed. *Arch. Oral. Biol.* 40, 507–512. doi: 10.1016/0003-9969(95)00004-9
- Sakamoto, K., Nakata, H., Inui, K., Perrucci, M., Del Gratta, C., Kakigi, R., et al. (2010). A difference exists in somatosensory processing between the anterior and posterior parts of the tongue. *Neurosci. Res.* 66, 173–179. doi: 10.1016/j.neures.2009.10.013
- Sanders, I., and Mu, L. (2013). A three-dimensional atlas of human tongue muscles. *Anat. Rec.* 296, 1102–1114. doi: 10.1002/ar.22711

- Sanders, I., Mu, L., Amiral, A., Su, H., and Sobotka, S. (2013). The human tongue slows down to speak: muscle fibers of the human tongue. *Anat. Rec.* 296, 1615–1627. doi: 10.1002/ar.22755
- Sasaki, M., Onishi, K., Stefanov, D., Kamata, K., Nakayama, A., Yoshikawa, M., et al. (2016). Tongue interface based on surface EMG signals of suprahyoid muscles. *Robomech. J.* 3:9. doi: 10.1186/s40648-016-0048-0
- Sawczuk, A., and Mosier, K. (2001). Neural control of tongue movement with respect to respiration and swallowing. *Crit. Rev. Oral. Biol. Med.* 12, 18–37. doi: 10.1177/10454411010120010101
- Schumacher, S. (1927). “Die Zunge,” in *Verdauungsapparat. Handbuch der Mikroskopischen Anatomie des Menschen*, eds T. Hellman, S. Schumacher, E. Seifert, and K. Zimmermann (Berlin; Heidelberg: Springer), 35–60. doi: 10.1007/978-3-642-51336-7_2
- Shellikeri, S., Green, J., Kulkarni, M., Rong, P., Martino, R., Zinman, L., et al. (2016). Speech movement measures as markers of bulbar disease in amyotrophic lateral sclerosis. *J. Speech Lang. Hear. Res.* 59, 887–899. doi: 10.1044/2016_JSLHR-S-15-0238
- Shen, D., Cui, L., Cui, B., Fang, J., Li, D., and Ma, J. (2015). A systematic review and meta-analysis of the functional MRI investigation of motor neuron disease. *Front. Neurol.* 6:246. doi: 10.3389/fneur.2015.00246
- Shinagawa, H., Ono, T., Ishiwata, Y., Honda, E., Sasaki, T., Taira, M., et al. (2003). Hemispheric dominance of tongue control depends on the chewing-side preference. *J. Dent. Res.* 82, 278–283. doi: 10.1177/154405910308200407
- Simonyan, K., and Fuertinger, S. (2015). Speech networks at rest and in action: interactions between functional brain networks controlling speech production. *J. Neurophysiol.* 113, 2967–2978. doi: 10.1152/jn.00964.2014
- Small, D. (2010). Taste representation in the human insula. *Brain Struct. Funct.* 214, 551–561. doi: 10.1007/s00429-010-0266-9
- Smith, S. (2002). Fast robust automated brain extraction. *Hum. Brain Mapp.* 17, 143–155. doi: 10.1002/hbm.10062
- Smith, S., Fox, P., Miller, K., Glahn, D., Fox, P., Mackay, C., et al. (2009). Correspondence of the brain's functional architecture during activation and rest. *Proc. Natl. Acad. Sci. U.S.A.* 106, 13040–13045. doi: 10.1073/pnas.0905267106
- Smith, S., Jenkinson, M., Woolrich, M., Beckmann, C., Behrens, T., Johansen-Berg, H., et al. (2004). Advances in functional and structural MR image analysis and implementation as FSL. *Neuroimage* 23, S208–S219. doi: 10.1016/j.neuroimage.2004.07.051
- Sörös, P., Bose, A., Sokoloff, L., Graham, S., and Stuss, D. (2011). Age-related changes in the functional neuroanatomy of overt speech production. *Neurobiol. Aging* 32, 1505–1513. doi: 10.1016/j.neurobiolaging.2009.08.015
- Sörös, P., Hoxhaj, E., Borel, P., Sadohara, C., Feige, B., Matthies, S., et al. (2019). Hyperactivity/restlessness is associated with increased functional connectivity in adults with ADHD: a dimensional analysis of resting state fMRI. *BMC Psychiatry* 19:43. doi: 10.1186/s12888-019-2031-9
- Sörös, P., Inamoto, Y., and Martin, R. (2009). Functional brain imaging of swallowing: an activation likelihood estimation meta-analysis. *Hum. Brain Mapp.* 30, 2426–2439. doi: 10.1002/hbm.20680
- Sörös, P., Lalone, E., Smith, R., Stevens, T., Theurer, J., Menon, R., et al. (2008). Functional MRI of oropharyngeal air-pulse stimulation. *Neuroscience* 153, 1300–1308. doi: 10.1016/j.neuroscience.2008.02.079
- Sörös, P., Macintosh, B., Tam, F., and Graham, S. (2010). fMRI-compatible registration of jaw movements using a fiber-optic bend sensor. *Front. Hum. Neurosci.* 4:24. doi: 10.3389/fnhum.2010.00024
- Sörös, P., Sokoloff, L., Bose, A., McIntosh, A., Graham, S., and Stuss, D. (2006). Clustered functional MRI of overt speech production. *Neuroimage* 32, 376–387. doi: 10.1016/j.neuroimage.2006.02.046
- Svoboda, K., and Li, N. (2018). Neural mechanisms of movement planning: motor cortex and beyond. *Curr. Opin. Neurobiol.* 49, 33–41. doi: 10.1016/j.conb.2017.10.023
- Takai, O., Brown, S., and Liotti, M. (2010). Representation of the speech effectors in the human motor cortex: somatotopy or overlap. *Brain Lang.* 113, 39–44. doi: 10.1016/j.bandl.2010.01.008
- Tourville, J., Nieto-Castañón, A., Heyne, M., and Guenther, F. (2019). Functional parcellation of the speech production cortex. *J. Speech Lang. Hear. Res.* 62, 3055–3070. doi: 10.1044/2019_JSLHR-S-CSMC7-18-0442
- Tremblay, P., Sato, M., and Deschamps, I. (2017). Age differences in the motor control of speech: an fMRI study of healthy aging. *Hum. Brain Mapp.* 38, 2751–2771. doi: 10.1002/hbm.23558
- Turesky, T., Turkeltaub, P., and Eden, G. (2016). An activation likelihood estimation meta-analysis study of simple motor movements in older and young adults. *Front. Aging Neurosci.* 8:238. doi: 10.3389/fnagi.2016.00238
- Turner, B., Paul, E., Miller, M., and Barbey, A. (2018). Small sample sizes reduce the replicability of task-based fMRI studies. *Commun. Biol.* 1:62. doi: 10.1038/s42003-018-0073-z
- Tustison, N., Cook, P., Klein, A., Song, G., Das, S., Duda, J., et al. (2014). Large-scale evaluation of ANTs and FreeSurfer cortical thickness measurements. *Neuroimage* 99, 166–179. doi: 10.1016/j.neuroimage.2014.05.044
- Tustison, N. J., Avants, B. B., Cook, P. A., Zheng, Y., Egan, A., Yushkevich, P. A., et al. (2010). N4ITK: improved N3 bias correction. *IEEE Trans. Med. Imaging* 29:1310. doi: 10.1109/TMI.2010.2046908
- Van Lieshout, P., Steele, C., and Lang, A. (2011). Tongue control for swallowing in Parkinson's disease: effects of age, rate, and stimulus consistency. *Mov. Disord.* 26, 1725–1729. doi: 10.1002/mds.23690
- Veale, J. (2014). Edinburgh Handedness Inventory–Short Form: a revised version based on confirmatory factor analysis. *Laterality* 19, 164–177. doi: 10.1080/1357650X.2013.783045
- Watanabe, J., Sugiura, M., Miura, N., Watanabe, Y., Maeda, Y., Matsue, Y., et al. (2004). The human parietal cortex is involved in spatial processing of tongue movement—an fMRI study. *Neuroimage* 21, 1289–1299. doi: 10.1016/j.neuroimage.2003.10.024
- Weirich, M., Lancia, L., and Brunner, J. (2013). Inter-speaker articulatory variability during vowel-consonant-vowel sequences in twins and unrelated speakers. *J. Acoust. Soc. Am.* 134, 3766–3780. doi: 10.1121/1.4822480
- Wexler, B., Fulbright, R., Lacadie, C., Skudlarski, P., Kelz, M., Constable, R., et al. (1997). An fMRI study of the human cortical motor system response to increasing functional demands. *Magn. Reson. Imaging* 15, 385–396. doi: 10.1016/S0730-725X(96)00232-9
- Wong, D., Dziedzic, M., Talavage, T., Romito, L., and Byrd, K. (2011). Motor control of jaw movements: an fMRI study of parafunctional clench and grind behavior. *Brain Res.* 1383, 206–217. doi: 10.1016/j.brainres.2011.01.096
- Woolrich, M., Behrens, T., Beckmann, C., Jenkinson, M., and Smith, S. (2004). Multilevel linear modelling for FMRI group analysis using Bayesian inference. *Neuroimage* 21, 1732–1747. doi: 10.1016/j.neuroimage.2003.12.023
- Woolrich, M., Jbabdi, S., Patenaude, B., Chappell, M., Makni, S., Behrens, T., et al. (2009). Bayesian analysis of neuroimaging data in FSL. *Neuroimage* 45, S173–S186. doi: 10.1016/j.neuroimage.2008.10.055
- Woolrich, M., Ripley, B., Brady, M., and Smith, S. (2001). Temporal autocorrelation in univariate linear modeling of FMRI data. *Neuroimage* 14, 1370–1386. doi: 10.1006/nimg.2001.0931
- Xu, A., Larsen, B., Baller, E. B., Scott, J. C., Sharma, V., Adebimpe, A., et al. (2019). Convergent neural representations of acute nociceptive pain in healthy volunteers: a large-scale fMRI meta-analysis. *bioRxiv* 779280. doi: 10.1101/779280
- Yeo, B., Krienen, F., Sepulcre, J., Sabuncu, M., Lashkari, D., Hollinshead, M., et al. (2011). The organization of the human cerebral cortex estimated by intrinsic functional connectivity. *J. Neurophysiol.* 106, 1125–1165. doi: 10.1152/jn.00338.2011
- Ziegler, W. (2003). Speech motor control is task-specific: evidence from dysarthria and apraxia of speech. *Aphasiology* 17, 3–36. doi: 10.1080/729254892
- Zuo, X., and Xing, X. (2014). Test-retest reliabilities of resting-state FMRI measurements in human brain functional connectomics: a systems neuroscience perspective. *Neurosci. Biobehav. Rev.* 45, 100–118. doi: 10.1016/j.neubiorev.2014.05.009

Conflict of Interest: The authors declare that the research was conducted in the absence of any commercial or financial relationships that could be construed as a potential conflict of interest.

Copyright © 2020 Sörös, Schäfer and Witt. This is an open-access article distributed under the terms of the Creative Commons Attribution License (CC BY). The use, distribution or reproduction in other forums is permitted, provided the original author(s) and the copyright owner(s) are credited and that the original publication in this journal is cited, in accordance with accepted academic practice. No use, distribution or reproduction is permitted which does not comply with these terms.



A Systematic Review of Physical Rehabilitation of Facial Palsy

Annabelle Vaughan^{1,2,3*}, Danielle Gardner¹, Anna Miles⁴, Anna Copley², Rachel Wenke^{1,3} and Susan Coulson⁵

¹ Speech Pathology Service, Gold Coast University Hospital, Gold Coast, QLD, Australia, ² School of Health and Rehabilitation Sciences, University of Queensland, Brisbane, QLD, Australia, ³ School of Allied Health Sciences, Griffith University, Gold Coast, QLD, Australia, ⁴ Speech Science, The University of Auckland, Auckland, New Zealand, ⁵ School of Health Sciences, Discipline of Physiotherapy, The University of Sydney, Camperdown, NSW, Australia

OPEN ACCESS

Edited by:

Limor Avivi-Arber,
University of Toronto, Canada

Reviewed by:

Meg E. Morris,
La Trobe University, Australia
Orlando Guntinas-Lichius,
University Hospital Jena, Germany
Adriaan Grobbelaar,
University College London,
United Kingdom

*Correspondence:

Annabelle Vaughan
annabelle.vaughan@health.qld.gov.au

Specialty section:

This article was submitted to
Neurorehabilitation,
a section of the journal
Frontiers in Neurology

Received: 27 September 2019

Accepted: 10 March 2020

Published: 31 March 2020

Citation:

Vaughan A, Gardner D, Miles A,
Copley A, Wenke R and Coulson S
(2020) A Systematic Review of
Physical Rehabilitation of Facial Palsy.
Front. Neurol. 11:222.
doi: 10.3389/fneur.2020.00222

Background: Facial palsy is a frequent and debilitating sequela of stroke and brain injury, causing functional and aesthetic deficits as well as significant adverse effects on quality of life and well-being. Current literature reports many cases of acquired facial palsy that do not recover spontaneously, and more information is needed regarding the efficacy of physical therapies used in this population.

Methods: A systematic search of eight electronic databases was performed from database inception to December 2018. Gray literature searches were then performed to identify additional articles. Studies were included if they addressed physical rehabilitation interventions for adults with acquired facial palsy. Reasons for exclusion were documented. Independent data extraction, quality assessment, and risk of bias assessment followed the Preferred Reporting Items for Systematic Reviews and Meta-Analyses (PRISMA) guidelines.

Results: Following abstract screening, a total of 13 full-text articles were identified for independent screening by two reviewers. This included four randomized control trials, two non-randomized control trials, one cohort study, and six prospective case series studies. Twelve out of the 13 included studies reported on facial palsy as a sequela of stroke. A total of 539 participants received intervention for facial palsy across the 13 included studies. Therapy design, length and frequency of intervention varied across the studies, and a wide range of outcome measures were used. Improvement on various outcome measures was reported across all 13 studies. The quality of the evidence was low overall, and most studies were found to have high risk of bias.

Conclusions: All the studies in this review report improvement of facial movement or function following application of various methods of physical rehabilitation for facial palsy. Methodological limitations and heterogeneity of design affect the strength of the evidence and prevent reliable comparison between intervention methods. Strong evidence supporting physical rehabilitation was not found; well-designed rigorous research is required.

Keywords: central facial palsy, rehabilitation, exercise, systematic review, therapy

INTRODUCTION

The facial nerve (CNVII) plays a critical role in multiple complex functions of human life including mastication, speech, and successful social communication through expression of mood and emotion (1–4). Central facial palsy (CFP) results from damage to the central segment of this nerve (facial nucleus in the pons, motor cortex, or connections between the two) (5) and manifests typically as a unilateral impairment of movement opposite to the side of the injury, with predominance in the lower face (6). In contrast, peripheral facial palsy (PFP) results from injury or damage to extratemporal segments of the facial nerve (7), for example in idiopathic “Bell’s” palsy, surgery such as mastoidectomy, or inflammation such as herpes zoster (Ramsay Hunt syndrome) (8).

CFP is a frequent initial symptom in patients after stroke and other neurological injury. A study conducted by Cattaneo and Pavesi (9) found that 60% of patients with first-time ischemic cortical stroke (MCA and ACA territories) presented with CFP. Other studies of stroke populations have reported a prevalence of approximately 45% (6). It is evident from multiple searches of libraries and online evidence repositories during clinical management of CFP that most of the available literature relates to rehabilitation of peripheral facial palsy (PFP), and there is very little evidence available to guide therapists working with people suffering from CFP. Whilst systematic reviews have evaluated physical rehabilitation and other management for PFP (10–12), the different etiopathogenesis of CFP suggests that rehabilitation approaches should be specifically modified for this group (13).

Spontaneous recovery of CFP has been reported in two-thirds of people at 6 months post-stroke, with approximately one-third of patients after stroke continue to present with persisting facial palsy after 6 months (14). More recently, differing opinions are emerging in the literature regarding rates of spontaneous resolution of CFP (including associated functional and QOL deficits), with some authors noting that in the absence of rehabilitation, symptoms seem unlikely to improve (15). In their study, Volk et al. (6) reported that a high percentage of patients continued to present with CFP 3 weeks post-onset, and over 60% of these patients were discharged from sub-acute rehabilitation with deficits persisting for more than 41 days post-stroke. As the available literature suggests that CFP can persist past the initial acute phase of stroke and not resolve spontaneously, people with CFP may benefit from access to a specific rehabilitation program aimed at maximizing recovery of facial movement and function (6, 13, 16).

Facial palsy can be distressing and debilitating for those affected, causing both functional and aesthetic deficits (16). Functional deficits may be characterized by facial asymmetry and weakness of the lower half of the face, drooping of the corner of the mouth, dribbling from the corner of the mouth at rest or during oral intake, reduced masticatory force and efficiency, asymmetrical smile and dysarthria (slurring or reduced clarity of speech) (15). It is well-recognized in the literature that in addition to functional deficits, facial palsy has a negative effect on quality of life (QOL) and emotional well-being (7, 17–21). In their 2016 study comparing QOL between individuals with pure CFP post

stroke vs. pure dysarthria, Chang et al. (21) found that the CFP group had significantly worse scores on QOL and depression scales. Interestingly, it has been found that the presence of facial palsy alone regardless of its severity has a detrimental effect on the psychological well-being of those who experience it (19).

Rationale

Currently, there is minimal evidence available to guide clinical decision-making in the rehabilitation of CFP (22, 23) and very little information available regarding the effectiveness of popular intervention techniques (21, 23). As mentioned above, CFP may not resolve spontaneously and the negative impacts of CFP on people who experience this disorder can be wide-ranging. Rehabilitation may maximize functional recovery and improve the quality of life and psychological well-being of people with CFP (6, 13, 16) however there is currently no comprehensive or systematic review of the literature specific to this disorder to inform therapy planning and provision. This has significant implications for patient management, as it is still not clear to health professionals whether physical rehabilitation techniques work, or which technique is most effective.

Objective

The purpose of this review is to identify and examine the available literature specifically relating to physical rehabilitation of CFP. This review aims to (1) identify the types of physical rehabilitation methods used in remediation of CFP; (2) review the effectiveness of various methods of physical rehabilitation, and (3) review the methodological quality of the studies retrieved. The findings will be pertinent to clinicians working with patients with CFP as this is the only review that the authors are aware of that systematically evaluates the evidence base for rehabilitation of this disorder.

Research Question

What is the effectiveness of physical rehabilitation for acquired central facial palsy in adults?

METHODS

Study Design and Search Strategy

This review follows the Preferred Reporting Items for Systematic Reviews and Meta-Analyses (PRISMA) statement. The review protocol is registered on PROSPERO (CRD42018115303). A systematic search strategy was devised in conjunction with a senior librarian, using the core concepts of facial paralysis, central nervous system disease, and physical rehabilitation. The Medical Subject Headings (MeSH) database was used to obtain terms that were related to these concepts to ensure a comprehensive search of the literature was performed. The search strategy was designed and performed using Medline (Ovid) terminology (see **Appendix 1**). No limitations were used for year published, language, or publication type. The search strategy was then translated for searching the following databases: Embase (Elsevier), CINAHL (Ebsco), Cochrane Central Register of Controlled Trials, Proquest Dissertations and Theses Global, PEDro, Speechbite, and Web of Science (Clarivate).

Gray literature searches included searches of WHO ICTRP (3) and ANZCTR (0) using the terms *central facial pa**, with no completed studies (3 currently registered trials) retrieved. ClinicalTrials.gov was searched using the heading *facial palsy* with 18 completed studies retrieved, however all retrieved studies either pertained to peripheral facial palsy or did not have results available and were therefore not included in this review. Clinical practice guidelines and best practice statements were searched for relevant literature/references, including Clinical Guidelines for Stroke Management 2017 (24), United Kingdom National Clinical Guideline for Stroke (25), and American Speech and Hearing Association Evidence Maps ([https://www.asha.org/MapLanding.aspx?id=\\$8589947062](https://www.asha.org/MapLanding.aspx?id=$8589947062)).

Further hand-searching of library and clinical databases were conducted. Specialists from facial therapy services in Australia and internationally were asked to provide any relevant literature which informs their current clinical practice. The reference lists of articles eligible for inclusion following full text screening were searched, and any titles that appeared to fit the criteria set were retrieved.

Participants, Interventions, Comparators

The inclusion and exclusion criteria for the review are presented in Table 1.

Systematic Review Protocol

The systematic search strategy is presented in Figure 1. A senior health service librarian performed database searching. Articles retrieved in the database searches were deduplicated using the Bond University CREB SRA deduplicating tool (<http://crebp-sra.com>) and then further screened to remove other duplicates. Abstracts of all articles remaining following deduplication were then collated into an Endnote library, which was then uploaded

to Covidence (Veritas Health Innovation Ltd, Melbourne, Australia) for blind review by two independent reviewers (AV and DG). Titles and abstracts were screened against the predetermined inclusion/exclusion criteria and subsequently added to full text screening lists. Articles included by both independent reviewers and articles that were marked as “maybe” by one or both reviewers were considered eligible for further review. Full texts of eligible studies were then retrieved and independently assessed for inclusion/exclusion. Any conflicts that arose during eligibility assessment were resolved by (a) discussion between reviewers, or where agreement could not be reached, by (b) discussion with the review team and relevant experts in the field.

Data Extraction

For all included articles, a range of variables including study population/participant details, selection criteria, methodology, interventions (therapy approach, intensity, follow-up) and outcomes were extracted and are presented in a descriptive summary in Table 2. These variables were identified as most relevant to our clinical question. Data extraction was performed initially by the second author (DG), and then amended and expanded where necessary by the first author (AV) using Google Sheets (Google, CA, USA). Due to heterogeneity in the included studies a meta-analysis was not able to be performed.

Quality Assessment

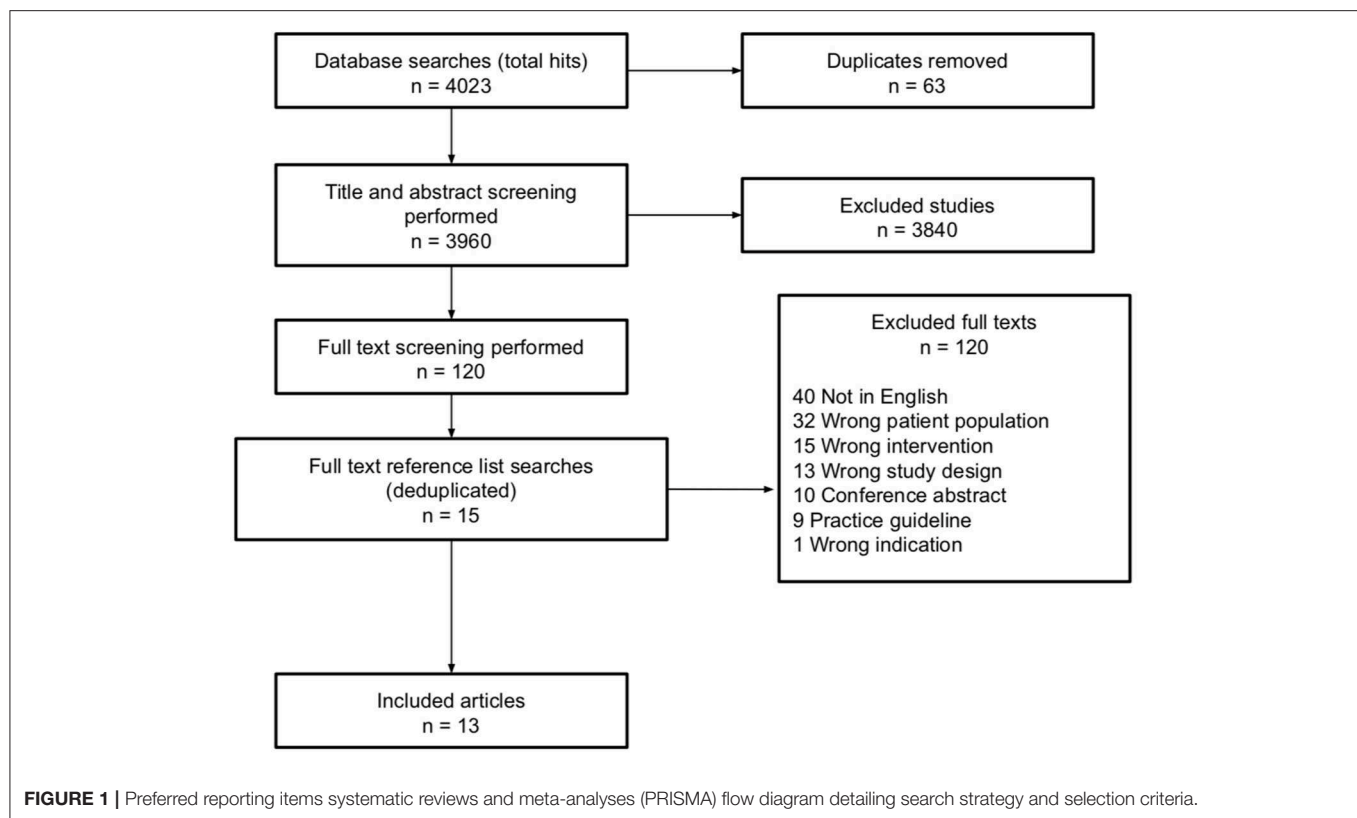
Risk of bias was assessed using tools appropriate to the study methodology determined during the data extraction process: case series reports were assessed using the JBI Critical Appraisal Checklist for Case Series (35), cohort studies were assessed using the JBI Critical Appraisal Checklist for Cohort Studies (35), and control trials were assessed using the Physiotherapy Evidence Database—Psychbite scale (PEDro-P) (36). No mixed-method studies were identified during the search, therefore the tools used to assess risk of bias were altered from the original PROSPERO protocol to be more appropriate to the various study designs retrieved (control trials, case series, cohort study). Risk of bias analyses were performed independently by two reviewers (AV and RW) and discrepancies were discussed by the two authors until consensus was achieved.

Data Analysis

Meta-analysis of the results was not indicated due to the clinical diversity of the studies retrieved, as recommended by the Cochrane Handbook for Systematic Reviews of Interventions (37). Each of the studies retrieved described differing experimental designs, treatment protocols, and methods of outcome measurement, and there was inadequate reporting of data and statistics necessary for appropriate and meaningful meta-analysis. Types of physical rehabilitation used in CFP have been broadly grouped as having used either an active approach (recipients actively move their own muscles or structures to perform exercises or volitional muscle movements), passive approach (movement is facilitated by external force, person or device e.g., massage/stretching, acupuncture, electrical

TABLE 1 | Selection criteria.

| Selection Criteria | Inclusion Criteria | Exclusion Criteria |
|----------------------------|--|--|
| Participant | Adults with acquired CFP | Pediatrics (<18 yrs) |
| Intervention | Physical rehabilitation of CFP | Surgical or pharmacological intervention with no physical rehabilitation component |
| Comparator | None or placebo treatment, drug/surgical treatment, or other physical rehabilitation | No outcomes reported |
| Outcomes | Quantitative or qualitative outcomes in subjective or objective measures of motor function or symmetry/appearance or QOL | |
| Other: Methodology | Case series Separate data for CFP and PFP | Single case study design, secondary research (i.e., reviews) Combined data for CFP and PFP or unclear delineation |
| Other: Publication details | Articles from research journals Articles in English | Book chapters, thesis publications, opinion pieces Articles not in English |



stimulation), or a combination of the two. The effectiveness of physical rehabilitation has been determined by the examination of the reported results in those studies that provided sufficient data and is discussed in the context of the various grouped approaches. Rating of the overall quality of the evidence has been performed by applying relevant sections of the Grades of Recommendation, Assessment, Development, and Evaluation (GRADE) approach to individual studies (38).

RESULTS

Study Selection

The results from database searching and selection processes are shown in **Figure 1**.

Study Characteristics

Six case series (total no. of subjects = 108) one cohort study (total no. of subjects = 112), and six control trials (total no. of subjects = 133) were identified. Methodological details are outlined in **Table 2**. Of the four RCTs, two appeared to use identical participant populations and outcome data and are subsequently discussed as one study in parts of this review ($n = 99$ (13, 16)). All the included studies used a pre-test post-test design.

Participant Demographics

Participant demographics for all included studies are reported in **Table 2**. Twelve out of the 13 included studies reported on facial palsy as a sequela of stroke, and one study reported facial palsy secondary to acquired brain injury. A total of 539 participants

received intervention for facial palsy in the 13 studies included in this review (age range 48–88 yr old). There was a large range in time post-onset of facial palsy from acute (e.g., “days”) to chronic (e.g., 6–10 years) stages of recovery.

Types of Physical Rehabilitation for Facial Palsy

There was a high degree of heterogeneity in physical rehabilitation methods described for adults with CFP. Seven studies reported interventions aimed at remediation of facial palsy as their primary objective (6, 26–29, 31, 33), and six reported targeting lip function or movement in the context of post-stroke dysphagia therapy (13, 16, 23, 30, 32, 34). Four studies reported on active intervention methods for remediation of oromotor function or facial palsy (23, 26–28); two used muscle strengthening exercises alone (26, 27) and the other two used biofeedback (via mirror or device) while performing orofacial exercises (23, 28). Four studies reported on passive intervention techniques such as massage, stretching or electrical stimulation for the remediation of facial muscle strength or facial palsy (13, 16, 29, 30). Acupuncture is classified in this review as passive rehabilitation; one study (30) reported on the use of scalp acupuncture compared to a group that received “western medicine.” Five studies combined active and passive approaches in the rehabilitation of CFP (6, 31–34); therapy varied across these studies but all included elements of active exercise, massage, stretching or passive manipulation, or application of various devices (**Table 2**).

TABLE 2 | Extracted data.

| Study ID [References] | Participants N Dx time post onset | Methodology | | Interventions | | Intensity length of Tx freq duration | Outcome measures | Results |
|--------------------------|---|--|---------------------|--|--------------------------------------|---|---|---|
| | | | | Group A | Group B | | | |
| Hagg and Anniko (26) | 30 (24 with UFP) Stroke 2 days–10yrs | Retrospective case series | Active Therapy | Lip muscle training | N/A | >5 weeks 3 × 3/day 5–10 s | Swallowing capacity (ml/s) Lip force | Stat sig improvement in both OMs ($p < 0.05$) FP 'improved' |
| Hee-Su et al. (27) | 10 Stroke <6 mths | Prospective case series | | Traditional therapy + resistance training of OO | N/A | 4 weeks 5×/wk <i>not stated</i> | Orbicularis oris strength Lip closure (VDS) | Stat sig improvement in both OMs ($p < 0.05$) |
| Huffman (28) | 4 Brain injury >2 mths | Prospective non-randomized control trial | | Mirror therapy | Mirror therapy + EMG | 10 days (in 2 week period) Daily 30min | Muscle grade | Improvement in both pairs although 3× greater in EMG vs. mirror |
| Kang et al. (23) | 21 Stroke <12 wks | Prospective RCT | | Orofacial exercises | Orofacial exercises + mirror therapy | 14 days 2×/day 15 min | HBGS Facial movement difference (m-dif) Facial movement ratio (m-rat) | Stat sig improvement in all OMs ($p < 0.05$), greater in mirror vs. control |
| Choi (29) | 9 Stroke <3 mths | Prospective case series | Passive Therapy | Neuromuscular ES + dysphagia therapy | N/A | 4 weeks 5×/wk 30 min/session | Max cheek strength (MCS) Max lip strength (MLS) Dysphagia (VDS) | Stat sig improvement in MCS and MLS Stat sig decrease on VDS ($p < 0.05$) |
| Konecny et al. (16) | 99 Stroke 1–2wks | Prospective RCT | | SSRI, SP/OT/PT | SSRI, SP/OT/PT + orofacial therapy | 4 weeks Daily <i>not stated</i> | HBGS Distance measure BDI-II | Stat sig improvement in all OMs ($p < 0.05$), greater in experimental vs. control |
| Konecny et al. (13) | 99 Stroke 1–2wks | Prospective RCT | | SSRI, SP/OT/PT | SSRI, SP/OT/PT + orofacial therapy | 4 weeks Daily <i>not stated</i> | As above + Bartel index Mod. Rankin score | Stat sig improvement in both QOL OMs ($p < 0.05$), greater in experimental vs. control |
| Zhou and Zhang (30) | 165 Stroke 1day–6yrs | Prospective RCT | | Scalp acupuncture | Western medicine | 24 days? Daily ~50 min | Clinical indexes / function grading scales | Improvement in 88.57% of acupuncture group and 76.67% of western medicine group |
| Hagg and Larsson (31) | 7 Stroke 6 mths–4 yrs | Prospective case series | Combination Therapy | Body regulation, manual orofacial regulation, palatal plate activation + velopharyngeal closure training | N/A | 5 weeks 5×/wk 120 min/session + HEP | Swallowing capacity (ml/s) Meal observation Oral motor performance Orofacial sensory function Velopharyngeal closure VFSS Self-assessment | Improvement on raw scores in at least one variable for all OMs |
| Hagg Tibbling (32) | 31 Stroke Days–10 yrs | Prospective non-randomized control trial | | Palatal Plate (PP) | Oral IQoroR screen (IQS) | 3 months 3×/day PP 10–30 min; IQS 30 s | Swallowing capacity (ml/s) Facial Activity Testing (FAT) | Stat sig improvement in both OMs for both groups ($p < 0.05$) Improvements maintained at 1 yr f/up |
| Noor et al. (33) | 50 Stroke <i>Not stated</i> | Prospective case series | | Massage, ES, KOBAT | N/A | ?3 weeks 3×/wk <i>not stated</i> | Spasticity grade | Reduction in spasticity grade for all participants |
| Van Gelder et al. (34) | 2 Stroke 2mths | Prospective case series | | Neuro Developmental Treatment | N/A | 9–12 weeks Weekly <i>not stated</i> | Mimic expressions Orofacial function Asymmetry and adequacy | 2/2 improved mimic expressions + symmetry 1/2 improved orofacial function + adequacy |
| Volk et al. (6) | 112 Stroke 20 days (median) | Prospective cohort study | | Physical training of related muscles, tapping, mirror therapy | N/A | 21 days (median) <i>not stated not stated</i> | Bartel index HBGS Sunnybrook FGS Stennert index Action units (AU) FaCE questionnaire FDI | Stat sig improvement in activity, facial nerve motor function, self-reported non/motor abilities ($p < 0.05$) |

Dx, Diagnosis; EMG, Electromyography; ES, Electrical stimulation; HBGS, House Brackmann Grading Scale; FGS, Facial Grading System; FDI, Facial Disability Index; FP, Facial palsy; HEP, Home exercise program; OM, Outcome measures; OO, Orbicularis oris; OT, Occupational therapist; PT, Physiotherapist; QOL, Quality of life; SP, Speech pathologist; SSRI, Selective serotonin reuptake inhibitor; Tx, Therapy; UFP, Unilateral facial palsy; VDS VFSS, Dysphagia Scale; VFSS, Videofluoroscopic Swallow Study.

Dosage

Length and frequency of therapy varied across the studies, with participants receiving multiple therapy sessions per week for between 10 days and 9 weeks. Details relating to intensity of therapy (length, frequency, and duration of intervention) are presented in **Table 2**.

Outcome Measures

A wide range of outcome measures for muscle strength and facial movements were used including measures of muscle strength, facial movement, and symmetry; details are outlined in **Table 2**. No validated outcome measurement tools were used. The majority of studies did not provide detailed descriptions of grading scales; only three studies (6, 13, 16, 23) used well-known outcome measures specific to facial palsy. Facial palsy was often measured in conjunction with other deficits of speech, swallowing, emotional and psychological well-being.

Effectiveness of Physical Rehabilitation of Facial Palsy

Four RCTs and nine observational studies reported improvements in various measures of facial palsy or facial motor function, which are outlined below in the context of the rehabilitation approach used (active, passive or combination). Eight of the 13 studies included comments about the statistical significance of the results (*p*-values), however none performed calculations of effect size, and therefore none of the studies provided sufficient data to assess imprecision or inconsistency as outlined in the GRADE approach. There were also insufficient data reported to facilitate judgement of indirectness; the nine observational studies do not undertake comparison with an alternative therapy or control group, and none of the RCTs provided calculations of risk ratio or effect size that would enable meaningful direct comparison.

Active Therapy

Four studies reported on active therapy methods; one RCT (23), one nRCT (28), and two case series' (26, 27). All four studies reported improvements in treatment variables measured. Kang et al. (23) reported improvement in HBGS scores and functional measures (facial movement ratios) in both the control group and the experimental group (both groups performed the exercise protocol with the experimental group receiving mirror feedback as the experimental condition). Huffman (28) also reported improvement in all subjects on an unvalidated 'muscle grade' rating scale mentioned but not detailed by the authors; as well as improvements three times greater for the subjects receiving EMG feedback compared to mirror feedback. Both the case series' implemented protocols of lip strengthening using instrument-based exercise. Hee-su et al. (27) reported improvements in orbicularis oris muscle strength and lip closure function during swallowing; no outcomes specific to facial palsy (e.g., measures of movement or symmetry) were used. Hagg and Anniko (26) also reported improvement in raw scores of lip force from baseline measures taken using a Lip Force Meter instrument however did not specifically report on outcomes for facial palsy.

Passive Therapy

Four studies reported on passive therapy methods, including a case series study (29) and three RCTs (13, 16, 30); two RCTs are discussed together (13, 16) for reasons mentioned previously. All four reported improvements in relevant measures. Choi (29) reported changes in facial muscle strength compared to baseline measures however did not explicitly report outcomes for facial palsy. Zhou and Zhang (30) reported a larger change in all outcome measures (including a facial movement grading scale not described in the study) for the group receiving acupuncture compared to those receiving "western medicine." There was no detail provided regarding the method for administration of this grading scale. Konecny et al. (13, 16) reported improvements in formal facial nerve assessment measures (HBGS) as well as in a variety of other functional and quality-of-life scales.

Combination Therapy

Five studies reported on therapy protocols that combined passive and active methods (e.g., massage/manipulation with active exercise regime). These included three case series' (31, 33, 34), one non-randomized control trial (32) and one cohort study (6). One case series (33) reported improvements in spasticity of facial muscles; this was demonstrated by reporting the number of participants per scoring level (grade I–V) pre and post treatment on an unnamed grading tool. There were no individual assessment outcomes reported and there was an absence of statistical analysis of the data. One (31) reported improvements in raw scores of orofacial motility on an informal four-point scale as well as improvement in mean severity score of oral motor performance. The authors provided raw pre and post assessment data for each participant as rated by multiple assessors; there was an absence of further analysis of this data and overall outcomes were focused on dysphagia rather than facial palsy. The case series reported by Volk (6) reported improvements in three well-known tools to assess facial palsy [HBGS (39), Sunnybrook Grading Scale (40), and Stennert Index (41)], two validated quality of life instruments [FaCE Questionnaire (42) and FDI (43)], and a system of automated facial movement analysis described in the study.

Maintenance of Therapeutic Effects

Eleven of the 13 included studies did not report any follow up assessment, and therefore no evaluation of the maintenance of therapeutic effects was available. One study (32) reported maintenance of improved facial activity at follow-up assessment at least 1 year post treatment in both groups. Van Gelder et al. (34) reported on follow-up assessment 9 weeks post treatment in only one of the two participants. Their results showed a decline in function between completion of treatment and re-assessment, which the authors interpreted as showing treatment effects were not maintained.

Methodological Quality and Risk of Bias

A summary of the consensus ratings for methodological assessment is shown using modified harvest plots, which have been used previously in systematic reviews to present data that is not able to be graphed using traditional methods (44, 45).

TABLE 3 | PEDro-P and JBI ratings.

| Condensed category | PEDro-P Item | Condensed category | JBI item (Case series) | Condensed category | JBI item (Cohort) |
|--------------------|---|--------------------|--|--------------------|---|
| Participant | Eligibility criteria specified Concealed allocation | Participant | Eligibility criteria specified Standard, reliable measurement of condition Valid identification of condition | Participant | Both groups similar, recruited from same population |
| Intervention | Prognostic similarity at baseline between intervention groups | Design | Consecutive inclusion Complete inclusion Participant demographics Participant clinical information Outcomes or follow-up | Design | Exposures measured similarly Standard, reliable measurement of exposure Confounding factors identified Groups/participants free of outcome initially Outcome measurement valid and reliable |
| Blinding | Subject blinding Therapist blinding Assessor blinding | | | | |
| Outcomes | >85% of the subjects followed up for at least 1 key outcome Intention-to-treat analysis Between group statistical analysis for at least 1 key outcome | Site | Site demographics | Follow-up | Follow up sufficient and reported Complete follow up Incomplete follow up managed |
| Variability | Point estimates of variability provided for at least 1 key outcome | Statistics | Appropriate statistical analysis | Statistics | Appropriate statistical analysis |

These modified harvest plots were created by grouping similar criteria together for each appraisal tool, as detailed in **Table 3**. As in previous studies where modified harvest plots have been used, methodological quality is represented by bar height (45). “Unclear” consensus ratings have been scored as zero when calculating scores for each criterion on the JBI tools.

Control Trials

Across the control trials, scores on the PEDRO-P ranged from 3 to 9 with an average of 5.5 out of 11 (see **Figure 2**). Of the RCTs, 2 of the 4 specified eligibility criteria for inclusion in the study, and while the majority allocated subjects randomly to interventions only one concealed this allocation. Blinding was an area of significant risk across the RCTs, with 1 of 4 studies blinding subjects and assessors and no blinding of therapists in any study. The nRCTs showed similar shortcomings in allocation and blinding items. The intervention groups were similar at baseline regarding the most important prognostic indicators in >90% of the studies. Outcome measurement was an area of strength for all the control studies; 100% obtained measures of at least one key outcome from >85% of subjects and demonstrated that all subjects for whom outcome measures were available received the treatment or control condition. Overall the quality of the control trials is low due to the significant limitations present in the majority of studies.

Case Series and Cohort Study

Scores on the JBI tool for case series evaluation ranged from 2 to 7 with an average of 3.8 out of 10 (see **Figure 3**). Four (27, 29, 33, 34) of the six case studies were judged to be at high risk of bias; 2 of the 6 of studies failed to outline clear criteria, only 30% used

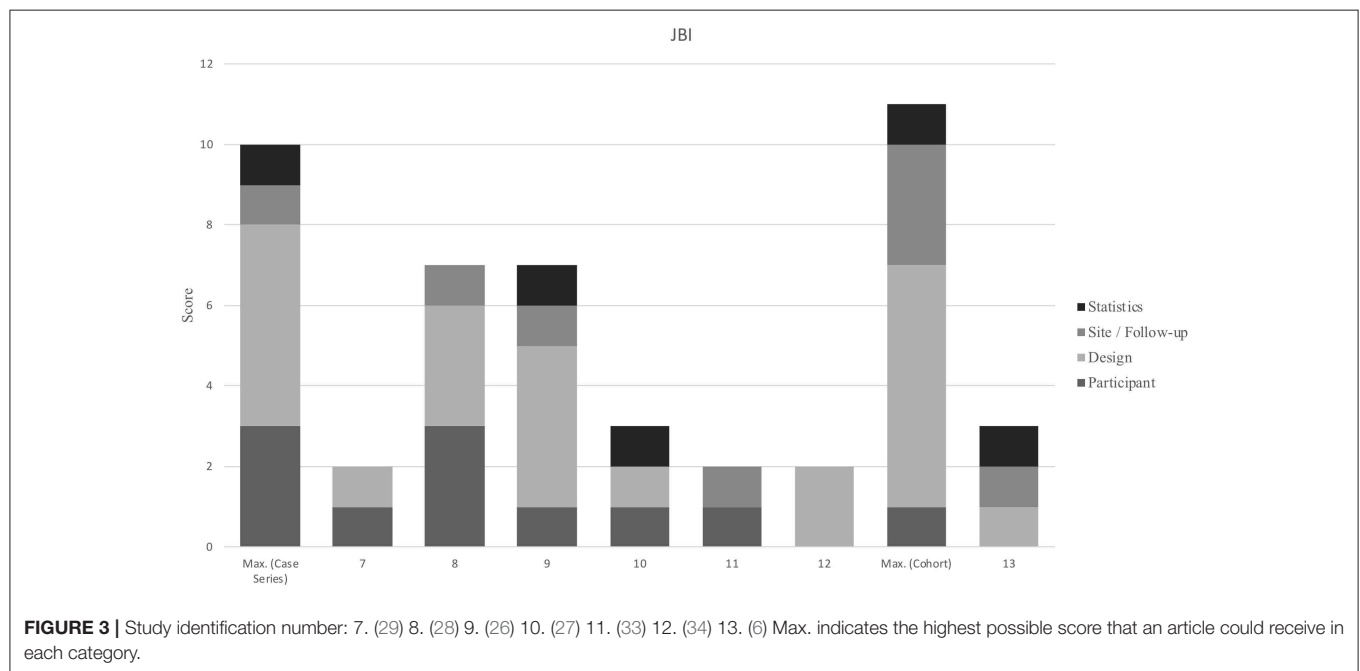
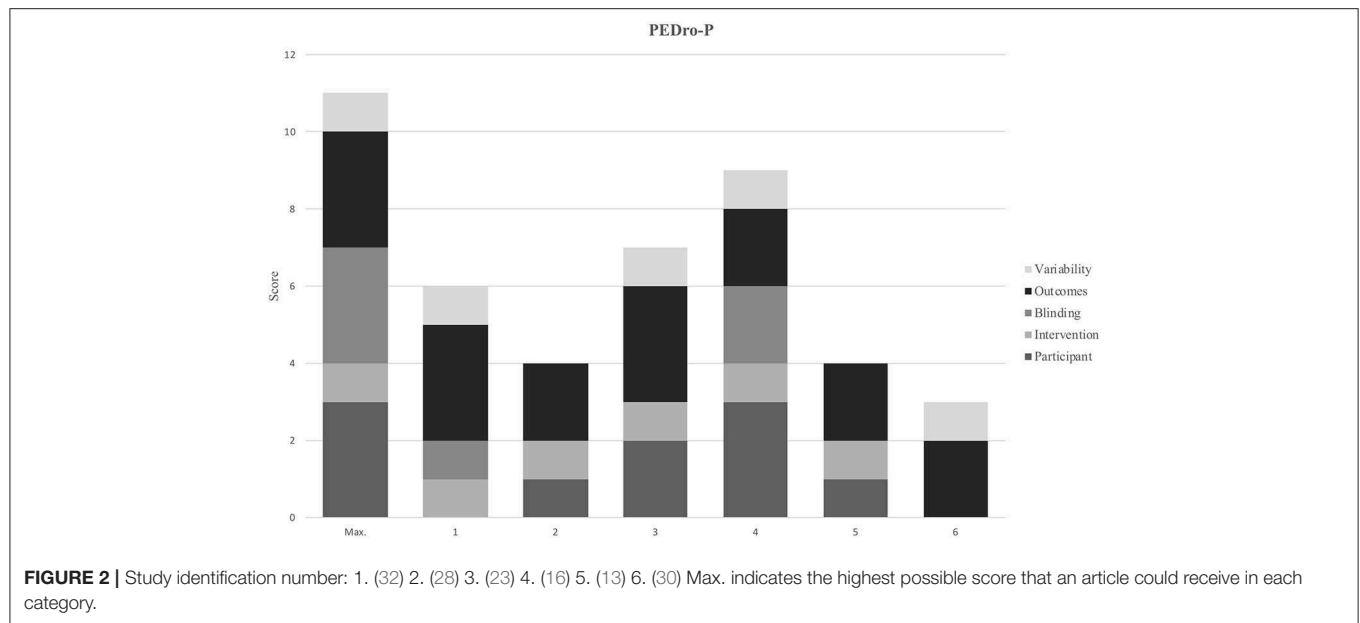
valid methods for identification of the condition, >80% did not report consecutive recruitment of subjects and failed to clearly report clinical information of the participants. Two case studies were judged to have an unclear risk of bias (26, 31); strengths of both these studies were found in reliable condition measurement and clear reporting of participant demographics. Limitations of the case series’ judged as “unclear risk of bias” were varied—in one (31) it was not clear if the study included consecutive and complete inclusion and methods of statistical analysis were ambiguous; in the other (26) criteria were not clearly defined and it was not possible to determine if valid methods for identification of the condition were used.

DISCUSSION

This review has shown that despite trends demonstrating improvement in CFP following various types of physical rehabilitation, there is a lack of high-quality evidence currently available to inform clinical practice. Many questions remain for clinicians planning and providing therapy for this population. Literature is emerging which recognizes CFP as an impairment in its own right (separate to its impact on speech or swallowing function), and therapies specifically targeting this disorder are being investigated with increasing frequency. All the studies in this review report improvement on various parameters of facial movement or function and, although lacking in rigor, indicate potential benefit from using physical rehabilitation approaches.

Effectiveness of Therapy

Improvement in facial muscle strength or movement was reported across all 13 studies, and positive changes in other



outcome measures such as swallow function and quality of life were also shown (where measured). Only one study provided data for maintained effects of therapy at >1 year post intervention (32), and while this study had comparative strengths in methodology, its lack of overall rigor reduced the strength of the data. All 13 studies reported statistically significant improvements from baseline measures, however none performed calculations of optimal sample size or treatment effect measures. It is therefore unclear if the improvements reported can be attributed to the physical therapy provided or if other variables influenced the outcomes. Overall, the studies included in this

review provide insufficient evidence to draw strong conclusions regarding the effectiveness of physical rehabilitation for CFP.

Comparison of the effectiveness of differing therapy approaches remains unclear following this review. Of the four studies that were found to be the most methodologically sound (as per risk of bias assessments), two provided active therapy (one involved strengthening exercises only) (23, 26), one provided passive therapy (16), and one described a combination of these two approaches (32). Active and passive approaches were explored by only a small number of methodologically weak RCTs, and there were no RCT designs that investigated

a combination of approaches. As well as insufficient reporting of treatment effect size or precision, there was a large amount of variation in all aspects of the design of the studies—each study described different participant variables (e.g., time post onset), dosage and treatment duration. These factors restrict any meaningful comparison being made between outcomes, which leads to a lack of support for one method of rehabilitation over another.

This review highlights the need for further well-designed and rigorous research to examine the efficacy of physical rehabilitation of CFP. The trend of improvement across various outcome measures reported in all studies provides some indication that physical therapy may be of benefit, however overall there were significant limitations that impact on confident application of these findings to current clinical practice. These include a lack of comprehensive reporting and analysis of data in all studies, and methodological limitations (e.g., lack of RCT designs, lack of concealed allocation, minimal use of blinding, and lack of follow-up assessment). The majority of studies also failed to use standardized, reliable outcome measurements, which creates questions about the validity of findings and makes any comparison of outcomes difficult. Future studies should aim for more rigor in their design, for example by using RCTs to minimize risk of bias and strengthen the validity of findings and including follow-up assessment to measure maintenance of therapeutic effect.

Assessment

A major challenge for evaluation of methods of physical rehabilitation of CFP is the heterogeneity of assessment tools (and subsequently outcome measures) described. Only four of the 13 included studies utilized any standardized method of assessing facial palsy (6, 13, 16, 23, 32) and only three of these used widely-accepted quantitative outcome measures (6, 13, 16, 23). The remainder of the studies described a variety of informal clinical measures of muscle strength or facial movement and function. As such, comparison of findings between the studies in an effort to establish which methods were more effective is not able to be reliably performed.

Clinical Implications

Positive trends in favor of physical rehabilitation were found. All the studies retrieved by this review process do appear to show improvements in facial palsy with rehabilitation, which lends support to the rationale for continuation of therapy provision as well as ongoing research. The strength of the evidence is low overall, which should be considered when planning intervention for this population.

Future Directions

Future studies should aim to use objective and standardized assessment tools. Objective assessment of facial palsy is notoriously difficult (42, 46). Due to the lack of published, validated assessment tools available specific to CFP, further validation of tools designed for broader use (including peripheral types of facial palsy) may be indicated. Literature specific to PFP recommends use of the Sunnybrook Facial Grading System (40), and the House-Brackmann Grading Scale (39), and these

tools have been used with some effectiveness to measure CFP in studies by Volk et al. (6), Kang et al. (23), and Konecny et al. (13, 16). There are limitations in both tools including subjective ordinal grading systems with limited items (47, 48). The Electronic Facial Paralysis Assessment (eFACE) was developed to provide clinicians with a tool that “has greater sensitivity and objectivity when assessing incomplete paralysis and post-interventional improvement...in cases of both acute peripheral nerve palsy and recovery” (49). This tool has been found to have high test-retest reliability (50), have high validity and reliability (49), and had positive feedback from a panel of international facial nerve experts (51). The tool needs further validation in a CFP population. In addition to measuring facial function, the inclusion of reliable outcome measures that evaluate the emotional and psychological impact of CFP would enable a broader assessment of the holistic impacts of rehabilitation. Two examples of validated patient-graded tools that are referenced in current CFP literature are the Facial Clinometric Evaluation (FaCE Scale) (42) and the Facial Disability Index (FDI) (43). Studies of CFP should include use of one of these tools, as non-motor impacts of facial palsy have been shown to be as important as motor function to people with this impairment (52).

It would be beneficial to have a comprehensive picture of current clinical practice to incorporate into future studies. Clinical physiotherapists and speech pathologists provide rehabilitation for CFP for using principles derived from peripheral nerve damage literature due to the lack of studies specific to CFP, despite these therapies also having low quality supporting evidence (12) and varying significantly in mechanism of impairment. A comprehensive survey of current practice would enable “expert opinion” to be integrated into the development of a gold standard of evidence-based physical rehabilitation, along with stronger evidence from well-designed clinical trials.

Exercise-based physical rehabilitation for facial palsy must be performed in a controlled and precise manner, and repeated sufficient times to induce long-term synaptic change (53). These exercises are often performed using some method of biofeedback (e.g., mirror); primarily relying on the visual system to obtain accurate proprioceptive information about position of facial muscles during slow, controlled movements that focus on symmetry (54). Without some form of external proprioceptive feedback, it is extremely difficult for patients to precisely and effectively judge and monitor the movements of facial structures (54). Exercise protocols can therefore be difficult for people to perform accurately if they have concomitant visual-perceptual, cognitive or behavioral changes secondary to stroke. Well-designed research which evaluates the effectiveness of interventions which are accessible to a wider clinical population would be of great benefit to people suffering from central facial palsy whose other impairments prevent them from engaging in strict exercise-based protocols. Regardless of the intervention strategy employed, clear and detailed reporting should be ensured to enable replicable therapeutic protocols.

Further investigation of physical rehabilitation methods for CFP is required to determine effective types and approaches for therapy and to guide clinical decision-making. There is a gap in services currently available for people wishing to access therapy

for CFP and is not possible to base a strong case for clinical input on the current literature, even though trends have been identified that indicate potential benefit of physical rehabilitation.

LIMITATIONS

Although every effort was made to ensure database and other searches were comprehensive it is possible that some records were not retrieved via the search methods. Due to the difficulties and cost associated with obtaining verified and reliable document translation, this review was unable to include articles where the full text was not available in English. This may have resulted in some studies being missed; the authors are aware of at least one non-English study (14) which may have contributed toward this review. Our systematic review also had limitations relating to methodological quality and available data in the existing literature; only four RCTs were retrieved, which were of low quality, and the observational studies all lacked sufficient data to draw strong conclusions or perform calculation of treatment effect size. It is recognized that in many areas of health care, some interventions are supported by evidence from RCTs and others are not (55). It is also acknowledged in medical research literature that decision-making is often necessary even when there is imperfect evidence (56). As clinicians who provide assessment and therapy to patients with central facial palsy, we included the smaller observational studies due to a lack of larger or more well-designed trials—as per Balshem et al. “in the absence of high-quality evidence, clinicians must look to lower quality evidence to guide their decisions” (57). While we are aware that the limitations in methodology affect the reliability of these studies, and thus also affect the strength of recommendations that can be drawn from their findings, the reality is that there are not enough large well-designed RCTs available to rely solely on this level of evidence for clinical decision-making and intervention.

CONCLUSIONS

The studies in this review report improvement of facial movement or function following application of various methods

of physical rehabilitation for CFP. Methodological limitations and heterogeneity of design affect the strength of the evidence and prevent reliable comparison between intervention methods. Strong conclusions regarding the effectiveness of intervention cannot be drawn using the studies identified by this review as good quality, robust evidence supporting physical rehabilitation of central facial palsy was not found.

DATA AVAILABILITY STATEMENT

The datasets generated for this study are available on request to the corresponding author.

AUTHOR CONTRIBUTIONS

AV and DG conceived the idea for this review. AV, DG, RW, AM, and SC formulated the question for review and designed the search strategy. AV and DG performed the abstract screening, full text review, and extracted data from included studies. AV and RW performed the risk of bias assessments. AV analyzed and interpreted the data and drafted the manuscript. AC and AM provided overall supervision of the project and final approval of the version to be published. All authors provided critical feedback and helped shape the research, analysis, and manuscript.

FUNDING

This study was undertaken with support from a Gold Coast Health Allied Health Clinical Backfill for Research grant, which provided AV and DG with four weeks of funded offline time. Assistance with funding open-access publication was granted via the Gold Coast Health Study, Education and Research Trust.

ACKNOWLEDGMENTS

The review team thanks Sarah Thorning for her valuable assistance with database searching and deduplication of search results. We also thank the Speech Pathology and Audiology Service (Allied Health Services|Gold Coast Health).

REFERENCES

1. Takezawa K, Townsend G, Ghabriel M. The facial nerve: anatomy and associated disorders for oral health professionals. *Odontology*. (2018) 106:103–16. doi: 10.1007/s10266-017-0330-5
2. Perry ES, Potter NL, Rambo KD, Short R. Effects of strength training on neuromuscular facial rehabilitation. *Dev Neurorehabil*. (2011) 14:164–70. doi: 10.3109/17518423.2011.566595
3. Owusu JA, Boahene KD. Management of long-standing flaccid facial palsy: midface/smile: locoregional muscle transfer. *Otolaryngol Clin North Am*. (2018) 51:1119–28. doi: 10.1016/j.otc.2018.07.008
4. Krippel M, Karim AA, Brechmann A. Neuronal correlates of voluntary facial movements. *Front Hum Neurosci*. (2015) 9:598. doi: 10.3389/fnhum.2015.00598
5. Adour KK. Current concepts in neurology: diagnosis and management of facial paralysis. *N Eng J Med*. (1982) 307:348–51. doi: 10.1056/NEJM198208053070605
6. Volk G, Steinerstauch A, Lorenz A, Modersohn L, Mothes O, Denzler J, et al. Facial motor and non-motor disabilities in patients with central facial paresis: a prospective cohort study. *J Neurol*. (2019) 266:46–56. doi: 10.1007/s00415-018-9099-x
7. Wax MK. *Facial Paralysis: A Comprehensive Rehabilitative Approach*. San Diego, CA: ProQuest, Plural Publishing Inc. (2015).
8. Roob G, Fazekas F, Hartung HP. Peripheral facial palsy: etiology, diagnosis and treatment. *Eur Neurol*. (1999) 41:3–9. doi: 10.1159/000007990
9. Cattaneo L, Pavesi G. The facial motor system. *Neurosci Biobehav Rev*. (2014) 38:135–59. doi: 10.1016/j.neubiorev.2013.11.002
10. Pereira LM, Obara K, Dias JM, Menacho MO, Lavado EL, Cardoso JR. Facial exercise therapy for facial palsy: systematic review and meta-analysis. *Clin Rehabil*. (2011) 25:649–58. doi: 10.1177/0269215510395634
11. Cardoso JR, Teixeira EC, Moreira MD, Fávero FM, Fontes SV, Bulle De Oliveira AS. Effects of exercises on Bell's Palsy: systematic review of randomized controlled trials. *Otol Neurotol*. (2008) 29:557–60. doi: 10.1097/MAO.0b013e31816c7bf1

12. Teixeira L, Soares B, Vieira VP, Prado G. Physical therapy for Bell's palsy (idiopathic facial paralysis). *Cochrane Database Syst Rev.* (2008) CD006283. doi: 10.1002/14651858.CD006283.pub2
13. Konecny P, Elfmark M, Horak S, Pastucha D, Krobot A, Urbanek K, et al. Central facial paresis and its impact on mimicry, psyche and quality of life in patients after stroke. *Biomed Pap Med Fac Univ Palacky Olomouc Czech Repub.* (2014) 158:133–7. doi: 10.5507/bp.2013.014
14. Svensson BH, Christiansen LS, Jepsen E. [Treatment of central facial nerve paralysis with electromyography biofeedback and taping of cheek. A controlled clinical trial]. *Ugeskrift Laeger.* (1992) 154:3593–6.
15. Schimmel M, Ono T, Lam OL, Muller F. Oro-facial impairment in stroke patients. *J Oral Rehabil.* (2017) 44:313–26. doi: 10.1111/joor.12486
16. Konecny P, Elfmark M, Urbanek K. Facial paresis after stroke and its impact on patients' facial movement and mental status. *J Rehabil Med.* (2011) 43:73–5. doi: 10.2340/16501977-0645
17. Ho AL, Scott AM, Klassen AF, Cano SJ, Pusic AL, Van Laeken N. Measuring quality of life and patient satisfaction in facial paralysis patients: a systematic review of patient-reported outcome measures. *Plast Reconstr Surg.* (2012) 130:91–9. doi: 10.1097/PRS.0b013e318254b08d
18. Ishii LE, Nellis JC, Boahene KD, Byrne P, Ishii M. The importance and psychology of facial expression. *Otolaryngol Clin North Am.* (2018) 51:1011–17. doi: 10.1016/j.otc.2018.07.001
19. Walker DT, Hallam MJ, Ni Mhurchadha S, McCabe P, Nduka C. The psychosocial impact of facial palsy: our experience in one hundred and twenty six patients. *Clin Otolaryngol.* (2012) 37:474–7. doi: 10.1111/coa.12026
20. Dai R, Lam OL, Lo EC, Li LS, Wen Y, McGrath C. Orofacial functional impairments among patients following stroke: a systematic review. *Oral Dis.* (2015) 21:836–49. doi: 10.1111/odi.12274
21. Chang WH, Sohn MK, Lee J, Kim DY, Lee SG, Shin YI, et al. Impact of central facial palsy and dysarthria on quality of life in patients with stroke: the KOSCO study. *Neurorehabilitation.* (2016) 39:253–9. doi: 10.3233/NRE-161355
22. Morgan Stuart JR, Byrne JP. The importance of facial expression and the management of facial nerve injury. *Neurosurg Q.* (2004) 14:239–48. doi: 10.1097/00013414-200412000-00009
23. Kang JA, Chun MH, Choi SJ, Chang MC, Yi YG. Effects of mirror therapy using a tablet PC on central facial paresis in stroke patients. *Ann Rehabil Med.* (2017) 41:724. doi: 10.5535/arm.2017.41.4.724
24. Stroke Foundation. *Clinical Guidelines for Stroke Management.* Melbourne, VIC: Stroke Foundation (2019).
25. Rudd AG, Bowen A, Young G, James MA. *National Clinical Guideline for Stroke*, 5th ed. (2016) London: Clinical Medicine. (2017).
26. Hagg M, Anniko M. Lip muscle training in stroke patients with dysphagia. *Acta Otolaryngol.* (2008) 128:1027–33. doi: 10.1080/00016480701813814
27. Hee-Su P, Park JY, Kwon YH, Choi Hee SU, Kim Hee J. Effect of orbicularis oris muscle training on muscle strength and lip closure function in patients with stroke and swallowing disorder. *J Phys Ther Sci.* (2018) 30:1355–6. doi: 10.1589/jpts.30.1355
28. Huffman AL. Biofeedback treatment of orofacial dysfunction: a preliminary study. *Am J Occup Ther.* (1978) 32:149–54.
29. Choi JB. Effect of neuromuscular electrical stimulation on facial muscle strength and oral function in stroke patients with facial palsy. *J Phys Ther Sci.* (2016) 28:2541–3. doi: 10.1589/jpts.28.2541
30. Zhou J, Zhang F. A research on scalp acupuncture for cerebral infarction. *J Tradition Chin Med.* (1997) 17:194–7.
31. Hägg M, Larsson B. Effects of motor and sensory stimulation in stroke patients with long-lasting dysphagia. *Dysphagia.* (2004) 19:219–30. doi: 10.1007/s00455-004-0016-3
32. Hagg M, Tibbling L. Effect of oral IQoro R and palatal plate training in post-stroke, four-quadrant facial dysfunction and dysphagia: a comparison study. *Acta Otolaryngol.* (2015) 135:962–8. doi: 10.3109/00016489.2015.1042043
33. Noor R, Ghazanaffar M, Neelam H, Bashir MS. Role of physiotherapy in rehabilitation of facial muscles in facial palsy due to hemorrhagic stroke. *Rawal Med J.* (2014) 39:389–91.
34. Van Gelder RS, Philippart SMM, Hopkins B. Treatment of facial paralysis of CNS-origin: initial studies. *Int J Psychol.* (1990) 25:213–28. doi: 10.1080/00207599008247858
35. Moola S, Munn Z, Tufanaru C, Aromataris E, Sears K, Sfetcu R, et al. Chapter 7: Systematic reviews of etiology and risk. In: Aromataris E, Munn Z, editors. *Joanna Briggs Institute Reviewer's Manual.* The Joanna Briggs Institute (2017). Available online at: <https://reviewersmanual.joannabriggs.org/>
36. Tate R, Perdices M, McDonald S, Togher L, Moseley A, Winders K, et al. Development of a database of rehabilitation therapies for the psychological consequences of acquired brain impairment. *Neuropsychol Rehabil.* (2004) 14:517–34. doi: 10.1080/09602010343000182
37. Higgins JPT. *Cochrane Handbook for Systematic Reviews of Interventions.* 2nd ed. Hoboken, NJ: Wiley-Blackwell, Cochrane Collaboration (2019).
38. Meader N, King K, Llewellyn A, Norman G, Brown J, Rodgers M. A checklist designed to aid consistency and reproducibility of GRADE assessments: development and pilot validation. *Syst Rev.* (2014) 3:82. doi: 10.1186/2046-4053-3-82
39. House JW, Brackmann DE. Facial nerve grading system. *Otolaryngol Head Neck Surg.* (1985) 93:146–7. doi: 10.1177/019459988509300202
40. Ross BR, Fradet G, Nedzelski JM. Development of a sensitive clinical facial grading system. *Otolaryngol Head Neck Surg.* (1994) 114:380–6.
41. Stennert E, Limberg CH, Frentrup KP. An index for paresis and defective healing—an easily applied method for objectively determining therapeutic results in facial paresis (author's transl). *HNO.* (1977) 25:238–45.
42. Kahn JB, Gliklich RE, Boyev KP, Stewart MG, Metson RB, McKenna MJ. Validation of a patient-graded instrument for facial nerve paralysis: the FaCE scale. *Laryngoscope.* (2001) 111:387–98. doi: 10.1097/00005537-200103000-00005
43. Vanswearingen JM, Brach JS. The Facial Disability Index: reliability and validity of a disability assessment instrument for disorders of the facial neuromuscular system. *Phys Ther.* (1996) 76:1288–98. doi: 10.1093/ptj/76.12.1288
44. Crowther M, Avenell A, MacLennan G, Mowatt G. A further use for the Harvest plot: a novel method for the presentation of data synthesis. *Res Synth Methods.* (2011) 2:79–83. doi: 10.1002/jrsm.37
45. Finch E, Copley A, Cornwell P, Kelly C. Systematic review of behavioral interventions targeting social communication difficulties after traumatic brain injury. *Arch Phys Med Rehabil.* (2016) 97:1352–65. doi: 10.1016/j.apmr.2015.11.005
46. Banks AC, Bhama KP, Park RJ, Hadlock AC, Hadlock AT. Clinician-graded electronic facial paralysis assessment: the eFACPlastic. *Reconstruct Surg.* (2015) 136:223e–30e. doi: 10.1097/PRS.0000000000001447
47. Coulson SE, Croxson GR, Adams RD, O'Dwyer NJ. Reliability of the “Sydney,” “Sunnybrook,” and “House Brackmann” facial grading systems to assess voluntary movement and synkinesis after facial nerve paralysis. *Otolaryngol Head Neck Surg.* (2005) 132:543–9. doi: 10.1016/j.otohns.2005.01.027
48. Kang ST, Vrabec TJ, Giddings JN, Terris JD. Facial nerve grading systems (1985–2002): beyond the House-Brackmann scale. *Otol Neurotol.* (2002) 23:767–71. doi: 10.1097/00129492-200209000-00026
49. Chong HLS, Evison JT, Low TH, Hasmat ES, Coulson RS, Clark RJ. Validation of the clinician-graded electronic facial paralysis assessment. *Plastic Reconstruct Surg.* (2017) 140:159–67. doi: 10.1097/PRS.00000000000003447
50. Banks CA, Jowett N, Hadlock TA. Test-retest reliability and agreement between In-Person and Video assessment of facial mimetic function using the eFACE facial grading system. *JAMA Facial Plastic Surg.* (2017) 19:206–11. doi: 10.1001/jamafacial.2016.1620
51. Banks CA, Jowett N, Azizzadeh B, Beurskens C, Bhama P, Borschel G, et al. Worldwide testing of the eFACE facial nerve clinician-graded scale. *Plastic Reconstruct Surg.* (2017) 139:491e. doi: 10.1097/PRS.00000000000002954
52. Volk GF, Granitzka T, Kreysa H, Klingner CM, Guntinas-Lichius O. Initial severity of motor and non-motor disabilities in patients with facial palsy: an assessment using patient-reported outcome measures. *Eur Arch Otorhinolaryngol.* (2017) 274:45. doi: 10.1007/s00405-016-4018-1
53. Dorion J. Facial neuromuscular retraining. *Perspect Swallow Swallow Disord.* (2005) 14:18–23. doi: 10.1044/sasdl4.2.18
54. Lindsay RW, Robinson M, Hadlock TA. Comprehensive facial rehabilitation improves function in people with facial paralysis: a 5-year experience at the Massachusetts Eye and Ear Infirmary. *Phys Ther.* (2010) 90:391–7. doi: 10.2522/ptj.20090176
55. Schünemann HJ, Higgins JPT, Vist GE, Glasziou P, Akl EA, Skoetz N, et al. Chapter 14: Completing ‘Summary of findings’ tables and grading the

- certainty of the evidence. In: Higgins JPT, Thomas J, Chandler J, Cumpston M, Li T, Page MJ, Welch VA, editors. *Cochrane Handbook for Systematic Reviews of Interventions version 6.0*. Cochrane (2019). Available online at: www.training.cochrane.org/handbook
56. O'Neil M, Berkman N, Hartling L, Chang S, Anderson J, Motu'Apuaka M, et al. Observational evidence and strength of evidence domains: case examples. *Syst Rev.* (2014) 3:35. doi: 10.1186/2046-4053-3-35
 57. Balshem H, Helfand M, Schünemann HJ, Oxman AD, Kunz R, Brozek J, et al. GRADE guidelines: 3. rating the quality of evidence. *J Clin Epidemiol.* (2011) 64:401–6. doi: 10.1016/j.jclinepi.2010.07.015

Conflict of Interest: The authors declare that the research was conducted in the absence of any commercial or financial relationships that could be construed as a potential conflict of interest.

Copyright © 2020 Vaughan, Gardner, Miles, Copley, Wenke and Coulson. This is an open-access article distributed under the terms of the Creative Commons Attribution License (CC BY). The use, distribution or reproduction in other forums is permitted, provided the original author(s) and the copyright owner(s) are credited and that the original publication in this journal is cited, in accordance with accepted academic practice. No use, distribution or reproduction is permitted which does not comply with these terms.

APPENDIX

Search Strategy (Example)

Database: Ovid MEDLINE(R) ALL <1946 to December 31, 2018>

1. exp Facial Paralysis/ (11721)
2. ((facial or orofacial or oro-facial) adj3 (paralys* or paresis or droop* or palsy or asymmetr* or impair*)).tw. (14536)
3. ((facial or orofacial or oro-facial) adj3 (express* or nerve* or muscle* or move* or reanimat*)).tw. (26746)
4. or/1-3 (38981)
5. exp Physical Therapy Modalities/ (140199)
6. (exercis* or therap* or physiotherap* or rehabilit* or retrain* or train* or treat* or manag* or intervention*).tw. (7745138)
7. (mime* or miming or mirror* or tap* or massag* or stretch* or acupunctur* or needling* or biofeedback or neuromuscular* or kinesio* or cryo*).tw. (382977)
8. (electric* adj2 stimul*).tw. (62989)
9. (e-stim* or electromyograph* or semg).tw. (39537)
10. or/5-9 (8084566)
11. 4 and 10 (15595)
12. exp Central Nervous System Diseases/ (1342443)
13. (central nervous system adj2 (diseas* or injur* or infect*)).tw. (9406)
14. upper motor neuron.tw. (1424)
15. stroke*.tw. (218936)
16. brain injur*.tw. (57635)
17. tbi.tw. (21035)
18. (central adj3 (facial.tw. adj2 (paralys* or paresis or palsy or palsies))).tw. (144)
19. or/12-18 (1463675)
20. 11 and 19 (1970).



Masticatory Adaptation to Occlusal Changes

Pierre Bourdiol¹, Martine Hennequin^{1,2}, Marie-Agnes Peyron³ and Alain Woda^{1*}

¹ CROC EA 4847, Faculty of Dentistry, Université Clermont Auvergne, Clermont-Ferrand, France, ² CHU Clermont-Ferrand, Clermont-Ferrand, France, ³ Human Nutrition Unit, Institut National de la Recherche Agronomique, Paris, France

This review deals with the frequent wide variability of masticatory capacity/incapacity. Neither researchers nor clinicians have taken sufficient account of this variability despite its implications for nutrition. Mastication in normal healthy oral conditions is first described, followed by a short presentation of the mechanisms of masticatory adaptation in the nervous system. Capacity, incapacity, and successful compensatory adaptation of mastication are then defined, along with the different methods used for their evaluation. Examples of adaptation needs are given, such as those concomitant with dental wear or occlusal changes. Finally, given its vital importance for deeply impaired mastication/deglutition function, the impact of masticatory adaptation processes on nutrition is examined.

OPEN ACCESS

Edited by:

Limor Avivi-Arber,
University of Toronto, Canada

Reviewed by:

Alexandros E. Tsouknidas,
University of Western Macedonia,
Greece
Edwin M. Ongkosuwito,
Radboud University Medical Center,
Netherlands

*Correspondence:

Alain Woda
wodaalain@gmail.com;
alain.woda@uca.fr

Specialty section:

This article was submitted to
Craniofacial Biology and Dental
Research,
a section of the journal
Frontiers in Physiology

Received: 31 October 2019

Accepted: 09 March 2020

Published: 03 April 2020

Citation:

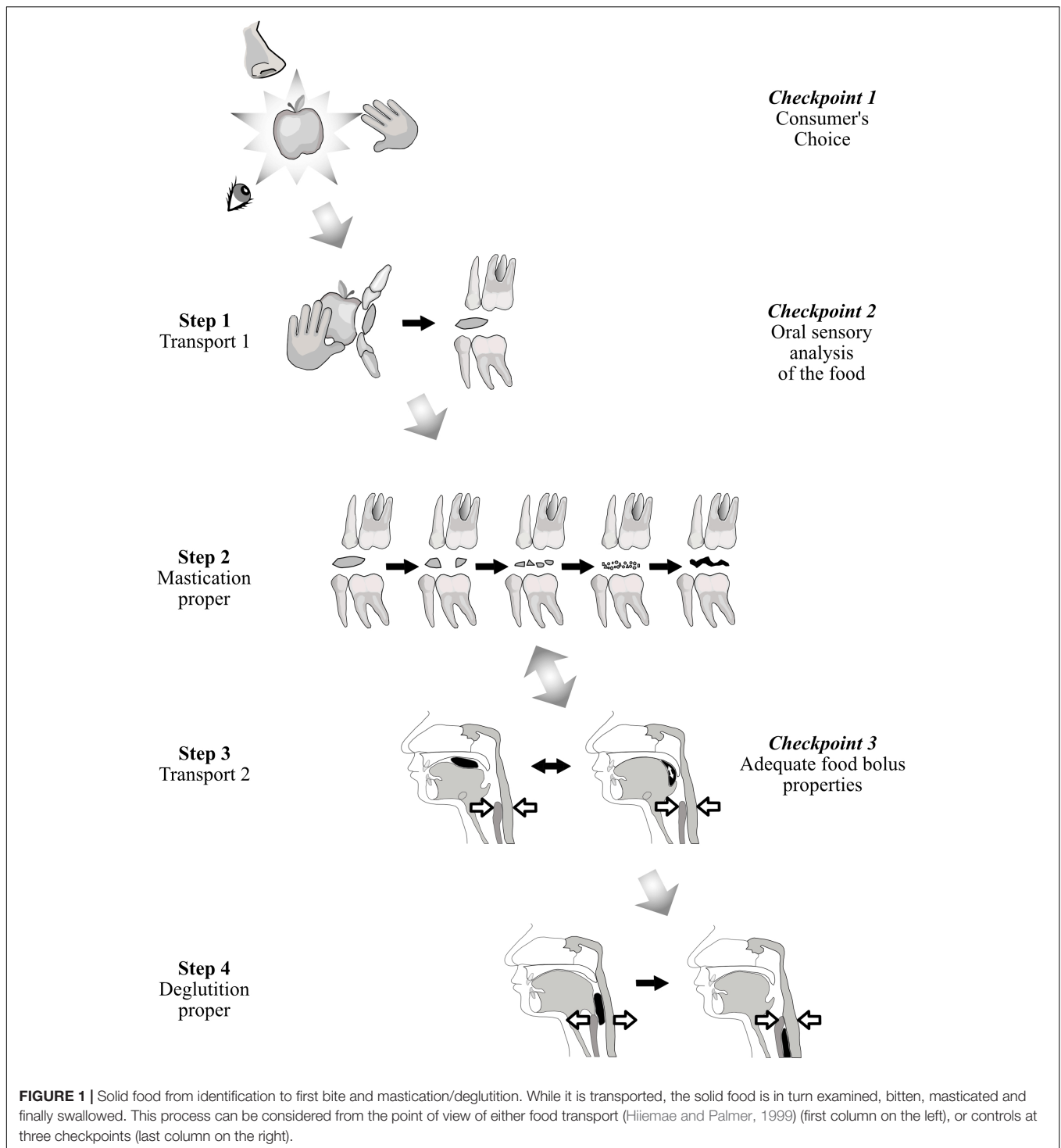
Bourdiol P, Hennequin M,
Peyron M-A and Woda A (2020)
Masticatory Adaptation to Occlusal
Changes. *Front. Physiol.* 11:263.
doi: 10.3389/fphys.2020.00263

Keywords: masticatory adaptation, occlusion, dental wear, masticatory test, disability, tooth loss

PHYSIOLOGY OF NORMAL MASTICATION

Ingestion starts with the choice and selection of a food and ends with its passage through the upper esophageal sphincter during deglutition. A first model, based on common observation, considers that ingestion is controlled at three checkpoints, each of which can cancel ingestion. The first checkpoint is food selection before ingestion. The second consists of sensory cues from food. The third is deglutition. A second model is the four-step sequence described by Hiimeae and Palmer (1999) for the fate of solid or semi-solid foods in the mouth.

Figure 1 relates these two models. At the first checkpoint, individuals express their personal choice when they shop for food, and when they accept or decline food they are proffered. After selection, solid or semi-solid foods are portioned into mouthfuls, typically with the front teeth or with eating utensils. This portion is then transported from the front teeth to the molars (Hiimeae and Palmer's Stage I transport). During this phase, each mouthful is analyzed by taste, retro-nasal olfaction and oral receptors of the somatosensory system. If this second checkpoint is successfully crossed, then (i) the central pattern generators of mastication located in the cerebral cortex and in the brainstem are activated, and (ii) the required physiological responses are anticipated to prepare digestion of the food in the digestive tract post-esophagus (cephalic phase). This cephalic phase also occurs during mastication proper (Hiimeae and Palmer's second step), when the food is transformed into a food bolus by the actions of the teeth through the exertion of lingual, facial and masticatory muscles and with the aid of saliva. In the third step, Hiimeae and Palmer's Stage II transport, the chewed food moved rearward along the oropharyngeal tongue surface, crosses the fauces isthmus and collects in pharyngo-epiglottic folds. The fourth step, acting as a third checkpoint, is deglutition proper, with opening of the upper esophageal sphincter. Steps 2 and 3 often occur simultaneously, the bolus being moved cyclically upward and forward on the tongue surface, returning through the fauces isthmus into the oral cavity while the mastication proper



is taking place. After passing through this third checkpoint, chewed food is irreversibly delivered to the gastro-intestinal tract, from which it can then be expelled only by vomiting. To cross this last checkpoint, a deglutition center's "go-ahead" is needed, signaling that the bolus is sufficiently well prepared to be easily and safely swallowed. Many studies have shown that the particle size of the bolus just before swallowing is a determining factor

(van der Bilt et al., 1993; Jalabert-Malbos et al., 2007; N'Gom et al., 2007). Particle size below a ceiling is one necessary condition for swallowing to be triggered. Particle size acts as a cofactor with saliva and food juice to reach the required rheological properties for the food bolus. To be safely swallowed, the bolus must possess certain physical and rheological properties. It must be slippery, cohesive and plastic (Prinz and Lucas, 1995).

Plasticity allows the deformation of the bolus during its passage through the digestive tract. Slipperiness helps it slide along the mucous membranes and down the narrow alimentary canal to the stomach. Cohesiveness means that the bolus must behave like a unit (Hutchings and Lillford, 1988; Palmer and Hiimeae, 2003). This is essential to avoid aspiration, which can happen if food particles disperse and enter the airways when the bolus crosses the aerodigestive junction. It is noteworthy that subjects neither stop chewing nor trigger deglutition when the required mean particle size has been reached (Peyron et al., 2011). They masticate longer, increasing the number of cycles, to obtain all the necessary rheological conditions described above (Prinz and Lucas, 1995; Seo et al., 2007; Mishellany-Dutour et al., 2011) by mixing the solid particles with saliva and juice expelled from the crushed food. This probably accounts for the weak correlation between number of cycles and pre-swallow median particle size (van der Bilt et al., 1993; Fontijn-Tekamp et al., 2000; Mishellany-Dutour et al., 2011).

Hiimeae and Palmer's Step 2 consists of a chewing sequence comprising a variable number of masticatory cycles (Fontijn-Tekamp et al., 2004; Peyron et al., 2004; Lund and Koltá, 2005). Food placed in the mouth acts as a stimulus for sensory receptors. This stimulation by food occurs both at the start and then throughout the masticatory sequence as the food is progressively transformed. Through this continuous sensory input, the mastication generating centers adjust several parameters, such as number of cycles before swallowing, muscular force exerted, and shape of the mandibular movement (see Table 1 in Woda et al., 2006). These parameters are adjusted to (i) continuously adapt to food properties inside the mouth and (ii) obtain required final food bolus properties. The need to reach a final state of the boluses, which is similar for all healthy individuals, is met using all the available means. This drive for adaptation produces strong inter-individual differences in the masticatory sequence. If the right bolus properties cannot be attained, subjects either swallow insufficiently comminuted foods, or avoid eating the food, which they deem difficult to chew. We note that only in experimental conditions can refusal of food types be assessed (Hennequin et al., 2015; Depeyre et al., 2019).

MECHANISMS OF MASTICATION ADAPTATION

Variation of the mastication parameters allows adaptation to several types of changes deriving from either the environment (extrinsic) or the individual (intrinsic). Four adaptation/variability situations can be distinguished: (i) the cycles of mastication vary during a single sequence to adapt to the changes in the food during its transformation into a food bolus, (ii) the programming of mastication varies to adapt to food types, (iii) mastication undergoes slow reprogramming to adapt to evolving conditions such as orthodontic movements, dental wear or aging, and (iv) mastication must also adapt to discontinuities such as tooth loss or prosthodontic occlusal rehabilitation. There is neuroscientific evidence for these different types of adaptation/variability.

All the forms taken by mastication adaptation have a common foundation, namely the rhythmicity and coordination of masticatory muscles, tongue, lips, and cheeks, which depend on a central pattern generator located in the brainstem (Lund and Koltá, 2005). Central to this rhythmicity is the presence of neurons with rhythmogenic properties in one area of the central pattern generator: the rostro-dorsal part of the trigeminal sensory complex. These neurons have intrinsic calcium- and voltage-dependent bursting abilities. The integration of peripheral and cortical inputs by these neurons could partly explain the first type of variability/adaptation, i.e., the instantaneous variations in cycles occurring while mastication proper is progressively transforming the food into a food bolus (see review in Morquette et al., 2012). Chewing patterns can also change suddenly in response to events caused during mastication, such as pain (temporo-mandibular joint, dental, or mucosal), or foods sticking to gums or teeth. Periodontal, muscle spindle, mucosal and other peripheral receptors all act to adapt to hardness and other rheological modifications of the food during mastication and to protect the apparatus from unexpected perturbations, which may be of a nociceptive nature. Responses reach the brainstem central pattern generator directly, but also through cortical areas, which form part of a feedback loop. That the cortex plays a role is indicated by the fact that if the masticatory area is suppressed, mastication, though still possible, becomes awkward and slowed (see Lund and Koltá, 2005; Avivi-Arber and Sessle, 2018; Kumar et al., 2018).

The second type of adaptation, i.e., adaptation of mastication to each food type, is probably programmed before the mastication sequence starts. Cortical inputs seem essential to activate, directly or indirectly, the brainstem central pattern generator with the program appropriate to a given type of food, as suggested by the representation, at specific locations within the cortex, of maps of the various patterns of mastication (Lin et al., 1998; Lund and Koltá, 2005). This pre-ingestive programming can also be inferred from the fact that cognitive, visual and olfactory information about food type reaches the cortex before the first bite, while somato-sensory, retronasal olfactory and taste information is collected during the initial transport of food in the mouth and before the beginning of mastication proper (see Lund and Koltá, 2005, 2006; Kumar et al., 2018).

Cortical plasticity seems to underlie the adaptation of mastication accompanying evolving conditions such as orthodontic movements, dental wear or aging, and more sudden events such as tooth loss or chance injuries of the orofacial area (see recent and complete reviews in Avivi-Arber and Sessle, 2018; Kumar et al., 2018). The plasticity of the central nervous system has long been known, but it is only recently that the role of this plasticity has been studied in detail for cortical areas devoted to orofacial function in the primary somato-sensory cortex and in the primary motor cortex. Among other techniques and experimental designs, intracortical micro-stimulation allows the observation of adaptive changes in some oral functional tasks in rats. Functional magnetic resonance imaging or transcranial magnetic stimulation have been used in humans for related purposes. Reorganization of sensory and motor representation and/or modification of the excitability of

the orofacial cortical region have been shown following events such as occlusal grinding, tooth extraction and nerve injury (Avivi-Arber et al., 2011), but also after gradual changes such as orthodontic movements (Sood et al., 2015). This adaptive plasticity can be positive by helping mastication adapt to the new conditions, thereby limiting the dysfunction, but may also lead to new maladaptive motor habits, either postural or kinetic. Cortical plasticity is also involved when a subject is learning a new task or receiving a new complete denture. Adaptation to a new complete denture correlated with plasticity of cortical motor area in a time-dependent manner (Luraschi et al., 2013). Neuroplasticity induced by tooth extraction can be reversed by replacement with an implant-supported crown, although it does not return to its initial state before extraction (Avivi-Arber et al., 2015). As pointed out by Avivi-Arber and Sessle (2018) “Such information has clinical significance as cortical changes may underlie the mechanisms by which humans adapt (or not) to intra-oral manipulation.” Finally, these new scientific data reinforce the old insufficiently applied clinical concept that training of oral motor tasks or relearning of initial masticatory praxis after occlusal rehabilitation would help users adapt to their new dental prosthesis.

The swallowing function also adapts to the food bolus. The activation of the relevant oropharyngeal muscles occurs in an invariable order, but the intensity of muscle activities and the overall temporal aspects of muscle events are influenced by bolus characteristics such as volume (Kahrilas and Logemann, 1993; Lazarus et al., 1993), viscosity (Lazarus et al., 1993; Smith et al., 2006) and taste (Ding et al., 2003). In normal conditions, swallows frequently occur intermittently during the chewing sequence until the final food bolus is swallowed (Hiieae et al., 1996; Okada et al., 2007).

CAPACITY WITH OR WITHOUT COMPENSATORY ADAPTATION, INCAPACITY

The main question when evaluating the masticatory function in a subject or group of subjects is whether this function achieves its purpose. In other words, whether subjects are able to make an acceptable food bolus or whether the food texture has to be changed. This tells us how well the mastication centers adapt to the characteristics of both the food and the eater. In some individuals, the mastication process may lie close to the border of normal healthy functioning. In these situations, adaptation may be difficult and costly, though still possible. It may be impossible in other situations. These three conditions: totally healthy, moderately impaired and totally impaired, determine masticatory capacity, compensatory adaptation, and masticatory incapacity (Feldman et al., 1980; Woda et al., 2010, 2011). Capacity means that chewing is perfectly achieved, and the masticatory capacity is fully intact. The food bolus meets all the requirements for deglutition as established with an indicator of normal food bolus such as MNI (see next section). Compensatory adaptation occurs when mastication is slightly disturbed, but the individual concerned can implement a physiological adaptation,

mainly an increase in the number of cycles, that makes a normal bolus. Compensatory adaptation implies extra effort, but normal values of MNI are reached. Incapacity means the function is largely deficient, because the individual fails to make a proper food bolus or refuses it in some way. In such subjects, adaptability is overstretched; they are unable to masticate correctly as shown by the MNI value, which is above the ceiling. The subjects have to develop a strategy that enables them to feed themselves despite their incapacity. The main strategies are: changing diets, avoiding foods that are difficult to chew, and swallowing unchewed food. In all cases, negative nutritional consequences and/or excessive workload inflicted on the digestive tract are likely. The morbid outcomes of this situation are still under-researched but appear more and more probable and serious (El Osta et al., 2014). These three conditions are summarized in **Figure 2**. Compensatory adaptation or incapacity can be found in many settings such as craniofacial dysmorphism, neurological diseases, traumatic or surgical sequelae, temporomandibular disorders and other conditions leading to occlusal changes including partial or complete edentulousness.

Epidemiological evaluation of the prevalence of mastication incapacity in the general population is incomplete. Prevalence of mastication incapacity is almost totally lacking for persons with neuromotor and cognitive disorders such as Parkinson disease, stroke, congenital or acquired brain damage and other neurological disorders. It can, however, be inferred to be high since these conditions are common and concern both young and aged individuals. In addition, epidemiology of mastication inability in cognitive and neuromotor disorders has been hidden by the emphasis placed on dysphagia which showed very high values, up to 80% of stroke patients and 81% of Parkinson disease patients (Takizawa et al., 2016). It is worth noting that the major role of mastication incapacity in the dysphagia states was never considered. Epidemiology of mastication deficiency in the elderly is better known. However, the respective role of neurological disorders and of edentulousness in this aging population is difficult to determine because, in these studies, elderly with cognitive and neurological disorders had been either discarded (Cavalcante et al., 2019) or not reported.

Fifty-three percents of a Brazilian population made up of 5,124 elderly individuals (aged 65–74; 59.2% wearing complete denture) declared they had poor mastication (Dias-da-Costa et al., 2010). In a group of 3,134 Japanese community dwelling elderly persons with a median age of 71, 20.7% could not eat one of the five test foods proposed (Okamoto et al., 2019). As concluded by the authors the subjects' difficulties were strongly correlated with the number of residual natural teeth. Indeed, a large proportion of them (786, 25%) had less than 10 teeth with a median of two teeth remaining. A similar value (21%) was reported in a cohort of Australian elderly persons aged over 78 years, who could not eat hard foods and reported both discomfort and meal interruption while eating. Only 14.6% wore complete denture but partial edentulousness was widespread. There was a 2.3 times greater likelihood that those with fewer than 21 natural teeth were not able to eat hard foods (Wright et al., 2019). These results are in line with the well-known fact that complete denture patients have mastication difficulties









| | FOOD BOLUS | PHYSIOLOGY | CONSEQUENCES |
|--------------------------------|---|---|---|
| CAPACITY | Particle size < 4 mm (MNI) & adequate plasticity, cohesiveness, slipperiness | When chewing a given food: Great inter-individual variability & low intra-individual variability |   |
| COMPENSATORY ADAPTATION | Particle size < 4 mm (MNI) & adequate plasticity, cohesiveness, slipperiness | Cycle number increase and / or force change and / or jaw movement change |   |
| INCAPACITY | Particle size > 4 mm (MNI) or insufficient plasticity, cohesiveness, slipperiness or saliva problems | Swallowing unprepared bolus and/or some food types refused |  Diet change and/or modified food   or  |

FIGURE 2 | Capacity, compensatory adaptation, and incapacity. Evaluation of food boluses is proposed through particle size measurement and a masticatory normative indicator (MNI) made with raw carrot. Main physiological characteristics at work during adaptation are indicated. Basic consequences are shown.

(van der Bilt, 2011; Peyron et al., 2017). In a cross-sectional study conducted in north-east Brazil with a random sample of 532 participants aged 20–59 years, the prevalence of declared chewing difficulties was 30.5% (Cavalcante et al., 2019) with 8.7% having less than nine remaining natural teeth.

TOOLS FOR MASTICATION EVALUATION

Maintaining or rehabilitating masticatory function is a dentist's main goal. Achieving it often relies on reconstructing normal anatomy using various criteria, such as bilateral symmetry. However, the underlying assumption that good morphology implies good physiology is somewhat specious. Given the importance of masticatory function, it is essential to be able to assess and quantify it simply and reproducibly, like any other function. Various methods are available to practitioners.

Number of Posterior Functional Units

A posterior functional unit (PFU) can be defined as a pair of antagonist posterior natural (or fixed prosthodontic) teeth with at least one contact during chewing. A fully dentate subject has eight PFUs in the form of premolar-molar contacts between maxillary and mandibular natural teeth. The number of PFUs may reach ten if third molars are included. Many malocclusions are morphologically based, although they may allow perfect functioning. For this reason, PFUs must be recorded *in vivo* using a functional test with interposed articulating paper bitten during simulated chewing movements (Hennequin et al., 2015). The role of opposing teeth in mastication is straightforward. Many studies have shown that mastication performance is reduced

by loss of posterior teeth, since these are the active tools in food comminution (Helkimo et al., 1978; Feldman et al., 1980; Kohyama et al., 2003; van der Bilt, 2011; Hennequin et al., 2015). The utility of recording PFUs is further illustrated by El Osta's study conducted in 200 aged individuals characterized by their nutritional status with the Mini-Nutritional Assessment questionnaire. Variations in PFU number largely explained nutritional status (El Osta et al., 2014). The precision of this PFU method has been criticized (Yurkstas and Manly, 1949). This may be an issue for basic experimental research, but in clinical experiments, the method is simple and useful.

Self-Administered Questionnaires

Masticatory function can be subjectively evaluated by self-administered questionnaires. Such questionnaires are often used in epidemiological surveys. They can also be useful when evaluating a change induced by a therapeutic intervention in a specific population. For example, a questionnaire of this type usefully evaluated the benefit for edentulous populations of wearing implants (Feine and Lund, 2006). However, their use is generally restricted to particular pathological and/or experimental situations, and they have no general validity for the whole population (Allison and Hennequin, 2000; Feine and Lund, 2006). In addition, these questionnaires tend to give an overly favorable result for chewing, and their results show little correlation with those of the objective evaluation methods (Slagter et al., 1992; de Lucena et al., 2011; Cusson et al., 2015). They may be useful when considering the overall oral function including swallowing, salivation and other oral functions. The Oral Health Impact Profile (OHIP), the Geriatric Oral Health Assessment Index (GOHAI), and the International Classification

of Functioning, Disability and Health (ICF) are examples of such frequently used questionnaires mostly related to oral quality of life or classification purposes (Atchinson and Dolan, 1990; Slade and Spencer, 1994; Faulks et al., 2013; Dougall et al., 2018).

Particle Size of the Food Bolus

The purpose of chewing is to reduce food to small particles and mix these with saliva. The size of the particles forming the food bolus just before swallowing is one deglutition triggering factor. Accordingly, measuring food bolus particle size is considered the “gold standard” for objective mastication evaluation. Test foods are most often carrots or peanuts as natural foods, and elastomeric compounds (Optosyl® or Optocal®). The median particle size (d50) is determined. The d50 corresponds to the mesh of a sieve that lets through one half of the mass of the particles and retains the other half. A *chewing test*, or chewing efficiency test, is based on determining the d50 at a predetermined number of cycles (usually 10 or 20 cycles). It gives an indication of chewing efficiency. We note the possibility of low efficiency in subjects with a healthy mastication made of long sequences composed of low power cycles. The *chewing test* must be differentiated from the *mastication test*, which gives a direct indication about the mastication capacity (Bonnet et al., 2019). In the mastication test, the d50 is evaluated from a bolus collected just before deglutition. A cut-off value for normality of 4 mm has been demonstrated with raw carrots (Woda et al., 2010) or artificial food (Witter et al., 2013). This value corresponds to the Masticatory Normative Indicator (MNI) beyond which the analyzed subject can adapt no further, the upper limit of capacitive adaptation being reached. Raw carrot was chosen as edible test food because it is hard to chew, and best reveals a subject's deficiency or difficulty in adapting. It may be refused by patients, clear evidence of deficiency (Depeyre et al., 2019). However, it may hide partial improvements during a therapeutic trial. Clearly, because of their relative complexity, particle size evaluation and other measurements of the rheological properties of the pre-swallowing bolus belong to experimental research.

Physiologic Methods of Evaluation

Chewing can be evaluated by electromyography, kinematics, force sensors or video (Hennequin et al., 2005; Nicolas et al., 2007). Muscular strength, amplitude and trajectory of the masticatory cycles of the mandible, duration of a mastication cycle, and frequency of chewing cycles can thus be evaluated. Owing to their characteristically complex nature, these methods are used in an experimental context only. Many experiments have studied the role of rheological properties of food, hardness, plasticity, viscosity or elasticity, to observe the adaptation of mastication to these extrinsic stimuli. One related question concerns the choice of the test food. Natural foods are a first choice because subjects can accept and swallow them easily. However, for better control of the rheological properties, several groups of experimenters have introduced model foods whose homogeneous and reproducible structure, controlled physical properties, and controlled size and shape, make it possible to observe the impact of a variation in hardness on the masticatory parameters (Nicolas et al., 2007; van der Bilt, 2011). The first

model foods were made from elastomers. More recently, edible model foods were introduced. They were made of gelatin, which offers the possibility of graduating hardness independently of the other rheological properties (Peyron et al., 2002).

Routine Clinical Evaluation of Masticatory Function

The color-mixing test could be used routinely to evaluate masticatory function. The advantage of this chewing test is that it can be easily used in daily dental practice to determine the masticatory capabilities of a subject before and after oral rehabilitation. The colorimetric test demonstrates the ability of an individual to homogenize an initially two-color support into a single monochrome phase, and thus to form a homogeneous bolus. Different materials have been used: two-tone chewing paste, two-tone wax and two-tone silicone (van der Bilt et al., 2010b). The most promising test material is a two-color chewing-gum that is chewed by the subject for a defined number of cycles and then spat out; the mixture of the two colors is evaluated either visually by direct observation or with analysis software (Schimmel et al., 2007, 2015; van der Bilt et al., 2012; Halazonetis et al., 2013). The method was validated by comparison with the results obtained by particle size measurement (van der Bilt et al., 2010b). This evaluation can also be visualized using a 5-stage color mixing reference scale (from Stage 1: unmixed chewing-gum, to Stage 5: perfectly mixed chewing-gum when the bolus color is uniform throughout). The simplicity in use of the colorimetric test lends it potential for clinical application (Elsig et al., 2015). Another attractive proposal relies simply on visual observation of food boluses immediately after they are produced. The bolus is compared with a chart composed of photographic pictures of 5 or 10 food boluses ranging from very well prepared to unprepared (Nokubi et al., 2013; Igarashi et al., 2019).

ADAPTATION OF MASTICATION TO DENTAL WEAR

The most obvious example of slowly occurring, directly visible changes of the dental arches is dental wear, which offers an example of a gradual, reciprocal adaptation of mastication and occlusion.

Normality of Dental Wear

Pioneer observations and more recent studies have amply shown that dental wear is normal. Dental wear is a general phenomenon found in all mammals, in every civilization, and at all ages (d'Incau et al., 2012). Its fullest extent is seen in ancient populations (d'Incau et al., 2012). It is also observed in populations who currently still have an “archaic” way of life and eat non-industrially processed natural foods (Campbell, 1925; Begg, 1954; Davies and Pedersen, 1955; Murphy, 1959b; Beyron, 1964). Examples of these populations include Australian Aborigines, Inuit, and native North Americans. The severity and shape of the worn surfaces in ancient populations or modern ones with “archaic” ways of life are mainly related to diet, with abrasive foods, the individual's natural environment, and food processing

technology (Kaifu et al., 2003; d'Incau et al., 2012). Dental wear is also found in all individuals in populations of developed countries, where it occurs at a slower pace (Woda et al., 1987). The low level of dental wear in modern civilization is probably due to more industrially processed foods that need less forceful mastication and are less abrasive (d'Incau et al., 2012). Whatever the population observed, all the occlusal wear facets are formed during the different masticatory cycles. For the incisors, some wear facets are associated with protrusion/retrusion movements. However, at the premolar/molar level, they are associated with lateral/medial movements, creating two types of facet: working and non-working, which are equally functional (Woda et al., 1979). When they are multiple and evenly distributed, they are superimposable on the occlusal contacts during maximum intercuspation. Finally, dental wear reshapes and adapts the morphology of the dental arches. Dental wear appears as a correlate of masticatory function, since dental wear facets guide masticatory movements, which in turn are the cause of dental wear (Hildebrand, 1936; Anderson and Picton, 1957; Beyron, 1964; Pameijer et al., 1969; Woda et al., 1987; Kim et al., 2001).

Tooth Displacement and Dental Wear

Reciprocal relationships link dental wear to several other phenomena. Loss of dental material due to dental wear results in tooth displacement to keep the continuity of contact between upper versus lower teeth and between adjacent teeth. In the vertical direction, wear of the occlusal table is compensated for by continuous active dental growth (Compagnon and Woda, 1991), without which an increase in facial vertical dimension may result (Begg, 1954; Tallgreen, 1957; Berry and Poole, 1976). Cementum apposition near the apical part of the dental root increases root length. Mesial drift of the posterior teeth ensures contact between adjacent teeth and compensates for the proximal wear. Lingual tilt of the anterior teeth accompanies the change from initial psalidodontia (with overlap) to labidodontia (end-to-end) with advanced wear (Kaifu, 1996) helping to maintain occlusal equilibrium (Kaifu et al., 2003; d'Incau et al., 2012; Garot et al., 2016).

One interesting condition is when there is an intercalated posterior tooth loss in an otherwise healthy dentition. Study of this situation showed that after their initial eruption, teeth continued to evolve in the occlusal direction during adulthood, through two mechanisms: egression, through an addition of alveolar bone, and eruption, by the tooth growing out of its socket (Murphy, 1959a; Compagnon and Woda, 1991). This latter component increases the ratio of crown to root length, the negative impact of which on biomechanical equilibrium is counterbalanced by the apposition of cementum at the apex of the root. These two components of vertical dental movement interact with different degrees of dental wear in a complex equilibrium that depends on the amplitude of masticatory or other external applied forces and physiological or pathological variations of dental arches. Several situations are possible. Weak masticatory forces lead to discrete occlusal wear, resulting in an enhanced occlusal vertical dimension due to the continuous egression of all teeth (Tallgreen, 1957). Conversely, intense masticatory forces are frequent in archaic civilizations. This

may enhance egression, resulting in the preservation of the occlusal vertical dimension despite abrasion of all dental crowns as observed in Inuit populations (Berry and Poole, 1976). Lack of antagonist teeth favors both permanent egression and permanent eruption, the latter phenomenon being preeminent in inflammatory conditions.

Balance between proximal wear and movements occurs between adjacent teeth. There is a migration of all teeth forward from the third molar toward the first incisor; this phenomenon is also called mesial migration. This movement maintains contact between adjacent teeth and reduces the frequency of malocclusion and crowding of anterior teeth by decreasing tooth size. More space is thus left for the eruption of the third molar (Begg, 1954).

Dental Wear Origin

The origin of dental wear evidences the relationship between mastication and dental wear. Several studies have shown that dental wear is due to abrasion caused by very small hard particles found in various parts of many plant species. These silicate particles are called phytoliths (Lanning and Eleuterius, 1985; Hart, 1988; Piperno, 1989). Other abrasive particles like sand grains or shed dental enamel may also serve as abrasive materials (Lewis and Dwyer-Joyce, 2005). The food itself may polish the pits and grooves made by these abrasive materials, whose mean half-life is very short, much less than 1 month (Morel et al., 1991).

Dental Wear May Be Abnormal

Although wear is less evident in modern civilization, it sometimes takes abnormal forms that can cause pain and alter function and/or esthetics. Marked occlusal wear can be due to parafunctional habits and/or dysfunctional behavior such as bruxism. When abrasion of occlusal surfaces is excessive, physiological egression may fail to compensate for loss of tooth height and may result in reduction of the facial vertical dimension and in accentuation of mandible closure in maximal intercuspation. With such excessive abrasion, anterior occlusion progresses toward an end-to-end anterior relationship and finally to mandible protrusion or prognathism, and sometimes a deep-bite face with advancement of the chin. This loss of vertical dimension has a progressive repercussion on soft tissue profile (Begg and Kesling, 1977; Richards, 1985; Planas, 1987; Kaifu et al., 2003; Kaidonis, 2008; d'Incau et al., 2012). Conversely, insufficient wearing, often found in modern populations, may have unwanted consequences: dental wear may be hidden or hindered by therapeutic reconstruction (Anderson and Myers, 1971; Woda et al., 1987). In addition, inconspicuous or insufficient occlusal dental wear, together with the continuing vertical egression of teeth, can result in an increase in the occlusal vertical dimension (Tallgreen, 1957). This may place periodontal tissues in an unfavorable condition. Also, a general decrease in occlusal wear explains the recourse to therapeutic occlusal management of interarch contacting surfaces (Planas, 1987; d'Incau et al., 2012), i.e., occlusal equilibration, in prosthetic cases and in cases of temporo-mandibular problems (Kurita et al., 2001; Pereira et al., 2009; van der Bilt, 2011). The disappearance of proximal tooth wear favors a tendency to crowding induced

by physiological mesial migration. This effect was the basis of an orthodontic technique promoting tooth reduction in material and number (Begg and Kesling, 1977; Planas, 1987; Kaifu et al., 2003). It has also been suggested that less dental wear gives free rein to functional disorders encountered in modern populations such as temporo-mandibular problems (van der Bilt, 2011).

Dental Wear and Masticatory Capacity/Efficiency

Dental wear increases the interarch contact area and participates actively in interarch adjustment. This in turn increases the efficiency of mastication (Yurkstas, 1965). Inversely, the decrease in functional occlusal surface may reflect a decrease in masticatory efficiency (Yurkstas and Manly, 1949; Julien et al., 1996). Occlusal contact area of the postcanine teeth is correlated with the small median particle size obtained at the end of a mastication sequence (Wilding, 1993; Julien et al., 1996; English et al., 2002; Lepley et al., 2011). This relation was also observed when chewing side preference in individuals was examined (Wilding, 1993). Direct measurement of worn facet areas on the arch occlusal surfaces revealed left-to-right area differences in approximately half of a sample of young adults, suggesting that about one individual in two had a preferred side of mastication (Bourdiol and Mioche, 2000). Dental wear differences are also found for both age and sex (Bourdiol et al., 2007). Increase in the number of mastication cycles was found when masticating on the side with fewer wear facets, suggesting a more difficult adaptation of the masticatory process (Bourdiol and Mioche, 2000).

Finally, dental abrasion is correlated with better oral health, fewer carious lesions due to dental plaque removal by an active mastication, Knychalska-Darman et al. (1972) and Taylor (1975) healthier periodontal tissues, Ainamo (1972) and good occlusal masticatory function. Masticatory function adapts to such slow, life-long gradual changes probably by plastic modifications of patterns in the central nervous system. The dental wear process, when normally progressive and evenly distributed along the dental arch, is thus physiological, at least for as long as the teeth and their supporting structures remain functional (Brace, 1977; Kaidonis, 2008).

ADAPTATION OF MASTICATION TO CHANGES IN FUNCTIONAL OCCLUSION

Here we consider malocclusion exclusively from a functional point of view. The question is to what extent malocclusion impacts chewing. It is claimed that malocclusion has little impact on chewing (Mohlin and Kurol, 2003). This appraisal is based on casual clinical situations but does not take full account of the broad variety of situations covered by the ill-defined term malocclusion. There is a huge difference between morphological malocclusion such as limited anterior dental crowding in which the disorder is purely esthetic, and major malocclusions resulting from maxillofacial oncological surgery or sudden severe cerebral palsy. All shades are possible between these two extremes. How does masticatory function adapt completely, partially or unsuccessfully to the various possibilities

across this broad malocclusion range? Whether patients have mastication characterized by compensatory adaptation or by incapacity has important clinical consequences that have still not been satisfactorily addressed. Mastication training could be proposed when compensatory adaptation is possible, and special food provision or a modified diet should be advised in cases of incapacity. A related question is the direction of the change: most often, spontaneous evolution, either gradual or sudden, tends toward a worsening of the occlusion conditions of mastication; a gradual or sudden change for the better is expected after therapeutic interventions. Apart from saliva, which must be of adequate quality and quantity, two factors seem to affect the extent of adaptation: (i) number of functional teeth and (ii) masticatory forces (Hatch et al., 2000; Kosaka et al., 2018). The presence of enough functional interarch posterior tooth-to-tooth contacts as indicated by the PFU concept is a determining factor (van der Bilt, 2011; Tanaka and Shiga, 2018). Below are two examples of the role of PFUs among many others. Firstly, shortened dental arches, i.e., dental arches with no more than one PFU in the molar area, have been proposed as a therapeutic solution (van der Bilt, 2011). Persons with shortened dental arches tend to be satisfied with their oral function. They are, however, in a situation of compensatory adaptation, since they need twice as many strokes to obtain the same bolus as they would with complete dental arches (Fontijn-Tekamp et al., 2000). Secondly, Decerle et al. (2013) studied young adults with multiple carious lesions causing a decrease in the number of PFUs. Maximum adaptive capacity was reached; they evidenced an impaired masticatory capacity with a d50 well above the MNI value of 4 mm. The presence of a healthy neuromuscular system is also a determining factor controlling mastication through changes in muscle strength and coordination. In Down syndrome, the neuro-muscular defect negatively impacts mastication, independently of a smaller number of PFUs (Hennequin et al., 1999). The mastication deficiency induced by Parkinson disease (Ribeiro et al., 2016) becomes more marked as the disease progresses (Bakke et al., 2011). Very advanced age is another possible factor in neuromuscular system decline (Osterberg et al., 1996). However, several studies have shown that outside extreme vital decline, elderly subjects were able to adapt to the age-induced changes provided there were not too many interfering problems (Peyron et al., 2017), and particularly if they had a sufficient number of PFUs (Kohyama et al., 2003; Kosaka et al., 2018). However, the effect of age is often one factor among many, where the specific role of any single one is difficult to specify. A good illustration is given by the effect of aging on mastication, as shown in **Figure 3**.

The adaptation of mastication to occlusion can also be observed in the opposite direction, i.e., as adaptation not to a worsened occlusal state but to an upgraded one. Therapeutic rehabilitation offers opportunities to study this adaptation. Occlusal rehabilitation diversely improves mastication efficiency. This clearly depends on the method of rehabilitation. Complete dentures do not fully correct food comminution compared with a healthy dentate state. Longer mastication time and more masticatory cycles are necessary to obtain acceptable food bolus comminution. In the overwhelming majority of

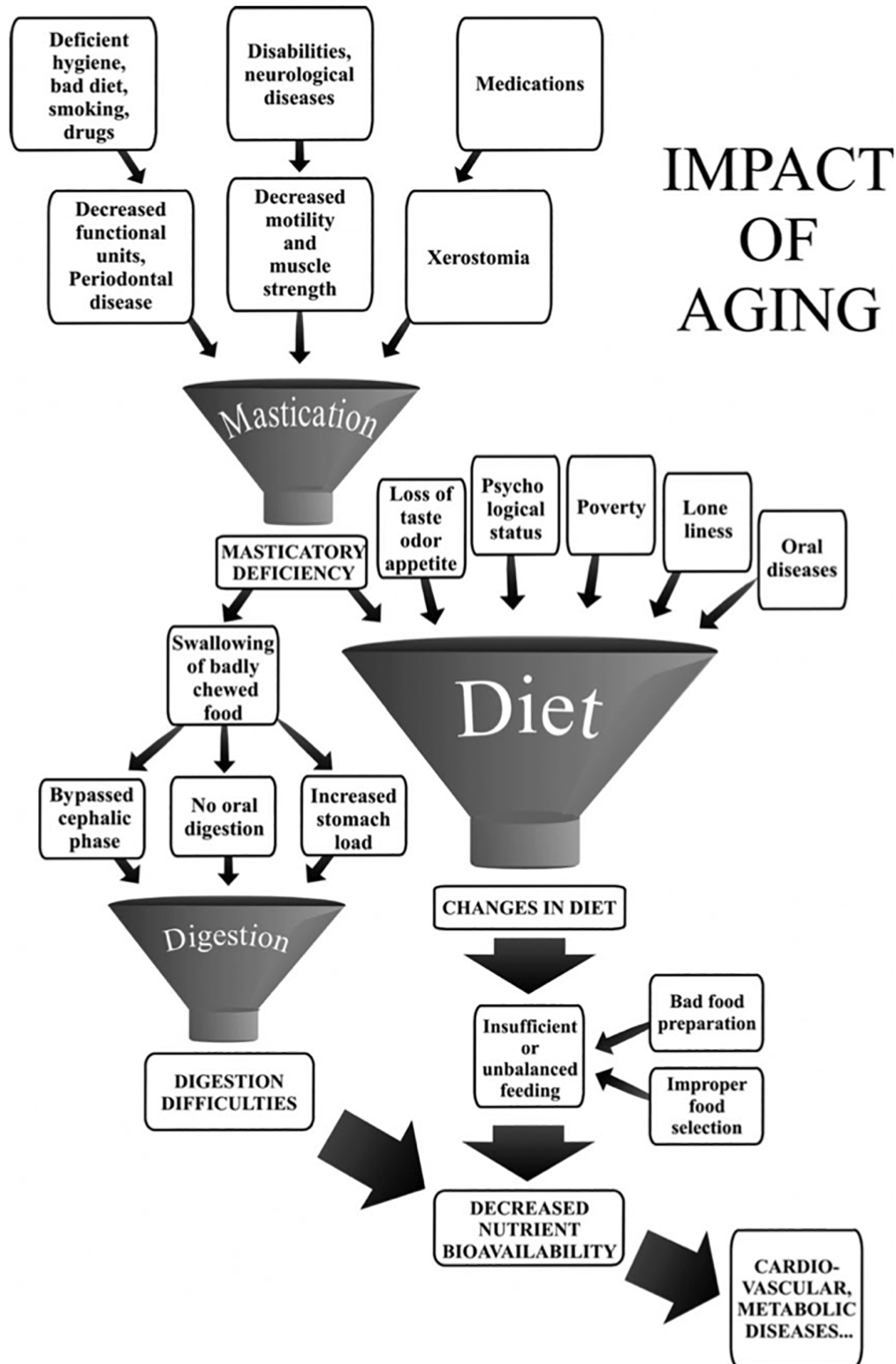
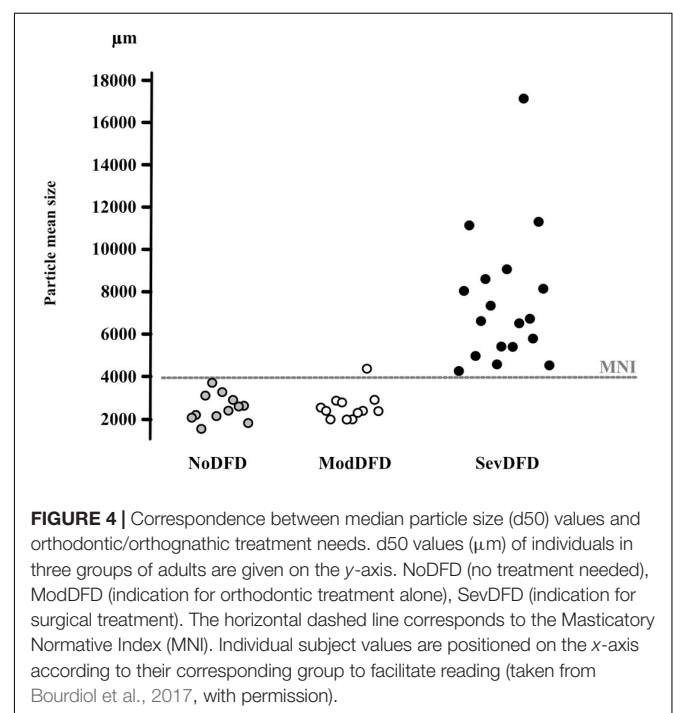


FIGURE 3 | Impact of aging on mastication-dependent nutrient bioavailability. Impaired mastication may cause decreased nutrient bioavailability through changes in diet. The diagram emphasizes that mastication deficiency is only one of the many factors that may induce a change in the diet. Similarly, mastication deficiency or digestion difficulties may have several causative factors. The multiplicity of factors liable to lead to decreased nutrient bioavailability rules out any fully convincing demonstration of an etiological relationship between masticatory deficiency and decreased nutrient availability (taken from Peyron et al., 2017, with permission).

cases, complete denture wearers are unable to reach the performance of naturally dentate individuals (Helkimo et al., 1978; Wayler and Chauncey, 1983; Veyrune et al., 2007; van der Bilt, 2011). Many complete denture wearers are clearly in a state of mastication incapacity, while others manage a compensatory adaptation (Mishellany-Dutour et al., 2008). Again, compensatory adaptation or incapacity should be differentiated to offer appropriate therapeutic advice. The quality of prosthodontics is another factor. Some authors have described a strong improvement after complete denture renewal (Gunne, 1985; Berteretche et al., 2015) and others have reported more nuanced observations (Garrett et al., 1996; Veyrune et al., 2005). In every case, it seems that complete denture wearers have first to adapt to their new prosthetic device first to control their mastication behavior, and second to improve its result in terms of mastication efficiency (Yurkstas and Emerson, 1964; Fontijn-Tekamp et al., 2000; Veyrune et al., 2005). Up to 1 year has been reported as the time needed for maximal recovery of mastication after delivery of a new denture (Goiato et al., 2010). This long time might be shortened, and the recovery made more complete with a training program aimed at relearning a masticatory praxis adapted to the new dental prosthesis.

Removable partial dentures offer only a poor addition to efficient occlusal contacts. Even with removable partial dentures, the number of residual natural PFUs controls chewing. For most authors, improved comminution performance is obtained with removable partial dentures (Liang et al., 2015), but it never reaches normality (Bessadet et al., 2013; Liang et al., 2015; Tanaka and Shiga, 2018), with some authors describing no difference in comminution performance with or without removable partial dentures being worn (Liedberg et al., 1995). Subjective feelings of patients about mastication may, however, be improved by removable partial dentures (Gunne, 1985). Many parameters point to incomplete mastication with removable partial dentures. Mastication frequency remains low, a mark of abnormal mastication. The modest improvement brought about by removable partial dentures, and the dominant role of natural PFUs in mastication, is well demonstrated by no difference (Fueki et al., 2011) or only a slight difference (Liang et al., 2015) between mastication efficiency with shortened dental arch and with adjunction of a removable partial denture. The decreased number of natural PFUs also determines diminished biting forces (Helkimo et al., 1977; Ikebe et al., 2010). Subjects tend to compensate for decreased mastication efficiency by increasing the number of strokes, which is compensatory adaptation, and by selecting a soft diet (Liedberg et al., 2004). The exclusion of hard food and selection of soft diet can have a demonstrable (Inomata et al., 2015), a small impact (Wallace et al., 2018) or no impact (Liedberg et al., 2004) on nutrition and health. We can expect very different results depending on contrasting conditions. For example, the number and distribution of missing teeth, the type of food tested, and the tests used to assess the mastication deficiency/adaptation are powerful factors explaining differences in results. In summary, depending on the individual condition, mastication may be characterized by compensatory adaptation or by incapacity.

There is an unsubstantiated belief that implant-supported bridges allow complete recovery of masticatory function. Pioneer papers using pre/post-treatment design showed a clear improvement of mastication (Lindquist and Carlsson, 1985; Carlsson and Lindquist, 1994) especially when the initial oral state was so degraded that it needed major oral rehabilitation. Many of these pioneer papers also reported an adaptation process after these new conditions were set, with a progressive enhancement of mastication parameters in the subsequent months or years (Lindquist and Carlsson, 1985; Lundqvist and Haraldson, 1992; Akeel et al., 1993; Lundqvist, 1993). A strong subjective satisfaction with mastication accompanied the improvement in objective criteria (Lindquist and Carlsson, 1985; Lundqvist and Haraldson, 1992; Carlsson and Lindquist, 1994; Veyrune et al., 2013). However, comparison with healthy dentate subjects was seldom made (Carlsson and Lindquist, 1994). It was long after the initial pioneer period that a careful controlled study compared mastication function of subjects receiving implant-supported bridges with a healthy full dentate group (Grigoriadis et al., 2011). Implant-supported bridges involved one or both jaws. The evaluation was done at least 1 year after treatment. Electromyographic recording while chewing model foods with progressively increasing hardness revealed that jaw movements were affected in the group of subjects with dental implants. Unlike the control subjects, who increased muscle activity with hardness and decreased it near the end of the masticatory sequence with related changes in jaw movements, the participants with implants used similar muscle activities and jaw movements irrespective of both food type and time in the masticatory sequence. For the authors, this lack of adaptation probably relates to a lack of neural



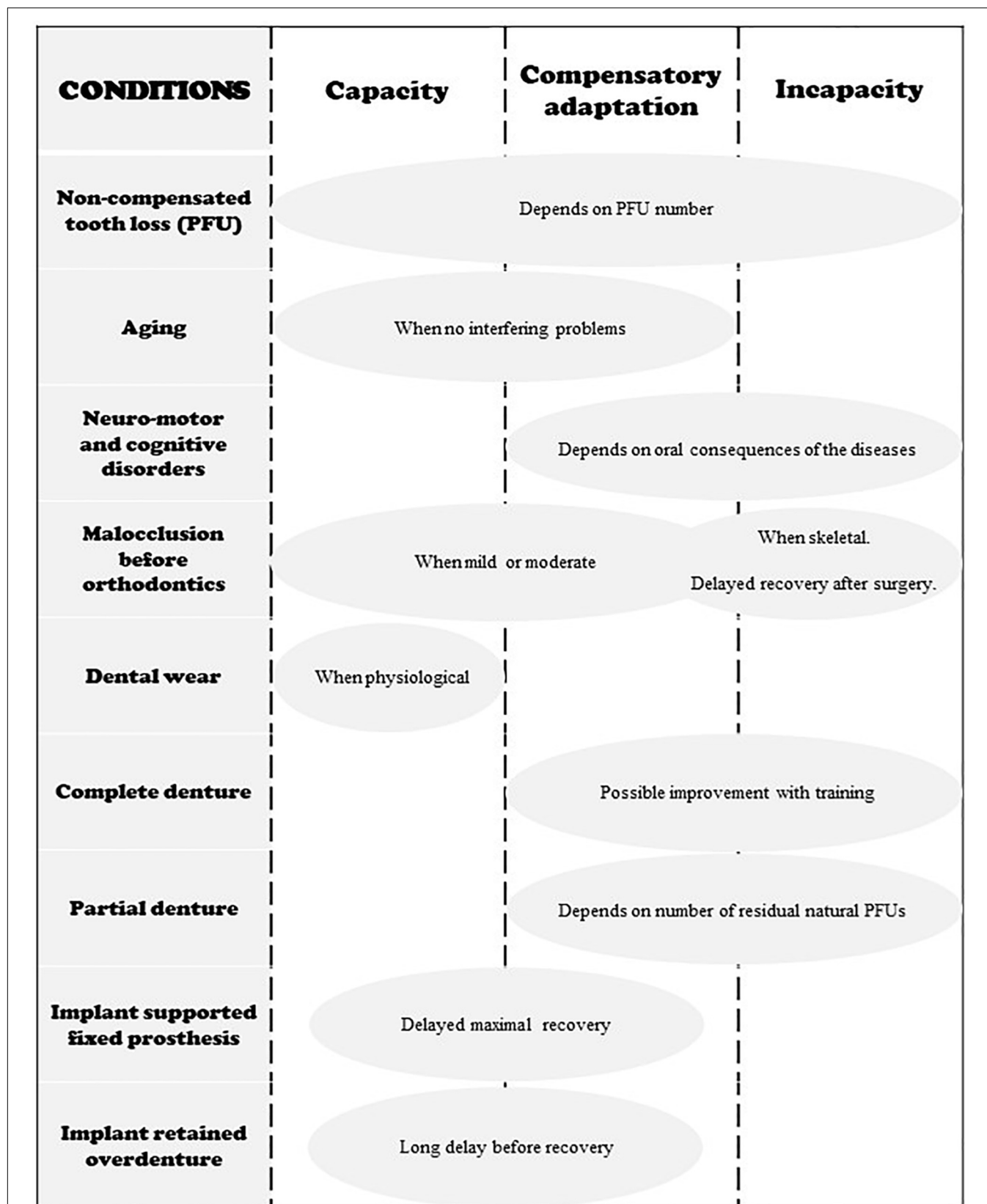


FIGURE 5 | Schematic representation of the three states of adaptation in regard to different occlusal conditions. Neuromotor and cognitive disorders include Down Syndrome, stroke, Parkinson disease and other neuro-degenerative disorders, facial damage, mental illness, etc.

control due to the absence of periodontal receptors (see review in Avivi-Arber and Sessle, 2018). Implant-retained overdentures also strongly ameliorated masticatory efficiency and patient satisfaction, which remained high for a long time (Awad et al., 2000; Bakke et al., 2002; van der Bilt et al., 2012). Mastication parameters were observed to approach the values obtained in normal dentate subjects (Haraldson et al., 1988; Heckmann et al., 2009). This also applies to different type of implant-retained overdentures (Tang et al., 1999; Feine et al., 2002; Awad et al., 2003; van der Bilt et al., 2012), including mini-implants (Batisse et al., 2016; Goiato et al., 2018; Yao et al., 2018). The improvement with implant-retained overdentures was delayed for more than 6 months after rehabilitation treatment. This is because deeply anchored chewing habits corresponding to the previous oral conditions may be maintained despite conditions that are more favorable (Garrett et al., 1998; van der Bilt et al., 2010a; Okoński et al., 2011; Batisse et al., 2016). Maladaptive neuroplasticity may explain deeply anchored chewing habits (Avivi-Arber and Sessle, 2018), and positive plasticity might have been enhanced by a training program (Kumar et al., 2018).

Subjects with dento-facial deformities and orthodontic needs may present a deficient masticatory function (Tate et al., 1994; van den Braber et al., 2001; English et al., 2002; Iwase et al., 2006; N'Gom et al., 2007; Magälhaes et al., 2010; Picinato-Pirola et al., 2012; Abrahamsson et al., 2013; Hennequin et al., 2015). These subjects often display an interarch discrepancy or inadequacy, as reflected by the significantly reduced functional area (Kobayashi et al., 1993; Henrikson et al., 1998; Magälhaes et al., 2010; Bourdiol et al., 2017). However, dento-facial deformities may lead to two quite different endpoints: satisfactory masticatory function through successful compensatory adaptation, or strongly impaired mastication because adaptation proves impossible (incapacity) (Mishellany et al., 2006; Woda et al., 2011). The relation between severity of dento-facial deformities and extent of mastication deficiency has been assessed (Bourdiol et al., 2017) (**Figure 4**). Subjects needing only orthodontic treatment, i.e., presenting with a moderate dento-facial deformity, succeeded in making a normal food bolus. They might have a lowered masticatory efficiency as indicated by food bolus particle size measured after a limited number of cycles. It can be inferred that they adapted their masticatory function, mostly by increasing the number of chewing cycles and the duration of the masticatory sequence. Members of this group thus achieved a normal functional result. By contrast, subjects confronted with severe dento-facial deformities and needing combined orthodontics and surgery, failed to adapt. They swallowed insufficiently prepared food or selected their diet. Both orthodontic treatment alone (Henrikson et al., 2009) and orthodontics associated with orthognathic surgery (Shiratsuchi et al., 1991; Kikuta et al., 1994; Zarrinkelk et al., 1995; van der Braber et al., 2005) improved masticatory performance, at least partially. It must be noted that after orthognathic surgery, improvement of masticatory efficiency does not occur immediately. The functional benefit of a combined orthodontic and surgical approach appears progressively in the course of at least 1 year (Kikuta et al., 1994; Iwase et al.,

2006; Magälhaes et al., 2010), but may never reach complete normality (van der Braber et al., 2006). The delayed recovery is probably due, at least in part, to the time needed to learn a new masticatory praxis enabling the patient to master the new anatomic conditions.

Rehabilitating intervention in patients with Down syndrome led to an increased number of PFUs. This increase improved chewing, with a decreased occurrence of food rejections, and a smaller median size of bolus particles and fewer masticatory cycles before bolus swallowing (Hennequin et al., 2015).

The conditions that govern capacity, compensatory adaptation and incapacity are summarized in **Figure 5**.

EFFECT OF ADAPTATION OF MASTICATION ON NUTRITION

One component of adaptation is behavioral adaptation through diet choice. When in a state of incapacity, subjects presenting with deficient mastication may exclude hard-to-chew food from their diet. For example, removable denture wearers reject hard foods and restrict themselves to those easy to chew (Liedberg et al., 2005). Others may shorten chewing time and swallow a coarse food bolus. In both cases, there may be negative health consequences, mostly on digestive function and nutrition as described below (see Peyron et al., 2017). There is overwhelming evidence of a correlation between masticatory deficiency and malnutrition (N'Gom and Woda, 2002; Hutton et al., 2002). However, a causal relationship remains to be demonstrated (Mioche et al., 2004; Rémond et al., 2015). Based on a systematic review with 11 studies using a multivariate approach, van Lancker et al. (2012) supported an independent association between oral health status and malnutrition. Changes in diet depended on masticatory function according to number of teeth. However, little modification was seen in nutrient concentrations in blood (Sheiham et al., 2001). A causal relationship between masticatory function and blood availability of nutrients was shown in a trial design comparing full dentures with and without supporting implants (Moraes et al., 2003). Further research is needed to seek evidence for a causal relationship between mastication, oral health and malnutrition. Several points, however, must be clarified for this approach. The common assumption that the oral stage of eating is a minor function gainsays the obvious vital role of food. Eating is so important that evolution has engineered overlapping functions shared by several segments of the upper digestive tract. In this way, failure of any one organ will not mean starvation. Mouth and stomach may thus be considered as performing multiple mechanical activities with built-in functional redundancy. Hence mouth function may have been underestimated.

CONCLUSION

Increasing knowledge about the processes by which mastication adapts in response to food properties or oral status is

challenging for researchers, clinicians and patients. This review describes the different adaptation processes for mastication that enable individuals to maintain healthy nutritional status. Any modification of dental status, saliva flow or neuromuscular apparatus can affect mastication and nutrition. Oral incapacities affect mastication for solid and semi-solid foods. Eating liquid foods or purées can facilitate deglutition but this bypasses the triggering of the cephalic phase and alters the digestive process. Dental professionals need to be alert to these concepts and to mastication evaluation.

REFERENCES

- Abrahamsson, C., Henrikson, T., Nilner, M., Sunzel, B., Bondemark, L., and Ekberg, E. C. (2013). TMD before and after correction of dentofacial deformities by orthodontic and orthognathic treatment. *Int. J. Oral. Maxillofac. Surg.* 42, 752–758. doi: 10.1016/j.ijom.2012.10.016
- Ainamo, J. (1972). Relationship between occlusal wear of the teeth and periodontal health. *Scand. J. Dent. Res.* 80, 505–509. doi: 10.1111/j.1600-0722.1972.tb00320.x
- Akeel, R., Fernandes, C. P., and Vassilakos, N. (1993). Masticatory efficiency of patients treated with implant retained fixed bridges in the upper jaw over a 2-year period. *Eur. J. Prosthodont. Restor. Dent.* 1, 131–133.
- Allison, P. J., and Hennequin, M. (2000). The oral assessment in down syndrome questionnaire (OADS): development of an instrument to evaluate oral health problems in individuals with down syndrome. *Community. Dent. Health.* 17, 172–179.
- Anderson, D. J., and Picton, D. C. (1957). Tooth contact during chewing. *J. Dent. Res.* 36, 21–26. doi: 10.1177/00220345570360011301
- Anderson, J. R., and Myers, G. E. (1971). Nature of contacts in centric occlusion in 32 adults. *J. Dent. Res.* 50, 7–13. doi: 10.1177/00220345710500013201
- Atchinson, K., and Dolan, T. A. (1990). Development of the geriatric oral health assessment index. *J. Dent. Educ.* 54, 680–687.
- Avivi-Arber, L., Lee, J. C., and Sessle, B. J. (2011). Chapter 9-face sensorimotor cortex neuroplasticity associated with intraoral alterations. *Prog. Brain Res.* 188, 135–150. doi: 10.1016/B978-0-444-53825-3.00014-0
- Avivi-Arber, L., Lee, J. C., Sood, M., Lakschevitz, F., Fung, M., Barashi-Goza, M., et al. (2015). Long-term neuroplasticity of the face primary motor cortex and adjacent somatosensory cortex induced by tooth loss can be reversed following dental implant replacement in rats. *J. Comp. Neurol.* 1, 2372–2389. doi: 10.1002/cne.23793
- Avivi-Arber, L., and Sessle, B. J. (2018). Jaw sensorimotor control in healthy adults and effects of ageing. *J. Oral Rehabil.* 45, 50–80. doi: 10.1111/joor.12554
- Awad, M. A., Locker, D., Korner-Bitensky, N., and Feine, J. S. (2000). Measuring the effect of intra-oral implant rehabilitation on health-related quality of life in a randomized controlled clinical trial. *J. Dent. Res.* 79, 1659–1663. doi: 10.1177/00220345000790090401
- Awad, M. A., Lund, J. P., Dufresne, E., and Feine, J. S. (2003). Comparing the efficacy of mandibular implant-retained overdentures and conventional dentures among middle-aged edentulous patients: satisfaction and functional assessment. *Int. J. Prosthodont.* 16, 117–122.
- Bakke, M., Holm, B., and Gotfredsen, K. (2002). Masticatory function and patient satisfaction with implant-supported mandibular overdentures: a prospective 5-year study. *Int. J. Prosthodont.* 15, 575–581.
- Bakke, M., Larsen, S. L., Lautrup, C., and Karlsborg, M. (2011). Orofacial function and oral health in patients with Parkinson's disease. *Eur. J. Oral. Sci.* 119, 7–32.
- Batisse, C., Bonnet, G., Bessadet, M., Veyrune, J. L., Hennequin, M., Peyron, M., et al. (2016). Stabilization of mandibular complete dentures by four mini implants: Impact on masticatory function. *J. Dent.* 50, 43–50. doi: 10.1016/j.jdent.2016.04.012
- Begg, P. R. (1954). Stone age man's dentition. *Am. J. Orthod. Dentofac. Orthop.* 40, 298–312. doi: 10.1016/0002-9416(54)90103-7
- Begg, P. R., and Kesling, P. C. (1977). *Begg Orthodontic-Theory and Technique*. Philadelphia: Saunders.

AUTHOR CONTRIBUTIONS

PB, MH, M-AP, and AW contributed to the concepts and bibliographic analysis. AW and PB made first writing which was later corrected by the four authors.

FUNDING

We have received no funding except by our Clermont Auvergne University.

- Berry, D. C., and Poole, D. F. G. (1976). Attrition: possible mechanisms of compensation. *J. Oral. Rehabil.* 3, 201–206. doi: 10.1111/j.1365-2842.1976.tb00945.x
- Berteretche, M. V., Frot, A., Woda, A., Pereira, B., and Hennequin, M. (2015). Different types of antagonists modify the outcome of complete denture renewal. *Int. J. Prosthodont.* 28, 270–278. doi: 10.11607/ijp.3916
- Bessadet, M., Nicolas, E., Sochat, M., Hennequin, M., and Veyrune, J. L. (2013). Impact of removable partial denture prosthesis on chewing efficiency. *J. Appl. Oral. Sci.* 21, 392–396. doi: 10.1590/1679-775720130046
- Beyron, H. (1964). Occlusal relations and mastication in Australian Aborigines. *Acta. Odontol. Scand.* 22, 597–678. doi: 10.3109/00016356409058580
- Bonnet, G., Batisse, C., Peyron, M. A., Nicolas, E., and Hennequin, M. (2019). Which variables should be controlled when measuring the granulometry of a chewed bolus? A systematic review. *J. Texture Stud.* 50, 194–216. doi: 10.1111/jtxs.12376
- Bourdiol, P., Abou ElKaram, S., Martin, J. F., Nicolas, E., and Mioche, L. (2007). Age and gender-related differences in premolar and molar functional areas. *J. Oral. Rehab.* 34, 251–258. doi: 10.1111/j.1365-2842.2007.01666.x
- Bourdiol, P., and Mioche, L. (2000). Correlations between functional and occlusal tooth-surface areas and food texture during natural chewing sequences in humans. *Arch. Oral. Biol.* 45, 691–699. doi: 10.1016/S0003-9969(00)00027-3
- Bourdiol, P., Soulier-Peigue, D., Lachaze, P., Nicolas, E., Woda, A., and Hennequin, M. (2017). Only severe malocclusion correlates with mastication deficiency. *Arch. Oral. Biol.* 75, 14–20. doi: 10.1016/j.archoralbio.2016.12.002
- Brace, C. L. (1977). "Occlusion to the anthropological eye," in *The Biology of Occlusal Development, Monograph no. 7, Craniofacial Growth Series*, ed. J. A. McNamara Jr. (Ann Arbor, MI: The University of Michigan), 179–209.
- Campbell, T. D. (1925). *Dentition and Palate of the Australian Aboriginal*. Adelaide: Hassell Press.
- Carlsson, G. H., and Lindquist, L. W. (1994). Ten-year longitudinal study of masticatory function in edentulous patients treated with fixed complete dentures on osseointegrated implants. *Int. J. Prosthodont.* 7, 448–453.
- Cavalcante, F. T., Moura, C., Perazzo, P. A. T., Cavalcante, F. T., and Cavalcante, M. T. (2019). Prevalence of chewing difficulty among adults and associated factors. *Cien. Saude. Colet.* 24, 1101–1110. doi: 10.1590/1413-81232018243.10122017
- Compagnon, D., and Woda, A. (1991). Supraeruption of the unopposed maxillary first molar. *J. Prosthet. Dent.* 66, 29–34. doi: 10.1016/0022-3913(91)90347-y
- Cusson, V., Caron, C., Gaudreau, P., Morais, J. A., Shatenstein, B., and Payette, H. (2015). Assessing older adults' masticatory efficiency. *J. Am. Geriatr. Soc.* 63, 1192–1196. doi: 10.1111/jgs.13443
- Davies, T. G., and Pedersen, P. O. (1955). The degree of attrition of the deciduous teeth and first permanent molars of primitive and urbanised Greenland natives. *Br. Dent. J.* 99, 35–43.
- de Lucena, S. C., Gomes, S. G., Da Silva, W. J., and Del Bel Cury, A. A. (2011). Patients' satisfaction and functional assessment of existing complete dentures: correlation with objective masticatory function. *J. Oral. Rehabil.* 38, 440–446. doi: 10.1111/j.1365-2842.2010.02174.x
- Decerle, N., Nicolas, E., and Hennequin, M. (2013). Chewing deficiencies in adults with multiple untreated carious lesions. *Caries. Res.* 47, 330–337. doi: 10.1159/000348397

- Depeyre, A., Pereira, B., Pham-Dang, N., Barthélémy, I., and Hennequin, M. (2019). Impairments in food oral processing in patients treated for tongue cancer. *Dysphagia*. doi: 10.1007/s00455-019-10054-5
- Dias-da-Costa, J. S., Galli, R., Oliveira, E. A., Backes, V., Vial, E. A., Canuto, R., et al. (2010). Prevalence of poor self-rated mastication and associated factors in Brazilian elderly. *Cad. Saude. Publica* 26, 79–88.
- d'Incau, E., Couture, C., and Maureille, B. (2012). Human tooth wear in the past and the present: tribological mechanisms, scoring systems, dental and skeletal compensations. *Arch. Oral. Biol.* 57, 214–229. doi: 10.1016/j.archoralbio.2011.08.021
- Ding, R., Logemann, J. A., Larson, C. R., and Rademaker, A. W. (2003). The effects of taste and consistency on swallow physiology in younger and older healthy individuals: a surface electromyography study. *J. Speech. Lang. Hear. Res.* 46, 977–989. doi: 10.1044/1092-4388(2003)076
- Dougall, A., Martinez Pereira, F., Molina, G., Eschevins, C., Daly, B., and Faulks, D. (2018). Identifying common factors of functioning, participation and environment amongst adults requiring specialist oral health care using the International classification of functioning, disability and health. *PLoS. One* 3:13. doi: 10.1371/journal.pone.0199781
- El Osta, N., Hennequin, M., Tubert-Jeannin, S., Abboud Naaman, N. B., El Osta, L., and Geahchan, N. (2014). The pertinence of oral health indicators in nutritional studies in the elderly. *Clin. Nutr.* 33, 316–321. doi: 10.1016/j.clnu.2013.05.012
- Elsig, F., Schimmel, M., Duvernay, E., Giannelli, S. V., Graf, C. E., Carlier, S., et al. (2015). Tooth loss, chewing efficiency and cognitive impairment in geriatric patients. *Gerodontology* 32, 149–156. doi: 10.1111/ger.12079
- English, J. D., Bushang, P. H., and Throckmorton, G. S. (2002). Does Malocclusion affect masticatory performance? *Angle. Orthod.* 72, 21–27.
- Faulks, D., Norderyd, J., Molina, G., Macgiolla Phadraig, C., Scagnet, G., Eschevins, C., et al. (2013). Using the international classification of functioning, disability and health (ICF) to describe children referred to special care or paediatric dental services. *PLoS. One* 16:8. doi: 10.1371/journal.pone.0061993
- Feine, J. S., Carlsson, G. E., Awad, M. A., Chehade, A., Duncan, W. J., Gizani, S., et al. (2002). The McGill consensus statement on overdentures. Mandibular two-implant overdentures as first choice standard of care for edentulous patients. *Gerodontology* 19, 3–4. doi: 10.1111/j.1741-2358.2002.00003.x
- Feine, J. S., and Lund, J. P. (2006). Measuring chewing ability in randomized controlled trials with edentulous populations wearing implant prostheses. *J. Oral. Rehabil.* 33, 301–308. doi: 10.1111/j.1365-2842.2006.01614.x
- Feldman, R. S., Kapur, K. K., Alman, J. E., and Chauncey, H. H. (1980). Aging and mastication: changes in performance and in swallowing threshold with natural dentition. *J. Am. Geriatr. Soc.* 28, 97–103. doi: 10.1111/j.1532-5415.1980.tb00240.x
- Fontijn-Tekamp, F. A., Slagter, A. P., van der Bilt, A., van't Hof, M. A., Witter, D. J., Kalk, W., et al. (2000). Biting and chewing in overdentures, full dentures, and natural dentitions. *J. Dent. Res.* 79, 1519–1524. doi: 10.1177/00220345000790071501
- Fontijn-Tekamp, F. A., van der Bilt, A., Abbink, J. H., and Bosman, F. (2004). Swallowing threshold and masticatory performance in dentate adults. *Physiol. Behav.* 83, 431–436. doi: 10.1016/j.physbeh.2004.08.026
- Fueki, K., Yoshida, E., and Igarashi, Y. (2011). A systematic review of prosthetic restoration in patients with shortened dental arches. *Jpn. Dent. Sci. Rev.* 47, 167–174. doi: 10.1016/j.jdsr.2011.03.003
- Garot, E., Rouas, P., d'Incau, E., Lenoir, N., Manton, D., and Couture-Veschambre, C. (2016). Mineral density of hypomineralised and sound enamel. *Bull. Group. Int. Rech. Sci. Stomatol. Odontol.* 28:53.
- Garrett, N. R., Kapur, K. K., Hamada, M. O., Roumanas, E. D., Freymiller, E., Han, T., et al. (1998). A randomized clinical trial comparing the efficacy of mandibular implant-supported overdentures and conventional dentures in diabetic patients. Part II. Comparisons of masticatory performance. *J. Prosthet. Dent.* 79, 632–640. doi: 10.1016/s0022-3913(98)70177-5
- Garrett, N. R., Kapur, K. K., and Perez, P. (1996). Effects of improvements of poorly fitting dentures and new dentures on patient satisfaction. *J. Prosthet. Dent.* 76, 403–413. doi: 10.1016/s0022-3913(96)90483-7
- Goiato, M. C., Garcia, A. R., Dos Santos, D. M., and Zuim, P. R. (2010). Analysis of masticatory efficiency in complete denture wearers. *J. Prosthodont.* 19, 10–13. doi: 10.1111/j.1532-849X.2009.00520.x
- Goiato, M. C., Sonego, M. V., Pellizzer, E. P., Gomes, J. M. L., da Silva, E. V. F., and Dos Santos, D. M. (2018). Clinical outcome of removable prostheses supported by mini dental implants. A systematic review. *Acta. Odontol. Scand.* 76, 628–637. doi: 10.1080/00016357.2018.1499958
- Grigoriadis, A., Johansson, R. S., and Trulsson, M. (2011). Adaptability of mastication in people with implant-supported bridges. *J. Clin. Periodontol.* 38, 395–404. doi: 10.1111/j.1600-051X.2010.01697.x
- Gunne, H. S. (1985). The effect of removable partial dentures on mastication and dietary intake. *Acta. Odontol. Scand.* 43, 269–278. doi: 10.3109/00016358509046507
- Halazonetis, D. J., Schimmel, M., Antonarakis, G. S., and Christou, P. (2013). Novel software for quantitative evaluation and graphical representation of masticatory efficiency. *J. Oral. Rehabil.* 40, 329–335. doi: 10.1111/joor.12043
- Haraldson, T., Jemt, T., Ståhlblad, P. A., and Lekholm, U. (1988). Oral function in subjects with Oral function in subjects with overdentures supported by osseointegrated implants. *Scand. J. Dent. Res.* 96, 235–242. doi: 10.1111/j.1600-0722.1988.tb01550.x
- Hart, D. M. (1988). The plant opal content in the vegetation and sediment of a swamp at Oxford Falls, New South Wales, Australia. *Aust. J. Bot.* 36, 159–170. doi: 10.1071/BT9880159
- Hatch, J. P., Shinkai, R. S. A., Sakai, S., Rugh, J. D., and Paunovich, E. D. (2000). Determinants of masticatory performance in dentate adults. *Arch. Oral. Biol.* 46, 641–648. doi: 10.1016/s0003-9969(01)00023-1
- Heckmann, S. M., Heussinger, S., Linke, J. J., Graef, F., and Pröschel, P. (2009). Improvement and long-term stability of neuromuscular adaptation in implant-supported overdentures. *Clin. Oral. Implants. Res.* 20, 1200–1205. doi: 10.1111/j.1600-0501.2009.01722.x
- Helkimo, E., Carlsson, G. E., and Helkimo, M. (1977). Bite force and state of dentition. *Acta. Odontol. Scand.* 35, 297–303. doi: 10.3109/00016357709064128
- Helkimo, E., Carlsson, G. E., and Helkimo, M. (1978). Chewing efficiency and state of dentition. A methodologic study. *Acta. Odontol. Scand.* 36, 33–41. doi: 10.3109/00016357809026364
- Hennequin, M., Allison, P. J., Veyrune, J. L., Faye, M., and Peyron, M. (2005). Clinical evaluation of mastication: validation of video versus electromyography. *Clin. Nutr.* 24, 314–320. doi: 10.1016/j.clnu.2004.11.010
- Hennequin, M., Faulks, D., Veyrune, J. L., and Bourdiol, P. (1999). Significance of oral health in persons with Down syndrome: a literature review. *Dev. Med. Child. Neurol.* 41, 275–283. doi: 10.1111/j.1469-8749.1999.tb00599.x
- Hennequin, M., Mazille, M. N., Cousson, P. Y., and Nicolas, E. (2015). Increasing the number of inter-arch contacts improves mastication in adults with Down syndrome: a prospective control trial. *Physiol. Behav.* 145, 14–21. doi: 10.1016/j.physbeh.2015.03.034
- Henrikson, T., Ekberg, E., and Nilner, M. (1998). Masticatory efficiency and ability in relation to occlusion and mandibular dysfunction in girls. *Int. J. Prosthodont.* 11, 125–132.
- Henrikson, T., Ekberg, E., and Nilner, M. (2009). Can orthodontic treatment improve mastication? A controlled, prospective and longitudinal study. *Swed. Dent. J.* 33, 59–65.
- Hiiemae, K., Heath, M. R., Kazazoglu, E., Murray, J., Sapper, D., and Hamblet, K. (1996). Natural bites, food consistency and feeding behaviour in man. *Arch. Oral. Biol.* 41, 175–189. doi: 10.1016/0003-9969(95)00112-3
- Hiiemae, K. M., and Palmer, J. B. (1999). Food transport and bolus formation during complete feeding sequences on foods of different initial consistency. *Dysphagia* 14, 31–42. doi: 10.1007/PL00009582
- Hildebrand, G. Y. (1936). Studies in mandibular kinematics. *Dent. Cosmos* 78, 449–458.
- Hutchings, J. B., and Lillford, P. J. (1988). The perception of food texture – The philosophy of the breakdown path. *J. Texture. Stud.* 19, 103–115. doi: 10.1111/j.1745-4603.1988.tb00928.x
- Hutton, B., Feine, J., and Morais, J. (2002). Is there an association between edentulism and nutritional state? *J. Can. Dent. Assoc.* 68, 182–187.
- Igarashi, K., Watanabe, Y., Kugimiya, Y., Shiobe, M., Edahiro, A., Kaneda, K., et al. (2019). Validity of a visual scoring method using gummy jelly for evaluating chewing efficiency in a large-scale epidemiological survey. *J. Oral. Rehabil.* 46, 409–416. doi: 10.1111/joor.12761
- Ikebe, K., Matsuda, K., Murai, S., Maeda, Y., and Nokubi, T. (2010). Validation of the Eichner index in relation to occlusal force and masticatory performance. *Int. J. Prosthodont.* 23, 521–524.

- Inomata, C., Ikebe, K., Okada, T., Takeshita, H., and Maeda, Y. (2015). Impact on Dietary Intake of Removable Partial Dentures Replacing a Small Number of Teeth. *Int. J. Prosthodont.* 28, 583–585. doi: 10.11607/ijp.4306
- Iwase, M., Ohashi, M., Tachibana, H., Toyoshima, T., and Nagumo, M. (2006). Bite force, occlusal contact area and mastication efficiency before and after orthognathic surgical correction of mandibular prognathism. *Int. J. Oral. Maxillofac. Surg.* 35, 1102–1107. doi: 10.1016/j.ijom.2006.08.014
- Jalabert-Malbos, M. L., Mishellany-Dutour, A., Woda, A., and Peyron, M. A. (2007). Particle size distribution in the food bolus after mastication of natural foods. *Food. Qual. Pref.* 18, 803–812. doi: 10.1016/j.foodqual.2007.01.010
- Julien, K. C., Bushang, P. H., Throckmorton, G. S., and Dechow, P. C. (1996). Normal masticatory performance in young adults and children. *Arch. Oral. Biol.* 41, 69–75. doi: 10.1016/0003-9969(95)00098-4
- Kahrilas, P. J., and Logemann, J. A. (1993). Volume accommodation during swallowing. *Dysphagia* 8, 259–265. doi: 10.1007/bf01354548
- Kaidonis, J. A. (2008). Tooth wear: the view of the anthropologist. *Clin. Oral. Invest.* 12(Suppl.1), 21–26. doi: 10.1007/s00784-007-0154-8
- Kaifu, Y. (1996). Edge-to-edge bite and tooth wear. *Bull. Natn. Sci. Mus. Tokyo. Ser. D* 22, 45–54.
- Kaifu, Y., Kasai, K., Townsend, G. C., and Richards, L. C. (2003). Tooth wear and the « design » of the human dentition: a perspective from evolutionary medicine. *Am. J. Phys. Anthropol.* 37, 47–61. doi: 10.1002/ajpa.10329
- Kikuta, T., Hara, I., Seto, T., Yoshioka, I., Nakashima, T., and Yasumitsu, C. (1994). Evaluation of masticatory function after sagittal split ramus osteotomy for patients with mandibular prognathism. *Int. J. Adult. Orthodon. Orthognath. Surg.* 9, 9–17.
- Kim, S. K., Kim, K. N., Chang, I. T., and Heo, S. J. (2001). A study of the effects of chewing patterns on occlusal wear. *J. Oral. Rehabil.* 28, 1048–1055. doi: 10.1111/j.1365-2842.2001.00761.x
- Knychalska-Darman, Z., Laskowska, L., Pelcowa, M., Szafraniec, I., and Wedler, A. (1972). Carie et abrasion dentaire. *Rev. Odontol. Stomatol.* 19, 471–472.
- Kobayashi, T., Honma, K., Nakajima, T., and Hanada, K. (1993). Masticatory function in patients with mandibular prognathism before and after orthognathic surgery. *J. Oral. Maxillofac. Surg.* 51, 997–1001. doi: 10.1016/s0278-2391(10)80043-6
- Kohyama, K., Mioche, L., and Bourdiol, P. (2003). Influence of age and dental status on chewing behavior studied by EMG recordings during consumption of various food samples. *Gerodontology.* 20, 15–23. doi: 10.1111/j.1741-2358.2003.00015.x
- Kosaka, T., Kida, M., Kikui, M., Hashimoto, S., Fujii, K., Yamamoto, M., et al. (2018). Factors Influencing the changes in masticatory performance: the suita study. *J. D. R. Clin. Trans. Res.* 3, 405–412. doi: 10.1177/2380084418785863
- Kumar, A., Kothari, M., Grigoriadis, A., Trulsson, M., and Svensson, P. (2018). Bite or brain: Implication of sensorimotor regulation and neuroplasticity in oral rehabilitation procedures. *J. Oral Rehabil.* 45, 323–333. doi: 10.1111/joor.12603
- Kurita, H., Ohtsuka, A., Kurashina, K., and Kopp, S. (2001). Chewing ability as a parameter for evaluating the disability of patients with temporomandibular disorders. *J. Oral. Rehabil.* 28, 463–465. doi: 10.1046/j.1365-2842.2001.00688.x
- Lanning, F. C., and Eleuterius, L. N. (1985). Silica and Ash in Tissues of Some Plants Growing in the Coastal Area of Mississippi, USA. *Ann. Bot.* 56, 157–172. doi: 10.1093/oxfordjournals.aob.a087000
- Lazarus, C. L., Logemann, J. A., Rademaker, A. W., Kahrilas, P. J., Lazar, T., and Halper, A. (1993). Effects of bolus volume, viscosity, and repeated swallows in nonstroke subjects and stroke patients. *Arch. Phys. Med. Rehabil.* 74, 1066–1070. doi: 10.1016/0003-9993(93)90063-g
- Lepley, C. R., Throckmorton, G. C., Ceen, R. F., and Bushang, P. H. (2011). Relative contributions of occlusion, maximum bite force, and chewing cycle kinematics to masticatory performance. *Am. J. Orthod.* 139, 605–613. doi: 10.1016/j.ajodo.2009.07.025
- Lewis, R., and Dwyer-Joyce, R. S. (2005). Wear of human teeth: a tribological perspective. *Proc. Inst. Mech. Eng.* 219, 1–18. doi: 10.1243/1350650053295394
- Liang, S., Zhang, Q., Witter, D. J., Wang, Y., and Creugers, N. H. J. (2015). Effects of removable dental prostheses on masticatory performance of subjects with shortened dental arches: a systematic review. *J. Dent.* 43, 1185–1194. doi: 10.1016/j.jdent.2015.05.008
- Liedberg, B., Norlén, P., Owall, B., and Stoltze, K. (2004). Masticatory and nutritional aspects on fixed and removable partial dentures. *Clin. Oral. Investig.* 8, 11–17. doi: 10.1007/s00784-003-0223-6
- Liedberg, B., Spiechowicz, E., and Owall, B. (1995). Mastication with and without removable partial dentures: an intraindividual study. *Dysphagia* 10, 107–112. doi: 10.1007/bf00440080
- Liedberg, B., Stoltze, K., and Owall, B. (2005). The masticatory handicap of wearing removable dentures in elderly men. *Gerodontology* 22, 10–16. doi: 10.1111/j.1741-2358.2004.00050.x
- Lin, L. D., Murray, G. M., and Sessle, B. J. (1998). Effects on non-human primate mastication of reversible inactivation by cooling of the face primary somatosensory cortex. *Arch. Oral Biol.* 43, 1331–1341.
- Lindquist, L. W., and Carlsson, G. E. (1985). Long-term effects on chewing with mandibular fixed prostheses on osseointegrated implants. *Acta. Odonto. Scand.* 43, 39–45. doi: 10.3109/00016358509064138
- Lund, J. P., and Kolta, A. (2005). Adaption of the central masticatory pattern to the biomechanical properties of food. *Int. Congr. Ser.* 1284, 11–20. doi: 10.1016/j.ics.2005.07.007
- Lund, J. P., and Kolta, A. (2006). Generation of the central masticatory pattern and its modification by sensory feedback. *Dysphagia* 21, 167–174. doi: 10.1007/s00455-006-9027-6
- Lundqvist, S. (1993). Speech and other oral functions. Clinical and experimental studies with special reference to maxillary rehabilitation on osseointegrated implants. *Swed. Dent. J. Suppl.* 91, 1–39.
- Lundqvist, S., and Haraldson, T. (1992). Oral function in patients wearing fixed prosthesis on osseointegrated implants in the maxilla: 3-year follow-up study. *Scand. J. Dent. Res.* 100, 279–283. doi: 10.1111/j.1600-0722.1992.tb01071.x
- Luraschi, J., Korgaonkar, M. S., Whittle, T., Schimmel, M., Müller, F., and Klineberg, I. (2013). Neuroplasticity in the adaptation to prosthodontic treatment. *J. Orofac. Pain.* 27, 206–216. doi: 10.11607/jop.1097
- Magalhães, I. B., Pereira, L. J., and Marques, L. S. (2010). Gameiro, G.H. The influence of malocclusion on masticatory performance. A systematic review. *Angle Orthod.* 80, 981–987. doi: 10.2319/011910-33.1
- Mioche, L., Bourdiol, P., and Peyron, M. A. (2004). Influence of age on mastication: effects on eating behaviour. *Nutr. Res. Rev.* 17, 43–54. doi: 10.1079/NRR200375
- Mishellany, A., Woda, A., Labas, R., and Peyron, M. A. (2006). The challenge of mastication: preparing a bolus suitable for deglutition? *Dysphagia* 21, 87–94. doi: 10.1007/s00455-006-9014-y
- Mishellany-Dutour, A., Peyron, A. M., Croze, J., François, O., Hartman, C., Alric, M., et al. (2011). Comparison of food boluses prepared in vivo and in vitro by the mastication simulator: AM2. *Food. Quality. Preference.* 22, 326–331. doi: 10.1016/j.foodqual.2010.12.003
- Mishellany-Dutour, A., Renaud, J., Peyron, M. A., Rimek, F., and Woda, A. (2008). Is the goal of mastication reached in young dentates, aged dentates and age denture wearers? *Br. J. Nutr.* 99, 121–128. doi: 10.1017/S0007114507795284
- Mohlin, B., and Kurok, J. (2003). To what extent do deviations from an ideal occlusion constitute a health risk? *Swed. Dent. J.* 27, 1–10.
- Morais, J. A., Heydecke, G., Pawliuk, J., Lund, J. P., and Feine, J. S. (2003). The effects of mandibular two-implant overdentures on nutrition in elderly edentulous individuals. *J. Dent. Res.* 82, 53–58. doi: 10.1177/154405910308200112
- Morel, A., Albuissou, E., and Woda, A. (1991). A study of human jaw movements deduced from scratches on occlusal wear facets. *Archs. Oral. Biol.* 36, 195–202. doi: 10.1016/0003-9969(91)90086-a
- Morquette, P., Lavoie, R., Fhima, M. D., Lamoureux, X., Verdier, D., and Kolta, A. (2012). Generation of the masticatory central pattern and its modulation by sensory feedback. *Prog. Neurobiol.* 96, 340–355. doi: 10.1016/j.pneurobio
- Murphy, T. (1959a). Compensatory mechanism in facial height adjustment to functional tooth attrition. *Aust. Dent. J.* 4, 312–323. doi: 10.1111/j.1834-7819.1959.tb03727.x
- Murphy, T. (1959b). The changing pattern of dentine exposure in human tooth attrition. *Am. J. Phys. Anthropol.* 17, 167–178. doi: 10.1002/ajpa.1330170302
- N'Gom, P. I., Diagne, F., Aidara-Tamba, A. W., and Sene, A. (2007). Relationship between orthodontic anomalies and masticatory function in adults. *Am. J. Orthod. Dentofacial. Orthop.* 31, 216–222. doi: 10.1016/j.ajodo.2005.03.027
- N'Gom, P. I., and Woda, A. (2002). Influence of impaired mastication on nutrition. *J. Prosthet. Dent.* 87, 667–673. doi: 10.1067/jmpr.2002.123229
- Nicolas, E., Veyrune, J. L., Lassauzay, C., Peyron, M. A., and Hennequin, M. (2007). Validation of video versus electromyography for chewing evaluation of the elderly wearing a complete denture. *J. Oral. Rehabil.* 34, 566–571. doi: 10.1111/j.1365-2842.2007.01696.x

- Nokubi, T., Yoshimuta, Y., Nokubi, F., Yasui, S., Kusunoki, C., Ono, T., et al. (2013). Validity and reliability of a visual scoring method for masticatory ability using test gummy jelly. *Gerodontology* 30, 76–82. doi: 10.1111/j.1741-2358.2012.00647.x
- Okada, A., Honma, M., Nomura, S., and Yamada, Y. (2007). Oral behavior from food intake until terminal swallow. *Physiol. Behav.* 90, 172–179. doi: 10.1016/j.physbeh.2006.09.032
- Okamoto, N., Amano, N., Nakamura, T., and Yanagi, M. (2019). Relationship between tooth loss, low masticatory ability, and nutritional indices in the elderly: a cross-sectional study. *BMC Oral Health* 13:110. doi: 10.1186/s12903-019-0778-5
- Okoński, P., Mierzwińska-Nastalska, E., and Janicka-Kostrzewa, J. (2011). Implant supported dentures: an estimation of chewing efficiency. *Gerodontology* 28, 58–61. doi: 10.1111/j.1741-2358.2009.00303.x
- Osterberg, T., Carlsson, G. E., Tsuga, K., Sundh, V., and Steen, B. (1996). Associations between self-assessed masticatory ability and some general health factors in a Swedish population. *Gerodontology* 13, 110–117. doi: 10.1111/j.1741-2358.1996.tb00162.x
- Palmer, J. B., and Hiemea, K. M. (2003). Eating and breathing: interactions between respiration and feeding on solid food. *Dysphagia* 18, 169–178. doi: 10.1007/s00455-002-0097-9
- Pameijer, J. H., Glickman, I., and Roeber, F. W. (1969). Intraoral occlusal telemetry. 3. Tooth contacts in chewing, swallowing and bruxism. *J. Periodontol.* 40, 253–258. doi: 10.1902/jop.1969.40.5.253
- Pereira, T. C., Brasolotto, A. G., Conti, P. C., and Berretin-Felix, G. (2009). Temporomandibular disorders, voice and oral quality of life in women. *J. Appl. Oral. Sci.* 17(Suppl.), 50–56. doi: 10.1590/s1678-77572009000700009
- Peyron, A., Lassauzay, C., and Woda, A. (2002). Effects of increased hardness on jaw movement and muscle activity during chewing of visco-elastic model foods. *Exp. Brain. Res.* 42, 41–51. doi: 10.1007/s00221-001-0916-5
- Peyron, M., Mishellany, A., and Woda, A. (2004). Particle size distribution of food boluses after mastication of six natural foods. *J. Dent. Res.* 83, 578–582. doi: 10.1177/154405910408300713
- Peyron, M. A., Gierczynski, I., Hartmann, C., Loret, C., Dardevet, D., Martin, N., et al. (2011). A likely role of physical bolus properties as sensory inputs in swallowing triggering. *Plos One* 6: e21167. doi: 10.1371/journal.pone.0021167
- Peyron, M. A., Woda, A., Bourdiol, P., and Hennequin, M. (2017). Age-related changes in mastication. *J. Oral. Rehabil.* 44, 299–312. doi: 10.1111/joor.12478
- Picinato-Pirola, M. N., Mestriner, W. Jr., Freitas, O., Mello-Filho, F. V., and Trawitzki, L. V. (2012). Masticatory efficiency in class II and class III dentofacial deformities. *Int. J. Oral. Maxillofac. Surg.* 41, 830–834. doi: 10.1016/j.ijom.2012.03.025
- Piperno, D. R. (1989). The occurrence of phytoliths in the reproductive structures of selected tropical angiosperms and their significance in tropical paleoecology, paleoethnobotany and systematics. *Rev. Paleobot. Palynol.* 61, 147–173. doi: 10.1016/0034-6667(89)90067-5
- Planas, P. (1987). *Rehabilitación Neuro-Occlusal (RNO)*. Barcelona: Salvat.
- Prinz, J. F., and Lucas, P. W. (1995). Swallow thresholds in human mastication. *Arch. Oral. Biol.* 40, 401–403. doi: 10.1016/0003-9969(94)00185-e
- Rémond, D., Shahar, D. R., Gille, D., Pinto, P., Kachal, J., Peyron, M. A., et al. (2015). Understanding the gastrointestinal tract of the elderly to develop dietary solutions that prevent malnutrition. *Oncotarget* 10, 13858–13898. doi: 10.18632/oncotarget.4030
- Ribeiro, G. R., Campos, C. H., and Rodrigues Garcia, R. C. M. (2016). Oral health in elders with Parkinson's disease. *Braz. Dent. J.* 27, 340–344. doi: 10.1590/0103-6440201600881
- Richards, L. C. (1985). Dental attrition and craniofacial morphology in two Australian aboriginal populations. *J. Dent. Res.* 64, 1311–1315. doi: 10.1177/00220345850640111201
- Schimmel, M., Christou, P., Herrmann, F., and Müller, F. (2007). A two-colour chewing gum test for masticatory efficiency: development of different assessment methods. *J. Oral. Rehabil.* 34, 671–678. doi: 10.1111/j.1365-2842.2007.01773.x
- Schimmel, M., Christou, P., Miyazaki, H., Halazonetis, D., Herrmann, F. R., and Müller, F. (2015). A novel colourimetric technique to assess chewing function using two-coloured specimens: Validation and application. *J. Dent.* 43, 955–964. doi: 10.1016/j.jdent.2015.06.003
- Seo, H. S., Hwang, I. K., Han, T. R., and Kim, I. S. (2007). Sensory and instrumental analysis for slipperiness and compliance of food during swallowing. *J. Food. Sci.* 72, 707–712. doi: 10.1111/j.1750-3841.2007.00544.x
- Sheiham, A., Steele, J. G., Marcenes, W., Lowe, C., Finch, S., Bates, C. J., et al. (2001). The relationship among dental status, nutrient intake, and nutritional status in older people. *J. Dent. Res.* 80, 408–413. doi: 10.1177/00220345010800020201
- Shiratsuchi, Y., Kouno, K., and Tashiro, H. (1991). Evaluation of masticatory function following orthognathic surgical correction of mandibular prognathism. *J. Craniomaxillofac. Surg.* 19, 299–303. doi: 10.1016/S1010-5182(05)80336-1
- Slade, G. D., and Spencer, A. J. (1994). Development and evaluation of the Oral Health Impact Profile. *Community. Dent. Health* 11, 3–11.
- Slagter, A. P., Olthoff, L. W., Bosman, F., and Steen, W. H. (1992). Masticatory ability, denture quality, and oral conditions in edentulous subjects. *J. Prosthet. Dent.* 68, 299–307. doi: 10.1016/0022-3913(92)90334-7
- Smith, C. H., Logemann, J. A., Wesley, R. B., Steven, G. Z., and Rademaker, A. W. (2006). Oral and oropharyngeal perceptions of fluid viscosity across the age span. *Dysphagia* 21, 209–217. doi: 10.1007/s00455-006-9045-4
- Sood, M., Lee, J. C., Avivi-Arber, L., Bhatt, P., and Sessle, J. B. (2015). Neuroplastic changes in the sensorimotor cortex associated with orthodontic tooth movement in rats. *J. Comp. Neurol.* 523, 1548–1568. doi: 10.1002/cne.23753
- Takizawa, C., Gemmell, E., Kenworthy, J., and Speyer, R. A. (2016). Systematic review of the prevalence of oropharyngeal dysphagia in stroke, Parkinson's disease, Alzheimer's disease, head injury, and pneumonia. *Dysphagia* 31, 434–441. doi: 10.1007/s00455-016-9695-9
- Tallgreen, A. (1957). Changes in adult face height due to ageing, wear and loss of teeth, and prosthetic treatment. *Helsinki: Acta. Odontol. Scand.* 15(Suppl.):24.
- Tanaka, Y., and Shiga, H. (2018). Masticatory performance of the elderly as seen from differences in occlusal support of residual teeth. *J. Prosthodont. Res.* 62, 375–378. doi: 10.1016/j.jpor.2018.01.007
- Tang, L., Lund, J. P., Tache, R., Clockie, C. M. L., and Feine, J. S. (1999). A within-subject comparison of mandibular long-bar and hybrid implant-supported prostheses evaluation of masticatory function. *J. Dent. Res.* 78, 1544–1553. doi: 10.1177/00220345990780090901
- Tate, G. S., Throckmorton, G. S., Ellis, E. III, and Sinn, D. P. (1994). Masticatory performance, muscle activity, and occlusal force in preorthognathic surgery patients. *J. Oral. Maxillofac. Surg.* 5, 476–481. doi: 10.1016/0278-2391(94)90344-1
- Taylor, R. M. S. (1975). The significance of tooth wear in Polynesians. A review. *J. Dental Assoc. South Afr.* 30, 241–244.
- van den Braber, W., van der Glas, H. W., van der Bilt, A., and Bosman, F. (2001). Chewing efficiency of pre-orthognathic surgery patients: selection and breakage of food particles. *Eur. J. Oral. Sci.* 109, 306–311. doi: 10.1034/j.1600-0722.2001.00092.x
- van der Bilt, A. (2011). Assessment of mastication with implications for oral rehabilitation: a review. *J. Oral. Rehabil.* 38, 754–780. doi: 10.1111/j.1365-2842.2010.02197.x
- van der Bilt, A., Abbink, J. H., Mowlana, F., and Heath, M. R. (1993). A comparison between data analysis methods concerning particle size distributions obtained by mastication in man. *Arch. Oral. Biol.* 38, 163–167. doi: 10.1016/0003-9969(93)90202-w
- van der Bilt, A., Burgers, M., van Kampen, F. M., and Cune, M. S. (2010a). Mandibular implant-supported overdentures and oral function. *Clin. Oral. Implants. Res.* 21, 1209–1213. doi: 10.1111/j.1600-0501.2010.01915.x
- van der Bilt, A., Mojet, J., Tekamp, F. A., and Abbink, J. H. (2010b). Comparing masticatory performance and mixing ability. *J. Oral. Rehabil.* 37, 79–84. doi: 10.1111/j.1365-2842.2009.02040.x
- van der Bilt, A., Speksnijder, C. M., De Liz Poczaruk, R., and Abbink, J. H. (2012). Digital image processing versus visual assessment of chewed two-colour wax in mixing ability tests. *J. Oral. Rehabil.* 39, 11–17. doi: 10.1111/j.1365-2842.2011.02229.x
- van der Braber, W., van der Bilt, A., van der Glas, H., Bosman, F., Rosenberg, A., and Koole, R. (2005). The influence of orthognathic surgery on masticatory performance in retrognathic patients. *J. Oral. Rehabil.* 32, 237–241. doi: 10.1111/j.1365-2842.2004.01436.x
- van der Braber, W., van der Bilt, A., van der Glas, H., Rosenberg, T., and Koole, R. (2006). The influence of mandibular advancement surgery on oral function

- in retrognathic patients: a 5-year follow-up study. *J. Oral. Maxillofac. Surg.* 64, 1237–1240. doi: 10.1016/j.joms.2006.04.019
- van Lancker, A., Verhaeghe, S., van Hecke, A., Vanderwee, K., Goossens, J., and Beeckman, D. (2012). The association between malnutrition and oral health status in elderly in long-term care facilities: a systematic review. *Int. J. Nurs. Stud.* 49, 1568–1581. doi: 10.1016/j.ijnurstu.2012.04.001
- Veyrune, J. L., Lassauzay, C., Nicolas, E., Peyron, M. A., and Woda, A. (2007). Mastication of model products in complete denture wearers. *Arch. Oral. Biol.* 52, 1180–1185. doi: 10.1016/j.archoralbio.2007.04.016
- Veyrune, J. L., Opé, S., Nicolas, E., Woda, A., and Hennequin, M. (2013). Changes in mastication after an immediate loading implantation with complete fixed rehabilitation. *Clin. Oral. Investig.* 17, 1127–1134. doi: 10.1007/s00784-012-0787-0
- Veyrune, J. L., Tubert-Jeannin, S., Dutheil, C., and Riordan, P. J. (2005). Impact of new prostheses on the oral health related quality of life of edentulous patients. *Gerodontology* 22, 3–9. doi: 10.1111/j.1741-2358.2004.00048.x
- Wallace, S., Samietz, S., Abbas, M., McKenna, G., Woodside, J. V., and Schimmel, M. (2018). Impact of prosthodontic rehabilitation on the masticatory performance of partially dentate older patients: can it predict nutritional state? Results from a RCT. *J. Dent.* 68, 66–71. doi: 10.1016/j.jdent.2017.11.003
- Wayler, A., and Chauncey, H. H. (1983). Impact of complete dentures and impaired natural dentition on masticatory performance and food choice in healthy aging men. *J. Prosthet. Dent.* 49, 427–433. doi: 10.1016/0022-3913(83)90289-5
- Wilding, R. J. (1993). The association between chewing efficiency and occlusal contact area in man. *Arch. Oral. Biol.* 38, 589–596. doi: 10.1016/0003-9969(93)90124-5
- Witter, D. J., Woda, A., Bronkhorst, E. M., and Creugers, N. H. J. (2013). Clinical interpretation of a masticatory normative indicator analysis of chewing function in subjects with different occlusal and prosthodontic status. *J. Dent.* 41, 443–448. doi: 10.1016/j.jdent.2013.02.004
- Woda, A., Foster, K., Mishellany, A., and Peyron, M. A. (2006). Adaptation of healthy mastication to factors pertaining to the individual or to the food. *Physiol. Behav.* 89, 28–35. doi: 10.1016/j.physbeh.2006.02.013
- Woda, A., Gourdon, A. M., and Faraj, M. (1987). Occlusal contacts and tooth wear. *J. Prosthet. Dent.* 57, 85–93. doi: 10.1016/0022-3913(87)90122-3
- Woda, A., Hennequin, M., and Peyron, A. (2011). Mastication in humans: finding a rationale. *J. Oral. Rehabil.* 38, 781–784. doi: 10.1111/j.1365-2842.2011.02235.x
- Woda, A., Nicolas, E., Mishellany-Dutour, A., Hennequin, M., Mazille, M.-N., Veyrune, J.-L., et al. (2010). The masticatory normative indicator. *J. Dent. Res.* 89, 281–285. doi: 10.1177/0022034509357022
- Woda, A., Vigneron, P., and Kay, D. (1979). Nonfunctional and functional occlusal contacts: a review of the literature. *J. Prosthet. Dent.* 42, 335–341. doi: 10.1016/0022-3913(79)90226-9
- Wright, F. A. C., Law, G. G., Milledge, K. L., Chu, S. K., Hsu, B., Valdez, E., et al. (2019). Chewing function, general health and the dentition of older Australian men: the concord health and ageing in men project. *Commun. Dent. Oral Epidemiol.* 47, 134–141. doi: 10.1111/cdoe.12435
- Yao, C. J., Cao, C., Bornstein, M. M., and Mattheos, N. (2018). Patient-reported outcome measures of edentulous patients restored with implant-supported removable and fixed prostheses: a systematic review. *Clin. Oral. Implants. Res.* 16, 241–254. doi: 10.1111/clr.13286
- Yurkstas, A., and Emerson, W. H. (1964). Decreased masticatory function in denture patients. *J. Prosthet. Dent.* 14, 931–934. doi: 10.1016/0022-3913(64)90021-6
- Yurkstas, A., and Manly, R. S. (1949). Measurement of occlusal contact area effective in mastication. *Am. J. Orthod.* 35, 185–195. doi: 10.1016/0002-9416(49)90028-7
- Yurkstas, A. S. (1965). The masticatory act a review. *J. Prosthet. Dent.* 15, 248–262. doi: 10.1016/0022-3913(65)90094-6
- Zarrinkelk, H. M., Throckmorton, G. S., Ellis, E. III, and Sinn, D. P. (1995). A longitudinal study of changes in masticatory performance of patients undergoing orthognathic surgery. *J. Oral. Maxillofac. Surg.* 53, 777–782. doi: 10.1016/0278-2391(95)90331-3 discussion 782-783,

Conflict of Interest: The authors declare that the research was conducted in the absence of any commercial or financial relationships that could be construed as a potential conflict of interest.

Copyright © 2020 Bourdiol, Hennequin, Peyron and Woda. This is an open-access article distributed under the terms of the Creative Commons Attribution License (CC BY). The use, distribution or reproduction in other forums is permitted, provided the original author(s) and the copyright owner(s) are credited and that the original publication in this journal is cited, in accordance with accepted academic practice. No use, distribution or reproduction is permitted which does not comply with these terms.



The Effect of Granisetron on Sensory Detection and Pain Thresholds in Facial Skin of Healthy Young Males

Malin Ernberg, Anna Wieslander Fältmars, Milad Hajizadeh Kopayeh, Sofia Arzt Wallén, Therese Cankalp and Nikolaos Christidis*

Division of Oral Diagnostics and Rehabilitation, Department of Dental Medicine, Karolinska Institutet, and Scandinavian Center for Orofacial Neuroscience (SCON), Huddinge, Sweden

OPEN ACCESS

Edited by:

Limor Avivi-Arber,
University of Toronto, Canada

Reviewed by:

Marcelo M. Valença,
Federal University of
Pernambuco, Brazil
Bright Nii Okine,
Independent Researcher, London,
United Kingdom
Parisa Gazerani,
Aalborg University, Denmark

*Correspondence:

Nikolaos Christidis
nikolaos.christidis@ki.se

Specialty section:

This article was submitted to
Headache Medicine and Facial Pain,
a section of the journal
Frontiers in Neurology

Received: 19 November 2019

Accepted: 12 March 2020

Published: 09 April 2020

Citation:

Ernberg M, Wieslander Fältmars A, Hajizadeh Kopayeh M, Arzt Wallén S, Cankalp T and Christidis N (2020) The Effect of Granisetron on Sensory Detection and Pain Thresholds in Facial Skin of Healthy Young Males. *Front. Neurol.* 11:237. doi: 10.3389/fneur.2020.00237

Background: The specific serotonin type 3 (5-HT₃)-receptor antagonist granisetron effectively reduces clinical as well as experimental muscle pain and hyperalgesia and with a duration that exceeds that of lidocaine. Hence, it may be an alternative to lidocaine as a local anesthetic. There are also some indications that granisetron in addition to 5-HT₃ receptors blocks sodium channels. Thus, the local anesthetic effect by granisetron may resemble that of lidocaine, but this has not been tested. The aim of this study was therefore to compare the effect granisetron has on facial skin sensitivity to the effect of lidocaine and isotonic saline.

Methods: This was a randomized, controlled, and double-blind study, in which 1 ml of either granisetron (test-substance), lidocaine (positive control), or isotonic saline (negative control) was injected into the skin over the masseter muscle at three different occasions in 18 healthy males (27.2 ± 5.8 years old). Skin detection thresholds and pain thresholds for thermal stimuli as well as mechanical detection thresholds and sensitivity to a painful mechanical (pinprick) stimulus were assessed before (baseline) and 5, 20, 40, and 60 min after injection. The quality and area of subjective sensory change over the cheek were assessed 20 min after injection.

Results: All substances increased the mechanical detection threshold (granisetron: $p = 0.011$; lidocaine: $p = 0.016$; saline: $p = 0.031$). Both granisetron and lidocaine, but not isotonic saline, increased the heat detection thresholds ($p < 0.001$ and $p < 0.02$, respectively), but not the cold detection thresholds. Granisetron and lidocaine also reduced pinprick pain ($p = 0.001$ for each comparison). There were no significant differences between granisetron and lidocaine for any of these variables. There was no effect on thermal pain thresholds for any substance.

Conclusion: The similar analgesic patterns on mechanical sensory and pain thresholds as well as thermal sensory thresholds over the facial skin by subcutaneous injection of granisetron and lidocaine shown in this study and the absence of paresthesia, in combination with the reduced pain intensity and pressure pain sensitivity shown in previous studies, indicate that granisetron might be a novel candidate as a local anesthetic.

Keywords: granisetron, sodium channels, lidocaine, human, mechanical thresholds, thermal thresholds

INTRODUCTION

Serotonin (5-HT) is an important neurotransmitter involved in many diverse functions in the body, for example, sleep and awakening, appetite, aggression, and pain. 5-HT exerts its effect by activating different receptors, grouped into 5-HT₁- to 5-HT₇-receptors (1). The 5-HT₃-receptor is widely distributed on neurons both in the brain and peripherally and participates in nociception supraspinally, spinally, and in the periphery (2–4).

5-HT₃-antagonists, such as granisetron, ondansetron, and tropisetron, are commonly used to treat radiotherapy- and chemotherapy-induced vomiting and nausea (5). In addition to this effect, several animal and human studies have shown that 5-HT₃-antagonists reduce inflammatory and clinical pain, e.g., in fibromyalgia (6–9). In chronic orofacial myalgia, tender-point injections of granisetron were reported to be a safe and effective treatment (10). Further, systemic and local administration of granisetron increase the mechanical pain threshold over healthy human muscles (11–13).

It has been shown that granisetron has a higher affinity to the 5-HT₃-receptor than ondansetron and tropisetron (1). However, there are also indications that granisetron and other 5-HT₃-antagonists block sodium channels (14–18). Sodium channels play a key role in the activation of peripheral nociceptive sensory neurons involved in transmission of noxious stimuli (19, 20).

Local anesthetics, such as lidocaine, non-specifically block sodium channels, e.g., on nociceptors, mainly by inhibiting the sodium influx into the neuronal cell membrane, thus suppressing the cell excitability (21). Sodium channels on all types of sensory neurons are affected, but A δ -fibers are most sensitive, followed by A β -fibers, and C-fibers (22, 23). This suppression leads to a transient loss of sensation in a circumscribed area of the body (24). In the orofacial region, local anesthetics are associated with paresthesia that lasts far beyond the duration of anesthesia (25). This paresthesia involves not just a perception of facial distortion (26) but also sensations of numbness, swelling, tingling, and itching (24). Based on this, a substance with local anesthetic effects, but without paresthesia would be desirable, especially for the orofacial region. Indeed, a previous *in vitro* and *in vivo* study showed that ondansetron blocked sodium channels in rat brain neurons, produced local analgesia in a dose-related manner, and caused numbness under the skin (16). Hence, 5-HT₃ antagonists may perhaps be used as a new class of local anesthetics.

One way to investigate if granisetron produce local anesthetic-like effects in humans could be to record changes in skin sensitivity to mechanical stimuli (A β -fibers), heat stimuli (C-fibers), and cold stimuli (A δ -fibers) after injection of the substance (16, 27–32). Hence, this study aimed to investigate the effect by granisetron on facial skin-sensitivity and comparing it to the effect of lidocaine and isotonic saline. We hypothesized that granisetron has a local-anesthetic like reduction of detection- and pain thresholds for mechanical and thermal stimuli.

MATERIALS AND METHODS

The present study was conducted at the Department of Dental Medicine, Karolinska Institutet, Huddinge, Sweden,

between March 2014 and November 2018. It followed the present guidelines according to the Declaration of Helsinki and was approved by the Regional Ethical Review Board in Stockholm, Sweden (Dnr 2013/932-31/4) and the Swedish Medical Products Agency (EudoraCT-number 2008-000746-32). Verbal and written information of the study was given to all participants, and their written consent was obtained before the study start.

Participants

The study is composed of 18 healthy male participants with a mean (SD) age of 27.2 (5.8) years. They were recruited by flyers posted at the Department of Dental Medicine, Karolinska Institutet, and at the library of Södertörn University, both in Huddinge, Sweden. According to the power calculation, based on the outcome from a previous study (10), inclusion of 17 participants would be sufficient to detect a difference of 30% (SD 30%) between interventions in order to reach a significance level (α) of 0.05 and a power (β) of 80%. In order to compensate for dropouts, one additional person was included.

Inclusion criteria were as follows: (a) age between 18 and 40 years, (b) good general health, and (c) male sex. Exclusion criteria were as follows: (1) any current pain from the orofacial region; (2) a diagnosis of temporomandibular disorders (TMD) according to the Diagnostic Criteria for TMD (DC/TMD) (33); (3) any type of headache; (4) diagnosed systemic muscular or joint diseases, such as fibromyalgia and rheumatoid arthritis; (5) whiplash-associated disorders; (6) neuropathic pain or neurological disorders; (7) pregnancy or lactation; (8) severe psychiatric conditions, including depression; (9) use of any kind of medication except for contraceptives 48 h preceding the study day; (10) use of any kind of medications, balms, or lotions affecting skin sensitivity; and (11) previous negative or allergic reactions to either of the injected substances (e.g., lidocaine or granisetron).

Experimental Protocol

The study used a randomized, controlled, and double-blind design with each participant as his own control. The study consisted of three separate sessions, with at least 1 week of washout between. The sessions, in which granisetron (test-substance), lidocaine (positive control), and isotonic saline (negative control) were subcutaneously injected into the skin over the masseter muscle, were performed in a random order. The injections were placed subcutaneously in order just to affect the skin sensitivity and not the surrounding tissues. To randomize the order of injection, a randomization list was generated using a web-based randomization tool (www.randomization.com) by one of the researchers not participating in data collection (NC). With this randomization tool, not just the order of the sessions but also the side for injections were randomized in a balanced order. The injections were administered on the same side in each participant for all three substances.

The test substances were prepared in syringes prior to the experiment by the same researcher (NC). The syringes all appeared identical since all three substances were clear

liquids, therefore making it impossible for the researchers collecting (SAW, TC) or registering (AW, MHK) the data, as well as for the participants to distinguish one substance from another.

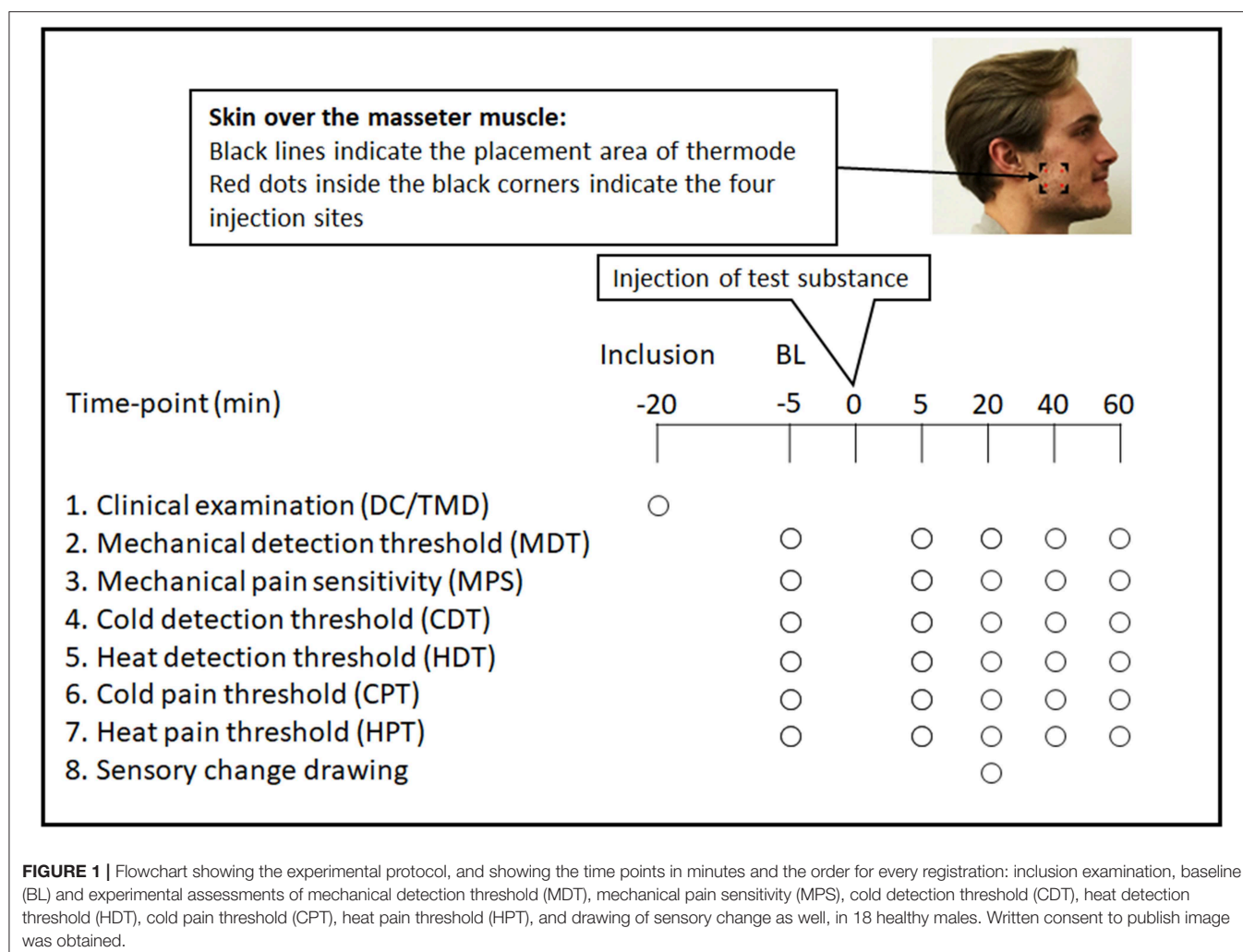
The participants sat in a conventional dental chair in a quiet environment during the entire experiment. Before the experiment started, they underwent a clinical examination according to the DC/TMD in order to screen for trial suitability and inclusion (33). Subsequently, after inclusion as well as in the beginning of each session, baseline recordings of mechanical detection threshold (MDT), mechanical pain sensitivity (MPS) to a pinprick stimulus, and detection as well as pain thresholds to cold (CDT and CPT, respectively) and heat (HDT and HPT, respectively) were recorded in the same order for all participants and sessions. The participant had his eyes closed during the recordings and was asked to concentrate on the task. After the baseline registrations, an injection of the test substance followed. The recordings were then repeated in the same order (MDT, MPS, CDT, HDT, CPT, HPT) after 5, 20, 40, and 60 min. Twenty minutes after the injection, the participants were also asked to make a drawing of the area of subjective sensory change over the

cheek at the site of injection. The experimental protocol is shown in **Figure 1**.

Injections

A felt pen was used to mark out the area of injection overlying the masseter muscle using a plastic patch cut to a size equivalent to the size of the thermal probe (3×3 cm), which was used for assessment of thermal sensitivity. The plastic patch was placed in the midline of the masseter muscle and 1 cm above the lower border of the mandible. This location was used for all sessions in order to ensure that the injections were placed at the same sites all three times. The skin overlying the masseter muscle was chosen since it is an easily accessible orofacial area that has been used in previous experiments by our research group.

The substances used in the present study were as follows: (a) the active test substance granisetron (Kytril® 1 mg/ml, Roche, Stockholm, Sweden, pH ranging from 4.0 to 6.0); (b) the positive control substance (for the possible analgesic effect) was lidocaine (Xylocain® 20 mg/ml, AstraZeneca AB, Södertälje, Sweden, pH ranging from 5.0 to 7.0); and (c) the negative control substance isotonic saline (NaCl 9 mg/ml B Braun, Melsungen, Germany,



pH ranging from 4.5 to 7.0). Isotonic saline was used as vehicle for both granisetron and lidocaine. One milliliter of the chosen substance was subcutaneously injected using a 19-mm needle (Neofly, BOC Ohmeda AB) with a 0.4-mm diameter from a 2-ml syringe. The solution was injected into four different sites, i.e., 0.25 ml in each site, 3 mm inside each corner of the marked area using the above-described plastic patch. This was done in order to allow the injected substance to diffuse into the entire area that was covered by the thermal probe. The spread of the substances caused an ischemic appearance and was homogeneous. One single bolus did not diffuse more than 1×1 cm, thus not covering the entire surface of the thermal probe. All substances had room temperature, i.e., 23°C.

Assessment of Mechanical Detection and Pain Level

The MDT was assessed using calibrated von Frey nylon monofilaments (Anesthesiometer, Somedic Sales AB, Hörby, Sweden) exerting bending forces ranging from 0.026 to 110 g according to the stepwise ascending–descending method in order to find the lowest detectable bending force. This means that the examiner started with the lightest monofilament by placing it perpendicular to the skin surface with a contact time of 1.5 s. If no sensation was reported, the examiner continued to apply filaments in ascending order in the same manner until the participant first reported a sensation. The weight of this filament was noted. The whole procedure was repeated twice and the mean value of the monofilament weight for the three assessments was calculated and used for statistical analysis. In order to assess MPS, the von Frey nylon monofilament 19 with a force of 110 g was used. The filament was applied three times during 1.5 s. Directly after each application, the intensity of the pinprick stimulus applied was assessed on a 0–100 numerical rating scale (NRS), where 0 means no sensation, 50 is just barely painful (pain threshold), and 100 represents the most painful sensation one can imagine (34). The mean value of the three ratings was used for further analysis.

Assessment of Thermal Detection and Pain Threshold

In order to assess the thermal detection as well as pain thresholds, an electronic thermo-test system was used (CHEPS thermo-test system, Medoc Ltd. Ramat Yishai, Israel). The measurements were done using an advanced thermal stimulator (ATS) with a contact area of 3×3 cm that was placed on the skin surface of the masseter. A preset automatic program was used in which the thermal stimulator had a baseline temperature of 32°C (skin temperature) and a minimum and maximum temperature of 0° and 55°C, in order not to cause frostbite or burn of the skin. The automatic program started with recording of the cold detection threshold (CDT), i.e., cooling of the skin. The participant was asked to press a stop button as soon as he experienced that the thermode started to get cold. The temperature then increased to 32°C to start a new cycle. This was done four times with an interstimulus interval (ISI) of 4 s and a decrease/increase rate of 1°C/s. The warmth detection threshold (WDT) was

then immediately assessed in the same manner. Directly after assessments of thermal detection thresholds, the cold pain threshold (CPT) and heat pain threshold (HPT) were recorded, i.e., the cooling/heating continued until the cold or heat became minimally painful. The pain thresholds were assessed three times, with an ISI of 10 s, and a decrease/increase rate of 1.5°C/s. The average of the repeated recordings was used in the analyses.

Assessment of Sensory Change Drawings

Twenty minutes after the injections, each participant was asked to mark out the maximum perceived area of subjective change in sensory experience over the injected cheek. The participants were instructed to encircle the area(s) where they perceived any kind of sensory change with a felt pen on a printed paper sheet with two images, one image displaying a lateral view of the head for the side of injection and one image displaying an intra-oral lateral view of the head highlighting the teeth and jaws for the side of injection (Figures 1, 3). Finally, the participants were asked to describe any type of sensory change.

For the analysis of the subjective sensory change drawings, each picture was scanned separately using a network printer (Ricoh MP C6004ex) having a resolution of 300 dpi. The area of subjective change in sensory experience was then calculated with an area calculation function in a photo editing program (Adobe Photoshop CS4 Extended version 11.0.2, Adobe Systems Incorporated USA). The areas of the sensory change drawings are expressed in arbitrary units (au).

Data Analysis and Statistics

Data were analyzed using the SigmaPlot for Windows version 14.0 software (Systat Software Inc., San Jose, CA, USA). The normality of the data was tested using the Shapiro–Wilk's test. Parametric statistical methods were used for normally distributed data on a continuous scale, while non-parametric statistics were used for data that were not normally distributed or on an ordinal scale. All pain sensitivity variables (MPS, CPT, and HPT) were normally distributed, so parametric statistical methods were used to analyze these data. All detection thresholds (MDT, CDT, and HDT) were not normally distributed. An attempt to log transform the data did not result in normal distribution of data; this is why non-parametric methods were used. Means and standard deviations (SD) were used for descriptive statistics for pain variables, whereas medians and interquartile ranges (IQRs) were used for detection thresholds. The level of significance was set at $p < 0.05$.

Two-way ANOVA for repeated measures (RM ANOVA) with time and substance as factors analyzed group differences in MPS, CPT, and HPT. When a significant difference was indicated, Tukey test for multiple comparisons vs. a control group (baseline) was used as *post hoc* test to test for differences between substances and time points. Changes of CDT, HDT, and MDT across times were analyzed using Friedman ANOVA with Dunn's test for multiple comparison vs. a control group (baseline) as *post hoc* test. Friedman test was also used to analyze differences between the substances at the different time points. As there were in total five comparisons made for these variables, Bonferroni

correction was done to compensate for multiple testing, giving a significance level of $p < 0.01$ in these analyses.

RESULTS

All 18 participants completed all three sessions, i.e., there were no dropouts.

There were no significant differences between the baseline values (means and medians) of MDT, MPS, CDT, HDT, CPT, or HPT across the three sessions, i.e., before injection of either granisetron, lidocaine, or isotonic saline (Table 1).

Mechanical Detection Threshold

Significant changes in MDT were recorded over time for all substances, as shown in Figure 2A.

MDT for granisetron increased with time ($p < 0.001$; Friedman ANOVA). The *post hoc* test showed that the increase was significant compared to baseline at all time points during 40 min after injection ($p < 0.011$; Dunn's test). The increase of MDT was 458% at 5 min after injection, 304% at 20 min after injection, and 313% at 40 min after injection. The lidocaine injection increased the MDT ($p < 0.001$; Friedman ANOVA). The increase of MDT after injection with lidocaine followed the same pattern as granisetron and was significant during 40 min ($p < 0.016$; Dunn's test) and was 1088% at 5 min after injection,

616% at 20 min, and 652% after 40 min. Also, isotonic saline injection increased the MDT ($p < 0.001$; Friedman ANOVA). The increase was significant from 20 min up to 60 min after injection ($p < 0.031$; Dunn's test) and was 347% at 20 min after injection, 253% at 40 min, and 228% at 60 min after injection.

There were no significant differences in MDT between the substances at the different time points ($p > 0.01$; Friedman ANOVA).

Mechanical Pain Sensitivity

Lidocaine and granisetron, but not isotonic saline, reduced the MPS. The two-way RM ANOVA showed a time effect ($df = 4$; $F = 23.03$; $p < 0.001$), but no difference between substances ($df = 2$; $F = 2.95$; $p = 0.066$). However, there was an interaction between time and substance ($df = 8$; $F = 5.06$, $p < 0.001$). The *post hoc* test showed that granisetron reduced the MPS 5 and 20 min after injection by 23 and 20%, respectively ($p = 0.001$, Tukey test) compared to baseline, while lidocaine reduced the MPS 5 min after injection ($p = 0.001$, Tukey test). No significant changes were found over time for isotonic saline (Figure 2B).

There were no significant differences in changes of MPS between the substances at the different time points ($p > 0.05$; Tukey test).

Cold Detection Thresholds

There were no significant differences in CDT over time for granisetron ($p = 0.065$; Friedman ANOVA) or lidocaine ($p = 0.839$; Friedman ANOVA), as shown in Figure 2C. A significant decrease of CDT was recorded for isotonic saline when compared to baseline ($p < 0.001$; Friedman ANOVA). According to the *post hoc* test, the decrease was significant at 5, 40, and 60 min after injection ($p < 0.005$; Dunn's test). The decrease was 4% at 5 min after injection, 5% at 40 min, and 5% at 60 min after injection.

There were no significant differences in changes of CDT between the substances at the different time points ($p > 0.059$; Friedman ANOVA).

Cold Pain Threshold

Three of the participants reached the minimum preset temperature without reporting any pain; i.e., they did not reach the CPT. Their data were therefore regarded as missing data, so the CPT results are based on 15 participants. None of the injected substances affected the CPT. The two-way RM ANOVA did not show any significant time effect ($df = 4$; $F = 0.28$; $p = 0.888$) or any difference between substances ($df = 2$; $F = 2.04$; $p = 0.146$). Neither was there any interaction between time and substance ($df = 8$; $F = 1.26$, $p = 0.269$) (Figure 2D).

Heat Detection Threshold

A significant increase in HDT was recorded over time for all substances, as shown in Figure 2E. HDT for granisetron increased significantly when compared to baseline ($p < 0.001$; Friedman ANOVA). The *post hoc* test showed that the increase was significant at all time points after injection ($p < 0.001$; Friedman ANOVA) and was 4.0% at 5 min after injection, 2.8% at 20 min after injection, 4.0% at 40 min after injection, and 3.5% at 60 min after injection. The lidocaine injection

TABLE 1 | Baseline values in mean (SD) and median (IQR) of cold detection threshold (CDT), heat detection threshold (HDT), and mechanical detection threshold (MDT), as well as cold pain threshold (CPT), heat pain threshold (HPT), and mechanical pain level (MPS) are presented.

| | Isotonic saline | Granisetron | Lidocaine |
|--|-----------------|-------------|-------------|
| DETECTION THRESHOLDS | | | |
| Mechanical detection (MDT) (g) | | | |
| Mean (SD) | 4.9 (3.1) | 6.4 (10.7) | 5.1 (3.7) |
| Median (IQR) | 3.4 (3.8) | 3.4 (3.8) | 3.4 (3.8) |
| Cold detection (CDT) (°C) | | | |
| Mean (SD) | 30.2 (1.3) | 30.0 (1.5) | 31.6 (1.9) |
| Median (IQR) | 30.5 (1.0) | 30.3 (1.4) | 31.0 (3.0) |
| Heat detection (HDT) (°C) | | | |
| Mean (SD) | 34.6 (1.6) | 34.0 (1.2) | 34.4 (2.0) |
| Median (IQR) | 33.8 (2.4) | 33.5 (1.1) | 33.6 (1.5) |
| PAIN THRESHOLDS | | | |
| Mechanical pain sensitivity (MPS) in NRS 0–100 | | | |
| Mean (SD) | 36.1 (14.6) | 39.2 (16.3) | 38.6 (14.5) |
| Median (IQR) | 37.5 (30.0) | 37.5 (24.5) | 40.0 (21.4) |
| Cold pain (CPT) (°C) | | | |
| Mean (SD) | 13.6 (11.0) | 14.1 (9.6) | 12.3 (9.8) |
| Median (IQR) | 15.4 (22.6) | 15.6 (20.9) | 11.3 (19.8) |
| Heat pain (HPT) (°C) | | | |
| Mean (SD) | 44.2 (4.6) | 44.0 (4.4) | 45.4 (4.0) |
| Median (IQR) | 45.2 (7.9) | 43.3 (6.9) | 46.1 (6.2) |

SD, standard deviation; IQR, interquartile range (75th percentile minus 25th percentile); °C, degrees in Celsius; g, gram; NRS, numeric rating scale. There were no significant differences in any aspect.

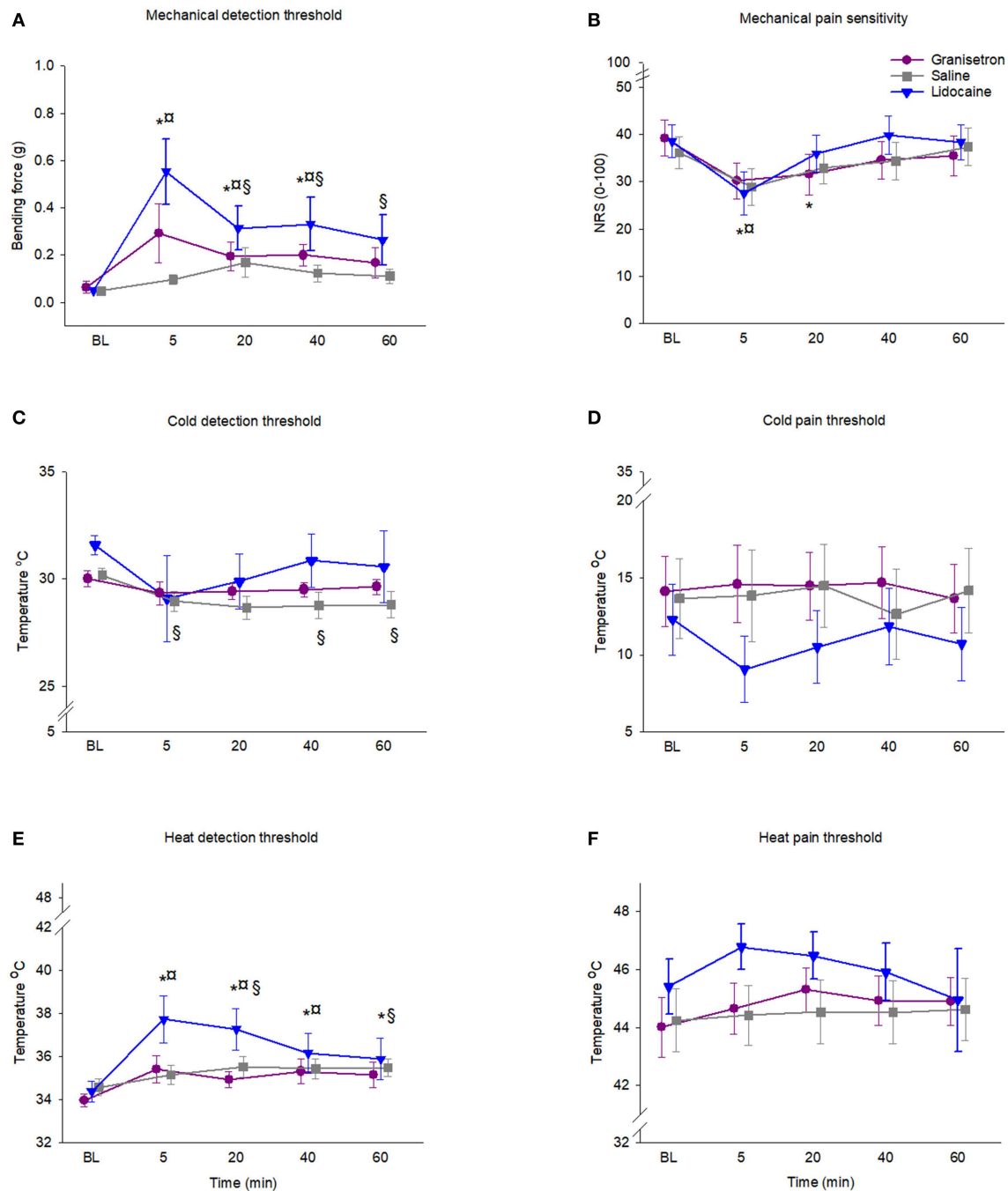


FIGURE 2 | Graph showing the changes in skin sensitivity after subcutaneous injection of granisetron (test substance), lidocaine (positive control), or saline (negative control) into the skin overlying the masseter muscle in 18 healthy males. **(A)** Mechanical detection threshold (MDT), **(B)** mechanical pain sensitivity (MPS), **(C)** heat detection threshold (HDT), **(D)** heat pain threshold (HPT), **(E)** cold detection threshold (CDT), and **(F)** cold pain threshold (CPT). Mean (SEM) values are presented. In order to clarify, the time points for each substance are differentiated. The special characters indicate significant differences compared to baseline ($p < 0.05$) for *granisetron, §lidocaine, and §saline.

significantly increased the HDT when compared to baseline ($p < 0.001$; Friedman ANOVA). The *post hoc* test showed that the increase was only significant at 40 min after injection ($p < 0.001$; Friedman ANOVA), and was 5.2%. There was a significant increase in HDT after injection of isotonic

saline, when compared to baseline ($p < 0.011$; Friedman ANOVA). The *post hoc* test showed that the increase was significant at 20 and 60 min after injection ($p < 0.031$; Friedman ANOVA), and was 2.7% after 20 min and 2.6% after 60 min.

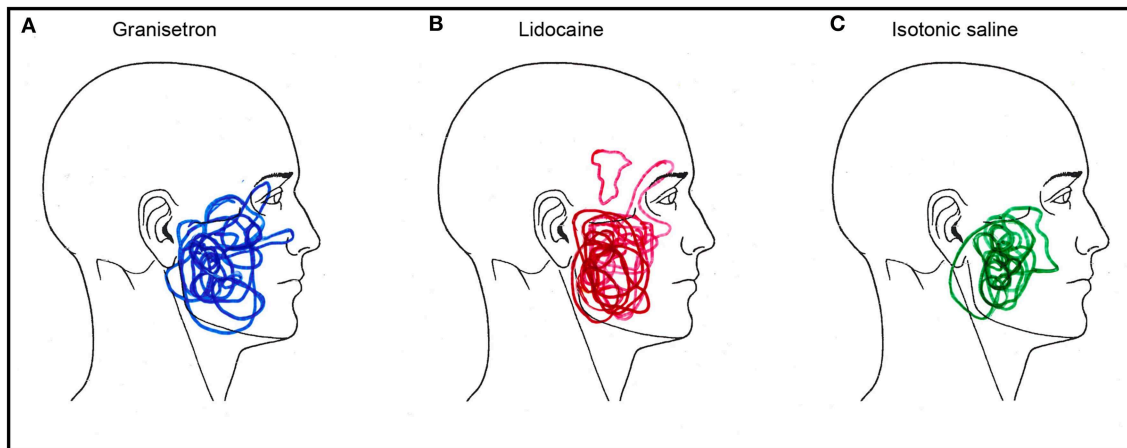


FIGURE 3 | Superimposed illustrations of the areas of the changes in sensory experience after subcutaneous injections of (A) granisetron (blue; active test substance), (B) lidocaine (red; positive control substance), and (C) isotonic saline (green; negative control substance) in 18 healthy males. Note that 16 male participants marked out their change in sensory experience after injection of granisetron, while all 18 did so after injection of lidocaine and 14 did so after injection with isotonic saline. These are not missing data, but a sign of no change in sensory experience.

There were no significant differences in the magnitude of the changes of HDT between the substances ($p > 0.01$; Friedman ANOVA).

Heat Pain Threshold

None of the injected substances affected the HPT. The two-way RM ANOVA did not show any significant time effect ($df = 4$; $F = 2.10$; $p = 0.090$) or any difference between substances ($df = 2$; $F = 1.80$; $p = 0.180$). Likewise, there was no interaction between time and substance ($df = 8$; $F = 1.18$, $p = 0.318$), as shown in Figure 2F.

Area of Sensory Changes

All injected test substances induced an experience of sensory change over the skin surface. The sensory experience was described by the participants as (a) numbness ($n = 15$) and tingling ($n = 10$) for granisetron; (b) numbness ($n = 18$), swelling ($n = 18$), tingling ($n = 16$), and itching ($n = 5$) for lidocaine; and (c) numbness ($n = 7$) and tingling ($n = 8$) for isotonic saline. Several of the participants experienced more than one sensory change. The area of subjective change in sensory experience over the skin overlaying the injections was 107.4 au after injection of lidocaine, 73.8 au after injection of granisetron, and 62.8 au after the isotonic saline injection. The perceived affected area 20 min after lidocaine injection was 159% larger than after isotonic saline ($p = 0.039$; Friedman ANOVA) and 91% larger than after granisetron (NS). The perceived affected area 20 min after granisetron was 35% larger than after isotonic saline (NS). Superimposed illustrations of the areas of the sensory changes are presented in Figure 3.

DISCUSSION

In this study, the effect on skin sensitivity by a subcutaneous injection of granisetron was compared to lidocaine and isotonic

saline. The main finding was that the effect by granisetron on facial skin sensitivity resembles that of lidocaine. Both substances decreased the sensitivity to mechanical stimuli and increased the sensitivity to heat. The changes in sensitivity were greater for lidocaine, but granisetron showed a somewhat longer duration. Thus, granisetron could therefore be considered a novel candidate for local anesthetics, without the bothersome side effect of traditional local anesthetics, such as lidocaine, in terms of facial distortion, i.e., swelling lasting beyond the duration of the anesthesia.

All substances significantly increased the MDT and HDT, while only lidocaine and granisetron increased the MPS. All substances also induced an area of perceived sensory change over the skin surface with a significant difference between lidocaine and isotonic saline, but not between granisetron and saline or lidocaine. The increase for all outcomes was the greatest for lidocaine and more pronounced for mechanical stimuli than for heat. The increase in MDT for granisetron showed a similar pattern to lidocaine. The effect of lidocaine was expected based on results from numerous previous studies showing a local anesthetic effect by lidocaine (35–37). The increase in HDT regarding lidocaine is further supported by another study using a similar methodology to ours (30) and by recent studies using quantitative sensory testing in the facial area of healthy participants after topical lidocaine application (38, 39). However, although a pain-reducing effect by granisetron has been reported in many previous human studies (10, 12, 40), the finding that granisetron showed a similar effect to lidocaine on skin sensitivity, even if it was less pronounced, is a new and interesting finding. This differs from findings in 5-HT₃ knock-out mice, where neither thermal, nor mechanical nociceptive thresholds were affected during physiologic conditions (41). An explanation to the difference could be additional blocking of other receptors and ion channels by granisetron (14–17). The fact that also isotonic saline showed weak effects on skin sensitivity could

perhaps be explained by a change of sodium and chloride ions in the tissue that was sufficient to minorly change nerve conduction.

Another interesting finding was that the duration of the reduced skin sensitivity was longer for granisetron than for lidocaine, regarding MDT, MPS, and HDT. For example, the decrease in MPS by lidocaine peaked at 5 min after injection and thereafter rapidly declined and was non-significant already after 20 min. In comparison, after injection of granisetron, the decrease in MPS lasted beyond 20 min. Similar results, with a longer pain-reducing effect by granisetron than lidocaine, have been reported in patients with rheumatic diseases using tropisetron (40). The results are also in accordance with a previous study from our group where granisetron injected into the masseter muscle increased the pressure pain threshold of healthy volunteers (12). One possible explanation to this could be differences in elimination half-times between the substances where granisetron has a half time of ~9 h (42) and lidocaine only 90–110 min (43). Another possible explanation for the longer duration of granisetron than lidocaine can be the effect on 5-HT₃-receptors, which reduces 5-HT-enhanced hyperalgesia to thermal stimuli (44). A third possible explanation is that calcium influx by granisetron, which causes longer-lasting phosphorylation of sodium channels promoting further activation (45).

Neither lidocaine nor granisetron significantly affected the CDT. We had expected an effect by lidocaine on CDT since this has been reported before (39). In that study, topical application of lidocaine reduced CDT with 8°C. However, in our study the changes were much smaller for all substances and both lidocaine and granisetron also showed minor changes with time, although not significant. Our findings are also consistent with findings by Krumova et al. where the change in CDT after lidocaine application, even if significant, were small (30). The reason for the diverging results regarding lidocaine could perhaps be methodological differences, such as selected dose and way of distribution. We used a single injection of lidocaine, while in the other studies, lidocaine cream was applied topically for 30 min and 6 h, respectively (30, 39). In contrast, isotonic saline reduced the CDT. This is an intriguing finding, since saline was used as negative control and thus not expected to evoke any changes in the variables. However, the changes of CDT were small for all substances, although the greatest for lidocaine. However, in comparison to isotonic saline, lidocaine showed much greater interindividual variation. Granisetron, on the other hand, showed a similar interindividual variation as isotonic saline and also a trend toward significance. This could therefore be a plausible explanation for the significant effect only for isotonic saline.

All substances had some effect on sensory thresholds and there were no significant differences between the substances at any time point. One explanation for this could be that the subcutaneous bolus of the injected substances increased the tissue pressure to such an extent that the bolus itself affected nerve signaling (46, 47), which then disguised any difference between substances.

Based on the similarities in local anesthetic effect between granisetron and lidocaine, it is tempting to speculate about

the mechanisms. Granisetron has a high affinity to the 5-HT₃ receptor, but there are also indications that it blocks, e.g., voltage-gated sodium channels (14–17). Hence, the local anesthetic-like effect by granisetron could be due to a dual blockage of both 5-HT₃-receptors and sodium channels. Lidocaine non-selectively blocks sodium channels, but it might be that granisetron in the periphery more selectively blocks sodium channels involved in pain transmission, i.e., Nav 1.8 and Nav 1.9. If so, this could hypothetically explain the lack of paresthesia. However, since the exact function of the different voltage-gated sodium channels is unknown, as well as the mechanisms behind paresthesia after lidocaine injection, these could be possible areas for future research. In addition, there are indications that 5-HT₃ antagonists also block other ion channels, such as potassium, calcium, and acid-sensing ion channels (48, 49), so the local anesthetic effect may not be limited to 5-HT₃ receptor and sodium channel blocking.

Study Strengths and Limitations

Some study strengths and limitations will be addressed. Firstly, there were two researchers performing the examinations and injections (SAW and TC), which could be considered as a limitation. However, in order to minimize any risk of bias, both investigators were trained by the same researcher (NC) and used the same plastic patch during all sessions to ensure that the injections were placed at the same spot. The bolus of an injected substance could increase the pressure in the tissue and affect the ability to mediate nerve signals (46, 47). Any such effect on the outcome in this study can be ruled out due to the study design since the same volume of all substances was injected and the injections were made in the same site and with the same (subcutaneous) depth. The latter also rules out any potential risk of activation of centrally mediated descending pain inhibitory pathways caused by tissue damage from the needle insertion (50–52), because it requires tissue damage of muscle fascia and tissue (53). Secondly, the present study only included young healthy males, which also could be seen as a limitation since the results cannot be extrapolated to females. Therefore, future studies including both genders are necessary. A third and final limitation was an observed difficulty regarding the methodology. Some of the participants found it difficult to identify the exact transition from non-painful to painful thermal sensation, especially regarding CPT. The consequence was that three of the participants reached the preset minimum temperature (0°C) for all of the three assessments and for all substances without reaching the CPT, why their data could not be included in the statistical analyses. One could argue that this would underpower the study leading to a type II error; however, this was not the case since power was checked for and reached over 90%. On the other hand, there were no significant changes of HPT either, although data were based on all participants. In addition, our results are in line with those of Krumova et al. (30), in which thermal pain thresholds did not even change significantly after application of a lidocaine patch for 6 h in 26 healthy participants. Finally, it would probably not affect the outcome regarding differences between substances.

CONCLUSION

In conclusion, the findings of this study suggest that a subcutaneous injection of granisetron into the facial skin decreases the sensory transmission, mainly concerning the painful mechanical and heat detection stimuli. The analgesic-like effects by granisetron lasted longer than for lidocaine and lacked the bothersome side effects in terms of numbness that outlasts the analgesic effect seen after lidocaine injection. Combined, these results strengthen the role of granisetron as a promising local anesthetic, especially for use in the orofacial area. However, further research with more subjects and with both sexes included is necessary for more profound conclusions.

DATA AVAILABILITY STATEMENT

The datasets generated for this study are available on request to the corresponding author.

REFERENCES

- Gyermek L. Pharmacology of serotonin as related to anesthesia. *J Clin Anesth.* (1996) 8:402–25. doi: 10.1016/0952-8180(96)00093-1
- Bradley PB, Engel G, Feniuk W, Fozard JR, Humphrey PP, Middlemiss DN, et al. Proposals for the classification and nomenclature of functional receptors for 5-hydroxytryptamine. *Neuropharmacology.* (1986) 25:563–76. doi: 10.1016/0028-3908(86)90207-8
- Costall B, Naylor RJ. 5-HT₃ receptors. *Curr Drug Targets CNS Neurol Disord.* (2004) 3:27–37. doi: 10.2174/1568007043482624
- Christidis N, Kang I, Cairns BE, Kumar U, Dong X, Rosen A, et al. Expression of 5-HT₃ receptors and TTX resistant sodium channels (Na(V)1.8) on muscle nerve fibers in pain-free humans and patients with chronic myofascial temporomandibular disorders. *J Headache Pain.* (2014) 15:63. doi: 10.1186/1129-2377-15-63
- Hindle AT. Recent developments in the physiology and pharmacology of 5-hydroxytryptamine. *Br J Anaesth.* (1994) 73:395–407. doi: 10.1093/bja/73.3.395
- Giordano J, Daleo C, Sacks SM. Topical ondansetron attenuates nociceptive and inflammatory effects of intradermal capsaicin in humans. *Eur J Pharmacol.* (1998) 354:R13–14. doi: 10.1016/S0014-2999(98)00492-0
- Farber L, Stratz TH, Bruckle W, Spath M, Pongratz D, Lautenschlager J, et al. Short-term treatment of primary fibromyalgia with the 5-HT₃-receptor antagonist tropisetron. Results of a randomized, double-blind, placebo-controlled multicenter trial in 418 patients. *Int J Clin Pharmacol Res.* (2001) 21:1–13.
- Appel H, Loddenkemper C, Rohweder J, Rudwaleit M, Zeitz M, Sieper J. Massive splenomegaly and hypersplenism in a young woman with primary Sjogren's syndrome. *J Rheumatol.* (2002) 29:2012–3.
- Haus U, Spath M, Farber L. Spectrum of use and tolerability of 5-HT₃ receptor antagonists. *Scand J Rheumatol Suppl.* (2004) 119:12–8. doi: 10.1080/03009740410006961
- Christidis N, Omrani S, Fredriksson L, Gjølset M, Louca S, Hedenberg-Magnusson B, et al. Repeated tender point injections of granisetron alleviate chronic myofascial pain—a randomized, controlled, double-blinded trial. *J Headache Pain.* (2015) 16:104. doi: 10.1186/s10194-015-0588-3
- Christidis N, Kopp S, Ernberg M. The effect on mechanical pain threshold over human muscles by oral administration of granisetron and diclofenac-sodium. *Pain.* (2005) 113:265–70. doi: 10.1016/j.pain.2004.10.016
- Christidis N, Nilsson A, Kopp S, Ernberg M. Intramuscular injection of granisetron into the masseter muscle increases the pressure pain threshold in healthy participants and patients with localized myalgia. *Clin J Pain.* (2007) 23:467–72. doi: 10.1097/AJP.0b013e318058abb1
- Christidis N, Ioannidou K, Milosevic M, Segerdahl M, Ernberg M. Changes of hypertonic saline-induced masseter muscle pain characteristics, by an infusion of the serotonin receptor type 3 antagonist granisetron. *J Pain.* (2008) 9:892–901. doi: 10.1016/j.jpain.2008.05.002
- Fruhstorfer H. Thermal sensibility changes during ischemic nerve block. *Pain.* (1984) 20:355–61. doi: 10.1016/0304-3959(84)90112-X
- Yarnitsky D, Ochoa JL. Differential effect of compression-ischaemia block on warm sensation and heat-induced pain. *Brain.* (1991) 114(Pt 2):907–13. doi: 10.1093/brain/114.2.907
- Ye JH, Mui WC, Ren J, Hunt TE, Wu WH, Zbuzek VK. Ondansetron exhibits the properties of a local anesthetic. *Anesth Analg.* (1997) 85:1116–21. doi: 10.1213/00000539-199711000-00029
- Ziegler EA, Magerl W, Meyer RA, Treede RD. Secondary hyperalgesia to punctate mechanical stimuli. Central sensitization to A-fibre nociceptor input. *Brain.* (1999) 122(Pt 12):2245–57. doi: 10.1093/brain/122.12.2245
- Kuryshv YA, Brown AM, Wang L, Benedict CR, Rampe D. Interactions of the 5-hydroxytryptamine 3 antagonist class of antiemetic drugs with human cardiac ion channels. *J Pharmacol Exp Ther.* (2000) 295:614–20.
- Catterall WA. From ionic currents to molecular mechanisms: the structure and function of voltage-gated sodium channels. *Neuron.* (2000) 26:13–25. doi: 10.1016/S0896-6273(00)81133-2
- Goldin AL. Resurgence of sodium channel research. *Annu Rev Physiol.* (2001) 63:871–94. doi: 10.1146/annurev.physiol.63.1.871
- Courtney KR. Mechanism of frequency-dependent inhibition of sodium currents in frog myelinated nerve by the lidocaine derivative GEA. *J Pharmacol Exp Ther.* (1975) 195:225–36.
- Tetzlaff JE. The pharmacology of local anesthetics. *Anesthesiol Clin North Am.* (2000) 18:217–33. doi: 10.1016/S0889-8537(05)70161-9
- Strichartz GR, Zhou Z, Sinnott C, Khodorova A. Therapeutic concentrations of local anaesthetics unveil the potential role of sodium channels in neuropathic pain. *Novartis Found Symp.* (2002) 241:189–201; discussion 202–185, 226–132.
- Boyce RA, Kirpalani T, Mohan N. Updates of topical and local anesthesia agents. *Dental Clin North Am.* (2016) 60:445–71. doi: 10.1016/j.cden.2015.12.001
- Malamed SF. *Handbook of Local Anesthesia - E-Book.* St. Louis, MO: Elsevier Health Sciences (2019).
- Kothari SF, Shimomasa M, Iida T, Komiyama O, Shibutani K, Svensson P, et al. Quantitative and qualitative assessment of sensory changes induced by

- local anesthetics block of two different trigeminal nerve branches. *Clin Oral Invest.* (2019) 23:2637–49. doi: 10.1007/s00784-018-2695-4
27. Mense S. Nociception from skeletal muscle in relation to clinical muscle pain. *Pain.* (1993) 54:241–89. doi: 10.1016/0304-3959(93)90027-M
 28. Cairns BE, Gambiarota G, Svensson P, Arendt-Nielsen L, Berde CB. Glutamate-induced sensitization of rat masseter muscle fibers. *Neuroscience.* (2002) 109:389–99. doi: 10.1016/S0306-4522(01)00489-4
 29. Lewis JS, Welch MJ, Tang L. Workshop on the production, application and clinical translation of “non-standard” PET nuclides: a meeting report. *Q J Nucl Med Mol Imaging.* (2008) 52:101–6.
 30. Krumova EK, Zeller M, Westermann A, Maier C. Lidocaine patch (5%) produces a selective, but incomplete block of Ad and C fibers. *Pain.* (2012) 153:273–80. doi: 10.1016/j.pain.2011.08.020
 31. Okeson JP. *Management of Temporomandibular Disorders and Occlusion*. St. Louis, MI: Mosby Inc, affiliate of Elsevier Inc (2013).
 32. Van't Klooster MP, Foadi N, Hage A, Stoetzer C, Wegner F, Eberhardt M, et al. Local-anesthetic like inhibition of the cardiac sodium channel Nav1.5 α -subunit by 5-HT₃ receptor antagonists. *Eur J Pharmacol.* (2016) 789:119–26. doi: 10.1016/j.ejphar.2016.07.020
 33. Schiffman E, Ohrbach R, Truelove E, Look J, Anderson G, Goulet JP, et al. Diagnostic criteria for temporomandibular disorders (DC/TMD) for clinical and research applications: recommendations of the international RDC/TMD consortium network* and Orofacial Pain Special Interest Groupdagdagger. *J Oral Facial Pain Headache.* (2014) 28:6–27. doi: 10.11607/jop.1151
 34. Svensson P, Graven-Nielsen T, Arendt-Nielsen L. Mechanical hyperesthesia of human facial skin induced by tonic painful stimulation of jaw muscles. *Pain.* (1998) 74:93–100. doi: 10.1016/S0304-3959(97)00156-5
 35. Dahl JB, Brennum J, Arendt-Nielsen L, Jensen TS, Kehlet H. The effect of pre- versus postinjury infiltration with lidocaine on thermal and mechanical hyperalgesia after heat injury to the skin. *Pain.* (1993) 53:43–51. doi: 10.1016/0304-3959(93)90054-S
 36. Eidelman A, Weiss JM, Lau J, Carr DB. Topical anesthetics for dermal instrumentation: a systematic review of randomized, controlled trials. *Ann Emerg Med.* (2005) 46:343–51. doi: 10.1016/j.annemergmed.2005.01.028
 37. Raeissadat SA, Rayegani SM, Sadeghi F, Rahimi-Dehghan S. Comparison of ozone and lidocaine injection efficacy vs dry needling in myofascial pain syndrome patients. *J Pain Res.* (2018) 11:1273–9. doi: 10.2147/JPR.S164629
 38. Okayasu I, Komiyama O, Ayuse T, De Laat A. Effect of 8% lidocaine spray on the sensory and pain thresholds of the skin of the face and hands evaluated by quantitative sensory testing. *J Dent Anesth Pain Med.* (2018) 18:361–5. doi: 10.17245/jdpm.2018.18.6.361
 39. Costa YM, Ferreira D, Conti PCR, Baad-Hansen L, Svensson P, Bonjardim LR. Topical anaesthesia degree is reduced in temporomandibular disorders patients: a novel approach to assess underlying mechanisms of the somatosensory alterations. *J Oral Rehabil.* (2020) 47:113–22. doi: 10.1111/joor.12874
 40. Muller W, Fiebich BL, Stratz T. [5-HT₃ receptor antagonist als analgetics in rheumatic diseases]. *Z Rheumatol.* (2006) 65:548–52. doi: 10.1007/s00393-005-0014-3
 41. Kayser V, Elfassi IE, Aubel B, Melfort M, Julius D, Gingrich JA, et al. Mechanical, thermal and formalin-induced nociception is differentially altered in 5-HT1A^{-/-}, 5-HT1B^{-/-}, 5-HT2A^{-/-}, 5-HT3A^{-/-} and 5-HTT^{-/-} knock-out male mice. *Pain.* (2007) 130:235–48. doi: 10.1016/j.pain.2006.11.015
 42. Cieslak GD, Watcha MF, Phillips MB, Pennant JH. The dose-response relation and cost-effectiveness of granisetron for the prophylaxis of pediatric postoperative emesis. *Anesthesiology.* (1996) 85:1076–85. doi: 10.1097/0000542-199611000-00016
 43. Collinsworth KA, Kalman SM, Harrison DC. The clinical pharmacology of lidocaine as an antiarrhythmic drug. *Circulation.* (1974) 50:1217–30. doi: 10.1161/01.CIR.50.6.1217
 44. Loyd DR, Henry MA, Hargreaves KM. Serotonergic neuromodulation of peripheral nociceptors. *Semin Cell Dev Biol.* (2013) 24:51–7. doi: 10.1016/j.semcdb.2012.09.002
 45. Riering K, Rewerts C, Zieglansberger W. Analgesic effects of 5-HT₃ receptor antagonists. *Scand J Rheumatol Suppl.* (2004) 119:19–23. doi: 10.1080/03009740410006970
 46. Graven-Nielsen T, McArdle A, Phoenix J, Arendt-Nielsen L, Jensen TS, Jackson MJ, et al. In vivo model of muscle pain: quantification of intramuscular chemical, electrical, and pressure changes associated with saline-induced muscle pain in humans. *Pain.* (1997) 69:137–43. doi: 10.1016/S0304-3959(96)03270-8
 47. Sørensen LB, Boudreau SA, Gazerani P, Graven-Nielsen T. Enlarged areas of pain and pressure hypersensitivity by spatially distributed intramuscular injections of low-dose nerve growth factor. *J Pain.* (2019) 20:566–76. doi: 10.1016/j.jpain.2018.11.005
 48. Scholtysik G, Imoto Y, Yatani A, Brown AM. 5-Hydroxytryptamine antagonist ICS 205-930 blocks cardiac potassium, sodium and calcium currents. *J Pharmacol. Exp Therap.* (1988) 245:773–8.
 49. Su YS, Mei HR, Wang CH, Sun WH. Peripheral 5-HT₃ mediates mirror-image pain by a cross-talk with acid-sensing ion channel 3. *Neuropharmacology.* (2018) 130:92–104. doi: 10.1016/j.neuropharm.2017.11.044
 50. Fields HL. Pain modulation: expectation, opioid analgesia and virtual pain. *Prog Brain Res.* (2000) 122:245–53. doi: 10.1016/S0079-6123(08)62143-3
 51. Millan MJ. Descending control of pain. *Prog Neurobiol.* (2002) 66:355–474. doi: 10.1016/S0301-0082(02)00009-6
 52. Hadjipavlou G, Dunckley P, Behrens TE, Tracey I. Determining anatomical connectivities between cortical and brainstem pain processing regions in humans: a diffusion tensor imaging study in healthy controls. *Pain.* (2006) 123:169–78. doi: 10.1016/j.pain.2006.02.027
 53. Ceccherelli F, Rigoni MT, Gagliardi G, Ruzzante L. Comparison of superficial and deep acupuncture in the treatment of lumbar myofascial pain: a double-blind randomized controlled study. *Clin J Pain.* (2002) 18:149–53. doi: 10.1097/00002508-20020500-00003

Conflict of Interest: The authors declare that the research was conducted in the absence of any commercial or financial relationships that could be construed as a potential conflict of interest.

Copyright © 2020 Ernberg, Wieslander Fältmars, Hajizadeh Kopayeh, Arzt Wallén, Cankalp and Christidis. This is an open-access article distributed under the terms of the Creative Commons Attribution License (CC BY). The use, distribution or reproduction in other forums is permitted, provided the original author(s) and the copyright owner(s) are credited and that the original publication in this journal is cited, in accordance with accepted academic practice. No use, distribution or reproduction is permitted which does not comply with these terms.



Swallow Motor Pattern Is Modulated by Fixed or Stochastic Alterations in Afferent Feedback

Suzanne N. King^{1,2}, Tabitha Y. Shen³, M. Nicholas Musselwhite³, Alyssa Huff^{2,4†}, Mitchell D. Reed^{2,4}, Ivan Poliaček^{3,5}, Dena R. Howland^{2,4,6}, Warren Dixon⁷, Kendall F. Morris⁸, Donald C. Bolser³, Kimberly E. Iceman^{2,4} and Teresa Pitts^{2,4*}

OPEN ACCESS

Edited by:

Kazutaka Takahashi,
The University of Chicago,
United States

Reviewed by:

Ivan M. Lang,
Medical College of Wisconsin,
United States
Mathias Dutschmann,
The University of Melbourne, Australia
Francois Gould,
Northeast Ohio Medical University,
United States

*Correspondence:

Teresa Pitts
t.pitts@louisville.edu

†Present address:

Alyssa Huff,
Center for Integrative Brain Research,
Seattle Children's Research Institute,
Seattle, WA, United States

Specialty section:

This article was submitted to
Motor Neuroscience,
a section of the journal
Frontiers in Human Neuroscience

Received: 19 November 2019

Accepted: 12 March 2020

Published: 09 April 2020

Citation:

King SN, Shen TY,
Musselwhite MN, Huff A, Reed MD,
Poliaček I, Howland DR, Dixon W,
Morris KF, Bolser DC, Iceman KE and
Pitts T (2020) Swallow Motor Pattern
Is Modulated by Fixed or Stochastic
Alterations in Afferent Feedback.
Front. Hum. Neurosci. 14:112.
doi: 10.3389/fnhum.2020.00112

¹ Department of Otolaryngology-Head and Neck Surgery, University of Louisville, Louisville, KY, United States, ² Kentucky Spinal Cord Injury Research Center, University of Louisville, Louisville, KY, United States, ³ Department of Physiological Sciences, College of Veterinary Medicine, University of Florida, Gainesville, FL, United States, ⁴ Department of Neurological Surgery, School of Medicine, University of Louisville, Louisville, KY, United States, ⁵ Department of Medical Biophysics, Jessenius Faculty of Medicine, Comenius University, Bratislava, Slovakia, ⁶ Robley Rex VA Medical Center, Louisville, KY, United States, ⁷ Department of Mechanical and Aerospace Engineering, Herbert Wertheim College of Engineering, University of Florida, Gainesville, FL, United States, ⁸ Department of Molecular Pharmacology and Physiology, Morsani College of Medicine, University of South Florida, Tampa, FL, United States

Afferent feedback can appreciably alter the pharyngeal phase of swallow. In order to measure the stability of the swallow motor pattern during several types of alterations in afferent feedback, we assessed swallow during a conventional water challenge in four anesthetized cats, and compared that to swallows induced by fixed (20 Hz) and stochastic (1-20Hz) electrical stimulation applied to the superior laryngeal nerve. The swallow motor patterns were evaluated by electromyographic activity (EMG) of eight muscles, based on their functional significance: laryngeal elevators (mylohyoid, geniohyoid, and thyrohyoid); laryngeal adductor (thyroarytenoid); inferior pharyngeal constrictor (thyropharyngeus); upper esophageal sphincter (cricopharyngeus); and inspiratory activity (parasternal and costal diaphragm). Both the fixed and stochastic electrical stimulation paradigms increased activity of the laryngeal elevators, produced short-term facilitation evidenced by increasing swallow durations over the stimulus period, and conversely inhibited swallow-related diaphragm activity. Both the fixed and stochastic stimulus conditions also increased specific EMG amplitudes, which never occurred with the water challenges. Stochastic stimulation increased swallow excitability, as measured by an increase in the number of swallows produced. Consistent with our previous results, changes in the swallow motor pattern for pairs of muscles were only sometimes correlated with each other. We conclude that alterations in afferent feedback produced particular variations of the swallow motor pattern. We hypothesize that specific SLN feedback might modulate the swallow central pattern generator during aberrant feeding conditions (food/liquid entering the airway), which may protect the airway and serve as potentially important clinical diagnostic indicators.

Keywords: deglutition, schluckatmung, diaphragm, facilitation, electrical stimulation, swallow, stochastic

INTRODUCTION

During ingestion, the pharyngeal phase of swallow is initiated and regulated by a host of sensory afferents in the oral, pharyngeal, and laryngeal cavities (Pommerenke, 1928; Kahrilas and Logemann, 1993; Ertekin et al., 2000; Hiss et al., 2001; Humbert et al., 2009; Pitts et al., 2013; Spearman et al., 2014; Huff et al., 2018). Changes in temperature, food size and texture, or taste can significantly modulate the swallow motor pattern, and are used by speech-language pathologists as therapeutic options to treat swallowing disorders (dysphagia) (Bushmann et al., 1989; DePippo et al., 1992; Hiss et al., 2001; Kendall, 2002; Butler et al., 2004; Daniels et al., 2004, 2007; Clave et al., 2008; Troche et al., 2008; Humbert et al., 2009; Yamamura et al., 2010). While the clinical literature demonstrating these effects is robust, very little is understood about their mechanism of action. If these mechanisms are elucidated, specific sensory treatment parameters could be optimized for maximal therapeutic effect.

Historically, much of the basic investigation into the swallow pattern generator has been performed under *fictive* conditions (deafferented and paralyzed) using fixed-frequency electrical stimulation of the superior laryngeal nerve (SLN) (Gia, 1958; Doty, 1968; Miller, 1982; Dick et al., 1993). The SLN branches off the vagus nerve and provides both sensory and motor innervation to the larynx. While its stimulation can readily evoke a series of rhythmic swallows, it also strongly suppresses breathing, and there is limited information about how that pattern compares to a more natural stimulus condition. The key features of the swallow in an experimentally reduced preparation are a burst on the hypoglossal nerve followed by a burst on the vagus nerve (Gestreau et al., 1996, 2000; Roda et al., 2002; Bautista and Dutschmann, 2014; Bautista et al., 2014; Hashimoto et al., 2019). However, natural deglutition is complex and involves variable motor sequences produced by an array of muscles, and also includes inspiratory (e.g., diaphragm) muscle activation (“*schluckatmung*”) that is thought to produce negative intra-thoracic pressure to aid in propelling the bolus through the esophagus (Pitts et al., 2013, 2015a,b; Spearman et al., 2014). During normal breathing and swallow, laryngeal afferents are stimulated, producing variable sensory frequency patterns with discharge rates from 10 – 184 Hz, which are transmitted by the SLN (Storey, 1968; Bradley et al., 1983). This corresponds to stochastic-like afferent nerve firing discharge which can stimulate multiple behavior responses including apnea, swallow, and cough. Recent work has also demonstrated short-term facilitation of swallow duration (Horton et al., 2018) in response to SLN stimulation, which contrasts with the classical view of swallow as a strictly stereotypical motor event (Miller and Scheeington, 1916; Doty and Bosma, 1956; Doty, 1968; Miller, 1982). Additionally, the SLN carries afferent fibers which, when stimulated, can ultimately evoke laryngeal closure during swallow (Jafari et al., 2003), however this activity is not essential for the onset of the normal swallow sequence (Kitagawa et al., 2002). The vallecular space near the epiglottis is also innervated by SLN afferents (except in humans), and when food/liquid accumulates in this space behind the tongue, reflexive swallow occurs. When swallow is induced by delivering milk to the vallecular space of

decerebrate piglets (Thexton et al., 2007, 2009), the motor pattern is modified by the presence of other rhythmic oral movements (suckling). This indicates that afferent feedback from natural stimuli can influence pharyngeal swallow motor pattern, and that this is brainstem-mediated.

Previous work has defined characteristics of swallow motor pattern based on deterministic repetitive SLN stimulation, and suggests that repetitive swallows are produced by changes in excitability of the swallow central pattern generator (CPG) (Jean, 2001). Previous studies have not systematically compared swallows evoked by electrical SLN stimulation to those evoked by a natural stimulus (e.g., water in the oropharynx or vallecula). Thus, it remains uncertain if the repetitive swallow motor patterns produced in response to SLN stimulation are directly comparable to a natural stimulus, or if the addition of variability in the stimulation parameters can be used experimentally to produce motor patterns akin to a natural stimulus. We tested the hypothesis that swallow-related upper airway and inspiratory (diaphragm and parasternal: *schluckatmung*) muscle activity is modified by use of fixed frequency and stochastic SLN electrical stimulation versus oral water infusion.

MATERIALS AND METHODS

Experiments were performed on four spontaneously breathing adult cats. Ethical approval of the protocol was confirmed by the University of Florida and University of Louisville Institutional Animal Care and Use Committees (IACUCs). The animals were initially anesthetized with sevoflurane (3–5%) via inhalation and then transitioned to sodium pentobarbital (35–40 mg/kg i.v.); supplementary doses were administered as needed (1–3 mg/kg i.v.). A dose of atropine sulfate (0.1–0.2 mg/kg, i.v.) was given at the beginning of the experiment to reduce airway secretions. Cannulas were placed in the femoral artery, femoral vein, and trachea. An esophageal balloon was placed via an oral approach to measure pressure in the mid-thoracic esophagus. Arterial blood pressure and end-tidal CO₂ were continuously monitored. Body temperature was monitored and maintained at 37.5 ± 0.5 °C using a pad. Arterial blood samples were periodically removed for blood gas analysis. PO₂ was maintained using air mixtures with enriched oxygen (25–60%) to maintain values above 100 mm Hg if needed.

Muscle activity was recorded via electromyography (EMG) using bipolar insulated fine wire electrodes according to the technique of Basmajian and Stecko (1962). Eight muscles were used to evaluate swallow occurrence: mylohyoid, geniohyoid, thyrohyoid, thyropharyngeus, thyroarytenoid, cricopharyngeus, parasternal, and costal diaphragm. These muscles span the actions during the pharyngeal phase of swallow: (a) mylohyoid, geniohyoid and thyrohyoid for hyolaryngeal elevation; (b) thyropharyngeus for inferior pharyngeal constriction; (c) cricopharyngeus for upper esophageal sphincter regulation; (d) thyroarytenoid for laryngeal adduction; and (e) parasternal and costal diaphragm for inspiratory (*schluckatmung*) activity (Pitts et al., 2013, 2015a,b; Spearman et al., 2014). As in our

previous publications, swallow duration was defined as onset of the mylohyoid burst to the end of the thyropharyngeus burst.

Surgical placement of EMGs proceeded as follows: the digastric muscles were blunt dissected away from the surface of the mylohyoid and electrodes were placed medially in the left mylohyoid. A small horizontal incision was made at the rostral end of the right mylohyoid followed by an incision down the midline for approximately 5 mm to reveal the geniohyoid muscle. Electrodes were placed 1 cm from the caudal insertion of the geniohyoid muscle. The thyroarytenoid muscle electrodes were inserted through the cricothyroid window into the anterior portion of the vocal folds, which were visually inspected post-mortem. Minor rotation of the larynx and pharynx counterclockwise revealed the superior laryngeal nerve, which facilitated placement of the thyropharyngeus muscle electrodes. The thyropharyngeus is a fan shaped muscle with the smallest portion attached to the thyroid cartilage; electrodes were placed in the ventral, caudal portion of the muscle overlaying thyroid cartilage within 5 mm of the rostral insertion of the muscle. To place electrodes within the cricopharyngeus muscle, the larynx and pharynx were rotated counterclockwise to reveal the posterior aspect of the larynx. The edge of the cricoid cartilage was located by palpation and electrodes were placed in the cricopharyngeus muscle just cranial to the edge of this structure. Thyrohyoid muscle electrodes were inserted approximately 5 mm rostral to the attachment to the thyroid cartilage; those for the parasternal muscle were placed in the third intercostal space, just adjacent to the sternum, and the costal diaphragm EMGs were placed transcutaneously just under the xiphoid process. The positions of all electrodes were confirmed by visual inspection (following electrode placement and post-mortem) and by EMG activity patterns during breathing and swallow, as we have previously published (Pitts et al., 2013, 2015b, 2018; Spearman et al., 2014).

The right SLN was unilaterally exposed and bipolar hook electrodes were placed on the intact nerve. Voltage thresholds for evoking swallow were determined at the beginning of the experiment using fixed frequency (20 Hz) stimulus, and for the experimental condition the voltage was set at 1.5 times higher than threshold necessary for producing at least one swallow (4.4 ± 0.7 V). Non-deterministic stimulation frequencies were produced by a custom MATLAB (MathWorks; Natick, MA) program that shuffled inter-pulse intervals instantaneously corresponding to 4–40 Hz. Pulse parameters were controlled from a host PC interfaced to a custom electrical stimulator through a commercial interface board (QPID terminal board, Quanser; Markham, ON, Canada).

Conditions

To initiate swallow via water, a bolus of approximately 3 ml was infused into the pharynx via a 1-inch long piece of polyethylene tubing (P.E. 90) (placed rostral to the faucial pillars) attached to 5 ml syringe. All water trials for each animal were performed by the same researcher to maintain stimulus consistency. Fixed frequency electrical stimulation was produced at 20 Hz, while the stochastic condition was produced across the range of 1–40 Hz (median of 20 Hz), each for 20 second series (see **Figure 1**).

All stimuli were presented three times, separated by a minimum inter-stimulus interval of one minute; the presentation was randomized within each animal and across animals.

Signal Analysis

Raw EMG signals were filtered (200–5000 Hz), rectified, and integrated with time constant of 20 ms. Swallow was identified by sequential bursts of the mylohyoid, geniohyoid, thyrohyoid, thyroarytenoid, and thyropharyngeus as well as a decline in tonic (followed by a burst) EMG activity of the cricopharyngeus (UES). Swallows that could not be differentiated from other behaviors (i.e., licking, cough, laryngeal elevation, laryngeal adductor reflex and aspiration reflex) were excluded from analysis. To avoid analyzing data from spontaneous swallow activity, the EMG activity was included in the analysis if the swallow occurred within 30 seconds of the initial water or within the stimulus duration. Reported maximum EMG values were calculated as a percentage of maximum for each muscle across the experiment for normalization across animals (i.e., the maximum EMG amplitude for each muscle was 100%).

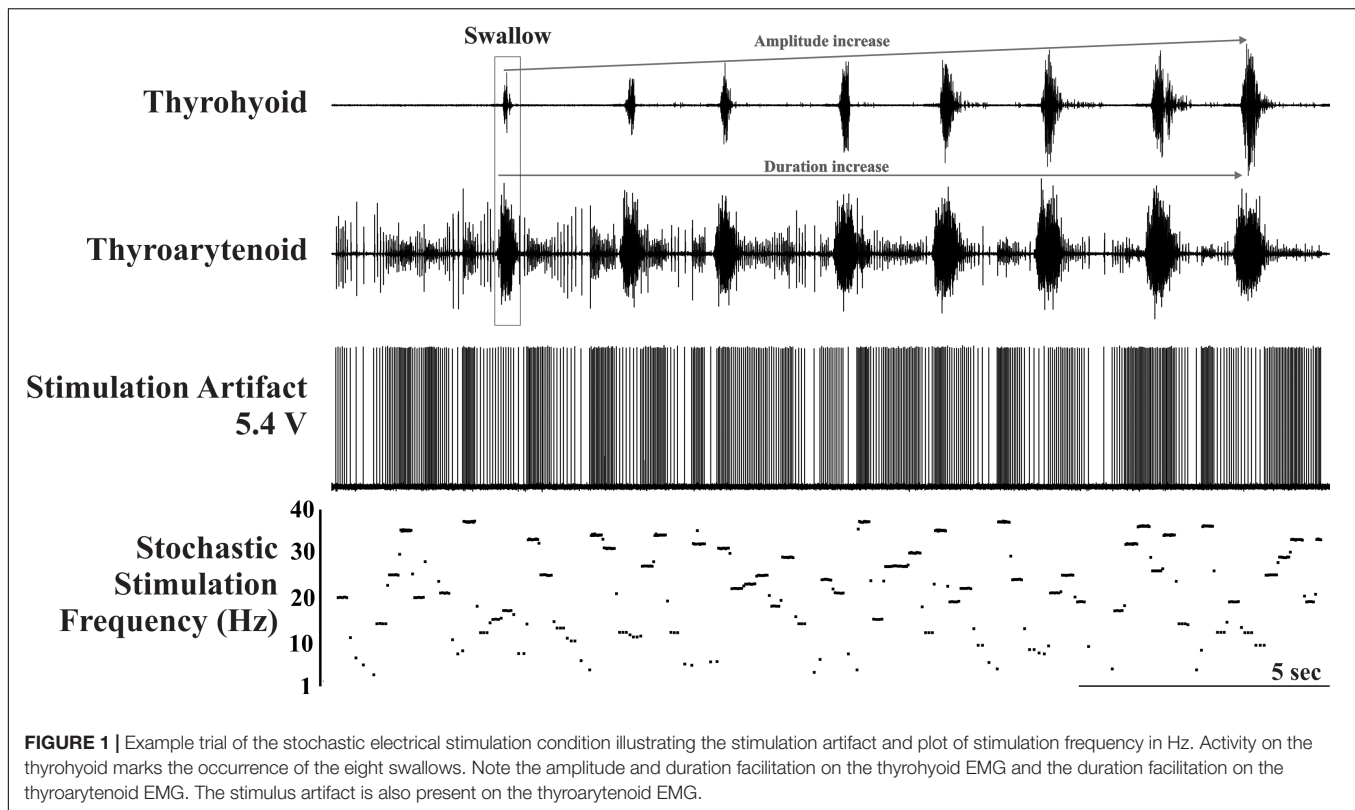
Statistical Analysis

A mean \pm standard deviation (SD) was calculated for each measure and animal including all induced swallows, and then averaged for each condition across animals (**Table 1**). For statistical analysis of group differences by *condition*, an ANOVA with Fisher's least significant difference *post hoc* tests were performed as appropriate (**Table 1**). To assess *short-term facilitation*, a repeated-measures ANOVA was performed comparing the first swallow in the series to each subsequent swallow with Fisher's least significant difference *post hoc* tests performed as appropriate, similar to procedures performed by Horton and colleagues (2018) (**Table 1**). A difference was considered significant if the *p*-value was less or equal to 0.05. To assess relationships between changes in EMG amplitude and duration during swallow, Pearson's product moment correlations (*r*) were calculated comparing all amplitude measures across conditions (**Table 2**).

RESULTS

All three stimulus conditions produced apnea and repetitive swallows: water (3.2 ± 0.5), fixed frequency (7.5 ± 2.6), and stochastic (9.2 ± 2.5) electrical stimulation. Of note, the stochastic stimulation produced significantly more swallows compared to the fixed frequency stimulation ($p = 0.005$), due to a difference in time from the initiation of the stimulation to the first swallow [fixed (4.2 ± 0.9 s), stochastic (2.7 ± 0.4 sec; $p = 0.01$)].

There was a significant effect of condition on the EMG amplitude (percent of maximum) of mylohyoid, geniohyoid, thyrohyoid, thyropharyngeus, parasternal, and costal diaphragm (**Table 1**). Electrical stimulation (fixed and stochastic) increased the mylohyoid ($\sim 120\%$), geniohyoid ($\sim 200\%$), and thyrohyoid (137%) amplitude compared to water (**Figures 1–3**). Stochastic stimulation also increased thyropharyngeus amplitude by 138% compared to water (**Figures 1–3**). Conversely, there was



significant depression of the costal diaphragm EMG amplitude by electrical stimulation (fixed and stochastic; $\sim 75\%$) and of the parasternal by fixed electrical stimulation (41%) compared to water (**Table 1** and **Figures 2, 3**). There was no significant effect of condition on swallow duration (**Table 1** and **Figure 3**).

There was evidence of short-term facilitation with fixed electrical stimulation (i.e., significant increase in EMG amplitude when compared to the first swallow in the series; see **Figure 3** and **Table 1**) on the mylohyoid ($p = 0.01$) with significant increases starting at the second swallow ($p = 0.004$), continuing through the third ($p = 0.006$), fourth ($p = 0.001$), and fifth ($p = 0.007$) in the series (**Table 1**). During stochastic stimulation there was evidence of short-term facilitation on the thyrohyoid ($p = 0.02$) starting at the third swallow ($p = 0.006$), continuing through the fourth ($p = 0.002$), fifth ($p = 0.01$) and sixth ($p = 0.01$); and the thyropharyngeus ($p = 0.05$) starting at the fourth swallow ($p = 0.05$), continuing through the fifth ($p = 0.008$) and sixth ($p = 0.02$) in the series (**Table 1**).

For swallow duration there was evidence of short-term facilitation with fixed and stochastic stimulation (**Figure 3**; **Table 1**). Significant increases in swallow duration with fixed stimulation ($p = 0.005$) started at the third swallow ($p = 0.02$), continuing through the fourth ($p = 0.02$) and fifth ($p = 0.005$); stochastic stimulation facilitation ($p = 0.03$) started at the third swallow ($p = 0.001$), continuing through the fourth ($p = 0.04$), fifth ($p = 0.04$) and sixth ($p = 0.01$) swallow in the series.

Table 2 is a matrix showing all Pearson Product moment correlations for EMG amplitudes and swallow duration

combined across all conditions. This analysis resulted in six moderate correlations: mylohyoid and geniohyoid ($r = 0.48$); mylohyoid and thyrohyoid ($r = 0.54$); UES (cricopharyngeus) and parasternal ($r = 0.49$); UES (cricopharyngeus) and costal diaphragm ($r = 0.54$); parasternal and costal diaphragm ($r = 0.61$); and geniohyoid to swallow duration ($r = 0.57$).

DISCUSSION

Modulation of afferent feedback is an important component in determining the stability of a reflexive motor pattern. This is the first study to demonstrate the differential effects of water infusion vs. electrical stimulation (stochastic or fixed) of the SLN on swallow production. The effects of electrical stimulation included significant increases in upper airway muscle (mylohyoid, geniohyoid, thyrohyoid, and thyropharyngeus) EMG amplitudes, and significant depression of the schluckatmung activity evidenced by the decreases in diaphragm (fixed and stochastic) and parasternal (fixed) EMG amplitudes. Additionally, there is evidence of short-term amplitude facilitation of the mylohyoid with fixed frequency stimulation, and of the thyrohyoid and thyropharyngeus with stochastic frequency stimulation.

Fixed Versus Stochastic Stimulation

Our observations suggest that the stochastic stimulation increased excitability in the swallow CPG as evidenced by a reduction in the time to the first swallow, increases in EMG

TABLE 1 | Means and standard deviations (SD) for EMG amplitude (% maximum) and total swallow duration changes across the three conditions (ANOVA) and evidence of short-term facilitation (repeated-measures ANOVA).

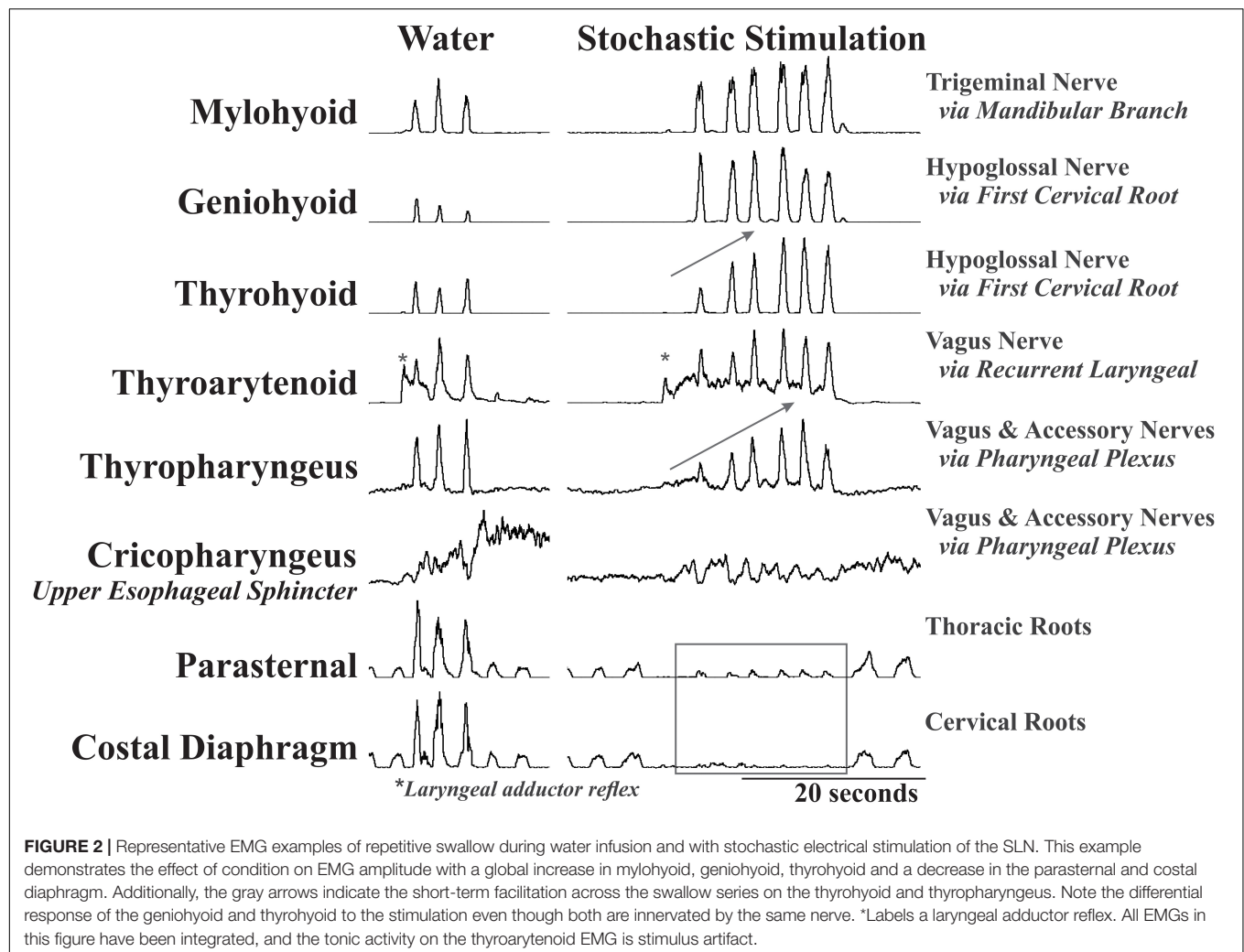
| | | Mylohyoid Mean ± SD | Geniohyoid Mean ± SD | Thyrohyoid Mean ± SD | Thyroarytenoid Mean ± SD | Thyropharyngeus Mean ± SD | UES (Cricopharyngeus) Mean ± SD | Parasternal Mean ± SD | Costal diaphragm Mean ± SD | Swallow duration Mean ± SD |
|----------------------|---------|------------------------|-------------------------|-------------------------|-----------------------------|------------------------------|------------------------------------|--------------------------|-------------------------------|-------------------------------|
| Water (W) | SW# | | | | | | | | | |
| | 1 | 63 ± 16 | 49 ± 33 | 59 ± 20 | 66 ± 12 | 44 ± 38 | 63 ± 28 | 77 ± 32 | 75 ± 23 | 588 ± 121 |
| | 2 | 69 ± 15 | 34 ± 23 | 57 ± 38 | 86 ± 19 | 49 ± 35 | 50 ± 16 | 70 ± 41 | 76 ± 28 | 561 ± 84 |
| | 3 | 55 ± 8 | 26 ± 19 | 42 ± 23 | 66 ± 12 | 54 ± 46 | 78 ± 20 | 50 ± 12 | 87 ± 15 | 423 ± 87 |
| | | 62 ± 13 | 36 ± 25 | 53 ± 27 | 73 ± 14 | 49 ± 39 | 64 ± 22 | 66 ± 28 | 79 ± 22 | 524 ± 98 |
| 20 Hz fixed (F) | 1 | 53 ± 10 | 72 ± 20 | 57 ± 17 | 71 ± 8 | 34 ± 28 | 37 ± 25 | 36 ± 23 | 20 ± 21 | 605 ± 81 |
| | 2 | 78 ± 10* | 68 ± 7 | 68 ± 7 | 63 ± 6 | 49 ± 37 | 39 ± 22 | 29 ± 13 | 22 ± 22 | 612 ± 95 |
| | 3 | 76 ± 10* | 75 ± 18 | 76 ± 6 | 64 ± 3 | 46 ± 31 | 46 ± 22 | 42 ± 23 | 20 ± 22 | 726 ± 122* |
| | 4 | 82 ± 13* | 74 ± 11 | 80 ± 10 | 73 ± 13 | 57 ± 37 | 51 ± 32 | 40 ± 23 | 20 ± 20 | 731 ± 95* |
| | 5 | 76 ± 7* | 82 ± 14 | 81 ± 15 | 66 ± 10 | 57 ± 29 | 49 ± 21 | 50 ± 35 | 19 ± 20 | 830 ± 120* |
| | | 73 ± 10 | 74 ± 14 | 73 ± 11 | 67 ± 8 | 49 ± 32 | 44 ± 24 | 39 ± 23 | 20 ± 21 | 701 ± 103 |
| 1–20 Hz variable (V) | 1 | 62 ± 17 | 72 ± 20 | 51 ± 4 | 63 ± 4 | 41 ± 29 | 42 ± 13 | 50 ± 31 | 21 ± 20 | 557 ± 29 |
| | 2 | 62 ± 13 | 67 ± 3 | 67 ± 3 | 69 ± 10 | 52 ± 22 | 46 ± 20 | 46 ± 30 | 21 ± 21 | 644 ± 69 |
| | 3 | 70 ± 17 | 76 ± 20 | 82 ± 17* | 68 ± 10 | 50 ± 22 | 52 ± 20 | 53 ± 36 | 20 ± 21 | 644 ± 38* |
| | 4 | 80 ± 14 | 78 ± 17 | 87 ± 13* | 79 ± 20 | 69 ± 13* | 53 ± 23 | 47 ± 33 | 19 ± 21 | 724 ± 116* |
| | 5 | 82 ± 6 | 76 ± 13 | 77 ± 15* | 72 ± 9 | 82 ± 16* | 52 ± 31 | 49 ± 29 | 19 ± 20 | 794 ± 160* |
| | 6 | 76 ± 9 | 77 ± 15 | 78 ± 10* | 75 ± 6 | 73 ± 5* | 57 ± 34 | 46 ± 36 | 19 ± 20 | 785 ± 90* |
| | | 74 ± 14 | 72 ± 13 | 73 ± 10 | 70 ± 10 | 68 ± 16 | 57 ± 23 | 51 ± 31 | 21 ± 21 | 691 ± 84 |
| <i>p</i> value** | | 0.01 | <0.001 | 0.001 | 0.8 | 0.03 | 0.2 | 0.01 | <0.001 | 0.08 |
| <i>Post hoc</i> | W vs. F | 0.003 | <0.001 | 0.001 | | 0.6 | | 0.003 | <0.001 | |
| | W vs. V | 0.008 | <0.001 | 0.001 | | 0.03 | | 0.2 | <0.001 | |
| | F vs. V | 0.6 | 0.6 | 0.9 | | 0.2 | | 0.3 | 0.9 | |

Swallow number (SW#) is expressed as 1 to *n*; condition means and SD are represented in bold below each condition; ANOVA *p*-values and significant post hoc tests are expressed at the bottom; significant short-term facilitation is expressed as a * to the right of the swallow measure. *Facilitation analysis: significant change compared to the first swallow in the series, **Significant change by condition. Significant if *p* < 0.05; significant values are bolded.

TABLE 2 | Pearson correlations comparing EMG amplitudes (% maximum) and the total swallow duration (ms).

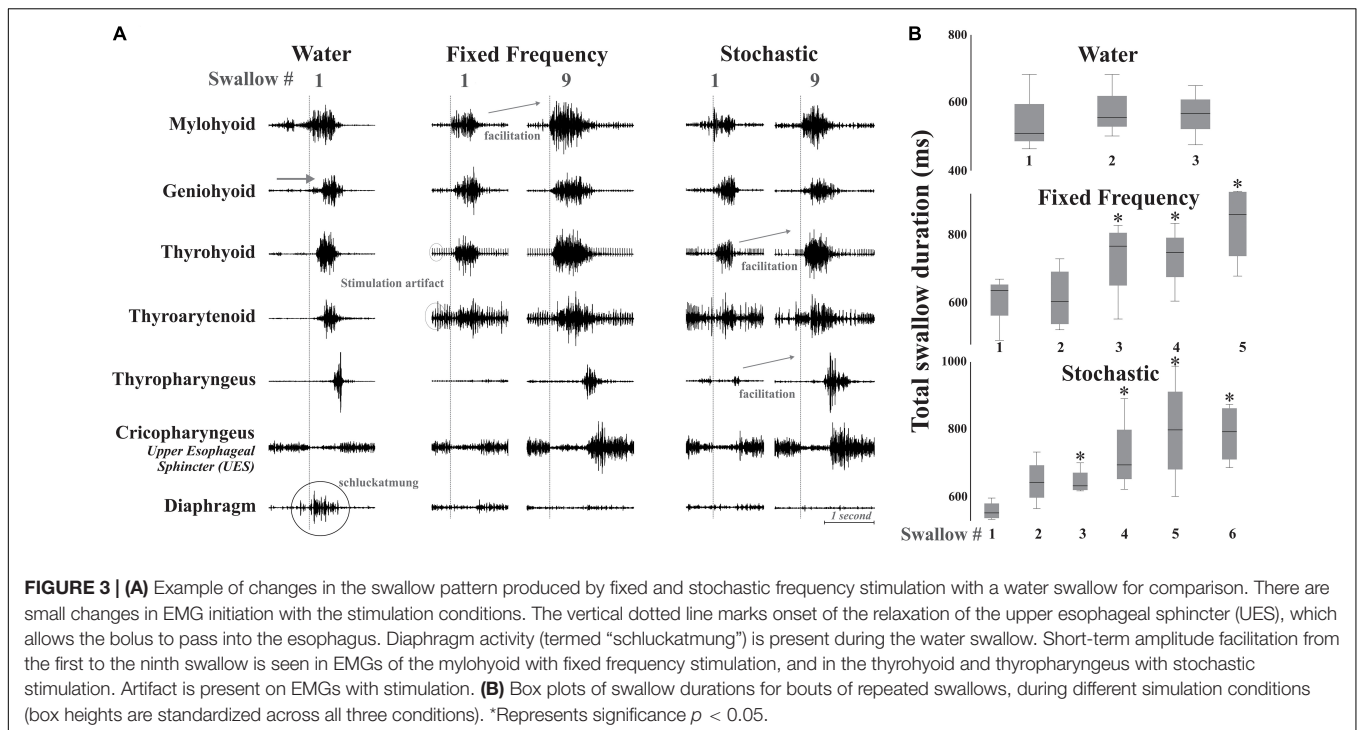
| | MyHy | GeHy | ThHy | ThAr | ThPh | UES | PS | Cos Dia | Duration |
|---------|------|-------------|-------------|------|-------|-------|-------------|-------------|-------------|
| MyHy | | 0.48 | 0.48 | 0.13 | 0.27 | 0.01 | −0.17 | −0.22 | 0.33 |
| GeHy | | | 0.39 | 0.09 | −0.06 | 0.01 | −0.24 | −0.39 | 0.57 |
| ThHy | | | | 0.27 | 0.12 | −0.11 | −0.32 | −0.38 | 0.29 |
| ThAr | | | | | −0.15 | −0.16 | −0.17 | −0.1 | 0.15 |
| ThPh | | | | | | −0.04 | −0.2 | −0.33 | 0.01 |
| UES | | | | | | | 0.54 | 0.49 | 0.09 |
| PS | | | | | | | | 0.61 | −1.7 |
| Cos Dia | | | | | | | | | 0.22 |

All data were pooled across the three conditions: water, fixed and stochastic electrical stimulation. Moderately strong relationships (in bold) are present among the upper airway muscles (geniohyoid and thyrohyoid with the mylohyoid) and among the inspiratory muscles (parasternal and costal diaphragm) with the upper esophageal sphincter. [MyHy = mylohyoid; GeHy = geniohyoid; ThHy = thyrohyoid; ThPh = thyropharyngeus; UES = upper esophageal sphincter (aka cricopharyngeus); PS = parasternal; Cos Dia = costal diaphragm; and Duration = total swallow duration in ms].



amplitudes, and an increase in number of swallows produced. Beyak et al. (1997) demonstrated that an increase in fixed stimulation frequency shortened latency and increased swallow number. Our data suggest that adding variance to the electrical stimulation signal works similarly, and maintains the overall

stimulation delivered. The variance (i.e., noise) in an electrical signal has been shown to both increase information content of a signal and increase detection of a weak signal in sensory systems (Moss et al., 2004). Potential applications that have been explored could include stabilizing breathing (Paydarfar et al., 1986, 2006)



and the suck-swallow patterns (Finan and Barlow, 1998) in pre-term infants, and in decreasing tremor and bradykinesia in parkinsonian patients and rats using deep brain stimulation (Grill et al., 2001; Brocker et al., 2017). Historically, studies in deglutition have used only fixed frequency stimulation between 5 and 30 Hz, with a range of 20–30 Hz optimally evoking rapid continuous swallow with short latencies and low threshold periods (Bieger et al., 1977; Kessler and Jean, 1985; Ezure et al., 1993; Oku et al., 1994; Ootani et al., 1995; Sang and Goyal, 2001; Kitagawa et al., 2009). In the current study, we chose the parameters to stimulate at a 20 Hz fixed frequency or with a stochastic pattern where the average was around 20 Hz using a custom electrical stimulator which appeared to add a sufficient amount of “noise” to the signal without degrading the sensory input.

In clinical dysphagia therapy, surface electrical stimulation (i.e., NMES) uses an 80 Hz fixed frequency (Poorjavat et al., 2014), and has been successful in short term sessions (Humbert et al., 2006; Ludlow et al., 2007), but has been unsuccessful for long term therapeutic uses (Carnaby-Mann and Crary, 2007; Shaw et al., 2007; Bülow et al., 2008; Bogaardt et al., 2009; Christiaanse et al., 2011). While the voltage and intensity of the stimulus have been scrutinized, the frequency parameters have not. We believe that the current study is the first of many that are needed to begin testing and optimizing alterations in stimulation frequency for effective swallow manipulation.

Diaphragm Activity During Swallow

Our recent work has extended the hypothesis that the swallow pattern generator activates motoneuron pools in the spinal cord for contraction of diaphragm and parasternal muscles (Spearman et al., 2014; Pitts et al., 2015a,b). This component of the swallow

pattern has been described by research groups since the 1800's, however, there have been very few studies in the modern era. Rosenthal (1861) was the first to report on the diaphragm contractions during SLN stimulation, and Arloing (1874) was the first to provide substantial evidence that these contractions form an active part of the swallow pattern by creating a negative deflection. The field termed this activity *schluckatmung*: a German word meaning “swallow-breath”. While this may not be the optimal term to describe this activity, it has continued to be used in the ensuing literature, for example Marckwald (1888) and Bosma (1957), Forester and colleagues (Feroah et al., 2002a,b; Bonis et al., 2011). In recent years, inspiratory motor drive during swallow has been reported in humans (Wilson et al., 1981; Hardemark Cedborg et al., 2009) and animals (Gestreau et al., 1996; Bonis et al., 2011). Previous work by our group showed that parasternal activity could be modulated through varying swallow stimuli, and that mechanical stimulation of the oropharyngeal wall produced parasternal EMG contractions with increased amplitude and duration (Spearman et al., 2014).

Our hypothesis is that breathing and swallow both involve an aspiration pump: they use negative pressure to “suck” air/bolus into the thoracic cavity (swallow also has significant positive pressure from above the bolus). This is consistent with McConnel's theory of the “hypopharyngeal suction pump” although we hypothesize this pressure is created by inspiratory muscle activation instead of laryngeal elevation (McConnel et al., 1987, 1988a,b,c,d; McConnel, 1988). Our current results demonstrating that electrical SLN stimulation depresses diaphragm activity during swallow reveal why this was previously regarded as a non-existent and/or un-remarkable portion of the swallow pattern, as it would not have been apparent to most investigators using those common experimental conditions.

This effect also mirrors what has been observed in the field of respiratory control. Bellingham and colleagues (Bellingham et al., 1989) were the first to demonstrate that SLN stimulation induced central apnea via a chloride-dependent oligo-synaptic pathway which hyperpolarizes phrenic motoneurons. More recently, Pilowsky and colleagues (Sun et al., 2011) demonstrated further effects in the core respiratory CPG by activation of expiratory-decrementing neurons in the ventral respiratory group, which in turn inhibit initiation of inspiration. However, we have demonstrated that using water as a stimulus for swallow can result in swallow occurrence across all phases of respiration (Pitts et al., 2013, 2015b; Spearman et al., 2014). We also previously reported that, in a non-paralyzed freely breathing animal with water as the stimulus, 16 of 18 inspiratory cells in the NTS were active during swallow and 7 of these increased their firing frequency (Pitts et al., 2018). We theorize that, while SLN stimulation does produce repetitive swallow, it may also through a secondary mechanism produce apnea (or inhibition of inspiratory neuronal activity).

Facilitation of Upper Airway Muscles

Short-term plasticity of excitatory synapses has been extensively studied in both invertebrates and vertebrates (Atwood and Karunanithi, 2002; Pan and Zucker, 2009). It is characterized by an enhancement of synaptic transmission after a prolonged period of stimulation, and can affect the function of neural circuitry. Potential mechanisms of short-term synaptic enhancement in swallow were elegantly explained in the recent paper by Horton et al. (2018). They propose that, because of the importance of the nucleus tractus solitarius (NTS) in the swallow motor pathway, several mechanisms could be involved, including glutamatergic axon terminals (Fortin et al., 1992), activation of N-methyl-D-aspartate receptors within the NTS (England et al., 1992), and neurotransmitters such as nicotine (Kalappa et al., 2011), serotonin, and/or glutamate (Bieger, 1981; Hashim and Bieger, 1987). The results from the current study also suggest that facilitation is present or modulated downstream from the NTS. Our selection of EMGs allows analysis of muscles that are innervated by the same cranial nerve(s). For example, geniohyoid and thyrohyoid are both innervated by the hypoglossal nerve via the first cervical root. While both had significant increases in EMG amplitude during SLN stimulation compared to water (geniohyoid by ~200% and thyrohyoid by 137%), the thyrohyoid also demonstrated short-term facilitation throughout the swallow series during variable stimulation (**Figure 1**). Of all the upper airway muscles measured, geniohyoid showed the greatest change in amplitude with SLN stimulation. Interestingly, in the decerebrate pig studies, geniohyoid was the only muscle that showed consistent modulation during swallow in the presence vs absence of natural background rhythmic oral feeding movements (Thexton et al., 2007, 2009).

Along with Horton et al. (2018), our current results contradict the classic view that SLN stimulus-induced swallows have a strictly stereotypical motor action, and instead suggest that swallow is strongly shaped by frequency and location-dependent afferent information. Many modern studies also report significant variance in swallow amplitude. Doty

and Bosma (1956), observed intra-muscle and inter-animal electromyography (EMG) variability with swallow evoked by mechanical or electrical stimulation in dogs, cats, and monkeys. Although not directly indicated, irregular EMG activity was also reported in certain muscles when attempts were made to alter the temporal pattern of swallow (e.g., fixing hyoid, applying lingual traction, opening mouth, etc.). Studies by Thexton et al. (2007, 2009) demonstrated that contractions of certain swallow muscles are prone to increased variability due to the diversity of fiber types and the multiple functions they serve throughout different phases of swallow, and that a “switch” between activation of fiber types/functions can be provoked by a change in stimulus condition. In light of these findings, interpretation of swallow data obtained under SLN electrical stimulation conditions may need to be re-examined.

While electrical SLN stimulation does trigger swallow, those swallows are highly modified compared to those of a naturally induced behavior. From a clinical perspective, stimulation of the larynx is aberrant, as it would occur if food or liquid had entered the airway. Thus, the depression of diaphragm activity and increase in the upper airway muscle activation that we observed during SLN stimulation may act as protective mechanisms that would reduce negative pressure on the bolus, increase pharyngeal clearance, and therefore decrease further aspiration risk. This is important for interpretation of studies on swallow using reduced animal preparations.

Limitations of the Experimental Design

The greatest limitation of the experimental design was the use of anesthesia, and the consequent potential suppression of airway reflexes. This was chosen because, in anesthetized animals, continuous SLN stimulation inhibits breathing (Donnelly and Haddad, 1986). Our choice of experimental preparation allowed for a train of swallows to be produced without potential interference from the breathing central pattern generator. Although it is clear that conditional modulation of the swallow motor pattern is possible in decorticate animals (Thexton et al., 2007, 2009), the current results cannot be directly extrapolated to swallow function in awake animals, because anesthesia reduces cortical function. Additionally, we did not directly record from any muscles which are innervated by the hypoglossal motor nucleus, because the geniohyoid is innervated via a cervical root. While we do see pre-swallow oral behaviors in response to water infusion, we did not observe such behaviors with electrical SLN stimulation, and do not know how they would have influenced swallow under those conditions.

CONCLUSION

Electrical stimulation of the SLN produces trains of swallows with evidence of short-term facilitation of specific EMG amplitudes and swallow duration. When compared to the fixed frequency stimulus, stochastic stimulation increased the excitability of the swallow pattern generator without changing overall current delivered. SLN stimulation significantly depressed diaphragm

and parasternal (inspiratory muscles) activity during swallow, implicating involvement of spinal pathways.

DATA AVAILABILITY STATEMENT

The datasets generated for this study are available on request to the corresponding author.

ETHICS STATEMENT

The animal study was reviewed and approved by the University of Louisville IACUC.

AUTHOR CONTRIBUTIONS

TS, MM, IP, WD, KM, DB, and TP conceptualized and designed the data. SK, TS, MM, AH, MR, IP, DH, KM, DB, KI, and TP

acquired, analyzed, and/or interpreted the data. SK, TS, MM, AF, MR, IP, DH, WD, KM, DB, KI, and TP drafted, revised, and/or approved the manuscript.

FUNDING

Supported by: NIH HL111215, NS110169, 1OT2OD023584, Craig H. Neilsen Foundation Pilot Research Grant 546714. The Kentucky Spinal Cord and Head Injury Trust, The Commonwealth of Kentucky Challenge for Excellence, the Rebecca F. Hammond Endowment, VEGA 1/0072/16, NSF award number 1762829, the Kentucky Spinal Cord and Head Injury Research Trust, and the Commonwealth of Kentucky Challenge for Excellence. Any opinions, findings and conclusions or recommendations expressed in this material are those of the author(s) and do not necessarily reflect the views of the sponsoring agency. The funders had no role in study design, data collection and analysis, decision to publish, or preparation of the manuscript.

REFERENCES

- Arloing, S. (1874). *Application de la Méthode Graphique à l'étude du Mécanisme de la Déglutition*. Available online at: <https://www.hachettebnf.fr/application-methode-graphique-letude-mecanisme-de-la-deglutition-chez-les-mammiferes-et-oiseaux> (accessed October 4, 2014).
- Atwood, H. L., and Karunanithi, S. (2002). Diversification of synaptic strength: presynaptic elements. *Nat. Rev. Neurosci.* 3, 497–516. doi: 10.1038/nrn876
- Basmajian, J., and Stecko, G. (1962). A new bipolar electrode for electromyography. *J. Appl. Physiol.* 17, 849–849. doi: 10.1152/jappl.1962.17.5.849
- Bautista, T. G., and Dutschmann, M. (2014). Ponto-medullary nuclei involved in the generation of sequential pharyngeal swallowing and concomitant protective laryngeal adduction in situ. *J. Physiol.* 592, 2605–2623. doi: 10.1113/jphysiol.2014.272468
- Bautista, T. G., Fong, A. Y., and Dutschmann, M. (2014). Spontaneous swallowing occurs during autoresuscitation in the in situ brainstem preparation of rat. *Respir. Physiol. Neurobiol.* 202, 35–43. doi: 10.1016/j.resp.2014.07.015
- Bellingham, M., Lipski, J., and Voss, M. (1989). Synaptic inhibition of phrenic motoneurons evoked by stimulation of the superior laryngeal nerve. *Brain Res.* 486, 391–395. doi: 10.1016/0006-8993(89)90530-1
- Beyak, M., Collman, P., Valdez, D., Xue, S., and Diamant, N. (1997). Superior laryngeal nerve stimulation in the cat: effect on oropharyngeal swallowing, oesophageal motility and lower oesophageal sphincter activity. *Neurogastroenterol. Motil.* 9, 117–127. doi: 10.1046/j.1365-2982.1997.d01-22.x
- Bieger, D. (1981). Role of bulbar serotonergic neurotransmission in the initiation of swallowing in the rat. *Neuropharmacology* 20, 1073–1083. doi: 10.1016/0028-3908(81)90099-x
- Bieger, D., Giles, S., and Hockman, C. (1977). Dopaminergic influences on swallowing. *Neuropharmacology* 16, 245–252. doi: 10.1016/0028-3908(77)90102-2
- Bonis, J., Neumueller, S., Marshall, B., Krause, K., Qian, B., Pan, L., et al. (2011). The effects of lesions in the dorsolateral pons on the coordination of swallowing and breathing in awake goats. *Respir. Physiol. Neurobiol.* 175, 272–282. doi: 10.1016/j.resp.2010.12.002
- Bosma, J. F. (1957). Deglutition: pharyngeal stage. *Physiol. Rev.* 37, 275–300. doi: 10.1152/physrev.1957.37.3.275
- Bradley, R. M., Stedman, H. M., and Mistretta, C. M. (1983). Superior laryngeal nerve response patterns to chemical stimulation of sheep epiglottis. *Brain Res.* 276, 81–93. doi: 10.1016/0006-8993(83)90550-4
- Brocker, D. T., Swan, B. D., So, R. Q., Turner, D. A., Gross, R. E., and Grill, W. M. (2017). Optimized temporal pattern of brain stimulation designed by computational evolution. *Sci. Transl. Med.* 9:eaa3532. doi: 10.1126/scitranslmed.aah3532
- Bogaardt, H., van Dam, D., Wever, N. M., Bruggeman, C., Koops, J., and Fokkens, W. (2009). Use of neuromuscular electrostimulation in the treatment of dysphagia in patients with multiple sclerosis. *Ann. Otol. Rhinol. Laryngol.* 118, 241–246. doi: 10.1177/000348940911800401
- Bülwö, M., Speyer, R., Baijens, L., Woisard, V., and Ekberg, O. (2008). Neuromuscular electrical stimulation (NMES) in stroke patients with oral and pharyngeal dysfunction. *Dysphagia* 23, 302–309. doi: 10.1007/s00455-007-9145-9
- Bushmann, M., Dobmeyer, S. M., Leeker, L., and Perlmuter, J. S. (1989). Swallowing abnormalities and their response to treatment in Parkinson's disease. *Neurology* 39, 1309–1314.
- Butler, S. G., Postma, G. N., and Fischer, E. (2004). Effects of viscosity, taste, and bolus volume on swallowing apnea duration of normal adults. *Otolaryngol. Head and Neck Surg.* 131, 860–863. doi: 10.1016/j.otohns.2004.06.006
- Carnaby-Mann, G. D., and Crary, M. A. (2007). Examining the evidence on neuromuscular electrical stimulation for swallowing: a meta-analysis. *Arch. Otolaryngol. Head Neck Surg.* 133, 564–571.
- Christiaanse, M. E., Mabe, B., Russell, G., Simeone, T. L., Fortunato, J., and Rubin, B. (2011). Neuromuscular electrical stimulation is no more effective than usual care for the treatment of primary dysphagia in children. *Pediatr. Pulmonol.* 46, 559–565. doi: 10.1002/ppul.21400
- Clave, P., Arreola, V., Romea, M., Medina, L., Palomera, E., and Serra-Prat, M. (2008). Accuracy of the volume-viscosity swallow test for clinical screening of oropharyngeal dysphagia and aspiration. *Clin. Nutr.* 27, 806–815. doi: 10.1016/j.clnu.2008.06.011
- Daniels, S. K., Corey, D. M., Hadskey, L. D., Legendre, C., Priestly, D. H., Rosenbek, J. C., et al. (2004). Mechanism of sequential swallowing during straw drinking in healthy young and older adults. *J. Speech and Hear. Res.* 47, 33–45. doi: 10.1044/1092-4388(2004)004
- Daniels, S. K., Schroeder, M. F., Degeorge, P. C., Corey, D. M., and Rosenbek, J. C. (2007). Effects of verbal cue on bolus flow during swallowing. *Am. J. Speech Lang. Pathol.* 16, 140–147. doi: 10.1044/1058-0360(2007)018
- DePippo, K. L., Holas, M. A., and Reding, M. J. (1992). Validation of the 3-oz water swallow test for aspiration following stroke. *Arch. Neurol.* 49, 1259–1261. doi: 10.1001/archneur.1992.00530360057018
- Dick, T., Oku, Y., Romaniuk, J., and Cherniack, N. (1993). Interaction between central pattern generators for breathing and swallowing in the cat. *J. Physiol.* 465, 715. doi: 10.1113/jphysiol.1993.sp019702

- Donnelly, D., and Haddad, G. (1986). Effect of graded anesthesia on laryngeal-induced central apnea. *Respir. Physiol.* 66, 235–245. doi: 10.1016/0034-5687(86)90076-9
- Doty, R. (1968). Neural organization of deglutition. *Handb. Physiol.* 4:6.
- Doty, R., and Bosma, J. (1956). An electromyographic analysis of reflex deglutition. *J. Neurophysiol.* 19, 44–60. doi: 10.1152/jn.1956.19.1.44
- England, S. J., Melton, J. E., Pace, P., and Neubauer, J. A. (1992). Nmda receptors mediate respiratory short-term potentiation in the nucleus-tractus-solitarius. *FASEB J.* 6, A1826–A1826.
- Ertekin, C., Kiyiloglu, N., Tarlaci, S., Keskin, A., and Aydogdu, I. (2000). Effect of mucosal anaesthesia on oropharyngeal swallowing. *Neurogastroenterol. Motil.* 12, 567–572. doi: 10.1046/j.1365-2982.2000.00232.x
- Ezure, K., Oku, Y., and Tanaka, I. (1993). Location and axonal projection of one type of swallowing interneurons in cat medulla. *Brain Res.* 632, 216–224. doi: 10.1016/0006-8993(93)91156-m
- Feroah, T. R., Forster, H., Fuentes, C. G., Lang, I. M., Beste, D., Martino, P., et al. (2002a). Effects of spontaneous swallows on breathing in awake goats. *J. Appl. Physiol.* 92, 1923–1935. doi: 10.1152/japplphysiol.01079.2000
- Feroah, T. R., Forster, H., Fuentes, C. G., Wenninger, J., Martino, P., Hodges, M., et al. (2002b). Contributions from rostral medullary nuclei to coordination of swallowing and breathing in awake goats. *J. Appl. Physiol.* 93, 581–591. doi: 10.1152/japplphysiol.01268.2001
- Finan, D. S., and Barlow, S. M. (1998). Intrinsic dynamics and mechanosensory modulation of non-nutritive sucking in human infants. *Early Hum. Dev.* 52, 181–197. doi: 10.1016/s0378-3782(98)00029-2
- Fortin, G., Velluti, J. C., Denavit-Saubie, M., and Champagnat, J. (1992). Responses to repetitive afferent activity of rat solitary complex neurons isolated in brainstem slices. *Neurosci. Lett.* 147, 89–92. doi: 10.1016/0304-3940(92)90781-2
- Gestreau, C., Grelot, L., and Bianchi, A. L. (2000). Activity of respiratory laryngeal motoneurons during fictive coughing and swallowing. *Exp. Brain Res.* 130, 27–34. doi: 10.1007/s002210050003
- Gestreau, C., Milano, S., Bianchi, A. L., and Grelot, L. (1996). Activity of dorsal respiratory group inspiratory neurons during laryngeal-induced fictive coughing and swallowing in decerebrate cats. *Exp. Brain Res.* 108, 247–256.
- Gia, P. (1958). [Superior laryngeal nerve & its role in deglutition]. *Fiziol. Zh. SSSR Im. I. M. Sechenova* 44, 141–147.
- Grill, W. M., Craggs, M. D., Foreman, R. D., Ludlow, C. L., and Buller, J. L. (2001). Emerging clinical applications of electrical stimulation: opportunities for restoration of function. *J. Rehabil. Res. Dev.* 38, 641–654.
- Hardemark Cedborg, A. I., Sundman, E., Boden, K., Hedstrom, H. W., Kuylenstierna, R., Ekberg, O., et al. (2009). Co-ordination of spontaneous swallowing with respiratory airflow and diaphragmatic and abdominal muscle activity in healthy adult humans. *Exp. Physiol.* 94, 459–468. doi: 10.1113/expphysiol.2008.045724
- Hashim, M. A., and Bieger, D. (1987). Excitatory action of 5-HT on deglutitive substrates in the rat solitary complex. *Brain Res. Bull.* 18, 355–363. doi: 10.1016/0361-9230(87)90013-x
- Hashimoto, K., Sugiyama, Y., Fuse, S., Umezaki, T., Oku, Y., Dutschmann, M., et al. (2019). Activity of swallowing-related neurons in the medulla in the perfused brainstem preparation in rats. *Laryngoscope* 129, E72–E79. doi: 10.1002/lary.27401
- Hiss, S. G., Treole, K., and Stuart, A. (2001). Effects of age, gender, bolus volume, and trial on swallowing apnea duration and swallow/respiratory phase relationships of normal adults. *Dysphagia* 16, 128–135. doi: 10.1007/s004550011001
- Horton, K. K., Segers, L. S., Nuding, S. C., O'Connor, R., Alencar, P. A., Davenport, P. W., et al. (2018). Central respiration and mechanical ventilation in the gating of swallow with breathing. *Front. Physiol.* 9:785. doi: 10.3389/fphys.2018.00785
- Huff, A., Day, T. A., English, M., Reed, M. D., Zouboules, S., Saran, G., et al. (2018). Swallow-breathing coordination during incremental ascent to altitude. *Respir. Physiol. Neurobiol.* 265, 121–126. doi: 10.1016/j.resp.2018.06.005
- Humbert, I. A., Fitzgerald, M. E., McLaren, D. G., Johnson, S., Porcaro, E., Kosmatka, K., et al. (2009). Neurophysiology of swallowing: effects of age and bolus type. *Neuroimage* 44, 982–991. doi: 10.1016/j.neuroimage.2008.10.012
- Humbert, I. A., Poletto, C. J., Saxon, K. G., Kearney, P. R., Crujido, L., Wright-Harp, W., et al. (2006). The effect of surface electrical stimulation on hyolaryngeal movement in normal individuals at rest and during swallowing. *J. Appl. Physiol.* 101, 1657. doi: 10.1152/japplphysiol.00348.2006
- Jafari, S., Prince, R. A., Kim, D. Y., and Paydarfar, D. (2003). Sensory regulation of swallowing and airway protection: a role for the internal superior laryngeal nerve in humans. *J. Physiol.* 550, 287–304. doi: 10.1113/jphysiol.2003.03.9966
- Jean, A. (2001). Brain stem control of swallowing: neuronal network and cellular mechanisms. *Physiol. Rev.* 81, 929–969. doi: 10.1152/physrev.2001.81.2.929
- Kahrilas, P. J., and Logemann, J. A. (1993). Volume accommodation during swallowing. *Dysphagia* 8, 259–265. doi: 10.1007/bf01354548
- Kalappa, B. I., Feng, L., Kem, W. R., Gusev, A. G., and Uteshev, V. V. (2011). Mechanisms of facilitation of synaptic glutamate release by nicotinic agonists in the nucleus of the solitary tract. *Am. J. Physiol. Cell Physiol.* 301, C347–C361. doi: 10.1152/ajpcell.00473.2010
- Kendall, K. A. (2002). Oropharyngeal swallowing variability. *Laryngoscope* 112, 547–551. doi: 10.1097/00005537-200203000-00025
- Kessler, J., and Jean, A. (1985). Identification of the medullary swallowing regions in the rat. *Exp. Brain Res.* 57, 256–263.
- Kitagawa, J., Nakagawa, K., Hasegawa, M., Iwakami, T., Shingai, T., Yamada, Y., et al. (2009). Facilitation of reflex swallowing from the pharynx and larynx. *J. Oral Sci.* 51, 167–171. doi: 10.2334/josn.51.167
- Kitagawa, J., Shingai, T., Takahashi, Y., and Yamada, Y. (2002). Pharyngeal branch of the glossopharyngeal nerve plays a major role in reflex swallowing from the pharynx. *Am. J. Physiol. Regul. Integr. Comp. Physiol.* 282, R1342–R1347.
- Ludlow, C. L., Humbert, I., Saxon, K., Poletto, C., Sonies, B., and Crujido, L. (2007). Effects of surface electrical stimulation both at rest and during swallowing in chronic pharyngeal dysphagia. *Dysphagia* 22, 1–10. doi: 10.1007/s00455-006-9029-4
- Marckwald, M. (1888). *The Movements of Respiration and their Innervation in the Rabbit*, trans. T. A. Haig (London: Blackie and Son).
- McConnel, F. M. (1988). Analysis of pressure generation and bolus transit during pharyngeal swallowing. *Laryngoscope* 98, 71–78.
- McConnel, F. M., Cerenko, D., Hersh, T., and Weil, L. J. (1988a). Evaluation of pharyngeal dysphagia with manofluorography. *Dysphagia* 2, 187–195. doi: 10.1007/bf02414425
- McConnel, F. M., Cerenko, D., Jackson, R. T., and Guffin, T. N. Jr. (1988b). Timing of major events of pharyngeal swallowing. *Arch. Otolaryngol. Head Neck Surg.* 114, 1413–1418. doi: 10.1001/archotol.1988.01860240063025
- McConnel, F. M., Cerenko, D., Jackson, R. T., and Hersh, T. (1988c). Clinical application of the manofluorogram. *Laryngoscope* 98, 705–711.
- McConnel, F. M., Cerenko, D., and Mendelsohn, M. S. (1988d). Manofluorographic analysis of swallowing. *Otolaryngol. Clin. North Am.* 21, 625–635.
- McConnel, F. M., Mendelsohn, M. S., and Logemann, J. A. (1987). Manofluorography of deglutition after supraglottic laryngectomy. *Head Neck Surg.* 9, 142–150. doi: 10.1002/hed.2890090303
- Miller, A. J. (1982). Deglutition. *Physiol. Rev.* 62, 129–184.
- Miller, F. R., and Scheeington, C. S. (1916). Some observations on the buccopharyngeal stage of reflex deglutition in the cat. *Q. J. Exp. Physiol.* 9, 147–186. doi: 10.1113/expphysiol.1915.sp000201
- Moss, F., Ward, L. M., and Sannita, W. G. (2004). Stochastic resonance and sensory information processing: a tutorial and review of application. *Clin. Neurophysiol.* 115, 267–281. doi: 10.1016/j.clinph.2003.09.014
- Oku, Y., Tanaka, I., and Ezure, K. (1994). Activity of bulbar respiratory neurons during fictive coughing and swallowing in the decerebrate cat. *J. Physiol.* 480, 309–324. doi: 10.1113/jphysiol.1994.sp020361
- Ootani, S., Umezaki, T., Shin, T., and Murata, Y. (1995). Convergence of afferents from the SLN and GPN in cat medullary swallowing neurons. *Brain Res. Bull.* 37, 397–404. doi: 10.1016/0361-9230(95)00018-6
- Pan, B., and Zucker, R. S. (2009). A general model of synaptic transmission and short-term plasticity. *Neuron* 62, 539–554. doi: 10.1016/j.neuron.2009.03.025
- Paydarfar, D., Eldridge, F. L., and Kiley, J. P. (1986). Resetting of mammalian respiratory rhythm: existence of a phase singularity. *Am. J. Physiol. Regul. Integr. Comp. Physiol.* 250, R721–R727.
- Paydarfar, D., Forger, D. B., and Clay, J. R. (2006). Noisy inputs and the induction of on-off switching behavior in a neuronal pacemaker. *J. Neurophysiol.* 96, 3338–3348. doi: 10.1152/jn.00486.2006

- Pitts, T., Gayagoy, A., Rose, M., Poliecek, I., Condrey, J., Musslewhite, M., et al. (2015a). Suppression of abdominal motor activity during swallowing in cats and humans. *PLoS One* 10:e0128245. doi: 10.1371/journal.pone.0128245
- Pitts, T., Poliecek, I., Rose, M. J., Reed, M. D., Condrey, J. A., Tsai, H.-W., et al. (2018). Neurons in the dorsomedial medulla contribute to swallow pattern generation: Evidence of inspiratory activity during swallow. *PLoS One* 13:e0199903. doi: 10.1371/journal.pone.0199903
- Pitts, T., Rose, M. J., Poliecek, I., Condrey, J., Davenport, P. W., and Bolser, D. C. (2015b). Effect of Laparotomy on the Swallow–Breathing Relationship in the Cat. *Lung* 193, 129–133. doi: 10.1007/s00408-014-9662-x
- Pitts, T., Rose, M. J., Mortensen, A. N., Poliecek, I., Sapienza, C. M., Lindsey, B. G., et al. (2013). Coordination of cough and swallow: a meta-behavioral response to aspiration. *Respir. Physiol. Neurobiol.* 189, 543–551. doi: 10.1016/j.resp.2013.08.009
- Pommerenke, W. T. (1928). A study of the sensory areas eliciting the swallow reflex. *Am. J. Physiol.* 84, 36–41. doi: 10.1152/ajplegacy.1928.84.1.36
- Poorjavad, M., Talebian Moghadam, S., Nakhoshtin Ansari, N., and Daemi, M. (2014). Surface electrical stimulation for treating swallowing disorders after stroke: A review of the stimulation intensity levels and the electrode placements. *Stroke research and treatment*
- Roda, F., Gestreau, C., and Bianchi, A. L. (2002). Discharge patterns of hypoglossal motoneurons during fictive breathing, coughing, and swallowing. *J. Neurophysiol.* 87, 1703–1711. doi: 10.1152/jn.00347.2001
- Rosenthal, J. (1861). De l'influence du nerf pneumogastrique et du nerf laryngé supérieur sur les mouvements du diaphragme. *C. R. Acad. Sci.* 52, 754–756.
- Sang, Q., and Goyal, R. K. (2001). Swallowing reflex and brain stem neurons activated by superior laryngeal nerve stimulation in the mouse. *Am. J. Physiol. Gastrointest. Liver Physiol.* 280, G191–G200.
- Shaw, G. Y., Sechtem, P. R., Searl, J., Keller, K., Rawi, T. A., and Dowdy, E. (2007). Transcutaneous neuromuscular electrical stimulation (VitalStim) curative therapy for severe dysphagia: myth or reality? *Ann. Otol. Rhinol. Laryngol.* 116, 36–44. doi: 10.1177/000348940711600107
- Spearman, D. G., Poliecek, I., Rose, M. J., Bolser, D. C., and Pitts, T. (2014). Variability of the pharyngeal phase of swallow in the cat. *PLoS One* 9:e106121. doi: 10.1371/journal.pone.0106121
- Storey, A. T. (1968). A functional analysis of sensory units innervating epiglottis and larynx. *Exp. Neurol.* 20, 366–383. doi: 10.1016/0014-4886(68)90080-0
- Sun, Q. J., Bautista, T. G., Berkowitz, R. G., Zhao, W. J., and Pilowsky, P. M. (2011). The temporal relationship between non-respiratory burst activity of expiratory laryngeal motoneurons and phrenic apnoea during stimulation of the superior laryngeal nerve in rat. *J. Physiol.* 589, 1819–1830. doi: 10.1113/jphysiol.2010.203794
- Thexton, A. J., Crompton, A. W., and German, R. Z. (2007). Electromyographic activity during the reflex pharyngeal swallow in the pig: Doty and Bosma (1956) revisited. *J. Appl. Physiol.* 102, 587–600. doi: 10.1152/japplphysiol.00456.2006
- Thexton, A. J., Crompton, A. W., Owerkowicz, T., and German, R. Z. (2009). Impact of rhythmic oral activity on the timing of muscle activation in the swallow of the decerebrate pig. *J. Neurophysiol.* 101, 1386–1393. doi: 10.1152/jn.90847.2008
- Troche, M. S., Sapienza, C. M., and Rosenbek, J. C. (2008). Effects of bolus consistency on timing and safety of swallow in patients with Parkinson's disease. *Dysphagia* 23, 26–32. doi: 10.1007/s00455-007-9090-7
- Wilson, S. L., Thach, B. T., Brouillette, R. T., and Abu-Osba, Y. K. (1981). Coordination of breathing and swallowing in human infants. *J. Appl. Physiol. Respir. Environ. Exerc. Physiol.* 50, 851–858. doi: 10.1152/jappl.1981.50.4.851
- Yamamura, K., Kitagawa, J., Kurose, M., Sugino, S., Takatsuji, H., Mostafaezur, R. M., et al. (2010). Neural mechanisms of swallowing and effects of taste and other stimuli on swallow initiation. *Biol. Pharm. Bull.* 33, 1786–1790. doi: 10.1248/bpb.33.1786

Conflict of Interest: The authors declare that the research was conducted in the absence of any commercial or financial relationships that could be construed as a potential conflict of interest.

Copyright © 2020 King, Shen, Musselwhite, Huff, Reed, Poliecek, Howland, Dixon, Morris, Bolser, Iceman and Pitts. This is an open-access article distributed under the terms of the Creative Commons Attribution License (CC BY). The use, distribution or reproduction in other forums is permitted, provided the original author(s) and the copyright owner(s) are credited and that the original publication in this journal is cited, in accordance with accepted academic practice. No use, distribution or reproduction is permitted which does not comply with these terms.



Characterizing Motor Control of Mastication With Soft Actor-Critic

Amir H. Abdi^{1*}, Benedikt Sagl², Venkata P. Srungarapu¹, Ian Stavness³, Eitan Prisman⁴, Purang Abolmaesumi¹ and Sidney Fels¹

¹ Electrical and Computer Engineering Department, University of British Columbia, Vancouver, BC, Canada, ² Department of Prosthodontics, University Clinic of Dentistry, Medical University of Vienna, Vienna, Austria, ³ Department of Computer Science, University of Saskatchewan, Saskatoon, SK, Canada, ⁴ Department of Surgery, University of British Columbia, Vancouver, BC, Canada

OPEN ACCESS

Edited by:

Teresa Lever,
University of Missouri, United States

Reviewed by:

Elmar Rueckert,
University of Lübeck, Germany
Greg Murray,
University of Sydney, Australia

*Correspondence:

Amir H. Abdi
amirabdi@ece.ubc.ca

Specialty section:

This article was submitted to
Motor Neuroscience,
a section of the journal
Frontiers in Human Neuroscience

Received: 01 January 2020

Accepted: 27 April 2020

Published: 26 May 2020

Citation:

Abdi AH, Sagl B, Srungarapu VP,
Stavness I, Prisman E,
Abolmaesumi P and Fels S (2020)
Characterizing Motor Control of
Mastication With Soft Actor-Critic.
Front. Hum. Neurosci. 14:188.
doi: 10.3389/fnhum.2020.00188

The human masticatory system is a complex functional unit characterized by a multitude of skeletal components, muscles, soft tissues, and teeth. Muscle activation dynamics cannot be directly measured on live human subjects due to ethical, safety, and accessibility limitations. Therefore, estimation of muscle activations and their resultant forces is a longstanding and active area of research. Reinforcement learning (RL) is an adaptive learning strategy which is inspired by the behavioral psychology and enables an agent to learn the dynamics of an unknown system via policy-driven explorations. The RL framework is a well-formulated closed-loop system where high capacity neural networks are trained with the feedback mechanism of rewards to learn relatively complex actuation patterns. In this work, we are building on a deep RL algorithm, known as the Soft Actor-Critic, to learn the inverse dynamics of a simulated masticatory system, i.e., learn the activation patterns that drive the jaw to its desired location. The outcome of the proposed training procedure is a parametric neural model which acts as the brain of the biomechanical system. We demonstrate the model's ability to navigate the feasible three-dimensional (3D) envelope of motion with sub-millimeter accuracies. We also introduce a performance analysis platform consisting of a set of quantitative metrics to assess the functionalities of a given simulated masticatory system. This platform assesses the range of motion, metabolic efficiency, the agility of motion, the symmetry of activations, and the accuracy of reaching the desired target positions. We demonstrate how the model learns more metabolically efficient policies by integrating a force regularization term in the RL reward. We also demonstrate the inverse correlation between the metabolic efficiency of the models and their agility and range of motion. The presented masticatory model and the proposed RL training mechanism are valuable tools for the analysis of mastication and other biomechanical systems. We see this framework's potential in facilitating the functional analyses aspects of surgical treatment planning and predicting the rehabilitation performance in post-operative subjects.

Keywords: mastication modeling, reinforcement learning, soft actor-critic, inverse dynamics, jaw, motor control, musculoskeletal modeling, computational biomechanics

1. INTRODUCTION

The stomatognathic or masticatory system is one of the most complex functional units in the human body. It is characterized by a multitude of skeletal components, teeth, soft tissues, muscles, tendons, ligaments, and fibrous disks. The mandible is at the heart of this complex and is connected to the skull via the mandibular condyles. The condyles of the mandible are located inside the glenoid fossa of the temporal bone and the collective of them forms the temporomandibular joint (TMJ), hence the name. The TMJ is a ginglymoarthrodial joint and enables the mandible to exhibit rotational and translational movements constrained by the passive tensions of the ligaments, muscles, and other passive factors (Gallo et al., 2000). Two TMJs form a functional masticatory system which enables the mandible to rotate and translate with six degrees of freedom across its limited domain of motion (Drake et al., 2014). The TMJs are among the most utilized joints in the human body and play an essential role in chewing and speaking functions.

During mastication, like any other biomechanical routine, a set of time-varying neural and muscular activations work in unison to enable kinematics. Motor control is a highly complex process that involves the nervous and musculoskeletal systems. The peripheral neurons innervate the muscles. Upon excitation of the neural pathways, the skeletal muscles are activated which generate forces to actuate the joints. Neural excitation patterns and, in turn, the muscle activation trajectories are often unknown.

An electromyograph is a highly sensitive voltmeter that detects the electric potential from the transmembrane current of the muscle fibers and a common research tool in many disciplines. The intramuscular electromyography examination (iEMG), which requires placement of small needles into several muscles to record their electrical activity, is an invasive procedure and is known to cause discomfort for the subject. If a robust electrode contact with the skin is feasible, electrical activities of shallow muscles can be, to some extent, captured via the non-invasive and convenient method of surface EMG (sEMG). However, sEMG suffers from a higher rate of crosstalk, i.e., misleading signals coming from adjacent muscles (Farina et al., 2004). Clearly, not every muscle is accessible for neither sEMG nor iEMG examination. Moreover, there are many concerns regarding the applicability, reliability, sensitivity, and reproducibility of EMG measurements (Vigotsky et al., 2018). Different segments of the same muscle do not generate consistent electrical signals (Ahamed et al., 2014), and the relationship between the recorded EMG signals and the generated muscle forces is deemed complex (Al Harrach et al., 2017). Due to the safety, ethical, and technical limitations of *in vivo* studies and limited accessibility to deep muscles and peripheral neurons, muscle dynamics cannot be directly measured on live human subjects. Therefore, the estimation of muscle activations and the resultant forces is a longstanding and active area of research. Computational biomechanics is considered, to a limited extent, as one of the few possibilities to understand the neural and muscular activation patterns of humans (Erdemir et al., 2007).

Building controllers for musculoskeletal systems is a challenging task as they are inherently underdetermined due to the disparity between the degrees of freedom of the rigid bodies and the number of skeletal muscles (Lee et al., 2014). The masticatory system is also shown, in theory, to be mechanically redundant; therefore, multiple muscle activation patterns can generate similar motion trajectories and bite forces (Osborn, 1996). This redundancy often results in non-unique solutions for the inverse dynamics problem. In computational modeling and computer animation, the joint torques and muscle excitations are estimated so that the model follows a given motion trajectory while, possibly, considering external forces. In the prior works, the inverse dynamics challenge has been tackled with numerical solvers which have either a static or dynamic viewpoint to the optimization problem.

In the static approach, the problem is solved for each timestep with the most likely set of activations which drive the model closer to the desired trajectory (Otten, 2003). Static optimization has been a popular choice in biomechanics thanks to its simplicity (Seireg and Arvikar, 1975; Pedersen et al., 1997; Thelen et al., 2003). The low computational costs of static solvers have extended their application to complex three-dimensional many-muscle models (Lee et al., 2014). However, this formulation is sensitive to the given trajectory and often results in non-smooth outcomes. An extension to the static optimization is the forward-dynamics assisted tracking where consecutive steps are collectively considered for temporal consistency. This allows for the inclusion of muscle contraction dynamics as a regularization factor to reduce sensitivity to the input kinematics (Erdemir et al., 2007). Dynamic optimization stands on the other end of the spectrum and considers muscle forces, among other performance criteria, as time-dependent variables. It optimizes an integral cost function to address a subset of the mentioned challenges (Anderson and Pandy, 1999, 2001). Even though inverse dynamic solvers are fairly straightforward, they have certain limitations including the inconsistencies between the measured external forces and the body kinematics (Faber et al., 2018), the need to solve complex differential equations, and many more (Kuo, 1998; Hatze, 2002; Fluit et al., 2014). When it comes to choosing solvers, there is always the trade-off between the accuracy and the computational cost. More importantly, any inverse dynamics solution inherently relies on the availability of motion trajectories as inputs; however, kinematics are not often easy to obtain from human and animal subjects and are susceptible to the sensor noise.

Reinforcement learning (RL) is an adaptive control strategy inspired by behavioral psychology where organisms' actions are encouraged or averted through antecedent stimuli. The RL paradigm is very similar to the habit development processes in the basal ganglia of the brain and it is suggested that understanding the RL-based control strategies is helpful in the analysis of human behavior (Yin and Knowlton, 2006). With the rise of deep learning and its integration into the RL framework, unprecedented solutions for control and decision making problems were introduced (Mnih et al., 2013). A deep reinforcement learning (Deep RL) solution is essentially a well-formulated closed-loop system where high capacity neural

networks are trained with the feedback mechanism of rewards to learn relatively complex actuation patterns. RL solutions are shown to scale well to high-dimensional state and action spaces for biomechanical control (Abdi et al., 2019a).

The main challenge when using RL solutions for motor control is to design a training algorithm, without much knowledge of the systems' dynamics, which teaches the agent to carry out complex musculoskeletal tasks and maximize a delayed reward signal. In computer graphics, where models are not muscle driven and their validity is not an issue, RL is used to teach agents to mimic locomotion tasks (Peng et al., 2018). In biomechanics, some RL-based solutions have been introduced for the motor control tasks either via muscle activations (Abdi et al., 2019b) or joint activations (Clegg et al., 2018). In human locomotion, most works have focused on arm movement (Golghou et al., 2005; Jagodnik et al., 2016) and gait control (Peng et al., 2017; Kidziński et al., 2018; Jiang et al., 2019). Recent interdisciplinary collaborations have helped to bridge the gap between reinforcement learning and motor control in biomechanics using the OpenSim and ArtiSynth modeling environments (Kidziński et al., 2018; Abdi et al., 2019a). These efforts gained more traction after the "learning to run" challenge of NeurIPS 2017 where variants of the policy gradient family of controllers were implemented to generate gait patterns (Kidziński et al., 2018).

In this work, we are demonstrating our deep reinforcement learning approach toward learning the neural excitation patterns of mastication. We implemented the Soft Actor-Critic (SAC) reinforcement learning algorithm with a domain-engineered reward function to teach the RL policy how to move the jaw in its 3D Posselt envelope of motion. To address the underdetermined nature of the system, we encourage the agent to minimize the generated muscle forces to reduce the metabolic energy expenditure. The outcome of the proposed training process is a parametric model that acts as the brain of the biomechanical system. Our contributions are 4-fold. Firstly, we design a physiologically accurate jaw model, based on the works of Sagl et al. (2019b), with a new take on the TMJ modeling suited for the computationally demanding training process of reinforcement learning. Secondly, we demonstrate the feasibility of training a neural network to estimate the efficient excitation patterns to drive the jaw model in its domain of motion. Thirdly, we conduct experiments to show the sensitivity of the model to the coefficients of the reward function. We also demonstrate how the model's neural excitations match the expected physiological patterns during standard jaw movements. Lastly, we introduce an analytical framework consisting of a set of quantitative metrics to assess the functional performance of a given masticatory system and report on the performance of different models.

2. MATERIALS AND METHODS

2.1. Data Acquisition

The biomechanical model used in this study is constructed based on the clinical data of a healthy male 30-years-old volunteer at the Medical University of Vienna. A single full-skull CT scan was acquired from the participant in the closed-mouth position to model the bony structures (Siemens Sensation 4). The in-slice

resolution of the scan was 0.3×0.3 mm with a slice thickness of 0.5 mm. A full-skull 3D MRI scan was also acquired to model the origin and insertion points of the masticatory muscles (Siemens Magnetom Prisma 3T with a 64-channel head coil). A coronal Double Echo Steady State T1-weighted sequence with water excitation was used for image acquisition, covering the maxillofacial region down to the shoulders. The resolution of the MRI scan was 0.3×0.3 mm with a slice thickness of 0.5 mm. Further details of the data acquisition process are discussed in a prior publication of our team (Sagl et al., 2019a).

Given the central role that teeth play in the masticatory system, and in order to obtain high-resolution dental surfaces, physical plaster models (dental casts) of the subject's dentition were created with Gypsum Stone IV. The dental casts were then digitized with an optical scanner (Ceramill map 400) with 3D accuracy of smaller than $20 \mu\text{m}$. The dental segment of the upper and lower jaws obtained from the CT scan was then replaced with the high-resolution 3D optical scans of the dentitions.

2.2. Modeling

We used the open-source mechanical modeling platform, ArtiSynth¹, to implement the 3D biomechanical model of the subject. The model used in this study is based on the validated model of Sagl et al. (2019b), with some alterations in the TMJs and the occlusal surfaces to lower the computational cost. This model consists of three rigid bodies: jaw, skull, and the hyoid bone. To speed up the training, the model is simplified with the fixed hyoid bone assumption. To make up for the loss in the range of mouth opening, the hyoid bone is moved about 10 mm inferiorly according to the values reported by Muto and Kanazawa (1994). The forward simulation steps are computed with the semi-implicit backward Euler method. For stability reasons, small timesteps of 0.001 s are used by the integrator across experiments.

Teeth are assumed to be rigidly attached to the mandible and the collective of them is referred to as the jaw rigid body with an estimated mass of 200 g (Langenbach and Hannam, 1999). The moment of inertia of the jaw is calculated based on its 3D geometry with the uniform density assumption.

2.2.1. Masticatory Muscles

Muscles are modeled as point-to-point Hill-type springs which provide a practical formulation of the muscle contraction mechanism (Hill, 1953). Considering the challenges with the estimation of tissue's biomechanical properties (Blümel et al., 2012), here, muscles' cross-sectional areas, length-tension function, and velocity-tension function are based on the parameters reported in the literature (Langenbach and Hannam, 1999; Peck et al., 2000; Hannam et al., 2008). Each modeled point-to-point muscle resembles a spring that only applies forces along its main axis. While we acknowledge the over-simplifying assumptions with the Hill-type point-to-point muscles, the designed model competes with other masticatory models in complexity, details, and biomechanically relevant intricacies (Koolstra and van Eijden, 2005; Choy et al., 2017).

¹www.artisynth.org

Large muscles (e.g., temporalis) and those with multiple heads (e.g., masseter and lateral pterygoid) are modeled with multiple actuators. One exciter is assigned to each point-to-point actuator. An exciter is the counterpart of the motor axons that innervate the skeletal muscle. In response to the neural excitation, the muscle contracts according to the Hill-type model's function along the muscle compartment's longitudinal axis. This process is referred to as the excitation-contraction coupling. All neural excitations are parameterized as the normalized ratios of their maximal activation in the 0 to 1 range.

The modeled masticatory system has 24 actuators and 24 associated exciters (12 on each side) associated with the following muscles: temporalis (3 actuators), lateral pterygoid (2 actuators), masseter (2 actuators), medial pterygoid, anterior digastric, geniohyoid, and mylohyoid (2 actuators on each side). All exciters are assumed to be disjoint, allowing for any excitation pattern to be deemed feasible. The muscle bundles and their exciters are demonstrated in **Figures 1A,B**.

2.2.2. Temporomandibular Joint

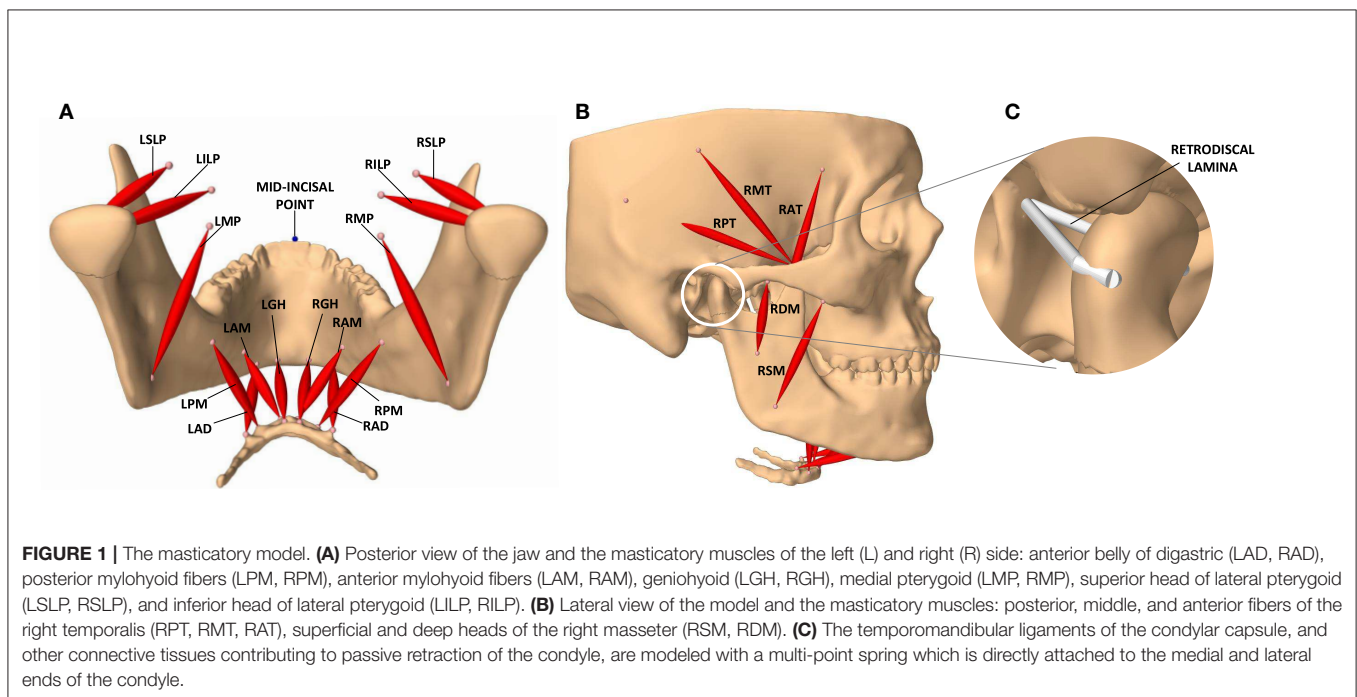
The 3D shape of the condyles and the mandibular fossae (glenoid fossae) are obtained from the CT scan. Given the high computational cost of finite element methods, and in order to speed up the computationally demanding process of reinforcement training, the condylar disks are excluded from the current jaw model. The forward and downward movement of the condyle is guided by a curved bilateral planar constraint mimicking the articular eminence's role during jaw opening. In absence of the condylar disc, and following the original design (Sagl et al., 2019b), the articular cartilage is modeled as an elastic foundation contact model with a thickness of 0.45 mm (Hansson et al., 1977). Based on the available literature, the Young's modulus and Poisson ratio of the elastic foundation

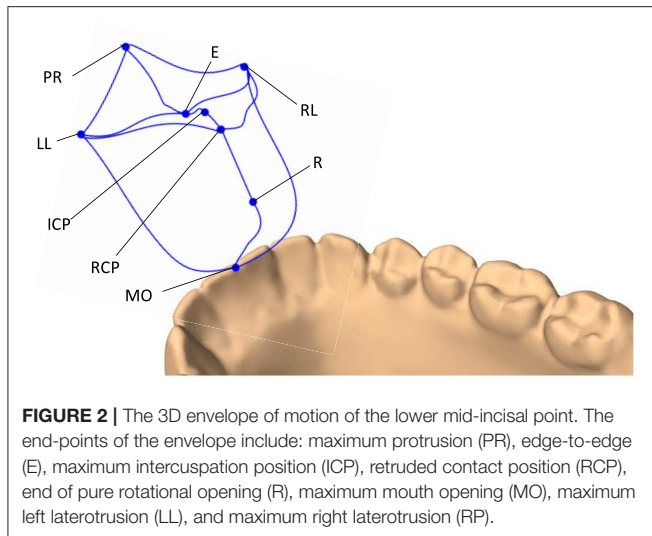
are set to 2.7 MPa and 0.49, respectively (Koolstra and van Eijden, 2005). For a fast and stable simulation, the elastic foundation is computed with the constraint regularization method of Servin et al. (2006).

The retrodiscal tissues, superior retrodiscal lamina, and the temporomandibular ligaments of the condylar capsule are modeled with a multi-point spring. This multi-point spring resembles a passive ligament which is wrapped around the condyle and connects its medial and lateral ends to the back of the mandibular fossa and the tympanic plate (**Figure 1C**). The ligaments grant passive stability to the TMJ. They are designed with a slack length of 7.5 mm longer than the closed jaw position. The Young's modulus of the ligaments is set to 2.45 MPa based on the recent work of Coombs et al. (2017) on the retrodiscal tissue. This design constrains the motion of the condyles inside the mandibular fossae, counters the forward pull of the superior head of the lateral pterygoid, and facilitates the posterior rotation of the condylar neck during jaw closure. It also allows the condyle to slightly reach beyond the summit of the articular eminence at its full stretch during mouth opening which matches that of a healthy subject (Muto et al., 1994).

2.3. 3D Envelope of Motion

The 3D envelope of motion was estimated through manual activation of the masticatory muscles in the simulation environment. To calculate the 3D envelope of the current model, a trained dentist used the graphical user interface of the simulation environment to set the excitation levels of the masticatory muscles and drive the jaw to the extremities. The excitations were slowly updated to move the jaw from one end-point to another and the 3D position of the lower mid-incisal point was tracked in between the boundary end-points.





The end-points of the envelope were decided based on the works of Posselt (1952) and Koolstra et al. (2001). The following jaw positions were used to form the 3D envelope of motion: maximum intercuspation position (ICP), edge-to-edge (E), maximum protrusion (PR), maximum left and right laterotrusion (LL and RL), retruded contact position (RCP), end of the pure rotational opening (R), and maximum mouth opening (MO). The trajectories of the boundary movements of the lower mid-incisal point are visualized in **Figure 2**.

The 3D envelope of motion is important for this research in three capacities. Firstly, the fact that the simulated 3D envelope of motion resembles that of Posselt's attests the validity of the designed jaw model for the current application. Secondly, it defines the feasible space of motion for the jaw which is necessary for the RL training of the model. Lastly, it defines the optimum motion domain of the non-pathological jaw which acts as a reference for further evaluation of the learned control policies (see section 4).

3. MOTOR CONTROL WITH SOFT ACTOR-CRITIC

In reinforcement learning, we often seek to train a policy, π , which maximizes the expected sum of the future rewards (J). A policy is simply a mapping from the state space to the action space, i.e., it tells the agent what to do at each situation. This is analogous to the brain's functionality in live subjects. The policy can be a deterministic mapping function or a probabilistic distribution over the possible set of actions. The optimal policy (π^*) is the one that achieves the maximum rewards and is defined as

$$\pi^* = \arg \max_{\pi} J(\pi), \quad (1)$$

$$J(\pi) = \mathbb{E}_{a_t \sim \pi(\cdot|s_t)} \left[\sum_t \gamma^t r(s_t, a_t) \right], \quad (2)$$

where a_t and s_t denote the action and the state at time t , respectively. In the jaw model, actions are the changes in the neural excitations. Here, γ is the factor that discounts the value of future rewards, i.e., near future rewards are worth more than far future rewards. As mentioned earlier, $J(\pi)$ is the expected sum of future rewards for the policy π , and $r(\cdot)$ is the reward function that determines the bonus or penalty associated with actions and state-transitions. The reward function to train the motor control of the jaw model is discussed in section 3.2.

The state-transitions (dynamics model), reward function, and the optimum trajectory to the desired goal are all unknown to the agent in the beginning. It is then the agent's responsibility to interact with the environment and gather information. In reinforcement learning, the agent switches between two strategies to learn about its space, namely, exploration and exploitation. When the agent keeps on pursuing what he believes to be the optimum solution, it is exploiting its learned policy. On the other hand, exploration is when the agent decides to try something new which is not in line with its learned policy. An RL algorithm should maintain a balance between its exploration and exploitation strategies for efficient training.

Different RL algorithms have different takes on how to search for the optimum policy. The Soft Actor-Critic (SAC) algorithm belongs to the family of model-free reinforcement learning. It is an off-policy solution that forms a bridge between stochastic policy optimization and deterministic policy gradient algorithms (Haarnoja et al., 2018a,b). Unlike its many alternatives, SAC is considered to be relatively insensitive to its hyper-parameters which makes it an intriguing option for our current biomechanical modeling setting.

The SAC algorithm contains an entropy term to improve the agent's exploration. The agent is rewarded with respect to the entropy (\mathcal{H}) of its learned policy which discourages a premature convergence to sub-optimal deterministic policies (Mnih et al., 2016). The agent is rewarded for randomness (higher entropy) which is also a popular phenomenon in nature (Eysenbach and Levine, 2019). The higher entropy results in more exploration of the environment. It also works as a regularizer that stabilizes the training and is shown to accelerate learning. The SAC formulation for the optimal policy can be summarized as

$$\pi^* = \arg \max_{\pi} \mathbb{E}_{a_t \sim \pi(\cdot|s_t)} \left[\sum_t \gamma^t (r(s_t, a_t) + \alpha \mathcal{H}(\pi(\cdot|s_t))) \right], \quad (3)$$

$$\mathcal{H}(\pi(\cdot|s_t)) = \mathbb{E}[-\log \pi(\cdot|s_t)], \quad (4)$$

which is similar to Equation (2), except for the added entropy term. Here, α is the temperature parameter that determines the relative strength of the entropy regularization term.

In our implementation of the deep SAC algorithm, two parametric models are trained simultaneously, each parameterized by a neural network: the policy function (π) and the action-value function (Q), parameterized by ϕ and θ , respectively. The policy function is the *actor* (brain) and the action-value function (Q) is its *critic* with the entropy *softening* the expectations, hence the name SAC. During training, at each simulation timestep t , the actor receives the current state of the environment s_t , processes it and takes the action a_t according to

its parametric policy π_ϕ . As a result of this action, the agent will end up in the new state s_{t+1} .

In the biomechanical model of the jaw, the state is formed of the current and the desired orientation of the jaw as well as the excitation levels of all the masticatory muscles. Given the constrained motion of the jaw, its orientation is abstracted as the position of the mid-incisal point. The muscle excitations are normalized to the $[0-1]$ range. During training, the history of interactions with the environment are stored in a random access memory (\mathcal{D}), known as the replay buffer. Each sample in the replay buffer, (s_t, a_t, s_{t+1}, r_t) , is a tuple of the current state, executed action, next state, and the reward associated with the transition. The buffer allows for a higher sample efficiency as each sample can contribute to the training of the Q and π networks multiple times (Lin, 1992; Mnih et al., 2013).

The action-value function, $Q_\theta(s_t, a_t)$, is the expected reward if, at timestep t , the agent takes the action a_t at the state s_t , and then continues acting according to the learned policy. In other words, the Q -function estimates the value of an action at a given state based on its prospective rewards. Due to the co-dependency of neighboring states, the Q -function of SAC can be computed recursively with the modified Bellman operator (Lagoudakis and Parr, 2003) as

$$Q_\theta(s_t, a_t) = r(s_t, a_t) + \gamma \mathbb{E}_{s_{t+1} \sim \mathcal{D}} [V_{\bar{\theta}}(s_{t+1})], \quad (5)$$

$$V_{\bar{\theta}}(s_t) = \mathbb{E}_{a_t \sim \pi_\phi(\cdot|s_t)} [Q_{\bar{\theta}}(s_t, a_t) - \alpha \log \pi(a_t|s_t)]. \quad (6)$$

Here, $V(\cdot)$ is the regularized (soft) *state-value* function which is simply called the *value* function. The value function is the expected future reward of a state. In the SAC formulation, this is equal to the value of a state and the expected entropy of the state. In the context of masticatory motor control, the value function roughly indicates how likely it is for the agent to reach its desired position and achieve high rewards if it started from the current jaw orientation and followed its learned policy. Substituting $V(\cdot)$ into Equation (5) would result in the recursive Bellman equation for the Q -function. While it is possible to learn the state-value function separately using a neural network with independent parameters, in our formulation, the value function is estimated based on the Q -function defined in Equation (5).

As discussed earlier, all neural networks are trained based on the randomly drawn samples from the replay buffer (\mathcal{D}). The parameters of the Q -function are updated with the stochastic gradient descent toward minimizing the mean squared error between the estimated Q values, calculated by the Q_θ function as $Q_\theta(s_t, a_t)$, and the *assumed* ground-truth Q value. The assumed ground-truth Q values are estimated based on the current reward (r_t) and the discounted future reward of the next state ($\gamma V_{\bar{\theta}}(s_{t+1})$). Accordingly, the mean squared error objective function of the Q_θ network can be summarized as:

$$J(Q_\theta) = \mathbb{E}_{(s_t, a_t, r_t, s_{t+1}) \sim \mathcal{D}, a_{t+1} \sim \pi_\phi} \left[\left(Q_\theta(s_t, a_t) - \left[r_t + \gamma \mathbb{E}_{s_{t+1} \sim \mathcal{D}} [V_{\bar{\theta}}(s_{t+1})] \right] \right)^2 \right]. \quad (7)$$

In Equation (6), and, consequently, in the nested expectation on the right-hand side of Equation (7), the parameters of the networks are denoted as $\bar{\theta}$. This change in notation is to highlight a stabilizing practice where the critic is modeled with two neural networks with the exact same architecture but independent parameters (Mnih et al., 2015). The secondary network, referred to as the target network and denoted as $Q_{\bar{\theta}}$, is the one that is used to calculate the *assumed* ground-truth value of the next state in Equations (6) and (7). The parameters of the target critic network ($Q_{\bar{\theta}}$) are iteratively updated with the exponential moving average of the parameters of the main critic network (Q_θ). This constrains the parameters of the target network to update at a slower pace toward the parameters of the main critic, which has shown to stabilize the training. It also transforms the ill-posed problem of learning the Q -function through bootstrapping (learning estimates from estimates) into a supervised learning problem that can be solved via the gradient descent optimization (Lillicrap et al., 2016).

Another enhancement which played a substantial role in the success of the current motor control solution is the double Q -learning (Hasselt, 2010; Van Hasselt et al., 2016). In this approach, two Q networks for both of the main and the target critic functions are maintained. When estimating the current Q values or the discounted future rewards, the minimum of the outputs of the two Q networks is used:

$$Q_\theta(s_t, a_t) = \min(Q_{\theta 1}(s_t, a_t), Q_{\theta 2}(s_t, a_t)). \quad (8)$$

This approach prohibits the estimated Q values to grow too large and is found to speed up the training and help achieve higher performing policies (Haarnoja et al., 2018a).

As for the optimal policy (Equation 3), the parameters of π_ϕ is updated to maximize the expected future return as well as the expected entropy. If the Q -function (critic) is assumed to be telling the truth, finding the optimal policy is the same as maximizing $\mathbb{E}_\pi [V_{\bar{\theta}}(s)]$. This can be expanded, based on Equation (6), as follows

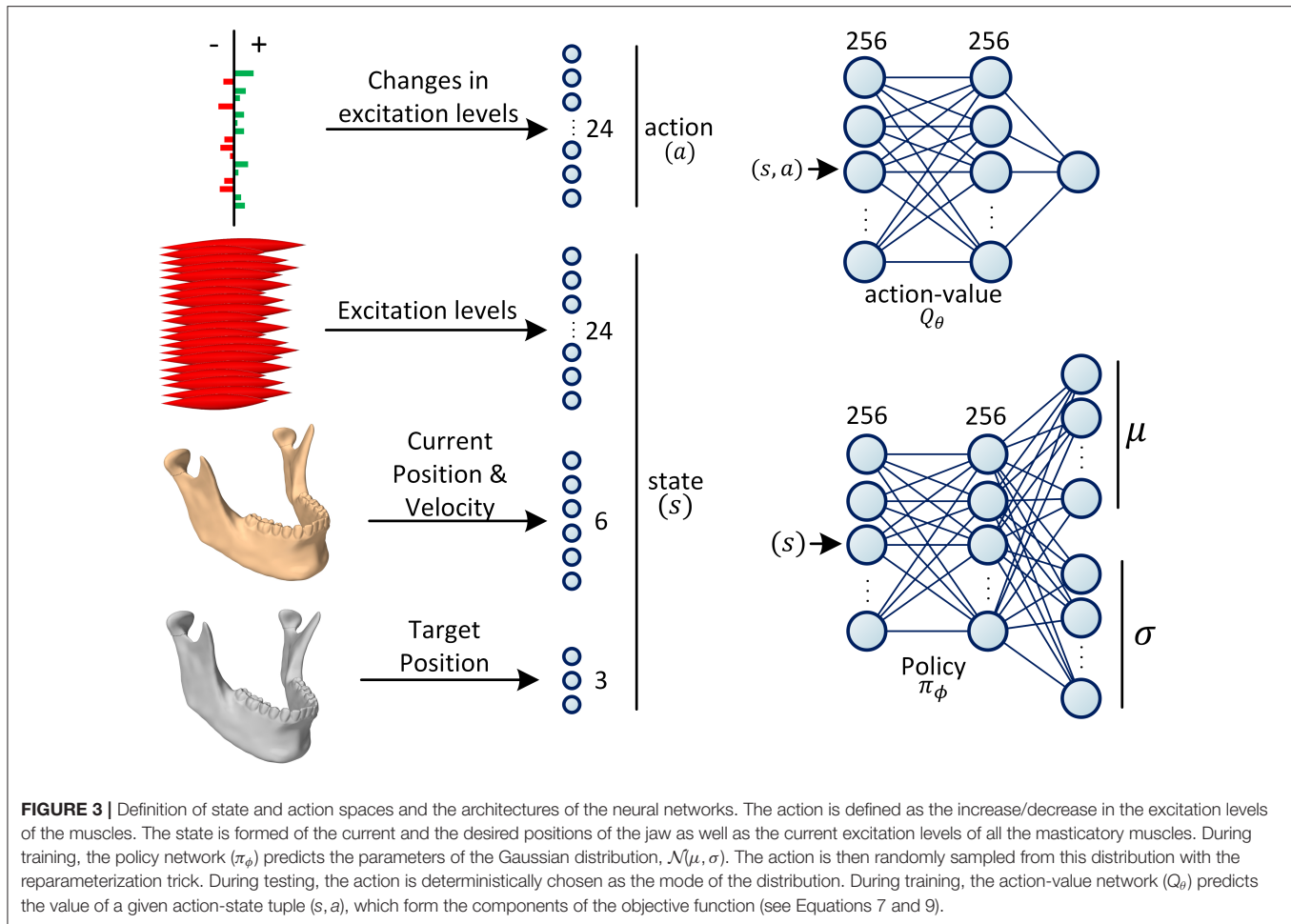
$$J(\pi_\phi) = \mathbb{E}_{a \sim \pi_\phi, s \sim \mathcal{D}} [Q_\theta(s, a) - \alpha \log \pi(a|s)]. \quad (9)$$

The objective is optimized using the stochastic gradient ascent based on the random samples drawn from the replay buffer (\mathcal{D}).

3.1. Neural Architectures and Space Definitions

The two functions, Q_θ and π_ϕ , are parameterized with neural networks. In all our experiments, the Q -network is designed as a 3-layer fully-connected (dense) neural architecture (multi-layer perceptron with two hidden layers) with Rectifier Linear Unit (ReLU) activations after the first two layers. As shown in **Figure 3**, the sizes of the middle (hidden) layers are set to 256. The Q_θ network estimates the action-value function denoted as $Q(s, a)$; therefore, its input size is the sum of the dimensionalities of the action space and the state space and its output size is 1.

The jaw model is formed of 24 masticatory muscles, hence, the action size of 24. In this context, an action is a command sent to the simulation environment to increase or decrease the



excitations of a subset of muscles. Change in each muscle's excitation level is capped to the maximum 10% of its excitation range. The jaw orientation is abstracted and approximately represented as the 3D position of the mid-incisal point. The state of the RL agent is then defined as the union of the current neural excitations for the muscles (24 values), the orientation (3 values) and velocity (3 values) of the jaw, and its desired orientation (3 values). Therefore, the size of the state space sums up to 33. In our experiments, the velocity of the desired mid-incisal point is always zero, i.e., the model is trained to reach a static target state.

The policy network is a probability density function estimator that predicts the distribution of actions conditioned on the state. The policy network is formed of two linear hidden layers of size 256, each followed by a ReLU activation function. In our design, we are assuming the policy to have a Gaussian distribution. Therefore, the last layer of the policy network is formed of two parallel linear layers which encode the mean and standard deviation of the $\mathcal{N}(\mu, \sigma)$ distribution, respectively (Figure 3). During training, the estimated distribution is sampled with the reparameterization trick for the sampling to be differentiable (Kingma and Welling, 2014). During inference (testing), the mode of the distribution is used for the optimal action selection.

3.2. Reward Function

At each timestep, the agent receives a reward value from the environment based on the executed action and its state transition from s_t to s_{t+1} . The success of an RL experiment heavily relies on the design of the reward function. Reward functions are counterparts to the objective functions (loss functions) in the optimization domain; however, in the realm of RL, the agents are trained to maximize the expectation of future rewards. The reward function used in this study is formed of three terms, each of which encourages the agent to pursue a certain goal. If the current position of the mid-incisal point is denoted as P_t , and its desired position as \hat{P} , the designed reward function can be formulated as:

$$r(s_t, a_t) = -w_u \log(\|\hat{P}P_{t+1}\|_2 + \epsilon) - w_r \|\mathbf{f}_{t+1}\|_2 - w_s \|e^I_{t+1} - e^r_{t+1}\|_1, \quad (10)$$

where $\|\hat{P}P_{t+1}\|_2$ is the second norm of the vector, i.e., the Euclidean distance (in millimeters) of the current mid-incisal point to its desired location. The first term incentivizes the

policy (brain) to drive the jaw toward its desired location. The logarithmic nature of this term mitigates the destructive growth of the penalty when the jaw is far away from its deemed target. On the other hand, when the jaw gets to the sub-millimeter distance of the target, the agent is highly positively rewarded. The ϵ value is to avoid the infinite reward in cases where P exactly resides at \hat{P} . In the second term, f is the vector of the muscle tensions. The second term acts as a regularizer which minimizes the energy expenditure of the collective of the masticatory muscles. In the third term, e^l and e^r are the neural excitations of the left and right side muscles, respectively. Accordingly, the third term calculates the first norm of the differences between the bilateral muscle pairs; thus, it is the non-symmetric penalty that punishes the action if the bilateral muscle pairs are not similarly activated. Finally, w_u , w_r , and w_s are coefficients that determine the relative weights of the target reaching, the force regularization, and the symmetry terms.

3.3. Training Details

The training process is partitioned into independent episodes. At each episode of training, the desired position of the mid-incisal point is randomly chosen from within the 3D envelope of motion (see section 2.3). The random target positioning alternates between two approaches. In 50% of the episodes, the target's position is set as the weighted linear combination of all of the envelope's end-points (Figure 2). The weights of this linear equation are randomly drawn for each episode. In the other 50% of episodes, two of the eight envelope end-points are randomly selected with replacement and the target's position is set as a random linear combination of the two points. This strategy asserts that the boundaries of the envelope are included in the training for the agent to learn the entire domain of motion. Moreover, since the end-point selection is done with replacement, in $0.5 \times 0.125 = 6.25\%$ of the episodes the desired jaw position is one of the end-points with the same point chosen in the random selection.

The training can continue for tens of thousands of episodes until no further improvement is noticed in the optimization of the objective functions. An episode runs for a maximum of T steps during which the agent interacts with the environment according to its learned policy. An episode ends with the jaw reaching the $100\ \mu\text{m}$ proximity of the desired position or with the agent running out of its maximum T allowed steps for the episode.

The parameters of the neural networks are primarily initiated to random values based on the Xavier initialization function (Glorot and Bengio, 2010). Consequently, the agent will start by randomly exploring the space. As the agent interacts with the environment, it collects experiences that eventually get stored in the replay buffer. The weights of Q_θ and the π_ϕ functions are updated at each timestep based on a batch of 256 samples randomly drawn from the replay buffer. As a result, the algorithm alternates between experiencing (filling the replay buffer) and updating the parameters of the Q_θ and π_ϕ networks based on the randomly drawn buffer samples. The parameters of the networks are updated to minimize their respective objective functions

(Equations 7 and 9). At the end of each timestep, the parameters of the target critic network, $Q_{\hat{\theta}}$, are updated as the exponential moving average of the parameters of the Q_θ network based on the target smoothing coefficient τ .

In all of the experiments, the learning rate starts at 0.001 and gradually decreased to 0.0004 at an exponential decay rate of 0.999995. The α value of the SAC algorithm and the reward discount value (γ) are consistently set to 0.3 and 0.99, respectively. The capacity of the replay buffer is generously set to include 1 million samples. The coefficient of the target reaching term, w_u , is not updated in between experiments, instead w_r and w_s are tuned. The target smoothing coefficient (τ) is set to 0.005. The maximum number of steps in an episode (T) was set to 100.

The training is continued until the objective functions of the actor and the critic converge to a steady-state and stop improving. In our experiments, and with the non-distributed implementation of the training procedure, it took an RL model a few days up to a week to converge. During this time period, the agent went through 10–30k episodes of training, equal to 2–4 million interactions with the environment.

The SAC learning algorithm and the training procedure were implemented in Python and used the ArtiSynth-RL plugin to interact with the ArtiSynth modeling environment (Abdi et al., 2019a). Our implementations of the jaw model and the training algorithm along with the scripts to reproduce the experiments are open-sourced at <https://github.com/amir-abdi/artisynth-rl>.

4. PERFORMANCE ANALYSIS OF MASTICATION

The performance of mastication can be quantified based on the chewing rhythm, velocity, range of mandible displacements, and the masticatory forces (Xu et al., 2008). The chewing process can be divided into cyclic jaw movements or gape cycles which can be measured through lateral and vertical tracking of the jaw (Laird et al., 2020). According to the literature, a high performing masticatory system is one with a high frequency of cycles, high velocity of mandibular movements, high maximum bite force, and potential for large mandibular displacements. These quantities can be measured with respect to some reference points, such as the lower mid-incisor point and the condylar centers (Ow et al., 1998; Tsuruta et al., 2002). Many studies have focused on the patterns of occlusion and chewing cycle excursions with different bolus types (Anderson et al., 2002; Peyron et al., 2002; Foster et al., 2006). The EMG measurements of muscular activities, albeit variable between subjects, are also shown to have sufficient correlation within a subject across experiments and have been suggested as an efficiency metric (Tortopidis et al., 1998).

The masticatory cycle can be simplified as a tear-drop movement where the mid-incisal point moves downward, then laterally toward the working side, and finally retracted medially to crush the bolus (Murray, 2016). Considering these masticatory movements, we propose a framework for masticatory performance evaluation. This framework is designed to quantify

the performance of a given masticatory system based on the following criteria.

4.1. Range of Motion (ROM)

To quantify the range of mandibular motion, the boundary envelope of the motion is approximated as a convex space and the volume of this assumed convex hull is calculated. The range of motion is then defined as the percentage of the feasible space achieved by the model. We rely on the reference (optimum) convex hull calculated in section 2.3 by setting the neural excitations.

4.2. Metabolic Efficiency (ME)

We are assuming a linear relationship between the muscle tensions and the amount of energy consumed by the muscle fibers. Accordingly, the metabolic efficiency is defined as the inverse of the average muscle tensions during a predefined set of masticatory movements, as follows

$$ME = \left(\frac{1}{T} \sum_t \bar{f}_t \right)^{-1}, \quad (11)$$

where T is the total number of steps in an episode, and \bar{f}_t is the mean of the muscle tension vector at timestep t .

4.3. Agility (Ag)

Agility is defined as the inverse of the time it takes for the masticatory system to translate the jaw in between a predefined set of locations in the 3D space.

4.4. Accuracy (Ac)

The ability of the trained RL policy in driving the body of the mandible toward the desired position is counted as the accuracy of the system. This metric is evaluated as the inverse of the Euclidean distance of the lower mid-incisal point to its desired target position, averaged over multiple episodes, and formulated as

$$Ac = \left\| \hat{P}P_T \right\|_2^{-1}, \quad (12)$$

where P_T is the location of the lower mid-incisal point after the very last iteration of the episode and \hat{P} is its desired location.

4.5. Symmetry (Sym)

The biomechanical system in question is not fully symmetric; however, the current metric is designed to evaluate the extent of symmetric behavior in the trained RL agent. In this context, symmetry is defined as the inverse of the first norm of absolute differences between corresponding excitations of the left and right muscles, averaged over multiple episodes:

$$Sym = \left(\frac{1}{T} \sum_t \left\| e_t^l - e_t^r \right\|_1 \right)^{-1}. \quad (13)$$

5. EXPERIMENTS AND RESULTS

After the reinforcement learning model is trained, the trained stochastic policy is queried with a state (as defined in **Figure 3**) and the agent executes the action associated with the mode of the returned distribution. Accordingly, the inference process is deterministic.

5.1. Force Regularization

In the first set of experiments, we investigate the impact of the regularization term in the reward function (Equation 10) in the metabolic efficiency of the trained agent. Here, we keep the w_u coefficient consistent across experiments and evaluate the converged model with respect to the w_r coefficient based on the performance metrics discussed in section 4. The non-symmetric coefficient, w_s was set to zero during these experiments.

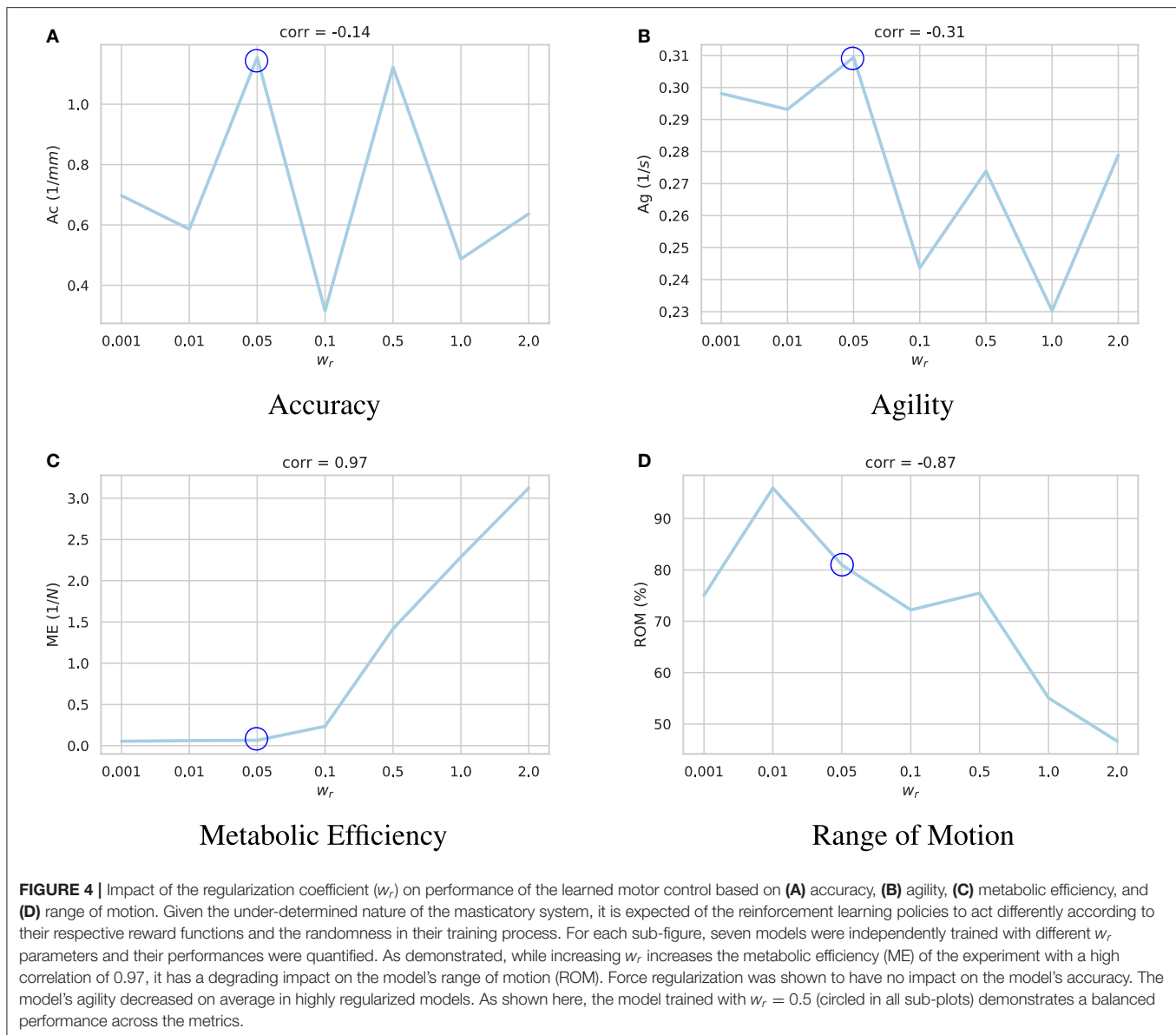
To test the trained model, a series of 21 target positions on the border and inside the envelope of movement were defined. The agent was then tested based on its ability to navigate the jaw model in between the predefined target locations. The position of the jaw, neural excitations, and muscle forces were tracked throughout the experiments.

The results of these experiments are summarized in **Figure 4**. As demonstrated, higher values of the regularization coefficient result in more metabolically efficient muscle activation trajectories according to the model's perception of metabolic efficiency, i.e., the muscular tensions (section 3.2). However, with the model thriving for the least amount of applied force, its agility slightly decays. For example, in highly regularized models, the agent delegates the responsibility of jaw elevation to the passive ligaments of the TMJ. Accordingly, mouth closing is carried out at a slower pace (see **Supplementary Video 1**).

A high negative correlation ($\rho = -0.87$) was also observed between w_r and the model's range of motion. It is our understanding that with an excessive force regularization, lowering the metabolic energy expenditure becomes a priority as the agent is highly penalized to activate its muscles. Since reaching the edges of the envelope of motion requires higher muscle activations, the agent decides not to reach the edges to save more energy.

5.2. Symmetric Behavior

Similar to live subjects, the masticatory model designed in ArtiSynth is not completely symmetric. Consequently, the RL agent as well does not learn symmetric excitation patterns for the left and right muscles. To explore the impact of the symmetry term of the reward function (Equation 10) in the RL training process and to understand the neuromuscular activation patterns, a set of models were trained with different w_s coefficient values. The models were trained with $w_r = 0.5$ as a balanced solution between speed, accuracy, range of motion, and the least neural excitations, based on the results presented in section 5.1. Given that the neural excitations have a value between 0 and 1, larger w_s values were used to incentivize symmetric activations compared to the w_r values. The values of the w_u and w_r coefficients were kept consistent in these sets of experiments.



The same series of target positions as the previous section were chosen and the trained models were tested based on the same performance criteria. As plotted in **Figure 5**, higher w_s values encourage the model to learn symmetric activation patterns for the left and right muscles. However, with more symmetric behavior, the model becomes damper and fails to explore its feasible domain of motion. Moreover, the non-symmetric penalty is shown to have a regularization effect, similar to the force regularization, which decreases the overall neural excitations and increases the metabolic efficiency (ME) of the model.

5.3. Muscle Activation Patterns

To understand the learned dynamic patterns, a trained agent was set to navigate in the 3D space in between a predefined series of positions. The neural excitation patterns were recorded during these movement. Here, we used the model trained

with $w_r = 0.5$ and $w_s = 10$ as it demonstrated the most balanced performance.

The neural excitation trajectories recorded in this experiment are visualized in **Figure 6**. As demonstrated, while some of the observations do not match perfectly with our expectations, they follow our knowledge of the masticatory system to a good extent. For example, in the right laterotrusion function (E to RL), the contralateral (left side) lateral pterygoid muscle (LILP) does the heavy lifting, assisted by the ipsilateral posterior temporalis muscle and slightly by the contralateral superficial masseter (Bakke, 2016). To return the jaw to the edge-to-edge position (RL to E), the left lateral pterygoid abruptly relaxes and the right lateral pterygoid (RILP) takes over. When the jaw arrives at the mid-sagittal position, RILP relaxes at a slower pace. This process is assisted by the ipsilateral masseter; consequently, to counterbalance the closing force

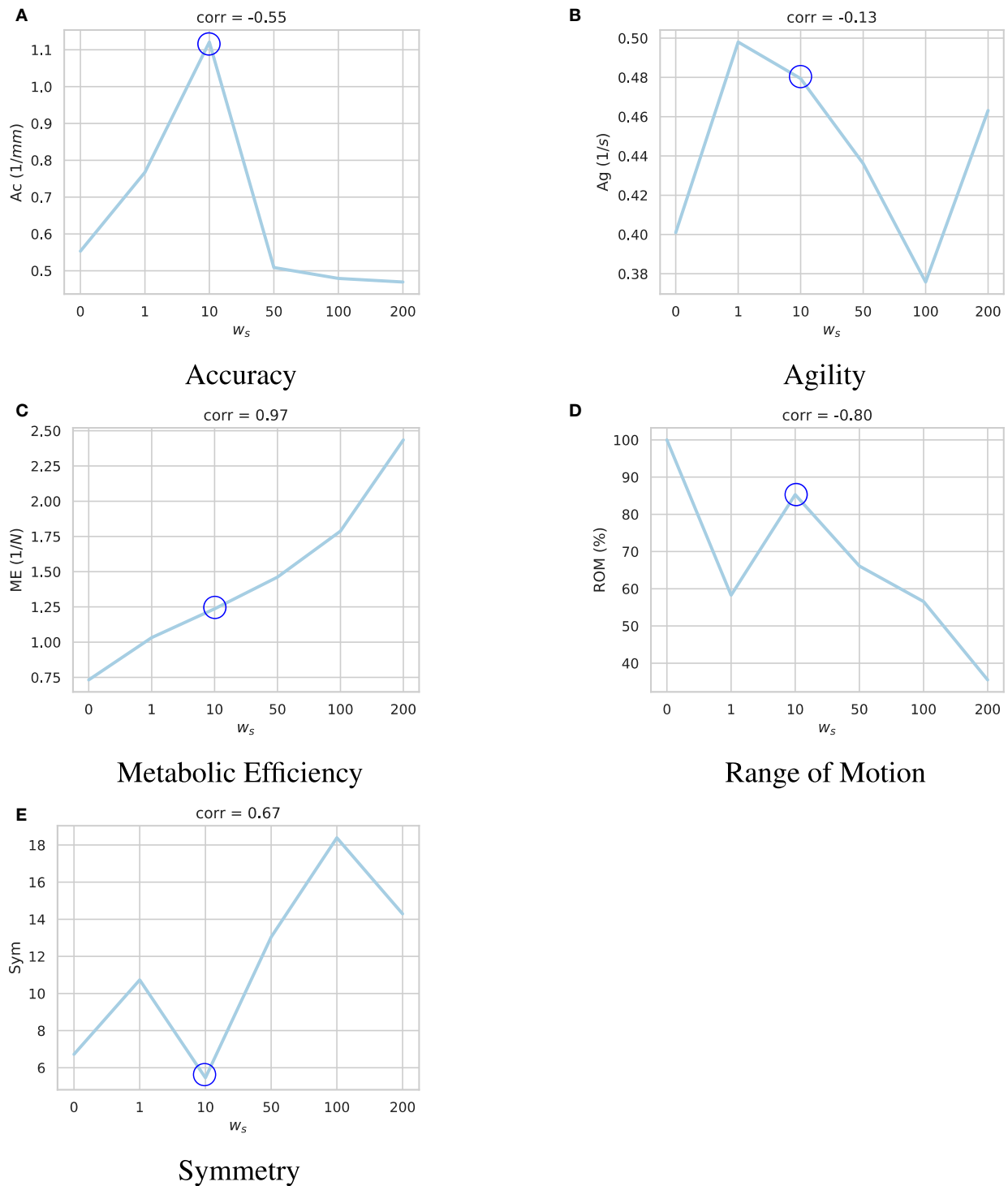
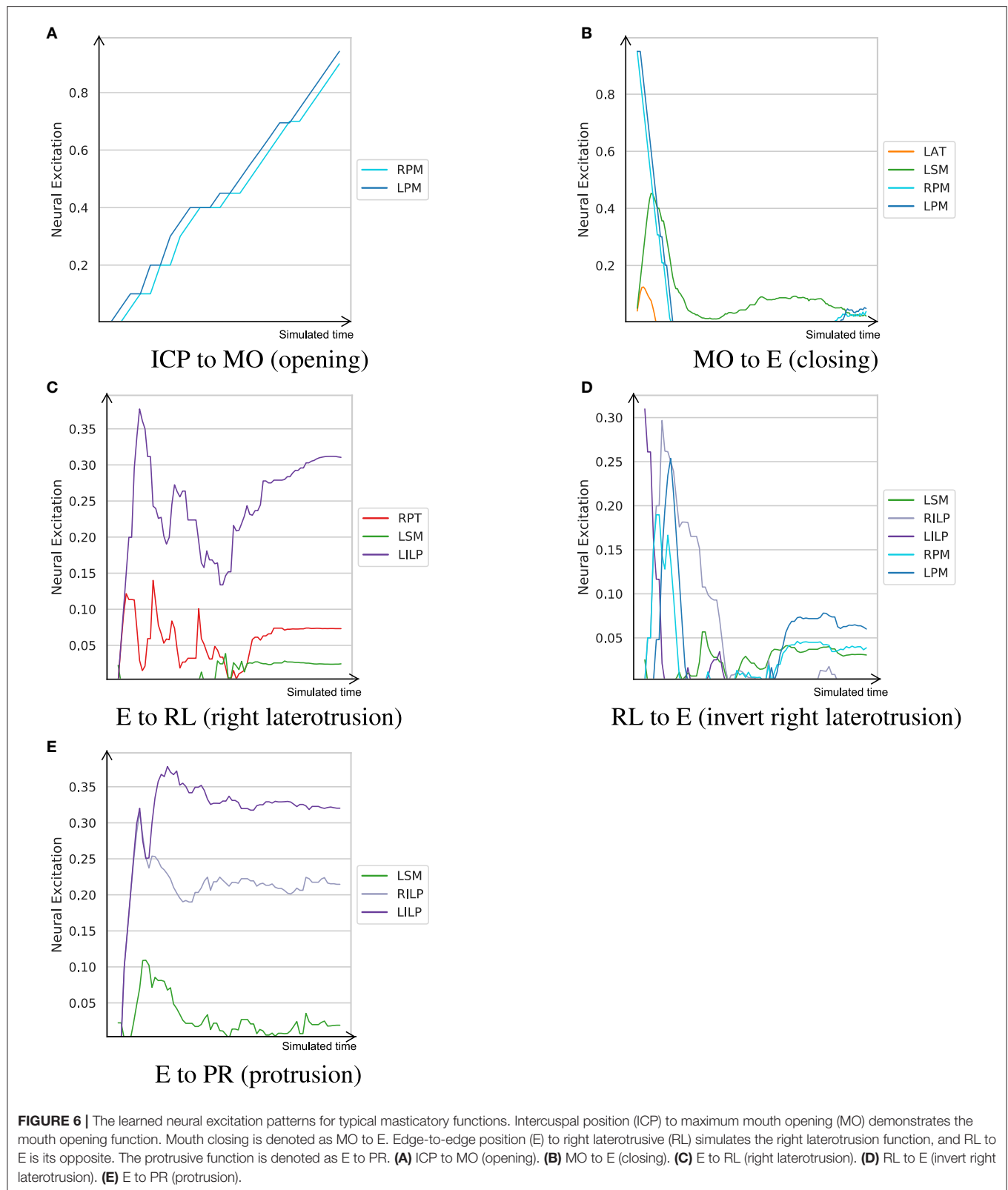


FIGURE 5 | Impact of the symmetry coefficient (w_s) on the learned motor control based on **(A)** accuracy, **(B)** agility, **(C)** metabolic efficiency, **(D)** range of motion, and **(E)** symmetry. For each sub-figure, six models were independently trained with different w_s parameters and their performances were quantified. As shown, bigger w_s coefficient incentivizes the agent to learn more symmetric activation patterns. However, such model is less accurate, and is not able to explore as much of the state space. Moreover, the non-symmetric penalty (Equation 10) has a regularization effect which decreases the overall neural excitations and increases the metabolic efficiency (ME). Accordingly, the model trained with $w_s = 10$ (circled in all sub-plots) demonstrates a balanced performance across the metrics.



of the left-side masseter, the posterior fibers of the right mylohyoid (RPM) are slightly (close to 3%) activated to keep the jaw in the edge-to-edge position. Similarly, the protrusive

movement of the mandible (E to PR in **Figure 6**) is driven by the bilateral contraction of the lateral pterygoid muscles (Ho, 2017).

Since smaller muscles tend to produce less force, and in turn, consume less energy, a metabolically efficient model (such as one trained with $w_r = 0.5$) prioritizes activation of small muscles over large ones for certain tasks. From the visualized experiments, the mouth opening task (ICP to MO) is carried out by activating the bilateral posterior mylohyoid fibers, while other muscles, such as the anterior digastric and inferior head of the lateral pterygoid, remain inactive. While this observation is not in sync with our understanding of the masticatory system, the model's decision is optimal according to its own understanding of the metabolic efficiency. This experiment was conducted to highlight that the proposed approach to learning neural excitation patterns is a good tool for generating hypotheses. However, without subject-specific models and rigorous studies of the reward functions and fine-tuning of the learning coefficients, it is not possible to establish a learning paradigm that mimics the human neural system.

Another example is jaw elevation (MO to E) where the mylohyoid muscles suddenly relax and the closing muscles, namely the temporalis and masseter, are activated to bring the condyle back to the glenoid fossa. The passive force of the condylar ligaments, modeled with the multi-point springs, play an important role in the jaw closure; therefore, once the translational phase of jaw closure is over, all muscles temporarily relax and then get slightly activated to establish the edge-to-edge relationship. Accordingly, the agent exploits the passive force of the condylar ligaments to minimize its energy expenditure during mouth closing.

Supplementary Video 1 captures the dynamics of the jaw during the experiments described in this section.

6. DISCUSSION

We present a reinforcement learning (RL) approach to estimate the neural excitations of the masticatory muscles. The implemented RL algorithm in this research is based on the Soft Actor-Critic (SAC) formulation which promotes policies with higher entropies. The SAC has demonstrated results that outperform other off-policy and on-policy state-of-the-art RL algorithms, such as the Deep Deterministic Policy Gradient (Lillicrap et al., 2016), Trust Region Policy Optimization (Schulman et al., 2015), and the Proximal Policy Optimization (Schulman et al., 2017), both in terms of performance and sample efficiency (Haarnoja et al., 2018a). In our design, the actor and critic functions of SAC were parameterized by relatively shallow neural networks. We also leveraged double Q-learning and used a separate target critic network to stabilize the learning process.

As demonstrated in section 5.3, the muscle excitation trajectories during opening, closing, laterotrusive, and protrusive movements matches the known physiological patterns (**Figure 6**). Accordingly, the left and right pterygoid muscles play a substantial role in laterotrusive and protrusive movements. We would like to highlight that, similar to live subjects, the jaw model in question is not symmetric. This asymmetry is apparent in muscle insertion sites, the location

of the curved bilateral planar constraints for the TMJ, and the shapes of the teeth. Accordingly, it is not expected to observe symmetric excitation patterns especially when the RL policy is mainly opting to minimize the metabolic cost of its actions. As a result, and as **Figure 6** represents, muscles of the left side are more predominantly activated even during symmetric movements, such as jaw closing and protrusion. The non-symmetry penalty term in the reward function mitigates this issue to some extent (**Figure 5**); however, this gain in symmetry comes with the cost of a lower range of motion. A smarter reward function is deemed necessary to achieve higher performing results.

There have been quite a few metabolic analyses of gait that consider ground reaction forces, motion trajectories of limbs, and pulmonary gas exchanges to estimate the metabolic cost of walking and running. Based on these metrics, multiple metabolic models are introduced which demonstrate consistent results in estimating the relative metabolic cost of different gait tasks (Koelewijn et al., 2019). However, the question of *what is being optimized in biomechanical systems during mechanical tasks* remains unanswered. Should efficiency be defined as the minimum metabolic cost or should the mechanical work be also included as a second indicator of efficient movements (Fetters and Holt, 1990)? Moreover, whether the fidelity requirements of the task play a role in the metabolic efficiency trade-off requires further investigations. In the neural excitation trajectories presented in **Figure 6**, small muscles seem to get activated more often while large muscles are seldomly activated and merely used for balancing. This is certainly the case for mouth opening where the entire task is handled by the posterior fibers of the left and right mylohyoid muscles.

As discussed earlier, motor control of biomechanical systems is often an underdetermined problem as there are more muscles than the collective of degrees of freedom of the bodies (Lee et al., 2014). Consequently, the local maxima that the model's policy in the RL training framework converges to is not unique either. From the trained agent's perspective, at any state, there is a distribution of actions to choose from. The agent can be instructed to act based on either the mode of the distribution or a randomly drawn sample from the distribution. Regardless, an infinite number of policies can be trained, differing in their respective reward functions and other aspects of their RL formulation, each of which could converge to a different, but to some extent justified, local maxima. Both the force regularization and symmetric terms of the reward function (Equation 10) constrain the solution space of the model; however, these constraints are rather soft and do not guarantee a unique solution.

The RL training procedure is computationally intensive and can take a few hours to a few days depending on the training algorithm, hardware, the parallel efficiency of the implementation, and the dimensionality of the action and the space states. However, once the policy is trained, it is faster than any inverse dynamics solvers as it does not require an iterative numerical method to estimate the excitation and forces at every simulation time step (Abdi et al., 2019a). In deep RL, a trained

policy is a feed-forward or recurrent neural network which has learned a deterministic or probabilistic mapping between the state space and the action space. Therefore, at a given state, the action can be inferred via a single feed-forward passing of the model which is quite fast for the shallow neural architectures used in the deep RL paradigm. In our experiments, the feed-forward pass of the policy network (see π_ϕ in **Figure 3**) took <1 ms running on a GeForce GTX 1080. This is one-tenth of the time needed for a single forward step of the jaw simulation in ArtiSynth, running on an Intel Core i7-8700K 3.70 GHz processor, without even taking into account the overhead of the iterative inverse dynamics solver.

Similar to other machine learning and RL settings, the hyper-parameter space was deemed bigger than what could be fully investigated with our limited computational resources. However, within the limitations of our study, we found the entropy coefficient (α in Equation 9) to play a substantial role in the rate of convergence. According to our findings, and due to the relatively high dimensional action space, an α value of <0.2 does not incentivize the agent to explore the environment with an adequate frequency which, in turn, slows down the learning process.

In a simulated mechanical system, it is possible to assess the feasibility of a hypothetical motion trajectory by estimating the motor control resulting in the given kinematics via forward or inverse dynamics solutions. Therefore, the proposed RL training framework along with the masticatory performance metrics can be a viable solution to predict the post-operative functionalities of a subject. Patients who come out of extensive jaw reconstructive surgeries suffer from impaired masticatory functions. The brain of a post-operative patient, who has just come to realize its altered masticatory system, is in the self-experimental phase, meaning that it interacts with the environment through experiments and makes predictions on the results of those interactions to decide the best trajectory. As the patient fails to predict the results of the sensorimotor predictions, it enters a self-repairing phase where it starts to adapt to new world dynamics and compensate for lost motor abilities by finding new paths and activation patterns. This brain is also self-growing as it rebuilds the dynamics model of the jaw via gathering new information through experiments (Corbacho, 2016). The reinforcement learning process designed in this study is in sync with the three qualities of the post-operative brain, namely, self-experience, self-repair, and self-grow. While the subject is going through rehabilitation, the clinical team is curious to know, in theory, the extent to which the subject is expected to regain masticatory performance. With the proposed approach, such questions can be answered through virtual surgical interventions in the simulation platform and retraining of the RL agent to evaluate its adaptation with the new environment. Moreover, if multiple surgical avenues are available at the time of treatment planning, the surgeon and, in turn, the patient would benefit from knowing if an alternative plan could result in a more optimal functional outcome. We see a future where the proposed training framework is coupled with subject-specific biomechanical models as a benchmarking platform and to answer the *what-if* questions which are often raised during treatment planning of surgeries.

7. LIMITATIONS AND FUTURE WORK

Although the main contribution of this work is not to present the most accurate and validated subject-specific jaw model, we acknowledge the simplifying assumptions made in the biomechanical modeling as well as the policy training procedure. We would like to elaborate on some of these limitations to highlight potential avenues for enhancement. We divide these details into two categories, namely, limitations of the biomechanical model and those of the reinforcement learning procedure.

In order to speed up the costly process of the RL training, no component was modeled as finite elements. Consequently, and in contrast to previous works of Sagl et al. (2019b), the condylar disks and other soft tissues associated with the stomatognathic system were excluded from the model. While we acknowledge that the condylar disks play a non-trivial role in the masticatory system, we compensated for the loss of accuracy by modeling the condylar capsule and the adjacent tissues as passive multi-point springs. The cartilages were also modeled with elastic foundations (Servin et al., 2006). Moreover, and similar to all the jaw models presented in the literature, teeth were assumed to be rigidly connected to the jaw bone with no periodontal ligaments (PDL). In a more favorable setting with an abundance of computational power and time, each tooth can be modeled separately with a PDL that enables a limited extent of physiological movement.

In the designed stomatognathic system, the hyoid bone was assumed to be static and was moved inferoposteriorly to compensate for the loss in the amount of jaw opening. Moreover, some ligaments which contribute to the passive retraction of the jaw were not modeled, such as the stylomandibular ligament and the sphenomandibular ligament.

Here, muscles were modeled as point-to-point axial springs and large muscles were represented with multiple actuators. This simplifying assumption matches the conventional wisdom of prior arts, yet is not in sync with reality. Moreover, the muscles are assumed homogeneous along their length and their force functions follow the well-known Hill-type model. As a result, the muscles ignore the impact of temporal dependency and the recent contractile conditions of the muscle on their generated force (Arslan et al., 2019).

Along the same lines, in the current formulation, the muscle activations were not delicately modeled. Firstly, no delays were considered between the neural stimulation and muscle contraction. Encoding such delay is deemed complex given the discrete temporal simulation with fixed timesteps of 0.001 s. Moreover, a monotonically increasing mapping was assumed between the excitation level and the muscle activation, i.e., higher neural excitation would always result in a higher muscular tension.

Last but not least, we would like to highlight that, similar to other biomechanical models, the current jaw model relies on the parameters reported in the literature, such as the mass of jaw, tissue materials, force-length properties of the muscles, properties of the condylar capsule, and many more. We cannot imagine this issue to be resolved in the near future with the

current imaging and sensing technologies. This limitation has an adverse impact on the validity of any subject-specific models designed for treatment planning. Considering the open-source nature of our research, we invite other researchers to join hands in improving upon the model by including more details and alleviating the above limitations.

As for the limitations of the learning procedure, we should highlight the sample inefficiency of model-free approaches, such as the Soft Actor-Critic algorithm. Although the implemented process leverages a replay buffer memory which holds 1 million samples, it is our understanding that the current training process does not efficiently use the gathered samples. In our implementation, after each environment interaction, a batch of 256 samples are drawn from the replay buffer to apply a single update on the weights of the actor and critic networks. Therefore, a viable next-step would be to dynamically adjust the number of parameter updates per environment interaction over time to achieve a faster and more sample-efficient training. Another enhancement is to change the paradigm toward model-based or hybrid reinforcement learning solutions (Nagabandi et al., 2018). Given the stationary state of the masticatory simulation environment, model-based approaches are expected to achieve the same performance with fewer environment interactions.

In the designed motor control paradigm, the neural pathways are assumed to be completely disjoint. This enables the reinforcement learning actor to activate each muscle independently. This assumption is not well-aligned with the reality of biomechanical systems and the reality of muscular synergies where co-activation of muscles that share the descending or afferent neural pathways produce the kinematic trajectories (Bizzi and Cheung, 2013). In a similar work by Ruckert and d'Avella (2013), a movement primitive representation was proposed which employed parameterized basis functions to exploit the hypothesized muscle co-activations. Accordingly, the shared knowledge between muscles simplified the policy search in high-dimensional action spaces. Coupling the neural excitations limits the degrees of freedom and decreases the dimensionality of action space; thus, it results in a more efficient exploration of the smaller action space which makes the job of the RL agent easier. On the other hand, it raises the concern of the *correctness* of neural couplings. Since Kutch and Valero-Cuevas (2012) have debated the assumption of same neural origins for the muscle synergies and argued that constraints arising from the biomechanics could also result in certain couplings across the muscles, we kept the neural pathways independent in this research. However, this avenue needs further exploration.

An important unanswered question in the training is centered around the reward function. As shown in **Figure 4**, different muscle force regularization coefficients would result in substantially different policies (brains). One policy could be more agile while the other one generates the least amount of muscle tensions. Finding the right balance between the agent's incentives and validating the outcomes with *in vivo* studies or against the available literature will be a valuable and enlightening research project.

Lastly, a fascinating next step would be to include the occlusal forces in the process and design the reward function for the agent to learn a complete chewing cycle. Such rewarding mechanism should be taking the masticatory rhythm and interocclusal forces into account. However, some version of bolus modeling might be necessary to achieve reliable results.

8. CONCLUSION

In this work, we present a new perspective into estimating the neural excitations of the masticatory musculoskeletal system based on the paradigm of reinforcement learning. In this approach, an RL agent is trained to drive the mandible across the 3D envelope of motion in the simulation environment. The proposed method does not require dynamic clinical measurements, such as EMG, kinematics, or joint force trajectories; instead, the model explores the feasible domain of motion via environment interactions and learns the right excitation patterns from its own experiments. We demonstrate that the agent can be trained to optimize over three objectives: minimizing the distance to the target, maximizing the metabolic efficiency of the movement, and maximizing the symmetric behavior of the left and right neural excitations. The trained models demonstrate excitation trajectories that match the known physiological patterns. The proposed approach does not rely on the availability of the recorded kinematics, therefore, it is deemed as an intriguing alternative for the inverse dynamics problem.

DATA AVAILABILITY STATEMENT

The biomechanical model, the reinforcement learning algorithm, and scripts to reproduce the reported results are publicly accessible at <https://github.com/amir-abdi/artisynth-rl>.

ETHICS STATEMENT

The ethics application for data collection involving human participants were reviewed and approved by the Institutional Review Board of the Medical University of Vienna. The participant provided his written informed consent to participate in this study. Data sharing agreements were signed between the participating institutions, namely the Medical University of Vienna, Austria, and the University of British Columbia, Canada.

AUTHOR CONTRIBUTIONS

AA and VS designed the study and the experiments based on comments from IS, BS, and SF. AA, BS, and IS developed the biomechanical model. AA and VS drafted the manuscript with valuable inputs from BS. BS, SF, and IS reviewed and edited the manuscript. PA and EP played a supervisory role in the research, overseeing the progress and commenting on important aspects.

FUNDING

This research was undertaken, in part, thanks to the funding from the Vanier Scholarship of the Natural Sciences and Engineering Research Council of Canada (NSERC) to AA, and a Collaborative Health Research Projects (CHRP) grant from NSERC and Canadian Institutes of Health Research (CPG-163974). We gratefully acknowledged the support of the Vancouver Coastal Health Authority.

REFERENCES

- Abdi, A. H., Malakoutian, M., Oxland, T., and Fels, S. (2019a). "Reinforcement learning for high-dimensional continuous control in biomechanics: an intro to artisynth-rl," in *Deep Reinforcement Learning Workshop, 33rd Conference on Neural Information Processing Systems NeurIPS* (Vancouver, BC).
- Abdi, A. H., Saha, P., Srungarapu, V. P., and Fels, S. (2019b). "Muscle excitation estimation in biomechanical simulation using NAF reinforcement learning," in *Computational Biomechanics for Medicine*, eds M. P. Nash, P. M. F. Nielsen, A. Wittek, K. Miller, and G. R. Joldes (Springer International Publishing), 133–141. doi: 10.1007/978-3-030-15923-8_11
- Ahamed, N. U., Sundaraj, K., Alqahtani, M., Altwijri, O., Ali, M. A., and Islam, M. A. (2014). EMG-force relationship during static contraction: effects on sensor placement locations on biceps brachii muscle. *Technol. Health Care* 22, 505–513. doi: 10.3233/THC-140842
- Al Harrach, M., Carriou, V., Boudaoud, S., Laforet, J., and Marin, F. (2017). Analysis of the sEMG/force relationship using HD-sEMG technique and data fusion: a simulation study. *Comput. Biol. Med.* 83, 34–47. doi: 10.1016/j.compbiomed.2017.02.003
- Anderson, F. C., and Pandey, M. G. (1999). A dynamic optimization solution for vertical jumping in three dimensions. *Comput. Methods Biomech. Biomed. Eng.* 2, 201–231. doi: 10.1080/10255849908907988
- Anderson, F. C., and Pandey, M. G. (2001). Dynamic optimization of human walking. *J. Biomech. Eng.* 123, 381–390. doi: 10.1115/1.1392310
- Anderson, K., Throckmorton, G. S., Buschang, P. H., and Hayasaki, H. (2002). The effects of bolus hardness on masticatory kinematics. *J. Oral Rehabil.* 29, 689–696. doi: 10.1046/j.1365-2842.2002.00862.x
- Arslan, Y. Z., Karabulut, D., Ortes, F., and Popovic, M. B. (2019). "Exoskeletons, exomusculatures, exosuits: dynamic modeling and simulation," in *Biomechatronics* (Elsevier), 305–331. doi: 10.1016/B978-0-12-812939-5.00011-2
- Bakke, M. (2016). "Jaw muscle disorders," in *Functional Occlusion in Restorative Dentistry and Prosthodontics*, eds I. Klineberg and S. E. Eckert (Elsevier), 173–187. doi: 10.1016/B978-0-7234-3809-0.00014-0
- Bizzi, E., and Cheung, V. C. K. (2013). The neural origin of muscle synergies. *Front. Comput. Neurosci.* 7:51. doi: 10.3389/fncom.2013.00051
- Blümel, M., Hooper, S. L., Guschlbauer, C., White, W. E., and Büschges, A. (2012). Determining all parameters necessary to build hill-type muscle models from experiments on single muscles. *Biol. Cybern.* 106, 543–558. doi: 10.1007/s00422-012-0531-5
- Choy, S. E. M., Lenz, J., Schweizerhof, K., Schmitter, M., and Schindler, H. J. (2017). Realistic kinetic loading of the jaw system during single chewing cycles: a finite element study. *J. Oral Rehabil.* 44, 375–384. doi: 10.1111/joor.12501
- Clegg, A., Yu, W., Tan, J., Liu, C. K., and Turk, G. (2018). Learning to dress. *ACM Trans. Graph.* 37, 1–10. doi: 10.1145/3272127.3275048
- Coombs, M., Petersen, J., Wright, G., Lu, S., Damon, B., and Yao, H. (2017). Structure-function relationships of temporomandibular retrodiscal tissue. *J. Dental Res.* 96, 647–653. doi: 10.1177/0022034517696458
- Corbacho, F. J. (2016). Towards the self-constructive brain: emergence of adaptive behavior. *arXiv* 1608.02229.
- Drake, R., Vogl, A. W., and Mitchell, A. (2014). *Gray's Anatomy for Students*. London: Churchill Livingstone.
- Erdemir, A., McLean, S., Herzog, W., and van den Bogert, A. J. (2007). Model-based estimation of muscle forces exerted during movements. *Clin. Biomech.* 22, 131–154. doi: 10.1016/j.clinbiomech.2006.09.005
- Eysenbach, B., and Levine, S. (2019). If maxent rl is the answer, what is the question? *arXiv* 1910.01913.

SUPPLEMENTARY MATERIAL

The Supplementary Material for this article can be found online at: <https://www.frontiersin.org/articles/10.3389/fnhum.2020.00188/full#supplementary-material>

Supplementary Video 1 | Demonstrates some of the muscle activation patterns of the masticatory system learned with the designed reinforcement learning approach.

- Faber, H., van Soest, A. J., and Kistemaker, D. A. (2018). Inverse dynamics of mechanical multibody systems: an improved algorithm that ensures consistency between kinematics and external forces. *PLoS ONE* 13:e0204575. doi: 10.1371/journal.pone.0204575
- Farina, D., Merletti, R., Indino, B., and Graven-Nielsen, T. (2004). Surface emg crosstalk evaluated from experimental recordings and simulated signals. *Methods Inform. Med.* 43, 30–35. doi: 10.1055/s-0038-1633419
- Fetters, L., and Holt, K. (1990). Efficiency of movement: biomechanical and metabolic aspects. *Pediatr. Phys. Ther.* 2, 155–159. doi: 10.1097/00001577-199002030-00008
- Fluit, R., Andersen, M., Kolk, S., Verdonschot, N., and Koopman, H. (2014). Prediction of ground reaction forces and moments during various activities of daily living. *J. Biomech.* 47, 2321–2329. doi: 10.1016/j.jbiomech.2014.04.030
- Foster, K. D., Woda, A., and Peyron, M. A. (2006). Effect of texture of plastic and elastic model foods on the parameters of mastication. *J. Neurophysiol.* 95, 3469–3479. doi: 10.1152/jn.01003.2005
- Gallo, L. M., Fushima, K., and Palla, S. (2000). Mandibular helical axis pathways during mastication. *J. Dental Res.* 79, 1566–1572. doi: 10.1177/00220345000790080701
- Glorot, X., and Bengio, Y. (2010). "Understanding the difficulty of training deep feedforward neural networks," in *Proceedings of the Thirteenth International Conference on Artificial Intelligence and Statistics* (Sardinia), 249–256.
- Golkhou, V., Parnianpour, M., and Lucas, C. (2005). Neuromuscular control of the point to point and oscillatory movements of a sagittal arm with the actor-critic reinforcement learning method. *Comput. Methods Biomech. Biomed. Eng.* 8, 103–113. doi: 10.1080/10255840500167952
- Haarnoja, T., Zhou, A., Abbeel, P., and Levine, S. (2018a). "Soft actor-critic: off-policy maximum entropy deep reinforcement learning with a stochastic actor," in *Proceedings of the 35th International Conference on Machine Learning, Volume 80 of Proceedings of Machine Learning Research*, eds J. Dy and A. Krause (Stockholm: Stockholmsmässan), 1861–1870.
- Haarnoja, T., Zhou, A., Hartikainen, K., Tucker, G., Ha, S., Tan, J., et al. (2018b). Soft actor-critic algorithms and applications. *arXiv* 1812.05905.
- Hannam, A., Stavness, I., Lloyd, J., and Fels, S. (2008). A dynamic model of jaw and hyoid biomechanics during chewing. *J. Biomech.* 41, 1069–1076. doi: 10.1016/j.jbiomech.2007.12.001
- Hansson, T., Öberg, T., Carlsson, G. E., and Kopp, S. (1977). Thickness of the soft tissue layers and the articular disk in the temporomandibular joint. *Acta Odontol. Scand.* 35, 77–83. doi: 10.3109/00016357709064126
- Hasselt, H. V. (2010). "Double q-learning," in *Advances in Neural Information Processing Systems* (Lake Tahoe), 2613–2621.
- Hatze, H. (2002). The fundamental problem of myoskeletal inverse dynamics and its implications. *J. Biomech.* 35, 109–115. doi: 10.1016/S0021-9290(01)00158-0
- Hill, A. V. (1953). The mechanics of active muscle. *Proc. R. Soc. Lond. B Biol. Sci.* 141, 104–117. doi: 10.1098/rspb.1953.0027
- Ho, S. (2017). "Temporomandibular joint," in *Orthopaedic Physical Therapy Secrets* (Elsevier), 490–494. doi: 10.1016/B978-0-323-28683-1.00061-8
- Jagodnik, K. M., Thomas, P. S., van den Bogert, A. J., Branicky, M. S., and Kirsch, R. F. (2016). Human-like rewards to train a reinforcement learning controller for planar arm movement. *IEEE Trans. Hum. Mach. Syst.* 46, 723–733. doi: 10.1109/THMS.2016.2558630
- Jiang, Y., Wouwe, T. V., Groote, F. D., and Liu, C. K. (2019). Synthesis of biologically realistic human motion using joint torque actuation. *ACM Trans. Graph.* 38, 1–12. doi: 10.1145/3306346.3322966
- Kidziński, Ł., Mohanty, S. P., Ong, C. F., Huang, Z., Zhou, S., Pechenko, A., et al. (2018). "Learning to run challenge solutions: adapting reinforcement learning methods for neuromusculoskeletal environments," in *The*

- NIPS '17 Competition: Building Intelligent Systems, eds S. Escalera and M. Weimer (Cham: Springer International Publishing), 121–153. doi: 10.1007/978-3-319-94042-7_7
- Kingma, D. P., and Welling, M. (2014). “Auto-encoding variational bayes,” in *2nd International Conference on Learning Representations, ICLR 2014, April 14–16, 2014, Conference Track Proceedings* (Banff, AB).
- Koelewijn, A. D., Heinrich, D., and van den Bogert, A. J. (2019). Metabolic cost calculations of gait using musculoskeletal energy models, a comparison study. *PLoS ONE* 14:e0222037. doi: 10.1371/journal.pone.0222037
- Koolstra, J., Naeije, M., and Eijden, T. V. (2001). The three-dimensional active envelope of jaw border movement and its determinants. *J. Dental Res.* 80, 1908–1912. doi: 10.1177/00220345010800100901
- Koolstra, J., and van Eijden, T. (2005). Combined finite-element and rigid-body analysis of human jaw joint dynamics. *J. Biomech.* 38, 2431–2439. doi: 10.1016/j.jbiomech.2004.10.014
- Kuo, A. D. (1998). A least-squares estimation approach to improving the precision of inverse dynamics computations. *J. Biomech. Eng.* 120, 148–159. doi: 10.1115/1.2834295
- Kutch, J. J., and Valero-Cuevas, F. J. (2012). Challenges and new approaches to proving the existence of muscle synergies of neural origin. *PLoS Comput. Biol.* 8:e1002434. doi: 10.1371/journal.pcbi.1002434
- Lagoudakis, M. G., and Parr, R. (2003). Least-squares policy iteration. *J. Mach. Learn. Res.* 4, 1107–1149. doi: 10.5555/945365.964290
- Laird, M. F., Ross, C. F., and O'Higgins, P. (2020). Jaw kinematics and mandibular morphology in humans. *J. Hum. Evol.* 139:102639. doi: 10.1016/j.jhevol.2019.102639
- Langenbach, G., and Hannam, A. (1999). The role of passive muscle tensions in a three-dimensional dynamic model of the human jaw. *Archiv. Oral Biol.* 44, 557–573. doi: 10.1016/S0003-9969(99)00034-5
- Lee, Y., Park, M. S., Kwon, T., and Lee, J. (2014). Locomotion control for many-muscle humanoids. *ACM Trans. Graph.* 33, 1–11. doi: 10.1145/2661229.2661233
- Lillicrap, T. P., Hunt, J. J., Pritzel, A., Heess, N., Erez, T., Tassa, Y., et al. (2016). “Continuous control with deep reinforcement learning,” in *International Conference on Learning Representations (ICLR)* (San Juan).
- Lin, L.-J. (1992). Self-improving reactive agents based on reinforcement learning, planning and teaching. *Mach. Learn.* 8, 293–321. doi: 10.1007/BF00992699
- Mnih, V., Badia, A. P., Mirza, M., Graves, A., Lillicrap, T., Harley, T., et al. (2016). “Asynchronous methods for deep reinforcement learning,” in *International Conference on Machine Learning* (New York, NY), 1928–1937.
- Mnih, V., Kavukcuoglu, K., Silver, D., Graves, A., Antonoglou, I., Wierstra, D., et al. (2013). Playing atari with deep reinforcement learning. *arXiv* 131.25602.
- Mnih, V., Kavukcuoglu, K., Silver, D., Rusu, A. A., Veness, J., Bellemare, M. G., et al. (2015). Human-level control through deep reinforcement learning. *Nature* 518, 529–533. doi: 10.1038/nature14236
- Murray, G. M. (2016). “Jaw movement and its control,” in *Functional Occlusion in Restorative Dentistry and Prosthodontics* (Elsevier), 55–66. doi: 10.1016/B978-0-7234-3809-0.00005-X
- Muto, T., and Kanazawa, M. (1994). Positional change of the hyoid bone at maximal mouth opening. *Oral Surg. Oral Med. Oral Pathol.* 77, 451–455. doi: 10.1016/0030-4220(94)90222-4
- Muto, T., Kohara, M., Kanazawa, M., and Kawakami, J. (1994). The position of the mandibular condyle at maximal mouth opening in normal subjects. *J. Oral Maxillofac. Surg.* 52, 1269–1272. doi: 10.1016/0278-2391(94)90049-3
- Nagabandi, A., Kahn, G., Fearing, R. S., and Levine, S. (2018). “Neural network dynamics for model-based deep reinforcement learning with model-free fine-tuning,” in *2018 IEEE International Conference on Robotics and Automation (ICRA)* (Long Beach, CA: IEEE), 7559–7566. doi: 10.1109/ICRA.2018.8463189
- Osborn, J. (1996). Features of human jaw design which maximize the bite force. *J. Biomech.* 29, 589–595. doi: 10.1016/0021-9290(95)00117-4
- Otten, E. (2003). Inverse and forward dynamics: models of multi-body systems. *Philos. Trans. R. Soc. Lond. B Biol. Sci.* 358, 1493–1500. doi: 10.1098/rstb.2003.1354
- Ow, R. K. K., Carlsson, G. E., and Karlsson, S. (1998). Relationship of masticatory mandibular movements to masticatory performance of dentate adults: a method study. *J. Oral Rehabil.* 25, 821–829. doi: 10.1046/j.1365-2842.1998.00325.x
- Peck, C., Langenbach, G., and Hannam, A. (2000). Dynamic simulation of muscle and articular properties during human wide jaw opening. *Archiv. Oral Biol.* 45, 963–982. doi: 10.1016/S0003-9969(00)00071-6
- Pedersen, D. R., Brand, R. A., and Davy, D. T. (1997). Pelvic muscle and acetabular contact forces during gait. *J. Biomech.* 30, 959–965. doi: 10.1016/S0021-9290(97)00041-9
- Peng, X. B., Abbeel, P., Levine, S., and van de Panne, M. (2018). DeepMimic. *ACM Trans. Graph.* 37, 1–14. doi: 10.1145/3197517.3201311
- Peng, X. B., Berseth, G., Yin, K., and Panne, M. V. D. (2017). DeepLoco. *ACM Trans. Graph.* 36, 1–13. doi: 10.1145/3072959.3073602
- Peyron, M. A., Lassauzay, C., and Woda, A. (2002). Effects of increased hardness on jaw movement and muscle activity during chewing of visco-elastic model foods. *Exp. Brain Res.* 142, 41–51. doi: 10.1007/s00221-001-0916-5
- Posselt, U. (1952). Studies in the mobility of the human mandible. *Acta Odontol. Scand.* 10, 19–160.
- Ruckert, E., and d'Avella, A. (2013). Learned parametrized dynamic movement primitives with shared synergies for controlling robotic and musculoskeletal systems. *Front. Comput. Neurosci.* 7:138. doi: 10.3389/fncom.2013.00138
- Sagl, B., Schmid-Schwab, M., Piehlinger, E., Kronnerwetter, C., Kundi, M., Trattning, S., et al. (2019a). *In vivo* prediction of temporomandibular joint disc thickness and position changes for different jaw positions. *J. Anat.* 234, 718–727. doi: 10.1111/joa.12951
- Sagl, B., Schmid-Schwab, M., Piehlinger, E., Kundi, M., and Stavness, I. (2019b). A dynamic jaw model with a finite-element temporomandibular joint. *Front. Physiol.* 10:1156. doi: 10.3389/fphys.2019.01156
- Schulman, J., Levine, S., Moritz, P., Jordan, M., and Abbeel, P. (2015). “Trust region policy optimization,” in *Proceedings of the 32nd International Conference on International Conference on Machine Learning, Volume 37, ICML'15* (Lille), 1889–1897.
- Schulman, J., Wolski, F., Dhariwal, P., Radford, A., and Klimov, O. (2017). Proximal policy optimization algorithms. *arXiv* 1707.06347.
- Seireg, A., and Arvikar, R. (1975). The prediction of muscular load sharing and joint forces in the lower extremities during walking. *J. Biomech.* 8, 89–102. doi: 10.1016/0021-9290(75)90089-5
- Servin, M., Lacoursière, C., and Melin, N. (2006). “Interactive simulation of elastic deformable materials,” in *Proceedings of SIGRAD Conference* (Skövde).
- Thelen, D. G., Anderson, F. C., and Delp, S. L. (2003). Generating dynamic simulations of movement using computed muscle control. *J. Biomech.* 36, 321–328. doi: 10.1016/S0021-9290(02)00432-3
- Tortopidis, D., Lyons, M. F., Baxendale, R. H., and Gilmour, W. H. (1998). The variability of bite force measurement between sessions, in different positions within the dental arch. *J. Oral Rehabil.* 25, 681–686. doi: 10.1046/j.1365-2842.1998.00293.x
- Tsuruta, J., Mayanagi, A., Miura, H., and Hasegawa, S. (2002). An index for analysing the stability of lateral excursions. *J. Oral Rehabil.* 29, 274–281. doi: 10.1046/j.1365-2842.2002.00904.x
- Van Hasselt, H., Guez, A., and Silver, D. (2016). “Deep reinforcement learning with double q-learning,” in *Thirtieth AAAI Conference on Artificial Intelligence* (Phoenix, AZ).
- Vigotsky, A. D., Halperin, I., Lehman, G. J., Trajano, G. S., and Vieira, T. M. (2018). Interpreting signal amplitudes in surface electromyography studies in sport and rehabilitation sciences. *Front. Physiol.* 8:985. doi: 10.3389/fphys.2017.00985
- Xu, W., Bronlund, J., Potgieter, J., Foster, K., Röhrle, O., Pullan, A., et al. (2008). Review of the human masticatory system and masticatory robotics. *Mech. Mach. Theory* 43, 1353–1375. doi: 10.1016/j.mechmachtheory.2008.06.003
- Yin, H. H., and Knowlton, B. J. (2006). The role of the basal ganglia in habit formation. *Nat. Rev. Neurosci.* 7:464–476. doi: 10.1038/nrn1919

Conflict of Interest: The authors declare that the research was conducted in the absence of any commercial or financial relationships that could be construed as a potential conflict of interest.

Copyright © 2020 Abdi, Sagl, Srungarapu, Stavness, Prisman, Abolmaesumi and Fels. This is an open-access article distributed under the terms of the Creative Commons Attribution License (CC BY). The use, distribution or reproduction in other forums is permitted, provided the original author(s) and the copyright owner(s) are credited and that the original publication in this journal is cited, in accordance with accepted academic practice. No use, distribution or reproduction is permitted which does not comply with these terms.



A Case of Recurrent Painful Ophthalmoplegic Neuropathy

Yaping Yan¹, Bo Zhang², Zhuocong Lou³, Kaiming Liu¹, Ming Lou¹, Meiping Ding¹ and Yongfeng Xu^{1*}

¹ Department of Neurology, Second Affiliated Hospital, College of Medicine, Zhejiang University, Hangzhou, China,

² Department of Surgery, Second Affiliated Hospital, College of Medicine, Zhejiang University, Hangzhou, China, ³ Department of Neurology, Affiliated Hospital of Shaoxing University, Shaoxing, China

OPEN ACCESS

Edited by:

Kazutaka Takahashi,
University of Chicago, United States

Reviewed by:

Marco Carotenuto,
University of Campania Luigi
Vanvitelli, Italy

Vivek Lal,
Post Graduate Institute of Medical
Education and Research
(PGIMER), India

*Correspondence:

Yongfeng Xu
xuyf925@zju.edu.cn

Specialty section:

This article was submitted to
Headache Medicine and Facial Pain,
a section of the journal
Frontiers in Neurology

Received: 09 October 2019

Accepted: 24 April 2020

Published: 04 June 2020

Citation:

Yan Y, Zhang B, Lou Z, Liu K, Lou M,
Ding M and Xu Y (2020) A Case of
Recurrent Painful Ophthalmoplegic
Neuropathy. *Front. Neurol.* 11:440.
doi: 10.3389/fneur.2020.00440

Ophthalmoplegic migraine (OM) is characterized by recurrent episodes of headache with unilateral ophthalmoplegia due to paresis of cranial nerve III, IV, or VI. The recent revision to the International Headache Classification has reclassified it as recurrent painful ophthalmoplegic neuropathy (RPON). However, it is of note that the presentation of oculomotor nerve tumors may mimic RPON. Here, we report the case of a patient presenting with recurrent migraine and oculomotor palsy with several specific magnetic resonance imaging (MRI) findings. The patient was initially diagnosed with migraine 15 years ago, but since 10 years ago, his symptoms had evolved to include repeated oculomotor paralyzes. Before this attack, the patient did eventually recover completely each time after the initial episode. MRI performed during this attack revealed a nodular enhancing lesion described as schwannoma of the left oculomotor nerve, and on diffusion-weighted imaging (DWI), the nerve was isointense to the midbrain. The nodular enhancement became weaker, and the nerve's signal on DWI disappeared 3 months later as the patient's symptoms resolved mostly. This is the first case of RPON demonstrating an obvious change in signal of the affected nerve on DWI during the attack and remission.

Keywords: migraine, repeated oculomotor paralyzes, diffusion weighted imaging (DWI), schwannoma, demyelination

INTRODUCTION

Ophthalmoplegic migraine (OM) was first reported by Charcot in 1890, described as migraine with oculomotor nerve palsy (1). More than 100 years later, OM was included as a migraine variant in the first edition of the International Headache Classification (IHCD- I) (2). Then, in 2004, the disorder was reclassified as one of the cranial neuralgias in ICHD-II due to the enhancement and thickening of the involved nerve in the brain as observed on magnetic resonance imaging (MRI) (3). In 2013, OM was replaced by recurrent painful ophthalmoplegic neuropathy (RPON) in IHCD-3 based on headache, subsequent cranial neuropathies, MRI features, and the fact that some cases showed response to corticosteroid treatment (4). However, the etiology remains controversial, but mainly involves schwannoma or recurrent bouts of demyelination of the affected nerve (5, 6).

Reduction or complete resolution of focal enhancement in the cisternal portion of the involved nerve is observed in most RPON patients and in rare patients with schwannoma (7–9). Instead, persistent nodular enhancement of the lesion is seen in most patients with schwannoma (10, 11). Here, we report a case of recurrent migraine and oculomotor palsy in which MRI showed enhancement of the oculomotor nerve with visible DWI signal at the midbrain exit while the patient was symptomatic. Follow-up MRIs more than 4 months after the resolution of the latest episode demonstrated reduced enhancement and resolution of the DWI signal.

CASE PRESENTATION

A 24-year-old man was admitted to our hospital with a complaint of diplopia. Before admission, he had been experiencing migraine and then concurrent oculomotor paralysis for 1 month. He was treated with prednisolone (40 mg/d) for 4 days but without any improvement. He denied a family history of migraine. General physical examination was normal. Neurological examination revealed a complete paralysis of the left third cranial nerve (**Figure 1**). Serologic and cerebrospinal fluid (CSF) studies were normal. MRI revealed focal enhancement of the cisternal segment of the left oculomotor nerve (**Figure 2A**). Meanwhile, the affected nerve was isointense to the midbrain on DWI and apparent diffusion coefficient (ADC) maps (**Figures 2B,C**). He received intravenous methylprednisolone (80 mg/d) for 8 days followed by prednisolone taper for 15 days but still experienced no immediate improvement. Gradually, over the course of the next 3 months, the patient's left-sided ptosis and diplopia showed complete resolution although the left pupil remained relatively dilated and poorly reactive to light (**Figure 3**). Repeated MRI revealed relatively weaker enhancement with no signal visible on DWI and ADC maps (**Figures 2D–F**).

Back to the patient's history, he had been suffering from monthly episodes of migraine for the past 15 years, lasting for 24 h each time. Then, 10-years ago, he started experiencing diplopia and a left-sided ptosis after resolution of the headache and nausea every 2 months, which persisted for 1 week each time. A review of a previous MRI performed at another hospital 9-years earlier, when the patient was aged 15, showed slight thickening of the left third cranial nerve at the site of exit from the midbrain, especially on T2 FLAIR (**Figure 4B**). At that time, the patient was able to prevent the development of oculomotor paralysis by taking aminopyrine-caffeine tablets immediately when the headache occurred. However, the time to resolution of the oculomotor paralysis had begun to increase to usually 2–3 weeks, and the frequency of the attacks was reduced to 3–4 times a year. During the past 15-years, although the symptoms resolved completely each time except for this attack, the lesion had increased in size on T1 since his initial presentation (**Figures 4A,C,D**).

DISCUSSION

As Carlow have reported, enhancement of the cisternal segment of the third nerve was usually detected during an attack, resolving several weeks later when the patient's symptoms had also been relieved. Based on this observation, Carlow proposed that the diagnostic criteria for oculomotor OM should include the presence of post-contrast enhancement on MRI and thickening of the third nerve during an attack with less dramatic enhancement observable during remission (12). Here, we report a male adolescent who had been suffering from recurrent painful ophthalmoplegic neuropathy (RPON) for 10-years. Consistently, several other similar cases have been reported recently. The image feature of these patients on MRI with contrast was quite similar to that in the present study (6, 13). Additionally, our case also displayed an obvious signal change in the affected nerve on DWI and ADC maps during the episode compared to that during remission. To our knowledge, this is the first reported case accompanied by such neuroimaging documentation.

With respect to the pathophysiology of this disease entity, the underlying mechanism remains controversial because of lack of autopsy or surgical resection (14). However, some possible theories have been proved histopathologically, mainly including infectious neuritis, ischemia of the third cranial nerve, recurrent demyelination-remyelination, and schwannoma (15–18). As the cerebrospinal fluid and serum test was normal, there was no evidence to support an infectious process in the current case. And the lesion on MRI image did not favor the ischemia mechanism.

The repeated demyelinating theory has gained favor in recent years (6, 16, 18), which is supported by features such as the recurrent episodes; nearly complete remission every time; and transient, reversible MRI contrast enhancement of the oculomotor nerve. Our patient refused biopsy as the symptom could resolve every time. Therefore, histopathological evidence to support this hypothesis was not available.

As for the tumor pathogenesis, it has been reported that transient or recurrent oculomotor nerve deficits may be the primary manifestation in some cases of cranial nerve schwannoma (10). Recently, Petruzzelli et al. have reported a case of a 16-year-old boy with a diagnosis of OM initially but which

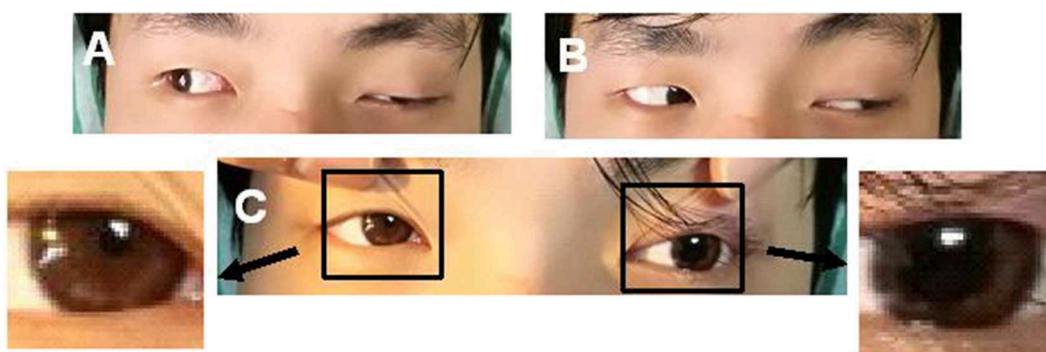


FIGURE 1 | A case of left ptosis, difficulty in seeing inward (**A**), and left pupil enlargement (**C**). The case had normal left abduction (**B**).

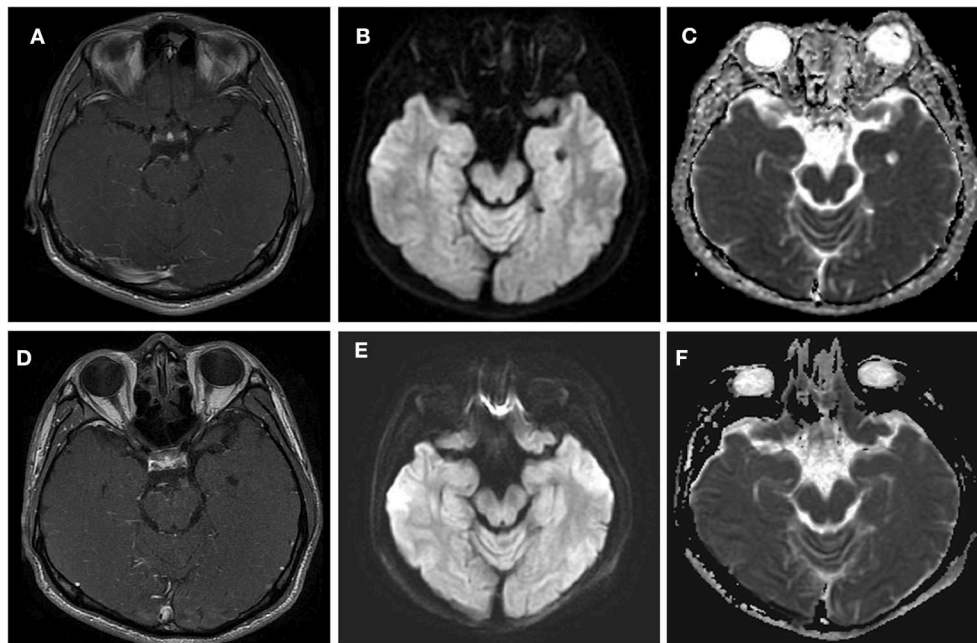


FIGURE 2 | Axial T1 contrast-enhanced MRI (44 days after headache) and DWI (30 days after headache) through the point at which the oculomotor nerve emerges from the midbrain in this patient with left oculomotor ophthalmoplegic migraine. **(A–C)** Acute phase. The MRI shows a nodular, enhancing lesion in the cisternal segment of the left third nerve (arrow) in **(A)**. In **(B,C)**, a signal was demonstrated at the midbrain of the left-sided third cranial nerve on DWI and ADC. **(D–F)** Quiescent phase, taken 7 weeks after the left ptosis and diplopia had resolved. **(D)** Demonstrates the decreased enhancement. **(E,F)** Demonstrate that the signal had disappeared at this point on DWI and ADC.

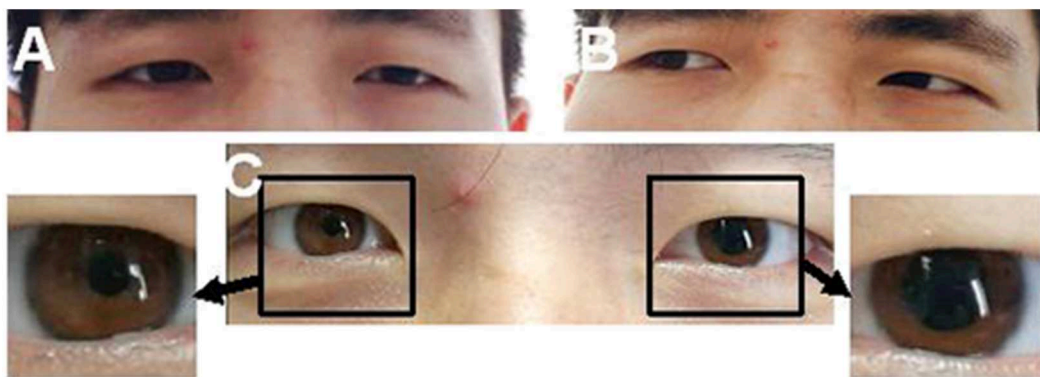


FIGURE 3 | Relatively dilated left pupil **(C)** with recovered extra-ocular movement **(A,B)**.

turned out to have the presentation of a schwannoma after 7-year follow-up (5). In her review, three cases of schwannoma of the affected nerve had been reported, which included a long history of follow-up, and only one was histologically proven (17). It was reported that more than 60% of patients with oculomotor schwannoma treated by surgery developed more severe ophthalmoplegia postoperatively (19). So few cases of RPON accept surgery (15–18). However, the increased thickening of the oculomotor nerve observed after 9 years of RPON attacks may serve as evidence in support of the tumor theory. This hypothesis extends the inflammatory theory,

proposing that repeated bouts of inflammation may lead to cycles of demyelination and remyelination of the affected nerve, and such a process may encourage the transformation of Schwann cells to schwannoma (5). Yet, as Kim et al., Akimoto et al., and Shin et al., have proposed, follow-up surveillance via MRI is required to exclude tumors, especially in patients with suspected RPON with persistent post-contrast enhancement during times of remission (10, 11, 20). However, the enhancement in this case that we describe is weaker during remission than that during the acute episode, which is similar to what was observed in another reported case in which a nodular enhancing lesion was already

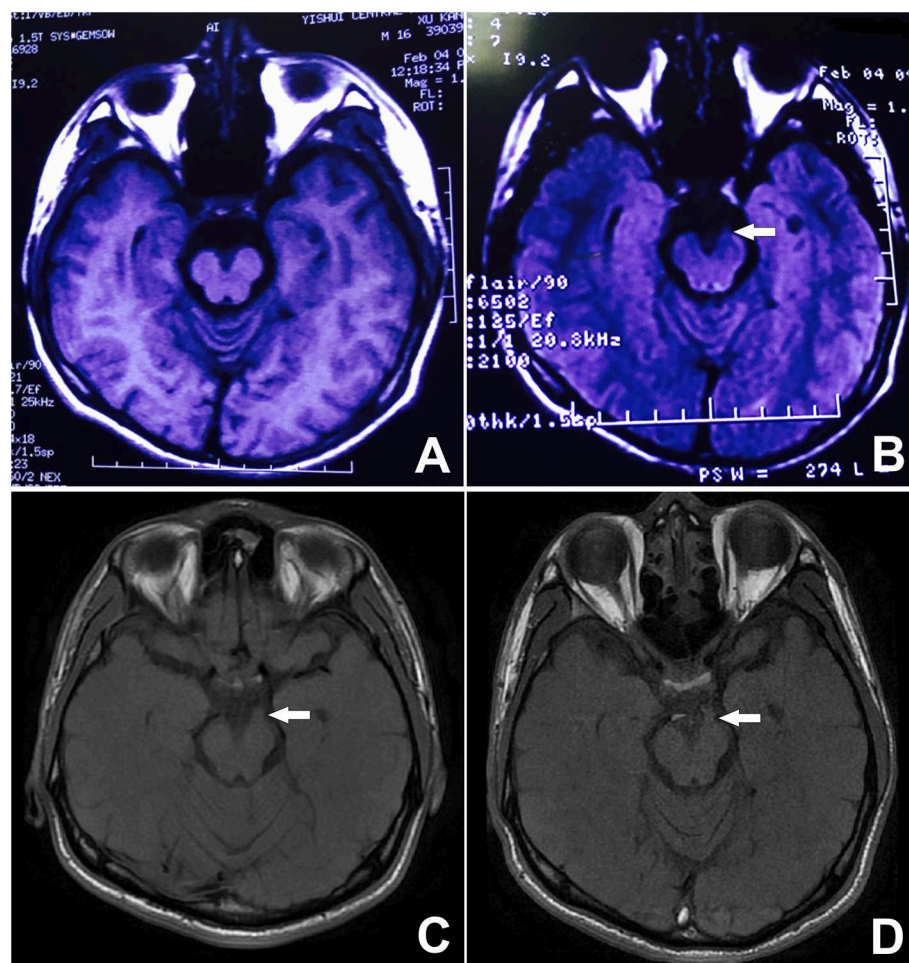


FIGURE 4 | Unenhanced MRI from 9 years prior showing minor thickening of the distal cisternal portion of the left-sided third cranial nerve on T2 FLAIR. See arrow (B). The signal on T1 is obvious, during both the attack and remission. See arrow (C,D) although it is not visible on the T1 image from 9 years ago (A).

visible and of similar size (8). As such, whether the nodular lesion in fact represented a schwannoma remains controversial.

In conclusion, the exact underlying nature of the findings in this patient remains unknown due to the lack of histopathological evidence. Further imaging studies incorporating DWI sequence analysis and serial MRI follow-up of a greater number of cases are required to clarify whether RPON may be a risk factor for the development of schwannoma over an extended period.

DATA AVAILABILITY STATEMENT

All datasets generated for this study are included in the article/supplementary material.

ETHICS STATEMENT

The studies involving human participants were reviewed and approved by The Second Affiliated Hospital, Zhejiang University

School of Medicine. The patients/participants provided their written informed consent to participate in this study. Written informed consent was obtained from the individual(s) for the publication of any potentially identifiable images or data included in this article.

AUTHOR CONTRIBUTIONS

YY, ZL, KL, ML, MD, and YX were responsible for diagnosis and clinical evaluation. YY, ML, MD, and YX collected and analyzed MRI data. YY and BZ wrote the manuscript. YY, BZ, and YX contributed to the revision of the manuscript.

FUNDING

This work was supported by grants from the National Natural Science Foundation of China (No. 81570698)

and (No.81200984), the Natural Science Foundation of Zhejiang Province (LY16H070003), the General medical and health project of Zhejiang Province (No. 2018RC004).

REFERENCES

- Charcot JM. Sur un cas de migraine ophtalmoplégique (paralysie oculomotrice périodique). *Prog Med.* (1890) 31:83–6.
- Classification and diagnostic criteria for headache disorders, cranial neuralgias and facial pain. Headache classification committee of the International Headache Society. *Cephalalgia.* (1988) 8(Suppl. 7):1–96.
- Headache Classification Committee of the International Headache Society. (2004). *The International Classification of Headache Disorders, 2nd edition. Cephalalgia.* 24(Suppl. 1):9–160. doi: 10.1111/j.1468-2982.2003.00824.x
- Headache Classification Committee of the International Headache Society (IHS). The International classification of headache disorders, 3rd edition (beta version). *Cephalalgia.* (2013) 33:629–808. doi: 10.1177/0333102413485658
- Petruzzi MG, Margari M, Furente F, Costanza MC, Legrottaglie AR, Dicuonzo F, et al. Recurrent painful ophthalmoplegic neuropathy and oculomotor nerve schwannoma: a pediatric case report with long-term MRI follow-up and literature review. *Pain Res Manag.* (2019) 2019:5392945. doi: 10.1155/2019/5392945
- Gelfand AA, Gelfand JM, Prabakhar P, Goadsby PJ. Ophthalmoplegic “migraine” or recurrent ophthalmoplegic cranial neuropathy: new cases and a systematic review. *J Child Neurol.* (2012) 27:759–66. doi: 10.1177/0883073811426502
- Mark AS, Casselman J, Brown D, Sanchez J, Kolsky M, Larsen TR, et al. Ophthalmoplegic migraine: reversible enhancement and thickening of the cisternal segment of the oculomotor nerve on contrast-enhanced MR images. *Am J Neuroradiol.* (1998) 19:1887–91.
- Bisdorff AR, Wildanger G. Oculomotor nerve schwannoma mimicking ophthalmoplegic migraine. *Cephalalgia.* (2006) 26:1157–9. doi: 10.1111/j.1468-2982.2006.01167.x
- Kobayashi Y, Kondo Y, Uchibori K, Tsuyuzaki J. Recurrent painful ophthalmoplegic neuropathy with residual mydriasis in an adult: should it be classified as ophthalmoplegic migraine? *Intern Med.* (2017) 56:2769–72. doi: 10.2169/internalmedicine.8842-17
- Kim R, Kim JH, Kim E, Yang HK, Hwang JM, Kim JS. Oculomotor nerve tumors masquerading as recurrent painful ophthalmoplegic neuropathy: report of two cases and review of the literature. *Cephalalgia.* (2015) 35:825–30. doi: 10.1177/0333102414558886
- Akimoto J, Fukami S, Hashimoto R, Haraoka J. Neuromuscular hamartoma is a possible primary pathology of oculomotor ophthalmoplegic migraine. *Cephalalgia.* (2012) 32:171–4. doi: 10.1177/0333102411431331
- Carlow TJ. Oculomotor ophthalmoplegic migraine: is it really migraine? *J Neuroophthalmol.* (2002) 22:215–21. doi: 10.1097/00041327-200209000-00006
- Sharifi A, Kayfan S, Clarke RL, Mehta A, Pfeifer CM. Recurrent painful ophthalmoplegic neuropathy: MRI findings in 2 patients. *Radiol Case Rep.* (2019) 14:1039–42. doi: 10.1016/j.radcr.2019.05.029
- Forderreuther S, Ruscheweyh R. From ophthalmoplegic migraine to cranial neuropathy. *Curr Pain Headache Rep.* (2015) 19:21. doi: 10.1007/s11916-015-0492-1
- Morimoto K, Nagatani M, Mogami H. A case simulating ophthalmoplegic migraine: clinicopathological study. *Headache.* (1985) 25:426–8. doi: 10.1111/j.1526-4610.1985.hed2508426.x
- McMillan HJ, Keene DL, Jacob P, Humphreys P. Ophthalmoplegic migraine: inflammatory neuropathy with secondary migraine? *Can J Neurol Sci.* (2007) 34:349–55. doi: 10.1017/S0317167100006818
- Murakami T, Funatsuka M, Komine M, Hirayama Y, Suzuki H, Shishikura K, et al. Oculomotor nerve schwannoma mimicking ophthalmoplegic migraine. *Neuropediatrics.* (2005) 36:395–8. doi: 10.1055/s-2005-873056
- van der Dussen DH, Bloem BR, Liauw L, Ferrari MD. Ophthalmoplegic migraine: migrainous or inflammatory? *Cephalalgia.* (2004) 24:312–5. doi: 10.1111/j.1468-2982.2004.00669.x
- Moloney P, Hughes NM, Killeen RP, O’Riordan S. A case of recurrent painful ophthalmoplegic neuropathy with associated oculomotor nerve tumour. *Neuroophthalmology.* (2020) 44:28–33. doi: 10.1080/01658107.2018.1534870
- Shin RK, Mejico LJ, Kawasaki A, Purvin VA, Moster ML, Younge BR et al. Transient ocular motor nerve palsies associated with presumed cranial nerve schwannomas. *J Neuroophthalmol.* (2015) 35:139–43. doi: 10.1097/WNO.0000000000000220

ACKNOWLEDGMENTS

We would like to thank the patient for their participation in this study.

Conflict of Interest: The authors declare that the research was conducted in the absence of any commercial or financial relationships that could be construed as a potential conflict of interest.

Copyright © 2020 Yan, Zhang, Lou, Liu, Lou, Ding and Xu. This is an open-access article distributed under the terms of the Creative Commons Attribution License (CC BY). The use, distribution or reproduction in other forums is permitted, provided the original author(s) and the copyright owner(s) are credited and that the original publication in this journal is cited, in accordance with accepted academic practice. No use, distribution or reproduction is permitted which does not comply with these terms.



Different Therapeutic Effects of CO₂ and Diode Laser Irradiation on Tooth Movement-Related Pain

Takako Tsuchiya¹, Naoya Hasegawa¹, Misato Yugawa¹, Au Sasaki¹, Naoto Suda¹ and Kazunori Adachi^{2*}

¹ Division of Orthodontics, Meikai University School of Dentistry, Sakado, Japan, ² Division of Pharmacology, Meikai University School of Dentistry, Sakado, Japan

OPEN ACCESS

Edited by:

Limor Avivi-Arber,
University of Toronto, Canada

Reviewed by:

Man-Kyo Chung,
University of Maryland, Baltimore,
United States
Sheng Wang,
University of Maryland, Baltimore,
United States

*Correspondence:

Kazunori Adachi
k-adachi@dent.meikai.ac.jp

Specialty section:

This article was submitted to
Neurorehabilitation,
a section of the journal
Frontiers in Neurology

Received: 01 November 2019

Accepted: 04 May 2020

Published: 05 June 2020

Citation:

Tsuchiya T, Hasegawa N, Yugawa M,
Sasaki A, Suda N and Adachi K (2020)
Different Therapeutic Effects of CO₂
and Diode Laser Irradiation on Tooth
Movement-Related Pain.
Front. Neurol. 11:481.
doi: 10.3389/fneur.2020.00481

Although orthodontic treatment is common, orthodontic force often induced pain. Low-level laser therapy (LLLT) has been investigated to improve therapeutic comfort. In dentistry, LLLT is mainly applied using two types of lasers, CO₂ and diode lasers, whose biological actions are thought to be associated with wavelength (CO₂: 10,600 nm; diode: 808 nm). The analgesic effect of LLLT on orthodontic treatment-related pain is widely reported but inconsistent. This study aimed to (1) determine whether irradiation with a CO₂ or diode laser attenuates orthodontic treatment-related pain using the jaw-opening reflex model, (2) elucidate the optimal irradiation protocol for both lasers to obtain the maximal analgesic effect, (3) evaluate the effects of laser irradiation on other biological features [e.g., tooth movement, glial fibrillary acidic protein (GFAP) expression, and temperature alterations] and (4) investigate the mechanism underlying the analgesic effect of laser irradiation. In this animal model, orthodontic treatment-induced pain manifested as a significantly reduced the threshold for inducing the jaw-opening reflex on the orthodontically treated side compared with the contralateral side. GFAP expression in the bilateral trigeminal ganglia (TGs) was significantly increased by the application of orthodontic force. CO₂ laser irradiation of the orthodontically treated region significantly increased the threshold for inducing the jaw-opening reflex and the peripheral temperature. Similar reductions in jaw-opening reflex excitability were induced by surface anesthesia and thermal stimulation but not, the diode laser. Neither CO₂ nor diode laser irradiation altered GFAP expression in the TGs. Infiltration anesthesia also significantly increased the threshold for inducing the jaw-opening reflex on each anesthetized side. Irradiation (30 s) by either laser immediately after orthodontic force application (preirradiation) significantly decreased jaw-opening reflex excitability and GFAP expression in the bilateral TGs the next day. However, thermal stimulation immediately after orthodontic force application failed to alter jaw-opening reflex excitability the next day. Laser irradiation did not alter tooth movement; however,

an optimized irradiation protocol for aiding tooth movement is suggested. In conclusion, both CO₂ and diode lasers are able to prevent orthodontic treatment-related pain. Furthermore, the involvement of temperature alterations and surface anesthesia in the analgesic effect induced by CO₂ laser irradiation is suggested.

Keywords: jaw-opening reflex, orthodontic pain, low-level laser therapy, CO₂ laser, diode laser

INTRODUCTION

Orthodontic force-induced pain, which appears within a day and lasts up to a week after the placement or reactivation of orthodontic force, is frequently observed in patients (1–4). Although inflammation in the periodontium is required to achieve accurate tooth movement (5, 6), pain sensation is an adverse effect for patients (1). In dentistry, acidic non-steroidal anti-inflammatory drugs (NSAIDs) are frequently used for severe orofacial pain (e.g., trauma caused by tooth extraction); however, acidic NSAIDs are not recommended for orthodontic patients because prostaglandin E₂, the eicosanoid that is inhibited by acidic NSAIDs, mediates the maturation of osteoclasts (7–10). To protect patients from this disadvantage of orthodontic therapy, alternative analgesic methods have been investigated, and low-level laser therapy (LLLT) is one of these approaches (11–15). Several types of lasers are available for therapeutic purposes and are classified based on wavelength (16, 17). Lasers in the near-infrared (700–1,200 nm) range (e.g., diode and Nd:YAG lasers) are able to penetrate surface tissue and reach deep tissue. On the other hand, lasers in the far-infrared (>1,200 nm) range (e.g., CO₂ lasers) are absorbed in the surface tissue and increase the tissue temperature. Despite these differences, both types of lasers have a photodynamic effect (e.g., photons activate mitochondria) (16, 17), which has been thought to be the basis of the therapeutic effect of laser irradiation. LLLT has been applied to treat temporomandibular disorder (18) and endodontic and periodontal diseases (17) in dentistry, and an analgesic effect of LLLT on orthodontic force-induced pain has been reported, although not consistently (11, 12, 19, 20). To evaluate the analgesic effect quantitatively and to elucidate the appropriate CO₂ or diode laser irradiation strategy for orthodontic force-induced pain, the changes in jaw-opening reflex excitability caused by laser irradiation were measured in the experimental tooth movement (ETM) animal model. In this animal model, the application of orthodontic force increases jaw-opening reflex excitability, which is inhibited by the repetitive administration of acidic NSAIDs (e.g., aspirin) (21). This result indicates that orthodontic force induces peripheral inflammation. Recently, a relationship between the presence of peripheral inflammation and morphological alterations in satellite glial cells (SGCs) was reported (22). In the trigeminal ganglia (TGs), SGCs surround the somata of neurons (23) and are excited by peripheral injury (22, 24) and/or inflammation (23, 25). Since the excitation of SGCs was evaluated by an increase in the expression of glial fibrillary acidic protein (GFAP) in those reports, the effect of laser irradiation on GFAP expression in the TGs was examined. Moreover, the distance of ETM was measured to evaluate the effects (adverse or beneficial)

of laser irradiation on the maturation of osteoclasts indirectly. Finally, the mechanism underlying the analgesic effect of laser irradiation was investigated by applying thermal stimulation and local anesthesia.

MATERIALS AND METHODS

Animals and Experimental Design

The experimental procedure in this study was approved by the Animal Experimentation Committee of Meikai University School of Dentistry. The animal treatments were performed in accordance with the Animal Research: Reporting of *In Vivo* Experiments (ARRIVE) guidelines and the institutional guidelines for the care and use of experimental animals described in the US National Institutes of Health's *Guide for the Care and Use of Laboratory Animals*. One hundred seventy-six 10-week-old male Wistar rats (273 ± 2.7 g, Sankyo Laboratory Service, Tokyo, Japan) were used in this study. The rats were maintained in a temperature-controlled ($23 \pm 1^\circ\text{C}$) environment under a 12 h light-dark cycle with free access to food and water. After the application of orthodontic force, the food was replaced with ground chow (MF, Oriental Yeast Co., Tokyo). The rats were divided into the intact and ETM groups ($n = 8$ each). Jaw-opening reflex excitability in the intact group was evaluated as an acute experiment, whereas jaw-opening reflex excitability in the ETM group was assessed at one (D1), three (D3), or seven (D7) days after the application of orthodontic force. Thirty or 600 s of CO₂ or diode laser irradiation was applied in the intact and D1 groups. Additional D1 animals received 15 s of CO₂ laser irradiation or 30 s of guide laser irradiation, local anesthesia (infiltration or surface) or thermal stimulation before the evaluation of jaw-opening reflex excitability. Thirty seconds of CO₂ or diode laser irradiation was applied immediately after the application of orthodontic force (preirradiation: PI) in another set of animals, and jaw-opening reflex excitability was evaluated one (PI-D1), three (PI-D3), or seven (PI-D7) days after the application of orthodontic force for comparison with that in the D1, D3, and D7 groups. Thermal stimulation was also applied in another set of animals immediately after the application of orthodontic force (preheating: PH), and jaw-opening reflex excitability was evaluated the next day.

Application of Experimental Orthodontic Force and Evaluation of Jaw-Opening Reflex Excitability

An orthodontic apparatus was applied in every group except the intact group. After anesthetization with isoflurane (3.0%, 1.0 L/min), a closed-coil titanium-nickel spring (855–180; American Orthodontics, WI, USA) was placed between the maxillary

incisors and the right first molar for continuous application of orthodontic force (**Figure 1A**). The right first molar was ligated by a wire (0.08 in. 506-01, Tommy, Tokyo, Japan), and the incisors were bonded to a mesh sheet (110-00, Tommy) by light-cured dental adhesive resin cement (Optiband Ultra 740-0293 KaVo Dental Systems Japan Co., Ltd., Tokyo, Japan). The force magnitude was confirmed by a tension gauge (DTN-150, Teclock, Tokyo, Japan), and the spring elongation was ~6 mm to obtain continuous orthodontic force (50 g) (21). For the evaluation of jaw-opening reflex excitability, the animals were anesthetized with isoflurane and underwent tracheal intubation. During surgery, the concentration of isoflurane was maintained at 2.0% (1.0 L/min) to eliminate expression of the nocifensive reflex. Pairs of Teflon[®]-insulated stainless-steel wires (40 gauge; Cooner wire, Chatsworth, CA, USA) were implanted to record the heart rate and the activity of the bilateral anterior digastric muscles by electromyography (EMG). Another pair of electrodes was placed in the buccal and palatal gingiva of the bilateral maxillary first molars for local electrical stimulation (21, 26). After surgery, the concentration of isoflurane was reduced (<1.25%, 1.0 L/min) until the toe-pinch reflex was detected. The animal's body temperature and heart rate were maintained at physiological levels of ~37°C and 330–430 beats/min, respectively. Passing currents (200 μ s) were ascendingly applied to the right and then to the left maxillary first molar region to evoke anterior digastric muscle activity, which was defined as the jaw-opening reflex when it exceeded the baseline muscle activity (mean amplitude of 100-ms duration before stimulation + 5 SD) with constant latency. The current stimulation intensity that induced anterior digastric muscle activity in more than three out of five trials was defined as the jaw-opening reflex threshold. Then, suprathreshold ($\times 1.5$, $\times 2$, and $\times 3$) stimulation was applied. The data were stored (6 kHz; CED 1401 Plus; Cambridge Electronic Design, Cambridge, UK) to analyze the latency, duration, and area under the curve (AUC) of the jaw-opening reflex (Spike2 ver. 7; Cambridge Electronic Design). In all experimental groups, excluding the preirradiation groups, jaw-opening reflex excitability was repetitively evaluated for 60 min at 30 min intervals.

Application of Laser Irradiation, Local Anesthesia and Thermal Stimulation

Laser irradiation was applied to the palatal mucosa of the maxillary right first molar region (**Figure 1B**). To exclude the spread of laser irradiation, a silicon rubber plate made of impression paste (682864, YOSHIDA, Tokyo, Japan) was used to cover the contralateral periodontium. CO₂ (OPELASER PRO, YOSHIDA, Tokyo, Japan) and diode (OPELASER Filio, YOSHIDA, Tokyo, Japan) lasers were used as described in **Table 1** to obtain a consistent laser output range. The distance between the tip of the laser fiber and the tissue surface and the irradiation time were determined using the following formula:

$$t \text{ (s)} = \frac{A \times \left\{ \pi \times \left[\left(\frac{B}{2} \right)^2 + x \times \tan \left(\frac{C}{2} \right) \right]^2 \right\}}{P}$$

where t is the duration of irradiation (sec), A is the energy density (J/mm²), B is the diameter of the output fiber tip (mm), C is the angle (radians) of the laser, and P is the heat capacity (J/sec). Laser irradiation was carried out immediately after the first jaw-opening reflex evaluation in the intact and D1 groups (**Figure 4A**). In the preirradiation groups, laser irradiation was applied immediately after the application of orthodontic force, and then jaw-opening reflex excitability was measured after one (PI-D1), three (PI-D3), or seven (PI-D7) days (**Figure 6A**).

Local anesthesia was applied to the palatal side of the maxillary first molar mucosa. Ethyl aminobenzoate (0.02 g; Benzocaine Dental Jelly 20%, Bee Brand Medico Dental Co., Ltd., Osaka, Japan) was applied to the mucosal surface for surface anesthesia, and lidocaine (0.10 ml; xylocaine injection 2% with epinephrine, AstraZeneca, Osaka Japan) was injected into the mucosa for infiltration anesthesia. After 5 min, jaw-opening reflex excitability was evaluated (**Figure 11A**).

Thermal stimulation was applied using a custom-made heat probe (diameter: 3.5 mm; screw and copper wire). A constant current (1.2 A at 2 V) was supplied to the copper wire to warm the probe tip to 45°C. The probe was brought into contact with the palatal surface mucosa of the right maxillary first molar for 30 s (**Figures 9A, 10A**).

Temperature Measurement of the Mucosal Surface and Gingival Sulcus

The surface temperature of the laser-irradiated oral mucosa was measured with an infrared thermometer (IT-545 NH, HORIBA, Kyoto, Japan) in intact animals before and after each 30 s of laser irradiation. The temperature of the gingival sulcus was continuously measured by using a digital thermometer (BWT-100A00A, Bio Research Center, Aichi, Japan) with a temperature microprobe (diameter: 0.14 mm; IT-23, Physitemp, NJ, USA) and was stored with the EMG data (CED 1401 Plus) for offline analysis. The temperature microprobe was inserted into the palatal side of the gingival sulcus (2.0 mm).

GFAP Immunostaining and Measurement of Neurons Encircled by GFAP-Immunoreactive (IR) Cells in the TGs

After the evaluation of jaw-opening reflex excitability, rats were administered an overdose of anesthetic and fixed via transcardial perfusion of isotonic saline followed by buffered 4% paraformaldehyde. The bilateral TG were removed from the animals in the intact, D1 (30 s of CO₂ or diode laser irradiation) and PI-D1 (30 s of CO₂ or diode laser irradiation) groups ($n = 5$ each). The removed tissue was kept in the same fixative solution for one additional day at 4°C and then kept in 0.01 M phosphate-buffered saline (PBS) containing 20% sucrose (w/v) for 12 h for cryoprotection. For cryosectioning, the specimens were embedded in Tissue Tek (Sakura Finetek Japan, Tokyo, Japan) and stored at –20°C. Ten-micron horizontal TG sections were obtained along the long axis. Every 15th section was thaw-mounted on MAS-GP glass microscope slides (Mastunami, Osaka, Japan) and dried overnight at room temperature. Four sections were chosen from each TG in each rat to be processed for

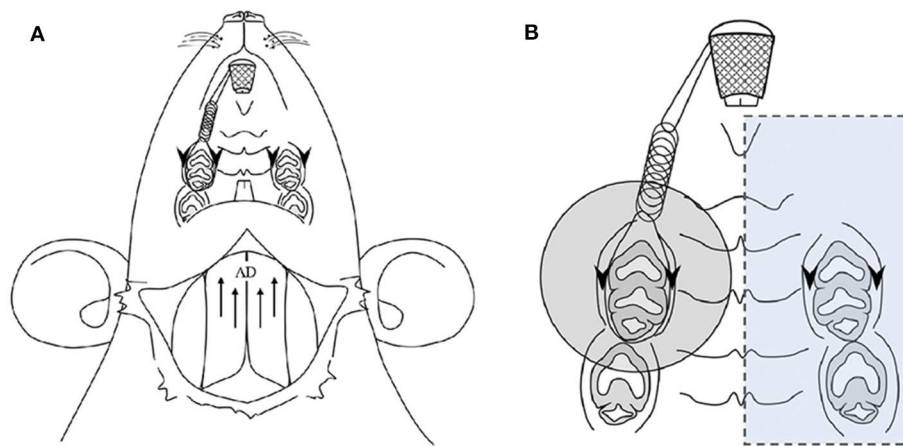


FIGURE 1 | Application of experimental orthodontic force and recording of the jaw-opening reflex **(A)** and the oral region targeted for laser irradiation **(B)**. **(A)** Schematic drawing of the application of experimental orthodontic force to the right maxillary first molar by the placement of a nickel-titanium closed-coil spring between the incisors. Electrodes were placed for recording the bilateral anterior digastric (AD) muscles by electromyography (EMG) as well as for electrical stimulation of the gingiva of the bilateral maxillary first molars. **(B)** The region targeted for laser irradiation is indicated by a shaded circle ($\phi 14.6$ mm, 1.67 cm²). The left molars and gingiva were covered with a silicone rubber impression material to avoid laser irradiation (blue square). Arrows: electrode insertion regions for EMG recording of AD muscles. Arrowheads: electrode insertion regions for electrical stimulation.

GFAP immunohistochemistry. The sections were incubated with a mouse anti-GFAP monoclonal antibody (Millipore, Billerica, MA, USA) after dilution at a concentration of 1:800 in 0.01 M PBS containing 4% normal goat serum (NGS) and 0.3% Triton X-100 (Millipore, Sigma, St. Louis, MO, USA) overnight at 4°C. After rinsing with 0.01 M PBS, the sections were incubated in Alexa Fluor 568 anti-mouse IgG (1:200 in 0.01 M PBS; Invitrogen, Paisley, U.K.) for 2 h at room temperature. After rinsing with 0.01 M PBS, the sections were coverslipped in mounting medium (Thermo Fisher Scientific, Fremont, CA, USA), examined under a fluorescence microscope and analyzed with MIPAR Base (MIPAR, Worthington, OH, USA). No specific labeling was observed in the absence of the primary antibody. TG neurons with more than 2/3 of the perimeter surrounded by GFAP-IR cells were defined as TG neurons encircled with GFAP-IR cells. The number of TG neurons encircled with GFAP-IR cells was counted in each rat, and the relative number was calculated by the following formula: $100 \times \text{number of neurons encircled with GFAP-IR cells} / \text{total number of neurons}$ (22).

Measurement of ETM

In each animal in the PI (PI-D1, PI-D3, and PI-D7) and nonirradiated (D1, D3, and D7) groups, an impression of the maxillary dental arch was obtained with silicone impression paste before spring application (pre-cast) and after jaw-opening reflex evaluation (post-cast) to obtain dental casts. In both casts, the distance between the mesial surface of the maxillary first molar and the distal surface of the second molar was measured by a Vernier caliper (resolution: 0.01 mm; model AD-10AX; Mitutoyo Corporation, Kanagawa, Japan), and the difference was defined as the amount of tooth movement (Figure 8A). The measurement was carried out by two blinded

TABLE 1 | Laser irradiation parameters.

| Type of laser | CO ₂ | Diode |
|-------------------------------------|-----------------|-----------|
| Output wavelength (nm) | 10,600 | 808 |
| Mean power output (W) | 0.5 | |
| Output mode | Continuous wave | |
| Irradiation time (sec) | 15, 30 or 600 | 30 or 600 |
| Distance (cm)* | 20 | 3.2 |
| Irradiation area (cm ²) | 1.67 | |
| Type of guide laser | Diode laser | |

*From the tip of the laser fiber to the tissue surface.

investigators (3 times each) for each cast, and the mean value was calculated (21).

Data Analysis and Expression

The right-side threshold for inducing the jaw-opening reflex and related EMG parameters were standardized to those obtained from left-side stimulation. For example, each threshold (%) is expressed as the threshold for inducing the jaw-opening reflex on the left and right sides (μA)/threshold for inducing the jaw-opening reflex on the left side that was obtained before treatment (e.g., irradiation, thermal stimulation and local anesthesia) (μA). Because the AUC was variable across animals, the suprathreshold intensity-induced AUC was standardized to that obtained by threshold stimulation in each animal. Data are expressed as the mean \pm SE. One-way ANOVA or two-way ANOVA was performed, followed by the Bonferroni *post hoc* test or Dunnett's *post hoc* test. Student's *t*-test or paired *t*-test was used for comparisons between two groups, as appropriate. A $p < 0.05$ was considered to be significant.

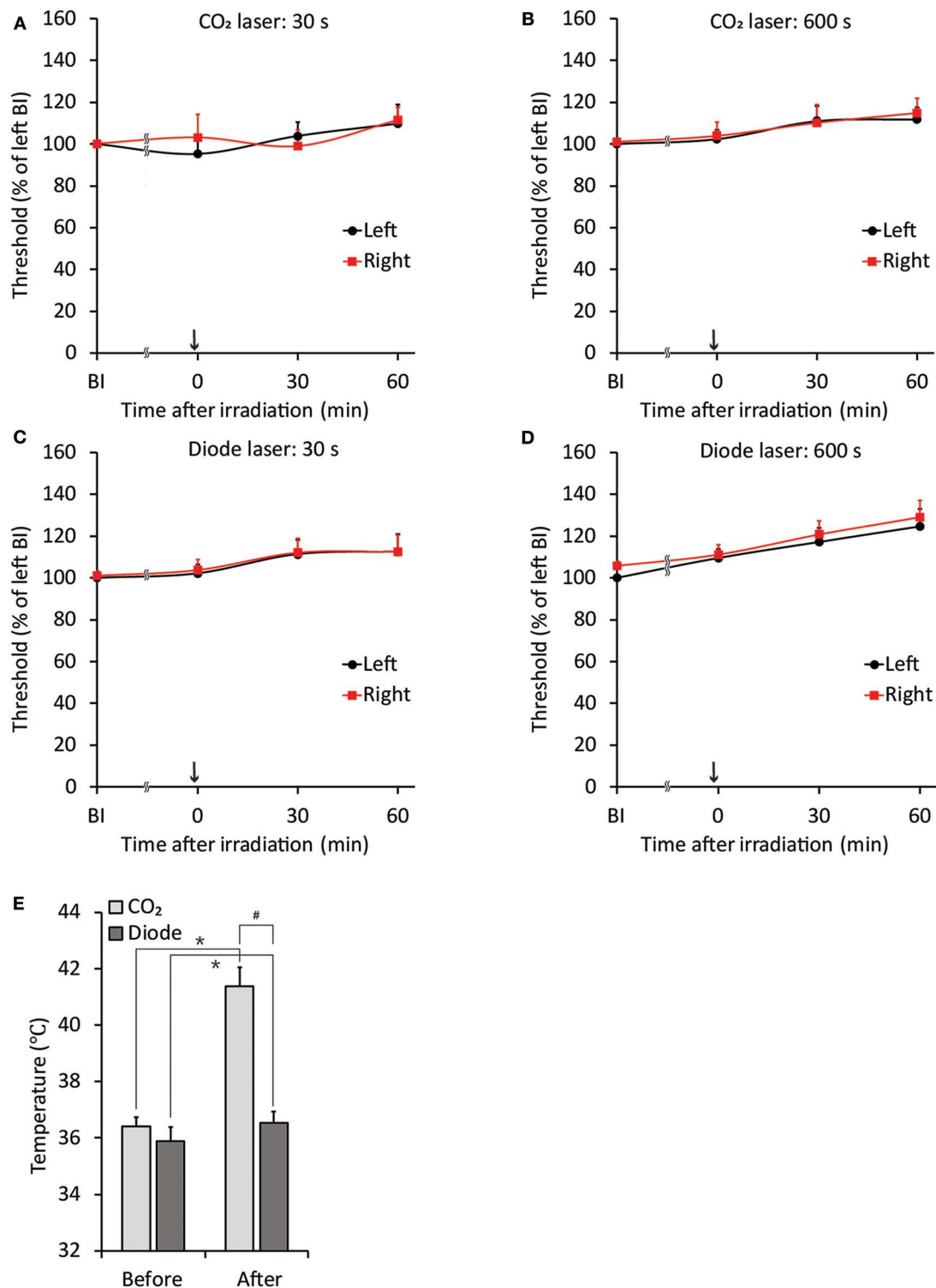
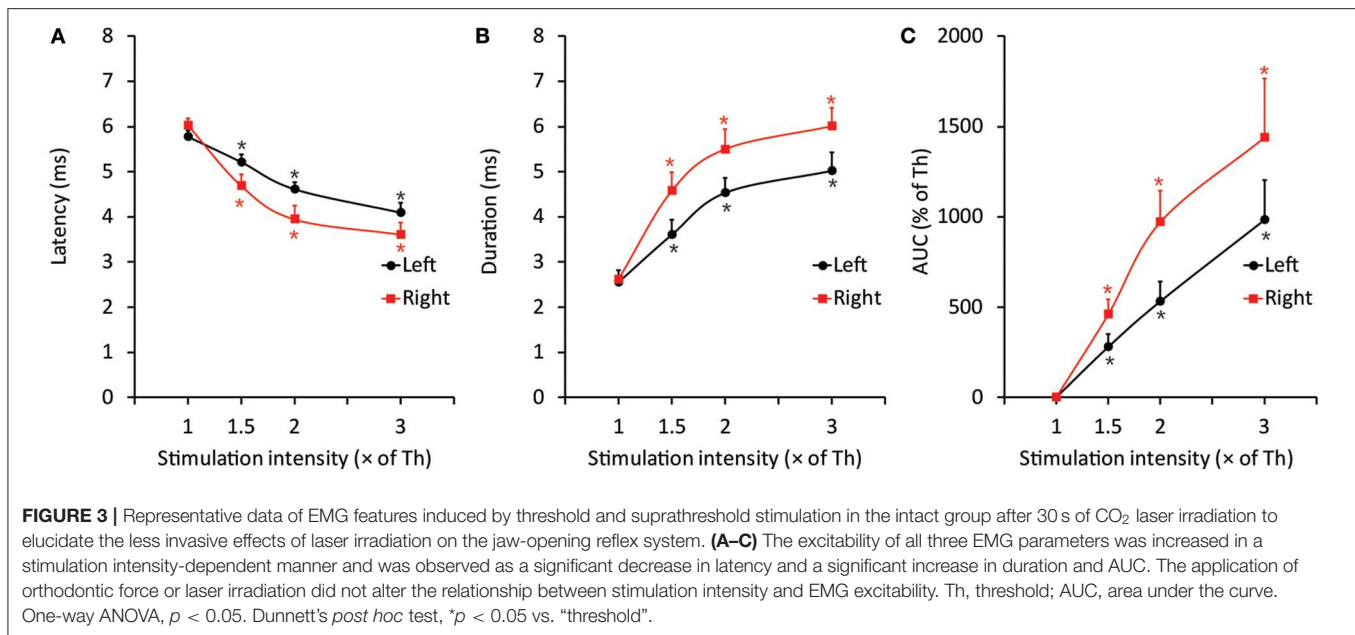


FIGURE 2 | Stability of jaw-opening reflex excitability and temperature alterations after laser irradiation in rats without application of orthodontic force. **(A–D)** There were no significant differences between the left- and right-side thresholds for inducing the jaw-opening reflex (BI). The application of CO₂ (**A**: 30 s, **B**: 600 s) or diode (**C**: 30 s, **D**: 600 s) laser irradiation did not alter jaw-opening reflex excitability. **(E)** CO₂ laser irradiation significantly increased the surface temperature of the right maxillary first molar gingiva. BI: before laser irradiation. Arrow: laser irradiation. Before: before irradiation. After: after irradiation. Paired *t*-test, **p* < 0.05, Student's *t*-test, #*p* < 0.05.



OriginPro 2018 (OriginLab, Northampton, MA, USA) was used for all statistical analyses.

RESULTS

Influence of Laser Irradiation on Jaw-Opening Reflex Excitability and Mucosal Temperature in Intact Animals

The threshold intensity for inducing the jaw-opening reflex varied among intact animals; however, the threshold intensity was quite stable within each animal, and there were no significant differences between left- and right-side stimulation (Figures 2A–D: BI). After CO₂ laser irradiation of the right maxillary first molar region, the threshold slightly increased (30 s: left: $< 9.7 \pm 9.0\%$, right: $< 11.1 \pm 6.3\%$; 600 s: left: $< 11.9 \pm 5.8\%$, right: $< 13.8 \pm 6.8\%$) for 60 min, and there were no significant differences between left- and right-side stimulation (Figures 2A,B, 0–60 min). Similar alterations were observed in the animals treated with diode laser irradiation (30 s: left: $< 12.5 \pm 8.4\%$, right: $< 11.4 \pm 7.9\%$; 600 s: left: $< 24.7 \pm 7.4\%$, right: $< 23.5 \pm 9.4\%$) (Figures 2C,D: 0–60 min). After 30 s of irradiation, the CO₂ laser significantly ($p < 0.05$) increased the temperature of the right maxillary mucosa (Figure 2E), while the diode laser did not alter the temperature significantly; there was a significant ($p < 0.05$) difference between CO₂ and diode laser irradiation. Significant alterations in jaw-opening reflex-related EMG parameters were observed as stimulation-dependent reductions in latency and increases in duration and AUC (Figure 3). These alterations of EMG parameters were similarly observed on left- and right-side stimulation in all experimental groups, including the ETM groups (not shown). Figure 3 shows the alterations observed in intact animals that received 30 s of CO₂ laser irradiation.

Influence of Laser Irradiation on Jaw-Opening Reflex Excitability in the ETM Groups

Because both the CO₂ and diode lasers were equipped with a guide laser (Table 1) to indicate the approximate range of irradiation, the effect of guide laser irradiation on jaw-opening reflex excitability was evaluated in D1 animals. One day of orthodontic force application to the right maxillary first molar significantly ($p < 0.05$) reduced the threshold for inducing the jaw-opening reflex on right-side stimulation compared with left-side stimulation (Figure 4B: BI). Thirty seconds of guide laser irradiation did not alter the significant reduction in the right-side threshold until 60 min after irradiation (Figure 4B: 0–60 min). Both 30 and 600 s of CO₂ laser irradiation significantly ($p < 0.05$) increased the right-side threshold at 30 min after irradiation. The analgesic effect lasted for 60 min (Figures 5B,C: 30–60 min); however, 15 s of CO₂ laser irradiation failed to alter the right-side threshold. The threshold for inducing the jaw-opening reflex on left-side stimulation was not altered by 15–600 s of CO₂ laser irradiation (Figures 5A–C). Thirty and 600 s of diode laser irradiation did not alter the threshold for inducing the jaw-opening reflex on either left- and right-side stimulation (Figures 5D,E). Prolonged application of orthodontic force induced temporal alterations in jaw-opening reflex excitability. The reduction in the right-side threshold for inducing the jaw-opening reflex was almost recovered on D3, and the threshold exceeded that on the left side on D7 (Figures 6B,C). The effects of laser irradiation immediately after orthodontic force application on the temporal alterations in jaw-opening reflex excitability were investigated in the preirradiated groups. Compared with the nonirradiated D1 group, preirradiation (30 s of CO₂ laser) significantly ($p < 0.05$) increased the threshold for inducing the jaw-opening reflex on right-side stimulation (Figure 6B) on D1. On D3 and D7, the threshold for inducing the jaw-opening

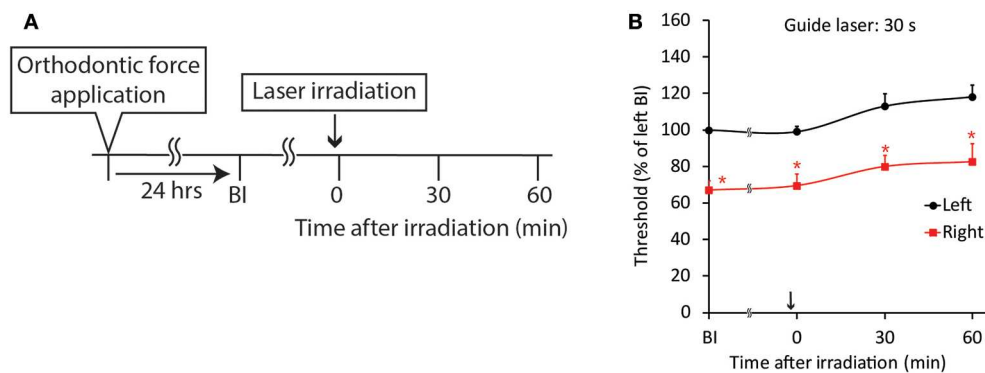


FIGURE 4 | Effect of guide laser irradiation on orthodontic treatment-induced excitation of the jaw-opening reflex. **(A)** Experimental procedure for the application of orthodontic force, guide laser irradiation and the evaluation of jaw-opening reflex excitability. **(B)** One day of orthodontic force application significantly reduced the right-side threshold for inducing the jaw-opening reflex, and guide laser irradiation of the maxillary first molar region for 30 s failed to alter the reduction in the threshold for 60 min. BI: before laser irradiation. Arrow: laser irradiation. Left vs. right: two-way ANOVA, side: $p < 0.05$, time: $p < 0.05$, side \times time: $p < 0.05$; Bonferroni *post hoc* test, * $p < 0.05$ vs. "BI of left".

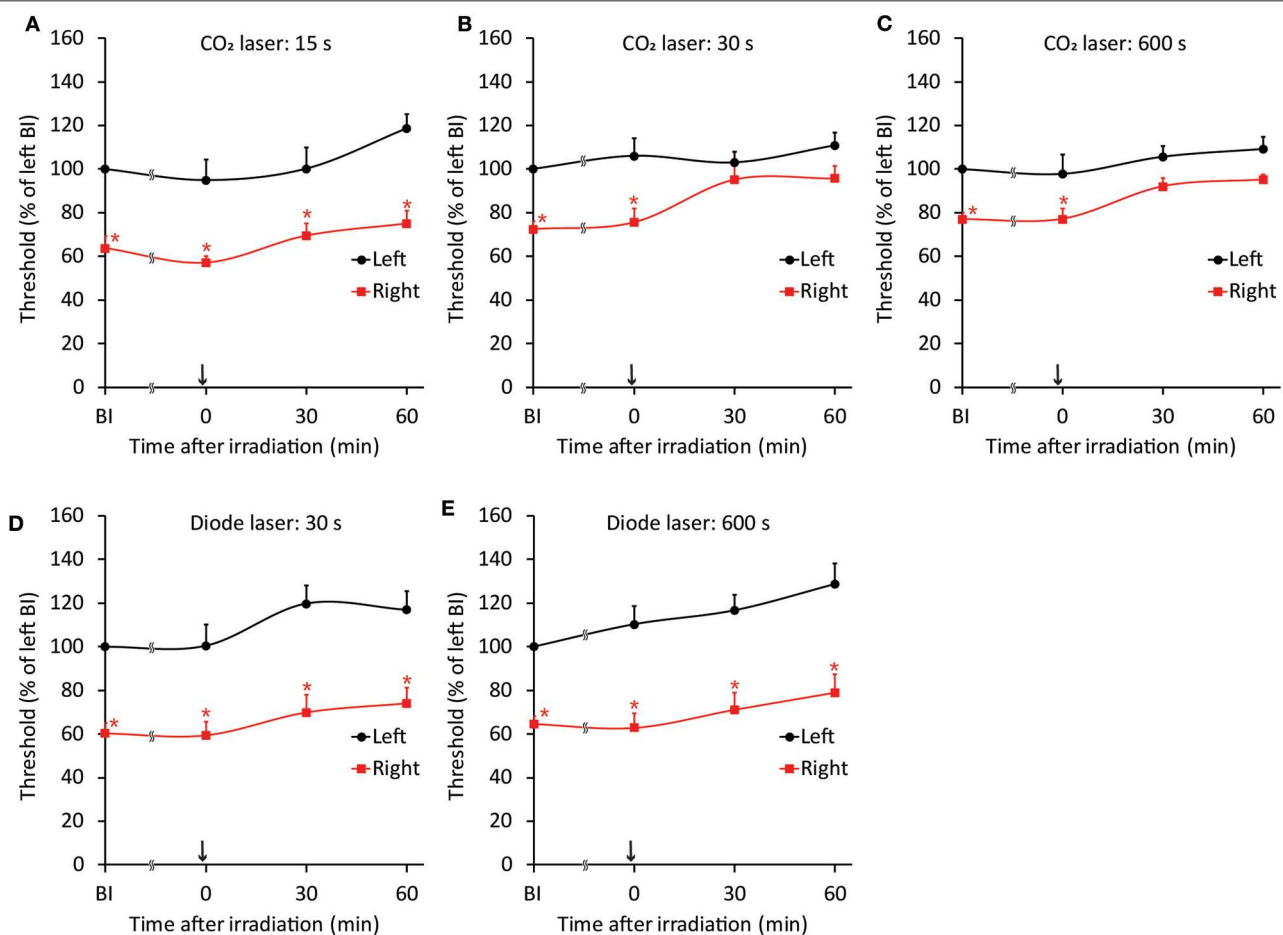


FIGURE 5 | Effects of CO₂ or diode laser irradiation on orthodontic treatment-induced excitation of the jaw-opening reflex. **(A–C)** One day of orthodontic force application significantly reduced the right-side threshold for inducing the jaw-opening reflex before irradiation. CO₂ laser irradiation of the maxillary first molar region for 15 s **(A)** failed to alter jaw-opening reflex excitability. However, 30 **(B)** and 600 **(C)** s of CO₂ laser irradiation significantly increased the right-side threshold for inducing the jaw-opening reflex. **(D,E)** Thirty seconds **(D)** or 600 s **(E)** of diode laser irradiation failed to increase the right-side threshold for inducing the jaw-opening reflex. BI: before irradiation. Arrow: laser irradiation. Two-way ANOVA, side: $p < 0.05$, time: $p < 0.05$, side \times time: $p < 0.05$; Dunnett's *post hoc* test, * $p < 0.05$ vs. "BI of left".

reflex was not significantly different from that in the non-irradiated groups. Interestingly, preirradiation prohibited the increase in the threshold for inducing the jaw-opening reflex on D7. Similar effects were observed in animals irradiated by a diode laser for 30 s immediately after the application of orthodontic force (Figure 6C). Compared with that in the non-irradiated D1 group, the threshold for inducing the jaw-opening reflex was significantly ($p < 0.05$) increased in the preirradiated group, and subsequent temporal alterations in jaw-opening reflex excitability were almost the same as those observed after preirradiation by a CO₂ laser (Figures 6B,C).

Alterations in GFAP-IR Cells Expression Induced by Orthodontic Force Application and Laser Irradiation

In comparison with the intact control, 1-day of orthodontic force application significantly ($p < 0.01$) increased the number of neurons encircled with GFAP-IR cells in the V₁ and V₂ branch regions of the bilateral TGs (Figures 7A,B). On the left but not the right side, the expression of GFAP-IR cells in the TG was also significantly ($p < 0.01$) increased in the V₃ branch region. Irradiation by a CO₂ or diode laser at 1 day after the application of orthodontic force failed to alter the number of TG neurons encircled with GFAP-IR cells (Figures 7C,D). On the other hand, preirradiation by either laser significantly reduced the number of neurons encircled with GFAP-IR cells in the V₁ ($P < 0.01$) and V₂ ($p < 0.05$) branch regions of the right TG. In addition, preirradiation with a diode laser significantly ($p < 0.05$) reduced the expression of GFAP-IR cells in the V₁ branch region of the left TG (Figures 7E,F).

Effect of Laser Irradiation on the Distance of ETM

Without laser irradiation, the application of orthodontic force induced a temporal increase in the distance of tooth movement, as previously described (21). Thirty s of irradiation by a CO₂ or diode laser did not alter the distance of tooth movement at any of the observation timepoints (D1, D3, or D7) (Figure 8B).

Effect of Thermal Stimulation on Jaw-Opening Reflex Excitability in the ETM Groups

Thermal stimulation (30 s, 45°C) of the palatal mucosa of the right maxillary first molar significantly ($p < 0.05$) increased the right-side threshold for inducing the jaw-opening reflex immediately after thermal stimulation, and the increase in the threshold was sustained until the termination of observation (Figure 9B). Thermal stimulation of the right molar region also increased the left-side threshold for inducing the jaw-opening reflex 30 min later. One day of orthodontic force application significantly ($p < 0.05$) increased the temperature of the gingival sulcus of the right maxillary first molar compared with that of the contralateral molar (Figure 9C: BH). Thermal stimulation of the right-side molar region significantly ($p < 0.05$) and promptly increased the temperature of the gingival sulcus of the right molar, and it returned to the previous level

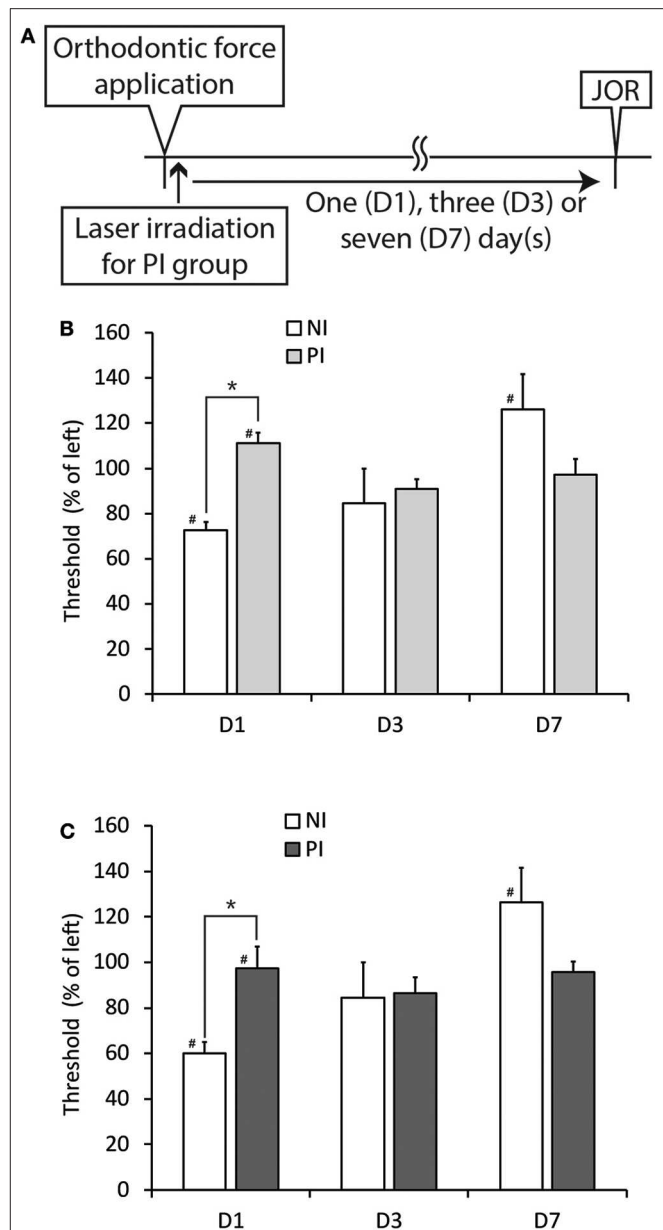
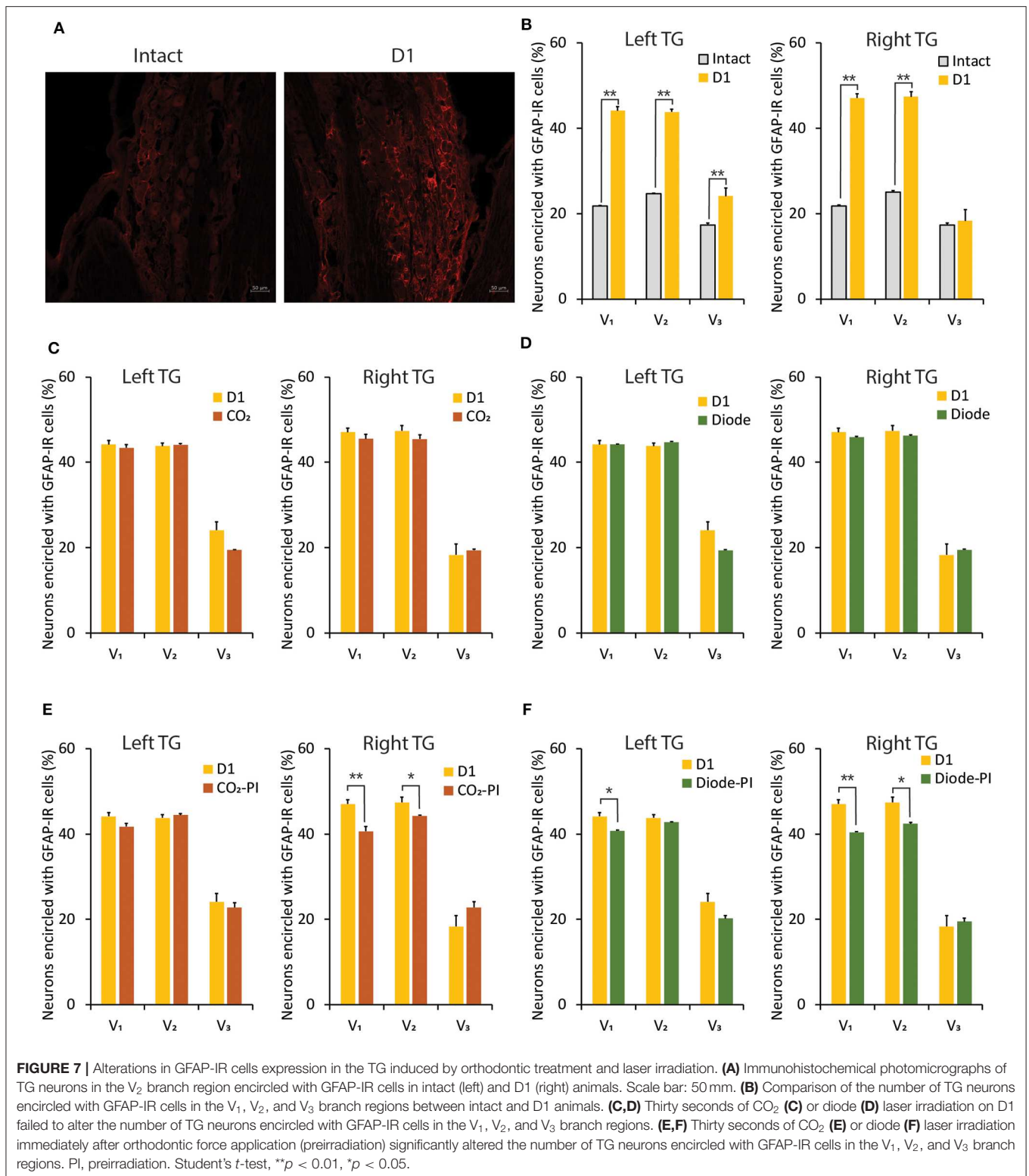


FIGURE 6 | Effects of CO₂ or diode laser irradiation immediately after the application of orthodontic force (preirradiation) on the development of orthodontic treatment-induced excitation of the jaw-opening reflex. **(A)** Experimental procedure for the application of orthodontic force, laser irradiation and the evaluation of jaw-opening reflex excitability. **(B)** Thirty seconds of CO₂ laser irradiation significantly increased the right-side threshold for inducing the jaw-opening reflex on D1, but this effect was not observed at three or seven days after PI (D3 and D7). **(C)** Thirty seconds of diode laser irradiation significantly increased the right-side threshold for inducing the jaw-opening reflex on D1, but this effect was not observed at 3 or 7 days after PI (D3 and D7). NI, non-irradiation; PI, preirradiation; JOR, evaluation of jaw-opening reflex excitability. Student's *t*-test, * $p < 0.05$: NI vs. PI. Paired *t*-test, # $p < 0.05$: left vs. right in the same group.

immediately after the termination of stimulation. Similarly, but to a much lesser extent, temporal alterations in the temperature of the gingival sulcus of the left molar were observed. Thermal



stimulation immediately after the application of orthodontic force failed to alter the right-side threshold for inducing the jaw-opening reflex on D1 (**Figure 10B**). In those animals, a

significant ($p < 0.05$) difference in the temperature of the gingival sulcus was observed between the left and right molars (**Figure 10C**).

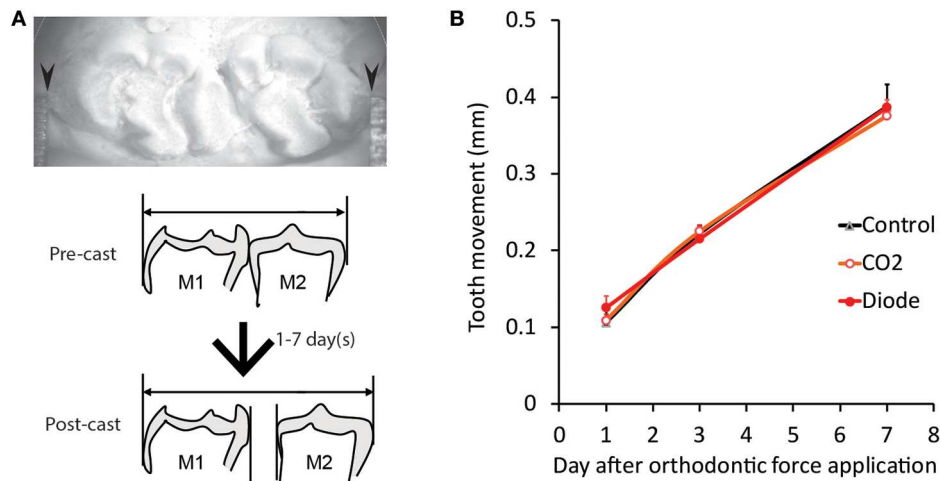


FIGURE 8 | Effects of laser irradiation on orthodontic force-induced ETM. **(A)** Representative photomicrograph of tooth movement measurement in the plaster model (post-cast) (top) and schematic drawing of the lateral view of the pre- and post-casts of the molars (bottom). **(B)** The distance of tooth movement at one (D1), three (D3) and seven (D7) days after the application of orthodontic force in each experimental group. Arrowheads: contact point between the molars of the plaster model and the Vernier caliper.

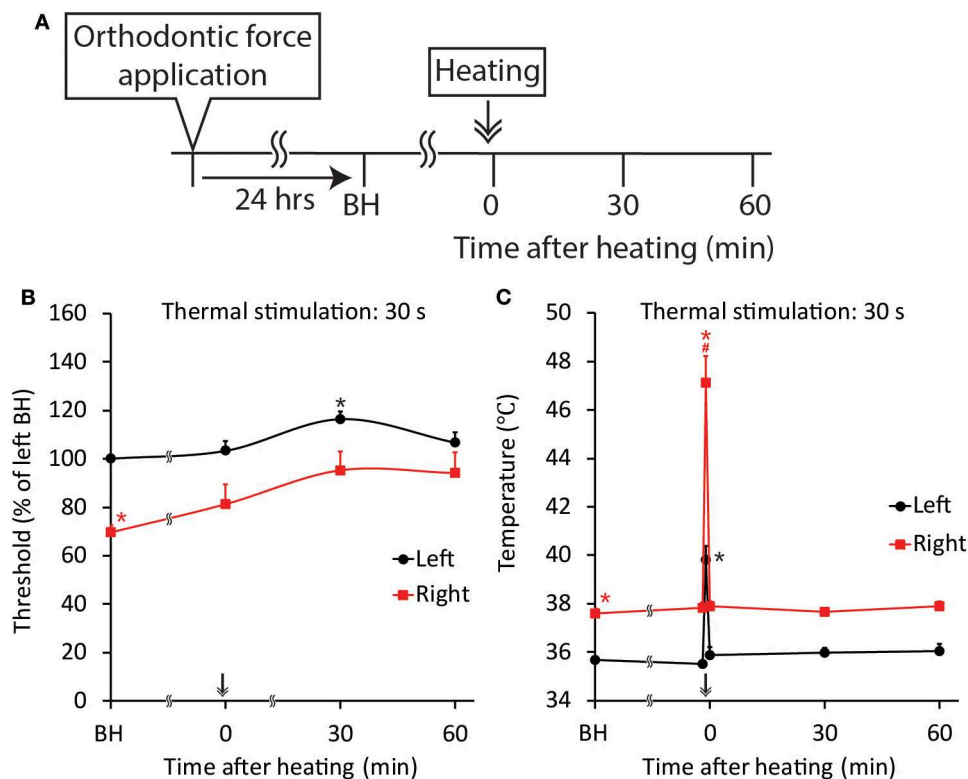


FIGURE 9 | Effect of thermal stimulation on orthodontic treatment-induced excitation of the jaw-opening reflex. **(A)** Experimental procedure for the application of orthodontic force, thermal stimulation and the evaluation of jaw-opening reflex excitability. **(B)** Thermal stimulation (30 s, 45°C) significantly increased the right-side threshold for inducing the jaw-opening reflex. **(C)** Thermal stimulation (30 s, 45°C) significantly increased the gingival sulcus temperature on both sides. BH, before heating (thermal stimulation). Arrow & Heating: thermal stimulation. Two-way ANOVA, side: $p < 0.05$, time: $p < 0.05$, side \times time: $p < 0.05$; Dunnett's *post hoc* test, * $p < 0.05$: vs. "BH of left," # $p < 0.05$: vs. "BH of right".

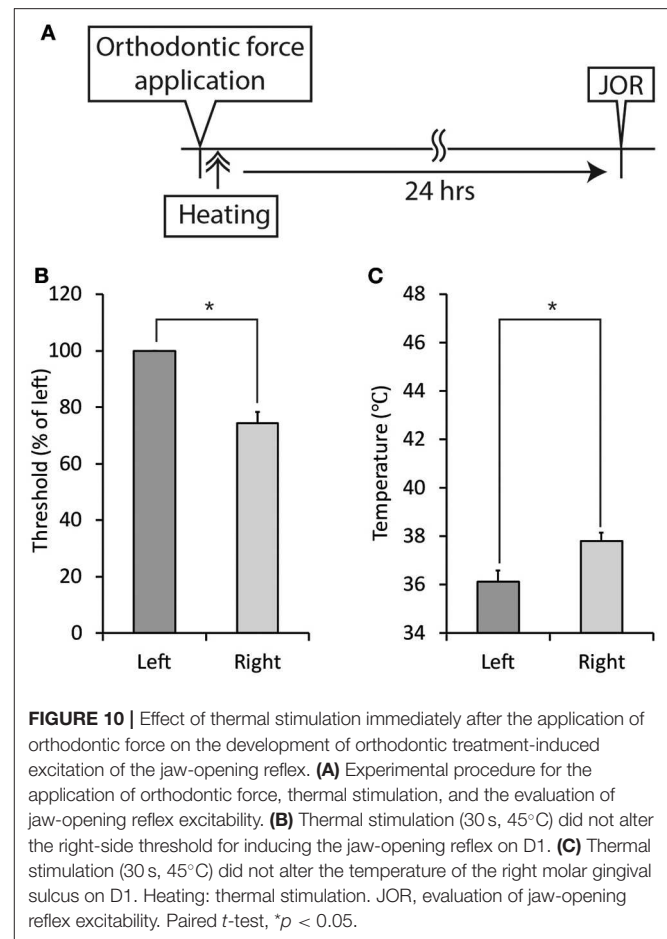
Effect of Local Anesthesia on Jaw-Opening Reflex Excitability in the ETM Groups

Both surface and infiltration anesthesia of the palatal mucosa of the right maxillary first molar significantly ($p < 0.05$) increased the right-side threshold for inducing the jaw-opening reflex, and the increase in the threshold was sustained until the termination of observation (Figures 11B,C). Although surface anesthesia of the left molar region did not alter the left-side threshold for inducing the jaw-opening reflex, infiltration anesthesia of the left molar region significantly ($p < 0.05$) increased the left-side threshold for inducing the jaw-opening reflex. The intensity of the left- and right-side thresholds after infiltration anesthesia were similar.

DISCUSSION

In this study, the beneficial effects of laser irradiation by common dental lasers using different light sources on the orthodontic pain-related reflex and ETM were examined. In this animal model, the threshold for inducing the jaw-opening reflex was significantly reduced on the right side, which was subjected to orthodontic force, compared to the left side, which remained intact. These findings are consistent with those of previous studies reporting that trigeminal (e.g., pulp and temporomandibular joint) noxious stimulation increases jaw-opening reflex excitability (27–29) and that orthodontic force-induced inflammation in the periodontium (e.g., the periodontal ligaments and alveolar bone) plays a crucial role in the excitability of the jaw-opening reflex (21). In addition, it has been confirmed previously that the application of an orthodontic apparatus without spring elongation did not alter the excitability of the jaw-opening reflex (21).

Two types of lasers are available for therapeutic usage: one is characterized by long wavelengths (1,064–10,600 nm) and is absorbed in surface tissue (e.g., CO₂ and Nd:YAG lasers); the other is characterized by short wavelengths (633–890 nm) and penetrates tissue (e.g., diode lasers) (16). The analgesic effect of laser irradiation has been investigated in humans and animals; however, the results of those investigations are not consistent. In humans, sufficient and insufficient effects of LLLT by either CO₂ (11, 15, 19) or diode laser (12, 20) irradiation have been reported. In animals, although CO₂ lasers have been used for noxious stimulation (30), analgesic effects of other lasers with long wavelengths have been reported (13, 31). To exclude invasive effects and to evaluate the beneficial effects of CO₂ laser irradiation, an appropriate irradiation distance between the tip of the laser fiber and the tissue surface had to be determined. We set the irradiation distance for the CO₂ laser as 20 cm away from the tissue surface because irradiation at this distance did not induce a pain sensation in human skin. Based on the irradiation distance of the CO₂ laser, the distance for the diode laser was calculated as 3.2 cm to obtain a consistent irradiation range. Under these conditions, neither CO₂ nor diode laser irradiation altered jaw-opening reflex excitability in intact animals, and a stimulation intensity-dependent increase in EMG parameters was observed, as reported in a previous study (21). These observations indicated



that laser irradiation by neither laser induced invasive effects on trigeminal sensation or muscle (e.g., anterior digastric and masseter) function under the current conditions. The wavelength of the CO₂ laser is in the far-infrared range (>1,200 nm). It has been reported that such lasers penetrate tissue only 20 μm (14) and are then absorbed by the moisture of the tissue, increasing the temperature (17). On the other hand, the wavelength of the diode laser is in the near-infrared range (700–1,200 nm) (14), and these lasers penetrate tissue 4 mm and are not absorbed by tissue moisture (17). Differences in the thermal effects of CO₂ and diode lasers may play a critical role in the acute analgesic effect in this model because the diode-sourced guide laser did not show an analgesic effect. Indeed, an increase in the local circulation of the CO₂ laser-irradiated area has been reported (11, 32), which may increase the clearance of inflammatory mediators in inflamed tissue. In humans, similar acute analgesic effects of CO₂ laser irradiation on tissue with mucosal disease (e.g., pemphigus vulgaris and aphthous stomatitis) have been reported (15, 33). Zand et al. applied a CO₂ laser through a thick layer of transparent, high-water-content gel, and there were no significant alterations in the mucosal temperature after irradiation (33). This result suggests the importance of evaluating the local anesthetic effect of CO₂ laser irradiation. In the present

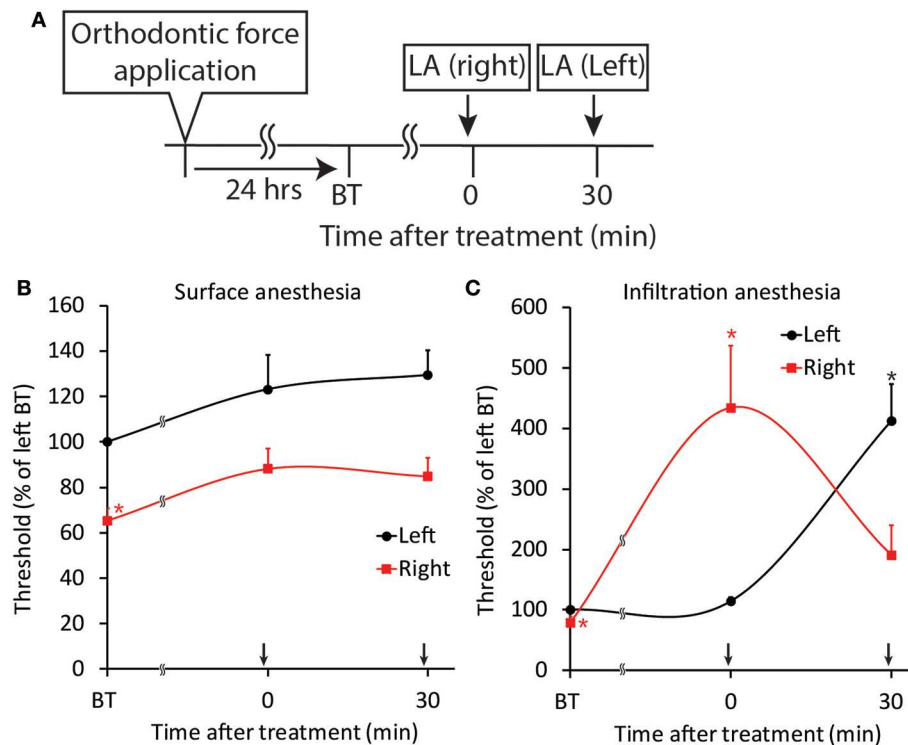


FIGURE 11 | Effect of local anesthesia on orthodontic treatment-induced excitation of the jaw-opening reflex. **(A)** Experimental procedure for the application of orthodontic force, local anesthesia, and the evaluation of jaw-opening reflex excitability. **(B)** Surface anesthesia applied to the right maxillary first molar region significantly increased the right-side threshold for inducing the jaw-opening reflex. **(C)** Infiltration anesthesia applied to the right maxillary first molar region increased the right-side threshold for inducing the jaw-opening reflex. LA, local anesthesia; BT, before treatment (local anesthesia). Arrow: local anesthesia. Two-way ANOVA, side: $p < 0.05$, time: $p < 0.05$, side \times time: $p < 0.05$; Dunnett's *post hoc* test, * $p < 0.05$: vs. "BT of left".

study, CO₂ but not diode laser irradiation, thermal stimulation and surface anesthesia increased the right-side threshold for inducing the jaw-opening reflex similarly on D1. From these results, the involvement of both temperature alterations and surface anesthetic effects in the acute analgesic effect of CO₂ laser irradiation was evident. Since infiltration anesthesia increased the threshold for inducing the jaw-opening reflex to a much higher level (400% of BI) on both sides, the surface anesthetic effect of the CO₂ laser might be related to the absorption rate of the longer laser wavelength. Moreover, the involvement of transient receptor potential vanilloid 1 (TRPV1) and transient receptor potential ankyrin 1 (TRPA1) in the acute analgesic effect of CO₂ laser irradiation has been suggested (34, 35). TRPV1 is a highly temperature-sensitive ($>42^{\circ}\text{C}$) non-selective cation ion channel (36, 37); however, it is rapidly (on the ms-to-s time scale) desensitized, and the molecular basis of the heat desensitization of TRPV1 has recently been reported (38). Moreover, the inhibition of acid-sensing ion channels by TRPV1 activation has also been reported (39). On the other hand, TRPA1 is a lower temperature-sensitive ($<20^{\circ}\text{C}$) non-selective cation ion channel and is also involved in pain sensation (37). Although the activating temperature of TRPA1 is different from that of TRPV1, agonist-activated TRPA1 is suppressed by warmth ($>40^{\circ}\text{C}$) (35). Since both CO₂ laser irradiation and thermal stimulation rapidly

increased the peripheral temperature in the present study in the range of the heat desensitization of TRPV1 and TRPA1, further investigation of the crucial role of TRPV1 and TRPA1 in orthodontic force-induced pain is emphasized. Nevertheless, effects other than those described above are likely involved in the preventive effects of both lasers on orthodontic force-induced excitation of the jaw-opening reflex in the preirradiation groups. Indeed, thermal stimulation immediately after orthodontic force application failed to alter jaw-opening reflex excitability on D1. Diode laser irradiation has been used for photodynamic therapy (17), and biologically relevant photochemical reactions are dependent on the generation of reactive oxygen species (ROS) (40, 41) and singlet oxygen ($^1\text{O}_2$) (42). One potential cause of the preventive effects of the diode laser on orthodontic force-induced excitation of the jaw-opening reflex in this study is ROS because laser irradiation at a wavelength $<800\text{ nm}$ is required to produce a therapeutic concentration of $^1\text{O}_2$ (17). Moreover, a recent report on the enhancement of ROS generation by CO₂ laser irradiation (43) suggested that ROS were also involved in the preventive effects of the CO₂ laser irradiation on orthodontic force-induced excitation of the jaw-opening reflex. ROS are involved in two different aspects of biological function: redox biology and oxidative stress (44). To elucidate whether ROS have beneficial effects on orthodontic force-induced pain,

further investigation into the functional relationship between laser irradiation-induced ROS generation and the production of inflammatory chemical mediators is required. Although the molecular basis of the preventive effects of both lasers on orthodontic force-induced excitation of the jaw-opening reflex is still unclear, the modulation of inflammation might play an important role. The increases in the gingival sulcus temperature and the number of TG neurons encircled with GFAP-IR cells induced by the application of orthodontic force on D1 indicated the presence of inflammation around the treated molar. An inhibitory effect of anti-inflammatory drugs, such as aspirin, on orthodontic treatment-induced excitation of the jaw-opening reflex has been reported (21). In the present study, the significant reduction in the number of TG neurons encircled with GFAP-IR cells was associated with a significant decrease in jaw-opening reflex excitability. These results suggest that the preventive effects of both lasers on orthodontic force-induced excitation of the jaw-opening reflex are associated with the attenuation of inflammation but do not alter tooth movement (see below). Nerve injury induces the expression of GFAP in dorsal root ganglionic SGCs within 4 h, and this effect is reduced in 3 weeks (45). This temporal pattern of GFAP expression is consistent with our results, such as the slight increase in the number of TG neurons encircled with GFAP-IR cells in intact animals compared with the results of a previous study (22), because those animals underwent the orofacial surgical procedure and the evaluation of jaw-opening reflex excitability before the histochemical procedure (e.g., perfusion). Furthermore, an attenuating effect of irradiation with either laser on GFAP expression is hypothesized to occur because preirradiation inhibits the increase in the threshold for inducing the jaw-opening reflex on D7. The alterations in GFAP-IR cell expression in the TG are related to the expression of referred pain (46). The application of orthodontic force significantly increased the number of neurons encircled with GFAP-IR cells in not only the V₂ but also the V₁ and V₃ branch regions in the bilateral TGs. SGCs are connected by gap junctions; thus, excitatory information might spread from the V₂ branch region to other regions in the unilateral TG. It has been documented that unilateral noxious stimulation of the orofacial region increased neural activity in the bilateral trigeminal spinal subnucleus caudalis (Vc), upper cervical spinal cord (C1/C2), and paratrigeminal nucleus (Pa5) (26), which are thought to organize somatotopic information related to orofacial pain. This result suggests the contribution of those nuclei to the increase in GFAP-IR cells in the contralateral TG.

The ETM was measured to assess another effect of laser irradiation. Recently, a significant increase in tooth movement mediated by irradiation with 660 or 830 nm lasers was reported

(47). Laser irradiation also significantly increased the expression of interleukin-1 β (IL-1 β), receptor activator of nuclear factor κ -B ligand (RANKL), and osteoprotegerin (OPG) and the activity of osteoclasts in a wavelength-dependent manner. Yang et al. applied laser irradiation almost every day for 1 week, and a significant increase in ETM was observed after 14 days. In the present study, neither CO₂ laser nor diode laser irradiation increased ETM. This inconsistency may be related to the irradiation procedure (e.g., frequency and period) and the observation period. However, this difference raises the possibility that the biological effect of short-wavelength lasers on the synthesis of IL-1 β , RANKL and OPG appears rapidly but does not last long enough to influence tooth movement.

DATA AVAILABILITY STATEMENT

All datasets generated for this study are included in the article/supplementary material.

ETHICS STATEMENT

The animal study was reviewed and approved by Animal Experimentation Committee of Meikai University School of Dentistry.

AUTHOR CONTRIBUTIONS

All authors had full access to all of the data in the present study and take responsibility for the integrity of the data and the accuracy of the data analysis. KA, NS, and TT: study concept and design and drafting of the manuscript. TT, MY, NH, AS, and KA: data acquisition. TT, MY, NH, NS, and KA: data analysis and interpretation. TT, MY, NS, NH, AS, and KA: critical revision of the manuscript. KA: study supervision.

FUNDING

This work was supported by the Japan Society for the Promotion of Science KAKENHI, Grant No. 18K09843 to NS and 16K20653 and 19K10411 to AS and the ONUKI FUND.

ACKNOWLEDGMENTS

We thank Prof. S. Yokose for providing advice regarding the experimental design and YOSHIDA for providing the CO₂ and diode laser equipment.

REFERENCES

1. Krukemeyer AM, Arruda AO, Inglehart MR. Pain and orthodontic treatment. *Angle Orthod.* (2009) 79:1175–81. doi: 10.2319/1213088-632R22RR.1
2. Ngan P, Kess B, Wilson S. Perception of discomfort by patients undergoing orthodontic treatment. *Am J Orthod Dentofacial Orthop.* (1989) 96:47–53. doi: 10.1016/08899-5406(89)90228-X
3. Shibazaki T, Yozgatian JH, Zeredo JL, Gonzales C, Hotokezaka H, Koga Y, et al. Effect of celecoxib on emotional stress and pain-related behaviors evoked by experimental tooth movement in the rat. *Angle Orthod.* (2009) 79:1169–74. doi: 10.2319/1211088-629R99RR.1
4. Wilson S, Ngan P, Kess B. Time course of the discomfort in young patients undergoing orthodontic treatment. *Pediatr Dent.* (1989) 11:107–10.

5. Li Y, Jacox LA, Little SH, Ko CC. Orthodontic tooth movement: the biology and clinical implications. *Kaohsiung J Med Sci.* (2018) 34:207–14. doi: 10.1016/j.kjms.2018.01.007
6. Proffit WR, Fields HW, Sarver DM, Ackerman JL. The biologic basis of orthodontic therapy. In: Proffit WR, and Sarver DM, editors. *Contemporary Orthodontics*. St. Louis: Mosby Elsevier (2013). p. 278–311.
7. Arias OR, Marquez-Orozco MC. Aspirin, acetaminophen, and ibuprofen: their effects on orthodontic tooth movement. *Am J Orthod Dentofacial Orthop.* (2006) 130:364–70. doi: 10.1016/j.jado.2004.12.027
8. Diravidamani K, Sivalingam SK, Agarwal V. Drugs influencing orthodontic tooth movement: an overall review. *J Pharm Bioallied Sci.* (2012) 4:S299–303. doi: 10.4103/09755-7406.100278
9. Fang J, Li Y, Zhang K, Zhao Z, Mei L. Escaping the adverse impacts of NSAIDs on tooth movement during orthodontics: current evidence based on a meta-analysis. *Medicine.* (2016) 95:e3e256. doi: 10.1097/MD.00000000000003256
10. Kehoe MJ, Cohen SM, Zarrinnia K, Cowan A. The effect of acetaminophen, ibuprofen, and misoprostol on prostaglandin E2E synthesis and the degree and rate of orthodontic tooth movement. *Angle Orthod.* (1996) 66:339–49.
11. Fujiyama K, Deguchi T, Murakami T, Fujii A, Kushima K, Takano-Yamamoto T. Clinical effect of CO₂ laser in reducing pain in orthodontics. *Angle Orthod.* (2008) 78:299–303. doi: 10.2319/0330077-153.1
12. Furquim RD, Pascotto RC, Rino Neto J, Cardoso JR, Ramos AL. Low-level laser therapy effects on pain perception related to the use of orthodontic elastomeric separators. *Dental Press J Orthod.* (2015) 20:37–42. doi: 10.1590/21766-9451.20.3.037-042.oar
13. Pozza DH, Fregapani PW, Weber JB, de Oliveira MG, de Oliveira MA, Ribeiro Neto N, et al. Analgesic action of laser therapy (LLLT) in an animal model. *Med Oral Patol Oral Cir Bucal.* (2008) 13:E6E48–E6E52. doi: 10.1016/S1010-5182(08)71950-4
14. van Gemert MC, Welch AJ. Clinical use of laser-tissue interactions. *IEEE Eng Med Biol Mag.* (1989) 8:10–3. doi: 10.1109/51.45950
15. Zand N, Mansouri P, Fateh M, Ataie-Fashtami L, Rezaee Khiabanloo S, Safar F, et al. Relieving pain in oral lesions of pemphigus vulgaris using the non-ablative, non-thermal, CO₂ laser therapy (NTCLT): preliminary results of a novel approach. *J Lasers Med Sci.* (2017) 8:7–12. doi: 10.15171/jlms.2017.02
16. Asnaashari M, Safavi N. Application of low level lasers in dentistry (endodontic). *J Lasers Med Sci.* (2013) 4:57–66. doi: 10.22037/jlms.v4i2.4187
17. Peng Q, Juzeniene A, Chen J, Svaasand LO, Warloe T, Giercksky KE, et al. Lasers in medicine. *Rep Prog Phys.* (2008) 71:056701. doi: 10.1088/00344-4885/71/5/056701
18. Sousa DFM, Goncalves MLL, Politti F, Lovisetto RDP, Fernandes KPS, Bussadori SK, et al. Photobiomodulation with simultaneous use of red and infrared light emitting diodes in the treatment of temporomandibular disorder: study protocol for a randomized, controlled and double-blind clinical trial. *Medicine.* (2019) 98:e1e4391. doi: 10.1097/MD.00000000000014391
19. Lippert BM, Werner JA. Comparison of carbon dioxide and neodymium: yttrium-aluminum-garnet lasers in surgery of the inferior turbinate. *Ann Otol Rhinol Laryngol.* (1997) 106:1036–42. doi: 10.1177/000348949710601207
20. Turhani D, Scheriau M, Kapral D, Benesch T, Jonke E, Bantleon HP. Pain relief by single low-level laser irradiation in orthodontic patients undergoing fixed appliance therapy. *Am J Orthod Dentofacial Orthop.* (2006) 130:371–7. doi: 10.1016/j.jado.2005.04.036
21. Sasaki A, Hasegawa N, Adachi K, Sakagami H, Suda N. Orthodontic treatment-induced temporal alteration of jaw-opening reflex excitability. *J Neurophysiol.* (2017) 118:2289–95. doi: 10.1152/jn.00379.2017
22. Katagiri A, Shinoda M, Honda K, Toyofuku A, Sessle BJ, Iwata K. Satellite glial cell P2PY2Y1Y2 receptor in the trigeminal ganglion is involved in lingual neuropathic pain mechanisms in rats. *Mol Pain.* (2012) 8:23. doi: 10.1186/17444-80699-8-23
23. Hanani M. Satellite glial cells: more than just ‘rings around the neuron’. *Neuron Glia Biol.* (2010) 6:1–2. doi: 10.1017/S15740925X55X1X0000104
24. Gunjigake KK, Goto T, Nakao K, Kobayashi S, Yamaguchi K. Activation of satellite glial cells in rat trigeminal ganglion after upper molar extraction. *Acta Histochem Cytochem.* (2009) 42:143–9. doi: 10.1267/ahc.09017
25. Chiang CY, Dostrovsky JO, Iwata K, Sessle BJ. Role of glia in orofacial pain. *Neuroscientist.* (2011) 17:303–20. doi: 10.1177/1073858410386801
26. Adachi K, Shimizu K, Hu JW, Suzuki I, Sakagami H, Koshikawa N, et al. Purinergic receptors are involved in tooth-pulp evoked nociceptive behavior and brainstem neuronal activity. *Mol Pain.* (2010) 6:59. doi: 10.1186/17444-80699-6-59
27. Chattipakorn SC, Light AR, Narhi M, Maixner W. The effects of noxious dental heating on the jaw-opening reflex and trigeminal Fos expression in the ferret. *J Pain.* (2001) 2:345–53. doi: 10.1054/jpai.2001.26173
28. Clarke RW, Matthews B. The thresholds of the jaw-opening reflex and trigeminal brainstem neurons to tooth-pulp stimulation in acutely and chronically prepared cats. *Neuroscience.* (1990) 36:105–14. doi: 10.1016/03066-4522(90)903544-7
29. Noguchi M, Kurose M, Yamamura K, Inoue M, Taguchi Y, Sessle BJ, et al. Unilateral application of an inflammatory irritant to the rat temporomandibular joint region produces bilateral modulation of the jaw-opening reflex. *Brain Res Bull.* (2005) 67:182–8. doi: 10.1016/j.brainresbull.2005.06.013
30. Seltzer Z, Dubner R, Shir Y. A novel behavioral model of neuropathic pain disorders produced in rats by partial sciatic nerve injury. *Pain.* (1990) 43:205–18. doi: 10.1016/03044-3959(90)91074-S
31. Zeredo JL, Sasaki KM, Takeuchi Y, Toda K. Antinociceptive effect of Er:YAG laser irradiation in the orofacial formalin test. *Brain Res.* (2005) 1032:149–53. doi: 10.1016/j.brainres.2004.11.010
32. Capon A, Mordon S. Can thermal lasers promote skin wound healing? *Am J Clin Dermatol.* (2003) 4:1–12. doi: 10.2165/001280711-2003040100-00001
33. Zand N, Ataie-Fashtami L, Djavid GE, Fateh M, Alinaghizadeh MR, Fatemi SM, et al. Relieving pain in minor aphthous stomatitis by a single session of non-thermal carbon dioxide laser irradiation. *Lasers Med Sci.* (2009) 24:515–20. doi: 10.1007/s10103-008-0555-1
34. Wang S, Kim M, Ali Z, Ong K, Pae EK, Chung MK. TRPV1V and TRPV1V-expressing nociceptors mediate orofacial pain behaviors in a mouse model of orthodontic tooth movement. *Front Physiol.* (2019) 10:1207. doi: 10.3389/fphys.2019.01207
35. Wang S, Lee J, Ro JY, Chung MK. Warmth suppresses and desensitizes damage-sensing ion channel TRPA1AA1. *Mol Pain.* (2012) 8:22. doi: 10.1186/17444-80699-8-22
36. Caterina MJ, Schumacher MA, Tominaga M, Rosen TA, Levine JD, Julius D. The capsaicin receptor: a heat-activated ion channel in the pain pathway. *Nature.* (1997) 389:816–24. doi: 10.1038/39807
37. Dai Y. TRPs and pain. *Semin Immunopathol.* (2016) 38:277–91. doi: 10.1007/s00281-015-05266-0
38. Luo L, Wang Y, Li B, Xu L, Kamau PM, Zheng J, et al. Molecular basis for heat desensitization of TRPV1V ion channels. *Nat Commun.* (2019) 10:2134. doi: 10.1038/s41467-019-099655-6
39. Blanchard MG, Kellenberger S. Effect of a temperature increase in the non-noxious range on proton-evoked ASIC and TRPV1V activity. *Pflugers Arch.* (2011) 461:123–39. doi: 10.1007/s00424-010-0844-3
40. Bayir H. Reactive oxygen species. *Crit Care Med.* (2005) 33(12 Suppl. 1):S4S98–501. doi: 10.1097/01.CCM.0000186787.64500.12
41. Halliwell B. Reactive oxygen species in living systems: source, biochemistry, and role in human disease. *Am J Med.* (1991) 91:14S–22S. doi: 10.1016/00022-9343(91)902799-7
42. Devasagayam TP, Kamat JP. Biological significance of singlet oxygen. *Indian J Exp Biol.* (2002) 40:680–92.
43. Constantin A, Dumitrescu M, Mihai Corotchi MC, Jianu D, Simionescu M. CO₂ laser increases the regenerative capacity of human adipose-derived stem cells by a mechanism involving the redox state and enhanced secretion of pro-angiogenic molecules. *Lasers Med Sci.* (2017) 32:117–27. doi: 10.1007/s10103-016-20933-6
44. Schieber M, Chandel NS. ROS function in redox signaling and oxidative stress. *Curr Biol.* (2014) 24:R4R53–R62. doi: 10.1016/j.cub.2014.03.034

45. Ji RR, Berta T, Nedergaard M. Glia and pain: is chronic pain a gliopathy? *Pain*. (2013) 154(Suppl. 1):S1S0–28. doi: 10.1016/j.pain.2013.06.022
46. Tsuboi Y, Takeda M, Tanimoto T, Ikeda M, Matsumoto S, Kitagawa J, et al. Alteration of the seconds branch of the trigeminal nerve activity following inferior alveolar nerve transection in rats. *Pain*. (2004) 111:323–34. doi: 10.1016/j.pain.2004.07.014
47. Yang H, Liu J, Yang K. Comparative study of 660 and 830 nm photobiomodulation in promoting orthodontic tooth movement. *Photobiomodul Photomed Laser Surg*. (2019) 37:349–55. doi: 10.1089/photob.2018.4615

Conflict of Interest: The authors declare that the research was conducted in the absence of any commercial or financial relationships that could be construed as a potential conflict of interest.

Copyright © 2020 Tsuchiya, Hasegawa, Yugawa, Sasaki, Suda and Adachi. This is an open-access article distributed under the terms of the Creative Commons Attribution License (CC BY). The use, distribution or reproduction in other forums is permitted, provided the original author(s) and the copyright owner(s) are credited and that the original publication in this journal is cited, in accordance with accepted academic practice. No use, distribution or reproduction is permitted which does not comply with these terms.



Differentiation of Feeding Behaviors Based on Masseter and Supra-Hyoid Muscle Activity

Fumiko Uehara¹, Kazuhiro Hori^{1*}, Kazuhiro Murakami^{1,2}, Jumpei Okawa¹ and Takahiro Ono¹

¹ Division of Comprehensive Prosthodontics, Faculty of Dentistry & Graduate School of Medical and Dental Sciences, Niigata University, Niigata, Japan, ² Department of Prosthodontics, Gerodontology and Oral Rehabilitation, Osaka University Graduate School of Dentistry, Osaka, Japan

OPEN ACCESS

Edited by:

Limor Avivi-Arber,
University of Toronto, Canada

Reviewed by:

Callum Ross,
University of Chicago, United States
Alain Woda,
Université Clermont Auvergne, France

*Correspondence:

Kazuhiro Hori
hori@dent.niigata-u.ac.jp

Specialty section:

This article was submitted to
Craniofacial Biology and Dental
Research,
a section of the journal
Frontiers in Physiology

Received: 24 January 2020

Accepted: 18 May 2020

Published: 12 June 2020

Citation:

Uehara F, Hori K, Murakami K,
Okawa J and Ono T (2020)
Differentiation of Feeding Behaviors
Based on Masseter and Supra-Hyoid
Muscle Activity.
Front. Physiol. 11:618.
doi: 10.3389/fphys.2020.00618

Older adults with disorders of mastication and swallowing are often fed soft foods such as jelly or puree. The texture of such semi-solid foods allows them to be squeezed between the tongue and palate rather than being chewed. However, it is difficult to visually identify such strategies for the oral processing of food. This study aimed to test the hypothesis that there is a difference in the sequential coordination between the masseter and supra-hyoid muscles, and to identify feeding behaviors such as chewing and squeezing using electromyography. Seventeen male subjects (mean age: 30.8 years) were recruited. Four kinds of gels were prepared (two kinds of fracture force and fracture strain) as test samples. Subjects were instructed to consume the gels in three ways: squeezing with the tongue, chewing with the teeth and eating freely until swallowing. The amount of squeezing/chewing and the consumption time was unlimited. The masseter and supra-hyoid muscle activity were recorded during the entire consumption time and videofluorography was simultaneously recorded during each ingestion. Lissajous figures were made from the electromyographic activity of the two groups of muscles during the first stroke, and a regression line was made to determine the gradient of each figure to compare squeezing and chewing using the Mann-Whitney *U*-test. The masseter and supra-hyoid muscles were active simultaneously during squeezing with the tongue. However, the masseter was active after the supra-hyoid during chewing. The gradient of the regression line from the Lissajous figures between the masseter and supra-hyoid muscle activity was positive during squeezing, but negative during chewing. Analysis of the ROC curve showed that the cutoff value of the gradient for differentiating feeding behaviors was 0.097, with a sensitivity of 95.3% and specificity of 98.4%. When we allocated 68 free intakes into squeezing and chewing according to this cutoff value, we could distinguish with good precision, and the accuracy, sensitivity, and specificity were 86.8, 91.1, and 66.7% respectively. These results suggest that certain aspects of muscle activity differed among oral processing methods. Lissajous analysis of muscle activity was useful for identifying ingestion behaviors.

Keywords: muscle activity, tongue, mastication, squeezing, Lissajous figure

INTRODUCTION

Accidental suffocation is the most common form of accidental death in older adults, and in Japan, half of these deaths are caused by respiratory obstruction resulting from food aspiration (Kiyohara et al., 2018; Cabinet Office Government of Japan, 2019). Therefore, providing meals for older adults that can be consumed safely without suffocation is an urgent issue. Risk factors related to suffocation in older adults can be divided into human factors and factors related to the physical properties of food. The cross-sectional area of the lower end of the oropharyngeal cavity is significantly smaller in older adults than in younger people (Ariyoshi et al., 2013) possibly as a result of changes in the shape of the pharyngeal cavity caused by age-related drooping of the larynx. Another study reported age-related weakness in muscles and deterioration of the swallowing reflex (Nishikubo et al., 2015). Risk factors for suffocation in aged care facility residents are related to cognitive function, the presence of meal independence, and the presence of molar occlusion (Ariyoshi et al., 2013). Swallowing without chewing and food thrusting are often seen in older adults with cognitive impairment even when they are capable of eating meals independently (Samuels and Chadwick, 2006). To prevent suffocation of older adults who need long-term care, it is necessary to assess their masticatory and swallowing function and provide appropriate assistance with meal planning, such as selecting the food type and adjusting the size and texture according to their masticatory ability.

Semi-solid food such as jelly tends to be squeezed between the tongue and palate rather than being chewed (Ishihara et al., 2014). However, it is difficult to identify such strategies for oral processing of food by visual observation. Additionally, self-reporting by older adults with cognitive decline may not match the actual feeding behaviors. Appropriate bolus formation is important for swallowing, and it is necessary to match the meal form with the feeding behavior. Mastication is defined as the process of chewing food for swallowing and digestion (Ferro et al., 2017) or the process of food ingestion, crushing, mixing with saliva, and finally forming a bolus. In the process mode developed by Palmer et al. (1992) the processes associated with mastication consist of food intake, transfer to the molars (stage I transport), food processing, and bolus transport to the oropharynx before swallowing (stage II transport) (Hiimeae and Palmer, 1999). If one of these processes fails, the most important masticatory purpose of forming a swallowable bolus cannot be achieved. There are many kinds of research on muscle activity during mastication, where the main research subjects were the masseter and temporal muscles with solid foods either natural or no edible as test foods (Foster et al., 2006; Iguchi et al., 2015; Révérend et al., 2016; Bilt and Abbink, 2017). However, few studies have investigated mastication of semi-solid foods (Kohyama et al., 2016).

Older adults with disorders in mastication and swallowing are often fed soft foods, such as jelly or puree, rather than solid foods. Compensatory strategies for oral processing of food, such as squeezing the food with the tongue and palate, have been observed in patients with reduced masticatory function

due to tooth loss (Ohta et al., 2017). Additionally, even healthy adults eating semi-solid foods can be observed to process the food by squeezing it with their tongue (Arai et al., 1992). In previous studies using electromyography (EMG), the activity of the suprahyoid muscles was observed when squeezing jelly with the tongue and elevating the tongue to the palate (Ishihara et al., 2011, 2013) and the activity of the suprahyoid muscles changed depending on the physical properties of the jelly.

A Lissajous figure expresses vector-synthesis on the Brownian X-axis and Y-axis. This method was able to describe the dynamic aspect of the muscle activity of two different muscles better than the level of myoelectric potential, and has been applied to express the sequential relationship between the two different muscles, for example the masseter and temporal muscles or bilateral muscles (Ferrario and Sforza, 1996; Ferrario et al., 1999, 2014). Moreover, the phase difference was obtained from Lissajous figure. We hypothesized that the Lissajous analysis should be able to clarify the differences in the sequential state of activity of the masseter and suprahyoid muscles caused by different feeding behaviors. This study aimed to test the hypothesis that there is a difference in sequential coordination between the masseter and suprahyoid muscles, and that feeding behaviors such as chewing and squeezing can be identified using EMG.

MATERIALS AND METHODS

Subjects

The subjects were 17 healthy adult males (average age = 30.8 ± 4.2 years). We recruited them from university staff and students as volunteers after we presented the details of the experiment. All subjects provided written consent after receiving full written and verbal explanations of the purpose and details of the experiment. Exclusion criteria included any history of eating or swallowing difficulties, dysphagia, neurological disorders, dental pain, periodontal problems, or temporomandibular joint syndromes. Regarding the exclusion criteria, we did an oral interview about their medical history and confirmed that they had no subjective symptoms nor abnormal findings. We set the target number at 20 subjects because this study is an observational study, and there is a risk of exposure due to VF. However, only 17 eligible volunteers who applied for recruitment, therefore we adopted the largest possible number of subjects. This experiment was approved by the ethics committee of the Faculty of Dentistry of Niigata University (28-R2-4-14).

Test Samples

As test samples, gels were prepared using a mixture of KELCOGEL™ (low-acylated gellan gum) and KELCOGEL LT-100™ (high-acylated gellan gum) (both from San-Ei Gen F.F.I., Inc., Osaka, Japan) (Ishihara et al., 2014; **Table 1**). Low-acylated gellan gum forms less deformable and more brittle gels than high-acylated gellan gum, and diverse textures can be obtained through blending of the two gums (Sworn, 2000). To mask the subtle flavor from these polysaccharides, which may have affected the results of sensory evaluation, sucrose was added at 10% (w/w) to all gel samples.

TABLE 1 | Physical properties of samples.

| Sample | Breaking load (N) | Breaking strain (%) |
|--------|-------------------|---------------------|
| A10 | 9.71 ± 0.13 | 43.31 ± 0.34 |
| A30 | 28.70 ± 1.00 | 46.16 ± 1.08 |
| C10 | 9.73 ± 0.94 | 74.34 ± 1.67 |
| C30 | 29.40 ± 0.99 | 78.71 ± 1.19 |

The mechanical characteristics of the gellan gels were measured using a TA.XTplus texture analyzer (Stable Micro Systems, Surrey, United Kingdom) through instrumental compression of the gel samples. We set the breaking load and strain of each gel samples. Breaking load and breaking strain were determined from the first peak (breaking point) of the compression curve as shown in **Supplementary Figure 1**. Breaking strain was calculated as the ratio of the deformation at breaking point to the initial height of gel. Breaking load and strain were measured by compressing these gels on a hard metal stage using a cylindrical aluminum plate 50 mm in diameter at a crosshead speed of 10 mm/s at 20°C. The gel sample was 20 mm in diameter and 10 mm in height. Compression rate was 90%. The average of the five samples was taken as the physical properties of each sample.

In this study, four kinds of prepared gel samples were used (A10, A30, C10, and C30). The breaking load was set to 30 N for A30 and C30, and 10 N for A10 and C10. The breaking strain was set to 45% for A10 and A30, and 75% for C10 and C30 (**Table 1**). In other words, A30 and C30 were formulated to have the same breaking load, and A10 and A30 to have the same breaking strain. The mechanical properties of the four test samples used in this experiment were as follows: A10 was soft and brittle, A30 was hard and brittle, C10 was soft and elastic, and C30 was hard and elastic. These gels were contrasted for videofluorography (VF) by 8.2 w/v% iopamiron 370® (Bracco Imaging, Milan, Italy) and the taste was corrected with granulated sucrose. Additionally, subjects were provided with the test samples with all the conditions coordinated, such as the form (semi-spherical), size, color, and smell, so that each test sample could not be distinguished from other test samples except for the oral sensation when eating.

Measurement Device

The EMG activity of the right masseter and supra-hyoid muscles was recorded during using a wired bipolar surface EMG system (NT-212u, Nihon Kohden, Tokyo, Japan). The two couples of electrodes were attached non-invasively to the skin surface over the part of corresponding to the masseter and supra-hyoid muscles at an inter-electrode distance of 20 mm so as not to restrict the subjects' movements, while a ground electrode was applied to the right ear. The same operator performed the work of attaching the electrodes so that there was no variation among the subjects. After placing the electrodes, each subject waited for a certain period until the potential stabilized. The subjects were asked to perform occlusal movement, tongue elevation, and swallowing, and we confirmed that the EMG was recorded normally. All muscle activity was recorded from the intake of

the test food to the initial swallowing at a sampling frequency of 1000 Hz. All signals were amplified with an amplifier (AB611-J, Nihon Kohden, Tokyo, Japan) and recorded on the computer through an analog to digital converter (Power Lab ML880, AD Instruments, Bella Vista, Australia). The EMG signals were then filtered (30–1000 Hz). The recorded EMG signals were analyzed after full-wave rectification waveform processing. To assess the feeding behavior during free ingestion, videofluorography (VF) was recorded at 30 frames/s (ARCADIS Avantic Gen2, Siemens, Germany) from the sagittal plane, and recorded on the computer through Power Lab ML880 simultaneously.

Data Collection and Feeding Behavior

A semi-spherical gel sample was put on each subject's tongue by the assistant in the same manner. The subjects sat on the examination chair and the headrest position was adjusted so that the subject's Frankfurt plane was parallel to the floor.

The subjects were instructed to consume the test products in one of three ways: squeezing, chewing, or eating freely. For squeezing, the subject was instructed "Don't chew but squeeze with your tongue." The instruction for chewing was "chew with your teeth," and the instruction for eating freely was simply "eat freely," with no specific instructions. Squeezing with the tongue and chewing were performed twice for each sample (8 times in total), and eating freely was performed once for each sample (4 times in total). For each method, the subject consumed the sample until swallowing, with no limit on the amount and time of chewing or squeezing, and the order of implementation was randomized using online random number generator (Research Randomizer)¹. The EMG activity was recorded when the test sample was ingested, and the VF was recorded from the sagittal plane at the same time.

Data Analysis

After recording the entire EMG activity of the masseter and suprahyoid muscles during chewing and squeezing with the tongue, only the first stroke of chewing or the first squeezing with the tongue were extracted as the target and analyzed. The first stroke of chewing or squeezing with the tongue was defined as the lowest value including one peak value to the next lowest value.

The Lissajous figures (scatter charts) were created by plotting the values of the EMG activity of the suprahyoid muscles on the X-axis and the values of the masseter muscle on the Y-axis. Then, a regression line was made on these Lissajous figures to determine the gradients (**Supplementary Figure 2**). Then the gradient of regression line of the EMG activity of the masseter and supra-hyoid muscles during the first stroke was calculated and compared between squeezing with the tongue and chewing using the Mann–Whitney *U*-test. Additionally, using the gradient values of regression line of squeezing and chewing data, the receiver operating characteristic (ROC) curve for distinguishing feeding behaviors was drawn. The optimum cutoff value for these behaviors was established using the receiver operating characteristic (ROC) curve.

¹<https://www.randomizer.org/>

The free intake was analyzed in the same manner. The free intake feeding behaviors were determined according to the cutoff value we obtained; in other words, the same analysis was performed during free intake, and the gradient of the regression line of the Lissajous figure was calculated and the feeding behaviors of squeezing with the tongue and chewing were compared. The consistency of the results was determined by observing the VF images. For the VF images, we focused on the gel's first movement after it had been placed on the tongue. Chewing was determined to start when the gel was moved by the tongue onto the dental arch at the start of consumption and squeezing with the tongue was determined to start when it was raised and squeezed between the palate and the tongue.

The analysis software used was SPSS Statistics (ver. 25 IBM Japan, Tokyo, Japan) with the significance defined at $P < 0.05$.

RESULTS

The masseter and supra-hyoid muscles were active almost simultaneously during squeezing (**Figures 1A,B**), whereas during chewing, the supra-hyoid and masseter muscles were active in turn during mastication (**Figures 1C,D**).

Analysis using the Lissajous figures of muscle activity showed that the gradient of the regression line was negative for chewing (**Figure 2A**), but positive for squeezing (**Figure 2B**). This tendency was common in all gel samples, and the value of inclination for squeezing was significantly greater than that for chewing (**Figure 3**). Examination of the cutoff value for the gradient of the regression line estimating the differences in feeding behavior using the ROC curve indicated that when the gradient was 0.097, the best sensitivity was 95.3% and the specificity was 98.4% (**Figure 4**).

Based on the cutoff value obtained, 68 free intakes were estimated and compared with the results of the VF determination (**Table 2**). The accuracy was 86.8%, the sensitivity was 91.1%, and the specificity was 66.7%. Additionally, only 2 out of 17 subjects performed squeezing with the tongue in more than half of the trials during free eating, and most subjects chewed when they ingested freely with all four test samples.

DISCUSSION

In this study, we were able to distinguish two types of feeding behaviors, squeezing with the tongue and chewing, by using a new method of analyzing Lissajous figures of the phase differences of the masseter and suprahyoid muscles. This method was a way to allow distinguishing between two gradients of regression lines, one for chewing and the other for squeezing. The regression line was obtained from the Lissajous figure, i.e., putting an EMG of supra hyoid muscles on the *X*-axis and the EMG of masseter on the *Y*-axis and determining the regression lines (**Supplementary Figure 3**). The results of this study show the feasibility of using a non-invasive method for differentiating feeding behaviors. This method could be used at facilities such as nursing homes where there is no professional

who can evaluate chewing and swallowing function, and where determination of the feeding behavior relies on self-reporting by the patient. Objective and quantitative assessment of feeding behavior could be helpful in determining the most appropriate food for patients, thus reducing the risk of suffocation during meals in disabled older adults.

Differences in Muscle Activity Between Chewing and Squeezing

During chewing, the masseter muscle was active during jaw-closing and the suprahyoid muscle was active during jaw-opening. As a result, masseter muscle activity was observed after suprahyoid muscle activity, and the Lissajous figure suggested the phase difference in the activity of the masseter and supra-hyoid muscles. In contrast, when squeezing with tongue, not only the supra-hyoid muscles were working, but also the masseters were active asynchronously. Therefore, it can be deduced that the tongue was raised while the mouth was closed and the food was being compressed during squeezing. In most subjects, the EMG data for the masseter tended to be smaller during squeezing with the tongue than when chewing (data not shown). During chewing, the masseter muscle contracts until the upper and lower teeth are firmly engaged, but when squeezing with the tongue, there is no need to bite deeply as is required during chewing. Thus, it can be deduced that the main role of the masseter muscle during squeezing with the tongue is to work in cooperation with the supra-hyoid muscle to close the mouth and fix the lower jaw in place.

In this study, we measured the masseter and suprahyoid muscles of the right side only. The jaw movement represented by mastication is an activity resulting from the cooperation of the paired left and right temporomandibular joints and the masticatory muscles. It is known that there is a slight left-right difference in that the muscle activity on the mastication side occurs first. In this study, the main purpose was to analyze the difference in cooperative EMG activity between different muscles related to feeding behavior. Therefore, we only analyzed the masseter and suprahyoid muscles on the right side, to determine their different roles in chewing and squeezing with the tongue.

Analysis of Free Intake

In the free ingestion task of the present study, only 2 out of 17 subjects performed squeezing with the tongue for more than half of the four types of samples, and most subjects performed chewing with most of the samples. All the test samples were classified as "food for people who have problems with chewing" according to the Smile Care Food classification, which is one of the standards for the classification of nursing home foods established by the Ministry of Agriculture, Forestry and Fisheries. A30 was a food that can be easily chewed (Smile Care Food 5), A10 and C30 were foods that can be crushed by the gums (Smile Care Food 4), and C10 was a food that can be crushed by the tongue (Smile Care Food 3). These four kinds of test foods were selected because we expected that the feeding behavior would change depending on the physical properties of the food. However, in reality, many subjects chewed all the test foods when

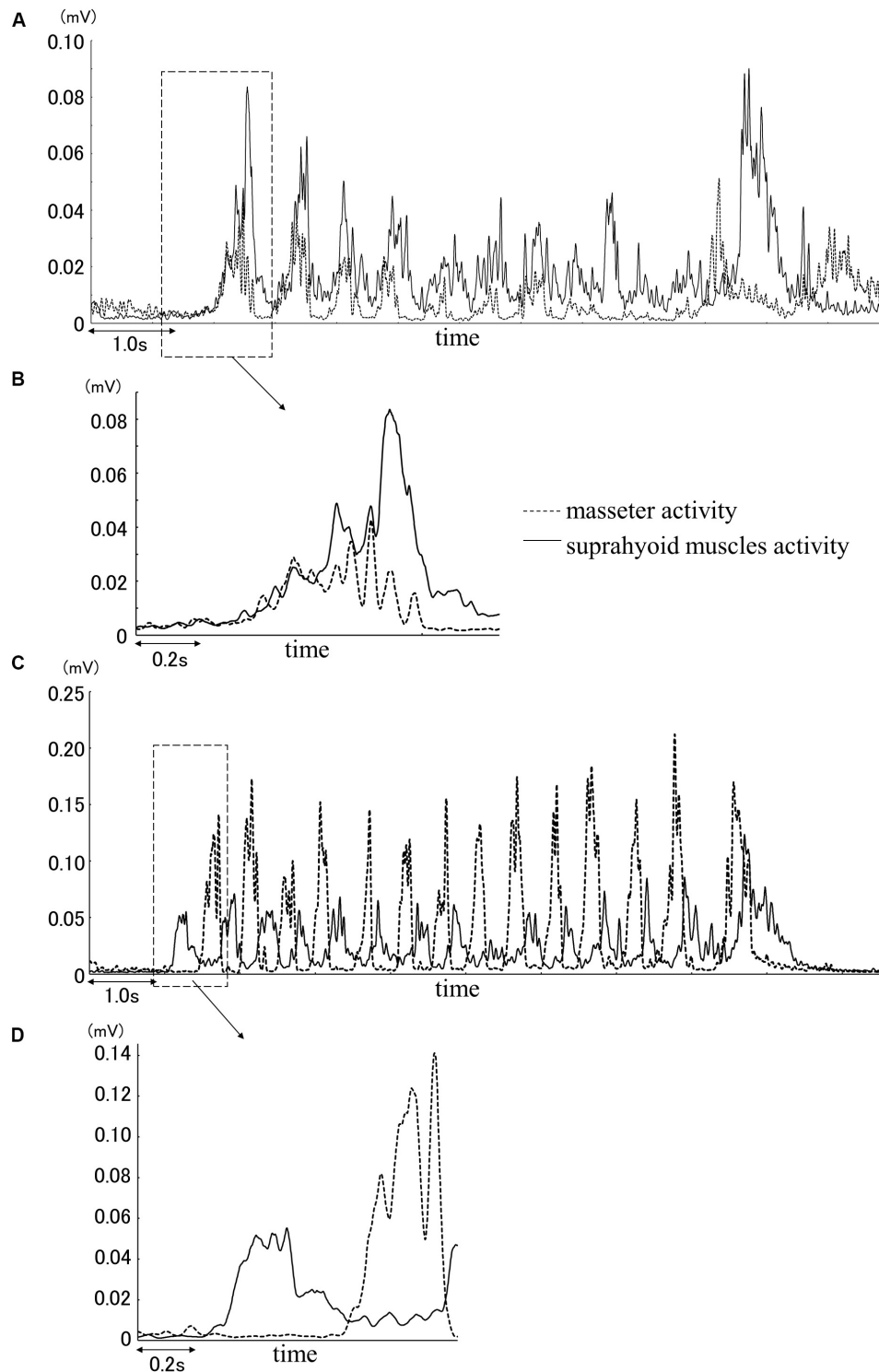
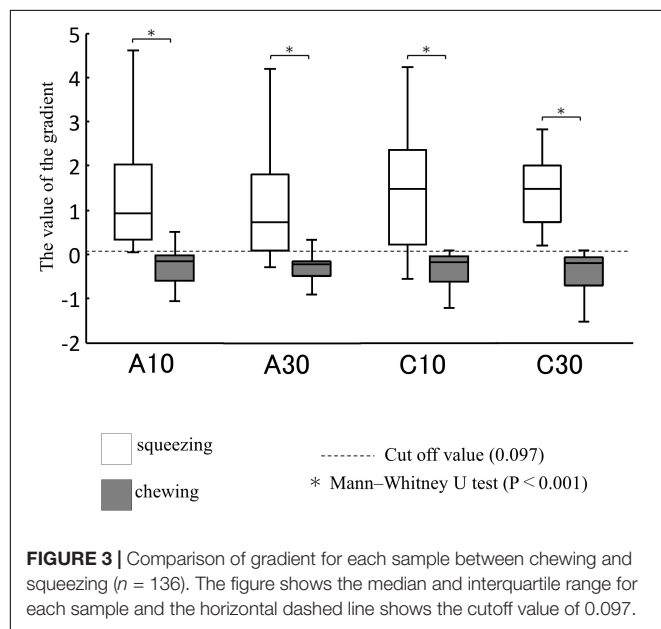
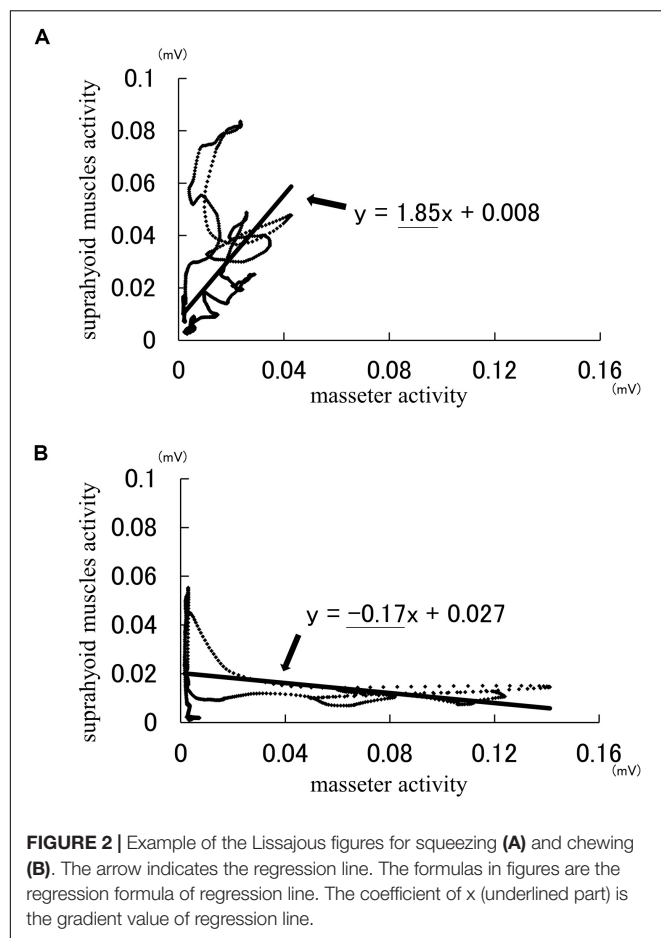


FIGURE 1 | Example of muscle activity during squeezing **(A)** and the first cycle from the muscle activity data of the masseter and suprahyoid muscles **(B)**. Example of muscle activity during chewing **(C)** and the first cycle from the muscle activity data of the masseter and suprahyoid muscles **(D)**.

they were ingested freely. These outcomes suggest that “food that can be eaten by squeezing with the tongue” was not necessarily “food that you want to eat by squeezing with the tongue” for all

subjects. The following factors were considered to have greatly affected the results: (1) all subjects were healthy dentulous adults; (2) there were no extreme differences in the physical properties



of the four test samples; and (3) gel sample had a slight bitterness due to contrast agents. Furthermore, these food were developed

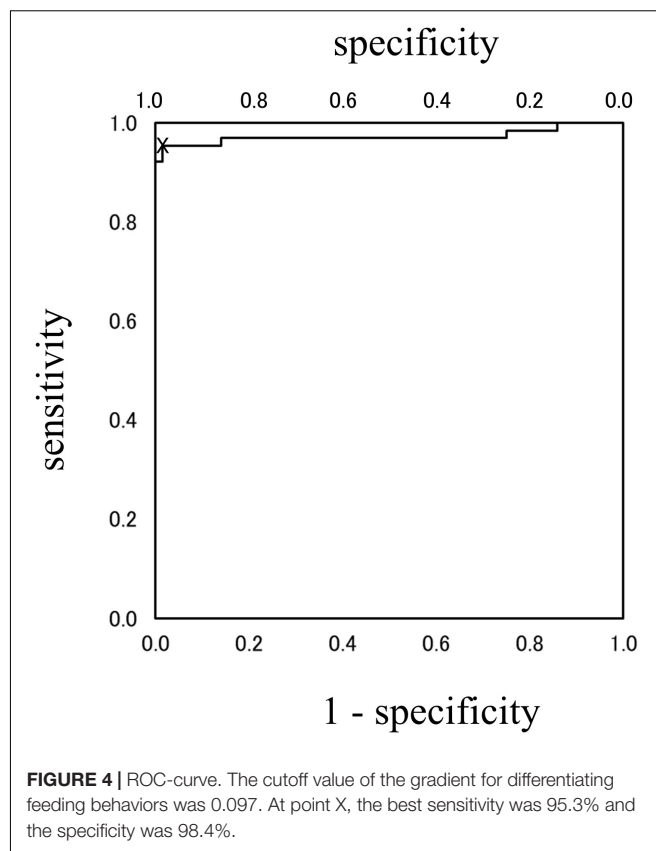


TABLE 2 | Differentiation of feeding behavior based on videofluorography (VF) and the cutoff value.

| Determined by cutoff value (0.097) | | | |
|------------------------------------|-----------|---------|-----------|
| | | Chewing | Squeezing |
| Determined by VF | Chewing | 51 | 5 |
| | Squeezing | 4 | 8 |

for elderly patients of the patients with dysphagia. Therefore, verification for the elderly is needed in the future.

It is speculated that these results might be due to the fact that the subjects were adults with healthy teeth and that there were no extreme differences in the physical properties of the four test samples used in this study. Past studies on mastication suggested that factors that affect masticatory movement include food size, food hardness, and the condition of the subject (Mizumori et al., 1985). In this study, all subjects were fed gel samples of the same size (volume) by the operator. According to a study by Arai et al. (1992) which investigated the effect of food shape on mastication, the most important factor for differentiating feeding behaviors when ingesting semi-solid foods such as agar gels was the size, rather than the physical properties of the gel. Additionally, when the test food was $15 \times 15 \times 15$ mm or less, all subjects ingested the sample by squeezing with the tongue and their hard palate, but when the test food was $20 \times 20 \times 15$ mm or more, the main ingestion pattern changed from squeezing

to chewing. They also reported that the food size threshold for changing feeding behavior was $20 \times 20 \times 15$ mm (Arai et al., 1992; Fueki et al., 2008). The test samples we used in this study were equivalent to one teaspoon (5 ml), with a diameter of 25 mm and height of 15 mm. This is slightly larger than the threshold of $20 \times 20 \times 15$ mm, as suggested by Arai et al. (1992) which may have increased the percentage of subjects who performed chewing during free eating.

Bellisle et al. found that the chewing time became shorter when subjects ate something delicious and enjoyed rolling the food on the tongue (Bellisle et al., 2000; Johansson et al., 2013). It is thought that the preferences and experience of each subject are key determinants in choosing whether to chew or squeeze a food with the tongue. However, although the test samples used in this study were flavored with granulated sugar, the characteristic bitter flavor of the iopamiron370® remained, and the food was never thought to be delicious. The effect of the bitter flavor of the test sample could be the reason why fewer subjects ingested by squeezing with the tongue.

Limitations and Clinical Significance

In this study, the number of subjects and experimental tasks was limited to minimize the radiation exposure. Because we analyzed only the first cycle of each feeding behavior in this study, we were able to discern the trend of the beginning of each feeding behavior. In this report we focused on developing and testing the methodology for using Lissajous figures to distinguish tongue squeeze and chew behaviors. We think that it is important to be able to objectively quantify the feeding behavior. To identify changes in the characteristics of each feeding behavior over time and to evaluate the strategy of oral processing of food, we should conduct an analysis using Lissajous figures with the EMG data from the masseter and suprahyoid muscles from the start of feeding to swallowing. Further analysis of these data might provide important insights in the future.

It is reported that cognitive function, occlusal support including dentures, and oral function are important for preventing choking (Ariyoshi et al., 2013). Some elderly people, even if they retain a complete dentition, eat with tongue squeezing instead of chewing. Preventing choking or aspiration and providing safe meals involving both behaviors are important goals for monitoring feeding by elderly patients (Jayatilake et al., 2015). In order to assess what kinds of foods might best be eaten by specific individuals, reliable discrimination of chewing and tongue squeezing is important. However, reliable discrimination by experienced observers might be difficult and error prone in a busy clinical environment. The methods proposed in this study for rapid and reliable assessment of food oral processing behavior would ideally be validated in elderly people, but it is difficult to measure VF and EMG synchronously in elderly people. Future research should compare the results of our experiment with those of a similar experiment with older adults with missing teeth. It would be expected that the ratio of chewing in free eating would be different from that of young subjects with healthy teeth.

A lot of work is needed to develop a clinical application of Lissajous figures to determine feeding behavior. However, a small electromyograph has been released recently

(Yamaguchi et al., 2018) and the data analysis method used in this report was not very complicated. It is important to be able to evaluate feeding behavior by objective numerical values, regardless of the caregiver's experience, in the care of the elderly. We consider this report to be the first step. Moreover, this method might also be applied in food engineering for designing food for the elderly requiring care.

CONCLUSION

By analyzing the muscle activity of the masseter and suprahyoid muscles using Lissajous figures, the cutoff value 0.097 was determined for the eating pattern of tongue crushing and mastication. These results suggest that this method may be a new means for non-invasive assessment of solid food consumption.

DATA AVAILABILITY STATEMENT

The datasets generated for this study are available on request to the corresponding author.

ETHICS STATEMENT

The studies involving human participants were reviewed and approved by the Ethics Committee of the Faculty of Dentistry of Niigata University. The patients/participants provided their written informed consent to participate in this study.

AUTHOR CONTRIBUTIONS

KH designed the study. FU, KM, JO, and KH collected the data. FU and JO analyzed the data. FU and KH drafted the manuscript. TO edited the manuscript.

FUNDING

This work was supported by the JSPS KAKENHI Grant Number JP15K11194.

ACKNOWLEDGMENTS

We express our deepest gratitude to Drs. Sayaka Ishihara, Makoto Nakauma, and Takahiro Funami for providing gel samples. We also thank Helen Jeays, BSc AE, from Edanz Group (<https://en-author-services.edanzgroup.com/>) for editing a draft of this manuscript.

SUPPLEMENTARY MATERIAL

The Supplementary Material for this article can be found online at: <https://www.frontiersin.org/articles/10.3389/fphys.2020.00618/full#supplementary-material>

REFERENCES

- Arai, E., Yamada, Y., and Nishisaka, T. (1992). Influences of size in soft foods on masticatory process in humans. *Jpn. J. Oral Biol.* 34, 221–229. doi: 10.2330/joralbiosci1965.34.221
- Ariyoshi, H., Shouji, H., Mami, M., Kentarou, I., Akiko, I., Takao, M., et al. (2013). Assessment of feeding and swallowing by cone beam computed tomography - changes in oropharyngeal airway shape with aging. *Dent. Med. Res.* 33, 81–87. doi: 10.7881/dentalmedres.33.81
- Bellisle, F., Guy-Grand, B., and Le Magnen, J. (2000). Chewing and swallowing as indices of the stimulation to eat during meals in humans: effects revealed by the edogram method and video recordings. *Neurosci. Biobehav. Rev.* 24, 223–228. doi: 10.1016/s0149-7634(99)00075-5
- Bilt, A. V. D., and Abbink, J. H. (2017). The influence of food consistency on chewing rate and muscular work. *Arch. Oral Biol.* 83, 105–110. doi: 10.1016/j.archoralbio.2017.07.011
- Cabinet Office Government of Japan (2019). *Annual Report on the Ageing Society*. Available online at: <https://www8.cao.go.jp/kourei/english/annualreport/2019/pdf/2019.pdf> (accessed January 10, 2020).
- Ferrario, V. F., and Sforza, C. (1996). Coordinated electromyographic activity of the human masseter and temporalis anterior muscles during mastication. *Eur. J. Oral Sci.* 104, 511–517. doi: 10.1111/j.1600-0722.1996.tb00134.x
- Ferrario, V. F., Sforza, C., and Serrao, G. (1999). The influence of crossbite on the coordinated electromyographic activity of human masticatory muscles during mastication. *J. Oral Rehabil.* 26, 575–581. doi: 10.1046/j.1365-2842.1999.00419.x
- Ferreira, C. L., Machado, B. C., Borges, C. G., Rodrigues Da Silva, M. A., Sforza, C., and De Felicio, C. M. (2014). Impaired orofacial motor functions on chronic temporomandibular disorders. *J. Electromyogr. Kinesiol.* 24, 565–571. doi: 10.1016/j.jelekin.2014.04.005
- Ferro, K. J., Morgano, S. M., Driscoll, C. F. M., Freilich, A., Guckes, A. D., Knoernschild, K. L., et al. (2017). The glossary of prosthodontic terms. Ninth edition GPT-9. *J. Prosthet. Dent.* 117:57.
- Foster, K. D., Woda, A., and Peyron, M. A. (2006). Effect of texture of plastic and elastic model foods on the parameters of mastication. *J. Neurophysiol.* 95, 3469–3479. doi: 10.1152/jn.01003.2005
- Fueki, K., Yoshida, E., Sugiura, T., and Igarashi, Y. (2008). Comparison of electromyographic activity of jaw-closing muscles between mixing ability test and masticatory performance test. *J. Prosthodont. Res.* 53, 72–77. doi: 10.1016/j.jpor.2008.09.003
- Hiimae, K. M., and Palmer, J. B. (1999). Food transport and bolus formation during complete feeding sequences on foods of different initial consistency. *Dysphagia* 14, 31–42. doi: 10.1007/PL00009582
- Iguchi, H., Magara, J., Nakamura, Y., Tsujimura, T., Ito, K., and Inoue, M. (2015). Changes in jaw muscle activity and the physical properties of foods with different textures during chewing behaviors. *Physiol. Behav.* 152, 217–224. doi: 10.1016/j.physbeh.2015.10.004
- Ishihara, S., Isono, M., Nakao, S., Nakauma, M., Funami, T., Hori, K., et al. (2014). Instrumental uniaxial compression test of gellan gels of various mechanical properties using artificial tongue and its comparison with human oral strategy for the first size reduction. *J. Text. Stud.* 45, 354–366. doi: 10.1111/jtxs.12080
- Ishihara, S., Nakao, S., Nakauma, M., Funami, T., Hori, K., Ono, T., et al. (2013). Compression test of food gels on artificial tongue and its comparison with human test. *J. Text. Stud.* 44, 104–114. doi: 10.1111/jtxs.12002
- Ishihara, S., Nakauma, M., Funami, T., Tanaka, T., Nishinari, K., and Kohyama, K. (2011). Electromyography during oral processing in relation to mechanical and sensory properties of soft gels. *J. Text. Stud.* 42, 254–267. doi: 10.1111/j.1745-4603.2010.00272.x
- Jayatilake, D., Ueno, T., Teramoto, Y., Nakai, K., Hidaka, K., Ayuzawa, S., et al. (2015). Smartphone-based real-time assessment of swallowing ability from the swallowing sound. *IEEE J. Transl. Eng. Health Med.* 3:2900310. doi: 10.1109/JTEHM.2015.2500562
- Johansson, A. S., Westberg, K. G., and Edin, B. B. (2013). Task-dependent control of the jaw during food splitting in humans. *J. Neurophysiol.* 111, 2614–2623. doi: 10.1152/jn.00797.2013
- Kiyohara, K., Sakai, T., Nishiyama, C., Nishiuchi, T., Hayashi, Y., Iwami, T., et al. (2018). Epidemiology of out-of-hospital cardiac arrest due to suffocation focusing on suffocation due to Japanese rice cake: a population-based observational study from the Utstein Osaka Project. *J. Epidemiol.* 28, 67–74. doi: 10.2188/jea.JE20160179
- Kohyama, K., Gao, Z., Ishihara, S., Funami, T., and Nishinari, K. (2016). Electromyography analysis of natural mastication behavior using varying mouthful quantities of two types of gels. *Physiol. Behav.* 161, 174–182. doi: 10.1016/j.physbeh.2016.04.030
- Mizumori, T., Kuwahara, T., Nishio, K., Miyauchi, S., and Maruyama, T. (1985). Clinical studies on chewing movements. -effects of foods size and hardness. *J. Jpn. Prosthodont. Soc.* 29, 1062–1069. doi: 10.2186/jjps.29.1062
- Nishikubo, K., Mise, K., Ameya, M., Hirose, K., Kobayashi, T., and Hyodo, M. (2015). Quantitative evaluation of age-related alteration of swallowing function: videofluoroscopic and manometric studies. *Auris. Nasus. Larynx* 42, 134–138. doi: 10.1016/j.anl.2014.07.002
- Ohta, M., Ueda, T., and Sakurai, K. (2017). Effect of chewing or compressing food on autonomic nervous activity in older adults. *Gerodontology* 34, 434–440. doi: 10.1111/ger.12284
- Palmer, J. B., Rudin, N. J., Lara, G., and Crompton, A. W. (1992). Coordination of mastication and swallowing. *Dysphagia* 7, 187–200. doi: 10.1007/bf02493469
- Réverend, B. L., Saucy, F., Moser, M., and Loret, C. (2016). Adaptation of mastication mechanics and eating behaviour to small differences in food texture. *Physiol. Behav.* 165, 136–145. doi: 10.1016/j.physbeh.2016.07.010
- Samuels, R., and Chadwick, D. D. (2006). Predictors of asphyxiation risk in adults with intellectual disabilities and dysphagia. *J. Intellect. Disabil. Res.* 50, 362–370. doi: 10.1111/j.1365-2788.2005.00784.x
- Sworn, G. (2000). “Gellan gum,” in *Handbook of Hydrocolloids*, eds G. O. Phillips and P. A. Williams (Cambridge: Woodhead Publishing), 117–135.
- Yamaguchi, T., Mikami, S., Saito, M., Okada, K., and Gotouda, A. (2018). A newly developed ultraminiature wearable electromyogram system useful for analyses of masseteric activity during the whole day. *J. Prosthodont. Res.* 62, 110–115. doi: 10.1016/j.jpor.2017.04.001

Conflict of Interest: The authors declare that the research was conducted in the absence of any commercial or financial relationships that could be construed as a potential conflict of interest.

Copyright © 2020 Uehara, Hori, Murakami, Okawa and Ono. This is an open-access article distributed under the terms of the Creative Commons Attribution License (CC BY). The use, distribution or reproduction in other forums is permitted, provided the original author(s) and the copyright owner(s) are credited and that the original publication in this journal is cited, in accordance with accepted academic practice. No use, distribution or reproduction is permitted which does not comply with these terms.



Toll-Like Receptor 4 in the Rat Caudal Medulla Mediates Tooth Pulp Inflammatory Pain

Helena F. Filippini^{1,2*}, Graziella R. Molska², Maryam Zanjir², Yamini Arudchelvan², Siew-Ging Gong², Maria M. Campos^{1,3}, Limor Avivi-Arber^{2,4} and Barry J. Sessle^{2,4,5}

¹ Programa de Pós-graduação em Odontologia, Escola de Ciência da Saúde e da Vida, Pontifícia Universidade Católica do Rio Grande do Sul, Porto Alegre, Brazil, ² Faculty of Dentistry, University of Toronto, Toronto, ON, Canada, ³ Centro de Pesquisa em Toxicologia e Farmacologia, Escola de Ciências da Saúde e da Vida, Pontifícia Universidade Católica do Rio Grande do Sul, Porto Alegre, Brazil, ⁴ Centre for the Study of Pain, University of Toronto, Toronto, ON, Canada, ⁵ Department of Physiology, Faculty of Medicine, University of Toronto, Toronto, ON, Canada

OPEN ACCESS

Edited by:

Teresa Lever,
University of Missouri, United States

Reviewed by:

Nikolaos Christidis,
Karolinska Institutet (KI), Sweden
Antoon De Laat,
KU Leuven, Belgium

*Correspondence:

Helena F. Filippini
helenaf.filippini@utoronto.ca;
helenafilippini@gmail.com

Specialty section:

This article was submitted to
Perception Science,
a section of the journal
Frontiers in Neuroscience

Received: 26 December 2019

Accepted: 25 May 2020

Published: 23 June 2020

Citation:

Filippini HF, Molska GR, Zanjir M, Arudchelvan Y, Gong S-G, Campos MM, Avivi-Arber L and Sessle BJ (2020) Toll-Like Receptor 4 in the Rat Caudal Medulla Mediates Tooth Pulp Inflammatory Pain. *Front. Neurosci.* 14:643. doi: 10.3389/fnins.2020.00643

The aims of this study were to investigate if Toll-like receptor 4 (TLR4) is expressed in the medullary dorsal horn (MDH) and if medullary application of a TLR4 antagonist (lipopolysaccharides from *Rhodobacter sphaeroides*, LPS-RS) can attenuate changes in nociceptive sensorimotor responses or TLR4 expression that might be evoked by mustard oil (MO) application to the right maxillary first molar tooth pulp. Of 41 adult male Sprague-Dawley rats used in the study, 23 received intrathecal application of the TLR4 antagonist LPS-RS (25 µg/10 µl; LPS-RS group) or isotonic saline (10 µl; vehicle control group) 10 min before pulpal application of MO (95%; 0.2 µl). Bilateral electromyographic (EMG) activities of the anterior digastric and masseter muscles were recorded continuously before and until 15 min after the MO application to the pulp. In 6 of these 23 rats and an additional 18 rats, the caudal medulla containing the ipsilateral and contralateral MDH was removed after euthanasia for subsequent Western Blot analysis of TLR4 expression in LPS-RS ($n = 8$) and vehicle ($n = 8$) groups and a naïve group ($n = 8$). The % change from baseline in the MO-evoked EMG activities within the anterior digastric muscles were significantly smaller in the LPS-RS group than the control group (two-way ANOVA, *post hoc* Bonferroni, $P < 0.0001$). Western Blot analysis revealed similar levels of TLR4 expression in the caudal medulla of the naïve, vehicle and LPS-RS groups. These novel findings suggest that TLR4 signaling in the caudal medulla may mediate MO-induced acute dental inflammatory pain in rats.

Keywords: mustard oil, tooth pulp inflammation, toll-like receptor – 4, electromyography, LPS, LPS-RS

INTRODUCTION

Tooth inflammatory pain is a common and debilitating condition with negative social and economic consequences that may result in an impaired quality of life if not appropriately treated. Regrettably, its underlying mechanisms are still not fully understood (Sessle, 2014; FDI World Dental Federation, 2015), and so studies aimed at enhancing understanding of its mechanisms are important for providing fundamental knowledge that could lead to improved management approaches to tooth inflammatory pain.

Several studies have shown that the medullary dorsal horn (MDH), which is often referred to as the trigeminal subnucleus caudalis, is an important caudal medullary site related to the processing and relaying of nociceptive information from the teeth and other orofacial structures to higher brain centers (for review, see Sessle, 1986, 2000, 2014; Byers and Närhi, 1999; Iwata et al., 1999, 2011; Chiang et al., 2011; Chichorro et al., 2017). For example, tooth pulp application of mustard oil (MO), an inflammatory irritant and transient receptor potential ankyrin 1 (TRPA1) agonist, can markedly enhance activity of MDH nociceptive neurons accompanied by nociceptive sensorimotor responses in jaw muscles reflected in MO-induced increases in electromyographic (EMG) activities (e.g., Chiang et al., 1998, 2007, 2011; Sunakawa et al., 1999; Narita et al., 2012). In addition, the MDH has been shown to be a critical interneuronal relay site in these reflex responses to MO and other noxious orofacial stimuli (Cairns et al., 1998, 2001; Tsai et al., 1999).

The neuronal hyperexcitability that can be induced in the MDH by MO or other noxious orofacial stimuli is considered to reflect a so-called central sensitization which involves the induction of neuroplastic changes in nociceptive processes in the central nervous system (CNS). In the trigeminal system, central sensitization has been documented to be an integral mechanism underlying acute and chronic pain states and to be dependent on the functional integrity of MDH microglia (Chiang et al., 2007, 2011; Iwata et al., 2011; Sessle, 2014; Chichorro et al., 2017). Microglial activation in pain states has been shown to involve the toll-like receptor 4 (TLR4) (Lehnardt et al., 2002; Olson and Miller, 2004; Guo and Schluesener, 2007; Kashima and Grueter, 2017; Bruno et al., 2018). TLR4 is a subtype of toll-like receptors involved in the recognition of lipopolysaccharides (LPS) present in the cell wall of gram-negative bacteria (Bryant et al., 2015; Gao and Li, 2016; Bruno et al., 2018). The stimulation of TLR4 results in the activation of two major intracellular signaling pathways: the myeloid differentiation primary response 88 (MyD88) dependent pathway and the TIR-domain-containing adapter-inducing interferon- β (TRIF) pathway. The first one induces nuclear factor- κ B (NF- κ B) translocation and expression of inflammatory cytokines as well as type I interferon genes, whereas the TRIF pathway activates type I interferon genes and delayed NF- κ B translocation and expression of inflammatory cytokines via interferon regulatory factor 3 (IRF-3) (Vaure and Liu, 2014; Bruno et al., 2018).

TLR4 has been shown to be expressed in the spinal dorsal horn, the spinal analog of the MDH (Sun et al., 2015; Yan et al., 2015b; Hu et al., 2018). There is evidence that TLR4 may play a critical link between the innate and adaptive immune response as well as the induction, conversion, and maintenance of chronic pain states (Takeda et al., 2003; Bruno et al., 2018). Previous studies have documented the involvement of TLR4 processes in several pain models (Tanga et al., 2005; Christianson et al., 2011; Ohara et al., 2013; Tramullas et al., 2014; Sun et al., 2015; Bruno et al., 2018). Some of these studies have included investigations showing that TLR4 is involved in the induction phase of behavioral hypersensitivity in rodent pain models (Tanga et al., 2005) and that TLR4 antagonists such as LPS from *Rhodobacter sphaeroides* (LPS-RS) can attenuate nociceptive

processes (Christianson et al., 2011; Sun et al., 2015). LPS-RS is a potent antagonist of toxic LPS in both human and murine cells, and also is effective in antagonizing effects attributed to TLR4 (Christianson et al., 2011; Sorge et al., 2011; Li et al., 2015; Sun et al., 2015). TLR4 expressed on microglia has been shown to contribute to spinal cord microglial activation and central sensitization (Lehnardt et al., 2002; Olson and Miller, 2004; Guo and Schluesener, 2007; Kashima and Grueter, 2017; Bruno et al., 2018). Microglial activation involving TLR4 processes leads to an increase of spinal inflammatory cytokines that maintain the proinflammatory environment within the spinal dorsal horn and thereby sustain central sensitization (Lehnardt et al., 2003; Tanga et al., 2005; Buchanan et al., 2010; Nicotra et al., 2012; Yan et al., 2015a; Bruno et al., 2018).

While the role of TLR4 in immune function, inflammation and spinal nociceptive mechanisms has been well established, knowledge of the role of this receptor in orofacial nociceptive processes is limited. It has been suggested that expression of TLR4 and its co-receptor CD14 in trigeminal sensory neurons may be related to the inflammatory pain resulting from tooth pulp infection (Wadachi and Hargreaves, 2006). LPS from gram-negative bacteria is the main exogenous TLR4 agonist during infection-associated dental pain and likely sensitizes the transient receptor potential vanilloid 1 (TRPV1) via TLR4 activation in the trigeminal sensory neurons (Diogenes et al., 2011; Green et al., 2016). There is also evidence that TRPV1 is co-expressed with TRPA1 in many sensory neurons, including those in tooth pulp, associated with small-diameter C-fibers in the trigeminal ganglion as well as in the dorsal root ganglion (Kobayashi et al., 2005; Sadofsky et al., 2014; Hargreaves and Ruparel, 2016; Gouin et al., 2017; Lee et al., 2019). This co-expression might lead to functional interactions between these two subtypes of TRP receptors (Fischer et al., 2014). However, although some studies (Ohara et al., 2013; Lin et al., 2015) have suggested the importance of TLR4 in orofacial pain states, the role of TLR4 in central mechanisms of dental pain is still unclear.

Some studies using pain models have shown increased expression of TLR4 in the spinal dorsal horn (Sun et al., 2015; Yan et al., 2015b; Hu et al., 2018). As noted above, the spinal dorsal horn is the spinal analog of the MDH, and earlier findings indicate that the MDH is a critical element in the neural circuitry underlying the reflex EMG activity that can be evoked in the jaw muscles by noxious orofacial stimuli. Therefore, the present study was initiated to use electrophysiological, pharmacological and molecular approaches to determine if TLR4 is expressed in the MDH and if medullary application of the TLR4 antagonist LPS-RS can attenuate these nociceptive sensorimotor responses or the increased TLR4 expression that might be evoked by MO stimulation of the rat tooth pulp.

MATERIALS AND METHODS

Animals

A total of 41 adult male Sprague-Dawley rats (250–350 g) were obtained from Charles River (Montreal, QC, Canada). Social interaction and appropriate environmental conditions

are important factors reducing anxiety and other emotions that can influence pain. Therefore, the rats were kept in their home cages (3 animals/cage) at the Department of Comparative Medicine (University of Toronto) under standard conditions of temperature ($22 \pm 2^\circ\text{C}$), light (12 h light-dark cycle) and humidity (50–70%) and provided with food and water *ad libitum*. The animals had an acclimatization time of 7 days before any experiment. All experimental procedures were carried out between 8:00 a.m. and 5:00 p.m. Twenty-three rats were used in the EMG experiments (6 of them were used in both the EMG and Western Blot experiments) and another 18 were used only in the Western Blot experiments described below. The sample sizes for the EMG experiments ($n = 10\text{--}13$ per group) and for Western Blot experiments ($n = 3\text{--}5$ per group) were established based on our previous studies documenting statistically significant findings in analogous experiments (Chiang et al., 1998, 2007; Sunakawa et al., 1999; Narita et al., 2012; **Figure 1**). All the procedures were approved by the Animal Care Committee of the University of Toronto (protocol number #20011420) and were accomplished in accordance with the regulations of the Ontario Animal Research Act (Canada).

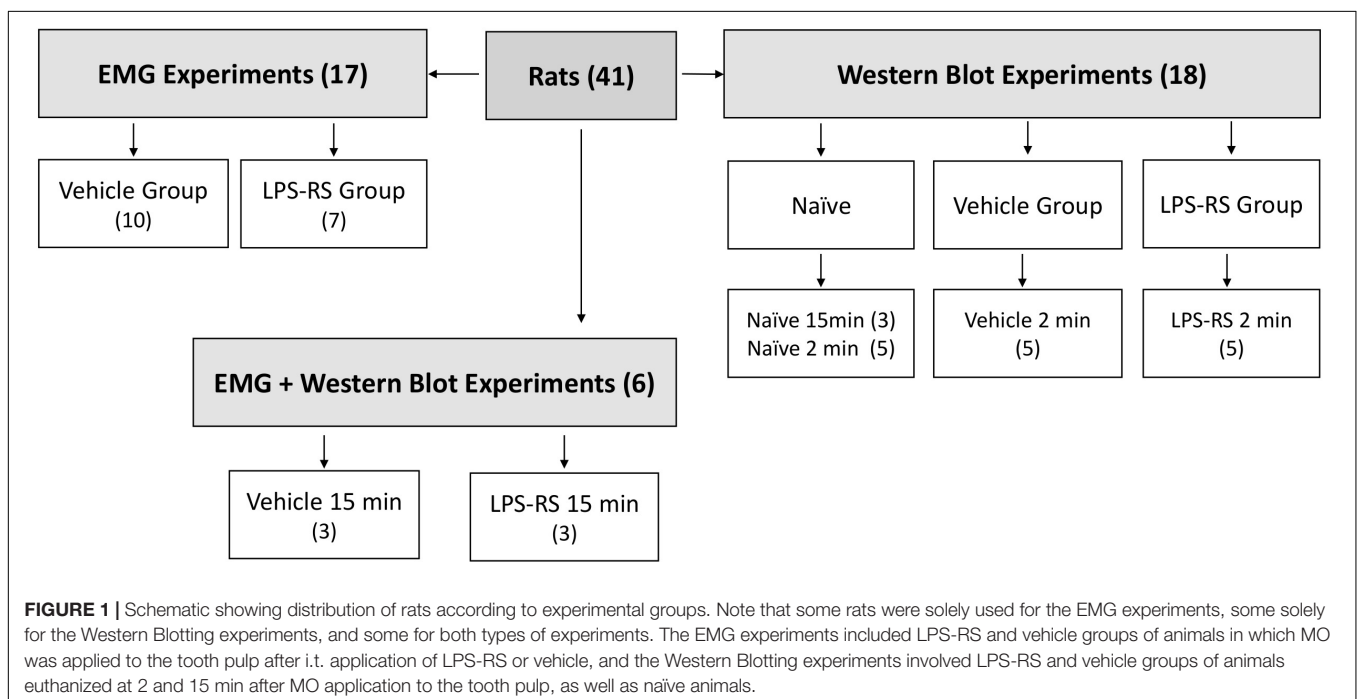
Drugs and Reagents

The inflammatory irritant and TRPA1 agonist mustard oil (MO – Allyl isothiocyanate, 95%; $0.2\ \mu\text{l}$, Aldrich-Sigma, CA, United States) was applied to the pulp of the right maxillary first molar to evoke EMG activities in the jaw muscles as previously described in detail (Chiang et al., 1998, 2007; Sunakawa et al., 1999; Narita et al., 2012). LPS from *Rhodobacter sphaeroides* (LPS-RS, InvivoGen, United States) was used as a TLR4 antagonist, as noted below. LPS-RS was dissolved in isotonic saline and it (or its vehicle – isotonic saline) was delivered by

intrathecal (i.t.) administration to the caudal medulla overlying the MDH at a dose of $25\ \mu\text{g}$ in a total volume of $10\ \mu\text{l}$, this dose of LPS-RS has been previously reported to be effective in attenuating mechanical allodynia when applied i.t. to L5/L6 in a spinal pain model (Sun et al., 2015). In preliminary experiments, Lipopolysaccharides (LPS) from *P. aeruginosa* (1 mg/ml and 5 mg/ml; Sigma, United States) (Shrestha et al., 2015) or from *E. coli* (10 mg/ml; Sigma, United States) (Renard et al., 2016) were applied to the pulp as a TLR4 agonist but were ineffective compared to MO in evoking EMG activities. Thus, the present study focused on the effects of the MO application to the pulp which has been well documented to induce jaw muscle EMG activity in rats (Sunakawa et al., 1999; Narita et al., 2012).

General Experimental Protocols

Procedures followed our previously published standardized protocols (Avivi-Arber et al., 2010, 2015; Awamleh et al., 2015; Pun et al., 2016). For femoral vein cannulation, rats were anesthetized with intramuscular (i.m.) administration of ketamine (175 mg/kg) and xylazine (25 mg/kg), and then placed in a supine position. After cannulation, general anesthesia was maintained by intravenous (i.v.) administration of ketamine (75 mg/kg/h) for pulp exposure, insertion of EMG electrodes, neck dissection, and exposure of the caudal medulla. Subsequently, for EMG recordings, ketamine dosage was set at 25–50 mg/kg/h, and noxious pressure was periodically applied to the hind paw to ensure that it could induce a weak flexion reflex, indicating that an adequate and stable level of general anesthesia was obtained throughout the experimental sessions. Consistent with earlier electrophysiological recording and/or stimulation studies by ourselves and others, we used ketamine as a general anesthetic since, as compared with other general anesthetics (e.g.,



isoflurane), it does not suppress muscle tone (Nudo et al., 2003; Tennant et al., 2011, 2012; Avivi-Arber et al., 2015; Awamleh et al., 2015; Pun et al., 2016). A heating blanket (Model 73A, YSI, OH, United States) regulated by a rectal thermometer was used to maintain the animal's body temperature (37–38°C), and a pulse oximeter monitored heart rate (333–430 beats/min) and oxygen saturation (90–100%).

Pulp Exposure

The right maxillary first molar pulp was exposed using a low-speed dental drill with a round tungsten carbide bur (#1) under water cooling, as previously described (Chiang et al., 1998; Sunakawa et al., 1999; Narita et al., 2012). The pulp surface was covered with a piece of cotton wool soaked with isotone saline until the MO was applied to the pulp.

EMG Electrode Insertion and Exposure of Medulla

EMG electrodes were made with 40-gauge, single-stranded, Teflon-insulated stainless-steel wires each with its final ~5 mm end formed into a hook and a ~1 mm exposed tip produced by stripping off its insulation (Cooner Wire, Chatsworth, CA, United States). After the pulp exposure, a pair of EMG electrodes (interpolated distance: ~5 mm) was inserted into each of the left and right masseter muscles (LM; RM) and left and right anterior digastric muscles (LAD; RAD). Then the animal was turned and placed in a stereotaxic apparatus and the dorsal surface of the caudal medulla overlying the MDH was surgically exposed at the obex level for medullary application of drug or vehicle, as described below. The hooked end of each electrode provided a stable position of the electrodes in the muscle before, during and after the re-positioning of the animal. Furthermore, we confirmed the placement of EMG electrodes in each muscle and ensured that the muscle preparation had not deteriorated during the experiment. As previously described (Awamleh et al., 2015), this was achieved by delivering a constant-current stimulus (33.2 ms, 12×0.2 ms pulses, 333 Hz) to the muscle via the EMG electrodes and observing muscle twitches evoked in the muscle at a threshold stimulation intensity of $\leq 200 \mu\text{A}$. This procedure was carried out immediately after EMG electrode placement, after positioning of the rat in the stereotaxic apparatus, and at the termination of the experiment.

EMG Recordings

A rest period of 30 min was allowed after the surgery to ensure stable EMG recordings. A baseline level of EMG activities was then recorded for 15 min in all four jaw muscles (LM, RM, LAD, and RAD), and then continuously from baseline until 15 min after MO application to the pulp; 15 min was chosen since previous studies have shown the duration of EMG activity evoked by MO application to the tooth pulp is <20 min (e.g., Sunakawa et al., 1999; Narita et al., 2012). The EMG activity of each muscle was amplified (gain: 1000–5000; bandwidth: 30–3000 Hz) by an AC amplifier (A-M system, Washington, DC, United States, model 1700) and displayed on an oscilloscope, and was directly processed (i.e., rectified and integrated) by a computer interface

1401/program Spike 2 (CED, Cambridge, United Kingdom). In accordance with previous studies (Sunakawa et al., 1999; Narita et al., 2012), increases in EMG activity evoked by the application of MO were regarded as significant if one or more EMG area bins (mV/min) increased at least two standard deviations (SD) above the mean baseline level. To conserve on animal numbers, no naïve group or group with vehicle control applied to the tooth pulp or with tooth pulp exposure alone were used since we have previously shown that naïve animals or animals with vehicle (mineral oil) application to the pulp do not show evoked EMG (or MDH neuronal) activities (Chiang et al., 1998, 2007; Sunakawa et al., 1999; Narita et al., 2012). All EMG activities during the experimental session were measured and transformed into percentage values, by the division of the averaged baseline activity (mV/min) for the first 5 min of the 15 min baseline (Narita et al., 2012).

Protocols of Treatment

LPS from *Rhodobacter sphaeroides* (LPS-RS) was selected based on previous studies of its effectiveness in antagonizing effects attributed to TLR4 (Christianson et al., 2011; Sorge et al., 2011; Li et al., 2015; Sun et al., 2015). The rats were divided into three groups (vehicle; LPS-RS; naïve) (see **Figure 1**). To address LPS-RS effects on MO-evoked EMG activities, the LPS-RS group was pre-treated by i.t. application of LPS-RS (25 $\mu\text{g}/10 \mu\text{l}$) to the caudal medulla at 10 min before the pulpal application of MO. The vehicle group received the vehicle (isotonic saline) by the same i.t. application procedures as for the LPS-RS group. All i.t. injections were carried out under i.v. ketamine general anesthesia, as described above. The dura overlying the ipsilateral MDH (obex +0.5 mm, lateral 0.5 mm) was punctured with a 30-gauge needle attached to a Hamilton syringe positioned on the stereotaxic apparatus to permit the precise injection into the subdural space overlying MDH (Chiang et al., 1998; Narita et al., 2012; Takeda et al., 2013). Ten minutes after the pre-treatment with vehicle or LPS-RS, MO was applied to the exposed pulp. For this purpose, a small piece of dental paper point (diameter, 0.3 mm; length 0.5 mm) was soaked with MO (0.2 μl ; 95%). The pulp cavity was then immediately sealed with temporary dental filling (Cavit, ESPE, Germany) to prevent any possible leakage of the chemical into other oral tissues.

Blotting to Detect TLR4 Expression

For the Western Blotting experiments, we used LPS-RS, vehicle, and naïve groups of animals. A goal was to test if MO caused any change in TLR4 expression in MDH during and soon after the period of any MO-evoked EMG activity changes. We also wanted to determine if any suppressive effects of LPS-RS that might be demonstrated on MO-evoked jaw EMG activity was associated with any change in TLR4 expression in MDH, the site of the interneuronal relay of nociceptive inputs to trigeminal motoneurons (Cairns et al., 1998, 2001; Tsai et al., 1999). Since we found that the increased EMG activity persisted for a few minutes after MO application to the tooth pulp before returning to baseline levels (see section “Results”), the Western Blot analyses included LPS-RS group and vehicle group animals euthanized at either 2 min (LPS-RS

group, $n = 5$; vehicle group, $n = 5$) or at 15 min (LPS-RS group, $n = 3$; vehicle group, $n = 3$) after application of MO to the pulp; naïve animals ($n = 8$) were also euthanized for the Western Blotting analysis (see **Figure 1**). The caudal medulla containing the ipsilateral and contralateral MDH was removed immediately after euthanasia for subsequent evaluation of TLR4 expression. The samples were homogenized on ice in 15 mmol/l Tris buffer containing a cocktail of proteinase and phosphatase inhibitors. The protein samples were separated via sodium dodecyl polyacrylamide gel electrophoresis (SDS-PAGE) and transferred onto polyvinylidene difluoride (PVDF) membranes. The membranes were placed in blocking buffer for 1 h at room temperature and incubated with a primary antibody against TLR4 (1:1000, Abcam, CA, United States) or Glyceraldehyde 3-phosphate dehydrogenase (GAPDH) (1:10,000, Cell Signaling, United States) overnight at 4°C. Then, the membranes were incubated in horseradish peroxidase-conjugated IgG (1:2000, Cell Signaling, United States). An enhanced chemiluminescence (ECL) solution (PierceTM Protein Biology, United States) was used to detect the immunocomplexes. Anti -GAPDH (Sigma-Aldrich, CA, United States) was used as loading control. The levels of TLR4 expression were quantified using GAPDH as an internal control as previously described (Sun et al., 2015).

Statistical Analyses

The data are expressed as the mean \pm the standard error. All EMG activities during the experimental session were measured and transformed into percentage values by the division of the averaged baseline activity (mV/min) recorded for the 5 min period prior to MO application in the experimental sessions. The data were normally distributed for RAD, LAD, RM, and LM in vehicle and LPS-RS groups, according to Agostino and Shapiro test or Kolmogorov-Smirnov test using GraphPad 8 software. A two-way analysis of variance (ANOVA), followed by Bonferroni test was used to test whether the independent variables (i.e., treatment with LPS-RS vs. vehicle and 1, 2, and 3 min time points after treatment) had any effect on the dependent variable (i.e., changes in EMG activities). For the Western Blotting analysis, data were evaluated by one-way ANOVA. P -values less than 0.05 were considered to indicate statistical significance.

RESULTS

EMG recordings in the control (vehicle) group revealed that MO application to the right maxillary molar tooth pulp resulted, within 2 s, in an increased EMG activity that was especially apparent in the LAD and RAD. The increased EMG activity persisted for up to 3 min before returning to baseline levels (**Figures 2A, 3A,B**). In contrast, in the LPS-RS group, i.t. application of LPS-RS 10 min prior to MO application to the tooth pulp, could attenuate the MO-evoked EMG responses (**Figure 2B**).

Statistical analysis revealed that there were statistically significant differences ($p < 0.0001$, 2-way ANOVA and *post hoc* Bonferroni) between the right and left masseter responses

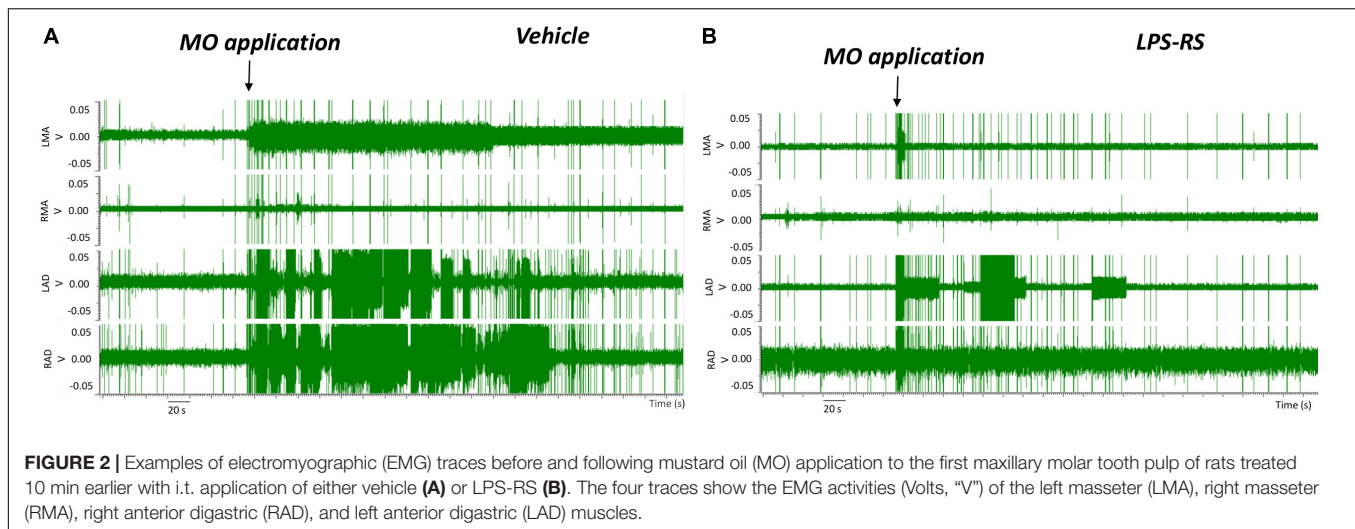
[vehicle group: $p < 0.0001$; $F_{(7, 161)} = 9.88$; LPS-RS group: $p < 0.0001$; $F_{(7, 126)} = 5.93$] and between right masseter and right anterior digastric responses, for both groups [vehicle group: $p < 0.001$; $F_{(7, 154)} = 13.89$; LPS-RS group: $p < 0.0001$; $F_{(7, 133)} = 11.68$]. In comparison with i.t. vehicle application, i.t. administration of LPS-RS could significantly attenuate the MO-evoked EMG responses only in the ipsilateral (RAD) and contralateral (LAD) anterior digastric muscles. In the RAD, decreased EMG activities were observed 1, 2, and 3 min following MO application to the tooth pulp [$p < 0.0001$; $F_{(7, 119)} = 6.27$] (**Figure 3A**). In the LAD, decreased EMG responses were observed only 2 and 3 min following MO application to the tooth pulp [$p = 0.0002$; $F_{(7, 147)} = 23$] (**Figure 3B**). No significant effects of LPS-RS were found in the masseter muscles (**Figures 3C,D**).

Western Blot analysis showed expression of TLR4 in the right (ipsilateral) and left (contralateral) MDH of naïve rats and at 2 and 15 min following MO application to the tooth pulp in the LPS-RS and vehicle groups. There were no significant differences ($p > 0.05$) in the levels of TLR4 expression between the naïve, vehicle and LPS-RS groups (**Figures 4A–C**).

DISCUSSION

The present investigation has provided the first documentation that medullary (i.t.) pre-treatment with the TLR4 antagonist LPS-RS attenuates nociceptive sensorimotor responses in a rat model of acute dental inflammatory pain. The findings that the application of MO to the tooth pulp of the maxillary first molar in the vehicle group evoked a marked increase of jaw muscle EMG activities are consistent with previous studies reporting that MO application to the rat maxillary tooth pulp induces sensorimotor responses reflected in increased EMG activities in the jaw muscles (Sunakawa et al., 1999; Narita et al., 2012). It has been shown that naïve animals or animals receiving application of vehicle to the tooth pulp do not show increased jaw EMG activity or central sensitization in the MDH (e.g., Chiang et al., 1998; Sunakawa et al., 1999; Narita et al., 2012). Therefore, to conserve on animal numbers, we did not include control groups with tooth pulp exposure alone, or with vehicle (i.e., mineral oil) application to the tooth pulp. These earlier studies, as well as others (Hu et al., 1993; Lam et al., 2005), have also shown a differential magnitude of evoked responses between anterior digastric and masseter muscles or left and right muscles, and significant differences were noted in the present study between the right and left masseter responses and right masseter and right anterior digastric responses. Like the authors of the earlier studies, we cannot give any clear explanation for some of these differential patterns of EMG activity; future studies monitoring jaw movements together with EMG recordings in anesthetized as well as unanesthetized preparations may help in clarifying the basis for these EMG patterns and the movement patterns with which they are associated.

In addition, it has previously been shown that the increased jaw muscle EMG activities evoked by application of MO or other noxious stimuli to the pulp (or other orofacial tissues)



have a reflex basis involving the activation of trigeminal pulp afferents and a relay via the MDH to the trigeminal motor nucleus where the trigeminal motoneurons supplying the jaw muscles are located (Yu et al., 1994; Cairns et al., 1998, 2001; Tsai et al., 1999; Sunakawa et al., 1999; Narita et al., 2012). Moreover, the short latency of the evoked EMG responses found in the present and previous studies suggest that they are initiated by direct excitatory action of MO on pulp afferents and a pauci-synaptic relay in brainstem (Sunakawa et al., 1999; Narita et al., 2012). The finding of increased EMG activities observed in the contralateral as well as ipsilateral anterior digastric muscles in the present study is in accordance with the findings of Cairns et al. (1998, 2001) and Tsai et al. (1999). These authors also revealed that the MDH plays an important role in the activation of contralateral as well as ipsilateral trigeminal motoneurons following the application of MO or other noxious stimuli to orofacial tissues.

Because the MDH is a critical element in neural pathways underlying the MO-evoked reflex responses (Cairns et al., 1998, 2001; Tsai et al., 1999), and TLR4 has been shown to be expressed in the spinal dorsal horn (Sun et al., 2015; Yan et al., 2015b) which is the spinal analog of MDH, the MDH was selected for i.t. administration of the TLR4 antagonist and for western blotting analysis. Our novel findings suggesting that TLR4 receptor processes in the rat caudal medulla may mediate nociceptive responses evoked by the TRPA1 agonist MO, which is a well-documented inflammatory irritant (Woolf and Wall, 1986; Hu et al., 1993; Yu et al., 1994; Cairns et al., 1998; Chiang et al., 1998), are consistent with previous studies documenting the presence of TRPA1 in the tooth pulp (Hargreaves and Ruparel, 2016; Lee et al., 2019) and the involvement of TLR4 and TRPA1 processes in several other pain models (Kobayashi et al., 2005; Christianson et al., 2011; Ohara et al., 2013; Fischer et al., 2014; Tramullas et al., 2014; Sun et al., 2015; Bruno et al., 2018). Some of these studies have included investigations showing that TLR4 antagonists such as LPS-RS can attenuate nociceptive processes (Christianson et al., 2011; Sun et al., 2015). LPS-RS is a potent LPS antagonist in murine and human cells and prevents inflammation mediated by TLR4. LPS-RS has two distinct mechanisms to block

LPS/TLR4 signaling. One mechanism involves direct competition between acylated lipid A and hexa-acylated lipid A for binding on Myeloid differentiation-2 (MD-2) and the other mechanism involves the ability of penta-acylated lipid A: MD-2 complexes to inhibit hexa-acylated endotoxin: MD-2 complexes and TLR4 functions (Saitoh et al., 2004; Coats et al., 2005; Teghanemt et al., 2005; Visintin et al., 2005; Brubaker et al., 2015). Additional studies including those incorporating molecular approaches are needed to determine which of these TLR4-related mechanisms may be involved in the findings documented in the present study.

The present study showed that LPS-RS (but not its vehicle) when applied to the caudal medullary surface overlying the MDH can attenuate for several minutes the jaw muscle EMG activities evoked by MO application to the tooth pulp. These novel findings suggest that TLR4 processes in the MDH, the major brainstem relay site for orofacial nociceptive afferent inputs (for review, see Byers and Närhi, 1999; Iwata et al., 1999, 2011; Sessle, 2000, 2014; Chiang et al., 2011; Chichorro et al., 2017), contribute to nociceptive mechanisms related to the development of dental pain and its modulation. The present study provided additional novel findings that TLR4 is expressed in the caudal medulla as evidenced by Western Blot analysis. Interestingly, although the LPS-RS group that received the TLR4 antagonist showed reduced MO-evoked EMG activities, the expression of this receptor did not differ significantly between the naïve, LPS-RS and vehicle groups when evaluated at 2 and 15 min after MO application to the tooth pulp. There have been no previous studies in an acute pain model assessing TLR4 expression in the caudal medulla by Western Blot to allow for comparison with these findings. Thus, it is possible that the MO-evoked increase in EMG activity could be associated with TLR4 activation without increased expression, or that the time interval (15 and 2 min) after MO application to the tooth pulp for assessment of TLR4 expression may have been too short to allow for a sufficient change in expression to be detected as a significant alteration by Western Blot analysis.

While there have been no studies of TLR4 expression in the MDH, there are some relevant studies evaluating TLR4

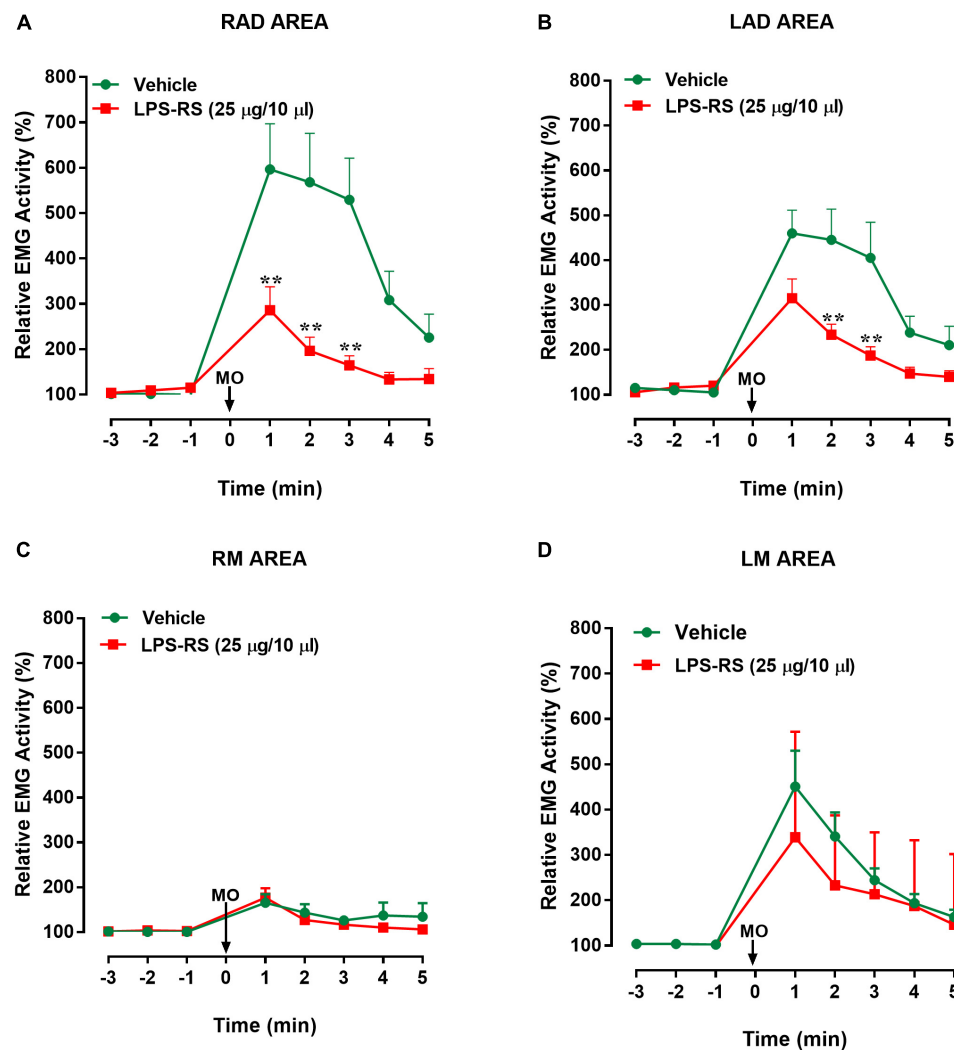
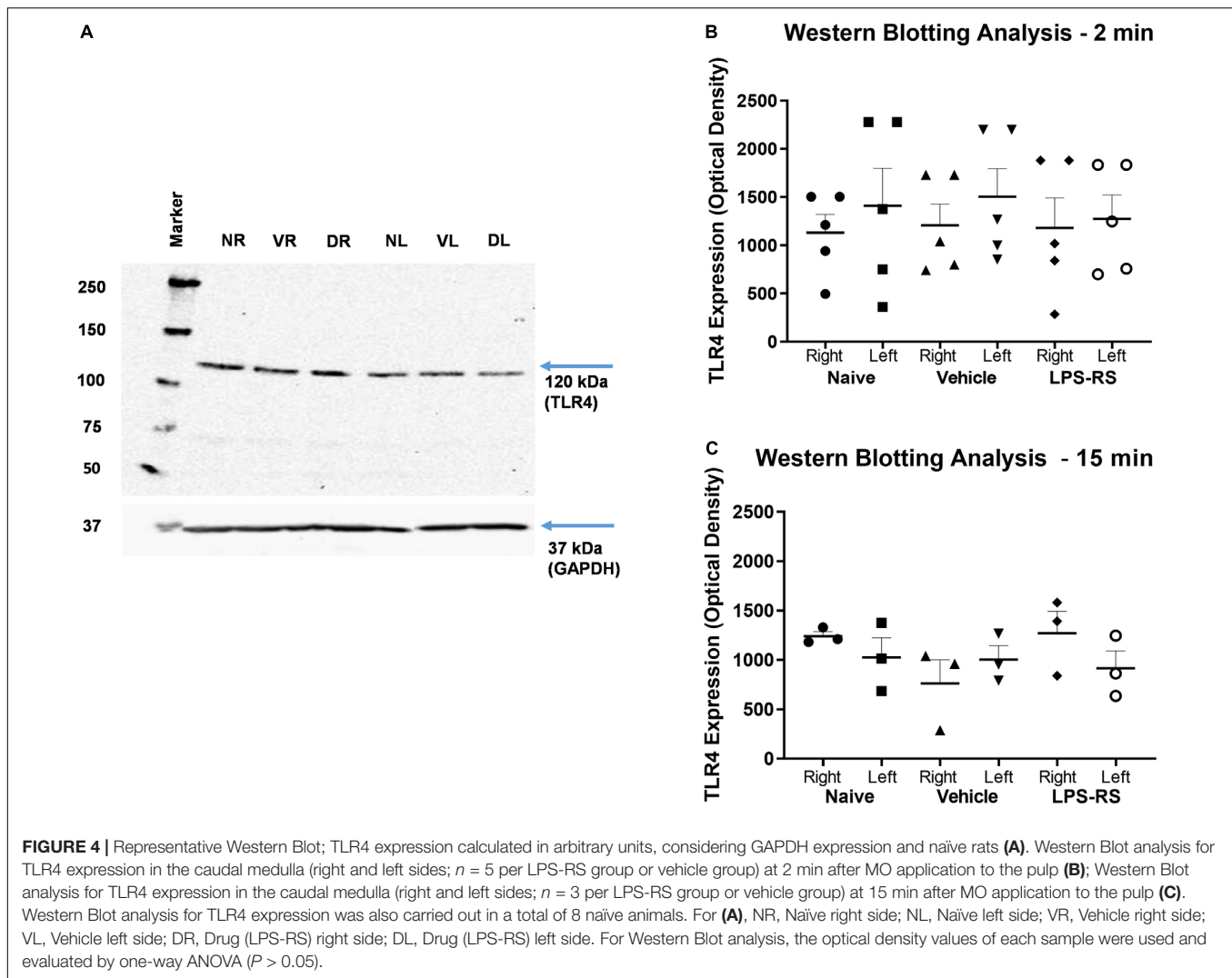


FIGURE 3 | Effects of i.t. application of LPS-RS on the MO-evoked EMG activity expressed as % change from baseline, following the application of MO to the pulp of the right maxillary first molar. Data show the relative EMG activity changes (%) in (A) right anterior digastric (RAD), (B) left anterior digastric (LAD), (C) left masseter (LM), (D) right masseter (RM). The circles indicate data obtained in vehicle-treated animals, and the squares show the effects of LPS-RS (that was applied at 10 min before the MO application). Each point represents the mean \pm standard error mean of 10–13 animals per group. $**P < 0.0001$ (two-way ANOVA followed by Bonferroni test).

expression elsewhere in the brainstem and in the spinal nociceptive system. A study by Ogawa et al. (2013) shows data from brainstem, but the anatomical region evaluated appears to be the rostral ventrolateral medulla and did not include the MDH. In spinal cord studies, Yan et al. (2015b) have reported that i.t. administration of Paclitaxel, a powerful anti-neoplastic drug, induces acute pain within 2 h via directly activating TLR4 and producing increased of tyrosine phosphorylation (p-TLR4) expression in the spinal dorsal horn within 1 h of its administration. At the same time, total TLR4 remained unchanged 4 h after i.v. injection of Paclitaxel (2 mg/kg). In addition, Sun et al. (2015) have evaluated TLR4 expression, albeit at a longer timeline, in the spinal dorsal horn, and reported upregulation of TLR4 expression in glial cells in the ipsilateral spinal dorsal horn in a skin/muscle incision retraction (SMIR)

model; this upregulation occurred on day 5 after SMIR and was maintained until the end of the experimental period (day 20) used in their study. However, a mouse visceral pain model has been reported to be associated with no significant change in TLR4 expression in the lumbar region of the spinal cord, although there was changed TLR4 expression in the prefrontal cortex and hippocampus (Tramullas et al., 2014). Hu et al. (2018) evaluated TLR4 expression in the medulla as well as L4/L5 spinal cord at 3, 7, 11, and 14 days after nerve surgery in neuropathic models of pain (partial infraorbital nerve transection; partial sciatic ligation). These chronic pain models are quite different from our dental pain model in which we evaluated TLR4 expression at 2 and 15 min after MO application to the tooth pulp. Furthermore, the medullary region examined is not clear in the study by Hu et al. in which they found no marked changes in TLR4 expression



after partial infraorbital nerve transection. Thus, the present study appears to be the first to check, by Western Blot analysis, for TLR4 expression in the region of the MDH at short time periods after noxious stimulation of peripheral tissues. Furthermore, this demonstration of TLR4 expression represents an important first step for understanding receptor signaling in MDH nociceptive processes related to TLR4 expression. It is also noteworthy that the LPS-RS dose ($25 \mu\text{g}/10 \mu\text{l}$) used in the LPS-RS group in the present study, although sufficient to attenuate the MO-evoked increased EMG activity, may have been too low a dose to produce significant differences between the experimental groups in TLR4 expression, or that it lacked sufficient specificity and sensitivity, as Nicotra et al. (2012) have suggested for TLR4 antibodies. The specificity and sensitivity of antibodies are important in biomarker research, and the lack of quality control tests may result in equivocal results (Signore et al., 2017). Sun et al. (2015) also used LPS-RS as a TLR4 antagonist in their SMR study, but they did not report if this antagonist had any effect on TLR4 expression. While LPS-RS is considered an LPS antagonist, its mechanism of action may not be related to TLR4 expression,

but rather to the prevention of TLR4 signaling, which could also involve other molecules such as heat shock proteins (Cognasse et al., 2015; Gao and Li, 2016; Yadav and Surolia, 2019). Further studies in orofacial pain models are needed to address these possibilities. The cell types (neurons, glia) expressing TLR4 in the MDH are also worthy of future investigation since previous studies have shown that pulpal application of MO can lead to trigeminal central sensitization of MDH nociceptive neurons that is dependent on MDH microglia (Chiang et al., 2011) and that TLR4 expressed on microglia contribute to spinal cord microglial activation and central sensitization (Lehnardt et al., 2002; Olson and Miller, 2004; Guo and Schluesener, 2007; Kashima and Grueter, 2017; Bruno et al., 2018).

The present results provide evidence that tooth pulp stimulation by the TRPA1 agonist and inflammatory irritant MO induces TLR4 activation in the caudal medulla. We show for the first time that central activation of TLR4 may contribute to the mechanisms in the CNS that underlie dental nociceptive transmission. While these mechanisms likely contribute to tooth inflammatory pain in humans, additional molecular and

pharmacological studies are needed to define the central role of TLR4 in dental pain and its translation to humans. An enhanced knowledge of TLR4 signaling pathways and interactions between TLR4 and other receptors promises to help guide future research aimed at developing effective drugs for controlling dental and other types of orofacial pain.

CONCLUSION

This study has shown that the application of the inflammatory irritant MO to the tooth pulp can evoke a marked bilateral increase of EMG activity in the anterior digastric muscles, consistent with earlier studies. The study has also provided novel findings that TLR4 is expressed in the caudal medulla and that the application of a TLR4 antagonist to the caudal medulla can significantly attenuate the MO-evoked EMG activities but not the expression levels of TLR4 within the rat MDH. The findings suggest that TLR4 may be an important pharmacological target for the control of acute inflammatory pain involving the teeth.

DATA AVAILABILITY STATEMENT

The datasets generated for this study are available on request to the corresponding author.

REFERENCES

- Avivi-Arber, L., Lee, J.-C., and Sessle, B. J. (2010). Effects of incisor extraction on jaw and tongue motor representations within face sensorimotor cortex of adult rats. *J. Comp. Neurol.* 518, 1030–1045. doi: 10.1002/cne.22261
- Avivi-Arber, L., Lee, J. C., Sood, M., Lakschevitz, F., Fung, M., Barashi-Goza, M., et al. (2015). Long-term neuroplasticity of the face primary motor cortex and adjacent somatosensory cortex induced by tooth loss can be reversed following dental implant replacement in rats. *J. Comp. Neurol.* 523, 2372–2389. doi: 10.1002/cne.23793
- Awamleh, L., Pun, H., Lee, J. C., and Avivi-Arber, L. (2015). Decreased face primary motor cortex (face-M1) excitability induced by noxious stimulation of the rat molar tooth pulp is dependent on the functional integrity of face-M1 astrocytes. *Exp. Brain Res.* 233, 1261–1272. doi: 10.1007/s00221-015-4198-8
- Brubaker, S. W., Bonham, K. S., Zanolini, I., and Kagan, J. C. (2015). Innate immune pattern recognition: a cell biological perspective. *Annu. Rev. Immunol.* 33, 257–290. doi: 10.1146/annurev-immunol-032414-112240
- Bruno, K., Woller, S. A., Miller, Y., Yaksh, T. L., Wallace, M., Beaton, G., et al. (2018). Targeting toll-like receptor-4 (TLR4)-an emerging therapeutic target for persistent pain states. *Pain* 159, 1908–1915. doi: 10.1097/j.pain.0000000000001306
- Bryant, C. E., Gay, N. J., Heymans, S., Sacre, S., Schaefer, L., and Midwood, K. S. (2015). Advances in Toll-like receptor biology: modes of activation by diverse stimuli. *Crit. Rev. Biochem. Mol. Biol.* 50, 359–379. doi: 10.3109/10409238.2015.1033511
- Buchanan, M. M., Hutchinson, M., Watkins, L. R., and Yin, H. (2010). Toll-like receptor 4 in CNS pathologies. *J. Neurochem.* 114, 13–27.
- Byers, M. R., and Närhi, M. V. (1999). Dental injury models: experimental tools for understanding neuroinflammatory interactions and polymodal nociceptor functions. *Crit. Rev. Oral Biol. Med.* 10, 4–39. doi: 10.1177/10454411990100010101
- Cairns, B. E., Sessle, B. J., and Hu, J. W. (1998). Evidence that excitatory amino acid receptors within the temporomandibular joint region are involved in the reflex activation of the jaw muscles. *J. Neurosci.* 18, 8056–8064. doi: 10.1523/jneurosci.18-19-08056.1998

ETHICS STATEMENT

The animal study was reviewed and approved by the Animal Care Committee of the University of Toronto (protocol number #20011420) and were accomplished in accordance with the regulations of the Ontario Animal Research Act (Canada).

AUTHOR CONTRIBUTIONS

HF designed, conducted the experiments, analyzed the data, wrote the drafts, and finalized the manuscript. GM and YA conducted the experiments. LA-A designed, conducted and supervised the experiments, and edited the manuscript. MZ analyzed the data. S-GG and MC designed the experiments and edited the manuscript. BS designed, supervised the experiments, and edited the manuscript. All authors contributed to the article and approved the submitted version.

FUNDING

This research was supported by Coordenação de Aperfeiçoamento de Pessoal de Nível Superior (CAPES). HF received a grant for an international Ph.D. internship from CAPES (99999.006931/2015-04).

- Cairns, B. E., Sessle, B. J., and Hu, J. W. (2001). Temporomandibular-evoked jaw muscle reflex: role of brainstem NMDA and non-NMDA receptors. *Neuroreport* 12, 1875–1878. doi: 10.1097/00001756-200107030-00022
- Chiang, C. Y., Dostrovsky, J. O., and Sessle, B. J. (2011). Role of glia in orofacial pain. *Neuroscientist* 17, 303–321.
- Chiang, C. Y., Park, S. J., Kwan, C. L., Hu, J. W., and Sessle, B. J. (1998). NMDA receptor mechanisms contribute to neuroplasticity induced in caudalis nociceptive neurons by tooth pulp stimulation. *J. Neurophysiol.* 80, 2621–2631. doi: 10.1152/jn.1998.80.5.2621
- Chiang, C. Y., Wang, J., Xie, Y. F., Zhang, S., Hu, J. W., Dostrovsky, J. O., et al. (2007). Astroglial glutamate-glutamine shuttle is involved in central sensitization of nociceptive neurons in rat medullary dorsal horn. *J. Neurosci.* 27, 9068–9076. doi: 10.1523/jneurosci.2260-07.2007
- Chichorro, J. G., Porreca, F., and Sessle, B. J. (2017). Mechanisms of craniofacial pain. *Cephalalgia* 37, 613–626.
- Christianson, C. A., Dumlao, D. S., Stokes, J. A., Dennis, E. A., Svensson, C. I., and Corr, M. (2011). Spinal TLR4 mediates the transition persistent mechanical hypersensitivity after the resolution of inflammation in serum-transferred arthritis. *Pain* 152, 2881–2891. doi: 10.1016/j.pain.2011.09.020
- Coats, S. R., Pham, T. T., Bainbridge, B. W., Reife, R. A., and Darveau, R. P. (2005). MD-2 mediates the ability of tetra-acylated and penta-acylated lipopolysaccharides to antagonize *Escherichia coli* lipopolysaccharide at the TLR4 signaling complex. *J. Immunol.* 175, 4490–4498. doi: 10.4049/jimmunol.175.7.4490
- Cognasse, F., Nguyen, K. A., Damien, P., McNicol, A., Pozzetto, B., Hamzeh-Cognasse, H., et al. (2015). The inflammatory role of platelets via their TLRs and Siglec receptors. *Front. Immunol.* 6:83. doi: 10.3389/fimmu.2015.00083
- Diogenes, A., Ferraz, C. C., Akopian, A. N., Henry, M. A., and Hargreaves, K. M. (2011). LPS sensitizes TRPV1 via activation of TLR4 in trigeminal sensory neurons. *J. Dent. Res.* 90, 759–764. doi: 10.1177/0022034511400225
- FDI World Dental Federation (2015). *The Challenge of Oral Disease – A Call for Global Action. The Oral Health Atlas*, 2nd Edn. Geneva: FDI World Dental Federation.

- Fischer, M. J., Balasuriya, D., Jeggle, P., Goetze, T. A., McNaughton, P. A., Reeh, P. W., et al. (2014). Direct evidence for functional TRPV1/TRPA1 heteromers. *Pflugers Arch.* 466, 2229–2241. doi: 10.1007/s00424-014-1497-z
- Gao, D., and Li, W. (2016). Structures and recognition modes of toll-like receptors. *Proteins* 85, 3–9. doi: 10.1002/prot.25179
- Gouin, O., L'Herondelle, K., Lebonvallet, N., Le Gall-Ianotto, C., Sakka, M., Buhé, R., et al. (2017). TRPV1 and TRPA1 in cutaneous neurogenic and chronic inflammation: pro-inflammatory response induced by their activation and their sensitization. *Prot. Cell* 8, 644–661. doi: 10.1007/s13238-017-0395-5
- Green, D., Ruparel, S., Gao, X., Ruparel, N., Patil, M., Akopian, A., et al. (2016). Central activation of TRPV1 and TRPA1 by novel endogenous agonists contributes to mechanical allodynia and thermal hyperalgesia after burn injury. *Mol. Pain* 12, 1–9.
- Guo, L. H., and Schluesener, H. J. (2007). The innate immunity of the central nervous system in chronic pain: the role of Toll-like receptors. *Cell Mol. Life Sci.* 64, 1128–1136. doi: 10.1007/s00018-007-6494-3
- Hargreaves, K. M., and Ruparel, S. (2016). Role of oxidized lipids and TRP channels in orofacial pain and inflammation. *J. Dent. Res.* 95, 1117–1123. doi: 10.1177/0022034516653751
- Hu, J. W., Yu, X. M., Vernon, H., and Sessle, B. J. (1993). Excitatory effects on neck and jaw muscle activity of inflammatory irritant applied to cervical paraspinal tissues. *Pain* 55, 243–250. doi: 10.1016/0304-3959(93)90153-g
- Hu, T. T., Wang, R. R., Tang, Y. Y., Wu, Y. X., Yu, J., Hou, W. W., et al. (2018). TLR4 deficiency abrogated widespread tactile allodynia, but not widespread thermal hyperalgesia and trigeminal neuropathic pain after partial infraorbital nerve transection. *Pain* 159, 273–283. doi: 10.1097/j.pain.0000000000001100
- Iwata, K., Imamura, Y., Honda, K., and Shinoda, M. (2011). Physiological mechanisms of neuropathic pain: the orofacial region. *Int. Rev. Neurobiol.* 97, 227–250. doi: 10.1016/b978-0-12-385198-7.00009-6
- Iwata, K., Tashiro, A., Tsuboi, Y., Imai, T., Sumino, R., Morimoto, T., et al. (1999). Medullary dorsal horn neuronal activity in rats with persistent temporomandibular joint and perioral inflammation. *J. Neurophysiol.* 82, 1244–1253. doi: 10.1152/jn.1999.82.3.1244
- Kashima, D. T., and Grueter, B. A. (2017). Toll-like receptor 4 deficiency alters nucleus accumbens synaptic physiology and drug reward behavior. *Proc. Natl. Acad. Sci. U.S.A.* 114, 8865–8870. doi: 10.1073/pnas.1705974114
- Kobayashi, K., Fukuoaka, T., Obata, K., Yamanaka, H., Dai, Y., Tokunaga, A., et al. (2005). Distinct expression of TRPM8, TRPA1, and TRPV1 mRNAs in rat primary afferent neurons with a delta / c - fibers and colocalization with trk receptors. *J. Comp. Neurol.* 26, 596–606. doi: 10.1002/cne.20794
- Lam, D. K., Sessle, B. J., Cairns, B. E., and Hu, J. W. (2005). Peripheral NMDA receptor modulation of jaw muscle electromyographic activity induced by capsaicin injection into the temporomandibular joint of rats. *Brain Res.* 1046, 68–76. doi: 10.1016/j.brainres.2005.03.040
- Lee, K., Lee, B. M., Park, C. K., Kim, Y. H., and Chung, G. (2019). Ion Channels Involved in Tooth Pain. *Int. J. Mol. Sci.* 20, 2266. doi: 10.3390/ijms20092266
- Lehnardt, S., Lachance, C., Patrizi, S., Lefebvre, S., Follett, P. L., Jensen, F. E., et al. (2002). The toll-like receptor TLR4 is necessary for lipopolysaccharide-induced oligodendrocyte injury in the CNS. *J. Neurosci.* 22, 2478–2486. doi: 10.1523/jneurosci.22-07-02478.2002
- Lehnardt, S., Massillon, L., Follett, P., Jensen, F. E., Ratan, R. P., Rosenberg, J. J., et al. (2003). Activation of innate immunity in the CNS triggers neurodegeneration through a Toll-like receptor 4-dependent pathway. *Proc. Natl. Acad. Sci. U.S.A.* 100, 8514–8519. doi: 10.1073/pnas.1432609100
- Li, Y., Zhang, H., Kosturakis, A. K., Cassidy, R. M., Zhang, H., Kennamer-Chapman, R. M., et al. (2015). MAPK signaling downstream to TLR4 contributes to paclitaxel-induced peripheral neuropathy. *Brain Behav. Immun.* 49, 255–266. doi: 10.1016/j.bbi.2015.06.003
- Lin, J. J., Du, Y., Cai, W. K., Kuang, R., Chang, T., Zhang, Z., et al. (2015). Toll-like receptor 4 signaling in neurons of trigeminal ganglion contributes to nociception induced by acute pulpitis in rats. *Sci. Rep.* 5:12549. doi: 10.1038/srep12549
- Narita, N., Kumar, N., Cherkas, P. S., Chiang, C. Y., Dostrovsky, J. O.,Coderre, T. J., et al. (2012). Systemic pregabalin attenuates sensorimotor responses and medullary glutamate release in inflammatory tooth pain model. *Neuroscience* 218, 359–366. doi: 10.1016/j.neuroscience.2012.05.016
- Nicotra, L., Loram, L. C., Watkins, L. R., and Hutchinson, M. R. (2012). Toll-like receptors in chronic pain. *Exp. Neurol.* 234, 316–329.
- Nudo, R. J., Larson, D., Plautz, E. J., Friel, K. M., Barbay, S., and Frost, S. B. (2003). A squirrel monkey model of poststroke motor recovery. *ILAR J.* 44, 161–174. doi: 10.1093/ilar.44.2.161
- Ogawa, K., Hirooka, Y., Kishi, T., Ide, T., and Sunagawa, K. (2013). Partially silencing brain toll-like receptor 4 prevents in part left ventricular remodeling with sympathoinhibition in rats with myocardial infarction-induced heart failure. *PLoS One* 8:e69053. doi: 10.1371/journal.pone.0069053
- Ohara, K., Shimizu, K., Matsuura, S., Ogiso, B., Omagari, D., Asano, M., et al. (2013). Toll-like receptor 4 signaling in trigeminal ganglion neurons contributes tongue-referred pain associated with tooth pulp inflammation. *J. Neuroinflamm.* 10:139. doi: 10.1186/1742-2094-10-139
- Olson, J. K., and Miller, S. D. (2004). Microglia initiate central nervous system innate and adaptive immune responses through multiple TLRs. *J. Immunol.* 173, 3916–3924. doi: 10.4049/jimmunol.173.6.3916
- Pun, H., Awamleh, L., Lee, J. C., and Avivi-Arber, L. (2016). Decreased face primary motor cortex (face-M1) excitability induced by noxious stimulation of the rat molar tooth pulp is dependent on the functional integrity of medullary astrocytes. *Exp. Brain Res.* 234, 645–657. doi: 10.1007/s00221-015-4448-9
- Renard, E., Gaudin, A., Bienvenu, G., Amiaud, J., Farges, J. C., Cuturi, M. C., et al. (2016). Immune cells and molecular networks in experimentally induced pulpitis. *J. Dent. Res.* 95, 196–205. doi: 10.1177/0022034515612086
- Sadofsky, L. R., Sreekrishna, K. T., Lin, Y., Schinaman, R., Gorka, K., Mantri, Y., et al. (2014). Unique responses are observed in transient receptor potential ankyrin 1 and vanilloid 1 (TRPA1 and TRPV1) co-expressing cells. *Cells* 3, 616–626. doi: 10.3390/cells3020616
- Saitoh, S., Akashi, S., Yamada, T., Tanimura, N., Kobayashi, M., Konno, K., et al. (2004). Lipid A antagonist, lipid IVA, is distinct from lipid A in interaction with Toll-like receptor 4 (TLR4)-MD-2 and ligand-induced TLR4 oligomerization. *Int. Immunol.* 16, 961–969. doi: 10.1093/intimm/dxh097
- Sessle, B. J. (1986). Recent developments in pain research: central mechanisms of orofacial pain and its control. *J. Endod.* 12, 435–444. doi: 10.1016/s0099-2399(86)80196-0
- Sessle, B. J. (2000). Acute and chronic craniofacial pain: brainstem mechanisms of nociceptive transmission and neuroplasticity, and their clinical correlates. *Crit. Rev. Oral Biol. Med.* 11, 57–91. doi: 10.1177/10454411000110010401
- Sessle, B. J. (2014). *Orofacial Pain*. Washington, DC: IASP Press.
- Shrestha, A., Cordova, M., and Kishen, A. (2015). Photoactivated polycationic bioactive chitosan nanoparticles inactivate bacterial endotoxins. *J. Endod.* 41, 686–691. doi: 10.1016/j.joen.2014.12.007
- Signore, M., Manganelli, A., and Hodge, A. (2017). Antibody validation by western blotting. *Methods Mol. Biol.* 1606, 51–70.
- Sorge, R., Lacroix-Fralish, M., Tuttle, A., Sotocinal, S., Austin, J. S., Ritchie, J., et al. (2011). Spinal cord toll-like receptor 4 mediates inflammatory and neuropathic hypersensitivity in male but not female mice. *J. Neurosci.* 31, 15450–15454. doi: 10.1523/jneurosci.3859-11.2011
- Sun, Y., Yang, M., Tang, H., Ma, Z., Liang, Y., and Li, Z. (2015). The overproduction of TNF- α via Toll-like receptor 4 in spinal dorsal horn contributes to the chronic postsurgical pain in rat. *J. Anesth.* 29, 734–740. doi: 10.1007/s00540-015-2011-2
- Sunakawa, M., Chiang, C. Y., Sessle, B. J., and Hu, J. W. (1999). Jaw electromyographic activity induced by the application of algescic chemicals to the rat tooth pulp. *Pain* 80, 493–501. doi: 10.1016/s0304-3959(98)00241-3
- Takeda, K., Kaisho, T., and Akira, S. (2003). Toll-like receptors. *Annu. Rev. Immunol.* 21, 335–376.
- Takeda, M., Takahashi, M., Kitagawa, J., Kanazawa, T., Nasu, M., and Matsumoto, S. (2013). Brain-derived neurotrophic factor enhances the excitability of small-diameter trigeminal ganglion neurons projecting to the trigeminal nucleus interpolaris/caudalis transition zone following masseter muscle inflammation. *Mol. Pain* 9:49. doi: 10.1186/1744-8069-9-49
- Tanga, F. Y., Natile-McMenemy, N., and DeLeo, J. A. (2005). The CNS role of toll-like receptor 4 in innate neuroimmunity and painful neuropathy. *Proc. Natl. Acad. Sci. U.S.A.* 102, 5856–5861. doi: 10.1073/pnas.0501634102
- Teghanemt, A., Zhang, D., Levis, E. N., Weiss, J. P., and Gioannini, T. L. (2005). Molecular basis of reduced potency of underacylated endotoxins. *J. Immunol.* 175, 4669–4676. doi: 10.4049/jimmunol.175.7.4669

- Tennant, K. A., Adkins, D. L., Donlan, N. A., Asay, A. L., Thomas, N., Kleim, J. A., et al. (2011). The organization of the forelimb representation of the C57BL/6 mouse motor cortex as defined by intracortical microstimulation and cytoarchitecture. *Cereb. Cortex* 21, 865–876. doi: 10.1093/cercor/bhq159
- Tennant, K. A., Adkins, D. L., Scalco, M. D., Donlan, N. A., Asay, A. L., Thomas, N., et al. (2012). Skill learning induced plasticity of motor cortical representations is time and age-dependent. *Neurobiol. Learn. Mem.* 98, 291–302. doi: 10.1016/j.nlm.2012.09.004
- Tramullas, M., Finger, B. C., Moloney, R. D., Golubeva, A. V., Moloney, G., Dinan, T. G., et al. (2014). Toll-like receptor 4 regulates chronic stress-induced visceral pain in mice. *Biol. Psychiatry* 76, 340–348. doi: 10.1016/j.biopsych.2013.11.004
- Tsai, C. M., Chiang, C. Y., Yu, X. M., and Sessle, B. J. (1999). Involvement of trigeminal subnucleus caudalis (medullary dorsal horn) in craniofacial nociceptive reflex activity. *Pain* 81, 115–128. doi: 10.1016/s0304-3959(99)00009-3
- Vaure, C., and Liu, Y. (2014). A comparative review of toll-like receptor 4 expression and functionality in different animal species. *Front. Immunol.* 5:316. doi: 10.3389/fimmu.2014.00316
- Visintin, A., Halmen, K. A., Latz, E., Monks, B. G., and Golenbock, D. T. (2005). Pharmacological inhibition of endotoxin responses is achieved by targeting the TLR4 coreceptor, MD-2. *J. Immunol.* 175, 6465–6472. doi: 10.4049/jimmunol.175.10.6465
- Wadachi, R., and Hargreaves, K. M. (2006). Trigeminal nociceptors express TLR-4 and CD14: a mechanism for pain due to infection. *J. Dent. Res.* 85, 49–53. doi: 10.1177/154405910608500108
- Woolf, C. J., and Wall, P. D. (1986). Relative effectiveness of C primary afferent fibers of different origins in evoking a prolonged facilitation of the flexor reflex in the rat. *J. Neurosci.* 6, 1433–1442. doi: 10.1523/jneurosci.06-05-01433.1986
- Yadav, S., and Suroolia, A. (2019). Lysozyme elicits pain during nerve injury by neuronal Toll-like receptor 4 activation and has therapeutic potential in neuropathic pain. *Sci. Transl. Med.* 11:504. doi: 10.1126/scitranslmed.aav4176
- Yan, X., Jiang, E., and Weng, H. R. (2015a). Activation of toll like receptor 4 attenuates GABA synthesis and postsynaptic GABA receptor activities in the spinal dorsal horn via releasing interleukin-1 beta. *J. Neuroinflamm.* 12:222. doi: 10.1186/s12974-014-0222-3
- Yan, X., Maixner, D. W., Yadav, R., Gao, M., Li, P., Bartlett, M. G., et al. (2015b). Paclitaxel induces acute pain via directly activating toll like receptor 4. *Mol. Pain.* 11:10. doi: 10.1186/s12990-015-0005-6
- Yu, X. M., Sessle, B. J., Vernon, H., and Hu, J. W. (1994). Administration of opiate antagonist naloxone induces recurrence of increased jaw muscle activities related to inflammatory irritant application to rat temporomandibular joint region. *J. Neurophysiol.* 72, 1430–1433. doi: 10.1152/jn.1994.72.3.1430

Conflict of Interest: The authors declare that the research was conducted in the absence of any commercial or financial relationships that could be construed as a potential conflict of interest.

The handling editor is currently organizing a Research Topic with one of the authors LA-A, and confirms the absence of any other collaboration.

Copyright © 2020 Filippini, Molska, Zanjir, Arudchelvan, Gong, Campos, Avivi-Arber and Sessle. This is an open-access article distributed under the terms of the Creative Commons Attribution License (CC BY). The use, distribution or reproduction in other forums is permitted, provided the original author(s) and the copyright owner(s) are credited and that the original publication in this journal is cited, in accordance with accepted academic practice. No use, distribution or reproduction is permitted which does not comply with these terms.



Functional Connectivity Between the Trigeminal Main Sensory Nucleus and the Trigeminal Motor Nucleus

Mohammed Slaoui Hasnaoui¹, Isabel Arsenault¹, Dorly Verdier¹, Sami Obeid¹ and Arlette Kolta^{1,2*}

¹Groupe de Recherche sur le Système Nerveux Central, Département de Neurosciences, Faculté de Médecine, Université de Montréal, Montréal, QC, Canada, ²Département de Stomatologie, Faculté de Médecine Dentaire, Université de Montréal, Montréal, QC, Canada

OPEN ACCESS

Edited by:

Teresa Lever,
University of Missouri, United States

Reviewed by:

Parisa Gazerani,
Aalborg University, Denmark
Donald C. Bolser,
University of Florida, United States

*Correspondence:

Arlette Kolta
arlette.kolta@umontreal.ca

Specialty section:

This article was submitted to Cellular Neurophysiology, a section of the journal *Frontiers in Cellular Neuroscience*

Received: 12 March 2020

Accepted: 19 May 2020

Published: 23 June 2020

Citation:

Slaoui Hasnaoui M, Arsenault I, Verdier D, Obeid S and Kolta A (2020) Functional Connectivity Between the Trigeminal Main Sensory Nucleus and the Trigeminal Motor Nucleus. *Front. Cell. Neurosci.* 14:167. doi: 10.3389/fncel.2020.00167

The present study shows new evidence of functional connectivity between the trigeminal main sensory (NVsnpr) and motor (NVmt) nuclei in rats and mice. NVsnpr neurons projecting to NVmt are most highly concentrated in its dorsal half. Their electrical stimulation induced multiphasic excitatory synaptic responses in trigeminal MNs and evoked calcium responses mainly in the jaw-closing region of NVmt. Induction of rhythmic bursting in NVsnpr neurons by local applications of BAPTA also elicited rhythmic firing or clustering of postsynaptic potentials in trigeminal motoneurons, further emphasizing the functional relationship between these two nuclei in terms of rhythm transmission. Biocytin injections in both nuclei and calcium-imaging in one of the two nuclei during electrical stimulation of the other revealed a specific pattern of connectivity between the two nuclei, which organization seemed to critically depend on the dorsoventral location of the stimulation site within NVsnpr with the most dorsal areas of NVsnpr projecting to the dorsolateral region of NVmt and intermediate areas projecting to ventromedial NVmt. This study confirms and develops earlier experiments by exploring the physiological nature and functional topography of the connectivity between NVsnpr and NVmt that was demonstrated in the past with neuroanatomical techniques.

Keywords: mastication, trigeminal, NVsnpr, NVmt, motoneurons, jaw muscles, burst firing

INTRODUCTION

Mastication is a vital behavior that allows the preparation of food for swallowing during feeding. This rhythmic movement can be initiated by repetitive stimulation of either the cortical masticatory area (CMA) or the trigeminal sensory afferents while its pattern of activity is shaped by a neuronal network in the brainstem known as the masticatory central pattern generator (CPG; Bremer, 1923; Dellow and Lund, 1971). Combined evidence from several *in vitro* studies suggests that the CPG is located in the pons near the trigeminal motor nucleus (NVmt; Kogo et al., 1996; Nakamura et al., 1999; Tanaka et al., 1999).

In rodents, motoneurons (MNs) innervating masticatory muscles are clustered in two distinct divisions in the NVmt, a large dorsolateral (DL) and a much smaller ventromedial (VM) containing respectively the jaw-closing and jaw opening MNs (Mizuno et al., 1975; Limwongse and DeSantis, 1977; Sasamoto, 1979; Jacquin et al., 1983; Lynch, 1985; Rokx and van Willigen, 1985). The DL division extends throughout the entire rostrocaudal length of the NVmt, while the VM division is limited to its caudal two thirds. Masticatory

muscles are often categorized as jaw opening and jaw-closing muscles, but many of them are subdivided in neuromuscular compartments allowing for the production of complex movements. These compartments represent the smallest anatomical muscular division which activation generates a unique movement (Widmer and Morris-Wiman, 2010). They are innervated independently and can be recruited either individually or in a group by the CPG. For instance, the rabbit masseter muscle was shown to be composed of at least 23 different neuromuscular compartments each innervated by axons of a single motor unit (English et al., 1999; Widmer et al., 2003). Thus, the differential recruitment of these compartments by the trigeminal pre-MNs would allow the production of diverse and precise jaw movements. This implies a much more complex myotopic organization of the NVmt paralleled by a functional topographical organization of the projections from the masticatory CPG.

Several lines of evidence suggest that the trigeminal main sensory nucleus (NVsnpr), one of the regions near NVmt, is likely to play a crucial role in either pattern and/or rhythm generation, placing it at the very heart of the masticatory CPG.

NVsnpr receives inputs from the CMA in the rat and trigeminal sensory afferents in rats and cats which allow respectively the initiation and adaptation of masticatory movements (Yasui et al., 1985; Shigenaga et al., 1986a,b, 1988; Yoshida et al., 2009). Bouts of masticatory movements increase blood flow to the NVsnpr nucleus in humans (Viggiano et al., 2015) and even bouts of fictive mastication in rabbits are associated to increased neural activity, as detected by C-Fos in its dorsal part (Athanasiadis et al., 2005a), and rhythmic firing of many of its neurons in phase with either the closing or opening motoneurons (Tsuboi et al., 2003). Furthermore, these dorsal neurons were shown to have intrinsic bursting properties in gerbils (Sandler et al., 1998) and rats (Brocard et al., 2006). In rats, this intrinsic bursting relies on a sodium persistent current (I_{NaP}) whose appearance coincides with the emergence of the first masticatory movements (Brocard et al., 2006). This voltage-dependent current is also sensitive to variations in extracellular Ca^{2+} -concentration (Li and Hatton, 1996; Su et al., 2001; Brocard et al., 2006, 2013; Tsuruyama et al., 2013; Morquette et al., 2015), and we have shown that small local extracellular applications of the Ca^{2+} -chelator BAPTA can trigger rhythmic firing in rats NVsnpr neurons.

Anatomical evidence in mice, rats, cats, and rabbits suggest that direct projections from NVsnpr to trigeminal MNs exist (Mizuno et al., 1983; Landgren et al., 1986; Li et al., 1993; Kolta et al., 2000) and in rats, these seem topographically organized with the dorsal and intermediate regions projecting respectively to the DL and VM regions of NVmt (Li et al., 1995). However, the size of tracer injections and the presence of fibers passing through the NVmt limit interpretation of the results of these anatomical studies. Besides these anatomical studies of connectivity, and an electrophysiological investigation led in newborn rats (Nonaka et al., 2012) little is known about the functional relationship between NVsnpr neurons and trigeminal MNs. Therefore, the purpose of this study was to investigate electrophysiologically functional connectivity between NVsnpr

and NVmt in more mature rats and to verify whether similar anatomical and electrophysiological findings can be obtained in mice to validate the use of transgenic mice expressing a genetically encoded Ca^{2+} -indicator (GECI) in motoneurons and NVsnpr neurons for mapping purposes.

Our results suggest that NVsnpr and NVmt are topographically connected in both rats and mice and that rhythmic firing in NVsnpr neurons can drive rhythmic activation of trigeminal MNs.

MATERIALS AND METHODS

All experiments were conducted according to the Canadian Institutes of Health Research rules and were approved by the Animal Care and Use Committee of Université de Montréal. Thirty-five Sprague–Dawley rats (Charles River, Montreal, QC, Canada) and 90 Thy1-GCaMP6f transgenic mice (C57BL/6J-Tg(Thy1-GCaMP6f)GP5.17Dkim/J, stock 025393, The Jackson Laboratory, Sacramento, CA, USA) were used in this study. The transgenic mice express a genetically encoded green fluorescent calcium indicator (GCaMP6f) used for imaging-based monitoring of neuronal activity in individual neurons (Chen et al., 2013).

Retrograde Labeling of Trigeminal Motoneurons in Rats

Pups (2–5 days old) were first injected with 5–10 μ l of the retrograde tracer Cholera Toxin conjugated with Alexa Fluor 488 (Molecular Probes, Eugene, OR, USA) into their digastric muscles under hypothermic anesthesia. Crystals of the carbocyanine dye 1,1'-diocetadecyl-3,3',3'-tetramethylindocarbocyanine perchlorate DiI [DiI_{C18} (3), Molecular Probes, Eugene, OR, USA] were then inserted within their masseter muscles using the tip of a needle. The tracers were allowed several days to diffuse (9–28 days) before the animals were used for experiments.

Brainstem Slice Preparations in Rats and Mice

Experiments were conducted on slices obtained from either the rats (aged P12–27) previously injected with the retrograde tracers or from Thy1-GCaMP6f mice (aged P8–26). The animals were anesthetized with isoflurane (Pharmaceutical Partners of Canada Inc., Richmond Hill, ON, Canada) before decapitation. Their brain was quickly extracted from the cranium and immersed in an ice-cold (4°C) sucrose-based artificial cerebrospinal fluid (ACSF) solution saturated with 95% O₂ and 5% CO₂ containing (in mM): 5, 3 KCl, 1.25 KH₂PO₄, 4 MgSO₄, 20, 26 NaHCO₃, 10 dextrose, 0.2 CaCl₂ and 225, 219 sucrose, pH 7.3–7.4, 300–320 mosmol/kg. Coronal sections (350–400 μ m thick) were performed in the same medium with a vibratome (Leica, Model VT 100S).

The rat brainstem slices were transferred to an interface-type chamber saturated with a humidified mixture of 95% O₂–5% CO₂. They were then perfused successively for 20 min with sucrose ACSF, then with a mixture (50–50%) of sucrose ACSF and normal ACSF (composition in mM: 124 NaCl, 5, 3 KCl,

1.25 KH_2PO_4 , 1.3 MgSO_4 , 26 NaHCO_3 , 25, 10 dextrose and 2.4, 1.6 CaCl_2 , pH 7.3–7.4, 290–300 mosmol/kg) for 20 more minutes and finally, only with normal ACSF at 29–31°C (1 ml/min). The experiments were performed under an epifluorescence microscope (Eclipse E600FN, Nikon) where the slices were viewed at low magnification (5 \times) and the pools of labeled motoneurons (either with cholera-toxin or DiI) were targeted for recording.

The mice brainstem slices containing both the trigeminal main sensory nucleus (NVsnpr) and the trigeminal motor nucleus (NVmt) were transferred at room temperature to a continuously perfused holding chamber filled with normal ACSF bubbled with a mix of 95% O_2 and 5% CO_2 . Slices were allowed to recover for at least 1 h when used to record from NVsnpr neurons, otherwise, they were directly transferred to a recording chamber perfused with ACSF (1.5 ml/min) when used to record from MNs due to their rapid deterioration.

Experiments using the Thy1-GCamp mice were performed under an epifluorescence microscope (Olympus BX50WI) equipped with an optiMOSTM Scientific CMOS camera (QImaging) and a 10 \times -air objective for visualization and precise positioning of the pipettes in either the NVsnpr or the NVmt.

Electroporation and Biocytin Labeling

Slices (350 μm) used for these experiments were acquired from 17 Thy1-GCaMP6f mice aged between 14 and 26 days. Electrophoresis pipettes were pulled from borosilicate glass capillaries (1.5 mm outside diameter, 1.12 mm inside diameter; World Precision Instruments, Sarasota, FL, USA) using the P-97 puller model (Sutter Instruments, Novato, CA, USA) and back-loaded with a solution of biocytin (Sigma; 1.5% in 0.5 M NaCl). A silver wire inserted inside the injection pipette was used to perform the electrophoresis. Positive pressure was applied before the descent to maintain the patency of the injection electrodes which were then guided on the surface of either the NVsnpr or the NVmt until a depression was formed. Biocytin was ejected from the pipette tip with positive rectangular pulses of current (1 μA , 7 s on, 7 s off) for 15 min. After electrophoresis, slices were kept in the chamber to recover for 2 h and then fixed for 24 h in 4% paraformaldehyde. Biocytin was revealed with streptavidin-Alexa 594 (Molecular Probes, no. S11227). The clearing was performed on the slices using the ClearT2 protocol (Kuwajima et al., 2013) to increase the imaging depth and resolution. Imaging was performed under an Olympus FluoView FV 1000 confocal microscope equipped with a 4 \times air and 20 \times water-immersion objectives (Olympus). Acquired images were processed and analyzed offline with FIJI ImageJ (NIH) and Illustrator CS4.

Electrophysiology

Intracellular recordings were performed with brainstem slices from 35 Sprague–Dawley rats using glass microelectrodes (1.0 mm OD, 80–200 M Ω) filled with potassium acetate (3 M). Synaptic responses were evoked by electrical stimulation of the medial part of three different regions (dorsal, intermediate and ventral) of the NVsnpr using bipolar

nichrome electrodes (25 μm diam) insulated except at the tip. The intensity (0.01–7 mA) and duration (0.05–0.3 ms) of the stimulus were varied to obtain optimal responses. Data were recorded using an Axoclamp 2B amplifier (Axon Instruments, Foster City, CA, USA) or a BVC-700 amplifier (Cornerstone by Dagan) through a bridge circuit and sampled at 20 kHz. Data were stored on a standard computer hard drive and analyzed using pClamp 6–8 software (Axon Instruments).

Whole-cell experiments were performed with brainstem slices from 31 Thy1-GCaMP6f mice aged between 8 and 26 days and were acquired at room temperature in a submerged recording chamber perfused with normal aCSF. Recordings of neurons from the NVsnpr and the NVmt were performed with microelectrodes pulled from borosilicate glass capillaries (1.5 mm outside diameter, 1.12 mm inside diameter; World Precision Instruments, Sarasota, FL, USA) using the P-97 puller model (Sutter Instruments, Novato, CA, USA). The microelectrodes had resistances of 5–10 M Ω and were filled with an internal solution containing (in mM) 140 potassium gluconate, 5 NaCl, 10 HEPES, 0.5 EGTA, 2 Tris ATP salt, 0.4 Tris GTP salt, pH 7.2–7.3, 280–300 mosmol/kg. Recordings were acquired in current-clamp mode using the pClamp8 software (Molecular Devices). Electrophysiological signals were amplified with the Axopatch 200B and digitized with the Digidata 1322A (Axon Instruments, Downingtown, PA, USA) and later on analyzed offline with Clampfit10.3 (Molecular Devices). Input resistance was measured using current-clamp recordings of the voltage in response to hyperpolarizing steps. Neuron viability was constantly monitored throughout the experiments with a step current-voltage protocol and only the recordings from neurons with stable resting membrane potential (RMP) of at least -45 mV and overshooting action potentials were analyzed.

Synaptic responses in trigeminal MNs were evoked by electrical stimulation (single pulse) of the NVsnpr using tungsten bipolar electrodes controlled by an Isostim A320 stimulator (WPI, Sarasota, FL, USA). Stimulation parameters were adapted for each cell to attain optimal responses except for pulse width that was kept at 0.2 ms to prevent any risk of direct stimulation of the recorded neuron. BAPTA (10 mM) was also applied locally in the dorsal NVsnpr to synaptically activate trigeminal MNs. As previously defined, we considered rhythmic bursting as a recurrent depolarization plateau over-ridden by at least three action potentials occurring at high frequency and separated by silent periods (Morquette et al., 2015). Based on the pattern and shape of both the plateau and their spikes, the bursts were classified as three different types (Ferraz-Pereira et al., 2015). Plateau potentials occurring regularly were classified as regular bursts (RB) when the spikes occurring within them are regular and perceived throughout all their extent and as adaptative bursts (AB) when the intraburst spiking is subject to an adaptation which leads to the progressive disappearance of the spikes. Finally, long-lasting plateaus occurring irregularly and with irregular spiking defined by the existence of smaller spike over-ridden plateaus were classified as irregular bursts (IB).

Calcium Imaging

Calcium imaging in slices from 47 transgenic mice (P8–23; five of which had also served for whole-cell recordings experiments) expressing GCaMP6f under the neuronal promoter Thy1 was performed using an epifluorescence microscope (Olympus BX50WI) equipped with air (10×) and water-immersion (20× and 40×) objectives (Olympus) and an optiMOSTM Scientific CMOS camera (QImaging) controlled by the open-source acquisition software Micro-Manager v1.4¹. Acute brain slices were prepared and observed the same as for electrophysiology experiments. Excitation of GCaMP6f (470 nm) was carried out with a mercury light source (Olympus U-HGLGPS) and emission was detected through a bandpass filter (535 nm). Slices were under continuous light exposure during the recordings and images were acquired at frequencies of 5–7 Hz with no interval delay between each frame. To assess the specific topographical connectivity, we recorded calcium response of trigeminal MNs responding to electrical or pharmacological (BAPTA at 10 mM for 20 s) stimulations delivered in NVsnpr at four different and equal regions in the dorsoventral orientation. Four electrical trains (500–900 ms at 40 Hz; every 5–10 s) were delivered at the center of each location using tungsten bipolar electrodes controlled by an Isostim A320 stimulator (WPI, Sarasota, FL, USA). A blue dye that can be seen in the acquired time-lapse images was added to the BAPTA solution as a control for any possible spread of the drug outside the desired region of application in the NVsnpr.

Drug Application

BAPTA tetrasodium salt (10 mM; Invitrogen) was locally applied with a glass pipette using the pressure pulses ejection system (Picospritzer III; Parker, Mayfield Heights, OH, USA) to induce bursting in NVsnpr neurons. In some experiments, a cocktail of blockers of excitatory and inhibitory amino-acid receptors was bath-applied with a Harvard 22 syringe pump at the following concentrations: 6-Cyano-7-nitroquinoxaline-2, 3-dione (CNQX; 10 μM; TOCRIS), D, L-2-amino-5-phosphonovaleric acid (APV; 26 μM; Sigma), GABAA Receptor Antagonist (Gabazine; 20 μM; TOCRIS).

Imaging Analysis

Time-lapse images obtained under either the 10× air lens (0.3 N.A.) or the 20× (0.5 N.A.) and 40× (0.80 N.A.) water immersion objectives were processed and analyzed offline with FIJI ImageJ (NIH) and Excel (Microsoft). Photo-bleaching was compensated using the Bleach Correction plugin in FIJI. Changes in fluorescence intensity of responsive cells were determined by measuring for each frame the average pixel values of defined regions of interest (ROIs) traced over the cell bodies using the freehand selection tool in FIJI. The dFoverFmovie FIJI plugin was also used to help to localize lower calcium responses that may have been concealed by higher background fluorescence. An extracellular ROI was also traced near each responsive neuron for background

subtraction. Calcium responses were quantified for each cell as relative changes in fluorescence intensity (ΔF) from the baseline fluorescence and were calculated in % as $\Delta F/F_0 = (F_t - F_0)/F_0$ where F_t is the fluorescence at a time t and F_0 is the fluorescence intensity averaged over a baseline period of 1 s before the start of the stimulations. Only the neurons with changes of at least 20% and which responded either at the same delay or in synchronization with the stimulation onset were considered as “responsive cells” and included in our analysis.

Mapping Analysis

Images acquired at 20× and 40× with traced ROIs of the responsive cells were saved in ImageJ and transferred to Adobe Illustrator to be resized and aligned over the 10× image of the nucleus of interest. For uniformity purposes, all the resulting 10× images were rotated in ImageJ so that the nuclei are vertically orientated with their dorsal and ventral poles positioned respectively at the top and bottom of the image. To produce our heatmaps, x- and y-coordinates were attributed for each responsive cell and their position was displayed in a referential normalized nucleus. To do so, the Polygon tool combined with the Bounding Rectangle option was used to trace an ROI over each nucleus to measure the size of the smallest rectangle surrounding their boundaries as well as their referential point coordinates defined as xBR and yBR. The mean width and height of rectangles measured for all the experiments were used to normalize the size of each nucleus (NVsnpr and NVmt). Afterward, we traced new ROIs over all the previously identified cells to obtain their coordinates with the 10X referential. The referential translation was used to express these coordinates in the nucleus referential using the following formula:

$$(xR, yR) = (x10X - xBR, y10X - yBR)$$

where (xR, yR) are the coordinates of the cell in the bounding rectangle referential; (x10X, y10X) are the coordinates of the cell in the 10× referential; and (xBR, yBR) are the coordinates of the bounding rectangle referential in the 10× image. These coordinates were then transferred in OriginPro 2019 (OriginLab) to create 2D Density plots and transform them into heatmaps using the Kernel Density estimation function.

Statistics

Data are expressed as mean \pm standard error (SEM) throughout the text. In all the experimental results, “N” represents the number of animals used while “n” represents the number of neurons tested unless otherwise specified. Statistical analysis was performed using the program Graphpad Sigma Stat 3.5. Paired Student’s *t*-tests were used for comparison of PSPs amplitude and frequency before and after electrical stimulation or BAPTA application. Fisher Exact tests were used for comparison of the distribution of retrogradely labeled cells or responsive neurons within NVsnpr or NVmt subdivisions. Statistical significance was defined as $P < 0.05$ in all cases.

¹<http://www.micro-manager.org>

RESULTS

Electrophysiological Evidence of Connectivity Between NVsnpr and NVmt

Intracellular Recordings of Trigeminal MNs in Rats

To investigate functional connections from NVsnpr to NVmt in rats, we recorded intracellularly, from different motoneuronal pools, responses elicited by stimulation of different portions of NVsnpr (as schematized in **Figure 1A**). In these initial studies, the emphasis was placed on the most dorsal third of NVsnpr because of earlier findings of Tsuboi et al. (2003) in the rabbit showing that NVsnpr neurons firing in phase with trigeminal MNs during fictive mastication were mostly confined to the most dorsal and medial third. Eighty recordings were made from the retrogradely labeled pool of cells (**Figures 1B,C**) in NVmt; 32 dorsally from masseteric MNs (MMNs) and 48 ventrally from digastric MNs (DMNs). The basic electrophysiological characteristics of MNs from the two pools did not differ remarkably from each other (RMP and input resistance = -61 ± 1 mV and 45 ± 2 M Ω and -65 ± 1 mV and 43 ± 2 M Ω for MMNs and DMNs, respectively). Electrical stimulation of dorsal NVsnpr evoked postsynaptic potentials (PSPs) in the majority of cases (19/30 of MMNs; latency 5.3 ± 2 ms and 26/35 of DMNs; latency 3.9 ± 0.3 ms) or direct activation (**Figure 1E**, right) in a few cases ($n = 6$ in MMNs; latency 0.6 ± 0.02 ms) presumably by current spread to their dendritic arbors which sometimes reach as far as NVsnpr. Most of these PSPs were excitatory as the ones shown in the left panel of **Figure 1E** (EPSPs; 15 in MMNs at a latency of 3.3 ± 0.3 ms and 21 in DMNs at a latency of 3.7 ± 1.3 ms) and many (3/16 in MMNs and 12/21 DMNs) had multiple peaks (**Figure 1E**, left, bottom trace) indicating either activation of other premotor neurons or perhaps responses to bursts of activity in NVsnpr. The remaining PSPs were either inhibitory, like the example shown in the middle panel (top trace) of **Figure 1E** (IPSPs, $n = 3$ in MMNs; latency 7.3 ± 0.8 ms) or biphasic, as illustrated in the middle panel (bottom trace) of **Figure 1E** ($n = 5$ in DMNs; latency 3.5 ± 0.7 ms). Stimulation of the middle portion of NVsnpr was slightly less efficient than that of the dorsal portion to elicit responses in MNs (roughly 50% success rate vs. about 66%) and evoked almost only excitatory responses (five EPSPs/9 MMNs at a latency of 3.7 ± 1.3 ms; 14 EPSPs occurring at a latency of 3.9 ± 0.6 ms and 1 biphasic PSP/31 DMNs at a latency of 3.2 ms). As was the case with EPSPs elicited by dorsal stimulation, many of these EPSPs had multiple peaks (three in MMNs and six in DMNs). Lastly, stimulation of the most ventral 3rd of NVsnpr did not elicit any response in eight MMNs and evoked nine EPSPs (at a latency of 3.4 ± 0.7 ms) in DMNs; seven of which had multiple peaks. The percentage of digastric and masseteric MNs responding to stimulation of each division of NVsnpr is depicted in **Figure 1C** and their number, types, and latencies are shown in **Figure 1D**.

In several cases (29 altogether), single-pulse stimulation in NVsnpr elicited a synaptically evoked EPSP followed by several mini EPSPs appearing at variable latencies (**Figure 1F**; four

trials for the same stimulation). This was observed in the two populations of MNs with all stimulation sites but more frequently with dorsal stimulation (23 cases vs. 5 for the middle part and 1 for the ventral part). Repetitive stimulation (trains of 250–300 ms, 20–80 Hz) causes long lasting (from 800 ms to up to 10 s tested) occurrence of these “randomly” occurring mini EPSPs (mean frequency of 18.5 ± 2.3 Hz) that were sometimes organized into recurrent repetitive clusters (**Figure 1G**).

Whole-Cell Recordings of Trigeminal MNs in Mice

To investigate whether similar evidence of functional connectivity between NVsnpr and NVmt exist in mice, we performed whole-cell recordings of responses of trigeminal MNs ($n = 32$ from 22 mice) to electrical stimulation of NVsnpr. Trigeminal MNs had a mean input resistance of 67 ± 12 M Ω and resting membrane potentials (RMP) ranging from -45 to -74 mV (mean of -56 ± 1 mV). Nearly half of the recorded MNs (44%, $n = 14$) exhibited spontaneous tonic firing at frequencies ranging from 1 to 41 Hz with a mean of 7.5 ± 2.1 Hz. Electrophysiological characteristics of trigeminal MNs are summarized in **Table 1**.

Electrical stimulation of dorsal NVsnpr evoked excitatory responses in 17 of the 32 MNs recorded. In 7 of the 17 cases (from 12 mice), these were EPSPs that occurred at a mean latency of 2.5 ± 0.2 ms and could follow frequency stimulations of 20–40 Hz suggesting that they resulted from mono- to di-synaptic connections. Their mean amplitude and duration were respectively 4.2 ± 0.7 mV and 40 ± 1 ms, and in five of these seven cases, they appeared as multiphasic and were composed of multiple overlapping synaptic events (see example in **Figures 2A–C**). In 5 MNs, high-frequency stimulation (40 Hz) of dorsal NVsnpr increased the frequency of spontaneous EPSPs (6.5 ± 2.3 Hz; **Figure 2D**). In three cases, the high-frequency stimulation also caused a sustained depolarization (6.5 ± 1.9 mV lasting 9.4 ± 3.2 s) at a mean latency of 1.0 ± 0.5 s that led (in two cases) to low frequency firing at a mean latency of 1.2 ± 0.6 s (**Figure 2E**). In the remaining 10 MNs, eight responded to the electrical stimulation with short-latency (1.0 ± 0.1 ms) action potentials (amplitude: 89 ± 7 mV; duration: 1.6 ± 0.3 ms; AHP amplitude: 10.6 ± 1.7 mV) that did not emerge from an underlying EPSP (**Figure 2F**) and display variable latency and amplitude with repetitive high-frequency stimulation (**Figure 2G**) indicating that they may result from direct activation of MNs through their dendrites which are known to extend far beyond the boundaries of NVmt, reaching NVsnpr (white arrows, **Figure 2H**), among other regions (Mong et al., 1988; Lingenhohl and Friauf, 1991).

Anatomical Evidence of Connectivity Between NVsnpr and NVmt in Mice

To document direct projections from NVsnpr to NVmt in mice, and to examine if these projections follow a topographic organization, we made injections of biocytin into the dorsal (NVmt-D) and ventral (NVmt-V) divisions of NVmt for retrograde labeling of NVsnpr neurons (**Figures 3A,B**) or into the dorsal and ventral divisions of NVsnpr for anterograde labeling to NVmt (**Figures 3D,E**). NVsnpr was arbitrarily divided

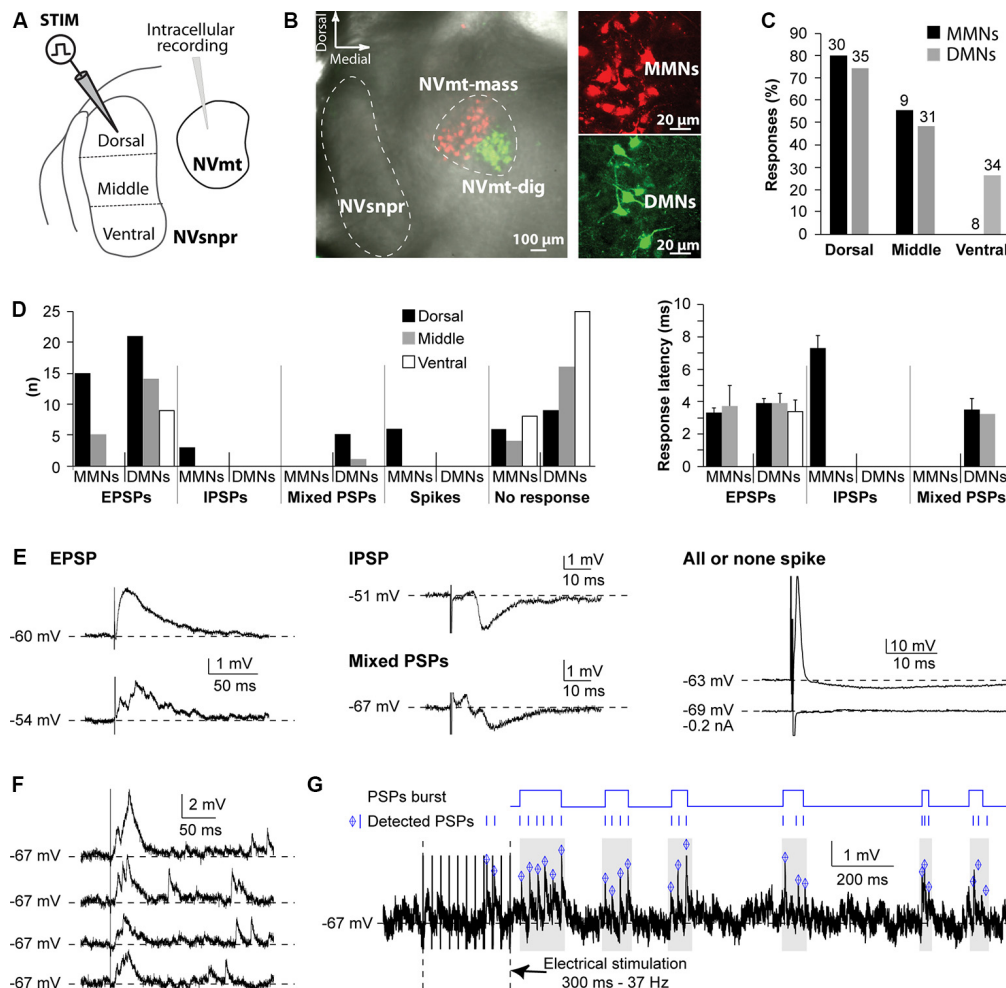


FIGURE 1 | Responses elicited in trigeminal motoneurons upon stimulation of different NVsnpr divisions in rats. **(A)** Schematic illustration of the recording and stimulation (in 3 NVsnpr divisions) arrangements. **(B)** Low (left) and high (right) magnification images of MNs retrogradely labeled in NVmt after injection of Dil (red) in masseter muscles and of Cholera toxin conjugated to Alexa Fluor 488 (green) in digastric muscles. **(C)** Histograms showing the success rate of stimuli applied to each of the NVsnpr divisions for MMNs and DMNs. **(D)** Number (left) and latency (right; mean \pm SEM) of each type of response elicited in the two motoneuronal pools by stimuli applied to each of the NVsnpr divisions shown in panel **(A)**. **(E)** Examples of monophasic (top) and multiphasic (bottom) EPSPs (left) and IPSPs (middle). Right: shows a typical, short latency, all or none response that results from direct activation of the recorded cell. **(F)** Long-lasting increase in the frequency of spontaneous mini EPSPs elicited by single-pulse stimulation in NVsnpr (four trials from the same stimulation site in one MN). **(G)** Top Rasters of PSPs detected in raw (bottom) traces showing clustering of PSPs that could potentially lead to burst firing in MNs after train stimulation in NVsnpr. Abbreviations: Stim, stimulation; NVsnpr, trigeminal main sensory nucleus; NVmt, trigeminal motor nucleus; NVmt-mass, masseter motoneuronal pool; NVmt-dig, digastric motoneuronal pool; MMNs, masseter motoneurons; DMNs, digastric motoneurons; EPSPs, excitatory postsynaptic potentials; IPSPs, inhibitory postsynaptic potentials; PSPs, post-synaptic potentials.

into four regions (R1, R2, R3, and R4; see **Figure 3B**) to count retrogradely labeled neurons as shown in insets of **Figures 3A,B**. Both injections sites in NVmt yielded roughly similar numbers (injections in NVmt-D yielded a total of 207 cells in five slices from five mice, and injections in NVmt-V labeled a total of 196 cells in three slices from three mice) and distribution patterns of retrogradely labeled cells among NVsnpr divisions (injection in NVmt-D vs. NVmt-V: R1/75 vs. 78 cells, R2/109 vs. 96 cells, R3/21 vs. 21 cells and R4/2 vs. 1 cell; **Figure 3C**; Fisher Exact Test, $P = 1$, R1+R2 vs. R3+R4). Thus, projections to both dorsal and ventral NVmt originated almost exclusively from the dorsal

$\frac{3}{4}$ of NVsnpr, with the highest number of retrogradely labeled neurons in R1 and R2, much fewer in R3 and nearly none in R4 (**Figure 3C**).

To further support these results, we injected biocytin into the dorsal (R1+R2, six slices from six mice) and ventral (R3+R4, four slices from three mice) divisions of NVsnpr to assess the direction of their axonal projections to NVmt. In three of the six slices tested, injections of biocytin in dorsal NVsnpr resulted in labeling of thin fibers projecting to or terminating in NVmt (white arrows and asterisks in **Figure 3D**), whereas injections in ventral NVsnpr resulted in labeling of thin

TABLE 1 | Electrophysiological characteristics of trigeminal MNs and NVsnpr neurons in mice. Values are mean \pm SEM.

| Electrophysiological characteristics | Motoneurons (<i>n</i> = 32) | NVsnpr neurons (<i>n</i> = 12) |
|--------------------------------------|---------------------------------|------------------------------------|
| Input resistance (M Ω) | 67 \pm 12 | 230 \pm 29 |
| RMP (mV) | −56 \pm 1 | −50 \pm 2 |
| Firing threshold (mV) | −42 \pm 2 | −40 \pm 1 |
| Spontaneous firing frequency (Hz) | 7.5 \pm 2.1 | 7.2 \pm 1.8 |
| AP amplitude (mV) | 85 \pm 4 | 60.8 \pm 8.6 |
| AP duration (ms) | 1.6 \pm 0.1 | 1.7 \pm 0.3 |
| AHP amplitude (mV) | 12.4 \pm 1.6 | 6.8 \pm 1.9 |

Abbreviations: MNs, motoneurons; NVsnpr, trigeminal main sensory nucleus; RMP, resting membrane potential; AP, action potential; AHP, after hyperpolarization.

fibers mostly in a region ventral to NVmt (white arrows and asterisks in **Figure 3E**) also known as the parvocellular reticular formation (PCrt).

However, retrograde and anterograde labeling can always result from the uptake of the tracer from passing by fibers. Thus, to further document direct connectivity between the two nuclei, we recorded Ca²⁺ and electrophysiological changes elicited in neurons of one of the two nuclei upon electrical stimulation of the other (as schematized in **Figures 4A, 5A**).

Functional Evidence of Connectivity Between NVsnpr and NVmt Revealed by Calcium Imaging

Electrical stimulation (500–900 ms train, 40 Hz) in either NVmt-D (*N* = 15) or NVmt-V (*N* = 13) elicited synchronized transient calcium responses ($261 \pm 20\% \Delta F/F_0$ lasting 2.2 ± 0.1 s; **Figure 4B**) in 161 NVsnpr neurons (in 23 slices from 12 of 14 mice tested). These neurons were distributed essentially throughout the dorsal $\frac{3}{4}$ of the nucleus (**Figure 4C**) with the highest density located mainly in its dorsomedial area (**Figure 4D**). Stimulation of NVmt-D elicited a higher number of responses in the most dorsal part of NVsnpr (R1) relative to stimulation of NVmt-V and both divisions elicited a comparable number of responses in R2 and R3. However, the distributions of the responsive NVsnpr neurons within R1 vs. R2+R3 in response to both stimulation sites in NVmt were not statistically different (Fisher Exact Test, *P* = 1).

Electrical stimulation (500–900 ms train, 40 Hz) in four different regions of the NVsnpr elicited a monophasic increase of intracellular calcium (as in **Figure 5C**) in 118 MNs (in a total of 60 slices from 35 mice. R1: 54 MNs in 18 of 30 mice, R2: 49 MNs in 10 of 15 mice, R3: 13 MNs in three of five mice and R4: 2 MNs in two of five mice; see **Figure 5E**), throughout the dorsal and ventral NVmt. These were mostly (68% of cases) transient responses ($160 \pm 15\% \Delta F/F_0$ lasting 3.4 ± 0.3 s; *n* = 80/118) characterized by a fast rise and a slow decay that out lasted the stimulation train (**Figures 5C,D**). The remaining 32% (38 out of 118 MNs) exhibited persistent calcium responses ($87 \pm 16\% \Delta F/F_0$) with a minimum duration ranging between 3 and 55 s (**Figures 5C,D**). To ensure that responses observed in NVmt did not result from direct activation of motoneuronal dendrites that sometimes reach NVsnpr, a cocktail was used in three animals to block glutamatergic and GABAergic receptors [6-Cyano-7-nitroquinoxaline-2,3-dione (CNQX) 10 μ M; D, L-2-amino-

5-phosphonovaleric acid (APV) 26 μ M; Gabazine; 20 μ M]. Bath-application of these blockers abolished calcium responses in four out of six (67%) responding MNs (not shown). In general, each (trial) electrical stimulation performed in NVsnpr elicited few responses in the NVmt (mean cells/trial: 2.29 for R1, 2.25 for R2, 2.00 for R3 and 1.00 for R4; **Figure 5F**). The highest number of responsive cells per stimulation was obtained with R1 which in one case activated a cluster of 11 MNs in the dorsolateral quadrant (see MNs positions in **Figure 5B**) of NVmt (an example is shown in **Figure 5C**). This region also holds the highest concentration and density of responsive cells which may reflect the highest level of connectivity with NVsnpr (**Figures 5E,G**). Stimulation of the first three regions (R1–R3, black, blue, and red circles in **Figure 5E**) of the NVsnpr generated nearly all the calcium responses elicited in trigeminal MNs. In five mice, only two MNs located in the dorsolateral quadrant responded to the stimulation of R4 (R4, green circles in **Figures 5E,G**, right panel).

In general, activated MNs were observed throughout NVmt but were more concentrated in certain areas depending on the stimulated site. Stimulation of the dorsal NVsnpr resulted mainly in the activation of MNs located dorsally [R1: 44 of 54 MNs (82%) and R2: 35 of 49 MNs (71%)]. However, there was a slight lateral and ventral shift of the cell clusters when R2 was stimulated compared to R1 where the clusters were mostly located dorsally (**Figure 5G**, 2 left panels). Of the four NVsnpr areas, stimulation of R2, which is also the area with the highest connectivity to NVmt (**Figures 3C, 4D**), produced the highest ratio (67% of tested mice) and number (4.9/animal) of calcium responses in NVmt. Fewer stimulation attempts were made in R3, but the number of elicited responses/trial was similar to that obtained with stimulation of more dorsal areas (**Figure 5F**). However, these tended to be located more ventrally in NVmt (red circles in **Figures 5E,G**, 2nd from right). A slight trend of connectivity pattern emerges from a comparison of the heatmaps of R1, R2 and R3 with the position of regions of the higher density of activated neurons in NVmt shifting in the same direction in the dorsoventral axis as the displacement of the stimulation in NVsnpr (**Figure 5G**). However, despite the obvious trend of connectivity between both nuclei, the distributions of the responsive MNs in response to stimulation of the dorsal vs. the ventral part of NVsnpr were not statistically different (Fisher Exact Test, *P* = 1).

We then questioned the pattern of activity elicited in MNs when NVsnpr neurons fire rhythmically.

Induction of Rhythmic Firing in NVsnpr Neurons and Transmission to MNs

BAPTA-Induced Bursting in NVsnpr Neurons

To induce rhythmic firing in NVsnpr we used local extracellular applications of BAPTA (10 mM) in NVsnpr of Thy1-GCaMP6f mice (*N* = 9, P10–19) as previously done in rats (Morquette et al., 2015). The basic electrophysiological characteristics of 12 dorsal NVsnpr neurons recorded for this purpose are summarized in **Table 1**. Ten of these had spontaneous activity as in **Figure 6A** (right, top trace) and a

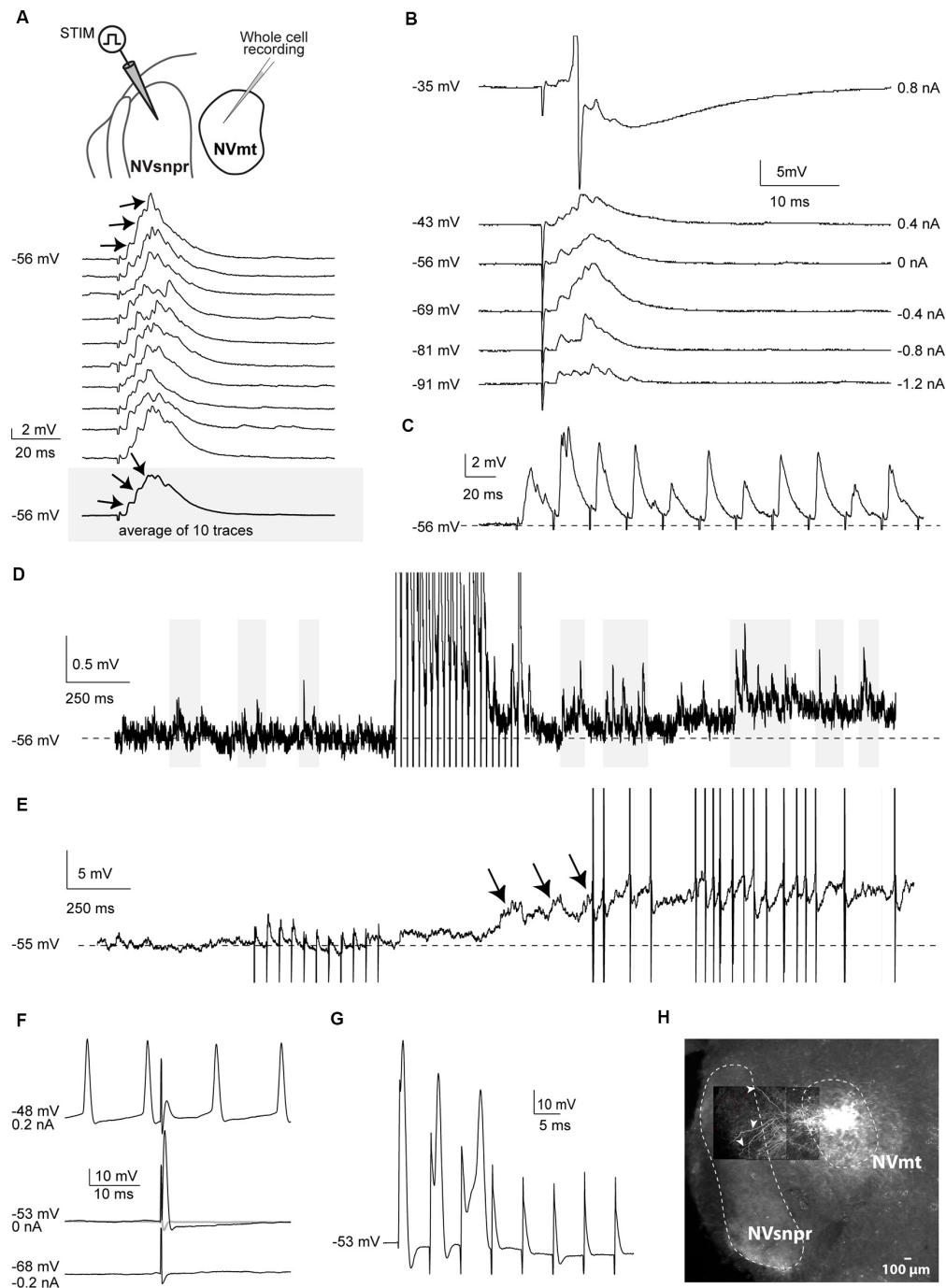


FIGURE 2 | Responses elicited in trigeminal motoneurons upon stimulation of dorsal NVsnpr in mice. **(A)** top: schematic drawing of the brainstem slice preparation and the experimental conditions used. Bottom: example of a multiphasic EPSP recorded in the NVmt following electrical stimulation in the dorsal NVsnpr. Responses to 10 single pulses are shown. Inset: average trace of 10 EPSPs still shows the multiphasic component. **(B)** Depolarization does not reveal a reversal of the response. With depolarization, the stimulation elicited an action potential (Top trace, truncated). **(C)** This EPSP followed stimulation of 40 Hz. **(D)** Train of repetitive stimulations (500 ms 40 Hz) in the dorsal NVsnpr causes a long-lasting increase in the frequency of spontaneous PSPs in the recorded motoneuron. **(E)** Train of repetitive stimulations (500 ms 40 Hz) in the dorsal NVsnpr causes action potentials firing in the recorded motoneuron that seems to emerge from the summation of the increased spontaneous PSPs. **(F)** Example of a short-latency action potential (middle) elicited in the motoneuron by electrical stimulation in the dorsal NVsnpr. Hyperpolarization does not reveal an underlying postsynaptic potential (PSP; bottom) and firing preceding the stimulation causes failure (top). **(G)** High-frequency stimulation (166 Hz) reveals an inconsistency in latency and amplitude of the spike suggesting direct activation of the recorded motoneuron. **(H)** Extracellular injection of biocytin in NVmt reveals the dendritic processes of MNs extending into dorsal NVsnpr. Abbreviations: Stim, stimulation; NVsnpr, trigeminal main sensory nucleus; NVmt, trigeminal motor nucleus.

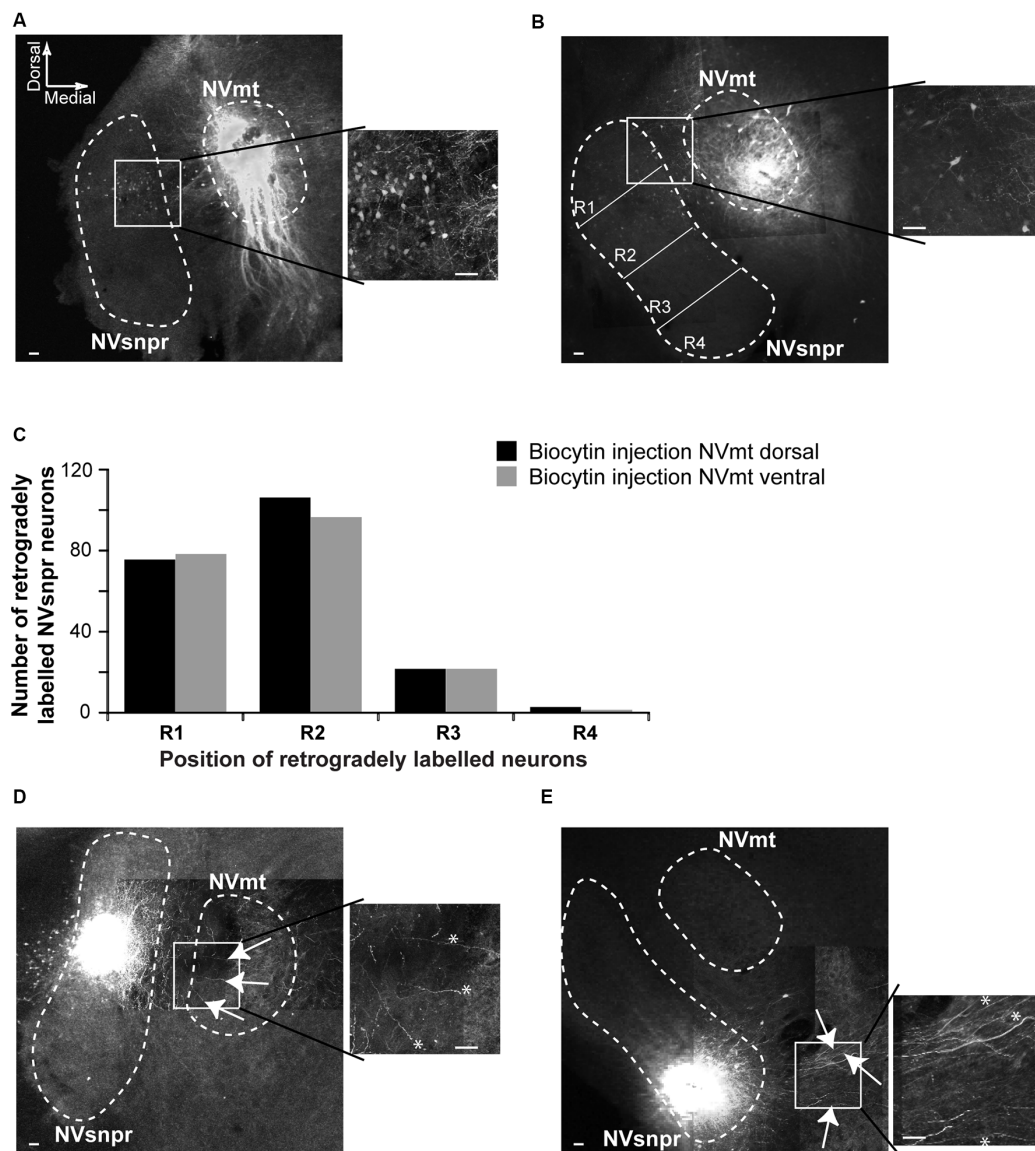


FIGURE 3 | Retrograde and anterograde labeling of projections from divisions of NVsnpr to dorsal and ventral divisions of NVmt. **(A)** Left: photomicrograph showing retrogradely labeled cell bodies in the NVsnpr following extracellular injection of biocytin in the dorsal part of the NVmt. Right: enlargement of the white square in left. Calibration bars 100 μ m. **(B)** Left: photomicrograph showing retrogradely labeled cell bodies in the NVsnpr following extracellular injection of biocytin in the ventral part of the NVmt. Right: enlargement of the white square in left. Calibration bars 100 μ m. **(C)** Vertical bars chart reporting the distribution of retrogradely labeled cells bodies within the four subdivisions of the NVsnpr. **(D)** Left: photomicrograph showing the presence of several fibers (white arrows) in the NVmt following extracellular injection of biocytin in the dorsal part of the NVsnpr. Right: enlargement of the white square in left (*fibers pointed by the arrows in right). Calibration bars 100 μ m. **(E)** Left: photomicrograph revealing the absence of fibers in the NVmt following extracellular injection of biocytin in the ventral part of the NVsnpr. Several fibers (white arrows) could be seen coursing ventrally to the nucleus. Right: enlargement of the white square in left (*fibers pointed by the arrows in right). Calibration bars 100 μ m. Abbreviations: NVsnpr, trigeminal main sensory nucleus; NVmt, trigeminal motor nucleus.

depolarizing sag upon hyperpolarization (Figure 6A, left, top traces) with nine of them displaying rebound spiking upon the termination of the current injection (see Figure 6A, right, bottom trace).

In 8 of the 12 neurons recorded, BAPTA applications at the RMP induced rhythmic bursting (Figures 6B,D, bottom traces), but in seven of these, there was first a depolarization (6.1 ± 1.6 mV) and/or an increase in firing frequency for those

that were spontaneously active, before the switch in firing pattern indicated by the abrupt drop of the inter-spike interval (ISI; occurring at a latency of 2.4 ± 0.8 s in the example shown in Figure 6B (top) and its oscillation between two levels; one reflecting the intra-burst frequency and one the inter-burst frequency. Recurrent bursting produced a hyperpolarization (7.2 ± 1.6 mV) in five cases lowering the neurons membrane potential to approximately -62 ± 3 mV. When tested at more

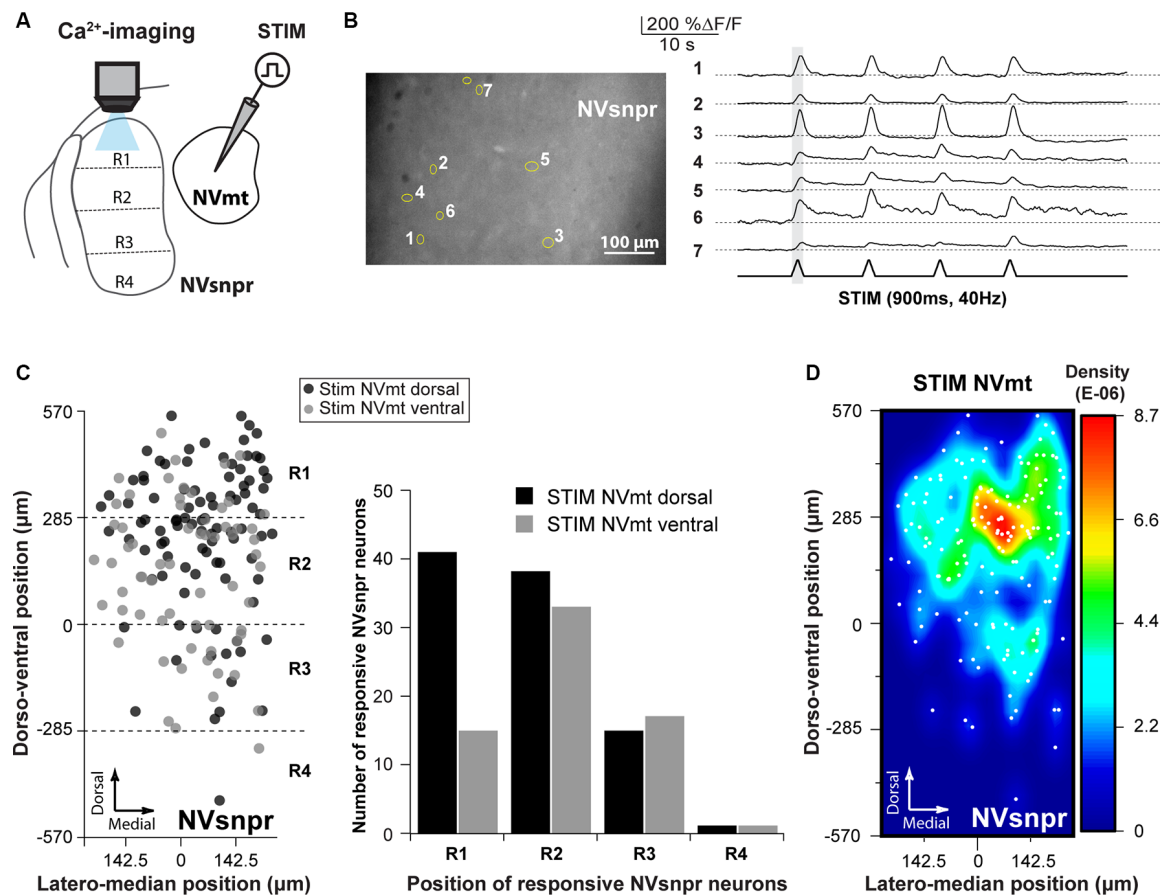


FIGURE 4 | Distribution of NVsnpr neurons activated by stimulation of NVmt. **(A)** Schematic drawing of the brainstem slice preparation and the experimental conditions used. **(B)** Photomicrograph showing the position of responsive cells in NVsnpr following electrical stimulation of dorsal NVmt and their synchronous Ca^{2+} responses. Gray vertical line indicates the length of the train of stimulation. The bottom trace shows a stimulus artifact. **(C)** Distribution of cells responding to stimulation of both NVmt-D and NVmt-V throughout NVsnpr (Left) and count of the number of cells per division in NVsnpr (Right). **(D)** Heatmap representing the density of responsive neurons in NVsnpr following stimulation of NVmt-D and NVmt-V pooled together. Abbreviations: Stim, stimulation; NVsnpr, trigeminal main sensory nucleus; NVmt, trigeminal motor nucleus.

hyperpolarized potentials (-61 ± 2 mV), BAPTA induced a depolarization ($n = 4$; 5.4 ± 1.7 mV at a latency of 2.8 ± 1.0 s) followed by a tonic firing ($n = 2$; 9 ± 4 Hz at a latency of 10.1 ± 1.2 s) or bursting ($n = 6$; at a latency of 7.0 ± 2.3 s) in 8 out of 11 tested NVsnpr neurons (see **Figures 6C,D**). The bursts elicited at the RMP consisted of three different types, the regular bursts (RB; $n = 4$; 50%), the adaptative bursts (AB; $n = 1$) and the irregular bursts (IB; $n = 3$; 38%). RB appeared at -60 ± 2 mV and were represented by recurrent short plateaus (10.3 ± 2.6 mV, lasting 384 ± 137 ms, 0.9 ± 0.4 Hz) with over-riding action potentials occurring regularly at a frequency of 69.3 ± 15.9 Hz. AB was elicited in only one neuron and was characterized by recurrent plateaus (0.4 Hz) of larger amplitudes (30.8 mV) and durations (1,200 ms) that set off at a potential of -62 mV. Finally, the three remaining neurons displayed IB characterized by an irregular occurrence (0.9 ± 0.4 Hz) of plateaus that set-off at an average potential of -48 ± 6 mV and that could be further subdivided into smaller plateaus. The bursts elicited upon membrane hyperpolarisation (occurring at -59 ± 2 mV with a

mean latency of 7.0 ± 2.3 s) were mainly RB ($n = 3$; plateaus of 9.4 ± 1.6 mV lasting 86 ± 22 ms, at 1.0 ± 0.2 Hz) with two IB (1.0 ± 0.1 Hz) and only one AB (plateaus of 30.9 mV lasting 1,700 ms, at 0.3 Hz). Interestingly, the majority of the bursts with irregular intra-burst spiking (two AB and three of five IB) were elicited in mice younger than P12 (P10 and P11) which coincides with the age of emergence of the first masticatory movements in the rat (Westneat and Hall, 1992).

Calcium Imaging of NVsnpr Neurons

Whole-cell recordings in the current-clamp configuration allow for real-time monitoring of electrophysiological activity and manipulation of the membrane potential of the recorded cell but do not provide information about the number, synchrony, and distribution of activated cells. Calcium imaging of NVsnpr neurons in Thy1-GCaMP6f mice was used for that purpose. Local BAPTA (10 mM, in two mice) applications in two slices from these mice elicited mainly transient calcium responses in 19 NVsnpr neurons located near the site of application with

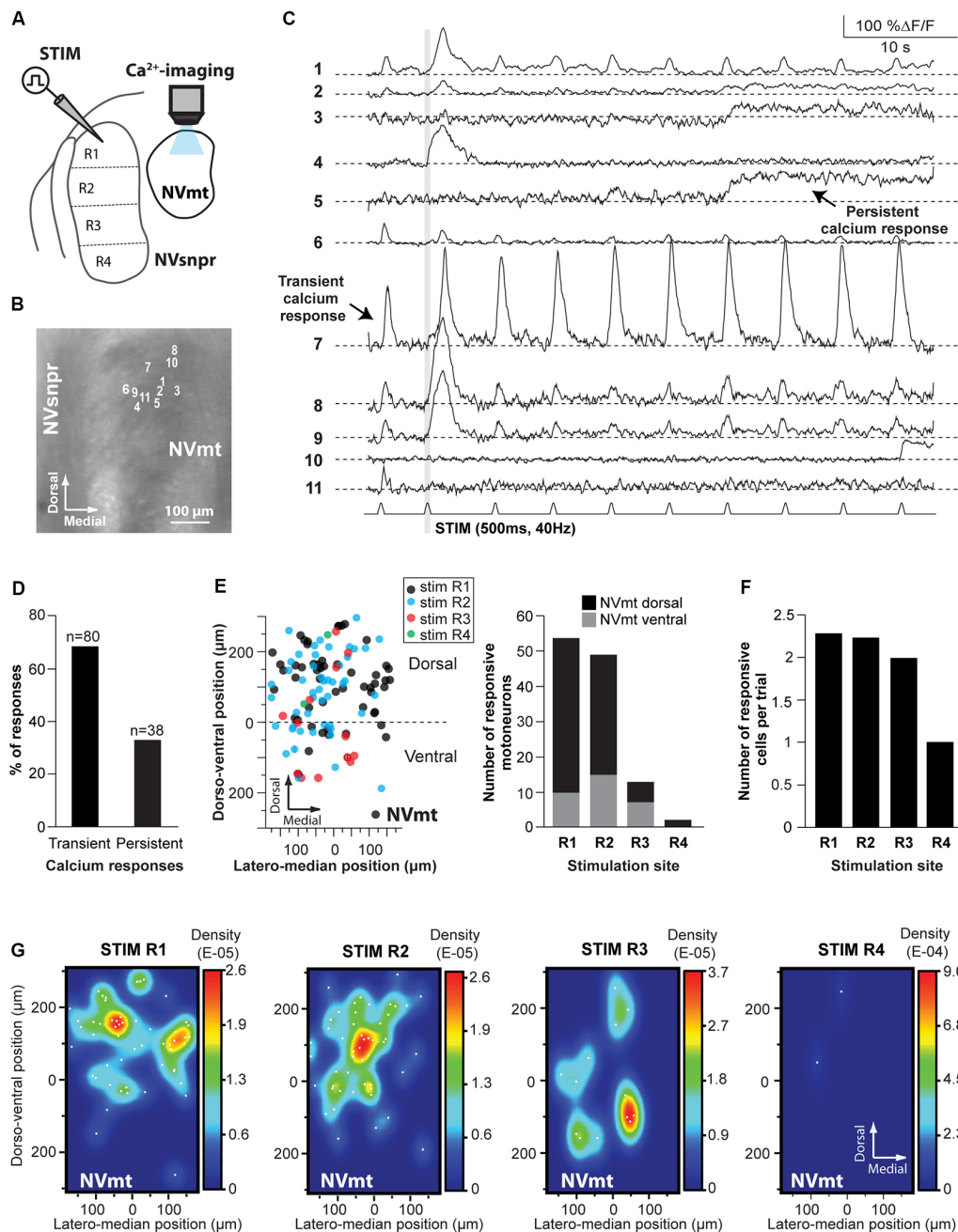


FIGURE 5 | Distribution of motoneurons activated by stimulation of different divisions of NVsnpr. **(A)** Schematic drawing of the brainstem slice preparation and the experimental conditions used. **(B)** Photomicrograph showing the position of the responsive cells in NVmt following electrical stimulation of the dorsal NVsnpr and their Ca^{2+} -responses in panel **(C)**. Some showed a transient response at every stimulation pulse (e.g., trace 7), while others had persistent responses (e.g., trace 5) or only one large transient response with or without a few much smaller ones afterward. Gray vertical line indicates the length of the train of stimulation. **(D)** Percentage of NVsnpr cells presenting transient vs. persistent responses. **(E)** Left: distribution of all responsive motoneurons according to the site of electrical stimulation in NVsnpr. Right: vertical bars chart reporting the number of responsive motoneurons according to the site of electrical stimulation in the NVsnpr. **(F)** Vertical bars chart reporting the number of responsive motoneurons per trial according to the site of electrical stimulation in the NVsnpr. **(G)** Heatmaps illustrating the location of responsive motoneurons within the NVmt according to the site of electrical stimulation in the NVsnpr. Abbreviations: Stim, stimulation; NVsnpr, trigeminal main sensory nucleus; NVmt, trigeminal motor nucleus.

a maximum radius of activation of approximately $420\ \mu\text{m}$ (distance between the tip of the BAPTA pipette and the farthest responsive NVsnpr neuron). Responses occurred at variable

latencies (mean of $17.3 \pm 4.0\ \text{s}$) depending on the distance from the pipette tip. NVsnpr neurons responded with either single or repetitive Ca^{2+} increases to single BAPTA applications.

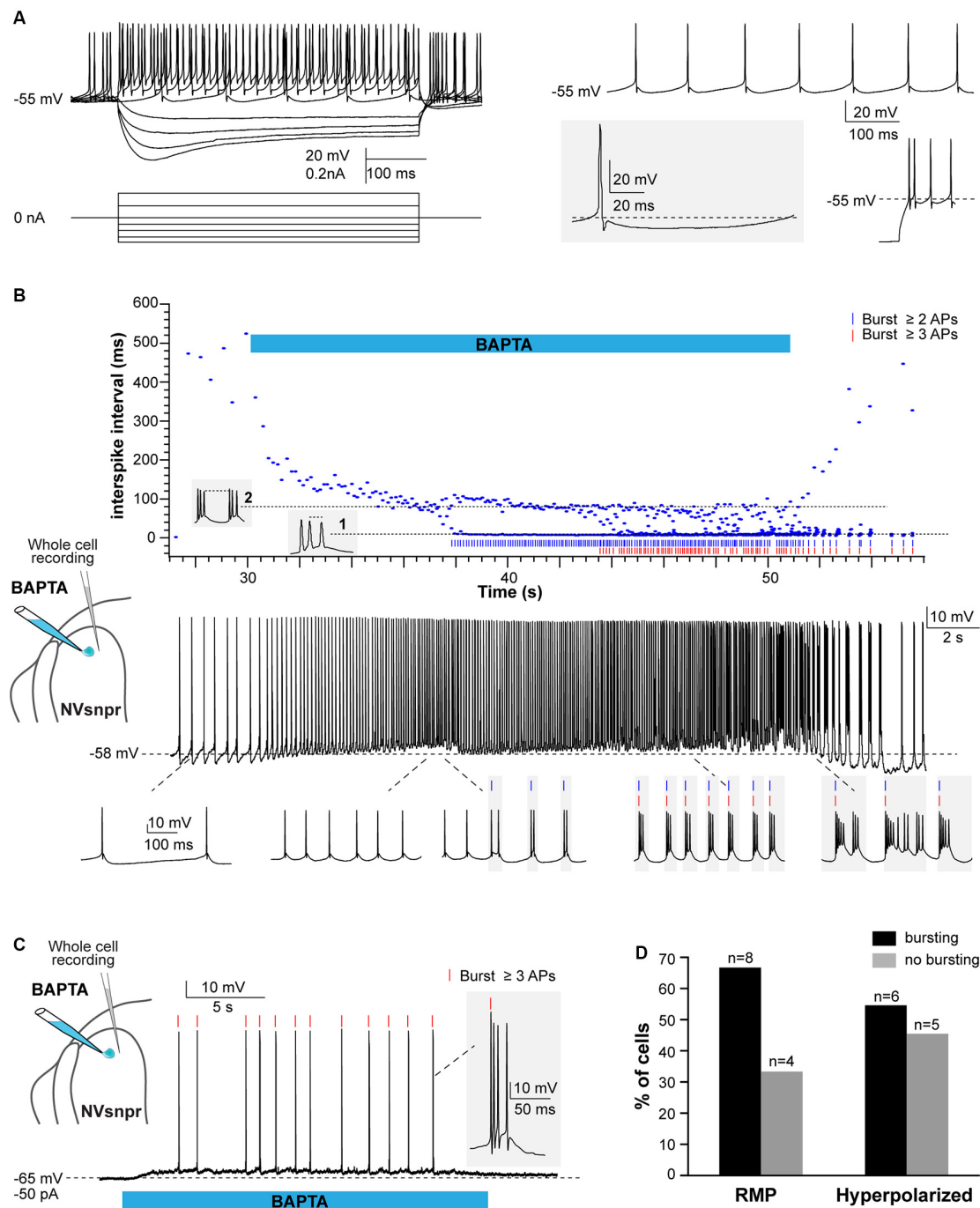


FIGURE 6 | Local applications of BAPTA induce rhythmic burst firing in NVsnpr neurons. **(A)** Left: membrane responses of an NVsnpr neuron (top traces) to injections of depolarizing and hyperpolarizing current pulses (bottom traces). Right top: spontaneous activity recorded in an NVsnpr neuron (inset bottom enlargement showing the biphasic after hyperpolarization (AHP)). Right bottom: example of the rebound firing observed at the offset of membrane hyperpolarization. **(B)** Top: scatter plot of the inter-spike interval prior, along with and after local application of BAPTA at the NVsnpr neuron resting potential. The pattern of firing gradually progresses from tonic to bursting along the course of BAPTA application (Bottom traces). **(C)** Upon membrane hyperpolarization, the BAPTA application directly causes burst firing (inset) in the NVsnpr neuron. **(D)** Percentage of NVsnpr cells in which bursting was induced by local BAPTA applications at their RMP or upon imposed hyperpolarization. Abbreviations: NVsnpr, trigeminal main sensory nucleus; APs, action potentials; RMP, resting membrane potential.

Single Ca^{2+} responses ($187 \pm 87\% \Delta F/F_0$) most often ($n = 6$) consisted of an initial fast rising phase followed by a slow decay period (Figure 7A, trace 1, and Figure 7B top trace) and lasted

8.6 ± 2.8 s. In two additional cases, the Ca^{2+} -response ($396 \pm 10\% \Delta F/F_0$) did not decay after the initial rise and persisted as a long-lasting plateau until the end of the BAPTA application

(as in **Figure 7B** middle trace). In the 11 other neurons (58%; **Figure 7C**), repetitive Ca^{2+} transients peaks ($110 \pm 12\% \Delta\text{F}/\text{F}_0$ lasting 4.2 ± 1.6 s) were observed (**Figure 7A**, traces 4–7) occurring at a mean frequency of 0.38 ± 0.04 Hz. In five of these cases, the repetitive Ca^{2+} transients peaks overrode a plateau-like calcium transient as in the examples shown in **Figure 7A**, trace 3, and **Figure 7B** (left, bottom trace). Very interestingly, many of these recurrent events occurred synchronously in several adjacent cells (see gray lines in **Figure 7A**).

Trigeminal MNs Respond to BAPTA-Induced Bursting in NVsnpr

Whole-Cell Recordings of MNs

Responses of trigeminal MNs to BAPTA applications in dorsal NVsnpr were first assessed electrophysiologically with recordings from 20 MNs distributed across the NVmt (as schematized in **Figures 8A, 9A**). No discernible effects were seen in 6 of the 20 recorded neurons following BAPTA applications in the NVsnpr. In the remaining 14, a clear effect was seen on the MNs spiking ability ($n = 7$) or its subthreshold activity ($n = 7$). In the former seven cases, BAPTA in NVsnpr induced firing in previously silent neurons ($n = 6$) and reduced the firing frequency in a single spontaneously active neuron (from 8.8 to 3.7 Hz as evidenced by the increased inter-spike interval upon BAPTA (bottom scatter plot; **Figure 8G**). Firing induced in the six other MNs upon BAPTA application in the NVsnpr occurred at a mean latency of 7.1 ± 0.8 s and is shown as raster plots aligned to the start of BAPTA application in **Figure 8B**. This spiking was preceded by depolarization (2.8 ± 1.6 mV occurring at a latency of 5.8 ± 2.2 s) that lead to either tonic firing of single-action potentials (**Figure 8C**; $n = 2$), doublets (**Figure 8D**; $n = 1$) of action potentials or rhythmic bursts at a frequency of 0.9 ± 0.4 Hz (**Figure 8E**; $n = 3$).

In the seven cases, where BAPTA applications in NVsnpr appeared to affect the MNs subthreshold activity, six were excitatory and one was inhibitory as above. The latter appeared as a long-lasting hyperpolarization (as in **Figure 8F**; 3.8 mV, lasting 49 s). The excitatory effects on the six other MNs are presented as raster plots of detected PSPs, aligned to the start of the BAPTA application in **Figure 9B**. BAPTA seemed to cause an increase in the amplitude of the spontaneous PSPs, as in the example shown in **Figure 9D**, but this effect was not significant when all the neurons were pooled (**Figure 9C**; 1.1 ± 0.5 mV vs. 1.2 ± 0.5 mV, paired t -test, $P = 0.09$). However, BAPTA application in the NVsnpr significantly increased the frequency of the spontaneous EPSPs (**Figure 9C**; 1.5 ± 0.5 Hz vs. 4.4 ± 2 Hz, paired Student's t -test, $P = 0.02$) and caused in many cases ($n = 4$) appearance of rhythmic clusters of PSPs (as in **Figure 9E**), that may be indicative of a direct rhythmic input that does not reach firing threshold. BAPTA also caused the appearance of recurrent depolarizations (as in **Figure 9F**; see arrows; 4.6 ± 0.9 mV lasting 1.0 ± 0.3 s) characterized by synchronized groups of high amplitude spontaneous EPSPs ($n = 4$). This type of response appeared at a mean latency of 11.5 ± 6.9 s with an average frequency of 1.1 ± 0.2 Hz and lasted for approximately 43 ± 10 s. In one MN, the appearance of spontaneous EPSPs combined with an increase of their frequency (0–40 Hz) following BAPTA

application can be observed preceding the occurrence of such repetitive depolarizations (see **Figure 9F** inset). In two out of four MNs, these repetitive depolarizations summated and lead to a transient depolarization of longer duration (4.5 ± 2.6 s) and greater amplitude (7.1 ± 2.5 mV). In the two remaining MNs, the repetitive depolarizations were overridden by APs (singlets or doublets as in the inset of **Figure 8D**) suggesting that each one of them may have resulted from bursting NVsnpr neurons near the BAPTA pipette.

These excitatory effects of BAPTA applied in the NVsnpr were more frequent in MNs at hyperpolarized holding potentials ($n = 7$, -65 ± 1 mV) compared to when it was tested at RMP ($n = 4$, -60 ± 3 mV). For instance, 4 out of 11 MNs exhibited rhythmic bursts or doublets (RB type as in **Figure 8E**) when tested at hyperpolarized potentials, with only two of them occurring when tested at their RMP.

Calcium Imaging of MNs

In calcium imaging experiments (as schematized in **Figure 10A**), local BAPTA application in the four regions of NVsnpr (R1, R2, R3, and R4) elicited calcium responses (as the examples shown in **Figure 10C**; see MNs positions in **Figure 10B**) in 27 MNs (in 12 of 25 mice) located mainly in the dorsal NVmt ($n = 21$) with only six cells responding ventrally (see **Figures 10E–G**). Dorsal BAPTA applications in NVsnpr induced more calcium responses in NVmt (1.4/animal) than ventral applications (0.6/animal; **Figure 10F**) with the highest ratio obtained by R2 (1.8/animal). Although, no clear distribution pattern of the responding MNs in NVmt was observed across stimulation sites in NVsnpr, there is no overlap between regions activated by R1 and R2 (**Figure 10G**).

The Ca^{2+} -responses elicited by BAPTA applications were either single or repetitive increases that occurred at a mean latency of 13.9 ± 2.2 s (**Figures 10C,D**). Single events were either transient ($n = 2$; $66 \pm 16\% \Delta\text{F}/\text{F}_0$ for 22.4 ± 9.0 s) or persistent and lasted as long ($n = 5$; $106 \pm 23\% \Delta\text{F}/\text{F}_0$) or longer than the BAPTA application ($n = 3$; $210 \pm 70\% \Delta\text{F}/\text{F}_0$). In the 17 remaining cases, BAPTA applications in NVsnpr produced repeated calcium transients in MNs ($83 \pm 27\% \Delta\text{F}/\text{F}_0$ for 2.9 ± 0.5 s, see trace 3 in **Figure 10C**) at a mean frequency of 0.4 ± 0.1 Hz and in 11 of these, the repetitive calcium transients overrode long plateaus calcium transients of 11.3 ± 2.9 s.

DISCUSSION

The present results provide new evidence of functional connectivity between the NVmt and the NVsnpr, thought to form the rhythmogenic core of the masticatory CPG (Athanasias et al., 2005a,b; Brocard et al., 2006; Kolta et al., 2007, 2010; Morquette et al., 2015). Our results indicate that neurons projecting to different parts of the NVmt are located in the dorsal $\frac{3}{4}$ region of NVsnpr (R1, R2, and R3). Electrical stimulation of the dorsal NVsnpr induced multiphasic excitatory synaptic responses in trigeminal MNs while BAPTA applications induced rhythmic firing in NVsnpr that translated in rhythmic activities in NVmt, further supporting the hypothesis that NVsnpr may drive the masticatory rhythmic motor

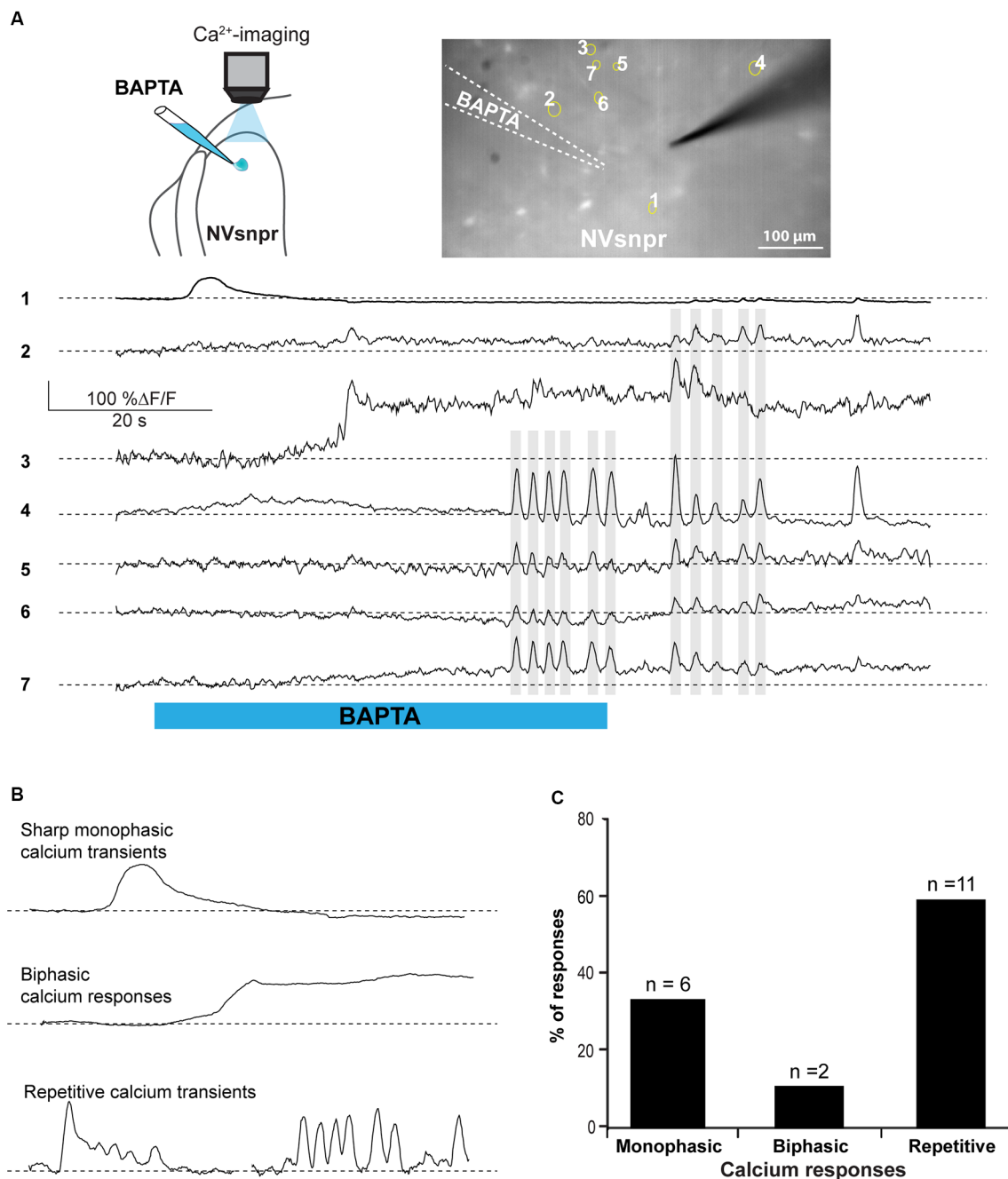


FIGURE 7 | BAPTA applications near NVsnpr neurons induce transient and recurrent Ca²⁺-responses that can sometimes occur synchronously in nearby neurons. **(A)** Right top: schematic drawing of the brainstem slice preparation and the experimental conditions used. Left top: photomicrograph showing the position of the responsive cells in the NVsnpr following local BAPTA application. Bottom: calcium responses of several NVsnpr neurons following the BAPTA application. Gray lines crossing several traces emphasize synchronicity between recurrent events occurring in different cells. **(B)** Illustration of the three main types of calcium responses observed in NVsnpr neurons following local application of BAPTA. **(C)** Vertical bars chart reporting the percentage (and number) of types of calcium responses observed in NVsnpr neurons following local applications of BAPTA. Abbreviation: NVsnpr, trigeminal main sensory nucleus.

pattern. Anatomical and functional mapping of projections from NVsnpr to NVmt suggests that dorsal NVsnpr projects preferentially to dorsal NVmt whereas intermediate parts of NVsnpr project more ventro-medially in NVmt. However,

the most ventral part of NVsnpr does not project to NVmt. This study confirms and expands earlier findings (Li et al., 1995, 1996; Stanek et al., 2014) by exploring the physiological nature and functional topography of the connectivity between

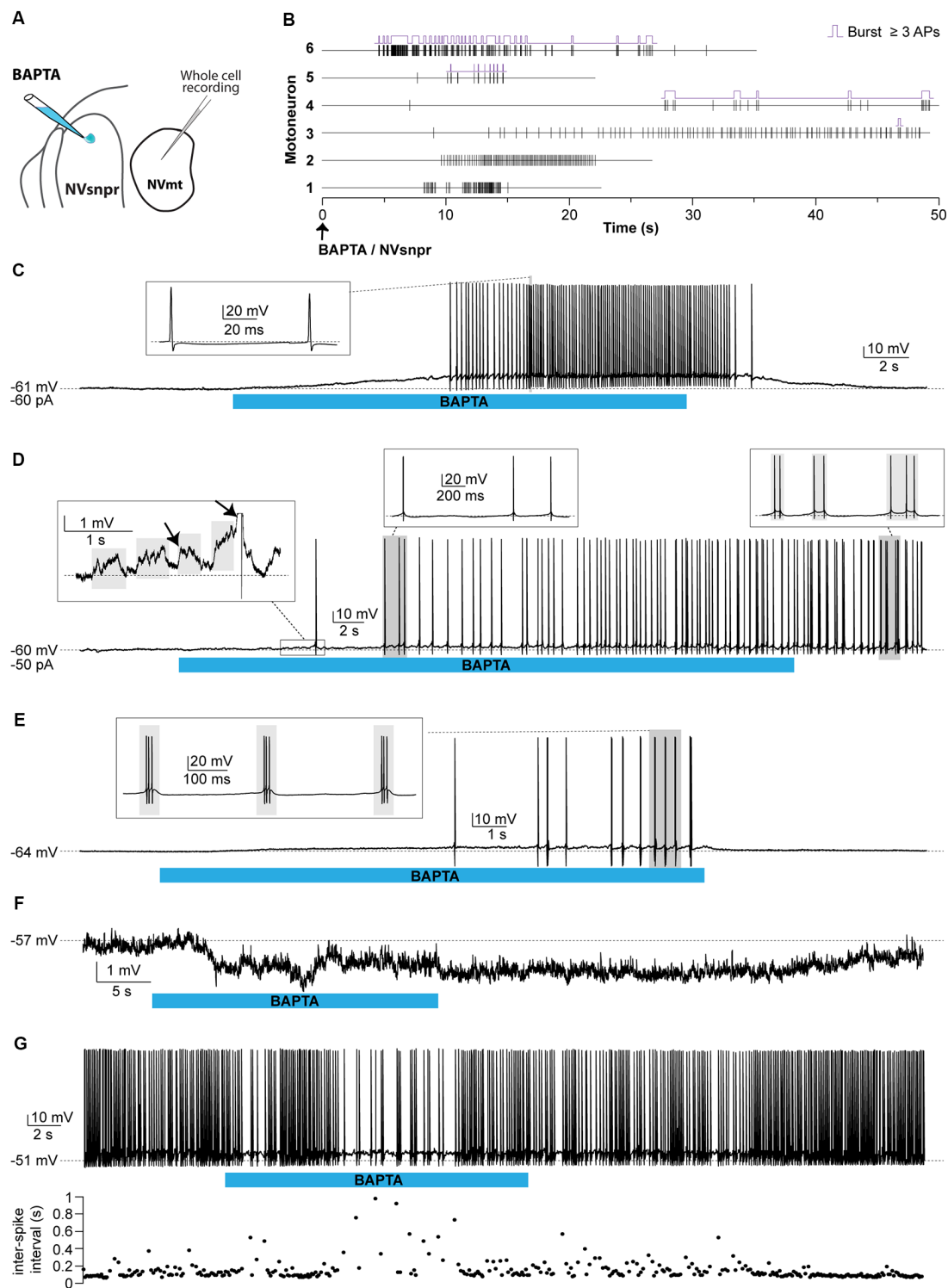


FIGURE 8 | Effects of local BAPTA applications in NVsnpr on motoneuronal firing. **(A)** Schematic drawing of the brainstem slice preparation and the experimental conditions used. **(B)** Raster plots of firing induced in six MNs that were silent before applications of BAPTA in NVsnpr. Traces are aligned on the BAPTA application. The firing patterns elicited in the MNs were single spikes as in panel **(C)**, that sometimes emerged from the summation of subthreshold PSPs (left inset in panel **D**), and progressed to doublets as in panel **(D)** (right inset). **(E)** BAPTA application in the dorsal NVsnpr also sometimes caused burst firing (left, inset) in the recorded motoneuron as in this case. **(F)** Long-lasting hyperpolarization or decrease in firing frequency **(G)** as indicated by the raw trace (top) or raster plot (bottom) of the inter-spike intervals were observed at a mean latency of 5.2 ± 2.8 s in two MNs. Abbreviations: NVsnpr, trigeminal main sensory nucleus; NVmt, trigeminal motor nucleus; APs, action potentials; RMP, resting membrane potential.

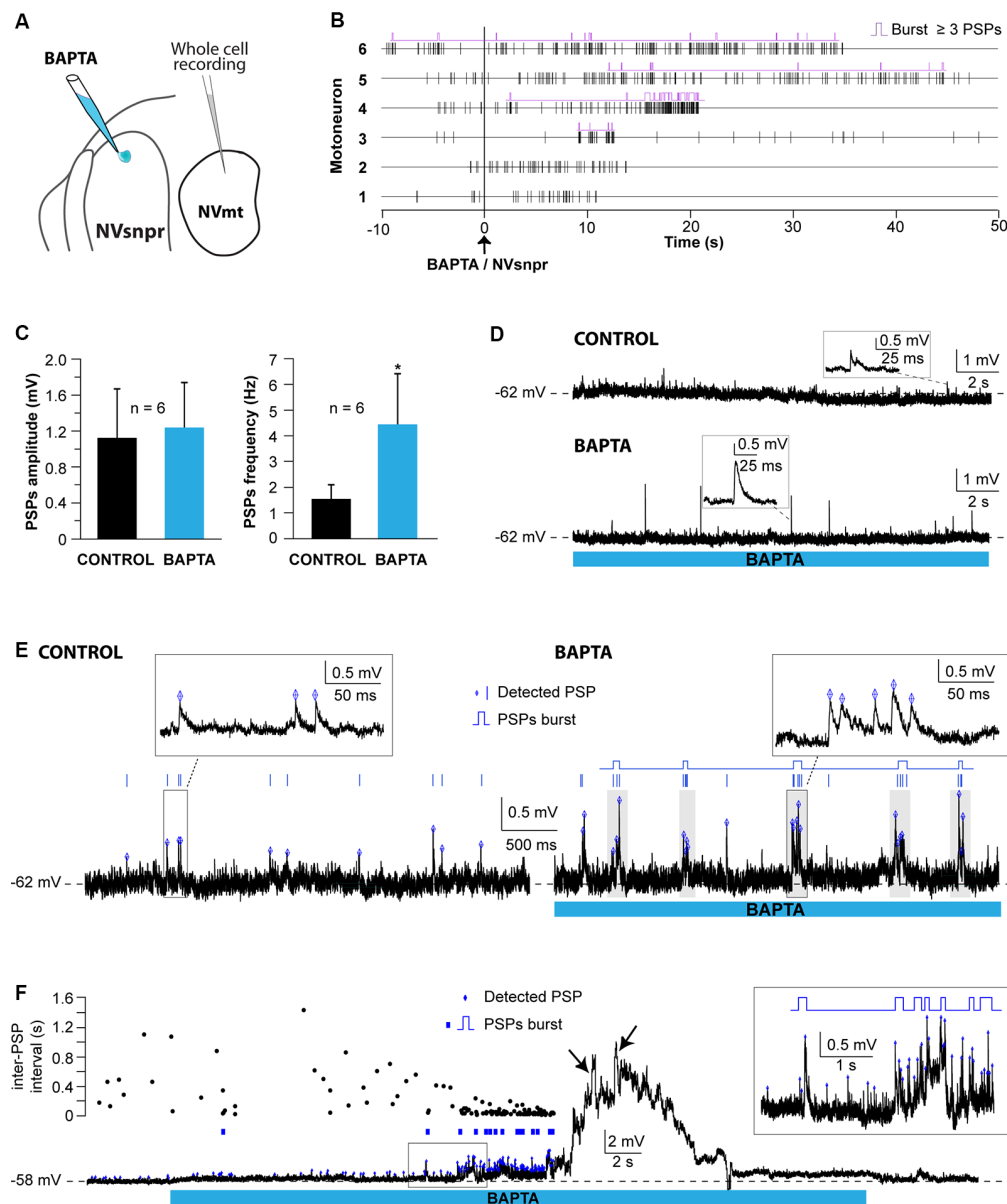


FIGURE 9 | Effects of local BAPTA applications in NVsnpr on subthreshold motoneuronal activity. **(A)** Schematic drawing of the brainstem slice preparation and the experimental conditions used. **(B)** Raster plots of detected PSPs in six MNs before and after the application of BAPTA in NVsnpr. Traces are aligned on the BAPTA application. **(C)** Effect of the BAPTA application on the amplitude (left) and frequency (right) of these PSPs. Data are mean \pm SEM; * $P < 0.05$, paired Student's *t*-test. **(D)** Example of a case where spontaneous PSPs recorded in the MN were of greater amplitude after BAPTA application in NVsnpr. **(E)** Example of a case where BAPTA application in NVsnpr induced rhythmic (right) clusters of PSPs (right inset) in the recorded MN. **(F)** BAPTA application in the dorsal NVsnpr elicited repetitive depolarizations caused by the summation of spontaneous PSPs (inset) in the recorded motoneuron. The raster plot above the raw trace shows a decrease of the inter-PSP intervals a few seconds before these large summation events. Abbreviations: NVsnpr, trigeminal main sensory nucleus; NVmt, trigeminal motor nucleus; PSPs, post-synaptic potentials.

NVsnpr and NVmt that was demonstrated in the past with neuroanatomical techniques.

Connectivity

Anatomical Evidence

Our anatomical experiments suggest that NVsnpr neurons projecting to both the dorsal or ventral NVmt emanate mostly

from the dorsal three-quarter region (R1, R2, and R3) of NVsnpr. In both cases, the highest number and density of retrogradely labeled NVsnpr neurons were found constricted within the dorsal half (R1 and R2) with very few observed in R3. Moreover, injections of biocytin within NVsnpr resulted in labeled fibers originating exclusively from the dorsal region and terminating both in the DL and VM divisions of NVmt further

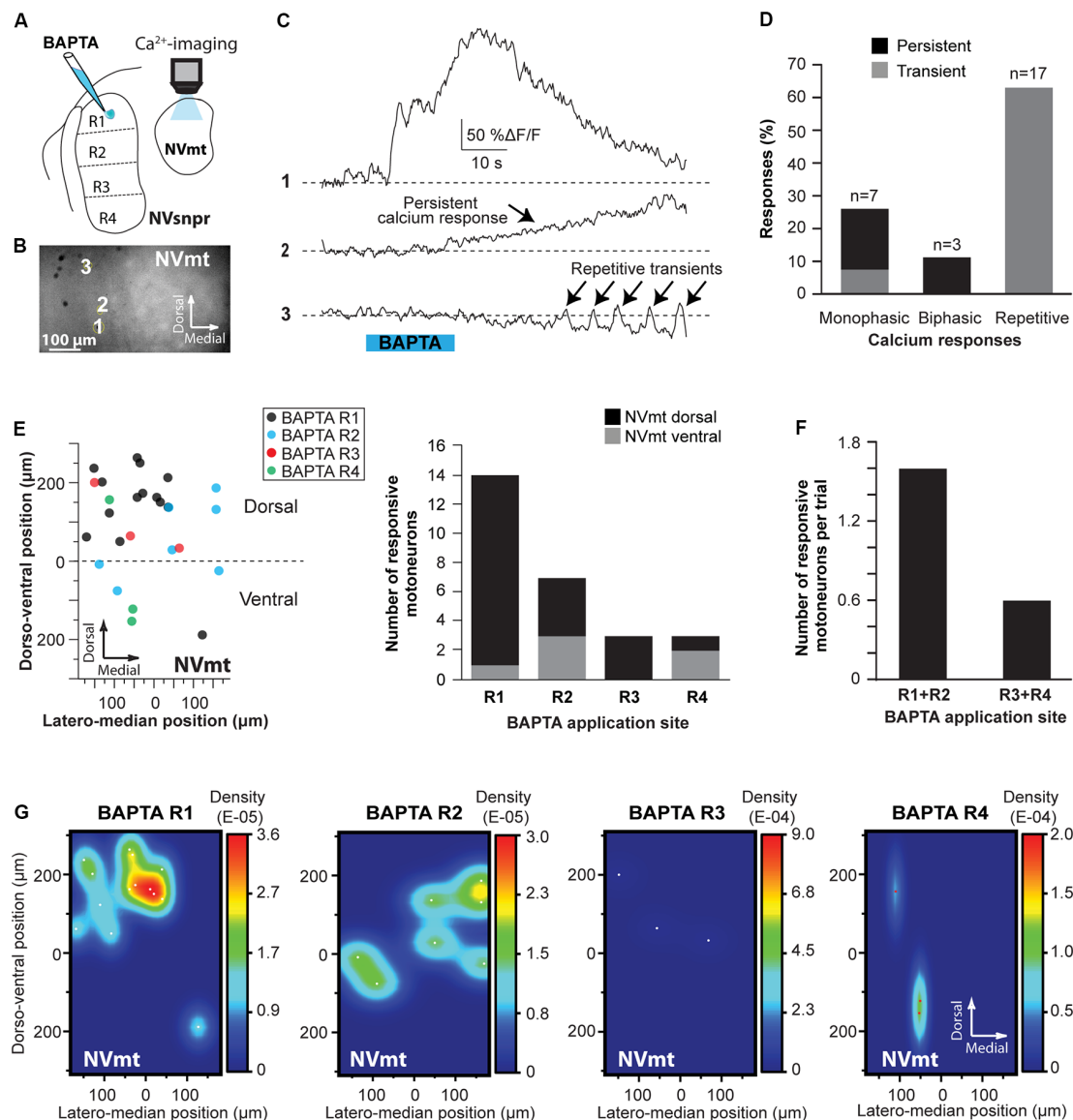


FIGURE 10 | Distribution and types of Ca^{2+} -responses elicited in NVmt by local applications of BAPTA in NVsnpr. **(A)** Schematic drawing of the brainstem slice preparation and the experimental conditions used. **(B)** Photomicrograph showing the position of the responsive cells in the NVmt following BAPTA application in the dorsal NVsnpr. **(C)** Types of Ca^{2+} -responses recorded in three different MNs after BAPTA applications in the dorsal NVsnpr. **(D)** Vertical bars chart representing the percentage of cells displaying each type of Ca^{2+} -response. **(E)** Left: distribution of all the responsive motoneurons according to the site of BAPTA application in the dorsal NVsnpr. Right: vertical bars chart reporting the number of responsive MNs according to the site of BAPTA application in the dorsal NVsnpr. **(F)** Vertical bars chart reporting the number of responsive motoneurons per trial according to the site of BAPTA application in the dorsal NVsnpr. **(G)** Heatmaps illustrating the location of the responsive motoneurons within the NVmt according to the site of BAPTA application in NVsnpr. Abbreviations: NVsnpr, trigeminal main sensory nucleus; NVmt, trigeminal motor nucleus.

supporting this connectivity evidence. This is consistent with previous anatomical studies demonstrating in both rats (Li et al., 1995, 1996) and mice (Stanek et al., 2014) that the majority of NVsnpr projections to NVmt arises from neurons located in the dorsal division.

Although labeled fibers originating from the ventral NVsnpr did not project to the NVmt, we observed multiple fibers terminating into PCrt, the region directly ventral to it. PCrt, a nucleus recently associated with hunger-driven mastication and

feeding modulation (Nakamura and Nakamura, 2018), is also known to form direct synaptic contact with both jaw-closing and jaw-opening MNs (Mogoseanu et al., 1993; Kolta et al., 2000; McDavid et al., 2006; Yoshida et al., 2009). In the same region but closer to the ventral division of the NVsnpr is the group k nucleus formed by small neurons organized in a column (Mukerji et al., 2009). This nucleus contains the tensor tympani MNs and is believed to be responsible for the attenuation of sounds generated during the mastication process (Mukerji et al.,

2010). Furthermore, there is additional evidence showing in the rabbit that masticatory muscles receive direct innervation from the group k nucleus (Donga et al., 1992; Saad et al., 1997, 1999). However caution should be used in the interpretation of these results since retrograde labeling may partly result from the uptake by fibers of passage inside NVmt, and because of the small size of the VM division and its proximity to the DL, the specific labeling of jaw-opening pre-MNs becomes even more challenging.

Electrophysiological Evidence

In the present study, nearly half of the trigeminal MNs evoked short-latency EPSPs following electrical stimulation of the dorsal NVsnpr suggesting a monosynaptic connection with NVmt. Moreover, these synaptic responses were for the majority multiphasic in nature which may have resulted from a convergence of monosynaptic glutamatergic inputs from multiple pre-MNs stimulated in NVsnpr or possibly from activation of polysynaptic pathways. Many anatomical studies demonstrated that the region in the lateral reticular formation surrounding NVmt [peritrigeminal area (PeriV) and PCRT] is home of the largest population of trigeminal pre-MNs (Mizuno et al., 1983; Landgren et al., 1986; Chandler et al., 1990; Stanek et al., 2014) which are known to form a complex network of interconnected excitatory and inhibitory neurons that could shape the final masticatory motor output (Kolta, 1997; Bourque and Kolta, 2001). NVsnpr has been shown to share reciprocal connectivity with both PeriV and PCRT, further supporting the implication of polysynaptic pathways originating from NVsnpr (Shammah-Lagnado et al., 1992; Kolta, 1997; Yoshida et al., 1998; Kolta et al., 2000; Athanassiadis et al., 2005b). An alternative explanation of such responses would be the convergence of multiple synaptic inputs received through the extensive dendritic arborization of trigeminal jaw-closing MNs known to extend beyond the boundaries of NVmt and even reaching inside the NVsnpr (Mong et al., 1988; Lingenhohl and Friauf, 1991). This type of connectivity is not unusual for trigeminal MNs where it was demonstrated in earlier electron microscopic studies that axon terminals of most trigeminal pre-MNs surrounding the NVmt make synaptic contact more often with the dendrites than with the soma of MNs (Mizuno et al., 1978, 1983; Mogoseanu et al., 1993).

Motoneurons Respond to High-Frequency Stimulation in NVsnpr

Stimulation of the dorsal NVsnpr at 40 Hz, a frequency close to the natural output of the sensory afferents during mastication (Trulsson and Johansson, 2002), evoked intracellular calcium transients in MNs located mainly in the DL division of NVmt. The persistence of these responses beyond the stimulation trains could be partially reflecting the slow calcium dissociation kinetics of GCaMP but is likely to also reflect real slow decay of the intracellular calcium concentration (Yoshida et al., 2001; Chen et al., 2013). In some cases, a long-lasting response was evoked in MNs following several electrical trains. In calcium imaging, these responses were characterized by a slow and persistent rise of calcium which could probably represent a gradual and slow

increase of the spike frequency while in whole-cell recordings the response represented a depolarization leading to an increasing spike discharge. This interpretation is based on evidence showing that GCaMP is mainly sensitive to spike discharge and not to smaller membrane potential changes (Grienberger and Konnerth, 2012; Chen et al., 2013; Badura et al., 2014; Helmchen and Tank, 2015). The slope and duration of the rising phase of the recorded calcium transients would then correspond to the spike frequency and firing duration, respectively (Yoshida et al., 2001). This comes from the fact that calcium transients from internal stores are not necessarily correlated with changes in membrane potential (Nakajima and Baker, 2018). Moreover, an increase in the frequency of spontaneous EPSPs was also induced, indicating a possible synaptic facilitation effect caused by the high-frequency stimulations. Alternately, the long-lasting responses and putative facilitation effects may also result from activation of the polysynaptic pathways referred to above which have been described as forming strong redundant connections (Bourque and Kolta, 2001) or from activation of astrocytic networks. Our previous work has shown that 40 Hz stimulation of inputs to NVsnpr activates NVsnpr astrocytes that release a Ca^{2+} -binding protein (S100 β) that decreases extracellular Ca^{2+} concentration (Morquette et al., 2015). This in turn potentiates a Na^{+} persistent current leading to burst-firing in NVsnpr neurons. This process occurs over hundreds to thousands of milliseconds and may explain the longer latency and duration of some of the responses elicited in MNs.

Topography

Biocytin injections and calcium imaging, used to investigate the specific organization of the projections from NVsnpr to the NVmt, revealed that the dorsal part of NVsnpr projects mostly to the DL division containing the jaw-closing MNs. The electrical stimulation of NVmt revealed that the dorsomedial part of NVsnpr, which coincides with the region known to innervate the masseter MNs, is the main region projecting to trigeminal MNs (Appenteng and Girdlestone, 1987). Interestingly, this region is also known to arbor the majority of neurons with intrinsic bursting properties (Athanassiadis et al., 2005b). Previous retrograde HRP labeling studies performed in rats and mice revealed the myotopical arrangement of jaw-closing and jaw-opening MNs within NVmt: (1) those innervating the masseter muscle are located in the lateral part of the DL division; (2) those innervating the temporal muscle are located in the dorsomedial part of the DL division; (3) those innervating the medial and lateral pterygoid muscles are located in the most ventral part of the NVmt; and (4) those innervating the mylohyoid and the anterior belly of the digastric muscle are located in the VM division of NVmt (Chen et al., 1988; Terashima et al., 1994; Setsu et al., 2001).

In our experiments, the masseter region was activated by the dorsal NVsnpr with R2 resulting in a larger activated region in the lateral part of NVmt. On the other hand, the temporal region was innervated most exclusively by R1 suggesting a smaller and more distinct representation of the temporal pre-MNs within NVsnpr compared to those of the masseter which cover the whole dorsal region. Interestingly, the jaw-closing

representations within NVmt are known to be proportional to the innervated muscle size (Maeda et al., 1993; Watson et al., 2012) and this seems to be also preserved within the NVsnpr. Although most NVsnpr regions (R1, R2, and R3) evoked responses in the ventral NVmt, our results revealed a dorso-ventral tendency where the activation ratio in the ventral NVmt was increasing and the recruited regions were shifting ventrally through NVmt. R3 was the only region exhibiting an exclusive ventral innervation of NVmt and activated the highest density of MNs within VM which suggests that it might preferentially innervate the lateral and medial pterygoid and the jaw-opening MNs. These observations are in line with an anterograde study conducted on the rat reporting that trigeminal pre-MNs located in the dorsal NVsnpr make axon contact preferentially to jaw-closing MNs while those located in the intermediate part of NVsnpr make axon contact primarily to jaw-opening MNs (Li et al., 1995).

BAPTA-Induced Rhythmic Activity in NVsnpr

We showed in previous studies performed in rats that bursting could be elicited in NVsnpr neurons with local BAPTA application and that this rhythmic discharge is I_{NaP} -dependent as it can be abolished by pharmacological blockade of the current (Brocard et al., 2006; Morquette et al., 2015). Therefore, BAPTA could be used as a burst-inducing stimulus in NVsnpr to experiment rhythm transmission toward NVmt. However, despite being currently the most commonly used animal model for fundamental research, there are still no reports investigating this mechanism in mice. We successfully evoked bursting with BAPTA in 67% of the recorded NVsnpr neurons at a membrane potential within the activation range of I_{NaP} (between -65 and -50 mV; Crill, 1996). In most cases, a depolarization followed by spiking preceded the bursts which occurred at frequencies ranging from 0.4 to 0.9 Hz.

The spatiotemporal activity pattern induced within the BAPTA application site in NVsnpr appeared as a circular wave with sequential activation of NVsnpr neurons. Not only NVsnpr neurons responded at variable latencies, but also the patterns evoked were not always rhythmic as expected. Indeed, BAPTA evoked single Ca^{2+} events in 42% and repetitive calcium transients in 58% of neurons which correspond approximately to the proportion of bursting response at RMP (67%) obtained in whole-cell recordings. Thus, it might suggest that those who responded with only one transient could be too depolarized to activate I_{NaP} knowing that BAPTA caused a depolarization in 60% of the recorded NVsnpr. Recurrent transients occurred at frequencies comparable to the bursts recorded electrophysiologically in whole-cell patch configuration but the duration of the peak was longer in calcium imaging which could be due to the slow calcium decay phase of GCaMP6f (Chen et al., 2013; Li et al., 2019). Earlier reports have demonstrated that neural rhythmic patterns are detectable with calcium imaging techniques and that their sensitivity highly depends on the decay kinetics of the calcium indicator (Yoshida et al., 2001; Lin et al., 2007; Chen et al., 2013). If the calcium decay phase is longer than the inter-spike interval, a

summation would occur and therefore, multiple action potentials would be represented by a long-lasting calcium transient. Thus, the long-lasting singular transients evoked in NVsnpr neurons with BAPTA could perhaps result from trains of action potentials while repetitive calcium transients would represent rhythmic bursting.

Motoneurons Respond to BAPTA-Induced Bursting in NVsnpr

BAPTA application in NVsnpr successfully induced rhythmic bursting in MNs at a membrane potential within the I_{NaP} activation range. Another rhythmic activity characterized by recurrent plateau potentials was evoked in MNs. It was shown in guinea pigs that trigeminal motoneurons have bistable membrane properties mediated by I_{NaP} and L-type Ca^{2+} currents required for the production of such plateau potentials (Hsiao et al., 1998). In our study, these plateau potentials occurred at frequencies resembling those evoked in NVsnpr in patch-clamp and were, in 50% of the cases, overridden by action potentials. Therefore, we think that these recurrent depolarizations might represent the bursts evoked in NVsnpr neurons with BAPTA.

In calcium imaging, BAPTA evoked rhythmic calcium transients occurring at similar frequencies than those obtained in NVsnpr neurons. Moreover, responding MNs upon BAPTA application were found mainly within the DL division of NVmt. These MNs responded mostly when BAPTA was applied within the dorsal NVsnpr. This result is consistent with our findings stipulating that the jaw-closing MNs receive most of their inputs from the dorsal NVsnpr where both the masseter and temporal pre-MNs are localized.

CONCLUSION

Mastication is the first step of nutrition, but has also been linked to many other functions including systemic health and cognitive performance (Yamamoto and Hirayama, 2001; Kamiya et al., 2016; Lin, 2018). In animal studies (reviewed in Weijenbergh et al., 2019) factors impacting mastication, such as molar loss or abrasion or soft food diets have been associated with poorer spatial memory and learning ability as well as decreased proliferation and differentiation of newborn neurons in the hippocampus. Both measures increase when molars are restored with crowns or when hard food is given back. In humans, mastication is compromised in several pathologies [e.g., Down syndrome (Faulks et al., 2008), Parkinson's (Ribeiro et al., 2017), Alzheimer's (Campos et al., 2017) and Huntington's diseases (Trejo et al., 2004)], and in the elderly where masticatory dysfunction is increasingly considered as an unrecognized risk factor contributing to the development of cognitive impairment (Tada and Miura, 2017). Thus, a better understanding of the circuitry and mechanisms responsible for mastication is important to help elaborate strategies to modify masticatory efficiency to slow the rate of cognitive decline and improve cognitive health during aging. Although the pattern of masticatory movements may vary across species, the mechanisms and general organization of the circuits generating them are likely to be similar. Human studies report an increase in

blood flow in NVsnpr during mastication (Viggiano et al., 2015), but cannot further address how the activity is triggered in this nucleus and how it is relayed to the motoneurons controlling the masticatory muscles. The results reported here suggest that projections from NVsnpr to NVmt are similarly organized in rats and mice with the dorsolateral region of NVmt receiving inputs from the dorsal NVsnpr (R1 and R2), and the ventromedial region receiving mostly inputs from R2 and R3. Knowing that different areas of NVsnpr receive topographically organized sensory inputs may help devise intervention strategies for reeducation. From a functional perspective, NVsnpr neurons were also shown to have the capacity to drive rhythmic activity in trigeminal MNs, thus reinforcing their potential role in masticatory rhythmogenesis (Athanasiadis et al., 2005a,b; Brocard et al., 2006; Kolta et al., 2007, 2010; Kadala et al., 2015; Morquette et al., 2015).

DATA AVAILABILITY STATEMENT

The datasets generated for this study are available on request to the corresponding author.

REFERENCES

- Appenteng, K., and Girdlestone, D. (1987). Transneuronal transport of wheat germ agglutinin-conjugated horseradish peroxidase into trigeminal interneurons of the rat. *J. Comp. Neurol.* 258, 387–396. doi: 10.1002/cne.902580307
- Athanasiadis, T., Olsson, K. A., Kolta, A., and Westberg, K. G. (2005a). Identification of c-Fos immunoreactive brainstem neurons activated during fictive mastication in the rabbit. *Exp. Brain Res.* 165, 478–489. doi: 10.1007/s00221-005-2319-5
- Athanasiadis, T., Westberg, K. G., Olsson, K. A., and Kolta, A. (2005b). Physiological characterization, localization and synaptic inputs of bursting and nonbursting neurons in the trigeminal principal sensory nucleus of the rat. *Eur. J. Neurosci.* 22, 3099–3110. doi: 10.1111/j.1460-9568.2005.04479.x
- Badura, A., Sun, X. R., Giovannucci, A., Lynch, L. A., and Wang, S. S. (2014). Fast calcium sensor proteins for monitoring neural activity. *Neurophotonics* 1:025008. doi: 10.1117/1.nph.1.2.025008
- Bourque, M. J., and Kolta, A. (2001). Properties and interconnections of trigeminal interneurons of the lateral pontine reticular formation in the rat. *J. Neurophysiol.* 86, 2583–2596. doi: 10.1152/jn.2001.86.5.2583
- Bremer, F. (1923). Physiologie nerveuse de la mastication chez le chat et le lapin. Reponses masticatrices corticales et centre corticale du gout. *Arch. Int. Physiol.* 21, 308–352.
- Brocard, F., Shevtsova, N. A., Bouhadjane, M., Tazerart, S., Heinemann, U., Rybak, I. A., et al. (2013). Activity-dependent changes in extracellular Ca^{2+} and K^{+} reveal pacemakers in the spinal locomotor-related network. *Neuron* 77, 1047–1054. doi: 10.1016/j.neuron.2013.01.026
- Brocard, F., Verdier, D., Arsenault, I., Lund, J. P., and Kolta, A. (2006). Emergence of intrinsic bursting in trigeminal sensory neurons parallels the acquisition of mastication in weanling rats. *J. Neurophysiol.* 96, 2410–2424. doi: 10.1152/jn.00352.2006
- Campos, C. H., Ribeiro, G. R., Costa, J. L., and Rodrigues Garcia, R. C. (2017). Correlation of cognitive and masticatory function in Alzheimer's disease. *Clin. Oral Invest.* 21, 573–578. doi: 10.1007/s00784-016-1923-z
- Chandler, S. H., Turman Jr, J., Salem, L., and Goldberg, L. J. (1990). The effects of nanoliter ejections of lidocaine into the pontomedullary reticular formation on cortically induced rhythmical jaw movements in the guinea pig. *Brain Res.* 526, 54–64. doi: 10.1016/0006-8993(90)90249-b

ETHICS STATEMENT

The animal study was reviewed and approved by Comité de déontologie de l'expérimentation sur les animaux/Université de Montréal.

AUTHOR CONTRIBUTIONS

MS, DV, and AK designed the research. MS, IA, and SO performed the research. MS, DV, and AK analyzed the data and wrote the article.

FUNDING

This work was supported by the Canadian Institutes of Health Research grant 14932 (to AK).

ACKNOWLEDGMENTS

We thank D. Veilleux for technical support, genotyping the mice, and maintaining the colony.

- Chen, T. W., Wardill, T. J., Sun, Y., Pulver, S. R., Renninger, S. L., Baohan, A., et al. (2013). Ultrasensitive fluorescent proteins for imaging neuronal activity. *Nature* 499, 295–300. doi: 10.1038/nature12354
- Chen, K. N., Wen, C. Y., Shieh, J. Y., and Tseng, T. M. (1988). The somatotopy of the masticatory neurons in the rat trigeminal motor nucleus as revealed by HRP study. *Proc. Natl. Sci. Coun. Repub. China B* 12, 146–155.
- Crill, W. E. (1996). Persistent sodium current in mammalian central neurons. *Annu. Rev. Physiol.* 58, 349–362. doi: 10.1146/annurev.ph.58.030196.002025
- Dellow, P. G., and Lund, J. P. (1971). Evidence for central timing of rhythmical mastication. *J. Physiol.* 215, 1–13. doi: 10.1113/jphysiol.1971.sp009454
- Donga, R., Dubuc, R., Kolta, A., and Lund, J. P. (1992). Evidence that the masticatory muscles receive a direct innervation from cell group k in the rabbit. *Neuroscience* 49, 951–961. doi: 10.1016/0306-4522(92)90371-8
- English, A. W., Carrasco, D. I., and Widmer, C. G. (1999). Torques produced by different compartments of the rabbit masseter muscle. *J. Appl. Biomech.* 15, 348–360. doi: 10.1123/jab.15.4.348
- Faulks, D., Collado, V., Mazille, M. N., Veyrune, J. L., and Hennequin, M. (2008). Masticatory dysfunction in persons with Down's syndrome. Part 1, aetiology and incidence. *J. Oral Rehabil.* 35, 854–862. doi: 10.1111/j.1365-2842.2008.01877.x
- Ferraz-Pereira, K. N., da Silva Aragao, R., Verdier, D., Toscano, A. E., Lacerda, D. C., Manhães-de-Castro, R., et al. (2015). Neonatal low-protein diet reduces the masticatory efficiency in rats. *Br. J. Nutr.* 114, 1515–1530. doi: 10.1017/s0007114515003062
- Grienberger, C., and Konnerth, A. (2012). Imaging calcium in neurons. *Neuron* 73, 862–885. doi: 10.1016/j.neuron.2012.02.011
- Helmchen, F., and Tank, D. W. (2015). A single-compartment model of calcium dynamics in nerve terminals and dendrites. *Cold Spring Harb. Protoc.* 2015, 155–167. doi: 10.1101/pdb.top085910
- Hsiao, C. F., Del Negro, C. A., Trueblood, P. R., and Chandler, S. H. (1998). Ionic basis for serotonin-induced bistable membrane properties in guinea pig trigeminal motoneurons. *J. Neurophysiol.* 79, 2847–2856. doi: 10.1152/jn.1998.79.6.2847
- Jacquin, M. F., Rhoades, R. W., Enfiejan, H. L., and Egger, M. D. (1983). Organization and morphology of masticatory neurons in the rat: a retrograde HRP study. *J. Comp. Neurol.* 218, 239–256. doi: 10.1002/cne.902180302
- Kadala, A., Verdier, D., Morquette, P., and Kolta, A. (2015). Ion homeostasis in rhythmogenesis: the interplay between neurons and astroglia. *Physiology* 30, 371–388. doi: 10.1152/physiol.00023.2014

- Kamiya, K., Narita, N., and Iwaki, S. (2016). Improved prefrontal activity and chewing performance as function of wearing denture in partially edentulous elderly individuals: functional near-infrared spectroscopy study. *PLoS One* 11:e0158070. doi: 10.1371/journal.pone.0158070
- Kogo, M., Funk, G. D., and Chandler, S. H. (1996). Rhythmical oral-motor activity recorded in an *in vitro* brainstem preparation. *Somatosens. Mot. Res.* 13, 39–48. doi: 10.1019/08990229609028910
- Kolta, A. (1997). *In vitro* investigation of synaptic relations between interneurons surrounding the trigeminal motor nucleus and masseteric motoneurons. *J. Neurophysiol.* 78, 1720–1725. doi: 10.1152/jn.1997.78.3.1720
- Kolta, A., Brocard, F., Verdier, D., and Lund, J. P. (2007). A review of burst generation by trigeminal main sensory neurons. *Arch. Oral Biol.* 52, 325–328. doi: 10.1016/j.archoralbio.2006.10.023
- Kolta, A., Morquette, P., Lavoie, R., Arsenault, I., and Verdier, D. (2010). Modulation of rhythmogenic properties of trigeminal neurons contributing to the masticatory CPG. *Prog. Brain Res.* 187, 137–148. doi: 10.1016/b978-0-444-53613-6.00009-5
- Kolta, A., Westberg, K. G., and Lund, J. P. (2000). Identification of brainstem interneurons projecting to the trigeminal motor nucleus and adjacent structures in the rabbit. *J. Chem. Neuroanat.* 19, 175–195. doi: 10.1016/s0891-0618(00)00061-2
- Kuwajima, T., Sitko, A. A., Bhansali, P., Jurgens, C., Guido, W. and Mason, C. (2013). ClearT: a detergent- and solvent-free clearing method for neuronal and non-neuronal tissue. *Development* 140, 1364–1368. doi: 10.1242/dev.091844
- Landgren, S., Olsson, K. A., and Westberg, K. G. (1986). Bulbar neurones with axonal projections to the trigeminal motor nucleus in the cat. *Exp. Brain Res.* 65, 98–111. doi: 10.1007/bf00243833
- Li, P., Geng, X., Jiang, H., Caccavano, A., Vicini, S., and Wu, J. Y. (2019). Measuring sharp waves and oscillatory population activity with the genetically encoded calcium indicator GCaMP6f. *Front. Cell. Neurosci.* 13:274. doi: 10.3389/fncel.2019.00274
- Li, Z., and Hatton, G. I. (1996). Oscillatory bursting of phasically firing rat supraoptic neurones in low- Ca^{2+} medium: Na^{+} influx, cytosolic Ca^{2+} and gap junctions. *J. Physiol.* 496, 379–394. doi: 10.1113/jphysiol.1996.sp021692
- Li, Y. Q., Takada, M., Kaneko, T., and Mizuno, N. (1995). Premotor neurons for trigeminal motor nucleus neurons innervating the jaw-closing and jaw-opening muscles: differential distribution in the lower brainstem of the rat. *J. Comp. Neurol.* 356, 563–579. doi: 10.1002/cne.903560407
- Li, Y. Q., Takada, M., Kaneko, T., and Mizuno, N. (1996). GABAergic and glycinergic neurons projecting to the trigeminal motor nucleus: a double labeling study in the rat. *J. Comp. Neurol.* 373, 498–510. doi: 10.1002/(sici)1096-9861(19960930)373:4<498::aid-cne3>3.0.co;2-x
- Li, Y. Q., Takada, M., and Mizuno, N. (1993). Identification of premotor interneurons which project bilaterally to the trigeminal motor, facial or hypoglossal nuclei: a fluorescent retrograde double-labeling study in the rat. *Brain Res.* 611, 160–164. doi: 10.1016/0006-8993(93)91789-u
- Limwongse, V., and DeSantis, M. (1977). Cell body locations and axonal pathways of neurons innervating muscles of mastication in the rat. *Am. J. Anat.* 149, 477–488. doi: 10.1002/aja.1001490405
- Lin, C. S. (2018). Revisiting the link between cognitive decline and masticatory dysfunction. *BMC Geriatr.* 18:5. doi: 10.1186/s12877-017-0693-z
- Lin, B. J., Chen, T. W., and Schild, D. (2007). Cell type-specific relationships between spiking and $[\text{Ca}^{2+}]_i$ in neurons of the *Xenopus* tadpole olfactory bulb. *J. Physiol.* 582, 163–175. doi: 10.1113/jphysiol.2006.125963
- Lingenhohl, K., and Friauf, E. (1991). Sensory neurons and motoneurons of the jaw-closing reflex pathway in rats: a combined morphological and physiological study using the intracellular horseradish peroxidase technique. *Exp. Brain Res.* 83, 385–396. doi: 10.1007/bf00231163
- Lynch, R. (1985). A qualitative investigation of the topographical representation of masticatory muscles within the motor trigeminal nucleus of the rat: a horseradish peroxidase study. *Brain Res.* 327, 354–358. doi: 10.1016/0006-8993(85)91535-5
- Maeda, N., Sugiyama, H., Suemune, S., Wakisaka, H., Niida, S., Ogata, K., et al. (1993). Sexual dimorphism in the trigeminal motor neurons innervating the mouse masseter muscle. *Brain Res.* 627, 177–180. doi: 10.1016/0006-8993(93)90763-d
- McDavid, S., Lund, J. P., Auclair, F., and Kolta, A. (2006). Morphological and immunohistochemical characterization of interneurons within the rat trigeminal motor nucleus. *Neuroscience* 139, 1049–1059. doi: 10.1016/j.neuroscience.2006.01.031
- Mizuno, N., Konishi, A., and Sato, M. (1975). Localization of masticatory motoneurons in the cat and rat by means of retrograde axonal transport of horseradish peroxidase. *J. Comp. Neurol.* 164, 105–115. doi: 10.1002/cne.901640109
- Mizuno, N., Nomura, S., Itoh, K., Nakamura, Y., and Konishi, A. (1978). Commissural interneurons for masticatory motoneurons: a light and electron microscope study using the horseradish peroxidase tracer technique. *Exp. Neurol.* 59, 254–262. doi: 10.1016/0014-4886(78)90154-1
- Mizuno, N., Yasui, Y., Nomura, S., Itoh, K., Konishi, A., Takada, M., et al. (1983). A light and electron microscopic study of premotor neurons for the trigeminal motor nucleus. *J. Comp. Neurol.* 215, 290–298. doi: 10.1002/cne.902150305
- Mogoseanu, D., Smith, A. D., and Bolam, J. P. (1993). Monosynaptic innervation of trigeminal motor neurones involved in mastication by neurones of the parvocellular reticular formation. *J. Comp. Neurol.* 336, 53–65. doi: 10.1002/cne.903360105
- Mong, F. S., Chen, Y. C., and Lu, C. H. (1988). Dendritic ramifications of trigeminal motor neurons innervating jaw-closing muscles of rats. *J. Neurol. Sci.* 86, 251–264. doi: 10.1016/0022-510x(88)90103-7
- Morquette, P., Verdier, D., Kadala, A., Fethiere, J., Philippe, A. G., Robitaille, R., et al. (2015). An astrocyte-dependent mechanism for neuronal rhythmogenesis. *Nat. Neurosci.* 18, 844–854. doi: 10.1038/nn.4013
- Mukerji, S., Brown, M. C., and Lee, D. J. (2009). A morphologic study of Fluorogold labeled tensor tympani motoneurons in mice. *Brain Res.* 1278, 59–65. doi: 10.1016/j.brainres.2009.04.035
- Mukerji, S., Windsor, A. M., and Lee, D. J. (2010). Auditory brainstem circuits that mediate the middle ear muscle reflex. *Trends Amplif.* 14, 170–191. doi: 10.1177/1084713810381771
- Nakajima, R., and Baker, B. J. (2018). Mapping of excitatory and inhibitory postsynaptic potentials of neuronal populations in hippocampal slices using the GEVI, ArcLight. *J. Phys. D Appl. Phys.* 51:504003. doi: 10.1088/1361-6463/aae2e3
- Nakamura, Y., Katakura, N., and Nakajima, M. (1999). Generation of rhythmical ingestive activities of the trigeminal, facial and hypoglossal motoneurons in *in vitro* CNS preparations isolated from rats and mice. *J. Med. Dent. Sci.* 46, 63–73.
- Nakamura, K., and Nakamura, Y. (2018). Hunger and satiety signaling: modeling two hypothalamomedullary pathways for energy homeostasis. *Bioessays* 40:e1700252. doi: 10.1002/bies.201700252
- Nonaka, M., Nishimura, A., Nakamura, S., Nakayama, K., Mochizuki, A., Iijima, T., et al. (2012). Convergent pre-motoneuronal inputs to single trigeminal motoneurons. *J. Dent. Res.* 91, 888–893. doi: 10.1177/0022034512453724
- Ribeiro, G. R., Campos, C. H., and Rodrigues Garcia, R. C. M. (2017). Parkinson's disease impairs masticatory function. *Clin. Oral Investig.* 21, 1149–1156. doi: 10.1007/s00784-016-1879-z
- Rokx, J. T., and van Willigen, J. D. (1985). Arrangement of supramandibular and suprahyoid motoneurons in the rat; a fluorescent tracer study. *Acta Anat.* 122, 158–162. doi: 10.1159/000145997
- Saad, M., Dubuc, R., Westberg, K. G., and Lund, J. P. (1999). Distribution of cholinergic neurons in cell group K of the rabbit brainstem. *Neuroscience* 88, 927–937. doi: 10.1016/s0306-4522(98)00212-7
- Saad, M., Dubuc, R., Widmer, C. G., Westberg, K. G., and Lund, J. P. (1997). Anatomical organization of efferent neurons innervating various regions of the rabbit masseter muscle. *J. Comp. Neurol.* 383, 428–438. doi: 10.1002/(sici)1096-9861(19970714)383:4<428::aid-cne3>3.0.co;2-4
- Sandler, V. M., Puil, E., and Schwarz, D. W. (1998). Intrinsic response properties of bursting neurons in the nucleus principalis trigemini of the gerbil. *Neuroscience* 83, 891–904. doi: 10.1016/s0306-4522(97)00415-6
- Sasamoto, K. (1979). Motor nuclear representation of masticatory muscles in the rat. *Jpn. J. Physiol.* 29, 739–747. doi: 10.2170/jjphysiol.29.739
- Setsu, T., Ikeda, Y., Woodhams, P. L., and Terashima, T. (2001). Branchiogenic motoneurons innervating facial, masticatory and esophageal muscles show

- aberrant distribution in the reeler-phenotype mutant rat, Shaking Rat Kawasaki. *J. Comp. Neurol.* 439, 275–290. doi: 10.1002/cne.1350
- Shammah-Lagnado, S. J., Costa, M. S., and Ricardo, J. A. (1992). Afferent connections of the parvocellular reticular formation: a horseradish peroxidase study in the rat. *Neuroscience* 50, 403–425. doi: 10.1016/0306-4522(92)90433-3
- Shigenaga, Y., Chen, I. C., Suemune, S., Nishimori, T., Nasution, I. D., Yoshida, A., et al. (1986a). Oral and facial representation within the medullary and upper cervical dorsal horns in the cat. *J. Comp. Neurol.* 243, 388–408. doi: 10.1002/cne.902430309
- Shigenaga, Y., Okamoto, T., Nishimori, T., Suemune, S., Nasution, I. D., Chen, I. C., et al. (1986b). Oral and facial representation in the trigeminal principal and rostral spinal nuclei of the cat. *J. Comp. Neurol.* 244, 1–18. doi: 10.1002/cne.902440102
- Shigenaga, Y., Sera, M., Nishimori, T., Suemune, S., Nishimura, M., Yoshida, A., et al. (1988). The central projection of masticatory afferent fibers to the trigeminal sensory nuclear complex and upper cervical spinal cord. *J. Comp. Neurol.* 268, 489–507. doi: 10.1002/cne.902680403
- Stanek, E., Cheng, S., Takatoh, J., Han, B.-X., and Wang, F. (2014). Monosynaptic premotor circuit tracing reveals neural substrates for oro-motor coordination. *Elife* 3:e02511. doi: 10.7554/elife.02511
- Su, H., Alroy, G., Kirson, E. D., and Yaari, Y. (2001). Extracellular calcium modulates persistent sodium current-dependent burst-firing in hippocampal pyramidal neurons. *J. Neurosci.* 21, 4173–4182. doi: 10.1523/jneurosci.21-12-04173.2001
- Tada, A., and Miura, H. (2017). Association between mastication and cognitive status: a systematic review. *Arch. Gerontol. Geriatr.* 70, 44–53. doi: 10.1016/j.archger.2016.12.006
- Tanaka, S., Kogo, M., Chandler, S. H., and Matsuya, T. (1999). Localization of oral-motor rhythmogenic circuits in the isolated rat brainstem preparation. *Brain Res.* 821, 190–199. doi: 10.1016/s0006-8993(99)01117-8
- Terashima, T., Kishimoto, Y., and Ochiishi, T. (1994). Musculotopic organization in the motor trigeminal nucleus of the reeler mutant mouse. *Brain Res.* 666, 31–42. doi: 10.1016/0006-8993(94)90279-8
- Trejo, A., Tarrats, R. M., Alonso, M. E., Boll, M. C., Ochoa, A., and Velasquez, L. (2004). Assessment of the nutrition status of patients with Huntington's disease. *Nutrition* 20, 192–196. doi: 10.1016/j.nut.2003.10.007
- Trulsson, M., and Johansson, R. S. (2002). Orofacial mechanoreceptors in humans: encoding characteristics and responses during natural orofacial behaviors. *Behav. Brain Res.* 135, 27–33. doi: 10.1016/s0166-4328(02)00151-1
- Tsuboi, A., Kolta, A., Chen, C. C., and Lund, J. P. (2003). Neurons of the trigeminal main sensory nucleus participate in the generation of rhythmic motor patterns. *Eur. J. Neurosci.* 17, 229–238. doi: 10.1046/j.1460-9568.2003.02450.x
- Tsuruyama, K., Hsiao, C. F., and Chandler, S. H. (2013). Participation of a persistent sodium current and calcium-activated nonspecific cationic current to burst generation in trigeminal principal sensory neurons. *J. Neurophysiol.* 110, 1903–1914. doi: 10.1152/jn.00410.2013
- Viggiano, A., Manara, R., Conforti, R., Paccone, A., Secondulfo, C., Lorusso, L., et al. (2015). Mastication induces long-term increases in blood perfusion of the trigeminal principal nucleus. *Neuroscience* 311, 75–80. doi: 10.1016/j.neuroscience.2015.10.017
- Watson, C., Provis, J., and Herculano-Houzel, S. (2012). What determines motor neuron number? Slow scaling of facial motor neuron numbers with body mass in marsupials and primates. *Anat. Rec.* 295, 1683–1691. doi: 10.1002/ar.22547
- Weijnenberg, R. A. F., Delwel, S., Ho, B. V., van der Maarel-Wierink, C. D., and Lobbezoo, F. (2019). Mind your teeth—the relationship between mastication and cognition. *Gerodontology* 36, 2–7. doi: 10.1111/ger.12380
- Westneat, M. W., and Hall, W. G. (1992). Ontogeny of feeding motor patterns in infant rats: an electromyographic analysis of suckling and chewing. *Behav. Neurosci.* 106, 539–554. doi: 10.1037/0735-7044.106.3.539
- Widmer, C. G., Carrasco, D. I., and English, A. W. (2003). Differential activation of neuromuscular compartments in the rabbit masseter muscle during different oral behaviors. *Exp. Brain Res.* 150, 297–307. doi: 10.1007/s00221-003-1464-y
- Widmer, C. G., and Morris-Wiman, J. (2010). Limb, respiratory and masticatory muscle compartmentalization: developmental and hormonal considerations. *Prog. Brain Res.* 187, 63–80. doi: 10.1016/b978-0-444-53613-6.00005-8
- Yamamoto, T., and Hirayama, A. (2001). Effects of soft-diet feeding on synaptic density in the hippocampus and parietal cortex of senescence-accelerated mice. *Brain Res.* 902, 255–263. doi: 10.1016/s0006-8993(01)02410-6
- Yasui, Y., Itoh, K., Mitani, A., Takada, M., and Mizuno, N. (1985). Cerebral cortical projections to the reticular regions around the trigeminal motor nucleus in the cat. *J. Comp. Neurol.* 241, 348–356. doi: 10.1002/cne.902410308
- Yoshida, A., Hiraga, T., Moritani, M., Chen, K., Takatsuki, Y., Hirose, Y., et al. (1998). Morphologic characteristics of physiologically defined neurons in the cat trigeminal nucleus principalis. *J. Comp. Neurol.* 401, 308–328. doi: 10.1002/(sici)1096-9861(19981123)401:3<308::aid-cne2>3.0.co;2-3
- Yoshida, R., Iwamoto, A., and Nagahama, T. (2001). Calcium imaging for detection and estimation of spike activities in aplysia neurons. *Zoolog. Sci.* 18, 631–643. doi: 10.2108/zsj.18.631
- Yoshida, A., Taki, I., Chang, Z., Iida, C., Haque, T., Tomita, A., et al. (2009). Corticofugal projections to trigeminal motoneurons innervating antagonistic jaw muscles in rats as demonstrated by anterograde and retrograde tract tracing. *J. Comp. Neurol.* 514, 368–386. doi: 10.1002/cne.22013

Conflict of Interest: The authors declare that the research was conducted in the absence of any commercial or financial relationships that could be construed as a potential conflict of interest.

Copyright © 2020 Slaoui Hasnaoui, Arsenault, Verdier, Obeid and Kolta. This is an open-access article distributed under the terms of the Creative Commons Attribution License (CC BY). The use, distribution or reproduction in other forums is permitted, provided the original author(s) and the copyright owner(s) are credited and that the original publication in this journal is cited, in accordance with accepted academic practice. No use, distribution or reproduction is permitted which does not comply with these terms.



Brain Cortex Activity in Children With Anterior Open Bite: A Pilot Study

Claudia Restrepo^{1*}, Paola Botero^{2*}, David Valderrama³, Kelly Jimenez¹ and Rubén Manrique¹

¹ CES-LPH Research Group, Universidad CES, Medellín, Colombia, ² GIOM Group, Universidad Cooperativa de Colombia, Envigado, Colombia, ³ Visión Integral, Medellín, Colombia

OPEN ACCESS

Edited by:

Teresa Lever,
University of Missouri, United States

Reviewed by:

Yoon Jeong Choi,
Yonsei University, South Korea
Kıymet Kübra Yurt,
Kastamonu University, Turkey

*Correspondence:

Claudia Restrepo
crestrepos@ces.edu.co
Paola Botero
paola.botero@ucc.edu.co

Specialty section:

This article was submitted to
Health,
a section of the journal
Frontiers in Human Neuroscience

Received: 03 March 2020

Accepted: 15 May 2020

Published: 30 June 2020

Citation:

Restrepo C, Botero P,
Valderrama D, Jimenez K and
Manrique R (2020) Brain Cortex
Activity in Children With Anterior Open
Bite: A Pilot Study.
Front. Hum. Neurosci. 14:220.
doi: 10.3389/fnhum.2020.00220

Anterior open bite (AOB) is related to functional alterations of the stomatognathic system. There are no studies concerning brain activation of the cortex comparing children with and without AOB during rest and activities such as deglutition and phonation. The aim of this study was to determine the activity of the brain cortex of children with AOB at rest and during phonation and deglutition and to evaluate the association of intelligence quotient (IQ), attention (Test of Variables of Attention, known as TOVA), beats per minute (BPM), and oxygen saturation measurement (SpO₂) with brain activity in subjects with AOB. Fourteen children (seven with AOB and seven without AOB) with mixed dentition, aged 10–13 years, underwent an IQ test, TOVA, SpO₂, and quantitative electroencephalography (QEEG). Electrodes were set in the scalp, according to the 10–20 protocol. Data were analyzed using statistical tests to assess comparisons between children with and without AOB. The results showed that IQ, TOVA, SpO₂, or BPM did not show any statistically significant differences between the groups, except for the response time (contained in TOVA) ($p = 0.03$). Significant differences were found for the brain activity during rest (Condition 1) of the tongue, between children with and without AOB ($p < 0.05$ for alpha/theta and alpha peaks), whereas there were no differences during function (Condition 2). The findings of this investigation provide insights about the cortex activity of the brain while the tongue is in the resting position in children with AOB. This may imply an altered activity of the brain cortex, which should be considered when diagnosing and treating AOB. Other diagnostic techniques derived from investigations based on neuroscience could develop new diagnostic and therapeutic techniques to give better solutions to children with malocclusions. Treatments should be focused not only on the teeth but also on the brain cortex.

Keywords: brain cortex, anterior open bite, children, deglutition, phonation

INTRODUCTION

Anterior open bite (AOB) is defined as the absence of vertical overlap between the maxillary and mandibular incisors (Subtelny and Sakuda, 1964). Its prevalence is about 2.7% in children between 8 and 16 years of age (Ocampo-Parra et al., 2015). It has a multifactorial etiology. The improper posture of the tongue at rest (Knösel et al., 2015) and its size and function (Zhou et al., 2016), as well as oral habits (Chen et al., 2015), neurological disturbances (Martinez-Mihi et al., 2014), and airway obstruction (Cazzolla et al., 2010), play a significant role in the origin of AOB.

It is well established that many functions of the tongue, such as deglutition and phonation (Ludlow, 2015; Xiao et al., 2017), depend on brain cortex regulation. Brain cortical representation of these functions has previously been investigated (Kober et al., 2015). It is well established that the central sulcus area, in which the ventral half of the sensorimotor cortex is located, is related to the tongue's functions of deglutition, movement, and coordinated movements of phonation (Breshears et al., 2015). These processes are influenced by cognitive performance (Burgaleta et al., 2014) and oxygen saturation (Rodriguez Moreno et al., 2015).

Previous investigations indicate that AOB is present in around 13% of mouth breathers (Pacheco et al., 2015). Electroencephalography (EEG) signals in mouth breathers present a brain activity involving lower theta and alpha powers at rest when compared with that of nose breathers. This activity comprises cognitive regions and involves decreased oxygen saturation during mouth breathing. This issue suggests that when cognition is required, mouth breathing can act as one of the variables that could cause alteration in brain function, especially in memory tasks (Lee et al., 2019).

Studies concerning brain activation when the tongue is at rest and during deglutition and phonation in children with AOB are not available and could be the answer to why orthodontic treatments of AOB are so unstable (Bondemark et al., 2007). To avoid a relapse of AOB treatments, changing the motor response must be permanently imprinted in the brain (trained) (Svensson et al., 2003). The learning process occurs because a movement that has been elicited repeatedly by successive stimuli may, after a while, be evoked without the need of the conditioning stimulus, because it has been imprinted in the cerebral cortex (Svensson et al., 2003). Based on this concept, other diagnostic techniques derived from neuroscience investigations could develop new diagnostic and therapeutic techniques to give better solutions to children with malocclusions. The approach from neuroscience in the case of AOB could give support as to why treatments relapse is less when myofunctional therapy is used than when only orthodontics is performed (Smithpeter and Covell, 2010).

According to the above statements, the aims of this study were to (1) determine the activity of the brain cortex of children with AOB at rest and during phonation and deglutition and (2) to evaluate the association of intelligence quotient (IQ), attention [Test of Variables of Attention (TOVA)], and oxygen saturation with brain activity in subjects with AOB.

MATERIALS AND METHODS

Approval and Design

This investigation was approved by the ethics committee of Universidad CES (file number 60-225). The children and their parents gave their written informed consent and assent to participate in the study.

The study was performed according to an exploratory design. Sequence and measurement procedures are shown in **Figure 1**.

Population and Sample

Children (10–13 years of age) with mixed dentition with fully erupted maxillary and mandibular incisors and with complete

posterior occlusion, with either primary or permanent molars or bicuspid, were included. Mixed dentition is defined as the transition stage between primary and permanent dentition, when the first molars erupt and the primary teeth are replaced by permanent teeth (Louly et al., 2011). The sample size was calculated based on the formula by Viechtbauer et al. (2015), assuming the highest difference between brain cortex activity of children with and without AOB. Data collection was performed from June 2015 to December 2015.

Children were selected from a previous study of 264 students, recruited from public schools of Envigado, Colombia (Ocampo-Parra et al., 2015). Subjects in this study were included on the basis of having normal facial morphology (no anatomical abnormalities, such as cleft lip); absence of neurological and/or psychiatric disorders previously diagnosed by a physician and known by the parents (including reading disorders or disabilities); absence of mouth breathing, related by parents and previously diagnosed by a physician; amelogenesis or dentinogenesis imperfecta, present in dental records and/or diagnosed by a pediatric dentist; history of anterior dentoalveolar trauma during the permanent dentition; absence of pretreatment and/or current speech therapy; and absence of previous and/or current preventive or corrective orthodontics or orthopedics. All children were required to present with a Nolla (1960) dental development stage of 10 (apical end of root completed) in permanent incisors and permanent first molars. Finally, 14 children were selected (seven with and seven without AOB).

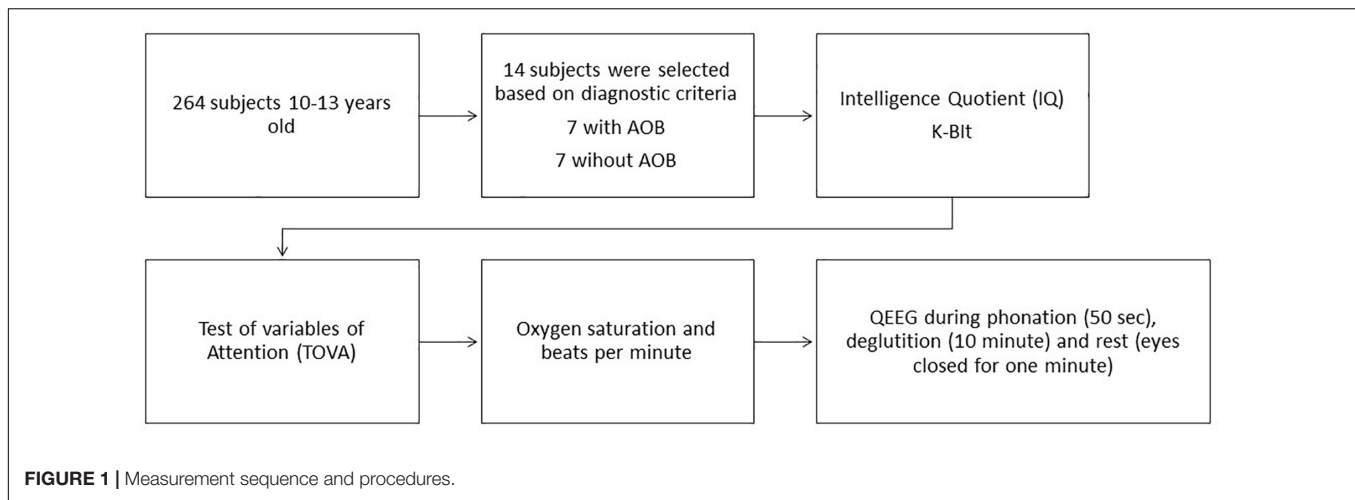
Clinical Evaluation of Anterior Open Bite

Subjects included in the study underwent a clinical examination to assess the presence of AOB, sitting in a dental chair, with the same conditions of light. The anterior bite was measured from the upper right central incisor to the lower right central incisor. AOB was considered present, when there was a vertical space >0.1 mm between the maxillary and mandibular teeth, whereas posterior teeth were in occlusion and absent when the vertical space between the maxillary and mandibular incisors was 0 or there was no AOB present (Subtelny and Sakuda, 1964).

Intelligence Quotient

A Fast IQ test was performed using the K-BIT, which is a Brief Intelligence Kaufman Test® (Kaufman and Kaufman, 2004), which assesses intellectual ability for ages 4–89 years. It evaluates verbal ability (vocabulary and definitions) and non-verbal reasoning ability (matrices). The K-BIT presents internal consistency reliability of 0.90 for verbal scale and 0.86 for non-verbal scale in children aged 4–18 years (Kaufman and Kaufman, 2004; Mervis et al., 2012). Its application takes 15–30 min, and it consists of two subtests:

1. Vocabulary and definitions: A measure of verbal skill that requires oral responses, language development, the formation of verbal concepts, and information flow.
2. Matrices: Measures non-verbal skills and the ability to solve new problems. Evaluates the ability to solve problems of reasoning through visual stimuli both figurative and abstract.



Test of Variables of Attention

The TOVA is a five-item, self-rated tool that assesses errors of omission (inattention), errors of commission (impulsivity rate), response time, the variability of response time, and double-clicks (error committed when differentiating two simple geometric figures, one of those determined as the target of attention). TOVA was designed for subjects between 8 and 80 years of age, with different scales for each age group. The evaluation takes approximately 22 min (Lawrence et al., 1993).

Attention was measured while responding to a geometric stimulus, which was considered the target of attention. For this investigation “target frequent” was considered when the child focused on the geometric stimuli and “target infrequent” when attention was not paid to the stimuli. The incorrect response to the target was called an “error of commission” or impulsivity, whereas the failure to respond to the designated target was measured as an “error of omission” or inattention. The mean time to respond correctly to the target stimulus and the variability of the response time was considered as “attentional variability.” The multiple and anticipatory responses to the target were designated as double-clicks. TOVA precisely measures reaction times (± 1 ms). Its reliability coefficient is 0.84 (Llorente et al., 2001).

Oxygen Saturation and Beats per Minute

Measurements of oxygen saturation (SpO_2) and beats per minute (BPM) of the children were performed with a pulse oximeter (Safe Heart FPO40, Beijing Safe Heart Technology, China). SpO_2 was considered as the measure of the percentage of hemoglobin binding sites in the bloodstream occupied by oxygen (normal SpO_2 should be between 96 and 99%), whereas BPM was the number of times that the heart beats per minute while it is at rest. Its mean value ranges from 60 to 80.

Quantitative Electroencephalography

Each child underwent a quantitative EEG (QEEG) at Instituto Psicotecnológico in Medellín, Colombia. QEEG is a validated technique for brain mapping (Thatcher, 2010), which allows

highly accurate measurement of the electrical activity of the brain cortex, at rest, and during the execution of specific tasks. The electrical activity was measured with a 2EB Hardware Clinical Brain Master® of Brainmaster System Technologies, Inc. (Ohio, OH, United States). Data were collected using the BioExplorer version 1.6® and BioReview 1.3® software (Cyber Evolution Inc., United States).

Each QEEG examination was performed with the child seated in a right position. Electrodes were set in specific points in the scalp. For that purpose, the scalp was cleaned with Nuprep® skin prepping gel (Weaver and Company, Colorado, CO, United States) to minimize interference with the electrical signals. Afterward, conductive paste (Ten20®, Weaver and Company, Colorado, CO, United States) was applied to each electrode. Surface electrodes were positioned on the scalp, following the international 10/20 system and set between the skull points nasion, inion, and preauricular, according to a validated technique (Jurkac et al., 2007).

The central sulcus (referred to herein as the letter C) divides the frontal and parietal lobes of the left and right cerebral hemispheres. The signal from this electrode aimed to measure the primary sensory cortex. The electrode with the even number 4 was positioned in the right hemisphere and the one with the odd number 3, in the left hemisphere (Mervis et al., 2012). In this investigation, only the central sulcus area of the left (C3; Zone 1) and right (C4; Zone 2) hemispheres were analyzed, which are the ones in the brain cortex related to the tongue at rest (Condition 1) and during function (Condition 2) involving deglutition and phonation.

Quantitative electroencephalography recordings were performed in three cases: (1) The children were asked to breathe softly and to close their eyes for 1 min (measurement at rest), and then they were asked to open their eyes for another minute; (2) children were asked to execute a phonation task for 50 s (reading the same text for every child). The reading included dental and alveolar consonants to evaluate the tongue function during phonation. Dental consonants are articulated in the Spanish language with the tongue against the upper teeth, such as /d/, /n/, /t/, and /l/, whereas the alveolars contact the tongue with the gum

ridge. (3) Finally, deglutition was recorded for 10 s. Each child was given a glass of water and asked to drink it continuously for 10 s. The test was done with water, to avoid any extrinsic stimulation of salivation.

The QEEG applies mathematical algorithms to transform the data obtained into the following frequency bands: theta/beta, alpha/theta, alpha, beta, and wavelength of 2–38 Hz. The magnitude corresponds to the amount of energy that the original QEEG possesses at each frequency, and it is measured in hertz.

An expert investigator read and analyzed the data and gave a diagnosis based on the guidelines given by the Othmer protocol (Oostenveld and Praamstra, 2001).

Control Parameters

Both the clinical classification (AOB/No AOB) and the QEEG examination were performed by expert trained investigators. In the previous study from which children were selected for this investigation (Ocampo-Parra et al., 2015), AOB was assessed by two researchers. The consensus was gathered in order to avoid evaluation bias. Kappa index and intraclass correlation coefficient (ICC) were obtained, and the results were 0.95 and 0.99, respectively. For this investigation, the presence or absence of AOB was confirmed before assessing the IQ, attention, oxygen saturation, and QEEG.

Acquiring a QEEG signal properly means avoiding errors and affecting the subject and the biosignal measurements. The goal is to obtain measurements secure for the individual and with high signal-to-noise ratio (SNR) and no data loss. The points that were considered in this investigation were as follows (Usakli, 2010):

1. Subject safety: Leakage currents were avoided by maintaining subjects and front-end circuitry and earth grounds as separate.
2. Electromagnetic interference protection: QEEG signals are distorted, and the signal is corrupted with noise when electrical or electronic devices are near the recording setup. Therefore, operation of those devices closed to the recording setup was prohibited. Additionally, the instrumentation amplifier was used.
3. Subject muscular movements: Muscular movements, different from the ones that were purposed for the investigation, could affect the QEEG signals. Therefore, children were encouraged to avoid those types of muscle activities.
4. Electrostatic discharge (ESD) protection: No ESD protection may cause damage of electronic components and QEEG signals and serious problem for subjects. Thus, active electronic components had greater than 2,000 V of ESD protection.
5. Efficient grounding: The lab where measurements were made had proper grounding techniques to help reduce noise, therefore increasing SNR.
6. Electrodes: Electrodes were dried before setting, and the position was controlled by locating the surface electrodes in a previously calibrated and validated position.
7. Electrode contact impedance: Less than 1 k Ω of contact impedance indicates probable shortcut between the

electrodes, and greater than 10 k Ω avoids acquiring EEG signals. Thus, the contact impedance value for electrodes was between 1 and 10 k Ω .

8. Digitization: Sufficient and optimal digital resolution was provided for analog-to-digital conversion in order to impede an increase in the quantization error.
9. Sampling instants: In a multichannel system, the time delay between channels could be a problem. This problem was controlled by using a digital multiplier.

All the QEEG interpretations were made by the same investigator who was blind to the AOB classification.

Statistical Analysis

A comparison of variables between the anterior AOB and No AOB group was performed, using Mann–Whitney *U* test or *T*-test, depending on the distribution of the variables.

Statistical analysis was performed using STATA version 14.0 (StataCorp LP, Texas, TX, United States).

RESULTS

This study included 14 child subjects (seven females and seven males; mean age 11.9 years; range 10–13 years old). The children with AOB presented with an open bite with a mean of 3.3 mm (SD 1.3). The distribution of children, according to vertical space (mm) between the maxillary and mandibular incisors, is presented in **Figure 2**.

When analyzing IQ, TOVA (response time, variability, inattention, commission, double-click), SpO₂ (mean 97%, SD 1.0), and BPM (mean 73, SD 2.8), no statistically significant differences were found between the groups with and without AOB, except for response time, which presents statistically significant differences when comparing both groups (**Table 1**).

When evaluating the brain activity, there are statistically significant differences in the variables frequency alpha/theta during rest in the central sulcus area of the left hemisphere (C3; Condition 1/Zone 1) ($p = 0.047$) and frequency alpha peak

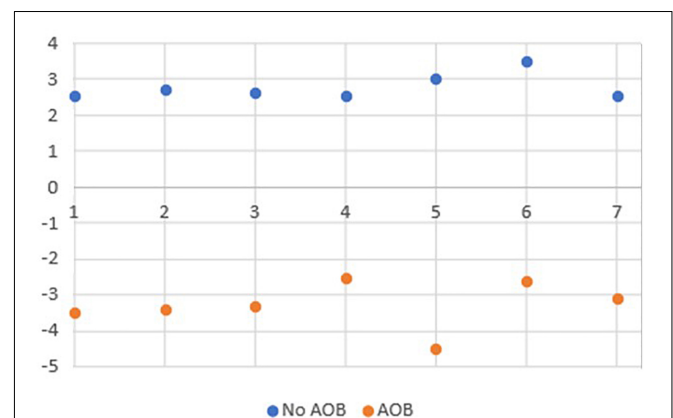


FIGURE 2 | Distribution of children according to vertical space (mm) between the maxillary and mandibular incisors.

TABLE 1 | Comparison of IQ, TOVA, SpO₂, and BPM between children with and without anterior open bite (AOB).

| Variable | Anterior open bite Rank sum | No anterior open bite Rank sum | p-Value |
|-------------------|--------------------------------|-----------------------------------|---------|
| IQ | 65 | 40 | 0.11 |
| Response time | 36 | 69 | 0.03 |
| Variability | 66.5 | 38.5 | 0.07 |
| Inattention | 65 | 40 | 0.11 |
| Commission | 54.5 | 50.5 | 0.80 |
| Double-click | 59.5 | 45.5 | 0.14 |
| Oxygen saturation | 57 | 48 | 0.56 |
| BPM | 57.5 | 47.5 | 0.52 |

All p-values were obtained with Student T-test. IQ, intelligence quotient; TOVA, Test of Variables of Attention; SpO₂, oxygen saturation measurement; BPM, beats per minute.

TABLE 2 | Comparison of cortex activity between children with and without anterior open bite during rest (Condition 1).

| Variable | Anterior open bite Rank sum | No anterior open bite Rank sum | p-Value |
|--------------------|--------------------------------|-----------------------------------|---------|
| Zone 1 | | | |
| Theta/beta | 53.5 | 51.5 | 0.90* |
| Alpha/theta | 68 | 37 | 0.05** |
| Alpha peak | 71 | 34 | 0.02** |
| Beta | 49 | 56 | 0.66* |
| Wavelength 2–38 Hz | 57.5 | 47.5 | 0.52* |
| Zone 2 | | | |
| Theta/beta | 57.5 | 47.5 | 0.52* |
| Alpha/theta | 60.5 | 44.5 | 0.31* |
| Alpha peak | 65 | 40 | 0.11* |
| Beta | 50 | 55 | 0.75* |
| Wavelength 2–38 Hz | 57 | 48 | 0.565* |

Zone 1, C3 (central sulcus area, left hemisphere). Zone 2, C4 (central sulcus area, right hemisphere). *p-value obtained with Student T-test. **p-value obtained with Mann–Whitney U test.

during rest in the central sulcus area of the left hemisphere (C3; Condition 1/Zone 1) ($p = 0.018$). The brain activity is higher in subjects with AOB than in subjects without AOB (Table 2). Comparing the frequency alpha/theta with alpha peak during rest in the central sulcus area of the left hemisphere (C3) within the groups, there are no differences between the AOB and control groups (Table 2).

When comparing the data of children with and without AOB, no statistically significant differences are found for any variable in C2 (function) (Table 3).

DISCUSSION

AOB is a complex malocclusion, often associated with functional alterations in the stomatognathic system. An improper tongue rest posture has been suggested as one of the primary contributing factors to AOB (Knösel et al., 2015). It is well established that the brain cortex, specifically the primary

TABLE 3 | Comparison of cortex activity between children with and without anterior open bite during function (Condition 2).

| Variable | Anterior open bite Rank sum | No anterior open bite Rank sum | p-Value |
|--------------------|--------------------------------|-----------------------------------|---------|
| Zone 1 | | | |
| Deglutition | | | |
| Theta/beta | 49 | 56 | 0.65* |
| Alpha/theta | 53.5 | 58.5 | 1.00* |
| Alpha peak | 52 | 49 | 0.55* |
| Beta | 49 | 56 | 0.43* |
| Wavelength 2–38 Hz | 44.5 | 60.5 | 0.31* |
| Phonation | | | |
| Theta/beta | 48.5 | 54.3 | 0.34* |
| Alpha/theta | 54.2 | 53.5 | 0.83* |
| Alpha peak | 46 | 49 | 0.46* |
| Beta | 52 | 56 | 0.45* |
| Wavelength 2–38 Hz | 53.5 | 60.5 | 0.21* |
| Zone 2 | | | |
| Deglutition | | | |
| Theta/beta | 54 | 61 | 0.33* |
| Alpha/theta | 66 | 59 | 0.06* |
| Alpha peak | 66 | 39 | 0.35* |
| Beta | 49 | 56 | 0.55* |
| Wavelength 2–38 Hz | 53.5 | 51.5 | 0.81* |
| Phonation | | | |
| Theta/beta | 45 | 60 | 0.329* |
| Alpha/theta | 66 | 39 | 0.083* |
| Alpha peak | 66 | 39 | 0.084* |
| Beta | 49 | 56 | 0.655* |
| Wavelength 2–38 Hz | 53.5 | 51.5 | 0.898* |

Condition 2, function (deglutition and phonation). Zone 1, C3 (central sulcus area, left hemisphere). Zone 2, C4 (central sulcus area, right hemisphere). *p-value obtained with Student T-test.

sensorimotor cortex, plays an important functional role in the regulation of tongue functions, such as deglutition and phonation (Kober et al., 2015; Ludlow, 2015). However, thus far, there have been no studies considering brain activation when the tongue is at rest or in function (deglutition and phonation) in children with AOB.

This exploratory investigation assessed the activation of the brain cortex activity of children with AOB at rest and during phonation and deglutition and evaluated the influence of the IQ, attention, and oxygen saturation on brain activity during those functions.

Efforts were made to use validated instruments and calibrated devices to assess IQ, attention, oxygen saturation, and brain activity and to test the influence of these variables on the brain cortex. Overall, the results of this investigation suggest that (1) IQ, attention, and oxygen saturation are not different between subjects with and without AOB and thus are not considered as confounding variables for the activity of the brain cortex in this study; (2) the activity of the brain cortex during rest was higher in subjects with AOB than with those with no AOB; and (3) the activity of the brain cortex during deglutition and phonation was not different between children with and without AOB.

Breathing disorders influence the cognitive and behavioral performance of children, including IQ and attention (Cazzolla et al., 2010; Lal et al., 2012). The present study did not demonstrate differences in oxygen saturation and TOVA between children with and without AOB. These findings disagree with the results of previous investigations (Blunden et al., 2000; Lal et al., 2012). Two major reasons for this disagreement must be analyzed. Firstly, children with mouth breathing or other breathing disorders were excluded from this exploratory study, in order to reduce the confounding variables that could affect the brain cortex activity as was previously demonstrated by other authors (Lee et al., 2019); and secondly, the results of the present investigation should be interpreted with caution, owing to the few subjects included in the sample, which could be considered a limitation of the study.

This was a study testing an original technique to evaluate brain activity in children with an AOB. As there are no data of previous investigations on the topic, it was recommended by the ethics committee of Universidad CES to test the new research hypothesis in a study with a pilot design in the first instance. The results of this hypothesis-generating study showed differences between the activity of brain cortex during rest, of children with and without AOB. Thus, obtained results are to be confirmed in a larger confirmatory study.

Differences in IQ and TOVA were not found between children with and without AOB. However, looking at the results yielded by the QEEG, higher alpha/theta activity was found, as well as a higher alpha peak during rest in children with AOB. These findings suggest possible differences in the brain cortex activity during cognitive demands (Usakli, 2010; Rodriguez-Larios and Alaerts, 2019), such as arithmetic tasks that were not measured with QEEG in this study. The correlation between the measurements of QEEG and clinical cognitive measurements in children with AOB deserves further attention for future investigations.

Regarding the effects of the tongue function on the anterior bite of children, several studies have measured forces of the tongue against the maxillary incisors and palate during rest and normal deglutition. The conclusions validated the hypothesis that the resting position of the tongue has a more significant role in the etiology of AOB than had deglutition and phonation functions (Shenoy et al., 2015). Furthermore, the cortical plasticity of individuals with incorrect tongue position during rest is different from the cortical plasticity of individuals whose tongue is in the palate during rest (Arima et al., 2011). The results of Arima et al. (2011) agree with those of this investigation, where an alteration in the sensorimotor cortex of subjects with AOB was found. In this context, therapies to establish correct rest position of the tongue, such as orofacial myofunctional therapy (OMT) (Van Dyck et al., 2016), could also influence the brain cortex plasticity, necessary to avoid relapse in orthodontic treatments of AOB. However, the quality of the evidence on this topic is still questionable (Koletsis et al., 2018).

When the function is analyzed, previous results demonstrated that during deglutition or phonation, incorrect position of the tongue can be observed in subjects with AOB. The reason could be a disturbed function of one or several afferent

neurons (Maezawa et al., 2016). According to the results of the present study, there is no difference in brain activity during phonation and deglutition, between subjects with and without AOB (Shenoy et al., 2015).

Even when evaluating the activity of the left and right hemispheres during rest, deglutition, and phonation was not an objective of this investigation, it is interesting to mention the findings regarding this topic. Differences were found between the left and right hemispheres in both Condition 1 (rest) and Condition 2 (function). For most brain functions, the two hemispheres are a “mirror” of each other. However, there is evidence that shows that speech production is one of the most important lateralized features of the brain (Raemaekers et al., 2018). In the case of this pilot study, it was observed (even when not statistically compared) that differences were present at rest and in deglutition and phonation. This issue requires further exploration in other studies.

To our knowledge, this is the first study using brain mapping, which demonstrates that the brain activity in subjects with AOB is higher than in subjects without AOB at rest. A possible explanation could be the altered tongue posture during rest in AOB children. Future studies to test this hypothesis are suggested in larger samples, where the classification of the severity of the AOB could be assessed.

CONCLUSION

The findings of this investigation provide insights about the cortex activity of the brain during the rest position of the tongue in children with AOB. This may mean an altered function, not only in the orofacial system but also in the central nervous system, that should be considered when diagnosing and treating AOB. Diagnosis of AOB should be focused not only on the teeth but also on the brain cortex.

DATA AVAILABILITY STATEMENT

The datasets generated for this study are available on request to the corresponding author.

ETHICS STATEMENT

The studies involving human participants were reviewed and approved by the Ethics committee of Universidad CES. Written informed consent to participate in this study was provided by the participants' legal guardian/next of kin.

AUTHOR CONTRIBUTIONS

CR and PB conceived the project. CR, PB, and KJ wrote the project. CR, PB, and DV were in charge of the control parameters. KJ and DV performed the measurements and collected the data. CR and PB were involved in planning and supervising the work.

RM processed the data and performed the analysis. All authors interpreted the results and worked on the manuscript. All authors drafted the manuscript and designed the tables. All authors discussed the results and commented on the manuscript.

REFERENCES

- Arima, T., Yanagi, Y., Niddam, D. M., Ohata, N., Arendt-Nielsen, L., Minagi, S., et al. (2011). Corticomotor plasticity induced by tongue-task training in humans: a longitudinal fMRI study. *Exp. Brain Res.* 212, 199–212. doi: 10.1007/s00221-011-2719-7
- Blunden, S., Lushington, K., Kennedy, D., Martin, J., and Dawson, D. (2000). Behavior and neurocognitive performance in children aged 5–10 years who snore compared to controls. *J. Clin. Exp. Neuropsychol.* 22, 554–568. doi: 10.1076/1380-3395(200010)22:5;1-9;ft554
- Bondemark, L., Holm, A. K., Hansen, K., Axelsson, S., Mohlin, B., Brattstrom, V., et al. (2007). Long-term stability of orthodontic treatment and patient satisfaction: a systematic review. *Angle Orthod.* 77, 181–191. doi: 10.2319/011006-16r.1
- Breshears, J. D., Molinaro, A. M., and Chang, E. F. (2015). A probabilistic map of the human ventral sensorimotor cortex using electrical stimulation. *J. Neurosurg.* 123, 340–349. doi: 10.3171/2014.11.jns.14889
- Burgaleta, M., Johnson, W., Waber, D. P., Colom, R., and Karama, S. (2014). Cognitive ability changes and dynamics of cortical thickness development in healthy children and adolescents. *Neuroimage* 84, 810–819. doi: 10.1016/j.neuroimage.2013.09.038
- Cazzolla, A. P., Lacarbonara, V., Pellegrino, B., Testa, N. F., Fidanza, F., and Lacaita, M. G. (2010). Sleep-disordered breathing in a sample of 495 children in Southern Italy. *Eur. J. Paediatr. Dent.* 11, 189–192.
- Chen, X., Xia, B., and Ge, L. (2015). Effects of breast-feeding duration, bottle-feeding duration and non-nutritive sucking habits on the occlusal characteristics of primary dentition. *BMC Pediatr.* 15:46.
- Jurkac, V., Tsuzuki, D., and Ippaita, D. (2007). 10/20, 10/10, and 10/5 systems revisited: their validity as relative head-surface-based positioning systems. *NeuroImage* 34, 1600–1611. doi: 10.1016/j.neuroimage.2006.09.024
- Kaufman, A. S., and Kaufman, N. L. (2004). *Kaufman Brief Intelligence Test*, 2nd Edn. Circle Pines, MN: American Guidance Services, 103.
- Knösel, M., Nüser, C., Jung, K., Helms, H. J., Engelke, W., and Sandoval, P. (2015). Interaction between deglutition, tongue posture, and malocclusion: a comparison of intraoral compartment formation in subjects with neutral occlusion or different types of malocclusion. *Angle Orthod.* 86, 697–705. doi: 10.2319/101615-699.1
- Kober, S. E., Gressenberger, B., Kurzmann, J., Neuper, C., and Wood, G. (2015). Voluntary modulation of hemodynamic responses in swallowing related motor areas: a near-infrared spectroscopy-based neurofeedback study. *PLoS One* 10:e0143314. doi: 10.1371/journal.pone.0143314
- Koletsis, D., Makou, M., and Pandis, N. (2018). Effect of orthodontic management and orofacial muscle training protocols on the correction of myofunctional and myoskeletal problems in developing dentition: a systematic review and meta-analysis. *Orthod. Craniofac. Res.* 21, 202–215. doi: 10.1111/ocr.12240
- Lal, C., Strange, C., and Bachman, D. (2012). Neurocognitive impairment in obstructive sleep apnea. *Chest* 141, 1601–1610. doi: 10.1378/chest.11-2214
- Lawrence, M., Greenberg, A., Urwin, D., and Waldman, F. (1993). Developmental normative data on the test variables of attention (T.O.V.A.). *J. Child Psychol. Psychiatr.* 34, 1019–1030. doi: 10.1111/j.1469-7610.1993.tb01105.x
- Lee, K. J., Park, C. A., Lee, Y. B., Kim, H. K., and Kang, C. K. (2019). EEG signals during mouth breathing in a working memory task. *Int. J. Neurosci.* 130, 425–434. doi: 10.1080/00207454.2019.1667787
- Llorente, A. M., Amado, A. J., Voigt, R. G., Berretta, M. C., Fraley, J. K., Jensen, C. L., et al. (2001). Internal consistency, temporal stability and reproducibility of individual index scores of the Test of Variables of Attention in children with attention-deficit/hyperactivity disorder. *Arch. Clin. Neuropsychol.* 16, 535–546. doi: 10.1016/s0887-6177(00)00065-2
- Louly, F., Nouer, P. R., Janson, G., and Pinzan, A. (2011). Dental arch dimensions in the mixed dentition: a study of Brazilian children from 9 to 12 years of age. *J. Appl. Oral. Sci.* 19, 169–174. doi: 10.1590/s1678-77572011000200014
- Ludlow, C. L. (2015). Central nervous system control of voice and swallowing. *J. Clin. Neurophysiol.* 32, 294–303. doi: 10.1097/wnp.0000000000000186
- Maezawa, H., Mima, T., Yazawa, S., Matsushashi, M., Shiraishi, H., and Funahashi, M. (2016). Cortico-muscular synchronization by proprioceptive afferents from the tongue muscles during isometric tongue protrusion. *Neuroimage* 128, 284–292. doi: 10.1016/j.neuroimage.2015.12.058
- Martinez-Mihi, V., Silvestre, F. J., Orellana, L. M., and Silvestre-Rangil, J. (2014). Resting position of the head and malocclusion in a group of patients with cerebral palsy. *J. Clin. Exp. Dent.* 6, 1–6.
- Mervis, C. B., Kistler, D. J., Jhon, A. E., and Morris, C. A. (2012). Longitudinal assessment of intellectual abilities of children with Williams syndrome: multilevel modeling of performance on the kaufman brief intelligence test-2. *Am. J. Intellect. Dev. Disabil.* 117, 134–141.
- Nolla, C. M. (1960). The development of permanent teeth. *J. Dent. Child.* 27, 254–266.
- Ocampo-Parra, A., Escobar-Toro, B., Sierra-Alzate, V., Rueda, Z. V., and Lema, M. C. (2015). Prevalence of dyslalias in 8 to 16 year-old students with anterior open bite in the municipality of Envigado. Colombia. *BMC Oral. Health* 15, 77–85. doi: 10.1186/s12903-015-0063-1
- Oostenveld, R., and Praamstra, P. (2001). The five percent electrode system for high-resolution EEG and ERP measurements. *Clin. Neurophysiol.* 112, 713–719. doi: 10.1016/s1388-2457(00)00527-7
- Pacheco, M. C., Fiorott, B. S., Finck, N. S., and Araújo, M. T. (2015). Craniofacial changes and symptoms of sleep-disordered breathing in healthy children. *Dental. Press J. Orthod.* 20, 80–87. doi: 10.1590/2176-9451.20.3.080-087.oar
- Raemaekers, M., Schellekens, W., Petridou, N., and Ramsey, N. F. (2018). Knowing left from right: asymmetric functional connectivity during resting state. *Brain Struct. Funct.* 223, 1909–1922.
- Rodriguez Moreno, D., Schiff, N. D., and Hirsch, J. (2015). Negative blood oxygen level dependent signals during speech comprehension. *Brain Connect* 5, 232–244. doi: 10.1089/brain.2014.0272
- Rodriguez-Larios, J., and Alaerts, K. (2019). Tracking transient changes in the neural frequency architecture: harmonic relationships between theta and alpha peaks facilitate cognitive performance. *J. Neurosci.* 39, 6291–6298. doi: 10.1523/jneurosci.2919-18.2019
- Shenoy, U., Hazarey, P., Akhare, P. J., and Mute, B. K. (2015). Cephalometric appraisal of tongue and related soft tissues in normal and open bite subjects at rest. *J. Clin. Diagn. Res.* 9, 16–20.
- Smithpeter, J., and Covell, D. Jr. (2010). Relapse of anterior open bites treated with orthodontic appliances with and without orofacial myofunctional therapy. *Am. J. Orthod. Dentofacial. Orthop.* 137, 605–614. doi: 10.1016/j.jado.2008.07.016
- Subtelny, J. D., and Sakuda, M. (1964). Open-bite: diagnosis and treatment. *Am. J. Orthod.* 50, 337–358. doi: 10.1016/0002-9416(64)90175-7
- Svensson, P., Romaniello, A., Arendt-Nielsen, L., and Sessle, B. J. (2003). Plasticity in corticomotor control of the human tongue musculature induced by tongue-task training. *Exp. Brain Res.* 152, 42–51. doi: 10.1007/s00221-003-1517-2
- Thatcher, R. (2010). Validity and reliability of quantitative electroencephalography. *J. Neurother.* 14, 122–152. doi: 10.1080/10874201003773500
- Usakli, A. (2010). Improvement of EEG signal acquisition: an electrical aspect for state of the art of front end. *Comput. Intel. Neurosci.* 1-7:630649.
- Van Dyck, C., Dekeyser, A., Vantricht, E., Manders, E., Goeleven, A., Fieuws, S., et al. (2016). The effect of orofacial myofunctional treatment in children with anterior open bite and tongue dysfunction: a pilot study. *Eur. J. Orthod.* 38, 227–234. doi: 10.1093/ejo/cjv044

FUNDING

This investigation was fully funded by Universidad CES and Universidad Cooperativa de Colombia.

- Viechtbauer, W., Smits, L., Kotz, D., Budé, L., Spigt, M., Serroyen, J., et al. (2015). A simple formula for the calculation of sample size in pilot studies. *J. Clin. Epidemiol.* 68, 1375–1379. doi: 10.1016/j.jclinepi.2015.04.014
- Xiao, F. L., Gao, P. Y., Qian, T. Y., Sui, B. B., Xue, J., Zhou, J., et al. (2017). Cortical representation of facial and tongue movements: a task functional magnetic resonance imaging study. *Clin. Physiol. Funct. Imaging* 37, 341–345. doi: 10.1111/cpf.12304
- Zhou, Z., Liu, F., Shen, S., Shang, L., Shang, L., and Wang, X. (2016). Prevalence of and factors affecting malocclusion in primary dentition among children in Xi'an, China. *BMC Oral. Health* 16, 91–98. doi: 10.1186/s12903-016-0285-x

Conflict of Interest: The authors declare that the research was conducted in the absence of any commercial or financial relationships that could be construed as a potential conflict of interest.

Copyright © 2020 Restrepo, Botero, Valderrama, Jimenez and Manrique. This is an open-access article distributed under the terms of the Creative Commons Attribution License (CC BY). The use, distribution or reproduction in other forums is permitted, provided the original author(s) and the copyright owner(s) are credited and that the original publication in this journal is cited, in accordance with accepted academic practice. No use, distribution or reproduction is permitted which does not comply with these terms.



Effect of Deep Brain Stimulation on Swallowing Function: A Systematic Review

Huiyan Yu^{1,2}, Kazutaka Takahashi³, Lisa Bloom^{2,4}, Samuel D. Quaynor² and Tao Xie^{2*}

¹ Department of Neurology, Beijing Hospital, National Center of Gerontology, Beijing, China, ² Department of Neurology, The University of Chicago Medicine, Chicago, IL, United States, ³ Department of Organismal Biology and Anatomy, The University of Chicago, Chicago, IL, United States, ⁴ Speech and Swallowing Service, The University of Chicago Medicine, Chicago, IL, United States

OPEN ACCESS

Edited by:

Steven Frucht,
Mount Sinai Hospital, United States

Reviewed by:

Adolfo Ramirez-Zamora,
University of Florida Health,
United States
Santiago Perez-Lloret,
Consejo Nacional de Investigaciones
Científicas y Técnicas
(CONICET), Argentina

*Correspondence:

Tao Xie
txie@neurology.bsd.uchicago.edu

Specialty section:

This article was submitted to
Movement Disorders,
a section of the journal
Frontiers in Neurology

Received: 10 February 2020

Accepted: 14 May 2020

Published: 17 July 2020

Citation:

Yu H, Takahashi K, Bloom L,
Quaynor SD and Xie T (2020) Effect of
Deep Brain Stimulation on Swallowing
Function: A Systematic Review.
Front. Neurol. 11:547.
doi: 10.3389/fneur.2020.00547

The effect of deep brain stimulation (DBS) on swallowing function in movement disorders is unclear. Here, we systematically reviewed this topic by searching keywords following PICOS strategy of problem (swallowing or swallow or dysphagia or aspiration) and intervention (deep brain stimulation, or DBS) in the PubMed and Web of Science in English in April 2020, with comparators [subthalamic nucleus (STN), globus pallidus interna (GPi), ventralis intermedius, (ViM), post-subthalamic area, or caudal zona incerta (PSA/cZi); ON/OFF DBS state/settings, ON/OFF medication state, Parkinson's disease (PD), dystonia, tremor], outcomes (swallowing function measures, subjective/objective) and study types (good quality original studies) in mind. We found that STN DBS at usual high-frequency stimulation could have beneficial effect (more so on subjective measures and/or OFF medication), no effect, or detrimental effect (more so on objective measures and/or ON medication) on swallowing function in patients with PD, while low-frequency stimulation (LFS) could have beneficial effect on swallowing function in patients with freezing of gait. GPi DBS could have a beneficial effect (regardless of medication state and outcome measures) or no effect, but no detrimental effect, on swallowing function in PD. GPi DBS also has beneficial effects on swallowing function in majority of the studies on Meige syndrome but not in other diseases with dystonia. PSA/cZi DBS rarely has detrimental effect on swallowing functions in patients with PD or tremor. There is limited information on ViM to assess. Information on swallowing function by DBS remains limited. Well-designed studies and direct comparison of targets are further needed.

Keywords: deep brain stimulation (DBS), dysphagia, swallowing function, subthalamic nucleus (STN), globus pallidus interna (GPi), post-subthalamic area (PSA), Parkinson's disease, movement disorders

INTRODUCTION

Dysphagia, or impaired swallow function, is one of the two major causes of mortalities in Parkinson's disease (PD) (along with falls related to the loss of balance). Dysphagia usually does not respond well to dopaminergic medication treatment (1, 2). Although deep brain stimulation (DBS) has significant beneficial effects in PD patients with motor fluctuation, dyskinesia, or medication refractory tremor (3–7), it has less benefits in axial symptoms of balance, speech, and swallowing function. Some studies even raise concerns about worsening of the axial symptom

after DBS, particularly with long-term DBS at the usual high-frequency stimulation (HFS) (8–13), while axial symptoms have been found to predict the mortality of PD patients with STN DBS (14). Low-frequency stimulation (LFS) has been reported to have beneficial effect on axial symptoms in patients with freezing of gait (FOG) at usual HFS (15–18). Most common DBS targets to treat PD are STN (subthalamic nucleus) or GPi (globus pallidus interna) (3–7). They both have a similar effect on motor function of PD, but different effects in non-motor symptoms, such as cognitive function and depression, with different extents in medication reduction after the surgery as well (5, 19). GPi also seems to have a better outcome on axial symptoms, particularly after more than 2-year stimulation compared to STN (12).

The effect of DBS on swallowing function has not been well-studied across various movement disorders and targets. There was a retrospective study on the effect of unilateral STN vs. unilateral GPi on swallowing function in PD patients, which demonstrated a better swallowing function in penetration–aspiration (PA) scores on the videofluoroscopic swallow study (VFSS) in GPi compared to STN at medication OFF status, although there was a difference in baseline swallowing function between these two groups (20). LFS of STN was found to have beneficial effect on dysphagia compared to HFS in patients with FOG refractory to usual HFS of STN (16, 17). DBS targeting the post-subthalamic area and caudal zona incerta (PSA/cZi) was thought to be associated with fewer side effects compared to ventralis intermedius (ViM) or STN (21), including the swallowing function (22–24). GPi DBS has also been used to treat various dystonia (25–28), including Meige syndrome (29–32), and its effect on the swallowing function is also of interest to review compared to that in PD.

Besides diseases and targets, ON/OFF DBS state and stimulation frequencies, ON/OFF medication state, outcome measures for swallowing function (subjective questionnaires or scales vs. objective assessments, such as VFSS), and study designs (randomized double blind vs. open label retrospective or prospective) could also affect the swallowing function.

There was only one review article specifically focusing on the effect of DBS on swallowing function comparing different targets in the literature, mainly on unilateral GPi to STN DBS in patients with PD (33), which was published about 7 years ago. Therefore, it is necessary to have a comprehensive review with updated information on the effect of DBS on swallowing function covering various targets and movement disorders to reflect recent advances in the field, which will help guide our clinical practice in applying DBS for movement disorders.

METHODS

We systematically searched the PubMed and the Web of Science in April 2020 for all available publications in English by keywords following PICOS concepts: problem = (dysphagia or swallowing or swallow or aspiration) and intervention = (DBS or deep brain stimulation) to include all pertinent articles, with comparators [subthalamic nucleus (STN), globus pallidus interna (GPi), ventralis intermedius (ViM), post-subthalamic area or caudal

zona incerta (PSA/cZi), ON/OFF DBS state/settings (ON/OFF) medication state; Parkinson's disease (PD), dystonia, tremor], outcomes (swallowing function measures, subjective/objective) and study types (good quality original studies) in mind during the search. We followed PRISMA guideline for systematic review, and the flow chart of the literature search and selection process of the review is depicted in **Figure 1** (34, 35). A total of 145 publications were found from PubMed and 169 from Web of Science. After removing the duplicate entries, screening was performed to narrow down to 177 articles by excluding reviews, comments, viewpoints, author responses, letters, book chapters, single case reports with insufficient information, and meeting abstracts. Then the full texts were assessed, and we removed studies without clear outcome measures on swallowing function by DBS. We finally identified 32 unique articles. We included DBS studies targeting STN, GPi, ViM, or PSA/cZi on patients with PD, various dystonia (including Meige syndrome), and essential tremor (ET), and compared swallowing function measures (subjective vs. objective) at ON/OFF DBS state under different settings (including stimulation frequencies), or post-operative to pre-operative baseline, at ON/OFF medication state. Basic demographics and types of study designs (retrospective vs. prospective, open vs. blind) were also taken into consideration in assessments.

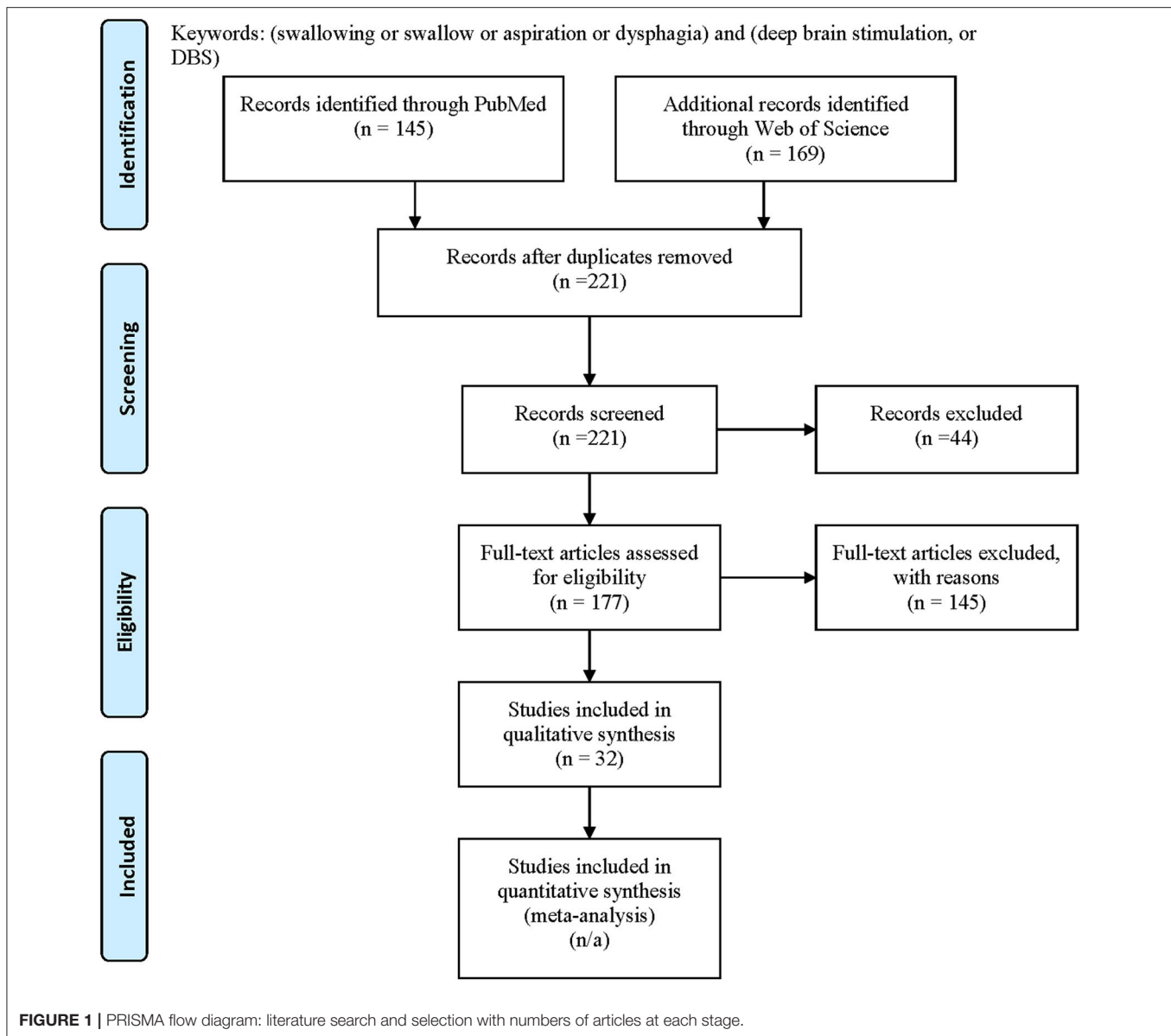
RESULTS

Each pertinent publication is listed in detail in **Table 1**, with information on references, diseases, DBS targets, basic demographics, study designs (randomized double blind vs. open label retrospective or prospective), outcome measures (subjective vs. objective measures) on swallowing functions at ON/OFF DBS or post-operational vs. pre-operational state under different DBS settings (if available) and ON/OFF medication state, and major conclusions. Among the 32 articles identified, 22 articles were on PD patients, with 19 targeting STN, 3 targeting GPi, and 3 targeting PSA/cZi, as some studies were targeting more than one target. There were six articles on Meige syndrome and five on non-Meige dystonia or dyskinesia (including primary generalized dystonia, segmental dystonia, and cerebral palsy), all targeting GPi. There was only one article on ET targeting PSA and none on ET targeting ViM on swallowing function. The majority of the studies used HFS of 125–210 Hz, but two studies used LFS of 60 Hz (16, 17). The assessments included subjective measures, such as swallowing questionnaires or scales, and objective measures, such as VFSS and fiberoptic endoscopic evaluation of swallowing (FEES).

We summarized the result as below, based on the diseases and targets.

PD With STN DBS

STN DBS in patients with PD can have no effects (36–38). Kitashima et al. reported no improvement in swallowing function in 18 PD patients assessed by VFSS at ON medication state 6 months after the bilateral STN DBS (37). Olchik et al. found no change in swallowing function 6 months after bilateral STN DBS



in 10 PD patients assessed by anamnesis, functional oral intake scale, and clinical swallowing function (38).

STN DBS in patients with PD can also have detrimental effects on the swallowing function. STN DBS impaired the jaw opening and closing velocities by scales 6 months after DBS compared to baseline regardless of ON/OFF medication state in a randomized double blind study in 14 patients with bilateral STN DBS (39). Xu et al. did not find any improvement on swallowing function based on the item on Unified Parkinson's Disease Rating Scale (UPDRS) Part II in 85 PD patients assessed on an average of 4.9 years after STN DBS (mixed unilateral and bilateral STN DBS) at ON/OFF medication state (and the swallowing function was even worse ON DBS) (40). Troche et al. reported significantly worse in the PA score of VFSS in 14 PD 6 months after unilateral STN DBS at ON medication state (20). Kraus reported that at least three

patients developed worsening dysphagia or new dysphagia after bilateral STN DBS in a group of 27 PD patients during a mean of 30 months follow-up, based on the assessment for adverse effect, with unclear medication state though (8). Add-on stimulation of substantia nigra reticular (SNr) to STN did not have beneficial effect (41). Worsening of the dysphagia could be related to the suboptimal placement of the DBS electrodes or suboptimal programming in some cases, as turning off or reprogramming of the DBS made the swallowing symptoms better or go away in these cases (42, 43).

Some studies even reported beneficial effects on the swallowing function but mostly at OFF medication status, on subjective measures, or at LFS. Ciucci et al. reported significantly improved pharyngeal composite score and transit time by VFSS in ON DBS compared to OFF DBS at OFF medication status

TABLE 1 | The effect of DBS on swallowing functions.

| References | Diseases, targets (STN vs. GPi vs. PSA/cZi) and side (Unil vs. Bil) | Age at study, and/or disease duration (Mean \pm Std, unless noted) (Years) | Design and assessment | DBS settings | Outcome (ON/OFF medication, ON/OFF DBS) |
|------------|---|--|--|---|---|
| (8) | PD, Bil STN | Age of 57.7 ± 8.4 yo, PD duration of 14.4 ± 5.8 years | Retrospective chart review, in 27 PD, unknown M/F ratio, assessed dysphagia after DBS, as adverse effect, in a mean of 30 months after DBS, unclear ON or OFF medication status when and how the dysphagia was assessed. Medication dose was also reduced by 39% at 12 months and 30% at 30 months. | Unknown | At least three patients developed worsening or new dysphagia after the DBS, in a mean of 30 months post-operation (post-op). |
| (16) | PD, Bil STN | Age of 64.0 ± 8.0 yo and PD duration of 12.9 ± 4.9 years, s/p Bil STN-DBS for 4.4 ± 4.9 years. | Prospective, sequence randomized, crossover, double-blind study in seven PD patients with refractory FOG at HFS of 130 Hz and ON medication, each received VFSS under DBS of 130, 60 Hz, or OFF DBS, all ON medication. The laryngeal PA events and a swallowing questionnaire were assessed. UPDRS-III motor score, axial subscore, tremor subscore, and FOG by a questionnaire and stand-walk-sit test were also assessed. DBS condition with the least FOG (60 Hz) was maintained for 6 weeks on average, and patients were assessed again then (at 60 Hz). Changes in measurements between the 60 Hz and 130 Hz at initial assessment, and between 60 Hz of 6 weeks apart were analyzed, with swallowing function as primary and the remainder as secondary outcomes. Changes between other DBS conditions were also explored. | Amplitudes: Rt 3.1 ± 0.4 V; Lt 3.2 ± 0.4 V. Pulse widths: Rt 81.4 ± 14.6 μ s; Lt 90.0 ± 24.5 μ s. Frequencies: 130, 60 Hz, OFF Configurations: 13 active contacts on monopolar and one active contact on bipolar configurations. | Compared with the routine 130, 60 Hz significantly reduced aspiration frequency by 57% on VFSS and reduced the perceived swallowing difficulty by 80% on questionnaire. It also significantly reduced FOG, overall axial symptoms and parkinsonism. The benefits at 60 Hz stimulation persisted over the 6-week assessed. |
| (17) | PD, Bil STN | 68.5 ± 5.9 yo, PD duration of 14.2 ± 5.7 years and DBS duration of 3.5 ± 4.0 years | A prospective, sequence randomized, crossover, double-blind study, PD patients with DBS refractory FOG at 130 Hz and ON medication were randomized to sequences of 130, 60 Hz, or OFF DBS to assess swallowing function by VFSS, FOG severity (stand-walk-sit test and FOG questionnaire) and motor function (UPDRS-III) at initial visit (V1) and follow-up visit (V2, after being on 60 Hz stimulation for an average of 14.5 months), in usual ON medication state. The frequency of aspiration events, perceived swallowing difficulty and FOG severity at 60 Hz compared with 130 Hz at V2, and their corresponding changes at V2 compared with V1 at 60 Hz were set as primary outcomes, with similar comparisons in UPDRS-III and its subscores as secondary outcomes. | Amplitudes: L: 3.0 ± 0.4 V, R: 2.9 ± 0.3 V. Pulse widths: L: 76.0 ± 24 μ s, R: 68.0 ± 14 μ s Frequencies: 130, 60 Hz, OFF Configurations: 20 leads on monopolar, 2 leads on bipolar; 16 on dorsal and 6 on ventral active contacts. | All 11 participants completed V1 and 10 completed V2. They found benefits of 60 Hz compared to 130 Hz in reducing aspiration frequency, perceived swallowing difficulty, FOG severity, bradykinesia and overall axial and motor symptoms at V1, with persistent benefits on all of them except dysphagia at V2, with overall decreasing efficacy when comparing V2 to V1. |

(Continued)

TABLE 1 | Continued

| References | Diseases, targets (STN vs. GPi vs. PSA/cZi) and side (Unil vs. Bil) | Age at study, and/or disease duration (Mean \pm Std, unless noted) (Years) | Design and assessment | DBS settings | Outcome (ON/OFF medication, ON/OFF DBS) |
|------------|---|---|--|--|--|
| (20) | PD, Unil STN or GPi | PD duration 11.21 \pm 5.21 years for STN, 12.11 \pm 4.15 years for GPi | Retrospective chart review, 33 PD, M/F 28/5, 14 on Unil STN, 19 on Unil GPi, before and 6 months after DBS on PA score of VFSS and SWAL-QOL scores. The assignment on the target was not randomized. | Unknown | PA scores significantly worsened in STN but not in GPi at ON DBS state and ON medications state. No change in SWAL-QOL scores before and after the DBS for either group. However, the GPi group had worse swallowing function at the baseline than the STN before the DBS. |
| (22) | PD, Bil cZi | Age 49–71 yo, median 62 yo; disease duration 6.1 \pm 2.8 years. | Open label, prospective longitudinal study, 8 PD patients, M/F 6/2, Bil cZi, swallowing function before and 6 and 12 months after DBS on any of the swallowing parameters, assessed by FEES and self-assessment questionnaire. Pre-op patients were examined ON (1.5 times of the ordinary levodopa equivalent) and OFF meds. Post-op ON medication, with ON/OFF DBS. | Unknown | No clear-cut effect of DBS at 6 and 12 months on any of the swallowing parameters except the pre-swallow spillage that was slightly worsened ON DBS at 12 months post-op. Overall no negative effect on swallowing function. |
| (23) | PD, Bil cZi | Median 53 yo for PD and 54 yo for controls. | Open label, prospective, longitudinal study, 9 PD, M/F 7/2, compared to 9 controls in SWAL-QOL scale and VA scale before (ON and OFF meds) and 12 months after Bil cZi DBS (ON medications, ON/OFF DBS) | Unknown, except 125–160 Hz | No significant differences between the pre- or post-op scores. No difference between PD and controls. cZi not negatively affecting the swallowing QOL. |
| (24) | PD, Bil cZi | Median 57 yo, with median disease duration of 6 years | Open label, prospective longitudinal study on 14 PD patients with Bil cZi, M/F 12/2, extending their previous report on swallowing function using FEES, before (ON medications, 1.5 \times of the original dose) and 12 months after DBS at ON medications (original dose) and ON DBS On vs. OFF DBS state, on PA scale, secretion severity scale, premature spillage and pharyngeal residual. | Unknown, except 125–160 Hz | cZi DBS was found not to have a negative impact on swallowing safety, with no changes on PA, pharyngeal residual or premature spillage. Speech function noted to be worse. |
| (25) | DYT6, Bil GPi | Age at DBS 8–57 yo. Disease duration before DBS 2–19 years. Length follow up after the DBS: 1–16 years 4 months. | Retrospective multiple centers case serials of medical records in 14 DYT6 patients, 9F, 5M, with BFMDRS and the sub-scores as the outcome measures at a median of 4 year 10 months post-surgery compared to that before the surgery | Stimulation frequency 90–180 Hz at their last follow up visit. Details unknown. | No improvement in swallowing and speech function in 10/14, and some improvement in 4/14. |
| (26) | Primary general or segmental dystonia, Bil GPi | 20 neurostim (13 M) and 20 sham stim (14 M), age 40.5 \pm 13.5 and 38.4 \pm 13.8 yo, respectively; disease duration 21.8 \pm 8.1 and 17.2 \pm 7.5 years, respectively | A randomized, controlled trial, with 40 patients randomly assigned either to neurostim or sham stim for 3 months. Primary end point was the change from baseline to 3 months on BFMDRS. Subsequently all patients received open label neurostim; blinded assessment was repeated after 6 months of active treatment. | Neurostim: 3 months 3.2/122.2/139.5 (V/ μ s/Hz) 6 months: 3.2/123.7/135.7 Sham stim: 3 months: N/A 6 months: 3.2/131.3/132.8 unknown contacts, xyz (mm): 20 to 21/2/–2 to –6 | Significantly benefit in dystonia on neurostim than sham stim at 3 months. No improvement in swallow and speech after 6 months neurostim. |

(Continued)

TABLE 1 | Continued

| References | Diseases, targets (STN vs. GPi vs. PSA/cZi) and side (Unil vs. Bil) | Age at study, and/or disease duration (Mean \pm Std, unless noted) (Years) | Design and assessment | DBS settings | Outcome (ON/OFF medication, ON/OFF DBS) |
|------------|---|--|--|--|--|
| (27) | Dystonia, Bil GPi | 19 patients (12 M); Age at surgery 47.3 ± 12 yo; mean disease duration 13.7 ± 10.9 years, with isolated generalized ($n = 10$), segmental ($n = 4$) or cervical dystonia ($n = 5$) and chronic GPi DBS for up to 16 years (11 ± 2.6 years) for follow up. | Retrospective analysis in 19 patients, analyzing BFMDRS at baseline, short-term (range 3–36 months) and long-term follow-up (range 93–197 months). Quality of life and mood were evaluated using the SF-36 and Beck Depression Index questionnaires. | Unknown | GPi DBS is a safe and efficacious long-term treatment for dystonia with sustained effects on motor impairment and disability, accompanied by a robust improvement in mood and quality of life. The most common stim-related side effects were dysarthria ($n = 4$), swallowing difficulties ($n = 1$) and bradykinesia ($n = 2$), which were all partially reversible with adjustment of stimulation settings. |
| (28) | Dyskinetic CP, Bil GPi | Age 30 ± 6.8 yo at study, about 4 years after the surgery | Eight patients with dyskinetic CP, s/p Bil GPi were openly assessed by BFMDR Scale. Subjective impression of the extent of postoperative change as well as gait, speech and swallowing performances (by fiberoptic laryngoscopy) also assessed during ON/OFF DBS. | 1.2–3.8 V/90–210 μ s /all 120–180 Hz, except one 5 Hz. Active contacts: 0, 8, 0, 8, 0, 8, 3, 7, 2, 5, 0, 4, 0, 4, 1, 5. | No change in objective assessment of speech and swallowing function after DBS compared to baseline, but patients reported subjective improvement. |
| (29) | Meige Syndrome, Bil GPi | Age at surgery 64.5 ± 4.4 yo, mean PD duration 8.3 ± 4.4 years | Retrospective study, in 12 patients with Meige syndrome, M/F 6/6, followed up to 78 mon after Bil GPi. BFMDR speech and swallowing subscore in short-term (4.4 ± 1.5 months) and long-term (38.8 ± 21.7 months) follow-up. | Rt 2.4–5.0 V/60–210 μ s/130–210 Hz, Lt 2.2–4.9 V/90–210 μ s/130–210 Hz. Most of them on bipolar or monopolar | BFMDR speech and swallowing subscore improved by 44 and 64% respective in short-term and long-term assessment. |
| (30) | Meige syndrome, Bil GPi | Age 58.0 ± 7.8 yo, duration: 8.7 ± 7.6 years. | Retrospective study in 11 cases, unknown M/F, Meige syndrome, Bil GPi DBS, on BFMDRS, f/u for more than 12 months (mean 23.1 ± 6.4 months). | 3.4 ± 0.6 V/ 133.6 ± 576.4 μ s/ 143.1 ± 38.1 Hz (last follow up), xyz 21.6/2.8/– 4, unknown contacts | Improved by 68.4% for speech and swallowing subscore at 12 months after DBS. No difference between 12 and 24 months |
| (31) | Meige syndrome, Bil GPi | Mean age 58.5 yo, disease duration 12.5 years | Open label, prospective follow up study, in 6 cases of Meige syndrome, M/F 2/4 Bil GPi, BFMDRS assessed before and after DBS compared to the baseline scores in short-term (3 months) and long-term (6–60 months) post-op follow up. | 3.4–4.1 V or 2.5–3.2 mA, 117–120 μ s, 130–160 Hz; 9 on double monopolar. | Speech/swallowing subscore improved by 49% in short-term and 39% in long-term assessment. |
| (32) | Meige syndrome, | Age: 41.5 yo, Bil GPi | Retrospective study, 40 patients (M/F 16/24), Bil GPi with Meige syndrome. Motor functions were assessed using the BFMDRS and subscores. The severity of patients' dystonia was evaluated before surgery and at follow-up DBS. | All 40 patients received monopolar stimulation with the average voltage of 2.6 ± 0.8 V, pulse width of 90.0 ± 21.1 μ s, and frequency of 88.0 ± 21.3 Hz. | At 6, 12, and 24 months after surgery, the BFMDRS subscores of eyes, mouth, speech, and swallowing and mouth movement were significantly better. The overall improvement rate was 83% |
| (36) | PD, Unil and Bil STN | Median 61 yo (41–72), disease course unknown | Open label, prospective study, 11 patients (5 Unil and 6 Bil STN) evaluated before and 6 and 12 months after DBS, using self-estimation on a VA scale (11 patient) and FEES (8 patient) including PA scale, secretion severity scale, pre-swallow spillage, pharyngeal residue and clearance, ON/OFF DBS, at ON medication | Unknown | Subjectively improved with DBS on self-assessments, but no improvement on objective FEES. |

(Continued)

TABLE 1 | Continued

| References | Diseases, targets (STN vs. GPi vs. PSA/cZi) and side (Unil vs. Bil) | Age at study, and/or disease duration (Mean \pm Std, unless noted) (Years) | Design and assessment | DBS settings | Outcome (ON/OFF medication, ON/OFF DBS) |
|------------|---|--|--|--|---|
| (37) | PD, Bil STN | Age of 66.6 ± 6.2 yo, with 11.6 ± 5.7 years of PD | Open label study, 18 patients, M/F 8/10, Bil STN, with clinical swallowing impairments, evaluated at pre- and 6 month post-DBS, using VFSS comparing ON DBS ON medication to pre-op ON medication (though with more LED than post-op) on oropharyngeal transit times, speed of tongue movement and laryngeal elevation delay time and dysphagia scale score, and comparing ON DBS to OFF DBS at ON medication post-op as well. | Unknown | STN-DBS may not significantly improve overall swallowing function, but may improve tongue movement and laryngeal elevation |
| (38) | PD, Bil STN | Age of 57.3 ± 4.7 yo; disease duration 13.0 ± 2.4 years | Longitudinal prospective descriptive study, 10 PD, M/F 10/0, Bil STN DBS, clinical assessment of anamnesis, Functional Oral Intake Scale, and clinical swallowing function before and 6 months after the DBS | Unknown DBS configurations and parameters, or medication status (but no changes in levodopa equivalent dose pre and post-DBS). | No change in swallowing function 6 months after DBS compared that before DBS. |
| (39) | PD, Bil STN and Bil GPi | 27 PD, 14 with 16.8 ± 6.2 years of PD for STN, 13 with 15.1 ± 10.2 years of PD for GPi. 27 age and gender matched healthy control subjects. | Randomized, double-blind, longitudinal study, with matched healthy controls, in 14 PD with Bil STN and 13 PD with Bil GPi, M/F 25/2, assessed before (OFF/ON medication) and 6 months after DBS (OFF/ON medication and OFF/ON DBS) on self-scaled and externally-scaled jaw peak velocity. | Mean amplitude 3.28 V, with 70% of the patients on 90 μ s of pulse width (60, 120, and 150 in two subjects each), and 71% on 185 Hz (the rest was between 130 and 150 Hz). xyz for STN: 12/–4/–4 mm; xyz for GPi: 20–21/2/–4 mm. No specific contact settings available. | OFF medications: DBS in STN worsened while GPi improved jaw velocities by self-scale 6 months after DBS compared to baseline. ON medications: velocities in STN still worse than the baseline, but no difference in GPi. Similar results also revealed by external scale. No benefit of STN or GPi on jaw velocity in PD compared to the best medication therapy. STN could even be harmful |
| (40) | PD, Bil or Unil STN | Age of 57.9 ± 9.6 yo, disease duration 8.3 ± 3.7 years | Retrospective study, in 85 PD, M/F 52/33, Bil (51) or Unil (34) STN DBS, assessed before (ON/OFF meds) and 4.9 years after DBS (ON/OFF medication and ON/OFF DBS) on UPDRS-II (swallowing) and UPDRS-III (speech) | 2.9–3.1 V/86–88 μ s/163–174 Hz | Long-term STN DBS failed to improve swallowing and speech (swallowing and speech parameters even worsened with DBS). |
| (41) | PD, Bil STN, | Age of 63.4 ± 6.7 yo (10 M), disease duration unknown. DBS duration at least 6 months post-op. Healthy control (HC) age of 68.1 ± 10.7 yo (16 M) | Controlled, randomized, double blind, crossover trial, 15 PD patients were assessed with DBS Stim OFF, STN-DBS, STN + SNr- DBS. Patients and 32 age-matched HC were examined clinically and by FEES to evaluate the swallowing function. The primary end point was the assessment of residues, secondary endpoints were penetration/aspiration, leakage, retained pharyngeal secretions, drooling, and assessments of the patient's self-perception of swallowing on a VA scale. | The tip of the electrodes >4.5 mm below to AC-PC line. Various DBS parameters. All at HFS 125–130 Hz. | Eleven completed the study. Four dropped out from STN/SNr Stim due to side effects. Compared with HC, PD patients showed significantly more pharyngeal residues in Stim OFF and both DBS modes. Residues or aspiration events were found in 80% of the patients under STN-Stim. STN + SNr-Stim had no additional positive effect on swallowing function compared to STN-DBS. |

(Continued)

TABLE 1 | Continued

| References | Diseases, targets (STN vs. GPi vs. PSA/cZi) and side (Unil vs. Bil) | Age at study, and/or disease duration (Mean \pm Std, unless noted) (Years) | Design and assessment | DBS settings | Outcome (ON/OFF medication, ON/OFF DBS) |
|------------|---|--|--|---|--|
| (42) | PD, Bil STN | 74 yo, male, PD of 14 years | Case report. The patient experienced stridor and dysphagia with pulmonary restriction and aspiration, which started 4 months after Bil STN DBS, and significantly improved when the DBS was OFF. | Initial left: monopolar(unknown exact contact) 1.6 V/90 μ s/130 Hz; right: monopolar, 1.6 V/60 μ s/130 Hz. Final left: bipolar, 1.5 V/60 μ s/160 Hz; right: bipolar 2.1 V/60 μ s/160 Hz | All his symptoms improved after DBS turned off or adjusted to bipolar settings, suggesting that the initial dysphagia was related to suboptimal placement or programming. |
| (43) | PD, Unil STN (R), followed by Unil GPi (L) DBS | PD since 29 yo, age of 51 yo had Rt STN DBS sub-optimally placed. | Case report. A 62 yo male PD, VFSS after Bil DBS (Rt STN first, followed by Lt GPi), with dysphagia confirmed by VFSS, which improved when the suboptimal Rt STN was OFF. Reassessed with improvement after DBS parameters optimized. | Rt STN, 3.8 V/90 μ s/135 Hz, Lt GPi, 2.9 V/120 μ s/135 Hz | Marked, immediate improvement with optimizing DBS settings compared to previous DBS settings. |
| (45) | PD, Bil STN | 2 women (62 and 76 yo) and 12 men (mean 59 yo; range 41–75 yo) | Open label, prospective study, 14 patients, M/F 12/2, Bil STN, VFSS pre- and 3- and 12-mon post-DBS, ON/OFF DBS and ON/OFF medication, with DHI being assessed as well at each time. | Unknown | Subjective but no objective improvement in swallowing function. Specifically, there was a trend toward improved swallowing response for solid intake and oral preparation of thin liquid in OFF meds with ON/OFF 12 mon later. The remaining swallowing parameters showed no change regardless of the DBS or medications states. DHI revealed improved self-perception of swallowing 3 and 12 months post-op compared with the baseline. |
| (46) | PD, Bil STN, | Age of 61.2 ± 6.2 yo at surgery, the duration of PD 16.7 ± 4.4 years | Open label, prospective study, in 36 PD, M/F 22/12, pre-op (ON and OFF meds) and 12 and 24 months post-op. Post-op ON medications (but with reduced dosage) and ON DBS, comparing with pre-op OFF/ON medications baseline, on salivation, swallowing and sensory complaints in UPDRS-II corresponding items. | 3.2 ± 0.4 V; 63.3 ± 9.5 μ s; 136 ± 14.8 Hz at 12 mon; 3.3 ± 0.3 V; 65.0 ± 11.3 μ s; 136.1 ± 12.5 Hz at 24 mon. Most of them on mono polar setting | Salivation, swallowing and sensory complaints ameliorated by ON DBS with reduced meds compared to pre-op OFF medication, but no changes compared to pre- op ON medication status. (Levodopa equivalent dosage 60 and 59% reduction at 12 and 24 months, respectively) |
| (47) | PD, Bil STN | PD onset age of 49.3 ± 10.2 yo. PD duration at time of surgery 135.3 ± 68.7 months | Retrospectively collected data for a prospective study in 18 PD, M/F 11/7, ON medication, before and 20 months after DBS (medication reduced by 50%), comparing swallowing before vs. after DBS and ON vs. OFF DBS using VFSS and "New Zealand Index for Multidisciplinary Evaluation of Swallowing Subscale One" for qualitative and "Logemann-MBS-Parameters" for quantitative evaluation. | 0.5–6.0 V/60–120 μ s/65–180 Hz. Configurations: 26 of the leads were monopolar; the rest were bipolar, double bipolar and double monopolar. | Postoperatively, medications reduced by 50%. No clinically relevant effect of DBS on swallowing was observed using qualitative parameters. However, quantitative parameters found significant changes of pharyngeal parameters with ON DBS as compared to pre-op and OFF DBS mostly with fluid consistency. They concluded that DBS modulates the pharyngeal phase but has no clinically relevant influence on overall deglutition. |

(Continued)

TABLE 1 | Continued

| References | Diseases, targets (STN vs. GPi vs. PSA/cZi) and side (Unil vs. Bil) | Age at study, and/or disease duration (Mean \pm Std, unless noted) (Years) | Design and assessment | DBS settings | Outcome (ON/OFF medication, ON/OFF DBS) |
|------------|---|---|--|---|--|
| (48) | PD, Bil STN | Age of 58.0 ± 6.5 yo, disease duration 10.9 ± 4.7 years | Open label study in 20 PD, M/F 15/5, Bil STN DBS, The frequency and severity of gastrointestinal symptoms (including dysphagia) based on a structured gastrointestinal dysfunction questionnaire also assessed, at OFF medication state. | Unknown configuration but 1–2 V/60 μ s/130 Hz | DBS improves gastric motility and symptoms. Gastrointestinal dysfunction questionnaire improved by > 50% with dysphagia 3 months post-op, at OFF medication but ON DBS |
| (49) | PD, Bil STN | Age of 67.5 ± 6.5 yo, disease duration 15.2 ± 4.8 years. DBS median duration of 13 months | Open label study in 34 PD (M/F 23/11), OFF medication state, ON DBS compared to OFF, in subjective VAS for non-motor symptoms, including dysphagia in the study | Unknown | DBS improved the dysphagia. |
| (50) | Meige syndrome, Bil and Unil GPi | Median ages 61 (41–72) yo, and median duration 6.5 (1–13) years. | Retrospective review of videos and charts in 6 cases, M/F 4/2, 1 Unil and 5 Bil GPi, evaluated 6 months and 12 months for UDRS and BFMDR including speech and swallowing function. | 1.5–3.5 V/60–450 μ s/10–185 Hz. Configurations: 9 monopolar, 1 bipolar, and 1 double monopolar | Swallowing and speech did not improve in this cohort. |
| (51) | Dystonia (Meige syndrome and crural dystonia), Bil GPi | Mean age 42.8 (30–67) yo, mean disease duration 18.5 (12–25) years | Retrospective analysis, 11 segmental dystonia (9 Meige syndrome, 2 crural type dystonia), M/F 3/8, Bil GPi, assessed pre-op and post-op 6–12–24–36 months, by BFMDRS | 3.2 ± 0.5 V/150 \pm 60 μ s/130 Hz. Monopolar configuration in all patients, with ventral contacts in all except two patients. | Speech and swallowing function improved significantly at 6 months and 36 months post-op. |
| (52) | ET, PSA, 19 patients with ET had Unil and 2 had Bil PSA DBS. | Age of 63.6 ± 14.8 yo, ET duration of 20.3 ± 13.7 years. | A prospective study in 21 patients (M/F 14/7) with ET were included in this study for the efficacy and safety of PSA DBS. Eight patients presented a postoperative mild dysphasia that regressed within days to weeks. | The mean stim parameters: 2.5 \pm 0.8 V, 61.4 \pm 6.0 μ s, 165 \pm 21 Hz, and monopolar stim in 78% leads. | Effective and safe in tremor control, with transiently mild dysphagia regressed within days to week |

STN, subthalamic nucleus; GPi, globus pallidus interna; ViM, ventralis intermedius; PSA, post-subthalamic area; cZi, caudal zona incerta; M, male; F, female; yo, year-old; FOG, freezing of gait; s/p, status post; Bil, Bilateral; Unil, unilateral; HFS, high frequency of stimulation; LFS, low frequency of stimulation; VFSS, videofluoroscopic swallow study; FEES, fiberoptic endoscopic evaluation of swallowing; PA, penetration-aspiration; UPDRS, Unified Parkinson's Disease Rating Scale; V, voltage; L, left; R, right; SWAL-QOL, swallowing related quality of life; VA, visual analogue; DYT6, dystonia by the THAP1 mutation; BFMDR, Burke-Fahn-Masden Dystonia Rating Scale; neurostim, neuronal stimulation; stim, stimulation; SNr, substantia nigra reticular; DHI, Dysphagia Handicap Index; UDRS, Unified Dystonia Rating Scale; ET, essential tremor.

in 14 PD patients assessed at least 3 months after STN DBS (44). Kulnef et al. reported a subjective improvement in a self-assessment of swallowing function, but not on objective FEES, at ON DBS compared to OFF DBS at ON medication state in 11 PD patients 6 and 12 months after STB DBS (a mixed bilateral and unilateral DBS) (36). A similar result was also reported by Silbergleit et al. in 14 PD patients 3 and 12 months after bilateral STN DBS assessed by VFSS who found subjective but not objective improvement in swallowing function at ON/OFF medication state (45). Zibetti et al. found improved salivation and swallowing function in 36 patients with PD and bilateral STN DBS at 12 and 24 months after DBS at OFF medication state but no difference at ON medication compared to the pre-operational state (although the levodopa dosage was also reduced then) (46). Lengerer et al. reported no clinically relevant influence of DBS on swallowing function using qualitative parameters in 18 PD patients with bilateral STN DBS, but quantitative parameters found improved pharyngeal parameters with ON DBS compared to preoperative condition or OFF DBS, mostly with fluid consistency (47). Krygowska-Wajs et al. reported a 50% improvement on dysphagia on the gastrointestinal dysfunction questionnaire in 20 PD patients, assessed 3 months after bilateral STN DBS at ON DBS but OFF medication state (48). Wolz et al. studied 34 PD patients at a median of 13 months after the bilateral STN DBS and found improved dysphagia in subjective visual analog (VA) scale at ON DBS compared to OFF DBS and OFF medication state (49). Xie et al. reported acute and short-term improvement of objective and subjective swallowing function on PD patients with bilateral STN DBS in randomized double blind crossover studies under LFS (60 Hz) compared to those under HFS (130 Hz) in patients with HFS and medication refractory FOG at ON medication state (16, 17). However, the long-term (more than a year) benefit of LFS on the swallowing function was not demonstrated (17).

PD With GPi DBS, and Compared to STN as Well

Troche et al. performed a retrospective chart review in 33 PD patients, with unilateral GPi DBS in 19 and unilateral STN DBS in 14 patients, looking at PA score of VFSS and patient-reported swallowing-related quality of life (SWAL-QOL) before and 6 months after DBS (20). PA scores significantly worsened in STN but not in GPi DBS assessed at ON medication state. No change in SWAL-QOL score was found before and after the DBS in either group of patients. The GPi group patients had worse swallowing function than the STN group at baseline. Robertson et al. randomized the PD patients to STN or GPi in double-blind study in 14 PD with bilateral STN and 13 PD with bilateral GPi, assessed before (OFF medication vs. ON) and 6 months after DBS (OFF medication vs. ON medication and OFF DBS vs. ON DBS) on self-scaled and externally scaled jaw peak velocity (39). At OFF medication state, DBS in STN worsened, while GPi improved the jaw velocities after DBS compared to baseline. At ON medication state, the velocities in STN were worse than the baseline, but no difference in GPi. The authors concluded that there was

no benefit of STN or GPi on jaw velocity in PD compared to the best medication therapy, and that STN could even be harmful.

PD With PSA/cZi DBS

The swallowing function of eight PD patients with bilateral cZi DBS was assessed before and after DBS by FEES and questionnaire (22). There was no clear-cut effect of DBS at 6 and 12 months on any of the swallowing parameters except for the pre-swallow spillage, which was slightly worse in the ON stimulation state 12 months after DBS, although the medication was cut down by one-third post-operatively. Sundstedt et al. found no significant difference in SWAL-QOL score and VA scale score 12 months after the DBS at ON medication state in nine PD patients with bilateral cZi (23). Sundstedt et al. also did a prospective longitudinal study on 14 PD patients with bilateral cZi, extending their previous report on swallowing function, before and after DBS at ON medications and ON DBS vs. OFF DBS state by FEES (24). They found that cZi DBS did not have a negative impact on swallowing function, with no changes on PA scores, pharyngeal residual or premature spillage, although the medication was cut down by one-third post-operatively.

Dystonia and Meige Syndrome With GPi DBS

Bilateral GPi DBS has been shown to improve the swallowing function in majority of the studies in patients with Meige syndrome, as demonstrated by improved Burke-Fahn-Masden Dystonia Rating Scale (BFMDRS) speech and swallowing scores in 12 patients who followed up to 38 months on average (29), in 11 patients who followed up for 23 months on average (30), in 6 patients who followed up to 60 months (31), and in 40 patients who followed up at 6, 12, and 24 months after surgery (32). There was one study by Limotai et al. in six patients with Meige syndrome, with one unilateral and five bilateral GPi, evaluated 6 and 12 months after DBS for Unified Dystonia Rating Scale (UDRS) and BFMDR speech and swallowing function, but they did not find improvement in speech and swallowing function in this cohort (50). Bilateral GPi also has been used in patients with 11 non-Meige dystonia patients and 9 Meige syndrome patients (51), with significantly improved swallowing and speech scores in BFMDR up to 36 months after the DBS. Bilateral GPi also has been used in primary generalized dystonia and segmental dystonia patients (25–27), and dyskinetic cerebral palsy patients (28), but no changes or just slightly worsening in speech and swallowing function after DBS compared to baseline were reported.

ET With ViM or PSA/cZi DBS

There is no specifically designed study on the evaluation of dysphagia in ET by ViM or PSA/cZi DBS, although transient mild dysphagia after the DBS implantation surgery was reported, which usually resolved within several weeks (21, 52).

DISCUSSIONS

The majority of the studies were open label, retrospective or prospective, small-size studies, with subjective and/or objective assessments of swallowing function, at ON DBS compared to OFF DBS and ON/OFF dopaminergic medication state. There were only a few prospective randomized double blind studies (16, 17, 39), a few on comparing different targets (20, 39), and a few on comparing different frequency stimulations (16, 17). Most studies used bilateral targets although some were unilateral or mixed targets, as bilateral DBS is more likely to affect the axial symptoms, including dysphagia. Some of them were not fairly compared, as there were reduced dopaminergic medications post-operatively. Although the medications probably would not have a major impact on the objective swallowing functions (1, 2), beneficial effect of dopaminergic medication was also reported in a small proportion of patients (53). Taking dopaminergic medications could also affect the subjective measure with overall improvement of the parkinsonism. Therefore, it probably could explain why some studies showed improved swallowing function at subjective measures but not objective measures at ON medication state, and why the beneficial effect of DBS is more appreciated at OFF medication state or less appreciated at ON medication state.

We found that STN DBS at usual HFS could have beneficial effect (more so on subjective measures of scales, questionnaires, or swallowing item in UPDRS-II, and/or OFF medication state), no effect, or detrimental effect (more so on objective measures of VFSS or FEES, and/or ON medication state) on swallowing function in patients with PD. The effect of LFS stimulation on FOG has been consistently reported positively by many studies, as summarized in a review article (18). However, there have been only a few studies addressing its effect on dysphagia. Two studies of randomized double blinded crossover prospective studies in the short- and long-term effects did find significant benefit of LFS on acute and short-term studies (16, 17), but not the long-term benefits (17), although the long-term effect remains unclear given the small sample size and sub-clinical dysphagia in participants, which could limit the power to detect the potential difference. These studies were conducted at ON medication state in bilateral STN DBS patients with refractory FOG to HFS; hence, the beneficial effect should not necessarily be generalized to the whole PD population.

GPI DBS seems more likely to improve the swallowing function or process compared to the STN DBS, more so at OFF medication state (20, 39). In contrast to STN DBS, GPI DBS does not have detrimental effect on swallowing function or process at ON medication state (20, 39). Even though the non-matched baseline swallowing function in the two groups, and the retrospective and non-randomized design in assigning the targets could all affect the interpretation of the favorable PA scores in unilateral GPI compared to STN DBS (20), similar results were also obtained in a randomized, double-blind study comparing the effect of bilateral GPI to bilateral STN DBS on jaw velocity (39), suggesting that GPI DBS is

probably more favorable than STN DBS in overall swallowing function for PD patients, particularly at OFF medication state. Although there is no benefit of STN or GPI DBS on swallowing function in PD compared to the best medication therapy (at ON medication state), STN DBS could even be harmful at ON medication state, based on limited studies available so far.

Targeting GPI seemed to have positive results on Meige syndrome in the majority of the studies (29–32). One of the possibilities behind the benefit is the direct effect on the pharyngeal and laryngeal dystonia by GPI, which could help to improve dysphagia symptoms. There was no study on using STN in Meige syndrome and other dystonia on dysphagia. Hence, it is not certain if targeting STN would have similar benefit, as STN has also been found to be beneficial to dystonia in PD (54). There is no beneficial effect of GPI DBS on dysphagia in patients with primary generalized dystonia, segmental dystonia, and dyskinesic cerebral palsy patients, and there rarely is worsening effect either (25–28).

The PSA and cZi are relatively new targets. They have the potential to provide more efficient stimulations but fewer side effects due to their anatomic characteristics, with the fibers from both the basal ganglia and cerebellar merging together at the PSA/cZi area, and studies so far found that PSA/cZi DBS rarely has a detrimental effect on swallowing functions in patients with PD or tremor (21, 55). There has been limited information on the effect of ViM DBS on swallowing function to assess so far.

In summary, we found that STN DBS at usual HFS could have beneficial effect (more so on subjective measures and/or OFF medication state), no effect, or detrimental effect (more so on objective measures and/or ON medication state) on swallowing function in patients with PD, while LFS of STN could have beneficial effect on swallowing functions in PD patients with FOG refractory to HFS. GPI DBS could have a beneficial effect (regardless of medication state, and subjective or objective measures), or no effect (more so at ON medication state), but no detrimental effect (in contrast to STN DBS, even at ON medication state) on swallowing function in PD, suggesting that GPI DBS could be probably more favorable than STN DBS in overall swallowing function for PD patients, particularly at OFF medication state. GPI DBS also has beneficial effects on swallowing function in the majority of the studies on Meige syndrome but no beneficial effect on swallowing function in other dystonia. Stimulation of PSA/cZi rarely has detrimental effect on swallowing functions. The effect of ViM on swallowing function in ET patients is too limited to assess. Overall, most of them are retrospective, open label, small-size studies, with medication reduction post-operatively. There are only a few randomized, double blind studies, a few on direct comparisons among targets or between stimulation frequencies. The overall evidence levels of these studies are low, ranging from IV to III. Information on swallowing function by DBS remains limited. Well-designed studies and direct comparison of targets and stimulating parameters are further needed to gain more insights on the effect of DBS on swallowing function in movement disorders.

DATA AVAILABILITY STATEMENT

All datasets analyzed for this study are included in the article and the **Table 1**.

AUTHOR CONTRIBUTIONS

KT and TX initiated the study and made the study PRISMA compatible systematic review. HY, SQ, LB, and TX performed

search and initial writeup. All authors edited and worked on the submitted manuscript.

FUNDING

KT was partially supported by NIH R03DE028395. TX was partially supported by NIH U01 project and National Parkinson's Foundation.

REFERENCES

- Fuh J-L, Lee R-C, Wang S-J, Lin C-H, Wang P-N, Chiang J-H, et al. Swallowing difficulty in Parkinson's disease. *Clin Neurol Neurosurg.* (1997) 99:106–12. doi: 10.1016/S0303-8467(97)80006-6
- Hunter PC, Cramer J, Austin S, Woodward MC, Hughes AJ. Response of Parkinsonian swallowing dysfunction to dopaminergic stimulation. *J Neurol Neurosurg Psychiatry.* (1997) 63:579–83. doi: 10.1136/jnnp.63.5.579
- Deuschl G, Schade-Brittinger C, Krack P, Volkmann J, Schäfer H, Bötzel K, et al. A randomized trial of deep-brain stimulation for Parkinson's disease. *N Engl J Med.* (2006) 355:896–908. doi: 10.1056/NEJMoa060281
- Weaver FM, Follett K, Stern M, Hur K, Harris C, Marks WJ, et al. Bilateral deep brain stimulation vs best medical therapy for patients with advanced Parkinson disease: a randomized controlled trial. *JAMA.* (2009) 301:63–73. doi: 10.1001/jama.2008.929
- Follett KA, Weaver FM, Stern M, Hur K, Harris CL, Luo P, et al. Pallidal versus subthalamic deep-brain stimulation for Parkinson's disease. *N Engl J Med.* (2010) 362:2077–91. doi: 10.1056/NEJMoa0907083
- Williams A, Gill S, Varma T, Jenkinson C, Quinn N, Mitchell R, et al. Deep brain stimulation plus best medical therapy versus best medical therapy alone for advanced Parkinson's disease (PD SURG trial): a randomised, open-label trial. *Lancet Neurol.* (2010) 9:581–91. doi: 10.1016/S1474-4422(10)70093-4
- Schuepbach WMM, Rau J, Knudsen K, Volkmann J, Krack P, Timmermann L, et al. Neurostimulation for Parkinson's disease with early motor complications. *N Engl J Med.* (2013) 368:2038. doi: 10.1056/NEJMc1303485
- Krause M, Fogel W, Mayer P, Kloss M, Tronnier V. Chronic inhibition of the subthalamic nucleus in Parkinson's disease. *J Neurol Sci.* (2004) 219:119–24. doi: 10.1016/j.jns.2004.01.004
- Moro E, Lozano AM, Pollak P, Agid Y, Rehnchrona S, Volkmann J, et al. Long-term results of a multicenter study on subthalamic and pallidal stimulation in Parkinson's disease. *Mov Disord.* (2010) 25:578–86. doi: 10.1002/mds.22735
- Østergaard K, Aa Sunde N. Evolution of Parkinson's disease during 4 years of bilateral deep brain stimulation of the subthalamic nucleus. *Mov Disord.* (2006) 21:624–31. doi: 10.1002/mds.20776
- Romito LM, Contarino MF, Vanacore N, Bentivoglio AR, Scerrati M, Albanese A, et al. Replacement of dopaminergic medication with subthalamic nucleus stimulation in Parkinson's disease: long-term observation. *Mov Disord.* (2009) 24:555–61. doi: 10.1002/mds.22390
- St George RJ, Nutt JG, Burchiel KJ, Horak FB. A meta-regression of the long-term effects of deep brain stimulation on balance and gait in PD. *Neurology.* (2010) 75:1292–9. doi: 10.1212/WNL.0b013e3181f61329
- Rodriguez-Oroz MC, Obeso JA, Lang AE, Houeto J-L, Pollak P, Rehnchrona S, et al. Bilateral deep brain stimulation in Parkinson's disease: a multicentre study with 4 years follow-up. *Brain.* (2005) 128:2240–9. doi: 10.1093/brain/awh571
- Lau B, Meier N, Serra G, Czernecki V, Schuepbach M, Navarro S, et al. Axial symptoms predict mortality in patients with Parkinson disease and subthalamic stimulation. *Neurology.* (2019) 92:e2559–70. doi: 10.1212/WNL.00000000000007562
- Moreau C, Defebvre L, Destée A, Bleuse S, Clement F, Blatt JL, et al. STN-DBS frequency effects on freezing of gait in advanced Parkinson disease. *Neurology.* (2008) 71:80–4. doi: 10.1212/01.wnl.0000303972.16279.46
- Xie T, Vigil J, MacCracken E, Gasparaitis A, Young J, Kang W, et al. Low-frequency stimulation of STN-DBS reduces aspiration and freezing of gait in patients with PD. *Neurology.* (2015) 84:415–20. doi: 10.1212/WNL.0000000000001184
- Xie T, Bloom L, Padmanaban M, Bertacchi B, Kang W, MacCracken E, et al. Long-term effect of low frequency stimulation of STN on dysphagia, freezing of gait and other motor symptoms in PD. *J Neurol Neurosurg Psychiatry.* (2018) 89:989–94. doi: 10.1136/jnnp-2018-318060
- Xie T, Padmanaban M, Bloom L, MacCracken E, Bertacchi B, Dachman A, et al. Effect of low versus high frequency stimulation on freezing of gait and other axial symptoms in Parkinson patients with bilateral STN DBS: a mini-review. *Transl Neurodegener.* (2017) 6:13. doi: 10.1186/s40035-017-0083-7
- Ramirez-Zamora A, Hess CW, Nelson DR. Is interferon therapy for hepatitis c infection a treatable risk factor for parkinson disease? *JAMA Neurol.* (2019) 76:1006–7. doi: 10.1001/jamaneurol.2019.1377
- Troche MS, Brandimore AE, Foote KD, Morishita T, Chen D, Hegland KW, et al. Swallowing outcomes following unilateral STN vs GPi surgery: a retrospective analysis. *Dysphagia.* (2014) 29:425–31. doi: 10.1007/s00455-014-9522-0
- Xie T, Bernard J, Warnke P. Post subthalamic area deep brain stimulation for tremors: a mini-review. *Transl Neurodegener.* (2012) 1:20. doi: 10.1186/2047-9158-1-20
- Sundstedt S, Olofsson K, van Doorn J, Linder J, Nordh E, Blomstedt P, et al. Swallowing function in Parkinson's patients following Zona Incerta deep brain stimulation. *Acta Neurol Scand.* (2012) 126:350–6. doi: 10.1111/j.1600-0404.2012.01658.x
- Sundstedt S, Nordh E, Linder J, Hedström J, Finizia C, Olofsson K, et al. Swallowing quality of life after zona incerta deep brain stimulation. *Ann Otol Rhinol Laryngol.* (2017) 126:110–6. doi: 10.1177/0003489416675874
- Sundstedt S, Holmén L, Rova E, Linder J, Nordh E, Olofsson K, et al. Swallowing safety in Parkinson's disease after zona incerta deep brain stimulation. *Brain Behav.* (2017) 7:e00709. doi: 10.1002/brb3.709
- Danielsson A, Carecchio M, Cif L, Koy A, Lin J-P, Solders G, et al. Pallidal deep brain stimulation in DYT6 dystonia: clinical outcome and predictive factors for motor improvement. *J Clin Med.* (2019) 8:2163. doi: 10.3390/jcm8122163
- Kupsch A, Benecke R, Müller J, Trottenberg T, Schneider G-H, Poewe W, et al. Pallidal deep-brain stimulation in primary generalized or segmental dystonia. *N Engl J Med.* (2006) 355:1978–90. doi: 10.1056/NEJMoa063618
- Krause P, Völzmann S, Ewert S, Kupsch A, Schneider GH, Kühn AA, et al. Long-term effects of bilateral pallidal deep brain stimulation in dystonia: a follow-up between 8 and 16 years. *J Neurol.* (2020) 267:1622–31. doi: 10.1007/s00415-020-09745-z
- Koy A, Pauls KAM, Flossdorf P, Becker J, Schönaue E, Maarouf M, et al. Young adults with dyskinetic cerebral palsy improve subjectively on pallidal stimulation, but not in formal dystonia, gait, speech and swallowing testing. *Eur Neurol.* (2014) 72:340–8. doi: 10.1159/000360984
- Reese R, Gruber D, Schoenecker T, Bänzner H, Blahak C, Capelle HH, et al. Long-term clinical outcome in meige syndrome treated with internal pallidum deep brain stimulation. *Mov Disord.* (2011) 26:691–8. doi: 10.1002/mds.23549
- Ghang JY, Lee MK, Jun SM, Ghang CG. Outcome of pallidal deep brain stimulation in meige syndrome. *J Korean Neurosurg Soc.* (2010) 48:134–8. doi: 10.3340/jkns.2010.48.2.134
- Sobstyl M, Brzuszkiewicz-Kuzmicka G, Zaczynski A, Pasterski T, Aleksandrowicz M, Zabek M, et al. Long-term clinical outcome of bilateral pallidal stimulation for intractable craniocervical dystonia

- (Meige syndrome) Report of 6 patients. *J Neurol Sci.* (2017) 383:153–7. doi: 10.1016/j.jns.2017.10.017
32. Tian H, Yu Y, Zhen X, Zhang L, Yuan Y, Zhang B, et al. Long-term efficacy of deep brain stimulation of bilateral globus pallidus internus in primary meige syndrome. *Stereotact Funct Neurosurg.* (2019) 97:356–61. doi: 10.1159/000504861
 33. Troche MS, Brandimore AE, Foote KD, Okun MS. Swallowing and deep brain stimulation in Parkinson's disease: a systematic review. *Parkinsonism Relat Disord.* (2013) 19:783–8. doi: 10.1016/j.parkreldis.2013.05.001
 34. Moher D, Liberati A, Tetzlaff J, Altman DG. Preferred reporting items for systematic reviews and meta-analyses: the PRISMA statement. *J Clin Epidemiol.* (2009) 62:1006–12. doi: 10.1016/j.jclinepi.2009.06.005
 35. Moher D, Shamseer L, Clarke M, Ghersi D, Liberati A, Petticrew M, et al. Preferred reporting items for systematic review and meta-analysis protocols (PRISMA-P) 2015 statement. *Syst Rev.* (2015) 4:1. doi: 10.1186/2046-4053-4-1
 36. Kulneff L, Sundstedt S, Olofsson K, van Doorn J, Linder J, Nordh E, et al. Deep brain stimulation – effects on swallowing function in Parkinson's disease. *Acta Neurol Scand.* (2013) 127:329–36. doi: 10.1111/ane.12019
 37. Kitashima A, Umemoto G, Tsuboi Y, Higuchi M, Baba Y, Kikuta T, et al. Effects of subthalamic nucleus deep brain stimulation on the swallowing function of patients with Parkinson's disease. *Parkinsonism Relat Disord.* (2013) 19:480–2. doi: 10.1016/j.parkreldis.2012.10.023
 38. Olchik MR, Ghisi M, Ayres A, Schuh AFS, Oppitz PP, Rieder CR de M, et al. The impact of deep brain stimulation on the quality of life and swallowing in individuals with Parkinson's Disease. *Int Arch Otorhinolaryngol.* (2018) 22:125–9. doi: 10.1055/s-0037-1603466
 39. Robertson LT, St George RJ, Carlson-Kuhta P, Hogarth P, Burchiel KJ, Horak FB, et al. Site of deep brain stimulation and jaw velocity in Parkinson disease. *J Neurosurg.* (2011) 115:985–94. doi: 10.3171/2011.7.JNS102173
 40. Xu C, Zhuang P, Hallett M, Zhang Y, Li J, Li Y, et al. Parkinson's disease motor subtypes show different responses to long-term subthalamic nucleus stimulation. *Front Hum Neurosci.* (2018) 12:365. doi: 10.3389/fnhum.2018.00365
 41. Pflug C, Nienstedt JC, Gulberti A, Müller F, Vettorazzi E, Koseki J-C, et al. Impact of simultaneous subthalamic and nigral stimulation on dysphagia in Parkinson's disease. *Ann Clin Transl Neuron.* (2020) 7:628–38. doi: 10.1002/acn3.51027
 42. Fagbami OY, Donato AA. Stridor and dysphagia associated with subthalamic nucleus stimulation in Parkinson disease: case report. *J Neurosurg.* (2011) 115:1005–6. doi: 10.3171/2011.7.JNS11602
 43. Troche MS, Brandimore AE, Hegland KW, Zeilman PR, Foote KD, Okun MS, et al. Tailored deep brain stimulation optimization for improved airway protective outcomes in Parkinson's disease. *Interdiscip Neurosurg.* (2016) 5:3–5. doi: 10.1016/j.inat.2016.03.003
 44. Ciucci MR, Barkmeier-Kraemer JM, Sherman SJ. Subthalamic nucleus deep brain stimulation improves deglutition in Parkinson's disease. *Mov Disord.* (2008) 23:676–83. doi: 10.1002/mds.21891
 45. Silbergleit AK, LeWitt P, Junn F, Schultz LR, Collins D, Beardsley T, et al. Comparison of dysphagia before and after deep brain stimulation in Parkinson's disease. *Mov Disord.* (2012) 27:1763–8. doi: 10.1002/mds.25259
 46. Zibetti M, Torre E, Cinquepalmi A, Rosso M, Ducati A, Bergamasco B, et al. Motor and nonmotor symptom follow-up in Parkinsonian patients after deep brain stimulation of the subthalamic nucleus. *Eur Neurol.* (2007) 58:218–23. doi: 10.1159/000107943
 47. Lengerer S, Kipping J, Rommel N, Weiss D, Breit S, Gasser T, et al. Deep-brain-stimulation does not impair deglutition in Parkinson's disease. *Parkinsonism Relat Disord.* (2012) 18:847–53. doi: 10.1016/j.parkreldis.2012.04.014
 48. Krygowska-Wajs A, Furgala A, Gorecka-Mazur A, Pietraszko W, Thor P, Potasz-Kulikowska K, et al. The effect of subthalamic deep brain stimulation on gastric motility in Parkinson's disease. *Parkinsonism Relat Disord.* (2016) 26:35–40. doi: 10.1016/j.parkreldis.2016.02.010
 49. Wolz M, Hauschild J, Fauser M, Klingelhöfer L, Reichmann H, Storch A, et al. Immediate effects of deep brain stimulation of the subthalamic nucleus on nonmotor symptoms in Parkinson's disease. *Parkinsonism Relat Disord.* (2012) 18:994–7. doi: 10.1016/j.parkreldis.2012.05.011
 50. Limotai N, Go C, Oyama G, Hwynn N, Zesiewicz T, Foote K, et al. Mixed results for GPi-DBS in the treatment of cranio-facial and cranio-cervical dystonia symptoms. *J Neurol.* (2011) 258:2069–74. doi: 10.1007/s00415-011-6075-0
 51. Sensi M, Cavallo MA, Quatrone R, Sarubbo S, Biguzzi S, Lettieri C, et al. Pallidal stimulation for segmental dystonia: long term follow up of 11 consecutive patients. *Mov Disord.* (2009) 24:1829–35. doi: 10.1002/mds.22686
 52. Blomstedt P, Sandvik U, Tisch S. Deep brain stimulation in the posterior subthalamic area in the treatment of essential tremor. *Mov Disord.* (2010) 25:1350–6. doi: 10.1002/mds.22758
 53. Warnecke T, Oelenberg S, Teismann I, Hamacher C, Lohmann H, Ringelstein EB, et al. Endoscopic characteristics and levodopa responsiveness of swallowing function in progressive supranuclear palsy. *Mov Disord.* (2010) 25:1239–45. doi: 10.1002/mds.23060
 54. Ostrem JL, San Luciano M, Dodenhoff KA, Ziman N, Markun LC, Racine CA, et al. Subthalamic nucleus deep brain stimulation in isolated dystonia. *Neurology.* (2017) 88:25–35. doi: 10.1212/WNL.0000000000003451
 55. Ramirez-Zamora A, Smith H, Kumar V, Prusik J, Phookan S, Pilitsis JG, et al. Evolving concepts in posterior subthalamic area deep brain stimulation for treatment of tremor: surgical neuroanatomy and practical considerations. *Stereotact Funct Neurosurg.* (2016) 94:283–97. doi: 10.1159/000449007

Conflict of Interest: The authors declare that the research was conducted in the absence of any commercial or financial relationships that could be construed as a potential conflict of interest.

Copyright © 2020 Yu, Takahashi, Bloom, Quaynor and Xie. This is an open-access article distributed under the terms of the Creative Commons Attribution License (CC BY). The use, distribution or reproduction in other forums is permitted, provided the original author(s) and the copyright owner(s) are credited and that the original publication in this journal is cited, in accordance with accepted academic practice. No use, distribution or reproduction is permitted which does not comply with these terms.



Modulation of Intermuscular Beta Coherence in Different Rhythmic Mandibular Behaviors

Evan R. Usler^{1*†}, Xiaomei Wei^{2†}, Meg Simione³, Brian Richburg⁴, Kaila L. Stipancic⁴ and Jordan R. Green⁴

¹ Department of Communication Sciences and Disorders, College of Health Sciences, University of Delaware, Newark, DE, United States, ² Department of Rehabilitation Medicine, The Third Affiliated Hospital of Sun Yat-sen University, Guangzhou, China, ³ Department of Pediatrics, Massachusetts General Hospital, Boston, MA, United States, ⁴ Speech and Feeding Disorders Laboratory, MGH Institute of Health Professions, Boston, MA, United States

OPEN ACCESS

Edited by:

Kazutaka Takahashi,
The University of Chicago,
United States

Reviewed by:

Noman Naseer,
Air University, Pakistan
Hitoshi Maezawa,
Osaka University, Japan

*Correspondence:

Evan R. Usler
eusler@udel.edu

[†] These authors have contributed
equally to this work and share first
authorship

Specialty section:

This article was submitted to
Motor Neuroscience,
a section of the journal
Frontiers in Human Neuroscience

Received: 13 December 2019

Accepted: 08 July 2020

Published: 30 July 2020

Citation:

Usler ER, Wei X, Simione M,
Richburg B, Stipancic KL and
Green JR (2020) Modulation
of Intermuscular Beta Coherence
in Different Rhythmic Mandibular
Behaviors.
Front. Hum. Neurosci. 14:302.
doi: 10.3389/fnhum.2020.00302

Introduction: Jaw movement during chewing and speech is facilitated by neural activation patterns for opening and closing movements of the mandible. This study investigated anatomic- and task-dependent differences in intermuscular coherence (IMC) and their association with the parameters of jaw muscle activity using surface electromyography (sEMG).

Methods: We recorded sEMG activation from bilateral and ipsilateral jaw-closing muscle pairs during non-nutritive and nutritive chewing, and during a syllable repetition task. IMC and cross-correlational analyses between bilateral and ipsilateral muscle pairs were performed.

Results: Intermuscular coherence in the beta band was statistically significant between agonist jaw-closing muscle pairs, with beta IMC weaker for rapid syllable repetition compared to chewing tasks. Cross-correlational analysis of muscle co-activation, as well as sEMG burst amplitude, was positively associated with beta IMC strength.

Discussion: Beta IMC was influenced heavily by task-dependent behavioral goals and physiologic demands, which was interpreted as evidence of shared neural drive among jaw-closing muscles.

Keywords: intermuscular coherence, sensorimotor integration, beta band, mandible, chewing

INTRODUCTION

Learning to speak and chew involves the gradual tuning of the complex muscle group that control mandibular movements (Green et al., 1997; Simione et al., 2018). Although jaw closing is an integral component of both speech and chewing, the coordination of jaw-closing muscles varies significantly across these behaviors to accommodate their divergent behavioral goals and physiologic demands (Moore, 1993; Simione and Green, 2018). During speech, jaw-closing

Abbreviations: sEMG, surface electromyography; IMC, intermuscular coherence; LMxLT, left masseter x left temporalis pair; RMxLM, right masseter x left masseter pair; RMxRT, right masseter x right temporalis pair; RTxLT, right temporalis x left temporalis pair; RMS, root mean square.

movements transport the lower lip and tongue toward the palate through low-amplitude and relatively tonic muscle activation patterns (Barlow and Rath, 1985; Moore, 1993). During chewing, the jaw-closing muscles are activated in phasic bursts that alternate with those of the jaw-opening muscle. Task differences have not only been observed in the temporal coordination of jaw muscle activation patterns, but also in the intermuscular coherence (IMC) between jaw muscles (Smith and Denny, 1990; Steeve and Price, 2010).

Intermuscular coherence is a correlation of electromyographic activation in the frequency domain between two muscles. The strength of IMC is an indicator of common neural drive to motor neuron pools, which is hypothesized to be generated by shared or synchronized inputs from descending motor pathways (Farmer et al., 1993). In studies of limb muscle coordination, IMC specific to the beta band (~15–35 Hz) has been reported to be an indicator of coordinated neural drive across functionally linked muscles originating from the motor cortex (Reyes et al., 2017). In a large sample of typical adults (Jaiser et al., 2016), the strength of beta IMC was found to be consistent across adulthood and to be associated with motor performance. Stronger beta IMC may reflect greater synchrony in neural oscillations that are transmitted to motor neuron pools (Flood et al., 2019), resulting in motor unit synchronization driving the coordination of jaw muscles. According to Kerkman et al. (2018), beta IMC distribution patterns across the body indicate functional connectivity across muscles and are strongly shaped by (1) anatomical constraints such as muscle distance and homology, and (2) physical and cognitive demands of the task. Similar anatomical constraints and task-dependent effects on IMC may be evident between jaw muscles during mandibular movement.

Prior works on jaw muscle activation patterns have demonstrated task-dependent effects on IMC. Smith and Denny (1990), for example, found strong IMC between the bilateral masseter muscles of adults during various mandibular behaviors, with IMC between 20 and 60 Hz stronger during chewing than during speech or jaw clenching. Steeve and Price (2010) similarly reported stronger IMC in bilateral masseter and temporalis pairs in an infant and an adult for chewing compared to vocalization, suggesting chewing was facilitated by stronger IMC compared to speech-like behavior. Given that task- and muscle-related differences in the coordinative organization across jaw muscles has also been found in cross-correlational analyses of the degree of muscle co-activation, the strength of IMC during oromotor tasks may be an indicator of common drive to motor neuron pools from “a central command system” involving input from a central pattern generator (Lund, 1991) or reflex pathways (Moore et al., 1988; Moore, 1993; Steeve and Moore, 2009).

Beta IMC has been reported to be modulated by the extent to which a motor task engages afferent feedback, with coherence becoming weaker when afferent sensory feedback is restricted (Fisher et al., 2002). The contribution of afferent feedback to IMC strength suggests a role for sensorimotor integration between afferent sensory information and the efferent neural control of oromotor tasks. In regard to speech, the role of auditory and somatosensory feedback and feedforward mechanisms has been well established (Guenther, 2016). It remains unclear if

beta IMC is sensitive to task- and muscle-related differences in the reliance on sensory feedback underlying movement of the jaw. Compared to mandibular control during speech, the coordination of jaw muscles for the manipulation of an object or bolus (such as during chewing) arguably involves a greater reliance on somatosensory feedback (Lund and Kolta, 2006) and thus may be facilitated by strong IMC between synergistic jaw-closing muscles. IMC is also modulated by extramotor factors such as task-dependent cognitive demands. Kristeva-Feige et al. (2002) found beta corticomuscular coherence to weaken when attention is divided and motor precision is decreased during an isometric constant force task. During speech, Stepp et al. (2011) found beta IMC between anterior neck muscles to weaken when participants’ attention was divided (counting backward) compared to a normal speaking condition. Tasks that tax cognitive and motoric resources necessary for mandibular control, such as those characteristic of speech production, may weaken IMC relative to less demanding non-speech tasks such as chewing.

Our understanding of IMC in the beta band as an indicator of common neural input driving functional connectivity between jaw muscles will be strengthened by additional information about the influence of (1) anatomic relations (e.g., bilateral versus ipsilateral muscle pairs), and (2) task-dependent demands in sensorimotor integration and extramotor factors (e.g., chewing versus speech). We recorded muscle activation during non-nutritive (i.e., gum) and nutritive chewing (i.e., food) using sEMG from bilateral and ipsilateral jaw muscle pairs. IMC was also examined during a rhythmic speech-like behavior—a rapid syllable repetition task. Combined, these behaviors elicit a wide range of behavioral demands on agonist jaw muscles that likely result in across-task and within-task differences in beta IMC.

Given the likely influence of sensory input and cognitive demands on beta IMC strength mentioned above, we hypothesized that beta IMC would be stronger for chewing compared to speech-like rapid syllable repetition. We also hypothesized that differences in anatomical function would contribute to task-dependent differences in beta IMC. For example, gum chewing (which was restricted to the right working side) was expected to exhibit a strong beta IMC between right ipsilateral muscles (temporalis and masseter) compared to bilateral pairs. We also hypothesized that beta IMC strength between jaw muscles during these tasks would be correlated with cross-correlational measures of muscle co-activation (peak cross-correlation coefficient and temporal lag) underlying mandibular control. Lastly, as an exploratory analysis without an *a priori* hypothesis, we investigated the potential relationship between beta IMC and sEMG burst amplitude, to determine if this parameter contributed to beta IMC strength.

MATERIALS AND METHODS

Participants

Ten healthy volunteer participants (aged 18–45 years) including seven females and three males were recruited for this study. All participants had a negative history of speech, language,

or hearing disorders. All participants also had no history of neurological/musculoskeletal disease or dysfunction that would affect oromotor behavior. All procedures were approved by the Institutional Review Board of Spaulding Rehabilitation Hospital, and all participants gave informed consent. Two additional participants initially participated in the study; however, significant movement artifact during the repetition task resulted in the removal of their data from further analysis.

Surface Electromyography Recordings

Electromyography recordings were obtained from jaw-closing muscles including right and left masseter and the right and left temporalis. Electrode placement was similar to previous studies (e.g., Green et al., 1997) and determined by palpation of participants' muscle during jaw clenching. Electrodes were spaced approximately 0.5 cm apart and aligned parallel to muscle fiber orientation. A single ground electrode was placed on the mastoid process. Using the BIOPAC M150 system (BIOPAC Systems, Inc., Goleta, CA, United States), sEMG signals were digitized at a 7792 Hz sampling rate and amplified at a factor of 1000 (gain) with hardware high-pass (10 Hz) and low-pass (5000 Hz) filtering. Simultaneous video and audio signals from the sEMG samples were recorded and reviewed to aid in the removal of artifact and other non-chewing motor behaviors, such as swallowing.

Tasks

In one experimental session, participants conducted three jaw movement tasks: chewing gum, chewing food, and a rapid syllable repetition task. The ordering of these tasks was consistent across participants to accommodate other experimental conditions beyond the scope of the current study. This acknowledged limitation is discussed further in the Limitations section. Gum chewing was a self-paced and ipsilateral task (chewing only on the right side). A piece of gum was placed on the right molar, and participants were instructed to chew normally. The gum was softened before the task began to ensure consistency during chewing. Food chewing was a self-paced and adaptive bilateral task—three Cheerios (General Mills) were offered twice and participants voluntarily chewed the Cheerios at their own pace until they were ready to swallow. Cheerios were selected as the representative food because it was universally recognized and edible for our participants. Obtaining sEMG parameters for the chewing of Cheerios in typical adults is also important for future studies by our laboratory involving the safe consumption of this food by populations with motor speech and feeding disorders. For the rapid syllable repetition task, participants repeated the syllable/ba/ as clearly and quickly as possible on one breath. All the tasks were conducted without any visual or augmented auditory feedback. Each sEMG recording was seven seconds in length, regardless of the task (except for the repetition task for Participant #4 and gum chewing for Participant #3, whose recordings were less than seven seconds). This length of time allowed for a number of chewing cycles (i.e., sEMG bursts) is typical for the breakdown of soft solid foods (e.g., Fontijn-Tekamp et al., 2004). All recordings exhibited at least 10 chewing cycles (see **Figure 1A**), with the exception of gum chewing by

Participants #3 and #8 who produced less than 10 cycles. There was an approximately 3-min interval between each task.

Data Analysis

Intermuscular Coherence Analysis

The continuous sEMG recordings from each task were trimmed according to the reference video and analyzed using MATLAB (MathWorks, Inc., 2009). Audio recordings were used to aid in trimming the sEMG recordings for the rapid syllable repetition task. sEMG activity during vocalization, visible bolus positioning, and swallow movements were excluded from the dataset. The first and last sEMG burst of each recording was also removed from further analysis to remove any potential movement artifact not associated with the chewing cycles. IMC was calculated from continuous and non-rectified sEMG recordings for each task. sEMG recordings were low-pass filtered with an eighth-order Butterworth filter and linearly detrended and amplitude normalized to prevent any slow non-stationarity artifacts to influence calculation of IMC (Boonstra et al., 2009). For each muscle pair, an IMC estimate was calculated using a 2048-point fast Fourier transform and 1948-point Hamming window with 50% overlap. Muscle pairs were yielded, including bilateral agonists: right masseter x left masseter (RMxLM) and right temporalis x left temporalis (RTxLT), and ipsilateral agonists: right masseter x right temporalis (RMxRT) and left masseter x left temporalis (LMxLT). Auto-power and cross-power spectra were calculated using a cross power density ("d") function in MATLAB. IMC in the beta frequencies (15–35 Hz) was computed as the cross-spectra of the muscle pair normalized by the product of their autospectra (Halliday and Rosenberg, 1999; see **Figures 1C,D**). Visual inspection of raw sEMG recordings during data collection and analysis was done to ensure signal quality. For example, it was determined that none of the sEMG recordings from our participants exhibited significant noise or sEMG crosstalk (i.e., high degree of IMC across all frequencies).

sEMG Parameters and Cross-Correlational Analyses

Cross-correlational analyses—peak cross-correlation and temporal lag to peak cross-correlation coefficient—were also employed as measurements of co-activation between paired jaw muscles (e.g., Green et al., 1997). Participant data were analyzed using a custom MATLAB program (SMASH), which has been described in a previous study (Green et al., 2013). All raw sEMG signals were full-wave rectified, detrended, and low-pass filtered with cutoff of 30 Hz to generate an amplitude envelope for visualization of burst pattern. Pairwise cross-correlations were performed for each muscle pair in a spatiotemporal coupling window in SMASH (see **Figure 1B**). The peak cross-correlation coefficient was considered an estimate of the strength of activation coupling between the two muscles. Lag to the peak cross-correlation coefficient provided an indication of the temporal synchrony of related activity between the muscle pair. For each participant, burst amplitude of the muscle pairs were also calculated in SMASH as the average root mean square (RMS) across the rectified sEMG waveform. RMS values were normalized using standard z-scores for each participant prior to conducting statistical comparisons.

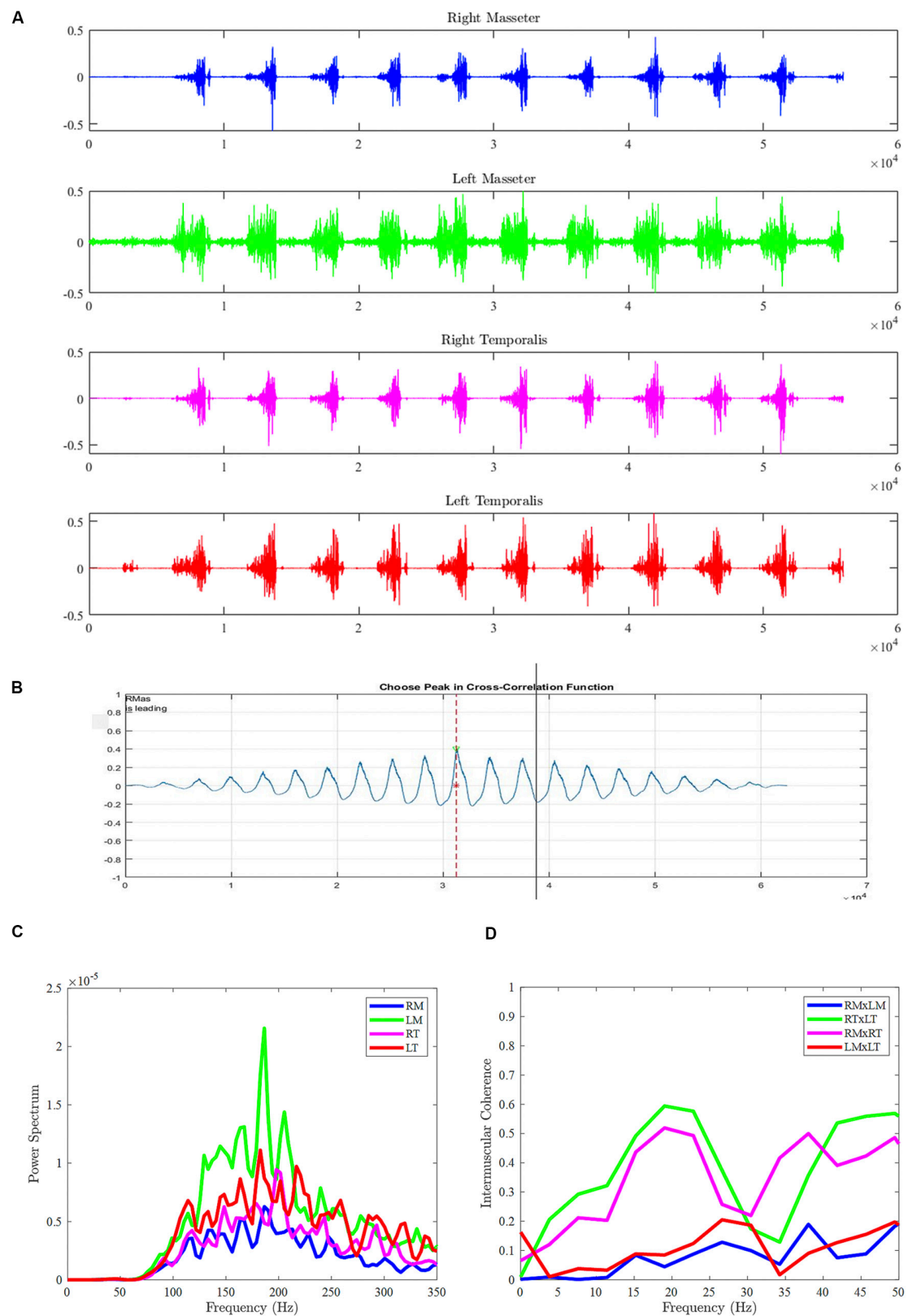


FIGURE 1 | Sample data from Participant #1 during gum chewing (food chewing and syllable repetition tasks not shown), including sEMG bursts across muscles **(A)**, cross-correlogram between right and left masseters **(B)**, power spectral density for each muscle **(C)**, and intermuscular coherence between muscle pairs **(D)**. RM, right masseter; LM, left masseter; RT, right temporalis; LT, left temporalis.

Statistical Analysis

Beta IMC, cross-correlational measures, and sEMG burst amplitude were all computed for the four muscle pairs of each participant. The IMC confidence limit (CL) was calculated based on the formula: $CL = 1 - 0.05^{1/(L-1)}$ by Rosenberg et al. (1989). The IMC confidence limit (CL) was calculated using the formula: $CL = 1 - 0.05^{1/(L-1)}$ by Rosenberg et al. (1989) that was modified by Terry and Griffin (2008) to account for the use of overlapping segments (L) in calculation of the auto- and cross-power spectra. Because the values of IMC and peak cross-correlation coefficient are both on a scale of 0 to 1, a Fisher's z transformation was used to normalize these data prior to conducting statistical comparisons across participants and across tasks, n represents the number of segments, $Coh(f)$ represents the coherence of corresponding frequency:

$$z = \sqrt{(2n)} * \text{Tanh}^{-1} \sqrt{Coh(f)}$$

Linear mixed models using restricted maximum likelihood fit were applied to determine the fixed effects of “task” and “muscle pair” on the dependent variable “beta IMC” (“lmer” function in R 3.5.2; R Core Team, 2013). “Participant” was entered as the random effect. These analyses were followed by Tukey's honest significant difference multiple comparisons using the multcomp package (“ghlt” function; Hothorn et al., 2008). In addition, linear mixed model analyses were conducted to determine potential differences in cross-correlational measures (peak coefficient and associated lag) and sEMG burst amplitude. Lastly, Pearson correlation coefficients were computed to determine if beta IMC strength was associated with cross-correlational measures and sEMG parameters. Statistical significance was determined using an alpha level of $p < 0.05$.

RESULTS

Intermuscular Coherence Comparisons Between Tasks

As illustrated in **Figure 2A**, the strength of beta IMC differed between tasks for the muscle pairs, with the exception of RMxLM. Overall, beta IMC differed between tasks, $F(2,108) = 35.35$, $p < 0.001$, and pairwise comparisons revealed beta IMC was weaker for rapid syllable repetition compared to chewing food ($p < 0.001$) and chewing gum ($p < 0.001$). The strength of beta IMC did not differ between chewing food and gum ($p = 0.18$). Beta IMC strength was significantly greater during chewing compared to rapid syllable repetition across the muscle pairs, except for RMxLM. Although the chewing of food appeared to exhibit a stronger beta IMC compared to chewing gum across most of the pairs, this difference was not statistically significant.

Comparisons Between Muscle Pairs

As illustrated in **Figure 2B**, beta IMC across muscle pairs was observed in each of the three tasks. Overall, beta IMC differed between muscle pairs for gum chewing, $F(3,27) = 10.37$, $p < 0.001$, and rapid syllable repetition, $F(3,27) = 3.28$, $p = 0.04$, but not for food chewing, $F(3,27) = 1.77$, $p = 0.18$. For gum

chewing, pairwise comparisons revealed beta IMC to be stronger for the right ipsilateral muscle pair (RMxRT) compared to left ipsilateral pair (LMxLT; $p < 0.001$) and bilateral masseter pair (RMxLM; $p < 0.001$). The bilateral temporalis pair (RTxLT) was also strong in beta IMC compared to the LMxLT ($p = 0.003$) and RMxLM ($p = 0.006$). For rapid syllable repetition, beta IMC was strong in the RMxLM pair compared to the left ipsilateral (LMxLT) pair ($p = 0.01$), which was relatively low for this task.

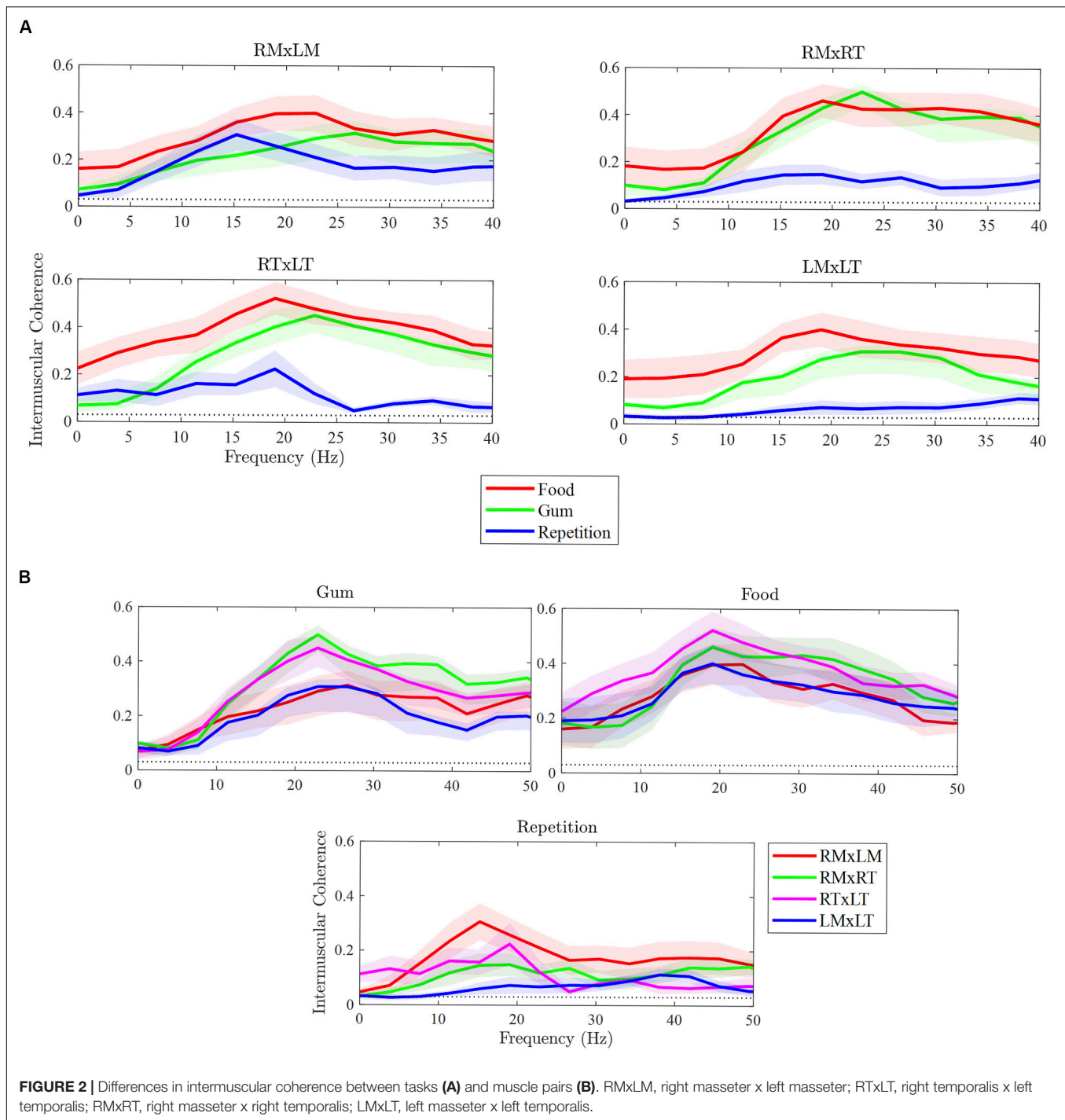
sEMG Parameters

Cross-correlational analyses revealed sEMG activation to be tightly coupled across muscle pairs during the chewing tasks (reflected by peak cross-correlation coefficients, $rs > 0.75$), but less so for rapid syllable repetition ($rs < 0.70$). As shown in **Figure 3A**, peak cross-correlation coefficients differed between tasks, $F(2,108) = 172.83$, $p < 0.001$, and were larger overall for the chewing of gum and food compared to repetition ($ps < 0.001$). Peak cross-correlation coefficients did not differ between the two chewing tasks ($p = 0.12$). Peak cross-correlation coefficients also did not differ between muscle pairs, $F(3,116) = 0.26$, $p = 0.86$. As illustrated in **Figure 3B**, the lag (or temporal synchrony) of muscle co-activation differed significantly between tasks, $F(2,111) = 3.33$, $p = 0.04$ ($p = 0.04$), but not between muscle pairs, $F(3,110) = 1.51$, $p = 0.22$. Pairwise comparisons between tasks revealed greater asynchrony (i.e., increased lag) for chewing food compared to chewing gum ($p = 0.03$). Lag during repetition did not differ significantly from that during food chewing ($p = 0.23$) and gum chewing ($p = 0.67$). sEMG burst amplitude of the muscle pairs (**Figure 3C**) differed significantly across tasks, $F(2,117) = 231.23$, $p < 0.001$, but not muscle pairs $F(3,116) = 1.71$, $p = 0.17$. Pairwise comparisons revealed burst amplitude to be lower for rapid syllable repetition compared to the chewing tasks ($ps < 0.001$). Amplitude did not differ between the chewing of food and gum ($p = 0.99$).

An exploratory analysis of potential associations between beta IMC and sEMG parameters was performed. Linear regression lines in **Figure 4** highlight task differences in the relationship between beta IMC and values of peak cross-correlation coefficient and sEMG burst amplitude. Overall, peak cross-correlation coefficients were positively correlated with beta IMC across the muscle pairs ($rs > 0.36$, $ps \leq 0.05$). Beta IMC was also positively correlated with RMS amplitude across the muscle pairs ($rs > 0.29$, $ps \leq 0.10$).

DISCUSSION

In this study, we recorded sEMG activation from bilateral and ipsilateral jaw-closing muscle pairs to examine differences in beta IMC between non-nutritive (i.e., gum) and nutritive chewing (i.e., food), as well as during rapid syllable repetition. The three tasks elicited differences in beta IMC, cross-correlational measures of muscle co-activation, and sEMG burst amplitude. Across the muscle pairs, beta IMC was moderately positively correlated with the peak cross-correlation coefficient and burst amplitude. These associations between IMC and sEMG activation allowed us to speculate about the functional significance of



IMC on mandibular control. Beta IMC in jaw-closing muscles was influenced heavily by task-dependent behavioral goals and physiologic demands. The observed task-dependency is consistent with prior findings on the task-dependency of jaw-muscle activation coupling (Moore, 1993; Steeve and Moore, 2009). Our findings on beta IMC extend this previous work by identifying the task demands that are driving these changes, which include the level of muscle activation, the synergistic and

anatomic relation between muscles, and possibly, the engagement levels of afferent feedback and cognition.

Differences in Jaw-Closing IMC Across Tasks and Muscles Within Tasks

Task- and muscle-dependent differences in coordinative organization were evident in the strength of beta IMC across

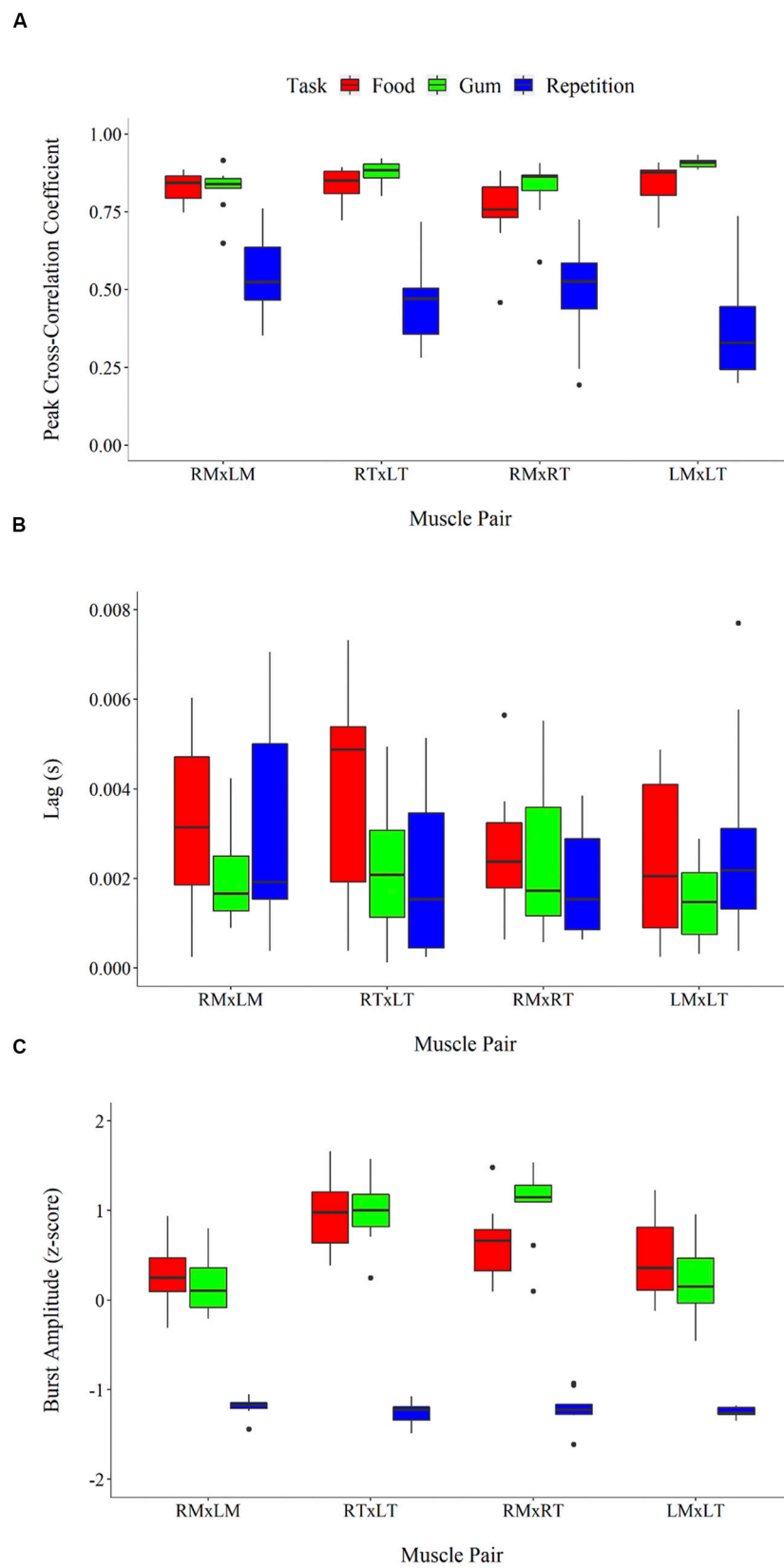
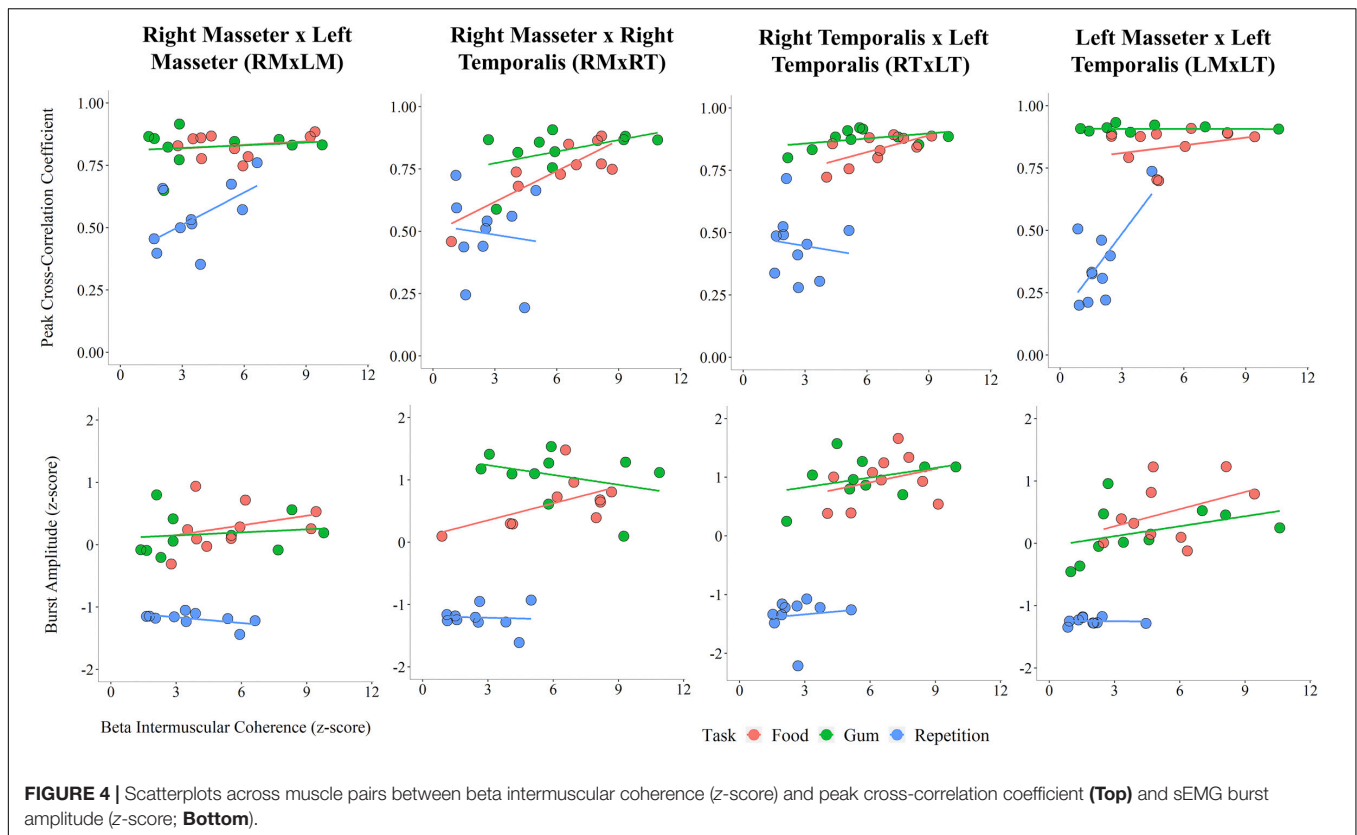


FIGURE 3 | sEMG parameters including peak cross-correlation coefficient **(A)**, associated lag (in seconds) **(B)**, and burst amplitude (z-score root mean square) **(C)**. Error bars represent standard error.



muscle pairs. The most salient task-related difference observed in this study, consistent with our hypothesis, was the considerably weaker beta IMC across all muscle pairs for rapid syllable repetition compared to the two chewing tasks. During rapid syllable repetition, beta IMC was strongest between the left and right masseters, which are the prime movers of the mandible during speech (Moore, 1993). As expected, during right-lateralized gum chewing, beta IMC was strong between the right temporalis and masseter muscle (the working side) compared to the left. Beta IMC was also particularly strong between the temporalis muscles during gum chewing. This is not surprising because the resistance of gum during chewing required activation of temporalis muscles for additional muscle force for jaw closing (Farella et al., 1999). This finding also corresponds with the high muscle coupling and burst amplitudes observed between the temporalis muscles during chewing gum. Beta IMC was similar in strength between the two chewing tasks and mandibular control during the two chewing tasks was characterized by similar jaw-muscle activation patterns (i.e., strong co-activation and high burst amplitude) compared to rapid syllable repetition. In contrast to gum chewing, food chewing was not restricted to the right working side, and as a result, beta IMC is more similar across all the muscle pairs. The chewing of food, relative to gum, was also reduced in muscle co-activation and synchrony. The more vertical and rhythmic cycles that characterized gum chewing (Simione and Green, 2018) was likely aided by a masticatory central pattern generator in the brainstem

that may be relatively isolated from the cortical motor drive associated with beta IMC.

The weaker beta IMC during rapid syllable repetition is congruent with previous findings of stronger IMC between masseter muscles during chewing compared to speech-like behavior (Smith and Denny, 1990; Steeve and Price, 2010). The co-activation of muscles (revealed by the peak cross-correlation coefficient) for chewing could be strong even with a relatively low beta IMC. Although speculative, the strong beta IMC characterizing the chewing tasks may be an indicator that jaw movement during chewing may be, at least in part, controlled by a brainstem central pattern generator (Smith and Denny, 1990). Unlike the chewing tasks, muscle activation during rapid syllable repetition was characterized by relatively weak muscle co-activation and reduced burst amplitude, all of which are characteristic of muscle activation during speech (Moore, 1993). Also characteristic of speech is the primary role of the bilateral masseters, evidenced by the strong beta IMC between these muscles during the repetition task compared to the other muscle pairs.

The moderate correlations observed between beta IMC and the parameters of sEMG co-activation and amplitude across the tasks provides evidence that task-dependent differences in sEMG co-activation and amplitude may be associated with beta IMC. More specifically, the sEMG activation patterns characteristic of chewing likely contributed to the relatively strong beta IMC that was observed, and vice versa for the relatively weak beta IMC during rapid syllable repetition. As indicated by higher sEMG

amplitudes, chewing required more force generation than speech (Barlow and Rath, 1985). Given that greater force generation is associated with stronger corticomuscular coherence in the beta frequency (Witte et al., 2007), the relatively greater force generation characteristic of chewing may have contributed to the task-dependent differences in beta IMC.

In addition, the weaker beta IMC observed during rapid syllable repetition compared to the chewing tasks may also have also been influenced by differences in cognitive demands (Simione and Green, 2018). The current findings raise the possibility that beta IMC may be stronger for tasks that are highly practiced, such as chewing, than for are motorically and cognitively demanding such as the rapid syllable repetition task, a task that is designed to elicit maximum performance. In sum, differences in neuromuscular activation, task dynamics, anatomical relations, and cognitive demands all likely contribute to differences in beta IMC, revealing varieties in the neural control of different mandibular behaviors.

Limitations and Future Research Considerations

The current study was limited by the consistent ordering of the tasks, which was done in order to accommodate other experimental conditions beyond the scope of the current study. However, the evidence provided of task-related effects in beta IMC between muscle pairs, which were not likely affected by any potential order effects, is suggestive that the observed differences in beta IMC were likely due to the task itself and not the order of their production. Still, future studies should randomize these tasks to prevent any order effects. The limited number of trials in the current study was necessary because (1) chewing of a simple food substance, such as Cheerios, prevented a large amount of chewing cycles, and (2) this was a preliminary study to determine the appropriateness of such a paradigm with populations with bulbar motor dysfunction who are not able to provide large numbers of chewing cycles without fatigue. Given that coherence values have been shown to either increase or remain stable with

the use of increasing segments for coherence calculation (van Asseldonk et al., 2014), future studies consisting of jaw movement tasks with a feasibly greater number of trials are necessary to determine the reliability of IMC as a marker of neural control of mandibular behavior.

DATA AVAILABILITY STATEMENT

The datasets for this article are not publicly available because prior approval to share the data was not obtained from the research participants. Requests to access the datasets should be directed to JG, jgreen2@mghihp.edu.

ETHICS STATEMENT

The studies involving human participants were reviewed and approved by the MGH Institutional Review Board. The participants provided their written informed consent to participate in this study.

AUTHOR CONTRIBUTIONS

Data interpretation and subsequent drafting of this article were conducted by EU, XW, and JG. Furthermore, data were collected by MS and XW. JG and MS provided the experimental conception and design of the study. All authors contributed to the article and approved the submitted version.

FUNDING

This work was supported by NIH-NIDCD under Grants K24DC016312 (PI: JG) and T32 DC013017 (PI: Christopher Moore).

REFERENCES

- Barlow, S. M., and Rath, E. M. (1985). Maximum voluntary closing forces in the upper and lower lips of humans. *J. Speech Lang. Hear. Res.* 28, 373–376. doi: 10.1044/jshr.2803.373
- Boonstra, T. W., Daffertshofer, A., Roerdink, M., Flipse, I., Groenewoud, K., and Beek, P. J. (2009). Bilateral motor unit synchronization of leg muscles during a simple dynamic balance task. *Eur. J. Neurosci.* 29, 613–622. doi: 10.1111/j.1460-9568.2008.06584.x
- Farrella, M., Bakke, M., Michelotti, A., Marotta, G., and Martina, R. (1999). Cardiovascular responses in humans to experimental chewing of gums of different consistencies. *Arch. Oral Biol.* 44, 835–842. doi: 10.1016/s0003-9969(99)00074-6
- Farmer, S. F., Bremner, F. D., Halliday, D. M., Rosenberg, J. R., and Stephens, J. A. (1993). The frequency content of common synaptic inputs to motoneurons studied during voluntary isometric contraction in man. *J. Physiol.* 470, 127–155. doi: 10.1113/jphysiol.1993.sp019851
- Fisher, R. J., Galea, M. P., Brown, P., and Lemon, R. N. (2002). Digital nerve anaesthesia decreases EMG-EMG coherence in a human precision grip task. *Exp. Brain Res.* 145, 207–214. doi: 10.1007/s00221-002-1113-x
- Flood, M. W., Jensen, B. R., Malling, A.-S., and Lowery, M. M. (2019). Increased EMG intermuscular coherence and reduced signal complexity in Parkinson's disease. *Clin. Neurophysiol.* 130, 259–269. doi: 10.1016/j.clinph.2018.10.023
- Fontijn-Tekamp, F., Vanderbilt, A., Abbink, J., and Bosman, F. (2004). Swallowing threshold and masticatory performance in dentate adults. *Physiol. Behav.* 83, 431–436. doi: 10.1016/j.physbeh.2004.08.026
- Green, J. R., Moore, C. A., Ruark, J. L., Rodda, P. R., Morveie, W., and Vanwittenburg, M. J. (1997). Development of chewing in children from 12 to 48 months: longitudinal study of EMG patterns. *J. Neurophysiol.* 77, 2704–2716. doi: 10.1152/jn.1997.77.5.2704
- Green, J. R., Wang, J., and Wilson, D. L. (2013). *SMASH: A Tool for Articulatory Data Processing and Analysis*. Shanghai: Interspeech, 1331–1335.
- Guenther, F. H. (2016). *Neural Control of Speech*. Cambridge, MA: MIT Press.
- Halliday, D. M., and Rosenberg, J. R. (1999). "Time and frequency domain analysis of spike train and time series data," in *Modern Techniques in Neuroscience Research*, eds U. Windhorst and H. Johansson (Berlin: Springer).
- Hothorn, T., Bretz, F., and Westfall, P. (2008). Simultaneous inference in general parametric models. *Biometr.* J. 50, 346–363. doi: 10.1002/bimj.200810425

- Jaiser, S. R., Baker, M. R., and Baker, S. N. (2016). Intermuscular coherence in normal adults: variability, and changes with age. *PLoS One* 11:e0149029. doi: 10.1371/journal.pone.0149029
- Kerkman, J. N., Daffertshofer, A., Gollo, L. L., Breakspear, M., and Boonstra, T. W. (2018). Network structure of the human musculoskeletal system shapes neural interactions on multiple time scales. *Sci. Adv.* 4:eaat0497. doi: 10.1126/sciadv.aat0497
- Kristeva-Feige, R., Fritsch, C., Timmer, J., and Lücking, C. H. (2002). Effects of attention and precision of exerted force on beta range EEG-EMG synchronization during a maintained motor contraction task. *Clin. Neurophysiol.* 113, 124–131. doi: 10.1016/S1388-2457(01)00722-2
- Lund, J. P. (1991). Mastication and its control by the brain stem. *Crit. Rev. Oral Biol. Med.* 2, 33–64. doi: 10.1177/10454411910020010401
- Lund, J. P., and Kolta, A. (2006). Generation of the central masticatory pattern and its modification by sensory feedback. *Dysphagia* 21, 167–174. doi: 10.1007/s00455-006-9027-6
- Moore, C. A. (1993). Symmetry of mandibular muscle activity as an index of coordinative strategy. *J. Speech Hear. Res.* 36, 1145–1157. doi: 10.1037/a0030561
- Moore, C. A., Smith, A., and Ringel, R. L. (1988). Task-specific organization of activity in human jaw muscles. *J. Speech Lang. Hear. Res.* 31, 670–680. doi: 10.1044/jshr.3104.670
- R Core Team (2013). *R: A Language and Environment for Statistical Computing*. Vienna: R Foundation for Statistical Computing.
- Reyes, A., Laine, C. M., Kutch, J. J., and Valero-Cuevas, F. J. (2017). Beta band corticomuscular drive reflects muscle coordination strategies. *Front. Comput. Neurosci.* 11:17. doi: 10.3389/fncom.2017.00017
- Rosenberg, J. R., Amjad, A. M., Breeze, P., Brillinger, D. R., and Halliday, D. M. (1989). The Fourier approach to the identification of functional coupling between neuronal spike trains. *Prog. Biophys. Mol. Biol.* 53, 1–31. doi: 10.1016/0079-6107(89)90004-7
- Simione, M., and Green, J. R. (2018). An exploratory investigation of the effects of whole-head vibration on jaw movements. *Exp. Brain Res.* 236, 897–906. doi: 10.1007/s00221-018-5183-9
- Simione, M., Loret, C., Le Révérend, B., Richburg, B., Del Valle, M., Adler, M., et al. (2018). Differing structural properties of foods affect the development of mandibular control and muscle coordination in infants and young children. *Physiol. Behav.* 186, 62–72. doi: 10.1016/j.physbeh.2018.01.009
- Smith, A., and Denny, M. (1990). High-frequency oscillations as indicators of neural control mechanisms in human respiration, mastication, and speech. *J. Neurophysiol.* 63, 745–758. doi: 10.1152/jn.1990.63.4.745
- Steeve, R. W., and Moore, C. A. (2009). Mandibular motor control during the early development of speech and nonspeech behaviors. *J. Speech Lang. Hear. Res.* 52, 1530–1554. doi: 10.1044/1092-4388(2009/08-0020)
- Steeve, R. W., and Price, C. M. (2010). Investigating the use of coherence analysis on mandibular electromyograms to investigate neural control of early oromandibular behaviours: a pilot study. *Clin. Linguist. Phonet.* 24, 485–501. doi: 10.3109/02699200903506312
- Stepp, C. E., Hillman, R. E., and Heaton, J. T. (2011). Modulation of neck intermuscular Beta coherence during voice and speech production. *J. Speech Lang. Hear. Res.* 54, 836–844. doi: 10.1044/1092-4388(2010/10-0139)
- Terry, K., and Griffin, L. (2008). How computational technique and spike train properties affect coherence detection. *J. Neurosci. Methods* 168, 212–223. doi: 10.1016/j.jneumeth.2007.09.014
- van Asseldonk, E. H., Campfens, S. F., Verwer, S. J., van Putten, M. J., and Stegeman, D. F. (2014). Reliability and agreement of intramuscular coherence in tibialis anterior muscle. *PLoS One* 9:e88428. doi: 10.1371/journal.pone.0088428
- Witte, M., Patino, L., Andrykiewicz, A., Hepp-Reymond, M.-C., and Kristeva, R. (2007). Modulation of human corticomuscular beta-range coherence with low-level static forces. *Eur. J. Neurosci.* 26, 3564–3570. doi: 10.1111/j.1460-9568.2007.05942.x

Conflict of Interest: The authors declare that the research was conducted in the absence of any commercial or financial relationships that could be construed as a potential conflict of interest.

Copyright © 2020 Usler, Wei, Simione, Richburg, Stipanovic and Green. This is an open-access article distributed under the terms of the Creative Commons Attribution License (CC BY). The use, distribution or reproduction in other forums is permitted, provided the original author(s) and the copyright owner(s) are credited and that the original publication in this journal is cited, in accordance with accepted academic practice. No use, distribution or reproduction is permitted which does not comply with these terms.



Chewing Efficiency, Global Cognitive Functioning, and Dentition: A Cross-sectional Observational Study in Older People With Mild Cognitive Impairment or Mild to Moderate Dementia

Suzanne Delwel^{1,2*}, Andrea B. Maier^{3,4}, Donya Parvaneh², Jesse Meijers⁵, Erik J. A. Scherder¹ and Frank Lobbezoo²

¹Department of Clinical Neuropsychology, Faculty of Behavioral and Movement Sciences, Vrije Universiteit Amsterdam, Amsterdam, Netherlands, ²Department of Orofacial Pain and Dysfunction, Academic Centre for Dentistry Amsterdam (ACTA), University of Amsterdam and Vrije Universiteit Amsterdam, Amsterdam, Netherlands, ³Department of Medicine and Aged Care, The Royal Melbourne Hospital, University of Melbourne, Melbourne, VIC, Australia, ⁴Department of Human Movement Sciences, Faculty of Behavioural and Movement Sciences, Amsterdam Movement Sciences, Vrije Universiteit Amsterdam, Amsterdam, Netherlands, ⁵Independent Researcher, Amsterdam, Netherlands

OPEN ACCESS

Edited by:

Limor Avivi-Arber,
Faculty of Dentistry, University of
Toronto, Canada

Reviewed by:

Antonina Luca,
University of Catania, Italy
Kaija Hiltunen,
University of Helsinki, Finland
Eef Hogervorst,
Loughborough University,
United Kingdom

*Correspondence:

Suzanne Delwel
s.delwel@vu.nl

Received: 02 December 2019

Accepted: 25 June 2020

Published: 09 September 2020

Citation:

Delwel S, Maier AB, Parvaneh D, Meijers J, Scherder EJA and Lobbezoo F (2020) Chewing Efficiency, Global Cognitive Functioning, and Dentition: A Cross-sectional Observational Study in Older People With Mild Cognitive Impairment or Mild to Moderate Dementia. *Front. Aging Neurosci.* 12:225. doi: 10.3389/fnagi.2020.00225

Introduction: Previous studies suggest an association between poor mastication and cognitive impairment. The role of chewing efficiency and dentition in this relation is unclear. The aim was to examine global cognitive functioning and dentition as predictors for chewing efficiency, in older people with mild cognitive impairment (MCI) or dementia.

Methods: In this observational cross-sectional study, 136 people with MCI or dementia were included. The chewing efficiency was assessed with a two-colored chewing gum and analyzed with the Chewing Efficiency Analysis software. The level of global cognitive functioning was measured with the Mini Mental State Examination (MMSE) by trained clinical staff. An oral examination was performed by a dentist and included the number of present teeth, the number of occluding pairs, and the presence of prostheses. Age, gender, and educational years were derived from the medical records. Univariate and multivariate backward stepwise linear regression analyses were used to evaluate global cognitive functioning and dentition as predictors for chewing efficiency.

Results: The mean age of the participants was 82.1 (SD 5.8) years, and 74 (54.4%) were female. The participants had a median MMSE score of 22.4 (IQR 18.0–26.0) and a median Chewing Efficiency Analysis score of 0.46 (IQR 0.14–0.59). The median number of teeth was 13.0 (IQR 0.0–23.0), and the median number of occluding pairs was 0.0 (IQR 0.0–7.0). Sixty-four (47.4%) of the participants wore full prosthesis in the upper jaw. In univariate linear regression analyses, predictive factors for the Chewing Efficiency Analysis score were age, MMSE score, full prosthesis in the

upper jaw, number of present teeth, and number of occluding pairs. In the multivariate model, full prosthesis in the upper jaw and number of occluding pairs were significant predictors for the Chewing Efficiency Analysis score. Participants with full prosthesis in the upper jaw had a lower Chewing Efficiency Analysis score than participants with natural dentition in the upper jaw.

Conclusion: Better mastication is associated with a higher number of occluding pairs. Full prosthesis in the upper jaw is related to a lower chewing efficiency. Global cognitive functioning is not associated with mastication in older people with MCI or mild-to-moderate dementia. This might be explained by sufficient capacity for compensation of reduced mastication in this group.

Keywords: mastication, chewing, cognitive impairment, cognitive dysfunction, dementia, aged, geriatric dentistry, gerodontology

INTRODUCTION

Worldwide, around 48 million people have dementia, and this number is estimated to increase to 1.25 billion by 2050 (Prince et al., 2013). Dementia is a clinical syndrome, characterized by memory loss and impairment in language (aphasia or dysphasia), motor function (apraxia), visual recognition (agnosia), and executive functioning, resulting in difficulties during activities in daily life (Kester and Scheltens, 2009). Mild cognitive impairment (MCI) is characterized by a mild impairment of cognition, more than can be expected from age alone, at which daily functioning is largely unaffected (Petersen et al., 2014). The prevalence of MCI increases with age and varies between 6.7% in people aged 60–64 years and 25.2% for 80–84 years (Petersen et al., 2018). Older people with MCI are at higher risk for developing dementia, among which Alzheimer's disease (AD; Petersen et al., 2018).

At the same time, currently aging individuals maintain their natural dentition until a higher age as a result of better prevention of oral disease and improved professional dental care (Petersen, 2003). However, throughout an individual's life, teeth are lost, mainly as a result of caries and periodontitis (Tonetti et al., 2017), especially in people with dementia, who show a decrease in oral hygiene self-care and professional dental care utilization (Fereshtehnejad et al., 2017). Interestingly, several studies examined the relation between periodontitis, tooth loss, and cognitive impairment (Wu et al., 2016; Delwel et al., 2017, 2018; Tonsekar et al., 2017). Although some of these studies indicate such a relation, the combined results are inconclusive (Wu et al., 2016; Tonsekar et al., 2017). Most of the studies concerning cognition and mastication used the number of present teeth as a measure for mastication (Tada and Miura, 2017). Only a few studies included an objective assessment of chewing efficiency for mastication, such as a mixing ability test (Kimura et al., 2013; Elsig et al., 2015; Weijenberg et al., 2015).

The aim of the current study was to examine global cognitive functioning and dentition as predictors for chewing efficiency, in older people with MCI or dementia. Dentition was represented by the number of teeth, occluding pairs, and the presence of prosthesis.

MATERIALS AND METHODS

Study Design, Setting, and Participants

In this cross-sectional study, the relation between chewing efficiency, global cognitive functioning, and dentition was examined in participants with MCI or dementia. The participants were recruited at the geriatric outpatient clinics of the Amsterdam UMC and the Amstelland Hospital in Amstelveen and the psychogeriatric wards of ten nursing homes in Amsterdam and the surrounding area, as part of the Pain in Dementia Amsterdam, or PainDemiA study. The study protocol was approved by the Medical Ethics Review Committee of the Amsterdam UMC (approval number NL 43861.029.13) and was described elsewhere (van Kooten et al., 2015). The study protocol article describes the inclusion and exclusion criteria, power calculation, and procedure to establish the dementia diagnosis. Participants who met the following criteria included: aged 60 or older; diagnosis of MCI or dementia, i.e., AD, vascular dementia (VaD), frontotemporal dementia (FTD), and dementia with Lewy bodies (DLB); and a signed informed consent by the participant or legal representative. In the outpatient memory clinics at the hospitals, the MCI or dementia diagnosis was established by a multidisciplinary team of medical doctors, nurses, neuropsychologists, and neurologists, based on the National Institute of Neurological and Communicative Disorders and Stroke (NINCDS) and the AD and Related Disorders Association (ADRDA) criteria for Alzheimer dementia (McKhann et al., 2011), the National Institute of Neurological Disorders and Stroke Association (NINDS) and Association Internationale pour la Recherche et l'Enseignement en Neurosciences (AIRESN) criteria for vascular dementia (Román et al., 1993), the revised criteria for FTD (Rascovsky et al., 2011), the revised criteria for DLB (McKeith et al., 2005), and the revised criteria for MCI (Petersen et al., 2014). At the nursing homes, the formal dementia diagnosis in the medical chart was used, which was usually based on the Diagnostic and Statistical Manual of Mental Disorders (DSM-IV) criteria for dementia (American Psychiatric Association, 2000). Participants without a MCI or dementia diagnosis were excluded. The data was collected between April 2014 and December

2015, in accordance with the STrengthening the Reporting of OBservational Studies in Epidemiology (STROBE) statement (Sanderson et al., 2007). The demographic characteristics, gender, date of birth, and educational status were derived from the medical records of the participants.

Global Cognitive Functioning

The global cognitive functioning of the participants was measured with the Mini Mental State Examination (MMSE) by trained clinical staff at the outpatient clinics of the hospitals and a neuropsychologist at the nursing homes (Folstein et al., 1975). The MMSE screens different cognitive domains: orientation in time and place (10 points), immediate recall (3 points), attention and calculation (5 points), delayed recall (3 points), language (8 points), and visual construction (1 point). The minimum score is 0, and the maximum total score is 30. Participants with an MMSE score of lower than 14 points were excluded, because understanding of the instructions could not be assumed (Hadjistavropoulos et al., 2010).

Chewing Efficiency

The chewing efficiency was tested with a two-colored chewing gum, consisting of blue and pink Bubblicious® bubble gum (Cadbury Nederland B.V., Breda, Netherlands). The participants were instructed to chew on the two-colored chewing gum as normally as possible for 1 min. After 60 s, the dentist asked the participants to return the chewing gum, after which it was placed between two clear cellophane sheets to be flattened between two connected acrylic plates. Thereafter, the flattened chewing gum was photographed in a standard setting with a digital Canon 450D® camera (Canon Inc., Tokyo, Japan; Weijnenberg et al., 2013).

The chewing gum photos were analyzed with the Chewing Efficiency Analysis software, according to the algorithm described in Table 1. The minimum Chewing Efficiency Analysis score was 0.00, and the maximum possible score was 1.00. The mixture of the two colors was ~25% for score 0.25, ~50% for score 0.50, and ~75% for score 0.75.

Dentition

All oral examinations took place by one dentist, experienced in gerodontology, who was blind to the MMSE score at the

moment of the examination. The standardized examination took place at the outpatient clinics and nursing homes, with a mouth mirror and head light (Black Diamond, UT, USA). The oral examination included counting of the number of present teeth and the number of occluding pairs (Käyser, 1990). For the number of occluding pairs, a natural premolar contact between the upper and lower jaw counted as one occluding pair and a full natural molar contact as two occluding pairs, resulting in a minimum of 0 occluding pairs and a maximum of 14 occluding pairs. Furthermore, the presence of prosthesis was recorded. At least three occluding pairs or the presence of replacing prosthesis were considered acceptable for chewing ability (Gerritsen et al., 2013).

Statistical Analysis

The data were analyzed with IBM Statistics SPSS 26 (SPSS Inc., Chicago, IL, USA). The continuous variables were expressed as means and standard deviations (SD) for parametric data and as medians and interquartile ranges (IQR) for nonparametric data. The categorical variables were presented as numbers and percentages. Normality of distribution was assessed with the Shapiro–Wilk test. The means of two continuous dependent variables of two categorical independent variables were compared with the independent *t*-test for parametric data and the Mann–Whitney *U* test for nonparametric data. The means of two categorical variables were compared with the Pearson chi-square test.

Univariate and multivariate linear regression analyses were performed to identify predictors for Chewing Efficiency Analysis score. Variables with $p < 0.10$ in the univariate regression were included in the multivariate backward stepwise analysis to identify the predictors. $p < 0.05$ was considered statistically significant. Multicollinearity was identified with the correlation matrix ($r < 0.90$), variance inflation factor (>10), and tolerance statistics (<0.10).

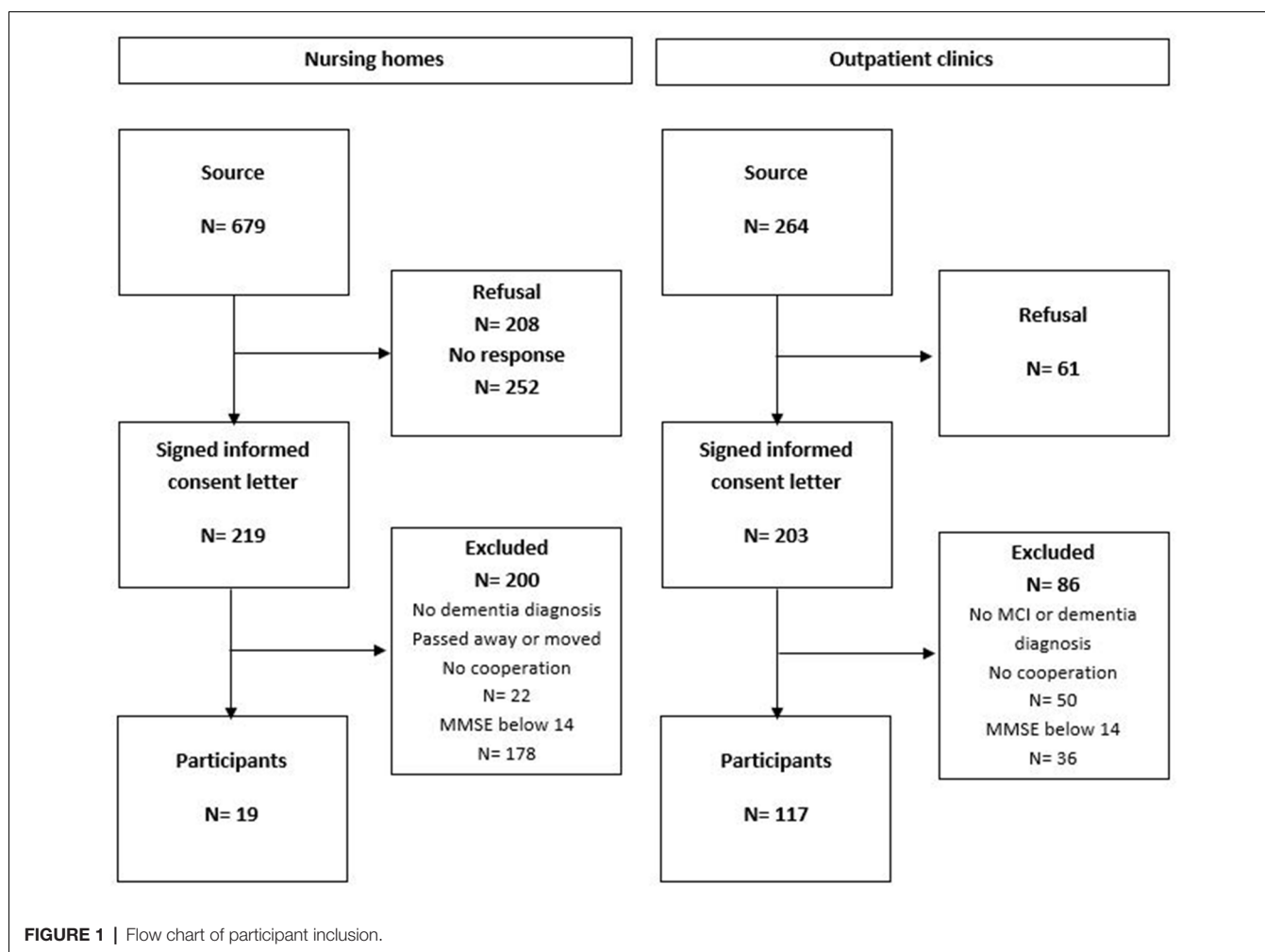
RESULTS

Participants

Of the individuals visiting the hospitals, 264 were approached for participation, 203 signed the informed consent letter, and

TABLE 1 | Algorithm of the chewing efficiency analysis.

- (1) Divide the photo into squares of 20×20 pixels each.
- (2) For each square:
 - (a) For each pixel in the square:
 - (i) Get the R(ed), G(reen), B(lue) values of the color of the pixel.
 - (ii) Calculate the 3-dimensional spatial distance of the pixel's color and the reference colors Blue, Magenta, Gray, and White, by adding up the absolute difference between the R, G, and B values of both colors being compared.
 - (iii) Classify the pixel as Blue, Magenta, Gray, or White based on the shortest spatial distance.
 - (b) Assign a value to the square, based on the categorized pixels in the square:
 - (i) None—If $>50\%$ of pixels is White, the square is not counted
 - (ii) 0.00—If $>75\%$ of pixels is Blue
 - (iii) 0.00—If $>75\%$ of pixels is Magenta
 - (iv) 0.50—If $>25\%$ of pixels is Blue and $>25\%$ of pixels is Magenta
 - (v) 0.75—If $>25\%$ of pixels is Gray and $>25\%$ of pixels is Blue
 - (vi) 0.75—If $>25\%$ of pixels is Gray and $>25\%$ of pixels is Magenta
 - (vii) 1.00—If $>50\%$ of pixels is Gray
- (3) Calculate the average of the scored squares as the final Chewing Efficiency Analysis score. The value is between 0.00 and 1.00.



117 were included in this study (**Figure 1**). The main reason for refusal was the expected burden for the participants, and the main reasons for exclusion were the absence of an MCI or dementia diagnosis or an MMSE score lower than 14. For 679 nursing home residents, an informed consent letter was sent to the legal representatives. Following this, 252 did not respond and 208 refused participation. The main reason for refusal was the expected burden for the participants, and the main reason for exclusion was an MMSE score lower than 14. Nineteen nursing home residents remained. In total, 136 persons were included in this study.

Descriptive Data

Table 2 shows the descriptive data of the 136 participants. The mean age of the participants was 82.1 (SD 5.8) years, and 74 (=54.4%) were female. The median number of educational years was 11.0 (IQR 9.0–12.0). The majority of the participants were home-dwelling: 117 (86.0%).

The participants had a median MMSE score of 23.0 (IQR 18.0–26.0) and a median Chewing Efficiency Analysis score of 0.46 (IQR 0.14–0.59). The median number of teeth was 13.0

(IQR 0.0–23.0), and the median number of occluding pairs was 0.0 (IQR 0.0–7.0). Sixty-four (47.4%) of the participants wore full prosthesis in the upper jaw. Seventy-one (52.2%) of the participants had 0–2 occluding pairs and wore full or partial prostheses. Thirty-eight (27.9%) participants had six or more occluding pairs.

On average, the group with full prosthesis in the upper jaw (FPU) was significantly older (mean 84.1, SD 5.6) than the group without FPU, or a dentate upper jaw (mean 80.4, SD 5.5), T -test (df 134) = -3.93 , $p = 0.000$. The groups were not significantly different concerning gender, $\chi^2_{(1)} = 2.08$, $p = 0.150$. In addition, the group with FPU included significantly more nursing-home residents than the group without FPU did, $\chi^2_{(1)} = 9.0$, $p = 0.003$.

The group with FPU had no occluding pairs and less present teeth than the group without FPU. The MMSE score was not significantly different for the group with FPU (median 22.0, IQR 18.0–26.0) and the group without FPU (median 23.0, IQR 19.0–27.0). The group with FPU had a significantly lower chewing analysis score (median 0.15, IQR 0.09–0.38) than the group without FPU (median 0.57, IQR 0.46–0.68), $U = 532.0$, $p = 0.000$.

TABLE 2 | Descriptive data.

| Variable | All (n = 135) | Full prosthesis upper (n = 64) | No full prosthesis (e.g., dentate) upper (n = 72) |
|--|------------------|--------------------------------|---|
| Age, mean (SD) years | 82.1 (5.8) | 84.1 (5.7)*** | 80.4 (5.5)*** |
| Gender, female (%) | 74 (54.4%) | 39 (60.9%) | 35 (48.6%) |
| Education, median (IQR) years | 11.0 (9.0–12.0) | 9.5 (8.0–11.8)*** | 12.0 (10.0–14.0)*** |
| Living environment, number home dwelling (%) | 117 (86.0%) | 49 (76.6%)** | 68 (94.4%)** |
| Cognition, median (IQR) MMSE score | 23.0 (18.0–26.0) | 22.0 (18.0–26.0) | 23.0 (19.0–27.0) |
| Present teeth, median (IQR) | 13.0 (0.0–23.0) | 0.0 (0.0–6.0)*** | 22.5 (18.3–26.0)*** |
| Occluding pairs, median (IQR) | 0.0 (0.0–7.0) | n/a | 6.0 (2.0–9.0) |
| Oral function | | | |
| 0–2 OP and no prosthesis, N (%) | 7 (5.1%) | n/a | 7 (9.7%) |
| 0–2 OP and prosthesis, N (%) | 71 (52.2%) | 58 (90.6%) | 13 (18.1%) |
| 3–5 OP, N (%) | 13 (9.6%) | n/a | 13 (18.1%) |
| ≥6 OP, N (%) | 38 (27.9%) | n/a | 38 (52.8%) |
| Chewing efficiency, median (IQR) score | 0.46 (0.14–0.59) | 0.15 (0.09–0.38)*** | 0.57 (0.46–0.68)*** |

IQR, interquartile range; MMSE, Mini Mental State Examination; N, number; ** $p < 0.01$, *** $p < 0.001$, OP, occluding pairs; SD, standard deviation.

TABLE 3 | Predictors of the Chewing Efficiency Analysis score in univariate linear regression analysis.

| Variable | R | R ² | B | t | p | 95% CI Lower | 95% CI Upper |
|-----------------------|------|----------------|-------|--------|-------|--------------|--------------|
| Age | 0.35 | 0.12 | −0.02 | −4.30 | 0.000 | −0.02 | −0.01 |
| Gender | 0.16 | 0.03 | 0.08 | 1.89 | 0.061 | −0.00 | 0.17 |
| Education | 0.15 | 0.02 | 0.01 | 1.51 | 0.134 | −0.00 | 0.03 |
| Cognition | 0.18 | 0.03 | 0.01 | 2.10 | 0.038 | 0.00 | 0.02 |
| Full prosthesis upper | 0.67 | 0.44 | −0.33 | −10.35 | 0.000 | −0.40 | −0.27 |
| Present teeth | 0.66 | 0.44 | 0.02 | 10.21 | 0.000 | 0.01 | 0.02 |
| Occluding pairs | 0.62 | 0.39 | 0.04 | 9.18 | 0.000 | 0.03 | 0.05 |

Note: N = 135, B, unstandardized B; CI, confidence interval; p, level of significance; R, variance; t, test value.

Main Results

Table 3 shows the predictors of Chewing Efficiency Analysis score in univariate linear regression analysis. The variables age, gender, cognition, full prosthesis upper jaw, number of present teeth, and number of occluding pairs were eligible for the multivariate regression model ($p < 0.10$). The covariate education was excluded ($p = 0.134$).

The correlation matrix (**Table 4**) indicates a very strong, negative correlation between the number of present teeth and the presence of full prosthesis in the upper jaw ($r = -0.89$) and a very strong, positive correlation between the number of present teeth and the number of occluding pairs ($r = 0.83$). To avoid multicollinearity, the number of present teeth was excluded from the multivariate regression model.

In multivariate linear backward regression analysis (**Table 5**), significant predictors for Chewing Efficiency Analysis score were full prosthesis in the upper jaw ($p < 0.000$) and the number of occluding pairs ($p < 0.003$). The final model explained 52% ($R^2 = 0.52$) of the variance in Chewing Efficiency Analysis score, $F_{(3,131)} = 47.23$, $p < 0.000$.

DISCUSSION

The aim of this cross-sectional observational study was to examine global cognitive functioning and dentition as predictors for chewing efficiency in older people with MCI or dementia. One of the main findings was that full prosthesis in the upper jaw and number of occluding pairs were significant predictors for Chewing Efficiency Analysis score. After adjusting

for these two predictors and age, the MMSE score was not a significant predictor.

In the current study, a strong, positive correlation was found between the chewing efficiency and the number of teeth present. In a study of Ikebe et al. (2011), a comparable correlation ($r = 0.57$) was found between masticatory performance and the number of residual teeth in a sample of 1,288 community-dwelling, independently living people over the age of 60 years. Furthermore, there was a moderate, negative correlation between age and chewing efficiency in the current study, while there was a weak, negative correlation between age and masticatory performance in the study by Ikebe et al. (2011). In the latter study, gummy jellies were used to measure masticatory performance. Previous research showed a decline in masticatory performance with age, although this decline was not gradual, but stronger in older age (Lin et al., 2017). With aging, the integrity of the white matter of the brain might show a decline, resulting in a lower signal transmission between brain regions (Malykhin et al., 2011). Consequently, neural systems, including the frontal lobe, the striatum, and the cerebellum, involved in mastication among others, may show an age effect (Sesay et al., 2000). Therefore, a reduced masticatory function as part of general aging effect can be expected (Taubert et al., 2020). Additionally, the study by Ikebe et al. (2011) showed that masticatory performance was significantly associated with occlusal bite force and stimulated salivary flow rate. However, the level of global cognitive functioning was not reported.

A study by Kim et al. (2017) involved the level of cognitive impairment, measured with the MMSE of Dementia

TABLE 4 | Correlation matrix of the Chewing Efficiency Analysis (CEA) score and the predictors.

| Correlations | CEA score | Age | Gender | MMSE | FPU | PT | OP |
|-----------------------------|-----------|-------|--------|-------|-------|-------|-------|
| CEA score | 1.00 | −0.35 | 0.15 | 0.16 | −0.68 | 0.69 | 0.62 |
| Age | −0.35 | 1.00 | −0.26 | −0.35 | 0.33 | −0.32 | −0.30 |
| Gender | 0.15 | −0.26 | 1.00 | 0.19 | −0.13 | 0.17 | 0.12 |
| Cognition (MMSE) | 0.16 | −0.35 | 0.19 | 1.00 | −0.08 | 0.10 | 0.05 |
| Full prosthesis upper (FPU) | −0.68 | 0.33 | −0.13 | −0.08 | 1.00 | −0.89 | −0.71 |
| Present teeth (PT) | 0.69 | −0.32 | 0.17 | 0.10 | −0.89 | 1.00 | 0.83 |
| Occluding pairs (OP) | 0.62 | −0.30 | 0.12 | 0.05 | −0.71 | 0.83 | 1.00 |

Note: $N = 135$.

TABLE 5 | Predictors of the Chewing Efficiency Analysis score in multivariate linear backward regression analysis.

| Variable | B | t | p | 95% CI Lower | 95% CI Upper |
|-----------------------|-------|-------|-------|--------------|--------------|
| Step 1 | | | | | |
| (Constant) | 0.66 | | | | |
| Age | 0.00 | −1.21 | 0.227 | −0.01 | 0.00 |
| Gender | 0.01 | 0.39 | 0.695 | −0.05 | 0.07 |
| Cognition | 0.00 | 1.21 | 0.228 | 0.00 | 0.01 |
| Full prosthesis upper | −0.23 | −5.26 | 0.000 | −0.31 | −0.14 |
| Occluding pairs | 0.02 | 3.06 | 0.003 | 0.01 | 0.03 |
| Step 2 | | | | | |
| (Constant) | 0.68 | | | | |
| Age | 0.00 | −1.31 | 0.193 | −0.01 | 0.00 |
| Cognition | 0.00 | 1.27 | 0.207 | 0.00 | 0.01 |
| Full prosthesis upper | −0.23 | −5.29 | 0.000 | −0.31 | −0.14 |
| Occluding pairs | 0.02 | 3.08 | 0.003 | 0.01 | 0.03 |
| Step 3 | | | | | |
| (Constant) | 0.89 | | | | |
| Age | 0.00 | −1.87 | 0.064 | −0.01 | 0.00 |
| Full prosthesis upper | −0.23 | −5.30 | 0.000 | −0.31 | −0.14 |
| Occluding pairs | 0.02 | 3.01 | 0.003 | 0.01 | 0.03 |

B, unstandardized B; CI, confidence interval; p, level of significance; R, variance; t, test value. $R^2 = 0.53$ and $F = 28.64$ ($p < 0.000$) for Step 1. $\Delta R^2 = 0.00$ and $F = 35.99$ ($p < 0.000$) for Step 2. $\Delta R^2 = 0.01$ and $F = 47.23$ ($p < 0.000$) for Step 3. $N = 135$.

Screening (MMSE-DS), and found a significant association with chewing efficiency, measured with a color-changing gum. Furthermore, the study by Kim et al. (2017) reported that participants with a lower chewing efficiency had poorer nutritional status. At the same time, no oral health examination could be done and no correlation could be determined with dentition.

Lexomboon et al. (2012) examined chewing efficiency and tooth loss and the association with cognitive impairment in older people. The study found a significant relation between self-reported chewing efficiency and cognitive function, after adjusting for age, gender, and level of education. The association between tooth loss and cognition was mainly explained by age and education. Both the study by Lexomboon et al. (2012) and the current study found that global cognition had a stronger correlation with age than with the number of teeth present. The difference in chewing efficiency could be explained by the measuring methods of both studies: the study by Lexomboon et al. (2012) used self-reported dental status and chewing difficulty, while the current study included a dental examination by a dentist and a standardized chewing efficiency test. Another explanation might be that people with mild to moderate cognitive impairment still have sufficient capacity for compensation of impairments, such as a reduction in

mastication, while this might not be the case in people with severe dementia (Henskens et al., 2018).

People with FPU had a lower chewing efficiency score than people without FPU in the present study, which might be explained by an actual lower chewing efficiency or, alternatively, by the sticking of the chewing gum to the prosthesis. Furthermore, people with prosthesis might also take more time and chewing cycles to achieve the same chewing result (Gonçalves et al., 2014). In addition, people with full prosthesis make smaller vertical and lateral chewing movements than people with natural dentition do (Gonçalves et al., 2014).

Although it is known that age is a risk factor for cognitive decline and tooth loss (Beydoun et al., 2014; Kossioni et al., 2018; Müller et al., 2017), it could also be a risk factor for deterioration in chewing efficiency (Lin et al., 2017; Avivi-Arber and Sessle, 2018).

Strengths and Limitations

One of the major limitations of this study was that the chewing gum stuck to the prosthesis. Therefore, it was decided to split the data into a group with full prosthesis in the upper jaw and a group without full prosthesis in the upper jaw, or a dentate upper jaw.

Furthermore, the MMSE does not specifically test loss of spatial memory and learning capacity, although these cognitive

functions might be reduced in relation to reduced masticatory activity (Weijenberg et al., 2011). However, the MMSE tests memory (among other cognitive functions), which is related to the hippocampus as part of a complex memory network. The hippocampus showed degeneration in animal studies after reduced masticatory activity (Yamamoto and Hirayama, 2001; Watanabe et al., 2002; Tsutsui et al., 2007). Another limitation of this study was the MMSE cutoff score of 14. Consequently, people with severe cognitive impairment were excluded, while it could be hypothesized that the chewing efficiency in this group could be affected the most.

At the same time, the MMSE cutoff score of 14 can be seen as a strength, because the participants could be expected to understand the instructions (Hadjistavropoulos et al., 2010). The MMSE is a widely used instrument to screen global cognitive functioning, which makes comparison with other studies and interpretation easier (Folstein et al., 1975). In addition, the non-response rate of the current study was clearly described.

Another strength was that all participants were examined by the same dentist, who had experience in geriatric dentistry and was not informed about the MMSE score of the participants during the dental examination. A structured dental examination took place, instead of using questionnaires to assess the number of teeth present, the number of occluding pairs, and the presence of prostheses. Moreover, the chewing efficiency was measured objectively with a standardized two-colored gum and analyzed with an algorithm programmed specifically for this purpose.

Generalizability

The current study included a sample of participants with mild to moderate cognitive impairment or mild to moderate dementia, living in the community (86%) or nursing homes (14%) in the Netherlands. Following the inclusion criteria of MCI or dementia and the MMSE cutoff score of 14 or higher, it did not include people without cognitive impairment or people with severe cognitive impairment.

Clinical Relevance

This study showed a strong, positive correlation between the chewing efficiency and the number of teeth present and the number of occluding pairs, indicating that their maintenance is important to maintaining a good chewing efficiency. Tooth loss can lead to chewing difficulties and food deficiencies, affecting general health (Kossioni et al., 2018). The oral health-related quality of life (OHRQoL) and chewing efficiency might be restored partially with removable prostheses in people with cognitive impairment or dementia (Campos et al., 2018).

Oral health is important in maintaining food intake, general health, and quality of life (Niesten et al., 2012; Furuta et al., 2013; Peres et al., 2019; van de Rijt et al., 2019). The maintenance of oral health in older people with cognitive impairment requires specialized care (Janssens et al., 2018b; Marchini et al., 2019), including oral health-care assistance by formal and informal caregivers, knowledge about oral health, general health, and cognitive impairment, as well as a multidisciplinary collaboration (Delwel et al., 2018; Jablonski et al., 2018; Janssens et al., 2018a).

Future Research

For future studies, it is recommended to use an objective measurement for the assessment of chewing efficiency (Weijenberg et al., 2011). For this purpose, a two-colored chewing gum could be used, which is a validated method to evaluate chewing efficiency (Weijenberg et al., 2013). An advantage of the chewing gum is the sweet taste, which could encourage cooperation of study participants. Our clinical observation was that the chewing gum could stick to full prosthesis in the upper jaw. At the same time, Silva et al. specifically studied the reliability of chewing gum in participants with full prosthesis in the upper and lower jaw and concluded that it can be used reliably to assess mastication in this group (Silva et al., 2018). An alternative method to evaluate chewing efficiency in participants with prosthesis is the use of red and blue wax (Speksnijder et al., 2009) or gummy jellies (Ikebe et al., 2011). The Chewing Efficiency Analysis software that was used in the current study is also suitable for the analysis of other materials with contrasting colors (see algorithm in **Table 1**). In addition to a mixing ability test, the evaluation of maximum voluntary bite force is important to assess the level of functioning of the masticatory system (Speksnijder et al., 2009; Ikebe et al., 2011; Weijenberg et al., 2011).

For the screening of global cognitive functioning, the MMSE is suitable and widely used (Nilsson et al., 2014). In order to study the relation between chewing and cognitive functioning, more specific cognitive tests seem interesting, such as tests for spatial memory and learning capacity (Teixeira et al., 2014; Weijenberg et al., 2018). Moreover, a multifactorial approach is needed, including age, socioeconomic status, cognition, dentition, general health, nutrition, chewing efficiency, inflammatory factors, and stress levels (Azuma et al., 2017; Weijenberg et al., 2018).

CONCLUSION

Better mastication is associated with a higher number of occluding pairs. Moreover, full prosthesis in the upper jaw is related to a lower chewing efficiency, compared to natural dentition in the upper jaw. Furthermore, global cognitive functioning is not associated with mastication in older people with MCI or mild to moderate dementia, after adjusting for age and dentition. This might be explained by sufficient capacity for compensation of reduced mastication in this group.

DATA AVAILABILITY STATEMENT

The datasets generated for this study are available on request to the corresponding author.

ETHICS STATEMENT

The study protocol was reviewed and approved by the Medical Ethics Review Committee of the Amsterdam UMC

(approval number NL 43861.029.13). The participants or their legal representatives provided written informed consent for participation in this study.

AUTHOR CONTRIBUTIONS

ES, FL, and SD designed the study. JM developed the Chewing Efficiency Analysis software. SD collected and analyzed the data. SD and DP drafted the manuscript. All authors contributed to the article and approved the submitted version.

FUNDING

This study was supported by grants from Alzheimer Nederland (WE.09-2012-02), Amstelring (RVB U-9107-2013/HM/wb), Arnold Oosterbaan Hersenstichting, Fonds NutsOhra (1130-046), Roomsche Catholiek Oude Armen Kantoor (U-9128-2012 HM/lw), Stichting Beroepsopleiding Huisartsen (SBOH), and Stichting Henriëtte Hofje. FL reports grants from Sunstar Suisse, SomnoMed, Goedegebuure, and Airway Management, outside the submitted work.

REFERENCES

- American Psychiatric Association. (2000). *Diagnostic and Statistical Manual of Mental Disorders, Fourth Edition, Text Revision (DSM-IV-TR)*. 3rd Edn. Arlington, VA: American Psychiatric Association.
- Avivi-Arber, L., and Sessle, B. J. (2018). Jaw sensorimotor control in healthy adults and effects of ageing. *J. Oral Rehabil.* 45, 50–80. doi: 10.1111/joor.12554
- Azuma, K., Zhou, Q., Niwa, M., and ya Kubo, K. (2017). Association between mastication, the hippocampus and the HPA axis: a comprehensive review. *Int. J. Mol. Sci.* 18:1687. doi: 10.3390/ijms18081687
- Beydoun, M. A., Beydoun, H. A., Gamaldo, A. A., Teel, A., Zonderman, A. B., and Wang, Y. (2014). Epidemiologic studies of modifiable factors associated with cognition and dementia: systematic review and meta-analysis. *BMC Public Health* 14:643. doi: 10.1186/1471-2458-14-643
- Campos, C. H., Ribeiro, G. R., and Rodrigues Garcia, R. C. M. M. (2018). Mastication and oral health-related quality of life in removable denture wearers with Alzheimer disease. *J. Prosthet. Dent.* 119, 764–768. doi: 10.1016/j.prosdent.2017.07.010
- Delwel, S., Binnekade, T. T., Perez, R. S. G. M., Hertogh, C. M. P. M., Scherder, E. J. A., and Lobbezoo, F. (2017). Oral health and orofacial pain in older people with dementia: a systematic review with focus on dental hard tissues. *Clin. Oral Investig.* 21, 17–32. doi: 10.1007/s00784-016-1934-9
- Delwel, S., Binnekade, T. T., Perez, R. S. G. M., Hertogh, C. M. P. M., Scherder, E. J. A., and Lobbezoo, F. (2018). Oral hygiene and oral health in older people with dementia: a comprehensive review with focus on oral soft tissues. *Clin. Oral Investig.* 22, 93–108. doi: 10.1007/s00784-017-2264-2
- Elsig, F., Schimmel, M., Duvernay, E., Giannelli, S. V., Graf, C. E., Carlier, S., et al. (2015). Tooth loss, chewing efficiency and cognitive impairment in geriatric patients. *Gerodontology* 32, 149–56. doi: 10.1111/ger.12079
- Fereshtehnejad, S.-M., Garcia-Plata, S., Religa, D., Holmer, J., Buhlin, K., Eriksdotter, M., et al. (2017). Dental care utilization in patients with different types of dementia: a longitudinal nationwide study of 58,037 individuals. *Alzheimers Dement.* 14, 10–19. doi: 10.1016/j.jalz.2017.05.004
- Folstein, M. F., Folstein, S. E., and McHugh, P. R. (1975). “Mini-mental state”. A practical method for grading the cognitive state of patients for the clinician. *J. Psychiatr. Res.* 12, 189–198. doi: 10.1016/0022-3956(75)90026-6
- Furuta, M., Komiya-Nonaka, M., Akifusa, S., Shimazaki, Y., Adachi, M., Kinoshita, T., et al. (2013). Interrelationship of oral health status, swallowing

ACKNOWLEDGMENTS

We thank the participants and their care providers for their cooperation with the study. Furthermore, we thank the staff of the outpatient clinics at the VU Medical Center and the Amstelland Hospital, the staff at the 10 participating nursing homes of Amstelring, Cordaan, and Zonnehuisgroep Amstelland for their cooperation. Moreover, we thank Tarik Binnekade of the Department of Clinical Neuropsychology, Vrije Universiteit Amsterdam, and Janine van Kooten of the Department of General Practice and Elderly Care Medicine, VU University Medical Center, for their help with the acquisition of the participants and the demographic and neuropsychological data collection. Furthermore, we thank the students of the Department of Clinical Neuropsychology, Vrije Universiteit Amsterdam, and the Department of Orofacial Pain and Dysfunction, Academic Centre for Dentistry Amsterdam (ACTA), for their assistance. In addition, we thank Irene Aartman of the Department of Social Dentistry and Maurits van Selms of the Department for Orofacial Pain and Dysfunction, Academic Centre for Dentistry Amsterdam (ACTA), for their statistical support.

- function, nutritional status and cognitive ability with activities of daily living in Japanese elderly people receiving home care services due to physical disabilities. *Community Dent. Oral Epidemiol.* 41, 173–181. doi: 10.1111/cdoe.12000
- Gerritsen, A. E., Witter, D. J., Bronkhorst, E. M., and Creugers, N. H. J. (2013). An observational cohort study on shortened dental arches-clinical course during a period of 27–35 years. *Clin. Oral Investig.* 17, 859–866. doi: 10.1007/s00784-012-0765-6
- Gonçalves, T. M. S. V., Vilanova, L. S. R., Gonçalves, L. M., and Rodrigues Garcia, R. C. M. (2014). Effect of complete and partial removable dentures on chewing movements. *J. Oral Rehabil.* 41, 177–183. doi: 10.1111/joor.12125
- Hadjistavropoulos, T., Fitzgerald, T. D., and Marchildon, G. P. (2010). Practice guidelines for assessing pain in older persons with dementia residing in long-term care facilities. *Physiother. Can.* 62, 104–113. doi: 10.3138/physio.62.2.104
- Henskens, M., Nauta, I. M., Drost, K. T., and Scherder, E. J. A. (2018). The effects of movement stimulation on activities of daily living performance and quality of life in nursing home residents with dementia: a randomized controlled trial. *Clin. Interv. Aging* 13, 805–817. doi: 10.2147/cia.s160031
- Ikebe, K., Matsuda, K., Kagawa, R., Enoki, K., Yoshida, M., Maeda, Y., et al. (2011). Association of masticatory performance with age, gender, number of teeth, occlusal force and salivary flow in Japanese older adults: is ageing a risk factor for masticatory dysfunction? *Arch. Oral Biol.* 56, 991–996. doi: 10.1016/j.archoralbio.2011.03.019
- Jablonski, R. A., Kolanowski, A. M., Azuero, A., Winstead, V., Jones-Townsend, C., and Geisinger, M. L. (2018). Randomised clinical trial: efficacy of strategies to provide oral hygiene activities to nursing home residents with dementia who resist mouth care. *Gerodontology* 35, 365–375. doi: 10.1111/ger.12357
- Janssens, B., Vanobbergen, J., Lambert, M., Schols, J. M. G. A., and De Visschere, L. (2018a). Effect of an oral healthcare programme on care staff knowledge and attitude regarding oral health: a non-randomised intervention trial. *Clin. Oral Investig.* 22, 281–292. doi: 10.1007/s00784-017-2110-6
- Janssens, B., Vanobbergen, J., Petrovic, M., Jacquet, W., Schols, J. M., and De Visschere, L. (2018b). The impact of a preventive and curative oral healthcare program on the prevalence and incidence of oral health problems in nursing home residents. *PLoS One* 13:e0198910. doi: 10.1371/journal.pone.0198910

- Käyser, A. F. (1990). How much reduction of the dental arch is functionally acceptable for the ageing patient? *Int. Dent. J.* 40, 183–8.
- Kester, M. I., and Scheltens, P. (2009). Dementia: the bare essentials. *Pract. Neurol.* 9, 241–251. doi: 10.1136/jnnp.2009.182477
- Kim, E.-K., Lee, S. K., Choi, Y.-H., Tanaka, M., Hirotsu, K., Kim, H. C., et al. (2017). Relationship between chewing ability and cognitive impairment in the rural elderly. *Arch. Gerontol. Geriatr.* 70, 209–213. doi: 10.1016/j.archger.2017.02.006
- Kimura, Y., Ogawa, H., Yoshihara, A., Yamaga, T., Takiguchi, T., Wada, T., et al. (2013). Evaluation of chewing ability and its relationship with activities of daily living, depression, cognitive status and food intake in the community-dwelling elderly. *Geriatr. Gerontol. Int.* 13, 718–725. doi: 10.1111/ggi.12006
- Kossioni, A. E., Hajto-Bryk, J., Janssens, B., Maggi, S., Marchini, L., McKenna, G., et al. (2018). Practical guidelines for physicians in promoting oral health in frail older adults. *J. Am. Med. Dir. Assoc.* 19, 1039–1046. doi: 10.1016/j.jamda.2018.10.007
- Kossioni, A. E., Hajto-Bryk, J., Maggi, S., McKenna, G., Petrovic, M., Roller-Wirnsberger, R. E., et al. (2018). An expert opinion from the European college of gerodontology and the European geriatric medicine society: European policy recommendations on oral health in older adults. *J. Am. Geriatr. Soc.* 66, 609–613. doi: 10.1111/jgs.15191
- Lexomboon, D., Trulsson, M., Wårdh, I., and Parker, M. G. (2012). Chewing ability and tooth loss: Association with cognitive impairment in an elderly population study. *J. Am. Geriatr. Soc.* 60, 1951–1956. doi: 10.1111/j.1532-5415.2012.04154.x
- Lin, C., Wu, C., Wu, S., Lin, H.-H., Cheng, D., and Lo, W. (2017). Age-related difference in functional brain connectivity of mastication. *Front. Aging Neurosci.* 9:82. doi: 10.3389/fnagi.2017.00082
- Malykhin, N., Vahidy, S., Michielse, S., Coupland, N., Camicioli, R., Seres, P., et al. (2011). Structural organization of the prefrontal white matter pathways in the adult and aging brain measured by diffusion tensor imaging. *Brain Struct. Funct.* 216, 417–431. doi: 10.1007/s00429-011-0321-1
- Marchini, L., Ettinger, R., Caprio, T., and Jucan, A. (2019). Oral health care for patients with Alzheimer's disease: an update. *Spec. Care Dent.* 39, 262–273. doi: 10.1111/scd.12375
- McKeith, I. G., Dickson, D. W., Lowe, J., Emre, M., O'Brien, J. T., Feldman, H., et al. (2005). Diagnosis and management of dementia with Lewy bodies: third report of the DLB consortium. *Neurology* 65, 1863–1872. doi: 10.1212/wnl.65.12.1992-a
- McKhann, G. M., Knopman, D. S., Chertkow, H., Hyman, B. T., Jack, C. R., Kawas, C. H., et al. (2011). The diagnosis of dementia due to Alzheimer's disease: recommendations from the National Institute on Aging-Alzheimer's Association workgroups on diagnostic guidelines for Alzheimer's disease. *Alzheimers Dement.* 7, 263–269. doi: 10.1016/j.jalz.2011.03.005
- Müller, F., Shimazaki, Y., Kahabuka, F., and Schimmel, M. (2017). Oral health for an ageing population: the importance of a natural dentition in older adults. *Int. Dent. J.* 67, 7–13. doi: 10.1111/idj.12329
- Niesten, D., Van Mourik, K., and Van Der Sanden, W. (2012). The impact of having natural teeth on the QoL of frail dentulous older people. A qualitative study. *BMC Public Health* 12:1. doi: 10.1186/1471-2458-12-839
- Nilsson, H., Berglund, J., and Renvert, S. (2014). Tooth loss and cognitive functions among older adults. *Acta Odontol. Scand.* 72, 639–644. doi: 10.3109/00016357.2014.882983
- Peres, M. A., Macpherson, L. M. D., Weyant, R. J., Daly, B., Venturelli, R., Mathur, M. R., et al. (2019). Oral diseases: a global public health challenge. *Lancet* 394, 249–260. doi: 10.1016/S0140-6736(19)31146-8
- Petersen, P. E. (2003). The World Oral Health Report 2003: continuous improvement of oral health in the 21st century--the approach of the WHO global oral health programme. *Community Dent. Oral Epidemiol.* 31, 3–23. doi: 10.1046/j.2003.com122.x
- Petersen, R. C., Caracciolo, B., Brayne, C., Gauthier, S., Jelic, V., and Fratiglioni, L. (2014). Mild cognitive impairment: a concept in evolution. *J. Intern. Med.* 275, 214–228. doi: 10.1111/joim.12190
- Petersen, R. C., Lopez, O., Armstrong, M. J., Getchius, T. S. D., Ganguli, M., Gloss, D., et al. (2018). Practice guideline update summary: mild cognitive impairment. *Neurology* 90, 126–135. doi: 10.1212/WNL.00000000000006038
- Prince, M., Bryce, R., Albanese, E., Wimo, A., Ribeiro, W., and Ferri, C. P. (2013). The global prevalence of dementia: a systematic review and metaanalysis. *Alzheimers Dement.* 9, 63–75.e2. doi: 10.1016/j.jalz.2012.11.007
- Rascovsky, K., Hodges, J. R., Knopman, D., Mendez, M. F., Kramer, J. H., Neuhaus, J., et al. (2011). Sensitivity of revised diagnostic criteria for the behavioural variant of frontotemporal dementia. *Brain* 134, 2456–77. doi: 10.1093/brain/awr179
- Román, G. C., Tatemichi, T. K., Erkinjuntti, T., Cummings, J. L., Masdeu, J. C., García, J. H., et al. (1993). Vascular dementia: diagnostic criteria for research studies. Report of the NINDS-AIREN International Workshop. *Neurology* 43, 250–60. doi: 10.1212/wnl.43.2.250
- Sanderson, S., Tatt, I. D., and Higgins, J. P. T. (2007). Tools for assessing quality and susceptibility to bias in observational studies in epidemiology: a systematic review and annotated bibliography. *Int. J. Epidemiol.* 36, 666–676. doi: 10.1093/ije/dym018
- Sesay, M., Tanaka, A., Ueno, Y., Lecaroz, P., and De Beaufort, D. G. (2000). Assessment of regional cerebral blood flow by xenon-enhanced computed tomography during mastication in humans. *Keio J. Med.* 49, A125–A128.
- Silva, L. C., Nogueira, T. E., Rios, L. F., Schimmel, M., and Leles, C. R. (2018). Reliability of a two-colour chewing gum test to assess masticatory performance in complete denture wearers. *J. Oral Rehabil.* 45, 301–307. doi: 10.1111/joor.12609
- Speksnijder, C. M., Abbink, J. H., Van Der Glas, H. W., Janssen, N. G., and Van Der Bilt, A. (2009). Mixing ability test compared with a comminution test in persons with normal and compromised masticatory performance. *Eur. J. Oral Sci.* 117, 580–586. doi: 10.1111/j.1600-0722.2009.00675.x
- Tada, A., and Miura, H. (2017). Association between mastication and cognitive status: a systematic review. *Arch. Gerontol. Geriatr.* 70, 44–53. doi: 10.1016/j.archger.2016.12.006
- Taubert, M., Roggenhofer, E., Melie-Garcia, L., Muller, S., Lehmann, N., Preisig, M., et al. (2020). Converging patterns of aging-associated brain volume loss and tissue microstructure differences. *Neurobiol. Aging* 88, 108–118. doi: 10.1016/j.neurobiolaging.2020.01.006
- Teixeira, F. B., Pereira Fernandes, L. M., Noronha, P. A. T., dos Santos, M. A. R., Gomes-Leal, W., Ferraz Maia, C. S., et al. (2014). Masticatory deficiency as a risk factor for cognitive dysfunction. *Int. J. Med. Sci.* 11, 209–14. doi: 10.7150/ijms.6801
- Tonetti, M. S., Bottenberg, P., Conrads, G., Eickholz, P., Heasman, P., Huysmans, M.-C., et al. (2017). Dental caries and periodontal diseases in the ageing population: call to action to protect and enhance oral health and well-being as an essential component of healthy ageing - Consensus report of group 4 of the joint EFP/ORCA workshop on the boundaries be. *J. Clin. Periodontol.* 44, S135–S144. doi: 10.1111/jcpe.12681
- Tonsek, P. P., Jiang, S. S., and Yue, G. (2017). Periodontal disease, tooth loss and dementia: is there a link? A systematic review. *Gerodontology* 34, 151–163. doi: 10.1111/ger.12261
- Tsutsui, K., Kaku, M., Motokawa, M., Tohma, Y., Kawata, T., Fujita, T., et al. (2007). Influences of reduced masticatory sensory input from soft-diet feeding upon spatial memory/learning ability in mice. *Biomed. Res.* 28, 1–7. doi: 10.2220/biomedres.28.1
- van de Rijt, L. J. M., Stoop, C. C., Weijenberg, R. A. F., de Vries, R., Feast, A. R., Sampson, E. L., et al. (2019). The influence of oral health factors on the quality of life in older people: a systematic review. *Gerontologist* XX, 1–17. doi: 10.1093/geront/gnz105
- van Kooten, J., Delwel, S., Binnekade, T. T., Smalbrugge, M., Van Der Wouden, J. C., Perez, R. S. G. M., et al. (2015). Pain in dementia: prevalence and associated factors: protocol of a multidisciplinary study. *BMC Geriatr.* 15:29. doi: 10.1186/s12877-015-0025-0
- Watanabe, K., Ozono, S., Nishiyama, K., Saito, S., Tonosaki, K., Fujita, M., et al. (2002). The molarless condition in aged SAMP8 mice attenuates hippocampal Fos induction linked to water maze performance. *Behav. Brain Res.* 128, 19–25. doi: 10.1016/S0166-4328(01)00268-6
- Weijenberg, R. A. F., Delwel, S., Ho, B., Van van der Maarel-Wierink, C. D., and Lobbezoo, F. (2018). Mind your teeth—The relationship between mastication and cognition. *Gerodontology* 36, 2–7. doi: 10.1353/book.49273

- Weijenberg, R. A. F., Lobbezoo, F., Visscher, C. M., and Scherder, E. J. A. (2015). Oral mixing ability and cognition in elderly persons with dementia: a cross-sectional study. *J. Oral Rehabil.* 42, 481–486. doi: 10.1111/joor.12283
- Weijenberg, R. A. F., Scherder, E. J. A., and Lobbezoo, F. (2011). Mastication for the mind—The relationship between mastication and cognition in ageing and dementia. *Neurosci. Biobehav. Rev.* 35, 483–497. doi: 10.1016/j.neubiorev.2010.06.002
- Weijenberg, R. A. F., Scherder, E. J. A., Visscher, C. M., Gorissen, T., Yoshida, E., and Lobbezoo, F. (2013). Two-colour chewing gum mixing ability: digitalisation and spatial heterogeneity analysis. *J. Oral Rehabil.* 40, 737–743. doi: 10.1111/joor.12090
- Wu, B., Fillenbaum, G. G., Plassman, B. L., and Guo, L. (2016). Association between oral health and cognitive status: a systematic review. *J. Am. Geriatr. Soc.* 64, 739–51. doi: 10.1111/jgs.14572
- Yamamoto, T., and Hirayama, A. (2001). Effects of soft-diet feeding on synaptic density in the hippocampus and parietal cortex of senescence-accelerated mice. *Brain Res.* 902, 255–63. doi: 10.1016/s0006-8993(01)02410-6
- Conflict of Interest:** The authors declare that the research was conducted in the absence of any commercial or financial relationships that could be construed as a potential conflict of interest.

Copyright © 2020 Delwel, Maier, Parvaneh, Meijers, Scherder and Lobbezoo. This is an open-access article distributed under the terms of the Creative Commons Attribution License (CC BY). The use, distribution or reproduction in other forums is permitted, provided the original author(s) and the copyright owner(s) are credited and that the original publication in this journal is cited, in accordance with accepted academic practice. No use, distribution or reproduction is permitted which does not comply with these terms.



Small Posterior Cranial Fossa and Cerebellopontine Cistern Volumes Are Associated With Bilateral Trigeminal Neuralgia

Jiayu Liu^{1†}, Ruen Liu^{1,2*}, Bo Liu¹, Jingru Zhou¹, Cungang Fan¹, Feng Jiao¹, Dongliang Wang¹, Fang Li¹ and Bo Hei¹

¹ Department of Neurosurgery, Peking University People's Hospital, Beijing, China, ² Department of Neurosurgery, Jiangxi provincial People's Hospital Affiliated to Nanchang University, Nanchang, China

OPEN ACCESS

Edited by:

Teresa Lever,
University of Missouri, United States

Reviewed by:

Marcelo M. Valença,
Federal University of
Pernambuco, Brazil
Yohannes W. Woldeamanuel,
Stanford University, United States

*Correspondence:

Ruen Liu
liuruen@pku.edu.cn

†ORCID:

Jiayu Liu
orcid.org/0000-0001-6976-4568

Specialty section:

This article was submitted to
Headache Medicine and Facial Pain,
a section of the journal
Frontiers in Neurology

Received: 16 June 2020

Accepted: 11 September 2020

Published: 15 October 2020

Citation:

Liu J, Liu R, Liu B, Zhou J, Fan C,
Jiao F, Wang D, Li F and Hei B (2020)
Small Posterior Cranial Fossa and
Cerebellopontine Cistern Volumes Are
Associated With Bilateral Trigeminal
Neuralgia. *Front. Neurol.* 11:573239.
doi: 10.3389/fneur.2020.573239

Objective: To investigate whether small volumes of the posterior cranial fossa and cerebellopontine cisterns are associated with bilateral trigeminal neuralgia (BTN) and to provide further knowledge regarding the etiology and treatment of this rare disease.

Methods: We retrospectively analyzed clinical data and imaging examination results for 30 BTN patients between January 2009 and December 2019. Thirty age- and sex-matched healthy individuals and 30 patients with unilateral trigeminal neuralgia (UTN) were selected as two control groups. The volume of the posterior cranial fossa (VPCF) and volumes of the cerebellopontine cisterns were measured using ITK-SNAP 3.0, which considers the cerebrospinal fluid (CSF) volume based on the region of interest (ROI). Preoperative and postoperative statuses were based on visual analog scale (VAS) pain scores and Barrow Neurological Institute (BNI) scores.

Results: A total of 30 patients (11 males; 19 females) were included, and the age of the BTN participants ranged from 41 to 77 (59.93 ± 9.89) years. The duration of TN ranged from 1 to 20 (5.36 ± 3.92) years, and the interval between the two sides ranged from 0 to 3 (1.10 ± 0.79) years. Three patients (10%) in the BTN group had familial trigeminal neuralgia, with no other hereditary history of neurological disorders. In BTN patients, with 25 (83.3%) cases on the left side and 26 (86.7%) on the right side, veins were identified in the operative field and regarded as the individual or offending vessel. The mean VPCF was significantly lower in the patients with BTN than in the healthy controls ($4,813 \pm 1,155 \text{ mm}^3$ vs. $5,127 \pm 1,129 \text{ mm}^3$, $p = 0.008$). The volumes of the cerebellopontine cisterns on both sides were significantly smaller in the BTN patients than in the healthy controls ($477 \pm 115 \text{ mm}^3$ vs. $515 \pm 112 \text{ mm}^3$ on the left side, $p = 0.001$; and $481 \pm 114 \text{ mm}^3$ vs. $515 \pm 110 \text{ mm}^3$ on the right side, $p = 0.007$). There was no significant difference between the BTN group and the UTN group in terms of the VPCF ($4,843 \pm 1,184 \text{ mm}^3$ vs. $4,813 \pm 1,155 \text{ mm}^3$, $p = 0.402$), and there was also no significant difference between the two groups in terms of preoperative VAS pain scores or BNI scores.

Conclusion: Overcrowding in the posterior fossa will lead to closer neurovascular relations and, a higher incidence of NVC, and ultimately may be more likely to lead to TN. Veins are the common offending vessels that cause BTN; they might be associated with abnormal vascular development leading to NVC. Microsurgical vascular decompression (MVD) is a safe and effective method for the treatment of BTN, similar to UTN.

Keywords: bilateral trigeminal neuralgia, posterior cranial fossa, cerebellopontine cisterns, microvascular decompression, neurovascular conflict

INTRODUCTION

Trigeminal neuralgia (TN) is recurrent and intense pain in the region of the trigeminal nerve innervation (1). The pathogenesis of TN is believed to comprise neurovascular conflict (NVC) between the trigeminal nerve and adjacent blood vessels (2). By eliminating NVC, microsurgical vascular decompression (MVD) can successfully relieve pain. Several studies have shown that the small space of the posterior cranial fossa is associated with NVC, suggesting a correlation between overcrowding of the posterior cranial fossa and TN (3, 4).

In general, bilateral trigeminal neuralgia (BTN) is rare in clinical practice (5), though its occurrence has been reported as early as the 18th century (6). The pathogenesis remains controversial. Some scholars believe that the pathogenesis of this disease is different from that of UTN (7), but most consider that it is the same type of disease. Although one study showed that the mean MRI volumetry of the posterior cranial fossa was smaller in a BTN group than in a unilateral trigeminal neuralgia (UTN) (8), volume measurement does not fully consider individual differences. Indeed, this measurement is susceptible to the influence of head circumference and body shape. Moreover, as a limitation, the number of cases was small in that study. Cerebrospinal fluid volume (CSFV) is an effective space for the posterior cranial fossa. The CSFV in the posterior cranial fossa can be used to evaluate the effective space in this region, and can accurately reflect the degree of crowding. In this study, we measured and compared the degree of posterior cranial fossa crowding in Chinese patients with BTN and investigated whether small volumes of the posterior cranial fossa and cerebellopontine cisterns are associated with BTN. Additionally, clinical data for patients with BTN were analyzed to provide further knowledge regarding the etiology and treatment of this rare disease.

METHODS

Patients

Clinical data for 30 patients with bilateral trigeminal neuralgia who received MVD were collected between January 2009 and December 2019 at the Department of Neurosurgery, Peking University People's Hospital, the Seventh Medical Center of PLA General Hospital and Characteristic Medical Center of Strategic Support Force. Patients with secondary or atypical TN and incomplete clinical data were excluded. Operations were carried out by the corresponding author Ruen Liu.

Age- and sex-matched healthy individuals and patients with UTN were selected as two control groups. Written informed consent was obtained from each participant, and the study was approved by the institutional review board of the hospitals.

Magnetic Resonance Imaging

A preoperative MRI examination was performed in all cases, including 3D T1- and T2-weighted high-resolution sequences, for clear visualization of the trigeminal nerve and all vascular structures. The use of 3D time-of-flight magnetic resonance angiography (MRA) allowed the visualization of only vessels with high flow, which are principally arteries.

Imaging was conducted using a Discovery 750 3.0T (GE Healthcare, Waukesha, WI) MRI scanner. T1-weighted anatomical images in the sagittal plane were collected with a 3D fast spoiled gradient-echo sequence: repetition time (TR) = 4.9 ms, echo time (TE) = 2 ms, flip angle = 15°, field of view (FOV) = 240 mm, in-plane resolution = 1 × 1 mm², slice thickness = 1 mm, and 170 slices. All scans were performed by the same imaging physician.

Image Data Analysis

VPCF was measured using ITK-SNAP 3.0 (Cognitica, Philadelphia, PA, USA, <http://www.itksnap.org>) that considered the cerebrospinal fluid (CSF) volume, as based on the region of interest (ROI), as well as the thickness and number of the individual layers. The measurement was limited to the region from the root entry zone (REZ) of the trigeminal nerve to that of the vagus nerve of the medulla oblongata and included only the fluid space of the precerebellar cistern, prepinal cistern and cerebellopontine cisterns (Figure 1). To minimize the influence of cerebellar atrophy, the CSF volume from behind the pontocerebellar cisterns, laterally, and from behind the cerebellar hemisphere as well as in the fourth ventricle were not considered for the determination of VPCF. The ROI was automatically marked on each layer in the 3D sequences and corrected manually by the radiologist, if necessary.

Operative Technique

After the induction of general anesthesia, the patient was placed in the lateral park bench position with three-point fixation, and a retrosigmoid craniotomy was performed. The rostral edge of the craniotomy was extended until the caudal edge of the transverse sinus was visible and the junction between the transverse and posterior edges of the sigmoid sinus was adequately exposed. After opening the dura mater, the cerebellar horizontal fissure



FIGURE 1 | An example of ROI views on MRI. **(A)** cerebellopontine cisterns, **(B)** precerebellar cistern, **(C)** prepinal cistern.

was carefully dissected to minimize retraction of the acoustic nerve. With maximum protection of the petrosal veins, the trigeminal nerve was observed, and we inserted a Teflon prosthesis between the offending vessels and the affected nerve to separate the neurovascular conflict. If the arcuate eminence of the petrosal bone was found to compress the trigeminal nerve during the operation, the abnormal bone was removed.

If no neurovascular conflict was observed during the operation, the patient underwent microvascular decompression with nerve combing. For nerve combing, the trigeminal nerve itself was then longitudinally divided along its fibers using a special nerve combing knife with a cutting edge of 0.90 mm into 4–5 bundles from the REZ to the petrous bone (9). For concomitant patients, we believe that the side with more severe symptoms should be treated first. Contralateral surgery should be performed if the contralateral side still has pain or aggravation after the first surgery (At least 3 months).

Data Collection

Baseline and medical history data were obtained from medical records. The baseline data included age, sex, and preoperative and postoperative pain status according to visual analog scale (VAS) pain scores. VAS pain scores were recorded on a 11-point scale, with zero indicating no pain and 10 indicating maximal pain. Postoperative outcomes of TN were assessed by the Barrow Neurological Institute (BNI) pain intensity score and the BNI facial numbness score, and the total of both scores was considered for further analysis (10) (Table 1).

Statistical Analysis

SPSS statistical software 19.0 (IBM Corp., Armonk, NY, USA) was used for data analysis. Numerical variables are expressed as the mean \pm SD. Qualitative variables are described as the absolute value of cases in the distinctive group. Statistical significance between quantitative variables was assessed by the χ^2 test, with Yates's or Fisher's correction, if necessary. Student's *t*-test was performed to evaluate the data and to follow a normal distribution. Bonferroni correction was applied for

TABLE 1 | Barrow Neurological Institute (BNI) pain intensity score, facial numbness score, and total evaluation of the results.

(P) Evaluation of pain relief by the BNI pain intensity score

1. No pain, no medication
2. Occasional pain, not requiring medication
3. Some pain, adequately controlled with medication
4. Some pain, not adequately controlled with medication
5. Severe pain/no pain relief

(N) Evaluation of numbness by the BNI facial numbness score

1. No facial numbness
2. Mild facial numbness, not bothersome
3. Facial numbness, somewhat bothersome
4. Facial numbness, very bothersome

(T) Total evaluation of results = (P) + (N)

- 2 Excellent
- 3 Good
- 4 Fair
- ≥ 5 Poor

multiple comparisons. Significant differences between groups were indicated at $p < 0.05$.

RESULTS

Baseline Characteristics

A total of 30 patients (11 males; 19 females) were included, and the age of the BTN participants ranged from 41 to 77 (59.93 ± 9.89) years. Thirty age- and sex-matched healthy individuals and 30 patients with UTN were selected as two control groups. In the BTN group, 14 patients were initially affected on the left side and 16 on the right side. The duration of TN ranged from 1 to 20 (5.36 ± 3.92) years, and the interval between the two sides ranged from 0 to 3 (1.10 ± 0.79) years. Three patients (10%) in the BTN group had familial trigeminal neuralgia, but there was no other hereditary history of neurological disorders.

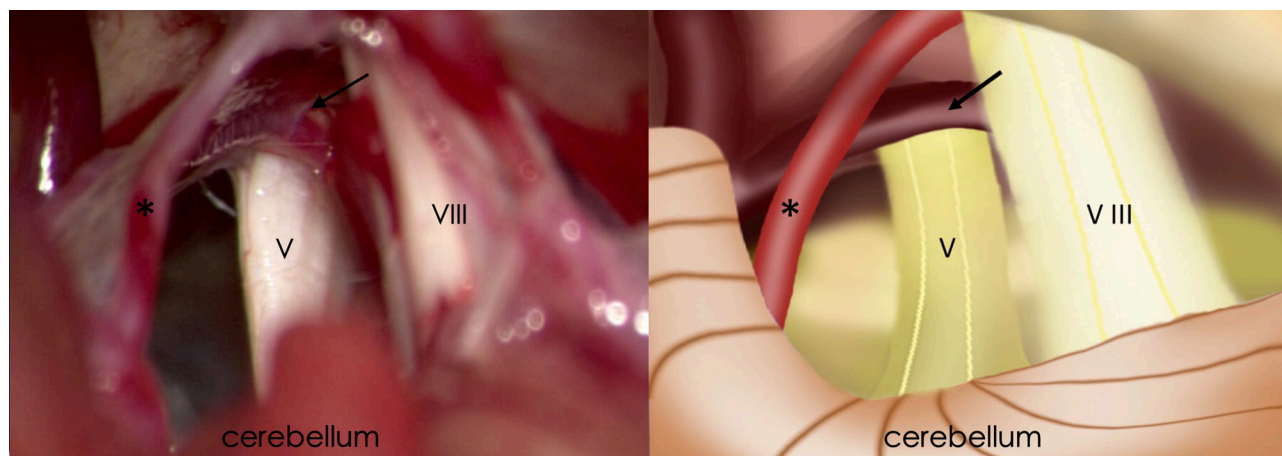


FIGURE 2 | Intraoperative findings of retrosigmoid craniotomy (**Left**) and corresponding schematic diagram (**Right**). Black arrow, the petrosal vein; Asterisk, superior cerebellar artery; V, trigeminal nerve; VIII, vestibulocochlear nerve.

TABLE 2 | Clinical characteristics of the groups.

| Group | BTN (Left) | BTN (Right) | UTN |
|-------------------|-------------|-------------|-------------|
| VAS | 9.17 ± 0.99 | 9.33 ± 0.76 | 9.23 ± 1.04 |
| BNI | | | |
| 2 | 25 | 24 | 26 |
| 3 | 5 | 6 | 4 |
| Offending vessels | | | |
| SCA | 2 | 1 | 19 |
| AICA | 1 | 0 | 3 |
| SCA + AICA | 0 | 1 | 3 |
| Only Vein | 18 | 19 | 3 |
| Vein + SCA | 4 | 3 | 0 |
| Vein + AICA | 2 | 2 | 0 |
| Vein + SCA + AICA | 1 | 2 | 0 |
| None | 2 | 2 | 2 |

Preoperative VAS scores were 9.17 ± 0.99 for the left side and 9.33 ± 0.76 for the right side. Among the BTN patients, 25 (83.3%) cases for the left side and 26 (86.7%) for the right side, veins were identified in the operative field and were regarded as the individual or offending vessel (**Figure 2**). In the other patients, the offending vessels were the anterior inferior cerebellar artery (AICA), superior cerebellar artery (SCA), SCA and AICA or none of these. The offending vessels in all three familial patients were veins. The follow-up period ranged from 6 to 110 months. For left-side cases, postoperative BNI scores were excellent ($T = 2$) in 25 patients (83%) and good ($T = 3$) in 5 (17%). For right-side cases, 24 (80%) patients had excellent outcomes, and 6 (20%) had good outcomes (**Table 2**). All the offending vessels in this study corresponded to TN on the same side. There is no case with bilateral neuralgia that improved bilaterally only with unilateral decompression.

No mortality, complete facial paralysis, intracranial haematoma, or postoperative hearing loss occurred, and

there were no other serious complications. Two patients had scalp tingling, five had facial numbness, and one had transient vertigo, all of whom were cured by symptomatic and supportive treatment. In the follow-up period, no recurrence or any dysfunction of cranial nerves was found on either side. Furthermore, there was no significant difference between the two sides in terms of preoperative VAS pain scores ($p = 0.316$), offending vessels ($p = 0.960$) or BNI scores ($p = 0.739$).

Volumes of the Posterior Cranial Fossa and Cerebellopontine Cisterns

VPCF was defined as the volumes of the precerebellar cistern, prepinal cistern and cerebellopontine cisterns on both sides in BTN patients. The mean VPCF was significantly lower in the patients with BTN than in the healthy controls ($4,813 \pm 1,155 \text{ mm}^3$ vs. $5,127 \pm 1,129 \text{ mm}^3$, $p = 0.008$). Additionally, the volumes of the cerebellopontine cisterns on both sides were significantly smaller in the BTN patients than in the healthy controls ($477 \pm 115 \text{ mm}^3$ vs. $515 \pm 112 \text{ mm}^3$ on the left side, $p = 0.001$; and $481 \pm 114 \text{ mm}^3$ vs. $515 \pm 110 \text{ mm}^3$ on the right side, $p = 0.007$). In contrast, there was no significant difference between the BTN and control groups in terms of the precerebellin cistern volume ($3,084 \pm 743 \text{ mm}^3$ vs. $3,148 \pm 721 \text{ mm}^3$, $t = -0.9$, $p = 0.370$) or the prepinal cistern volume ($771 \pm 185 \text{ mm}^3$ vs. $787 \pm 180 \text{ mm}^3$, $t = -1.0$, $p = 0.400$) (**Table 3**).

In the UTN group, the mean VPCF was significantly lower than that in the healthy control group ($4,843 \pm 1,184 \text{ mm}^3$ vs. $5,127 \pm 1,129 \text{ mm}^3$, $t = -2.61$, $p = 0.014$). Moreover, the volumes of the cerebellopontine cisterns on the affected side were significantly smaller than those on the healthy side ($472 \pm 116 \text{ mm}^3$ vs. $482 \pm 121 \text{ mm}^3$, $t = -2.46$, $p = 0.020$). However, there was no significant difference between the BTN group and the UTN group in terms of VPCF ($t = -0.85$, $p = 0.402$). There was also no significant difference between the BTN group and the UTN group in terms of the precerebellin cistern volume ($3,084 \pm$

TABLE 3 | Comparison of the volumes of the posterior cranial fossa and cerebellopontine cisterns between the BTN and healthy control groups.

| Group | BTN | Healthy controlled | Statistically significance |
|--|---------------|--------------------|----------------------------|
| Posterior fossa vol, mm ³ | 4,813 ± 1,155 | 5,127 ± 1,129 | $t = -2.8; p = 0.008$ |
| CPA cistern vol, mm ³ | | | |
| Left | 477 ± 115 | 515 ± 112 | $t = -3.5; p = 0.001$ |
| Right | 481 ± 114 | 515 ± 110 | $t = -2.9; p = 0.007$ |
| Precerebellin cistern vol, mm ³ | 3,084 ± 743 | 3,148 ± 721 | $t = -0.9; p = 0.370$ |
| Prespinal cistern vol, mm ³ | 771 ± 185 | 787 ± 180 | $t = -1.0; p = 0.400$ |

743 mm³ vs. 3,087 ± 759 mm³, $t = -0.119$, $p = 0.906$) or the prespinal cistern volume (771 ± 185 mm³ vs. 772 ± 190 mm³, $t = -0.120$, $p = 0.900$).

Comparison Between the Bilateral TN and UTN Groups

For the 30 age- and sex-matched UTN patients, the preoperative VAS score was 9.23 ± 1.04 . The superior cerebellar artery (SCA) was identified in the operative field in 26 (87%) patients, though veins were identified in only 3 (10%) patients. Postoperative BNI scores were excellent ($T = 2$) in 26 patients (87%) and good ($T = 3$) in 4 (13%) (Table 2). Conversely, there was no significant difference between the two groups in terms of preoperative VAS pain scores ($p = 0.698$ on the left side, $p = 0.237$ on the right side) or BNI scores ($p = 0.718$ on the left side, $p = 0.488$ on the right side).

DISCUSSION

Trigeminal neuralgia (TN), also known as painful convulsion, is mainly characterized by paroxysmal tearing and acute pain that occurs repeatedly in the trigeminal nerve distribution area on one side of the face (11), with an incidence of 8/100,000 (12). Currently, the theory of peripheral lesions has been accepted by most scholars (13). Regarding the pathogenesis of TN, it is believed that the trigeminal nerve becomes chronically compressed by abnormal twisted microvessels in the REZ area, resulting in inflammation and demyelination changes in the root of the trigeminal nerve and thus in a “short circuit” of membrane potential and neuropathic pain in the trigeminal nerve distribution area (14). One study (4) showed that the size, shape, and structure of the skull varies according to race and sex. Asians, especially women, have a higher incidence of TN and more crowding in the posterior fossa. The space occupied by tissues of the posterior fossa is small, resulting in NVC of the trigeminal nerve and clinical symptoms. However, for people with a large posterior fossa volume, there will be no symptoms of compression, clinical pain or other discomfort, even if the blood vessels are in contact with the nerve (15). In our study, the mean VPCF in the UTN group was significantly lower than that in the healthy control group ($p < 0.05$). The volumes

of the cerebellopontine cisterns on the affected side were also significantly smaller than those on the healthy side ($p < 0.05$), similar to the results obtained by Rasche et al. (16) and Park et al. (17) based on two-dimensional measurement of the coronal plane and cross-section.

Bilateral TN is rare in clinical practice, and the proportion of BTN in TN patients is reported to be 0.6–5.3% (5). In the present study, patients with BTN often presented with paroxysmal needling, knife cutting or radiating excruciating pain on both sides, and the pain symptoms were similar to those of UTN. Furthermore, there was no significant difference between the two groups in terms of preoperative VAS pain scores ($p > 0.05$). BTN is often characterized by simultaneous or alternating attacks on both sides, and in our study, the interval between the two sides ranged from 0 to 3 years.

The pathogenesis of BTN is not clear, but several studies have suggested that BTN is significantly related to microvascular compression of the trigeminal nerve, which is consistent with unilateral pathogenesis (5–7). In this study, neurovascular conflict during surgery was recorded for 93% (28/30) of the patients (Table 2). The offending vessels observed were the AICA, SCA and veins. Some studies to date have linked BTN to multiple sclerosis (MS). For example, research by Brisman et al. reported the presence of MS in 4–10% of BTN patients (18), and Gale et al. found that ~8% of 210 patients with multiple sclerosis have trigeminal neuralgia (19). However, no patients in this study were found to have MS, which is consistent with the findings of another study of patients with BTN in the Chinese population (8). We also observed that the mean MRI volumetry of the posterior cranial fossa was smaller in the BTN group than in the UTN group, though with no significant difference between the groups for VPCF ($p > 0.05$). We believe that the reason for this conflicting outcome is that the measurement of volume did not fully consider individual differences. This measurement is susceptible to the influence of head circumference and body shape, and the number of cases was small, which is a limitation. As one study showed, the mean posterior fossa volume in ipsilateral TN patients was not different from that in controls, even though smaller cisterns were found in these patients (20). In contrast to our study, the method of measuring posterior fossae volume in the study by Park and Ha involved manual measurement by invasive image-guided surgery technology. In our study, the CSFV was used to evaluate the effective space of the posterior cranial fossa, accurately reflecting the degree of crowding. According to our results, the mean VPCF was significantly lower in the patients with BTN than in healthy controls, and the volumes of the cerebellopontine cisterns on both sides in BTN patients were significantly smaller (Table 3). Although previous studies have demonstrated that reduced posterior fossa volume is associated with UTN, our study is the first to find that small volumes of the posterior cranial fossa and cerebellopontine cisterns are associated with BTN. This finding strengthens the theory that BTN, similar to UTN, is the cause of neurovascular conflict. As mentioned above, trigeminal nerve compressed by vessels, resulting in inflammation and demyelination changes in the root of the trigeminal nerve and thus in a “short circuit” of membrane potential and neuropathic

pain in the trigeminal nerve distribution area. Furthermore, 3 (10%) patients in the BTN group in our study had familial trigeminal neuralgia. Previous studies (5, 21) have shown that familial trigeminal neuralgia accounts for 7–17% of patients with BTN, which is consistent with the present results. In fact, anatomical abnormalities of the skull base may explain the familial incidence of TN (22). Takada et al. (23) reported 1 case of achondroplasia with TN, an autosomal inherited disease. The disease in this patient was due to skull dysplasia, which led to crowding of the posterior fossa and the production of NVC. Ugur et al. (24) described a case of Dandy Walker malformation with TN. Dandy Walker malformation is a congenital central nervous system malformation characterized by posterior fossa cysts and cerebellar vermis dysplasia, and it is considered a multifactorial genetic disease. This suggests that TN may have been caused by a small posterior fossa volume due to genetic factors in this patient. Although further study of familial BTN is needed, the results of this study suggest that a small posterior fossa volume is an important factor in the pathogenesis of BTN.

Although few patients have small pontine arteries or veins near the trigeminal nerve REZ that cause NVC, most cases of TN are caused by the SCA (25). UTN patients, 26 (87%) patients, the SCA was identified in the operative field in our study, which is consistent with the above finding. It is worth mentioning that in 25 (83.3%) left-side cases and 26 (86.7%) right-side cases, veins were identified in the operative field and were regarded as the individual or offending vessel. Moreover, the offending vessels in all three familial patients were veins. Smyth et al. (26) purported that familial TN is related to autosomal inherited vascular variant diseases. This study showed that the vascular variation of familial TN is different from known autosomal inherited vascular malformations, which might be related to variation of the vascular system in the posterior cranial fossa (26). Combined with the results of this study, BTN may also be associated with abnormal vascular development leading to NVC. However, further research is needed to address this possibility.

The significance of exploring the pathogenesis of BTN is to determine the surgical treatment strategy. Current studies suggest that MVD and radiofrequency thermocoagulation (RFT) are the most effective treatments (5–7). However, RFT of the bilateral trigeminal nerves inevitably results in a series of complications, particularly numbness in the bilateral trigeminal nerve distribution and decreases in masticatory function, which are often concerning to surgeons and patients. As NVC due to the small volume of the posterior fossa is the cause of BTN, we believe that MVD is the preferred effective treatment for patients who can tolerate craniotomy. Takada et al. (23) found that in patients with familial TN, MVD could achieve a better therapeutic effect in those with a small CPA caused by abnormal skull development. Additionally, MVD can preserve the function of the trigeminal nerve and reduce permanent dysfunction. Regardless, the disadvantage is the high recurrence rate. Combining the trigeminal nerve root in MVD is helpful to cure TN and reduce recurrence. In this study, microvascular decompression and nerve combing were used, and the clinical efficacy was satisfactory (9). Although some patients experienced mild facial numbness, they recovered within half a year. In

addition, postoperative BNI scores were excellent ($T = 2$) in 25 patients (83%) with BTN on the left side and in 24 (80%) with BTN on the right side. Therefore, we believe that MVD is a safe and effective method for the treatment of BTN, similar to UTN. It is worth noting that as shown by our study, patients with BTN tend to have smaller cerebellopontine cisterns. The region of the cerebellopontine angle is the MVD operation area. When the posterior cranial fossa is crowded, the space decreases, and the operation becomes more difficult. Excessive traction of the cerebellar exposure field may damage nerves and blood vessels and increase postoperative complications. Venous compression is characterized by the fact that veins often adhere closely to nerves. Complete separation may cause blood vessel rupture, massive hemorrhage or, after cutting off blood vessels, cerebellar stem vein infarct hemorrhage; it may also injure nerves. Therefore, adhesion release should not be performed during the process, but removing the NVC is necessary. To better assess the difficulty of surgery and to help neurosurgeons develop the best treatment plan, it is recommended that the degree of posterior fossa crowding be evaluated before MVD.

In summary, overcrowding in the posterior fossa will lead to closer neurovascular relations and a higher incidence of NVC and ultimately may be more likely to lead to TN. The purpose of MVD is to separate the NVC by the surgical method and use Teflon for decompression. Therefore, we believe that MVD is an effective treatment for BTN compared with other treatment methods. However, the difficulty of surgery and postoperative complications will increase when the posterior fossa space, as the operating area of MVD, is crowded. Therefore, we recommend that the degree of posterior cranial fossa crowding should be evaluated before MVD to help the neurosurgeon determine the optimal surgical procedure. As described above, all patients in this study achieved satisfactory surgical results. Nonetheless, although this is the largest clinical study of this rare disease, BTN, to date, we must admit that the sample size was too small to enable comparison of the safety and availability of different treatments. In the future, multi-center large-sample studies or meta-analyses are necessary to obtain effective conclusions.

CONCLUSION

TN is a common and frequently occurring disease in neurosurgery, but BTN is rare in clinical practice. The etiology and treatment of BTN are still controversial. Although cases of bilateral trigeminal neuralgia have been reported, clinical studies on the etiology, diagnosis and treatment of BTN are currently lacking. Our study is the first to retrospectively analyze the clinical data, imaging examination results, surgical methods, and treatment efficacy for 30 Chinese patients. First, we found small volumes of the posterior cranial fossa and cerebellopontine cisterns to be associated with BTN. This finding strengthens the theory that BTN is the cause of neurovascular conflict. Second, veins were commonly the offending vessels that caused BTN, which might be associated with abnormal vascular development leading to NVC. Finally, our results show that MVD is a safe and effective method for the treatment of BTN.

DATA AVAILABILITY STATEMENT

The raw data supporting the conclusions of this article will be made available by the authors, without undue reservation.

ETHICS STATEMENT

Written informed consent was obtained from the individual(s) for the publication of any potentially identifiable images or data included in this article.

REFERENCES

- Koopman JS, Dieleman JP, Huygen FJ, de Mos M, Martin CG, Sturkenboom MC. Incidence of facial pain in the general population. *Pain*. (2009) 147:122–7. doi: 10.1016/j.pain.2009.08.023
- Crucchi G, Finnerup NB, Jensen TS, Scholz J, Sindou M, Svensson P, et al. Trigeminal neuralgia: New classification and diagnostic grading for practice and research. *Neurology*. (2016) 87:220–8. doi: 10.1212/WNL.0000000000002840
- Horinek D, Brezova V, Nimsky C, Belsan T, Martinkovic L, Masopust V, et al. The MRI volumetry of the posterior fossa and its substructures in trigeminal neuralgia: a validated study. *Acta Neurochir*. (2009) 151:669–75. doi: 10.1007/s00701-009-0283-8
- Reinard K, Nerenz DR, Basheer A, Tahir R, Jelsema T, Schultz L, et al. Racial disparities in the diagnosis and management of trigeminal neuralgia. *J Neurosurg*. (2017) 126:368–74. doi: 10.3171/2015.11.JNS.151177
- Pollack IF, Jannetta PJ, Bissonette DJ. Bilateral trigeminal neuralgia: a 14-year experience with microvascular decompression. *J Neurosurg*. (1988) 68:559–65. doi: 10.3171/jns.1988.68.4.0559
- Cherrick HM. Trigeminal neuralgia. Report of a bilateral case. *Oral Surg Oral Med Oral Pathol*. (1972) 34:714–26. doi: 10.1016/0030-4220(72)90289-7
- Brisman R. Bilateral trigeminal neuralgia. *J Neurosurg*. (1987) 67:44–8. doi: 10.3171/jns.1987.67.1.0044
- Zhao H, Wang XH, Zhang Y, Zhang X, Tang YD, Zhou P, et al. Management of primary bilateral trigeminal neuralgia with microvascular decompression: 13-case series. *World Neurosurg*. (2018) 109:e724–30. doi: 10.1016/j.wneu.2017.10.072
- Liu J, Wu G, Jiang Y, Li L, Wang D, Liu R. Relationship between arterial blood pressure during trigeminal nerve combing and surgical outcome in patients with trigeminal neuralgia. *World Neurosurg*. (2020) 137:e98–105. doi: 10.1016/j.wneu.2020.08.067
- Rogers CL, Shetter AG, Fiedler JA, Smith KA, Han PP, Speiser BL. Gamma knife radiosurgery for trigeminal neuralgia: the initial experience of The Barrow Neurological Institute. *Int J Radiat Oncol Biol Phys*. (2000) 47:1013–9. doi: 10.1016/S0360-3016(00)00513-7
- Eboli P, Stone JL, Aydin S, Slavin KV. Historical characterization of trigeminal neuralgia. *Neurosurgery*. (2009) 64:1183–6; discussion 1186–7. doi: 10.1227/01.NEU.0000339412.44397.76
- Spatz AL, Zakrzewska JM, Kay EJ. Decision analysis of medical and surgical treatments for trigeminal neuralgia: how patient evaluations of benefits and risks affect the utility of treatment decisions. *Pain*. (2007) 131:302–10. doi: 10.1016/j.pain.2007.02.009
- Barker FG II, Jannetta PJ, Bissonette DJ, Larkins MV, Jho HD. The long-term outcome of microvascular decompression for trigeminal neuralgia. *N Engl J Med*. (1996) 334:1077–83. doi: 10.1056/NEJM199604253341701
- Zakrzewska JM, McMillan R. Trigeminal neuralgia: the diagnosis and management of this excruciating and poorly understood facial pain. *Postgrad Med J*. (2011) 87:410–6. doi: 10.1136/pgmj.2009.080473

AUTHOR CONTRIBUTIONS

JL and RL contributed to the writing of this manuscript, study conception and design, and the editing of the manuscript. BL, JZ, CF, FJ, DW, FL, and BH contributed to the editing of the manuscript. All authors contributed to the article and approved the submitted version.

FUNDING

This study was supported by Peking University People's Hospital (2017-T-01).

- de Almeida Holanda MM, Pereira Neto NG, de Moura Peixoto G, Pinheiro Santos RH. Trigeminal neuralgia secondary to basilar impression: a case report. *J Craniovertebr Junction Spine*. (2015) 6:76–8. doi: 10.4103/0974-8237.156062
- Rasche D, Kress B, Stippich C, Nennig E, Sartor K, Tronnier VM. Volumetric measurement of the pontomesencephalic cistern in patients with trigeminal neuralgia and healthy controls. *Neurosurgery*. (2006) 59:614–20; discussion 614–20. doi: 10.1227/01.NEU.0000228924.20750.D4
- Park SH, Hwang SK, Lee SH, Park J, Hwang JH, Hamm IS. Nerve atrophy and a small cerebellopontine angle cistern in patients with trigeminal neuralgia. *J Neurosurg*. (2009) 110:633–7. doi: 10.3171/2008.8.JNS08522
- Brisman R. Treatment of trigeminal neuralgia associated with multiple sclerosis. *World Neurosurg*. (2014) 81:497–8. doi: 10.1016/j.wneu.2013.10.018
- Gale D, Prime S, Campbell MJ. Trigeminal neuralgia and multiple sclerosis. A complex diagnosis. *Oral Surg Oral Med Oral Radiol Endod*. (1995) 79:398–401. doi: 10.1016/S1079-2104(05)80235-5
- Park YS, Ha SM. Does a small posterior fossa increase nerve vascular conflict in trigeminal neuralgia? *Acta Radiol*. (2015) 56:1514–8. doi: 10.1177/0284185114561914
- DiCorato MP, Pierce BA. Familial trigeminal neuralgia. *South Med J*. (1985) 78:353–4. doi: 10.1097/00007611-198503000-00030
- Auld AW, Buermann A. Trigeminal neuralgia in six members of one generation. *Arch Neurol*. (1965) 13:194. doi: 10.1001/archneur.1965.00470020084011
- Takada Y, Morimoto T, Sugawara T, Ohno K. Trigeminal neuralgia associated with achondroplasia. Case report with literature review. *Acta Neurochir*. (2001) 143:1173–6. doi: 10.1007/s007010100010
- Ugur HC, Torun F, Yilmaz E, Kanpolat Y. Trigeminal neuralgia in a patient with Dandy-Walker malformation. *J Clin Neurosci*. (2005) 12:815–7. doi: 10.1016/j.jocn.2004.09.032
- Granata F, Vinci SL, Longo M, Bernava G, Caffo M, Cutugno M, et al. Advanced virtual magnetic resonance imaging. (MRI) techniques in neurovascular conflict: bidimensional image fusion and virtual cisternography. *Radiol Med*. (2013) 118:1045–54. doi: 10.1007/s11547-013-0928-9
- Smyth P, Greenough G, Stommel E. Familial trigeminal neuralgia: case reports and review of the literature. *Headache*. (2003) 43:910–5. doi: 10.1046/j.1526-4610.2003.03172.x

Conflict of Interest: The authors declare that the research was conducted in the absence of any commercial or financial relationships that could be construed as a potential conflict of interest.

Copyright © 2020 Liu, Liu, Liu, Zhou, Fan, Jiao, Wang, Li and Hei. This is an open-access article distributed under the terms of the Creative Commons Attribution License (CC BY). The use, distribution or reproduction in other forums is permitted, provided the original author(s) and the copyright owner(s) are credited and that the original publication in this journal is cited, in accordance with accepted academic practice. No use, distribution or reproduction is permitted which does not comply with these terms.



Hyperalgesia and Central Sensitization in Subjects With Chronic Orofacial Pain: Analysis of Pain Thresholds and EEG Biomarkers

Andrea Baroni^{1,2*}, Giacomo Severini^{3,4}, Sofia Straudi², Sergio Buja², Silvia Borsato² and Nino Basaglia^{1,2}

¹ Translational Neurosciences and Neurotechnologies, Ferrara University, Ferrara, Italy, ² Department of Neuroscience and Rehabilitation, University Hospital of Ferrara, Ferrara, Italy, ³ School of Electrical and Electronic Engineering, University College Dublin, Dublin, Ireland, ⁴ Centre for Biomedical Engineering, University College Dublin, Dublin, Ireland

OPEN ACCESS

Edited by:

Kazutaka Takahashi,
University of Chicago, United States

Reviewed by:

Joel D. Greenspan,
University of Maryland, Baltimore,
United States

Laura Petrini,

Aalborg University, Denmark
César Fernández-de-las-Peñas,
Rey Juan Carlos University, Spain

*Correspondence:

Andrea Baroni
a.baroni@ospfe.it

Specialty section:

This article was submitted to
Perception Science,
a section of the journal
Frontiers in Neuroscience

Received: 16 April 2020

Accepted: 20 October 2020

Published: 12 November 2020

Citation:

Baroni A, Severini G, Straudi S, Buja S, Borsato S and Basaglia N (2020) Hyperalgesia and Central Sensitization in Subjects With Chronic Orofacial Pain: Analysis of Pain Thresholds and EEG Biomarkers. *Front. Neurosci.* 14:552650. doi: 10.3389/fnins.2020.552650

Introduction: The presence of a temporomandibular disorder is one of the most frequent causes of orofacial pain (OFP). When pain continues beyond tissue healing time, it becomes chronic and may be caused, among other factors, by the sensitization of higher-order neurons. The aim of this study is to describe psychological characteristics of patients with chronic OFP, their peripheral pain threshold, and electroencephalography (EEG) recording, looking for possible signs of central sensitization (CS).

Materials and methods: Twenty-four subjects with chronic OFP caused by temporomandibular disorder were evaluated using the Research Diagnostic Criteria for Temporomandibular Disorders Axis I and Axis II. Pain intensity, catastrophizing, and presence of CS were assessed through self-reported questionnaires. Pressure pain threshold (PPT) was recorded in facial and peripheral sites; EEG activity was recorded during open and closed eyes resting state and also during the pain threshold assessment. Pain thresholds and EEG recordings were compared with a cohort of pain-free age- and sex-matched healthy subjects.

Results: Patients with chronic OFP showed a significant reduction in their pain threshold compared to healthy subjects in all sites assessed. Greater reduction in pain threshold was recorded in patients with more severe psychological symptoms. Decreased alpha and increased gamma activity was recorded in central and frontal regions of all subjects, although no significant differences were observed between groups.

Discussion: A general reduction in PPT was recorded in people who suffer from chronic OFP. This result may be explained by sensitization of the central nervous system due to chronic pain conditions. Abnormal EEG activity was recorded during painful stimulation compared to the relaxed condition in both chronic OFP subjects and healthy controls.

Keywords: chronic pain, orofacial pain, central sensitization, pain threshold, EEG

INTRODUCTION

Chronic pain is defined as pain that lasts for more than 3 months beyond the normal healing time (Treede et al., 2015). Chronic pain impacts working life, somatic, emotional and social well-being, and quality of life of the affected individuals and is recognized as a major health care problem in Europe (Breivik et al., 2006). Involvement of cerebral circuits in chronic pain development has been broadly documented (Apkarian et al., 2004; Kim et al., 2013; Ferdek et al., 2019). Chronic pain seems to be associated with pain related to central networks, and neuroplastic changes in these circuits may change perception of pain independent of peripheral neural activation (Camfferman et al., 2017). The thalamus appears to play a key role in several chronic pain conditions, and its connection with cerebral cortex seems imputable to maintenance of pain (Llinás et al., 1999; Stern et al., 2006). Many studies have tried to identify an electroencephalography (EEG) pattern related to pain development and maintenance beyond physiological tissue healing time (Prichep et al., 2011; Jensen et al., 2013; Pinheiro et al., 2016). Despite the lack of certainty around cortical markers of chronic pain, a reduction in alpha activity in frontal lobes and increased theta activity in the posterior parietal cortex have been recorded in subjects who experience chronic pain in various conditions (Sarnthein et al., 2006; Sarnthein and Jeanmonod, 2008; Jensen et al., 2013; Camfferman et al., 2017). Recently, the International Association for the Study of Pain (IASP) distinguished between “chronic primary pain” and “chronic secondary pain.” In the first category, chronic pain is conceived as a disease in its own right; in the second, pain is a consequence of an underlying disease and may be initially conceived as a symptom (Treede et al., 2019). Orofacial pain (OFP) is usually classified as chronic secondary pain because, in most cases, it can be attributed to an underlying cause (Benoliel et al., 2019). Frequently, the pain starts from a problem with the temporomandibular joint (TMJ), outlasts the initiating event, and becomes the leading cause for ongoing treatment (Benoliel et al., 2019). Patients, following temporomandibular disease (TMD) resolution, no longer exhibit peripheral tissue damage but continue to feel pain, suggesting an abnormal functioning of the somatosensory system (Sarlan and Greenspan, 2005). This process may be due to an induced sensitization of higher-order neurons, a phenomenon well described by the central sensitization (CS) process (Campi et al., 2017). According to the IASP definition, CS is characterized by an increased responsiveness of nociceptive neurons in the central nervous system (CNS) to their normal or subthreshold afferent input (Loeser and Treede, 2008). With the introduction of the CS concept, pain starts to reflect a functional state of circuits in the CNS instead of being exclusively peripherally driven (Woolf, 2011). Injury or inflammation in peripheral tissue can alter the properties of somatic sensory pathways. This induced peripheral sensitization could trigger CS, leading to pathological pain states (Harte et al., 2018). Evidence for CS has been described in patients with TMD by Dworkin (1995), who found no correlation between physical signs of jaw dysfunction and levels of pain in a 3-year follow-up study. Quantitative sensory testing, such as pressure

pain threshold (PPT), can be used to document the patient's somatosensory profile (Svensson et al., 2011). A generalized state of pain sensitivity can justify low PPT, linked to altered sensory processing, dysregulated endocrine function, hyperinflammatory states, or psychological processes (Lautenbacher et al., 1994). In a large prospective study, the OPPERA (Orofacial Pain: Prospective Evaluation and Risk Assessment) study, Slade et al. (2014) observed that PPT fluctuated in synchrony with the course of painful TMD. Further, a reduction of PPT in sites related to the TMJ has been identified as sign of peripheral sensitization (Campi et al., 2017). In case of sensitization due to supraspinal pathways, the local threshold is further reduced at the local site, but it is also reduced in more distant body sites not related to TMD. The comparison of a TMD cohort with a healthy and pain-free sample may be the only way to evaluate the degree of localized and spreading sensitization (Arendt-Nielsen et al., 2018). We can assume that changes in EEG activity and signs of sensitization can be recorded in people who suffer from long-lasting pain due to TMD. The objective of this study is therefore to describe features of chronic OFP through the analysis of patients' psychological profile, peripheral pain threshold, and EEG recordings, looking for possible signs of CS.

MATERIALS AND METHODS

This cross-sectional observational study describes factors related to chronic OFP and characteristics of patients in a cohort of 24 subjects with OFP due to TMD. This study has been reviewed by the Ferrara University Hospital Ethics Committees. All the procedures described have been carried out in accordance with the Code of Ethics of the World Medical Association (Declaration of Helsinki) for experiments involving humans. Written informed consent was obtained before all procedures. The study meets the STROBE Guidelines for observational studies (von Elm et al., 2014).

Patients who underwent rehabilitation for TMD at Ferrara Rehabilitation Hospital between January 2018 and January 2019 were assessed for eligibility. Age, sex, occupation, side and duration of TMD, past treatment for the TMJ, comorbidities, and medications were recorded. All subjects with a Numeric Pain Rating Scale (NPRS) of less than 3 in the 2 weeks prior to assessment or who took pain relief medication were excluded from the study (Jensen et al., 2013). The other exclusion criteria were impaired cognitive functioning (score < 24 on the Mini-Mental Status Examination), neurological or psychiatric disorders, or pregnancy.

A medical doctor with an expertise in temporomandibular rehabilitation evaluated all subjects included in the study, following the Research Diagnostic Criteria for Temporomandibular Disorders (RDC/TMD) Axis I (Schiffman et al., 2014).

The RDC/TMD Axis II was used to assess psychological distress and pain-related disability (Schiffman et al., 2014). For the purpose of this analysis, depression, anxiety, and non-specific physical symptoms (NSPS) were treated as dichotomous variables, and patients were classified as minimal/mild if their

total score was lower than 10; patients with a higher score were classified as moderate/severe (Campi et al., 2017). All subjects included were evaluated using a self-reported questionnaire for subjective description of pain and PPT for objective assessment of pain perception (Dworkin et al., 2005). Neural activity linked to pain sensation was recorded using EEG. PPT and EEG were also evaluated in a sample of age- and sex-matched healthy controls.

Self-Reported Questionnaire

Catastrophizing has been defined as “an exaggerated negative orientation toward actual or anticipated pain experiences” and reflects a tendency to misinterpret or exaggerate apparently threatening situations (Sullivan et al., 1995). The Pain Catastrophizing Scale (PCS) was used to assess the tendency to magnify the threat value of pain stimulus and to feel helpless in the context of pain (Quartana et al., 2009). A PCS score ≥ 30 was used to detect the presence of catastrophizing (Sullivan et al., 1995).

Central sensitization was assessed using the Italian version of the Central Sensitization Inventory (CSI-I) (Chiarotto et al., 2018). A CSI score ≥ 40 has been suggested as the cutoff score to determine if patients display CS (Neblett et al., 2013, 2015; Nijs et al., 2014).

Pressure Pain Threshold

Pressure pain threshold is defined as the minimum pressure applied to anatomical regions that can induce pain (Fischer, 1987). PPT measurement was performed with a handled digital dynamometer (Commander Algometer, JTECH Medical, United States), consisting of a device with a 1-cm² flat circular tip used to apply pressure on subjects' skin. A researcher was trained to apply increasing pressure of approximately 1 lb/cm²/s perpendicular to the skin using the dynamometer, following a protocol well described in literature (Campi et al., 2017). The stimulus intensity increased from zero, and the subject was instructed to stop the stimulation at the first perception of pain by pushing a button. At that moment, the pressure was removed, and the value of pressure applied was recorded. The sites of the stimulation were the muscle belly of the temporal and masseter muscles, the surface of the mandibular condyle, the middle part of the upper trapezius, and the center of the thenar eminence (Figure 1). During examinations subjects were in a comfortable sitting position with muscles relaxed. The researcher stabilized the subject's head gently applying manual resistance contralateral to the point of pressure application. This procedure was repeated three times for every site, on both sides, with an interstimulus interval of 30 s (Nie et al., 2009). The PPT value of the painful side was used for the analysis. When symptoms were present bilaterally, the value of the more affected side was used. This side was matched in measuring PPT in healthy subjects.

EEG Recording

Electroencephalography assessment was performed using an electrode montage of 32 Ag/AgCl pellet pin electrodes (Easy Cap GmbH, Herrsching, Germany) placed according to the 10–20 International System on a Fast'n Easy cap. A BrainAmp amplifier (Brain Products, Munich, Germany) was used to record

EEG activity. All scalp electrodes were referenced to nasion and grounded at AFz during recordings. Horizontal and vertical eye movements were detected, respectively, with electrodes placed at the left and right outer canthi at Fp1 and below the eye at the non-painful side. The impedance of all the electrodes was kept below 10 k Ω . The EEG signals were recorded with a 1,000-Hz sampling rate with a low cutoff frequency of 0.1 Hz and a high cut-off of 1,000 Hz.

Electroencephalography data were recorded during a 5-min resting state task with open eyes and a 5-min resting state task with closed eyes. Participants were instructed to stay relaxed and keep their eyes fixed on a cross in front of them during open-eyes recording. EEG was also recorded during the PPT assessment at the thenar eminence following the aforementioned protocol.

EEG Preprocessing

The EEG data were preprocessed in MATLAB, using the EEGLab toolbox (Delorme and Makeig, 2004). A notch filter centered around 50 Hz was applied in post-processing for eliminating the power noise. Then, data were re-referenced to the average reference. Eye movement artifacts were removed by means of an independent component analysis (ICA) procedure. ICA was used to determine the independent components. A visual analysis was used to discard components that were characterized by high-amplitude fluctuations and were mostly located at or close to the eye electrodes.

EEG Spectral Analysis

The spectral power in the different EEG bands (delta 1–4 Hz, theta 4–7 Hz, alpha 7–13 Hz, beta 13–30 Hz, gamma 30–60 Hz) was calculated, during both resting state tasks, in the middle minute of the 5 min of each recording. The power spectral density (PSD) was calculated using Welch's method, using 1-s windows and 80% of overlap over successive windows (Welch, 1967). The PSDs of all subjects during each trial were then transformed into z-scores to improve comparability of PSD values across subjects and conditions. For the pain stimulus trials, the PSD was calculated from the 3-s window before reaching the sensory threshold. The z-score of the PSD was calculated for each electrode of each subject during each condition by subtracting by each PSD spectrum its mean and dividing by its standard deviation. For the statistical analyses, in order to minimize the number of comparisons, we calculated the average PSD in the different bands for clusters of electrodes centered around locations F3, C3, P3, and their homologous on the right side of the scalp. For each location, the PSD in each band was calculated as the average PSD in the band among the central and directly adjacent electrodes. To visually assess for relative differences in EEG activity due to the pain, the z-score PSD calculated during the pain stimulus trials was expressed as a percentage of the average PSD calculated from the resting state trials with the eyes open of all subjects. This choice for normalization was dictated by the fact that subjects had their eyes open during the pain stimulus trials. These data were then plotted for both groups for visual comparison.

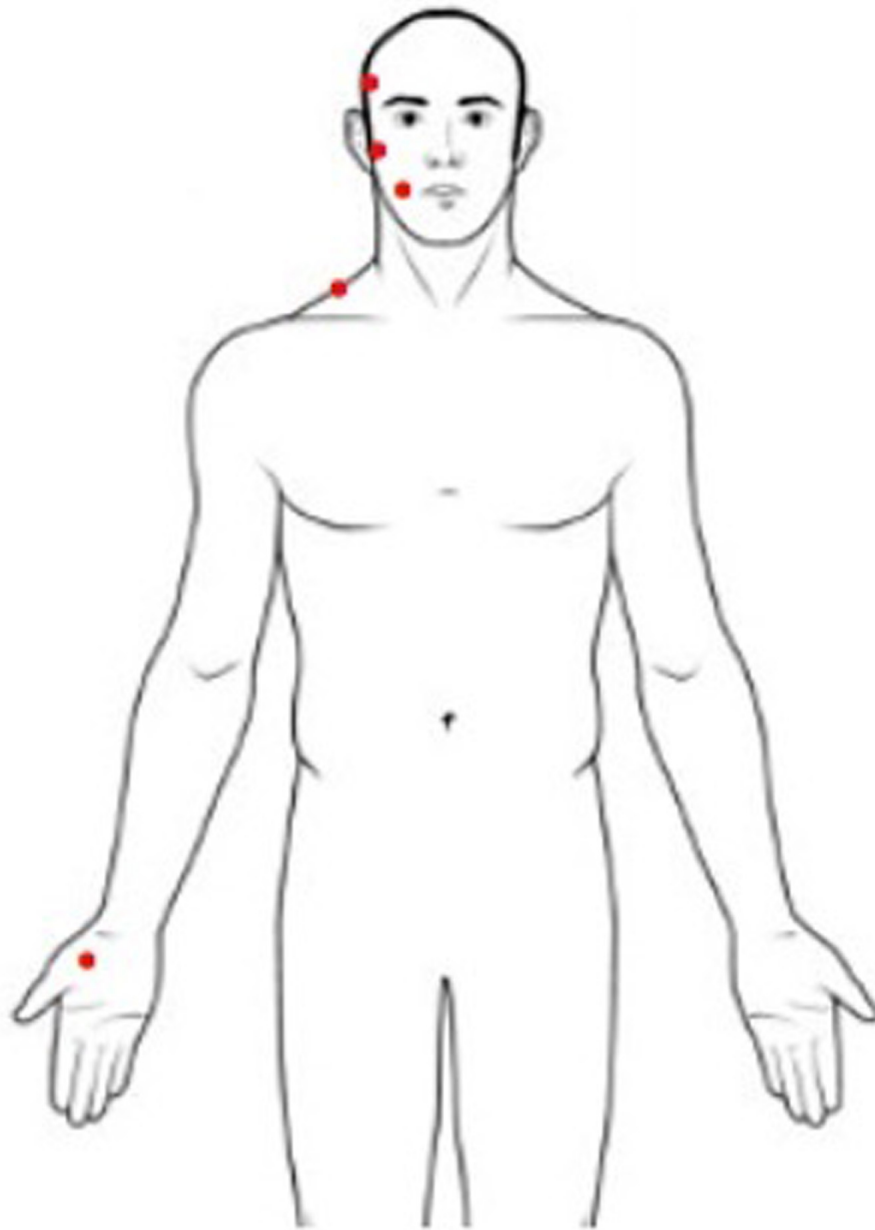


FIGURE 1 | Sites for pressure pain threshold assessment (right body sites for illustrative purposes only).

Statistical Analysis

Descriptive statistics were used for characterizing the sample. Continuous variables are reported as means and standard deviations, non-continuous variables as counts and percentages. Differences in PPT between patients with OFP and healthy subjects were assessed using the Wilcoxon rank-sum test due to non-normal data distribution. Patients with OFP were also divided according to intensity of pain, presence of psychological disorders, catastrophizing, and CS, and differences between groups were analyzed. Spearman rank correlation coefficient was used to measure strength and

direction of association between psychological scores and self-reported questionnaires.

This statistical analysis was performed using STATA 13.1 software with significance set at $p < 0.05$. Statistical analysis was also performed on the clustered EEG data. In this analysis, we compared the z-score PSD of the OFP and the healthy subjects in the eyes open and pain stimulus conditions for each band and electrode cluster. This analysis was based on a two-way analysis of variance (ANOVA) test. The significance level was set to 0.05. All the statistical analysis on the EEG data was performed in MATLAB using custom-made scripts.

RESULTS

The sample consisted of 19 women and 5 men. The mean age was 49.8 years, with a minimum of 23 and a maximum of 77 years. Detailed demographic and clinical features of the sample are summarized in **Table 1**. Most of the sample was classified as myofascial pain with spreading following the Axis I of DC/TMD. The mean pain intensity during the 24 h before at the NPRS was 6.42 (1.72 SD), with a minimum of 3 and a maximum of 9. Twenty-four age- and sex-matched healthy subjects were recruited. The assessment of PPT revealed a reduction in pain threshold in subjects with OFP in all the sites of assessment compared to healthy subjects. Differences between groups were statistically significant (**Figure 2**). Reduction in PPT in subjects with OFP compared to healthy subjects was observed even after removing people with fibromyalgia from the analysis ($p < 0.05$ for all the sites of assessment). Stratifying patients according to psychological assessment performed with RDC/TMD Axis II, we observed differences in PPT between groups of subjects with moderate or severe symptoms compared to those with low or mild; significant differences were recorded only for pain-related disability and depression ($p = 0.045$ and $p = 0.023$, respectively) (**Table 2**). No significant differences in pain threshold were identified in patients with CS signs. Positive correlations were found between CS and psychological disorders for every class of impairment $\rho = 0.331$ for depression, $\rho = 0.575$ for NSPS, $\rho = 0.365$ for catastrophizing), without reaching significant level.

EEG Results

The average PSD z -score values for OFP and healthy individuals for both conditions are presented in **Table 3**. We did not notice specific qualitative trends in the PSD values between OFP and healthy controls, which translated in the absence of statistically significant differences in the ANOVA in the PSD calculated from all electrode clusters in all frequency bands among the two groups (**Table 4**). However, we observed a marked decrease in PSD values for both groups between the two conditions in the alpha and beta bands. This observed decrease in PSD translated in statistically significant differences in the ANOVA between the two conditions for all clusters in the alpha band and for clusters F3 and C3 in the beta band. In the gamma band, we observed a general qualitative trend of increased PSD values in both groups in most clusters. This trend translated in statistically significant differences in the ANOVA for all clusters (with the exception of P4) in the gamma band. The interaction analysis (**Table 4**) suggests that the differences observed in the gamma band are group-specific. We then analyzed the group-specific relative changes in PSD values due to the pain stimulus. This was done by expressing the z -score PSD values extracted during the PS trial and expressed as percentage changes with respect to the same values extracted during the EO trial. We observed a qualitative increase in the relative PSD values (with respect to the eyes open trial) in the gamma band in the controls that were localized mostly in the occipital region. In the patients, differently than the controls, increased values of PSD in the gamma band were instead observed in the central and frontal regions (C3/C4 F3/F4 electrodes) (**Figure 3**).

TABLE 1 | Descriptive data for the sample.

| | Sample ($n = 24$) Mean (SD) or n (%) |
|--|---|
| Age (years) | 49.8 (13.1) |
| Sex (n) | |
| Male/female | 5 (21)/19 (79) |
| Occupation (n) | |
| Employed/unemployed | 14 (58)/10 (42) |
| Principal comorbidities (n) | |
| Fibromyalgia | 5 (21) |
| Hypertension | 4 (17) |
| Enteric disease | 3 (12) |
| Diabetes mellitus | 1 (4) |
| Other rheumatic disease | 1 (4) |
| None | 10 (42) |
| Drug use (n) | |
| Non-steroidal anti-inflammatory drugs | 5 (21) |
| Antidepressants | 2 (8) |
| Muscle relaxants | 2 (8) |
| Analgesics | 3 (11) |
| None | 12 (50) |
| Symptoms duration (months) | 49.21 (68.59) |
| Symptoms frequencies (n) | |
| Continuous/episodic recurrent | 7 (35)/17 (65) |
| Pain side (n) | |
| Right/left/bilateral | 3 (10)/3 (15)/18 (75) |
| Previous treatment | |
| Physiotherapy | 11 (45) |
| Arthrocentesis | 10 (35) |
| Byte use | 16 (65) |
| DC/TMD Axis I | |
| Myofascial pain | 21 (90) |
| Myalgia | 1 (5) |
| Arthralgia | 2 (5) |
| DC/TMD Axis II | |
| Pain-related disability (n) | |
| Low | 9 (37.5) |
| High | 15 (62.5) |
| Depression (n) | |
| Minimal–mild | 16 (66.7) |
| Moderate–severe | 8 (33.3) |
| Anxiety (n) | |
| Minimal–mild | 19 (79) |
| Moderate–severe | 5 (21) |
| Non-specific physical symptoms (n) | |
| Minimal–mild | 13 (54) |
| Moderate–high | 11 (46) |
| NPRS | 6.42 (1.72) |
| Catastrophizing (n) | |
| Not present | 12 (50) |
| Present | 12 (50) |
| Central sensitization (n) | |
| Subclinical–mild | 12 (50) |
| Moderate–severe | 12 (50) |

n, number; SD, standard deviation; DC/TMD Axis I and Axis II, Diagnostic Criteria for Temporomandibular Disorders Axis I and Axis II; NPRS, Numeric Pain Rating Scale.

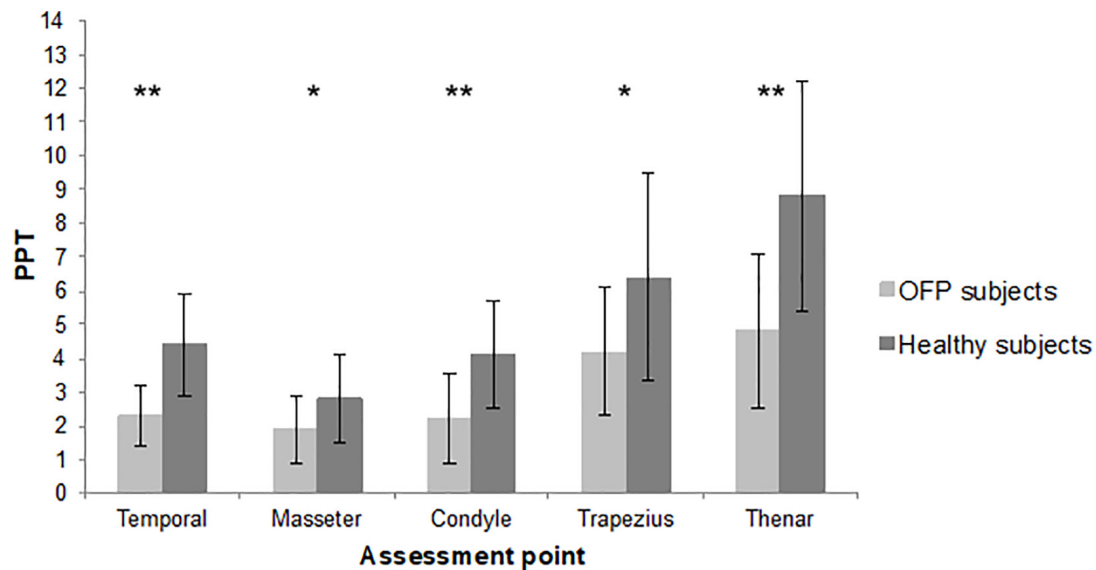


FIGURE 2 | Mean pressure pain threshold of the two samples. PPT, pressure pain threshold; lb, libra; OFP, orofacial pain; * $p < 0.01$; ** $p < 0.001$.

DISCUSSION

In this observational study, we tried to describe features and clinical signs of people with chronic OFP due to TMD by comparing them with healthy controls. Our main finding revealed that people who suffer from this debilitating condition present a generalized reduction in PPT. This reduction in pain threshold was observed not only in facial sites but also in areas not

involved by pathology, such as the upper trapezius and the thenar eminence. The phenomenon we observed may be due to CS, an increased responsiveness of nociceptive neurons to subthreshold input (Loeser and Treede, 2008). Fillingim et al. (2018) in their longitudinal study found that individuals who transitioned from being TMD-free to a TMD state tended to show reduction in PPT limited to the orofacial region and not to other body sites. The discrepancy between these and our results may be explained by the difference in time elapsed between OFP onset and PPT assessment in the two studies.

Fillingim et al.'s (2018) research did, in fact, involve a long-term follow-up, in which years separated original and follow-up assessments.

Again from the OPPERA study, Greenspan et al. (2011) found that people with chronic TMD were more pain-sensitive than controls to many mechanical and thermal stimuli, with particular sensitivity to pressure stimulation, applied to symptomatic and asymptomatic body sites.

In our study, PPT was assessed in patients with OFP from a median time of 33 months. Chronic pain, critical in development of CS, has to last for more than 3 months to be defined as such (Treede et al., 2015). Pain lasting for a shorter time may not contribute to hyperexcitability of the CNS, one of the main features of sensitization process (den Boer et al., 2019). In our study, we included patients with fibromyalgia, and this may represent a confounding factor in PPT assessment (Maquet et al., 2004). However, the analysis performed on the sample after exclusion of fibromyalgia patients showed no differences compared with the whole sample. Stratification of people with OFP based on psychological disorder severity revealed that subjects with moderate or severe depression and high level of pain-related disability showed generalized reduction in PPT. A large systematic review on pain sensitivity and depression found uncertain results about mechanisms underlying their

TABLE 2 | Pressure pain threshold for classes of impairment.

| | | Mean (SD) | <i>p</i> |
|--------------------------------|------------------------------------|-----------|----------|
| DC/TMD Axis II | | | |
| Pain-related disability | Low (<i>n</i> = 9) | 3.8 (1.3) | 0.045* |
| | High (<i>n</i> = 15) | 2.6 (1.1) | |
| Depression | Minimal–mild (<i>n</i> = 16) | 3.5 (1.3) | 0.023* |
| | Moderate–severe (<i>n</i> = 8) | 2.3 (1.0) | |
| Anxiety | Minimal–mild (<i>n</i> = 19) | 3.1 (1.3) | 0.749 |
| | Moderate–severe (<i>n</i> = 5) | 2.9 (1.3) | |
| Non-specific physical symptoms | Minimal–mild (<i>n</i> = 13) | 3.4 (1.4) | 0.213 |
| | Moderate–severe (<i>n</i> = 11) | 2.7 (1.1) | |
| NPRS | Mild–moderate 3–6 (<i>n</i> = 12) | 3.0 (1.3) | 0.954 |
| | Severe 7–10 (<i>n</i> = 12) | 3.1 (1.3) | |
| Catastrophizing | Not present (<i>n</i> = 12) | 3.2 (1.4) | 0.427 |
| | Present (<i>n</i> = 12) | 2.8 (0.9) | |
| Central sensitization | Subclinical–mild (<i>n</i> = 12) | 3.3 (1.5) | 0.564 |
| | Moderate–severe (<i>n</i> = 12) | 2.9 (0.9) | |

n, number; SD, standard deviation; DC/TMD Axis II, Diagnostic Criteria for Temporomandibular Disorders Axis II; NPRS, Numeric Pain Rating Scale. * $p < 0.05$.

relationship (Thompson et al., 2016). However depression and pain sensitivity frequently occur together (Von Knorring et al., 1983; Von Korff et al., 1988; Bair et al., 2003; Lépine and Briley, 2004; Agüera-Ortiz et al., 2011), probably due to dysfunction at the level of the serotonergic and noradrenergic neurons that affects not only psychological and somatic symptoms of depression but also physical painful symptoms (Stahl and Briley, 2004). Another possible explanation of the aforementioned results is that depressed people react negatively to painful

stimulation with stronger emotional involvement. A reduction in PPT as sign of CS may explain the link between sensitization of the CNS and emotional comorbidities. Smart et al. (2012) in their study on patients with low back pain reported significantly greater levels of pain-related disability, depression, and anxiety in people with signs of CS compared to those with nociceptive or neuropathic pain. Strong relationship between CS and psychological symptoms is confirmed by our analysis. What needs to be clarified is the causal link between them, establishing

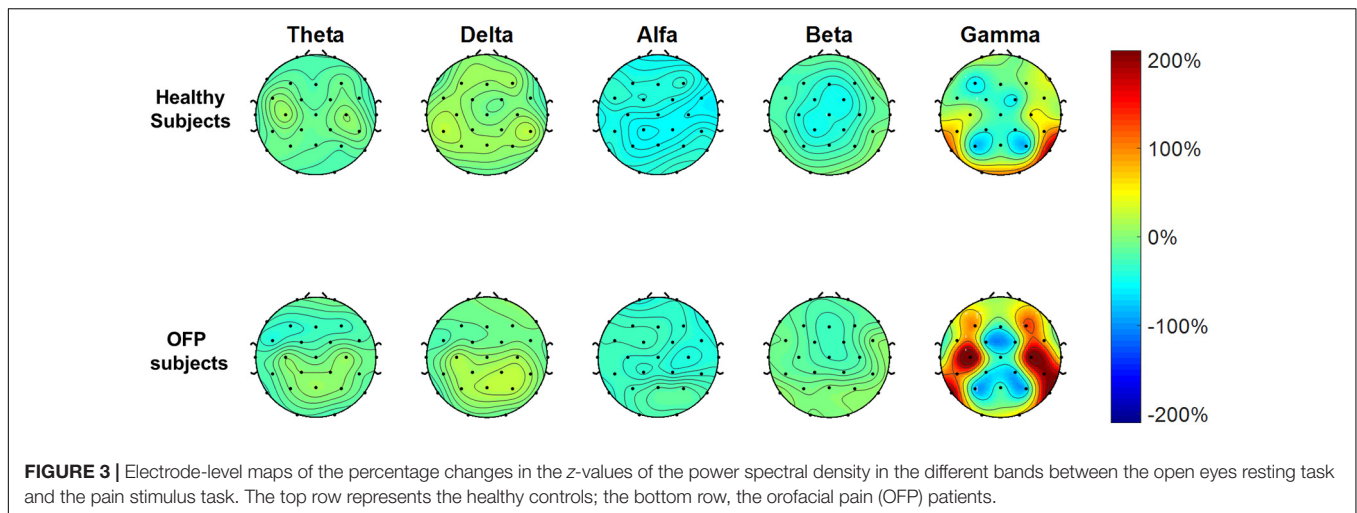
TABLE 3 | PSD values, expressed as mean (standard deviation) of the z-scores, for the different clusters, across all frequency bands, for the orofacial pain (OFF) patients and the healthy controls (HC) for the eyes open (top table) and pain stimulus (bottom table) conditions.

| Eyes Open | | | | | | | | | | |
|---------------|--------------|-------------|--------------|------------|-------------|-------------|--------------|----------------|---------------|---------------|
| Cluster | Theta OFF | HC | Delta OFF | HC | Alfa OFF | HC | Beta OFF | HC | Gamma OFF | HC |
| F3 | 0.67 (0.73) | 0.75 (0.72) | 1 (0.74) | 1.2 (0.62) | 0.78 (0.94) | 0.78 (0.99) | 0.15 (0.35) | 0.21 (0.37) | −0.46 (0.11) | −0.5 (0.12) |
| F4 | 0.68 (0.66) | 0.77 (0.58) | 1.1 (0.64) | 1.2 (0.63) | 0.83 (0.91) | 0.78 (0.89) | 0.1 (0.35) | 0.25 (0.38) | −0.42 (0.099) | −0.51 (0.13) |
| C3 | 0.52 (0.67) | 0.66 (0.6) | 1 (0.75) | 1.2 (0.54) | 1.1 (0.93) | 1.1 (0.97) | 0.18 (0.42) | 0.22 (0.3) | −0.45 (0.095) | −0.47 (0.088) |
| C4 | 0.54 (0.65) | 0.62 (0.5) | 1.1 (0.7) | 1.2 (0.6) | 1.1 (0.93) | 1.1 (0.95) | 0.14 (0.45) | 0.24 (0.32) | −0.41 (0.16) | −0.49 (0.098) |
| P3 | 0.67 (0.53) | 0.8 (0.45) | 1.1 (0.62) | 1.3 (0.44) | 1.5 (1) | 1.3 (0.83) | 0.16 (0.41) | 0.16 (0.23) | −0.45 (0.077) | −0.47 (0.054) |
| P4 | 0.67 (0.55) | 0.76 (0.42) | 1.1 (0.69) | 1.2 (0.48) | 1.5 (1) | 1.3 (0.85) | 0.13 (0.42) | 0.16 (0.21) | −0.43 (0.1) | −0.47 (0.072) |
| Pain stimulus | | | | | | | | | | |
| F3 | 0.3 (0.52) | 0.58 (0.51) | 0.86 (0.68) | 1.2 (0.55) | 0.38 (0.69) | 0.27 (0.5) | 0.049 (0.3) | 0.016 (0.24) | −0.4 (0.11) | −0.39 (0.11) |
| F4 | 0.43 (0.53) | 0.55 (0.45) | 1.1 (0.71) | 1.1 (0.49) | 0.31 (0.57) | 0.19 (0.43) | 0.067 (0.38) | 0.03 (0.28) | −0.41 (0.13) | −0.39 (0.14) |
| C3 | 0.4 (0.37) | 0.54 (0.5) | 1.1 (0.57) | 1.2 (0.62) | 0.57 (0.8) | 0.34 (0.5) | 0.092 (0.33) | −0.0018 (0.17) | −0.41 (0.11) | −0.36 (0.12) |
| C4 | 0.44 (0.48) | 0.47 (0.5) | 1.2 (0.6) | 1.1 (0.6) | 0.45 (0.56) | 0.25 (0.38) | 0.086 (0.35) | 0.036 (0.21) | −0.41 (0.12) | −0.36 (0.14) |
| P3 | 0.57 (0.36) | 0.59 (0.5) | 1.1 (0.43) | 1.3 (0.52) | 0.82 (0.77) | 0.51 (0.47) | 0.12 (0.33) | 0.035 (0.19) | −0.44 (0.088) | −0.39 (0.085) |
| P4 | 0.57 (0.38) | 0.52 (0.54) | 1.3 (0.57) | 1.2 (0.59) | 0.86 (0.79) | 0.55 (0.59) | 0.084 (0.3) | 0.062 (0.18) | −0.43 (0.074) | −0.4 (0.087) |

TABLE 4 | Results of the ANOVA two-way analysis performed between groups [orofacial pain (OFF) and healthy controls (HC)], conditions [eyes open (EO) and pain stimulation (PS)], and the interaction between group and condition, expressed as *p*-value and the relative *F* statistic in parenthesis.

| Group (OFF vs. HC) | Theta | Delta | Alpha | Beta | Gamma |
|-----------------------|------------------|-----------------|----------------|-----------------|-----------------|
| F3 | 0.1977 (1.7) | 0.1311 (2.3) | 0.7615 (0.093) | 0.8753 (0.025) | 0.5755 (0.32) |
| F4 | 0.4174 (0.66) | 0.6626 (0.19) | 0.5988 (0.28) | 0.4876 (0.49) | 0.2082 (1.6) |
| C3 | 0.2479 (1.4) | 0.1819 (1.8) | 0.6626 (0.19) | 0.7346 (0.12) | 0.6789 (0.17) |
| C4 | 0.6331 (0.23) | 0.8776 (0.024) | 0.5007 (0.46) | 0.7181 (0.13) | 0.5621 (0.34) |
| P3 | 0.4754 (0.51) | 0.1828 (1.8) | 0.1597 (2) | 0.5297 (0.4) | 0.4509 (0.57) |
| P4 | 0.8361 (0.043) | 0.8711 (0.026) | 0.141 (2.2) | 0.9361 (0.0065) | 0.9474 (0.0044) |
| Condition (EO vs. PS) | | | | | |
| F3 | 0.0582 (3.7) | 0.4898 (0.48) | 0.0131 (6.5) | 0.0441 (4.2) | 0.0006 (13) |
| F4 | 0.0649 (3.5) | 0.5521 (0.36) | 0.0010 (12) | 0.1152 (2.5) | 0.0203 (5.6) |
| C3 | 0.3325 (0.95) | 0.7877 (0.073) | 0.0008 (12) | 0.0337 (4.7) | 0.0022 (10) |
| C4 | 0.3194 (1) | 0.8800 (0.023) | <0.0001 (20) | 0.1013 (2.8) | 0.0369 (4.5) |
| P3 | 0.1313 (2.3) | 0.7745 (0.083) | 0.0001 (16) | 0.2514 (1.3) | 0.0141 (6.3) |
| P4 | 0.1263 (2.4) | 0.6303 (0.23) | 0.0005067 (13) | 0.3014 (1.1) | 0.0513 (3.9) |
| Interaction | | | | | |
| F3 | 0.4889 (0.48) | 0.5522 (0.36) | 0.7887 (0.072) | 0.5419 (0.38) | 0.3114 (1) |
| F4 | 0.8997 (0.016) | 0.9310 (0.0076) | 0.8260 (0.049) | 0.2483 (1.4) | 0.0498 (4) |
| C3 | 0.9984 (<0.0001) | 0.9528 (0.0035) | 0.4226 (0.65) | 0.3287 (0.97) | 0.1078 (2.6) |
| C4 | 0.8429 (0.04) | 0.4403 (0.6) | 0.6146 (0.26) | 0.3170 (1) | 0.0452 (4.1) |
| P3 | 0.6290 (0.24) | 0.6967 (0.15) | 0.7160 (0.13) | 0.5159 (0.43) | 0.0438 (4.2) |
| P4 | 0.5279 (0.4) | 0.4067 (0.7) | 0.8331 (0.045) | 0.6767 (0.18) | 0.1012 (2.8) |

The three different shades of green represent three *p*-value threshold, specifically *p* < 0.05 (lightest shade), *p* < 0.01 and *p* < 0.001 (darkest shade).



if psychological disorders are involved in causing sensitization or whether they are a consequence of a sensitized system.

To our knowledge, the current study is the first investigating EEG PSD during PPT assessment in people with OFP vs. healthy control subjects. In this study, we found no differences between patients and control subjects during resting and pain stimulus trials. Our results about the reduction in the EEG alpha power during pain stimulation, which we observed in both cohorts, had already been observed in literature, without distinction between phasic or tonic pain (Chang et al., 2002; Peng et al., 2015). We observed also an increase in gamma band activity across all the electrodes between the two conditions. This translated, in the OFP patients, in a qualitative relative (with respect to the resting condition) increase in the central and prefrontal activity in the gamma band during peripheral stimulation just before stimulus was perceived as painful. Other studies investigating resting state EEG in people with chronic pain described significant overactivation of regions involved in the pain network. Prichep et al. (2018) recorded overactivity in insula areas, parietal lobule, thalamus, and the dorsolateral prefrontal cortex; significant differences between normal and pain patients were found in mid and posterior cingulate. Generalized overactivity was described in all areas belonging to the “pain matrix.” Our findings of an increase in gamma activity in the prefrontal areas may further support the model proposed by Baliki and Apkarian (2015) on dissociation in processing of longer lasting pain and nociceptive information. The authors described a dissociation of prefrontal component of the default mode network (DMN) in different types of chronic pain (Baliki and Apkarian, 2015). In fMRI studies, the DMN was described as one of the three brain systems that, with their dynamic interactions, are involved in spontaneous attentional fluctuations toward and away from pain (Kucyi and Davis, 2015). The DMN is activated when subject attention is not engaged by sensations from the external world (Andrews-Hanna et al., 2014). In opposition to the DMN, a system known as the salience network (SN) works to track how external stimuli capture attention (Downar et al., 2000, 2001, 2002, 2003; Mouraux et al., 2011; Uddin, 2015). Prefrontal areas,

in particular dorsolateral prefrontal cortex, are part of the SN (Seeley et al., 2007; Kucyi et al., 2012). Although in our study we did not observe statistically significant differences between patients and controls, an overactivity of the prefrontal cortex recorded in patients with OFP due to TMD may be representative of an exaggerated engagement of SN in people with long-lasting pain and a general tendency to focus attention on external stimuli that could generate pain. Similar results of increased prefrontal gamma activity were reported in chronic back pain patients (May et al., 2019) and patients with postherpetic neuralgia and fibromyalgia (Lim et al., 2016; Zhou et al., 2018). The association between gamma oscillations and involuntary attentional effects of pain has been well described in literature (Hauck et al., 2007; Tiemann et al., 2010; Schulz et al., 2015; Hansen et al., 2017) and has great relevance in cortical networks for behavioral and cognitive phenomena (Uhlhaas et al., 2009).

Increased activity of the primary motor cortex (M1) area in people with chronic pain has been previously described in literature in various musculoskeletal conditions (Di Pietro et al., 2013; Schabrun et al., 2015, 2017; Te et al., 2017). A recent systematic review found inconclusive results with regard to abnormal M1 activation in pain conditions due to the heterogeneity of studies and assessment tools (Chang et al., 2018). Our results seem to underlie abnormal brain activity recorded by C3/C4 electrodes just before the peripheral stimulus became painful. Increased gamma activity may indicate increased muscle activity during pain, which contaminates EEG signal during pain stimulation. However, we did not record muscular activity during pain threshold assessment (Whitham et al., 2007; Dowman et al., 2008). Furthermore, muscular activation would also be highlighted by altered EEG signal during the recording.

Movement dysfunction such as unnecessary protective behavior may justify our findings, when patients received a stimulus perceived as threatening. The primary motor cortex has already been target of brain stimulation treatment, with a positive impact on pain relief (Fregni et al., 2006; Straudi et al., 2018). Abnormal function of motor and prefrontal cortex during stimulus perception may be due to neuroplastic changes

that occur in the human brain subjected to long-lasting pain. Neurophysiological adaptations occur and seem to persist over peripheral tissue healing time in presence of emotional and behavioral aspects of pain that cause maladaptive changes in areas not normally involved in pain perception (Mansour et al., 2014). Structural as well as functional changes have been described in frontal and motor areas of patients with chronic pain due to coxarthrosis (Rodriguez-Raecke et al., 2013).

Interpretation of our findings is subject to several limitations. First, the small sample size does not allow us to confirm our results on PPT and EEG recordings. Even though CS may be hypothesized looking at our results, we cannot draw any definitive conclusion on the mechanism underlying sensitization of CNS. Second, interpretation of our results must consider the inclusion in our sample of fibromyalgia patients whose sensitivity to pain may influence their PPT.

CONCLUSION

In a convenience sample of patients with OFP due to TMD we observed generalized reduction in PPT compared to age- and sex-matched healthy controls, not limited to facial sites. Generalized decrease of pain threshold seems to be linked to the severity of psychological symptoms such as depression and perceived health-related disability. Abnormal EEG activity was recorded during painful stimulation of non-painful sites of patients with OFP due to TMD. This observational study tried to identify potential signs of CS through the analysis of patients' sensory and psychological profiles and brain activity. Our results can

open doors to new strategies for the assessment and treatment of patients with CS due to chronic pain conditions.

DATA AVAILABILITY STATEMENT

The raw data supporting the conclusions of this article will be made available by the authors, without undue reservation.

ETHICS STATEMENT

The studies involving human participants were reviewed and approved by the Ferrara University Hospital Ethics Committees. The patients/participants provided their written informed consent to participate in this study.

AUTHOR CONTRIBUTIONS

AB, SS, SBu, and NB conceived the study and participated in its design. AB and SBo performed the instrumented and clinical data collections. AB and GS analyzed the data. AB, GS and SS interpreted the results, and drafted and revised the manuscript. All authors approved the submitted version.

ACKNOWLEDGMENTS

Gloria Mura and Serena Modenese helped with subjects' recruitment.

REFERENCES

- Agüera-Ortiz, L., Failde, I., Mico, J. A., Cervilla, J., and López-Ibor, J. J. (2011). Pain as a symptom of depression: prevalence and clinical correlates in patients attending psychiatric clinics. *J. Affect. Disord.* 130, 106–112. doi: 10.1016/j.jad.2010.10.022
- Andrews-Hanna, J. R., Smallwood, J., and Spreng, R. N. (2014). The default network and self-generated thought: component processes, dynamic control, and clinical relevance. *Ann. N.Y. Acad. Sci.* 1316, 29–52. doi: 10.1111/nyas.12360
- Apkarian, A. V., Sosa, Y., Sonty, S., Levy, R. M., Harden, R. N., Parrish, T. B., et al. (2004). Chronic back pain is associated with decreased prefrontal and thalamic gray matter density. *J. Neurosci.* 24, 10410–10415. doi: 10.1523/JNEUROSCI.2541-04.2004
- Arendt-Nielsen, L., Morlion, B., Perrot, S., Dahan, A., Dickenson, A., Kress, H. G., et al. (2018). Assessment and manifestation of central sensitization across different chronic pain conditions. *Eur. J. Pain* 22, 216–241. doi: 10.1002/ejp.1140
- Bair, M. J., Robinson, R. L., Katon, W., and Kroenke, K. (2003). Depression and pain comorbidity: a literature review. *Arch. Intern. Med.* 163, 2433–2445. doi: 10.1001/archinte.163.20.2433
- Baliki, M. N., and Apkarian, A. V. (2015). Nociception, Pain, Negative Moods, and Behavior Selection. *Neuron* 87, 474–491. doi: 10.1016/j.neuron.2015.06.005
- Benoliel, R., Svensson, P., Evers, S., Wang, S.-J., Barke, A., Korwisi, B., et al. (2019). The IASP classification of chronic pain for ICD-11: chronic secondary headache or orofacial pain. *Pain* 160, 60–68. doi: 10.1097/j.pain.0000000000001435
- Breivik, H., Collett, B., Ventafridda, V., Cohen, R., and Gallacher, D. (2006). Survey of chronic pain in Europe: prevalence, impact on daily life, and treatment. *Eur. J. Pain* 10, 287–333. doi: 10.1016/j.ejpain.2005.06.009
- Camfferman, D., Moseley, G. L., Gertz, K., Pettet, M. W., and Jensen, M. P. (2017). Waking EEG Cortical Markers of Chronic Pain and Sleepiness. *Pain Med.* 18, 1921–1931. doi: 10.1093/pm/pnw294
- Campi, L. B., Jordani, P. C., Tenan, H. L., Camparis, C. M., and Gonçalves, D. A. G. (2017). Painful temporomandibular disorders and central sensitization: implications for management—a pilot study. *Int. J. Oral. Maxillofac. Surg.* 46, 104–110. doi: 10.1016/j.ijom.2016.07.005
- Chang, P.-F., Arendt-Nielsen, L., and Chen, A. (2002). Dynamic changes and spatial correlation of EEG activities during cold pressor test in man. *Brain Res. Bull.* 57, 667–675. doi: 10.1016/S0361-9230(01)00763-8
- Chang, W.-J., O'Connell, N. E., Beckenkamp, P. R., Alhassani, G., Liston, M. B., and Schabrun, S. M. (2018). Altered Primary Motor Cortex Structure, Organization, and Function in Chronic Pain: A Systematic Review and Meta-Analysis. *J. Pain* 19, 341–359. doi: 10.1016/j.jpain.2017.10.007
- Chiarotto, A., Viti, C., Sulli, A., Cutolo, M., Testa, M., and Piscitelli, D. (2018). Cross-cultural adaptation and validity of the Italian version of the Central Sensitization Inventory. *Musculoskelet. Sci. Pract.* 37, 20–28. doi: 10.1016/j.msksp.2018.06.005
- Delorme, A., and Makeig, S. (2004). EEGLAB: an open source toolbox for analysis of single-trial EEG dynamics including independent component analysis. *J. Neurosci. Methods* 134, 9–21. doi: 10.1016/j.jneumeth.2003.10.009
- den Boer, C., Dries, L., Terluin, B., van der Wouden, J. C., Blankenstein, A. H., van Wilgen, C. P., et al. (2019). Central sensitization in chronic pain and medically unexplained symptom research: A systematic review of definitions, operationalizations and measurement instruments. *J. Psychosom. Res.* 117, 32–40. doi: 10.1016/j.jpsychores.2018.12.010
- Di Pietro, F., McAuley, J. H., Parkitny, L., Lotze, M., Wand, B. M., Moseley, G. L., et al. (2013). Primary motor cortex function in complex regional pain

- syndrome: a systematic review and meta-analysis. *J. Pain* 14, 1270–1288. doi: 10.1016/j.jpain.2013.07.004
- Dowman, R., Rissacher, D., and Schuckers, S. (2008). EEG indices of tonic pain-related activity in the somatosensory cortices. *Clin. Neurophysiol.* 119, 1201–1212. doi: 10.1016/j.clinph.2008.01.019
- Downar, J., Crawley, A. P., Mikulis, D. J., and Davis, K. D. (2000). A multimodal cortical network for the detection of changes in the sensory environment. *Nat. Neurosci.* 3, 277–283. doi: 10.1038/72991
- Downar, J., Crawley, A. P., Mikulis, D. J., and Davis, K. D. (2001). The effect of task relevance on the cortical response to changes in visual and auditory stimuli: an event-related fMRI study. *Neuroimage* 14, 1256–1267. doi: 10.1006/nimg.2001.0946
- Downar, J., Crawley, A. P., Mikulis, D. J., and Davis, K. D. (2002). A cortical network sensitive to stimulus salience in a neutral behavioral context across multiple sensory modalities. *J. Neurophysiol.* 87, 615–620. doi: 10.1152/jn.00636.2001
- Downar, J., Mikulis, D. J., and Davis, K. D. (2003). Neural correlates of the prolonged salience of painful stimulation. *Neuroimage* 20, 1540–1551.
- Dworkin, R. H., Turk, D. C., Farrar, J. T., Haythornthwaite, J. A., Jensen, M. P., Katz, N. P., et al. (2005). Core outcome measures for chronic pain clinical trials: IMMPACT recommendations. *Pain* 113, 9–19. doi: 10.1016/j.pain.2004.09.012
- Dworkin, (1995). "Personal and societal impact of orofacial pain," in *Orofacial Pain and Temporomandibular Disorders*. eds J. R. Friction, and R. Dubner, (New York: Raven Press), 15–32.
- Ferde, M. A., Oosterman, J. M., Adamczyk, A. K., van Aken, M., Woudsma, K. J., Peeters, B. W. M. M., et al. (2019). Effective Connectivity of Beta Oscillations in Endometriosis-Related Chronic Pain During rest and Pain-Related Mental Imagery. *J. Pain* 113:9–19. doi: 10.1016/j.jpain.2019.05.011
- Fillingim, R. B., Slade, G. D., Greenspan, J. D., Dubner, R., Maixner, W., Bair, E., et al. (2018). Long-term changes in biopsychosocial characteristics related to temporomandibular disorder: findings from the OPFERA study. *Pain* 159, 2403–2413. doi: 10.1097/j.pain.0000000000001348
- Fischer, A. A. (1987). Pressure algometry over normal muscles. Standard values, validity and reproducibility of pressure threshold. *Pain* 30, 115–126. doi: 10.1016/0304-3959(87)90089-3
- Fregni, F., Boggio, P. S., Lima, M. C., Ferreira, M. J. L., Wagner, T., Rigonatti, S. P., et al. (2006). A sham-controlled, phase II trial of transcranial direct current stimulation for the treatment of central pain in traumatic spinal cord injury. *Pain* 122, 197–209. doi: 10.1016/j.pain.2006.02.023
- Greenspan, J. D., Slade, G. D., Bair, E., Dubner, R., Fillingim, R. B., Ohrbach, R., et al. (2011). Pain Sensitivity Risk Factors for Chronic TMD: Descriptive Data and Empirically Identified Domains from the OPFERA Case Control Study. *J. Pain* 12 (Suppl. 1), T61–T74. doi: 10.1016/j.jpain.2011.08.006
- Hansen, T. M., Mark, E. B., Olesen, S. S., Gram, M., Frøkjær, J. B., and Drewes, A. M. (2017). Characterization of cortical source generators based on electroencephalography during tonic pain. *J. Pain Res.* 10, 1401–1409. doi: 10.2147/JPR.S132909
- Harte, S. E., Harris, R. E., and Clauw, D. J. (2018). The neurobiology of central sensitization. *J. Applied Biobehav. Res.* 23:e12137. doi: 10.1111/jabr.12137
- Hauck, M., Lorenz, J., and Engel, A. K. (2007). Attention to Painful Stimulation Enhances γ -Band Activity and Synchronization in Human Sensorimotor Cortex. *J. Neurosci.* 27, 9270–9277. doi: 10.1523/JNEUROSCI.2283-07.2007
- Jensen, M. P., Sherlin, L. H., Gertz, K. J., Braden, A. L., Kupper, A. E., Gianas, A., et al. (2013). Brain EEG activity correlates of chronic pain in persons with spinal cord injury: clinical implications. *Spinal Cord* 51, 55–58. doi: 10.1038/sc.2012.84
- Kim, J.-Y., Kim, S.-H., Seo, J., Kim, S.-H., Han, S. W., Nam, E. J., et al. (2013). Increased power spectral density in resting-state pain-related brain networks in fibromyalgia. *Pain* 154, 1792–1797. doi: 10.1016/j.pain.2013.05.040
- Kucyi, A., and Davis, K. D. (2015). The dynamic pain connectome. *Trends Neurosci.* 38, 86–95. doi: 10.1016/j.tins.2014.11.006
- Kucyi, A., Hodaie, M., and Davis, K. D. (2012). Lateralization in intrinsic functional connectivity of the temporoparietal junction with salience- and attention-related brain networks. *J. Neurophysiol.* 108, 3382–3392. doi: 10.1152/jn.00674.2012
- Lautenbacher, S., Rollman, G. B., and McCain, G. A. (1994). Multi-method assessment of experimental and clinical pain in patients with fibromyalgia. *Pain* 59, 45–53. doi: 10.1016/0304-3959(94)90046-9
- Lépine, J.-P., and Briley, M. (2004). The epidemiology of pain in depression. *Hum. Psychophar.* 19(Suppl. 1), S3–S7. doi: 10.1002/hup.618
- Lim, M., Kim, J. S., Kim, D. J., and Chung, C. K. (2016). Increased Low- and High-Frequency Oscillatory Activity in the Prefrontal Cortex of Fibromyalgia Patients. *Front. Hum. Neurosci.* 10:111. doi: 10.3389/fnhum.2016.00111
- Llinás, R. R., Ribary, U., Jeanmonod, D., Kronberg, E., and Mitra, P. P. (1999). Thalamocortical dysrhythmia: A neurological and neuropsychiatric syndrome characterized by magnetoencephalography. *Proc. Natl. Acad. Sci. U S A.* 96, 15222–15227. doi: 10.1073/pnas.96.26.15222
- Loeser, J. D., and Treede, R.-D. (2008). The Kyoto protocol of IASP Basic Pain Terminology. *Pain* 137, 473–477. doi: 10.1016/j.pain.2008.04.025
- Mansour, A. R., Farmer, M. A., Baliki, M. N., and Apkarian, A. V. (2014). Chronic pain: the role of learning and brain plasticity. *Restor. Neurol. Neurosci.* 32, 129–139. doi: 10.3233/RNN-139003
- Maquet, D., Croisier, J.-L., Demoulin, C., and Crielaard, J.-M. (2004). Pressure pain thresholds of tender point sites in patients with fibromyalgia and in healthy controls. *Eur. J. Pain* 8, 111–117. doi: 10.1016/S1090-3801(03)00082-X
- May, E. S., Nickel, M. M., Ta Dinh, S., Tiemann, L., Heitmann, H., Voth, I., et al. (2019). Prefrontal gamma oscillations reflect ongoing pain intensity in chronic back pain patients. *Hum. Brain Mapp.* 40, 293–305. doi: 10.1002/hbm.24373
- Mouraux, A., Diukova, A., Lee, M. C., Wise, R. G., and Iannetti, G. D. (2011). A multisensory investigation of the functional significance of the "pain matrix." *Neuroimage* 54, 2237–2249. doi: 10.1016/j.neuroimage.2010.09.084
- Neblett, R., Cohen, H., Choi, Y., Hartzell, M. M., Williams, M., Mayer, T. G., et al. (2013). The Central Sensitization Inventory (CSI): establishing clinically significant values for identifying central sensitivity syndromes in an outpatient chronic pain sample. *J. Pain* 14, 438–445. doi: 10.1016/j.jpain.2012.11.012
- Neblett, R., Hartzell, M. M., Cohen, H., Mayer, T. G., Williams, M., Choi, Y., et al. (2015). Ability of the central sensitization inventory to identify central sensitivity syndromes in an outpatient chronic pain sample. *Clin. J. Pain* 31, 323–332. doi: 10.1097/AJP.0000000000000113
- Nie, H., Graven-Nielsen, T., and Arendt-Nielsen, L. (2009). Spatial and temporal summation of pain evoked by mechanical pressure stimulation. *Eur. J. Pain* 13, 592–599. doi: 10.1016/j.ejpain.2008.07.013
- Nijs, J., Torres-Cueco, R., van Wilgen, C. P., Girbes, E. L., Struyf, F., Roussel, N., et al. (2014). Applying modern pain neuroscience in clinical practice: criteria for the classification of central sensitization pain. *Pain Physician.* 17, 447–457.
- Peng, W., Babiloni, C., Mao, Y., and Hu, Y. (2015). Subjective pain perception mediated by α rhythms. *Biol. Psychol.* 109, 141–150. doi: 10.1016/j.biopsycho.2015.05.004
- Pinho, E. S., dos, S., de Queirós, F. C., Montoya, P., Santos, C. L., do Nascimento, M. A., et al. (2016). Electroencephalographic Patterns in Chronic Pain: A Systematic Review of the Literature. *PLoS One* 11:e0149085. doi: 10.1371/journal.pone.0149085
- Prichep, L. S., John, E. R., Howard, B., Merkin, H., and Hiesiger, E. M. (2011). Evaluation of the pain matrix using EEG source localization: a feasibility study. *Pain Med.* 12, 1241–1248. doi: 10.1111/j.1526-4637.2011.01191.x
- Prichep, L. S., Shah, J., Merkin, H., and Hiesiger, E. M. (2018). Exploration of the Pathophysiology of Chronic Pain Using Quantitative EEG Source Localization. *Clin. EEG Neurosci.* 49, 103–113. doi: 10.1177/1550059417736444
- Quartana, P. J., Campbell, C. M., and Edwards, R. R. (2009). Pain catastrophizing: a critical review. *Expert Rev. Neurother.* 9, 745–758. doi: 10.1586/ern.09.34
- Rodriguez-Raecke, R., Niemeier, A., Ihle, K., Ruether, W., and May, A. (2013). Structural brain changes in chronic pain reflect probably neither damage nor atrophy. *PLoS One* 8:e54475. doi: 10.1371/journal.pone.0054475
- Sarlani, E., and Greenspan, J. D. (2005). Why look in the brain for answers to temporomandibular disorder pain? *Cells Tissues Organs* 180, 69–75. doi: 10.1159/000086200
- Sarnthein, J., and Jeanmonod, D. (2008). High thalamocortical theta coherence in patients with neurogenic pain. *NeuroImage* 39, 1910–1917. doi: 10.1016/j.neuroimage.2007.10.019
- Sarnthein, J., Stern, J., Aufenberg, C., Rousson, V., and Jeanmonod, D. (2006). Increased EEG power and slowed dominant frequency in patients with neurogenic pain. *Brain* 129, 55–64. doi: 10.1093/brain/awh631
- Schabrun, S. M., Elgueta-Cancino, E. L., and Hodges, P. W. (2017). Smudging of the Motor Cortex Is Related to the Severity of Low Back Pain. *Spine* 42, 1172–1178. doi: 10.1097/BRS.0000000000000938

- Schabrun, S. M., Hodges, P. W., Vicenzino, B., Jones, E., and Chipchase, L. S. (2015). Novel adaptations in motor cortical maps: the relation to persistent elbow pain. *Med. Sci. Sports Exerc.* 47, 681–690. doi: 10.1249/MSS.0000000000000469
- Schiffman, E., Ohrbach, R., Truelove, E., Look, J., Anderson, G., Goulet, J.-P., et al. (2014). Diagnostic Criteria for Temporomandibular Disorders (DC/TMD) for Clinical and Research Applications: recommendations of the International RDC/TMD Consortium Network and Orofacial Pain Special Interest Group†. *J. Oral. Facial Pain Headac.* 28, 6–27. doi: 10.11607/jop.1151
- Schulz, E., May, E. S., Postorino, M., Tiemann, L., Nickel, M. M., Witkovsky, V., et al. (2015). Prefrontal Gamma Oscillations Encode Tonic Pain in Humans. *Cereb. Cortex* 25, 4407–4414. doi: 10.1093/cercor/bhv043
- Seeley, W. W., Menon, V., Schatzberg, A. F., Keller, J., Glover, G. H., Kenna, H., et al. (2007). Dissociable intrinsic connectivity networks for salience processing and executive control. *J. Neurosci.* 27, 2349–2356. doi: 10.1523/JNEUROSCI.5587-06.2007
- Slade, G. D., Sanders, A. E., Ohrbach, R., Fillingim, R. B., Dubner, R., Gracely, R. H., et al. (2014). Pressure pain thresholds fluctuate with, but do not usefully predict, the clinical course of painful temporomandibular disorder. *Pain* 155, 2134–2143. doi: 10.1016/j.pain.2014.08.007
- Smart, K. M., Blake, C., Staines, A., and Doody, C. (2012). Self-reported pain severity, quality of life, disability, anxiety and depression in patients classified with “nociceptive”, “peripheral neuropathic” and “central sensitisation” pain. The discriminant validity of mechanisms-based classifications of low back (\pm leg) pain. *Man. Ther.* 17, 119–125. doi: 10.1016/j.math.2011.10.002
- Stahl, S., and Briley, M. (2004). Understanding pain in depression. *Hum. Psychophar.* 19(Suppl. 1), S9–S13. doi: 10.1002/hu.p.619
- Stern, J., Jeanmonod, D., and Sarnthein, J. (2006). Persistent EEG overactivation in the cortical pain matrix of neurogenic pain patients. *Neuroimage* 31, 721–731. doi: 10.1016/j.neuroimage.2005.12.042
- Straudi, S., Buja, S., Baroni, A., Pavarelli, C., Pranovi, G., Fregni, F., et al. (2018). The effects of transcranial direct current stimulation (tDCS) combined with group exercise treatment in subjects with chronic low back pain: a pilot randomized control trial. *Clin. Rehabil.* 32, 1348–1356. doi: 10.1177/0269215518777881
- Sullivan, M. J. L., Bishop, S. R., and Pivik, J. (1995). The Pain Catastrophizing Scale: Development and validation. *Psychol. Assess.* 7, 524–532. doi: 10.1037/1040-3590.7.4.524
- Svensson, P., Baad-Hansen, L., Pigg, M., List, T., Eliav, E., Ettlin, D., et al. (2011). Guidelines and recommendations for assessment of somatosensory function in oro-facial pain conditions—a taskforce report. *J. Oral. Rehabil.* 38, 366–394. doi: 10.1111/j.1365-2842.2010.02196.x
- Te, M., Baptista, A. F., Chipchase, L. S., and Schabrun, S. M. (2017). Primary Motor Cortex Organization Is Altered in Persistent Patellofemoral Pain. *Pain Med.* 18, 2224–2234. doi: 10.1093/pm/pnx036
- Thompson, T., Correll, C. U., Gallop, K., Vancampfort, D., and Stubbs, B. (2016). Is Pain Perception Altered in People With Depression? A Systematic Review and Meta-Analysis of Experimental Pain Research. *J. Pain* 17, 1257–1272. doi: 10.1016/j.jpain.2016.08.007
- Tiemann, L., Schulz, E., Gross, J., and Ploner, M. (2010). Gamma oscillations as a neuronal correlate of the attentional effects of pain. *Pain* 150, 302–308. doi: 10.1016/j.pain.2010.05.014
- Treede, R.-D., Rief, W., Barke, A., Aziz, Q., Bennett, M. I., Benoliel, R., et al. (2015). A classification of chronic pain for ICD-11. *Pain* 156, 1003–1007. doi: 10.1097/j.pain.000000000000160
- Treede, R.-D., Rief, W., Barke, A., Aziz, Q., Bennett, M. I., Benoliel, R., et al. (2019). Chronic pain as a symptom or a disease: the IASP Classification of Chronic Pain for the International Classification of Diseases (ICD-11). *Pain* 160, 19–27. doi: 10.1097/j.pain.0000000000001384
- Uddin, L. Q. (2015). Salience processing and insular cortical function and dysfunction. *Nat. Rev. Neurosci.* 16, 55–61. doi: 10.1038/nrn3857
- Uhlhaas, P. J., Pipa, G., Lima, B., Melloni, L., Neuenschwander, S., Nikolić, D., et al. (2009). Neural synchrony in cortical networks: history, concept and current status. *Front. Integr. Neurosci.* 3:17. doi: 10.3389/neuro.07.017.2009
- von Elm, E., Altman, D. G., Egger, M., Pocock, S. J., Götzsche, P. C., Vandenbroucke, J. P., et al. (2014). The Strengthening the Reporting of Observational Studies in Epidemiology (STROBE) Statement: guidelines for reporting observational studies. *Int. J. Surg.* 12, 1495–1499. doi: 10.1016/j.ijsu.2014.07.013
- Von Knorring, L., Perris, C., Eisemann, M., Eriksson, U., and Perris, H. (1983). Pain as a symptom in depressive disorders: I. Relationship to diagnostic subgroup and depressive symptomatology. *Pain* 15, 19–26. doi: 10.1016/0304-3959(83)90003-9
- Von Korff, M., Dworkin, S. F., Le Resche, L., and Kruger, A. (1988). An epidemiologic comparison of pain complaints. *Pain* 32, 173–183. doi: 10.1016/0304-3959(88)90066-8
- Welch, P. D. (1967). The use of fast Fourier transform for the estimation of power spectra: a method based on time averaging over short, modified periodograms. *IEEE Trans. Aud. Electroacoust.* 15, 70–73. doi: 10.1109/TAU.1967.1161901
- Whitham, E. M., Pope, K. J., Fitzgibbon, S. P., Lewis, T., Clark, C. R., Loveless, S., et al. (2007). Scalp electrical recording during paralysis: quantitative evidence that EEG frequencies above 20 Hz are contaminated by EMG. *Clin. Neurophysiol.* 118, 1877–1888. doi: 10.1016/j.clinph.2007.04.027
- Woolf, C. J. (2011). Central sensitization: implications for the diagnosis and treatment of pain. *Pain* 152, S2–S15. doi: 10.1016/j.pain.2010.09.030
- Zhou, R., Wang, J., Qi, W., Liu, F.-Y., Yi, M., Guo, H., et al. (2018). Elevated Resting State Gamma Oscillatory Activities in Electroencephalogram of Patients With Post-herpetic Neuralgia. *Front. Neurosci.* 12:750. doi: 10.3389/fnins.2018.00750

Conflict of Interest: The authors declare that the research was conducted in the absence of any commercial or financial relationships that could be construed as a potential conflict of interest.

Copyright © 2020 Baroni, Severini, Straudi, Buja, Borsato and Basaglia. This is an open-access article distributed under the terms of the Creative Commons Attribution License (CC BY). The use, distribution or reproduction in other forums is permitted, provided the original author(s) and the copyright owner(s) are credited and that the original publication in this journal is cited, in accordance with accepted academic practice. No use, distribution or reproduction is permitted which does not comply with these terms.



The Pain-to-Well-Being Relationship in Patients Experiencing Chronic Orofacial Pain

Kanokporn Bhalang^{1*}, Beat Steiger², Nenad Lukic³, Aleksandra Zumbrunn Wojczyńska³, Ray S. Hovijitra⁴ and Dominik A. Ettlin^{3,5,6}

¹ Department of Oral Medicine, Faculty of Dentistry, Chulalongkorn University, Bangkok, Thailand, ² Department of Psychiatry and Psychotherapy, Psychiatric Services Aargau, Aarau, Switzerland, ³ Orofacial Pain Unit, Center of Dental Medicine, University of Zurich, Zurich, Switzerland, ⁴ Dental Center, Bumrungrad International Hospital, Bangkok, Thailand, ⁵ São Leopoldo Mandic Institute and Research Center, São Paulo, Brazil, ⁶ Department of Reconstructive Dentistry and Gerodontology, School of Dental Medicine, University of Berne, Berne, Switzerland

OPEN ACCESS

Edited by:

Limor Avivi-Arber,
University of Toronto, Canada

Reviewed by:

Harold Avila,
Indiana University, United States
Vishal Aggarwal,
University of Leeds, United Kingdom
Konstantinos Kotsis,
University of Ioannina, Greece

*Correspondence:

Kanokporn Bhalang
cudent70@gmail.com

Specialty section:

This article was submitted to
Headache Medicine and Facial Pain,
a section of the journal
Frontiers in Neurology

Received: 07 May 2020

Accepted: 26 October 2020

Published: 03 December 2020

Citation:

Bhalang K, Steiger B, Lukic N,
Zumbrunn Wojczyńska A, Hovijitra RS
and Ettlin DA (2020) The
Pain-to-Well-Being Relationship in
Patients Experiencing Chronic
Orofacial Pain.
Front. Neurol. 11:557415.
doi: 10.3389/fneur.2020.557415

Introduction: Orofacial pain features may negatively influence a person's well-being and vice versa. Some aspects of well-being can be measured with axis II instruments that assess patients' psychosocial and behavioral status. The aim of this study was to investigate associations between pain features and psychosocial variables as indicators of well-being.

Materials and Methods: Seven hundred ninety-nine anonymized datasets collected using the Web-based Interdisciplinary Symptom Evaluation (WISE) of patients reporting to the Interdisciplinary Orofacial Pain Unit, University of Zurich, between March 19, 2017 and May 19, 2019, were analyzed. Pain features including intensity, number of locations, impact, and duration were evaluated. Psychometric measures assessed pain-related catastrophizing and disability, illness perception, distress, anxiety, depression, injustice experience, dysmorphic concerns, and insomnia.

Results: Most patients were between 30 and 59 years old (58.3%), female (69.8%), working (66.0%), and experienced pain for more than 6 months (68.5%). Pain intensities were higher in women than men and higher in disabled than working patients. Scores indicating elevated stress and depression were also observed in disabled patients. The sample prevalence rates of clinically relevant axis II instrument scores were as follows: Graded Chronic Pain Scale for the Head (GCPS-H), 27%; Patient Health Questionnaire 4 (PHQ4), 21%; PHQ9, 21%; Pain Catastrophizing Scale (PCS), 20%; General Anxiety Disorder 7 (GAD7), 15%; Insomnia Severity Index (ISI), 15%; Injustice Experience Questionnaire (IEQ), 14%; GCPS for the Body (GCPS-B), 13%; PHQ for Stress (PHQstr), 6%; and Dysmorphic Concern Questionnaire (DCQ), 2%. Noteworthy results of correlation analysis of the clinically relevant axis II scores and pain measures were as follows: the PHQstr had moderate associations (0.34–0.43) with the sum of pain intensity at rest and during function, number of pain locations, and typical pain intensity. The IEQ scores were moderately associated with typical pain intensity at 0.39. The DCQ scores were moderately associated with pain extension at 0.41.

Conclusions: Moderate correlations of certain pain and well-being measures were found in patients reporting clinically relevant stress, injustice experience, and dysmorphic concern, all of which reflect impaired well-being. PHQ4 is suitable for routine distress screening in the clinical setting.

Keywords: injustice, stress, well-being, orofacial pain, dysmorphic

INTRODUCTION

Pain is a complex, multidimensional construct that includes features such as intensity (at rest and during movements), spread, symmetry, chronicity, and impact of pain. Analogous to pain in any other body region, orofacial pain (OFP) negatively influences well-being and *vice versa* (1). Well-being can be conceptualized as a spectrum, with happiness, minimal distress, and high well-being at one end and elevated depression, anxiety, and low well-being at the other (2). Diverse psychometric instruments exist for indirectly measuring well-being, e.g., the Hospital Depression and Anxiety Scale, the General Health Questionnaire, the Perceived Stress Scale, and the Positive and Negative Affect Schedule (3). Accordingly, a well-being proxy measure may consist of a diverse set of psychometric instruments that offer information on a patient's psychological and behavioral status. From a pain management perspective, well-being proxy measures, such as anxiety, depression, catastrophizing, and others, are all relevant in influencing treatment outcomes in patients experiencing OFP and temporomandibular disorders (TMDs) (4–7). Another important negative influence on well-being is unemployment, resulting in feelings of worry, insecurity, and stress due to changes in the patient's financial situation (8, 9).

Pain and well-being are interrelated. Hence, a dual-axis diagnostic system has been proposed for evaluating patients experiencing OFP and TMD (10). This system differentiates physical diagnoses (which can be grouped into axis I) from the patients' psychosocial and behavioral status (known as axis II) reflecting their well-being. Notably, axis I diagnoses are categorical in nature, such as temporomandibular joint disc displacement or arthritis, while axis II construct measures have ordinal values. According to an international expert panel, axis II instruments aim at assessing the psychosocial and behavioral status (including pain-related disability) (11). For the purpose of this paper, we refer to pain as a symptom and not as a diagnosis or psychological status *per se*. Sleep has been proposed as an additional axis II construct because a strong relationship between self-assessed sleep disturbances, OFP, and TMD has been observed (12, 13). Perceived injustice, anger, illness perception, catastrophization, and dysmorphophobia are additional potential moderators of the pain-to-well-being relationship (14–17).

The Web-based Interdisciplinary Symptom Evaluation (WISE) is an online tool based on self-reports that assists clinicians in the comprehensive assessment of patients with OFP or TMD (18). WISE records sex, age, and employment status. This evaluation further combines a description of pain features with widely available in-depth psychometric measures. The automatically generated summary report supports clinicians

in identifying case complexity and disability levels. WISE thus facilitates resource planning for the initial consultation, such as allocation of time and appropriate healthcare specialists. Anonymized WISE data can be extracted for research purposes.

Using anonymous data collected by the WISE tool, the aim of this study was to correlate pain features with other axis II construct measures reflecting well-being in patients experiencing OFP of mixed etiologies. Further, we analyzed whether known confounders such as sex, age, employment status, and pain duration influenced psychometric scores and pain features.

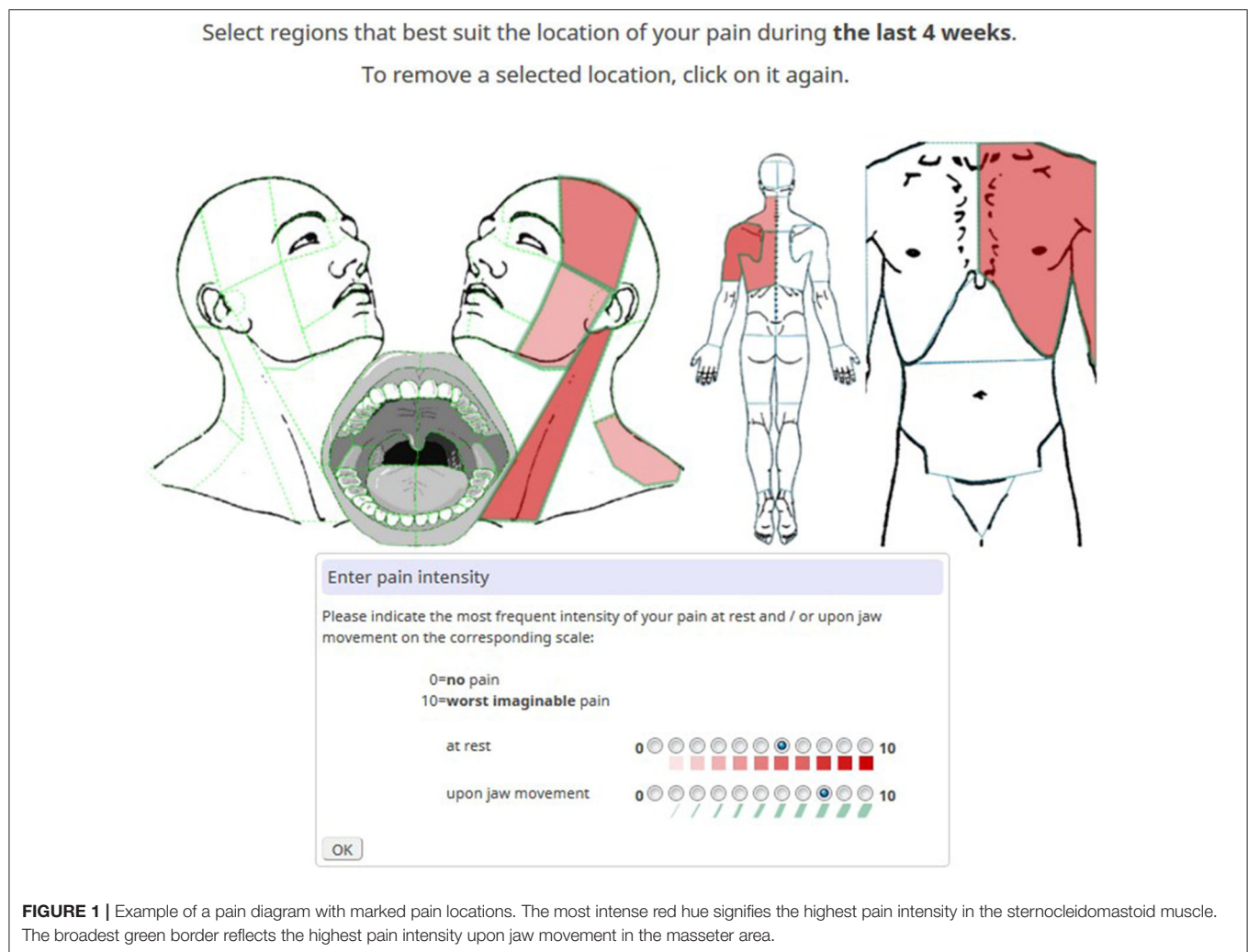
MATERIALS AND METHODS

Subjects

This study included 799 anonymized WISE datasets of patients reporting to the Interdisciplinary Orofacial Pain Unit, Center of Dental Medicine, University of Zurich, Switzerland, between March 19, 2017 and May 19, 2019. The spectrum of axis I diagnoses encountered in this unit has been reported elsewhere (16). Patients completed the WISE questionnaire prior to their first clinical appointment. Anonymized data were retrieved from a server located at Hof University of Applied Science, Germany, and exported in csv format for statistical analysis. According to Swiss law, researchers can use strictly anonymized data and do not require approval by an ethics committee. Only fully completed WISE datasets of patients reporting OFP were analyzed, given that the subjects consented to the use of their anonymized data for research. Data related to non-painful symptom reports were excluded.

Web-Based Interdisciplinary Symptom Evaluation Datasets

The WISE system is a Web-based instrument for interdisciplinary subject-tailored symptom evaluation in patients experiencing OFP and TMD (18). WISE combines a symptom-oriented checklist with validated in-depth questionnaires, also referred to as case finding instruments. The questionnaires are presented when the checklist scores exceed threshold values and thus indicate a burden related to the screening item. Graphical maps offer patients the opportunity to indicate their pain location, intensity, and duration in various defined oral and cranial tissues as well as other body regions. In addition to pain measures, several other psychometric instruments are integrated. Only German and English versions of the WISE were completed. German versions of the applied measures are available. The following variables from the WISE datasets were used in this study.



Pain Features

Pain features were captured by detailed interactive pain maps of the head and neck and front/back view maps of the rest of the body. Pain locations were differentiated by 93 selectable anatomical areas across the entire body and 72 areas across the head and neck region (**Figure 1**). Patients marked painful areas by clicking on a defined area and reported the typical pain intensity at rest and upon movement. Both were reported for the last 4 weeks on an 11-point numeric rating scale (NRS) for pain. Different pain intensities at rest were represented by gradients of red, and different pain intensities upon movement were captured by graded widths of anatomical green borders.

Using the same NRS, typical (PI-typ) and maximum (PI-max) pain intensities of the chief complaint were additionally reported. Pain extension for the body (P-ext-B) was defined as the total number of pain locations across the entire body and pain extension for the head (P-ext-H) was defined as the number of pain locations across the head and neck region (left part of **Figure 1**). Pain impact at rest and pain impact upon movement were calculated as the sum scores of pain intensities across the head and neck region at rest (\sum -PI-rest-H) and upon movement

(\sum -PI-move-H), respectively. The duration of OFP (P-dur) as a measure of chronicity was grouped by intervals: <3 months, 3–6 months, 6 months–2 years, 2–5 years, >5 years.

Axis II Psychometric Measures

Brief Illness Perception Questionnaire

The Brief Illness Perception Questionnaire (B-IPQ) (19–21) assesses cognitive and emotional representations of illness and health threat. Eight questions covering different aspects of illness perception were rated on an NRS ranging from 0 to 10. The maximum score is 80. No cutoff score has been reported for this questionnaire. Test–retest reliability of the single items of the B-IPQ ranged from 0.48 to 0.70; a coefficient alpha value was not reported.

Dysmorphic Concern Questionnaire

The Dysmorphic Concern Questionnaire (DCQ) (22, 23) assesses excessive preoccupation with an imagined or a real minimal defect in appearance that is associated with a significant impact on psychosocial functioning. The questionnaire consists of seven items that cover different aspects of dysmorphic concern. Each

item is rated on an ordinal scale ranging from 0 to 3, resulting in a maximum sum score of 21. A cutoff score of nine indicates a possible body dysmorphic disorder. The following coefficient alpha for the DCQ has been reported: 0.85; test–retest reliability was not reported.

Graded Chronic Pain Scale Version 2.0 for the Head or for the Body

The Graded Chronic Pain Scale (GCPS) (24) consists of three pain intensity scales ranging from “no pain” (=0) to “pain as bad as it could be” (=10) assessing current, worst, and average pain intensity for the last 30 days. The disability days report the number of days being kept from daily activities by pain for the last 3 months. The number of days determines a disability score ranging from 0 to 3. Three additional scales measure the interference by pain during (1) daily activities, (2) recreational, social, and family activities, and (3) working ability on a scale from “no interference” (=0) to “unable to carry on any activities” (=10) for the last 30 days. The average value of these three disability scales yields a disability score ranging from 0 to 3. Combining the pain activity interference score with the disability day score results in a disability sum score ranging from 0 to 6. Two separate disability scores due to pain in the head (GCPS-H) or the body (GCPS-B) were calculated. Scores ≥ 3 are considered as high disability and severely limiting. The following coefficient alpha has been reported: 0.71 for TMD pain; test–retest reliability has not been reported.

General Anxiety Disorder 7

The General Anxiety Disorder 7 (GAD7) (25) assesses general anxiety in primary care patients. Seven items cover different aspects of general anxiety. For the question “Over the last 2 weeks, how often have you been bothered by the following problems?” items are scored on a four-point scale from not at all” (=0), “several days” (=1), “half of the days” (=2), and “nearly every day” (=3). Summary scores range from 0 to 21 and indicate anxiety levels of “none/minimal” (0–4), “mild” (5–9), “moderate” (10–14), or “severe” (>14). The following coefficient alpha has been reported: 0.92; for test–retest reliability: 0.83.

Injustice Experience Questionnaire

The Injustice Experience Questionnaire (IEQ) (26–28) assesses injustice experienced due to accidents, injuries, or maltreatment. Twelve items reflect the frequency of thoughts, beliefs, and emotions associated with injury. They are rated on a scale with the following response options: “never” (=0), “rarely” (=1), “sometimes” (=2), “often” (=3), to “all the time” (=4). The maximum score is 48. Scores ≥ 18 indicate the need for professional evaluation. The following coefficient alpha has been reported: 0.92; for test–retest reliability: 0.90.

Insomnia Severity Index

The Insomnia Severity Index (ISI) (29, 30) screens for sleep disorders by measuring the severity of insomnia problems, sleep-related satisfaction, and interference on a scale of “none” (=0), “mild” (=1), “moderate” (=2), “severe” (=3), and “very severe” (=4) for the items falling asleep, staying asleep, and

waking up too early over the past 2 weeks. On a scale from “very satisfied” (=0), “satisfied” (=1), “moderately satisfied” (=2), “dissatisfied” (=3), to “very dissatisfied” (=4), the patient indicates how satisfied/dissatisfied he/she perceives his/her current sleep pattern. On three additional scales from “not at all” (=0), “a little” (=1), “somewhat” (=2), “much” (=3), to “very much” (=4), the patient is asked how much he/she considers his/her sleep problem to interfere with daily activities, how noticeable the interference by his/her sleep problem is to others, and how worried/distressed the patient is because of his/her sleep problem. The maximum score is 28, with scales of “none” (0–7), “subthreshold” (8–14), “moderate” (15–21), or “severe” (>21). The following coefficient alpha has been reported: 0.74; test–retest reliability was not reported.

Pain Catastrophizing Scale

The Pain Catastrophizing Scale (PCS) (31, 32) assesses catastrophizing thoughts and corresponding behavior. The questionnaire has 13 items that are scored on a five-point ordinal scale [“not at all” (=0), “to a slight degree” (=1), “to a moderate degree” (=2), “to a great degree” (=3), or “all the time” (=4)]. Scores can also be calculated for three subscales of helplessness, maximizing, and ruminating. The maximum value is 52 for the entire questionnaire. The corresponding cutoff values are 13 for helplessness, five for maximizing, 13 for ruminating, and 30 for the entire questionnaire. These cutoff values correspond to the 75th percentile. The following coefficient alpha has been reported: 0.87; for test–retest reliability: 0.75.

Patient Health Questionnaire 4

The Patient Health Questionnaire 4 (PHQ4) (33) screens for anxiety and depression. This questionnaire consists of two subscales, GAD2 (items one and two of the GAD7) and PHQ2 (items one and two of the PHQ9). Items are scored on an ordinal scale ranging from 0 to 3 using the same labels as the GAD7. Scores can be calculated for the two subscales (maximum score = 6) and overall (maximum score = 12). Scores ≥ 6 for the total score and three for the sub-scores indicate expert evaluation referral. The following coefficient alpha has been reported: 0.87; for test–retest reliability: 0.81.

Patient Health Questionnaire 9

The PHQ9 (34, 35) assesses the severity of depression. Nine items covering different aspects of depression are scored on an ordinal scale ranging from 0 to 3 using the same labels as the GAD7. Summary scores range from 0 to 27, indicating depression levels of “none/minimal” (0–4), “mild” (5–9), “moderate” (10–14), “moderately severe” (15–19), or “severe” (>19). A cutoff score range of 8–11 has been recommended for expert evaluation referral. The following coefficient alpha has been reported: 0.89; for test–retest reliability: 0.84.

Patient Health Questionnaire for Stress

The Patient Health Questionnaire for Stress (PHQstr) (34, 36) is a 10-item subscale of the Primary Care Evaluation of Mental Disorders (PRIME-MD) Patient Health Questionnaire that addresses psychosocial stress burden. Items are scored on an ordinal scale ranging from “not at all” (=0), “a little” (=1),

TABLE 1 | Sample characteristics ($N = 799$).

| Gender | Age group | | | | | | | | | Employment status | | | | Pain duration | | | | | |
|--------|-----------|-----|-------|-------|-------|-------|-------|-------|------|-------------------|---------|---------|----------|---------------|-----------|------------|------------------|-----------|----------|
| | | | 10-19 | 20-29 | 30-39 | 40-49 | 50-59 | 60-69 | ≥70 | Training | Working | Retired | Disabled | No job | <3 months | 3-6 months | 6 months-2 years | 2-5 years | >5 years |
| | M | F | | | | | | | | | | | | | | | | | |
| | | | 53 | 122 | 148 | 162 | 156 | 92 | 66 | 80 | 527 | 113 | 52 | 27 | 124 | 128 | 248 | 149 | 150 |
| | 558 | 241 | 6.6% | 15.3% | 18.5% | 20.3% | 19.5% | 11.5% | 8.2% | 10.0% | 66.0% | 14.1% | 6.5% | 3.4% | 15.5% | 16.0% | 31.0% | 18.6% | 18.8% |

TABLE 2 | Descriptive statistics of pain measures used in the study ($N = 799$).

| Pain measures | Maximum possible score | Mean | SD |
|--|------------------------|------|------|
| Number of pain locations across the entire body (P-ext-B) | 93 | 8.69 | 9.56 |
| Number of pain locations across the head and neck region (P-ext-H) | 72 | 5.54 | 6.91 |
| Typical pain intensity (PI-typ) | 10 | 4.91 | 2.44 |
| Maximum pain intensity (PI-max) | 10 | 7.10 | 2.49 |
| Pain intensity sum score at rest across the head and neck region (\sum PI-rest-H) | 720 | 33.4 | 48.7 |
| Pain intensity sum score upon movement across the head and neck region (\sum PI-move-H) | 720 | 38.2 | 51.3 |

to “a lot” (=2). Summary scores range from 0 to 20 indicating the degree of psychosocial stress burden by the following levels: “none/minimal” (0–4), “mild” (5–9), “medium” (10–14), or “severe” (>14). No coefficient alpha nor test–retest reliability was reported.

Statistical Analysis

The data were analyzed using SPSS (Version 22, Armonk, New York). Descriptive statistics were used to characterize the datasets. Spearman rank correlation was used for correlation analysis. To determine the effect size, small ($0.1 < r < 0.3$), moderate ($0.3 < r < 0.5$), and strong ($r \geq 0.5$) were used for the different association levels (37). Analysis of variance was used with a Bonferroni or Tamhane correction for *post hoc* testing depending on whether the variances were equal or not. A significance level of ≤ 0.05 was considered statistically significant.

RESULTS

Most patients were female ($N = 558$; 69.8%), with a female-to-male ratio of 2.3:1. Among the patients, 73.6% ($N = 588$) were 20–59 years old, 66.0% were working ($N = 527$), and 84.4% suffered from pain for more than 3 months ($N = 675$) (Table 1).

The descriptive statistics of various pain measures are shown in Table 2. On average, patients had 8.69 pain sites across the entire body and 5.54 pain sites across the head region. The mean typical pain intensity was 4.91, and the mean maximum pain intensity was 7.10. With an average of 33.4, the intensity sum score at rest was lower compared with upon movement (38.2).

We determined the influence of patient characteristics (sex, age, employment status, and pain duration) on the mean of the assessed pain features. Sex had a significant influence on PI-typ, PI-max (Figure 2), and \sum -PI-rest-H, with women reporting higher mean values. Effects of age were found for P-ext; patients aged 30–39 years indicated more pain locations compared with older patients (>60 years old). Employment status demonstrated significant effects on all pain-related

measures. Disabled patients significantly indicated more pain locations compared to employed patients, patients in training, or retired patients. Working patients presented more pain locations compared to retired patients. The highest typical and maximum pain intensities were reported by patients without a job and by disabled patients (**Figure 2**). The \sum -PI-rest-H was highest in disabled patients. Pain duration had significant effects on all pain-related measures, except for PI-typ and PI-max. The number of pain locations, \sum -PI-rest-H, and \sum -PI-move-H increased with the duration of pain.

The number of patients who completed one of the case finding questionnaires ranged from 216 (GAD7) to 799 (PCS, PHQ4, and PHQstr). The percentage of patients reaching a clinically relevant score (cutoff) ranged from 5.1% (DCQ) to 73.7% (PHQ9) (**Table 3**).

The analysis of variance of the selected mean axis II domain scores grouped by selected patient characteristics (age group and employment status) is shown in **Figure 3**. There were no significant effects of age on axis II measures, except that older patients (>60 years) had lower PHQstr scores than those aged 30–59 years, and patients in the middle age groups had a higher PHQ4 score than those in the younger age groups and in older patients. Employment status had a significant effect on several measures. GCPS-H scores were higher among disabled patients or patients with no job than among trainees, working, or retired patients; GCPS-B scores were higher in disabled patients than in trainees, working, or retired patients. PCS and PHQ4 values were higher in disabled patients or patients with no job compared with trainees, working, or retired patients. PHQ9 scores were higher in disabled than in retired or working patients, and PHQstr scores were higher in disabled patients than in trainees, working, or retired patients. Pain duration had no significant effect on psychosocial variables except for PHQ4 and PHQstr, where patients experiencing pain longer than 5 years had higher mean values compared with patients with a pain duration of <3 months.

For the correlations between various pain features and axis II measures (**Figure 4A**), the following five pain features showed moderate correlation effects ($r \geq 0.30$; $P < 0.50$) with other axis II measures: (1) \sum -PI-rest-H with PCS, PHQ4, PHQstr, GAD7, IPQ, GCPS-H, and GCPS-B; (2) \sum -PI-move-H with PCS, PHQ4, GCPS-H, and GCPS-B; (3) PI-max with PCS, IPQ, and GCPS-H; (4) PI-typ with PCS and GCPS-H; and (5) P-ext-B with PHQ4 and PHQstr. Pain duration showed only weak or no correlations with all pain measures. All other axis II measures (IEQ, ISI, and DCQ) only had weak or no correlations with pain features.

From **Figure 4B**, when correlation analyses were performed after dichotomizing questionnaire scores into above and below cutoff values, we found that PHQstr scores above nine ($N = 46$) significantly correlated with levels of P-ext, PI-typ, \sum -PI-rest-H, and \sum -PI-move-H ($r = 0.34$ – 0.47 ; $P < 0.05$). GCPS-B scores above cutoff level ($N = 107$) significantly correlated with P-ext-B and \sum -PI-move-H ($r = 0.30$ and 0.31 , respectively; $P < 0.001$). DCQ scores above cutoff level ($N = 22$) moderately correlated ($r = 0.32$ – 0.41) with P-ext, PI-max, \sum -PI-rest-H, and \sum -PI-move-H. IEQ scores above cutoff level ($N = 93$)

significantly correlated with PI-typ ($r = 0.39$; $P < 0.001$). ISI scores above 14 ($N = 121$) significantly correlated with PI-typ ($r = 0.31$; $P < 0.001$).

DISCUSSION

The aim of this study was to further understand the pain-to-well-being relationship in patients experiencing OFP. Thus, the relationships between various pain features and other psychometric measures as indicators of well-being were analyzed. Furthermore, pain features and psychometric scores were analyzed with regard to patient characteristics, such as gender, age group, employment status, and pain duration.

Data Origin and Sample Characteristics

Anonymized data were derived from a large clinical cohort of 799 patients who completed the WISE between March 19, 2017 and May 19, 2019. This comprehensive evaluation tool is routinely used in the Orofacial Pain Unit of the Center of Dental Medicine, University of Zurich, to plan the resources for the initial consultation, such as allocation of time and appropriate healthcare specialists. **Table 1** indicates that the gender proportion and age distribution matched those reported in other studies on patients seeking care for OFP (16, 38–40). Three quarters of our sample were in training or working, while 6.5% of patients were disabled. Most patients were considered chronic pain sufferers since more than 80% of them experienced pain longer than 3 months (41).

Pain Scores and Relation to Patient Characteristics

On average, patients reported pain in ~ 9 of possible 93 locations as defined in the diagrams in **Figure 1**, indicating that the majority experienced locoregional pain. On the 11-point numerical pain scale, the reported mean pain intensity was moderate (4.9), with a mean maximum intensity of 7.1. As expected, pain was more intense upon movement compared to at rest (**Table 2**). Pain intensities were higher in women than men and higher in disabled than working patients (**Figure 2**). As was previously reported, pain is generally more prevalent in females in the head and neck areas (42, 43). Somewhat counterintuitively, pain extension decreased from middle to old age as was reported in fibromyalgia patients (44). This may be due to the observation that OFP origins shift across age from myogenic to neurogenic (e.g., trigeminal neuralgia) and the latter being typically a localized pain (45, 46). This may also explain why working subjects indicated more pain locations than those retired. Recent findings do not indicate that OFP mediates the relationship between socioeconomic inequalities (linked to disability) and the impacts of oral conditions on daily life (47).

Well-Being Scores

Table 3 summarizes the axis II questionnaire scores serving as proxies for well-being. The PHQ4 is part of the WISE checklist and was therefore completed by all patients. All patients were also asked to complete the PCS due to relevant associations of pain

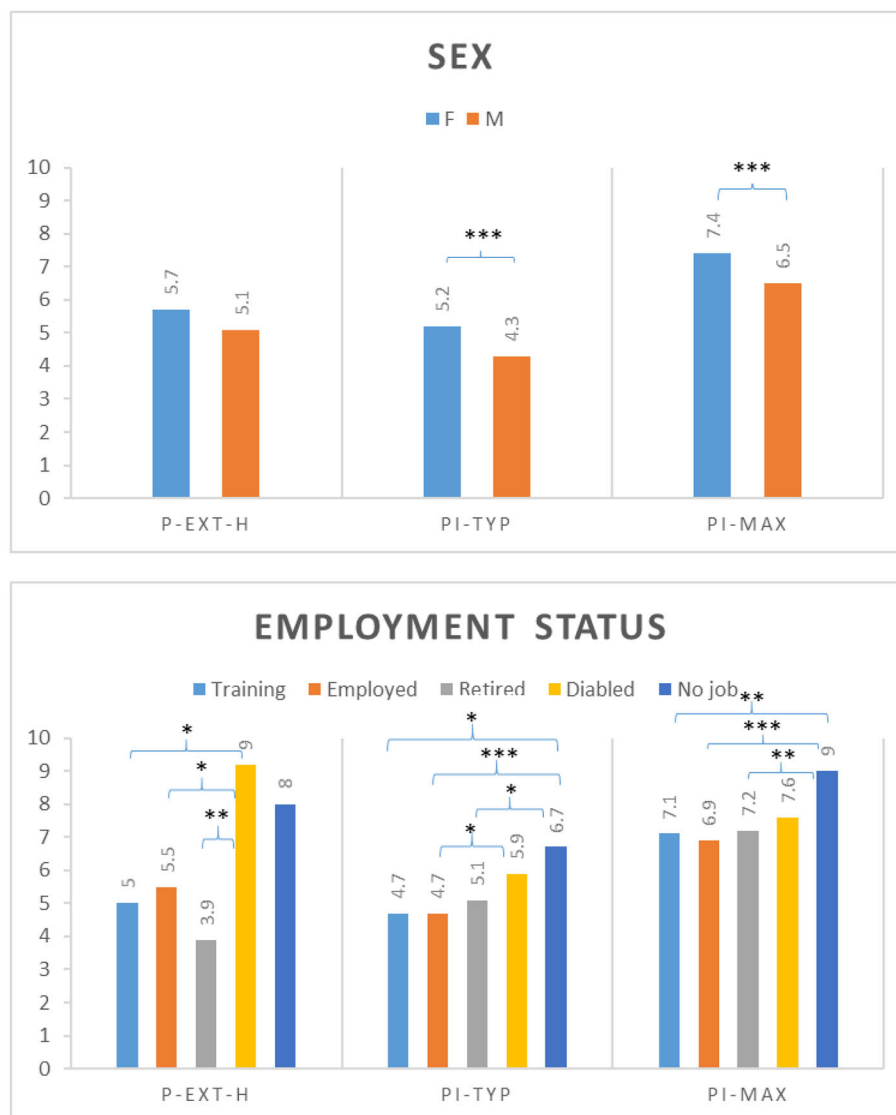


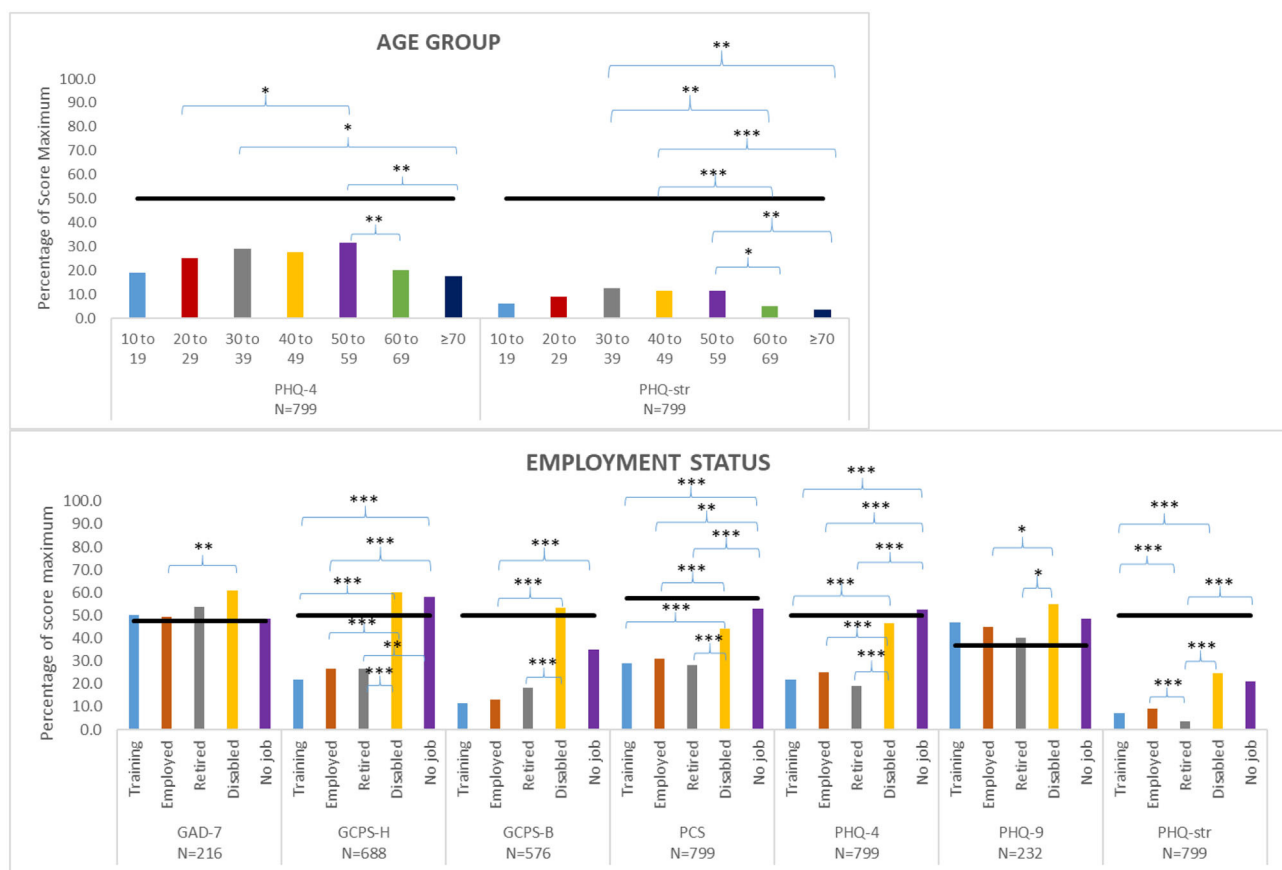
FIGURE 2 | Analysis of variance between selected patient characteristics (sex, employment status) and selected pain features (P-ext-H, number of pain locations across the head and neck region; PI-typ, typical pain intensity; PI-max, maximum pain intensity); *Post hoc* tests with Bonferroni correction or Tamhane correction (* $P \leq 0.05$ ** $P \leq 0.01$ *** $P \leq 0.001$).

catastrophizing with pain-related disability, number of painful body sites, and pain-related impact (7). The sample prevalence rates of clinically relevant axis II instrument scores (above cutoff) in descending order were as follows: GCPS-H, 27%; PHQ4 and PHQ9, 21%; PCS, 20%; GAD7, 15%; ISI, 15%; IEQ, 14%; GCPS-B, 13%; PHQstr, 6%; and DC, 3%. No cutoff value has been reported for the IPQ. The GCPS can predict the healthcare utilization cost for chronic OFP patients (48). Approximately one in four patients experienced moderate or severe impairment due to craniofacial pain (and 13% due to bodily pain). Almost as many had PHQ scores that warrant further evaluation for depression, whereas 15% experienced symptoms characteristic of a GAD. The 20% of patients reporting pain catastrophizing scores above

29 might have an elevated risk of delayed pain recovery (49). Pain catastrophizing was demonstrated to mediate the effects of distress in OFP patients, which was attributed to the helplessness component of the PCS (50). Due to the sample overlap, the prevalence of moderate and severe grades of insomnia (15%) confirms the 16% we previously reported (13). A novel finding of this study is that approximately one in seven patients (14%) perceived injustice of a clinically relevant level. It is noteworthy that patients concerned about injustices in the treatment they receive are vulnerable to greater emotional distress, prolonged work disability, invalidating or stigmatizing reactions of others, and poor pain-related outcomes (51–53). According to Sullivan (54), blame cognitions may have an impact on feelings of

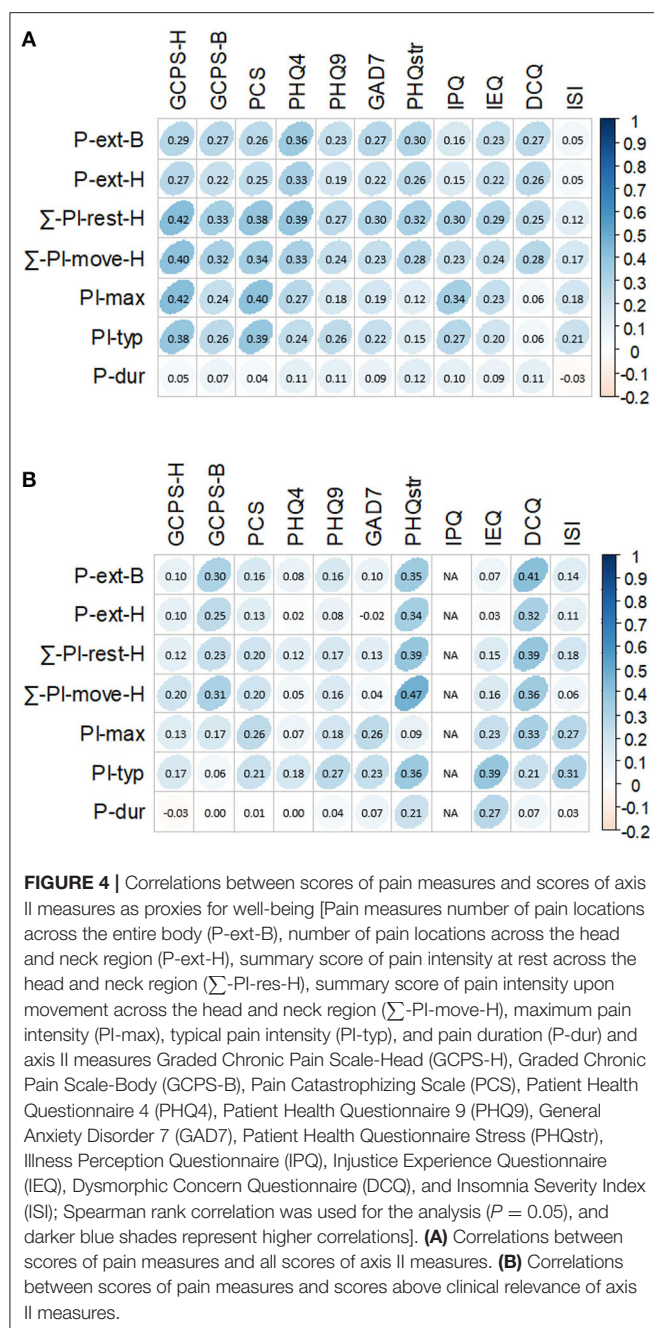
TABLE 3 | Scores of the axis II psychometric measures [Note that \geq cutoff score (CO) indicates clinical relevance].

| Domains (alphabetical order) | N | Max | Mean | SD | \geq cut-off score CO | | | |
|--|-----|-------|------|------|-------------------------|-----|----------|-------------------|
| | | | | | CO | N | % domain | % of study sample |
| Dysmorphic Concern Questionnaire (DCQ) | 432 | 21/21 | 1.45 | 3.35 | 9 | 22 | 5.10 | 3 |
| General Anxiety Disorder 7 (GAD7) | 216 | 21/21 | 10.8 | 3.81 | 10 | 120 | 55.6 | 15 |
| Graded Chronic Pain Scale-Head (GCPS-H) | 688 | 6 | 1.79 | 0.84 | 3 | 218 | 31.7 | 27 |
| Graded Chronic Pain Scale-Body (GCPS-B) | 576 | 6 | 1.04 | 1.62 | 3 | 107 | 18.5 | 13 |
| Illness Perception Questionnaire (IPQ) | 566 | 78/80 | 44.5 | 11.5 | | | | |
| Injustice Experience Questionnaire (IEQ) | 302 | 48/48 | 14.1 | 11.3 | 18 | 108 | 35.8 | 14 |
| Insomnia Severity Index (ISI) | 296 | 28/28 | 13.5 | 5.58 | 15 | 121 | 40.9 | 15 |
| Pain Catastrophizing Scale (PCS) | 799 | 51/52 | 16.6 | 12.6 | 30 | 157 | 19.6 | 20 |
| Patient Health Questionnaire 4 (PHQ4) | 799 | 12/12 | 3.13 | 3.10 | 6 | 165 | 21.0 | 21 |
| Patient Health Questionnaire 9 (PHQ9) | 232 | 25/27 | 12.5 | 4.81 | 10 | 171 | 73.7 | 21 |
| Patient Health Questionnaire Stress (PHQstr) | 799 | 20/20 | 6.24 | 3.74 | 10 | 46 | 18.9 | 6 |

**FIGURE 3 |** Analysis of variance between selected patient characteristics (age group, employment status) and selected axis II measures [Patient Health Questionnaire 4 (PHQ4), Patient Health Questionnaire Stress (PHQstr), General Anxiety Disorder 7 (GAD7), Graded Chronic Pain Scale-Head (GCPS-H), Graded Chronic Pain Scale-Body (GCPS-B), Pain Catastrophizing Scale (PCS), Patient Health Questionnaire 9 (PHQ9)]; *Post hoc* tests with Bonferroni correction or Tamhane correction ($^*P \leq 0.05$ $^{**}P \leq 0.01$ $^{***}P \leq 0.001$). Maximum scores are listed in **Table 3**. Black bars indicated cutoff scores of the respective psychometric instrument.

anger and revenge motives that warrant interventions to alter the individual's perceptions of the offender. Although perceived stress has been reported to predict the incidence of painful TMDs, the number of patients (6%) reporting medium to severe stress on

the PHQstr was rather low in this sample, likely due to the broad variety of pain origins (16, 18, 29). And only 2% reached clinically relevant DCQ scores. Health anxiety questionnaire was reported to have good association with OFP and other related syndromes



(55) and was found to be a strong predictor of chronic OFP (56). However, we only observed moderate correlation between GAD7 score and Σ -PI-res-H in our subjects. The inclusion of patients experiencing various types of disorders in this study is justified by the pain associations with axis II psychological and psychosocial variables independent of pain origin (57).

Well-Being Scores in Relation to Patient Characteristics

Women not only experienced significantly more intense pain than men (Figure 2) but also suffered significantly severer impairment (data not shown). A multitude of mechanisms

has been proposed to explain sex differences in pain and emotional processing, including the effects of sex hormones, differences in endogenous opioid function, cognitive/affective influences, coping patterns, and contributions of social factors such as stereotypic gender roles (58, 59). In our sample, PHQ4 and PHQstr scores were highest in 50–59-year-old subjects, which is consistent with a Japanese study reporting PHQ scores being low in young adulthood, increasing in middle age (peaking during age 50–59), and then decreasing again in older age (60). The relationship between employment-related factors and chronic pain lacks adequate research (61). Our findings that being disabled and/or unemployed was negatively associated with various axis II instrument scores emphasize the need for routine collection of information on employment status to optimize clinical care and future research (62). It is noteworthy that daily activities are negatively influenced not only by pain itself but also by pain-related fear (63).

Correlations Between Pain and Well-Being Scores

As the structure of the WISE instrument is modular, not all 799 patients completed each axis II instrument or each pain-related questionnaire. However, everyone was requested to complete questions related to pain locations, intensities, and duration. None of the calculated correlations was strong ($r \geq 0.5$). The fact that the PCS, PHQ4, and PHQstr were completed by all patients and the GCPS-H by nearly 90% of them largely explains their highest correlation levels with pain intensity variables and pain extension for the entire sample (Figure 4A). Such effects reversed when only cases with clinically relevant scores (above cutoff) were analyzed (Figure 4B). Our data thus support the routine use of PHQ4 as a screener for anxiety and depression in the clinical setting, as recommended by international expert panels (11). PEG, a three-item scale measuring pain intensity (P), interference with enjoyment of life (E), and interference with general activity (G), is another tool available for initial pain patient evaluation (64). Psychological comorbidity has been shown to influence patients' illness perceptions by means of pain ratings, treatment-seeking behavior, and treatment adherence, as well as recovery after surgical procedures (65–67).

The well-being of patients is more likely compromised when we defined compromised well-being by axis II scores at or above cutoff values. Figure 4B reveals that patients experiencing widespread pain and high sum intensity scores suffered high distress levels (PHQstr scores ≥ 10 ; $N = 46$; $r = 0.34$ – 0.47 ; all P -values < 0.05). This confirms previous findings that self-reported stress independent of its origin (pain or non-pain-related) can initiate or exacerbate the impact of TMDs, chronic pain, and disability (68, 69). However, further research is needed to clarify the amount, timing, severity, and type of stress that is needed to contribute, maintain, and exacerbate persistent pain (70). While stress is often comorbid with anxiety, depression, as well as pain catastrophizing and persistence, clinically relevant scores of these domains did not significantly

correlate with any pain measure in our study (6, 71–73). The low number of patients experiencing dysmorphic features (DCQ scores ≥ 9 ; $N = 22$) makes it difficult to interpret correlations with pain features. Still, this may be an interesting topic for further exploration.

A new and highly significant finding was that typical pain intensity moderately correlated with high scores on the IEQ (scores >17 ; $N = 93$). The IEQ has proven to be a good predictor for delayed healing in patients experiencing pain and post-traumatic stress (6, 74, 75). However, we are unaware of the use of this questionnaire in the OFP domain, except for its German-language validation (28). Notably, patients perceiving injustice also had pain for a longer duration compared to subjects with lower IEQ scores ($r = 0.27$; $P < 0.001$).

Although patients with OFP report sleep disturbances disproportionately more often compared with the general population (13), clinically relevant insomnia only associated with typical pain intensity at a moderate level, which is in line with previous observations (ISI scores >15 ; $N = 121$) (76). This finding indicates that other psychosocial variables likely contribute more to insomnia than the selected pain features, and it supports the notion that sleep impairment is more likely a predictor of OFP than pain is of sleep impairment (77). Surprisingly to us, pain duration did not correlate with any of the axis II measures employed in our study, except for a weak correlation with perceived injustice.

A key difference of this study as compared to the OPPERA studies (78) is that our sample is a pure clinical sample and therefore more likely represents a clinical population that most dentists encounter in their practices. Taken together, our results support Schiffman et al. (11) for the use of GCPS and PHQ4 as screening tools in clinical practice; however, for comprehensive assessments of orofacial patients' well-being, not only PHQ9 and GAD7 but also PHQstr, DCQ, IEQ, and ISI should be utilized by specialists to obtain a more in-depth evaluation of these patients.

Although it was not the main objective of this study, we also explored the correlations between various axis II instruments (data not shown) and, interestingly, found that IPQ and IEQ strongly correlated with PCS and PHQ4 ($r = 0.55$ – 0.61 ; $P < 0.001$).

Study Limitations

Since this is a cross-sectional study, we cannot draw definite causal conclusions regarding the relationship between pain and well-being. The WISE pain drawing allows patients to report on pain intensities in every region marked on the body diagram. When a person experienced pain in multiple locations, the limitation to a single numeric value for the typical (PI-typ) and maximum (PI-max) pain intensity characteristic of his/her chief complaint may have made the choice difficult. We did not attempt to capture psychological factors that influence pain intensity and distribution on pain drawings (79, 80), although

we are aware of their importance in understanding the somatic awareness present in chronic pain conditions (81). Since the DC/TMD axis II measures currently do not cover some of the biopsychosocial aspects of interest in this study, which included a broad variety of OFP complaints beyond TMDs, we have incorporated several additional psychometric instruments in our data analyses. Most patients in this study had moderate pain intensities, which may explain why no strong correlation levels were detected in our analyses. The low prevalence of DCQ likely explains the lack of correlation between the DCQ and the assessed pain dimensions. Nevertheless, the fact that the correlation between dysmorphic concern and pain has not previously been reported warrants further investigations. This study did not examine the presence of additional painful comorbidities, although patients experiencing prolonged painful TMDs are at increased risk of suffering from other painful conditions (82). Furthermore, we did not employ a specific instrument for measuring well-being, such as the Warwick–Edinburgh Mental Well-Being Scale (83). Rather, our well-being proxy measures included the set of axis II constructs listed in the Materials and Methods section.

CONCLUSIONS

Due to the modular structure of the WISE that questions patients according to their symptom burden, a variable number of the 799 patients completed the axis II instruments. Pain intensities were higher in women than men and highest in patients with disabilities or no job. The latter group also had the highest scores for pain-related disability, pain catastrophizing, stress, and depression. Older patients (60+ years) had significantly lower stress scores and were less likely to report symptoms of anxiety or depression. When correlating pain and well-being measures, moderate associations were observed in patients reporting clinically relevant stress, insomnia severity, injustice experience, and dysmorphic concern. Surprisingly, compromised well-being in the form of anxiety, depression, and pain catastrophizing (clinically relevant scores of GAD7, PHQ9, and PCS) did not correlate with any of the pain measures. The results of this study support the clinical usefulness of the DC/TMD core assessment instruments, but also suggest measuring of sleep, catastrophizing, injustice experience, and dysmorphic concern as important dimensions for patients suffering from OFP symptoms. Further studies are needed to determine how pain and well-being influence each other, i.e., to clarify whether there are direct causal influences or influences mediated by other variables not investigated in this study. Preferably this would be related to a theoretical framework about relations between OFP, well-being, psychiatric disorders, and socioeconomic status.

DATA AVAILABILITY STATEMENT

The raw data supporting the conclusions of this article will be made available by the authors, without undue reservation.

ETHICS STATEMENT

Ethical review and approval was not required for the study on human participants in accordance with the local legislation and institutional requirements. Written informed consent to participate in this study was provided by the participants' legal guardian/next of kin.

AUTHOR CONTRIBUTIONS

All authors listed have made substantial, direct and intellectual contribution to the work, and approved it for publication.

REFERENCES

- Ohrbach R, Durham J. Biopsychosocial aspects of orofacial pain. In: Farah CS, et al. editors. *Contemporary Oral Medicine*. Cham, Switzerland: Springer Nature (2019). p. 1797–818. doi: 10.1007/978-3-319-72303-7_37
- Johnson J, Wood AM. Integrating positive and clinical psychology: viewing human functioning as continua from positive to negative can benefit clinical assessment, interventions and understandings of resilience. *Cognitive Ther Res*. (2016) 41:1–15. doi: 10.1007/s10608-015-9728-y
- Hall LH, Johnson J, Wattl, Tsipa A, O'Connor DB. Healthcare staff wellbeing, burnout, and patient safety: A systematic Review. *PLoS ONE*. (2016) 11:e0159015. doi: 10.1371/journal.pone.0159015
- Von Korff M, Dunn KM. Chronic pain reconsidered. *Pain*. (2008) 138:267–76. doi: 10.1016/j.pain.2007.12.010
- Fillingim RB, Slade GD, Greenspan JD, Dubner R, Maixner W, Bair E, et al. Long-term changes in biopsychosocial characteristics related to temporomandibular disorder: findings from the OPPERA study. *Pain*. (2018) 159:2403–13. doi: 10.1097/j.pain.0000000000001348
- Durham J, Raphael KG, Benodiel R, Ceusters W, Michelotti A, Ohrbach R. Perspectives on next steps in classification of oro-facial pain - part 2: role of psychosocial factors. *J Oral Rehabil*. (2015) 42:942–55. doi: 10.1111/joor.12329
- Miller VE, Poole C, Golightly Y, Barrett D, Chen DG, Ohrbach R, et al. Characteristics associated with high-impact pain in people with temporomandibular disorder: a cross-sectional study. *J Pain*. (2019) 20:288–300. doi: 10.1016/j.jpain.2018.09.007
- Winkelmann R. Unemployment and happiness. *IZA World Labor*. (2014) 94:1–10. doi: 10.15185/izawol.94
- Hiswäls AS, Marttila A, Mälstam E, Macassa G. Experiences of unemployment and well-being after job loss during economic recession: results of a qualitative study in east central Sweden. *J Public Health Res*. (2017) 6:995. doi: 10.4081/jphr.2017.995
- Dworkin SF, LeReche L. Research diagnostic criteria for temporomandibular disorders: review, criteria, examinations and specifications, critique. *J Craniomandib Disord*. (1992) 6:301–55.
- Schiffman E, Ohrbach R, Truelove E, Look J, Anderson G, Goulet JP, et al. Diagnostic criteria for temporomandibular disorders (DC/TMD) for clinical and research applications: recommendations of the international RDC/TMD consortium network and orofacial pain special interest group. *J Oral Facial Pain Headache*. (2014) 28:6–27. doi: 10.11607/jop.1151
- Renner-Sitar K, John MT, Pusalavidyasagar SS, Bandyopadhyay D, Schiffman EL. Sleep quality in temporomandibular disorder cases. *Sleep Med*. (2016) 25:105–12. doi: 10.1016/j.sleep.2016.06.031
- Meira EC, Lukic N, Wojczynska A, Steiger B, Guimarães AS, Ettlin EA. Insomnia in patients seeking care at an orofacial pain Unit. *Front Neurol*. (2019) 10:542. doi: 10.3389/fneur.2019.00542
- Yakovov E, Suso-Ribera C, Vranceanu T, Adams H, Sullivan MJ. Trait perceived injustice is associated with pain intensity and pain behavior in participants undergoing an experimental pain induction procedure. *J Pain*. (2019) 20:592–9. doi: 10.1016/j.jpain.2018.11.007

FUNDING

KB travel was supported by the Chulalongkorn University Office of International Affairs Scholarship for Short-term Research.

ACKNOWLEDGMENTS

We would like to thank Prof. Martin Tyas, Dr. Joao Ferreira, Dr. Kevin Tompkins, and Dr. Vera Colombo for manuscript editing. The translation of the WISE in various languages was kindly sponsored by the Digital Society Initiative of the University of Zurich.

- Sommer I, Lukic N, Rössler W, Ettlin DA. Measuring anger in patients experiencing chronic pain - A systematic review. *J Psychosom Res*. (2019) 125:109778. doi: 10.1016/j.jpsychores.2019.109778
- Galli U, Ettlin DA, Palla S, Ehler U, Gaab J. Do illness perceptions predict pain-related disability and mood in chronic orofacial pain patients? A 6-month follow-up study. *J Eur J Pain*. (2010) 14:550–8. doi: 10.1016/j.ejpain.2009.08.011
- Sullivan MJ, Thorn B, Haythornthwaite JA, Keefe F, Martin M, Bradley LA, et al. Theoretical perspectives on the relation between catastrophizing and pain. *Clin J Pain*. (2001) 17:52–64. doi: 10.1097/00002508-200103000-00008
- Ettlin DA, Sommer I, Brönnimann B, Maffioletti S, Scheidt J, Hou MY, et al. Design, construction, and technical implementation of a web-based interdisciplinary symptom evaluation (WISE) - a heuristic proposal for orofacial pain and temporomandibular disorders. *J Headache Pain*. (2016) 17:77. doi: 10.1186/s10194-016-0670-5
- Broadbent E, Petrie KJ, Main J, Weinman J. The brief illness perception questionnaire. *J Psychosom Res*. (2006) 60:631–7. doi: 10.1016/j.jpsychores.2005.10.020
- Gaab J, Bunschoten SL, Sprött H, Ehler U. Psychometric evaluation of a German translation of the illness perception questionnaire. In: *Paper Presented at the 62nd Annual Scientific Meeting of the American Psychosomatic Society (APS)*. Orlando, USA (2004).
- Gaab J, Latanzia-Bunschoten S, Sprött H. Illness Perception Questionnaire. In: Begel, Wirtz, Zwimgmann, Hrsg. *Kompandium: Diagnostische Verfahren in der Rehabilitation*. Göttingen: Hogrefe Verlag (2008). S. 109–111.
- Mancuso SG, Knoesen NP, Castle DJ. The Dysmorphic Concern Questionnaire: a screening measure for body dysmorphic disorder. *Aust N Z J Psychiatry*. (2010) 44:535–42. doi: 10.3109/00048671003596055
- Schieber K, Kollei I, de Zwaan M, Martin A. The Dysmorphic Concern Questionnaire in the German general population: psychometric properties and normative data. *Aesth Plast Surg*. (2018) 42:1412–20. doi: 10.1007/s00266-018-1183-1
- Visscher CM, Baad-Hansen L, Durham J, Goulet JP, Michelotti A, Roldán Barraza C, et al. Benefits of implementing pain-related disability and psychological assessment in dental practice for patients with temporomandibular pain and other oral health conditions. *JADA*. (2018) 149:422–31. doi: 10.1016/j.adaj.2017.12.031
- Löwe B, Decker O, Müller S, Brähler E, Schellberg D, Herzog W, et al. Validation and standardization of the Generalized Anxiety Disorder Screener (GAD-7) in the general population. *Medical Care*. (2008) 46:266–74. doi: 10.1097/MLR.0b013e318160d093
- Sullivan MJL, Adams H, Horan S, Maher D, Boland D, Gross R. The role of perceived injustice in the experience of chronic pain and disability: scale development and validation. *J Occup Rehabil*. (2008) 18:249–61. doi: 10.1007/s10926-008-9140-5
- Niederstrasser N, Steiger B, Welsch K, Hartmann S, Nilges P, Ljutow A, et al. Deutsche transkulturelle Übersetzung des Injustice Experience Questionnaire [German transcultural translation of the Injustice Experience Questionnaire]. *Schmerz*. (2018) 32:442–8. doi: 10.1007/s00482-018-0329-z
- Steiger B, Welsch K, Niederstrasser N, Hartmann S, Nilges P, Ljutow A, et al. Validierung der deutschen Übersetzung des Injustice Experience

- Questionnaire (IEQ) in 5 ambulanten Schmerzbehandlungseinrichtungen [Validation of the German-language version of the Injustice Experience Questionnaire (IEQ) in five outpatient clinics]. *Schmerz*. (2019) 33:106–15. doi: 10.1007/s00482-018-0345-z
29. Bastien CH, Vallières A, Morin CM. Validation of the Insomnia Severity Index as an outcome measure for insomnia research. *Sleep Med*. (2001) 2:297–307. doi: 10.1016/S1389-9457(00)00065-4
 30. Gerber M, Lang C, Lemola S, Colledge F, Kalak N, Holsboer-Trachsler E, et al. Validation of the German version of the insomnia severity index in adolescents, young adults and adult workers: results from three cross-sectional studies. *BMC Psychiatry*. (2016) 31:174. doi: 10.1186/s12888-016-0876-8
 31. Sullivan MJL, Bishop SR, Pivik J. The Pain Catastrophizing Scale: development and validation. *Psychol Assess*. (1995) 7:524–32. doi: 10.1037/1040-3590.7.4.524
 32. Meyer K, Sprött H, Mannion AF. Cross-cultural adaptation, reliability, and validity of the German version of the Pain Catastrophizing Scale. *J Psychosom Res*. (2008) 64:469–78. doi: 10.1016/j.jpsychores.2007.12.004
 33. Löwe B, Wahl I, Rose M, Spitzer C, Glaesmer H, Wingenfeld K, et al. A 4-item measure of depression and anxiety: validation and standardization of the Patient Health Questionnaire-4 (PHQ-4) in the general population. *J Affect Disord*. (2010) 122:86–95. doi: 10.1016/j.jad.2009.06.019
 34. Gräfe K, Zipfel S, Herzog W, Löwe B. Screening for psychiatric disorders with the patient health questionnaire (PHQ). *Res Ger Validation Study Diagnostica*. (2004) 50:171–81. doi: 10.1026/0012-1924.50.4.171
 35. Kroenke K, Spitzer RL, Williams JB. The PHQ-9: validity of a brief depression severity measure. *J Gen Intern Med*. (2001) 16:606–13. doi: 10.1046/j.1525-1497.2001.016009606.x
 36. Spitzer RL, Williams JB, Kroenke K, Hornyak R, McMurray J. Validity and utility of the PRIME-MD Patient Health Questionnaire in assessment of 3000 obstetric-gynecologic patients: The PRIME-MD Patient Health Questionnaire Obstetrics-Gynecology Study. *Am J Obstet Gynecol*. (2000) 183:759–69. doi: 10.1067/mob.2000.106580
 37. Gignac GE, Szodorai ET. Effect size guidelines for individual differences researchers. *Pers Individ Differ*. (2016) 102:74–8. doi: 10.1016/j.paid.2016.06.069
 38. Slade GD, Bair E, Greenspan JD, Dubner R, Fillingim RB, Diatchenko L, et al. Signs and symptoms of first-onset TMD and socio-demographic predictors of its development: the OPFERA prospective cohort study. *J Pain*. (2013) 14 (Suppl. 2):T20–32. doi: 10.1016/j.jpain.2013.07.014
 39. Goldfarb EV, Seo D, Sinha R. Sex differences in neural stress responses and correlation with subjective stress and stress regulation. *Neurobiol Stress*. (2019) 11:100177. doi: 10.1016/j.ynstr.2019.100177
 40. Hodes GE, Epperson CN. Sex differences in vulnerability and resilience to stress across the life span. *Biol Psychiatry*. (2019) 86:421–32. doi: 10.1016/j.biopsych.2019.04.028
 41. Treede RD, Rief W, Barke A, Aziz Q, Bennett MI, Benoliel R, et al. A classification of chronic pain for ICD-11. *Pain*. (2015) 156:1003–7. doi: 10.1097/j.pain.0000000000000160
 42. Shaefer JR, Khawaja SN, Bavia PF. Sex, gender, and orofacial pain. *Dent Clin North Am*. (2018) 62:665–82. doi: 10.1016/j.cden.2018.06.001
 43. Slade GD, Rosend RD, Ohrbach R, Greenspan JD, Fillingim RB, Parisien M, et al. Anatomical selectivity in overlap of chronic facial and bodily pain. *Pain Rep*. (2019) 4:e729. doi: 10.1097/PR9.0000000000000729
 44. Cronan TA, Serber ER, Walen HR, Jaffe M. The influence of age on fibromyalgia symptoms. *J Aging Health*. (2002) 14:370–84. doi: 10.1177/08964302014003004
 45. Okeson JP. *Orofacial Pain: Guidelines for Assessment, Diagnosis, and Management*. Chicago: Quintessence Publishing Company, Inc (1996).
 46. De Toledo IP, Conti Réus J, Fernandes M, Porporatti AL, Peres MA, Takaschima A, et al. Prevalence of trigeminal neuralgia: a systematic review. *J Am Dent Assoc*. (2016) 147:570–76. doi: 10.1016/j.adaj.2016.02.014
 47. Joury E, Bernabe E, Gallagher JE, Marcenes W. Burden of orofacial pain in a socially deprived and culturally diverse area of the United Kingdom. *Pain*. (2018) 159:1235–43. doi: 10.1097/j.pain.0000000000001203
 48. Durham J, Shen J, Breckons M, Steele J, Araújo-Soares V, Exley C, et al. Healthcare cost and impact of persistent orofacial pain. *J Dent Res*. (2016) 95:1147–54. doi: 10.1177/0022034516648088
 49. Riddle DL, Wade JB, Jiranek WA, Kong X. Preoperative pain catastrophizing predicts pain outcome after knee arthroplasty. *Clin Orthop Relat Res*. (2010) 468:798–806. doi: 10.1007/s11999-009-0963-y
 50. Jang HH, Kim ME, Kim HK. Pain catastrophizing mediates the effects of psychological distress on pain interference in patients with orofacial pain: a cross-sectional study. *J Oral Facial Pain Headache*. (2018) 32:409–17. doi: 10.11607/ofph.2067
 51. De Ruddere L, Goubert L, Stevens MAL, Deveugele M, Craig KD, Crombez G. Healthcare professional reactions to patient pain: impact of knowledge about medical evidence and psychosocial influences. *J Pain*. (2014) 15:262–9. doi: 10.1016/j.jpain.2013.11.002
 52. Cano A, Williams AC. Social interaction in pain: reinforcing pain behaviors or building intimacy? *Pain*. (2010) 149:9–11. doi: 10.1016/j.pain.2009.10.010
 53. Scott W, Yu L, Patel S, McCracken LM. Measuring stigma in chronic pain: preliminary investigation of instrument psychometrics, correlates, and magnitude of change in a prospective cohort attending interdisciplinary treatment. *J Pain*. (2019) 20:1164–75. doi: 10.1016/j.jpain.2019.03.011
 54. Sullivan MJL. *User manual for the Injustice Experience Questionnaire (IEQ)*. (2008). Available online at: <http://sullivan-painresearch.mcgill.ca/pdf/ieq/IEQManual.pdf> (accessed April 1, 2020).
 55. Aggarwal VR, Macfarlane GJ, Farragher TM, McBeth J. Risk factors for onset of chronic oro-facial pain—results of the North Cheshire oro-facial pain prospective population study. *Pain*. (2010) 149:354–9. doi: 10.1016/j.pain.2010.02.040
 56. Aggarwal VR, McBeth J, Zakrzewska JM, Lunt M, Macfarlane GJ. The epidemiology of chronic syndromes that are frequently unexplained: do they have common associated factors? *Int J Epidemiol*. (2006) 35:468–76. doi: 10.1093/ije/dyi265
 57. Gustin SM, Wilcox SL, Peck CC, Murray GM, Henderson LA. Similarity of suffering: equivalence of psychological and psychosocial factors in neuropathic and non-neuropathic orofacial pain patients. *Pain*. (2011) 152:825–32. doi: 10.1016/j.pain.2010.12.033
 58. Fillingim R. Individual differences in pain: understanding the mosaic that makes pain personal. *Pain*. (2017) 158(Suppl. 1):S11–8. doi: 10.1097/j.pain.0000000000000775
 59. El-Shormilisy N, Strong J, Meredith PJ. Associations among gender, coping patterns and functioning for individuals with chronic pain: a systematic review. *Pain Res Manag*. (2015) 1:48–55. doi: 10.1155/2015/490610
 60. Tomitaka S, Kawasaki Y, Ide K, Akutagawa M, Ono Y, Furukawa TA. Stability of the distribution of Patient Health Questionnaire-9 scores against age in the general population: data from the National Health and Nutrition Examination survey. *Front Psychiatry*. (2018) 9:390. doi: 10.3389/fpsy.2018.00390
 61. Teasell RW, Bombardier C. Employment-related factors in chronic pain and chronic pain disability. *Clin J Pain*. (2001) 17:S39–45. doi: 10.1097/00002508-200112001-00010
 62. Rajamani S. Representation of occupational information across resources and validation of the occupational data for health model. *J Am Med Inform Assoc*. (2015) 25:197–205. doi: 10.1093/jamia/ocx035
 63. Somers TJ, Keefe FJ, Pells JJ, Dixon KE, Waters SJ, Riordan PA, et al. Pain catastrophizing and pain-related fear in osteoarthritis patients: relationships to pain and disability. *J Pain Symptom Manage*. (2009) 37:863–72. doi: 10.1016/j.jpainsymman.2008.05.009
 64. Krebs EE, Lorenz KA, Bair MJ, Damush TM, Wu J, Sutherland JM, et al. Development and initial validation of the PEG, a three-item scale assessing pain intensity and interference. *J Gen Intern Med*. (2009) 24:733–8. doi: 10.1007/s11606-009-0981-1
 65. Bair MJ, Robinson RL, Katon W, Kroenke K. Depression and pain comorbidity: a literature review. *Arch Intern Med*. (2003) 163:2433–45. doi: 10.1001/archinte.163.20.2433
 66. du Fort GG, Newman SC, Bland RC. Psychiatric comorbidity and treatment seeking: sources of selection bias in the study of clinical populations. *J Nerv Ment Dis*. (1993) 181:467–74. doi: 10.1097/00005053-199308000-00001
 67. Häggman-Henrikson B, Ekberg EC, Ettlin DA, Michelotti A, Durham J, Goulet JP, et al. Mind the gap: a systematic review of implementation of screening for psychological comorbidity in dental and dental hygiene education. *J Dent Educ*. (2018) 82:1065–76. doi: 10.21815/JDE.018.104

68. Sanders AE, Akinkugbe AA, Fillingim RB, Ohrbach R, Greenspan JD, Maixner W, et al. Causal mediation in the development of painful temporomandibular disorder. *J Pain.* (2017) 18:428–36. doi: 10.1016/j.jpain.2016.12.003
69. Hall AM, Kamper SJ, Maher CG, Latimer J, Ferreira ML, Nicholas MK. Symptoms of depression and stress mediate the effect of pain on disability. *Pain.* (2011) 152:1044–51. doi: 10.1016/j.pain.2011.01.014
70. Rodero B, Luciano JV, Montero-Marín J, Casanueva B, Palacin JC, Gili M, et al. Perceived injustice in fibromyalgia: psychometric characteristics of the injustice experience questionnaire and relationship with pain catastrophizing and pain acceptance. *J Psychosom Res.* (2012) 73:86–91. doi: 10.1016/j.jpsychores.2012.05.011
71. Lunde CE, Sieberg CB. Walking the tightrope: a proposed model of chronic pain and Stress. *Front Neurosci.* (2020) 14:270. doi: 10.3389/fnins.2020.00270
72. McWilliams LA, Cox BJ, Enns MW. Mood and anxiety disorders associated with chronic pain: an examination in a nationally representative sample. *Pain.* (2003) 106:127–33. doi: 10.1016/S0304-3959(03)00301-4
73. Reiter S, Eli I, Mahameed M, Emodi-Perlman A, Friedman-Rubin P, Reiter MA, et al. Pain catastrophizing and pain persistence in temporomandibular disorder patients. *J Oral Facial Pain Headache.* (2018) 32:309–20. doi: 10.11607/ofph.1968
74. Sullivan MJL, Thibault P, Simmonds MJ, Milioto M, Cantin A-P, Velly A. Pain, perceived injustice and the persistence of post-traumatic stress symptoms during the course of rehabilitation for whiplash injuries. *Pain.* (2009) 145:325–31. doi: 10.1016/j.pain.2009.06.031
75. van Leeuwen WF, van der Vliet QMJ, Janssen SJ, Heng M, Ring D, Vranceanu A-M. Does perceived injustice correlate with pain intensity and disability in orthopaedic trauma patients? *Injury.* (2016) 47:1212–6. doi: 10.1016/j.injury.2016.02.018
76. Wei Y, Blanken TF, Van Someren EJW. Insomnia really hurts: effect of a bad night's sleep on pain increases with insomnia severity. *Front Psychiatry.* (2018) 9:377. doi: 10.3389/fpsy.2018.00377
77. Finan PH, Goodin BR, Smith MT. The association of sleep and pain: an update and a path forward. *J Pain.* (2013) 14:1539–52. doi: 10.1016/j.jpain.2013.08.007
78. Slade GD, Ohrbach R, Greenspan JD, Fillingim RB, Bair E, Sanders AE, et al. Painful temporomandibular disorder: decade of discovery from OPPERA studies. *J Dent Res.* (2016) 95:1084–92. doi: 10.1177/0022034516653743
79. Egloff N, Cámara RJ, von Känel R, Klingler N, Marti E, Ferrari MG. Pain drawings in somatoform-functional pain. *BMC Musculoskelet Disord.* (2012) 13:257. doi: 10.1186/1471-2474-13-257
80. Boudreau SA, Badsberg S, Christensen SW, Egsgaard LL. Digital pain drawings: assessing touch-screen technology and 3D body schemas. *Clin J Pain.* (2016) 32:139–45. doi: 10.1097/AJP.0000000000000230
81. Fillingim RB, Ohrbach R, Greenspan JD, Knott C, Diatchenko L, Dubner R, et al. Psychological factors associated with development of TMD: The OPPERA prospective cohort study. *J Pain.* (2013) 14:T75–90. doi: 10.1016/j.jpain.2013.06.009
82. Nguyen TT, Vanichanon P, Bhalang K, Vongthongsri S. Pain duration and intensity are related to coexisting pain and comorbidities present in temporomandibular disorder pain patients. *J Oral Facial Pain Headache.* (2018) 33:205–12. doi: 10.11607/ofph.2088
83. Tennant R, Hiller L, Fishwick R, Platt S, Joseph S, Weich S, et al. The Warwick-Edinburgh Mental Wellbeing Scale (WEMWBS): development and UK validation. *Health Qual Life Outcomes.* (2007) 5:63. doi: 10.1186/1477-7525-5-63

Conflict of Interest: The authors declare that the research was conducted in the absence of any commercial or financial relationships that could be construed as a potential conflict of interest.

Copyright © 2020 Bhalang, Steiger, Lukic, Zumbunn Wojczyńska, Hovijitra and Ettlin. This is an open-access article distributed under the terms of the Creative Commons Attribution License (CC BY). The use, distribution or reproduction in other forums is permitted, provided the original author(s) and the copyright owner(s) are credited and that the original publication in this journal is cited, in accordance with accepted academic practice. No use, distribution or reproduction is permitted which does not comply with these terms.



Adaptive Stress Coping in Awake Bruxism

Xabier Ander Soto-Goñi^{1†}, Francisco Alen^{1*†}, Leticia Buiza-González¹,
Danielle Marcolino-Cruz¹, Teresa Sánchez-Sánchez², Ignacio Ardizzone-García²,
Fernando Aneiros-López² and Laura Jiménez-Ortega^{1,3*}

¹ Department of Psychobiology and Behavioral Sciences Methods, Faculty of Odontology, Complutense University of Madrid, Madrid, Spain, ² Department of Conservative and Prosthetic Dentistry, Faculty of Odontology, Complutense University of Madrid, Madrid, Spain, ³ Centre for Human Evolution and Behaviour, Instituto de Salud Carlos III, Complutense University of Madrid (UCM-ISCIII), Madrid, Spain

OPEN ACCESS

Edited by:

Limor Avivi-Arber,
University of Toronto, Canada

Reviewed by:

Ephraim Winocur,
Tel Aviv University, Israel
Helena Martynowicz,
Wroclaw Medical University, Poland
Marc Schmitter,
Julius Maximilian University of
Würzburg, Germany
Akira Nishiyama,
Tokyo Medical and Dental
University, Japan

*Correspondence:

Laura Jiménez-Ortega
laurajim@ucm.es
Francisco Alen
falenfar@ucm.es

[†]These authors have contributed
equally to this work

Specialty section:

This article was submitted to
Headache Medicine and Facial Pain,
a section of the journal
Frontiers in Neurology

Received: 21 May 2020

Accepted: 19 November 2020

Published: 09 December 2020

Citation:

Soto-Goñi XA, Alen F,
Buiza-González L, Marcolino-Cruz D,
Sánchez-Sánchez T,
Ardizzone-García I, Aneiros-López F
and Jiménez-Ortega L (2020)
Adaptive Stress Coping in Awake
Bruxism. *Front. Neurol.* 11:564431.
doi: 10.3389/fneur.2020.564431

Numerous studies have analyzed the relationship between psychological factors and bruxism. However, the data are often obscured by the lack of precise diagnostic criteria and the variety of the psychological questionnaires used. The purpose of this study is to determine the association between awake bruxism and psychological factors (anxiety, depression, sociability, stress coping, and personality traits). With this aim, 68 participants (13 males) completed a battery of psychological questionnaires, a self-reported bruxism questionnaire, and a clinical examination. Based on their scores on the bruxism questionnaire and the clinical examination, subjects were divided into two groups. Subjects who met the criteria for “probable awake bruxism” were assigned to the case group ($n = 29$, five males). The control group ($n = 39$, nine males) was composed of subjects who showed no signs or symptoms of bruxism in the examination nor in the questionnaire. The probable awake bruxism group presented significantly higher levels of trait and state anxiety, symptoms of somatization, and neuroticism than the control group. Despite this, and when their problem coping strategies were considered, awake bruxers showed higher levels in Positive Reappraisal ($p < 0.05$), a strategy generally considered as adaptive. In conclusion, although awake bruxers in our study showed larger levels of anxiety, somatization, and neuroticism, they also displayed more adapted coping strategies, while according to previous data TMD patients (which generally also present high levels of anxiety, somatization and neuroticism) might tend to present less adaptive coping styles. Thus, awake bruxism may play a positive role in stress coping, which would be compatible with the hypothesis of mastication as a means of relieving psychological tension. This finding should be further confirmed by future research comparing TMD patients with definitive awake bruxers and controls and using larger and more representative samples.

Keywords: bruxism, anxiety, temporomandibular disorder (TMD), psychological factors, neuroticism, stress coping

INTRODUCTION

Awake bruxism is a masticatory muscle activity during wakefulness that is characterized by repetitive or sustained tooth contact and/or by bracing or thrusting of the mandible. Sleep bruxism is a masticatory muscle activity during sleep that is characterized as either rhythmic (phasic) or non-rhythmic (tonic) (1). Mixed episodes are formed by awake and sleep bruxism. Recent studies

found a prevalence of 5.0% for awake bruxism and of 16.5% for sleep bruxism (2). However, its prevalence among the young college population is much higher, reaching 37.9% for awake bruxism and 31.8% for sleep bruxism (3). Recently, it has been argued that the mere presence of awake or sleep bruxism should not be considered pathological on its own in otherwise healthy individuals, but rather as a risk for other negative health consequences. Moreover, in some individuals, it could even have positive consequences for the bruxer (e.g., mediating the recovery from respiratory arousals or reducing teeth wear due to gastro-esophageal reflux by increasing salivation) (1).

Patients with awake bruxism are more likely to experience jaw pain and/or limitations of movement than patients with sleep bruxism, which highlights the importance of considering this distinction (4, 5). Furthermore, the etiology of bruxism is not completely clear. While it is thought that morphological and pathophysiological factors may be related to bruxism, the importance of psychosocial factors in its etiology is becoming clearer, particularly in the case of awake bruxism (6, 7). Indeed, psychological and social factors appear to be critical in the transition from non-symptomatic bruxism or teeth clenching to a painful disorder (8). Thus, traditional approaches centered on occlusal interventions are being replaced by more comprehensive approaches which place special emphasis on psychosocial factors which are considered by some authors to be the most important etiopathological factor in bruxism (8–10).

Among the psychological factors influencing bruxism, a recent exhaustive review singles out anxiety, sensitivity to stress, depression, and some personality characteristics while pointing out that the impact of these factors has been clearly demonstrated for awake bruxism, whereas evidence linking psychosocial factors and sleep bruxism is less clear (7). Thus, an accurate diagnosis of bruxism, along with a clear distinction between awake and sleep bruxism, appears of paramount importance. In addition, more detailed investigations underline the importance of perceived stress in relation to bruxism (1, 11). Furthermore, perceived stress is strongly related to poor stress coping strategies (12). Generally, stress-related coping can be defined as the predictable cognitive and behavioral efforts to manage environmental and internal demands or conflicts (13), and data point out that stress coping influences perceived stress, anxiety and depression, among other factors (14, 15). Maladaptive coping strategies have, in turn, been linked to negative pain experiences in TMD (10). However, there is a lack of studies exploring the role of different stress coping strategies in bruxism.

Therefore, the objective of this study was to investigate the role of coping in awake bruxism by studying the following psychological factors: depression, anxiety, stress, coping styles, and personality traits.

MATERIALS AND METHODS

Subjects

A total of 68 students (14 males, 54 females) were selected from a pool of 109 students who volunteered to participate in this study at the faculty of Dentistry, Complutense University of Madrid. The age of participants ranged between 17 and 31

(mean age = 19.6 years, SD = 2.6). All subjects underwent a clinical exploration and completed a self-assessed bruxism questionnaire. The case group ($n = 29$, 5 males, mean age = 20.0, SD = 3.4), was composed of participants classified as awake bruxers in the clinical examination and the bruxism questionnaire (see materials section), but did not fulfill TMD criteria. Taken together, the case group met criteria for diagnosis of probable awake bruxism, according to the recent international consensus (16). The control group ($n = 39$, nine males, mean age = 19.2, SD = 1.8) was composed of participants who did not present symptoms either signs of awake bruxism nor sleep bruxism in the clinical examination, and who showed no self-reported bruxism in the questionnaire. Student t analyses did not detect significant differences in the mean age between awake bruxism and control groups [$t_{(66)} = 1.23$, $p = 0.22$]. The number of males and females in the two groups could not be exactly matched (23 and 17.2% of males for control and case groups, respectively). However, a gender proportion analyses did not produce significant differences when comparing the ratio of males to females per group between the case and control groups ($\chi^2 = 0.34$, $p = 0.76$). Participants suffering from TMD and/or showing inconsistent results in the clinical exploration and self-assessment questionnaire were excluded. Among participants in the awake bruxism group, 16 (three males) presented probable sleep bruxism according to bruxism questionnaire and 15 participants (three males) presented mild tenderness to palpation (1 kg) but did not meet DC/TMD local myalgia criteria.

All participants were duly informed and gave their consent, the study has the approval of the ethics committee of the “Hospital Clínico Universitario,” UCM, Madrid, Spain (Reference: 12/043-E).

Materials

Psychological Questionnaires

The battery of selected questionnaires included: the State and Trait Anxiety Inventory (STAI), the State and Trait Depression Inventory (ST-DEP), the Brief Symptom Inventory: Anxiety, Depression and Somatization (BSI-18), the Coping Response Inventory—Adult form (CRI-A), and the NEO Personality Inventory (NEO-FFI). All used questionnaires have high levels of reliability and validity in all their scales (>0.8) (17–21) and have been largely used in research [e.g., (22–24)].

Anxiety was measured using the STAI (17). It is composed of 10 items assessing state anxiety STAI-E (transient emotional state) and another 10 items for trait anxiety STAI-R (anxious, relatively stable propensity of the participant in general). The ST-DEP was used to assess depression (18). This 20-items questionnaire has a construction similar to the STAI, includes depression scales for state and trait depression, and within each one includes two euthymia and dysthymia subscales.

In addition, to further assess symptoms of depression, anxiety and somatization we included the BSI-18 questionnaire (19), which is a short questionnaire consisting of 18 items. Stress coping was assessed using the CRI-A (20). This questionnaire contains 48 items and provides eight scales assessing different coping strategies: logical analysis, positive reappraisal, seeking

guidance and support, problem solving, cognitive avoidance, acceptance or resignation, seeking alternative rewards, and emotional discharge. Lastly, personality variables were assessed using the NEO-FFI questionnaire (21); which includes 60 items abbreviated as five major dimensions of personality: neuroticism, extraversion, openness, agreeableness, and conscientiousness.

Self-Reported Bruxism Questionnaire

To evaluate bruxism, we used the Pintado et al. questionnaire (25), which consists of six items: (1) Has anyone heard you grinding your teeth at night? (2) Is your jaw ever fatigued or sore on awakening in the morning? (3) Are your teeth or gums ever sore on awakening in the morning? (4) Do you ever experience temporal headaches on awakening in the morning? (5) Are you ever aware of grinding your teeth during the day? (6) Are you ever aware of clenching your teeth during the day?

In addition, three questions were added to assess the sensations of tension or stiffness in the jaw muscles, thereby increasing diagnosis certainty: (1) How would you rate your jaw muscle stiffness or tension at the present time? (2) What was the greatest jaw muscle tension or stiffness felt in the last 6 months? (3) What was the average jaw muscle intensity or stiffness felt during the last 6 months? The questions included a scale similar to the visual analog scale, ranging from 0 to 10 points, where 0 would indicate the “absence of tension” and 10 would mean “the highest possible tension.” Patients were classified as probable awake bruxers when they answered “Yes” to items 5 or 6 in the Pintado questionnaire, which both refer to the awareness of clenching or grinding teeth during wakefulness, and showed a score equal or >4 regarding to the intensity of the tension and stiffness experienced in the last 6 months. Probable sleep bruxers were evaluated based on items 1–4 of Pintado questionnaire, which refer to sleep bruxism.

Clinical Examinations

Following the questionnaires, the participants underwent clinical examinations. Firstly, we assessed the potential bruxism in each participant by asking about grinding, clenching, presence of headaches, discomfort and/or jaw tension when waking up and during the day. Likewise, for exclusion and control purposes a clinical examination of the temporomandibular joint (TMJ) was also conducted, following DC/TMD axis I criteria (26). Thus, the clinical examination included pain location, incisal relationships, opening pattern, opening movements, lateral and protrusive movements, TMJ noises, joint locking, muscle and TMJ palpation, and supplementary muscles palpation (posterior mandibular area, submandibular region, lateral pterygoid, and temporal tendon).

Procedure

All participants were dentistry students. After receiving instructions, they filled out the questionnaires at the same time in a quiet environment. Although no time limit was set, it took participants around 60 min on average to complete all the questionnaires. The questionnaires were scheduled so that they were administered outside of university exam periods, which might increase stress levels. Due to space and trained

personal limitations that could not be avoided at that moment, the clinical exploration took place 2 months later. They were carried out in the dentistry room of the faculty by 4th year dentistry students under the supervision of three calibrated Odontology faculty teachers of Craniomandibular Dysfunction and Orofacial Pain subjects. Therefore, three calibrated dentists in DC/TMD protocol (co-authors of this study), supervised and validated the adequacy of the students' explorations. It was a double-blind design, since dentists in charge of the clinical examination were not aware of the psychological assessment results and psychologists and participants did not know to which group each participant belonged.

Statistical Analysis

Since a multivariate study was conducted, sample size was calculated with the method described in Naing, et al. (27), assuming an awake bruxism prevalence of 5% in the general population (2), a level of confidence of 0.95 and a precision of 0.07. Sample size calculation resulted in 19 subjects per group, that is a total of 38 participants. The statistical analyses were calculated using SPSS 24 Statistics Software (IBM) and R, including the package MVN for Mardia's multivariate analysis (28). Items multivariate normality was assessed via Mardia's multivariate kurtosis and skewness coefficients (29). In order to compare the psychological variables between bruxers and control groups, a one-way MANOVA was carried out including direct scores from all the scales of each questionnaire. The response to the three questions included in the self-reported bruxism questionnaire on mandibular tension or stiffness (see detailed description above) was also included in the data analysis.

RESULTS

The estimates of Mardia's multivariate kurtosis and skewness coefficients were statistically non-significant (949.7, $p = 0.66$ and -1.31 , $p = 0.18$, respectively), indicating that normality can be assumed for MANOVA analyses calculations.

State anxiety levels (transient emotional state) were significantly greater ($p < 0.05$) in the awake bruxism group ($M = 17.8$, $SD = 6.8$) than in the control group ($M = 13.7$, $SD = 6.8$). Additionally, trait anxiety levels (general propensity to anxiety) were also higher in the awake bruxism group ($M = 22.6$, $SD = 7.4$) than in the control group ($M = 18.1$, $SD = 9.2$) ($p < 0.05$). Accordingly, anxiety symptoms, as assessed with the BSI-18 questionnaire, were significantly higher ($p < 0.01$) in the awake bruxism group ($M = 9.1$, $SD = 3.9$) than in the control group ($M = 5.8$, $SD = 4.1$). In regard to the somatization scale, significant differences were also present between groups ($p < 0.05$), with higher scores appearing among the awake bruxers participants ($M = 8.5$, $SD = 4.8$) with in comparison to the healthy ones ($M = 5.9$, $SD = 3.9$). However, despite the fact that the awake bruxer's group displayed higher depression scores than the control group, ($M = 7.5$, $M = 5.6$ and $SD = 4.4$, $SD = 3.9$, respectively) the statistical analysis revealed that this difference was statistically non-significant, showing only a weak trend ($p = 0.09$) (Figure 1). Furthermore, the ST-DEP depression questionnaire failed to show significant differences between the

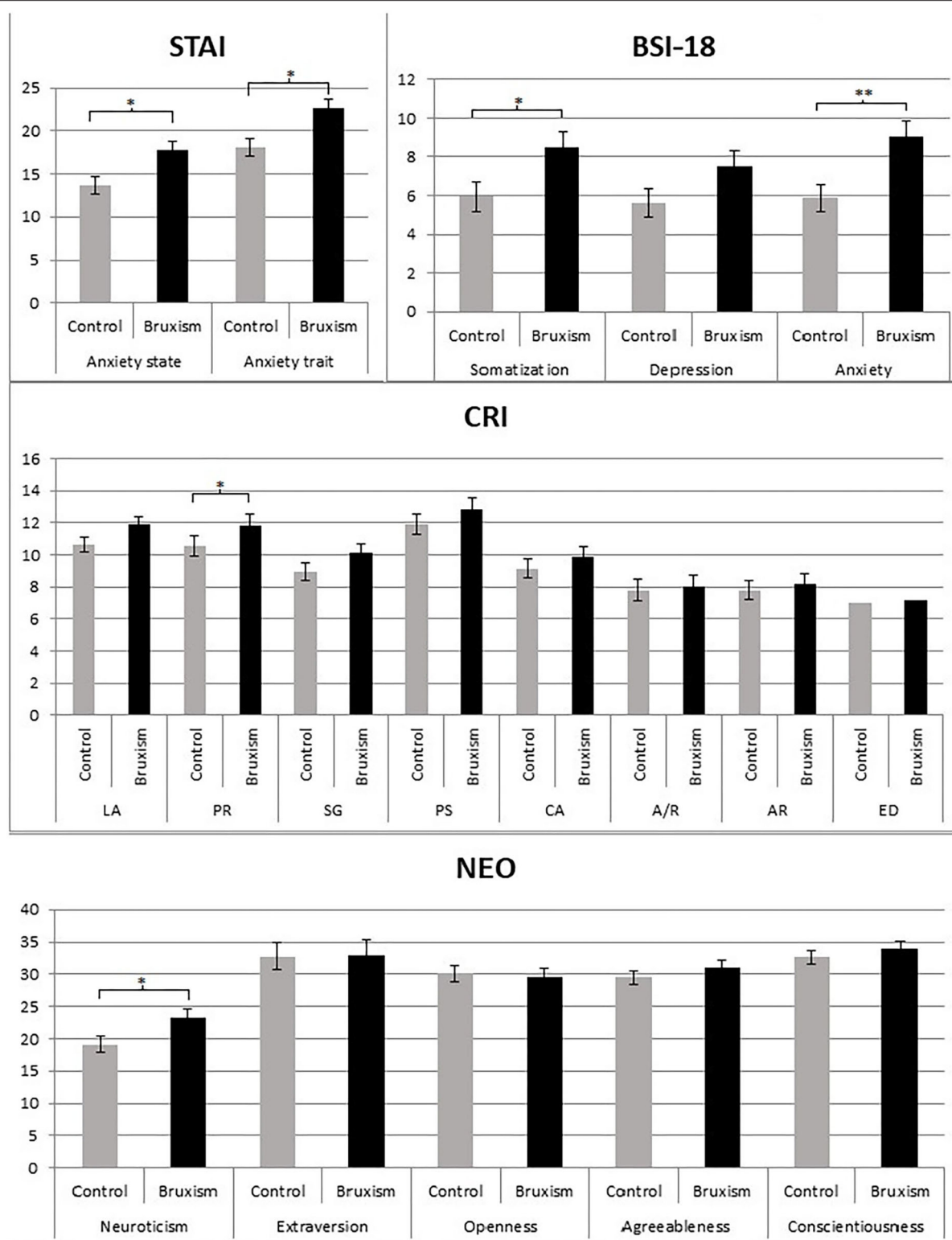


FIGURE 1 | Averages and standard errors of STAI (State and Trait Anxiety Inventory); BSI-18 (Brief Symptom Inventory), CRI-A (Coping Responses Inventory—Adult form), and NEO-FFI (NEO Personality Inventory) scales for control and bruxers groups. Graphics for ST-DEP (State and Trait Depression Inventory) are not included due to the lack of significant results, however, means and statistical analyses can be seen in **Table 1**. LA, logical análisis; PR, positive reappraisal; SG, seeking guidance and support; PS, problem solving; AV, cognitive avoidance; A/R, acceptance and resignation; AR, seeking alternative rewards; ED, emotional discharge. * $p < 0.05$; ** $p < 0.001$. Bars represent the standard error of the mean.

TABLE 1 | STAI (State and Trait Anxiety Inventory), ST-DEP (State and Trait Depression Inventory), BSI-18 (Brief Symptom Inventory), CRI-A (Coping Responses Inventory—Adult form), and NEO—FFI (NEO Personality Inventory) multiple analyses of variances (MANOVAs).

| Questionnaires | Scale | Group | Mean | Std. | DF | F | p | ηp^2 | θ |
|------------------------|------------------------|---------|-------|-------|------|------|-------|------------|----------|
| STAI (Anxiety) | Anxiety state | Control | 13.69 | 6.77 | 1.57 | 5.25 | 0.03* | 0.08 | 0.61 |
| | | Bruxism | 17.76 | 6.78 | | | | | |
| | Anxiety trait | Control | 18.12 | 9.24 | 1.57 | 4.15 | 0.04* | 0.07 | 0.52 |
| | | Bruxism | 22.65 | 7.39 | | | | | |
| ST/DEP (Depression) | Euthymia state | Control | 10.88 | 2.85 | 1.57 | 0.07 | 0.79 | 0.00 | 0.06 |
| | | Bruxism | 11.08 | 2.95 | | | | | |
| | Dysthymia trait | Control | 6.45 | 1.87 | 1.57 | 0.89 | 0.35 | 0.02 | 0.15 |
| | | Bruxism | 7.00 | 2.55 | | | | | |
| | Euthymia state | Control | 11.24 | 3.64 | 1.57 | 1.17 | 0.28 | 0.02 | 0.18 |
| | | Bruxism | 10.27 | 3.16 | | | | | |
| | Dysthymia trait | Control | 6.73 | 1.72 | 1.57 | 0.34 | 0.56 | 0.01 | 0.09 |
| | | Bruxism | 7.00 | 1.85 | | | | | |
| BSI-18 (symptoms) | Somatization | Control | 5.94 | 3.98 | 1.57 | 4.83 | 0.03* | 0.08 | 0.58 |
| | | Bruxism | 8.46 | 4.84 | | | | | |
| | Depression | Control | 5.61 | 3.96 | 1.57 | 2.97 | 0.09 | 0.05 | 0.39 |
| | | Bruxism | 7.50 | 4.47 | | | | | |
| | Anxiety | Control | 5.88 | 3.86 | 1.57 | 9.51 | 0.00* | 0.14 | 0.86 |
| | | Bruxism | 9.08 | 4.07 | | | | | |
| CRI (Coping) | Logical Analysis | Control | 10.62 | 2.85 | 1.57 | 3.17 | 0.08 | 0.05 | 0.42 |
| | | Bruxism | 11.9 | 2.59 | | | | | |
| | Positive Reappraisal | Control | 10.55 | 2.55 | 1.57 | 4.06 | 0.04* | 0.07 | 0.51 |
| | | Bruxism | 11.85 | 2.34 | | | | | |
| | Seeking Guidance | Control | 8.94 | 3.98 | 1.57 | 1.53 | 0.22 | 0.03 | 0.23 |
| | | Bruxism | 10.08 | 2.78 | | | | | |
| | Problem Solving | Control | 11.92 | 3.26 | 1.57 | 1.28 | 0.26 | 0.02 | 0.20 |
| | | Bruxism | 12.81 | 2.56 | | | | | |
| | Cognitive Avoidance | Control | 9.12 | 3.61 | 1.57 | 0.59 | 0.45 | 0.01 | 0.12 |
| | | Bruxism | 9.85 | 3.58 | | | | | |
| | Acceptance/Resignation | Control | 7.79 | 3.14 | 1.57 | 0.06 | 0.81 | 0.00 | 0.06 |
| | | Bruxism | 8.00 | 3.65 | | | | | |
| | Alternative Reward | Control | 7.77 | 3.88 | 1.57 | 0.15 | 0.70 | 0.00 | 0.07 |
| | | Bruxism | 8.15 | 3.56 | | | | | |
| | Emotional Discharge | Control | 6.97 | 3.72 | 1.57 | 0.05 | 0.81 | 0.00 | 0.06 |
| | | Bruxism | 7.17 | 2.66 | | | | | |
| NEO (Personality) | Neuroticism | Control | 19.09 | 7.31 | 1.57 | 5.14 | 0.03* | 0.08 | 0.61 |
| | | Bruxism | 23.27 | 6.65 | | | | | |
| | Extraversion | Control | 32.79 | 14.46 | 1.57 | 0.00 | 0.95 | 0.00 | 0.05 |
| | | Bruxism | 33.00 | 8.09 | | | | | |
| | Openness | Control | 30.12 | 7.49 | 1.57 | 0.12 | 0.73 | 0.00 | 0.06 |
| | | Bruxism | 29.46 | 6.92 | | | | | |
| | Agreeableness | Control | 29.48 | 6.61 | 1.57 | 0.87 | 0.35 | 0.01 | 0.15 |
| | | Bruxism | 31.04 | 5.98 | | | | | |
| | Conscientiousness | Control | 32.64 | 6.148 | 1.57 | 0.58 | 0.45 | 0.01 | 0.12 |
| | | Bruxism | 33.88 | 6.37 | | | | | |

Std., Standar deviation; DF, degree of freedom; ηp^2 , Effect size; θ , power. * < 0.05.

two groups in any of the scales or subscales. For detailed analyses see **Table 1**.

Regarding the coping questionnaire (CRI-A), of eight scales analyses revealed significant differences between the groups in

positive reappraisal ($p < 0.05$) and a tendency toward logical analysis ($p = 0.08$), suggesting that awake bruxer participants used more positive reappraisal strategies (RP) and logical analysis (AL) than healthy control participants (RP: $M = 8.1$, $M = 10.5$,

and $SD = 2.3$, $SD = 2.5$, respectively; AL: $M = 11.9$, $M = 10.6$, and $SD = 2.6$, $SD = 2.8$, respectively). The remaining coping scales did not show any significant difference (Table 1, Figure 1).

The analysis of the Personality Questionnaire (NEO) yielded statistically significant results for neuroticism ($p < 0.05$), specifically indicating that the level of neuroticism was higher for the awake bruxism group ($M = 23.3$, $SD = 7.3$) than for the control group ($M = 19.1$, $SD = 6.9$). Other personality dimensions failed to yield significant differences between the two groups.

Finally, in the self-reported bruxism questionnaire, there were significant differences on all the items regarding stiffness intensity and muscular tension, affirming that the awake bruxers scored significantly higher in these variables: At the questionnaire moment ($p < 0.01$) (Case group: $M = 4.7$, $SD = 2.2$; Control group: $M = 2.0$, $SD = 1.9$), maximum in the last 6 months ($p < 0.01$) (Case group: $M = 7.2$, $SD = 1.6$; Control group: $M = 4.0$, $SD = 2.7$), and average over the last 6 months ($p < 0.01$) (Case group: $M = 5.0$, $SD = 1.6$; Control group: $M = 2.6$, $SD = 2.3$).

DISCUSSION

The awake bruxer group showed significantly higher levels of state and trait anxiety, symptoms of anxiety, symptoms of somatization and neuroticism than the control group. With respect to coping strategies, the awake bruxer participants used positive reappraisal to a greater extent (Figure 1).

The data are consistent with previous studies that found an association between awake bruxism and anxiety, sensitivity to stress, and various personality factors (30, 31). As in the present study, most of these investigations adopted a clinical or self-reported diagnosis of bruxism. According to Loobezoo et al. (16), the fact that bruxism is significantly associated with some psychological conditions such as stress and anxiety (both assessed using validated methods) as well as muscle and joint pain, makes self-reported bruxism worthy of further exploration. Nonetheless, in the present study we tried to add self-reports by including three questions about tension or stiffness in the jaw muscles on a 0–10 scale. In addition, during clinical inspection participants were assessed again in order to improve the reliability and validity of the probable bruxism diagnosis as much as possible. Nonetheless electromyographic assessment would have helped to increase diagnosis certainty.

Although anxiety appears to be the most consistent psychological factor involved in awake bruxism, questionnaires that differentiate between state (transient) and trait (general propensity) anxiety are seldom used. The significant relationship between state anxiety and awake bruxism might reflect a very common observation in everyday clinical practice, which is noted when patients are questioned about the presence of mandibular tension or tightening: they often answer that it is not always present, but it is frequent in stressful situations. This observation indirectly supports the notion of bruxism as a continuum without a clear cut-off point between neutral or beneficial and pathological behavior (1). In addition to the suggested beneficial function of bruxist behavior during sleep, for example, in

mediating the recovery from respiratory arousals or reducing teeth wear due to gastro-oesophageal reflux by increasing salivation, bruxism during the day seems to be inherently related to facial emotional displays. Darwin in the book “The Expression of the Emotions in Man and Animals” already stated that “the grinding of the teeth, and the uttering of piercing shrieks, all give relief under an agony of pain” (32). More recently, animal models pointed out that chewing might reduce stress response, since biting on a wooden stick during a restraint situation reduced blood pressure, core temperature, suppression of hippocampal long-term potentiation, and serum chemical mediators of stress (33–36). Additionally, evidence in humans also supports the notion that mastication might reduce negative mood, cortisol release, and the production of salivary chromogranin, a marker of mental stress that reflects sympathetic activity (37–39). As a result, it has been hypothesized that bruxism might play a role in stress reduction (40, 41). It is well-known that emotional expression, including face expression, are preferable to their repression in relation to stress, particularly acute and chronic pain severity is related to anger inhibition (42). In fact, many stress reduction programs use techniques favoring emotional expression (43).

In our study we find significantly elevated levels of trait anxiety in our awake bruxer sample, as opposed to other authors (44), who failed to find such significant differences although their patients did show higher levels than the controls in this variable. This difference may be explained by the use of different cut-off points for the selection of participants. Thus, it is possible that our subjects, who were selected based on both the clinical exploration and the self-reported questionnaire, comprised a more constricted sample, avoiding the inclusion of doubtful or milder cases. Whatever the case, it has been shown that people with elevated trait anxiety tend to perceive situations as more threatening or stressful, therefore favoring the more frequent presence of awake bruxism. The higher levels of neuroticism found in the personality questionnaire and in previous research (45), could be interpreted in a similar manner as the neuroticism personality trait is characterized by emotional instability, including tendency for anxiety and excessive preoccupation over daily situations, which could, in turn, relate to the presence of awake bruxism. Thus, more research is needed which takes into account the different degrees of bruxism and their relation to psychosocial factors.

Previous studies have found high levels of depression and somatization in awake bruxer patients while our data showed only a weak tendency for higher depression in these patients. The depression variable is not always included in studies on bruxism and, when specific questionnaires are used, as in our case, higher levels of depression do not always appear (46). As in the case of anxiety, the strict inclusion criteria, a different study population and other sample characteristic such as age may explain the divergent data.

Finally, the awake bruxer participants showed higher levels of adaptive coping strategies like positive reappraisal. Positive reappraisal is a strategy used to cope with negative events by attempting to see a problem in a positive way while still accepting the reality of the situation (20). This strategy is

generally considered as an adaptive cognitive strategy in stress coping models. However, TMD patients tend to show negative stress coping strategies (47, 48). While awake bruxers displayed higher levels of positive coping strategies, TMD patients would use more negative ones. On the one hand, it is possible that awake bruxism may be playing a positive psychological role in those patients, allowing them to partly discharge some of the psychological tension (40, 41), which would enable them to display more adaptive coping strategies. On the other hand, recent investigations demonstrate that arousal reappraisal (encouraging individuals to interpret heightened physiological arousal as a tool that can help maximize performance) benefits cardiovascular and cognitive responses to stress (49, 50). Furthermore, short-term stress responses can enhance immune function (51). Therefore, larger levels of positive reappraisal in awake bruxism might indeed prevent the adverse effects of stress on health. It is possible that awake bruxism could constitute a risk factor for TMD only when accompanied by maladaptive coping strategies and/or the lack of adaptive ones (positive reappraisal) that might increase perceived stress, which, in turn, has been described as the strongest psychological predictor of TMD (52). Logical Analysis showed a trend toward significance, so it is possible that in larger samples, other adaptive strategies besides positive reappraisal could emerge. Therefore, more research in awake bruxist and TMD patients is needed in order to clarify the validity of this hypothesis and to allow for an adequate understanding and treatment of both conditions.

The awake bruxism group showed significantly higher scores in anxiety (state and trait), somatization and neuroticism than the control group. Our data are in line with the majority of previous studies. In relation to stress coping, the awake bruxism group showed higher levels of positive reappraisal (adaptive coping strategy), which might prevent negative effects of stress on health, such as the onset or worsening of TMD. Furthermore, when adaptive coping strategies are present, awake bruxism may be playing a positive psychological role, allowing for a partial discharge of some of the psychological tension, as some authors hypothesize (40, 41). In this line, chewing gum alleviates negative mood and reduces cortisol during acute laboratory psychological stress (37). Furthermore, according to Ono's review (2010) mastication during stress conditions in animal models, might increase stress-induced hippocampal neurogenesis, synaptic plasticity, and cognitive function by attenuating stress hormones and their receptors by activating serotonin neurons in the dorsal raphe nucleus (41).

Although, data support the implication of psychological factors in bruxism, more research is needed acknowledging the dimensional nature of bruxism, distinguishing between definitive sleep and awake subtypes, and relating them to the various psycho-sociological factors, including coping strategies. In addition, the sample selection (a cohort of university students) favored the homogeneity of the samples in terms of age, sociological, cultural and environmental variables. However, further research including a larger and more representative sample of participants (not only students), selected also using electromyographic assessment could enhance the generalizability of the results and increase diagnosis certainty. Additionally,

clinical and psychological explorations should be done at the same time. Finally, it should be noticed that the proportion of males and females per group did not match exactly. Although, a proportion analyses did not find significant differences in the ratio of males to females between cases and controls, further research may benefit from using paired samples with an equal number of males and females, since gender is an important variable that should be controlled in psychological assessment.

In conclusion, despite the limitations of the study, the findings may have clinical significance. It was observed that bruxers showed larger levels of anxiety, somatization, and neuroticism, similarly to previous studies on TMD patients. Nonetheless, they also displayed more adapted coping strategies while, frequently, TMD patients tend to present less adaptive coping styles. Thus, awake bruxism might play a positive role in stress coping, which would be compatible with the hypothesis of mastication as a means of relieving psychological tension. This hypothesis should be further validated by future research comparing TMD patients with definitive awake bruxers and controls using larger and more representative samples.

DATA AVAILABILITY STATEMENT

The raw data supporting the conclusions of this article will be made available by the authors, without undue reservation.

ETHICS STATEMENT

The studies involving human participants were reviewed and approved by Comité Ético de Investigación Clínica Hospital Clínico San Carlos. The patients/participants provided their written informed consent to participate in this study.

AUTHOR CONTRIBUTIONS

LJ-O, IA-G, and TS-S designed, directed the experiment, participated in patient assessment, and data discussion. XS-G, LB-G, FA, and DM-C participated in the clinical explorations, data collection, and data processing. LJ-O, FA, and XS-G also collaborated in the writing and review process of the article. All authors contributed to the article and approved the submitted version.

FUNDING

This article was funded by the Faculty of Odontology (Psychobiology, Behavioral Sciences Methods Department) of Complutense University of Madrid.

ACKNOWLEDGMENTS

We thank all the students of the 4th year of the Craniomandibular Dysfunction and Orofacial Pain Course, at the Faculty of Dentistry of the UCM, who have collaborated in the clinical analysis of the participants in this research. We are very grateful to Clara Hinchcliffe to correct the manuscript in record time.

REFERENCES

- Lobbezoo F, Ahlberg J, Raphael KG, Wetselaar P, Glaros AG, Kato T, et al. International consensus on the assessment of bruxism: report of a work in progress. *J Oral Rehabil.* (2018) 11:837–44. doi: 10.1111/joor.12663
- Wetselaar P, Vermaire E, Lobbezoo F, Schuller AA. The prevalence of awake bruxism and sleep bruxism in the Dutch adult population. *J Oral Rehabil.* (2019) 46:617–23. doi: 10.1111/joor.12787
- Cavallo P, Carpinelli L, Savarese GJB. Perceived stress and bruxism in university students. *BMC Res Notes.* (2016) 9:514. doi: 10.1186/s13104-016-2311-0
- Lavigne G, Palla S. Transient morning headache: recognizing the role of sleep bruxism and sleep-disordered breathing. *J Am Dental Assoc.* (2010) 141:297–9. doi: 10.14219/jada.archive.2010.0163
- Svensson P, Jadidi F, Arima T, Baad-Hansen L, Sessle BJ. Relationships between craniofacial pain and bruxism. *J Oral Rehabil.* (2008) 35:524–47. doi: 10.1111/j.1365-2842.2008.01852.x
- Reddy SV, Kumar MP, Sravanthi D, Mohsin AHB, Anuhya V. Bruxism: a literature review. *J Int Oral Health.* (2014) 6:105–9.
- Manfredini D, Lobbezoo F. Role of psychosocial factors in the etiology of bruxism. *J Orofac Pain.* (2009) 23:153–66.
- Manfredini D, Poggio CE. Prosthodontic planning in patients with temporomandibular disorders and/or bruxism: a systematic review. *J Prosthetic Dentistry.* (2017) 117:606–13. doi: 10.1016/j.prosdent.2016.09.012
- Suvinen TI, Reade PC, Kempainen P, Könönen M, Dworkin SF. Review of aetiological concepts of temporomandibular pain disorders: towards a biopsychosocial model for integration of physical disorder factors with psychological and psychosocial illness impact factors. *Eur J Pain.* (2005) 9:613–33. doi: 10.1016/j.ejpain.2005.01.012
- Wieckiewicz M, Paradowska-Stolarz A, Wieckiewicz W. Psychosocial aspects of bruxism: the most paramount factor influencing teeth grinding. *BioMed Res Int.* (2014) 2014:469187. doi: 10.1155/2014/469187
- Winocur E, Uziel N, Lisha T, Goldsmith C, Eli I. Self-reported Bruxism-associations with perceived stress, motivation for control, dental anxiety and gagging. *J Oral Rehabil.* (2011) 38:3–11. doi: 10.1111/j.1365-2842.2010.02118.x
- Por J, Barriball L, Fitzpatrick J, Roberts J. Emotional intelligence: its relationship to stress, coping, well-being and professional performance in nursing students. *Nurse Educ Today.* (2011) 31:855–60. doi: 10.1016/j.nedt.2010.12.023
- Lazarus RS, Folkman S. *Stress, Appraisal and Coping.* New York, NY: Springer (1984).
- Kasi PM, Naqvi HA, Afghan AK, Khawar T, Khan FH, Khan UZ, et al. Coping styles in patients with anxiety and depression. *ISRN Psychiatry.* (2012) 2012:128672. doi: 10.5402/2012/128672
- Bittner JG, Khan Z, Babu M, Hamed O. Stress, burnout, and maladaptive coping: strategies for surgeon well-being. *Bull Am Coll Surg.* (2011) 96:17–22.
- Lobbezoo F, Ahlberg J, Glaros A, Kato T, Koyano K, Lavigne G, et al. Winocur E. Bruxism defined and graded: an international consensus. *J Oral Rehabil.* (2013) 40:2–4. doi: 10.1111/joor.12011
- Spielberger CD, Gorsuch RL, Lushene RE. *STAI: Cuestionario de ansiedad Estado-Rasgo, 9th Edn.* Madrid: Tea ediciones (2011).
- Spielberger CD. *IDER. Inventario de depresión estado-rasgo.* Madrid: Tea Ediciones. (2008).
- Derogatis LR. *Brief Symptom Inventory (BSI)-18. Administration, Scoring and Procedures manual.* Minneapolis: NCS Pearson (2001).
- Moos RH. *CRI-A: Inventario de Respuestas de Afrontamiento Para Adultos.* Madrid: Tea ediciones (2010).
- Costa PT, McCrae RR. *Inventario de Personalidad Neo - Revisado (NEO-PI-R) e Inventario Neo - Reducido de cinco factores (NEO-FFI).* Madrid: Tea Ediciones (2008).
- Alegre A, Pérez-Escoda N, López-Cassá E. The relationship between trait emotional intelligence and personality. Is trait ei really anchored within the big five, big two and big one frameworks? *Front Psychol.* (2019) 10:866. doi: 10.3389/fpsyg.2019.00866
- Kirchner T, Santacana M, Muñoz D, Pereda N. Psychometric properties and dimensional structure of the Spanish version of the coping responses inventory-adult form. *Psicothema.* (2008) 20:902–9.
- Gustems-Carnicer J, Calderón C. Coping strategies and psychological well-being among teacher education students. *Eur J Psychol Educ.* (2013) 28:1127–40. doi: 10.1007/s10212-012-0158-x
- Pintado MR, Anderson GC, DeLong R, Douglas WH. Variation in tooth wear in young adults over a two-year period. *J Prosthetic Dentistry.* (1997) 77:313–20. doi: 10.1016/S0022-3913(97)70189-6
- Schiffman E, Ohrbach R, Truelove E, Look J, Anderson G, Goulet JP, et al. Diagnostic Criteria for Temporomandibular Disorders (DC/TMD) for clinical and research applications: recommendations of the International RDC/TMD consortium network and orofacial pain special interest group. *J Oral Facial Pain Headache.* (2014) 28:6–27. doi: 10.11607/jop.1151
- Naing L, Winn T, Rusli BN. Practical issues in calculating the sample size for prevalence studies. *Arch Orofac Sci.* (2006) 1:9–14.
- Korkmaz S, Goksuluk D, Zararsiz G. MVN: an R package for assessing multivariate normality. *R J.* (2014) 6:151–62. doi: 10.32614/RJ-2014-031
- Mardia KV. Measures of multivariate skewness and kurtosis with applications. *Biometrika.* (1970) 57:519–30. doi: 10.1093/biomet/57.3.519
- Ahlberg J, Lobbezoo F, Ahlberg K, Manfredini D, Hublin C, Sinisalo J, et al. Self-reported bruxism mirrors anxiety and stress in adults. *Med Oral Patol Oral Cir Bucal.* (2013) 18:e7–11. doi: 10.4317/medoral.18232
- Van Selms MK, Muzalev K, Visscher CM, Kouttris M, Bulut M, Lobbezoo F. Are pain-related temporomandibular disorders the product of an interaction between psychological factors and self-reported bruxism? *J Oral Facial Pain Headache.* (2017) 31:331–8. doi: 10.11607/ofph.1909
- Darwin C. *The Expression of the Emotions in Man and Animals.* New York, NY: D. Appleton (1896).
- Ono Y, Kataoka T, Miyake S, Cheng S-J, Tachibana A, Sasaguri K-I, et al. Chewing ameliorates stress-induced suppression of hippocampal long-term potentiation. *Neuroscience.* (2008) 154:1352–9. doi: 10.1016/j.neuroscience.2008.04.057
- Ono Y, Kataoka T, Miyake S, Sasaguri K, Sato S, Onozuka M, et al. Chewing rescues stress-suppressed hippocampal long-term potentiation via activation of histamine H1 receptor. *Neurosci Res.* (2009) 64:385–90. doi: 10.1016/j.neures.2009.04.011
- Okada S, Hori N, Kimoto K, Onozuka M, Sato S, Sasaguri K. Effects of biting on elevation of blood pressure and other physiological responses to stress in rats: biting may reduce allostatic load. *Brain Res.* (2007) 1185:189–94. doi: 10.1016/j.brainres.2007.09.030
- Tanaka T, Yoshida M, Yokoo H, Tomita M, Tanaka M. Expression of aggression attenuates both stress-induced gastric ulcer formation and increases in noradrenaline release in the rat amygdala assessed by intracerebral microdialysis. *Pharmacol Biochem Behav.* (1998) 59:27–31. doi: 10.1016/S0091-3057(97)00312-2
- Scholey A, Haskell C, Robertson B, Kennedy D, Milne A, Wetherell M. Chewing gum alleviates negative mood and reduces cortisol during acute laboratory psychological stress. *Physiol Behav.* (2009) 97:304–12. doi: 10.1016/j.physbeh.2009.02.028
- Okamura M, Yoshida A, Saruta J, Tsukinoki K, Sasaguri K, Sato S. Effect of bruxism-like activity on the salivary chromogranin a as a stress marker. *Stomatologie.* (2008) 105:33–9. doi: 10.1007/s00715-008-0049-6
- Tahara Y, Sakurai K, Ando T. Influence of chewing and clenching on salivary cortisol levels as an indicator of stress. *J Prosthodont.* (2007) 16:129–35. doi: 10.1111/j.1532-849X.2007.00178.x
- Sato S, Sasaguri K, Ootsuka T, Saruta J, Miyake S, Okamura M, et al. Bruxism and Stress Relief. Onozuka M, Yen CT, editors. In: *Novel Trends in Brain Science.* Tokyo: Springer (2008). p. 183–200.
- Ono Y, Yamamoto T, Kubo KY, Onozuka M. Occlusion and brain function: mastication as a prevention of cognitive dysfunction. *J Oral Rehabil.* (2010) 37:624–40. doi: 10.1111/j.1365-2842.2010.02079.x
- Burns, JW, Quartana, PJ, Bruhl, S. Anger inhibition and pain: conceptualizations, evidence and new directions. *J Behav Med.* (2008) 31:259–79. doi: 10.1007/s10865-008-9154-7
- Landsman-Dijkstra JJ, van Wijck R, Groothoff JW. The long-term lasting effectiveness on self-efficacy, attribution style, expression of emotions and quality of life of a body awareness program for chronic a-specific psychosomatic symptoms. *Patient Educ Couns.* (2006) 60:66–79. doi: 10.1016/j.pcc.2004.12.003

44. Alves AC, Alchieri JC, Barbosa GA. Bruxism: masticatory implications and anxiety. *Acta Odontol Latinoamericana*. (2013) 26:15–22.
45. Cruz-Fierro N, Martínez-Fierro M, Cerda-Flores RM, Gómez-Govea MA, Delgado-Enciso I, Martínez-De-Villarreal LE, et al. The phenotype, psychotype and genotype of bruxism. *Biomed Rep*. (2018) 8:264–8. doi: 10.3892/br.2018.1041
46. Gungormus Z, Erciyas K. Evaluation of the relationship between anxiety and depression and bruxism. *J Int Med Res*. (2009) 37:547–50. doi: 10.1177/147323000903700231
47. Ferrando M, Andreu Y, Galdón MJ, Durá E, Poveda R, Bagán JVJOS. Psychological variables and temporomandibular disorders: distress, coping, and personality. *Oral Med Oral Pathol Oral Radiol Endodontol*. (2004) 98:153–60. doi: 10.1016/j.tripleo.2003.12.030
48. Reissmann DR, John MT, Schierz O, Seedorf, H, Doering SJJ. Stress-related adaptive versus maladaptive coping and temporomandibular disorder pain. *J Orofac Pain*. (2012) 26:181.
49. Jamieson JP, Nock MK, Mendes WB. Mind over matter: reappraising arousal improves cardiovascular and cognitive responses to stress. *J Exp Psychol*. (2012) 141:417–22. doi: 10.1037/a0025719
50. Moore LJ, Vine SJ, Wilson MR, Freeman P. Reappraising threat: how to optimize performance under pressure. *J Sport Exerc Psychol*. (2015) 37:339–43. doi: 10.1123/jsep.2014-0186
51. Dhabhar FS, Malarkey WB, Neri E, McEwen BS. Stress-induced redistribution of immune cells—from barracks to boulevards to battlefields: a tale of three hormones—Curt Richter Award winner. *Psychoneuroendocrinology*. (2012) 37:1345–68. doi: 10.1016/j.psyneuen.2012.05.008
52. Fillingim RB, Ohrbach R, Greenspan JD, Knott C, Diatchenko L, Dubner R, et al. Psychological factors associated with development of TMD: the OPPERA prospective cohort study. *J Pain*. (2013) 14(Suppl.12):T75–90. doi: 10.1016/j.jpain.2013.06.009

Conflict of Interest: The authors declare that the research was conducted in the absence of any commercial or financial relationships that could be construed as a potential conflict of interest.

Copyright © 2020 Soto-Goñi, Alen, Buiza-González, Marcolino-Cruz, Sánchez-Sánchez, Ardizzone-García, Aneiros-López and Jiménez-Ortega. This is an open-access article distributed under the terms of the Creative Commons Attribution License (CC BY). The use, distribution or reproduction in other forums is permitted, provided the original author(s) and the copyright owner(s) are credited and that the original publication in this journal is cited, in accordance with accepted academic practice. No use, distribution or reproduction is permitted which does not comply with these terms.



Neuromotor Speech Recovery Across Different Behavioral Speech Modifications in Individuals Following Facial Transplantation

Marziye Eshghi¹, Bridget J. Perry¹, Brian Richburg¹, Hayden M. Ventresca¹, Bohdan Pomahac² and Jordan R. Green^{1*}

¹ Speech and Feeding Disorders Lab, MGH Institute of Health Profession, Boston, MA, United States, ² Plastic Surgery, Brigham and Women's Hospital, Harvard Medical School, Boston, MA, United States

OPEN ACCESS

Edited by:

Teresa Lever,
University of Missouri, United States

Reviewed by:

Vijayalakshmi P,
SSN College of Engineering, India
Christopher Dromey,
Brigham Young University,
United States

*Correspondence:

Jordan R. Green
jgreen2@mghihp.edu

Specialty section:

This article was submitted to
Neurorehabilitation,
a section of the journal
Frontiers in Neurology

Received: 09 August 2020

Accepted: 04 December 2020

Published: 06 January 2021

Citation:

Eshghi M, Perry BJ, Richburg B,
Ventresca HM, Pomahac B and
Green JR (2021) Neuromotor Speech
Recovery Across Different Behavioral
Speech Modifications in Individuals
Following Facial Transplantation.
Front. Neurol. 11:593153.
doi: 10.3389/fneur.2020.593153

Despite signs of facial nerve recovery within a few months following face transplantation, speech deficits persist for years. Behavioral speech modifications (e.g., slower-than-normal speaking rate and increased loudness) have shown promising potential to enhance speech intelligibility in populations with dysarthric speech. However, such evidence-based practice approach is lacking in clinical management of speech in individuals with facial transplantation. Because facial transplantation involves complex craniofacial reconstruction and facial nerve coaptation, it is unknown to what extent individuals with face transplant are capable of adapting their motor system to task-specific articulatory demands. The purpose of this study was to identify the underlying articulatory mechanisms employed by individuals with face transplantation in response to speech modification cues at early and late stages of neuromotor recovery. In addition, we aimed to identify speech modifications that conferred improved speech clarity. Participants were seven individuals who underwent full or partial facial vascularized composite allografts that included lips and muscles of facial animation and were in early (~2 months) or late (~42 months) stages of recovery. Participants produced repetitions of the sentence “Buy Bobby a puppy” in normal, fast, loud, and slow speech modifications. Articulatory movement traces were recorded using a 3D optical motion capture system. Kinematic measures of average speed (mm/s) and range of movement (mm³) were extracted from the lower lip (\pm jaw) marker. Two speech language pathologists rated speech clarity for each speaker using a visual analog scale (VAS) approach. Results demonstrated that facial motor capacity increased from early to late stages of recovery. While individuals in the early group exhibited restricted capabilities to adjust their motor system based on the articulatory demands of each speech modification, individuals in the late group demonstrated faster speed and larger-than-normal range of movement for loud speech, and slower speed and larger-than-normal range of movement for slow speech. In addition, subjects in both groups showed overreliance on jaw rather than lip articulatory function across all speech modifications, perhaps as a compensatory strategy to optimize articulatory stability and maximize speech function. Finally, improved speech clarity was associated with loud speech in both stages of recovery.

Keywords: facial transplantaion, speech modifications, kinematics, neural recovery, speed of movement, range of movement

INTRODUCTION

With over 40 facial transplantation surgeries completed worldwide, this procedure is now considered an effective reconstructive option for restoring a patient's facial appearance and oromotor functions after a traumatic injury. Despite evidence of facial nerve recovery within a few months post-surgery (1–3), speech deficits persist for years (4, 5). Although the existing literature on long-term outcomes is sparse, improvement of neuromotor function following facial transplantation has been documented in at least three studies (2, 6, 7). Recently, Tasigiorgos et al. (6) conducted a 5-year follow-up of motor recovery in six patients with full and partial facial transplants using Daniels and Worthingham Muscle Testing. Findings of their study revealed that motor function showed rapid improvement during the 1st year after transplantation and continued to improve at a slower rate after the 1st year. At 5 years of follow-up, motor recovery had reached a mean of 60% of maximal motor function. Similarly, De Letter and colleagues (2) reported that facial motor function improved over 38 months post-surgery as indicated by gains in lip motor function scores and increased muscle activation levels based on electromyography (EMG) during a speech task (i.e., a sentence completion task). In addition to these longitudinal studies, a case study conducted by Grigos et al. (7) reported increases in vertical jaw and lip movements during speech and non-speech (e.g., lip opening, closure, retraction, and protrusion) tasks over 13 months post-transplant. The same study also reported several negative findings such that the same gains were not seen for lip spreading, and jaw and lip movement variability were greater than the controls, which may in part explain continued mild functional speech impairments in this population.

One untested hypothesis is that the impact of these residual facial motor impairments on speech may be minimized using speech modification techniques that are commonly used in speech treatment, such as decreasing rate, increasing loudness, or intentionally speaking as clearly as possible. These modifications have been demonstrated to enhance speech intelligibility in a wide-variety of speech impairments (8–17). Each speech modification differs in the demands they place on the speech motor system. As compared to the normal (habitual) speech, increasing the rate of speech (i.e., fast speech) tends to elicit greater movement speeds but smaller articulatory displacements (18–23). During fast speech, speakers typically truncate articulatory displacement rather than alter the speed of movement as a strategy to economize effort (21, 24, 25). Slow speech, in contrast, tends to elicit larger articulatory displacement, slower movement speed, and longer movement duration (26, 27). Some research suggests that the longer duration associated with slow speech enhances articulatory precision (28, 29) or phoneme distinctiveness (9, 30–32) and improves speech intelligibility (33, 34); however, findings are mixed. Several studies have found that slow speech did not promote more precise articulation, but rather clear speech allowed speakers to maintain control over jaw opening movements and improved speech intelligibility (10, 35).

Much of the research on loud speech interventions has been focused on testing the efficacy of the Lee Silverman Voice Treatment (LSVT^R) program (36, 37), which was initially developed to improve speech in individuals with Parkinson disease (PD). Loud speech, in comparison to normal speech, elicits global gains across the speech system such as larger articulator displacements and faster movement speeds (9, 17, 38–41), greater respiratory drive (42, 43), greater subglottal air pressure (44), and improved vocal fold function (45). These physiologic changes can have the overall effect of enhancing speech accuracy, speech clarity, and speech intelligibility (12, 44, 46–48).

To our knowledge, the efficacy of speech modification techniques for improving speech following facial transplantation has not been evaluated. Although research exploring the impact of facial nerve repair on speech motor control is sparse (7), impairments in motor control for facial expression have been reported for populations undergoing unilateral facial nerve coaptation (49). A recent systematic review and meta-analysis exploring recovery of facial movement following masseteric facial nerve transfer in patients with facial paralysis found that the mean time to initial movement of smile excursion was 4.95 months (49). Additionally, differences in recovery of purposeful vs. spontaneous facial expressions have been documented, with spontaneous smiles found to be present in only 25/108 (23%) patients (49). Therefore, as a result of facial nerve coaptation during surgery, individuals after face transplant may exhibit limited ability to perform different motoric demands of fast, loud, and slow speech modifications, particularly in the early stages of recovery. As such, examining the efficacy of behavioral speech modifications in deriving articulatory functional gain in individuals with facial transplants at different time points in recovery to improve speech clarity and intelligibility is warranted.

The purpose of this study was to determine (1) the extent to which patients recovering from facial transplantation surgery can adapt their motor system to various articulatory demands of different speech modifications using measures of facial biomechanics, and (2) the comparative effects of these adaptations on speech clarity. Based on limited available literature, we hypothesized that motor adaptation to articulatory demands of speech modifications will be restricted during the early stages of neural recovery and that loud speech would confer improved speech clarity. This information is needed to identify optimal articulatory strategies to promote oromotor functional gain throughout the course of neural recovery and to provide an assessment technique to monitor the rate of neural recovery following facial transplant surgery.

METHOD

Participants

Seven participants who had undergone full or partial facial vascularized composite allografts were included in this study. Participants were at varying phases of recovery. Three (three males) participants were between 0 and 3 months post-surgery (mean = 2 months, SD = 1.73) and were grouped as the early post-surgery group, whereas, four participants (two females, two

males) were between 41 and 43 months post-surgery (mean = 42 months, SD = 10.12) and were grouped as the late post-surgery group. Surgeries were performed at Brigham and Women's Hospital. Subjects in the early post-surgery group received osteomyocutaneous transplantations of the mid-face which included facial tissue and musculature, the nose, mandible, upper and lower lips. Bilateral buccal and marginal mandibular branches of the facial nerve coaptations were completed for this group. In the late post-surgery group, three of the subjects received myocutaneous full facial transplantations which included facial tissue and musculature including the upper and lower lips. One subject in the late post-surgery group received an osteomyocutaneous full transplantation which included facial tissue and musculature, the nose, maxilla, upper and lower lips. One of these subjects received bilateral frontal, zygomatic, buccal, and marginal mandibular branches of facial nerve coaptation. One received unilateral frontal, zygomatic, buccal, and marginal mandibular branches of facial nerve coaptation and unilateral temporal and cervical branch coaptation. Two received bilateral buccal and marginal mandibular branch of facial nerve coaptation. Patients in the early group were seen by the speech-language pathologist following surgery for the management of speech and swallowing deficits, including diet modifications and communication strategies (repetition, writing, text to speech) as necessary. For various reasons, including patient proximity to the hospital, social support systems and patient preference, at the time of these assessments, no patient had received consistent speech therapy targeting speech deficits. The study was approved by the Institutional Review Board of Partners HealthCare and all subjects provided written informed consent to participate in the study. **Table 1** summarizes each participant's demographic and clinical information.

Speech Samples

Participants were instructed to produce a total of 19 repetitions of the sentence "Buy Bobby a puppy" in four different speech modifications that varied in the degree of loudness (intensity)

or rate. Because the utterance was produced on one breath, the likelihood of pauses occurring was low. Ten of the repetitions were produced at a normal rate and loudness, and three repetitions were produced at each of the three speech modifications loud, fast, and slow. The production of speech samples in the four speech modifications were blocked by task (each speech modification) and were presented in a fixed order. Audio recordings were collected using a lapel microphone (Model Countryman B3P4FF05B) with a sampling frequency of 44,100 Hz located approximately 15 cm from the participant's mouth. The duration of each task was measured to validate task performance (i.e., presumably, a slow task should take a longer time to complete and a fast task should take shorter time to complete).

Speech Severity of the Participants

Audio recordings of five subjects were used to assess speech severity by two expert listeners (i.e., speech language pathologists) using the visual analog scale ranged from 0 (normal) to 100 (profoundly severe). Subjects showed varying levels of speech severity based on the perceptual ratings of the two listeners. The perceptual paradigm for clinical rating of speech severity will be discussed in Section Clinician Ratings of Speech Severity and Clarity. Two subjects in the early post-surgery group, P01, and P02, exhibited speech severity ratings of 84 and 57. Three subjects in the late post-surgery group, P04, P05, and P06 demonstrated speech severity of 14, 17, and 11, respectively. The quality of audio recordings obtained from participants P03 and P07 was poor, thereby, perceptual assessment of speech severity was not feasible for these participants. The poor quality of the audio recordings was due to the ambient noise and assessor cross-talk, which can be avoided if audio samples are recorded in a laboratory setting, rather than clinical setting.

Biomechanical Assessment

Movement traces were recorded using an eight-camera 3D optical motion capture system (Motion Analysis, Rohnert Park, CA). An array of 17 retroreflective facial markers were positioned on different locations of participants' faces following a standard procedure (**Figure 1**). We limited our kinematic analyses to data obtained from the jaw and lips because these structures are primer movers during speech—unlike the cheeks, which are more active during facial expressions.

Kinematic measures were extracted from three markers: the NTC marker which stands for "nose top center" and refers to the marker at the top of the nose dorsal bridge; the CLL marker which stands for "center lower lip" and refers to the midline lower lip marker; and the VJC marker which stands for "virtual jaw center" and refers to the virtual midline jaw marker. The NTC, CLL, and VJC acronyms were created by our lab to label the corresponding markers on the face. To distinguish the contribution of jaw-driven lower lip movement from lower lip autonomous movement during production of speech tasks, movement of CLL was represented in two ways: one that included movements of the underlying jaw (lower lip + jaw) and one that was independent from the movements of the jaw (lower lip -

TABLE 1 | Participants' demographic and clinical information.

| | Participant | Sex | Age | Type of facial transplantation | Months post-surgery | Speech severity* |
|--------------------|-------------|--------|-----|--------------------------------|---------------------|------------------|
| Early Post-surgery | P01 | Male | 60 | Osteomyocutaneous | 0 | 84 |
| | P02 | Male | 33 | Osteomyocutaneous | 3 | 57 |
| | P03 | Male | 38 | Osteomyocutaneous | 3 | N/A |
| Late Post-surgery | P04 | Female | 47 | Myocutaneous | 43 | 14 |
| | P05 | Male | 28 | Myocutaneous | 42 | 17 |
| | P06 | Male | 33 | Myocutaneous | 41 | 11 |
| | P07 | Female | 61 | Osteomyocutaneous | 48 | N/A |

*Speech severity was rated on a scale of 0–100 with 0 representing normal and 100 representing profoundly severe. N/A was assigned to participants whose audio recordings had poor quality and, hence were not used in the perceptual assessment of speech severity.

jaw). In the first approach, the Euclidean distance between NTC to CLL markers was measured to calculate kinematic properties of the combined movement of the lip and jaw lip movement (i.e., lower lip + jaw). In the second approach (i.e., lower lip - jaw), a virtual marker for the center of the jaw was calculated in CORTEX (Motion Analysis, Rohnert Park, CA) as the linear distance between the right and left jaw markers protruded 30% perpendicular to the line that connects left and right lower lip markers. The VJC was consistently used for all participants because some patients with facial transplantation had facial hair on the chin which did not allow for the placement of a marker on the underside of the body of the mandible. Subsequently,

the Euclidean distance between the VJC and the center of lower lip was measured to calculate the kinematic measures of the lip movement independent of the jaw (Figure 2).

A four-sensor head marker was used to subtract head movement (translation and rotation) from the facial markers. Motion capture recordings were cut and labeled using the CORTEX Motion Analysis software (Motion Analysis, Rohnert Park, CA). To extract kinematic measures, the initial segmentation landmark was placed on the first trough associated with the lip closure for /b/ in /bat/ and the final landmark was placed on the last trough associated with the second /p/ in /papi/. The outcome kinematic measures, thus, included all bilabial closures and vowels averaged together between the two segmentation landmarks. Subsequently, the data were transferred to SMASH, a customized MATLAB-based software program (50), to calculate two kinematic measures of average speed of movement (mm/s) and range of movement (mm³) from the movement time series of the lower lip independent of the jaw. Each 3D positional time series was represented as the 3D Euclidean distance between the markers. Average speed was calculated as the average value in the first derivative of the 3D Euclidean distance movement time history. Range of motion was measured by the change in distance in mm between the maximum opening and maximum closing positions during speech. Values obtained across the repetitions of the “Buy Bobby a puppy” in each speech modifications were averaged.

Clinician Ratings of Speech Severity and Clarity

Two speech-language pathologists rated the speech severity and speech clarity of five participants (two from the early post-surgery group and three from the late post-surgery group) who had

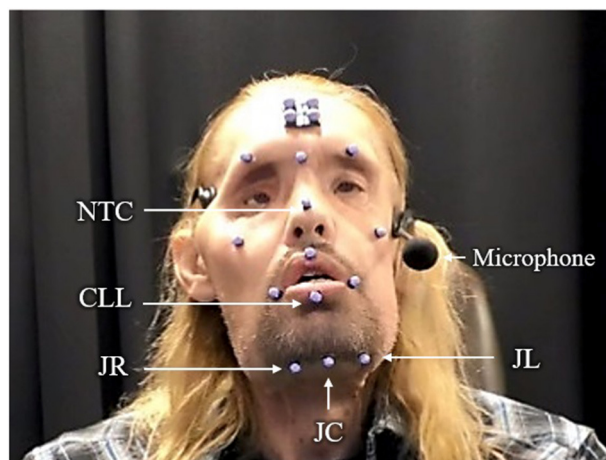


FIGURE 1 | Placement of retroreflective markers on a participant's face.

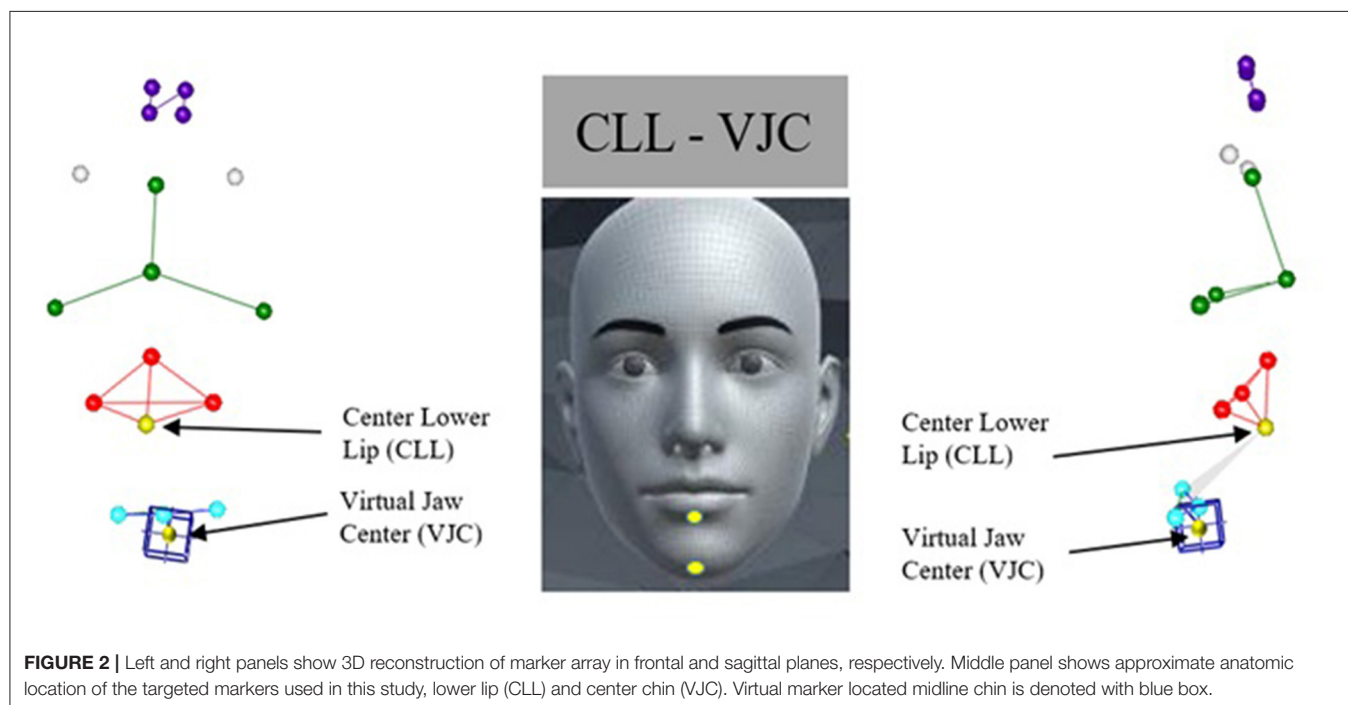


FIGURE 2 | Left and right panels show 3D reconstruction of marker array in frontal and sagittal planes, respectively. Middle panel shows approximate anatomic location of the targeted markers used in this study, lower lip (CLL) and center chin (VJC). Virtual marker located midline chin is denoted with blue box.

good quality audio recordings. The speech stimuli were the same samples (i.e., “Buy Bobby a puppy”) from which the kinematic measures were extracted. Perceptual evaluation of speech severity and speech clarity were conducted separately. Two different listening paradigms were designed for the perceptual judgment of speech severity and speech clarity using a computerized continuous visual analog scale (VAS). Written instructions were provided for each paradigm and each speaker completed the perceptual tasks blindly and independently.

Ratings of Speech Severity

Clinical ratings were performed to index the overall severity of speech impairment in individuals at early and late stages of neural recovery. These measures are important for documenting the range of impairment in our cohort and provide a metric for evaluating the potential effects of baseline severity and response to speech modifications. For speech severity, listeners were instructed to rate the overall speech naturalness and prosody, resonance and voice qualities, and articulatory precision. The speech severity paradigm consisted of five blocks (one block for each subject) presented to each listener in a random order. Each block included three repetitions of the sentence “Buy Bobby a puppy” in normal speech produced by a study participant, and the same sentence produced by a normal speaker of the participant’s same sex as the reference sample. Speech stimuli in each block were also presented to the listeners in a random order. Listeners were asked to listen to the reference sample prior to the rating of each stimulus and using the computer mouse, drag the corresponding slider vertically anywhere along a continuous 100 mm scale (0 for normal severity and 100 profound severe) to indicate their responses. Each listener was able to listen to each stimulus up to five times. Upon the completion of the listening tasks for speech severity, the program converted responses to numerical values ranging from 0 (normal) to 100 (profoundly severe).

The average intraclass correlation coefficient (ICC) between the ratings of the listeners was 0.99 ($p = 0.0001$) and the single measures ICC was 0.98 ($p = 0.0001$), indicating excellent interrater reliability. The Pearson product correlation coefficients of ratings of speech severity ranged from 0.96 to 0.99 for the Listener 1, with a mean of 0.97 ($SD = 0.015$). For Listener 2, correlations ranged from 0.96 to 0.99 with a mean of 0.98 ($SD = 0.015$).

Ratings of Speech Clarity

Clinical ratings of speech clarity were conducted to compare the effectiveness of different behavioral speech modifications in deriving a clearer-than-normal speech (aim 2 of the study). Speech clarity refers to how well and clear speech samples are enunciated and can be assessed in both connected and isolated speech utterances. Speech intelligibility, on the other hand, is defined as how well speech samples are understood and is usually assessed in connected speech. Because our participants did not have severe speech impairments and had high baseline intelligibility, speech clarity is the preferred metric of functional speech as ceiling effects would render intelligibility data unusable.

For speech clarity, listeners were instructed to rate how clear and well-enunciated the speech sample in a given speech modification is relative to the same sample produced in a normal speech. The listening paradigm for speech clarity also consisted of five blocks (one for each subject) that were randomly presented to the listeners. Each block included 10 speech stimuli: three repetitions of the sentence “Buy Bobby a puppy” in each of the fast, loud, and slow speech modifications and the same sentence in normal speech as the reference sample. The scale for VAS was a 100 mm continuum ranged from -50 to 50 . The speech clarity of the reference sample was set as 0 (baseline). Listeners were instructed to replay the reference sample prior to the rating of each stimulus and drag the corresponding slider vertically anywhere above the baseline 0 if they judged that the speech clarity of the stimulus in a given speech modification is improved relative to the reference or drag the slider below the baseline 0 if the clarity decreased relative to the reference stimulus. Similar to the speech severity paradigm, listeners were able to listen to each stimulus up to 5 times. If listeners needed to replay a sample to make perceptual judgement, they were instructed to replay the reference sample prior to the rating of the stimulus in each repetition. Therefore, in each repetition, they basically compare the clarity of the sample to the reference sample rather than replaying the sample multiple times. The combined presentation of the reference (auditory anchor) and the speech sample has been implemented in the previous perceptual studies and have been shown to significantly increase the effectiveness and reliability of the perceptual judgment (51–53). Although we did not keep track of the number of listening attempts, listeners rarely listened to the samples five times. Upon the completion of the listening tasks for speech clarity, the program converted responses to numerical values ranging from -50 to 50 .

Statistical Analysis

Separate one-way analysis of variance (ANOVA) with Tukey *post hoc* tests were used for early and late post-surgery groups to compare the duration of speech samples in the four speech modifications. Mann-Whitney *U* tests were used to compare the average speed and range of lower lip movement in the early and late post-surgery groups across the four speech modifications (between-group comparisons). Additionally, to compare the lip articulatory performance across speech modifications, Mann-Whitney *U* tests were performed separately for each pair of speech modifications in each group (within-group comparisons). Finally, descriptive statistics for listeners’ ratings of the speech severity and clarity of the “Buy Bobby a puppy” sentence produced by five subjects were calculated to perceptually identify (1) the speech modification with potential to derive articulatory precision and clear speech and (2) the degree to which participants were able to adapt their motor system to various articulatory demands of speech modifications. The intraclass correlation coefficient (ICC) test was applied to assess the consistency between speech clarity ratings of the two listeners, using a two-way mixed effects. Intrarater reliability was examined using Pearson correlation product. All statistical analyses were performed in SPSS statistical software version 25 and the α -level

of 0.05 was set as the level of significance. Bonferroni corrections were applied to manage family-wise multiple comparisons.

RESULTS

Task Effects on Speech Duration

Among the four speech modifications, speech samples produced in the slow speech modification were the longest in duration compared to the other speech modifications in both early and late post-surgery groups. In addition, speech productions in the fast speech modification were the shortest in duration as expected in individuals in the late post-surgery group. Individuals in the early post-surgery group, however, were observed to produce speech productions in the loud speech modification in the shortest duration of time (**Figure 3**). Results of one-way ANOVA indicated significant differences across the duration of speech samples produced by individuals in the early post-surgery group ($p = 0.03$) as well as individuals in the late post-surgery group ($p = 0.0001$). Tukey *post hoc* tests revealed that individuals in the late post-surgery group produced samples in the slow speech modification significantly longer than samples in normal, fast, and loud speech modifications ($p = 0.0001$). Individuals in the early post-surgery group, exhibited significant differences between the duration of samples produced in slow and normal speech modifications ($p = 0.03$) and between the duration of samples produced in slow and loud speech modifications ($p = 0.04$).

Between-Group Comparisons (Early vs. Late Post-surgery)

For kinematic measures extracted from the lower lip + jaw movement, the late post-surgery group had a significantly (adjusted p -value = 0.0125) faster speed and larger range of movement compared to those in the early post-surgery group across all speech modifications except slow (**Table 2, Figure 4**).

For kinematic measures extracted from the lower lip – jaw movement, Mann-Whitney U tests revealed a significantly greater average speed of movement in the late post-surgery group compared to the early post-surgery group (adjusted p -value =

0.0125). The observed between-group difference was during the normal speech only (**Table 3, Figure 5**).

Within-Group Comparisons (Task Effect)

In the early post-surgery group, no significant differences were observed across the speech modifications using kinematic measures extracted from the lower lip + jaw movement. In the late post-surgery group, however, significant between-task differences were observed using kinematic measures extracted from both the lower lip + jaw movement and lower lip – jaw movement (**Table 4**).

Speech Clarity

Qualitative analyses of listener's judgment of speech clarity indicated that among fast, loud, and slow speech modifications, speech loudness consistently improved speech clarity compared to the baseline (speech clarity of normal speech) in the five subjects incorporated in the perceptual component of the study

TABLE 2 | Comparison of average speed (mm/s) and range (mm³) of lower lip + jaw movement in early and late post-surgery groups.

| Kinematic measure | Speech modification | Speech modification | | Mann-Whitney U test P -value |
|--------------------------------------|----------------------|------------------------------|-----------------------------|----------------------------------|
| | | Early post surgery Mean (SD) | Late post surgery Mean (SD) | |
| lower lip + jaw | | | | |
| | Average speed (mm/s) | | | |
| | Normal | 17.01 (6.26) | 46.75 (13.44) | 0.0001 |
| | Fast | 24.01 (9.81) | 49.66 (14.14) | 0.0001 |
| Range of movement (mm ³) | Loud | 22.64 (9.30) | 59.79 (15.34) | 0.0001 |
| | Slow | 15.21 (10.76) | 24.06 (11.05) | 0.110 |
| | Normal | 5.39 (1.92) | 9.89 (1.63) | 0.0001 |
| | Fast | 5.82 (2.09) | 9.82 (1.46) | 0.0001 |
| | Loud | 6.11 (2.01) | 11.97 (1.68) | 0.0001 |
| | Slow | 5.55 (1.37) | 11.76 (1.94) | 0.0001 |

Gray areas represent significant comparisons at the adjusted p -value ($\alpha = 0.0125$).

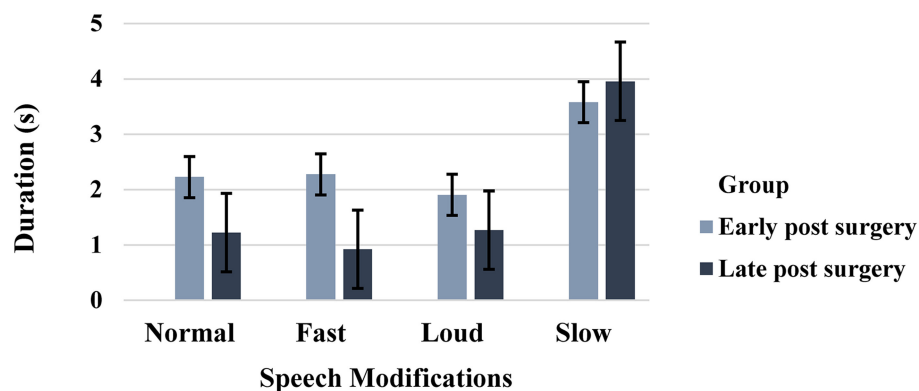


FIGURE 3 | Duration (s) of speech samples produced in normal, fast, loud, and slow speech modifications in early and late post-surgery groups (error bars represent the standard error (SE) of the mean).

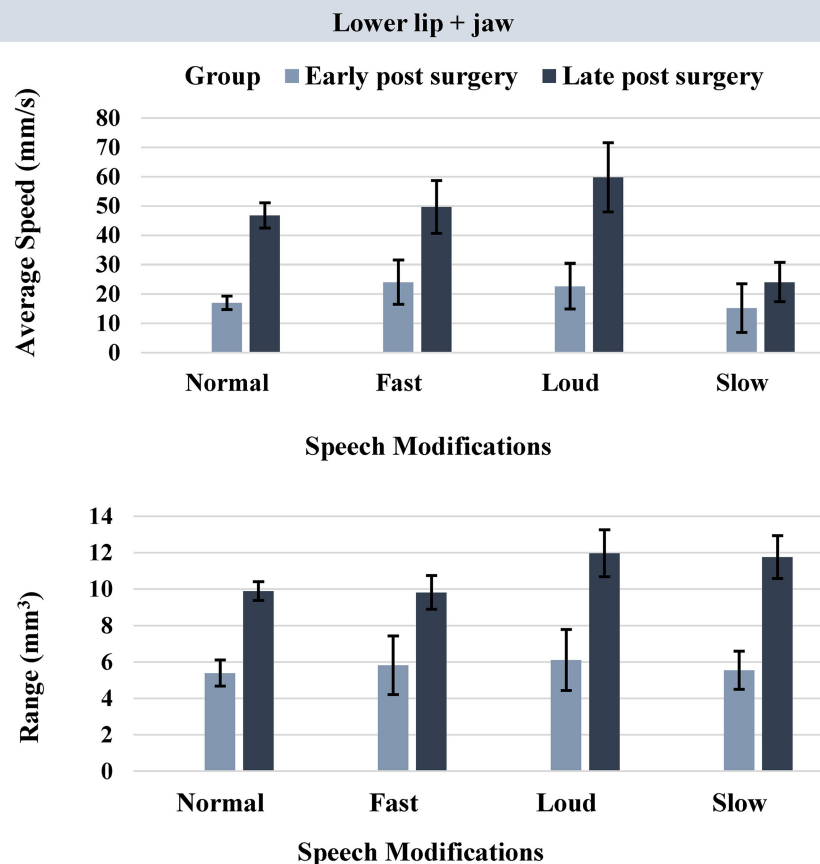


FIGURE 4 | Bar plots representing the average speed (mm/s) and range (mm³) of lower lip + jaw movement in early and late post-surgery groups (error bars represent the standard error (SE) of the mean).

TABLE 3 | Comparison of average speed (mm/s) and range (mm³) of lower lip - jaw movement in early and late post-surgery groups.

| Kinematic measure | Speech modification | | | Mann-Whitney <i>U</i> test <i>P</i> -value |
|--------------------------------------|---------------------|------------------------------|-----------------------------|--|
| lower lip - jaw | | Early post surgery Mean (SD) | Late post surgery Mean (SD) | |
| Average speed (mm/s) | Normal | 8.10 (2.02) | 11.87 (3.07) | 0.0001 |
| | Fast | 10.59 (3.34) | 14.35 (5.55) | 0.136 |
| | Loud | 10.13 (2.89) | 16.69 (6.32) | 0.059 |
| | Slow | 6.77 (3.61) | 7.19 (3.06) | 0.243 |
| Range of movement (mm ³) | Normal | 2.93 (1.06) | 2.99 (0.69) | 0.260 |
| | Fast | 2.60 (1.17) | 3.02 (0.55) | 0.190 |
| | Loud | 2.83 (1.19) | 3.97 (0.92) | 0.081 |
| | Slow | 2.57 (0.76) | 3.19 (0.64) | 0.079 |

The gray area represents the significant comparison at the adjusted p-value ($\alpha = 0.0125$).

(Figure 6). In this figure, P01 and P02 belong to the early post-surgery group and the three other participants (P04, P05, and P06) belong to the late post-surgery group. The baseline 0 was

assigned to the clarity of speech stimuli produced in the normal speech (i.e., reference). Accordingly, scale values above baseline 0 indicate relatively better speech clarity, whereas values below the baseline 0 represent relatively poorer speech clarity. Slowed speech improved speech clarity in participants in the late post-surgery group but decreased speech clarity in participants in the early post-surgery group. Rating of speech clarity across the three speech modifications (fast, loud, and slow) indicated that participants in the early post-surgery group (P01 and P02) showed improvement in speech clarity about eight units on the scale for the loud speech modification. In this group, the speech clarity decreased about five and nine units on the scale for the fast and slow speech modifications, respectively. In the late post-surgery group (P04, P05, and P06), the average rating of speech clarity across the three speech modifications (fast, loud, and slow) indicated improved speech clarity (17 units on the scale) for the loud and slow speaking modes and decreased speech clarity (eight units on the scale) for the fast speaking mode.

For the observed perceptual ratings of speech clarity, the average intraclass correlation coefficient (ICC) was 0.75 ($p < 0.05$) and the single measures ICC was 0.74 ($p < 0.05$), indicating fair interrater reliability. The average Pearson product correlation coefficients of ratings of speech clarity across fast, loud, and slow

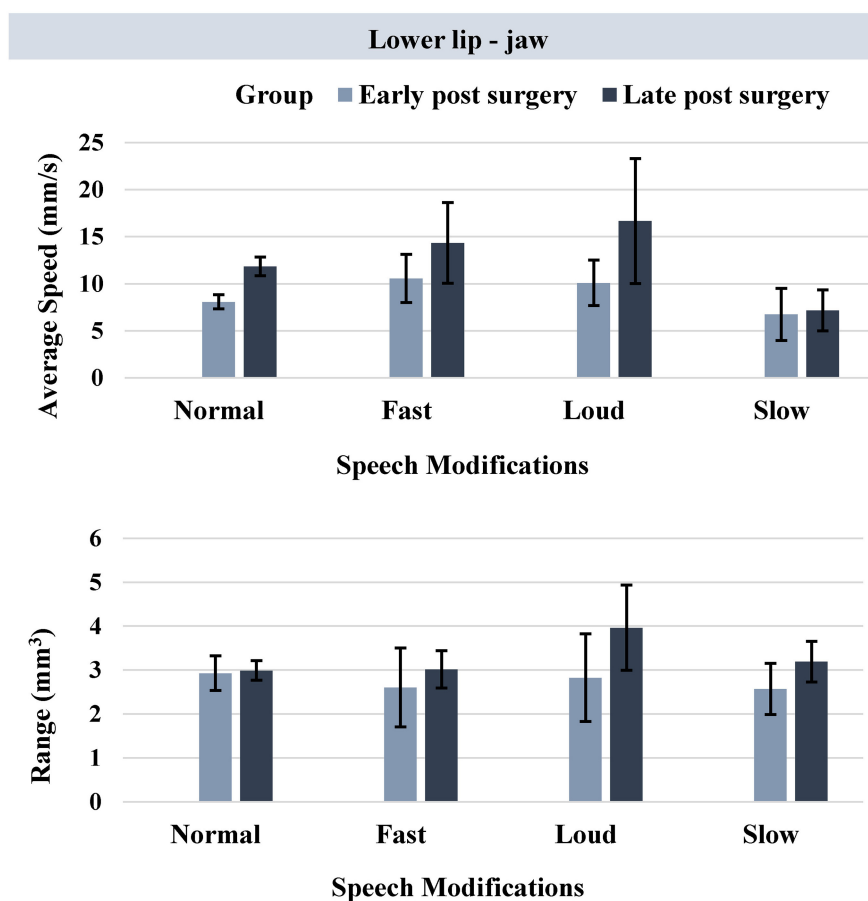


FIGURE 5 | Bar plots representing the average speed (mm/s) and range (mm³) of lower lip - jaw movement in early and late post-surgery groups (error bars represent the standard error (SE) of the mean).

TABLE 4 | Pairwise comparisons of speech modifications in terms of kinematic measures extracted from lower lip ± jaw movement in the late post-surgery group.

| Kinematic measure | Pairwise comparison | Mann-Whitney <i>U</i> test <i>P</i> -value | |
|--------------------------------------|---------------------|--|--------------------------|
| | | lower lip + jaw movement | lower lip - jaw movement |
| Average speed (mm/s) | Normal vs. Fast | 0.550 | 0.339 |
| | Normal vs. Loud | 0.007 | 0.075 |
| | Normal vs. Slow | <0.001 | 0.000 |
| | Fast vs. Loud | 0.219 | 0.328 |
| | Fast vs. Slow | <0.001 | 0.001 |
| | Loud vs. Slow | <0.001 | 0.002 |
| Range of movement (mm ³) | Normal vs. Fast | 0.931 | 0.810 |
| | Normal vs. Loud | 0.003 | 0.017 |
| | Normal vs. Slow | 0.004 | 0.436 |
| | Fast vs. Loud | 0.009 | 0.036 |
| | Fast vs. Slow | 0.011 | 0.604 |
| | Loud vs. Slow | 0.948 | 0.093 |

Gray areas represent significant comparisons at the adjusted *p*-value ($\alpha = 0.008$).

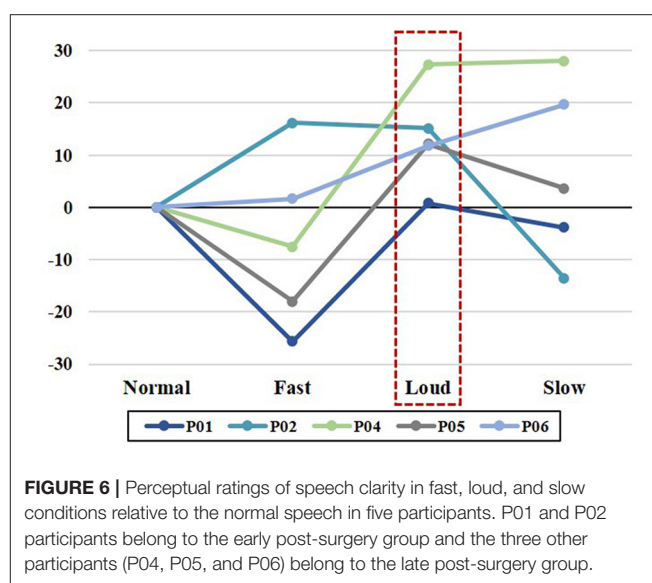


FIGURE 6 | Perceptual ratings of speech clarity in fast, loud, and slow conditions relative to the normal speech in five participants. P01 and P02 participants belong to the early post-surgery group and the three other participants (P04, P05, and P06) belong to the late post-surgery group.

speech modifications for listener 1 and 2 were 0.88 ($p < 0.05$) and 0.70 ($p < 0.05$) respectively. **Table 5** summarizes the average of speech clarity ratings performed by each listener for fast, loud, and slow speech modifications in reference to the normal speech (baseline 0).

DISCUSSION

The purpose of this study was to determine (1) the extent to which patients recovering from facial transplantation surgery can adapt their motor system to various articulatory demands of different speech modification using measures of facial biomechanics, and (2) the comparative effects of these adaptations on speech clarity. Results from our study suggest that (1) motor adaptation to articulatory demands of speech modifications increased from 2 to 42 months post-surgery as an indication of neural recovery; (2) across the four speech modifications, loud speech modification most consistently improved speech clarity during early and late stages of neuromotor recovery; and (3) individuals in early and late stages of neuromotor recovery over-rely on jaw for the lip articulatory function across all speech modifications. These findings help improve our understanding of underlying mechanisms of motor speech recovery following facial transplantation and offer a speech modification strategy that may help improve speech intelligibility in this patient population particularly in the early stages of recovery.

Facial Motor Capacity for Speech Demands Increased From 2 to 42 Months Post-surgery

Our participants' ability to accommodate the varying motoric demands required by the speech modifications significantly improved from early (~2 months) to late (~42 months) post-surgery. Restricted facial motor capacity in the early post-surgery group was demonstrated by (1) the lack of difference in the duration of speech samples produced by this group in normal, fast, and loud speech modifications, and (2) no differences between speed and range of lower lip movement during these various speech modifications. In contrast, individuals in the late post-surgery group were able to make modification-specific articulatory adjustments in speed and range of lip movement, as the magnitude of speed and range of lip movement during production of all speech modifications were significantly larger

in the late post-surgery group compared to values of their corresponding modification in the early post-surgery group. Improvement in facial motor function in the later stage of neural recovery supports findings reported by Grigos et al. (7), who observed significant increase in jaw displacement and lip aperture in the vertical plane over a 13-month period for nonspeech and speech tasks produced by a single facial transplant patient. These findings are also consistent with the prior longitudinal case study conducted by De Letter et al. (2) in which improved functional neuromotor recovery were observed up to 38 months post-surgery in a patient who underwent facial allotransplantation.

Loud Speech Modification Consistently Improved Speech Clarity During Early and Late Stages of Neuromotor Recovery

Perceptual evaluations of speech produced during normal, fast, loud, and slow speech modifications in our study demonstrated that relative to normal speech, increased speech loudness resulted in enhanced speech clarity across the recovery spectrum. Additionally, for those is the late-recovery group, slow speech resulted in improved speech clarity. These findings are supported by prominent gains in range of lip movements observed during the loud and slow speech modifications in our study. Consistent gain in speech clarity during loud speech support previous findings as well as the LSVT^R program that advocate loud speech intervention to improve speech motor system and overall intelligibility in populations with dysarthria (8, 9, 12, 37, 54). These findings provided empirical evidence for potential benefits of implementing loud speech modification as an intervention technique to enhance clarity and most possibly intelligibility in individuals with facial transplantation. More studies with interventional research design are warranted to test the efficacy of loud speech on speech intelligibility in individuals post facial transplant surgery.

Individuals in Early and Late Stages of Neuromotor Recovery Over-Rely on Jaw for the Lip Articulatory Function Across All Speech Modifications

Although all subjects in the early-post surgery group and one subject in the late post-surgery group underwent osteomyocutaneous transplantations, jaw-dependent lip movements outperformed jaw-independent lip movements in deriving articulatory distinctions between groups and across speech modifications, as kinematic measures extracted from lip + jaw movement showed greater differences between speech modifications than the ones obtained from the lip – jaw movement. In addition, greater between-group differences were captured using kinematic measures extracted from lip + jaw movement, rather than the lip – jaw movement.

Unlike the lip + jaw movement, which demonstrated significant improvement in speed and range of movement across all speech modifications over the course of neuromotor recovery, lip movements that were decoupled from those of the jaw (lip – jaw) were similar regardless of the type of speech modification in both early and late post-surgery groups. For the purposes of

TABLE 5 | The average of speech clarity ratings by listeners 1 and 2 for participants in early (P01 and P02) and late (P04, P05, and P06) post-surgery groups during fast, loud, and slow speech modifications.

| | Early post-surgery Group | | | Late post-surgery Group | | |
|------------|--------------------------|------|------|-------------------------|------|------|
| | Fast | Loud | Slow | Fast | Loud | Slow |
| Listener 1 | –5 | 3 | –10 | –8 | 13 | 5 |
| Listener 2 | –5 | 13 | –8 | –8 | 21 | 30 |

Ratings are in reference to the normal speech (baseline 0).

functional speech, it appears that neuromotor recovery of the lips is limited, at least for the participants who participated in this study. In the absence of recovery of lip motor control, individuals with face transplant may depend on the jaw as an articulatory strategy to enhance speech function. These findings provide value when considering functional outcomes for potential surgical candidates, as patients requiring surgical techniques that impede jaw movement may experience worse functional speech outcomes than those who do not. Similar findings have been reported in populations with impaired speech motor control such as multiple sclerosis (55) and amyotrophic lateral sclerosis (56, 57) or during normal speech motor development in neurotypical children (58).

CONCLUSION

Our findings suggest that the articulatory kinematic adaptations to speech modifications are significantly restricted in individuals at the early stage of neuromotor recovery post facial transplant surgery but improve over time. In addition, our findings provide empirical evidence for the overreliance of the jaw to support lip articulatory functions during speech over the course of neural recovery. Despite speech motor restrictions on speech modifications and jaw reliance during speech, loud speech may result in increased lip and jaw movement and increased speech clarity as early as 2-months post-surgery, and therefore, may be beneficial as a behavioral speech modification to improve functional speech in this population.

Two limitations of this study need to be acknowledged. First, the sample size in each group was small. Second, the elicitation procedure for speech modification tasks was not in a random order. Future studies with larger sample size and longitudinal design are warranted to further substantiate the findings of this study. It should be noted that the current study examined the effect of speech modifications on articulatory movements over one session, and results cannot be over-interpreted as treatment outcomes of loud or slow speech modifications. Further work is required to understand the effect of these approaches when applied during intervention and to identify speech kinematic profiles of speakers who benefit from different speech treatment approaches. In addition, in this study, speech samples were not produced in clear speech modification (i.e., hyperarticulated speech). Given that several perceptual studies have shown significant improvement to speech intelligibility during clear speech compared to normal speech (10, 59–62),

future studies are encouraged to implement cues for clear speech and compare the effectiveness of that to those of loud and slow speech modifications.

DATA AVAILABILITY STATEMENT

The raw data supporting the conclusions of this article will be made available by the authors, without undue reservation.

ETHICS STATEMENT

The studies involving human participants were reviewed and approved by Partners health care IRB. The patients/participants provided their written informed consent to participate in this study. Written informed consent was obtained from the individual(s) for the publication of any potentially identifiable images or data included in this article.

AUTHOR CONTRIBUTIONS

ME had a major role in study conceptualization and design, data analyses, interpretation of the findings, and writing the manuscript. BJP contributed to data collection and interpretation of the findings, reviewed the manuscript, and provided feedback. BR contributed to data collection and data analyses. HV contributed to data analyses. BP reviewed the manuscript and provided feedback. JG had a major role in the study conceptualization and design, interpretation of the findings, and manuscript preparation. All authors contributed to the article and approved the submitted version.

FUNDING

This research was supported by the National Institutes of Health (NIH-NIDCD) under award numbers R21DC01666401 and K24DC016312.

ACKNOWLEDGMENTS

The views and content expressed herein are solely the responsibility of the authors and does not necessarily represent the official views of the National Institute of Health. The authors would like to thank Kaila Stipancic and Sarah Gutz for their assistance with the perceptual judgment of speech.

REFERENCES

- Lantieri L, Hivelin M, Audard V, Benjoar MD, Meningaud JP, Bellivier F, et al. Feasibility, reproducibility, risks and benefits of face transplantation: a prospective study of outcomes. *Am J Transplant.* (2011) 11:367–78. doi: 10.1111/j.1600-6143.2010.03406x
- De Letter M, Vanhoutte S, Aerts A, Santens P, Vermeersch H, Roche N, et al. Facial nerve regeneration after facial allotransplantation: a longitudinal clinical and electromyographic follow-up of lip movements during speech. *J Plast Reconstr Aesthetic Surg.* (2017) 70:729–33. doi: 10.1016/j.bjps.2017.02025
- Petruzzo P, Testelin S, Kanitakis J, Badet L, Lengelé B, Girbon J-P, et al. First human face transplantation. *Transplantation.* (2012) 93:236–40. doi: 10.1097/TP0b013e31823d4af6
- Perry BJ, Pomahac B, Bueno EM, Su P, Richburg B, Green JR. Characteristics of speech following facial transplantation. In: *18th International Congress of Phonetic Sciences (ICPhS)*. Glasgow (2015).
- Van Lierde KM, Roche N, De Letter M, Corthals P, Stillaert F, Vermeersch H, et al. Speech characteristics one year after first Belgian facial transplantation. *Laryngoscope.* (2014) 124:2021–7. doi: 10.1002/lary.24585

6. Tasigiorgos S, Kollar B, Turk M, Perry B, Alhefzi M, Kiwanuka H, et al. Five-year follow-up after face transplantation. *N Engl J Med*. (2019) 380:2579–81. doi: 10.1056/NEJMc1810468
7. Grigos MI, LeBlanc É, Hagedorn C, Diaz-Siso JR, Plana N, Rodriguez ED. Changes in articulatory control pre- and post-facial transplant: a case report. *J Speech Lang Hear Res*. (2019) 62:297–306. doi: 10.1044/2018_JSLHR-S-18-0147
8. Yorkston KM, Hakel M, Beukelman DR, Fager S. Evidence for effectiveness of treatment of loudness, rate, or prosody in dysarthria: a systematic review. *J Med Speech Lang Pathol*. (2007) 15:xi–xxxvi.
9. Tjaden K, Wilding GE. Rate and loudness manipulations in dysarthria. *J Speech Lang Hear Res*. (2004) 47:766–83. doi: 10.1044/1092-4388(2004/058)
10. Tjaden K, Sussman JE, Wilding GE. Impact of clear, loud, and slow speech on scaled intelligibility and speech severity in Parkinson's disease and multiple sclerosis. *J Speech Lang Hear Res*. (2014) 57:779–92. doi: 10.1044/2014_JSLHR-S-12-0372
11. Tjaden K, Lam J, Wilding G. Vowel acoustics in Parkinson's Disease and multiple sclerosis: comparison of clear, loud, and slow speaking conditions. *J Speech Lang Hear Res*. (2013) 56:1485–502. doi: 10.1044/1092-4388(2013/12-0259)
12. Sapir S, Spielman JL, Ramig LO, Story BH, Fox C. Effects of intensive voice treatment (the Lee Silverman Voice Treatment [LSVT]) on vowel articulation in dysarthric individuals with idiopathic parkinson disease: acoustic and perceptual findings. *J Speech Lang Hear Res*. (2007) 50:899–912. doi: 10.1044/1092-4388(2007/064)
13. Park S, Theodoros D, Finch E, Cardell E. Be clear: a new intensive speech treatment for adults with nonprogressive dysarthria. *Am J Speech-Language Pathol*. (2016) 25:97–110. doi: 10.1044/2015_AJSLP-14-0113
14. McAuliffe MJ, Fletcher AR, Kerr SE, O'Beirne GA, Anderson T. Effect of dysarthria type, speaking condition, and listener age on speech intelligibility. *Am J Speech-Language Pathol*. (2017) 26:113–23. doi: 10.1044/2016_AJSLP-15-0182
15. Hustad KC, Weismer G. Interventions to improve intelligibility and communicative success for speakers with dysarthria. In: *Motor Speech Disorders*. San Diego, CA: Plural Publishing Inc (2007). p. 217–28. doi: 10.1159/000091735
16. Blanchet PG, Snyder GJ. Speech rate treatments for individuals with dysarthria: a tutorial. *Percept Mot Skills*. (2010) 110:965–82. doi: 10.2466/pms.110.3965-982
17. Kearney E, Giles R, Haworth B, Faloutsos P, Baljko M, Yunusova Y. Sentence-level movements in parkinson's disease: loud, clear, and slow speech. *J Speech Lang Hear Res*. (2017) 60:3426–40. doi: 10.1044/2017_JSLHR-S-17-0075
18. Adams SG, Weismer G, Kent RD. Speaking rate and speech movement velocity profiles. *J Speech Lang Hear Res*. (1993) 36:41–54. doi: 10.1044/jshr.360141
19. Flege JE. Effects of speaking rate on tongue position and velocity of movement in vowel production. *J Acoust Soc Am*. (1988) 84:901–16. doi: 10.1121/1396659
20. Hertrich I, Ackermann H. Lip-jaw and tongue-jaw coordination during rate-controlled syllable repetitions. *J Acoust Soc Am*. (2000) 107:2236–47. doi: 10.1121/1428504
21. Kuehn DP, Moll KL. A cineradiographic study of VC and CV articulatory velocities. *J Phon*. (1976) 4:303–20. doi: 10.1016/S0095-4470(19)31257-4
22. Ostry DJ, Munhall KG. Control of rate and duration of speech movements. *J Acoust Soc Am*. (1985) 77:640–8. doi: 10.1121/1391882
23. Shaiman S. Kinematics of compensatory vowel shortening: the effect of speaking rate and coda composition on intra- and inter-articulatory timing. *J Phon*. (2001) 29:89–107. doi: 10.1006/jpho.20010133
24. Mefferd AS, Green JR. Articulatory-to-acoustic relations in response to speaking rate and loudness manipulations. *J Speech Lang Hear Res*. (2010) 53:1206–19. doi: 10.1044/1092-4388(2010/09-0083)
25. Westbury JR, Dembowski J. Articulatory kinematics of normal diadochokinetic performance. In: *Annual Bulletin of the Research Institute of Logopedics and Phoniatrics*. Faculty of Medicine, University of Tokyo (1993). p. 13–36.
26. Berry J. Speaking rate effects on normal aspects of articulation: outcomes and issues. *Perspect Speech Sci Orofac Disord*. (2011) 21:15–26. doi: 10.1044/ssod.21.115
27. Berry J, Weismer G. Speaking rate effects on locus equation slope. *J Phon*. (2013) 41:468–78. doi: 10.1016/j.wocn.2013.09002
28. Southwood H. The use of prolonged speech in the treatment of apraxia of speech. In: *Clinical Aphasiology*. Lake of the Ozarks, MO (1987). p. 277–87.
29. Wambaugh JL, Martinez AL. Effects of rate and rhythm control treatment on consonant production accuracy in apraxia of speech. *Aphasiology*. (2000) 14:851–71. doi: 10.1080/026870300412232
30. Tjaden K, Turner GS. Spectral properties of fricatives in amyotrophic lateral sclerosis. *J Speech Lang Hear Res*. (1997) 40:1358–72. doi: 10.1044/jshr.40061358
31. Turner GS, Tjaden K, Weismer G. The influence of speaking rate on vowel space and speech intelligibility for individuals with amyotrophic lateral sclerosis. *J Speech Lang Hear Res*. (1995) 38:1001–13. doi: 10.1044/jshr.38051001
32. Weismer G, Laures JS, Jeng J-Y, Kent RD, Kent JF. Effect of speaking rate manipulations on acoustic and perceptual aspects of the dysarthria in amyotrophic lateral sclerosis. *Folia Phoniatr Logop*. (2000) 52:201–19. doi: 10.1159/000021536
33. Yorkston KM, Beukelman DR. Ataxic dysarthria: treatment sequences based on intelligibility and prosodic considerations. *J Speech Hear Disord*. (1981) 46:398–404. doi: 10.1044/jshd.4604398
34. Yorkston KM, Hammen VL, Beukelman DR, Traynor CD. The effect of rate control on the intelligibility and naturalness of dysarthric speech. *J Speech Hear Disord*. (1990) 55:550–60. doi: 10.1044/jshd.5503550
35. Mefferd AS. Effects of speaking rate, loudness, and clarity modifications on kinematic endpoint variability. *Clin Linguist Phon*. (2019) 33:570–85. doi: 10.1080/02699206.20191566401
36. Ramig LO, Pawlas A, Countryman S. *The Lee Silverman Voice Treatment (LSVT): A Practical Guide to Treating the Voice and Speech Disorders in Parkinson Disease*. Iowa City, IA: National Center for Voice and Speech (1995).
37. Ramig LO. Intensive voice treatment (LSVT(R)) for patients with Parkinson's disease: a 2 year follow up. *J Neurol Neurosurg Psychiatry*. (2001) 71:493–8. doi: 10.1136/jnnp.71.4493
38. Darling M, Huber JE. Changes to articulatory kinematics in response to loudness cues in individuals with Parkinson's disease. *J Speech Lang Hear Res*. (2011) 54:1247–59. doi: 10.1044/1092-4388(2011/10-0024)
39. Dromey C, Adams S. Loudness perception and hypophonia in Parkinson disease. *J Med Speech Lang Pathol*. (2000) 8:255–9.
40. Huber JE, Chandrasekaran B. Effects of increasing sound pressure level on lip and jaw movement parameters and consistency in young adults. *J Speech Lang Hear Res*. (2006) 49:1368–79. doi: 10.1044/1092-4388(2006/098)
41. Wong MN, Kuruvilla-Dugdale M, Ng ML. Differential effects of increased loudness on tongue kinematics in individuals with PD? Analyses of two cases. *Speech Lang Hear*. (2017) 20:49–56. doi: 10.1080/2050571X.20161206694
42. Huber JE, Stathopoulos ET, Ramig LO, Lancaster SL. Respiratory function and variability in individuals with Parkinson disease: pre- and post-lee silverman voice treatment. *J Med Speech Lang Pathol*. (2003) 11:185–202.
43. Huber JE, Chandrasekaran B, Wolstencroft JJ. Changes to respiratory mechanisms during speech as a result of different cues to increase loudness. *J Appl Physiol*. (2005) 98:2177–84. doi: 10.1152/jappphysiol.012392004
44. Ramig LO, Dromey C. Aerodynamic mechanisms underlying treatment-related changes in vocal intensity in patients with parkinson disease. *J Speech Lang Hear Res*. (1996) 39:798–807. doi: 10.1044/jshr.3904798
45. Smith ME, Ramig LO, Dromey C, Perez KS, Samandari R. Intensive voice treatment in parkinson disease: Laryngostroboscopic findings. *J Voice*. (1995) 9:453–9. doi: 10.1016/S0892-1997(05)80210-3
46. Dromey C, Ramig LO, Johnson AB. Phonatory and articulatory changes associated with increased vocal intensity in parkinson disease: a case study. *J Speech Lang Hear Res*. (1995) 38:751–64. doi: 10.1044/jshr.3804751
47. Sapir S, Spielman J, Ramig LO, Hinds SL, Countryman S, Fox C, et al. Effects of intensive voice treatment (the Lee Silverman Voice Treatment [LSVT]) on ataxic dysarthria. *Am J Speech-Language Pathol*. (2003) 12:387–99. doi: 10.1044/1058-0360(2003/085)
48. Watson PJ, Hughes D. The relationship of vocal loudness manipulation to prosodic F0 and durational variables in healthy adults. *J Speech Lang Hear Res*. (2006) 49:636–44. doi: 10.1044/1092-4388(2006/040)

49. Murphey AW, Clinkscales WB, Oyer SL. Masseteric nerve transfer for facial nerve paralysis. *JAMA Facial Plast Surg.* (2018) 20:104–10. doi: 10.1001/jamafacial.20171780
50. Green JR, Wang J, Wilson DL. SMASH: a tool for articulatory data processing and analysis. In: *Interspeech*. Lyon (2013). p. 1331–5.
51. Chan KMK, Yiu EM-L. The effect of anchors and training on the reliability of perceptual voice evaluation. *J Speech Lang Hear Res.* (2002) 45:111–26. doi: 10.1044/1092-4388(2002/009)
52. Eadie TL, Kapsner-Smith M. The effect of listener experience and anchors on judgments of dysphonia. *J Speech Lang Hear Res.* (2011) 54:430–47. doi: 10.1044/1092-4388(2010/09-0205)
53. Awan SN, Lawson LL. The effect of anchor modality on the reliability of vocal severity ratings. *J Voice.* (2009) 23:341–52. doi: 10.1016/j.jvoice.2007.10006
54. Neel AT. Effects of loud and amplified speech on sentence and word intelligibility in Parkinson disease. *J Speech Lang Hear Res.* (2009) 52:1021–33. doi: 10.1044/1092-4388(2008/08-0119)
55. Mefferd AS, Lai A, Bagnato F. A first investigation of tongue, lip, and jaw movements in persons with dysarthria due to multiple sclerosis. *Mult Scler Relat Disord.* (2019) 27:188–94. doi: 10.1016/j.msard.2018.10116
56. Lee J, Bell M, Simmons Z. Articulatory kinematic characteristics across the dysarthria severity spectrum in individuals with amyotrophic lateral sclerosis. *Am J Speech-Language Pathol.* (2018) 27:258–69. doi: 10.1044/2017_AJSLP-16-0230
57. Rong P, Green JR. Predicting speech intelligibility based on spatial tongue–jaw coupling in persons with amyotrophic lateral sclerosis: the impact of tongue weakness and jaw adaptation. *J Speech Lang Hear Res.* (2019) 62:3085–103. doi: 10.1044/2018_JSLHR-S-CSMC7-18-0116
58. Green JR, Moore CA, Higashikawa M, Steeve RW. The physiologic development of speech motor control. *J Speech Lang Hear Res.* (2000) 43:239–55. doi: 10.1044/jslhr.4301239
59. Beukelman DR, Fager S, Ullman C, Hanson E, Logemann J. The impact of speech supplementation and clear speech on the intelligibility and speaking rate of people with traumatic brain injury. *J Med Speech Lang Pathol.* (2002) 10:237–42.
60. Lam J, Tjaden K. Intelligibility of clear speech: effect of instruction. *J Speech Lang Hear Res.* (2013) 56:1429–40. doi: 10.1044/1092-4388(2013/12-0335)
61. Smiljanić R, Bradlow AR. Speaking and hearing clearly: talker and listener factors in speaking style changes. *Lang Linguist Compass.* (2009) 3:236–64. doi: 10.1111/j.1749-818X.2008.00112x
62. Uchanski RM. Clear speech. In: *The Handbook of Speech Perception*. Oxford, UK: Blackwell Publishing Ltd (2005). p. 207–35. doi: 10.1002/9780470757024ch9

Conflict of Interest: The authors declare that the research was conducted in the absence of any commercial or financial relationships that could be construed as a potential conflict of interest.

Copyright © 2021 Eshghi, Perry, Richburg, Ventresca, Pomahac and Green. This is an open-access article distributed under the terms of the Creative Commons Attribution License (CC BY). The use, distribution or reproduction in other forums is permitted, provided the original author(s) and the copyright owner(s) are credited and that the original publication in this journal is cited, in accordance with accepted academic practice. No use, distribution or reproduction is permitted which does not comply with these terms.



Electromyographic Patterns and the Identification of Subtypes of Awake Bruxism

Ubirakitan Maciel Monteiro, Vinicius Belém Rodrigues Barros Soares, Caio Belém Rodrigues Barros Soares, Tiago Coimbra Costa Pinto, Rosana Christine Cavalcanti Ximenes* and Marcelo Araújo Cairrão Rodrigues

Federal University of Pernambuco, Recife, Brazil

OPEN ACCESS

Edited by:

Teresa Lever,
University of Missouri, United States

Reviewed by:

Riccardo Rosati,
University of Milan, Italy
Jari Ahlberg,
University of Helsinki, Finland

*Correspondence:

Rosana Christine Cavalcanti Ximenes
rosanaximenes1@gmail.com

Specialty section:

This article was submitted to
Motor Neuroscience,
a section of the journal
Frontiers in Human Neuroscience

Received: 01 September 2020

Accepted: 29 December 2020

Published: 28 January 2021

Citation:

Monteiro UM, Soares VBRB, Soares CBRB, Pinto TCC, Ximenes RCC and Araújo Cairrão Rodrigues M (2021) Electromyographic Patterns and the Identification of Subtypes of Awake Bruxism. *Front. Hum. Neurosci.* 14:601881. doi: 10.3389/fnhum.2020.601881

The future of awake bruxism assessment will incorporate physiological data, possibly electromyography (EMG) of the temporal muscles. But up to now, temporal muscle contraction patterns in awake bruxism have not been characterized to demonstrate clinical utility. The present study aimed to perform surface EMG evaluations of people assessed for awake bruxism to identify possible different subtypes. A 2-year active search for people with awake bruxism in three regions of the country resulted in a total of 303 participants (223 women, 38 ± 13 years, mean and SD). Their inclusion was confirmed through non-instrumental approaches for awake bruxism: self-reported questionnaire and clinical exam, performed by three experienced and calibrated dentists (Kappa = 0.75). Also, 77 age- and sex-matched healthy controls were recruited (49 women, 36 ± 14 years). Temporalis surface EMG was performed with a portable device (Myobox; NeuroUp, Brazil). EMG signals were sent to a computer via Bluetooth 4.0 at a sampling rate of 1,000 Hz. Digital signal processing was performed using the commercial neuroUP software, transformed in RMS and then normalized for peak detection (EMG peaks/min), in a 10 min session. Cluster analysis revealed three distinct subtypes of awake bruxism: phasic, tonic, and intermediate. Individuals with a predominance of EMG peaks/min were classified as the “phasic” subtype (16.8%). Those with the highest EMG rest power were classified as the “tonic” subtype (32.3%). There was also an “intermediate” subtype (50.8%), when both variables remained low. Characterization of awake bruxism physiology is important for future establishment of instrumental assessment protocols and treatment strategies.

Keywords: awake bruxism, electromyography, temporal muscle, cluster analysis, tonic contraction, phasic contractions

INTRODUCTION

Bruxism is an umbrella term for different motor phenomena/behaviors of the masticatory muscles. An international consensus defined awake bruxism as a masticatory muscle activity behavior during wakefulness that is characterized by repetitive or sustained tooth contact and/or by bracing or thrusting of the mandible (Lobbezoo et al., 2018). Awake bruxism is not defined as a disease by the current consensus (Lobbezoo et al., 2018) and does not necessarily present with pain at the time it is identified. But it is important to study this phenomenon because it is known that people with

awake bruxism have a greater probability of suffering from temporomandibular pain and diseases in the future (Maltarollo et al., 2020; Wetselaar et al., 2020).

The prevalence of awake bruxism in the general population is high (8–31%), and is influenced by psychological factors, such as stress and anxiety, a quite common situation in the post COVID-19 pandemic (Manfredini et al., 2013a, 2015; Lobbezoo et al., 2018; Winocur et al., 2019). The new consensus in bruxism (Lobbezoo et al., 2018) states that assessment of this condition in the future will need to go beyond clinical evaluation. Physiological parameters are needed, and electromyography (EMG) was identified as an alternative, despite the fact that no protocols have been suggested yet. Also, a recent review of literature (Yamaguchi et al., 2020) stated that masticatory muscle EMG can be easily and precisely recorded during the daytime by using a wearable EMG device that improves the assessment of awake bruxism. However, there are no studies regarding the physiology of awake bruxism using EMG. This knowledge is necessary to advance the field and for future long-term follow-up studies of awake bruxism based on physiological data.

Surface EMG is a widely used non-invasive technique capable of amplifying electrical signals captured on the skin above superficial muscles. The signals, which are conducted through the tissues and captured by electrodes, represent the temporal and spatial summation of a population of nearby motor units (Rainoldi et al., 2004). Therefore, the present study aimed to perform EMG evaluations of people included in the assessment of awake bruxism. Our hypothesis is that there are different patterns of activation of the masticatory muscles in awake bruxism and that these profiles can be unveiled by EMG assessment. We also hypothesized that pain intensity levels would be different among the EMG-based profiles for awake bruxism, such that participants with tonic temporal muscle contractions would report the highest pain intensity levels.

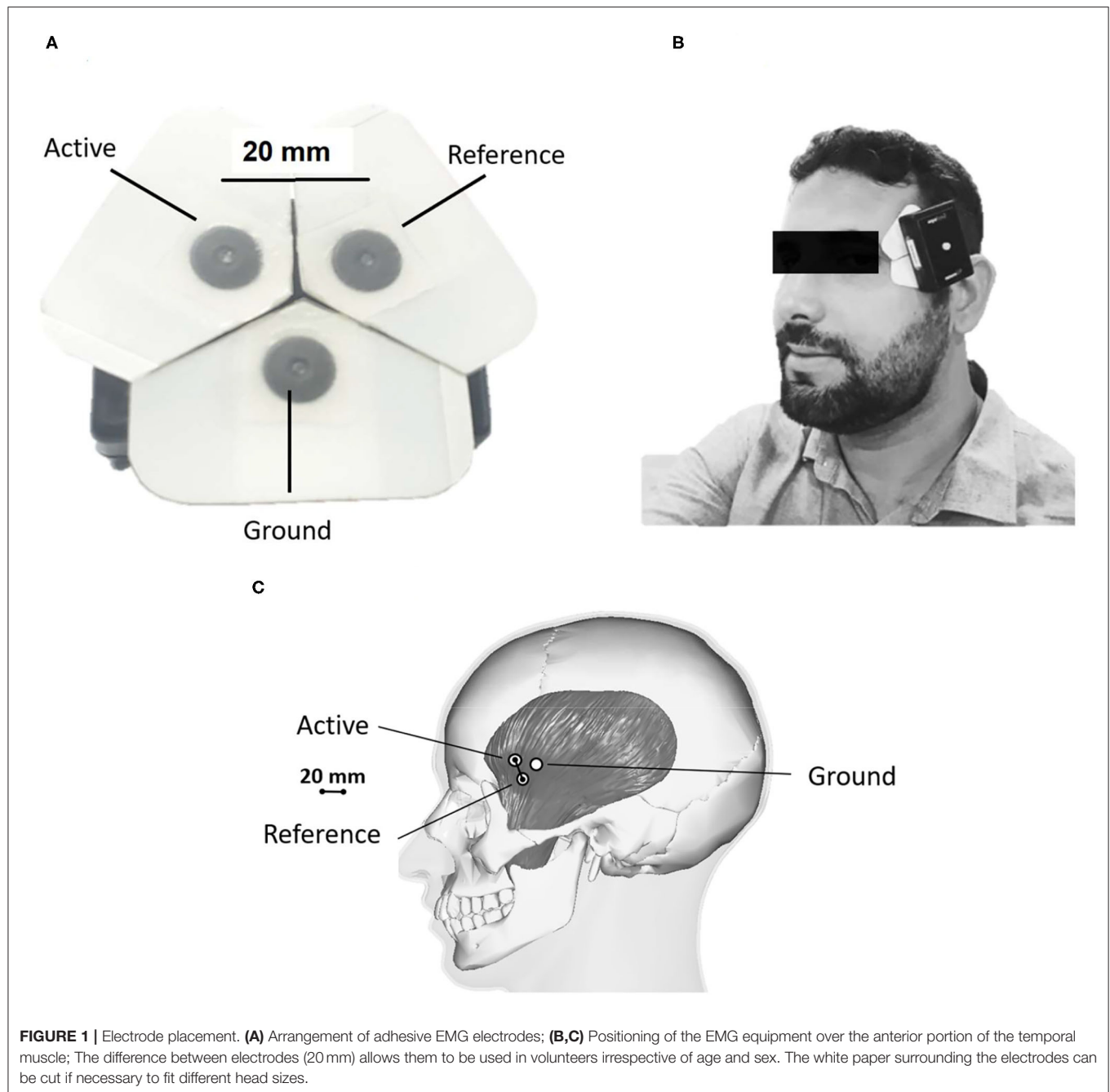
METHODS

An observational, analytic, and cross-sectional study was conducted. The participants were recruited by convenience from private healthcare services over 2 years (2017–2019) in the northeastern, central-western, and southeastern regions of Brazil. An active search was conducted in all centers to recruit subjects with a high probability of awake bruxism. The clinical signs of awake bruxism were disclosed. Possible candidates to the research study came spontaneously or were recruited by clinicians for an evaluation by a specialist. Only those volunteers compatible with the international consensus (Lobbezoo et al., 2018) were included in the awake bruxism group ($n = 303$, 38 ± 14 years, mean, and standard deviation, both sexes). A control group consisted of 77 healthy, age-matched volunteers (36 ± 14 years, both sexes) who were evaluated by the same specialists. All volunteers signed a statement of informed consent in compliance with Resolution n° 466/12 of the National Board of Health, and this study received approval from the human research ethics committee of the Center of Health Sciences of the Federal University of Pernambuco (process 65515417.1.0000.5208).

The inclusion criteria for the awake bruxism group was clinical and followed the international consensus (1): presence of self-reported jaw movements with or without associated pain symptoms, and (2) orofacial clinical signs identified by a dentist. The study exclusion criteria were: history of head trauma, presence of degenerative neurological diseases, stroke, open lesions in the region of the anterior temporal muscle, severe visual or hearing impairment, previous botulinum toxin injection in the masticatory muscles (masseter and temporal), or having undergone other concomitant rehabilitation treatments in the previous month.

All subjects completed a self-reported questionnaire on oral history and masticatory muscle activity, jaw/teeth clenching and bracing/thrusting, and teeth touching during non-swallowing behaviors. Also, a clinical exam was performed by 3 dentists with at least 5 years of experience in clinical assessment of awake bruxism to visually identify masticatory muscle hypertrophy, indentations on the tongue or lip and/or a *linea alba* on the inner cheek, damage to the dental hard tissues, failures of restorative work/prosthetic constructions, or mechanical wear of the teeth. The Tooth Wear Evaluation System (TWES), recommended by Wetselaar and Lobbezoo (2016), was used as reference. Despite all three specialists being experienced, a calibration procedure was executed as a guarantee that all evaluations would be compatible. The consensus (Lobbezoo et al., 2018), examination criteria, sequence of the examination, and the written specifications were reviewed again. Then, a pre-calibration session included a visual data bank with 30 images of oral alterations of awake bruxism or healthy controls obtained from previous work of the group (Ximenes et al., 2010). After that, a clinical practice calibration session was performed in patients assessed for awake bruxism and controls ($n = 30$ in each group). The three dentists examined the same patients. The data were analyzed, reviewed, and discussed; discrepancies in the data were re-examined. Finally, a reliability session was conducted, and the kappa index was calculated. The calibration procedure continued until a kappa index of 0.75 was reached, indicating an excellent agreement among the three dentists (Landis and Koch, 1997).

Surface EMG was performed using the Myobox device (neuroUP, Brazil). EMG signals were sent to a computer via Bluetooth 4.0 at a sampling rate of 1,000 Hz. Digital signal processing was performed using commercial software (neuroUP, Brazil), with a 60-Hz Notch filter to avoid electrical artifacts and a Butterworth bandpass filter (30–500 Hz) to reduce low frequencies artifacts (e.g., cardiac activity) and to guarantee a reading of up to half of the sampling rate (Nyquist Theorem). The signals were transformed in real-time to calculate the root mean square (RMS). Before the evaluation, an automatic measurement of the signal quality was performed in the software. EMG data were also processed by an algorithm that automatically calculates the amount of electric field gradients per minute. The counting of peaks per minute was based on individualized normalization, not on absolute values. Sudden increases in EMG signal above 80% of the patient's own basal was identified as a peak. This cutoff value was defined in a pilot project carried out prior to the



research and was the most accurate value in the identification of phasic contractions.

Standard disposable surface adhesive electrodes with Ag/AgCl sintered composition were used. These electrodes were placed with a distance of 20 mm between them (Figure 1A). In addition, a ground electrode was positioned 20 mm away from each active electrode (triangulation between them). The sensor was positioned on the anterior portion of the temporal muscle on the right or left side (Figures 1B,C). The side was chosen based on the following criteria: pain upon palpation (first criteria); self-reported habitual chewing side (second criteria). This approach

was for operational purposes, as there is no description that awake bruxism has a unilateral effect. Also, a study has shown that people with unilateral masticatory muscle pain show no significant difference in muscle electrical activity of painful and non-painful muscles (Manfredini et al., 2013b).

The EMG procedure lasted ~10 min. Pilot studies from our group (data not shown) and also studies from other laboratories have shown that this period suffices for an EMG evaluation (Prasad et al., 2019). The participant was seated in a comfortable armchair, legs uncrossed, shoulders relaxed, teeth not in contact, back erect, shoulders in external rotation, forearms in supination,

and hands resting on the thighs. During the instrumental approach, the EMG signals were observed only by the examiners; the participants did not receive EMG biofeedback.

The Visual Analog Scale (VAS) for pain was used to measure pain intensity. The VAS used was unidimensional, and the volunteer marked the intensity of pain, from zero (no pain) to ten

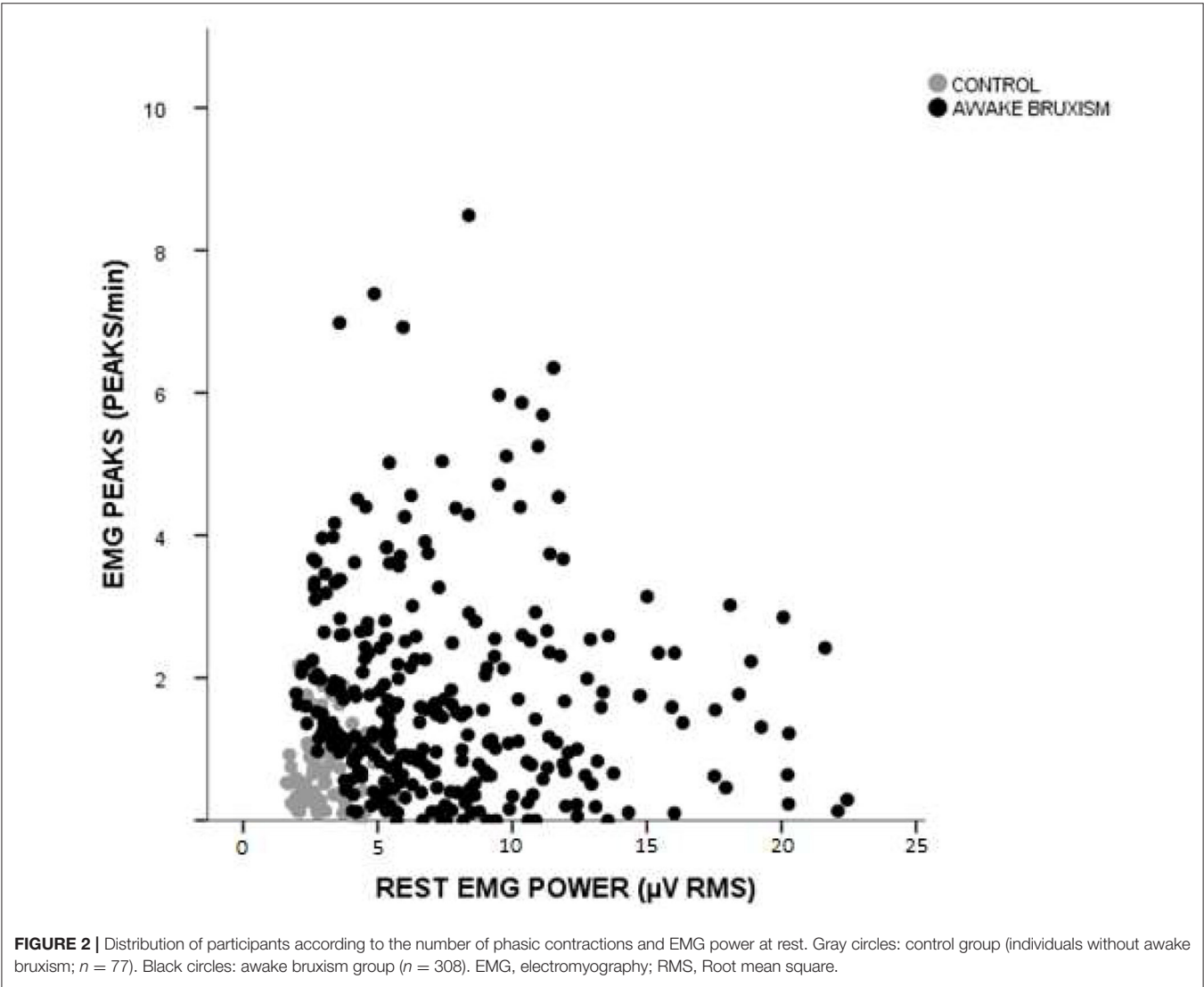
(intense pain). This scale was applied before palpation to avoid trigger points being activated, and participants were instructed to respond about the current painful perception felt at the time of the assessment.

As the objective of present work was to search for profiles of EMG markers in volunteers with awake bruxism, it was decided

TABLE 1 | Descriptive statistics of the study participants.

| Group | Age (mean ± SD) | Min/Max (years) | 95% CI lower/upper | VAS (arbitrary units 0–10) | Rest EMG Power (µV RMS) | EMG peaks (peaks/min) | n (male/female) |
|--------------|--------------------|--------------------|-----------------------|-------------------------------------|-------------------------------|-----------------------------|--------------------|
| Phasic | 36 ± 14 | 6/65 | 32/40 | 3.5 ± 3.2 | 6.4 ± 2.9 | 4.4 ± 1.3 | 51 (14/37) |
| Tonic | 39 ± 14 | 12/75 | 36/42 | 3.9 ± 3.1 | 13.1 ± 4.1 | 1.1 ± 0.9 | 98 (22/76) |
| Intermediate | 38 ± 13 | 11/70 | 33/39 | 4.1 ± 3.1 | 5.1 ± 1.6 | 1.2 ± 0.7 | 154 (44/110) |
| Controls | 36 ± 14 | 13/75 | 36/39 | 0.5 ± 0.4 | 2.9 ± 0.1 | 0.7 ± 0.5 | 77 (28/49) |

Values represent mean and standard deviation; 95% CI: confidence interval, interval where 95% of data is located; VAS, visual analog pain scale (0 means no pain); n, group sample size.



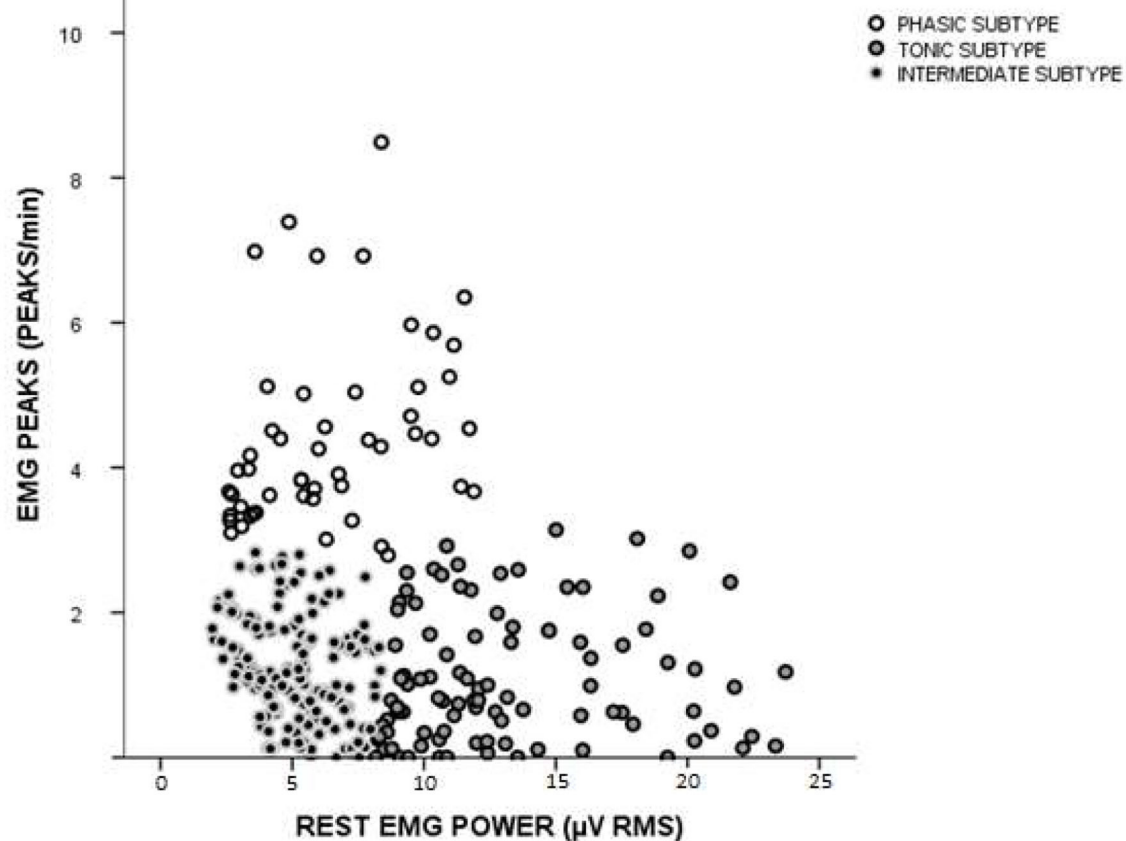


FIGURE 3 | Cluster analysis of individuals with awake bruxism. Three clusters emerged from analysis: phasic (increased EMG peaks/min and less rest muscle tonus), tonic (increased rest muscle tonus and decreased EMG peaks/min), and an intermediary group.

to perform a cluster analysis. Cluster analysis is a statistical method for organizing data into relatively homogeneous groups that differ from each other according to the variables of interest. All data were plotted in a 2D chart with phase contractions (EMG peaks/min, y) against their rest EMG power (μV RMS). These data were inserted in the automatic cluster analysis of SPSS software, using hierarchical cluster analysis (Crum et al., 2020). The level of significance was set to 5% ($p < 0.05$), and 95% confidence intervals were calculated.

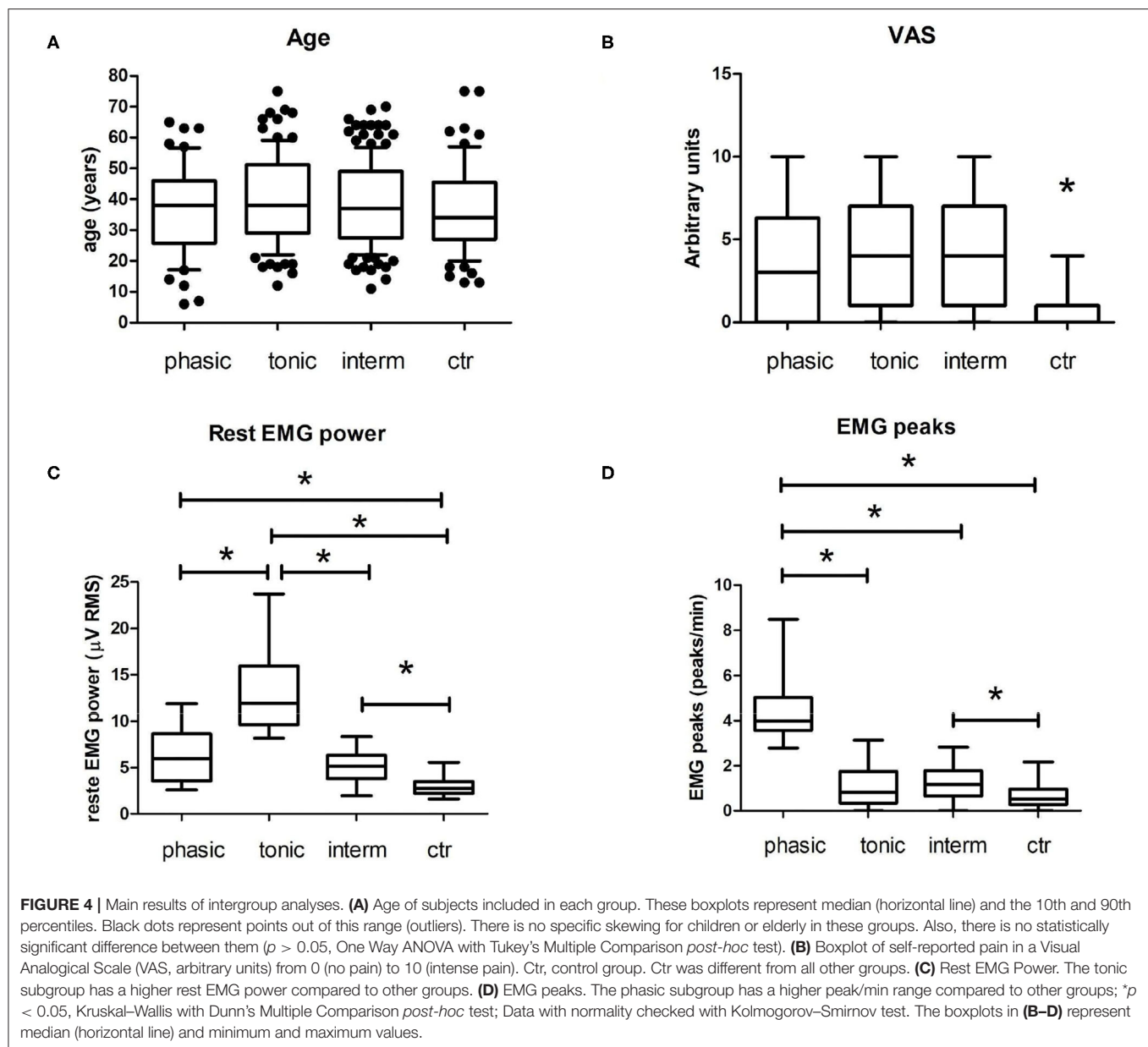
RESULTS

The age of the 380 participants with and without a clinical evidence of bruxism ranged from 11 to 75 years and included both sexes. The 303 participants with awake bruxism, with or without pain, were considered the participant group. The remaining 77 participants were considered the control group. There were no statistically significant differences among the control and participant groups relative to gender and age

(Table 1). Figure 2 shows the EMG peaks per minute and rest muscle power from participant and control groups.

Analyzing the EMG data of only the 308 participants with awake bruxism, as determined by clinical evaluation, revealed three clusters (Figure 3) representing three distinct subtypes of awake bruxism. The measure of cohesion and separation was 0.6 and considered good for cluster analysis. Individuals with the highest number of phasic contractions per minute and lowest EMG power were classified as the “phasic” subtype (51 participants—16.8%). Those with the highest rest EMG power and the smallest number of phasic contractions were classified as the “tonic” subtype (98 participants—32.3%). Those in whom both variables remained low were classified as the “intermediate” subtype (154 participants—50.8%).

Figure 4 and Table 1 show the descriptive statistics for all groups included in the study. With respect to age (Figure 4A), there is no statistically significant difference between groups. Also, no skewing was detected regarding child or teenage incidence between the groups. This can be seen in the boxplot of 10th to 90th percentiles. Pain intensity (Figure 4B), measured by the VAS, did not differ between awake bruxism subgroups



(phasic, tonic, and intermediate); however, all three subgroups were significantly higher than the control group. The rest EMG power (**Figure 4C**) was significantly higher in the tonic subgroup compared to all other groups (including controls), but also the phasic and intermediary subgroups had significantly higher values than controls. With regard to the EMG peaks/min (**Figure 4D**), the phasic subgroup had significantly higher values than all groups, but also the intermediary subgroup was higher than controls.

Table 1 contains the participant characteristics. The 95% confidence interval (CI) unveils that all groups had similar distribution with regard to age, but also that we found a higher prevalence of bruxism in the female gender.

DISCUSSION

The main finding of the present study is that individuals included in the assessment of awake bruxism can be classified based on surface EMG characteristics into three different subtypes: phasic, tonic, and intermediate. However, if one looks at **Figures 2, 3**, it can be seen that some overlap exists between the intermediate subtype and control group. But the authors do not believe that EMG could be overidentifying patients. First, in the present work, EMG was not used for awake bruxism identification. Second, VAS pain data are statistically different between these two groups (4.1 ± 3.1 for intermediate awake bruxism and 0.48 ± 0.9 for controls, see also **Figure 4B**). We cannot rule out that

some controls may be subclinical notifications of awake bruxism. When looking at the raw data, there was only one VAS score 4 in the control group. The upper limit of the 95% confidence interval (CI) of the mean in the control group is 0.68, quite below the apparently spurious score 4 occasionally found. With regard to pain, all three awake bruxism subtypes can be associated with some moderate pain; there is no difference between them, but all are higher than controls (see **Figure 4B**). One lesson that can be learned from this finding is that EMG alone is not (and will not) be the sole evaluation parameter of awake bruxism, as the clinical analysis is not (and will not be), either. Both approaches must be combined to gain a greater comprehension of what is most important: accurately evaluate the patient with regard to his/her physiology and possible awake bruxism assessment and predict the most suitable clinical approach for the best outcome possible, regardless if the patient has pain or not at the present time.

We believe that the side of sensor positioning can be aleatory. The criteria adopted here had just operational purposes. There is no description of laterality in awake bruxism. Also, people with unilateral masticatory muscle pain show no significant difference in muscle electrical activity of painful and non-painful muscles (Manfredini et al., 2013b). Furthermore, we compared right and left side EMG in 10 subjects of different subtypes, and did not find any difference (data not shown).

In a review of current methods for the assessment of bruxism, Pigozzi et al. (2019) point out the need for novel, more effective techniques. Current clinical methods require rigorous standardization and training and are still influenced by the subjective opinion of the examiner. According to Guillot et al. (2019), there is considerable disparity among health professionals regarding the assessment of bruxism, which results from different and often erroneous approaches to treatment. Inexperienced examiners, for example, may induce false pain when vigorously performing palpation on the muscle being evaluated.

Methods using portable devices (Yamaguchi et al., 2020), similar to those employed in the present study, have been gaining ground due to the increasing preference for evaluating individuals in their daily settings outside the clinic, which can alter the state of wakefulness and stress. Comparing EMG recordings under laboratory conditions to natural environment conditions, Prasad et al. (2019) found that differences in the amplitude of masseter muscle contractions were small and certainly not clinically relevant (0.94–1.00 to 0.82–1.00, respectively). Thus, the difference in evaluation setting does not exert influence over the degree of wakefulness, making surface EMG a reliable method in both situations (Prasad et al., 2019).

In the present study, no differences were found among the tonic, phasic, and intermediate subtypes regarding VAS scores. This finding contradicts our initial hypothesis that the tonic subgroup would have higher pain intensity values. However, individuals in the phasic and intermediate groups may have increased perceptions regarding pain symptoms, as individuals of different age groups and sexes were included in the sample. But a limitation of the present study was that the VAS score is subjective. We believe that further studies with a more

specific methodology of pain evaluation (e.g., digital algometer) are necessary.

Future studies will be able to identify whether different psychomotor profiles and different brain circuits can influence the prevalence of phasic and tonic contractions in people with awake bruxism. In addition, understanding the different EMG patterns may assist in choosing specific treatments in cases where bruxism causes harmful consequences. According to Wetselaar et al. (2020), bruxism can be a risk factor with possible negative oral health outcomes, such as severe masticatory muscle pain or temporomandibular joint pain, extreme mechanical tooth wear, cracked teeth, and/or prosthodontic complications. It is also important to note that some of these oral changes are irreversible and progressive, such as tooth wear and cracked teeth. When tooth wear reaches advanced stages, it can cause pain, hypersensitivity, problems with function (e.g., chewing), and negative aesthetics (Maltarollo et al., 2020).

The international consensus in bruxism states that assessment of this condition may be performed by non-instrumental and instrumental approaches, such as physiological parameters acquired by EMG (Lobbezoo et al., 2018). There is also a recent review of the literature stating that masticatory EMG is important for the assessment of bruxism, which can be easily and precisely recorded during the daytime using a wearable EMG device (Yamaguchi et al., 2020). Here, we showed novel evidence that people included in the assessment of awake bruxism have different EMG patterns. The resultant EMG-based subtype classification may help establish new approaches for awake bruxism assessment, identifying effective treatment strategies, and improving outcome prognostication.

CONCLUSIONS

The use of surface EMG enabled the identification of three distinct subtypes of awake bruxism (tonic, phasic, and intermediate), with no significant differences in VAS scores between them.

DATA AVAILABILITY STATEMENT

The raw data supporting the conclusions of this article will be made available by the authors, without undue reservation.

ETHICS STATEMENT

The studies involving human participants were reviewed and approved by Comitê de ética em pesquisa com seres humanos—CEP UFPE. Written informed consent to participate in this study was provided by the participants' legal guardian/next of kin.

AUTHOR CONTRIBUTIONS

UM and VS: term, conceptualization, methodology, formal analysis, investigation, data curation, writing - original draft,

writing - review and editing, and project administration. CS and TP: validation, investigation, and writing - review and editing. RX: term, conceptualization, methodology, validation, resources, writing- original draft, and writing - review and editing. MA: conceptualization, methodology, resources, writing - review and editing, and funding acquisition.

FUNDING

This study was financed in part by the Coordenação de Aperfeiçoamento de Pessoal de Nível Superior—Brasil (CAPES)—Finance Code 001.

REFERENCES

- Crum, M., Nelson, T., de Borst, J., and Byrnes, P. (2020). The use of cluster analysis in entrepreneurship research: review of past research and future directions. *J. Small Bus. Man.* 1:40. doi: 10.1080/00472778.2020.1748475
- Guillot, M., Jungo, S., Maniere, A., Laplanche, O., Tillier, Y., and Ehrmann, E. (2019). Diagnosis and management of bruxism: evaluation of clinical practices in France. *Cranio*. 11, 1–12. doi: 10.1080/08869634.2019.1661657
- Landis, J. R., Koch, G. G. (1997). The measurement of observer agreement for categorical data. *Biometrics*. 33, 159–174. doi: 10.2307/2529310
- Lobbezoo, F., Ahlberg, J., Raphael, K. G., Wetselaar, P., Glaros, A. G., Kato, T., et al. (2018). International consensus on the assessment of bruxism: report of a work in progress. *J. Oral Rehabil.* 45, 837–844. doi: 10.1111/joor.12663
- Maltarollo, T. H., Pedron, I. G., Medeiros, J. M. F., Kubo, H., Martins, J. L., and Shitsuka, C. (2020). The dental erosion is a problem! *Res. Soc. Dev.* 9:3. doi: 10.33448/rsd-v9i3.2723
- Manfredini, D., Ahlberg, J., Winocur, E., and Lobbezoo, F. (2015). Management of sleep bruxism in adults: a qualitative systematic literature review. *J. Oral Rehabil.* 42:11. doi: 10.1111/joor.12322
- Manfredini, D., Cocilovo, F., Stellini, E., Favero, L., and Guarda-Nardini, L. (2013b). Surface electromyography findings in unilateral myofascial pain patients: comparison of painful vs. non painful sides. *Pain Med.* 14, 1848–1853. doi: 10.1111/pme.12159
- Manfredini, D., Winocur, E., Guarda-Nardini, L., Paesani, D., and Lobbezoo, F. (2013a). Epidemiology of bruxism in adults: a systematic review of the literature. *J. Orofac. Pain.* 27:2. doi: 10.11607/jop.921
- Pigozzi, L., Rehm, D., Fagundes, S., Pellizzer, E., and Grossi, M. (2019). Current methods of bruxism diagnosis: a short communication. *Int. J. Prosthodont.* 32:3. doi: 10.11607/ijp.6196
- Prasad, S., Paulin, M., Cannon, R. D., Palla, S., and Farella, M. (2019). Smartphone-assisted monitoring of masticatory muscle activity in freely moving individuals. *Clin. Oral Investig.* 23:3601–3611. doi: 10.1007/s00784-018-2785-3

ACKNOWLEDGMENTS

The authors would like to thank the patients for participating in this study. We would also like to acknowledge the NeuroUp® for their support.

SUPPLEMENTARY MATERIAL

The Supplementary Material for this article can be found online at: <https://www.frontiersin.org/articles/10.3389/fnhum.2020.601881/full#supplementary-material>

- Rainoldi, A., Melchiorri, G., and Caruso, I. (2004). A method for positioning electrodes during surface EMG recordings in lower limb muscles. *J. Neurosci. Methods*. 134:1. doi: 10.1016/j.jneumeth.2003.10.014
- Wetselaar, P., and Lobbezoo, F. (2016). The tooth wear evaluation system (TWES): a modular clinical guideline for the diagnosis and management planning of worn dentitions. *J. Oral Rehabil.* 43:1. doi: 10.1111/joor.12340
- Wetselaar, P., Vermaire, J., Lobbezoo, F., and Schuller, A. (2020). The prevalence of awake bruxism and sleep bruxism in the Dutch adolescent population. *J. Oral Rehabil.* 1–7. doi: 10.1111/joor.13117
- Winocur, E., Messer, T., Eli, I., Emodi-Perlman, A., Kedem, R., Reiter, S., et al. (2019). Awake and sleep bruxism among Israeli adolescents. *Front. Neurol.* 10:4. doi: 10.3389/fneur.2019.00443
- Ximenes, R., Couto, G., and Sougey, E. (2010). Eating disorders in adolescents and their repercussion in oral health. *Int. J. Eat. Disord.* 43:1. doi: 10.1002/eat.20660
- Yamaguchi, T., Mikami, S., Maeda, M., Saito, T., Nakajima, T., Yachida, W., et al. (2020). Portable and wearable electromyographic devices for the assessment of sleep bruxism and awake bruxism: a literature review. *Cranio* 1:9. doi: 10.1080/08869634.2020.1815392

Conflict of Interest: The authors declare that the research was conducted in the absence of any commercial or financial relationships that could be construed as a potential conflict of interest.

Copyright © 2021 Monteiro, Soares, Soares, Pinto, Ximenes and Araújo Cairrão Rodrigues. This is an open-access article distributed under the terms of the Creative Commons Attribution License (CC BY). The use, distribution or reproduction in other forums is permitted, provided the original author(s) and the copyright owner(s) are credited and that the original publication in this journal is cited, in accordance with accepted academic practice. No use, distribution or reproduction is permitted which does not comply with these terms.



Functional Magnetic Resonance Connectivity in Patients With Temporomandibular Joint Disorders

Felice Festa¹, Chiara Rotelli¹, Antonio Scarano², Riccardo Navarra³, Massimo Caulo³ and Monica Macri^{1*}

¹ Department of Medical, Oral, and Biotechnological Sciences, University of G. d'Annunzio Chieti-Pescara, Chieti, Italy,

² Department of Medical, Oral, and Biotechnological Sciences and CeSi Met, University of G. d'Annunzio Chieti-Pescara, Chieti, Italy, ³ Department of Clinical Sciences and Bio-imaging, University of G. d'Annunzio Chieti-Pescara, Chieti, Italy

OPEN ACCESS

Edited by:

Teresa Lever,
University of Missouri, United States

Reviewed by:

Marco Carotenuto,
University of Campania Luigi
Vanvitelli, Italy
Antonio Orlacchio,
Santa Lucia Foundation (IRCCS), Italy

*Correspondence:

Monica Macri
m.macri@unich.it

Specialty section:

This article was submitted to
Headache and Neurogenic Pain,
a section of the journal
Frontiers in Neurology

Received: 13 November 2020

Accepted: 01 March 2021

Published: 12 April 2021

Citation:

Festa F, Rotelli C, Scarano A,
Navarra R, Caulo M and Macri M
(2021) Functional Magnetic
Resonance Connectivity in Patients
With Temporomandibular Joint
Disorders. *Front. Neurol.* 12:629211.
doi: 10.3389/fneur.2021.629211

Myofascial pain in the masticatory region, generally referred to as headache, is a common temporomandibular disorder (TMD) characterized by the hypersensitive regions of the contracted skeletal muscle fibers. A correct clinical treatment of myofascial pain has the potential to modify the functional activation of cerebral networks associated with pain and unconscious teeth clenching, specifically the pain network (PN) and default mode network (DMN). In this study, research is presented as a case series of five patients with myofascial pain: three were diagnosed with intra- and extra-articular disorders, and two were diagnosed with only extra-articular disorders. All five patients received gnathological therapy consisting of passive splints and biofeedback exercises for tongue–palatal vault coordination. Before and after treatment, patients underwent pain assessments (through measures of visual analog scales and muscular palpation tests), nuclear magnetic resonance of the temporomandibular joint, and functional nuclear magnetic resonance of the brain. In each patient, temporomandibular joint nuclear magnetic resonance results were similar before and after the gnathological treatment. However, the treatment resulted in a considerable reduction in pain for all patients, according to the visual analog scales and the palpation test. Furthermore, functional nuclear magnetic resonance of the brain clearly showed a homogeneous modification in cerebral networks associated with pain (i.e., PN and DMN), in all patients. In conclusion, gnathological therapy consisting of passive aligners and biofeedback exercises improved myofascial pain in all five patients. Most importantly, this study showed that all five patients had a homogeneous functional modification of pain and default mode networks. Using passive splints in combination with jaw exercises may be an effective treatment option for patients with TMD. This research could be a starting point for future investigations and for clinicians who want to approach similar situations.

Keywords: TMD, TMJ, teeth clenching, trigger points, fMRI, facial pain management, myofascial pain, headache

INTRODUCTION

Temporomandibular disorder (TMD) is a general term used for several clinical issues involving the masticatory muscles and the temporomandibular joint (TMJ), and is one of the most common pathologies of the maxillofacial region in patients between 20 and 40 years. About 33% of the population has at least one symptom of TMD, and between 3.6 and 7.0% require prompt treatment. Furthermore, the concomitant incidence of anxiety and stress in patients exacerbate the TMD symptoms. TMD etiology is related to chronic pain, teeth grinding, and cervical spine problems. Signs and symptoms of TMD include pain, malocclusion, TMJ dysfunction, joint noises, deviation in opening or closing, and restricted jaw movement. Therefore, as an analgic mechanism, the patient limits their own mandibular movements (1).

Unconscious teeth clenching constitutes a persistent microtrauma of muscles and articulation and is one of the main etiological factors of myofascial pain. It is characterized by regions of contracted motor fibers, defined as “trigger points,” which are the source of constant deep pain and can cause central excitatory effects, commonly referred by patients as headache. The diagnosis of myofascial pain is easily made through medical history and physical examination. The diagnostic suspicion is based on a history of chronic daily headaches and facial pain without evidence of neurological or intracranial abnormalities.

The goals of TMD treatment are to alleviate and/or reduce pain to improve mandibular function. Several procedures have been used as treatment methods, such as drug therapies, surgical and non-surgical procedures, dental appliances, physical therapy, and behavioral and psychosocial interventions. The guidelines of the Royal College of Dental Surgeons of Ontario recommend applying irreversible procedures (e.g., surgical interventions) only after the failure of conservative treatments, if the symptoms are severe and persistent (1).

Functional magnetic resonance imaging (fMRI), by taking the endogenous oxyhemoglobin as a contrast mean, allows inferring functional information on the metabolic activity of different cerebral regions (cerebral networks). Several fMRI studies have shown a permanent modification of pain and behavioral-associated cerebral networks following jaw-related therapeutic interventions (2, 3).

fMRI assesses neural functional activity by measuring the level of intra-tissutal oxyhemoglobin and deoxyhemoglobin, indices of regional blood supply and metabolic activity. The blood oxygenation level-dependent (BOLD) signal can be measured during the execution of a task (task-evoked fMRI) or during rest as a measure of brain functional connectivity (fcMRI). In our setting, we evaluated the fcMRI of two networks, the pain network (PN), and the default mode network (DMN). The PN is the cortical network of the physiology of pain, and the DMN is the network used in the processing of the unconscious processes.

Abbreviations: TMD, temporomandibular disorder; TMJ, temporomandibular joint; fMRI, functional magnetic resonance imaging; BOLD, blood oxygenation level dependent; fcMRI, functional connectivity magnetic resonance imaging; MRI, magnetic resonance imaging; PN, pain network; DMN, default mode network; LPAS, lower passive aligner splint; UPAS, upper passive aligner splint; T1, time one (is for time-points); T2, time two (is for time-points).

DMN is also involved in pain perception. These two cortical networks were analyzed in terms of functional connectivity. This study investigated the neural network activity at rest, in the absence of stimuli. Functional network connectivity is defined as the temporal correlation at rest in cortical networks. The resting functional connectivity represents 80% of the oxygen consumed by brain activities (4).

In this research study, a case series of five patients diagnosed with myofascial pain and treated with passive aligners and biofeedback exercises to teach the patient not to clench their teeth is presented. All the patients underwent quantitative pain assessments and fMRI before and after the gnathological treatment.

MATERIALS AND METHODS

The study was performed in the Oral Sciences Department of the University of Chieti G. D’Annunzio. Ethics approval (number 23) was obtained by the hospital’s Independent Ethics Committee of Chieti. The study protocol was drawn in accordance with the European Union Good Practice Rules and with the Helsinki Declaration. The sample consisted of a group of five patients who were treated at the Orthodontics and Orofacial Pain Department for TMD disorders. Each patient signed an informed consent form before the study.

The study lasted 1 year: 6 months were used to recruit the patients, 3 months for follow-up of the recruited subjects, and 3 months for data processing.

Inclusion Criteria

- 1) At least 18 years of age.
- 2) Diagnosis of chronic myofascial pain syndrome of the masticatory muscles.
- 3) Pain in the jaw muscles at least four times a week and for at least 12 weeks.
- 4) Average pain severity of 4 on a 10-point scale for at least 1 h per day.
- 5) Pain in the jaw, temples, face, pre-auricular area, or in the ear during rest or function.
- 6) Diagnosis of TMDs using MR imaging of the TMJ to evaluate the articular disk, or meniscus, in terms of its morphologic features and its location related to the condyle in both closed- and open-mouth positions.

Exclusion Criteria

- 1) Pregnancy.
- 2) Current opioid use.
- 3) Claustrophobia.
- 4) Moderate or severe psychiatric disorder or current use of psychiatric medications.
- 5) Presence of fibromyalgia or other chronic pain disorder.
- 6) Diagnosis of metabolic disease, coagulopathy, neurological disorder, vascular disease, or neoplasia.
- 7) Family history of arthritis or gout.

Also, participants taking non-steroidal anti-inflammatory drugs or paracetamol (acetaminophen) stopped those medications at least 1 day prior to their study appointment.

Measurements

VAS

The pain intensity ratio was estimated by using a visual analog scale (VAS), which consisted of a graphic representation of the patient's face. The patient had to highlight painful areas, specifying the intensity (quantifying it with a value from 0 = No Pain to 10 = Maximum Pain) and frequency of the disturbance, and how it affected everyday life (5).

Palpation

Palpation of the temporal, masseter, sternocleidomastoid, digastric, and pterygoid muscles and TMJ was made bilaterally with constant pressure. It consisted of searching for trigger points in the masticatory muscles. Accordingly, these trigger points, once stimulated, tend to produce and provoke headaches through central excitatory effects.

The sensations of pain were classified on a scale from 0 to 3:

- 0: the absence of pain;
- 1: mild pain or apparent discomfort with muscle contraction;
- 2: moderate pain or discomfort with muscle contraction;
- 3: severe pain; the patient "draws back" or "drops in tears" (6).

MRI of the TMJ

MRI evaluated the integrity of the temporomandibular joint, disc dislocations, and condyle positions to diagnose intra-articular or extra-articular disorders and to assess changes in the condyle-disc relationship associated with clinical treatment. Each patient underwent TMJ MRI procedures with open-mouth and closed-mouth postures, before and after the treatment.

fMRI of the Brain

fMRI of the brain analyzed the functional resting connectivity of the pain network (PN) and default mode network (DMN). The PN represents the cortical network of the physiology of pain, whereas the DMN is the system that processes the unconscious mechanisms involved in pain perception.

The DMN areas that were studied:

- Right occipital lobe (DMN-RIGHT-OCC);
- Left occipital lobe (DMN-LEFT-OCC);
- Right temporal lobe (DMN-RIGHT-TEMP);
- Left temporal lobe (DMN-LEFT-TEMP);
- Posterior cingulate cortex (DMN-PCC);
- Precuneus (DMN-PRECUNEUS);
- Medial pre-frontal cortex (DMN-MPFC).

The PN areas that were studied:

- Anterior cingulate cortex (PAIN-ACC);
- Right insula (PAIN-RIGHT-INSULA);
- Left insula (PAIN-LEFT-INSULA);
- Right somatosensory cortex 1 (PAIN-RIGHT-S1);
- Left somatosensory cortex (PAIN-LEFT-S1);
- Right somatosensory cortex 2 (PAIN-RIGHT-S2).

- Left somatosensory cortex 2 (PAIN-LEFT-S2).

The fMRI of the brain allowed assessment of the *average functional connectivity* concerning PN and DMN networks from the *different functional connectivity matrices*, obtained from the difference between the connectivity matrix at T2 (posttreatment) and the connectivity matrix at T1 (baseline), for each subject. In the matrices, each node corresponds to the numerical value of the interaction of two specific ROIs (regions of interest): the ROI of the row with the ROI of the column. In the difference matrix of each patient, the algebraic sum of all the nodes in each network was calculated. A positive value of average functional connectivity corresponds to a greater functional connectivity at rest in that network after treatment. A negative value corresponds to a lower functional connectivity at rest after treatment.

MR Data Acquisition and Processing

The MRI data were collected using a GE Medical Systems 3.0 Tesla system with an eight-channel brain-receiving coil.

The protocol used a fast 3D-SPGR sequence with the following parameters:

- TR = 6.9 ms,
- TE = 1.6 ms,
- TI = 450 ms,
- flip angle = 15°,
- matrix = 256 × 256,
- field of view = 25.6 × 25.6 cm,
- 156 axial slices with 1 mm thickness, yielding a voxel size of 1 × 1 × 1 mm.

The scanning parameters provided complete coverage of the brain, midbrain, pons, and cerebellum regions.

CNS abnormalities associated with M-TMD were assessed using several MRI tools.

The first step was the brain extraction and parcellation by using FreeSurfer (7). Then, the 1000 Functional Connectomes Project was followed to obtain residuals from the BOLD images



FIGURE 1 | Passive splints made of hard polycarbonate with thickness not exceeding 0.7 mm.

TABLE 1 | Clinical and demographical characteristics of the patients and the impact of the gnathological treatment.

| | Age | Gender | Kind of TMD | VAS at T1 | VAS at T2 | Painful areas at T1 | Painful areas at T2 | Duration of symptoms | Evolution of symptoms |
|-----------|-----|--------|-----------------|-----------|-----------|---|---------------------|----------------------|---|
| PT1 (CS) | 41 | Female | Intra-articular | 8 | 4 | Neck, under eyes, shoulders, TMJ, mandible | Neck, shoulders | About 2 years | The symptoms worsened during this period |
| PT 2 (SS) | 22 | Female | Intra-articular | 8 | 1 | TMJ, around eyes, trapezoids | TMJ | About 1 year | The symptoms worsened during this period |
| PT 3 (RF) | 26 | Male | Extra-articular | 5 | 1 | Mandible, neck, lumbar area, head | Neck | About 2–3 years | Symptomatology remained constant during this period |
| PT 4 (AN) | 41 | Female | Intra-articular | 7–8 | 4 | Sinusitis-like symptoms, TMJ, neck, shoulders, pelvis | TMJ | About 15 years | The symptoms worsened during this period |
| PT 5 (CT) | 55 | Female | Extra-articular | 6 | 0 | Masseter, mandible, maxilla | | About 5 years | The symptoms worsened during this period |

TABLE 2.1 | Masseter, temporal, and sternocleidomastoid palpation test after treatment compared with baseline.

| | Masseter palpation at T1 | Masseter palpation at T2 | Temporal palpation at T1 | Temporal palpation at T2 | Sternocleidomastoid palpation at T1 | Sternocleidomastoid palpation at T2 |
|-----------|--------------------------|--------------------------|--------------------------|--------------------------|-------------------------------------|-------------------------------------|
| PT 1 (CS) | 3 | 1 | 2 | 1 | 3 | 1 |
| PT 2 (SS) | 3 | 1 | 3 | 1 | 3 | 0 |
| PT 3 (RF) | 2 | 0 | 2 | 0 | 3 | 1 |
| PT 4 (AN) | 3 | 2 | 2 | 0 | 3 | 1 |
| PT 5 (CT) | 2 | 0 | 2 | 1 | 2 | 0 |

(8). Thereafter, the residuals were registered to MNI template (9), and the FSL toolbox (10) was used to extract the time-course from the selected ROI (11). The functional connectivity matrices and treatment timepoint (T2–T1) differences were calculated using a Python in-house script (12).

Treatment Protocol

Each patient received two passive splints made of hard polycarbonate that covers all the teeth without pre-established mandibular positions (13) (**Figure 1**). There was a lower passive aligner splint (LPAS) and an upper passive aligner splint (UPAS). The PAS was made of polycarbonate and was adjusted intraorally, as described by Sears, to avoid the impact of soft tissues. The LPAS was used during the daytime and the UPAS during the night.

While wearing the LPAS, patients performed a biofeedback exercise for 2 min, three times a day (prior to breakfast, lunch, and dinner), with a minimum of 3 h between each exercise, 7 days a week. Biofeedback exercises of the tongue serve to enhance patient awareness of the palatal arches' spatial positioning associated with jaw clenching so that patients can learn to stop or refrain from doing this maladaptive behavior.

During the exercise, patients assumed an upright position or reclined on a hard, flat surface, and were required to follow the accorded three steps:

TABLE 2.2 | Digastric and pterygoid palpation test after treatment compared with baseline.

| | Digastric palpation at T1 | Digastric palpation at T2 | Pterygoid palpation at T1 | Pterygoid palpation at T2 |
|-----------|---------------------------|---------------------------|---------------------------|---------------------------|
| PT 1 (CS) | 1 | 0 | 3 | 1 |
| PT 2 (SS) | 2 | 0 | 3 | 0 |
| PT 3 (RF) | 2 | 0 | 3 | 1 |
| PT 4 (AN) | 0 | 0 | 3 | 2 |
| PT 5 (CT) | 1 | 0 | 2 | 0 |

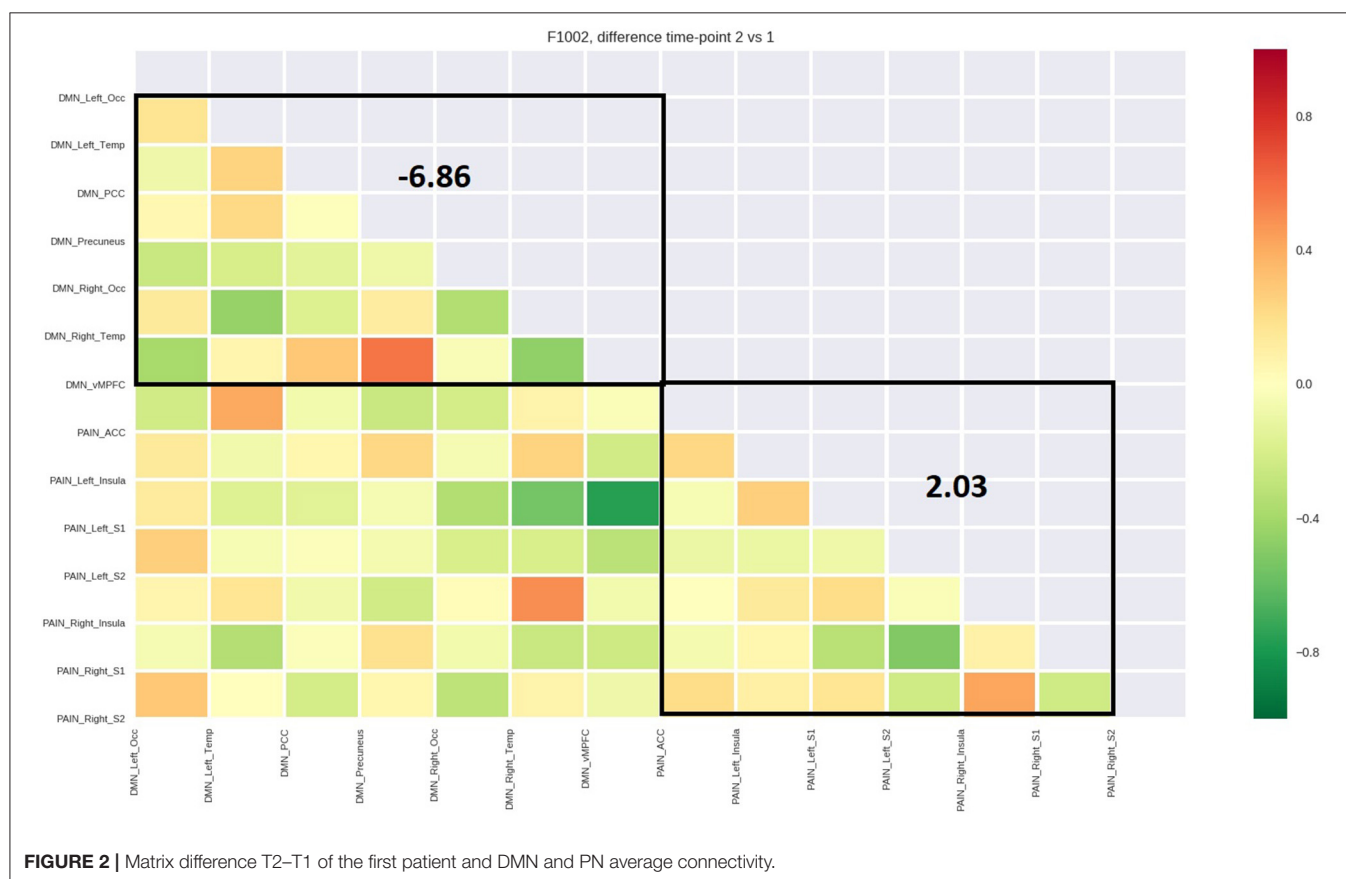
TABLE 3 | Average connectivity of the DMN and PN.

| | DMN average connectivity: T2–T1 | PN average connectivity: T2–T1 |
|-----------|---------------------------------|--------------------------------|
| PT 1 (CS) | 15.83 | 1.14 |
| PT 2 (SS) | 6.86 | 2.03 |
| PT 3 (RF) | 7.34 | 20.24 |
| PT 4 (AN) | 6.76 | 13.41 |
| PT 5 (CT) | 8.93 | 0.20 |

1. In the first phase, the patient clenched their teeth to fully contract the masseter bilaterally. A light touch with the forefinger on the contracted masseter was applied

TABLE 4 | Statistical results.

| | Masseter palpation | Temporal palpation | Sternocleidomastoid palpation | Digastric palpation | Pterygoid palpation at T1 | VAS | DMN | PN |
|-----------------|--------------------|--------------------|-------------------------------|---------------------|---------------------------|-------------|--------------|-------------|
| t.stat (paired) | 9 | 6.531972647 | 11 | 3.207134903 | 6.32455532 | 7.90569415 | −0.601279077 | 1.848546182 |
| df | 4 | 4 | 4 | 4 | 4 | 4 | 4 | 4 |
| t-crit | 2.776445105 | 2.776445105 | 2.776445105 | 2.776445105 | 2.776445105 | 2.776445105 | 2.776445105 | 2.776445105 |
| p | <0.001 | <0.1 | <0.001 | <0.05 | <0.01 | <0.01 | >0.05 | <0.05 |
| sig | sig | sig | sig | sig | sig | sig | no. sig | no. sig |

**FIGURE 2 |** Matrix difference T2-T1 of the first patient and DMN and PN average connectivity.

during maximum contraction. The patient visualized the muscle's volume in a mirror as a swollen tennis ball for 5 s.

- In the second phase, the patient clenched their teeth to partially contract (~50%) the masseter bilaterally; a light touch with the forefinger was applied during the contraction force, which is about halfway. The patient visualized the muscle's volume in a mirror as a semi-deflated tennis ball for 5 s.
- In the third phase, the patient was instructed to fully relax their jaw by opening it ~1 mm and applying a light touch with the forefinger on the utterly relaxed masseter. The patient visualized the muscle's volume in a mirror as a completely deflated tennis ball for 5 s.

- In the fourth phase, the patient touched the tip of the tongue on the top of the palatine vault, approximately between the palatine wrinkles and the flat palate for 5 s.

Then, the patient removed the LPAS for breakfast.

The same exercise was repeated before lunch and before dinner with the LPAS inserted. Biofeedback was timed to occur immediately prior to meals because masseter activation during meals typically causes pain levels to worsen.

The treatment lasted ~3 months. In the 6 months follow-up, a new assessment was made using the VAS and palpation test of temporal, masseter, sternocleidomastoid, digastric, pterygoid muscles, and TMJ MRI, and fMRI of the brain was repeated to evaluate the treatment effect.

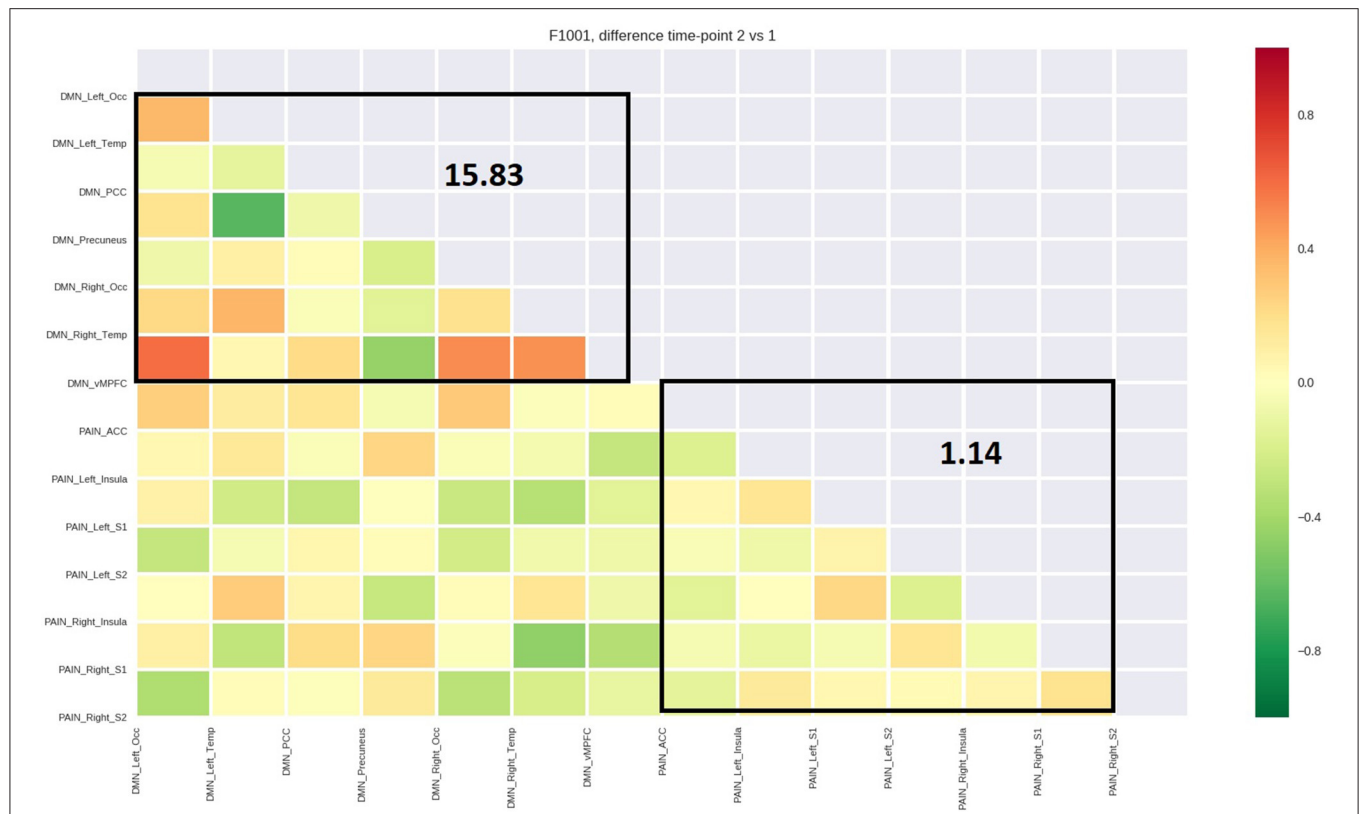


FIGURE 3 | Matrix difference T2-T1 of the second patient and DMN and PN average connectivity.

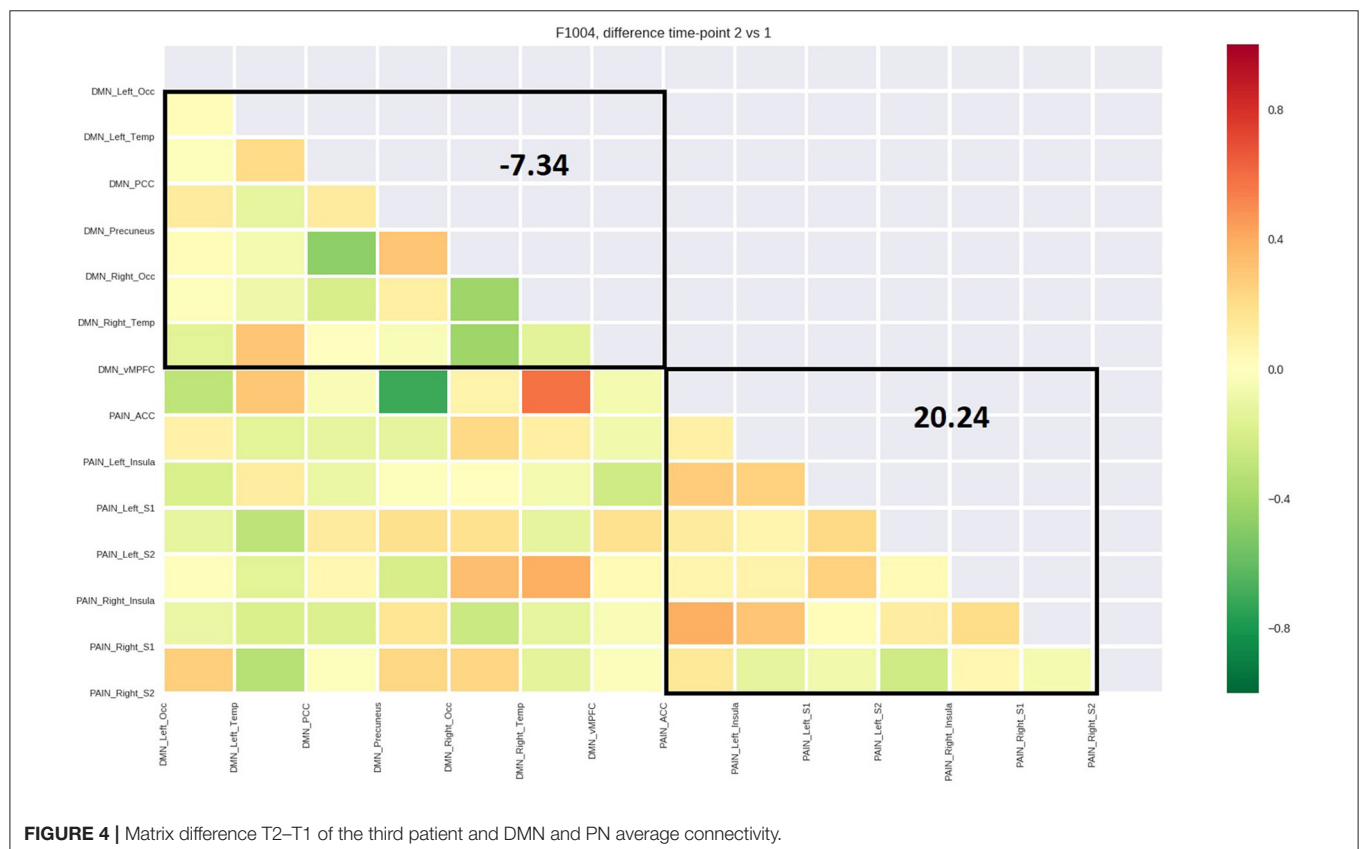
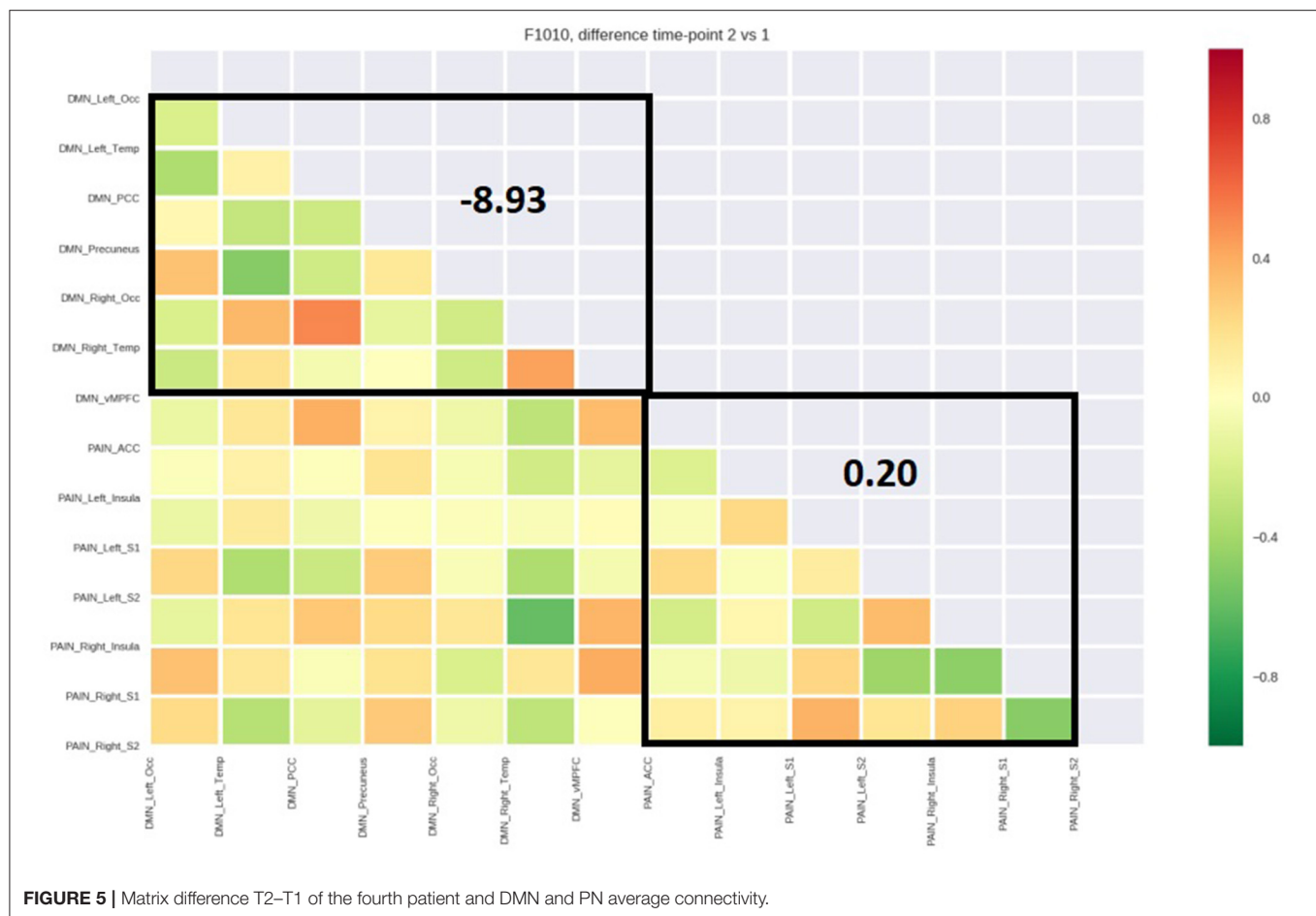


FIGURE 4 | Matrix difference T2-T1 of the third patient and DMN and PN average connectivity.



Throughout the entire study duration, every patient continued to record in their diaries the extent and intensity of their pain during headaches and treatment sessions/compliance.

Study Protocol

The study included five patients, three with intra-articular and extra-articular disorders and two with only extra-articular disorders, who were diagnosed by magnetic resonance imaging of the TMJ. All patients were treated using gnathological therapy consisting of passive aligners and biofeedback exercises. The study's patient selection was founded on the diagnosis of TMD based on a standardized and complete clinical examination that fulfills the Research Diagnostic Criteria (RDC TMDs) (14).

In the first phase of the study, all the patients underwent the palpation test and VAS to diagnose myofascial pain disorders. After recruitment in the study, the patients underwent TMJ MRI to assess the TMJ condition and fMRI of the brain to assess functional response.

During the second phase of the study, lasting 6 months, all five patients were treated by gnathological therapy consisting of passive aligners and biofeedback exercises for 2 min, three times a day (prior to breakfast, lunch, and dinner), with a minimum of 3 h between each exercise, 7 days a week.

Patients underwent follow-up appointments once a month, in which the VAS and the palpation test were repeated.

After 3 months, all patients underwent a second TMJ MRI and fMRI of the brain.

All the clinical examinations, splint fitting, and follow-up appointments were performed by the same examiner.

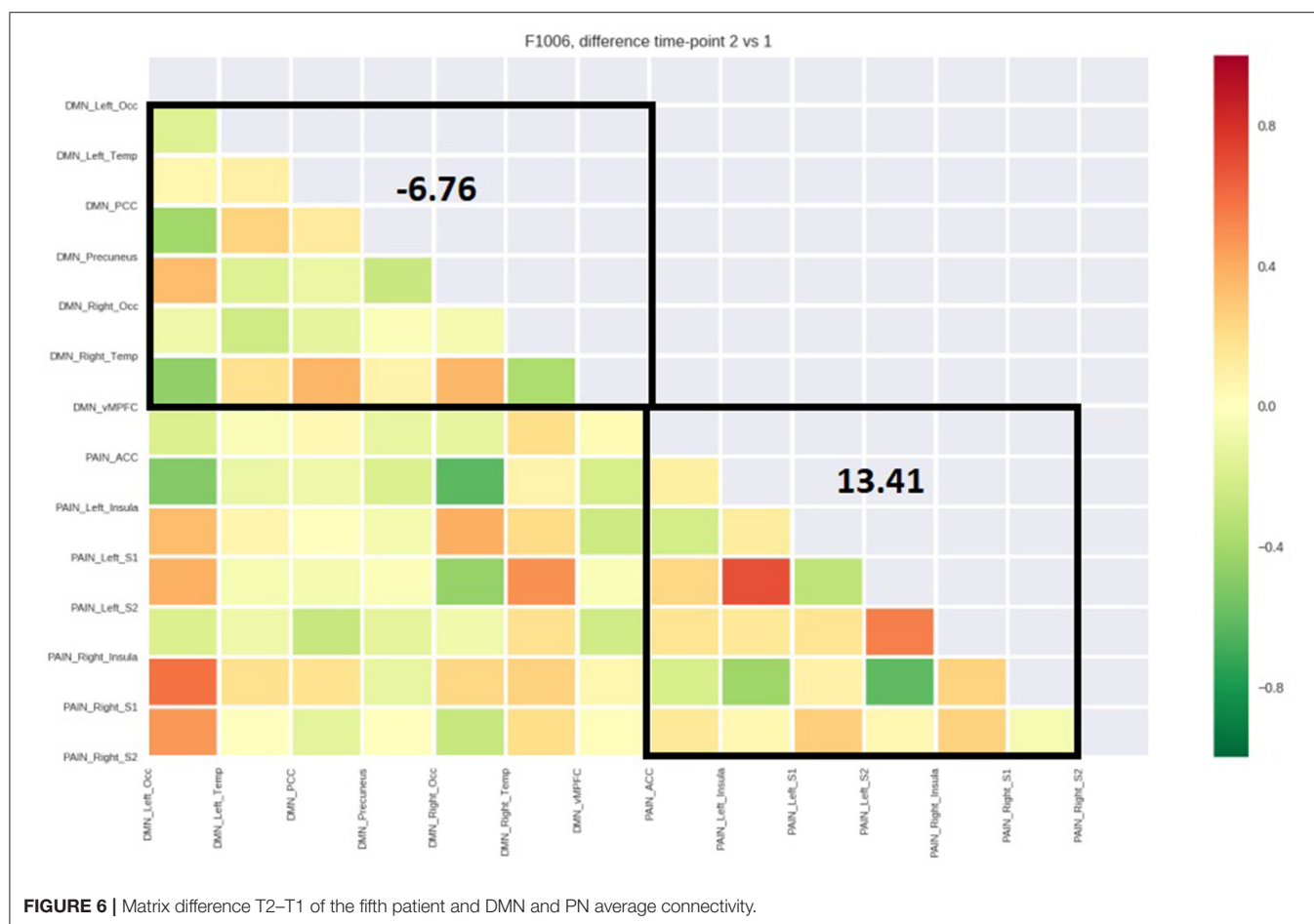
Statistical Analysis

Paired Student t-tests (pre- and posttreatment, T2-T1) were used to understand the impact of the treatment protocol on VAS scores and PN and DMN average connectivity. The significance threshold for all tests was set at 0.05.

RESULTS

All five patients exhibited forms of tension headaches but no sort of migraines, diagnosed according to the criteria of the International Classification of Headache Disorders 3rd edition (ICHD-III beta) (15).

In **Table 1**, the impact of gnathological treatment on pain is reported (VAS and painful areas). Most importantly, by comparing the baseline values (T1) with posttreatment values (T2), the pain symptomatology decreased both in terms of intensity and number of painful areas for each patient.



Furthermore, the patients sufficiently complied with the program to constitute a treatment effect.

The improvements were independent of age and gender but dependent on symptom intensity and chronicity at T1. Patient 1, patient 2, and patient 4 had intra-articular and extra-articular disorder; patient 3 and patient 5 had only extra articular disorder. Patient 1 exhibited, after treatment only, residual symptomatology (VAS 4) on the neck and shoulder region, but had a long-standing spinal disc herniation detected by MRI of the spine. In patients 2 and 3, the symptomatology almost disappeared in each painful area (VAS 1). In patient 4, there was only residual symptomatology on the TMJ (VAS 4). In patient 5, the symptomatology completely disappeared in each painful area (VAS 0). There was a significant effect for VAS [$t(4) = 7.9$, $p = 0.0013$] (Table 4).

Each of the patients was fully compliant with the “prescribed” home treatment program.

Tables 2.1, 2.2 summarize the impact of the gnathological treatment concerning trigger points (palpation). Compared with baseline (T1), posttreatment (T2) pain extent and intensity during palpation of the masseter, temporal, sternocleidomastoid, digastric, and pterygoid decreased in all patients.

According to the VAS data for patients 2, 3, and 5, the pain evoked by masseter, temporal, and sternocleidomastoid muscle

palpation almost disappeared (PALPATION TEST 0–1). Patient 1 exhibited the presence of spinal disc herniation; it caused no persistency in terms of pain upon palpation of the masseter, temporal, and sternocleidomastoid muscles (PALPATION TEST 1). Patient 4 exhibited persistent pain at the masseter muscle upon palpation (PALPATION TEST 2) due to the residual pain experienced in the TMJ.

Pain on palpation in the digastric muscle region disappeared in all patients (PALPATION TEST 0). Pain on palpation in the pterygoid muscle region was relevant only in patient 4 (PALPATION TEST 2) with residual TMJ pain. There was a significant effect for palpation of the masseter [$t(4) = 9$, $p < 0.001$], temporalis [$t(4) = 6.5$, $p = 0.0028$], sternocleidomastoid [$t(4) = 11$, $p < 0.001$], digastric [$t(4) = 3.2$, $p = 0.0326$], and pterygoid [$t(4) = 6.3$, $p = 0.0032$] (Table 4).

Table 3 reports the average functional connectivity, which in the PN had a positive value for all five patients while in the DMN had a negative value for four of five patients. The variations of fMRI within each network were uniform among the five patients. Only patient 1’s DMN behaved differently, possibly due to the detected spinal disc herniation. Figures 2–6 show the matrix difference T2-T1 for all ROIs of PN and DMN for each patient; the algebraic sum of the functional connectivity values of each ROI in this matrix was represented as the average

connectivity of each network. There was no significant effect for the DMN average connectivity [$t(4) = -0.6, p = 0.5801$] and for the PN average connectivity [$t(4) = 1.8, p = 0.1382$] (Table 4).

DISCUSSION

In this case series of five patients with myofascial pain in the masticatory region due to unconscious clenching reflexes, we investigated the impact of gnathological therapies on pain and associated arrangement of pain and default mode neural networks. Teeth clenching is an unconscious behavior that represents the etiology of all TMDs, which have complex and multifactorial etiology outcomes. A scientific review reveals the TMDs' major causal factors including occlusion, trauma, emotional stress, deep nociceptive stimuli, and parafunctional activities (bruxism and clenching). If there are substantial loads (e.g., unconscious clenching), slight flexion in the mandible causes tension in the disc ligaments and intracapsular disorders. The unconscious clenching and bruxism cause microtrauma against the teeth, muscles, and joints.

The most frequent TMD associated with unconscious clenching is myofascial pain syndrome, the fourth stage of muscular pathology in TMD (16). Tooth clenching diagnosis is made when the patient reports problems such as tension headaches, neck pain, back pain, tenderness of the masticatory muscles, and fatigue of the masticatory muscles when chewing hard food, difficulty opening the mouth completely, muscle tenderness on waking, and muscular tension in the head-neck region. Myofascial pain is different compared with migraine pain because headaches respond to anti-inflammatories and are independent of noises and lights. Also, myofascial pain can have bilateral involvement, and it is not excessively debilitating.

Biofeedback has been used for over 50 years in muscle rehabilitation to facilitate standard movement patterns after injury. This technique provides biological information, which would not otherwise be known by the patient in real-time (17). A systematic review of the literature concludes that biofeedback can be useful in helping to manage masticatory muscle activity. Most of the studies showed a significant correlation between the use of biofeedback and the reduction of masticatory muscle activity (18).

The study outlined a significant decrease in the symptomatology (Tables 1, 2.1, 2.2, 4), both in terms of the referred pain (VAS) and in terms of trigger points detected (assessed by muscle palpation). The TMJ MRI did not highlight any modification in the disc-condyle relation in patients diagnosed with either combined intra- and extra-articular disorder or only extra-articular disorder. However, the treatment was equally effective for both subgroups of patients in terms of reduction of pain, unconscious teeth clenching, and muscular tension. fMRI of the brain revealed that in all the patients, the average fcMRI of the pain network tended to increase, whereas after the treatment, the average fcMRI of the DMN

tended to decrease in four out of five patients (Tables 3, 4, and Figures 2–6). It is proposed to increase the sample size to permit exploration of the data using robust statistical methods.

Our finding of lower functional connectivity of the DMN, associated with a greater functional connectivity of the PN after the treatment, is consistent with the results of a recent study showing that DMN and the PN are functionally connected but show an inverse temporal modulation (19). It is important to emphasize that a decrease or increase in functional connectivity at rest within a neural network does not correspond to an increase or decrease in the physiological activity of that network; it may instead indicate an increase or decrease of the task-evoked activity.

This study research outlines limits concerning low sample sizes; therefore, the aim for the future is to increase the sample size; furthermore, another limit is the no use of EMG, on which inclusion in future studies will be relevant. Based on our qualitative and quantitative clinical and fcMRI evaluation of five patients, our data suggest that a gnathological treatment protocol based on a splint and associated biofeedback exercises is effective and repeatable in future studies. Moreover, we showed the neurophysiological impact of the gnathological therapy, assessed as qualitative clinical/quantitative fMRI PN and DMN measurements of improvement. After the treatment was completed, the functional connectivity of the brain networks showed homogeneous changes in all the five patients.

DATA AVAILABILITY STATEMENT

The original contributions presented in the study are included in the article/supplementary material, further inquiries can be directed to the corresponding author/s.

ETHICS STATEMENT

The studies involving human participants were reviewed and approved by University of Chieti Ethics Committee. The patients/participants provided their written informed consent to participate in this study.

AUTHOR CONTRIBUTIONS

MM and CR submitted the study protocol to the ethics committee and wrote the manuscript. FE, MM, and CR selected the sample. MC and RN performed the fMRI and analyzed the radiological data. FE, MM, AS, and CR analyzed the clinical data. All authors read and approved the final manuscript.

FUNDING

This study was supported by the University Gabriele D'Annunzio of Chieti, Italy.

REFERENCES

1. Brett K, Wells C, Sinclair A, Tenenbaum H, Freeman B, Spry C. *Interventions for Temporomandibular Joint Disorder: An Overview of Systematic Reviews*. Ottawa, ON: Canadian Agency for Drugs and Technologies in Health. (2018).
2. Andreescu C, Aizenstein H. Predicting treatment response with functional magnetic resonance imaging. *Biol Psychiatry*. (2016) 79:262–3. doi: 10.1016/j.biopsych.2015.11.017
3. Oda M, Yoshino K, Tanaka T, Shiiba S, Makihara E, Miyamoto I, et al. Identification and adjustment of experimental occlusal interference using functional magnetic resonance imaging. *BMC Oral Health*. (2014) 14:124. doi: 10.1186/1472-6831-14-124
4. Raichle ME, Mintun MA. Brain work and brain imaging. *Annu Rev Neurosci*. (2006) 29:449–76. doi: 10.1146/annurev.neuro.29.051605.112819
5. Nishiyama A, Otomo N, Tsukagoshi K, Tobe S, Kino K. The true-positive rate of a screening questionnaire for temporomandibular disorders. *Open Dent J*. (2014) 8:236–40. doi: 10.2174/1874210601408010236
6. Nixdorf DR, John MT, Wall MM, Friction JR, Schiffman EL. Psychometric properties of the modified Symptom Severity Index (SSI). *J Oral Rehabil*. (2010) 37:11–20. doi: 10.1111/j.1365-2842.2009.02017-x
7. Fischl B, Salat DH, Busa E, Albert M, Dieterich M, Haselgrove C, et al. Whole brain segmentation: automated labeling of neuroanatomical structures in the human brain. *Neuron*. (2002) 33:341–55. doi: 10.1016/s0896-6273(02)00569-x
8. Mennes M, Biswal BB, Castellanos FX, Milham MP. Making data sharing work: the FCP/INDI experience. *Neuroimage*. (2013) 82:683–91. doi: 10.1016/j.neuroimage.2012.10.064
9. Brett M, Johnsrude IS, Owen AM. The problem of functional localization in the human brain. *Nat Rev Neurosci*. (2002) 3:243–9. doi: 10.1038/nrn756
10. Jenkinson M, Beckmann CF, Behrens TE, Woolrich MW, Smith SM. FSL. *Neuroimage*. (2012) 62:782–90. doi: 10.1016/j.neuroimage.2011.09.015
11. Nebel MB, Folger S, Tommerdahl M, Hollins M, McGlone F, Essick G. Temporomandibular disorder modifies cortical response to tactile stimulation. *J Pain*. (2010) 11:1083–94. doi: 10.1016/j.jpain.2010.02.021
12. van Rossum G. *Python tutorial, Technical Report CS-R9526, Centrum voor Wiskunde en Informatica (CWI)*. Amsterdam (1995).
13. Lundh H, Westesson PL, Eriksson L, Brooks SL. Temporomandibular joint disk displacement without reduction. Treatment with flat occlusal splint versus no treatment. *Oral Surg Oral Med Oral Pathol*. (1992) 73:655–8. doi: 10.1016/0030-4220(92)90003-9
14. Dworkin SF, LeResche L. Research diagnostic criteria for temporomandibular disorders: review, criteria, examinations and specifications, critique. *J Craniomandib Disord*. (1992) 6:301–55
15. Headache Classification Committee of the International Headache Society (IHS). The International Classification of Headache Disorders, 3rd edition (beta version). *Cephalalgia*. (2013) 33:629–808. doi: 10.1177/0333102413485658
16. Okeson JP. *Management of Temporomandibular Disorders and Occlusion-E-Book*. Elsevier Health Sciences (2019).
17. Giggins OM, Persson UM, Caulfield B. Biofeedback in rehabilitation. *J Neuroeng Rehabil*. (2013) 10:60. doi: 10.1186/1743-0003-10-60
18. Florjanski W, Malysa A, Orzeszek S, Smardz J, Olchoway A, Paradowska-Stolarz A, et al. Evaluation of biofeedback usefulness in masticatory muscle activity management—a systematic review. *J Clin Med*. (2019) 8:766. doi: 10.3390/jcm8060766
19. Mantini D, Caulo M, Ferretti A, Romani GL, Tartaro A. Noxious somatosensory stimulation affects the default mode of brain function: evidence from functional MR imaging. *Radiology*. (2009) 253:797–804. doi: 10.1148/radiol.2533090602

Conflict of Interest: The authors declare that the research was conducted in the absence of any commercial or financial relationships that could be construed as a potential conflict of interest.

Copyright © 2021 Festa, Rotelli, Scarano, Navarra, Caulo and Macrì. This is an open-access article distributed under the terms of the Creative Commons Attribution License (CC BY). The use, distribution or reproduction in other forums is permitted, provided the original author(s) and the copyright owner(s) are credited and that the original publication in this journal is cited, in accordance with accepted academic practice. No use, distribution or reproduction is permitted which does not comply with these terms.



Risk Score for Predicting Dysphagia in Patients After Neurosurgery: A Prospective Observational Trial

Li Zeng^{1,2†}, Yu Song^{3†}, Yan Dong^{3,4}, Qian Wu², Lu Zhang², Lei Yu⁵, Liang Gao^{3*} and Yan Shi^{2*}

OPEN ACCESS

Edited by:

Teresa Lever,
University of Missouri, United States

Reviewed by:

Jun Lyu,
First Affiliated Hospital of Jinan
University, China
Kendra Garand,
University of South Alabama,
United States

*Correspondence:

Liang Gao
lianggaoh@126.com
Yan Shi
594907113@qq.com

[†]These authors have contributed
equally to this work

Specialty section:

This article was submitted to
Neurorehabilitation,
a section of the journal
Frontiers in Neurology

Received: 14 September 2020

Accepted: 12 April 2021

Published: 11 May 2021

Citation:

Zeng L, Song Y, Dong Y, Wu Q,
Zhang L, Yu L, Gao L and Shi Y (2021)
Risk Score for Predicting Dysphagia in
Patients After Neurosurgery: A
Prospective Observational Trial.
Front. Neurol. 12:605687.
doi: 10.3389/fneur.2021.605687

¹ Neurosurgical Intensive Care Unit, Shanghai Tenth People's Hospital, School of Medicine, Tongji University, Shanghai, China, ² Department of Nursing, Shanghai Tenth People's Hospital, School of Medicine, Tongji University, Shanghai, China, ³ Department of Neurosurgery, Shanghai Tenth People's Hospital, School of Medicine, Tongji University, Shanghai, China, ⁴ Clinical Medicine Scientific and Technical Innovation Park, Shanghai Tenth People's Hospital, Shanghai, China, ⁵ Department of Anesthesiology, Dongfang Hospital Affiliated to Tongji University, Shanghai, China

Background: Acquired dysphagia is common in patients with tracheal intubation and neurological disease, leading to increased mortality. This study aimed to ascertain the risk factors and develop a prediction model for acquired dysphagia in patients after neurosurgery.

Methods: A multicenter prospective observational study was performed on 293 patients who underwent neurosurgery. A standardized swallowing assessment was performed bedside within 24 h of extubation, and logistic regression analysis with a best subset selection strategy was performed to select predictors. A nomogram model was then established and verified.

Results: The incidence of acquired dysphagia in our study was 23.2% (68/293). Among the variables, days of neurointensive care unit (NICU) stay [odds ratio (OR), 1.433; 95% confidence interval (CI), 1.141–1.882; $P = 0.005$], tracheal intubation duration (OR, 1.021; CI, 1.001–1.062; $P = 0.175$), use of a nasogastric feeding tube (OR, 9.131; CI, 1.364–62.289; $P = 0.021$), and Acute Physiology and Chronic Health Evaluation (APACHE)-II C score (OR, 1.709; CI, 1.421–2.148; $P < 0.001$) were selected as risk predictors for dysphagia and included in the nomogram model. The area under the receiver operating characteristic curve was 0.980 (CI, 0.965–0.996) in the training set and 0.971 (0.937–1) in the validation set, with Brier scores of 0.045 and 0.056, respectively.

Conclusion: Patients who stay longer in the NICU, have a longer duration of tracheal intubation, require a nasogastric feeding tube, and have higher APACHE-II C scores after neurosurgery are likely to develop dysphagia. This developed model is a convenient and efficient tool for predicting the development of dysphagia.

Keywords: prediction, neurointensive care unit, nomogram, neurosurgery, dysphagia

INTRODUCTION

Post-extubation dysphagia is a common complication in mixed intensive care units (ICUs), causing aspiration pneumonia, malnutrition, and dehydration, and increasing the length of hospital stay and mortality (1–5). The prevalence of post-extubation dysphagia ranges from 3 to 62%, which leads to increased healthcare-related costs (6, 7). The condition is even worse in patients with neurological diseases. In addition to neuromuscular disease, acquired neurological disease is also a high risk for dysphagia. According to reports, 28–65% of patients with acute stroke experience difficulty in swallowing (8), same as brain tumors (9). Even in patients with a non-traumatic subarachnoid hemorrhage, the incidence of dysphagia is 16.33% (10). In fact, previous clinical studies have identified neurological diseases as a significant risk factor for the development of dysphagia (11, 12).

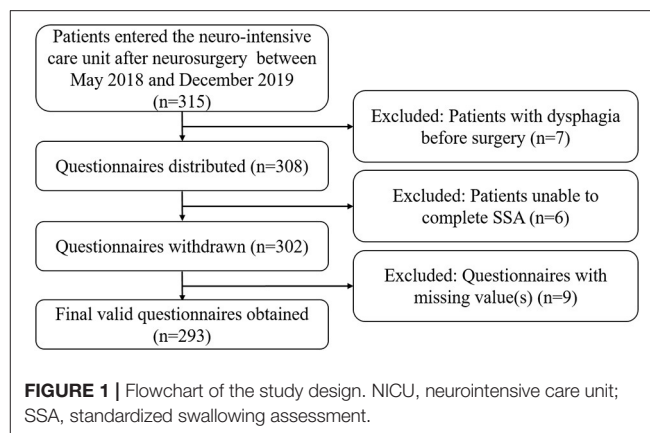
Therefore, early and timely assessment of whether the patient has dysphagia can significantly reduce the occurrence of pneumonia and further reduce mortality (13). Although dysphagia has a high incidence rate in patients with neurological diseases and is an important predictor of poor prognosis, few relevant predictive studies have been conducted over the past few decades. A nomogram is a graphical statistical device that makes it possible to qualify individual prediction probability based on patients' characteristics. Currently, nomograms have been widely used in the medical field, helping to guide clinical decision-making.

In the present study, we performed a multicenter prospective observational study to identify risk factors for acquired dysphagia in patients after neurosurgery. Additionally, we developed and validated a simple and reliable model for predicting dysphagia in patients after neurosurgery.

METHODS

Study Design and Participants

A multicenter prospective observational study was performed in the neurointensive care unit (NICU) of three tertiary care teaching hospitals. The prerequisites for extubation in patients after undergoing neurosurgery included having spontaneous breathing, s' hemodynamics, and presumably protecting the airway (positive cough reflex, less tracheobronchial secretions, and normal consciousness level). Eligible patients were consecutively included in our study between May 2018 and December 2019. Inclusion criteria were as follows: (1) age >18 years; (2) admitted to the NICU after neurosurgery. Exclusion criteria were as follows: (1) patients with primary laryngopharyngeal diseases, laryngopharyngeal mass, or any other situation leading to dysphagia before enrollment; (2) patients who could not be extubated or with tracheotomy; (3) patients who rejected to participated in standardized swallowing assessment (SSA) for any reason; and (4) patients who failed to finish the first SSA (e.g., Some patients were not allowed to drink or eat due to their condition) or failed to complete all the follow up (e.g., Some patients were thought that the SSA was cumbersome and they were unwilling to participate again after



the first test). This study was approved by the Ethics Committees of Shanghai Tenth People's Hospital, affiliated with Tongji University (Shanghai, China).

Data Collection

Questionnaire Design and Distribution

Data collection was performed using a self-designed questionnaire (**Supplementary Materials**), which mainly comprised three sections: patients' demography, past medical history, and clinical features. The nurses in our research team have strict criteria: (a) work for at least 5 years; (b) with a master's degree; (c) training and testing of SSA by one nurse manager. Questionnaires were distributed to qualified nurses in the NICU. All eligible patients underwent systematic bedside screening and filled out the questionnaires, which were then reviewed by a neurologist. **Figure 1** shows a flowchart of the experimental design.

Parameters Acquisition

After collecting all the questionnaires, data were extracted. Demographic features, past medical history, and clinical features were collected. Dysphagia was evaluated by SSA within 24 h of extubation, as previously reported (14) (**Supplementary Materials**). Briefly, the SSA scale comprised three parts, including clinical examination, a stage 1 water swallow test (WST), and a stage 2 WST. Patients with an abnormal consciousness level, breath pattern, lip closure, palate movement, laryngeal function, gag reflex, voluntary cough, or loss of control of the head and trunk were valued as dysphagia, and SSA was terminated. In stage 1 WST, the patient was given 5 ml of water three times consecutively. If the patient finished stage 1 WST two out of three times without dribbling water, laryngeal movements on the attempted swallow, "repeated movements" felt, coughing, stridor, or any abnormal laryngeal function after swallowing, they then proceeded to the stage 2 WST. In stage 2 WST, the patient was instructed to drink 60 ml of water. If the patient did not display coughing, stridor, aspiration, or any abnormal laryngeal function after swallowing, the patient was considered not having dysphagia. In the present study, patients had normal consciousness levels and normal breathing

TABLE 1 | Baseline characteristics comparison between patients with dysphagia or not.

| Variables | Overall | Dysphagia screening negative | Dysphagia screening positive | p-value |
|---|----------------------|------------------------------|------------------------------|---------|
| | N = 293 | N = 225 | N = 68 | |
| Age, years | 53.0 [44.0, 63.0] | 51.0 [42.0, 62.0] | 60.5 [53.0, 66.0] | <0.001 |
| Male, n (%) | 151 (51.5) | 118 (52.4) | 33 (48.5) | 0.669 |
| Height, cm | 165.0 [160.0, 170.0] | 165.0 [160.0, 171.0] | 162.5 [158.0, 170.0] | 0.074 |
| Weight, kg | 68.0 [60.0, 75.0] | 68.0 [60.0, 75.0] | 68.0 [60.0, 75.0] | 0.813 |
| BMI | 24.5 [22.0, 26.6] | 24.5 [21.9, 26.6] | 24.4 [22.0, 27.0] | 0.577 |
| Diagnostic Category (%) | | | | 0.001 |
| Neurovascular disease | 132 (45.1) | 105 (46.7) | 27 (39.7) | |
| Central nervous system tumor | 146 (49.8) | 115 (51.1) | 31 (45.6) | |
| Traumatic brain injury | 12 (4.1) | 4 (1.8) | 8 (11.8) | |
| Others | 3 (1.0) | 1 (0.4) | 2 (2.9) | |
| Past medical history | | | | |
| Diabetes mellitus, n (%) | 31 (10.6) | 23 (10.2) | 8 (11.8) | 0.891 |
| Hypertension, n (%) | 88 (30.0) | 52 (23.1) | 36 (52.9) | <0.001 |
| Heart failure, n (%) | 48 (16.4) | 34 (15.1) | 14 (20.6) | 0.378 |
| Arrhythmia, n (%) | 30 (10.2) | 24 (10.7) | 6 (8.8) | 0.833 |
| Chronic renal failure, n (%) | 19 (6.5) | 15 (6.7) | 4 (5.9) | 1 |
| Previous stroke, n (%) | 174 (59.4) | 141 (62.7) | 33 (48.5) | 0.052 |
| Clinical features | | | | |
| NICU stay, days | 2.0 [1.0, 3.0] | 2.0 [1.0, 2.0] | 6.0 [3.0, 10.0] | <0.001 |
| Mechanical ventilation, hours | 4.0 [3.0, 5.0] | 3.0 [2.5, 5.0] | 5.0 [3.2, 6.0] | <0.001 |
| Protective restraint, n (%) | 9 (3.1) | 1 (0.4) | 8 (11.8) | <0.001 |
| Nasogastric feeding tube, n (%) | 47 (16.0) | 9 (4.0) | 38 (55.9) | <0.001 |
| Tracheal intubation type (%) | | | | 0.171 |
| 6.5 | 84 (28.7) | 62 (27.6) | 22 (32.4) | |
| 7.0 | 113 (38.6) | 94 (41.8) | 19 (27.9) | |
| 7.5 | 38 (13.0) | 29 (12.9) | 9 (13.2) | |
| 8.0 | 58 (19.8) | 40 (17.8) | 18 (26.5) | |
| Tracheal intubation duration, hours | 4.0 [3.0, 7.0] | 3.0 [2.5, 5.0] | 29.5 [7.8, 95.8] | <0.001 |
| Sedation, hours | 3.5 [3.0, 5.0] | 3.0 [2.3, 5.0] | 5.0 [3.8, 7.0] | <0.001 |
| Relaxants, hours | 4.0 [3.0, 6.0] | 3.0 [2.0, 5.0] | 6.0 [4.0, 8.0] | <0.001 |
| Muscle strength grade III and IV, n (%) | 44 (15.0) | 7 (3.1) | 37 (54.4) | <0.001 |
| RASS score | 0.0 [0.0, 0.0] | 0.0 [0.0, 0.0] | 0.0 [-1.0, 0.0] | <0.001 |
| APACHE-II score | 20.0 [19.0, 21.0] | 20.0 [19.0, 21.0] | 23.0 [21.0, 29.2] | <0.001 |
| APACHE-IIA | 2.0 [0.0, 3.0] | 2.0 [0.0, 3.0] | 3.0 [2.0, 5.0] | <0.001 |
| APACHE-IIB | 2.0 [2.0, 2.0] | 2.0 [2.0, 2.0] | 2.0 [2.0, 5.0] | <0.001 |
| APACHE-IIC | 0.0 [0.0, 1.0] | 0.0 [0.0, 0.0] | 6.0 [2.0, 8.0] | <0.001 |
| APACHE-IID | 15.0 [13.0, 17.0] | 15.0 [14.0, 17.0] | 13.5 [9.0, 17.0] | 0.001 |

NICU, neurointensive care unit; BMI, body mass index; RASS, richmond agitation-sedation scale; APACHE, acute physiology and chronic health evaluation. Continuous variables present with median and inter-quartile range; Categorical variables present with frequencies.

patterns at the first evaluation (the prerequisites for extubation). Patients were screened every 8 h until dysphagia was diagnosed or they were discharged from the hospital. The baseline severity of the disease was assessed using Acute Physiology and Chronic Health Evaluation (APACHE)-II scores at admission, and each item was listed separately. The Richmond Agitation-Sedation Scale (RASS) was used to assess the sedation state of patients when assessing SSA. Days in the NICU, hours on mechanical ventilation, hours with tracheal intubation, and hours with sedation relaxant usage were recorded. Questionnaires with missing values were discarded.

Statistical Analyses

All data were randomly divided into a training set and a validation set at a ratio of 7:3. The continuous variables were checked for normal distribution using a Shapiro-Wilk test. Data are expressed as medians and interquartile ranges for continuous variables and *n* (%) for categorical variables. Univariate analysis between the two groups in terms of categorical variables and continuous variables was conducted using a chi-squared test or Mann-Whitney *U*-test, respectively. The variance of inflation factors (VIF) was calculated to determine multicollinearity. Factors with VIF >10 were considered as serious collinearity,

were excluded from further analyses. A logistic regression analysis was then performed to identify the risk factors for predicting dysphagia. Only variables with $P < 0.05$ in the univariate analysis were included in the next analysis. The best subset selection strategy was employed to construct a logistic regression model, and the Bayesian Information Criteria (BIC) was used to select the best model from all possible subsets. Then, a nomogram was developed based on the results of the logistic regression, which was validated using the validation set. The model was also internally validated using all the data by performing 10-fold cross-validation. The area under the receiver operating characteristic curve (AUC) was calculated to measure the discrimination performance. The calibration curve was used to test the reliability with bootstraps of 1,000 resamples, which described the degree of fit between the actual and nomogram-predicted probability. The Brier score was used to measure the accuracy of probabilistic predictions, which ranged from 0 to 1. The lower the Brier score, the better the predictions of dysphagia were calibrated. Decision curve analysis was used to evaluate the model's profitability. All statistical analyses were performed using R statistical software (version 4.0.0; R Foundation for Statistical Computing, Vienna, Austria).

RESULTS

Demographic and Clinical Characteristics

After screening according to our exclusion criteria, we collected 293 valid questionnaires in this study. In total, 206 patients (48 patients with dysphagia, 23.3%) were included in the training set, while 87 patients (20 patients with dysphagia, 23.0%) were included in the validation set.

The demographics and clinical characteristics of patients with and without dysphagia are shown in **Table 1**. Considering that the APACHE-II score includes patients' age, we listed the four items separately. Among all the variables, age, diagnostic category, hypertension, NICU stay, mechanical ventilation, protective restraint, nasogastric feeding tube, tracheal intubation, sedation, relaxants, muscle strength grade, RASS score, and APACHE II score were significantly different between the two groups.

Risk Factors of DG

All variables were included in the multivariate logistic regression analysis. The best subset was chosen based on the smallest BIC. Days of NICU stay, tracheal intubation duration, the existence of a nasogastric feeding tube, and APACHE-II C score were selected as risk predictors for dysphagia. No variables were meeting the criteria for multicollinearity ($VIF > 10$). The results of multivariable analyses for dysphagia in the training set are shown in **Table 2**.

Establishment and Verification of a Nomogram for DG

According to the results of multivariate logistic regression analysis, four variables, including days of NICU stay, tracheal intubation duration, the existence of a nasogastric feeding tube, and APACHE-II C score were ultimately chosen as predictors to

TABLE 2 | Model for prediction of dysphagia.

| Variables | Coefficient | OR (CI) | p-value |
|--|-------------|----------------------|---------|
| NICU stay, days | 0.360 | 1.433 (1.141–1.882) | 0.005 |
| Tracheal intubation duration, hours | 0.021 | 1.021 (1.001–1.062) | 0.175 |
| Nasogastric feeding tube, <i>n</i> (%) | 2.212 | 9.131 (1.364–62.289) | 0.021 |
| APACHE-II C | 0.536 | 1.709 (1.421–2.148) | <0.001 |

NICU, neurointensive care unit; APACHE, acute physiology and chronic health evaluation; OR, odds ratio.

develop a nomogram model (**Figure 2**). In this model, tracheal intubation duration showed the greatest effect on dysphagia, followed by APACHE-II C score and then days of NICU stay. The existence of a nasogastric feeding tube was the smallest risk factor for dysphagia. The risk of dysphagia for patients after neurosurgery was found to be positively correlated with the sum of the four predictors' points in the nomogram model.

AUC was used to assess the discriminative performance of the nomogram model in the training set [0.980, 95% confidence interval (CI): 0.965–0.996, **Figure 3A**] and externally validated in the validation set (0.971, 95% CI: 0.937–1, **Figure 3B**). Using 10-fold cross-validation in the total data, we further evaluated the predictive accuracy of the model. The max AUC was 0.994 (95% CI: 0.977–1).

Considering that discrimination alone was insufficient to assess the prediction capability of the model, we verified the performance of calibration using a calibration plot and the Brier score. A calibration plot with 1,000 bootstraps suggested good prediction performance in both the training set (**Figure 4A**) and validation set (**Figure 4B**), with mean absolute errors of 0.048 and 0.057, respectively. The Brier score can quantify the calibration performance. The Brier scores in the two sets were 0.045 and 0.056, respectively. A decision curve analysis was developed to evaluate the prognostic value of the prediction model. **Figure 5** shows the decision curve analysis of the two sets. This indicates that patients can benefit from our nomogram model.

DISCUSSION

In the present study, we performed a multicenter prospective observational study in the NICU. Days of NICU stay, tracheal intubation duration, the existence of a nasogastric feeding tube, and APACHE-II C score were identified as risk factors for dysphagia in patients after neurosurgery. Using these four variables, we developed a nomogram model to calculate the risk of dysphagia in these patients.

Tracheal intubation and neurological diseases are the two main risk factors for acquired dysphagia (6, 8). Tracheal intubation often causes mechanical injury, such as mucosal abrasion, laryngeal edema, or a decrease in laryngeal sensation. Prolonged intubation can lead to tongue, pharynx, and larynx muscles disuse atrophy (15, 16). Patients with a neurological disease or critical illness often have damage to the cortex and subcortical structures, which decreases the coordination of the swallowing reflex (8, 17, 18). Acute phase admission is also

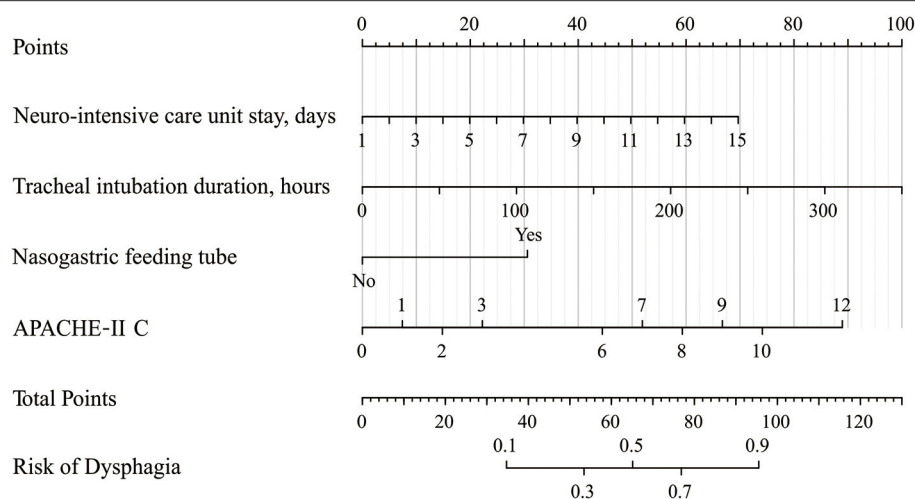


FIGURE 2 | Nomogram for predicting the risk of dysphagia. Points are assigned for NICU stay, tracheal intubation duration, nasogastric feeding tube, and APACHE-II C score. The “Points” displays prognostic points. The “total points” are calculated as the sum of the individual score of each variable, which is then used to find the appropriate position on the “Risk of Dysphagia” axis to determine the patient’s individual risk of dysphagia. For example, if one patient now stayed in NICU for 7 days (about 30 points), the tracheal intubation lasted for 35 h (about 10 points), without the nasogastric feeding tube (0 points), the APACHE-II C score was 2 at admission (about 15 points), the total points for this patient were 55 points. The risk of dysphagia for this patient was about 33%. NICU, neurointensive care unit; APACHE-II, Acute Physiology and Chronic Health Evaluation.

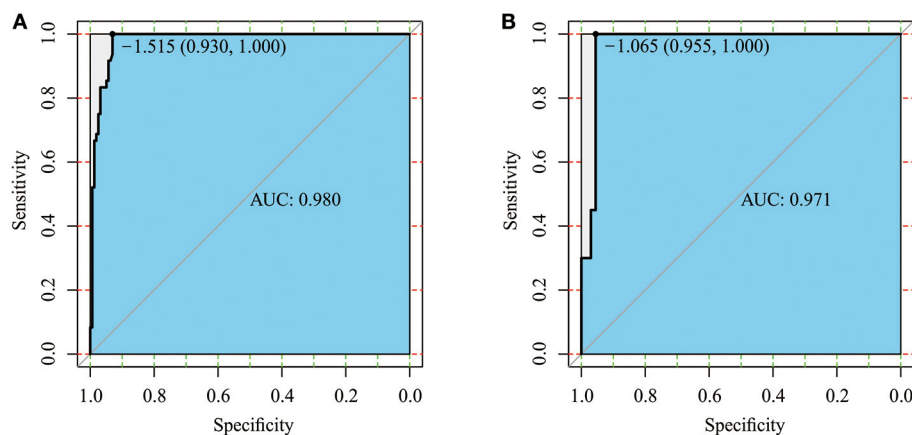


FIGURE 3 | Receiver operating characteristic (ROC) curve of the training set (A) and validation set (B).

a crucial factor for dysphagia (11, 12), concentrating on the main diseases with less attention to nutrition and activity (19). However, there are few studies on patients after neurosurgery, which contains all three factors. In our study cohort, the incidence of dysphagia was 23.2% (68/293), which is relatively low compared with other studies (6, 7). The reason why there were fewer positive patients may be due to fewer emergency patients (47/293 patients with APACHE-II B score of 5) and a higher baseline APACHE-II C score (the median of the patient’s APACHE II C score is 0) in our institutes.

The SSA was first proposed by Smithard et al. in 1996 (14), and also validated by other patients with neurological diseases

(20). In the meantime, it’s easy to perform at the bedside than videofluoroscopy or fiberoptic endoscopy and safer than Kubota Water Swallowing Test. It is a good tool for screening dysphagia at the bedside (20, 21). However, it still requires a well-trained nurse and is time-intensive. Our prediction model only included four factors; however, it demonstrated excellent discrimination and calibration. Using our nomogram tool, clinicians or nurses can easily perform bedside screening in the NICU to screen patients who are at high risk for acquired dysphagia. Patients with a high score should further undergo a systematic examination and measures should be taken to prevent the complication of acquired dysphagia. Aspiration pneumonia is

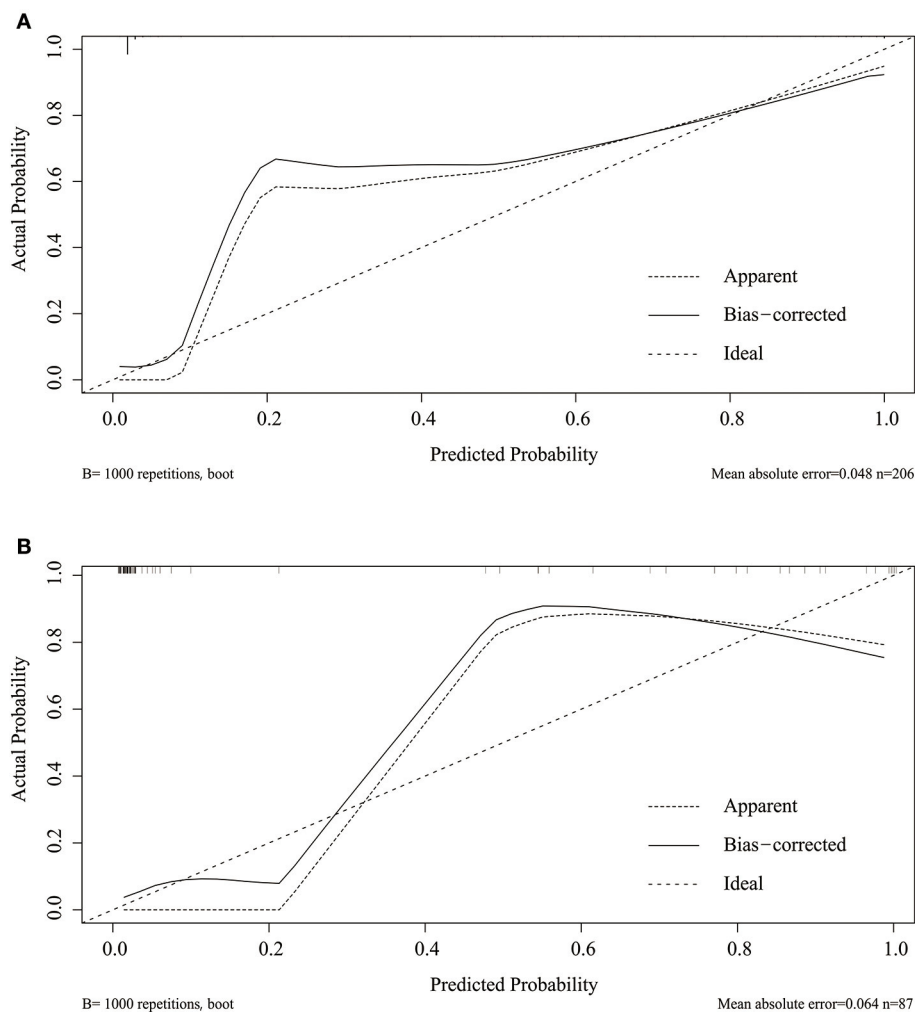


FIGURE 4 | Calibration plot of the nomogram in the training (A) and validation set (B). Predictions generated from the model are plotted against actual patient outcomes. The 45-degree line represents the perfect model calibration. The dotted line (apparent) indicates calibration when the model is applied to each set, and the solid line (bias-corrected) indicates calibration when the model is applied to the bootstrap set.

a serious consequence of dysphagia, affecting 37–55% of patients with stroke (22). Screening and timely assessment of dysphagia could significantly decrease the risk of pneumonia. In fact, the incidence of pneumonia increases by 1% every day the evaluation is delayed (13). For people with acute stroke, dysphagia increases the risk of malnutrition by up to 12 times. Therefore, patients with a high risk of dysphagia should be assessed thoroughly for the risk of malnutrition, and enteral nutrition or parenteral nutrition should be considered (23).

These four variables are all routine and easy to obtain. A longer ICU stay has been previously proposed as a potential risk factor for post-extubation dysphagia (10), which was further confirmed in our study. The existence of a nasogastric feeding tube can cause mechanical damage to the pharyngeal mucosa, laryngopharyngeal edema, sensory deficits, and swallowing-related muscle atrophy, which decreases

swallowing function (24). Several studies have also reported the risk of feeding tube exposure (11, 25). In addition, the long-term existence of the feeding tube can increase the risk of aspiration (26, 27). Although swallowing can be achieved without conscious input, cortical control plays a critical role in the swallowing process (18). The baseline APACHE-II C score was calculated using the Glasgow Coma Scale (GCS), which is used to evaluate the state of a patient's consciousness. Patients with decreased GCS are likely to have dysphagia and aspiration (10, 28).

Importantly, our primary goal was to build a prediction model. Therefore, we attempted to achieve the best discriminatory ability and calibration possible. So although tracheal intubation duration is not statistically significant ($p > 0.05$), it also stays in our final model. Tracheal intubation duration was previously reported as a risk factor for dysphagia

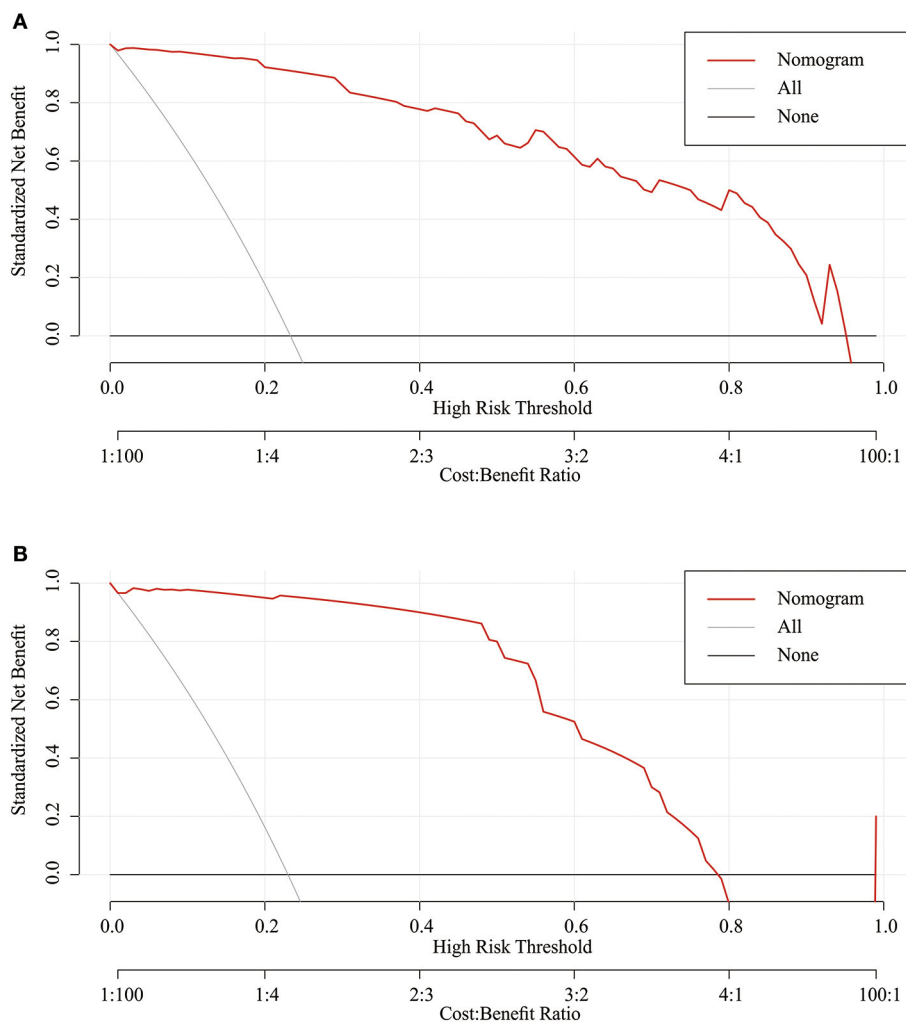


FIGURE 5 | Decision curve analysis of the nomogram in the training set (A) and validation set (B). The red line displays the net benefit of our model. The gray line assumes that all patients develop dysphagia. The black line assumes that no patients develop dysphagia.

(29). The tracheal tube can directly lead to trauma in normal anatomic structures and compress the laryngeal nerve, which leads to swallowing dysfunction (30).

Nevertheless, there are some limitations to our study. First, our study cohort was relatively small for prediction model development. Second, we did not include other previously reported risk factors in our model, such as advanced age (31–33), emergency admission (11, 12), and previous stroke (4, 18, 29, 34). Therefore, the discrimination and calibration of our model need to be further validated by an external cohort from other centers. Third, we didn't set the exclusion criteria for patients with pneumonia, obstructive sleep apnea, gastroesophageal reflux et al. However, these diseases share dysphagia as common sequelae, which may increase the positive rate of dysphagia. In the meantime, our questionnaire lacks information during the perioperative period. This could also bias our results. Lastly, there were relatively few patients positive for dysphagia in our study cohort, which may come from SSA. This screening tool cannot

definitively rule out silent aspiration and laryngeal dysfunction. Few numbers of positive events may cause the model's prediction accuracy to be too high and thus not stable enough. In the future, more patients from different levels of medical institutions are needed to verify our model.

CONCLUSIONS

Longer NICU stay, longer tracheal intubation duration, the existence of a nasogastric feeding tube, and higher APACHE-II C score were the main risk factors for acquired dysphagia in patients undergoing neurosurgery. Our model has good performance in terms of discrimination and calibration in predicting acquired dysphagia. It allows clinicians to screen patients with a high risk of dysphagia, thus providing them the ability to take timely preventative measures to reduce the complications associated with dysphagia.

DATA AVAILABILITY STATEMENT

The raw data supporting the conclusions of this article will be made available by the authors, without undue reservation.

ETHICS STATEMENT

The studies involving human participants were reviewed and approved by Ethics Committee of Shanghai Tenth People's Hospital. The patients/participants provided their written informed consent to participate in this study.

AUTHOR CONTRIBUTIONS

LG and YSh: conception, design, and revising the article critically for intellectual content. LY and LZ: acquisition of data. LZ and YSo: analysis, interpretation of data, and drafting the article. LZ, YSo, YD, QW, LZ, LY, LG, and YSh: final approval of the version to be published and Agreement to be accountable for all aspects of the work in ensuring that questions related to the accuracy or integrity of any part of the work are appropriately investigated

and resolved. All authors contributed to the article and approved the submitted version.

FUNDING

This study was supported by the projects of Young Scientists Fund, National Natural Science Foundation of China (No. 72004162), the projects of National Natural Science Foundation of China (No. 81671227), the Fundamental Research Funds for the Central Universities (No. 22120170003), and Shanghai Sheng Kang Hospital Development Center (No. SHDC12017X17).

ACKNOWLEDGMENTS

All of the authors appreciate the agreement of the participants and their families.

SUPPLEMENTARY MATERIAL

The Supplementary Material for this article can be found online at: <https://www.frontiersin.org/articles/10.3389/fneur.2021.605687/full#supplementary-material>

REFERENCES

- Guyomard V, Fulcher RA, Redmayne O, Metcalf AK, Potter JF, Myint PK. Effect of dysphasia and dysphagia on inpatient mortality and hospital length of stay: a database study. *J Am Geriatr Soc.* (2009) 57:2101–6. doi: 10.1111/j.1532-5415.2009.02526.x
- Macht M, Wimbish T, Clark BJ, Benson AB, Burnham EL, Williams A, et al. Postextubation dysphagia is persistent and associated with poor outcomes in survivors of critical illness. *Crit Care.* (2011) 15:R231. doi: 10.1186/cc10472
- Reber E, Gomes F, Dahn IA, Vasiloglou MF, Stanga Z. Management of dehydration in patients suffering swallowing difficulties. *J Clin Med.* (2019) 8:1923. doi: 10.3390/jcm8111923
- Zuercher P, Moret C, Schefold JC. Dysphagia in the intensive care unit in Switzerland (DICE) - results of a national survey on the current standard of care. *Swiss Med Wkly.* (2019) 149:w20111. doi: 10.4414/smw.2019.20111
- Marin S, Serra-Prat M, Ortega O, Clave P. Healthcare-related cost of oropharyngeal dysphagia and its complications pneumonia and malnutrition after stroke: a systematic review. *BMJ Open.* (2020) 10:e031629. doi: 10.1136/bmjopen-2019-031629
- Skoretz SA, Flowers HL, Martino R. The incidence of dysphagia following endotracheal intubation: a systematic review. *Chest.* (2010) 137:665–73. doi: 10.1378/chest.09-1823
- McIntyre M, Doeltgen S, Dalton N, Koppa M, Chimunda T. Post-extubation dysphagia incidence in critically ill patients: a systematic review and meta-analysis. *Aust Crit Care.* (2021) 34:67–75. doi: 10.1016/j.aucc.2020.05.008
- Cohen DL, Roffe C, Beavan J, Blackett B, Fairfield CA, Hamdy S, et al. Post-stroke dysphagia: a review and design considerations for future trials. *Int J Stroke.* (2016) 11:399–411. doi: 10.1177/1747493016639057
- Park DH, Chun MH, Lee SJ, Song YB. Comparison of swallowing functions between brain tumor and stroke patients. *Ann Rehabil Med.* (2013) 37:633–41. doi: 10.5535/arm.2013.37.5.633
- Dunn K, Rumbach A, Finch E. Dysphagia following non-traumatic subarachnoid haemorrhage: A prospective pilot study. *Int J Lang Commun Disord.* (2020) 55:702–11. doi: 10.1111/1460-6984.12554
- Schefold JC, Berger D, Zurcher P, Lensch M, Perren A, Jakob SM, et al. Dysphagia in mechanically ventilated ICU patients (DYnAMICS): a prospective observational trial. *Crit Care Med.* (2017) 45:2061–9. doi: 10.1097/CCM.0000000000002765
- Zuercher P, Schenk NV, Moret C, Berger D, Abegglen R, Schefold JC. Risk factors for dysphagia in ICU patients after invasive mechanical ventilation. *Chest.* (2020) 158:1983–91. doi: 10.1016/j.chest.2020.05.576
- Bray BD, Smith CJ, Cloud GC, Enderby P, James M, Paley L, et al. The association between delays in screening for and assessing dysphagia after acute stroke, and the risk of stroke-associated pneumonia. *J Neurol Neurosurg Psychiatry.* (2017) 88:25–30. doi: 10.1136/jnnp-2016-313356
- Smithard DG, O'Neill PA, Parks C, Morris J. Complications and outcome after acute stroke. Does dysphagia matter? *Stroke.* (1996) 27:1200–4. doi: 10.1161/01.STR.27.7.1200
- DeVita MA, Spierer-Rundback L. Swallowing disorders in patients with prolonged orotracheal intubation or tracheostomy tubes. *Crit Care Med.* (1990) 18:1328–30. doi: 10.1097/00003246-199012000-00004
- Feng X, Todd T, Lintzenich CR, Ding J, Carr JJ, Ge Y, et al. Aging-related geniohyoid muscle atrophy is related to aspiration status in healthy older adults. *J Gerontol A Biol Sci Med Sci.* (2013) 68:853–60. doi: 10.1093/gerona/gls225
- Goldsmith T. Evaluation and treatment of swallowing disorders following endotracheal intubation and tracheostomy. *Int Anesthesiol Clin.* (2000) 38:219–42. doi: 10.1097/00004311-200007000-00013
- Macht M, Wimbish T, Bodine C, Moss M. ICU-acquired swallowing disorders. *Crit Care Med.* (2013) 41:2396–405. doi: 10.1097/CCM.0b013e31829caf33
- Nagano A, Nishioka S, Wakabayashi H. Rehabilitation nutrition for iatrogenic sarcopenia and sarcopenic dysphagia. *J Nutr Health Aging.* (2019) 23:256–65. doi: 10.1007/s12603-018-1150-1
- Brodsky MB, Suiter DM, Gonzalez-Fernandez M, Michtalik HJ, Frymark TB, Venediktov R, et al. Screening accuracy for aspiration using bedside water swallow tests: a systematic review and meta-analysis. *Chest.* (2016) 150:148–63. doi: 10.1016/j.chest.2016.03.059
- Bours GJ, Speyer R, Lemmens J, Limburg M, de Wit R. Bedside screening tests vs. videofluoroscopy or fiberoptic endoscopic evaluation of swallowing to detect dysphagia in patients with neurological disorders: systematic review. *J Adv Nurs.* (2009) 65:477–93. doi: 10.1111/j.1365-2648.2008.04915.x
- Martino R, Foley N, Bhogal S, Diamant N, Speechley M, Teasell R. Dysphagia after stroke: incidence, diagnosis, and pulmonary complications. *Stroke.* (2005) 36:2756–63. doi: 10.1161/01.STR.0000190056.76543.eb
- Sabbouh T, Torbey MT. Malnutrition in stroke patients: risk factors, assessment, and management. *Neurocritical Care.* (2017) 29:374–84. doi: 10.1007/s12028-017-0436-1

24. Wang ZY, Chen JM, Ni GX. Effect of an indwelling nasogastric tube on swallowing function in elderly post-stroke dysphagia patients with long-term nasal feeding. *BMC Neurol.* (2019) 19:83. doi: 10.1186/s12883-019-1314-6
25. Zhou XD, Dong WH, Zhao CH, Feng XF, Wen WW, Tu WY, et al. Risk scores for predicting dysphagia in critically ill patients after cardiac surgery. *BMC Anesthesiol.* (2019) 19:7. doi: 10.1186/s12871-019-0680-3
26. Dzievas R, Ritter M, Schilling M, Konrad C, Oelenberg S, Nabavi DG, et al. Pneumonia in acute stroke patients fed by nasogastric tube. *J Neurol Neurosurg Psychiatry.* (2004) 75:852–6. doi: 10.1136/jnnp.2003.019075
27. Schwarz M, Coccetti A, Murdoch A, Cardell E. The impact of aspiration pneumonia and nasogastric feeding on clinical outcomes in stroke patients: a retrospective cohort study. *J Clin Nurs.* (2018) 27:e235–41. doi: 10.1111/jocn.13922
28. Metheny NA. Risk factors for aspiration. *JPEN J Parenter Enteral Nutr.* (2002) 26(Suppl. 6), S26–31; discussion S32–23. doi: 10.1177/014860710202600605
29. Barker J, Martino R, Reichardt B, Hickey EJ, Ralph-Edwards A. Incidence and impact of dysphagia in patients receiving prolonged endotracheal intubation after cardiac surgery. *Can J Surg.* (2009) 52:119–24.
30. Sue RD, Susanto I. Long-term complications of artificial airways. *Clin Chest Med.* (2003) 24:457–71. doi: 10.1016/S0272-5231(03)00048-0
31. Dehing-Oberije C, De Ruyscher D, Petit S, Van Meerbeeck J, Vandecasteele K, De Neve W, et al. Development, external validation and clinical usefulness of a practical prediction model for radiation-induced dysphagia in lung cancer patients. *Radiother Oncol.* (2010) 97:455–61. doi: 10.1016/j.radonc.2010.09.028
32. Kwok AM, Davis JW, Cagle KM, Sue LP, Kaups KL. Post-extubation dysphagia in trauma patients: it's hard to swallow. *Am J Surg.* (2013) 206:924–7; discussion 927–928. doi: 10.1016/j.amjsurg.2013.08.010
33. Teguh DN, Levendag PC, Ghidry W, van Montfort K, Kwa SL. Risk model and nomogram for dysphagia and xerostomia prediction in head and neck cancer patients treated by radiotherapy and/or chemotherapy. *Dysphagia.* (2013) 28:388–94. doi: 10.1007/s00455-012-9445-6
34. Rousou JA, Tighe DA, Garb JL, Krasner H, Engelman RM, Flack JE, 3rd, et al. Risk of dysphagia after transesophageal echocardiography during cardiac operations. *Ann Thorac Surg.* (2000) 69:486–9; discussion 489–490. doi: 10.1016/S0003-4975(99)01086-3

Conflict of Interest: The authors declare that the research was conducted in the absence of any commercial or financial relationships that could be construed as a potential conflict of interest.

Copyright © 2021 Zeng, Song, Dong, Wu, Zhang, Yu, Gao and Shi. This is an open-access article distributed under the terms of the Creative Commons Attribution License (CC BY). The use, distribution or reproduction in other forums is permitted, provided the original author(s) and the copyright owner(s) are credited and that the original publication in this journal is cited, in accordance with accepted academic practice. No use, distribution or reproduction is permitted which does not comply with these terms.



The Role of White Matter in the Neural Control of Swallowing: A Systematic Review

Ann Alvar^{1†}, Rachel Hahn Arkenberg^{1†}, Bethany McGowan², Hu Cheng³ and Georgia A. Malandraki^{1,4*}

¹ I-EaT Swallowing Research Laboratory, Speech Language and Hearing Sciences, Purdue University, West Lafayette, IN, United States, ² Libraries and School of Information Studies, Purdue University, West Lafayette, IN, United States, ³ Psychological and Brain Sciences, Imaging Research Facility, Indiana University, Bloomington, IN, United States, ⁴ Weldon School of Biomedical Engineering, Purdue University, West Lafayette, IN, United States

OPEN ACCESS

Edited by:

Teresa Lever,
University of Missouri, United States

Reviewed by:

Pere Clavé,
Hospital de Mataró, Spain
Emilia Michou,
University of Patras, Greece
Antonio Schindler,
University of Milan, Italy

*Correspondence:

Georgia A. Malandraki
malandraki@purdue.edu

[†]These authors have contributed
equally to this work

Specialty section:

This article was submitted to
Health,
a section of the journal
Frontiers in Human Neuroscience

Received: 17 November 2020

Accepted: 26 March 2021

Published: 28 June 2021

Citation:

Alvar A, Hahn Arkenberg R, McGowan B, Cheng H and Malandraki GA (2021) The Role of White Matter in the Neural Control of Swallowing: A Systematic Review. *Front. Hum. Neurosci.* 15:628424. doi: 10.3389/fnhum.2021.628424

Background: Swallowing disorders (dysphagia) can negatively impact quality of life and health. For clinicians and researchers seeking to improve outcomes for patients with dysphagia, understanding the neural control of swallowing is critical. The role of gray matter in swallowing control has been extensively documented, but knowledge is limited regarding the contributions of white matter. Our aim was to identify, evaluate, and summarize the populations, methods, and results of published articles describing the role of white matter in neural control of swallowing.

Methods: We completed a systematic review with a multi-engine search following PRISMA-P 2015 standards. Two authors screened articles and completed blind full-text review and quality assessments using an adapted U.S. National Institute of Health's Quality Assessment. The senior author resolved any disagreements. Qualitative synthesis of evidence was completed.

Results: The search yielded 105 non-duplicate articles, twenty-two of which met inclusion criteria. Twenty were rated as Good (5/22; 23%) or Fair (15/22; 68%) quality. Stroke was the most represented diagnosis ($n = 20$; 91%). All studies were observational, and half were retrospective cohort design. The majority of studies (13/22; 59%) quantified white matter damage with lesion-based methods, whereas 7/22 (32%) described intrinsic characteristics of white matter using methods like fractional anisotropy. Fifteen studies (68%) used instrumental methods for swallowing evaluations. White matter areas commonly implicated in swallowing control included the pyramidal tract, internal capsule, corona radiata, superior longitudinal fasciculus, external capsule, and corpus callosum. Additional noteworthy themes included: severity of white matter damage is related to dysphagia severity; bilateral white matter lesions appear particularly disruptive to swallowing; and white matter adaptation can facilitate dysphagia recovery. Gaps in the literature included limited sample size and populations, lack of in-depth evaluations, and issues with research design.

Conclusion: Although traditionally understudied, there is sufficient evidence to conclude that white matter is critical in the neural control of swallowing. The reviewed studies

indicated that white matter damage can be directly tied to swallowing deficits, and several white matter structures were implicated across studies. Further well-designed interdisciplinary research is needed to understand white matter's role in neural control of normal swallowing and in dysphagia recovery and rehabilitation.

Keywords: white matter, swallowing, dysphagia, deglutition, neurophysiology, diffusion weighted imaging, diffusion tensor MRI

INTRODUCTION

Swallowing is an essential biological function governed by both peripheral and central sensorimotor pathways. Damage in these pathways can cause swallowing disorders, also known as dysphagia. Dysphagia is a frequent consequence of many neurological and anatomical conditions or diseases (e.g., stroke, cerebral palsy, Parkinson's disease, dementia, head and neck cancer, trauma, etc.), and is very common. In the US alone, four percent of adults are reported to experience dysphagia per year (Bhattacharyya, 2014). For those individuals, the impact can be profound. Dysphagia affects quality of life (Leow et al., 2010), nutrition (Namasivayam and Steele, 2015), hydration (Reber et al., 2019), respiratory function, and overall health (Langmore et al., 1998). Because of its impact and relatively high prevalence, developing effective interventions for the management of dysphagia has been a longstanding goal of clinicians and researchers. Central in these efforts has been the attempt to increase our knowledge and understanding of the underlying physiological and neurophysiological mechanisms that govern swallowing, and which can be targeted in treatment.

This knowledge base has been growing over the past 100 years, with much of the literature focused on the role of cortical and brainstem gray matter areas involved in the neural control of swallowing. In the early 1900's, neuroscience research relied heavily on animal models and focused on the reflexive nature of swallowing (Miller and Sherrington, 1915). This animal work revealed the essential role that brainstem nuclei, specifically a group of medullary nuclei, play in triggering the pharyngeal response (Doty, 1951, 1968; Car and Roman, 1969; Jean et al., 1975; Amri et al., 1984; Kessler and Jean, 1985). In the mid 1900's, some attention was directed to the cortex (Car, 1970; Sumi,

1972), as researchers found that swallowing or mastication were evoked when specific cortical regions (i.e., the lateral pericentral and superior sylvian cortex) were stimulated with electrical pulses in patients under seizure evaluation (Penfield and Welch, 1949; Penfield, 1955). This same response was also seen in animals during intracranial microelectrode stimulation (Sumi, 1972; Martin et al., 1999). Despite these findings, the theory that swallowing is primarily *reflexive* (i.e., brainstem mediated) predominated from the early 1900's even into the 1980's (Bosma, 1957; de Lama Lazzara et al., 1986). During this time period, this notion started being challenged with the advent of new imaging techniques that allowed researchers to non-invasively look at changes in brain structures in living humans.

Clinical studies reporting swallowing deficits in patients with cortical and subcortical lesions provided the first clear support that the role of the cerebrum was essential in swallowing (Meadows, 1973; Gordon et al., 1987; Martin and Sessle, 1993; Robbins et al., 1993; Daniels et al., 1996). This was then further delineated through novel neuroimaging techniques that enabled the study of metabolic correlates of brain activation during swallowing *in vivo* (e.g., Hamdy et al., 1999; Martin et al., 2001, 2004; Suzuki et al., 2003; Toogood et al., 2005; Malandraki et al., 2009, 2011). This growing body of literature was critical in shifting our appreciation of swallowing from a simple brainstem mediated reflex to a highly complex sensorimotor function relying on all levels of the central nervous system (CNS) (Malandraki et al., 2011).

Undoubtedly, identifying the gray matter regions that play a role in swallowing was a significant contribution. However, the specifics on how these regions communicate and connect with each other to achieve this complex control remains largely unexplored, i.e., there is little insight on the role of white matter tracts. One early computed tomography (CT) study reported that damage to subcortical white matter (the internal capsule and within the brainstem) caused dysphagia, likely due to disruption in the sensorimotor pathways of the corticobulbar tract (Logemann et al., 1993). Additional early CT/MRI work showed that lingual discoordination and dysphagia were common in patients with periventricular white matter lesions (Daniels et al., 1999).

Despite the relatively limited focus on the role of white matter for swallowing, it is evident from broader neurophysiology work that white matter is highly relevant to the study of all human functions. White matter is the CNS component composed primarily of myelinated axons of neurons, provides the connections between cells, and functions as the information highway between distinct brain regions. These connections bundle together to form three primary types of white matter

Abbreviations: CNS, central nervous system; NGT, nasogastric tube; DWI, diffusion weighted imaging; FA, fractional anisotropy; TV, tract volume; VFSS, videofluoroscopic swallow study; PAS, penetration aspiration scale; FOIS, functional oral impact scale; CBT, corticobulbar tract; CD, cannot determine; GUSS, Gugging Swallow Screen; LA, leukoaraiosis (hyperintensity around ventricles); ASHA, NIOS American Speech Language Hearing Association National Outcome Measurement System; OR, odds ratio; WM, white matter; MCA, middle cerebral artery; NIHSS, national institute of health stroke scale; VLSM, voxel based lesion symptom mapping; ROI, regions of interest; MBSIMPTM, Modified Barium Swallow Impairment Profile; CNS, Canadian Neurological Scale; MRI, magnetic resonance imaging; SLP, speech language pathologist; NR, Not Rated; FEES, Fiberoptic Endoscopic Evaluation of Swallowing; GMFCS, gross motor function classification scale; MACS, manual ability classification scale; RD, radial diffusivity; MD, mean diffusivity; FC, fibers count; DDS, Dysphagia Disorder Survey; DMSS, dysphagia management staging scale; fMRI, functional magnetic resonance imaging; BODS-2, Bogenhausen Dysphagia Score Part 2; FEDSS, fiberoptic endoscopic dysphagia severity scale; SMA, supplementary motor area; PVWM, periventricular white matter.

tracts. First, association tracts connect areas of the cortex within the same hemisphere (Schmahmann et al., 2007). One prominent association tract is the superior longitudinal fasciculus which contains many branches, most notably the arcuate fasciculus, which connects the Broca's and Wernicke's areas in the left hemisphere (Breier et al., 2008). Damage to these structures in each hemisphere can lead to different symptoms, due to the lateralization of functions. Secondly, commissural tracts are the tracts that connect the right and left hemispheres, and include the corpus callosum, and the anterior and posterior commissures. Damage to these inter-hemispheric structures can cause frontal lobe dysfunction and spatial deficits (Buklina, 2005). Lastly, projection tracts connect areas in the cortex with lower centers such as deep nuclei or the brainstem. An example of projection tracts/structures are the internal capsules, which carry motor and sensory information between the cortex and sub-cortical areas. Damage to projection fibers can result in motor or sensory deficits throughout the body (Puig et al., 2011; Emos and Agarwal, 2020).

Scientific and clinical interest in these white matter tracts has been increasing. In a PubMed search using the key word "white matter," we identified a 400% increase in relevant articles since 1999. This increase is most likely due to the emergence of a new field devoted to understanding the full network of these tracts in humans, known as the human connectome (Sporns et al., 2005). This field has evolved through imaging advancements in diffusion weighted imaging (DWI), and in analysis techniques, such as tractography (Huisman, 2010). Diffusion weighted imaging senses the diffusion of water across tissue materials. Notably, white matter tracts have a unique diffusion property; they are anisotropic, i.e., water diffuses predominantly along the fiber (Frank, 2001). This characteristic (captured with DWI) allows us to identify and describe white matter structures and their properties with simple metrics such as fractional anisotropy (Alexander et al., 2007).

Although our understanding of the role of white matter for many biological functions is increasing, our understanding of these pathways in the neural control of swallowing remains scarce. Further, it is unclear to what extent newer imaging techniques such as DWI/DTI have been used for the study of the swallowing control. Identifying and addressing these gaps will provide critical insight on the structural neural connections involved in swallowing and has the potential to improve our ability to accurately identify and treat patients with neurological disease and dysphagia. Further, white matter is highly adaptable as shown by studies on recovery of sensorimotor functions after neurotrauma (Schlaug et al., 2009; Kou and Iraj, 2014; Sampaio-Baptista and Johansen-Berg, 2017), and may hold potential for maximizing swallowing recovery, but it is unclear to what extent this has been investigated. As a first step to informing future research in this line of work, it is necessary to systematically evaluate the quality of existing evidence and compare results across studies. Therefore, this systematic review aimed to identify all published research articles describing the role of white matter in the neural control of swallowing, and summarize and evaluate them to determine answers to four primary research questions:

- (1) What patient populations are represented in the available evidence?
- (2) What white matter imaging techniques and swallowing evaluation techniques have been utilized to investigate the role of white matter in the neural control of swallowing?
- (3) Does the available evidence provide definitive information on specific white matter tracts that are implicated in the neural control of swallowing and their role?
- (4) What are the main gaps in the investigation of the role of white matter tracts in the neural control of swallowing that need to be addressed in future research?

METHODS

Systematic Review Protocol

This review was conducted systematically and the detailed protocol was developed a priori in accordance with the PRISMA-P 2015 (Preferred Reporting Items for Systematic Reviews and Meta-Analyses) guidelines (Moher et al., 2009). Further, it was registered with the international prospective register of systematic reviews (PROSPERO ID: CRD 42020191453). Throughout the process, Rayyan data management software was utilized for blinding and tracking (Ouzzani et al., 2016).

Literature Search Strategy

A health sciences librarian (third author, BM) performed literature searches from May 2020 through July 2020, in the following databases: MEDLINE (*via* PubMed), Cochrane Library Database of Systematic Reviews, CINAHL, and Web of Science. Searches included a combination of controlled vocabulary terms, when applicable, and free text keywords. No filters were used during the search process. The literature was searched using combinations of terms including the following: "magnetic resonance imaging," OR "MRI," OR "white matter," AND "deglutition disorders," OR "dysphagia." Terms were nominated by the senior/last author (GAM) and were further discussed and agreed upon with the entire team, including an MRI physicist and experienced imager (fourth author; H.C.). Both initial and final searches included a back-chained search of the reference lists of all identified articles. The final search was executed in November 2020, just before manuscript submission, to capture new publications. The precise search strategies, databases searched, and the number of results retrieved per database, are available in **Supplementary Table A**.

Inclusion and Exclusion Criteria

Studies were included in this review if they met the following criteria: (1) included human subjects of all ages, (2) were peer-reviewed research articles, scientific abstracts, case studies, or reviews, (3) were written in English language, (4) reported aberration of white matter microstructure/pathways and/or documentation of damage to white matter resulting in dysphagia, (5) used one or more of the following methods: MRI, diffusion MRI (dMRI), diffusion-weighted imaging (DWI), diffusion tensor imaging (DTI), tractography, and/or structural brain network (connectome), and (6) included swallowing/dysphagia as a primary outcome.

Consequently, studies were excluded if they: (1) included only animal models, (2) were not in English, (3) did not specifically document white matter aberration, or (4) did not include swallowing as a primary outcome measure.

The two first authors (AA and RHA) independently screened all titles and abstracts identified with the search strategy for inclusion/exclusion, and any disagreements were resolved by the senior/last author (GAM). Then, the same two authors (AA and RHA) reviewed the full text of all qualifying articles to make the final decision of eligibility, with disagreements, again, resolved by the senior/last author (GAM).

Bias Assessment

In order to compare results across studies, it is essential to assess study quality and risk of bias. Because the majority of the studies identified in this review were observational cohort studies, study quality was assessed using an adapted version of the U.S. Department of Health and Human Services National Institute of Health's (NIH) Quality Assessment protocol for observational cohort and cross-sectional studies (National Heart, Lung, and Blood Institute, 2019). This 12-item tool was developed to assist reviewers in critically appraising the internal validity of studies through a structured evaluation of sources of bias, diagnosis and outcome measures, and statistical components. For the purpose of this study, three of 12 original assessment items in the protocol were not considered in the quality assessment, because they were consistently not reported or not applicable in the studies reviewed (these were: sufficient timeframe to see exposure effect, repeated exposure assessment, and follow-up rate). See **Table 1** for a full list of items assessed, and **Supplementary Table B** for details on the final adapted quality assessment tool.

Each study was independently evaluated by the two first authors (AA and RHA) using the NIH Quality Assessment protocol and was given a cumulative rating of Good, Fair, or Poor, that summarized the risk of bias in the study. According to the NIH Quality Assessment guidelines for the cumulative ratings, research studies are rated as "Good" if they have the least risk of bias, although they may not be free from all potential biases (Study Quality Assessment Tools | NHLBI, NIH, 2019). Bias in papers rated as "Good" is minimal and is discussed and accounted for in analysis. A study rated as "Fair" is still considered valid, with useful information, but may have some clear risk of bias that is not addressed. For example, a fair study may be underpowered due to limited sample size and not including blinding, both of which increase risk of bias. Finally, studies rated as "Poor" have substantial methodological limitations across multiple categories that limit interpretation of results. This tool does not determine precise cut-offs between these quality categories, but instead helps the evaluators rate the overall risk of internal bias based on key items/questions (see **Supplementary Table B**). To maximize objectivity, we used two independent raters (first two authors, AA and RHA), who participated in a 3-h practice training on this tool led by the senior author (GAM), before starting its use. Any disagreements in quality ratings were planned to be resolved through discussion with the senior/last author (GAM), though no disagreements occurred.

Data Extraction and Qualitative Synthesis

After completion of the bias assessment, the two first authors (AA and RHA) independently extracted data from all articles. Information extracted from each paper included study type and population characteristics, white matter techniques and information, swallowing evaluation methods, outcome measurements, and main findings from each study.

Extracted data on study type and population characteristics included: study design [classified in accordance with (Mann, 2003)], number of patients, number of participants in control group (if applicable), underlying diagnosis/disease of patient group or subgroups, severity/state of disease, age, sex, race, and ethnicity. Data extracted on white matter measurement included: scan type, scanner model and strength, head coil type, b-values, and number of directions (for DWI scans), scan settings, analysis type, and analysis method.

We also extracted details on how the primary outcome variable (swallowing) was assessed in order to compare clinical findings across studies. Data extracted included swallowing measurement method (e.g., instrumental or clinical assessment) and analysis of swallowing components (e.g., use of Penetration Aspiration Scale (Rosenbek et al., 1996), temporal measures, binary clinical ratings, etc.). Finally, information was extracted on the studies' main findings, which included implicated white matter areas and their suggested role in swallowing (including the statistical descriptions of that relationship), and limitations of each study.

Due to the wide variety of study types, patient populations, and imaging and swallowing evaluation methods, it was not possible to analyze the data across studies quantitatively at this time. Instead, a qualitative synthesis of the findings across studies was completed while critically evaluating the risk of bias of their methods and results.

RESULTS

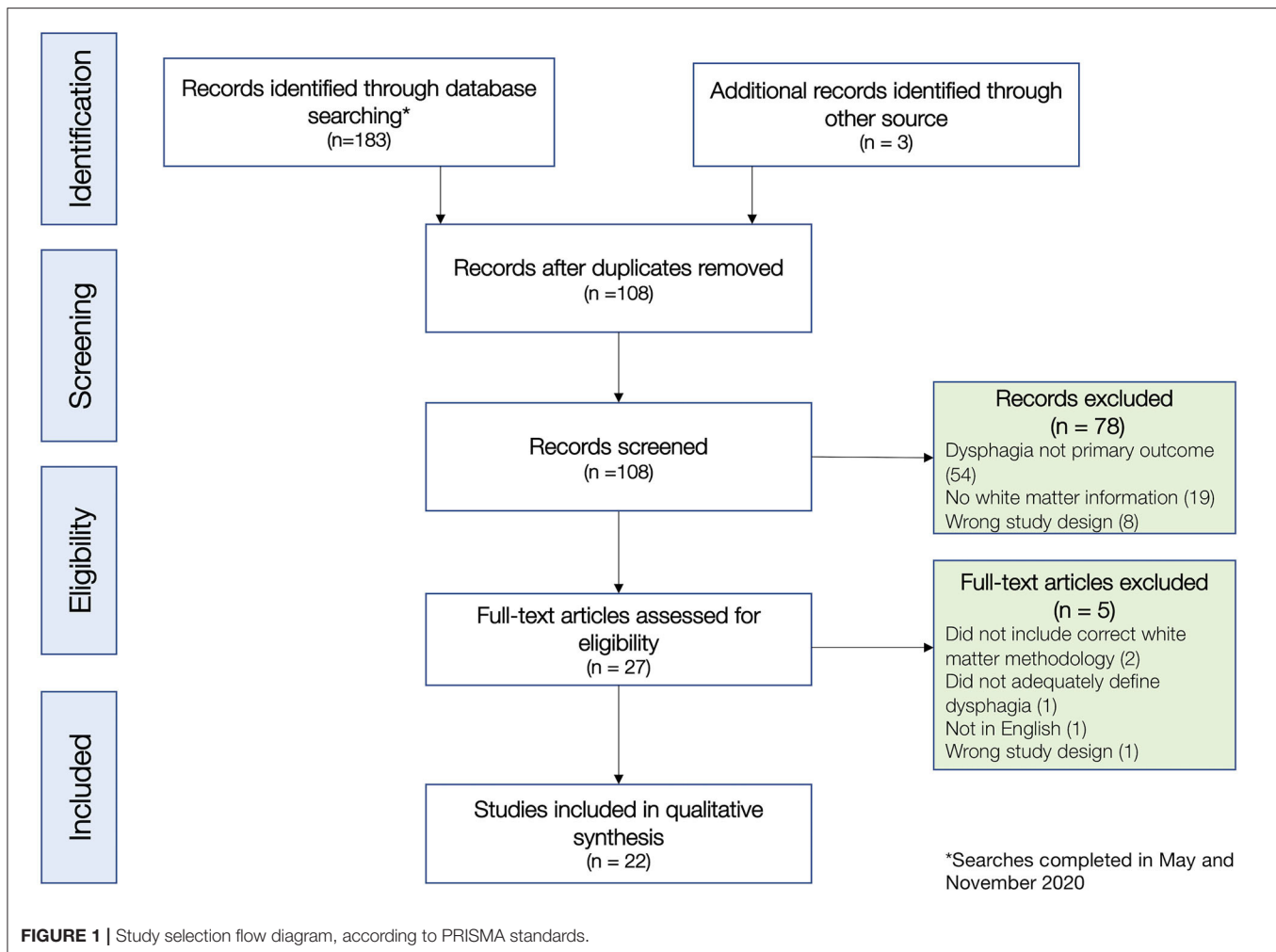
Study Selection and Data Extraction

The initial search of four databases in May-July 2020 retrieved a total of 182 titles, including 78 duplicates and 104 unique titles. Two articles were identified *via* backward citation chaining, and two additional articles (Jang et al., 2020b; Lee et al., 2020) were identified in a search verification in September 2020. A final search was conducted on November 8th, before submission, which revealed three novel articles, none of which met inclusion criteria. In total, this resulted in a subset of 108 non-duplicate articles, which all had full abstracts. Two independent reviewers (first two authors; AA and RHA) reviewed the titles and abstracts, and after this review, 27 articles met our inclusion criteria for full text review. Following a detailed full text review, 22 articles were selected for inclusion (see **Figure 1** for CONSORT diagram and exclusion reasons). There was disagreement on three articles at the screening stage, which was resolved by the senior/last author (GAM), and there were no other author disagreements on article review and inclusion. After study selection, the two first authors (AA and RHA) extracted data independently with agreement on 91% of extracted items and reached consensus on the remaining 9% of items extracted.

TABLE 1 | Study quality parameters rated using the modified NIH quality assessment for observational cohort and cross-sectional studies.

| First author date | Research question and hypotheses | Study population | Uniform eligibility criteria | Sample size justification | Primary diagnoses determined before outcome | Different levels of severity of diagnosis | Diagnosis measures (white matter integrity) | Outcome measures (swallowing) | Blinding of outcome measures | Statistical analysis (confounding variables) | Overall rating |
|----------------------------|----------------------------------|------------------|------------------------------|---------------------------|---|---|---|-------------------------------|------------------------------|--|----------------|
| Cola et al. (2010) | + | + | + | – | + | + | + | + | + | + | Good |
| Galovic et al. (2013) | + | + | + | – | + | + | + | p | CD | + | Good |
| Galovic et al. (2016) | + | + | + | – | + | + | + | + | – | p | Good |
| Mihai et al. (2016) | + | + | + | + | + | + | + | p | – | p | Good |
| Wilmskoetter et al. (2019) | + | + | + | + | + | + | + | + | CD | + | Good |
| Jang et al. (2020b) | + | + | + | – | + | – | + | + | – | – | Fair |
| Jang et al. (2020a) | + | + | + | – | + | – | + | + | – | – | Fair |
| Lee et al. (2020) | + | + | + | – | + | + | p | p | CD | + | Fair |
| Fandler et al. (2018) | + | + | + | – | + | + | + | p | – | – | Fair |
| Fandler et al. (2017) | p | + | + | – | + | + | + | p | CD | + | Fair |
| Flowers et al. (2017) | + | + | + | – | CD | + | p | – | CD | + | Fair |
| Galovic et al. (2017) | p | + | + | – | + | – | + | + | + | p | Fair |
| Jang et al. (2017) | + | + | NA | NA | + | + | + | – | – | – | Fair |
| Ko et al. (2019) | p | + | + | – | + | + | p | p | CD | + | Fair |
| Kumar et al. (2012) | + | + | + | – | CD | + | p | p | CD | + | Fair |
| Levine et al. (1992) | p | + | + | – | NA | + | p | p | CD | p | Fair |
| Li et al. (2014) | + | + | + | – | + | – | + | + | CD | – | Fair |
| Moon et al. (2017) | p | + | + | – | + | + | + | p | – | + | Fair |
| Mourão et al. (2017) | + | + | + | – | + | + | + | p | – | p | Fair |
| Suntrup et al. (2015) | p | + | + | – | + | + | p | p | + | – | Fair |
| Kim et al. (2014) | p | – | + | CD | CD | – | p | + | – | – | Poor |
| Wan et al. (2016) | p | + | + | – | CD | – | – | + | CD | – | Poor |

+ yes (adequately addressed), –no (not adequately addressed), p, partially addressed; CD, cannot determine; NA, not applicable.



Study Types and Characteristics

Of the 22 articles included in the review, one was a case study (Jang et al., 2017), and 21 included multiple participants and were observational, i.e., there was no intervention assessed (Table 2). The most frequent observational study design employed was retrospective cohort ($n = 11$), followed by three case control studies, and one prospective cohort study. Six studies did not neatly fit into one of the main observational study categories (Mann, 2003). Four of these were closest to a prospective cohort design (Li et al., 2014; Suntrup et al., 2015; Galovic et al., 2016, 2017). However, instead of examining whether an outcome of interest (i.e., dysphagia) would develop *over time*, these four studies included only participants who had *already* failed a dysphagia screening or were diagnosed with dysphagia. One study identified a convenience sample with a common diagnosis (cerebral palsy, CP) and used observational methods to determine dysphagia status (Mourão et al., 2017), and one study recruited healthy individuals to look at both a risk factor (i.e., aberrations in white matter) and changes in swallowing (Levine et al., 1992). Because these six studies did not fit into a specific pre-defined study type, but all involved carefully defined groups of subjects, we identified them broadly as “cohort design.”

Participant Characteristics and Clinical Classifications

Demographic and clinical diagnosis data (Research Question 1) of all reviewed studies are also included in Table 2. Ages of participants ranged from five to 96 years old, and only one study included patients under 18, children with CP, ages 5.11–17.6 (Mourão et al., 2017). One study did not report age of the participants (Kim et al., 2014). Only two studies reported race (Cola et al., 2010; Wilmskoetter et al., 2019), and one also reported ethnicity (Wilmskoetter et al., 2019). The number of participants across studies ranged from a single subject to 322 (mean = 92.77), and 40.88% of all subjects were female, though one study did not report sex (Kim et al., 2014). One article included exclusively healthy participants, and 21 articles included patients. Of these 21 articles, seven also included groups of healthy adults, four as control groups and three for white matter mapping and modeling, not for comparison.

The majority of subjects were adult patients post stroke (20 articles) and, as already mentioned, one study focused on children with CP (Mourão et al., 2017). Thirteen studies included a clinical rating of the underlying diagnosis of their subjects (Table 2). For stroke, the most frequent clinical rating scale used

TABLE 2 | Demographics and participant characteristics across studies.

| | Number of participants (groups) | Age and sex | Race and ethnicity | Inclusion criteria and underlying diagnosis | Clinical rating of diagnosis |
|--|---|--|--|---|---|
| Jang et al. (2020b) Retrospective Cohort | 40 (20 controls; 16 pts w/dysphagia and NGT < 6 mos; 4 pts w/dysphagia and NGT > 6 mos) | Control: 56 ± 10 (55% female) NGT < 6 mos: 60.6 ± 12.4 (37.5% female). NGT > 6 mos: 63.2 ± 14.7 (75% female) | NR | Stroke: Lateral medullary infarct with dysphagia and NGT placement | NR |
| Jang et al. (2020a) Retrospective cohort | 64 (22 controls; 42 pts w/dysphagia; 10 pts w/dysphagia and NGT < 2 days; 27 pts w/dysphagia and NGT < 6 mos; 5 pts w/dysphagia with NGT > 6 mos) | Control: 51 ± 11 (50% female) NGT < 2 days: 51 ± 15 (40% female) NGT < 6 mos: 60 ± 8.9 (52% female) NGT > 6 mos: 59 ± 10 (40% female) | NR | Stroke: Supratentorial intra-cerebral and intra-ventricular hemorrhage with dysphagia and NGT placement | NR |
| Lee et al. (2020) Retrospective cohort | 137 | 68.7 ± 14 (49.6% female) | NR | Stroke: acute ischemic stroke and referred for VFSS | NIHSS |
| Ko et al. (2019) Case control | 87 (20 pts with LA in contralateral CBT; 67 LA not in ipsilateral CBT) | 64.6 ± 11.5 (36% female) | NR | Stroke: First unilateral corona radiata infarct involving CBT with LA | NIHSS, Korean mini mental, motricity index of limbs |
| Wilmskoetter et al. (2019) Retrospective cohort | 68 | 68.21 ± 15.23 (53% female) | White 45 (66%), Black 21 (31%), Asian 1 (1.5%), Other 1 (1.5%); Not Hispanic/Latino: 68 (100%) | Stroke: First (and only) hemispheric stroke of the MCA | NIHSS (mean 12.57 ± 6.97), Rankin Scale (median 0, range 0–4) |
| Fandler et al. (2018) Retrospective cohort | 243 (196 pts w/o dysphagia; 47 pts w/dysphagia) | Pts w/o dysphagia: 67.1 ± 12.4 (37.2% female) Pts w/dysphagia: 70.8 ± 10.8 (30% female); | NR | Stroke: Recent small subcortical infarct | NIHSS 0–4 (263, 79.2%), NIHSS > 5 (69, 20.88%) |
| Fandler et al. (2017) Retrospective cohort | 322 (249 pts w/o dysphagia; 83 pts w/dysphagia) | Pts w/o dysphagia: 67 ± 12.4 (7.2% female) Pts w/dysphagia: 70.8 ± 10.8 (29.8% female) | NR | Stroke: Recent small subcortical infarct | NIHSS: Dysphagia 3 (1–10) No dysphagia 3 (0–9) |
| Flowers et al. (2017) Retrospective cohort | 160 (84 pts w/o dysphagia; pts w/76 dysphagia) | Total: 66.7 ± 15 (43.1% female) Pts w/o dysphagia: 63.6 ± 15.6 (46.4% female) Pts w/dysphagia: 69.9 ± 13.8 (39.5% female) | NR | Stroke (no other specifications) | Rankin scale, CNS score |
| Galovic et al. (2017) Cohort | 62 pts (24 additional controls for white matter modeling) | Pts: 75 ± 21 years (55% female). Controls: 63 ± 9 (42% female) | NR | Stroke: First hemispheric stroke leading to impaired oral intake | NR |
| Jang et al. (2017) Single case study | 1 pt (3 additional controls for modeling) | 59 (Male) | White | Stroke (no other specifications) | NR |

(Continued)

TABLE 2 | Continued

| | Number of participants (groups) | Age and sex | Race and ethnicity | Inclusion criteria and underlying diagnosis | Clinical rating of diagnosis |
|---|---|---|--|--|------------------------------------|
| Moon et al. (2017) Retrospective cohort | 63 (49 mild lesions, 14 severe lesions) | 77.24 ± 7.22 (50.8% female) | NR | Stroke: Mild first stroke, had dysphagia symptoms and completed VFSS. | NIHSS-K <5, mean = 2.83, SD = 1.42 |
| Mourão et al. (2017) Cohort | 20 (13 left hemisphere; 7 right hemisphere) | 5.11–17.6 (45% female) | NR | Unilateral spastic cerebral palsy | GMFCS, MACS |
| Galovic et al. (2016) Cohort | 119 (107 tube independent; 12 tube dependent) | Tube independent: 71 ± 19 (45% female) Tube dependent: 76 ± 9 (50% female) | NR | Stroke: First hemispheric stroke who failed dysphagia screening | NIHSS |
| Mihai et al. (2016) Case control | 36 (18 patients; 18 control) | Pts: 56.6 ± 15.3 (27.8% female) Control: 61.94 ± 9.78 (77.8% female) | NR | Stroke: Single ischemic stroke (recovered from Severe dysphagia w/in last 3 years) | NR |
| Suntrup et al. (2015) Cohort | 200 (35 pts w/o dysphagia; 85 pts w/mild dysphagia; 80 pts w/severe dysphagia) | 73.7 years (49.5% female) Pts w/o dysphagia: (72 ± 10.7) Pts w/mild dysphagia: (73.5 ± 13.1) Pts w/severe dysphagia: (74.8 ± 11.9) | NR | Stroke: First stroke; failed dysphagia screening and completed FEES | NIHSS |
| Li et al. (2014) Cohort | 36 (12 pts w/dysphagia; 12 pts w/o dysphagia; 12 controls) | Pts w/o dysphagia: 66.5 ± 5.2 (41.7% female) Pts w/dysphagia: 65.2 ± 4.3 (50% female) Control: 65.8 ± 3.3 (50% female) | NR | Stroke: First (and only) hemispheric stroke of the MCA | NR |
| Galovic et al. (2013) Prospective Cohort | 94 (34 acute risk; 60 no risk; 7 days later within the acute risk group; 17 transient risk; 17 extended risk) | Acute risk: 74 ± 19 (59% female) No risk: 71.5 ± 16 (43% female) | NR | Stroke: First | NIHSS, Rankin scale |
| Kumar et al. (2012) Retrospective cohort | 77 | Median = 76 (64.9% female) | NR | Stroke: Acute ischemic stroke and severe dysphagia | NIHSS (median 8) |
| Cola et al. (2010) Case Control | 45 (10 RHD; 10 LHD; 25 control) | RHD: 62.3 ± 12.1 (10% female) LHD: 62.3 ± 8.7 (0% female) Control: 67.2 ± 9.1 (8% female) | RHD: 7 black (70%) LHD: 8 black (80%) Control: 4 black (16%) | Stroke: Acute unilateral ischemic stroke | NIHSS |
| Levine et al. (1992) Cohort | 49 controls (25 MRI score 0-1; 24 MRI score 2-3) | Mean = 66 (40.8% female) [*] | NR | NA | NA |
| *Wan et al. (2016) Retrospective cohort | 12 | 66 ± 10 (25% female) | NR | Stroke: Basal ganglia and/or centrum semiovale | NR |
| *Kim et al. (2014) Retrospective cohort | 103 (62 anterior infarcts; 19 posterior infarcts; 22 WM disease) | NR | NR | Stroke: First unilateral ischemic stroke within 3 months; had dysphagia symptoms and completed VFSS in last 3 months | NR |

^{*}Received a modified NIH Quality Assessment rating of "poor".

Order of appearance: pts, patients; w/with; mos, months; w/o, without; NGT, naso-gastric tube; NR, not reported; NIHSS, national institute of health stroke scale; NIHSS-K, national institute of health stroke scale Korean version; VFSS, videofluoroscopic swallow study; RHD, right hemisphere disease; LHD, left hemisphere disease; MRI, magnetic resonance imaging; LA, leukoaraiosis (hyperintensity around ventricles); CBT, corticobulbar tract; CNS, Canadian Neurological Scale; GMFCS, gross motor function classification scale; MACS, manual ability classification scale; NA, not applicable.

was the National Institute for Health Stroke Scale (NIHSS; $n = 10$). Three studies used the Rankin Scale ($n = 3$), one used the Canadian Neurological Scale ($n = 1$), one used the Korean mini mental ($n = 1$), and one used the motility index of limbs ($n = 1$) (Table 2). The clinical ratings used for CP were the Gross Motor Function Classification System (GMFCS) and the Manual Ability Classification System (MACS) (Mourão et al., 2017).

Notably, within the studies that focused on stroke (20/22), inclusion criteria varied substantially. One study listed broad criteria of stroke diagnosis without further specification, eleven required that it was the first stroke, six required damage to a specific region, such as the middle cerebral artery, and nine required varying degrees of dysphagia severity for inclusion (Table 2).

Imaging Parameters and Analysis

Data Acquisition

Imaging specifications (Research Question 2) used in all reviewed studies are detailed in Table 3. All studies used MR imaging, however, specifics on scanner models and strength, scan types, settings, and analysis methods varied.

Scanner strength is reported in tesla (T), and scanners with higher tesla values allow for a stronger MR signal and may increase the speed of scan acquisition. Fourteen of the 22 reviewed studies provided information on scanner strength (Table 3). Of those 14, three reported using exclusively 3T MRI scanners, two of which were Siemens models, and one GE. Eight reported using exclusively 1.5T, including models from GE (2), Siemens (1), and Philips (4). Three studies utilized scans from both 1.5 and 3T Siemens scanners. Finally, eight studies did not report scanner strength, brand, or model. Only five studies reported information on head coils utilized. Two reported using a 6 channel coil, two reported using a 32 channel coil, and one reported using a quadrature head coil.

In addition to scanner strength and types, a wide variety of scan sequences and parameters were also reported across studies (Table 3), with three studies not reporting scan types at all. Of the studies that did report scan types (19/22), ten acquired a T2-weighted scan (most commonly a T2 FLAIR sequence), and seven a T1-weighted scan. Eighteen studies reported acquiring a DWI/DTI sequence, i.e., the state-of-the-art non-invasive technique to explore white matter integrity (Chanraud et al., 2010). However, it is noteworthy that DWI/DTI scans were not necessarily collected for the studies' white matter analysis, but as standard-of-care protocols for stroke patients (Leiva-Salinas and Wintermark, 2010).

Of the 18 papers that acquired a DWI/DTI sequence, eleven reported their b values (i.e., the diffusion-sensitive gradient factor that helps create different types of contrast between tissues). The most frequently reported b-value was 1,000 s/mm² which has been reported to be the optimal b-value for assessing stroke in the acute phase (Kingsley and Monahan, 2004). Additionally, one pediatric study (CP) reported a b-value of 800 s/mm² (Mourão et al., 2017).

Another important parameter to consider when acquiring DWI scans is the number of directions in which diffusion is measured (i.e., the greater the number of directions, the greater

the number of details that can be mapped in tractography) (Vos et al., 2016). Of the eighteen studies that reported acquiring DWI scans, only four reported the number of directions. Two reported 64 directions, one reported 15, and one three directions (see Table 3).

Data Analysis

As expected, given the variety of scan models and specifications utilized, there was also considerable variability in the methods used for white matter data analysis. However, some common themes emerged. The major observation was that researchers followed one of two paths for analysis. Either they examined the **damage/lesions** to white matter by investigating the size and characteristics of these lesions; or they evaluated **white matter integrity** by measuring and describing characteristics of the tissue. Most studies followed the first approach and used qualitative rating scales or quantitative measurements to measure lesions. Studies using this (lesion-based) approach are discussed first followed by studies using the second option (white-matter integrity).

Lesion-based analysis: qualitative methods

Eight studies utilized qualitative scales to describe damage to white matter. The most commonly cited scale ($n = 6$) (Fandler et al., 2017; Flowers et al., 2017; Moon et al., 2017; Ko et al., 2019; Jang et al., 2020b; Lee et al., 2020) was the 4-point Fazekas scale (Fazekas et al., 1987). To determine ratings using the Fazekas scale, clinicians or researchers visually examine the amount and size of white matter hyperintensities [i.e., brighter spots on T2-weighted scans that relate to damage to small blood vessels or decrease in myelination (Wardlaw et al., 2015)] in two domains: the periventricular white matter and the deep white matter, and provide a rating of these hyperintensities. An earlier study (Levine et al., 1992) used another 4-point/grade scale developed by Awad et al. using size, multiplicity, and location to rate subcortical incidental lesions (Awad et al., 1986). Further, one study employed a rather indirect approach (Kim et al., 2014), using an adapted scale which categorizes damage to the brain's vascular territories (Rovira et al., 2005), to indirectly infer lesions to white matter.

Lesion-based analysis: quantitative methods

Ten of the 22 reviewed studies used a quantitative volume and voxel-based approach to record the location and size of lesions. These studies quantified damage by measuring lesion volume with voxels or mm² lesioned (Galovic et al., 2013, 2016, 2017; Suntrup et al., 2015; Mihai et al., 2016; Flowers et al., 2017; Fandler et al., 2018; Ko et al., 2019; Wilmskoetter et al., 2019; Jang et al., 2020a) or they used these units to derive the amount of area or proportion (%) of an area that is lesioned (Suntrup et al., 2015). Three studies used a technique called voxel-based lesion symptom mapping (VLSM) (Bates et al., 2003), which enables calculation of correlations between locations of the "damaged" voxels and behavioral scores (Galovic et al., 2016, 2017; Wilmskoetter et al., 2019).

TABLE 3 | MR imaging specifications across studies.

| | Scan type | Scanner model and head coil | Diffusion settings and directions | MRI scans settings | Analysis type | Analysis specifications |
|-----------------------|--|---|-----------------------------------|---|---|--|
| Jang et al. (2020b) | DWI | 1.5T Phillips Gyroscan Intera 6 channel head coil | b = 1,000 s/mm ² | Acquisition matrix = 96 × 96; reconstructed matrix = 192 × 192; FOV = 240 × 240 mm; TR = 10,398 ms; TE = 72 ms; EPI factor = 59; slice thickness=2.5 mm | Seed based Tractography FA; TV; Fazekas Grade | FMRIB Diffusion Software with routines option (0.5 mm step lengths, 5,000 streamline samples, curvature threshold = 0.2) used for fiber tracking |
| Jang et al. (2020a) | DWI | 1.5T Phillips Gyroscan Intera 6 channel head coil | b = 1,000 s/mm ² | Acquisition matrix=96 × 96; reconstructed to matrix = 192 × 192; FOV = 240 × 240 mm ² ; TR = 10,398 ms; TE = 72 ms; SENSE factor = 2; EPI factor = 59; slice thickness = 2.5 mm. | Seed based Tractography FA; TV; Modified Graeb Score | FMRIB Diffusion Software with routines option (0.5 mm step lengths, 5,000 streamline samples, curvature thresholds = 0.2) used for fiber tracking; analysis done by expert w/3 years of experience |
| Lee et al. (2020) | DWI, FLAIR | NR | NR | NR | Fazekas grade (manual rating) | Two physiatrists completed analysis |
| Fandler et al. (2017) | T2- axial fast spin echo, axial T2 FLAIR, sagittal T1 spin echo, gradient echo T2, axial diffusion-weighted single shot echo planar axial | 1.5T Siemens Symphony | NR | All axial slices slice thickness = 5 mm | Manual lesion identification; Fazekas Grade | Two independent experts used standards for reporting vascular changes on neuroimaging consensus criteria |
| Fandler et al. (2018) | T2- axial fast spin echo sequence, FLAIR sequence-axial, gradient echo T2, DWI single-shot echo planar with ADC maps (axial) and TOP angiography | 1.5 T | NR | Axial T2-weighted fast spin echo sequence (0.5 × 0.5 × 5 mm); FLAIR sequence (0.4 × 0.4 × 5 mm); sagittal T1-weighted spin echo sequence (0.6 × 0.6 × 5 mm); gradient echo T2* weighted sequence (0.4 × 0.4 × 5 mm); axial DWI single-shot echo planar imaging sequence (1.2 × 1.2 × 5 mm) with apparent diffusion coefficient ADC maps and a 3D time of flight (TOF) angiography. Axial slices; slice thickness = 5 mm with 0.5 mm gap | Lesion probability mapping; tractography analysis | RSSI manually marked by two neuroimaging experts |
| Moon et al. (2017) | T2 FLAIR and DWI | NR | NR | NR | Fazekas scale (using diffusion images with FLAIR MRI); unspecified localization | Physician rating |

(Continued)

TABLE 3 | Continued

| | Scan type | Scanner model and head coil | Diffusion settings and directions | MRI scans settings | Analysis type | Analysis specifications |
|----------------------------|--|---|---|---|---|--|
| Li et al. (2014) | Resting state fMRI, DTI | 3T MRI GE Signa EXCITE | b = 1,000 s/mm ² reference scan with b = 0 (no diffusion gradient) 15 non-collinear directions | NR | Seed-based functional connectivity maps (from primary motor and supplementary motor to the brain); swallowing-related functional connectivity for 20 ROIs; mean FA between the SMA and M1 | Whole brain fiber tracking using "Diffusion Toolkit" software |
| Mihai et al. (2016) | DWI, T1-weighted, fMRI | 3T Siemens Verio, 32-channel head coil | b = 1,000 s/mm ² ; 64 gradient directions | Gradient echo (34 slices 2 × 2 × 2 mm); functional EPI (96 × 96 oblique); structural T1 (1 × 1 × 1) | FA lateralization index; T1 lesion size | FSL, MNI, and bedpostx were used for probabilistic tractography; researchers manually drew borders for lesions for lesion size, for detailed description of other programs used see paper. |
| Galovic et al. (2017) | Transverse T2, T1, FLAIR, sagittal T2, isotropic DWI | 1.5T Siemens Avanto, 1.5T Siemens Symphony, or 3T Siemens Verio MRI | DWI (b = 1,000 s/mm ² with 4 mm transverse slices) | FLAIR slice thickness = 5 mm; T2 sagittal slice thickness = 4.5 mm; transverse DWI slice thickness = 4 mm | Voxel-based lesion symptom mapping (VLSM); ROI analysis; Probabilistic Tractography for healthy individuals | VLSM: ICBM standard brain template, NPM software. Tractography: FMRIB Diffusion toolkit, FSL FLIRT algorithm |
| Flowers et al. (2017) | Sagittal T1, T2 FLAIR, isotropic axial diffusion | 1.5 T Signa EchoSpeech MR scanner (GE), quadrature head coil | b = 1,000 s/mm ² | T1: 7.5 mm slice thickness 2 mm space; T2: 5 mm slice thickness = 2 mm spacing; diffusion slice thickness = 5 mm slice w/0 mm spacing | Fazekas scale for periventricular hyperintensities and deep hyperintensities in 12 ROIs | Manually traced lesions on each DWI slice with MRICron and calculated volumes |
| Galovic et al. (2013) | T2, T1, FLAIR, Sagittal T2, isotropic DWI, with TOF sequence | 1.5T Siemens Avanto 1.5T Siemens Symphony or 3T Siemens Verio | b = 1,000 s/m ² | FLAIR slice thickness = 5 mm; sagittal T2 slice thickness = 4.5 mm; DWI slice thickness = 4 mm | Lesion mapping with ROI | MICRON with MNI space for model. Semi-automatic image analysis by 1 neurologist using MIPAV to Talairach (used Brodmann areas) and visually noted lesions with binomial scale. ImageJ used for lesion size. Age-related white matter documented by Wahlund et al. (2001) |
| Wilmskoetter et al. (2019) | DWI | NR | NR | Voxel-wise resolution ranged from 0.9375 × 0.9375 × 3 mm to 1.4458 × 1.4458 × 6 mm | Manually drawn lesions; VLSM; ROI when there were no significant findings from VLSM | Lesions drawn by a researcher using MRICron; reviewed by neurologist with expertise in VLSM; custom MATLAB script for lesion symptom mapping |
| Levine et al. (1992) | T2 | 1.5T GE Signa | n/a | NR | T2 scales graded according to Awad et al. (1986); number of unidentified bright objects | NR |
| Kumar et al. (2012) | DWI | NR | NR | NR | Lesion volume and location on DWI | Image J; brain atlas |

(Continued)

TABLE 3 | Continued

| | Scan type | Scanner model and head coil | Diffusion settings and directions | MRI scans settings | Analysis type | Analysis specifications |
|-----------------------|--|--|--|---|---|---|
| Jang et al. (2017) | DTI (at both 5 and 9 weeks) | 1.5T Philips Gyroscan Intera | 1,000 s/mm ² | 60 continuous slices; 76 ms; 2.5 mm thickness for each of the 32 gradients | Probabilistic tractography; ROI | FSL FMRI |
| Cola et al. (2010) | DWI | NR | b = 1,000 s/mm ² ; 3 directions | Slice thickness = 6 mm axial images; | Lesion volumes semi-manually tracked | Image J (semiautomatic threshold) |
| Ko et al. (2019) | NR | NR | NR | Slice thickness = 3-5 mm | Lesion size using Sims et al. (2009) method; Fazekas scale | Expert |
| Mourão et al. (2017) | T1 NPrAGE, MRI, DTI | 3T Siemens Magnetom Trio; 32-channel head coil | b = 800 s/mm ² ; 64 directions | T1 and DTI: slice thickness = 2 mm, 75 slices | Tractography; fractional anisotropy; radial diffusivity; mean diffusivity; fibers count | DTI studio |
| Suntrup et al. (2015) | DWI, T2 FLAIR, | MRI: 1.5T Intera Gyroscan, Philips. CT: somatom Definition AS+ Siemens | b = 1,000 s/m ² ** | MRI: slice thickness = 5 mm transverse. reconstruction, 1 mm increment | Atlas-based regional analysis (% of brain affected) | Completed by neuroradiologist using FSL FLIRT, FMRI and FNIRT |
| Galovic et al. (2016) | T2 (transverse and sagittal), T1, FLAIR, and DWI | 1.5T Siemens Avanto, 1.5T Siemens Symphony or 3T Siemens Verio | b = 1,000 s/m ² | DWI transverse slices 4 mm; T2: T1: FLAIR slice thickness = 5 mm; Sagittal T2: slice thickness = 4.5 mm | Voxel-based lesion symptom mapping (VLSM) | VLSM was calculated using MRICron software |
| Wan et al. (2016)* | MRI (no details given) | NR | NR | NR | NR, Though presence of stroke was determined by scans | NR |
| Kim et al. (2014)* | MRI (no details given) | NR | NR | NR | Determined vascular territory with modified Rovira et al. (2005) method | NR |

*Received a modified NIH Quality Assessment rating of "poor".

**The authors reported this as "b = 0 and 1.9 mm/s²" which we standardized to b = 1,000 s/m².

Order of appearance: DWI, diffusion weighted imaging; FA, fractional anisotropy; TV, tract volume; FMRI, Functional Magnetic Resonance Imaging of the Brain; FLAIR, fluid attenuated inversion recovery; NR, not rated; RSSI, MRI magnetic resonance imaging; fMRI, functional magnetic resonance imaging; DTI, diffusion tensor imaging; SM, Supplementary motor area and M1; EPI, Echo-planar imaging; FSL, FMRI Software Library; MNI, Montreal Neurological Institute; VLSM, voxel-based lesion symptom mapping; ICBM, International Consortium for Brain Mapping; NPM, FLIRT FMRI's Linear Image Registration Tool; MR, Magnetic resonance; MPAGE, magnetization-prepared rapid gradient-echo; ADC, Apparent Diffusion Coefficient; FACT, Fiber Assignment by Continuous Tracking, apparent diffusion coefficient A.

White matter integrity analysis

Seven of the 22 studies included in this review utilized analysis techniques that provided information on the structural integrity of the white matter, instead of focusing only on lesions. The main quantitative measure reported was fractional anisotropy (FA; $n = 5$) (Table 3). Higher FA values are associated with greater white matter integrity, due to more coherent diffusion of water across tissue (De Erausquin and Alba-Ferrara, 2013). Six studies generally reported using tractography, an analysis method that creates a 3D map of the white matter tracts in the brain, and two of the seven studies measured tract volumes (TV). Of those six, only one reported additional diffusion-based analysis measures, including radial diffusivity, mean diffusivity, and fibers count (Mourão et al., 2017). These measures give more in-depth information on the integrity of white matter, such as strength of connection and anisotropy of the diffusion (Mori and Zhang, 2006; Clark et al., 2011; de Figueiredo et al., 2011). One study used a different quantitative approach that indirectly informs us about connections in the brain, known as functional connectivity (Li et al., 2014), using the synchrony of the blood oxygen level dependent signals between areas of gray matter to give us indirect insight about how these areas are connected.

Swallowing Evaluation Methods and Analysis

Swallowing Evaluation Methods

All, but one study (Jang et al., 2017), reported details on how swallowing was evaluated (Research Question 2; Table 4). It is commonly accepted that the gold standard for comprehensively evaluating swallowing involves radiologic or endoscopic imaging, i.e., Videofluoroscopic Swallow Studies (VFSS) or Fiberoptic Endoscopic Evaluations of Swallowing (FEES). These evaluation methods allow differing degrees of visualization of the oropharyngeal area, upper airway and upper esophagus, and allow clinicians to make subjective judgments or objective measurements of symptoms, and/or kinematic, temporal and bolus flow events. Fifteen of the 21 studies that reported swallowing evaluation methods used some imaging modality (VFSS and/or FEES; Table 4). Specifically, nine reported use of VFSS for all patient participants, and four reported using VFSS for a subset of subjects (e.g., they included some patients who had received a VFSS while hospitalized post-stroke and others who had only received clinical bedside swallowing evaluations). FEES was used in three studies: one used only FEES (Suntrup et al., 2015), one used FEES in addition to VFSS (Wan et al., 2016), and a third study used FEES for a subset of subjects (Galovic et al., 2017).

Eight studies used a clinical (bedside) swallowing evaluation (CSE), which typically includes a case history, a detailed cranial nerve assessment, oropharyngeal mechanism exam, and oral trials of foods and liquids. One study used a CSE in addition to VFSS (Li et al., 2014), four studies used a CSE for all patients, while reporting that a portion of subjects also received instrumental assessments (Kumar et al., 2012; Mihai et al., 2016; Galovic et al., 2017; Ko et al., 2019), and three studies used only a CSE (Galovic et al., 2013, 2016; Mourão et al., 2017). Lastly, in two

studies the researchers performed only a swallow screening, i.e., a brief evaluation determining the risk for a diagnosis of dysphagia (Fandler et al., 2017, 2018).

Analysis of Swallowing Parameters

Table 4 also summarizes each study's swallowing analysis methods (see Supplementary Table C for more extensive detail). Of the studies that included VFSS for all subjects ($n = 9$), six used the Penetration Aspiration Scale (PAS) which rates the level of airway invasion and patients' response to penetration or aspiration events (Rosenbek et al., 1996), five studies employed temporal/timing measures, and Wilmskoetter et al. (2019) used the Modified Barium Swallow Impairment Profile (MBSImP[®]; Martin-Harris et al., 2008), a standardized protocol that enables clinicians to quantify physiological swallowing impairments. Of the studies that used FEES, one study used a tool to rate dysphagia severity from FEES, the fiberoptic endoscopic dysphagia severity scale (FEDSS).

Five of the eight studies that included CSEs used standardized tools to interpret the assessment. Mourão et al. (2017) used the Dysphagia Disorder Survey, a validated clinical assessment of swallowing and feeding function for individuals with intellectual and developmental disability (Sheppard et al., 2014); three studies used the Bogenhausen Dysphagia Score, Part 2 (BODS-2) (Bartolome, 2006), which is a German assessment of oral intake; and two used the Functional Oral Intake Scale (FOIS) (Crary et al., 2005), i.e., a description of levels of oral intake, retrospectively. Three studies reported mixed methods for swallowing analysis, such as a variety of different clinical scales (see details on all methods in Supplementary Table C).

White Matter Areas Implicated in the Neural Control of Swallowing

Quality of Evidence and Bias Assessment

In order to determine if there is definitive evidence implicating specific white matter areas in the control of swallowing (Research Question 3), we first critically assessed the quality of the available evidence using the modified NIH quality assessment (results in last column of Table 1). Five articles were rated as "Good," fifteen articles were classified as "Fair," and two articles were classified as "Poor."

The most common risk of bias (found in 20 of the 21 studies with greater than one participant) involved failing to justify sample size (i.e., not reporting power analysis or variance/effect estimates) (Table 1). Sample size was frequently limited by the clinical setting and/or by the retrospective design. The second most frequent item impacting quality assessment was blinding. Twenty of the 22 studies did not describe blinding of assessors (e.g., whether swallowing assessors were blinded to MRI results/diagnoses). Other elements negatively affecting quality ratings were related to the measurement methods used to evaluate swallowing and/or white matter. For example, studies frequently included the use of a non-validated and/or non-standardized swallowing assessment tool (15 of 22 studies) or reported limited details on MRI methodology/imaging. Lastly, for 13 studies, ratings were affected by not including confounding variables in statistical analysis. Although handling of missing data

TABLE 4 | Summary of methods, major findings and limitations of studies included in qualitative synthesis ($n = 20$ studies).

| Study type | Underlying diagnosis | White matter method | Swallow measurement method | Swallowing analysis | Implicated WM areas | Associations with swallowing | Limitations |
|---|--|----------------------------------|--------------------------------------|--|---|--|--|
| Jang et al. (2020b) Retrospective cohort | Stroke: lateral medullary w/dysphagia and NGT | DWI FA TV Fazekas grade | VFSS | PAS; FOIS | Corticobulbar tract | FA in CBT was significantly reduced in pts w/longer compared to shorter NGT use or controls ($p < 0.05$), but was not significantly different between patients w/dysphagia and NG for <6 mos and controls. Fazekas ratings were not significantly different between patient groups. | CD blinding; did not account for confounding variables in statistical analyses; no sample size justification |
| Jang et al. (2020a) Retrospective cohort | Stroke: supratentorial intra-cerebral and intra-ventricular hemorrhage w/dysphagia and NGT | DWI FA TV | GUSS, VFSS | PAS; residue scale | Corticobulbar tract | Patients who had NGT removed w/in 2 days had milder CBT injury (only FA decreased, not TV). FA in CBT for each patient group was lower than controls ($p < 0.05$). CBT TV was lower than controls in both hemispheres for patients with NGT <6 mos, and lower for both hemispheres for patients with NGT > 6 mos. TV of the CBT in the affected hemisphere was negatively correlated with length of time until NGT removal in < 6 mos group ($r = 0.430$, $p < 0.05$). NGT removed within 6 mos for individuals with unilateral but not bilateral injuries. | CD blinding; did not account for confounding variables in statistical analyses; no sample size justification |
| Lee et al. (2020) Retrospective cohort | Stroke: acute ischemic, VFSS | DWI; FLAIR Fazekas grade | VFSS | Clinical dysphagia scale | Corona radiata/internal capsule/basal ganglia | Bilateral lesions at the corona radiata/internal capsule/basal ganglia were significant prognostic factors for persistent dysphagia ($p < 0.001$). | CD blinding; no sample size justification; no details on white matter or swallowing analysis methods; collapsing brain areas into one category |
| Ko et al. (2019) Case control | Stroke: first unilateral involving corona radiata, CBT | NR Lesion size, Fazekas grade | Clinical swallow, VFSS for a portion | Feeding method, clinical judgement, dysphagia scale, PAS, NOMS, bolus timing | Corticobulbar tract | LA involving contralateral CBT was a significant predictor of feeding method at discharge ($b = -3.95$, $OR = 0.02$, $p < 0.01$) and NOMS score ($b = 1.56$, $p = 0.03$). | Limited information on WM assessment, Age was a confounding factor, no sample size justification, inconsistent use of video swallowing |

(Continued)

TABLE 4 | Continued

| Study type | Underlying diagnosis | White matter method | Swallow measurement method | Swallowing analysis | Implicated WM areas | Associations with swallowing | Limitations |
|--|--|--|--|---|--|--|--|
| Wilmskoetter et al. (2019) Retrospective cohort | Stroke: first hemispheric of the MCA | DWI VLSM ROI | VFSS | MBSIMP [®] ™ and PAS | Corona radiata, sup. longitudinal fasciculus, external capsule, ansa lenticularis, lenticular fasciculus | Regions surviving corrected threshold ($z < -2.78$) for impaired laryngeal elevation: Right external capsule (8.2%), right superior longitudinal fasciculus (0.1%), right superior corona radiata (0.2%); laryngeal vestibule closure ($z < -3.43$): right superior corona radiata (0.1%), right external capsule (5.5%); pharyngeal residue ($z < -3.33$): right superior corona radiata (1.2%), right posterior corona radiata (12.5%), right tapatum (1.7%), posterior limb of right internal capsule (0.2%), retrolenticular part of right internal capsule (3.9%), right superior longitudinal fasciculus (8.8%); PAS ($z < -4.36$): right superior longitudinal fasciculus (1.7%). | Statistical power higher in some brain regions (more damaged areas), missing data, limited discussion of power, CD blinding of outcome assessors |
| Fandler et al. (2018) Retrospective cohort | Stroke: recent small subcortical infarct | Lesion probability | GUSS | SLP GUSS rating: absent, mild, moderate, severe | Pyramidal tract, contralateral lacune, contralateral WM hypersensitivities (unspecified) | All patients with moderate or severe dysphagia had damage along the pyramidal tract, compared to 86% of patients without dysphagia. Patients with moderate to severe dysphagia more frequently had damage to the pyramidal tract and a contralateral pyramidal tract lacune (77.8 vs. 19.9%, $p < 0.001$). | Limited details on WM analysis, used a screener to identify dysphagia, did not incorporate confounds in stats, no sample size justification |
| Fandler et al. (2017) Retrospective cohort | Stroke: recent small subcortical infarct | MRI, DWI Lesion identification Fazekas grade | GUSS | SLP GUSS rating: absent, mild, moderate, severe | Unspecified | More severe WM hyperintensities were an independent predictor of dysphagia ($p < 0.03$), but that association was lost when analysis was restricted to patients with supratentorial damage ($p < 0.27$). | Screener for dysphagia, unspecified WM locations, no sample size justification, CD blinding for swallowing |
| Flowers et al. (2017) Retrospective cohort | Stroke | MRI, DWI ROI Fazekas grade | Clinical instrumental, or feeding method | NR | Internal capsule, | Internal capsule had an OR = 2.9 for dysphagia. | Did not give assessment details for swallowing, no sample size justification, heterogeneous sample, broadly defined regions, CD blinding |

(Continued)

TABLE 4 | Continued

| Study type | Underlying diagnosis | White matter method | Swallow measurement method | Swallowing analysis | Implicated WM areas | Associations with swallowing | Limitations |
|--|---|---|--|---|--|---|--|
| Galovic et al. (2017) Cohort | Stroke: first hemispheric, impaired oral intake | MRI, DWI VLSM ROI Tractography | Clinical Swallow. FEES if results “indeterminate” | Clinical Swallow (50 mL swallow test, Any 2 Scale, Gugging), FOIS | Sup. Corona Radiata, sup. longitudinal fascicle, external capsule, thalamic and cortico-bulbar projection fibers, fibers to contralateral thalamus | Statistical map of voxels associated with impaired oral intake after 7 days affected 89% WM with a center of maximum overlap over superior corona radiata with location immediately anterior to facial fibers (65% superior corona radiata, 12% superior longitudinal fascicle, 8% external capsule). Proportion of damaged voxels in the superior corona radiata was negatively correlated with degree of oral intake after 7 days ($p = 0.001$). After 4 weeks, the statistical lesion map covered 76% gray matter. | No classification of stroke severity, telephone assessment for last phase, no sample size justification |
| Jang et al. (2017) Single case study | Stroke | DWI ROI Tractography | NR | Severe dysphagia, fed by Levin tube | Corticobulbar tract | At the 5-week follow-up, the right CBT was discontinued at the subcortical right matter (Severe narrowing), left was not reconstructed. Right CBT recovered after rehabilitation and cranioplasty: thickened and extended to cerebral cortex. Resolution of dysphagia. | No details on swallowing measurement, limited demographic details, no discussion of power, no statistical analysis, CD blinding |
| Moon et al. (2017) Retrospective cohort | Stroke: mild first stroke, dysphagia symptoms, VFSS | MRI, DWI Fazekas grade | VFSS | Clinician description, bolus timing, penetration, aspiration | Unspecified | WM lesions are correlated with prolonged oral transit time ($r = 0.384$, $p = 0.003$) and increased penetration ($r = 0.322$, $p = 0.015$), even controlling for confounding variables. Mean oral transit time (OR = 3.082, $p = 0.03$) and penetration (OR = 2.521, $p = 0.015$) were significantly different in the severe WM lesion group than in the mild group. Left lesions associated with mastication ($p = 0.039$). | Unspecified WM lesions, subjective measures, no specific hypotheses, limited validated swallowing outcomes, no reliability testing, no sample size justification, CD blinding for swallow assessment |
| Mourão et al. (2017) Cohort | Unilateral spastic cerebral palsy | MRI, DWI, FA, RD, MD, FC | Clinical Swallow | DDS, DMSS | Anterior, middle, posterior corpus callosum | Left hemisphere group (less severe): As FA ($r = -0.667$, $p = 0.013$) and FC decreased ($r = -0.829$, $p < 0.001$) and RD increased ($r = 0.594$, $p = 0.032$) (i.e., reduced structural integrity of the corpus callosum), dysphagia increased. Reduced FC in middle ($r = -0.762$, $p = 0.002$) and posterior ($r = -0.739$, $p = 0.004$) CC was associated with increased (worse) DDS. Right hemisphere group was more severe, and no significant correlations were observed. | Heterogeneous groups did not account for confounding variables in statistical analyses, no sample size justification |

(Continued)

TABLE 4 | Continued

| Study type | Underlying diagnosis | White matter method | Swallow measurement method | Swallowing analysis | Implicated WM areas | Associations with swallowing | Limitations |
|---|--|--|---|---|---|--|--|
| Galovic et al. (2016) Cohort | Stroke: first hemispheric stroke, failed dysphagia screening | MRI VLSM | Clinical Swallow | BODS-2 | Sup. corona radiata, external capsule, sup. longitudinal fascicle | Mildly impaired oral intake was correlated with a widespread gray and white-matter network shown by a statistical map that included the superior corona radiata (12%), the external capsule (10%) and the superior longitudinal fascicle (8%). | No discussion of blinding, no sample size justification, limited accounting for confounding variables |
| Mihai et al. (2016) Case control | Stroke: first ischemic (recovered from Severe dysphagia w/in 3 years) | fMRI, DWI FA Lesion size | Clinical Swallow and VFSS for a portion | BODS-2, Neurogenic Oral Dysphagia test, water swallowing test | Pyramidal track laterality (between tongue and posterior limb of internal capsule) | Overall laterality of fractional anisotropy differed between patients and controls [$t_{(32)} = 3.21, p < 0.005$]. Patients showed asymmetric laterality of the pyramidal tract between tongue area and posterior limb of internal capsule. The larger the lesion, the more asymmetric ($r = -0.676, p < 0.001$). Laterality index was positively associated with compliance, meaning less compliant patients were less symmetric ($r = 0.65, p < 0.009$). | Lesions were heterogeneous, not all patients had VFSS, they each had individualized therapy which varied, hard to control for compliance, CD blinding |
| Wan et al. (2016) Retrospective cohort | Stroke: basal ganglia and/or centrum semiovale | MRI NR | VFSS FEES | Bolus timing, residue, physiologic observation | Centrum semiovale in conjunction with basal ganglia | 83% of 12 patients had dysphagia. | No hypotheses, Small heterogeneous sample, no sample size justification, no diagnosis levels of severity, no MRI information, minimal participant information, no blinding, no confounding variables in analysis |
| Suntrup et al. (2015) Cohort | Stroke: first, failed dysphagia screening, FEES | MRI, DWI Regional lesion analysis | FEES | FEDSS ranking 1-6 | Sup. longitudinal fasciculus (right and right temporal part), corticospinal tract (right) | Patients with dysphagia had a significant difference of mean percentage lesioned volume in the following areas: superior longitudinal fasciculus (right; $p < 0.021$, OR = 4.52), superior longitudinal fasciculus temporal part (right; $p < 0.028$, OR = 4.17), corticospinal tract (right; $p < 0.044$, OR = 2.79). | No sample size justification, limited methodology for WM and swallowing measures, unclear MRI settings, no confounding variables in analysis |
| Kim et al. (2014) Retrospective cohort | Stroke: first unilateral ischemic w/in 3 mos, dysphagia symptoms, VFSS | MRI Vascular white matter territory | VFSS | Physiologic observation, bolus timing, residue, penetration, aspiration | Unspecified | Excessive vallecular residue observed most frequently in the WM group ($p < 0.002$). | Unspecified WM lesions, no participant information, no assessment of stroke severity, no MRI specifications, no sample size justification, no confounding variables in analyses. CD blinding |

(Continued)

TABLE 4 | Continued

| Study type | Underlying diagnosis | White matter method | Swallow measurement method | Swallowing analysis | Implicated WM areas | Associations with swallowing | Limitations |
|---|---|--|-------------------------------|---|--|--|--|
| Li et al. (2014) Cohort | Stroke: first hemispheric stroke of MCA | fMRI, DWI ROI, FA, seed-based connectivity | Clinical Swallow and VFSS | Logemann's indicators, PAS | Bilateral Corticospinal tract, Corpus Callosum | Reduced FA for left SMA to right SMA (corpus callosum), left SMA to internal capsule (corticospinal tract), and right SMA to internal capsule (corticospinal) in pts with dysphagia compared to controls. There were clear differences between stroke patients with dysphagia and healthy controls, but not between patients with and without dysphagia. | Limited detail on MRI, No sample size justification, no stroke severity, CD blinding, no confounding variables in statistical analyses, placed seeds for WM tracking close to cortex |
| Galovic et al. (2013) Prospective cohort | Stroke: first | MRI, DWI ROI lesion mapping | Clinical Swallow | Daniels et al. (1996) aspiration risk scale and BODS-2 | Internal capsule, PVWM | Acute findings: internal capsule (OR = 7.6, $p < 0.001$), PVWM (OR = 4.8, $p < 0.001$). When adjusted for NIHSS and lesion size, internal capsule (OR = 6.2, $p < 0.002$) and now PVWM OR = 2.7, $p < 0.06$. Model accuracy 76%. No WM areas were associated with extended risk of aspiration. | No sample size justification, CD blinding, Clinical "risk of aspiration" with no instrumental, no mild strokes, only analyzed early subacute phase |
| Kumar et al. (2012) Retrospective cohort | Stroke: ischemic, severe dysphagia | DWI Lesion volume | Clinical and/or video swallow | Severe dysphagia = absence of oral intake or significant aspiration | Unspecified | In univariate analysis PVWM was not a significant predictor of PEG placement. In a multivariate analysis with age, NIHSS score, lesion volume, and brain locations, PVWM approached significance ($p < 0.057$ with OR = 3.829). NIHSS score and Bihemispheric lesions were significant predictors. | Unspecified white matter lesions, only participants with severe dysphagia, limited details on measurement methods, no sample size justification, CD blinding |
| Cola et al. (2010) Case control | Stroke: unilateral ischemic subcortical | DWI Lesion volume | VFSS | Bolus timing, PAS, bolus clearance | Unspecified | Significant interaction between peri-ventricular WM lesions and hemisphere (chi square = 9.85, $p = 0.002$). 100% had dysphagia in LH PVWM group, 0% dysphagia for RHD. No association was detected for those without PVWM damage. | Unspecified WM lesions, Small n, no MRI in healthy subjects, controls were not matched for race, no sample size justification |
| Levine et al. (1992) Cohort | n/a | MRI MRI score | VFSS | Bolus timing | Unspecified | Total swallow duration ($p < 0.009$) and oral transit duration ($p < 0.047$) significantly differed by MRI score (total number of WM unidentified bright objects). | Unspecified WM lesions, only healthy controls, no sample size justification, limited participant details, old imaging methods |

Order of appearance: NGT, nasogastric tube; DWI, diffusion weighted imaging; FA, fractional anisotropy; TV, tract volume; VFSS, videofluoroscopic swallow study; PAS, penetration aspiration scale; FOIS, functional oral impact scale; CBT, corticobulbar tract; CD, cannot determine; GUSS, Gugging Swallow Screen; LA, leukoaraiosis (hyperintensity around ventricles); ASHA, NOMS American Speech Language Hearing Association National Outcome Measurement System; OTT, Oral Transit Time; PTT, Pharyngeal Transit Time; OR, odds ratio; WM, white matter; MCA, middle cerebral artery; NIHSS, national institute of health stroke scale; VLSM, voxel based lesion symptom mapping; ROI, regions of interest; MBSIMP[®], Modified Barium Swallow Impairment Profile; Sup, Superior CNS Canadian Neurological Scale; MRI, magnetic resonance imaging; SLP, speech language pathologist; NR, Not Rated; FEES, Fiberoptic Endoscopic Evaluation of Swallowing; GMFCS, gross motor function classification scale; MACS, manual ability classification scale; RD, radial diffusivity; MD, mean diffusivity; FC, fibers count; DDS, Dysphagia Disorder Survey; DMSS, dysphagia management staging scale; fMRI, functional magnetic resonance imaging; BODS-2, Bogenhausen Dysphagia Score Part 2; FEDSS, fiberoptic endoscopic dysphagia severity scale; SMA, supplementary motor area; PVWM, periventricular white matter.

was not quantified by the NIH quality assessment tool we used, we noted that few studies described whether they had missing data and how they handled it.

Robust statistical analysis was a common element among all papers that received a quality rating of “Good.” Although only five papers received this highest rating, 20 of 22 papers were of at least “Fair” quality. Therefore, to answer Research Question 3 we qualitatively synthesized the findings of these 20 studies. The two studies rated as “Poor” were not included in this synthesis, due to significant risk of bias, but their information is presented in the tables for the sake of completeness.

Specific White Matter Tracts of Interest and Their Roles

Six of the twenty “Good” or “Fair” quality studies discussed “periventricular white matter” without further location specificity, and fourteen provided information on specific white matter regions implicated in swallowing control (Table 4; see **Supplementary Table C** for more detailed summary), albeit with differing levels of specificity. The most commonly implicated white matter tracts across studies were the pyramidal tracts ($n = 8$), followed by more specific tract sections, such as the internal capsule ($n = 4$), the superior longitudinal fasciculus ($n = 3$), the corona radiata ($n = 3$), the corpus callosum ($n = 2$), the external capsule ($n = 2$), and the ansa lenticularis/lenticular fasciculus ($n = 1$).

Pyramidal tracts and subdivisions

Eight studies identified the pyramidal tracts as important in swallowing control. The pyramidal tracts are the projection fibers carrying motor information from the cortex to the brainstem and spinal cord. Although these fibers are frequently subdivided into the corticobulbar and corticospinal tracts (Lohia and McKenzie, 2020a), two studies referred to the pyramidal tract as a whole. Specifically, Fandler et al. (2018) examined 243 patients with dysphagia and found that all patients (100%) with moderate or severe dysphagia had damage along the pyramidal tracts, compared to 86% of patients without dysphagia (Fandler et al., 2018). Further, patients with moderate to severe dysphagia more frequently presented with damage to one pyramidal tract (left or right) and a white matter hyperintensity on the contralateral pyramidal tract than those without dysphagia (77.8 vs. 19.9% respectively, $p < 0.001$). In a study by Mihai et al. (2016), both clinical swallowing assessments and task-based fMRI and DWI scans were performed in 18 patients who had recovered from clinically determined post-stroke dysphagia and 18 healthy controls. Results of the DWI-based FA analysis revealed that, in comparison with the control group, the patient group had an asymmetric laterality index of the pyramidal tract FA with reduced FA mostly ipsilesionally. This indicated involvement of pyramidal tract lesions in the development of dysphagia, but also some neuroplastic capacity that played a role in recovery.

Two additional studies implicated one division of the pyramidal tract, the corticospinal tract. Li et al. (2014) found that stroke patients with dysphagia had reduced FA in the corticospinal tracts bilaterally when compared to healthy controls, but their FA was not statistically different than

stroke patients without dysphagia. This finding may have been influenced by the small sample size ($n = 12$ in each group) (Li et al., 2014). In a larger study ($n = 200$), patients with damage to the right corticospinal tract had significantly higher odds of being diagnosed with dysphagia than patients without damage to the same area (OR = 2.79, $p < 0.044$; Suntrup et al., 2015).

The other division of the pyramidal tract, the corticobulbar tract (CBT), is critical for bulbar functions such as swallowing and speech and was implicated in four papers. Three of these papers directly aimed to investigate the contribution of the CBT in swallowing control. Two studies evaluated the predictive value of CBT damage on prognosis for dysphagia recovery (Jang et al., 2020a,b). Specifically, Jang et al. (2020a) used tractography to measure FA and TV of the CBT in 42 patients with intracerebral hemorrhage and subsequent dysphagia requiring nasogastric tube (NGT) placement. Patients who recovered swallowing within 2 days had relatively minor damage to the CBT (only reduced FA, not reduced TV), whereas patients with longer NGT placement had more extensive damage to the CBT (both reduced FA and TV). In patients with longer NGT placement (2 days to 6 months), CBT volume in the affected hemisphere was negatively correlated ($r = -0.430$, $p < 0.05$) with length of time until NGT removal. Finally, none of the patients who had bilateral damage to the CBT were able to have their NGT removed within 6 months (Jang et al., 2020a). In a separate study using similar methodology, Jang et al. (2020b) examined 20 patients with lateral medullary infarctions and found that CBT FA was significantly lower in patients with prolonged NGT placement (<6 months) compared to controls and to patients with shorter NGT placement durations (Jang et al., 2020b, p. 20). Ko et al. (2019) examined the impact of unilateral vs. bilateral damage to the corticobulbar tract (CBT) on swallowing (Ko et al., 2019). They investigated two groups of stroke patients with lesions involving the CBT: one group with unilateral CBT damage and one group with bilateral CBT involvement [defined as damage to the CBT in one hemisphere and *additional* CBT leukoaraiosis (i.e., white matter hyperintensity) contralaterally]. As expected, bilateral CBT involvement independently predicted worse performance on functional swallowing measures (Ko et al., 2019).

Finally, the involvement of the CBT in swallowing was also reported in a single case study including a stroke patient with damage to the middle cerebral artery and subsequent intracerebral hemorrhage (Jang et al., 2017). At 5 weeks post-stroke, the patient was reported to exhibit severe dysphagia and extensive brain swelling, accompanied by a severely narrowed right CBT, which was not extending to the cortex, and no identifiable left CBT. After decompressive craniotomy at 8 weeks post-stroke, dysphagia symptoms resolved and imaging showed decreased swelling, and a more “normal appearing” right CBT that now extended to the cortex. This indirectly suggests the role of CBT fibers in connecting areas of the swallowing network.

Internal capsule

The internal capsule is a white matter structure which contains both ascending (i.e., thalamocortical) and descending (i.e., pyramidal) fibers, and therefore carries both sensory and motor

information. Damage to the internal capsule was associated with dysphagia or aspiration risk in four studies. Flowers et al. (2017) retrospectively reviewed 160 stroke patients to examine neuroanatomical factors that predict the diagnosis of dysphagia, aphasia, and/or dysarthria. They identified seventy-six patients with post stroke dysphagia, and they reported that damage to the internal capsule increased odds of being diagnosed with dysphagia by an average of 3 times (OR = 2.9; 95% CI 1.2–6.6) (Flowers et al., 2017). Galovic et al. (2013) examined lesion location as a predictor of aspiration risk [assessed using the Daniels' et al. clinical evaluation method (Daniels et al., 2000)] in 94 patients within 48 h post stroke and at ~1-week post-stroke. They found that patients with internal capsule lesions had increased odds of aspiration risk in the acute phase (OR = 4.8, $p < 0.001$), but not at 1-week post-stroke [OR = 1.3, $p = 1.0$; (Galovic et al., 2013; Flowers et al., 2017)]. Further evidence for the involvement of the internal capsule in swallowing control derives from Mihai et al. DWI-based FA analysis (Mihai et al., 2016). Similar to the results involving the pyramidal tracts, their patient group had an asymmetric laterality index of the posterior limb of the internal capsule FA with reduced FA ipsilaterally, also suggesting involvement of this specific white matter area in the recovery of swallowing function. Lastly, Lee et al. (2020) found that bilateral internal capsule/corona radiata/basal ganglia lesions (all grouped together) were significant prognosticators for persistent dysphagia ($p < 0.001$) (Lee et al., 2020).

Superior longitudinal fasciculus

The superior longitudinal fasciculus, an association tract, connects multiple brain regions including the frontal, occipital, parietal, and temporal lobes, creating the networks needed for the regulation of motor behavior and conveyance of somatosensory information. Involvement of the superior longitudinal fasciculus was reported in three studies. In two of these, the Galovic group used VLSM to examine lesion locations and connectivity patterns as predictors of impaired oral intake in the acute stroke phase (~2 days post-stroke) (Galovic et al., 2016) and at ~1 and 4 weeks post stroke (Galovic et al., 2017). Their results showed that the statistical map of voxels associated with impaired oral intake involved the superior longitudinal fasciculus to a small extent (8 and 12% of voxels), in the acute and ~1-week phases, respectively (Galovic et al., 2016, 2017). Further, Suntrup et al. (2015) also used voxel-based imaging analysis to examine whether stroke location is associated with dysphagia in 200 acute stroke patients. They reported that damage to the right superior longitudinal fasciculus or the temporal part of the right superior longitudinal fasciculus increased the odds of dysphagia diagnosis by ~4 times. This tract was also reported in a more recent retrospective study that investigated the association between lesion location (using VLSM) and physiological aspects of swallowing (rated using the MBSIMP[®] and the PAS) in 68 acute stroke patients (Wilmskoetter et al., 2019). After controlling for age, time between measurements, and lesion volume, this study found that lesions including the superior longitudinal fasciculus were associated (to a small extent) with impairment in three physiological components. Specifically, the superior longitudinal fasciculus was implicated in 1.7% of lesioned voxels

associated with increased PAS scores, 8.8% of voxels associated with pharyngeal residue, and 0.1% of voxels associated with impaired laryngeal elevation (Wilmskoetter et al., 2019).

Corona radiata

The corona radiata is a collection of both ascending and descending white matter tracts that spread toward the cortex and connect with the internal capsule. Three studies found that damage to the corona radiata was associated with some swallowing deficits. Galovic et al. reported two interesting findings regarding this region in their 2017 study examining the associations between lesion locations and impaired oral intake at ~1 and 4 weeks post stroke. First, they found that at ~1-week post-stroke, the statistical map of voxels associated with impaired oral intake included lesions in the superior corona radiata to a greater extent than any other area (65% of lesioned voxels). Secondly, at the same time point, the percent of damage in this area was negatively correlated with the degree of oral intake and the majority of patients with lesions in more >50% of the corona radiata had impaired oral intake (Galovic et al., 2017). In the 2016 study by the same research group, the corona radiata was identified in 12% of lesioned voxels associated with decreased oral intake at 48 h post-stroke (Galovic et al., 2016), further implicating this tract in swallowing control. The Wilmskoetter et al. study (2019) also reported that lesions including the right superior corona radiata were associated to a small extent with impaired laryngeal elevation (voxel overlap of 0.2%), impaired laryngeal vestibular closure (voxel overlap of 0.1%), and pharyngeal residue (voxel overlap of 1.2%). Lesions including the right posterior corona radiata were associated to a slightly larger extent with pharyngeal residue scores (voxel overlap of 8.8%) (Wilmskoetter et al., 2019). Finally, as reported previously, Lee et al. (2020) found that bilateral internal capsule/corona radiata/basal ganglia lesions (all grouped together) were prognosticated persistent dysphagia (Lee et al., 2020).

Corpus callosum

The corpus callosum (CC) was identified in two papers as important in swallowing control. In children with CP and left hemisphere lesions affecting primarily the sensorimotor cortex area ($n = 13$), increased clinical signs of dysphagia were correlated with reduced structural integrity of the corpus callosum quantified by FA decrease ($r = -0.667$, $p = 0.013$), fiber count decrease ($r = -0.829$, $p < 0.001$), and radial diffusivity increase ($r = 0.594$, $p = 0.032$) (Mourão et al., 2017). In particular, reduced fiber count in the middle ($r = -0.762$, $p = 0.002$) and posterior ($r = -0.739$, $p = 0.004$) corpus callosum was associated with increased (worse) total score on the Dysphagia Disorder Survey for this group of children. A similar pattern was not observed for the group of children with right hemisphere lesions ($n = 7$), however the vast majority of these children had subcortical or peri-ventricular white matter (PVWM) lesions affecting intra-hemispheric connections. The authors concluded that CC integrity and inter-hemispheric communication might be more critical for swallowing control when the sensorimotor

cortex is impacted, and not as critical when subcortical intra-hemispheric connections are disrupted (Mourão et al., 2017). In the study by Li et al. (2014) including stroke patients with and without dysphagia and healthy controls, mean FA for the corpus callosum was significantly decreased in stroke patients with dysphagia when compared to the healthy controls, but when these stroke patients were compared to the group of patients without dysphagia, this difference was not significant.

External capsule

The external capsule, a series of association tracts between the putamen and claustrum, was reported in three studies. In the 2016 Galovic et al. study, 10% of lesioned voxels associated with impaired oral intake at the acute stroke phase (<48 h after imaging) overlapped the external capsule (Galovic et al., 2016). In the 2017 study by the same group, 8% of lesioned voxels associated with impaired oral intake at 1-week post-stroke overlapped this white matter area (Galovic et al., 2017). Finally, Wilmskoetter et al. (2019) reported that damage to the right external capsule was associated to some extent with impaired laryngeal elevation (voxel overlap of 8.2%) and impaired laryngeal vestibule closure (voxel overlap of 5.5%) in their sample of 68 patients post stroke (Wilmskoetter et al., 2019).

Three Additional Themes

In addition to insights on specific white matter tracts, there were several studies that generally investigated white matter and its role in swallowing control, without specifying tract locations. Three themes emerged from this literature and were reinforced by some previously discussed studies. These were topics on lesion severity, hemispheric involvement, and time post-stroke.

Lesion Severity

Although lesion severity was not consistently reported in all studies included in this synthesis, six studies indicated that severity of the white matter lesion impacts components of swallowing. In a retrospective study of 63 mild stroke patients (NIHSS ≤ 5), severity of white matter lesions (measured using the Fazekas scale) was correlated with prolonged oral transit time ($r = 0.384, p = 0.003$) and increased penetration occurrences ($r = 0.322, p = 0.015$), even after controlling for variables such as age, sex, initial stroke severity, lesion laterality, and lesion location (Moon et al., 2017). In addition, a larger retrospective study including 322 stroke patients found that a higher NIHSS score (indicating higher stroke severity) and more severe white matter hyperintensities identified in MRI scans were both identified as risk factors for suspected dysphagia as measured with the Gugging Swallow Screen. However, when the analysis was restricted to patients with supratentorial damage, white matter hyperintensities did not remain significant risk factors (Fandler et al., 2017). Further, severity of damage to one specific white matter tract, the CBT, predicted prognosis for dysphagia recovery in two studies by Jang et al. (2020a,b).

In another study, by Kumar et al. (2012), the aim was to examine the influence of age, NIHSS score, time post stroke, and lesion characteristics in predicting placement of a percutaneous endoscopic gastrostomy (PEG) tube in 77 patients with severe

dysphagia resulting from an acute-subacute hemispheric lesion. Baseline NIHSS score and bilateral hemispheric involvement were the most significant predictors of PEG tube placement in this cohort (Kumar et al., 2012). Further, as reported earlier, in the study by Galovic et al. (2017) the amount of damage in the superior corona radiata was negatively correlated with the degree of oral intake, further implicating that white matter lesion load or severity plays a role in the development of swallowing difficulties (Galovic et al., 2017).

Finally, in a prospective study of 49 healthy adults (43 to 79 years of age), VFSS evaluations and a brain MRI scan were performed in order to examine the effect of subtle changes to white matter, or “unidentified bright objects,” on temporal/durational aspects of swallowing. Results showed that total swallow duration ($p < 0.009$) and oral transit duration ($p < 0.047$) differed significantly by MRI score, i.e., by number of “unidentified bright objects” in white matter (Levine et al., 1992). This was the only study included in this review that indicated that even in healthy individuals, small changes/aberrations to white matter might be influential for swallowing control.

Hemispheric Involvement

Three studies found a potential effect of lateralization of a white matter lesion to dysphagia diagnosis and/or severity. Cola et al. (2010) investigated 20 acute stroke patients, ten with left subcortical damage and ten with right subcortical damage. They found a significant statistical interaction between hemisphere and lesion location (chi square = 9.85, $p = 0.002$) and concluded that lesions to the left PVWM may be more disruptive to swallowing than right PVWM lesions. On the other hand, the study by Wilmskoetter et al. (2019) found that the majority of gray and white matter areas implicated in swallowing dysfunction in their post-stroke sample were in the right hemisphere. However, they also observed that two of four pharyngeal components of the MBSIMPTM were associated with some lesions to the left hemisphere, thus concluding that although both hemispheres play a role in swallowing control, the control of the right hemisphere appears to be more prominent (Wilmskoetter et al., 2019). Similarly, the study by Mourão et al. (2017) reported that children with CP and right hemisphere lesions (the majority of which were in the PVWM area) presented with more severe clinical dysphagia compared to children with CP with left hemisphere lesions (Mourão et al., 2017). However, the majority of children in the left hemisphere group did not have PVWM lesions and there was a relatively small sample of children in each subgroup (13 left hemisphere, 7 right hemisphere), limiting the interpretation of this finding. Regardless of the individual contributions of left and right hemispheres, there is evidence that bilateral lesions, particularly to the pyramidal tract, tend to be more disruptive than unilateral lesions (Kumar et al., 2012; Ko et al., 2019; Jang et al., 2020a,b).

Time Post-stroke

Additionally, two studies demonstrated that white matter damage may have particular clinical relevance in the acute post-stroke phase. Galovic et al. (2017) reported that the map of lesioned areas associated with impaired oral intake at 1-week

post-stroke affected white matter structures in 89% (of the voxels), whereas the respective map for patients with persistent dysphagia at 4 weeks post stroke covered mostly gray matter areas, and only 24% white matter (Galovic et al., 2017). Similarly, the same research team previously (2013) reported that patients with damage to PVWM had higher aspiration risk at 48 h post-stroke compared to patients without PVWM damage ($OR = 4.8$, $p < 0.001$) (Galovic et al., 2013). Both studies indicate that disruptions in white matter areas early post-stroke likely disrupt the communication between gray matter areas that are critical in swallowing, but also that recovery of these connections can occur quickly and can be essential in helping restore swallowing function.

Gaps in the Investigation of White Matter and Swallowing

The last research question (Research Question 4) sought to identify specific gaps in the literature in order to help guide future research in this area. Through our qualitative synthesis three major gaps were identified. These gaps were: (1) limited representation of populations, (2) imaging and swallowing methodology, and (3) research design and statistical rigor.

Limited Representation of Populations

Two clinical populations were represented in the available literature: patients post stroke (20 studies) and children with cerebral palsy (1 study), along with one study examining variability within healthy adults (Levine et al., 1992). Representation across age, race, and ethnicity was significantly limited (Table 2). Only one study included pediatric patients; all other studies included wide adult age ranges, often without accounting for effects of age in their statistical analysis. Finally, only two studies reported race, and one reported ethnicity.

Imaging and Swallowing Methodology

Studies included in this review greatly varied in both imaging and swallowing methodology used, and critically few used current gold standard methodology for both measures. Specifically, most identified articles measured white matter lesions and rarely used methods to measure white matter integrity, such as tractography, fractional anisotropy, radial diffusivity, mean diffusivity, and fibers count. There were also inconsistencies in the reporting of imaging parameters (such as signal strength or scanner type), which limits interpretation of findings. However, clinical scales that were reported across multiple studies, such as the Fazekas scale, improved comparability between those studies. In regard to swallowing evaluation and analysis, relatively few papers used gold-standard swallowing measurement methods (VFSS or FEES) in conjunction with validated analysis tools (Table 4). Even when VFSS or FEES methodologies were utilized, the measures used to analyze the data were often limited or not validated (Table 4).

Research Design and Statistical Rigor

Finally, issues with research design or statistical rigor were observed across many studies (see Tables 1, 4). Several retrospective studies included inconsistent assessment methods

or lacked carefully controlled research protocols. Further, few studies provided evidence of adequate power or reported blinding outcome assessors, and less than half of the studies thoroughly controlled for the potential impact of confounding variables in their statistical analysis. One key area that should also be highlighted in future studies is incorporation of confounding factors in research design and analysis.

These identified gaps in representation, methodology, and study design are important and need to be carefully considered in future research.

DISCUSSION

The majority of swallowing neurophysiology work has focused on the contributions of CNS gray matter in the control of human swallowing, and much less attention has been given to the white matter tracts that form connections between gray matter areas. These tracts hold promise for patients with dysphagia because, in addition to being communication highways, they are also known to be primary drivers of recovery after injury or disease and are highly capable of adaptation with rehabilitation and re-learning (Trivedi et al., 2008; Schulz et al., 2014; Kato and Izumiyama, 2017, p. 201; Barghi et al., 2018).

In this systematic review, we sought to identify and systematically evaluate the literature describing the role of white matter in the neural control of swallowing in order to answer four primary questions: what patient populations have been studied in this literature; what methodologies have been used to assess white matter integrity and swallowing; what specific white matter tracts are implicated in swallowing control; and what are the main gaps in the literature that need to be addressed in future research.

To summarize, we identified 22 articles that fit our inclusion criteria. All studies were observational, i.e., there was no intervention assessed, and almost half followed a retrospective cohort design, with the other half being either case control studies or variations of prospective cohort designs. Using a modified NIH quality assessment protocol (Study Quality Assessment Tools | NHLBI, NIH, 2019) (Table 1), five studies were rated as having “Good” quality, 15 studies were of “Fair” quality; and two studies were rated as “Poor” and were excluded from the qualitative synthesis used to answer question 3 of this review.

Regarding the first research question (populations), stroke was by far the most represented diagnosis in the identified literature. Only two of the 22 reviewed papers examined different populations; one study examined children with CP, and one focused on healthy older adults. The majority of studies included acute adult stroke patients, with almost exclusively first strokes with no prior infarcts or comorbidities, and a mix of types of strokes (see Table 4). This proportionally high representation of one diagnosis in the literature is likely due to relevance and convenience. Patients post stroke often exhibit white matter damage with subsequent deficits, and also have readily available neuroimaging scans that can be studied retrospectively. Since neuroimaging is costly, it is unsurprising that research on this topic has started with a population who has existing scans and related damage. However, white matter damage has been

documented in other populations that are also at high risk for developing swallowing difficulties, including people with traumatic brain injury (Herrera et al., 2016), dementia (Love and Miners, 2015), chronic drug abuse (Narayana et al., 2014), multiple sclerosis (Tassorelli et al., 2008), and gestational hypoxia (Baud et al., 2004; Kaur and Ling, 2009), as well as in typical aging (Metzler-Baddeley et al., 2019). In addition to a gap in representation of clinical populations, few of the reviewed studies included healthy control participants or focused on white matter integrity measures in healthy participants, leaving an additional gap in our understanding of white matter connections in normal swallowing.

In regard to the second question (methodologies to assess white matter and swallowing), we observed an interesting dichotomy. The majority of studies that measured characteristics of the white matter structures themselves (e.g., FA, tract volume, mean diffusivity, etc.), evaluated swallowing *via* clinical methods or screenings, instead of using instrumental tools. On the other hand, most of the studies that examined swallowing physiology in some depth or with validated tools tended to utilize the more crude (or lesion-based) white matter imaging techniques (e.g., lesion volume calculations, lesion severity scales, etc.).

Imaging advancements in the use of DWI/DTI have allowed for a significant increase in our understanding of brain connections and their role in recovery and rehabilitation in related fields (Trivedi et al., 2008; Schlaug et al., 2009; Huber et al., 2018). For this reason, we expected to find these methodologies used in swallowing neurophysiology literature as well. However, we observed that very few of the reviewed studies utilized these sequences to investigate white matter integrity in their samples, despite the fact that many research groups had access to the relevant DWI scans. Instead, they relied on lesion-based methods, which are useful when examining patients with stroke or another pathology with specific lesions, but do not quantifiably measure white matter itself. Since lesions often affect multiple brain areas at once this approach can result in unspecified conclusions. Alternatively, techniques that measure and describe characteristics of white matter, such as FA, radial diffusivity, mean diffusivity, or fibers count, reveal changes specific to the white matter structures. These techniques are sensitive enough to detect differences even within healthy populations (Madden et al., 2008; Ziegler et al., 2010; Bennett et al., 2011; Schulz et al., 2014). The few studies in this review that used these techniques indicated that these metrics could be valid predictors for swallowing outcomes post stroke (Jang et al., 2020a,b), and they helped identify more specific white matter tracts of interest for swallowing control (Mourão et al., 2017; Wilmskoetter et al., 2019).

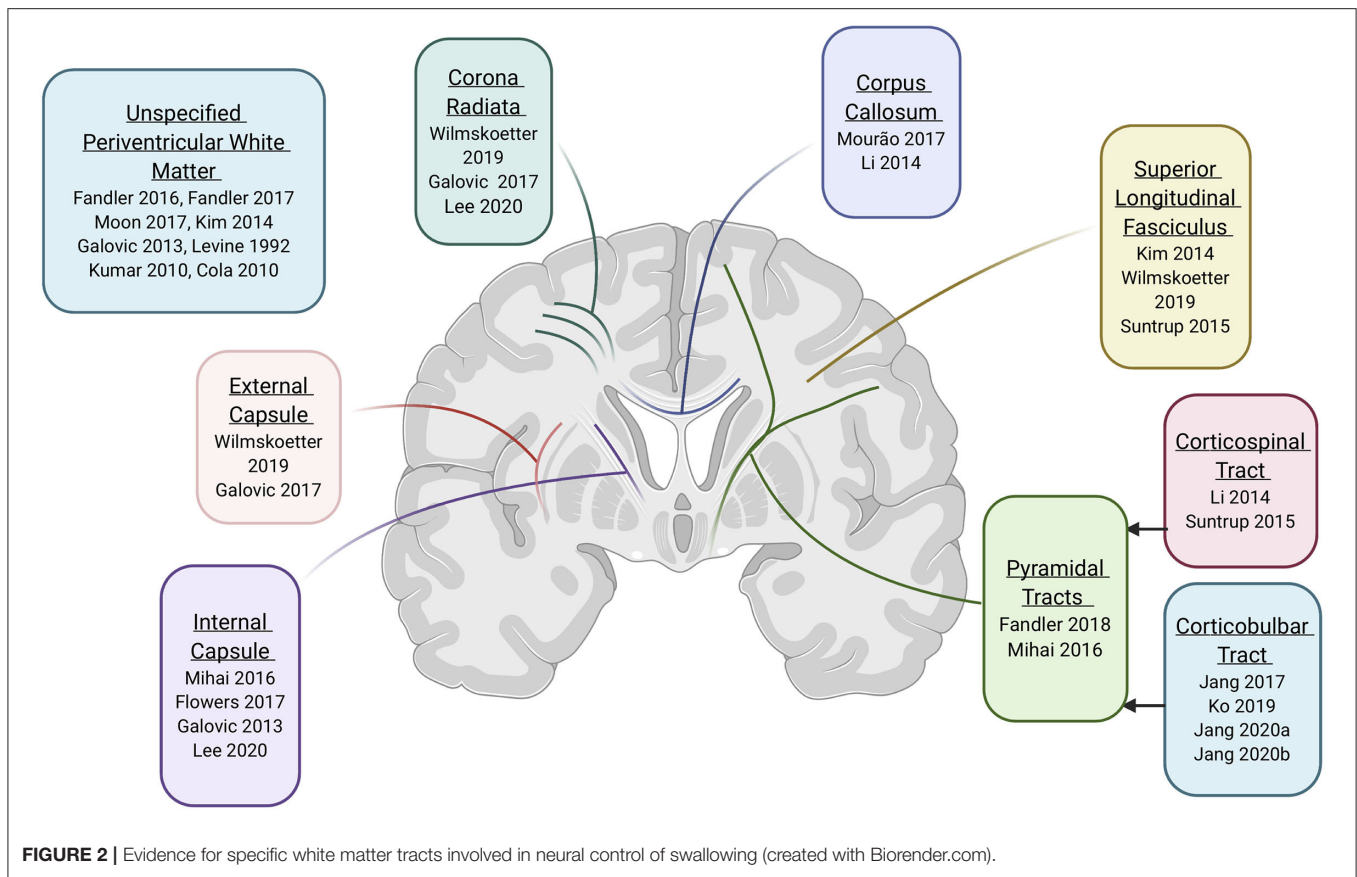
To further delineate elements critical to advancing these efforts, we also reviewed these studies' swallowing methodology. Fifteen of the identified studies used gold-standard measures that allow in-depth evaluation of the oropharyngeal swallowing phases (VFSS or FEES). Further, several of these studies used timing/temporal measures to quantify imaging analysis, and one study used the MBSIMP[®] to standardize clinical

interpretation. This allowed for more in-depth discussion of subcomponents of swallowing in relation to nervous system damage. For the remaining studies that did not use instrumental methods, it is difficult to adequately characterize the underlying mechanisms of dysphagia in their participants. This was, in some cases, partially ameliorated with the use of validated and standardized clinical assessments. Our understanding of swallowing physiology in relation to white matter integrity could be improved through detailed kinematic or morphometric analysis methods (Molfenter and Steele, 2014; Pearson et al., 2016), which help assess aspects of swallowing physiology more objectively.

Our findings on question 2 highlight the importance of combining high quality neuroimaging and swallowing physiology expertise to comprehensively investigate the neural control of swallowing. The need for strong interdisciplinary collaborations that will enable the combination of recent advanced imaging methods with in-depth swallowing evaluation and analysis techniques is apparent.

Given the methodological issues described above, for question 3 (i.e., white matter tracts implicated in swallowing control), we completed a synthesis of the findings of 20/22 studies that had a quality rating of at least Fair. Since the methods and results of the studies reviewed were heterogeneous, we cannot definitively describe the specific role of white matter in the neural control of swallowing. However, through our synthesis, the following white matter tracts or structures were frequently reported (**Figure 2**): the pyramidal tract (as a whole) and some of its subparts like the corticospinal and corticobulbar tracts, the internal capsule, the superior longitudinal fasciculus, the corona radiata, the corpus callosum, and the external capsule.

Fibers in three of these tracts/structures are categorized as projection fibers. Projection fibers were implicated in four of five studies that received a "Good" quality rating. Projection fibers connect the cortex with deep nuclei, lower parts of the brain (i.e., the brainstem), and the spinal cord. The role of the cortex and brainstem are extensively documented in animal and human studies of the neural control of swallowing (e.g., Jean, 1984; Robbins et al., 1993; Hamdy et al., 1997; Malandraki et al., 2011), so it logically follows that disruptions in the connections between these areas could affect swallowing. Specifically, dysphagia was frequently associated with bilateral damage to the pyramidal tracts, internal capsule, or corona radiata. The pyramidal tract originates in the bilateral supplementary motor area and dorsal premotor area (Wang et al., 2019) and ends at the brainstem (corticobulbar tract) or spinal cord (corticospinal tract) (Lohia and McKenzie, 2020b), and was the most clearly implicated projection tract. This is unsurprising since the supplementary motor area (SMA) has been repeatedly implicated in volitional swallowing, particularly in the preparatory phase (Huckabee et al., 2003; Satow et al., 2004; Hamdy, 2006; Malandraki et al., 2009), and communication between the SMA and subcortical areas (e.g., the basal ganglia and brainstem) is needed for swallow initiation (Hamdy et al., 1996). A subpart of the pyramidal tract, the corticobulbar tract, was reported in five reviewed papers, with two papers finding that severity of CBT injury appears to have



prognostic value for predicting swallowing recovery post-stroke (Jang et al., 2020a,b).

Fibers in the superior longitudinal fasciculus and external capsule are categorized as association fibers and connect brain regions within the same hemisphere. In two of the papers rated as “Good,” damage to these fibers was also associated with swallowing deficits. The superior longitudinal fasciculus carries input from parietal sensorimotor centers to frontal motor areas influential for swallowing coordination and initiation (Schmahmann et al., 2008). The external capsule connects the pre-frontal cortex and the supplementary motor area with the basal ganglia, and it has been hypothesized to be the key for the engagement of the basal ganglia in swallowing motor control (Schmahmann et al., 2008). Damage to these tracts was associated with impaired oral intake post-stroke and was associated (to a small extent) with deficits in specific pharyngeal subcomponents of swallowing in one study (Wilmskoetter et al., 2019).

Finally, one commissural tract, the corpus callosum, was identified in two studies. It is established that swallowing involves bilateral cerebral control (Hamdy et al., 1999; Malandraki et al., 2009), and the main pathway connecting the hemispheres is the corpus callosum. Although direct evidence is scarce, it has been theorized that the corpus callosum may be involved in communications between swallowing areas in the right and left hemispheres (Mourão et al., 2017). In the Mourão et al.’ study (2017), which included a relatively small sample of children with CP ($n = 20$), it was concluded that disruptions in the

corpus callosum were more influential for swallowing control when lesions affected cortical MCA areas, thus suggesting some influential disruptions in interhemispheric connections. Given that the quality of the studies implicating the corpus callosum was “Fair,” further research is needed to elucidate the role of inter-hemispheric connectivity for swallowing control.

In addition to insight on specific white matter tracts/structures of interest, there were three common themes regarding severity, hemispheric contribution, and time post-stroke that emerged from this literature. First, studies provided evidence that severity of white matter lesions was predictive of dysphagia severity and/or recovery (Jang et al., 2020a,b). Further, even among healthy individuals, changes to white matter were associated with changes in swallowing control (i.e., total swallow duration and oral transit duration) (Levine et al., 1992). This finding is consistent with prior literature, supporting that severity of impairment from stroke (NIHSS score) moderately predicts clinically relevant dysphagia (Jeyaseelan et al., 2015), and lesion severity also predicts post-stroke dysphagia (Otto et al., 2016; Cabib et al., 2017; Rofes et al., 2018) and warrants further investigation.

The second theme involved the role of each hemisphere’s white matter in swallowing control. White matter lesions of both hemispheres were reported to correlate with swallowing deficits, but more evidence pointed to the potential influence of the right hemisphere’s white matter areas (Mourão et al., 2017; Wilmskoetter et al., 2019). This finding is not surprising, as

several prior neuroimaging studies have also shown that gray matter areas of the right hemisphere play a more prominent role in the pharyngeal phase of swallowing compared to areas in the left hemisphere (Robbins et al., 1993; Daniels et al., 1996, p. 199; Hamdy et al., 1996; Malandraki et al., 2010; Wilmskoetter et al., 2018). In addition, there was consistent evidence that bilateral white matter damage is particularly disruptive to the neural control of swallowing (Kumar et al., 2012; Ko et al., 2019; Jang et al., 2020a,b), also paralleling related literature on bilateral gray matter damage and dysphagia (Ickenstein et al., 2003).

Finally, two studies (Galovic et al., 2013, 2017) indicated that disruptions in white matter connections are particularly disruptive to swallowing in the early post-stroke phase (i.e., within a week post stroke), but have quick recovery potential and can help restore swallowing function. The critical role of white matter in swallowing recovery was further highlighted in two additional studies that showed swallowing recovery upon white matter tracts adaptations post stroke (Mihai et al., 2016; Jang et al., 2017). These studies prompt questions surrounding the critical role that white matter plasticity may play in swallowing recovery. They also identify an area in need of rigorous exploration and with high potential impact for swallowing recovery and rehabilitation.

Limitations

A systematic review is always limited by the available evidence. We identified only twenty-two studies that met our inclusion criteria, even though our inclusion criteria were rather broad. Another limitation is that meta-analysis was not possible due to heterogeneous study designs, and all synthesis of findings was qualitative. Finally, in order to synthesize data, we used a quality assessment, but we had to modify the most relevant quality assessment available because not all components applied to this type of observational research, which we acknowledge introduces some bias.

Conclusion

This systematic review highlighted the critical role of white matter in the neural control of swallowing, which is an area that has been significantly understudied. Findings indicated that white matter damage can be directly tied to swallowing deficits, and several white matter tracts (such as the pyramidal tracts, internal capsule, superior longitudinal fasciculus, corona

radiata, corpus callosum, and external capsule) were implicated across studies. Despite these findings, several methodological limitations were also identified in most reviewed studies and need to be addressed in the future. It is our hope that this systematic review will serve as a starting point for future research that will build a more thorough understanding of the role of white matter in the neural control of normal swallowing, and, more critically, will inspire future work on delineating its role in dysphagia recovery and rehabilitation.

DATA AVAILABILITY STATEMENT

The raw data supporting the conclusions of this article will be made available by the authors, without undue reservation.

AUTHOR CONTRIBUTIONS

GM conceptualized the study, study design, and is the guarantor of the study. GM, AA, and RH designed the study and wrote the article. BM designed and performed the search, with input from all other authors. HC provided input on the methods. AA and RA screened, read, and assessed all studies. GM resolved disagreements and trained AA and RA in qualitative review. All authors read and revised manuscript drafts, and approved the final manuscript version.

FUNDING

This study was partially supported by the National Institute on Deafness and Other Communication Disorders Early Investigator R21 Grant (Grant 1R21DC015867-01A1, PI: Malandraki). Publication of this article was funded in part by the Purdue University Libraries Open Access Publishing Fund.

ACKNOWLEDGMENTS

Figure 2 was created with Biorender.com.

SUPPLEMENTARY MATERIAL

The Supplementary Material for this article can be found online at: <https://www.frontiersin.org/articles/10.3389/fnhum.2021.628424/full#supplementary-material>

REFERENCES

- Alexander, A. L., Lee, J. E., Lazar, M., and Field, A. S. (2007). Diffusion tensor imaging of the brain. *Neurotherapeutics* 4, 316–329. doi: 10.1016/j.nurt.2007.05.011
- Amri, M., Car, A., and Jean, A. (1984). Medullary control of the pontine swallowing neurones in sheep. *Exp. Brain Res.* 55, 105–110. doi: 10.1007/BF00240503
- Awad, I. A., Johnson, P. C., Spetzler, R. F., and Hodak, J. A. (1986). Incidental subcortical lesions identified on magnetic resonance imaging in the elderly. II. Postmortem pathological correlations. *Stroke* 17, 1090–1097. doi: 10.1161/01.STR.17.6.1090
- Barghi, A., Allendorfer, J. B., Taub, E., Womble, B., Hicks, J. M., Uswatte, G., et al. (2018). Phase II randomized controlled trial of constraint-induced movement therapy in multiple sclerosis. Part 2: effect on white matter integrity. *Neurorehabil. Neural Repair.* 32, 233–241. doi: 10.1177/1545968317753073
- Bartolome, G. (2006). "Kapitel 10 - Grundlagen der funktionellen Dysphagietherapie (FDT)," in *Schluckstörungen (Dritte Ausgabe)*, eds. G. Bartolome, H. Schröter-Morasch, D. Buchholz, H. Feussner, C. Hannig, S. Neumann, et al. (Munich: Urban and Fischer), 245–370.
- Bates, E., Wilson, S. M., Saygin, A. P., Dick, F., Sereno, M. I., Knight, R. T., et al. (2003). Voxel-based lesion-symptom mapping. *Nat. Neurosci.* 6, 448–450. doi: 10.1038/nn1050

- Baud, O., Daire, J.-L., Dalmaz, Y., Fontaine, R. H., Krueger, R. C., Sebag, G., et al. (2004). Gestational hypoxia induces white matter damage in neonatal rats: a new model of periventricular leukomalacia. *Brain Pathol.* 14, 1–10. doi: 10.1111/j.1750-3639.2004.tb00492.x
- Bennett, I. J., Madden, D. J., Vaidya, C. J., Howard, J. H., and Howard, D. V. (2011). White matter integrity correlates of implicit sequence learning in healthy aging. *Neurobiol. Aging* 32, 2317.e1–2317.e12. doi: 10.1016/j.neurobiolaging.2010.03.017
- Bhattacharyya, N. (2014). The prevalence of dysphagia among adults in the United States. *Otolaryngol. Head Neck Surg.* 151, 765–769. doi: 10.1177/0194599814549156
- Bosma, J. F. (1957). Deglutition: pharyngeal stage. *Physiol. Rev.* 37, 561–561. doi: 10.1152/physrev.1957.37.4.561-s
- Breier, J. I., Hasan, K. M., Zhang, W., Men, D., and Papanicolaou, A. C. (2008). Language dysfunction after stroke and damage to white matter tracts evaluated using diffusion tensor imaging. *Am. J. Neuroradiol.* 29, 483–487. doi: 10.3174/ajnr.A0846
- Buklina, S. B. (2005). The corpus callosum, interhemisphere interactions, and the function of the right hemisphere of the brain. *Neurosci. Behav. Physiol.* 35, 473–480. doi: 10.1007/s11055-005-0082-5
- Cabib, C., Ortega, O., Vilardell, N., Mundet, L., Clavé, P., and Rofes, L. (2017). Chronic post-stroke oropharyngeal dysphagia is associated with impaired cortical activation to pharyngeal sensory inputs. *Eur. J. Neurol.* 24, 1355–1362. doi: 10.1111/ene.13392
- Car, A. (1970). [Cortical control of the bulbar swallowing center]. *J. Physiol.* 62, 361–386.
- Car, A., and Roman, C. (1969). Deglutitions and oesophageal reflex contractions induced by electrical stimulation of the medulla oblongata. *Exp. Brain Res.* 11, 75–92.
- Chanraud, S., Zahr, N., Sullivan, E. V., and Pfefferbaum, A. (2010). MR diffusion tensor imaging: a window into white matter integrity of the working brain. *Neuropsychol. Rev.* 20, 209–225. doi: 10.1007/s11065-010-9129-7
- Clark, K. A., Nuechterlein, K. H., Asarnow, R. F., Hamilton, L. S., Phillips, O. R., Hageman, N. S., et al. (2011). Mean diffusivity and fractional anisotropy as indicators of disease and genetic liability to schizophrenia. *J. Psychiatr. Res.* 45, 980–988. doi: 10.1016/j.jpsychires.2011.01.006
- Cola, M. G., Daniels, S. K., Corey, D. M., Lemen, L. C., Romero, M., and Foundas, A. L. (2010). Relevance of subcortical stroke in dysphagia. *Stroke* 41, 482–486. doi: 10.1161/STROKEAHA.109.566133
- Crary, M. A., Mann, G. D. C., and Groher, M. E. (2005). Initial psychometric assessment of a functional oral intake scale for dysphagia in stroke patients. *Arch. Phys. Med. Rehabil.* 86, 1516–1520. doi: 10.1016/j.apmr.2004.11.049
- Daniels, S. K., Ballo, L. A., Mahoney, M.-C., and Foundas, A. L. (2000). Clinical predictors of dysphagia and aspiration risk: outcome measures in acute stroke patients. *Arch. Phys. Med. Rehabil.* 81, 1030–1033. doi: 10.1053/apmr.2000.6301
- Daniels, S. K., Brailey, K., and Foundas, A. L. (1999). Lingual discoordination and dysphagia following acute stroke: analyses of lesion localization. *Dysphagia* 14, 85–92. doi: 10.1007/PL00009592
- Daniels, S. K., Foundas, A. L., Iglesia, G. C., and Sullivan, M. A. (1996). Lesion site in unilateral stroke patients with dysphagia. *J. Stroke Cerebrovasc. Dis.* 6, 30–34. doi: 10.1016/S1052-3057(96)80023-1
- De Erausquin, G. A., and Alba-Ferrara, L. (2013). What does anisotropy measure? Insights from increased and decreased anisotropy in selective fiber tracts in schizophrenia. *Front. Integr. Neurosci.* 7:9. doi: 10.3389/fnint.2013.00009
- de Figueiredo, E. H. M. S. G., Borroni, A. F. N. G., and Doring, T. M. (2011). Basic concepts of MR imaging, diffusion mr imaging, and diffusion tensor imaging. *Magn. Reson. Imaging Clin. N. Am.* 19, 1–22. doi: 10.1016/j.mric.2010.10.005
- de Lama Lazzara, G., Lazarus, C., and Logemann, J. A. (1986). Impact of thermal stimulation on the triggering of the swallowing reflex. *Dysphagia* 1, 73–77. doi: 10.1007/BF02407117
- Doty, R. W. (1951). Influence of stimulus pattern on reflex deglutition. *Am. J. Physiol.* 166, 142–158. doi: 10.1152/ajplegacy.1951.166.1.142
- Doty, R. W. (1968). Neural organization of deglutition. *Alimentary Canal* 1861. Available online at: <https://ci.nii.ac.jp/naid/10011018245/> (accessed July 31, 2020).
- Emos, M. C., and Agarwal, S. (2020). “Neuroanatomy, Internal Capsule,” in *StatPearls* (Treasure Island, FL: StatPearls Publishing). Available online at: <http://www.ncbi.nlm.nih.gov/books/NBK542181/> (accessed July 29, 2020).
- Fandler, S., Gattringer, T., Eppinger, S., Doppelhofer, K., Pinter, D., Niederkorn, K., et al. (2017). Frequency and predictors of dysphagia in patients with recent small subcortical infarcts. *Stroke* 48, 213–215. doi: 10.1161/STROKEAHA.116.015625
- Fandler, S., Gattringer, T., Pinter, D., Pirpamer, L., Borsodi, F., Eppinger, S., et al. (2018). Dysphagia in supratentorial recent small subcortical infarcts results from bilateral pyramidal tract damage. *Int. J. Stroke* 13, 815–819. doi: 10.1177/1747493018778141
- Fazekas, F., Chawluk, J. B., Alavi, A., Hurtig, H. I., and Zimmerman, R. A. (1987). MR signal abnormalities at 1.5 T in Alzheimer's dementia and normal aging. *AJR Am. J. Roentgenol.* 149, 351–356. doi: 10.2214/ajr.149.2.351
- Flowers, H. L., AlHarbi, M. A., Mikulis, D., Silver, F. L., Rochon, E., Streiner, D., et al. (2017). MRI-based neuroanatomical predictors of dysphagia, dysarthria, and aphasia in patients with first acute ischemic stroke. *Cerebrovasc. Dis. Extra* 7, 21–34. doi: 10.1159/000457810
- Frank, L. R. (2001). Anisotropy in high angular resolution diffusion-weighted MRI. *Magn. Reson. Med.* 45, 935–939. doi: 10.1002/mrm.1125
- Galovic, M., Leisi, N., Müller, M., Weber, J., Abela, E., Kägi, G., et al. (2013). Lesion location predicts transient and extended risk of aspiration after supratentorial ischemic stroke. *Stroke* 44, 2760–2767. doi: 10.1161/STROKEAHA.113.001690
- Galovic, M., Leisi, N., Müller, M., Weber, J., Tettenborn, B., Brugger, F., et al. (2016). Neuroanatomical correlates of tube dependency and impaired oral intake after hemispheric stroke. *Eur. J. Neurol.* 23, 926–934. doi: 10.1111/ene.12964
- Galovic, M., Leisi, N., Pastore-Wapp, M., Zbinden, M., Vos, S. B., Mueller, M., et al. (2017). Diverging lesion and connectivity patterns influence early and late swallowing recovery after hemispheric stroke. *Hum. Brain Mapp.* 38, 2165–2176. doi: 10.1002/hbm.23511
- Gordon, C., Hewer, R. L., and Wade, D. T. (1987). Dysphagia in acute stroke. *Br. Med. J. (Clin. Res. Ed)* 295, 411–414. doi: 10.1136/bmj.295.6595.411
- Hamdy, S. (2006). *Role of Cerebral Cortex in the Control of Swallowing*. GI Motility online.
- Hamdy, S., Aziz, Q., Rothwell, J. C., Hobson, A., Barlow, J., and Thompson, D. G. (1997). Cranial nerve modulation of human cortical swallowing motor pathways. *Am. J. Physiol. Gastro. Liver Physiol.* 272, G802–G808. doi: 10.1152/ajpgi.1997.272.4.G802
- Hamdy, S., Aziz, Q., Rothwell, J. C., Singh, K. D., Barlow, J., Hughes, D. G., et al. (1996). The cortical topography of human swallowing musculature in health and disease. *Nat. Med.* 2, 1217–1224. doi: 10.1038/nm1196-1217
- Hamdy, S., Mikulis, D. J., Crawley, A., Xue, S., Lau, H., Henry, S., et al. (1999). Cortical activation during human volitional swallowing: an event-related fMRI study. *Am. J. Physiol. Gastro. Liver Physiol.* 277, G219–G225. doi: 10.1152/ajpgi.1999.277.1.G219
- Herrera, J. J., Bockhorst, K., Kondraganti, S., Stertz, L., Quevedo, J., and Narayana, P. A. (2016). Acute white matter tract damage after frontal mild traumatic brain injury. *J. Neurotrauma* 34, 291–299. doi: 10.1089/neu.2016.4407
- Huber, E., Donnelly, P. M., Rokem, A., and Yeatman, J. D. (2018). Rapid and widespread white matter plasticity during an intensive reading intervention. *Nat. Commun.* 9:2260. doi: 10.1038/s41467-018-04627-5
- Huckabee, M.-L., Deecke, L., Cannito, M. P., Gould, H. J., and Mayr, W. (2003). Cortical control mechanisms in volitional swallowing: the bereichschaftspotential. *Brain Topogr.* 16, 3–17. doi: 10.1023/A:1025671914949
- Huisman, T. A. G. M. (2010). Diffusion-weighted and diffusion tensor imaging of the brain, made easy. *Cancer Imaging* 10, S163–S171. doi: 10.1102/1470-7330.2010.9023
- Ickenstein, G. W., Kelly, P. J., Furie, K. L., Ambrosi, D., Rallis, N., Goldstein, R., et al. (2003). Predictors of feeding gastrostomy tube removal in stroke patients with dysphagia. *J. Stroke Cerebrovasc. Dis.* 12, 169–174. doi: 10.1016/S1052-3057(03)00077-6
- Jang, S., Kim, J., Seo, Y., and Kwak, S. (2017). Recovery of an injured corticobulbar tract in a patient with stroke: a case report. *Medicine* 96:e7636. doi: 10.1097/MD.00000000000007636
- Jang, S. H., Kwak, S. Y., Chang, C. H., Jung, Y. J., Kim, J., Kim, S. H., et al. (2020a). Prognostic prediction of dysphagia by analyzing the corticobulbar tract in the early stage of intracerebral hemorrhage. *Dysphagia* 35, 985–992. doi: 10.1007/s00455-020-10093-3
- Jang, S. H., Lee, J., and Kim, M. S. (2020b). Dysphagia prognosis prediction via corticobulbar tract assessment in lateral medullary infarction: a diffusion tensor tractography study. *Dysphagia*. doi: 10.1007/s00455-020-10182-3. [Epub ahead of print].

- Jean, A. (1984). Brainstem organization of the swallowing network. *BBE* 25, 109–116. doi: 10.1159/000118856
- Jean, A., Car, A., and Roman, C. (1975). Comparison of activity in pontine versus medullary neurones during swallowing. *Exp. Brain Res.* 22, 211–220. doi: 10.1007/BF00237690
- Jeyaseelan, R. D., Vargo, M. M., and Chae, J. (2015). National Institutes of Health Stroke Scale (NIHSS) as an early predictor of poststroke dysphagia. *PMR* 7, 593–598. doi: 10.1016/j.pmrj.2014.12.007
- Kato, H., and Izumiyama, M. (2017). Damage to the pyramidal tract leads to post-stroke reorganization of brain motor network. *J. Neurol. Sci.* 381, 598–599. doi: 10.1016/j.jns.2017.08.1687
- Kaur, C., and Ling, E. A. (2009). Periventricular white matter damage in the hypoxic neonatal brain: Role of microglial cells. *Progress Neurobiol.* 87, 264–280. doi: 10.1016/j.pneurobio.2009.01.003
- Kessler, J. P., and Jean, A. (1985). Identification of the medullary swallowing regions in the rat. *Exp. Brain Res.* 57, 256–263. doi: 10.1007/BF00236530
- Kim, S. Y., Kim, T. U., Hyun, J. K., and Lee, S. J. (2014). Differences in videofluoroscopic swallowing study (VFSS) findings according to the vascular territory involved in stroke. *Dysphagia* 29, 444–449. doi: 10.1007/s00455-014-9525-x
- Kingsley, P. B., and Monahan, W. G. (2004). Selection of the optimum b factor for diffusion-weighted magnetic resonance imaging assessment of ischemic stroke. *Magn. Res. Med.* 51, 996–1001. doi: 10.1002/mrm.20059
- Ko, E. J., Choi, K. H., and Kwon, S. U. (2019). The relationship between leukoaraiosis involving contralateral corticobulbar tract and dysphagia in patients with acute unilateral corona radiata infarction with corticobulbar tract involvement. *Dysphagia* 34, 654–664. doi: 10.1007/s00455-018-9963-y
- Kou, Z., and Iraj, A. (2014). Imaging brain plasticity after trauma. *Neural Regen. Res.* 9, 693–700. doi: 10.4103/1673-5374.131568
- Kumar, S., Langmore, S., Goddeau, R. P., Alhazzani, A., Selim, M., Caplan, L. R., et al. (2012). Predictors of percutaneous endoscopic gastrostomy tube placement in patients with severe dysphagia from an acute-subacute hemispheric infarction. *J. Stroke Cerebrovasc. Dis.* 21, 114–120. doi: 10.1016/j.jstrokecerebrovasdis.2010.05.010
- Langmore, S. E., Terpenning, M. S., Schork, A., Chen, Y., Murray, J. T., Lopatin, D., et al. (1998). Predictors of aspiration pneumonia: how important is dysphagia? *Dysphagia* 13, 69–81. doi: 10.1007/PL00009559
- Lee, W. H., Lim, M. H., Seo, H. G., Seong, M. Y., Oh, B.-M., and Kim, S. (2020). Development of a novel prognostic model to predict 6-month swallowing recovery after ischemic stroke. *Stroke* 51, 440–448. doi: 10.1161/STROKEAHA.119.027439
- Leiva-Salinas, C., and Wintermark, M. (2010). Imaging of ischemic stroke. *Neuroimaging Clin. N. Am.* 20, 455–468. doi: 10.1016/j.nic.2010.07.002
- Leow, L. P., Huckabee, M.-L., Anderson, T., and Beckert, L. (2010). The impact of dysphagia on quality of life in ageing and Parkinson's disease as measured by the swallowing quality of Life (SWAL-QOL) questionnaire. *Dysphagia* 25, 216–220. doi: 10.1007/s00455-009-9245-9
- Levine, R., Robbins, J. A., and Maser, A. (1992). Periventricular white matter changes and oropharyngeal swallowing in normal individuals. *Dysphagia* 7, 142–147. doi: 10.1007/BF02493446
- Li, S., Ma, Z., Tu, S., Zhou, M., Chen, S., Guo, Z., et al. (2014). Altered resting-state functional and white matter tract connectivity in stroke patients with dysphagia. *Neurorehabil. Neural Repair.* 28, 260–272. doi: 10.1177/1545968313508227
- Logemann, J. A., Shanahan, T., Rademaker, A. W., Kahrilas, P. J., Lazar, R., and Halper, A. (1993). Oropharyngeal swallowing after stroke in the left basal ganglion/internal capsule. *Dysphagia* 8, 230–234. doi: 10.1007/BF01354543
- Lohia, A., and McKenzie, J. (2020a). "Neuroanatomy, Pyramidal Tract Lesions," in *StatPearls* (Treasure Island, FL: StatPearls Publishing). Available online at: <http://www.ncbi.nlm.nih.gov/books/NBK540976/> (accessed July 31, 2020).
- Lohia, A., and McKenzie, J. (2020b). "Neuroanatomy, Pyramidal Tract Lesions," in *StatPearls* (Treasure Island, FL: StatPearls Publishing). Available at: <http://www.ncbi.nlm.nih.gov/books/NBK540976/> (accessed September 7, 2020).
- Love, S., and Miners, J. S. (2015). White matter hypoperfusion and damage in dementia: post-mortem assessment. *Brain Pathol.* 25, 99–107. doi: 10.1111/bpa.12223
- Madden, D. J., Spaniol, J., Costello, M. C., Bucur, B., White, L. E., Cabeza, R., et al. (2008). Cerebral white matter integrity mediates adult age differences in cognitive performance. *J. Cogn. Neurosci.* 21, 289–302. doi: 10.1162/jocn.2009.21047
- Malandraki, G. A., Johnson, S., and Robbins, J. (2011). Functional MRI of swallowing: from neurophysiology to neuroplasticity. *Head Neck* 33, S14–S20. doi: 10.1002/hed.21903
- Malandraki, G. A., Sutton, B. P., Perlman, A. L., and Karampinos, D. C. (2010). Age-related differences in laterality of cortical activations in swallowing. *Dysphagia* 25, 238–249. doi: 10.1007/s00455-009-9250-z
- Malandraki, G. A., Sutton, B. P., Perlman, A. L., Karampinos, D. C., and Conway, C. (2009). Neural activation of swallowing and swallowing-related tasks in healthy young adults: an attempt to separate the components of deglutition. *Hum. Brain Mapp.* 30, 3209–3226. doi: 10.1002/hbm.20743
- Mann, C. J. (2003). Observational research methods. Research design II: cohort, cross sectional, and case-control studies. *Emerg. Med. J.* 20, 54–60. doi: 10.1136/emj.20.1.54
- Martin, R. E., Goodyear, B. G., Gati, J. S., and Menon, R. S. (2001). Cerebral cortical representation of automatic and volitional swallowing in humans. *J. Neurophysiol.* 85, 938–950. doi: 10.1152/jn.2001.85.2.938
- Martin, R. E., Kempainen, P., Masuda, Y., Yao, D., Murray, G. M., and Sessle, B. J. (1999). Features of cortically evoked swallowing in the awake primate (Macaca fascicularis). *J. Neurophysiol.* 82, 1529–1541. doi: 10.1152/jn.1999.82.3.1529
- Martin, R. E., MacIntosh, B. J., Smith, R. C., Barr, A. M., Stevens, T. K., Gati, J. S., et al. (2004). Cerebral areas processing swallowing and tongue movement are overlapping but distinct: a functional magnetic resonance imaging study. *J. Neurophysiol.* 92, 2428–2443. doi: 10.1152/jn.01144.2003
- Martin, R. E., and Sessle, B. J. (1993). The role of the cerebral cortex in swallowing. *Dysphagia* 8, 195–202. doi: 10.1007/BF01354538
- Martin-Harris, B., Brodsky, M. B., Michel, Y., Castell, D. O., Schleicher, M., Sandridge, J., et al. (2008). MBS measurement tool for swallow impairment-MBSImp: establishing a standard. *Dysphagia* 4, 392–405. doi: 10.1007/s00455-008-9185-9
- Meadows, J. C. (1973). Dysphagia in unilateral cerebral lesions. *J. Neurol. Neurosurg. Psychiatry* 36, 853–860. doi: 10.1136/jnnp.36.5.853
- Metzler-Baddeley, C., Mole, J. P., Sims, R., Fasano, F., Evans, J., Jones, D. K., et al. (2019). Fornix white matter glia damage causes hippocampal gray matter damage during age-dependent limbic decline. *Sci. Rep.* 9:1060. doi: 10.1038/s41598-018-37658-5
- Mihai, P. G., Otto, M., Domin, M., Platz, T., Hamdy, S., and Lotze, M. (2016). Brain imaging correlates of recovered swallowing after dysphagic stroke: a fMRI and DWI study. *Neuroimage Clin.* 12, 1013–1021. doi: 10.1016/j.nicl.2016.05.006
- Miller, F. R., and Sherrington, C. S. (1915). Some observations on the buccopharyngeal stage of reflex deglutition in the cat. *Quarterly J. Exp. Physiol.* 9, 147–186. doi: 10.1113/expphysiol.1915.sp000201
- Moher, D., Liberati, A., Tetzlaff, J., Altman, D. G., and Group, T. P. (2009). Preferred reporting items for systematic reviews and meta-analyses: the PRISMA statement. *PLoS Med* 6:e1000097. doi: 10.1371/journal.pmed.1000097
- Molfenter, S. M., and Steele, C. M. (2014). Kinematic and temporal factors associated with penetration-aspiration in swallowing liquids. *Dysphagia* 29, 269–276. doi: 10.1007/s00455-013-9506-5
- Moon, H. I., Nam, J.-S., Leem, M. J., and Kim, K. H. (2017). Periventricular white matter lesions as a prognostic factor of swallowing function in older patients with mild stroke. *Dysphagia* 32, 480–486. doi: 10.1007/s00455-017-9788-0
- Mori, S., and Zhang, J. (2006). Principles of diffusion tensor imaging and its applications to basic neuroscience research. *Neuron* 51, 527–539. doi: 10.1016/j.neuron.2006.08.012
- Mourão, L. F., Friel, K. M., Sheppard, J. J., Kuo, H.-C., Luchesi, K. F., Gordon, A. M., et al. (2017). The role of the corpus callosum in pediatric dysphagia: preliminary findings from a diffusion tensor imaging study in children with unilateral spastic cerebral palsy. *Dysphagia* 32, 703–713. doi: 10.1007/s00455-017-9816-0
- Namasivayam, A. M., and Steele, C. M. (2015). Malnutrition and dysphagia in long-term care: a systematic review. *J. Nutr. Gerontol. Geriatr.* 34, 1–21. doi: 10.1080/21551197.2014.1002656
- Narayana, P. A., Herrera, J. J., Bockhorst, K. H., Esparza-Coss, E., Xia, Y., Steinberg, J. L., et al. (2014). Chronic cocaine administration causes extensive white matter damage in brain: diffusion tensor imaging and immunohistochemistry studies. *Psychiatry Res. Neuroimaging* 221, 220–230. doi: 10.1016/j.pscychres.2014.01.005

- National Heart, Lung, and Blood Institute (2019). Study quality assessment tools. Available online at: <https://www.nhlbi.nih.gov/health-topics/study-quality-assessment-tools>
- Otto, D. M., Ribeiro, M. de C., Barea, L. M., Mancopes, R., Almeida, S. T. de, Otto, D. M., et al. (2016). Association between neurological injury and the severity of oropharyngeal dysphagia after stroke. *CoDAS* 28, 724–729. doi: 10.1590/2317-1782/20162015139
- Ouzzani, M., Hammady, H., Fedorowicz, Z., and Elmagarmid, A. (2016). Rayyan—a web and mobile app for systematic reviews. *Syst. Rev.* 5:210. doi: 10.1186/s13643-016-0384-4
- Pearson, W. G., Taylor, B. K., Blair, J., and Martin-Harris, B. (2016). Computational analysis of swallowing mechanics underlying impaired epiglottic inversion. *Laryngoscope* 126, 1854–1858. doi: 10.1002/lary.25788
- Penfield, W. (1955). The twenty-ninth maudslay lecture: the role of the temporal cortex in certain psychical phenomena. *J. Mental Sci.* 101, 451–465. doi: 10.1192/bjp.101.424.451
- Penfield, W., and Welch, K. (1949). Instability of response to stimulation of the sensorimotor cortex of man. *J. Physiol.* 109, 358–365. doi: 10.1113/jphysiol.1949.sp004399
- Puig, J., Pedraza, S., Blasco, G., Daunis-i-Estadella, J., Prados, F., Remollo, S., et al. (2011). Acute damage to the posterior limb of the internal capsule on diffusion tensor tractography as an early imaging predictor of motor outcome after stroke. *Am. J. Neuroradiol.* 32, 857–863. doi: 10.3174/ajnr.A2400
- Reber, E., Gomes, F., Dähn, I. A., Vasiloglou, M. F., and Stanga, Z. (2019). Management of dehydration in patients suffering swallowing difficulties. *J. Clin. Med.* 8:1923. doi: 10.3390/jcm8111923
- Robbins, J., Levine, R. L., Maser, A., Rosenbek, J. C., and Kempster, G. B. (1993). Swallowing after unilateral stroke of the cerebral cortex. *Arch. Phys. Med. Rehabil.* 74, 1295–1300. doi: 10.1016/0003-9993(93)90082-L
- Rofes, L., Muriana, D., Palomeras, E., Vilardell, N., Palomera, E., Alvarez-Berdugo, D., et al. (2018). Prevalence, risk factors and complications of oropharyngeal dysphagia in stroke patients: A cohort study. *Neurogastroenterol Motil.* 30:e13338. doi: 10.1111/nmo.13338
- Rosenbek, J. C., Robbins, J. A., Roecker, E. B., Coyle, J. L., and Wood, J. L. (1996). A penetration-aspiration scale. *Dysphagia* 11, 93–98. doi: 10.1007/BF00417897
- Rovira, A., Grivé, E., Rovira, A., and Alvarez-Sabin, J. (2005). Distribution territories and causative mechanisms of ischemic stroke. *Eur. Radiol.* 15, 416–426. doi: 10.1007/s00330-004-2633-5
- Sampaio-Baptista, C., and Johansen-Berg, H. (2017). White matter plasticity in the adult brain. *Neuron* 96, 1239–1251. doi: 10.1016/j.neuron.2017.11.026
- Satow, T., Ikeda, A., Yamamoto, J., Begum, T., Thuy, D. H. D., Matsushashi, M., et al. (2004). Role of primary sensorimotor cortex and supplementary motor area in volitional swallowing: a movement-related cortical potential study. *Am. J. Physiol. Gastro. Liver Physiol.* 287, G459–G470. doi: 10.1152/ajpgi.00323.2003
- Schlaug, G., Marchina, S., and Norton, A. (2009). Evidence for plasticity in white matter tracts of chronic aphasic patients undergoing intense intonation-based speech therapy. *Ann. N. Y. Acad. Sci.* 1169, 385–394. doi: 10.1111/j.1749-6632.2009.04587.x
- Schmahmann, J. D., Pandya, D. N., Wang, R., Dai, G., D'Arceuil, H. E., de Crespigny, A. J., et al. (2007). Association fibre pathways of the brain: parallel observations from diffusion spectrum imaging and autoradiography. *Brain* 130, 630–653. doi: 10.1093/brain/awl359
- Schmahmann, J. D., Smith, E. E., Eichler, F. S., and Filley, C. M. (2008). Cerebral white matter. *Ann. N. Y. Acad. Sci.* 1142, 266–309. doi: 10.1196/annals.1444.017
- Schulz, R., Zimmerman, M., Timmermann, J. E., Wessel, M. J., Gerloff, C., and Hummel, F. C. (2014). White matter integrity of motor connections related to training gains in healthy aging. *Neurobiol. Aging* 35, 1404–1411. doi: 10.1016/j.neurobiolaging.2013.11.024
- Sheppard, J. J., Hochman, R., and Baer, C. (2014). The dysphagia disorder survey: validation of an assessment for swallowing and feeding function in developmental disability. *Res. Dev. Disabil.* 35, 929–942. doi: 10.1016/j.ridd.2014.02.017
- Sims, J. R., Gharai, L. R., Schaefer, P. W., Vangel, M., Rosenthal, E. S., Lev, M. H., et al. (2009). ABC/2 for rapid clinical estimate of infarct, perfusion, and mismatch volumes. *Neurology* 72, 2104–2110. doi: 10.1212/WNL.0b013e3181aa5329
- Sporns, O., Tononi, G., and Kötter, R. (2005). The human connectome: a structural description of the human brain. *PLoS Comput. Biol.* 1, 0245–0251. doi: 10.1371/journal.pcbi.0010042
- Study Quality Assessment Tools | NHLBI, NIH (2019). Available online at: <https://www.nhlbi.nih.gov/health-topics/study-quality-assessment-tools> (accessed July 31, 2020).
- Sumi, T. (1972). Reticular ascending activation of frontal cortical neurons in rabbits, with special reference to the regulation of deglutition. *Brain Res.* 46, 43–54. doi: 10.1016/0006-8993(72)90004-2
- Suntrup, S., Kemmling, A., Warnecke, T., Hamacher, C., Oelenberg, S., Niederstadt, T., et al. (2015). The impact of lesion location on dysphagia incidence, pattern and complications in acute stroke. Part 1: dysphagia incidence, severity and aspiration. *Eur. J. Neurol.* 22, 832–838. doi: 10.1111/ene.12670
- Suzuki, M., Asada, Y., Ito, J., Hayashi, K., Inoue, H., and Kitano, H. (2003). Activation of cerebellum and basal ganglia on volitional swallowing detected by functional magnetic resonance imaging. *Dysphagia* 18, 71–77. doi: 10.1007/s00455-002-0088-x
- Tassorelli, C., Bergamaschi, R., Buscone, S., Bartolo, M., Furnari, A., Crivelli, P., et al. (2008). Dysphagia in multiple sclerosis: from pathogenesis to diagnosis. *Neurol. Sci.* 29, 360–363. doi: 10.1007/s10072-008-1044-9
- Toogood, J. A., Barr, A. M., Stevens, T. K., Gati, J. S., Menon, R. S., and Martin, R. E. (2005). Discrete functional contributions of cerebral cortical foci in voluntary swallowing: a functional magnetic resonance imaging (fMRI) “Go, No-Go” study. *Exp. Brain Res.* 161, 81–90. doi: 10.1007/s00221-004-2048-1
- Trivedi, R., Gupta, R. K., Shah, V., Tripathi, M., Rathore, R. K. S., Kumar, M., et al. (2008). Treatment-induced plasticity in cerebral palsy: a diffusion tensor imaging study. *Pediatr. Neurol.* 39, 341–349. doi: 10.1016/j.pediatrneurol.2008.07.012
- Vos, S. B., Aksoy, M., Han, Z., Holdsworth, S. J., Maclaren, J., Viergever, M. A., et al. (2016). Trade-off between angular and spatial resolutions in *in vivo* fiber tractography. *Neuroimage* 129, 117–132. doi: 10.1016/j.neuroimage.2016.01.011
- Wahlund, L. O., Barkhof, F., Fazekas, F., Bronge, L., Augustin, M., Sjögren, M., et al. (2001). A new rating scale for age-related white matter changes applicable to MRI and CT. *Stroke* 32, 1318–1322. doi: 10.1161/01.STR.32.6.1318
- Wan, P., Chen, X., Zhu, L., Xu, S., Huang, L., Li, X., et al. (2016). Dysphagia post subcortical and supratentorial stroke. *J. Stroke Cerebrovasc. Dis.* 25, 74–82. doi: 10.1016/j.jstrokecerebrovasdis.2015.08.037
- Wang, Z.-M., Shan, Y., Zhang, M., Wei, P.-H., Li, Q.-G., Yin, Y.-Y., et al. (2019). Projections of brodmann area 6 to the pyramidal tract in humans: quantifications using high angular resolution data. *Front. Neural Circ.* 13:62. doi: 10.3389/fncir.2019.00062
- Wardlaw, J. M., Valdés Hernández, M. C., and Muñoz-Maniega, S. (2015). What are white matter hyperintensities made of? *J. Am. Heart Assoc.* 4:e001140. doi: 10.1161/JAHA.114.001140
- Wilmskoetter, J., Bonilha, L., Martin-Harris, B., Elm, J. J., Horn, J., and Bonilha, H. S. (2019). Mapping acute lesion locations to physiological swallow impairments after stroke. *Neuroimage Clin.* 22:101685. doi: 10.1016/j.nicl.2019.101685
- Wilmskoetter, J., Martin-Harris, B., Pearson, W. G., Bonilha, L., Elm, J. J., Horn, J., et al. (2018). Differences in swallow physiology in patients with left and right hemispheric strokes. *Physiol. Behav.* 194, 144–152. doi: 10.1016/j.physbeh.2018.05.010
- Ziegler, D. A., Piguet, O., Salat, D. H., Prince, K., Connally, E., and Corkin, S. (2010). Cognition in healthy aging is related to regional white matter integrity, but not cortical thickness. *Neurobiol. Aging* 31, 1912–1926. doi: 10.1016/j.neurobiolaging.2008.10.015

Conflict of Interest: The authors declare that the research was conducted in the absence of any commercial or financial relationships that could be construed as a potential conflict of interest.

Copyright © 2021 Alvar, Hahn Arkenberg, McGowan, Cheng and Malandraki. This is an open-access article distributed under the terms of the Creative Commons Attribution License (CC BY). The use, distribution or reproduction in other forums is permitted, provided the original author(s) and the copyright owner(s) are credited and that the original publication in this journal is cited, in accordance with accepted academic practice. No use, distribution or reproduction is permitted which does not comply with these terms.



Coordination of Respiration, Swallowing, and Chewing in Healthy Young Adults

Naohito Hao, Anna Sasa, Sirima Kulvanich, Yuta Nakajima, Kouta Nagoya, Jin Magara, Takanori Tsujimura and Makoto Inoue*

Division of Dysphagia Rehabilitation, Niigata University Graduate School of Medical and Dental Sciences, Niigata, Japan

OPEN ACCESS

Edited by:

Limor Avivi-Arber,
University of Toronto, Canada

Reviewed by:

Jeffrey Palmer,
Johns Hopkins University,
United States
Ivy Cheng,
The University of Manchester,
United Kingdom

*Correspondence:

Makoto Inoue
inoue@dent.niigata-u.ac.jp

Specialty section:

This article was submitted to
Craniofacial Biology and Dental
Research,
a section of the journal
Frontiers in Physiology

Received: 16 April 2021

Accepted: 15 June 2021

Published: 13 July 2021

Citation:

Hao N, Sasa A, Kulvanich S,
Nakajima Y, Nagoya K, Magara J,
Tsujimura T and Inoue M (2021)
Coordination of Respiration,
Swallowing, and Chewing in Healthy
Young Adults.
Front. Physiol. 12:696071.
doi: 10.3389/fphys.2021.696071

Examining the coordination of respiration and swallowing is important for elucidating the mechanisms underlying these functions and assessing how respiration is linked to swallowing impairment in dysphagic patients. In this study, we assessed the coordination of respiration and swallowing to clarify how voluntary swallowing is coordinated with respiration and how mastication modulates the coordination of respiration and swallowing in healthy humans. Twenty-one healthy volunteers participated in three experiments. The participants were asked to swallow 3 ml of water with or without a cue, to drink 100 ml of water using a cup without breathing between swallows, and to eat a 4-g portion of corned beef. The major coordination pattern of respiration and swallowing was expiration–swallow–expiration (EE type) while swallowing 3 ml of water either with or without a cue, swallowing 100 ml of water, and chewing. Although cueing did not affect swallowing movements, the expiratory time was lengthened with the cue. During 100-ml water swallowing, the respiratory cycle time and expiratory time immediately before swallowing were significantly shorter compared with during and after swallowing, whereas the inspiratory time did not differ throughout the recording period. During chewing, the respiratory cycle time was decreased in a time-dependent manner, probably because of metabolic demand. The coordination of the two functions is maintained not only in voluntary swallowing but also in involuntary swallowing during chewing. Understanding the mechanisms underlying respiration and swallowing is important for evaluating how coordination affects physiological swallowing in dysphagic patients.

Keywords: electromyography, mastication, respiration, suprahyoid muscles, swallowing

INTRODUCTION

Swallowing is essential not only to propel a food bolus into the stomach but also to protect the upper airway and prevent pulmonary aspiration. During swallowing, several mechanisms function simultaneously; the tongue and soft palate elevate to propel the bolus posteriorly and open the fauces, respectively, accompanied by the elevation of the hyolaryngeal complex and pharyngeal muscle contraction to transport the bolus, laryngeal closure to serve as airway protection, and finally, relaxation of the upper oesophageal sphincter to allow the bolus to enter the esophagus

(Jean, 2001). Most of these structures also serve as a common pathway for other behaviors, such as mastication, respiration, and vocalization.

Breathing and swallowing are tightly coupled to perform safe and effective coordination (Martin-Harris and McFarland, 2013). Both the respiratory and swallowing neural networks, which generate and coordinate muscle activities, are located in the lower brainstem (Amri et al., 1984; Bianchi and Gestreau, 2009). Previous studies have suggested that within the swallowing neural network in the brain stem, some neurons, such as interneurons and motor neurons, may also participate in the respiratory activity. The respiratory central pattern generator (CPG) consists of the dorsal respiratory group and the ventral respiratory column in the medulla and pneumotactic centers in the pons (Bianchi and Gestreau, 2009). In contrast, the swallowing CPG is located in the medulla oblongata and includes a dorsal swallowing group (DSG) in the nucleus tractus solitarius and a ventral swallowing group (VSG) within the ventrolateral medulla above the nucleus ambiguus (Jean, 2001). Both CPGs receive afferent sensory inputs from the pharynx and larynx *via* the vagal nerves (Bianchi and Gestreau, 2009). Furthermore, ambiguous, trigeminal, and hypoglossal motoneurons are activated in both situations (Sumi, 1963; Larson et al., 1994; Shiba et al., 1999), which indicates that these motoneurons may receive inputs from these CPGs. Thus, it can be assumed that there is a substantial amount of cross talk between them.

Regarding coordination of respiration and swallowing in animals, swallowing reflexes are reported to operate during the different phases of respiration. Doty and Bosma (1956) first demonstrated that most swallowing evoked by the superior laryngeal nerve stimulation occurred during the inspiratory phase in anesthetized dogs and monkeys. In addition, Kawasaki et al. (1964) reported that spontaneous swallowing occurred during the inspiratory phase in anesthetized dogs. In contrast, in awake animals, Feroah et al. (2002) reported that around half of spontaneous swallows occurred during the inspiratory phase (45%) followed by the expiratory phase (28%) or the transition from expiration to inspiration (26%) in awake goats. McFarland et al. (McFarland and Lund, 1993) reported that more than half of swallowing reflexes were recorded during the first half of the inspiratory phase in awake rabbits. Several studies reported that the occurrence of the swallowing reflex coincided with the expiratory phase in anesthetized cats (Doty and Bosma, 1956; Dick et al., 1993).

In humans, most swallows occur during the expiratory phase (Nishino et al., 1985; Smith et al., 1989; McFarland et al., 1994). While most swallows are readily evoked by pharyngeal or laryngeal stimulation, humans are thought to be the only species that can voluntarily initiate swallowing. Thus, it is impossible to evaluate how the coordination of respiration and swallowing is achieved during voluntary swallowing in animal studies. Previous studies have investigated the coordination of respiration and swallowing during voluntary swallowing (Shaker et al., 1992; Martin-Harris et al., 2003; Ouahchi et al., 2019). Shaker et al. (1992) investigated the coordination of respiration and voluntary swallowing in healthy young and older adult volunteers. In both groups, the pre- and post-respiratory phase

was most commonly found to be the expiratory phase, which was more frequent during 5-ml water swallowing compared with during dry swallowing. The authors also demonstrated that tachypnoea resulted in an increase in the occurrence rate of EE-type swallowing. Shaker et al. (1992); Martin-Harris et al. (2003), Ouahchi et al. (2019) reported that the most frequent pattern during 5-ml water swallowing was the EE type, although the temporal pattern of events, such as bolus transport, hyoid excursion, laryngeal closure, or opening of the upper oesophageal sphincter varied among subjects. The swallowing task in these studies was the command swallow task, in which the subject was instructed to swallow when the examiner presented a cue (Nagy et al., 2013; Kurosu et al., 2020). Nagy et al. (2013) conducted a videofluoroscopy (VF) study in healthy adults to compare swallowing behavior between cued and non-cued 10-ml water swallowing. They found that the pharyngeal transit time was significantly longer and that the bolus was more distally advanced in the pharynx at swallowing initiation with non-cued swallowing compared with cued swallowing. These results suggest that command swallowing may modulate swallowing physiology.

Coordination of respiration and swallowing during mastication should also be considered, because the food bolus must be transported into the esophagus safely during swallowing to protect the upper airway. Previous studies have reported the modulation of respiratory rhythm as well as coordination of respiration and swallowing during chewing in healthy humans (Smith et al., 1989; McFarland and Lund, 1995; Palmer and Hiimeae, 2003; Matsuo et al., 2008). Although these previous studies have demonstrated that most swallowing was evoked during the expiratory phase, some studies have produced conflicting results. Palmer and Hiimeae (2003) recorded electromyography (EMG) activity and VF images during solid food chewing, reporting that the respiratory cycle time changed between individuals and was significantly longer during banana chewing than cookie chewing. The authors suggested that bolus aggregation and hypopharyngeal transport occurred during the expiratory plateau phase, which seems to be one of the reasons for the prolonged respiratory cycle time. These results were, however, inconsistent with the findings of several other studies. Smith et al. (1989) reported no difference in respiratory cycle time, such as expiratory and inspiratory cycle time, among resting, solid food swallowing, and water drinking. Matsuo et al. (2008) reported a decrease in respiratory cycle time during chewing. Thus, the way in which the respiratory cycle is affected during chewing and its underlying mechanisms remains unclear.

In this study, we assessed the coordination of respiration and swallowing in healthy humans to clarify how cueing, drinking, and mastication modulate the coordination of respiratory and swallowing in healthy humans. For this purpose, we recorded EMG activity in the masseter (Mas, jaw closer), suprahyoid (Supra, hyoid elevator), and infrahyoid muscles (Infra, thyroid elevator) to evaluate chewing and swallowing movements and nasal temperature to monitor breathing as well as videoendoscopic (VE) images. We hypothesized that there would be a difference in swallowing physiology between cued and non-cued voluntary swallowing, and that chewing or drinking

would reduce the respiratory cycle time during chewing to compensate for the narrowing of the pharyngeal cavity.

MATERIALS AND METHODS

Participants

In this study, 21 healthy volunteers (10 men, 11 women) whose age ranged from 22 to 35 years [average age \pm standard deviation (SD), 28.4 ± 3.7 years] participated. Before data collection, a dentist (NH) confirmed that all the participants had no abnormalities or temporomandibular disorders, occlusal abnormalities, masticatory problems, or swallowing problems. No participant had a history of alimentary, pulmonary, or neurological disease, structural or speech disorders, or voice problems. Informed consent was obtained from all the participants after receiving information about the experimental procedure. This study was approved by the Ethics Committee of the Niigata University Graduate School of Medical and Dental Sciences (2020-0131). The experiments were performed in accordance with the Declaration of Helsinki (2008) for humans.

Recordings

Surface EMGs were recorded from both the right and left Mas muscle, right Supra muscles, and left Infra muscles. Electrodes (ZB-150H; Nihon Kohden, Tokyo, Japan) were attached to the skin over the center of the Mas, the anterior belly of the right digastric muscle for Supra, and the center of the left thyrohyoid muscle for Infra with an inter-electrode distance of 2 cm. EMG signals were filtered and amplified (high pass, 60 Hz) (WEB-1000; Nihon Kohden, Tokyo, Japan). A thermo-sensor system (MLT415 and ML309; Nihon Kohden, Tokyo, Japan) was used to record nasal temperature during respiration. A nasal probe was attached below the external nares to measure the temperature. Increases and decreases of temperature indicated expiration and inspiration, respectively. Since there was a difference between room temperature (around 20°C) and the nasal cavity temperature, the nasal temperature gradually increased, even during breath-holding. We calculated the rate of temperature increase in one participant. At several randomly determined temperatures, the participant was asked to hold her breath for 10 s, and changes in temperature were measured (**Supplementary Figure 1**). Although the rate of temperature increase was negatively correlated with the initial temperature, it was relatively small compared with that during respiration.

VE images were recorded in 11 participants (six men, five women; age range from 24 to 32 years, average age \pm SD, 29 ± 2.7 years) to measure the distance between the posterior wall of the pharynx and epiglottis and between the lateral walls of the pharynx in Protocol 3 (see below). A fiber-optic endoscope (FNL-10RP3; Pentax, Tokyo, Japan) was inserted through the nasal passage and into the mid pharynx.

All signals were collected *via* an interface board (PowerLab; ADInstruments, Colorado Springs, CO, United States) and stored on a personal computer. The sampling rate was 10 kHz for EMGs, 100 Hz for nasal temperature, and 33 Hz for VE images. Data synchronization and analysis were performed using the

PowerLab software package (Video Module and LabChart 8; ADInstruments, Colorado Springs, CO, United States), which automatically aligned the data at different sampling rates.

Data Recordings

The participants were instructed not to eat or drink for at least 1 h before the experiment. They were asked to sit in a chair with their head vertical to the Frankfort plane. In this study, we carried out three experiments on the same day for each individual. In the first experiment (Protocol 1), 3 ml of water was inserted into the mouth *via* a syringe; the participants were asked to keep the water on the floor of the mouth, then swallow it when prompted by a cue as quickly as possible (with cue) or whenever they wanted to (without cue) in a single swallow [dipper-type swallow (Cook et al., 1989)]. In the second experiment (Protocol 2), the participants were asked to drink 100 ml of water using a cup without breathing between swallows. In the third experiment (Protocol 3), the participants were asked to eat a 4-g portion of corned beef (Echigo Uonuma low fat corned beef, Forica Foods, Horinouchi, Japan) using a spoon in their usual manner. The time interval between trials was at least 2 min, and the participants were able to rinse their mouths with distilled water whenever they wished between the trials.

Data Analysis

The onset and offset of EMG activity, following smoothing of the rectified EMGs (time constant 20 ms), were determined. Mean value \pm SD of EMGs at rest for 5 s was obtained as a control for each participant. When the values exceeded the control + 2 SDs during the trials, the EMG burst was considered active.

Swallowing activity was evaluated by Supra and Infra EMG burst duration (time) and area. Time and area of these muscles were defined as the time interval between onset and offset, and area under the curve (area) of rectified and smoothed EMG burst, respectively. The amplitude of EMGs was normalized to the mean amplitude of rectified and smoothed EMG burst during 3-s maximum jaw closing for Mas and during 3-s maximum jaw opening for Supra and Infra.

First, we recorded the five respiratory cycles at rest for all the participants to obtain the mean respiratory cycle time, such as the expiratory and inspiratory time. Respiratory cycle time (respiratory time) was defined as the time from the start of one inspiration to the start of the next inspiration. Respiratory time was then divided into inspiratory and expiratory times. The duration of the inspiratory phase (inspiratory time) and expiratory phase (expiratory time) were defined as the time from the onset of inspiration to the end of inspiration and the time from the end of inspiration to the onset of the next inspiration, respectively. Each respiratory cycle had inspiratory and expiratory phases, sometimes with a pause after expiration. To identify each time duration, we included these short plateau phases in the expiratory phase. Furthermore, swallowing apnoea was commonly observed during swallowing and was measured in accordance with previous studies (Martin-Harris et al., 2003; Butler et al., 2004; Matsuo et al., 2008).

The swallowing pattern was determined based on the respiratory phase immediately before and after swallowing. When

the onset of pharyngeal swallowing, defined as the onset of Supra EMG burst, was preceded and followed by the expiratory phase, we designated the swallow as expiration–swallow–expiration type (EE type). When the onset of swallowing was preceded by the inspiratory phase and followed by the expiratory phase, we designated the swallow as inspiration–swallow–expiration type (IE type). When the onset of swallowing was preceded by the expiratory phase and followed by the inspiratory phase, we designated the swallow as expiration–swallow–inspiration type (EI type). When the onset of swallowing was preceded by and followed by the inspiratory phase, we designated the swallow as inspiration–swallow–inspiration type (II type). Previous studies have defined other criteria, such as swallows occurring at the transition between inspiration and expiration, which were designated inspiratory–expiratory (I–E) transition swallows, and swallows occurring at the transition between expiration and the inspiratory phase of the next breath, which were designated expiratory–inspiratory (E–I) transition swallows (Kijima et al., 1999). In this study, we did not use these terms, because we intended to simplify the pattern of coordination between respiration and swallowing.

In Protocol 1, the mean values of Supra and Infra time and area were compared between with and without cue conditions. Next, the occurrence frequency of coordination between respiration and swallowing (EE, IE, EI, or II type) was compared between with and without cue conditions. For the major pattern of coordination, changes in respiratory time, such as inspiratory and expiratory time, were compared among before, during, and after swallowing. It can be assumed that the coordination pattern was dependent on the timing of cueing. Therefore, the onset time of the expiratory phase was defined as the reference time “0,” and the time of cueing, onset, and offset of swallowing determined by the Supra EMG burst was calculated in the “with cue” session.

In Protocol 2, the coordination pattern was determined by the same procedure in Protocol 1. During 100-ml water swallowing, breath-holding must be performed until drinking is finished. We determined whether the swallowing apnoea time affected the coordination pattern in this protocol. Next, changes in respiratory time, such as inspiratory and expiratory time, were compared among before, during, and after swallowing.

In Protocol 3, we selected the data of masticatory sequence until the first swallow for analysis. The number of respiratory cycles and respiratory time, such as inspiratory and expiratory time of each respiratory cycle, were measured during mastication, and the coordination pattern of respiration and swallowing was determined. Respiratory, inspiratory, and expiratory times were compared between the conditions; at rest vs. during chewing. These times were also compared between the first and last respiratory cycles. In this session, changes in airway size at the pharynx during chewing were evaluated using VE images (Supplementary Figure 2). Since we did not measure the real size on the endoscopic view, the width of the epiglottis was determined as a reference. The normalized distance between the right and left walls of the oropharynx (width) and between the posterior wall of the oropharynx and posterior edge of the epiglottis (A–P distance) was measured three times at the inspiratory–expiratory and expiratory–inspiratory transition at

rest, and mean values were obtained for each participant. Width and A–P distance were also measured at the third peak of Mas EMG burst and Supra EMG burst, and at the third last peak of Mas EMG burst and Supra EMG burst during chewing.

All the data were analyzed by two experts (NH and AS). To estimate the inter-rater reliability, the intraclass correlation coefficient (ICC) was obtained, and the average was used for the subsequent analysis. Statistical analyses were performed using the SigmaPlot software (SigmaPlot 14.0, Systat Software Inc., San Jose, CA, United States) and Bell Curve for Excel (Social Survey Research Information Co., Ltd., Tokyo, Japan). Tests for normality and equality of variances were initially performed, followed by a paired *t*-test or Wilcoxon signed rank test to analyze differences between two paired groups, or by a *t*-test or Wilcoxon’s rank-sum test to analyze differences between two groups. Further, for multiple comparisons, we performed a one-way repeated measures analysis of variance (ANOVA) or one-way repeated measures ANOVA on ranks according to the results of test for normality. This was followed by Tukey’s test. The relationship between the two data sets was evaluated using Spearman’s rank order correlation. *P*-values < 0.05 were considered significant.

RESULTS

Reliability of the Data

The ICCs for parameters were calculated (Table 1) and were significant, although the ICCs of EMG data were relatively small. This was expected, because the threshold differed between the raters. Of the participants in the third experiment (Protocol 3), the VE data for the width of the pharynx were excluded in two participants because the whole view of the pharynx was not observed.

Protocol 1: 3-ml Water Swallowing

Figure 1 shows examples of raw data of recordings. In both the “with cue” and “without cue” conditions, the most frequent coordination pattern was EE type (Table 2). We evaluated how quickly the participants responded to cueing to initiate swallowing. There was no difference in the time from cueing to onset of Supra EMG burst between the coordination patterns (*t*-test); 0.83 ± 0.37 s ($n = 15$) for EE type vs. 0.7 ± 0.2 s ($n = 6$) for IE type. EMG duration time and area, as well as swallowing apnoea time, were no different between the “with

TABLE 1 | Intraclass correlation coefficients.

| | | <i>F</i> value | ICC | <i>P</i> value |
|-------------|------------|----------------|--------|----------------|
| EMG | Supra time | 3.6083 | 0.7229 | $P < 0.001$ |
| | Infra time | 3.6259 | 0.7242 | $P < 0.001$ |
| Respiration | Insp time | 21.2420 | 0.9529 | $P < 0.001$ |
| | Exp time | 12.3628 | 0.9191 | $P < 0.001$ |

EMG, electromyography; Exp time, expiratory time; ICC, intraclass correlation coefficient; Infra time, infrahyoid electromyographic burst duration; Insp time, inspiratory time; Supra time, suprahyoid electromyographic burst duration.

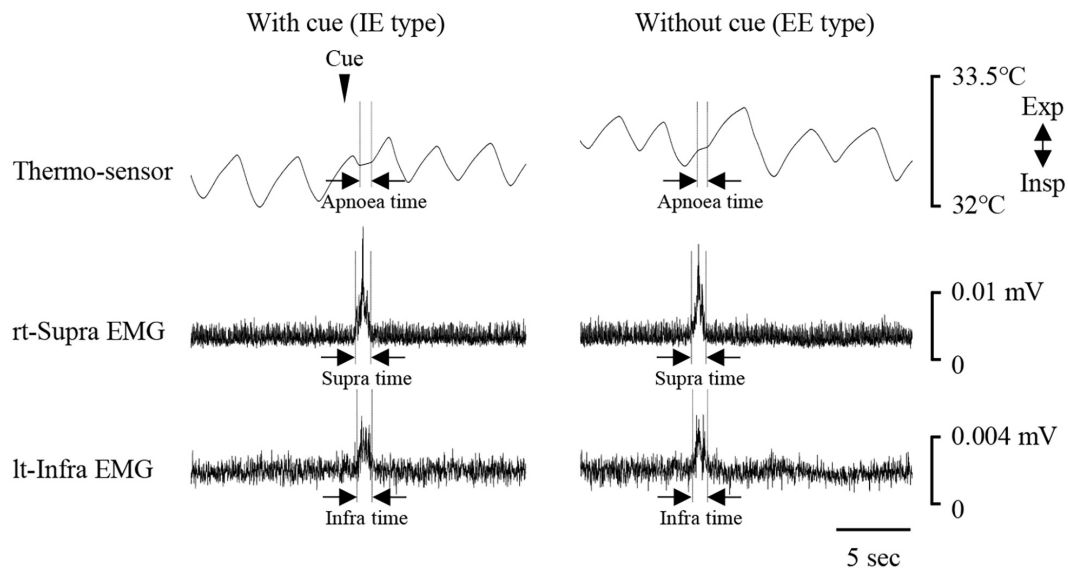


FIGURE 1 | Examples of respiratory and swallowing recordings during 3-ml water swallowing with (left) and without cue (right). Electromyography (EMG) waveforms were rectified and smoothed. Periods of swallowing apnoea and EMG burst are shown by dotted lines. The coordination pattern was inspiration–swallow–expiration (IE) with cue (left), and expiration–swallow–expiration (EE) without cue. The timing of cueing is indicated by an arrowhead. lt-Infra, left infrahyoid, rt-Supra, right suprahyoid.

cue” and “without cue” conditions (**Figure 2A**). This was also the case in the temporal pattern of muscle activity, in that the Supra EMG bursts always preceded the Infra EMG burst and swallowing apnoea in both cases (**Figure 2B**). Since the major pattern of coordination was EE type, we also compared those parameters for EE type between the “with cue” and “without cue” conditions. These findings were consistent with the overall results (**Figure 3**). These results indicated that command swallowing did not change the swallowing pattern, at least when swallowing 3 ml of water.

Next, we investigated why the most frequent pattern of coordination was EE type in both the “with cue” and “without cue” conditions. In this study, the mean respiratory cycle time was 4.7 ± 1.4 s ($n = 21$), and the inspiration–expiration ratio (IE ratio) was 1:1.63 ($n = 21$). In EE type with cue, the cue was provided from the last stage of inspiratory phase to the expiratory phase (**Figure 4**). In contrast, the cue was given from the last stage of expiratory phase to the inspiratory phase in IE type (**Figure 4**). It was likely that the coordination pattern was dependent on the

timing of the cue. EE type was the most frequent without cue as well as with cue. However, the subset of participants who showed EE type with cue was not identical to the subset of those who showed EE type without cue. Comparing the ratio of expiratory time to the respiratory time between the participant group in EE and IE types without cue revealed no difference; 0.62 ± 0.06 in EE type ($n = 15$) vs. 0.58 ± 0.04 in IE type ($n = 4$).

Next, we compared the coordination between respiration and swallowing in the group with EE type between with and without cue. While the inspiratory time was not affected by cueing, the respiratory cycle time and expiratory time were significantly longer during swallowing compared with those before and after swallowing only during 3-ml swallowing with cue, while there was no difference in any of the times without cue (**Figure 5**). These results suggest that the modulation of respiratory cycle time was affected by command.

Based on these results, we speculate that not only the difference in the time duration between the inspiratory and expiratory phases but also other factors may be responsible for determining the coordination pattern of respiration and swallowing.

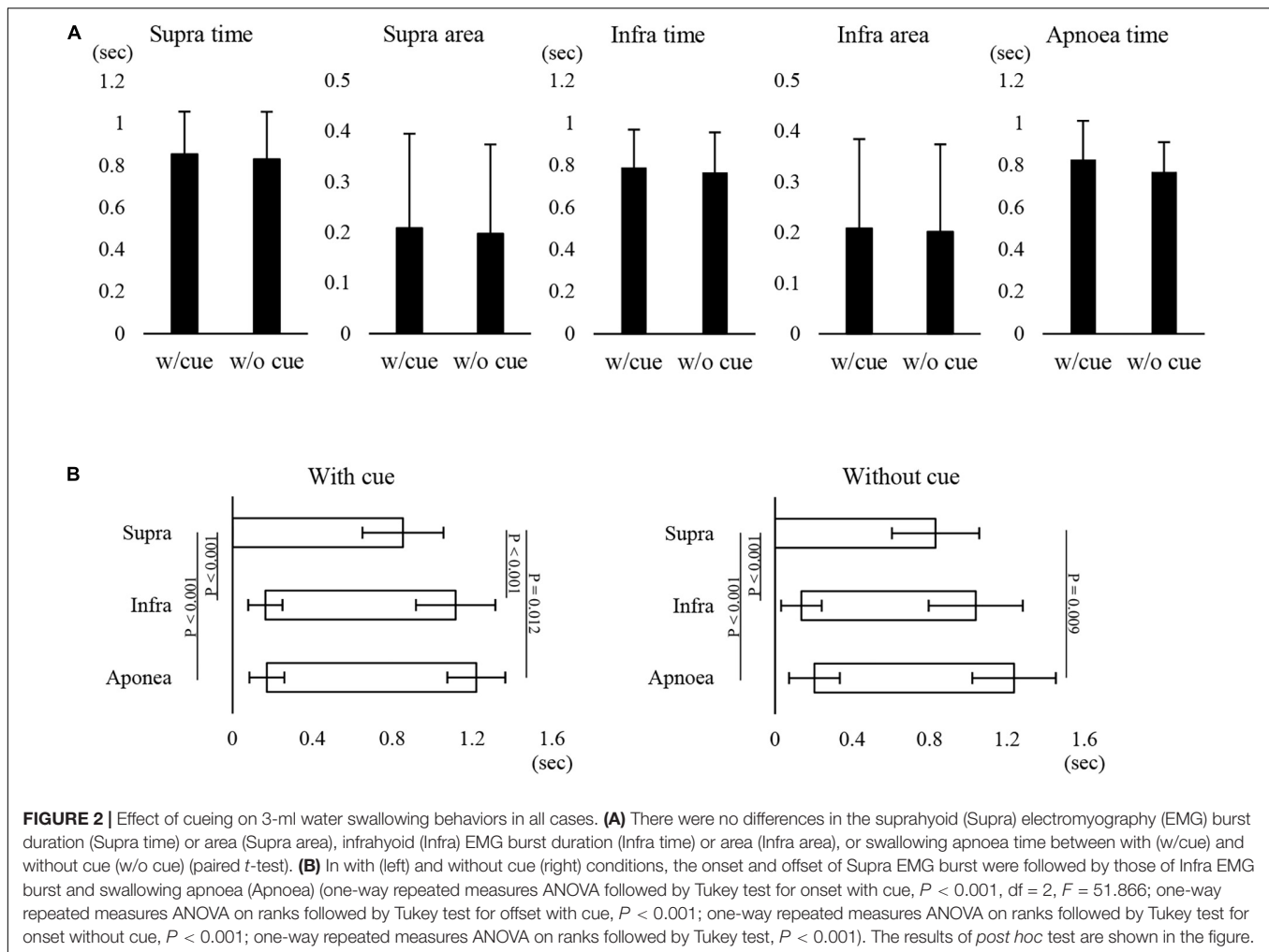
TABLE 2 | Coordination pattern of respiration and swallowing.

| | EE | IE | EI | NA |
|------------------------|----|----|----|----|
| 3-ml water with cue | 15 | 6 | 0 | 0 |
| 3-ml water without cue | 15 | 4 | 2 | 0 |
| 100-ml water | 11 | 3 | 2 | 5 |
| Chew and swallow | 14 | 1 | 1 | 5 |

EE, expiration–swallow–expiration type; EI, expiration–swallow–inspiration type; IE, inspiration–swallow–expiration type. NA indicates cases of subjects who failed to swallow 100 ml with breath holding for the 100-ml water swallowing task and the case of subjects who held their breath while chewing in the chew and swallow task.

Protocol 2: 100-ml Water Swallowing

Figure 6 shows examples of raw data of recordings. Of all the participants, five could not complete the 100-ml swallowing with breath-holding task, so their data were excluded from analysis. As in the 3-ml water swallowing task, the most common coordination pattern was EE type (**Table 2**). The total number of swallows was 8.8 ± 2.5 swallows, and the duration of swallowing apnoea was 10.7 ± 3.2 s ($n = 16$). The results indicated that it was unlikely that swallowing apnoea time was associated with the



coordination type (10.9 ± 3.4 s for EE type, $n = 10$; 9 ± 1.3 s for IE type, $n = 3$; 11.5 ± 4 s for EI type, $n = 3$). The mean Supra and Infra areas per swallow were not significantly different from those during 3-ml water swallowing; 0.2 ± 0.13 /swallow ($n = 16$) during 100-ml swallowing vs. 0.21 ± 0.19 /swallow during 3-ml swallowing with cue ($n = 21$) for Supra area, and 0.21 ± 0.18 /swallow ($n = 16$) during 100 ml swallowing vs. 0.3 ± 0.21 /swallow during 3-ml swallowing with cue ($n = 21$) for Infra area, respectively (Mann–Whitney Rank Sum Test).

We then investigated the modulation of respiratory movements. The respiratory cycle time and expiratory time immediately before swallowing were significantly shorter than those during swallowing (Figure 7). Inspiratory time was no different throughout the recording period. These results suggest that modulation of respiratory cycle time occurred before swallowing by shortening the expiratory time.

Protocol 3: Chewing and Swallowing

Figure 8 shows an example of raw data of recordings. The mean number of chewing cycles, chewing duration, and chewing cycle time until the first swallow were 17.1 ± 7.9 cycles, 11.9 ± 5.8 s, and 0.7 ± 0.11 s/cycle, respectively ($n = 21$). The number of

chewing cycles and chewing duration ranged widely among the participants; the number of chewing cycles ranged from 6 to 29 cycles, and the duration ranged from 4.6 to 30 s. Of the all participants, five participants held or inhibited their breathing during chewing (Figure 9). In this group, the number of chewing cycles was 10.8 ± 4.1 cycles ($n = 5$), and the chewing duration was 8.3 ± 3.3 s ($n = 5$), which tended to be smaller compared with the whole group. We excluded those participants from the subsequent analysis. In the remaining 16 participants, the mean respiratory cycle time, expiratory time, and inspiratory time were significantly smaller during chewing compared with at rest (Figure 10A). Further, comparing them between the first and last respiratory cycles, the respiratory cycle time and expiratory time were significantly smaller at the former than the latter (Figure 10B). There was no relationship between respiratory cycle time at rest and chewing rate (cc, -0.188 , $P = 0.476$), between respiratory cycle time at rest and during chewing (cc, -0.206 , $P = 0.364$), and between chewing rate and respiratory cycle time during chewing (cc, -0.122 , $P = 0.640$).

Since the size of the pharynx changes because of the dynamic movements of posterior tongue during chewing, we compared

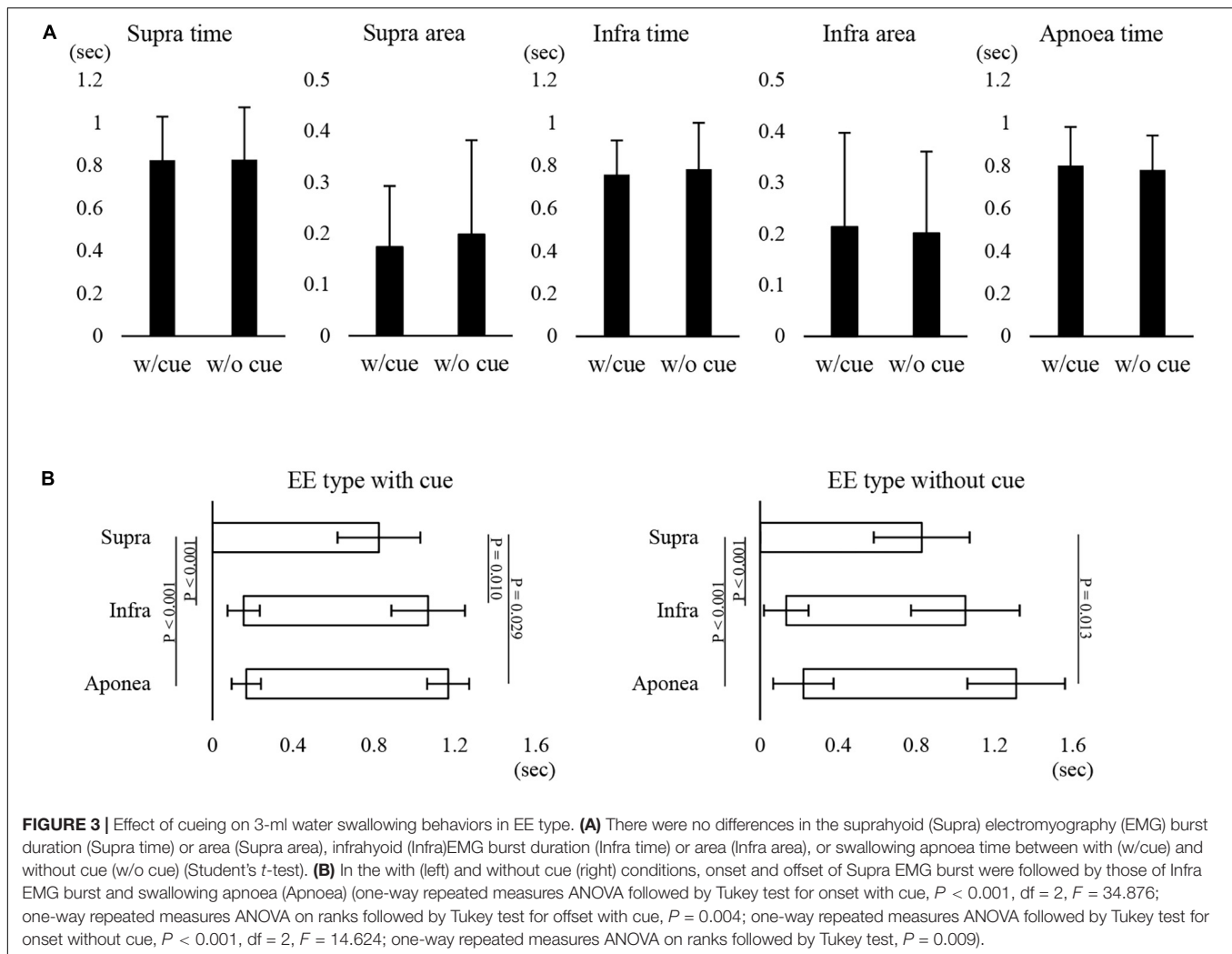


FIGURE 3 | Effect of cueing on 3-ml water swallowing behaviors in EE type. **(A)** There were no differences in the suprahyoid (Supra) electromyography (EMG) burst duration (Supra time) or area (Supra area), infrahyoid (Infra) EMG burst duration (Infra time) or area (Infra area), or swallowing apnoea time between with (w/cue) and without cue (w/o cue) (Student's *t*-test). **(B)** In the with (left) and without cue (right) conditions, onset and offset of Supra EMG burst were followed by those of Infra EMG burst and swallowing apnoea (Apnoea) (one-way repeated measures ANOVA followed by Tukey test for onset with cue, $P < 0.001$, $df = 2$, $F = 34.876$; one-way repeated measures ANOVA on ranks followed by Tukey test for offset with cue, $P = 0.004$; one-way repeated measures ANOVA followed by Tukey test for onset without cue, $P < 0.001$, $df = 2$, $F = 14.624$; one-way repeated measures ANOVA on ranks followed by Tukey test, $P = 0.009$).

the width and A-P distance of the pharynx between before and during chewing. There was no difference between the conditions (Supplementary Figure 3). These results suggest that respiratory cycle time gradually decreased during chewing, which was unlikely to have been caused by changes in the size of the pharynx.

DISCUSSION

Effect of Cueing on Swallowing

We intended to clarify how single swallow was affected by cueing. Therefore, we first determined the bolus volume in the preliminary experiment. We used 3-ml water in the experiment, because this amount of water was found to be suitable for all the participants to keep the bolus in the mouth. As a result, all the participants completed a 3-ml water swallowing task. As previously reported, most coordination patterns were EE type in single voluntary swallows in both the with and without cue conditions (Shaker et al., 1992; Martin-Harris et al., 2003; Ouahchi et al., 2019). In the with cue condition, although the participants were asked to swallow as quickly as possible after

the cue, they may have determined the timing of swallowing in accord with the respiratory phase (i.e., the expiratory phase). In this respect, the latency was 0.83 ± 0.37 s for EE type and 0.7 s for IE type. Michou et al. (2012) also measured the fast-swallowing reaction time when participants were asked to perform swallowing of 5-ml boluses of liquids delivered into the mouth as quickly as possible while the latency between the delivery time of the electrical cue to the onset of the pharyngeal swallow was measured. The mean time is reported to be 0.886 s, which is consistent with the results of this study. We suggest that the participants in this study completed 3-ml swallowing with the cue regardless of the respiratory phase.

In this study, the mean respiratory cycle time was 4.7 ± 1.4 s, and the IE ratio was 1:1.6, which was within the normal range (Boyle, 2001). The occurrence ratio of EE type was much higher (EE type, 15 vs. IE type, 6) compared with the IE ratio (inspiration 1.6 vs. expiration 1). We found that in the “with cue” condition, most EE type swallows were initiated when cues were given from the very late inspiratory phase to the expiratory phase, while most IE type swallows were initiated when cues were given from the very late expiratory phase to the inspiratory

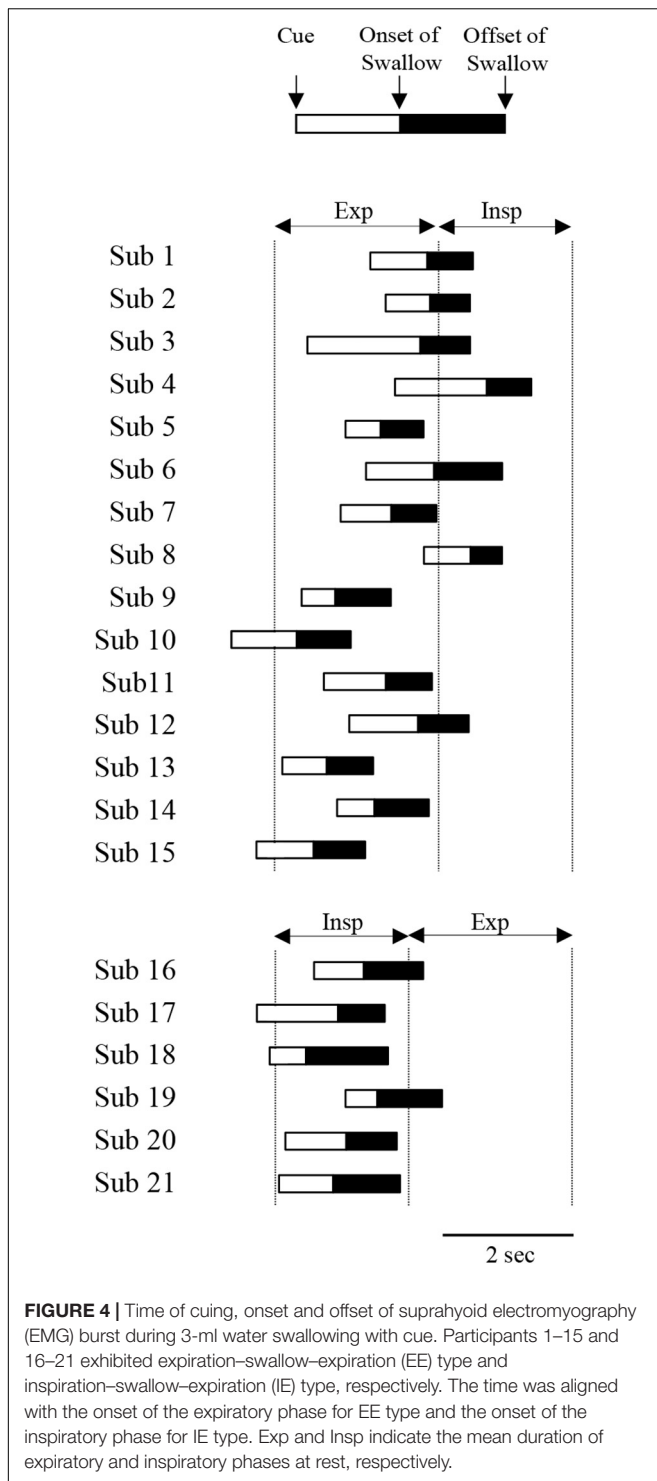
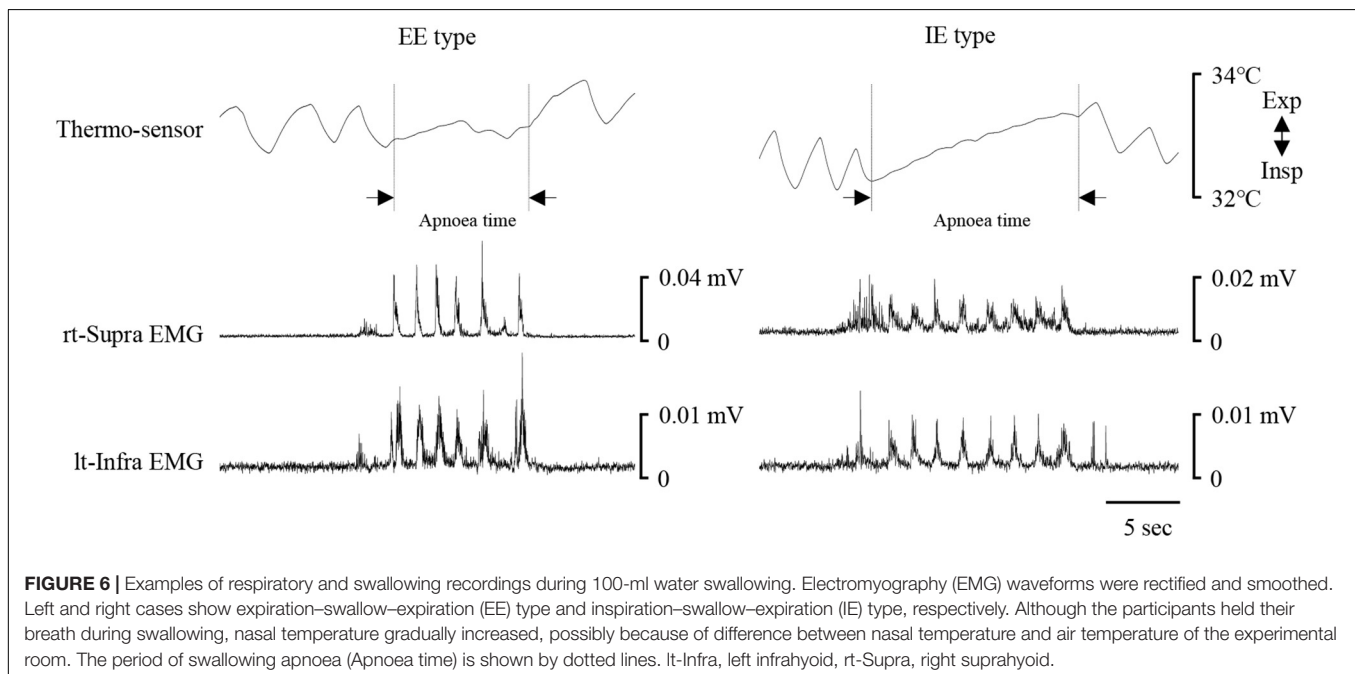
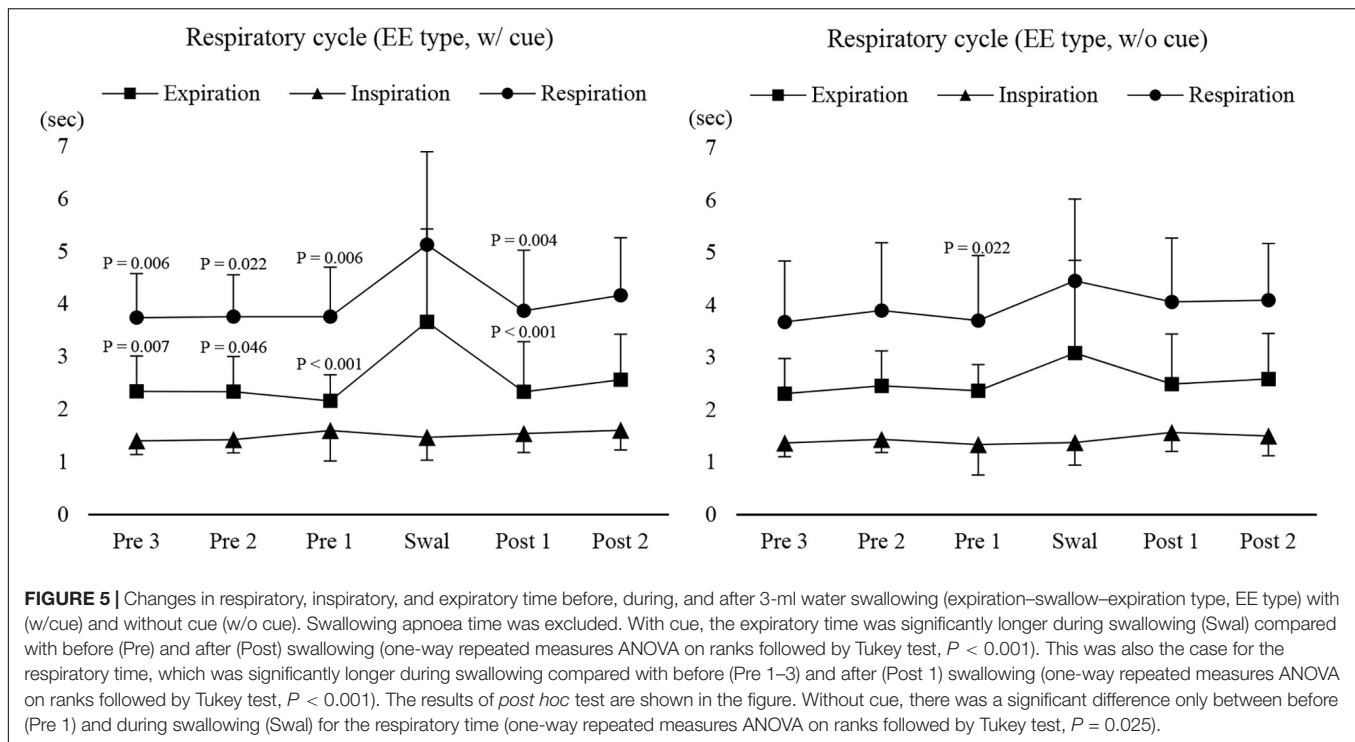


FIGURE 4 | Time of cueing, onset and offset of suprahyoid electromyography (EMG) burst during 3-ml water swallowing with cue. Participants 1–15 and 16–21 exhibited expiration–swallow–expiration (EE) type and inspiration–swallow–expiration (IE) type, respectively. The time was aligned with the onset of the expiratory phase for EE type and the onset of the inspiratory phase for IE type. Exp and Insp indicate the mean duration of expiratory and inspiratory phases at rest, respectively.

phase. We speculated that the timing of cueing affected the coordination pattern of respiration and swallowing. However, this raises the question of why the frequency of occurrence of EE type swallows was dominant in the without cue condition. There are substantial differences in the timing of swallowing initiation across species and experimental conditions. In most mammals,

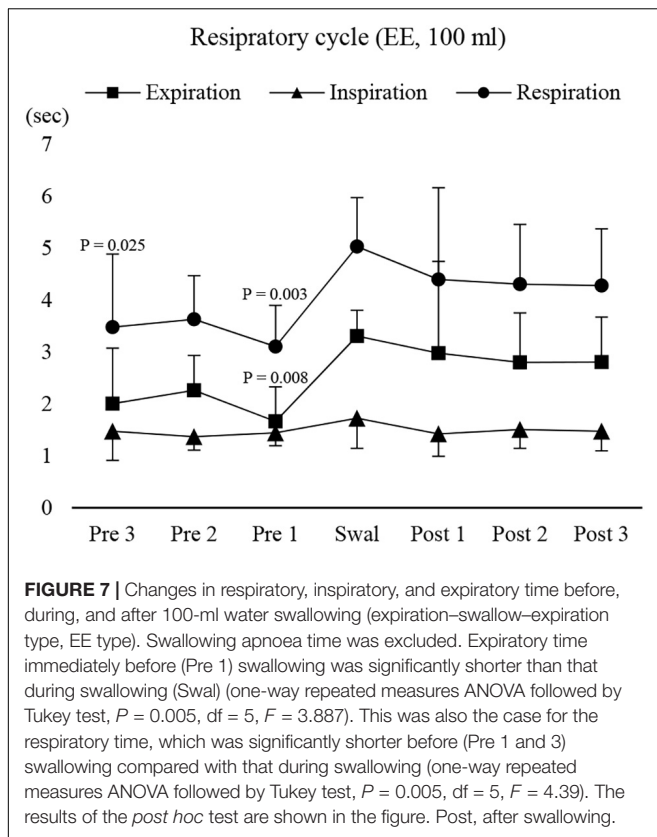
such as dogs, monkeys, and rabbits, swallowing reflexes are typically evoked during the inspiratory phase (Doty and Bosma, 1956; Kawasaki et al., 1964; McFarland and Lund, 1993; Feroah et al., 2002). In contrast, as shown in this study, most swallows are evoked during the expiratory phase either involuntarily or voluntarily in humans, as in anesthetized cats (Doty and Bosma, 1956; Nishino et al., 1985; Smith et al., 1989; Dick et al., 1993; McFarland et al., 1994). One potential cause of the difference in swallowing between humans and other species is the anatomical characteristics of the location of the hyolaryngeal complex. In most non-human mammals, the hyolaryngeal complex is located in a relatively high position (Laitman and Reidenberg, 1993). Furthermore, the height of the mid-pharynx is very small, and the tongue lies within the oral cavity and never forms the posterior part of the pharynx. This unique anatomical configuration enables the epiglottis to pass up the soft palate, allowing the larynx to open directly into the nasopharynx. Thus, the food way from the oral cavity to the esophagus and the airway from the nasal cavity to the trachea are separated, which means that these animals do not need strict coordination of respiration and swallowing movements to prevent pulmonary aspiration. When a single swallow occurs during the inspiratory phase, inspiration must be interrupted by swallowing apnoea, which is followed by a shortened duration of the expiratory phase. In contrast, if a swallow is evoked during the expiratory phase, the duration of entire expiratory phase including pre and post swallowing is lengthened. In either case, the tidal volume of the post-swallow period is increased, although the latter may be more effective than the former (Nishino et al., 1985). Possible advantages of swallowing initiation during the inspiratory phase include the facilitation of bolus transport by inhalation, and minor effects of respiration after swallowing in this situation, because the shortened duration of inspiration is less effective for activating stretch receptors in the trachea or lung (Davis et al., 1956; Bartlett et al., 1976; Bradley et al., 1987). Humans, however, need to protect their airway because of the lower position of the hyolaryngeal complex, as described above. The action of the diaphragm, which is a major inspiratory muscle, and the Infra muscles, which are all inspiratory muscles, appear to be counteracted by contraction of the Supra muscles during swallowing, at least in humans (McFarland et al., 1994).

The results revealed no significant difference in swallowing movements in terms of Supra and Infra EMG time and area, as well as swallowing apnoea, which represents pharyngeal swallowing between the with and without cue conditions. The temporal features of swallowing events were also similar to each other. These results suggest that voluntary swallowing of a small amount of bolus does not affect swallowing motor actions, regardless of swallowing command and type of coordination of respiration and swallowing. Several previous studies have compared swallowing behaviors between cued and non-cued swallows (Daniels et al., 2007; Nagy et al., 2013). Nagy et al. (2013) compared 10-ml liquid swallows between cue and non-cue conditions. When bolus transport was measured using 10 ml of ultrathin barium by VF, the results revealed that during cued swallowing, bolus advancement to the pyriform sinuses prior to swallow initiation was seen significantly less frequently, and



pharyngeal transit time and response time were both significantly longer than those during non-cued swallowing (Nagy et al., 2013). Considering the difference in the effect on swallowing movements, we evaluated only Supra and Infra EMG activities. Although Supra EMG activity during swallowing represents pharyngeal swallowing, with a previous study having reported a significant linear relationship between the passage of the bolus tail at the upper oesophageal sphincter and offset of the Supra

EMG burst (Tsukada et al., 2009), we only recorded muscle function and not bolus passage. In addition, the bolus volume was different among previous studies. A small amount of water (3 ml) might cause a failure to modulate swallowing physiology. Furthermore, Nagy et al. (2013) did not measure the response latency to swallowing initiation. If the participant had responded to cueing more quickly than the participants in this study, bolus transport would be expected to be affected.



We did not expect to find a difference in respiratory time during swallowing between the with and without cue conditions, because the most frequent coordination type exhibited no difference between the with and without cue conditions. Although most previous studies have reported that the duration of expiratory phase is lengthened during swallowing, they all included swallowing apnoea. In this study, however, we excluded this period in the calculations. Paydarfar et al. (1995) investigated the relationship between respiration and swallowing dynamics in humans. They studied three types of swallowing tasks: spontaneous swallowing, evoked swallowing by water injection, and cued swallowing. The authors found that the smaller the time interval between the onset of the expiratory phase and the onset of the Supra EMG burst, the longer the time between the onset of the Supra EMG burst to the onset of the inspiratory phase after swallowing, without any effects on the duration of swallowing apnoea, in all swallowing tasks. Since swallowing was recorded only once in each condition in this study, we were unable to clarify how the timing of swallowing initiation affected the subsequent phase. However, it should be noted that there was a significant difference in the whole duration of the expiratory phase between the with and without cue conditions. Changes in duration in the expiratory phase without swallowing apnoea were smallest in the without cue condition. Thus, we speculate that voluntary swallowing with cue may modulate the coordination of respiration and swallowing by lengthening the expiratory phase duration.

Coordination of Respiration and Swallowing During 100-ml Water Swallowing

All but five participants successfully completed the 100-ml water swallowing task with breath-holding. As expected, the most frequent coordination pattern was EE type, as in the 3-ml water swallowing task. Therefore, we evaluated how sequential 100-ml swallowing affected the coordination of respiration and swallowing in EE type.

In animal studies, high-frequency repetitive swallowing has been reported to be evoked by continuous electrical stimulation applied to the superior laryngeal nerve (Fukuhara et al., 2011; Tsuji et al., 2014; Suzuki et al., 2018; Yoshihara et al., 2020) or capsaicin application to the vocal folds (Tsuji et al., 2016, 2017; Tsuji et al., 2020). In these cases, both the rhythm and amplitude of breaths are reported to be increased after cessation of repetitive swallows (Doty, 1968; Dick et al., 1993). However, the findings of these animal studies are not comparable to the results of this study because the animals were anesthetized and did not control the rhythmicity or swallowing movements by themselves. Numerous previous studies have investigated how sequential swallowing affects respiration pre- and post-swallowing in humans (Dozier et al., 2006; Daniels et al., 2007; Wheeler Hegland et al., 2011; Lederle et al., 2012). However, the respiratory pattern at pre- and post-swallowing has varied between previous studies. For example, the percentage of occurrence of the expiratory phase immediately before and after sequential swallowing (i.e., the EE type) was reported to be 33% for 100 ml (Wheeler Hegland et al., 2011) and 38.6% for 50 ml (Dozier et al., 2006), while it was 52.4% (11/21 participants) in this study.

Since the duration of swallowing apnoea was long and the respiration was inhibited during repetitive swallowing, the respiratory drive could be facilitated, at least after swallowing. Based on this perspective, we recorded several respiratory cycles before and after swallowing. The duration of the expiratory phase immediately before swallowing was smaller than that following swallowing, whereas the duration of the inspiratory phase remained unchanged. Although we did not measure oxygen saturation and tidal volume, it could be assumed that breath-holding for several seconds during 100-ml water swallowing facilitated respiratory drive. Strohl and Altose (1984) observed a decrease in oxygen saturation during 10–20-s breath-holding, although the rate of fall of oxygen saturation was relatively small. Decreased oxygen saturation leads to a decrease in oxygen partial pressure as well as an increase in carbon dioxide partial pressure. Changes in respiratory frequency have been reported under experimental conditions, such as hypoxia or hypercapnia (Rebuck et al., 1976; Gardner, 1980; Cunningham and Robbins, 1984; Dozier et al., 2006). Rebuck et al. (1976) reported that the inspiratory time remained constant during hypercapnia until tidal volume had increased during hypercapnia, consistent with the results of this study. However, the authors found that the respiratory rate increased with shortening expiratory time when the tidal volume increased 3–5 times of the eupneic value. Jennett et al. (1981) reported that following a brief

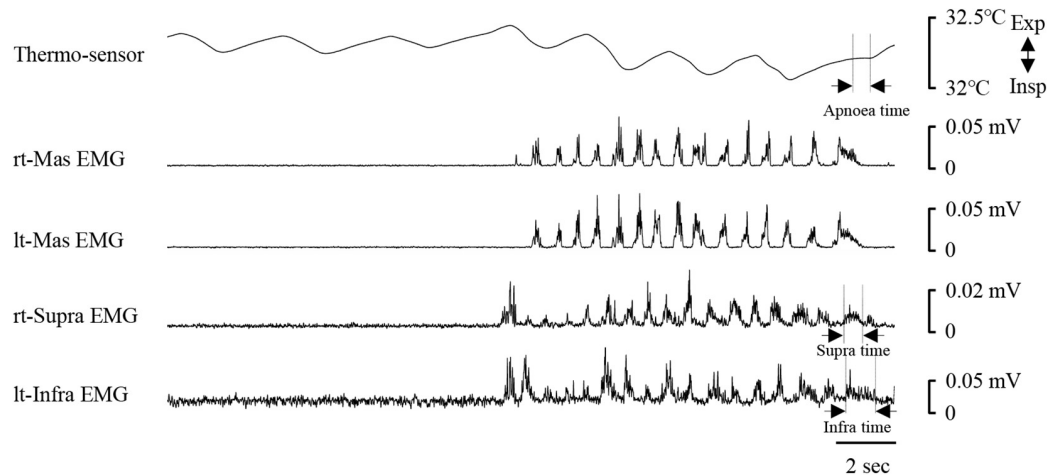


FIGURE 8 | Example of respiratory and electromyography (EMG) recordings during chewing. EMG waveforms were rectified and smoothed. Note that the respiratory cycle time decreased once mastication started. The coordination pattern of respiratory and swallowing was expiration–swallow–expiration type. Periods of swallowing apnoea (Apnoea time) and swallow-related EMG burst (suprahyoid EMG time duration, Supra time; infrahyoid EMG time duration, Infra time) are shown by dotted lines. rt-Mas, right masseter; lt-Mas, left masseter; rt-Supra, right suprahyoid; lt-Infra, left infrahyoid.

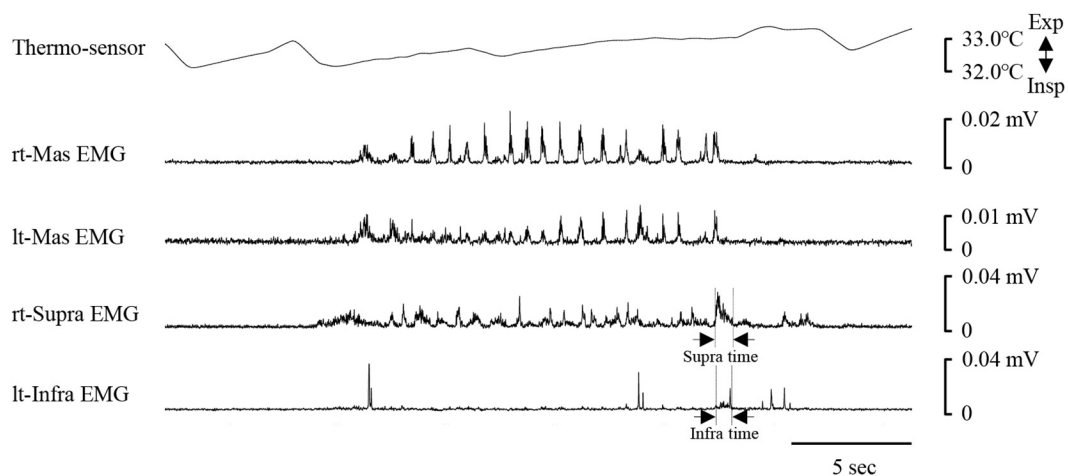


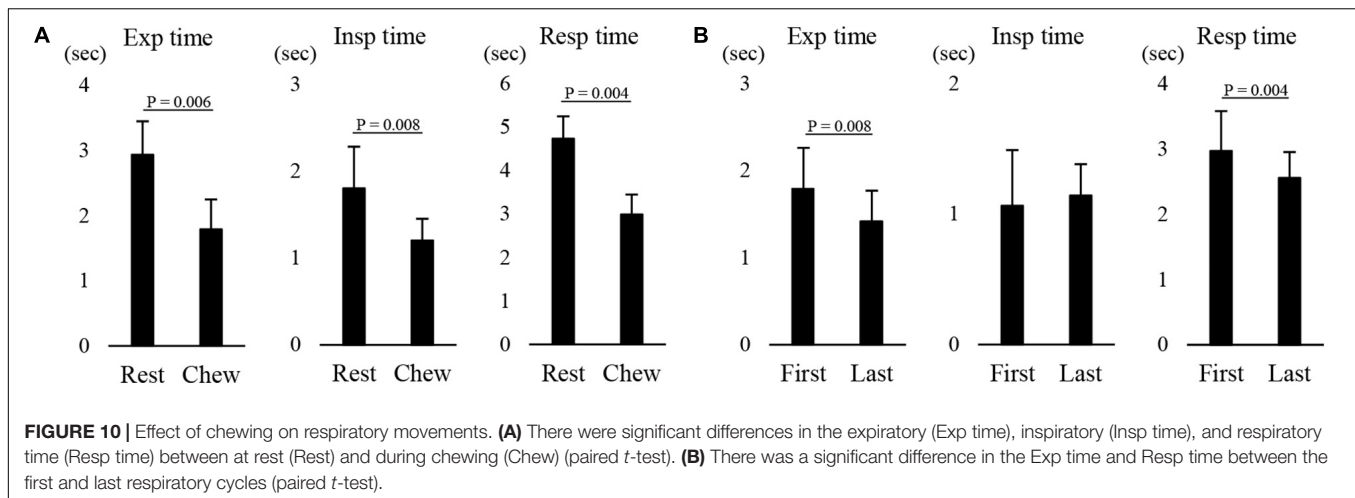
FIGURE 9 | Example of respiratory and electromyography (EMG) recordings in one participant who inhibited her breath during chewing. In this case, no clear period of swallowing apnoea could be identified. Infra time, infrahyoid EMG burst duration; rt-Mas, right masseter; lt-Mas, left masseter; rt-Supra, right suprahyoid; lt-Infra, left infrahyoid; Supra time, suprahyoid EMG burst duration.

hypoxic stimulus, frequency changes resulted from alterations in the two phases; when total respiratory time decreased, it was always linked to a decrease in expiratory time, and an increase in the respiratory cycle time was due to an increase in the inspiratory time. In this study, it can be assumed that changes in respiratory rhythm were not due to hypoxia or hypercapnia but can be attributed to voluntary behaviors to maintain the oxygen level in the lungs. Most of the participants understood how to swallow a large amount of water (100 ml) with breath-holding. Thus, the participants would be expected to aim to maintain a sufficient oxygen level to hold their breath during swallowing. We did not find evidence of strong inspiratory effort but observed a significantly shortened duration of the expiratory phase before swallowing compared with that after swallowing.

Future studies should measure tidal volume, including expired and inspired volume, to clarify how respiratory effort is affected by sequential swallowing.

Coordination of Respiration and Swallowing During Chewing

The results revealed that the most frequent coordination pattern was EE type during chewing, in accord with previous studies (Mead and Reid, 1988; McFarland and Lund, 1995; Matsuo et al., 2008). Mechanisms of swallowing initiation at the expiratory phase during chewing different from those in a single or sequential swallow should be considered. During chewing, a person does not determine the timing of



swallowing by themselves. In this process, the triturated food bolus is transported into the mid-pharynx, where the bolus is accumulated (Palmer et al., 1992). Once the pharyngeal mucosa, which is innervated by the pharyngeal branch of the vagal nerve or the superior laryngeal nerve, is stimulated by the bolus, the swallowing reflex is readily evoked. Swallowing initiation would be expected to be determined dominantly by the bolus condition, such as the location or texture, rather than the respiratory phase. Matsuo et al. (2008) reported that pharyngeal bolus aggregation started 1.27 s before the end of the inspiratory phase and lasted until the end of this phase, which was followed by the expiratory phase and swallowing. Mead and Reid (1988) found expiratory muscle activation when airflow was interrupted at the glottis. It is likely that bolus propulsion initiates expiration followed by the swallowing reflex. Further, during pharyngeal swallowing, when hyolaryngeal elevation contributes to passive opening of upper oesophageal sphincter, infrahyoid muscles, such as the thyrohyoid, omohyoid, sternohyoid, and sternothyroid muscles, are also activated. These are all inspiratory muscles and are activated synchronously with the diaphragm (Mitchinson and Yoffey, 1947; Megirian et al., 1985). During the inspiratory phase, contraction of the diaphragm caused pulling of the trachea and larynx inferiorly, and the contraction of all infrahyoid muscles resulted in pulling down of the hyoid and thyroid cartilages, which have antagonistic functions for swallowing. Thus, it is possible that bolus stimulation applied to the pharyngeal and laryngeal region activates expiratory muscle activity and then initiates the swallowing reflex during the expiratory phase.

The effects of mastication on respiratory function have not yet been clarified; although one study reported no effect (Smith et al., 1989). Other studies reported a decrease in respiratory cycle time (Fontana et al., 1992; McFarland and Lund, 1995; Matsuo et al., 2008). The results are consistent with the latter finding and reveal that the respiratory cycle time, as with the expiratory and inspiratory time, significantly decreased during chewing. In addition, there was a significant difference in the expiratory time between the first and last respiration before swallowing.

We initially predicted the spatial interruption of the upper airway by the bolus during chewing. During chewing, dynamic

movements of the tongue body are needed not only in the anterior but also in the posterior region, which was observed by a VF study (Palmer et al., 1997; Hiimae et al., 2002). Since the posterior tongue forms the anterior wall of the mid-pharynx, tongue movements might be expected to interfere with respiration by narrowing the airway in the pharynx. This was, however, not the case in this study, as the results revealed no significant differences in the width or A-P distance of the pharynx between the control and chewing conditions.

It is well documented that exercise causes increased respiratory function. Exercise may cause metabolic demand, which causes hyperpnea. Although mastication is not a kind of exercise but can be considered a natural behavior in human life, chewing has been found to decrease the respiratory cycle time depending on the chewing speed (Formiga et al., 2005), and to decrease the tidal volume with an increase in respiratory frequency (Fontana et al., 1992; McFarland and Lund, 1995). Furthermore, as previously reported, changes in respiratory cycle time can result from alterations either when total respiratory time decreased with a decrease in expiratory time or increased respiratory cycle time with an increase in the inspiratory time under hypoxic conditions (Jennett et al., 1981). We speculate that the decrease in respiratory cycle time and gradual decrease throughout the chewing process may have been due to changes in metabolic demand.

It is possible that the pattern of respiration was irregular during chewing, which could also have important implications. In this study, there was no relationship between the respiratory cycle time between at rest and during chewing in each individual. The pattern of breathing is regulated by the respiratory CPG, so that normal ventilation can be achieved with the lowest work output or energy expenditure. Performing a chewing task may cause deviation from this optimal pattern, and, hence, an increase in the work of breathing. Thus, irregularity in the modulation of respiratory function may be associated with individual dependent increased loads.

Five participants exhibited markedly inhibited respiration during chewing, in accord with the findings of previous studies

(McFarland and Lund, 1995; Matsuo et al., 2008). Although we were not able to clarify the mechanisms underlying this finding, it is possible that the result was caused by the experimental conditions. In this study, a videoendoscopic fiber was inserted into the nasal cavity of the participants on either side, which may have interfered with nasal air flow during chewing. Future studies should clarify whether the inhibition was caused by this condition in some participants, or if it represents an exaggerated response, as suggested by Matsuo et al. (2008).

Clinical Implications

Understanding the coordination of respiration and swallowing is particularly important in clinical situations. For example, respiratory impairment is defined as an age-related reduction in ventilatory control, and weakened respiratory muscle strength and respiratory mechanics (Chen and Kuo, 1989; Enright et al., 1994; Sachs et al., 2009), as well as ineffective gas exchange (Vaz Fragoso and Gill, 2012). Parreira et al. (2010) suggested that thoracoabdominal motion, rather than breathing pattern, was affected by age. Furthermore, older people have been reported to exhibit reduced responses to hypoxia or hypercapnia compared with young people (Kronenberg and Drage, 1973; Peterson et al., 1981). Previous studies have reported an effect of aging on swallowing and the coordination between respiration and swallowing (Selley et al., 1989; Robbins et al., 1992; Sonies, 1992; Wang et al., 2015). Wang et al. (2015) reported that older people exhibited delayed onset latency of the swallowing reflex and longer swallowing apnoea duration, which depended on the bolus volume. The authors also noted that older people exhibited less EE-type swallowing during dry and water swallowing compared with young people. In this study, the results revealed that command swallowing in response to a cue affected expiratory duration. If pulmonary function is impaired in patients, collapse of coordination may be associated with a risk of bolus penetration or aspiration. In addition, impaired chewing function may lead not only to longer chewing duration but also to collapse of coordination among chewing, respiration, and swallowing. Clinicians should pay attention to swallowing in patients with stroke, Parkinson's disease, and any other conditions that potentially cause swallowing disorders (Wirth et al., 2016). Future studies should investigate how aging itself or diseases affect swallowing function and coordination between respiration and swallowing.

Limitations

Several limitations should be considered when interpreting the findings of this study. First, we recruited only 21 healthy participants. In a future study, it would be useful to evaluate how aging or other personal factors affect not only swallowing but also coordination between respiratory and swallowing functions. Second, we recorded only 3- and 100-ml water swallowing as well as solid food chewing and swallowing in a pre-determined order. Bolus volume or order may affect the coordination between respiration and swallowing. Third, we measured nasal temperature to monitor respiration because this method was convenient and easy for combining the data for analysis. Plethysmography is a system for measuring

respiratory function, enabling three-dimensional assessment of absolute chest wall volumes. Matsuo et al. (2008) concluded that plethysmography was better than nasal manometry for determining the respiratory phase during chewing and swallowing. Future studies should clarify tidal volume and pulmonary ventilation using plethysmography. Finally, we only calculated pharyngeal volume by two-dimensional measurement. The methods of this study should be validated in future studies using VF or three-dimensional computed tomography images.

Conclusion

The major coordination pattern of respiration and swallowing was EE type during 3-ml water swallowing, either with or without cue, and during 100-ml water swallowing and chewing. Although cueing did not affect swallowing movements, the expiratory time was lengthened by the cue. During 100-ml swallowing, the respiratory cycle time and expiratory time immediately before swallowing were significantly smaller than those during and after swallowing, while the inspiratory time did not differ throughout the recording period. During chewing, the respiratory cycle time was decreased in a time-dependent manner, probably because of metabolic demands. The coordination of the two functions is maintained not only in voluntary swallowing but also in involuntary swallowing during chewing. Understanding the mechanisms underlying respiration and swallowing is important for evaluating the coordination required to complete safe swallowing in older people and patients with dysphagia.

DATA AVAILABILITY STATEMENT

The original contributions presented in the study are included in the article/**Supplementary Material**, further inquiries can be directed to the corresponding author.

ETHICS STATEMENT

This study was approved by the Ethics Committee of the Niigata University (2020-0131). The patients/participants provided their written informed consent to participate in this study.

AUTHOR CONTRIBUTIONS

NH and MI were involved in the conception and design of this study. NH, AS, SK, YN, KN, JM, TT, and MI were involved in the acquisition of the data, and drafting and critical revision of the study for important intellectual content. NH, AS, and MI were involved in the analysis or interpretation of the data. All authors approved the final version of the manuscript submitted for publication and agreed to be accountable for all aspects of the work in ensuring that questions related to the accuracy or integrity of any part of the study are appropriately investigated and resolved.

ACKNOWLEDGMENTS

The authors would like to thank Benjamin Knight, M.Sc., from Edanz (<https://jp.edanz.com/ac>) for editing a draft of this manuscript.

REFERENCES

- Amri, M., Car, A., and Jean, A. (1984). Medullary control of the pontine swallowing neurones in sheep. *Exp. Brain Res.* 55, 105–110.
- Bartlett, D. Jr., Sant'ambrogio, G., and Wise, J. C. (1976). Transduction properties of tracheal stretch receptors. *J. Physiol.* 258, 421–432. doi: 10.1113/jphysiol.1976.sp011428
- Bianchi, A. L., and Gestreau, C. (2009). The brainstem respiratory network: an overview of a half century of research. *Respir. Physiol. Neurobiol.* 168, 4–12. doi: 10.1016/j.resp.2009.04.019
- Boyle, J. I. (2001). "Respiratory physiology," in *Physiology (National Medical Series for Independent Study)*, eds J. Bullock, B. J. Iii, and M. B. Wang (Russia: Harwal).
- Bradley, D. J., Pascoe, J. P., Paton, J. F., and Spyer, K. M. (1987). Cardiovascular and respiratory responses evoked from the posterior cerebellar cortex and fastigial nucleus in the cat. *J. Physiol.* 393, 107–121. doi: 10.1113/jphysiol.1987.sp016813
- Butler, S. G., Postma, G. N., and Fischer, E. (2004). Effects of viscosity, taste, and bolus volume on swallowing apnea duration of normal adults. *Otolaryngol. Head Neck Surg.* 131, 860–863. doi: 10.1016/j.ototns.2004.06.706
- Chen, H. I., and Kuo, C. S. (1989). Relationship between respiratory muscle function and age, sex, and other factors. *J. Appl. Physiol.* (1985) 66, 943–948. doi: 10.1152/jappl.1989.66.2.943
- Cook, I. J., Dodds, W. J., Dantas, R. O., Kern, M. K., Massey, B. T., Shaker, R., et al. (1989). Timing of videofluoroscopic, manometric events, and bolus transit during the oral and pharyngeal phases of swallowing. *Dysphagia* 4, 8–15. doi: 10.1007/bf02407397
- Cunningham, D. J., and Robbins, P. A. (1984). The pattern of breathing in man in response to sine waves of alveolar carbon dioxide and hypoxia. *J. Physiol.* 350, 475–486. doi: 10.1113/jphysiol.1984.sp015213
- Daniels, S. K., Schroeder, M. F., Degeorge, P. C., Corey, D. M., and Rosenbek, J. C. (2007). Effects of verbal cue on bolus flow during swallowing. *Am. J. Speech Lang. Pathol.* 16, 140–147. doi: 10.1044/1058-0360(2007/018)
- Davis, H. L., Fowler, W. S., and Lambert, E. H. (1956). Effect of volume and rate of inflation and deflation on transpulmonary pressure and response of pulmonary stretch receptors. *Am. J. Physiol.* 187, 558–566. doi: 10.1152/ajplegacy.1956.187.3.558
- Dick, T. E., Oku, Y., Romaniuk, J. R., and Cherniack, N. S. (1993). Interaction between central pattern generators for breathing and swallowing in the cat. *J. Physiol.* 465, 715–730. doi: 10.1113/jphysiol.1993.sp019702
- Doty, R. W. (1968). "Neural organization of deglutition," in *Handbook of Physiology. The Alimentary Canal*, ed. C. F. Code (Washington DC: American Physiological Society), 1861–1902.
- Doty, R. W., and Bosma, J. F. (1956). An electromyographic analysis of reflex deglutition. *J. Neurophysiol.* 19, 44–60. doi: 10.1152/jn.1956.19.1.44
- Dozier, T. S., Brodsky, M. B., Michel, Y., Walters, B. C. Jr., and Martin-Harris, B. (2006). Coordination of swallowing and respiration in normal sequential cup swallows. *Laryngoscope* 116, 1489–1493. doi: 10.1097/01.mlg.0000227724.61801.b4
- Enright, P. L., Kronmal, R. A., Manolio, T. A., Schenker, M. B., and Hyatt, R. E. (1994). Respiratory muscle strength in the elderly: correlates and reference values. cardiovascular health study research group. *Am. J. Respir. Crit. Care Med.* 149, 430–438. doi: 10.1164/ajrcm.149.2.8306041
- Feroah, T. R., Forster, H. V., Fuentes, C. G., Lang, I. M., Beste, D., Martino, P., et al. (2002). Effects of spontaneous swallows on breathing in awake goats. *J. Appl. Physiol.* (1985) 92, 1923–1935. doi: 10.1152/japplphysiol.01079.2000
- Fontana, G. A., Pantaleo, T., Bongianini, F., Cresci, F., Violi, L., and Saragó, G. (1992). Changes in respiratory activity induced by mastication in humans. *J. Appl. Physiol.* (1985) 72, 779–786. doi: 10.1152/jappl.1992.72.2.779
- Formiga, F., Chivite, D., Mascaro, J., Ramon, J. M., and Pujol, R. (2005). No correlation between mini-nutritional assessment (short form) scale and clinical outcomes in 73 elderly patients admitted for hip fracture. *Aging Clin. Exp. Res.* 17, 343–346. doi: 10.1007/bf03324620
- Fukuhara, T., Tsujimura, T., Kajii, Y., Yamamura, K., and Inoue, M. (2011). Effects of electrical stimulation of the superior laryngeal nerve on the jaw-opening reflex. *Brain Res.* 1391, 44–53. doi: 10.1016/j.brainres.2011.03.065
- Gardner, W. N. (1980). The pattern of breathing following step changes of alveolar partial pressures of carbon dioxide and oxygen in man. *J. Physiol.* 300, 55–73. doi: 10.1113/jphysiol.1980.sp013151
- Hiiemae, K. M., Palmer, J. B., Medicis, S. W., Hegener, J., Jackson, B. S., and Lieberman, D. E. (2002). Hyoid and tongue surface movements in speaking and eating. *Arch. Oral. Biol.* 47, 11–27. doi: 10.1016/s0003-9969(01)00092-9
- Jean, A. (2001). Brain stem control of swallowing: neuronal network and cellular mechanisms. *Physiol. Rev.* 81, 929–969. doi: 10.1152/physrev.2001.81.2.929
- Jennett, S., McKay, F. C., and Moss, V. A. (1981). The human ventilatory response to stimulation by transient hypoxia. *J. Physiol.* 315, 339–351. doi: 10.1113/jphysiol.1981.sp013751
- Kawasaki, M., Ogura, J. H., and Takenouchi, S. (1964). Neurophysiologic observations of normal deglutition. i. its relationship to the respiratory cycle. *Laryngoscope* 74, 1747–1765.
- Kijima, M., Isono, S., and Nishino, T. (1999). Coordination of swallowing and phases of respiration during added respiratory loads in awake subjects. *Am. J. Respir. Crit. Care Med.* 159, 1898–1902. doi: 10.1164/ajrcm.159.6.9811092
- Kronenberg, R. S., and Drage, C. W. (1973). Attenuation of the ventilatory and heart rate responses to hypoxia and hypercapnia with aging in normal men. *J. Clin. Invest.* 52, 1812–1819. doi: 10.1172/jci107363
- Kurosu, A., Pratt, S. R., Palmer, C., and Shaiman, S. (2020). Investigation of embodied language processing on command-swallow performance in healthy participants. *J. Speech Lang. Hear. Res.* 64, 75–90. doi: 10.1044/2020_jslhr-20-00048
- Laitman, J. T., and Reidenberg, J. S. (1993). Specializations of the human upper respiratory and upper digestive systems as seen through comparative and developmental anatomy. *Dysphagia* 8, 318–325. doi: 10.1007/bf01321770
- Larson, C. R., Yajima, Y., and Ko, P. (1994). Modification in activity of medullary respiratory-related neurons for vocalization and swallowing. *J. Neurophysiol.* 71, 2294–2304. doi: 10.1152/jn.1994.71.6.2294
- Lederle, A., Hoit, J. D., and Barkmeier-Kraemer, J. (2012). Effects of sequential swallowing on drive to breathe in young, healthy adults. *Dysphagia* 27, 221–227. doi: 10.1007/s00455-011-9357-x
- Martin-Harris, B., Brodsky, M. B., Price, C. C., Michel, Y., and Walters, B. (2003). Temporal coordination of pharyngeal and laryngeal dynamics with breathing during swallowing: single liquid swallows. *J. Appl. Physiol.* (1985) 94, 1735–1743. doi: 10.1152/japplphysiol.00806.2002
- Martin-Harris, B., and McFarland, D. H. (2013). "Coordination of deglutition and respiration," in *Principles of Deglutition*, eds R. Shaker, P. C. Belafsky, G. N. Postma, and C. Easterling (Berlin: Springer), 55–113.
- Matsuo, K., Hiiemae, K. M., Gonzalez-Fernandez, M., and Palmer, J. B. (2008). Respiration during feeding on solid food: alterations in breathing during mastication, pharyngeal bolus aggregation, and swallowing. *J. Appl. Physiol.* (1985) 104, 674–681. doi: 10.1152/japplphysiol.00527.2007
- McFarland, D. H., and Lund, J. P. (1993). An investigation of the coupling between respiration, mastication, and swallowing in the awake rabbit. *J. Neurophysiol.* 69, 95–108. doi: 10.1152/jn.1993.69.1.95
- McFarland, D. H., and Lund, J. P. (1995). Modification of mastication and respiration during swallowing in the adult human. *J. Neurophysiol.* 74, 1509–1517. doi: 10.1152/jn.1995.74.4.1509
- McFarland, D. H., Lund, J. P., and Gagner, M. (1994). Effects of posture on the coordination of respiration and swallowing. *J. Neurophysiol.* 72, 2431–2437. doi: 10.1152/jn.1994.72.5.2431

SUPPLEMENTARY MATERIAL

The Supplementary Material for this article can be found online at: <https://www.frontiersin.org/articles/10.3389/fphys.2021.696071/full#supplementary-material>

- Mead, J., and Reid, M. B. (1988). Respiratory muscle activity during repeated airflow interruption. *J. Appl. Physiol.* (1985) 64, 2314–2317. doi: 10.1152/jappl.1988.64.6.2314
- Megirian, D., Hinrichsen, C. F., and Sherrey, J. H. (1985). Respiratory roles of genioglossus, sternohyoid, and sternohyoid muscles during sleep. *Exp. Neurol.* 90, 118–128. doi: 10.1016/0014-4886(85)90045-7
- Michou, E., Mastan, A., Ahmed, S., Mistry, S., and Hamdy, S. (2012). Examining the role of carbonation and temperature on water swallowing performance: a swallowing reaction-time study. *Chem. Senses* 37, 799–807. doi: 10.1093/chemse/bjs061
- Mitchinson, A. G., and Yoffey, J. M. (1947). Respiratory displacement of larynx, hyoid bone and tongue. *J. Anat.* 81, 118–120.1.
- Nagy, A., Leigh, C., Hori, S. F., Molfenter, S. M., Shariff, T., and Steele, C. M. (2013). Timing differences between cued and noncued swallows in healthy young adults. *Dysphagia* 28, 428–434. doi: 10.1007/s00455-013-9456-y
- Nishino, T., Yonezawa, T., and Honda, Y. (1985). Effects of swallowing on the pattern of continuous respiration in human adults. *Am. Rev. Respir. Dis.* 132, 1219–1222.
- Ouahchi, Y., Ben Salah, N., Mjid, M., Hedhli, A., Abdelhedi, N., Beji, M., et al. (2019). Breathing pattern during sequential swallowing in healthy adult humans. *J. Appl. Physiol.* (1985) 126, 487–493. doi: 10.1152/japplphysiol.00150.2018
- Palmer, J. B., and Hiimeae, K. M. (2003). Eating and breathing: interactions between respiration and feeding on solid food. *Dysphagia* 18, 169–178. doi: 10.1007/s00455-002-0097-9
- Palmer, J. B., Hiimeae, K. M., and Liu, J. (1997). Tongue-jaw linkages in human feeding: a preliminary videofluorographic study. *Arch. Oral. Biol.* 42, 429–441. doi: 10.1016/s0003-9969(97)00020-4
- Palmer, J. B., Rudin, N. J., Lara, G., and Crompton, A. W. (1992). Coordination of mastication and swallowing. *Dysphagia* 7, 187–200. doi: 10.1007/bf02493469
- Parreira, V. F., Bueno, C. J., França, D. C., Vieira, D. S., Pereira, D. R., and Britto, R. R. (2010). Breathing pattern and thoracoabdominal motion in healthy individuals: influence of age and sex. *Rev. Bras. Fisioter.* 14, 411–416.
- Paydarfar, D., Gilbert, R. J., Poppel, C. S., and Nassab, P. F. (1995). Respiratory phase resetting and airflow changes induced by swallowing in humans. *J. Physiol.* 483, 273–288. doi: 10.1113/jphysiol.1995.sp020584
- Peterson, D. D., Pack, A. I., Silage, D. A., and Fishman, A. P. (1981). Effects of aging on ventilatory and occlusion pressure responses to hypoxia and hypercapnia. *Am. Rev. Respir. Dis.* 124, 387–391.
- Rebuck, A. S., Rigg, J. R., and Saunders, N. A. (1976). Respiratory frequency response to progressive isocapnic hypoxia. *J. Physiol.* 258, 19–31. doi: 10.1113/jphysiol.1976.sp011404
- Robbins, J., Hamilton, J. W., Lof, G. L., and Kempster, G. B. (1992). Oropharyngeal swallowing in normal adults of different ages. *Gastroenterology* 103, 823–829. doi: 10.1016/0016-5085(92)90013-o
- Sachs, M. C., Enright, P. L., Hinckley Stukovsky, K. D., Jiang, R., and Barr, R. G. (2009). Performance of maximum inspiratory pressure tests and maximum inspiratory pressure reference equations for 4 race/ethnic groups. *Respir. Care* 54, 1321–1328.
- Selley, W. G., Flack, F. C., Ellis, R. E., and Brooks, W. A. (1989). Respiratory patterns associated with swallowing: Part 1. the normal adult pattern and changes with age. *Age Ageing* 18, 168–172. doi: 10.1093/ageing/18.3.168
- Shaker, R., Li, Q., Ren, J., Townsend, W. F., Dodds, W. J., Martin, B. J., et al. (1992). Coordination of deglutition and phases of respiration: effect of aging, tachypnea, bolus volume, and chronic obstructive pulmonary disease. *Am. J. Physiol.* 263, G750–G755.
- Shiba, K., Satoh, I., Kobayashi, N., and Hayashi, F. (1999). Multifunctional laryngeal motoneurons: an intracellular study in the cat. *J. Neurosci.* 19, 2717–2727. doi: 10.1523/jneurosci.19-07-02717.1999
- Smith, J., Wolkove, N., Colacone, A., and Kreisman, H. (1989). Coordination of eating, drinking and breathing in adults. *Chest* 96, 578–582. doi: 10.1378/chest.96.3.578
- Sonies, B. C. (1992). Oropharyngeal dysphagia in the elderly. *Clin. Geriatr. Med.* 8, 569–577. doi: 10.1016/s0749-0690(18)30465-8
- Strohl, K. P., and Altose, M. D. (1984). Oxygen saturation during breath-holding and during apneas in sleep. *Chest* 85, 181–186. doi: 10.1378/chest.85.2.181
- Sumi, T. (1963). The activity of brain-stem respiratory neurons and spinal respiratory motoneurons during swallowing. *J. Neurophysiol.* 26, 466–477. doi: 10.1152/jn.1963.26.3.466
- Suzuki, T., Yoshihara, M., Sakai, S., Tsuji, K., Nagoya, K., Magara, J., et al. (2018). Effect of peripherally and cortically evoked swallows on jaw reflex responses in anesthetized rabbits. *Brain Res.* 1694, 19–28. doi: 10.1016/j.brainres.2018.05.002
- Tsuji, K., Tsujimura, T., Magara, J., Sakai, S., Nakamura, Y., and Inoue, M. (2014). Changes in the frequency of swallowing during electrical stimulation of superior laryngeal nerve in rats. *Brain Res. Bull.* 111C, 53–61. doi: 10.1016/j.brainresbull.2014.12.008
- Tsuji, K., Tsujimura, T., Sakai, S., Suzuki, T., Yoshihara, M., Nagoya, K., et al. (2020). Involvement of capsaicin-sensitive nerves in the initiation of swallowing evoked by carbonated water in anesthetized rats. *Am. J. Physiol. Gastrointest. Liver Physiol.* 319, G564–G572.
- Tsujimura, T., Sakai, S., Suzuki, T., Ujihara, I., Tsuji, K., Magara, J., et al. (2017). Central inhibition of initiation of swallowing by systemic administration of diazepam and baclofen in anaesthetized rats. *Am. J. Physiol. Gastrointest. Liver Physiol.* 312, G498–G507.
- Tsujimura, T., Tsuji, K., Magara, J., Sakai, S., Suzuki, T., Nakamura, Y., et al. (2016). Differential response properties of peripherally and cortically evoked swallows by electrical stimulation in anesthetized rats. *Brain Res. Bull.* 122, 12–18. doi: 10.1016/j.brainresbull.2016.02.015
- Tsukada, T., Taniguchi, H., Ootaki, S., Yamada, Y., and Inoue, M. (2009). Effects of food texture and head posture on oropharyngeal swallowing. *J. Appl. Physiol.* 106, 1848–1857. doi: 10.1152/japplphysiol.91295.2008
- Vaz Frago, C. A., and Gill, T. M. (2012). Respiratory impairment and the aging lung: a novel paradigm for assessing pulmonary function. *J. Gerontol. A Biol. Sci. Med. Sci.* 67, 264–275. doi: 10.1093/gerona/glr198
- Wang, C. M., Chen, J. Y., Chuang, C. C., Tseng, W. C., Wong, A. M., and Pei, Y. C. (2015). Aging-related changes in swallowing, and in the coordination of swallowing and respiration determined by novel non-invasive measurement techniques. *Geriatr. Gerontol. Int.* 15, 736–744. doi: 10.1111/ggi.12343
- Wheeler Hegland, K., Huber, J. E., Pitts, T., Davenport, P. W., and Sapienza, C. M. (2011). Lung volume measured during sequential swallowing in healthy young adults. *J. Speech Lang. Hear Res.* 54, 777–786. doi: 10.1044/1092-4388(2010/09-0237)
- Wirth, R., Dziewas, R., Beck, A. M., Clavé, P., Hamdy, S., Heppner, H. J., et al. (2016). Oropharyngeal dysphagia in older persons - from pathophysiology to adequate intervention: a review and summary of an international expert meeting. *Clin. Interv. Aging* 11, 189–208. doi: 10.2147/cia.s97481
- Yoshihara, M., Tsujimura, T., Suzuki, T., Nagoya, K., Shiraishi, N., Magara, J., et al. (2020). Sustained laryngeal transient receptor potential vanilloid 1 activation inhibits mechanically induced swallowing in anesthetized rats. *Am. J. Physiol. Gastrointest. Liver Physiol.* 319, G412–G419.

Conflict of Interest: The authors declare that the research was conducted in the absence of any commercial or financial relationships that could be construed as a potential conflict of interest.

Copyright © 2021 Hao, Sasa, Kulvanich, Nakajima, Nagoya, Magara, Tsujimura and Inoue. This is an open-access article distributed under the terms of the Creative Commons Attribution License (CC BY). The use, distribution or reproduction in other forums is permitted, provided the original author(s) and the copyright owner(s) are credited and that the original publication in this journal is cited, in accordance with accepted academic practice. No use, distribution or reproduction is permitted which does not comply with these terms.



Event-Related Desynchronization and Corticomuscular Coherence Observed During Volitional Swallow by Electroencephalography Recordings in Humans

Satoko Koganemaru^{1,2*}, Fumiya Mizuno³, Toshimitsu Takahashi², Yuu Takemura⁴, Hiroshi Irisawa⁴, Masao Matsushashi⁵, Tatsuya Mima⁶, Takashi Mizushima⁴ and Kenji Kansaku²

OPEN ACCESS

Edited by:

Kazutaka Takahashi,
The University of Chicago,
United States

Reviewed by:

Atsushi Noritake,
National Institute for Physiological
Sciences (NIPS), Japan
Pantelis Lioumis,
Aalto University, Finland

*Correspondence:

Satoko Koganemaru
kogane@kuhp.kyoto-u.ac.jp

Specialty section:

This article was submitted to
Motor Neuroscience,
a section of the journal
Frontiers in Human Neuroscience

Received: 04 January 2021

Accepted: 29 October 2021

Published: 26 November 2021

Citation:

Koganemaru S, Mizuno F, Takahashi T, Takemura Y, Irisawa H, Matsushashi M, Mima T, Mizushima T and Kansaku K (2021) Event-Related Desynchronization and Corticomuscular Coherence Observed During Volitional Swallow by Electroencephalography Recordings in Humans. *Front. Hum. Neurosci.* 15:643454. doi: 10.3389/fnhum.2021.643454

¹ Department of Regenerative Systems Neuroscience, Human Brain Research Center, Graduate School of Medicine, Kyoto University, Kyoto, Japan, ² Department of Physiology, Dokkyo Medical University, Mibu, Japan, ³ Division of Rehabilitation Medicine, Dokkyo Medical University Hospital, Mibu, Japan, ⁴ Department of Rehabilitation Medicine, Dokkyo Medical University, Mibu, Japan, ⁵ Department of Epilepsy, Movement Disorders and Physiology, Graduate School of Medicine, Kyoto University, Kyoto, Japan, ⁶ The Graduate School of Core Ethics and Frontier Sciences, Ritsumeikan University, Kyoto, Japan

Swallowing in humans involves many cortical areas although it is partly mediated by a series of brainstem reflexes. Cortical motor commands are sent to muscles during swallow. Previous works using magnetoencephalography showed event-related desynchronization (ERD) during swallow and corticomuscular coherence (CMC) during tongue movements in the bilateral sensorimotor and motor-related areas. However, there have been few analogous works that use electroencephalography (EEG). We investigated the ERD and CMC in the bilateral sensorimotor, premotor, and inferior prefrontal areas during volitional swallow by EEG recordings in 18 healthy human subjects. As a result, we found a significant ERD in the beta frequency band and CMC in the theta, alpha, and beta frequency bands during swallow in those cortical areas. These results suggest that EEG can detect the desynchronized activity and oscillatory interaction between the cortex and pharyngeal muscles in the bilateral sensorimotor, premotor, and inferior prefrontal areas during volitional swallow in humans.

Keywords: swallowing, event-related (de-) synchronization, healthy subject, coherence, electroencephalogram

INTRODUCTION

Swallow is a fundamental behavior to maintain life in animals. Although it is partly mediated by reflexive neuronal activities at the brainstem level, multiple areas in the cerebral cortices, such as primary motor and somatosensory cortices and supplemental and premotor cortices, are involved in swallow (Jean, 2001; Ertekin and Aydogdu, 2003; Michou and Hamdy, 2009). Recently, event-related desynchronizations (ERDs) involved in the process of swallow have been reported in bilateral sensorimotor areas using magnetoencephalography (MEG) (Dziewas et al., 2003;

Suntrup et al., 2013, 2014, 2015). Generally, ERDs are a decrease of the power in the alpha and beta frequency bands during voluntary movements when compared with that during the rest (nonmovement) (Pfurtscheller and Lopes da Silva, 1999; Li et al., 2018; Chen et al., 2020; Spadone et al., 2020; Xie et al., 2021). They are supposed to reflect cortical activities during voluntary movements (Pfurtscheller and Lopes da Silva, 1999). In the previous works using MEG by the same research group, ERDs were observed in the alpha and beta frequency bands during volitional swallows in the bilateral sensorimotor, premotor, and prefrontal areas (Dziewas et al., 2003; Suntrup et al., 2013, 2014, 2015; Suntrup-Krueger et al., 2018). The emergence of the ERDs detected by their methods was changed in patients with Parkinson's disease without dysphagia (Suntrup et al., 2013), in patients with functional dysphagia without organic abnormality (Suntrup et al., 2014), in patients with poststroke dysphagia after transcranial direct current stimulation therapy (Suntrup-Krueger et al., 2018), mildly and severely in patients with dysphagic amyotrophic lateral sclerosis, and in healthy subjects after electrical stimulation on the pharynx (Suntrup et al., 2015). There have been few analogous works in electroencephalography (EEG) (Cuellar et al., 2016), whereas EEG is an easier and more economical method for evaluating cortical activities, compared with MEG. In addition to ERDs during voluntary movements, corticomuscular coherence (CMC) has been reported in EEG works using motor tasks of the upper and lower extremities (Mima and Hallett, 1999). CMC is supposed to indicate both corticomotoneuronal activities that projecting the anterior horn cell in the spinal cord (Mima and Hallett, 1999) and ascending sensory feedback from muscles to motor cortex (Witham et al., 2011; Liu et al., 2019). Transcranial magnetic stimulation (TMS) works showed changes in corticomotoneuronal activities by the evaluation of motor-evoked potentials in the pharyngeal muscles in the resting state after repetitive TMS, which increased the cortical excitability of the stimulated area (Michou et al., 2014). In the previous works using MEG, significant CMCs in theta, alpha, and beta frequency bands have been found during tongue protrusion task, which suggests that cortical motor commands can be evaluated in oral apparatus by CMC (Maezawa et al., 2014, 2016; Maezawa, 2017). Although it is important to evaluate the corticomotoneuronal activities during swallow movements with activated submental group muscles and pharyngeal muscles (Ding et al., 2002), there has been no analogous work on them. If ERD and CMC can be detected by EEG recordings using a similar way with the previous MEG studies, it would be easily applicable in clinical practice for the evaluation of swallow dysfunction in neurological patients. Therefore, we investigated them based on the hypothesis that ERDs and CMCs could be measured in the bilateral sensorimotor, premotor, and prefrontal areas as reported by the previous MEG works (Dziewas et al., 2003; Suntrup et al., 2013, 2014, 2015; Maezawa et al., 2014, 2016; Maezawa, 2017). The submental group muscle activity was used to differentiate the swallow activation from the baseline according to the previous MEG works (Dziewas et al., 2003; Suntrup et al., 2013, 2014, 2015) because the onset of the activity was close to the start of the pharyngeal phase (Ding et al., 2002). This work is the observational and descriptive one to investigate the EEG change such as ERD and CMC associated with swallowing.

MATERIALS AND METHODS

Experimental Protocol

Participants

Eighteen healthy volunteers (six women and 12 men, mean age 34.2 ± 13.9 years) were recruited for this work. The inclusion criteria were the absence of history of swallow dysfunction and the absence of chronic or acute neurological, psychiatric, or medical diseases. Seventeen subjects were right-handed, and one subject was left-handed according to the Edinburgh Handedness Inventory (Oldfield, 1971). The work protocol was approved by the Committee of Medical Ethics of Dokkyo Medical University, Japan (No. 30008), and written informed consent was obtained from all subjects.

Electroencephalography and Electromyogram Recordings

Participants were comfortably seated in an armchair during the recordings. EEG signals were recorded with 32 electrodes. The EEG electrodes, which were the eegoTMsports active electrodes (ANT Neuro, Netherlands), attached inside the EEG cap were positioned according to the 10–20 international electrode system. The EEG signals were amplified using the eegoTMsports amplifier. The CPz electrode was selected as the reference electrode. Impedance of all electrodes was <15 k Ω . Data were recorded and saved at a sampling rate of 1 kHz with bandpass filter of the hardware from DC to 260 Hz (ANT Neuro, Netherlands).

Participants were asked to perform volitional swallow without head movements at their own pace with a waiting time of greater than 3 s after 3 mL of water was infused into the oral cavity via a flexible plastic tube with 3.3-mm diameter connected with a syringe pressed by an experimenter. The tip of the tube was randomly placed in the left or right corner of the mouth between the buccal part of the teeth and cheek and gently fixed to the skin with tape similar to those in previous MEG works (Suntrup et al., 2014, 2015; Suntrup-Krueger et al., 2018). In the process of the volitional swallow, they were asked to send a small bolus of water deeply to the dorsum of tongue, to have a rest (no tongue movement), and then to perform one time of volitional swallow, and to have a rest (no tongue movement) for a few seconds after the volitional swallow ends. Volitional swallow was repeated for 1 h.

We concurrently recorded surface electromyogram (EMG) with two pairs of bipolar silver electrodes placed on the right and left submental group muscles and unilateral orbicularis oris muscle contralateral to the tube (Okitsu et al., 1998; Nederkoorn et al., 1999; Ding et al., 2002; Vaiman, 2007). The electrodes were connected to a bipolar eegoTMsports amplifier, and the EMG data were recorded with a sampling rate of 1 kHz and an input range of 150 mV_{peak-to-peak} (ANT Neuro, Netherlands). Swallowing vibrations were recorded with a triple-axis accelerometer (ANT Neuro, Netherlands) which is positioned on the anterior part of the participant's neck based on the previous works (Suntrup et al., 2014, 2015; Jestrovic et al., 2018; Suntrup-Krueger et al., 2018).

The head movements were monitored by video recordings using two cameras.

Data Analysis

Preprocessing

We removed the artifacts of the blink and electrooculographic activities from the EEG signals using the independent component analysis (ICA) algorithm (Hyvarinen and Oja, 2000) using EEGLAB MATLAB toolbox (Delorme and Makeig, 2004) (MathWorks Inc., United States). The EEG signals were removed with the power spectral density over $1 \times 10^{-8} \mu V^2/Hz$ mainly in the frequency domain from 0.01 to 4 Hz as EOG activities (Jung et al., 2000) and with the 50 Hz data as powerline noise in the continuous data from the start to the end of the recording using ICA. EEG signals were segmented based on the onset and offset of separate swallows as determined by EMG signals from the submental group muscles as follows: the beginning of the main muscle activation (M1) and end of the swallow-specific muscle activity (M2) were identified for separate swallows from the submental group muscles. M1 was defined as the time to produce a sustained activity greater than 100% increase in amplitude or frequency of the averaged EMG signal in the resting state. M2 was defined as the time to decrease greater than 50% of the activity in amplitude or frequency of the averaged EMG signal in the resting state according to the previous works (Suntrup et al., 2014, 2015; Suntrup-Krueger et al., 2018). For the analyses of the event-related EEG data, time intervals were defined from -0.4 to 0.6 s in reference to M1 (from "M1-0.4" to "M1+0.6" seconds) as an activation stage and from 2 to 3 s in reference to M2 (from "M2" to "M2+1" seconds) as the resting stage (Figure 1). A third marker (M0) was manually set to distinguish background activity from the onset of swallowing preparation in the EMG to determine mean total swallow duration (from M0 to M2) per subject according to the previous work (Dziewas et al., 2009; Suntrup et al., 2015).

Electroencephalography Analyses

Event-Related Desynchronization

We computed the power spectral density of the denoised EEG data using fast Fourier transform (FFT) for both activation and resting stages. We applied FFT using a boxcar window to 1,000 ms (1,000 points) segments spanning the activation stage (M1 - 0.4 to M1 + 0.6 s), where M1 are the timing of multiple swallowing movements when EMG activity grew larger than the predefined threshold and 1,000 ms segments spanning the resting stage (M2 to M2 + 1.0 second), where M2 is the timing of multiple swallowing movements when EMG activity grew lower than the predefined threshold at each swallowing trial. The FFT data were converted to their absolute value and then averaged across M1 and M2 events. The upper and lower limits of the FFT were 500 and 1 Hz, respectively. The evaluated frequency ranged from 1 to 60 Hz. As we applied FFT to 1,000 ms (1,000 points) segments, 1–60 Hz band was covered by 60 steps using 1 Hz frequency step in the FT computation. We obtained the logarithm of the estimated power spectral densities from 1 to 60 Hz and calculated ERD by subtracting the logarithm of the power spectral densities during the resting stage from that during the activation stage in nine channels (C3, Cz, C4, FC1, FC2, FC5, FC6, CP1, and CP2), which represents the frontal and parietal regions according to the previous works, in which a region of interest was predefined with exclusion of the inferior temporal areas because of tongue movements (Suntrup et al., 2013, 2015). The ERDs of the nine channels were averaged in all subject in the theta (4–7 Hz), alpha (8–14 Hz), and beta (15–25 Hz) frequencies.

To investigate the frequency and temporal properties during swallow, we performed the time-frequency analysis using short-time FT according to the previous works (Kobayashi et al., 2015; Samiee et al., 2015; Usami et al., 2015; Inada et al., 2021). The FT

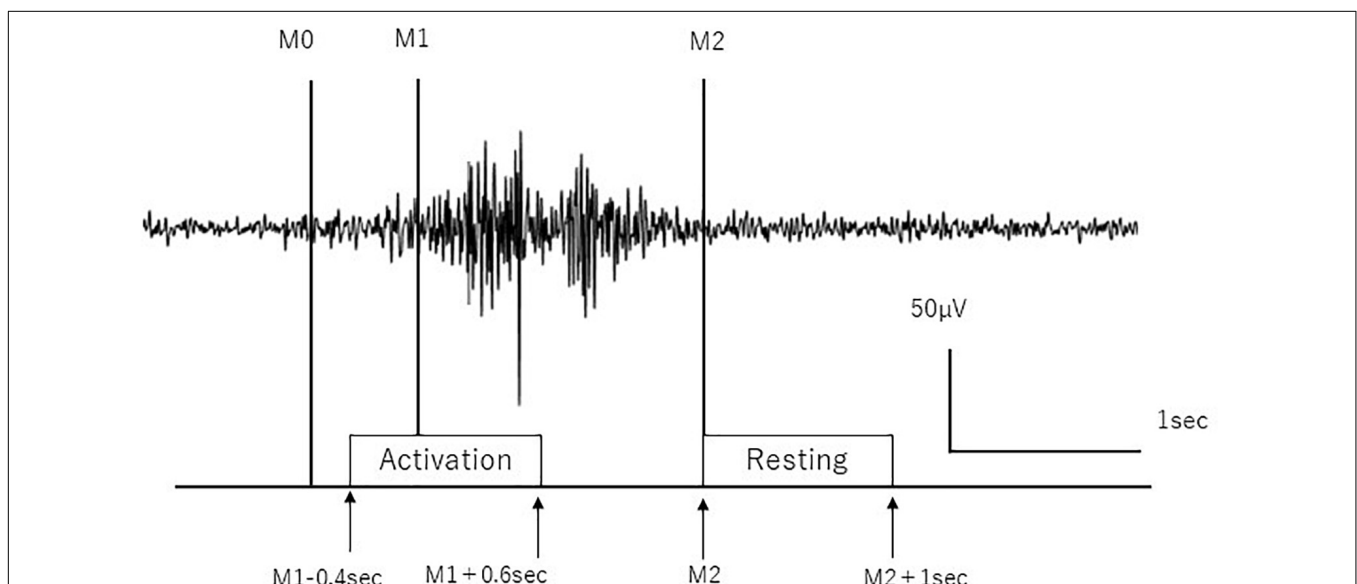


FIGURE 1 | Definition of activation and resting stages. Activation and resting stages are defined according to swallow-related submental group muscle activities. M0 is the time to initiate swallow, M1 is the time to start main muscle activation, and M2 is the time to return to baseline. The surface EMG trace during a single swallow is shown.

size was 200 points using a boxcar window to 200 ms (200 points) segments and the time shift was 50 ms. The analyzed time period was from 0.5 s before the start of the activation stage $\{(M1 - 0.4) - 0.5 = M1 - 0.9 \text{ s}\}$ to 2.5 s after the start of the activation stage $\{(M1 - 0.4) + 2.5 = M1 + 2.1 \text{ second}\}$ and averaged across all the swallow trials. Then, all the subjects' data of the same nine channels were averaged. The upper and lower limits of the FT were 500 and 5 Hz. The evaluated frequency ranged from 5 to 60 Hz. As the FT size was 200 points with the sampling rate of 1,000 Hz (1,000 points), 5 to 60 Hz band was covered by 12 steps using 5 Hz frequency step in the FT computation.

Corticomuscular Coherence

Using the FFT, we computed the cross- and autospectra in the frequency domain of the EEG in each of nine channels (C3, Cz, C4, FC1, FC2, FC5, FC6, CP1, and CP2) and the submental EMG signals segmented for 1 s in the activation stage. The EMG signals were rectified by calculating the root mean square values as the rectified EMG was better to represent the motor unit firing times which reflected the cortical motor inputs (Elble and Randall, 1976; Halliday and Farmer, 2010). The properties of the FFT were the same as those of ERD calculation. The coherence was defined with crossspectra normalized by autospectra in the following equation, in which $f_{xx}(j)$, $f_{yy}(j)$, and $|f_{xy}(j)|$ are the values of auto- and cross-spectra, respectively, at a given frequency j (Mima and Hallett, 1999):

$$|R_{xy}(j)|^2 = \frac{|f_{xy}(j)|^2}{f_{xx}(j) \cdot f_{yy}(j)}.$$

We calculated the coherence and detected the maximal (peak) one in nine channels, each in theta (4–7 Hz), alpha (8–14 Hz), and beta (15–25 Hz) frequency bands.

To investigate the frequency and temporal properties in the CMC during swallow, we performed time-frequency analysis of the CMC using short-time FT in the same way as the ERDs (FT size was 200 points using a boxcar window to 200 ms (200 points) segments and the time shift was 50 ms). The time period was from 0.5 s before the start of the activation stage to 2.5 s after the start of the activation stage. The properties of the short-time FT were the same as those of ERD calculation in time-frequency analysis. We calculated the inverted hyperbolic tangent of the coherence values to make them normally distributed by the following equation:

$$\tanh^{-1} |R_{xy}(j)| = \frac{1}{2} \ln \left(\frac{1 + |R_{xy}(j)|}{1 - |R_{xy}(j)|} \right).$$

Then, all the subjects' data were averaged each in the nine channels, and the grand average of the averaged subjects' data were calculated over the nine channels.

Statistical Analysis

As for the ERDs, the averaged ERDs were subjected to one-sample t -test (two-sided). The null hypothesis was that the average was zero. As for the CMC, the 95% confidence limit was calculated for the number of trials (n) in each subject in the

following equation (Mima and Hallett, 1999):

$$\text{Confidence limit (95\%)} = 1 - (0.05)^{1/(n-1)}.$$

The existence of CMC was evaluated by the binomial test for each channel in theta, alpha, and beta frequency bands. The null hypothesis was that no subject had a peak of CMC greater than 95% confidence limit in any channel, each in theta, alpha, and beta frequency bands. The Bonferroni correction was used for the multiple comparisons. Effects were considered significant at a p -value < 0.05 . All data were expressed as mean \pm SD unless otherwise indicated. The JMP statistical package (JMP Pro 12.2, SAS Institute Inc., United States) was used in each analysis unless otherwise described.

RESULTS

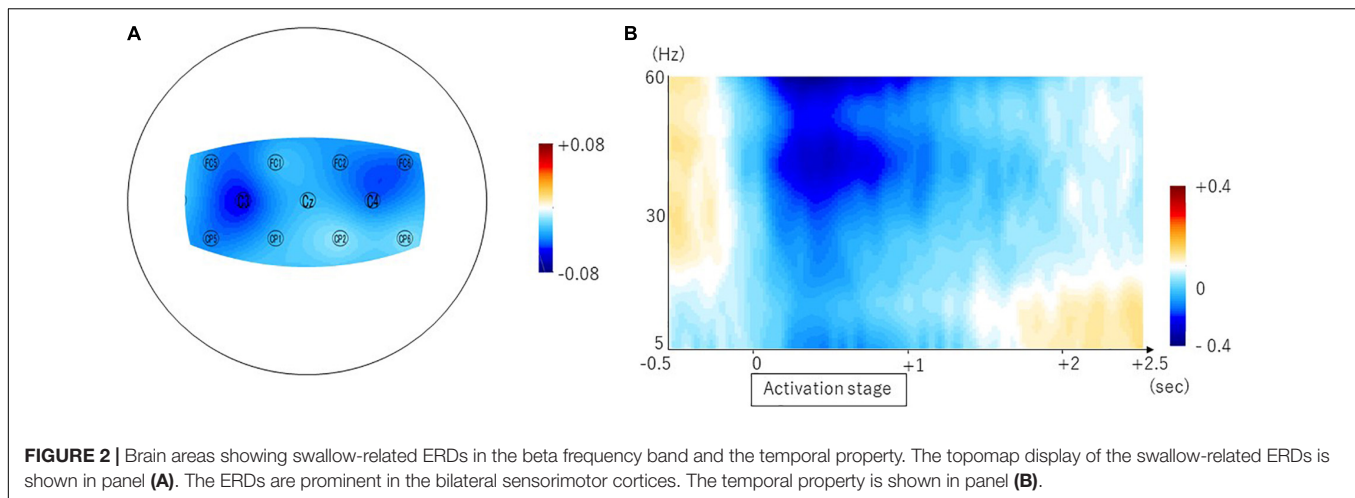
The numbers of volitional swallows were 206 ± 14.4 times during EEG recordings. The participants' EMG swallowing parameters were as follows: swallow duration, 1.95 ± 0.69 s and EMG peak-to-peak amplitude, $72.8 \pm 36.6 \mu\text{V}$. Head movement during EEG recordings was visually inspected. We found the ERDs by EEG recordings similar to the previous works using MEG recordings and CMC during swallow movements.

Event-Related Desynchronization

We found the ERD in the frontal and parietal areas in the beta frequency band (**Figure 2A**). The averaged ERDs for the nine channels (C3, Cz, C4, FC1, FC2, FC5, FC6, CP1, and CP2) were significantly different with zero in the beta frequency band (-0.034 ± 0.048 , 95% CI $[-0.05 - 0.01]$, $p = 0.0074$) but not in the theta (0.006 ± 0.067 , 95% CI $[-0.028 0.039]$, $p = 0.7190$) and alpha (0.017 ± 0.041 , 95% CI $[-0.003 0.038]$, $p = 0.0917$) frequency bands (**Figure 2A**). The **Table 1A** shows the difference calculated by subtracting the logarithm of the power spectral densities during the resting stage from that during the activation stage (ERD or event-related synchronization (ERS)) in the 31 channels. The **Figure 2B** shows the temporal modulation of the averaged ERD values of the nine channels during the time period from 0.5 s before the start of the activation stage to 2.5 s after the start of the activation stage. The ERDs emerged immediately before the activation stage and maintained during the activation stage.

Corticomuscular Coherence

The representative result of the CMC is shown in **Figure 3A**. In the frontal and parietal areas, we found significant CMC in theta, alpha, and beta frequency bands in all nine channels (theta frequency band, C3, C4, FC2, FC5, FC6, and CP2, $p < 0.0001$, and FC1, Cz, and CP1, $p = 0.0010$; alpha frequency band, Cz, C4, FC1, FC2, FC5, FC6, and CP1, $p < 0.0001$, and C3 and CP2, $p = 0.0018$; and beta frequency band, C3, Cz, FC1, FC2, FC5, FC6, CP1, and CP2, $p < 0.0001$, and C4, $p = 0.0002$). The ratio of the subjects who had the peak of CMC greater than 95% confidence limit was represented in **Table 1B** and in the topographical mapping in **Figures 3B–D**. The **Figure 3E** shows the temporal modulation of the averaged CMC values of the nine channels. The CMC in



relatively low-frequency band including alpha frequency band emerged at the early phase of the activation stage, whereas the CMC in relatively high-frequency band including beta frequency band emerged at the late phase of the activation stage.

DISCUSSION

We found the ERDs during the volitional swallow by EEG recordings in the bilateral sensorimotor, premotor, and prefrontal areas in a consistent way as previously reported in MEG works. Furthermore, we found the significant CMC in those areas during the volitional swallow movement.

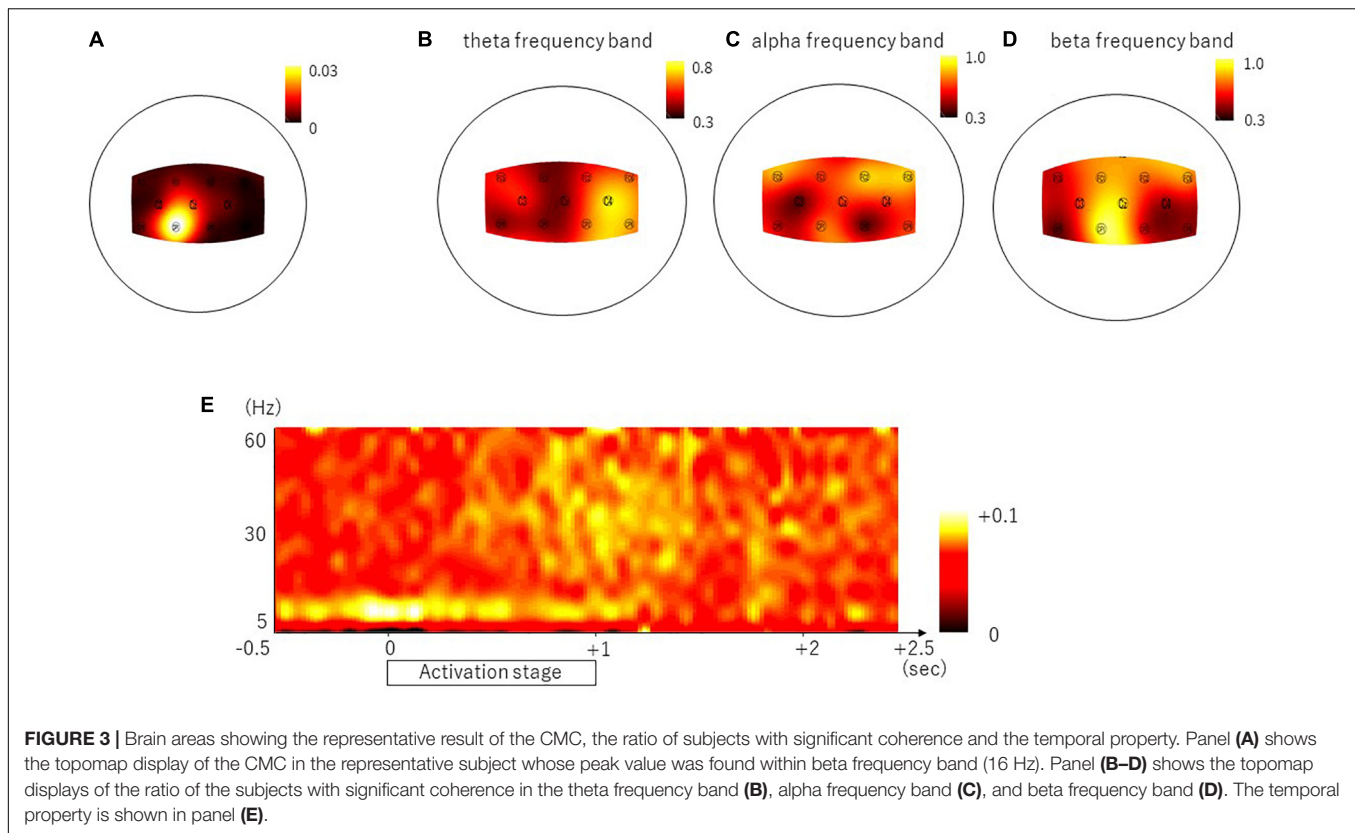
Event-related desynchronizations in the beta frequency band were most evident in C3 and C4, which corresponds to the middle precentral gyrus in this work. The somatotopy for pharyngeal muscles is arranged in a more medial part than that for tongue muscles (Hamdy et al., 1996; Dziewas et al., 2003). The previous MEG work reported the ERDs during volitional swallow in more medial parts, compared with the ERDs during tongue movement (Dziewas et al., 2003), whereas the previous TMS work showed that pharyngeal muscles were arranged more medial and oral muscles were more lateral in the cortical representations (Hamdy et al., 1996). Our findings indicate cortical activities related to pharyngeal muscles during swallow.

The other brain imaging works also showed swallow-related cortical areas (Kern et al., 2001; Martin et al., 2001; Kober et al., 2015; Kober and Wood, 2018). The bilateral primary sensorimotor cortices, insula, cingulate, and parietal regions were represented during volitional swallow in the fMRI works (Kern et al., 2001; Martin et al., 2001). Although the activity of deep brain structure is difficult to measure with the EEG recordings, it may have influenced the observed sensorimotor activities by the EEG recordings. The previous fNIRS works showed the increased blood flow of the bilateral inferior frontal gyri (Kober et al., 2015; Kober and Wood, 2018), which were included in the analyzed areas for the ERDs in this work.

Event-related desynchronizations in the sensorimotor area are associated with the neuronal activities in not only the

production of appropriate motor outputs but also in the processing of somatosensory information from the moving muscle (Pfurtscheller and Lopes da Silva, 1999). Processing of oropharyngeal sensation and complex motor execution are essential during swallow to prevent aspiration (Dziewas et al., 2003; Ertekin and Aydogdu, 2003). Therefore, alteration in ERDs can occur according to the dysphagia symptoms and recovery process (Suntrup et al., 2014; Suntrup-Krueger et al., 2018).

In the process of swallow, the tongue movement is important. To transit a bolus of water posteriorly at the oral phase, the apex of the tongue elevates and contacts with the hard palate and the bolus is propelled posteriorly in the oral cavity. At the pharyngeal phase, the tongue is retracted posteriorly to keep the oropharynx closed at the same time with the elevation and closure of the larynx. After the bolus transits pharynx, the tongue is relaxed and returned to the resting position (Logemann, 1988). In the previous work using the ROIs that covering the lateral areas from the C3 and C4, the tongue thrust execution induced the alpha ERD in the left hemisphere whether the tongue thrust left or right, and beta band ERD in the left hemisphere when the tongue thrust right, suggesting the left-sided dominance in the tongue movement (Sakihara and Inagaki, 2015). In our work, beta band ERD during the swallow was induced in the bilateral sensorimotor cortices. As the tongue movement is not lateralized during swallow, the side-dominance may not have been found. In the other previous work, ERD, ERS, or nothing was induced during the press of the tongue on the roof of the mouth in the primary motor cortex (Morash et al., 2008). The ERD may depend on how the tongue moves. In the previous MEG work that using the tongue electrical sensory stimulation, 20-Hz ERD was shown around 400 ms after the stimulation in the bilateral temporoparietal areas. The sensory inputs to the tongue also induced the beta band ERD. In our work, the ERD during swallow was induced in more medial and rostral parts probably because it was mixed with motor efferents and sensory afferents to the tongue and pharynx. Swallow movement itself requires various muscle activities in the tongue and the pharynx. It is difficult to differentiate specific brain activities for a specific muscle because complex activities of various muscles are necessary for swallow



movement. The ERDs found in this work are brain activities during swallow including tongue and pharyngeal movements.

Event-related desynchronizations are detected by comparison with brain activity during a specific event with that during baseline (nonevent) period in the event-related design, instead of comparison with a control task. ERDs have been reported in motor and cognitive tasks without control experiments (Pfurtscheller and Lopes da Silva, 1999; Li et al., 2018; Spadone et al., 2020; Xie et al., 2021). According to the previous works, we detected the brain activity during swallow movements by subtracting that during rest. The ERDs in work emerged at the immediately preceding time of the swallow movements and disappeared around the end time of the swallow movements (the end of the submental EMG activities). The ERDs showed prior to movement onset over the contralateral sensorimotor region and ended after the motor execution in the hand and foot movements in the previous report (Pfurtscheller and Lopes da Silva, 1999). The temporal property of the ERDs during the swallow was similar with the previous finding.

We did not investigate relationships between the ERD and swallow movements because they are beyond the scope of this EEG descriptive work. It is the limitation of this work. The next step would be necessary to investigate relationships between the ERD and swallow movements using correlation, decoding, or validation methods.

We have found that the significant CMC existed in all nine channels covering the lateral and medial parts of the sensorimotor area in theta, alpha, and beta frequency bands

in accordance with the previous works (Maezawa et al., 2014, 2016; Maezawa, 2017). For the finger muscles, CMC was not consistently observed in the theta and alpha frequency bands (Mima and Hallett, 1999). However, the previous MEG works reported the CMC in the beta band at 15–35 Hz and the low-frequency band at 2–10 Hz and its contralateral side-dominance in both sides of the tongue during the 2-min tongue protrusion mainly contracting genioglossus muscle (Maezawa et al., 2014, 2016). The CMC in the low-frequency band was suggested to be oscillatory proprioceptive feedback from the tongue muscles to the primary sensory cortex (Maezawa et al., 2016). Swallow consists of a complex series of the pharyngeal and tongue movements. The CMC during swallow may have been partly produced by tongue motion because the submental group muscles included the suprahyoid muscles attached to the hyoid although the muscles working during the swallow are different from those during the tongue protrusion.

As for the temporal property of the CMC, the CMC in low-frequency band was dominant in the early swallow stage with low activity of the submental group muscles and the CMC in beta band frequency was shown with the high activity of the submental group muscle in the late part of the swallow. Previous works showed that the CMC in the beta band frequency reflected the cortical motor commands during a steady tonic muscle contraction and that it did not appear during the initial parts of the movement before the steady contraction (Kilner et al., 1999; Mima and Hallett, 1999). It suggests that the CMC in the beta band may indicate the neural state during a few

TABLE 1 | The ERD or ERS (mean \pm SD) is calculated by subtracting the logarithm of the power spectral densities during the resting stage from that during the activation stage in all channels in Table A.

| (A) | | | | | |
|-------------|----------------------|----------------------|---------------------|-------------|--------------------|
| EEG channel | ERD/ERS | EEG channel | ERD/ERS | EEG channel | ERD/ERS |
| Fp1 | -0.002 \pm 0.062 | FC6 | -0.008 \pm 0.080 | CP6 | -0.050 \pm 0.077 |
| Fpz | -0.010 \pm 0.067 | M1 | 0.013 \pm 0.061 | P7 | -0.013 \pm 0.061 |
| Fp2 | -0.004 \pm 0.069 | T7 | -0.018 \pm 0.066 | P3 | -0.026 \pm 0.062 |
| F7 | 0.009 \pm 0.071 | C3 | -0.043 \pm 0.069 | Pz | -0.015 \pm 0.056 |
| F3 | -0.013 \pm 0.053 | Cz | -0.026 \pm 0.054 | P4 | -0.038 \pm 0.071 |
| Fz | -0.025 \pm 0.048 | C4 | -0.044 \pm 0.060 | P8 | -0.022 \pm 0.063 |
| F4 | -0.024 \pm 0.064 | T8 | -0.041 \pm 0.072 | POz | 0.003 \pm 0.037 |
| F8 | 0.011 \pm 0.098 | M2 | 0.017 \pm 0.074 | O1 | 0.008 \pm 0.078 |
| FC5 | -0.009 \pm 0.069 | CP5 | -0.039 \pm 0.065 | Oz | 0.009 \pm 0.077 |
| FC1 | -0.025 \pm 0.050 | CP1 | -0.033 \pm 0.045 | | |
| FC2 | -0.030 \pm 0.043 | CP2 | -0.051 \pm 0.049 | | |
| (B) | | | | | |
| EEG channel | Theta frequency band | Alpha frequency band | Beta frequency band | | |
| Fp1 | 0.28 | 0.61 | 0.56 | | |
| Fpz | 0.67 | 0.67 | 0.61 | | |
| Fp2 | 0.39 | 0.72 | 0.72 | | |
| F7 | 0.39 | 0.72 | 0.50 | | |
| F3 | 0.39 | 0.72 | 0.67 | | |
| Fz | 0.39 | 0.50 | 0.72 | | |
| F4 | 0.39 | 0.61 | 0.78 | | |
| F8 | 0.39 | 0.61 | 0.50 | | |
| FC5 | 0.44 | 0.72 | 0.50 | | |
| FC1 | 0.33 | 0.61 | 0.72 | | |
| FC2 | 0.44 | 0.78 | 0.67 | | |
| FC6 | 0.50 | 0.78 | 0.72 | | |
| M1 | 0.44 | 0.61 | 0.78 | | |
| T7 | 0.39 | 0.56 | 0.56 | | |
| C3 | 0.39 | 0.39 | 0.61 | | |
| Cz | 0.33 | 0.61 | 0.78 | | |
| C4 | 0.61 | 0.61 | 0.44 | | |
| T8 | 0.44 | 0.56 | 0.44 | | |
| M2 | 0.56 | 0.72 | 0.61 | | |
| CP5 | 0.33 | 0.50 | 0.39 | | |
| CP1 | 0.39 | 0.67 | 0.89 | | |
| CP2 | 0.44 | 0.39 | 0.50 | | |
| CP6 | 0.50 | 0.61 | 0.44 | | |
| P7 | 0.56 | 0.78 | 0.56 | | |
| P3 | 0.50 | 0.50 | 0.50 | | |
| Pz | 0.50 | 0.72 | 0.83 | | |
| P4 | 0.61 | 0.67 | 0.50 | | |
| P8 | 0.44 | 0.67 | 0.39 | | |
| POz | 0.72 | 0.72 | 0.67 | | |
| O1 | 0.72 | 0.67 | 0.61 | | |
| Oz | 0.44 | 0.50 | 0.39 | | |

n = 18, mean \pm SD.

The ratio of the subjects with a significant coherence in all 18 subjects is presented in Table B. *n* = 18.

hundred milliseconds after the pharyngeal movements reached the maximum, that is, the peak of laryngeal elevation. Moreover, it may reflect sensory afferents to motor related areas (Baker et al., 2006). Therefore, the CMC in the beta band frequency might

reflect both of motor commands and of sensory afferents in the late part of the swallow. The CMC in the low-frequency band was shown in the early part of the swallow. The previous MEG works showed that the CMC in the low-frequency band reflected the sensory feedback to M1 area with a delay of about 80 ms after CMC in the beta frequency band. However, the CMC in the low-frequency band was only shown without the CMC in the beta frequency band in the early part of the swallow. It might suggest that different networks activate in the early part and in the late part of the swallow. Swallow is a complex motion with multiple muscles working at various timings. Therefore, it is difficult to differentiate precisely the timing of cortical commands with that of the muscle contraction unlike previous MEG works. A future work would be necessary to reveal it.

Corticomuscular coherence does not inform us of the directionality of signals between the EEG and the EMG (Liu et al., 2019). Although it is beyond the scope of this EEG descriptive work, the next step would be to investigate the directionality using causality analyses such as Granger causality analysis (Witham et al., 2011).

The relationship between the submental EMG activities and the phases of the swallow movement was reported by using electroglottography (EGG) in the previous work (Nederkoorn et al., 1999; Ding et al., 2002). Although the submental EMG activities indicate the final oral and pharyngeal phases, it is difficult to differentiate the end of the oral phase from the start of the pharyngeal phase only by the EMG activity. In future, the relationship between swallow phases and EEG activity is to be revealed with the concurrent EEG and EGG recordings.

In conclusion, this work reported that EEG recordings with a small number of electrodes can detect ERDs in the bilateral sensorimotor cortices and oscillatory interaction between the cortex and pharyngeal muscles during volitional swallow in humans. The EEG is an easy and economical equipment for the clinical use compared with MEG, which is available in community hospitals. It might be a useful technology for the evaluation of cortical function during swallow in both healthy subjects and patients with dysphagia.

DATA AVAILABILITY STATEMENT

The raw data supporting the conclusions of this article will be made available by the authors, without undue reservation.

ETHICS STATEMENT

The studies involving human participants were reviewed and approved by the Committee of Medical Ethics of Dokkyo Medical University. The participants provided their written informed consent to participate in this study.

AUTHOR CONTRIBUTIONS

SK designed the work, collected and interpreted the data, and wrote the initial draft of the manuscript. TMima contributed to

interpretation of data and assisted in the preparation of the manuscript. All other authors have contributed to data collection and interpretation and critically reviewed the manuscript. All authors approved the final version of the manuscript.

FUNDING

This work was supported by Grant-in-Aid for Exploratory Research (20K21770), and Grants-in-Aid for Scientific Research (B) (21H03308) (SK), Grants-in-Aid for Scientific

Research (A) (19H01091) (TMima), and Grants-in-Aid for Scientific Research (A) (19H01126) and (B) (19H03939) (KK) from the Japan Society for the Promotion of Science.

ACKNOWLEDGMENTS

The authors would like to thank S. Sugawara and M. Hayakawa for the technical assistance with the experiments.

REFERENCES

- Baker, S. N., Chiu, M., and Fetz, E. E. (2006). Afferent encoding of central oscillations in the monkey arm. *J. Neurophysiol.* 95, 3904–3910. doi: 10.1152/jn.01106.2005
- Chen, S., Li, Y., Shu, X., Wang, C., Wang, H., Ding, L., et al. (2020). Electroencephalography mu rhythm changes and decreased spasticity after repetitive peripheral magnetic stimulation in patients following stroke. *Front. Neurol.* 11:546599. doi: 10.3389/fneur.2020.546599
- Cuellar, M., Harkrider, A. W., Jenson, D., Thornton, D., Bowers, A., and Saltuklaroglu, T. (2016). Time–frequency analysis of the eeg mu rhythm as a measure of sensorimotor integration in the later stages of swallowing. *Clin. Neurophysiol.* 127, 2625–2635. doi: 10.1016/j.clinph.2016.04.027
- Delorme, A., and Makeig, S. (2004). EEGLAB: an open source toolbox for analysis of single-trial EEG dynamics including independent component analysis. *J. Neurosci. Methods* 134, 9–21. doi: 10.1016/j.jneumeth.2003.10.009
- Ding, R., Larson, C. R., Logemann, J. A., and Rademaker, A. W. (2002). Surface electromyographic and electroglottographic studies in normal subjects under two swallow conditions: normal and during the Mendelsohn maneuver. *Dysphagia* 17, 1–12. doi: 10.1007/s00455-001-0095-3
- Dziewas, R., Sörös, P., Ishii, R., Chau, W., Henningsen, H., Ringelstein, E. B., et al. (2003). Neuroimaging evidence for cortical involvement in the preparation and in the act of swallowing. *Neuroimage* 20, 135–144. doi: 10.1016/s1053-8119(03)00285-4
- Dziewas, R., Teismann, I. K., Suntrup, S., Schiffbauer, H., Steinstraeter, O., Warnecke, T., et al. (2009). Cortical compensation associated with dysphagia caused by selective degeneration of bulbar motor neurons. *Hum. Brain Mapp.* 30, 1352–1360. doi: 10.1002/hbm.20603
- Elble, R. J., and Randall, J. E. (1976). Motor-unit activity responsible for 8- to 12-Hz component of human physiological finger tremor. *J. Neurophysiol.* 39, 370–383. doi: 10.1152/jn.1976.39.2.370
- Ertekin, C., and Aydogdu, I. (2003). Neurophysiology of swallowing. *Clin. Neurophysiol.* 114, 2226–2244. doi: 10.1016/s1388-2457(03)00237-2
- Halliday, D. M., and Farmer, S. F. (2010). On the need for rectification of surface EMG. *J. Neurophysiol.* 103:3547. doi: 10.1152/jn.00222.2010 author reply 3548–3549
- Hamdy, S., Aziz, Q., Rothwell, J. C., Singh, K. D., Barlow, J., Hughes, D. G., et al. (1996). The cortical topography of human swallowing musculature in health and disease. *Nat. Med.* 2, 1217–1224. doi: 10.1038/nm1196-1217
- Hyvarinen, A., and Oja, E. (2000). Independent component analysis: algorithms and applications. *Neural Netw.* 13, 411–430. doi: 10.1016/s0893-6080(00)00026-5
- Inada, T., Kobayashi, K., Kikuchi, T., Matsuhashi, M., Matsumoto, R., Takahashi, Y., et al. (2021). Effects of a stable concentration of propofol on interictal high-frequency oscillations in drug-resistant epilepsy. *Epileptic Disord.* 23, 299–312. doi: 10.1684/epd.2021.1264
- Jean, A. (2001). Brain stem control of swallowing: neuronal network and cellular mechanisms. *Physiol. Rev.* 81, 929–969. doi: 10.1152/physrev.2001.81.2.929
- Jestrovic, I., Coyle, J. L., Perera, S., and Sejdic, E. (2018). Influence of attention and bolus volume on brain organization during swallowing. *Brain Struct. Funct.* 223, 955–964. doi: 10.1007/s00429-017-1535-7
- Jung, T. P., Makeig, S., Humphries, C., Lee, T. W., Mckeown, M. J., Iragui, V., et al. (2000). Removing electroencephalographic artifacts by blind source separation. *Psychophysiology* 37, 163–178. doi: 10.1111/1469-8986.3720163
- Kern, M. K., Jaradeh, S., Arndorfer, R. C., and Shaker, R. (2001). Cerebral cortical representation of reflexive and volitional swallowing in humans. *Am. J. Physiol. Gastrointest. Liver Physiol.* 280, G354–G360. doi: 10.1152/ajpgi.2001.280.3.G354
- Kilner, J. M., Baker, S. N., Salenius, S., Jousmäki, V., Hari, R., and Lemon, R. N. (1999). Task-dependent modulation of 15–30 Hz coherence between rectified EMGs from human hand and forearm muscles. *J. Physiol.* 516(Pt 2), 559–570. doi: 10.1111/j.1469-7793.1999.0559v.x
- Kobayashi, K., Matsumoto, R., Matsuhashi, M., Usami, K., Shimotake, A., Kunieda, T., et al. (2015). Different mode of afferents determines the frequency range of high frequency activities in the human brain: direct electrocorticographic comparison between peripheral nerve and direct cortical stimulation. *PLoS One* 10:e0130461. doi: 10.1371/journal.pone.0130461
- Kober, S. E., Gressenberger, B., Kurzmann, J., Neuper, C., and Wood, G. (2015). Voluntary modulation of hemodynamic responses in swallowing related motor areas: a near-infrared spectroscopy-based neurofeedback study. *PLoS One* 10:e0143314. doi: 10.1371/journal.pone.0143314
- Kober, S. E., and Wood, G. (2018). Hemodynamic signal changes during saliva and water swallowing: a near-infrared spectroscopy study. *J. Biomed. Opt.* 23, 1–7. doi: 10.1117/1.jbo.23.1.015009
- Li, H., Huang, G., Lin, Q., Zhao, J.-L., Lo, W.-L. A., Mao, Y.-R., et al. (2018). Combining movement-related cortical potentials and event-related desynchronization to study movement preparation and execution. *Front. Neurol.* 9:822. doi: 10.3389/fneur.2018.00822
- Liu, J., Sheng, Y., and Liu, H. (2019). Corticomuscular coherence and its applications: a review. *Front. Hum. Neurosci.* 13:100. doi: 10.3389/fnhum.2019.00100
- Logemann, J. A. (1988). Swallowing physiology and pathophysiology. *Otolaryngol. Clin. North Am.* 21, 613–623. doi: 10.1016/S0030-6665(20)31488-2
- Maezawa, H. (2017). Cortical mechanisms of tongue sensorimotor functions in humans: a review of the magnetoencephalography approach. *Front. Hum. Neurosci.* 11:134. doi: 10.3389/fnhum.2017.00134
- Maezawa, H., Mima, T., Yazawa, S., Matsuhashi, M., Shiraishi, H., and Funahashi, M. (2016). Cortico-muscular synchronization by proprioceptive afferents from the tongue muscles during isometric tongue protrusion. *Neuroimage* 128, 284–292. doi: 10.1016/j.neuroimage.2015.12.058
- Maezawa, H., Mima, T., Yazawa, S., Matsuhashi, M., Shiraishi, H., Hirai, Y., et al. (2014). Contralateral dominance of corticomuscular coherence for both sides of the tongue during human tongue protrusion: an MEG study. *Neuroimage* 101, 245–255. doi: 10.1016/j.neuroimage.2014.07.018
- Martin, R. E., Goodyear, B. G., Gati, J. S., and Menon, R. S. (2001). Cerebral cortical representation of automatic and volitional swallowing in humans. *J. Neurophysiol.* 85, 938–950. doi: 10.1152/jn.2001.85.2.938
- Michou, E., and Hamdy, S. (2009). Cortical input in control of swallowing. *Curr. Opin. Otolaryngol. Head Neck Surg.* 17, 166–171. doi: 10.1097/MOO.0b013e32832b255e
- Michou, E., Mistry, S., Jefferson, S., Tyrrell, P., and Hamdy, S. (2014). Characterizing the mechanisms of central and peripheral forms of neurostimulation in chronic dysphagic stroke patients. *Brain Stimul.* 7, 66–73. doi: 10.1016/j.brs.2013.09.005

- Mima, T., and Hallett, M. (1999). Corticomuscular coherence: a review. *J. Clin. Neurophysiol.* 16, 501–511. doi: 10.1097/00004691-19991000-00002
- Morash, V., Bai, O., Furlani, S., Lin, P., and Hallett, M. (2008). Classifying EEG signals preceding right hand, left hand, tongue, and right foot movements and motor imageries. *Clin. Neurophysiol.* 119, 2570–2578. doi: 10.1016/j.clinph.2008.08.013
- Nederkoorn, C., Smulders, F. T., and Jansen, A. (1999). Recording of swallowing events using electromyography as a non-invasive measurement of salivation. *Appetite* 33, 361–369. doi: 10.1006/appe.1999.0268
- Okitsu, T., Arita, M., Sonoda, S., Ota, T., Hotta, F., Honda, T., et al. (1998). The surface electromyography on suprahyoid muscles during swallowing. *Jpn. J. Rehabil. Med.* 35, 241–244. doi: 10.2490/jjrm1963.35.241
- Oldfield, R. C. (1971). The assessment and analysis of handedness: the Edinburgh inventory. *Neuropsychologia* 9, 97–113. doi: 10.1016/0028-3932(71)90067-4
- Pfurtscheller, G., and Lopes da Silva, F. H. (1999). Event-related EEG/MEG synchronization and desynchronization: basic principles. *Clin. Neurophysiol.* 110, 1842–1857. doi: 10.1016/s1388-2457(99)00141-8
- Sakihara, K., and Inagaki, M. (2015). Mu rhythm desynchronization by tongue thrust observation. *Front. Hum. Neurosci.* 9:501. doi: 10.3389/fnhum.2015.00501
- Samiee, K., Kovács, P., and Gabbouj, M. (2015). Epileptic seizure classification of EEG time-series using rational discrete short-time fourier transform. *IEEE Trans. Biomed.* 62, 541–552. doi: 10.1109/TBME.2014.2360101
- Spadone, S., Croce, P., Zappasodi, F., and Capotosto, P. (2020). Pre-stimulus EEG microstates correlate with anticipatory alpha desynchronization. *Front. Hum. Neurosci.* 14:182. doi: 10.3389/fnhum.2020.00182
- Suntrup, S., Teismann, I., Bejer, J., Suttrup, I., Winkels, M., Mehler, D., et al. (2013). Evidence for adaptive cortical changes in swallowing in Parkinson's disease. *Brain* 136(Pt 3), 726–738. doi: 10.1093/brain/awt004
- Suntrup, S., Teismann, I., Wollbrink, A., Warnecke, T., Winkels, M., Pantev, C., et al. (2014). Altered cortical swallowing processing in patients with functional dysphagia: a preliminary study. *PLoS One* 9:e89665. doi: 10.1371/journal.pone.0089665
- Suntrup, S., Teismann, I., Wollbrink, A., Winkels, M., Warnecke, T., Pantev, C., et al. (2015). Pharyngeal electrical stimulation can modulate swallowing in cortical processing and behavior - magnetoencephalographic evidence. *Neuroimage* 104, 117–124. doi: 10.1016/j.neuroimage.2014.10.016
- Suntrup-Krueger, S., Ringmaier, C., Muhle, P., Wollbrink, A., Kemmling, A., Hanning, U., et al. (2018). Randomized trial of transcranial direct current stimulation for poststroke dysphagia. *Ann. Neurol.* 83, 328–340. doi: 10.1002/ana.25151
- Usami, K., Matsumoto, R., Kobayashi, K., Hitomi, T., Shimotake, A., Kikuchi, T., et al. (2015). Sleep modulates cortical connectivity and excitability in humans: direct evidence from neural activity induced by single-pulse electrical stimulation. *Hum. Brain Mapp.* 36, 4714–4729. doi: 10.1002/hbm.22948
- Vaiman, M. (2007). Standardization of surface electromyography utilized to evaluate patients with dysphagia. *Head Face Med.* 3:26. doi: 10.1186/1746-160X-3-26
- Witham, C. L., Riddle, C. N., Baker, M. R., and Baker, S. N. (2011). Contributions of descending and ascending pathways to corticomuscular coherence in humans. *J. Physiol.* 589(Pt 15), 3789–3800. doi: 10.1113/jphysiol.2011.211045
- Xie, J., Peng, M., Lu, J., Xiao, C., Zong, X., Wang, M., et al. (2021). Enhancement of event-related desynchronization in motor imagery based on transcranial electrical stimulation. *Front. Hum. Neurosci.* 15:635351. doi: 10.3389/fnhum.2021.635351

Conflict of Interest: The authors declare that the research was conducted in the absence of any commercial or financial relationships that could be construed as a potential conflict of interest.

Publisher's Note: All claims expressed in this article are solely those of the authors and do not necessarily represent those of their affiliated organizations, or those of the publisher, the editors and the reviewers. Any product that may be evaluated in this article, or claim that may be made by its manufacturer, is not guaranteed or endorsed by the publisher.

Copyright © 2021 Koganemaru, Mizuno, Takahashi, Takemura, Irisawa, Matsuhashi, Mima, Mizushima and Kansaku. This is an open-access article distributed under the terms of the Creative Commons Attribution License (CC BY). The use, distribution or reproduction in other forums is permitted, provided the original author(s) and the copyright owner(s) are credited and that the original publication in this journal is cited, in accordance with accepted academic practice. No use, distribution or reproduction is permitted which does not comply with these terms.



Effectiveness of Standard Oral Care Plan During Hospital Stay in Individuals With Brain Injury

Simple F. Kothari^{1,2}, Gustavo G. Nascimento³, Mille B. Jakobsen¹, Jørgen F. Nielsen¹ and Mohit Kothari^{1,4*}

¹ Department of Clinical Medicine, Hammel Neurorehabilitation Centre and University Research Clinic, Aarhus University, Hammel, Denmark, ² Section of Orofacial Pain and Jaw Function, Department of Dentistry and Oral Health, Aarhus University, Aarhus, Denmark, ³ Section of Periodontology, Department of Dentistry and Oral Health, Aarhus University, Aarhus, Denmark, ⁴ JSS Dental College and Hospital, JSS Academy of Higher Education and Research, Mysore, India

Objective: To investigate the effectiveness of an existing standard oral care program (SOCP) and factors associated with it during hospitalization in individuals with acquired brain injury (ABI).

Material and Methods: A total of 61 individuals underwent a SOCP for 4 weeks in a longitudinal observational study. Rapidly noticeable changes in oral health were evaluated by performing plaque, calculus, bleeding on probing (BOP) and bedside oral examination (BOE) at weeks 1 and 5. Individuals' brushing habits, eating difficulties, and the onset of pneumonia were retrieved from their medical records. Association between oral-health outcomes to systemic variables were investigated through multilevel regression models.

Results: Dental plaque ($P = 0.01$) and total BOE score ($P < 0.05$) decreased over time but not the proportion of dental calculus ($P = 0.30$), BOP ($P = 0.06$), and tooth brushing frequency ($P = 0.06$). Reduction in plaque and BOE over time were negatively associated with higher periodontitis scores at baseline (coef. -6.8 ; -1.0), respectively, which in turn were associated with an increased proportion of BOP (coef. ≈ 15.0). An increased proportion of calculus was associated with eating difficulties (coef. 2.3) and the onset of pneumonia (coef. 6.2).

Conclusions: Nursing care has been fundamental in improving oral health, especially reducing dental plaque and BOE scores. However, our findings indicate a need for improving the existing SOCP through academic-clinical partnerships.

Clinical Relevance: Early introduction of oral care program to brain-injured individuals is beneficial in reducing plaque accumulation and improving oral health.

Keywords: hospitalization, neurorehabilitation, nursing, oral health, oral hygiene, periodontitis, stroke, traumatic brain injury

INTRODUCTION

Oral care is essential to maintain oral health and prevent complications such as periodontal diseases and tooth loss in patients with acquired brain injury (ABI) (1–5). Poor oral hygiene among dependent hospitalized patients could lead to severe complications such as poor nutritional intake, increased length of hospital stays, and pneumonia (5–7). Concerning oral health, stroke can cause

OPEN ACCESS

Edited by:

Kazutaka Takahashi,
University of Chicago, United States

Reviewed by:

Adriana Sant'Ana,
Universidade de São Paulo,
Bauru, Brazil
Daniel Demetrio Faustino-Silva,
Conceição Hospital Group, Brazil

*Correspondence:

Mohit Kothari
mohkot@rm.dk

Specialty section:

This article was submitted to
Neurorehabilitation,
a section of the journal
Frontiers in Neurology

Received: 24 May 2021

Accepted: 10 November 2021

Published: 15 December 2021

Citation:

Kothari SF, Nascimento GG,
Jakobsen MB, Nielsen JF and
Kothari M (2021) Effectiveness of
Standard Oral Care Plan During
Hospital Stay in Individuals With Brain
Injury. *Front. Neurol.* 12:714167.
doi: 10.3389/fneur.2021.714167

hemiparesis and hemiplegia to the facial muscles and the muscles of the pharynx, tongue, palate, and mastication, resulting in impaired oral clearance (8, 9). Medications prescribed for patients after stroke may further impact oral health resulting in, for example, dry mouth, oral ulcers, and stomatitis (10). Acquired brain injury individuals with swallowing difficulties have compromised oral clearance that may lead to increased bacterial load (5). Swallowing impairment, along with poor oral health has a significant impact on an individual's nutritional intake (11), increasing the risk of aspirational pneumonia (6, 12), which in turn has a negative impact on rehabilitation and other functional outcomes (6, 13).

Evidence suggests that stroke survivors with an increased plaque and bacterial load experience a deterioration of the periodontal conditions (1, 14). Recently, a study showed that 40% of the ABI population had an abundant amount of dental plaque and increased bleeding on probing (BOP), a finding that may indicate an acute hospitalization effect (2). In addition, 74% of the ABI individuals also had severe periodontitis, a condition, supported by their poor sociobehavioral and medical history, representing a chronic stage of an oral health disease (2).

Post ABI, many patients are reliant on nursing staff to assist them with oral hygiene. Despite indications that healthcare staff is interested in improving this aspect of care, a recent survey conducted with >250 health professionals showed that oral care had not been their prime focus due to barriers such as lack of time due to prioritizing other emergency tasks and unfocused oral care policies, and absence of training and evidence-based continuing education (15).

In the light of the current evidence on the importance of oral health among individuals with ABI, oral care management through oral care providers could play an important role in this area (11). It is not clear whether the existing oral care provided by healthcare professionals has any effect on the oral health of hospitalized patients with ABI in a neurorehabilitation setting (2, 15, 16). New knowledge on the topic may provide an overview to promote and manage oral health in these individuals. Accordingly, this study aimed to investigate the effectiveness of the existing oral care program over time (5 weeks) and its associated factors during hospitalization in patients with ABI. We hypothesized that the current standard oral care provision requires further structural improvement and modifications.

METHODS

Participants and Recruitment

All individuals with ABI admitted between February and June 2019 to the Hammel Neurorehabilitation and Research Centre (HNRC), Denmark, were recruited for this longitudinal observational study. Patients admitted reasons other than ABI were excluded, so were pregnant women. As some patients moved in and out from the HNRC due to medical emergencies or the need for other facilities unavailable at the center, they were included in the study if re-admitted within 5 days to the HNRC from their first day of admission. The readmission day was counted as their first day of admission. Individuals with ABI who prevented the examination for reasons such as

fatigue/cognition/ limited mouth opening/stress/infection were rescheduled within 1 week and excluded from the study if it was not possible to re-examine within the week 1 window. In total, 132 individuals with ABI were screened and examined within the first week (baseline) from the admission day and later at week 5, re-examined to assess the acute changes in oral health (**Figure 1**). Out of 132 individuals, 90 were eligible for the week 1 assessment, and 61 individuals were eligible for the week 5 assessment after fulfilling all the above-mentioned eligibility criteria (**Figure 1**). The strengthening the reporting of observational studies in epidemiology guidelines were used to guide the reporting of the study.

Procedures and Measures

Medical Records

Each individual's *main diagnosis, medical history, the onset of brain injury, and length of stay in acute care* were documented at week 1, and *onset of pneumonia during hospitalization, clinically measured body mass index, eating difficulties, dysphagia, and feeding status* were documented at weeks 1 and 5 from the e-journal of the patients (2, 3, 6).

Demographics and Sociobehavioral History

A structured questionnaire was used to elicit general and oral health-related social and behavioral history. The questionnaire elicited information on *age, sex, education level, profession, living status, smoking habits, and brushing and dental appointment frequencies*, which were recorded by a nurse (MBJ) at week 1 and in addition *brushing frequency during hospitalization* was again recorded at week 5 (2, 3, 6).

Motor and Cognitive Deficits Related to Orofacial Function Parameters

Motor and cognitive domains related to orofacial function were collected from the subset of the following brain injury scales at both baseline and at week 5: the early functional ability (EFA) scale (17), the functional independent measure (FIM) (18), the functional oral intake scales (FOIS) (19), and the Rancho Los Amigos scale (RLAS) (20).

Early Functional Ability Scale

The EFA scale (17) evaluates the early functional abilities in terms of basic everyday functions with increasing wakefulness and at the same time yet significant functional motor limitations. The scale comprises of 20 items, which are scored on a five-point Likert scale with 1 = "no function," 2 = "severe disturbance," 3 = "moderate disturbance," 4 = "slight disturbance," and 5 = "normal." In this study, four items from EFA were taken as markers of orofacial dysfunction: (1) orofacial stimulation, (2) swallowing, (3) tongue movements/chewing, and (4) facial expressions/mimic.

Functional Independent Measure

Functional independent measure (18) assess ADL in patients with ABI 24, 25. Functional Independent Measure scale assesses motor and cognitive disability. The scale includes 18 items, of which 13 items are motor domains. Eating motor items were taken as markers of orofacial function whereas all five items of cognition,

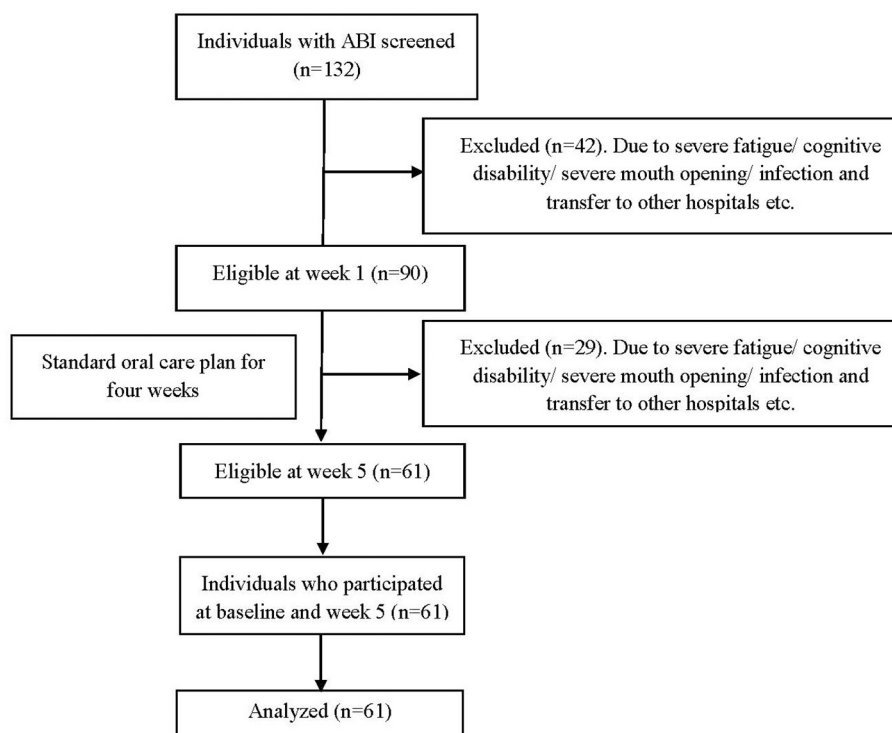


FIGURE 1 | Flow chart.

problem-solving, social interaction, comprehension, expression, and memory were included. Each item is scored from 1 to 7 based on level of independence, where 1 represents total dependence and 7 indicates complete independence.

Functional Oral Intake Scale

Functional Oral Intake scale (19) documents the functional level of oral intake of food and liquid in patients with stroke. This scale consists of seven items: tube dependent (levels 1–3): 1—no oral intake, 2—tube dependent with minimal/inconsistent oral intake, and 3—tube supplements with consistent oral intake 26; total oral intake (levels 4–7): 4—total oral intake of a single consistency, 5—total oral intake of multiple consistencies requiring special preparation, 6—total oral intake with no special preparation, but must avoid specific foods or liquid items, and 7—total oral intake with no restrictions.

Rancho Los Amigos Scale

Rancho Los Amigos scale (20) assesses the cognitive function in patients with post-coma. Patients are scored according to the levels: 1—response, 2—generalized response, 3—localized response, 4—confused, agitated response, 5—confused, inappropriate, non-agitated response, 6—confused, appropriate response, 7—automatic, appropriate response, and 8—purposeful, appropriate response.

In our previous study, by employing a factor analysis approach on the questionnaire data, we were able to identify two different factors, which were later dubbed as the “motor” domain based

on their orofacial health and entire “cognitive” domain (6). Accordingly, a “motor” factor was defined based on the scores of the eating domain of the FIM questionnaire, the total score of the FOIS questionnaire, and the orofacial stimulation, and swallowing domains of the EFA questionnaire. The “cognitive” factor, comprised the total score of cognitive FIM which included, problem-solving, social interaction, comprehension, expression, and memory domain, and the total score of the RLAS questionnaire (6). As the tongue and mimic domains of the EFA questionnaire loaded in both the factors, they were not included in either of the factors (6).

Comprehensive Oral Health Assessment

The clinical oral examination was conducted by a trained dentist (SFK) during week 1 and week 5 of hospitalization. This examination consisted of (1) *BOP examination*: was performed at six sites of each tooth (starting from the distal to the mesial end of each tooth buccally and palatally/lingually, respectively) by tipping a University of North Carolina-15 periodontal probe (PCPUNC15, Hu-Freidy, Chicago, IL, USA) until light resistance offered by the gingival tissues could be perceived (21). Bleeding on probing was recorded as absent or present. (2) *Plaque, and calculus detection*: was performed at six sites of each tooth using the tip of the periodontal probe at the dentogingival junction as recommended by O’Leary et al. (22, 23). Each condition was recorded as a dichotomous variable, based on its presence or absence. (3) *Bedside Oral Examination (BOE)*: After permission from the author, BOE parameters were included (24). It has

TABLE 1 | Standard oral care program at HNRC.

| Individuals at HNRC | Standard oral-care (recommended clinical guidelines) | Supplemental oral-care (case-dependent) |
|--|--|--|
| All ABI individuals (self-oral care) | Instruction to brush twice a day, preferably after each meal. Free to have any toothbrush they bring from home (small head/big head/electric soft bristle toothbrush) with fluoride toothpaste (min. 1,450 ppm). | Chlorhexidine mouth wash (0.12%). Oral mucosal care. Dental floss once a day. Lip moisturizer for dry or cracked lips. |
| ABI individuals with eating or cognitive difficulties (oral care by caregivers) | Orofacial stimulation (face, lip, gum, and tongue) before every meal. Cleaning of mouth for food debris and secretions before and after each intake of food and drinks. Use of small head soft bristle toothbrush and fluoridated non-foaming toothpaste (min. 1,450 ppm). Tooth brushing in circulatory motion starting buccally, palatally, and then to occlusal table twice a day after each meal. | Chlorhexidine mouth wash (0.12%). Oral mucosal care. Lip moisturizer for dry or cracked lips. |
| Tracheotomized ABI individuals (oral care by caregivers) | Oral care in recline or side wise position. Orofacial stimulation (face, lip, gum, and tongue) 2–3 times/day. Cleaning of mouth for food debris and secretions 2–3 times/day. Individual who are unable to spit, the oral cavity is cleaned by mouthwash having amylglucosidase and fluoride (Zendium) with the help of sponge or swabs. | Carbonated water for patients with dry mouth. Mouthwash containing both chlorhexidine (0.05%) and fluoride (0.05%) for bleeding gums. Lip moisturizer for dry or cracked lips. |

eight categories and three numerical and descriptive ratings (1—normal; 2—moderate dysfunction; and 3—severe dysfunction). Total BOE scores ranged from 8 (excellent oral health) to 24 (poor oral health). Bedside oral examination scores ranging from 8 to 10 are considered as indicative of excellent oral health, from 11 to 14 as moderately impaired oral health, and from 15 to 24 as significantly impaired oral health (24).

In addition, at baseline, we also assessed probing depth, gingival margin level, and clinical attachment level (CAL) with the use of the aforementioned probe. The baseline periodontal data was also submitted to factor analysis, which allowed us to identify two periodontal phenotypes, dubbed as “moderate” (number of sites with CAL = 3 or 4 mm, Periodontal Pocket Depth (PPD) = 3 or 4 mm, and the number of sites with BOP) and “severe” (number of sites with CAL \geq 5 mm, the number of sites with PPD \geq 5 mm, and the number of sites with suppuration) periodontitis. Detailed information about the identification of the periodontal phenotypes using the baseline periodontal data can be found elsewhere (2, 4).

Standard Oral Care Program at HNRC

Based on the Danish national clinical guidelines for oral care, the healthcare professionals follow the standard oral care program (SOCP) in all the individuals admitted at HNRC (25). The SOCP was supplemented by additional oral care depending on the individual needs. See **Table 1** for details.

Data Analyses

Data on the proportion of plaque, calculus, BOP, BOE scores, and frequency of tooth brushing were submitted to descriptive analyses. In addition, paired analyses (*t*-test for normally distributed variables and Wilcoxon signed-rand test for non-normally distributed variables) were also conducted. Using multilevel mixed-effects regression models, we were able to investigate the association between changes in oral health outcomes (proportion of plaque, calculus,

BOP, and BOE scores) with both time-varying, collected at both baseline and week 5, and non-varying (elicited at baseline only) variables (sociodemographic and behavioral factors, systemic diseases, and motor and cognitive deficits related to orofacial function parameters). Variable selection was performed using the “backward” stepwise procedure, in which all variables were entered in the model, and then subsequently removed. Only variables with a *P*-value < 0.20 were maintained in the model and those with a *P*-value < 0.05 were considered statistically significant. The data analysis was carried out using the software Stata 14.2 (StataCorp., College Station, TX, USA).

RESULTS

Of the 90 patients included at baseline, 61 provided data for the 5-week follow-up (**Figure 1**). The mean age was 55.1 years (± 14.0), and 64% of patients were male. More information about the sociodemographic data of the participants can be found elsewhere (2). A *post-hoc* sample size power revealed that using the BOP and plaque data at baseline and week 5 and assuming a correlation between the paired estimates of 0.7, our sample reached a power of 81%.

Paired analysis revealed that the proportion of sites with visible dental plaque ($P = 0.01$) significantly decreased over time but BOP ($P = 0.06$), calculus ($P = 0.30$), and the frequency of tooth brushing ($P = 0.06$) did not achieve statistically significant changes after 5 weeks of hospitalization. In addition, the total BOE score ($P < 0.001$) significantly improved over time, and most of the BOE domains like, swallow, saliva, mucosa, teeth, and odor ($P < 0.05$) (**Table 2**).

Mixed-effects regression models indicated that individuals with “moderate” periodontitis at baseline (coef. -6.8) and those hospitalized at the regional ward (coef. -15.6) had decreased proportion of sites with dental plaque. In addition, the number

TABLE 2 | Changes in oral health parameters during hospitalization.

| Items | Baseline (Week 1) | Week 5/Discharge | P-value |
|--|----------------------|------------------|---------|
| 1. % Plaque^b | 50.6 (27.1) | 42.2 (30.4) | 0.01 |
| 2. % BOP^b | 41.9 (42.7) | 30.4 (37.3) | 0.06 |
| 3. % Calculus^b | 5.5 (12.5) | 4.7 (11.9) | 0.29 |
| 4. BOE^a | | | |
| a. Swallow | 1 (1–2) | 1 (1–1) | <0.01 |
| b. Lips | 1 (1–2) | 1 (1–1) | 0.10 |
| c. Tongue | 1 (1–2) | 1 (1–2) | 0.29 |
| d. Saliva | 1 (1–2) | 1 (1–2) | 0.03 |
| e. Mucosa | 1 (1–2) | 1 (1–1) | <0.01 |
| f. Gingiva | 1 (1–2) | 1 (1–1) | 0.07 |
| g. Teeth | 1 (1–2) | 1 (1–1) | <0.01 |
| h. Odor | 1 (1–2) | 1 (1–1) | 0.05 |
| Total | 11 (9–13) | 9 (8–11) | <0.001 |
| 5. Frequency of toothbrushing^a | 1.8 (0.6) | 2.0 (0.5) | 0.06 |

BOE, bedside oral examination; BOP, bleeding on probing.

^aWilcoxon signed ranked test.

^bPaired t-test.

TABLE 3A | Mixed effect regression model comparing plaque and systemic findings.

| Variables | % Plaque | | |
|--|------------------------------|-------------|----------|
| | Coefficient (β) ^a | 95% CI | P-values |
| “Moderate” periodontitis at baseline | −6.8 | −12.1; −1.5 | 0.012 |
| Regional ward (Reference: high-specialized ward) | −15.6 | −27.3; −3.9 | 0.009 |
| # Extracted teeth at baseline | −1.0 | −1.9; −0.1 | 0.05 |
| % Calculus | −0.5 | −0.9; 0.0 | 0.032 |
| Time | −8.8 | −15.4; −2.2 | 0.009 |

a: Adjusted for age, BMI, and ‘severe’ periodontitis at baseline and variables in the model.

of extracted teeth (coef. −1.0), the proportion of calculus (coef. −0.5), and the time (coef. −8.8) were also associated with a reduction in the proportion of plaque (**Table 3A**).

Patients with higher scores of both “moderate” (coef. 14.3) and “severe” (coef. 15.6) periodontitis at baseline had an increase in the proportion of sites with BOP over the study period (**Table 3B**), whereas those who improved their “cognitive” domain (coef. −6.6) had a decrease in the proportion of BOP. The number of extracted teeth at baseline (coef. 0.5) and increased proportion of plaque over the study period (coef. 0.4) were also associated with an increased proportion of BOP after the 5-week follow-up. As displayed in **Table 3C**, those who developed pneumonia during hospitalization (coef. 6.2) and those with eating difficulties over the study period (coef. 2.3) had an increase in the proportion of sites with dental calculus.

Finally, mixed-effects regression models indicated that the individuals with higher scores of “moderate” periodontitis at

TABLE 3B | Mixed effect regression model comparing BOP with systemic findings.

| Variables | % BOP | | |
|--|------------------------------|-------------|----------|
| | Coefficient (β) ^a | 95% CI | P-values |
| “Moderate” periodontitis at baseline | 14.3 | 9.6; 19.0 | <0.001 |
| “Severe” periodontitis at baseline | 15.6 | 11.6; 19.5 | <0.001 |
| # Extracted teeth at baseline | 0.5 | 0.1; 1.1 | 0.045 |
| “Cognitive” domain over the study period | −6.6 | −11.6; −1.6 | 0.010 |
| % Plaque | 0.4 | 0.2; 0.7 | 0.001 |

^aAdjusted for #Decayed teeth, FIM scores and variables in the model.

TABLE 3C | Mixed effect regression model comparing calculus with systemic findings.

| Variables | % Calculus | | |
|---|------------------------------|----------|---------|
| | Coefficient (β) ^a | 95% CI | P-value |
| Onset of pneumonia during hospitalization | 6.2 | 1.4; 9.9 | 0.009 |
| Eating difficulty | 2.3 | 0.6; 4.0 | 0.007 |

^aAdjusted for ward, age, ‘Cognitive’ domain over the study period and variables in the model.

TABLE 3D | Mixed effect regression model comparing BOE data with systemic findings.

| Variables | BOE—total score | | |
|--|------------------------------|------------|---------|
| | Coefficient (β) ^a | 95% CI | P-value |
| “Moderate” periodontitis at baseline | −1.0 | −1.3; −0.5 | <0.001 |
| Regional ward (Reference: high-specialized ward) | −1.7 | −2.8; −0.5 | 0.006 |
| “Motor” domain over the study period | −0.6 | −1.0; −0.1 | 0.010 |
| Dysphagia at baseline | 0.5 | 0.1; 1.1 | 0.043 |
| Age | 0.04 | 0.0; 0.1 | 0.016 |

^aAdjusted for variables in the model.

baseline (coef. −1.0), those hospitalized at the regional ward (coef. −1.7), and those who improved their “motor” skills during the study period (coef. −0.6) had a reduction in their total BOE score, whereas those with dysphagia at baseline (coef. 0.5) and the old individuals (coef. 0.04) had an increased total BOE score after 5 weeks (**Table 3D**).

DISCUSSION

The main finding of the study was that the oral health parameters such as visible plaque and BOE scores significantly improved during a 5-week stay at neurorehabilitation setting following the current SOCP. Although a reduction in the proportion of sites with BOP and frequency of tooth brushing over time (5-week stay) was observed, it did not reach statistical significance. These findings demonstrate that although there was an improvement in the oral health status in hospitalized individuals, it was not

substantiated, indicating a need for further development in the oral care program.

A significant reduction in the amount of dental plaque was observed over time. Dental plaque is a biofilm that comprises a diverse community of microorganisms formed regularly on the tooth surface and can be disrupted with proper toothbrushing and interdental cleaning (5, 26, 27). Individuals with less severe ABI are usually admitted to the regional ward at HNRC instead of the highly-specialized ward due to their better motor and cognitive functions, which makes them more co-operative than severely affected individuals with ABI (28). It was also evident from the mixed regression analysis that individuals admitted to the “regional ward” showed a strong association in reducing plaque compared to individuals from the highly specialized ward (25). This finding indicates that the poorest oral health conditions and the least oral health improvements occurred in moderate and severe ABI cases, i.e., those requiring most caregivers’ attention. Hence, it is of utmost importance to properly train these professionals to improve oral health and, consequently, the quality of life of individuals with ABI. Interestingly, the proportion of plaque was also reduced in individuals with “moderate” periodontitis and with an increased proportion of calculus and BOP, indicating that there are also other factors such as the host immune response (6), which were not taken into account in this study, that might have influenced BOP.

Bleeding on probing is a sign of inflammation that occurs as a response to plaque accumulation on the periodontal tissues (29). In general, good oral hygiene practices are sufficient to control and reduce gingival bleeding (24, 27), which was also shown in the current study with a strong association between plaque and BOP (Table 3C). However, despite the significant plaque reduction, the proportion of sites with BOP did not reduce in the same individuals over the study period, as it probably originated from deep pocket rather than from the gingival tissues. It is also important to discuss that the SD values of BOP were probably quite high as few individuals had a very low BOP, while some (especially those with periodontitis) accumulated most of the BOP burden. Such a finding suggests that factors other than plaque might play a role in the onset and progression of gingival inflammation. It has been shown that a more exacerbated and rapid immune response, acute hospitalization, and cognitive and systematic complications are linked to a higher neutrophilic activity, which mounts an immediate gingival inflammatory response when exposed to plaque (30–32). Interestingly, our findings demonstrated that BOP decreased over time in individuals who showed an improvement in their “cognitive” function, indicating a reduction in confusion and agitation leading to increased cooperation with oral care, which very well-correlates with previous research (6). It has been shown that BOP is closely associated with “severe” periodontitis, which in addition to an already existing cognitive impairment, may contribute to other chronic conditions that share a common biological background to ABI (6, 33). Assuming that such an exacerbated immune response is not restricted to the oral cavity, this may interfere with other inflammatory processes, especially in a hospital setting and in the presence

of other comorbidities, explaining partially our findings (6). On the other hand, the proportion of sites with BOP increased over time among patients with both “moderate” and “severe” periodontitis, despite the increase in toothbrushing frequency over the same period. This finding indicates that the oral health status in these patients was poor and tooth brushing alone may not be enough to tackle periodontitis, which can only be treated using scaling and root planning performed by dental professionals. In addition, toothbrushing is unable to remove calculus, a factor that contributes to further plaque accumulation, inflammation of gingival tissues, and progression of periodontitis. Furthermore, brushing is also thought to be more optimal for cleaning facial surfaces of teeth compared to interproximal/interdental surfaces that present a higher risk of plaque accumulation and developing periodontal lesions (34). Thus, interdental cleaning aids such as dental floss, and interdental brushes may prove to help decrease BOP as interdental cleaning has shown to be associated with less plaque, calculus, and gingivitis (35). Nevertheless, despite the efforts made by nurses to maintain oral hygiene, there was still deterioration of the inflammatory periodontal condition (5). This suggests a need for the involvement of dental personnel in hospitals for providing adequate oral care to patients with ABI (2).

Calculus, defined as hard deposit around the gingiva as a result of long-term plaque accumulation, showed no significant improvement over time, indicating that the amount of calculus identified was already present when the individuals were hospitalized. It is important to highlight that calculus does not indicate disease, but it makes oral hygiene more difficult to maintain and works as a plaque-retaining factor (36). It is known that periodontal pockets can be the focus of infection and calculus removal can improve the clinical condition of patients and reduce the length of hospital stay (37). Even though the removal of calculus is not possible without professional dental assistance, it is possible to maintain proper oral hygiene by preventing calculus formation. Such a finding supports the idea that chronic oral changes require professional help from dental personnel and changes in sociobehavioral factors for the improvement of oral health (29).

Our findings also revealed that individuals with eating difficulty and those who developed pneumonia during hospitalization had an increase in the proportion of sites with dental calculus. One may speculate whether the combination of dental calculus and eating difficulties may influence the onset of pneumonia. A recent study on patients with ABI has shown a robust association between periodontitis and debilitating conditions like dysphagia, dependency on a feeding tube, which is a major concern, as they lead to pneumonia (6). Although our study does not allow us to disentangle the causal relationship between these conditions, our overall findings suggest the need for increased focus on oral care especially for ABI individuals with conditions like eating difficulties and severe cognitive disturbances.

Interestingly, BOE scores decreased in individuals with higher scores of “moderate” periodontitis. As discussed, “moderate” periodontitis originates essentially from neglected oral hygiene,

so do most of the BOE domains (2, 6, 24, 38). Thus, the combined effect of plaque reduction and increased frequency of oral hygiene can explain this association. It should be noted that, although BOE is a simple and easy-to-use tool in hospital settings, especially in intensive care units, its usefulness is questioned in patients with ABI, and therefore, the BOE results may be carefully interpreted (2, 4). This is because the instrument seems not to reflect the real clinical conditions of patients with ABI, thus, affecting the treatment plan. Furthermore, it has been shown that “aging” patients have more compromised function than young individuals, making them more vulnerable to dysphagia and unable to perform and maintain good oral hygiene procedures (2, 6).

A recent survey conducted among 157 oral caregivers at HNRC showed that the majority of oral caregivers were aware of the existing “Danish National Clinical Guidelines for Oral Care” (25). However, a significant number of oral care providers did not follow the guidelines systematically, expressing it as ineffective, time-consuming, and difficult to follow (15). Professionals were aware that patients with eating difficulties have challenges and different requirements (15) and on top, cognitive, and motor deficits add an extra challenge to oral hygiene maintenance (6). In addition, there is always a professional dilemma to maintain oral hygiene standards whilst respecting the autonomy of patients once they refuse oral hygiene care, even if it is required. Therefore, all these factors should be considered while formulating and designing oral care training and guidelines to improve oral care in a neurorehabilitation setting.

Methodological Considerations

The current study sample originates from a single hospital setting, and therefore, our findings may have limited external validity. However, it is worth mentioning that this hospital is a reference center for the treatment of patients with ABI and receives patients from most regions of Denmark. In addition, a limited sample size and 30% lost to follow-up might have reduced the analytical power, as can be noted by borderline *P*-values. However, as aforementioned, our sample reached a power of 80%, which can be considered an acceptable value for this study. Future studies with large samples originating from several centers are needed. Another limitation of the study was the short follow-up time, given the chronicity of the most common oral diseases, i.e., dental caries and periodontitis. However, treatment of these conditions demands the involvement of dental personnel with appropriate armamentarium, which was not within the scope of the study. As our purpose was to observe the effect of an existing oral care program during hospitalization on oral health, we decided to evaluate conditions such as the proportion of dental plaque and BOP, as those parameters can rapidly change. We also need to be aware that few patients were excluded due to extreme fatigue, agitation, motor-cognitive deficits, leaving us with no opportunity for clinical examination, which might be a bias in representing the entire oral health status. Finally, since different oral care measures were implemented depending on the patients’ condition, the distinct levels of care might have impacted our

results. However, our main goal was to evaluate whether the standard oral care plan delivered during hospitalization was effective to improve oral health rather than to evaluate the most effective plan. Hence, further studies are needed to elucidate this aspect.

CONCLUSIONS

A significant reduction in dental plaque and total BOE score was observed over time. However, non-significant improvements in gingivitis, the proportion of calculus, and brushing frequency indicate the need to further develop oral care programs for individuals with ABI keeping motor-cognitive deficits and eating difficulties in consideration. This study also enforces the need for the involvement of dentists in educating and supervising non-dental professionals at an early stage to provide a better and integrated oral care program for ABI individuals in hospital settings.

DATA AVAILABILITY STATEMENT

The raw data supporting the conclusions of this article will be made available by the authors, without undue reservation.

AUTHOR CONTRIBUTIONS

JFN and MK: conceptualization and methodology. SFK, GGN, and MK: validation and writing—original draft preparation. GGN: formal analysis. MJB and SFK: investigation and data curation. SFK, GGN, JFN, and MK: writing—review and editing. MK: resources, visualization, supervision, project administration, and funding acquisition. All authors have read and agreed to the published version of the manuscript.

FUNDING

MK received grant from Health Research Fund of Central Denmark Region for the current study with grant number A1407. The authors’ salary was supported by their respective institution.

ACKNOWLEDGMENTS

The authors would like to thank Lena Aadal, Associate Professor in Nursing, Hanne Møller Nielsen, neurorehabilitation specialized nurse, Katje Bjerrum, neurorehabilitation specialized occupational therapist, and the entire nursing staff at HNRC, who were integral in potential participant identification, clinical, and scientific critical discussions. A special thanks to Helle Leegård, Head Nurse and Ole Hovgaard, Clinical Head, Department of Dentistry and Oral Health, AU for providing dental instruments for the study. The author would also like to express his gratitude to Mr. Olaf Westening, country manager of Hu-Freidy (www.hu-friedy.eu) for donating 14 UNC-15 periodontal probes to perform the periodontal clinical examination and without saying to all the participants who gave their time generously.

REFERENCES

- Pillai RS, Iyer K, Spin-Neto R, Kothari SF, Nielsen JF, Kothari M. Oral health and brain injury: causal or casual relation? *Cerebrovasc Dis Extra*. (2018) 8:1–15. doi: 10.1159/000484989
- Kothari SF, Nascimento GG, Jakobsen MB, Nielsen JF, Kothari M. Oral health: something to worry about in individuals with acquired brain injury? *Brain Inj*. (2020) 34:1264–9. doi: 10.1080/02699052.2020.1795720
- Kothari SF, Nascimento GG, De Caxias FP, Jakobsen MB, Nielsen JF, Kothari M. Changes in oral health related quality of life and its associated factors in individuals with brain injury. *Brain Inj*. (2021) 35:718–24. doi: 10.1080/02699052.2021.1891289
- Kothari M, Spin-Neto R, Nielsen JF. Comprehensive oral-health assessment of individuals with acquired brain-injury in neuro-rehabilitation setting. *Brain Inj*. (2016) 30:1103–8. doi: 10.3109/02699052.2016.1167244
- Kothari M, Pillai RS, Kothari SF, Spin-Neto R, Kumar A, Nielsen JF. Oral health status in patients with acquired brain injury: a systematic review. *Oral Surg Oral Med Oral Pathol Oral Radiol*. (2017). 123:205.e7–19.e7. doi: 10.1016/j.oooo.2016.10.024
- Kothari SF, Nascimento GG, Jakobsen MB, Nielsen JF, Kothari M. Periodontitis and orofacial health-related systemic impairment in patients with brain injury: a factor analysis approach. *Brain Inj*. (2020) 35:96–102. doi: 10.1080/02699052.2020.1858497
- Brady M, Furlanetto D, Hunter RV, Lewis S, Milne V. Staff-led interventions for improving oral hygiene in patients following stroke. *Cochrane Database Syst Rev*. (2006) 4:CD003864. doi: 10.1002/14651858.CD003864.pub2
- Ajwani S, Jayanti S, Burkolder N, Anderson C, Bhole S, Itaoui R, et al. Integrated oral health care for stroke patients - a scoping review. *J Clin Nurs*. (2017) 26:891–901. doi: 10.1111/jocn.13520
- Mortensen J, Pedersen AR, Nielsen JF, Kothari M. Construct and content validity of the Functional Oral Intake Scale; analyses from a cohort of patients with acquired brain injury. *Brain Inj*. (2020) 34:1257–63. doi: 10.1080/02699052.2020.1800094
- Janket SJ, Jones JA, Rich S, Meurman J, Garcia R, Miller D. Xerostomic medications and oral health: the Veterans Dental Study (Part I). *Gerodontology*. (2003) 20:41–9. doi: 10.1111/j.1741-2358.2003.0041.x
- Bailey RL, Ledikwe JH, Smiciklas-Wright H, Mitchell DC, Jensen GL. Persistent oral health problems associated with comorbidity and impaired diet quality in older adults. *J Am Diet Assoc*. (2004) 104:1273–6. doi: 10.1016/j.jada.2004.05.210
- Dickinson H. Maintaining oral health after stroke. *Nurs Stand*. (2012) 26:35–39. doi: 10.7748/ns2012.08.26.49.35.c9233
- Adams HP Jr, del Zoppo G, Alberts MJ, Bhatt DL, Brass L, Furlan A, et al. Guidelines for the early management of adults with ischemic stroke: a guideline from the American Heart Association/American Stroke Association Stroke Council, Clinical Cardiology Council, Cardiovascular Radiology and Intervention Council, and the Atherosclerotic Peripheral Vascular Disease and Quality of Care Outcomes in Research Interdisciplinary Working Groups: the American Academy of Neurology affirms the value of this guideline as an educational tool for neurologists. *Stroke*. (2012) 38:1655–711. doi: 10.1161/STROKEAHA.107.181486
- Pow EH, Leung KC, Wong MC, Li LS, McMillan AS. A longitudinal study of the oral health condition of elderly stroke survivors on hospital discharge into the community. *Int Dent J*. (2005) 55:319–24. doi: 10.1111/j.1875-595X.2005.tb00330.x
- Odgaard L, Kothari M. Survey of oral nursing care attitudes, knowledge and practices in a neurorehabilitation setting. *J Oral Rehabil*. (2019) 46:730–7. doi: 10.1111/joor.12799
- Kwok C, McIntyre A, Janzen S, Mays R, Teasell R. Oral care post stroke: a scoping review. *J Oral Rehabil*. (2015) 42:65–74. doi: 10.1111/joor.12229
- Hankemeier A, Rollnik JD. The Early Functional Abilities (EFA) scale to assess neurological and neurosurgical early rehabilitation patients. *BMC Neurol*. (2015) 15:207. doi: 10.1186/s12883-015-0469-z
- Nichol AD, Higgins AM, Gabbe BJ, Murray LJ, Cooper DJ, Cameron PA. Measuring functional and quality of life outcomes following major head injury: common scales and checklists. *Injury*. (2011) 42:281–7. doi: 10.1016/j.injury.2010.11.047
- Crary MA, Mann GD, Groher ME. Initial psychometric assessment of a functional oral intake scale for dysphagia in stroke patients. *Arch Phys Med Rehabil*. (2005) 86:1516–20. doi: 10.1016/j.apmr.2004.11.049
- Lin K, Wroten M. *Ranchos Los Amigos*. In: StatPearls. Treasure Island, FL: StatPearls Publishing LLC (2020).
- Trombelli L, Farina R, Silva CO, Tatakis DN. Plaque-induced gingivitis: case definition and diagnostic considerations. *J Periodontol*. (2018) 89(Suppl 1):S46–73. doi: 10.1002/JPER.17-0576
- O'Leary TJ, Drake RB, Naylor JE. The plaque control record. *J Periodontol*. (1972) 43:38. doi: 10.1902/jop.1972.43.1.38
- Ainamo J, Bay I. Problems and proposals for recording gingivitis and plaque. *Int Dent J*. (1975) 25:229–35.
- Prendergast V, Kleiman C, King M. The bedside oral exam and the barrow oral care protocol: translating evidence-based oral care into practice. *Intensive Crit Care Nurs*. (2013) 29:282–90. doi: 10.1016/j.iccn.2013.04.001
- Trosborg I, Christensen L, Konradsen H. *Klinisk Retningslinje til Identifikation af Behov for Mundpleje og Udførelse af Tandbørstning hos Voksne Hospitalsindlagte Patienter. [Clinical Guideline for Identification of Oral Care Needs and Tooth-Brushing in Adult Hospitalized Patients]*. Aarhus: Center for Kliniske Retningslinjer. Afdeling for Sygeplejevidenskab (2010).
- Cabre M, Serra-Prat M, Palomera E, Almirall J, Pallares R, Clave P. Prevalence and prognostic implications of dysphagia in elderly patients with pneumonia. *Age Ageing*. (2010) 39:39–45. doi: 10.1093/ageing/afp100
- Ortega O, Parra C, Zarcero S, Nart J, Sakwinska O, Clave P. Oral health in older patients with oropharyngeal dysphagia. *Age Ageing*. (2014) 43:132–7. doi: 10.1093/ageing/aft164
- Sundhedsstyrelsen S, editor. *Hjerneskaderehabilitering: En Medicinsk Teknologivurdering (Brain Injury Rehabilitation: A Medical Technology Assessment)*. Copenhagen: DACEHTA (2011).
- Dai R, Lam OL, Lo EC, Li LS, Wen Y, McGrath C. A systematic review and meta-analysis of clinical, microbiological, and behavioural aspects of oral health among patients with stroke. *J Dent*. (2015) 43:171–80. doi: 10.1016/j.jdent.2014.06.005
- Nascimento GG, Leite FRM, Vestergaard P, Scheutz F, Lopez R. Does diabetes increase the risk of periodontitis? A systematic review and meta-regression analysis of longitudinal prospective studies. *Acta Diabetol*. (2018) 55:653–67. doi: 10.1007/s00592-018-1120-4
- Nascimento GG, Peres MA, Mittinty MN, Peres KG, Do LG, Horta BL, et al. Diet-induced overweight and obesity and periodontitis risk: an application of the parametric G-formula in the 1982 pelotas birth cohort. *Am J Epidemiol*. (2017) 185:442–51. doi: 10.1093/aje/kww187
- Nascimento GG, Danielsen B, Baelum V, Lopez R. Identification of inflammatory response patterns in experimental gingivitis studies. *Eur J Oral Sci*. (2019) 127:33–9. doi: 10.1111/eos.12588
- Nascimento PC, Castro MML, Magno MB, Almeida AN, Fagundes CF, et al. Association between periodontitis and cognitive impairment in adults: a systematic review. *Front Neurol*. (2019) 10:323. doi: 10.3389/fneur.2019.00323
- Christou V, Timmerman ME, Van der Velden U, Van der Weijden FA. Comparison of different approaches of interdental oral hygiene: interdental brushes versus dental floss. *J Periodontol*. (1998) 69:759–64. doi: 10.1902/jop.1998.69.7.759
- Crocombe LA, Brennan DS, Slade GD, Loc DO. Is self interdental cleaning associated with dental plaque levels, dental calculus, gingivitis and periodontal disease? *J Periodontol Res*. (2012) 47:188–97. doi: 10.1111/j.1600-0765.2011.01420.x
- Jepsen S, Deschner J, Braun A, Schwarz F, Eberhard J. Calculus removal and the prevention of its formation. *Periodontol 2000*. (2011) 55:167–88. doi: 10.1111/j.1600-0757.2010.00382.x
- Manresa C, Sanz-Miralles EC, Twigg J, Bravo M. Supportive periodontal therapy (SPT) for maintaining the dentition in adults treated for periodontitis. *Cochrane Database Syst Rev*. (2018) 1:CD009376. doi: 10.1002/14651858.CD009376.pub2
- Nascimento GG, Baelum V, Dahlen G, Lopez R. Methodological issues in assessing the association between periodontitis and caries among adolescents.

Community Dent Oral Epidemiol. (2018) 46:303–9. doi: 10.1111/cdoe.12367

Conflict of Interest: The authors declare that the research was conducted in the absence of any commercial or financial relationships that could be construed as a potential conflict of interest.

Publisher's Note: All claims expressed in this article are solely those of the authors and do not necessarily represent those of their affiliated organizations, or those of the publisher, the editors and the reviewers. Any product that may be evaluated in

this article, or claim that may be made by its manufacturer, is not guaranteed or endorsed by the publisher.

Copyright © 2021 Kothari, Nascimento, Jakobsen, Nielsen and Kothari. This is an open-access article distributed under the terms of the Creative Commons Attribution License (CC BY). The use, distribution or reproduction in other forums is permitted, provided the original author(s) and the copyright owner(s) are credited and that the original publication in this journal is cited, in accordance with accepted academic practice. No use, distribution or reproduction is permitted which does not comply with these terms.



Functional Role of Suprahyoid Muscles in Bolus Formation During Mastication

Anna Sasa¹, Sirima Kulvanich^{1,2}, Naohito Hao¹, Reiko Ita¹, Masahiro Watanabe³, Taku Suzuki¹, Jin Magara¹, Takanori Tsujimura¹ and Makoto Inoue^{1*}

¹Division of Dysphagia Rehabilitation, Niigata University Graduate School of Medical and Dental Sciences, Niigata, Japan,

²Department of Community Dentistry and Gerodontology, Faculty of Dentistry, Thammasat University, Klongluang, Thailand,

³Department of Special Needs Dentistry, Division of Hygiene and Oral Health, Showa University School of Dentistry, Tokyo, Japan

OPEN ACCESS

Edited by:

Limor Avivi-Arber,
University of Toronto, Canada

Reviewed by:

Teresa Pitts,
University of Louisville, United States
Satoshi Iwase,
Aichi Medical University, Japan

*Correspondence:

Makoto Inoue
inoue@dent.niigata-u.ac.jp

Specialty section:

This article was submitted to
Craniofacial Biology and Dental
Research,
a section of the journal
Frontiers in Physiology

Received: 23 February 2022

Accepted: 16 May 2022

Published: 08 June 2022

Citation:

Sasa A, Kulvanich S, Hao N, Ita R,
Watanabe M, Suzuki T, Magara J,
Tsujimura T and Inoue M (2022)
Functional Role of Suprahyoid Muscles
in Bolus Formation During Mastication.
Front. Physiol. 13:881891.
doi: 10.3389/fphys.2022.881891

It still remains unclear how the suprahyoid muscles function in bolus formation during mastication. This study aimed to investigate the contributory role of the suprahyoid muscles during mastication. A total of 20 healthy young volunteers were asked to perform tongue pressure generation tasks and unilateral mastication tasks using peanuts and two different types of rice crackers. Surface electromyographic (EMG) activity of the masseter and suprahyoid muscles and mandibular kinematics were recorded. Suprahyoid activity increased with increasing tongue pressure. Masticatory duration until the first deglutition differed significantly among the different foods; the harder the food, the longer the duration. This was also the case in masseter activity per masticatory cycle. Masticatory rate and suprahyoid activity per masticatory cycle were significantly higher during soft rice cracker mastication. Masseter activity was higher on the masticatory side than on the non-masticatory side, however, there was no difference in suprahyoid activity between the sides. Suprahyoid activity and jaw gape showed significant positive correlation in the early stage on both the masticatory and non-masticatory sides. The suprahyoid muscles functioned dominantly for jaw-opening during peanut mastication, and for bolus formation, especially in the late stage during soft rice cracker mastication. Bolus formation was performed dominantly on the masticatory side during rice cracker mastication. These findings clearly demonstrate a functional role of the suprahyoid muscles during mastication of solid foods from assessments using both EMG activity and mandibular kinematic recordings.

Keywords: bolus formation, electromyography, suprahyoid muscles, mastication, mandibular kinematics

1 INTRODUCTION

Mastication is essential for the adequate intake of solid foods in most mammals (Hiemae et al., 1996). During mastication, food is crushed and mixed with saliva by the actions of the teeth and masticatory muscles while the tongue, palate, and cheeks contribute to forming a food bolus. Although underlying digestive motor actions such as mastication and deglutition are triggered and controlled by a central pattern generator in the brainstem (Jean, 2001; Lund and Kolta, 2006), sensory information from the bolus in terms of its size, temperature, texture, or moisture, changes from moment to moment, and motor patterns can adapt to these changing characteristics. Previous studies demonstrated a relationship between masticatory muscle activity and the mechanical

properties of food during mastication; masticatory movements are affected by bolus property, primarily the hardness of the food and bolus hardness changed masticatory force, mandibular movement and masticatory cycles, and masticatory cycle times (Horio and Kawamura, 1989; Bishop et al., 1990; Hiimeae et al., 1996; Lassauzay et al., 2000; Peyron et al., 2002; Grigoriadis et al., 2014; Takei et al., 2020).

Once the food is broken down by the masticatory muscles, the differences in these properties decrease, and the changes in food consistency affect the movements required to make the bolus suitable for deglutition. In this regard, some properties of the bolus other than hardness should also be considered. In a previous study, we compared masticatory behaviors between different rice products using steamed rice and rice cake (Iguchi et al., 2015). We found that masseter and suprahyoid electromyographic (EMG) activity per masticatory cycle was higher for rice cake than for steamed rice although the hardness of the boluses was similar throughout the masticatory process. Because cohesiveness and adhesiveness were significantly higher for the latter than the former, we suggested that a difference in cohesiveness also has a critical effect on masticatory performance as previously reported (Kohyama et al., 2005). In addition, we evaluated masticatory activity using rice crackers with different physical properties (Takei et al., 2020). As expected, the harder/larger the rice cracker, the longer the masticatory duration and the higher the number of masticatory cycles. Conversely, the suprahyoid EMG activity was much higher for the soft rice cracker than for the others. We also found that the water absorption rate of the bolus was significantly higher for the rice cracker with the lowest hardness and density compared with other rice crackers. It would likely have been more difficult to transport the bolus that had high water absorption compared with others in the late stage of the masticatory cycle. In those studies, however, only the average suprahyoid muscle activity was compared among the foods, thus, it remains unclear how the bolus properties affected masticatory behaviors.

As with recordings of EMG activity, numerous studies have assessed the functional contribution of intraoral structures such as the tongue to bolus formation and transport during mastication using videofluorography (Palmer et al., 1992; Palmer et al., 1997). This is because movements of the bolus and intraoral structures cannot be directly visualized. Palmer et al. (1992) reported on bolus propulsion during mastication where the bolus was moved toward the pharynx during the late stage of mastication, that is, stage II transport. The authors also demonstrated that the patterns of mandibular and tongue movements during stage II transport were characterized by exaggerated upward movements of the tongue that compress food against the palate during the jaw-closing phase. The tongue is attached to the hyoid bone and several mastication-related muscles are attached to the hyoid itself including the suprahyoid muscles, which keep the tongue in place. The suprahyoid muscles are also known to be jaw-opening muscles. Therefore, it is plausible that changes in tongue muscle activity may be accompanied by changes in suprahyoid muscle activity, and hence mandibular movements can also change depending on

the masticatory stage. Nonetheless, our knowledge of the functional contribution of the suprahyoid muscles to bolus formation and the differences in these activities and mandibular kinematics among foods is rather limited.

This study was designed: 1) to investigate the contribution of the suprahyoid muscles to bolus formation during mastication; 2) to clarify how suprahyoid muscle activity for bolus formation differs among foods; and 3) to elucidate the difference in suprahyoid muscle activity between the masticatory and non-masticatory sides. We hypothesized that the ratio of suprahyoid muscle activity to vertical distance of jaw opening represents the functional role of these muscles in bolus formation, and thus differs depending on bolus properties and masticatory stage.

2 MATERIALS AND METHODS

2.1 Participants

This study involved 20 healthy volunteers (12 men, eight women), ranging from 23 to 44 years (average age \pm standard deviation [SD], 31.0 ± 6.1 years). Prior to obtaining recordings, an attending dentist confirmed that all participants had no missing teeth except the third molar teeth, no temporomandibular disorder and no masticatory or deglutition problems at meal. Written informed consent was obtained from all participants, and the study was approved by the Ethics Committee of Niigata University (approval no. 2020-0039). All experiments were performed in accordance with the Declaration of Helsinki guidelines for studies involving human participants (2008).

2.2 Test Foods

In this study, we used two commercially available rice cracker products and peanuts (Nuts) as test foods (**Figure 1**). The rice crackers were Happy-Turn (Happy) and Haihain (Kameda Seika Co. Ltd., Niigata, Japan). Peanuts are one of the most common solid foods used in dental research to evaluate masticatory function (Gonçalves et al., 2014; Goto et al., 2015; Yamasaki et al., 2016; Oki et al., 2021). We believe that rice crackers are also a suitable sample food to evaluate masticatory function because they are typically hard and brittle. Eating rice crackers requires many steps of the process in the oral cavity, including function not only of the masticatory muscles but also the tongue and cheek muscles to crush and mix the bolus with saliva. As previously described, the thickness of one piece of Happy and Haihain was 8.9 ± 0.2 mm and 6.4 ± 0.2 mm, and the density was 0.397 ± 0.021 g/ml and 0.115 ± 0.002 g/ml, respectively (Takei et al., 2020). Both properties were significantly higher for Happy than Haihain. The hardness of the food was measured using a creep meter (RE2-33005S, YAMADEN CO., LTD., Tokyo, Japan). The maximum load was 39.9 ± 13.0 N for Nuts, 26.5 ± 10.5 N for Happy, and 8.7 ± 2.6 N for Haihain. Happy characteristically had a higher fat content (28.9%) than Haihain (1.2%). Mouthful volume for each trial was determined as 3 g except for Haihain, which was 0.85 g. Haihain had a very low density, and so the volume was adjusted to the same volume as that of Happy.

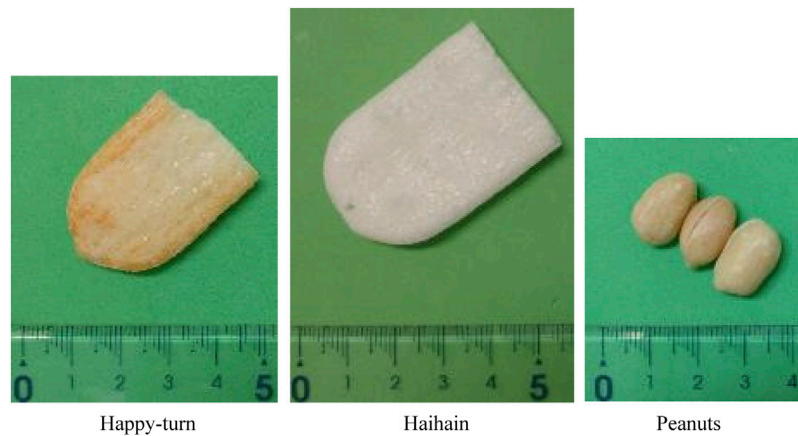


FIGURE 1 | Photograph showing the food samples, Happy-turn (Happy), Haihain, and peanuts (Nuts).

2.3 EMG Activity and Videoendoscopic Recordings

The methodology was precisely as described in our previous study (Takei et al., 2020). Briefly, surface EMG activities were recorded from the masseter and suprahyoid muscles on both the left and right sides. Electrodes (NT-611T; Nihon Kohden, Tokyo, Japan) were attached to the skin over the masseter muscle and the anterior belly of the digastric muscle for the suprahyoid muscles. The suprahyoid musculature comprises the geniohyoid, mylohyoid, and the anterior belly of the digastric muscle. Using surface electrode, EMG activities of all these muscles were recorded (Palmer et al., 1999). Signals were filtered and amplified to remove movement-related artifacts (low-pass and high-pass cut-off frequency, 30 Hz and 2 kHz, respectively) (AB-611J; Nihon Kohden).

VE images were recorded to identify deglutition. A fibre-optic endoscope (FNL-10RP3; Pentax, Tokyo, Japan) was inserted through the nasal passage and into the midpharynx. All signals, including EMG and VE data, were stored through an interface board (PowerLab; ADInstruments, Colorado Springs, CO) on a personal computer (2 kHz for EMG and 33 Hz for VE images). Data analysis was performed using the PowerLab software package (LabChart 8; ADInstruments).

2.4 Mandibular Kinematics

Mandibular kinematics were recorded using a 10-camera Vicon motion capture system (Vicon Motion Systems, Oxford, United Kingdom), which documented three-dimensional coordinates of reflective markers on the skin covering maxillary and mandibular bones. First, laboratory-fabricated adhesive frame housing markers were placed on the scalp. Next, three reflective markers were placed at specific cephalometric landmarks, namely the nasion and the left and right gonions, in a plane parallel to the Frankfort horizontal plane. Another marker was placed on the pogonion. These signals were stored on a personal computer at 100 Hz and were extracted in csv format using a software program (MATLAB, R2021a;

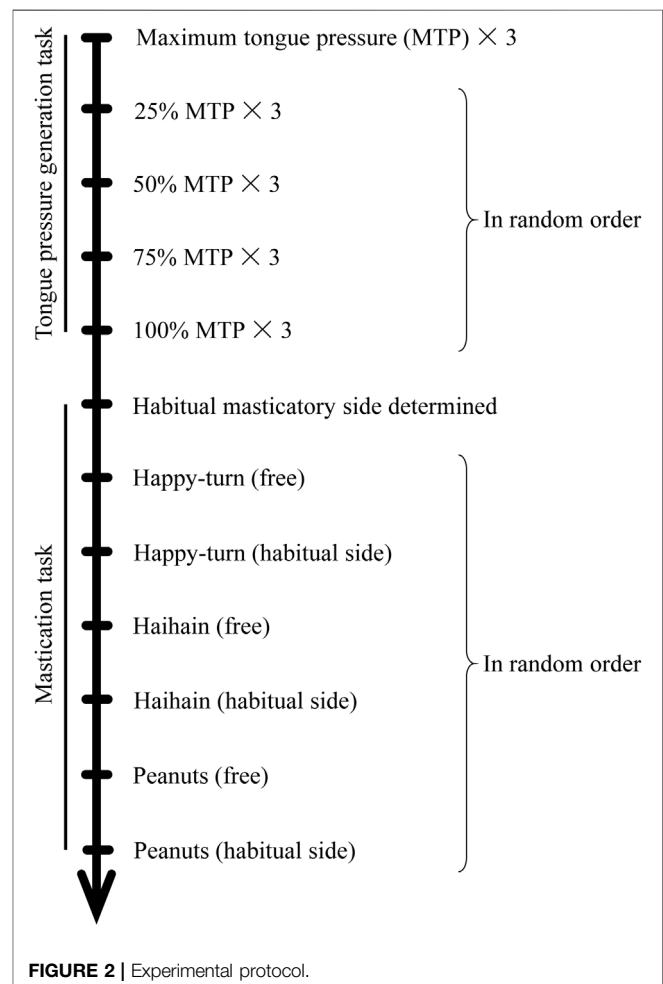


FIGURE 2 | Experimental protocol.

Mathworks, Natick, MA). Finally, mandibular kinematics data was synchronized off-line with EMG activities and VE images using LabChart 8 (ADInstruments).

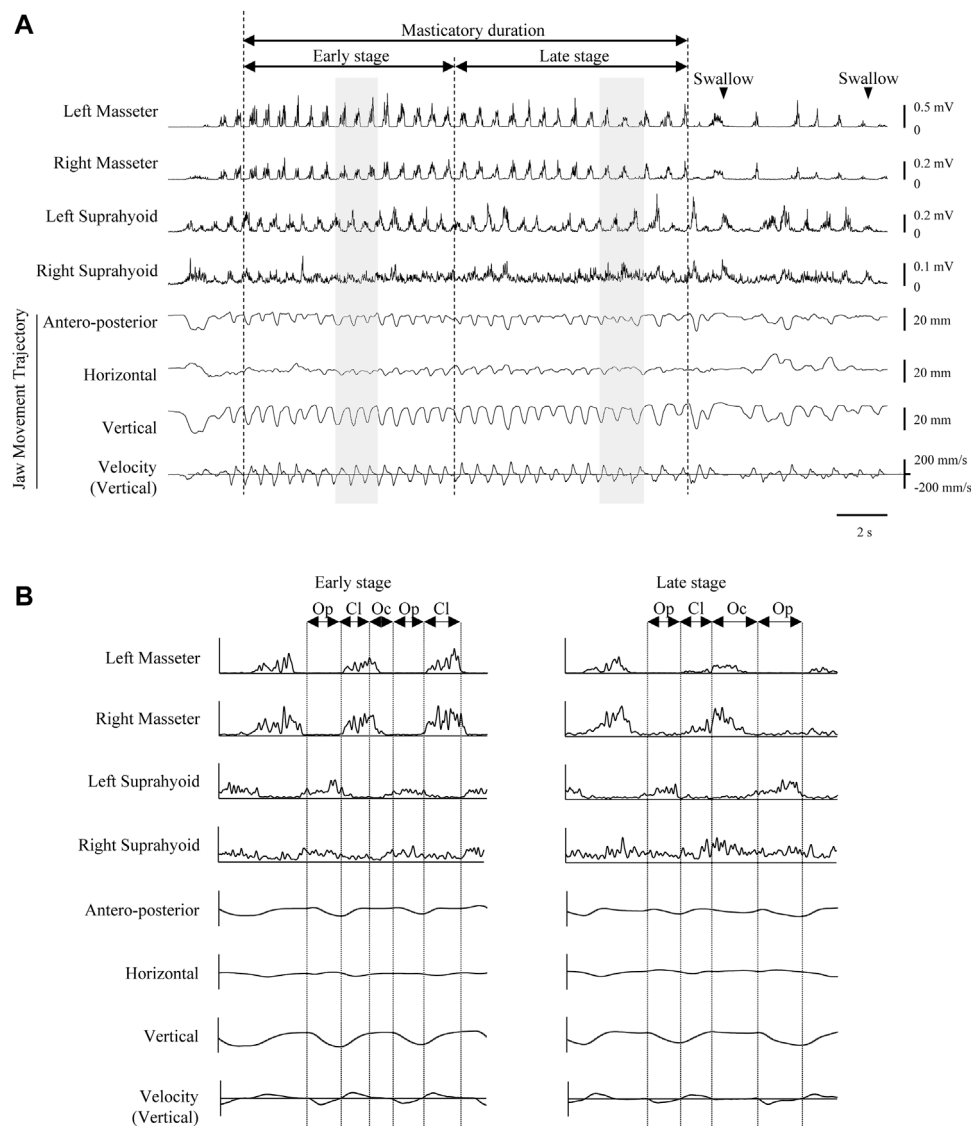


FIGURE 3 | Representative electromyographic (EMG) activity recording and mandibular movement trajectories during Happy mastication on the habitual (right) side. Rectified and smoothed EMG waveforms are shown. **(A)** Vertical dotted lines indicate masticatory onset, border between early and late stages, and offset of masticatory duration. **(B)** Expanded view of shaded areas in recordings A. Reciprocal EMG bursts commonly observed in masseter and suprahyoid muscles on both sides in the early stage. Vertical dotted lines indicate the border between phases. Cl, jaw-closing phase; Oc, occlusal phase; Op, jaw-opening phase.

2.5 Data Processing

Participants were instructed not to eat or drink for at least 1 h prior to the experiment to avoid the situation in that the participants eat any foods immediately before the experiment and are on a full stomach. They were seated in an upright sitting position without headrests throughout the duration of the experiment. In this study, we conducted two tests involving specific tasks: tongue pressure generation followed by food mastication tasks (Figure 2).

In the tongue pressure generation task, each participant was first asked to maximally open the jaw three times for 5 s each to normalize the suprahyoid EMG activity. They were then asked to

press the tongue as hard as possible against the anterior aspect of the hard palate for 7 s each three times; this maximum tongue pressure (100%) was measured by using a balloon-type tongue pressure instrument (JM-TPM02, JMS Co., Japan). To obtain the stable EMG burst in one trial, it took several seconds so that we determined 5-s jaw opening task and 7-s tongue pressure generation. Further, from the three data, we confirmed the EMG activity was reproducible (data not shown).

In the procedure, they lightly held the probe in 4-mm diameter. We confirmed that no apparent EMG activity was observed during only holding the probe. The average of 100% tongue pressure was calculated and then participants were asked

to repeat the task at 25, 50, 75, and 100% pressure for 7 s in random order. Visual feedback was provided during recordings and suprahyoid EMG activities on the left and right sides were recorded. An interval of at least 1 min was allowed between trials.

In the masticatory task, participants were asked to unilaterally masticate and then ingest three different types of test foods (Happy, Haihain, and Nuts) in a random order. Subjects were asked to masticate on their preferred/habitual masticatory side that was determined in a previous study (Sano and Shiga, 2021; Shiga et al., 2021), where subjects were asked to masticate on a gummy jelly test food and report the side on which mastication appeared to be easier.

During these tasks, masseter and suprahyoid EMG activities, VE images, and mandibular kinematics were recorded simultaneously (Figure 3A). Each trial ended with a right hand raise when the participant had finished eating. The interval between trials was set to at least 1 min, and participants could rinse their mouths with water whenever they wished between the trials.

2.6 Data Analysis

To determine the threshold of EMG activity, all EMG waveforms were first full-wave rectified and smoothed (time constant 20 ms).

2.6.1 Tongue Pressure Generation Task

Using the data recorded during both maximum jaw-opening and tongue pressure generation, the mean amplitude of the area under the curve of the rectified suprahyoid EMG activities for 1 s, which was obtained by averaging the left and right EMG data, was calculated for each task (25, 50, 75, and 100%). Regarding the relationship between the maximal mouth opening and the position of the mandibular condyle, when the maximal mouth opening is wide, the mandibular head shifts towards the anterior, and next the condyle is located anterior to the articular tubercle. This suggests that not only on the jaw distance but also the size of the mandibula affects the mandibular head/condyle movement and suprahyoid EMG activity. Because mouth-opening capacity was different among the participants, we decided to use the EMG values normalized to those recorded maximum jaw-opening. Normalized mean activity of suprahyoid EMG burst was compared using one-way repeated measures ANOVA followed by Tukey's honestly significant difference (HSD) test for further analysis.

2.6.2 Mastication Task

During mastication, each masticatory cycle had three components, namely the jaw-opening, jaw-closing, and occlusal phases, which were determined based on the speed and direction of the vertical and horizontal jaw movements, respectively (Figure 3B). The jaw-opening phase began at the uppermost mandibular position and ended at the point of maximum opening. At the onset of the jaw-opening phase, the speed of jaw-opening in the vertical direction was 0. The jaw-closing phase was followed by the occlusal phase. The latter phases were demarcated from the jaw-closing phase by the most lateral position of the jaw-closing path.

We previously reported that a mouthful of solid food is swallowed during the first deglutition during mastication, and that any residual food becomes aggregated by the intra-oral structures into a bolus before being swallowed in the last deglutition (Maeda et al., 2020; Kochi et al., 2021). This suggests that the process of bolus formation before the first deglutition occurs is critical. We first measured the masticatory duration between the onset of the first masticatory cycle and the offset of the masticatory cycle immediately before the first deglutition. Deglutition was identified as an advancing whitish appearance on VE images.

For analysis, masticatory duration, number of masticatory cycles, and masticatory rate in this period were compared among the foods using one-way repeated measures ANOVA followed by Tukey's HSD test for further analysis. Further, masseter and suprahyoid EMG activities per masticatory cycle was also compared using two-way repeated measures ANOVA (masticatory side vs. non-masticatory side, foods) followed by Tukey's HSD test for further analysis.

The relationship between suprahyoid EMG activity and the vertical distance of the mouth (jaw gape) per masticatory cycle was examined using data obtained during mastication before the first deglutition. Because the suprahyoid muscles are known to contribute to jaw-opening during rhythmic mandibular movements, the correlation coefficient (CC) between them in masticatory duration was first calculated in each task for each participant. Unexpectedly, in some participants there was no statistically significant positive correlation in some tasks, which suggested that the suprahyoid muscles did not mainly function for jaw-opening. Subsequently, we divided the masticatory period until the first deglutition into two stages, namely early and late stages depending on the number of masticatory cycles. After collating all the data, including Happy, Haihain, and Nuts mastication in each participant, the CC in the early stage was also calculated for each participant. Because significantly high positive correlation was noted in the early stage in all cases, the regression line and 95% confidence intervals were obtained (Supplementary Table S1, Figure 4). Figure 4 shows the plotted data for one representative participant. Although the plotted data were few during Haihain mastication, there was a clear significant positive correlation among them in the early stage for all test foods; this was also the case for all participants (data not shown). If the plotted data was located between the intervals, we determined that the suprahyoid muscles were activated mainly for jaw-opening. In contrast, if the data was plotted right to the intervals, we determined that the suprahyoid muscles were activated mainly for bolus formation. The former cycle was designated the jaw-opening dominant cycle and the latter the deviation-dominant cycle. The number of these cycles was compared using two-way repeated measures ANOVA on ranks (masticatory side vs. non-masticatory side, among foods) followed by Tukey's HSD test for further analysis. In addition, the rate of occurrence of these cycles in the masticatory duration was compared in the same manner.

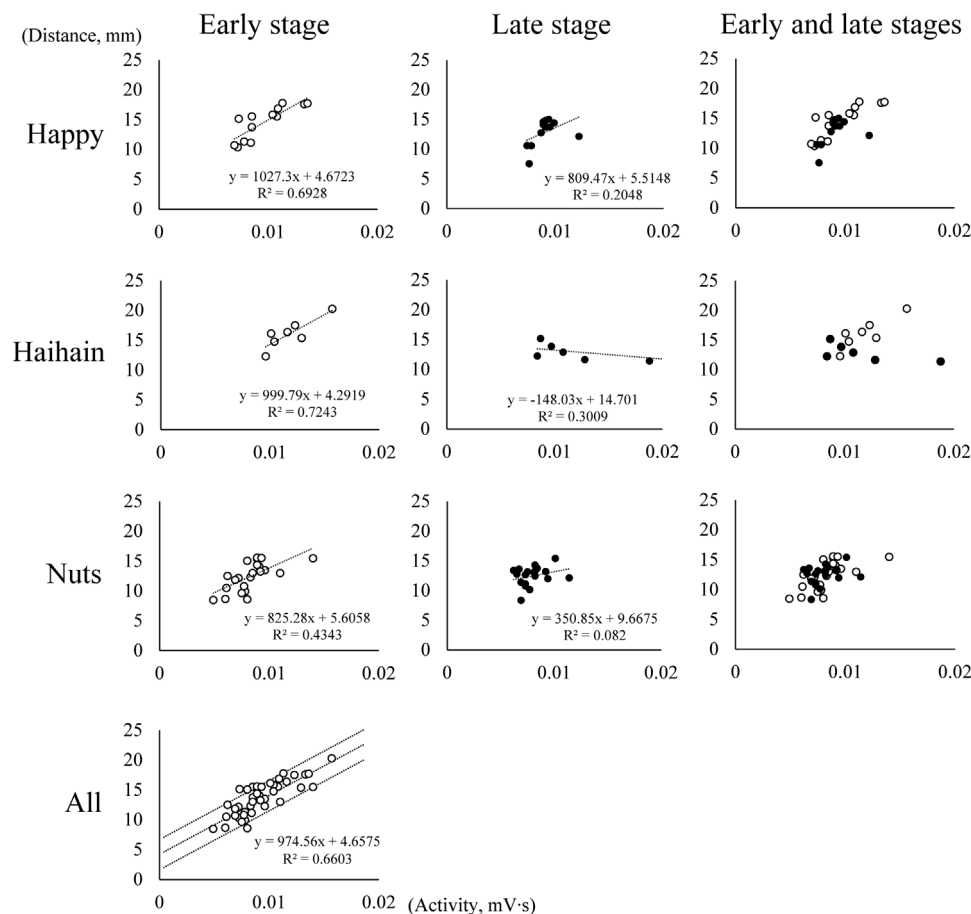


FIGURE 4 | Relationship between suprahyoid electromyographic activity and maximum vertical jaw distance (jaw gape) in one participant. Each graph shows the relationship between suprahyoid activity and jaw gape in one masticatory cycle. The number of masticatory cycles in the masticatory duration was 26 during Happy mastication, 14 during Haihain mastication, and 41 during Nuts mastication with significant positive correlation among them in all test foods in the early stage. Dotted lines indicate the regression line and 95% confidence intervals obtained (All).

Finally, the magnitude of suprahyoid EMG activity was examined. In each task, suprahyoid EMG activity was divided by jaw gape in each masticatory cycle, and was designated modified suprahyoid activity. For each food, the mean modified suprahyoid activity was compared using two-way repeated measures ANOVA (early vs. late, masticatory vs. non-masticatory side) followed by Tukey's HSD test for further analysis.

2.6.3 Statistical Analysis

The sample size was calculated using G*Power 3.1 30, indicating that at least 18 healthy participants with complete data sets would be needed to achieve a statistical power of 95% and a p -value of <0.05 , assuming an effect size of 40%. Statistical analysis was performed using SigmaPlot software (SigmaPlot 13.0, Systat Software Inc., San Jose, CA) and BellCurve for Excel (Social Survey Research Information Co., Ltd., Tokyo, Japan). p values <0.05 were considered significant. All values are expressed as mean \pm SD except those for modified suprahyoid activity (mean \pm SEM).

3 RESULTS

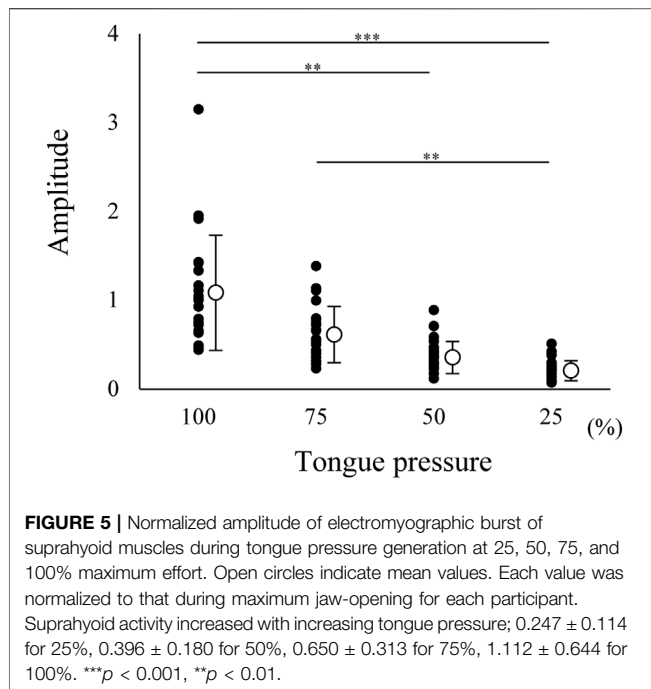
All participants performed the masticatory task and did not report any discomfort.

3.1 Suprahyoid EMG Activity During Tongue Pressure Generation

Suprahyoid EMG activity was measured during tongue pressure generation at several force levels, ranging from 25 to 100%. Suprahyoid EMG activity increased with increasing tongue pressure (Figure 5). This indicated that the suprahyoid muscles contribute to elevating the tongue body and/or generating tongue pressure against the hard palate.

3.2 General Feature of EMG Activity During Mastication

Representative data of EMGs during unilateral Happy mastication on the habitual side are shown in Figure 3. After



mastication started, masticatory rate gradually decreased in the late stage towards the first deglutition. It was apparent that the rhythmic pattern of masseter and suprahyoid EMG burst in the early stage was stable on both sides, and reciprocal masseter and suprahyoid EMG bursts were observed. In the late stage, however, reciprocal patterns were sometimes collapsed such that considerable activity was observed in the suprahyoid EMG activity during the jaw-closing phase (**Figure 3B**).

For the masticatory duration, number of masticatory cycles, and masticatory rate, one-way repeated measures ANOVA revealed significant difference between Happy and Haihain ($p < 0.001$ for masticatory duration, $p < 0.001$ for number of masticatory cycles, $p = 0.003$ for masticatory rate) and between Haihain and Nuts ($p < 0.001$) (**Figures 6A–C**).

We also compared the masseter and suprahyoid EMG activity per masticatory cycle among the conditions. For masseter EMG activity, two-way repeated measures ANOVA with Masticatory side \times Food revealed a significant main effect of Side ($F(1, 19) = 25.738$, $p < 0.001$) with significant interaction ($F(2, 38) = 8.362$, $p < 0.001$) (**Figure 6D**). On further post-hoc testing, masseter EMG activity was significantly higher on the masticatory side than that on the non-masticatory side ($p < 0.001$). In addition, masseter EMG activity on the masticatory side was significantly lower during Hahain mastication than Happy and Nuts mastication ($p = 0.013$ for Happy, $p = 0.014$ for Nuts). Regarding suprahyoid EMG activity, a significant main effect was noted only in Food ($F(2, 38) = 29.575$, $p < 0.001$) without significant interaction ($F(2, 38) = 2.484$, $p = 0.097$) (**Figure 6E**). On post-hoc testing, suprahyoid EMG activity during Nuts mastication was significantly lower than that during Happy and Haihain mastication ($p < 0.001$).

Suprahyoid activity during Happy mastication was also significantly lower than that during Haihain mastication ($p = 0.005$).

Taken together, these results indicate that the harder the food, the longer the masticatory duration. The change in duration was generally dependent on changes in the number of masticatory cycles but not on the masticatory rate; the masticatory rate during Haihain mastication was significantly higher than Happy and Nuts mastication. It can also be presumed that the difference in masseter EMG activity was affected by the initial hardness of food or by masticatory behaviors in that the harder the food the higher the masseter EMG activity; this was apparent on the masticatory side. Conversely, suprahyoid EMG activity was significantly higher during Haihain mastication than Happy and Nuts mastication. Contrary to masseter EMG activity, no difference in suprahyoid EMG activity was observed between the sides. These results suggest that suprahyoid EMG activity was neither dependent on the initial hardness of the food nor on mastication side.

3.3 Correlation Between Suprahyoid EMG Activity and Jaw Gape

The CC between suprahyoid EMG activity and jaw gape per masticatory cycle was obtained for each food. As mentioned above, in some participants there was no significant correlation between these parameters on both the masticatory and non-masticatory sides, however, a strongly significant positive correlation was noted in the early stage on both sides. Further, a significant correlation of CC was also observed between the masticatory and non-masticatory sides (**Figure 7**). These results suggest that the suprahyoid muscles contribute not only to jaw-opening but also to other functions such as bolus formation, and at least in the early stage, these muscles mainly function for jaw-opening on both sides.

To clarify the function of suprahyoid EMG activity pattern during mastication, we plotted suprahyoid EMG activity and maximum jaw-opening distance (maximum jaw gape) per masticatory cycle. We counted the number of jaw-opening dominant cycles, the data plotted between the intervals, and that of deviation-dominant cycles, the data plotted right to the intervals, in the masticatory duration for each food. For the number of jaw-opening dominant cycles, two-way repeated measures ANOVA with Food \times Side (masticatory side vs. non-masticatory side) revealed a significant main effect of Food ($F(2, 38) = 38.745$, $p < 0.001$) but not Side ($F(1, 19) = 1.307$, $p = 0.267$) with significant interaction ($F(2, 38) = 7.704$, $p = 0.002$) (**Figure 8A**). On post-hoc testing, the effect of Food was apparent on both the masticatory and non-masticatory sides ($p < 0.001$ for all but $p = 0.004$ for Happy vs. Haihain with the non-masticatory side). The difference between the sides was observed only during Nuts mastication ($p = 0.025$). The results were as expected because the order of masticatory duration and number of masticatory cycles was Nuts $>$ Happy $>$ Haihain. Regarding the occurrence rate of jaw-opening dominant cycles, two-way repeated measures ANOVA with Food \times Side revealed a significant main effect of Food ($F(2, 38) = 13.441$, $p < 0.001$) but not

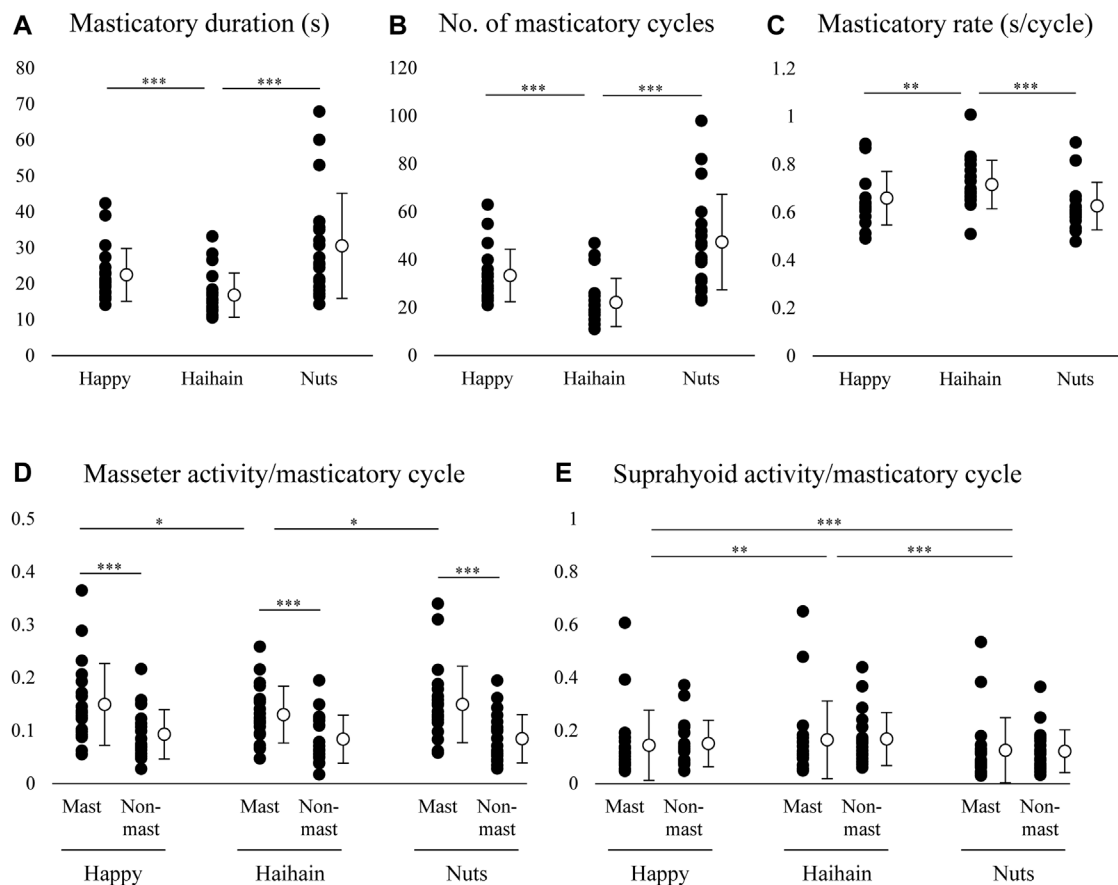


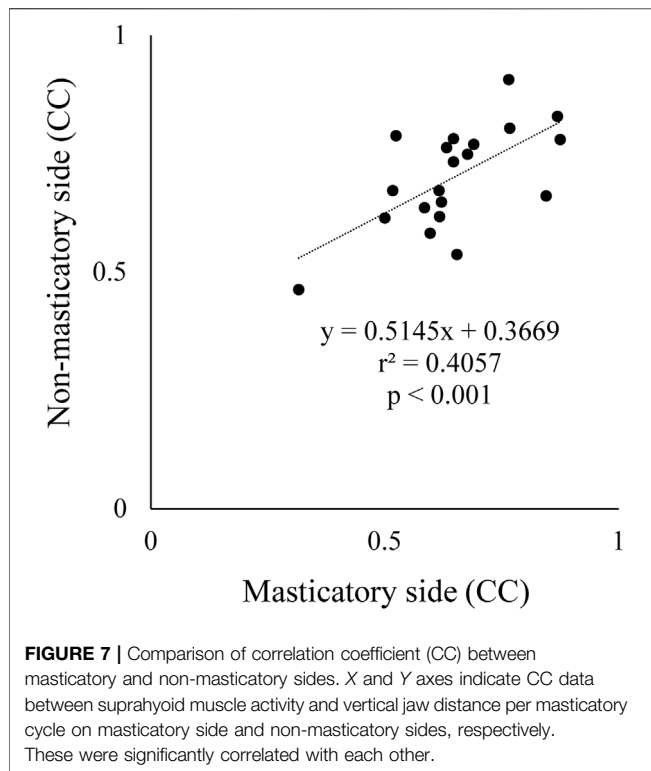
FIGURE 6 | Masticatory duration, number of masticatory cycles, masticatory rate, masseter and suprahyoid electromyographic activity per masticatory cycle. Open circles indicate mean values. **(A)** Masticatory duration was significantly different between Happy and Haihain mastication and between Haihain and Nuts mastication. **(B)** Significant difference in the number of masticatory cycles between Happy and Haihain mastication and between Haihain and Nuts mastication. **(C)** Significant difference in the masticatory rate between Happy and Haihain mastication and between Haihain and Nuts mastication. **(D)** Significantly higher masseter activity on the masticatory side (Mast) than that on the non-masticatory side (Non-mast). There was also a significant difference on the masticatory side between Happy and Haihain and between Haihain and Nuts. **(E)** Difference in suprahyoid activity noted between Happy and Haihain, between Happy and Nuts, and between Haihain and Nuts. There was no difference between the sides. *** $p < 0.001$, ** $p < 0.01$, * $p < 0.05$.

Side ($F_{1, 19} = 0.704$, $p = 0.412$) with significant interaction ($F_{2, 38} = 4.931$, $p = 0.012$) (**Figure 8B**). Post-hoc testing revealed a significantly lower occurrence rate of jaw-opening dominant cycle on the masticatory side in Haihain than Happy ($p < 0.001$) and Nuts ($p < 0.001$). In addition, that on the non-masticatory side was also significantly lower in Haihain than in Nuts ($p < 0.001$).

For the number of deviation-dominant cycles, two-way repeated measures ANOVA with Food \times Side revealed a significant main effect of Food ($F_{2, 38} = 7.800$, $p < 0.001$) but not Side ($F_{1, 19} = 0.034$, $p = 0.856$) with significant interaction ($F_{2, 38} = 4.299$, $p = 0.021$) (**Figure 8C**). On post-hoc testing, a significantly higher number of deviation-dominant cycles was noted both on the masticatory and non-masticatory sides in Nuts than Happy ($p = 0.002$ for both). In addition, that during Nuts mastication was also significantly higher on the non-masticatory side than that on the masticatory side ($p = 0.008$). Regarding the occurrence rate

of deviation-dominant cycles, two-way repeated measures ANOVA with Food \times Side revealed a significant main effect of Food ($F_{2, 38} = 18.661$, $p < 0.001$) but not Side ($F_{1, 19} = 0.044$, $p = 0.836$) with significant interaction ($F_{2, 38} = 6.074$, $p = 0.005$) (**Figure 8D**). Post-hoc testing revealed significantly higher occurrence rate of deviation-dominant cycles on both the masticatory and non-masticatory sides in Haihain than in Happy ($p < 0.001$ on the masticatory side, $p = 0.002$ non-masticatory sides) and Nuts ($p < 0.001$ on the masticatory side, $p = 0.016$ non-masticatory sides). In addition, that during Haihain mastication was also significantly higher on the masticatory side than that on the non-masticatory side ($p = 0.021$).

We further compared the modified suprahyoid EMG activity between the sides and between the early and late stages in each food. For Happy, two-way repeated measures ANOVA with Side \times Stage (early vs. late) revealed a significant main effect of Side ($F_{1, 19} = 6.808$, $p = 0.017$) but not Stage ($F_{1, 19} = 0.816$, $p = 0.378$)



with significant interaction ($F_{1, 19} = 6.544$, $p = 0.019$) (**Figure 9A**). Post-hoc testing revealed significantly higher suprahyoid EMG activity at the early stage during Happy mastication on the non-masticatory side than on the masticatory side ($p = 0.005$). For Haihain, two-way repeated measures ANOVA revealed a significant main effect of Stage ($F_{1, 19} = 28.267$, $p < 0.001$) but not Side ($F_{1, 19} = 3.461$, $p = 0.078$) without significant interaction ($F_{1, 19} = 2.835$, $p = 0.109$) (**Figure 9B**). On further post-hoc testing suprahyoid EMG activity at the early stage was significantly lower than that at the late stage on both sides ($p < 0.001$). For Nuts, two-way repeated measures ANOVA revealed a significant main effect of Side ($F_{1, 19} = 5.237$, $p = 0.034$) but not Stage ($F_{1, 19} = 0.033$, $p = 0.858$) without significant interaction ($F_{1, 19} = 1.495$, $p = 0.236$) (**Figure 9C**). On post-hoc testing, suprahyoid EMG activity on the masticatory side was significantly higher than that on the non-masticatory side ($p = 0.034$).

Finally, changes in modified suprahyoid EMG activity were compared among the foods and between the masticatory and non-masticatory sides. Two-way repeated measures ANOVA with Food \times Side revealed a significant main effect of Food ($F_{2, 38} = 22.814$, $p < 0.001$) and Side ($F_{1, 19} = 19.303$, $p < 0.001$) with significant interaction ($F_{2, 38} = 4.698$, $p = 0.015$) (**Figure 9D**). On post-hoc testing, the increasing rate of suprahyoid EMG activity on both the masticatory and non-masticatory side was significantly higher in Haihain than Happy ($p < 0.001$ both on the masticatory and non-masticatory sides) and Nuts ($p < 0.001$ both on the masticatory and non-masticatory sides). In addition, that on the masticatory side was also significantly higher in Happy and Haihain than that on the non-masticatory side ($p < 0.001$ for both).

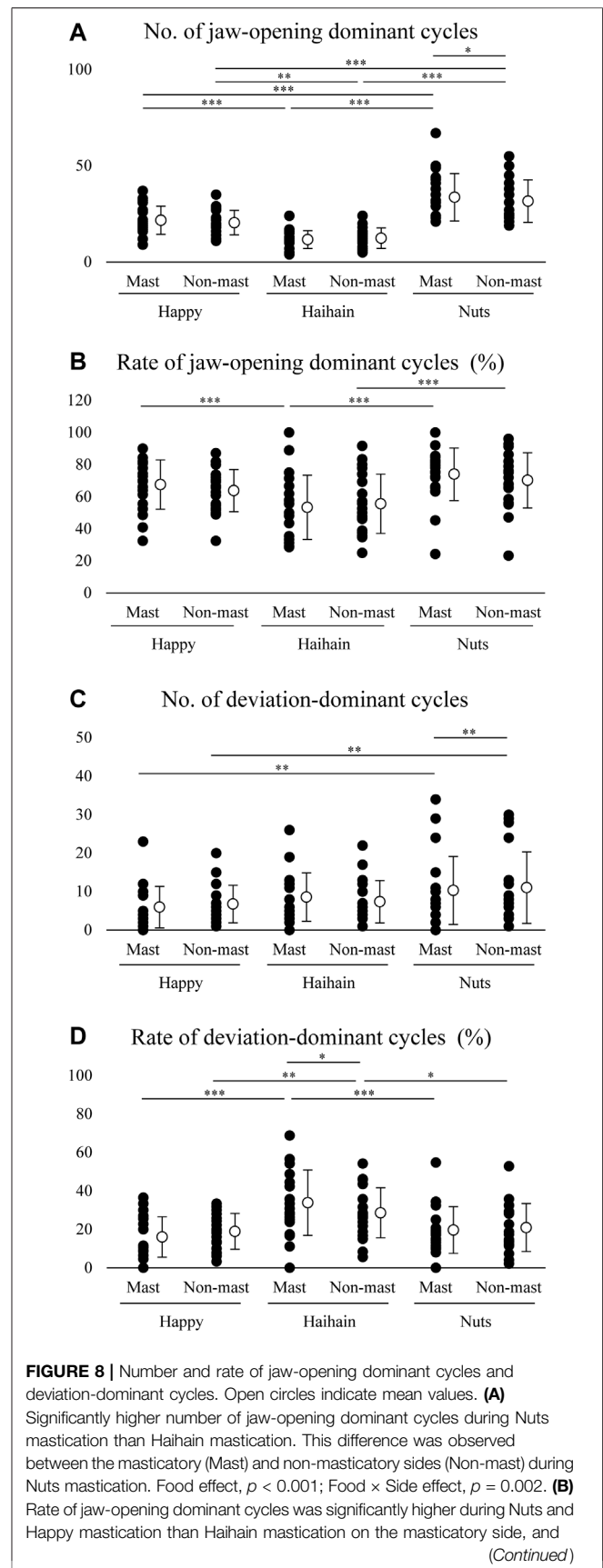


FIGURE 8 | during Nuts mastication than Haihain mastication on the non-masticatory side. Food effect, $p < 0.001$; Food \times Side effect, $p = 0.012$. **(C)** Significantly higher number of deviation-dominant cycles during Nuts mastication than Happy mastication on both sides. This difference was also observed between the masticatory and non-masticatory sides during Nuts mastication. Food effect, $p < 0.001$; Food \times Side effect, $p = 0.021$. **(D)** Significantly higher rates of deviation-dominant cycles were seen during Haihain mastication than Happy and Nuts mastication on both sides. This difference was also observed between the masticatory and non-masticatory sides during Haihain mastication. Food effect, $p < 0.001$; Food \times Side effect (Free vs. Habitual), $p = 0.005$. *** $p < 0.001$, ** $p < 0.01$, * $p < 0.05$.

4 DISCUSSION

4.1 Functional Contribution of the Suprahyoid Muscles to Tongue Movements

The process of mastication involves the several intra-oral structures including the lips, tongue, and the hard and soft palates, which function for intake and size-reduction of ingested food *via* the mastication-related muscles. Specifically, the tongue plays a critical role in that it generates pressure against the palate to move the food bolus from side to side within the oral cavity or to propel it posteriorly for deglutition (Logemann, 2014). Further, patterns of tongue movements adjust to sensory information based on location and physical properties such as hardness, cohesiveness, or viscosity of the bolus from cycle to cycle. As with the tongue, the suprahyoid muscles help in manipulating the bolus. When the tongue muscles are activated to form the bolus, the base of the tongue may also need to be elevated and rotated to collect the food together with saliva and/or keep the food positioned in the oral cavity with the cheeks (Abd-El-Malek, 1955). In other words, the suprahyoid muscles must be activated during mastication not only for jaw-opening but also for bolus formation.

Our findings have shown increased suprahyoid EMG amplitude with increasing magnitude of tongue pressure such that maximum tongue pressure generation resulted in larger amplitude suprahyoid EMG bursts, almost the same as that generated during maximum jaw-opening. This strongly suggests that suprahyoid EMG bursts function for both jaw-opening and tongue elevation.

It is possible that the suprahyoid EMG activities were not an accurate outcome measure of contraction of these muscles but also included recordings of activity in surrounding muscles such as the muscles of the tongue, because of the proximity of these muscles to the suprahyoid muscles. In this regard, Palmer et al. (1999) recorded EMG activity from the mylohyoid, anterior belly of the digastric, geniohyoid, and genioglossus muscles and found that the contributions of the genioglossus to EMG activity of the other muscles were quite minimal. Further, we previously demonstrated that the surface EMG activity patterns of the genioglossus and suprahyoid muscles differed from each other in terms of function (Tsukada et al., 2009). Thus, the possibility of contamination of these signals can be excluded.

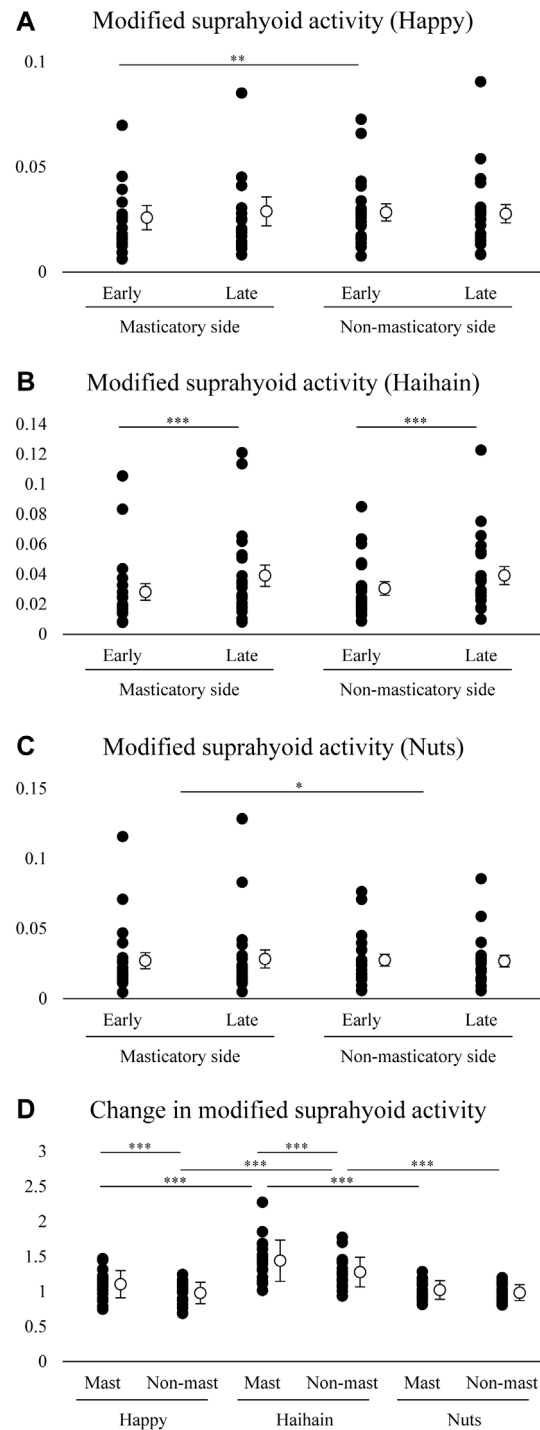


FIGURE 9 | Modified suprahyoid activity and changes in modified suprahyoid activity. Open circles indicate mean values. Modified suprahyoid activity was defined as suprahyoid electromyographic activity divided by maximal vertical jaw distance per masticatory cycle. There was no significant difference between early and late stages on both sides during Happy **(A)** and Nuts **(C)** mastication but during Haihain mastication **(B)**. Side effect, $p = 0.017$; Food \times Stage effect, $p = 0.019$ for A. Stage effect, $p < 0.001$ for B. Side effect, $p = 0.034$ for C. **(D)** Increasing rate of modified suprahyoid activity was significantly higher on both the masticatory (Mast) and non-masticatory (Non-mast) sides. (Continued)

FIGURE 9 | masticatory sides (Non-mast) during Haihain mastication than Happy and Nuts. The difference between the sides was observed during Happy and Haihain mastication. Food effect, $p < 0.001$; Food \times Side effect, $p = 0.005$. *** $p < 0.001$, ** $p < 0.01$, * $p < 0.05$.

4.2 Difference in Performance Among Test Foods

The muscles of mastication are broadly divided into jaw-closers and jaw-openers. Jaw-closer muscles consist of the masseter, temporalis, and medial pterygoid muscles. These muscles do most of the work of mastication during the jaw-closing power stroke. In contrast, the suprahyoid muscles, which include the mylohyoid, anterior belly of the digastric, and the geniohyoid muscles, are known as the jaw-opener muscles that depress the mandible. Human studies typically utilize surface masseter and suprahyoid EMG activity, due to preferred non-invasiveness of the procedures and ease of recordings. These represent jaw-closer and jaw-opener muscle activity although many other muscles such as the lingual and facial muscles are activated as well (Palmer et al., 1992; Yamada et al., 2005). Therefore, we recorded both masseter and suprahyoid surface EMG activities during mastication in this study.

It is well-known that masticatory behavior adapts to changes in the hardness of the bolus or particle size resulting in altered numbers of masticatory cycles, sequence duration, and masticatory EMG activity (Diaz-Tay et al., 1991; Takada et al., 1994; Hiemae et al., 1996; Peyron et al., 1997; Miyawaki et al., 2001; Anderson et al., 2002; Peyron et al., 2002; Foster et al., 2006). Thus, the harder or larger the bolus, the more the masticatory cycles, the longer the sequence duration, and the greater the masseter EMG activity, especially on the masticatory side. Our current results were quite consistent with theirs in that masticatory duration, number of masticatory cycles, as with masseter EMG activity were dependent on the initial hardness.

In this study, masticatory rate was significantly higher during Haihain mastication than Happy and Nuts mastication; and suprahyoid activity was significantly higher during Haihain mastication than Happy and Nuts. In our previous study, it was found that the difference in masticatory rate was caused by the difference in suprahyoid activity among the foods (Takei et al., 2020). In addition, we suspect that because of the small size of one piece of Nuts, participants were not required to open the mouth widely during mastication, which led to relatively low masticatory rates. This raises the question as to why the masticatory rate differed between Happy and Haihain. As described above, Happy characteristically had a high fat content as compared with Haihain. We previously found that the water absorption rate and water content were higher for Haihain than Happy, which might affect the force required to move the food bolus in the late stage of mastication (Takei et al., 2020). Thus, the difference in suprahyoid activity patterns among the foods may not have resulted from only one property.

Further, there was no difference in suprahyoid activity between the masticatory and non-masticatory sides. The suprahyoid muscle group includes the mylohyoid, anterior belly of the digastric, and the geniohyoid muscles; the geniohyoid functions in jaw-opening. In addition, they also function with the tongue muscles to form the bolus during mastication (Khan and Bordoni, 2021). Considering the results obtained from EMG data in that suprahyoid activity differed among the foods but not between sides or between masticatory tasks, suprahyoid muscle activity does not seem to be affected by masticatory side. However, these results were obtained from EMG data only. We therefore simultaneously recorded mandibular kinematics in our experiment (see next section).

4.3 Difference in Sequence Changes Among Foods

The suprahyoid muscles, particularly the anterior belly of the digastric and the mylohyoid, dominantly contribute to jaw-opening (Khan and Bordoni, 2021). The digastric muscle helps in depressing and retracting the mandible functionally but is less involved in deglutition, at least in animals (Doty and Bosma, 1956; Tsujimura et al., 2012). Conversely, the mylohyoid muscle also functions to elevate the floor of the mouth and the tongue during deglutition or speaking while the geniohyoid muscle contributes to upward and forward movements of the hyoid, and hence widening of the passage for the bolus during deglutition. Thus, assessment using only EMG data makes it difficult to precisely identify the functional role of each EMG burst during mastication.

A major focus of our study was to clarify the possibility of determining how the suprahyoid muscles function throughout the masticatory sequence. During mastication, the food bolus is manipulated differently depending on the masticatory stage, early, middle, or late. In the early stage, jaw-closing muscles mainly participated in reducing bolus size, and the food bolus hardness rapidly decreased (Iguchi et al., 2015; Maeda et al., 2020; Kochi et al., 2021). Conversely, in the late stage the tongue and suprahyoid muscles are dominantly activated possibly to gradually alter bolus properties such as adhesiveness or cohesiveness by mixing it with saliva (Peyron et al., 2011; Maeda et al., 2020; Takei et al., 2020; Kochi et al., 2021). From this perspective, we hypothesized that the role of the suprahyoid muscles differed between the early and late stages. In fact, there was an excellent positive correlation between suprahyoid activity and jaw gape in the early stage during all mastication in all participants. We therefore decided to use the suprahyoid activity/jaw gape per masticatory cycle ratio in the early stage as a reference. When the suprahyoid muscles mainly contribute to elevating the floor of the mouth and the tongue for bolus formation, the ratio must increase. Thus, we compared the number and occurrence ratio of jaw-opening dominant and deviation-dominant phases and the amplitude of the suprahyoid activity/jaw gape ratio among the foods. We found that the suprahyoid muscles primarily function for jaw-opening during

Nuts mastication and for bolus formation during Haihain mastication, especially in the late stage.

Numerous studies have used Nuts as a test food to investigate masticatory movements because of its toughness (Wilding and Lewin, 1994; Agrawal et al., 2000; Mishellany et al., 2006; van der Bilt and Abbink, 2017; Capuano et al., 2020). The advantage of using Nuts is likely because peanuts are a naturally hard food with dimensional stability. During mastication, the bolus gradually changes in size and rheological properties such as hardness, cohesiveness, and adhesiveness. Previous studies suggested that deglutition cannot be initiated when bolus particles remain above a certain size, which is considered the deglutition threshold (Feldman et al., 1980; Hutchings and Lillford, 1988; Prinz and Lucas, 1995). Further, the size distribution of the bolus particles is a determining factor in making the bolus sufficiently cohesive to enable deglutition to occur safely (Mishellany et al., 2006). Thus, the focus of masticatory performance using Nuts might be the breakdown of the bolus by the masticatory muscles. It can be concluded that the suprahyoid muscles were dominantly activated for jaw-opening during Nuts mastication regardless of the side although a minor but significant difference was noted between sides.

As compared with Happy mastication in which the deviation-dominant phase was relatively shorter, during Haihain mastication, the number of deviation-dominant phases was not significantly lower and the rate of deviation-dominant phases was significantly higher than Happy and Nuts even though the number of masticatory cycles was lowest during Haihain mastication. Further, during Haihain mastication, modified suprahyoid activity was significantly higher in the late than in the early stage on both the masticatory and non-masticatory sides; a difference was noted between the masticatory and non-masticatory sides. In a previous study, we found that the increasing ratio of masticatory cycle time in the late stage was highest in Haihain mastication vs. the other rice cracker suggesting that the longer masticatory cycle time and higher suprahyoid activity can be attributed to the water absorption rate of the bolus, and not hardness (Takei et al., 2020). That study also found that there was no difference in the adhesiveness and cohesiveness of the bolus at deglutition initiation between Happy and Haihain. These results suggest that bolus properties, as well as oral conditions such as dryness, significantly affect suprahyoid activity. A negative impact of oral dryness on mastication can thus be presumed. Shinkawa et al. (2009) reported that poor masticatory ability is associated with lower mucosal moisture in elderly individuals. These results suggest the need to consider that masticatory behavior is affected by both bolus properties and oral conditions such as salivary flow rate or oral dryness.

To our knowledge, ours is the first report to have demonstrated the difference in the contribution of the suprahyoid muscles to bolus formation between the masticatory and non-masticatory sides. Previous studies introduced a new method to record neck surface EMG

activities, which represents the force of posterior tongue lifting (Manda et al., 2016; Mori et al., 2021). The authors demonstrated that neck EMG activity was significantly higher on the masticatory side than on the non-masticatory side although there was no difference among the stages. Our findings in this study are partly consistent with theirs in that the EMGs recorded on the masticatory side dominantly contributed to bolus manipulation during mastication. In their study, however, they evaluated only the peak amplitude of EMG bursts. In addition, as described, the suprahyoid muscles are activated not only during jaw opening but also during tongue-lifting. Because particle size gradually decreases in a masticatory sequence, it is vital to consider how the muscle activity changes with changes in bolus size and jaw gape during mastication. In this respect, it is noteworthy that the change in modified suprahyoid activity was observed only during Happy and Haihain mastication in this study. Future studies, should precisely clarify which conditions determine the asymmetry of these functions.

4.4 Limitations

Several limitations of this study should be considered when interpreting the findings. First, we recruited only healthy young male and female participants, and so these findings could not be generalized to other/older populations. Considering the effects of age, particularly regarding the effects of dental status or oral dryness, recruiting other populations would help clarify how these conditions affect masticatory behaviors. In addition, gender difference should also be considered. Although our previous study reported difference in the masticatory function between the genders (Maeda et al., 2020), we believe that the nature of masticatory movements is not much different between them. In our future study, we will focus on the effect of age and gender on the masticatory kinematics as well as EMG activity. Second, only two rice crackers and peanuts were used, and so we could not determine specifically which factors, including the shape, size, or taste of the foods, were critical for determining the masticatory movements. Third, although the focus was on only jaw gape to determine the function of the suprahyoid muscles, other parameters such as the duration or speed of mandibular movements should also be evaluated. Although there was a mild correlation between EMG activity and the duration of each phase, the CC was always lower than that between EMG activity and jaw gape (data not shown). Fourth, we analyzed the EMG signals using only the area under the curve, but did not consider timing such as onset, offset, and peak time nor the changes in these values between conditions. Fifth, we did not directly visualize bolus transport in the oral cavity and pharynx. Our future study will involve simultaneous recordings of EMG activity and imaging.

Despite these limitations, our findings clearly demonstrate a functional role of the suprahyoid muscles during mastication of solid foods with different initial consistencies by analyzing both EMG activity and mandibular kinematics. This provides a useful modality for evaluating the masticatory physiology of a range of solid foods.

5 CONCLUSION

This study showed the difference in suprahyoid EMG activity during mastication of solid foods with different initial properties. We demonstrated that the suprahyoid muscle activity increased not for jaw opening, but for bolus formation especially on the masticatory side during the late stage of soft rice cracker (Haihain) mastication. These findings were obtained from assessments using both EMG activity and mandibular kinematic recordings. In a clinical situation, not only hardness but also other characteristics of the solid food should be considered to evaluate masticatory function.

DATA AVAILABILITY STATEMENT

The original contributions presented in the study are included in the article/**Supplementary Material**, further inquiries can be directed to the corresponding author.

ETHICS STATEMENT

The studies involving human participants were reviewed and approved by the Ethics Committee of Niigata University. The patients/participants provided their written informed consent to participate in this study.

REFERENCES

- Abd-El-Malek, S. (1955). The Part Played by the Tongue in Mastication and Deglutition. *J. Anat.* 89, 250–254.
- Agrawal, K. R., Lucas, P. W., and Bruce, I. C. (2000). The Effects of Food Fragmentation Index on Mandibular Closing Angle in Human Mastication. *Archives Oral Biol.* 45, 577–584. doi:10.1016/s0003-9969(00)00019-4
- Anderson, K., Throckmorton, G. S., Buschang, P. H., and Hayasaki, H. (2002). The Effects of Bolus Hardness on Masticatory Kinematics. *J. Oral Rehabil.* 29, 689–696. doi:10.1046/j.1365-2842.2002.00862.x
- Bishop, B., Plesh, O., and McCall, W. D., Jr. (1990). Effects of Chewing Frequency and Bolus Hardness on Human Incisor Trajectory and Masseter Muscle Activity. *Archives oral Biol.* 35, 311–318. doi:10.1016/0003-9969(90)90048-f
- Capuano, E., Pellegrini, N., Van Bommel, R., and Stieger, M. (2020). The Effect of a Bread Matrix on Mastication of Hazelnuts. *Food Res. Int.* 137, 109692. doi:10.1016/j.foodres.2020.109692
- Diaz-Tay, J., Jayasinghe, N., Lucas, P. W., McCallum, J. C., and Jones, J. T. (1991). Association Between Surface Electromyography of Human Jaw-Closing Muscle and Quantified Food Breakdown. *Archives oral Biol.* 36, 893–898. doi:10.1016/0003-9969(91)90120-j
- Doty, R. W., and Bosma, J. F. (1956). An Electromyographic Analysis of Reflex Deglutition. *J. Neurophysiology* 19, 44–60. doi:10.1152/jn.1956.19.1.44
- Feldman, R. S., Kapur, K. K., Alman, J. E., and Chauncey, H. H. (1980). Aging and Mastication: Changes in Performance and in the Swallowing Threshold with Natural Dentition†. *J. Am. Geriatrics Soc.* 28, 97–103. doi:10.1111/j.1532-5415.1980.tb00240.x
- Foster, K. D., Woda, A., and Peyron, M. A. (2006). Effect of Texture of Plastic and Elastic Model Foods on the Parameters of Mastication. *J. Neurophysiology* 95, 3469–3479. doi:10.1152/jn.01003.2005
- Gonçalves, T. M. S. V., Vilanova, L. S. R., Gonçalves, L. M., and Rodrigues Garcia, R. C. M. (2014). Effect of Complete and Partial Removable Dentures on Chewing Movements. *J. Oral Rehabil.* 41, 177–183. doi:10.1111/joor.12125

AUTHOR CONTRIBUTIONS

MI and MW conceived the design and wrote the first draft of the article; AS, SK, NH, and RI collected the data; MI, SK, and JM conducted the literature review and analyzed the data; MI, TT, and JM revised the first draft. All authors approved the final version of the manuscript.

FUNDING

The authors declare that this study received funding from Kameda Seika Co., Ltd. This study was supported in part by JSPS KAKENHI Grant 20K10265.

ACKNOWLEDGMENTS

We thank Florence Ene (Platinum Medical Consulting Jp) for editing a draft of this manuscript.

SUPPLEMENTARY MATERIAL

The Supplementary Material for this article can be found online at: <https://www.frontiersin.org/articles/10.3389/fphys.2022.881891/full#supplementary-material>

- Goto, T., Nakamichi, A., Watanabe, M., Nagao, K., Matsuyama, M., and Ichikawa, T. (2015). Influence of Food Volume Per Mouthful on Chewing and Bolus Properties. *Physiology Behav.* 141, 58–62. doi:10.1016/j.physbeh.2015.01.007
- Grigoriadis, A., Johansson, R. S., and Trulsson, M. (2014). Temporal Profile and Amplitude of Human Masseter Muscle Activity Is Adapted to Food Properties During Individual Chewing Cycles. *J. Oral Rehabil.* 41, 367–373. doi:10.1111/joor.12155
- Hiiemae, K., Heath, M. R., Heath, G., Kazazoglu, E., Murray, J., Sapper, D., et al. (1996). Natural Bites, Food Consistency and Feeding Behaviour in Man. *Archives Oral Biol.* 41, 175–189. doi:10.1016/0003-9969(95)00112-3
- Horio, T., and Kawamura, Y. (1989). Effects of Texture of Food on Chewing Patterns in the Human Subject. *J. Oral Rehabil.* 16, 177–183. doi:10.1111/j.1365-2842.1989.tb01331.x
- Hutchings, J. B., and Lillford, P. J. (1988). The Perception of Food Texture - the Philosophy of the Breakdown Path. *J. Texture Stud.* 19, 103–115. doi:10.1111/j.1745-4603.1988.tb00928.x
- Iguchi, H., Magara, J., Nakamura, Y., Tsujimura, T., Ito, K., and Inoue, M. (2015). Changes in Jaw Muscle Activity and the Physical Properties of Foods with Different Textures During Chewing Behaviors. *Physiology Behav.* 152, 217–224. doi:10.1016/j.physbeh.2015.10.004
- Jean, A. (2001). Brain Stem Control of Swallowing: Neuronal Network and Cellular Mechanisms. *Physiol. Rev.* 81, 929–969. doi:10.1152/physrev.2001.81.2.929
- Khan, Y. S., and Bordoni, B. (2021). “Anatomy, Head and Neck, Suprahyoid Muscle,” in StatPearls (Treasure Island, FL: StatPearls Publishing LLC). Available at: <https://www.ncbi.nlm.nih.gov/books/NBK546710/>.
- Kochi, I., Takei, E., Maeda, R., Ito, K., Magara, J., Tsujimura, T., et al. (2021). Changes of Bolus Properties and the Triggering of Swallowing in Healthy Humans. *J. Oral Rehabil.* 48, 592–600. doi:10.1111/joor.13151
- Kohyama, K., Yamaguchi, M., Kobori, C., Nakayama, Y., Hayakawa, F., and Sasaki, T. (2005). Mastication Effort Estimated by Electromyography for Cooked Rice of Differing Water Content. *Biosci. Biotechnol. Biochem.* 69, 1669–1676. doi:10.1271/bbb.69.1669
- Lassauzay, C., Peyron, M.-A., Albuissou, E., Dransfield, E., and Woda, A. (2000). Variability of the Masticatory Process During Chewing of Elastic Model Foods. *Eur. J. Oral Sci.* 108, 484–492. doi:10.1034/j.1600-0722.2000.00866.x

- Logemann, J. A. (2014). Critical Factors in the Oral Control Needed for Chewing and Swallowing. *J. Texture Stud.* 45, 173–179. doi:10.1111/jtxs.12053
- Lund, J. P., and Kolta, A. (2006). Generation of the Central Masticatory Pattern and its Modification by Sensory Feedback. *Dysphagia* 21, 167–174. doi:10.1007/s00455-006-9027-6
- Maeda, R., Takei, E., Ito, K., Magara, J., Tsujimura, T., and Inoue, M. (2020). Inter-Individual Variation of Bolus Properties in Triggering Swallowing During Chewing in Healthy Humans. *J. Oral Rehabil.* 47, 1161–1170. doi:10.1111/joor.13044
- Manda, Y., Maeda, N., Pan, Q., Sugimoto, K., Hashimoto, Y., Tanaka, Y., et al. (2016). New Method of Neck Surface Electromyography for the Evaluation of Tongue-Lifting Activity. *J. Oral Rehabil.* 43, 417–425. doi:10.1111/joor.12389
- Mishellany, A., Woda, A., Labas, R., and Peyron, M.-A. (2006). The Challenge of Mastication: Preparing a Bolus Suitable for Deglutition. *Dysphagia* 21, 87–94. doi:10.1007/s00455-006-9014-y
- Miyawaki, S., Ohkuchi, N., Kawakami, T., and Sugimura, M. (2001). Changes in Masticatory Muscle Activity According to Food Size in Experimental Human Mastication. *J. Oral Rehabil.* 28, 778–784. doi:10.1046/j.1365-2842.2001.00702.x
- Mori, K., Manda, Y., Kitagawa, K., Nagatsuka, H., Furutera, H., Kodama, N., et al. (2021). Coordination of Surface Electromyography Activity in the Posterior Tongue Region During Mastication of Differently Textured Foods. *J. Oral Rehabil.* 48, 403–410. doi:10.1111/joor.13135
- Oki, K., Ogino, Y., Tsukiyama, Y., Yamasaki, Y., and Koyano, K. (2021). The Impacts of Prosthetic Interventions on Mastication Predominance in Kennedy Class II Patients. *J. Prosthodont Res.* 65, 327–331. doi:10.2186/jpr.jpr_d_20_00055
- Palmer, J. B., Hiemae, K. M., and Liu, J. (1997). Tongue-Jaw Linkages in Human Feeding: A Preliminary Videofluorographic Study. *Archives Oral Biol.* 42, 429–441. doi:10.1016/s0003-9969(97)00020-4
- Palmer, J. B., Rudin, N. J., Lara, G., and Crompton, A. W. (1992). Coordination of Mastication and Swallowing. *Dysphagia* 7, 187–200. doi:10.1007/bf02493469
- Palmer, P. M., Luschei, E. S., Jaffe, D., and McCulloch, T. M. (1999). Contributions of Individual Muscles to the Submental Surface Electromyogram During Swallowing. *J. Speech Lang. Hear Res.* 42, 1378–1391. doi:10.1044/jslhr.4206.1378
- Peyron, M.-A., Gierczynski, I., Hartmann, C., Loret, C., Dardevet, D., Martin, N., et al. (2011). Role of Physical Bolus Properties as Sensory Inputs in the Trigger of Swallowing. *PLoS One* 6, e21167. doi:10.1371/journal.pone.0021167
- Peyron, M. A., Lassauzay, C., and Woda, A. (2002). Effects of Increased Hardness on Jaw Movement and Muscle Activity During Chewing of Visco-Elastic Model Foods. *Exp. Brain Res.* 142, 41–51. doi:10.1007/s00221-001-0916-5
- Peyron, M. A., Maskawi, K., Woda, A., Tanguay, R., and Lund, J. P. (1997). Effects of Food Texture and Sample Thickness on Mandibular Movement and Hardness Assessment During Biting in Man. *J. Dent. Res.* 76, 789–795. doi:10.1177/00220345970760031201
- Prinz, J. F., and Lucas, P. W. (1995). Swallow Thresholds in Human Mastication. *Archives Oral Biol.* 40, 401–403. doi:10.1016/0003-9969(94)00185-e
- Sano, M., and Shiga, H. (2021). Inter-Measurement Variation of Masticatory Performance Test Using Gummy Jelly. *Odontology* 110, 212–215. doi:10.1007/s10266-021-00640-1
- Shiga, H., Nakajima, K., Uesugi, H., Komino, M., Sano, M., and Arai, S. (2021). Reference Value of Masticatory Performance by Measuring the Amount of Glucose Extraction From Chewing Gummy Jelly. *J. Prosthodont Res.* [Epub Ahead of Print] doi:10.2186/jpr.JPR_D_21_00154
- Shinkawa, T., Hayashida, N., Mori, K., Washio, K., Hashiguchi, K., Taira, Y., et al. (2009). Poor Chewing Ability Is Associated with Lower Mucosal Moisture in Elderly Individuals. *Tohoku J. Exp. Med.* 219, 263–267. doi:10.1620/tjem.219.263
- Takada, K., Miyawaki, S., and Tatsuta, M. (1994). The Effects of Food Consistency on Jaw Movement and Posterior Temporalis and Inferior Orbicularis Oris Muscle Activities During Chewing in Children. *Archives Oral Biol.* 39, 793–805. doi:10.1016/0003-9969(94)90009-4
- Takei, E., Kulvanich, S., Tsujimura, T., Magara, J., Ito, K., Takei, R., et al. (2020). Age-Related Changes in Functional Adaptation to Bolus Characteristics During Chewing. *Physiology Behav.* 225, 113102. doi:10.1016/j.physbeh.2020.113102
- Tsujimura, T., Yamada, A., Nakamura, Y., Fukuhara, T., Yamamura, K., and Inoue, M. (2012). The Digastric Muscle Is Less Involved in Pharyngeal Swallowing in Rabbits. *Dysphagia* 27, 271–276. doi:10.1007/s00455-011-9363-z
- Tsukada, T., Taniguchi, H., Ootaki, S., Yamada, Y., and Inoue, M. (2009). Effects of Food Texture and Head Posture on Oropharyngeal Swallowing. *J. Appl. Physiology* 106, 1848–1857. doi:10.1152/japplphysiol.91295.2008
- Van der Bilt, A., and Abbink, J. H. (2017). The Influence of Food Consistency on Chewing Rate and Muscular Work. *Archives Oral Biol.* 83, 105–110. doi:10.1016/j.archoralbio.2017.07.011
- Wilding, R. J. C., and Lewin, A. (1994). The Determination of Optimal Human Jaw Movements Based on Their Association with Chewing Performance. *Archives Oral Biol.* 39, 333–343. doi:10.1016/0003-9969(94)90125-2
- Yamada, Y., Yamamura, K., and Inoue, M. (2005). Coordination of Cranial Motoneurons During Mastication. *Respir. Physiology Neurobiol.* 147, 177–189. doi:10.1016/j.resp.2005.02.017
- Yamasaki, Y., Kuwatsuru, R., Tsukiyama, Y., Oki, K., and Koyano, K. (2016). Objective Assessment of Mastication Predominance in Healthy Dentate Subjects and Patients with Unilateral Posterior Missing Teeth. *J. Oral Rehabil.* 43, 575–582. doi:10.1111/joor.12403

Conflict of Interest: The authors declare that the research was conducted in the absence of any commercial or financial relationships that could be construed as a potential conflict of interest.

Publisher's Note: All claims expressed in this article are solely those of the authors and do not necessarily represent those of their affiliated organizations, or those of the publisher, the editors and the reviewers. Any product that may be evaluated in this article, or claim that may be made by its manufacturer, is not guaranteed or endorsed by the publisher.

Copyright © 2022 Sasa, Kulvanich, Hao, Ita, Watanabe, Suzuki, Magara, Tsujimura and Inoue. This is an open-access article distributed under the terms of the Creative Commons Attribution License (CC BY). The use, distribution or reproduction in other forums is permitted, provided the original author(s) and the copyright owner(s) are credited and that the original publication in this journal is cited, in accordance with accepted academic practice. No use, distribution or reproduction is permitted which does not comply with these terms.



A Strength Endurance Exercise Paradigm Mitigates Deficits in Hypoglossal-Tongue Axis Function, Strength, and Structure in a Rodent Model of Hypoglossal Motor Neuron Degeneration

OPEN ACCESS

Edited by:

Cassie S. Mitchell,
Georgia Institute of Technology,
United States

Reviewed by:

John Russell,
University of Wisconsin–Madison,
United States
Miranda Jane Cullins,
University of Wisconsin–Madison,
United States

*Correspondence:

Nicole L. Nichols
Nicholsn@missouri.edu
Teresa E. Lever
Lever@health.missouri.edu

Specialty section:

This article was submitted to
Neurodegeneration,
a section of the journal
Frontiers in Neuroscience

Received: 04 February 2022

Accepted: 23 May 2022

Published: 30 June 2022

Citation:

Murphy ER, Thompson R,
Osman KL, Haxton C, Brothers M,
Lee L, Warncke K, Smith CL,
Keilholz AN, Hamad A, Golzy M,
Bunyak F, Ma L, Nichols NL and
Lever TE (2022) A Strength
Endurance Exercise Paradigm
Mitigates Deficits
in Hypoglossal-Tongue Axis Function,
Strength, and Structure in a Rodent
Model of Hypoglossal Motor Neuron
Degeneration.
Front. Neurosci. 16:869592.
doi: 10.3389/fnins.2022.869592

Erika R. Murphy¹, Rebecca Thompson^{2,3}, Kate L. Osman², Chandler Haxton², Margaret Brothers¹, Li Lee^{4,5}, Kristen Warncke^{4,5}, Catherine L. Smith³, Amy N. Keilholz³, Ali Hamad⁶, Mojgan Golzy⁷, Filiz Bunyak⁶, Lixin Ma^{4,5}, Nicole L. Nichols^{3,8*} and Teresa E. Lever^{1,2,3*}

¹ Department of Speech, Language and Hearing Sciences, School of Health Professions, University of Missouri, Columbia, MO, United States, ² Department of Otolaryngology-Head and Neck Surgery, School of Medicine, University of Missouri, Columbia, MO, United States, ³ Department of Biomedical Sciences, College of Veterinary Medicine, University of Missouri, Columbia, MO, United States, ⁴ Department of Radiology, School of Medicine, University of Missouri, Columbia, MO, United States, ⁵ Research Division, Biomolecular Imaging Center, Harry S. Truman Memorial Veterans' Hospital, Columbia, MO, United States, ⁶ Department of Electrical Engineering and Computer Science, University of Missouri, Columbia, MO, United States, ⁷ Biostatistics Unit, Department of Family and Community Medicine, University of Missouri, Columbia, MO, United States, ⁸ Dalton Cardiovascular Research Center, University of Missouri, Columbia, MO, United States

The tongue plays a crucial role in the swallowing process, and impairment can lead to dysphagia, particularly in motor neuron diseases (MNDs) resulting in hypoglossal-tongue axis degeneration (e.g., amyotrophic lateral sclerosis and progressive bulbar palsy). This study utilized our previously established inducible rodent model of dysphagia due to targeted degeneration of the hypoglossal-tongue axis. This model was created by injecting cholera toxin B conjugated to saporin (CTB-SAP) into the genioglossus muscle of the tongue base for retrograde transport to the hypoglossal (XII) nucleus via the hypoglossal nerve, which provides the sole motor control of the tongue. Our goal was to investigate the effect of high-repetition/low-resistance tongue exercise on tongue function, strength, and structure in four groups of male rats: (1) control + sham exercise ($n = 13$); (2) control + exercise ($n = 10$); (3) CTB-SAP + sham exercise ($n = 13$); and (4) CTB-SAP + exercise ($n = 12$). For each group, a custom spout with adjustable lick force requirement for fluid access was placed in the home cage overnight on days 4 and 6 post-tongue injection. For the two sham exercise groups, the lick force requirement was negligible. For the two exercise groups, the lick force requirement was set to ~40% greater than the maximum voluntary lick force for individual rats. Following exercise exposure, we evaluated the effect on hypoglossal-tongue axis function (via videofluoroscopy), strength (via force-lickometer), and structure [via Magnetic Resonance Imaging (MRI) of the brainstem and tongue in a subset of rats]. Results showed that sham-exercised CTB-SAP rats had significant deficits in

lick rate, swallow timing, and lick force. In exercised CTB-SAP rats, lick rate and lick force were preserved; however, swallow timing deficits persisted. MRI revealed corresponding degenerative changes in the hypoglossal-tongue axis that were mitigated by tongue exercise. These collective findings suggest that high-repetition/low-resistance tongue exercise in our model is a safe and effective treatment to prevent/diminish signs of hypoglossal-tongue axis degeneration. The next step is to leverage our rat model to optimize exercise dosing parameters and investigate corresponding treatment mechanisms of action for future translation to MND clinical trials.

Keywords: motor neuron disease (MND), hypoglossal, tongue, dysphagia, exercise, rodent model

INTRODUCTION

Tongue weakness and atrophy are pervasive symptoms of motor neuron diseases (MNDs) (Brooks et al., 2000; Bruijn et al., 2004; Gonzalez de Aguilar et al., 2007; Mitchell and Borasio, 2007; Ravits et al., 2013; Turner et al., 2013; Waito et al., 2017) particularly amyotrophic lateral sclerosis (ALS), spinobulbar muscular atrophy/Kennedy's disease, and progressive bulbar palsy (Baumer et al., 2014; Tiriyaki and Horak, 2014; National Institute of Neurological Disorders and Stroke [NIH], 2019). For reasons that remain largely unknown, hypoglossal lower motor neurons (XII LMNs) innervating the tongue progressively degenerate in these patients, often resulting in life-threatening swallowing (dysphagia) and breathing (dyspnea) impairment (Hadjikoutis and Wiles, 2001; Corcia et al., 2008; Kurian et al., 2009; Kiernan et al., 2011). Treatments aimed at preventing XII LMN degeneration to preserve tongue function have not yet been identified, thus palliative/supportive intervention currently remains the standard of care. We propose that targeted tongue exercise may be a candidate treatment to significantly improve the quality and duration of life for MND patients.

Data on tongue exercise in MNDs are limited to only a few case studies (Dworkin and Hartman, 1979; Watts and Vanryckeghem, 2001) and animal model investigations (Ma et al., 2017) with variable findings, providing insufficient evidence to conclude whether tongue exercise is beneficial or harmful to MND patients (Plowman, 2015; Sheikh and Vissing, 2019). However, research outside the MND field has shown that tongue exercise improves upper airway/swallowing deficits caused by stroke (Robbins et al., 2007; Cullins et al., 2019), traumatic brain injury (Steele et al., 2013), Parkinson's disease (Argolo et al., 2013; Ciucci et al., 2013; Wang et al., 2018), and biological aging (Connor et al., 2009; Kletzien et al., 2013) via putative neuroplastic mechanisms that are not yet well understood. Moreover, a growing body of evidence has emerged over the past two decades in favor of exercise training in general (i.e., not tongue-specific) in MND patients (Sheikh and Vissing, 2019). However, the optimal dose of time, intensity, and duration of exercise therapy remains to be identified for different MNDs as well as the different clinical stages of disease progression (Sheikh and Vissing, 2019; Tsitkanou et al., 2019).

To facilitate research in this area, we recently developed an inducible rat model of dysphagia due to selective degeneration of XII LMNs in the hypoglossal nucleus of the brainstem

medulla, which provides the sole motor innervation to the tongue via the hypoglossal nerve. This model was created by injecting cholera toxin B conjugated to saporin (CTB-SAP) into the genioglossus muscle in the tongue base for retrograde transport to XII LMNs. Upon entering XII LMN cell bodies, CTB-SAP dissociates, leaving SAP free to bind to ribosomes and consequently halt protein synthesis, resulting in apoptotic cell death (Llewellyn-Smith et al., 2000; Lujan et al., 2010). Our recent investigations with this model revealed that a single CTB-SAP injection into the midline genioglossus of adult rats resulted in ~60% XII LMN cell death within 9 days (Lind et al., 2018), with corresponding "downstream" degenerative changes in the XII nerve (i.e., denervation atrophy) and genioglossus (i.e., myofiber atrophy) (Lind et al., 2021) as well as development of swallowing-related deficits (slower lick and swallow rates) (Lind et al., 2018). In contrast, when control rats were tongue-injected with unconjugated CTB and SAP (CTB + SAP), only CTB was uptaken by XII nerve terminals for retrograde transport to XII LMNs, without resultant neuromuscular degenerative changes and corresponding swallowing-related deficits (Lind et al., 2018, 2021). Thus, our inducible rat model selectively involves the hypoglossal-tongue axis and provides a unique platform for studying the effects of targeted tongue exercise on tongue-related function, strength, and structure.

Here, we leveraged our rat model of hypoglossal-tongue axis degeneration to test the hypothesis that targeted tongue exercise can beneficially alter the clinical deficits we previously observed in this model. For this study, we developed a customized force-lickometer system to measure spontaneous lick force in rats during unrestrained drinking, and a tongue exercise spout that permits individualized resistance training overnight in the rat's home cage. We utilized a high-repetition/low-resistance (i.e., strength endurance) exercise paradigm designed for muscle growth (Anderson and Kearney, 1982), which consisted of two non-consecutive overnight sessions. Following the exercise program, we evaluated the effect of targeted tongue exercise on hypoglossal-tongue axis function (*via* videofluoroscopy), strength (*via* force-lickometer), and structure (*via* MRI of the brainstem and tongue). These non-invasive to minimally invasive diagnostic tests were chosen because of their translatability to human medicine. Specifically, we hypothesized that: (1) sham exercise-treated CTB-SAP rats would develop behavioral evidence of dysphagia (i.e., reduced lick and swallow rates as previously shown (Lind et al., 2018), in addition to longer

lick-swallow ratios and longer pharyngeal transit times, PTT) and reduced tongue strength (i.e., reduced lick force during drinking); (2) these behavioral-based deficits in tongue/swallow function and strength would be prevented by tongue exercise in CTB-SAP rats; (3) sham exercise-treated CTB-SAP rats would have degenerative structural changes that correspond to neuronal loss in the hypoglossal nucleus (i.e., enlarged 4th ventricle), as well as changes in the tongue (i.e., hyperintensity indicative of muscle fiber inflammation and fat infiltration and increased tongue thickness and volume) compared to control groups; and (4) these structural deficits would be prevented by tongue exercise in CTB-SAP rats. Results from this study may provide novel insight into translationally relevant clinical indicators of XII LMN degeneration and response to treatment. Moreover, demonstrating a beneficial effect of tongue exercise in this model would support its ongoing use in research to develop and optimize translationally feasible therapeutic strategies for MNDs.

MATERIALS AND METHODS

Animals

Forty-eight male Sprague Dawley rats (Envigo Colony 208; Indianapolis, IN, United States) between 3 and 4 months of age (335–416 g) were included in this study. Rats were pair-housed in standard vivarium conditions (ambient temperature 20–26°C, humidity 30–70%, and standard 12-h light cycle) with unlimited access to food pellets (Purina Lab Diet 5008) and filtered tap water (pH adjusted to 3.5), except during experimental testing (described below). Daily health monitoring and routine surveillance for common rodent illnesses were performed by veterinary staff. All experimental procedures were approved by our Institutional Animal Care and Use Committee and conducted in accordance with the Guide for the Care and Use of Laboratory Animals within our USDA-licensed and AAALAC-accredited academic institution.

Experimental Procedures

Rats were randomly allocated to 4 experimental groups to study the effects of tongue resistance exercise on tongue-related function, strength, and structure, as summarized in **Table 1**. All rats received an intralingual injection of either unconjugated CTB + SAP (i.e., control) or conjugated CTB-SAP, followed by exposure to either tongue exercise (i.e., treatment) or sham exercise (i.e., sham treatment), as described

in detail below. Before tongue injections and after exercise/sham exercise exposure, rats underwent behavioral testing of tongue function (*via* videofluoroscopy) and tongue strength (*via* force-lickometer). At the study endpoint (i.e., 9 days after tongue injection), a subset of 16 rats (1) control + sham exercise ($n = 5$); (2) control + exercise ($n = 2$); (3) CTB-SAP + sham exercise ($n = 6$); and (4) CTB-SAP + exercise ($n = 3$) underwent MRI of the brainstem and tongue to investigate corresponding structural changes that may correlate with behavioral findings. This study endpoint is the same as our previous studies (Lind et al., 2018, 2021), which was determined based on pilot data showing that other time points either did not result in dysphagia (4 days post tongue injection) or resulted in severe dysphagia (11–14 days post tongue injection). A summary of the 9-day experimental timeline is shown in **Figure 1**. All rats were euthanized on Day 9 using approved methods.

Intralingual Injections to Create an Inducible Rat Model of Targeted Hypoglossal Motor Neuron Degeneration

Our rat model was created as previously described (Lind et al., 2018, 2021). In brief, rats were anesthetized via 5% isoflurane in an induction chamber and immobilized in ear bars in the supine position on a custom-built tilt table to stabilize the head during tongue injections. For the remainder of the procedure, isoflurane (2–3%) was delivered via nose cone to extinguish hindlimb and jaw reflexes. The jaw was gently held open by a custom-built weighted pulley-mechanism looped around the mandibular incisors for unobstructed access to the tongue. Under light guidance (LED Stereotaxic Light, #59290, Stoelting; Wood Dale, IL, United States), fine forceps were used to gently lift the tongue for visualization of the frenulum, which was the anatomical landmark for targeted injection into the midline genioglossus muscle in the tongue base. Each rat received a single “control” injection (20 μ g CTB + 25 μ g SAP; unconjugated CTB + SAP) or CTB-SAP injection (25 μ g of CTB conjugated to SAP) using a 50 μ L Luer tip syringe (Microliter #705, Hamilton; Reno, NV, United States) and 26-gauge Luer lock needle (26G3/8, Becton, Dickinson and Company; Franklin Lakes, NJ, United States). The needle was angled at 45-degrees during insertion into the midpoint of the frenulum, with half of the bolus delivered at ~ 8 mm depth (i.e., near maximum needle insertion) and the remainder at ~ 4 mm (i.e., half the needle insertion depth) during needle retraction. All injections were performed by the same investigator for replicability of results. Rats were recovered from anesthesia and closely monitored for several hours to ensure resumption of food and water intake before being returned to standard vivarium conditions and daily health monitoring.

Behavioral Assessments of Tongue Motility, Swallowing Function, and Tongue Strength

Behavioral assessments included videofluoroscopic swallow study (VFSS) to assess tongue motility and swallowing function, and force-lickometer testing to assess tongue strength. Testing occurred at baseline (i.e., prior to tongue injection) and Day 8 (i.e., endline behavioral test point after exercise/sham exercise treatment). An extensive behavioral conditioning program

TABLE 1 | Experimental group assignment.

| Experimental groups | | Group name | Sample size |
|---------------------|---------------|---------------------------|-------------|
| Control | Sham Exercise | ‘Control + Sham Exercise’ | 13 |
| | Exercise | ‘Control + Exercise’ | 10 |
| CTB-SAP | Sham Exercise | ‘CTB-SAP + Sham Exercise’ | 13 |
| | Exercise | ‘CTB-SAP + Exercise’ | 12 |
| Total | | | 48 |

Sham Exercise = negligible (<4 g) lick force requirement; Exercise target = 50% greater than maximum voluntary lick force (MVLf).

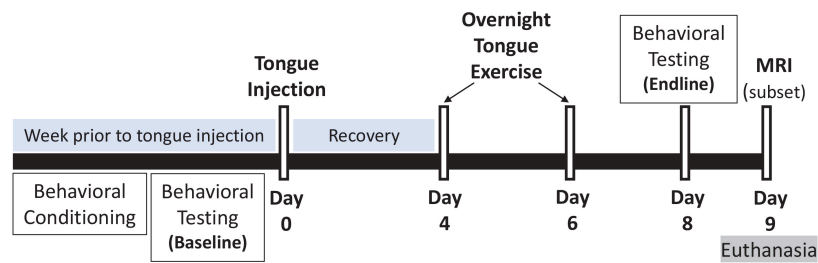


FIGURE 1 | Experimental timeline. Our inducible rat model of targeted hypoglossal motor neuron degeneration has a 9-day timeline. On Day 0, rats received a single tongue injection of either control (unconjugated CTB + SAP) or conjugated CTB-SAP solution into the midline genioglossus. The week preceding tongue injection, rats underwent behavioral conditioning and baseline behavioral testing: (1) videofluoroscopic study (VFSS) to assess tongue motility and swallow function, and (2) force-lickometer testing to determine each rat's maximum voluntary lick force (MVLf) during drinking. At Days 4 and 6, rats underwent an overnight (12-h) tongue exercise program consisting of low intensity (50% > MVLf) or sham (≤ 4 g) exercise. Endline behavioral testing occurred on Day 8, followed by MRI (on a subset of 16 rats) and euthanasia on Day 9 (i.e., study endpoint).

was performed prior to baseline testing to ensure optimal performance during both tests at both timepoints. The behavioral conditioning and corresponding test protocols are described in detail below.

Behavioral Conditioning in Preparation for Behavioral Testing

All rats underwent 4 consecutive days of behavioral conditioning prior to baseline testing to ensure optimal performance on test days. For the first 2 days of conditioning, rats were exposed to the VFSS test solution (described below, but without radiographic contrast added) via standard vivarium bottles and a custom polycarbonate test chamber (with both end-caps removed for unimpeded pass-through exploration) for 2 h in the home cage. The final 2 days of conditioning took place in the actual test environment. For VFSS acclimation, rats were individually enclosed in a custom VFSS test chamber (described below) and placed on the remote-controlled platform within our miniature fluoroscope (described below). The remote-controlled platform was moved up/down and forward/backward for ~ 10 min to simulate test conditions, without turning on the X-ray beam. Following VFSS acclimation, rats were individually contained in a custom force-lickometer chamber (described below) placed within the force-lickometer system (described below) for ~ 10 min. During this time, rats had free access to the test solution (described below) from the force-lickometer spout (described below). Rats with drinking bouts of ≥ 20 s (i.e., continuous drinking from the spout) were considered adequately acclimated for force-lickometer testing. Rats not meeting this criterion were returned to the home cage for up to one hour before undergoing a 2nd 10-min trial. Following each day of behavioral conditioning, rats were returned to the vivarium in the home cage.

Videofluoroscopic Swallow Study Testing

Videofluoroscopic swallow study testing was performed as previously described (Lind et al., 2018). Briefly, rats underwent an overnight (12–16 h) water restriction prior to VFSS testing to motivate participation. During the water restriction period, a VFSS test chamber (clear polycarbonate, 25 cm long \times 7.5 cm

wide \times 10 cm high) without end-caps was placed in the home cage for exploration. Only water was restricted; rats continued to have free access to food pellets. The following morning, rats were individually enclosed in the same home cage VFSS test chamber by attaching both end-caps; rats readily entered the test chamber when suspended by the tail over the chamber opening. The chamber (with enclosed rat) was positioned on the remote-controlled platform within our miniature low energy fluoroscope (The LabScope, Glenbrook Technologies; Randolph, NJ, United States), as shown in **Figure 2A**. With the continuous X-ray beam set to maximum power (40 kilovolts and 0.2 milliamperes), rats underwent videofluoroscopy in the lateral view while spontaneously drinking thin liquid contrast (by volume, 74.7% of 30% sucrose in DI water, 0.3% non-alcoholic vanilla extract, and 25% Omnipaque 350; GE Healthcare, Marlborough, MA, United States) from a peg-bowl inserted into an end-cap ~ 2 mm above the chamber floor. The contrast solution was delivered to the peg-bowl using a custom syringe delivery system, which permitted undisturbed refilling (~ 1.5 mL maximum volume) as needed between drinking bouts. The X-ray beam was turned on only when the rat was drinking from the bowl. Fluoroscopic videos were captured at 30 frames per second (fps) using video editing software (Pinnacle Studio 18, Pinnacle Systems, Inc.; Mountain View, CA, United States) on a desktop computer. Up to three 5-min trials were conducted per rat (spaced ~ 15 –30 min apart) until ~ 2 min of drinking was recorded. Following testing, rats remained water restricted in preparation for force-lickometer testing (described below).

The fluoroscopic videos were analyzed in two steps. Step one entailed randomly selecting and splicing three non-overlapping 3–5-s clips of uninterrupted drinking from the peg-bowl using Pinnacle software. Step two entailed semi-automated analysis of jaw motion and bolus flow utilizing our custom jaw tracking software, JawTrackTM (see **Supplementary Video 1**), as previously described (Welby et al., 2020). Outcome measures included lick rate (i.e., number of licks per second; measured in cycles per second or Hertz, Hz) and swallow rate (i.e., number of swallows per second; measured in Hz), which we previously showed are impaired in our rat model (Lind et al., 2018). We also included two additional VFSS-measures for additional

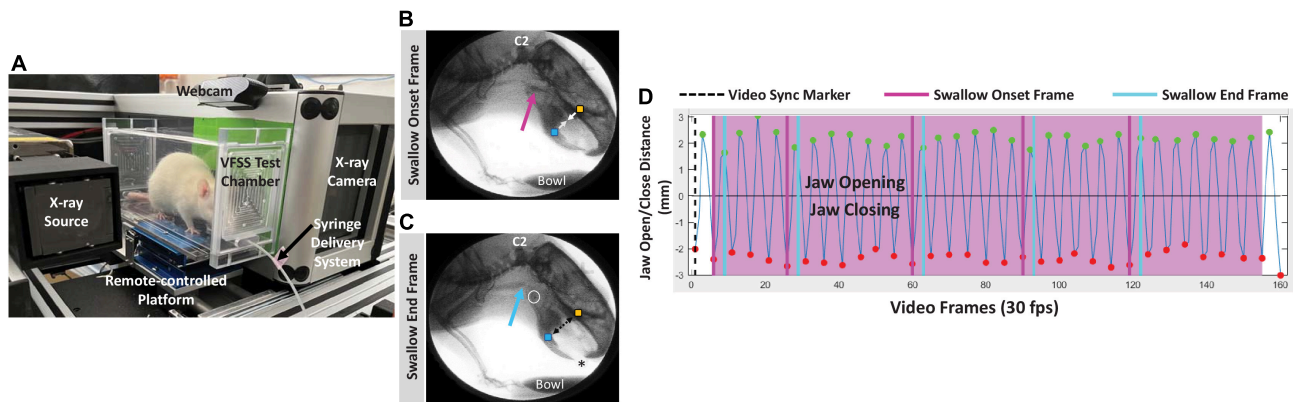


FIGURE 2 | VFSS methods. (A) A rat undergoing VFSS testing in our miniature c-arm designed for use with rodents, with labeled components. (B,C) Representative lateral view radiographic images depicting the swallow onset frame (B) and swallow end frame (C) during VFSS testing. Note the bolus filling the vallecular space at swallow onset (pink arrow), and the bolus in the proximal esophagus (blue arrow) at the swallow end frame. The yellow and blue square markers on the upper and lower jaw, respectively, automatically tracked jaw open/close motion via our JawTrack™ software. Image contrast was adjusted to accentuate the bolus rather than soft tissue; the asterisk indicates the location of the tongue protruding toward the bowl (filled with liquid contrast agent) during drinking. C2 = 2nd cervical vertebra; white open circle = hyoid bone. The cross in the upper right quadrant is a 1 cm calibration marker. (D) Representative graph generated by our JawTrack™ software showing 5 s (@ 30 frames per second, fps) of uninterrupted licking based on jaw motion tracking (B,C). The positive peaks (green dots) indicate maximum jaw opening/gape, whereas the negative peaks (red dots) indicate maximum jaw closure; the time stamp of each positive peak was used to calculate lick rate (Hz). Manually added event markers superimposed on the jaw motion graph indicate each pharyngeal swallow onset frame (pink lines) and pharyngeal swallow end frame (blue lines), which were used to calculate swallow rate (Hz) and pharyngeal transit time (PTT, ms). The black dashed line (i.e., video sync marker) moves in synchrony with the corresponding video frame when viewing video clips in our JawTrack™ interface.

characterization of swallowing function: lick-swallow ratio (i.e., number of licks per swallow; a unitless measurement) and PTT (i.e., time between the swallow onset and swallow end frames; measured in milliseconds, ms). Quantification of these four outcome measures is explained in Figures 2B–D. The baseline and endline values were used to determine the exercise treatment effect on tongue motility and swallowing function.

Force-Lickometer Testing

The maximum voluntary lick force (MVLf) of individual rats was measured using a modified force-lickometer system (Force Lickometer for Rat, Med Associates; Fairfax, VT, United States), as shown in Figure 3. Modifications included: (1) adding a site-built vertical lift platform for manual height positioning of individual rats at the lickometer spout, (2) substituting the pin-spout for a double ball-bearing spout that mimics our standard vivarium sipper tubes, and (3) substituting the data acquisition hardware and software with a PowerLab digitizer and LabChart software (ADInstruments; Colorado Springs, CO, United States) to permit graphic display of lick force data in synchrony with video recording of drinking behavior.

Rats underwent force-lickometer testing immediately following VFSS at each timepoint. During testing, rats were individually enclosed in a custom lickometer chamber (clear polycarbonate, 25 cm long × 8 cm wide × 15 cm high) positioned on a custom vertical lift platform within the lickometer system (Figure 3A). Rats readily entered the test chamber when suspended by the tail over the chamber opening. One end-cap has a centered vertical slip opening (5 cm) through which the lickometer spout is inserted to reach the chamber interior; this slit also accommodates raising/lowering of the lickometer

platform for optimal height positioning of each rat during testing (Figure 3B). For each rat, the lickometer funnel reservoir was filled with 30% sucrose to motivate drinking from the spout. The spout was customized with a force-tension mechanism

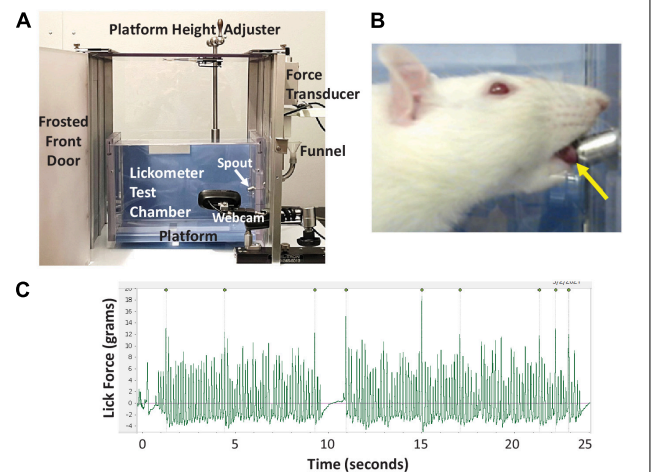


FIGURE 3 | Lickometer methods. (A) Our custom force-lickometer system for use with rodents, with labeled components. During testing, the funnel is filled with a 30% sucrose solution, which rats drink from the spout. (B) Close-up image of a rat drinking from the spout, recorded via the lickometer webcam. Note the protruded tongue contacting the spout (yellow arrow). (C) Representative lick force graph generated by LabChart software showing 25 s of drinking. Peaks with the highest lick forces are automatically labeled; 9 peaks in this case. For this rat, each labeled peak is followed by 10–30 lower force licks (i.e., ~1:20 ratio).

(described in the Tongue Exercise Paradigm subsection below) set to ≤ 4 g as a minimum force requirement during licking to obtain water access. This negligible force requirement was essential to prevent the spout from leaking during testing; however, it was well below the typical lick force of rats and thus did not prevent water access. Tongue contact against the spout was measured in grams (g) by the lickometer's force transducer and digitized (PowerLab 8/30, ADInstruments) for recording and real-time graphic display (LabChart version 8, ADInstruments) on a dedicated computer. A webcam (V-u0018, Logitech; Newark, CA, United States) positioned within the lickometer system (but outside the test chamber) permitted synchronous video recording of drinking behaviors and lick force data via LabChart (**Figures 3A–C**). Up to three 5-min trials were conducted per rat (spaced ~ 15 – 30 min apart) until ~ 2 min of drinking was recorded. Following testing, rats were returned to the home cage with free access to food and water.

Calculation of MVLF for each rat began by identifying the 3–5 longest drinking bouts lasting at least 15 s in the LabChart files. Only lick-force data verified as actual licking at the spout in the synchronized videos were included in data analysis. Additionally, the initial ~ 0.5 s of each bout (~ 3 – 5 licks) was excluded to control for confounding extraneous head/body motion as the rat approached the spout to begin licking, which may artificially inflate the lick force values. From the identified drinking bouts, the peak-to-peak amplitude (g) of individual licks was automatically detected via LabChart (**Figure 3C** and **Supplementary Video 2**) and the corresponding data exported into a Microsoft Excel file. The 10 highest values across the multiple bouts were averaged to obtain each rat's MVLF (Connor et al., 2009; Behan et al., 2012; Krekeler et al., 2020; Glass et al., 2021). As such, this approach is similar to measuring peak plantar pressure while walking at a natural, self-selected speed during kinematic gait analysis (Hessert et al., 2005; Nandikolla et al., 2017; Jasiewicz et al., 2022). The baseline MVLF value was used to determine the individualized exercise program for each rat (described below). MVLF values also were used to determine the exercise treatment effect.

Tongue Exercise Paradigm

Rats participated in a strength endurance tongue exercise paradigm on Day 4 and Day 6 post-tongue injection (see **Figure 1** timeline), which necessitated single housing for the remainder of the study to ensure a personalized medicine approach. On both days, a custom exercise spout (i.e., resisto-spout, **Figure 4**) containing 30% sucrose solution was placed in the home cage of individually housed rats for 12 h overnight (i.e., $\sim 8:00$ PM – $8:00$ AM), coinciding with peak activity in these nocturnal rodents. The spout was customized with a manually adjustable tension spring mechanism (**Figure 4A**) with a force range of ~ 2 – 50 g to accommodate sham exercise (≤ 4 g) and exercise (~ 20 – 35 g, based on unpublished pilot testing) conditions. Each resisto-spout force setting was calibrated immediately prior to use with one of two analog tension force meters (**Figure 4C**): low range (0–10 g; model GD-1, Jonard Tools, Elmsford, NY, United States) for sham exercise or high range (0–50 g; model GD-5, Jonard Tools) for exercise.

For rats in the two exercise groups (i.e., 'control + exercise' and 'CTB-SAP + exercise'), the resisto-spout was set to 50% greater than baseline MVLF (i.e., $50\% > \text{MVLF}$) throughout the overnight exercise period. For example, a rat with a MVLF of 20 g would have the resisto-spout set to 30 g during exercise. Pilot testing (unpublished) revealed that CTB-SAP-injected rats were readily able to overcome this added low-force requirement to access the sucrose solution. Moreover, this $50\% > \text{MVLF}$ target is well below the reported 100–150% increase in tongue force (during voluntary drinking) achieved by rats following an 8-week tongue resistance exercise program (Ma et al., 2017; Cullins et al., 2019; Glass et al., 2021). An important distinction here is that our approach is based on percent effort *above natural drinking behavior*, whereas most other research groups utilized force lickometer systems that permit estimation of maximum lick force capability (Connor et al., 2009; Behan et al., 2012; Cullins et al., 2019; Krekeler et al., 2020; Glass et al., 2021), thereby allowing the exercise target intensity level to be set to a percentage *below maximum effort* (i.e., 50–80% of maximum effort), similar to the maximum bench press test to estimate training intensity percentages for weight-lifting (Grgic et al., 2020). Here, we were interested in the effect of low intensity exercise; therefore, as a starting point, we chose a relatively low effort requirement above MVLF (i.e., $50\% > \text{MVLF}$) as our target for low intensity tongue resistance exercise. Resistospouts for rats in the two sham exercise groups (i.e., 'control + sham exercise' and 'CTB-SAP + sham exercise') were set to ≤ 4 g, consistent with the negligible force setting used during force-lickometer testing. Resistospout force settings for all four groups were recorded for comparisons with and between groups.

Rats had free access to standard food pellets and enrichment materials during exercise/sham exercise, thus, the only cage-level difference was the substitution of the resisto-spout bottle (containing 30% sucrose solution) for the standard vivarium water bottle. Overnight fluid intake (in grams) was measured for each exercise night to estimate the level of exercise participation (i.e., lick frequency). We hypothesized that overnight fluid intake would be similar within and between rats over time, thus any identified exercise treatment effects would be due to differences in exercise level and group assignment (control vs. CTB-SAP) rather than lick frequency.

Live Magnetic Resonance Imaging of the Brainstem and Tongue

In vivo MRI scans were performed on a subset of 20 rats on Day 9 to determine the absence or presence of degeneration in the brainstem and tongue using a 7 T Bruker AVANCE III BioSpec MRI scanner (Bruker BioSpin Inc., Billerica, MA, United States) and a four-element phased-array radiofrequency (RF) coil. Rats were anesthetized with 1.0–3.5% isoflurane in oxygen via a nose cone and placed in supine (for brainstem imaging) or prone (for tongue) position. A physiological monitoring and gating system (SA Instruments, Inc., Stony Brook, NY, United States) was used to monitor vital signs and for triggering respiratory-gated MRI scans. Body temperature was maintained at 36 – 37°C with warm air circulating in the magnet bore. T2-weighted (T2W) MRI coronal and axial brain scans and axial tongue

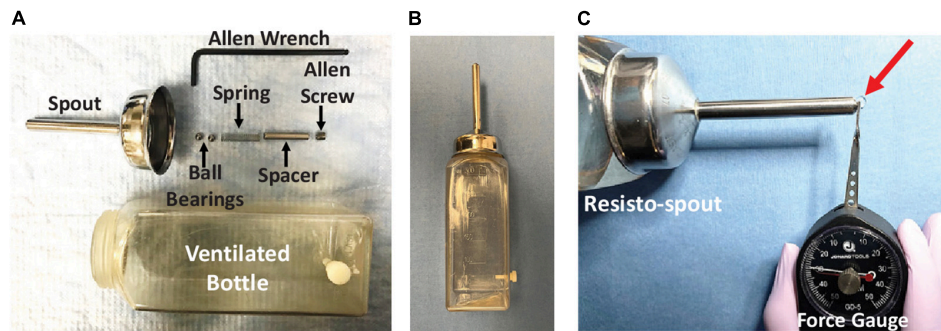


FIGURE 4 | Resisto-spout design and calibration. **(A)** Our custom exercise spout (i.e., resisto-spout) with disassembled components (labeled), designed for home-cage use by individual rats. **(B)** The assembled resisto-spout replaces the standard vivarium water bottle during the overnight (12 h) exercise period. **(C)** Demonstration of lick force calibration (in grams) using a hand-held analog tension force meter (gauge). The spout force setting is manually adjusted to the target level for an individual rat by turning the Allen screw further in/out of the spout shaft, followed by re-testing with the force gauge. To measure the resisto-spout force setting, the resisto-spout and force gauge are secured in each hand and positioned perpendicular on an immovable tabletop. The tip of the gauge lever is precisely positioned to contact only the ball bearing that slightly protrudes from the spout tip. Pressure is incrementally applied to the ball bearing by manually moving the gauge dial slowly toward the resisto-spout in a single smooth, uninterrupted manner. The “reading” on the dial at which liquid begins to leak from the spout tip (red arrow) corresponds with the resisto-spout force setting.

scans were performed with fat-suppression using multi-slice RARE (rapid acquisition with relaxation enhancement) spin echo sequence with a b -value of 0 or smaller than 30 s/mm^2 . Diffusion-weighted (DW) MRI sagittal scans of the brainstem were acquired using standard spin-echo DW sequence with a b -value of $750\text{--}1200 \text{ s/mm}^2$. Respiratory gating was used to trigger each scan. Other imaging parameters included: 15–30 slices, slice thickness = 0.8 mm , in-plane resolution of $70\text{--}140 \mu\text{m}$, TR (repetition time) = 2 s , TE (echo time) = 35 ms , RARE factor = 2, and 2 averages. Image analysis and processing were performed in ParaVision 6.0.1 software (Bruker BioSpin Corporation). The volume (mm^3) of the brain 4th ventricle was measured as the sum of the areas multiplied by the slice thickness on the brain DW and T2W sagittal images at Bregma position – $0.8, 0.0$, and 0.8 mm . Axial T2W MRI was utilized to capture the oral tongue volume (cm^3), which consisted of the anterior (mobile) body from the apex of the tongue to the root of the lower incisor teeth. Tongue volume was measured as the sum of the areas multiplied by the slice thickness on the tongue T2W axial images. The thickness (mm) of the tongue body was measured as the distance from dorsal to ventral surface of the tongue on three T2W axial images at $4.0\text{--}5.6 \text{ mm}$ from the anterior apex of the tongue and calculated with an average value for each rat. Similarly, the width (mm) of the tongue blade was measured as the distance from left to right lateral surface of the tongue on five images at $3.2\text{--}6.4 \text{ mm}$ from the apex of the tongue and calculated with an average value for each rat. The width (mm) of the tongue root was measured on the axial T2W image at the level of the root of the lower incisor teeth. Segmentations were performed for quantification of the volume of the brain 4th ventricle and tongue volume, thickness, and width using Segment (Medviso AB, Lund, Sweden) or ImageJ.

Statistical Analysis

Investigators involved with data collection were blinded to experimental group assignment until the study databases were

created in either IBM SPSS Statistics 24 or SAS/STAT® 13.1 software, which were used to perform statistical analyses. Data outliers for each variable were identified and re-checked for accuracy, but not removed from the dataset. The following dependent variables were assessed: (1) VFSS – lick rate (Hz), swallow rate (Hz), and PTT (ms); (2) force-lickometer – MVLF (g); (3) exercise intensity (g); (4) overnight fluid intake (g) during exercise; and (5) MRI – brain 4th ventricle volume (mm^3), tongue volume (cm^3), tongue thickness (mm), tongue blade width (mm), and tongue root width (mm). Averaged values for each animal were used for VFSS, force-lickometer, and MRI tongue (thickness and width) data, whereas raw/unaveraged data were used for fluid intake and MRI volume data (i.e., single value per animal per time point). Data for each variable were normally distributed (Shapiro–Wilk test, $p > 0.05$) and thus appropriate for parametric statistics. However, non-parametric statistics were used for MRI data to accommodate the small and unbalanced sample sizes (4–6 rats per group).

Resisto-spout force settings and corresponding exercise intensity were compared between groups using one-way analysis of variances (ANOVAs) and visualized using overlaid boxplots and dot plots. Overnight fluid intake was compared between experimental groups using a mixed (group \times time) repeated measures ANOVA (RMANOVA) and visualized using overlay plots (boxplots and dot plots). A separate Generalized Linear Regression Model (GLM) was fitted to assess the effect of exercise treatment on lick/swallow function and MVLF outcomes at Day 8 when controlling for baseline values. Interaction effects between baseline values and experimental groups were explored for each dependent variable to verify the identified treatment effects were not influenced by baseline values (i.e., no significant interactions). Bonferroni *post hoc* multiple comparison tests were performed to create 95% confidence intervals (CIs) and corresponding p -values for all pairwise differences between groups while controlling the familywise Type 1 error rate. The R^2 scoring metric was used to measure the goodness of fit

for the GLM models. Results were visualized via scatterplots with fitted regression lines from the GLM models. Additionally, overlay plots (boxplots and dot plots) were used to illustrate and summarize the descriptive statistics of lick/swallow function and MVLF outcomes at Day 8, with asterisks denoting the significant GLM findings. For MRI data, the non-parametric Kruskal–Wallis test (one-way ANOVA on ranks) was used to explore statistically significant differences between experimental groups for each outcome measure, followed by *post hoc* Dwass–Steel–Critchlow–Fligner multiple comparisons based on pairwise rankings. For all statistical tests, the significance threshold was set at $\alpha = 0.05$.

RESULTS

All rats tolerated the experimental procedures without developing signs of stress or morbidity. As is expected with behavioral experiments, missing data occurred for each dependent variable for a variety of reasons (e.g., behavioral non-compliance, leaky resisto-spouts, technical difficulties, etc.). However, the group sample sizes for each behavioral test remained between 7 and 12 rats (summarized in each subsection below), which our prior studies have demonstrated is sufficient to detect statistical differences between groups (Lind et al., 2018).

Tongue Exercise Paradigm

Meaningful exploration of potential treatment effects warrants full transparency of the rats' participation in the treatment paradigm in order to draw appropriate conclusions. Thus, we have summarized essential details and data below.

Baseline Maximum Voluntary Lick Force and Corresponding Exercise Intensity Level

Rats with inconclusive baseline MVLF values ($n = 3$) were allocated to sham exercise (i.e., ≤ 4 g force setting), leaving 45 rats for MVLF assessment. There was no significant difference in baseline MVLF between the four experimental groups ($F_{3,41} = 0.605$, $p = 0.616$), as shown in **Figure 5A** and summarized in **Table 2**. As expected (data not shown), there was a significant difference in exercise intensity between the four experimental groups ($F_{3,44} = 1,017.71$, $p < 0.001$), with *post hoc* comparisons revealing statistically significant differences between sham exercise and exercise groups ($p < 0.001$ for all comparisons) but not within each exercise group ($p = 1.000$ for all comparisons). As shown in **Figure 5B** and **Table 2**, the mean resisto-spout force setting was ~ 29 g for both groups of exercise-treated rats, which corresponded to $\sim 40\%$ > MVLF exercise intensity level (also shown in **Figure 5C** and **Table 2**).

Importantly, exercise intensity varied between rats in the two exercise groups ('control + exercise' and 'CTB-SAP + exercise'), ranging from 10 to 53% higher than baseline MVLF values. While our initial plan was to use 50% > MVLF intensity for all rats, we elected to reduce the force requirement for rats that immediately began biting the spout at the onset of the overnight exercise period (i.e., 6 'control + exercise' rats and 5 'CTB-SAP + exercise' rats). For these cases, the threshold force requirement was reduced until stereotypical

licking behavior resumed. Additionally, the analog technology of our resisto-spout allowed us to get close to, but typically a few grams away from, the target force setting; thus, some rats had slightly above or below the target 50% > MVLF value. Despite this variability, there was no significant difference in exercise intensity between the two groups ($F_{1,20} = 0.078$, $p = 0.783$). The mean (standard error) exercise intensity levels were 40.1% (3.62) for the 'control + exercise' group and 38.5% (4.27) for the 'CTB-SAP + exercise' group. Graphic display of the data distribution is shown in **Figure 5C**. As a reminder, the resisto-spout for the two sham-exercise groups ('control + sham exercise' and 'CTB-SAP + sham exercise') was set to a negligible (≤ 4 g) force requirement for fluid access, which was well below each rat's MVLF and thus did not constitute exercise for these two groups.

Overnight Fluid Intake to Estimate Exercise Participation

Of the two exercise nights (Days 4 and 6), rats consumed more 30% sucrose solution on the 2nd night (i.e., main effect of time; $F_{1,31} = 6.533$, $p = 0.016$). However, there was no significant difference in overnight fluid intake between experimental groups (main effect, $F_{3,31} = 0.320$, $p = 0.811$), nor was there a time \times group interaction ($F_{3,31} = 0.316$, $p = 0.813$). Thus, fluid intake (30% sucrose) was similar between groups at both exercise timepoints (Day 4 and Day 6). Prior to this study, we determined that naïve (non-injected, non-exercised) rats weighing ~ 350 g consumed an average of 14 g water during a 12-h overnight period (unpublished), which is consistent with published values of 9–12 g water per 100 g rat per 24 h (Holdstock, 1973). The rats in this study drank an average of 29 g sucrose solution per night (**Table 3**), which equates to ~ 32 mL (i.e., 1.1 g/mL 30% sucrose solution). Thus, the rats consumed ~ 2 times more volume than normal each night, which demonstrates the added value of providing sucrose rather than plain water to motivate enhanced participation (i.e., higher lick frequency) during the exercise program. Moreover, using published data of 200 licks per mL sucrose solution in naïve rats (Hsiao and Fan, 1993), we estimated that our rats licked approximately 6,400 times (i.e., 32 mL average overnight intake \times 200 licks per mL sucrose solution) per night. However, their stereotypical lick pattern consisted of intermittently higher lick forces to obtain water from the spout, followed by multiple lower lick forces to "manage" the dispensed water (i.e., $\sim 1:20$ ratio, as shown in **Figure 3**). This equates to an estimated 320 "forceful" licks per rat (i.e., $6,400 \div 20$) to access the sucrose solution during each 12-h exercise period, which is consistent with a high repetition exercise paradigm.

Tongue Exercise Treatment Effect on Behavioral Videofluoroscopic Swallow Study Measures of Lick/Swallow Function

As summarized in **Table 4**, three of the four VFSS outcome measures were significantly different between the four

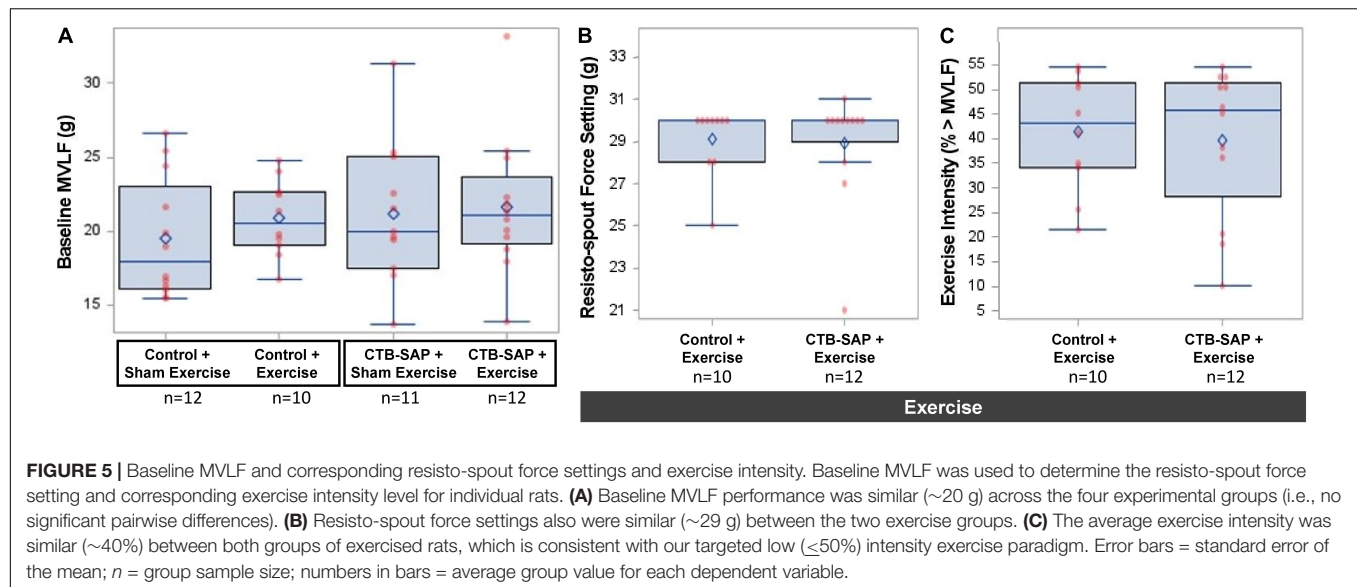


TABLE 2 | Descriptive statistics for baseline maximum voluntary lick force (MVLF) and corresponding resisto-spout force settings and exercise intensity by experimental group.

| Experimental group | Sample size | Baseline MVLF (g) | | Resisto-spout force setting (g) | | Exercise intensity (% > MVLF) | |
|---------------------------|-------------|-------------------|------|---------------------------------|-------|-------------------------------|------|
| | | Mean | SEM | Mean | SEM | Mean | SEM |
| 'Control + Sham Exercise' | 12 | 19.5 | 1.18 | | | | |
| 'Control + Exercise' | 10 | 20.9 | 0.82 | 29.05 | 0.54 | 40.1 | 3.62 |
| 'CTB-SAP + Sham Exercise' | 11 | 21.2 | 1.44 | | | | |
| 'CTB-SAP + Exercise' | 12 | 21.7 | 1.37 | 28.92 | 0.783 | 38.5 | 4.27 |

SEM, standard error of the mean. Exercise intensity (i.e., % > MVLF) is applicable only to the two exercise groups because the sham exercise groups had a negligible (i.e., ≤ 4 g) lick force requirement that was below their spontaneous lick force during voluntary drinking.

TABLE 3 | Descriptive statistics for overnight fluid intake during exercise by experimental group and exercise time point (Days 4 and 6).

| Experimental group | Sample size | Fluid intake (grams) | | | | | |
|---------------------------|-------------|----------------------|-----|-------|-----|-------------|------------|
| | | Day 4 | | Day 6 | | Average | |
| | | Mean | SEM | Mean | SEM | Mean | SEM |
| 'Control + Sham Exercise' | 7 | 29.3 | 4.4 | 33.7 | 3.5 | 31.5 | 3.4 |
| 'Control + Exercise' | 8 | 23.2 | 4.2 | 30.9 | 3.2 | 27.0 | 3.2 |
| 'CTB-SAP + Sham Exercise' | 9 | 27.3 | 3.9 | 30.6 | 3.1 | 29.0 | 3.0 |
| 'CTB-SAP + Exercise' | 11 | 28.2 | 3.5 | 31.5 | 2.8 | 29.9 | 2.7 |
| Grand total | | | | | | 29.3 | 3.1 |

SEM, standard error of the mean. Fluid = 30% sucrose in standard vivarium water (pH 3.5).

experimental groups when controlling for baseline values: lick rate ($F_{4,40} = 9.97$, $p < 0.001$), swallow rate ($F_{4,37} = 9.59$, $p < 0.0001$), and inter-swallow interval ($F_{4,36} = 6.28$, $p = 0.0006$). The model for PTT was weak ($R^2 = 0.28$) and not statistically significant ($F_{4,37} = 1.29$, $p = 0.2924$). Importantly, there was no significant interaction effect of baseline and experimental group for the VFSS outcome measures, thus confirming that any subsequently identified treatment effects via *post hoc* testing (summarized separately below for each

VFSS outcome measure) were not influenced by baseline values. **Figures 6A–D** summarizes the GLM data for each VFSS outcome measure as regression plots with baseline versus endline values for individual animals within each experimental group. **Figures 6E–H** shows overlay plots summarizing the corresponding descriptive statistics for each outcome measure at Day 8 to highlight the identified treatment effects. Descriptive statistics for each VFSS outcome measure are presented in **Table 5**.

TABLE 4 | GLM fitted model summary table for behavioral outcome measures at day 8 when controlling for baseline values.

| Outcome measure | Parameter | Estimate | Standard Error of Estimate | t-Value | Pr > t |
|--|-----------------------------|----------|-------------------------------|---------|-------------------|
| Lick Rate (Hz) ($R^2 = 0.50$) $p < 0.0001$ | Intercept | 4.796 | 0.910 | 5.27 | <0.0001 |
| | Lick Rate Baseline Value | 0.293 | 0.127 | 2.31 | 0.0261 |
| | Control + Exercise | 0.058 | 0.111 | 0.52 | 0.6054 |
| | CTB-SAP + Sham Exercise | -0.511 | 0.105 | -4.85 | <0.0001 |
| | CTB-SAP + Exercise | -0.197 | 0.106 | -1.87 | 0.0689 |
| | Control + Sham Exercise | 0 | . | . | . |
| Swallow Rate (Hz) ($R^2 = 0.51$) $p < 0.0001$ | Intercept | 0.722 | 0.184 | 3.93 | 0.0004 |
| | Swallow Baseline Value | 0.441 | 0.132 | 3.33 | 0.002 |
| | Control + Exercise | -0.037 | 0.086 | -0.44 | 0.6651 |
| | CTB-SAP + Sham Exercise | -0.282 | 0.083 | -3.39 | 0.0017 |
| | CTB-SAP + Exercise | -0.283 | 0.085 | -3.31 | 0.0021 |
| | Control + Sham Exercise | 0 | . | . | . |
| Lick-Swallow Ratio ($R^2 = 0.41$) $p = 0.0006$ | Intercept | 1.471 | 1.650 | 0.89 | 0.3785 |
| | Lick-Swallow Ratio Baseline | 0.656 | 0.289 | 2.27 | 0.0293 |
| | Control + Exercise | 0.514 | 0.807 | 0.64 | 0.5284 |
| | CTB-SAP + Sham Exercise | 2.413 | 0.803 | 3.01 | 0.0048 |
| | CTB-SAP + Exercise | 2.335 | 0.819 | 2.85 | 0.0072 |
| | Control + Sham Exercise | 0 | . | . | . |
| PTT (ms) ($R^2 = 0.12$) $p = 0.2924$ | Intercept | 56.027 | 17.118 | 3.27 | 0.0023 |
| | PTT Baseline Value | 0.299 | 0.194 | 1.54 | 0.1314 |
| | Control + Exercise | 3.701 | 4.376 | 0.85 | 0.4031 |
| | CTB-SAP + Sham Exercise | 8.638 | 4.388 | 1.97 | 0.0565 |
| | CTB-SAP + Exercise | 3.373 | 4.272 | 0.79 | 0.4348 |
| | Control + Sham Exercise | 0 | . | . | . |
| MVLF (g) ($R^2 = 0.28$) $p = 0.0183$ | Intercept | 18.602 | 3.338 | 5.57 | <0.0001 |
| | MVLF Baseline Value | 0.073 | 0.164 | 0.44 | 0.6602 |
| | Control + Exercise | 0.094 | 1.598 | 0.06 | 0.9535 |
| | CTB-SAP + Sham Exercise | -4.181 | 1.607 | -2.6 | 0.0135 |
| | CTB-SAP + Exercise | 1.214 | 1.612 | 0.75 | 0.4565 |
| | Control + Sham Exercise | 0 | . | . | . |

'Control + Sham Exercise' was considered as the reference for experimental group pairwise comparisons for each outcome measure. Statistically significant pairwise comparisons are bolded and highlighted in yellow.

Tongue Exercise Mitigates Deficits in Lick Rate but Not Swallow Timing Measures in Cholera Toxin B Conjugated to Saporin-Injected Rats

Lick Rate

As hypothesized, lick rate was significantly slower in the 'CTB-SAP + sham exercise' group compared to the 'control + sham exercise' group [$d = 0.51$, 95% CI = (0.23, 0.80), $p < 0.001$], thus demonstrating that CTB-SAP causes impaired tongue motility congruent with our prior study (Lind et al., 2018). Also as hypothesized, lick rate in the 'CTB-SAP + exercise' group was not statistically different from the 'control + sham exercise' group [$d = 0.21$, 95% CI = (-0.065, 0.50), $p = 0.0689$] but was significantly faster than the 'CTB-SAP + sham exercise' group [$d = 0.29$, 95% CI = (0.02, 0.58) $p < 0.042$], thus providing evidence of a beneficial exercise treatment effect. Interestingly, the exercise intensity training was sufficiently low to result in no significant difference in lick rate between the two control groups: 'control + sham exercise' and 'control + exercise' [$d = 0.25$, 95% CI = (-0.035, 0.54), $p = 0.6054$]. These findings, summarized

in **Table 4** and **Figure 6E**, demonstrate that targeted tongue resistance exercise in CTB-SAP-injected rats mitigates tongue motility dysfunction.

Swallow Rate

As hypothesized, swallow rate was significantly slower in the 'CTB-SAP + sham exercise' group compared to 'control + sham exercise' rats [$d = 0.28$, 95% CI = (0.05, 0.50), $p = 0.0017$], thus demonstrating that CTB-SAP causes impaired swallow function congruent with our prior study (Lind et al., 2018). However, swallow rate also was significantly slower for the 'CTB-SAP + exercise' group compared to 'control + sham exercise' rats [$d = 0.34$, 95% CI = (0.11, 0.57), $p < 0.0021$], but there was no significant difference in swallow rate between the two CTB-SAP groups [$d = 0.06$, 95% CI = (-0.15, 0.28, $p = 0.9969$]. Thus, contrary to our hypothesis, tongue exercise had no apparent beneficial treatment effect on swallow rate in our model. Additionally, there was no significant difference in swallow rate between the two control groups: 'control + sham

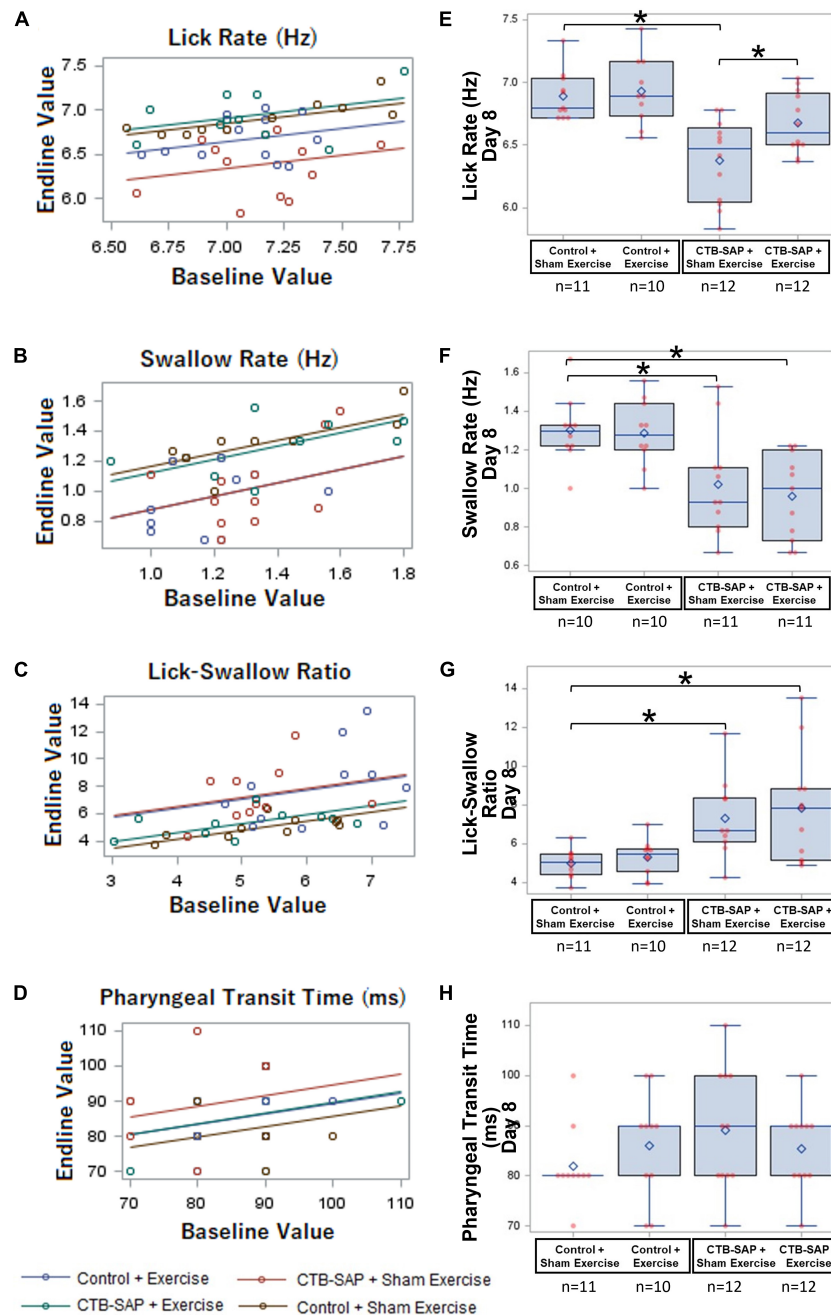


FIGURE 6 | Effect of tongue exercise on VFSS-based lick and swallow function. **(A–D)** Scatter plots of baseline vs. endline values and the regression lines from the fitted generalized regression model are shown for each VFSS outcome measure. The estimated difference between any pair of groups is the vertical distance between the corresponding lines. Significant differences between the regression lines are summarized in **(E–H)** as corresponding overlay boxplots (median, quartiles, and whiskers; mean = diamond) and dot plots (individual data points) to highlight the significant treatment effects at the Day 8 time point in our CTB-SAP model. Data points outside the whiskers are considered mild outliers; there were no extreme outliers. Note that only 3 of the 4 VFSS outcome measures (i.e., lick rate, swallow rate, and lick-swallow-ratio) were significantly impaired in the ‘CTB-SAP + sham exercise’ group, but only lick rate was significantly improved in the ‘CTB-SAP + exercise’ group. Specifically, compared to the ‘control + sham exercise’ group (lick rate was significantly slower in the ‘CTB-SAP + sham exercise’ group ($p < 0.001$) but not the ‘CTB-SAP + exercise’ group ($p = 0.0689$)). Moreover, lick rate was significantly different between the two CTB-SAP groups (i.e., faster for the ‘CTB-SAP + exercise’ group; $p < 0.042$). Thus, our CTB-SAP model develops impaired lick motility that is beneficially improved by targeted tongue exercise. **(B)** Swallow rate was significantly slower in both CTB-SAP groups (‘CTB-SAP + sham exercise’: $p = 0.0017$; ‘CTB-SAP + exercise’: $p = 0.0021$) compared to the ‘control + sham exercise’ group, but targeted tongue exercise had no effect on this VFSS outcome measure. **(C)** Lick-swallow ratio was significantly lower in both CTB-SAP groups (‘CTB-SAP + sham exercise’: $p = 0.0048$; ‘CTB-SAP + exercise’: $p = 0.0072$) compared to the ‘control + sham exercise’ group but was unaffected by tongue exercise. **(D)** Pharyngeal transit time was not significantly different between experimental groups. Error bars = standard error of the mean; n = group sample size; asterisks indicate significant difference ($p < 0.05$) between pairwise groups.

TABLE 5 | Descriptive statistics for behavioral outcome measures by experimental group at day 8.

| Outcome Measures | CTB SAP + Exercise | | CTB SAP + Sham Exercise | | Control + Exercise | | Control + Sham Exercise | |
|--------------------|--------------------|------|-------------------------|------|--------------------|------|-------------------------|------|
| | Mean | SEM | Mean | SEM | Mean | SEM | Mean | SEM |
| Lick Rate (Hz) | 6.67 | 0.07 | 6.38 | 0.1 | 6.93 | 0.09 | 6.89 | 0.06 |
| Swallow Rate (Hz) | 0.96 | 0.07 | 1.02 | 0.08 | 1.29 | 0.05 | 1.3 | 0.06 |
| Lick Swallow Ratio | 7.86 | 0.86 | 7.33 | 0.6 | 5.3 | 0.29 | 4.99 | 0.23 |
| PTT (ms) | 85.45 | 2.47 | 89.09 | 3.68 | 86 | 3.4 | 82 | 2.49 |
| MVLF (g) | 21.37 | 1.4 | 15.96 | 0.76 | 20.22 | 1.32 | 20 | 0.68 |

exercise' and 'control + exercise' [$d = 0.014$, 95% CI = (-0.22, 0.25), $p = 0.6651$]. These findings are summarized in **Table 4** and **Figure 6F**.

Lick-Swallow Ratio

As hypothesized, lick-swallow ratio was significantly higher in the 'CTB-SAP + sham exercise' group compared to the 'control + sham exercise' group [$d = 2.34$, 95% CI = (0.18, 4.5), $p = 0.0048$], which provides a new outcome measure for assessing treatment effects in this rat model. However, lick-swallow ratio also was significantly higher for the 'CTB-SAP + exercise' group compared to 'control + sham exercise' rats [$d = 0.34$, 95% CI = (0.11, 0.57), $p < 0.0072$], but there was no significant difference in lick-swallow ratio between the two CTB-SAP groups [$d = 0.52$, 95% CI = (-1.58, 2.63), $p = 0.9254$] or the two control groups [$d = 0.31$, 95% CI = (-1.92, 2.55), $p = 0.5284$]. Thus, similar to the results of swallow rate, tongue exercise had no apparent beneficial treatment effect on lick-swallow ratio. These findings are summarized in **Table 4** and **Figure 6G**.

Pharyngeal Transit Time

Although not significant, the 'CTB-SAP + sham exercise' group had the longest PTT. Moreover, the PTT distribution for the 'CTB-SAP + exercise' group was similar to the two control groups, suggesting a potential beneficial effect of tongue exercise may emerge with larger group sample sizes. These findings are summarized in **Table 4** and **Figure 6H**.

Lick Force Deficit During Voluntary Drinking in Cholera Toxin B Conjugated to Saporin-Injected Rats Is Mitigated by Targeted Strength Endurance Exercise

As summarized in **Table 4**, MVLF was statistically different between the four experimental groups at Day 8 when controlling for baseline values ($F_{4,35} = 3.42$, $p = 0.0183$), as shown in **Figure 7A**. As hypothesized, the 'CTB-SAP + sham exercise' group performed significantly worse (i.e., had lower MVLF values) than the 'control + sham exercise' group [$d = 5.405$, 95% CI = (1.16, 9.65), $p = 0.0135$], thus providing novel evidence of a lick force deficit in this model. Also as hypothesized, MVLF was significantly higher in the 'CTB-SAP + exercise' group compared to the 'CTB-SAP + sham exercise' group [$d = 5.405$, 95% CI = (1.161, 9.649), $p = 0.0016$]. Interestingly, MVLF for the 'CTB-SAP + exercise' group was significantly higher than

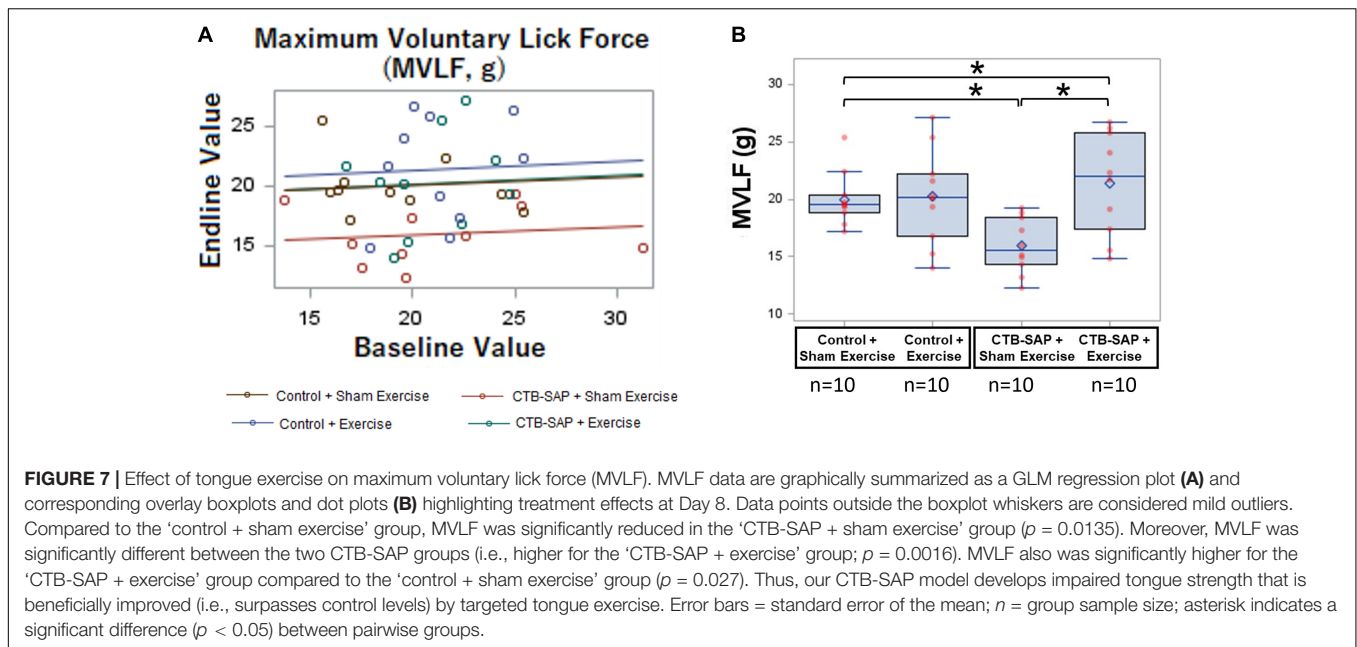
the 'control + sham exercise' group [$d = 1.4$, 95% CI = (-2.87, 5.6), $p = 0.027$] but was not significantly different from the 'control + exercise' group [$d = 1.15$, 95% CI = (-3.1, 5.39), $p = 0.4818$]. Moreover, there was no significant difference between the two control groups: 'control + sham exercise' and 'control + exercise' [$d = 0.218$, 95% CI = (-4.03, 4.46), $p = 0.9535$]. Collectively, these results demonstrate that our CTB-SAP rat model develops impaired tongue strength (i.e., lick force), and a strength-endurance tongue exercise paradigm preserves tongue strength at/above control levels. **Figure 7B** graphically summarizes these findings, and descriptive statistics are presented in **Table 5**.

Tongue Exercise Mitigates Structural Degeneration in the Brainstem and Tongue of Cholera Toxin B Conjugated to Saporin-Injected Rats

Magnetic Resonance Imaging of the brainstem and tongue suggest further degenerative changes in the hypoglossal-tongue axis; however, statistical significance was reached only for some of the tongue but not brainstem MRI measures. Descriptive statistics for all MRI outcome measures are presented in **Table 6**.

For MRI of the brain, no significant differences in the 4th ventricle volume were identified across experimental groups ($p = 0.075$). However, as shown in **Figure 8**, 4th ventricle volume was notably higher in 'CTB-SAP + sham exercise' rats compared to the other three groups, suggesting significance may emerge with larger group sample sizes that permit application of more robust statistical analysis approaches.

For MRI of the tongue, statistically significant differences were identified for tongue volume ($p = 0.029$) and thickness ($p = 0.0395$) but not for tongue width measured at either the blade ($p = 0.251$) or root ($p = 0.1805$) regions. As shown in **Figure 9**, tongue volume and thickness were notably greater in the 'CTB-SAP + sham exercise' group compared to the other three groups. Specifically, tongue volume was significantly greater in the 'CTB-SAP + sham exercise' group compared to 'control + exercise' rats ($p = 0.05$). Although not significant, tongue volume was greater in 'CTB-SAP + sham exercise' rats compared to 'CTB-SAP + exercise' ($p = 0.08$) and 'control + sham exercise' ($p = 0.18$) groups. Tongue thickness was significantly greater in 'CTB-SAP + sham exercise' compared to 'control + sham exercise' ($p = 0.05$) groups. We also qualitatively observed increased bilateral hyperintensity in the intrinsic muscles (i.e., verticalis



and transversus muscles) of the anterior tongue in 'CTB-SAP + sham exercise' rats vs. controls. The diffuse-pattern of the hyperintensity is clearly visible and is indicative of muscle fiber inflammation and infiltrations of fatty replacement of atrophied muscle fibers in 'CTB-SAP + sham exercise' rats. Collectively, these preliminary results suggest hypertrophy of the tongue and a beneficial treatment effect of tongue exercise on tongue volume and thickness in CTB-SAP-injected rats.

DISCUSSION

The main findings from this study were that: (1) sham exercise-treated CTB-SAP rats had behavioral evidence of dysphagia (i.e., reduced lick and swallow rates as previously shown, (Lind et al., 2018) and longer lick-swallow ratios) and reduced tongue strength (i.e., lick force); (2) our strength endurance tongue exercise program resulted in preserved lick rate and lick force in CTB-SAP rats but had no effect on swallow timing deficits; (3) structural degeneration in the brainstem and tongue in sham exercise-treated CTB-SAP rats was observed via *in vivo* MRI; and (4) tongue exercise appears to mitigate this structural degeneration in CTB-SAP rats. These novel findings collectively suggest that a strength endurance exercise program targeting the tongue may be a feasible treatment for hypoglossal-tongue axis degeneration in motor neuron diseases such as ALS.

Importantly, we purposely chose to start the tongue exercise program on Day 4 based on published work showing it takes 3 days following intrapleural injection of CTB-SAP (or unconjugated CTB in controls animals) for retrograde labeling of phrenic motor neurons (Mantilla et al., 2009). We estimate a similar (but likely shorter) time frame for XII MN labeling following CTB-SAP (or unconjugated CTB) injection into the tongue. Moreover, pilot data from a few rats at Day 4 showed that

XII degeneration has already started, yet VFSS and lickometer testing at Day 4 did not reveal any significant changes in licking/swallowing function. This collective preliminary data suggest the underlying XII degenerative process at Day 4 precedes the clinical onset of behavioral licking/swallowing deficits, as previously reported in the MND literature (Kiernan et al., 2011; Rattray et al., 2017; Salvadores et al., 2017). Thus, by starting the exercise program on Day 4, we were specifically attempting to prevent clinical onset and progression of dysphagia while also beneficially altering the underlying degenerative disease process in this model.

Tongue Exercise Has a Beneficial Treatment Effect on Tongue Motility and Strength but Not Swallow Timing Measures

Here, we hypothesized that tongue exercise would preserve hypoglossal-tongue axis function and strength in CTB-SAP rats. This hypothesis held true for lick rate (i.e., tongue motility) and lick force (i.e., tongue strength), but not for swallow timing measures. Specifically, the swallow rate and lick-swallow ratio deficits identified in sham exercise-treated CTB-SAP rats were not any different from the exercised CTB-SAP rats; thus, there was no beneficial or harmful effect of tongue exercise on VFSS-derived swallow timing measures. These results perhaps can be attributed to lick versus swallow pattern generators (CGSs) in the brainstem (Jean, 2001; Boughter et al., 2007; Moore et al., 2014). Licking mainly involves the muscles of the tongue which are innervated by CN XII (hypoglossal) and the muscles of the jaw which are innervated by CN V (trigeminal), whereas the act of swallowing is more complex and extends beyond CNs V and XII to include CN VII (facial), CN IX (glossopharyngeal), CN X (vagus), CN XI (spinal accessory), and cervical spinal nerves.

TABLE 6 | Descriptive statistics for MRI outcome measures by experimental group at day 9.

| Outcome Measures | CTB SAP + Exercise | | CTB SAP + Sham Exercise | | Control + Exercise | | Control + Sham Exercise | |
|---|--------------------|-------|-------------------------|-------|--------------------|-------|-------------------------|-------|
| | Mean | SEM | Mean | SEM | Mean | SEM | Mean | SEM |
| Tongue Volume (cm ³) | 0.495 | 0.008 | 0.543 | 0.014 | 0.489 | 0.012 | 0.488 | 0.015 |
| Tongue thickness (mm) | 5.123 | 0.117 | 5.791 | 0.237 | 5.097 | 0.302 | 4.815 | 0.112 |
| Tongue width at root (mm) | 7.233 | 0.231 | 7.404 | 0.275 | 7.693 | 0.115 | 7.086 | 0.231 |
| Tongue width at blade (mm) | 8.462 | 0.280 | 8.836 | 0.167 | 8.160 | 0.249 | 8.604 | 0.251 |
| 4th Ventricle volume (mm ³) | 3.893 | 0.402 | 5.052 | 0.337 | 3.431 | 0.393 | 3.729 | 0.279 |

While the selective hypoglossal motor neuron degeneration in our rat model negatively impacts both lick and swallow CPGs, tongue exercise appears to have a beneficial effect mainly on the relatively simplistic CPG for licking. This suggests that our tongue exercise paradigm is highly specific for targeting the lick CPG but not the swallow CPG, even though rats were swallowing while performing “forceful licks” against the resisto-spout throughout the overnight exercise session. While this finding may simply be a limitation of behavioral research with rats (and laboratory animals in general), this species nonetheless provides an invaluable tool for improving the scientific understanding of normal and disordered swallowing to accelerate the advancement of personalized dysphagia treatment.

Translational Methodology for Advancing Personalized Dysphagia Treatment

In this study, we used our rat model of dysphagia to develop translational methodology for a personalized strength endurance tongue exercise to ultimately benefit patients with MNDs. Specifically, rats performed an estimated 320 forceful licks against the exercise spout (i.e., resisto-spout) for fluid access per night of exercise. Importantly, the exercise program took place in each rat’s home cage, without water restriction, in an attempt to mimic personalized home exercise programs traditionally utilized for dysphagia rehabilitation. The resisto-spout force requirement during exercise was based on each individual rat’s MVLF at baseline force-lickometer testing. Thus, our approach resembled the dysphagia rehabilitation literature in which each patient’s baseline tongue force is measured by compressing a pneumatic pressure sensor between the tongue and hard palate, which is then used to develop a personalized tongue strengthening program (Lazarus et al., 2003, 2014; Robbins et al., 2005; Lazarus, 2006; Yeates et al., 2008; Steele et al., 2013; Park et al., 2015). Importantly, these prior clinical studies used a low-repetition/high-resistance exercise paradigm with long rest intervals (Lazarus et al., 2003, 2014; Robbins et al., 2005; Lazarus, 2006; Yeates et al., 2008) that resembles a body builder’s workout to increase muscle mass (Mangine et al., 2015).

A low-repetition/high-resistance tongue exercise paradigm has also been tested in a variety of rat models (e.g., ALS, primary aging, and Parkinson’s disease). The approach requires an extensive behavioral conditioning program (via water restriction) to train rats to press the tongue progressively harder against a force transducer to receive water rewards, typically 50–80% of maximum lick force for ~20 “tongue presses” during brief

(<10-min) treatment sessions, 3–5 days/week (Smittkamp et al., 2010; Ciucci et al., 2011, 2013; Kletzien et al., 2013; Cullins et al., 2018; Krekeler et al., 2018). Though beneficial effects were shown for rat models of primary aging (Kletzien et al., 2013; Cullins et al., 2018; Krekeler et al., 2018) and Parkinson’s disease (Ciucci et al., 2011, 2013), this tongue exercise training paradigm in the ALS rat model was detrimental, causing further reduction in lick rate during drinking and no discernable improvement in tongue strength (Ma et al., 2017). For this reason, we chose to investigate a high-repetition/low-resistance (~40% greater than MVLF) exercise paradigm designed for strength endurance and flexibility (Anderson and Kearney, 1982) that may be more tailored to prevent the characteristic weakened, slowed, fatigued, and limited tongue motion caused by MNDs. Our results thus far show beneficial treatment effects in our rat model, without any harmful outcomes. Moreover, the exercise intensity level was sufficiently low that it did not produce any beneficial effects in control animals (i.e., ‘control’ + ‘sham exercise group’), thus providing evidence that this high-repetition/low-resistance training paradigm is uniquely tailored for degenerating motor neurons. However, given the degenerative underpinnings of our model as well as motor neuron diseases in general, frequent re-evaluation and adjustment of the tongue exercise intensity benchmark will likely be essential to optimize personalized treatment outcomes.

Magnetic Resonance Imaging Detection of Degenerative Changes in the Hypoglossal-Tongue Axis

Here, we hypothesized that structural degeneration in the brainstem and tongue would be detectable with *in vivo* MRI and present in sham exercise-treated CTB-SAP rats based on our previous findings (i.e., hypoglossal motor neuron degeneration and genioglossal myofiber atrophy; Lind et al., 2021), and would be prevented or decreased with tongue exercise. While our observations thus far are based on a small subset of rats and treatment groups, MRI did provide evidence of degeneration in the hypoglossal-tongue axis (i.e., a trend for 4th ventricle enlargement, significantly increased tongue volume and thickness, and marked hyperintensity of the tongue) in response to genioglossal myofiber atrophy (Lind et al., 2021), and these pathological MRI features were somewhat mitigated via tongue exercise in CTB-SAP rats. Importantly, fourth ventricle enlargement is a common feature of neurodegenerative diseases and is correlated with degeneration of the surrounding brain

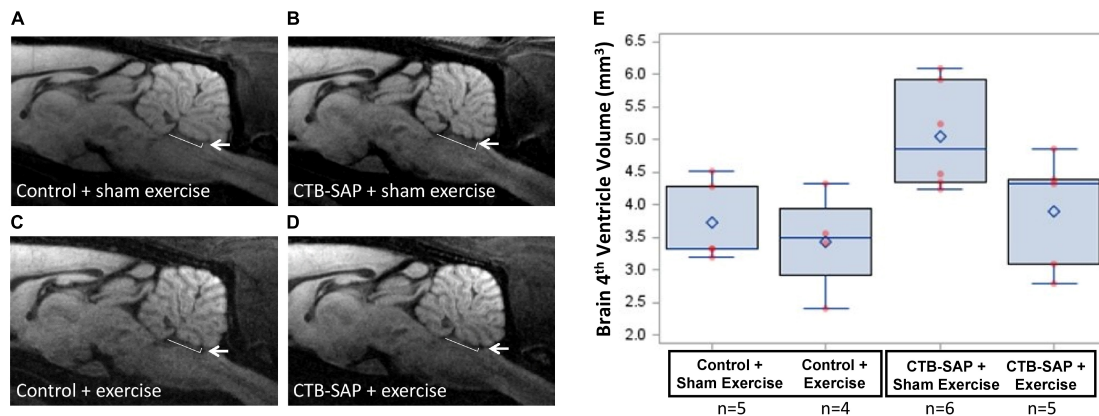


FIGURE 8 | Structural changes in the brainstem in the absence and presence of tongue exercise. **(A–D)** *In vivo* diffusion weighted MRI of brainstem sagittal slice at Bregma position 0.0 mm shows a trend for an enlargement of the 4th ventricle in sham exercise-treated CTB-SAP rats **(B)**, denoted by white arrow) vs. sham exercise-treated controls **(A)**, suggesting degeneration of neighboring brainstem tissue (i.e., XII nucleus). Following tongue exercise, the size of the 4th ventricle (denoted by white arrow) in CTB-SAP rats **(D)** appeared to resemble that of sham exercise-treated **(A)** and exercise-treated **(C)** control rats, suggesting that tongue exercise may prevent or decrease/slow degeneration in CTB-SAP rats and provides sufficient preliminary evidence to continue collecting these non-invasive translational measurements with larger group sample sizes. **(E)** MRI segmented 4th ventricle volume showed no significant differences across groups ($p = 0.075$). Error bars = standard error of the mean; n = group sample size.

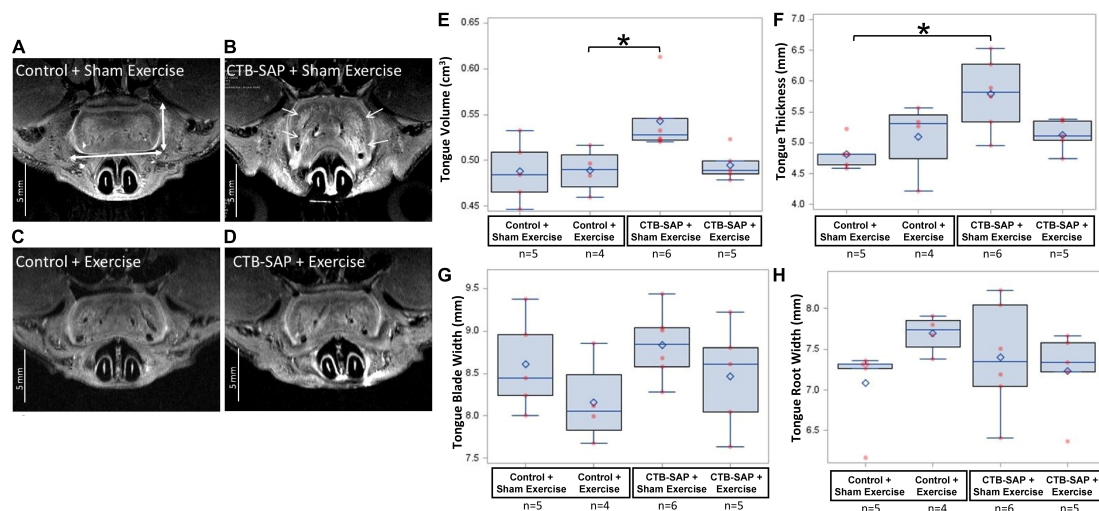


FIGURE 9 | Structural changes in the tongue in the absence and presence of tongue exercise. **(A–D)** *In vivo* T2-weighted MRI of the axial images at the A-P position 4.8 mm from the anterior apex of the tongue shows hyperintensity (i.e., increased brightness, denoted by white arrows) and increased tongue thickness and volume in sham exercise-treated CTB-SAP rats **(B)** vs. sham exercise-treated controls **(A)**, suggesting hypertrophy of the tongue and is consistent with muscle fiber inflammation and fatty replacement of atrophied muscle fibers. Following tongue exercise, tongue thickness, volume, and intensity in CTB-SAP rats **(D)** resembled that of sham exercise-treated and exercise-treated control rats **(A,C)**, suggesting that tongue exercise may prevent or decrease/slow degenerative structural changes in CTB-SAP rats. Tongue thickness and width are indicated by vertical and horizontal double arrows, respectively in **(A)**. **(E)** MRI segmentation of tongue volume showed a significant increase in the 'CTB-SAP + sham exercise' group vs. the 'control + exercise' group ($p = 0.05$) but was not significantly different compared to 'CTB-SAP + exercise' ($p = 0.08$) and 'control + sham exercise' ($p = 0.18$) groups. **(F)** Tongue thickness was significantly increased in the 'CTB-SAP + sham exercise' group vs. the 'control + sham exercise group' ($p = 0.05$). **(G,H)** The tongue blade and root widths were not significantly different across groups ($p = 0.251$ and $p = 0.1805$, respectively). Error bars = standard error of the mean; n = group sample size.

structures (Westeneng et al., 2015; Bede et al., 2019). In the case of ALS, 4th ventricle enlargement is attributed to atrophy of the floor of the fourth ventricle due to degeneration of the hypoglossal and vagal trigones, which are formed by the underlying hypoglossal and vagal nuclei, respectively (Westeneng et al., 2015; Bede et al., 2019). In our CTB-SAP model, only

the hypoglossal nucleus undergoes neurodegeneration (Lind et al., 2018); thus, it is intuitive to speculate that the observed 4th ventricle enlargement is solely due to degeneration of the hypoglossal trigone along the floor of the 4th ventricle. However, we will need to conduct MRI and corresponding histological experiments with larger group sample sizes to

specifically test this hypothesis. Moreover, our MRI findings of diffuse hyperintensity and increased volume and thickness of the tongue are indicative of muscle fiber inflammation and fat infiltrations, which are consistent with denervation atrophy as a consequence of hypoglossal motor neuron degeneration (Alves, 2010; Borges, 2010). These pathological tongue-based MRI findings in our CTB-SAP model remarkably resemble macroglossia in ALS patients (McKee et al., 2013; Hensiek et al., 2020). Thus, our model may be particularly suited for studying pathological muscle changes that remain poorly understood in ALS and other neuromuscular disorders (Theret et al., 2021).

The ability of MRI to detect early degenerative changes in the entire XII axis (brainstem and tongue) of our rat model suggests early MRI detection may likewise be possible in patients with MNDs. Our findings therefore suggest that this non-invasive imaging modality may have untapped clinical potential to facilitate early differential diagnosis of MNDs from other neurological disorders, thus providing opportunity for earlier intervention and objective treatment monitoring when effective treatments become available. Because of its non-invasive nature and wide availability in hospitals, MRI of the tongue and brainstem is readily translatable to future MND clinical trials.

Limitations

Several limitations must be considered when interpreting the results of this study. First, we used overnight water consumption as an indirect measure of lick frequency (i.e., exercise repetitions). We are currently working on incorporating home-cage contact lickometer technology to permit direct measurement of lick frequency for individual rats. Second, we calculated each rat's MVLF during spontaneous drinking in our force-lickometer system, which does not provide a lick-force challenge during testing. In other words, we cannot incrementally increase the force setting to identify each rat's maximum tongue force capacity, which is a capability of other systems (Ciucci et al., 2011, 2013; Cullins and Connor, 2019). As a solution, our future research with this model will include tongue force strain gauge measurements (Nagai et al., 2008; Ciucci et al., 2013) at the study endpoint (Day 9) to determine each rat's maximum lick force for correlation with behavioral findings. Third, the exercise intensity in our study was not strictly controlled between rats, as it ranged from 20 to 53%. This was due to some rats not tolerating the 50% > MVLF setting, as evidence by switching to biting rather than licking behavior. For these cases, we reduced the resisto-spout force setting until rats resumed drinking. To overcome this limitation in future studies, we have been conducting pilot testing using a built-in "exercise force ramp up" period at the start of each overnight treatment, whereby the force setting is increased from 20% to 50% > MVLF in 10% increments every 15–30 min during the first 1.5 h. Our preliminary results suggest this approach prevents conversion to biting behaviors at higher force settings. Thus, we will use this approach to reduce the variability in exercise intensity in our future studies. Fourth, we were surprised to find that tongue exercise did not preserve swallow rate or lick-swallow ratio in CTB-SAP rats. The persistent slower swallow rate and higher lick-swallow ratios suggest that CTB-SAP rats take

longer to accumulate a sufficiently large bolus in the vallecular space to trigger the pharyngeal swallow reflex. While we did not measure bolus size, we could certainly include this VFSS-based outcome measure (Lever et al., 2015a,b; Osman et al., 2020) in our future studies with this model to determine if tongue exercise in CTB-SAP rats results in larger, more normal-sized boluses. Fifth, we did not identify PTT deficits in CTB-SAP rats, which we suspect is a limitation of fluoroscopy frame rate (i.e., 30 fps) in rodents (Lever et al., 2015a,b; Osman et al., 2020). Although not significant, the sham exercise-treated CTB-SAP rats had the longest PTT, and the PTT distribution in exercised CTB-SAP rats was similar to the two control groups, suggesting a potential beneficial effect of tongue exercise on this swallow timing measure. Therefore, we are currently investigating if 60 fps imaging capability may unmask significant PTT deficits in this model to provide another translational outcome measure to objectively quantify treatment response. Finally, we have thus far focused on drinking-related measures of tongue and swallowing function. The tongue is also essential for mastication (Palmer et al., 1992); thus, we expect our rat model of XII LMN degeneration will also develop deficits in mastication and dyscoordination between mastication and swallowing. We will therefore include mastication-based VFSS measures in our future studies with this model.

Significance

This study provides novel evidence in support of tongue exercise as a treatment for dysphagia in MNDs, which currently remains highly controversial in the absence of high rigor investigations (Dworkin and Hartman, 1979; Watts and Vanryckeghem, 2001; Plowman, 2015; Ma et al., 2017). Thus, we will continue utilizing our rat model to optimize tongue exercise dosing parameters and investigate corresponding treatment mechanisms of action for future translation to MND clinical trials. The next step is to leverage our rat model of XII LMN degeneration to optimize dosing parameters that are translatable to humans. While we started this scientific exploration using a 12-h exercise program in rats, we fully acknowledge that translation to humans will require much shorter treatment durations. Thus, our rat model will provide a suitable platform for high throughput investigations of exercise dosing parameters as well as investigations of treatment mechanisms of action for future translation to MND clinical trials. Moreover, we will utilize this model to determine whether targeted tongue exercise is directly impacting the dying versus surviving XII motor neurons, or a combination thereof, which may lead to the discovery of mechanistic targets to effectively delay, slow, or even reverse XII motor neuron degeneration to achieve more impactful clinical outcomes. As such, this research may have scalability to other cranial and/or spinal nerves affected by motor neuron diseases.

DATA AVAILABILITY STATEMENT

The raw data supporting the conclusions of this article will be made available by the authors, without undue reservation.

ETHICS STATEMENT

The animal study was reviewed and approved by University of Missouri Animal Care and Use Committee.

AUTHOR CONTRIBUTIONS

NN, TL, CS, and AK worked on developing and maintaining the model. NN and TL designed the study. EM, RT, KO, NN, and TL organized and maintained the study databases. TL and NN prepared and performed all intralingual injections. EM, RT, KO, and CH performed the behavioral conditioning. EM, RT, KO, and TL performed the videofluoroscopic swallow study (VFSS) testing. EM, RT, MB, CH, AK, and TL analyzed VFSS videos. AH, FB, and TL validated the JawTrack™ software data. EM, RT, and TL performed the force-lickometer testing, analyzed the data, and calculated maximum voluntary lick force (MVLf) percentages. EM, RT, KO, AK, and TL performed overnight exercise. LM, KW, LL, NN, TL, CS, and AK performed the MRI. MG and TL performed the statistical analysis. TL, EM, and NN wrote the initial draft of the manuscript. TL prepared **Figures 1–7** and corresponding figure legends. LM, KW, LL, NN, MG, and TL prepared **Figures 8, 9** and corresponding legends. TL and RT prepared the **Supplementary Videos**. All authors reviewed and approved the manuscript.

REFERENCES

- Alves, P. (2010). Imaging the hypoglossal nerve. *Eur. J. Radiol.* 74, 368–377. doi: 10.1016/j.ejrad.2009.08.028
- Anderson, T., and Kearney, J. T. (1982). Effects of three resistance training programs on muscular strength and absolute and relative endurance. *Res. Q. Exerc. Sport* 53, 1–7. doi: 10.1080/02701367.1982.10605218
- Argolo, N., Sampaio, M., Pinho, P., Melo, A., and Nobrega, A. C. (2013). Do swallowing exercises improve swallowing dynamic and quality of life in Parkinson's disease? *NeuroRehabilitation* 32, 949–955. doi: 10.3233/NRE-130918
- Baumer, D., Talbot, K., and Turner, M. R. (2014). Advances in motor neurone disease. *J. R. Soc. Med.* 107, 14–21.
- Bede, P., Chipika, R. H., Finegan, E., Li Hi Shing, S., Doherty, M. A., Hengeveld, J. C., et al. (2019). Brainstem pathology in amyotrophic lateral sclerosis and primary lateral sclerosis: a longitudinal neuroimaging study. *Neuroimage Clin.* 24:102054.
- Behan, M., Moeser, A. E., Thomas, C. F., Russell, J. A., Wang, H., Levenson, G. E., et al. (2012). The effect of tongue exercise on serotonergic input to the hypoglossal nucleus in young and old rats. *J. Speech Lang. Hear. Res.* 55, 919–929. doi: 10.1044/1092-4388(2011/11-0091)
- Borges, A. (2010). Imaging of denervation in the head and neck. *Eur. J. Radiol.* 74, 378–390. doi: 10.1016/j.ejrad.2009.06.034
- Boughter, J. D. Jr., Baird, J. P., Bryant, J., St John, S. J., and Heck, D. (2007). C57BL/6J and DBA/2J mice vary in lick rate and ingestive microstructure. *Genes Brain Behav.* 6, 619–627. doi: 10.1111/j.1601-183X.2006.00293.x
- Brooks, B. R., Miller, R. G., Swash, M., and Munsat, T. L. (2000). Diseases WFO NRGo MN. El Escorial revisited: revised criteria for the diagnosis of amyotrophic lateral sclerosis. *Amyotroph. Lateral Scler Other Motor Neuron Disord.* 1, 293–299. doi: 10.1080/146608200300079536
- Bruijn, L. I., Miller, T. M., and Cleveland, D. W. (2004). Unraveling the mechanisms involved in motor neuron degeneration in ALS. *Annu. Rev. Neurosci.* 27, 723–749. doi: 10.1146/annurev.neuro.27.070203.144244

FUNDING

This work was funded by a multi-PI (NN and TL) grant from the National Institutes of Health (HL153612), the University of Missouri Research Board (NN, TL, and FB), and the University of Missouri College of Veterinary Medicine Committee on Research (NN and TL). The 7-T MRI equipment was funded by the US Department of Veterans Affairs (VA) – Shared Equipment Evaluation Program (ShEEP) and jointly supported by the University of Missouri and the Harry S. Truman Veterans Memorial Hospital (Columbia, MO, United States).

ACKNOWLEDGMENTS

We graciously thank Sophia Kington for assisting with behavioral testing and health monitoring and providing environmental enrichment for our rats.

SUPPLEMENTARY MATERIAL

The Supplementary Material for this article can be found online at: <https://www.frontiersin.org/articles/10.3389/fnins.2022.869592/full#supplementary-material>

- Ciucci, M. R., Russell, J. A., Schaser, A. J., Doll, E. J., Vinney, L. M., and Connor, N. P. (2011). Tongue force and timing deficits in a rat model of Parkinson disease. *Behav. Brain Res.* 222, 315–320. doi: 10.1016/j.bbr.2011.03.057
- Ciucci, M. R., Schaser, A. J., and Russell, J. A. (2013). Exercise-induced rescue of tongue function without striatal dopamine sparing in a rat neurotoxin model of Parkinson disease. *Behav. Brain Res.* 252, 239–245. doi: 10.1016/j.bbr.2013.06.004
- Connor, N. P., Russell, J. A., Wang, H., Jackson, M. A., Mann, L., and Kluender, K. (2009). Effect of tongue exercise on protrusive force and muscle fiber area in aging rats. *J. Speech Lang. Hear. Res.* 52, 732–744. doi: 10.1044/1092-4388(2008/08-0105)
- Corcia, P., Pradat, P. F., Salachas, F., Bruneteau, G., Forestier, N., Seilhean, D., et al. (2008). Causes of death in a post-mortem series of ALS patients. *Amyotroph. Lateral Scler.* 9, 59–62. doi: 10.1080/17482960701656940
- Cullins, M. J., and Connor, N. P. (2019). Reduced tongue force and functional swallowing changes in a rat model of post stroke dysphagia. *Brain Res.* 1717, 160–166. doi: 10.1016/j.brainres.2019.04.023
- Cullins, M. J., Krekeler, B. N., and Connor, N. P. (2018). Differential impact of tongue exercise on intrinsic lingual muscles. *Laryngoscope* 128, 2245–2251. doi: 10.1002/lary.27044
- Cullins, M. J., Wenninger, J. M., Cullen, J. S., Russell, J. A., Kleim, J. A., and Connor, N. P. (2019). Tongue force training induces plasticity of the lingual motor cortex in young adult and aged rats. *Front. Neurosci.* 13:1355. doi: 10.3389/fnins.2019.01355
- Dworkin, J. P., and Hartman, D. E. (1979). Progressive speech deterioration and dysphagia in amyotrophic lateral sclerosis: case report. *Arch. Phys. Med. Rehabil.* 60, 423–425.
- Glass, T. J., Figueroa, J. E., Russell, J. A., Krekeler, B. N., and Connor, N. P. (2021). Progressive protrusive tongue exercise does not alter aging effects in retrusive tongue muscles. *Front. Physiol.* 12:740876. doi: 10.3389/fphys.2021.740876
- Gonzalez de Aguilar, J. L., Echaniz-Laguna, A., Fergani, A., Rene, F., Meininger, V., Loeffler, J. P., et al. (2007). Amyotrophic lateral sclerosis: all roads lead to Rome. *J. Neurochem.* 101, 1153–1160.

- Grgic, J., Lazinica, B., Schoenfeld, B. J., and Pedisic, Z. (2020). Test–retest reliability of the one-repetition maximum (1RM) strength assessment: a systematic review. *Sports Med. Open* 6:31. doi: 10.1186/s40798-020-00260-z
- Hadjikoutis, S., and Wiles, C. M. (2001). Respiratory complications related to bulbar dysfunction in motor neuron disease. *Acta Neurol. Scand.* 103, 207–213.
- Hensiek, N., Schreiber, F., Wimmer, T., Kaufmann, J., Machts, J., Fahlbusch, L., et al. (2020). Sonographic and 3T-MRI-based evaluation of the tongue in ALS. *NeuroImage Clin.* 26:102233. doi: 10.1016/j.nicl.2020.102233
- Hessert, M. J., Vyas, M., Leach, J., Hu, K., Lipsitz, L. A., and Novak, V. (2005). Foot pressure distribution during walking in young and old adults. *BMC Geriatrics* 5:8. doi: 10.1186/1471-2318-5-8
- Holdstock, T. L. (1973). Body weight and water consumption in rats. *Physiol. Psychol.* 1, 21–23.
- Hsiao, S., and Fan, R. J. (1993). Additivity of taste-specific effects of sucrose and quinine: microstructural analysis of ingestive behavior in rats. *Behav. Neurosci.* 107, 317–326. doi: 10.1037//0735-7044.107.2.317
- Jasiewicz, B., Klimiec, E., Guzek, P., Kolaszczynski, G., Piekarski, J., Zaraska, K., et al. (2022). Investigation of impact of walking speed on forces acting on a foot-ground unit. *Sensors (Basel)* 22:3098. doi: 10.3390/s22083098
- Jean, A. (2001). Brain stem control of swallowing: neuronal network and cellular mechanisms. *Physiol. Rev.* 81, 929–969. doi: 10.1152/physrev.2001.81.2.929
- Kiernan, M. C., Vucic, S., Cheah, B. C., Turner, M. R., Eisen, A., Hardiman, O., et al. (2011). Amyotrophic lateral sclerosis. *Lancet* 377, 942–955.
- Kletzien, H., Russell, J. A., Levenson, G. E., and Connor, N. P. (2013). Differential effects of targeted tongue exercise and treadmill running on aging tongue muscle structure and contractile properties. *J. Appl. Physiol.* (1985) 114, 472–481. doi: 10.1152/japplphysiol.01370.2012
- Krekeler, B. N., Levenson, G., and Connor, N. P. (2018). Tongue exercise and ageing effects on morphological and biochemical properties of the posterior digastric and temporalis muscles in a Fischer 344 Brown Norway rat model. *Arch. Oral Biol.* 89, 37–43. doi: 10.1016/j.archoralbio.2018.02.002
- Krekeler, B. N., Weycker, J. M., and Connor, N. P. (2020). Effects of tongue exercise frequency on tongue muscle biology and swallowing physiology in a rat model. *Dysphagia* 35, 918–934. doi: 10.1007/s00455-020-10105-2
- Kurian, K. M., Forbes, R. B., Colville, S., and Swingler, R. J. (2009). Cause of death and clinical grading criteria in a cohort of amyotrophic lateral sclerosis cases undergoing autopsy from the Scottish Motor Neurone Disease Register. *J. Neurol. Neurosurg. Psychiatry* 80, 84–87. doi: 10.1136/jnnp.2008.149708
- Lazarus, C. (2006). Tongue strength and exercise in healthy individuals and in head and neck cancer patients. *Semin. Speech Lang.* 27, 260–267. doi: 10.1055/s-2006-955116
- Lazarus, C. L., Husaini, H., Falciglia, D., DeLacure, M., Branski, R. C., Kraus, D., et al. (2014). Effects of exercise on swallowing and tongue strength in patients with oral and oropharyngeal cancer treated with primary radiotherapy with or without chemotherapy. *Int. J. Oral Maxillofac. Surg.* 43, 523–530. doi: 10.1016/j.ijom.2013.10.023
- Lazarus, C., Logemann, J. A., Huang, C. F., and Rademaker, A. W. (2003). Effects of two types of tongue strengthening exercises in young normals. *Folia Phoniatr. Logop.* 55, 199–205. doi: 10.1159/000071019
- Lever, T. E., Braun, S. M., Brooks, R. T., Harris, R. A., Littrell, L. L., Neff, R. M., et al. (2015a). Adapting human videofluoroscopic swallow study methods to detect and characterize dysphagia in murine disease models. *J. Vis. Exp.* 97:52319. doi: 10.3791/52319
- Lever, T. E., Brooks, R. T., Thombs, L. A., Littrell, L. L., Harris, R. A., Allen, M. J., et al. (2015b). Videofluoroscopic validation of a translational murine model of Presbyphagia. *Dysphagia* 30, 328–342. doi: 10.1007/s00455-015-9604-7
- Lind, L. A., Lever, T. E., and Nichols, N. L. (2021). Tongue and hypoglossal morphology after intralingual cholera toxin B-saporin injection. *Muscle Nerve* 63, 413–420. doi: 10.1002/mus.27131
- Lind, L. A., Murphy, E. R., Lever, T. E., and Nichols, N. L. (2018). Hypoglossal motor neuron death via intralingual CTB-saporin (CTB-SAP) injections mimic aspects of amyotrophic lateral sclerosis (ALS) related to dysphagia. *Neuroscience* 390, 303–316. doi: 10.1016/j.neuroscience.2018.08.026
- Llewellyn-Smith, I. J., Martin, C. L., Arnolda, L. F., and Minson, J. B. (2000). Tracer-toxins: cholera toxin B-saporin as a model. *J. Neurosci. Methods* 103, 83–90. doi: 10.1016/s0165-0270(00)00298-3
- Lujan, H. L., Palani, G., Peduzzi, J. D., and DiCarlo, S. E. (2010). Targeted ablation of mesenteric projecting sympathetic neurons reduces the hemodynamic response to pain in conscious, spinal cord-transected rats. *Am. J. Physiol. Regul. Integr. Comp. Physiol.* 298, R1358–R1365. doi: 10.1152/ajpregu.00755.2009
- Ma, D., Shuler, J. M., Kumar, A., Stanford, Q. R., Tungtur, S., Nishimune, H., et al. (2017). Effects of tongue force training on bulbar motor function in the female SOD1-G93A rat model of amyotrophic lateral sclerosis. *Neurorehabil. Neural Repair.* 31, 147–156. doi: 10.1177/1545968316666956
- Mangine, G. T., Hoffman, J. R., Gonzalez, A. M., Townsend, J. R., Wells, A. J., Jajtner, A. R., et al. (2015). The effect of training volume and intensity on improvements in muscular strength and size in resistance-trained men. *Physiol. Rep.* 3:e12472. doi: 10.14814/phy2.12472
- Mantilla, C. B., Zhan, W. Z., and Sieck, G. C. (2009). Retrograde labeling of phrenic motoneurons by intrapleural injection. *J. Neurosci. Methods* 182, 244–249. doi: 10.1016/j.jneumeth.2009.06.016
- McKee, H. R., Escott, E., Damm, D., and Kasarskis, E. (2013). Macroglossia in amyotrophic lateral sclerosis. *JAMA Neurol.* 70, 1432–1435.
- Mitchell, J. D., and Borasio, G. D. (2007). Amyotrophic lateral sclerosis. *Lancet* 369, 2031–2041.
- Moore, J. D., Kleinfeld, D., and Wang, F. (2014). How the brainstem controls orofacial behaviors comprised of rhythmic actions. *Trends Neurosci.* 37, 370–380. doi: 10.1016/j.tins.2014.05.001
- Nagai, H., Russell, J. A., Jackson, M. A., and Connor, N. P. (2008). Effect of aging on tongue protrusion forces in rats. *Dysphagia* 23, 116–121. doi: 10.1007/s00455-007-9103-6
- Nandikolla, V. K., Bochen, R., Meza, S., and Garcia, A. (2017). Experimental gait analysis to study stress distribution of the human foot. *J. Med. Eng.* 2017:3432074. doi: 10.1155/2017/3432074
- National Institute of Neurological Disorders and Stroke [NIH] (2019). Motor Neuron Diseases Fact Sheet. Available online at: <https://www.ninds.nih.gov/Disorders/Patient-Caregiver-Education/Fact-Sheets/Motor-Neuron-Diseases-Fact-Sheet> (accessed August 13, 2019).
- Osman, K. L., Kohlberg, S., Mok, A., Brooks, R., Lind, L. A., McCormack, K., et al. (2020). Optimizing the translational value of mouse models of ALS for dysphagia therapeutic discovery. *Dysphagia* 35, 343–359. doi: 10.1007/s00455-019-10034-9
- Palmer, J. B., Rudin, N. J., Lara, G., and Crompton, A. W. (1992). Coordination of mastication and swallowing. *Dysphagia* 7, 187–200.
- Park, J. S., Kim, H. J., and Oh, D. H. (2015). Effect of tongue strength training using the Iowa Oral Performance Instrument in stroke patients with dysphagia. *J. Phys. Ther. Sci.* 27, 3631–3634. doi: 10.1589/jpts.27.3631
- Plowman, E. K. (2015). Is there a role for exercise in the management of bulbar dysfunction in amyotrophic lateral sclerosis? *J. Speech Lang. Hear. Res.* 58, 1151–1166. doi: 10.1044/2015_JSLHR-S-14-0270
- Rattray, I., Smith, E. J., Crum, W. R., Walker, T. A., Gale, R., Bates, G. P., et al. (2017). Correlations of behavioral deficits with brain pathology assessed through longitudinal MRI and histopathology in the HdhQ150/Q150 mouse model of Huntington's disease. *PLoS One* 12:e0168556. doi: 10.1371/journal.pone.0168556
- Ravits, J., Appel, S., Baloh, R. H., Barohn, R., Brooks, B. R., Elman, L., et al. (2013). Deciphering amyotrophic lateral sclerosis: what phenotype, neuropathology and genetics are telling us about pathogenesis. *Amyotroph. Lateral Scler. Frontotemporal Degener.* 14(Suppl. 1), 5–18. doi: 10.3109/21678421.2013.778548
- Robbins, J., Gangnon, R. E., Theis, S. M., Kays, S. A., Hewitt, A. L., and Hind, J. A. (2005). The effects of lingual exercise on swallowing in older adults. *J. Am. Geriatr. Soc.* 53, 1483–1489. doi: 10.1111/j.1532-5415.2005.53467.x
- Robbins, J., Kays, S. A., Gangnon, R. E., Hind, J. A., Hewitt, A. L., Gentry, L. R., et al. (2007). The effects of lingual exercise in stroke patients with dysphagia. *Arch. Phys. Med. Rehabil.* 88, 150–158. doi: 10.1016/j.apmr.2006.11.002
- Salvadores, N., Sanhueza, M., Manque, P., and Court, F. A. (2017). Axonal degeneration during aging and its functional role in neurodegenerative disorders. *Front. Neurosci.* 11:451. doi: 10.3389/fnins.2017.00451
- Sheikh, A. M., and Vissing, J. (2019). Exercise therapy for muscle and lower motor neuron diseases. *Acta Myol.* 38, 215–232.
- Smittkamp, S. E., Spalding, H. N., Brown, J. W., Gupta, A. A., Chen, J., Nishimune, H., et al. (2010). Measures of bulbar and spinal motor function, muscle

- innervation, and mitochondrial function in ALS rats. *Behav. Brain Res.* 211, 48–57. doi: 10.1016/j.bbr.2010.03.007
- Steele, C. M., Bailey, G. L., Polacco, R. E., Hori, S. F., Molfenter, S. M., Oshalla, M., et al. (2013). Outcomes of tongue-pressure strength and accuracy training for dysphagia following acquired brain injury. *Int. J. Speech Lang. Pathol.* 15, 492–502. doi: 10.3109/17549507.2012.752864
- Theret, M., Rossi, F. M. V., and Contreras, O. (2021). Evolving roles of muscle-resident fibro-adipogenic progenitors in health, regeneration, neuromuscular disorders, and aging. *Front. Physiol.* 12:673404. doi: 10.3389/fphys.2021.673404
- Tiryaki, E., and Horak, H. A. (2014). ALS and other motor neuron diseases. *Continuum (Minneapolis)* 20, 1185–1207.
- Tsitkanou, S., Della Gatta, P., Foletta, V., and Russell, A. (2019). The role of exercise as a non-pharmacological therapeutic approach for amyotrophic lateral sclerosis: beneficial or detrimental? *Front. Neurol.* 10:783. doi: 10.3389/fneur.2019.00783
- Turner, M. R., Hardiman, O., Benatar, M., Brooks, B. R., Chio, A., de Carvalho, M., et al. (2013). Controversies and priorities in amyotrophic lateral sclerosis. *Lancet Neurol.* 12, 310–322. doi: 10.1016/S1474-4422(13)70036-X
- Waito, A. A., Valenzano, T. J., Peladeau-Pigeon, M., and Steele, C. M. (2017). Trends in research literature describing dysphagia in motor neuron diseases (MND): a scoping review. *Dysphagia* 32, 734–747.
- Wang, C. M., Shieh, W. Y., Ho, C. S., Hu, Y. W., and Wu, Y. R. (2018). Home-based orolingual exercise improves the coordination of swallowing and respiration in early Parkinson disease: a quasi-experimental before-and-after exercise program study. *Front. Neurol.* 9:624. doi: 10.3389/fneur.2018.00624
- Watts, C. R., and Vanryckeghem, M. (2001). Laryngeal dysfunction in Amyotrophic Lateral Sclerosis: a review and case report. *BMC Ear Nose Throat Disord.* 1:1. doi: 10.1186/1472-6815-1-1
- Welby, L., Caudill, H., Yitsege, G., Hamad, A., Bunyak, F., Zohn, I. E., et al. (2020). Persistent feeding and swallowing deficits in a mouse model of 22q11.2 deletion syndrome. *Front. Neurol.* 11:4. doi: 10.3389/fneur.2020.00004
- Westeneng, H. J., Verstraete, E., Walhout, R., Schmidt, R., Hendrikse, J., Veldink, J. H., et al. (2015). Subcortical structures in amyotrophic lateral sclerosis. *Neurobiol. Aging* 36, 1075–1082.
- Yeates, E. M., Molfenter, S. M., and Steele, C. M. (2008). Improvements in tongue strength and pressure-generation precision following a tongue-pressure training protocol in older individuals with dysphagia: three case reports. *Clin. Interv. Aging* 3, 735–747. doi: 10.2147/cia.s3825
- Conflict of Interest:** The authors declare that the research was conducted in the absence of any commercial or financial relationships that could be construed as a potential conflict of interest.
- Publisher's Note:** All claims expressed in this article are solely those of the authors and do not necessarily represent those of their affiliated organizations, or those of the publisher, the editors and the reviewers. Any product that may be evaluated in this article, or claim that may be made by its manufacturer, is not guaranteed or endorsed by the publisher.

Copyright © 2022 Murphy, Thompson, Osman, Haxton, Brothers, Lee, Warncke, Smith, Keilholz, Hamad, Golzy, Bunyak, Ma, Nichols and Lever. This is an open-access article distributed under the terms of the Creative Commons Attribution License (CC BY). The use, distribution or reproduction in other forums is permitted, provided the original author(s) and the copyright owner(s) are credited and that the original publication in this journal is cited, in accordance with accepted academic practice. No use, distribution or reproduction is permitted which does not comply with these terms.

Advantages of publishing in Frontiers



OPEN ACCESS

Articles are free to read
for greatest visibility
and readership



FAST PUBLICATION

Around 90 days
from submission
to decision



HIGH QUALITY PEER-REVIEW

Rigorous, collaborative,
and constructive
peer-review



TRANSPARENT PEER-REVIEW

Editors and reviewers
acknowledged by name
on published articles

Frontiers

Avenue du Tribunal-Fédéral 34
1005 Lausanne | Switzerland

Visit us: www.frontiersin.org

Contact us: frontiersin.org/about/contact



REPRODUCIBILITY OF RESEARCH

Support open data
and methods to enhance
research reproducibility



DIGITAL PUBLISHING

Articles designed
for optimal readership
across devices



FOLLOW US

@frontiersin



IMPACT METRICS

Advanced article metrics
track visibility across
digital media



EXTENSIVE PROMOTION

Marketing
and promotion
of impactful research



LOOP RESEARCH NETWORK

Our network
increases your
article's readership